American Society of Biomechanics

FOUNDED IN 1977

ABSTRACT BOOK

ASB Annual Meeting

AUGUST 8 – 11 2023

Knoxville Convention Centre

Knoxville, TN

www.asbweb.org

THE EFFECT OF CONCUSSION AND ANTERIOR CRUCIATE LIGAMENT INJURY HISTORY ON THIGH MUSCULATURE MOTOR CONTROL

April L. McPherson[1,2*], Nathaniel A. Bates[1], Takashi Nagai[3], Christopher V. Nagelli,[4] Nathan D. Schilaty[5]
[1]The Ohio State University, Columbus, OH; [2]Emory SPARC, Flowery Branch, GA; [3]United States Army Research Institute of Environmental Medicine, Natick, MA; [4]Mayo Clinic, Rochester, MN; [5]University of South Florida, Tampa, FL
*Corresponding author's email: April.mcpherson@osumc.edu

Introduction: An estimated >1.6 million sports-related concussions (SRC) annually comprise 13% of all sports injuries. Recent literature has established an increased risk of lower extremity musculoskeletal (LE MSK) injury after SRC.[1] This increased risk of LE MSK injury suggests there is a gap in return to sport protocols after SRC that fail to identify an apparent lingering motor control or neuromuscular deficit that contribute to future injury risk. Additional studies have demonstrated altered biomechanics in concussed individuals compared to control subjects[2], but there lacks prospective longitudinal studies that indicate any potential mechanism linking SRC to future LE MSK injury risk. However, it has been suggested that SRC alters motor control, in addition to neuroanatomic and neurophysiological function, and may be associated with LE MSK injury risk.[3]

Previous work has demonstrated altered motor control via assessment of motor unit (MU) activity in ACL-injured populations [4] and in healthy athletes after subconcussive head impacts.[5] However, to do date, no study has investigated the effect of each injury (SRC, ACL tear) independently on motor control strategies, and the combined effect of both injuries (SRC+ACL). The purpose of this study was to investigate motor control of the LE via decomposed electromyography, which allows for analysis of motor unit (MU) activity. We hypothesized that subjects with history of SRC (CONC) would have decreased motor control compared to healthy controls (CTRL).

Methods: Participants' health history was assessed for SRC history to determine groups after obtaining consent (assent if applicable): CTRL (18.8±3.4 years; 173.4±8.2 cm; 65.3±12.2 kg), CTRL+CONC (18.8±1.6 years; 176.3±10.4 cm; 76.7±15.5 kg; time from SRC 2127 [641,2707] days), ACL (19.6±2.7 years; 175.8±9.5 cm; 80.0±16.0 kg; time from ACL 32 [19,135] days), and CONC+ACL (18.9±3.4 years; 172.8±8.6 cm; 75.8±14.9 kg; time from SRC 1608 [725,2262] days; time from ACL 51 [21,196] days). Data collections were performed with subjects positioned in a dynamometer (HumacNORM; CSMi, Stoughton, MA, USA). A custom load cell apparatus (MLP-300; Transducer Techniques, Temecula, CA, USA) was affixed to the dynamometer torque arm to measure subjects' isometric force production required for EMG decomposition software (*dEMG Analysis*; Delsys, Natick, MA, USA). dEMG electrodes (Bagnoli; Delsys, Natick, MA, USA) were placed on the muscle belly of quadriceps and hamstrings musculature for extension and flexion testing (10-50% maximal effort). Statistical analyses were performed with *JMP Pro 16* (SAS Institute Inc., Cary, NC, USA). We calculated an interaction variable (AvgFR*MUAP) to represent overall MU function that was compared between groups by recruitment threshold with standard least squares regression and least square means ANOVA. Tukey's HSD post-hoc comparisons were utilized. Significance was set *a priori* at $p<0.05$.

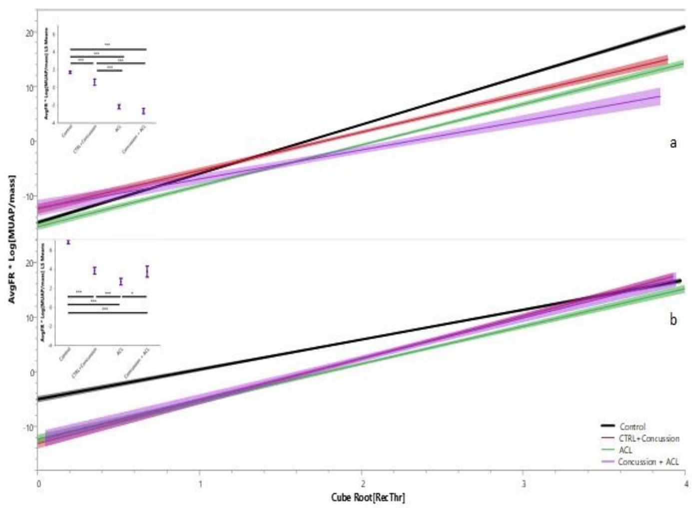

Figure 1: a) Quadriceps and b) Hamstrings AvgFR*MUAP by Recruitment Threshold. (* = $p<0.05$; *** = $p<0.001$; line shading and error bars denote 95% confidence intervals of the mean.)

Results & Discussion: All groups demonstrated decreased motor control for quadriceps (**Fig. 1a**, $R^2=0.39$, p<0.001) and hamstrings (**Fig. 1b**, $R^2=0.\ 27$, p<0.01) compared to CTRL. For quadriceps, motor control was significantly worse for ACL and CONC+ACL compared to CTRL+CONC (p<0.001), but there was no significant difference between ACL and CONC+ACL (p=0.09). For hamstrings, motor control was significantly worse for ACL compared to CTRL+CONC (p<0.001), but there was no significant difference between CTRL+CONC and CONC+ACL (p=0.99).

The results support the hypothesis and demonstrate altered motor control of the LE musculature in previously concussed participants, despite being years removed from SRC, compared to those with no previous history of SRC. This may suggest that SRC causes neuroplastic changes that influence motor control long-term. These findings are an important consideration for future investigations that seek to identify mechanisms that contribute to the increased risk of LE MSK injury after SRC.

Significance: This study begins to address the gap in knowledge necessary to advance clinical understanding of LE motor control changes that follow SRC. Future studies could investigate how interventions could target altered motor control patterns and the impact on subsequent LE MSK injury risk after SRC.

Acknowledgements: The authors acknowledge the support of NIH grants R01AR056259, K12HD065987, L30AR070273, the Florida Department of State Center for Neuromusculoskeletal Research, and the Mayo Clinic Ultrasound Research Center.

References: [1] McPherson (2019) *Am J Sports Med* 47(7); [2] Avedesian (2020) *J Appl Biomech* 36(5); [3] Chmieklewski (2021) *J Sport Health Sci* 10(2). [4] McPherson (2022) *Eu J Sport Sci* epub.; [5] Di Virgilio (2019) *Front Hum Neurosci* 13.

COMPARING JOINT MECHANICS AND MUSCLE ACTIVITY BETWEEN LEVEL AND INCLINE WALKING IN CEREBRAL PALSY

Ying Fang[1*], Zachary F. Lerner[1,2]
[1]Department of Mechanical Engineering, Northern Arizona University, Flagstaff, AZ 86011, USA
[2]Department of Orthopaedics, the University of Arizona College of Medicine-Phoenix, Phoenix, AZ 85004, USA
*Corresponding author's email: ying.fang@rosalindfranklin.edu

Introduction: Cerebral palsy (CP) is the most common childhood disability [1]. It often causes lower limb muscle weakness and dysfunction that affects mobility and quality of life [2]. Incline walking is a promising gait rehabilitation exercise [3]. However, existing gait analyses on inclines are limited to healthy individuals [4]. Before incline walking is safely and effectively implemented in clinical settings, a thorough biomechanical evaluation is needed for people with impairment, including CP. The **purpose** of this study is to compare joint mechanics and lower limb muscle activity between level and incline walking in CP. We hypothesize that people with CP would walk with greater joint moment and power, and increased lower limb muscle activity on inclines compared to level ground.

Methods: Twelve participants with CP (Table 1) completed two one-minute walks at preferred speed on a treadmill (Bertec), one on level ground and one on 5° incline. We collected motion, force, and muscle activity of the soleus, medial gastrocnemius, tibialis anterior, vastus lateralis, rectus femoris, and biceps femoris for the more affected limb. Joint angles and moments were derived in OpenSim 3.3. Stance phase average positive joint power and integrated electromyography (iEMG) for a gait cycle were calculated. Outcomes were averaged by all gait cycles within the trial. Paired two-tailed t-tests ($\alpha \leq 0.05$) were used to assess differences between the two conditions.

Table 1. Participant Characteristics.

GMFCS Level	Number	Sex (male/female)	Age (years)	Mass (kg)	Height (m)	Speed (m)	Affected Side (R/L)
I	5	4/1	14 ± 3.4	48.3 ± 15.8	1.56 ± 0.2	0.88 ± 0.19	4/1
II	5	5/0	23.1 ± 11.3	58.6 ± 11	1.68 ± 0.1	0.98 ± 0.13	4/1
III	2	0/2	18.9 ± 7.5	39.8 ± 20.3	1.2 ± 0.74	0.55 ± 0.35	1/1

GMFCS: Gross Motor Function Classification System.

Results & Discussion: Participants walked with greater peak ankle dorsiflexion and smaller peak ankle plantarflexion on inclines compared to level ground ($p \leq 0.028$). This is expected because an inclined surface put ankle joint at a more dorsiflexed position throughout the gait cycle. Peak hip extension and ankle plantarflexion moment increased by 22% and 6% ($p \leq 0.001$), respectively, for incline compared to level walking. This was consistent with findings from healthy adults (20% and 13% increased moment for hip and ankle, respectively) [5]. Similarly, our CP participants walked with greater hip, knee, and ankle power during incline compared to level walking ($p \leq 0.011$; Fig. 1), which was similar to unimpaired findings (113%, 68%, and 29% increase in hip, knee, and ankle power, respectively) [6]. The increases in ankle moment and power were smaller in CP versus healthy population, supporting literature that ankle dysfunction is common in CP and should be targeted in gait training [2].

Participants had increased muscle activity in incline vs level walking for major muscles around ankle and knee joints ($p \leq 0.014$; Fig. 2). This is consistent with unimpaired findings [4] and supports the use of incline walking to target muscle weakness.

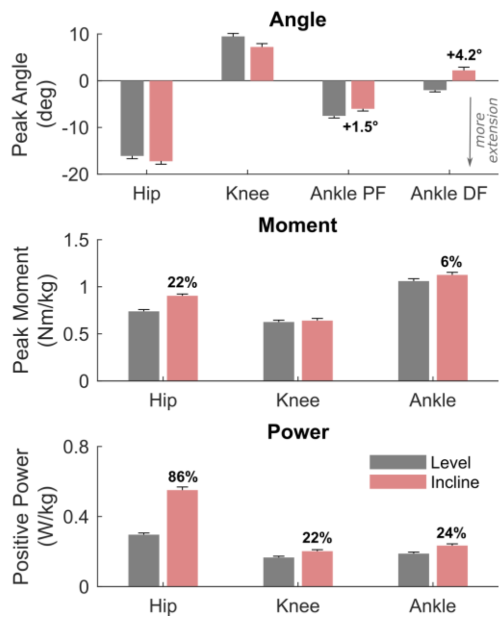

Figure 1: Lower limb peak extension angle and moment, and stance phase average positive power in level and incline walking. PF: plantarflexion; DF: dorsiflexion. Values indicate significant differences between incline and level walking. Error bar represents standard error.

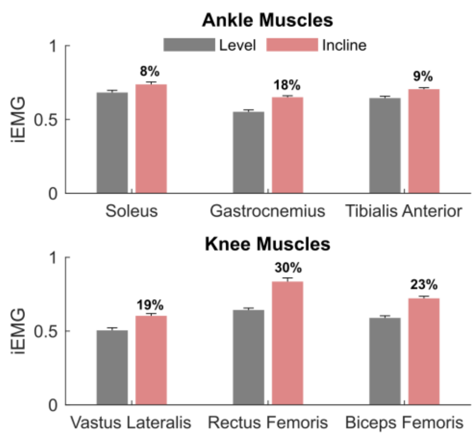

Figure 2: Integrated electromyography (iEMG) of lower limb muscles in level and incline walking. Values indicate significant differences between incline and level walking.

Significance: Understanding incline gait mechanics in CP is fundamental to designing an effective rehabilitation protocol. Our data suggested that incline walking could be a functional gait training exercise that also improves muscle strength and power. Some other tools (coaching or biofeedback) may be needed to help patients maintain a proper gait, i.e., focusing on engaging the ankle joint.

Acknowledgments: This project was supported by the National Institutes of Health under Award Number F32HD109018.

References: [1]Stavsky et al. (2017), *Front Pediatr* 5(21). [2]Riad et al. (2008), *Gait Posture* 27(4). [3]Willerslev-Olsen et al. (2014), *NeuroRehabilitation* 35(4). [4]Franz et al. (2012), *Gait Posture* 35(1). [5] Haggerty et al. (2014), *Gait Posture* 38(4). [6]Nuckols et al. (2020), *PLoS One* 15(8).

THE RELATIVE IMPACT OF CARBON FIBER PLATES AND FIT ON PERFORMANCE

Adam Luftglass[1*], Eric Honert[1], Daniel Feeney[1]
[1]Performance Fit Laboratory, BOA Technology Inc., Denver, Colorado, USA
*Corresponding author's email: adam.luftglass@boatechnology.com

Introduction: Carbon fiber plates [1] and the fit of footwear [2,3] impact biomechanical performance in running and agility movements, however, the relative impact of these technologies have not been examined together. The purpose of this study was to understand the relative impact that a carbon plate and improved fit through alteration of the upper has on biomechanical outcomes in running and agility movements.

Figure 1: The Speedland HSV modified with laces (left) and the dual dial Speedland (right)

Methods: Twelve male runners with a recent 5K time faster than 20 min and 12 male athletes that participate in sports requiring agility movements participated in this study on separate days. We tested four footwear conditions built around the Speedland HSV: dual-dial BOA with the carbon plate (DDP), dual-dial BOA without the carbon plate (DD), laced with the carbon plate (LaceP), and laced without the carbon plate (Lace). For run testing, subjects ran at 3.0 m/s for six minutes in each shoe a randomized counterbalanced order (i.e., A-B-C-D-D-C-B-A). Energy expenditure per minute was estimated using indirect calorimetry and averaged over the final two minutes of each trial. During agility testing, the subjects completed 8 lateral skater jumps in each shoe twice in a randomized counterbalanced order while collecting lower limb kinematics (Vicon) and ground reaction forces (AMTI). Peak propulsive force, peak positive distal foot, and positive distal ankle powers were calculated from the lateral skater jumps. Qualitative rankings were taken to determine the preferred footwear conditions for each participant. All dependent variables were entered into a hierarchical linear mixed effects model with random intercepts for each subject and random slopes for each condition (i.e., Biomechanical Outcome ~ Shoe Condition + (Shoe Condition|Subject). The estimated marginal mean, standard error, and 95% confidence intervals are presented for each coefficient relative to the baseline Lace condition. Additionally, we examined interaction effect between fit and carbon plate in each model.

Results & Discussion: During running, the Lace with no plate condition increased the energy expenditure relative to the other conditions by approximately 1%. There were no meaningful differences between the LaceP, DDP, and DD conditions in energetic expenditure. Improving the fit of a shoe has a similar impact to energetic expenditure to adding a plate. Optimization of shoe fit and its interaction with the geometry of a carbon plate could lead to improved metabolic performance. Taken together, the impact of carbon-fiber plates in agility movements increased peak propulsive force modestly while the impact of going from lace to dual dial increased peak propulsive force by a larger margin. The increased force observed with improved fit and carbon fiber plate depended on the upper configuration. Athletes generated the greatest peak propulsive force in the DDP condition, and had the highest ratio of ankle power to foot power. In DD alone, athletes generated the most distal rearfoot power. Both laced conditions were similar: athletes generated most of their power at the ankle relative to the foot. No interactions were observed between fit and carbon plate in the outcomes. Qualitatively, the DDP ranked the highest, followed by DD; Lace and LaceP ranked similarly as the worst. In agility-based movements, the combination of a plate and improved fit leads to improved lateral propulsive force. These results indicate improved fit increases lateral agility performance more than simply adding a plate. Adding a plate does not impact distal rearfoot power in laced conditions, while a plate decreases distal rearfoot power and increases ankle power in the dual dial conditions. We hypothesize that improving performance through footwear requires optimizing the timing, rate, and direction of force relevant to a given task. Exploring the power that the foot shoe complex produces (i.e., distal rearfoot power) during lateral movements is important to consider when analysing the effects of footwear on agility performance. The magnitude of power production at the foot can give an indication of strategy changes and biomechanical adaptations to movement in a lateral direction.

Table 1: Estimated Marginal Means, Standard Errors, and Confidence Intervals for Outcome Variables

	Running	Skater		
Configuration	Energetic Expenditure (kcal/min)	Peak Propulsive Force (N)	Peak Positive Distal Foot Power (W)	Peak Positive Ankle Power (W)
DDP	14.8 (0.33) 14.65 – 14.92)	1234 (31.3) 1220.2 – 1248.3)	134 (11.1) (119 – 146.8)	465 (35.3) (451.5 – 478.3)
DD	14.7 (0.33) (14.6 – 14.88)	1231(31.3) (1217.1 – 1245)	155 (11) (132.2 – 175)	447 (35.3) 439.5 – 473.1)
LaceP	14.8 (0.33) (14.65 – 14.92)	1227 (31.3) 1213.4 – 1241.4)	140 (11) (118.5 – 146.2)	476 (35.3) (464.5 – 497.9)
Lace	14.9 (0.33) (14.2 – 15.5)	1225 (31.3) (1160.1 – 1289.2)	140 (11.1) (125.3 - 176.4)	473 (35.3) (398.0 – 538.2)

Significance: This research explores the effects of both the fit of the upper and adding a carbon-fiber plate to the midsole in agility-based movements and running. The results support previous research that alternative shoe uppers positively impact performance [2,3]. Improving fit and adding a carbon plate results in similar improvements in running economy. In agility movements, adding a plate may be useful, but the impact of fit was more important.

References: 1. Joubert et al. (2022), *Footwear Science* 14(2) 2. Harrison et al. (2021), *Footwear Science* 13(1), 3. Honert et al. (2023), *Frontiers in Sports and Active Living*

STABILITY ANALYSIS FOR QUANTITATIVE ASSESSMENT OF PROGRESSIVE SUPRANUCLEAR PALSY AFFECTED GAIT

Sandesh G. Bhat Ph.D.[1*], Farwa Ali M.B.B.S. [1], Cecilia A. Hogen M.S.[1], Keith A. Josephs M.D. [1], Jennifer Whitwell Ph. D. [1], Kenton R. Kaufman Ph.D.[1]
[1]Mayo Clinic, Rochester, MN
*Corresponding author's email: bhat.sandesh@mayo.edu

Introduction: Progressive Supranuclear Palsy (PSP), is a rapidly progressing, fatal neurodegenerative disease characterized by early onset of severe gait and balance abnormalities. Gait and balance abnormalities in PSP are currently assessed using clinical scales such as the Unified Parkinson's Disease Rating scale (UPDRS) part III and the PSP rating scale (PSPRS). These scales provide an aggregated assessment of overall disease severity. However, there is a lack of objective metrics that specifically quantify imbalance which is the most disabling manifestation of PSP. Gait is a dynamical system which can be modeled as an inverted pendulum with perturbations [1]. Dynamical system analysis techniques like the Lyapunov-Floquet (L-F) theory have been applied to quantify dynamic stability during walking [2, 3] and the stability of abnormal gait [4]. L-F theory provides an objective method of assessing gait instability in the PSP population. Hence, we hypothesize that the metrics derived by applying the L-F theory are different for healthy gait compared to PSP affected gait and are correlated to the current clinical outcome measures used for assessing PSP.

Methods: 9 healthy subjects (Control group) and 10 PSP patients (PSP group) were studied. 3D trajectory data for the markers placed on the heel (RHEE, LHEE), and posterior and anterior iliac crest on both sides (RPSI, LPSI, RASI, and LASI) were collected at 120Hz with a 10-camera motion capture system (Raptor 12HS, Motion Analysis Corporation, Rohnert Park, CA) while subjects walked on level ground (10m in length) for 6 trials. The average of the RPSI, LPSI, RASI, and LASI markers was considered a surrogate center of mass (sCoM) and the average of the RHEE and LHEE markers was considered a surrogate center of pressure (sCoP) [5]. The lateral trajectory for the sCoM relative to the average lateral trajectory of the sCoP was calculated and mean normalized ($y_{pendulum}$). All 6 trials were stitched together (matching the value of the data and its derivative between the end of one trial to the start of the next trial) and filtered for noise (lowpass Butterworth filter with a cutoff of 10 Hz) to form a longer dataset ($Y_{pendulum}$). The UPDRS-III and PSPRS scores were collected for the PSP group. The $Y_{pendulum}$ and its derivative were assumed to be periodic with a period of one gait cycle. The system was defined as $m(t) = [Y_{pendulum}, \dot{Y}_{pendulum}]$. Using time-delayed embedding, system estimation was performed to obtain the system $M(t) = [m(t), m(t+\tau), m(t+2\tau), \ldots, m(t+n\tau)]$ where τ was the time delay, and n was the embedding dimension. The monodromy matrix for the system was calculated as $\Phi(T) = M(T)M^{-1}(0)$. The absolute value of the Floquet multipliers (FM; eigenvalues of $\Phi(T)$) and the real part of the Floquet exponents (eigenvalues of $R = (\log(\Phi(T))/T)$), called the Lyapunov exponents (LE), were calculated. A dynamical system is considered stable if $|FM| \leq 1$. The LE is used to analyze the chaotic behaviour of dynamical systems and the rate at which the system approaches/diverges from its attractor/repeller respectively. Both FM and LE were compared between groups using the Kruskal Wallis test. Correlation between the FM and LE compared to UPDRS-III and PSPRS scores was tested using the Spearman's rank correlation coefficient.

Results & Discussion: The $|FM|_{avg}$ and LE_{avg} for the Control group were 0.761 and -0.274, and for the PSP group were 0.682 and -0.318 respectively. The FM was significantly different for the control group compared to the PSP group (χ^2 = 4.945; p = 0.026). The LE was similar for both groups (χ^2 = 2.4967; p = 0.114). Hence, the gait of healthy individuals was more stable and closer to an asymptotically stable system compared to the PSP patients. Since the LE was similar and negative, the gait for both the Control and PSP groups was converging towards the attractor event (standing still). Within the PSP group, the UPDRS-III scores were moderately correlated to both the FM (rho = 0.473; p = 0.035) and LE (rho = 0.479; p = 0.033). PSPRS was not significantly correlated to either FM (rho = 0.370; p = 0.109) or LE (rho = 0.436; p = 0.055). Therefore, the FM may offer a novel quantifiable measure of gait instability and imbalance in PSP. It also correlates with disease severity as measured by UPDRS. It offers the benefit of purely representing gait instability as opposed to clinical scales that are an aggregated score of various motor domains (slowness, tremor, rigidity). L-F theory has been shown to capture imbalance in other neurological gait disorders such as multiple sclerosis [6] and cerebellar ataxia [7] and has been shown to identify fall-prone individuals [8]. Existing objective measures of imbalance in PSP include measures of static balance such as postural sway, which do not capture dynamic balance while walking where most falls occur [9]. In this pilot study, we describe a novel application of the L-F theory to the PSP patient population and identify a measure of gait instability.

Significance: Current methods to assess imbalance and postural instability in PSP are largely qualitative clinical scales with subjective assessments of balance. We present a novel metric of gait instability in PSP which could serve as a clinical outcome measure to specifically assess imbalance in PSP.

Acknowledgements: The study was supported by the grants NIH NINDS R01 NS089757 and NIH NINDS K23 NS124688.

References: [1] Kuo, A.D.(2007) Hum. Mov. Sci., 26(4): 617-656; [2] Bhat, S.G., et al.(2021) J. of Mech. & Robotics, 13(6); [3] Dingwell, J., et al.(2001) J. Biomech. Eng., 123(1): 27-32; [4] Bruijn, S.M., et al.(2013) J. R. Soc. Interface, 10(83): 20120999; [5] Granata, K.P., et al.(2008) J. Electromyogr. Kinesiol., 18(2): 172-178; [6] Caronni, A., et al.(2020) IEEE T. Neur. Sys. Reh., 28(6): 1389-1396; [7] Chini, G., et al.(2017) The Cerebellum, 16(1): 26-33; [8] Reynard, F., et al.(2014) PloS one, 9(6): e100550; [9] Dale, M.L., et al.(2022) Front. Neurol., 13: 801291.

FINITE ELEMENT ANALYSIS OF ACROMIAL FRACTURE RISK AFTER REVERSE SHOULDER ARTHROPLASTY

Joshua E. Johnson[1], Maria F. Bozoghlian[1], Brendan M. Patterson[1], Donald D. Anderson[1*]
[1]Department of Orthopedics & Rehabilitation, University of Iowa, Iowa City, IA
*Corresponding author's email: don-anderson@uiowa.edu

Introduction: Traditional reverse shoulder arthroplasty (RSA) designs medialize and distalize the center of rotation of the reconstructed glenohumeral joint.[1] Contemporary RSA designs have focused on increased glenoid lateralization to improve impingement-free range of motion. Humeral stem designs now also feature onlay constructs that can further distalize and lateralize the humerus. As a result, surgeons have more options for maximizing range of motion and functional outcome following RSA, but the effects of combined glenoid and humeral lateralization and distalization on acromial stresses are poorly understood. Increased soft tissue tensions may increase the risk of acromial stress fractures.[2] The purpose of this study was to define the relative changes in acromial stresses and risk of fracture for variations in glenoid lateralization with inlay versus onlay humeral constructs in RSA.

Methods: A validated finite element model of RSA [3] was modified to incorporate the Stryker/Tornier Perform Humeral Stem in both inlay and onlay configurations (Figure 1). A 36 mm glenosphere was used, and variations in glenoid lateralization from 3 mm to 9 mm were evaluated. Deformable soft tissues were assigned isotropic, linear elastic homogenous properties as reported previously.[3] The deltoid muscle was held fixed at its bony origin/insertion sites. The subscapularis tendon was tensioned and wrapped around the glenohumeral joint prior to motion simulation by pulling its proximal end back to the pre-RSA origin. The acromion was assigned representative scapula-specific cortical and trabecular bone material properties.[4] Acromial stresses were assessed following virtual implantation of the glenoid and humeral components, as well as after subsequent simulation of external rotation from neutral to 50°. A Hoffman failure criterion incorporating differences in tensile and compressive failure strengths of bone [5,6] was used to estimate failure risk in the acromion.

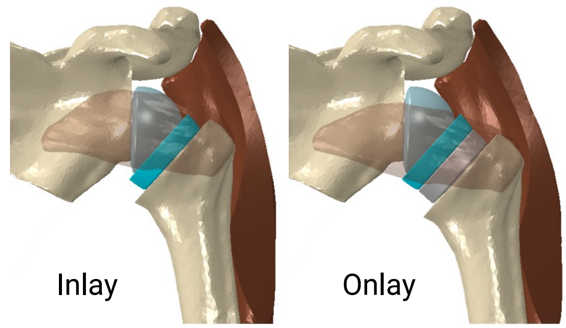

Figure 1: Finite element model of RSA inlay and onlay configurations for the 3 mm glenoid lateralization case. The spacer behind the humeral component effectively further lateralizes and distalizes the humerus.

Hoffman Failure Criterion: $$\frac{1}{2\sigma_{yt}\sigma_{yc}}[(\boldsymbol{\sigma}_1-\boldsymbol{\sigma}_2)^2+(\boldsymbol{\sigma}_1-\boldsymbol{\sigma}_3)^2+(\boldsymbol{\sigma}_2-\boldsymbol{\sigma}_3)^2]+\left[\frac{1}{\sigma_{yt}}-\frac{1}{\sigma_{yc}}\right](\boldsymbol{\sigma}_1+\boldsymbol{\sigma}_2+\boldsymbol{\sigma}_3)\geq 1$$

where $\boldsymbol{\sigma}_1$, $\boldsymbol{\sigma}_2$, and $\boldsymbol{\sigma}_3$ ($\boldsymbol{\sigma}_1>\boldsymbol{\sigma}_2>\boldsymbol{\sigma}_3$) represent element principal stresses in bone, while $\boldsymbol{\sigma}_{yt}$ and $\boldsymbol{\sigma}_{yc}$ represent the yield stress of bone in tension and compression, respectively. Element failure is assumed to occur when the Hoffman Failure Criterion equalled or exceeded 1.

Results & Discussion: Glenoid lateralization alone (inlay) caused progressive stretching of the deltoid after implantation (15% increase over baseline for most lateralized case). Deltoid stretching was more severe with the onlay construct (60% increase for most severe case) due to additional stretching along the primary muscle axis. Progressive stretching of the deltoid produced corresponding increases in acromial stress with increasing glenoid lateralization. For each level of glenoid lateralization, there were additional increases in deltoid and acromial stresses with use of an onlay stem as compared to inlay stem constructs (Figure 2), both at implantation and during subsequent external rotation. For each level of glenoid lateralization tested, the addition of an onlay stem increased the torque required to externally rotate the shoulder. The construct with 9 mm of glenoid lateralization and an onlay stem design required the largest torque to externally rotate the humerus due to greater tensioning of the subscapularis tendon compared to the other combinations.

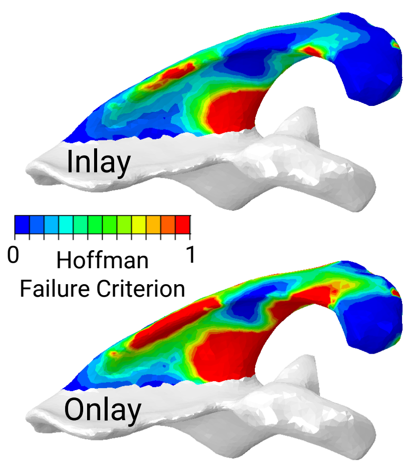

Figure 2: Bone failure criteria suggests elevated risk of stress fracture in the onlay configuration with 9 mm lateralization.

Significance: For a given glenoid component lateralization, using an onlay stem construct increased acromial stresses compared to inlay constructs. Increased soft tissue tension from glenoid lateralization and humeral distalization led to increased torque requirements for external rotation, which would make it more difficult for patients to complete activities of daily living. Limitations in the model are that only one motion was simulated, and scapula motion was not modeled. These limitations notwithstanding, the results suggest that surgeons should use caution when combining glenoid component lateralization and humeral distalization in RSA, especially for patients with osteoporotic bone that likely puts them at increased risk of stress fracture.

Acknowledgements: This research was funded by a grant from Stryker Orthopaedics.

References: [1] Boileau et al. (2005), *J Shoulder Elbow Surg* 14(1 Suppl S):147S-161S; [2] Wong et al. (2016), *J Shoulder Elbow Surg* 25(11):1889-95; [3] Johnson et al. (2021), *Semin Arthroplasty: JSES* 31(1):36-44; [4] Chae et al. (2016), *J Orthop Res* 34(6):1061-8; [5] Bayraktar et al. (2004), *J Biomech* 37(1):27-35; [6] Edwards & Troy (2012), Med Eng Phys 34(3):290-8.

ESTIMATING TENDON LOAD AND WALKING SPEED USING AN INSTRUMENTED IMMOBILIZING BOOT

Michelle P. Kwon*, Todd J. Hullfish, Lorraine A.T. Boakye, Josh R. Baxter
Department of Orthopaedic Surgery, Pearlman School of Medicine, University of Pennsylvania, Philadelphia, PA
*michelle.kwon@pennmedicine.upenn.edu

Introduction: Rehabilitative loading is a critical period for healing outcomes in musculoskeletal injuries or surgical treatments especially in lower extremity injuries [1,2]. Throughout the healing process of lower extremity injuries, providers typically prescribe gradual progression of loading in an immobilizing boot. Understanding loading during the period spent in an immobilizing boot is needed to identify beneficial biomechanical forces early in healing. However, early rehabilitative loading is most often observed in controlled, in-lab settings for short periods of time due to our limited ability to take accurate measurements in the field for prolonged times [3]. Expanding our capability to monitor loading in real world settings for extended periods is necessary to optimize rehab therapies to promote tissue growth and restore function. The purpose of our study is to assess if Achilles tendon loading and walking speed in an immobilizing boot can be accurately estimated through a machine learning model trained on inertial measurement unit (IMU) data. We expected to successfully predict tendon loading and walking speed because human kinematics and loading are closely correlated with metrics that can be extracted from IMU data. A robust paradigm will allow us to transition away from complicated lab base sensors and instead use IMUs which will reduce patient burden and increase data fidelity for long-term monitoring projects in real-world settings.

Methods: We recruited ten healthy subjects (3 females, age: 25 ± 2.4 yrs, BMI: 23.9 ± 6.56) to walk across our lab in an immobilizing boot in a range of walking speeds, stride patterns, and immobilization angles. In this abstract, we will focus on the neutral immobilization angle for brevity. Subjects were instructed to walk 10.5-meter spans in an immobilizing boot for 4 different speeds: pathological (uneven gait cycle), slow, medium, and fast. 8-16 trials were collected for each speed resulting in 1984 steps across all 10 subjects. The immobilizing boot (*Formfit® Walker Air CAM*) was worn on the right leg with an IMU (Opal) rigidly attached to the lateral shank of the boot. Both the boot and shoe were outfitted with an instrumented insole (*Loadsol*) to estimate Achilles tendon loading [4,5]. We measured other segment motions using IMUs placed on the left wrist, left foot, and left shank and monitored walking speed using markerless motion capture (*Theia3D*). We manually confirmed the data integrity and rejected any trials that were not synchronized. Every step (heel contact to heel contact) was isolated and the max, min, and impulse of every IMU channel were extracted. Walking speed for each trial was calculated from the motion capture data. Max tendon load and walking speed were target metrics while the max, min, and impulse of each IMU channel were used as training features. We selected LASSO regression as the machine learning model because it has shown good performance when used with IMU data to predict biomechanical proxies [6-8]. We also created models to compare the effects of different sampling frequencies and different combinations of sensors to prepare for implementing these sensors in the clinic.

Results & Discussion: The model for a neutral boot condition to predict tendon load had a mean absolute percentage error (MAPE) of 28.5 ± 5.2%, while the model to predict walking speed had a MAPE of 9.2 ± 0.5% (Fig. 1). Walking speed is better estimated by IMU data than by tendon load given that the model has a reduced percent error by 19.3%. The R squared value for IMU predicting tendon load in a neutral immobilizing boot was 0.728 while the R squared value for the IMU predicting walking speed was 0.854. This reaffirms that the LASSO model trained on the IMU data can give us more accurate predictions of walking speed than of tendon load. While both models have low MAPE values, the MAPE values could be overexaggerated by the steps with tendon loads or walking speeds that are close to 0.

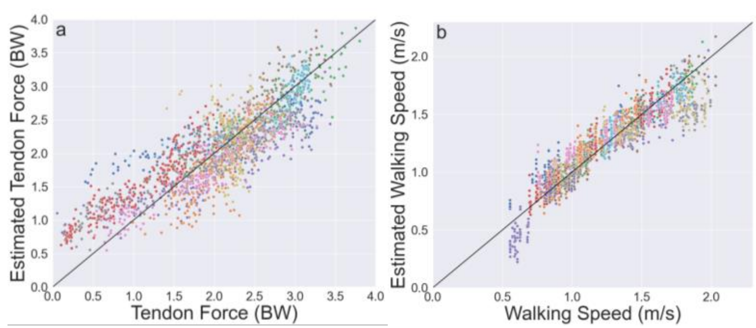

Figure 1: Boot worn IMU predicts tendon loading and walking speed. a) Predicted max tendon force has moderate spread away from the reference line. Reference line indicates 0 error b) Predicted walking speed demonstrates minimal spread, indicating more accurate estimates.

Significance: Many lab-grade wearables are not designed for out-of-lab settings, with their limited battery life and complex user interfaces. These limitations often impose a burden on subjects, making them an unrealistic option for long-term monitoring purposes. Fortunately, the rapid advancement in wearables has recently reduced some wearable constraints. In particular, the AX6 (*Axivity*) a wearable, 6-axis IMU is compact, requires no subject handling, water and dust resistant, and has 7-140 days of battery, making it ideal to capture measurements of human motion without jeopardizing data fidelity. With wearables that can feasibly be deployed into the field, we can understand tendon loading during periods outside of controlled lab settings in early-stage Achilles healing, enabling us to make recommendations that optimize the therapeutic effects of rehabilitative loading.

Acknowledgements: We thank the NIH/NIAMS R01AR078898 and P50AR080581 for supporting this research.

References: [1] Jielile et al. (2015), *Orthopedics* 39(1); [2] Malliaras et al. (2013), *Sports Med.* 43(4); [3] Fan et al. (2022), *Healthcare (Basel)* 10(7); [4] Hullfish & Baxter (2022), *Gait Pos.* 79; [5] Hullfish et al. (2020), *J Biomech.* 109; [6] Halilaj et al. (2018), *J Biomech.* 81; [7] Kammoun et al. (2022), *Annu Int Conf IEEE EMBS*; [8] Matijevichet al. (2020), *Hum Mov Sci.* 74.

EFFECTS OF HIGH GLYCATION DUE TO DIABETES ON FRACTURE BEHAVIOR OF HUMAN CORTICAL BONE UNDER DYNAMIC LOADING

Ebrahim Maghami[1], Ahmad R. Najafi[1,*]
[1]Department of Mechanical Engineering and Mechanics, Drexel University, Philadelphia, PA 19104, USA
Email: *arn55@drexel.edu

Introduction: Bone has a hierarchical structure of collagenous protein and minerals in multiple length scales that can activate various toughening mechanisms under normal conditions. In incidents such as car collisions or sports accidents, bone undergoes different loading regimes. Studies on the mechanical behavior of bone depict that the mechanical properties of bone are influenced by a change in the rate of dynamic loading. The risk of bone-related fracture under high loading rates increases with aging and diabetes. One of the alterations in bone tissue with diabetes is advanced glycation end-products (AGEs) due to non-enzymatic glycation that accumulates in bone [1]. It is widely found that the accumulation of AGEs in bone tissue increases with aging. Despite many studies on the influence of AGEs on bone tissue, there is not adequate in-depth and detailed information yet on how the microstructure of human bone with a high level of AGEs responds to high loading rate events such as accidents or falls where the main loading condition is dynamic.

In the present study, the objective is to investigate the effects of high levels of AGEs on damage initiation and propagation in human cortical under dynamic loading. In order to capture different toughening mechanisms at the microscale, we use a brittle model of the phase-field method to analyze the crack growth under dynamic loading.

Methods: At the microscale level, the human Haversian (osteonal) cortical bone has been considered as a composite material and modeled as a fiber-ceramic matrix. We consider osteons as fibers and the interstitial tissue as the matrix. We also define the interface between the osteons and interstitial tissue as the cement line. We use human microscopic images obtained from the tibias of female donors (60 and 81 year old) to create 2D plain-strain models (Fig. 1). we assume that high AGEs levels can deteriorate the material properties of bone and bone fragility by decreasing the global fracture toughness. To simulate crack growth trajectories, we implement a phase field fracture method with a brittle framework under dynamic loading [2]. The boundary conditions of the models are shown in Figure 1. We aim to observe how damage propagation changes with increasing AGEs through the cortical samples under dynamic loading.

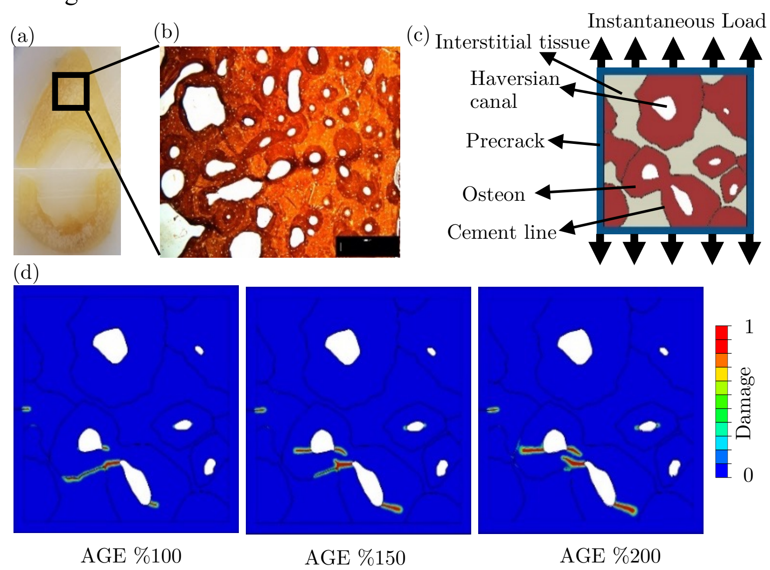

Figure 1. (a) A cross-section of the cortical bone in 60-year-old human tibia, (b) a microscopy image from the cross-section, (c) the 2D model of the cortical bone microstructure, and (d) the influence of different AGE levels on the fracture response of cortical bone under dynamic loading. There are a few damaged cement lines in the lower levels of AGEs. Damage with 1.0 shows the crack path and the zero value presents that there is no damage.

Results & Discussion: Our results show the crack growth trajectory in the cortical bone microstructure is highly dependent on the reduced critical energy release rate of the osteons due to increased AGEs contents. The difference between the fracture toughness of the osteons and the interstitial bone also affects damage growth. The results depict that there are fewer damaged cement lines in the simulated models with high AGEs levels under dynamic loading. In addition, more microcracks form and more osteons are damaged under dynamic loading by increasing AGEs levels. The dynamic loading in cortical bone with high AGEs levels can activate and deactivate the toughening mechanisms and crack growth trajectories. For instance, we observe crack branching in our models. Crack branching is determined as one of the toughening mechanisms in the simulations. However, changing the levels of AGEs can affect the formation of crack branching.

The results from the present simulations also show that the post-yielding features such as damage accumulation and crack growth trajectories can be influenced by changing the mismatch ratio between the fracture properties of microstructural features under dynamic loading.

Significance: The findings of the present study show that activation and deactivation of toughening mechanisms depend on the levels of AGEs in the samples. Such studies on micromechanics of studies can be used to predict the probability of failure in human cortical bone diagnosed with diabetes.

Acknowledgements: The authors acknowledge the high-performance computing resources (Picotte: the Drexel Cluster) and support at the Drexel University. We would like to express our special thanks to Dr. Lamya Karim and Taraneh Rezaee for providing us with the cortical bone samples from human tibias. We also thank Dr. Theresa Freeman for using her facilities and providing invaluable support with the staining and imaging process.

References: [1] Vashishth D. *Ibms Bonekey*, 2009, 6(8):268; [2] Molnár G, et al. *Finite Elements in Analysis and Design*, 130, pp.27-38, 2017.

KINEMATICS ASSOCIATED WITH ELBOW VARUS TORQUE IN BASEBALL PITCHERS

Glenn S. Fleisig[1*], Thomas W. McCutcheon[1], Jonathan S. Slowik[1]
[1]American Sports Medicine Institute
*Corresponding author's email: glennf@asmi.org

Introduction: The rates of ulnar collateral ligament (UCL) injuries and surgeries in baseball pitching continues to rise. This is because the tension in the UCL providing elbow varus torque for elite pitchers is near the tissue's physiologic limit. Numerous studies have investigated pitching kinematics associated with elbow varus torque,[1-7] but these studies were limited in the parameters analyzed, skill level of pitchers, and/or number of pitchers tested. The purpose of this work was to evaluate numerous parameters in a large sample of elite adult pitchers. It was hypothesized that several kinematic parameters are associated with varus torque.

Methods: Biomechanical data were analyzed for 523 professional and collegiate healthy baseball pitchers. A total of 39 reflective markers were placed on each subject before testing. After unrestricted warmup, the pitcher threw 5 to 10 full-effort fastballs from a mound to a catcher or target strike zone above home plate at regulation distance from the pitching rubber (18.44 m). Fastball velocity was recorded with a radar gun (Stalker Sports Radar, Plano, TX, USA) while motion of the reflective markers was measured with a 12-camera, 240 Hz automated motion capture system (Motion Analysis Corporation, Santa Rosa, CA, USA). For each pitch, 21 kinematic variables were calculated as previously described.[8] Elbow varus torque was calculated using inverse dynamics.[9,10] Elbow varus torque was then divided by body weight and by height to normalize into a unitless variable.[8] Subjects were separated into high (n=174), medium (n=175), and low (n=174) torque groups based upon their normalized elbow varus torque. Because a Shapiro-Wilk test suggested a deviation from normality, kinematic data for the high torque group and low torque group were compared with Mann-Whitney U tests. All analyses were conducted in SPSS (Version 29.0, IBM, USA) with an *a priori* level of significance of $\alpha=0.05$.

Results & Discussion: The high torque group produced greater ball velocity than the low torque group (38.0±1.7 vs 37.1±2.0 m/s). In addition, there were 9 kinematic differences between torque groups (Table 1). If results from this study are to be used by coaches and biomechanists to adjust the mechanics of pitchers to lower their elbow torque mechanics, it is encouraging that nearly half of these differences were at the instant of foot contact as flaws earlier in the pitching motion are easier to change.[11] One of the most analyzed parameters in pitching is shoulder external rotation at foot contact, as countless news stories, coaches, and scientists have written about how this parameter or "late arm" or "inverted W" leads to higher elbow torque and risk of injury.[12,13] This study supports this theory as the high torque group demonstrated less shoulder external rotation at foot contact than the low torque group. Recently, some pitching coaches and experts have advocated increased elbow flexion at foot contact. However, the current study showed that the higher torque group had greater elbow flexion, which is consistent with previous research correlating increased elbow flexion with increased varus torque.[14] Interestingly, the high torque group produced greater ball velocity with less maximum external rotation of the shoulder. From a physics perspective, it makes sense that decreased range of shoulder rotation to generate greater velocity requires greater torque. At ball release, the high torque group had greater trunk contralateral tilt (i.e. towards the glove side), which is consistent with many previous studies,[3,4,5,6,8,15] but in contrast to one study.[1] While the high torque group had greater trunk tilt, they also had less shoulder abduction at ball release. Previous research has shown that trunk contralateral tilt and shoulder abduction usually increase together,[15] thus the high torque and low torque group demonstrated significantly different mechanics.

Table 1. Significant differences between normalized torque groups

	High Torque (n=174)	Low Torque (n=174)
Instant of Front Foot Contact		
Upper trunk tilt (º)	7.2 ± 7.3	9.0 ± 7.6
Shoulder external rotation (º)	53.9 ± 25.7	59.8 ± 27.8
Elbow flexion (º)	99.3 ± 16.0	93.6 ± 16.5
Shoulder abduction (º)	91.3 ± 9.5	86.1 ± 11.2
Instant of Maximum External Rotation		
Shoulder external rotation (º)	160.1 ± 10.6	165.5 ± 12.1
Arm Acceleration Phase		
Max knee extension velocity (º/s)	361 ± 152	264 ± 118
Max elbow extension velocity (º/s)	2704 ± 314	2509 ± 304
Instant of Ball Release		
Trunk contralateral tilt (º)	23.2 ± 8.6	19.4 ± 13.9
Shoulder abduction (º)	86.5 ± 7.7	88.9 ± 8.4

Significance: With a robust analysis of a large, elite database, this study identified kinematic parameters associated with high elbow varus torque. The results are consistent with and build upon findings from smaller previous studies. Results from this investigation provide objectives for modification of pitching mechanics to reduce elbow torque and risk of injury, particularly kinematics in the early phase of the pitching motion.

References: [1] Aguinaldo & Chambers (2009), *AJSM* 37(10); [2] Cohen et al. (2019), *AJSM* 47(12); [3] Manzi et al. (2022), *JSES* 31(9); [4] Matsuo et al (2006), *J Appl Biomech* 22(2); [5] Oyama et al. (2013), *AJSM* 41(10); [6] Solomito et al. (2015), *AJSM* 43(5); [7] Solomito et al. (2018), *AJSM* 46(1); [8] Crotin et al. (2022), *AJSM* online ahead of print; [9] Fleisig et al. (1995), *AJSM* 23(2); [10] Zheng et al. (2004), *Biomed Eng Princ in Sports*, Kluwer Academic; [11] Fleisig et al. (2018), *Sports Biomech* 17(3); [12] Fleisig GS. (1994), *UAB dissertation*, pp 92-113; [13] Douoguih et al. (2015), *OJSM* 3(4). [14] Werner et al. (2002), *JSES* 11(2); [15] Escamilla et al. (2018), *J Appl Biomech* 34(5).

TWO MINUTES IS SUFFICIENT TO CHARACTERIZE THE VISCOELASTIC PROPERTIES OF THE HUMAN LOWER BIRTH CANAL DURING THE FIRST STAGE OF LABOR

Mariana Masteling[1*], John DeLancey[2], James Ashton-Miller[3]
Departments of [1]Biomedical Engineering, [2]Obstetrics and Gynecology, [3]Mechanical Engineering, University of Michigan
*Corresponding author's email: mastelin@umich.edu

Introduction: Up to 19% of nulliparous women sustain lower birth canal and pelvic muscle injuries while giving birth vaginally. These injuries are the primary cause of pelvic organ prolapse that requires surgery in over 200,000 women each year. If we could identify women at high risk of injury before it occurs, preventative strategies might be considered to avoid pelvic floor damage. From a biomechanical perspective, it seems reasonable that if women have unusually stretch-resistant lower birth canals they should expect a higher risk for pelvic floor injury. In the present work, a novel vaginal dilator (PREP, Maternal Medical, LLC, Mountain View, CA) was used during the first stage of labor to pre-stretch the birth canal to facilitate delivery during the second stage. We used the data from this device to quantify inter-individual differences in lower birth canal hoop tension and lower birth canal viscoelastic properties, using a Fractional viscoelastic Zener Model (FZM). The current analysis evaluates the feasibility of predicting resistance to dilation based on a 90 second test that can be done before injury occurs.

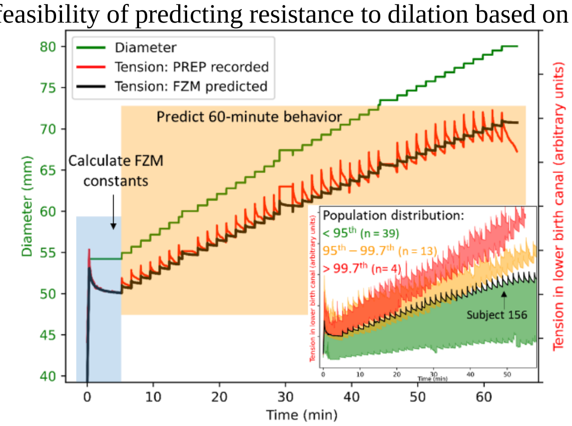

Figure 1: An example of *in vivo* PREP data from subject 156. With insert showing the 56 subject population distribution.

Methods: This is a secondary analysis of data from the ongoing multicenter EASE clinical trial (NCT 03973281) during which the PREP dilator was introduced into the first 4 cm of the lower vaginal canal in the region where injuries occur in women having their first birth during the first stage of labor. Its semi-automatic, displacement-controlled, actuation system was programmed to mechanically expand the lower canal to ~ 80 mm diameter over ~60 minutes in 0.9 mm steps (Fig. 1). Given the dilation force, diameter and time are all recorded, we were able to calculate the hoop tension, T, in the lower birth canal tissues during the dilation. During trial design, we requested the initial 20 s ramp dilation to 55 mm be followed by a 5-minute hold, after which the step-wise ramp dilation proceeded to the final 80 mm diameter (Fig. 1). That 20 s ramp-and-5-minute-hold enabled us to characterize the tissue response to dilation using a Fung quasilinear viscoelastic model, similar to what we previously used in processing data from a constant-force vaginal dilator during the first stage of labor [1]. Unfortunately, it had no predictive power after the fitted interval. Considering the strong linear relationship seen after the 5-minute hold (Fig. 1), we also tried several classical viscoelastic models, but they also had poor predictive power. We discovered that using a fractional approach, the simplest model with predictive power was the fractional viscoelastic Zener Model (FZM, a SpringPot (constants C_α and α) in series with a spring in one arm (k_β), lying in parallel with a spring (k_γ) in the other arm). For each subject, RHEOS.jl [2] was used to obtain the four FZM constants. First, dilation diameter and lower birth canal hoop tension data from the 'hold' tissue relaxation were used to obtain the constants. Then using the four constants, the time course of the equivalent lower birth canal hoop tension, T, was predicted for the remainder of the dilation to 80 mm using the experimentally recorded dilation diameter and temporal data (Fig. 1). The relative error of the prediction was calculated as the squared error relative to the maximum hoop tension, T, for each subject. Data management and statistical analyses were performed using Julia and Python.

Results & Discussion: In the 56 women with PREP data, we found that when the four FZM constants were calculated from the 20 s ramp-and-5-minute-hold data, the relative fit error was 8 ± 4%, and the relative prediction error of T after 60 minutes of dilation was 10 ± 5 %. But, when the FZM constants were instead calculated from the 20 s ramp ***and the initial 90 s*** of the 5-min-hold, the error was acceptable: 13 ± 4 % for relative fit and 13 ± 18 % for relative prediction. This suggests that the initial 90 s of the 5-min-hold is actually sufficient to characterize the 60-minute dilation behavior over the wide range of values. For the 5-minute estimate, the FZM constants varied 742, 64 and 23-fold for C_α, k_β, and k_γ; α varied between its acceptable range of 0 and 1. Importantly from a clinical perspective, k_β was 33% larger in older (age ≥ 30 years) than younger women. T, at a diameter of 55 mm, varied 5.5-fold and was 22% greater in older women while tissue stiffness during the initial 20 s ramp varied 6.8-fold and was 31% higher in older women (Fig. 1-insert). These age effects may help explain why the risk of pelvic muscle injury is higher, and second stage of labor longer, in older women [3,4].

Significance: These biomechanical results demonstrate that the PREP can be used with the FZM to characterize, in less than 2 minutes, the viscoelastic properties of the lower birth canal to identify women with abnormally stiff birth canal tissues (i.e., those with stiffnesses greater than 3*SD above the mean) during their 1st stage of labor. This can occur quickly enough to be useful in decision-making during labor. When combined with the obstetric variables collected during the EASE trial, the PREP dilator may eventually prove useful in decision-making to mitigate the risks of a difficult vaginal delivery.

Acknowledgements: MM, JAAM and JOLD received salary support from NICHD R44 HD 096987 and NIDDK 1 RC2 DK122379. MM received funding from the Portuguese Foundation of Science and Technology under grant number SFRH/BD/138822/2018.

References: [1] Tracy *et al.*, J *Mech Behav Biomed Mater*,79:213-218, 2018; [2] Kaplan *et al.*, *J Open Source Softw*, 4:1700, 2019; [3] Doxford-Hook *et al.*, *Midwifery*, 115:103494, 2022; [4] Papadias *et al.*, *Ann N Y Acad Sci*, 1092:414-417, 2006

EVALUATING GAIT SYMMETRY 6 MONTHS AFTER ACL RECONSTRUCTION WITH QUADRICEPS TENDON AUTOGRAFT USING WIRELESS FORCE SENSING INSOLES IN THE CLINICAL ENVIRONMENT

Rachel E. Cherelstein, BS[1*], Christopher M. Kuenze, PhD, ATC[1,2], Michelle C. Walaszek, PT, DPT, MS[2], Emily R. Brumfield, ATC[1], Jennifer N. Lewis, PT, DPT[1], Garrison A. Hughes, BS[1], Edward S. Chang, MD[1]
[1]Inova Sports Medicine, Fairfax, VA, United States
[2]Department of Kinesiology, University of Virginia, Charlottesville, VA, United States
*Corresponding author's email: rachel.cherelstein@inova.org

Introduction: Alterations in lower extremity walking biomechanics can persist for years after anterior cruciate ligament reconstruction (ACLR) despite rehabilitative efforts of the patient and healthcare team. Asymmetries in gait at 6 months post-ACLR are associated with delayed return to play [1], worse knee-related function 1-year post-ACLR [2], and incident radiographic knee osteoarthritis 5 years post-ACLR [3]. However, most post-ACLR gait symmetry research thus far has focused on patients who receive bone-patellar tendon-bone (BPTB) autograft and assessments have been completed in biomechanics labs that lack feasibility of translation to the clinical environment. As a result, there is a gap in knowledge concerning biomechanical outcomes after ACLR with quadriceps tendon (QT) autograft, as QT autografts have been increasing in popularity since 2014 [4]. Therefore, the purpose of this study was to evaluate limb loading symmetry during gait 6 months post-ACLR with QT autograft using methods that can be translated to the clinic. Compared to patients who receive BPTB autograft, patients who receive QT autograft experience less strength asymmetry [5] and report less anterior knee pain [6], both of which are associated with limb loading asymmetry [7]. Because of this, we expected that patients with QT autograft would not experience significant gait asymmetry at 6 months post-ACLR.

Methods: 20 patients (75% female) aged 14-32 years (average 20.51) who underwent unilateral, primary ACLR with QT autograft completed biomechanical gait assessment, the International Knee Documentation Committee (IKDC) survey and the ACL-Return to Sport after Injury (ACL-RSI) survey at 6.20±0.43 months post-ACLR. Participants walked on a treadmill at a self-selected pace for 30 seconds and ground reaction force data was collected at 100Hz using loadsol® (Novel Electronics, St. Paul, MN, USA) single sensor insoles, which have been validated for the collection of ground reaction forces during overground and treadmill walking [8]. Peak loading phase vertical ground reaction force (vGRF; Nm), loading response instantaneous loading rate (ILR; Nm*s^{-1}), and loading response average loading rate (ALR; Nm*s^{-1}) were calculated. Variables were compared between limbs using paired samples t-tests. Limb symmetry indices (LSI; %) were calculated and reported for each variable. The relationships between gait variable LSI and patient-reported outcome measures were characterized using Pearson correlation coefficients. A-priori alpha level was $p < 0.05$. Statistical analysis was completed using an open-source statistical package (v 1.2, Jamovi).

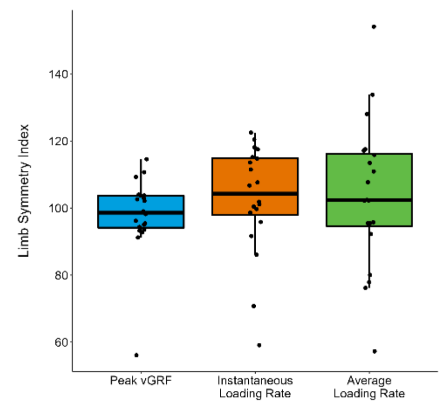

Figure 1. Limb symmetry indices (%) for gait vertical ground reaction force and loading rate variables in the sample of individuals with QT ACLR.

Results & Discussion: Patients who undergo primary, unilateral ACLR with QT autograft did not experience asymmetry in gait biomechanics at 6 months post-ACLR (Fig. 1). There was no significant between limb difference in peak loading phase vGRF ($p = 0.35$), ALR ($p = 0.99$), or ILR ($p = 0.55$) during 30 seconds of treadmill walking gait. These results support our hypothesis that QT autograft preserves gait biomechanics post-ACLR, given that BPTB patients at this time point typically experience asymmetry when compared to uninjured controls [9]. Additionally, while patients reported generally low IKDC (73.07±9.69) and ACL-RSI (50.55±20.91) scores compared to previous studies including healthy controls and those who return to preinjury sport [10-11], there was no association between either score with peak loading phase vGRF (IKDC $r = 0.26$, $p = 0.27$; ACL-RSI $r = -0.10$, $p = 0.68$) or ALR (IKDC $r = 0.24$, $p = 0.32$; ACL-RSI $r = 0.11$, $p = 0.66$). Conversely, IKDC score was correlated with ILR (IKDC $r = 0.48$, $p = 0.03$; ACL-RSI $r = 0.26$, $p = 0.27$). This may suggest that self-reported function and psychological readiness are not primary predictors of gait biomechanics at this time, which was unexpected, given that individuals who report worse symptoms typically exhibit more gait asymmetry as compared to those without symptoms [2].

Significance: To our knowledge, this is the first study evaluating gait symmetry post-ACLR in a cohort of patients who have undergone ACLR with QT autograft. Of note, loadsol® single sensor insoles are a less expensive option than traditional force plates and do not require advanced training, making our assessments clinically replicable. Given that post-ACLR gait asymmetry is associated with several negative long-term outcomes [1-3], use of the loadsol® in rehabilitation programs can inform the patient and healthcare team of asymmetry and allow for early intervention to ultimately improve health outcomes and quality of life.

Acknowledgements: Funding for this project was provided by an internal grant awarded to E.S.C. by Inova Health System.

References: [1] Di Stasi et al. (2013), *Am J Sports Med* 41(6); [2] Pietrosimone et al. (2018), *J Orthop Res* 36(11); [3] Wellsandt et al. (2017), *J Orthop Res* 35(3); [4] Arnold et al. (2021), *Knee Surg Sports Traumatol Arthrosc* 29(11); [5] Johnston et al. (2021), *Knee Surg Sports Traumatol Arthrosc* 29(9); [6] Galan et al. (2020), *J Exp Orthop* 7(1); [7] Paterno et al. (2010), *Am J Sports Med* 38(10); [8] Renner et al. (2019), *Sensors (Basel)* 19(2); [9] Davis-Wilson et al. (2020), *Med Sci Sports Exerc* 52(4); [10] Anderson et al. (2006), *Am J Sports Med* 31(1); [11] Sadeqi et al. (2018), *Orthop J Sports Med* 6(12)

THE EFFECT OF AN EXOSUIT ON TRUNK MUSCLE ACTIVITIES DURING PROLONGED CONSTRUCTION-RELATED HOLDING TASKS

Yu Song[1], Haylen Cordova[2], Zhichen Feng[1], Ling Li[1], Maja Goršič[3], Boyi Dai[1], Vesna D. Novak[4*]
[1] Division of Kinesiology and Health, University of Wyoming, Laramie, WY, USA
*Corresponding author's email: novakdn@ucmail.uc.edu

Introduction: Low back pain is a leading cause of disability worldwide and is commonly caused by repetitive lifting of heavy objects and prolonged postures with a bent trunk [1]. Exoskeletons and exosuits are a strategy, providing external forces and moments to decrease low back loading for workers in physically demanding occupations [2]. The positive effects of an exosuit in reducing erector spinae (ES) muscle activities have been found in leaning and lifting tasks [2, 3]. However, previous studies focused on the effect of the exosuit in controlled tasks such as lifting a box or holding a dumbbell. It is unclear if an exosuit may help reduce muscle activities in prolonged holding tasks performed in an actual work environment. Therefore, this study aimed to quantify the effects of a passive exosuit on trunk muscle activities during two prolonged construction-related holding tasks.

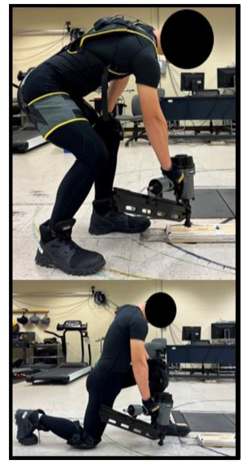

Figure 1: Standing (top) and kneeling (bottom) tasks.

Methods: Twenty male volunteers (age: 26.6 ± 4.7 years, height: 1.75 ± 0.07 m, mass: 76.5 ± 11.9 kg, and all right-hand dominant) with no previous history of chronic back pain/injury/surgery participated in this study. Participants performed static standing and kneeling tasks by holding a nail gun (4.54 kg) to mimic common construction postures for 3 minutes with and without wearing an exosuit (the Apex from HeroWear, Nashville, TN) (Fig. 1) [1]. Electromyography (EMG) was assessed on the left and right ES and rectus abdominis (RA) by using the Delsys Trigno Avanti system at 1926 Hz, as previously described [1]. The tasks (standing vs. kneeling) and exoskeleton status (with vs. without) were counterbalanced among participants. The EMG data were collected at the initiation of the task (Phase 1), the end of the first minute (Phase 2), the end of the second minute (Phase 3), and the end of the third minute (Phase 4). The independent variables were exoskeleton status and four phases. The dependent variables were the mean values of each muscle's EMG for 5 seconds, which were expressed as percentages of the maximum voluntary contraction (MVC) test. Paired t-tests were applied with a Type I error equal to 0.05.

Results & Discussion: Regarding the exosuit status, wearing the exosuit resulted in decreased muscle activities for left ES during Phases 3 and 4 and for left RA during Phase 1 in the kneeling task (Table 1). The increased muscle activities of the left ES compared to the right ES were likely caused by participants holding the nail gun in their right hands. Regarding the phases, decreased left ES activities were found at Phases 3 and 4 compared to Phases 1 and 2 in the kneeling task. In addition, greater muscle activities were found for left ES during Phases 1 and 2 and for right RA during Phases 3 and 4 when wearing the exosuit in the standing task. Right ES and left RA demonstrated greater muscle activities during Phase 1 and Phase 4, regardless of exosuit status in the standing task. Overall, the magnitudes of muscle activities observed were much less than the muscle activities observed in dynamic lifting tasks [2]. The decreased muscle activities were likely due to the other free hand on the knee supporting the trunk to decrease the overall low back moment. Furthermore, the low muscle activities were likely related to the flexion-relaxation phenomenon (FRP), as ES muscle activities typically decrease during prolonged static trunk bending [1]. The decreased ES muscle activities over the four phases were also consistent with the FRP [3]. In summary, the two holding tasks impose low demands on low back muscle activities, while the exosuit resulted in small decreases in left ES activities during the later phases of the kneeling task. While the loading on passive tissue was expected to decrease as the exosuit provided an external supporting moment, future studies that directly quantify passive tissue loading are needed.

Significance: The exosuit slightly reduced ES EMG during the later phases of the kneeling task, but the ES EMG was generally low during the two holding tasks. Passive tissue loading and dynamics construction-related tasks need to be examined in future studies.

Acknowledgements: NSF, China Scholarship Council, and Wyoming INBRE (NIH).

References: [1] Hu et al., 2014. *Clin Biomech*, 29(3); [2] Goršič et al., 2021. *J Biomech.* 126; [3] Lamers et al., 2020. *Sci Rep*, 10(1).

Table 1. Means ± standard deviations of muscle activities (% of MVC) and the results of t-tests among four phases with and without the exosuit.

		Standing				Kneeling			
		Phase 1	Phase 2	Phase 3	Phase 4	Phase 1	Phase 2	Phase 3	Phase 4
Left ES	Without Exosuit	4.4 ± 5.1	3.2 ± 3.1	3.2 ± 3.0	2.5 ± 2.6	11.1 ± 5.0	11.0 ± 4.5	10.9 ± 4.3*	11.0 ± 5.2*
	With Exosuit	4.5 ± 4.0^{A}	4.0 ± 3.6^{A}	3.1 ± 3.2^{B}	2.9 ± 2.7^{B}	10.1 ± 6.4^{AB}	9.8 ± 5.9^{A}	9.1 ± 5.1^{BC*}	8.3 ± 5.0^{C*}
Right ES	Without Exosuit	2.8 ± 2.5^{A}	2.3 ± 2.0^{AB}	1.9 ± 1.2^{AB}	1.8 ± 1.4^{B}	3.7 ± 2.2	3.9 ± 2.0	4.2 ± 2.5	4.7 ± 3.7
	With Exosuit	3.4 ± 3.2^{A}	2.8 ± 2.5^{AB}	2.3 ± 1.6^{AB}	2.1 ± 1.4^{B}	4.7 ± 4.2	4.6 ± 3.6	4.3 ± 3.1	4.3 ± 3.1
Left RA	Without Exosuit	1.2 ± 1.0^{B}	1.4 ± 1.0^{AB}	1.5 ± 1.2^{A}	1.5 ± 1.0^{A}	1.2 ± 0.9*	1.5 ± 1.9	1.5 ± 1.5	1.4 ± 1.4
	With Exosuit	1.1 ± 0.7^{C}	1.4 ± 1.2^{AB}	1.5 ± 1.1^{B}	1.6 ± 1.3^{A}	1.0 ± 0.7*	1.2 ± 0.9	1.2 ± 0.9	1.2 ± 0.8
Right RA	Without Exosuit	1.2 ± 1.4	1.3 ± 1.4	1.3 ± 1.3	1.3 ± 1.2	1.1 ± 1.3	1.4 ± 1.7	1.3 ± 1.3	1.4 ± 1.5
	With Exosuit	1.1 ± 1.0^{C}	1.3 ± 1.1^{BC}	1.3 ± 1.1^{AB}	1.4 ± 1.2^{A}	1.0 ± 0.8	1.1 ± 0.9	1.1 ± 0.8	1.1 ± 0.9

Note. * Significant differences between exoskeleton status (with vs. without); $^{A, B, \text{and } C}$: A is greater than B and C, and B is greater than C among phases at each task and phase, with no significant differences for the phases with the same letter.

TAKE-OFF TECHNIQUE IS ASSOCIATED WITH PEAK SPINE EXTENSION IN THE BACK HANDSPRING STEP OUT ON THE BALANCE BEAM

Gabriella H. Small* and Richard R. Neptune
Walker Department of Mechanical Engineering, The University of Texas at Austin, Austin, TX
*Corresponding author's email: gsmall@utexas.edu

Introduction: The back handspring step out (BHS) in women's artistic gymnastics is a foundational skill that occurs in balance beam routines starting at skill level 5 (out of 10 levels) through the collegiate and Olympic levels [1]. Given the importance of the BHS across a gymnast's career, determining the optimal technique is crucial. Furthermore, back injuries are highly prevalent in gymnastics due to the combination of spine extension and loading in skills such as the BHS [4]. There are multiple variations in technique that can lead to a successful BHS on a balance beam, but they remain largely understudied [2]. Given the unique biomechanical demands and high repetitions of skills in gymnastics, a better understanding of the variations in techniques is crucial for coaching and targeted muscle training routines. Specifically, the countermovement jump in the take-off of the BHS requires the gymnast to produce angular momentum as well as vertical and backward momentum. There are multiple ways a gymnast can use their legs and trunk to successfully produce these momentum components which can lead to differences in body segment kinematics, including the spine extension angle [1]. While some studies have looked into different techniques of hand position [5] and elbow flexion [6] at hand contact in a BHS, fewer studies have investigated the take-off technique in a BHS and how that affects the peak spine extension during the skill. Therefore, the purpose of this study was to determine how the take-off technique affects the spine extension angle. We hypothesize that the gymnasts' peak spine extension angle will be directly related to body segment kinematics at take-off.

Methods: A 12 camera system (Vicon, Oxford) recorded 3D full body kinematics for 20 gymnasts (age: 16.7 ± 4 years, skill level: 8.1 ± 1) during 3 BHS on a 9' long 4'' wide balance beam mounted on the floor. Motion data was then analysed in Visual3D (C-Motion, MD) and MATLAB (Mathworks Inc., MA). Trials where the gymnast fell off the beam were not included in the analyses. Peak trunk flexion, peak knee flexion and knee flexion when the trunk reaches its maximum flexion (representing differing take-off techniques) were calculated as well as peak spine extension, defined as the angle between the thorax and the abdomen. Linear regressions were performed between the knee and trunk flexion angles and spine extension angle to determine if correlations exist between the take-off technique and peak spine extension.

Results & Discussion: Neither peak trunk flexion ($r^2 = 0.06$) nor peak knee flexion alone ($r^2 = 0.05$) during the countermovement take-off were sufficient to describe the variation in peak spine extension seen during the BHS. However, there was a significant linear correlation between the knee flexion angle when the trunk reached its maximum flexion and peak spine extension (Fig. 1), suggesting that the lower body kinematics as a whole is more informative of spine extension angle than knee or trunk angle alone. Interestingly, this correlation was not affected by the skill level of the gymnast (Fig. 1), suggesting the differences in take-off technique are self-selected as opposed to changing with the skill level of the gymnast. Overall, these results suggest that differing take-off techniques can lead to large differences in peak spine extension. High repetitive spine extension can lead to back pain and injuries in gymnasts [7], and so understanding what biomechanical factors in common skills such as the BHS lead to higher spine angles is crucial to reducing injuries.

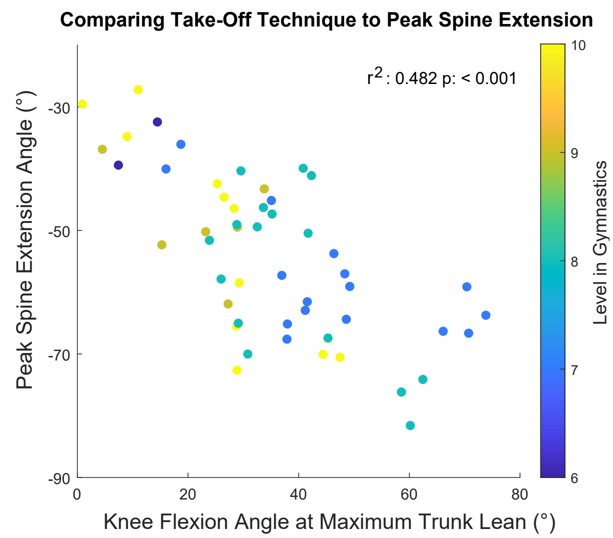

Figure 1: Relationship between take-off technique, measured by the knee flexion at maximum trunk flexion, and peak spine extension during the back handspring step out. The color represents the skill level of the gymnast (1-10, where 10 is the highest level).

Significance: Given the importance of the BHS as a foundational skill on the balance beam, a better understand of the underlying BHS biomechanics is necessary. We found that variations in the take-off of the BHS lead to differences in the spine extension during the skill. Reducing spine extension, especially in a skill that is repeated as frequently as the BHS, is an important step in reducing injury risk in gymnasts [8]. Given that only the coordination between the knee and trunk flexion correlated with the spine kinematics, these results provide further insight into the coordination necessary to control a BHS to help instruct training regimens, with implications for other countermovement jumps and skills as well.

Acknowledgements: This project was supported in part by the National Science Foundation Graduate Research Fellowship Program.

References: [1] FIG Code of Points (2022); [2] Farana et al., (2023), *Sports Biomech.* 22; [4] Pimentel et al., (2020) *Clin Biomech* 76; [5] Richter & Boucher (2017), *J. Athl. Train.* 52; [6] Koh et al., (1992), *Am. J. Sports Med.* 20; [7] Kruse & Lemmen (2009) *Curr Sports Med Rep.* 8; [8] Jackson et al., (1976) *Clin. Orthop. Relat. Res.* 117.

POSITIVE STEP LENGTH ASYMMETRY DURING SPLIT-BELT WALKING REDUCES JOINT WORK IN OLDER ADULTS

Russell T Johnson, Tara Cornwell, Ryan Novotny, James M Finley
University of Southern California
*Corresponding author's email: rtjohnso@usc.edu

Introduction: A comprehensive understanding of how people adapt to novel environments during gait, and the role of metabolic cost, can assist researchers in designing new assistive devices or rehabilitation protocols that reduce the metabolic cost of walking. One paradigm for studying gait in novel environments involves walking on a split-belt treadmill, where each belt moves at a different speed [1,2]. Adopting a positive step length asymmetry (SLA) during split-belt walking (taking a longer step on the fast belt than the slow belt) reduces the positive work performed by the legs on the center of mass and reduces metabolic cost relative to walking with negative asymmetries [3,4]. The reduction in positive work on the center of mass has previously been computed via an individual-limbs method, where each limb is treated as a massless piston performing work on the whole-body center of mass. However, the individual-limbs method does not provide insight into how the work is distributed across joints. Additionally, joint moments and joint work are more strongly associated with muscular work and therefore may better explain the mechanisms for how and why the metabolic cost is reduced when walking with a positive SLA on a split-belt treadmill [5]. Therefore, the purpose of this study is to quantify the relationship between positive and negative joint work rates with SLA when older adults walk on a split-belt treadmill. We hypothesized positive work would reduce across joints when walking with a positive SLA and that the largest reduction would be observed for the ankle joint of the leg on the fast belt, as plantar flexors of the fast-belt limb exhibit the largest reductions in EMG during adaptation [6].

Methods: We measured the whole-body kinematics of 14 older adults (8 F; 70±5 years; 73.4±13.4 kg; 1.67±0.08 m) walking on a split-belt treadmill with one belt moving at 1.00 m/s (left) and the other belt at 0.5 m/s (right). Each participant was given visual feedback of their SLA while walking on the treadmill for five target conditions: -10, -5, 0, +5, and +10% SLA. We computed the SLA, lower limb joint angles, and joint moments during 21 strides for each condition for each subject. We calculated joint powers from the kinematic and joint moment data, integrated joint powers over the stride, and divided the resulting joint work by stride time to compute the joint work rate for the hip, knee, and ankle for both limbs in the sagittal plane. To assess the relationship between joint work rate and SLA, we used a set of linear mixed-effects models with a fixed effect of SLA and a random effect of intercept.

Results & Discussion: The total positive joint work rate (sum of sagittal plane hip, knee, and ankle work rates for both limbs) decreased as SLA increased (slope = -6.3×10^{-5}; $R^2 = 0.71$). This indicates that, just as with the individual-limbs method reported in previous literature, positive work is reduced when walking with a positive SLA on the split-belt treadmill. The total slow-limb joint work rate (sum of hip, knee, and ankle) was not significant ($p=0.24$), because there were decreases at the hip and knee but an offsetting increase in ankle work with increasing SLA (Figure 1, left column). There was a significant decrease in fast-limb joint work rate with increasing SLA, with the greatest decrease in the ankle joint (slope = -3.02×10^{-5}; $R^2 = 0.73$). This indicates that the fast-limb ankle joint is primarily driving the decrease in positive work performed when walking with a positive SLA on the split-belt treadmill, which supports our hypothesis (Figure 1, bottom of right column). We also computed the negative work rate for each limb and found greater negative work performed by both the fast and slow limb with increasing SLA. This is due to a substantial increase in negative work rate (more negative) for both the fast and the slow ankles as SLA increases.

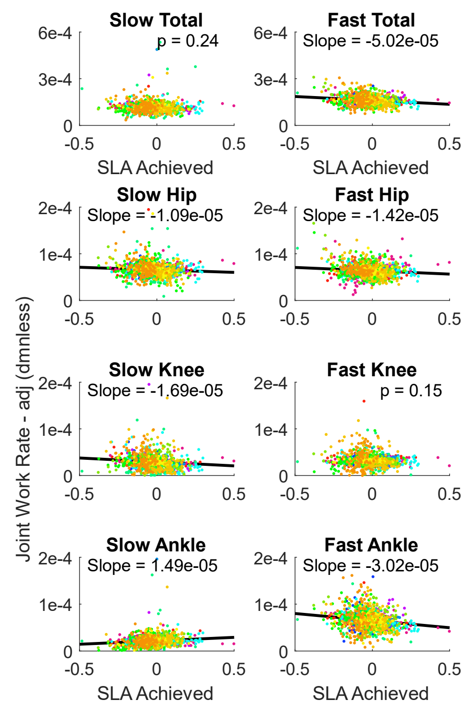

Figure 1: Positive joint work rate for each limb (slow is right limb, fast is left limb). The top row is the sum of the joint work of the hip, knee, and ankle for each limb. Colors represent individual subject data. Step length asymmetry (SLA) achieved is computed as the actual SLA during each stride. Solid black lines show a group-level slope for each variable that was statistically significant. Subject-specific intercepts were removed to adjust the data before plotting to remove the random effect in the model.

Significance: Our findings of reduced hip and ankle positive work rates with increasing SLA correspond with the joints that have been hypothesized to consume the most metabolic energy during gait [7]. Overall, these data suggest that participants improve economy when walking on a split-belt treadmill by reducing the amount of work performed by the ankle on the fast belt, thereby reducing the total metabolic cost of walking in this novel environment.

Acknowledgements: Funding provided by NIH NICHD R01 HD091184

References: [1] Dietz et al., 1994 *Exp Brain Res.* 101; [2] Prokop et al., 1995 *Exp Brain Res.* 106; [3] Sánchez et al., 2019 *J. Physiol.597(15);*[4] Sánchez et al., 2021 J. Neurophysiol.125(2); [5] Sasaki et al., 2009 *J Exp Biol.* 212(5); [6] Finley et al., 2013, *J. Physiol.* 591(4); [7] Umberger & Rubenson, 2011 *Exerc Sport Sci Rev.* 39(2).

EFFECT OF A BACK EXOSUIT ON LIFTING ENDURANCE AND LOW BACK DISORDER RISK FACTORS

Paul R. Slaughter*, Katherine M. Rodzak, Derek N. Wolf, Shimra J. Fine, Chad C. Ice, Karl E. Zelik
Center for Rehabilitation Engineering and Assistive Technology, Vanderbilt University, Nashville, TN
*Corresponding author's email: paul.r.slaughter@vanderbilt.edu

Introduction: Back overexertion injuries are common, especially among people who frequently perform heavy lifts as a part of their job. Back exos are one emerging technology that can reduce certain musculoskeletal disorder risk factors including back muscle activity, spinal compression force, and lumbar moment [1]. Back exos may also increase lifting performance (e.g., endurance), however existing evidence is mixed and limited [2,3]. For instance, studies have not quantified the effect of a back exo during heavy lifting tasks, such as those experienced by Soldiers in the field artillery, as well as others in civilian material handling jobs. The primary objective of this study was to address this gap by testing whether participants were able to perform more heavy lift repetitions when wearing a back exo compared to not wearing one. If so, then the secondary objective was to assess whether this increase in lifting repetitions would negate the injury risk reduction benefits of the back exo.

Methods: We tested how many heavy lifts participants were able to perform with vs. without wearing a back exo. The back exo used was a quasi-passive (unpowered, mode-switching) exosuit which uses elastic bands to generate an extension moment about the low back as the participant flexes their trunk or hips. Before testing, participants were fitted with the exosuit, instructed on its use, and given 10-20 minutes of practice lifting using the exosuit.

Eight field artillery Soldiers from the 101st Airborne Division participated. They were consented under a protocol approved by the Vanderbilt University IRB and the U.S. Army Human Research Protections Office. Each participant performed repetitive lifts using objects they commonly handle in their job. The first four participants performed an AB protocol in which they lifted a 46 kg artillery round every 6 seconds until failure. First, they did this without the back exosuit ("A" trial). They were given 20-30 minutes of rest afterward. Then they repeated this lifting task with the back exosuit ("B" trial). The remaining four participants performed an ABA protocol in which they lifted a 54.5 kg artillery box every 6 seconds until failure. Between each lifting trial, participants were given 20-30 minutes of rest. For all trials, the number of lifts was recorded. To assess the primary objective, we computed the change in lifting repetitions when wearing the exosuit ("B" trials) relative to not wearing an exosuit ("A" trials) to determine if this increased.

An ergonomic assessment tool, Exo-LiFFT [4] was used to evaluate low back disorder risk of each lifting trial. Exo-LiFFT uses lifting repetitions, the exosuit's lumbar extension moment, and the peak load moment of the object being lifted as inputs. We measured the exosuit's lumbar extension moment and the load moment for each participant during a practice lift performed before the evaluated lifting trials. Exo-LiFFT outputs cumulative damage to the low back for each trial, which is an indicator of wear-and-tear on the back based on mechanical fatigue failure principles. To assess the secondary objective, we computed the change in cumulative damage when wearing the exosuit ("B" trials) vs. not wearing one ("A" trials) to determine if it decreased.

Results and Discussion: Seven out of the eight participants increased their lift repetitions when wearing an exosuit, by 8%-75% (mean: 43%). The single remaining participant performed 37% fewer lifts. These results suggest that a back exosuit can increase lifting endurance (number of repetitions) for most users. These findings corroborate and extend lab-based studies that found back exosuits can reduce back muscle fatigue [5].

Cumulative damage to the back was 41-91% (mean: 67%) lower when wearing the exosuit (i.e., when comparing B vs. A trials), indicating reduced low back disorder risk while wearing the exosuit. This risk reduction was found even though most participants performed more lifts while wearing the exosuit. This suggests that back exosuits are able to provide reductions in injury risk even if the number of lifts a user performs increases.

These findings relate to the effects on individuals who performed more lifting repetitions of a fixed weight. In contrast, using exosuits to lift heavier weights (as opposed to increasing the number of lifts) could offset the risk reduction benefits.

Significance: While exosuits should still primarily be used to decrease injury risk, these results suggest that it is feasible for exosuits to simultaneously increase heavy lifting endurance and reduce low back disorder risk factors. These findings are relevant to individuals who often perform repetitive heavy lifting and who are at risk of back overexertion injuries.

Acknowledgements: Funded by U.S. Army Research Lab W911NF-21-2-0078. Views in this document do not represent the views or policies of the U.S. Army.

References: [1] Kermavnar et al. (2021), Ergonomics 64(6); [2] So et al. (2022), J of Safety Research 83; [3] Tan et al. (2019), Front. Hum. Neurosci 13. [4] Zelik et al. (2022), App. Ergonomics 99. [5] Lamers et al. (2020), Scientific Reports

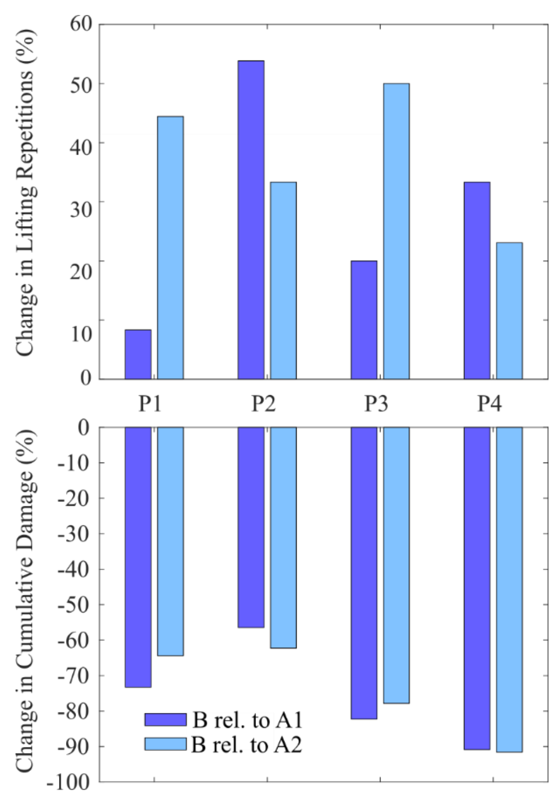

Figure 1: The exosuit increased lifting repetitions (top) and reduced cumulative damage (bottom) for all 4 participants in the ABA protocol.

FUNCTIONAL COVERAGE FOLLOWING PERIACETABULAR OSTEOTOMY SURGERY FOR DYSPLASTIC HIPS

Christina A. Bourantas*, John C. Clohisy, Michael D. Harris
Washington University in St. Louis, St. Louis, MO
*Corresponding author's email: bourantas@wustl.edu

Introduction: Developmental dysplasia of the hip (DDH) is an arthritis-causing disorder that involves reduced hip stability due to insufficient coverage of the femoral head. [1,2] Current treatment for DDH focuses on reorienting the acetabulum (pelvis socket) using periacetabular osteotomy (PAO) surgery to improve lateral femoral head coverage. [3] Coverage before, during, and after surgery is most often measured using 2D radiographs. Two key limitations with 2D radiographic measures are that they cannot capture 3D femoral anatomy and are limited to static hip positions. To fully assess how PAO surgery changes femoral coverage it is important to quantify coverage in 3D and during functional activities, like gait, that are cited by patients with DDH as being painful. [4–6] The first objective of this study was to calculate 3D femoral coverage changes after PAO over the entire femoral head and in the lateral regions targeted during surgery. The second objective was to compare 3D coverage in a neutral position to coverage during gait at the times of peak hip joint loading. We hypothesized that total femoral coverage would not change after PAO, but coverage in the lateral regions would increase. We also hypothesized that coverage measured in a neutral position would not match coverage during the functional gait task.

Methods: Using pre- and post-PAO computed tomography scans (0.74 x 0.74 x 0.6 mm voxels), femur and pelvis bones from patients with DDH (N=5) who underwent PAO were segmented with IRB approval. The femurs and pelvises were aligned to a neutral anatomical position and segment coordinate systems were established. The femoral head was objectively isolated and split into four anatomic regions (Fig 1). [7] Coverage was determined by projecting the lunate surface of the acetabulum to the nearest points on the femoral head (Fig 1). To isolate the effects of geometry, gait in each subject was simulated by rotating the femur in the acetabulum using the average hip joint angles of 20 previous patients with DDH. [8,9] Coverage was calculated pre- and post-PAO in the neutral position and at the time of peak joint reaction forces during midstance (17% gait, 15.6° flexion, 9.5° adduction, 0.1° rotation) and late stance (52% gait, -18.5° flexion, -0.04° adduction, 4.1° rotation). The percent of the anterolateral (AL) and posterolateral (PL) head sections covered at these time points was also calculated because these regions are a focus during PAO. Coverage pre- and post-PAO was compared, as was the change in coverage in the neutral position versus change in coverage at the time points during gait.

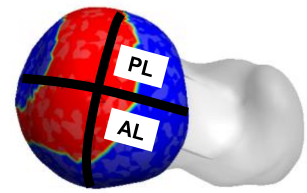

Figure 1: Example of femoral head regionalization and coverage. Red area indicates coverage of the lunate surface of the acetabulum. This study focused on total head coverage and coverage in the anterolateral (AL) and posterolateral (PL) regions.

Results & Discussion: As hypothesized, total femoral head coverage remained similar pre- and post-PAO (Table 1). Coverage in the AL and PL regions increased for all patients, but changes in the PL region were larger and more variable than changes in the AL region (Table 1). Our results are similar to previous research that found significantly greater 3D coverage in the lateral and anterior regions following surgery. [10,11] In the neutral position, total head coverage matched total head coverage at the two gait time points (Table 1), which is similar to previous findings in healthy hips. [12] However, neutral coverage in the AL and PL regions did not match AL and PL coverage at the gait time points (Table 1). These differences in regional coverage during gait compared to neutral, even in the range of 2-7% could have important effects on biomechanical loading. For example, it is known that acetabular edge loading induced by joint reaction forces is high during gait before PAO [8], and in pilot data we have found that edge loads are reduced after PAO. Future work will quantify the relationships between the magnitude of regional coverage changes and edge loading responses. Limitations of this study include a small sample size and using average hip joint angles of previous patients for the gait cycle. Thus, a larger sample and more variable kinematic inputs, including a range of activities, as well as comparison to healthy controls is warranted.

Table 1. Average ± standard deviation increase in percent of region covered after PAO

	Neutral	At first joint reaction force peak	At second joint reaction force peak
Total head	1.7 ± 0.9%	2.0 ± 0.8%	1.7 ± 1.1%
AL region	7.6 ± 2.8%	9.2 ± 3.5%	4.0 ± 1.7%
PL region	16.3 ± 10.4%	11.3 ± 6.0%	18.9 ± 10.3%

Significance: Changes in regional coverage in a neutral position do not match and are not indicative of changes in coverage during gait. This finding is important given that surgeons often target regional changes during surgery based on a patient's initial coverage deficiencies and intend to create coverage that improves stability for all activities of daily living, not just a neutral position. Going forward, the influence of regional coverage change on biomechanics should be quantified. Also, more comprehensive measures that use 3D methods and include simulation of multiple functional activities should be developed to aid with surgical planning.

Acknowledgements: Funding provided by the National Institute of Health T32007434, K01AR072072, and R01AR081881.

References: [1]Wyles *Clin Orthop* 2017. [2]Ganz *Clin Orthop* 2008. [3]Clohisy *JBJS* 2005. [4]Reijman *Arthritis Rheum* 2005. [5]Hampton *Bone Jt J 2019.* [6]Reddy *BMC Musculoskelet Disord* 2020. [7]Harris *Ann Biomed Eng* 2013. [8]Song *Front Sports Act Living* 2021. [9]Song *J Orthop Res* 2022. [10]Tanaka *Int Orthop* 2018. [11]Uemura *Arch Orthop Trauma Surg* 2023. [12]Uemura *Clin Anat* 2018.

KINEMATICS AND KINETICS DURING RUNNING IN DYSPLASTIC HIPS

Molly C. Shepherd[1*], Michael D. Harris[1]
[1]Washington University in St. Louis
*email: mollycshepherd@wustl.edu

Introduction: Developmental dysplasia of the hip (DDH) is an orthopaedic condition characterized by a shallow hip socket that lateralizes hip joint centers and increases loading on the joint.[1,2] The increased loads can lead to chondrolabral damage and early onset osteoarthritis.[3] Many patients with symptomatic DDH are young, active individuals who regularly participate in demanding exercise or sport but become limited by pain that increases with activity.[4] Additionally, symptom onset tends to occur at younger ages in patients with high activity scores than those who are less active.[4] This younger presentation of symptoms is thought to occur due to the repeated high impact loading that comes with participation in exercise or sports.[5] However, most studies of hip joint loading in DDH have been limited to the lower impact activities of gait or squatting.[6–8] It remains unknown if there is abnormal hip loading such as elevated joint reaction forces (JRFs) in dysplastic hips during high impact activities, and their potential effect on symptoms remains unclear. Therefore, the objective of this study was to compare hip JRFs and joint angles between patients with DDH and healthy controls during running.

Methods: Five female patients with DDH (age = 24.4±6.7, BMI = 24.3±1.7) and five healthy controls (age = 20.4±1.9, BMI = 23.2±1.8) were included with IRB approval and informed consent. Patients were diagnosed with DDH by an orthopaedic surgeon based on a lateral center edge angle <20° and unilateral hip/groin pain for 3+ months. Kinematic running gait data (200 Hz) was collected using 70 reflective markers and 10 infrared cameras (Vicon) at 2.5 m/s after a 90 second acclimation period. Ground reaction forces (2000 Hz) were collected from an instrumented treadmill (Bertec). A baseline OpenSim musculoskeletal model was updated for each subject with three-dimensional reconstructions of the pelvis and femurs from MRI.[6] OpenSim Moco was used to calculate joint angles, muscle forces, and hip JRFs.[9] All JRFs were normalized to bodyweight (xBW) and JRFs and joint angles from representative running cycles (foot strike to foot strike) were compared between the DDH and control groups. Inter-group differences were tested for significance across the running cycle using one-dimensional independent samples t-test statistical parametric mapping.[10]

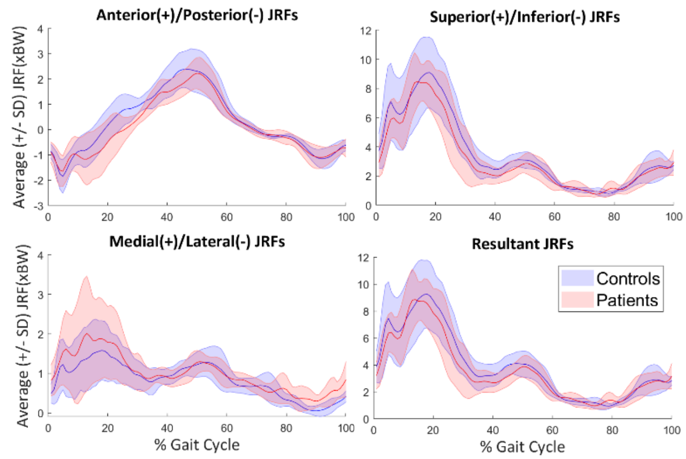

Figure 1: Average ± standard deviation hip JRF components across the running gait cycle. All forces were normalized to bodyweight (xBW).

Results & Discussion: Average running JRF peaks for DDH patients were 2.23±0.62 xBW in the anterior direction, 8.48±1.67 xBW in the superior direction, 2.01±1.45 xBW in the medial direction, and 8.86±1.91xBW overall (Fig. 1). For controls, JRF peaks were 2.38±0.72 xBW anteriorly, 9.10±2.42 xBW superiorly, 1.58±0.75 xBW medially, and 9.26±2.51 xBW overall (Fig. 1). There were no statistically significant differences between patients and controls in hip JRFs or joint angles during the running gait cycle (Fig. 1&2).

Hip JRF magnitudes and joint angles were consistent with previous reports of running kinematics and kinetics in healthy hips.[11] Despite the lack of significance, the higher medial JRFs during running in DDH hips are of interest as similar trends have been found in walking and are thought to contribute to medial femoral head cartilage damage in these patients.[1,6,7] However, it is important to note the small sample size and the possibility that differences would appear when the sample is increased, an area of future work.

Significance: Studying activities such as running that are frequently performed by symptomatic DDH patients are important to contribute knowledge on mechanisms of damage. Identifying abnormal loading during this high impact activity may contribute to understanding of symptom onset and can inform activity modifications and optimal treatment techniques in patients with DDH.

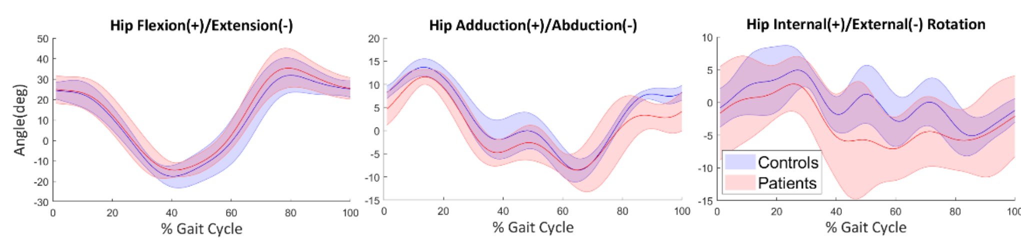

Figure 2: Average ± standard deviation hip joint angles across the running gait cycle.

Acknowledgements: Stanford Restore and Mobilize Center for their assistance with OpenSim Moco. Funding was provided through NIH grants R01AR081881, K01AR072072, and T32HD007434.

References: [1] Harris *J. Orthop. Res.* 2022. [2] vanBosse *Clin. Orthop. Relat. Res.* 2015. [3] Murphy *J. Bone Jt. Surg.* 1995. [4] Matheney *J. Bone Jt. Surg.* 2016. [5] Kapron *J. Sports Med.* 2015. [6] Song *J. Biomech.* 2020. [7] Harris *J. Biomech.* 2017. [8] Song *Front. Sport Act. Living* 2021. [9] Dembia *PLoS Comput. Biol.* 2020. [10] Pataky *Comput. Methods Biomech. Biomed. Engin.* 2012. [11] Giarmatzis *J. Bone Miner. Res.* 2015.

KINETIC ADAPTATIONS TO RESTRICTING SPINE MOTION DURING LIFTING

Danielle R. Carnegie*, Steven Hirsch[1], Tyson A. C. Beach[2], Samuel J. Howarth[3]
[1]Faculty of Kinesiology & Physical Education, University of Toronto, Toronto, ON
[2]Department of Kinesiology and Health Sciences, University of Waterloo, Waterloo, ON
[3] Division of Research and Innovation, Canadian Memorial Chiropractic College, Toronto, ON
*Corresponding author's email: danielle.carnegie@mail.utoronto.ca

Introduction: Physically restraining spine motion is an approach to investigate the necessary biomechanical redistribution of joint demands to achieve recommended "safe" lifting techniques. When lumbar spine flexion is physically restricted, greater lower extremity motion is required to complete the same lifting task [1]. However, the kinetic effects of altered lower extremity joint motion in the presence of restricted spine motion have not been documented. Mechanical energy expenditure (MEE) is useful for this endeavour because it provides a high-level approximation of joint demands while reducing dimensionality of the data. Thus, the objective of this study was to compare ankle, knee, hip, low-back, and total MEE between spine flexion-restricted and self-selected lifting across a variety of lifting tasks that varied by combinations of lift origin height and object mass. Since joint range-of-motion demands are increased in lower extremity joints when spine motion is restricted [1], it was expected that restricting spine flexion would result in a concomitant increase in MEE at the hips, knees and ankles and a reduction in lumbar spine MEE when restricting lumbar spine flexion compared to self-selected lifting. Further, it was expected that the nature and magnitude of redistributed joint demands would depend on task constraints (i.e., lift origin height, object mass).

Methods: Twenty participants (10 female) (mean ± SD: age: 26 ± 1.54 years, height: 1.77 ± 0.1 m, mass: 76 ± 14.4 kg), performed 8 different barbell lifting tasks that varied by all combinations of three task factors: 1) spine posture (presence or absence of spine flexion-restricting harness); 2) lift origin height (high = knee height, low = mid shank height); and 3) object mass (light: females = 20kg; males = 34kg and heavy: females = 34kg; males = 58kg). Five repetitions for each lifting task were performed. An optoelectronic motion capture system (VICON, Oxford, UK), and two spatially synced in-ground force plates (AMTI BP400600-OP, MA, USA) were used to record segment mechanics during all lifts. Bottom-up inverse dynamics analyses were conducted using standard methods to quantify lower extremity and spine kinematics and kinetics, which were used to quantify absolute and relative MEE. Repeated measures ANCOVAs were conducted using R to compare all dependent variables between spine restriction, lift origin height, and object mass conditions [2]. Time taken to complete lifts was used as a covariate to account for potential differences in self-selected movement speed.

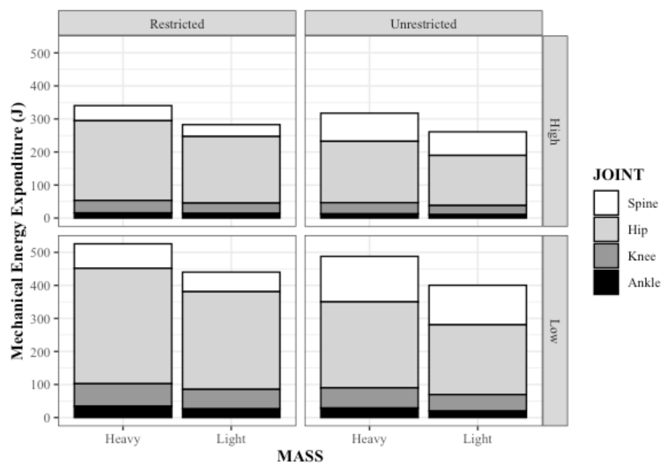

Figure 1: Total MEE depicted on the vertical axis, and stacked bars show contribution of MEE from each joint to the total in each lifting task.

Results & Discussion: Figure 1 depicts results obtained for MEE. Total MEE was higher when lifting from a lower origin or a heavier mass (p <0.001). Joint-level MEE differences for the spine and hip, when lifting from a lower height, were greater when spine flexion was restricted ($p \leq 0.050$). Similarly, the difference in MEE for the ankle between lift origin heights was greater for the heavier mass (p = 0.050). A lower height also increased MEE at the knee compared to a higher height (p <0.001). On average, restricting spine flexion decreased the relative contribution of the spine to total MEE by 13%, which was countered by 12% increase in the relative contribution from the hips (p <0.001) (Table 1). The higher lift origin increased the hip's contribution to total MEE by 5% (p = 0.010). Conversely, the lower lift origin increased the ankle's contribution to MEE by 1% (p <0.001). Thus, to reduce spine flexion during lifting, spine MEE appears to be redistributed to place greater demands on the hips, which is consistent with joint motion redistributions in kinematic analyses [1]. The redistribution of MEE contribution throughout the body appears to be affected mainly by spine posture and lift height.

Significance: Restricting lumbar spine flexion can reduce MEE at the spine. Since total MEE is unaffected by spine posture, when spine flexion is restricted, the reduction in MEE at the spine is predominately accounted for by an increase in hip MEE. Individuals lacking the capacity to meet further increases in mechanical demands imposed on hips by lifting task conditions (i.e., heavier masses, lower lift origins) may not have the capacity to redistribute MEE to the lower extremity and thus be obliged to flex the lumbar spine when lifting. This may provide one possible explanation for why some lifters, in some lifting conditions, resort to increased spine flexion.

References: [1] Carnegie, D et al. (2022). *J Electromyogr Kinesiol* 67; 102716. [2] R Core Team (2019).

Table 1. Percent (SD) contribution of each joint to total MEE. Statistically significant effects (p <0.05) indicated by bold font.

CONTRIBUTION TO TOTAL MECHANICAL ENERGY EXPENDITURE (%)

JOINT	SPINE POSTURE		LIFT ORIGIN HEIGHT		MASS	
	RESTRICTED	UNRESTRICTED	LOW	HIGH	HEAVY	LIGHT
SPINE	**13.1 (3.6)**	**25.6 (9.7)**	20.5 (10.0)	19.1 (9.9)	19.8 (9.5)	19.9 (10.4)
HIP	**69.6 (8.3)**	**57.6 (10.7)**	**61.5 (11.5)**	**65.7 (10.7)**	63.5 (11.0)	63.6 (11.6)
KNEE	12.0 (6.0)	11.3 (5.7)	12.5 (6.9)	10.8 (4.3)	11.6 (5.3)	11.7 (6.4)
ANKLE	5.4 (2.6)	4.5 (2.1)	**5.5 (2.4)**	**4.4 (2.3)**	5.1 (2.4)	4.8 (2.5)

REDUCTIONS IN SHOULDER FUNCTION FOLLOWING MASTECTOMY AND BREAST RECONSTRUCTION

Joshua Pataky[1*], Jared Heitzenrater[2], Kathryn H. Schmitz[3], Daleela Dodge[2], John Potochny[2], Kristine Widders[2], Melody Paulishak[2], Dino Ravnic[2], Cathy R. Henry[2], Timothy S. Johnson[2], Kavita Vakharia[2], Meghan E. Vidt[1,2]
[1]Pennsylvania State University, University Park, PA, USA
[2]Penn State College of Medicine, Hershey, PA, USA
[3]University of Pittsburgh, Pittsburgh, PA, USA
*Corresponding author's email: jjp6192@psu.edu

Introduction: Breast cancer affects 14.8% of women with a 5-year survival rate of 90% [1]. As part of their treatment, 35.5% of patients undergo mastectomy, with 36.4% also undergoing breast reconstruction [2]. Breast reconstruction surgery is performed using either an implant or autologous flap [3]. Following mastectomy and reconstruction, many women experience reduced shoulder strength and mobility, resulting in reduced overall quality of life and difficulty performing daily functional tasks [4-6]. Our objective is to determine if surgical treatment and reconstruction approach influences objective and patient-perceived shoulder function for breast cancer patients.

Methods: Objective and patient-perceived measures of shoulder function were collected from 29 women (age: 56±12 yrs.) diagnosed with breast cancer who had either: lumpectomy with no reconstruction surgery (pre-/post-surgery: n=8/6), or mastectomy followed by implant (n=14/6) or autologous flap (n=7/2) reconstruction. Objective measures included range of motion (ROM) and isometric joint moment to assess strength. Patient-perceived function was assessed with the Penn Shoulder Score questionnaire. Measures were taken before surgery and 3 months after the terminal (lumpectomy or final reconstruction) surgery. Pre- and post-surgical timepoints were compared using one-way ANOVA (strength, Penn Shoulder Score) and Kruskal-Wallis test (ROM) across groups. Analyses were performed using SAS software (v.9.4, SAS, Inc., Cary, NC), with $p<0.05$ considered significant.

Results & Discussion: No age differences were seen between groups ($p>0.05$). Pre-surgery, there were no differences between any groups for any measure of function (all $p>0.05$). Post-surgery, active external rotation for the implant group was 64°, which was trending towards a significant reduction when compared to the 70.7° active external rotation for the lumpectomy group ($p=0.0685$) (Fig. 1A). There was also a trend towards reduced passive external rotation ($p=0.0579$) for the implant group (72.2°) compared to the lumpectomy group (80.5°). No differences were seen when the lumpectomy or implant groups were compared to the flap group ($p>0.05$). There were no differences between any group in measured isometric joint moment post-surgery. For patient-perceived function post-surgery, no differences were seen between groups for any domains assessed by the Penn Shoulder Score ($p>0.05$) (Fig. 1b). Pre-surgery, all groups had comparable shoulder function which was expected. Post-surgery, however, trends are emerging towards reduced ROM in both active and passive external rotation for the implant group compared to the lumpectomy group. This may suggest that implant reconstruction approach could negatively impact objective function, despite no patient-perceived differences.

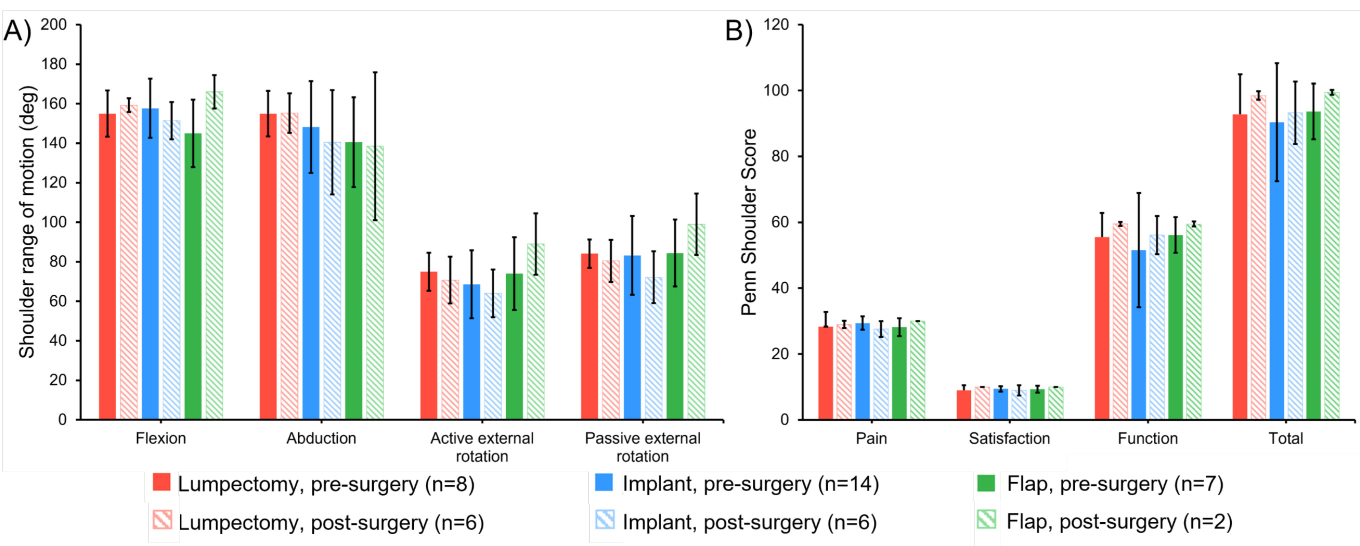

Figure 1: Shoulder (A) range of motion and (B) self-reported Penn Shoulder Score recorded before surgery (solid bars) and 3 months after (striped bars) the terminal surgery for the lumpectomy (red), reconstruction with implant (blue), and reconstruction with autologous flap (green) groups.

Significance: These data are part of an ongoing study to determine the impact of mastectomy and breast reconstruction on shoulder function and survivorship. Emerging trends suggest function may be impacted differently depending on approach. It is important to understand the functional impacts of reconstruction approach to limit functional deficits and improve overall quality of life for survivors.

Acknowledgements: Penn State College of Medicine, Junior Faculty Development Program Seed Grant (Vidt)

References: [1] National Cancer Institute, Cancer stat facts: Female breast cancer (2021); [2] Kummerow et al. (2015), *JAMA Surg* 150(1):9-16; [3] Panchal & Matros (2017), *Plast Reconstr Surg* 14:7S-13S; [4] Nesvold et al. (2017), *J Cancer Surviv* 5(1):62-67; [5] de Haan et al. 2007, *Ann Plast Surg* 59(6):605-610; [6] Andersen & Kehlet (2011), *J Pain* 12(7):725-746.

FEMALES WIH HIP PAIN DISPLAY DECREASED KINETICS AT THE HIP AND ANKLE DURING GAIT

Madeline Grosklos[1,2*], Cara L. Lewis[3], Elizabeth Ceballos[2], Jennifer Perry[2], Stephanie Di Stasi[2,4]
[1]The Ohio State University Department of Biomedical Engineering [2]The Ohio State University Sports Medicine Research Institute
[3]Boston University Department of Physical Therapy [4]The Ohio State University Department of Physical Therapy
*Corresponding author's email: madeline.grosklos@osumc.edu

Introduction: Hip-related pain (HRP) is a debilitating, non-arthritic condition characterized by motion-related pain, and can occur in the presence or absence of structural variants in bony morphology. [1] Over half of individuals with HRP conditions report pain with walking. [2,3] Individuals with HRP display abnormal gait mechanics and muscle forces (e.g. altered sagittal plane kinetics and lower hip muscle forces) that are associated with worse hip joint pain and function, [5] and are sex specific. [6,7] The hip flexors and ankle plantar flexors are key contributors to the forward progression of the body during gait.[8] Increasing ankle push-off during terminal stance decreases sagittal plane hip moments and anterior hip joint loading in healthy individuals. [9] The purpose of this study was to compare hip and ankle kinetics during gait between individuals with HRP and healthy controls (HCs), focusing on interlimb asymmetries and sex-specific differences. Due to the described hip-ankle relationship, we hypothesized that individuals with HRP would show increased peak internal ankle plantarflexion moment (pPFM) and angular impulse and decreased internal peak hip flexion moment (pHFM) and angular impulse during terminal stance on their affected limb compared to both their unaffected limb and to healthy controls. This hypothesis assumes a compensatory gait strategy to reduce forces on the painful hip. Secondly, due to previous findings of sex-specific biomechanics in this population, [6,7] we expected that these differences would be unique between males and females.

Methods: 42 patients with HRP (23F, 19M) and a comparable group of 20 healthy controls (9F, 11M) between the ages of 14-50 underwent 3D motion analysis of overground gait at their self-selected pace. Marker trajectories and ground reaction forces (GRF) were sampled at 240Hz and 1200Hz respectively, and lowpass filtered in Visual3D software (C-Motion Inc. Rockville, MD) using a 4th order Butterworth filter at 20Hz and 50Hz respectively. Data were analyzed during terminal stance, defined as the phase from peak knee extension during midstance to toe off (vertical GRF $\leq$ 10N). All moments and impulses were reported as internal. Custom code in MATLAB was used to extract variables of interest including: pPFM, pHFM, ankle plantarflexion angular impulse, and hip flexion angular impulse. Moments were normalized to participant mass and height (Nm/kg*m). Angular impulse was calculated as the area under the timeseries moment curve. The mean values from the three gait trials for each limb was used for analysis. The involved limb for HCs was randomly selected to match the distribution of dominant and nondominant involved limb in the HRP group. Group (HRP, HC) by limb interactions, with gait speed as a covariate, were analyzed with General Estimating Equations (GEE) for males and females separately. Sex by limb interactions within the HRP group were then analyzed with GEEs to investigate if limb mechanics differed based on sex. Significance was defined as $p \leq 0.05$ and data were reported as means with 95% confidence interval.

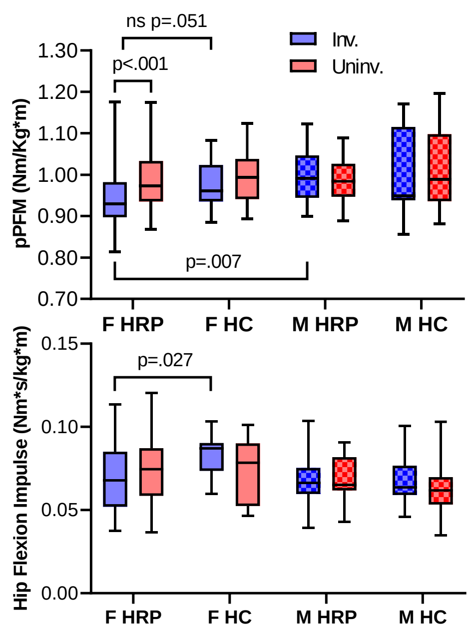

Figure 1: pPFM and hip flexion impulse on the involved and uninvolved limb in females (F) and males (M) with HRP compared to HCs.

Results & Discussion: Age, BMI, and sex distribution were not different between groups ($p \geq .374$); individuals with HRP walked slower than HCs (1.45m/s, 1.54m/s; p=.042). Females with HRP demonstrated decreased pPFM on their involved limb compared to their uninvolved limb and decreased hip flexion angular impulse on their involved limb compared to HC females (Fig. 1). There were no limb asymmetries or group differences in males ($p \geq .220$). In contrast to our primary hypothesis, a compensatory relationship between the ankle and hip was not observed, rather the decrease in kinetics at both joints may indicate an overall offloading of the painful limb during terminal stance in females. To the authors' knowledge, this is the first focused investigation of the relationship between the hip and ankle in this population. That biomechanical differences were present only in females supports the second hypothesis. This agrees with previous studies in this population and is especially relevant considering that females report worse symptoms and poorer treatment outcomes than males. [10]

Significance: This study indicates that females with HRP likely do not use their ankle to compensate for the painful hip during gait but may have an overall offloading strategy for the entire involved limb. Future work should evaluate the effect of gait cues to "push off at the ankle" to understand if individuals with HRP, especially females, can improve terminal stance push-off and therefore decrease anterior hip forces during gait [9]. These findings further emphasize the need for continued sex-specific study of biomechanics and symptoms in HRP as the most effective treatment options may be different for males and females.

Acknowledgements: This work was supported in part by the American Academy of Sports Physical Therapy.

References: [1] Reiman et al. (2020), *Br J Sports Med.* 54(11) [2] Nunley et al. (2011), *JBJS* 93(Suppl 2). [3] Philippon et al. (2007) *Knee Surg Sports Traumatol Arthrosc.* 15(8). [5] Samaan et al. (2019) *J Biomech* 84. [6] King et al (2019) *Clin Biomech* 68. [7] Lewis et al. (2018) *JOSPT* 48(8). [8] Sadeghi et al. (2001) *Clin Biomech*. 16(8). [9] Lewis & Garibay (2015) *J Biomech.* 48(1). [10] Westermann et al. (2017) Orthop J Sports Med. 5(9).

COMPARISON OF GLENOHUMERAL KINEMATICS BETWEEN INDIVIDUALS WITH INSTABILITY AND HEALTHY CONTROLS

Oliver A. Silverson[1*], Gaura Saini[1], William L. Christenson[1], Paula M. Ludewig[1], Justin L. Staker[1].
[1] University of Minnesota, Minneapolis, MN
*Corresponding author's email: silve567@umn.edu

Introduction: Individuals clinically diagnosed with glenohumeral joint multidirectional instability (MDI) are thought to possess altered glenohumeral joint kinematics during dynamic arm activity compared to individuals with stable shoulders. While prior research suggests that some glenohumeral joint kinematic differences may exist between individuals with MDI and healthy controls,[1,2] the magnitude of differences is unclear. Factors surrounding motion capture methods used in prior research ultimately confound these results. Therefore, the purpose of this analysis was to compare glenohumeral joint kinematics captured during dynamic arm activity between individuals clinically classified with MDI and healthy, matched, controls using novel variables to quantify joint instability (Fig. 1). Based on the clinical construct of MDI,[3] we hypothesized that there would be significantly greater average magnitudes of contact path length (CPL) for the humerus traveling on the glenoid and humeral instantaneous helical axis (IHA) positional dispersion in individuals clinically diagnosed with MDI compared to controls (Fig. 1- dashed box).

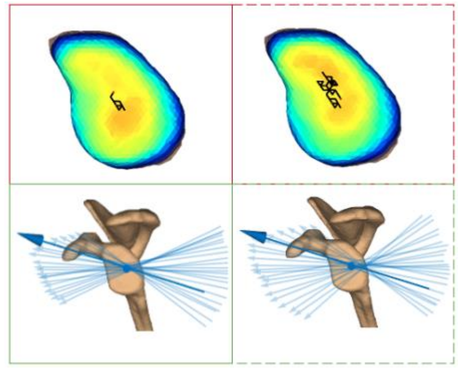

Figure 1: *Top row*: Black lines represent CPL of the humerus on the glenoid across SAB. *Bottom row*: Scattered IHAs (light arrows) depicting dispersion from an optimal IHA (dark arrow) and location (dark dot) across SAB. *Dashed outline*: hypothesized increase in variables.

Methods: Twenty individuals clinically classified with MDI via a comprehensive clinical examination[4] (BMI: 23.3; 13 females) and 10 healthy matched controls with stable shoulders (BMI: 23.6; 6 females) were enrolled. Active, unweighted, scapular plane abduction (SAB) was recorded with dynamic biplane video radiography at 60Hz. Glenohumeral joint kinematics were tracked with 2D/3D shape-matching.[5] Data for the CPL and humeral IHA positional dispersion were extracted between 30-65 degrees of glenohumeral elevation and normalized to glenoid height. Based on the 2:1 humeral elevation:scapular upward rotation ratio expected during arm raising,[6] 35 degrees of glenohumeral elevation relates to roughly 60-130 degrees of humerothoracic elevation. Following checks for equal variances, each variable was independently compared between groups with two sample *t*-tests (alpha < 0.05).

Results: There was no significant difference in either CPL or humeral IHA positional dispersion between groups (Table 1). There were small to moderate effect sizes observed for each comparison.

Table 1: Summary of Group Comparisons

Outcome Variable	MDI N = 20	Control N = 10	Mean Difference	*p*-value	95% CI	Cohen's *d*
CPL (%)	44.95 (17.07)	47.57 (23.04)	2.64	0.75	-14.99-20.27	0.13
IHA positional dispersion (%)	19.60 (8.01)	23.37 (9.98)	3.77	0.32	-3.97-11.51	0.42

Values represent mean ± standard deviation values.

Discussion: Results from this analysis did not detect significant differences in either CPL or humeral IHA positional dispersion between individuals clinically diagnosed with MDI and healthy controls with stable shoulders during active SAB. These findings do not support our hypothesis or the clinical construct of MDI.[3] Instead, our results may suggest that CPL and humeral IHA positional dispersion variables are not sensitive enough to identify the suspected differences in glenohumeral joint stability between groups. The lack of significant findings could be caused by the relatively small range of glenohumeral elevation that data was extracted. Therefore, perhaps larger differences in both variables may exist at higher angles of arm elevation or across larger ranges of motion. Additionally, the movement task of unweighted SAB may not have been provocative enough to elicit kinematic differences between groups. Future studies investigating the kinematics of glenohumeral joint instability may employ potentially more sensitive methods to quantify instability, such as total helical translation, along with more strenuous testing conditions to distinguish kinematic differences between groups, should they exist.

Significance: Our results question if the variables of CPL and humeral IHA positional dispersion are sensitive enough to capture underlying differences in glenohumeral joint instability associated with MDI. Furthermore, our findings offer consideration to what magnitude of difference is necessary to identify differences in either variable kinematics or represent a clinically meaningful difference. The true kinematic differences in CPL and helical dispersion variables between individuals clinically classified with MDI and individuals with stable shoulders may be apparent during participation in more strenuous activities. Researchers conducting future examinations of glenohumeral joint instability may need to consider a combination of variables including such as angular and positional data to fully quantify the clinical construct of MDI.

Acknowledgements: The authors would like to thank Dr. Lawrence for her data processing assistance.

References: [1] Ogston & Ludewig. (2007), *AJSM* 35(8). [2] Illyés & Kiss. (2006), *KSSTA* 14(7). [3] Matsen et al. (2006), *JBJS-A 88(3)*.[4] Staker et al. (2017) *Int. Biomech* 4(2). [5] Bey et al. (2008), *J Biomech* 41(3). [6] Ludewig et al. (2009), *JSBS-A* 91(2).

EVALUATING EYE DROP INSTILLATION BIOMECHANICS WITH AN INSTRUMENTED BOTTLE

Daniel Duque Urrego[1*], Andrew P. Droste[2], Tanner T. Trenary[2], Alanson P. Sample[2], David T. Burke[2], Susan H. Brown[2], Paula Anne Newman-Casey[2], and Stephen M. Cain[1]
[1]West Virginia University, Morgantown, WV and [2]University of Michigan, Ann Arbor, MI
*Corresponding author's email: dd00055@mix.wvu.edu

Introduction: Glaucoma remains the leading cause of blindness among Black Americans and is the second leading cause of irreversible blindness in the United States. As the American population over 65 is expected to grow in the next four decades, so is the population of Americans with glaucoma [1]. To prevent vision loss, glaucoma patients must take daily eye drop medications; unfortunately, at least 40% of patients do not do this, and 20% are unable to instill the drops into their eyes successfully [2]. A better understanding of why people are unable to instill drops successfully is needed to inform better interventions. This study aimed to evaluate the relationships between the stability or sway of the eye drop bottle during eye drop instillation, instillation success (number of drops needed before a drop went into the eye), and instillation posture (standing, sitting, or supine), where bottle motion was captured by a bottle-mounted inertial measurement unit (IMU). We hypothesized that 1) posture would have a significant effect on eye drop bottle stability measures and 2) the number of drops needed to get a drop in the eye would have a significant relationship with eye drop bottle stability measures.

Methods: Seventeen older adults (6M/10F/1Prefered not to answer, age: 70.1 ± 3.7 years) who do not use eye drops daily participated in this University of Michigan IRB-approved study. Participants applied eye drops with their dominant hand into both eyes during three different body postures: standing, sitting, and supine, performing at least three attempts in each eye in each position (18 total instillation attempts). An IMU secured to the bottom of the eye drop bottle (Fig. 1) measured the bottle's linear acceleration and angular velocity. The velocity and displacement of the bottle were calculated from the measured data using a Zero Velocity Update (ZUPT) algorithm [3]. The instillation period (Fig. 1), or the time during which a participant was attempting to instill eye drops, was defined using the bottle velocity where the start/end time was the point at which the bottle's velocity was less/greater than 5% of the peak bottle's velocity during the movement toward/away from the face. Using the data measured during the instillation period, we extracted measures of bottle stability using an approach similar to that used to quantify postural sway [4] and calculated the mean, standard deviation, and coefficient of variation of the linear acceleration and angular velocity magnitudes. We used one-way ANOVAs to compare the effects of body posture, and the number of drops dispensed during each attempt on bottle stability measures; bottle stability measures were normalized with a sinh-arcsinh (SHASH) distribution prior to analysis.

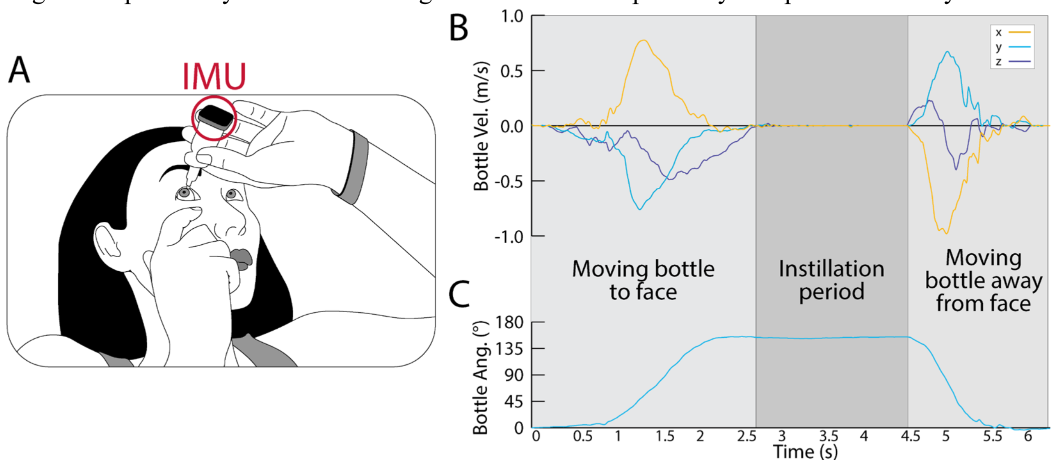

Figure 1. A) Eye drop instillation using the instrumented bottle. **B)** Linear velocity and **C)** bottle angle of the bottle during a sample instillation. Bottle angle is 0° when the bottle is upright and 180° when fully inverted.

Results & Discussion: A one-way ANOVA revealed that there were significant differences in measures of bottle stability depending on posture: acceleration magnitude mean [$F(2,302)=12.09$, $p<.0001$], acceleration magnitude standard deviation [$F(2,302)=5.13$, $p=0.0064$], acceleration magnitude coefficient of variation [$F(2,302)=5.86$, $p=0.0032$], angular velocity magnitude coefficient of variation [$F(2,302)=4.89$, $p=0.0081$], mean distance [$F(2,302)=7.03$, $p=0.001$], RMS distance [$F(2,302)=3.86$, $p=0.0221$], 95% confidence circle area [$F(2,302)=3.46$, $p=0.0326$], and 95% confidence ellipse area [$F(2,302)=4.57$, $p=0.0110$]. A one-way ANOVA also found that there were significant differences in measures of bottle stability depending on how many drops were needed for a successful instillation: acceleration magnitude mean [$F(5,302)=3.24$, $p=0.007$], instillation duration [$F(5,302)=6.73$, $p<.0001$], and total excursions [$F(5,302)=6.05$, $p<.0001$]. Overall, the eye drop bottle was most stable and exhibited the least sway when participants were supine and needed only a single drop for a successful instillation; it was less stable and exhibited the most sway when participants were standing or sitting and needed multiple drops for a successful instillation.

Significance: Our results demonstrate that data from a single bottle mounted IMU can be useful for understanding eye drop instillation biomechanics. Measures of bottle stability or sway during the instillation period can help identify postures and techniques that improve bottle stability or patients needing additional assistance to improve instillation success.

Acknowledgments: Supported by the NIH National Institute of Biomedical Imaging and Bioengineering (R01EB032328).

References: [1] Vajaranant et al. (2012), *Investigative Ophthalmology & Visual Science* 53, 2464-2466; [2] GRF. National Survey Reveals Glaucoma Has Significant Impact on Patients' and Caregivers' Daily Lives and Well-Being (2019); [3] Rebula et al. (2013), *Gait & posture*, 38(4), 974-980. [4] Mancini et al. (2012), *Journal of neuroengineering and rehabilitation*, 9, 1-8.

DAILY RUNNING CONSISTENCY REDUCES ODDS OF RUNNING-RELATED INJURY

Kiara M. Chan[1*], Jennifer Sumner[2], Isaac Loegering[2], Jessica Thompson[2], Jeff Moreno[3], Allison H. Gruber[1]
[1]Department of Kinesiology, Indiana University, Bloomington, IN, USA
[2]Brooks Sports, Inc., Seattle, WA, USA
[3]DashLX, Santa Cruz, CA, USA
*Corresponding author's email: kiachan@iu.edu

Introduction: Running is an accessible and effective form of physical activity; however, a high number of runners suffer running-related injuries (RRI), causing a temporary or permanent stop of running. While the historical perspective has been more training leads to more injuries, there are conflicting reports as to whether greater training increases or decreases RRI risk [1,2]. Thus, there is no clear consensus on how to prevent training errors leading to RRIs. The goal of this study is to identify and explore risk factors for RRI based on daily consistency metrics.

	Pre-Challenge		During Challenge	
	Injured	**Uninjured**	**Injured**	**Uninjured**
Average speed/session (m/s)	2.73 [2.62; 2.84]	2.78 [2.74; 2.83]	2.72 [2.61; 2.83]	2.80 [2.75; 2.85]
Average distance/session (m)	7684.8 [6989.7; 8380.0]	8301.5 [7961.6; 8641.4]	8230.8 [7321.3; 9140.4]	8467.6 [8117.8; 8817.3]
# sessions	44.9 * [39.1; 50.6]	57.6 * [54.0; 61.1]	22.6 * [18.8; 26.5]	60.5 * [57.2; 63.7]

Table 1: Training characteristics (mean and 95% CI) for injured and uninjured participants prior to and during the challenge. * Indicates difference between injured and uninjured participants. Note: challenge workouts recorded after RRI were not included in the analysis.

Methods: Running workout data was collected with the DashLX platform for 16 weeks prior to and during a 16-week gamified running challenge (Brooks 191.4 Challenge) via GPS device. Participants' responses to weekly surveys determined injury status, where a RRI was defined as modified training due to lower limb pain. Workouts recorded after RRI were not included in the analysis. Survey and device data were processed by assessing survey compliance, removing participants who did not meet the minimum data threshold, and removing non-lower limb pain reports.

Training characteristics (speed/session, distance/session, and number of sessions) were calculated for each participant before and during the challenge and student's T-tests were used to compare injured and uninjured participants. Training consistency was determined based on running frequency and distribution; for each day in the 16 weeks prior to the challenge and the 16 weeks during the challenge (or until the first injury occurred), participants received a daily consistency score (integer between 0-7) based on the number of active running days in the prior seven days. Participants were classified as "consistent" if ≥75% of total days had a daily consistency score ≥3, or classified as "inconsistent" if <75% of total days had a daily consistency score ≥3. Odds ratios (OR) were calculated to compare the odds participants sustained an injury based on demographic exposure variables and running consistency. The Fisher's Exact Test was used to determine whether the OR was equal to or greater/less than 1 ($p<0.05$).

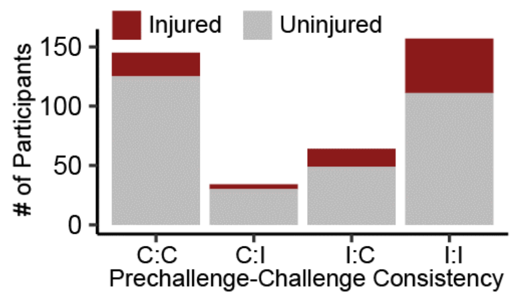

Figure 1: Injury status based on change in consistency classification between pre-challenge and challenge periods: C:C=Consistent-Consistent, C:I=Consistent-Inconsistent, I:C=Inconsistent-Consistent, I:I=Inconsistent-Inconsistent.

Results & Discussion: After data processing, 400 participants were included in the analysis, with 85 injured and 315 uninjured. The ORs for becoming injured were 1 for sex (male/female), injury history (yes/no previous injury), BMI (normal/overweight), and age (above/below 40 years old), indicating none of these exposures were associated with greater injury risk.

There was no difference in average speed/session or average distance/session between injured and uninjured participants prior to and during the challenge. Uninjured participants recorded more sessions compared to injured participants prior to the challenge, suggesting more training sessions did not lead to more injuries (Table 1). For daily consistency, the OR for becoming injured was less than 1 for inconsistent runners compared to consistent runners prior to and during the challenge (pre-challenge: OR=0.41 [0.24;0.68], $p<0.001$ and challenge: OR=0.57 [0.35;0.92], $p<0.05$). Moreover, when comparing consistency between the pre-challenge and challenge periods (Fig. 1), the OR for becoming injured was <1 for inconsistent participants before and during the challenge compared to consistent participants before and during the challenge (OR=0.39 [0.21;0.69], $p<0.005$). These results suggest inconsistency may be a risk factor for RRI while consistency may be protective against RRI. However, the OR for becoming injured was not greater or less than 1 for inconsistent participants before the challenge who then became consistent during the challenge (OR=0.52 [0.25;1.12]), signifying running more frequently and increasing running consistency alone is not sufficient to reduce RRI risk.

Significance: While traditional training metrics of running speed and distance were the same between injured and uninjured participants, inconsistent runners were more likely to become injured than consistent runners. This work identifies a link between daily consistency and injury risk, but these findings do not indicate that becoming consistent alone reduces injury risk. Nevertheless, identifying inconsistent running patterns may highlight runners who are at increased risk of injury.

Acknowledgements: This work was funded by Brooks Sports, Inc. GPS watch data was collected in collaboration with DashLX.

References: [1] Nielsen et al. (2012), *Int. J. Sports Phys. Ther.* 7(1); [2] Edwards. (2018), *Exerc. Sport Sci. Rev.* 46(4).

BIOINSPIRED HORN SHAPED OSCILLATORS FOR MITIGATING THE EFFECTS OF IMPACT

Jake M. Schaefer[1], Aaron M. Drake[2], Benjamin B. Wheatley[1]*
[1]Department of Mechanical Engineering, Bucknell University, Lewisburg, PA, [2]Function First Innovative Design, LLC, Denver, CO
*bbw008@bucknell.edu

Introduction: Over time, repeated head trauma can lead to Chronic Traumatic Encephalopathy (CTE), which can cause short-term memory loss and impaired judgment. Male Bighorn sheep, however, participate in repeated seasonal ramming bouts and exhibit mild to moderate signs of CTE biomarkers found in humans [1]. Structures in the bighorn sheep skull and horns contribute to reduced brain cavity accelerations during ramming events [2], such as the velar bone horn core [3] and the unique tapered spiral of the keratin-rich horns [4]. Specifically, we have shown that an impact model with a ~50% reduced horn length experiences brain cavity accelerations that are 20% higher than a fully intact horn model, and that altering the cross-sectional geometry of the horns can increase the head injury criterion (HIC_{15}) by more than 100% [2, 4]. The mechanisms of energy dissipation in these structures is directional oscillations of the horn tip [4]. However, little work has been conducted to leverage these tapered oscillators (horns), specifically exploring how the number, orientation, size, geometry, and material properties of horns could be optimized to maximize energy dissipation. The goal of this work was to determine the extent to which the number of horns reduced the head injury criterion (HIC_{15}) in an impactor model. It was hypothesized that increasing the number of horns would decrease HIC_{15}.

Methods: A finite element model was created in ABAQUS finite element software of a half sphere impactor with variable number of horns (Figure 1). A drop test experiment was simulated in ABAQUS/Explicit between the keratin ($E = 2$ MPa, $\nu = 0.3$, $\rho = 1.3$ g/cm^3) impactor and a keratin plate at an impact velocity of 4.24 m/s. Four different model geometries were developed: zero horns, two horns, five horns, and 22 horns. The mesh was constructed of second order tetrahedral elements and mesh convergence analyses were performed to determine appropriate mesh density. HIC_{15}, which is a function of translational acceleration and has been used to assess the likelihood of head injury resulting from an impact, and maximum translational acceleration was compared across each model.

Results & Discussion: While the impact direction was vertical, horizontal horn tip oscillations were observed (Figure 1), which agrees with our previous findings [2, 4]. This mechanism converts kinetic energy from the vertical impact direction to horizontal horn tip oscillations (kinetic and strain energy), thus reducing accelerations at the impactor. Maximum acceleration and HIC_{15} results (Table 1) show that the 22-horn model exhibited the greatest impact mitigating qualities, with reductions in maximum acceleration and HIC_{15} of 82% and 47% relative to the 0-horn model.

Table 1. Model maximum acceleration and HIC_{15} results.

Number of Horns	0	2	5	22
Max Accel (g) (% diff from 0 model)	*9790* *(-)*	*8360* *(-15%)*	*6800* *(-31%)*	*1780* *(-82%)*
HIC_{15} (s-g$^{2.5}$) (% diff from 0 model)	*171* *(-)*	*401* *135%*	*584* *241%*	*90.2* *-47%*

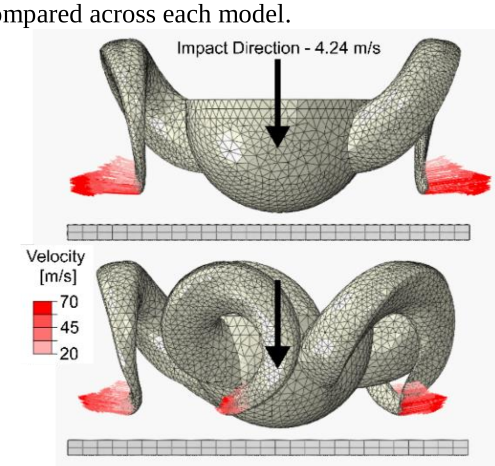

Figure 1: Impactors with two horns (top) and five horns (bottom). The impact direction is shown in the black arrow. The 4.24 m/s vertical impact results in horizontal tip oscillations at high velocities (approaching

Interestingly, while both the 2-horn and 5-horn models exhibited lower maximum acceleration values than the baseline condition (reductions of 15% and 31%, respectively), they exhibited higher HIC_{15} values than the baseline condition (increases of 135% and 241%, respectively). These findings are due to the cumulative nature of HIC_{15} and what we believe to be a superposition of synchronized horn tip oscillations that contributed to greater impactor oscillation after impact. This superposition causes a reverberating effect, which leads to higher overall HIC_{15} values despite a lower maximum acceleration. The reduced horn size and increased horn number in the 22-model likely prevents this phenomenon by introducing a greater number of structures that are thus less likely to synchronize. This observation suggests that the horn orientation and horn size of the horns are key variables in the design of impact mitigating structures. Compared to our previous work on bighorn sheep biomechanics [2-4], this study modified horns organization for impact mitigation, specifically by using horns as secondary oscillating structures that are not directly contacted during impact. The 22-horn model in particular shows promise for the use of horn-like structures in this manner. Further work is ongoing to determine the effect of material properties and horn orientation on impact mitigation.

Significance: This study presents new insight into impact mitigating structures inspired by bighorn sheep horns. Specifically, we have shown that the number and size of horns as secondary oscillating structures can reduce the effects of impact. The findings from this work could lead to new designs across a broad range of impact applications, such as helmets, vehicle bumpers, and athletic equipment. These structures dissipate energy through elastic deformations, thus exhibiting reusability in comparison to mechanisms such as a car bumper. However, the size, material properties, and organization of these structures would benefit from application-specific optimization before they can reliably be used to mitigate the effects of impact.

References: [1] Ackermans et al. (2022), *Acta Neuropathol* 144(1). [2] Drake et al. (2016), *Acta Biomaterilia* 44. [3] Aguirre et al. (2021) *Scientific Reports* 10(1). [4] Wheatley et al. (2023), *Bioinspir Biomim* 18(2).

EXPERIENCE WITH A CANE IMPACTS BRAKING FORCE DURING WALKING IN POST-STROKE

Martins E. Amaechi[1*], Emily Steffenson[1], Oluwaseye Odanye[1], Lindsey Remski[1], Brian Knarr[1]
[1]Department of Biomechanics, University of Nebraska at Omaha, Omaha, NE USA
*Email : mamaechi@unomaha.edu

Introduction: During steady-state walking, the succession of propulsive and braking phases at each leg contributes to the control of the forward progression of the body's center of mass (COM) by regulating its acceleration and deceleration. However, the coordination of braking and propulsion is impaired in post-stroke individuals [1]. Hemiplegic post-stroke individuals are often prescribed a cane to improve stability, and gait, and to reduce postural sway by increasing the base of support and shifting the body COM toward the paretic limb [2] Individuals post-stroke often use the paretic limb for braking and the unaffected limb for propulsion, which is correlated with impaired control of walking speed. To generate a reasonably constant velocity they must generate propulsive and braking impulse of equal amounts [3]. However, while a cane provides a braking effort on the paretic limb, the individuals' interaction with the cane is not usually considered and quantitively reported. Therefore, understanding the relationship between the braking force on the paretic limb and the cane is needed. The purpose of this study is to determine how the braking force generated on the paretic limb relates to the force generated on the cane. We hypothesize individuals with no experience with a cane will have a greater difference between the braking force on the paretic limb and the cane due to greater reliance on the cane for braking.

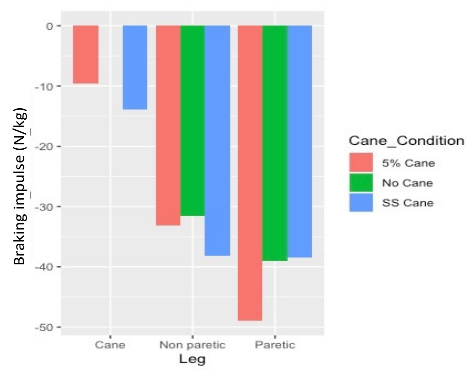

Figure 1: Paretic, non-paretic, and cane breaking impulse for 5%, self-selected and no cane use conditions during overground walking. Negative values indicate greater breaking impulse.

Methods: 20 post-stroke participants (8 males, 12 females, age 60.72 ±12.6 yrs., mass = 87.9±17.62 kg) were recruited: no history of assistive device use (N=8), history of assistive device use (N=5), and current dependence on an assistive device (N=7). Participants were included if they met the following criteria: age 19-80, single-chronic stroke, and ambulatory. Kinetic and kinematic analysis using a full-body, 65-marker set was completed using motion capture, in-ground force plates and an instrumented cane. Subjects completed three conditions: walking with a cane using 5% of their body weight (5%BW), walking with a cane comfortably (self-selected BW), and walking without a cane. Real-time feedback of the cane forces was displayed for the 5% bodyweight condition on a monitor in front of the walkway. Paretic breaking impulse and walking speed were calculated for the level of experience with a cane and the walking speed in cane conditions were determined. Statistical analysis included a two-way repeated measures ANOVA.

Results & Discussion: The mean braking impulse generated on the cane in the self-selected BW condition was significantly more than with 5% BW ($p<0.001$). Canes majorly provide support for the affected limb [3], which may be why individuals applied less braking force on the cane when asked not to use more than 5% BW. The mean braking impulse generated on the paretic limb in the self-selected condition was less than the 5% BW and no cane condition when compared with results from the contralateral limb (Fig. 1). This suggests that individuals used the paretic foot for braking function when using reduced or no cane support. Individuals that had no history of assistive device use had significantly higher walking speed than current users and users with prior history of cane usage ($p<0.01$) (Fig. 2). This is consistent with Chen et al's findings, where they showed hemiplegic stroke individuals that require a cane have relatively slower walking speed than unassisted people with hemiplegic stroke [3]. Paretic breaking impulse in current users (-17.7N/kg ±13.9) was lesser than individuals with experience (-23.5N/kg ±7.5) and no experience (-21.6N/kg ±7.4). Because braking impulse considers the time to generate the force in addition to its magnitude [1], this suggests that current cane users may have lesser magnitude and take longer time to generate braking force. Further analysis with a one-way ANCOVA ($F(1, 152) = 4.05$, $p = 0.046$) showed a significant interaction with walking speed as the covariant. Therefore, an individual's prior experience with assistive devices could impact the braking force generated by the limb thereby influencing walking speed.

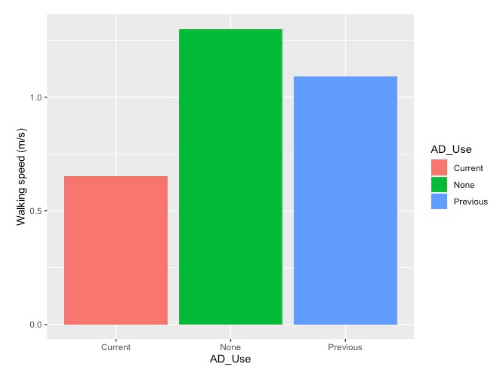

Figure 2: Walking speed for each cane use group: current users, no history and previous history with cane. Positive values indicate greater walking speed.

Significance: These results suggest that assistive device use and prior experience with assistive devices can influence how these devices affect breaking force generation in the paretic limb of individual's post-stroke. How this difference may change through the rehabilitation process may be a quantitative way to progress and guide clinical decision-making regarding transitions to independent walking.

Acknowledgements: This research was funded by the NIH(R15HD094194).

References: [1] Duclos et al. (2019), *Gait Posture*, vol. 68, pp. 483–487; [2] Kuan et al. (1999), *Arch Phys Med Rehabil*, vol. 80, no. 7, pp. 777–784; [3] Chen et al. (2001), *Arch Phys Med Rehabil*, vol. 82, pp. 43–48.

ACCELEROMETRY-BASED ANALYSIS OF POSTURAL SWAY IN PARKINSON'S DISEASE PATIENTS WITH LEVODOPA-INDUCED DYSKINESIA

Carolin Curtze[1*], Chandler Brock[1], Joseph A. Aderonmu[1]
[1]Department of Biomechanics, University of Nebraska at Omaha, Omaha, NE USA
*Corresponding author's email: ccurtze@unomaha.edu

Introduction: Parkinson's disease (PD) is a progressive neurodegenerative disorder, with patient numbers projected to double to 12 million in the next 20 years. While dopamine replacement therapy and dopamine agonists are standard of care and most effective in treating the slowness of movement in PD, side effects can occur. Levodopa-induced dyskinesia (LID) is a major problem associated with the long-term use of levodopa for symptomatic treatment of PD. These involuntary hyperkinetic movements can become disabling and may interfere with quality of life. Our prior research showed that PD w/ LID were less stable while standing (i.e., increased postural sway) and had a higher incidence of falls [1]. The aim of this study is to determine if postural sway properties are altered by LID via decomposing the sway signal. We hypothesize that in the on-state, LID will exaggerate the postural sway properties seen in both the signals without the dyskinesia frequency bands (w/o 1-3 Hz) and those with the dyskinesia frequency bands (signal).

Methods: Individuals with idiopathic PD (n = 26; 14 PD w/ LID) and healthy controls (HC) (n = 10) performed 30 seconds of postural sway under two conditions: (1) a single task: standing quietly with arms along their sides, and (2) a cognitive dual task: standing while performing a serial subtraction task. PD individuals were tested in their off-state (i.e., after withholding their anti-parkinsonian medication for at least 12 hours) and on-state (i.e., about 1 hour after intake of a levodopa challenge dose, approximately 1.25x their regular medication dosage). Inertial sensors (Opals V1, APDM) were attached to the head, lumbar, left/right foot, and trunk while the lumbar data was of primary interest. The acceleration signal from the lumbar sensor was decomposed using empirical mode decomposition (EMD) and reconstructed w/ or w/o the 1-3 Hz dyskinesia band (Figure 1) [2]. Subsequently, the root mean square (RMS) sway was calculated for each of the recomposed signals.

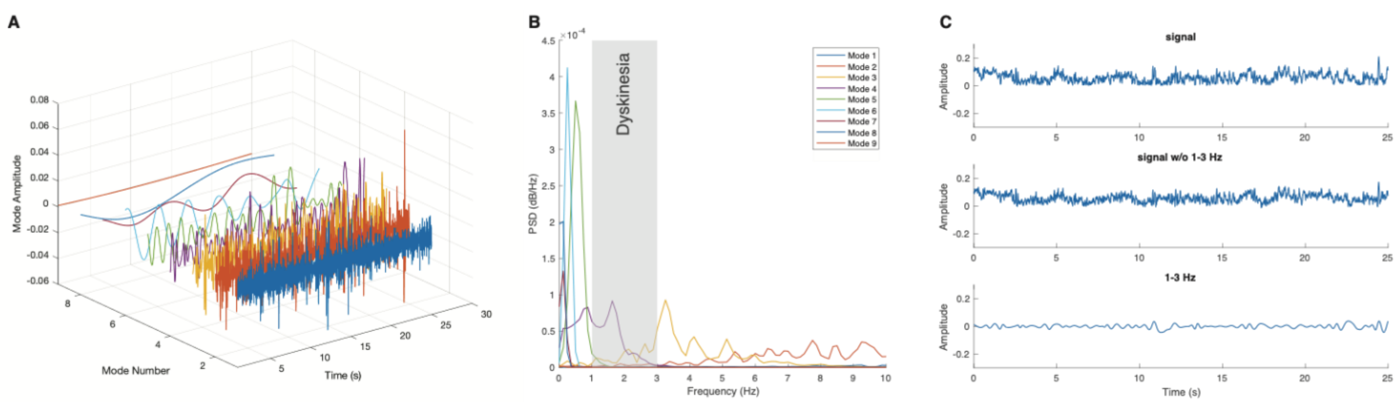

Figure 1: A) Signal decomposition, B) mode selection, and C) sway signal reconstruction w/ and w/o the 1-3 Hz dyskinesia bands.

Results & Discussion: In the on-state, we observed dyskinesia in 14 PD subjects with clinical ratings spanning a range from 1-9 (mild to moderate). Non-parametric group comparisons (Kruskal-Wallis) showed significance in AP RMS sway for the on-state dual task condition, only. Specifically, in the on-state dual-task condition, significance was seen between groups for all three signal subgroups: 1) signal (chi- squared = 9.93, $p < 0.01$), 2) w/o 1-3 Hz (chi-squared = 8.03, $p < 0.05$), and 3) 1-3 Hz (chi-squared = 14.46, $p < 0.001$).

Significance: The results indicate that after decomposing postural sway signals and removing dyskinesia frequency band content using EMD method, AP RMS sway values are still elevated when comparing PD w/ LID to PD w/o LID, especially in the on-state. In conclusion, dyskinesia alters postural sway and should be taken into consideration when conducting postural sway analysis.

Acknowledgements: This research is supported by the Medical Research Foundation of Oregon, NIH P20 GM109090, and UNO GRACA.

References: [1] Curtze C, et al. Movement Disorders 30, 1361-1370, 2015. [2] Mellone, S., et al. IEEE transactions on biomedical engineering 58, 1752-1761, 2011.

KNEE EXCURSION IS WEAKLY ASSOCIATED WITH IMPACT LOADS IN RUNNING AND LOADED WALKING

Torstein E. Dæhlin[1]*, Caleb D. Johnson[2], Lauren K. Sara[3], Stephen A. Foulis[2], Julie M. Hughes[2], Irene S. Davis[1]
[1]School of Physical Therapy & Rehabilitation Sciences, Morsani College of Medicine, University of South Florida
[2]Military Performance Division, U.S. Army Research Institute of Environmental Medicine
[3]Spaulding National Running Center, Spaulding Rehabilitation Hospital
*Corresponding author's email: daehlin@usf.edu

Introduction: Impact loads are associated with running and loaded walking injuries commonly experienced by military personnel [1, 2]. It is therefore important to understand the factors that influence impact loads during these tasks. In running and walking, the knee of the stance limb flexes during the load acceptance phase to attenuate the impact [3]. Increasing the amount of knee flexion that occurs during load acceptance could increase the compliance of the stance limb, thereby decreasing impact loads. However, little is known about the relationship between knee excursion during stance and common measures of impact load, such as tibial acceleration [2]. This study aimed to investigate how knee excursion relates to tibial acceleration and ground reaction force load rate during running and loaded walking in military trainees. As the stance limb compliance may increase with greater knee excursion, we hypothesized that greater knee excursion would be associated with lower load rates and peak tibial accelerations.

Methods: 311 U.S. Army trainees (sex[F/M] = 122/189, age = 21 ± 4 yrs., height = 1.70 ± 0.10 m, mass = 71.9 ± 14.2 kg; (mean ± standard deviation)) were recruited for this study. Only those that ran with a rearfoot strike pattern were included in this analysis. Prior to the gait assessment, inertial measurement units (IMUs; BlueTrident, AMTI, Watertown, MA) were affixed to participants' distal tibias. For the loaded walking, an 18.1 kg backpack was worn by participants. Each participant completed steady state loaded walking (3.0 mph) and running (6.5 mph) on an instrumented treadmill (AMTI, Watertown, MA) that recorded their ground reaction forces. Additionally, sagittal plane video recordings were obtained using 2 GoPro Hero 9 (GoPro, San Mateo, CA) cameras. DeepLabCut™ was used to automatically digitize points of interest from the 2D video recordings, allowing knee flexion excursion from foot strike to peak knee flexion to be computed [4]. Vertical average load rates (VALR) and peak vertical tibial accelerations (VTA) were extracted from ground reaction force and IMU data, respectively. Pearson's correlation coefficients (r) were computed to investigate the association between knee flexion excursion, load rates, and tibial accelerations. Statistical significance was accepted for $p < 0.05$, as determined *a priori*.

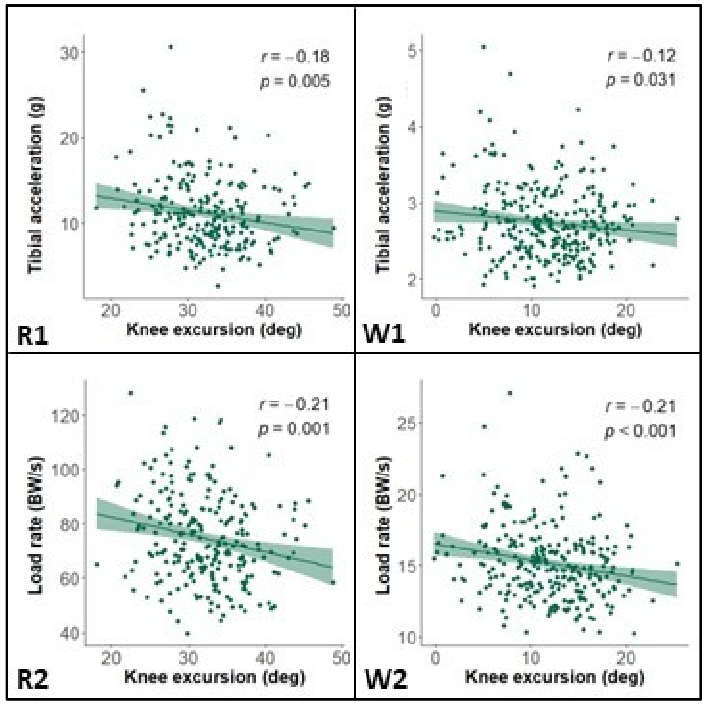

Figure 1. Scatter plots illustrating the association between knee excursion and tibial acceleration (1) or load rate (2) during running (R) and loaded walking (W). Solid lines and shaded regions represent the line of best fit and its 95% confidence interval,

Results & Discussion: Knee excursion and VTA were weakly correlated during both running (Figure 1, R1) and loaded walking (Figure 1, W1). Similarly, knee excursion was weakly correlated to VALR during running (Figure 1, R2) and loaded walking (Figure 1, W2). As hypothesized, these results suggest that as knee excursion increases during running and loaded walking, impact loading is reduced. However, the weakness of the relationships may be related to the relative timing of the outcome variables. For example, during running, both peak VTA and VALR are typically confined to the first 20% of stance while knee flexion continues to 50% of stance [5]. As a result, most of the knee flexion excursion may occur later in stance. In support of this notion, one study reported a strong association between VALR and knee excursion from foot strike until 1st peak ground reaction force during running [6]. It may be more informative for future studies to investigate these relationships during the window from foot strike until peak impact loads occur.

Significance: The weak association between knee joint excursion and impact loads during running and loaded walking suggests that knee excursion plays a small role in determining the compliance of the stance limb. These results are important for researchers and practitioners designing exercise programs aiming to reduce injuries associated with impact loads during running and loaded walking, such as tibial stress fractures. Specifically, increasing knee joint excursion may not be the most effective way to reduce impact loads.

Acknowledgements: This study was supported with a research grant from the Department of Defense (W81XWH-20). The views expressed in this abstract are those of the authors and do not reflect the official policy of the Department of Defense.

References: [1] Jensen et al. (2019). *Mil Med.* 184(suppl. 1); [2] Milner et al. (2006). *Med Sci Sports Exerc.* 38(2); [3] McMahon, (1987). *J Appl Physiol*. 62(6); [4] Mathis et al. (2018). *Nat Neurosci.* 21; [5] Lafortune et al. (1994). *J Biomech.* 28(8); [6] Shih et al. (2019) *Med Sci Sports Exerc.* 51(1).

ADVERSE EFFECTS OF A PASSIVE LEG-SUPPORT EXOSKELETON ON REACTIVE BALANCE AFTER SIMULATED SLIPS AND TRIPS

Stephen Dooley*, Sunwook Kim, Maury A. Nussbaum, Michael L. Madigan
Grado Department of Industrial and Systems Engineering, Virginia Tech
*Corresponding author's email: stepd17@vt.edu

Introduction: Occupational exoskeletons (EXOs) are an emerging ergonomic control to reduce the physical demands of manual material handling [1]. However, using these EXOs could lead to undesirable and unintended effects that may increase fall risk. For example, passive leg-support EXO users can be more susceptible to loss of balance following external perturbations while seated [2]. The purpose of this exploratory study was to investigate the effects of a passive leg-support EXO (Chairless Chair®, Noonee, Germany) on reactive balance after simulated slips and trips. We hypothesized that the EXO would adversely affect reactive balance after simulated slips and trips.

Methods: Six young adults (age: 19-25 years, 3 males and 3 females) completed the study. Each participant completed three experimental conditions: not wearing the EXO, wearing the EXO at a high-seat setting, and wearing the EXO at a low-seat setting (Figure 1). During each condition, the participants were exposed to two replications of each of 14 treadmill perturbations. Perturbations started from a standing posture, involved a step-function change in treadmill belt speed, and required participants to step to recover balance and establish a stable gait. Forward speed changes (0.4-1.6 m/s) induced a backward loss of balance similar to a slip, whereas backward speed changes (0.75-2.25 m/s) induced a forward loss of balance similar to a trip. Perturbation direction and speed were presented in a random order within each experimental condition. Dependent variables included perturbation outcome (successful or failed recovery when harness force exceeded 30% body weight) and measures of stepping/trunk kinematics at initial recovery step touchdown in the anterior-posterior direction.

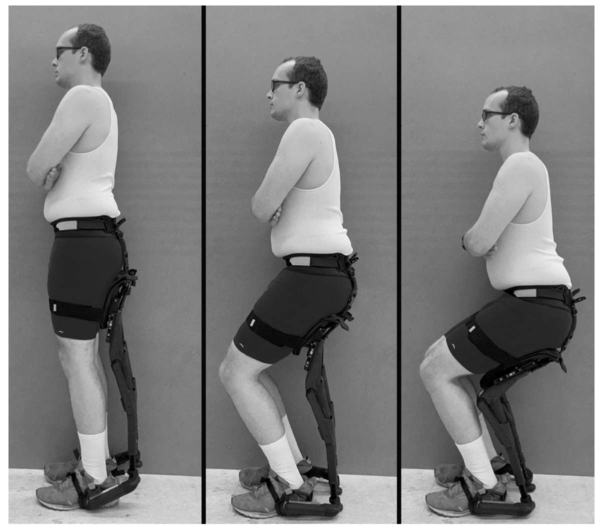

Figure 1: An EXO user while standing (left), sitting in the high-seat setting (middle), and sitting in the low-seat setting (right).

Results & Discussion: After simulated slips, the probability of a failed recovery was higher in the low-seat setting (odds ratio or OR = 2.85; p=0.035) and high-seat setting (OR = 11.78; p=0.002) compared to the no EXO condition (Figure 2). Moreover, the high-seat setting caused a 3.9 cm shorter step length (p=0.019), 0.12 m/s slower step speed (p=0.002), and stepping toe 4.5 cm more anterior to the posterior superior iliac spine (PSIS; p=0.003) when compared to the no EXO condition. After simulated trips, the probability of a failed recovery was not affected by condition (p=0.265). However, the high-seat setting caused a 3.3 cm shorter step length (p=0.002) and a 2.4 degree larger trunk angle (p=0.001) compared to the no EXO condition. These results supported our hypothesis. Reasons for these results may have been the posterior position of the EXO on the lower-limbs – which caused inadvertent ground contact of the EXO when attempting to step backwards after slip perturbations with lowered hips after slip perturbations, and the added mass and mechanical constraint or resistance imposed by the EXO – which made stepping more difficult. Study limitations included: 1) a small sample size that limits generalizability to working-age adults and strong conclusions regarding sex differences, 2) limited participant experience with the EXO, 3) the use of simulated slips and trips, instead of over-ground slips and trips, to enhance experimental control, and 4) challenges in systematically discerning the specific underlying mechanisms behind the adverse effects identified.

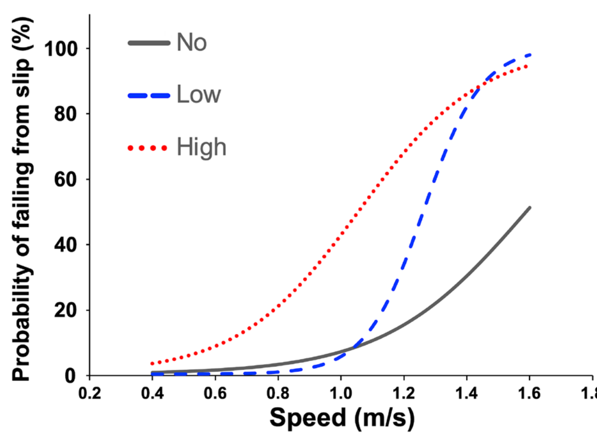

Figure 2: Separate generalized logistic regression models of slip-recovery probabilities of failure at

Significance: We believe this is the first study to investigate the effects of EXOs on responses to large postural slip- and trip-like perturbations. Our results indicate that caution is warranted when using a leg-support EXO in some applications due to a potential increased risk of slip and trip-induced falls, and may inform EXO design modifications and usage policies to mitigate the adverse effects reported here.

Acknowledgements: Johns Hopkins Education and Research Center for Occupational Safety and Health (T42 OH0008428).

References: [1] Kong et al. (2022), *Int J Environ Res Public Health* 19(13), 8088; [2] Steinhilber et al. (2022), *Hum Factors* 64(4), 635-648; [3] Yang and Pai (2011), *J Biomech* 44(12), 2243-2249.

QUANTIFYING THE IMPACTS AND CHALLENGES OF UNDERGRADUATE RESEARCH

Brooke M. Odle[1*], Craig M. Goehler[2], Allison R. Altman-Singles[3], David A. Phillips[4], Michael V. Potter[5], Mukul C. Talaty[6], Jacob W. Hinkel-Lipsker[7], and Kimberly E. Bigelow[8]
[1]Hope College; [2]University of Notre Dame; [3]Penn State Berks; [4]Oregon State University; [5]Francis Marion University; [6]Penn State Abington; [7]California State University, Northridge; [8]University of Dayton
*Corresponding author's email: odle@hope.edu

Introduction: Inclusion of undergraduate students in research can yield many benefits to not only the students in question, but faculty and higher education institutions as a whole. In the case of the students, working alongside a faculty mentor on research yields an increase in academic confidence, a higher likelihood to pursue graduate education, greater self-efficacy and sense of belonging at the university, increased passion for the field, greater enthusiasm for learning, improved academic success, and solidified identity as a scientist, researcher, and scholar [1,2]. For faculty, working with undergraduate researchers may provide new perspectives and unbiased insights when designing research methodology [3] while at the institutional level a commitment to undergraduate research (UR) can foster broader collaborations, improve institutional reputation, attract top talent and donor funding, meet graduation and equity goals, and drive student retention [4].

However, while the studies above that discuss the benefits of UR were in STEM-related fields, relatively little has specifically focused on inclusion of undergraduate researchers in biomechanics. Of those studies in the biomechanics domain that do exist, much attention has been paid to student-related outcomes (e.g., [5]). Biomechanics is a unique area of research given its multidisciplinary nature, and therefore inclusion of undergraduates in research may require unique considerations. Thus, it is important to take a holistic perspective in understanding how involvement of undergraduates in research tangibly benefits not only students but also faculty, who may have to spend additional time reviewing biomechanics concepts with undergraduate researchers. Therefore, the purpose of this work was to better understand the degree to which undergraduate students are involved in the research groups of biomechanics researchers. Such work would lead to a better understanding of UR in biomechanics may help to identify challenges in including this group of students in future research efforts, advancing the American Society of Biomechanics (ASB) 2020-2025 Strategic Plan, particularly with respect to Member Engagement as well as Education, Outreach, and Advocacy.

Methods: The authors desired to obtain quantitative data pertaining to UR at different universities that would aid in exploring the benefits of UR and how it should be assessed differently than standard graduate research metrics. To that end, an IRB-approved Qualtrics survey was generated with questions broken down into five categories: PI/institution demographics, laboratory/group demographics, UR compensation/involvement methods, conference productivity, and percent of PI productivity that involved UR students. Our poster at NACOB'22 included a QR code to this survey. Additionally, the survey was shared with the authors' networks via email blasts, Slack, and social media. This abstract presents the results from the 50 survey participants that had 100% completion (partial submissions and test submissions by the authors were omitted).

Results & Discussion: From among our survey respondents, the majority of which are PIs at research institutions (R1 or R2), 85% reported engaging undergraduates in research. This suggests that it is common for PIs in the field of biomechanics to at least occasionally include undergraduates in their research laboratory, though the full scope of engagement was not probed in this survey. The mechanisms by which undergraduates engage in laboratories are diverse, but the survey results suggest that more PIs engage undergraduate students in research through course credit and course project opportunities rather than paid research experiences (63% vs. 32%). This may be helpful insight in guiding future efforts to increase undergraduate engagement: PIs may want to consider and formalize increased opportunities for research-based coursework and projects that encourage students to engage in biomechanics labs, while institutions and organizations like ASB may wish to explore new initiatives that provide funding, particularly in the summer, to students hoping to engage in research. Efforts like the B-SURE program are a step toward addressing this.

Results of the survey also show that undergraduates are generally productive, though their relative scientific contributions as a proportion of overall PI productivity was fairly low. Undergraduates are authors on 13% of all peer-reviewed publications, presented at 12% of all national/international conferences, and surprisingly presented at only 16% of all local/regional conferences. This suggests a possible opportunity to better promote and support undergraduate attendance at the ASB regional meetings, as these meetings are intended to be student-centered events occurring annually at different sites across the nation. It is envisioned that this could be an excellent outlet for undergraduate students to present, one that seems to be a missed opportunity for some right now.

Significance: This study presents survey results that provide us with a glimpse of how undergraduate research is occurring in biomechanics. There remains a need to ask much deeper questions to continue to better understand the opportunities and challenges PIs have recognized through their experience engaging undergraduates in research, and specifically how this compares to engaging graduate students. As we learn more, we believe this could help to increase the engagement of undergraduates overall, helping diversify and grow the field.

Acknowledgements: Thanks to all survey participants for sharing their experiences and helping us to learn more about this topic.

References: [1] Bauer & Bennett (2003), *J Higher Ed 74*(2); [2] Lopatto (2004), *Cell Bio Ed 3*(4); [3] Bass et al. (2018), *ASEE SE Section Conference*; [4] Malachowski (2020), *Council Undergrad Res Q 3*(2); [5] McErlain-Naylor (2020, *J Appl Biomech 36*(5)

MATCHING STEP LENGTHS & WIDTHS TO THE CURVILINEAR PATHS WE WALK ON

Jonathan B. Dingwell[1*], Anna C. Render[1], David M. Desmet[1], Joseph P. Cusumano[2]
[1] Department of Kinesiology, Pennsylvania State University, University Park, PA, USA
[2] Department of Engineering Science & Mechanics, Pennsylvania State University, University Park, PA, USA
*Corresponding author's email: dingwell@psu.edu

Introduction: Stepping parameters (e.g., length, width, etc.) offer simple variables to assess gait function. Such parameters can predict important gait impairments like fall risk in older adults [1]. These parameters are clearly defined for straight walking. Indeed, most gait labs presume a pre-defined constant forward direction along a straight path [2]. However, real humans only rarely walk in straight lines [3]. Surprisingly, however, how to quantify step lengths / widths etc. during *non*-straight walking, where direction of forward progression changes at each step, has received scant attention. The most prevalent approach is that of Huxham et al. [2]. They take the line connecting any 2 ipsilateral foot placements (i.e., 1 stride) to define the direction of progression, with the intermediate contralateral foot placement denoting the step of interest (e.g., **Fig. 1A**, top). Although simple, Huxham's convention entirely disregards that *goal*-directed humans walk along *paths* that define specific goals to achieve (i.e., 'stay on the path') [4]. Here, we assert that measures of step length and width should account for how people step relative to their path. Specifically, we hypothesize that if we do so, this will yield step lengths and widths that are consistently more *accurate* and meaningful across a range of non-straight walking tasks.

Methods: We defined several non-straight walking tasks: turn at 1 step, walk around a circle, make a lateral lane-change [5], walk along an arbitrary curvilinear path [6]. To deliberately avoid confounds inherent in experimental data, we constructed step sequences defining perfect performance (zero error) in each task, where every step had *a priori* known step width $\boldsymbol{W}$ = 0.15m & length $\boldsymbol{L}$ = 0.60m [7].

We used Huxham's convention [2] to compute step lengths ($\boldsymbol{l_H}$) and so-called "stride widths" ($\boldsymbol{w_H}$).

For our proposed convention, we define each step from only its 2 consecutive foot placements [4]. We then just rotate the lab coordinate system, $[\boldsymbol{x},\boldsymbol{y}]$, to be tangent to the walking path at the mid-point between the two feet [8] (e.g., $[\boldsymbol{x'},\boldsymbol{y'}]$ in **Fig. 1A**) at each step. Step lengths ($\boldsymbol{l_P}$) and widths ($\boldsymbol{w_P}$) are then defined in the normal way, except in rotated $[\boldsymbol{x'},\boldsymbol{y'}]$ coordinates.

For each, we directly compared the computed values to the known, unequivocal *true* values ($\boldsymbol{W}$, $\boldsymbol{L}$).

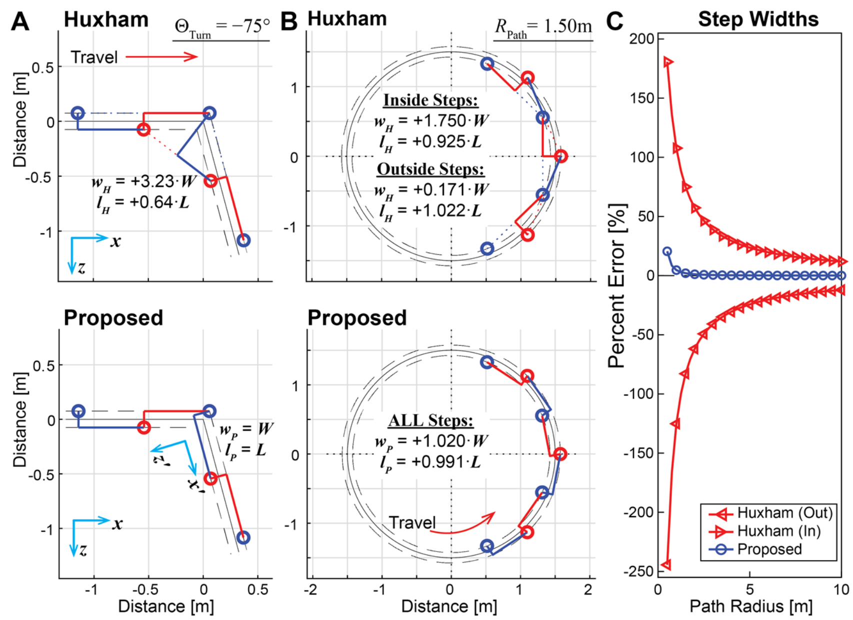

Figure 1: A: Example single-step turn; [Top] Huxham convention step length ($\boldsymbol{l_H}$) and "stride width" ($\boldsymbol{w_H}$); [Bottom] Proposed convention step length ($\boldsymbol{l_P}$) and step width ($\boldsymbol{w_P}$), each relative to *true* step width ($\boldsymbol{W}$=0.15m) and length ($\boldsymbol{L}$=0.60m). **B:** Example walking (counter-clockwise) on a circular path. **C:** Percent Errors from known true values ($\boldsymbol{W}$, $\boldsymbol{L}$) for walking on circular paths of varying radii (R_{Path}) (errors for step widths shown).

Results & Discussion: For single-step turns (**Fig. 1A**), Huxham's convention gives highly distorted values at the turn step. Conversely, our proposed convention returns exactly correct values. For walking on a circular path (**Fig. 1B**), Huxham's convention yields also dramatically different errors for "inside" vs. "outside" steps, despite *all* steps being (by construction) exactly equidistant from the path center. Conversely, our proposed convention yields far smaller errors that are consistent across *all* steps. These discrepancies increase approximately exponentially with decreasing path radius, R_{Path} (**Fig. 1C**). Similar findings were obtained for both simulated lateral lane changes (as in [5]) and arbitrary curvilinear paths (as in [6]) (results not shown). In all cases, for all posited tasks, the proposed convention yielded far more (i.e., order-of-magnitude more) *accurate* results relative to unequivocally known *a priori* values.

Here, we purposefully analyzed pre-defined "perfect" steps to compute *accuracy* relative to known *true* values ($\boldsymbol{W}$, $\boldsymbol{L}$). Findings and conclusions would be the same for any reasonable ($\boldsymbol{W}$, $\boldsymbol{L}$) values or with deviations (noise) added to simulate experimental data, etc.

Significance: The significance here is not just methodological, but conceptual. Humans almost never "just walk" (aimlessly) as [2] (inadvertently) assumes. People walk *purposefully* to achieve some *task* (e.g., to reach a destination) and thus, on some *path* [4-6]. Just as we regularly transform local coordinate systems between body segments (e.g., foot, shank, thigh, etc.), we should do the same for the walking *tasks* we perform. In a lab, such paths can be imposed by experiments [5-6]. In "the world", wearables offer numerous possibilities for defining paths from tracking where people actually go [3]. The proposed approach is applicable to all such scenarios.

Acknowledgements: Partly supported by NIH / NIA Grants # R01-AG049735 & R21-AG053470.

References: [1] Morag et al. (2013), *Gait Post.* 37(1); [2] Huxham et al. (2006), *Gait Post.* 23(2); [3] Glaister et al. (2007), *Gait Post.* 25(2); [4] Dingwell et al. (2019), *PloS Comp. Bio.* 15(3); [5] Desmet et al. (2022), *PloS Comp. Bio.* 18(11); [6] Render et al. (2022), *N. Am. Congr. Biom.*; [7] Herssens et al. (2020), *J. Roy. Soc. Interf.* 17(166); [8] Orendurff et al. (2004), *J. Rehab. Res. Dev.* 41(6).

PREDICTION OF MEDIAL KNEE JOINT CONTACT FORCE DURING WALKING AND RUNNING USING CUSTOM INSTRUMENTED INSOLE AND DEEP LEARNING IN YOUNG FEMALE INDIVIDUALS

Samantha J. Snyder[1*], Edward Chu[1], Yun Jung Heo[2], Ross H. Miller[1], and Jae Kun Shim[1,2]
[1]Department of Kinesiology, University of Maryland, College Park, MD, USA
[2]Department of Mechanical Engineering, Kyung Hee University, Yong-in, South Korea
*email: snyder36@umd.edu

Introduction: Knee osteoarthritis is a painful chronic disease that disproportionately affects women (Blagojevic et al., 2010; Hart et al., 1999) and causes an inability to perform activities throughout the day. Currently, there is no cure for this complex disease, but there is an association between larger knee adduction moment during walking and greater risk of development and progression of knee osteoarthritis (Miyazaki et al., 2002; Sharma et al., 1998). Knee adduction moment is a surrogate measure for the forces on the medial side of the knee, but the correlation between knee adduction moment and the actual medial knee joint contact force (JCF) varies (Miller et al., 2015; Trepczynski et al., 2014). Model-based estimates of medial JCF can indicate the magnitude of mechanical loads on the medial knee, but these estimates have historically been restricted to a gait analysis lab. Measuring medial JCF outside of a lab setting utilizing wearable sensors and machine learning will allow future research to analyze the effects of reduced medial JCF on knee osteoarthritis rates and to predict biomechanical variables outside of a lab with greater validity (Halilaj et al., 2018). Here we used a novel tri-axial piezoresistive force sensing insole and a convolutional neural network (CNN) to predict musculoskeletal modeling calculated values of medial JCF during walking and running in young healthy women. Based on our previous research that predicted knee adduction moment during walking using CNN and our instrumented insoles (Snyder et al., 2023), we hypothesize that the models will predict medial JCF during walking and running with high correlation coefficients and low mean squared error.

Methods: Nine young female individuals were recruited from the local population. Motion capture, force plate, and custom instrumented insole data was synchronously collected during walking and running trials. The custom insole consists of five tri-axial piezoresistive force sensors located under high pressure areas of the foot. Eight walking and eight running trials were performed at various speeds based on random assignment. In Visual3D software, stance phases of the gait cycle were extracted through automatic gait detection, knee moments were calculated through inverse dynamics, and each stance phase was normalized to 101 time points. Using a reduction modeling approach in MATLAB, medial JCF were calculated (Morrison, 1968). Muscle cross sectional areas were selected based on data summarized in Miller (2016). The muscle forces were assigned based on typical activations during the stance phase, with the quadriceps accounting for knee extension moments, the hamstring for knee flexion moments early in stance, and gastrocnemius for knee flexion moments later in stance. Muscle moment arms and muscle orientations were expressed as quadratic functions of the knee flexion angle using average female values (Wretenberg et al., 1996). Lateral collateral, medial collateral, anterior cruciate, and posterior cruciate ligaments were calculated based on methods in Morrison (1968) to satisfy dynamic equilibrium in the resultant knee kinetics, and moment arms and orientations for anterior and posterior cruciate ligaments were based on results in Herzog and Read (1993). The total medial joint contact force was calculated by taking the moment about the lateral aspect of the knee (Miller & Krupenevich, 2020). The insole sensor data during each activity was input to the respective running and walking 3-layer, hyperparameter tuned CNN and leave-one-group out cross validation was applied to reduce prediction bias (Halilaj et al., 2018). Total waveform predicted medial JCF and peak medial JCF were compared to musculoskeletal modeled medial JCF values using Pearson's correlation coefficient (r) and mean squared error (MSE).

Results & Discussion: Running and walking CNN models predicted medial JCF with correlation coefficients greater than 0.97 and mean squared error (MSE) less than 0.55 %bodyweight (BW). While both models predicted peak and medial JCF with similar correlation coefficients, the walking CNN performed with lower mean squared errors compared to the running CNN. Peak and total medial JCF predicted values were compared to musculoskeletal model peak and total waveform medial JCF, and results are shown in Table 1. Our results demonstrate the ability to estimate stance phase medial JCF with a lower cost, more accessible wearable machine learning setup while maintaining a high validity. We found that both models overall estimated medial JCF with high success compared to similar inertial measurement based research (Konrath et al., 2019), but the walking model outperformed the running model for peak medial JCF with stronger correlation coefficients.

Table 1. Accuracy of models measured as Pearson's correlation coefficient and mean squared error.

	Total Medial JCF		Peak Medial JCF	
	r	**MSE (%BW)**	***r***	**MSE (%BW)**
Walk	0.97	0.03	0.91	0.09
Run	0.97	0.40	0.90	0.55

Significance: In conclusion, this research used a novel combination of CNNs and instrumented insole sensors to predict medial JCF during walking and running. In the future, this data can be collected on a larger population, possibly in real-world settings outside of gait labs, and be used to provide instantaneous biofeedback to allow for gait modifications to reduce medial JCF.

References: Blagojevic et al. (2010) *Osteoarthr Cartil*. 18(1); Halilaj et. al (2018) *Biomech*. 81(16); Hart et al. (1999) *Arthritis Rheum*. 42(1); Herzog & Read (1993) *J. Anat.* 182; Konrath et al. (2019) *Sensors* 19(1681); Miller (2016) *bioRxiv*; Miller et al. (2015) *Knee*. 22(6); Miller & Krupenevich (2020) *PeerJ* 8; Miyazaki et al. (2002) *Ann. Rheum. Dis.* 61(7); Morrison et al. (1968) *Biomed Eng* 3; Sharma et al. (1998) *Arthritis Rheum*. 41(7); Snyder et al. (2023) *Knee.* 41; Trepczynski et al. (2014) *Arthritis Rheumatol*. 66(5); Wretenberg et al. (1996) *Clin Biomech*. 11(8)

THUMB OSTEOARTHRITIS PROGRESSION IS ASSOCIATED WITH DECREASES IN CARPOMETACARPAL ARTHROKINEMATICS AND ARTICULAR SURFACE OVERLAP

Joseph J. Crisco[1*], Amy Morton[1], Douglas C. Moore[1], Arnold-Peter C. Weiss[1], Amy L. Ladd[2]
[1]Department of Orthopaedics, Warren Alpert Medical School of Brown University and Rhode Island Hospital, Providence, RI [2]Robert A. Chase Hand & Upper Limb Center, Department of Orthopaedic Surgery, Stanford University School of Medicine, Stanford, CA
*Email: joseph_crisco@brown.edu

Introduction: Thumb carpometacarpal (CMC) osteoarthritis (OA) affects 15% of adults over age 30, and 66% of women over the age of 55, leading to significant impairment of the upper extremity due to the thumb's central role in nearly all grasp and handling maneuvers. While the pathophysiology of osteoarthritis is multifactorial, abnormal joint kinematics and altered cartilage contact trigger and sustain the disease via the production of non-physiologic contact stresses, which in turn lead to chondrocyte derangement, necrosis, and cartilage degradation. Numerous studies have documented changes in first metacarpal (MC1) ROM with thumb OA progression, but these studies are limited in that they are based on goniometer or optical motion capture measurement systems that are unable to quantify changes in ROM at the trapezio-metacarpal articulation (CMC arthrokinematics). Similarly, subluxation of the MC1 with respect to the trapezium (TPM) has been well documented in OA progression with plain x-rays; however, the complex anatomy of the CMC joint and the limitations of planar imaging with x-rays make precise, true measurements of the subluxation extremely challenging. The aims of this study were to determine if CMC arthrokinematics decreases with early osteoarthritis (EOA) progression and to determine if subluxation, quantified herein by decreased overlap of the MC1 and TPM articular surfaces, increased with osteoarthritis progression.

Methods: Ninety patients with early thumb CMC OA and 24 age-matched Control subjects were recruited into an IRB-approved study Patient data were collected at baseline (time 0), and at 1.5, 3, 4.5, and 6-year follow-up, and at the baseline and year 6 time points of the dominant hand of the Controls. At each visit, CT scans were acquired of the hand and wrist during a braced neutral pose and 4 active thumb poses: flexion, extension, adduction, and abduction. Bone models of the MC1 and TPM were semi-automatically segmented from the neutral CT scan and the bone positions were resolved in each pose using an established markerless registration pipeline. The articular facets on the MC1 and TPM were manually delineated. MC1 ROM was defined as the phi angle of the helical axis of motion, calculated with respect to the mathematically fixed TPM. TPM articular overlap was computed as the union of all projected MC1 overlaps and expressed as a percentage of the TPM articular facet surface area. Osteophyte volume and rate of growth was computed and used to stratify patients into Stable and Progressive EOA groups. Differences in CMC ROM and articular overlap among the groups at baseline and 6-year time points were assessed with an ordinary two-way (Group x Time) ANOVA and Tukey's multiple comparison tests.

Results & Discussion: At the 6-year follow-up time point, thumb CMC flexion ROM was significantly less in the Progressive EOA group than in the Controls and the Stable EOA subjects, by means of -6.1° and -17.6°, respectively (Figure 1). CMC extension ROM decreased less over the study period, with mean differences of -4.8° and -7.0° for the Controls and Stable EOA groups compared to the Progressive EOA group, respectively. However, extension of the Progressive EOA group was only significantly less that the baseline Control extension ROM, with a mean difference of -7.0°. Decreases in the articular surface overlap with OA progression were most notable (Figure 2). At baseline (time 0), the Progressive EOA group was significantly less articular overlap than the Controls and the Stable EOA group. Articular overlap decreased over the study period in all groups. Articular overlap in the Progressive EOA group was significantly less than the overlap in both the Controls and the Stable EOA group at the 6-year follow-up. Prior studies have reported decreases in thumb ROM with OA, but this is the first study to quantify reductions in ROM specifically at the CMC joint. This study is limited to the observations reported. The mechanisms behind the reduction in CMC ROM, which may include loss of neuromuscular control, ligament/soft tissue contracture, and/or osteophyte growth, remain to be determined. Similarly, it is unclear whether CMC subluxation is a cause or a result of OA progression.

Significance: Thumb CMC OA is a highly prevalent disease associated with loss of hand function and pain, and an unknown etiology. The findings described here provide new insight into the functional changes in the thumb CMC joint as early OA progresses.

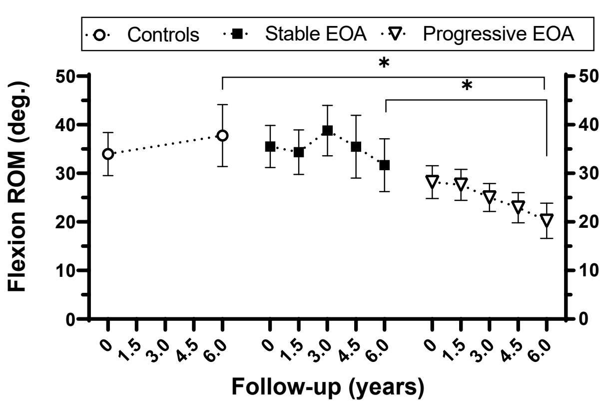

Figure 1. CMC joint flexion ROM significantly decreased over the six year study period with EOA progression.

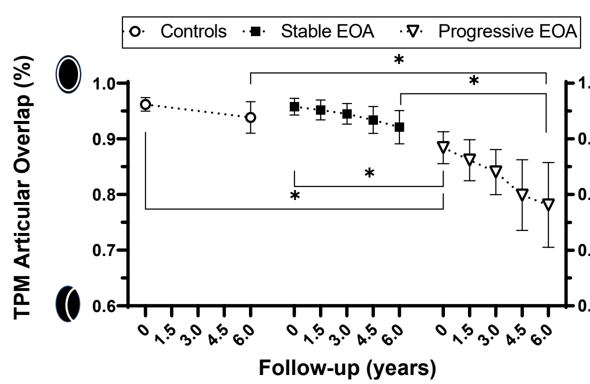

Figure 2. Overlap of the articular surfaces of the CMC joint, a measure of joint subluxation, decreased significantly with disease progression.

Acknowledgements: This research was supported in part by funding from NIH/NIAMS AR059185. Portions of the data have been previously presented at the 2022 Annual Meeting of the Orthopaedic Research Society.

USE OF SUBJECT-SPECIFIC PARAMETERS FOR PREDICTING PASSIVE FORCE IN MUSCULOSKELETAL MODELS: AN INVESTIGATION OF THEIR ACCURACY

Lomas S. Persad[1], Benjamin I. Binder-Markey[2], Alexander Y. Shin[1], Richard L. Lieber[3,4] and, Kenton R. Kaufman[1]
[1]Mayo Clinic, Rochester, MN, [2]Drexel University, Phila., PA, [3]Shirley Ryan AbilityLab, [4]Hines VA Medical Center, Chicago, IL
Email: Kaufman.Kenton@mayo.edu

Introduction

Musculoskeletal modeling has been proposed to inform clinical decision-making. However, generic musculoskeletal modeling parameters do not accurately reflect the unique anatomical and physiological characteristics of the individual being modeled. Therefore, incorporating subject-specific parameters into musculoskeletal models is proposed to lead to assessments of musculoskeletal function that are more accurate [1] and reliable. These individualized parameters may include muscle mass, bone length, joint angles, and other anatomical characteristics that vary among individuals. Due to the large amount of data and time required to create a complete subject-specific model, it is common to use both measured subject-specific data and data derived from the literature. The purpose of this study was to compare benefits and limitations of incorporating subject-specific variables into two popular muscle models often used to predict passive muscle force.

Methods

Intraoperative data were collected from 21 patients (4 female, age: 33 ± 13years, mass: 85 ± 26kg, height: 175 ± 9cm) who provided written informed consent. *In situ* gracilis muscle-tendon unit (MTU) length, passive sarcomere length (measured from clamped biopsies) and passive tension (measured with a buckle transducer) were obtained at four joint configurations (JC1-JC4) that gradually lengthen the gracilis muscle. Gracilis muscle volume, MTU slack length and external tendon slack length were measured from the harvested muscle.

Subject-specific values for maximum isometric force (P_0), optimal fiber length (l_{opt}), and tendon slack length (l_{ts}) were derived from experimental data. Measured muscle volume was divided by l_{opt} to yield physiological cross-sectional area (PCSA). Maximum isometric force was calculated using PCSA and a specific tension of 22.5 N cm^{-2} [2]. Muscle fiber length was estimated using the fiber length-to-muscle length ratio of 0.79 [3]. Fiber lengths were normalized by the experimental sarcomere length:optimal sarcomere length of 2.7 μm ratio to yield optimal fiber length.

Musculotendon parameters obtained experimentally were used to investigate the effect subject-specific values on passive force predictions using two muscle models. Model 1 was the Millard model [4] and Model 2 was the Thelen model [5]. In addition to subject-specific parameters listed above, the characteristic passive force-length (FL) curve (F_p curve) in both models was adjusted to match the passive FL relationship for the human gracilis [6]. A total of five modelling variations were tested, each using a different combination of subject-specific and default values that ranged from linearly scaled default generic parameters to all measured subject-specific modelling parameters (Figure 1).

Results and Discussion

Experimental passive tension ranged from 1.3 ± 0.9 N at JC1 to 21.7 ± 13.2 N at JC4 (knee fully extended). In variation 1, Model 1 overestimated passive force by 92%P_0 while Model 2 underestimated passive force by 9%P_0 in JC4. Model 1 fiber length error was 7% vs 22% for Model 2. The difference in errors observed between models were due to the default l_{opt} and l_{ts} values for each model.

In variation 2, when the strength of the muscle was adjusted, Model 1 passive force errors exceeded 40%P_0 at JC4. When our passive FL relationship was used (variation 3), the error was reduced to 29%P_0 at JC4. These results highlight the improvement of using the individual muscle strength and our human passive FL relationship in Model 1.

Surprisingly, when all subject-specific values were used (variation 4) passive force errors exceeded 80%P_0 at JC4. However, in variation 5 when the tendon slack length value included aponeurosis slack length, there was a seven-fold reduction in passive force error and average fiber length error decreased from 28% to 12%. Even with these improvements, force errors still exceeded 34%P_0. When 'tendon slack length' included aponeurosis length, it resulted in significant error reduction. *Researchers need to be aware of this misnomer*.

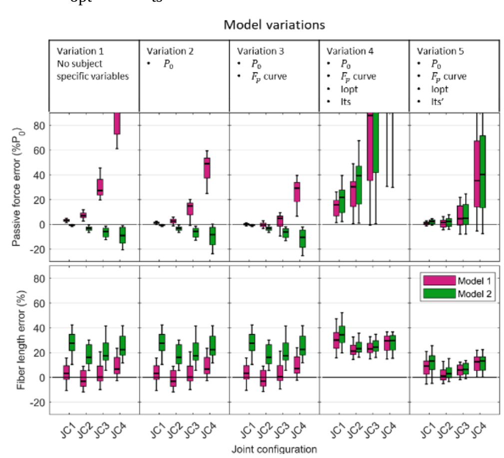

Figure 1: Passive force and fiber length error. Each column shows a variation in modeling while the upper and lower data rows show passive force and fiber length error respectively. Subject-specific parameters used for each model variation is shown at the top of each column ($l_{ts'}$ = external tendon slack length + aponeurosis slack length).

Significance

Use of subject specific modeling parameters significantly reduced musculoskeletal modeling errors. However, large errors (>35%P_0) between measured and predicted passive force remained. The magnitude of these force and fiber length errors are functionally significant.

Acknowledgments

Supported by VA grants I01 RX002462 and IK6 RX003351.

References

[1] Akhundov *et al.* (2022) PLoS One. **17**(1):0262936. [2] Powell *et al.* (1984) *J. Appl Physiol*. **57**(6):1715-21 [3] Ward *et al.* (2009) Clin. Orthop. Relat. Res. **467**(4):1074-1082 [4] Millard *et al.* (2013) *J. Biomech Eng*. **135**(2):1-11 [5] Thelen (2003) *J. Biomech Eng*. **125**(1):70-77 [6] Persad *et al.* (2021), *J Exp Biol*. doi: 10.1242/jeb.242722.

HIP JOINT FORCES DURING GAIT INCREASE WITH GREATER ILIOPSOAS STRENGTH: A SIMULATION STUDY

Madeline Grosklos[1,2*], Cara L Lewis[3], Jay R Patel[2], Jil B Patel[2], Siddharth Fernandes[2], Jennifer Perry[2], Stephanie Di Stasi[2,4]
[1]The Ohio State University Department of Biomedical Engineering [2]The Ohio State University Sports Medicine Research Institute
[3]Boston University Department of Physical Therapy [4]The Ohio State University Department of Physical Therapy
*Corresponding author's email: madeline.grosklos@osumc.edu

Introduction: Musculoskeletal modeling is a powerful analysis technique that enhances traditional assessments of kinetics and kinematics by investigating muscle properties and intra-articular forces. Uniquely, musculoskeletal modeling can simulate rehabilitation before it is tested in real patients. For example, in patients with joint pain, we can model the effects of both muscle weakness and strengthening on the forces experienced by the joint. Hip flexor weakness is common in individuals with femoroacetabular impingement syndrome (FAIS),[1] a condition associated with pain, symptoms, and structural variants of the hip joint; yet, flexor strengthening is often avoided for fear of increasing the patient's symptoms.[2] The anterior region of the joint is a primary location of structural damage in FAIS, and the flexors (iliacus and psoas) are a major contributor to anterior joint forces during gait.[3] Weakness of the hip flexors is associated with worse patient reported outcomes, decreased range of motion, and increased severity of labrum and articular cartilage damage.[4,5] The purpose of this exploratory study was to use musculoskeletal modeling to investigate the effects of hip flexor strength on hip joint reaction forces (JRFs) during terminal stance of gait, when anterior JRFs are at their highest. Observational simulation studies have found decreased iliopsoas forces and decreased JRFs during gait in individuals with FAIS;[6] thus, we hypothesized that hip JRFs would decrease under decreased flexor strength conditions and increase under increasing flexor strength conditions.

Methods: Eight females with FAIS ages 18-40 underwent 3D motion capture of overground gait at their self-selected pace. Marker trajectories and ground reaction forces (GRFs) were sampled at 240Hz and 1200Hz, respectively, and lowpass filtered using a 4th order Butterworth filter at 6Hz and 50Hz respectively. A participant specific model was scaled, and joint motion was tracked with inverse kinematics in Visual3D (C-Motion Inc. Rockville, MD). Scaling, kinematics, and GRF data were imported into OpenSim 4.4 and a 23°-of-freedom, 92-actuator model Gait2392 was scaled based on calculations from Visual3D. The Residual Reduction Algorithm (RRA) tool was used to adjust model masses until residual forces and moments were <5N and <15Nm respectively, ensuring that changes in rotations and translations were <2° and <2cm respectively. The scaled, RRA adjusted model was saved with five different conditions of iliacus and psoas maximum isometric force; 50%, 70%, 100% ("natural"), 130%, and 150% to simulate both weakening and strengthening of the iliopsoas flexor muscle group. Kinematics were constrained to the experimentally observed gait patterns in 3D motion capture. For each model, muscle forces were calculated using the Computed Muscle Control (CMC) tool, and RRA and CMC results were used in the JointReaction tool to estimate femur-on-acetabulum forces in the anterior (JRFx), superior (JRFy), and medial (JRFz) directions. The resultant force (JRFr) was the vector summation of all three components. All data were analyzed during terminal stance, defined as the phase from the local minima of the vertical GRF to toe off (vertical GRF ≤ 10N). Forces were normalized to be expressed as a percentage of body weight (BW). Peak JRF values were used for analysis. A one-way repeated measures ANOVA with custom contrasts was used to compare differences in JRFs between each level of flexor force capacity alteration and the 100% condition. Where sphericity was violated, Greenhouse and Geisser epsilon was calculated and used to correct the one-way repeated measures ANOVA. Bonferroni corrections for multiple comparisons were not utilized as this was an exploratory analysis of a small data set intended to be hypothesis-generating for future work. Data were reported as mean ± standard deviation.

Results & Discussion: In support of our hypothesis, JRFx, JRFy, and JRFr increased with increasing levels of hip flexor strength ($p \leq .017$); unexpectedly, there was no difference in JRFz ($p=0.972$). Compared to the 100% condition, JRFx was lower in the 50% and 70% conditions ($p<.001$, $p=.002$) and higher in the 150% condition ($p=.035$), but not different between the 100% and 130% conditions ($p=.093$). JRFy was lower in the 50% and 70% conditions ($p=.001$, $p=.018$), but not different between the 100% and 130% or 150% conditions ($p \geq .066$). JRFr was lower in the 50% and 70% conditions ($p<.001$, $p=.018$) and higher in the 150% condition ($p=.049$) but not different between the 100% and 130% conditions ($p=.438$). JRF values appeared more affected by the weakened versus strengthened conditions, indicating that even small amounts of flexor weakness may alter forces experienced by the joint. A previous study established the importance of flexor strength for normal gait, demonstrating that weakness of the hip flexors is not well tolerated and causes large increases in total muscle cost.[7] To our knowledge, this is the first study to model the cause-and-effect relationship between different flexor strength conditions and hip JRFs during gait in FAIS.

	JRFx	JRFy	JRFz	JRFr
50%	1.77 ± .26	4.92 ± .60	1.40 ± .46	5.38 ± .76
70%	2.07 ± .25	5.02 ± .55	1.36 ± .31	5.57 ± .57
100%	2.49 ± .32	5.50 ± .58	1.38 ± .38	6.15 ± .77
130%	2.73 ± .42	5.63 ± .70	1.35 ± .29	6.38 ± 1.06
150%	2.97 ± .46	6.03 ± .69	1.39 ± .29	6.89 ± 1.13

Table 1: Peak JRFs ± standard deviation as percent body weight at each hip flexor strength condition

Significance: These preliminary results show that flexor strength can directly impact hip JRFs and should be a focus of future research in individuals with FAIS. Flexor strength may be an important but overlooked element of rehabilitation; of 31 post-hip arthroscopy protocols available online, none included hip flexor strengthening explicitly or justification for its exclusion.[8] Model-based studies such as this can be a data-driven source of development for effective rehabilitation protocols.

References: [1] Kierkegaard et al. (2017) *JSAMS.* 20(12). [2] Pennock et al. (2018) *AJSM.* 46(14). [3] Correa et al. (2010) *J Biomech.* 43(8). [4] Samaan et al. (2019) *J. Biomech* (84). [5] Nepple et al. (2015) *Arthroscopy.* 31(11). [6] Ng et al (2018) *AJSM* 46(11). [7] Van der Krogt et al. (2012) Gait *Posture.* 36(1). [8] Cvetanovich et al. (2017) *Arthroscopy.* 33(11)

TEMPOROSPATIAL GAIT PARAMETERS DIFFER BASED ON PROLONGED STANDING AND KNEE PAIN

Abigail C. Schmitt[1*], Ellie Mueller[2], Gary Austin[1], Kaitlin M. Gallagher[1]
[1]University of Arkansas, Fayetteville, AR [2]New York Institute of Technology, Jonesboro, AR
*email: acs063@uark.edu

Introduction: Prolonged standing is a common occupational task in service-based jobs and is becoming more common in the office with standing desks. While prolonged standing may seem less demanding than other occupational tasks (such as heavy lifting), remaining upright still requires physical effort. A 2-hour bout of prolonged standing resulted in poorer balance during single-leg stance[1] and increased center of pressure regularity[2]. Pain development is also common in prolonged standing, with low back pain most commonly assessed[1]; however, mild knee pain development can influence gait patterns[3]. Thus, the main objective of this study is to assess the influence of knee pain development during a 75-minute prolonged standing occupational simulation on temporospatial gait characteristics. We hypothesize that while prolonged standing will alter temporospatial variables, those with knee pain development during standing will see greater changes after standing.

Methods: Thirteen participants between 18-40 years old were recruited from a convenience sample. After providing written informed consent, participants performed six walking trials at a self-selected pace along a 28 m hallway through an 8-camera markerless motion capture system (SONY RX0 II, ~6 m long). Participants then entered into a 75-minute prolonged standing protocol where they completed standardized computer tasks. The computer workstation was set up individually for each participant. Every 15 minutes, participants completed a 100 mm visual analog scale (VAS) to document knee pain intensity. After standing, the participant completed six walking trials at a self-selected pace. Motion capture data were processed with Theia software (Kingston, ON, Canada). Temporospatial variables were calculated in Visual3D (v6). Participants were classified as developing knee pain during standing if their VAS score measured 10 mm or greater for one knee during standing. This threshold has been used previously to assess transient pain during standing[1]. A two-way repeated measures ANOVA was performed on the outcome measures (Table 1), with a repeated factor of time (pre-/post-standing) and a between factor of knee pain development (yes/no). Significance was set at $p < .05$.

Results & Discussion: Five participants (38%) were characterized as knee pain developers in standing, with an average maximum VAS score of 15.3 (5.9) mm for the left knee and 19.8 (4.2) mm for the right knee. Those who did not develop pain had an average maximum of 0.2 (0.6) mm and 0.63 (1.8) mm for the left and right, respectively. There was a significant effect of standing on gait cycle time ($p= .047$), gait speed ($p= .004$), and stride length ($p= .008$). Cycle time increased after standing, while speed and stride length decreased (Table 1). This aligns with previous work showing that musculoskeletal fatigue can alter gait speed and stride length[4]. Finally, there was a significant main effect of knee pain development during standing on stride length standard deviation ($p= .003$). Participants who developed knee pain had greater stride length variability than those who did not. While stride width standard deviation was not significant for knee pain development ($p= .067$), the Cohen's d effect size was .87, with a larger standard deviation for those who developed knee pain. These outcomes align with work showing that increased gait variability and lower gait complexity are related to a higher likelihood of mild unilateral knee pain[3]. Our results show that a potential adaptation to the presence of pain may already be evident in individuals who develop knee pain during standing. Future research will investigate if this pain alters joint angles.

Significance: Prolonged standing for 75 minutes altered temporospatial gait patterns. The changes in linear gait variability in those who develop knee pain during standing measures could be of concern if these results are similar for older adults. Many who have knee osteoarthritis also have knee pain[5], and an increase in gait variability is linked to falls in this age group[6]. With the workforce participation rates of those 55 or older continuing to increase[7], understanding how working postures, such as standing, affect older adults will be important to assess potential risks they face at work for trips and falls.

Acknowledgments: A U of A Honors College Research Grant and ADHE Undergraduate Research Fellowship funded this project.

References: [1] Nelson-Wong et al., 2010. *Ergonomics,* 53. [2] Fewster et al., 2020. *Gait Pos*, e1-6. [3] Bacon et al., 2022. *Sci Reports,* 12. [4] Granacher et al., 2010. *J Neuro Eng Rehab,*. 7 [5] Debi, R., et al., 2009. BMC Musculoskel, *10*(1). [6] Hausdorff et al., 2001. Arch Phys Med Rehabil, 82. [7] US Bureau of Labor Statistics. https://www.bls.gov/emp/tables/civilian-labor-force-summary.htm

Table 1: Mean (standard deviation) for temporospatial gait parameters. *= main effect of prolonged standing; += main effect of knee pain.

	Knee Pain (n=5)		**No Knee Pain (**n = 8)	
	Pre	**Post**	**Pre**	**Post**
Cycle Time (s)*	1.08 (.05)	1.09 (.05)	1.07 (.06)	1.08 (.07)
Speed (m/s)*	1.42 (.13)	1.39 (.12)	1.38 (.08)	1.34 (.08)
Stride Length (m)*	1.53 (.08)	1.51 (.07)	1.47 (.10)	1.45 (.11)
Stride Length Std Dev (m)$^{+}$	0.037 (.010)	0.033 (.005)	0.025 (.006)	0.030 (.004)
Stride Width (m)	0.13 (.02)	0.14 (.02)	0.14 (.04)	0.14 (.03)
Stride Width Std Dev (m)	0.018 (.005)	0.018 (.005)	0.014 (.003)	0.016 (.003)

Reduced Muscle Coordination Complexity Alters Walking Balance Control Across a Diverse Range of Perturbations in Older Adults

Grant T Maddox[1*], Andrew D Shelton[2,3], Vicki S Mercer[2], Jeremy R Crenshaw[4], Jason R Franz[2,3], Jessica L Allen[1]
[1] University of Florida, USA, [2] UNC Chapel Hill, USA, [3] NC State University, USA, [4] University of Delaware, USA
email: grantmaddox@ufl.edu

Introduction: Older adults are at an exceptionally high risk of falls, with most falls occurring during walking. Appropriately coordinating muscle recruitment during walking plays an important role in preventing falls. Indeed, we recently provided initial evidence that the complexity of muscle coordination during walking was reduced in older adults and associated with increased susceptibility to walking balance challenges [1]. In that previous work, we focused only on perturbations that elicited the visual perception of instability. This study aimed to examine whether that discovery generalizes to a broader range of perturbation contexts that more fully represent the variety of balance challenges encountered in the real world, e.g., slips/trips and center-of-mass balance loss. We hypothesized that individuals with lower muscle coordination complexity during unperturbed walking as measured using motor module analysis [2] would be more susceptible to walking balance challenges, characterized by lower margin-of-stability (MoS) [3] in response to the perturbations.

Methods: 14 older adults (6F; 71.1±5.5yrs) walked on a split-belt treadmill at their preferred walking speed (1.24±0.16 m/s) under four different conditions [4]: (1) unperturbed walking, (2) treadmill-induced slip perturbations (200 m/s duration, 6 m/s^2) applied randomly 5 times bilaterally at heel strike, (3) impulsive lateral waist pulls (100 m/s duration, 5% body weight) applied bilaterally toward the swing leg at toe-off, and (4) two minutes of continuous mediolateral optical flow perturbations using a nominal amplitude of 35 cm. Surface electromyography (EMG) was collected from eight lower limb muscles on the right leg spanning the ankle, hip, and knee: tibialis anterior, soleus, medial gastrocnemius, vastus lateralis, rectus femoris, medial hamstring, gluteus maximus, and gluteus medius. Motor modules were extracted from the EMG data during unperturbed walking using non-negative matrix factorization and muscle coordination complexity was defined as 100 – the variability accounted for by one motor module (100 – VAFby1) [2]. Subjects also wore 36 motion capture markers on their feet, legs, pelvis, and trunk from which we calculated MoS during the perturbation conditions. MoS was calculated in both the anterior-posterior (MoS_{AP}) and mediolateral (MoS_{ML}) directions at the instant of heel-strike in the step directly following perturbation onset for the discrete slips and waist pulls and across all steps for the continuous optical flow perturbations. To test our hypothesis that lower muscle coordination complexity would be associated with increased susceptibility to walking balance challenges, we performed Pearson's correlation between our measure of muscle coordination complexity and both MoS_{AP} and MoS_{ML} in the three different perturbation conditions. We interpreted moderate to large positive correlations ($r > 0.30$ [5]) as evidence that lower muscle coordination complexity is associated with lower MoS.

Results & Discussion: We identified a moderate relationship between muscle coordination complexity and MoS in all perturbation conditions, but only in the direction of the perturbation (Fig. 1).

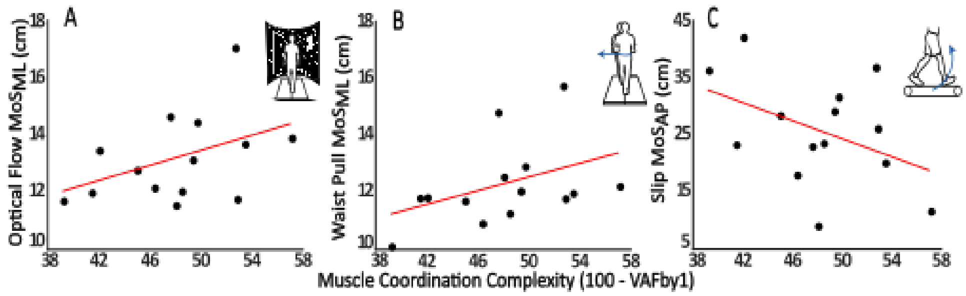

Figure 1: There was a relationship between muscle coordination complexity and MoS in the direction of the perturbation. (A) Optical flow and (B) waist pulls had a positive relationship, while (C) slips had a negative one.

Consistent with our hypothesis, we found a positive correlation between unperturbed muscle coordination complexity and MoS_{ML} in the lateral waist-pull and mediolateral optical flow perturbations ($r = 0.42$ and $r = 0.43$) but no correlation with MoS_{AP} ($r = -0.06$, and $r = 0.19$). Specifically, individuals with lower muscle coordination complexity had a lower MoS_{ML}. We interpret this finding as evidence that lower muscle coordination complexity in straight-line walking constrains the ability to respond to a broad range of balance perturbations faced in everyday life.

Interestingly, the treadmill-induced slips that occurred in the anteroposterior direction had the opposite trend; individuals with lower muscle coordination complexity had *higher* MoS_{AP} ($r = -0.42$). There was no correlation with MoS_{ML} ($r = 0.06$). Future work is needed to unravel the source of this paradoxical relationship. Since MoS can be modulated by controlling center-of-mass (CoM) kinematics and/or step placement, it is possible that lower muscle coordination complexity represents a proactive strategy helpful for preventing large CoM motion or, conversely, that participants with lower muscle coordination complexity have an altered reactive response in which they take longer recovery steps.

Significance: These results provide evidence that muscle coordination complexity alters walking balance control across diverse perturbations in older adults. Increasing muscle coordination complexity through rehabilitation may therefore be beneficial to help reduce the risk of falls during daily life.

Acknowledgments: Supported by NIH 1R21AG067388.

References: [1] Allen and Franz (2018), *J Neurophysiol* 120(5), [2] Steele et al. (2015), *Dev Med Child Neurol* 57(2), [3] McAndrew et al (2012). *J Biomech* 45(6), [4] Shelton et al (2022). *North American Congress on Biomechanics*, [5] Cohen et al. (1992), *Psychol Bull* 112(1)

MOTOR MODULES ARE LARGELY UNAFFECTED BY DIFFERENT WALKING BIOMECHANICS

Mohammad RahimiGoloujeh* and Jessica L. Allen
University of Florida, Gainesville, FL, USA
*Corresponding author's email: rahimig.mohammad@ufl.edu

Introduction: Motor module (a.k.a. muscle synergy) analysis has frequently been used to provide insight into changes in muscle coordination associated with declines in walking performance. The number of motor modules recruited during walking can provide a measure of muscle coordination complexity, with reduced complexity reflected by fewer modules. Reduced complexity is often correlated with impaired walking performance, such as slower walking speeds and more asymmetrical step lengths in stroke survivors [1]. The purpose of this study was to explore to what extent such reductions in complexity are simply emergent from biomechanics. Or in other words, does walking with slower speeds, asymmetric step widths, and/or wider step widths *require* a reduction in muscle coordination complexity? We hypothesize that there is a neural origin to these reductions, such that they cannot be explained by biomechanics alone. We tested this hypothesis using a computational modeling approach as described below**.**

Methods: We designed a series of 27 different simulations to model different walking biomechanics, including three speeds (0.8, 1.1, and 1.45 m/s), step length asymmetry levels (0, 15, and 30%), and step widths (0.1, 0.2, and 0.3 m). For each simulation, optimal muscle recruitment over a single gait cycle was identified using OpenSim MoCo [2] using a 3D musculoskeletal model with 23 degrees of freedom and 94 muscles. An initial reference simulation (1.45 m/s, 0% asymmetry, and 0.1 m step width) was attained by tracking motion capture data of normal walking [3]. The remaining simulations were derived by using the reference solution as the initial guess and a cost function that included deviation from reference motion, deviation from desired step length asymmetry, and minimizing muscle activity. Constraints were imposed to achieve target speeds and step widths. Subsequently, non-negative matrix factorization was applied to the optimal muscle activation patterns from each simulation to extract motor modules. Two sets of motor modules were identified on each leg: (1) from all muscles, and (2) from a subset of muscles commonly examined experimentally [1,4]. The number and structure of these motor modules were compared to those of the reference solution. Based on our hypothesis, we predicted that the number and structure of motor modules would not differ across these simulations despite their different walking biomechanics. Motor module numbers were chosen such that the variability accounted for across all muscles was greater than 95% within a simulation and Pearson's correlations were used to compare motor module structure back to the reference simulation.

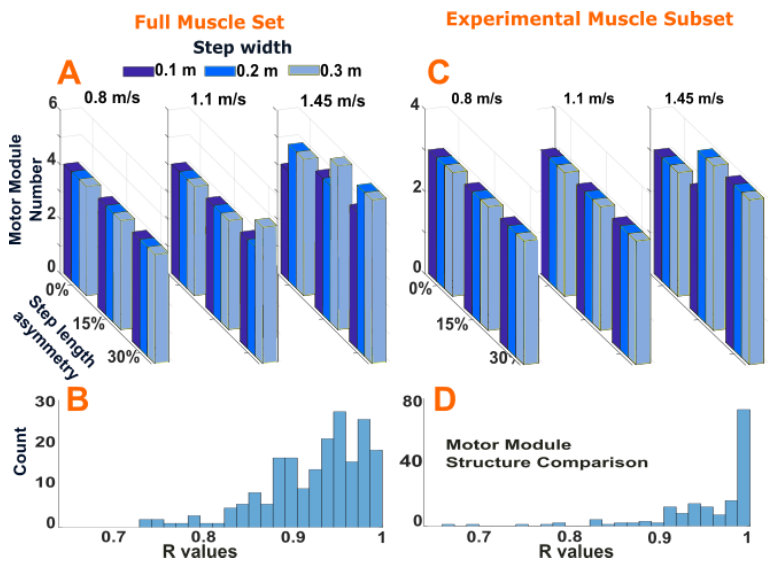

Figure 1: A and C: motor module numbers across all conditions for full muscle and reduced subset respectively. B and D: histograms of motor modules structure comparisons to the reference solution.

Results & Discussion: In support of our hypothesis, impaired gait was feasible with the same number of motor modules regardless of whether we looked at all muscles or a reduced experimental subset (Fig. 1A,C). The number of motor modules was equal to 4 in almost every simulation in case of all muscles and 3 in case of the reduced experimental subset. Interestingly, we found that walking at the fastest speed with asymmetric and wide steps required an increase in complexity. However, such a combination of biomechanical factors is not commonly observed as people exhibiting asymmetric or wide steps tend to walk at slower not faster speeds. Our simulations suggest that reduced muscle coordination complexity observed in neurological populations such as stroke survivors reflects at least to some extent an impairment in their nervous system rather than only changes in their spatiotemporal gait biomechanics.

We also found that motor module structure did not substantially differ between simulations ($r = 0.92\pm0.06$ for full set and $r = 0.95\pm0.06$ for reduced set, Fig. 1B,D). We do observe some minor changes to motor module structure with walking biomechanics. For example, the simulation with the most distinct structure from the full muscle set ($r=0.73$) was the one at the slowest speed with 30% step length asymmetry and 0.3 m step width. Such a value corresponds to relatively high similarity to the reference solution, suggesting that different walking biomechanics are feasible by not only the same number of motor modules, but also the same motor module structure.

Significance: This study supports our hypothesis that reductions in the number of motor modules during walking in stroke survivors cannot be explained purely by walking biomechanics. Such reductions may therefore reflect to some extent a variation in their underlying nervous system and be a good indicator of impairment neuromuscular control.

Acknowledgements: Supported by NSF/DARE 2245260.

References: [1] Clark et al. (2010), *J Neurophysiol* 103(2)*;*[2] Dembia et al. (2020), *PLOS Comput Bio.*, *16*(12), [3] Miller et al. (2014), *Med Sci Sports Exerc 46*(3); [4] De Groote et al. (2014) *Front. Comput Neurosci 8(115).*

BALANCE CONFIDENCE AND WALKING MARGIN OF STABILITY SYMMETRY AFTER LOWER-EXTREMITY PROSTHESIS OSSEOINTEGRATION: A CASE SERIES

James B. Tracy[1*], Mohamed E. Awad, Danielle H. Melton, Jason W. Stoneback, Brecca M. M. Gaffney, Cory L. Christiansen
[1] University of Colorado, Anschutz Medical Campus, Aurora, CO
*Corresponding author's email: james.tracy@cuanschutz.edu

Introduction: Lower-limb amputation significantly increases fall risk and is associated with between-limb gait asymmetries and reduced quality of life **[1-3]**. One factor affecting fall risk and movement impairments is the high number of reported socket prosthesis fit issues (e.g., discomfort, skin irritation) that are associated with reductions in quality of life **[3].** Today, prosthesis osseointegration (OI) is a secondary procedure that uses a bone-anchored implant to directly connect the prosthesis to the residual limb **[4]** with early evidence demonstrating improved balance confidence **[5,6]** and standing balance **[6]**. It is not known how prosthesis OI impacts walking stability symmetry. This investigation explored the effect of prosthesis OI on balance confidence (Activity-specific Balance Confidence (ABC) scores **[7]**) and walking stability symmetry (between-limb symmetry of margins of stability (MoS)). We hypothesized that prosthesis OI would improve (1) balance confidence and (2) walking stability symmetry, compared to pre-OI using a socket prosthesis.

Methods: This IRB-approved study includes a case series of 10 participants (5F/5M; Age: 51.7(12.4) yrs; BMI: 28.1(4.5) kg·m^{-2}) who underwent unilateral transfemoral (n=5) or transtibial (n=5) prosthesis OI and 2 test sessions (Pre-OI: within 5 days prior to surgery using a socket prosthesis; Post-OI: 12 months after surgery). In addition to completing the ABC, participants completed whole-body motion capture (Vicon, 120 Hz) during overground walking at self-selected speeds. The MoS (distance between the base of support edge and the whole-body center of mass position plus a scaled center of mass velocity) **[8]** was calculated to indirectly measure limb control. The anterior MoS was measured just before foot contact (i.e., the state of stability just before a phase of gait when a loss of balance could potentially occur during the initial contact phase of gait prior to limb loading). The lateral MoS value was measured as the minimum value reached during stance (i.e., the state of least lateral stability). The anterior and lateral MoS were measured for each step and the between-limb symmetry calculated using the Normalized Symmetry Index (NSI) **[9]**. Zero represents full symmetry and ±100 full asymmetry. ABC scores and NSI absolute values were compared between time points using Cohen's *d* effect sizes (SPSS).

Results & Discussion: In agreement with our hypothesis and other studies **[5,6]**, ABC scores increased (Table 1, *d*=1.21) showing increased balance confidence after prosthesis OI. Contrary to our hypothesis, we observed only small effects for both anterior (*d*=0.28) and lateral (*d*=0.21) MoS symmetry and high degrees of symmetry (i.e., NSI near zero) for the MoS measures at both timepoints. Both quasi-static and dynamic postural control mechanisms could account for improvements in balance confidence. Recently, in a comparable sample of participants before and after prosthesis OI, we found a medium-sized effect of decreased center of pressure path length and path ellipse area during quiet standing with eyes closed, representing improved standing postural control **[6]**. This previously reported magnitude of effect for standing (i.e., quasi-static) postural control was larger than that noted in the current analysis of walking (i.e., dynamic) MoS symmetry, potentially indicative of different mechanisms across postural control domains **[10]**. A systematic review of MoS during pathologic gait reported mixed results for lateral MoS measures using a socket prosthesis showing inconsistent differences between intact and prosthetic limbs and between individuals with and without a unilateral amputation **[11].** These mixed results highlight the heterogeneity of this population and a potential limitation of the MoS to differentiate stability between limbs or between individuals with and without an amputation. Three primary limitations in this case-series data were (1) a small sample, (2) a sample of high-functioning participants (i.e., minimal walking issues and high symmetry pre-OI), and (3) not accounting for osseoperception and proprioception, among other possible confounding variables. Further research is needed to evaluate the effects of prosthesis OI on reactive postural control under additional dynamic conditions.

Significance: In this case-series, we indirectly assessed limb control through MoS during walking showing minimal change in between-limb symmetry from before to after prosthesis OI. It is possible that metrics of postural control other than walking MoS are more relevant to balance and balance confidence following prosthesis OI (e.g., reactive responses to postural disturbances).

Acknowledgements: Funding: CU Osseointegration Research Consortium. Data collection: Gary Schneider and Tony Johnson.

References: **[1]** Kulkarni et al., 1996. *Physiotherapy.* 82(2). **[2]** Sadeghi et al., 2000. *Gait Posture*, 12. **[3]** Hagberg et al., 2001. *Prosth Orth Inter*, 25(3). **[4]** Hebert et al., 2017. *JBJS Reviews*, 5. **[5]** Davis-Wilson et al., 2022. *Prosth Ortho Inter*. **[6]** Gaffney et al., 2023. *Gait Posture*, 100. **[7]** Powell and Myers, 1995. *J Geron*, 50A(1). **[8]** Hof et al., 2005. *J Biomech*, 38. **[9]** Queen et al., 2020. *J Biomech*, 99. **[10]** Horak et al., 2009, *Phys Ther*, 89. **[11]** Watson et al., 2021. *BMC Mus Dis*, 22.

Table 1 – Pre- and post-OI ABC, anterior and lateral MoS, absolute value of NSI, and gait speed (mean (SD)), and between-timepoint effect sizes.

**Large Effect*		**Anterior Margin of Stability**			**Lateral Margin of Stability**			
Timepoint	**ABC Score**	**Intact Limb (%height)**	**Prosthetic Limb (%height)**	**|NSI| (%)**	**Intact Limb (%height)**	**Prosthetic Limb (%height)**	**|NSI| (%)**	**Gait Speed (m/s)**
Pre-OI	61.4 (28.8)	-27.2 (6.1)	-27.9 (6.2)	5.8 (5.7)	4.37 (0.74)	3.70 (1.14)	12.9 (14.3)	1.04 (0.21)
Post-OI	78.8 (19.0)	-27.1 (5.3)	-27.4 (5.4)	4.6 (3.6)	4.14 (0.76)	4.15 (0.78)	9.1 (9.4)	1.03 (0.17)
Cohen's *d*	**1.21*	0.03	0.10	0.28	0.26	0.41	0.21	0.09

MUSCLE-DRIVEN, IMPLANTED FOOT-ANKLE ENDOPROSTHESIS RECOVERS GAIT KINEMATICS

Katrina L. Easton[1*], Caleb Stubbs[1], Caroline Billings[2], Kristin M Bowers[2], Stacy M. Stephenson[3], Cheryl B. Greenacre[2], David E. Anderson[2], and Dustin L. Crouch[1]

[1]College of Engineering, [2]College of Veterinary Medicine, [3]Graduate School of Medicine; University of Tennessee-Knoxville

*Corresponding author's email: keaston@utk.edu

Introduction: About 2 million people in the US are affected by limb amputation [1]. All existing prostheses must be worn externally, and even the state-of-the-art devices fail to restore natural sensorimotor function, leading many patients to reject external prostheses [2]. To improve sensorimotor function, we propose to completely internalize the prosthesis within living skin, enabling direct muscle-prosthesis attachment. In an ongoing *in vivo* study, we are testing a prototype of a muscle-driven, articulated, foot-ankle implanted endoprosthesis in a rabbit model of hindlimb below-knee amputation. For this prototype, we previously reported that vertical ground contact force on the endoprosthetic limb during hopping gait increased over time post-surgery [3]. The objective of the current study was to quantify the hindlimb kinematics of rabbits with the endoprosthesis prototype during hopping gait.

Methods: Foot and shank segments of the endoprosthesis prototype were 3D-printed in 316 stainless steel and joined by a polyethylene hinge pin to create an ankle joint (Fig. 1). To improve biocompatibility, the prosthesis was overmolded in medical-grade silicone (BIO M360, Elkem Silicones). The *in vivo* study was approved by our Institutional Animal Care and Use Committee. Three 18- to 27-week-old female New Zealand White rabbits underwent surgical amputation of the left hindlimb under general anesthesia. Briefly, the skin surrounding the foot and ankle was preserved by retracting it proximally. The musculoskeletal tissues were amputated approximately 2 cm proximal to the distal end of the tibia. After amputation, the prosthesis was anchored in the intramedullary canal of the tibia and immobilized using bone cement. The tibialis cranialis and triceps surae muscles were attached to eyelets on the foot segment using polyester-based artificial tendons in Rabbit 1 (R1) and the native tendons in Rabbits 2 (R2) and 3 (R3). The skin was replaced and sutured over the prosthesis.

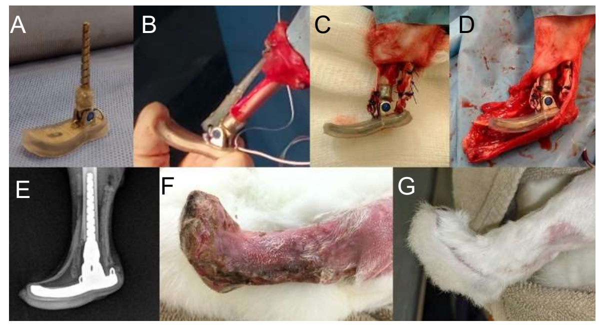

Fig. 1: A) Jointed prosthesis. B) Intra-op endoprosthesis with artificial tendons. C) Intra-op endoprosthesis with native tendons. D) Intra-op just prior to skin closure. E) Lateral radiograph post-surgery with artificial tendons. F) Eight and G) thirty days post-op.

Once bandages were removed (3 - 7 weeks post-surgery), we recorded sagittal plane motion video with 3 high-speed cameras (Prime 13, OptiTrack, NaturalPoint, Inc) placed parallel along a 2.6 m long walkway. Reflective 7.5 mm flat circular markers were placed on the lateral aspect of the left limb at the hip (greater trochanter), knee, ankle (lateral malleolus), and 5th metatarsophalangeal joint to facilitate tracking of the joint centers. Data was collected weekly for weeks 4-16 post-surgery for R2 and R3 and for weeks 3-24 post-surgery for R1; the start of data collection depended on when bandages could be removed. DeepLabCut [4] and custom MATLAB scripts were used to obtain marker positions, calculate sagittal-plane joint angles for the knee and ankle joints, and combine the data from the 3 cameras into one curve for the entire length of the walkway.

Results & Discussion: Maximum ankle extension angle and ankle range of motion (difference between max and min angles over gait cycle) was reduced across all post-surgery timepoints compared to baseline. In all rabbits, the endoprosthetic ankle was more flexed post-surgery compared to baseline throughout both stance and swing phases of gait; in contrast, the knee joint was more extended throughout the gait cycle possibly to compensate for the more flexed ankle posture. At 3-weeks post-surgery, there was minimal ankle rotation throughout the gait cycle (Fig 2, solid grey line) and minimal knee flexion during stance. However, both knee and ankle flexion and extension increased over time post-surgery. By 24-weeks post-surgery, ankle kinematics for R1 had recovered substantially (Fig 2; swing phase ROM: 67° (baseline); 13° (3 weeks); 44° (24 weeks)). The extent to which the attached muscles contributed to post-surgical kinematic recovery is unknown but will be assessed by electromyography in future studies. The study duration was relatively short; given sufficient time and neuromuscular re-education, more normal gait patterns may be achieved.

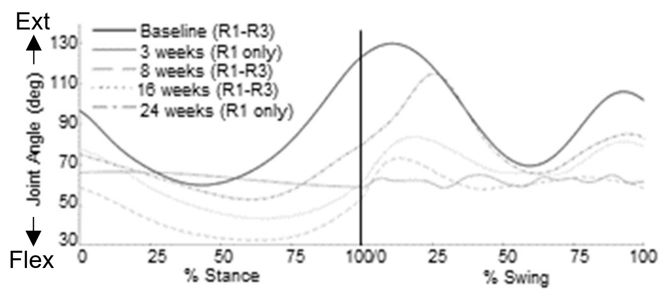

Figure 2: Ankle joint angle over stance and swing phase of gait for different timepoints. Three and 24-weeks post-surgery are for rabbit 1 only. The other timepoints are averages for the 3 rabbits.

Significance: Promisingly, our preliminary data demonstrated partial recovery of hindlimb joint kinematics during hopping gait with our foot-ankle endoprosthesis prototype, supporting the potential of muscle-driven endoprostheses to restore motor function.

Acknowledgements: Funding: NIH (R61AR078096), NSF (1944001). Thanks to Kaitlyn Stephens, Sarah Clabo, Victoria Theobald, and Nicholas Ray for help with data collection; and to Ivy Milligan, Dylan Marler, and Carter Hatch for help with data processing.

References: [1] Ziegler-Graham, 2008. *Arch Phys Med Rehabil.* 89(3):422; [2] Biddiss, 2007. *Am J Phys Med Rehabil.* 86(12):977; [3] Easton, 2022, NACOB; [4] Mathis, 2018, *Nat Neurosci*. 21(9):1281.

PREDICTIVE SIMULATION OF POSTSTROKE ADAPTIVE TREADMILL GAIT

Kayla M. Pariser[1*], Jill S. Higginson[1, 2]
University of Delaware [1]Mechanical and [2]Biomedical Engineering, Newark DE, USA
*Corresponding author's email: pariserk@udel.edu

Introduction: Standard fixed-speed treadmill rehabilitation paradigms improve walking speed and function in only 50% of stroke survivors [1, 2]. To address this concern, we developed an adaptive treadmill (ATM) that adjusts belt speed in real-time via changes in user step length and propulsion, promoting natural stride-to-stride variability [3]. Healthy young adults increase speed and propulsion on the ATM versus fixed-speed treadmill, signifying that the ATM may be a good rehabilitation tool [3]. But while all individuals poststroke tolerated the ATM, their responses were mixed [4], possibly due to lack of controller customization. Computational treatment design with predictive simulations may allow for more efficient customization of ATM paradigms compared to fatiguing trial-and-error experiments. We have developed a novel predictive simulation framework of ATM gait that captures changes in gait mechanics and speed observed experimentally in a study of healthy young adults walking on variations of the ATM [5, 6]. The goal of this study was to adapt the simulation framework to predict the response of stroke survivors with various ATM controllers. We hypothesized that as we increased the weight on the step length or propulsive impulse term in the simulated ATM cost function, we would predict increased paretic step length or propulsive impulse and that the increases would be greater when strength was preserved (e.g. high functioning).

Methods: We modified a 2D lower limb fixed-speed treadmill gait model [7] to make the treadmill belt motion a free parameter chosen by the simulation instead of prescribed. We modelled hemiparesis severity by uniformly decreasing the maximum isometric strength values of all muscles of the left limb by 25% and 50% to represent high and low functioning individuals poststroke. Treadmill gait was simulated using direct collocation optimal control methods in OpenSim Moco [8]. A prior tracking simulation solution was the initial guess for the predictive problem that minimized the controls (u), error between simulated and reference belt speed (e_{vbelt}) multiplied by a constant (c) for scaling, and maximized step length (SL) and propulsive impulse (PI, Eq 1). We modified the values of the weights on the step length and propulsive impulse terms to generate five simulated ATM controllers: Baseline ($w_{SL} = w_{PI}$), Low & High SL ($w_{SL} > w_{PI}$), and Low & High PI ($w_{SL} < w_{PI}$). In total we ran 10 simulations, one for each of the two weakness conditions on each of the five simulated ATMs. Predicted step length, propulsive impulse, and walking speed were compared to suggest who may benefit from which ATM controller.

$$J = \int_{t_0}^{t_f} (w_{control}\|u\|^3 + w_{vbelt}(c)\|e_{vbelt}\| + w_{SL}\|SL\| + w_{PI}\|PI\|)dt \quad (1)$$

Results & Discussion: For both the low and high functioning models, paretic step length decreased as w_{SL} increased, (Fig. 1a) and paretic propulsive impulse increased as w_{PI} increased (Fig 1b). The high functioning model exhibited larger changes in paretic step length and paretic propulsive impulse than the low functioning model between ATM conditions. Self-selected belt speed was slower for the low functioning model for all ATM control conditions, which is consistent with literature defining a strong negative correlation between hemiparesis severity and walking speed [9]. There was no clear trend in belt speed with increases in w_{SL} or w_{PI}. These predictive simulation results suggest that increasing w_{PI} may improve the efficacy of the ATM as a rehabilitation tool to increase paretic propulsion for stroke survivors, especially for high functioning individuals. Additionally, the differences in responses between the high functioning and low functioning models to the ATM controllers further justifies customization of the ATM control based on patient-specific impairments.

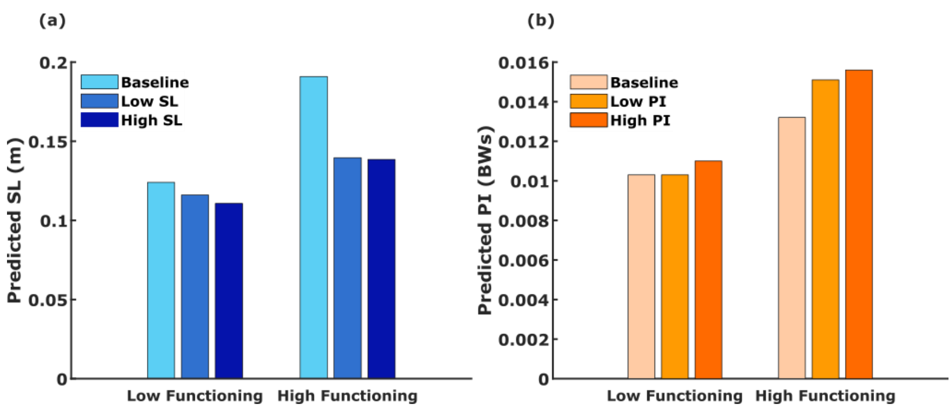

Fig 1. Predicted changes in paretic limb (a) step length as w_{SL} was increased and (b) propulsive impulse as w_{PI} was increased for both the low and high functioning models.

Significance: A major challenge in neurorehabilitation is that due to the heterogeneity of many patient populations it is can be difficult to determine who will benefit from which rehabilitation protocol or to tailor treatments to individuals. This is the first study to show how computational modelling can be used to inform the development and personalization of novel ATM controllers.

Acknowledgements: This work was financially supported by NSFGRFP, University of Delaware Helwig Mechanical Engineering Fellowship, University Dissertation Fellowship, Delaware Space Grant College and Fellowship Program.

References: [1] Reisman et al. (2009), *Neurorehab & Neur Rep* 23(6); [2] Duncan et al. (2011), *N Eng J Med* 364(21); [3] Ray et al. (2018), *J Biomech* 78; [4] Ray et al. (2020) *J Biomech* 101; [5] Pariser et al. (in progress); [6] Pariser et al. (2022), *J Biomech* 133; [7] Pariser & Higginson (2022), *J Biomech Eng* 144; [8] Dembia et al. (2020), *PLOS Comp Bio*; [9] Perry et al. (1995), *Stroke* 26(6).

ENERGETICS OF WALKING WITH WITHIN-STRIDE CHANGES IN TREADMILL SPEED

Caitlin L. Banks[1,2*], Junyao Li[2], Jan Stenum[1,2], Ryan T. Roemmich[1,2]
[1]Center for Movement Studies, Kennedy Krieger Institute
[2]Department of Physical Medicine and Rehabilitation, Johns Hopkins University
*Corresponding author's email: cbanks32@jhmi.edu

Introduction: Millions of people in the United States walk with asymmetric gait patterns due to a variety of neurologic and orthopedic conditions [1]. Unfortunately, most rehabilitation approaches that aim to restore symmetric walking require specialized equipment that is not available in most clinics [2,3]. Our lab developed a novel dynamic treadmill controller than can induce a split-belt-like adaptation using a standard single belt treadmill [4]. This controller can be used to selectively modify gait parameters of importance to gait rehabilitation such as step length, trailing limb angle, and propulsion. Additionally, since the controller runs the treadmill at a fast speed for 50% of the gait cycle and a slower speed for the remaining 50%, this paradigm could be less metabolically demanding on individuals that are not capable of sustained fast walking. Here, we sought to compare the metabolics of walking with the dynamic controller to that of fast walking. Our hypothesis was that the metabolic power needed for walking with the dynamic controller would fall between the power required for walking at the faster speed and walking at the slower speed, suggesting that this strategy could be used to target gait asymmetry in patients who may not be able to tolerate fast treadmill walking (a common gait rehabilitation approach for many clinical conditions).

Methods: Eleven healthy young adults (age 25±3 years, 5 male, 6 female) walked on an instrumented treadmill at speeds of 0.75 m/s, 1.125 m/s, and 1.50 m/s. They were then exposed to the dynamic treadmill controller, which alternated the treadmill between 0.75 m/s and 1.50 m/s for 50% of each gait cycle. Each participant performed four trials where a metronome was used to target stepping at different timings relative to the treadmill belt speed changes. Participants wore a mask connected to a Parvomedics TrueOne 2400 metabolic system, and we sampled breath-by-breath oxygen consumption and carbon dioxide production to calculate net metabolic power during the last two minutes of each walking bout.

Results: Each of the four metronome-timed Dynamic Treadmill blocks produced similar results ($F(3,28)=0.729$, $p=0.54$), so we will present the subject average data here. We performed a one-way ANOVA to compare net metabolic power across the following conditions: baseline walking at each of the three speeds (Baseline 0.75 m/s, Baseline 1.125 m/s, and Baseline 1.50 m/s) and walking with the dynamic controller (Dynamic Treadmill). Net power varied significantly by condition ($F(3,30)=93.48$, $p<0.001$) and a Tukey HSD post-hoc test revealed significant differences between each of the three baseline walking speeds (all p's<0.001) as well as between the Dynamic Treadmill condition and each of the baseline speeds (all p's<0.001) (Fig. 1).

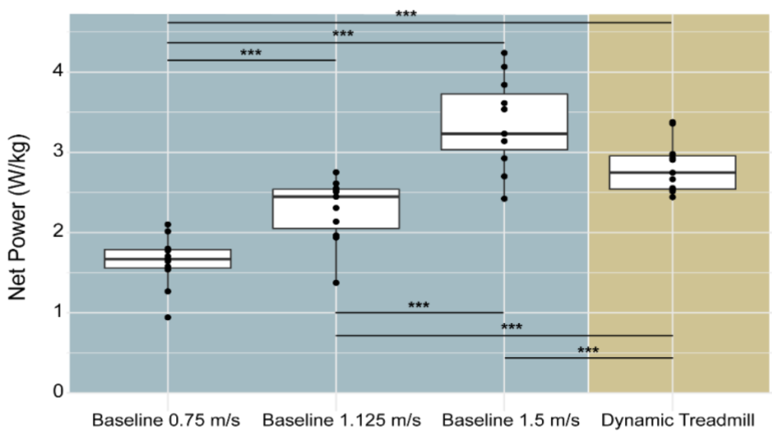

Figure 1. Net metabolic power in each walking condition. Baseline walking is standard, tied-belt treadmill walking with listed speeds. Dynamic Treadmill utilizes a controller that alternates belt speeds between 0.75 and 1.50 m/s.

Discussion: Our observation that net metabolic power increases with increasing walking speed aligns well with the literature and indicates that our metabolic methodology is sound [5]. The observation that walking with the dynamic treadmill controller requires more metabolic power than walking at the controller's slow speed but less power than fast walking aligns well with our hypothesis, as well as the mechanics of the task. These findings, coupled with our previous work showing that the controller can drive selective changes in gait symmetry [4], synergistically demonstrate that this technique has potential to deliver asymmetric gait training at a reduced metabolic demand (relative to fast walking). Our future work will focus on applications in clinical populations.

Significance: Gait asymmetry remains a difficult challenge for researchers and clinicians, and response rates from clinical trials have led the field to prioritize precision medicine to target specific impairments that may respond best to a given treatment [6]. This dynamic treadmill controller offers clinically feasible promise for individuals with gait asymmetries, and future research will explore personalized application of the controller to subject-specific gait asymmetries. These results in healthy individuals add insight that therapeutic use of this controller may be ideal for those individuals who cannot tolerate fast walking, a popular rehabilitation strategy for individuals with better cardiovascular fitness.

Acknowledgements: This research was supported by AHA grant # 935556 (PI Roemmich). Caitlin Banks is supported by a T32 training grant (#T32HD007414-29, PI Bastian).

References: [1] Hollis et al. (2020), *Disabil Health J* 13(3); [2] Reisman et al. (2013), *Neurorehabil Neural Repair* 27(5); [3] Aycardi et al. (2019) *J Neuroeng Rehabil* 16(1); [4] Browne et al (2022), *bioRxiv* ; [5] Pimentel et al. (2022), *Front Sports Act Living* 4 :942498 ; [6] Duncan et al. (2011), *New Engl J Med* 364 (21).

VISUOSPATIAL COGNITION PREDICTS BIOFEEDBACK-DRIVEN LOCOMOTOR PERFORMANCE IN INDIVIDUALS POST-STROKE

Sarah A. Kettlety[1]*, Kristan A. Leech[1]
[1]Division of Biokinesiology and Physical Therapy, University of Southern California
*kettlety@usc.edu

Introduction: Visual biofeedback targets post-stroke biomechanical gait impairments, such as reduced paretic propulsion [1]. Using visual biofeedback to alter gait parameters is an explicit, cognitively demanding motor learning approach [2]. Cognitive impairment is common post-stroke [3], making it important to consider how cognitive function may impact motor learning approaches. Previous work has demonstrated that overall cognitive function is related to biofeedback-driven improvements in walking patterns post-stroke [4]; however, it is unknown which cognitive domains drove this result. Here, we aim to understand which cognitive domains predict performance during a paretic propulsion biofeedback task in individuals post-stroke. Because there is little research informing our understanding of the relationship between cognition and biofeedback-driven changes in gait parameters, we performed an exploratory analysis to better understand which cognitive domains may contribute to locomotor performance during a visual biofeedback task.

Methods: Twenty-eight participants post-stroke completed one day of paretic propulsion biofeedback training. Before training, participants completed two cognitive tests, the Repeatable Battery for the Assessment of Neuropsychological Status (RBANS) and the Trail Making B test. The RBANS provided scores for immediate memory, visuospatial, language, attention, and delayed memory, and the Trail Making B test provided a score for executive function. Next, we collected treadmill-walking data for two minutes without biofeedback and twenty minutes with biofeedback (Figure 1). Our primary outcome measure was normalized propulsion error (distance from the propulsion goal, normalized to baseline) averaged over the final thirty strides of biofeedback training. We then performed best-subsets selection with terms for Lower-Extremity Fugl-Meyer (LEFM) and all cognitive test scores. Each model in the selection process included a LEFM term to account for motor impairment. The model with the lowest BIC score was chosen as the final model. We excluded participants whose average baseline propulsion error was smaller than the minimal detectable change for propulsion [5]. This ensured that the error we measured was larger than the error of the force measurement.

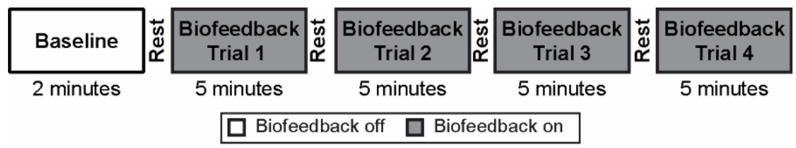

Figure 1: Experimental paradigm.

Results & Discussion: After removing participants with an average baseline error smaller than the minimal detectable change, we included seventeen participants in this analysis. Visuospatial cognition and LEFM scores best-predicted normalized propulsion error during the final thirty strides of biofeedback training (adjusted $R^2 = 0.54$, $p = 0.001$; Figure 2). Participants with better visuospatial cognition were able to use the biofeedback more effectively to reduce their propulsion error. Our results suggest that visuospatial cognition is important when learning to use a visual biofeedback task to increase paretic propulsion.

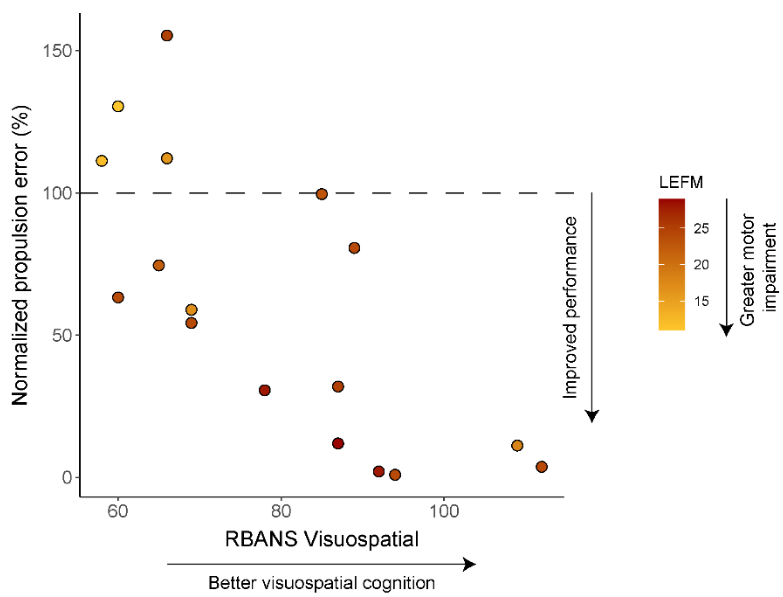

Figure 2: Visuospatial cognition vs. normalized propulsion error. A normalized propulsion error of 100% is equivalent to participants' average error at baseline (dashed line). A normalized propulsion error closer to zero represents a reduction in error from baseline. Abbreviations: LEFM, Lower-Extremity Fugl-Meyer; RBANS, Repeatable Battery for the Assessment of Neuropsychological Status.

Significance: We found that visuospatial cognition may be an important factor in acquiring an explicit locomotor skill. This suggests that it may be beneficial to understand the specific cognitive domains that are impaired in individuals post-stroke to aid in developing personalized motor learning approaches.

Acknowledgments: NIH R03 HD104217-01 and Magistro Family Foundation Research Grant from the Foundation for Physical Therapy Research supported this work.

References: [1] Genthe et al. (2018), *Top in Stroke Rehabil* 25(3); [2] Leech et al. (2022), *Phys Ther* 102(1). [3] Nys et al. (2007), *Cerebrovasc Dis* 23(5-6). [4] French et al. (2021), *Neurorehabil Neural Repair* 35(5). [5] Kesar et al. (2011), *Gait & Posture* 33(2).

A PILOT STUDY MEASURING HEAD KINEMATICS DURING LAB-INDUCED LADDER FALLS

Gabrielle M. Ferro[1], Steve Rowson[2], Michael L. Madigan[1*]
[1]Grado Department of Industrial and Systems Engineering, Virginia Tech, Blacksburg, VA, USA
[2]Department of Biomedical Engineering and Mechanics, Virginia Tech, Blacksburg, VA, USA
*Corresponding author's email: mlm@vt.edu

Introduction: Falls from ladders are a major source of traumatic brain injuries in construction [1]. Improving the ability of hard hats to attenuate head impacts from falls may help to mitigate these injuries. Epidemiological studies have used accident reports, hospital records, and worker interviews to identify environmental and behavioral factors contributing to ladder falls [2]. Human subjects studies have investigated the biomechanics of the initial loss of balance. A small number of studies have also used computational modeling to determine fall kinematics [3]. No human subjects studies we are aware of have measured head kinematics during lab-induced ladder falls involving impact with the ground. Therefore, the purpose of this descriptive study was to characterize head kinematics of human subjects during lab-induced ladder falls to the ground.

Methods: 18 young adults (7 female; height 1.7 m ± 0.1 m; mass 71.4 kg ± 13.6 kg) were recruited and formed two groups receiving different instructions and number of trials. Both groups were instructed to simulate overhead work while on a step ladder, and lateral reaching while on an extension ladder. Trials were at three feet heights ranging from 0.8 m to 1.8 m above rock-climbing crash pads covering the floor of the fall area, and while wearing a hockey helmet and wrist braces. Group 1 (n = 14; 6 female) completed three trials at each height/ladder combination and was instructed to extend as far back overhead as possible on the step ladder and as far laterally as possible on the extension ladder without falling. During a randomly selected trial at each ladder/height condition, the investigator pushed the ladder to simulate the ground shifting under the ladder to induce a loss of balance. Group 2 (n = 4; 1 female) was only exposed to one trial at each ladder/height condition and was instructed to not resist the loss of balance or ground impact. Ladder/height conditions were presented in a counterbalanced order using a balanced Latin square.

Results & Discussion: Group 1 experienced 98 falls with 68 of these involving landing on the feet and maintaining balance on the feet. The other 30 falls involved first landing on the feet but then falling onto the pads. One of these falls involved a head impact (from step ladder). Group 2 experienced 17 falls with all involving first contacting the pads with the feet but then falling onto the pads (Figure 1). 15 of these falls involved a head impact (10 from step ladder and 5 from extension ladder). Eliciting falls from ladders that resulted in falling onto the pads (not landing and standing on the feet), as well as falls resulting in head impact, were challenging to achieve when limiting perturbation severity for safety and when instructing participants to not fall (as would be their desire during a real fall). Head kinematics immediately prior to head contact with the pads (Figure 2) were of primary interest because these can be used to inform hard hat drop testing. The highest downward head speed immediately before head impact was 4.2 m/s and the highest angular velocity about a mediolateral axis through head was 1153 deg/s, both during the same fall from a step ladder at feet height of 1.8 meters.

Significance: Data such as these can inform the development of hard hat testing standards and improve hard hat design to mitigate traumatic brain injuries.

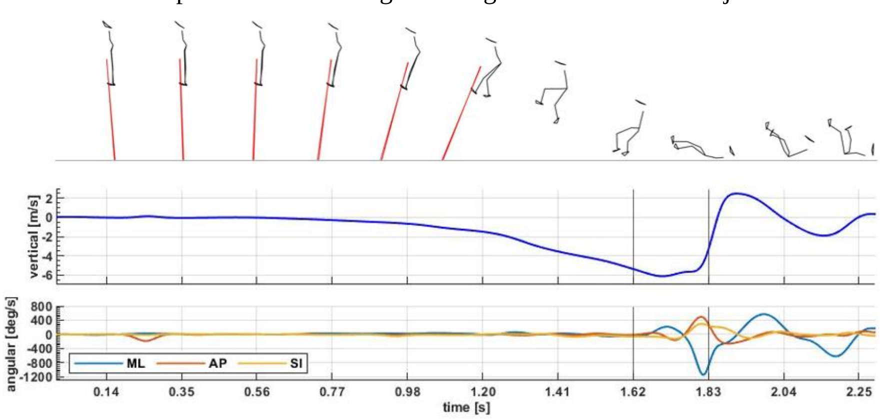

Figure 1: Sample data during a 1.8 m fall from step ladder including head vertical and angular velocities. Back vertical lines indicate first foot impact and head impact, respectively.

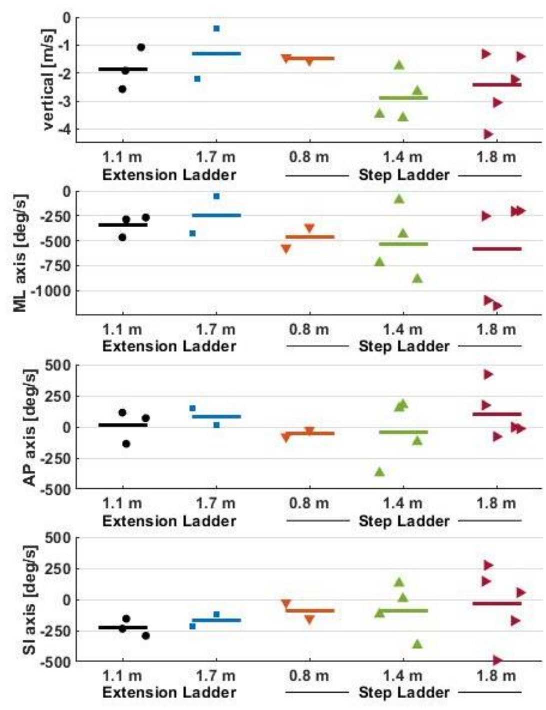

Figure 2: Head velocities at the instant before impact in every trial (points) and the mean velocity (line).

Acknowledgements: We would like to thank Tanner Upthegrove and Institute for Creativity, Arts, and Technology at Virginia Tech for their contributions and the use of their facility for data acquisition.

References: [1] Tiesman, et al. (2011), *Am J Prev Med;* [2] Lombardi, et al. (2011), *Scand J Work Environ Health*; [3] Wiechel et al. (2013) *Proceedings of ASME-IMECE*

A ROBOT-ACTUATED IN VITRO TESTING APPROACH FOR QUANTIFYING PASSIVE RANGE OF MOTION IN THE THUMB CMC JOINT

Josephine M. Kalshoven[1,2*], Rohit Badida[1], Amy M. Morton[1], Douglas C. Moore[1], Joseph J. Crisco[1,2]
[1]Department of Orthopaedics, Warren Alpert Medical School of Brown University and Rhode Island Hospital, Providence RI
[2] Brown University Center for Biomedical Engineering
*Corresponding author's email: josephine@brown.edu

Introduction: Studies have found that active and passive ranges of motion (ROM) are reduced in thumb carpometacarpal (CMC) joint osteoarthritis (OA), yet the underlying causes remain unclear [1]. Osteophyte growth and ligament property changes associated with progressive disease have been hypothesized to affect CMC ROM, yet no study has confirmed a causal relationship. An *in vitro* ROM assessment would eliminate neuromuscular influence and allow for prescribed, directional load application, shedding light on inherent stabilizing structures.

The aim of this work was to develop an approach to determine the multi-directional biomechanics of the CMC joint *in vitro* and demonstrate its implementation in six pilot specimens spanning a wide age range.

Methods: Six fresh-frozen human forearms (4M, 2F, 27-63 yrs.) were sectioned proximally at the midshaft of the radius/ulna. All bones distal to the carpus were removed, except for the first metacarpal (MC1) and the proximal head of the second metacarpal (MC2).

A cluster of 6 infrared markers (NDI) was rigidly mounted via k-wires to the radial portion of the trapezium (TPM) to track the motion of the TPM. A CT scan of each specimen was acquired and segmented using previously described methodology[2]. Exterior bone surface meshes and fiducial point coordinates were exported. MC1 and TPM bone coordinate systems (CS) were computed based on directions of principal curvature of the articular surfaces [3] and, for the MC1, its proximal-distal inertial axis. CS were directed volarly (+x), proximally (+y), and radially (+z) with anatomical rotations about each axis.

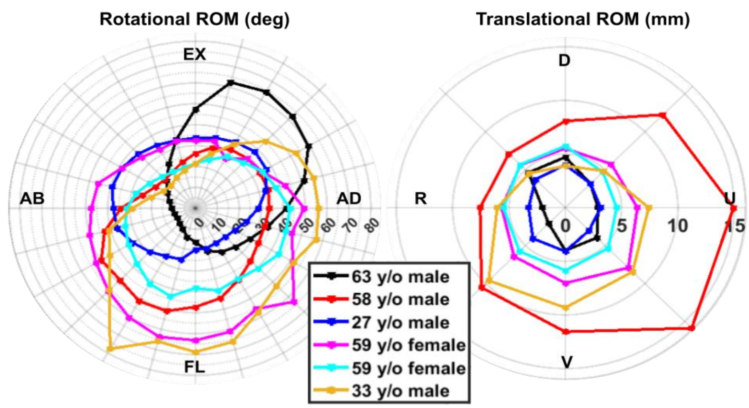

Figure 1. Rotational (left, degrees) and Translational (right, mm) ROM envelopes for 6 CMC specimens.
Flexion (FL), Extension (EX), Abduction (AB), Adduction (AD), Volar (V), Dorsal (D), Radial (R), Ulnar (U)

During ROM testing, each thumb CMC joint specimen was mounted to a six axis industrial robot (KUKA KR 6 R700) with the radius/ulna affixed to the robot base and the MC1 to the robot end effector. The CS were imported and registered to robot space [2], for testing MC1 motion with respect to the TPM in anatomical CS:

- Maximum ROM in flexion, extension, abduction, and adduction, and in 20 coupled directions (15-degree increments of flexion-adduction, extension-abduction, etc.)
  - 1 º/s until resultant torque (RMS of 3 rotational DOF) = 1 Nm
- Translation of the MC1 on the trapezium volarly, dorsally, radially, ulnarly, and in four combined directions
  - 1 mm/s until resultant force (RMS of 2 translational DOF: volar/dorsal and radial/ulnar) = 30 N

For each test, force-displacement and torque-rotation curves were analyzed from 6 DOF kinematics and kinetics. Polar plots of ROM envelopes were generated from max ROM in each direction in the plane of the articular surfaces.

Results & Discussion: Data demonstrated the variability of ROM across individuals, with an average standard deviation of 14º in rotations (max SD of 23.7º in abduction-flexion) and 3mm in translation (max SD of 4.7 mm in volar-ulnar translation) (Fig. 1). For 4/6 specimens, the greatest rotational ROM was in flexion and flexion-coupled regions, which are most utilized for grips. Additionally, for three of those specimens, as much as 8mm less translation in the dorsal and radial regions than volar and ulnar regions suggested greater stability in these directions, which may support the joint against common dorsoradially-directed grip forces. Two specimens presented roughly symmetrical translational ROM. The oldest specimen (only one with documented hand OA) demonstrated a small translational ROM oriented along the functional dorsoradial-volar/ulnar path exercised in most grips, as well as a distinctly larger extension ROM and smaller flexion ROM than other specimens. The youngest specimen's ROM was most like the oldest specimen. Additionally, the 58-year-old male specimen had a rotational ROM like age-matched specimens, yet a remarkably large translational ROM (up to 8mm larger than the next greatest ROM in the volar-ulnar direction). These results underscore the need for additional data and motivate future studies on ligament integrity and osteophyte volume as structural influences on ROM.

Our ROM values are larger than those reported in previous thumb CMC ROM studies [1]. This difference may be due to specimen preparation (i.e., missing MC2, tendon loads), the nature of passive assessment (vs. active), and variations in neutral position definition (joint surface congruence vs. anatomical).

Significance: These results support the feasibility of determining *in vitro* CMC biomechanics across a spectrum of joint conditions, such as OA presentation. Such data would build a more-complete understanding of the interplay of pathology and joint integrity, which will inform our understanding of disease progression, as well as appropriate tactics for prevention, identification, and treatment.

References: [1] Gehrmann, *J Hand Surg Am*, 2010. [2] Badida, *J Biomech Eng*, 2020. [3] Halilaj, *J Biomech*, 2013.

ASSOCIATIONS BETWEEN VERTICAL STIFFNESS AND WAIST MOUNTED ACCELERATION DURING HOPPING

FJ Goodwin[1*]
[1]Physical Therapy, Charleston Southern University
*Corresponding author's email: jgoodwin@csuniv.edu

Introduction: Vertical stiffness (K_{Leg}) during dynamic activities is associated with performance and injury risk [1,2]. K_{Leg} describes the ability of the lower extremity to resist flexion during ground contact and associated shock absorption capabilities. It is typically measured in a controlled motion capture laboratory environment. However, recent advancements in technology have allowed for more data collections in a more "real-world" setting. Skin-mounted accelerometers have been recently utilized to determine estimated kinetics and kinematic during dynamic activities [3].

However, minimal research has been conducted looking at associations between K_{Leg} and peak accelerations to determine if skin-mounted accelerometers could be utilized to estimate K_{Leg} in a more variable "real-world" environment compared to a motion capture laboratory. Due to both motion capture laboratory and skin-mounted accelerometers attempting to assess similar kinetics values, we expected greater K_{Leg} would be significantly associated with greater peak vertical accelerations during single leg hopping.

Methods: Twenty-three Division-1 athletes (15F, 8M, 1.73±0.08 m, 68.07±8.84 kg, 19±0.9 y.o.) volunteered for participation in this study. Subjects were required to be injury-free and cleared for participation. Subjects reported to the motion capture laboratory and were fit with retroreflective markers on the feet, legs, pelvis, and torso to collect three-dimensional kinematics. Additionally, 1 Delsys skin-mounted accelerometer was mounted to the sacrum to assess acceleration data.

Subjects completed a shod single leg hopping protocol for 20 seconds at a self-selected frequency on an embedded force plate [4]. This was completed for both legs. During the hopping protocol, ground reaction forces, whole-body kinematics and accelerations were collected via Qualisys. Data were processed via Visual 3D. K_{Leg} was calculated as the maximum vertical force divided by the change in center of mass depression during ground contact ($F_{max}/\Delta y$) and averaged over 10 successive hops. Additionally, peak vertical accelerations were averaged across the same 10 hops.

Data were analyzed in SPSS. A paired t-test was utilized to determine if there were significant differences in K_{Leg} between legs (i.e., right vs left, dominant vs non-dominant with dominance determined via preference to kick a ball). Additionally, a Pearson correlation was utilized between K_{Leg} of the dominant limb and peak vertical acceleration during hopping. An *a priori* alpha value of p=0.05 was utilized for all calculations.

Results & Discussion: There was no statistically significant difference in K_{Leg} between right vs left legs (p=0.06) or dominant vs non-dominant (p=0.19). There was a weak, negative correlation (r = -0.135) that was not statistically significant (p=0.539) between dominant leg K_{Leg} and peak acceleration collected at the sacrum.

Given these findings in this population, peak acceleration measured at the sacrum was not a valid measure for determining $K_{Leg.}$ However, accelerometers at different body positions (e.g., foot, shin, sternum) may yield different results [3,5,6]. Additionally, we utilized both males and females in our analysis that participated within 2 sports (17 soccer players and 6 tennis players). A more specific analysis involving a single sex, single sport cohort may yield stronger associations. Additionally, an analysis involving a sport that involves repetitive jumping such as basketball may also yield stronger associations.

One interesting finding is that between limb differences in K_{Leg} were approaching significance (p=0.06) when assessing right (15.89±3.45 KN/m) vs left leg (16.5±3.09 KN/m) within this healthy athletic population. Previous data indicates K_{Leg} asymmetries may predispose athletes to higher risk of soft-tissue injury [7].

Significance: In this current population, a sacrum mounted accelerometer was not associated with K_{Leg} however placement of the accelerometer closer to the ground interface (i.e., foot) may yield more robust results highlighting the importance of precision of placement for accelerometers during analysis of dynamic activities. The additional finding of near statistically significant differences between legs regarding K_{Leg} continues to highlight the need for athletic injury risk screening and potential therapeutic exercise implementation. These screenings could potentially assist with shifting rehabilitation to a more proactive vs reactive model in order to reduce injury risk and subsequent injury burden.

Acknowledgements: The author acknowledges Kimmie Wong, Nick Messina, and Elon University for their assistance with data collection and processing.

References: [1] Watsford et al. (2010), *Am J Sports Med* 38(10); [2] Maquirriain (2012), *Int J Spor Med* 33(7); [3] Wundersitz et al. (2015), *Eur J Spor Sci* 15(5); [4] Padua et al. (2005), *J Mot Behav* 37(2); [5] Watari et al. (2016), *J App Biom* 32(3); [6] Liikavainio et al (2007), *Arch Phys Med Rehab* 88(7); [7] Sporri et al. (2019), *J Spor Sci* 37(21).

COMPARING STANDARD AXILLARY CRUTCHES WITH MOBILEGS® CRUTCHES IN HEALTHY ADULTS

Yunju Lee[1,2*], Kendall Bird[2], Cassie Esch[2], Allison Sneller[2], Meri Goehring[2]
[1]School of Engineering, Grand Valley State University, Grand Rapids, MI, USA
[2]Department of Physical Therapy and Athletic Training, Grand Valley State University, Grand Rapids, MI, USA
*Corresponding author's email:leeyun@gvsu.edu

Introduction: An assistive device (AD) is required when normal walking is compromised due to the lower extremities loss of ability to withstand the stresses of conventional gait either due to a mechanical or neurological disability [1]. Advances in crutch designs have made light weight versions, such as aluminum, titanium, and carbon fiber, the gold standard in design. Wooden crutches are no longer in use due to their increased weight and lack of effectiveness for long term use. The energy expenditure is greatly increased anywhere from 33% to 75% with the use of standard axillary crutches during partial weight bearing gait when compared to normal walking [2]. Martin et al. stated that using crutches resulted in twice as much oxygen consumption when compared to baseline and doubled the participants heart rate [3]. This is especially important to consider when prescribing assistive devices to individuals with respiratory or cardiovascular problems. If there was a crutch that required less energy expenditure, patients would have more energy for daily activities and rehabilitation participation. The purpose of this study was to determine if there is a significant difference in the physiological response to the 6-minute walk test (6MWT) when using standard axillary crutches or Mobilegs® crutches. The 6MWT measures submaximal functional exercise capacity and reflects activities of daily living. The 6MWT has been used in similar studies that compared different crutch types and has been found to demonstrate reliability and construct validity [4].

Methods: The Grand Valley State University Institutional Review Board (IRB) approved the study protocol. Twenty-six subjects (21 females, 5 males; 24.15±1.1 yrs.; 65.81±11.3kg; 165.8±3.0cm) between 18 and 55 were recruited and completed the study. Subjects met at two times to complete the research protocol. At the initial session, subjects were fit for both pairs of crutches by the same two individuals with a third individual present. The axillary crutches were fit based on standard practice and the Mobilegs® crutches were fit based on the instructions that came with the Mobilegs® crutches. After initial session, subjects sat for 10 minutes and repeated their second session 6MWT. A 6MWT with a randomly chosen crutch type using a 3-point gait while heart rate (HR) via the Polar Heart Rate monitor, systolic blood pressure (SBP) taken by an automated machine, Modified Borg rating of perceived exertion (RPE), and distance were measured. Every two minutes the subject's heart rate and RPE were recorded. At the end of the 6-minutes, the subject's blood pressure, heart rate, RPE, and distance crutched was recorded. Subjects' preferred crutch type was documented. We compared the change in heart rate, the change in systolic blood pressure, and the change in RPE between the two pairs of crutches. A matched pairs t-test was used to statistically analysed the data. A significance level of $p < 0.05$ was used for all statistical analyses using SAS JMP Pro16.

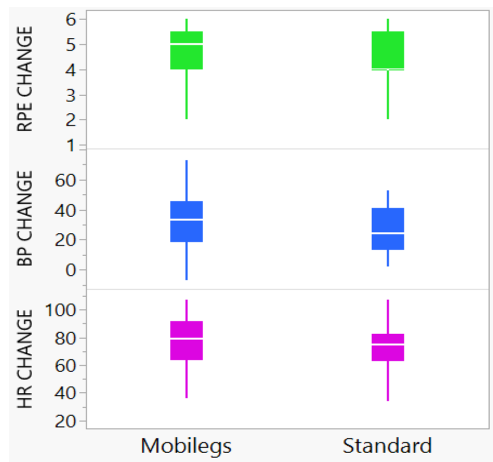

Figure 1: Box and Whisker plot of the changes in heart rate, systolic blood pressure, and RPE by two difference crutches (Mobilegs® vs. Standard)

Results & Discussion: The change in systolic blood pressure during the 6MWT between the two pairs of crutches was statistically significant (33.1±3.4 vs. 25.8±3.3, p=0.0339) however; there was no significant difference between the change in heart rate (75.8±3.9 vs. 72.9±4.0, p=0.3679) or RPE (p=0.8696) between the two crutches (Fig. 1). The difference in systolic blood pressure showed that with use of the Mobilegs® there was a greater change in SBP from the beginning to the end of the 6MWT, more specifically the average change in SBP was higher for Mobilegs® than standard crutches. This could be due to the fact that Mobilegs® crutches have a swivel-pivot saddle that moves with the person, therefore, offering less stability and requiring more upper extremity use. It is known that upper extremity exercises result in higher blood pressure and heart rate when compared to lower extremity exercises. However, there was the lack of statistical significance in heart rate and RPE which were adverse findings that heart rate and systolic blood pressure would increase at a similar rate. Participants often preferred the standard crutches to Mobilegs® crutches as 61% (16 participants) preferred standard crutches, 31% (8 participants) preferred Mobilegs®, and 8% (2 participants) had no preference; because standard crutches are inherently more stable due to axillary crutches having a more central anchor at the individual's chest level which provides trunk rotation stability. This likely decreased the potential effort used during ambulation with standard crutches with further distance (291.43±48.72m vs. 275.46±74.43m) compared to Mobilegs®.

Significance: This study provides evidence that Mobilegs® are no more ergonomic than standard axillary crutches. The significance is important when considering cost differences between different types of crutches and the importance of keeping costs for durable medical equipment under control. Additionally, the changes in blood pressure that occurred with Mobilegs® crutches indicates that care should be taken if these are used with individuals with blood pressure problems. As the population of older adults with potential blood pressure problems increases, use of Mobilegs® could be problematic. Further research is needed to fully assess the ergonomics of standard and Mobilegs® crutches.

References: [1] Goehring & Kenyon (2011), *JACPT. 2;* pp72-76.
[2] Annesley et al. (1990), *Phys Ther.70(1);* pp18-23.
[3] Martin et al. (2019), *Foot Ankle Orthop.40(10);* pp1203-1208.
[4] Kocher et al. (2016), *Foot Ankle Int 37(11);* pp1232-1237.

Interosseous proximity maps of the distal radioulnar joint during pronosupination using 4DCT

Cesar Lopez[1*], Taylor P. Trentadue[1,2], Robert Foley[1], Andrew Thoreson[1], Shuai Leng[3], Sanjeev Kakar[5], Kristin D. Zhao[1,4]

[1]Assistive and Restorative Technology Laboratory, Rehabilitation Medicine Research Center, Department of Physical Medicine and Rehabilitation, Mayo Clinic, Rochester, MN; [2]Mayo Clinic Medical Scientist Training Program, Mayo Clinic, Rochester, MN; [3]Department of Radiology, Mayo Clinic, Rochester, MN; [4]Deparment of Physiology and Biomedical Engineering, Mayo Clinic, Rochester, MN; [5]Department of Orthopedic Surgery, Mayo Clinic, Rochester, MN
*Corresponding author's email: lopez.cesar@mayo.edu

Introduction: The distal radioulnar joint (DRUJ) is an articulation in the wrist that allows pronosupination.[1, 2] DRUJ stability arises from bony constraints and multiple soft tissues, including the triangular fibrocartilage complex.[3-6] Instability of this joint alters forearm kinematics and results in ulnar-sided wrist pain. Due to the static nature of standard clinical imaging, dynamic instabilities are missed.[5, 7, 8] Given the challenges of detecting these injuries, patients may require invasive surgical procedures to confirm the diagnosis.[9] The purpose of this study is to use non-invasive, dynamic imaging—four-dimensional computed tomography (4DCT)—to assess DRUJ instabilities. We hypothesize that DRUJ instability is reflected in the magnitude of interosseous proximity distances between the ulna and radius.

Figure 1: Forearm fixture with participant in neutral position

Methods: Seven participants (all female) with clinically-diagnosed symptomatic unilateral DRUJ pain and/or instability were recruited (Institutional Review Board Protocol 20-009305). Exclusion criteria included a previous diagnosis of wrist osteoarthritis, inability to be appropriately positioned in the scanner for imaging, and an age under 18 years. A dual-source photon-counting-detector CT scanner (Siemens NAEOTOM Alpha) was used to acquire bilateral static and dynamic 4DCT images.[10-12] Dynamic images were acquired while participants performed unresisted and resisted pronosupination bilaterally. The forearm was restrained in a padded support channel to prevent arm rotation and limit shoulder motion without affecting forearm rotation. A custom-made fixture was designed to provide bidirectional torque resistance during pronosupination (**Figure 1**).[13] The device includes two single-hand grips mounted on an acrylic frame that can also be configured for grip in a locked neutral wrist position. Fifteen CT volumes were collected over a 1.5-second acquisition interval (temporal resolution: 66 ms). Image volumes were reconstructed using a commercially-implemented dual source cardiac reconstruction algorithm, resulting in a voxel dimensions of 0.234 mm × 0.234 mm × 0.600mm. All images were stored in DICOM format. Bones were segmented in Analyze software and used to create 3D meshes for each bone. Data were processed with a custom, validated MATLAB algorithm to yield osteokinematics.[14, 15] Proximity maps were calculated based on nearest mesh-vertex distances between nearest vertices on adjacent bone meshes within surface-normal angular (60°) and interosseous distance (5 mm) thresholds.

Results & Discussion: Interosseous proximity maps of the ulna and radius were created for the whole motion arc (pronosupination) (**Figure 2**). These data demonstrate increased interosseous proximity (greater distances) in pronation versus supination. The colormap transitions from 2 mm to 5 mm volarly. These data demonstrate how DRUJ interosseous proximities change during a dynamic task.

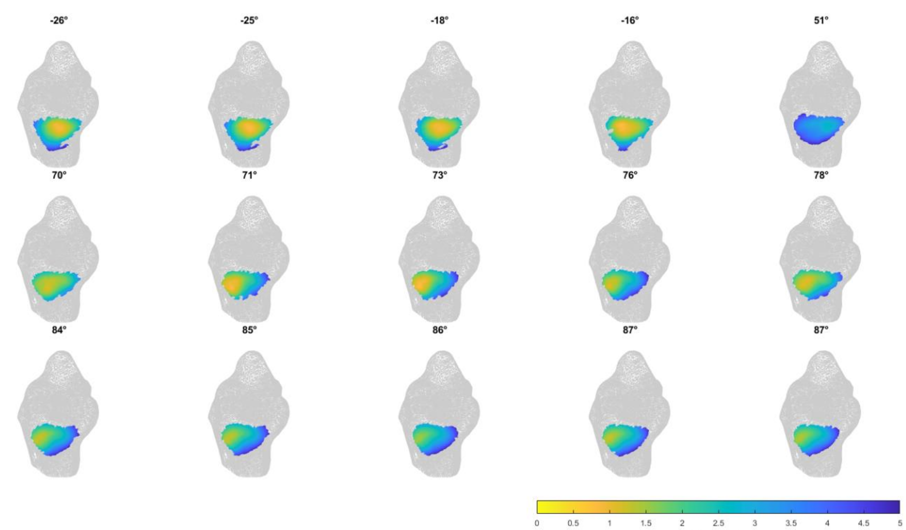

Figure 2: Demonstrative interosseous proximity map of the radius relative to the ulna during unresisted pronosupination of the right (uninjured) hand for a single participant. Supination (-) and Pronation (+).

Significance: Preliminary data suggest 4DCT-derived proximities within a motion arc reveals changes in DRUJ mechanics, both functionally and quantitatively. Future work will rigorously quantify differences between uninjured, injured, and postoperative (repaired) wrists to discern injury-related changes in arthrokinematics.

Acknowledgements: This work is partially supported by the generosity of W. Hall Wendel, Jr, Mayo Clinic Department of Radiology, NIH NIGMS T32 GM065841, and NIH NIAMS T32 AR056950.

References: [1] af Ekenstam. Clin Orthop Relat Res. 1992(275). [2] Linscheid. Clin Orthop Relat Res. 1992(275). [3] Kihara. J Hand Surg Am. 1995;20(6). [4] Ward. J Hand Surg Am. 2000;25(2). [5] Flores. Radiographics. 2023;43(1). [6] Haugstvedt. J Hand Surg Eur Vol. 2017;42(4). [7] Squires. AJR Am J Roentgenol. 2014;203(1). [8] Kakar. J Hand Surg Am. 2016;41(4). [9] Atzei. Tech Hand Up Extrem Surg. 2008;12(4). [10] Baffour. AJR Am J Roentgenol. 2023 [11] Leng. Radiographics. 2019;39(3). [12] Rajendran. Skeletal Radiol. 2023;52(1). [13] Amrami. Hand Clin. 2010; 26(4). [14] Trentadue. J Wrist Surg. 2023. [15] Zhao. J Biomech Eng. 2015;137(7).

COMPARING JUMP LANDING KINETICS AFTER A SOCCER HEADER MOTION IN DIFFERENT SITUATIONS

Chase S. Cycenas, Alex Lotts, Hayleigh Young, Mostafa A. Hegazy*
Science Department, Southwest Minnesota State University
*Corresponding author's email: Mostafa.hegazy@smsu.edu

Introduction: Soccer is the most popular sport in the world and continues to grow, particularly in females. This growth is associated with an increase in the number of injuries. A common mechanism for injury involves players landing after jumping for a header. To better understand injury mechanism, several studies have investigated jump landings following jumps that included a heading motion considering the cognitive load during a header makes it different from a typical jump.

Previous studies [1,2] investigated landing patterns following a heading motion that included a suspended ball. In both studies, landings following a heading motion showed an increase in ground reaction force compared to no heading motion. When players jump for a header in a game situation, they need to visually track a ball projected into the air. They also need to account for ball speed, angle, height, and point of contact. A suspended ball removes these variables, thus, may not reflect a real game like heading situation. A recent study [3] reported greater peak ground reaction force normalized to body weight (nGRF) and peak loading rate (LR) on the dominant side only when players jumped and headed a ball projected into the air compared to other scenarios. However, a suspended ball was not included in this comparison. Thus, the purpose of this study was to compare landing kinetics following a heading motion when a ball is suspended to that when a ball is projected.

Methods: Twelve Division II female soccer players (Age: 20.33±1.3 years; Mass: 66.3±10.3 kg; Height:162±3.9 cm) participated in this study. Loadsol force insoles (Novel, Munich, Germany) were inserted into participants' cleats to measure ground reaction forces. Participants performed four jump types, each performed three times on an artificial turf rug. Participants started with the vertical jump (VJ) to determine target jump height for the rest of the jumps. Participants then performed the other three jump types in a counterbalanced order. These jumps included: 1) Jump Header Stationary (JHS) during which participants jumped and headed a suspended ball; 2) Jump Air Header (JAH) during which participants jumped and performed a heading motion while keeping their eye on the suspended ball; 3) Jump Header Throw-in (JHT) during which players jumped and headed a ball that was thrown-in towards them.

A one-way 1×4 ANOVA was used to compare landing height between the four conditions. A series of two-way 3×4 repeated measures ANOVAs were performed with trial (3) and jump type (4) as the independent variables to compare peak nGRF and peak LR for the dominant and non-dominant sides. A Bonferroni correction was used for all post-hoc analyses.

Results & Discussion: Our analysis showed a significantly lower landing height for the JHT condition (0.15 m; $p<0.05$) compared to VJ (0.21 m), VHS (0.19 m) and JAH (0.19 m). As the jump task got more complex, there was a loss in jump height, which is likely an indication of increased cognitive loading when performing multiple tasks. This is in disagreement with previous research [2, 4] showing a higher or similar jump height when heading a ball compared to a jump without heading a ball. This may be related to player level considering previous studies used professional players compared to DII athletes in our study. With experience, the efficiency of performance when multitasking increases [5].

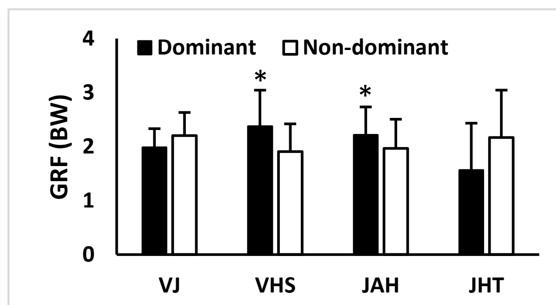

Figure 1: Peak ground reaction force normalized to body weight for the vertical jump, jump header stationary, jump air header, and jump header throw-in. * indicates significantly greater than VJ & JHT.

Our analysis showed significantly greater nGRF (Fig. 1) and LR on the dominant side for the VHS and JAH conditions ($p<0.05$) compared to VJ and JHT. In addition, VHS showed significantly greater LR compared to the JAH ($p<0.05$) as well as greater nGRF with a difference that approached significance ($p=0.055$). Similar to jump height, as the task became more complex, nGRF and LR also increased. This held true despite a lower landing height in VHS and JAH compared to VJ. The exception to the rule was JHT which showed lower values than all other conditions. In addition to the lower jump height, participants were also inconsistent as to which foot they landed on, which directly impacted mean values on both sides.

Landing following a header when tracking a ball in the air is different from those when heading a stationary ball or just performing a header motion without ball impact. Controlling landing height given the variability of ball movement in the air remains a challenge.

Significance: There has been growing interest in how cognitive loading affects landing mechanics after jumping for a header in soccer. However, most studies tend to focus on heading a stationary ball and not factor in the effects of visually tracking a moving ball. A stationary ball is more attractive as it eliminates the variability associated with a moving ball (speed, angle, height, ..etc). In this study, these jump types were compared. Our findings indicate that landing kinetics from these conditions are different, thus, performing a jumping and heading motion (with and without a ball) should not be used a substitute to performing a jump and heading motion in response to a real throw-in. However, controlling variables associated with a throw-in is difficult.

Acknowledgements: We would like to thank the Southwest Minnesota State Soccer team for participating in our study

References: [1] Butler et al.(2013), *Clin J Sport Med* 23(1); [2] Alfayyadh (2018), Master's Thesis; [3] Hoselton et al. (2022), *NACOB*, Ottawa, Aug 22-25.;[4] Fílter et al. (2022), *Sci Med Footb*, *6*(2); [5] Rémy et al.(2011), *Neuropsychologia*, *48*(9).

CAPACITIVE SENSING FOR REAL-TIME ESTMATION OF MUSCLE BULGING IN NATURAL ENVIRONMENTS

Owen Pearl[1*], Nataliya Rokhmanova[1], Louis Dankovich[2], Sarah Bergbreiter[1], Eni Halilaj[1]
[1]Mechanical Engineering, Carnegie Mellon University, Pittsburgh, USA
[2]University of Maryland College Park, College Park, USA
*Email: owen.pearl@cmu.edu

Introduction: Inexpensive wearable sensors are expected to transform both research and clinical practice by monitoring patient movement outside of the laboratory and helping personalize the treatment of mobility impairments. However, sensing muscle excitations with surface electromyography (EMG) is not feasible for multi-day natural environment applications, since EMG is prone to physiological noise and drift over long durations, requires expert placement with direct contact between the electrode and the skin, is uncomfortable for prolonged wear, and has limited battery life. Modern textile EMG wearables lead to crosstalk and timing artifacts, making results difficult to interpret [1]. Capacitive sensing (CS) is a mature, versatile, cost-effective, and power-efficient sensing modality that enables lightweight portable technologies such as touch screens and proximity sensors [2]. However, previous use of CS in humans has only emphasized basic activity classification with machine learning [3]. Here we characterize capacitive touch sensing in terms of the physiological phenomena it captures. Because CS measures cross-sectional proximity changes in the body segment due to muscle bulging, we hypothesized that CS would correlate with changes in (1) muscle cross-sectional area, (2) muscle excitations measured with EMG, and (3) muscle forces predicted with biomechanical simulations (SIM).

Methods: We developed affordable CS-based circumferential sleeves for the shank and thigh and benchmarked them against EMG and musculoskeletal simulations [4] of muscle area change and force production using marker-based motion capture. We derived muscle areas and forces with OpenSim and static optimization. Our $35 (USD) custom-built CS sleeves measure the circumferential capacitive profiles of each body segment. Shank signals are primarily governed by bulging of the gastrocnemius, soleus, and tibialis anterior (Fig 1), while thigh signals are primarily governed by the vastus lateralis, vastus medialis, rectus femoris, semitendinosus, and biceps femoris. Expansion in cross-sectional area decreases the distance between four copper tape electrodes in the CS sleeve and the subject's skin, resulting in an increase in their capacitive coupling. We benchmarked the CS sleeve on 20 adults (12 males, 8 females; mean ± std age of 25.2 ± 2.2 years; 18:2 right-left foot dominance). We compared CS to EMG and SIM during walking at each subject's preferred speed, both indoors and outdoors [5], to test the leading hypothesis that CS would correlate with traditional measures of muscle behaviour. After confirming our initial hypothesis, we further evaluated our CS wearable for its robustness to (1) electrical drift over time, (2) misplacement on the body, and (3) changes in design parameters.

Results & Discussion: CS measurements were highly correlated with changes in the cross-sectional area of the shank muscles ($r = 0.95$; Fig 1) and thigh muscles ($r = 0.89$; Fig 1). The shank CS signal was also significantly correlated with EMG ($r = 0.69$) and simulated muscle forces ($r = 0.84$). These results confirm the associations between CS and other measures of muscle behaviour while reinforcing that CS captures a different physical phenomenon. CS measures composite muscle bulging, EMG measures neural drive, and models infer muscle force based on measured kinematics and ground reaction forces. While EMG may be better suited for intent prediction, CS is likely better suited for monitoring muscle function and thereby adherence to prescribed rehabilitative therapies and human-in-the-loop assistive technologies. Additional analysis revealed that (1) CS had 14x less electrical drift than EMG after 6 hours of measurement, (2) CS was 2x more robust to misplacement artifacts than EMG, and (3) CS maintained consistency with its own measurements ($r \geq 0.89$) over various designs, even when the surface area, A, and the thickness of the fabric on the skin, d¸ were scaled to 0.25 and 4, respectively. This robustness makes CS uniquely suitable for natural environment applications.

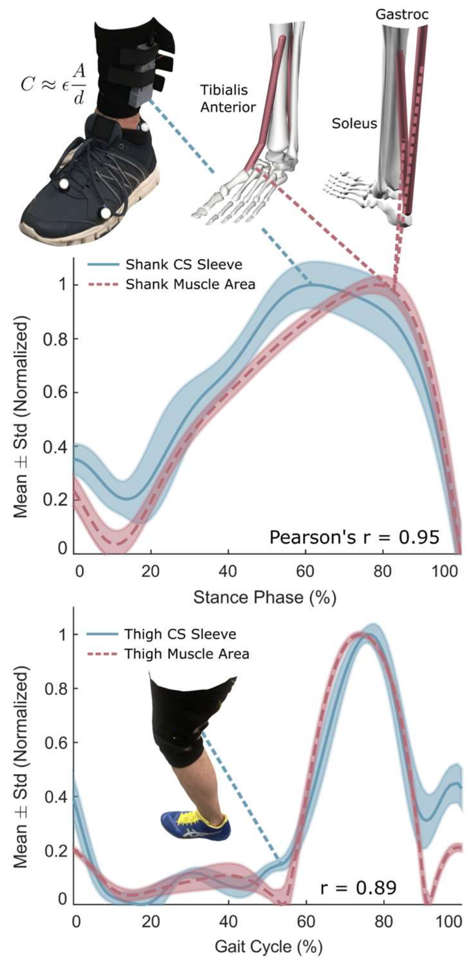

Figure 1: Biomechanical Characterization of Capacitive Sensing Wearables. Shank and thigh capacitive sensing wearables captures the change in cross-sectional area due to muscle bulging.

Significance: CS brings muscle tracking and smart rehabilitation with sensorized garments closer to reality. This affordable, easy-to-fabricate, and comfortable wearable could also improve human-in-the-loop control of assistive devices and help usher in a new wave of fundamental studies on the mechanical behaviour of muscles in the wild.

Acknowledgements: Our work was graciously supported by NSF DGE1745016 and NSF DGE2140739.

References: [1] Colyer, S. & McGuigan, P. *J. Sports Sci. & Med.* 2018. [2] Grosse-Puppendahl, T., et al. *CHI.* 2017. [3] Cheng, J., et al. *Pervasive Computing*. 2010. [4] Delp, S., et al. *IEEE Trans.* 2007. [5] Uhlrich, S., et al. *J. Biomech.* 2018.

GAIT DIFFERENCES BETWEEN CLINICAL SUBTYPES OF PARKINSON DISEASE

Sidney T. Baudendistel[1*], Allison M. Haussler[1], Kerri S. Rawson[1], Meghan C. Campbell[2], Gammon M. Earhart[1]
[1]Program in Physical Therapy, Washington University in St. Louis School of Medicine, St. Louis, MO, USA.
*Corresponding author's email: bsidney@wustl.edu

Introduction: As the number of people with PD is expected to double by 2040, there is a critical need to develop cost-effective, clinically meaningful, objective assessments that can accurately predict disease course and allow for tailored treatment for a range of future disabilities including psychiatric, cognitive, and mobility. Subtyping individuals based on common characteristics and investigating how these specific subgroups predict long-term disability is imperative to early introduction of targeted therapeutics. Among people with Parkinson disease (PD), spatiotemporal gait features are not just associated with disabling motor symptoms such as freezing of gait and falling, but also with cognitive impairment and depression [1]. Indeed, gait characteristics more accurately predict cognitive decline than tests of cognition [2]. As spatiotemporal gait data can be collected relatively quickly and easily and are related to multiple signs and symptoms of PD, including neuropsychological symptoms, gait measures could act as an objective and quantitative assessment to identify meaningful subtypes. We hypothesize gait characteristics may differ across clinical subtypes related to neuropsychological impairment in PD, and prospectively identifying the specific gait signatures of these subtypes may allow for earlier intervention. A first step in testing this hypothesis is to determine whether people with different clinical subtypes of PD exhibit different gait signatures.

Methods: For this cross-sectional study, we used an existing research database that included gait at preferred pace and basic clinical and neuropsychiatric tests. We separated individuals into clinically based subtypes similar to those described in Campbell et al. 2020 [3]: MOTOR (individuals without depressive symptoms and without cognitive impairment), DEPR (with depressive symptoms and without cognitive impairment), and COG (with cognitive impairment and without depressive symptoms). Individuals (n=256) were categorized based on the Geriatric Depression Scale (GDS) or the Hospital Anxiety and Depression Scale-Depression Subscale (HADSd) in combination with the Montreal Cognitive Assessment (MoCA) using published, disease-specific cut-offs. Individuals with other conditions that may affect walking or individuals with a diagnosis of dementia were excluded. Clinical characteristics (Unified Parkinson Disease Rating Scale – Motor section (UPDRSm)), basic demographics, and sixteen quantified spatiotemporal gait variables encompassing the domains of pace, rhythm, variability (standard deviation (SD)), postural control, and asymmetry [4] were identified. Differences between the three clinical subtypes were tested using ANOVAs with Dunn-Bonferroni corrections (p<.05).

Results & Discussion: Demographics between subtypes are in Table 1. Differences between PD subtypes were significant for step velocity (p<.001), step length (p<.001), step time (p=.014), and stance time (p=.004), as well as step-to-step variability of swing time (p=.015) and step length asymmetry (p=.020). MOTOR walked with faster step velocity, longer steps, and reduced stance time compared to DEPR and COG (p≤.021). MOTOR had reduced step time compared to COG (p=.028) but not compared to DEPR (p=.128) There were no significant differences between DEPR and COG for velocity, step length, step time, or stance time (p>.985). Swing time SD was higher in COG than MOTOR (p=.020). DEPR displayed intermediate values between MOTOR and COG, but was not significantly different from either subtype (p>.226). Step length asymmetry was significantly lower in the DEPR group compare to the COG group (97.56% vs 101.14%, p=.016; 100% indicating perfect symmetry, <100% the "more affected side" had shorter steps, >100% "less affected side" had shorter steps;). MOTOR (100.16%) was not significantly different from DEPR or COG (p=.105).

Table 1. Characteristics of Clinical Subtypes. Mean ± SD *indicates univariate significance, [C] indicates significantly different than COG, [D] indicates significantly different than DEPR

	n	Age*	Disease Duration	UPDRSm*	MoCA*	GDS*	HADSd*
MOTOR	132	66 ± 8[C]	5 ± 4	22 ± 9[C]	28 ± 1[C]	2 ± 1[D]	3 ± 2[D]
DEPR	32	65 ± 6[C]	5 ± 3	25 ± 10	27 ± 1[C]	7 ± 2	7 ± 3
COG	92	70 ± 8	5 ± 4	28 ± 10	22 ± 3	2 ± 1[D]	3 ± 2[D]

Across the spatiotemporal variables, those in the MOTOR subtype displayed less gait impairment than DEPR or COG. The only gait variable significantly different between DEPR and COG was step length asymmetry. Alterations in step length asymmetry may represent a compensation strategy between the more affected and less affected side. Future studies will include a more thorough neuropsychiatric battery to confirm these findings as related to other psychiatric symptoms such as anxiety. Longitudinal observation of the progression of gait impairment across these subtypes would also be of interest.

Significance: Herein, we identify specific gait variables that demonstrate differences between clinical subtypes. These results represent an important first step in determining the viability of gait signatures relating to the prediction and progression of non-motor symptoms. As gait changes may emerge prior to neuropsychological symptoms, correctly categorizing individuals into clinical subtypes based on gait could facilitate earlier implementation of personalized rehabilitation strategies addressing motor and neuropsychiatric impairment as indicated.

Acknowledgements: This project was supported by the National Institutes of Health (T32-HD007434 & NS097437).

References: [1] Mirelman et al. (2019), *Lancet Neurol.* 18(7); [2] Morris et al. (2017), *J Gerontol A Biol Sci Med Sci* 72(12); [3] Campbell et al. (2020), *Ann Clin Transl Neurol* 7(8); [4] Lord et al. (2013) *Mov Disord*. 28(11); [5] Bryant et al. (2012) *Eur Neurol* 67.

Characterizing the muscle activity of postpartum mothers during three infant lifting tasks

Safeer F Siddicky[1*], Yuhang Cai[2], Yunsheng Zou[2], Kathryn L Havens[2]
[1]Department of Kinesiology and Health Education, The University of Texas at Austin, Austin, TX
[2]Division of Biokinesiology and Physical Therapy, University of Southern California, Los Angeles, CA
email: *safeer.siddicky@austin.utexas.edu

Introduction: Infant caregiving requires individuals to frequently bend and lift their child. Throughout the day, mothers may lift their baby from the floor for tummy time; lift from a changing table after a diaper change; and lift baby who is strapped in a car seat to transport them to and from a car. Ergonomic studies have demonstrated that individuals who frequently perform lifting and bending tasks are more likely to develop low back pain. [1] The postpartum population is already vulnerable to lumbopelvic pain. [2-4] Thus, these lifting caregiving tasks are not only ecological but also potentially deleterious.

Current research on caregiver lifting mechanics is limited. One study found that when healthy young men lifted heavier infant dummies, their hip and lumbar joint moments increased, indicating that the demands on these areas of the body increase with heavier lifting loads [5]. Additionally, when healthy nulliparous women wore an infant dummy in a baby carrier while performing trunk bending tasks to simulate lifting, there was increased muscle activity of erector spinae, biceps femoris, and rectus femoris with increased trunk flexion [6]. While these studies provide some insight into caregiving mechanics during infant lifting tasks, no study has investigated the activation of gluteal muscles, nor asked mothers and infant pairs to participate.

The purpose of this study was to investigate muscle activity of mothers during infant lifting tasks. We aimed to identify patterns of activation of the gluteal and erector spinae muscles of postpartum mothers during 3 infant lifting tasks: lifting baby off the floor, from a changing table, and lifting off the floor within an infant car seat. We hypothesized that greater levels of activation would be identified with the larger task demand during car seat lifting, for all muscle groups, and that greater activation would also be identified for the gluteal muscles during lifting infants off the floor compared to the changing table.

Methods: 9 healthy mothers (34.0 ± 2.2yr, 1.7 ± 0.09m, 67.5 ± 14.5kg) lifted their own infants (14.8 ± 2.9wks, 6.3 ± 0.6kg) during three lifting tasks: from the floor, from a changing-table height counter, and from the floor while the baby was strapped into an infant car seat (9.3 ± 2.2kg). Five semi-continuous repetitions were performed. Mothers also stood still for baseline EMG, and performed maximal voluntary isometric contractions (MVIC) for each muscle group. Surface electromyography was collected from bilateral gluteus maximus, gluteus medius, and lumbar erector spinae muscles (Noraxon Wireless EMG, Scottsdale AZ, 1500Hz). Raw EMG was band-pass filtered (4th order Butterworth, 35-500Hz), demeaned, and full wave rectified. Overall muscle activity amplitude was identified as mean processed EMG over the repetitions and normalized to MVIC. Descriptive statistics were performed due to low sample size.

Results & Discussion: In line with our hypothesis, the greater relative weight of baby within the carseat resulted in higher median activation of the erector spinae muscles and the gluteus maximus, compared to lifting them from the floor or the table. The higher median gluteus medius activation when lifting infants from the floor, compared to lifting infants within the carseat and the table, may be attributed to greater frontal plane motion (hip abduction). Low level activity was identified for all of the muscles studied (<20% of MVIC). This indicates that these tasks were overall not highly demanding to these muscle groups. It is possible that other muscle groups, like the knee extensors or the hamstrings could have contributed more to these tasks. Overall, our findings indicate a trend of increasing lumbar erector spinae and gluteal muscle activation with larger task demands. Future work will involve recruiting more participants and exploring lower extremity muscle activation timing for these lifting tasks.

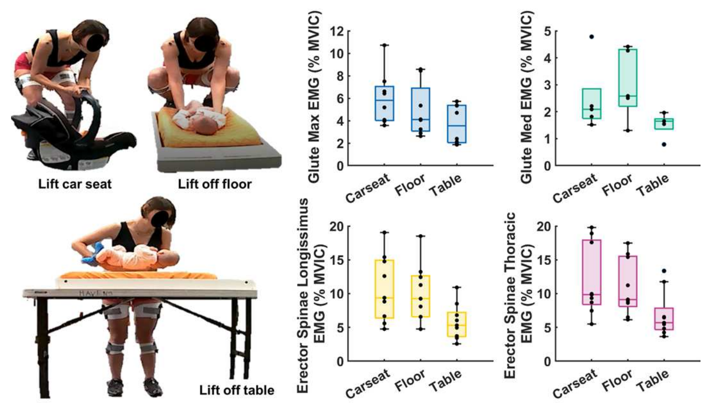

Figure 1: Photos of infant carriage methods (left). Box plots of average gluteal and erector spinae EMG, normalized to MVIC (right).

Significance: While infants are the focus of significant medical attention during the first months of life, mothers' health is given much less attention. This study adds to the limited biomechanical data available of the mother-infant dyad, using ecological tasks with implications for ergonomics and clinical practice. While the muscle activity of the selected muscles was relatively low, these strains over many daily repetitive cycles could be potentially deleterious, especially as the infant grows. A better understanding of muscular demands postpartum can help maternal health care practitioners develop educational tools for best lifting practices, create specific strength and conditioning protocols for expectant mothers, and develop more targeted rehabilitation protocols for new mothers and caregivers.

Acknowledgements: We thank the mother-infant pairs who participated in our study.

References: [1] Frymoyer et al., 1980, Spine 5: 419-23. [2] Havens et al., 2022, J Womens Health PT, 46: 25 [3] Ojukawa et al., 2017, J Obstet Gynecol, 37: 855. [4] Christopher et al., 2019, J Womens Health PT, 43:127. [5] Kim, Eom, Kwon, 2022, Technol Health Care, 30:441-450. [6] Park, Shin, Nam, 2020, Phys Ther Rehabil Sci, 9:36-42.

GAIT SYMMETRY AND FUNCTIONAL MOBILITY IN SERVICE MEMBERS WITH TRANSFEMORAL AND CONTRALATERAL TRANSTIBIAL LIMB LOSS AFTER BILATERAL AND UNILATERAL OSSEOINTEGRATION

Julian C. Acasio[1,2]*, Clare A. Severe, Brad D. Hendershot, Christopher L. Dearth,
Julio A. Rivera, Jonathan A. Forsberg, Benjamin K. Potter
[1]Defense Health Agency: Extremity Trauma and Amputation Center of Excellence, Falls Church, VA, USA
[2]Walter Reed National Military Medical Center, Bethesda, MD, USA
*Corresponding author's email: julian.c.acasio.civ@health.mil

Introduction: Nearly 1500 Service members (SMs) have sustained traumatic lower limb loss during the Global War on Terror, ~28% (n=418) of which have bilateral lower limb loss [1]. Bilateral (vs. unilateral) lower limb amputation generally results in worse outcomes, including diminished mobility, prosthesis use, and overall quality of life [2]. Among individuals with a combined transfemoral (TF) and contralateral transtibial (TT) amputation, specifically, though evidence is limited (to older individuals with dysvascular disease), poor functional and mobility outcomes are reported due, in large part, to limited prosthesis use [3]. Osseointegration (OI) – the direct skeletal attachment of a prothesis – aims to mitigate complications associated with prosthesis use and has been shown to improve functional and mobility outcomes in cases of unilateral TF amputation [4,5]. Thus, the purpose of this case series was to compare preliminary outcomes of gait symmetry and functional mobility in three SMs with TF/TT bilateral amputation following either bilateral or unilateral (i.e., TF-limb only) OI. We hypothesized SM with bilateral vs. unilateral OI would demonstrate greater symmetry and mobility following OI.

Methods: Three SMs (age: 41.3 [10.7] yr, body mass: 82.7 [9.8] kg, stature: 180.6 [5.4] cm, time since amputation: 94.0 [36.5] mo) with TF/TT bilateral amputation underwent a two-stage OI procedure (OPRA™ implant system): one received OI bilaterally, while two received OI on their TF limb only. Each SM completed overground biomechanical gait evaluations at a self-selected pace, in socket prostheses (pre-OI) and again twelve months post-stage II surgery (post-OI). Walking speed, bilateral step length and time, and first peak vertical ground reaction forces (VGRFs) and GRF loading rates (GRF LR) were determined and symmetry indices (SI) calculated relative to the TT limb (i.e., positive SI indicates larger value for TT side). Kinetic measures were normalized to body mass. Mobility was assessed using the timed up and go (TUG).

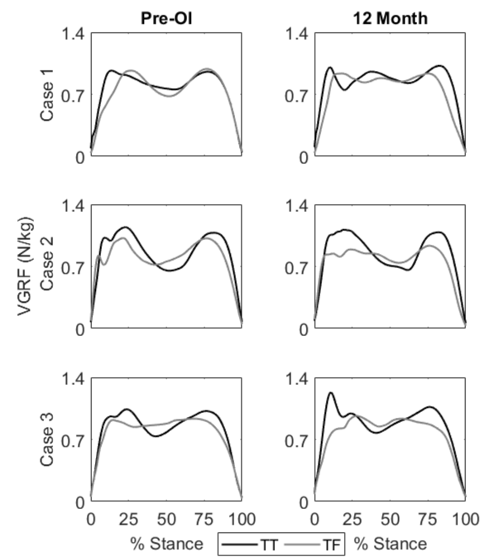

Figure 1: Mean vertical ground reaction forces (VGRF) during stance for the TT (black) and TF (gray) limbs for each case

Results & Discussion: In partial support of our hypothesis, post-OI, both SMs with unilateral OI demonstrated less symmetry in peak VGRFs and GRF LR, with larger forces on the TT limb (Figure 1). Larger peak VGRF and GRF LR in the TT vs. TF limb following OI (Figure 1), despite similar (or decreased) walking speeds (Table 1), suggest an over reliance on the TT-limb and may result in future overuse injuries [6]. Notably, in all cases, the observed SI are larger than those previously reported in cases of unilateral TF limb loss [7]. Additionally, TUG times increased with bilateral OI and decreased with unilateral OI (Table 1), suggesting increases in TT GRF are a means to improve functional mobility.

Significance: Current results emphasize the apparent trade-off(s) between functional mobility and quality of movement, likely requiring additional monitoring throughout the post-OI rehabilitation process. In particular, greater biomechanical demand on the TT limb poses a risk for secondary musculoskeletal injury and thus may eventually reduce functional outcomes or quality of life over the longer term.

Table 1: Walking speed, timed up and go (TUG) times, and symmetry indices (SI) for step length and time, and peak vertical ground reaction force (VGRF) loading rate (GRF LR).

Case	OI	Walking Speed (m/s)		TUG (s)		Step Length SI		Step Time SI		VGRF SI		GRF LR SI	
	Limb	Pre-OI	Post-OI	Pre-OI	Post-OI	Pre-OI	Post-OI	Pre-OI	Post-OI	Pre-OI	Post-OI	Pre-OI	Post-OI
1	Both	1.28	1.14	6.2	8.8	9.95	9.41	0.52	-16.49	3.30	5.55	51.18	36.45
2	TF	1.37	1.37	6.6	5.5	9.30	7.85	-14.17	-3.22	10.83	18.03	32.49	56.92
3	TF	1.17	1.07	9.9	9.5	6.09	11.89	-1.54	-5.13	10.98	23.75	-2.48	56.90

Acknowledgements: This work was supported by Award W81XWH-17-2-0060. The authors also acknowledge the DoD OI program, and specifically those who supported biomechanical evaluations (JME, JRG, BRK, CEM, MLT, MLO, KFA and HSM). The views expressed herein are those of the authors and do not reflect the views of HJF, USUHS, the Department of Defense, Departments of the Army/Navy/Air Force, nor the U.S. Government.

References: [1] Farrokhi et al. *MSMR* 2018 **25**(7): 10-6 [2] Penn-Barwell *Injury* 2011 **42**(12):1474-9 [3] Bhangu et al. *Prosthet Orthot Int.* 2009; **33**(1): 33–40 [4] Hagberg K et al. *Arch Phys Med Rehabil.* 2014; **95**(11):2120–7. [5] Van De Meent H et al. *Arch Phys Med Rehabil*. 2013; **94**(11):2174–8. [6] Farrokhi et al. *Arch Phys Med Rehabil.* **99**(2): 348-54. [7] Rutkowska-Kucharska et al. *Appl Bionics Biomech.* 2018; Article ID 5190816

A NEED FOR SPEED: OBJECTIVELY IDENTIFYING KINEMATIC STRATEGIES ASSOCIATED WITH FASTER SPRINT VELOCITIES

Chris L. Vellucci, Shawn M. Beaudette
Department of Kinesiology, Brock University, St. Catharines, ON

Introduction: Sprint velocity is a result of an athlete coordinating multiple body segments in a rhythmic fashion to accelerate their body forward. This suggests whole-body intersegmental coordination may be associated with improved sprint velocities. Despite this, many studies have assessed specific sub-regions[1,2] of the body and have selected discrete parameters a-priori. Such studies disregard the highly intricate and co-dependent nature of whole-body movements. These approaches have led to a substantial number of publications to focus on the lower extremity dynamics during sprinting, which has resulted in a reduced emphasis of the mechanics of the upper extremities and trunk. PCA is a powerful data reduction algorithm that identifies the main modes of variation in a dataset. In biomechanics, this has been previously used to analyze differences in whole-body movement strategies in ski technique[3] and to classify athletes as novice or advanced[4]. Therefore, the purpose of this study is to use wearable sensors and data-driven tools to objectively assess the whole-body kinematic and determinants of sprint velocity. This hypothesis-generating study will serve as the basis for future work on the development of an objective athletic performance scoring tool.

Methods: 41 healthy university aged athletes were recruited for this study. Participants were asked to run three maximal 60 m sprints while wearing a 17-sensor IMU motion capture suit (XSENS MTw Awinda, Netherlands). The five strides about the point of peak velocity were, drift corrected, stride segmented, time-normalized, and ensemble averaged before being input into the PCA matrix (40 participants*64 markers*3axes*101 data points). Following the application of PCA to the matrix, PCs that explained >95% of the variance in the dataset were retained and used as inputs into a stepwise multivariate linear regression ($p<0.10$) to assess relationships with sprint velocity. Multi-component reconstruction was used to reconstruct an upper and lower limit of the functional meaning of the multivariate linear regression models.

Results & Discussion: The first 21 PCs were retrained, which explained 95.4% of the cumulative variance in the data set. The stepwise multivariate model displayed an R^2=0.795 with a root mean squared error (RMSE) = 0.351 and a p-value<0.0001. The functional interpretation of the PCs revealed that faster sprint velocity was associated with improved coordination between the upper and lower body, a lowered horizontal head acceleration, a dynamic trunk extension, and various lower limb kinematic differences. The findings of this study suggest that a variety of key time-varying coordinative features are associated with improved sprint velocity (**Figure 1**).

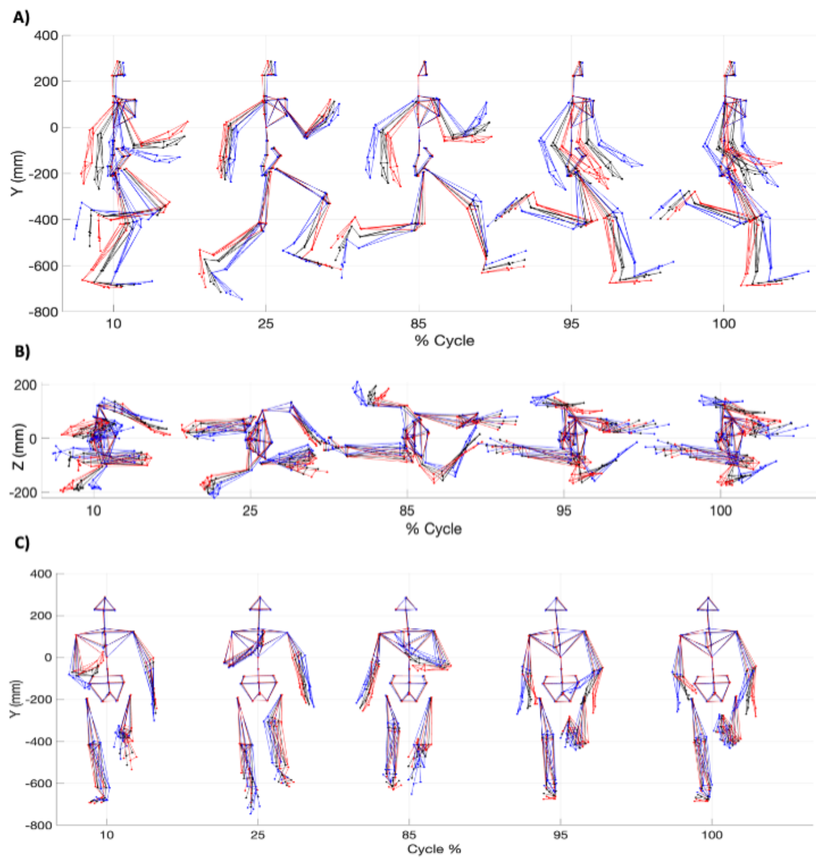

Figure 1: Depiction of the PCs correlated with max sprint velocity. Slow is represented in red, fast is represented in blue

Significance: This study is amongst the first to identify coordinative differences associated with objective continuous performance outputs. This provides athletes and coaches with objective feedback regarding coordinative features associated with improved sprint velocity. This work can inform coaching practices by providing objective performance benchmarking.

Acknowledgements: This research was funded, in part by the Natural Sciences and Engineering Research Council (NSERC) of Canada (RGPIN-2020-05195). The authors wish to thank Robin McKenzie and Nicholas Eck for their contributions to the research project.

References:[1] Bushnell et al. (2007). *Sports Biomech*. 6, (3); p. 261-268., [2] Muyashiro et al. (2019). *Front Sports Act living*. 1, (37). [3] Gløersen et al (2018). *J of Sports Sci 36*, 229–237. [4] Ross et al. (2018). *Medi & Sci in Sports & Exercise 50*, 1457–1464.

BIOMECHANICAL AND MOBILITY OUTCOMES OF SERVICE MEMBERS WITH BILATERAL TRANSFEMORAL AMPUTATION BEFORE AND 12 MONTHS AFTER OSSEOINTEGRATION

Clare A. Severe[1,2*], Julian C. Acasio, Brad D. Hendershot, Christopher L. Dearth,
Julio A. Rivera, Jonathan A. Forsberg, Benjamin K. Potter
[1]Henry M. Jackson Foundation, Bethesda, MD; [2]Walter Reed National Military Medical Center, Bethesda, MD
*clare.a.severe.ctr@health.mil

Introduction: Functional outcomes generally decline with increasing severity of lower limb trauma (i.e., more proximal and bilateral vs. unilateral amputation) [1]. Persons with bilateral transfemoral amputation (BTFA) are seemingly most susceptible to poor prosthesis fit [2], resulting in substantially diminished biomechanical and mobility outcomes. Osseointegration (OI) – the direct skeletal attachment of a prothesis – aims to eliminate complications of traditional socket prostheses [3-5], and thus may be especially beneficial for persons with BTFA. The purpose of this analysis was to compare biomechanical and mobility outcomes among Service members (SM) with BTFA receiving bilateral OI. We hypothesized that functional outcomes among SM with BTFA will improve after bilateral OI, evidenced by improved biomechanical outcomes (i.e., faster walking speed, reduced stride width, hip abduction angle, and lateral trunk lean) and improved mobility outcomes (i.e., six-minute walk test [6MWT] and timed up and go [TUG]), as well as improvements in self-reported outcomes (corresponding to prosthesis use and walking ability).

Methods: Fourteen male SM with BTFA (mean±SD age: 34±5yr, stature: 1.74±0.14m, body mass: 89.2±19.1kg, time since amputation: 98±20mo) underwent a two-stage OI procedure (OPRA™ implant system) simultaneously on both lower limbs. Before (baseline, traditional socket prostheses) and 12 months after OI, participants completed biomechanical and functional (6MWT and TUG) evaluations. For the biomechanical evaluation, participants walked overground at a self-selected speed, while full-body kinematics were tracked (120Hz) using an 18-camera motion capture system. We computed key temporal-spatial (walking speed, stride width) and joint kinematic (hip abduction and trunk lateral range of motion) features of gait commonly reported among persons with bilateral amputations (bilateral metrics were averaged between sides). SMs completed the Questionnaire for Persons with a Transfemoral Amputation (Q-TFA) [7] at both evaluations; the prosthesis use and mobility scores (0-100 scale each) are included in this analysis. All outcomes were compared baseline vs. 12 months post-OI using paired t-tests ($p<0.05$). Note, SM who were not walking or using (an) assistive device(s) other than a prosthesis were excluded from biomechanical analyses.

Results & Discussion: Before OI, nearly half (6 of 14) SM were unable to walk using full-length prostheses and were therefore unable to complete biomechanical or functional evaluations. One additional SM was walking, but unable to complete the full 6MWT due to pain in both the lower back and residual limb. 12 months after OI, four of the original six non-ambulatory SM were now walking. All four, plus the additional SM previously limited by excessive pain, completed biomechanical, 6MWT, and TUG evaluations. One SM who was walking at baseline was not yet walking with full-length prostheses at 12-month evaluation. In total, biomechanical outcomes are reported for four SM who were walking without an assistive device at baseline and 12-month evaluations; mobility outcomes are reported for five SM, regardless of assistive device use. There were no differences baseline vs. 12 months ($p>0.11$) in biomechanical outcomes (Table 1); thus, our primary hypothesis was not supported. 12 months after OI, Q-TFA prosthesis use scores increased ($p=0.002$), but the mobility scores were similar ($p=0.83$); thus, our secondary hypothesis was only partially supported.

Table 1. Mean±SD self-selected walking velocity (SSWV), stride width, hip abduction, trunk lateral range of motion (ROM), 6 Meter Walk Test (6MWT), Timed Up and Go (TUG), and Q-TFA sub-scores at baseline in full-length prostheses (pre-OI) and 12 months post-OI (*=significant change).

	SSWV (m/s)	**Stride Width** (m)	**Hip Abduction** (°)	**Trunk Lat. ROM** (°)	**6MWT** (m)	**TUG** (s)	**Q-TFA** (Prosthesis Use)	**Q-TFA** (Mobility)
Baseline	1.16±0.09	0.23±0.08	5.4±1.4	13.8±3.3	324.7±71.0	10.5±2.7	19±23	56±20
12 months	1.05±0.11	0.21±0.04	4.9±2.4	12.3±2.3	386.6±41.4	10.4±2.9	55±33*	57±23

Significance: Although no differences were observed in biomechanical characteristics of gait as of 12 months post-OI, the greater proportion of those walking at 12 months vs. baseline (79% vs. 57%) emphasizes the practical benefits of OI not captured by biomechanical analyses alone, particularly within a relatively acute stage of rehabilitation. Moreover, greater Q-TFA prosthesis use scores are encouraging, despite similar walking ability and mobility (noting the "walking habits" component of the mobility score was the only to not increase). In addition to monitoring through the 24-month timepoint, combining these biomechanical and mobility outcomes with other outcomes will facilitate a more comprehensive understanding of the benefits of (bilateral) OI for SM with BTFA.

Acknowledgements: This work was supported by Award W81XWH-17-2-0060. The authors also acknowledge the DoD OI program, and specifically those who supported biomechanical evaluations. The views expressed herein are those of the authors and do not reflect the views of HJF, USUHS, the Department of Defense, Departments of the Army/Navy/Air Force, nor the U.S. Government.

References: [1] Penn-Barwell (2011) *Injury* 42(12):1474-9; [2] Turner and McGregor (2020) *Arch Rehabil Res Clin Transl* 2: 100059. [3] Hagberg & Brånemark (2011), *Prosthet Orthot Int* 25, 815-23; [4] Hagberg et al. (2014) *Arch Phys Med Rehabil* 95(11):2120-7; [5] Van De Meent et al. (2013) *Arch Phys Med Rehabil* 94(11):2174-8; [6] Su et al. (2007) *JRRD* 44(4): 491-502; [7] Hagberg et al. (2004) *J Rehabil Res Dev* 41(5):695-706.

BODY MASS INDEX AND WALKING BIOMECHANICS PREDICT TROCHLEAR CARTILAGE STRAIN IN INDIVIDUALS WITH ANTERIOR CRUCIATE LIGAMENT RECONSTRUCTION

Steven A., Garcia*[1,2], McKenzie White[1,2], Seth Kahan[1,2], Jovanna Gallegos[1,2], Isabella Balza[1,2], Riann M., Palmieri-Smith[1,2]
[1]School of Kinesiology, University of Michigan, Ann Arbor MI
[2]Orthopaedic Rehabilitation Biomechanics Laboratory, University of Michigan, Ann Arbor MI
*Corresponding author's email: stevenag@umich.edu

Introduction: Individuals with previous anterior cruciate ligament reconstruction (ACLR) are at high risk for post-traumatic osteoarthritis (PTOA) as between 30-50% of patients are diagnosed with the disorder within 10-20 years [1]. A multitude of risk factors are implicated in PTOA development but high body mass index (i.e., BMI > 25.0 kg/m^2) is one of the strongest predictors of PTOA after ACLR [2]. High BMI is hazardous for cartilage health as increased body mass and adiposity are linked with poor walking biomechanics and systemic inflammation which together promote cartilage breakdown [3]. Indeed, recent work suggests higher BMI post-ACLR influences worsening of patellofemoral cartilage defects post-surgery [4] and is associated with increases in cartilage turnover biomarkers [5], suggesting those with high BMI may display earlier PTOA-related joint changes. Recently, it has been suggested that evaluating cartilage thickness changes post-exercise (i.e., strain) can be used to non-invasively assess cartilage health *in vivo* as the magnitude of cartilage strain after acute loading is associated with cartilage matrix composition [6]. Nonetheless, few studies to date have evaluated cartilage strain after ACLR and it remains relatively unclear how BMI, and knee mechanics influence cartilage function *in vivo*. Here we aimed to evaluate how BMI, and knee mechanics influence femoral cartilage strain in response to acute walking via ultrasonography (US) in those with previous ACLR. We hypothesized that higher BMI and reduced knee flexion moments (KFM), and knee flexion/extension excursions (KFE, KEE) would be associated with increased femoral cartilage strain post-walking.

Methods: We recruited 48 participants with ACLR (Age: 24.1 ± 5.8 yr., BMI: 26.0 ± 4.8 kg/m^2, Time Post-Op: 31.6 ± 11.1 mo.). Gait biomechanics (i.e., KFM, KFE, KEE) were captured using an instrumented treadmill (2000 Hz) synced with a 12-camera Qualisys motion capture system (200Hz) as participants walked at a standard speed of 1.3 m/s to minimize the effects of speed on gait metrics. Gait biomechanics were calculated by combining marker and force data from the treadmill using Visual 3D and filtered using a fourth-order Butterworth filter at 6 Hz and 10 Hz, respectively. Knee moments were resolved in the proximal femoral coordinate system and reported as external. Peak external KFM was defined as the moment in the first 50% of stance. KFE was defined as the change in angle from heel-strike to peak KFA (°) while KEE was defined as the change in angle from peak KFA to the minimum angle in late stance. The average excursion value from all stance phases identified was used for statistical analyses. Prior to ultrasound assessments for assessment of cartilage thickness, participants rested supine for 45 minutes with their knees at full extension to unload the femoral cartilage. Following rest, US images were acquired bilaterally at 140° of knee flexion. After baseline images, participants completed a standard 30-minute incline walking exercise (5° slope). Immediately following walking, US images were acquired bilaterally to evaluate post-exercise cartilage thickness. A custom MATLAB app was used to segment cartilage into medial, lateral, and intercondylar (IC) trochlear regions to measure cartilage thickness changes post-exercise. Cartilage thickness was evaluated as the Euclidean distance between deep (cartilage-bone) and superficial (cartilage-synovium) borders at each point across the entire contour. The average % Δ thickness (i.e., strain) across all images was used for analyses. Paired t-tests were used to compare cartilage strain between limbs. Linear regressions controlling for sex were used to evaluate the associations between BMI and gait outcomes on trochlear cartilage strain. Significance was set at $\alpha = 0.05$ for all tests.

Results & Discussion: We observed greater cartilage strain post-exercise in the medial femoral trochlea in the ACLR limb compared to the contralateral limb (-2.6% mean difference, $t = 2.2$, $p = 0.036$) but no differences were detected elsewhere. After controlling for sex, we observed that higher BMI ($\Delta R^2 = 0.16$, $p < 0.01$) and lesser KEE ($\Delta R^2 = 0.08$, $p = 0.04$) were associated with greater strain in the medial femoral trochlea in the ACLR limb but not the contralateral limb. Similarly, higher BMI ($\Delta R^2 = 0.08$, $p = 0.04$) was associated with greater strain in the lateral femoral trochlea in the ACLR limb but not in the contralateral limb. BMI and gait biomechanics were not associated with femoral cartilage stain in the contralateral limb in any cartilage region ($p > 0.05$).

Early cartilage degeneration is common in those with ACLR, often surfacing as changes in cartilage composition (i.e., reduced proteoglycan content, collagen disorganization) that impact the tissue's load-bearing capacity. Indeed, we observed greater medial trochlear strain in the ACLR limb compared to the uninjured contralateral limb. Given that greater magnitudes of cartilage strain post-exercise are thought to be influenced by poorer cartilage composition [6], our findings may suggest that the ACLR limb may be exhibiting tissue alterations consistent with early PTOA. Further, we observed that higher BMI and reduced knee extension excursions during midstance may contribute to greater magnitudes of femoral cartilage strain in the ACLR limb. Reduced KEE in midstance may shift the regions of cartilage loaded during walking to more localized areas, while higher BMI may influence cartilage breakdown via pro-inflammatory mediators and alter knee loading.

Significance: Cartilage in the ACLR limb may exhibit poorer tissue function compared to the contralateral limb, evidence by higher trochlear strain post-walking. Higher BMI and reduced excursions may contribute to greater cartilage strain in the medial femur. Future work should evaluate if increased cartilage strain in those with higher BMI may be linked with poorer cartilage composition markers.

References: [1] Barenius, B., et al., Am J Sports Med, 2014. [2] DiSilvestro, K.J., et al., Clinical Journal of Sport Medicine, 2019. [3] Blazek, K., et al. J Orthop Res, 2014. [4] Patterson, B.E., et al., Am J Sports Med, 2018. [5] Lane, A.R., et al., J Athl Train, 2019. [6] Collins, A.T., et al. Arthritis Res Ther, 2018.

SEX DIFFERENCES IN WALKING BIOMECHANICS AND FEMORAL CARTILAGE PROPERTIES IN THOSE WITH ANTERIOR CRUCIATE LIGAMENT RECONSTRUCTION

Jovanna Gallegos [2*], Isabella Balza[2], Steven A. Garcia[1, 2], Riann M. Palmieri-Smith[1, 2], McKenzie White[1, 2], Seth Kahan[1, 2]
[1] University of Michigan: School of Kinesiology, Ann Arbor
[2] Orthopaedic Rehabilitation and Biomechanics Laboratory, Ann Arbor
* jovanna@umich.edu

Introduction: Those with an anterior cruciate ligament injury often undergo reconstruction surgery (ACLR) to restore joint stability. After their operation, they often develop altered walking patterns [1] which may contribute to cartilage degeneration and knee osteoarthritis (OA) development within two decades of injury and surgery [2]. Interestingly, females are two to five times more likely to experience an ACL injury and are at greater risk for developing knee OA compared to males [3]—representing a large proportion of patients at risk for this debilitating disease. Walking patterns have been shown to differ between sexes in uninjured populations and some data suggests females with ACLR exhibit greater walking asymmetries than males—which may underlie higher risks of developing post-traumatic knee OA after ACLR in females [3]. These sex-specific differences in walking are important given that walking biomechanics are thought to strongly influence cartilage composition and function. For example, in healthy populations, larger knee loads are related to thicker femoral cartilage and lower T1ρ and T2 relaxation times–compositional biomarkers related to articular cartilage biomechanical function [4, 5]. Changes to cartilage composition are some of the earliest indicators of knee OA and can be indirectly evaluated by assessing the change in cartilage thickness after exercise. Given that habitual walking mechanics differ between sexes and females may exhibit poorer gait biomechanics post-ACLR, it is possible that cartilage health outcomes are disproportionately affected in females with ACLR. Therefore, the purpose was to evaluate differences in walking biomechanics and cartilage properties between males and females after ACLR.

Methods: Thirty-six participants with primary unilateral ACLR (Age: 24.0±4.4, Time-Post Op: 31.1±8.5 months, Weight: 71.85±11.10 kg, Height: 1.71±0.08m) completed one testing session involving gait biomechanical assessments and femoral cartilage ultrasound before and after an incline walking exercise. Each participant was equipped with 48 retroreflective markers on their lower extremities. Walking biomechanics were evaluated using a 12-camera Qualisys motion capture system (200Hz) synchronized with a force sensing Bertec treadmill (2000Hz). Participants completed three, 1-minute walking trials at a standardized speed of 1.3 m/s. Gait biomechanics were calculated by combining marker and force data and filtered using a fourth-order Butterworth filter at 6Hz and 10Hz, respectively. Standard inverse dynamics procedures were employed, and moments were reported as external. Peak external knee flexion (KFM) and adduction moments (KAM) were calculated from the first 50% of stance. Following gait assessments, participants rested supine for 45-minutes with their legs fully extended to unload the femoral cartilage and minimize the effects of preceding activity. Ultrasound was used to evaluate cartilage thickness bilaterally with the knee placed at 140° before and immediately after a 30-min incline walk (5° slope, 1.3 m/s). Images were processed via a custom MATLAB application to assess cartilage thickness across the medial (MED), lateral (LAT) and intercondylar (IC) regions. Cartilage strain (%Δ thickness) for each cartilage region was evaluated as the change in cartilage thickness between baseline and post-exercise time points and the average was used for analyses. Independent t-tests were used to compare gait and cartilage outcomes bilaterally. Significance was evaluated as $\alpha = 0.05$.

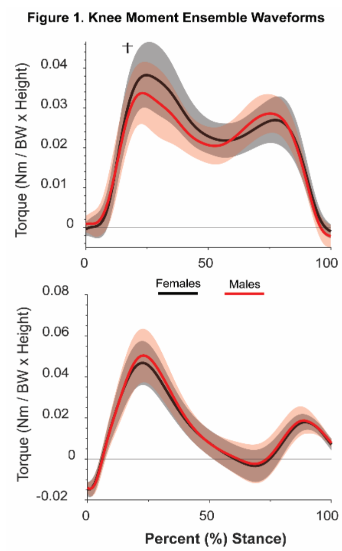

Figure 1. Ensemble averages for knee adduction (top) and flexion (bottom) moments for both sexes. † represents significant difference between groups.

Results & Discussion: Females had greater KAM compared to males bilaterally ($t_{1, 34} = 2.53 - 3.36$, $p < 0.05$) but KFM was similar between sexes ($p > 0.05$). Females had thinner cartilage compared to males in LAT and IC regions ($t_{1, 34} = 2.05 - 3.05$, $p < 0.05$) in both limbs. Females exhibited increases in LAT cartilage thickness after exercise in the ACLR limb ($t_{1, 34} = 2.68$, $p < 0.05$), whereas males did not. Few studies to date have compared walking mechanics and cartilage outcomes between sexes in those recovering from ACLR, but our findings are consistent with observations in uninjured individuals wherein cartilage structure and knee mechanics are different in females relative to males [6, 7]. Further, the sex-differences in post-exercise cartilage strain we observed in the lateral trochlea was similar to previous findings in the lateral tibia post-running which may be reflective of poorer cartilage composition in females [7]. It is plausible that there are sex differences in the gait features that influence cartilage health post-ACLR.

Significance: We observed that gait biomechanics differ between sexes, wherein females walk with greater KAM and have thinner cartilage compared to males. Females may also exhibit differences in cartilage strain in the surgical knee after ACLR. As such, it may be beneficial that future studies aim to understand if the associations between walking mechanics and cartilage health/function are moderated by sex in those with ACLR. Such knowledge is essential to understanding if targets for rehabilitation should be individualized on a sex-specific basis to optimize recovery and mitigate knee OA risk after ACLR.

References: [1] Kaur, M., et al. (2016). *Sports medicine*, 46 (12), [2] Cheung, E. C., et al. (2020). *Current reviews in musculoskeletal medicine*, *13*(1) [3] Lohmander, L. S., et al. (2004). *Arthritis and rheumatism*, 50(10). [4] Collins, A. T., et al. (2018). *Arthritis research & therapy*, *20*(1) [5] Andriacchi, T. P., et al. (2009). *The Journal of bone and joint surgery. 91*(Suppl 1), [6] Garcia, S.A., et al. (2021) *Gait & posture 83* [7] Brenneman Wilson, E.C., et al. (2021) *Magma 34*(4)

IMPACT OF VARIOUS OCCUPATIONAL FOOTWEAR ON POSTURAL STABILITY USING BALANCE TRACKING SYSTEM

Hunter Derby[1]*, Sachini Kodithuwakku Arachchige[2], Adam Knight[1], & Harish Chander[1]
[1] *Neuromechanics Laboratory, Department of Kinesiology, Mississippi State University*
[2] *Department of Exercise & Nutrition Sciences, Weber State University*
*Correspondence: Hunter Derby, hcd89@msstate.edu

Introduction: Falls and fall-related injuries due to postural instability are highly prevalent among the occupational population and are one of the leading causes of both fatal and non-fatal injuries in the workplace. Footwear that serves as the interface between the human foot and the environment has been shown to impact postural stability and the impact can vary among various footwear worn. While previous research has shown the effects of athletic footwear on postural stability and balance performance, literature in regard to various types of occupational footwear is limited, but constantly growing. Moreover, because occupational footwear is primarily designed for safety and protection, they may not be best designed for optimal human performance during occupational tasks, that involves upright balance maintenance. Because of this, certain design features of various occupational footwear may have negative impacts on postural stability and balance performance in an occupational environment [1]. The balance tracking system (BTrackS™) is an affordable low-cost force platform used to assess postural stability through center of pressure (COP) parameters and has been validated against gold standard force plates to provide accurate and reliable balance testing during unshod conditions. Therefore, the purpose of this study is to determine the influence of various occupational footwear on postural stability and balance performance using BTrackS™.

Methods: Twenty healthy males and females [age: 21±1.2 years, height: 178±8.3 cm, mass: 84±14.9 kg] completed the balance and fall risk (BFR) and the modified clinical test of sensory integration of balance (mCTSIB) [eyes open firm (EO), eyes closed firm (EC), eyes open foam (EOF), eyes closed foam (ECF)] on the BTrackS in seven different footwear conditions [steel-toed work boot (ST), tactical work boot (TB), slip resistant shoe (SR), standard military boot (SMB), minimalist work boot (MMB), firefighter boot (FF), and the participant's personal habitual athletic footwear (AF)]. Upon arrival, each participant completed informed consent, PAR-Q, and a brief familiarization regarding the protocol with general anthropometrics then recorded. The footwear tested was selected in a in a counterbalanced order for each participant. COP postural sway path length (cm) from both BFR and mCTSIB were analyzed independently using a one-way repeated measures analysis of variance (RM-ANOVA) to compare all seven footwear conditions at an alpha level of 0.05.

Results & Discussion: Results of this study revealed significant a significant difference among footwear conditions during the EO (p=0.003), EC (p=0.048), and ECF (p=0.037) trials of the mCTSIB. Post hoc comparison revealed that during EO trails, greater postural stability was seen with minimalist military boots when compared to both slip-resistant shoes (p=0.01) and the participants' habitual athletic footwear (p=0.017) (Fig. 1). However, post hoc comparison did not reveal any significance among footwear conditions in the EC and ECF trials of the mCTSIB. Additionally, no significance was observed during the ECF trial of the mCTSIB or the BFR. Based on the current findings, MMB elicited greater postural stability when compared to SR and AF footwear during the EO trials, which can be attributed to the design characteristics. The MMB has a higher boot shaft when compared to SR and AF, which has been shown in previous literature to increase proprioceptive/somatosensory feedback around the ankle joint due to mild compression around the ankle [2]. The MMB also has a minimalistic heel-to-toe drop design along with a thin firm midsole, further promoting proprioceptive feedback to improve postural stability [4]. During the EC and ECF trials of the mCTSIB, post hoc comparison did not show any significance among footwear, but followed a similar trend of observations during EC with better performance from MMB compared to AF, but was reversed in ECF, suggesting that the benefits of the MMB may not be preserved when standing on an unstable surface. Lack of significant differences among the rest of the footwear may also be attributed to the fact that only acute postural stability with no workload or fatiguing protocol was tested for this study, but previous research with the same footwear have shown that workload and fatigue impact balance performance differently with different occupational footwear [3]. Based on the current study, MMB show greater postural stability than SR and AF predominantly during EO trials of the mCTSIB, suggesting that MMB may only provide more postural stability in stable surface environment.

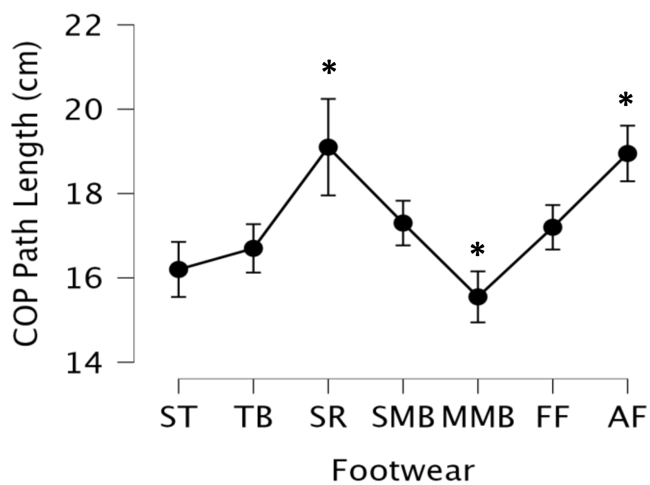

Figure 1: Results of the eyes open (EO) trial of the mCTSIB showing significance among SR, MMB, and AF. * represents significant difference and bars represent standard errors.

Significance: The current study revealed the significant effects of various occupational footwear has on postural stability when tested with a low-cost affordable and portable force platform. Findings can aid in occupational footwear design and manufacturing.

References: [1] Derby et al., (2023), *Applied Sciences*, 13(1), 116; [2] Dobson et al., (2017), *Applied Ergonomics*, 61, 53-68; [3] Chander et al., (2014), *Footwear Science*, 6(1), 59-66; [4] Chander et al. (2019), *Ergonomics*, 62(1), 103-114.

SIGNIFICANT INTRAMUSCULAR COMPLIANCE IS REQUIRED TO ACCOUNT FOR SARCOMERE SHORTENING IN THE IN SITU HUMAN GRACILIS MUSCLE

Benjamin I. Binder-Markey[1*], Lomas S. Persad[2], Alexander Y. Shin[2], William Litchy[2], Kenton R. Kaufman[2], and Richard L. Lieber[3,4]
[1]Drexel University, Phila., PA, [2]Mayo Clinic, Rochester, MN, [3]Shirley Ryan Ability Lab, [4]Hines VA Medical Center, Chicago, IL
Corresponding Author: bb983@drexel.edu

Introduction: Computational musculoskeletal models are helpful to predict muscle function. However, direct measurements of human muscle properties are extremely rare, and thus, many computational musculoskeletal models are never explicitly validated on human muscle. We recently measured human gracilis isometric contractile properties, resting sarcomere length, and muscle dimensions during a free functioning gracilis surgical transfer [1] and thus created a high-resolution data set that allows testing of current musculoskeletal modeling approaches. The current study uses the anatomical and physiological data previously acquired to attempt to validate using a standard Hill type-muscle model to predict human gracilis muscle active contractile properties.

Methods: After IRB approval and patient consent (n=12), intraoperative data were collected as the lower limb was placed in four joint configurations (JC1 to JC4), gradually lengthening the gracilis through its anatomical range. At each JC, we measured *in-situ* muscle-tendon unit (MTU) length, passive sarcomere length, passive tension, and active tetanic tension (Fig. 1A) [1,2]. After muscle removal from the thigh, we measured external MTU slack length, tendon length, and muscle volume. The active sarcomere length-tension curve was calculated for each subject using their measured active tension relationship and the human muscle force-length relationship that assumes maximum tension occurs at sarcomere length of 2.7 µm [3].

Subject-specific standard Hill type-muscle models for each subject were constructed [4]. Experimentally determined optimal fiber length was input and tendon slack length adjusted so optimal fiber length occurred at either the measured MTU slack length, matching passive sarcomere length (Model 1), or MTU length where maximal force was produced, as commonly done (Model 2).

Next, Hill type-muscle models (Model 3) were developed to include a compliant internal connective tissue (ICT) structure. External tendon slack length was input as the experimentally measured length, and ICT slack lengths were adjusted so optimal fiber length occurred at slack MTU. ICT compliance was optimized by scaling the normalized tendon stress-strain curve [4] to minimize the differences between experimental and modelled active and passive sarcomere lengths and forces.

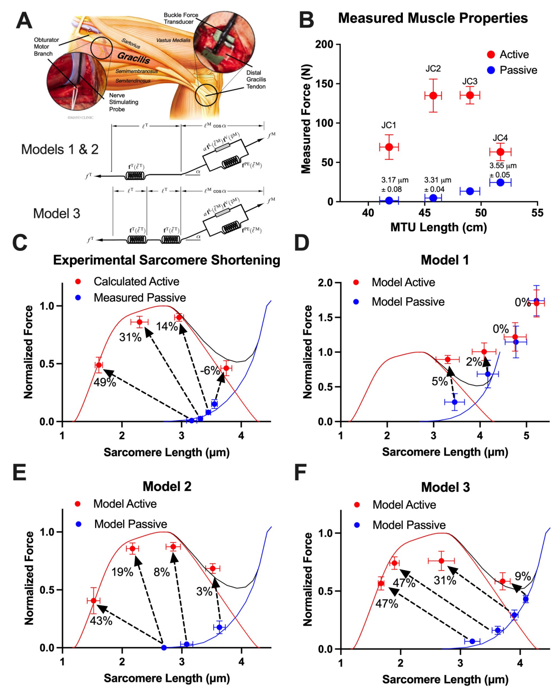

Figure 1: A) Illustration of the gracilis muscle within the thigh with buckle force transducer and stimulator probe inserts and model schematics B) Intraoperative data collected at each of four joint configurations (JC) in the passive state and stimulated active state. C) Measured passive force and sarcomere length with estimated active sarcomere lengths with estimated sarcomere shortening percentages, overlaid on the normalized muscles force v sarcomere length curves. Modeled normalized force, sarcomere lengths, and sarcomere shortening using Models 1(D), 2(E), or 3(F). (n=12 mean±SEM).

Results & Discussion: As previously reported, muscle length and passive force increased as the limb was moved from JC1 to JC4 (Fig. 1B). Measured passive sarcomere lengths increased from an average of 3.2 µm to 3.5 µm (Fig. 1B). Where the active force demonstrated the approximate shape of an active length-tension curve (Fig. 1B). The predicted sarcomere operating range covered the ascending and descending portions of the curve (Fig. 1C). Predicted sarcomere shortening was greatest for the shortest sarcomere length (49±9%) while at the longest sarcomere length, no shortening was predicted (-6±10%).

When using a standard Hill muscle model in which bulk muscle is in series with bulk tendon, it is impossible to create the active length-tension curve given the measured resting sarcomere lengths (Fig. 1D). This is because there is not enough tendon compliance for the sarcomeres to shorten the required magnitude (Fig. 1D). When the Hill muscle model is optimized for active force, the active length-tension curve is observed but passive sarcomere lengthening is not observed in JC 1 and 2 (Fig 1E). To match our experimental data, it was necessary to "insert" a compliant internal connective tissue in series with the muscle fibers, allowing significant sarcomere shortening to occur (Fig. 1F). The current source of this compliance and the precise anatomical arrangement of muscle fibers that would be required for this effect is not known.

Significance: This study actually measured *in-situ* gracilis force and sarcomere length and then modeled the mechanics deterministically. These data demonstrate that very large sarcomere length changes must occur to reproduce the measured data. Such changes are not compatible with current lumped-parameter Hill muscle models.

Acknowledgements: Supported by VA grants: I01 RX002462 and IK6 RX003351.

References: [1] Persad *et al.* (2022). *Sci Rep* **12:**6095 [2] Binder-Markey *et al.* (2023) *J. Physiol.* (in press) [3] Lieber *et al.* (1994). *J. Neurophysiol*. **71**:874. [4] Millard *et al.* (2013) *J. Biomech. Eng.* **135**:021005

CARRYING A BUNDLE OF JOY: A COMPARATIVE BIOMECHANICAL ANALYSIS OF INFANT TRANSPORTATION IN MOTHERS AND NON-MOTHERS

Kathryn L. Havens[1*], Sarah Goldrod[2], Erin Mannen[2]
[1]Division of Biokinesiology and Physical Therapy, University of Southern California
[2]Department of Mechanical and Biomedical Engineering, Boise State University
Corresponding author's email: khavens@usc.edu

Introduction: Load carriage has been the focus of extensive military biomechanics research to improve efficiency and prolong musculoskeletal health of our military personnel [1]. But considering a load that is not only heavy, but alive, moving, and incredibly precious to its carrier has not systematically explored. Yet, carriage of infants is essential to the survival of the human race, as infants are helpless during their early months of life and rely on their caregiver to transport them. Caregivers may do so in multiple ways, including carrying in their arms or using an ergonomic aid via babywearing.

Recently, researchers have started to explore the impact of carrying an infant on walking biomechanics. Holding an infant mannequin in a baby carrier on the body alters ground reaction forces, trunk mechanics, and lower extremity joint loading compared to walking without a load [2-6]. Although these studies indicate that carrying infants affects biomechanics, it remains unclear how this relates to the health of mothers, as the research has mainly focused on healthy young adults carrying weighted infant mannequins. Therefore, it is uncertain how these findings can be applied to mothers who have gone through the unique experience of pregnancy and childbirth.

The purpose of our study was to investigate the ground reaction force (GRF) and kinematic differences during gait between mothers carrying their infants and nulliparous women (non-mothers) carrying infant mannequins under three conditions: carrying nothing (unloaded), carrying in arms (arms) and carrying in a structured baby carrier (babywearing). We hypothesized that we would identify differences in mechanics between carrying conditions and between groups.

Methods: Ten healthy postpartum women (34.5±2.6 years; 68.5±14.2 kg; 1.7±0.1 m) and ten healthy nulliparous women (27.4±4.1 years; 62.6±12.2 kg; 1.7±0.1 m) walked overground for 20 m (average speed = 1.33±0.20 m/s) under the 3 conditions described above (Figure 1, top). For carrying conditions, nulliparous women held an infant mannequin (5 kg, Dietz, Freiburg, Germany) and mothers held their own baby (6.2±0.6 kg, 15.5±3.3 weeks old).

Lower extremity and trunk movements were identified using marker-based motion capture (100 Hz; Vicon & Qualisys systems) and ground reaction forces (GRFs) were collected using force plates embedded into the lab floor (900Hz; AMTI & Bertec plates). Peak GRF and GRF impulse, and ankle, knee, hip and trunk sagittal plane kinematics were compared using Mixed 2 x 3 (parity x carrying) ANOVA ($\alpha <= 0.05$). Post-hoc comparisons were done with t-tests using Bonferroni corrections for multiple comparisons (SPSS, Version 19, Chicago IL).

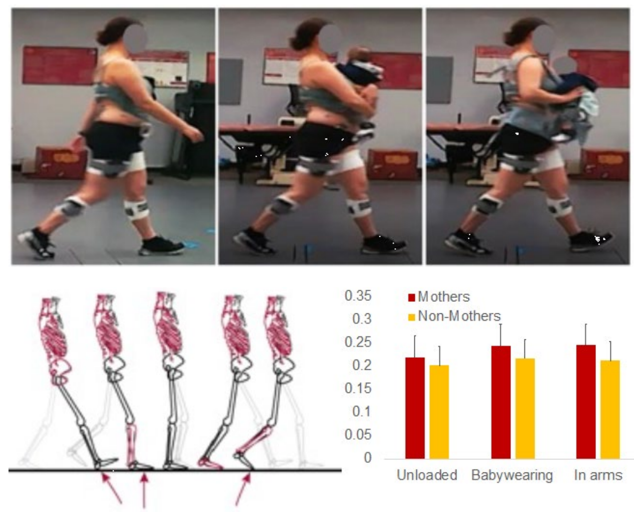

Figure 1: Top: Mother walking unloaded (left), carrying her baby in arms (middle), babywearing (right); Bottom left demonstrates differences between carrying conditions: in arms and babywearing resulted in greater anteroposterior and vertical loads, kinematic differences at trunk, and lower extremity demonstrated with thicker red segments. Bottom right demonstrates differences in peak propulsive GRF (unit: body weight) between conditions and groups

Results & Discussion: The largest differences occurred between carrying conditions: compared to unloaded walking, carrying in arms or babywearing increased vertical (Figure 1, bottom right) GRFs proportional to the 10% increased load and smaller increases in anteroposterior GRFs ($p<0.05$). Kinematic differences included increased trunk extension, hip flexion, ankle dorsiflexion, knee flexion at midstance and pre-swing ($p<0.05$; Figure 1, bottom left). We found few differences between the arms and babywearing conditions. Compared to non-mothers, mothers exhibited mechanics consistent with a greater propulsion at the end of stance, including less ankle plantarflexion, less knee flexion, and trends towards differences in propulsive impulse. We theorize that these mechanics may be used to maintain stability during gait by prioritizing double limb support and effectively controlling the altered center of mass over a larger base of support.

Significance: Infant carrying results in large differences in vertical and anteroposterior forces and smaller changes in trunk and lower extremity kinematics, which together suggest alterations in joint loading for both mothers and non-mothers. Our study contributes a novel understanding of postpartum health by demonstrating alterations in anterior forces, and ankle and knee mechanics, suggesting that mothers carrying their own infants choose different propulsive strategies than non-mothers carrying mannequins during gait. These preliminary results provide a justification for further exploration of postpartum mechanics as they relate to infant carrying techniques.

Acknowledgements: We would like to thank the participants.

References: [1] Birrell et al., *Gait & Posture,* 2007, [2] Junqueira et al., *Gait & Posture,* 2015, [3] Schmid et al., *Gait & Posture,* 2019, [4] Williams et al., *Gait & Posture,* 2019, [5] Brown et al., *Human Factors,* 2015, [6] Havens et al., *Gait & Posture,* 2020

THE USE OF HEELLESS TECHNOLOGY FOOTWEAR AS AN OFFLOADING INTERVENTION

Robert W. Gregory*, Marc I. Robertson
Department of Health & Movement Sciences, Southern Connecticut State University
*Corresponding author's email: gregoryr3@southernct.edu

Introduction: Footwear potentially plays an important role in managing repetitive external mechanical loads applied to the musculoskeletal system [1]. Therapeutic footwear can be used to offload these mechanical stresses to reduce plantar pressures in the diabetic foot [2,3] and treat overuse disorders such as plantar fasciitis and metatarsal stress fractures [1,3]. A novel footwear design using Heelless Technology™ (HT; see Figure 1) has been developed to inhibit heel landings and rearfoot strikes and, therefore, reduce lower extremity loading [4]. To better understand the potential clinical applications of HT footwear for treating a variety of conditions related to excessive loading of the plantar surface of the foot, it is necessary to understand the effects of this footwear on gait mechanics and in-shoe pressures. The purpose of this study was to determine the efficacy of HT shoes as therapeutic footwear based on the potential offloading benefits. Due to an anticipated anterior shift of initial foot contact during the stance phase of gait, it was hypothesized that wearing HT footwear would lead to decreased loading on the foot.

Methods: Twenty-one participants (10 M, 11 F; age: 38.1±15.8 years, height: 168.5±7.3 cm, mass: 74.8±12.6 kg) walked for 15 min at an age-based speed between 4.4-4.8 km·hr^{-1} while wearing both standard (Pegasus 30; Nike Inc.; Beaverton, OR) and HT (Sports Medicine The Difference, Inc.; Leominster, MA) athletic footwear. An instrumented treadmill (FDM-T; Zebris Medical GmbH; Isny, Germany) was used to measure walking kinematics (stride length, stride rate, stride width, stride time, and stance phase %) and kinetics (peak vertical ground reaction force [vGRF], peak rearfoot/midfoot/forefoot vGRFs, and average rate of vertical force development [RFD]). In addition, in-shoe sensors (Stridalyzer Prism; ReTiSense, Inc.; Bangalore, India) were used to collect plantar pressures for the heel, arch, metatarsal, and toe regions of the foot. Data was collected for 30 strides during the last 60 s of each trial; only right lower extremity data are presented. A repeated-measures MANOVA was used to determine the effects of footwear on the kinematic, kinetic, and pressure variables; the level of significance was set at $P<.05$.

Figure 1: Heelless Technology™ footwear (Sports Medicine The Difference, Inc.; Leominster, MA).

Results & Discussion: There were no notable changes in walking kinematics and plantar pressures when wearing HT footwear. However, there were several significant differences in kinetics between the footwear conditions. The only change in walking kinematics when wearing HT footwear was a moderate decrease in stance phase % (P=.02, d=0.75) (see Table 1). There was a moderate decrease in midfoot vGRF ($P<.03$, d=0.67), a large decrease in average RFD ($P<.001$, d=1.06), and a large increase in rearfoot vGRF ($P<.001$, d=1.08) when wearing HT footwear (see Table 2). While not statistically significant, decreased peak vGRF ($P<.06$, d=0.57) and forefoot GRF ($P<.08$, d=0.55) when wearing HT footwear were associated with moderate effect sizes (see Table 2). There were no differences in plantar pressures of the heel, arch, metatarsal, and toe regions of the foot between the footwear conditions (see Table 3).

Table 1: Walking kinematics in control and Heelless Technology™ footwear.

Footwear	Stride Length (m)	Stride Rate (Hz)	Stride Width (cm)	Stride Time (s)	Stance Phase (%)
Control	1.37±0.06	1.87±0.08	10.6±2.6	1.07±0.04	64.4±1.1
HT	1.36±0.06	1.88±0.08	11.3±2.5	1.07±0.04	63.5±1.2

Table 2: Walking kinetics in control and Heelless Technology™ footwear.

Footwear	Peak vGRF (BW)	Rearfoot vGRF (BW)	Midfoot vGRF (BW)	Forefoot vGRF (BW)	Avg. RFD (BW/s)
Control	1.17±0.04	0.56±0.08	0.62±0.06	1.03±0.08	5.79±0.43
HT	1.13±0.06	0.66±0.08	0.56±0.09	0.99±0.08	4.98±0.82

Table 3: In-shoe pressures in control and Heelless Technology™ footwear.

Footwear	Inner Heel (kPa)	Outer Heel (kPa)	Medial Arch (kPa)	Lateral Arch (kPa)	Metatarsals 1-2 (kPa)	Metatarsals 3-5 (kPa)	Hallux (kPa)	Toes 2-5 (kPa)
Control	36.4±7.2	27.0±5.4	17.6±8.1	15.6±6.2	46.5±15.1	33.5±10.5	8.6±3.1	14.6±6.1
HT	35.6±8.2	27.4±6.8	19.3±8.0	17.7±6.9	49.0±15.3	36.5±9.5	9.5±3.1	16.2±6.3

Significance: There is anecdotal evidence that HT footwear is an effective offloading intervention that can be used to reduce plantar pressures in diabetic foot patients. The decreased peak midfoot/forefoot vGRFs and average RFD when wearing HT footwear suggest that it may be suitable for treating some lower extremity overuse injuries. However, there is no efficacy for the use of HT footwear in ulcer prevention/treatment in diabetic persons due to the lack of reduction in plantar pressures when compared to regular footwear.

References: [1] Malisoux & Theisen (2020), *J Athl Train* 55(12); [2] Bus et al. (2008), *Diabetes Metab Res Rev* 24(Suppl 1); [3] Nigg et al. (2005), *Proc 7th Footwear Biomech Symposium*; [4] Davis et al. (2017), *J Sport Health Sci* 6(2).

HIP BELTS REDUCE LUMBAR SPINE COMPRESSIVE IMPULSE WHEN WALKING DOWNHILL

Jordan T. Sturdy[1*], Hedaya N. Rizeq[2,3], Amy Silder[2], Pinata H. Sessoms[2], Anne K. Silverman[1]
[1]Colorado School of Mines, Department of Mechanical Engineering, USA
[2]Naval Health Research Center, San Diego, CA, USA; [3]Leidos, Inc., San Diego, CA, USA
*Corresponding author's email: sturdy@mines.edu

Introduction: Musculoskeletal overuse injuries in the lumbar spine are prevalent among military service members and are causatively linked to occupational load carriage such as hiking with heavy backpacks [1]. Carrying heavy backpacks and walking on sloped surfaces require altered torso and pelvis postures relative to level, unloaded walking [e.g., 2,3]. The combination of flexed postures and axial compression in the spine can create stress gradients in intervertebral discs that increase the risk of injury [4]. However, lumbar joint contact forces during sloped and loaded walking, and how they are affected by different backpack attachments such as the hip belt, are unknown. Thus, the purpose of this study was to quantify lumbar joint contact forces during sloped and loaded walking while using different backpack implementations.

Methods: Optical motion capture (120 Hz), ground reaction forces (1200 Hz), and electromyography (EMG; 1260–2222 Hz) from six participants (5M, 1F) were used to develop and validate loaded walking simulations. Participants (height: 1.74±0.08 m, mass: 78.5±9.5 kg, age: 29±7 y) walked on −10 (Down), 0 (Level), and +10 (Up) degree slopes at a fixed speed of 1.15 m/s. Each walking slope was performed in three load conditions, including wearing body armor and a helmet totaling ~6.5 kg (No Pack) and two 40% body weight conditions where the remaining mass was added to a backpack supported by shoulder straps only (Shoulder) or shoulder straps and a hip belt (Hip Belt).

A musculoskeletal model containing the lower limbs [5] and a detailed torso with lumbar rhythm [6] with torque-driven arms [5] was developed in OpenSim 4.3 [7] (simtk.org) for the No Pack condition. A backpack attachment model [8] represented the Shoulder and Hip Belt conditions. Inverse kinematics and ground reaction forces from Visual3D were used to drive movement simulations of calibrated models of each participant and backpack condition. After reducing residual errors [9] computed muscle control was used to solve for muscle states. Then, a joint reaction analysis was used to quantify 3D lumbar joint contact forces.

Compressive force impulse over right strides was evaluated for both L1L2 and L4L5 joints. Analysis of variance ($\alpha = 0.05$) was used to test for main effects of backpack, slope, and the Backpack × Slope interaction. Pairwise comparisons using Tukey's honestly significant difference were performed when indicated by main effects.

Results & Discussion: Simulation quality was verified to ensure low residuals and kinematic tracking errors, and agreement between model muscle activations and EMG of 11 muscles was validated. Backpack × Slope interactions were significant for both L1L2 (p = .031) and L4L5 (p = .049) compressive impulse. Significance of pairwise results are indicated in Figure 1. L1L2 and L4L5 impulses (Fig. 1) were greater during Up compared with Level and Down in all backpack conditions; however, Level resulted in greater impulses than Down only within the Hip Belt condition. While walking on Level or Up slopes, L1L2 and L4L5 impulses were greater with both Shoulder and Hip Belt backpacks compared with No Pack. However, during Down only, Shoulder resulted in a greater L1L2 and L4L5 impulse compared with No Pack, and the L1L2 impulse during Shoulder was greater than during Hip Belt.

Walking uphill and with 40% body weight backpacks caused high compressive forces in the lumbar spine, which likely could increase the risk of low back pain and injury. The benefit from a hip belt was dependent on slope, with less compressive force than with shoulder straps only when walking downhill.

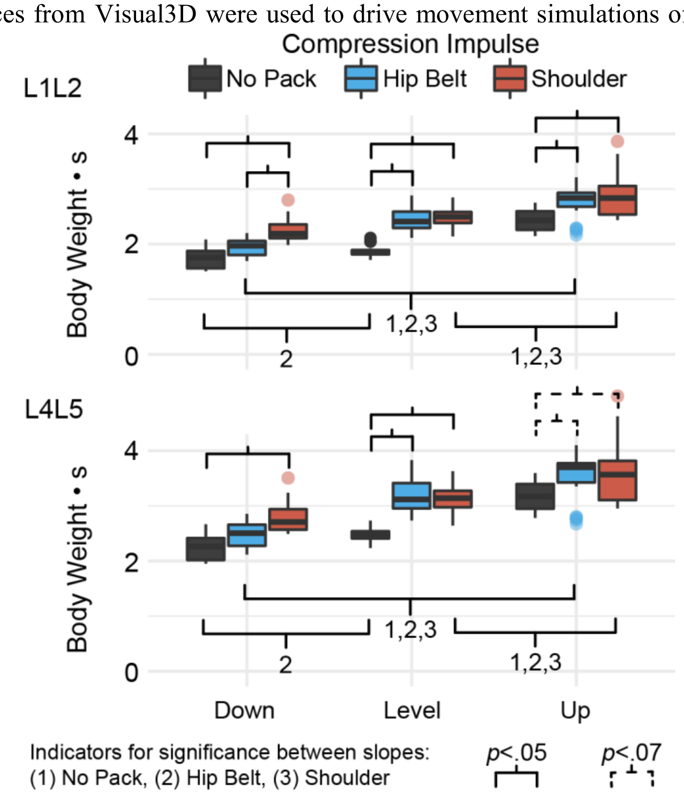

Figure 1. Box and whisker plots showing compressive force impulse in L1L2 (top) and L4L5 (bottom) joints while walking on slopes. Brackets indicate significant between backpack (above boxes) and between slope (below boxes) comparisons.

Significance: These findings illustrate the benefit of using a hip belt to support backpack weight and reduce lumbar loading, especially when walking downhill, and suggest that backpack design can be improved for level and uphill walking.

References: [1] Schuh-Renner et al. (2017) *J. Sci. Med. Sport*, 20, S28-S33; [2] Goh et al. (1998) *Clin. Biomech*., 13(1), S26-S31;
[3] Kimel-Naor et al. (2017) *J. Biomech*., 60, 142-149; [4] Stefanakis et al. (2014) *Spine*, 39(17), 1365-1372;
[5] Lai et al. (2017) *Ann. Biomed. Eng*., 45(12), 2762-2774;
[6] Christophy et al. (2012) *Biomech. Model. Mechanobiol*., 11(1-2), 19-34; [7] Seth et al. (2018) *PLoS Comput. Biol*., 14(7);
[8] Sturdy et al. (2021) *Appl. Ergon*., 90, 103277; [9] Sturdy et al. (2022) *J. Biomech*., 137(April), 111087;

THE GAIT LAB SYNDROME: HOW LABORATORY ENVIRONMENTS MASK GAIT DIFFERENCES BETWEEN HEALTHY SUBJECTS AND PATIENTS WITH ANTERIOR CRUCIATE LIGAMENT RECONSTRUCTION

Lauren Parola[1*] and Eni Halilaj[1]
[1]Department of Mechanical Engineering, Carnegie Mellon University, Pittsburgh, PA
*Corresponding author's email: lparola@andrew.cmu.edu

Introduction: Understanding of gait abnormalities following anterior cruciate ligament reconstruction (ACLR) has been primarily established from studies conducted in the laboratory, where participants are on their best behavior. The white coat syndrome, where patients exhibit higher blood pressure in the presence of a clinician than they do at home, is documented extensively in the cardiovascular literature, but the same phenomenon is not yet confirmed in gait analysis, although evidence in support is emerging. For example, a recent study found that in a gait laboratory participants adapted their speed, cadence, and stride length proportionally with the number of researchers present [1]. Accordingly, the aim of this study was to determine if laboratory environments cloud understanding of post-ACLR gait. We hypothesized that ACLR patients would exhibit higher gait cycle time, reliance on double support, and gait asymmetry in natural environments than in the laboratory. We also hypothesized that differences between ACLR patients and healthy individuals would be higher in natural environments than in laboratory.

Methods: Twelve subjects (6 post-ACLR 16.83 ± 2.48 years old; 6 healthy 22.83 ± 2.78 years old; balanced by sex) were recruited after IRB approval and informed consent to complete gait analysis both remotely and in the lab (Fig. 1A) with inertial measurement units (IMUs; MC10, Cambridge, MA). In the laboratory, they were monitored with four IMUs worn on the thighs and shanks and optical motion capture (OMC), while walking on a treadmill and overground at a self-selected speed. Participants also completed 5 days of remote monitoring while wearing four IMUs.

Walking bouts were segmented by using thresholding to identify stance (< 2 rad/sec) and swing (> 2 rad/sec) peaks from angular velocity data. Temporal and asymmetry outcomes were then computed by identifying toe off and heel contact from the shank angular velocities [2]. To test our leading hypotheses, we used multiple repeated measures ANOVAs followed by multiple t tests post hoc. A Bonferroni correction was used to account for multiple comparisons ($p_{sig} < 0.0166$).

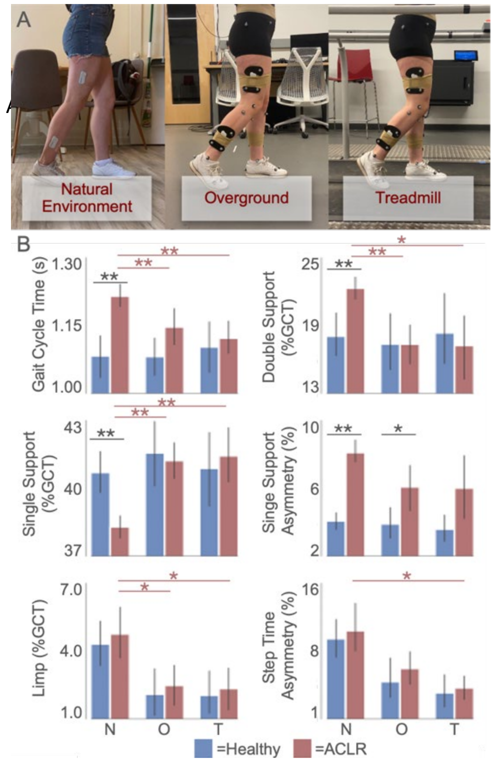

Figure 1: Study Overview. A) Monitoring took place in three environments: Natural Environments (N), Overground (O), and Treadmill (T). B) ACLR subjects walked asymetrically and limped more in natural environments than in the laboratory. Differences between ACLR and healthy subjects were more salient in natural environments than in the laboratory. (* $p < 0.05$; ** $p < 0.0166$; red bars = ACLR differences across environments; black bars = differences between groups)

Results & Discussion: ACLR patients walked with higher asymmetry and limp in natural environments than in the laboratory (Fig. 1B). Limp was 92.28% ($p = 0.045$) and 103.98% ($p = 0.044$) higher in natural environments than during overground and treadmill walking, respectively. Additionally, step time asymmetry was 62.94% higher ($p = 0.025$) in natural environments than the laboratory treadmill trial. Gait cycle time and double support in natural environments were 6.14% ($p = 0.011$) and 28.76% ($p = 0.003$) higher compared to overground walking and 8.54% ($p = 0.007$) and 29.66% ($p = 0.014$) higher compared to treadmill walking. These differences were greater than the respective mean absolute error of the IMU-derived outcome compared to the OMC-derived one, indicating that these differences were both statistically significant and meaningful.

ACLR patients walked similarly to healthy subjects in the laboratory, but in natural environments they demonstrated higher gait cycle time, double support time, and single support asymmetry than healthy subjects. In natural environments, differences between the two groups were 12.59% ($p = 0.001$), 23.67% ($p = 0.006$), and 8.95% ($p < 0.0001$) higher than in the laboratory. As noted above, these differences were also greater than the mean absolute error of IMUs-derived outcomes compared to OMC-derived ones.

These results suggest that our understanding of post-surgical gait until now may have been confounded by the effect of the laboratory. While this study was limited to temporal parameters of gait, they provide compelling evidence on the existence of a phenomenon akin to the white coat syndrome, motivating the move of biomechanics studies to natural environments.

Significance: Gait adaptation patterns following ACLR, and how they contribute in the progression of post-traumatic osteoarthritis, are still not fully understood, partly because of the limited tools we have had at our disposal. Wearable technologies now offer new opportunities for patient monitoring, promising to improve basic understanding of gait adaptation longitudinally, offering clinicians new information to adapt physical therapy accordingly, and forming the backbone of future smart-rehabilitation technologies with the patient in the loop, including biofeedback systems.

Acknowledgements: This work was partly supported by NIH R01AR080310. We thank Alexander Nguyen, Owen Pearl, and Mikayla Schneider for their help during data collection.

References: [1] Friesen et al., 2020, [2] Salarian et al 2004

PLANTARFLEXOR WEAKNESS AND LESSER ACHILLES TENDON STIFFNESS ASSOCIATE WITH GREATER VULNERABILITY TO WALKING BALANCE PERTURBATIONS

[1]Ross E. Smith*, [1]Andrew D. Shelton, [2]Gregory S. Sawicki, [1]Jason R. Franz
[1]Biomedical Engineering, UNC Chapel Hill and NC State University, Chapel Hill, NC, USA
[2]Mechanical Engineering, Georgia Tech, Atlanta, GA, USA
*Corresponding author's email: rsmit@ad.unc.edu

Introduction: Falls among older adults are a significant public health concern and can result in severe injuries with high healthcare costs. Intuitively, the ability to accommodate the instability elicited by walking balance challenges that could precipitate a fall can be impaired through age-related declines in sensory acuity and neuromuscular integrity. Foremost, sensory information from muscle stretch receptors requires rapid transmission of an unanticipated change in joint position. Age-related differences in sensory transmission are well-documented. However, tendon stiffness also decreases with age, which could delay and reduce the velocity of muscle spindle stretch and slow balance perturbation detection. Older adults also experience age-related decreases in muscle strength and power. Thus, even with requisite detection of a balance perturbation, weakness is likely to hinder older adults' ability to produce the requisite forces needed to mitigate instability. Ultimately, the association between tendon stiffness, muscle strength, and vulnerability to walking balance perturbations is not well understood [1]. Treadmill-induced slip perturbations emulate a situation in which falls among older adults are more likely. Moreover, given their proximity to the onset of those perturbations, factors associated with the integrity of muscle-tendon units spanning the ankle – namely Achilles tendon stiffness (k_{AT}) and plantarflexor muscle strength – are first line defenses against instability. Thus, the purpose of our study was to determine whether k_{AT} and plantarflexor strength were associated with vulnerability to treadmill-induced slip perturbations across a cohort of younger and older adults. We first hypothesized that older adults would exhibit lesser kAT and reduced plantarflexor strength compared to younger adults. We also hypothesized reduced k_{AT} and plantarflexor weakness would correlate with a greater vulnerability to perturbations. Data in support of our second hypothesis would provide evidence for potentially-modifiable factors and thus targets for intervention to mitigate falls risk.

Methods: 21 younger (21.7 ± 2.0 years, 66.4 ± 8.6 kg) and 22 older (74.0 ± 6.0 years, 69.5 ± 18.6 kg) adults participated. We first quantified subject's plantarflexor strength via peak torque values obtained from a series of two maximal voluntary isometric contractions in a Biodex dynamometer at a neutral ankle joint angle (0°) and at 20° knee flexion, which we normalized to body mass. We also used the dynamometer to quantify k_{AT} during passive, isokinetic ankle rotations from 20° plantarflexion to 30° dorsiflexion. Here, we record cine ultrasound images through a longitudinal cross section of the musculotendinous junction (MTJ) between the medial gastrocnemius and Achilles tendon (AT). We manually tracked time series of the MTJ position, which we transformed into a common marker coordinate system with a marker on the posterior calcaneus to estimate AT length change. We calculated AT force by dividing ankle torque during the passive rotations by a generalized moment arm length [2]. Finally, we calculated k_{AT} from the slope of the linear best fit relationship between AT force and tendon elongation between 20-80% of passive range. The same subjects also completed two treadmill walking trials. Specifically, in randomized order, participants walked for 2 minutes normally and again while responding to a series of treadmill-induced slip perturbations (200 ms duration, 6 m/s^2) applied randomly 5 times bilaterally at heel strike. We collected 3D motion capture from the trunk, pelvis, and legs and used scaled musculoskeletal models to estimate two balance outcomes - namely: (i) 3D whole-body angular momentum (WBAM), and (ii) anterior and lateral margins of stability (MoS).

Results & Discussion: Older adults had lesser k_{AT} during passive rotation than younger adults (4.33 ± 1.78 N/m vs. 6.12 ± 2.82 N/m, p = 0.016), but indistinguishable values of plantarflexor strength (p=0.865). We found no significant associations between k_{AT} and WBAM. However, across our study cohort, higher values of k_{AT} associated with lesser perturbation-induced changes in ML MoS (r=-0.303, p=0.048). Similarly across our study cohort, we found that lower plantarflexor strength associated with higher frontal (r=-0.350, p=0.021) and transverse (r=-0.402, p=0.008) WBAM range. Those latter correlations were also evident but moderately stronger in the older adult cohort alone. Finally, only in older adults, we found that lower plantarflexor strength associated with larger lateral MoS (r=-0.521, p=0.016).

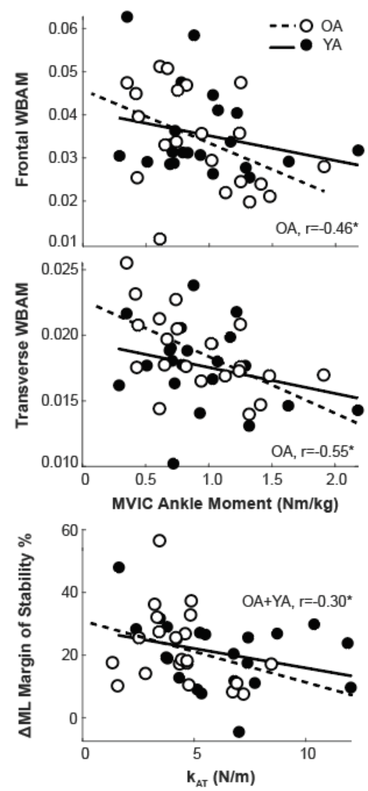

Figure 1. WBAM in the frontal (top) and transverse (middle) planes versus peak ankle torque for young adults in light grey (YA) and older adults in dark grey (OA). Mediolateral MoS (bottom) versus Achilles tendon stiffness (k_{AT}). Lines of best fit plotted for YA, OA, and Combined (black) with significant correlations (a=0.05) denoted by r-values.

Significance: This study points to potentially-modifiable factors (i.e., ankle strength and k_{AT}), that could help older adults mitigate walking instability following a perturbation.

Acknowledgements: This study was supported by grants from the NIH (R21AG067388, R01AR081287, R01AG058615).

References: [1] Granacher, et al. (2012), *J of Aging Res*.; [2] Rasske & Franz (2018), *J Biomech*, 77, 34-39.

IMPACT OF A COMPLEX NEUROMOTOR IMPAIRMENT ON LOCOMOTOR CONTROL AND EXECUTIVE FUNCTION DURING TREADMILL WALKING

Julia Manczurowsky[1*], Trevor L. Cline[2], Charles H. Hillman[1,2], Christopher J. Hasson[1]
Departments of [1]Physical Therapy, Movement and Rehabilitation Sciences, and [2]Psychology, Northeastern University
*Corresponding author's email: manczurowsky.j@northeastern.edu

Introduction: In rehabilitation science, biomechanics, sensorimotor control, and cognition are inexorably linked. As such, neuromotor impairments often act across these domains. For example, a stroke can impair muscular coordination, alter the normal distribution of muscle forces, introduce central and/or peripheral neuropathic pain, and disrupt executive function (EF) [1]. EF embodies a collection of cognitive processes that regulate goal-directed thoughts and actions and can be organized on a cold-hot axis according to logical (cold) and affective (hot) content [2]. Patients engaged in gait rehabilitation are asked to face this constellation of physiologic alterations while responding to feedback from a therapist or robotic system. Here, we aim to understand how the discoordinative and nociceptive aspects of a locomotor impairment affect cold and hot EF by testing the hypothesis that discoordination and nociception selectively tax cold and hot EF, respectively.

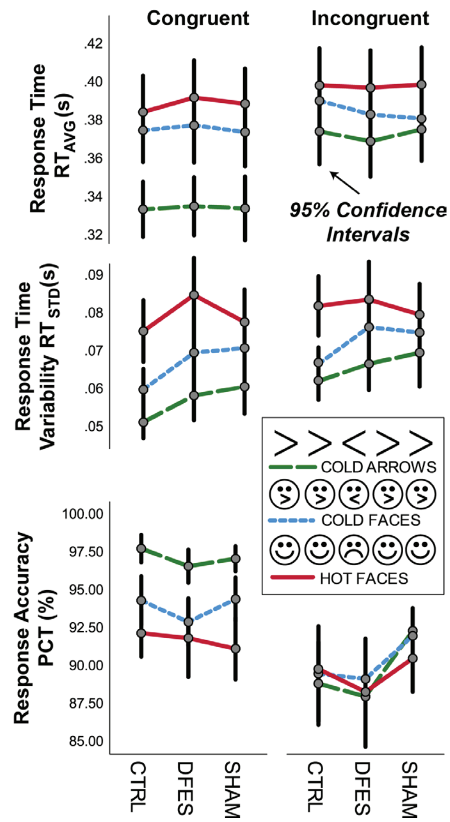

Figure 1: Effects of the artificial impairment and flanker type on flanker RT and PCT.

Methods: Twenty-four healthy participants (18-30 yrs.; 13 female) walked on a motorized treadmill at their preferred speed while experiencing dysfunctional electrical stimulation (DFES), which is a nociceptive disruption in muscular coordination that involuntarily activates the right hamstrings at the early swing phase. They were instructed to try to walk normally during counterbalanced blocks of trials with DFES, without stimulation (CTRL), and while receiving electrical stimulation to their right shoulder bony prominences (SHAM). During each walking condition, participants performed three types of flanker tasks, cold arrows, cold faces, and hot faces (Fig. 1), that required selective attention and inhibitory control. They were instructed to correctly identify, via button presses, the centrally presented image flanked by congruent (identical) or incongruent (opposite) distractors. The cold faces served as an affect-less control with a similar structure to the hot faces. Each flanker type was presented for 100 trials of equal congruent and incongruent versions. Dependent variables were stride-to-stride variability based on heel-strike timing (SV; an operationalized measure of locomotor control), reaction time mean and standard deviation across flanker types (RT_{AVG} and RT_{STD}, respectively), and flanker response accuracy (PCT). Flanker interferences were calculated within-subjects as the difference between incongruent and congruent values for each flanker performance metric. Statistical analyses were performed with SPSS using generalized linear mixed-effects models with walking condition (CRTL, DFES, SHAM), flanker type (cold arrows, cold faces, hot faces), and flanker congruency (congruent, incongruent) as within-subjects independent factors.

Results: For brevity, differences are reported only when $p < .05$. Pairwise comparisons using Holm-Bonferroni corrections followed significant omnibus tests. SV was higher in DFES than CTRL and SHAM, but there was no flanker type main effect or interaction. Compared to CTRL, walking with either DFES or SHAM made subjects more variable in their RTs on the flanker task (↑RT_{STD}; Fig. 1), but did not affect the response time (RT_{AVG}) or accuracy (PCT). The cold face flankers had worse flanker performance than the cold arrows, and the hot faces were worse than the cold face flankers (i.e., ↓RT_{AVG}, ↑RT_{STD}, and ↓PCT). As expected, across all flanker types, reaction times were longer (↑RT_{AVG}), more variable (↑RT_{STD}), and less accurate (↓PCT) for incongruent compared to congruent trials. The cold and hot faces had lower accuracy (↓PCT) than the cold arrows for congruent trials but were not different for incongruent trials. Interference effects were not different between CTRL and DFES for any of the flanker performance measures (RT_{AVG}, RT_{STD}, and PCT).

Discussion: DFES disrupted locomotor control as evident by an increase in stride-to-stride variability, but this variability was unaffected by performance of the three flanker tasks. We did not observe the hypothesized differential effect, i.e., discoordination (from DFES) and nociception (from DFES or SHAM) did not selectively tax the cold and hot ends of the EF spectrum, respectively. Neither DFES nor SHAM appreciably impacted flanker response time or accuracy; however, both perturbations increased response time variability. Since nociception is common to both DFES and SHAM, it seems that the painful part of the stimulation is the common driver of increased response time variability. The hot faces (affective flankers) had the lowest accuracy, but only for the congruent trials; this may be because of the greater visual complexity of the hot faces.

Significance: This was the first study investigating cold and hot executive function while walking with an artificial neuromotor impairment. Our paradigm provides the opportunity to study the interaction between motor adaptation and cognition in the same individuals with and without an experimentally controlled impairment. These results suggest that control processes associated with adaptation to a neuromotor impairment does not impact cold or hot executive function more than walking without the impairment. Administration of pain during walking appears to increase the variability associated with responding to visual stimuli, impacting executive function. Analysis is ongoing to examine covariates, such as variations in muscular/pain responses to the electrical stimulation.

References: [1] Tasseel-Ponche et al. (2022), *Eur J Neurol*; [2] Salehinejad et al. (2021), *Brain Neurosci Adv*

MEDIAL LONGITUDINAL ARCH ANGLE MEASURED DURING WALKING GAIT USING FLUOROSCOPIC RADIO-STEREOMETRIC ANALYSIS SHOWS DIFFERENCES BETWEEN BAREFOOT AND SHOED FEET

Kristen Bushey[1], Emma Smart[2] Thomas Jenkyn[1,2*]
[1]Department of Mechanical and Materials Engineering, Faculty of Engineering, University of Western Ontario
[2]School of Biomedical Engineering, Faculty of Engineering, University of Western Ontario
*Corresponding author's email: tjenkyn@uwo.ca

Introduction: The medial longitudinal arch (MLA) is a fundamental foot structure. Through its rise and fall during stance phase of gait, biomechanical forces are moderated and controlled. Two foot pathologies are defined by MLA behaviour [1]. When MLA fails to fall sufficiently one has pes cavus (high arches). When it fails to rise and stiffen the foot one has pes planus (flat feet). Measurement of the MLA during dynamic activity is therefore of clinical importance in diagnosing foot pathology. Typically the MLA is measured statically during quiet standing. It has recently become possible to measure MLA while dynamically loaded using fluoroscopic radio-stereometric analysis (fRSA) [2]. fRSA can be done while either barefoot or wearing shoes. This study measures the angle between the long axes of calcaneus and first metatarsal [3]. When the MLA falls this angle tends toward 180 degrees. When the MLA rises, this angle becomes smaller. It is hypothesized that MLA behaviour shows greater differences between pes cavus, normal and per planus feet when measured dynamically since the biomechanical loading is greater. It is also hypothesized that these differences are greater while barefoot since the foot in not constrained by footwear.

Methods: Test subjects walked along a raised platform above two x-ray fluoroscopes (Siemens Siremobil Compact-L). During each dynamic walking trial, the left foot landed at the spot where the two x-ray views converged giving two simultaneous views of the foot during stance phase. Each test subject also placed the left foot on this spot during quiet standing for the static condition. Each test subject was tested barefoot and with running shoes. The radio-stereometric analysis method was used to determine the three-dimensional pose of the calcaneus, navicular and first metatarsal bones in each frame of fluoroscopic data (Figure 1). Images were captured at 60 Hz. Six test subjects were recruited for the pes cavus, normal and per planus groups as diagnosed by a certified Canadian Pedorthist.

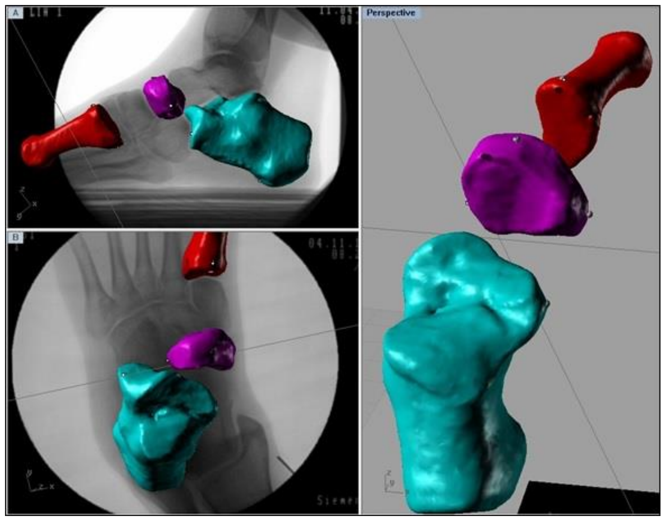

Figure 1: Tracking the calcaneus, navicular and first metatarsal bones during walking gait using fRSA allows the MLA angle to be measured during dynamic loading.

Results & Discussion: Table 1 shows average MLA angles (and range) for barefoot and shoe conditions during both static standing and dynamic gait. Pes cavus had the smallest mean MLA angle for static and dynamic loading. Pes planus had the largest static and dynamic angles. These both differed from the normal MLA angles. Ranges of motion were the smallest in the pes planus group. As hypothesized, dynamic walking gait resulted in a greater mean MLA angle for the normal group compared to static. However, the pes cavus and pes planus foot types did not see a significant difference between static and dynamic conditions. Mean MLA angles increased during barefoot compared to shoed conditions for all foot types and during both static and dynamic loading as hypothesized, except for normal feet during static loading. This perhaps shows the importance of assessing the behaviour of the MLA during dynamic loading since static loading does not challenge the MLA sufficiently for diagnosis.

MLA Angle Measurement	STATIC			DYNAMIC		
	Cavus (n=5)	Normal (n=5)	Planus (n=5)	Cavus (n=5)	Normal (n=5)	Planus (n=4)
Barefoot	**120** (5.6)	**129** (6.8)	**141** (4.4)	**119** (8.1)	**133**(7.7)	**141** (4.7)
Shoe	**118** (9.1)	**130** (7.0)	**140** (4.4)	**119**(9.1)	**132** (8.3)	**139** (4.7)
Mean angle difference	**-1.59** (3.8)	**0.80** (1.7)	**-0.87** (1.9)	**-0.11** (2.4)	**-1.14** (2.6)	**-1.80** (1.8)

Table 1: MLA angle was greater with pes planus and smaller with pes cavus compared to normal feet. The range of motion of the MLA was greater during dynamic loading compared to static.

Significance: The study suggests that clinical assessment of the MLA and the diagnosis of pes cavus and pes planus feet should be done during dynamic loading conditions rather than during quiet standing, which is static.

Acknowledgements: This research is supported by the Canada Foundation for Innovation (CFI)

References: [1] Franco AH. (1987), *Physical Therapy 67(5)*; [2] Balsdon ME et al (2016), *J Biomed Eng 138(10)*; [3] Tome J et al (2006), *J Orthop Sports Physical Therapy 36(9)*.

EFFECTS OF SUBMAXIMAL TREADMILL RUNNING ON PLANTAR FASCIA PROPERTIES IN RESOLVED PLANTAR FASCIITIS INDIVIDUALS

Lukas Krumpl[1*], Joshua P. Bailey[1]
[1]Department of Movement Sciences, University of Idaho, Moscow, ID, USA
*Corresponding author's email: lkrumpl@uidaho.edu

Introduction: The underlying mechanisms of plantar fasciitis are still unknown. Theories regarding the mechanical sequence of tissue creep suggest that repetitive loading leads to an initial thinning of the plantar fascia (PF), followed by an inflammatory reparative process. As theorized, PF thickness and stiffness decrease after one running bout, but approximate pre-exercise values after 30 minutes of recovery in individuals without history of plantar fasciitis [1]. The decrease in PF thickness and stiffness after running indicates that the PF behaves viscoelastically in plantar fasciitis asymptomatic individuals. Yet, little is known as to whether these PF property mechanics maintain after injury and pain have subsided.

Individuals with plantar fasciitis show increased thickness and decreased stiffness of PF [2,3]. The etiological relationship between these mechanical property differences and the development of plantar fasciitis are however unknown. Additionally, it is unclear how the PF responds once the pain is resolved compared to tissue that has not been previously injured in response to a running stimulus. Thus, the purpose of this study was to evaluate the effects of a 30-minute submaximal treadmill run on PF thickness and stiffness in individuals with resolved plantar fasciitis versus those with no history of plantar fasciitis.

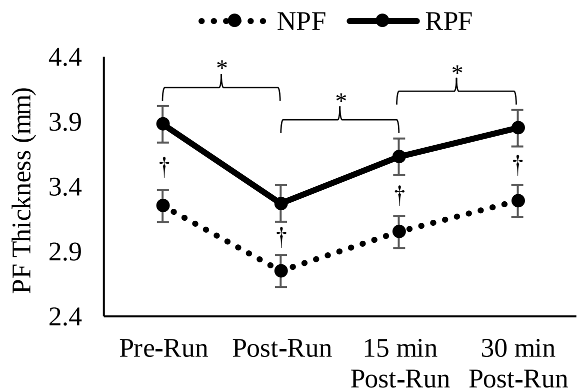

Figure 1: PF Thickness (mm) measurements for the no plantar fasciitis (NPF) and resolved plantar fasciitis groups (RPF). *Denotes a significant difference between the two adjacent PF measurements regardless of group. †Denotes a significant difference in PF thickness measurements between the two groups.

Methods: Twenty healthy individuals participated in this study. Eight participants had resolved plantar fasciitis (RPF) (4 females; age: 25.1yrs [±9.8]; mass: 69.4kg [±12.2], height 180.2cm [±11.3]). Resolved plantar fasciitis was defined as having had no symptoms for at least one month [4]. Twelve participants had no plantar fasciitis (NPF) history (2 females; age: 23.7yrs [±5.4]; mass: 70.8kg [±8.5], height 177.5cm [±7.1]). Participants performed a maximal effort graded exercise test prior to determine ventilatory threshold 2 (VT2). 80% of the speed at VT2 was used as relative velocity for the 30-minute submaximal run. PF thickness and stiffness were recorded with ultrasonography (LOGIQ S8, GE, Boston, MA, USA) at four time points (before, immediately after, 15 minutes after, and 30 minutes after the run). Thickness was captured via B-mode and stiffness was measured via shear wave elastography. Three live images for each property were taken per time point. Thickness was measured in mm, while stiffness was measured in m/s. Data were analyzed via mixed model (2 group x 4 time) repeated measures ANOVAs, and significant findings were explored with *post-hoc* t-tests. Statistical analyses were completed via SPSS (v.29.0) with alpha levels set at .05.

Results & Discussion: Analyses showed a significant main effect of time (p<0.001), and a significant main effect of group for PF thickness (p=0.042). Regardless of group, *post-hoc* t-tests revealed that thickness decreased between pre- and post-run (p<0.001; 3.4 to 2.9mm) & increased from post- to 15 min post-run (p<0.001; 2.9 to 3.25mm) and from 15 min post- and 30 min post-run (p<0.001; 3.25 to 3.49mm) (Fig 1). Between groups, *post-hoc* t-tests revealed that the RPF group had a greater PF thickness compared to the NPF group at the pre-run (p=0.016; 3.84 vs. 3.21mm), the post-run (p=0.041; 3.28 vs. 2.65mm), the 15 min post-run (p=0.035; 3.58 vs. 2.93mm), and the 30 min post-run (p=0.045; 3.81 vs. 3.18) measurements (Fig 1). There was a significant main effect of time (p<0.001) and for group for PF stiffness (p=0.018). Regardless of group, *post-hoc* t-tests revealed that PF stiffness decreased from pre- to post-run (p<0.001; 4.11 to 3.13m/s), increased from post- to 15 min post-run (p<0.001; 3.13 to 3.81m/s) but did not change from 15 min post-run to 30 min post-run measurements. Between groups, *post-hoc* t-tests revealed that the RPF group had a greater PF stiffness compared to the NPF group at the pre-run (p=0.03; 4.54 vs. 3.68m/s) and the 30 min post-run (p=0.002; 4.7 vs 3.62m/s) measurements only.

These findings indicate that the properties of the PF of both asymptomatic and resolved plantar fasciitis individuals behave similarly in response to submaximal treadmill running stimuli. However, mean thickness and stiffness were greater in the RPF group compared to the NPF group for most measurements. This suggests that previous plantar fasciitis alters the morphology of the tissue long term, yet its viscoelastic properties and responses maintain. However, this is a retrospective study and the tissue behavior of the RPF group is unknown prior to their injury history.

Significance: To the knowledge of the authors, this is the first study to evaluate PF tissue response to submaximal running in individuals with resolved plantar fasciitis. The results indicate that tissue response to mechanical loading, as well as the acute recovery period, do not change with injury history once resolved. This outcome provides essential information for understanding how previously injured PF tissue reacts to mechanical loading, and potentially creates new avenues to evaluate PF injury prevention strategies.

References: [1] Shiotani et al. (2020), *Scand J Med & Sc Sports* 30(8); [2] Baur et al. (2021), *J Clin Med* 10(11); [3] Goff et al. (2011), *Am Fam Physician* 84(6); [4] Wiegand et al. (2022), *Clin Biomech* 97.

CHRONIC LOW BACK PAIN IS ASSOCIATED WITH LARGER SPINAL COMPRESSIVE LOADS DURING WALKING WITH UNILATERAL TRANSTIBIAL AMPUTATION

Courtney M. Butowicz[1-3*], Pawel R. Golyski[1,2], Julian C. Acasio[1,2], Brad D. Hendershot[1-3]
[1]Defense Health Agency: Extremity Trauma and Amputation Center of Excellence, Falls Church, VA, USA
[2]Walter Reed National Military Medical Center, Bethesda, MD, USA
[3]Uniformed Services University of the Health Sciences, Bethesda, MD, USA
*Corresponding author's email: courtney.m.butowicz.civ@health.mil

Introduction: Chronic low back pain (cLBP) is highly prevalent among persons with lower limb amputation and is strongly associated with reduced quality of life [1]. After amputation, cLBP risk is often linked to repeated exposures to aberrant trunk-pelvic motions and trunk muscle activations during walking [2], corresponding to 50% larger spinal loads among persons with vs. without amputation [3]. Recent work has reported a higher percentage of persons with transtibial (TTA) vs. transfemoral amputation within cLBP groups [4], despite relatively smaller trunk-pelvic motions, potentially challenging the biomechanical contributions to LBP onset/recurrence. Therefore, the purpose of this study was to use a TTA-specific model to investigate the influence of cLBP (i.e., pain > 3 months and ≥ half the days in the last 6 months) on spinal loads during walking among persons with TTA. We hypothesized that those with vs. without cLBP would demonstrate larger peak L5-S1 compression and mediolateral shear forces.

Methods: Full-body kinematics and bilateral ground reaction forces during level-ground walking were collected at three speeds (self-selected [1.25±0.7], 1.0, and 1.6m/s) for ten males with unilateral TTA: 4 with no cLBP (age: 34±6yrs, stature: 1.8±0.1m, time since TTA: 112.5±57.4mo) and 6 with cLBP (age: 40±7yrs, stature: 1.8±0.1m, time since TTA: 79.8±26.7mo). A full-body, unilateral TTA-specific model was developed from validated OpenSim models [5,6] with muscle forces estimated using static optimization in OpenSim 4.4, to calculate peak (i.e., maximum absolute value) compressive, mediolateral, and anteroposterior spinal loads at L5-S1. A linear mixed model with a fixed effect of pain status (cLBP or no pain) and a covariate of walking speed during each trial was used determine the main and interactive effects of pain status and walking speed ($p<0.05$).

Results & Discussion: There was a significant main effect of cLBP ($p=0.02$) and interaction between cLBP and walking speed ($p<0.001$) on L5S1 peak compressive force, where larger differences between groups (cLBP vs. no cLBP) were noted at faster walking speeds (Figure 1). However, there were no effects of cLBP on anteroposterior ($p=0.3$) or mediolateral ($p=0.7$) shear forces. These findings partially support our hypothesis that spinal loads would be larger among TTA with vs. without cLBP; of note, the similar mediolateral shear forces between groups are inconsistent with previous work [4,7]. Larger compressive loads with cLBP support previous evidence suggesting these individuals freeze degrees of freedom during walking to minimize shear forces on the spine [4]. A secondary analysis confirms that the cLBP group walked with smaller or similiar trunk ranges of motion in the axial (~1°) and mediolateral (~5°) directions, and in a ~15° more extended trunk posture.

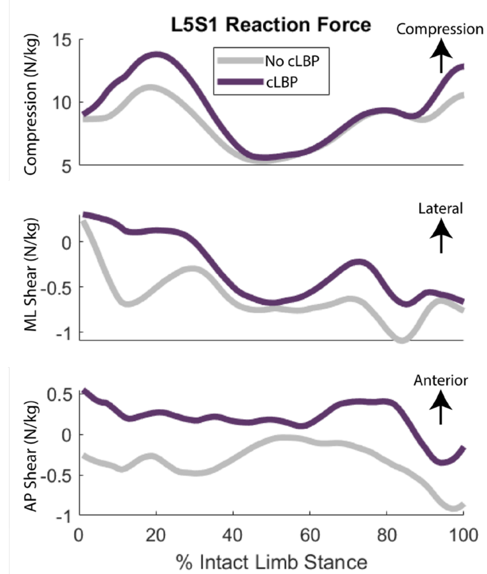

Figure 1: Ensemble mean (across all speeds and participants) compressive, mediolateral (ML), and anteroposterior (AP) forces on L5S1 vertebrae during walking among persons with unilateral transtibial amputation, with and without chronic low back pain (cLBP). Values were normalized to participant body mass.

Significance: Understanding potential mechanisms underlying pain recurrence, particularly among persons with TTA (the majority of lower limb amputations in the last 20 years), during activities such as walking is important given ambulation is a key outcome after amputation and is associated with independence and community reintegration. Moreover, those with TTA (vs. more proximal or bilateral amputations) are typically more active, which may elevate exposures to biomechanical risk factors and thus expansion to other activities is likely warranted. Establishing links between these factors and the implications on tissue or structural degeneration of the spine will allow practitioners to proactively mitigate persistence of pain (e.g., gait retraining, trunk neuromuscular control) as part of a comprehensive rehabilitation program that addresses the multifactorial nature of cLBP. Ultimately, reducing the onset or recurrence of pain will help maximize long-term quality of life, especially for younger persons with traumatic amputations (e.g., Service members) who have several decades of remaining life expectancy.

Acknowledgements: This work was supported, in part, by the National Center for Medical Rehabilitation Research (NIH-NICHD; award #5R03HD086512-02) and the Peer Reviewed Orthopaedic Research Program (PRORP; award #W81XWH-14-2-0144). The views expressed are those of the authors, and do not reflect the official policy of the USUHS, U.S. Departments of the Army, Navy, Defense, nor the U.S. Government.

References: [1] Taghipour (2009) *J Ortho Trauma* 23(7); [2] Butowicz (2018) *JEK* 40(48); [3] Hendershot (2018) *J Biomech* 70(249); [4] Acasio (2022) *J Biomech* 135(111); [5] Raabe (2016) *J Biomech* 49(7); [6] Willson (2022) *Comp Meth Biomech Biomed Eng*; [7] Yoder et al. (2015) *Gait Posture* 41(3).

SHEAR WAVE TENSIOMETRY REVEALS INDIVIDUAL ADAPTATIONS TO PASSIVE PLANTARFLEXOR ASSISTANCE DURING WALKING

Dylan G. Schmitz[1*], Sara E. Harper[1], Alex J. Reiter[1], Darryl G. Thelen[1]
[1]University of Wisconsin–Madison, Department of Mechanical Engineering, Madison, WI, USA
*dgschmitz@wisc.edu

Introduction: Exoskeletons which assist plantarflexion during walking can reduce energy cost [1,2]. Individualized assistance is key to the success of these devices, but the nuances of how an individual adapts to assistance is an open question. Motion analysis can characterize kinetic responses to exoskeletons, e.g., biological torque, computed by subtracting the external exoskeleton torque from the net ankle torque computed via inverse dynamics [2]. This is often used to understand the contributions of ankle assistance to plantarflexion torque during walking, but this simple additive model cannot distinguish between co-agonist and antagonist muscles. As such, ankle assistance consistently reduces net biological torque [3,4], while individual muscles contribute to variability at the whole-body metabolic level. Tissue-level measures are achievable using shear wave tensiometry, which tracks wave speed in biological tissues (e.g. the Achilles tendon) as a proxy for muscle-tendon loading [5]. In this study, we use shear wave tensiometry to delineate individual biomechanical adaptations to passive exoskeleton assistance during walking.

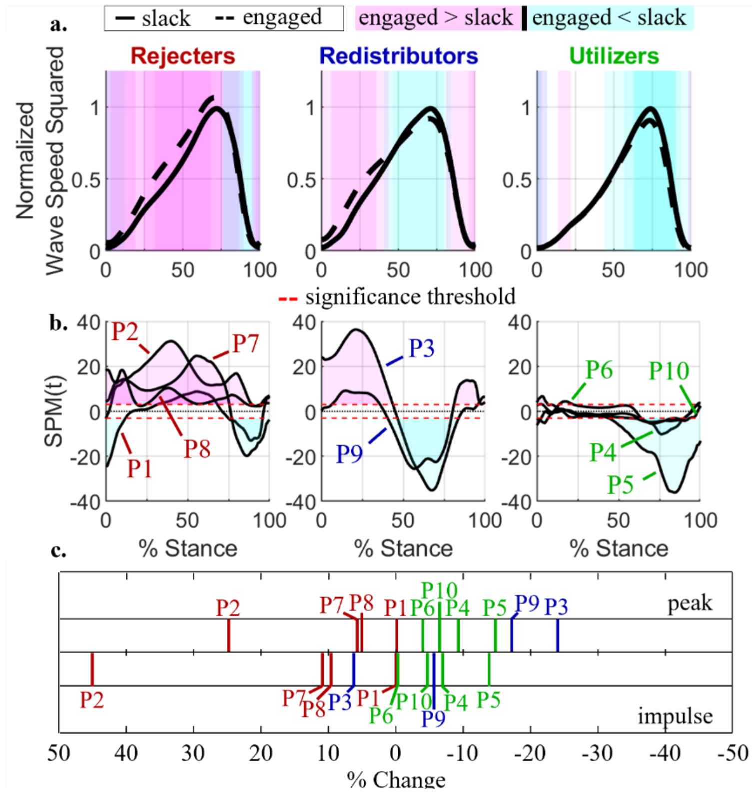

Figure 1: (a) Mean slack and engaged wave speed squared for each group. (b) SPM for each participant. (c) Average percent change in peak and impulse (mean*duration) loading by participant.

Methods: A passive elastic exoskeleton was designed and constructed to provide external supplementary plantarflexion torque during the propulsive phase of walking. The device was inspired by the designs published in [1,6], with a net angular stiffness of ~20 N-m/rad when engaged. After a brief, separate training session, healthy young adult participants ($n = 10$) walked on a treadmill at 1.25 m/s with the exoskeleton slack (zero angular stiffness) and engaged. Kinematics (inertial measurement units), exoskeleton force, triceps surae and tibialis anterior muscle activity (right limb), and Achilles tendon wave speeds (right limb) were recorded simultaneously. Statistical parametric mapping (SPM) quantified significance between conditions ($\alpha = 0.05$).

Results & Discussion: Participants exhibited varied changes in Achilles tendon loading patterns to the engaged exoskeleton assistance, from which three categories of adaptation were identified: utilizers, rejecters, and redistributors (Fig. 1a,b). Utilizers successfully harnessed the supplementary plantarflexion torque, maintaining near normal levels of Achilles loading through the first half of stance, but diminished Achilles tendon loading at pushoff by up to 15% at peak. Rejecters exhibited elevated loading (up to 25% at peak) throughout much of stance when compared to the slack condition. These utilizer/rejecter responses were similar to responder/non-responder behaviors observed in literature [7], respectively. Interestingly, the third category (redistributors) achieved the greatest reductions in peak force by preloading the triceps surae in early stance. We recognize that individual adaptations to exoskeletons fall on a continuum (Fig. 1c), while also finding value in classifying individual responses. For example, the training strategies required to help a rejecter become a utilizer (or redistributor, based on desired outcomes) are likely to vary between individuals and depend on the baseline characterization.

Significance: This study demonstrates the potential to characterize individual adaptations to an exoskeleton based on tendon loading patterns. We used the approach to delineate rejectors, redistributors, and utilizers of an exoskeleton. Such information could enable tuning of an exoskeleton device or controller for an individual, or be used as real-time biofeedback to train a successful adaptation strategy.

Acknowledgements: This work was funded by the NSF GRFP (DGE-1747503), NSF DARE (CBET-2019621), NIH TL1 (TL1TR002375), and DoD (129866603). Thank you, Elizabeth Schmida and Karen Walker for assisting data collection and analysis.

References: [5] Collins+ (2015). *Nature*, 522(7555). [2] Nuckols+ (2020). *Sci Rep*, 10(1). [3] Jackson+ (2015). *J Appl Phys*, 119(5). [4] Durandau+ (2022). *IEEE Trans Rob*, 38(3). [5] Martin+, (2018). *Nat Comm*, 9(1). [6] Yandell+ (2019). *IEEE Trans Neural Sys Rehab Eng*, 27(4). [7] Lee+ (2021). *IEEE Trans Biomed Eng*, 68(9).

MODULATION OF PATELLAR TENDON LOADING DURING RUNNING WITH REAL-TIME BIOFEEDBACK

Elizabeth A. Schmida[1*], Sara E. Harper[2], Darryl G. Thelen[1]
[1]Department of Mechanical Engineering, [2]Department of Biomedical Engineering, University of Wisconsin-Madison
*schmida@ortho.wisc.edu

Introduction: Increasing step rate during running has been shown to decrease loading at the knee and is thus a common gait retraining strategy used to treat and prevent anterior knee pain [1]. However, quantifying knee loads to ensure a particular change in step rate has a meaningful change in loading for an individual generally requires full motion analysis and is therefore rarely used as biofeedback. Patellar tendon (PT) shear wave speeds can be measured in real-time using a wearable tensiometer and may serve as a proxy for tendon loading [2]. Tensiometry thus has the potential to evaluate intervention efficacy and to further reinforce the value of gait retraining to runners. The purpose of this study was to 1) determine if real-time PT tensiometry can track changes in PT loading with modulation of step rate and 2) assess if visual feedback from real-time tensiometry can facilitate further decreases in PT loading during running.

Methods: A tensiometer [3] was placed over the PT of each runner's dominant limb. A MATLAB app was used to record and display live wave speeds (Fig. 1A). Lower body inertial measurement units simultaneously captured joint kinematics. Three healthy adults (2F, 29±5 years) participated in 2 blocks of testing. Each block consisted of three randomly ordered treadmill running trials (2.68 m/s) at +0%, +5%, and +10% preferred step rate. In Block 1, a metronome guided the target step rate. In Block 2, visual wave speed feedback supplemented the metronome. The wave speed display included a target line representing the average peak wave speed from the corresponding step rate in Block 1. Runners were asked to keep step with the metronome and adapt their running to decrease wave speed below the target line, with no further instructions. Runners practiced running at each step rate with the prescribed feedback, before a 15-second trial was recorded. For analysis, wave speeds were normalized to each runner's peak wave speed at their preferred step rate from Block 1. Time series data were averaged across runners for each condition.

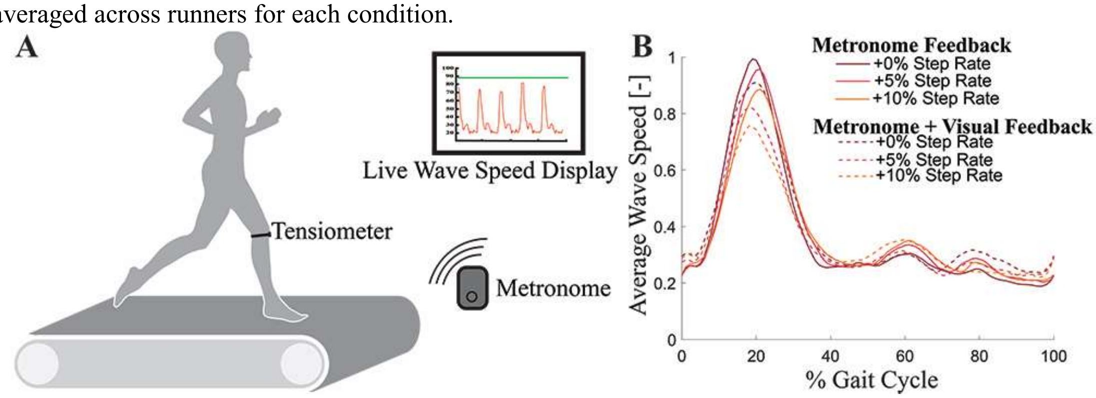

Figure 1: (A) Test setup with visual and audio feedback. **(B)** Average normalized patellar tendon wave speed for each feedback modality and step rate condition while running at 2.68 m/s.

Results & Discussion: As expected, peak PT wave speed decreased with 5% (-4%) and 10% (-11%) increases in step rate (Fig. 1B). The reduction in PT loading was accompanied by less peak knee flexion and vertical center of mass (vCOM) motion (Table 1). All runners further reduced peak PT wave speed when provided real-time biofeedback. For example, running at a +5% step rate with real-time biofeedback achieved an additional 14% reduction in peak wave speed from the nominal condition. To do this, runners ran with a more extended knee (+3.5°) and substantially greater plantar flexion (+6.8°) at foot strike.

Table 1: Summary of patellar tendon (PT) wave speeds and kinematics (mean(standard deviation)) at each step rate condition across testing blocks (Block 1 = metronome only feedback; Block 2 = metronome + visual feedback).

Percent of Preferred Step Rate	Peak Normalized PT Wave Speed [-]		Peak Knee Flexion Angle (stance phase) [°]		Plantar Flexion Angle (foot strike) [°]		Vertical Center of Mass Excursion [cm]	
	Block 1	Block 2	Block 1	Block 2	Block 1	Block 2	Block 1	Block 2
+0%	0.99(0.06)	0.91(0.17)	33.7(2.53)	32.7(3.58)	2.3(6.51)	10.3(5.53)	5.71(0.54)	5.61(0.70)
+5%	0.96(0.06)	0.82(0.11)	32.3(2.91)	30.2(3.88)	1.8(5.49)	9.1(6.60)	4.95(0.66)	5.01(0.80)
+10%	0.89(0.08)	0.76(0.11)	30.7(2.16)	27.3(3.57)	1.2(4.86)	9.7(4.36)	4.57(0.48)	4.63(0.75)

This study suggests that wave speed can quantify the effect of a running gait intervention on anterior knee loads. The reductions with step rate are consistent with metrics obtained via conventional motion analysis and biomechanical modeling [1,4]. The more salient finding is that real-time feedback of wave speed can facilitate further decreases in anterior knee loading. When provided visual feedback, the runners adopted a more forefoot strike pattern and extended knee to reduce PT wave speed. We note that our collection trials were relatively short, such that runners were likely continuing to explore the solution space. Further, our study was only designed to assess if runners could modulate PT loading with real-time biofeedback. Additional testing is needed to assess whether such adaptations in PT loading are warranted given the potential for compensatory strategies to alter injury risk elsewhere.

Significance: This study demonstrates the potential for tensiometry biofeedback to both reinforce and facilitate reductions in knee loading by modifying running gait patterns. Such interactive technology could empower clinicians and runners to assess the benefits of gait retraining through personalized quantitative results.

Acknowledgements: Funded by NIH STTR grant R42AR074897. Dylan Schmitz and Karen Walker contributed to the technology.

References: [1] Lenhart et al. (2014), *Med Sci Sports Exerc*. 46(3); [2] Martin et al. (2018), *Nat Commun*. 9(1592); [3] Schmitz et al. (2022), *Sensors*. 22(6); [4] Heiderscheit et al. (2011), *Med Sci Sports Exerc*. 43(2).

AGE AFFECTS MECHANICAL TRANSMISSION BETWEEN METATARSAL PHALANGEAL JOINT EXTENSION AND PLANTARFLEXOR MUSCLE LENGTHENING

Aubrey Gray[1*], Rebecca L. Krupenevich[1], Kota Takahashi[2], Jason R. Franz[1]
[1]Joint Department of Biomedical Engineering at University of North Carolina Chapel Hill and North Carolina State University
[2]Department of Health & Kinesiology, University of Utah
*Corresponding author's email: graaj@email.unc.edu

Introduction: Neuromechanical interaction between the human foot and ankle is critical for generating an effective push-off during walking. Reduction of walking independence in older adults has principally been attributed to a reduction in push-off power due to a deficit in ankle plantarflexor force-generating capacity [1]. Recent cadaveric studies describe a structural connection between the plantar aponeurosis (PA) and Achilles tendon (AT) [2]. Although there is some debate on whether the structural connection is only present in fetal/neonatal populations or whether it is present throughout the lifespan [2], we interpret those discoveries to suggest that foot-ankle interaction during functional activities such as walking may be more valuable and complex than previously appreciated. Indeed, Singh et al. found experimental evidence for force transmission spanning this connection [2]. Moreover, there is additional evidence that this connection ossifies with advanced age, which could weaken force transmission between the foot and ankle. The purpose of this study was to introduce a novel measure of the capacity for mechanical transmission between the metatarsal phalangeal joint (MTP joint) and the plantarflexor muscles most responsible for push-off power generation, and to compare that measure between younger and older adults. Specifically, we introduce FAMT (foot-ankle mechanical transmission), a measure of mechanical transmission defined as the ratio of medial gastrocnemius fascicle length to change in MTP joint angle during isolated contractions. We hypothesized that FAMT would be lesser in older adults than in younger adults.

Methods: 14 healthy younger (25±6 yrs, 73.2±9.5 kg, 1.78±0.10 m, 7M/7F) and 15 healthy older (71±5 yrs, 75.1±13.6 kg, 1.72±0.12 m, 7M/8F0) adults participated after being screened for lower extremity injuries in the last 6 months and neurological disorders affecting the lower extremity. Data collections consisted of one barefoot walking trial on an instrumented treadmill and a series of maximum voluntary isometric contractions (MVICs) on a custom MTP joint dynamometer. MVICs were performed at a combination of 9 combinations of 3 ankle angles (20° dorsiflexion, 0°, and 20° plantarflexion) and 3 MTP joint angles (0°, 30°, and 60° MTP extension). We block randomized postures and *in vivo* cine B-mode images of the medial gastrocnemius were recorded using a 10 MHz, 60 mm linear array ultrasound transducer (LV7.5/60/128Z-2, Telemed Echo Blaster 128, Lithuania). We processed ultrasound images using UltraTrack to obtain time series of gastrocnemius fascicle lengths [3]. We have thus far calculated mechanical transmission at a neutral ankle angle of 0°, which we did both at rest and at maximum activation. We used a three-way ANOVA to analyze differences in FAMT due to activation, age, and range of motion (i.e., 0-30° and 30-60° MTP extension).

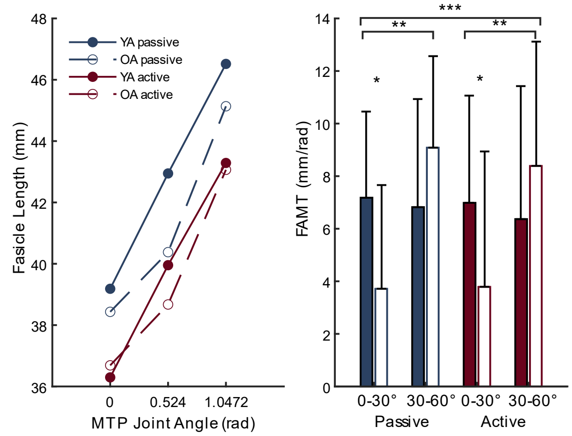

Figure 1. *Mechanical transmission in a neutral ankle position while changing MTP joint angle across younger and older adult groups (*age, **range of motion, ***age×range of motion interaction, p<0.05).*

Results & Discussion: As hypothesized, older adults exhibited lower FAMT than younger adults for both passive (-48.3%, p=0.010) and active (-45.8%, p=0.042) conditions during initial lengthening of the PA from 0-30° MTP extension. However, supported by a significant age × range of motion interaction (p=0.001) and the nonlinear FAMT behavior exclusively found in older adults, we found no age difference as the PA was further lengthened from 30° to 60° MTP extension, at least at the neutral ankle angle. This primary discovery could be explained by at least two age-related differences to the structures that govern foot-ankle mechanical transmission – namely, ossification of the structural connection between the PA and AT or increased compliance if the respective tendinous tissues. We also found a significant range of motion effect (p=0.007) (Fig. 1), which showed that FAMT in older adults increased significantly from 0-30° MTP extension to 30°-60° MTP extension. Despite some differences due to MTP range of motion, we find that older adults have a reduced capacity for mechanical transmission between the foot and ankle during fixed contractions. Ongoing work as a part of this immediate study will correlate FAMT across younger and older adults and across varying ankle postures with biomechanical outcomes such as ankle joint power output measured during walking.

Significance: This work contributes in novel ways toward better understanding age-related differences in foot and ankle joint mechanics to include insight into the role and functional relevance of a structural connection between the PA and AT.

Acknowledgements: We would like to acknowledge Dr. Ross Smith and Yujin Kwon for their assistance in data collections. This study was funded by NIH (R01AR081287).

References: [1] Krupenevich, R.L., et. al. (2021) *Journal of Biomechanics*, **123**(110499) [2] Singh, A., et. al. (2021) *Scientific Reports*, **11**(5986) [3] Farris, D.J., et. al. (2016) *Comput Methods Programs Biomed*, **128**(111-8)

UTILIZING WEIGHT BEARING CT TO EVALUATE PTOA RISK AFTER ACL RECONSTRUCTION

Tyce C. Marquez[1*], Shannon Ortiz[1], Brian R. Wolf[1], Donald D. Anderson[1]
[1]University of Iowa, Iowa City, IA
tyce-marquez@uiowa.edu

Introduction: The risk of post-traumatic osteoarthritis (PTOA) after ACL injury is high, with around 50% of individuals experiencing symptoms 10 to 20 years after injury [1]. ACL reconstruction (ACLR) is performed to restore function but does not reduce PTOA risk. Efforts to mitigate PTOA risk after ACL injury have been challenged by the lack of a sensitive, specific, and affordable early imaging marker. However, recent reports have linked the load-bearing pose of the knee following ACLR to early compositional MRI changes in articular cartilage consistent with PTOA [2]. We are investigating the potential for weight bearing CT (WBCT) to provide PTOA-predictive knee pose information and 3D joint space width (JSW) measures that are objective, affordable, and easy to collect. We recently developed a fully automated method to measure tibiofemoral 3D JSW from WBCT [3] that may be useful in this context. This study reports the preliminary cross-sectional results of automated 3D JSW measurements for intact and ACLR knees.

Methods: Twenty-one subjects ≥14 years old with a unilateral isolated partial or complete ACL tear reconstructed by one of three surgeons were recruited to participate in this IRB-approved study. Bilateral WBCT knee scans were acquired at 3 months after ACLR surgery for all subjects, with the knee in a semi-flexed (~30°) position [4]. Additional WBCT scans were acquired for 6 subjects at the same visit with the knee in a fully extended position. Maps of the 3D JSW, which depict the bone-to-bone distances across the apposed tibiofemoral surfaces, were generated for both intact contralateral and ACLR knees using the fully automated 3D JSW measurement methods [3]. The margins of the tibiofemoral articulation were defined as regions with JSW<10 mm. Portions of the tibiofemoral articulation with JSW<5 mm were identified as a meaningful approximation of the contact patch and an eventual indicator of joint space narrowing. Each subject's ACLR and intact knee 3D JSW distribution was graphed for comparison on a subject-to-subject basis.

Results & Discussion: On a subject-to-subject basis, the ACLR and intact knees demonstrated similar JSW distributions in the semi-flexed position (Fig. 1). The average percentage of JSW values below the 5 mm threshold for the semi-flexed WBCT scans were less than for the fully extended WBCT scans for both the medial and lateral tibiofemoral compartments (Fig. 2). The difference between semi-flexed and fully extended WBCT scans in average percentage of JSW values below the threshold was 5.52±13.69% for the lateral compartment and 7.29±29.92% for the medial compartment. As a result of a more conservative JSW distribution from the semi-flexed WBCT scans, comparison of ACLR and intact knee JSW distribution was limited to only semi-flexed WBCT scans. Additionally, subject-to-subject JSW distribution for ACLR and intact knees was limited to the medial compartment due to its greater percentage of JSW values below the set threshold. These findings suggest comparing JSW distributions for ACLR and intact knees using semi-flexed WBCT scans may be a useful tool for monitoring PTOA.

Significance: WBCT provides a cost-effective and easy method to evaluate PTOA progression following ACLR surgery.

Acknowledgements: This research was supported by a grant from the Arthritis Foundation (Award #851789).

References: [1] Lohmander LS, et al. Am J Sports Med. (2007), 35(10):1756-69. [2] Lansdown DA, et al. J Orthop Res. (2020), 38(6):1289-95. [3] McFadden EJ et al. Osteoarthritis Cartilage. (2022), 30(S1):S284-5. [4] Segal NA, et al. Osteoarthritis Cartilage. (2023), 31(3):406-13.

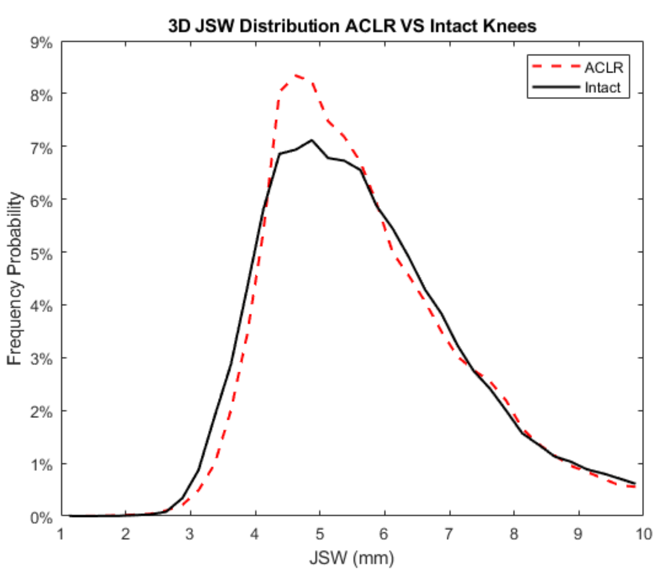

Figure 1: 3D JSW Distribution Comparison Between ACLR and Intact Knees

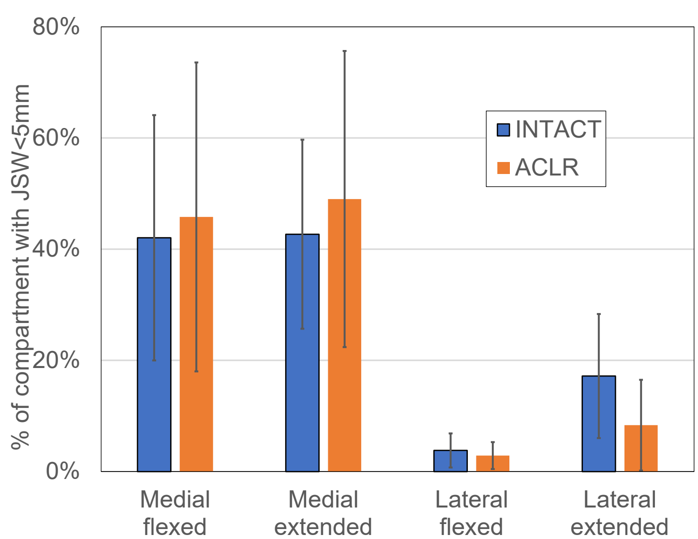

Figure 2: Comparison of Percentage of 3D JSW Distribution below 5 mm Between Flexed and Extended Scans

THE EFFECTS OF AGE AND TASK DEMAND ON DYNAMIC MEAN ANKLE MOMENT ARM DURING WALKING

Aubrey Gray[1*], Peter Adamczyk[2], Jason R. Franz[1]

[1]Joint Department of Biomedical Engineering at University of North Carolina Chapel Hill and North Carolina State University

[2]Department of Mechanical Engineering, University of Wisconsin-Madison

*Corresponding author's email: graaj@email.unc.edu

Introduction: Compared to younger adults, older adults walk with diminished mechanical output from muscle-tendon units spanning the ankle and more mechanical energy losses per step via distal foot structures. Moreover, these age-related differences vary by task demand, becoming more prevalent with higher demands for forward net propulsion (i.e., walking faster or with horizontal impeding forces). Given the neuromechanical complexity of the various factors that could precipitate these differences, the purpose of this study was to explore a summary outcome that captures gross changes in the control of the human foot-ankle complex due to age across a range of task demands. Specifically, the dynamic mean ankle moment arm (DMAMA), calculated as the ratio of sagittal ankle moment impulse to ground reaction force impulse on a single limb during stance phase, has been shown to summarize changes in ankle control across walking and running speeds in younger adults. We hypothesized that DMAMA would: (*i*) be smaller in older adults than younger adults during habitual walking and (*ii*) be more sensitive to increases in the demand for net propulsion (i.e., walking faster or with horizontal impeding forces) in older than in younger adults.

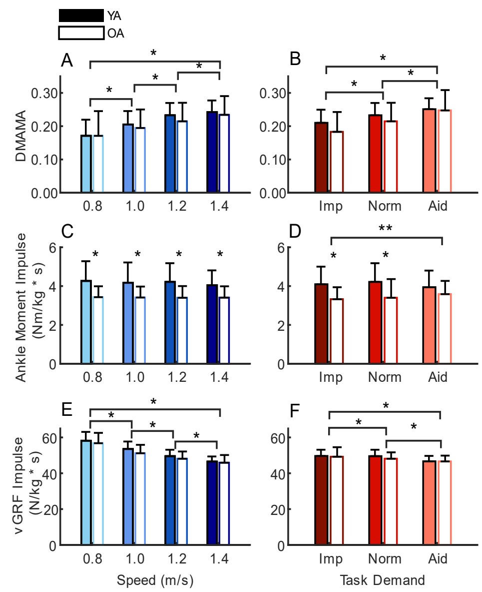

***Figure 1.** DMAMA and its determinants across speeds and horizontal forces in younger and older adults (*p< 0.05; ** age×condition interaction, p<0.05).*

Methods: We enrolled 12 healthy younger adults (18-35 years) and 10 healthy older adults (65-79 years). Exclusion criteria included a lower extremity injury in the last 6 months, use of an assistive device or prosthesis, and use of a medication that causes dizziness[1]. Subjects walked on an instrumented treadmill for 2 min at each of 4 speeds (0.8, 1.0, 1.2, 1.4 m/s) and again at 1.2 m/s attached to a motor-driven system that delivered, in two trials, constant 5% body weight horizontal forces aiding or impeding their motion. For all trials, 12 cameras (Motion Analysis Corporation, Santa Rose, CA) collected motion capture data from a lower limb marker set and ground reaction forces were recorded using an instrumented treadmill (Bertec Corp., Columbus, OH). Optimal fitting of a human body motion model calculated ankle joint moment impulse (Nm/kg * s) and vertical ground reaction force impulse (N/kg * s). From this kinetic data, DMAMA was calculated as described previously [2]. DMAMA and its determinants (namely, ankle moment impulse and vertical ground reaction impulse), were analyzed using a mixed factorial ANOVA for differences across conditions.

Results & Discussion: DMAMA was not significantly affected by age (across speed trials, p=0.663; across horizontal forces trials, p=0.416). Conversely, independent of age, DMAMA increased significantly with faster speed (Fig. 1A, p<0.001) and with lower demands for net propulsion (Fig. 1B, p<0.001). Adamczyk (2020) previously found that DMAMA decreased with faster walking speed; however, those changes were driven by effects at speeds faster than those studied here. For ankle moment impulse, we found a significant main effect of age (speed, p=0.025; horizontal forces, p=0.037) but not speed (p=0.206) or horizontal forces (p=0.120) (Fig. 1B-C). Specifically, largely independent of condition, older adults walked with a smaller ankle moment impulse than younger adults. Conversely, vertical ground reaction force impulse demonstrated a significant main effect of speed (p<0.001) but not horizontal force (p=0.733) nor age (p=0.478) (Fig. 1D-E). Here, participants walked with smaller vertical ground reaction force impulses with faster speed. This result implies a higher step frequency. We did find a significant age×horizontal force interaction effect (p=0.029) on ankle moment impulse, which showed that older adults walked with significantly smaller ankle moment impulses than younger adults during normal walking and in the presence of horizontal impeding forces, but not in the presence of horizontal aiding forces.

Significance: DMAMA is a simple composite measure that summarizes changes in ankle control due to changes in gait with varied demands in younger adults and older adults. However, DMAMA is generally unaffected by age, at least in our relatively small cohort of otherwise healthy participants. This outcome is despite age-related reductions in ankle moment impulse – one of the two determinants of DMAMA. Although we cannot recommend DMAMA be used on its own to characterize age-related differences in ankle joint control, that its sensitivity to varied task demands during walking generalizes between younger and older adults is a promising outcome. Indeed, prior work has suggested that DMAMA be used to inform the selection and optimization of control parameters for assistive devices such as prostheses, orthoses, and exoskeletons. It appears likely that this composite measure may apply equally well to younger and older adults with needs for those devices.

Acknowledgements: We would like to acknowledge William Clark for data acquisition. This study was funded by NIH (R01AG058615, F31AG060675).

References: [1] Clark, W.H., et. al. (2021) *Scientific Reports*, **11**(1) p.21264 [2] Adamczyk, P.G. (2020) *J Biomech Eng*, **142**(7)

THE TIMESCALES OF MEDIOLATERAL STABILITY AND ENERGETIC COST DURING GAIT ADAPTATION

Sarah A. Brinkerhoff[1*], Jaimie A. Roper[2]
[1]Auburn University School of Kinesiology
*Corresponding author's email: sbrinkerhoff@auburn.edu

Introduction: Adjusting gait to meet environmental demands is a critical and inherent feature of bipedal walking, accomplished through trial-and-error adaptation of typical walking patterns [1]. For example, the asymmetry between left and right step lengths adjusts over two timescales during continuous gait adaptation, when one leg is made to walk at a faster speed than the other leg [2-5]. However, the signal that drives the responses to a gait perturbation is unknown. Recently, it has been posited that gait adaptation in response to a continuous perturbation is driven by improving stability and reducing metabolic cost [6]. While the asymmetry between faster and slower step lengths adapts over two timescales, the timescale of mediolateral stability and energetic cost are yet to be determined in a neurotypical, young adult population. The primary purpose of this abstract was to determine the timescale(s) of adaptation of mediolateral stability, metabolic work rate, and mechanical work rate during 20 minutes of gait adaptation in neurotypical young adults.

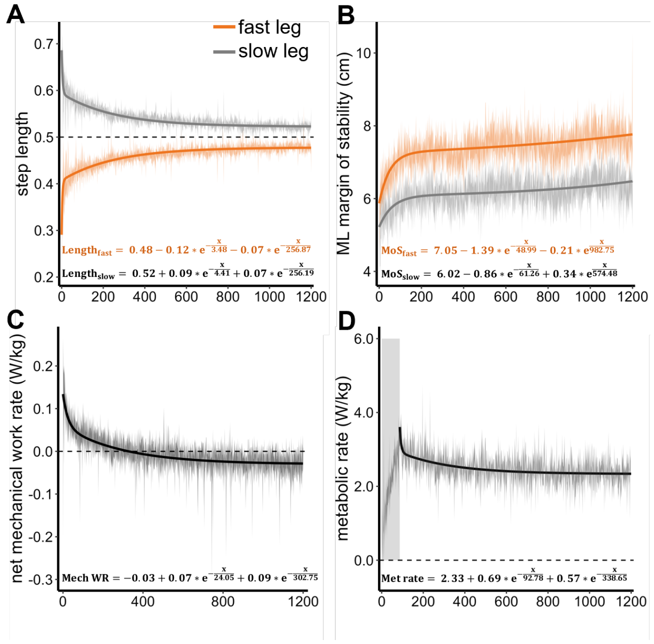

Figure 1. Model estimated two-exponent adaptation curves and equations. Shaded ribbons indicate standard error of the actual data. Orange = fast-leg, grey = slow-leg. A) Step lengths (normalized) , B) ML MoS (cm), C) net mechanical work rate (W/kg), D) metabolic rate (W/kg), where the vertical grey shaded rectangle indicates the metabolic rate that has been removed from analysis.

Methods: 16 sedentary adults walked for 20 minutes on an instrumented split-belt treadmill with the belt under one leg moving at 1.5 m/s and the belt under the other leg moving at 0.5 m/s. We measured step length at foot-strike, mediolateral margin of stability (ML MoS) at contralateral foot-off, net mechanical work rate by the legs, and metabolic rate through indirect calorimetry. Two- exponent mixed effects models were fit to each outcome measure (Eq. 1).

$$Outcome = plateau - a_{fast} * e^{-\frac{seconds}{r_f}} + a_s * e^{-\frac{seconds}{s}} \qquad 1$$

The model was then evaluated to determine the timescales of adaptation of each measure, where a_f and r_f are the initial value and the growth rate of the fast timescale, and a_s and r_s are the initial value and the growth rate of the slow timescale.

Results & Discussion: The plateau, both initial values, and both growth rates were significant for fast- and slow-leg step lengths, slow-leg ML MoS, net mechanical work rate, and net metabolic work rate. The plateau, both initial values, and only the fast growth rate of ML MoS of the fast leg. Thus, all measures except for fast-leg ML MoS adapted over two distinct timescales. The modelled exponential curves and equations of adaptation of each measure are shown in Figure 1.

Fast- and slow-leg step lengths adapted over similar timescales. Modelled fast timescale of adaptation of step lengths reached a plateau within 5 seconds and slow timescale reached a plateau after 257 seconds (4.3 min) for both legs. The slow timescale of net mechanical work rate reached a plateau just 46 seconds after that of step lengths (5 min), and plateaued at a significantly negative work rate (-0.03 W/kg). This supports Sanchez and colleagues' position that neurotypical young adults would try to take advantage of the work done by the treadmill on the legs to do more net negative work during split-belt treadmill walking [5]. The slow timescale of metabolic rate reached a plateau 82 seconds after that of step lengths (1.4 min), which also coincided with the on-kinetics of metabolic rate (86 seconds). It is therefore reasonable to estimate that metabolic cost lags behind kinematics by about 90 seconds during gait adaptation at 1.5 and 0.5 m/s belt speeds. ML MoS primarily adapted withing 60 seconds of gait adaptation, and was consistently higher in the fast-leg. While fast-leg ML MoS of the fast-leg adapted over only one timescale, slow-leg ML MoS adapted over two timescales, and began to exponentially increase during later gait adaptation. It may be that fast-leg ML MoS reaches some ceiling around 7-8 cm, and given more time, neurotypical young adults may adapt the slow-leg ML MoS to reach a similar ceiling.

Significance: Measuring the timescales of neurotypical adult gait adaptation will serve as a baseline population without nervous system or musculoskeletal insults against which to compare injured or disordered populations. However, caution should be taken, as this sample of 16 young adults was sedentary, and active young adults adapt step length mechanics over different timescales than sedentary young adults [7]. Future work will establish baseline norms for active neurotypical adults, and together these findings will provide insight into the timescales and mechanisms that different neurological or orthopaedic insults affect gait adaptation.

Acknowledgements: Participants were paid from an AU School of Kinesiology grant to S.A.B.

References: [1] Martin, et. al. (1996), *Brain, 119*(4). [2] Darmohray et. al. (2019), *Neuron, 102*(1). [3] Mawase et. al. (2013), *J Neurophys, 109*(8). [4] Roemmich et. al. (2016*), Current biology, 26*(20). [5] Sánchez et. al. (2021), *J Neurophys, 125*(2). [6] Seethapathi et. al. (2021), *bioRxiv*. [7] Brinkerhoff et. al. (2022), *bioRxiv*.

DISENTANGLING THE ROLES OF PAIN AND PAIN-RELATED PSYCHOLOGICAL FACTORS IN GAIT FOR CHRONIC LOW BACK PAIN: A PRELIMINARY STUDY

Bailes AH[1,2], McKernan GP, Greco C, Redfern M, Sowa G, Bell KM, Piva S, Brach JS, Cham R, LB3P Investigators
1) Bioengineering, University of Pittsburgh, Pittsburgh, PA, 2) Physical Therapy, University of Pittsburgh, Pittsburgh, PA
Corresponding author email: anb254@pitt.edu, sowaga@upmc.edu

Introduction: Chronic low back pain (cLBP) affects 13% of adults in the United States and is impacted not only by pain itself, but also pain-related psychological factors (e.g., fear-avoidance, pain catastrophizing) [1]. Individuals with cLBP move differently than their peers, but the relative contributions of pain intensity and pain-related psychological factors remain unclear. Much of the research has focused on small samples performing simple tasks (e.g., maximum forward flexion), while failing to consider larger samples performing functional tasks. This study moves beyond simple movements through the use of a wearable sensor to examine gait in a large sample of individuals with cLBP. Gait is one of the most prevalent functional tasks, yet is rarely studied in this population. Based on previous literature [2,3], it was hypothesized that individuals with high pain intensity, fear-avoidance (FA), and/or pain catastrophizing (PC) would demonstrate impairments in clinically relevant gait quality metrics (i.e., gait speed, variability, and symmetry).

Methods: Three hundred and fifty-eight participants (57.8±16.1 years; 38% M / 61% F / <1% non-binary) with cLBP (≥ 3 months, at least 50% of days with symptoms) were included in this preliminary analysis as part of a larger, ongoing study. Participants completed an IRB-approved protocol, including a two-minute-walk test around a 37.5-meter indoor oval track. Participants were fitted with an inertial measurement unit (Lifeware Labs, LLC, Pittsburgh, PA) placed over the L5 spinous process to capture relevant gait events. Gait speed was calculated based on distance walked during the two-minute task. Stride time variability and gait symmetry—by harmonic ratio—were derived from linear trunk accelerations in the sagittal plane. Participants completed the Pain Enjoyment and General Activity scale (PEG—scale 0-10) to quantify pain intensity; the Fear Avoidance Behavior Questionnaire – Physical Activity sub-scale (FABQ-PA—scale 0-24) to quantify FA; and the 6-item Pain Catastrophizing Scale (PCS—scale 0-24) to PC. Higher scores indicate higher symptom severity on all scales. Participants were divided into mild (0-3, N=140), moderate (4-6, N=126), and high (7-10, N=92) pain intensity groups based on the PEG; low (0-13, N=145) and high (14-24, N=213) FA groups based on the FABQ-PA; and low (0-15, N=303) and high (16-24, N=55) PC groups based on the PCS. One-way ANOVAs and independent t-tests were used to compare gait speed, variability, and symmetry between groups.

Results/Discussion: Participants scored an average of 4.8±2.3 on the PEG, 9.0±5.6 on the FABQ-PA, and 13.9±5.5 on the PCS. Individuals who reported moderate-severe pain (4-10), high fear avoidance (≥14), or high pain-catastrophizing (≥16) exhibited slower gait speeds (***Figure 1***) compared to those with mild pain ($p<0.0001$), low FA ($p=0.01$), and low PC ($p=0.001$). There were no differences in variability or symmetry. Results suggest that both pain and pain-related psychological factors impact gait quality in cLBP. Note that gait speed in the study sample was 1.5±0.3 m/s, a speed suitable for 'community ambulation,' suggesting that participants in this sample lack clinically-relevant gait impairments despite statistically significant differences in speed. Surprisingly, there were no differences in gait variability and symmetry metrics between groups. These unexpected results suggest that gait speed may be sufficient for detecting movement alterations during ambulation in this population. Nonetheless, results should be interpreted with caution given that—as evidenced by the high mean population gait speed—most study participants did not demonstrate clinically relevant gait impairments. A more gait-impaired population may exhibit differences in variability or symmetry based on pain intensity, FA, and PC. Limitations to this study include heterogeneity of the cLBP population. Future analysis should statistically account for factors known to impact gait quality, such as age, body size, and certain medical comorbidities.

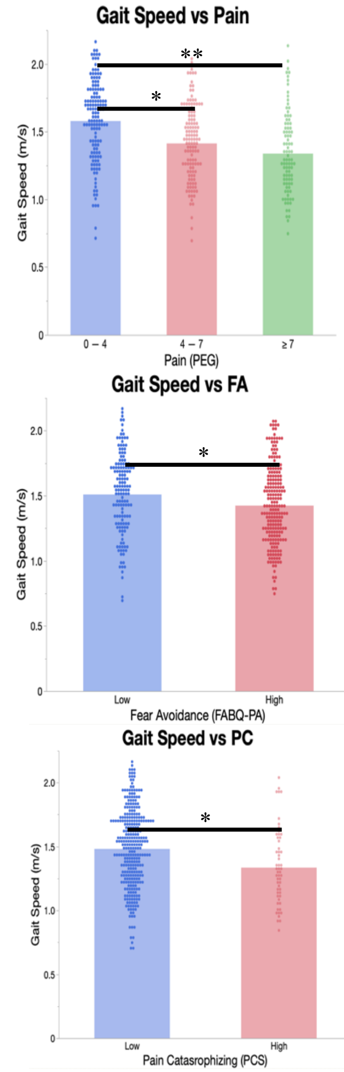

Figure 1: *Bars represent mean gait speed values, with individual points representing gait speed for each of the 358 participants. *p=0.01, **p<0.01*

Significance: This study provides a novel contribution to the literature because: 1) it is a first step toward disentangling the movement-related contributions of pain intensity and pain-related psychological factors; 2) it investigates gait, a functionally important yet understudied movement in cLBP; and 3) it incorporates innovative technological solutions (i.e., wearables sensors) to examine functional movement strategies. Results suggest that both pain and pain-related psychological factors are related to gait speed impairments in cLBP. Future studies should seek to examine the functional implications of such gait quality differences in these cLBP subgroups.

Acknowledgements: The Back Pain Consortium Research Program is administered by the National Institute of Arthritis and Musculoskeletal and Skin Diseases. This research was supported by the National Institutes of Health through the NIH HEAL Initiative under award number U19AR076725-01. The content is solely the responsibility of the authors and does not necessarily represent the official views of the National Institutes of Health or its NIH HEAL Initiative.

References: [1] Lethem J, et al. (1983), *I. Behav Res Ther.* 21(4); [2] O'Sullivan P. (2005), *Man Ther.*10(4); [3] Ippersiel P, et al. (2022), *Phys Ther*. 102(2).

TOWARDS GAIT SYMMETRY IMPROVEMENT USING AUTOMATIC ROBOTIC ASSISTANCE PERSONALIZATION CONTROL FOR ACTIVE HIP EXOSKELETONS

Qiang Zhang[1], Ming Liu[1], Xikai Tu[2], Jennie Si[3], Michael D. Lewek[4*], He (Helen) Huang[1*]

[1]The Joint Department of Biomedical Engineering, North Carolina State University and the University of North Carolina at Chapel Hill, Raleigh, NC 27695 USA. *Corresponding authors' email: michael_lewek@med.unc.edu and hhuang11@ncsu.edu

Introduction: Exoskeletons can be designed to assist the hip joints in providing stability and enhancing mobility during locomotion and other activities. In addition to their mechanical importance during gait, the hips may represent a good target because they are close to the torso, such that actuators can be arranged close to the joint to improve mechanical efficiency without affecting the mass distribution among body segments. Hip exoskeletons can be used to improve gait symmetry, a common clinical goal, through three main approaches: joint trajectory-tracking, finite-state-machine (FSM)-based assistance, and adaptive frequency oscillator-based assistance. However, most studies either generate unsmooth assistive torque trajectories (like FSM approach), lack an adaptive personalization procedure, or can be disturbed easily due to inaccurate user intent interpretation [1]. Although recent studies have demonstrated the promising performance of automatic control parameters tuning of exoskeletons/exosuits by using human-in-the-loop (HIL) optimization [2,3] or reinforcement learning (RL) approaches [4,5], very few studies have focused on maximizing gait symmetry by providing adaptive optimal assistance from hip exoskeletons [6]. Therefore, in this study, we propose a hierarchical control framework to optimally personalize robotic assistance for the hip joint that is gait phase detection-free and with a control objective of achieving a desired/reference gait symmetry.

Methods: The proposed hierarchical control framework has three levels (see Fig. 1). The high-level control automatically tunes three control parameters by using a least-square policy iteration (LSPI) RL approach, the middle-level control defines the assistance torque profile with the three control parameters and left and right hip joint trajectories' sinusoidal projections as

$$\tau_d(t) = k * \left[\sin\left(q_l(t-\Delta t)\right) - \sin\left(q_r(t-\Delta t)\right)\right] + A,$$

and the low-level control achieves accurate torque profile tracking. The cost function in this adaptive optimal control problem is defined as the summation of quadratic forms of gait symmetry errors and control parameter updates.

The treadmill walking protocol was approved by the IRB of North Carolina State University (# 24671). Five participants (mass: 73.9 ± 8.1 kg, height: 170.2 ± 3.7 cm, age: 26.6 ± 5.6 years old) without any neurological disorders were recruited in this study. Each participant conducted four treadmill walking conditions, including (1) transparent mode/zero assistance on both hip joints (C1), (2) induced gait asymmetry by adding consistent unilateral assistance on the left hip with the right hip joint remaining unassisted (C2), (3) RL-based control parameters tuning on the right hip joint while keeping the consistent assistance on the left hip (C3), (4) Parameters optimized in C3 on the right hip with the consistent assistance on the left (C4). Under C1, C2, and C4, each participant walked for 100 gait cycles separately. In C3, a < 10-minute RL-based control parameters tuning procedure was conducted on each participant.

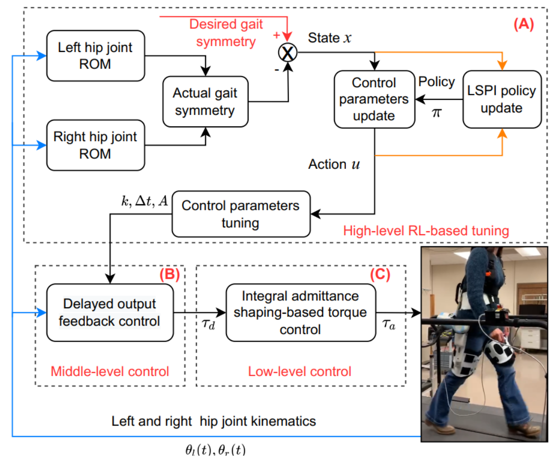

Figure 1: The hierarchical control framework that enables the personalization of hip exoskeleton assistance to walk. (A) The high-level RL-based control learns to personalize control parameters. (B) The middle-level delayed output feedback control during walking generates the desired torque profile. (C) The low-level intrinsic torque controller tracks desired assistive torque generated from the middle-level control.

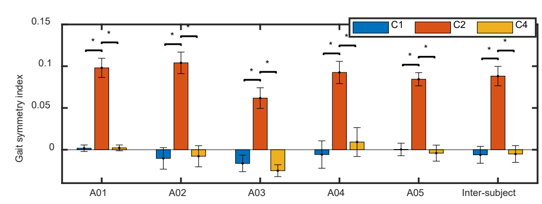

Figure 2: Gait symmetry results under conditions C1, C2, and C4. Individual data were averaged across 100 gait cycles for each condition. * represents the significant difference levels at p <0.05.

Results & Discussion: The tuning duration in condition C3 varied from person to person, as the iteration numbers were 38, 28, 28, 48, and 28 for the five participants. Correspondingly, the control parameters' tuning times were 178, 129, 135, 213, and 139 seconds, respectively. Fig. 2 summarizes the gait symmetry results (mean±SD) across 100 gait cycles under conditions C1, C2, and C4 intra-subject and inter-subject. The gait symmetry index under C2 showed a significant increase when compared to C1 and C4 due to the induced asymmetry; however, it did not show any significant difference between conditions C1 and C4, both intra-subject and inter-subject. On average, the personalized optimal assistance in condition C4 effectively reduced the gait symmetry index from 8.8% to -0.5%.

Significance: This study is the first attempt to tune control parameters for wearable exoskeletons that can provide robust, smooth gait assistance, which can adapt to users' needs. The developed online optimization procedure possibly opens a new avenue for the HIL optimization problem in real-world locomotion activities. Compared to the existing HIL optimization approach, RL-based automatic control tuning is more time efficient and can easily be scaled when meeting various walking conditions. The initial policy for each participant was set the same in condition C3, which was obtained from a pre-training procedure on one participant. The results in the current study indicate that after tuning on one human participant under one condition, the optimal policy usually possesses higher robustness and can be directly applied to the same walking condition on a new participant or a new condition on the same participant.

Acknowledgements: This work was partly supported by NIDILL \#90ARHF0004 and \#90REGE0017, NIH \#R21HD098570, and NSF \#2211739, \#2211740, \#1926998, and \#1808752. We would like to thank all participants for their involvement in the study.

References: [1] Lim et al. (2019), *IEEE Trans. Robot.* 35(4); [2] Zhang et al. (2017), *Science* 356(6344); [3] Ding et al. (2018), *Sci. Robot.* 3(15); [4] Tu et al. (2021), *ICRA*; [5] Zhang et al. (2022), *IEEE Robot. Autom. Lett.* 7(4); [6] Zhang et al. (2022), *IEEE Trans. Autom. Sci. Eng.*

INDIVIDUALS POST-STROKE DO NOT SELF-OPTIMIZE TO NOVEL AFO USE AFTER ONE MONTH

Jacob T. Skigen[1*], Corey Koller[2], Adrienne Henderson[3], Luke Nigro[4], Elisa S. Arch[3,5]
[1]Department of Biomedical Engineering, University of Delaware, Newark, DE
[3]Biomechanics & Movement Science Program, [5]Department of Kinesiology & Applied Physiology, University of Delaware, Newark, DE
email: *jtskigen@udel.edu

Introduction: Passive-dynamic ankle-foot orthoses (PD-AFOs) are commonly prescribed to individuals post-stroke to supplement weakened plantar flexor muscles in their paretic limb. Our previous research demonstrated stiffness-customized PD-AFOs can reduce lower extremity mechanical cost-of-transport (COT) for individuals post-stroke when walking compared to walking with No AFO or with their standard-of-care (SOC) AFO, although the magnitude of improvement varied among participants. [1] Furthermore, despite improvements in COT, biomechanical variables showed substantial variability across participants with PD-AFO use. Given this variability, we wanted to know if giving users time to acclimate to PD-AFO use would result in more consistent and improved outcomes. We focused on self-optimization for this initial study as there is no established method to train individuals to use an AFO. Therefore, the purpose of this study was to investigate if individuals post-stroke self-optimized walking performance with a newly prescribed PD-AFO during one month of wearing the PD-AFO in the free-living environment. We hypothesized that over the one-month period, participants would: increase their self-selected walking speed (SS WS), increase their peak ankle dorsiflexion (DF) angle during stance, increase their peak plantar flexion (PF) moment during stance, and decrease their total COT.

Methods: Nine individuals (mean (SD) age 64.8 (6.5) years; height 1.73 (0.12) m; mass 85.2 (16.3) kg; 4 male, 5 female) with single chronic stroke took part in this study. Data were collected at three time points for this study: immediately after being given the PD-AFO (Week 0), two weeks (Week 2), and four weeks (Week 4) later. Participants wore the PD-AFO instead of their SOC AFO in their free-living environment during the entire four-week period. At each data collection, gait analysis was conducted using an instrumented treadmill and motion capture cameras as participants walked with their customized PD-AFO at their self-selected walking speed determined via a 10 Meter Walk Test without an AFO. [2] After the treadmill walking, the participants completed an additional 10 Meter Walk Test to determine their self-selected walking speed with the PD-AFO for that visit. Biomechanical data were processed and analyzed in Visual 3D. Peak paretic dorsiflexion angle during stance and peak paretic plantar flexion moment during stance were computed using standard inverse dynamics and averaged across trials within each visit for each participant. COT was calculated per limb as positive limb work (summed hip, knee, ankle, and distal foot, all normalized by body mass) summed with the absolute value of negative limb work over the gait cycle, scaled by stride length. [3] A repeated measures ANOVA ($\alpha = 0.05$, with a Bonferroni correction of $P = 0.0125$) was performed for each variable to determine whether there was a significant difference between the different time points.

Results & Discussion: Overall, there were no significant differences in any of the outcome variables for any of the time point comparisons. The average self-selected walking speed did increase between Weeks 0 and 4, but an even higher average was seen at Week 2 ($P = 0.063$). Mean peak ankle dorsiflexion was higher than typical at Week 0 and did decrease (closer to typical) at Week 2, but then increased slightly at Week 4 ($P = 0.309$). Peak plantar flexion moment increased from Week 0 to Week 2 but did not change from Week 2 to Week 4 ($P = 0.0997$). The total COT decreased from Week 0 to Week 2, and then further decreased from Week 2 to Week 4 although differences were not statistically significant ($P = 0.354$). Overall, while some trends were seen in the mean values, results were not significant as there was large inter-participant variability. Via inspection of the results on a subject-by-subject basis, there did not appear to be any meaningful and consistent improvements in the outcome measures over the three time points, and individual results often did not mirror the group trends. As such, these results indicate that individuals do not continue to self-optimize their walking performance with a new PD-AFO over a one-month period. It is possible that participants intuitively optimized their walking performance immediately when given the orthosis, but it is more likely that they quickly settle into a given walking strategy and then do not explore alternative (and potentially more effective) strategies.

Table 1. Mean (SD) values of gait parameters at Week 0, Week 2, and Week 4 visits.

	SS WS (m/s)	*Peak Ankle DF (deg)*	*Peak PF Moment (N*m)*	*Total COT (J/kg/m)*
Week 0	0.76 (0.28)	17.44 (5.98)	-0.89 (0.25)	2.34 (0.40)
Week 2	0.81 (0.25)	15.11 (6.82)	-0.95 (0.31)	2.33 (0.42)
Week 4	0.79 (0.27)	16.22 (5.66)	-0.95 (0.24)	2.29 (0.42)

Significance: This study provided valuable insight into the adaptability of walking strategies of post-stroke individuals when given a new orthotic device. As results from this study appear to indicate that individuals post-stroke do not enhance their use of a PD-AFO via self-optimization, future research should develop and test formal training paradigms to determine if such paradigms can elicit more optimal walking strategies for individuals post-stroke using new orthotic devices. This study lays the foundation for continued work in the realm of training individuals to use new orthotic devices and the best way to optimize patient function with orthotic devices.

Acknowledgements: This work was supported by USAMRAA through the Orthotics & Prosthetics Outcomes Research Program under Award No. W81XWH-18-1-0502. Opinion, interpretations, conclusions, and recommendations are those of the author and not necessarily endorsed by USAMRAA.

References: [1] Koller, C. et al. Proc. ASB Annual Meeting, 2021; [2] Arch, E.S. et al. Journal of Prosthetics and Orthotics, 28(2), 60, 2016; [3] Ebrahimi, A. et al. Gait & Posture, 56, 49-53, 201, 2017

MAPPING FROM PERFORMANCE CRITERIA TO HUMAN GAIT BEHAVIOR

Matthew Mulligan[1*], Wenxin Zhou[1], Brian R. Umberger[1]
[1]University of Michigan School of Kinesiology, University of Michigan Ann Arbor, MI
*Corresponding author's email: mbmulli@umich.edu

Introduction It has been proposed that our gait behaviors result in part from optimizing performance criteria (e.g., metabolic cost, neuromuscular effort, stability) inherent to the task being completed. Experimental observations demonstrate that humans tend to select gait parameters that optimize these criteria [e.g., 1]. However, it is unclear: 1) how the central nervous system modulates the importance of these criteria, and 2) how these criteria lead to the resulting gait behaviors. Gait behavior may be characterized with qualitative descriptors (e.g., gait style) [1] and quantitative measures (e.g., speed, cost) [2]. Experimental studies have shown that manipulating these criteria leads to changes in gait [4, 5], yet there has been no means for mapping performance criteria modulation to a particular gait behavior. It is also difficult to solve the inverse problem, where given a particular gait behavior, we reconstruct the set of performance criteria leading to that behavior. Here, using musculoskeletal simulation, importance sampling, and machine learning techniques we demonstrate that is possible to: 1) predict a particular gait behavior from performance criteria alone, and 2) recover performance criteria combinations that may correspond to a single gait observation. This knowledge will improve our understanding of how the importance placed on performance criteria influences human gait and aid our ability to develop assistive devices that account for the priorities of human users.

Methods: To evaluate the effects of modulating multiple performance criteria (metabolic cost, muscular effort, head stability, and movement vigor) on gait behavior, we generated 1379 optimal control gait simulations with different combinations of weights on the criteria using OpenSim Moco [3]. Each simulation was classified according to one of four gait styles by two independent observers. We separated our gait styles into Normal, Short Step (similar to festinating gait), Trunk Oscillation (similar to posterior lurch gait) and a Hybrid gait pattern that included characteristics of two or more of the classified gaits. Classifications were validated using Cohen's Kappa to assess inter- and intra-rater reliability. Objective measures included gait speed and metabolic cost. To map from weights on performance criteria to gait style, we employed six different classification algorithms including a neural network, random forest, decision tree, logistic regression, k-nearest neighbors, and naive Bayes using k-folds cross-validation. To evaluate our ability to predict objective measures, we employed implementations of a decision tree, a random forest, a neural network, k-nearest neighbors, Bayesian ridge regression, and linear regression using k-folds cross-validation. To determine possible performance criteria weight combinations, we constructed a convex hull for each classification of gait using Delauney simplices. We then randomly sampled performance criteria combinations for each hull that had not been previously observed to determine if we could reconstruct the same gait behavior.

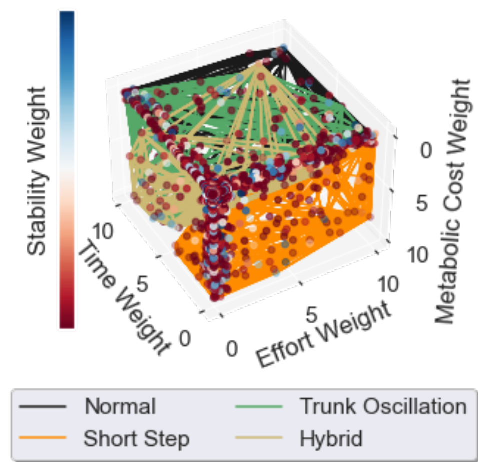

Figure 1: Performance criteria clusters by gait styles. Different weight combinations on our terms for vigor (time), effort, metabolic cost, and stability lead to different gait styles including Normal, Short Step, Trunk Oscillation, and Hybrid gaits.

Results & Discussion: We found the neural network and random forest algorithms produced classification accuracy of greater than 93% in identifying the correct pattern, with all algorithms being able to correctly identify gait style better than 85% of the time. This indicates a mapping from performance criteria to gait classifications. We were able to predict gait speed and metabolic cost values within 0.08 m/s and 0.6 W/kg respectively in the best case (k-nearest neighbors, random forest) as well as predict within 0.2 m/s and 1 W/kg respectively for all algorithms.

As demonstrated in Fig 1, we found that gait style separated spatially in terms of performance criteria. To examine the inverse problem of determining possible performance criteria corresponding to a given observation, we were able to reproduce Normal gait with 95% accuracy, Short Step gait with 92% accuracy, and Trunk Oscillation gait with 69% accuracy. Decreased accuracy for Trunk Oscillation may result from fewer cases being observed relative to Short Step and Normal in the random sample in training.
Thus, our approach demonstrates an ability to map performance criteria to a desired gait behavior. We show the ability to recreate gait behavior that approximates commonly studied gait parameters, while simultaneously matching qualitative descriptions. We further characterize gait changes in the context of quantities presumably important to the central nervous system in the control of gait.

Significance: Recent work has used performance criteria [e.g., neuromuscular effort] to understand human gait selection [6]. The two-way map between performance criteria and quantitative and qualitative aspects of gait selection demonstrated here provide unique insights regarding the control of locomotion. Though we focus on gait, we may use the same approach for other human movements.

Acknowledgements: Supported by a Fellowship from the Michigan Institute for Computational Discovery and Engineering.

References: [1] Montepare, et al (1987), *J. Nonverb Behav.* 11; [2] Ralston (1958), *Int. Z. angew. Physiol.* 17(4).; [3] Dembia et al (2020), *PLoS Comput. Biol.* 16(12); [4] Selinger et al (2015), *Curr Bio.* 25(18); [5] McDonald et al (2019), *J R Soc Interface* 16(158) [6] Han et a. (2021), *IEEE T Neur Sys Reh* 29.

KNEE JOINT BIOMECHANICS BEFORE AND AFTER TRANSTIBIAL PROSTHESIS OSSEOINTEGRATION

Amanda L. Vinson[1*], Nicholas W. Vandenberg[1], Mohamed E. Awad[2], Danielle Melton[2], Cory L. Christiansen[2,3], Jason W. Stoneback[2], Brecca M. M. Gaffney[1,2]
[1]University of Colorado Denver, [2]University of Colorado Anschutz Medical Campus, [3]VA Eastern Colorado Health Care System
*Corresponding author's email: amanda.vinson@ucdenver.edu

Introduction: Patients with transtibial amputation (TTA) who use a socket prosthesis demonstrate asymmetric gait patterns that most commonly overload the intact limb and underload the residual limb [1]. Asymmetric joint loading is linked to joint pain, reduced mobility, and increased risk of osteoarthritis [2]. Osseointegrated prostheses are an alternative to socket prostheses that involve a direct attachment of the prosthesis to the residual limb via a bone-anchored implant. While this type of TTA prosthesis offers a more direct axial loading of the residual limb compared to the distributed load by socket prostheses, its influence on knee joint loading is unknown. Our objective was to determine the impact of osseointegrated prostheses on knee joint biomechanics (joint angle, joint reaction forces (KJRF)) during walking for people with TTA. We hypothesized the peak KJRF would decrease in the intact limb and increase in the residual limb at 12-months post-osseointegration compared to pre-osseointegration.

Methods: With Institutional Review Board approval, six patients scheduled to undergo transtibial prosthesis osseointegration were enrolled (4M, 2F; Age: 49±14.4 y/o; BMI: 29.3±2.79 kg/m^2, OTNi custom press-fit implant). Motion capture data (kinematics, ground reaction forces (Fs = 120 and 2,160 Hz, respectively)) were collected during overground walking at self-selected speeds at two time points relative to osseointegration (~2-days prior and 12-months following). Musculoskeletal models were developed in OpenSim by modifying an existing generic model [3], with changes to the residual limb including removal of distal foot and ankle musculature, simulating a myodesis procedure by inserting the gastrocnemius to the distal end of the residual tibia, and updating limb inertial properties [4-5]. The baseline socket model included a 6 degree-of-freedom joint at the residuum-socket interface to account for motion between the residual limb and socket [5]. The osseointegrated model used a rigid connection between the residual limb and implant. Joint angles were calculated using Inverse Kinematics and Residual Reduction Analysis to ensure dynamic consistency between model and experimental data [6]. Muscle forces were estimated using Computed Muscle Control, and then used to calculate the KJRFs over three stance periods, bilaterally. Peak bilateral knee joint angles, muscle forces, and KJRFs in early (KJRF1) and late (KJRF2) stance before- and after- osseointegration were compared using Cohen's *d* effect size (medium: $0.5 \leq d < 0.8$; large: $d \geq 0.8$).

Results & Discussion: Self-selected gait speed slightly increased 12-months after osseointegration (pre: 1.0±0.2 m/s; post: 1.1±0.3 m/s, *d* = 0.75). There was no difference in the residual limb peak knee flexion angle during loading before or after osseointegration (pre: 14±6.9°; post: 12±6.5°, *d* = 0.20). However, peak vasti muscle force on the residual limb decreased during loading after osseointegration (pre: 0.9±0.4 BW; post: 0.6±0.3 BW, *d* = 0.56) (Fig. 1), which was also associated with a decrease in resultant KJRF1 (*d* = 0.54) (Fig. 1). Quadriceps avoidance is a known strategy used by socket users to shift the loading demand from the knee to the hip for greater stability during ambulation [7]. Thus, these results may suggest this habituation continues post-osseointegration, and this population may benefit from more extensive quadriceps strengthening and movement pattern training. On the intact limb, the peak knee flexion angle decreased during loading after osseointegration (pre: 22±9.4°; post: 15±5.1°, *d* = 0.78). Similarly, the peak vasti muscle force decreased (pre: 1.7±1.1 BW; post: 1.0±0.5 BW, *d* = 0.51), and the peak biceps femoris muscle force increased (pre: 0.4±0.1 BW; post: 0.5±0.2 BW, *d* = 0.59). Surprising, the intact limb KJRF1 was not changed in any direction (*d* = 0.24). As increased knee flexion and quadriceps muscle force is often observed in response to 'falling' on the intact limb [8], these results may indicate an improved load transfer strategy across limbs after osseointegration. However, a larger sample size is needed to support this conclusion as the heterogeneity of all internal and external forces contributing to the KJRF are amplified in a small sample size.

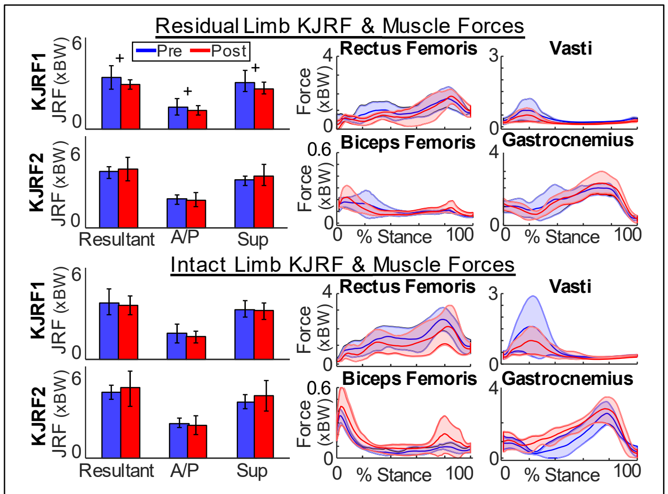

Figure 1: Mean ±1 SD maximum KJRF in early ('KJRF1') & late stance ('KJRF2') for baseline socket (pre, blue) and post-osseointegration (red), and muscle forces. + indicates a medium effect size ($0.5 \leq d < 0.8$). A/P: Anteroposterior, Sup: Superior.

Significance: This is the first investigation to quantify the impact of osseointegrated prosthesis on knee joint loading in people with TTA. As force transmission to the residual limb is different than a socket prosthesis, it is important to quantify its influence on joint biomechanics to understand the impact on overuse injuries.

Acknowledgements: This work is supported by the University of Colorado Osseointegration Research Consortium.

References: [1] Sanderson et al., (1996) *Gait Posture* [2] Struyf et al., (2009) *Arch Phys Med Rehabil* [3] Lai delp et al., (2017) *Annals of Biomed Eng* [4] Silverman et al., (2012) *J Biomech* [5] LaPre et al., (2017) *Int J Numer Meth Biomed Eng* [6] Delp et al., (2007) *IEEE Trans Biomed Eng* [7] Lloyd et al., (2010) *Gait Posture* [8] Hendershot et al., (2014) *Clin Biomech*

A LOW-COST MOVEMENT-BASED CONCUSSION DIAGNOSIS TOOL: PRELIMINARY RESULTS FROM A PILOT STUDY

Jacob M. Thomas[1*], Rebecca Bliss, Trent M. Guess
[1]School of Health Professions, University of Missouri
*Corresponding author's email: jmt2mb@missouri.edu

Introduction: Currently, most tools designed to diagnose concussion are subjective and are not based on movement tasks which simulate the demands of sport. For these reasons, recent research has identified the need for an objective and cost-efficient measurement device which accurately assesses neuromotor control using a combination of multiple assessments following concussion. [1-3] Therefore, the purpose of this study was to assess the ability of a novel motion-based concussion diagnosis tool (MPASS) which combines an Azure Kinect depth-sensing camera, a custom force plate, and an Arduino-based interface board to detect movement differences between individuals with and without concussion [Figure 1].

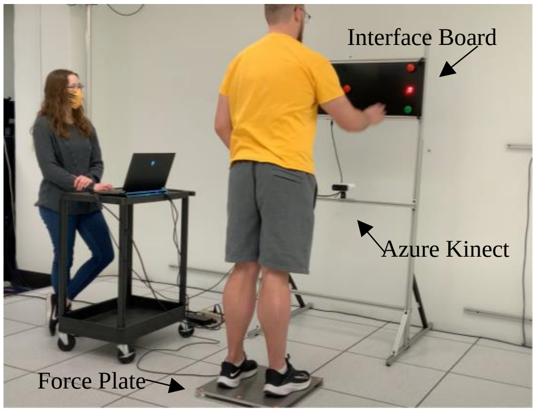

Figure 1: Reaction time test with the MPASS. Center of pressure and reaction time are simultaneously measured.

Methods: 19 individuals (22.59±1.66 yrs., 13 females) participated in this study. Seven participants suffered a concussion within 1-month before data collection. Twelve had not suffered a concussion within the past year. All participants completed the same battery of functional tasks: walking (normal and head shaking), Romberg balance tests (firm surface and foam surface with eyes open, eyes closed, and eyes closed head shaking), and reaction time. For walking tasks lower extremity spatiotemporal parameters and discrete kinematics were collected via Kinect depth-sensing camera [4]. For balance tasks, a force plate recorded center of pressure and Kinect recorded center of mass. For the reaction time task, reaction time was recorded using an Arduino-based interface board and center of pressure was recorded via force plate. Ensemble averages for each participant and each discrete measurement were calculated. This resulted in 125 unique variables for each participant. Principle component analysis (PCA) was used to reduce the dimensionality of the data. All statistical analyses were complete in RStudio (v4.2.0).

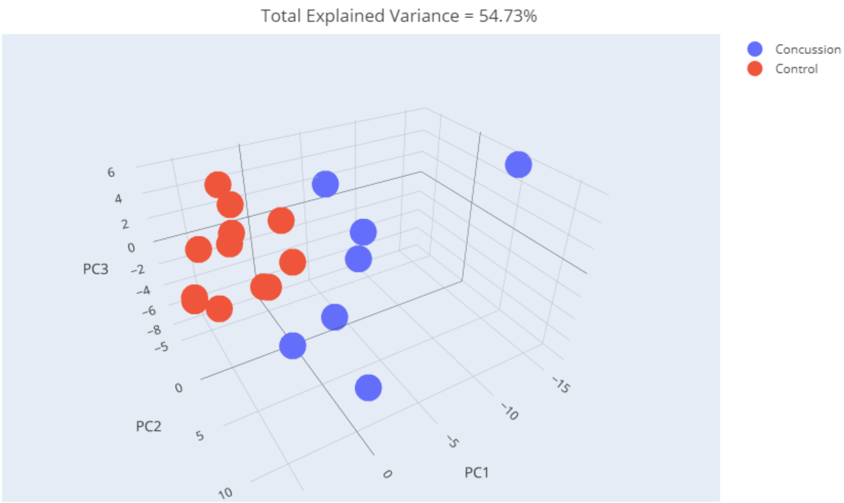

Figure 2: 3-dimensional PCA graph demonstrating separation between concussion and control groups.

Results & Discussion: Three principal components were retained using Horn's Parallel Analysis for component retention. These 3 principal components explained 54.73% of variance within the dataset. Visual analysis of these 3 principal components demonstrated clear separation between the two groups (concussion and control) [Figure 2]. Analysis of each variable's contribution to the retained principal components revealed significant contributions from center of mass data during balance tasks, stride and step length during walking, and step length during head-shaking walking.

The promising initial results from this pilot study indicate MPASS outcome measures can be used to discriminate between those with and without concussion. Additionally, multidimensional outcome measures of MPASS, such as center of mass during balance, may be important contributors to this discriminatory ability. However, greater sample size and more stringent sample-matching will be required before this can be determined. For these reasons, our future studies will aim to recruit college athletes within 72-hours of concussion and compare them to sport and sex-matched control participants from their teams.

Significance: Initial results indicate MPASS may provide an objective, low-cost, multidimensional, and movement-based concussion diagnosis tool. If these results continue throughout larger future studies MPASS represents a practical answer to the need for affordable and objective tools to inform clinical decision-making surrounding concussion diagnosis.

Acknowledgements: This study was funded in part by the University of Missouri Coulter Biomedical Accelerator.

References: [1] Lee et al. (2013), *J Sci Med Sport* 16(1); [2] Buckley et al. (2016), *J Sport Heal Sci* 5(1); [3] Howell et al. (2018), *Sport Med* 48(5); [4] Guess et al. (2022), *Gait & Posture* 96.

THE SPRING-LIKE FUNCTION OF THE FOOT'S ARCH REDUCES THE METABOLIC COST OF SIMULATED GAIT IN A GAIT MODE SPECIFIC MANNER

Daniel J. Davis*, John H. Challis
[1]The Biomechanics Laboratory, The Pennsylvania State University, University Park, PA
*Corresponding author's email: DanielJDavis@psu.edu

Introduction: The ability to passively store and return energy during gait helps humans reduce the metabolic energy required to locomote, and the foot's arch has been credited with aiding in this spring-like function [1]. While many computational musculoskeletal models of the human body have been developed to investigate the mechanisms underlying the metabolic cost of gait, the foot's arch is commonly ignored in these models and instead the foot is frequently represented as a single rigid segment. *In vivo* studies indicate that modelling the foot as a single segment in this manner alters the measured kinematics and kinetics of the ankle joint [2]. Given the importance assigned to the ankle joint and the muscles which cross it in propelling the body's center of mass forward and upward during gait, improperly modelling the foot not only precludes researchers from understanding the function of the foot's arch in locomotion, but also obscures the underlying mechanisms of ankle joint function which allow for efficient locomotion.

The present study examined the sensitivity of the metabolic cost of walking and running to the inclusion of the foot's midtarsal joint (i.e., arch) in a whole-body computational musculoskeletal model. Davis & Challis [3] recently demonstrated *in vivo* that the arch is more spring-like in walking compared with running and in non-rearfoot strike running compared with rearfoot strike running, therefore it is hypothesized that there will be a greater difference in metabolic cost in running compared with walking simulations and in non-rearfoot strike running vs rearfoot strike running simulations.

Methods: Two planar computational musculoskeletal models were developed in OpenSim [v4.4; 4]. Both models comprised two multi-segment feet along with shanks, thighs, and a pelvis, head, arms, and trunk segment. The version of the model with a midtarsal joint had a rearfoot and forefoot segment connected by the midtarsal joint and a metatarsophalangeal joint which connected the forefoot and toe segments. In the model without the midtarsal joint, each foot comprised only two segments connected by the metatarsophalangeal joint. Twenty-six muscles actuated the model's joints. The plantar aponeurosis was modelled using a path spring along the plantar surface of the foot, and a torsional spring at the midtarsal joint represented other passive structures. The midtarsal joint torsional spring stiffness was a parameter allowed to vary between simulation iterations.

Walking and running data from 15 participants [3] was used to inform computational musculoskeletal simulations performed in OpenSim Moco [5]. Inverse kinematics was used to generate joint angles from the stance phase of experimental walking, rearfoot strike running, and non-rearfoot strike running trials for both model versions scaled to a subset of three representative participants for which bilateral marker data was collected (2M/1F, 65.8 ± 10.6 kg, 1.72 ± 0.11 m). Simulations were performed which minimized the sum of muscle excitations squared, and the discrepancies with experimental joint angles, joint angular velocities, and ground reaction forces. The metabolic cost of the muscles of the right leg during the stance phase was estimated using the model of Koelewijn et al. [6].

Results & Discussion: Gait simulations with the model which included the midtarsal joint had lower metabolic costs than simulations with the model without the joint (Fig. 1). The mean decreases in metabolic cost in the model with the midtarsal joint were 1.6%, 3.7% and 6.4% in walking, rearfoot strike running, and non-rearfoot strike running, respectively. These results provide support for the current hypothesis that running, specifically non-rearfoot strike running, would result in greater differences in metabolic cost when the midtarsal joint is not modelled. This is in line with Stearne et al [7], who found increases in the metabolic cost of running, but not walking, when participants used a rigid insole that substantially reduced arch compression. Given that the arch is more spring-like in running [3], removing this spring-like function would be expected to have a greater influence on running compared with walking trials.

The metabolic cost of the gastrocnemius and soleus muscles were altered the most by the inclusion of the midtarsal joint in the model. The mean muscle fiber shortening velocities during the second half of stance in these muscles were reduced in the midtarsal joint model simulations compared with those using the model without the midtarsal joint. Further, these differences followed the same pattern as the mean differences in metabolic cost (i.e., mean between model differences increased from walking to rearfoot strike running to non-rearfoot strike running).

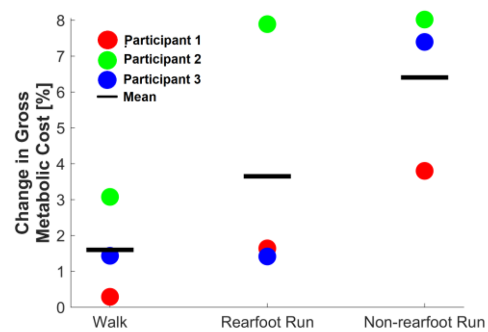

Figure 1: Simulations with the model that included the midtarsal joint resulted in lower gross metabolic costs than simulations with the model with no the midtarsal joint.

Significance: That the difference in metabolic cost was sensitive to the gait mode provides evidence that the spring-like function of the foot's arch, which also varies according to gait mode, influences the metabolic cost of locomotion. Differences in triceps surae muscle fiber shortening velocities when using the model which incorporated the foot's midtarsal joint highlight mechanisms by which the arch can contribute to metabolically efficient locomotion. Researchers aiming to uncover the mechanisms underlying locomotor energetics should consider the influence of the foot's arch when employing computational musculoskeletal models.

References: [1] Ker et al. (1987), *Nature* 325(6100); [2] Zelik & Honert (2018), *J Biomech* 75; [3] Davis & Challis (2023), *J Biomech* 151; [4] Delp et al. (2007) *IEEE Trans Biomed Eng* 54(11); [5] Dembia et al. (2020) *PLoS Comput Biol* 16(12); [6] Koelewijn et al (2018) *Comput Methods Biomech Biomed Engin* 21(8); [7] Stearne et al. (2016), *Sci Reports* 6(1).

MULTIVARIATE TIME-SERIES CLUSTERING IDENTIFIES SUBGROUPS OF INDIVIDUALS FOLLOWING ACL RECONSTRUCTION BASED ON MIDSTANCE DEFICITS

Willa Ma[1*], Susan Sigward[1]
[1]University of Southern California, Division of Biokinesiology and Physical Therapy
*Corresponding author's email: willama@usc.edu

Introduction: Clinically, gait is expected to normalize by 3 months following anterior cruciate ligament reconstruction (ACLr); however, biomechanical data suggests that altered knee mechanics, particularly reduced knee flexion excursion and knee extensor moment during loading response, persist long term [1-4]. These mechanics are considered maladaptive as they are thought to contribute to progression of knee osteoarthritis (OA) [5-6]. Traditional analyses of average between limb differences in mechanics identified at discrete time points limit our ability to understand how patient-specific mechanics vary across this population. A clearer understanding may allow for identification of patterns that are at greater risk for progression of OA. This study aimed to describe subgroups of individuals within the ACLr population that exhibit similar mechanical profiles using a data-driven clustering analysis that considers stance phase kinematics and kinetics attributed to OA. We hypothesized two clusters would distinguish altered gait mechanics of the surgical (Sx) limb from mechanics of the non-surgical (NSx) limb, and these clusters would be formed primarily based on differences during loading response of gait.

Methods: Forty individuals 101 ± 17 days post-ACLr (21 female, 19 male; mean ± SD: age, 26 ± 10.4 years; height, 1.72 ± 0.1 m; weight, 72.1 ± 15.1 kg) were included. Kinematic and kinetic data were collected (3D motion capture system) while individuals walked 10 meters overground at a self-selected speed. Data were normalized to 101 data points and averaged across 3 trials for Sx and NSx limbs. Multivariate time series clustering created clusters (2) based on variation in sagittal plane knee angle and moment and frontal plane knee moment waveforms of 80 limbs (40 Sx and 40 NSx). Time-series variables were compared between clusters through 100% of stance using statistical parametric mapping (SPM). Finally, individuals were grouped based on between-limb cluster assignments using a 2x2 classification matrix.

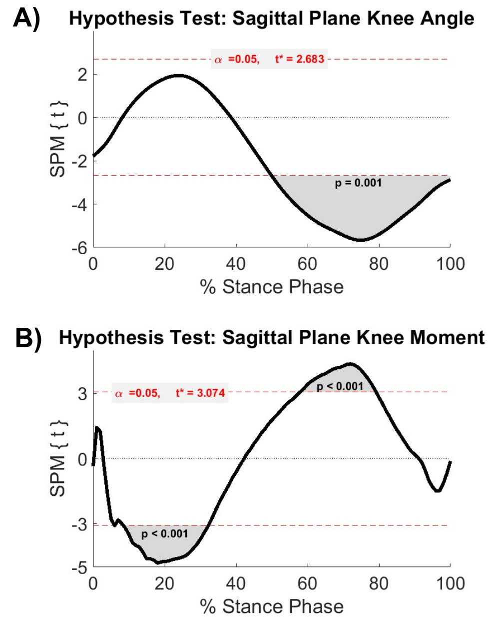

Figure 1: Two-tailed independent t-test using SPM for sagittal plane knee A) angle and B) moment through 100% of stance phase. The red dashed line is the critical t-value.

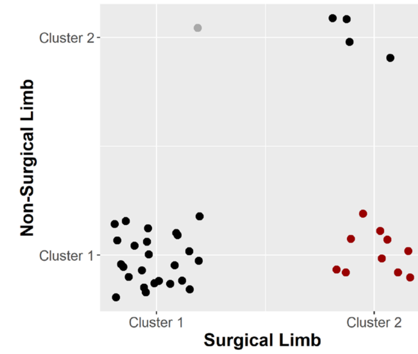

Figure 2: Each dot represents a participant. Black dots represent both limbs in the same cluster. Red and gray dots represent limbs in different clusters.

Results & Discussion: Most of the limbs (61/81) fell in cluster 1 (Sx = 26; NSx = 35), fewer (19/80) fell in cluster 2 (Sx = 14; NSx = 5). Almost 90% of NSx limbs clustered in 1 suggesting that it reflects more typical/healthy knee mechanics. SPM analyses revealed significant differences in flexion at 50-100% of stance ($p = 0.001$; Figure 1A), and extensor moments at 9-32% ($p < 0.001$) and 59-79% ($p < 0.001$) of stance (Figure 1B). Similar to previous analyses, limbs in cluster 2 exhibited lower extensor moments during loading response but without limitations in knee flexion. Interestingly, less knee extension and lower flexor moments were observed during midstance as differences in midstance mechanics have received less attention in the literature. No differences were observed for knee abductor moment. This suggests that this variable, typically attributed to progression of OA, was not a primary contributor to cluster assignments in this sample. When considering cluster assignments for each limb, both limbs classified in the same cluster for 29 (n = 25 cluster 1, n = 4 cluster 2) and different clusters for 11 (n = 10; Sx cluster 2/NSx cluster 1) individuals (Figure 2), resulting in three subgroups based on limb symmetry: 1) symmetrical cluster 1, n = 25; 2) symmetrical cluster 2, n = 4; and 3) asymmetrical, Sx cluster 2/NSx cluster 1, n = 10. Further steps are needed to understand how these cluster patterns and subgroups translate to joint loading variables and risk of early development of knee OA.

Significance: Data-driven clustering analyses of time series variables highlighted different sagittal plane mechanical patterns in early recovery post-ACLr. Consideration of data across stance phase versus discrete points exposed differences during midstance. Considering between limb differences in cluster assignment, revealed a smaller subgroup of individuals who clustered asymmetrically. It is not clear if this subgroup represents individuals who have slower recovery or who are more vulnerable to persistent deficits. Identifying movement patterns subgroups or phenotypes is the first step in understanding the variation in gait adaptations across this population allowing for exploration of a more personalized understanding of recovery and risk for knee OA.

References: [1] Kaur et al. (2016), *Sports Med* 46; [2] Adams et al. (2012), *J Orthop Sports Phys Ther* 42(7); [3] Sigward et al. (2016), *Clin Biomech* 32; [4] Perry & Burnfield (2010) Gait Analysis: Normal and Pathological Function, 2nd Ed; [5] Pfeiffer et al. (2019) *Med Sci Sports Exerc* 51(4); [6] Khandha et al. (2017), *J Orthop Res* 35(3).

The interactive effects of biological tendon and ankle exoskeleton stiffnesses on walking metabolic cost

Ricky Pimentel[1], Lindsey Trejo[2], Katherine Saul[3], Gregory Sawicki[2], & Jason R. Franz[1*]
[1]Biomedical Engineering, UNC Chapel Hill and North Carolina State University
[2]George W. Woodruff School of Mechanical Engineering, Georgia Institute of Technology
[3]Mechanical and Aerospace Engineering, North Carolina State University
*Corresponding author's email: jrfranz@email.unc.edu

Introduction: Passive-elastic ankle exoskeletons (EXOs) aim to improve walking economy by facilitating the storage and release of elastic energy during push off, which reduces biological ankle moments and requisite activation. EXO energy storage and return is governed by spring stiffness (k_{EXO}), which intuitively interacts with biological tendon stiffness (k_T) to influence overall device efficacy. Biological k_T has substantial effects on walking economy [1] and can change considerably with age [2]. Using experimental approaches alone, it can be challenging to document the interaction between k_T and k_{EXO}. Musculoskeletal modelling may streamline EXO tuning and personalization by identifying a candidate k_{EXO} that yields the most favorable interaction with k_T to reduce walking metabolic cost.

Our goal was to document the metabolic cost landscape across a physiological range of simulated k_T while walking at various k_{EXO} in a representative younger and older adult. We first hypothesized that ankle EXOs would reduce ankle extensor metabolic cost by decreasing requisite activation. We also hypothesized that ankle EXOs would elicit maximal reductions in ankle extensor metabolic cost at different k_T and k_{EXO} combinations for a representative younger versus older participant.

Methods: Two adults (*younger (YA):* 22 years, 1.84 m, 79.1 kg; o*lder (OA):* 70 years, 1.65 m, 61.1 kg) walked at 1.25 m/s in *Dephy ExoBoots* emulating a passive-elastic device with k_{EXO}s of 50, 150, and 200 Nm/rad. Participants received over 60 minutes of walking habituation across the various k_{EXO}s. We recorded whole body motions and forces as well as ground truth metabolic cost via indirect calorimetry. We measured k_T via isometric contractions and ultrasound of the Achilles tendon. We then customized scaled gait2392 OpenSim models for each participant to include a point mass with EXO inertial properties welded to each lateral tibia segment. We represented each EXO as an external torque applied bilaterally to the talus and tibia. We modified k_T in each model by simulating different tendon strains at maximum isometric force (ε_0) by performing simulations at participants measured ε_0 (YA: 3.4%; OA: 6.7%) and at 2, 4, 6, and 8% ε_0. We determined muscle-level metabolic costs using a bioenergetic model [3] and iterated simulations across each k_T and k_{EXO} combination to determine effects on ankle extensor and whole-body metabolic cost during walking.

Results & Discussion: YA and OA exhibited similar profiles of measured metabolic cost across k_{EXO} (Fig. 1A). Consistent with previous work [4], lower stiffnesses were most economical for both participants and increasing k_{EXO} raised walking metabolic cost. EXOs reduced measured metabolic cost to values below walking without the device in OA but not YA.

In silico, walking with increasing k_{EXO} reduced peak ankle dorsiflexion, moment, and activation for the ankle extensors. Walking with an EXO increased soleus metabolic cost for the YA (Fig. 1B) but decreased soleus metabolic cost for the OA (Fig. 1C). Increasing k_T (reducing ε_0) also decreased soleus metabolic cost across all k_{EXO}s. We found similar cost landscapes for the gastrocnemii.

Significance: Our simulations suggest that passive-elastic ankle EXOs may be more effective at reducing ankle extensor metabolic costs for older adults than for younger adults. One interpretation may be that younger adult muscle-tendon unit function and coordination during walking is likely to be sufficiently cost-optimized compared to older adults. One example of this is growing evidence that older adults exhibit lesser Achilles tendon stiffness than younger adults, which can disrupt ankle muscle mechanics.

Acknowledgements: Supported by a grant from NIH (R01AG058615).

References: [1] Sawicki et al. Exerc Sport Sci Rev. 2009 [2] Stenroth et al. J Gerontolog A Biol Sci Med Sci. 2015. [3] Umberger et al. Comp Meth Biomech Biomed Eng. 2003. [4] Collins et al. Nature. 2015.

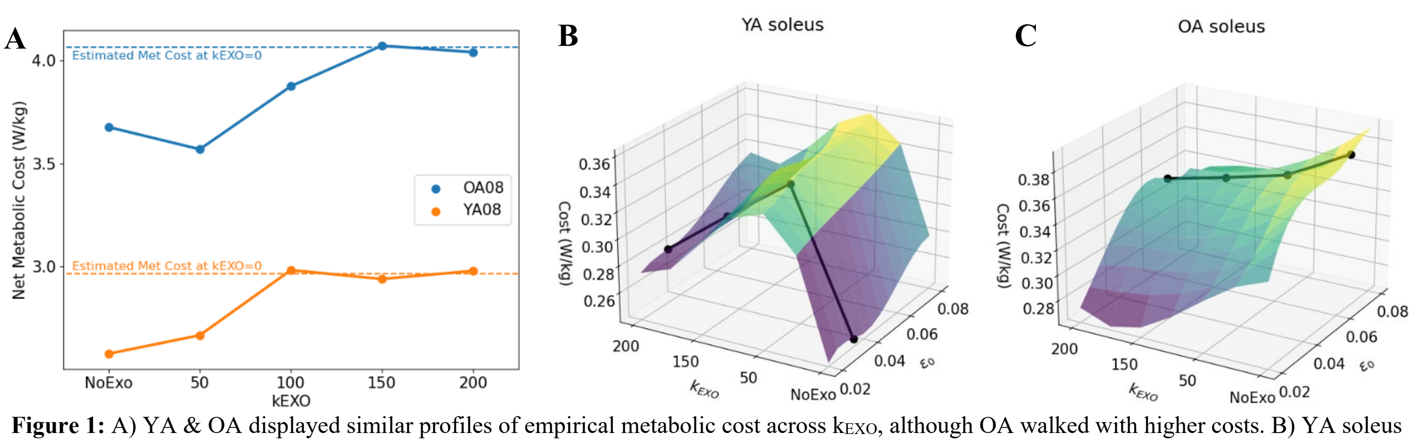

Figure 1: A) YA & OA displayed similar profiles of empirical metabolic cost across k_{EXO}, although OA walked with higher costs. B) YA soleus metabolic cost increased when wearing the EXO. C) OA soleus cost decreased when wearing the EXO. Black dots indicate cost at biological k_T.

THE EFFECTS OF CONTACT SPORT ON CORTICAL NEUROPHYSIOLOGY DURING COGNITIVE-MOTOR TASKS

Samuel R Zeff[1*], Richard van Emmerik[1], Douglas N Martini[1]
[1] Department of Kinesiology, University of Massachusetts Amherst, Massachusetts, USA
*Corresponding author's email: szeff@umass.edu

Introduction: Contact sport exposes athletes to sub-concussive head impacts, defined as mechanical energy transfer to neural tissue which disrupts axonal and/or neuronal integrity, but does not result in symptomology warranting a concussion diagnosis [1]. Contact sport participation has been associated with postural control deficits [2], as well as cognitive deficits and altered frontal cortex activity [3]. However, the relationship between cortical neurophysiology and motor performance deficits remains poorly understood due to the limited knowledge regarding cortical activity changes during cognitive-motor tasks in contact sport athletes. Theoretical approaches suggest increased cortical resource utilization may serve as a compensatory mechanism to maintain cognitive and/or motor task performance in individuals following neurotrauma [4]. From this perspective, increased cortical activity under low-level, motor task demands (e.g., standing posture) may provide insights into whether underlying impairment exists during more challenging sport specific motor tasks. Similarly, dual-tasking (DT), which involves the addition of a cognitive task during a motor task, may further increase task difficultly compared to motor tasks without a secondary cognitive task (single-task (ST)).

Functional near-infrared spectroscopy (fNIRS) is a mobile neuroimaging device that quantifies changes in blood oxygenated haemoglobin (HbO_2) levels within the cortex. fNIRS can be implemented to assess how sub-concussive head impacts influence cortical activity during ST and DT motor and cognitive tasks, and provide insight into the neurophysiological underpinnings associated with performance changes associated with contact sport participation. Therefore, we sought to determine the effect a season of contact sport participation would have on cortical neurophysiology, motor task performance, and cognitive performance. We hypothesized contact sport participation would negatively impact motor and cognitive performance. Similarly, we hypothesized that a season of contact sport would increase frontopolar prefrontal cortex activation during ST and DT motor tasks, with greater changes in cortical activity under DT conditions.

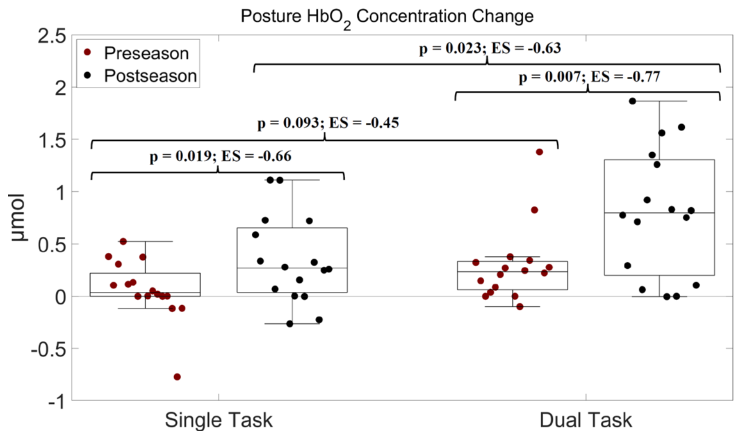

Figure 1: Box and scatter plots of changes in HbO_2 (in µmol) concentrations throughout a season of contact sport. Greater values indicate a larger increase in cortical activity relative to a quiet standing period. DT posture significantly increased cortical activity compared to ST at both timepoints. Separately, participating in a season of contact sport significantly increased cortical activity during both ST and DT posture.

Methods: 16 male collegiate hockey athletes (Age: 20.75 [1.53] yrs.) completed 2-minute quiet standing tasks while fitted with an inertial measurement unit on their sacrum and an fNIRS cap covering their frontopolar cortex (Broadman Area 10). Participants completed ST and DT standing tasks with their eyes closed at pre-season training and again following the season (30.94±3.28 days since last contact exposure; 283.38±6.30 days between testing sessions). During DT conditions, the cognitive task consisted of participants counted backwards by 7 from a random number between 900-999. Frontopolar cortex HbO_2 concentration changes were quantified relative to a baseline quiet standing period with eyes closed. HbO_2 changes, postural sway area (m^2/s^4), jerk (m^2/s^5), RMS sway area (m/s^2), and errors and percentage correct (correct attempts/total attempts) served as dependent variables. Our hypotheses were tested using two-way (Condition X Time) RM GLM modelled using Pillai's trace ($\alpha = 0.05$) for each dependent variable. Cohen's d effect sizes (ES) are presented.

Table 1: Means and standard deviations for postural variables

	Single Task		Dual Task	
	Preseason	**Postseason**	**Preseason**	**Postseason**
Sway Area	0.17±0.09	0.14±0.11	0.33±0.37	0.22±0.12
Jerk	16.56±16.94	14.83±7.08	45.52±56.51	37.46±31.84
RMS Sway	0.14±0.05	0.13±0.06	0.21±0.13	0.19±0.05

Results & Discussion: While no time (preseason-postseason) effects were observed ($p>0.05$), completing a cognitive task while standing significantly increased postural sway ($F_{(1,30)} = 7.51$, $p = 0.010$), jerk ($F_{(1,30)} = 7.48$, $p = 0.010$) and RMS sway ($F_{(1,30)} = 9.90$, $p = 0.004$; **Table 1**). There were no significant changes in the number of cognitive task errors ($p = 0.362$; ES = 0.39) or % correct ($p = 0.377$; ES = 0.37) following a season of contact sport during DT. A season of collegiate varsity hockey significantly increased frontal cortex oxyhaemoglobin concentration ($F_{(1,30)} = 16.28$, $p < 0.001$; **Figure 1**), with larger increases during dual-task conditions ($F_{(1,30)} = 8.744$, $p = 0.006$). Following neurotrauma, increased cortical resource utilization may serve as a compensatory mechanism to maintain task outcome performance (e.g., cognitive, motor) [4]. Cortical neurophysiologic assessments may provide an avenue to assess neurologic impairment in absence of cognitive and motor performance deficits. The results from this study are the first of their kind and suggest that contact sport participation appears to alter PFC activity in a way that may be detrimental, but further study is needed.

Significance: While a season of contact sport participation did not modify cognitive or postural task performance, systematic changes in cortical activity were observed from preseason to postseason testing sessions, further increased during DT conditions.

References: [1] Bailes et al., (2013), *J Neurosurgery* 119(5); [2] Bonke et al., (2021), *J Sci & Med in Sport* 24(3); [3] Talavage et al., (2014), *J Neurotrauma* 31; [4] Reuter-Lorenz & Cappell (2008), *Current directions in Psych Sci* 17(3)

THE EFFECTS OF CHEERLEADING SURFACES ON VERTICAL AND FLIP LANDING MECHANICS

Anthony V. Nguyen[1*], Brooke A. Slavens[2], Stephen C. Cobb[1], Kristian M. O'Connor[1]
University of Wisconsin-Milwaukee, Department of Kinesiology
*Corresponding author's email: nguyenav@uwm.edu

Introduction: Cheerleading is a growing sport that is linked to high risks of ankle injuries, particularly during tumbling landing activities [1]. Cheerleaders perform on a variety of surfaces, often on one that is not compliant, which may increase injury risk. Cushioned surfaces are more protective against injuries due to lower loading rates at landing [2]. Most studies investigating landing dynamics have only evaluated simple vertical drop/jump tasks. However, cheerleaders typically land from flipping tasks that have an added angular velocity component [3]. The use of simple vertical landing tasks to represent acrobatic landings remains questionable, and the effects of rotational task differences and potential surface interaction on impact characteristics remain unclear. The purpose of this study was to compare the effects of two cheerleading surfaces (hard vs. matted) between vertical drop and flip landing tasks on impact characteristics. We expected riskier landing dynamics during flips and when landing over a harder surface based on the findings of other landing-surfaces studies and the added angular velocity component [2,3].

Methods: Twelve collegiate cheerleaders (7 females, 5 males; age 20.8 ± 2.1 y; 62.0 ± 13.0 kg; 1.7 ± 0.1 m) participated in this study. A Bertec force plate collected kinetic data and a Motion Analysis Eagle System tracked reflective markers of the right lower extremity as participants landed from a vertical box drop (VERT) and a round-off, back tuck (FLIP) task. The drop height of an adjustable box was matched to each participant's center of mass displacement during the flip task. The center of mass displacement during flight was approximated by tracking a reflective marker on the posterior superior iliac spine. Both tasks were performed over the bare force plate (HARD) and a 1-3/8" cheerleading mat (MAT). The landing phase was defined as the point of initial contact (IC) to the point of maximal knee flexion during landing before recovery. Group averages were computed for impact peaks (IP) and maximal loading rates (LR), as well as sagittal and frontal plane contact angles, ranges of motion, and peak moments during landing. Repeated-measures ANOVAs with a 2x2 design for tasks and surfaces were conducted ($p < 0.05$).

Results & Discussion: The foot's vertical velocity at IC was almost doubled during the FLIP task compared to the VERT task (-5.0 m/s vs. -2.6 m/s, respectively). When comparing the vertical foot and pelvis velocity during the FLIP task, ~70% of this difference (~1.7m/s) was due to the body's angular velocity. The remaining difference was due to imperfections in matching the vertical drop height to the FLIP peak height during the experimental protocol. The foot impact velocity difference challenges the validity of substituting simple vertical landing tasks to represent acrobatic landings.

There were no task*surface interactions for IP or LR (Figure 1). IP values were ~76% greater, and LR values were more than doubled during the FLIP task. Other flip-landing studies also showed greater impact peaks compared to vertical-landing studies even though the vertical studies had landing tasks from higher heights [2,4]. The loading differences in our study, and between other studies, may relate back to the discrepancy in foot impact velocities between tasks. The higher impact velocities during FLIP tasks due to the added angular velocity likely caused significantly greater initial forces and loading rates. These loading differences further challenge equating these tasks. Next, LR was significantly greater on the HARD surface, although there were no surface differences in IP. These results were similar to other landing studies that demonstrated a cushioning effect on LR but not on IP [2]. High LR has been linked to increased injury risks [5,6]. Thus, performing flipping tasks on a harder surface may increase injury risk.

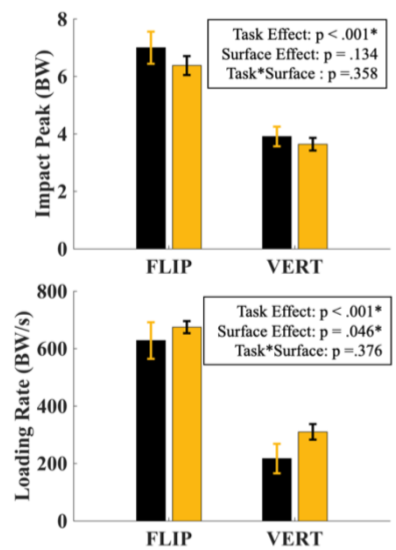

Figure 1. Impact peak forces (BW) and peak loading rates (BW/s). Black bar = MAT; gold bar = HARD. * Denotes significant effect/interaction.

Sagittal and frontal plane ankle mechanics were significantly affected by both the task and the surface. The ankle was ~19° less plantarflexed at impact, and the peak plantarflexion and eversion moments were each more than double for the FLIP task. Landing on the HARD surface placed the foot in a ~3° more inverted position at impact, which could increase ankle injury risks [7]. In addition, landing from a FLIP on the HARD surface increased the peak plantarflexion moment by ~10% as compared to the MAT. These results demonstrate that landing from a FLIP, especially on a hard surface, can place the ankle at greater risk of injury.

Significance: Mechanics during flip landings differed considerably from vertical landings. There is a greater foot velocity at impact, increased loading, and substantially different ankle joint mechanics when landing from a flip. While the effect of cushioning on ground reaction forces were similar for hard and matted surfaces, the effects on ankle joint mechanics were task dependent. These results indicate that using vertical landings as a proxy for the types of landings that occur during cheerleading and gymnastics may not be appropriate. These results also reinforce the greater risks faced by cheerleaders when landing on hard surfaces.

Acknowledgments: Special thanks to the local collegiate cheerleaders that volunteered for this study.

References: [1] Shields & Smith (2011), *Am. J. Emerg. Med* 29(9); [2] McNitt-Gray et al. (1993), *J. Appl. Biomech* 9(3); [3] Xiao et al. (2017), *Acta Bioeng Biomech* 19(1); [4] Wu et al. (2019), *Math Biosci Eng* 16(5); [5] Barrett et al. (1998), *J Sci Med Sport* 1(1); [6] Radin & Paul (1971), *Arthritis Rheumatol.* 14(3). [7] Wright et al. (2000), *J. Biomech.* 33(5).

HOW CAN LOWER BODY JOINT WORK BE USED TO ESTIMATE ENERGETIC COST OF WALKING?

Evan A. Dooley[1, 2*], Katherine R. Knaus[3], Allison M. Lehmann[1, 4], Shawn D. Russell[1, 2, 5]
[1]University of Virginia, Motion Analysis & Motor Performance Laboratory, Charlottesville, VA, USA
*Corresponding author's email: dooley@virginia.edu

Introduction: Locomotion results from work by skeletal muscles to move the segments of the body. As locomotion varies between individuals particularly those with pathologic gaits, it is of interest how muscles expend energy to perform this work. Current methods to capture this energy expenditure rely on indirect calorimetry or muscle modeling. Indirect calorimetry provides a measurement related to metabolic processes of muscles to convert chemical energy into mechanical work but is cumbersome and time-consuming to measure while requiring individuals to perform the activity continuously for ~5 minutes. Models of muscle energy expenditure generate predictions using optimization following rigid body modeling, but as these models are sensitive to parameters used, these parameters would need to be known in the case of pathologies. The mechanical work performed during walking can be calculated with inverse dynamics, however, there are challenges in relating that mechanical work to the corresponding chemical energy expenditure of muscles. Previous attempts to use mechanical work to capture energy expenditure during walking were limited by understanding of how energy transfers between segments of the model used to calculate work [1,2,3]. Additionally, these attempts have ignored negative work done by the system to avoid a net zero summation across the gait cycle [1,3]. This approach is problematic considering both concentric and eccentric muscle contractions, or positive and negative muscle mechanical work, both require a positive, though unequal, chemical energy cost. We aim to address the question of how we can account for both the positive and negative work for a mechanical formulation for the energetic cost of walking. Using indirect calorimetry, researchers have repeatedly found a U-shaped relationship between speed and cost of walking [4,5,6], with a minimum cost occurring near an individual's preferred walking speed (1-1.2 leg lengths (LL)/sec). In this work, we propose a method to estimate energetic cost of walking using mechanical joint work and explore weightings that account for differing costs of concentric and eccentric muscle work to best match indirect calorimetry measurements during the same task.

Methods: 16 people (23±2.7y.o.; 68±14.2 kg; 1.7±0.13 m; 11F, 5M) walked continuously over level-ground at 6 speeds relative to their preferred walking speed. Real-time audio feedback kept participants within 0.1 m/s of target speeds. Metabolic energy expenditure was collected at each speed via indirect calorimetry (Cosmed K5). Walking kinematics were captured using an 18-camera motion capture system (Vicon) and ground reaction forces were captured by 5 in-ground force plates (Bertec). Joint kinematics and kinetics were calculated in OpenSim using subject-specific full-body models [7]. Joint work was calculated through the stride as joint moment times change in joint angle. Positive joint work was assumed to be concentric dominant work while negative work was eccentric dominant. Net joint work is separated into concentric and eccentric work then weighted to investigate differing energy expenditure requirements. 54 combinations of con- and eccentric weighting were used including the current method of ignoring eccentric contractions [1,3], as well as relative cost of eccentric versus concentric contractions found in literature [8,9]. Weighted work of the hips, knees, and ankles was then summed to give lower body joint work. Mechanical work under each weighted condition was correlated to the matched VO2 measurements found for the same 96 walking events (16 people x 6 speeds each), then ranked by resulting R-value.

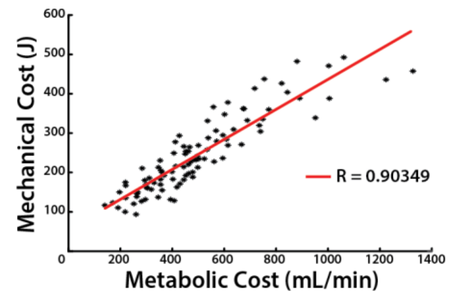

Figure 1: Best correlation between metabolic cost and mechanical cost per event weighted by 85% eccentric and 200% concentric work.

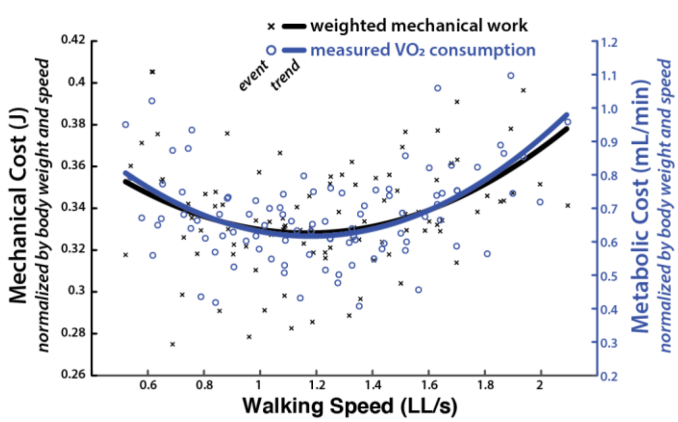

Figure 2: Mechanical & metabolic cost of walking at different speeds.

Results & Discussion: Mechanical cost of walking calculated as lower body joint work with eccentric and concentric work weighted to 85% and 200% respectively is highly correlated to metabolic cost as measured by VO2 consumption (R = 0.90349, *Fig 1*). This correlation is higher than using the weighting suggestion [8] of eccentric/concentric work at 85%/400% or having eccentric/concentric work weighted equally [9]. Also, this approach captures the relationship between energy cost and walking speed better than common practice of only considering the contribution of concentric work. Although eccentric contractions expend less energy than concentric contractions, they are not negligible. The results of these weighted energetic calculations indicate the importance of accounting for positive and negative muscle work to better estimate the energy expended as captured by indirect calorimetry (*Fig 2*).

Significance: This work explores use of mechanical work calculations to estimate the energetic cost of walking by accounting for the different costs of eccentric and concentric muscle work. Identifying the appropriate eccentric and concentric weightings enables an estimate of energy expenditure related to walking speed that can be measured by indirect calorimetry. This approach presents great opportunities to better understand energetics in clinical populations for which current measurements and models are not well suited.

References: [1] Mian (2006), *Acta Physiol* 86:127-39; [2] Russell (2011), *J Appl Biomech* 27:96-107; [3] Willems (1995), *J Exp Biol* 198:379-93; [4] Workman (1986), *J Physiol* 1369-74; [5] Holt (1991), *MSSE* 23:4; [6] Umberger (2007), *J Exp Biol* 210:3255-65; [7] Hamner (2010), *J Biomech* 43:2709-16; [8] Margaria (1968), *Int Physiol* 25:339-51; [9] Russell (2012), *Sports Tech* 5:120-33.

MOTOR CONTROL AND LEARNING OF A TRUNK TRACKING TASK ARE SIMILAR IN INDIVIDUALS WITH AND WITHOUT CHRONIC LOW BACK PAIN

Lee S. Chou[1], Nicholas E. Bray[1], Angela S. Lee[1], John M. Popovich, Jr.[1]*
[1]Center for Neuromusculoskeletal Clinical Research, College of Osteopathic Medicine, Michigan State University, East Lansing, MI
*Corresponding author's email: popovi16@msu.edu

Introduction: Individuals with chronic low back pain (CLBP) have deficits in trunk motor control, but the influence of CLBP on motor learning is not well understood. While pain is considered to influence motor control processes [1], conflicting results exist [2] and there is no consensus with respect to the effect of neuromusculoskeletal pain on motor learning [3]. Assessment of motor control and learning in those with CLBP is important for quantifying treatment outcomes and investigating mechanisms of CLBP. Therefore, the purpose of this study was to compare trunk motor control and learning in individuals with and without a history of CLBP. We hypothesized that individuals with CLBP would demonstrate deficits in performance when compared to individuals with no history of CLBP.

Methods: Individuals between the ages of 18-65 years old were recruited for this study. Participants with CLBP had symptoms lasting >3 months, while asymptomatic participants had no CLBP lasting more than 3 days over the past year. Participant in the asymptomatic group were age- and body mass index-matched to individuals enrolled with CLBP. Exclusion criteria were disorders affecting balance, blindness, neurological disorders, or significant spinal/postural deformity. Participants performed a seated trunk position tracking task that required moving the trunk in the sagittal plane (flexion/extension) to follow a time-varying input signal displayed on a monitor (Figure 1). The trunk tracking input signal was a 30-second long pseudorandom square wave that varied in amplitude as well as hold period [4]. Trunk position was recorded with string potentiometers (model SM2, Measurement Specialties, Inc., Chatsworth, CA). Participants performed a total of 20 trials during each of two laboratory sessions (separated by a minimum of 48 hours). Root mean square error (RSME) between the input signal and participants' output (i.e., trunk position) quantified performance of each trial. Learning was assessed over the acquisition of 20 trials and retention was determined using the average of the first five trials in the second testing session. Statistical comparisons within (paired) and between (independent) groups were conducted using SPSS® (Armonk, NY: IBM Corp), with significance set at $p<0.05$.

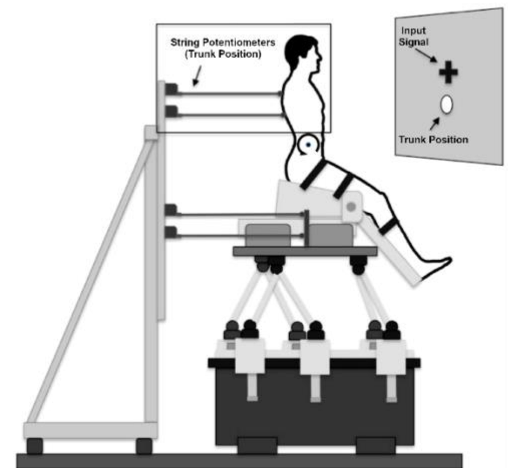

Figure 1. Experimental set-up of the trunk tracking task. Adapted from Reeves et al. [4].

Results & Discussion: A total of 34 participants enrolled in this study; however, 31 completed the required laboratory testing sessions and were included in this analysis. Of the 31 participants, 16 were categorized in the CLBP group (12 women, 4 men) and 15 in the asymptomatic group (11 women, 4 men). Average pain across the two testing sessions was 5.6±1.4 (out of 10) for participants with CLBP. While both groups demonstrated improvements (reduced RMSE) in performance with successive trials ($p<0.05$), there was no statistically significant difference in performance between the asymptomatic group versus the CLBP group across the 20 trials during session 1 or session 2 (Figure 2). There was also no statistically significant difference ($p>0.05$) in retention between the asymptomatic and CLBP groups (Figure 2). While this trunk-specific motor control task was sensitive to improvements in performance with successive trials (i.e., RMSE reduction), contrary to our hypothesis, CLBP did not seem to have a significant effect on trunk motor control or learning as assessed during the trunk-specific motor task. Considering musculoskeletal pain has been shown to affect learning strategies during gait [5], it is possible that individuals with CLBP and asymptotic individuals perform the task with different movement strategies while maintaining similar performance; however, this would warrant further investigation.

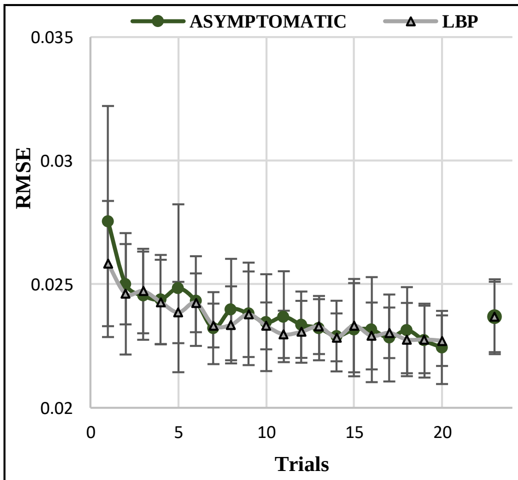

Figure 2. Acquisition (trials 1-20, 1st session) and retention (mean of 5 trials, 2nd session) performance.

Significance: The results of this study suggest that individuals with CLBP do not exhibit significant deficits in motor learning compared to asymptomatic individuals during a trunk-specific motor task. This finding has important clinical implications, as it suggests that interventions designed to improve trunk motor control and learning may be equally effective for individuals with and without CLBP. Overall, the findings of this study may help guide the development of effective treatment strategies for this prevalent and debilitating condition. The results of this study may also have implications beyond the field of CLBP, as the assessment of motor learning is a critical component of understanding and improving motor control in a range of clinical populations.

References: [1] Kantak et al., (2022), *Phys Ther*, 102(4); [2] Matthews et al., (2022), *PLoS One*, 17(9); [3] Izadi et al., (2022), *Front Hum Neurosci*, 16; [4] Reeves et al., (2014), *J Biomech*, 47(1).; [5] Dupuis et al., (2022), *BMC Musculoskelet Disord*, 23(1).

DIFFERENCES IN MIDDLE-AGED AND YOUNG ADULTS' HIP JOINT QUASI-STIFFNESS DURING WALKING

Shanpu Fang[1], Vinayak Vijayan[1], Megan E. Reissman[1], Allison L. Kinney[1], Timothy Reissman[1]*
[1]EMPOWER Lab, Department of Mechanical and Aerospace Engineering, University of Dayton, Dayton, OH, USA
*Corresponding author's email: treissman1@udayton.edu

Introduction: Joint quasi-stiffness represents the relationship between a person's internal moment and angular change for a certain plane of a joint [1]. This relationship has been often used to inform exoskeleton design [2]. Further understanding of hip quasi-stiffness is needed to design hip exoskeletons (exos). A hip exo is designed to provide assistance by altering the resultant torque at the wearer's hip joint. Thus, depending on the design, the change in the resultant torque can alter the stiffness felt by the hip exo wearer. Hip exo designs can benefit from knowing the wearer's hip joint quasi-stiffness at different phases of the gait cycle.

Overall, quasi-stiffness studies have been focused primarily on the ankle and knee and less on the hip, and those studies evaluating hip joint quasi-stiffness have been mostly focused on young adults [3-5]. As middle-aged or older adults are more likely to be the target population of hip exos, it would be valuable to examine whether such age groups adopt similar hip joint quasi-stiffness relationships as young adults. One prior study compared young and middle-aged adults walking at multiple speeds and found no significant difference between the two age groups in hip/knee/ankle joint quasi-stiffness during the braking phase of stance [6]. However, it is unknown how age influences quasi-stiffness in other phases of the gait cycle. Therefore, the purpose of this study was to analyze the sagittal plane hip joint quasi-stiffness during hip extension and flexion for both young and middle-aged, healthy adults. We hypothesized that quasi-stiffness would increase at higher walking speeds.

Methods: 13 young adults (age 22.5±3.9 years) and 16 middle-aged adults (age 44.6±8.9 years) participated in this IRB approved study. Participants performed three continuous 60-second treadmill walking trial collections, during which the treadmill speed was randomized to 100%, 115%, and 130% participant-specific speed. Marker trajectories (at 150 Hz) and ground reaction forces (at 1500 Hz) were collected using a 10-camera Vicon motion capture system (Vicon Motion Systems Ltd., Oxford, UK) and Bertec instrumented split-belt treadmill (Bertec Corporation, Columbus, Ohio, USA) according to [7]. Each participant's left and right sagittal plane hip joint angles and moments were calculated in Visual3D (C-Motion Inc., Germantown, Maryland, USA). Hip joint quasi-stiffness was calculated in two phases modified from definitions in [4]. The hip extension phase starts at 0 radian hip joint angle and ends at maximum hip extension angle. The hip flexion phase starts at maximum hip extension angle and ends at toe-off. For each gait cycle, the quasi-stiffness for each phase was determined from the slope of a linear curve fit to the moment-angle relationship. A repeated measures ANOVA compared quasi-stiffness between age group and walking speed levels (NCSS, LLC, Kaysville, Utah, USA). F-Tests with Geisser-Greenhouse Adjustments were run first, followed by Tukey-Kramer Pairwise Comparisons.

Results & Discussion: Compared to young adults, middle-aged adults showed consistently higher hip quasi-stiffness during both hip extension and flexion (Fig. 1). These differences, 3-7% during extension and 11-21% during flexion, were all significant ($p < 0.0001$) except for the condition at 115% Speed during hip extension. The larger differences in flexion quasi-stiffness can be attributed to greater differences in the hip angle at toe-off between the two age groups. Apart from the mean, higher variability was observed in middle-aged adults' hip quasi-stiffness. Their standard deviations during extension ranged from 0.75-0.80 Nm/kg/rad and 1.11-1.33 Nm/kg/rad during hip flexion, as opposed to young adults' 0.46-0.54 Nm/kg/rad during extension and 0.66-0.94 Nm/kg/rad during flexion.

For both young and middle-aged adults, increased walking speed significantly and consistently increased extension and flexion quasi-stiffness (all $p < 0.0001$, Fig. 1). This is consistent with prior studies of predominantly healthy, young adults [4-5]. Thus, the hypothesis that walking faster increases quasi-stiffness is further validated in this study with both age groups. The increases can be attributed to the increases in hip flexion moment that occurred at the transition point between the extension and flexion phases.

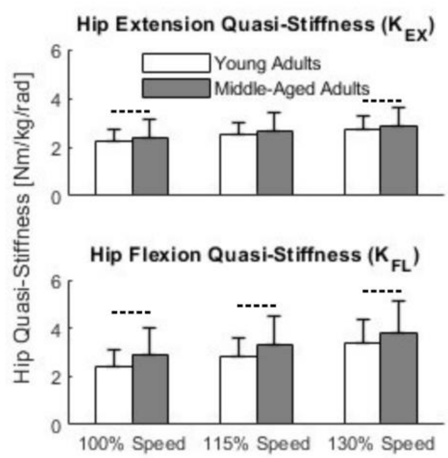

Figure 1: Mean and standard deviation of hip extension and flexion quasi-stiffness for young and middle-aged adults at 3 walking speed levels. $p < 0.0001$ for both speed comparisons and the comparisons connected by dashed lines.

Significance: This study found middle-aged adults had higher hip extension and flexion quasi-stiffness and overall higher extension and flexion quasi-stiffness variabilities. Such results highlight the importance of including studies beyond the behavior of only young adults. Designing hip exo control strategies based on only information from young adults is not necessarily translational to older populations, even those as close in age as middle-aged. With that being said, this study also furthers understanding of the relationship between walking speed and quasi-stiffness. Specifically, it finds that the general relationship of increasing waking speed increases hip quasi-stiffness is consistent across both age groups. This suggests that a hip exo should increase its stiffness support during the extension stage to help absorb the kinetic energy. Similarly, a hip exo should increase its joint stiffness to provide hip flexion assistance in order to propel the center of body mass.

References: [1] Rouse et al. (2013), *IEEE Trans Biomed Eng* 60(2); [2] Brahmi et al. (2021), *ASA Trans* 108; [3] Frigo et al. (1996) *J Electromyogr Kinesiol* 6(3); [4] Shamaei et al. (2013), *PLoS One* 8(12); [5] MacLean & Ferris (2022), *PLoS One* 17(8); [6] Jin & Hahn (2019), *Sci Rep* 9(1); [7] Vijayan et al. (2022), *Sensors* 22(16).

WEARABLE ESTIMATES OF PATELLAR TENDON LOADING WHILE NAVIGATING OUTDOOR TERRAINS

Alex J. Reiter[1]*, Dylan G. Schmitz[1], Sara E. Harper[2], Yiteng Ma[1], Peter G. Adamczyk[1], Darryl G. Thelen[1]
[1]Department of Mechanical Engineering, [2]Department of Biomedical Engineering, University of Wisconsin–Madison, Madison, WI
*alex.j.reiter@wisc.edu

Introduction: Wearable sensors are becoming increasingly popular to assess movement biomechanics in real-world environments. However, conventional wearables (e.g., inertial measurements units or instrumented insoles) can only provide indirect measures of the internal loading of the tissue of interest. Shear wave tensiometers [1] are non-invasive sensors capable of directly assessing changes in muscle-tendon loading. Prior studies have used wearable tensiometry to assess Achilles tendon loading while walking outdoors [2]. The purpose of this study was to estimate relative loading changes in the patellar tendon (PT) while navigating an outdoor course with multiple terrain types. Quantifying relative changes in PT loading directly with a wearable sensor opens the door to assessing performance and injury risk, tracking recovery, and defining return-to-activity or sport criteria in real-world environments.

Methods: With the approval of the University of Wisconsin Institutional Review Board, three healthy, young adults (2F/1M, 23.0 ± 1.6 years) have been tested in this on-going study. Shear wave tensiometers were placed bilaterally over the PT of each participant ($n = 6$). Signal generation and data acquisition were managed by a Raspberry Pi 4B and Measurement Computing Corps MCC172 HATs [3] secured to a running-style backpack worn by the participant. Synchronously, location data were acquired by a GPS antenna. After donning the equipment, participants walked at a self-selected pace along an approx. 1600m outdoor course consisting of *level pavement*, *uphill pavement*, *downhill pavement*, *level packed dirt*, and *level grass*. Wave speed data were segmented into strides, and the corresponding GPS data were used to match strides with course location and incline. Inclines were binned in 2° increments (i.e., 3° to 5° → +4° bin, -3° to -5° → -4° bin); *uphill pavement* and *downhill pavement* were the +4° incline bin and -4° decline bin, respectively. Wave speeds were normalized to the median peak wave speed during *level pavement* for each participant. Statistical parametric mapping was used to identify regions of the gait cycle where the various conditions were different ($p < 0.05$). Repeated measures analysis of variance with Dunnett's test was used to compare normalized peak wave speed of each condition to *level pavement* ($p < 0.05$).

Results & Discussion: Normalized wave speed showed significant differences among a subset of the five terrain conditions for the 0-27% ($p < 0.001$), 38-40% ($p = 0.049$), 43-52% ($p = 0.005$), and 96-100% ($p = 0.025$) portions of the gait cycle (Fig. 1). The *uphill pavement* reached ~25% higher values during the 0-27% portion of the gait cycle compared to the three level terrains, and the *downhill pavement* reached values ~50% higher during the same period. Normalized peak wave speed was significantly dependent on the terrain condition ($p = 0.008$). *Level packed dirt* (95CI = [0.94, 1.03], $p = 0.918$) and *level grass* (95CI = [0.93, 1.07], $p = 0.999$) were similar to *level pavement* (95CI = [0.98, 1.01]), but *uphill pavement* (95CI = [1.14, 1.32], $p = 0.004$) and *downhill pavement* (95CI = [1.21, 1.86], $p = 0.022$) were significantly higher than *level pavement*. *Downhill pavement* induced the largest PT wave speeds, which were 55% larger than the *level pavement*.

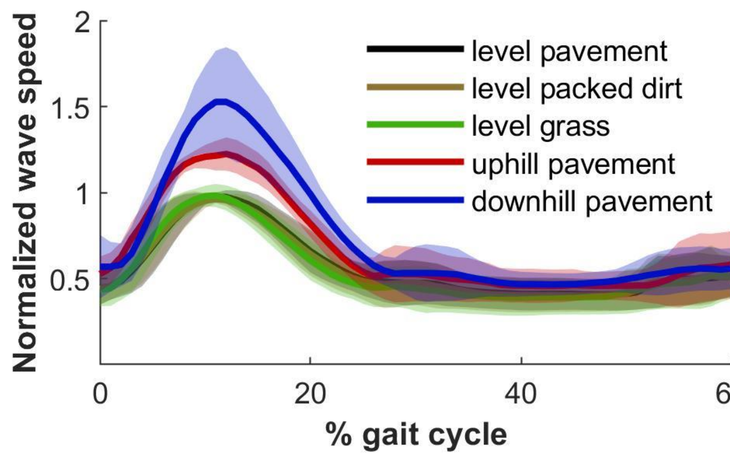

Figure 1: Normalized patellar tendon wave speed for approx. stance phase of gait to highlight the largest differences during early stance. (mean ± SD)

Walking on *level grass* and *level packed dirt* showed similar peak loading and profiles throughout gait compared to *level pavement*. Interestingly, the larger variability during peak loading in grass compared to pavement may suggest that the uneven grass surface causes ankle perturbations which trigger compensatory knee muscle forces to maintain balance. Future work may reveal important distinctions in loading variability while navigating more severe uneven terrains not fully captured by peak loading alone.

It is exciting to note that these wearable measures of loading are comparable to laboratory-based assessments. For example, in past tests of walking on +/-6° indoor ramps, participants also generated the larger forces on the declined (-6°) ramp condition [4]. Going forward, it is feasible to couple tensiometry metrics with IMUs to estimate joint power and work in real-world environments [3], as has been done in the laboratory [5]. Such metrics could prove crucial for identifying injury risk or recovery.

Significance: This study demonstrates the feasibility for a wearable system to monitor metrics of PT loading while navigating an outdoor course across various terrains. Future work will calibrate the relative loading metrics presented here to an absolute measure of PT loading. When combined with wearable kinematic data to characterize joint work and power, these measures may enable objective assessments of performance, injury risk, and recovery during real-world activity.

Acknowledgements: Funding from the DOD CDMRP (129866603), NSF DARE (2019621), and NIH STTR (R42AR074897).

References: [1] Martin+, *Nat Comm*, 9(1), 2018. [2] Harper+, *Sensors*, 20(17), 2020. [3] Harper+, *Sensors*, 22(4), 2022. [4] Alexander+, *Gait and Post*, 47, 2016. [5] Alexander+, *J of Biomech*, 61, 2017.

ASSOCIATION OF PHYSICAL ACTIVITY AND BODY MASS INDEX WITH SKELETAL MUSCLE MASS INDEX AFTER MENOPAUSE

Emma Fortune[1*], Omid Jahanian[1], Stacey Winham[1], Ekta Kapoor[1], Walter A. Rocca[1], Nathan LeBrasseur[1], Kejal Kantarci[1], Melissa M. Morrow[2], Michelle M. Mielke[3]
[1]Mayo Clinic, MN, [2]The University Medical Branch Texas, TX, [3]Wake Forest University School of Medicine, NC
*Corresponding author's email: Fortune.Emma@mayo.edu

Introduction: One in eight women have their ovaries removed before reaching natural menopause (premenopausal bilateral oophorectomy; PBO) for cancer prevention [1]. This may contribute to accelerated aging processes and is associated with a higher risk of multimorbidity compared to women who undergo natural menopause [2]. A recent study reported that women who undergo PBO, particularly before 45 years old, have an elevated risk of sarcopenia (characterized by loss of skeletal muscle mass, strength, and function) compared to women who undergo natural menopause [3]. Physical activity is associated with a lower risk of sarcopenia in postmenopausal women [4]. However, there is limited information regarding physical activity and its relationship with low skeletal muscle mass in women with PBO. Therefore, we investigated the differences in daily step counts and skeletal muscle mass index (SMI; appendicular skeletal muscle mass (ASM) normalized to body weight [5]), and the association of daily step counts with SMI in women with PBO and referent women. We hypothesized that women with PBO would have lower daily step counts and poorer SMI, and that daily step counts would be positively associated with SMI.

Methods: Fifty women with a history of PBO and 50 age-matched referent women (median ages of 66 and 65 years, respectively) received DEXA scans to estimate SMI and wore ankle accelerometers for 7 days. Daily step counts were calculated for each participant from acceleration data [6]. Differences between women with and without history of PBO were assessed using paired Wilcoxon Mann Whitney U-tests. Only descriptive statistics were presented for subgroup analyses because of the small sample sizes. Associations of daily step count with SMI were assessed using linear regression. Covariates included age, BMI, type of menopause (PBO or natural), age at menopause, and hormone replacement therapy (HRT; ever vs. never used).

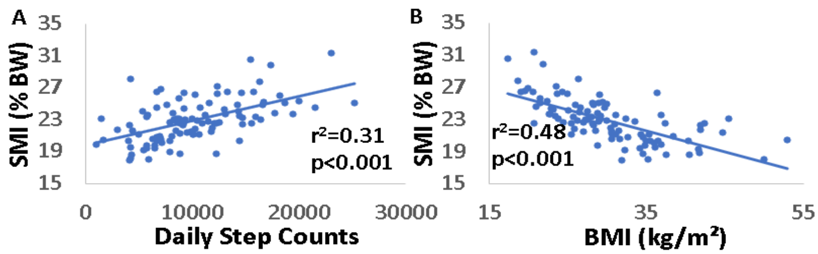

Fig. 1: Scatter plots of daily step counts (A) and BMI (B) vs. skeletal muscle mass index (SMI).

Results & Discussion: BMI was higher, and SMI was lower for PBO versus referent groups (p=0.02 and 0.04, respectively; Table 1). Although the daily step count was lower for PBO versus referent groups, the difference was not statistically significant (p=0.22). The lack of significance was partly due to insufficient statistical power for the observed effect sizes. In addition, referent women with HRT use history had lower step counts and younger age at menopause compared to referent women with no HRT use history. Sixteen percent of referent women were younger than 45 years at menopause. This frequency is much higher than previously reported for in the general population [7]. Our working hypothesis is that some of these women experienced estrogen deficiency-related health issues which resulted in physical activity declines and HRT prescription. In the linear regression model, daily step count (β=0.125, ρ=0.014) and BMI (β=0.217, ρ=0.001) were significant predictors of SMI, explaining 51% of the variability (Fig. 1).

Significance: Higher daily step count and lower BMI are associated with larger SMI. Larger sample sizes are needed to determine if PBO history results in lower daily step counts. Given the elevated risk of sarcopenia for women with PBO history, remote monitoring of daily step counts could provide a means to guide physical activity-based interventions for sarcopenia prevention.

Acknowledgements: This study was supported by funding from the NIH National Institute on Aging Grant U54 AG044170, K12 HD065987, and UL1 TR002371, and the Robert D. and Patricia E. Kern Center for the Science of Health Delivery.

References: [1] Howe (1984), Am J Public Health, 74; [2] Mucowski et al. (2014), Fertil Steril, 101; [3] Karia (2021), Cancer Epidemiol Biomarkers Prev, 30(7); [4] Keller (2019), Wien Med Wochenschr, 169; [5] Kim (2016), J Intern Med, 31; [6] Fortune (2014), Med Eng Phys, 36(6); [7] Rocca (2023), Maturitas, 170.

Table 1: Sample sizes (N) according to group (referent versus premenopausal bilateral oophorectomy (PBO)) and hormone replacement therapy (HRT) use history, median (first – third quartile) age, BMI, step count, and skeletal muscle mass index (SMI).

Group	HRT Use	N	Age (years)	BMI (kg/m^2)	Menopause Age (years)	Daily Step Count	SMI (% BW)
Referent	All	50	65 (62-69)	29 (24-32)*	50 (48-51)*	10717 (6519-14663)	23.4 (20.9-25.1)*
	No	33	63 (60-68)	28 (24-32)	50 (49-52)	12309 (7019-14743)	23.6 (21.6-25.6)
	Yes	17	67 (65-69)	29 (26-32)	48 (43-51)	7897 (5708-11820)	23.1 (20.6-24.6)
PBO	All	50	66 (62-68)	30 (27-36)*	44 (41-47)*	9178 (7080-11639)	22.5 (21.2-23.6)*
	No	4	63 (61-64)	35 (33-38)	48 (47-48)	9822 (9470-10530)	21.7 (21.3-23.1)
	Yes	46	66 (62-69)	29 (26-35)	44 (41-47)	8820 (6793-11825)	22.6 (21.1-23.6)

*p<0.05 for between group differences of all women with PBO history and all referent women.

DIFFERENCES IN GLENOHUMERAL JOINT CONTACT FORCES BETWEEN RECOVERY HAND PATTERNS

Shelby L. Walford[1*], Jeffery W. Rankin[2], Richard R. Neptune[1]
[1]Walker Department of Mechanical Engineering, The University of Texas at Austin, Austin, TX
[2]Pathokinesiology Laboratory, Rancho Los Amigos National Rehabilitation Center, Downey, CA
*Corresponding author's email: shelbywalford@utexas.edu

Introduction: Manual wheelchair users (MWCU) are susceptible to developing injuries such as subacromial impingement due to the repetitive load placed on the upper limbs during wheelchair propulsion [1]. The recovery hand pattern (i.e., the trajectory of the hand during the propulsion cycle) used influences propulsion mechanics, with the semi-circular (SC) and double-loop (DL) patterns typically recommended over arcing (ARC) and single-loop (SL) patterns [e.g., 2]. The purpose of this study was to identify how glenohumeral joint contact forces (GJCFs) vary across hand patterns to gain insight into shoulder pain and injury mechanisms. We hypothesized that hand patterns with higher anterior and middle deltoid forces, which elevate the humeral head (e.g., SL and ARC), would be accompanied by higher GJCFs**.**

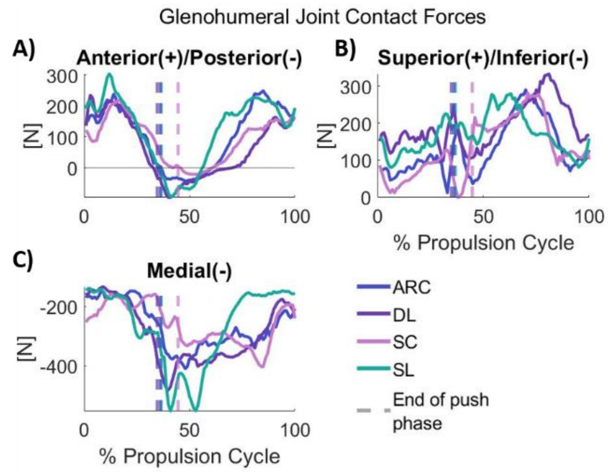

Figure 1: (A) anterior-posterior, (B) superior-inferior, and (C) medial glenohumeral joint contact forces (GJCFs) over the full cycle for the arcing (ARC), double-loop (DL), semi-circular (SC) and single-loop (SL) simulations.

Methods: Previously collected kinematic and kinetic data were used for the simulations [3]. MWCU propelled their own wheelchair during steady-state propulsion. A representative propulsion cycle from one representative subject of each hand pattern group was chosen for simulation and subsequent analysis.

Simulations were performed using OpenSim 4.0 [4] using an upper extremity model [5, 6] that was scaled to each subject. Joint angles were calculated using inverse kinematics [4], and computed muscle control determined the muscle excitations [7]. GJCFs for each simulation were determined using OpenSim's JointReaction analysis and were transformed into the glenoid reference frame [8]. The peak and impulse of the three components of the GJCF were determined over the propulsion cycle and compared between hand patterns.

Results & Discussion: Our hypothesis that hand patterns with increased anterior and middle deltoid forces would correspond to higher GJCFs was partially supported. The SL and DL patterns had the highest anterior deltoid forces and highest superior GJCFs. However, the middle deltoid forces were very similar between all patterns. The SC pattern had the lowest anterior and middle deltoid forces, lowest peak anterior GJCF and second-lowest superior GJCF, and the second-highest medial (i.e., compressive) GJCF impulse.

Anterior-posterior GJCFs: The SL and ARC patterns had higher peak anterior GJCF and impulses compared to the DL and SC patterns (Fig. 1A). Increases in anterior joint contact forces act to decrease shoulder joint stability [9]. Thus, both the DL and SC patterns had more favorable GJCFs compared to the other patterns. They also had the lowest peak posterior force during the push-to-recovery transition phase.

Superior-inferior GJCFs: The DL and ARC patterns had the highest peak superior GJCFs and the DL and SL patterns had the highest superior GJCF impulses, whereas SC had the second-lowest superior GJCF peak and impulse (Fig 1B). Increased superior force is often associated with the potential for subacromial impingement and rotator cuff tears [e.g., 10], making SC more preferable in this direction.

Medial GFCJs: Unlike the anterior-posterior and superior-inferior directions, having increased medial force is preferred because they keep the humeral head compressed against the glenoid fossa, allowing the glenohumeral joint to withstand more shear force [11]. The SC pattern had the second-highest compressive GJCF impulse, but had the lowest compressive force during the push-to-recovery transition phase (Fig 1C). In contrast, the DL pattern had the highest compressive GJCF impulse and the second-highest peak compressive force, which occurred during the transition. Although the DL pattern had more favorable compressive forces, these results suggest that using this pattern comes at the cost of having much higher superior GJCFs than the other patterns.

Significance: This study found that overall, the SC pattern required lower anterior and superior GJCFs and had high compressive GJCF throughout most of the cycle, suggesting that using this pattern will make the shoulder less susceptible to injuries than the other patterns. The only exception was in the late push to early recovery transition region, when the compressive GJCF decreased. Therefore, rehabilitation programs for MWCU should seek to increase rotator cuff muscle activity to increase joint stability during this region to help prevent shoulder injuries.

Acknowledgements: This study was supported in part by NIH Grant R01 HD049774.

References: [1] Bayley et al. (1987), *J Bone Jt Surgery-American* 69(5); [2] Kwarciak et al. (2012), *Disabil Rehabil Assist Technol*, 7(6); [3] Mulroy et al. (2015), *Phys Ther* 95(7); [4] Delp et al. (2007), *IEEE Trans Biomed Eng* 54(11);[5] Saul et al. (2015), *Comput Methods Biomech Biomed Engin* 18(13); [6] McFarland et al. (2019), *J Biomech Eng* 141(5); [7] Thelen et al. (2003), *J Biomech* 36(3); [8] Vidt et al. (2018), *Clin Biomech* 60; [9] Labriola et al. (2005), *J Shoulder Elb Surg* 14(1); [10] Veeger et al. (2002), *Clin Biomech* 17(3); [11] Lippitt et al. (1993), *J Shoulder Elb Surg* 2(1).

PREDICTING THE EFFECTS OF HIP STRENGTH CHANGES ON GAIT DYNAMICS IN PATIENTS WITH TRANSFEMORAL AMPUTATION

Nicholas W. Vandenberg[1*], Benjamin Wheatley[2], Mohamed E. Awad[3], Danielle H. Melton[3], Cory L. Christiansen[3,4], Jason W. Stoneback[3], Brecca M. M. Gaffney[1,3]
[1]University of Colorado Denver, Denver, CO, [2]Bucknell University, Lewisburg, PA, [3]University of Colorado Anschutz Medical Campus, Aurora, CO, [4]VA Eastern Colorado Healthcare System, Aurora, CO
*Corresponding author's email: nicholas.vandenberg@ucdenver.edu

Introduction: Patients with transfemoral (TF) amputation using socket prostheses adopt compensatory movement patterns during gait (e.g., compensated Trendelenburg) that are associated with muscle weakness and the development of secondary comorbidities (e.g., osteoarthritis) [1-3]. Osseointegration is an alternative to socket prostheses involving direct fixation of the prosthesis to the residual bone [4]. Although hip muscle strengthening is a primary component of rehabilitation protocols after osseointegration [5], it is unknown how this influences movement patterns. Musculoskeletal modeling driven by optimal control theory is a novel tool providing a powerful framework for utilizing predictive simulations to determine the effects of various simulated interventions in a dynamically consistent manner [6]. Such modeling allows a low-cost, non-invasive method to robustly examine potential rehabilitative interventions without physical stress on a patient. However, such methods have not been applied to patients with TF amputation. Given the paucity of existing evidence pertaining to rehabilitation efficacy in patients with TF amputation, particularly for those with osseointegrated prostheses, accurate prediction of rehabilitation outcomes *in silico* could be used to aid the evolution of rehabilitation protocols in this novel population. Therefore, our objective was to determine the feasibility of predicting gait mechanics in a patient with TF amputation while also examining the effects of perturbations in hip abductor muscle strength on movement pattern changes.

Methods: With IRB approval, motion capture data were collected from one patient with a unilateral TF osseointegrated prosthesis (Female, 37 y/o, 27.8 kg/m^2, OTNi press-fit implant) during overground walking. A previously developed TF amputee musculoskeletal model [7] was implemented into the optimal control software OpenSim Moco by adding torque actuators to prosthesis joints and six Hunt-Crossley contact sphere elements to each foot [8]. Direct collocation, a gradient-based optimization method, was used to predict a baseline solution of walking dynamics (kinematics, muscle forces) by solving an optimal control problem during the amputated limb stance phase; minimizing an objective function that combined experimental joint angle errors and ground reaction forces, muscle activations, and an upright torso goal [6,8]. Feasibility and validity of the baseline solution was established by comparing predicted kinematics to experimental inverse kinematics with root mean squared error (RMSE). Strengths of the amputated limb hip abductors (Gluteus Medius, Gluteus Minimus, and Tensor Fascia Latae) were then systematically perturbed by scaling the baseline model maximum isometric force values by 5, 50, 75, 125, 150, and 200%. Walking dynamics were predicted with perturbed strengths by solving the same optimal control problem, using the baseline predicted solution as an initial guess. Absolute differences in predicted peak kinematics from each perturbed solution were then calculated relative to the baseline solution.

Results & Discussion: The baseline solution converged in 6.13 hours on an 8-core 2.5 GHz processor (32 GB memory) with a solution that closely matched experimental kinematics (mean RMSE (lumbopelvic, hip, knee DOF) = 2.3±1.2°, max RMSE = 5.1° (intact knee)). Weakened hip abductors increased hip abduction angles and lateral lumbar bending over the amputated limb in early and mid-stance. The largest increases in peak hip and lumbar angles (1.6° and 9.6°, respectively) occurred when abductors were weakened to 5% baseline strength, with the opposite trend observed in strengthening (Fig. 1). These results follow prior evidence where weakened hip abductors were associated with a compensated Trendelenburg pattern [2]. While we did not incorporate subject-specific strength values in this model as dynamometry data was not collected, the fact that perturbing model muscle strengths resulted in expected movement pattern changes is promising. Given the computational and dynamic complexity caused by the lack of ankle and knee musculature in this population, establishing the feasibility of accurately predicting gait dynamics is an important step forward. Notably, this tool provides the platform that can be used to accurately predict gait dynamics in cases where direct biomechanical data may not exist, such as quantifying the effects of rehabilitation before it occurs. This is a critical first step to determine future viability of this tool in subject-specific rehabilitative planning, with the overall goal of improving intervention efficacy.

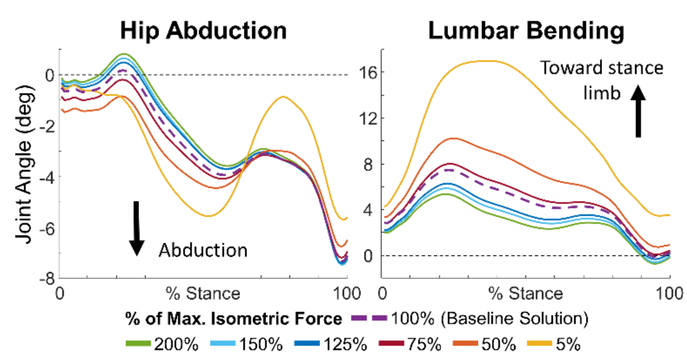

Figure 1. Kinematic changes from perturbed strength simulations

Significance: Establishing the feasibility of using predictive *in silico* modeling in patients with TF amputation may be beneficial in determining rehabilitative interventions to target patient-specific clinical outcomes.

Acknowledgements: This work is supported by the University of Colorado Osseointegration Research Consortium.

References: [1] Goujon-Pillet et al *Arch PM&R* (2008) [2] Gilliss et al *JAOA* (2010) [3] Morgenroth et al *PM&R* (2012) [4] Branemark et al *JRRD* (2001) [5] Leijendekkers et al *Physiotherapy Theory & Practice* (2017) [6] Dembia et al *PLoS* (2020) [7] Vandenberg et al *ORS* (2022) [8] Miller & Esposito *PeerJ* (2021)

TENDON INJURY PROPAGATES FROM THE ENTHESIS-BONE JUNCTION

Lilla Caton[1*], Chris Curry[1], Coleman Cush[1], Sujata Khandare[1], Julianna C. Simon[2], Meghan E. Vidt[1,3]
[1]Biomedical Engineering, Pennsylvania State University, University Park, PA, USA
[2]Acoustics Engineering, Pennsylvania State University, University Park, PA, USA
[3]Physical Medicine & Rehabilitation, Penn State College of Medicine, Hershey, PA, USA
*Corresponding author's email: lhc5111@psu.edu

Introduction: Tendon injury is the primary source of clinical musculoskeletal complaints [1]. Traditional conservative treatments for tendon injury include rest, non-steroidal anti-inflammatory medication, and physical therapy [1]. Dry needling (DN) is a more invasive therapy that is also used, but DN is inconsistent between practitioners, can cause tendon rupture, and has been shown to reduce tendon mechanical properties in a murine model [2]. Novel tendon treatments using focused ultrasound (fUS) have been shown to preserve mechanical properties of tendon better than DN [2]. However, it is unclear how the different treatments and resulting tendon mechanical properties influence injury propagation and healing. The goal of this study is to develop a finite element model to evaluate injury propagation across different treatments by assessing the tendon principal stress distribution in response to loading.

Methods: In our prior work, 50 healthy rat supraspinatus tendons were treated with DN (n=10), 3 different fUS parameters (n=10/group), or sham (n=10), and mechanical properties were measured and implemented in the model [2]. The 3 fUS groups (fUS-1, fUS-2, fUS-3) had varied pulse duration, pulse repetition, duty cycle and treatment time, as described previously [2]. Five separate models were developed in COMSOL Multiphysics® software (v.6.0, COMSOL, Stockholm, Sweden) using geometry derived from magnetic resonance images of a single rat [3]. Image segmentations included: supraspinatus muscle, tendon, and humerus bone. Geometry of segmented tissues was imported into COMSOL, and aponeurosis and enthesis geometry were included using literature values [4,5]. The model was meshed with quadratic tetrahedral elements ≤1.01 mm [3]. Muscle, tendon, and bone sections of each model were defined using elastic modulus determined from literature and experimental stress-strain curves [2,6,7]. Aponeurosis and enthesis were fit with equations to transition Young's modulus throughout the region [3]. Model simulations applied tensile body loads to the tendon belly and aponeurosis regions of each model. A range of loads (2.5 N; 5 N; 7.5 N; 10 N) were applied in-line with muscle line of action along the y- (lateral-medial) axis and at several rotations (2.5°; 5°; 7.5°; 10°) in positive and negative directions along x- (dorsal-ventral), y- (lateral-medial), and z- (caudal-cranial) axes. Additional applied loads represented average experimental force during load-to-failure tests for each group (Sham: 12.32 N; DN: 17.41 N; fUS-1: 18.88 N; fUS-2: 16.40 N; fUS-3: 17.92 N). Predicted principal stress in the tendon was transformed from the global to the tendon coordinate system. Heat maps of principal stress in the enthesis-bone junction were developed to evaluate location and distribution of stress and compared between groups.

Results & Discussion: For all uniaxial (0° rotation) loads, the maximum principal stress was located at the perimeter of the tendon enthesis-bone junction. Peak principal stress under ultimate tensile loading was 11.0 MPa (sham), 14.03 MPa (DN), 10.03 MPa (fUS-1), 13.24 MPa (fUS-2), and 13.42 MPa (fUS-3). Heat maps of the enthesis-bone junction for the same loading condition **(Fig. 1)** indicate that high stress concentrations are localized on the medial side. The range of stress in the enthesis was -1.69-11.0MPa (sham), -4.12-21.8 MPa (DN), -3.45-16.6 MPa (fUS-1), -3.89-20.6 MPa (fUS-2), and -3.24-17.9 MPa (fUS-3). In off-axis loading, peak principal stress is localized near the outer boundary of the enthesis-bone junction and features of on-axis loading heat maps are maintained. Propagation of stress through the cross section occurs in the opposite direction than the rotated force was applied. The distribution of stress under applied loads with lateral rotations showed greater stresses than simulations of the same load in other rotations. For a 10N load in all rotations, peak principal stress ranged from 5.35-8.17 MPa (sham), 7.08-10.28 MPa (DN), 5.10-7.99 MPa (fUS-1), 7.09-10.29 MPa (fUS-2), and 5.85-9.40 MPa (fUS-3). In each group, except for fUS-1, the maximum stress occurs with 10° lateral rotation.

Significance: These data suggest that tendon injury is likely to originate and propagate from the medial aspect of enthesis-bone junction perimeter. Stress magnitude in the enthesis at failure for fUS-1 and fUS-3 resemble the sham group for fUS-1 and fUS-3. Calculation of compressive stress was not expected, presence of these values is likely due to mathematical artifact from the modeling procedures. The fUS-1 and fUS-3 groups have low predicted peak stress and peak stress range, suggesting that after these treatments, tendon has greater ability to resist loading than the other tested treatments. These results also indicate that tendon injury is more likely to occur in lateral loading. More work is needed to understand how different loading parameters influence tissue loading and injury propagation characteristics.

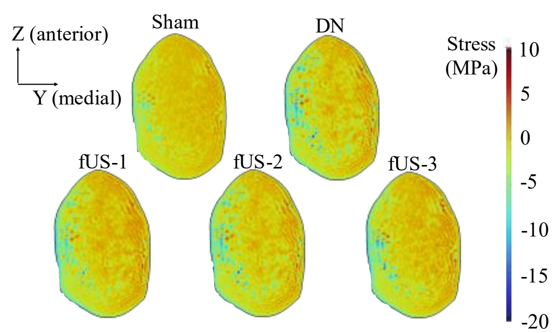

Figure 1. Heat maps of the enthesis-bone junction showing the third principal stress (MPa) for the maximum load in 0° rotation (Sham: 12.32N; DN: 17.41N; fUS-1: 18.88N; fUS-2: 16.40N; fUS-3: 17.92N).

Acknowledgements: Biomedical Acoustics Simon Lab (BASiL); NIH R21EB027886.

References: [1] Kaux et al. (2011) *J. Sports Sci. Med.* 10(2), 238–253. [2] Khandare et al. (2022) *J. Biomech.* 132, 110934. [3] Khandare (2022) PhD Dissertation. [4] Wopenka et al. (2008) *Appl. Spectrosc.* 62(12):1285-94. [5] Grega et al. (2020) *J. Mech. Behav. Biomed. Mater.* 110:103889. [6] Nie et al. (2011) *J. Appl. Mech. Trans. ASME* 78,1-5. [7] Rho et al. (1993) *J. Biomech.* 26(2):111-9.

HEALTHY ROTATOR CUFF MUSCLE CHARACTERISTICS ACROSS AGE AND SEX FROM CLINICAL MRI SCANS

Lara Riem, PhD[1*], Matthew Cousins, BS[1], Olivia DuCharme, ME[1], Elizabeth B. Leitch MEd, ATC[2], Mikalyn Defoor MD[3], Andrew J. Sheean MD[3], Brian C. Werner MD[2], Silvia S. Blemker, PhD[1,4]
[1]Springbok Analytics, Charlottesville, VA; [2]University of Virginia Medical School, Charlottesville, VA; [3]Brooke Army Medical Center, San Antonio, TX; [4]University of Virginia, Charlottesville, VA,
*Corresponding author's email: lara.riem@springbokanalytics.com

Introduction: Rotator cuff (RC) tears remain a challenging clinical problem causing functional impairments including pain, limited active range of motion, and weakness [1]. Current assessments of muscle atrophy and fat infiltration (FI) in the RC musculature rely on subjective grading [2] or analysis of a singular CT/MRI image [3] but fail to objectively characterize the full musculature. New innovations trend towards complete, objective 3D preoperative planning [4] and FI [5]/atrophy quantification. However, clinical MRI scans often only capture the lateral portion of the entire RC structure. Correcting for variation in scan coverage between patients is difficult because total scapula length is unknown. The primary objective of this study was to develop and validate a novel method of quantifying the volume, FI, and morphology of all four RC muscles and bones from clinically obtained MRI scans with typical limited coverage range by: (1) predicting total scapula length from features of the scapula captured and (2) determining RC characteristics as a function of predicted scapula length. Using this method, the study aimed to aggregate healthy RC data across differing ages and sex to create a reference database, providing expected measurements of each RC muscle's size, relative contribution to the RC unit, and FI percentage as a function of location along the scapula. Age and sex-specific control databases increase understanding of the RC unit's expected musculoskeletal characteristics, and in conjunction with the proposed methodology, can help create presurgical assessment of RC health to guide in surgical decision making. This study hypothesized: (1) characteristics of the lateral scapula correlate with the total scapula length, and (2) comparison across a large range of subjects will demonstrate that RC FI is higher in females as compared to males and that RC muscle size is lower in older adults as compared to younger adults.

Methods: 227 clinical shoulder MRI scans were analysed, of which 47 also had full scapula CT scans. The datasets were separated into two groups: (1) scapula length prediction group (n = 47, matched partial MRI/full CT scans), and (2) a control group (n = 180, no diagnosed RC injuries). The control database was split into subgroups of 15 patients for each sex (male, female) for each age group (15-29, 30-39, 40-49, 50-59, 60-69, 70-79 years). *Total Scapula Length Prediction:* The scapula was manually segmented on both the MRI and CT images for all patients in the matched dataset. Four features (1 - sagittal distance from peak cross-sectional area (CSA) to most lateral point on scapula, 2 - peak CSA, 3/4 - the vertical and horizontal bounding length of the scapula) were measured on the lateral portion of the partially captured MRI scapula and were correlated/trained to the total length of the CT scapula using a multivariable linear regression in 33 patients and validated in 14 patients. *Creation & Analysis of Healthy Database Across Age/Sex*: For all MRI scans, segmentation of the RC musculature (supraspinatus, infraspinatus, teres minor, subscapularis), fatty infiltration, and bones (scapula, humerus, clavicle) from the clinical MRI was performed automatically using 3D artificially intelligent segmentation and was vetted to ensure accuracy by trained segmentation engineers [6]. The volume of each segmentation as a function of sagittal distance moving medially was measured from where the lateral end of the scapula first appears. To allow for interscan comparison, the volume was expressed as a function of the location along the scapula (expressed as a percentage) using the predicted scapula length from above. Finally, the muscle volume (normalized by scapula volume to account for patient size [5]), relative contribution, and FI was found for each RC muscle as a function of percent distance along scapula. All data was capped at 40% along the scapula coverage. A two-way ANOVA spatial parametric mapping (SPM) analysis was used to statistically compare each muscle's metrics between patient sex and age groupings. The F-statistic (SPM {F}) was calculated at each point of the scapula location-series, and where SPM {F} crossed a threshold equivalent to $\alpha = 0.05$ post-hoc analysis was performed.

Results & Discussion: *Scapula Length Prediction:* The resulting linear regression relating scapula length from features of the lateral scapula in the training group (n=33) was significant ($r = 0.93$, $p < .001$). When applied to the test group (n=14) the absolute error in prediction was low (2.92% ± 1.68%). *Creation & Analysis of Healthy Database Across Age/Sex*: SPM analysis revealed significantly higher FI in females than males in the infraspinatus ($p < .01$) and subscapularis ($p < .05$). Relative muscle contribution of the supraspinatus ($p < .01$) and infraspinatus ($p < .05$) were lower in the older groups. Muscle size was lower in the older groups in the supraspinatus ($p < .001$) and subscapularis ($p < .05$).

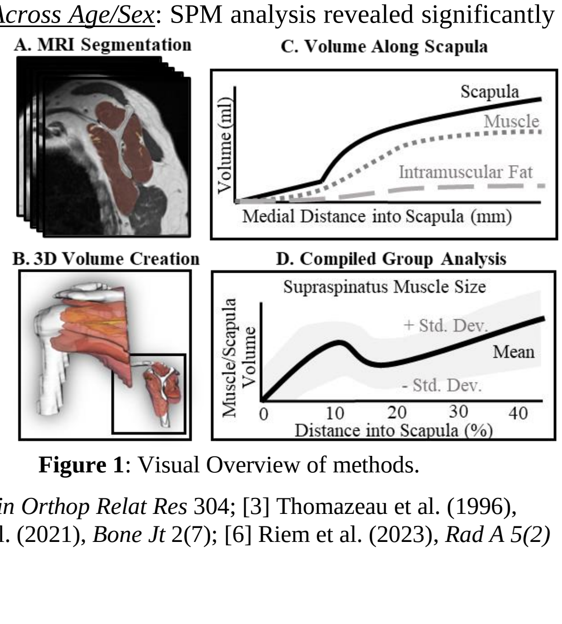

Figure 1: Visual Overview of methods.

Significance: Clinically obtained MRIs can be utilized for 3D analysis of the entire RC unit as a function of location along scapular length, even when scapula length is unknown, by using features of the lateral scapula. Application of methodology in a large healthy population revealed lateral changes to the RC musculature with age (lower muscle size/contribution with age) and FI level with sex (higher FI in females). This large database can be used to reference expected RC muscle characteristics as a function of scapula location.

Acknowledgements: Funding from: NIH-NIAMS Grant # 5R41AR078720

References: [1] Alaia et al. (2020), *MRI Clin N Am*. 28(2); [2] Goutallier et al. (1994), *Clin Orthop Relat Res* 304; [3] Thomazeau et al. (1996), *Acta Orthop Scand* 67(3); [4]Iannotti et al. (2019), *J Bone Joint Am* 101(5); [5] Werthel et al. (2021), *Bone Jt* 2(7); [6] Riem et al. (2023), *Rad A 5(2)*

LEVERAGING A COMMON THEME FOR ASSISTIVE DEVICE DESIGN PROJECTS IN A COURSE

Allison L. Kinney[1*] and Kimberly E. Bigelow[1]
[1]Department of Mechanical and Aerospace Engineering, University of Dayton, Dayton, OH, USA
*Corresponding author's email: akinney2@udayton.edu

Introduction: Engineering design courses including senior capstone or first-year cornerstone design courses are common. While these courses are similar in the general goal to provide engineering students with a hands-on design experiences, the implementation details vary. Design projects can come from many sources with the most popular sources being industry or government and a more recent emergence in service learning. In particular, design courses in biomedical disciplines are more concentrated on service learning projects [1]. Service or community-engaged learning experiences are emerging in engineering design courses and are beneficial to both students and the community [2]. Community-engaged learning is particularly effective in engaging students from historically underrepresented groups in engineering who desire to apply their engineering skills to make a positive impact on society [2, 3].

One example of community-engaged learning that is of interest to biomechanics students involves designing assistive and adaptive devices that meet the needs of individuals with disabilities. An ongoing challenge for faculty coordinating engineering design project courses is sourcing projects [1]. Engineering faculty do not have a direct means to identify clients with disabilities who have unmet needs and therefore, it is difficult to sustain the goal supporting multiple design projects yearly. Therefore, identifying a community partner organization with direct interaction to clients with disabilities is critical for engineering faculty. However, sourcing multiple clients yearly is an ongoing challenge. We have successfully coordinated courses at the senior and sophomore level for the past four years and our goal is to share our process for working alongside a community partner organization to regularly identify design projects.

Methods: Dr. Kinney and Dr. Bigelow have received funding for the past four years from a National Institutes of Health (NIH) R25 educational grant to support design projects in two engineering courses at the University of Dayton (UD). The projects focused on the design of devices that meet the needs of individuals with disabilities identified in a partnership between UD faculty and our community partner, United Rehabilitation Services of Greater Dayton (URS). URS focuses on the physical, social, and emotional needs of children, adults, and seniors with developmental and acquired disabilities throughout the Greater Dayton, Ohio area. Design projects are completed by undergraduate engineering students in two courses, a one-semester sophomore-level Introduction to Biomechanics course and a two-semester senior-level Design Capstone course sequence. A total of ten design projects are completed each year with six projects in the sophomore-level course and four projects in the senior-level course. The remainder of this abstract aims to describe how we leverage a common theme for projects specifically for the sophomore-level course.

Results & Discussion: Each year, the UD faculty meet with our main point of contact at URS, the Director of Operations, to discuss potential design projects for both courses. URS identifies everyday needs that their clients with disabilities have either at home, work, and/or the URS facility. Working closely with URS for many years has improved our ability to identify and appropriately scope projects that will be beneficial for the engineering students and ultimately, result in the delivery of successful final products to help the clients with disabilities. For the senior-level courses, the teams are assigned unique projects that serve the needs of an individual client or an identified need for the URS facility. The senior-level projects are more advanced and require more technical expertise. For the sophomore-level course, we have been most successful in having all of the student teams work on projects that have a common theme and meet a need for the URS facility and require simple and less technical engineering design solutions. Examples of these common needs are interactive elements for a sensory-garden and activity boards for adult and youth clients.

Having student teams work design projects focused on a common theme benefits the faculty, the students, and our community partner in many ways. This clearly reduces the number of unique projects that need to be identified yearly, which addresses challenges for both the faculty and community partner. Additionally, this allows us to sustain engagement of ~30 sophomore-level students and delivery of ~6 successful final products to the URS facility each year (in addition to projects at the senior level). At the beginning of the course, student teams are given a broad problem definition (e.g., design interactive, stimulating activity boards that can engage youth and/or adult clients in learning or practicing a skill) and meet with the URS Director of Operations to begin identifying specific needs that would benefit the URS clients. The broad problem definition allows the student teams to develop unique and creative solutions that address the common need. Throughout the semester, the teams get feedback and support on their design process from the faculty and the URS Director of Operations which is critical for developing successful final designs. Due to the common theme, these feedback sessions are streamlined and can be accomplished during a few class sessions. An added benefit of the common project theme is that the student teams can collaborate, share ideas, and provide more enriching peer-to-peer feedback. In addition, there is an element of friendly competition with the common theme that provides motivation to student teams to produce high-quality final products.

Significance: By leveraging a common theme for assistive device design projects for sophomore-level students, we have successfully engaged students in meaningful design experiences while addressing the challenge of sustaining the efforts involved in carrying out multiple projects yearly. The benefits of this process allow students to learn from each other and lead to creative, unique, and high-quality final products. We hope that others can leverage similar approaches in their own design courses.

Acknowledgements: Funded by NIH Award #1R25HD101096. We thank Rachel Zidaroff, the URS staff and clients for their support.

References: [1] Howe & Goldberg (2019), in *Design Education Today* pgs 115-148; [2] Mollica et al. (2021), *Adv Eng Educ* 8(3); [3] Canney & Bielefeldt (2015), *J Women Minor Sci Eng* 21(3).

EXOSKELETON USE ON SHOULDER MUSCLE ACTIVITY IN OVERHEAD-WORK WITH VIBRATIONS

Parisa Torkinejad Ziarati[1], Ting Xia[1*], Simon Kudernatsch[1], Donald R. Peterson[1]
[1]Mechanical Engineering, Northern Illinois University (NIU), DeKalb, Illinois
*Corresponding author's email: txia@niu.edu

Introduction: Many industries are interested in the use of occupational exoskeleton systems to increase the workers' performance and reduce the physical load and musculoskeletal injuries. The current dominant application of those occupational exoskeletons is providing upper-extremity support in overhead tasks, particularly those tasks with the use of vibratory, percussive, and torqueing tools. Exposure to vibrating hand tools can lead to a series of health disorders generally referred to as Hand-Arm Vibration Syndrome (HAVS). As a result of its significant health and financial implications, safety standards and guidelines have been established to protect against HAVS, including ISO 5349 [1] and ISO 10819 [2]. It has been reported in the literature that Upper-extremity Musculoskeletal Disorders (MSDs) like shoulder injuries are more likely to happen in the overhead postures [3]. There are many studies on the impact of upper-extremity exoskeleton devices on human performance. However, the effect of these supportive systems on the shoulder during use of vibratory power-hand tools has not been explored, which may introduce some unintended risks such as more exposure to vibrations. Currently, there are no safety standards and guidelines for use of tool-induced vibration while wearing an exoskeleton. To understand this issue more closely, a method was developed to investigate the influence of posture and tool-induced vibrations on the shoulder while wearing upper-extremity supporting exoskeletons under controlled conditions.

Methods: A laboratory-based experiment was conducted using ISO 10819, which is a standard protocol for measuring and evaluating the transmissibility of vibration reducing gloves. A random vibration spectrum from 3 Hz to 1,600 Hz modified from the one defined in the ISO-10819 was generated using an electrodynamic exciter placed in the front-of-body (FOB) position and the overhead (OH) position (Fig.1) [3]. The handle was instrumented with a tri-axial accelerometer to precisely control the vibration spectrum. A scissor lift was used to adjust the subject height for both testing postures in order to maintain the elbow flexion at 90°. In addition, grip force and push force were controlled at 30N and 50N, respectively using live-feedback on a pc monitor. Nine surface electromyography (EMG) sensors were adhered over the shoulder and arm muscles typically involved in the overhead work. These muscles included anterior (AD), medial (MD), and posterior (PD) deltoids, upper trapezius (UT), latissimus dorsi (LD), pectoralis major (PM), serratus anterior (SA), biceps brachii (BC), and triceps brachii (TC). Data were collected on six right-handed healthy male subjects with the mean (standard deviation) of the age 33 (11), height 163.5cm (12.9), and weight 69.7kg (9.6), who either wore a vest-type exoskeleton, a strap-type exoskeleton, or not wearing an exoskeleton when exposed to overhead and front-of-body vibrations. Muscle activity was normalized to maximum voluntary contraction collected prior to the experiment. None of these subjects were experienced in the use of exoskeleton. The study was approved by NIU Institutional Review Board.

Figure 1: Overhead setup

Results & Discussion: The study results (Fig.2) indicated that except for BC and PM, muscle activities were generally higher in the overhead posture, especially for AD, SA, and UT which are considered agonist muscles in the overhead tasks. Additionally, the shoulder muscle activities were slightly higher when subject is exposed to vibration. The use of exoskeleton decreased muscle activities in AD and SA; however, there was a slight increase in UT muscle activity when wearing the strap-type exoskeleton.

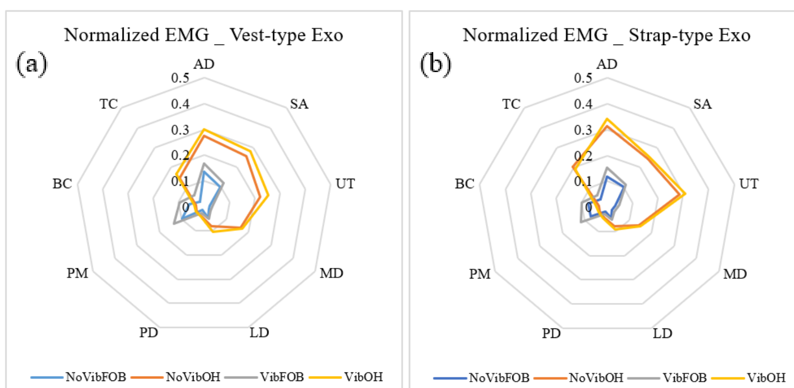

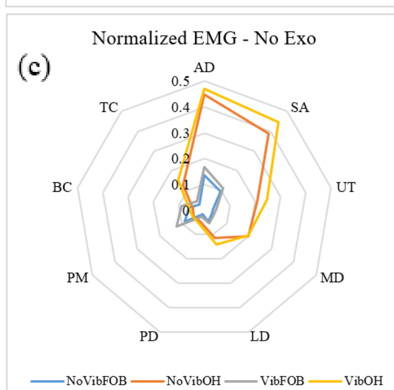

Figure 2: The effects of posture and vibration on shoulder and arm muscle activities under three exoskeleton conditions; (a) Vest-type exoskeleton (Vest-type Exo), (b) Strap-type exoskeleton (Strap-type Exo), (c) not wearing exoskeleton (No Exo)

Significance: The use of upper extremity supporting exoskeletons can have different impact on shoulder muscle activities during vibration exposure. Future work will involve a wider array of measurements and analyses, such as testing with exo-experienced workers, longer overhead and vibration exposure durations, varying overhead postures based and taking into account when an exoskeleton engages its support of the upper extremity, and joint loading analyses using musculoskeletal modeling in order to understand potential injury mechanisms.

Acknowledgements: The present study was in part supported by Northern Illinois University Great Journey's scholarship.

References: [1] ISO 5349, Parts 1 and 2, (2001); [2] ISO 10819, (2013); [3] Ziarati et al., *Proc 7th Intl C Dig Hum Mod Sym* (2022)

TORSO-DYNAMICS ESTIMATION SYSTEM (TES) FOR HANDS-FREE BALLBOT NAVIGATION

Seung Yun Song, Nadja Marin, Chentai Yuan, Yixiang Guo, Chenzhang Xiao, Joao Ramos, Elizabeth T. Hsiao-Wecksler
Mechanical Science & Engineering, University of Illinois at Urbana-Champaign
*Corresponding author's email: ethw@illinois.edu

Introduction: Our group is developing a novel self-balancing, omnidirectional, riding ball-based robot called PURE (Personalized Unique Rolling Experience) as a revolutionary option for manual wheelchair users. The intent of PURE is to allow navigation using intuitive hands-free (HF) control based only on torso motions. The HF control uses torso kinetic and kinematic signals that are scaled according to the rider's preference and used to control the direction and velocity of the ballbot. We developed a Torso-dynamics Estimation System (TES) that can estimate upper body motion (3D torso angles (θ), 3D seat-rider reaction forces ($\vec{\mathbf{F}}$) and torques ($\vec{\mathbf{T}}$), and 2D center of pressure (COP)). Human subject tests were conducted to assess the estimations by TES compared to gold-standard equipment (i.e., research-grade force plate and motion capture system).

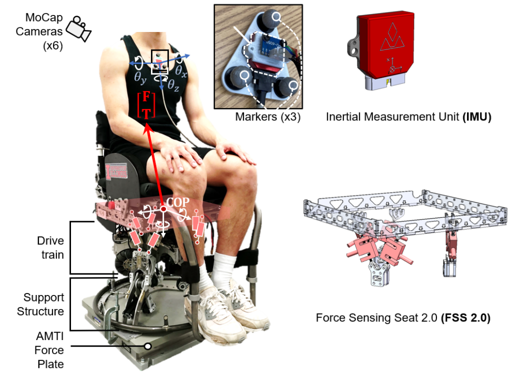

Figure 1: Torso-dynamics Estimation System (TES) consists of an IMU to estimate 3D torso angles and a Force Sensing Seat (FSS 2.0) to estimate 2D COP, 3D forces, and 3D torques.

Methods: The second-generation TES estimates torso rotational kinematics using a commercially-available inertial measurement unit (IMU) and torso kinetics using a custom Force Sensing Seat (FSS 2.0) (Figure 1). A 9-axis IMU (VN-100, VectorNav, USA) was attached to the subject's manubrium and estimated the 3D Euler angles of the rider's torso using the IMU's Relative Heading Mode algorithm with minimal reliance on magnetometers; thus reducing interference when operating indoors and near the robot. The seat plate of the FSS 2.0 was attached to six load cells (CZL301C, Hualanhai, China) arranged in a Stewart platform formation [1], i.e., making the seat into a portable force plate. The Stewart platform's semi-regular hexagonal structure and symmetrically arranged legs allow for more isotropic FSS estimations. The FSS 2.0 was connected to the structural frame that also housed the drive train for PURE (i.e., three sets of quasi-direct drive motor + omniwheel); the spherical wheel (a.k.a. ball) was not included in this test. The FSS was mounted on a force plate (OR6-7-2000, AMTI). Motion capture (Oqus 500+, Qualisys) markers were placed at four corners of the FSS seat and on the IMU module.

A convenience sample of eight able-bodied users (ABUs, 3F:3M, 26.8±1.5 yrs) and manual wheelchair users (mWCUs, 1F:1M, 20.5±2.1 yrs, 17.5±2.5 yrs WC use) were recruited for an IRB-approved protocol. mWCUs were included to assess their smaller and less dynamic torso motions and potentially unique movement patterns. Subjects performed a series of 10 torso movements for 4 cycles per motion (e.g., leaning forward/backwards, left/right, diagonal left/right, twisting, leaning + twisting, leaning diagonally + twisting).

TABLE 1. ACCURACY OF FSS 2.0 AND IMU FOR ABLE-BODIED USERS (ABUs) & MANUAL WHEELCHAIR USERS (mWCUs)

	ABU		mWCU	
	$\overline{RMSE}$	[min, max]	$\overline{RMSE}$	[min, max]
$\vec{\mathbf{F}}_x$ (N)	8.7 (2.4)	[-40.0, 27.2]	5.1 (2.8)	[-23.3, 6.2]
$\vec{\mathbf{F}}_y$ (N)	7.1 (1.2)	[-20.0, 51.1]	7.7 (1.9)	[-3.3, 43.0]
$\vec{\mathbf{F}}_z$ (N)	12.6 (1.2)	[395.2, 857.9]	10.1 (2.3)	[399.4, 682.7]
$\vec{\mathbf{T}}_x$ (Nm)	2.7 (0.4)	[-88.1, 108.1]	2.5 (1.4)	[-66.8, 68.9]
$\vec{\mathbf{T}}_y$ (Nm)	4.0 (1.0)	[-99.6, 200.0]	2.6 (1.6)	[-28.9, 78.7]
$\vec{\mathbf{T}}_z$ (Nm)	1.5 (0.4)	[-25.0, 53.8]	1.7 (1.2)	[-2.1, 14.2]
COP_x (mm)	6.0 (1.5)	[-313.7, 131.4]	4.1 (1.8)	[-125.1, 44.4]
COP_y (mm)	4.5 (1.0)	[-129.7, 168.7]	4.0 (1.8)	[-107.7, 104.6]
θ_{yaw}^{IMU} (°)	1.6 (0.4)	[-63.9, 58.1]	1.3 (0.7)	[-51.9, 55.1]
θ_{pitch}^{IMU} (°)	1.3 (0.6)	[-45.7, 44.4]	0.8 (0.4)	[-21.0, 17.3]
θ_{yaw}^{IMU} (°)	1.6 (0.4)	[-34.5, 34.4]	1.3 (0.7)	[-31.0, 38.2]

[a]Standard Errors from TES (in parentheses)

Results & Discussion: TES estimates displayed high consistency compared to gold-standard measurements when performing torso movements that mimicked motions used to navigate PURE (Table 1). The average RMSE of 3D forces, 3D torques, and 2D COP were approximately 8.6 N, 2.5 Nm, and 4.7 mm, respectively. All three IMU angles (yaw, pitch, and roll) displayed RMSE less than 2°, which is below the 6° maximum allowable RMSE for quantifying human joint angles [2]. The differences in the FSS estimates are likely caused by inherent mechanical compliance in the system and the height difference between the FSS and force plate due to the support structure and drivetrain. The design can be iterated to improve its accuracy, versatility in design, as well as user experience. Despite these limitations, the TES can be sufficiently practical to be used for HF control of powered mobile devices such as PURE and will be demonstrated for navigation performance in future studies.

Significance: The vision of PURE is to create a compact and lightweight ridable ballbot that has a footprint approximately as wide as the rider's hips. Both the FSS and IMU provided sufficiently accurate and sensitive kinetic and kinematic estimations of torso motion, while satisfying strict spatial and inertial design criteria. Future TES designs could have additional applications that use torso motions of seated users during human-robot interactions. Examples could include hands-free control for teleoperation or remote control of physical or virtual mobile robots, or portable applications that could benefit from sensing seat reaction forces-torques and COP.

Acknowledgements: NSF NRI #2024905. Thanks to Coach Adam Bleakney, Dr. Jeannette Elliot, Prof. Deana McDonagh, Prof. Bob Norris, Dr. Patricia Malik, and Shayna Talpallikar.

References: [1] R. Ranganath et. al, Mech Mach Theory, 39(9): 971–998, 2004. [2] T. Seel et. al, Sensors, 14(4): 6891-6909, 2014.

NEUROMUSCULAR CONTROL OF THE STANCE LIMB IS RELATED TO ANTERIOR REACTIVE STEPPING KINEMATICS IN CHRONIC STROKE

Grace K. Kellaher[1*], Jamie Pigman[2], Darcy S. Reisman[1], and Jeremy R. Crenshaw[1]
[1]University of Delaware, Newark, DE; [2]Monmouth University, West Long Branch, NJ
*Corresponding author's email: gkk@udel.edu

Introduction: Individuals with chronic stroke experience balance, mobility, and neuromuscular impairments that put them at an increased risk of falling [1]. This population is characterized by impaired reactive stepping in response to a perturbation [2]. This skill requires the ability to both generate torques about the ankle and take a rapid step in order to arrest a fall and regain stability [3]. The purpose of this study was to determine if there is a relationship between stance-leg muscle activation and recovery-step kinematics during anterior reactive stepping.

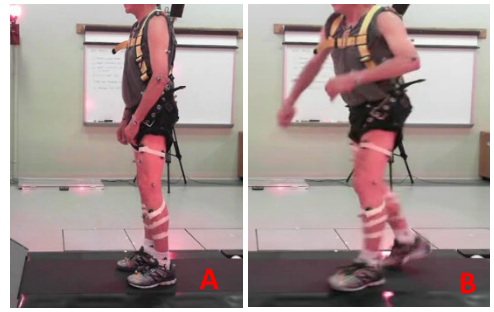

Figure 1. Panel A: Experimental set-up pre-disturbance; Panel B: Typical first-step response to standing perturbation.

Methods: This study is a secondary analysis of data collected as part of a larger study [4]. Ten individuals with chronic stroke (3F/7M; age: 57.1(13.2) years; time since stroke: 5.6(4.1) years) were included in this analysis. Participants were outfitted with a safety harness. From a standing position, rapid treadmill belt accelerations were delivered that induced anterior falls (Figure 1). Kinematic data and muscle activity were simultaneously recorded for each trial. Medial gastrocnemius (MG) activity was recorded using wireless, bipolar surface EMG electrodes. EMG signals were de-meaned, band-pass filtered (10 - 300 Hz), rectified, and low-pass filtered (8th order Butterworth) at 50 Hz for muscle onset latency and 4 Hz for peak activation. Two perturbation trials (one paretic stepping and one non-paretic stepping limb) for each participant were selected for analysis. Our EMG outcomes of interest were peak MG activity relative to pre-perturbation activity, as well as MG onset latency after the beginning of the perturbation. Kinematic outcomes, selected because they could they could be altered with greater plantar flexor torque of the stance limb, included trunk forward rotation angle at first heel strike, first step length, and the anterior and lateral distances between the whole-body COM and stepping-foot toe. The relationships between EMG and kinematic variables, specific to paretic and non-paretic steps, were evaluated using Spearman's rank correlation coefficients (r_S).

Results & Discussion: When stepping with the paretic limb, muscle onset latency of the non-paretic MG in stance was positively correlated with trunk forward rotation angle at first heel strike (Figure 2). This evidence suggests that a more rapid response from the plantar flexors may help arrest forward trunk rotation when taking a recovery step.

When stepping with the non-paretic limb, peak MG activity of the paretic stance limb was positively correlated with trunk forward rotation angle at first heel strike ($p = .021$, $r_S = 0.733$). In non-impaired limbs, we would expect more plantar flexor activity to be associated with less trunk rotation (i.e. a negative correlation). Perhaps the paretic-limb impairment was so severe that plantar flexor muscle activation had little meaningful effect on recovery kinematics.

No other correlations between EMG measures and kinematic measures were significant (p range: 0.087–0.973; r_S range: -0.479–0.575).

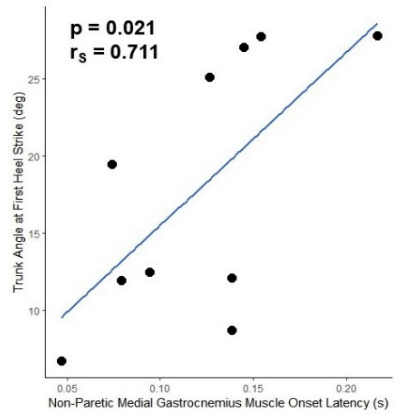

Figure 2. Relationship between non-paretic MG muscle onset latency and trunk angle at first heel strike when stepping with the paretic limb. r_S: Spearman's rank correlation coefficient.

Significance: These results infer a meaningful role of the non-paretic limb in stance during paretic-limb recovery steps during a forward fall. In this cross-sectional study, we could not detect a meaningful role of paretic-limb muscle activity when in stance while, stepping with the non-paretic limb. The stepping response of those with chronic stroke can be improved with perturbation-based balance training [4-6]. However, the ability of perturbation-based balance training to improve paretic stance limb muscle activity has been mixed [7-8]. It is likely, then, that such interventions improve reactive balance with increased compensation from the non-paretic limb muscle activity, rather than enhancing paretic limb muscle responses.

Acknowledgements: This work was supported by the National Institutes of Health (P30 GM103333), the Delaware Rehabilitation Institute/DRI, the University of Delaware Research Foundation, the American Society of Biomechanics Junior Faculty Research Award, and the National Institute of General Medical Sciences (2P20GM103446) from the National Institutes of Health and the State of Delaware.

References: [1] Batchelor et al. (2012) *Intl J Stroke* 7(482-490), [2] Patel & Bhatt (2018) *Exp Brain Res* 236(619-628), [3] Maki & McIroy (2006) *Age & Ageing* 35(12-18), [4] Pigman et al. (2019) *Clin Biomech* 69(205-214), [5] Nevisipour et al. (2019) *Gait & Posture* 70(222-228), [6] Dusane & Bhatt (2021) *Brain Sci* 11(894), [7] Pigman et al. (2021) *Clin Biomech* 82(105249), [8] Staring et al. (2022) *Front Sports Act Living* 4(1008236)

MUSCLE VOLUMES RELATE TO PERFORMANCE DIFFERENTLY IN COLLEGIATE SOCCER AND BASKETBALL ATHLETES

Matthew Cousins, BS[1*], Olivia DuCharme, ME[1], Vi Tran, PhD[2], Silvia S. Blemker, PhD[1,2], Joe Hart, PhD[1,3], Lara Riem, PhD[1]
[1]Springbok Analytics, Charlottesville, VA. [2]University of Virginia, Charlottesville VA. [3]University of North Carolina, Chapel Hill VA
*Corresponding author's email: matthew.cousins@springbokanalytics.com

Introduction: The purpose of this study was to examine how muscle development patterns distinct of athletes in soccer and basketball relate to performance characteristics of speed and jump heights. Soccer and basketball are both characterized by rapids movements, ballistic sprint demands, and prolonged agility. Lower extremity muscle volume development is important for performance, demonstrated by high correlations with sprint speed, squat jump height, and torque generation [1][2]. Our previous work has illustrated non-uniform hypertrophy patterns in athletes based on performance needs. Specifically, large knee flexors and knee extensors are advantageous for fast running in collegiate track athletes [3], and a developed vastus medialis and semimembranosus are crucial for jumping in collegiate basketball athletes [4]. In this study, the muscle volume and distribution of muscle size was examined in collegiate soccer and basketball players [4] and. 20-meter sprint time and jump height were recorded. We combined these measurements to examine the relationship between muscle development and performance output. It is hypothesized that the relationships between muscle volumes and performance metrics vary across muscles and differs between sports.

Methods: A total of 19 adult males (19.9 ± 1.4 years) participated in this study, specifically 9 soccer and 10 basketball varsity NCAA division 1 athletes. For all subjects, an MRI scan was performed on a 3T Siemen Trio MRI Scanner using a 2D multi-slice gradient-echo pulse sequence with an interleaved spiral k-space trajectory. The data collected for the basketball players were part of a previously published study [4]. Proton-density weighted images of the entire lower limb from T12 to the fibular maleoli were acquired with multiple stacks. Automated segmentation was performed to quantify 27 muscle's volumes bilaterally and final segmentations were vetted by a team of trained segmentation engineers to ensure consistency and accuracy across participants [5]. Muscle volumes were calculated by summing voxel volumes from segmented images. The average between the patient's left and right side was taken for all muscle volumes. To account for body size, muscle volume was normalized by the product of height and mass [6]. The following performance assessments were taken: (1) jump (jump height averaged from four vertical jump attempts) and (2) sprint (best 20-meter sprint time of three attempts). Linear regressions were used to evaluate which normalized muscle volumes most strongly correlated with jump and sprint metrics. For tests that were repeated over 27 muscles, a Holm–Bonferroni family-wise error rate correction was used with a statistical significance level of $\alpha = 0.05$.

Results & Discussion: Overall the relationship between muscle volume and performance differed between basketball and soccer players (Fig. 1). Similar to the findings from Xi et al [4] in basketball players, semimembranosus ($r = 0.86$, $p < 0.05$) and vastus medialis ($r = 0.84$, $p = 0.06$) muscle volumes most strongly correlated with jump height, while the vastus medialis ($r = -0.91$, $p < 0.01$) and gluteus maximus ($r = -0.71$, $p = 0.55$) muscle volumes most strongly correlated with sprint time. These relationships are different from soccer players: different muscles most strongly related to performance and overall, the correlations did not reach significance. In soccer players, the biceps femoris long head ($r = 0.62$, $p = 1.00$) and gastrocnemius medial head ($r = 0.53$, $p = 1.00$) most strongly correlated with jump height, while the adductor longus ($r = -0.74$, $p = 0.65$) and gluteus maximus ($r = -0.71$, $p = 0.92$) most strongly correlated with sprint time. This information signifies a need for individualized, sport-specific strength and conditioning approaches to isolate muscle development as needed for a sport's performance demands. Our ongoing work includes increasing the sample size and examining possible sex differences in these relationships.

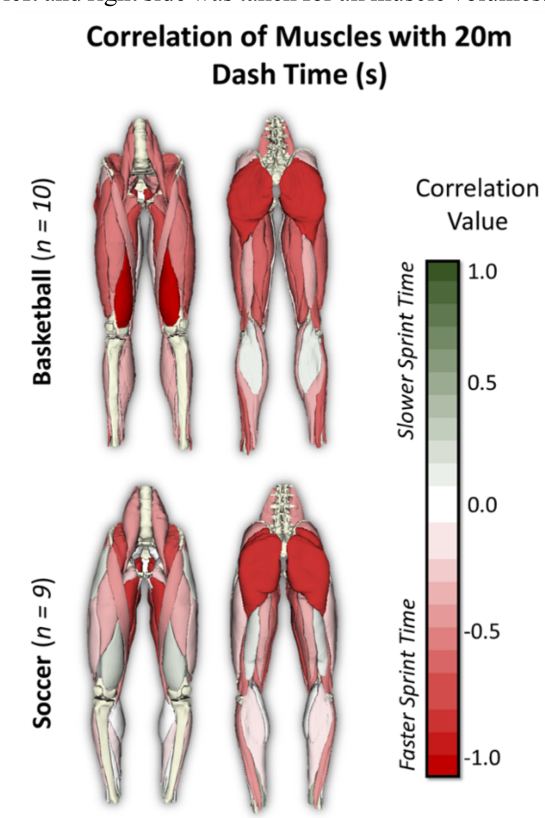

Figure 1: Visual color mapping of correlation between normalized muscle volume to 20m sprint times in basketball and soccer players.

Significance: The lower extremity musculature exhibits unique, non-uniform muscle development patterns depending on athlete demands. Individual muscles most correlated with task performance vary depending on sport. In this study, soccer athletes exhibit high correlations of the adductor longus and biceps femoris long head for sprint and jump performance respectively, while basketball players exhibit strong correlations of the vastus medialis and semimembranosus for sprint and jump performance respectively.

Acknowledgements: We wish to acknowledge Katie Knaus, Dan Podnisy, and Craig Meyer for aid in gathering the data as well as funding from the National Science Foundation and the UVA-Coulter Translational Partnership.

References: [1] Chelly et al. (2010), *J Strength Cond Res 24*; [2] Chelly et al. (2001), *Med Sci Sports Exerc* 33; [3] Handsfield et al. (2017), *Scand J Med Sci Sport* 27; [4] Xie et al. (2019), *J Strength & Cond Res* 34(3); [5] Ni et al. (2019), *J Med. Img*. 6(4); [6] Handsfield et al. (2014), *J Biomech* 4

DIFFERENCES IN WALKING BIOMECHANICS AND CARTILAGE FUNCTION DURING SLOPED AND LEVEL WALKING IN PERSONS WITH ANTERIOR CRUCIATE LIGAMENT RECONSTRUCTION

Isabella Balza[1,2*], Jovanna Gallegos[1,2], Steven A. Garcia[1,2], Seth Kahan[1,2], McKenzie White[1,2], Riann M. Palmieri-Smith[1,2]
[1] University of Michigan: School of Kinesiology, Ann Arbor
* ibalza@umich.edu

Introduction: Individuals with anterior cruciate ligament reconstruction (ACLR) are at greater risk for post-traumatic knee osteoarthritis (PTOA), a progressive disease resulting in degeneration of the cartilage matrix that impairs the tissue's ability to bear load [1]. Thus, it has been proposed that non-invasively assessing how cartilage responds to load or exercise (i.e., walking) may help uncover health of the cartilage matrix [2]. Previous work has shown cartilage thickness changes post-exercise (i.e., strain) are associated with poorer body composition and reduced proteoglycan density providing support for non-invasive assessments to identify early OA-related changes in cartilage properties [3]. Yet, most non-invasive assessments evaluating exercise-induced changes in cartilage generally assess level slope conditions. Walking is a one of the most common forms of exercise in which slopes of various grades are encountered in free-living conditions. Walking at an incline typically increases knee loads, particularly in the patellofemoral (PF) joint [4], which may be advantageous when assessing the PF cartilage matrix. It is currently unclear if inclined walking induces greater strain compared to level walking, but it remains plausible that inclined walking may improve sensitivity in detecting early deleterious changes in PF cartilage. As such, we assessed how sloped walking impacted cartilage strain after exercise and how knee joint mechanics (knee flexion moments [KFM], angles [KFA], and excursions [KFE]) differed across slope conditions. We hypothesized incline walking would lead to greater cartilage strain (i.e., Δ thickness), larger peak KFM, KFA, and reductions in KFE compared to level walking.

Methods: We recruited 10 participants with ACLR (Age: 24.6 ± 7.2 yr., BMI: 25.2 ± 2.5 kg/m^2, Time Post-Op: 27.3 ± 7.8 mo.). Walking biomechanics were captured using an instrumented split-belt treadmill (2000 Hz) synced with a 12-camera motion capture system (200Hz) on both level (0°) and inclined slopes (5°) at a predetermined speed of 1.3 m/s. Gait biomechanics were calculated by combining marker and force data and filtered using a fourth-order Butterworth filter at 6 Hz and 10 Hz, respectively. Peak external KFM, KFA and KFE were calculated from the first 50% of stance phase. Peak KFE was defined as the change in angle from heel-strike to peak KFA (°). Prior to ultrasound (US) assessments, participants rested supine for 45 minutes to unload the femoral cartilage. Following rest, US images were acquired bilaterally at 140° of knee flexion followed by a standard 30-minute walk, either at the incline or level slope (on separate days). Immediately after completing the 30-min walk, US images were again acquired. A custom MATLAB app was used to segment cartilage into medial, lateral, and intercondylar (IC) trochlear regions to measure cartilage thickness changes post-exercise (%Δ). Cartilage thickness for each region was evaluated as the Euclidean distance between deep (cartilage-bone) and superficial (cartilage-synovium) borders across all points on the contour. The average thickness across all three images was used to calculate cartilage strain post-exercise (%Δ thickness). Separate 2 (limb) x 2 (slope) repeated measures ANOVAs were used to compare gait and US metrics ($\alpha = 0.05$).

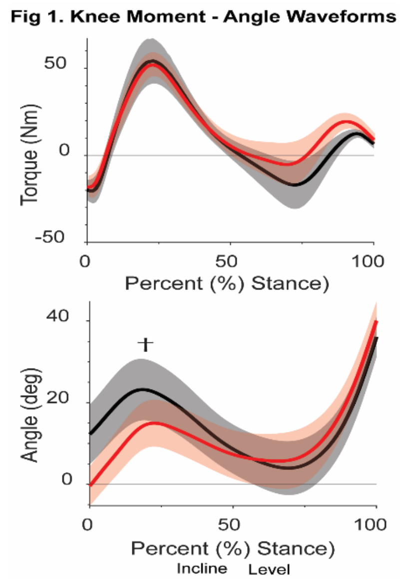

Figure 1. Ensemble averages for knee flexion moment (top) and angle (bottom). † represents differences between incline and level walking.

Results & Discussion: Walking at an incline produced a 3.5% increase in lateral cartilage thickness for both limbs post-exercise ($F = 21.06$, $p < 0.01$) compared to normal walking, but no significant differences were observed in the medial or intercondylar regions ($p > 0.05$). Walking at an incline also increased peak KFA and decreased KFE bilaterally (Fig. 1: F = 50.39 and 23.70, $p < 0.01$), but no differences were observed between slopes in peak KFM ($p > 0.05$). Lastly, we observed smaller peak KFE and KFM in the ACLR limb compared to contralateral limb ($p < 0.04$), but cartilage thickness changes post-exercise between limbs was similar across all regions.

Here, we found that inclined walking led to larger changes in cartilage thickness in the lateral femoral trochlea compared to level walking. In general, inclined walking is thought to increase sagittal plane knee demands, partly due to larger knee angles [5]. Although external KFM did not change in our cohort, increased peak KFA's and KFE were reduced. It is plausible greater changes in lateral thickness could be attributed to changes in peak knee angle and excursions which may lead to more concentrated load applications about the trochlea. Further, despite observing smaller KFM and KFE in the ACLR limb, cartilage thickness and strain post-exercise were similar compared to the contralateral limb. Both thinning and thickening occurs in PF cartilage within the first 5 years post-ACLR, though, previous work in a similar time phase post-op (i.e., approx. 2.5 yrs.) did not show any differences in trochlear cartilage thickness in ACLR knees compared to controls [6] which may suggest cartilage in these regions are more resistant to early tissue degeneration.

Significance: Sloped walking alters sagittal plane knee kinematics that may concentrate load applications about the PF joint and may contribute to greater cartilage strain compared to level walking. Our findings suggest using incline walking protocols may help better differentiate PF cartilage pathology in ACLR populations.

References: [1] Wang et al. (2020), *Arthritis Res Ther* 21(1); [2] Paranjape et al. (2019), *Sci Rep* 9(1); [3] Tamayo et al. (2022), *J Biomech* 134; [4] Alexander & Schwameder (2016), *Gait posture* 45(137-42); [5] Dewig et al. (2021), *Clin Biomech* 84; [6] Li et al. (2013), *Arthroscopy* 29(12)

HEADFORM FRICTION COEFFICIENTS AND IMPLICATION ON OBLIQUE HELMET TESTING

Nicole E-P. Stark[1*], Mark Begonia[2], Steve Rowson[1]
[1]Department of Biomedical Engineering and Mechanics, Virginia Tech Blacksburg, VA
[2]Institute for Critical Technology and Applied Science (ICTAS), Virginia Tech Blacksburg, VA
*Corresponding author's email: nestark@vt.edu

Introduction: Helmet-testing headforms are used to replicate the human head impact response, enabling the assessment of helmet protection and evaluation of injury risk. Accurate representation of rotational kinematics is critical as they are key predictors for injury risk [1]. Studies have suggested that peak rotational acceleration (PRA) and peak rotational velocity (PRV) are sensitive to individual headforms' friction during oblique impacts [2-5]. However, there has been no quantification or comparison of the overall effect across the three commonly used headforms in helmet testing: EN960, Hybrid III, and NOCSAE. Each headform also has different frictional characteristics, and only one study has compared headforms with different moments of inertia (MOI) and frictional coefficients, finding alterations in PRV and PRA [6]. Nonetheless, there was no specification if the response changes were from friction or MOI differences in the headforms [6], and MOI plays a crucial role in oblique impact response [7-8]. Therefore, the actual effect of friction on oblique impact measures is unknown, and recommendations for which headform is most biofidelic have not been made. This study aimed to quantify the influence of headform coefficient of friction (COF) and inertial properties on oblique impact response. Due to the grabbing interaction of a high COF material, we hypothesized that increased headform COF would increase PRV and PRA, but not affect peak linear acceleration (PLA). We also hypothesized that inertial properties would have a larger effect than COF on PRV and PRA.

Methods: Oblique impact testing was completed using guided drop tests of a helmeted headform (helmet, KASK S.p.A Protone Icon) onto a 45-degree anvil with 80-grit sandpaper. Each headform (EN960, Hybrid III, NOCSAE, Hybrid III with skull cap, NOCSAE with skull cap) was tested at two speeds (4.8 and 7.3 m/s) and two orientations (y-axis and x-axis rotation). Using a specially designed tribometer, the static COF of each headform was measured against the helmet's lining material. Each headform was instrumented with a six-degree-of-freedom sensor package at its center of gravity. Data were collected at a sampling rate of 20 kHz and filtered using a 4-pole Butterworth low-pass filter with cut-off frequencies of 1650 Hz (CFC 1000) for accelerometer signals and 289 Hz (CFC 175) for angular rate sensor signals. Resultant PLA, PRA, and PRV were calculated for each test. ANOVAs with type II sums of squares (SS) were used to assess the influence of COF, inertia (published [7-9]), and location on PLA, PRA, and PRV at the two different impact speeds.

Results & Discussion: Against the helmet lining material, the static COF were 0.92±0.04 NOCSAE, 0.83±0.03 Hybrid III, 0.48±0.04 EN960, 0.38±0.02 NOCSAE with skull cap, and 0.37±0.02 Hybrid III with skull cap, Fig. 1. In a previous study we determined that the EN960, NOCSAE with a skull cap, and Hybrid III a with skull cap have COFs closest to a human head. Partly agreeing with our hypothesis, friction statically significantly impacted all measures at high-speed impacts, but friction had a smaller effect than inertial properties for PRA and PRV, but not PLA (Table 1). Our model suggests that a 0.1 COF change alters PLA by 3.5 g, PRA by 204 rad/s^2, and PRV by 0.43 rad/s, while a 25 kg*cm^2 change in MOI alters PRA by 1379 rad/s^2 and PRV by 4.1 rad/s. However, at the low-speed impacts, friction only had a statically meaningful effect on PRV, agreeing with previous literature indicating that the effect of friction is based on tangential velocity [3]. Though MOI still had large effects on PRA and PRV at the low-speed impacts (Table 1). Also, at the low-speed impacts, a 0.1 COF change alters PRV by 0.23 rad/s, while a 25 kg*cm^2 change in axial MOI alters PRA by 729 rad/s^2 and PRV by 3.0 rad/s. The alterations from friction were all within the mean standard deviation of the measures, but the alterations from MOI exceeded the mean standard deviation for both PRV and PRA. Therefore, headform friction is not the most critical variable; MOI is for oblique impact response.

Table 1: Percent of Variance COF and Inertia Accounted for in Each Response Measure (*P<0.05)

	4.8 m/s		7.3 m/s	
	COF	Inertia	COF	Inertia
PLA	3%	0.5%	32%*	3%
PRA	2%	48%*	4%*	53%*
PRV	1%*	53%*	2%*	53%*

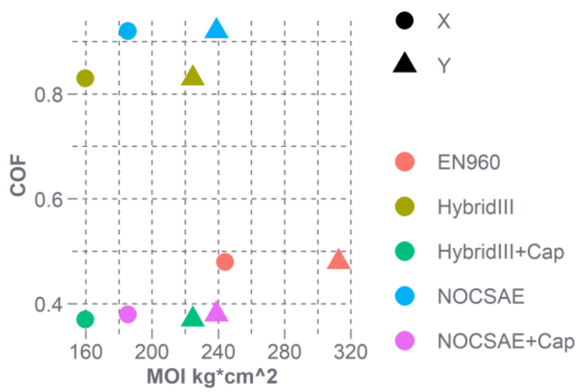

Figure 1: COF and axial MOI kg*cm2 for each headform. The NOCSAE and H3 have high COF that is reduced with skull caps. The EN960 has a low COF but higher MOIs.

Significance: Overall, we recommend that helmet testing protocols consider headform MOI for rotational measures and friction for linear acceleration when interpreting and comparing their results. This recommendation is based on the strong relationship between rotational impact response and injury prediction.

Acknowledgments: KASK S.p.A. ad Unico socio provided funding support for the completion of this project.

References: [1] Rowson (2013) *Ann Biomed Eng* 41(5), [2] Aare (2003), *Traffic Inj Prev* 4(3); [3] Juste-Lorente (2021) *App. Sci.* 11(23) [4] Ebrahimi (2015), *Traffic Inj Prev* 16(4); [5] Trotta (2018), *J Biomech* 75; [6] Yu (2022), *Front Bioeng Biotech* 10; [7] Connor (2019), *Inter J Crashworth* 24(6); [8] Kendall (2012), *Instit Mechanical Engineers* 3(226); [9] Funk (2018), *J Biomech* 140(6).

IMU-BASED MEASURES OF STABILITY REVEAL DIFFERENCES IN BALANCE PERFORMANCE BETWEEN GYMNASTS WITH AND WITHOUT A HISTORY OF SPORT RELATED CONCUSION

Daniel Duque Urrego[1*], Kathylee Pinnock Brandford[1], Gerard Aristizábal Pla[1], Hunter M. Robinson[1], Hailee A. Settle[1], Kate N. Jochimsen[1] and Stephen M. Cain[1]
[1]West Virginia University, Morgantown WV
*Corresponding author's email: dd00055@mix.wvu.edu

Introduction: In collegiate gymnastics, sport-related concussions (SRCs) are common injuries that can result in balance deficits [1], and that increases the chance of future injuries [2]. The Balance Error Scoring System (BESS) is a widely used test to evaluate balance and assist in determining return-to-play (RTP) decisions after SRCs. Although the BESS is a reliable clinical tool for assessing balance, it may not be sufficiently sensitive to identify deficits in athletes who are highly skilled in balance tasks. Previously, we found that force plate-derived measures of stability were different between gymnasts with and without a history of SRC, even though no significant differences were found in the clinical scoring for the BESS [3]. Our objective was to replicate our prior analysis using data from inertial measurement units (IMUs) positioned on the gymnasts' bodies instead of force plate measurements. We hypothesized that IMU-derived stability measures would significantly differ between BESS trials and between gymnasts with and without a history of SRC.

Methods: Seventeen Division I collegiate gymnasts (17F) participated in this study; ten reported a history of SRC. Participants completed the BESS on a force plate (used for a prior analysis [3]) while wearing IMUs on the pelvis and torso (Fig.1). The BESS involves three postures [double leg stance, single leg stance (non-dominant limb), and tandem stance (non-dominant limb behind)] and two surfaces (firm and foam), yielding a total of 6 trials. In each trial, athletes aimed to maintain the prescribed posture for 20 seconds while minimizing overall movement. IMU data were resolved into anatomically relevant reference frames using a functional alignment ([4]; anteroposterior, mediolateral, and longitudinal). We calculated postural sway measures [5] for each participant in each trial using the torso and pelvis IMU acceleration data in the anatomical transverse plane. We used two-way ANOVAs to compare the effects of BESS trial and the history of SRC on the stability measures, which were normalized with a sinh-arcsinh (SHASH) distribution prior to analysis.

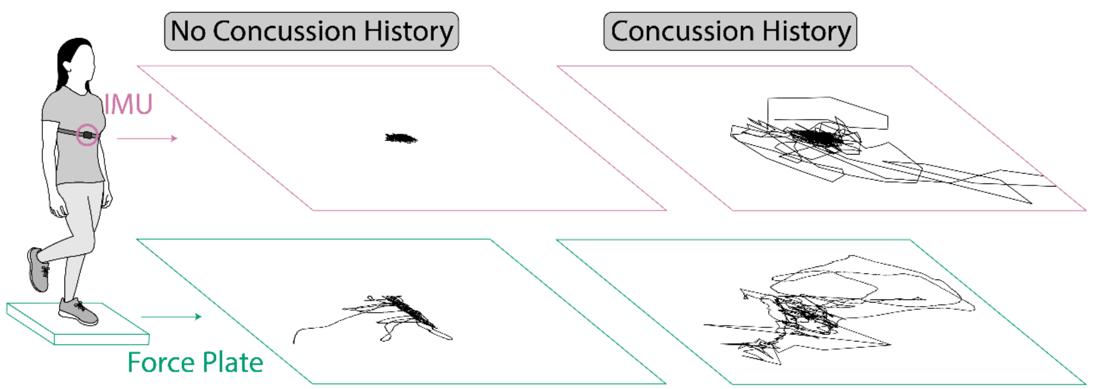

Figure 1. Sample results from single leg stance trials on a foam surface for a gymnast with a history of SRC (right) and without a history of SRC (left). Acceleration data captured from a torso worn IMU (purple, top plots) is similar to center of pressure data from a force plate (green, bottom plots).

Results & Discussion: A two-way ANOVA for the pelvis IMU revealed no statistically significant interaction between the effects of the BESS trial and concussion history. However, the main effects analysis showed that there were significant differences in measures of stability depending on concussion history: total excursions [$F(1,101)=7.43$, $p=0.0077$], mean velocity [$F(1,101)=7.43$, $p=0.0077$], anteroposterior mean velocity [$F(1,101)=8.84$, $p=0.0038$] and sway area [$F(1,101)=5.76$, $p=0.0185$]. Additionally, A two-way ANOVA for the torso IMU revealed that there was a significant interaction between the effects of the BESS trial and concussion history: anteroposterior mean distance [$F(5, 101)= 2.64$, $p= 0.0285$], RMS distance [$F(5, 101)=2.40$, $p=0.0433$], anteroposterior RMS distance [$F(5, 101)=2.76$, $p=0.023$], 95% confidence circle area [$F(5, 101)=2.52$, $p=0.0351$] and 95% confidence ellipse area[$F(5, 101)= 2.34$, $p=0.0478$]. For both sensors, simple main effects analysis showed significant differences in stability measures depending on the BESS trial for all the measurements of stability ($p<0.0001$). Overall, the gymnasts were most stable and exhibited the least sway on a firm surface using both legs; gymnasts were less stable and exhibited the most sway when using only one leg on the foam surface. In both cases, gymnasts with a history of SRC were less stable than the ones that did not have a history of SRC.

Significance: Our results demonstrate that postural stability measures calculated from data captured by body-worn IMUs during the Balance Error Scoring System (BESS) test are sensitive enough to reveal performance differences between gymnasts with and without a history of sport-related concussion (SRC). Notably, no significant differences between groups (history versus no history of SRC) were found in an analysis of the clinical scoring for the BESS [3]. Therefore, athletic training staff can utilize IMUs, which are inexpensive and relatively simple to use, to obtain measures of balance performance that are higher resolution and have higher sensitivity compared to the standard BESS assessment, which provides a discrete and limited measure. Measures of gymnasts' stability or sway during BESS trials can be incorporated to inform return-to-play decision-making.

References: [1] Chandran et al. (2021), *J Athl Train* 56(7):688-694; [2] Chmielewski et al.(2021), *J Sport Health Sci* 10(2):154-161. [3] Robinson et al. (2023), *74th NATA Clinical Symposia & AT Expo*. [4] Cain et al. (2016), *Gait & Posture*, 43: 65-69. [5] Mancini et al. (2012), *J NeuroEngineering Rehabil*, 9(1):59.

ENCOURAGING GROWTH MINDSETS IN UNDERGRADUATE KINESIOLOGY

Brian P. Selgrade*, Stephanie Scoville
Department of Sports Medicine and Human Performance, Westfield State University
*Corresponding author's email: bselgrade@westfield.ma.edu

Introduction: A growth mindset is a belief that intelligence can be shaped by practice, whereas someone with a fixed mindset believes intelligence is innate and unchangeable. Students with a growth mindset tend to perform better academically [1], but mindsets of students in challenging science courses can become more fixed [2]. Kinesiology is a challenging science course for Movement Science and Athletic Training majors. Thus, the purpose of this study was to teach a growth mindset intervention to improve kinesiology students' mindsets and their academic performance. We hypothesized that students in the mindset intervention group would (1) shift to more of a growth mindset and (2) improve their academic performance in kinesiology class, particularly in math-intensive parts of the class.

Methods: We compared kinesiology classes taught in the fall of 2022, which was the control group, and in the spring of 2023. In the first class of the semester for both classes, the professor encouraged students to ask questions. The spring 2023 class (intervention group) had a lesson during the second day of class about growth mindsets. In defining growth mindset, the 1-hour lesson compared the mind to a muscle that gets "stronger" with practice. The lesson stated benefits of growth mindset and emphasized behaviors that students with growth mindsets practice, such as asking for help, asking questions and seeing errors as opportunities to learn. The lesson ended with a video interview in which the professor and a former student discussed the importance of a growth mindset in kinesiology class. This class also completed a "letter to self" assignment, in which they encouraged their future selves to adopt a growth mindset and persevere through a challenging class. This assignment was based on a writing assignment from a previous growth mindset study that caused students to improve their mindsets and GPAs [3]. At the beginning of the course, students in both groups took a modified Implicit Theories of Intelligence Self Scale (ITI-SS) with questions added to understand specific mindsets towards math, writing and computer skills [4]. This survey had 20 questions with answers on a Likert Scale ranging from 1-5. Two weeks later, after the intervention, the mindset intervention group retook the same survey. No variables were normally distributed, so we used Mann-Whitney U tests for pairwise comparisons.

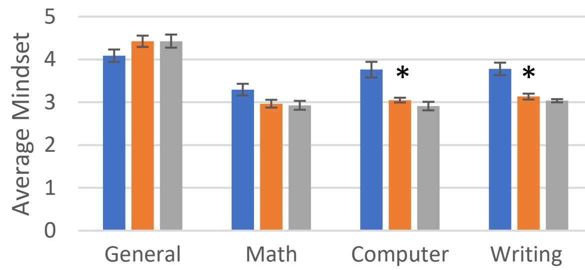

Figure 1: Students' mindsets toward each academic category. * means significant difference from control group pre-semester values for that category. Bar colors signify control group, pre-semester survey, intervention group, pre-semester and intervention group, post-intervention.

Results & Discussion: For the spring 2023 class, which had 18 students, there were no significant differences in survey responses between the first and second surveys, indicating that the growth mindset intervention did not cause students to adopt more of a growth mindset (Figure 1). Pre-semester, the 2 groups had similar general mindsets and mindsets towards math, although the control group, which had 22 students, started out with more of a growth mindset towards computer skills and writing than the intervention group ($p=0.002$ and $p=0.003$, respectively). The intervention group performed significantly better than the control group on the first test of the class ($p=0.015$), supporting the second hypothesis (Figure 2). The intervention group's grade of 71.7 was the highest class average on this test in the 4 years this professor has taught this course. Math grades, which were based on open-response math questions on the first test and normalized to a maximum possible score of 100, were not *significantly* higher for the intervention group than the controls (67.7 ± 31.7 vs 54.5 ± 29.5, $p=0.22$). Given that the mindset intervention did not change students' mindsets, it is surprising that their test grades were so much higher than the controls' grades. A possible reason for this difference may be the emphasis on helpful in-class and study behaviors during the mindset lesson, which emphasized asking for help, and viewing errors and difficult assignments as learning opportunities. These points were stressed by both by the professor and the student interviewed during the lesson. Both courses included encouragement to ask questions, but perhaps the repeated emphasis or hearing this advice from a former student in a more engaging presentation caused students in the intervention group to better internalize and act on this advice. Anecdotally, the intervention group asked more questions in class and during the professors office hours.

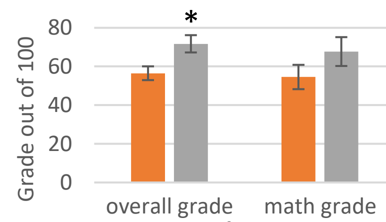

Figure 2: Academic performance on the first test and math-specific portions of this test. * means significant difference from the control group. Bar colors signify control group and intervention group. Error bars denote standard error.

Significance: This work suggests that a growth mindset intervention may help improve students' performance in kinesiology by encouraging helpful behaviors, but a major limitation is that the study is still ongoing. Future work will compare the two groups' grades through the entire semester. Although we cannot currently rule out that the improved grades were due to stronger students in the intervention group, the present academic performance data are promising enough to warrant continued research, which could inform techniques used to teach behaviors like asking for help in first-year undergraduate courses or other science courses.

Acknowledgements: We thank Westfield State for funding this work through a Scholarship of Teaching and Learning Grant.

References: [1] Hacisalihoglu, G. et al. (2018), *Education Sci.* [2] Limeri et al. (2020), *Int J STEM Ed*. 7 (35). [3] Aronson et al. (2002), *J Exp Soc Psych*. [4] De Castella, K., Byrne, D. (2015), *Eur J Psychol Ed*. 30 (245);

SHEAR WAVE SPEEDS PREDICT FATIGUE-INDUCED MICRODAMAGE IN TENDONS

Jonathon L. Blank[1*], Soniya A. Patel[2], Darryl G. Thelen[1,2], Joshua D. Roth[1,3]
[1]Department of Mechanical Engineering, [2]Department of Biomedical Engineering, [3]Department of Orthopedics and Rehabilitation
University of Wisconsin-Madison, Madison, WI
*Corresponding author's email: jlblank@wisc.edu

Introduction: Tendons are fibrous soft tissues that contain highly aligned type 1 collagen fibers. Tendinopathy is a painful condition where the fibrous structure is locally disrupted,[1] and is commonly linked to overuse.[2] It is hypothesized that tendinopathy arises initially from sub-rupture, fatigue-related damage to the tendon microstructure.[3] It is not feasible to detect microdamage *in vivo* using conventional imaging modalities. However, it may be feasible to detect the mechanical ramifications of microdamage, which will shift greater stress onto intact structures. Shear wave tensiometry is a technique for gauging stress based upon shear wave speed (SWS) in the tissue.[4] The objective of this study was to investigate the shear wave speed-stress relationship in fascicles subjected to fatigue loading. Our hypothesis was that fatigue loading would induce microdamage and result in greater stress, and hence wave speed, in the tissue.

Methods: <u>*Mechanical Testing:*</u> We harvested n=9 rat tail tendon fascicles from 32-month F334xBN rats. We secured fascicles in waveform grips in a custom loading device (Aerotech PRO165LM) in a 0.9% saline bath (Fig. 1a). We preloaded fascicles to 0.05 N and recorded the gauge length. We then preconditioned and loaded fascicles axially at 1 Hz from 3-6% strain for 10 cycles followed by 1000 cycles of fatigue loading at the same levels. Transient shear waves were induced via an impulsive tap and tracked via two laser vibrometers (Polytec PDV-100). SWS was computed using a Kalman-filtered cross-correlation of transverse motion measurements.[5] We measured SWS at 20 Hz for 10 seconds after every 100 cycles. <u>*Fatigue Damage Assessment:*</u> We imaged an intact fascicle and representative fascicle following 1000 fatigue cycles in 0.9% saline on a second harmonic generation (SHG) microscope. We imaged with a 60x water-immersed objective lens using an 800 nm excitation. We assessed damage qualitatively based on prior methods.[6] <u>*Statistical Analysis:*</u> We assessed the relationship between axial tension and SWS-squared using linear regression. We made comparisons of change in tension-SWS^2 slopes (in $N/m^2/s^2$) across fatigue levels using a repeated measures analyses of variance (ANOVA) (α=0.05).

Results & Discussion: We observed strong linear SWS^2-tension relationships in all fascicles ($R^2_{avg} > 0.98$) (Fig. 1b). The SWS^2-tension slope decreased with increasing fatigue cycles ($p < 0.001$) (Fig. 1c), which is consistent with plastic region microscopic failure. This was confirmed by imaging, where fascicles exhibited moderate damage following our fatigue loading protocol, with increased fibril kinking and breakage observed at 1000 fatigue cycles (Fig. 1d).

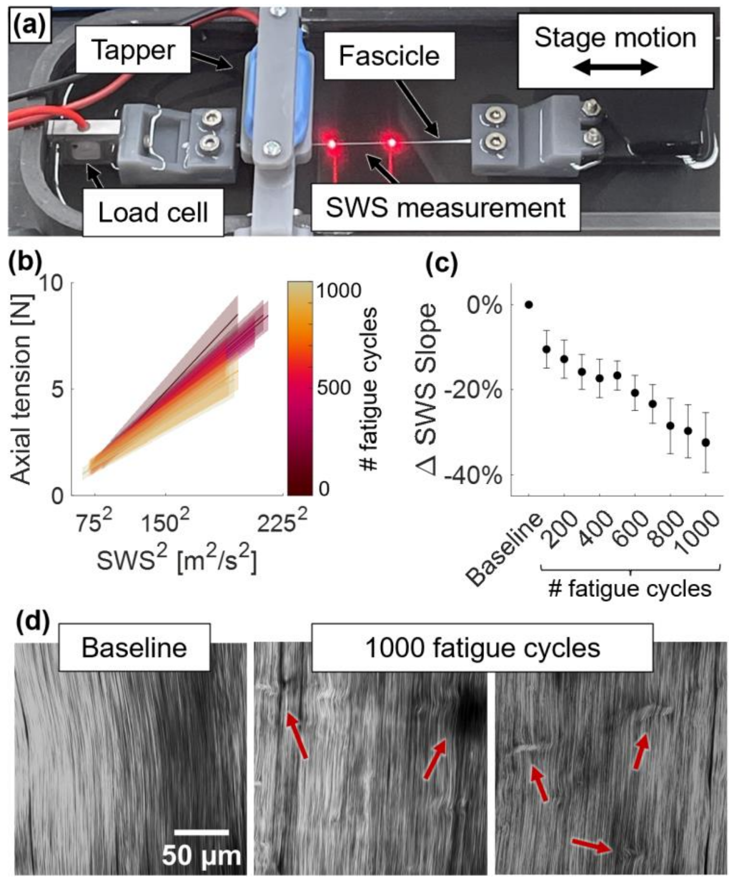

Figure 1: (a) Fascicle testing fixture. (**b)** Linear fits of compiled SWS^2-tension relationships. **(c)** The slope of the SWS^2-tension relationship decreased with fatigue. Error bars=SE. **(d)** SHG images. Red arrows show fibril kinks, breakage, and damage.

The salient observation in this study is that fascicles exhibited elevated SWSs despite an overall reduction in tension following a fatigue loading protocol. The elevated wave speeds were accompanied by identifiable microdamage within the fascicle. It is conjectured that the intact fibrils are carrying the remaining load, and thus the effective axial stress in the intact region is higher due to a decrease in load-bearing cross-sectional area. Future work will use SHG to determine if damaged area corresponds to the reduction in area needed to achieve the increase axial stress quantified using SWS. Overall, these experiments support prior findings of sub-rupture damage accumulation[3] in tendon fascicles and offer a novel technique for gauging microstructure-informed axial stress and damage accumulation during fatigue loading. Ongoing studies are investigating using this technique to probe age-related tendon injuries.

Significance: This study suggests that tensiometry may provide an assessment of the effects of tendon microdamage due to fatigue loading. While further work is needed, these promising results could provide an avenue for noninvasively assessing microdamage in early stages of tendinopathy.

Acknowledgements: NSF GRFP DGE-1747503. We thank Sinan Candan, Dr. Jing Zhang, and Dr. Christian Franck (SHG).

References: [1] Alfredson, *Clinic. Sport. Med.*, 2003. [2] Renström, *Sports Medicine*, 1985. [3] Fung, *J. Orthop. Res.*, 2009. [4] Martin, *Nat. Commun.*, 2018. [5] Schmitz, *Sensors*, 2022. [6] Ros, *J. Biomech.*, 2013.

DO ANKLE INVERTORS AND EVERTORS CONTRIBUTE SUBSTANTIALLY TO PUSHOFF POWER DURING GAIT?

Jack A. Martin[1,2*], Lauren Welte[1], Alex J. Reiter[1], Keith A. Knurr[2], Darryl G. Thelen[1,2]
Departments of [1]Mechanical Engineering and [2]Orthopedics & Rehabilitation, University of Wisconsin-Madison
*Corresponding author's email: jamartin8@wisc.edu

Introduction: It is typically understood that the triceps surae muscles play a dominant role in powering locomotion [1]. The soleus and gastrocnemius muscles have substantially larger cross-sectional areas [2] and moment arms [3] than auxiliary plantarflexor muscles such as the invertors and evertors (e.g., tibialis posterior, peroneus longus). However, the shorter moment arms of auxiliary plantarflexors may be advantageous in situations like the late stance phase of walking that require force production at high angular velocity. In this case, shorter moment arms allow muscles to act at lower shortening velocities, which allows them to function closer to their maximal force production capacity [4]. Contributions of auxiliary plantarflexors can be estimated with musculoskeletal modeling, but remain difficult to validate [5].We previously used shear wave tensiometry to characterize the triceps surae force transmitted by the Achilles tendon across a range of speeds [6]. This analysis leverages those tensiometry results and inverse dynamics analysis to estimate auxiliary muscle contributions to ankle moment and power during walking. We investigated the hypothesis that auxiliary plantarflexors make substantial contributions to pushoff, and that such contributions scale with walking speed.

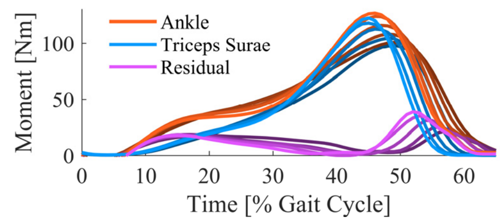

Figure 1: Inverse dynamics estimates of net ankle plantarflexion moment and shear wave tensiometry estimates of triceps surae contributions during the stance phase of walking reveal a substantial residual moment that is unaccounted for. The residual moment exhibits a peak in late stance that modulates with walking speed, and appears to be the result of contributions from the auxiliary plantarflexor muscles. Brighter colors indicate faster walking speeds (1.00-2.00 m·s^{-1}).

Methods: This analysis coupled Achilles tendon tensiometry and inverse dynamics analysis during walking [6]. Shear wave tensiometry was used to track wave speed in the Achilles tendon in 12 subjects during walking (1.00, 1.25, 1.50, 1.75, 2.00 m·s^{-1}) on an instrumented treadmill. Kinematics were tracked using optical motion capture. Inverse kinematics and inverse dynamics (ID) procedures were used to determine joint angles, moments, and powers. Squared Achilles tendon shear wave speeds were calibrated to ID-derived ankle plantarflexion moments, with the constraint that tensiometry-based moment estimates did not exceed ID-derived estimates at any point during the stance phase. This constraint assumes the maximum possible triceps surae loading given no antagonist co-contraction during mid- to late stance phase. Residual moments were calculated by subtracting tensiometry-based estimates from ID-derived estimates. Power was estimated using the product of moment and angular velocity, and positive work was estimated by integrating the positive portion of the power curve during stance.

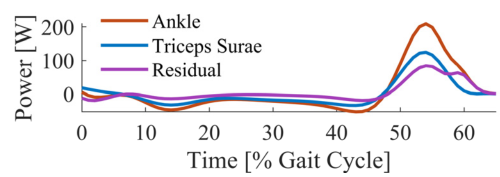

Figure 2: ID-derived ankle power, tensiometry-derived triceps surae power about the ankle, and residual ankle power during walking at 1.50 m·s^{-1}.

Results & Discussion: Achilles tendon wave speed declined before net ankle moment in late stance, resulting in a residual moment unaccounted for by the triceps surae (Fig. 1). The peak residual moment during pushoff ranged from 22-32% of the peak moment generated by the triceps surae. The peak residual power and work were even more substantial, equalling 49-86% and 66-85% of that produced by the triceps surae, respectively (Figs. 2,3). Interestingly, stance phase residual moment patterns are consistent with the timing of tibialis posterior and peroneus longus EMG activity and their modulation with walking speed [7]. These results raise the question of whether it is within the capacity of auxiliary plantarflexor muscles to account for the residuals described. Using a generic OpenSim model, we estimate that the auxiliary plantarflexors can generate approximately 12% of the maximal sagittal moment achievable by the triceps surae at zero degrees plantarflexion under isometric conditions. However, walking is not expected to require maximal force production. Hence, our data suggests that plantarflexors with shorter moment arms may supplement power generation at the high angular velocities seen during the late stage of pushoff in walking.

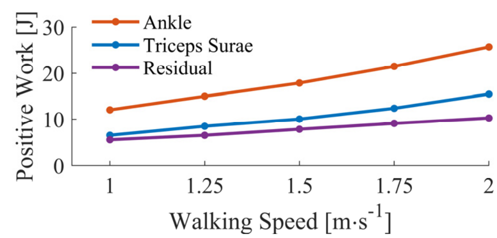

Figure 3: Ankle work estimates reveal a significant portion unaccounted for by the triceps surae, and potentially attributable to auxiliary plantarflexors.

Significance: This analysis highlights the insights that can be gained from more direct measures of muscle-tendon loading during locomotion. For example, the importance of auxiliary plantarflexors in generating pushoff power could shape the way we think about propulsive deficits occurring with aging. Additionally, these results have potential clinical relevance, indicating that injuries to muscles such as the peroneus longus or tibialis posterior may have greater effects on sagittal plane power generation than expected. Notably, the effect observed here is unlikely to be unique to the ankle: trade-offs between moment- and power-generating capacity with differing moment arms may partially explain the evolutionary benefits of muscle redundancy throughout the body.

Acknowledgements: Supported by NIH HD092697, AR074897, T32AG000213, and NSERC PDF 558140-2021.

References: [1] Zelik+ 2016 *JExpBiol*219(23); [2] Fukunaga+ 1996 *JApplPhysiol*80(1); [3] McCullough+ 2011 *FootAnkleInt*32(3); [4]Josephson1999*JExpBiol*202(23);[5]Herzog2017 *JNeuroengRehabil*14;[6]Keuler+2019 *SciRep*9;[7]Murley+2014 *GaitPosture*39(4).

A NEW WAY TO PHASE: USING TRANSLATIONAL KINEMATICS TO ESTIMATE PARETIC LIMB GAIT PHASE

Austin L. Mituniewicz[1], Helen Huang[1], Michael D. Lewek[1, 2]
[1]Joint Department of Biomedical Engineering, University of North Carolina at Chapel Hill and North Carolina State University
[2]Division of Physical Therapy, Department of Health Sciences, University of North Carolina at Chapel Hill
*Corresponding author's email: amituniewicz@unc.edu

Introduction: Current training programs do little to prevent intrinsically generated trips that can lead to falls in people recovering from stroke [1]. However, these gait-related trips could be prevented and eliminated if they were predicted early enough for an assistive device to intervene. Crucial to this solution is the real-time estimation of the paretic limb's gait cycle. This information would be used by the prediction algorithm to discern between normal and abnormal kinematics, and by a device controller to determine when the prediction must be made and when to intervene. Here, we present a potential solution to this task that estimates gait phase timing using the anterior-posterior (AP) translational kinematics of the shank's distal end, relative to the pelvis.

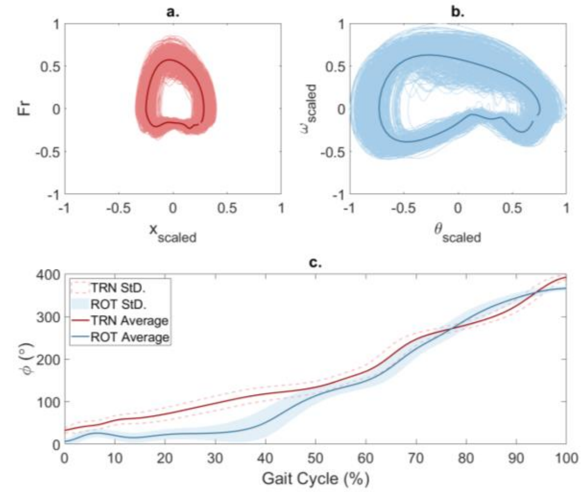

Figure 1: Phase portraits and angles of both methods tested from a representative participant. a.) Phase portrait of our novel method, TRN. b.) Conventional phase portrait, ROT, of the same subject. Dark lines here and in a. represent the averages, while the lighter lines depict individual gait cycles. c.) Average and standard deviation envelopes each method's phase angles.

Methods: Motion capture and GRF data were collected from 10 individuals recovering from stroke walking on a split-belt treadmill, at various speeds (0.2-1.0m/s), with and without a cognitive distraction (e.g. conversation). We started with ground truth gait cycle identification (i.e., initial contact: vGRF>20N). We then determined lower extremity segmental rotational kinematics in the sagittal plane, relative to the lab coordinate system, from subject scaled models in Visual3D. We used these rotations, their first derivatives, and the lengths of the paretic thigh and shank, to compute the AP translational kinematics of the shank's distal end, relative to the pelvis. The position of this point (i.e. ankle) and its velocity were then normalized by the combined thigh-shank length (L) and to the Froude number ($Fr=v/\sqrt{gL}$), respectively, to create our method's translational phase portrait (TRN), Fig 1a. For comparison, we created another phase portrait using shank rotation (ROT), normalized with the technique described by Burgess-Limerick [2], Fig 1b. Phase angles were then computed from each method's respective phase portrait by taking the four-quadrant arctangent and using Matlab's "unwrap" function, Fig 1c.

We assessed method consistency by calculating the standard deviations of each method, within each participant, and then averaging these values across the full gait cycle and stance phase. Next, we linearly fit each subject's phase angles from both methods to gait cycle specific "benchmarks" [3]. Both the full gait cycle and stance phase models began at each gait cycle's 0% phase angle and increased linearly from there at a rate of 3.6° phase/1% gait cycle until their respective termination points. We then acquired the root mean square error (RMSE) and R^2 from these models to assess method accuracy and linearity, respectively. All metrics were analysed using two-sided, paired t-tests at a 0.05 significance level.

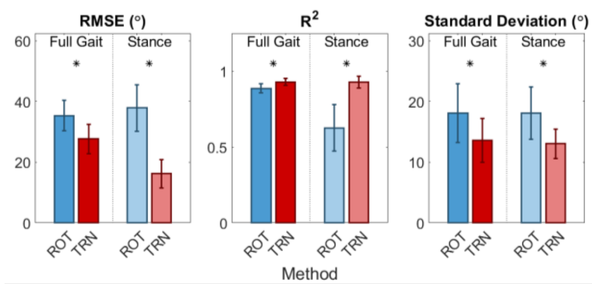

Figure 2: The root mean square error, R^2, and standard deviation results for five people recovering from stroke. Significant differences indicated with a '*'.

Results & Discussion: Implementing a system that can predict and prevent trips before they occur in people post-stroke requires a continuous estimation of gait. Current approaches that do so are often untested on any clinical population [4] or may not translate well to people recovering from stroke, due to increased movement variability within and across people [3]. Additionally, these techniques often require person-specific *a priori* data to train on or derive coefficients from [2-4], potentially increasing clinical burdens during real-world use.. We have avoided these issues by creating an algorithm that requires minimal and easily obtained prior information (i.e., thigh and shank lengths) and by testing our approach offline with data from our target population. These encouraging results, presented in Fig 2, from our first 5 participants demonstrate that our gait cycle detection method appears to be an accurate, linear, and consistent predictor of gait phase across multiple speeds, cognitive loads, and levels of impairment. In particular, the considerable improvement in stance phase results is suggestive of our approach's future success during online monitoring of gait.

Significance: Our novel estimator accurately, linearly, and consistently estimated paretic limb gait phase timing, particularly in stance, which make it ideal for a future system to predict and prevent intrinsically generated trips in people recovering from stroke. Additionally, its simple and interpretable formulation will be easy to implement. We believe this approach represents an improvement upon past methods for both its designed purpose and those of other researchers investigating gait in clinical populations.

Acknowledgements: NSF Graduate Research Fellowship, NIH Grant # R21 HD098570

References
[1] Weerdesteijn et al. (2008), *JRRD* 45(8); [2] Burgess-Limerick et al. (1993), *J Biomech* 26(1); [3] Yan et al. (2017), *Auton Robot* 41(3); [4] Prasanth et al (2021), *Sensors*

IMPLEMENTATION OF THE BLACK BIOMECHANICS SPEAKER SERIES AT THE UNIVERSITY OF DAYTON

Jordan Wilson[1] and Kimberly E. Bigelow[1]
[1] Department of Mechanical and Aerospace Engineering, University of Dayton, Dayton, Ohio, USA
*wilsonj36@udayton.edu kbigelow1@udayton.edu

Introduction: In 2022, we created a, now annual, Black Biomechanics Speaker Series in an effort to recognize and provide a platform for Black biomechanists. Historically in the United States underrepresented minority groups have experienced discrimination in academia and the workforce which have led to implementation of legal frameworks such as affirmative action. This trickles down to access to opportunities for minority groups to speak in the science field. "Giving a talk confers recognition and prestige, particularly for students and early-career researchers." [1] While this is true, studies have shown, authors from minority groups (especially women) are invited to speak less often than white counterparts at these student and early-career stages at conferences. [1] The creation of the Black Biomechanics Speaker Series works to elevate Black scientists who are less likely to be asked to give invited lectures and inspire a more diverse future within biomechanics by facilitating Black student empowerment in efforts to support underrepresented minorities in STEM. [2] This abstract summarizes our initiative so that others might appreciate the issues underrepresented scientists face and how we as a biomechanics community can advocate for and elevate our colleagues.

Figure 1: Black Biomechanics Speaker Series Flyers for 2022 and 2023.

Methods: We envisioned the series to highlight specific attributes of Black leaders in the biomechanics community; therefore, we began by developing a theme for each of the speaker series. Our themes evolved around both research expertise and also leadership and outreach accomplishments. Then we began to find leaders in biomechanics we thought were strong suitors. This was done by taking a deep dive into social media outlets of well-known black biomechanists and professional organizations such as the Black Biomechanist Association to find potential speakers for the series. Next, we contacted our chosen leaders, recognizing that a leader could be someone at any stage of their career. We found emails from official university or industry webpages, or through networking with professionals. Once we reached out to potential speakers through email and we began scheduling them to be a part of the series via webinar (Zoom). This was found to be the best medium for our speakers to present because our current initiative was student-driven and did not include funding for travel. Once a date and time were agreed upon, we scheduled for speakers to present on a topic of their choice in any format they prefer to a student body. We sought out six speakers over two series and all, but one accepted the invitation. Next, we advertised the event to all students, faculty, and biomechanics alumni. Advertising (See Figure 1) was posted and sent to faculty and staff in the School of Education & Health Sciences and the School of Engineering. This targets biomechanics-like majors such as sports and wellness, heath science, physical therapy, engineering etc. Finally, we conducted the event. The day of the event an introduction of the speaker was announced. After the session, the floor was opened to Q&A from the audience.

Results & Discussion: The Black Biomechanics Speaker Series is an interactive informational event that benefit both the speakers and our student body. For invited speakers, this series serves for some, another platform for technical research presentation and for others an opportunity to share their academic or career journey through biomechanics. It also serves as a platform for our speakers to share their leadership efforts in supporting youth, marginalized groups, or low-income communities with the hope to inspire outreach in students. Over 50 current University of Dayton students have come to the series as well as UD alumni and faculty. The information shared in these series have provided not only outstanding science, but also guidance on alternative and non-traditional career paths in a variety of specialties within biomechanics. Engagement with these speakers has led to conversations around useful resources, networking connections, advice on pivotal points in the academic career, post-collegiate career guidance, inspiration to explore sectors of biomechanics research, and more, which has impacted all of our students, including those from underrepresented groups.

Significance: The need for these types of events are important in order to inspire young adults at this stage in their college career. At universities especially Predominantly White Institutions (PWIs) representation of minorities in select fields are low and this makes the pursuit of STEM hard to visualize without a form of exposure. Some Persons of Color (POC) find goals more attainable when they see other POC have already achieved the same or a similar goal, making this speaker series important for multi-ethnic students who are unaware or fairly new to biomechanics. This initiative will continue to empower and acknowledge current black biomechanists for their contributions to the field while inspiring students to explore and get more involved in biomechanics.

References: [1] Ford, H. L., et.al. (2019). *Nature*, *576*(7785), (32-34).; [2] Arif, S., et.al. (2021). *PLOS Computational Biology*, *17*(9), e1009313.

TENOTOMY AND TENODESIS SURGICALLY 'SLACKEN' THE BICEPS: A SIMULATION STUDY

Jorie D. Budzikowski[1,2*], Gabriela C. Hernandez[1], Wendy M. Murray[1,2,3]
[1]Northwestern University, [2]Shirley Ryan AbilityLab, [3]Department of Veterans Affairs
*Corresponding author's email: Jorie.Budzikowski@u.northwestern.edu

Introduction: Shoulder pain is a common orthopedic complaint with a lifetime prevalence of 26-67%, often involving injury to the long head of the biceps (LHB) tendon [1]. Type II SLAP lesions, characterized by tearing of the superior glenoid labrum with detachment of the tendon from its glenoid origin, are a common injury and require surgical intervention to alleviate pain. Three surgical repair options exist: SLAP repair reattaches the labrum and tendon to the glenoid, restoring the LHB muscle-tendon unit to native length, tenodesis reattaches the tendon to the humerus and resects excess tendon [2], [3], and tenotomy releases the tendon to retract and adhere in the bicipital groove [4]. There is widespread debate on which repair is best. Here, we use musculoskeletal modeling to explore the functional implications of different tendon repair strategies for SLAP lesions.

Methods: We simulated Type II lesion repair by altering the origin of the LHB muscle path in a unimanual upper limb musculoskeletal model [5] based on anatomical landmarks and surgical descriptions. The threshold length for passive force generation (l_P) was defined as the sum of the muscle's default optimal fascicle length and tendon slack length [6]; l_P and the corresponding elbow joint posture (θ_P) were computed for each surgical model. For biceps tenodesis, tendon resection (Δl_T) was also simulated by reducing tendon slack length ($l_T^* = l_T - \Delta l_T$; l_T is tendon slack length in the healthy model, l_T^* is slack length induced by the surgery). The operating range of the fascicles of the LHB on the isometric force-length curve was also computed for each surgical simulation.

Results & Discussion: Simulations of biceps tenotomy and tenodesis suggest shorter origin-to-insertion distances impose "slack" muscle-tendon units (Fig. 1). For example, the simulated origin-to-insertion distance imposed by a tenotomy is less than l_P for the full range of elbow motion. For tenodesis, whether the biceps is "slack" depends on a combination of surgical attachment site and resection length. Based on existing model parameters and skeletal dimensions, resection lengths described in surgical literature (~3-5 cm, the length of intra-articular tendon), tenodesis would leave the LHB "slack" for both supra- and sub-pectoralis attachment sites.

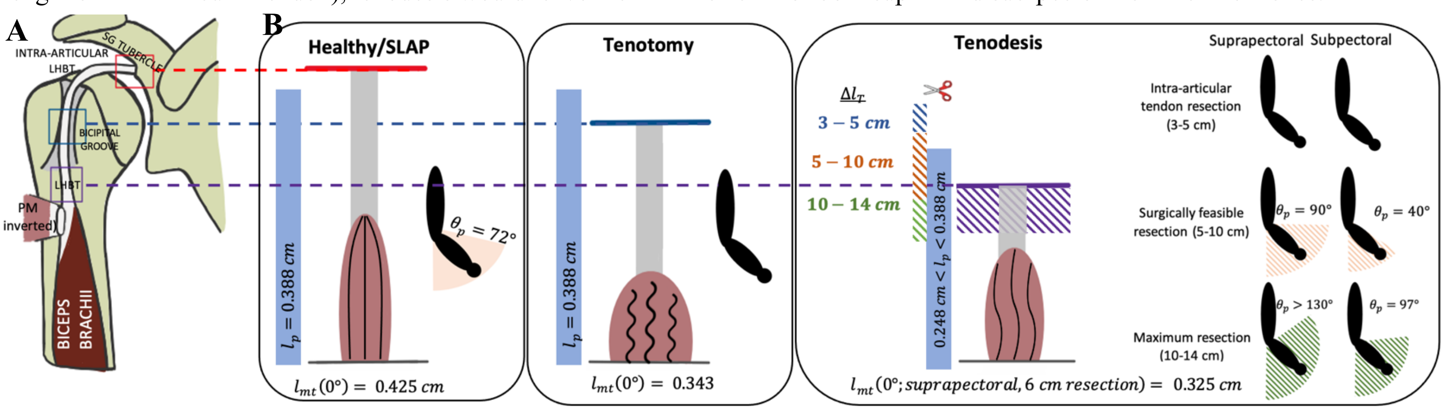

Figure 1: A. Anatomy of the LHB; origin at the supra-glenoid tubercle (outlined in red). SLAP repair maintains this attachment site. In tenotomy, the detached tendon frequently adheres in the bicipital groove (outlined in blue). In tenodesis, the tendon is detached, resected, and reattached on the proximal humerus (outlined in purple). **B.** Graphics compare l_P (blue bar) to l_{mt} at full elbow extension. The range of elbow postures over which the LHB produces passive forces are highlighted. For tenotomy and tenodesis with resection lengths described in the surgical literature, $l_{mt} < l_P$ for the full range of elbow motion, suggesting these surgical approaches "slacken" the muscle.

The functional consequences of surgical approaches that impose "slack" muscle-tendon units are not fully understood. Without adaptation, fascicle shortening needed to take up slack in the tendon during active force generation shifts the operating range substantially, severely compromising force production (Fig. 2). For tenodesis, these effects are sensitive to choices for surgical attachment site and tendon resection. However, restoring nominal fascicle operating range on the isometric force-length curve (Fig. 2) involved resection that exceeded current surgical descriptions, and often exceeded proximal tendon length. Thus, we conclude it is likely both tenotomy and tenodesis "slacken" the LHB.

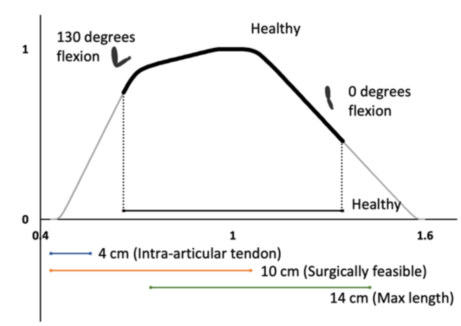

Figure 2: Operating range of LHB for elbow flexion in subpectoral tenodesis. Black curves: operating range of healthy LHB. Normalized fiber lengths predicted for a range of resection lengths are displayed in color below.

Significance: Surgical decisions for SLAP lesions are made based on patient satisfaction and return to activity reports; outcomes of muscle function have not been sufficiently differentiated. Simulations indicate that comparing active and passive force-generating ability across different repairs, as well as whether fascicle lengths adapt post-operatively may help differentiate outcomes and help guide surgical decision-making.

Acknowledgements: This research has been funded by NSF GRFP.

References: [1] Hodgetts, et al. (2021), *Archives of Physio*, [2] Kovack, et al. (2014), *Orth J Sports Med*, [3] Mirzayan, et al. (2017) *J of Arthroscopic*, [4] Karataglis, et al. (2012), *J of Bone and Joint Surgery*, [5] Saul, et al. (2015), *Comput Meth Biomech* [6] Binder-Markey, et al. (2017), *J of Biomech*

EFFECTS OF CUSTOM DYNAMIC ORTHOSIS POSTERIOR STRUT STIFFNESS ON FOOT LOADING

Jason M. Wilken[1*], Sara Magdziarz[1], Kirsten M. Anderson[1], Molly S. Pacha[1], Donald D. Anderson[2]
[1]Department of Physical Therapy and Rehabilitation Science, The University of Iowa, Iowa City, IA
*Corresponding author's email: jason-wilken@uiowa.edu

Introduction: Carbon fiber custom dynamic orthoses (CDOs) consist of a proximal cuff that wraps around the leg just below the knee, a carbon fiber posterior strut that stores and returns energy, and a semi-rigid carbon fiber footplate. During gait the posterior strut deflects to store and return energy, and forces can be transferred from the forefoot to the proximal cuff during mid to terminal stance.[1] CDOs have been shown to offload the forefoot, reduce pain, and improve function for individuals with lower extremity impairments.[1,2] Offloading can be achieved by transferring forces from the footplate to the proximal cuff via the posterior strut, however, the effect of posterior strut stiffness on offloading is unknown. Up to 60% offloading has been reported with a stiff CDO purposely designed for offloading.[1] However, it is unknown if more compliant CDOs can offload the foot by supporting the limb, reducing moments about the ankle, and thereby reducing forefoot forces. In this study, the effects of posterior strut stiffness on peak and cumulative foot loading during gait were investigated as participants walked in three different CDOs.

Figure 1: Participants completed testing while wearing no CDO, and 3 CDOs with different posterior struts.

Methods: Activities were approved by the local Institutional Review Board, and all participants provided written informed consent. Individuals who had experienced an intra-articular ankle fracture in the last six years were recruited (5Male/1Female; age 36.5(10.9)yrs, height 1.81(0.04)m, weight 93.7(20.8)kg). Participants completed weight bearing CT scans, were found to have harmfully elevated contact stress in the affected ankle,[3] and were then cast and fit for the study CDOs. Participants completed testing without a CDO (NoCDO) and with three CDOs of differing posterior strut stiffness in a randomized order (Figure 1): a stiff posterior strut (CDO1, 6.9(2.6)Nm/°) a moderate stiffness posterior strut (CDO2, 5.4(1.5)Nm/°) and a compliant posterior strut (CDO3, 3.8(1.8)Nm/°). *Procedures*: Loadsol wireless insoles (Novel Electronics) were used to measure forces acting on the foot as participants walked at a controlled speed.[4] Loadsol insoles were placed between the foot and shoe for the NoCDO condition and between the foot and CDO footplate for CDO conditions. *Data Analysis*: Data were processed in Visual 3D (C-motion Inc.) and Matlab R2020 (The MathWorks Inc.). Peak and cumulative loading were calculated for the hindfoot, midfoot, and forefoot (proximal 30%, middle 30% and distal 40% of insole, respectively), and all regions combined (total foot). Cumulative loading was calculated as the indefinite integral over the stance phase.

Results & Discussion: On average, compared to walking without a CDO, peak forefoot forces decreased more than 19% and peak hindfoot forces decreased more than 10% with each CDO (Figure 2A). The change in cumulative loading, compared to walking without a CDO, was mixed (Figure 2B). A systematic effect of stiffness was not observed for peak or cumulative loading. CDOs are used to transfer forces away from the foot to the tibia during gait to support the limb, reduce pain, and improve function. The study CDOs reduced forces under the foot, but to a lesser extent than previously reported with stiffer devices designed for the purpose of offloading.[1] Cumulative foot loading has not been investigated previously, but other work has shown that the distance travelled by the center of pressure is shorter when walking with a CDO than without, which may explain the increased cumulative loading of the midfoot and hindfoot seen in some conditions.[1]

Significance: Posterior strut stiffness did not systematically influence foot loading, however, all study CDOs reduced peak forefoot loading, supporting their potential use for reducing forefoot forces in individuals experiencing pain with limb loading. Cumulative loading was shown to increase for multiple CDO conditions, suggesting caution should be used when considering CDOs for individuals with poor sensation or tissue health.

Acknowledgements: This work was supported by a Department of Defense grant (W81XWH-18-1-0658).

References: [1] Stewart, et al. (2020), *JPO* 32(1). [2] Bedigrew, et al. (2014), *CORR* 472. [3] Anderson, et al. (2011), *J Orthop Res* 29(1). [4] Renner, et al. (2019), *Sensors* 19(2).

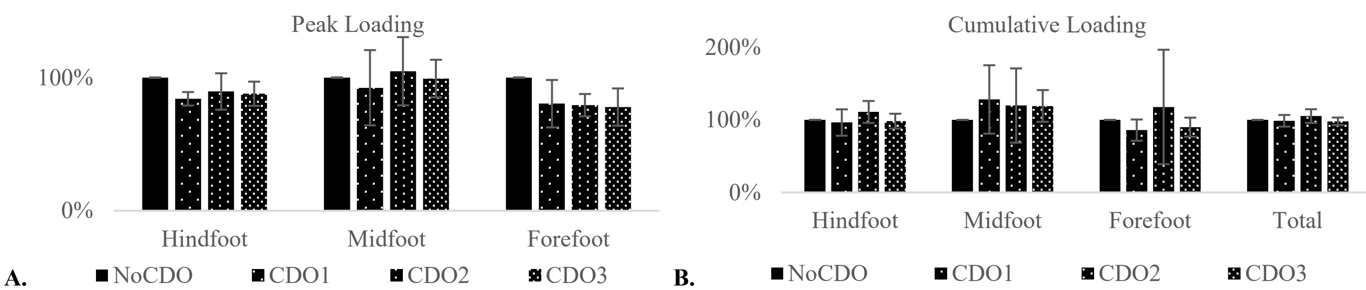

Figure 2: Peak (A) and cumulative loading (B) on the hindfoot, midfoot, forefoot, and total for NoCDO and CDO conditions (CDO1/2/3).

DOES FOOT STRIKE TYPE INFLUENCE CUMULATIVE LOAD DURING RUNNING?

Tamarie Trotter[1], Dustin Bruening[1], Joshua Sponbeck[1], Sarah T. Ridge[2*]
[1] Brigham Young University, Provo, UT [2] University of Hartford, West Hartford, CT
*Corresponding author's email: ridge@hartford.edu

Introduction: Although a plethora of research has been conducted related to the cause and incidence of running injuries, we still lack many definitive relationships between biomechanics and injury. Many studies suggest that aspects of ground reaction forces such as loading rate (LR) and peak vertical ground reaction forces (vGRF) may influence injury rate. Foot strike type has been shown to influence LR and vGRF impact peak; a rearfoot strike (RFS) pattern results in higher LR and peak vGRF during impact than a non-rearfoot strike (NRFS) pattern [1]. Theoretically, this would result in greater injury rates in runners using a RFS pattern. Recent literature suggests that while NRFS may decrease injury rates, it may also change a common site of injury from the knee to the ankle and/or forefoot due to changes in loading patterns [2,3]. There are often temporospatial differences between NRFS and RFS runners. Previous research has shown that stride length and foot strike type are coupled; NRFS is associated with shorter step length [4]. Shorter step lengths could result in more loading cycles during a run compared to a RFS runner. Based on this, it is possible that the benefit of decreased LR and peak vGRF during each step may be offset by an increased number of loading cycles. Therefore, the purpose of this study is to determine if cumulative load is different between NRFS and RFS runners. A secondary purpose of this study was to compare cumulative load measurements at based on data collected from different periods during the run.

Methods: Thirty male recreational runners participated in this study. Participants were recruited based on age, frequency of running, the ability to run 5 km in under 24 minutes, and foot strike type (16 RFS, 14 NRFS). Habitual foot strike type was determined visually using high speed video while participants ran on an instrumented treadmill at the test pace (3.15 m/s). After this, participants ran on the treadmill for 28.5 min (2.98 m/s for 3 min, then at the test pace for 25.5 min) while wearing Nike Pegasus shoes. Kinematic and kinetic data was collected in 30 sec increments at the 3-, 13-, and 23-minute marks. Per step (average of all right steps during the 30 sec increment) and cumulative (per step data was extrapolated to 1 km based on number of steps taken) metrics were calculated in Visual3D. These metrics were compared between groups and across time points using a 2x3 mixed model ANOVA ($\alpha = 0.05$). Mauchly's test for sphericity was tested and corrected for using Greenhouse-Geisser corrections when necessary. When significant main effects were found, Holm post-hoc tests were run to determine pairwise comparisons.

Results & Discussion: There were no significant interactions between group and time for any of the reported variables (Table 1). One somewhat surprising finding was the lack of group difference in number of steps per km. Significant differences in cumulative impulse across time points may be due to insufficient warm up prior to collection at Time 1. This also represents an interesting characteristic of this data – average impulses per step were nearly identical throughout the run, however when extrapolated to 1 km, average impulse significantly decreased over time. LR differences by group were as expected, while the significant decrease over time was unexpected.

Significance: These data show that foot strike type does not influence cumulative load. However, this study also suggests that caution should be used when calculating cumulative variables by extrapolating from short duration data collection.

Table 1 Group averages compared by strike type. Bolded values are cumulative per km, values in regular font are per stride, averaged over the 30 s collection interval. Cumulative LR was not calculated. [a] corrected for sphericity. [b] Significant differences between times 1 & 2 and between times 1 & 3 [c] Significant difference between times 1 & 3

	Metric	Strike Type	Time 1	Time 2	Time 3	p values		
						Time	Group	Interact
vGRF	# Steps	RFS	**437.8 (29.1)**	**436.3 (29.9)**	**433.8 (27.9)**	**0.10**	**0.682**	**0.173**
		NRFS	**440.3 (19.5)**	**438.8 (17.9)**	**429.8 (17.2)**			
	Impact Peak[a] (BW)	RFS	1.64 (0.31) **714.6 (130.9)**	1.58 (0.28) **686.7 (108.1)**	1.57 (0.27) **679.1 (104.2)**	0.756 **0.591**	0.407 **0.411**	0.111 **0.089**
		NRFS	1.48 (0.29) **647.1 (110.2)**	1.53 (0.37) **666.1 (138.9)**	1.52 (0.32) **662.7 (124.5)**			
	Absolute Peak (BW)	RFS	2.46 (0.21) **1073.6 (98.3)**	2.47 (0.19) **1076.4 (107.3)**	2.48 (0.20) **1074.7 (102.6)**	0.654 **0.94**	0.063 **0.051**	0.493 **0.912**
		NRFS	2.62 (0.22) **1151.7 (93.7)**	2.63 (0.24) **1150.9 (103.5)**	2.62 (0.25) **1149.1 (110.5)**			
	Impulse (BW*s)	RFS	0.36 (0.03) **158.1 (11.9)**	0.36 (0.03) **157.8 (12.1)**	0.36 (0.03) **157.4 (11.6)**	0.946 **<.001[b]**	0.671 **0.893**	0.147 **0.645**
		NRFS	0.36 (0.03) **157.9 (5.98)**	0.36 (0.02) **157.1 (6.14)**	0.36 (0.02) **156.9 (6.32)**			
	LR (BW/s)	RFS	90.0 (28.3)	85.6 (24.7)	83.0 (27.1)	0.035[c]	0.040	0.179
		NRFS	68.2 (20.9)	69.2 (20.0)	66.5 (18.1)			

References:
[1] Almeida et al. (2015), *JOSPT* 45(10); [2] Boyer & Derrick (2015), *Am J Sports Med* 43(9); [3] Nordin et al. (2017) *J Sport Health Sci* 6(4).); [4] Thompson et al., (2022) *Front Sport Act Living* 4.

INVESTIGATION OF PITCHING MECHANICS TO REDUCE INJURY RISK USING OPTIMAL CONTROL

Tylan Templin[1*], Sakiko Oyama[2], Travis Eliason[1], Daniel Nicolella[1]
[1]Southwest Research Institute, San Antonio, TX
[2]University of Texas San Antonio, San Antonio, TX
*Corresponding author's email: ty.templin@swri.org

Introduction: The application of experimental biomechanical methods to the understanding of baseball pitching over the past several decades has resulted in significant insights into pitching mechanics. However, injury rates remain high [1] particularly in youth pitchers [2]. Consequently, there are still many open questions regarding the underlying mechanisms driving pitching injury and how alterations in an individual's pitching biomechanics may lead to reduced risk of injury while maintaining pitching performance. Many of these questions remain unanswered because it is difficult to determine the effect of isolated changes to pitching mechanics parameters experimentally. However, optimal control-based biomechanical simulations offer insight into these cause-effect relationships by creating novel movement patterns that best satisfy an objective analogous to the human neuromuscular system [3]. Previously, optimal control simulations have been limited to simple models due to their high computational complexity [4]. However, advances in computational techniques have resulted in more efficient optimal control algorithms more widely available in biomechanics simulation software [3]. Recent studies using optimal control simulations have mainly been focused on investigating optimal mechanics of human walking [4]. An increased understanding of the underlying principles of pitching mechanics through predictive simulations would benefit coaches and athletes by giving them the information regarding not only of who is "at-risk" of suffering an injury but how modifications to technique can be made to reduce injury risk. Thus, our goal is to develop an optimal control framework that can be used to investigate the cause-effect relationship between biomechanical model parameters and mechanics on pitching performance (peak hand velocity) and injury risk (peak joint torque on shoulder).

Methods: We collected video and force plate data from one male pitcher throwing 15 fastball pitches using four synchronized Sony (DSC-RX0M2) cameras and a force instrumented pitching mound. The video data was processed using the ENABLE markerless system to derive a scaled model and the full body kinematics of the pitcher. The scaled model and kinematics were used in combination with the force plate measured ground reactions forces (GRFs) to determine joint moments using the OpenSim inverse dynamics tool [5]. Joint moments from one representative pitch were used as an initial guess to a torque-driven optimal control problem in OpenSim Moco [1] with the objective of minimizing peak shoulder internal rotation moment while penalizing deviations from measured kinematics, GRFs, and peak hand speed.

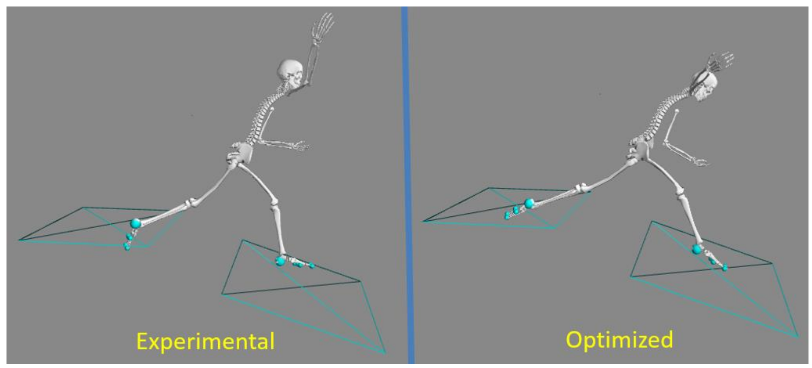

Figure 1: Visualization of experimental kinematics and optimized kinematics at release point

Results & Discussion: The optimization converged on a solution that reduced peak shoulder internal rotation by 27.1% while maintaining peak hand velocity within 1.7%. Two key differences were observed in the resulting optimized pitching mechanics relative to the measured experimental mechanics: the optimized pitching mechanics exhibited 1) increased hip external rotation in the drive leg and 2) greater knee extension for the stride leg at the time of ball release. These findings support previous research that suggest energy flow through the trunk is critical to pitching efficiency [6]. The increased hip external rotation of the drive leg generates more propulsion to the trunk that accelerates it forward. Conversely, the greater knee extension of the stride leg at ball release resulted in greater deceleration of the trunk resulting in more efficient transfer of the propulsion generated by the drive leg to the throwing shoulder.

Significance: Musculoskeletal model derived optimal control simulations of pitching mechanics with input from markerless motion capture can provide information not only into who may be at-risk of developing an injury but how individual pitchers can alter their mechanics to reduce injury risk. This combination of markerless motion capture and optimal control simulations has substantial potential to impact pitching analysis and coaching. Future studies should focus on implementing the findings from optimizations for individual pitchers as a means to validate results.

Table 1: Peak hand velocity, shoulder torque, hip torque, and knee flexion at release for the experimental and optimization conditions

Condition	Peak Hand Velocity (m/s)	Peak Shoulder Torque (N*m)	Peak Hip Torque (N*m)	Knee Flexion (degrees)
Experimental	23.0	106.1	19.9	30.5
Optimized	22.6	77.3	96.4	23.5

References:
[1] Zaremski et al. (2017) *Orthop J Sports Med.* 5(10); [2] Lyman et al. (2001). Med Sci Sports Exerc. 33(11) [3] Dembia et al. (2020), *PLos Comput Biol.* 16(12); [4] De Groote & Falisse (2021), *Proc Biol Sci.* 288(1946); [5] Delp et al. (2007), *IEEE Biom. Eng.* 54(11); [6] Howenstein et al. (2019), *Med Sci Sports Exerc.* 51(3)

USER-ADAPTIVE WALKING SPEED ESTIMATION FOR SCALING PROSTHETIC ASSISTANCE

Jairo Y. Maldonado-Contreras[1*], Aaron J. Young[2]
[1]School of Mechanical Engineering, College of Engineering, Georgia Institute of Technology, Atlanta, GA USA
[2]Institute of Robotics and Intelligence Machines, Georgia Institute of Technology, Atlanta, GA USA
*Corresponding author's email: jairoymc@gatech.edu

Introduction: Powered prostheses provide positive joint work that enable individuals with lower-limb amputations to emulate able-bodied biomechanics. Able-bodied biomechanics, such as ankle push-off moment, have been shown to scale with walking speed. Specifically, we found that ankle push-off moment increases with walking speed with a factor of 0.4898 Nm/kg/m/s [1]. This scaling factor and accurate walking speed estimators are necessary to enable powered prostheses to similarly scale assistance in a biomimetic fashion. Without proper assistance, prosthesis users may experience asymmetric gait, joint degradation, high energy consumption during walking, and further health complications.

Machine learning approaches to walking speed estimation are potentially beneficial for continuous and fast estimation as they can output new predictions of walking speed in real-time (RT). Prior work have primarily focused on 'user-dependent' (DEP) systems which means they require substantial training data from each prosthesis user. While this helps to ensure high accuracy within-subject, this approach is not easily translatable to clinical practice where gathering lots of user specific data is infeasible. Thus, we focus on a newer class of user-independent (IND) machine learning systems that are capable of predicting user intent such as walking speed on a novel subject without any user-specific data. One major goal of this study was to compare the usability of a prosthesis system that is capable of predicating walking speed in a IND manner, compared to more traditional DEP systems in real-time tests.

The disadvantage of a IND system is that it typically has a higher error rate associated with predicting the novel subject. To counter this limitation, we performed analyses on adaptive learning, which has shown benefit previously for mode classification [2]. Here, we consider the problem of walking speed estimation where we have a smoothed backward label to update our forward estimation of walking speed. This strategy could enable IND systems to achieve the accuracy and capability of DEP systems automatically over time, without the need of dedicated training data sessions for a new prosthesis user. The completion of this work can improve walking speed estimation for novel users, enable appropriate scaling of prosthetic assistance, and save prosthesis users, clinicians, and researchers valuable time and resources.

Methods: We collected training data from 10 individuals with transfemoral amputations as they walked on a treadmill at different walking speeds wearing a knee-ankle powered prosthesis known as the Open-Source Leg (OSL) (Fig.1 A). Seven of the ten participants returned for a real-time evaluation of IND, forward estimators. In a separate pilot study (N=1), the efficacy of IMU integration approaches for backward estimation was validated for an able-bodied individual.

The resulting forward and backward estimators were used to evaluate our adaptive learning methods offline. IND forward estimators were updated with labelled user specific data every three gait cycles. Walking speed labels were generated by a backwards estimator with errors modelled after piloted errors.

Results & Discussion: Offline evaluation of forward estimators yielded an average estimation error of 0.06 ± 0.02 and 0.09 ± 0.03 MAE (m/s) for DEP and IND estimation, respectively. The IND error rate was 50% higher than DEP. However, real-time evaluation of forward estimators yielded an average estimation error of 0.08 ± 0.01 and 0.09 ± 0.03 MAE (m/s) for DEP and IND estimation, respectively. This is likely due to the IND system being less reliant on specific user data, and thus more robust to different sessions, compared to the DEP system which suffered in accuracy over time. Offline adaptation of IND forward estimators decreased the IND error from a rate to an average adapted error rate of 0.07 ± 0.01 MAE (m/s), indicating that adaptation may with moderately noisy labels still outperforms purely IND or DEP systems (Fig.1 B). Future work will evaluate the real-time efficacy of adaptive learning for walking speed estimation.

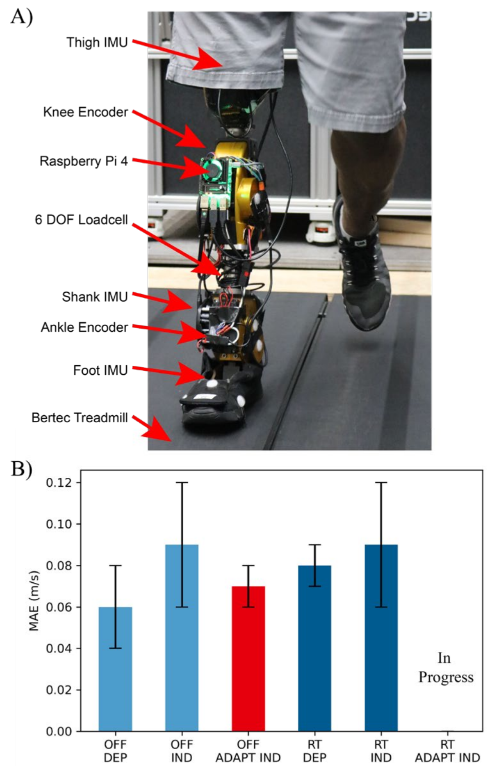

Figure 1: (A) Participant ambulating on a Bertec split-belt treadmill with the OSL. (B) Forward estimation error comparison across offline and real-time cases. Real-time adaptation errors are currently being investigated.

Significance: This work is the first attempt to implement adaptive walking speed estimation. Prostheses equipped with adaptive estimators enable accurate, continuous, and IND walking speed estimation. Adaptive walking speed estimation is needed if we are to deliver appropriate scaled assistance across real-world environments at a highly accurate degree across a wide range of amputee users.

Acknowledgements: We thank all our participants who have taken part in this study to date. Funding: Orthotics and Prosthetics Outcomes Research Program - Prosthetics Outcomes Research Award No. W81XWH-17-1-0031 (AY).

References: [1] Camargo et al. (2021), *J. Biomech.* 119; [2] Woodward et al. (2022), *TBME* 69(3).

COUPLED EXPERIMENTS AND MECHANICAL MODELS HIGHLIGHT THE ROLE OF COLLAGEN ORGANIZATION ON PASSIVE MUSCLE TISSUE PROPERTIES BY MEDIATING NONUNIFORM STIFFNESS AND STRAINS ACROSS EXTRACELLULAR MATRIX LAYERS

Ridhi Sahani[1*], C. Hunter Wallace[2], Silvia Blemker[1]
[1]University of Virginia, Department of Biomedical Engineering, Charlottesville, VA, USA
*Corresponding author's email: rs8te@virginia.edu

Introduction: Collagen is essential for the structural integrity and tensile properties of the extracellular matrix (ECM), but its role on passive muscle properties is debated. *Mdx* (dystrophin null) mouse diaphragm muscle replicates increased passive stiffness seen in Duchenne muscular dystrophy, but tissue stiffness and collagen amount do not correlate [1]. The diaphragm sustains biaxial loads along (longitudinal, 3+) and perpendicular (transverse, 1+) to muscle fibers and our equibiaxial mechanical tests found increased passive tissue stiffnesses in *mdx* relative to WT diaphragm tissue [2], with *mdx* stiffnesses best predicted by collagen distribution between ECM surrounding (epimuscular) and within muscle (intramuscular) [3]. We also found that collagen was oriented transverse to muscle fibers in epimuscular ECM (**Fig. 1A**), with increased alignment in *mdx* relative to healthy diaphragm [4]. However, we cannot determine how changes in ECM-level structure contribute to tissue-level properties from experiments alone. **Here we developed a novel framework coupling experimental measurements of tissue properties and microstructure with multiscale finite element models to investigate how collagen organization within the epimuscular and intramuscular ECM influences skeletal muscle tissue properties.**

Methods: Our initial framework leverages image-based and mechanical measurements in 6-month-old *mdx* mice (n=4). Epimuscular models represented a *100x100x1um* ECM region. Intramuscular models represented a *150x150x150um* region of muscle and ECM based on a diaphragm muscle cross-section (1-2 plane). Voronoi tessellation and Delaunay triangulation were used to assign an initial surface mesh and extruded along 3+ (MATLAB). Equibiaxial stretch (1+, 3+) was applied in both models (FEBio) to replicate experimental conditions (**Fig 1A**) [2]. Material definition (transversely isotropic) for muscle elements represented the passive behaviour of skeletal muscle [5], and for ECM elements, an ellipsoidal fiber distribution represented collagen with an isotropic ground matrix. Total collagen fiber stiffness ($\xi_{tot}= \xi_{e1}+\xi_{e2}+\xi_{e3}$) was constant across ECM elements and we varied the ratio of ξ_{e1}/ξ_{e2} with $\xi_{e2}=\xi_{e3}$ to scale the ellipsoidal fiber distribution based on the material axes. Epimuscular ECM was oriented transverse to muscle fibers with $\xi_{e1}/\xi_{e2}=1.77$ [3]. The intramuscular ECM was oriented along the muscle fiber direction [6] and we varied the intramuscular ratio of ξ_{e1}/ξ_{e2}. Bulk properties were calculated assuming layers act in parallel, such that stresses add based on their thickness (**Fig 1A**). Average element stresses and strains were used to calculate bulk stiffnesses at 3% tissue strain and compared with experimental values. 1st principal strain orientations were output per element to determine the average value ($\theta_{p,avg}$) and strength of alignment (0<SA<1, 1=high alignment).

Results & Discussion: Increased transverse relative to longitudinal stiffness was measured experimentally and reflected in our calibrated model (ξ_{total}=2 MPa, intramuscular ξ_{e1}/ξ_{e2}=0.3) (**Fig 1B**), suggesting intramuscular collagen fibers also have transverse alignment and that collagen regulates the ratio of transverse/longitudinal stiffness. The highest stiffness was seen in the epimuscular ECM, while the greatest distribution in principal strain orientation occurred in the intramuscular ECM (**Fig 1B**), highlighting nonuniformity across ECM.

Significance: Our findings challenge assumptions of transverse isotropy within muscle tissue, suggesting that instead, collagen organization regulates the amount of anisotropy. We can now incorporate data from additional mechanical tests and imaging experiments we have conducted to elucidate differences between *mdx* and healthy mice during loading scenarios mimicking *in vivo* strains. This framework can also be applied across muscle groups and diseases where changes in passive muscle properties contribute to dysfunction.

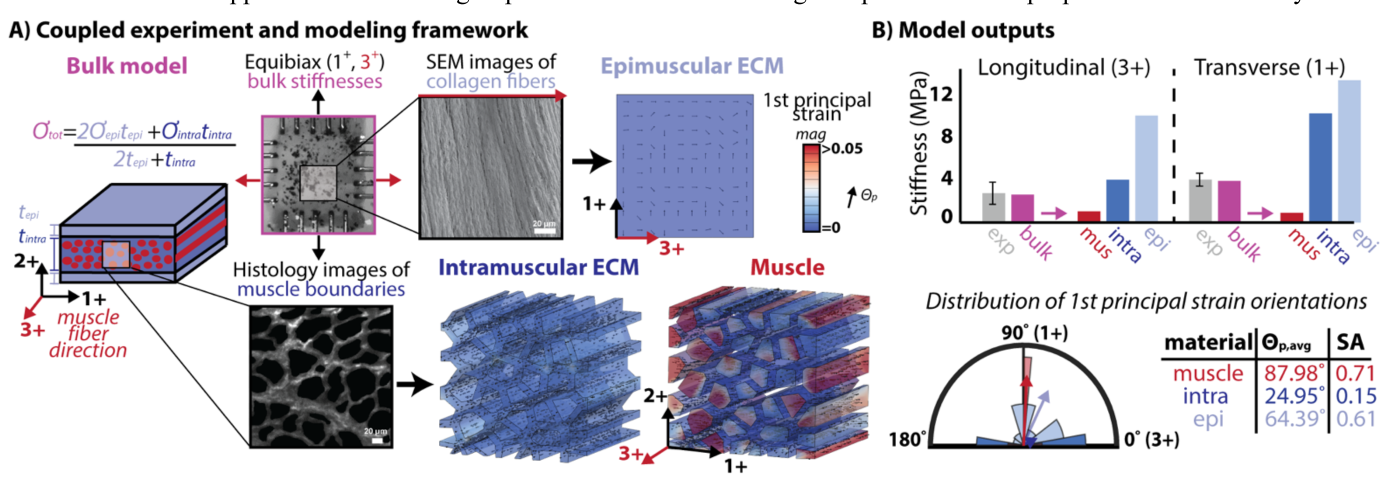

Figure 1: A) Coupled experiment and modelling framework. B) Experimental and model outputs of stiffness and principal strain orientations.

Acknowledgements: Thank you to our funding sources (Grant # U01AR06393, Grant # T32GM136615).

References: [1] Smith et al, 2014. Am J. Phys. [2] Wallace, 2021. [PhD Thesis] Univ. of Virginia. [3] Sahani et al, 2022. J. Appl. Phys. [4] Sahani et al, 2022. NACOB [5] Blemker et al, 2005. J. Biomech. [6] Brashear et al, 2022. PLOS ONE.

HIGH INTENSITY GAIT AND BALANCE TRAINING IMPROVES CONTROL OF CENTER OF MASS MOTION DURING WALKING IN PEOPLE WITH INCOMPLETE SPINAL CORD INJURY

Anna Shafer[1], Shamali Dusane[2], Heather Henderson[2], Keith E. Gordon[1, 2]
[1]Research Services, Edward Hines Jr. VA Hospital, Hines, IL 60141; [2]Department of Physical Therapy and Human Movement Sciences, Northwestern University Feinberg School of Medicine, Chicago, IL 60611
anna.shafer@northwestern.edu

Introduction: Impaired control of lateral balance during walking is common among ambulatory people with incomplete spinal cord injury (iSCI) [1, 2]. The ability to control lateral whole-body center-of-mass (COM) motion during walking is correlated with clinical gait and balance measures in people with iSCI [3]. This finding suggests the ability to control lateral COM motion could be a contributing factor to gait and balance function in people with iSCI. Current clinical practice guidelines strongly recommend high intensity gait training (HIGT) (i.e., repetitive stepping practice at a target heart rate (HR)) for improving walking distance and speed for people with iSCI [4]. However, the effect of this intervention on walking balance is not established. This study aimed to determine whether a HIGT intervention that uses a mix of treadmill-based speed training (fast walking intervals) and balance training (walking activities that challenge balance) improves clinical measures of gait speed and balance and the ability to control lateral COM motion during walking in people with iSCI. We hypothesized that following this 20-session HIGT intervention, people with iSCI would improve clinical measures of walking speed and balance and their ability to control lateral COM excursion during walking.

Methods: Eighteen ambulatory people with chronic iSCI (American Spinal Injury Association Impairment Scale D) from a subset of a larger clinical trial participated in twenty, 45-min sessions (~2x/week) of HIGT. Target HR during each session was 70-85% of estimated HR max. We conducted clinical outcomes measures Pre- and Post-training including a 10-meter walk test (10MWT) at participants' fastest speed to determine walking speed and a Functional Gait Assessment (FGA), a ten-item test to evaluate dynamic balance during gait. We also conducted a biomechanical assessment of lateral COM control during a treadmill walking task. The task used visual feedback to challenge participants to control (minimize) their lateral motion during forward walking. We project the participant's real-time medio-lateral COM position and a target lane on the treadmill (Fig. 1a). Participants were asked to maintain their COM position (white line) within the target lane (green lines). If successful, the target lane width progressively decreased, making the task more challenging. Stepping outside of the target lane prompted an immediate visual cue and lane width increase. Participants did not use handrails or assistive devices during the task. Minimum lateral COM excursion over a three-stride average was extracted as a measure of ability to control COM motion. The assessment was performed at both the Pre- and Post-training preferred treadmill speed. This data is from an ongoing clinical trial. We conducted a power analysis with plans for statistical comparisons to be made at the completion of the full trial. As such, descriptive statistics are used here to avoid making multiple comparisons.

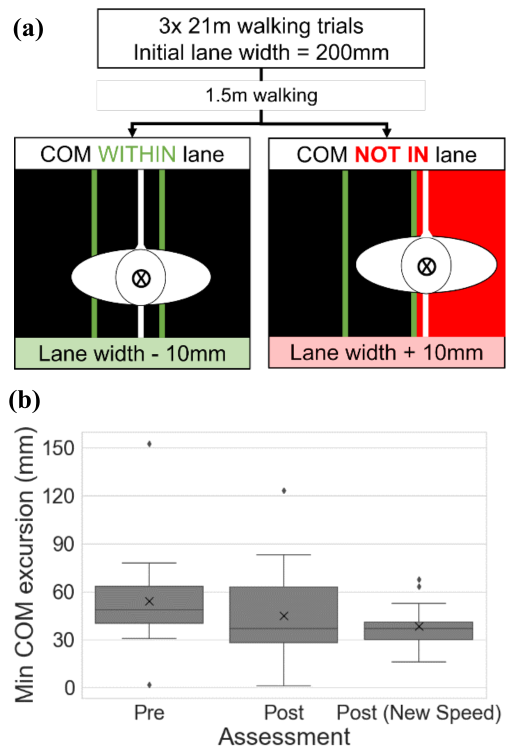

Figure 1: (a) Walking task to assess ability to control (minimize) COM lateral motion during walking. **(b)** Minimum lateral COM excursion during the walking task. X indicates mean.

Results & Discussion: Clinical measures of speed and balance improved for all participants after training. 10MWT speed increased by 0.13±0.17 m/s (which exceeded the minimally clinically important difference of 0.06 m/s) and FGA score improved by 4±7 points. Lateral COM excursion was reduced by 19% or 22% Pre- to Post-training (Fig. 1b). The larger reduction in COM excursion occurred at the preferred Post-training treadmill speed (which was substantially faster than the Pre-training preferred treadmill speed). These findings demonstrate that after HIGT participants improved their capacity to control lateral motion during walking.

Significance: Our findings suggest that HIGT may be an effective intervention to train both gait speed and balance in persons with iSCI. Improvements in the ability to control lateral COM during walking may translate to a range of balance-challenging walking activities.

Acknowledgements: This study was funded by the U.S. Department of Veteran Affairs #1 I01 RX003371. The authors thank Shay Pinhey, Jordan Dembsky, Mackenzie Mattone, Yuchan Choi, Keri Han, Wendy Ochs and Tara Cornwell for assisting with this study.

References: [1] Zwijgers et al. (2022), *J of Neuroengineering and Rehabilitation* 19(1); [2] Ochs et al. (2021), *J of Neuroengineering and Rehabilitation*, 18(1); [3] Dusane et al. (2023), *medRxiv*; [4] Hornby et al. (2020), *J of Neurologic Physical Therapy,* 44(1).

SENSITIVITY OF SIMULATED GAITS TO ASSUMED MUSCLE MASS AND SPECIFIC TENSION

Sheeba Davis[1*], Matthew C. O'Neill[2], Brian R. Umberger[1]
[1]School of Kinesiology, University of Michigan, Ann Arbor, MI
[2]Department of Anatomy, Midwestern University, Glendale, AZ
*Corresponding author's email: sheeba@umich.edu

Introduction: Musculoskeletal modeling and simulation are widely used to study the mechanics and energetics of locomotion. Even a modestly complex musculoskeletal model requires assigning values to hundreds of model parameters. Among them, peak isometric muscle force (F_0) is a critical parameter as it determines the strength of the model and is representative of muscle size. Muscle mass and specific tension (force per area) are not directly represented in most muscle models, yet F_0 is often based, in part, on muscle masses (or volumes) drawn from a variety of sources in the literature [1, 2, 3], combined with an assumed value for specific tension [1, 4]. Thus, model strength is often based on assumptions about the percentage of total body mass that the modeled muscles represent, and the intrinsic strength of muscle tissue, both of which vary considerably in the literature. Muscle mass and specific tension also are critical parameters directly represented in many models of muscle energy consumption [6, 7]. In order to use musculoskeletal modeling and simulation techniques effectively, it is important to understand the sensitivity of model predictions to the underlying modeling assumptions. Therefore, the purpose of this study was to evaluate the sensitivity of predicted walking gaits and the associated metabolic cost to the assumed muscle mass and specific tension in musculoskeletal simulations of human walking.

Methods: Predictive simulations of walking at 1.3 m/s were generated using OpenSim Moco with a 2-D sagittal plane musculoskeletal model (9 segments, 11 degrees of freedom, 18 muscle-tendon actuators) [5]. The objective function for the predictive simulations was the sum of cubed muscle excitations. Metabolic cost was estimated using two muscle energetics models [6, 7]. The total lower limb muscle mass as a percentage of whole body mass was separately set to 6%, 14%, and 20%, based on a range of muscle mass data sets in the literature [1, 2, 3]. For each case, individual muscle F_0 values and metabolic energy consumption were determined assuming specific tension of 31.5 N/cm^2 [4], and again using specific tension of 61 N/cm^2 [1]. Metabolic cost was also calculated using specific tension of 25 N/cm^2 because that is the default value in OpenSim, regardless of the value used for determining F_0, and it is consistent with specific tension measurements in single muscle fibers [8]. We evaluated the effects of muscle mass and specific tension by comparing predicted kinematics, ground reaction forces, muscle activations, and metabolic cost of walking.

Results & Discussion: The trends in predicted costs obtained with both muscle energy models were similar; results for [6] are shown in Fig. 1. The overall kinematics, kinetics and muscle activations were generally similar across the models with 6%, 14% and 20% muscle mass (M_{mus}). However, the kinematics and muscle activations differed slightly for the model with 14% M_{mus} and 31.5 N/cm^2 specific tension resulting in a greater metabolic cost (Fig. 1). M_{mus} and specific tension both had a considerable effect on predicted cost. For M_{mus} there was a more than proportional increase in cost, while for specific tension the increase in cost was less than proportional (Fig. 1). Thus, M_{mus} has a larger effect on the net metabolic cost of transport than the specific tension.

It is preferable to use consistent specific tension values for determining F_0 and metabolic cost; however, assuming a specific tension of 25 N/cm^2 in the metabolic energy model only resulted in a moderately greater cost prediction in the musculoskeletal model where F_0 was based on 61 N/cm^2.

The combined effects of muscle mass and specific tension on cost predictions can be considerable. There was a 4.5-fold greater predicted metabolic cost for the strongest model (20% M_{mus} & 61 N/cm^2) compared with the weakest model (6% M_{mus} & 31.5 N/cm^2). The overall results suggests that metabolic cost of transport is highly sensitive to muscle mass and specific tension in musculoskeletal simulations of human walking.

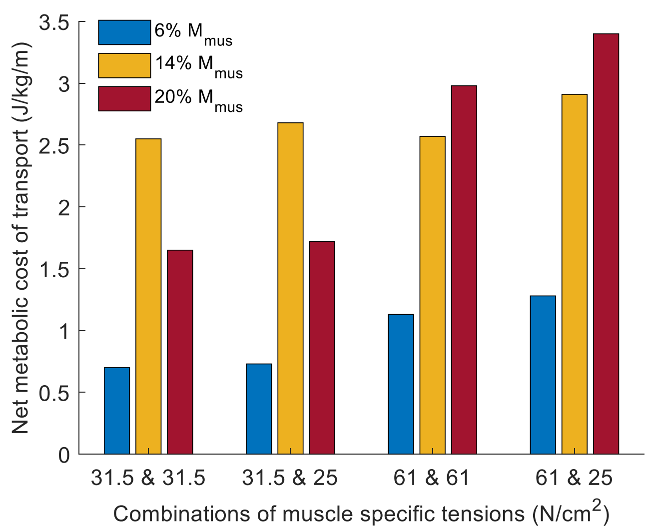

Figure 1: Net metabolic cost of transport predicted for muscle mass percentages (6%, 14% & 20% M_{mus}) using specific tensions 31.5, 61 & 25 N/cm^2. Experimental value = 2.2 J/kg/m [9].

Significance: Due to the high sensitivity of predicted metabolic cost of walking to muscle mass and specific tension, careful consideration should be paid to the selection of these model parameters in predictive simulations of walking.

References: [1] Ward et al. (2009), *Clin Ortho Rel Res* 467; [2] Handsfield et al. (2014), *J Biomech* 47(3); [3] Zihlman et al. (2015), *PNAS* 112(24); [4] O'Neill et al. (2013), *J Exp Biol* 216(19); [5] Nguyen et al. (2019), *IEEE TNSRE* 27(7); [6] Bhargava et al. (2004), *J Biomech* 37(1); [7] Umberger (2010), *J Roy Soc Int* 7(50); [8] O'Neill et al. (2017), *PNAS* 114(28); [9] Umberger & Martin (2007), *J Exp Biol* 210(18).

INFLUENCE OF PRESEASON WORKLOADS ON NEUROMUSCULAR PERFORMANCE AND PATELLAR TENDON PROPERTIES IN WOMEN COLLEGIATE VOLLEYBALL ATHLETES

Brian M. Guthrie[1,2*], Erica L. King[1,3,4], Parag V. Chitnis[3,4], Qi Wei[3], Siddhartha Sikdar[3,4], and Margaret T. Jones[1,2]

[1]Frank Pettrone Center for Sports Performance, George Mason University, Fairfax, VA; [2]Sport, Recreation, and Tourism Management, George Mason University, Fairfax, VA; [3]Bioengineering, George Mason University, Fairfax, VA; [4]Center for Brain and Body Interactions, George Mason University, Fairfax, VA
*Corresponding author's email: bguthri@gmu.edu

Introduction:
Patellar tendinopathy (PT) is a common overuse pathology in the sport of volleyball, which leads to impaired performance and structural abnormalities in the patellar tendon [1]. These abnormalities are a result of mechanical fatigue and result in microdamage to the tissue, decreased load tolerance, and increased risk of sustaining a more severe injury [2]. Excessive workload is a primary risk factor in the development of PT [3]. Athlete workload monitoring enables fatigue management through assessment of dose dependent responses to training. Subjective measures of workload represent a surrogate measure of psychophysiological load that is characterized as the culmination of psychological and physiological stress in response to training, where session rating of perceived exertion (sRPE) is most common [4]. However, the influence of workload on patellar tendon properties and neuromuscular performance remains unclear. Therefore, the purpose of this study was to: 1) evaluate whether changes in patellar tendon properties and neuromuscular performance occur across a preseason phase of training, 2) determine if surrogate measures of internal workload can predict such changes, and 3) determine if these findings differed among sport-position groups. It was hypothesized that time would predict neuromuscular performance and patellar tendon properties, internal workload would predict these changes, and findings would differ by position group.

Methods: 20 National Collegiate Athletic Association Division-I women volleyball athletes (age = 20.26 ± 1.13 yrs, height = 179.59 ± 3.98 cm, body mass = 76.10 ± 7.05 kg, body fat % = 28.15 ± 4.34 %) participated across a 2-week preseason (Figure 1a.). Sport position categories were: libero (L; n=3), middle blocker (MB; n=5), setter (S; n=3), and outside/right side hitter (OH; n = 9). Athletes reported RPE post session for all training and matches. sRPE was calculated as RPE*duration (i.e., minutes). Predictors included total, average, and standard deviation of sRPE across the entire preseason. At the beginning of each week, dominant (D) and non-dominant (ND) limbs were assessed for thickness (TH), echogenicity (EC), and entropy (EN) of the proximal portion of the patellar tendon using B-mode ultrasound. Myotonometry was used to assess stiffness (ST) of the patellar tendon. Countermovement jump (CMJ) was used to measure jump height (JH), reactive strength index modified (RSImod) and net vertical impulse (NetIMP). Individual changes in patellar tendon properties and neuromuscular performance across 3 timepoints were evaluated via multilevel modelling (Figure 1b-c.).

Results & Discussion: Time was a significant predictor of RSImod (β = -0.42, p = 0.03) across all position groups except L (p > 0.05). Decreased RSImod was indicative of an altered movement strategy in the CMJ characterized by lower ratio between contraction time and flight time. No other CMJ variables were predicted by time indicating movement strategy was altered. Time predicted proximal TH-ND (β = -2.83, p < 0.01) in OH and S; where S decreased and OH increased. This may be a result of differing demands between positions S and OH [5]. Standard deviation of sRPE was a predictor of the change in TH-D (β = 0.01, p < 0.01), ST-D (β = 1.55, p =0.01), and ST-ND (β = 2.41, p < 0.01). Additionally, average (β = -2.07, p = 0.02), and total (β = 63.88, p = 0.04) sRPE changed in ST-ND across week. The results provide evidence supporting sRPE as useful in predicting tendon property changes, which may be position dependent. Further, magnitude and variability of training parameters may provide insight into training-induced changes in patellar tendon properties.

Significance: Monitoring workload, performance, and patellar tendon properties may provide useful information to assess risk of overuse injury. Changes in movement strategy and patellar tendon properties were present across a preseason phase. These changes should be examined at the position level with particular interest in how magnitude and variability of workload influence these changes.

Acknowledgements: This research was supported by the National Strength and Conditioning Association Foundation grant GRD-2021-02. Additional support was provided in part by the NSF grant DGE:1922598.

References: [1] Kabacinski et al. (2022), *J. Strength Cond. Res* 36(8); [2] Edwards (2018), *Exerc. Sport Sci. Rev.* 46(4); [3] Visnes & Bahr (2013), *Scand J Med Sci Sports* 23(5); [4] Pisa et al., *J Sports Med Phys Fitness* 62(0); [5] García-de-Alcaraz et al. *J. Sports Sci. Med* 23(10)

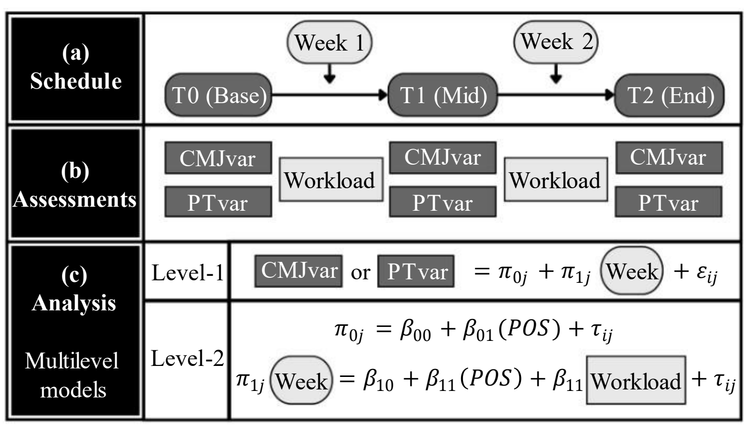

Figure 1: Data collection schedule, assessments, and equation used for analysis.
CMJvar = countermovement jump variable [JH, RSImod, NetIMP]
PTvar = patellar tendon variable [TH, EC, EN, ST]
Workload = sRPE [total, average, standard deviation]
POS = sport position

FEMALES WITH LOW BACK PAIN DEMONSTRATE ASYMMETRICAL SHOCK ATTNEUATION DURING RUNNING

Joshua D. Winters[1*], Tatiana E. Djafar[1], Nicholas R. Heebner[1], Alexa K. Johnson[2]
[1]Sports Medicine Research Institute, College of Health Sciences, University of Kentucky, Lexington, KY
[2]School of Kinesiology, University of Michigan, Ann Arbor, MI
*Corresponding author's email: joshua.winters@uky.edu

Introduction: Chronic low back pain (LBP) is becoming increasingly common among active populations, with approximately 15% of female athletes experiencing LBP in a given season, compared to 6% of males [1]. Among runners, LBP accounts for up to 22% of musculoskeletal injuries [2]. During running, individuals with LBP present with an increased knee joint stiffness, or reduced knee flexion during stance phase, disrupting the dissipation of load throughout the kinetic chain [3]. This inability to adequately attenuate shock likely impedes recovery, increasing the risk of an additional musculoskeletal injury.
Recent research has focused on utilizing innovative strategies to incorporate wearable technologies, such as inertial measurement units (IMUs) to assess loading patterns experienced by the participants in real-world environments. Shock attenuation, calculated from the dissipation of accelerations across multiple segments, is just one example of how IMUs are being used to identify altered loading patterns during running. Therefore, the purpose of this study was to determine if IMUs could identify altered loading patterns during running in females who suffer from LBP compared to healthy females. We hypothesized that females with LBP would present with a reduced capacity to attenuate shock and increased shock attenuation asymmetry during running.

Methods: Eighteen physically active females with chronic LBP (LBP; Age=23.8±3.6yrs; Mass=66.7±8.4 kgs; Height=1.7±0.05m; Duration of Pain=4.0±2.4 years; Oswestry Disability Index=15.7±3.5%) and 17 healthy female controls (CTRL; Age=23.5±3.9yrs; Mass=66.8±8.5kgs; Height=1.7±0.04m) completed this study. Individuals in the LBP group reported experiencing chronic LBP (for a minimum of four months) while those in the CTRL group had no reported history of LBP. Individuals completed one testing session that included an overground running biomechanical analysis. Individuals ran over a 50m runway at their self-selected speed. IMUs (IMeasureU, Vicon, Oxford, UK) were placed over the sacrum (between right and left posterior superior iliac spines) and bilaterally on the medial aspect of the tibia to primarily measure accelerations (streamed at 2000 Hz) during overground running. Peak tibial and sacral accelerations were identified during ground contact for each limb. Shock attenuation (in the time domain) was calculated for each limb as 1-(peak sacral acceleration/peak tibial acceleration)*100 [4]. A 2x2 (group x limb) repeated measures analysis of variance with post-hoc t-tests were used to assess group and limb differences in impact accelerations and shock attenuation during running. Significance was set a priori at $p < 0.05$.

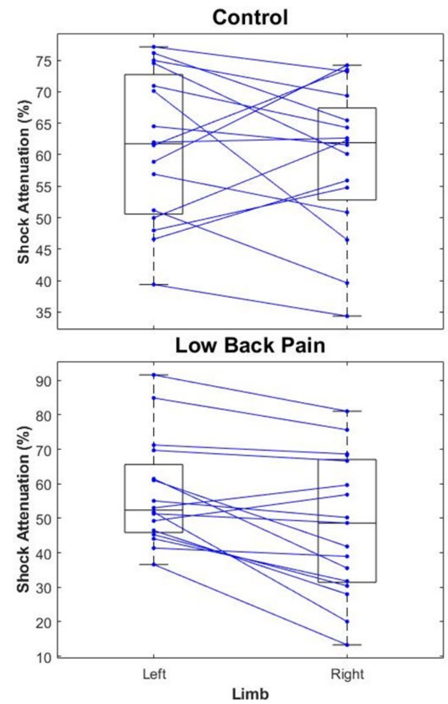

Figure 1: Boxplots with individual overlay of the shock attenuation calculated on each limb within the LBP and healthy control individuals.

Results & Discussion: There was a significant group by limb interaction for shock attenuation (p=0.041) with those in the LBP group demonstrating greater between limb asymmetries in shock attenuation than individuals in the CTRL group (Figure 1). In those with LBP, post-hoc paired samples t-tests identified significantly lower impact accelerations occurring at the right tibia (p=0.004) and higher impact accelerations occurring at the right pelvis (p=0.007) leading to a reduced shock attenuation with the right limb compared to the left limb (p=0.002). There was also a significant overall effect of limb on the impact accelerations at the pelvis (p=0.002) with higher pelvis impact accelerations occurring on the right side compared to the left. There were no limb effects for peak tibial accelerations. Though both groups demonstrated similar impact acceleration magnitudes, LBP demonstrated asymmetrical shock attenuation patterns that were not present within healthy individuals. Individuals with LBP demonstrated a reduced capacity to attenuate shock on the right limb, with greater impact accelerations measured at the pelvis from the right foot strike, even though the impact accelerations occurring at the right tibia are smaller than the impact accelerations on the left.

Significance: The inability to adequately attenuate shock symmetrically through the kinetic chain while running may lead to altered loading patterns within the lower back, increasing the likelihood of pain, and reducing overall performance. The cumulative effects of asymmetrical loading overtime may influence the progression of LBP severity throughout an individual's lifetime. Further research is needed to better understand how strength and mechanics are related to the impact accelerations and the asymmetrical loading patterns identified within this study. These relationships will contribute to the development of more effective evidence-based low back injury/pain prevention and rehabilitation strategies focused on improving recovery and performance in active individuals with LBP.

Acknowledgements: This research was supported by the American Society of Biomechanics Student Grant-in-Aid to Alexa Johnson. Content is the responsibility of the authors and does not represent the views of ASB.

References: [1] Nadler at al. 1998. *Spine.* (23)7; [2] Taunton et al. 2003. *Br J Sports Med.* 36(2); [3] Hamil et al. 2009. *Res Sports Med.* 17(4); [4] Reenalda et al. 2019. *Gait & Posture.*

THE IMPACT OF VARIOUS HELMET LOADS ON WARFIGTHER DISMOUNT STRATEGIES

Aidan Gross B.S.[1*], Martin Flament Fultot PhD[1], Brian Higginson PhD[1]
Galvion Ballistics Ltd., Warfigther Systems Integration Laboratory
*Email: aidan.gross@galvion-usa.com

Introduction: The use of external physical loads, such as helmets, night vision goggles (NVGs), counterweights (CW), etc., are essential aspects of modern military operations[2]. While these loads provide necessary protection and enhance situational awareness, they also impose additional physical and cognitive demands on the warfighter, which may negatively impact their performance and safety[3]. Such questions and concerns have been the subject of extensive research in the field of biomechanics, with studies exploring the effects of head-borne loads on various aspects of soldier performance, including, mobility, stability, accuracy, and perception-action coupling[12345].

One of the primary concerns regarding additional external head-borne loads in a military application is the resultant impact on the warfighters balance and stability[12]. Several studies have reported that things like helmets and NVGs can increase inertial and interactive forces which can alter the center of mass and the distribution of body weight, leading to increased postural sway and reduced stability during ambulatory tasks[12]. As such it is important to note that any disruption in normal segmental control and coordination during movement in combat directly impacts the warfighters survivability[3]. To begin addressing these challenges we present pilot research aimed at determining the impact of various helmet configurations on warfighter dismount strategies from an elevated surface during a simulated combat task. We posit that increasing external load on a helmet in the form of NVGs and CWs will limit the warfighters functional capacity leading to longer dismount durations where airtime (i.e., both feet in the air at the same time) is reduced to a minimum. We believe increasing factors like perceptual encapsulation and greater inertial forces due to additional external load will be detrimental to the warfighters capabilities resulting in more guarded dismount strategies.

Methods: Six healthy and experienced shooters (4=Police & 2=Military) participated in this study. Participants were instructed to complete a move and shoot task as quickly and accurately as possible. Included in this course was a one-meter box dismount where participants had to fire two shots on target from the box, immediately dismount, and then fire another two shots on target. Participants completed this task four times for each of the three different helmet conditions. Helmet conditions were randomized to limit the role of task learning across trials. The Helmet conditions included a naked helmet (HEL_NOCW), a helmet with deployed NVGs (DEP_NOCW), and a helmet with deployed NVG's and a counterweight (DEP_CW). Each participant was fitted with markers on each of their heels. Markers were tracked using a Vicon Nexus Motion Capture system with 12 infrared cameras. From the position data we calculated the elapsed time of the entire event (time from max vertical position of the first heel marker to min vertical position of second heel marker) denoted as (TD), the airtime (time from max vertical position of the second heel to min vertical position of the first heel) denoted as (AT) and the ratio of AT to TD denoted as (AT/TD). Repeated measures ANOVAs were used to test for significant differences in mean TD, AT, and AT/TD between the three helmet conditions. Post-hoc testing with Bonferroni adjustment were completed where significant main effects were found.

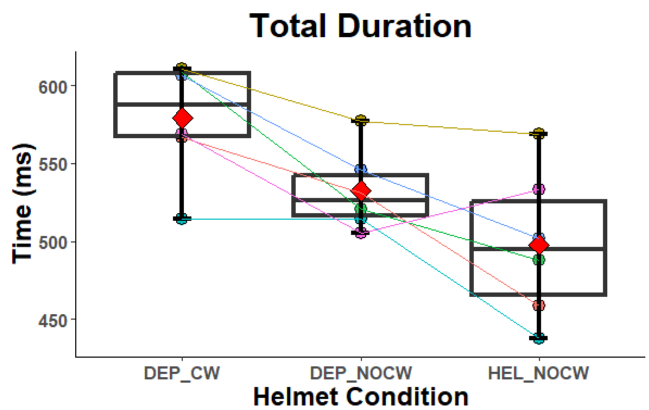

Figure 1: Mean event durations during a one-meter box dismount between three different helmet configurations. Statistical comparisons between conditions with p-value < 0.05 denoted by (*): (DEP_CW-DEP_NOCW) (p=0.01*) (DEP_CW-HEL_NOCW) (p=0.003*) (DEP_NOCW-HEL_NOCW) (p=0.08)

Results & Discussion: There was a main effect of helmet configuration for TD (p=0.0008). There were no main effects for helmet configuration for either AT or AT/TD. Post-hoc testing showed significant differences in TD between the DEP_CW and DEP_NOCW conditions suggesting an impact of increased absolute helmet load and inertial forces. Significant differences in TD were also found between the DEP_CW and HEL_NOCW suggesting further affects for increased helmet forces which may have been further exacerbated by NVG induced perceptual encapsulation. Comparisons between DEP_NOCW and HEL_NOCW were not statistically significant (p=0.08) which may be an affect of our small pilot sample size. While we see no significant differences between AT and AT/TD we do see significant differences in TD for both the DEP_CW and DEP_NOCW conditions compared to a naked helmet. Our data partly supports our initial hypothesis in that additional loads on the warfighter increase the event duration of the dismount.

Significance: To truly understand these findings we must consider them within the context of the modern combat environment. It is important to realize that in this realm very acute differences can alter survivability and as such rigorous helmet design and development should reflect this. Here we demonstrate differences within a single dismounting movement, but these findings can largely be extrapolated out too many situations and thus underscore the importance of minimizing physical load on the warfighter.

References: **[1]** Hagel et al. (2018), *Gait & Posture* 175-187; **[2]** Orr et al. (2020), *Sports Medicine* 417-447; **[3]** Palmer et al. (2013), *Journal of Applied Physiology* 697-704; **[4]** Knapik et al. (2015), *Military Medicine* 82-97; **[5]** Sanders et al. (2019), *Sports Medicine* 633-649

PATELLAR SHAPE STRONGLY DISCRIMINATES ADULT WITH RECURRENT PATELLAR DISLOCATION

Paras Shah, Barry P Boden, Frances T. Sheehan*
*Rehabilitation Medicine, Clinical Center, National Institutes of Health
*Corresponding author's email: gavellif@cc.nih.gov

Introduction: Lateral patellar dislocation (LPD) affects approximately 6/100,000 individuals annually [1], with the standard of care being non-operative for primary LPD. These rates jump to 29/100,000 annually for adolescents. Twenty to forty percent of patients will suffer a recurrence, with many requiring surgery [2]. Research has primarily focused on how femoral shape, tibiofemoral alignment, and soft tissue forces influence the likelihood of an LPD. There remains a paucity of information regarding the patella's role in LPD. Recent predictive algorithms [3] show promise in identifying individuals who will most likely experience recurrent dislocations and might benefit from early surgical intervention. To improve patient-specific interventional planning, these algorithms require enhanced accuracy. Thus, to enrich our understanding of LPD and potentially improve recurrence-predicting algorithms, we quantified patellar morphology in patients with recurrent LPD and matched asymptomatic controls. We hypothesized that: 1) patients would have decreased patellar width and volume, and 2) patellar morphologic parameters would accurately discriminate cohort membership.

Methods: Twenty-one adults with recurrent LPD (age=29.7±11.1 years, height=170.8±9.9 cm, weight=76.1±17.5 kg, 52% female) and 21 sex and height-matched controls (age=27.2±6.7 years, height=172.0±10.6 cm, weight=71.1±12.8 kg, 52% female) formed the basis of this study. Using 3D axial fat-saturated MRI images, acquired for each participant, we measured patellar volume, width, depth, height, medial/lateral facet length and Wiberg index (Fig 1), and previously validated patellofemoral alignment and femoral shape measurements. Each study variable was compared between groups using a 2-sided Student's t-test. A multi-variate step-wise discrimination analysis was used to determine the equation that best predicted cohort membership based on all study variables. A discriminant analysis was run for each variable independently to determine its discriminatory ability in isolation.

Results & Discussion: We found a larger Wiberg index along with a smaller patellar width and volume in our patients with recurrent LPD, relative to controls (Fig 1, Δ=0.05, p<0.001; Δ=-3.2 mm, p=0.009; Δ=-2.76 cm3, p=0.025, respectively). These results are both supported [4] and refuted [5] in the literature. This conflict likely arises because previous studies have not enrolled fully asymptomatic controls, with no history of lower limb pathology or disease, nor did they compensate for the influence of demographics. As the current study did both these things, our results provide greater clarity into the role of patellar shape in LPD.

Compared to the control group, our patients with LPD had decreased medial patellar width and facet length, along with no differences in lateral patellar width and facet length (Fig 1). This indicates that the larger Wiberg index and smaller patellar width are due primarily to a hypoplastic medial patellar [4] and not a hyperplastic lateral patellar [6]. Although a larger Wiberg index is associated with recurrent LPD, logically we do not see this as a direct contributor to patellar instability. The hypoplastic medial patella indicates decreases in medial soft tissue and contact forces acting on the patella. This is substantiated by a recent study demonstrating that the patella width in adolescents with LPD was decreased, but returned to normative values once the medial forces were re-established through a medial patellar ligament repair [6].

The Wiberg index combined with lateral patellar displacement has the strongest discriminatory ability (81% & 90% accuracy for controls and patients), whereas an increased patellar to femoral-trochlear depth ratio had the highest independent ability to discriminate LPD patients into their correct cohort (95% accuracy for patients). This strong ability to discriminate cohorts based on patellar shape further supports the importance of considering patellar morphological measures when evaluating therapeutic intervention after an LPD.

Significance: The current research enriches our understanding of the etiology of LPD and provides a pathway for advancing current predictive LPD algorithms for interventional decision making. Although rarely evaluated in patients with LPD, patellar morphology is associated with recurrent LPD and more accurately discriminates than traditional femoral shape and joint alignment measures. The Wiberg index was a key variable, likely due to its indirect relationship to reduced medial patellar stabilization. A loss of medial patellar forces, indicated by a hypoplastic medial patellar would support recurrent dislocation. Thus, adding patellar morphological and/or patellofemoral alignment measures to the current predictive algorithms will likely improve decision making and patient education regarding recurrence risk, as well as the therapeutic interventional planning.

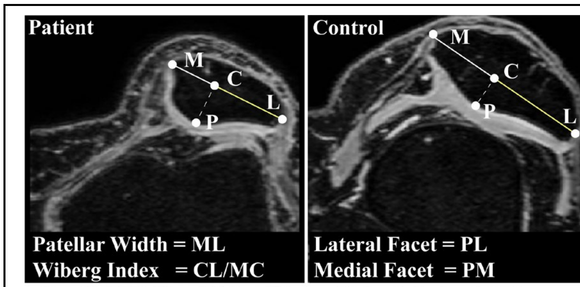

	Patient	Control	
Patellar Width	= 40.0 ± 4.8	= 43.2 ± 3.4	(p=0.009)
Wiberg Index	= 0.62 ± 0.04	= 0.57 ± 0.04	(p<0.001)
Medial Facet	= 18.0 ± 2.6	= 21.7 ± 2.7	(p<0.001)
Lateral Facet	= 26.8 ± 4.5	= 27.0 ± 2.2	(p=0.868)

Figure 1: Sample Patellar Shape Measures. Mid-patellar axial 3D FS GRE images for a patient and control whose patellar width are approximately equal to the cohort they represent.

Acknowledgements: This work was funded by the Intramural Research Program of the National Institutes of Health Clinical Center, Bethesda, MD, USA and the Medical Research Scholars Program

References: [1] Fithian et al (2005) *AJSM* 32(5) [2] Jain 2011 *Sports Health* 3(2) [3] Arendt et al (2017) *KSSTA* 25 [4] Fucentese et al. (2006), *The Knee* 13(2); [5] Li et al (2021) *Ortho Surg* 13(2); [6] Li et al (2021) *J Orthop Surg* 16

USE OF POSTUROGRAPHY INCREASES BALANCE-RELATED DIAGNOSES IN PHYSICIAN CLINIC SETTINGS

Ajit M.W. Chaudhari[*1,2], Virginia M. Yazzie[1], Daniel Richie[1], Carmen E. Quatman[2], Jennifer H. Garvin[1]
[1]School of Health and Rehabilitation Sciences & [2]Department of Orthopaedic Surgery, The Ohio State University
*chaudhari.2@osu.edu

Introduction: Falls are a significant source of early morbidity and mortality in the aging population [1], and several organizations including the Centers for Disease Control and Prevention (CDC) have released clinical practice guidelines and algorithms to identify individuals at elevated risk of falls [2]. However, challenges persist in adopting the guidelines into practice. Many providers report that they do not know how to conduct a fall risk assessment [3], and they report being overloaded when the average visitor has several health problems to address in a very short encounter (10 minutes or less). Moreover, guideline algorithms depend on patient subjective recall, which could be unreliable especially in the case of a very gradual decline, as well as observation by the clinical team. Less than half of older individuals who fall report having discussed the risk of falls with their provider at a previous visit, suggesting that the lack of use of standard algorithms may contribute to under-diagnosing patients with elevated fall risk. Quantitative posturography has been used in research settings for more than 50 years [4], it can be done more quickly than standard clinical assessments, and it can predict future falls [5]. Our previous work demonstrated that posturography can be easily used in the physician clinic setting [6]. This study tested the hypothesis that physicians and advanced practice providers who use a balance device instead of a standard weight scale are more likely to diagnose patients with a balanced-related problem than those who do not have access to posturography.

Methods: Forty-one physicians and nurse practitioners at 16 clinics were randomized by clinic into two groups after providing IRB-approved informed consent. Eight clinics received a weight scale that also provided the root-mean-squared medial-lateral deviation of the center of pressure (RMSml) for a single 30-second eyes closed quiet standing trial with feet 5cm apart. Participants were also provided interpretation guidelines based on previously-reported within-subject variability of RMSml [7]. All participants and their clinic staff were trained in how to use the device and how to document balance scores in their electronic health record (EHR). The other 8 clinics received an identical-appearing weight scale whose balance measurement capability was disabled. After 9 months, the scales were switched so that the other 8 clinics could measure balance and the first 8 clinics could only measure weight.

At completion of the 18-month intervention period, de-identified EHR data from participating providers were collected through an honest broker for the intervention period (November 2020-April 2022) as well as from a historical control period (March 2019-February 2020). All ICD-10 diagnosis codes used and referrals made by the participants were identified as likely balance-related or not likely balance-related, and each unique patient visit was then labelled as including a balance-related diagnosis or a balance-related referral. Visits where a balance measurement was recorded in the EHR were also identified. Mixed-effects models were used to test whether the monthly rate of balance-related diagnoses and referrals differed between intervention periods and the historical period, with the rate of balance measurement utilization as a co-variate.

Results & Discussion: During the 18-month intervention period, 79,962 unique patient visits were recorded in the EHR, while 69,224 were recorded during the 12-month historical control period. 41,726 visits occurred in clinics where the Balance+Weight device was available, and balance was recorded in 1364 of these visits. As shown in Fig. 1, no significant increase in the percentage of visits with a balance-related diagnosis across all participants, but 35/41 participants never recorded a balance measurement in the EHR. For the 6 participants who recorded balance at least 5 times per month, a significant increase in balance-related diagnoses was observed (B:40.0±9.6% vs. W:36.8±9.6%). This difference was even larger for the two participants who recorded balance in at least 1/3 of their visits (B:40.8±5.9% vs. W:34.6±5.9%). No significant differences were observed between the H, W, and B periods for the percent of visits with a relevant referral.

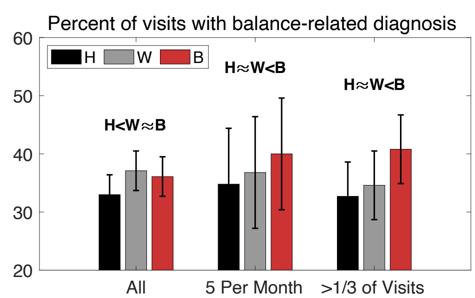

Figure 1: Percent of unique patient visits including a balance-related diagnosis code during Historical period (H), with Weight-Only device (W), and with Balance+Weight device (B). Results shown for all 41 providers, for 6 providers who recorded balance at least 5 times per month, and for the two providers who recorded balance in more than 1/3 of visits. Notations indicate significant differences with "<" and non-significant differences with "≈".

These results were consistent with our hypothesis that providers who use posturography are more likely to diagnose patients with a balance-related problem. The very low utilization of the balance measurement, however, indicates that much more work needs to be done to make posturography a standard screening tool like other vital signs commonly measured in physician clinic settings. Interviews confirmed that some providers were unable to use it because of time. Other providers reported that it provided more information than other assessments, and it was a useful conversation starter on fall risk or concrete tool to reinforce the need for further treatment.

Significance: This study demonstrates that it is possible to incorporate posturography into busy physician clinic settings to better screen patients for balance-related problems. However, usability needs to be improved to achieve widespread utilization.

Acknowledgements: National Institute of Aging (R42AG062065) awarded to Bertec Corporation and The Ohio State University.

References: [1] World Health Organization (2007), *WHO Global Report on Falls Prevention in Older Age*; [2] Stevens (2013), *HIS Primary Care Provider* 39(9); [3] Chou et al. (2006), *J Gen Int Med* 21(2); [4] Murray et al. (1967), *J Appl Phys* 23(6); [5] Maki et al. (1994), *J Geront* 49(2); [6] Chaudhari et al. (2020), *ASB Annual Meeting* 208.

COMPARISON OF COST FUNCTIONS FOR ESTIMATING INDIVIDUAL-MUSCLE ACTIVATIONS IN HUMAN AND CHIMPANZEE BIPEDAL WALKING

Aravind Sundararajan[1*], Susan G. Larson[2], Brian R. Umberger[3], Matthew O'Neill[1]
[1]Department of Anatomy, College of Graduate Studies, Midwestern University, Glendale, AZ, USA 85012
[2]Department of Anatomical Sciences, Stony Brook University, Stony Brook, NY, USA
[3]School of Kinesiology, University of Michigan, Ann Arbor, MI, USA
*Corresponding author's email: asunda@midwestern.edu

Introduction: Musculoskeletal modeling in combination with optimal control permits estimation of a wide range of individual-muscle parameters that can be difficult or impractical to measure directly, including muscle force, strain, and activations. Several distinct physiologically based cost functions have been used to solve the system's redundancy problem and estimate these parameters [e.g. 1, 2], but assessments of their accuracies have been limited to human studies. As musculoskeletal modeling emerges as an important tool for comparative biomechanics, the extensibility of these cost functions to other species has become important to understand. Here, we compare three distinct cost functions for predicting lab-based measurements of human and bipedal chimpanzee kinematics, ground reaction forces and muscle activation patterns.

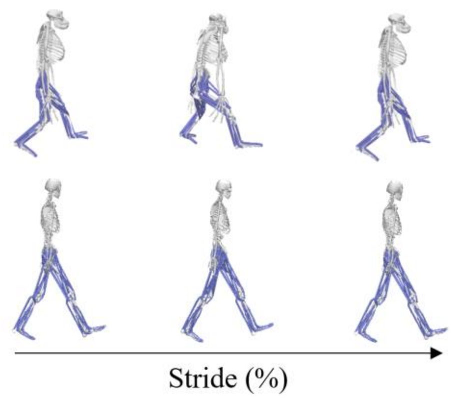

Figure 1: Chimpanzee (upper) and human (lower) generic models bipedally walking at dimensionless speeds of 0.56. The chimpanzee model has a mass of 55 kg and 44 muscles per limb, while the human model has a mass of 75 kg, and 41 muscles per limb.

Methods: Marker and force data were collected from three humans and three chimpanzees walking at the same dimensionless speed [3,4], and integrated with existing generic human [5] and chimpanzee [6] musculoskeletal models (Figure 1). Optimal control simulations were developed in OpenSim Moco that tracked 3-D kinematic and ground reaction force data and minimized one of three cost functions to estimate individual muscle state variables. The three cost function objectives were: minimum control effort by distance (J_1), metabolic cost of transport [7] (J_2), and a multi-objective function based on squared effort by distance, squared metabolic cost of transport, and squared coordinate accelerations (J_3).

Optimal control problems were solved with bilateral symmetry using 25 mesh intervals at convergence and constraint tolerances 1e-3 to generate full stride simulations containing 101 points. Optimal control problems were hot-started from initial guesses created using a torque-driven bilaterally symmetric simulation and converged in 1 to 9 hours. Root mean square error (RMSE) of the kinematics, ground forces and muscle activations were calculated from the experimental data and each cost function. Muscle activation data were compared to speed-specific electromyographic predictions from Hof et al. [8] for humans and indwelling electromyographic data for bipedal chimpanzees [9] for 14 pelvis and lower limb muscles in each species.

Results & Discussion: All simulations compared favourably with the experimental data. The average RMSEs for the three cost functions were broadly similar within and across species. Among the results, the metabolic cost of transport had the lowest average RMSE, and therefore the best correspondence to EMG data in both human and bipedal chimpanzees, at least for the speed and 14 muscles investigated here (Table 1). For both humans and chimpanzees, the single-objective functions, using effort or cost of transport enabled better tracking of the kinematics and ground reaction forces. In contrast, the multi-objective function underperformed both effort and cost of transport in average RMSE for the kinematics, ground reaction forces and muscle activations. Further comparisons using a greater walking speed range and more pelvis and lower/hind limb muscles in both species would provide further assessments of the generality of these results.

		RMSE		
		KIN	**GRF**	**ACT**
Human	J_1, effort	0.437	**0.050**	0.404
	J_2, COT	**0.420**	0.052	**0.401**
	J_3, multi	**0.420**	0.053	0.404
Chimp	J_1, effort	**0.123**	**0.041**	0.474
	J_2, COT	0.151	**0.041**	**0.449**
	J_3, multi	0.147	0.043	0.459

Table 1: 3-D kinematics (KIN) in radians, dimensionless contact forces (GRF), and dimensionless activations (ACT) RMSE for the 3 cost functions. $J_1 = 1/d$ (eff), $J_2 = 1/d$ (met), and $J_3 = 1/d\ (\text{eff}^2 + \text{met}^2 + \text{acc}^2)$, where d = distance. Lowest RMSE in bold.

Significance: These results suggest that similar cost functions may be used in both species and be expected to generate similar quality results. Comparisons of additional cost functions would be helpful in guiding future tracking and predictive simulations of both species. These results are relevant to researchers interested in simulating walking in other living or extinct animals.

Acknowledgements: This research was funded by NSF-BCS 0935327, 0935321, 2018436, 2018523.

References: [1] Ackermann M & van den Bogert AJ, J Biomech, 2010; [2] Veerkamp K et al., J. Biomech., 2021; [3] O'Neill MC et al. J. Hum Evol 2015; [4] O'Neill MC et al. J Hum Evol 2022; [5] Rajagopal et al., 2016; [6] O'Neill MC et al. J Exp Biol 2013; [7] Bargahava et al. 2004; [8] Hof AL, et al. Gait Posture. 2002; [9] Larson SG, et al. Am. J Phys Anthopol 2016.

EVALUATION OF A SOFT ROBOT PROTOTYPE FOR FINGER FLEXION REHABILITATION

Brittany Heintz Walters*[1], Katie Landwehr[1], Alissa Muñoz[1], Yen-Lin Han[2]
[1]Kinesiology Department, Seattle University, Seattle, WA, USA
[2]Mechanical Engineering Department, Seattle University, Seattle, WA, USA
*Email: bwalters1@seattleu.edu

Introduction: Hand motor impairments are well-documented in stroke survivors [1] and associated with difficulties performing activities of daily living and decreased quality of life [2]. Rehabilitation involving high-frequency, high-duration repetitive movements guided by a licensed therapist decreases hand motor impairments though this is labor-intensive, time-consuming and requires frequent travel to specialized clinics [3]. Robotic devices have been developed to supplement traditional rehabilitation by assisting repetitive movements, but many are costly, complex, and made of rigid materials [4], decreasing widespread use. To overcome these barriers, Han et al. recently developed a thermally actuated soft robot for finger flexion that is lightweight, easily fabricated, and costs approximately 1/10 the price of other devices [5] though it had not been tested in humans. The purpose of this study was to evaluate the performance of the soft robot in healthy adults.

Methods: The soft robot was designed based on Pneumatic Network Actuator architecture, consisting of two layers (Fig. 1). Layer 1 is composed of an inextensible material. Layer 2 is composed of an extensible material with small compartments. Increased pressure within the compartments causes them to inflate, leading to device actuation and bending. In the thermally actuated soft robot, compartments are filled with a phase changing material that changes from a liquid to gas when heated, increasing pressure. In this design, patients would place their hand in warm water while wearing the soft robot. Increased compartment pressure would cause bending of the soft robot and finger flexion. The robot would return to its natural state when removed from the water. This series would be repeated for rehabilitation. Preliminary testing and simulations of the thermally actuated soft robot demonstrate bending motions that mimic finger flexion [5,6].

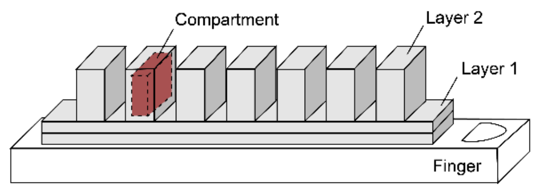

Figure 1: General prototype design. The prototype is fixed to a glove and positioned on the dorsal side of the finger. Adapted from Cabrera et al. [5].

To test geometry changes and inform continued development of the thermally actuated soft robot while preserving phase changing materials, a pneumatic soft robot was tested in 8 healthy adults (age 18-27 years; 4 f, 4 m). In the pneumatic soft robot, compartments are injected with air to increase pressure (Fig. 2). Participants were seated with their forearm supported in neutral. A finger flexion task was performed under active and passive conditions. For the active condition, participants flexed their right index finger voluntarily through the full range of motion. For the passive condition, the pneumatic soft robot was placed on the right index finger until full actuation was achieved. Participants were instructed to relax their hand and not assist the device. Range of motion was assessed at the metacarpophalangeal (MCP), proximal interphalangeal (PIP), and distal interphalangeal (DIP) joints using motion analysis software (Kinovea). Muscle activity was recorded from the flexor digitorum superficialis using electromyography (Delsys Trigno) [7]. Muscle activity was recorded for 5 s prior to the start of the passive task while the participant relaxed their hand to establish a baseline.

Results & Discussion: Actuation of the pneumatic device successfully resulted in index finger flexion for all participants (Fig. 2). Range of motion with device actuation was 30.76 ± 13.75 degrees, 66.41 ± 13.27 degrees, and 62.16 ± 13.49 degrees at the MCP, PIP, and DIP joints, respectively. The percentage of active range of motion from device actuation was 34.03% at the MCP, 66.16% at the PIP, and 78.53% at the DIP joints. Range of motion produced by the pneumatic soft robot was within the range of motion needed to perform activities of daily living based on previous research [8]. There was no difference in muscle activity of the flexor digitorum superficialis during baseline compared to the passive task, demonstrating that range of motion occurred from soft robot actuation versus voluntary muscle activation. Given the potential for reduced neuromuscular function post stroke [1], the ability of the soft robot to produce motion without voluntary muscle activation was important in demonstrating efficacy.

Figure 2: Pneumatic soft robot and finger flexion during actuation.

Significance: Results demonstrate efficacy of the soft robot in terms of finger flexion range of motion. This study is a step towards realization of an accessible, low-cost device for hand rehabilitation in stroke survivors. Future research will seek continued development of a thermally actuated soft robot through prototype testing, including use of different phase changing materials and a finger extension device.

Acknowledgements: The authors thank the American Society of Biomechanics Junior Faculty Research Award for the generous support, the Seattle University Summer Faculty Fellowship and College of Arts and Sciences Student Assistantship Award, and students Manilyn Cabrera, Noah Turoski, Arden Wong, and Andrew Scocozza.

References: [1] Raghavan (2015), *Phys Med Rehabil Cli* 26(4); [2] Carod-Artal & Egido (2009), *Cerebrovasc Dis* 27(Suppl. 1); [3] Nakayama et al. (1994), *Arch Phys Med Rehab* 75(4); [4] Balasubramian et al. (2012), *Am J Phys Med Rehab* 91(11); [5] Taylor et al. (2020), *IMECE2020;* [6] Cabrera et al. (2022), *ICAMechS2022*; [7] Hermens et al. (2000), *J Electromyogr Kines* 10(5); [8] Bain et al. (2015), *J Hand Surg* 40E(4).

HOP, SKIP, AND A JUMP: INVESTIGATING WHY PEOPLE JUMP IN RESPONSE TO WALKING PERTURBATIONS

Jennifer K. Leestma[1,2*], Vibha Iyer[3], Aaron J. Young[1,2], Gregory S. Sawicki[1,2,4]
[1]George W. Woodruff School of Mechanical Engineering, [2]Institute for Robotics and Intelligent Machines, [3]Wallace H. Coulter Department of Biomedical Engineering, [4]School of Biological Sciences, Georgia Institute of Technology
*Corresponding author's email: jleestma@gatech.edu

Introduction: What causes people to fall in the real world? Despite a vast amount of literature investigating balance metrics in response to perturbations, it may be the strategy that is required for balance recovery that causes people to fall rather than the magnitude of imbalance itself. In our recent work, we studied the balance and recovery strategies used to respond to perturbations that varied in magnitude, direction, and timing [1]. As a result of studying a thorough sweep of these variables (96 conditions), we observed a niche set of conditions that elicited an extreme balance recovery strategy; in over 20% of responses to some conditions, individuals jumped. Here, we took a closer look at the jump responses in our data set by analyzing two situations that we hypothesized would elicit a jump response and the three jump mechanisms that we observed.

Methods: We used our previously published data set; 11 participants walked while being exposed to ground perturbations that varied in magnitude, direction, and timing [1]. We hypothesized that **H1)** participants jumped to avoid a **collision** of the swing limb with the stance limb, typically elicited during a crossover step (Fig. 1A). We quantified this using the velocity vectors of the swing foot in the 150 ms leading to the jump; we classified a projected collision if the velocity vector of any swing foot marker was projected to collide with the region defined by the stance foot markers. If this was not the case, we hypothesized that **H2)** remaining jumps occurred if the required step width was **too narrow** and fell outside the capabilities of the participant (Fig. 1B). To quantify this, we fit a participant-specific center of mass-driven model [2] to the four steps after each non-jump perturbation trial. We used this model and center of mass mechanics leading up to the jump to project the required step width had the participant not jumped. We quantified three mechanisms that individuals use to jump (Fig. 1C); 1) a lateral **skip** strategy involves pushing off of the stance foot and landing on that same foot lateral to the original position, 2) a **foot replacement** strategy involves hopping into the air with the stance foot and landing in the same location with your swing foot, and 3) a **leap** strategy involves hopping into the air with the stance foot and landing anteriorly with the swing foot.

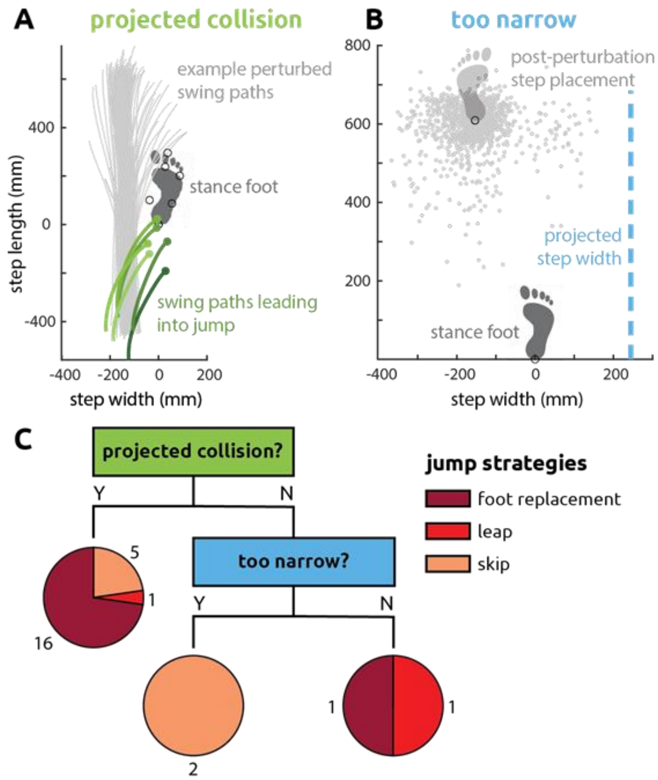

Figure 1: (A) Lines show swing foot heel marker relative to stance foot; grey lines are non-jump responses, green lines are swing phase leading up to jump. **(B)** Grey dots show non-jump post-perturbation steps, blue line shows a trial's projected step width from the linear model, which is a narrower step than any successfully executed step by the participant. **(C)** Decision tree showing the jump strategies used in response to projected collisions and too narrow steps.

Results & Discussion: Of the 26 trials with jump responses analyzed from the data set, 22 trials were projected to have a limb collision. In the jumps that followed the projected limb collision, 16/22 used a foot replacement strategy, 5/22 used a skip strategy, and 1/22 used a leap strategy. In the remaining 4 trials that did not include a projected limb collision, 2/4 were projected to require too narrow of a step. In both of these trials, individuals used a skip strategy. In the remaining 2 trials that did not present a collision or too narrow of a step, the foot replacement and leap strategies were both used once. Broadly, this work identifies potential limb collisions during a narrowing step maneuver as the leading cause of jump responses following perturbations. In these situations, participants dominantly reacted by using a foot replacement strategy; in addition to preventing a collision, this strategy effectively turns a narrowing step into a widening step, which may set up the participant to a wider range of maneuvers on the subsequent step. The lateral skip strategy effectively does the same, which is executed for the remaining steps that are too narrow.

Significance: Here, we identified some of the more demanding balance recovery mechanisms that have been reported, with only two other studies that we are aware of reporting jump responses [3,4]. The perturbation conditions that caused jumps could be a useful tool to study highly destabilizing scenarios, especially those that may cause a fall in balance-impaired individuals. These responses are also important to consider in the development of wearable robots, as these strategies may present edge cases for existing control architectures. Lastly, these responses pose an interesting stance/swing limb constraint challenge that should also be considered in bipedal robotics.

Acknowledgements: This work was supported by the NSF NRT ARMS Program Award #1545287 and NSF GRFP Award #1324585.

References: [1] Leestma et al. (2023), *J Exp Biol* [2] Joshi, Srinivasan (2019), *J R Soc Interface* [3] Eveld et al. (2020), *Mid-South Biomechanics Conference* [4] Pijnappels et al. (2004), *J Biomech*

DEVELOPMENTAL PLASTICITY OF MUSCLE ARCHITECTURE IN RESPONSE TO CHRONIC LIMB LOADING

Kavya Katugam-Dechene[1]*, Talayah Johnson[2], Stephen J. Piazza[1], and Jonas Rubenson[1]
[1]Biomechanics Laboratory, Dept. of Kinesiology, The Pennsylvania State University, University Park, PA, USA.
*kavya@psu.edu

Introduction: How muscles adapt to changes in load environment during growth has important implications for child development. Controlled longitudinal studies in humans are, however, lacking. To overcome practical and ethical constraints of human experimentation, our laboratory has adopted a bipedal animal model (guinea fowl; *numida meleagris*) to study the effect of altered growth-period activity on muscle architecture and locomotor mechanics and energetics [e.g., 1, 2]. Recently, we demonstrated that chronic lower limb loading (added mass) during development allows animals to carry the additional mass remarkably more economically as adults [3]. Here, we test the hypothesis that lower energetic cost of walking after growth-period limb loading arises due to adaptations in muscle architecture that allow for efficient production of mechanical work.

Methods: To study the effect of increased load stimulus during development on muscle architecture, we chronically applied a mass equal to 4.0% body mass unilaterally to the lower right limb of guinea fowl from 1-16 wks of age (n = 10; protocols approved by Penn State IACUC). At 16 wks, after locomotor and energetic analyses conducted for companion studies, animals were euthanized and immediately frozen (-20°C) for muscle analyses. Because limb loading causes a substantial increase in ankle flexion work during the swing phase in guinea fowl, and because the tibialis cranialis (TC) is the sole muscle responsible for ankle flexion, the TC is a muscle of choice for addressing load-induced plasticity. To study the TC, each animal was positioned with ~ 90° knee angle and a fully extended ankle (0°). Muscles were affixed to a 3D printed PLA splint *in situ* using 4-0 silk sutures, and then carefully dissected from the pelvic limb. Splinted muscles were placed in neutral buffered formalin for fixation. After formalin fixing, muscles were split into three compartments [anterior (crossing knee), middle, and posterior], and architecture parameters were measured for each compartment. Mass-weighted averages were computed for each architecture parameter. The mass of each compartment was measured to the nearest mg, and then split longitudinally to expose the arrangement of fascicles. Fascicle length (L_F) was measured by digitizing fascicles under a microscope with a digitizing arm (Microscribe, Immersion Inc.), taking 3D fascicle curvature into account. Pennation angles (θ) were measured from high-resolution digital photographs. A small bundle of fascicles was cut away from each muscle compartment and placed in 30% nitric acid for digestion. Small bundles of fascicles were teased apart for sarcomere length (L_S) measurement using laser diffraction analysis [4]. L_F, θ, and L_S were measured across three locations per muscle segment and averaged. Optimal fascicle length (L_O) and normalized L_S were computed using L_F, L_S and the known optimal sarcomere length of guinea fowl muscle [5]. Pennation angle at L_O (θ_O) was computed following [6]. Physiological cross-sectional area was computed as PCSA = $\text{mass} \cdot \cos\theta_0 / \rho \cdot L_0$, where ρ is muscle density (1.056g/cm^3). Parameters were analysed using Shapiro-Wilk hypothesis tests and paired t-tests.

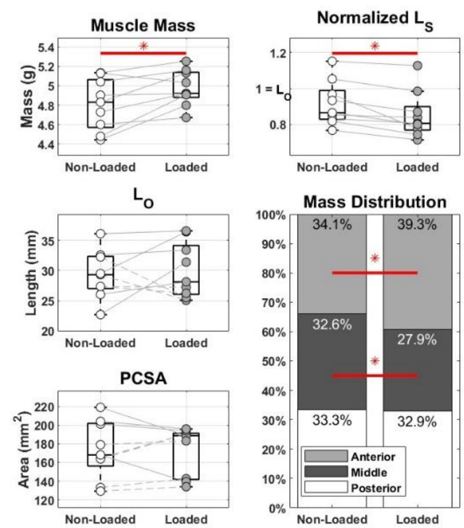

Figure 1: TC architecture variables. *($p < 0.05$).

Results & Discussion: Loaded-limb muscles had 3.5% greater mass than muscles of the contralateral non-loaded limb ($p = 0.02$), with 5.2% more mass distributed to the anterior compartment ($p < 0.01$) and 4.7% less mass distributed to the middle compartment ($p = 0.04$) (Fig. 1). It is possible that allocating proportionately more mass to the anterior compartment that crosses the knee allows for greater energy transfer between the knee and the ankle joints, a mechanism that could reduce the energy required to move the additional mass. The locus of increased mass in limb-loaded TC muscles varied: For 5 animals, increased mass was attributed to increased L_O (Fig. 1: solid lines); for 4 animals, increased mass was attributed to increased PCSA (Fig. 1: dashed lines). The lack of consistency in architecture plasticity was surprising and suggests that adaptation to achieve increased efficiency is not highly constrained. Increasing muscle length may lead to an improved efficiency of moving added mass by mitigating force-length-velocity constraints. On the other hand, increasing PCSA will reduce costs associated with high muscle activation. It is possible that skeletally mature animals display more uniform muscle adaptations to increased loading. Muscles splinted in the same posture had significantly shorter L_S in loaded-limb muscles ($p < 0.01$), indicating that loaded muscles may be more compliant, although passive forces are expected to be small due to relatively short L_S (Fig. 1). The short L_S may reflect priority for preventing TC overstretch injury, given that only a single muscle contributes to ankle flexion.

Significance: Growth-period adaptations to increased loading lead to increased muscle mass, but specific muscle architecture changes are not easily predictable. The present results suggest multiple adaptive strategies exist, even within the same species.

Acknowledgements: Supported by NIH Grants R21AR071588 and R01AR080711.

References: [1] Salzano et al. (2018), *J Biomech*; [2] Cox et al. (2021), *J Exp Biol* ; [3] Johnson (2021), *PSU KINES Master's Thesis*. [4] Lieber & Fridén (2000), *Musc Nerve*; [5] Carr et al. (2011), *J Exp Biol*; [6] Buchanan et al. (2015) *J. Appl. Physiol*.

KNEE CARTILAGE STRESS INTERLIMB DIFFERENCES THROUGHOUT GAIT 3 AND 6 MONTHS AFTER ACL RECONSTRUCTION: A FINITE ELEMENT ANALYSIS

Kelsey Neal[1*], Jack R Williams[1,2], Ashutosh Khandha[1], Lynn Snyder-Mackler[1], Thomas S. Buchanan[1]
[1]University of Delaware, Newark DE, [2]Northern Arizona University, Flagstaff AZ
*kaeneal@udel.edu

Introduction: Altered gait mechanics after ACL reconstruction (ACLR) are thought to be a leading mechanism for the development of post traumatic osteoarthritis (OA). Underloading of the involved limb's medial tibiofemoral compartment of the knee (vs. uninvolved), as assessed by medial compartment force, is present 3 months after ACLR but is found to become more symmetric by 6 months[1]. Additionally, many individuals develop a stiff gait during this early time period resulting in less range of motion within the involved limb compared to the uninvolved[1,2]. While alterations in gait mechanics are well documented during this early time points after surgery, it is unknown how these changes impact load distribution and the stress environment at the tissue level within the joint. Finite element models hold the potential to provide deeper insights into this tissue level loading environment. Thus, the purpose of this study was to analyze and compare interlimb differences (ILD=IN-UN) in stress maps of the medial femoral cartilage at 3- and 6-months post ACLR. We hypothesized that the medial cartilage in the involved limb will experience lower stress values throughout gait at both time points and that greater ILD will be seen during the 3-month time point compared to the 6-month time point.

Methods: 15 subjects (7 female, age: 23 ± 6 years, BMI: 24.5 ± 3.4 kg/m²) underwent gait analysis at 3 and 6-months after ACLR. Subjects walked at an identified self-selected speed that was held consistent across time points. During walking, kinematic (120 Hz), kinetic (1080 Hz), and surface electromyography (1080 Hz) data were collected bilaterally. These data were used to calculate subject-specific joint contact forces for the medial and lateral joint compartments via a validated EMG-informed neuromusculoskeletal model[3]. Using magnetic resonance imaging scans, a FE model was developed from the healthy knee of one subject (female, age:19)[4]. Model inputs included medial (MCF) and lateral (LCF) compartment forces and knee flexion angles (KFA) throughout gait. Instead of scaling the geometry of the model to each individual, joint forces were normalized to the body weight (BW) of the model's primary subject allowing us to create a scale factor for the load of each individual. This allowed for direct comparison of mesh results and drastically reduced model development time and validation. Simulations were executed in three steps for each subject's involved and uninvolved limbs in Abaqus CAE (Dassault Systems Simulia Corp., Providence, USA). Step 1 initialized contact between all contact surfaces (1 second), Step 2 applied the initial conditions (1 second), and Step 3 simulated the gait cycle (100 seconds). KFA was applied to a reference point placed at the center of the transepicondylar axis, while compartment forces were applied quasi-statically to reference points placed at the center of medial and lateral compartments along the transepicondylar axis. Von Mises stress was found throughout the entirety of the stance phase of walking gait (step three) for both the medial tibial and femoral cartilage. We then calculated mean von Mises stress maps and interlimb difference (ILD) at each point of the stance phase of gait at both 3 and 6 months.

Results & Discussion: Different stress patterns were present between limbs at both 3- and 6-months. The involved limb experienced less stress than the uninvolved limb throughout gait at both time points. The greatest ILDs occurred around 20-25% of stance which is when peak KFA and peak medial compartment force occurred. These differences were most pronounced on the medial edge of the femoral cartilage and occurred over a larger area of cartilage at 3 months than 6 months (**Figure 1**). The bone-cartilage interface experienced higher ILD than the cartilage-cartilage interface. This is of interest since previous biochemical findings in this cohort showed worse cartilage health in the deep layer of cartilage[5].

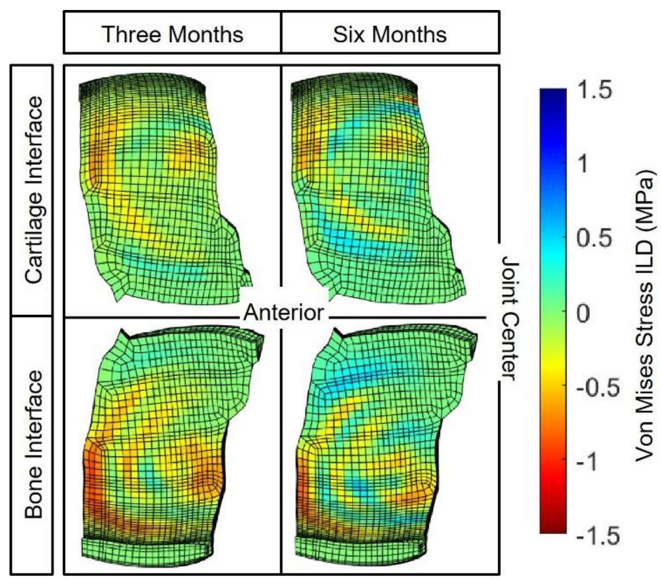

Figure 1: Von Mises Stress ILD at 20% of stance for the medial femoral cartilage at 3 and 6 months after ACLR. Cartilage is oriented with the joint center on the right of the figure and the anterior pointing toward the center of the figure.

Significance: The involved limb's medial femoral cartilage experienced a more varied stress environment after ACLR compared to the uninvolved limb. This work is among the first to provide insight into how changes in joint load and kinematics impact the stress patterns within the cartilage after ACLR. These reduced stresses within cartilage early after ACLR could be a mechanism for eventual development of OA. Future work will assess if these regions of high interlimb differences are associated with long-term cartilage degeneration.

Acknowledgements: NIH: R01-HD087459

References: [1] Neal et al. (2022), *J Orthop. Res.* 40(9); [2] Shabani et al. (2016), *Int Orthop* 39(6); [3] Manal, Buchanan (2013), *J Biomech Eng* 135(2); [4] Neal et al. (2022), *NACOB;* [5] Williams et al. (2021), *J Orthop. Res.* 40(1)

DIVERGENCE OF TRUNK-HIP MOVEMENT CONTROL STRATEGIES IN PERSISTENT LOW BACK PAIN

John R. Gilliam[1*], Ahyoung Song[1], Jennifer MC Vendemia[2], Sheri P Silfies[1]
University of South Carolina, [1]Department of Exercise Science, [2]Department of Psychology, Columbia, SC
*Corresponding author's email: jrg15@email.sc.edu

Introduction: Low back pain is the leading cause of years lost to disability worldwide.[1] Altered trunk-hip movement control is a well-documented impairment in persons with persistent low back pain (pLBP). Emerging evidence suggests rather than a single altered movement pattern, movement control may be better represented as a spectrum with multiple phenotypes including *loose* and *tight* control strategies.[2] Furthermore, it has been proposed that these strategies may be driven by changes in brain sensorimotor dynamics.[3] To test this, we compared movement control strategies between individuals with pLBP and matched healthy controls (HC). We then stratified participants with pLBP into groups based on movement strategy during unilateral bridging tasks to explore the existence of multiple movement control phenotypes.

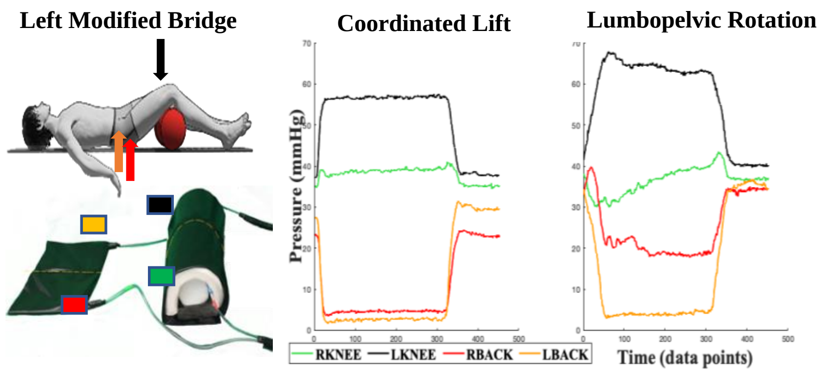

Figure 1. Top left: Left (L) unilateral bridging task performed by pushing the L knee down to initiate hip extension and simultaneously slightly raising the buttocks and lumbar spine. **Bottom left:** The system developed to assess movement control strategies during task-based neuroimaging. The system independently senses pressure changes under the knees (black and green) and lumbar spine (orange and red) on both the L and Right (R). **Right:** Times series data from 2 study participants. Coordinated Lift: Coordinated and simultaneous pressure increase in L knee sensor with decrease of the L and R back sensors. Lumbopelvic Rotation: Poor coordination and phase delay between the back sensors during task.

Methods: 30 individuals (20F; Age: 34+/-14 years) including 15 with pLBP and 15 age-, sex- and BMI-matched HC were included. An MRI-safe instrumented system was developed to record movement via pressure changes and assess trunk-hip movement strategies during task-based neuroimaging (Fig.1). Modified unilateral bridging tasks were performed by pushing one knee down into an instrumented bolster and slightly raising the lumbopelvic region off pressure sensors on the scanner bed. To quantify movement strategies, we derived peak cross-correlation (R_{xy}) and phase delay (τ^*) values[4] for time-series pressure changes between L_{back} and R_{back} pressure sensors. These values represent coordination of the lumbar spine and pelvis to lift both sides simultaneously without transverse plane lumbopelvic rotation (Fig.1). Peak R_{xy} and τ^* values were compared between groups (pLBP/ HC). The mean and SD of HC performance were used to determine individual control strategy types (*proficient*, *loose*, *tight*) in the pLBP group. *Loose* control was defined as less coordinated lumbopelvic movement (R_{xy} 1 SD < HC). *Tight* control was defined as a pattern of co-contraction and increased stiffness, which manifests in simultaneous movement of segments (R_{xy} 1 SD > HC). Consistent with a spectrum, *proficient* control lies between *loose* and *tight*. We expected that higher τ^* values would align with a *loose* control strategy. One participant with pLBP was excluded as an outlier. R_{xy} values were Fisher-Z transformed. Two-tailed t-tests (Z) and Mann-Whitney U tests (τ^*) were used to compare pLBP and HC. Descriptive statistics were calculated for each control strategy type.

Results & Discussion: Differences in Z values were found between pLBP and HC groups for the R bridge (p=0.01). No differences were observed between groups for Z values for the L bridge task (p=0.75), or for τ^* in either the R (p=0.201) or L (p=0.477) tasks (Table). 57% of persons with pLBP demonstrated a *loose* or *tight* control pattern. Consistent with a *loose* control strategy segmental lag (τ*) values were higher in the *loose* group. 4/7 individuals in the *loose* group were classified as *loose* for both tasks. There were no instances of individuals demonstrating a *loose* control strategy on one task and a *tight* control strategy on another. We did not find consistent differences between trunk-hip movement strategies when comparing pLBP as one homogenous group with HC. However, Z and τ^* values support the presence of a spectrum of movement strategies and align with the constructs of *loose*, *proficient*, and *tight* control.

Table 1.		**LEFT BRIDGE**				**RIGHT BRIDGE**			
		Z - R_{xy}		**τ***		**Z - R_{xy}**		**τ***	
Group	n	Mean	SD	Mean	SD	Mean	SD	Mean	SD
pLBP	14	1.87	0.47	0.06	0.17	1.70	0.45	-0.07	0.18
HC	15	1.93	0.39	0.00	0.01	2.11	0.34	0.00	0.00
Loose	7	1.62	0.41	0.12	0.24	1.37	0.37	-0.15	0.24
Proficient	6	2.04	0.37	0.01	0.02	2.01	0.23	0.00	0.00
Tight	1	2.66	NA	0.00	0.00	2.22	NA	0.00	0.00

Mean and SD of Z-transformed R_{xy} values and phase delays (τ*).

Significance: If subgroups demonstrating different movement control strategies exist in pLBP, identifying these subgroups and their features could drive more precise diagnosis and treatment. When looking at movement patterns across individuals with pLBP the large variability in motor control is likely reflected in variability in sensorimotor brain dynamics driving task performance.

Acknowledgments: Financial support: R01HD095959; T32GM081740

References: [1] Wu et al. (2020), *Ann Transl Med* 8(6); [2] Van Dien et al. (2019), *JOSPT* 49(6). [3] Meier et al. (2019), *Neuroscientist* 25(6); [4] Nelson-Wong et al. (2008), *Clin Biomech* 23(5).

ARE CHANGES IN RUNNING GAIT DURING A TYPICAL RUN ASSOCIATED WITH OVERUSE INJURY?

James J. McDonnell[1*], Kathryn A. Davel[1], Kai W. Chien[1], Max R. Paquette[2], Allison H. Gruber[1]
[1]Department of Kinesiology, Indiana University, Bloomington, USA
[2]College of Health Sciences, University of Memphis, Memphis, TN, USA
*Corresponding author's email: jimcdon@iu.edu

Introduction: Traditional running related injury (RRI) studies typically compare injured and uninjured runners to identify which multifactorial risk factors may be associated with RRI. However, meta-analyses indicate that there is currently no strong evidence for reliable or consistent RRI risk factors[1], particularly for gait-related risk factors[2]. Thus, the current approach to RRI research has not been effective if gait-related risk factors indeed exist, possibly due to the inability of lab-based measures to capture gait representative of real world running. Gait characteristics change during exhaustive prolonged runs[3,4,5], yet RRI studies typically capture gait after only a brief warm-up, which may not reflect the changes in gait occurring during a typical training run. Additionally, the level of exertion experienced during a typical training run is likely less than more intense or longer duration runs performed in prolonged running studies [3,4,5]. Therefore, the purposes of this study were to establish (1) if gait changes after a typical training run simulated in the lab and (2) if changes in gait were related to training compliance, pain, and subjective feelings of fatigue. Knee flexion and ankle rearfoot eversion were examined because of their role in active shock attenuation[7,8]. Based on previous research[3,6], knee flexion and rearfoot eversion were hypothesized to increase following a typical run.

Methods: 20 recreational runners between the age of 18-40yrs enrolled in a 12-week training program. Daily surveys recorded training and pain and subjective fatigue on a 0-10 scale. Subjects completed an in-lab gait analyses prior to beginning the program in which 3D overground running gait at typical training speed (mean±1SD: 2.9±0.4 m/s) was collected ('pre-run'). Next, subjects completed a treadmill run at the same speed and their typical duration (24.2±8.4 min). Borg rate of perceived exertion (RPE, 6-20) was collected every 5-minutes and the last minute. Immediately after the treadmill run, the subjects completed additional overground trials to measure 'post-run' gait as quickly as possible to minimize the effects of recovery. Rearfoot eversion and knee flexion angles at initial contact and peak angles were averaged across trials and compared between pre-run and post-run conditions using paired t-tests (α=0.05) and Hedge's g effect sizes. Individual regression models will test the association of pre-run and post-run gait and RPE to training compliance, pain and subjective fatigue experienced during the 12-week training program once follow-up is completed in May 2023.

Results: Maximum RPE reported during the simulated typical run was 14.3±1.7 for the n=17 gait data analysed to date. There was no significant difference pre-run versus post-run knee flexion angle at contact (p = 0.303, g = 0.163) or peak knee flexion angle (p = 0.803, g = 0.027). Both rearfoot eversion angle at contact (p = 0.042, g = 0.168) and peak eversion angle (p = 0.031, g = 0.384) were significantly different between pre-run and post-run (Fig 1). To date, 10 subjects have reported at least two unplanned days off from running due to pain, injury, or illness. Pain and lower-body fatigue, and overall fatigue levels were 3.3±1.3, 2.9±2.3, and 4.4±3.0 respectively on missed training days.

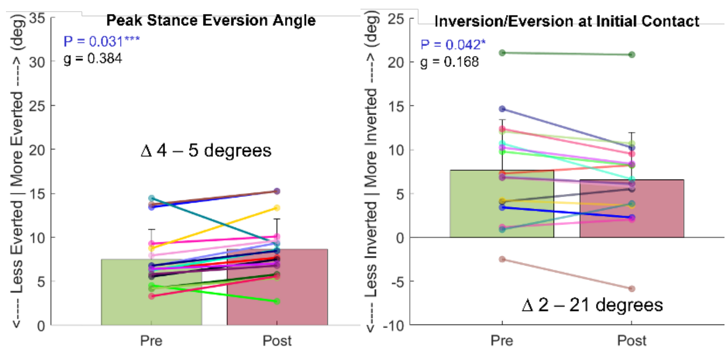

Fig. 1: Mean rearfoot eversion angle at initial contact and peak angle during stance for pre-run (green) and post-run (pink) conditions. Error bars are 1SD. Colored lines represent individual subject response (n=17).

Discussion: In support of our hypothesis, muscles crossing the ankle joint may fatigue faster than muscles crossing the knee[9], which may have contributed to increased initial contact and peak eversion angles observed after a simulated typical run. Large eversion is coupled with tibial abduction, knee valgus, and patellofemoral pain[6], but magnitudes associated with RRI risk may not emerge with a 'fresh' gait. Contrary to our hypothesis, similar pre- vs. post-run knee flexion was consistent with some previous prolonged running studies but not others[4,6,10]. Conflicting findings may be due to the 'typical' duration and exertion of our protocol if subjects stopped running prior to experiencing excessive exertion, knee extensor fatigue, or increased knee flexion observed previously[4,10,11].

Significance: While several studies have documented the kinematics effects of prolonged exerted running, none to our knowledge have compared the magnitude of changes across typical running intensities or durations within the same runner. This study demonstrates the importance of capturing kinematics before and after a typical training run to estimate the gait a runner experiences during typical training but in a lab environment. RRI risk factors may not emerge until after a runner has reached a certain level of exertion. Regression analyses to be performed after follow-up will provide preliminary data to generate hypotheses and sample size estimates for future prospective studies examining the role of typical gait changes and RRI.

References: [1]Willwacher et al., (2022), *Sports Med*. [2]Ceyssens et al., (2019), *Sports Med.* [3]Willwacher et al., (2019), *Gait & Posture.* [4]Derrick et al., (2002), *Med Sci Sports Exerc*. [5]Sanno et al., (2020), *Med Sci Sports Exerc* [6]Dierks et al., (2010), *J Biomech*. [7]Edwards et al., (2012), *J Biomech*. [8]Hintermann et al., (1998), *Sports Med*. [9]Weir et al., (2020), *Med Sci Sports Exerc*. [10]Mizrahi, J. et al., (2000), *Hum Mov Sci*. [11]Noakes, (2000), *Scand J Med Sci Sports Sports.*

Plantarflexor Central Drive Symmetry is Associated with Poststroke Walking Function in Community Ambulators

Ashley N. Collimore[1], Jonathan T. Alvarez[2], David A. Sherman[1,2], Conor J. Walsh[1,2], Louis N. Awad[1*]
[1]College of Health and Rehabilitation Sciences, Boston University, Boston, Massachusetts, USA; [2] Harvard John A. Paulson School of Engineering and Applied Sciences, Harvard University, Cambridge, MA
*Corresponding author's email: louawad@bu.edu

Introduction: Poststroke walking is slow and asymmetric[1], which ultimately leads to reduced community participation[2]. Determination of the most efficacious gait intervention for each individual patient requires identifying their primary neuromotor impairment. The lower extremity portion of the Fugl-Meyer Assessment of Motor Recovery after Stroke (FM-LE) is considered the clinical gold-standard for assessing neuromotor impairment[3], yet its application is limited by a known ceiling effect[3] and it is not well correlated to walking performance measures, such as propulsion symmetry[4]—which is an emerging focus of poststroke gait rehabilitation programs[5]. In contrast, plantarflexor central neural drive has emerged as an alternative measure of neuromotor impairment associated with walking performance[6]. While technological limitations have hindered widespread clinical adoption of central drive, our group has recently developed a system to improve its clinical accessibility[7].

Assessed by superimposing a burst of supramaximal stimulation during a maximum voluntary contraction, central drive can identify if muscle weakness is the result of deficits in neural control (i.e., reduced voluntary activation) or muscle strength (i.e., reduced force-generating capacity). As the plantarflexors are the primary contributors to gait propulsion[8] and paretic plantarflexor central drive moderates the relationship between gait propulsion and walking function[6], central drive to the paretic plantarflexors may be a better metric for identifying specific poststroke neuromotor impairments limiting walking function than the FM-LE. However, because poststroke gait deficits are commonly observed bilaterally, a measure of just one limb's neuromotor function may not accurately predict functional deficits in the bilateral activity of walking; symmetry of central drive across limbs may more fully capture the interlimb neuromotor coordination deficits underlying impaired walking function after stroke. The aim of this study is to investigate how well the FM-LE, paretic plantarflexor central drive, and central drive symmetry each explain the variance in the six-minute walk test distances of community ambulators poststroke[2]. We hypothesized that central drive symmetry would explain more variance in six-minute walk test distances than either the FM-LE or paretic plantarflexor central drive.

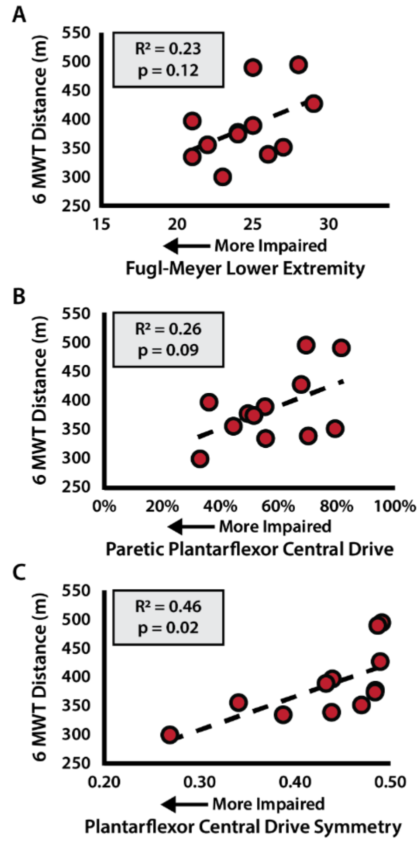

Figure 1: Plantarflexor central drive symmetry explains more variance in six-minute walk test distances than Fugl-Meyer lower extremity scores or paretic plantarflexor central drive.

Methods: 12 participants with six-minute walk test distances of at least 288m (i.e., the threshold for community ambulation[2]) were included in this study and completed assessments of six-minute walk test distance, FM-LE, and bilateral plantarflexor central drive. Central drive was assessed using the CEntral DRive System (CEDRS), an accurate and portable plantarflexor central drive measurement system previously validated[7]. CEDRS attaches to any standard clinical table and consists of two components: a force measurement component that isolates the force produced by the plantarflexors and an electrical stimulation component that delivers supramaximal electrical stimulation to the plantarflexors once voluntary strength has plateaued. Central drive for each limb was calculated as the average of three tests. Central drive symmetry was calculated as (Lowest Central Drive / Sum of Both Limbs), with 0.5 representing perfect symmetry. Three linear regressions were conducted in SPSS v27 between FM-LE scores, paretic central drive, and central drive symmetry and six-minute walk test distances. Median ± semi-IQR are reported. The study is ongoing; preliminary findings are reported below and a full analysis will be presented.

Results & Discussion: Participants were 58.87 ± 6.4 yrs. old with stroke chronicity of 7.11 ± 3.28 yrs. Participants had a median six-minute walk test distance of 375.67 ± 13.30 meters, FM-LE score of 24.5 ± 1.75, paretic plantarflexor strength of 35.0 ± 6.72 ft-lbs, and nonparetic plantarflexor strength of 62.75 ± 11.64 ft-lbs. With paretic and nonparetic central drive of 55 ± 11% and 79 ± 13%, respectively, the median central drive symmetry was 0.45 ± 0.04. Whereas FM-LE and paretic central drive respectively explained 23% ($p = 0.12$) and 26% ($p = 0.09$) of the variance in six-minute walk test distances, central drive symmetry explained 46% ($p = 0.02$).

Significance: These results suggest that central drive to the plantarflexors may be a better metric than the commonly used FM-LE for identifying the specific neuromotor impairments poststroke that limit walking function. Moreover, by identifying the nature of an individual's strength deficit as either impaired voluntary activation or muscle strength capacity, central drive assessments inform clinical interventions in a way the FM-LE cannot. Interestingly, an interlimb metric (i.e., central drive symmetry) explained more variance than the singular limb (i.e., paretic central drive), suggesting that functional metrics are impacted by bilateral impairments.

Acknowledgements: Funding sources include a Boston University Ignition Award and an NIH grant (F31HD106777).

References: **[1]** Chen et al. (2005), *Gait Posture* 22(1) **[2]** Perry et al. (1995), *Stroke* 26(6) **[3]** Gladstone et al. (2002), *Neurorehab & Neur Rep* 16(3) **[4]** Bowden et al. (2010), *Neurorehab & Neur Rep* 24(4) **[5]** Awad et al. (2020), *J. Neuroeng. Rehabil.* 17(139) **[6]** Awad et al. (2020), *J. Neurol. Phys. Ther.* 44(1) **[7]** Collimore et al. (2023), *CSM* **[8]** Zelik et al. (2016), *J Exp Biol.* 219(23)

THE EFFECT OF SERIAL LIGAMENT REMOVAL ON THE KINEMATIC BEHAVIOR OF A FUNCTIONAL UNIT SPINAL FINITE ELEMENT MODEL

Isaac K. Kumi, Michael Polanco, Sebastian Bawab, Stacie I. Ringleb
Department of Mechanical and Aerospace Engineering, Old Dominion University, Norfolk, VA USA
Email: sringleb@odu.edu

Introduction: In spine biomechanics, finite element (FE) models have been used to evaluate healthy and pathological conditions within the spine [1] and to provide information difficult to obtain from both *in vitro* and *in vivo* experimentations [2]. For these models to accurately simulate joint mechanics and predict clinical treatment outcomes while also minimizing time to create and run a model, understanding the effects of ligaments and their properties should be investigated. Moreover, since the kinematic behavior of the spine has been associated with the ligaments [3], it is necessary to evaluate the kinematic compatibility of ligament datasets before their application in FE spine models. The motion results of functional spinal units after ligament transection have been studied *in vitro* [4][5], yet their effects have yet to be evaluated using FE modeling. Therefore, this study aims to test the sensitivity of a functional unit FE model to a particular dataset of ligament properties by serially removing the ligaments while comparing the results to available *in vitro* data.

Methods: Quasi-static analyses were performed with a L4-L5 functional unit (Fig.1) obtained from SimTK [2] using FEBio (FEBio, Salt Lake City, UT). Vertebral and disc properties were acquired from literature [6]. Intervertebral ligaments were characterized as tension-only springs using linear elastic material properties obtained from literature [7]. A pure moment of 7.5N-m was applied in flexion and extension on the superior endplate of the L4 vertebra, while the inferior endplate of L5 was constrained in all degrees of freedom. The kinematics of the L4-L5 functional unit were initially assessed with all ligaments intact, then by serially removing specific ligaments in accordance with experimental protocol [3]. The ligaments were removed in the following sequence: supraspinous ligaments (SSL), interspinous ligaments (ISL), flaval ligaments (LF), facet capsules (FC), vertebral arch (VA), posterior longitudinal ligaments (PLL), and anterior longitudinal ligaments (ALL). The vertebral arches were removed for the purposes of validation to compare the results to the *in vitro* study [3]. Range of motion (ROM) values were recorded for flexion and extension during each ligament removal step.

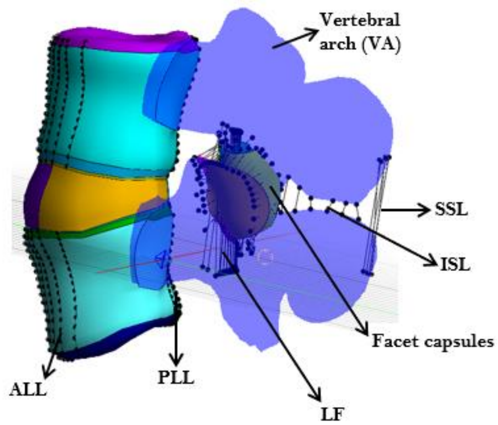

Figure 1: Sagittal view of the L4-L5 functional unit showing the vertebral arch and the ligaments.

Results & Discussion: The first four ligament removal steps saw a minimal effect on the range of motion for flexion and extension in both the published experimental results and the model (Fig. 2). The removal of the facet capsules had the most overall impact on ROM during flexion, producing about an 80% increase following the prior ligaments' removal. In extension, the ALL removal had the most significant impact on the ROM, resulting in a 47% increase in ROM, similar to that observed in the *in vitro* study [3]. This observation was expected since the ALL limits extension motions because of its higher cross-sectional area, leading to higher stiffness compared to the other ligaments [8]. Its removal was therefore expected to produce a significant extension rotation.

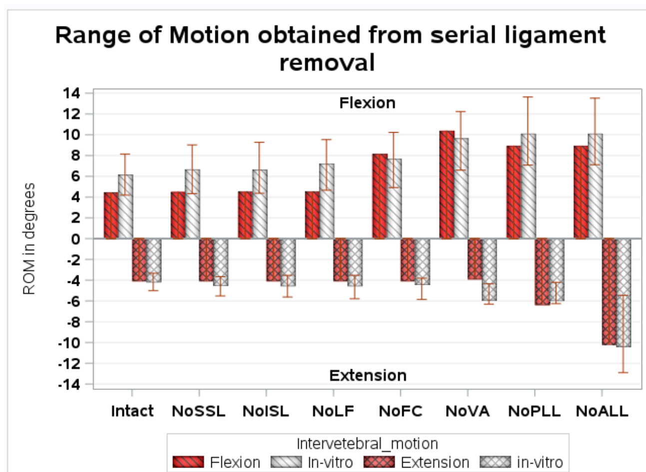

Figure 2: ROM obtained from serial ligament removal for 7.5Nm torque for the L4-L5 functional unit. The *in vitro* data reports the median value, where the error bars represent max and min values.

By following the ligament removal steps prescribed in the *in vitro* study, ROM values obtained for flexion and extension fell within the range of the *in vitro* data [3]. Future works can expand this study to include other planes of motion and utilise ligament datasets with viscoelastic properties. In addition, the model and this ligament dataset can be applied to clinical investigations interested in using FE modelling to explore procedures such as osteotomy and probe joint instabilities.

Significance: As FE modelling is gaining prominence in spine biomechanics, accurate ligament property datasets must be utilised in FE models such that *in vitro* studies can be replicated and validated. The ligament data set [7] and the functional spinal unit FE model in this study can be utilised to provide insights into clinical studies targeting ligament removal and exploring novel surgical treatments of spinal deformities and fractures.

References: [1]. Wilke, H.J. et al. *Eur Spine J* **29**(1), 179-85, 2020; [2] Finley, S. et al. *Comp. Method in Biom*. **21**(6), 444-52, 2018;
[3] Heuer, F et al. *Biomechanics* 40, 271-80, 2007; [4] Panjabi, M.M. et al. *Biomechanics* 8, 327-36, 1975;
[5] Gillespie, K.A. et al. *Spine* 29, 1208-16, 2004; [6] Naserkhaki et al. *Biomechanics* 70, 33-42, 2018;
[7] Rohlmann, A. et al. *Biomechanics* 39, 2484-90, 2016; [8] Myklebust, J.B. et al. *Spine* **13**(5), 526-31, 1988.

DYNAMIC COMPLIANCE VECTOR: UTILITY FOR QUANTIFYING SPINAL MECHANICS

Matthew R. MacEwen[1], Rebecca E. Abbott[1], Victor H. Barocas[1], and Arin M. Ellingson[1*]
[1]University of Minnesota – Twin Cities; *ellin224@umn.edu

Introduction: The spine is required to perform diametrically opposed roles: permit large ranges of motion while protecting neurological tissue. As a result, biomechanics play a critical role in both spinal health and function. Traditional measures, such as range of motion (ROM), stiffness, neutral zone, and hysteresis, have been extensively investigated, but are simple scalar values that don't capture the highly dynamic, non-linear, and multi-planar aspects of the spine. An instantaneous helical axis (IHA) approach overcomes these limitations but is a purely kinematic metric. The purpose of this study is to explore the utility of a primary dynamic compliance vector (DCV) approach in quantifying spinal kinetics.

Methods: Eight cadaveric osteoligamentous lumbar specimens (Age: 37-88 / 62±16 yrs) were obtained from the Anatomy Bequest program. The L4-L5 segment was isolated, potted, and loaded into a Spine Kinetic Simulator (8821 Biopuls, Instron) equipped with two 6DOF load cells (AMTI). Pure moments up to 7Nm were applied in flexion/extension, lateral bending, and axial rotation. Retroreflective markers were rigidly attached to each vertebra to quantify spinal kinematics (MX-40, Vicon). Kinetic and kinematic data were filtered using a lowpass Butterworth filter with cutoff of 10Hz and 0.4 Hz, respectively.

IHA were calculated throughout each planar motion and averaged over each 1Nm of applied moment [1] – yielding the mean IHA orientation and rotation magnitude (phi) throughout the full envelope of motion. The primary DCV was derived from the moment-angle relationship by calculating the principal eigenvector of the compliance matrix and averaged over the same regions as the IHA analysis – similarly yielding the mean DCV orientation and compliance magnitude throughout the full envelope of motion [2]. To quantify the agreement between vector orientations, the angle between IHA and DCV was computed (DCV deviation). Lastly, the relationship between compliance magnitude (DCV) and phi (IHA) was assessed using a linear regression.

Results & Discussion: Phi and DCV magnitude exhibit similar patterns throughout each of the planar motions (**Fig 1**) and were found to be correlated to each other (R>0.83). Interestingly, there is an apparent angular deviation, or offset, between IHA and DCV that requires further investigation. Analysis currently underway incorporates multi-planar motions with efforts to identify how tissue health and morphology impact these patterns.

Significance: This study demonstrates the utility of a 3D methodology to quantify spinal mechanics using a similar paradigm as the IHA approach with the added benefit of being kinetic derived, rather than based solely on kinematics. These data are spatially and temporally rich and can be powerful tools for detecting changes with spinal health and/or in response to various treatments.

Acknowledgements: This work was funded by the following NIH grants: U01AT010326, UL1TR002494, and TL1R002493.
References: [1] Ellingson et al. *J Biomech.* 2015. [2] Leeman et al. *J. Mechanisms Robotics.* 2019.

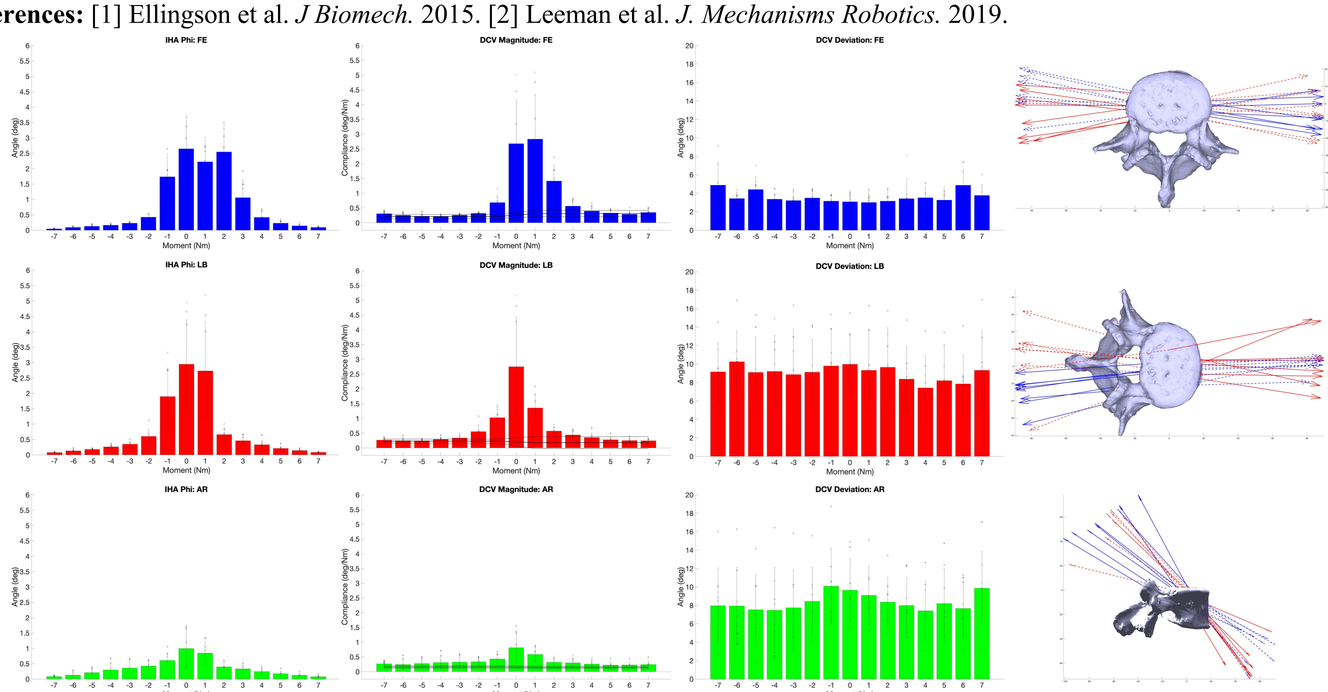

Figure 1: Flexion-Extension, Lateral Bending, and Axial Rotation (top to bottom) Summary Data. Bar Graphs display Mean and SD the following metrics throughout the full envelop of motion: IHA Phi (*left*), DCV Magnitude (*middle*), and DCV Deviation (*right*). Each specimen's data is represented by an individual symbol. Lines across DCV magnitude represent the mean (solid) and standard deviation (dashed) compliance calculated through traditional methods. **Right:** IHA (solid quiver) and DCV (dashed quiver) patterns from a representative healthy specimen. Red arrow = Flexion, Right LB, Right AR. Blue arrow = Extension, Left LB, Left AR.

INTERPRETING COMMON PATIENT SENSATIONS TO IMPROVE PROSTHESIS PRESCRIPTION

Brittany M Moores[1*], Harrison L Bartlett[2], Brian E Lawson[3], Max K Shepherd[4]
*Corresponding author's email: moores.b@northeastern.edu

Introduction: Over 150,000 people a year receive a lower extremity amputation in the United States and the prevalence will only increase due to the aging population and high rates of dysvascular conditions among U.S. adults [1-2]. For these individuals, a prosthesis will be prescribed to maximize their functional level by matching their abilities to available prosthetic components [3]. Matching and fitting these patients with appropriate componentry becomes a skill acquired by prosthetists from years of experience, however, there is a lack of consensus between clinicians and researchers on how to best optimize the various prosthetic characteristics (e.g., prosthetic foot alignment, stiffness, or energy return) [4]. Prosthetists use visual gait assessment and patient feedback to fine tune these variables, but formal research on patient and prosthetist perceptions are largely lacking since it can be difficult to rigorously understand qualitative feedback [4]. Our goal is to use a novel prosthetic foot prescription tool, called the Footropter, to better understand patient perception and the meaning behind commonly used clinical phrases (Fig. 1a). This prosthetic foot is completely passive and allows for independent adjustment of the forefoot and heel stiffnesses by the prosthetist or researcher. The forefoot stiffness is adjusted by clamping fiberglass layers together at different locations along its length with a socket wrench and the heel stiffness is adjusted by a sliding support under the heel spring with a M4 Allen key. Here, we present results from a pilot experiment in which the Footropter is used to understand how forefoot stiffness, hindfoot stiffness, and sagittal plane alignment can induce certain sensations. Our goal is to develop a better understanding of the combinations of these parameters that elicit these sensations, which could ultimately assist prosthetists with fittings in clinic.

Methods: A single subject with a below-knee amputation walked on a treadmill while wearing the Footropter. After a short practice trial with neutral ankle alignment and stiffnesses, the researchers modified sagittal plane ankle alignment (dorsiflexed, neutral, plantarflexed, via standard pyramid adaptor adjustments), forefoot stiffness (soft, neutral, stiff, via repositionable forefoot spring clamp), and heel stiffness (soft, neutral, stiff, via repositionable heel spring support) until the subject walked on all 27 combinations (3x3x3; randomized order). During each trial, the subject was presented with a "Dictionary" list of common clinical phrases and was asked to verbally indicate what sensations he felt with the present foot settings. The dictionary list includes 10 phrases like "scuffing my toe," "foot is slapping," "falling forward," and "knee collapsing." During each of the 27 trials, the subject was also asked to rate how much they like the setting via Likert scale.

Results & Discussion: Figure 1c shows the location in parameter space of the subject's two most frequently used clinical phrases: "knee hyperextending" and "feel like I'm falling forward." This n = 1 data collection indicates a likely correlation between Likert scale selection and the dictionary terms chosen, e.g., when the subject felt their knee hyperextending, they had a very low Likert scale rating. Our results also show that this specific subject preferred a neutral ankle alignment but with a "softer" forefoot and heel stiffness. Certain sensations may be elicited by more than one variable, e.g., knee hypertension can be caused not only by an overly plantarflexed foot but also an overly stiff forefoot. These results, along with future data, can provide the location of these sensations in the foot's parameter space, informing prosthetists on adjustments to make, given certain verbal feedback.

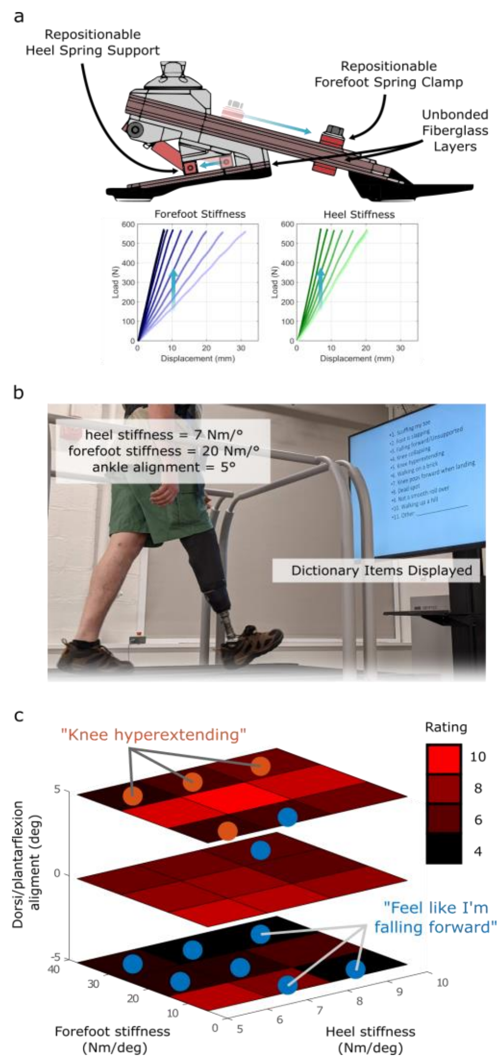

Figure 1: (a) The Footropter prosthesis, which is able to vary forefoot and heel stiffness. (b) Photo of the subject walking on the Footropter while presented with a list of "Dictionary" phrases (e.g., "knee hyperextending"). (c) Patient perceptions as a function of dorsi/plantarflexion alignment, forefoot stiffness, and heel stiffness. Likert scale values shown as shades of red.

Significance: During the prosthetic prescription and fitting process, patients do not have the option of testing multiple prosthetic feet. This results in patients not fully understanding how they feel about the stimuli they are receiving from the chosen componentry. With a clinical tool like the Footropter, a quantified dictionary of common phrases and an efficient prescription protocol, both prosthetists and patients could gain a better understanding of the mapping from foot characteristics to patient perceptions. The dictionary could also assist prosthetists, residents, and students in the fitting process.

Authors Bartlett, Lawson, and Shepherd are inventors on a patent for the Footropter.

References: [1] Molina & Faulk (2022), *StatPearls*; [2] Ziegler-Graham et al. (2008), *Archives of physical medicine and rehabilitation* 89(3); [3] Hofstad et al. (2004), *The Cochrane database of systematic reviews, 2004*(1); [4] Shepherd & Rouse (2020), *Scientific Reports* 10(1).

Hip moments differ by walking speed – but not group – in individuals with and without hip pain

Ria Rao[1*], Lauren Sara[1], Cara Lewis[1]
[1]Human Adaptation Lab, Boston University, Boston, MA, USA
*Corresponding author's email: riaprao@bu.edu

Introduction: Individuals with hip pain from femoroacetabular impingement syndrome (FAIS) or acetabular dysplasia have been reported to walk with decreased internal hip extension and hip abduction moments compared to healthy controls [1,2]. However, these data were collected only at the participants' self-selected walking speeds, and speed was either included as a covariate or not considered in analyses. Since many biomechanical variables are sensitive to walking speed [3] and individuals with hip pain typically walk slower than healthy controls [4], we hypothesized that hip moments would be similar between groups when walking at the same speed and would increase with faster speeds. To test our hypothesis, we compared peak sagittal and frontal plane hip moments of individuals with and without hip pain at three walking speeds.

Methods: Individuals with hip pain (N=137, 100F, 37M, age=27.5±8.8 years, height=1.70±.07 m, mass=70.4±10.3 kg, and preferred walking speed=1.27±.18 m/s) and without hip pain (N=60, 35F, 25M, age=23.7±5.5 years, height=1.70±.07 m, mass=68.1±10.1 kg, and preferred walking speed=1.28±.17) were recruited for this study. Kinetic data were collected while walking on an instrumented treadmill (Bertec) at three walking speed conditions: preferred, prescribed (1.25 m/s), and fast (1.25x preferred). Peak internal hip extension, flexion, abduction, and adduction moments (Nm) were calculated at each speed condition in Visual3D and normalized by body mass (kg). Moments were calculated on the more painful side in the hip pain group and averaged between limbs in the control group. A repeated measures ANOVA with a Geisser correction was used to observe within and between group differences. Post-hoc t-tests were conducted following the omnibus test as indicated; the alpha level was 0.05 for all tests.

Results & Discussion: There was a significant within-group effect of walking speed condition on all peak internal hip moments (all $p<.001$); the interaction effect of condition and group was not significant. There were no between-group differences in moments within walking speed conditions: extension ($p=.483$), flexion ($p=.554$), abduction ($p=.531$), and adduction ($p=.816$). Post-hoc pairwise t-tests revealed within-group differences. All peak moments were greater at the fast speed condition compared to the preferred or prescribed conditions (**Figure 1**). There were no differences in moments between preferred and prescribed speed conditions; the walking speeds in these conditions were similar. Therefore, walking speed, and not hip pain, produced differences in hip moments in this study, demonstrating that walking speed should be considered when comparing hip moments between groups.

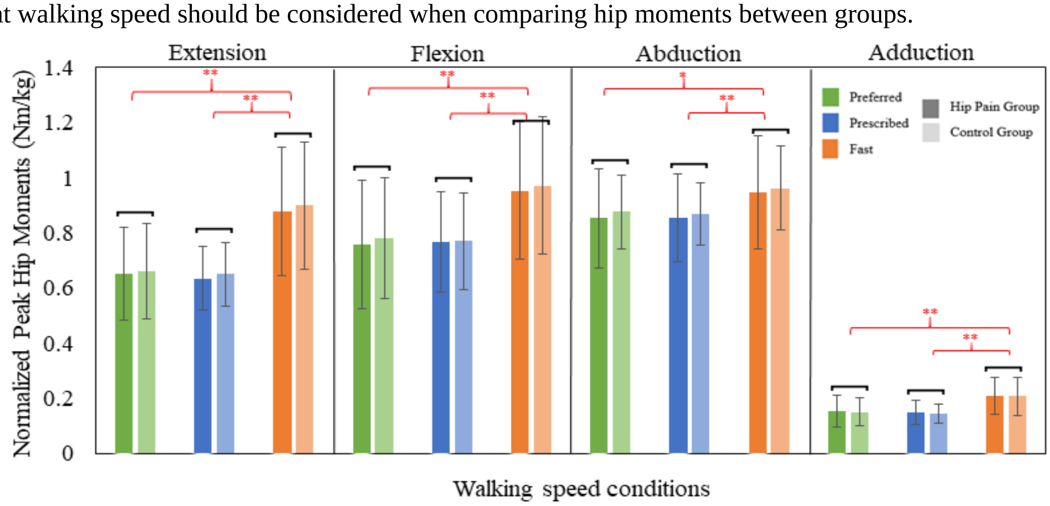

Figure 1. Means and standard deviations of peak internal hip moments for the hip pain and control groups at preferred, prescribed, and fast walking speed conditions. Significant p-values from the post-hoc t-tests are noted (*$p<.01$, **$p<.001$)

Significance: When walking at similar speeds, individuals with hip pain have similar peak hip moments compared to individuals without pain. This finding contrasts with other studies; however, in those studies, individuals with hip pain walked slower than individuals without hip pain. This finding emphasizes the impact of gait speed on joint moments.

Acknowledgements: This work was supported by NIH R21 AR061690 and K23 AR063235.

References: [1] Savage et al. (2021), *Gait & Posture*.; [2] Jacobsen et al. (2013), *Acta Orthop.;* [3] Lelas et al. (2003), *Gait & Posture;* [4] Ng et al. (2022), *Am J Sports Med*.

CHARACTERIZING POSTURAL CONTROL DYSFUNCTION AMONG BREAST CANCER SURVIVORS WITH CHEMOTHERAPY-INDUCED NEUROPATHY

Lise Worthen-Chaudhari[1*], Patrick Schnell, Jaqueline Wilder[1], Courtney Bland[1], Kristen Lantis[1], Craig Vargo, Madeleine Hackney, Maryam Lustberg
[1]The Ohio State University, Department of Physical Medicine and Rehabilitation
*Corresponding author's email: lise.worthen-chaudhari@osumc.edu

Introduction: Chemotherapy-induced neuropathy (CIN) is a highly prevalent adverse effect of neurotoxic chemotherapy treatment that degrades motor control[1], sensory function[1], quality of life[2] and increases fall risk[3]. Typically diagnosed based on patient self-report, better understanding of the quantified neuromotor functional deficits associated with CIN may inform diagnosis and treatment of the condition. To begin to characterize CIN-related neuromotor deficits, biomechanically, we measured postural control among breast cancer (BC) survivors with CIN.

Methods: This research protocol was approved by the Ohio State University Institutional Review Board. ***Participant screening:*** Within electronic medical records, we identified 804 clients diagnosed with breast cancer (stage I-III) who were 40+ years of age and had undergone at least 1 dose of taxane-based chemotherapy in the last 8 years. We used chart review to identify 156 of these survivors who met inclusion criteria: (a) CIN symptoms reported within their last clinic visit on record, (b) no vestibular or neurologic disorder other than CIN, (c) no uncontrolled diabetes (A1C<8.0), (d) not currently participating in physical therapy, and (e) lived no more than 1 hour away from the medical center campus. We contacted each these individuals to inquire whether CIN symptoms persisted and, if so, to determine interest and availability in participating in this study. Those able and interested to participate (n=26) underwent in-person screening of postural control as previously reported[4]. Briefly, screening involved standing on a balance plate (Bertec Corp, Columbus, OH) quietly and bilaterally for 30 seconds with eyes closed (QEC). Center of pressure (COP) variables of interest were calculated per [5] and [6]. Survivors who demonstrated postural control function outside of the estimated 70% confidence interval (CI)[7] of healthy, age-equivalent normative values in (1) COP ellipse area, (2) medial-lateral variability, (3) medial-lateral velocity or outside of the estimated 95% CI in terms of (4) COP complexity were enrolled in this study (n=23). ***Participant testing:*** In a repeated measures design, postural control data (30s QEC) were collected on 3-4 different days over the span of 2 weeks. Descriptive data were calculated. Log-transformed data were assessed regarding effect of visit number.

Results & Discussion: Twenty-three BC survivors (22 female/1 male) showed postural control dysfunction and consented to participate in the study. Descriptive data are reported in Table 1. No effect of visit number was demonstrated.

Table 1: Postural control norms among n=23 breast cancer survivors with CIN and balance dysfunction.

Variable	Age	Years since last taxane exposure	COP Ellipse Area	COP Med-Lat variability	COP Med-Lat velocity	COP Complexity
Mean	60.3	2.6	1086	5.74	11.02	0.47
SD	10.0	2.0	1162	3.04	6.35	0.16
Min	40	0.25	113	1.54	2.75	0.18
Max	78	6.2	6886	16.8	34	1.02
Inclusion Threshold	≥40	≥0.25	>400	>4.0	>11	<0.6
% cohort who met inclusion criteria	100%	100%	75%	70%	34%	84%

Significance: We found that BC survivors reported persistent symptoms of CIN as much as 6 years after last exposure to taxane-based agents and demonstrated postural control deficits far outside of typical normal bounds. Loss of complexity was the most commonly detected postural control deficit (84%) followed by increased COP ellipse area (75%) and variability (70%). Dysfunction in COP velocity was only noted in about a third of those tested. We noted no evidence of a training effect when testing postural control repeatedly over 3-4 days. These data begin to characterize the biomechanical deficits that persist years after chemotherapy exposure ends. Survivors continue to report CIN as one of their most common, unmet, highest priorities[8] with limited management options; more study is needed to determine best practices to rehabilitate these quantifiable deficits.

Acknowledgements: This study was funded by R21-AG068831 and supported by the National Center for Advancing Translational Sciences, Grant UL1TR001070

References:

[1] Monfort, et al., Gait and Posture. 48 (2016) 237–242. https://doi.org/10.1016/j.gaitpost.2016.06.011.
[2] Song, et al., Support Care Cancer. 25 (2017) 2241–2248. https://doi.org/10.1007/s00520-017-3631-x.
[3] M.H. Huang, Rehabilitation Oncology. 37 (2019) E7–E9.
[4] Reed, et al., Plos One. 15 (2020) e0237246.
[5] Prieto, et al., Transactions of Biomedical Engineering. 43 (1996) 965–966.
[6] Roerdink, et al., Human Movement Science. 30 (2011) 203–212.
[7] Worthen-Chaudhari, et al., Gait & Posture. 64 (2018) 141–146.
[8] 2022 State of Cancer Survivorship Survey, NCCS - National Coalition for Cancer Survivorship. (2022). https://canceradvocacy.org/2022-state-of-cancer-survivorship-survey/.

WEARING HIGH HEELS REMODELS LEG MUSCLE-TENDONS AND IMPROVES WALKING ECONOMY

Owen N. Beck[1*], Jordyn N. Schroeder[2], Gregory S. Sawicki[2]
[1]Department of Kinesiology and Health Education, University of Texas at Austin, Austin, Texas, USA
[2]Woodruff School of Mechanical Engineering, Georgia Institute of Technology, Atlanta, Georgia, USA
*Corresponding author's email: owen.beck@austin.utexas.edu

Introduction: Each morning people wake up and put on clothing and footwear, and a assistive devices (*e.g.,* prostheses). Most of these items improve user physical function, convention misses an opportunity to use wearables to alter muscle-tendon structure and after the item is removed from the body.

Cross-sectional- and modeling-studies suggest that the habitual use of high-heeled shortens calf muscles by ≥9-14% and stiffens Achilles tendons by 22% [1]. Shorter leg theoretically enable people to walk using less metabolic energy (walk more because shorter muscles have the same force-producing capabilities as longer muscles housing fewer energy consuming sarcomeres in-series (↓length), and stiffer tendons shortening per unit force production (x=F/↑k) [2]. Considering that calf muscles produce most of stance while expending ~27-40% of the body's metabolic energy during walking and stiffening the Achilles tendon may reduce a person's metabolic energy expenditure Accordingly, we hypothesized that the habitual use of high heels would reduce a person's expenditure during walking in flat-soled footwear.

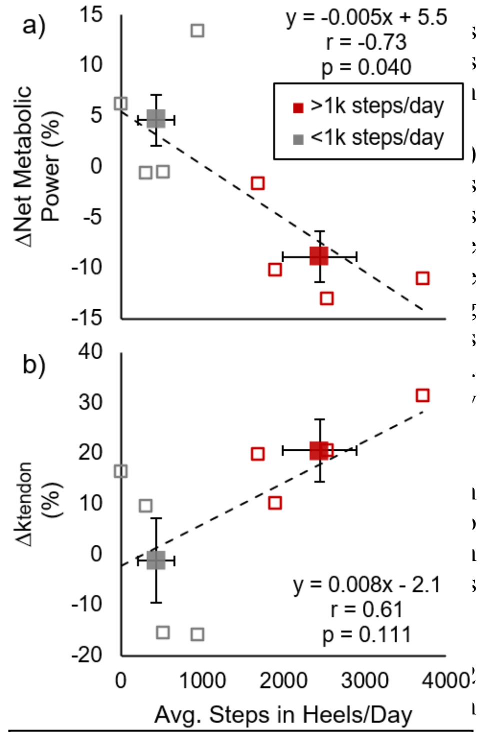

Figure 1. (a) Δnet metabolic power during walking at 1.3 m/s and (b) ΔAchilles tendon stiffness versus average steps in high heels per day over 12-16 weeks. Dashed lines indicate linear regressions on individual data (open symbols). Closed symbols represent Avg. ±SE values for participants who took >1k and <1k steps/day in high heels, respectively.

Methods: Eight young adults agreed to wear custom high heels as their everyday shoes heels placed participant ankles at 104° during standing. Throughout the protocol, log their daily steps with and without their high heels. Immediately before and after 12- heels, we conducted laboratory testing that involved treadmill walking at 1.3 m/s in flat- well as multiple ankle plantarflexion trials on a dynamometer at different joint angles.

Results: Participants varied in the amount that they wore their high heels (daily steps in ± 1257 steps/day; range: ~0 to 3704 steps/day). Participants who took more daily steps in heels stiffened their Achilles tendons and improved their walking economy in flats; supporting our hypothesis. For every 1000 steps/day that participants averaged wearing high heels, their Achilles tendon stiffness increased 7-8% (β= 19 kN/m; p=0.008) and their net metabolic power during treadmill walking decreased 3% (β=-0.09 W/kg; p=0.004) (Fig. 1). ΔTendon stiffness did not correlate with Δnet metabolic power during walking (r=-0.64; p=0.086) (Fig. 2). Moreover, post-hoc analyses suggest that averaging >1k steps/day in high heels is necessary to reduce net metabolic power during walking (p=0.018). Participants who averaged >1k steps/day in high heels reduced their net metabolic power during walking in flats by 9±3% (avg ± sd) (n=4; red symbols), whereas participants who averaged <1k steps/day in high heels consumed 5±7% (avg ± sd) more metabolic power during walking in flats post intervention (n=4; grey symbols) (Fig. 1).

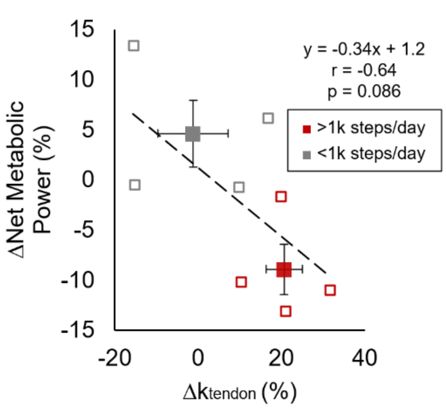

Figure 2. Δnet metabolic power during walking at 1.3 m/s versus ΔAchilles tendon stiffness. Dashed line indicates linear regressions on individual data (open symbols). Closed symbols represent Avg. ±SE values for participants who took >1k and <1k steps/day in high heels, respectively.

Discussion: Participants who took >1000 steps/day in high heels for 12-16 weeks reduced their metabolic energy expenditure during walking in flats. While we are still analysing the data to uncover which physiological changes contributed to the more economical walking following habitual high heel use, increased Achilles tendon stiffness may have contributed. Despite not reaching statistical significance with 8 participants (p=0.086) (Fig. 2), the moderate correlation between ΔAchilles tendon stiffness and Δnet metabolic power (r=-0.64) supports with the notion that increasing tendon stiffness enables in-series muscles to produce force more economically [2]. Further, habitual high heel use may have also shortened calf muscle fascicles [1] and/or elicited neuromechanical changes that contributed to the improved walking economy following high heel use.

Significance: The strategic design of everyday wearable items can improve user morphology and function *after* items are removed from the body. Because muscle-tendons take weeks to remodel, modifying leg muscle-tendon structure using high heels may improve user walking economy for multiple weeks after the high heels are last worn. Our study aims to inform the design of wearable items that can improve user physical function and mobility while the item is worn as well as after the device is removed from the body.

References: [1] Csapo et al. *J Exp Biol* 2010, [2] Krupenevich et al. *Gerontol* 2022,
[3] Umberger & Rubenson *Ex Sport Sci Rev* 2011.

Physiological Storage Solution Decreases Whole Muscle Passive Mechanical Properties

Timothy McGinley[1] and Benjamin I Binder-Markey[1,2]
[1]School of Biomedical Engineering, Science and Health Systems & [2]Department of Physical Therapy & Rehabilitation Sciences, Drexel University, Philadelphia Pa
Corresponding email: tm3292@drexel.edu

Introduction:

Understanding muscle structure and function relationships are essential to determining muscle performance and recovery following injury or disease. Muscle active force generating mechanics have been widely characterized to scale linearly across muscle tissue's scales from the whole muscle down to the single muscle fiber [1]. However passive muscle mechanics (the muscle's elastic properties) are less well understood for their properties do not scale linearly. Additionally, it is unknown the sources of passive mechanics across scales. One problem contributing to this dearth of knowledge is multiscale mechanical testing cannot be completed in a single day due to the time required to test the samples before rigor sets in the muscle. Thus, samples are often stored in a physiological storage solution to preserve the sample. This storage solution preserves the active mechanics; however, it is unknown how the storage solution affects the passive mechanics of the muscle. Therefore, the purpose of this study is to begin to understand how a commonly used glycerinated physiological storage solution affects whole muscle passive mechanical properties.

Methods:

Passive mechanical characteristics of fresh and stored samples were collected across four muscles, differing in structure and function, from 12 to 16-week C57BL6 mice. Muscles collected were the lateral gastrocnemius (LG), rectus femoris (RF), semimembranosus (SM) and tibialis anterior (TA). Fresh muscles were dissected from origin to insertion, placed in a physiological bath, and mechanically tested. Stored muscle samples were also dissected from origin to insertion, placed in a glycerinated physiological storage solution [2] and stored for 2-weeks at -20°C prior to testing. For mechanical testing, the samples were fastened to a 5N force transducer and muscle slack length determined. Each muscle was lengthened in ~5% fiber strain increments from 0%-40% being held for 3-minutes at each strain. Force and displacement at the end of each hold were recorded. Following testing the samples were weighed. Muscle passive forces were normalized to physiological cross-sectional area (PCSA), and muscle strain was converted to fiber strain using fiber length-ratio [2]. The normalized passive stress-strain data were fit to a linear regression rather than an exponential regression due to the linear nature of the data. The stiffness (slope) was compared across muscles: fresh vs. storage solution.

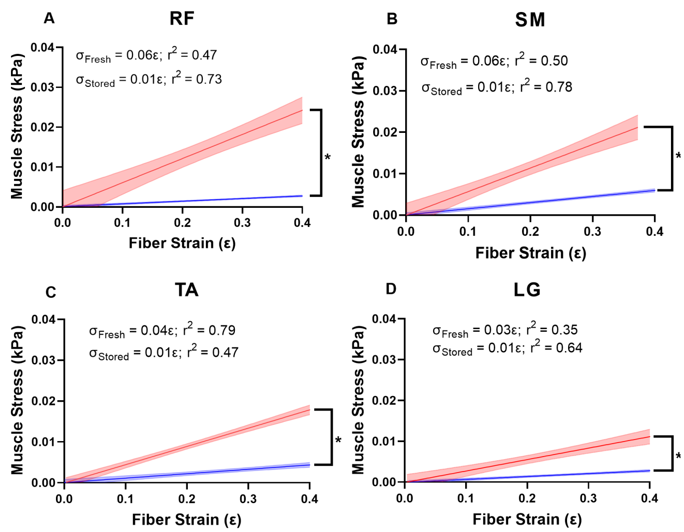

Figure 1: Normalized Stress-Strain Curve for fresh (red) and stored (blue) of the A) RF, B) SM, C) TA, & D) LG. Data shown as averages±SD. n_{fresh}=7-9; n_{stored}=6-7

Results & Discussion:

Muscles stored in glycerinated storage solution demonstrated significant swelling in the RF, SM, and LG (Table 1), swelling an average of ~140% across all muscles. Normalized stress-strain curves shown, demonstrates moderate to good fits with significant decreases in stiffness following storage in all muscles (Fig. 1). Stored RF stiffness was 857% less stiff than the fresh tissue. Likewise, the stiffness of stored SM was 600%, TA 400%, and LG 429% less than their respective fresh counterparts.

The ~400-850% decrease in muscle stiffness following storage cannot be accounted for by the ~140% increase in PCSA because of muscle swelling. This points to a decrease in structural integrity of the muscle following storage in a glycerinated storage solution. Since passive fiber mechanics remain intact following storage in a glycerinated solution [3], it is likely that this storage solution damages the connective tissue in the extracellular matrix, reducing the stiffness of the muscle tissue.

*Table 1: Physiological Properties of Fresh and Stored Muscle *p<0.05 compared to fresh*

	Mass (mg)		**% Swelling**
	Fresh	**Stored**	
RF	69.53 ± 9.07	116.07 ± 6.63*	166.93%
SM	92.91 ± 21.87	131.16 ± 13.16*	141.15%
TA	50.66 ± 12.95	57.57 ± 6.30	113.64%
LG	77.59 ± 18.46	106.4 ± 9.81*	137.15%

Significance:

Glycerinated physiological storage solution does not preserve the passive mechanics of muscle at the whole muscle scale. Following storage, muscles demonstrate swelling and reduce muscle stiffness. Future studies will explore other types of physiological storage solutions that do not contain glycerol. Additional studies should explore the sources of decreased in passive mechanics by further studying the mechanics at the fascicle and single fiber scale.

References:

[1] Winters, T.M et al. J. Biomech. 2011. **(44) 109–115**. [2] Eastwood A.B. et. al., Tissue & Cell 1979. **11 (3) 553-566** [3] Einarsson, F. et al. J. Ortho Surg., 2008. 3:22

MUSCLE SHEAR MODULUS IS GREATER IN THE PLANE PARALLEL TO MUSCLE FIBERS COMPARED TO THE PERPENDICULAR PLANE

Daniel Ludvig[1,2], William Reyna[1,2], Eric J. Perreault[1,2,3]
[1]Department of Biomedical Engineering, Northwestern University, Evanston, IL
[2]Shirley Ryan AbilityLab, Chicago, IL, [3]Department of Physical Medicine and Rehabilitation, Northwestern University, Chicago, IL
*Corresponding author's email: daniel.ludvig@northwestern.edu

Introduction: The shear modulus, quantifying a material's resistance to shear deformation, is thought to be essential for lateral force transmission within muscle [1]. Lateral loads can arise from internal deformations associated with active or passive muscle function, or external pressures including those that cause injury [1]. The shear deformations within a muscle are resisted by the passive components of the extracellular matrix connecting muscle fibers and fascicles. While several studies have investigated the passive material properties of muscle in tension [2-4], there is a dearth of data describing how muscle responds to shear, particularly across all directions relevant to the multidirectional deformations that can arise during normal functions. The objective of this study was to quantify the shear moduli of skeletal muscle in the two directions necessary to characterize its transversely isotropic structure. Our primary hypothesis was that the shear modulus would be greater in the plane parallel to the fibers than the plane perpendicular to the fibers. This is an important step towards evaluating shearing forces in muscle and further understanding the role of muscle material properties in force transmission and muscle injury.

Methods: Shear moduli were measured from 3 muscles harvested from rat hindlimb: extensor digitorum longus, tibialis anterior, and soleus. Muscles were sectioned into rectangular cubes (~9 x 9 x 4 mm) aligned with the muscle fibers. Shear measurements were made with the cubes oriented both parallel and perpendicular to the muscle fibers, allowing us to obtain shear modulus in both directions (Fig. 1A). Data were collected from a total of 106 specimens. Shear modulus was measured using an Instron mechanical tester (Instron 5942; Instron Corp., Canton, MA). Data were collected at a strain rate of 0.05 per minute until failure, as indicated by a sudden drop in force and tearing of the muscle. Shear modulus was calculated from measures of shear stress and shear strain. Tissue shear stress was calculated as the applied force divided by the initial cross-sectional area. Tissue shear strain was calculated as the inverse tangent of displacement divided by initial thickness. Instantaneous shear modulus was computed as the slope of the stress-strain curve. We simultaneously estimated shear and Young's moduli, allowing us to remove the effect of any normal strain and stress on our measures [5]. We tested our primary hypothesis that shear modulus would be greater in the parallel than the perpendicular direction by using a Bootstrap method to generate probability distributions.

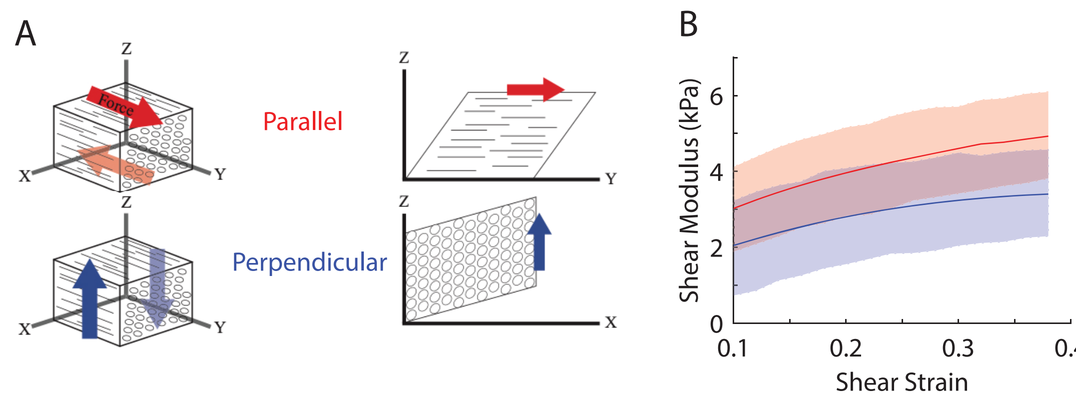

Figure 1: (A) The shear modulus of rat muscle was measured in two different planes: parallel and perpendicular to the muscle fibers. (B) The shear modulus was approximately 1.5 times bigger in the parallel plane compared to the perpendicular plane. Shaded areas show 95% confidence intervals.

Results & Discussion: The shear modulus was approximately 1.5 times greater in the parallel direction than the perpendicular direction across all levels of shear strain. Both directions of shear moduli increased with increasing strain (Fig 1B). At low levels of strain (~0.1), the difference between the two directions did not reach significance ($p=0.12$). However, with increasing strain, the moduli in the two different directions began to differ significantly (all $p < .05$ above a strain of 0.34). Despite architectural differences between muscles, we did not observe any difference in shear moduli with different muscles of the hindlimb.

Significance: Our results are the first direct measures of two-dimensional shear moduli in skeletal muscle. They show that the shear modulus measured in the plane parallel to muscle fibers was greater than those in the perpendicular plane. This demonstrates that the anisotropic properties of muscle is also reflected in its response to shear strain. Additionally, the shear modulus increased with increasing strain, indicative of a nonlinear elastic material. The quantitative measures reported here can be used to describe the mechanical properties of muscle in shear, which adds to the growing knowledge of muscle material properties as are needed to develop computational models of how muscle responds to the complex stresses and strains essential to its use in the control of movement and posture.

Acknowledgements: NIH R01 AR071162

References: [1] Huijing (1999), *J Biomech* 32; [2] Bosboom et al (2001), *J Biomech* 34; [3] Lieber & Friden (2019), *J Appl Physiol* 126; [4] Morrow et al. (2010), *J Mech Behav Biomed Mater* 3; [5] Crutison et al. (2022), *J Acoust Soc Am* 151.

INCREASED ANKLE PUSHOFF ALTERS FRONTAL PLANE HIP MECHANICS

Avery L. Kratzer[1*], Cara Lewis[1]
[1]Boston University Sargent College of Health and Rehabilitation Sciences
*Corresponding author's email: averyk@bu.edu

Introduction: Gait propulsion at a constant speed is powered by a tradeoff between an impulsive push along the trailing limb (similar to ankle plantar flexion) and a torque at the hip [1]. Increasing ankle pushoff is often recommended to populations with anterior hip pain, as this gait modification increases the ankle contribution and decreases hip moments and joint forces in the sagittal plane [1,2]. However, it is unknown if increased ankle pushoff also alters hip mechanics in the frontal plane and thus may be beneficial for individuals with lateral hip pain. The purpose of this study was to investigate the effect of increased ankle pushoff on frontal plane hip joint mechanics. We hypothesized that an increase in ankle pushoff would lead to a decreased abduction moment at the hip.

Methods: Thirty-seven healthy young adults (24 female, 13 male; age: 23.7 ± 4.9 years; height: 1.7 ± 0.1 m; mass: 63.2 ± 10.4 kg) participated in this study. Participants completed two walking conditions (NAT and PUSH) at a prescribed speed of 1.25 m/s while barefoot on a split-belt instrumented treadmill (Bertec®). During the NAT condition, participants were asked to walk as they would naturally. During the PUSH condition, participants were instructed to "push more with [their] feet when [they] walk." Participants walked for two minutes in each condition while kinematic and kinetic data were recorded using a 10-camera motion capture system (VICON®) and the instrumented treadmill. Data were analyzed in Visual3D (C-Motion, Inc.). Ankle and hip moments as well as ground reaction forces in the sagittal and frontal planes were extracted.

For each individual, time series data were segmented by right and left strides and normalized to 101 timepoints (0-100% of the gait cycle). Moment and force magnitudes were normalized to body mass, and the average across all strides was calculated for each individual. A Statistical Parametric Mapping (SPM) analysis with 2-tailed paired t-tests was conducted to explore differences in internal joint moments between the two walking conditions across the entire gait cycle. This analysis identified time points in the gait cycle when joint moments during the PUSH condition were significantly different from the joint moments in the NAT condition. Statistical significance was determined with alpha set to 0.05. This analysis method was also applied to detect differences in ground reaction force between the two walking conditions across the stance phase of the gait cycle.

Results & Discussion: The analysis confirmed that ankle moment was greater in the PUSH condition than in the NAT condition from 7 to 36% if the gait cycle (Figure 1A). In agreement with the ankle-hip tradeoff and our hypothesis, hip abduction moments were lower in the PUSH condition than in the NAT condition from 44 to 52% of the gait cycle (Figure 1B). However, the hip abduction moment was higher in the PUSH condition than in the NAT condition at its largest peak from 3 to 14% of the gait cycle. This initial peak in hip abduction is likely attributed to the increased medial force that occurs in the first 15% of the gait cycle (Figure 1C).

Significance: While increased pushoff may be effective in decreasing hip moments in the sagittal plane, this gait modification results in compensations in frontal plane hip moments. Because the hip abduction moment increases during the initial peak with increased pushoff, this modification may not be recommended for individuals with lateral hip pain.

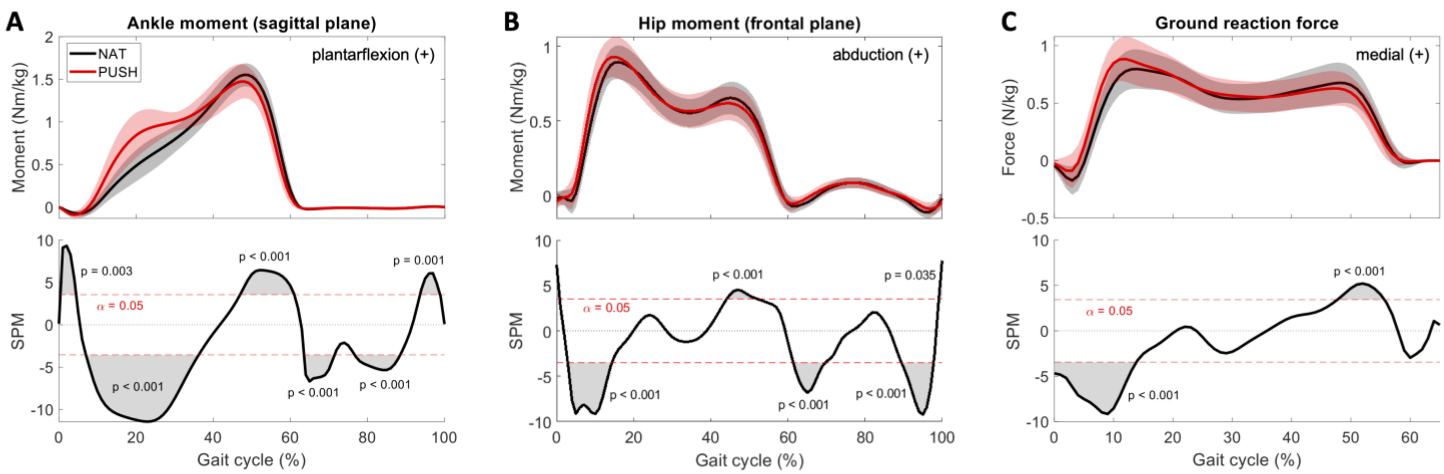

Figure 1: (A) Sagittal plane ankle moments and SPM analysis. (B) Frontal plane hip moments and SPM analysis. (C) Mediolateral ground reaction force and SPM analysis. PUSH condition in red and NAT condition in black. Time points with significant SPM shaded gray ($p < 0.05$).

Acknowledgements: This research was supported by the Dudley Allen Sargent Research Fund and the NIH K23 AR063235.

References: [1] Lewis et al. (2008), *J Biomech;* [2] Lewis et al. (2015) *J Biomech*.

RELIABILITY OF THREE EXTRAPOLATION METHODS FOR ULTRASOUND-BASED ESTIMATION OF GASTROCNEMIUS FASCICLE LENGTHS

Logan K. Faux-Dugan[1*] and Stephen J. Piazza[1]
[1]Dept. of Kinesiology, The Pennsylvania State University, University Park, PA, USA.
*Corresponding author's email: fauxdugan@psu.edu

Introduction: Muscle architecture parameters are key determinants of muscle force and thus muscle function. Muscle fascicle length is one of these parameters that is often estimated *in vivo* from ultrasound images. For many muscles, however, unless the ultrasound probe has an extended field of view, entire fascicles may not be contained within a single image. To find fascicle lengths in such cases, extrapolation is required and various methods for this have been proposed. The choice of extrapolation method may affect the repeatability and accuracy of fascicle length estimation [1]. One common method relies on trigonometry: The fascicle is modeled as the hypotenuse of a right triangle whose length is found from muscle thickness and pennation angle (TRIG). A variation on this method has been proposed that corrects for the angle between the superficial and deep aponeuroses (TRIG-CORR) [2]. A third method that finds the fascicle length by identifying fascicle-aponeurosis intersections (INTERSECT) has been found to be more reliable than the TRIG method for quadriceps fascicle lengths [3]. The purpose of the present study was to compare the reliability of these three methods when employed for estimating fascicle lengths in the lateral and medial heads of the gastrocnemius (LG and MG). Because of the superior reliability previously found for INTERSECT in the quadriceps [3], we hypothesized that this method would have higher inter-rater reliability than TRIG or TRIG-CORR when used to estimate gastrocnemius fascicle lengths.

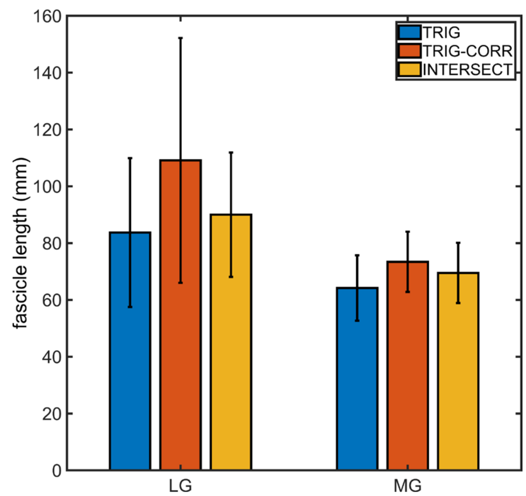

Figure 1: Mean fascicle lengths (n=16) for LG and MG estimated using three extrapolation methods.

Methods: Images of LG and MG were collected in 16 healthy participants (9M,7F) using an ultrasound scanner (LogicScan 128, Telemed) operating in B-mode and equipped with a 60 mm linear probe. Five static sagittal images of the central region of each muscle were made with participants standing in anatomical position. On each image, two raters selected points defining the superficial and deep aponeuroses boundaries and three fascicles. The points selected were used to estimate muscle thickness (MT) and aponeurosis angle (θ_a), as well as the pennation angle (θ_p) for each fascicle. For the TRIG method, fascicle length was estimated by $L_f = MT/\sin(\theta_p)$ [4]. For TRIG-CORR, fascicle length was found as $L_f = \sin(\theta_p+90°)*MT/\sin(180°-(\theta_a+180°-\theta_p)$ [2]. For INTERSECT, fascicle length was estimated as the distance between intersections of the extension of the fascicle and extensions of each aponeurosis [3]. A single measure of fascicle length was then calculated for each muscle by finding the average of all estimated fascicle lengths found across the five images. Inter-rater reliability was calculated for each method and each muscle using the *icc()* function in R (R Core Team), specifying a two-way random effects model and absolute agreement with a single rater as the base unit of measurement.

Results & Discussion: The reliability of all three extrapolation methods was found to be excellent (ICC ≥ 0.928; Table 1) for LG, but only moderate-to-good for MG. Our hypothesis that INTERSECT would provide the most reliable estimates of gastrocnemius fascicle length was not supported. The TRIG method was found to have the greatest reliability, perhaps due to high reliability of pennation angle and muscle thickness (Table 1) and lesser reliability in establishing the orientation of the superficial aponeurosis. The ICC values found here are consistent with those reported earlier for lower extremity muscles, and our finding that fascicle length estimation was generally less reliable for MG than for LG is consistent with previous reports comparing reliability for these two muscles [5].

Table 1: Inter-rater reliability for LG and MG muscle architecture parameters as assessed using intraclass correlation coefficient (ICC).

	Fascicle Length			θ_p	MT
	TRIG	TRIG-CORR	INTERSECT		
LG	0.952	0.929	0.928	0.955	0.974
MG	0.809	0.707	0.737	0.913	0.995

Fascicle length estimates made using the TRIG-CORR method were slightly longer than for the other two methods (Figure 1). Future work should include the use of a larger probe or comparison to measurements made in cadaver specimens in order to establish which method has the highest accuracy for estimation of gastrocnemius fascicle length.

Significance: Reliable *in vivo* techniques for estimation of plantarflexor muscle fascicle lengths is critical to investigations of how plantarflexor structure relates to locomotor function, as in the pushoff phase of human walking gait. The TRIG method was found to have the highest reliability and is also the simplest to implement as it does depend on identification of the superficial aponeurosis.

References: [1] May et al. (2021), *PloS One* 16(9); [2] Blazevich et al. (2006), *J Anat* 209(3); [3] Ando et al. (2014), *J Electromyogr Kinesol* 24(2); [4] Abe et al. (2000), *Med Sci Sports Exerc* 32(6); [5] Kwah et al. (2013), *J Appl Physiol (1985)* 114(6).

Rhythmic Movement Training Improves Spatiotemporal Modulation Of Gait In Older Adults With And Without Mild Cognitive Impairment

Meghan E. Kazanski[1*], Michael C. Rosenberg, Laura Emmery, J. Lucas McKay, Trisha M. Kesar, Madeleine E. Hackney[1]
[1]Department of Medicine, Division of Geriatrics and Gerontology, Emory University, Atlanta, GA
*email: m.e.kazanski@emory.edu

Introduction: Cognitive impairment induced by typical, healthy aging and as a precursor to Alzheimer's Disease contributes to degraded motor-cognitive integration [1]. During walking, motor-cognitive integrative processes are critical for producing complex, robust gait patterns that can be flexibly modulated in task and context-dependent ways. Impaired motor-cognitive integration manifests as functional gait limitations and falls risk in older adults, both with and without cognitive impairment [2].

Movement (e.g., dance) and music-based therapies effectively target motor-cognitive integration and improve gait function in older adults with cognitive impairment [3]. However, it remains unclear how to optimize the systematic design and administration of such therapies to maximize intervention-induced improvements in motor-cognition in older adults.

We recently developed *Rhythmic Movement Sequences* (RMS), a library of complex, multi-step movements comprising non-stereotypical gait patterns. Each RMS modulates distinct *spatial* (*S*; e.g., modified lower-extremity swing/ stance coordination), *temporal* (*T*; e.g., modified step timing), or both *spatiotemporal* (*ST)* features of gait. These RMS reveal gait-specific deficits in motor-cognition that present as spatiotemporal movement limitations, which are differentially impacted by typical aging and cognitive status [4].

Here, we evaluated the extent that two RMS training programs improve spatiotemporal gait modulation in older adults with and without mild cognitive impairment (MCI). We predicted that training effects would be sensitive to cognitive status and RMS complexity.

Methods: 8 healthy older adults (HOA; 72.5 ± 6.1 yrs., 8F/0M) and 7 adults with mild cognitive impairment (MCI; 74.9 ± 3.8 yrs., 4F/3M) received RMS training during three, 1-hour group classes. Participants were randomly assigned to an RMS program that induced either spatial and temporal modifications separately, in isolation (ISO), or spatiotemporal modifications coupling spatial and temporal features (COU). The COU training program offered more-complex RMS, challenging participants to modify their gait to achieve spatial and temporal accuracy, simultaneously.

Before and after the RMS training classes, participants were administered a gait modulation assessment battery consisting of 9 spatial, 9 temporal, and 4 spatiotemporal RMS *not* presented in the training classes. Lower extremity joint kinematics were recorded using wearable sensors.

Each RMS had discrete biomechanical (i.e., peak joint angles) and/or temporal (i.e., step timing) targets. Participants' RMS performance was computed as average percent error in their kinematics relative to corresponding targets. We computed overall RMS performance errors for spatial, temporal, and spatiotemporal gait modifications. We tested for performance differences between groups (HOA vs. MCI) and training programs (ISO vs. COU) using one-way ANOVAs. We quantified effect magnitudes using Cohen's *d*.

Results & Discussion: Overall deviations from RMS performance targets (Fig. 1A) indicate that ISO and COU RMS training improved participants' *temporal* modulation of gait (Fig. 1C; $p_T = 0.004$; $d_S = 0.2$, $d_T = 0.7$, $d_{ST} = 0.3$).

Prior to RMS training, MCI presented impaired gait modulation relative to HOA (Fig. 1B; all p<0.05; $d_S = 1.4$, $d_T = 0.7$, $d_{ST} = 0.9$), as expected [4]. MCI exhibited a trend toward *greater* improvements in gait modulation after RMS training compared to HOA, although these effects did not reach significance (Fig. 1D; all p > 0.05; $d_S = 0.3$, $d_T = 0.4$, $d_{ST} = 0.4$). Compared to the ISO group, the COU group exhibited a trend toward greater improvements across all gait domains following RMS training, although these effects did not reach significance (Fig. 1E; all p > 0.05; $d_S = 0.1$, $d_T = 0.5$, $d_{ST} = 0.3$).

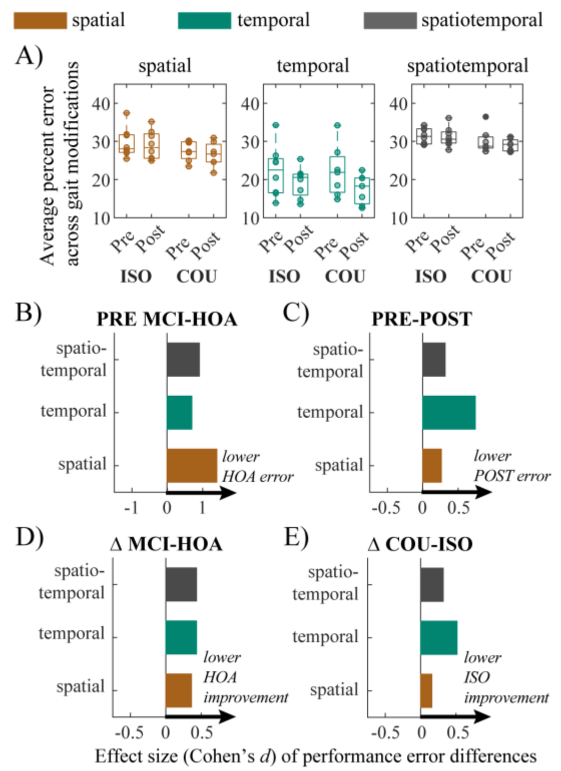

Figure 1: RMS performance for 8 isolated (ISO; 4HOA/ 4MCI) and 7 coupled (COU; 4 HOA/ 3 MCI) participants at pre- and post-RMS training for spatial, temporal, and spatiotemporal gait modifications **(A)**. Effect size (*d*) of RMS performance error differences between: MCI and HOA at pre-RMS training **(B)**, all participants at pre- and post-RMS training **(C)**, MCI and HOA **(D)** and COU and ISO RMS improvement following training **(E)**.

Significance: Our novel RMS therapy successfully targets the motor-cognition processes impaired due to aging and MCI. We demonstrate that RMS not only challenges distinct spatial and/ or temporal gait features [4], but that multi-day RMS training can improve the ability to modulate these features. Older adults, especially those with MCI, may benefit from RMS training programs that harness complex rhythms and challenging, yet functional movement patterns. This work informs our continued development of RMS therapy as an innovative, efficacious, and engaging approach to enhancing gait robustness and mobility in older adults with MCI.

Acknowledgements: Goizueta AD Research Center CEP Innovation Accelerator Seed Grant; NICHD/ NIA Grant #F32HD108927.
References: [1] Montero-Odasso et al. (2017). *JAMA Neurol.* 74(7).; [2] Ansai et al. (2019). *JGPT* 42(3).; [3] Hackney et al. (2015), *J Am Geriatr. Soc.* 63(10).; [4] Rosenberg et al. (2023), *Frontiers Hum. Neuro.* 17.

THE RELATIONSHIP BETWEEN DEEP BRAIN STIMULATION AND FALLS IN PARKINSON'S DISEASE

Christopher P Hurt[1*], Alyson Moll[1], Natasha Brooks[1], Daniel J Kuhman[1], Harrison C Walker[2]
[1]Department of Physical Therapy, University of Alabama Birmingham
[2] Department of Neurology, University of Alabama Birmingham
*Corresponding author's email cphurt@uab.edu

Introduction: Parkinson's disease (PD) is a progressive neurologic disease. For some, disease progression results in dopaminergic medication intolerance necessitating other therapeutic strategies to PD[1]. Deep brain stimulation (DBS) is an effective treatment for most cardinal symptoms of Parkinson's Disease (PD). Although for some individuals, axial symptoms like balance may not improve, which is problematic because individuals with PD are already at a higher fall risk[2]. It is equivocal whether fall risk increases with DBS implantation[3,4]. The current study is a secondary analysis of a longitudinal randomized control trial to assess biomarkers for DBS programming. We assessed fall incidence for a group of individuals who were candidates for deep brain stimulation surgery retrospectively and 1-year prospectively. We also assessed the extent that baseline variables collected prior to DBS implantation relate to fall incidence. This data will inform future trials to improve axial symptoms of PD in those with DBS.

Methods: Thirty-two individuals with PD (mean age: 58 ±8 years, MDS-UPDRS OFF MEDS 49±13) came to the lab for baseline motor testing prior to implantation of a deep brain stimulator as part of the SUNDIAL Trial (NCT03353688). At baseline testing we assessed single and multiple retrospective fall history, falls self-efficacy via the ABC scale and freezing of gait via the FOG scale. We also assessed functional domains with multiple outcome variables. We assessed quasi-static balance (stand quiet, stand feet together, stand semi-tandem, stand tandem), gait function (comfortable, maximum, and backward walk speed), mobility (timed up and go), and dexterity (9-hole pegboard and a novel lower limb dexterity task[5]) in the practically defined off medication state (≥12 hours medication withdrawal) and on medication. We also tracked single and multiple prospective falls for the year after DBS implantation. Data was gathered at a two-, four-, six-, and 12-month follow-up data collections. We performed a chi-square test to compare retrospective vs. prospective single and multiple falls. We also performed a logistic regression for the collected data to try to predict who may be at higher risk of prospective falls after DBS surgery.

Results & Discussion: Thirty-eight percent (12/32) of participants reported falling once in the year prior to surgery. Of those fallers, 8 reported falling more than once. After DBS implantation, 72% (23/32) reported falling once and while 8 of those individuals fell more than once. We observed a statistically significant increase in single ($p=0.03$) and multiple ($p=0.01$) prospective falls compared to retrospective falls. The retrospective fall data was similar to what currently exists in the literature for individuals with PD[2]. For the logistic regression, baseline data for comfortable walk speed and semi-tandem balance on medication correctly predicted 95.5% ($p<0.01$) of prospective fallers and correctly classify 90.3% of all participants (i.e., prospective fallers and nonfallers). Surprisingly previous falls were not predictive of future falls in this sample as is typical in this population.[6] Of particular interest in this sample are the 11 individuals who reported being nonfallers at baseline that became fallers prospectively. This study was not designed to test the causal mechanism related to fall risk; thus, it is unclear the extent that the falls we observed are primary or secondary to DBS and require future study. Future work will continue to explore the extent that baseline continuous or discrete data collected prior to neurosurgery can inform scientists and clinicians on those that may be at risk for worsening of axial symptoms that worsen balance.

Significance: The results of this study suggest that some individuals may require additional therapeutic intervention, such as physical therapy, after DBS to ensure optimal benefit of the therapeutic modality is achieved in addition to known benefit of reduced tremor, bradykinesia and rigidity.

Acknowledgements: Funding Dr. Walker receives research funding from the National Institutes of Health (1UH3NS100553-38401), the Michael J. Fox Foundation (MJFF 15098).

References: [1] Walker et al. (2009), *Neurosurgery*, 65(2); [2] Bloem et al. (2001), *J Neurology* 248. [3] Nilsson et al. (2010), *Acta Neurologica* 123 [4] Follet et al. (2010), *N Engl. J. Med* 362. [5] Kuhman et al. (2023), *Dis and Rehab* 45. [6] Yasuyuki (2014) *J of Parkinson's Disease*, 4.

SHEAR WAVE VELOCITY OF LOWER LIMB TENDONS IS NOT CORRELATED WITH METABOLIC POWER IN HUMAN LOCOMOTION

Alex N. Denton*, Susann Wolfram, David B. Lipps, Brian R. Umberger
School of Kinesiology, University of Michigan, Ann Arbor, MI.
*Corresponding author's email: alxdent@umich.edu

Introduction: Tendons are a key element of the musculoskeletal system and are responsible for transferring the force generated by our muscles to the skeleton to produce movement. The mechanical properties of tendon, such as stiffness, affect the metabolic energy cost of movement by influencing the storage and release of elastic energy and muscle fiber dynamics. Tendon stiffness is susceptible to long-term changes associated with aging [1] and disease [2], and it is responsive to physical training [3]. It is challenging to measure tendon stiffness *in vivo*, but we can non-invasively estimate soft tissue stiffness using ultrasound shear wave elastography [4]. Tendon stiffness is broadly relevant to a wide range of circumstances, however, our understanding of how lower limb tendon stiffness affects muscle and whole-body performance is still incomplete. Therefore, the purpose of this study was to explore the relationships of *in vivo* tendon stiffness of several major lower limb tendons, measured using shear wave elastography, with the metabolic energy cost of locomotion. We expect lower limb tendon stiffness to affect the metabolic energy cost of locomotion in muscle-specific ways. Based on existing literature [3], greater Achilles tendon stiffness is expected to lead to lower metabolic energy cost due to enhanced storage and release of elastic energy in young healthy adults; however, we lack a theoretical basis or prior data for predicting the relationships for other tendons.

Methods: Thirty-six young healthy adults (18M/18F, mean±SD 25.7±5.9 yr, 170.9±9.8 cm, 69.6±14.7 kg) participated after providing informed consent and reporting their habitual physical activity. Metabolic power was estimated using indirect calorimetry [5] during 5 minutes of rest, walking (1.0, 1.3, 1.6 m/s), and running (2.5 m/s), where the order of locomotion trials was randomized. Tendon stiffness was estimated using shear wave velocity (SWV) for the tibialis anterior (TA) tendon, Achilles tendon (AT), patellar tendon (PT), and semitendinosus tendon (ST) at rest. Images were acquired after positioning the corresponding lower limb joint angles to ensure sufficient tendon slack. Tendons were imaged in a randomized order. The relationships among lower limb tendon stiffness, based on mean SWV, on the metabolic energy cost of locomotion at each speed were examined using multiple linear regression.

Results & Discussion: The net metabolic power for each locomotion speed was significantly different from every other speed (all $p<0.001$, Fig. 1A) and the mean SWV for each tendon was significantly different from every other tendon (all $p<0.001$, Fig. 1B). The mean SWV of the ankle tendons (TA & AT) was greater than for the knee tendons (PT & ST). Lower limb tendon stiffness was not a significant predictor of the net metabolic power at any of the examined locomotion speeds in the overall regression models (all $p>0.13$), or for any bivariate correlations (Fig. 1C). There also were no significant differences between males and females (all $p>0.05$) or for activity levels across measurements (all $p>0.10$).

It is difficult to link the characteristics of any single element of the musculoskeletal system to whole-body metabolic cost in locomotion. Despite including stiffness measures from several major knee and ankle flexor and extensor tendons, the variation in tendon stiffness within our sample may not be sufficient to explain a significant portion of the metabolic cost. In summary, lower limb tendon stiffness measured using shear wave elastography at rest is not associated with the net metabolic power of walking or slow running.

Significance: While measuring tendon stiffness through SWV at rest is common, it may not adequately capture the mechanical behavior of tendon and the interaction with muscle during dynamic contractions during locomotion.

Acknowledgments: Funding was provided by a University of Michigan Rackham Graduate Student Research Grant.

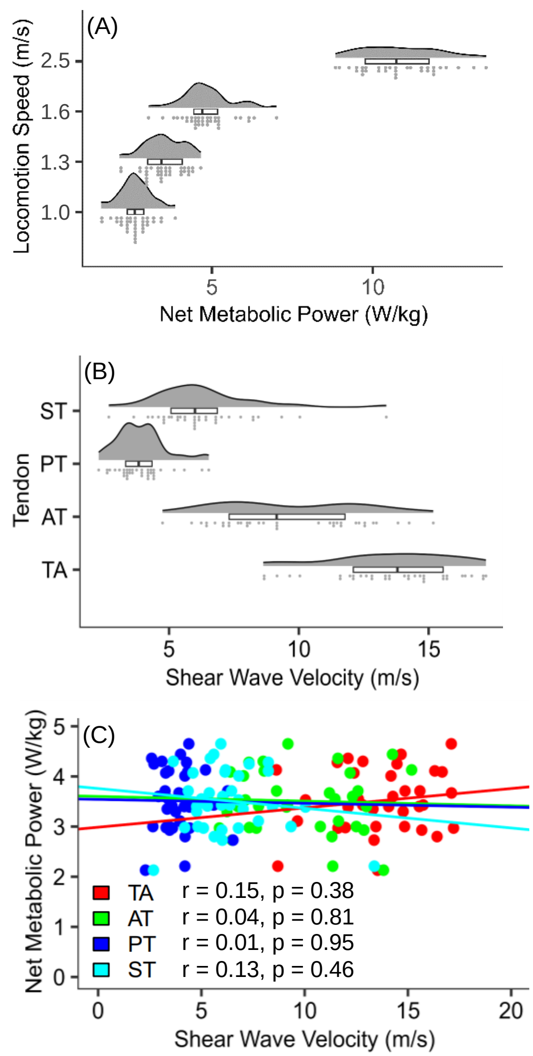

Figure 1: Net metabolic power during different speeds of locomotion (**A**), mean SWV of lower limb tendons at rest (**B**), and the bivariate correlations for each tendon and net metabolic power during normal speed walking in young healthy adults (**C**).

References: [1] Onambele et al. (2006), *J Appl Physiol* 100(6); [2] Arya & Kulig (2010), *J Appl Physiol* 108(3); [3] Fletcher et al. (2010), *Eur J Appl Physiol* 110(5); [4] Arda et al. (2011), *AJR Am J Roentgenol* 197(3); [5] Brockway (1987), *Sci Transl Med* 41(6)

GAIT VARIABILITY OF REAL-WORLD VS TREADMILL WALKING WITH BILATERAL ROBOTIC ANKLE EXOSKELETONS WITH PROPORTIONAL MYOELECTRIC CONTROL

Rachel L. Hybart[1*] and Daniel P. Ferris[1]
[1]J. Crayton Pruitt Department of Biomedical Engineering, University of Florida
*Corresponding author's email: rhybart@ufl.edu

Introduction: Gait variability can be an important indicator of functional ability or disability with aging or neurological insult, but it is also an important factor in gait adaptation [1]. Although most studies on gait biomechanics with robotic exoskeletons study participants walking on treadmills, the end goal of the device is usually to function during overground locomotion in the real world. Gait variability without an exoskeleton increases during outdoor walking compared to treadmill walking [2], and this may affect adaptation and exoskeleton dynamics. In this study, we assessed gait variability while walking with robotic ankle exoskeletons (Dephy, Inc.) under proportional myoelectric control both indoors on a treadmill and outdoors overground. We hypothesized that measures of gait variability would be higher during outdoor walking with robotic ankle exoskeletons compared to treadmill walking with robotic ankle exoskeletons.

Methods: We recruited 12 healthy subjects (5 female, 7 male) with the following characteristics: age 22.6 (8.66) yrs.; height 1.73 (0.751) m; and body mass 69.3 (10.2) kg; mean (s.d.). Participants trained for 30 minutes on three separate days walking with bilateral ankle exoskeletons with a proportional myoelectric controller using soleus EMG [3]. On the fourth day subjects walked both indoors on a treadmill and outdoors overground at a self-selected speed chosen on the first day of training of 1.15 (0.13) m/s with conditions randomized. Participants wore inertial measurement units on the shanks and feet. We used the final 45 strides of each condition on the final day of training and measured spatiotemporal gait and exoskeleton assistance variability.

We measured stride time, stance time, swing time and stride length from the inertial measurement units. We also measured exoskeleton power, ankle angle, and exoskeleton torque. We calculated the variability of the measurements of interest using the coefficient of variation (CoV=standard deviation/mean). We performed paired t-tests to determine significance between indoor and outdoor conditions (α=0.05).

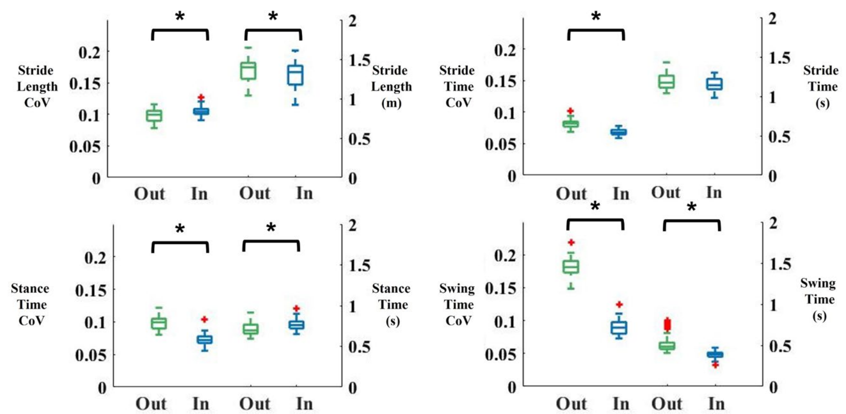

Figure 1: Box plots showing indoor (blue) and outdoor (green) coefficient of variation data (left axes and left two boxes) and average parameter data (right axes and right two boxes) for stride length, stride time, stance time, and swing time. * indicates a significant difference between conditions ($p<0.05$). Red + indicates outliers.

Results & Discussion: As hypothesized, the coefficients of variation for stance time, stride time, and swing time for the outdoor condition were all significantly higher compared to the indoor treadmill condition ($p<0.05$) (Figure 1, left axes). Unexpectedly, stride length coefficient of variation was actually slightly less for the outdoor condition compared to the indoor treadmill condition ($p<0.05$). There were significant increases in stride length and swing time, and a significant decrease in stance time, when walking outside compared to inside ($p<0.05$) (Figure 1, right axes). The exoskeletons supplied an average maximum torque of 0.25 Nm/kg on the indoor treadmill and 0.20 Nm/kg overground outdoors.

Our findings indicate that walking with robotic ankle exoskeletons using proportional myoelectric control overground outdoors leads to significantly different spatiotemporal gait variability compared to indoors on a treadmill. This alteration in gait variability, even when maintaining a similar constant average speed, indicates that exoskeleton dynamics may be affected by the altered gait kinematics. As an example, the decrease in torque supplied by the exoskeleton during outdoors condition compared to the indoor condition may be a result of the greater stance time variability in that condition.

Significance: The results showed significant differences in gait variability when walking with robotic ankle exoskeletons on a treadmill compared to outside. These results should inform lower limb exoskeleton training paradigms intended for new users. Training with robotic exoskeletons outside may provide increased benefits compared to treadmill training due to higher gait variability overground.

Acknowledgements: This work was supported in part by the U.S. National Institutes of Health under Grant R01 NS104772.

References: [1] S. Ulman et al., (2019) "Using Gait Variability to Predict Inter-individual Differences in Learning Rate of a Novel Obstacle Course," *Ann. Biomed. Eng.*, vol. 47, no. 5, pp. 1191–1202; [2] A. C. Schmitt, et al. (2021), "Walking indoors, outdoors, and on a treadmill: Gait differences in healthy young and older adults," *Gait Posture*, vol. 90; [3] G. S. Sawicki and D. P. Ferris, (2008) "Mechanics and energetics of level walking with powered ankle exoskeletons," *J. Exp. Biol.*, vol. 211, no. 9.

ANTROPOMETRIC DEFORMITIES IN FOOT AND ANKLE STRUCTURE AMONG INDIVIDUALS WITH CHRONIC STROKE

Hogene Kim[1*], Ji-Eun Cho[2], Kyeongjun Seo[2], Joo-Young Lee[3]
[1]Dept. of Clinical Rehabilitation Research, National Rehabilitation Center, Seoul, South Korea
[2]Dept. of Rehabilitative & Assistive Technology, National Rehabilitation Center, Seoul, South Korea
[3]Department of Applied Statistics, Chung-Ang University, Seoul, South Korea
*Corresponding author's email: hogenekim@gmail.com

Introduction: Chronic stroke victims suffer from a persistent inequivalence between their major ankle muscles, i.e., the spastic triceps surae and ankle dorsiflexors. This inequivalence is responsible for the geometric deformities of a foot [1]. A spastic equinus foot causes foot drop during gait and balance impairments.
Recent advances in scanned 3D digital imaging technology have been successfully introduced to clinical practice to enable the treatment of various pathological deformities. This study evaluates the validation of using 3D scanned surface images of the feet of stroke patients to visually assess the deformities of a hemiparetic foot. Anthropometric measurements that locate foot landmarks can sh,ow characteristic of hemiparetic foot abnormalities and are easier to obtain when using 3D scanning technology. Thus, we hypothesized that there is difference in the foot and ankle structure between the hemiparetic sides of chronic stroke patients and age- and gender-matched healthy controls, then difference between paretic and non-paretic sides using the geometric morphometrics method (GMM).

Methods: We defined four conventional (1~4) and three custom (5~7) foot landmarks as follows: (1) the first metatarsal joint head, (2) the fifth metatarsal joint head, (3) medial malleolus, and (4) lateral malleolus, (5) the medial and (6) the lateral outmost point of the heel ground-contact-area while standing, (7) the tip of index toe, and the origin as the most posterior point of the foot along the line between the calcaneus centre and index toe on this plane. Using the measurements of these landmarks of participants (Figure 1), a statistical shape analysis using GMM was performed (R package geomoph v.4.0.0). A Procrustes Analysis of variance(ANOVA) on Procrustes distances was conducted to test the significant foot shape differences between the stroke patients and healthy controls. The patterns of overall shape variation were visualized using Principal Component Analysis(PCA). The shape analysis of bilateral symmetry was performed using a Procrustes ANOVA with individual and side (as the paretic and non-paretic foot of each stroke patient) and individual*side interaction. In ANOVA, directional asymmetry(DA) corresponded to the main effect of the side and fluctuating asymmetry(FA) corresponded to the individual*side interaction. PCA was also performed to visualize the patterns of fluctuating asymmetry variations for testing the ANOVA effects with a significance level of 0.05.

Results & Discussion: A total of 30 subjects with stroke-induced hemiparesis (age: 65.6±8.7 years, Female: 11, onset: 10.2±8.7 years) and 11 age-matched healthy controls (age: 62.9±5.6 years, Female:7) participated in this study. The foot shapes of stroke patients significantly differed in the paretic side (F=3.298,p=0.001) and the non-paretic side (F=2.184,p=0.034) compared to the dominant side in healthy controls. The foot shape group differences showed results of a smaller degree of change in the medial malleolus for the paretic and non-paretic sides of stroke patients than the healthy controls.
The Procrustes ANOVA done for testing bilateral symmetry showed no significant variations among individuals (symmetry: SS=0.190,df=29, F=1.147,p=0.123) and no significant foot shape variations between the paretic and non-paretic sides (directional asymmetry: SS=0.009, df=1,F=1.622,p=0.116). However, The shape directional asymmetry showed a subtle foot shape difference in the first metatarsal joint head, the medial malleolus, and the index toe. The first principal component(PC1) explained that 31.8% of fluctuating asymmetry was related to overall locations. Our study successfully showed that using 3D scanning technology, the foot morphometric changes in the feet if chronic stroke patients and their anthropometric measurements identified significant hemiparetic deformities in ankle and foot structures between the paretic and non-paretic sides as well as between the chronic stroke patients and healthy controls.

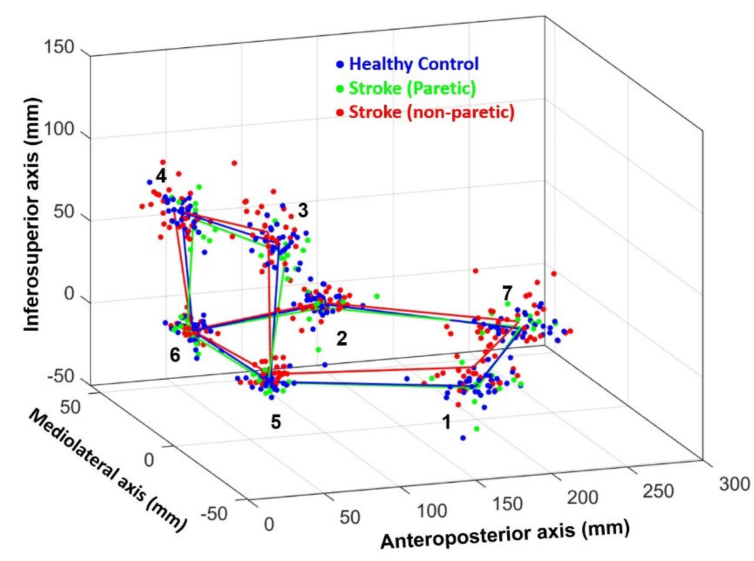

Figure 1 3D scatter plots of foot landmarks

Significance: 3D scanned measurements identified differences in typical foot landmarks in deformed hemiparetic ankle and foot structure.

Acknowledgements: This study was supported by Translational Research Center for Rehabilitation Robots, Korea National Rehabilitation Center, Ministry of Health & Welfare, Korea. (Award Number: #NRCTR-IN20003, Grant Recipient: Hogene Kim, PhD)

References: [1] A. Picelli, G. Vallies, E. Chemello, P. Castellazzi, A. Brugnera, M. Gandolfi, et al., Is spasticity always the same? An observational study comparing the features of spastic equinus foot in patients with chronic stroke and multiple sclerosis, J Neurol Sci 380 (2017) 132-136.

RELATING MUSCLE PHYSIOLOGICAL CHARACTERISTICS TO *IN VIVO* MUSCLE DYNAMICS

M. Janneke Schwaner[1*], Dean L. Mayfield[2], Emmanuel Azizi[1], Monica A. Daley[1]
[1]Department of Ecology and Evolutionary Biology, University of California, Irvine, Irvine CA
[2]Department of Evolution, Ecology and Organismal Biology, University of California, Riverside, Riverside CA
*Corresponding author's email: mjschwan@uci.edu

Introduction: A muscle's mechanical function is strongly influenced by the intrinsic physiological properties characterized by the force-length (F-L) and force-velocity (F-V) relationships. These relationships derive specific lengths and velocities that maximize the force and power output of a muscle. Work loop analyses can characterize mechanical actuation of muscles during dynamic *in vivo* tasks, with variations in stimulation and length trajectory [1]. Work loops are used to characterize muscle work, mechanics, and muscle function. The F-L and F-V relationships suggest optimal ranges for muscles for force or power production. Here, we investigate the relationship between muscle physiological characteristics, specifically the F-L and F-V relationships, and in vivo muscle function in the guinea fowl (*Numida Meleagris*) main ankle extensor, the lateral gastrocnemius (LG) muscle during walking and running. We compare muscle physiological characteristics across individuals and map each individual birds' *in vivo* work loops during walking and running to their individual force-length and force-velocity relationships. We hypothesize that muscles operate near optimal conditions for force or power production, respectively, during walking and running tasks. In support of this hypothesis, we expect to see that muscles operate around optimal lengths during force production (F-L), shorten across the optimal length plateau (F-L), and shorten near optimal velocities for power output during force production (F-V).

Methods: We collected *in vivo* muscle length, force, and activation (through EMG recordings) from 6 Guinea fowl LG muscles during level and steady walking (0.8 ms^{-1}) and running (1.56 ms^{-1}) on a treadmill. Sagittal videos were recorded at 200 Hz, *in vivo* muscle dynamics were recorded at 5000 Hz. To characterize muscle physiological properties, we collected *in situ* isometric force length (F-L) and isotonic force velocity (F-V) data from 11 birds according to previously used protocols [2]. We plotted *in vivo* muscle force (F/F_{max}) against length (L/L_0) to create work loops for each gait condition. In total we analysed 529 strides, with an average of 42 strides per bird per gait condition. From these work loops we obtained stress and strain at time of EMG onset (EMG_{on}), foot on (T_{on}), 50% force rise ($50preF_{pk}$), peak force (F_{pk}), and 50% force decay ($50postF_{pk}$). We also obtained strain rates at T_{on} and F_{pk}.

Results & Discussion: Muscles start shortening on the descending shoulder of the F-L plateau (± 5% F_{max}), but significant force development occurs entirely on the ascending limb of the F-L relationships curve around T_{on} in both walking and running (Fig 1.A). Peak force for both gaits occur around ~0.8 L_0. Muscles operate at low strain rates at peak force, and at higher strain rates during lower forces (Fig 1.B.). These findings only partly support our hypothesis: *in vivo* LG velocities are consistent with optimizing force and power according to the F-V relationship, but LG does not operate on the force plateau (F-L) during force production.

These data suggest that muscles shorten across the optimal length to optimize muscle force production potential in late swing. This may provide some resistance against potential unexpected perturbations which may require rapid force production at foot contact. We also found evidence of passive (i.e., in absence of EMG activity) force rise early in the swing phase of both gaits at lengths where passive force was not observed in isolated muscles. This suggests that history dependent and viscoelastic effects alter *in vivo* force production beyond the predictions of the F-L relationship.

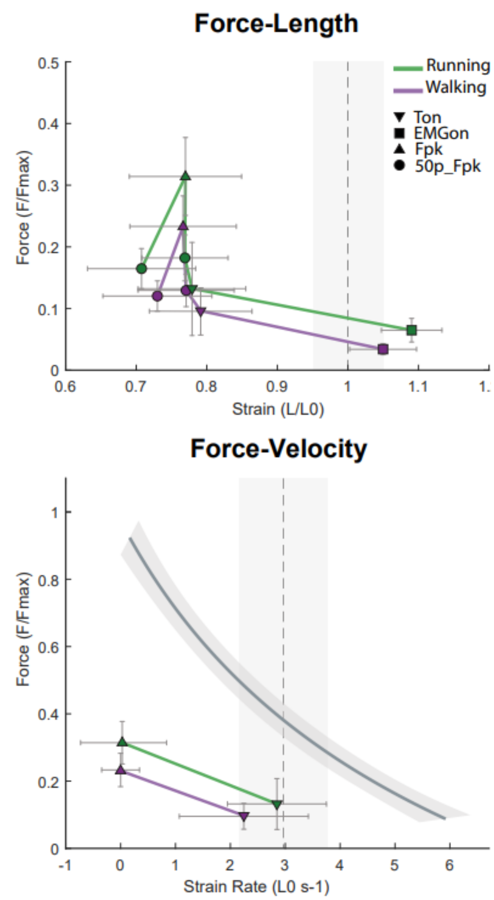

Figure 1: Average stress and strain of the LG during walking (purple) and running (green) mapped onto the force-length relationship (A). Average strain rate and stress of the LG mapped onto the force velocity relationships (B). Mean values of stress, strain, and strain rate at different time points were obtained from work loops across birds. Error bars indicate 95% CI. Vertical lines indicate L_0 (A) or V_{opt} (B), respectively, corresponding grey shading indicates a 10% plateau for L_0 and V_{opt}.

Significance: This study provides a novel comparison of *in vivo* muscle operating forces, lengths, and velocities to *in situ* characterized lengths and velocities. Direct comparison of *in vivo* work loops and physiological operating ranges suggest the need for further examination of how physiological properties of muscle influence dynamic tasks *in vivo*, in particular during navigating complex terrain.

Acknowledgements: This work is funded by the National Science Foundation (NSF), grant number: 2016049 (to M.A.D).

References: [1] Josephson (1985), *J Exp Biol* 114(1); [2] Holt & Azizi (2016), *Proc R Soc B* 232(20152832).

INFLUENCE OF FIREFIGHTER HELMETS ON NECK MUSCLES FATIGUE

Felipe Z. Santos[1], S. Sudeesh[1], Suman K. Chowdhury[1*]
[1]Department of Industrial, Manufacturing and Systems Engineering, Texas Tech University, Lubbock, Texas, United States
*email: suman.chowdhury@ttu.edu

Introduction: Generally, firefighter helmets are designed to give protection from fire and impact from falling debris. The influence of helmet designs on neck muscle fatigue should also be explored to reduce neck muscle fatigue and injuries [1]. According to the U.S. Fire Administration's National Fire Incident Reporting System (NFIRS), 40% of the injuries to the head and neck during firefighting operations are due to strains/overexertion [2]. In addition, functional accessories in modern firefighter helmets, such as communication device, face shield, thermal imaging, and lighting equipment, increase the net weight and shift the center of mass (COM) of the helmet system, thereby raising the risk of injuries and fatigue of the neck muscles. In the present study, we analyzed the effect of two different firefighter helmet designs, US traditional helmet (UTH) and jet-style helmet (JSH), on the neck muscles during sustained flexion and extension. The UTH weighs about 1.78 kg and have a high-profile (i.e., distance from the top of the head to the top of the helmet) geometry, while JSH weighs 2.02 kg and have a low-profile geometry. Due to the high-profile nature, the COM of the UTH is superior to the JSH by 5.8 cm. The objective of the study was to understand how different mass and COM of the helmet affect the neck muscles and thereby obtain insights for the development of firefighter helmets that not only provide fire and impact protection but also reduce neck fatigue. We have hypothesized that the COM has more influence on the neck fatigues than the overall mass of the helmet. Thus, the UTH could increase muscle fatigues than the JSH.

Methods: We recruited 36 firefighters (18 male and 18 female) for this study. Surface electromyography (EMG) sensors were used to acquire muscle activity at neck extensor (Cervical trapezius and Upper trapezius) and flexor (Sternocleidomastoid and Infra hyoid) muscles. Raw EMG signals were recorded with a sampling frequency of 2222 Hz with wireless sensors (Delsys, Massachusetts, U. S.). At first, firefighters were instructed to force flexion and extension while restraining their head in neutral posture to measure maximum voluntary contractions (MVC). Following this, they performed sustained flexion and extension till the maximum possible time. Three cases were performed for both flexion and extension: 1) without any helmet, 2) With UTH (UST series, Bullard, Kentucky, U.S.) 3) with JSH (Cairns XF1, MSA, Pennsylvania, U.S.). To analyse the neck muscle fatigue, only nine males and 12 females EMG normalized (by MVC) mean absolute values (NMAV) and time duration for each case were used. The institutional review board and ethics committee of Texas Tech University approved this study.

Results & Discussion: In this study, both UTH and JSH shortened the sustained extension time duration by 34% and 32%, respectively. During sustained flexion, it was 40 % for UTH and 36% for JSH. The effects of these helmets on individual muscles are presented in Table 1. During sustained extension, both the helmets elevated NMAV for all muscles studied here, where UTH increased 9% more than JSH. The increments were prominent on the extensor muscles for both male and female firefighters. On the contrary, no drastic differences were observed in the neck flexor muscle activity during sustained flexion, which could be due to the weight of the helmet assisting neck flexion. Overall, this study indicates that the muscle activity and time duration with UTH is more affected than the JSH, which agree with our initial hypothesis that helmet COM location influences neck muscles fatigue more than the overall weight. Therefore, the firefighter helmets should be designed to have lower COM.

Table 1: Comparison of averaged NMAV (average ± SD) with different helmets and without helmets on firefighters.

Male Firefighters								
	Cervical Trapezius		Upper Trapezius		Sternocleidomastoid		Infra Hyoid	
	Extension	Flexion	Extension	Flexion	Extension	Flexion	Extension	Flexion
No helmet	29.0 ± 16.0	20.1 ± 16.1	41.7 ± 28.7	44.2 ± 31.0	7.2 ± 5.2	12.2 ± 5.1	4.1 ± 4.0	9.8 ± 7.9
UTH	42.1 ± 31.3	19.2 ± 16.6	53.5 ± 43.0	37.6 ± 32.9	11.8 ± 7.3	6.1 ± 4.0	8.5 ± 9.8	4.8 ± 4.2
JSH	32.3 ± 18.1	18.1 ± 12.2	43.8 ± 34.3	39.3 ± 29.1	10.0 ± 7.8	7.9 ± 4.5	8.9 ± 9.7	4.9 ± 3.3
Female Firefighters								
	Cervical Trapezius		Upper Trapezius		Sternocleidomastoid		Infra hyoid	
	Extension	Flexion	Extension	Flexion	Extension	Flexion	Extension	Flexion
No helmet	26.2 ± 24.0	11.3 ± 5.2	51.6 ± 49.2	25.6 ± 29.6	7.6 ± 7.0	6.8 ± 5.7	5.2 ± 8.1	5.6 ± 5.2
UTH	31.8 ± 24.9	22.9 ± 10.1	58.8 ± 40.1	33.3 ± 35.8	15.1 ± 11.8	6.9 ± 11.5	12.4 ± 13.2	2.5 ± 1.6
JSH	30.6 ± 29.1	22.5 ± 10.5	56.3 ± 37.3	29.2 ± 29.1	14.2 ± 15.1	6.0 ± 13.1	14.2 ± 12.1	2.2 ± 1.7

Significance: Our study suggests that a more superior helmet COM increases neck muscle fatigue. Therefore, helmet COM is an important design metric when developing firefighter helmet.

Acknowledgements: We acknowledge the Department of Homeland Security & Technology (70RSAT21CB0000023) for funding this study.

References: [1] Harrison et al. (2016), *Aerospace medicine and human performance*, 87(1); [2]. NFIRS (2019), *Fire-Related Firefighter Injuries Reported to the National Fire Incident Reporting System (2015-2017)*.

A FRESH TECHNICAL LOOK AT FOOT POSTURE VS DYNAMIC FOOT FUNCTION IN HEALTHY GAIT

Dustin A. Bruening[1*], Kirk E. Bassett[2], Sarah T. Ridge[3]
[1]Brigham Young University
[2]University of Hartford
*Corresponding author's email: dabruening@byu.edu

Introduction: Clinically, dynamic foot function is often inferred from static or passive foot postural measurements; however, there is little evidence that foot posture can predict foot motion during walking gait. Significant relationships have been found when looking at dynamic position, for instance between medial longitudinal arch (MLA) height and stance phase peak eversion [1]. However, these relationships disappear when analyzing dynamic range of motion (RoM) [2].

While the lack of evidence against static-dynamic relationships is compelling, there are several limitations that may impede our ability to capture this long-theorized relationship. First, research has focused primarily on kinematics, with very little consideration for the forces present during gait. Second, motion measurements have been primarily planar, and may not fully capture the tri-planar nature of the midfoot joints. Thus, the purpose of this study was to re-analyze the static-dynamic relationship by focusing on advanced comprehensive measurements including kinetics. We hypothesized that static and dynamic stiffness would finally yield a significant correlation.

Methods: Foot posture and gait data were collected on 40 healthy participants selected to representing a range of foot postures (24M/16F, 1.74±0.09m, 73.6± 13.84 kg, 24.8 ± 3.9 yrs). MLA height and stiffness were measured using the Arch Height Measurement System. Participants were grouped into high (n=9), normal (n=14), or low (n=17) MLA heights based on standing MLA height, as well as stiff (n=17), normal (n=7), or flexible (n=16) MLA stiffnesses based on sit-to-stand differences [3]. A multi-segment foot model was used to quantify midfoot pronation and supination RoM using a novel signed helical axis algorithm [4]. Midfoot moments were also calculated from shear and pressure distribution measurements [5], and then used to calculate pronation and supination dynamic stiffness (slope of midfoot motion vs resultant midfoot joint moment) [4]. Between group differences in RoM and dynamic stiffness were evaluated using one-way ANOVAs ($\alpha = 0.05$). A multiple regression model was then created with MLA height, stiffness, and their interaction to predict the dynamic measurements of pronation ROM and stiffness, supination ROM and stiffness, and peak hindfoot eversion ($\alpha = 0.05$).

Results & Discussion: There were no significant differences in pronation or supination RoM or in pronation or supination dynamic stiffness for either arch height or arch stiffness grouping (Table 1, Figure 1). There were no statistically significant correlations in any of the multiple linear regression models, with just 13% of the total variance captured in the best predicted measure (pronation stiffness).

The novelty of this study was the use of a tri-planar measure of midfoot motion and in the addition of a stiffness measure that includes kinetics. The lack of correlations even with these new measurements suggests that foot posture is not the primary driver of dynamic motion or stiffness in the general asymptomatic population. Rather, the active role of foot musculature is beginning to emerge as an overriding influence in foot mechanics [3].

Significance: Future studies should pivot to focusing on how muscles modulate foot posture and function during dynamic movements as well as seek new recommendations to replace those commonly given for footwear, orthotics, etc. in the general population.

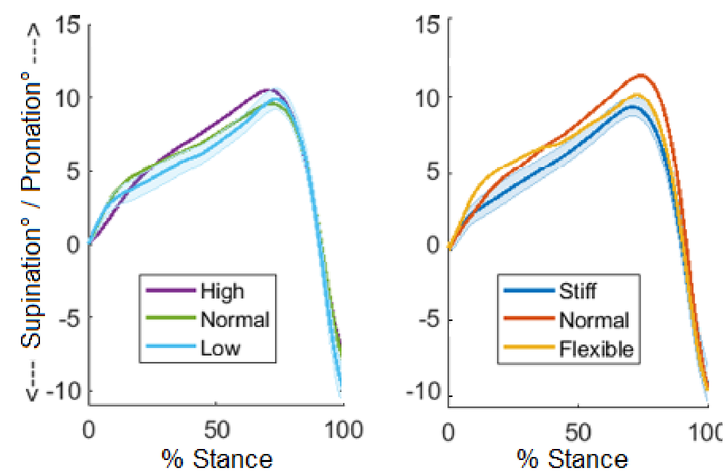

Figure 1: A novel signed helical angle measurement was developed to capture the tri-planar midfoot joint motion as a single angle during stance. The first ~70% of stance was termed pronation, while the final ~30% was termed supination. MLA height and stiffness groupings are shown with stdev bands only on the low/stiff group for clarity.

Table 1: Range of motion (RoM) and dynamic stiffness values during pronation and supination for each postural grouping.

	High	Normal	Low	*p-value*	Stiff	Normal	Flexible	*p-value*
Pronation RoM(°)	11.8±1.4	11.2±2.3	11.0±2.9	*0.701*	10.9±2.6	12.0±2.7	11.3±2.1	*0.573*
Supination RoM(°)	18.2±4.6	18.4±	19.9±5.0	*0.548*	18.2±4.5	19.9±5.1	19.4±4.2	*0.633*
Pronation Stiffness(Nm/°)	0.18±0.148	0.122±0.100	0.175±0.130	*0.409*	0.180±0.111	0.123±0.054	0.150±0.157	*0.579*
Supination Stiffness(Nm/°)	0.074±0.018	0.077±0.019	0.068±0.020	*0.427*	0.079±0.020	0.065±0.018	0.069±0.018	*0.196*

Acknowledgements: Work partially supported by the National Science Foundation (CBET – 2032190).

References: [1] Levinger et al. (2010), *Gait Post* 32(4); [2] Hunt & Smith (2004), *Clin Biomech* 19(4); [3] Williams et al. (2022), *J Foot Ankle Res* 15(1); [4] Bassett (2022), *Published Thesis, BYU*. [5] Petersen (2020), *Published Thesis, BYU.*

TIBIAL ACCELERATIONS, INTEGRALS, AND SYMMETRY VIA IMUS ON VARIOUS TURF SURFACES

Joshua M. Lardie[1*], Rebecca C. Waite[1], Kyley H. Dickson[2], John C. Sorochan[2], Joshua T. Weinhandl[1]
[1]Kinesiology, Recreation, and Sport Studies, University of Tennessee, Knoxville, TN
[2]Department of Plant Sciences, University of Tennessee, Knoxville, TN

*Corresponding author's email: jlardie@vols.utk.edu

Introduction: The use of synthetic turf fields has increased over recent years due to increased durability, decreased maintenance, and reduced environmental effects compared to natural turfgrasses [1]. A consensus has not been reached, however, on the impact of synthetic turf on musculoskeletal injury rates [2]. Overuse injuries are believed to be caused by excessive and repetitive loads, such as impacts with the ground during running or change of direction [3]. Vertical and resultant tibial accelerations have been associated with running injuries across all foot strike patterns using inertial measurement units (IMU) [4]. Therefore, the purpose of this study was to examine the effect of different turf surfaces on tibial accelerations during athletic movements. We hypothesize that there will be no differences between tibial accelerations or acceleration derived variables on different surfaces for a variety of movement drills.

Methods: 24 healthy participants (13 males, mass: 71.15kg ± 12.98, height: 1.73m ± 0.11) performed a variety of drills to show dynamic sprinting, change of direction, lateral agility, and single leg bounding. This included a self-selected jog (DNB), the M-drill, the 5-10-5 drill, and triple hop (TH). The M-drill navigated 5 cones, 5 meters from one another, in the shape of an uppercase M with focus on change of direction at each vertex, completed in both directions. The 5-10-5 consisted of a lateral shuffle 5 meters to the right, then 10 meters to the left, followed by 5 meters back to the original starting position. Triple hop began on a single leg and 3 bounds were taken, with the final landing position maintained, completed on both legs as well. Each set of drills were completed on 3 different surfaces: synthetic turf, warm season turfgrass, and cool season turfgrass. The synthetic turf (SYN) was a 3rd generation synthetic turf with a crumb rubber infill and a foam-based shock pad underneath. The warm season turfgrass was Bermuda (BER) and the cool season turfgrass was Kentucky Blue Grass (KBG). IMUs (IMeasureU, Auckland, New Zealand) were used with a rubber strap secured to the medial & distal tibia, superior to the medial malleolus (Figure 1). Participants were shown a demonstration of the drill and provided with verbal instructions. All drills were performed in participants non-provided athletic shoes. Data processing and statistical analysis took place in Python (3.10.7). Acceleration due to gravity was removed and oversaturation of the low G sensors was replaced with the output of the high G sensors [5]. A 4th order, zero-lag, recursive Butterworth lowpass filter with a 50Hz cut-off frequency was applied. The peak acceleration per trial was an average of all peaks following manual visual assessment of trial. Acceleration integrals were taken using these peaks. Symmetry was defined as the difference of the right and left leg divided by the average of the right and left leg. Multiple repeated measures ANOVA ($\alpha = 0.05$) were conducted to compare the effect of SYN, KBG, and BER on peak tibial accelerations, acceleration integrals, and symmetries.

Results & Discussion: There were no significant differences between tibial resultant acceleration variables for surfaces for all tasks for both legs. The DNB AccP did show significant differences between surfaces for the right leg [$F(2,46) = 10.55$, $p = 0.0002$]. Following Tukey's HSD post hoc, KBG and BER were not significantly different ($p = 0.08$). KBG and BER had a mean difference of -1.70 gs, compared to a mean difference of 1.22 gs between SYN and KBG (Table 1). In general, this agrees with our hypothesis that there would be no differences between SYN, KBG, and BER.

Table 1: Acceleration variables mean and standard deviation of right leg by task and surface type.

	5-10-5	DNB	M Drill	TH
Peak Acceleration (g)				
SYN	13.58 ± 4.18	9.06 ± 2.33	14.27 ± 3.56	19.54 ± 5.23
KBG	13.58 ± 4.01	10.28 ± 3.28	14.35 ± 3.02	18.65 ± 5.66
BER	13.84 ± 4.18	8.58 ± 2.33	14.55 ± 3.56	20.76 ± 5.23
Acceleration Integral (g*S)				
SYN	20.43 ± 4.01	32.89 ± 3.14	21.36 ± 3.76	N/A
KBG	20.07 ± 5.37	32.63 ± 5.53	22.51 ± 4.96	N/A
BER	21.14 ± 5.75	32.87 ± 3.98	22.33 ± 4.83	N/A
Acceleration Symmetry				
SYN	-0.01 ± 0.23	0.04 ± 0.11	0.04 ± 0.18	0.09 ± 0.25
KBG	0 ± 0.16	0.06 ± 0.15	0.02 ± 0.16	-0.03 ± 0.33
BER	0.03 ± 0.22	0.02 ± 0.13	0.07 ± 0.2	0.12 ± 0.27
Acceleration Integral Symmetry				
SYN	0.03 ± 0.14	0.01 ± 0.09	0.03 ± 0.13	N/A
KBG	-0.04 ± 0.2	-0.01 ± 0.08	0.03 ± 0.16	N/A
BER	0.09 ± 0.29	-0.02 ± 0.08	0.01 ± 0.15	N/A

Significance: Our findings help support that synthetic turf does not significantly alter the tibial accelerations during change of direction movements, lateral shuffling, or single leg support during dynamic athletic movement. A significant alteration of acceleration variables may be indicative of a potential injury causing element being introduced or an alteration of impact with the ground and attenuation of loading. Vertical tibial accelerations have shown sensitivity to changes in health states, but more longitudinal research is necessary to further extrapolate. Future research is needed on more heavily trafficked surfaces, more athletically trained populations, as well as additional drills and surface types.

References: [1] Elvidge et al. (2022), *Footwear Science* 14(3). [2] Gould et al. (2022), *Foot & Ankle Ortho* 7(1). [3] McGhie et al. (2013), *American J of Sport Med* 41(1). [4] Tenforde et al. (2020), *PM&R* 12(7). [5] van Hees et al. (2013), *PLOS* 8(4).

CHARACTERIZATION OF UNILATERAL SLIL INJURY USING 4DCT METRICS

Erica A. Bell[1*], Cesar Lopez[1], Taylor Trentadue[1], Robert Foley[1], Shuai Leng[1], David Holmes III[1], Sanjeev Kakar[1], Steven L. Moran[1], Ryan Breighner[2], Andrew R. Thoreson[1], Kristin D. Zhao[1]
[1]Mayo Clinic, Rochester, MN, U.S.A.
[2]Hospital for Special Surgery, New York City, NY, U.S.A
*Corresponding author's email: bell.erica@mayo.edu

Introduction: The scapholunate interosseus ligament (SLIL) is the primary stabilizer and most commonly injured ligament in the wrist [1,2]. While SLIL injury is of a progressive nature, the true incidence of SLIL injury is still largely unknown. Injury to the SLIL leads to motion abnormalities of the scaphoid and lunate carpal bones and can lead to a predictable pattern of wrist instability, pain, and arthritis when left untreated [3]. Thus, prompt and accurate diagnosis is critical to provide the most effective intervention. Static imaging modalities, such as plain radiographs, cannot detect alterations in carpal motion [4] and often appear normal in subtle or early injuries. Wrist arthroscopy, which directly examines ligament integrity and space between the scaphoid and lunate (Geissler grade, 0-4), remains the gold standard to diagnose SLIL injury. However, arthroscopy is invasive and involves risk of infection, nerve injury, pain, and stiffness, with scoring that is subjective and prone to interobserver variability.

Due to the diagnostic challenges of noninvasive clinical evaluation and the risk/cost of arthroscopy, SLIL injuries can be overlooked or improperly treated with surgical reconstructions that do not appropriately target the type and nature of the tear. Accurate diagnosis of the location of SLIL injuries is important to determine the appropriate surgical approach (volar, dorsal, or both) to correct the injury and interrupt the disease continuum that ultimately results in radioscaphoid osteoarthritis. **Thus, there is a critical need for a noninvasive, quantitative, diagnostic metric that accurately identifies the location of SLIL injuries to allow for more appropriate treatment and intervention to restore normal wrist function before the onset of arthritis.**

The purpose of the present study is to characterize unilateral SLIL injury using a summary 4DCT metric during wrist motion. **The primary hypothesis** is that a summary biomarker based on 4DCT-derived scapholunate (SL) and radioscaphoid (RS) interosseus proximities (gapping distance) during wrist motion will allow prediction of the presence and location of injury in patients diagnosed with SLIL injury. **The secondary hypothesis** is that patients with similar injury profiles will exhibit similar biomarker values.

Methods: The present IRB-approved study uses a rigorously validated 4DCT imaging technique that allows volumetric imaging of carpal bone motion in real-time, as previously described [6,7]. This method has been shown to enable accurate quantification of key metrics during wrist motion in patients with unilateral SLIL injury. The data presented represent a subset of data of nine patients (8M, 1F) with a Geissler score of III or IV, and a confirmed volar-only (VSL, n=2) or volar-with-dorsal SLIL injury (VSL+DSL, n=7) from a larger cohort of 29 patients, the remainder of which had different injury profiles.

In brief, each patient underwent a bilateral static CT scan followed by bilateral dynamic CT scans while performing flexion/extension (FE) and radioulnar deviation (RUD) motions (4 dynamic scans total). The forearm was stabilized to keep the wrist in the imaging field of interest. Proximity maps, color representations of the distances calculated between two bones, at the SL and RS joints, were generated using a custom MATLAB program. Median proximity values were extracted from dynamic volumes for each motion. Median proximities of all dynamic volumes, deviated in the same direction from neutral (e.g. flexion vs. extension), were calculated and normalized to the median proximity of the neutral position of the contralateral limb (Fig. 1).

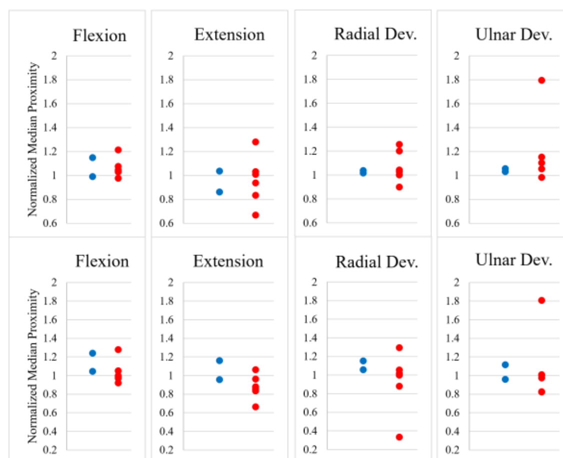

Figure 1: Comparison of normalized proximities for the SL (top) and RS (bottom) joints. VSL (blue), VSL+DSL (red).

Results & Discussion: Compared to their contralateral control limb, patients with a VSL+DSL injury had decreased median proximities at the RS joint in most motion positions, with the exception of ulnar deviation. This was consistent with the expectation that the RS joint proximity would decrease with increasing injury severity. However, when comparing between injury types, median proximities were similar at the SL joint (Fig. 1) for FE (and varied for RUD), contrary to the expected increase in proximity with increasing injury severity. Compared to their contralateral control limb, patients with a VSL injury had similar median proximities at both joints for all motions, whereas VSL+DSL patients exhibited wide variability.

Significance: These preliminary results of a limited dataset demonstrate there are differences in behavior of arthrokinematics between SLIL injury severity. These differences may not be clearly demonstrated when characterized by interosseous proximity using the current summary metric. Additional analysis, such as comparisons of the entire time series of proximity distributions, should be considered with dynamic evaluation of SLIL injury to further distinguish both location and severity of injury.

Acknowledgements: Funding by NIH NIAMS R01AR071338, NIH NIAMS T32AR056950, & NIH NIGMS T32GM065841.

References: [1] Kitay & Wolfe (2012), *J Hand Surg* 37(10); [2] Short et al. (2007), *J Hand Surg* 32(3); [3] Ruby et al. (1987) *J Hand Surg* 12(5 Pt 1); [4] Schadel-Hopfner et al. (2001), *J Hand Surg Eur Vol* 26(1); [5] Manuel & Moran (2007), *Orthop Clin N Am* 38(2); [6] Leng et al. (2011), *Med Phys 38(Suppl. 1;*, [7] Zhao et al. (2015), *J Biomech Eng* 137(7).

CORTICAL RESPONSE TO BALANCE PERTURBATION IS GREATER IN MODERN DANCERS THAN NONDANCERS

Kennedy G. Kerr[1*], Scott E. Boebinger[2], Jasmine L. Mirdamadi[3], Lena H. Ting[2,3]
[1]Emory College of Arts and Sciences Neuroscience and Behavioral Biology Program, Department of Computer Science, Atlanta, GA
[2]The Wallace H. Coulter Department of Biomedical Engineering, Emory University and the Georgia Institute of Technology, Atlanta, GA
[3]Emory University School of Medicine, Department of Rehabilitation Medicine, Division of Physical Therapy, Atlanta, GA
*Corresponding author's email: kgkerr@emory.edu

Introduction: Understanding when and how cortical resources are engaged in balance recovery may be crucial to understanding balance health prior to diagnosed balance impairments. Reactive balance control is generally considered to be an automatic, brainstem-mediated behavior [1]. However, cortical resources are engaged even in healthy adults as the level of challenge increases [2]. Following a balance perturbation, a large negative peak (N1) can be recorded by electroencephalography (EEG) (Fig. 1AB). The cortical N1 is localized to the supplementary motor area [4] and may be reflective of the varying reliance on cortical resources because N1 is thought to be an error assessment signal [5]. Previous work has shown the N1 scales with balance challenge and balance ability in healthy young adults (HYA) [5]. Here, we investigate whether the N1 response differs in a cohort with fine-tuned sensorimotor integration and balance ability – professional modern dancers. Because modern dance training emphasizes responding to sensory information and correcting balance errors without missing a beat, we predicted N1 amplitudes following balance perturbations would be smaller in modern dancers than HYA controls and scale with perturbation difficulty.

Methods: We collected data from 7 HYA and 3 professional modern dancers recruited from Emory University and the surrounding community. Exclusion criteria included history of neurologic, musculoskeletal, and/or visual impairments. Participants completed a challenging beam walking task [6]; balance ability was quantified as a BEAM score, or the mean distance traveled across 6 trials. EEG was used to record cortical activity throughout a series of support-surface perturbations. There were two difficulty levels across participants: perturbations in which a step was not needed to maintain balance and perturbations in which a step was needed. First, participants' step threshold was determined, which is the magnitude at which an individual must take an unplanned step to regain balance 50% of the time. The step threshold was then used to inform subsequent perturbation magnitudes. The "small" perturbation magnitude is equivalent to 60% of the participant's step threshold and the "large" perturbation magnitude was 140% of participant's step threshold. Participants were told to either step or not step in response to perturbations, and perturbations above step threshold were only delivered when the instruction was not to step, ensuring trials with unplanned steps. We then compared BEAM score with N1 amplitudes in both cohorts and in no step and unplanned step perturbation conditions.

Results & Discussion: Within groups, N1 amplitudes were smaller in no-step perturbations as seen in an exemplar HYA and dancer (Fig. 1B). In contrast to our prediction, dancers had larger N1 amplitudes than the median in both the small (no step) and large (unplanned step) conditions (Fig. 1B). Surprisingly, dancers also did not have higher step thresholds than HYA, so they did not receive larger magnitude perturbations. All 3 dancers had BEAM scores at or above the median, which did not show a relationship with N1 amplitude (Fig. 1C). Our data suggest that dancers may prioritize upright posture, leading to larger cortical N1 responses after a perturbation. This is slightly different from previous interpretations of N1, where larger amplitudes were thought to reflect perceived threat of the perturbation.

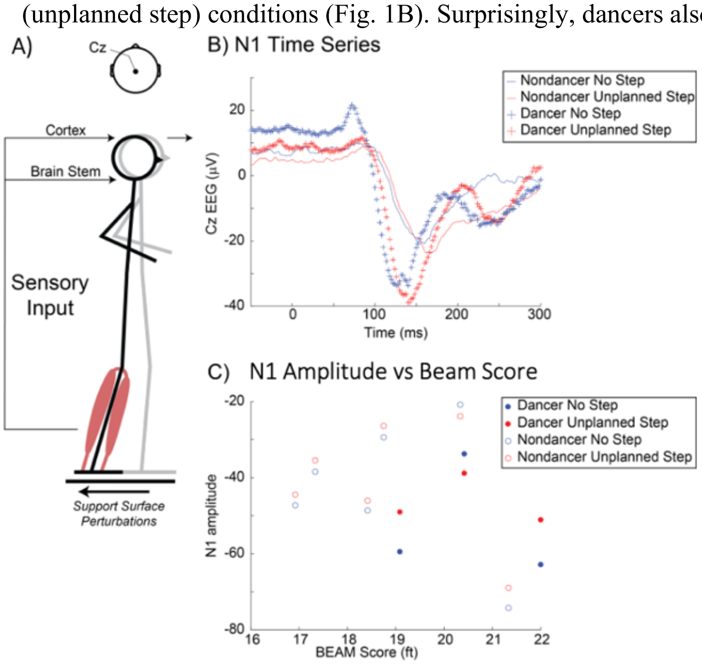

Fig 1. (A) Ascending pathway for the sensory feedback loop governing cortical and subcortical balance control while EEG is recorded. (B) EEG traces following a perturbation at time = 0 from the Cz electrode over the supplementary motor area. The N1 is the first negative peak in each trace. (B) Peak N1 amplitudes for each participant in both perturbation conditions against mean distance travelled along the beam, where higher scores indicate better balance.

Significance: The N1 response has been thought to be a potential biomarker of increased cortical engagement indicating worse balance ability. While dancers may not fear a fall, they may be more responsive to small threats to their balance and respond accordingly. Therefore, N1 amplitude may be an indicator of attentiveness to postural perturbation, and increased in both professional and HYA with poor balance potentially creating a U-shaped function across balance ability.

Acknowledgements: This research was funded by NIH R01 HD46922 (L.H.T.) and Emory Center for Mind Brain and Culture Fellowship (K.G.K.).

References: [1] Maki and McIlroy (2007), *J Neural Transm (Vienna)* 114(10); [2] Jacobs and Horak (2007), *J Neural Transm (Vienna)* 114(10); [3] Peterson and Ferris (2019) *NeuroImage* 198; [4] Marlin et al. (2014), *J Neurophysiol* (111)23; [5] Payne and Ting (2020), *Gait and Posture* 80; [6] Sawers and Ting (2015), *Gait Posture* 41(2)

"PUT ME IN THE ZOO": RESEARCH AND OUTREACH AT A ZOO BIOMECHANICS DAY

Cassie Shriver[1], Audra Davidson[1], Young-Hui Chang[1], David Hu[1,2], Joseph Mendelson III[1,3], Stacy Wiech[3], Andrew Schulz[4]
School of Biological Sciences[1] and Mechanical Engineering[2], Georgia Tech, Atlanta, GA;
Zoo Atlanta[3], Atlanta, GA; Max Planck Institute for Intelligent Systems[4], Stuttgart, Germany
*Email: aschulz@is.mpg.de

Introduction: National Biomechanics Day (NBD) occurs every spring and has traditionally focused on human-interfaced biomechanical demonstrations like wearable robotics [1]. Less attention has been given to comparative biomechanics that emphasize exotic, non-human species and their movement [2], but comparative research can be difficult without access to multitudes of different species. In this work, we sought to capitalize on an existing zoo-university collaborative relationship to showcase comparative research with NBD. We created a Zoo Biomechanics Day known as **Biomechanics Day: Animals in Motion**, with the goal of increasing total outreach for biomechanics. In 2018, NBD hosted 151 events, incorporated 539 biomechanists, and reached over 11,000 students internationally [3]. For our event, we collaborated with Zoo Atlanta and the Atlanta Science Festival, which has reached more than 300,000 people since its inception in 2014 [4]. We hypothesized that utilizing an existing research relationship between Georgia Tech and Zoo Atlanta and collaborating with the local science festival would increasing public attendance and participation in biomechanics outreach events.

Methods: Atlanta Science Festival is a yearly event during March in Atlanta, Georgia which hosts around 125-150 events in the metro Atlanta area. In 2020, Zoo Atlanta and Georgia Tech worked to develop a zoo biomechanics event to highlight zoo-university collaborative research, which would be hosted with Atlanta Science Festival 2020. Due to COVID-19, this event was delayed to Atlanta Science Festival 2023. We worked in the Fall of 2022 to submit a proposal to Atlanta Science Festival to host a significant zoo biomechanics event that coincided with Zoo Atlanta's Educator Appreciation Day. In December of 2022, our proposal was accepted to host "Biomechanics Day: Animals in Motion" at Zoo Atlanta. The event occurred for four hours in the late morning and early afternoon on Saturday, March 11th [5]. Research volunteers were recruited from three universities (Georgia Institute of Technology, Clemson University, and The University of Akron). Participation numbers for the event are from data collected by ticket sales at Zoo Atlanta.

Results & Discussion: Zoo Biomechanics Day was held Saturday, March 11th with the assistance of approximately 50 volunteers including students, faculty, and Zoo Atlanta affiliates. The goal was to highlight and compare the biomechanics of several species, with diversity ranging from a slingshot spider to tendons in humans to bio-inspired robotics based on snakes. Interactive stations also encouraged the public to compare their own human biomechanics to animals, such as trying to stand like a flamingo (Fig 1). In total, we hosted 8 lab groups from three universities, with 11 booths representing over 20 species with comparative biomechanics demos. An example of a demo is included below:

"The Many Uses of Elephant Trunks": This demo featured African elephant trunk biomechanics at Zoo Atlanta's elephant center. Keepers had the elephants perform elongation and shortening to display the mechanical capabilities and limitations of the trunk. During the demos, nearby research volunteers used various handhelds and visual displays to explain the biomechanics to the public. Zoo education staff were assigned to help explain the demonstration to younger audiences and discuss the conservation aspect of the zoo-research collaborations.

Zoo Biomechanics Day in 2023, as a single event, had an attendance of 8,241 members of the public spanning from toddlers to educators.

Figure 1: Zoo Biomechanics Day map with the locations of the 11 stations within Zoo Atlanta. Four example stations are shown in greater detail with images taken during the event.

Significance: Zoo Biomechanics Day marked the establishment of a new type of biomechanics event that utilized an existing research relationship between Georgia Tech and Zoo Atlanta. Zoos, botanical gardens, and aquariums can provide excellent opportunities for studying comparative biomechanics if academics foster effective relationships [6]. The success of this Zoo Biomechanics Day, with a total participation of over 8,000 for a single NBD event, encourages developing more collaborations with non-academic institutions to expand biomechanics research and achieve growing outreach goals.

Acknowledgements: We acknowledge the assistance from the 8 different PIs who volunteered to present their research and the 24 graduate and undergraduate research presenters. We thank the Zoo Atlanta education and interpretation staff for their assistance during Zoo Biomechanics Day. We thank Atlanta Science Festival's support and for providing volunteers for the event. Finally, we thank Zoo Atlanta, Georgia Tech, Atlanta Science Festival, and the festival's sponsors for funding the project.

References: [1] Devita P. (2018), *Journal of Biomechanics* 71(1-3). [2] Vogel S. (2013), *Princeton University Press* 113(110845). [3] Shultz et al. (2019), *Elsevier* 88(9). [4] Science ATL (2022), *2022 Festival Report* 18. [5] Science ATL (2023), *2023 Science Festival Booklet* 12. [6] Shriver et al. (2022), *Int. & Comp. Biology* 62(5).

DOES THE RELATIONSHIP BETWEEN WHOLE-BODY ANGULAR MOMENTUM AND STEP PLACEMENT CHANGE IN INDIVIDUALS POST-STROKE?

Jennifer K. Leestma[1,2*], Gregory S. Sawicki[1,2,3], Aaron J. Young[1,2]
[1]George W. Woodruff School of Mechanical Engineering, [2]Institute for Robotics and Intelligent Machines, [3]School of Biological Sciences, Georgia Institute of Technology
*Corresponding author's email: jleestma@gatech.edu

Introduction: Individuals post-stroke typically have impaired balance and are at an increased risk of falling [1]. Gaining a more thorough understanding of how balance recovery strategies are altered post-stroke could drive more effective rehabilitation strategies and improve the function of assistive devices for a post-stroke population. Here, we aimed to investigate how step width is modulated in response to frontal plane instability in neurotypical and post-stroke individuals. We hypothesized that H1) neurotypical individuals would display a weaker correlation between balance and step placement compared to post-stroke individuals, as post-stroke individuals typically have weaker ankles, which inhibit the ankle strategy that neurotypical individuals use to combat small perturbations. We also hypothesized that H2) correlations would be stronger for steps where the non-paretic limb is in stance in comparison to the paretic limb, due to the higher joint moment demand on the stance limb in comparison to the swing limb when making step width adjustments.

Methods: One post-stroke participant walked on a treadmill at 0.8 m/s while being exposed to ground translation perturbations. We applied 5 cm perturbations that varied in direction (anteroposterior, mediolateral) and onset timing (double stance; early, mid, late single stance). We applied each perturbation condition 3 times to the paretic and non-paretic limbs. We collected a full-body marker set and identified gait events using a kinematic method [2]. We calculated integrated frontal whole-body angular momentum (WBAM) using OpenSim and custom Matlab scripts. We calculated step width using the mediolateral distance between heel markers. We also used our previously collected open-source data set to provide 11 neurotypical participants with condition-matched perturbation trials for comparison [3]. We evaluated the correlation between integrated frontal WBAM and step width in the perturbed and recovery steps.

Results & Discussion: We expected low R^2 values for neurotypical individuals, as lateral ankle strategy is typically sufficient to combat minor amounts of instability whereas step width modulation is required for more severe perturbations. However, we still saw moderately strong correlations in the perturbed (R^2=0.46) and recovery (R^2=0.20) steps, which were roughly equal to or greater than the paretic and non-paretic comparison; this did not support H1. In the perturbed step, there is a stronger correlation in non-paretic stance steps (R^2=0.48) than in the paretic stance steps (R^2=0.27), supporting H2. However, in the recovery step, there was a stronger correlation in paretic stance steps (R^2=0.05) than in non-paretic stance steps (R^2=0), which does not support H2. These results are preliminary and only include a single stroke participant; we have collected and are analyzing additional post-stroke participants to incorporate in this analysis.

Significance: Understanding how individuals' balance and recovery strategies are affected following a stroke could enable therapy strategies that target more comparable balance responses to a neurotypical population. Additionally, uncovering asymmetries and insufficiencies in post-stroke balance recovery could help inform controllers for wearable robots that alter assistance between the paretic and non-paretic limbs or customize assistance to individual post-stroke users.

Acknowledgements: This work was supported by NSF NRT ARMS Program Award #1545287, NSF GRFP Award #1324585, NIH Director's New Innovator Award DP2-HD111709. Thank you to Dr. Yi-Tsen (Amy) Pan for her help with data collection.

References: [1] Weerdesteyn et al. (2008), *JRRD* [2] Zeni et al. (2008), *Gait Posture* [3] Leestma et al. (2023), *J Exp Biol*

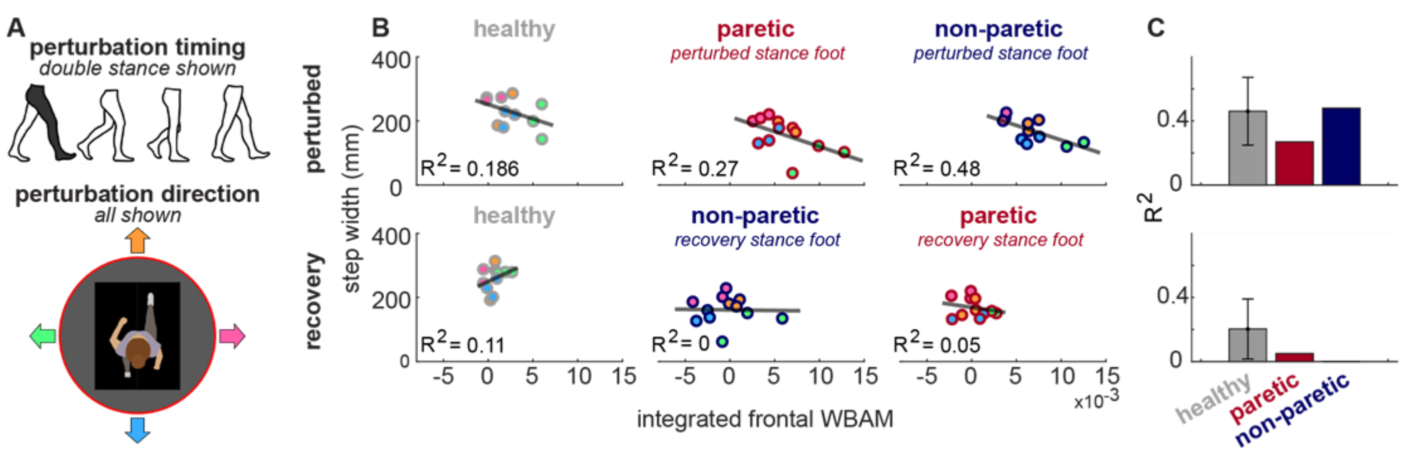

Figure 1: (A) Data shown in plots are for the double stance onset time across all perturbation directions. **(B)** Correlations between integrated frontal whole-body angular momentum (WBAM) and step width during the perturbed (top row) and recovery (bottom row) steps; grey outlines are for a representative healthy participant, red outlines indicate the paretic foot is in stance, navy outlines indicate the non-paretic foot is in stance. **(C)** The R^2 value for the relationships in the plots. The healthy group (grey) contains the mean and standard deviation for R^2 values from 11 participants, the paretic (red) and non-paretic (navy) data shows the R^2 value for a single stroke participant.

EMBEDDING ENTREPRENEURIALLY-MINDED LEARNING INTO UNDERGRADUATE RESEARCH EXPERIENCES

Kimberly E. Bigelow[1*]
[1]Department of Mechanical and Aerospace Engineering, University of Dayton, Dayton, Ohio, USA
*Corresponding author's email: kimberly.bigelow@udayton.edu

Introduction: Entrepreneurially-minded learning (EML) approaches have become common in the engineering classroom, and have also found their way into biomechanics education. The goal is to develop students who possess not only technical skills, but also an entrepreneurial mindset, which includes being curious, making connections, and creating values (the 3 C's) [1]. Entrepreneurially-minded learning has generally been integrated into formal course structures, particularly courses like engineering capstone design. However, almost any course can benefit from an EML approach.

After attending a Kern Entrepreneurship Engineering Network (KEEN) workshop on EML and Student Research, I was inspired to redesign the undergraduate research experiences I engage my biomechanics students in to better emphasize EML-infused activities. Here, I present the approach I took and the unexpected outcomes that came from trying this new approach.

Methods: Each semester I have approximately 10 – 15 undergraduate students engage in biomechanics research with me through a zero-credit research experience. Students generally devote approximately two hours per week to being in the lab, and we coordinate small groups of students to come to the lab at the same time, since because of the independent study nature of the course there is not a standing course meeting time.

While redesigning, I took a three-pronged approach to embedding EML into the research experience: 1) Students experienced EML through various, standalone activities that focused on one of the 3 C's, for example being assigned a Flipgrid video experience to give a "pitch" about what they bring to the lab; 2) Students experienced a more sustained semester-long deeper dive into EML when they participated in a shared experience of reading a common article and then were tasked with regularly incorporating and practicing the 3C's as they went step by step in building a presentation that would summarize the work; and 3) Students took ownership of individual initiatives based on their passions and ways they envisioned creating value for others, for example by coordinating an adaptive toy making event or alumni speaker series. In addition to the EML activities, students continued to do "traditional" research as well. Our course learning management site provided a structure, utilized in a rather unique way, that assisted with implementation of the various activities, especially when students were not all together as they would be in a course.

The developed activities and more information about the structure of the "course" and the implementation of the course learning management system have been made freely and widely available through the Engineering Unleashed website [2]. Through the piloting of this work, I received a KEEN Fellowship to continue to expand on, refine, grow, and disseminate this approach, which is currently underway.

Results & Discussion: The implementation of the new approach, to date, has resulted in some notable surprises and successes. Examples of student work and outcomes are also available through the Engineering Unleashed website [2]. Notably, the most impactful "prong" of the approach was the student-led initiatives – or "passion projects". Empowered by the freedom to pursue something they were passionate about, while being curious, making connections, and seeking to create value, my students truly became leaders of projects that far exceeded my expectations. Most of these initiatives were things that we might not have otherwise done through the lab, but that were very complementary to our lab's goals and desired outreach. For example, two students created a Black Biomechanics Seminar Series. Another small group started an adaptive toy making event to provide toys to our community-partners' clients. Another student created an Alumni Lab series, while another took the lead on our National Biomechanics Day event. These undergraduates elevated what we did in the lab and increased our impact substantially. They also seemed to feel more closely connected to the biomechanics field, and to each other through carrying out these activities. A record number of my undergraduates from the cohort participating in these activities pursued graduate programs in biomechanics.

One challenge of the approach is the PI effort that does go in to incorporating this approach and how this type of approach also can mean less time for students to engage in traditional research tasks. I have sought to find a balance, with my undergraduate students benefitting from the professional development and leadership opportunities related with the EML-type activities while also gaining skills through traditional data collections and analyses. Again, the benefits of the "extras" that have been generated by these students and what this has meant for the overall outreach of our lab at the university and the beyond have been notable.

The project is now in the stage of soliciting feedback from other PIs engaged with undergraduate researchers to see how they might envision adopting, and adapting, some of the developed activities.

Significance: Entrepreneurially-minded learning has received attention for the benefits it has for students as they learn to be more curious, make connections, and create value. Such an approach has not often been integrated into student research experiences, but has the potential to be beneficial if done so. With the materials described here being freely available, it enables those wishing to try such an approach to do so more easily.

Acknowledgements: The author is supported by the Kern Entrepreneurship Engineering Network (KEEN) through a KEEN Fellowship.

References: [1] LeBlanc et al. (2018), *IEEE Frontiers in Education Conference*; [2] EngineeringUnleashed.com

INTER-JOINT MONOSYNAPTIC FEEDBACK REDUCES SENSITIVITY TO PERTURBATION DIRECTION

Thendral Govindaraj[1*], Gregory S. Sawicki[1,2] , T. Richard Nichols[2]
[1] George Woodruff School of Mechanical Engineering, Georgia Institute of Technology, Atlanta, Ga
[2]School of Biological Sciences, Georgia Institute of Technology, Atlanta, Ga
*Corresponding author's email: tgovindaraj3@gatech.edu

Introduction: Most muscle spindle pathways are relatively localized, but some are inter-joint and asymmetric [1]. Inter-joint asymmetric pathways may play a role in regulating whole limb properties [2]. The goal of this study was to understand how asymmetric muscle spindle feedback influences limb impedance and inter-joint coordination (limb mechanics). Intrinsic impedance (inertia + musculoskeletal +feedforward activation at yield) follows a high proximal and low distal gradient. The masses of the limb segments and muscles also follow a high proximal to low distal gradient, matching the impedance gradient. Despite these strong coupled gradients, joint excursions across the cat hindlimb appear equally distributed over many conditions, such as up and down slope walking [3]. Cats have excitatory spindle pathways from the hip to knee and knee to ankle [1], leading us to hypothesize that these feedback pathways *increase* whole limb impedance and inter-joint coordination and *decrease* sensitivity to the direction of limb force perturbations.

Methods: To evaluate how inter-joint, asymmetric spindle feedback influences whole limb impedance and inter-joint coordination, we used a two joint, two segment model in Simulink with parameters taken from feline biomechanical [4] and neurophysiological data [5], with asymmetric spindle feedback modelled as off-diagonal stiffness and damping terms. We applied a varying direction ($\phi = -20^{\circ}\, to + 20^{\circ}$, [6]) sinusoidal endpoint force with an average value of 60N to the end of the distal segment. We fit 10 steady state cycles of the output to an impedance equation that includes apparent K, B, and M [7] and calculated the amplitude of the hip angle divided by the amplitude of the knee angle at steady state to evaluation proportionality of joint excursions.

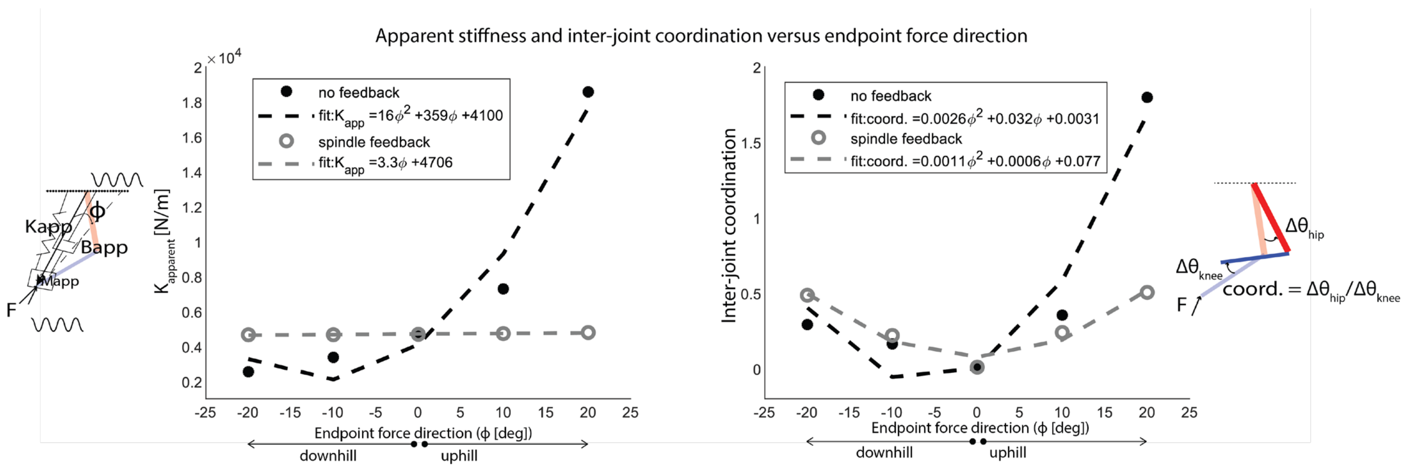

Figure 1: Apparent stiffness (left panel) and inter-joint coordination (right panel) versus endpoint force direction for no feedback (black) and spindle feedback (grey).

Results & Discussion: As shown in Figure 1, the apparent stiffness was higher with spindle feedback than with no feedback for endpoint force directions posterior to the hip (downhill). While the apparent stiffness changed significantly with respect to endpoint force direction (quadratic fit) without feedback, asymmetric spindle feedback caused the apparent stiffness to stay relatively constant (linear fit with high constant). Similarly, inter-joint coordination was higher with spindle feedback than with no feedback for endpoint force directions posterior to the hip (downhill). With no feedback, inter-joint coordination changed more significantly with respect to endpoint force direction than with spindle feedback (the first two quadratic fit parameters are higher without feedback). Therefore, in partial support of our hypothesis, asymmetric spindle feedback increases apparent stiffness and inter-joint coordination for endpoint force directions posterior to the hip and decreases sensitivity of both parameters to endpoint force direction.

Significance: Inter-joint coordination is important for maintaining muscles within their optimal (i.e., lengths best for force output) operating range of motion. Humans have extensive and bi-directional spindle pathways [8], so these pathways should be considered for diagnosis and treatment. Sensory pathways become disrupted after injury, and this leads to impaired inter-joint coordination (e.g., stroke [9]). Therefore, implementation of these feedback architectures in circuitry of assistive exoskeletons or FES support systems could better assist in recovery from injuries by providing adaptable forces and motions across many locomotor contexts.

Acknowledgements: I01 RX002316, R01 NS097781

References: [1] Eccles & Lundberg (1957), *J Physiol* 137(1); [2] Nichols, T. R. (2021) *Physics of Life Reviews* 37; [3] Abelew, et al. (2000), *J Neurophys* 84(5); [4] Hoy & Zernicke (1985), *J Biomech* 18(1); [5] Nichols & Houk (1976), *J Neurophys* 39(1); [6] Gregor, et. al. (2006), *J Neurophys* 95(3); [7] Rouse, et al. (2018), *IEEE Trans Neur Sys Rehab Eng* 22(4); [8] Pierrot-Deseilligny and Burke (2012) *The Circuitry of the Human Spinal Cord*: Cambridge; [9] Hsiao, et al. (2020), *J NeuroEng and Rehab* 17(1)

FOOT POWER DECREASES WITH RESTRICTED FIRST METATARSOPHALANGEAL JOINT RANGE OF MOTION

Adrienne D. Henderson[1*], Lauren R. Williams[2], Dustin A. Bruening[2], Elisa S. Arch[1]
[1]University of Delaware, Newark, DE; [2]Brigham Young University, Provo, UT
*Corresponding author's email: ahendo@udel.edu

Introduction: Osteoarthritis of the first metatarsophalangeal joint (1st MTP OA) is characterized by pain and a significant decrease in dorsiflexion range of motion [1]. This decreased dorsiflexion typically results in a rapidly off-loaded hallux and earlier toe-off during gait [1]. Common footwear treatments center on pain management by increasing padding as well as further limiting the MTP dorsiflexion motion [2]. However, this additional restraint likely affects mechanics of other foot joints and overall gait function. Specifically, recent research shows that the foot's MTP and midtarsal joints actively work together kinematically [3] and kinetically [4] to contribute to gait mechanics. Restricted MTP dorsiflexion range of motion may affect whole foot power, a critical component of forward propulsion. Foot power can be quantified either by summing rotational power across the joints of the foot or by calculating the net unified deformable (UD) power of all tissues distal to the hindfoot. The purpose of this study was to mimic the energetic implications of 1st MTP OA by restricting dorsiflexion, using this to probe whole foot joint and UD power. We hypothesized that this restriction would reduce propulsive power and that a comparison of methods would provide additional insight into foot energetics.

Figure 1: Markers for the multisegment foot as well as the brace used on the first metatarsophalangeal joint (ValguLoc II, Bauerfeind, Inc. Atlanta, GA, USA).

Methods: 26 healthy participants (age: 24.6±4.4yr, height: 1.74±0.09m, weight: 71.2± 10.7kg) walked across a 5.5 m walkway under two randomized conditions: with an unlocked brace on the left 1st MTP joint (UN), and with the brace locked with the joint in a neutral position (LOCK; Figure 1). A multisegment foot marker set was applied to the left foot and defined hindfoot, forefoot, and hallux segments separated by midtarsal and 1st MTP joints [5]. Participants walked at 1.3 m/s for both conditions while kinematic and kinetic (shear and pressure distributions) data were collected. A custom LabView code constructed separate segmental ground reaction forces for each foot segment before time normalized 1st MTP range of motion, unified deformable foot power, 1st MTP power, and midtarsal power were calculated in Visual 3D. Midtarsal and first MTP power were summed and peak positive and negative power as well as work metrics were extracted from all power curves. Paired t-tests compared all calculated metrics.

Results & Discussion: Peak 1st MTP dorsiflexion angle was significantly reduced by 6.7° ($p<0.001$) in the LOCK condition indicating that the brace successfully limited the 1st MTP range of motion during gait. Additionally, regardless of the method used for calculating power, foot positive power decreased in LOCK. When considering the individual joint rotational powers (Figure 2A), there was a decrease in MTP negative work ($p<0.001$) with a concomitant decrease in midtarsal peak positive power ($p=0.01$) in LOCK, which agrees with the reported theory of kinetic coupling between foot joints [4]. Interestingly, there is no change in the midtarsal negative work ($p=0.39$) in LOCK indicating that foot joint kinetic coupling may influence midtarsal positive but not negative power. This is also reflected in the decreased summed foot power ($p<0.001$, Figure 2B) and UD ($p=0.01$, Figure2C) peak positive powers in LOCK, with no significant difference in either negative power. The combination of these findings suggests that the foot acts more as a damper than a spring, potentially dissipating a greater portion of energy (rather than storing and returning that energy) as energy dissipation at the MTP joint decreases. However, it is impossible to distinguish between energy storage versus energy dissipation within the foot. Alternatively, altering MTP mechanics may inhibit the foot's ability to fully engage its active components and thus prevent energy generation within the foot.

Theoretically, the summed foot power and UD power curves should be very similar with only slight differences due to distal foot soft tissue mechanics. Despite this, there are larger than expected differences between power calculation methods, especially when considering negative power. This may indicate the continued need to include a multi-segment foot model when analyzing foot energetics.

Significance: Individuals with 1st MTP OA likely experience limited energetic contribution from the foot to propulsion in gait due to reduced foot positive power. However, the specific insights into foot energetics varied slightly by the analysis employed. Future research is needed to explain the discrepancy between summed foot power and UD power.

Acknowledgements: This work was supported by the National Science Foundation (Award #s: 2032155 & 2032190).

References: [1] Canseco et al. (2008), *J Orthop Res* 26(4); [2] Roddy et al. (2018), *Ther Adv Musculoskelet Dis* 10(4). [3] Sichting et al. (2021), *PLoS ONE* 16(4). [4] Takahashi et al. (2017), *Sci Rep* 7(1). [5] Bruening et al. (2012), *Gait Posture* 35(4).

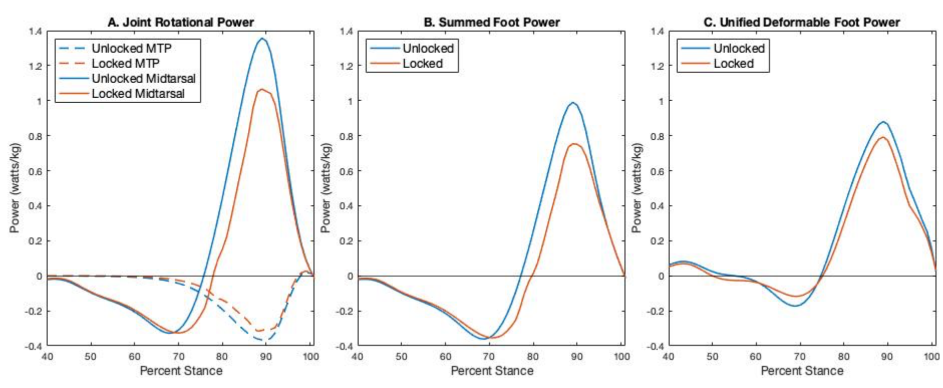

Figure 2 A) Unified deformable foot power B) The summation of midtarsal and MTP joint rotational power C) Individual foot joint rotational power for the midtarsal (solid) and MTP (dashed) joints under the UN (blue) and LOCK (orange) conditions for the last 60% of stance.

IMPACT OF TRICEPS-SURAE OPERATING LENGTHS ON WHOLE BODY METABOLIC COST

Jordyn N. Schroeder[1*], Owen N. Beck[2], Jason Franz[3], Gregory S. Sawicki[1]
[1]Georgia Institute of Technology, George W. Woodruff School of Mechanical Engineering
*Corresponding author's email: jschroeder9@gatech.edu

Introduction: Lower-limb exoskeletons have been shown to reduce metabolic cost of walking by reducing muscle-tendon (MT) force [1,2]. Even passive ankle exoskeletons that do not add net mechanical energy to the user have shown energy cost reductions [3]. These devices may reduce costs by altering MT dynamics of the largest contributor to ankle push off, the triceps-surae [4]. Previously, we showed that during isometric ankle plantarflexion, decreasing soleus fascicle operating length by 17%, increased metabolic cost by 208% [5]. These isolated muscle contractions indicate that increasing the force potential of calf muscle reduces the metabolic cost of producing force by reducing the volume of muscle activated to perform a task [6].

The purpose of this study was to determine the impact of shifting triceps-surae operating lengths, during walking, on whole body metabolic cost. We used modified footwear, to systematically shift incur more plantar-flexing and more dorsi-flexing via raised heels and raised toes, respectively. We hypothesized that force on the MT would increase in high heels and decrease in high toes due to shifts in COP [7]. We hypothesized that walking in raised heels would decrease triceps-surae operating lengths, leading to an increase in whole body metabolic cost compared to walking in flat shoes. Similarly, we hypothesized the raised toes would increase triceps-surae operating lengths, leading to a decrease in whole body metabolic cost compared to flat shoes.

Methods: We recruited n=7 in high toe group and n=8 in high heel group. We instrumented participants with B-mode ultrasound over the medial gastrocnemius (MG) and soleus (SOL) muscle belly, a full body 3D motion capture marker set, and a metabolic mask. Participants walked for 5-minutes at 0.5, 0.9, 1.3, and 1.7 m/s in both experimental and mass matched flat shoes on a dual-belt Instrumented treadmill. We randomized trial order.

Results & Discussion: Both high heels and high toes increased the metabolic cost of walking compared to mass matched flat shoes (Fig. 1A). As expected, heels decreased SOL and MG operating lengths and toes increased operating lengths (Fig. 1B). High toes increased calf MT peak forces by 8%, while high heels decreased forces by 21% (Fig. 1C).

As expected, raised heel shoes increased metabolic operating cost, and decreased triceps-surae operating lengths. Even though high heels decreased force demand on the calf MT, the decrease in force potential via less optimal operating lengths may drive the metabolic cost increases [5]. Contrary to our hypothesis, raised toes also increased metabolic cost of walking despite increasing triceps-surae force potential via longer operating lengths. Increased force demand may contribute to the overall raised metabolic cost.

These results highlight tradeoffs in force demand and force potential at the ankle. Further analysis of more proximal muscles and joints can provide insight on how changes in triceps-surae force potential impact whole body energy expenditure during walking.

Significance: Metabolic cost reduction is a key outcome measure for lower limb wearables. Increased understanding on how triceps-surae MT dynamics impact whole body energy cost can inform the wearables field on how to build better, more effective devices. Furthermore, insights on how force demand and force potential impact energy expenditure can guide device design, control, and interventions.

Acknowledgements: NIH Award Number R01AG058615.

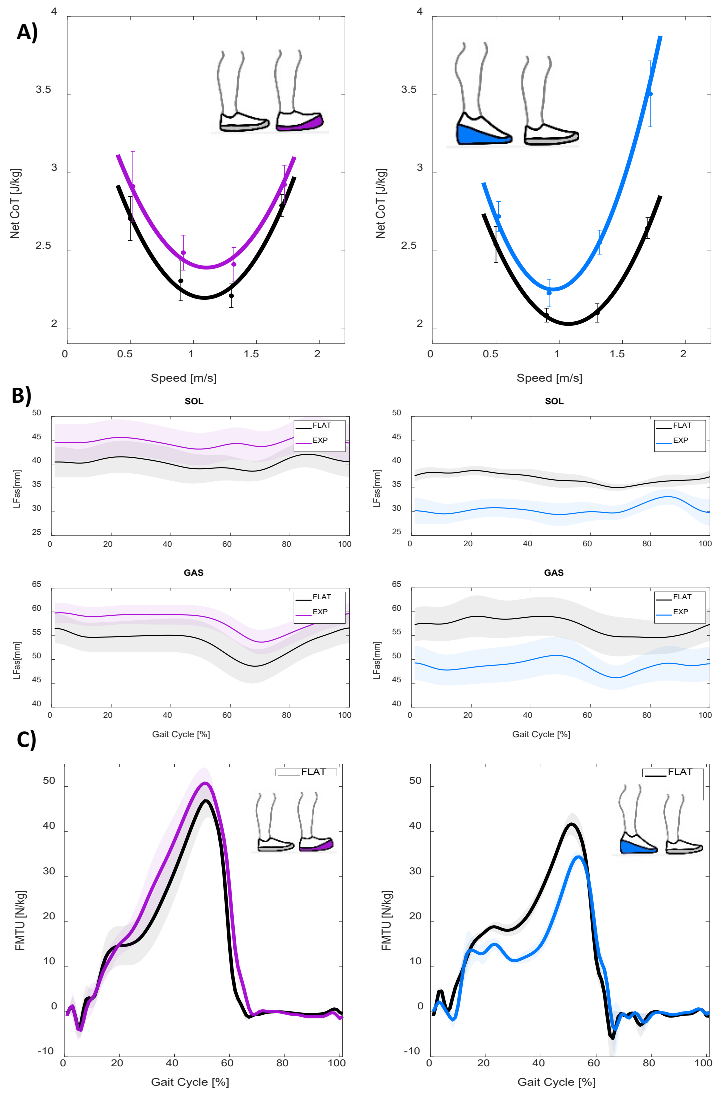

Figure 1: A) Metabolic cost of transport curves in toe shoes vs flat shoes (n=7) and heel shoes vs flat shoes (n=8)
B) Soleus and gastrocnemius fascicle operating lengths during walking in flat and modified shoes at 1.3 m/s, for toe group (n=5) and heel group (n=5)
C) Triceps-surae MT force in flat and experimental shoes at 1.3 m/s, for toe group (n=5) and heel group (n=5)

References: [1] Mooney and Herr (2016), *J NeuroEng Rehab* [2] Sawicki et. al (2020), *J NeuroEng Rehab* [3] Collins et al. (2015) *Nature* [4] Nuckols et. al (2020) *Sci Reports* [5] Beck et. al (2022), *JAppl* [6] Beck et. al (2019), *ESSR* [7] Shang et al. (2020) *J. Orthop. Surgery*

TOO MUCH EXOSKELETON “ASSISTANCE” CAN DISRUPT USER BALANCE CORRECTION

Rish Rastogi[1*], Kristen L. Jakubowski[1], Giovanni Martino, Owen N. Beck, Max K. Shepherd, Gregory S. Sawicki, Lena H. Ting[1]
[1]Walter H. Coulter Department of Biomedical Engineering, Emory University & Georgia Institute of Technology, Atlanta, GA, USA
*Corresponding author’s email: rrasto5@emory.edu

Introduction: Wearable robotics such as exoskeletons have the potential to enhance balance [1,2,3,4]. We previously showed that providing humans with ankle exoskeleton torque before muscle response in backward support surface standing balance perturbations could increase balance capacity. In large perturbations, 30 Nm of plantar-flexing exoskeleton torque provided to the user’s ankles reduced center of mass (CoM) kinematics, improving balance capacity [1]. However, it remains unclear whether such exoskeleton assistance improved balance following smaller perturbations. As users will experience a variety of perturbation outside the laboratory, appropriately tuning assistance magnitude is important for designing a controller for balance-improving wearable robotics. In this study, we sought to evaluate whether the amount of torque given before human response, beginning around 150ms after perturbation onset, affects balance in smaller balance perturbations.

Because these perturbations typically elicit an ankle strategy for balance recovery, we hypothesized that, given the same perturbation and timing of assistance, higher levels of ankle assistance would improve balance more than lower levels of assistance. Thus, we predicted that greater torque delivered before the muscle response would reduce CoM acceleration, velocity, and displacement more than a moderate amount of torque.

Methods: Ten healthy adults (26 ± 2 yrs) wore ankle exoskeletons (Dephy ExoBoot, Dephy Inc.) and were instructed to maintain standing balance during backward support-surface perturbations (Fig 1A). An accelerometer on the exoskeleton detected perturbation onset in ~40ms, after which the exoskeleton was commanded to either provide 15Nm or 30Nm of plantarflexion torque (50ms rise time, followed by a decline to 0 Nm over 150ms) immediately (*15Nm Fast & 30Nm Fast*) or to provide no torque (*Off*). To prevent adaptation to the magnitude of exoskeleton assistance, conditions were randomized. In all perturbations, the support-surface traveled 15cm over 500ms. To confirm the delivery of exoskeleton torque, center of pressure (CoP) displacement was calculated from force plate data 100ms after perturbation onset. CoM kinematics were calculated from recorded motion capture and force plate motion data. To separate immediate effects of exoskeleton torque (<150ms) and the later response of the nervous system after assistance (>150ms), the integral of acceleration & velocity was computed in two time-bins: 0-200ms (initial phase) and 200-500ms (later phase) following perturbation onset. Within-subjects repeated measures ANOVA statistics were run on to evaluate differences between conditions.

Results & Discussion: Considering CoM kinematics as a metric of balance performance, early exoskeleton assistance improved balance during the initial phase of perturbation. CoP was shifted anteriorly 1.7cm ± 0.8cm more in *15Nm* and 1.6 ± 1.0cm in *30Nm* compared to *Off* ($p<0.01$), confirming that torque was delivered earlier than human response. The integral of CoM velocity reduced by 2.45 ± 0.2 mm in *15Nm* and by 2.4 ± 2mm in *30Nm* compared to *Off* ($p<0.01$ & $p=0.03$); was no difference between *15Nm* and *30Nm* (Fig1B &C).

However, in some individuals, 30Nm of assistance made their balance worse, as evidence in the late phase (Fig 1B right vs left pane). In the *30Nm* condition, six participants had 5.5 ± 0.8 mm lower integral of CoM velocity (Fig1B, left) while 4 participants had 8.3 ± 0.6 mm higher integral of CoM velocity in the only (Fig1B, right). Comparing the 30Nm to the 15Nm condition, 6 poeple had 0.90±0.5 mm lower integrated velocity while 4 had 2.3±0.4 mm higher integrated velocity ($p<0.01$, Fig1B&D).

Significance:

Wearable robotics can actually have a negative impact on balance recovery if they provide too much assistance, and that this effect does not apply similarly to everyone.

The appropriate level of balance-correcting torque in response to perturbed balance may differ from person to person, possibly due to an increased reliance on hip strategy. If inappropriately high, torque may end up becoming a balance perturbation itself to the user.

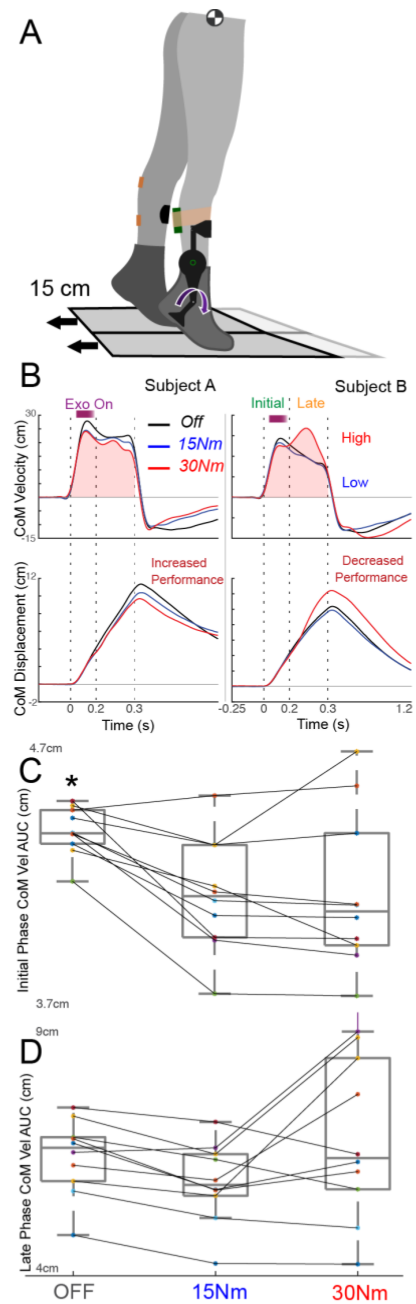

Figure 1: A) Experimental setup. B) CoM acceleration (top), velocity (mid), and displacement (bot) traces from two C) CoM travel in the initial and D) late phase for each condition. Each line represents a participant.

Acknowledgements: NIH F32 AG063460, R01 HD46922, R01 AG058615, R01 HD90642, R01 HD90642, McCamish Parkinson Disease Innovation Program

References: [1] Beck et al. (2023), *Sci Rob* 8(75); [2] Bayón et al. (2022), *Journal of NeurEngr & Rehab* 19); [3] Farkhatdinov et al. (2019) *IEEE Rob & Auto Let* 4(2); [4] Monaco et al. (2017) *Sci Rep* 7(1);

OFFSETTING THE LOAD: CAN EXOSKELETONS MITIGATE INJURY RISK DURING INDUSTRIAL LIFTING TASKS?

Felicia R. Davenport[1*], Jennifer K. Leestma[1], Christoph Nuesslein[1], Josh Fernandez[1], Raymond Kim[1], Ryan Casey[1], Jason Wheeler[2], Anirban Mazumdar[1], Aaron J. Young[1], Gregory Sawicki[1]
[1]George W. Woodruff School of Mechanical Engineering, Georgia Institute of Technology, Atlanta, GA, USA
[2]Sandia National Laboratories, Albuquerque, NM, USA
*Corresponding author's email: fdavenport6@gatech.edu

Introduction: Exoskeletons have been shown to reduce user joint loading [1] and metabolic cost [2] during manual labor tasks. These findings have influenced the slow adoption of such devices in workplaces where manual labor tasks that involve twisting and lifting high loads are associated with high worker injury rates [3]. Both active and passive commercial exoskeletons are designed to offset joint loading by providing assistive torque either in parallel or perpendicular to the body. Such assistance reduces user muscle forces and activations [4]. Previous research has proposed that joint kinematics, joint kinetics, and muscle activity can indicate injury predisposition; however, few studies have investigated how exoskeletons affect joint and muscle loading in manual labor tasks. Further, the impact of exoskeletons on internal joint contact forces is largely unknown due to the inability to measure *in vivo* and the complex computations required for estimation. Our experimental protocol addressed this gap by recreating industry-relevant lifting conditions in-lab to understand joint and muscle-level demands. We hypothesized that an active knee exoskeleton and a passive back exoskeleton will reduce user back and knee extensor muscle activity while performing assisted lifts versus unassisted.

Methods: Ten participants lifted a 11.3 kg. weight during a symmetrical (0°- no turn) and asymmetrical (90° - rotational turn) task which varied in starting and ending lift height (Fig 1A). The weight was lifted from knee-to-waist (KW) height (ascension) and waist-to-knee (WK) height (descension). Participants performed each task 10 times. Participants wore an active knee exoskeleton, a passive back exoskeleton (HeroWear), and a no-exoskeleton case. We collected ground reaction forces, a full-body marker set, 16 inertial measurement units (IMUs) for segment orientation, and surface electrodes to record muscle activity via electromyography (EMG). We analyzed our data using OpenSim 4.0 and custom MATLAB scripts.

Results & Discussion: Contrary to our hypothesis, we found that assistance from the passive back exoskeleton, HeroWear, reduced back flexor (rather than extensor) peak muscle activity (rectus abdominis) by ~5% during symmetric lifting (Fig 1B). Compared to unassisted lifting, HeroWear's passive assistance reduced peak net back flexion moments (~10% symmetric and asymmetric), lateral bending (~20% symmetric), and axial rotation (~40% symmetric, ~10% asymmetric) (Fig 1C). In support of our hypothesis, we found that the active knee device reduced the peak muscle activity in the knee extensor (rectus femoris) [5] by ~20% and ~10% in symmetrical and asymmetrical lifting, respectively (Fig 1B). The peak net knee flexor moment only showed a ~5% decrease in asymmetric lifting (Fig 1C). Changes in the net joint moments imply that participants used different overall kinematic strategies to perform the given tasks. The elastic band design of the HeroWear and rigid interface of the knee exo may have constrained users' movement to operate in the sagittal plane, thus altering their lifting strategies. In lifting with fixed foot placements, asymmetric lifting could induce rotation and shear about the joints. Constrained motion with devices may add out of plane stability to help mitigate risks in asymmetric motions.

Significance: Our research suggests that both passive back and active knee exoskeletons may be able to mitigate injuries during lifting tasks. However, internal loading within joints (i.e., contact forces) cannot be captured from these data alone. Ultimately, we intend to use information about the external joint loads, muscle activity, and kinematic patterns to compute knee and back joint contact forces and study whether they are influenced by exoskeleton design. Until then, the observed reduced muscle activity with exoskeletons indicates that muscle forces may also be reduced [6], potentially lowering internal joint loads during lifting tasks and further reducing injury risk.

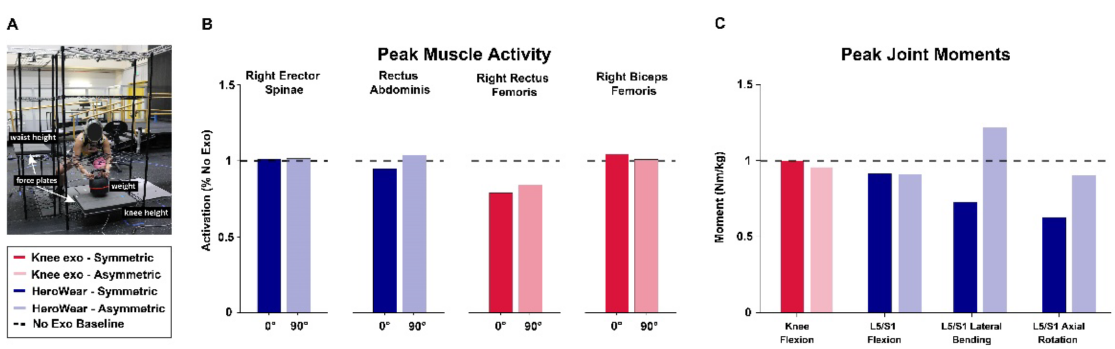

Figure 1: (A) Participant performing a lifting task. **(B)** Peak muscle activity normalized to the peak no exo muscle activity in symmetric (0°) and asymmetric (90°) lifting. **(C)** Peak net joint moments (exoskeleton + biological moments) in symmetric (0°) and asymmetric (90°) lifting. All values are normalized to the no-exo peak net joint moment. Each bar represents averaged ascension and descension conditions.

Acknowledgements: Supported by US Department of Energy (DOE), Sandia National Labs, DE-NA0003525.

References: [1] Kermavnar et al. (2020), *Ergonomics*; [2] Baltrusch et al. (2020), *Ergonomics*; [3] Matijevich et al. (2021), *Sensors*; [4] Medrano et al. (2021), *IEEE*; [5] Ranaweera et al. (2018). *JRNAL*; [6] Uhlrich et al. (2022), *Sci Rep*.

HOW TO IMPLEMENT WEARABLE ULTRASOUND FOR PROSTHETIC HAND CONTROL

Samuel A. Acuña*, Ahmed Bashatah, Siddhartha Sikdar
Department of Bioengineering, George Mason University, Fairfax, VA
*Corresponding author's email: sacuna2@gmu.edu

Introduction: Advanced upper limb prostheses, such as multi-degree-of-freedom prosthetic hands, are controlled by inferring a user's intentions (e.g., to grasp an object) to derive the control signals sent to the prosthesis actuators. Inferring user intent is typically done by assessing the residual muscle activities which arise from the descending motor commands that control the limb. Electromyography has become the primary clinical approach for evaluating residual muscle activity, which uses surface electrodes placed over the residual musculature [1]. However, surface electrodes can only examine a portion of the descending motor commands that control the residual limb, because the electrical activities of deep musculature are either not detected or diffused as cross-talk. Sonomyography, the ultrasound-based sensing of muscle deformation, is an emerging alternative sensing modality for upper limb prosthesis control [2]. Sonomyography enables spatiotemporal characterization of both superficial and deep muscle activity, making it possible to distinguish the contributions of a larger set of muscles when deriving prosthesis control signals. Previously, sonomyography was not feasible for prosthesis control due to high power requirements and large transducer sizes. However, our research lab has recently incorporated a new ultrasound imaging approach that borrows from techniques in the radar literature, which enables miniaturization of ultrasound instrumentation using low-voltage commodity hardware and low-frequency processing speeds [3]. We present a 4-channel wearable ultrasound system capable of tracking in vivo muscle interfaces that can feasibly be used to control a prosthetic hand (Fig 1).

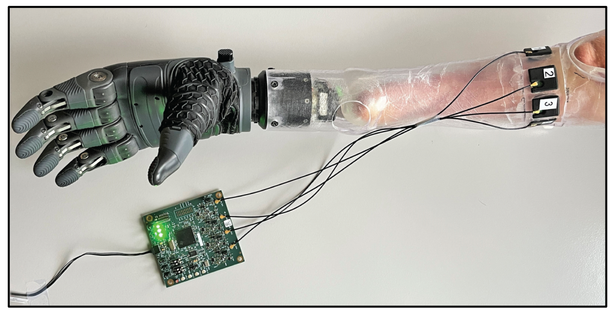

Figure 1: Controlling a prosthesis is feasible using a wearable sonomyographic system, as shown in our proof-of-concept prototype. The circuit board shown here contains all the ultrasound instrumentation and an embedded microprocessor to derive and send prosthesis control signals. Ongoing work includes embedding this instrumentation with a prosthetic socket for real-time testing during functional tasks.

Methods: Our implementation employs frequency-modulated continuous wave (FMCW) ultrasound imaging instead of conventional pulse-echo approaches. A key feature of FMCW imaging is the use of a linear chirp signal to encode the depth of ultrasound reflections as a range of frequencies, which bypasses the need to transmit short-duration high amplitude pulses to create a depth-resolved map of muscle tissue. Our system consists of a chirp generator, four single element ultrasound transducers (7mm diameter, 0.5 mm thick), a power regulation subsystem providing ± 5 V, and microprocessor for signal processing. Our system uses M-mode ultrasound images to assess the motion and timing of the internal structures, which are used to derive the prosthesis control signals (Fig. 2). We are currently using machine learning to recognize the patterns of user intent (analogous to pattern recognition for myoelectric control).

Results & Discussion: We anticipate that our implementation of low-power ultrasound imaging will serve as the foundation for future prosthetic and exoskeleton designs. One of the primary benefits of the sonomyographic sensing modality is that muscle activity can be sensed with high spatial specificity, even in deep-seated muscle compartments. This presents opportunity to derive more independent control signals than electromyographic sensing can provide. Our previous benchtop testing with able-bodied participants revealed that sonomyography can distinguish up to 15 unique hand grasps with 91% cross-validation accuracy [3]. The high spatial and temporal resolution of our approach shows promise for generating reliable control signals that are intuitively executed by the user and require minimal training. We found that transradial amputees could achieve 96% classification accuracy for 5 unique hand grasps after only a few minutes of training the algorithm [3].

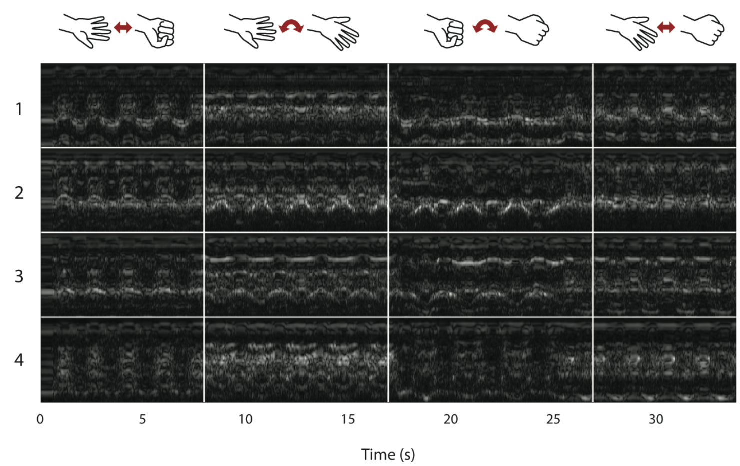

Figure 2: Example M-mode ultrasound images from the four single element transducers. Data is from an able-bodied participant cyclically performing hand open/close and wrist rotations. The cyclic motions are evident within the unique spatiotemporal patterns of tissue deformation.

Significance: Wearable ultrasound can now feasibly be implemented to control a prosthesis by analysing patterns of residual muscle activities. However, this technology could be applied to a broad range of applications, including exoskeleton control, muscle monitoring, wearables, and biofeedback devices.

Acknowledgements: This study is supported by NIH award 5U01EB027601 and CDMRP RESTORE award W81XWH2010817.

References: [1] Resnik et al. (2018), *Neuroeng. & Rehab.*; [2] Engdahl et al. (2022), *Front. Bioeng. & Biotech.*; [3] Acuña et al. (2022), *Myoelec. Contr. & Upper Limb Prosth. Symp.*

An investigation into seasonal changes of power and fatigue in collegiate baseball pitchers

Suzanne Konz[1], Chris Laple[2], Brand Anders[2]
Biomechanics, School of Kinesiology, Marshall University[1]
Athletic Training, Department of Orthopedics, Marshall University[2]
*Corresponding author's email: konz@marshall.edu

Introduction: Baseball pitching is a fatiguing process, not only for a single throwing session but over the season. As a complex and coordinated movement requiring a transfer of force throughout the whole body, the overall performance of a baseball pitcher is dependent on the ability to generate and transfer force onto a baseball at a high velocity (Lin et al., 2003). The overhand pitching motion in baseball is particularly susceptible to muscular fatigue, subsequent negative performance changes, and increased injury risk (Fortenbaugh et al., 2009). Muscular fatigue can drastically decrease performance and lead to serious injury if not regulated (Stone & Schilling, 2020). Muscular fatigue is the most common deterrent to continued performance, directly affecting the power output and resulting torque about the joint, impacting the consistency of throwing at high velocity during a single game and throughout a season (Oliver et al., 2016; Stone & Schilling, 2020). The impact of injuries occurs throughout all levels of baseball competition, and evidence of the need for consistent monitoring for muscular fatigue and power changes to determine the athlete's status. Current monitoring programs are not effective in detecting power changes and fatigue effectively. A more dynamic and whole-body approach to monitoring will better detect power changes and allow appropriate intervention. This study investigated the ability to detect fatigue-related performance decreases throughout a season using total body power-related measurements.

Methods: The isokinetic and field testing records of 21 male baseball pitchers (20.66 + 1.24 year; 1.88 + 0.07 m; 94.06 + 12.46 kg) from an NCAA Division I baseball team were accessed initially. The group consisted of 18 right-handed and 3 left-handed pitchers. Eighteen of the 21 participants were tested three times during the season and had their data included in this study, leaving 15 right-handed and 3 left-handed pitchers in the data set. Testing was done before preseason training, the start of the season, and before conference play. Participants performed three successful trials of the following hop tests: single-leg 6-meter hop jump, single-leg triple hop, and single-leg crossover triple hop. Participants performed the following medicine ball tests: seated medicine ball throw and kneeling medicine ball throw. Participants were tested using a calibrated isokinetic device (Cybex Humac Norm, Computer Sports Medicine, Inc., Stoughton, MA, USA) using the standing isokinetic shoulder internal (IR) and external rotation (ER) test. The isokinetic test consisted of 3 velocities of concentric testing in the order of 60º/sec, 180 º/sec, and 240 º/sec. Isokinetic and floor test variables were analyzed through a one-way analysis of variance with post-hoc testing to examine differences from baseline (October) throughout two in-season time points (January and March). All statistical analyses were performed using SPSS software (Version 26, SPSS, Inc., IMB Inc., Chicago, IL) with an a priori alpha level set at p # 0.05.

Results & Discussion: Our results provide insight into the relationships between field and isokinetic testing and athlete performance. Our hypotheses were that field, and isokinetic testing performance outcomes would decrease at each testing point. Statistical analysis determined that all testing outcomes decreased from October to March test points; not all decreases were significant. Field testing outcomes for the kneeling medicine ball throw and the 6-meter single-leg hop test of both legs decreased significantly. The distance the pitchers threw decreased from the initial test across the remaining test points in January and March for the kneeling medicine ball throw. Athletes significantly took longer to complete a 6-meter single-leg hop over the test points compared to the initial test in October. Multiple isokinetic outcomes at all three speeds significantly decreased at the testing time points.

Significance: Overall, this study determined that conducting field and isokinetic testing throughout the season can monitor the onset of fatigue by detecting decreases in testing measures. Using a combination of medicine ball throws, hop testing, and isokinetic testing at specific times during a season may provide insight into the overall fatigue level and injury risk within baseball pitchers. Routine monitoring of non-pitching-related testing measures is warranted and may add to the evidence to either rest the athlete or intervene with preventative treatment.

References: [1] Fortenbaugh et al. (2009) *Sports Health*; [2] Lin et al. (2003) *J Chinese Inst Engineers;* [3] Oliver et al. (2016) *J Str & Cond Res;* [4] Stone & Schilling (2020) *J Str & Cond Res;* [5] Urbin et al. (2013) *Amer J Sports Med.*

COMPARISON OF TWO FOAM SURFACES ON POSTUROGRAPHY OUTCOMES

Kimberly E. Bigelow[1*], Ajit M.W. Chaudhari[2], Daniel M. Merfeld[3]
[1]Department of Mechanical and Aerospace Engineering, University of Dayton, Dayton, Ohio, USA
[2]School of Health & Rehabilitation Science, The Ohio State University, Columbus, Ohio, USA,
[3]Department of Otolaryngology, The Ohio State University, Columbus, Ohio, USA
*Corresponding author's email: kimberly.bigelow@udayton.edu

Introduction: The inclusion of a foam pad for balance testing is important as it challenges balance by reducing somatosensory input; by manipulating the sensory inputs contributing to balance, underlying deficits can be revealed. When an individual is standing on a foam pad with their eyes closed, their resulting balance is largely attributable to their vestibular function and poor performance on this testing condition may provide particular insight. The 2001-2004 National Health and Nutrition Examination Survey (NHANES) currently serves as one of the largest (n > 5,000) and most compelling studies regarding the relationship between balance and falls [1]. The study found that individuals who were unable to successfully balance with eyes closed while standing on a foam pad had an odds ratio of 6.3 for having trouble with falls. The strength of these findings suggests the NHANES balance protocol be a model for the field, particularly as a detailed manual covering all aspects of the testing protocol is available on the CDC website [2]. However, to date, the foam specified for the NHANES protocol does not seem to be commonly utilized in balance testing. While there is an overall lack of standardization in foam choice, a commercially-available foam pad commonly used for balance training and rehabilitation (Airex™ balance pad) has been widely utilized in testing. The objective of this work was to compare posturography outcomes while standing on these two foam surfaces, with a focus on the "vestibular" testing condition, in order to provide guidance for future balance testing protocol development. A secondary objective was to determine if there was a correlation between body mass and postural sway and if so, how this differed between the foam pads. It was hypothesized that individuals would experience increased sway on the NHANES foam because of the memory foam like nature of the pad that can create inconsistent perturbations as individuals "sink" into the foam. Because of this, it was also hypothesized that there would be a greater relationship between body mass and sway on this foam pad.

Methods: Participants completed a balance assessment as part of two larger study protocols. During the assessment, participants completed a series of balance testing conditions while standing on a force plate in a narrowed stance with arms across their chest. Each trial lasted 60 seconds. For the eyes closed, foam pad condition, participants stood in a random order on the Airex balance pad (Airex Balance Pad Standard, 16" x 20" x 2.5") and the NHANES memory foam pad (Sunmate™ medium density foam pad, 16" x 18" x 3" with washable cover). If they could not complete their first attempt, a second attempt was allowed. A total of 93 individuals, aged 18 – 84 (mean age: 30.52 ± 14.5 years old, mean body mass: 73.87 ± 17.5 kg) attempted this testing condition. Data was collected from a force plate (Bertec Corp., Columbus OH) at 1000 Hz and filtered with a fourth-order low-pass Butterworth filter with 20 Hz cut-off. Based on past findings, Medial-Lateral (M/L) and Anterior-Posterior (A/P) Root Mean Square (RMS) were calculated as the primary outcomes of interest. SPSS statistical software was used to conduct a linear Mixed Model analysis ($p<0.05$). Correlations between body mass and sway outcomes for each foam pad were also examined using Pearson correlation coefficients.

Results & Discussion: Contrary to the hypothesis, it was found that while RMS outcomes were slightly higher on the NHANES foam as compared to the Airex foam, there were no significant differences (Table 1). The number of participants who were unsuccessful completing the test were comparable (n=7 for the NHANES foam; n=5 for the Airex foam). Pearson correlation coefficients for body mass and RMS were higher on the NHANES Memory foam (M/L RMS, r=.249; A/P RMS, r=.383) than Airex foam (M/L RMS, r=.180; A/P RMS, r=.155), as hypothesized; however, these low coefficients suggest that body mass is not highly correlated with balance performance on either foam pad. While prior research suggests that the choice of foam may matter in balance testing [3], these findings suggest that for these two strong candidate foams, researchers and clinicians may choose their preferred foam pad when interested in the "vestibular" condition across a diverse population.

Significance: These findings guide future balance assessment and provide guidance for researchers and clinicians seeking to determine what foam pad to use. Because there were no significant differences in sway between the Airex foam pad and the NHANES foam pad, and neither were highly correlated to body mass, researchers and clinicians could choose either of these strong candidate foams. However, we do highlight the underlying need for clearer reporting of all protocol choices in balance testing, including specifications of the foam used.

Acknowledgements: This work is supported by funding through grants from CDMRP (#W81XWH1920003) and NIH (1 R01 AG073113-01).

References: [1] Agrawal et al. (2009), *Arch Int Med* 169(10); [2] NHANES Balance Procedures Manual: http://www.cdc.gov/nchs/data/nhanes/ba.pdf; [3] Gosselin and Fagan. (2015), *Chiropr Man Ther 23*

Table 1. Results for the Eyes Closed, Foam Pad ("Vestibular") Testing Condition

	Airex Foam Pad	NHANES Foam Pad	Sig.	Effect Size (Cohen's d)
M/L RMS (mm)	11.535 ± 2.77	12.329 ± 3.21	.232	.26 (small)
A/P RMS (mm)	11.511 ± 2.71	12.619 ± 4.54	.134	.30 (small)

THE INFLUENCE OF STOCHASTIC VIBRATORY STIMULATION ON BALANCE RECOVERY

Karam Elali[1], Mehran Asghari[1], Alexis Sullivan[1], Nima Toosizadeh[1,2*]
[1]Department of Biomedical Engineering, College of Engineering; University of Arizona, Tucson, Arizona, USA
[2]Arizona Center on Aging, Department of Medicine, College of Medicine, University of Arizona, Tucson, Arizona, USA
*Corresponding author's email: ntoosizadeh@arizona.edu

Introduction: Human balance is a complex mechanism that involves sensory units, muscle reflexes, and the central nervous system. Among older adults, falls are the primary cause of traumatic injuries, and the leading cause of falls is tripping [1]. Strong evidence shows that proprioception deficits are highly associated with poor balance recovery [2]. Based on muscle activity assessment, previous research suggests that proprioceptive signals from the proximal musculature associated with the hip joint are responsible for initiation of the recovery response, while distal proprioception associated with the ankle joint is responsible for completing the recovery step [4]. All these conclusions are based on the hypothesis that muscle activity onset is directly associated with proprioceptive performance. In this regard, a methodology for directly manipulating proprioceptive performance would provide more insights regarding the contribution of each proprioceptive area (ankle vs. hip) on balance control. Stochastic vibratory stimulation (SVS) applied to lower extremity have shown effects on upright balance sway, because mechanical vibration of muscle can increase excitement of type Ia afferents in spindles. This extra excitement can influence both the short-latency reflexive mechanism and long-latency feedback to the central nervous system [3]. The goal of the current study was to identify the effects of altering proprioceptive information from the ankle and hip muscles on balance recovery. By altering the joint muscle proprioceptive performance using SVS applied to muscles corresponding to each joint, we investigated the individual contribution of ankle and hip proprioceptive information in balance recovery among a healthy young sample. We implement a modified treadmill setup to impose a trip-like perturbation and study the kinematics behaviours (Figure 1) in response to this perturbation. We hypothesized that SVS would affect balance recovery, with different effects when applied at the ankle compared to the hip musculature.

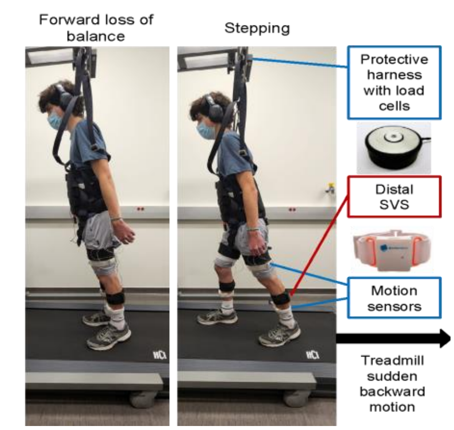

Figure 1: Treadmill trip-like perturbation.

Methods: 20 healthy young participants (18-30 years) were recruited, which were exposed to either ankle (n=10, five males and five females) or hip stimulation (n=10, four males and six females). Participants went through 15 trials of treadmill perturbation within three bouts (No stimulation, 40 Hz and 80 Hz vibrations). Each bout includes five randomized order of treadmill speeds (two with max speed at 0.35m/s and two with f max speed at 0.7m/s, reaching the max speed in 40 msec). Three-dimensional acceleration and angular velocity of shins, thighs, and the trunk were measured using five motion sensors. Balance recovery outcomes included response time, recovery step length, and required time for full recovery (time to reach steady-state walking based on standard deviations of stride times). Repeated measures mixed effects model was used to examine the association between balance recovery outcomes and vibration conditions.

Results & Discussion: Ankle SVS elicited main effects on reaction time and recovery step length (p<0.002). Reaction time increased by 21.2% on average with no significant difference between the 40 Hz and 80 Hz at the slow speed and increased by 24.8% for the fast speed with a significantly greater increase for 80 Hz in comparison to 40 Hz frequency. Hip SVS only elicited significant increase in the full recovery time and showed an increase of 61.4% for 40 Hz and 99.7% for 80 Hz for the slow speed. Similarly for the fast speed, full recovery time increased by 30.8% for 40 Hz and 29.2% for 80 Hz SVS (p=0.019). As hypothesized, the main finding of this study was that local SVS on ankle and hip muscles significantly influence recovery performance among healthy young adults. Within our sample, SVS caused a negative impact on the balance recovery performance, which was observed as a delayed reaction time when the stimulation was applied to the ankle muscles. Further, our findings suggest that SVS on the hip joint may compromise balance refinement after the recovery stepping.

Significance: Current findings demonstrated the role of ankle and hip muscle proprioceptive information in balance recovery. Our next step is to test SVS on older adults who are at high risk of fall. Our hypothesis is that SVS improves balance recovery by enhancing the proprioceptive afferent signal. This is based on our previous work showing that SVS can improve upright standing balance and timed-up-and-go test among high fall risk older adults [5,6]. This will ultimately guide us to engineer an easy-to-use sleeve/device that would help high fall risk older adults in performing strenuous tasks.

Acknowledgements: This project was supported by a grant from the Acceleration for Success (AFS) program at the University of Arizona. The views represented in this work are solely the responsibility of the authors and do not represent the views of sponsors.

References: [1] Gillespie et al. (2009), *Prevention of falls and fall-related injuries in older people. Injury Prevention* 15(5); [2] Flanders et al. (1992), *Early stages in a sensorimotor transformation 15(2)*; [3] Burke et al. *(1976), The responses of human muscle spindle endings to vibration during isometric contraction 261(3)*; [4] Čapičikova et al. (2006). *Human postural response to lower leg muscle vibration of different duration. Physiological research.* [5] N Toosizadeh et al (2018), *Proprioceptive impairments in high fall risk older adults: the effect of mechanical calf vibration on postural balance* 17; [6] N Toosizadeh et al (2020), *The effect of vibratory stimulation on the timed-up-and-go mobility test: a pilot study for sensory-related fall risk assessment* 69(4).

STOCHASTIC RESONANCE INFLUENCES HEAVINESS PERCEPTION

Alli A. Grunkemeyerr[1*], Aaron Likens[1], Joel Sommerfeld[1]
[1]University of Nebraska at Omaha, Department of Biomechanics
*Corresponding author's email: agrunkemeyer@unomaha.edu

Introduction: Heaviness perception is the ability to use haptic feedback from effortful touch to determine the weight of a wielded object [1]. When an object is wielded, torques and moments of inertia are produced. The inertia tensor provides information about how mass is distributed in a rigid body. The corresponding eigenvalues and eigenvectors of the inertia tensor have been related to an object's perceived magnitudes (e.g., weight) and directions (e.g., orientation with respect to hand), respectively (Fig 1) [2]. In this study, we sought to improve the perception of an object via wielding. Recent studies have provided evidence that adding noise to a weak stimulus can enhance a person's ability to detect it [2]. Introducing a subthreshold stimulus embedded with noise may, in some cases, improve sensations gained from limb movements [1]. Due to previous literature supporting gait and posture related benefits attributed to the stochastic resonance phenomenon, we hypothesized that subthreshold noise of various statistical structures and mass will influence accuracy in perceiving heaviness of a wielded object.

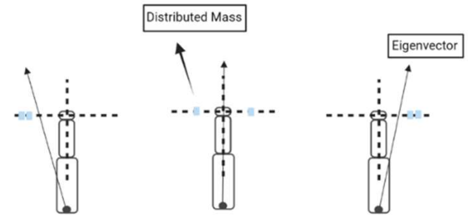

Figure 1. Effect of varying mass loads on eigenvectors.

Methods: Ten adults (above 19 years of age) were seated for the duration of the trial with a haptic device fastened to their wielding arm, as seen in Figure 2. Subjects wielded an occluded object with varying masses. Subthreshold stimuli were introduced via a haptic device with different signals of colored noise, or signals produced by stochastic processes varying in power spectral slope. Noise (3) × mass (4) combinations were presented. Subjects rated the heaviness of the object in relation to a standard object by marking their perceived heaviness on a scale presented at the end of each trial. We calculated the percent error based on the physical scale markings. For statistical analysis, we fit a series of linear mixed effect (LME) models with percent error as the outcome variable and fixed effects of mass, noise, and their interaction. Subsequent models were compared by likelihood ratio tests for model improvement.

Results: The best fitting model included all three terms, [$\chi^2(2) = 9.6415$, $p = 0.0081$]. Overall, the model produced an $r^2 = 0.378$ and an ICC = 0.34, suggesting that 38% of the variability in percent error is explained by the model, with 34% explained by the individual differences. A simple slope analysis was used to understand the interaction and revealed that the relationship between mass and percent error depended on noise. For the no noise and pink noise conditions, percent error decreased with increasing mass (Estimate = -0.227, CI = -0.5271 – 0.0731; Estimate = -0.229, CI = -0.592 – 0.0710, respectively). In contrast, the white noise condition produced a positive relationship (Estimate = 0.347, CI = 0.0468 – 0.6470). Comparing across conditions, we found slope relating mass and percent error did not differ between pink noise and no noise (Estimate = 0.00211, p = 0.9999). However, that relationship did differ between white noise and no noise (Estimate = -0.57389, p = 0.0230), as well as between white noise with pink noise (Estimate = -0.576, p = 0.0224).

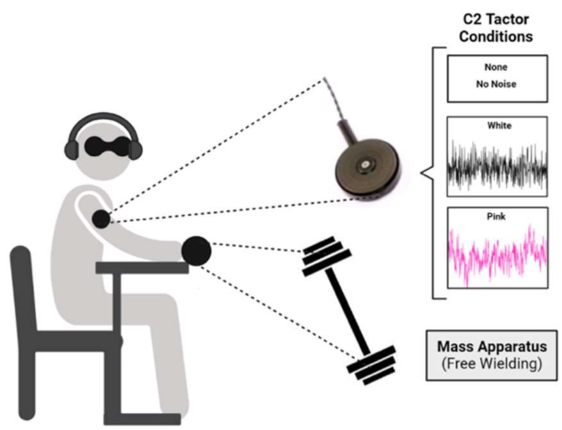

Figure 2. Experimental set up.

Discussion: As a general summary of the results, we found that percent error decreased as a function of mass in the no noise and pink noise conditions, at nearly identical rates. In contrast, the white noise condition produced qualitatively different results such that the presence of white noise appears to degrade one's ability to perceive weight, especially at larger masses. Hence, as we predicted, our results suggest that introducing subthreshold noise influences one's ability to perceive the weight of an occluded object. Importantly, the direction of influence depends on the statistical structure of the subthreshold noise. Somewhat contrary to our predictions, pink noise does not appear to influence the relationship between mass and percent error.

Significance: In the near future, we aim to replicate the finding concerning white noise while providing insight into the ineffectiveness of pink noise. One possibility for the findings concerning pink noise is that all subjects were young, healthy adults. So, we will include clinical groups that have altered sensitivity to test the generality of our current results. Other next steps involve including a larger range of masses added to the apparatus while varying locations of subthreshold stimulation.

Acknowledgements: This research was supported by an UNO GRACA to AG, and NASA Nebraska Space Grant FY23 Fellowship to AG.

References:
[1] Pagano et al. Journal of Applied Biomechanics, 14: 331-359, 1998.
[2] Nozaki et al. Physical Review Letters, 82: 2402-2405, 1999.

REPRODUCIBILITY OF GAZE AND MOVEMENT ASSESSMENT OF UPPER LIMB FUNCTION

Samuel Acuña[1*], Maddie Krotine[1], Gabriel Gibson[1], Quinn Boser[2], Jacqueline Hebert[2], Siddhartha Sikdar[1]
[1]Biomedical Imaging Laboratory, George Mason University, Fairfax, VA
[2]BLINC Lab (Bionic Limbs for Improved Natural Control), University of Alberta, Edmonton, AB
*Corresponding author's email: sacuna2@gmu.edu

Introduction: Functional assessments are often used to evaluate upper limb performance and track improvement during rehabilitation [1]. However, current clinical assessments may not adequately capture or evaluate the subtle differences in performance that underlie hand-object interaction, such as joint and trunk movements and hand-eye coordination. Quantifying these features may be essential to fully understand visuomotor behavior and develop new clinical treatment methods. For example, comprehensive measures of upper limb performance during object manipulation tasks could inform the design and control of new upper limb prostheses [2]. Recently, a Gaze and Movement Assessment (GaMA) protocol was developed at the University of Alberta that uses motion capture and eye tracking to quantify how participants move objects during functional tasks [3]. This protocol shows promise for accurately quantifying hand function, trunk and joint kinematics, and visuomotor behavior. The purpose of this study was to examine the reproducibility of the GaMA protocol at a new testing site.

Methods: We recruited 10 able-bodied participants (9 male, 1 female) to perform the GaMA protocol within the Biomedical Imaging Laboratory at George Mason University. Participants were fitted with markers on their head, limbs, and trunk for a full-body motion capture system (OptiTrack, NaturalPoint, Corvallis, OR). Participants also wore an eye tracking system (Pupil Core, Pupil Labs GmbH, Berlin, Germany) to record gaze and pupil dilation (Fig. 1). The protocol involved two functional tasks: relocating a pasta box between a side table and tiered shelves in front of the participant, and transferring a deformable cup filled with beads over a barrier on a tabletop [4]. Participants repeated each task 20 times to fully account for variability in their performance. Duration, hand movement, angular joint kinematics, and eye gaze measures were calculated for each trial. Summary outcome measures were then compared against the normative data collected at the Univ. of Alberta.

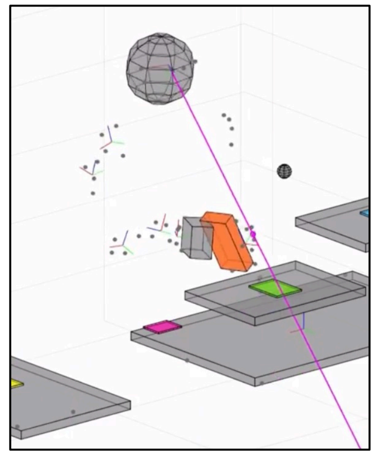

Figure 1: Gaze and motion data of a participant moving a pasta box (orange) to a target (green) while looking at the target (purple line).

Results & Discussion: We collected 200 repeated trials for each object manipulation task. The functional outcomes recorded fell within the acceptable bounds of normative data defined by the University of Alberta, confirming we could successfully execute the complex protocol at George Mason University (Table 1). The movement and duration parameters did not show any bias, but the eye fixation parameters were slightly lower (not significant) in our experiments compared to the normative values recorded by the University of Alberta. These results are consistent with a previous reproducibility study across two independent groups of non-disabled participants [3], supporting the utility of the GaMA protocol as a valid assessment of upper limb function.

The GaMA protocol is designed to evaluate the intuitiveness of grasp control during object manipulation. George Mason University will soon recruit individuals with upper limb loss to compare grasp control using different prosthetic hand control strategies, and the reproducibility data we collected will be used as a comparative normative dataset.

Significance: Many performance measures focus on outcomes (e.g., completing the task) and might not account for any compensatory movements or mental fatigue associated with performing the task. The GaMA protocol measures task performance in many domains (e.g., trunk kinematics, gaze fixation, range of motion, etc) to capture the subtle differences in performance that represent a user's experience. Normative data resulting from using the GaMA protocol with non-disabled participants will support future assessments for participants with upper limb loss.

Acknowledgements: This study is supported by NIH award 5U01EB027601.

References: [1] Velstra et al. (2011), *PM&R*; [2] Hebert et al. (2019), *JAMA Network Open*; [3] Williams et al. (2019), *PLOS One*; [4] Valevicius et al. (2018), *PLOS One.*

Table 1: Representative summary measures of normative data for a cup transfer task, one of the functional tasks. *Note: "Current" refers to the current area of interest as the task is executed, such as the cup or target location.*

	Movement Duration (seconds)		**Eye Fixation to Current (%)**	
	GMU	UofA	GMU	UofA
Reaching	0.69 ± 0.15	0.64 ± 0.10	73.3 ± 19.9	80.8 ± 11.3
Grasping	0.25 ± 0.11	0.20 ± 0.05	78.3 ± 26.6	86.3 ± 19.4
Transport	1.04 ± 0.20	1.01 ± 0.10	74.8 ± 14.1	82.9 ± 10.8
Release	0.27 ± 0.09	0.30 ± 0.07	49.5 ± 22.1	65.0 ± 20.2

FEMALE ATHLETE JOINT COORDINATION IS UNSTABLE DURING THE ECCENTRIC PHASE OF A JUMP LANDING

Kayla M. Kowalczyk[1*], Eric J. Shumski[1], Robert C. Lynall[1]
[1]UGA Biomechanics Laboratory, Department of Kinesiology, University of Georgia, Athens, GA, USA
*Corresponding author's email: Kayla.Kowalczyk@uga.edu

Introduction: Jump landings play a critical role in many sporting activities and the force from ground impact may reach values more than 4.5 times an individual's body weight [1,2]. Many lower extremity injuries, such as an anterior cruciate ligament tear, have been linked to the rapid deceleration involved in dissipating forces and the change in direction (transition from eccentric to concentric phases) during the landing portion of the jumping task [3]. Previous studies examined lower extremity biomechanics during a jump landing task and found that altered mechanics increased injury risk [4]. Proper coordination and mechanics of the lower extremity joints are essential to performing the landing task and attenuating high impact forces. Although peak and initial ground contact joint mechanics have received extensive analysis, understanding joint coordination during a jumping task may provide greater insights as to why rapid deceleration and change in direction places an athlete at risk for injury.

Continuous relative phase (CRP) and the variability of this value (CRP_V) have been used to analyze joint coordination and stability during movements from a dynamic systems perspective [5]. The CRP value provides information about whether two segments are moving in-phase or out-of-phase with each other. CRP_V provides information about the variability (stability) of coordination, or rather, the ability to repeat the same coordination pattern. Lower extremity sagittal plane coordination patterns and stability may play a role in the deceleration (eccentric) phase during a jump landing task [3] that has been linked to lower extremity injuries.

The purpose of this study was to examine how sagittal plane CRP_V differs between the eccentric and concentric phases of the jump landing task. Due to the increased risk for injuries during eccentric movements, we hypothesized that the eccentric phase of the jump landing would have a larger sagittal plane CRP_V, and thus decreased stability, compared to the concentric phase.

Methods: Twenty-two Division I female athletes (64.4 ± 9.2 kg, 170 ± 10 cm; soccer: 68%, gymnastics: 18%, volleyball: 14%) without a self-reported history of lower extremity injury or concussion were included in the analysis. Each athlete completed three jump landing trials. The athletes started on a 30 cm box half their height away from two force plates. They were instructed to jump forward with both feet, land on the force plates, and then immediately jump vertically as high as possible. Landing phase was defined as initial force plate contact (> 20 N) until take-off for the maximum vertical jump (< 20 N).

An 8-camera Qualisys system recorded kinematic data at 240 Hz. Kinetic data were collected from two Bertec force plates at 1200 Hz. We used Visual 3D and MATLAB to process raw data and calculate sagittal plane thigh-shank and shank-foot CRP_V of the dominant limb according to Hamill et al. [5]. The eccentric phase of the jump landing was defined as initial contact to maximum knee flexion while the concentric phase was defined as maximum knee flexion to take-off. CRP_V values were averaged across the three trials for each phase. We performed one-way repeated measures ANOVAs in R to compare the phases (*a priori* alpha 0.05)

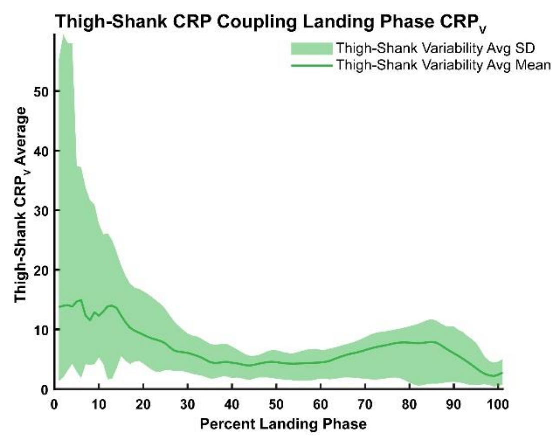

Figure 1: Thigh-Shank CRP_V Across the Landing Phase. 0 = no variability.

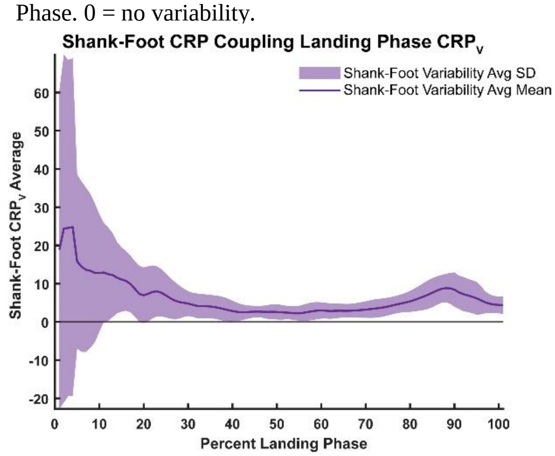

Figure 2: Shank-Foot CRP_V Across the Landing Phase. 0 = no variability.

Results & Discussion: There were significant CRP_V differences between phases for the thigh-shank ($p = 0.002$, Cohen's $d = 0.75$, Figure 1) and the shank-foot ($p = 0.019$, Cohen's $d = 0.54$, Figure 2) couplings. Joint coordination during the eccentric phase was significantly more variable (unstable) than during the concentric phase. Both sagittal plane couplings displayed this decreased stability early in the eccentric phase. The lower extremities must dissipate a large amount of force to change direction during a jump landing. A combination of increased internal muscle forces and an unstable, significantly more variable coordination environment may explain the increased risk of injury during the eccentric phase. Perhaps the large forces may be more injurious if coordination patterns are more variable. With decreased stability and increased force, the structures around a joint may fail.

Significance: Our results suggest that the eccentric phase of the jump landing task is significantly more unstable than the concentric phase. Future research should examine how joint coordination stability relates to previous injury history and how stability changes when athletes return to play following injury. A prospective approach may help determine if significantly more variability is an injury risk factor in landing tasks.

References: [1] Dufek & Bates (1991), *Sports Medicine* 12(5); [2] McNair & Prapavessis (1999), *J Sci Med Sport* 2(1); [3] Borden et al. (2000), *Orthopedics* 23(6); [4] Hewett et al. (2005), *Am J Sports Med* 33(4); [5] Hamill et al. (1999), *Clin Biomech* 14(5)

Does step descent while wearing a mask influence muscle activity?

[1] Kaitlin Kremsky and [1] Emily Gerstle
[1] University of Scranton, Scranton, PA, USA
email: emily.gerstle@scranton.edu

INTRODUCTION: Information from the field of vision allows for the safe navigation of steps. Steps are frequently encountered throughout many activities of daily living. Decreasing the visual field while descending a staircase creates an increased risk of injury, as vision influences step descent [1]. A study by Klatt et. al 2021 examined that while wearing a face mask, your lower visual field is compromised. When participants descended a five-step staircase in a step-over-step (SOS) pattern with a full view of the steps, there were muscle activity differences between steps [3]. A study by Thomas et. al (2020) demonstrated increased co-activation when descending four different staircase scenarios in SOS with basketball goggles obstructing the view of the steps. The purpose of this study was to quantify differences with and without a mask in muscle co-activation and integrated EMG (iEMG) during SOS descent. It was hypothesized that there would be increased muscle activation across the entry, mid-staircase, and exit steps when participants wore an N95/KN95 mask compared to participants without [3].

METHODS: Nine individuals without a mask (age 20.33 ± 0.87 years, height 1.70 ± 0.07m, body mass 66.1 ± 9.34kg, 1 male) and nine individuals wearing an N95/KN95 mask (age 20.56 ± 1.33 years, height 1.66 ± 0.07m, body mass 62.6 ± 12.2kg, 9 female) volunteered for the study. Participants were generally healthy with no current/recent lower extremity injuries. Data was collected via Ag/AgCl surface electrodes placed on the right tibialis anterior (TA), peroneal muscles, medial gastrocnemius (MG), rectus femoris (RF), and biceps femoris (BF). Variables analyzed were lead and trail limb co-activation of the knee (RF/BF) and ankle (TA/MG) and iEMG of the peroneals. Participants descended the seven-step staircase (rise: 15.5cm, run: 30cm, width: 152cm) in a SOS pattern, beginning by level walking 1.6m from the top stair, leading with the right foot descending first, then continuing to walk forwards once the bottom of the staircase was reached. Subjects descended the staircase wearing their own athletic shoes at a self-selected pace. Trials were recorded with a reference video camera collected at 30 Hz used to determine gait events. Lead limb step activity was from lead limb swing, through weight acceptance at the end of double limb support. The trail limb step activity was single limb support through controlled lowering. Data was rectified, filtered (500Hz and 20Hz), smoothed (30ms moving window), and normalized to the maximum muscle activity across trials in Noraxon MyoResearch software, then exported to a customized MATLAB program. Two-way Repeated Measures of Analysis of Variance tests were conducted for both lead and trail limb co-activation and iEMG. In trials with no interactions, significant main effects of the steps were followed up with pairwise comparisons with Bonferroni corrections.

RESULTS & DISCUSSION The purpose of this study was to quantify differences in muscle co-activation and iEMG during step descent in an SOS pattern with and without a mask. Data from Thomas et. al, (2020) suggests that with blocked vision on stairs, muscle co-activation may be higher; however, no statistics were provided. The expected increase in muscle activity was not supported for the SOS condition while participants wore masks. There were no significant differences in lead knee co-activation or any of the trail limb variables. There were significant main effects of step number present in the lead limb in both the ankle co-activation and iEMG of peroneals (Fig. 1). Andriacchi et. al (1980) demonstrated there were muscle activity differences across steps in a staircase. In the current study, iEMG activity across steps was different at the peroneals regardless of mask status, further supporting differences in muscle activity across steps (Fig. 1).

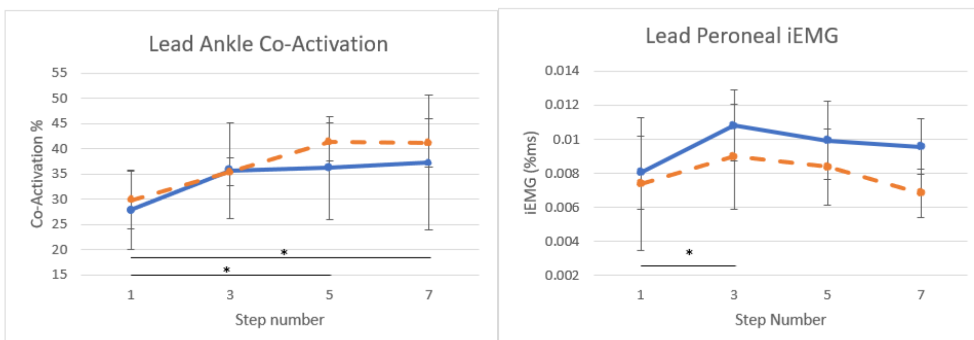

Figure 1: Blue solid lines = mask, orange dashed lines = no mask. Thin black lines with * indicate significant differences between steps.

SIGNIFICANCE: In conclusion, data from this study supports that in healthy young adults, wearing a mask does not appear to influence muscle activity during multi step descent. Differences were seen across step numbers in the lead limb ankle co-activation and iEMG activity of the lead limb peroneals. Although there were no muscle activity differences between mask and no mask when participants descended the staircase in an SOS pattern, further study could be conducted to analyze any potential kinematic differences from wearing a mask. The results of this study suggest further research is needed on muscle activity during multiple step descent.

ACKNOWLEDGEMENTS: Thanks to Emma Connolly, Julia LeMay, and Mary Kallberg for their contributions to this project.

REFERENCES: [1] Thomas et. al (2020), *Human movement science*, *73*, 102676. [2] Klatt et. al (2021), *J Neurol Physical Ther.*, 45(1), 36-40. [3] Andriacchi et. al (1980), *J Bone Joint Surg Am*, *62*(5), 749-757.

SCREENING COGNITIVE DECLINE: MULTISCALE ENTROPY ANALYSIS DURING DUAL-TASKING USING FUNCTIONAL NEAR INFRARED SPECTROSCOPY MEASUREMENTS

Kelsi Petrillo, B.S.[1], Hector Flores[1], Isabellah Mayoral-Ortega[1], Bilaval Javed, M.D. [1], Meenakshi Dagar, M.D., Nima Toosizadeh[*], Ph.D[1]
[1]Department of Biomedical Engineering, College of Engineering; University of Arizona
*Corresponding author's email: ntoosizadeh@arizona.edu

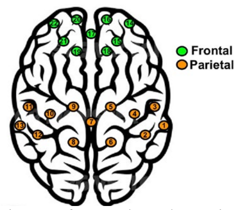

Figure 1: fNIRS Channel Locations

Introduction: Cognitive impairment is an increasingly relevant health concern, as data estimates predict that by 2060 the number of older adults with dementia will surpass 152 million globally, approximately a 200% increase compared to 2019[1]. Over half of patients with dementia never receive an evaluation, indicating that a quick and objective routine test for screening cognitive decline in older adults is needed[2]. Due to neural death and disconnections, Alzheimer's disease (AD) is associated with a low value of nonlinear complexity of the brain function, which can be quantified using entropy analysis (e.g., sample entropy/multiscale entropy)[3]. Our proposed solution was an upper extremity function (UEF) dual-task screening method combined with functional near-infrared spectroscopy (fNIRS), which measures brain function. The UEF motor task and cognitive component (dual-task procedure) were previously validated in older adults[4,5]. The aim of this study was to investigate fNIRS entropy data to assess its relationship with cognitive status and task condition (resting-state and dual-task).

Methods: MoCA scores stratified older adult participants into the following groups: cognitively normal (CN) (n=9, 69<age<90), mild cognitive impairment (MCI) (n=20, 65<age<97), and AD (n=8, 80<age<96). Healthy young (HY) participants were also included (n=15, 18<age<28). Participants performed a 3-minute dual-task with a 3-minute rest period before and after. The motor component of the dual-task was consistent elbow flexion while counting backwards by intervals of 3's. Measurements were taken over the frontal (right and left) and parietal (right and left) brain regions (Fig 1). Multiscale entropy was chosen as the complexity measure because higher scale factors can improve the signal-to-noise ratio in short time series. A MATLAB program was developed to use the following formula to calculate sample entropy, which was then used with a selected scale of 20 for calculating multiscale entropy:

$$SampEn(m,r,N) = -ln\frac{P_{m+1}(r)}{P_m(r)}$$

where N is the length of the time series, m is the pattern length for comparison, r is the tolerance for radius of similarity, and P is the probability of radius falling within the tolerance level r. A pattern length of m=2 was used and a tolerance of r = 0.2×SD, where SD is the standard deviation of the original time series (1 represents more complexity and 0 represents less complex signal). Multivariable repeated measures analysis using mixed effects modeling assessed the effect of cognitive status and task conditions on brain function entropy.

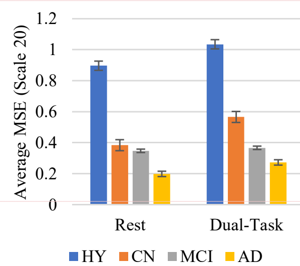

Figure 2: Average/Standard Error MSE for Groups Over Tasks

Results & Discussion: The cognitive status of participants was significantly associated with brain function entropy for all measured brain regions (Table 1). The task type was a significant factor affecting brain function for the left and right parietal regions (Table 1). Also, significant task and group interaction effects were observed for parietal regions (Table 1). The results of this study indicate potential for the use of fNIRS multiscale entropy analysis in combination with the UEF dual-task test as a screening tool for cognitive impairment. Identifying significant brain regions is critical for planning and understanding the behavioral response. It is known that that the frontal region is responsible for executive control including speaking and movement, while the parietal lobe and is involved in perception and sensory input.

Significance: Current findings suggest that combining measures of brain function and motor function may provide an accurate tool for screening and assessing cognitive impairment. Previous work has utilized finger tapping and gait as the motor component for dual-tasking. In our previous work, we showed the association between UEF and gait dual-task performance, within which, a better prediction of cognitive impairment (15% higher accuracy) was achieved using UEF motor variability parameters compared to gait measures[6]. These changes would increase the usability and convenience of the proposed methods for both patients and clinicians.

Fixed Effect Tests	Frontal Left Brain	Frontal Right Brain	Parietal Left Brain	Parietal Right Brain
Cognitive Group	**< 0.0001**	**< 0.0001**	**< 0.0001**	**< 0.0001**
Task	0.0869	0.0869	**0.0004**	**0.0002**
Cognitive Group*Task	0.6524	0.6524	**0.0127**	**0.0019**

Table 1. *p*-value results of Mixed Modeling Fixed Effect Tests. Bold is used to show significant difference.

Acknowledgements: Funding from the Arizona Alzheimer's Consortium and The University of Arizona BIO5 Institute support this project. The findings of this manuscript are those of the authors and not of the sponsor.

References: [1] Nichols et al. (2022), *Lancet Public Health* 7(e105-e135); [2] Lang et al. (2017), *BMJ Open* 7(e011146); [3] Pena et al. (2022) *J Neuroimaging* (1-13); [4] Ehsani et al. (2020), *Computers in Biology and Medicine* (103705); [5] Toosizadeh et al. (2019), *Scientific Reports* (10911); [6] Ehsani et al. (2019), *Clin Interv Aging* 14(659-669).

Commented [TN(1]: In your text you said you used scale 6 but here you presented scale 20.
Also use scale instead of W.

Also what would be good, is to do a post hoc analysis to show the significant differences between four groups. You can use different letters for groups that are significantly different.

Commented [TN-(2]: I think you should have some number showing the average values of MSE across groups and conditions. One or two sentences with effect sizes.

Effect of Waist Vibrotactile Feedback on Postural Balance under Dynamically Challenging Environments

Soubhagya Nayak, Kwanghee Jo, Anvitha Doddipalli, Soe Lin Paing, and Hyunglae Lee*
School for Engineering of Matter, Transport and Energy, Arizona State University, Tempe, AZ USA
Corresponding author's email: Hyunglae.Lee@asu.edu

Introduction: Achieving precise control of standing posture is critical for performing everyday activities effectively. However, this can become challenging when dealing with dynamic environments such as unstable terrain with unexpected perturbations. Among the various biofeedback methods available to improve postural balance control, vibrotactile feedback has the advantage of providing supplementary information about standing balance control without disturbing other core functions (e.g., visual perception). This study aims to investigate the effect of waist vibrotactile feedback on standing postural balance. The two questions that we would like to answer in this study are: whether the waist vibrotactile feedback can improve postural balance control under challenging ground conditions and secondly whether it is effective for the same purpose under fatigue conditions.

Methods: The study was performed with 10 young healthy participants (age: 20-30) who reported no history of neuromuscular injuries in the back and low extremities. We investigated the effectiveness of a waist vibrotactile feedback device for improving postural control during standing balance on a dynamically moving ground surface simulated by a twin multi-axis robotic balance platform [1]. Four vibration motors of the waist device applied vibrotactile feedback in the anterior-posterior (AP) and medio-lateral (ML) directions based on the 2-dimensional sway angle, measured by an inertia measurement unit (IMU). A custom-designed belt accommodated the integration of the vibration motors and an IMU sensor and it could comfortably fit the waist area of any participant (Figure 1A). The movement of the IMU sensor was presumed to be the movement of the participant's center of mass (COM). The experiment consisted of a threshold determination session, a pre-fatigue session, a fatigue exercise session, and a post-fatigue session. The threshold determination session was conducted to find threshold values of sway angle in AP and ML directions based on the criteria of the participant's COM should reside inside the threshold for 70% of the trial period of the experiment. The fatigue exercise (5 sets of calf raises, squats, and lunge forward exercises) was used to induce fatigue in the leg muscles. During both pre-fatigue and post-fatigue sessions, the participant was introduced to various trials of ground perturbations through the robotic balance platform. The perturbations were designed by a sequence of sine waves with randomly varying frequencies (0.5-1.5 Hz) and amplitudes (0-3°) for 90 seconds. The Shapiro-Wilk test was used to check the normality of the collected data set. Upon satisfaction of the normal distribution criterion, two-tailed paired t-tests were conducted for statistical analysis. The Wilcoxon signed-rank tests were used for the remaining data set.

Results & Discussion: Experimental results demonstrated that the waist vibrotactile feedback was effective in improving postural balance control under dynamically challenging environments, evidenced by the improvements in COM and center-of-pressure (COP) measures. In addition, this study confirmed the effectiveness of the waist vibrotactile feedback in improving standing balance control even under muscular fatigue induced by lower body exercise. The increased percentage of COM inside the threshold demonstrated a significant improvement in controlling the COM movement with the assistance of vibrotactile feedback (Figure 1B). In the pre-fatigue condition, there was a significant improvement in both the AP direction (148.0%; $p < 0.001$) and the ML direction (68.6%; $p < 0.001$). Similarly, in the post-fatigue condition, there was a significant improvement in both the AP direction (139.9%; $p < 0.001$) and the ML direction (102.0%; $p < 0.001$). Additionally, a reduction in the net angular velocity of the COM was achieved with the help of vibrotactile feedback (Figure 1C). There was a 14.7% reduction in the pre-fatigue condition ($p = 0.03$) and a 16.6% reduction ($p = 0.08$) in the post-fatigue condition. Consequently, vibrotactile feedback contributed to the reduction of COP sway area as well (Figure 1D). The reduction in the COP sway area was 21.2% for the pre-fatigue condition ($p = 0.003$) and 34.2% for the post-fatigue condition ($p = 0.02$).

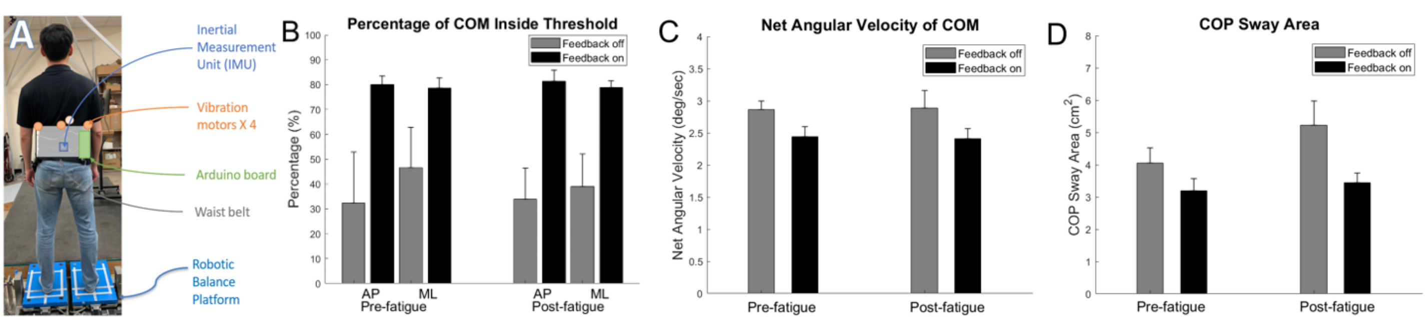

Figure 1: A) A subject stood on the platform with the waist vibrotactile belt on, B) Impact of vibrotactile feedback on the percentage of COM inside the respective threshold, C) Impact of vibrotactile feedback on net angular velocity of COM, and D) Impact of vibrotactile feedback on COP sway area.

Significance: The results of this study illustrate that vibrotactile feedback can be an invaluable tool in enhancing postural balance and reducing the risk of injury. This finding has important implications for a range of applications, including rehabilitation and sports performance. Further research is needed to explore the optimal parameters for delivering vibrotactile feedback, such as frequency and intensity of vibrations, as well as exploring its effects in different populations and in different types of balancing tasks.

References:

[1] Nalam, V., & Lee, H. (2019). Development of a two-axis robotic platform for the characterization of two-dimensional ankle mechanics. *IEEE/ASME Transactions on Mechatronics*, *24*(2), 459-470.

MODELLING OCCUPANT HEAD ACCELERATIONS DURING FAR-SIDE LATERAL IMPACTS

Minori Iizuka[1], Sean D. Shimada[1]
[1]Biomechanical Consultants of California
miizuka@ucdavis.edu

Introduction: While lateral impacts were the second most common and the second leading cause of passenger vehicle occupant deaths in 2020, lateral near-side and far-side impacts produce different occupant kinematics [1,2,3]. Typically, a crash will cause an occupant's torso to initially move toward the impact location, then rebound back toward the initial position. In a near-side impact, the occupant's body is closer to the impacted door and pillar. Conversely, in a far-side impact, the occupant has more space to move inboard and is less restricted by the interior structures, reducing the likelihood the occupant's head contacts the interior components [3]. Additionally, far-side occupants may be more susceptible to shoulder belt slip as the outboard shoulder belt design does not fully limit the inboard movement [2]. It is important for biomechanists, automotive safety engineers, and forensic experts to understand how crash dynamics and severity influence the occupant's kinematics and related injury risk. Previous studies have compared far-side vehicle dynamics and lateral head acceleration.

This study aimed to develop a mathematical relationship between peak lateral head acceleration and vehicle/sled lateral delta-V and lateral acceleration for far-side lateral impacts with the goal of creating a tool to estimate occupant kinematics and injury probability. An accurate model would contribute to the forensic literature, specifically used to determine injury threshold and injury analyses.

Methods: Data from various far-side lateral impact studies that measured peak lateral head linear acceleration and vehicle/sled lateral delta-V and/or lateral accelerations were collected [2-5]. To be included in the analysis, lateral impacts could be no more than ± 45° from the lateral direction. Commercial passenger vehicles and sled tests were included together in the analysis. Additionally, all occupant types (i.e., volunteers, post-mortem human subjects (PMHS), and anthropomorphic test devices (ATD)) as well as driver and non-driver occupants were included. Three-point restraints as well as lap belts were used in the analysis as the shoulder belt can fail to maintain the shoulder within the belt, playing a less significant role in far-side collisions [2]. Peak lateral head accelerations were plotted against the vehicle/sled lateral delta-V or acceleration. The plots were fitted with linear and second-order regressions with the y-intercept set at zero. The regression that yielded the higher R^2 was analyzed.

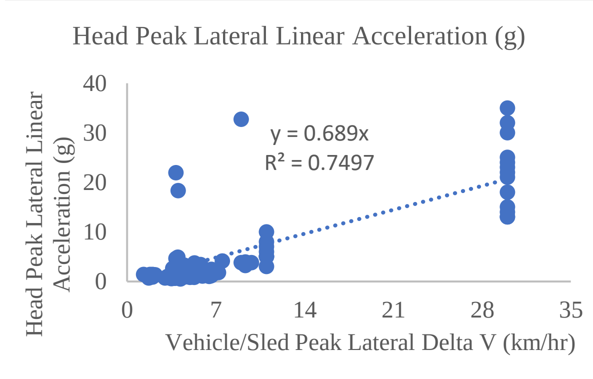

Figure 1: Head acceleration vs. far-side lateral delta-V

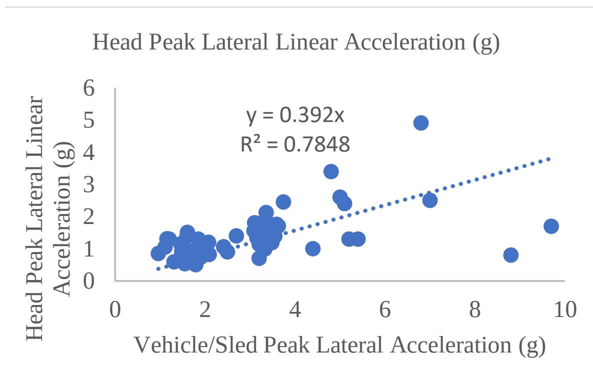

Figure 2: Head acceleration vs. far-side lateral acceleration

Results & Discussion: Lateral head acceleration during lateral impacts were collected from four studies [2-5]. Figure 1 (N=94, R^2 = 0.7497) and figure 2 (N=55, R^2 = 0.7848) show the positive linear regressions for head acceleration during far side impacts as a function of lateral delta-V and acceleration, respectively. The delta-V and acceleration regressions estimate the head accelerations for far-side lateral delta-Vs between 1.3-30 km/hr and accelerations less than 10g's.

Volunteers and PMHS occupants provide valuable physiological factors that ATDs may not accurately emulate. Approximately 80% of the head acceleration versus delta-V analysis included a volunteer or PMHS, while the head acceleration versus lateral acceleration analysis included only volunteer occupants. Since the data mostly included volunteer or PMHS tests, an accurate model for head accelerations was likely developed. Furbish et al. (2019) found that volunteers contacted the interior structure less often than the ATDs while the occupant sat in the rear, far-side seat, noting that the volunteers' ability to contract their muscles resisted the inertial motion caused by the collision [3]. The PMHS also has passive structures that provide resistance that the ATDs may fail to replicate due to their increased stiffness. Despite this, the ATDs provide valuable insight for more severe impacts where it would be unethical to use human volunteers.

Significance: Biomechanists and forensic experts may gain an appreciation for the reported regression models as part of a holistic analysis for estimating lateral head accelerations during far-side crashes. The estimated head accelerations can help determine whether the reported crash severity is consistent with the reported injuries. Furthermore, the improved understanding of head accelerations during far-side impacts provides automotive safety engineers valuable information for creating safety features that reduce injury potential. Additional tests should be investigated at delta-Vs between 11km/hr to 30km/hr to further enhance the delta-V model.

References: [1] Insurance Institute for Highway Safety Highway Loss Data Institute https://www.iihs.org/topics/fatality-statistics/detail/passenger-vehicle-occupants#Crash-types [2] Pintar et al. (2007), *Stapp Car Crash J*, 51, 313-360 [3] Furbish et al. (2019), *SAE Int J Advances & Curr Prac in Mobility*, 1(4), 1470-1490 [4] Fugger et al. (2002), SAE 2002 World Congress & Exhibition [5] Shibata et al. (2019), SAE Technical Paper, doi: 10.4271/2019-01-1030

SINGLE-LEG BACKWARD HOPPING CAN BETTER DETECT QUADRICEPS STRENGTH DEFICITS INDUCED BY A FATIGUE PROTOCOL COMPARED TO FORWARD AND VERTICAL HOPPING

Yu Song[1], Lauren Salsgiver[1], Kaden Van Valkenburg[1], Natalie Christofferson[1], Yessica Lo[1], Brenna McGuinness[2], Boyi Dai[1*]
[1] Division of Kinesiology and Health, University of Wyoming, Laramie, WY, USA
*Corresponding author's email: bdai@uwyo.edu

Introduction: Bilateral asymmetries in knee mechanics and quadriceps strength have been observed after anterior cruciate ligament (ACL) reconstruction and likely contribute to the high ACL re-injury risk to both previously injured and contralateral legs [1]. Effective rehabilitation, valid assessments, and safe return-to-play are essential for decreasing ACL re-injury risk. One of the common clinical assessments for knee strength following ACL reconstruction (ACLR) is single-leg hopping forward for distance. A symmetry index of 90% or greater has been recommended for return-to-play [2]. However, biomechanical studies showed that symmetrical forward hopping distances were insufficient to support symmetrical knee kinetics and strength in patients following ACLR [3]. In addition, a previous study showed that forward jumping demonstrated greater hip and ankle work than knee work, while knee work was the greatest in backward jumping [4]. From a mechanical perspective, knee extension moves the foot forward and generates a posterior ground reaction force, while ankle plantarflexion and hip extension mainly generate an anterior force. As such, forward hopping might not be a mechanically challenging task for the knee to detect its strength deficits. Therefore, this study aimed to quantify the effect of quadriceps deficits induced by a fatigue protocol on jumping performance and mechanics in single-leg forward, vertical, and backward hopping tasks.

Figure 1: Fatigue protocol (left); forward (top), vertical (middle), and backward (bottom) hopping.

Methods: Sixteen recreational athletes (7 females, 9 males, age: 23.1 ± 1.6 years, height: 1.7 ± 0.1 m, and mass: 75.6 ± 13.2 kg) performed ten practices of forward, vertical, and backward hopping on each leg to achieve a consistent performance (Fig. 1). Five official trials were collected for each condition before and after a quadriceps fatigue protocol on a pre-determined fatigue leg (holding 50% of the maximal weight at 60 degrees of knee flexion until exhaustion five times). The independent variables were three hopping tasks, fatigue status (before vs. after fatigue), and two legs (fatigued vs. non-fatigued leg). The dependent variables were hip/knee/ankle work and peak knee power during jumping, and hopping distance/height symmetry index (fatigued leg/non-fatigued leg). Paired t-tests were performed (Type I error rate = 0.05).

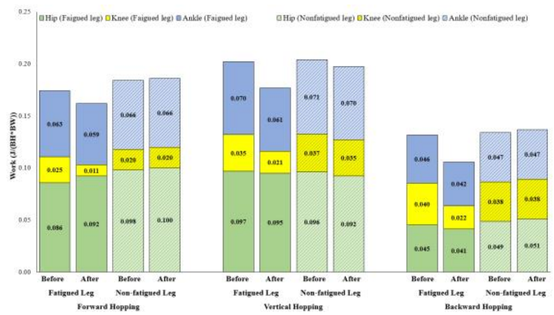

Figure 2: Hip (green), knee (yellow), and ankle (blue) work of bilateral legs for forward (left), vertical (middle), and backward (right) hopping before and after the fatigue protocol.

Results & Discussion: Knee and ankle work, peak knee power, and performance symmetry index of the fatigued leg significantly decreased after the fatigue protocol and was smaller compared to the non-fatigued leg for all three hopping tasks, supporting that the fatigue protocol simulated quadriceps strength deficits while the non-fatigue leg was not affected by the fatigue protocol (Fig. 2; Table 1). In addition, backward hopping showed significantly greater knee work and knee power and smaller hip and ankle work of both legs compared to forward hopping before and after the fatigue protocol, highlighting the more important role of the knee in backward hopping. Finally, participants demonstrated the least performance symmetry index for backward hopping compared to forward and vertical hopping, suggesting that decreased knee strength had a greater effect on backward hopping performance.

Significance: Backward hopping might be a more sensitive clinical assessment to detect quadriceps strength deficits in patients following ACL injuries due to greater knee involvement in generating the force toward the jumping direction.

Acknowledgements: NSF, China Scholarship Council, and Wyoming INBRE (NIH).

References: [1] Paterno et al., 2010. *Am J Sports Med.* 38:1968-78; [2] Nagai et al., 2020. *Knee Surg, Sports Traumatol, Arthrosc.* 28(3): 816-822; [3] Kotsifaki et al., 2020. *Br J Sports Med.* 54:139-153; [4] Hara et al., 2008. *J Biomech.* 41:2806-15.

Table 1. Means ± standard deviations and the results of t-tests.

		Forward Hopping		Vertical Hopping		Backward Hopping	
		Before	After	Before	After	Before	After
Peak knee power	Fatigued leg	$0.30 \pm 0.08^{*C}$	$0.17 \pm 0.07^{*C\wedge}$	$0.34 \pm 0.07^{*B}$	$0.22 \pm 0.07^{*B\wedge}$	$0.43 \pm 0.09^{*A}$	$0.31 \pm 0.10^{*A\wedge}$
(J/(BW*BH))	Non-fatigue leg	0.28 ± 0.09^{C}	$0.28 \pm 0.11^{C\wedge}$	0.35 ± 0.09^{B}	$0.34 \pm 0.10^{B\wedge}$	0.42 ± 0.11^{A}	$0.43 \pm 0.12^{A\wedge}$
Performance symmetry index (%)		1.01 ± 0.07*	$0.92 \pm 0.07*^{A}$	1.02 ± 0.06*	$0.90 \pm 0.15*^{AB}$	1.00 ± 0.07*	$0.85 \pm 0.09*^{B}$

Notes. *: significant difference between fatigue status (before vs. after); ^: significant difference between legs (fatigued vs. non-fatigued legs); $^{A, B, and C}$: A is greater than B and C, and B is greater than C among tasks at each fatigue status, with no significant differences for the task with the same letter.

AN OCCUPANT HEAD ACCELERATION MODEL DURING NEAR-SIDE LATERAL IMPACTS

Minori Iizuka[1], Sean D. Shimada[1]
[1]Biomechanical Consultants of California
miizuka@ucdavis.edu

Introduction: Near-side impacts are defined as lateral vehicle collisions where the occupant is seated on the side closest to the impacted area. Near-side impacts can cause occupants to contact their head on the vehicle pillar, interior, or the intruding vehicle [1]. These contacts can lead to serious head injuries or death, as these dangers are compounded by the limited time and space that safety systems can be applied to protect the occupant. It has been reported that near-side crashes cause more severe occupant injuries than far-side impacts. It is important for biomechanists, automotive safety engineers, and forensic experts to understand how crash dynamics and severity influence the occupant's kinematics and related injury risk.

This study compiled various studies with a goal of creating a mathematical model between peak lateral head acceleration and vehicle/sled lateral delta-V or acceleration. The final model would add to the existing literature and can be used to evaluate the consistency between crash dynamics and corresponding injuries.

Methods: A literature review was conducted for near-side lateral impacts that measured peak lateral head linear acceleration and lateral delta-V and/or acceleration [2-5]. Oblique impacts up to ± 45° from the lateral direction were included in the analysis. Additionally, tests involving volunteers, post-mortem human subjects, and anthropomorphic test devices (ATD) were all included in the analyses. Both drivers and non-drivers were included as well. Commercial passenger vehicles and sled tests were analyzed together. Studies with three-point restraints were only considered as the shoulder belt plays an important role in near-side collisions [3]. For vehicle tests, if the vehicles' center of mass kinematics were not reported, the vehicles' rear axle kinematics were recorded as the axle is a part of the main car structure and did not experience intrusion like those observed by the windowsill accelerometer locations. Lateral head acceleration was plotted against the vehicle/sled lateral delta-V or acceleration. The plot was fitted with linear, second-order, or exponential regressions with the y-intercept set at zero. The regression that yielded the higher R^2 was chosen for analysis.

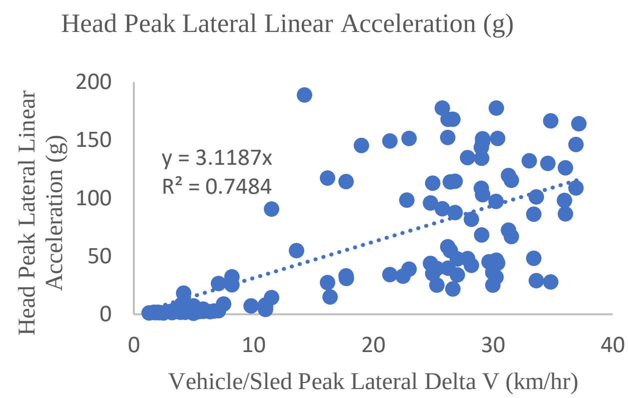

Figure 1: Head acceleration in relation to near-side lateral delta-V

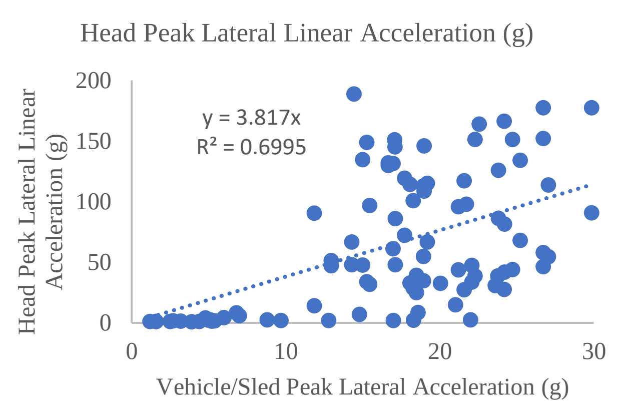

Figure 2: Head acceleration vs. near-side lateral acceleration

Results & Discussion: Lateral head acceleration during lateral accelerations were collected from three studies and 73 NHTSA crash tests [2-5]. Figure 1 (N=115, R^2 = 0.7484) and figure 2 (N=92, R^2 = 0.6995) demonstrate the positive linear regression for head acceleration during near side impacts as a function of lateral delta-V and acceleration, respectively. These regressions estimate the head accelerations for near-side lateral delta-Vs between 1.3-37.2 km/hr and accelerations less than 30g's.

Over 70% of the tests included in the subject study utilized ATDs for both regressions. ATD tests represent an upper bound for occupant kinematics during side impacts [3]. This proportion of occupant types likely influenced the resulting regressions. Furbish et al. (2019) found that while the ATDs demonstrate similar initial phase crash movements as the volunteers, the rebound phase showed that the ATD's had greater head acceleration magnitudes [3]. This increased head kinematics were attributed to the ATD's relatively higher stiffness, which was especially evident when the occupant contacted the vehicle interior [3]. Furthermore, not only were the occupant impact responses greater in ATDs, the ATDs were more likely to contact the interior compared to the volunteers as the ATDs lack the musculature necessary to resist inertial motion and prevent interior contacts [3]. Thus, the reported regression may overestimate the head accelerations experienced by human occupants.

Significance: The regression model provides a tool for biomechanists and forensic experts to estimate peak head accelerations during near-side lateral impacts. Ultimately, the model can be used to assess head injury probability from near-side impacts. Lastly, the model may help regulatory bodies place standards for allowable head accelerations during near-side impacts, prompting automotive safety engineers to create safety features that reduce head and brain injury risk. Future work should include additional volunteer and PMHS to support the current findings.

References: [1] Yoganandan et al. (2015), "Accidental Injury: Biomechanics and Prevention", doi: 10.1007/978-1-4939-1732-7 [2] Pintar et al. (2007), *Stapp Car Crash J*, 51, 313-360 [3] Furbish et al. (2019), *SAE Int J Advances & Curr Prac in Mobility*, 1(4), 1470-1490 [4] Fugger et al. (2002), SAE 2002 World Congress & Exhibition [5] "National Highway Traffic Safety Administration" https://www.nhtsa.gov/research-data/research-testing-databases#/vehicle

Quantifying the Effects of Perturbation Intensity on Slip Outcome in Young Adults

Sangwon Shin[1], Caroline Simpkins[1], Jiyun Ahn[1], Diané Brown[1], Laura Leigh Wentworth[1] and Feng Yang[1]
[1]Department of Kinesiology and Health, Georgia State University, Atlanta, GA, USA
Email: sshin33@student.gsu.edu

Introduction: Motorized treadmill has been widely used to examine the reactive balance control of the human body after an external perturbation [1, 2]. The profile of the treadmill-induced perturbation depends on the duration, velocity, acceleration, and displacement of the belt [3]. The intensity of the perturbation is affected by these interrelated factors. Dynamic stability is a novel way to quantify the responses to external perturbations, such as a slip [4]. Based on the Feasible Stability Region (FSR) theory (Fig. 1), dynamic stability is determined by the kinematic relationship between the body's center of mass (COM) and base of support (BOS) [5]. Although it was conceptually recognized that a higher slip intensity would lead to worse slip outcomes, no study has quantified how the perturbation intensity is related to slip outcome (fall vs. non-fall) and dynamic stability after an unexpected slip. This knowledge gap could be a barrier when designing slip-based assessment or intervention programs. The objective of this study was to quantify how the slip intensity, characterized by the belt's acceleration, affects slip outcome and dynamic stability with a controlled slip distance. We hypothesized that the increased acceleration level would increase the risk of slip-fall.

Methods: Eighteen healthy young adults (14 females / 4 males, age: 25.1 ± 4.4 years, height: 1.67 ± 0.1 m, mass: 71.8 ± 12.7 kg) were recruited. They were evenly and randomly assigned into three groups: low (group A), medium (group B), and high intensity (group C). After three normal standing trials without a slip on the ActiveStep treadmill (Simbex, NH), participants were instructed that they may or may not experience a slip on any of the forthcoming trials. Then, they experienced three more standing trials followed by a standing-slip with the assigned slip intensity, but the same slip distance (0.36 m). The acceleration level was 2.25 m/s^2 for group A, 4 m/s^2 for group B, and 9 m/s^2 for group C. The peak belt velocity and duration were 0.9 m/s and 0.8 s, 1.2 m/s and 0.6 s, and 1.8 m/s and 0.2 s, respectively, for groups A, B, and C. Full body kinematics were collected from the markers attached to the skin using a motion capture system (Vicon, UK). Another marker was placed on the treadmill belt to gather its movement. The slip trial was analyzed. Two time instants were identified: slip onset (ON) and recovery step liftoff (LO). ON was the moment when the belt's displacement is 3 standard deviations above its baseline. LO was determined using foot kinematics and verified against the video recordings. The slip outcome was the primary outcome measure. A slip was classified as a fall if the hip height dropped by more than 4.5% of body height from its height at ON during the slip. Dynamic stability (unitless) at ON and LO were the secondary outcomes. It was calculated using the FSR-based COM motion state at ON and LO. The two components of the COM motion state (position and velocity) were calculated relative to the BOS and normalized by foot length (l_{BOS}) and $\sqrt{g \times bh}$, respectively, where g is the gravitational acceleration and bh represents the body height. Chi-squared test was used to compare the slip outcome between groups. ANOVA models with post-hoc tests (independent t-test) compared dynamic stability at either event among groups. SPSS 27.0 (IBM) was used, and the significance level was 0.05.

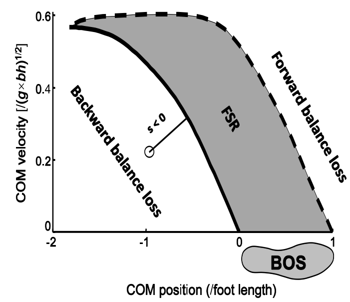

Fig. 1: Dynamic stability defined by the FSR theory. Dynamic stability (s) is calculated as the shortest distance (thin line) from the COM motion state to FSR's backward balance loss boundary. A larger stability value indicates a more stable state against backward falling.

Results & Discussion: The demographic and anthropometric information was comparable between groups ($p > 0.389$). The results supported our hypothesis. Chi-squared test results revealed that the fall incidence was closely related to the slip intensity ($p = 0.002$, Fig. 2a). Specifically, no one in the low-intensity group fell, 66% of participants in the medium group fell, and everyone in the high-intensity group experienced a fall after the slip. Although all groups showed comparable stability against backward balance loss at ON ($p = 0.678$, Fig. 2b), the low-intensity group was more stable than the high-intensity group at LO ($p < 0.001$, Fig. 2c). The medium group was also more stable than the high-intensity group ($p = 0.001$, Fig. 2c) at the same event. This study was conducted with healthy young adults and the perturbation was limited to slip. Therefore, it remains unknown how our findings can be generalized to other populations under different types of perturbations. More studies with large sample sizes are desired to address these questions.

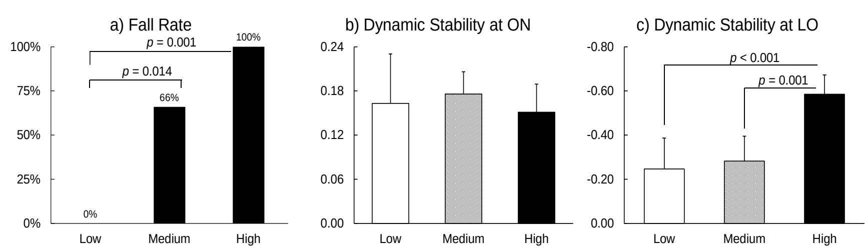

Fig. 2: Comparisons among groups (Low: 2.25 m/s^2, Medium: 4 m/s^2, and High: 9 m/s^2) of a) fall rate (%) and dynamic stability at b) ON and c) LO, after a standing-slip.

Significance: Our study, for the first time, quantified the relationship between perturbation intensity and slip outcome. The findings could provide some preliminary guidance to select perturbation intensity for adopting perturbation as either a training tool or assessment platform for rehabilitation and fall prevention.

References

[1] Yang et al., 2017. *J. Biomech.* 53: 148-153; [2] Kannan et al., 2022. *Neurosci. Lett.* 783: 136699; [3] Liu et al., 2015. *J. Biomech.* 49: 135-140; [4] Yang et al., 2009. *J Biomech*. 42: 1903-1908; [5] Yang et al., 2007. *J Biomech*. 40: 804-811.

EVALUATING THE EFFECTIVENESS OF NEUROMUSCULAR TRAINING TO REDUCE LOWER EXTREMITY INJURY RISK IN ATHLETES WITH A HISTORY OF CONCUSSION

April L. McPherson[1,2,3,4*], Taylor Zuleger[1,3,4,5], Kim D. Barber Foss[1,3,4], Jed A. Diekfuss[1,3,4], Gregory D. Myer[1,3,4,6]
[1]Emory Sports Performance And Research Center (SPARC), Flowery Branch, GA
[2]The Ohio State University, Columbus, OH
*Corresponding author's email: april.mcpherson@osumc.edu

Introduction: Sport-related concussion (SRC) increases the risk for future lower extremity musculoskeletal injury (LE MSKI).[1] Adolescent athletes are of particular concern for the concussion to LE MSKI sequalae, since an estimated 1.1-1.9 million SRCs occur annually in US athletes under 18 years old[2] and recovery periods are often longer in adolescent athletes than adult counterparts.[3] Moreover, adolescent athletes with a history of SRC demonstrate prolonged neuromuscular control deficits following symptomatic resolution, which may contribute to an increased risk of LE MSKI.[4] Neuromuscular training (NMT) interventions are gold standard for reducing the risk of LE MSKI in young athletes and recent evidence indicates that an 8-week NMT intervention reduced risk of future LE MSKI in athletes with recent concussion diagnosis.[5]

The purpose of this study was to determine if NMT reduced the risk of LE MSKI in female adolescent athletes with a self-reported history of SRC. We hypothesized that female high school athletes who reported any history of SRC, would have an increased risk of LE MSKI compared to controls, despite completion of a NMT intervention.

Methods: 83 female athletes (12-18 years old) were recruited from local high school athletic teams (volleyball (*n*=44), soccer (*n*=19), basketball *n*=20) prior to the start of the competitive season (14.0±0.7 years; BMI 23.4±0.7). Participants completed an SRC history questionnaire that queried history of head injuries for which they did and did not seek medical attention, to account for potentially unreported or medically undiagnosed SRCs.[6]

	CONC (n=29)	CTRL (n=54)
Injury Rate	5.0 (2.0-10.2)	1.1 (0.2-3.2)
Injury Risk (%)	24.1 (12.0-42.4)	5.6 (1.3-15.7)

Table 1: Injury rate and injury risk (95% confidence interval).

All participants completed a 6-week NMT intervention prior to the start of the competitive athletic season. The NMT intervention focused on lower extremity strength training, core, and plyometric abilities and was enhanced with additional total body and upper body pre-season training exercises.[7] After completion of the NMT intervention, participants were tracked for athletic exposures (AEs) and LE MSKIs for the first competitive sports season in which they participated. An LE MSKI was defined as any musculoskeletal injury (e.g., strain, sprain, tear, rupture) occurring at or inferior to the hip joint that required medical attention.

Epidemiologic data were analyzed using OpenEpi (Online Opensource, Version 3.01). Injury rates and injury risk were calculated between controls (CTRL) and those with a history of SRC (CONC) with 95% confidence intervals (CI). Significance was set *a priori* at $p<0.05$.

Results & Discussion: 54 female CTRL and 29 female CONC recorded 2,777 and 1,412 AEs respectively. Overall, 10 LE MSKI were recorded during the competitive athletic seasons. 7 LE MSKI were reported in the CONC group (62.5%) and 3 CTRL LE MSKI (37.5%). One athlete, in the CONC group, sustained 2 LE MSKI.

The overall LE MSKI rate was higher for participants with history of CONC compared to CTRL participants (**Table 1**), with a corresponding overall injury rate ratio of 4.6 (95% CI: 1.2-17.7, p=0.01). The risk of LE MSKI in the CONC group was higher than CTRL, with a corresponding an injury risk ratio of 4.3 (95% CI: 1.2-15.6; p=0.01).

This study found that female high school athletes with a self-reported history of SRC had a greater risk of LE MSKI compared to controls, even after completion of a 6-week NMT intervention. Completion of NMT immediately following an SRC (≤14 days) may have a greater impact on subsequent LE MSKI risk [4] than NMT beyond the initial immediate recovery period from an SRC. Future work could investigate the strategies to target specific lingering deficits and their responsiveness to NMT between athletes with a prolonged history of SRC (e.g., years) relative to athletes immediately recovering from an SRC. In addition, future work that considers inclusion of a post-concussion clinical standard-of-care treatment group would help to understand if NMT reduces a pre-existing elevated injury risk in participants with a history of SRC compared to non-concussed controls.

Significance: Results of this study support the hypothesis of an elevated risk of LE MSKI injury in athletes with a CONC relative to controls, despite both groups completing a NMT intervention. These data further highlight that concussion history can further magnify existing mechanisms that underly increased risk of LE MSKI for female adolescent. Identification of the mechanism(s) underlying elevated LE MSKI risk in athletes with a SRC and/or report history of SRC symptomology could support more personalized prevention strategies that uniquely target and restore lingering sources of dysfunction to preserve athlete health during competitive sport.

Acknowledgements: This research was directly supported by NIH/NIAMS research grants U01AR067997, R01AR077248, R01AR076153, and T32NS7453-20. This work was also partially funded by internal support from the Department of Orthopaedics at Emory University.

References: [1] McPherson (2019) *Am J Sports Med* 47(7); [2] Bryan (2016) *Ped* 138(1); [3] McCrory (2017) *Br J Sports Med* 51(11); [4] Chmielewski (2021) *J Sport Health Sci* 10(2); [5] Howell (2022) *Am J Sports Med* 50(4); [6] Lynall (2022) *Am J Sports Med* 50(12); [7] Myer (2005) *J Str Cond Res* 19(1)

FATIGABILITY AND PHYSICAL ACTIVITY LEVEL IN MIDDLE-AGED ADULTS WITH OBESITY

Julie S. Rekant[1*], Zachary J. Wilson[2], April J. Chambers[1,2]
[1]Department of Bioengineering, Swanson School of Engineering, University of Pittsburgh, Pittsburgh, PA, USA
[2]Health and Human Development, School of Education, University of Pittsburgh, Pittsburgh, PA, USA
*Corresponding author's email: julie.rekant@pitt.edu

Introduction: Middle-aged adults with obesity (MOB) have higher rates of measured fatigability compared to their normal weight counterparts.[1, 2] Research shows inefficiencies at the muscle level may contribute to this decreased activity capacity.[3] Adults with obesity demonstrate decreased fiber recruitment and slower fiber shortening during muscle contractions.[3] In particular, decreased endurance in the plantarflexors,[2] used for postural control, contributes to the prevalence of injuries and falls in aging adults and adults with obesity.[4] Regular physical activity is related to muscle hypertrophy, increasing the torque-producing capacity of muscles.[5] Further, participation in endurance-type physical activities like prolonged walking causes local muscle changes associated with greater fatigue resistance.[6, 7] The purpose of this research was to evaluate how daily physical activity level is associated with functional endurance and fatigability in MOB. Based on the known adaptations from physical activity participation on improved fatigue resistance, it was expected that MOB with higher levels of physical activity would also demonstrate less fatigability on a repeated plantarflexion contraction task. More active MOB were also expected to walk further on the 6-minute walk test (6MWT), a functional assessment of endurance. Finally, functional performance on the 6MWT was expected to relate with fatigability performance, where participants walking further during the 6MWT would also demonstrate plantarflexion fatigability resistance during a repeated contraction task.

Methods: Twenty-five MOB completed the 6-minute walk test (6MWT) and a maximum effort repeated plantarflexion isometric contraction task. MOB performed 4 second isometric contractions with interspersed 1 second rests for up to 5 minutes. Fatigability was assessed through features of torque production declines during the task (Fig. 1). An exponential decay function ($F = F_c + (100- F_c) * e^{-t/\tau}$ was fit to the peak torques during each 4-second contraction where F is the normalized torque, t is time, F_c is the asymptotic torque, and τ is the time when initiation of fatigue is observed and a flatter rate of torque decay begins.[2] Fatigue indexes (FIs) were also calculated as the area above the torque curve as a percentage of the summed area above and below the curve, representing the amount of torque decline that occurred over a given timeframe.[8] Physical activity level was quantified from one week of monitoring with a wrist-worn Actigraph activity monitor (ActiGraph, Pensacola, FL).

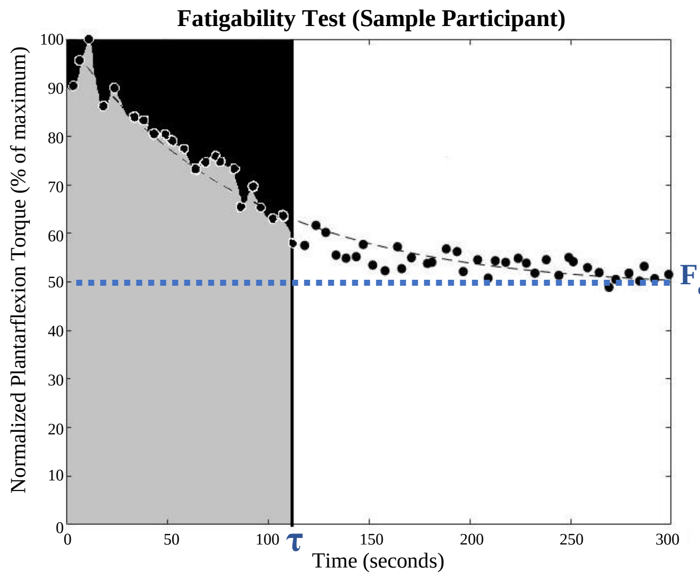

Figure 1. Exponential decay function fit to peaks of each 4-second contraction. Asymptotic torque (F_c), time to fatigue (τ), and fatigue index (FI) (black shaded area) were calculated.

Results & Discussion: Due to poor fit with the decay function ($R^2<0.75$, n=6), negative F_c values (n=2), and τ times after the end of the test (n=2), 15 participants were included in the final analysis (Age 52.8 ± 7.9, BMI 36.7 ± 4.2 kg/m^2). On average, torque production plateaued at 52.2 ± 9.3% of maximum torque (F_c). Onset of fatigue in MOB occurred after 111.1 ± 46.1 s (τ). Plantarflexion fatigability during a maximal effort repeated contraction task was not associated with physical activity level in MOB (Fc: ρ=-0.06 p=0.83 | τ: ρ=0.12 p=0.68 | $FI_{0-\tau}$: ρ=0.02 p=0.94 | $FI_{\tau\text{-end}}$: ρ=0.08 p=0.77). Further, 6MWT performance was not significantly related to physical activity level (ρ=0.11 p=0.70). However, 6MWT distance was inversely related with time to fatigue (6MWT & τ: ρ=-0.55 p=0.03). MOB who walked farther on the 6MWT also transitioned to fatigue earlier during the maximum effort repeated contraction task. This was unexpected, however may be explained by an ability sustain performance at a lower torque threshold for a longer period of time. This work was limited by the small sample size due to participant exclusion during pre-processing. Future work should explore the relationship between other measures of physical activity, particularly engagement in endurance activities, and fatigability, and evaluate measures of perceived fatigue in addition to objective measures of fatigability.

Significance: While overall physical activity level was not related to plantarflexion fatigability nor 6MWT performance in MOB, functional performance on the 6MWT was inversely related to plantarflexion fatigability. This work highlights the need for better classification of physical activity to quantify mode-specific adaptation in performance. Relatedly, general physical activity programs may not be sufficient for fatigability performance benefits. Future work should evaluate measures of muscle physiology like oxygenation dynamics and fiber types in addition to performance measures to understand mechanisms muscle performance in MOB.

Acknowledgements: This work was supported by NIH TL1TR001858 and the University of Pittsburgh Healthy Lifestyle Institute.

References: [1] Pajoutan et al. (2016), *Fatigue* 4(2); [2] Maktouf et al. (2020), *J Biomech* 105; [3] Bollinger (2017) *Gait Posture* 56; [4] King et al. (2012) *J Ger Phys Ther* 35(1)8-14; [5] Hall (2015) *Basic Biomechanics* p146-57; [6] Plotkin et al. (2021) *Sports* 9(9); [7] Coggan et al. (1985) *J Appl Phys* 72(5); [8] Surakka et al. (2004) *Clin Rehabil* 18(6)

EVALUATION OF A PNEUMATIC CYLINDER FOR ACTUATING AN ANKLE EXOSKELETON

David S. Bell[1*], Michael E. Zabala[2]
[1]Auburn University, Auburn, AL, USA
Email: dsb0029@auburn.edu

Introduction: Ankle exoskeletons are used to reduce the metabolic cost of walking by providing a force to assist plantarflexion and reduce the workload of the gastrocnemius muscle. An application of this device is to improve the mobility and endurance of workers who carry heavy equipment. Existing designs which have achieved a metabolic cost reduction are actuated by an electric motor on the joint, a pneumatic muscle actuator (PMA), or a Bowden cable driven by an external motor.[1] Controllers for these actuators have either followed the ankle angle of previous steps or used a predictive model.[2]

Pneumatic cylinders offer several potential advantages over more common designs and are heavily used in industrial applications. Unlike electric motors they are compliant while providing force and have no upper speed limit or overheating risk.[3] In addition, the limited range of motion provides natural safety stops. A major limitation of this actuator type is controllability. The control response is delayed, highly nonlinear, and difficult to model. Industrial applications often use on/off control between two positions. Precise position control has been achieved using a PID control method[3], however, this becomes unstable when applied to a speed optimized cylinder. There is no standard method for controlling the piston with a high velocity.[5] The objective of this work is to determine if a pneumatic cylinder can be used to actuate an ankle exoskeleton for walking based on speed, input delay, and control accuracy.

Methods: A double acting pneumatic cylinder with a 1.75 inch bore and four-inch stroke had four servo valves attached to control pressure input from a 130 psi source and exhaust to atmosphere for each direction. A potentiometer position sensor and generator velocity sensor were mounted on the end of the actuator rod to provide control feedback. The device, shown in Figure 1, uses low cost, consumer grade components and 3D printed PLA. The control algorithm was run on a microcontroller which read position commands from a computer and returned results.

The control algorithm was a velocity proportional controller with an overshoot predictor. Control gain was slowly adjusted for each direction based on position error to compensate for either changes in loading or control demands. The control design did not attempt to perfectly match positions but was optimized to follow the velocity profile of the input with the lowest possible delay.

First, a sine wave input was tested with an amplitude of 80% of the maximum stroke length at varying frequencies to determine the maximum operating frequency and speed of the actuator as well as to check controller stability. The maximum useful frequency was the highest one at which the actuator tracked the full amplitude of the input. Next, the actuator tracked a previously recorded ankle angle profile and the result was plotted to observe profile accuracy and stability.

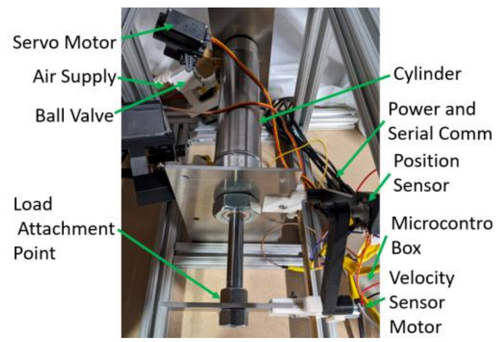

Figure 1: The actuator prototype as tested.

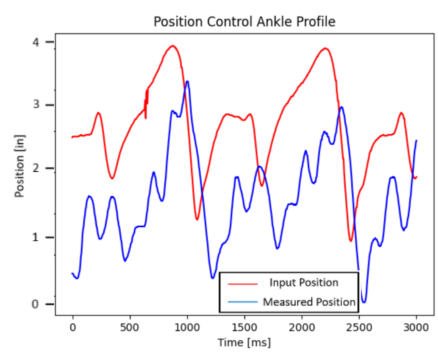

Figure 2: The actuator tracking an ankle angle at a real walking speed.

Results & Discussion: The cylinder was able to track the motion profile of sine waves up to 1.5 Hz and a recorded walking ankle angle at real speed. The ankle angle tracking is shown in Figure 2. In both cases the actuator had limited position drift away from the input but closely matched the velocity profile with a delay of 80 to 100 ms. There was a tendency to overshoot and oscillate, but it did not create instability in the controller.

The controller is able to provide assistive force at any point in the gait cycle without dangerous instability. Position drift and overshoot were substantial, likely because the actuator had no load or damping. Due to delay, the actuator would be expected to function optimally with an ankle angle prediction 80 ms into the future. Improved tracking could be achieved with more precise servo valves. Delay is primarily limited by the physics of airflow for a given cylinder size.[3]

Significance: The tests demonstrated that a pneumatic cylinder can reasonably track the movement of an ankle, although drift, overshooting and an offset was observed. It should be determined if it can provide assistive force through the entire gait cycle at the ankle. This design provides advantages over other actuators for exoskeleton design such as compliance, safety, and linear force output.

Acknowledgements: Thanks to Jakob Markham and Ethan Koenig for help with hardware design as well as Dr. Brenden Allen and Samuel Douglass for controls advice.

References: (1) Sawicki, Ferris, Journal of Experimental Biology, Vol 211. (2) Cao, Huang, IEEE/CAA Journal of Automatica Sinica, Vol 7. (3) Saravanakumar, Mohan, Precision Engineering, Vol 49. (4) Heo, Kim, IEEE Robotics and Automation Letters Vol 5. (5) Bone, Ning, IEEE/ASME Transactions on Mechatronics, Vol 12.

THE EFFECT OF USING AN EXTENSION ARM NAIL GUN ATTACHMENT ON MAXIMUM KNEE JOINT LOADING DURING A SIMULATED SLOPED SHINGLE INSTALLATION TASK

Kevin D. Moore[1*], John Z. Wu[1], Robert E. Carey[1], Scott P. Breloff[1,2]
[1]HELD, National Institute for Occupational Safety and Health, Morgantown, WV, USA *email: qcp5@cdc.gov
[2]DFSE, National Institute for Occupational Safety and Health, Cincinnati, OH, USA

Introduction: Residential roofing is a physically demanding job and requires working long hours in awkward postures, putting roofers at an increased risk for lower back and knee injuries such as musculoskeletal disorders (MSDs) and osteoarthritis (OA) [1,2,3]. To improve working posture and reduce MSD risks in roofers, interventions such as nail gun extension arms have been designed. While interventions like the nail gun extension arm may greatly improve working posture, their effect on knee joint loading is unknown. Since knee joint loading is linked to the initiation and development of knee OA and other MSDs [1,3], it is important to understand how working posture intervention-related devices affect knee joint loading. Therefore, the purpose of this study was to determine how the use of a nail gun extension arm aimed at improving working posture would affect maximum compressive and shear forces at the knee joint during a simulated sloped shingle installation task.

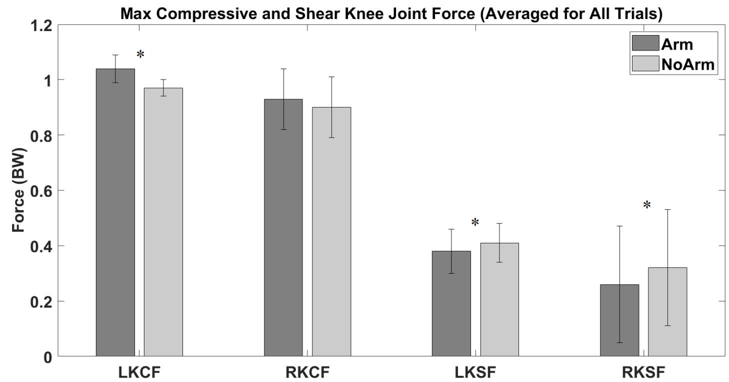

Figure 1: Average of max force values (BW) for all trials (Arm vs NoArm). *Significant difference. L-left, R-right, K-knee, C-compressive, S-shear, F-force.

Methods: Three healthy males (age: 24 ± 4 yrs, height: 1.84 ± 0.1 m, weight: 86.3 ± 10.9 kg) participated in this preliminary investigation and repeated a simulated shingle installation task five times on a roofing platform (at 14° incline) with and without an extension arm attached to a nail gun. Marker trajectories were captured using a 14-camera system (Vicon Inc.) at a sampling rate of 100 Hz and were synchronized with three force-plates (Bertec Corp.) sampling at 1000 Hz. Using the marker data, motions of the anatomical body segments were modelled in Visual3D (C-motion Inc.). The time histories of the shear and compressive forces at the right and left knee joints were then computed in Visual3D using inverse dynamics [4].

Bilateral knee maximum shear and compressive forces were calculated for every trial (normalized to Body Weight (BW) units). The maximum knee joint shear forces (MKSF) and maximum knee joint compressive forces (MKCF) for the trials with the extension arm (Arm) were compared to those without the extension arm (NoArm). The bilateral differences for MKSF and MKCF between the Arm and NoArm trials were compared statistically using a one-tailed paired t-test ($p < 0.05$).

Results & Discussion: Averages for the maximum left knee compressive forces (LKCF), right knee compressive forces (RKCF), left knee shear forces (LKSF), and right knee shear forces (RKSF) for the Arm and NoArm trials are shown in Fig. 1. Statistically significant differences for the maximum knee joint forces between the Arm and NoArm trials were identified for LKCF with the Arm trials being 0.065 BW larger on average ($p < 0.01$), LKSF with the NoArm trials being 0.031 BW larger on average ($p = 0.01$), RKSF with the NoArm trials being 0.055 BW larger on average ($p = 0.03$), and the only difference that was not significant was RKCF although the Arm trials were 0.03 BW larger on average (Fig. 1).

The Arm trials increased MKCF and decreased MKSF which may be caused by the changed working posture, as the center of mass is shifted forward when not using the arm (NoArm) since the roofer needs to bend/lean over, directing force anteriorly (shear). The MKCF for the Arm trials were larger than the NoArm trials; however, the magnitude of the Arm trials is still relatively small. The MKCF for the Arm trials are between those experienced during static standing and gait [5, 6], indicating that these joint contact forces are within normal physiological ranges and are not likely to result in an elevated risk for MSDs or OA. Additionally, the reduction in MKSF and increase in MKCF observed in the Arm trials, while relatively small, might have a cumulative effect which could increase knee stability over time, and this may potentially reduce the risk for reoccurring falls [7]. Based on the results, the nail gun extension arm should not have a negative impact on knee joint health and may increase knee stability for roofers over time.

Significance: The current study evaluated the variations of knee joint loading associated with the use of a nail gun extension arm during a simulated sloped shingle installation task. The current results suggest that the use of the extension arm should not negatively impact knee joint health, and the extension arm reduces the MKSF which may increase knee stability over time. The MKCF during the Arm trials are relatively small and are no larger than those experienced during activities of daily living [5, 6], indicating that the increased MKCF from the use of the extension arm is unlikely to pose an elevated risk for MSDs or knee OA.

Disclaimer: The findings and conclusions in this report are those of the authors and do not necessarily represent the official position of the National Institute for Occupational Safety and Health, Centers for Disease Control and Prevention. Mention of any company or product does not constitute endorsement by the National Institute for Occupational Safety and Health, Centers for Disease Control and Prevention.

References: [1] Wang et al. (2020), *Arth Care Res* 72(9); [2] Wang et al. (2017), *J Const Eng Man* 143(7); [3] Dutta et al. (2020), *Ergonomics* 63 (9); [4] Winter. (2009) *Biomechanics… 4th Edition*; [5] Messier et al. (2005) *Arch Phys Med Rehabil* 86 (4); [6] Harding et al. (2016), *Clin Biomech*; [7] Nevitt et al. (2016), *Arth Care Res* 68 (8);

Comparison of Fall Prevalence between Alzheimer's Disease and Mild Cognitive Impairment in Older Adults: A Meta-analysis

Sara Mahmoudzadeh Khalili[1], Caroline Simpkins[1], Debra Tann[2], Feng Yang[1*]

[1] Department of Kinesiology and Health, [2] Gerontology Institute, Georgia State University, Atlanta, GA USA

*Corresponding author's email: fyang@gsu.edu

Introduction: Falls present a serious health threat to older adults worldwide [1]. It is well recognized that the fall risk in older adults with Alzheimer's disease (AD) or mild cognitive impairment (MCI) is higher than their cognitively healthy counterparts [2]. In the literature, most of the studies merged AD and MCI groups when reporting their fall risk. This common practice could cause some potential issues as it assumes that the fall risk is similar between these two subgroups of population with dementia. However, it remains unknown whether such an assumption is accurate. If it is not, the combined fall risk assessment between people with AD and MCI may underestimate the fall risk for one group but overestimate it for the other group. This could provide misleading information to policymakers who oversee the distribution of limited healthcare resources for fall prevention and to researchers/clinicians who develop or implement fall prevention interventions for these populations. Therefore, it is essential to clarify if the fall risk is similar or different between people with MCI and AD. The annual fall prevalence is a common metric reflecting the fall risk. The purpose of this study was to meta-analyze the relevant literature and compare the annual fall prevalence between older adults with AD and MCI.

Methods: Our literature search was conducted within the following databases: APA PSYCINFO, CINAHL, EBSCO, Google Scholar, MEDLINE, and PUBMED based on the search terms related to the fall prevalence in people with AD or MCI. The search lasted between September and December 2022. No time range or region restrictions were applied. A study was included if it 1) was conducted in older adults aged 65 years or over with AD or MCI, and 2) was published in peer-reviewed English journals. The initial search obtained 5,828 publications. After duplicate removal and full-text screening based on the inclusion and exclusion criteria, 23 articles were selected for this meta-analysis. Among them, 17 (4) reported the fall prevalence for only older adults with AD (MCI). Two studies presented the fall prevalence data for both AD and MCI groups. Publication characteristics (author(s), year), sample characteristics (sample size, age, dementia type), and study characteristics (fall prevalence or the number of fallers) were extracted and input to Review Manager (RevMan) 5.3 (Nordic Cochrane Centre, Denmark) [3]. The annual fall prevalence was defined as the ratio of the number of fallers over 12 months to the total number of participants for each study. A participant was considered a faller if s/he has experienced at least one fall over the 12-month interval. Meta-analyses were conducted using the random-effects model with inverse variance weights to calculate the pooled annual fall prevalence for either population. The 95% confidence intervals (CI) of the fall prevalence were also estimated. χ^2 test was used to compare the pooled fall prevalence between people with AD and MCI. The significant level was set at $p < 0.05$.

Results & Discussion: For the included studies, the average age varied between 65 and 86.6 years for people with AD and between 71.9 and 76.7 years for MCI. Among 4,285 people with AD, 1,612 were fallers. The fall prevalence changed considerably between studies: 25% to 73.96%. The pooled annual fall prevalence was 44.32% (95% CI = [38.34%, 50.29%]) for people with AD. There were 1,166 people with MCI who enrolled in the studies included in this meta-analysis. Among them, 171 experienced at least one fall over the 12-month period. The fall prevalence also showed a drastic variance among studies: from 7.14% to 60%. The overall fall prevalence was 38.54% (95% CI = [13.92%, 63.17%]) for people with MCI. χ^2 test indicated that the pooled fall prevalence is significantly higher in people with AD than in people with MCI ($p < 0.001$). This difference in fall prevalence could be accounted for by the different stages of dementia between these two populations. This postulation should be further examined in future studies. Our meta-analysis had limitations. The number of studies included, especially for the MCI group, was small and the fall risk measurement was limited to the annual fall prevalence. It remains unknown if other fall risk-related metrics would follow the same trend as the annual fall prevalence. These could reduce the generalizability of our findings. More studies with larger sample sizes and involving more fall risk-related measurements should be conducted.

Significance: Our results suggested that people with AD experience a significantly higher fall prevalence than people with MCI. Such a difference in the annual fall prevalence implies that the fall risk is different between these two populations with dementia. Therefore, the underlying mechanism of falling could differ between them, and the fall prevention strategies should consider such differences and be designed specifically for each population. Our results also suggest that fall risk measurements should be reported separately for people with AD and MCI. The findings could provide useful information to stakeholders, such as policymakers, to distribute fall prevention resources between people with AD or MCI, to researchers and clinicians to develop fall prevention paradigms for people with dementia, and to individuals with AD or MCI and their caregivers about their fall risk.

Acknowledgements: This study was partially supported by the National Institutes of Health (1R21-AG077307-01) and the Alzheimer's Association (AARG-NTF-21-852145).

References: [1] James et al. (2020), *Injury Prevention*, 26. [2] Salari et al. (2022), *Journal of Orthopedic Surgery and Research*, 17. [3] Higgins et al. (2019), *Cochrane handbook for systematic reviews of interventions*.

JUST NOTICEABLE DIFFERENCE OF IMPEDANCE PARAMETERS WHILE WALKING IN AN ANKLE EXOSKELETON

Axl Maberry[1*], Anne E. Martin[1]
Mechanical Engineering, Penn State, University Park, PA, USA
*Corresponding author's email: akm6700@psu.edu

Introduction: Exoskeletons for civil, military, or rehabilitative use require appropriate control parameters that are tuned for optimal performance [1]. The just noticeable difference (JND) quantifies the minimum change in control parameters needed for the user to perceive a difference in exoskeleton assistance. Impedance control is often used in exoskeletons and typically requires multiple control parameters. The JND for static ankle impedance is 12% [2,3], but the JND has not been quantified while walking. Since JND studies typically only test one parameter, it is unknown if multiple parameters interact to alter the JND. This abstract tests two hypotheses, first that the starting value of one exoskeleton control parameter affects the JND of itself or the other parameter, and second that JNDs of the exoskeleton control parameters are higher while walking compared to static positions.

Methods: 13 subjects walked at a slow speed on a treadmill while wearing a pneumatically powered ankle exoskeleton on each leg. The exoskeleton was controlled via impedance control parameterized by a nondimensionalized gain, k_n, and ramp rate, m_n. Four pairs of nominal parameter values (k_n, m_n), each called a standard, were tested (Fig.1). Segments of unidirectional deviations, or comparisons, from the selected standard were tested to find the JND. The comparison consisted of magnitude changes of ±(0, 20, 30, 40, 60)%. During an experiment, the subject tested four pseudo-randomly chosen segments, and each comparison was randomly tested 10 times. During a trial, the subject took 5 strides with the standard and then up to 5 strides with the comparison [4]. The subject responded with a verbal "yes" if they detected a difference between the standard and the comparison and a "no" otherwise. The percentage of "yes" responses were used to curve fit a psychometric function with the JND defined as the midpoint between the false positive rate, α, and a 100% "yes" response rate or (100%+α)/2 [4]. Two one-way ANOVA tests ($p<0.05$) were used to determine if 1) a change in one of the parameters affected its own JND and 2) if a change in one of the parameters affects the JND of the other parameter.

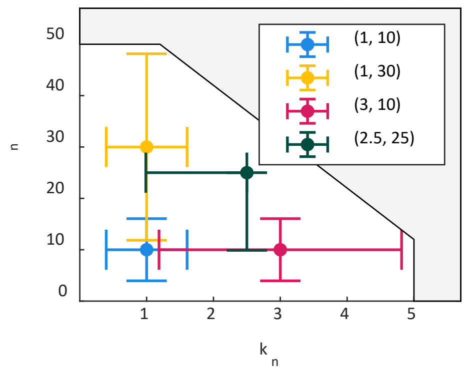

Figure 1: The selected standards (points) and range of comparisons (bars) for each standard. These were selected to test the full range of stable combinations for the ankle exoskeleton.

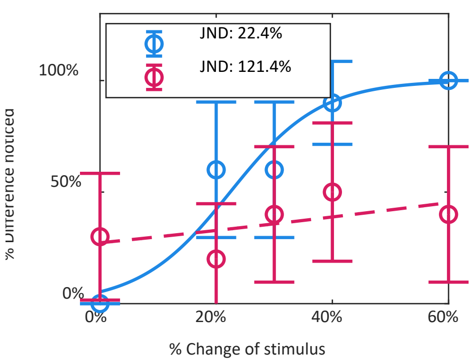

Figure 2: An example of an accurately captured JND (blue, solid) and a JND that was not captured by the test range (red, dashed). The tested standard was (3,10) testing a decrease in k_n magnitude.

Results & Discussion: 53.8% of the trials resulted in a JND in the tested 0-60% comparison range. The remaining trials had a JND either well above the tested range or below zero. In most cases, this occurred because the trials had very little difference in the response rate over the entire 0-60% comparison range (Fig. 2). This means the data only captured the flat portion of the curve and not the increase in slope that is typical for a logistic curve, preventing accurate estimation of the JND. Such cases were excluded from the statistical tests.

The ANOVA tests resulted in p-values > 0.29 and indicated that changing one parameter did not significantly affect the JND of either parameter. This suggests that we can combine the JND's from multiple standards to determine an overall mean and SD for each parameter. The combined means and SD of each parameter's JND were 36.01 (12.92)% for k_n, and 36.91 (11.16)% for m_n. This is approximately 3 times higher than the 12% JND for static position impedance [3]. The increased JND could be due to the increased cognitive load in dual-task walking i.e. detecting stimulus changes while walking produced competing demands, decreasing the performance of detection [5].

Significance: A quantified JND allows for more precise control of stimuli, which allows for better development of exoskeletons for civil, military, or rehabilitative use. If kept within the JND, parameters can be tuned to maximize an objective function without the user noticing significant changes to their gait. Since the JNDs for these impedance parameters are higher while walking than in a static position, the range that these parameters can be tuned is larger. Additionally, this also suggests that a significant parameter change is needed if a change in perception is desired while walking, such as changing the preference or comfort of a subject.

Acknowledgements: This work was supported by NSF awards 1943561 and 1930430.

References: [1] Young & Ferris (2017), *IEEE T Neur Sys Reh* 25(2); [2] Azocar et al. (2019), *IEEE T Neur Sys* 27(2); [3] Azocar & Rouse (2017), *IEEE Trans Biomed Eng* 64(12); [4] Peng et al. (2022) *IEEE T Neur Sys* 30; [5] Beurskens et al. (2016), *Neural Plast* 2016.

IN VIVO CERVICAL FACET CAPSULAR LIGAMENT MECHANICS: ESTIMATIONS BASED ON SUBJECT-SPECIFIC ANATOMY AND KINEMATICS

Maryam Nikpasand[1], Rebecca E. Abbott[1], Craig C. Kage[1], Sagar Singh[2], Beth A. Winkelstein[2], Victor H. Barocas[1], and Arin M. Ellingson[1*]

[1]University of Minnesota – Twin Cities; [2]University of Pennsylvania; *ellin224@umn.edu

Introduction: To understand the facet capsular ligament's (FCL) role in cervical spine mechanics, the interactions between the FCL and other spinal components must be examined [1]. One approach is to develop a subject-specific finite element (FE) model of the lower cervical spine, simulating the motion segments and their components' behaviors under physiological loading conditions. This approach can be particularly attractive when a patient's anatomical and kinematic data are available.

Methods: In this study, we developed and demonstrated a method to create 3D subject-specific models of the lower cervical spine (C4-C7), with a focus on FCL biomechanics [2]. The FCL geometries were generated using the knowledge that the ligament encloses the bilateral facet joints. As such, a surface was fitted to cover the estimated ligament-bone attachment regions on the joints' bony areas and across the joint space. Displacement-controlled boundary conditions were applied to the bones such that the vertebrae in the model mimicked the kinematics extracted from biplane videoradiography of different head motions, including axial rotation, lateral bending, and flexion-extension [3]. The fiber structure and material characteristics of the ligament tissue were extracted from available human cervical FCL data and were incorporated in a hybrid multiscale model to generate fiber characteristics that were used in FEBio to define tissue material. The method was demonstrated by application to the cervical geometry and kinematics of a healthy 23-year-old female subject.

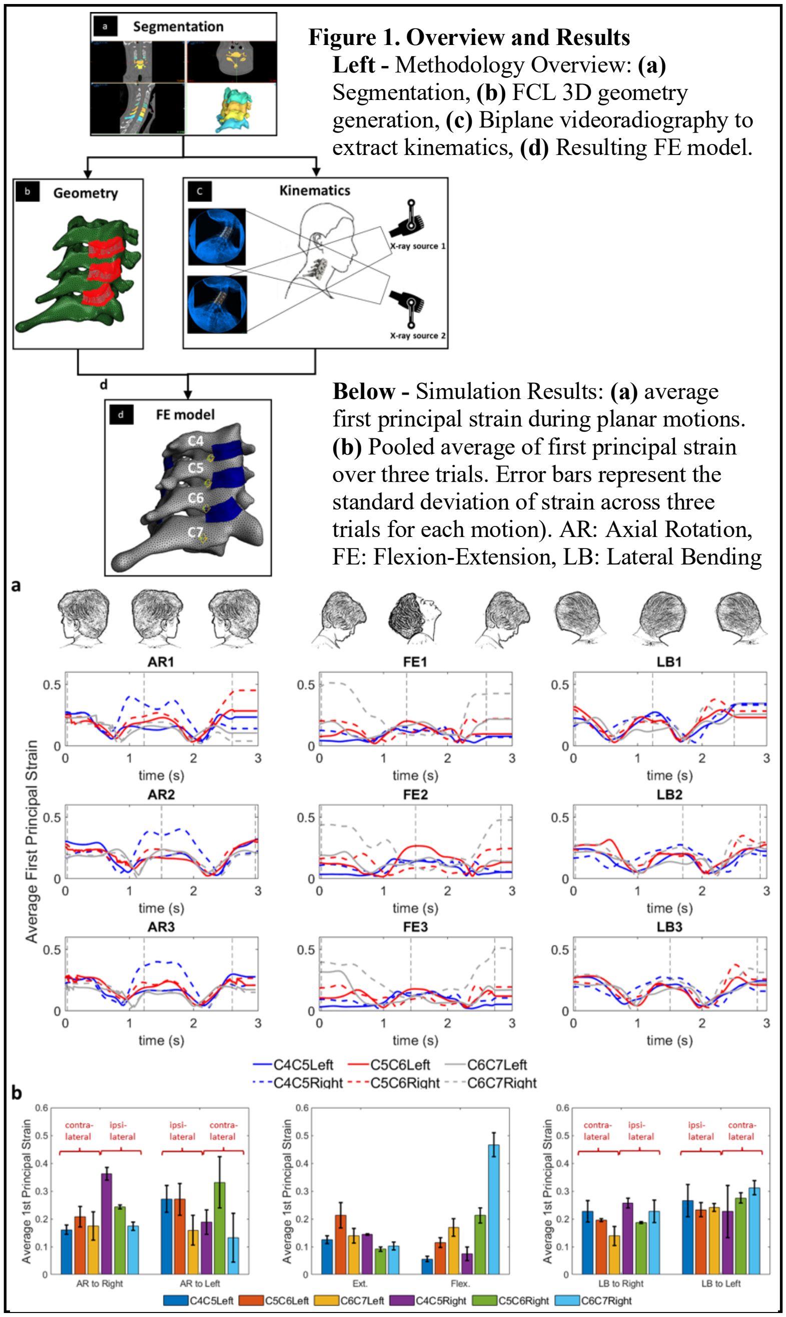

Figure 1. Overview and Results
Left - Methodology Overview: **(a)** Segmentation, **(b)** FCL 3D geometry generation, **(c)** Biplane videoradiography to extract kinematics, **(d)** Resulting FE model.

Below - Simulation Results: **(a)** average first principal strain during planar motions. **(b)** Pooled average of first principal strain over three trials. Error bars represent the standard deviation of strain across three trials for each motion). AR: Axial Rotation, FE: Flexion-Extension, LB: Lateral Bending

Results & Discussion: The strain maps within the FCL of the resulting subject-specific model were subsequently compared to models with generic: 1) geometry, 2) kinematics, and 3) material properties to assess the effect of model specificity on the FCL biomechanics. Asymmetry in both the kinematics and the anatomy led to asymmetry in the calculated strain fields, highlighting the importance of patient-specific models. A sensitivity study revealed that the qualitative form of the strain field was largely independent of the estimated ligament-bone contact area, but the strain in non-contact regions tended to increase with greater estimated contact area. We also found that the calculated strain field was largely independent of constitutive model and driven by vertebrae morphology and motion, but the stress field showed more constitutive-equation-dependence, as would be expected given the highly constrained motion of cervical FCLs.

Significance: The current study provides a methodology to create a subject-specific model of the cervical spine that can be used to investigate various clinical questions by coupling experimental kinematics with multiscale computational models.

Acknowledgements: This work was funded by the following NIH grants: U01AT010326, R03HD09771, K12HD073945, UL1TR002494, TL1R002493, and T32AR050938. Additionally, this work was supported by the Minnesota Partnership for Biotechnology and Medical Genomics (MHP IF #14.02). We gratefully acknowledge resources and support from the Minnesota Super Computing Institute.

References: [1] Steilen et al. *Open Orthop J.* 2014. [2] Zarei, et al., *J. R. Soc. Interface*, 2018. [3] Kage et al. *PLoS One* 2020.

BIODEX POSTURAL STABILITY TEST SCORES IN COLLEGIATE STUDENTS

Ben W. Meyer[1*]
[1]Shippensburg University
*Corresponding author's email: bwmeyer@ship.edu

Introduction: The purpose of this project was to assess the performance of collegiate students in the Biodex postural stability test. The Biodex Balance System SD allows a static platform setting, as well as dynamic settings from level 1 (most stable) to level 12 (least stable). Previous work found that dynamic (level 5) sway index values were over twice as large as values in static platform settings [1]. Other work has examined the differences in static balance performance between various footwear and barefoot conditions. No differences were found in left-to-right sway indices, but significant differences were found in front-to-back sway indices for athletic shoes, five-toed shoes, and barefoot conditions, with an overall sway index for the athletic shoes condition of 3.4, for the five-toed shoes 5.6, and barefoot 6.1 [2]. Previous work has also examined postural stability in single-leg conditions, with sway index values ranging from 2.2 to 3.5 on a static platform being found in the literature [3,4]. The small sway index values found in these studies indicates a large percentage of time spent near the center target of the postural stability test (e.g., in the closest "zone").

This project aimed to add to the body of literature for Biodex postural stability testing. Owing to the lack of information in the literature for balance tests performed at the largest dynamic setting (level 12), a protocol was developed to test collegiate students in both static and level 12 dynamic settings. Due to previous literature indicating that sway index values were over twice as large in level 5 dynamic settings as in static settings, it was hypothesized that participants in the present study would have level 12 dynamic sway index values well over twice as large as in the static setting. In addition, due to the large dynamic platform setting used in the current investigation, it was hypothesized that the percent time in the zone closest to the center target would be much smaller than in the static setting.

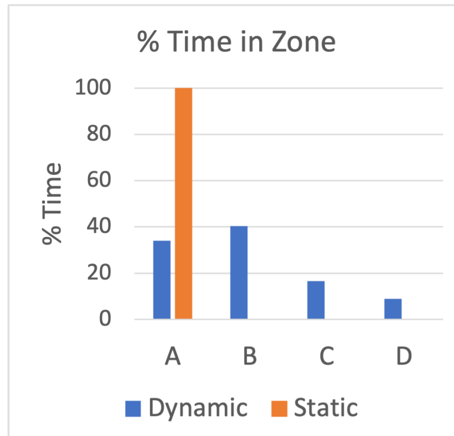

Figure 1: Average percent time in zone for dynamic and static conditions (Zone A represents best performance, Zone D worst performance).

Methods: Twenty males and fourteen females (age = 21 ± 1 yrs; mass = 80 ± 19 kg; height = 1.75 ± 0.11 m) participated in the study. Participants came from a variety of backgrounds (e.g., softball, football, track & field, recreational athlete, etc.). Each participant completed the postural stability tests using a Biodex Balance System SD. All participants wore athletic footwear, and the test order was randomized. The foot positioning recommendations provided by Biodex were used. All trials were completed with eyes open. Three attempts were completed using a static platform setting, and three attempts were completed using a level 12 dynamic setting. The best sway index value for each condition was used in the analysis.

The overall, front-to-back (F/B), and left-to-right (L/R) sway index scores were computed for each participant. Percent time in zone values were also recorded. The zones corresponded to concentric rings around the center target, with Zone A being the closest ring and Zone D being the outermost ring. The differences between static and dynamic sway index values and percent time in zones were assessed using ANOVA tests. Statistical significance was set at $\alpha = 0.05$.

Results & Discussion: Significant differences were found in the overall sway index value between the static condition (0.67 ± 0.17) and the level 12 dynamic condition (7.80 ± 2.76). The static platform sway index values were smaller than previous literature, while the level 12 dynamic sway index values were larger, in support of the study hypothesis. Figure 1 shows that significant differences were also found in the percent time in zone values: level 12 dynamic condition (34, 40, 17, 9) and static condition (100, 0, 0, 0) in Zones A-D, respectively. The differences in percent time in zone also support the study hypothesis, as the challenging level 12 dynamic condition led to only 34% of time in the closest zone compared to 100% in the static condition.

The relative difference between F/B sway index (dynamic 6.0 ± 2.0, static 0.6 ± 0.1) and L/R sway index values (dynamic 5.0 ± 2.0, static 0.3 ± 0.1) decreased going from static to level 12 dynamic conditions. In the easier static condition, participants primarily had F/B sway, while in the more challenging level 12 dynamic condition, participants more evenly distributed their sway between F/B and L/R directions.

Significance: The results of this study add to the literature for Biodex postural stability tests. Balance assessments are used extensively in clinical, research, and sport settings. Both in and out of the field of biomechanics, significant time and attention is given to the improvement of balance. Prior to this study, little was known about sway index values for postural stability tests at the largest dynamic setting. Now that we have baseline sway index values for young healthy individuals at the level 12 setting, future research can examine other populations at this most challenging dynamic setting.

Acknowledgements: The author would like to thank the College of Education and Human Services at Shippensburg University.

References: [1] Park et al. (2017), *J Phys Ther Sci* 29(2); [2] Smith et al. (2015), *Int J Sp Phys Ther* 10(1); [3] Hosp et al. (2017), *J Ath Train* 52(7); [4] Kara et al. (2018), *Mal J Mov* 7(2).

MUSCLE COACTIVATION DURING GAIT IN CHILDREN WITH CEREBRAL PALSY

Ippersiel P[1], Dussault-Picard C[1], Mohammadyari S.G[1], De Carvalho G, Vishnu D.C, Pal S, Dixon P.C [1]
[1] School of Kinesiology and Physical Activity Sciences, Faculty of Medicine, University of Montreal
Corresponding author email: Patrick.ippersiel@umontreal.ca

INTRODUCTION: Children with cerebral palsy (CP) present with impairments in the neuromuscular system, which often result in coordination difficulties during gait. Compared to their typically developing (TD) peers, children with CP walk with a more in-phase and less variable (i.e., "stiff") lower-limb coordination strategy [1]. This behavior may reflect an impaired ability to selectively activate muscles during gait. Muscular co-cactivation (MCa) is a biomechanical metric which provides insight into timing and activation levels of a pair of muscles surrounding a joint, wherein excessive or insufficient MCa is likened to poor motor control. Thus, studying MCa in children with CP may contextualize changes in coordination during gait and help guide management of CP. However, there are inconsistencies in reports of MCa in the CP literature, in-part related to differences in EMG normalization procedures [2]. Thus, our objective was to (i) compare lower extremity MCa during gait in children with, and without CP; and (ii) to determine if MCa is influenced by EMG normalization procedures.

METHODS: Data from 49 children (CP = 23, TD = 26) walking barefoot along a 10m walkway at their comfortable gait speed were extracted from two laboratory databases. Baseline demographics, EMG, and kinematic data were retained. EMG data were collected from rectus femoris, semitendinosus, lateral gastrocnemius, and tibialis anterior muscles, bilaterally, using a wireless Delsys system. Kinematic data were collected using a Vicon motion capture system and used to partition data and identify gait phases (i.e., stance and swing). Data were imported into Matlab (R2020a) and processed using biomechZoo (v1.9.7). EMG data were rectified and linear enveloped using a low-pass, 4th order Butterworth filter with frequency cut offs of 20 and 450 Hz, and a root mean squared (RMS) moving window. Data were then amplitude normalized to a local maximum, for each trial. MCa indices were calculated for the rectus femoris-semitendinosus (RF-S) and tibialis anterior-lateral gastrocnemius (TA-G) muscle pairs [3], using both amplitude normalized and RMS averaged data. Independent sample T-tests examined group differences for MCa, for both muscle pairs, across stance and swing phases. Statistical significance was set at $p < 0.05$. Effect size (Cohen's D) and confidence intervals (CI) are presented. Statistical analyses were carried out in SPSS.

RESULTS AND DISCUSSION: There were no statistical group differences in age, height, or BMI ($p > 0.05$). Using amplitude normalized data, the CP group had greater MCa for the TA-G muscle pair during stance ($\bar{x}$ difference = 15.3; 95% CI = [8.1, 22.6]; Cohen's D = 1.16). No other group differences were seen (Table 1). Using RMS averaged data, the CP group had greater MCa for TA-G during stance ($\bar{x}$ difference = 16.5; 95% CI = [9.1, 23.9]; Cohen's D = 1.20) and swing ($\bar{x}$ difference = 9.97; 95% CI = [1.8, 18.1]; Cohen's D = 0.778), and during swing for RF-S ($\bar{x}$ difference = 16.2; 95% CI = [6.0, 26.5]; Cohen's D = 0.793).

Table 1. Muscle coactivation differences in children with, and without CP during gait, for the tibialis anterior-gastrocnemius (TA-G) and rectus femoris-semitendinosus (RF-S) muscle pairs, using amplitude normalized (Norm) and RMS averaged data.

Muscle Pair	**Gait Phase**	**CP $\bar{x}$ (SD)**	**TD $\bar{x}$ (SD)**	**P-value**
TA-G (Norm)	Stance	67.4 (13.4)	52.1 (13.1)	**<0.01**
	Swing	42.7 (15.3)	38.4 (18.4)	0.38
RF-S (Norm)	Stance	60.1 (15.2)	54.8 (15.3)	0.21
	Swing	54.4 (17.9)	46.6 (18.3)	0.14
TA-G (RMS)	Stance	66.8 (12.7)	50.4 (14.5)	**<0.01**
	Swing	43.7 (13.5)	33.7 (14.0)	**0.017**
RF-S (RMS)	Stance	55.3 (17.2)	50.8 (19.3)	0.39
	Swing	51.8 (17.5)	35.8 (18.0)	**<0.01**

SIGNIFICANCE: Using normalized data, children with CP had greater MCa during stance phase in the TA-G muscle pair. Using RMS averaged data, greater MCa was seen during most of the gait cycle, in both muscle pairs. Greater MCa is aligned with an invariable coordination strategy, and likely reflects a less robust and flexible gait strategy. RMS averaged data may be more sensitive to detect change in MCa, perhaps due to normalization techniques removing between subject variability. Without a ground truth, however, this remains speculative, and it is hard to recommend one method.

REFERENCES: [1] Dussault C et al. *Clin Biomech* **98**: 105740, 2022; [2] Gagnat Y et al. *Front Neurol* **11**: 202, 2022; [3] Lo S et al. *Gait Posture* **53:** 110-114,

PREDICTING POSTURAL STABILITY FROM SKIN TEMPERATURE AFTER COLD-WATER IMMERSION IN FIELD CONDITIONS

Amy Silder[1*], Rebecca Weller[1,2], Rebecca McClintock[1,2], Timothy Dunn[1], Pinata H. Sessoms[1], Douglas Jones[1]
[1]Naval Health Research Center, San Diego, CA
[2]Leidos Inc, San Diego, CA
*Corresponding author's email: amy.b.silder.civ@health.mil

Introduction: Service members operating and training in cold environments are exposed to unique challenges. For example, a river crossing or accidental cold-water immersion can significantly impair operational performance and, in severe cases, may require life saving measures. Yet, unlike during similar civilian exposures, the need to engage with hostile forces, move location, or conduct necessary reconnaissance may prevent the warfighter from engaging in optimal recovery. An understanding of the body's physiological and physical response to extreme cold can mitigate the negative consequences associated with cold stress, expedite recovery, and increase safety. While numerous studies have investigated the effects of skin temperature and cold-induced shivering on upper extremity dexterity, fewer studies have considered the effects of cold exposure on balance and lower extremity function.

The primary purpose of this study was to explore the relationship between body temperature and postural stability following whole body cold-water immersion. We hypothesized that thigh and foot temperature would be highly predictive of worse postural stability, and that improvement in lower extremity temperature would be highly correlated with improved postural stability after rewarming.

Methods: Sixteen male service members (29 (8) years, 80 (7) cm, 86 (10) kg, mean (standard deviation)) who were enrolled in a Marine Corps cold-weather medicine course provided written informed consent to participate in this study. This course included a cold-water immersion and rewarming exercise.

Skin temperature: Before the cold-water immersion exercise, participants reported to an indoor classroom where skin temperature sensors (iButtonLink, Whitewater, WI) were secured to the thigh (mid-thigh; centered over the rectus femoris) and foot (dorsal surface). Skin temperature was recorded continuously at 1-minute intervals throughout the experiment.

Postural stability: Postural stability was measured a) the morning of the exercise in the indoor classroom (17°C), b) immediately after changing into dry clothes following cold-water immersion, and c) after rewarming. Center-of-pressure (COP) data (100Hz) were collected using a B-Tracks balance platform (Balance Tracking Systems, San Diego, CA). Participants were instructed to for 60 seconds with their feet approximately shoulder width apart, looking straight ahead, and with hands on their hips. The baseline indoor test was completed in socks and the post-cold-water immersion tests were completed wearing insulated booties that had a soft rubber sole. COP data were low pass filtered at 10Hz, then used to calculate path length and sway area from a 95% confidence ellipse.

Cold-water immersion (Figure 1): The exercise occurred in an outdoor pond located at 2100 m elevation. Air temperature was -3°C, wind speed was negligible, and water temperature was 1.6°C. Students wore t-shirt, shorts, socks, and athletic shoes into the water. They remained submerged up to their neck for 10. Medical staff (Figure 1, yellow dry suit) was in the water monitoring participants' safety and circulating water to maximize convective cooling. After immersion, participants changed into dry clothing and immediately performed the postural stability test outdoors (post-immersion). Participants then began passive rewarming in their sleeping system for ~45 minutes. The final postural stability test was completed outdoors after rewarming (post-rewarming).

Repeated measures ANOVA was used to test the effect of time on path length and sway. Linear regression was used to test if thigh and/or foot temperature significantly predicted postural stability. Finally, Pearson's correlation was used to test the hypothesis that recovery of skin temperature would be highly correlated with improved postural stability after rewarming.

Figure 1: Postural stability was measured at baseline, immediately after, and ~45 minute after a 10 minute immersion in 1.6°C water.

Results & Discussion: Compared to baseline indoor testing, sway area and path length increased after cold-water immersion and, despite large improvements, did not return to baseline levels after rewarming ($p<.001$, all comparisons).

Foot temperature post-immersion (i.e., after reclothing, at the time of the second postural stability test) significantly predicted postural sway area post-immersion ($r^2=0.295$, $p=.030$). When the regression model included both the minimum foot temperature recorded (i.e., during cold-water immersion) and foot temperature post-immersion, the predictive value of the regression equation improved substantially ($r^2=0.641$, $p=.004$). Note, the temperature of participants' feet increased from a minimum of 9.3 (2.8)°C during the cold-water immersion, to 15.0 (3.1)°C post-immersion, after exiting the water and donning insulated booties. No significant relationships were found between thigh temperature and postural stability measures.

The improvement in foot temperature from the minimum temperature recorded to post-rewarming was highly correlated with the improvement in sway area between post-immersion and post-rewarming ($r=0.785$, $p<.001$).

Significance: Accidental cold-water immersion has extreme negative effects on postural stability, which may hinder the ability to move to a safe location. Of equal importance is that postural stability did return to baseline after approximately 45 minutes of passive rewarming. It is important to consider how a reduction in stability may affect other operational tasks necessary for survival, such as starting a fire or handling a weapon. Current efforts are underway to quantify shivering and evaluate participants' ability to complete simple but operationally relevant tasks during recovery.

FOOT AND SHOE KINETICS ACROSS RUNNING GRADES AND FOOTWEAR UPPERS

Eric C. Honert[1*], Milena Singletary[1], Kathryn Harrison[1], Daniel Feeney[1]
[1]Peformance Fit Laboratory, BOA Technology Inc., Denver, Colorado, USA
*Corresponding author's email: eric.honert@boatechnology.com

Introduction: Understanding the interactions between foot and shoe is critical for advanced footwear technology [1] and for assistive devices that seek to replace or enhance the biological foot [2]. The net kinetic contribution from the foot and the shoe can be obtained from Distal Rearfoot power [1]. These contributions have been characterized at different running speeds on level terrain [3]. Because running outside-of-the-lab rarely happens on perfectly flat terrain, the kinetic contributions of the lower limb joints have been characterized at different gradients [4]. The primary purpose of this study was to understand how Distal Rearfoot work changes across different running grades.

Distal Rearfoot power can be used to understand the contributions of the shoe structures under the foot [1]. However, it is currently not known if this metric is sensitive to changes in the upper of footwear. A recent trail study demonstrated that a BOA Wrap upper improved shoe fit and speed for runners [5]. Yet, little is known about how changes in footwear uppers impact running kinetics. We sought to also understand how changes in footwear uppers impact Distal Rearfoot and Ankle work.

Methods: Ten (five male, five female) runners provided informed consent to participate in the study. Subjects ran on an instrumented treadmill (1000 Hz) at 3.0 m/s with motion capture (200 Hz) markers attached to their foot and shank. Subjects ran at 4° and 2° uphill and 6° downhill in the La Sportiva Cyklon (Wrap) and in a retrofitted lace version of the Cyklon (Lace). Marker and force data were low-pass filtered at 8 Hz and 20 Hz, respectively. Ankle and Distal Rearfoot work were extracted from the kinematics and force data.

To understand the effect of running grade and footwear on the work variables, we employed a series of linear mixed effects models. We evaluated running grade with a model that had independent slopes for running grade and independent intercepts for each subject (Outcome ~ Grade + (Grade|Subject)). Tukey's post-hoc tests were used for pairwise comparisons. As prior literature has shown that joint work changes with running grade, we used separate mix effects models for each running grade when evaluating the effects of the shoe upper. This model that had an independent slope for configuration and intercept for each subject (Outcome ~ Config + (Config|Subject)). Family-wise α was 0.05 for all models.

Results & Discussion: Negative foot work and positive ankle work increased with increasing running grade ($p<0.02$, Table 1). The positive foot work decreased between 2° uphill and 4° uphill ($p=0.02$), with no differences in positive foot work between running downhill and uphill ($p>0.4$). There was no difference in negative ankle work across running grades ($p>0.6$). Only the positive ankle work was decreased in the Wrap while running downhill ($p=0.04$). No other work metrics differed between the Lace and Wrap ($p>0.05$).

Previous studies have shown the foot to be energy neutral or net dissipative during gait [3]; however, when running uphill, there was net positive energy from the foot (Table 1). This can be interpreted as intrinsic foot muscles and multiarticular ankle-foot muscles play a greater active role while running uphill than running on level terrain. Biomemetic devices (e.g., ankle-foot prosthetics and orthotics) should account for this additional energy should they aim to restore physiological levels of push-off.

Interestingly, the only difference we observed between the two footwear configurations was a decrease in the positive ankle work. A decrement in positive ankle work during level ground running (along with a redistribution of work to proximal joints) can negatively impact running economy. Yet, while running downhill, the majority of lower limb joint work is negative [4] to slow the body's center-of-mass of the body rather than propel it from one step to the next. The effect of such a decrement in positive ankle work while running downhill is unknown. It is hypothesized that such a decrement would have negligible effects on running performance (e.g. metabolics).

Significance: This is the first study to characterize the Distal Rearfoot power across different slopes. This study demonstrated the Distal Rearfoot absorption increased with decreasing slope, with little change in the amount of generation. Changes in trail shoe uppers have little effect on this metric.

References: [1] Matijevich et al. (2022), *J Biomech* 141 (111217).; [2] Childers & Takahashi (2018), *Sci Rep* 8(5354).; [3] Kelly et al. (2018), *Sci Rep* 8(1).; [4] Baggaley et al. (2020), *Eur J Sport Sci* 20(6).; [5] Honert et al. (2023), *Front Sports Act Living* 4.

Table 1: Distal Rearfoot (Foot) kinetics across running grade and between a BOA Wrap and Lace upper. Presented are estimated means from linear mixed effects models (N=10). The superscript numbers indicate significant differences between the respective slopes. Superscript asterisks indicate significant different between the Wrap and Lace.

Running Grade	Downhill 6°		Uphill 2°		Uphill 4°	
Neg. Foot Work [J]	$-35.1^{+2,+4}$		$-24.0^{-6,+4}$		$-21.2^{-6,+2}$	
Pos. Foot Work [J]	29.5		35.3^{+2}		33.1^{+4}	
Neg. Ankle Work [J]	-34.7		-32.1		-31.7	
Pos. Ankle Work [J]	$24.5^{+2,+4}$		$40.9^{-6,+4}$		$45.0^{-6,+2}$	
Configuration	Wrap	Lace	Wrap	Lace	Wrap	Lace
Neg. Foot Work [J]	-31.5	-32.5	-23.8	-24.1	-21.5	-20.9
Pos. Foot Work [J]	29.0	29.3	35.4	35.2	34.1	32.3
Neg. Ankle Work [J]	-33.8	-35.8	-31.0	-33.2	-31.0	-32.5
Pos. Ankle Work [J]	22.7*	25.9*	39.7	42.6	44.1	46.4

USING A SINGLE INERTIAL MEASUREMENT UNIT TO RELATE Y-BALANCE REACH DISTANCE TO MOVEMENT COMPLEXITY IN U.S. MARINES

Amy Silder[1*], Brian Green[1,2], Nicole Heimark[1,2], Danielle M. Torp[3], Pinata H. Sessoms[1], John J. Fraser[1], Matthew Hoch[3]
[1]Naval Health Research Center, San Diego, CA
[2]Leidos Inc., San Diego, CA
[3]University of Kentucky, Lexington, KY
*Corresponding author's email: amy.b.silder.civ@health.mil

Introduction Poor neuromotor control is a well-established risk factor for a range of lower limb musculoskeletal injuries (MSKIs). Several studies have shown an association between lower limb MSKIs and dynamic balance performance, as measured by the Y-Balance Test (YBT). The YBT performance is traditionally assessed by reach distance, which may limit its ability to detect subtle alterations in neuromotor function. One solution is to leverage inertial measurement units (IMUs) to quantify movement control. IMUs enable the calculation of entropy, a representation of the amount of randomness, or complexity, of a signal. Although YBT reach distance is widely used to assess MSKI risk, it remains unknown if movement complexity is related to YBT reach distance.

The purpose of this study was to investigate the association between standard YBT reach distances and sample entropy, calculated from a lumbar-worn IMU. We hypothesized that for each of the YBT reach directions (anterior, posterior-lateral, posterior-medial), lower sample entropy (i.e., less randomness) would have a moderate to strong positive correlation with greater reach distance.

Methods: A total of 116 uninjured U.S. Marines (96 male, 17 female, 3 unreported; mean (standard deviation) age 19.8 (2.5) years; height 179 (9) cm; mass 75 (10) kg) provided informed consent to participate in this study. Participants were provided instructions on the YBT and allowed a maximum of four practice trials in each direction. Test order was not randomized and was conducted in the following order: non-dominant limb reaching in the anterior, posterior-lateral, and posterior-medial directions; followed by dominant limb in the anterior direction. The dominant limb was defined as the foot the participant would use to kick a ball. Three successful trials were completed in each direction. Reach distance was normalized to limb length, and the maximum reach distance across the three trials was used for analysis.

Angular velocity and linear acceleration were collected (60Hz) from single IMU (Xsens DOT) positioned on the lumbar spine (L4/5). Data were filtered at 20 Hz. The magnitude of tri-axis angular velocity and linear acceleration were computed and used to estimate sample entropy with an embedding dimension of 2, and a radius of similarity of 0.12 g's for linear acceleration and 2.30 deg/s for angular velocity. For each YBT trial, entropy values were calculated across 3 s epochs, moving forward every 0.1 s, and the maximum entropy value for each trial was used for analysis.

Movement complexity was related to YBT reach distance using Pearson correlations for the normalized maximum YBT reach distance in each direction and the sample entropy value for the corresponding trial. Repeated-measures ANOVA was used to compare the effect of reach direction on YBT reach distance and entropy. Paired t-tests were used to test the effect of limb on reach distance and entropy in the anterior direction only.

Results & Discussion: In contrast to our hypothesis, movement complexity was not strongly related to YBT reach distance. Weak, but significant correlations were found between reach distance and entropy calculated from angular velocity for the dominant limb in the anterior ($r=0.240$, $p=.010$) and posterior-lateral directions ($r=0.206$, $p=.027$). Reach distance was weakly correlated with entropy calculated from linear acceleration in only the posterior-lateral direction ($r=0.186$, $p=.045$).

YBT reach scores, but not movement complexity, were significantly different across reach directions. Normalized reach distance, expressed as a percentage of limb length, was farthest when standing on the dominant foot and reaching in the posterior-medial direction (79 (10) cm), followed by the posterior-lateral direction (75 (10) cm), and least in the anterior direction (67 (10) cm).

When reaching in the anterior direction, neither YBT reach scores nor movement complexity were significantly different between dominant and non-dominant limbs.

Significance: MSKIs pose a significant threat to the operational efficiency of the military. Historically, the YBT has been used to assess lower limb functional balance and symmetry. Sensor-based systems provide the unique opportunity to revolutionize clinical practice within military medicine by providing a complementary assessment of fine motor control during such tests. Our current study showed that among a group of over 100 uninjured U.S. Marines, normalized Y-balance test reach distance and associated test entropy were not strongly related. From a clinical and performance standpoint, this suggests that movement complexity may be independent of movement performance in healthy individuals.

Previous work has shown that movement complexity can differentiate healthy individuals from those recovering from traumatic brain injury or in those suffering from diseases that affect the neurological system, and that certain MSKIs can negatively affect neuromuscular control. Ongoing work of our project aims to determine if these same associations hold true among Marines with a current lower extremity MSKI and if YBT scores or movement complexity can predict those at risk for future injury. If true, the long-term impact of this work would allow targeted interventions to address the underlying risk factors contributing to MSKI incidence. Ultimately, this would improve military readiness, enhance short- and long-term personnel welfare, and reduce the financial impact of preventable MSKIs.

MUSCLE-DRIVEN ENDOPROSTHETIC LIMBS: RATIONALE, FEASIBILITY, AND CHALLENGES

Dustin L. Crouch[1*], David E. Anderson[2], Stacy M. Stephenson[3], Cheryl B. Greenacre[2], Katrina L. Easton[1], Patrick T. Hall[1], Caleb Stubbs[1], Obinna Fidelis[1], Morteza Asgari[1], Bryce Burton[2], Rebecca E. Rifkin[2], Remi M. Grzeskowiak[2], Alisha P. Pedersen[2], Caroline Billings[2], Kristin Bowers[2]

[1]College of Engineering, [2]College of Veterinary Medicine, [3]Graduate School of Medicine, University of Tennessee, Knoxville (UTK)
*Corresponding author's email: dustin.crouch@utk.edu

Introduction: Control, generation, and sensation of human movement are enabled by the physical link between muscles and limb segments. This link is severed following amputation, resulting in the complete loss of sensorimotor function of the missing limb. Modern myoelectric prostheses attempt to restore sensorimotor function by replacing the musculoskeletal structure of the missing limb with electromechanical systems. However, despite decades of significant technological advancements, modern myoelectric prostheses fail to restore natural, high-fidelity sensorimotor function; consequently, as many as 45% of amputees abandon prostheses [1].

Replicating biological musculoskeletal structure by physically attaching muscles to prostheses could restore natural sensorimotor function. This is because residual muscles that once crossed the missing limb still retain contractile and sensory functions. For example, residual muscles can be contracted forcefully [2] and in a coordinated manner [3]. Surgically connecting agonist-antagonist pairs of residual muscles restores proprioception of the missing limb [4]. Since all existing prostheses must be worn externally on the body, previous muscle-prosthesis attachment required the externalization of muscle force through skin via muscle tunnel cineplasty. Unfortunately, cineplasty has not been widely adopted due to poor mechanical output (i.e., force, range of motion) and cosmesis.

To address limitations of cineplasty and achieve more anatomically realistic muscle-prosthesis attachment, we propose to completely implant prostheses within living skin. Such a muscle-driven endoprosthesis (Fig. 1A) will require new research to understand how and the extent to which the interfacing neuromuscular system interacts and adapts to restore useful sensorimotor function. To enable this future research, we conducted a series of studies to develop and test muscle-driven endoprosthesis prototypes and surgical procedures for implanting them in an *in viv*o rabbit model. For select prototypes, we preliminarily quantified locomotor biomechanics.

Methods: Our muscle-driven endoprosthesis prototype was designed to replace the hindlimb foot and ankle in a New Zealand White rabbit model of hindlimb below-knee amputation. Foot and tibial segments of the prototype were modeled in computer-aided design software (Solidworks, Dassault Systemes), 3D printed in stainless steel, coated in silicone (BIO M340, Elkem), and joined with a polyethylene hinge pin to form the ankle joint. We tested three different prototypes in order of increasing size and complexity to assess skin wound healing: a linear, 2-cm-long unjointed endoprosthesis stem [5], an angled unjointed foot-ankle endoprosthesis [6], and a jointed foot-ankle muscle-driven endoprosthesis (Fig. 1B). The triceps surae and tibialis cranialis muscles were attached to the jointed endoprostheses using artificial tendons that consisted of braided, silicone-coated polyester suture; in other sub-studies, we tested artificial tendons for attaching the same muscles across the biological ankle joint. Endoprosthesis prototypes were implanted at the time of amputation and enclosed in a contiguous skin flap that was salvaged from the biological foot and ankle. In rabbits with jointed foot-ankle muscle-driven endoprostheses, we measured hindlimb biomechanics during hopping gait using an infrared motion capture system (Motive, OptiTrak) and pressure-sensitive mat (Strideway, Tekscan).

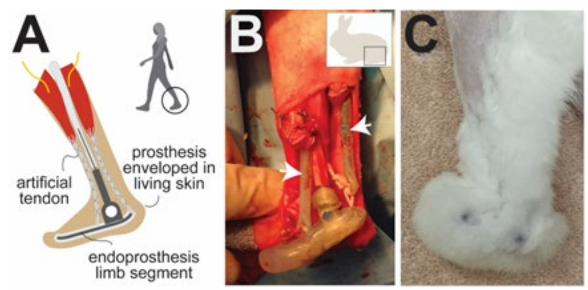

Figure 1: (A) Muscle-driven endoprosthesis concept in human lower extremity. Jointed foot-ankle muscle-driven endoprosthesis prototype in rabbit hindlimb ankle (A) intraoperatively and (B) 169 days post-surgery. Arrows indicate silicone-coated polyester artificial tendons.

Results & Discussion: The skin fully healed and closed in 3 of 6 rabbits with the unjointed endoprosthesis stem, in 3 of 3 rabbits with the angled unjointed foot-ankle endoprosthesis, and in 4 of 5 rabbits with the jointed foot ankle endoprosthesis (Fig. 1C). The biomechanical output of rabbits with artificial tendons only (biological ankle) during hopping gait supported the feasibility of using artificial tendons to attach muscles to endoprostheses [7]; improved artificial tendon design, interface with bone and muscle, surgical technique, and rehabilitation could potentially improve function. Rabbits with jointed foot-ankle muscle-driven endoprostheses demonstrated an increasing willingness and/or ability to use the operated limb during hopping gait, as vertical ground contact forces increased over time post-surgery. However, passive range of motion of the endoprosthetic ankle was limited due to fibrous encapsulation of the endoprosthesis [6]. Future research directions include (1) refining the endoprosthesis design and device-tissue interface, (2) quantifying functional recovery for different injury and treatment scenarios, and (3) developing and testing endoprosthesis designs for human clinical applications.

Significance: Muscle-driven endoprostheses could restore more natural limb structure and function to patients. The endoprosthesis concept will spur new research and innovation in biomechanics, orthopedics, biomaterials, plastic surgery, and other areas.

Acknowledgements: UTK Office of Laboratory Animal Care. NIH R61AR078096 and K12HD073945, NSF CAREER 1944001.

References: [1] Salminger et al. (2022), *Disabil Rehabil* 44(14); [2] Blaschke et al. (1952), *J Appl Physiol* 5(5); [3] Crouch and Huang. (2017) *J Neural Eng* 14(3); [4] Srinivasan et al. (2017) *Sci Robot* 2(6). [5] Hall et al. (2021) *Ann Biomed Eng* 49(3). [6] Crouch et al. (2022) *Bioeng* 9(8). [7] Hall et al. (Preprint) *bioRxiv* DOI: 10.1101/2022.01.25.477740.

AI SYSTEMS FOR IMPROVING BIOMECHANICS OF THE MOBILITY IMPAIRED WITH WEARABLE ROBOTS

Aaron. J Young[1*], Krishan Bhakta[2], Inseung Kang[3]
[1]Georgia Institute of Technology, Atlanta, GA
*Corresponding author's email: aaron.young@me.gatech.edu

Introduction: Robotic prostheses and exoskeletons that can personalize assistance through adaptation are of great value for individuals with mobility challenges, such as those with amputation or stroke. Studies show mobility is strongly linked to quality of life, participation and depression, and these technologies have significant ability to enhance human ambulation, reduce fall risk, and improve overall quality of life [1]. Control systems are still unable to handle community ambulation due to the difficulty of creating ubiquitous controllers that can handle both a wide range of human users with varying mobility capabilities. However, AI systems offer new possibilities to create data-driven systems that enable generalization of controllers to novel users while also personalizing to individual capabilities.

In the first study, we test the hypothesis that a user-independent machine learning system can enable scaling of biomimetic assistance similar to able-bodied biomechanics by recognizing a wide range of speeds and inclines for individuals with transfemoral amputation using a robotic knee/ankle system. In the second study, we test the hypothesis that a deep learning system that co-adapts its performance in real-time with human gait can enable personalization of robotic hip exoskeleton assistance for individuals with stroke.

Methods: In the first study, we recruited N=11 individuals with transfemoral amputation to walk on our robotic knee/ankle prosthesis (Open Source Leg – OSL [2]) across multiple speeds and inclines/declines. We trained a machine learning system (XGBoost) to recognize speed and ground slope on a novel user (user-independent) and provide biomimetic assistance that scaled ankle push-off and knee assistance based on able-bodied biomechanics [3]. We tested this system compared to a user-dependent system in real-time (N=7) during which the ML system fully modified the biomechanics of the OSL based on estimated speed and slope. In the second study, participants (N=8 able bodied & N=6 stroke) wore our robotic hip exoskeleton where a deep learning system (CNN) adapted a gait phase estimation system over 10 iterations which increased the accuracy of providing biomimetic hip flexion and hip extension assistance. After adaptation, a validation trial was performed compared the adapted profile to a generic user-independent system [4].

Results & Discussion: In the first study, the user-independent system achieved < 0.1 m/s average error in estimating walking speed and < 1° average error in estimating ground slope in real-time tests which was comparable in accuracy to a fully user-dependent system (Fig. 1). These accuracy levels enabled accurate biomimetic torque scaling of a mid-level controller for the knee and ankle.

In the second study, we first demonstrate that robotic hip exoskeleton in able-bodied controls, where AI personalization (N=10) increased performance by 40.9% where performance was measured as our ability to provide the correct timing of torque assistance. We then tested the framework in real-time tests of the robotic hip exoskeleton in individuals with stroke (n=6) which naturally had much worse baseline performance in the user-independent system trained on able-bodied individuals. However, after our novel AI adaptation routine was applied, the system increased performance by 65.9% (Fig. 1) yielding nearly identical final results as the able-bodied cohort. This demonstrates the capability of an AI system to adapt to an individual user over time from a generalized user-independent system.

Significance: These two studies together indicate that AI technology combined with wearable robotics has the potential to generalize controllers to novel subjects while simultaneously co-adapting over time to personalize assistance automatically. These generalization and personalization properties of data-driven systems can help improve and normalize biomechanics in impaired populations.

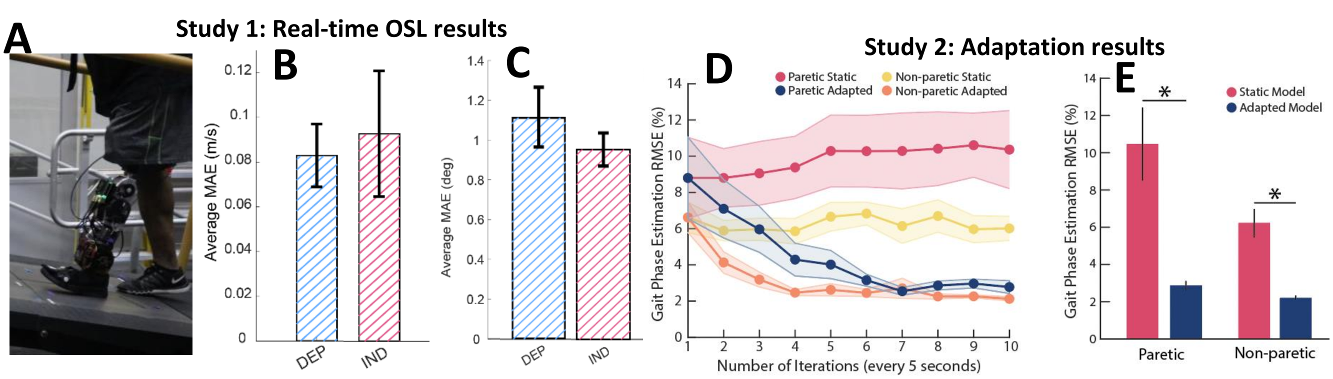

Figure 1: In the OSL study (A), N=7 individuals with TFA showed comparable performance with a user-independent (red) speed (B) and slope (C) ML estimation system for scaling biomimetic assistance compared to a user-dependent system (blue). In the stroke study, adaptation significantly improved gait phase estimation (D and E) on both paretic and non-paretic sides in N=6 individuals with stroke, but the magnitude of improvement was much greater for the paretic side.

Acknowledgements: These projects were funded by NSF NRI, CDMRP OPORP, and NIH New Innovator Award (DP2).

References: [1] Metz (2000), *Transport policy* 7(2); [2] Azocar et al. (2020) *Nature Biomedical*, 4(10); [3] Camargo et al. *Journal of Biomechanics* (2021) 119 (15); [4] Kang et al. (2021) *Robotics and Automation Letters* 6(2).

An initial set of reference values for the balance tracking system (BTracks) limits of stability protocol based on 800 healthy young adults

Nathan O. Conner[1*], Michael R. Nolff[2], Shweta Kapur[2], Daniel J Goble[2], Adam Knight[1] & Harish Chander[1]
[1]Neuromechanics Laboratory, Department of Kinesiology, Mississippi State University, Starkville, MS 39762
[2]Department of Human Movement Science, Oakland University, 433 Meadow Brook Road, Rochester, MI 48309
*Corresponding Author, Nathan Conner noc13@msstate.edu

Introduction: The ability to maintain upright stance in the presence and absence of perturbations can be described as postural stability. Stability is quantified by the ratio between center of mass (COM) location and base of support (BOS) size. The center-point of foot contact forces generated when standing on a force plate is known as center of pressure (COP). Postural stability involves the minimization of COP excursion from the origin point of upright stance in both normal and perturbed circumstances. Dynamic postural stability can be described as the controlled manipulation of the COP about the BOS. The most common way to measure dynamic postural control on a force plate is the Limits of Stability (LOS) protocol. The Balance Tracking Systems (BTrackS™) Balance Plate is a low-cost portable force plate for assessing and training balance. The BTrackS LOS protocol differs from traditional LOS methods as it instructs the participant to lean maximally in all directions as opposed to eight targets in cardinal directions. This alteration's advantage in balance assessment is twofold; it both allows for specific directional balance deficit diagnosis and controls for participant perception of self-balance ability. In this case, it would seem to be of particular importance to expand on this test to create reference data with percentiles. This is in order to examine the relationship between LOS area and pathological or biomechanical differences amongst ranks. To create accurate percentile rankings of LOS score, anthropometric variables that may affect balance must be accounted for. Proposed variables include height, weight, foot size, geographic location, and birth gender. From this, multiple pools of comparative data that more readily match participant characteristics can be created. To date, the extent to which LOS assessment is affected by these variables is unknown. Therefore, the purpose of this study was to collect a large set of data from multiple test sites to establish reference data and evaluate the variables that may influence the results of the assessment.

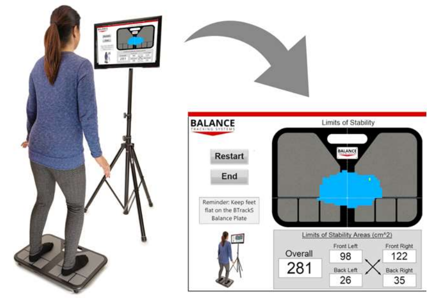

Figure 1: BTrackS LOS Assessment

Methods: Data was obtained from 800 healthy young adults (368 men, 432 women) with a mean age of 18-29 (21.4 ± 2.4) years using the BTrackS Balance Plate. Geographical locations in the United States included Michigan, Colorado, Northern Ireland, Mississippi, and Indiana. Data was collected from Universities, in-home testing, in fitness centers and others. Height, weight, and birth-assigned gender were recorded. The BTrackS LOS uses real time biofeedback on a screen in front of participants in the form of a yellow dot (COP) and a blue LOS area. Participants were not given time constraints and were instructed to continue until they felt they could no longer increase the blue area. The majority of assessments lasted under two minutes. The total LOS area is reported using cm^2. Strength of LOS score predictors were quantified using forward, stepwise linear regression of sex, height, and BMI. The threshold for model inclusion was set to $p < 0.05$.

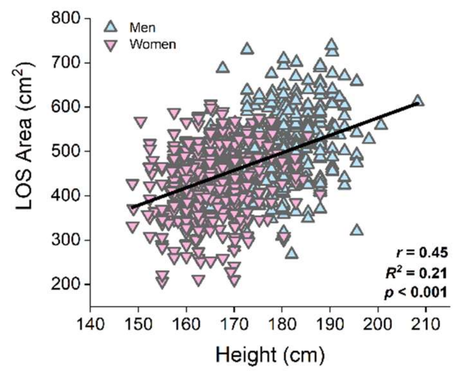

Figure 2: Relationship between Height (cm) and LOS Total area (cm^2)

Results & Discussion: Two significant predictors of BTrackS LOS area were identified. The largest predictor found was height (t = 7.1, p<0.001). These results are shown in Figure 2. The second predictor was birth assigned sex (t = 4.2, p <0.001). Percentile rankings were calculated in categories based on the results (Taller and shorter men and women). The cut off point for height was 180cm for men and 165 cm for women. While static balance assessments rarely show height effects, several studies utilizing dynamic movements to quantify postural control have found height as an influential variable. With the inverted pendulum model, increased lever arms allow for greater displacement of COM with equivalent ankle joint angular displacement. The mechanisms behind sex-based differences are more elusive. Woman traditionally have a more controlled static posture [1], which may reflect a lower COM in relation to BOS or greater tactile feedback per cross sectional area [2].

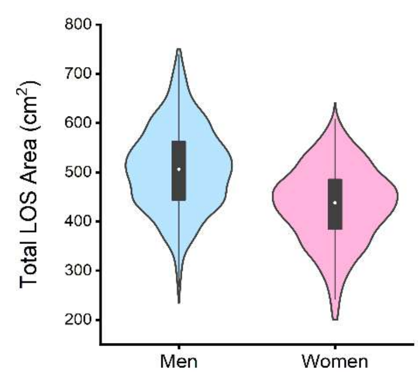

Figure 3: Distribution of both men's and women's LOS scores. highlighting both normality and gender based differences.

Significance: Clinicians, researchers, and sports performance industries can benefit through the implementation of this reference data set. These normative values can be used to assess pathological states, effects from interventions, and return to play status. The next step in this research is to add percentile ranks for the participants aged 30-59 years old. This will show us age trends in dynamic postural control.

References: [1] Goble and Baweja (2018), *Phys Ther* 98(9); [2] Era et al. (1996), *J Gerontol A Biol Sci Med Sci* 51(2).

DIFFERENCES OF NECK MUSCULATURE MOTOR UNIT CONTROL BETWEEN CONCUSSED AND CONTROLS

Nathan D. Schilaty,[1,*] Takashi Nagai,[2] April L. McPherson,[3] Nathaniel A. Bates[3]
[1]University of South Florida, Tampa, FL; [2]USARIEM, Natick, MA [3]The Ohio State University, Columbus, OH
*Corresponding author's email: nschilaty@usf.edu

Introduction: Concussion (CONC) encapsulates a constellation of transient clinical signs and symptoms of neurologic dysfunction following a mild traumatic brain injury due to biomechanical forces. From 2001-2012, sport- and recreation-related CONC accounted for 3.42M US emergency department visits, with individuals aged 0-19 years accounting for 70% of the visits.[1] Although CONC symptomology is expected to resolve within two weeks, there is evidence that associates CONC with longer-term ramifications.[2] For example, CONC can lead to cognitive deficits such as delay in reaction time, slower movement time, and reduced accuracy of movement.[3] In terms of possible protective factors, overall neck strength has been found to be a significant predictor of CONC, with every 1-pound increase in neck strength corresponding to 5% decrease odds of CONC in high school athletes.[4] While abundant literature on CONC exists, there has yet to be a study integrating the assessment of neuromotor control on neck muscles with CONC. Therefore, the purpose of this study was to assess the impact of CONC on motor unit (MU) control with age- and sex-matched controls (CTRL) in visual-elicited trials of neck movement. We hypothesized that CONC participants would have deficient MU activity compared to sex- and age-matched CTRLs in major neck musculature.

Methods: The study was approved by the Mayo Clinic IRB (17-006025). 26 adolescents / young adults (age 12-20), competitive in sports, participated in this study. When a medically diagnosed CONC participant was identified, they brought a teammate (similar sex and age) with no history of CONC as a CTRL. Exclusion criteria for participation were pre-existing conditions that prevented ability to perform neck motion or neck strength assessment. Subjects were seated in a custom-built isometric strength device and secured with a safety harness. A baseball helmet was placed on the head and a custom fixture directly secured it to a 6DOF load cell (45E15A; JR3 Inc). Surface 5-pin Galileo electrodes (Trigno; Delsys) were placed on bilateral sternocleidomastoid (SCM) and upper trapezius (UT) muscles according to SENIAM standards. Subjects were exposed to a visual stimulus using custom LabVIEW software (v2018; National Instruments). During each trial, a randomized arrow appeared in one of 4 cardinal directions (flexion, extension, or left/right lateral flexion) for 12 trials. Prior to recorded trials, at least 3 practice trials were performed to orient to the task. Subjects were asked to contract in the correct direction as 'fast and hard as possible' for 3 sec. MU action potential (MUAP) amplitude and average firing rates (AvgFR) were captured. The sEMG (2.2 kHz) was band-pass filtered (20-1750 Hz) then digitally filtered (high-pass; 50 Hz) before decomposition. In order to verify the decomposed signal, the algorithm performed a Decompose-Synthesize-Decompose-Compare test. Only MUs with an accuracy of ≥80% were included in analysis. Statistical analyses were performed with *JMP Pro 16* (SAS). *Log* MUAP and *cube root* Recruitment Threshold transformations were utilized to provide parametric data for linear regressions. MU data were normalized to mass and data were compared between groups with standard least square means Student's t-test. Significance was set *a priori* at $p<0.05$.

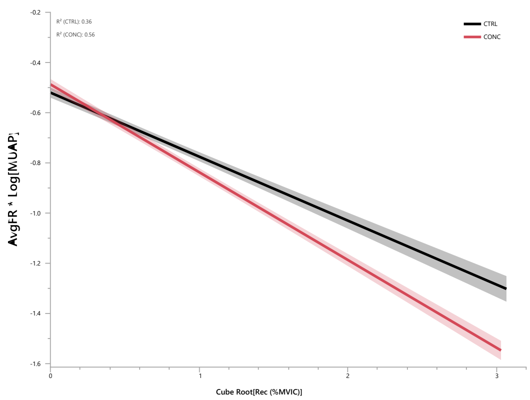

Figure 1: Upper Trapezius AvgFR * MUAP by Recruitment Threshold. (line shading: 95% confidence intervals of the mean.)

Results & Discussion: For UT, the linear regression (inclusive of all four directions; $R^2=0.56$) demonstrated lower MU activity than CTRLs, especially for later recruited MUs (**Fig. 1**; $p<0.001$). When isolated for extension only ($R^2=0.40$), UT demonstrated higher MU activity than CTRLs ($p<0.001$). For SCM, the linear regression (inclusive of all four directions; $R^2=0.24$) demonstrated higher MU activity for CONC than CTRLs, especially for later recruited MUs ($p<0.001$). When isolated for flexion only ($R^2=0.13$), the SCM demonstrated higher MU activity for CONC vs CTRL ($p<0.001$). With exception of the UT in isolated extension, the data demonstrates the opposite of our hypothesis. Previous lower extremity studies performed by our group similarly demonstrated decreased MU activity after injury.[5] However, the difference may lie in that we previously measured MU activity at a median of 28 days after anterior cruciate ligament injury. Thus, acute injury may cause an initial increase of MU activity in attempt to protect the body from further injury within the acute phase. However, these data also demonstrate that a CONC can have effects on motor control (either increased or decreased MU activity) of the axial musculature.

Significance: As a cross-sectional study, this data does not allow for evaluation of cause or effect. However, as pilot data, it demonstrates that differences exist between groups that could either be due to CONC or could be a risk factor for CONC to occur. Thus, further research is warranted in this arena, especially with a prospective clinical trial to follow MU control of neck musculature longitudinally.

Acknowledgements: The authors acknowledge support of the Florida Department of State Center for Neuromusculoskeletal Research and the Mayo Clinic Ultrasound Research Center.

References: [1] Taylor et al. (2017) *Surveillance Summaries* 66(9):1-16. [2] McPherson et al. (2020) *Sports Med* 50(6):1203-1210. [3] Brown et al. (2015) *BMC Sports Sci Med Rehabil*. 7:25. [4] Collins et al. (2014) *J Primary Prevention* 35(5):309-319. [5] Schilaty et al. (2022) *Eur J Sport Sci* 2:1-11.

DEPENDENCE OF TOTAL ANKLE TIBIAL COMPONENT STABILITY UPON BONE DENSITY

Gabriel A. Clarke,[1] Joshua E. Johnson[1], Cesar de Cesar Netto[1], Donald D. Anderson[1*]
[1]Department of Orthopedics & Rehabilitation, University of Iowa, Iowa City, IA
*Corresponding author's email: don-anderson@uiowa.edu

Introduction: The success of uncemented total ankle replacement (TAR) in improving patient outcomes is linked to its initial stability after implantation. Limiting early micromotion between implant and bone improves longer-term stability; micromotions below 20–50 µm promotes bone ingrowth, while those exceeding 150 µm instead promote fibrous tissue ingrowth.[1,2] Tibial component design fixation features play a critical role in determining early stability, with retention of medial and lateral bone sidewalls and interference press-fit both used to supplement fixation. However, tibial component stability is likely also influenced by regional bone density characteristics, and the exact relationship between the two is not adequately understood. The goal of this study was to investigate how bone density affects bone-implant interface micromotion between the tibial component of a specific TAR design and the distal tibia.

Methods: Micromotions of the tibial component during gait were evaluated using finite element analysis (FEA). A commercially available TAR tibial component baseplate (APEX 3D ARC, Paragon 28) was virtually inserted into a computer model of the distal tibias from two patients with end-stage ankle arthritis. These patients were selected based on having substantially different bone density profiles in the affected ankle. The tibia models were generated from patient CT scans, and a CT density-based inhomogeneous material distribution was assigned (Figure 1) that allowed for the modeling of plastic deformation (i.e., compaction) of bone with press-fit.[3] The tibial component was modeled as titanium alloy material. Two different fixation cases were simulated using FEA: (1) retained medial/lateral sidewalls + line-to-line fit, and (2) retained sidewalls + 50µm interference press-fit. FEA was performed using body weight-scaled kinetic (forces/moments) profiles representing the stance phase of gait, applied to the distal implant surface, while the proximal tibia was held fixed.[4] Press-fit was simulated prior to gait simulation (interference press-fit cases). Micromotions were defined as displacement differences between bone-implant closest nodal pairs, computed from FEA output.

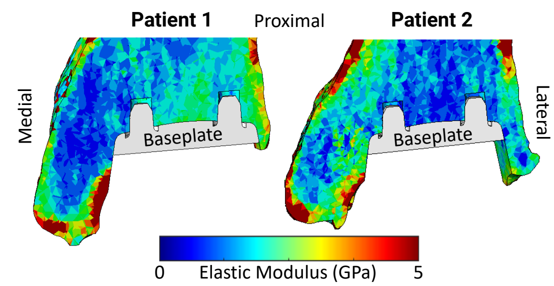

Figure 1: Coronal cross section through center of baseplate pegs showing assignment of elastic modulus based upon CT intensities.

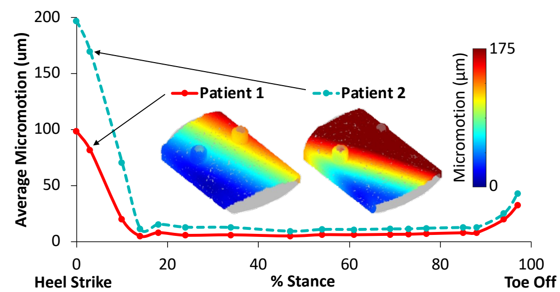

Figure 2: Micromotion During Stance with Sidewalls and Line-to-Line Fit.

Results & Discussion: For the case with sidewalls + line-to-line fit, micromotions were largest early and late in the stance phase of gait (Figure 2), with the largest micromotions observed at heel strike (0% stance). Dorsiflexion moment dominates in early stance with minimal proximally-directed forces, stressing the anterior edge of the tibia in contact with the implant, leading to relatively large posterior/lateral gapping (Figure 2, inset). The observed differences in micromotion between the two patients correlated with differences in bone quality at the tibia contact surface, particularly around the implant pegs (Figure 1). However, when interference press-fit was modeled, the differences in micromotion between the two subjects largely disappeared, as adequate bone compaction was generated around the interference regions with sufficient bone quality to resist micromotion (Figure 3).

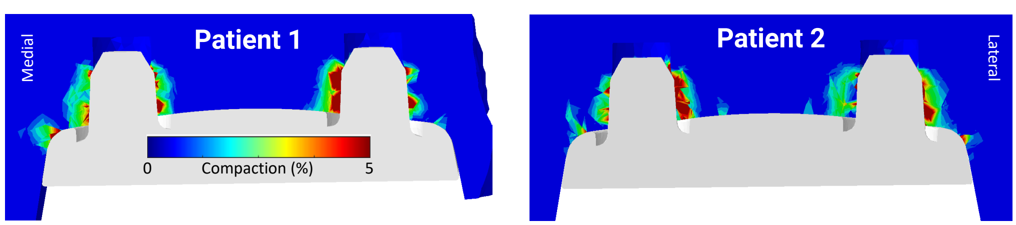

Figure 3: Coronal cross section through center of baseplate pegs showing compacted bone after interference press-fit.

Significance: This study presents novel insight into the effect of TAR fixation features and the associated micromotion at the bone-implant interface in patients with varying distal tibia bone density. While a more comprehensive understanding of TAR implant features and their performance is needed, we believe the results of this study clearly demonstrate the importance of bone quality and particularly implant interference press-fit in the stability of uncemented TAR implants.

Acknowledgements: Funding for this research was provided by Paragon 28, as were the CT scans and implant geometries. We thank Don Hume and Mathew Anderle from Paragon 28 for their scientific feedback.

References: [1] Jasty et al. (1997), *J Bone Joint Surg* 79(5):707-14; [2] Jasty et al. (1997), *J Arthroplasty* 12(1):106-13; [3] Bayraktar et al. (2004), *J Biomech* 37(1):27-35; [4] Quevedo Gonzalez et al. (2021) *J Orthop Res* 39(1):94-102.

PERTURBATION-BASED TRAINING ON COMPLIANT SURFACES TO ENHANCE POSTURAL BALANCE IN PEOPLE WITH NEUROLOGICAL DISORDERS USING A TWIN DUAL-AXIS ROBOTIC PLATFORM

Connor M. Phillips[1], Vu Phan[1], Kwanghee Jo[1], Omik Save[1], Joshua B. Russell[1], Kayla B Zeien[1], Megan C. Eikenberry[2], Carolyn L. Kinney[3], and Hyunglae Lee[1]*
[1]School for Engineering of Matter, Transport and Energy, Arizona State University, Tempe, AZ USA
[2]Department of Physical Therapy, Midwestern University, Glendale, AZ USA
[3]Physical Medicine and Rehabilitation, Mayo Clinic, Phoenix, AZ USA
Corresponding author's email: Hyunglae.Lee@asu.edu

Introduction: Neuromuscular diseases often greatly impair a patient's balance and may reduce an individual's ability to complete daily tasks. The standard of care for these diseases is physical therapy, which requires the presence of a trained therapist to assist the patient. In recent years, robotic systems are being introduced into clinical research settings to reduce the required human input for effective rehabilitation [1]. This study aimed to introduce a perturbation-based training method on compliant surfaces using a twin dual-axis robotic platform to improve balance in individuals with neurological disorders.

Methods: Approved by the ASU IRB, two cerebral palsy (CP) subjects (age: 11 and 14; gender: both males) and one stroke subject (age: 68; gender: female) were recruited. The training occurred over the course of 10 sessions, with visits twice a week for five weeks.

Subjects balanced on the twin dual-axis robotic platform system, while the system simulated a compliant surface (Fig 1A). Subjects were tasked with keeping the center-of-pressure (CoP) of each foot and their weight distribution within the boundaries shown on the screen (Fig. 1B). The platform system would randomly perturb in the sagittal or frontal plane to upset the balance of the subject after they stayed within the visual boundaries for two seconds consecutively. The more time the subjects stayed within the boundaries the more compliant the balancing surface became. The compliance of the system carried through to subsequent training sessions.

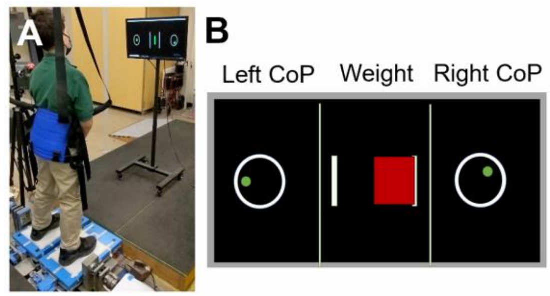

Figure 1: A) A subject stood on the platform, and B) the user interface used for the visuomotor task during the training phase. This example shows successful CoP modulation and unsuccessful weight modulation.

Clinical measures including Pediatric Balance Scale (PBS, or Berg Balance Scale where appropriate), 10 m Walk Test (10 MWT), and 5x Sit-to-Stand (5X STS) were assessed by a licensed physical therapist to evaluate subjects' functional balance and walking ability. CoP path length was used as the main experimental measure for evaluating postural balance. Subjects were tested under rigid (10,000 Nm/rad) and compliant (500 Nm/rad) conditions, with eyes-open (EO) and eyes-closed (EC). Prior to the calculation of the path length, the CoP displacement was obtained from low-pass filtered (5 Hz cut-off) CoP data under each foot.

Results and Discussion: At the completion of the training, we observed a decrease in the CoP displacement, represented by the CoP path length, in two CP subjects (S1 and S2) under both the rigid and compliant conditions (Table 1). For S3, our results showed no balance improvement while standing on the rigid ground. However, there was an improvement in postural balance control under the compliant condition. The higher scores in the clinical assessment of S1 and S2 confirmed the effectiveness of the training for these subjects who were both significantly impaired (Gross Motor Functions Classification Scale II and III, respectively), while only improvement in the 10 MWT was observed in S3. The lower improvement for this subject was attributed to lesser overall impairment.

Significance: This study highlighted that perturbation-based training on compliant surfaces could enhance postural balance of people with neurological disorders. Combined with existing work, our study contributed to the advancement of robot-aided rehabilitation for improving postural balance of balance-impaired populations.

Acknowledgments: This work was funded by Arizona Biomedical Research Centre (ABRC).

	Experimental				**Clinical**					
	Rigid		**Comp.**		**PBS**		**10 MWT (m/s)**		**5X STS (rep/s)**	
	Pre	**Post**	**Pre**	**Post**	**Pre**	**Post**	**Pre**	**Post**	**Pre**	**Post**
S1	38.1 (8.3)	21.2↓ (1.4)	45.6 (4.6)	35.5↓ (7.7)	45	52↑	SS: 1.06 Fast: 1.57	SS: 1.56↑ Fast: 2.31↑	0.35	0.66↑
	45.5 (7.3)	34.4↓ (4.0)	57.9 (6.4)	25.7↓ (3.4)						
S2	73.8 (113.0)	51.3↓ (4.8)	76.3 (27.3)	64.3↓ (15.1)	40	44↑	SS: 0.90 Fast: 1.17	SS: 1.06↑ Fast: 1.27↑	0.15	0.31↑
	112.9 (13.4)	80.6↓ (14.3)	149.6 (42.3)	76.5↓ (8.0)						
S3	36.0 (6.7)	39.8↑ (2.2)	62.0 (4.2)	58.0↓ (15.4)	53	52↓	SS: 1.41 Fast: 1.64	SS: 1.41 Fast: 1.86↑	0.47	0.41↓
	63.9 (30.8)	98.3↑ (25.5)	157.0 (6.9)	149.0↓ (24.3)						

Table 2: CoP path length (cm) of the net CoP data under different standing conditions is shown on the left. Results are presented as mean (standard deviation). White and shaded area represents EO and EC, respectively. Clinical measures are shown on the right. Where SS stands for self-selected walking speed.

References
[1] El-Kafy et al., 2014. *Am. J. Phys. Med. Rehabil*

A TWIN DUAL-AXIS ROBOTIC PLATFORM FOR THE QUANTIFICATION OF BILATERAL ANKLE IMPEDANCE

Connor M. Phillips, Joshua B. Russell, Matthew R. Auer, Vu Phan, Kwanghee Jo, Omik Save, Varun Nalam and Hyunglae Lee
School for Engineering of Matter, Transport and Energy, Arizona State University, Tempe, AZ USA
*Corresponding author's email: hyunglae.lee@asu.edu

Introduction: Detailed characterization of ankle impedance is key to understanding the contributions of the ankle during normal and altered postural balance control and locomotion. This information will allow us to better understand the effects of neuromuscular diseases on altered ankle mechanics and develop therapies or robotic devices to restore ankle function. However, existing systems for this purpose are unilateral which obscures the side-specific trends in ankle impedance common both for healthy and impaired populations. This paper presents a twin dual-axis robotic platform system designed to quantify bilateral ankle impedance in 2 degrees-of-freedom (DOF) during standing and walking, with the goal of assessing the level of symmetry between the dominant (D) and non-dominant (ND) ankles.

Methods: Approved by the ASU IRB, five young, healthy subjects (age: 22.7±4.2 years, height: 175.6±11.9 cm, weight: 70.7±12.0 kg) were recruited. The protocol for both experiments involved a series of perturbations in the dorsiflexion-plantarflexion (DP) or inversion-eversion (IE) directions applied to the subject's ankles. Each perturbation was 3° in magnitude, applied over 125 ms, with a peak velocity of 45°/sec and followed a minimum jerk velocity profile. Only one ankle and direction were perturbed at a time. Subjects were requested to stand or step on each platform with their ankles in-line with the DP motor axes, and as near the lateral midline as possible without altering their normal foot posture (Fig. 1A).

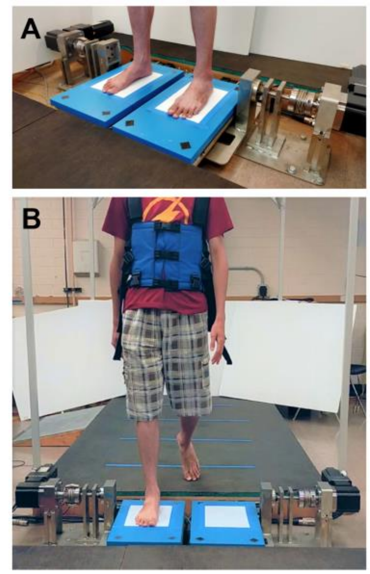

Figure 1. A subject on the platform during (A) standing and (B) walking experiments.

In the standing experiment, a perturbation occurred after satisfying the following conditions for 0.5 s consecutively: 1) the side-specific Center-of-Pressure (CoP) remained within a 0.5 cm radius of the nominal CoP and 2) the weight on that platform was within +/- 2 kg of half the subject's bodyweight. A visual display was placed in front of the subject that indicated the magnitude of the weight on the foot under test and the respective platform's local CoP. Kinematic data of the ankle and platforms as well as force data from each force plate were collected over 2 blocks with each block containing 15 trials for a total of 30 trials per foot per direction.

In the walking experiment, subjects were instructed to walk in sync with a metronome operating at 100 beats-per-minute. Perturbations were set to occur at ~45% of the stance phase. In this experiment, a trial consisted of one step onto the platform (Fig. 1B). To reduce the effect of anticipation, half of the trials had perturbations and the other half did not. Trials were grouped into 8 blocks each with 5 perturbation and 5 non-perturbation trials in a random order, thus leading to 40 perturbation and 40 non-perturbation trials per foot per direction.

For both standing and walking experiments, non-rejected trials were averaged. A 2nd order linear, time-invariant model was assumed for the ankle impedance model and constrained linear regression analysis was used to estimate the stiffness, damping, and inertial components of ankle impedance. The quality of the fit was assessed by the percentage of variance accounted for (%VAF) by the model when compared to the actual differential torque measurement. The level of symmetry between the ND and D limbs was calculated as the ratio of the ND stiffness to the D stiffness.

Results & Discussion: The results of ankle impedance characterization for both standing and walking were very reliable (Table I), evidenced by the high %VAF across all experimental conditions. The mean %VAF was higher than 95.5% for all 8 measurement conditions, i.e., ND/D, DP/IE, and standing/walking conditions. Only stiffness results were presented since it has been documented as the main contributor to the torque about the ankle that is induced by the perturbation [1]. As expected, for both standing and walking, the stiffness in the DP direction was higher than that in the IE. A wide range of symmetry across subjects indicates that the symmetry between dominant versus non-dominant ankles is highly subject-specific with no obvious trend in this sample of five subjects.

TABLE I. STANDING AND WALKING IMPEDANCE QUANTIFICATION RESULTS, STANDARD DEVIATIONS ARE SHOWN IN THE PARENTHESES.

	STANDING						WALKING					
	ND Stiff. (Nm/rad)	ND % VAF	D Stiff. (Nm/rad)	D % VAF	Symmetry	Symmetry Range	ND Stiff. (Nm/rad)	ND % VAF	D Stiff. (Nm/rad)	D % VAF	Symmetry	Symmetry Range
DP	207.3 (79.8)	99.4 (0.2)	240.1 (57.0)	99.6 (0.1)	0.87 (0.30)	0.60 - 1.34	403.5 (152.9)	99.3 (0.6)	359.9 (128.5)	99.2 (0.2)	1.11 (0.29)	0.76 - 1.48
IE	19.9 (3.8)	97.8 (0.4)	20.0 (8.1)	98.4 (1.1)	1.10 (0.37)	0.78 - 1.71	18.5 (8.2)	95.5 (3.6)	17.3 (7.4)	96.6 (3.2)	1.30 (0.84)	0.52 – 2.72

Significance: The robotic platform presented in this study serves as a tool to better understand the bilateral ankle impedance of both healthy and neurologically impaired individuals and to develop assistive robotics and rehabilitation training programs using this information.

Acknowledgements: This work was funded by the National Institute of Arthritis and Musculoskeletal and Skin Diseases of the National Institutes of Health under Award Number R01AR080826 and Arizona Biomedical Research Centre.

References: [1] V. Nalam et al., in *IEEE Trans. on Biomed. Eng.*, vol. 68, no. 6, pp. 1828-1837, 2021.

ANKLE STRESS ANALYSIS FOR BEGINNER PERFORMING THE ASYMMETRIC AND SYMMETRIC DUMBBELL FARMER'S WALK EXERCISE

Joyce Blandino[1*], Stephen J. Castle[1], Michael Krackow[2]
[1]Department of Mechanical Engineering, [2]Department of Human Performance and Wellness, Virginia Military Institute, Lexington, VA, USA
*Corresponding author's email: blandinojk10@vmi.edu

Introduction: Common daily functional activities require carrying loads (groceries) on one side of the body or on the back (backpack). Carrying loads while walking may affect a person's balance and alter the biomechanics of the trunk and lower limbs [1-4]. The farmer's walk exercise began as an event at Strongman competitions and has evolved to become part of regular exercise training program administered by coaches in many sports [5]. During this exercise, participants carry loads in both hands (symmetric), or one handed (asymmetric). Studies showed that this exercise may help improve strength in the core, lower extremity, and upper body musculature, improving trunk stability and balance during walking [6-7]. The farmer's walk when performed with a symmetric load produced greater vertical, anterior-propulsive, and medial lateral forces during gait [6], and increased strength ratio between the hamstrings, quadriceps, and gluteus medius activities [7]. However, these studies employed load with more than 50% of body weight (BW). An asymmetric load (15%-20% BW) resulted in an increase in hip abductor muscle activity and lateral trunk sway toward the non-loaded side to counteract load [8]. For beginners who want to incorporate the farmer's walk exercise as part of their fitness program, the appropriate weight to start the exercise without risk of injury should be considered. The purpose of this study was to examine the effect of symmetric and asymmetric farmer's walk at various load conditions on ankle forces and moments.

Methods: Fifteen healthy subjects (7 females, 8 males, aged 40.3±19.2 years) participated in the study. The average body weight was 82.40±19.18 kg. Subjects had between 0 to 25 years of weight or resistance training experience. Retro-reflective markers were placed on feet, shanks, thighs, chest, and lower back. Each subject performed three repetitions of the farmer's walk over 3 force platforms. Each subject walked with left leg first on the first force platform carrying no load, 10% or 15% body weight (BW) symmetrically and asymmetrically (left and right hand) (Figure 1). Eight VICON Vero cameras were used to gather kinematic data at 200Hz. Ground reaction force data were collected from the force platforms at 1000Hz. The Motion Monitor xGen software (TMMxGen) was used to collect data from both VICON cameras and the force platforms simultaneously. Subjects were given a one-minute rest period between tests. A one-way ANOVA was used to compare ankle forces and moments for symmetric and asymmetric loaded (left and right) tests. A post hoc analysis for pairwise comparisons with Bonferroni adjustment was followed to determine which two groups were different.

Figure 1: Asymmetric load with right hand (left), Symmetric load (right) for farmer's walk exercise.

Results & Discussion: With increasing load carrying (symmetrical or asymmetrical), it is expected that maximum stress at ankle would increase during the single leg stance phase of the gait cycle as compared to the no load condition. Results showed no statistical difference in maximum ankle forces and moments in all three directions (medial/lateral, anterior/posterior, and superior/inferior) among all groups (symmetrical and asymmetrical in either hand with 10% and 15% BW and no load). Results also indicated that the left leg ankle experienced statistically higher maximum moment in the anterior/posterior direction than that of the right ankle with and without loads during the single leg stance phase of the gait cycle. Conversely, the right leg moment was statistically higher than that of the left leg around the sagittal plane and transverse plane. This indicates that when the ankle absorbs more force in one direction, its moment (rotation) around the other two directions is reduced. This study demonstrated that for beginners who perform the farmer's walk, it is safe to start doing the exercise with symmetric or asymmetric loads at 15% body weight without altering the stress at the ankle. If subjects are not comfortable carrying 15% BW, a 10% BW is also an appropriate amount of weight to start the exercise.

Significance: Since many coaches incorporate the farmer's walk exercise as part of the training for athletes, similar exercises can be performed by non-athletes to strengthen the lower extremities, and trunk musculature. Stronger core muscles help improve balance and trunk stability. From a functional standpoint, it is very important for novices to select an appropriate weight to begin the farmer's walk exercise as part of a fitness program to minimize the risk of injury.

Acknowledgements: The VMI Institutional Review Board approved testing protocol. This project was supported by funding from the VMI Center for Undergraduate Research.

References: [1] Demura S et al. (2005), *Sport Science*, 5: 89-96; [2] DeVita, P et al. (1991), *J Biomech*, 24: 1119-1129. [3] Matsuo T et al. (2008), *Gait & Posture*, 28: 517-520. [4] Corrigan LP and Li JX (2014), *Res Sports Med*, 22: 23-35. [5] Winwood et al. (2014), *Int J Sports Sci Coach* 9(3): 1107-1125; [6] Winwood et al. (2014), *Int J Sports Sci Coach* 9(3): 1127-1143; [7] Stastny et al. (2015), *J Human Kinetics*, 45: 147-165; [8] Graber et al. (2021), *J Applied Biomech* 37(4): 351-358.

CHANGES TO MUSCLE FIBER MORPHOLOGY AND FIBROSIS FOLLOWING BRACHIAL PLEXUS BIRTH INJURY

Kyla B. Bosh[1,2*], Brooke K. Dunkley[1,2], Katherine R. Saul[1], Jacqueline H. Cole[1,2]
[1]North Carolina State University; [2]University of North Carolina at Chapel Hill
*Corresponding author's email: kbosh@ncsu.edu

Introduction: Brachial plexus birth injury (BPBI) is a common pediatric neuromuscular injury occurring during a difficult childbirth that causes paralysis, shoulder contracture, deformed scapular and humeral growth, and lifelong arm impairment[1-3]. Clinically, nerve damage presents as nerve rupture or avulsion[2] from the spinal cord. Nerve rupture (*postganglionic injury*) results in muscle paralysis, limb disuse, and elbow and shoulder contracture[4], while nerve avulsion (*preganglionic injury*) results in muscle paralysis and limb disuse without joint contracture[5]. Alterations to muscle fiber composition may contribute to these differences in functional losses due to muscle stiffening from increased fibrosis (*collagen* content)[6]. While musculoskeletal deformities have been well characterized following BPBI[6,7], little is known about the tissue-level changes that may drive deformity development. We hypothesize that the biceps brachii, supraspinatus, and subscapularis muscles, all thought to contribute to shoulder and elbow contracture[6-8], will have increased collagen content and decreased spindle number following both postganglionic and preganglionic injuries relative to sham.

Methods: Under an approved IACUC protocol, four groups of Sprague Dawley rat pups underwent surgery on postnatal day 3-6: postganglionic neurectomy[9] (n=20), preganglionic neurectomy[5] (n=20), forelimb disarticulation[6] (n=20), and sham (n=14). The C5-C6 nerve roots underwent postganglionic or preganglionic neurectomy or were left intact (sham), or one forelimb was amputated at the elbow to mimic unloading without neurectomy (disarticulation). The intact contralateral limb in each group served as an added control. Rats were sacrificed at 4 weeks after surgery. Injured and uninjured biceps brachii, subscapularis, and supraspinatus were harvested, embedded in OCT, snap-frozen, and stored at -80°C. Muscles were cryosectioned longitudinally at -24°C with 10-um thickness. Three sections were stained with Masson's trichrome to identify collagen I content (**Figure 1A**), and three sections were stained with hematoxylin and eosin to identify muscle spindles[5]. Stained muscle sections were imaged at 20x and analyzed for percent collagen content[6] or spindle number, respectively. Comparisons between injured and uninjured limbs were made with paired t-tests; group comparisons were made for injured/uninjured limb ratios of each metric using Kruskal Wallis tests ($\alpha = 0.05$).

Results & Discussion: Analyses are ongoing. A data subset is presented here for collagen content (postganglionic n=4, preganglionic n=2, disarticulation n=6, sham n=2) and spindle number (neurectomies and disarticulation n=2, sham n=1). Collagen Content: For the postganglionic group, injured biceps had greater collagen content than uninjured biceps (+31.9%, p=0.0400, **Figure 1B**), and supraspinatus and subscapularis muscles had similar collagen levels between injured and uninjured limbs. For preganglionic and disarticulation groups, all three muscles tended to have greater collagen content in the injured limbs than the uninjured limbs. While injured/uninjured ratios of collagen content were not significantly different among groups in this data subset, compared to sham, the mean ratios were consistently higher for the preganglionic group in all muscles and for the postganglionic group in the biceps. Mean values for the disarticulation group were similar to those in the sham group for each muscle. Spindle Number: Uninjured muscles tended to have greater muscle spindles, compared to the injured limb, in postganglionic (biceps and supraspinatus muscles), preganglionic (all three muscles), and disarticulation (all three muscles) groups (**Figure 1C**).

This study builds on our previous work[6] and another rodent BPBI study[5] and suggests that muscles affected by both postganglionic and preganglionic BPBI develop fibrosis by 4 weeks after injury. This study is the first to study collagen content in the supraspinatus muscle, which has been shown to be shorter and have decreased muscle mass following preganglionic BPBI[7], and to quantify spindle number in muscles surrounding the shoulder affected by BPBI. Previous studies have indicated that biceps brachii, subscapularis, and supraspinatus muscles have impaired longitudinal growth following postganglionic BPBI[4] and decreased muscle mass in preganglionic BPBI[7]; however, those studies only looked at macrostructural muscle changes that occurred once deformities were already developed at 8 weeks post-injury. This study suggests that tissue-level changes to muscles surrounding the shoulder occur at an earlier stage of deformity development.

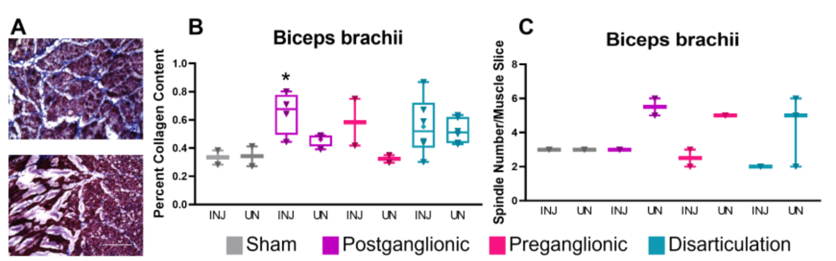

Figure 1. a) Sections of injured (top) and uninjured (bottom) limb biceps muscle in the postganglionic group (blue: collagen I). **b)** Collagen content was greater in the post-ganglionic injured (INJ) limb relative to the uninjured (UN) limb (*p<0.05) and tended to be greater for neurectomy injured limbs relative to sham. **c)** Spindle number tended to be greater for post- and preganglionic UN vs. INJ limb and similar in INJ limbs vs. sham.

Significance: Understanding when tissue-level changes in bones and muscles surrounding the shoulder initiate following BPBI will inform the selection and timing of treatments for patients to improve over the current wait-and-see approach.

Acknowledgments: Funding provided by NIH R01HD101406. We thank Drs. Kerry Danelson and Roger Cornwall for performing the surgeries and Jason Cox for muscle dissections.

References: [1] Hogendoorn, 2010 *J Bone Jt Surg Am* 92:935; [2] Poyhia, 2005 *J Pediatr Radiol* 35:402; [3] Defrancesco 2019 *J Pediatr Ortho* 39:e134; [4] Crouch, 2015 *J Bone Jt Surg Am* 97:1264; [5] Nikolaou 2015 *J Hand Surg Am* 40:2007; [6] Fawcett 2021 Doctoral Dissertation https://www.lib.ncsu.edu/resolver/1840.20/39052; [7] Dixit, 2021 *J Hand Surg Am* 46:e1; [8] Weekley, 2012 *J Orthop Res* 30:1335; [9] Li 2010 *J Bone Jt Surg Am* 92:2583

FACTORS ASSOCIATED WITH FALLS IN OLDER ADULTS: SECONDARY ANALYSIS OF A 12-MONTH RCT

Katherine L. Hsieh[1*], Jamie L. Speiser[2], Rebecca Neiberg[2], Anthony P. Marsh[3], Janet A. Tooze[4], Denise K. Houston[5]
[1]Department of Physical Therapy, College of Nursing and Health Professions, Georgia State University
*Corresponding author's email: khsieh5@gsu.edu

Introduction: Falls are a prevalent concern among adults 65 years and older, with one in four older adults falling per year [1]. Falls can result in serious health consequences, including fractures, hospitalizations, and death [2]. Due these consequences, many researchers have attempted to develop and validate fall prediction models and identify measures that best predict older adult fallers [3-5]. However, the sensitivity, specificity, and discrimination of these prediction models range from 0.65 to 0.74 [3-5].

Decline in physical function is an important predictor of falls in older adults [6]. However, there are multiple methods to assess physical function that range from routine clinical assessments to instrument-based assessments. While previous fall prediction models often included a measure of physical function because of its association with falls [7], it is unclear which measures should be included. Improving upon current fall prediction models can further help researchers and clinicians assess for fall risk with the proper tools while saving time, expenses, and resources. Thus, the purpose of this secondary analysis was to determine, among clinical and instrumented-based measures, which physical function and routinely collected clinical measures are associated with future falls in older adults.

Methods: This is a secondary analysis of the Exploring Vitamin D's Effects on Neuromuscular Endpoints (EVIDENCE; NCT02015611) study, a 12-month, double-blind randomized controlled trial comparing the effect of Vitamin D_3 supplementation to placebo on neuromuscular function in older adults. One hundred and thirty-six participants met all entry criteria and were enrolled in the trial.

At baseline, participants completed questionnaires related to demographics, medical history, and medication history. Participants also completed several physical performance measures, including the Short Physical Performance Battery (SPPB) and its expanded version, the Timed Up and Go, tests of muscle strength and power, standing on firm and foam surfaces on a force plate, and walking at usual and fast speeds over an instrumented walkway. Each month over 12 months, participants completed fall calendars, marking any falls that occurred on the calendar.

Unadjusted univariate analyses for each variable were assessed using logistic regression. Multivariable analyses were conducted for each of the clinical assessments and instrument-based assessments using logistic regression adjusted for age, sex, race, treatment assignment from the original trial, depression, and number of prescription medications. Multivariable models were further adjusted for a history of one or more falls over the past year. P-values of less than 0.05 were considered significant for univariate analysis. A conservative threshold considering p-values of less than 0.1 as significant in multivariable analysis adjusted for covariates.

Results & Discussion: A total of 124 participants had complete fall calendar data and were included in the analysis. The mean age was 73.0 years, 49% were female, 68% were white, all were Non-Hispanic, and average BMI was 30.3 kg/m^2. Sixty-one participants sustained one or more falls. In univariate analysis, white race, depression, fall history, SPPB, and postural stability on foam were significantly associated with future falls (all *p's* <0.05). In multivariable analysis, fall history (OR (95% CI): 3.20 (1.42-7.43)), SPPB (0.80 (0.62-1.01)), and postural stability on foam (3.01 (1.18-8.45)) were each significantly associated with future falls (Figure 1). After adjusting for fall history, only postural stability on foam was significantly associated with falls (2.50 (0.94-7.22)).

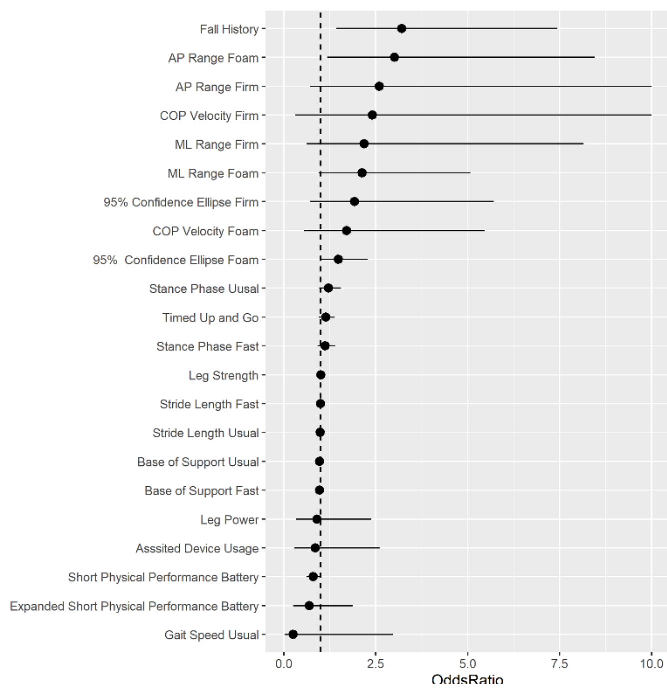

Figure 1. Association between baseline physical function measures and one or more falls over 12 months of follow-up. Odds ratios (95% confidence intervals). Abbreviations: AP=anteroposterior; ML=medio-lateral; COP=center of pressure

Significance: When developing future fall prediction models, researchers should consider collecting and including fall history, the SPPB, and postural sway measures from a force plate when standing on foam. If resources limit performing the SPPB or accessing postural sway with a force plate, fall history alone is useful to identify future older adult fallers. Including these measures in future fall prediction models may improve the accuracy of those models.

Acknowledgements: This work was supported by grants from the NIH (R01 AG042411, T32 AG033534, F32 AG077940, P30 AG021332, K25 AG068253).

References: [1] Bergen et al. (2016), *MMWR Morb Mortal Wkly Rep*. 65(37); [2] Haddad et al. (2020), *J Aging Health.* 32(10); [3] Dormosh et al. (2021), *Journals of Gerontology: Series A;* [4]. Glade et al. (2021), *BMC Geriatrics.* 21(1); [5] Oshiro et al. (2019), *JAGS.* 67(7); [6] Ambrose et al. (2013) *Maturitas*. 75(1); [7] Gadkaree et al. (2015). *Gerontology & Geriatric Med.*

INTRODUCING BIOMECHANICS IN AN UNDERGRADUATE MECHANISM DESIGN COURSE: A CASE STUDY

Michael V. Potter
Department of Physics and Engineering, Francis Marion University, Florence, SC, USA
Email: michael.potter@fmarion.edu

Introduction: Many engineering programs in the United States exclusively offer undergraduate degrees. Often with relatively few engineering faculty and engineering majors, many of these programs are unable to offer introductory courses entirely devoted to biomechanics. Thus, it is important to find other ways to reach students in these programs and expose them to topics in biomechanics. Additionally, research suggests that incorporating project-based learning within traditional courses can best satisfy the dual needs to help students obtain solid fundamental knowledge and prepare for real-world application [1]. This case study examines a final project aimed to introduce biomechanics to students in a traditional mechanism design course.

Methods: Five students enrolled in ENGR 401: Design of Mechanisms in Fall semester 2022 at Francis Marion University (FMU). The course is a required senior-level course for mechanical engineering majors at FMU and covers traditional topics for designing mechanisms and machines, focusing on kinematics and kinetics of mechanism and machine components. The course includes a final team design project for students to apply course concepts to a real-world problem. In Fall 2022, this project was designed to also expose students to biomechanics.

For the final project, students designed a mechanism-based powered exoskeleton to assist individuals with some movement impairment in performing an important task of daily living. The project focused on the kinematic and kinetic requirements of their design. Students applied human-centered design principles to identify a specific movement impairment to focus on and ensure that their design would meet intended user needs. Deliverables included a project proposal, final oral presentation, and final written report. At the conclusion of the project, students were given a brief IRB-approved survey to understand how well students felt the project met course objectives in addition to improving their understanding of and interest in biomechanics.

Results & Discussion: Survey statements (denoted S1, S2, etc.) and results are presented in Figure 1. Since this is a required core mechanical engineering course, it is critical that the project reinforce course fundamentals. All students felt that this project did improve their understanding of the course concepts (S3). Additionally, most students felt that the project improved specific course and general engineering concepts (S4, S5, S8).

Relating to the specific goal of this study it is notable that while students generally found the project to be interesting (S1), only one of the five students agreed that the project increased their interest in biomechanics (S7). However, it is important to remember that this was a small sample size (N=5) and that the course is a traditional required senior-level course in mechanical engineering (versus a biomechanics elective where students would be demonstrating some basic interest in the field by their enrollment). Most students did indicate that the project broadened their view of applications of the course material (S9) which is important for professional preparation.

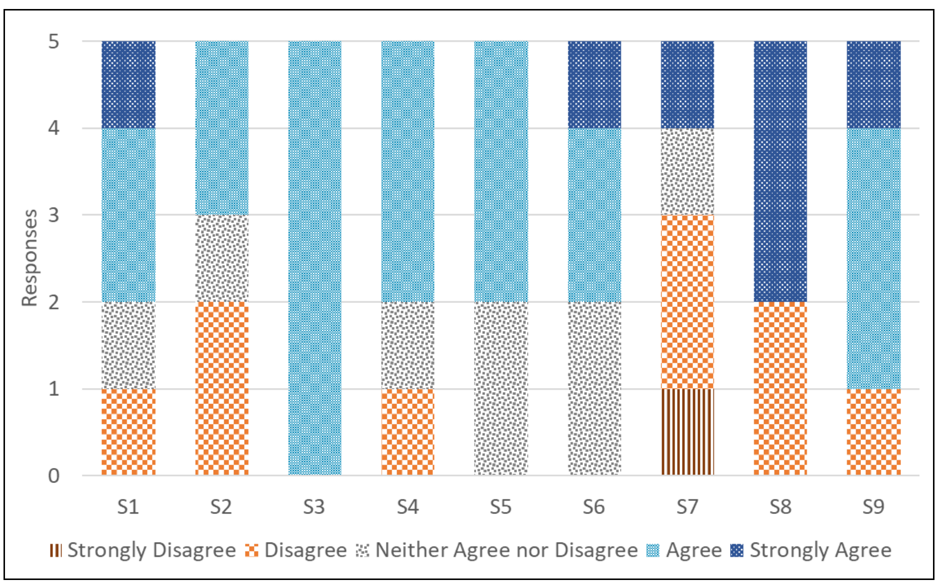

S1. This project was interesting.

S2. This project increased my interest in mechanism design.

S3. This project improved my understanding of course concepts generally.

S4. This project improved my understanding of function generation in mechanism design.

S5. This project improved my ability to solve complex engineering problems.

S6. The project improved my understanding of exoskeletons.

S7. This project increased my interest in biomechanics.

S8. This project improved my ability to do human-centered design.

S9. This project gave me a broader view of applications for mechanism design.

Figure 1: Distribution of responses from post-project survey.

Significance: This case study evaluates an approach for effectively introducing biomechanics in a traditional mechanical engineering course. This type of approach is critical to introducing biomechanics to students at small undergraduate-only programs that cannot support a course dedicated to the field. Such exposure to biomechanics within these programs could lead to improved diversity within the field of biomechanics at the graduate level and beyond. Future work should assess similar projects in other small undergraduate-only engineering programs and assess which specific elements of these projects produce successful outcomes.

References: [1] Mills & Treagust (2003), Aust. J. of Eng. Edu.

ERROR-STATE KALMAN FILTER FOR JOINT CENTER ESTIMATION FROM ADJACENT-LIMB IMU DATA

Michael V. Potter[1*], Stephen M. Cain, Lauro V. Ojeda, Reed D. Gurchiek, and Ryan S. McGinnis
[1]Department of Physics and Engineering, Francis Marion University, Florence, SC
*Corresponding author's email: michael.potter@fmarion.edu

Introduction: Inertial measurement units (IMUs) offer an attractive way of capturing human motion without many traditional laboratory constraints (e.g. limited capture volumes). However, an essential step for estimating human joint kinematics from body-worn IMU data is determining the sensor-to-segment (S2S) alignment parameters between segment anatomical frames and their corresponding IMU sense frames. In particular the S2S parameters for each body segment include the relative rotations and positions of the anatomical and IMU coordinate systems (i.e., origins and XYZ axes). S2S parameter estimation for IMU-based motion capture remains a largely unsolved problem and is particularly challenging for IMU-only methods that do not rely on additional equipment (e.g., optical motion capture) [1]. This study presents an error-state Kalman filter (ESKF) method for estimating individual joint center locations (in the IMU sense frames) from IMU data only. The study further evaluates the performance of this method compared to an optical motion capture assisted method for determining the same parameters on twenty human subjects.

Methods: An ESKF is utilized to estimate joint center locations in their adjacent IMU sense frames (e.g., estimating the ankle joint center location in the foot and shank IMU's coordinate systems). The mathematical formulation is similar to the ESKF developed in [2] for estimating lower-limb joint kinematics from seven IMUs (notably, requiring S2S parameters as an input). In the present method, an independent ESKF is utilized for each joint using only IMU data from the two adjacent limbs. The total state estimated consists of each IMU's quaternion orientation (in an arbitrary earth-fixed reference frame) and the position of the joint center in each IMU's coordinate system. Two measurement corrections are utilized to correct errors in the state estimates. First is a tilt correction which uses the IMU-measured acceleration to estimate the gravitational acceleration direction when the IMU is detected to be near-still. The second measurement leverages the fact that the world-resolved joint center acceleration should always be the same as estimated by each IMU using that IMU's state estimate (orientation and joint center location estimates) and data (acceleration and angular velocity).

IMU and marker-based motion capture data were previously collected from twenty healthy adult subjects performing a set of calibration movements designed to exercise all primary lower-limb joint degrees of freedom (about 1 minute trial). For each joint, the ESKF method described above estimates the joint center locations in the IMU frames as follows. Estimated joint center locations are initialized to zero and the ESKF updates state estimates at each time step via IMU data and measurement corrections. The final joint center estimate at the end of the trial is used as the estimated joint center location. ESKF-based estimates of the joint center locations are compared to marker-based estimates. Note that each joint center location estimate is a vector from the IMU sense axes to the joint center, resolved in the IMU reference frame. In this study, the magnitudes and angles of the joint center estimate vectors are compared.

Results & Discussion: Absolute differences between IMU and marker-based estimates of the joint center location vector magnitudes and directions are presented in Table 1. Each row presents the mean and standard deviation of these differences for each joint-IMU combination (e.g., the first row presents results for the foot-IMU estimates of the ankle joint center location).

Vector magnitude differences from foot and shank IMUs generally remain low indicating that the method accurately estimates the distances from the IMUs to the joint centers. Estimates from thigh and pelvis IMUs are generally larger which may be due to increased soft tissue under these IMUs and the relatively smaller accelerations of those segments during the calibration movements (i.e., lower signal-to-noise ratio). Remarkably, distances from the shank IMUs to the knee centers are estimated well even though the knee acts predominantly as a single degree of freedom joint making it more difficult to estimate the position of the joint center along the flexion axis from IMU data without additional corrections [3]. Angle estimates are generally poorer than magnitude estimates. However, poor angle estimates could be due to the small distances between some IMUs and their associated joint (e.g., between ankle and foot) where small positional errors could yield large angle errors. Further work is required to determine effective ways to improve these angle estimates.

Table 1: Comparison of IMU vs. marker-based estimated joint center location vectors (from IMU sense axes to joint center). Mean ± standard deviation of absolute differences between vectors magnitudes and angles (directions).

Joint	IMU	Magnitude Diff. (cm)	Angle Diff. (deg)
Ankle	Foot	0.61±0.41	16.9±3.07
	Shank	3.13±1.21	4.96±3.83
Knee	Shank	0.92±0.72	11.0±4.52
	Thigh	4.93±3.01	10.0±7.62
Hip	Thigh	8.64±4.40	12.0±8.94
	Pelvis	9.61±3.84	23.8±13.3

Significance: Advances in IMU-only sensor-to-segment parameter estimation will yield increased utilization of IMU-based methods for estimating human joint kinematics. Such advances are necessary to improve the accuracy and usability of IMU-based motion capture methods so that they can be effectively deployed to study and monitor human movement in natural settings without traditional laboratory-based motion capture equipment and restrictions. This study offers an important step towards this goal.

Acknowledgements: This work was funded by a Francis Marion University Summer Research Stipend award.

References: [1] Vitali and Perkins (2020), *J Biomech* 106:109832; [2] Potter et al. (2022) *Sensors* 22:8398; [3] Seel et al. (2014) *Sensors* 14(4).

Fit features of hike boots and their effects on walking biomechanics

Milena Singletary[1*], Daniel Feeney[1], Eric Honert[1]
[1]Performance Fit Lab BOA Technology Inc. Denver, CO
*Corresponding author's email: milena.singletary@boatechnology.com

Introduction: High-cut footwear is common in fields like workwear and recreation. Design features of high-cut footwear like mass, midsole flexibility, and shaft height can influence walking biomechanics [1]. There is limited work systematically evaluating the effect of cuff and midfoot fit on walking biomechanics, which can be assessed using wearable technologies. Plantar pressure metrics such as heel contact area [2] and metrics from an inertial measurement unit (IMU) such as foot eversion velocity are sensitive to footwear fit during running [3]. The purpose of this series of studies was to understand how different hike boot closures influence biomechanical fit features during gait.

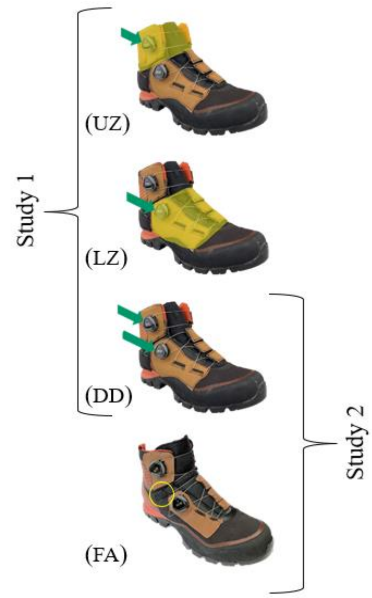

Figure 1: Configuration for the two studies. Study one: the top three boots - Upper Zone (UZ), Lower Zone (LZ), and Dual Dial (DD). Study two: the bottom two boots - Dual Dial (DD) and Dual Dial with a focus ankle guide (FA).

Methods: Nine male subjects participated in the first study and ten male subjects participated in the second study. Six subjects participated in both studies. For both studies a Tecnica Forge GTX boot was used (Fig 1). In the first study, three conditions on the same boot were tested: Upper Zone (UZ) – proximal dial engaged, Lower Zone (LZ) - distal dial engaged, and Dual Dial (DD) - both dials engaged. For the second study, conditions on two boots were tested: Dual Dial - both dials engaged on a boot without an ankle guide (DD) and Dual Dial on a boot with an ankle guide (FA) located between upper and lower zones designed to enhance heel fit. For both studies subjects walked on a treadmill at an incline and decline of 10 degrees for one minute. Subjects also traversed an indoor hiking pathway four times. The path is comprised of four eight-foot sections with different terrains in each section including: river rock, pea gravel, an eight-foot tree trunk, and an elevated obstacle with varying slopes. Data were collected using plantar pressure sensors (100 Hz, XSENSOR, Calgary, CAN), and an IMU attached to the heel counter of the left boot (±16 g and ±2,000°/sec at 1125 Hz, IMeasureU, Denver, USA). All data were processed in Python. The mean heel contact area during the last 50% of stance was computed from the pressure insole data. Gyroscope data from the IMU was filtered with a lowpass 30 Hz filter. Strides were detected using the accelerometer. Peak foot eversion velocity for each stride was then computed. Statistical analysis was performed in R. Linear mixed effect models were used to evaluate differences between configurations for the outcome metrics. Independent intercepts for each subject and independent slopes for each configuration were used. Tukey's test was run post-hoc to correct for multiple comparisons. Presented are estimated marginal means from the mixed effect models.

Results & Discussion: Study 1: On trail, the DD and UZ configurations had similar percent heel contact areas (≈ 57%, $p > 0.7$), and both were greater than the LZ (45.6%, $p < 0.001$). The DD and UZ configurations had similar peak foot eversion velocities (≈ 160 deg/s,, $p > 0.9$), and both were less than the LZ (183 deg/s, $p < 0.04$). Walking downhill, the DD and UZ configurations had similar heel contact areas (53.6% and 49.2%, respectively, $p > 0.06$), and both were greater than the LZ (32.4%, $p < 0.001$). Walking uphill, the heel contact area for DD, UZ, and LZ were all different (44.3%, 40.6%, and 29.8%, respectively, $p <0.006$). Foot eversion velocities were similar between all three configurations no matter the slope of the treadmill (downhill ≈ 135 deg/s, uphill ≈ 89 deg/s $p > 0.1$).

Study 2: On trail, the DD and FA configurations had similar percent heel contact areas (≈ 56%, $p > 0.5$). The configurations also had similar peak foot eversion velocities (≈ 162 deg/s, $p > 0.4$). Walking downhill, the DD and FA configurations had similar percent heel contact areas and peak eversion velocities (≈ 59% and ≈ 118 deg/s, respectively, $p > 0.4$). Walking uphill, FA had greater heel contact area than DD (49.6% and 46.2%, respectively, $p < 0.05$). The configurations had similar foot eversion velocities (≈ 90 deg/s., $p > 0.1$).

For both studies, walking uphill challenged heel fit the most likely due to greater demand at toe off potentially causing separation between the heel and the boot. Walking uphill, there was greater heel contact area with the FA configuration, suggesting that the added ankle guide better secures the heel in the cup of the boot. This feature should be considered when designing a hike boot as walking uphill is a common task during hiking. On trail the DD and UZ configuration had smaller eversion velocities than the LZ, similar reductions have been observed on-trail in better fitting low-cut shoes [2]. This suggests the upper zone of a hike boot may be relatively more important to fit than the lower zone during walking.

Significance: There is limited research on the impact closures of a hike boot play on fit. These findings can be further explored in areas that use high cut shoes like workwear. Next steps might include expanding on previous work by systematically altering design features like shaft height or sole stiffness [1]. This should be done by controlling for boot mass which can be accomplished with the materialization in mind.

References: [1] Dobson et al. (2017), *Applied Ergonomics* 61: 53-68 [2] Honert et al. (2023), *Frontiers in Sport and Active Living* [3] Hagen & Henning (2009) *Journal of Sports Sciences*; 27(3): 267–275

ADVERSE IMPACTS OF PARKINSON'S DISEASE AND DUAL-TASKING ON THE TEMPORAL AND CONTROL ASPECTS OF BALANCE INTEPRETED BY DIRECTIONAL VIRTUAL TIME-TO-CONTACT

Vu Phan[1], Daniel S. Peterson[2,3], and Hyunglae Lee[4,*]
[1]Department of Mechanical Engineering, Carnegie Mellon University, Pittsburgh, PA USA; [2]College of Health Solutions, Arizona State University, Phoenix, AZ USA; [3]Phoenix VA Medical Center, Phoenix, AZ USA; [4]School for Engineering of Matter, Transport and Energy, Arizona State University, Tempe, AZ USA
*Email: Hyunglae.Lee@asu.edu

Introduction: Virtual time-to-contact (VTC) is a promising approach for balance assessment, especially in populations with neurological diseases [1]. However, merely resultant measures, such as VTC mean, have been intensively used in the literature while directional components, namely anterior-posterior (AP) and medio-lateral (ML), may give more interesting insights into standing balance. To address this limitation of the standard VTC calculation, directional VTC was proposed in a recent work by Phan and colleagues [2]. Through multiple case studies, this variant of VTC was demonstrated to enable directional assessments and offer a means to enhance our understanding of posture biomechanics with provided spatial (e.g., which direction exhibits higher fall risks?) and control (e.g., how hard it is for one to perform balance adjustment?) information in addition to temporal information. However, further validation of the proposed method is imperative to draw more solid conclusions from this preliminary study. As an extension of a case study in the seminal work on directional VTC, we applied this novel approach to investigating balance of people with Parkinson's diseases (PwPD) and their healthy peers under single- and dual-task conditions.

Methods: Approved by ASU IRB, 14 PwPD and 13 healthy control (HC) individuals, >55 years, participated in this study. No participant had neurological diseases other than PD. Participants were instructed to perform single-task quiet standing, followed by standing with the auditory Stroop task (dual-tasking) on an instrumented, stationary treadmill. Each setup had two 50-second trials separated by a short break. Center-of-pressure (COP) data were low-pass filtered at 7 Hz. Base of support was reconstructed from motion capture data. Following [2], we derived directional VTC measures: AP/ML VTC mean to represent temporal aspects, AP/ML boundary contact (BC) to represent spatial aspects, and switching rate (SR) to represent control aspect of postural balance. A mixed ANOVA was used to examine the group (i.e., PD vs. HC) and task (i.e., single vs. dual) effects. No statistical test was performed on the spatial aspect.

Results & Discussion: While PD and dual-tasking had significant impacts on the temporal (specifically, ML VTC mean) and control (SR) aspects, their impacts on the spatial aspects (AP/ML BC) were negligible, as indicated in Fig. 1.

Temporal aspect: A decreasing trend in VTC mean measures in the dual-task condition (compared to single-task) was noticeable. Moreover, VTC mean values were higher (better) in HC participants compared to PwPD. This observation is anticipated as previous studies have demonstrated that ML rather than AP measures are especially affected by an additional cognitive task in PwPD [2, 3]. Statistical significance of group ($p = 0.03$) and task ($p < 0.001$) effects were observed in ML but not AP VTC (all p-values ≥ 0.24). No interaction between group and task effects was found (all p-values ≥ 0.34).

Spatial aspect: BC tended to be closer to 50% with PD and dual-tasking, yet the trend was not significant. This may be because our PD participants had mild-to-moderate balance impairment. With a more severe population, we envisioned the trend to be more obvious.

Control aspect: A clear distinction between the HC and PD participants ($p = 0.01$) was observed in either single- or dual-tasking. Decreasing SR values suggested PD participants may experience difficulty in adjusting their balance given the existence of a secondary cognitive task. However, this may not be the case in the HC cohort. For task effects ($p = 0.05$), the switching rate decreased in the PD but not HC group. The significant interaction was found ($p = 0.01$).

Significance: Directional VTC was further validated to be effective in assessing balance under challenging conditions across populations. It also showed the possibility of measuring spatial, temporal, and control aspects of postural balance simultaneously. Potential uses include clinical assessment and balance training. Future work will further investigate its applicability to other populations.

Acknowledgements: This work was funded by ASU-Mayo Seed Grant.

References: [1] Slobounov et al. (1997), *J Mot Behav* 29(3), [2] Phan et al. (2023), *J Biomech* 146, [3] Peterson et al. (2021), *Clin Biomech* 88.

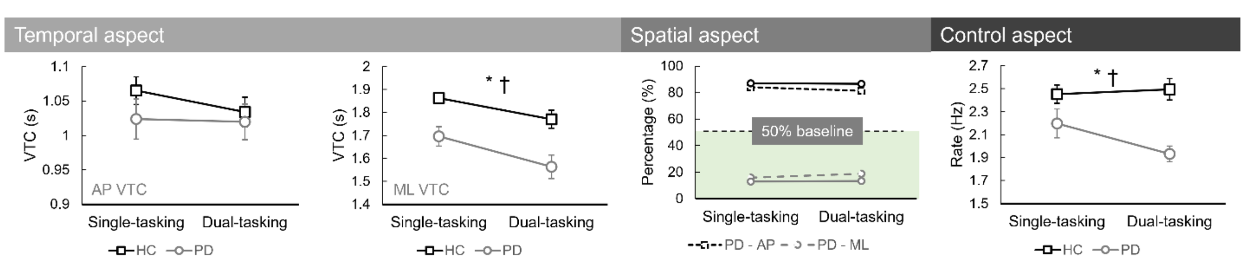

Figure 1: Effects of PD and a secondary cognitive task on (from left to right) AP/ML VTC (i.e., temporal aspect), predicted fall in the AP/ML direction (i.e., spatial aspect), and switching rate (i.e., control aspect). * and †, respectively, represents group and task effect.

EMG INFORMED MUSCULOSKELETAL MODELLING AND DEEP LEARNING TO ESTIMATE MUSCLE MOMENT

Ethan B. Schonhaut[1], Dean D. Molinaro[1,2], Keaton Scherpereel[1,2], and Aaron J. Young[1,2]
[1]George W. Woodruff School of Mech. Engineering, [2]Institute for Robotics and Intelligent Machines, Georgia Institute of Technology
Email: eschonhaut3@gatech.edu

Introduction: Understanding the internal joint biomechanics of the lower limbs during ambulation is potentially useful for augmenting human motion. Several deep learning (DL) approaches have been implemented to estimate biological joint moments [1]-[2] to generalize exoskeleton control across tasks. For instance, our previous study showed that using a temporal convolutional network (TCN), can effectively estimate biological joint moment during different ambulation modes [1]. These algorithms, however, fail to incorporate the underlying biomechanics occurring in the joint, such as muscle tendon unit (MTU) length, muscle force, or individual muscle moments, which may be beneficial for providing optimal assistance during rapid concentric muscle contractions [3]. This study uses a DL TCN with ground truth labels calculated using the Calibrated Electromyography (EMG) Informed Neuromusculoskeletal Modelling Toolbox (CEINMS) [4] and OpenSim [5] to estimate the internal muscle dynamics and joint moments surrounding the knee across a wide variety of ambulatory tasks and movements using common exoskeleton sensors, such as encoders, inertial measurement units (IMUs), and insoles (Fig 1A), calculated from the data in a virtual OpenSim environment [6]. Due to the accuracy of this approach shown in [1], we hypothesized that the TCN would be able to accurately estimate the flexion and extension components of the net joint moment, as well as individual muscle moments for the flexor and extensor muscles spanning the knee joint during human movement.

Methods: Twelve subjects were outfitted with motion capture markers and EMG sensors and were instructed to perform twenty-eight different cyclic and non-cyclic tasks, such as walking, running, jumping, squatting, and turning. Inverse dynamics, kinematics, and muscle analysis were calculated for each subject in OpenSim and EMG data were low pass filtered, rectified, and normalized by maximum contractions recorded across all tasks. The CEINMS Toolbox, normalized EMG activations, and OpenSim muscle moment arms were used to calculate ground truth internal muscle dynamics, such as muscle force, for the muscles spanning the knee which were identified by the OpenSim Gait 2354 model. Individual and combined flexion and extension muscle moments were calculated by multiplying muscle moment arm and muscle force (Fig. 1B) prior to estimation. To estimate muscle moments using the TCN, joint angles, virtual IMU outputs, and virtual insoles simulating ground reaction forces were modelled in OpenSim. These inputs, combined with the individual, flexion, and extension moments spanning the knee joint were fed into the TCN, where a two headed model estimated flexion and extension moment and a seven headed model estimated each individual muscle moment (Fig. 1C).

Results & Discussion: The R^2 of the TCN varied greatly across all muscles when compared to net flexion, net extension, and net biological joint moment (Fig. 1C). The TCN performed most accurately when estimating net biological joint moment with an R^2 of 0.897 ± 0.028, with a flexion moment R^2 of 0.250 ± 0.031, and an extension moment R^2 of 0.478 ± 0.036, with lower accuracy for the individual muscles. Overall, the DL TCN performed better when estimating knee extension rather than flexion, however this could be attributed to having more tasks in our dataset that emphasized extension vs. flexion (i.e., more non-cyclic tasks). In general, R^2 values tended higher in cases where the torque generated by a muscle or muscle group was higher, R^2 tracking was low when a muscle's torque contribution was low.

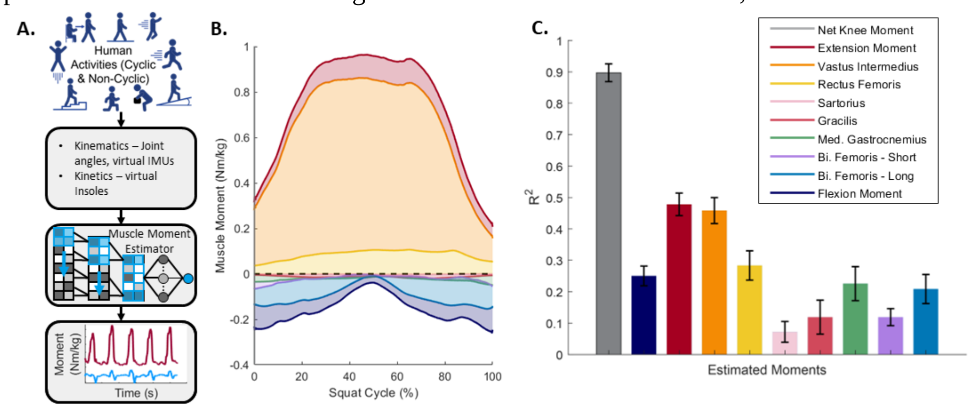

Figure 1: A. Flow chart showing path of data from human activity to muscle moment estimation. B. Contributions of individual muscle forces to net flexion and net extension in the knee for squatting. C. R^2 results from TCN estimation of net knee moment, flexion and extension moment, and individual muscle moment for all cyclic and non-cyclic tasks.

Significance: The purpose of this study was to determine the resolution of estimating an internal muscle characteristic such as muscle moment during several structured and unstructured tasks with a DL model. While previous studies have shown the efficacy of estimating net biological joint moment [1], little work has been done to estimate or calculate internal muscle dynamics without the use of invasive or intrusive sensor suites such as ultrasound or EMG. By targeting and estimating different internal muscle moments and states, exoskeleton assistance can potentially be fine-tuned to fill gaps between the user and the device, providing more beneficial assistance during ambulation. Likewise, the ability to separately estimate muscle dynamics such as flexion and extension moment can allow researchers to monitor joint health during different types of activities to better understand and prevent joint injury and degradation.

Acknowledgements: The authors would like to acknowledge x, the moonshot factory for their support. This work was funded by the X Scholarship (x, the moonshot factory), the NSF NRI Award #1830215, and the NSF GRFP #DGE-2039655.

References: [1] Molinaro et al. (2022) *IEEE T-MRB* (4), [2] Setter et al. (2020) *Front. Bioeng. Biotechnol.* (8), [3] Ryschon et al. (1997) *J. Appl. Physiol.* (83) [4] Pizzolato et al. (2015) *J. Biomech.*(48) [5] Delp et al. (2007) *IEEE TBME* (54) [6] Scherpereel et al. *In Review*

SEGMENT STABALIZATION FOR SAM AND FASTCAST SPLINTING OF COMPLETE TIBIA-FIBULA FRACTURES

Nathaniel A. Bates,[1*] C. Grace P. Hobayan,[1] John Heyniger,[1] Kenan Alzouhayli,[1] Franco Piscitani,[1] Clifton Haider,[2] Christopher Felton,[2] Adam T. Groth,[1] Kevin D. Martin[1]

[1] Department of Orthopaedics, The Ohio State University Wexner Medical Center, Columbus, OH, USA

[2] Special Purpose Processor Development Group, Mayo Clinic, Rochester, MN, USA

*Corresponding author's email: nathaniel.bates@osumc.edu

Introduction: Musculoskeletal injuries (MSKIs) are a burden to military readiness as 34.7% of service members report lost time due to non-combat injury, of which, 25-50% are fractures.[1] In Afghanistan, 40% of all MSKIs were fractures. Current standard of care for acute fracture stabilization in an austere environment includes SAM splints and external fixation. Splints are often unsuitable for deployment in complex or open fractures as they do not sufficiently stabilize the limb.[2] Conversely, external fixation is limited to application by field surgeons and not implementable in combat. Rapid, rigid stabilization of a fractured limb via one step spray-on FastCast foam can provide multiple direct benefits including minimized risk for secondary injury, infection, and fracture hemorrhage; management of pain control; and facilitation of medical evacuation. A critical military healthcare need exists to develop a product that couples the efficacious benefits of external fixation fracture stabilization with ease of deployment that matches a splint. Our hypothesis was that FastCast would increase stability of lower extremity fracture stabilization compared to SAM splints.

Methods: This study was performed on cadaveric specimens and was exempt from approval by The Ohio State University Wexner Medical Center Institutional Review Board. Ten cadaveric lower extremities disarticulated at the tibiofemoral joint underwent osteotomy in the transverse plane through the full thickness of the tibia and fibula at their midpoint. Two custom 6-axis sensors (Mayo Clinic, Rochester, MN) [3] were mounted superficial to the fibula on the medial aspect of the limb at the fibula head (superior) and lateral malleolus (inferior). Mounted sensors continuously recorded acceleration and angular displacement data at a 100 Hz throughout all Events. Specimen fractures were set by a medical professional and SAM (SP500-OB-EN, SAM Medical, Tualatin, OR) or FastCast spray foam (US Army Medical Research and Development Command, Fort Detrick, MD) splints were applied in a randomized order for stabilization. All splinting was performed by a single EMS squad. After splinting, specimens were transported up and down stairs, onto a gurney, and transferred onto an ambulance by an EMS team. Finally, a fall impact from a 1-meter height was simulated.

Discrete variables of (1) summation of change for acceleration and rotation, (2) cumulative difference between the superior and inferior mounted sensors were extracted along each axis of measurement. Nonparametric repeated-measures Freidman Tests were used to assess significance between factors of Material (SAM, FastCast) and Sensor (superior, inferior). Variables were assessed separately for each Event (Splinting, Transport, Impact). Significance was determined *a priori* at $\alpha < 0.05$.

Results & Discussion: The summation of change observed during Splinting was greater for SAM splint than FastCast with respect to acceleration and rotation on all three axes (Table 1, $p<0.01$). This was also true for the impact Event with respect to anterior and superior axes acceleration ($p\leq0.03$). No differences were observed for Transport ($p\geq0.50$). No differences were observed between superior and inferior sensors for FastCast during any Event ($p\geq0.10$). For the SAM splint, there were differences between sensors along medial-axis rotation for all Events ($p\leq0.03$), medial-axis acceleration for Splinting ($p<0.01$), and superior-axis acceleration for Transport ($p=0.01$)

The cumulative difference between the superior and inferior sensors during Splinting was greater for SAM splint than FastCast with respect to acceleration and rotation ($p<0.01$). This was also true for anterior-axis rotation during Impact ($p<0.05$). Anterior- and superior-axis acceleration and superior-axis rotation also approached significance ($p\leq0.07$). No differences were observed between splint Material during Transport ($p\geq0.60$).

Significance: These data support our hypothesis. SAM splints exhibited up to 14.8 times the acceleration and 14.6 times the rotation exhibited by FastCast splints. Thus, per our data, FastCast splints reduced acceleration and rotation versus SAM splints. This is true both cumulatively across the entire limb body as well as between both segments separated by the fracture site. Combat environments can necessitate extraction under duress, where impacts to the injured limb may occur. The reduced acceleration and rotation in FastCast splints indicate that they did a better job of maintaining rigid stability of the fractured limb than SAM splints. Furthermore, the actual splinting process for FastCast was less aggressive and traumatic to the limb specimens than SAM splints.

Acknowledgements: Surgical Skills Laboratory at The Ohio State University Wexner Medical Center.

References: [1] Belmont et al. (2016), *J Am Acad Orthop Surg* 24(6); [2] Pollak & Ficke (2008), *J Am Acad Orthop Surg* 16(628-634) [3] Gilbert et al. (2015), *Am J Biomed Eng* 5(2)

Table 1: Summation of change data for both Materials during the splinting Event, presented as median [interquartile range]

	Acceleration			Rotation (°)		
Axis	**Ant./Post.**	**Sup./Inf.**	**Med./Lat.**	**Ant./Post.**	**Sup./Inf.**	**Med./Lat.**
SAM splint	78.2 [71.2, 101.4]	128.4 [106.5, 152.2]	102.9 [70.9, 153.6]	19666 [17657, 25497]	31987 [26969, 37698]	24599 [17845, 38247]
FastCast foam	7.4 [3.6, 12.4]	8.7 [6.0, 16.7]	7.8 [4.1, 13.1]	1845 [890, 3122]	2195 [1490, 4119]	1919 [1049, 3258]

THIGH MUSCULATURE MOTOR CONTROL AFTER MULTIPLE ANTERIOR CRUCIATE LIGAMENT INJURIES

Nathaniel A. Bates,[1*] April McPherson,[1] Christopher Nagelli,[2] Takashi Nagai,[3] Nathan D. Schilaty[4]
[1] The Ohio State University Wexner Medical Center, Columbus, OH, USA; [2] Mayo Clinic, Rochester, MN, USA;
[3]United States Army Research Institute of Environmental Medicine, Natick, MA, USA; [4]University of South Florida, Tampa, FL, USA
*Corresponding author's email: nathaniel.bates@osumc.edu

Introduction: ACLRs fail to fully restore native knee mechanics and neuromuscular control (NMC), leading to secondary ruptures in 20-30% of patients.[1] Motor unit (MU) activation in relation to multiple injury incidence is not well understood. We have noted that after initial ACL injury, normative MU activation is disrupted for at least 12 months.[2] Specifically, in healthy subjects, muscle force generation is a product of both MU rate coding and quantity of MU recruitment, and an inverse relationship exists between MU firing rate and MU recruitment threshold.[3] After an ACL injury, there were decreases in size of recruited MUs and rate coding.[4] Despite this, a gap remains pertaining to longitudinal impact of multiple ACL injuries on MU control of the thigh. Thus, the purpose of this study was to investigate NMC of the thigh musculature via decomposed electromyography (dEMG), which allows for specific analysis of MU activity. We hypothesized that participants with multiple ACL injury (2ND) would demonstrate decreased NMC of the LE, with lower average firing rate (AvgFR) and decreased MU action potential (MUAP) peak-to-peak amplitude compared to both healthy controls (CTRL) and primary ACL injury (1ST) subjects.

Methods: 41 participants were recruited prior to ACL surgery. Participants were organized into three groups: CTRL (n=19, 18.9±3.5 years; 65.1±12.2 kg), 1ST (n=16 18.6±3.5 years; 76.0±16.1 kg), ACL (n=4, 20.5±2.9 years; 74.9±13.1 kg). All data collections were performed on a dynamometer (HumacNORM; CSMi). A custom load cell apparatus affixed to the torque arm measured isometric force production for the EMG decomposition (dEMG Analysis; Delsys). Surface 5-pin dEMG electrodes (Bagnoli; Delsys) were placed on the muscle belly of the quadriceps and hamstrings musculature, respectively, for extension and flexion testing (10-50% maximal effort). Data collections were repeated at three time points (pre-surgery, 6-months post-surgery, and 12-months post-surgery). As MU strategies are non-linear, log MUAP peak-to-peak amplitude and cube root Recruitment Threshold transformations were utilized to provide parametric data for linear regressions. MU data were normalized to force and mass for statistical analysis, when appropriate. We calculated an interaction variable (AvgFR * MUAP) to represent overall MU function (motor control) that was compared between groups by recruitment threshold with standard least squares regression and least square means ANOVA. Tukey's HSD post-hoc comparisons were utilized when appropriate. Significance was set a priori at $p<0.05$.

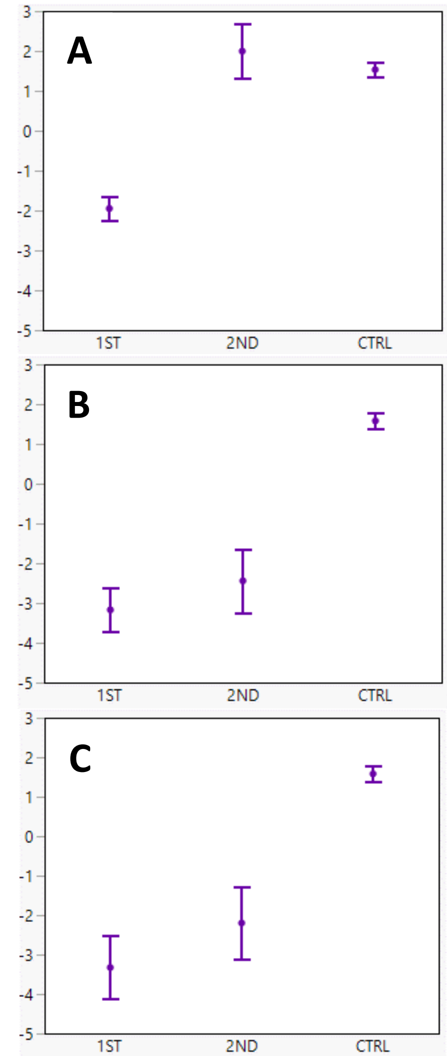

Figure 1: Progression of MU interaction (AvgFR*Log[MUAP]) by ACL injury Group from Pre-Surgery (A), 6 months (B), and 12 months (C)

Results & Discussion: Overall, for the hamstrings, the 1ST cohort exhibited decreased motor control than the 2ND cohort, which was decreased from CTRLs (R^2=0.27, $p<0.001$). This pattern was prevalent at pre-surgery ($p<0.001$) and 6-months (R^2=0.17, $p<0.04$). At 12-months, 2ND was decreased relative to 1ST, which was decreased relative to CTRLs ($p<0.001$). The 2ND cohort exhibited a decline in hamstrings motor control between 6-months and 12-months ($p<0.001$) Overall for the quadriceps, motor control was decreased in 1ST subjects and increased in 2ND subjects compared to CTRLs (R^2=0.41, $p<0.001$). At pre-surgery, the 1ST cohort exhibited decreased NMC compared to 2ND and CTRLs ($p<0.001$). At 6-months and 12-months, the 1ST and 2ND cohorts were decreased versus CTRLs ($p<0.001$). The 2ND cohort exhibited a decline in quadriceps NMC from pre-surgery to 6 months ($p=0.002$). The results partially supported the hypothesis as they demonstrated altered NMC in participants with ACL injuries compared to CTRLs. However, a cumulative effect of secondary ACL subjects expressing further reduced NMC relative to primary ACL subjects was not realized.

Significance: These data inform how multiple ACL injuries influence MU characteristics. Inconsistencies in MU characteristics between 1ST and 2ND injuries may indicate that MU characteristics are more difficult to regulate after 2ND injury. The 2ND cohort was worse than CTRLs, which perpetuates that NMC is disrupted after musculoskeletal injury. However, as dramatic worsening over time was not observed in the 1ST cohort, multiple injuries differentiated the NMC response. Investigations should target larger cohorts and interventions with the potential to restore normative NMC and MU characteristics to injured limbs. As large drops in NMC are observed in second injury patients, early implementation of NMC training should be emphasized to minimize deficits upon return to activity.

Acknowledgements: NIH NIAMS R01-AR055563.

References: [1] Bates et al. (2015), *Clin Biomech* 30(1); [2] Schilaty et al. (2022) *Eur J Sport Sci* 2:1-11; [3] Maffiuletti et al. (2016) *Eur J Appl Physiol* 116(6); [4] Di Virgilio et al. (2019), *Front Hum Neurosci* 13:294.

HAND-SPECIFIC SPECIALIZATION OF GRIP FORCE CONTROL DURING BIMANUAL PREHENSION

Anvesh S. Naik, Satyajit Ambike
Department of Health and Kinesiology, Purdue University, West Lafayette, Indiana
Email : naik20@purdue.edu

Introduction: Many activities of daily living require coordinated use of both hands to manipulate objects [1]. Yet, tasks requiring both hands to coordinate to either manipulate a common object (e.g., operating a steering wheel) or mechanically coupled objects (e.g., slicing bread) have not been studied well. Control of such tasks is complex because the grip force of each hand must account not only for the dynamics of the object that the hand manipulates, but also for the destabilizing forces arising from the actions of the other hand. The task can become more difficult if the effects of the other hand are modulated by the compliance of the intervening object (e.g., the bread). Understanding bimanual grip force control in such ecologically significant tasks will yield insights into prehensile control which cannot be obtained by studying unimanual prehension and bimanual prehension of a single object or of two unconnected objects. Hence, we studied bimanual grip force control during the manipulation of two objects that are coupled by a compliant spring.

According to the influential dynamic dominance theory that quantifies handedness in humans, each cerebral hemisphere specializes in different aspects of arm motion control [2]. The left hemisphere specializes in predictive control, producing well-coordinated dominant (right) arm movements by anticipating changes in arm dynamics. The right hemisphere specializes in impedance control, maintaining positional stability of the non-dominant (left) arm against disturbing forces induced by the right arm or the environment.

Our goal was to identify whether dynamic dominance extends to grip force control. As there is limited data on coupled bimanual prehension, we hypothesized that dynamic dominance extends to grip force control. Since the right arm is under predictive control, it would be better at modulating grip force by anticipating changes in load force. Therefore, the grip-load force coupling strength will be higher for the right hand than the left hand when manipulating an object (H1). Since the left hand is under impedance control, it would be more efficient than the right hand at exerting grip force to maintain an object's stability against perturbing forces imposed by the manipulating hand. Therefore, the left hand would use lower grip force to stabilize the object against the load generated by the moving hand compared to the grip force used by the right hand to stabilize the object (H2).

Methods: Healthy young adults (N=8, 3 female, 21.8±1.3 years, right-hand dominant) held two instrumented objects connected by a spring, one with each hand using pinch grasps. Force sensors on each object measured digit forces and a motion capture system recorded object movements. A computer screen displayed (1) a feedback cursor for each object's position in the frontal plane and (2) a red and a green target (Fig. 1A). Participants first held the objects in both hands and moved the objects apart in the mediolateral direction so that the spring was stretched. In this position, both cursors were inside the green target (Fig. 1A). Next, the green target oscillated vertically (amplitude=4cm, frequency=0.5Hz), and the red target remained fixed (Fig. 1B). Participants tracked the green target with a cursor by moving one object vertically, while simultaneously maintaining the other cursor static inside the red target by stabilizing the other object (Fig. 1B). The changing length of the spring due to continuous tracking induced disturbing loads on both objects. There were two tasks blocked by *hand* (order balanced), each with 10 repetitions, each lasting 20 seconds. In one block, the right hand moved, and the left hand stabilized respective objects, and hands switched roles in the other block. We quantified the grip force in each hand (sum of pinch forces) and the load force on the moving object (vector sum of the object's weight, spring and inertial forces). We computed Pearson's correlation coefficient between grip and load forces to quantify grip-load force coupling for the moving hand, and the mean grip force for the stabilizing hand, per trial in each *hand* block. We quantified task performance by computing RMSEs of tracking and stabilizing objects. We fit separate mixed-effects models to correlation coefficient, mean grip force, and RMSEs (significance level was $p<.05$).

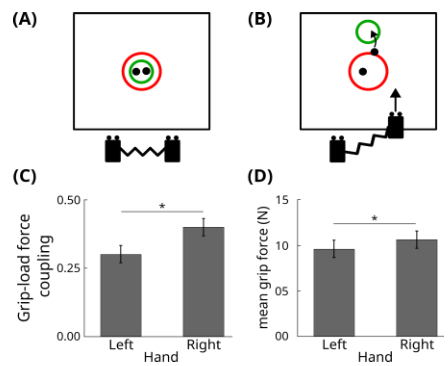

Figure 1: (A) Objects held in the frontal plane, (B) tracking with right object and stabilizing with left object, (C) grip-load force coupling, and (D) mean grip force comparisons between hands.

Results & Discussion: Compared to the left hand, the correlation coefficient (grip-load force coupling strength) was significantly greater (p=.01; Fig.1C) and tracking RMSE was significantly lower ($p<.01$) for the right hand indicating superior predictive control with the right hand (consistent with H1). Whereas, compared to the right hand, the mean grip force was significantly lower (p=.01; Fig.1D) for the left hand with no difference in RMSE for stabilizing the object with either hand ($p>.05$). The left hand achieved the same stabilization performance with lower grip force, indicating more efficient impedance control (consistent with H2). Thus, our results provide evidence for across-hand specialization of grip force control when both hands coordinate to manipulate mechanically coupled objects.

Significance: We present the first clear behavioral evidence of dynamic dominance in grip force control and thereby add to the fundamental understanding of bimanual prehension. This work informs future imaging- and modelling-based investigations for understanding inter-hemispheric specialization of neural pathways controlling prehension. Moreover, current upper-limb rehabilitation strategies for unilateral stroke survivors focus on training either the affected arm or both arms individually [1]. Our work could inform alternative interventions that use mechanically coupled bimanual prehensile activities encouraging the coordinated and simultaneous use of both hands. Such training may improve patient performance in activities of daily living.

References: [1] Kantak et al. (2017), Restor. Neurol. Neurosci., 35(4); [2] Sainburg (2002), Exp. Brain Res., 142.

UNCONTROLLED MANIFOLD ANALYSIS OF HAPTIC FEEDBACK DURING QUIET STANDING

Frankie Alcalá[1], Cara Painter[1], Andrew Meszaros[2], Kayt Frisch[1*]

[1]George Fox University, Department of Civil, Mechanical, & Biomedical Engineering
[2]George Fox University, Department of Physical Therapy
*Corresponding author's email: kfrisch@georgefox.edu

Introduction: It is well established that body center-of-mass (COM) control during quiet standing is a phenomenon that involves multi-segment coordination, rather than simple regulation at a single joint (i.e. ankle single-inverted pendulum model) [1]. Improvements in COM stability in patients have been demonstrated in patients while wearing a novel shirt that offers haptic input based upon trunk tilt during sway [2]. Understanding how such stability is mechanically accomplished across segments is difficult. Uncontrolled Manifold Analysis (UCM) characterizes variance in and contribution to the output of a multi-element system in order to identify elements prioritized for movement stabilization for a particular task [3], [4]. UCM defines two types of variability – good variability in motion (the UCM parallel space) which leads to the same values of task-level variables (e.g. position of the hand on the cup), while "bad" variability in motion (the UCM perpendicular space) destabilizes the task variables and thus the outcome. A ratio of these two variances can describe motor performance and stability [5], [6]. In this study we analyzed the UCM of subjects during quiet standing both with and without tactile feedback for their postural sway. We hypothesized that during the feedback condition, individuals would have less "bad variability" (i.e. be more stable) in their joint configurations.

Methods: *Experimental Data Collection:* 16 healthy normal subjects performed two quiet standing trials of 240s each. Motion data was collected using a standard full body marker set and 10 Qualisys cameras at 100Hz. Subjects wore a virtual reality headset showing a 180-deg view of the laboratory that was digitally manipulated for random motion in tilt and yaw for both trials. During the second trial, subjects were provided with directionally-specific haptic touch input in real-time when they exceeded 5-degrees of trunk tilt (IMU driven). Seven subjects were told that the vibrators in the shirt were a helper to keep them from losing their balance; the other nine were told that the vibrators were punitive, informing them they strayed too far.

UCM Geometric Model: A 3-segment geometric Matlab model was created for the task-level variable of sagittal plane center of mass (COM) position as a function of joint angles [1]. Hip joint centers were located using the CODA pelvis segment model and segment COMs using the Dempster tables. UCM analysis of each subject's data applied to the model followed the procedure described in [6] to produce a variance ratio for the middle 60s of each trial. The linearized null-space was calculated as described in [7]. To compare change within individual subjects, the difference between the baseline and haptic trials was calculated.

Results & Discussion: When COM performance with haptic assistance was contextualized as a "helper", 86% of the subjects (6/7) had increases in Variance Difference compared to baseline, indicating that the COM variable was stabilized by the haptics (Fig. 1). In contrast, when the haptics were put in a punitive "error" context, COM was only stabilized about half the time (56% of subjects, 5/9); in other words, haptic feedback embedded in an error context (as opposed to a helper context) had the effect of reducing COM stability in about half of subjects compared to their baseline (44%, 4/9). In fact, two subjects in the error condition experienced decreases into negative Variance Difference (#14, 15), suggesting that the haptics destabilized COM compared to baseline. Subjects in both conditions experienced changes to a varying degree, such that discernable group effects may be difficult to statistically demonstrate.

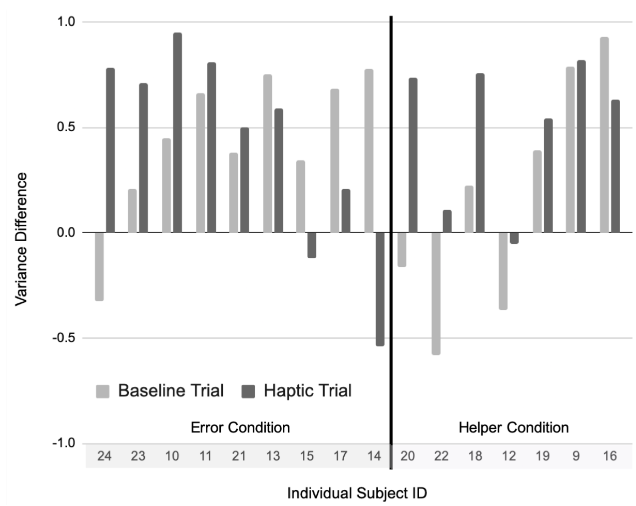

Figure 1: The UCM variance difference for baseline (no feedback) and feedback (haptic shirt) trials for each subject. Subjects to the left of the line were told the shirt vibrated when they made an error; Subjects on the right were told the shirt vibrated to help them maintain balance. Subjects are ordered based on change in variance difference between the two trials.

Significance: Because the haptic sensors provide feedback on excessive body sway, the shirt may help stabilize the wearer's motion, which could be particularly beneficial for stroke rehabilitation. UCM provides a potential way to assess these impacts and suggests that in this small sample that feedback is more likely to be beneficial if the subject views it as helpful.

Acknowledgements: The authors thank the Richter Summer Scholars Program for funding and Robin Dorociak for data collection.

References: [1] Hsu WL (2007), et al., *J Neurophys*, 97(4); [2] Meszaros, et al. (2019), *Int'l Soc Posture & Gait Research World Congress* - Oral presentation; [3] Latash (2010), *Motor Control* 14(3); [4] Latash, et al. (2002*), Exerc Sport Sci Rev* 30(1); [5] Qu (2012), *Gait Posture* 36(2); [6] Scholz (2003), *Exp Brain Res* 153(1); [7] de Freitas & Scholz (2010) *J Biomech* 43(4).

THE EFFECT OF ASYMMETRIC AND SYMMETRIC LOADING ON HIP AND LATERAL TRUNK SWAY WHILE PERFORMING THE DUMBBELL FARMER'S WALK EXERCISE

Michael Krackow[1*] and Joyce Blandino[2]
[1]Department of Human Performance and Wellness, [2]Department of Mechanical Engineering, Virginia Military Institute, Lexington, VA, USA
*Corresponding author's email: krackowms@vmi.edu

Introduction: Every day, people perform functional activities that require carrying loads on one side of the body (asymmetrical) or with two hands (symmetrical). Carrying these loads when walking can disturb the individual's stability and modify the biomechanics of the trunk and lower extremities [1-4]. One exercise, the farmer's walk, has become a routine exercise in training programs for individuals ranging from elite athletes to fitness enthusiasts [5]. When performing the farmer's walk, the person carries the load either in both hands (symmetric) or one handed (asymmetric). Research revealed that this exercise can increase core strength, as well as the strength in the upper and lower extremities. As a result, there is improvement in trunk stability and overall balance during walking [6-7]. It was found that an asymmetric load (15%-20% BW) resulted in an increase in hip abductor muscle activity and lateral trunk sway toward the non-loaded side to counteract load [8]. For novice strength training individuals who would like to add the farmer's walk exercise into their fitness regime, the safest weight to initiate this exercise without increasing the risk of injury should be considered. The purpose of this study was to examine the effect of the symmetric and asymmetric farmer's walk with various load conditions on hip and lateral trunk sway.

Methods: Eight healthy subjects (4 females, 4 males, aged 42.2±20.1 years) participated in the study. The average body weight was 81.27±25.70 kg. Subjects had between 0 to 25 years of weight or resistance training experience. Retro-reflective markers were placed on feet, shanks, thighs, chest, and lower back. Each subject performed three repetitions of the farmer's walk over 3 force platforms. Each subject walked with left leg first on the first force platform carrying no load, 10% or 15% body weight (BW) symmetrically and asymmetrically (left and right hand) (Figure 1). Eight VICON Vero cameras were used to gather kinematic data at 200Hz. Ground reaction force data were collected from the force platforms at 1000Hz. The Motion Monitor xGen software (TMMxGen) was used to collect data from both VICON cameras and the force platforms simultaneously. Subjects were given a one-minute rest period between tests. A one-way ANOVA was used to compare hip forces, moments, and thorax positions for symmetric and asymmetric loaded (left and right hip) tests. A post hoc analysis for pairwise comparison with Bonferroni adjustment was followed to determine which two groups were different.

Figure 1: Asymmetric load with right hand (left), Symmetric load (right) for Farmer's walk exercise

Results & Discussion: When the carrying loads are increased asymmetrically, it is assumed that lateral trunk sway would increase during the single leg stance phase of the gait cycle as compared to the no load or symmetrically loaded conditions. These preliminary findings demonstrated that there was no statistical difference in lateral trunk sway between all groups (symmetrical and asymmetrical in either hand with 10% and 15% BW and no load). The results of this study showed that for anyone who performs the farmer's walk exercise, it is safe to start the exercise with both symmetric and asymmetric loads of 15% body weight without significantly increasing lateral trunk sway. However, if subjects do not feel safe carrying 15% BW, a 10% BW load is also a suitable resistance to begin the exercise.

Significance: Results of this study indicated that there was no significant difference between the loads carried, both symmetrical and asymmetrical on lateral trunk sway. The preliminary findings suggest that it is safe for novice strength trainers to begin performing the farmer's walk exercise carrying 15% of their body weight symmetrically or asymmetrically without exhibiting compensatory movements. By conducting this exercise with a lower percentage of body weight, the individual can concentrate on the quality of the exercise execution, rather than quantity of weight carried.

Acknowledgements: The VMI Institutional Review Board approved testing protocol. This project was supported by funding from the VMI Center for Undergraduate Research.

References: [1] Demura S et al. (2005), *Sport Science*, 5: 89-96; [2] DeVita, P et al. (1991), *J Biomech*, 24: 1119-1129. [3] Matsuo T et al. (2008), *Gait & Posture*, 28: 517-520. [4] Corrigan LP and Li JX (2014), *Res Sports Med*, 22: 23-35. [5] Winwood et al. (2014), *Int J Sports Sci Coach* 9(3): 1127-1143; [6] Stastny et al. (2015), *J Human Kinetics*, 45: 147-165; [7] Graber et al. (2021, *J Applied Biomech* 37(4): 351-358; [8] Fowler et al. (2006), *Gait and Posture* 23: 133-141.

Increased instability during walking for individuals with Parkinson's disease is related to a loss of upper body and head control

Paphawee Prupetkaew[1*], Steven Morrison[1]
[1]School of Rehabilitation Sciences, Old Dominion University, Norfolk, VA 23529, USA
* Corresponding author's email: pprup001@odu.edu

Introduction Bradykinesia and rigidity are common motor symptoms for people with Parkinson's disease (PD). These symptoms can lead to changes in walking speed and often decreased stability [1-3]. As control of the head and trunk motion is critical during gait in order to ensure dynamic stability of visual, vestibular, and somatosensory information, increased rigidity in persons with PD may lead to declines in the control of walking. The aim of the current study was to assess the impact of this disease process on the control of the upper body and head for individuals with PD and the implications for overall walking stability.

Methods Walking patterns were assessed for twenty-five older persons with PD and 25 age-healthy elderly controls, who were asked to perform at their preferred and fast walking speeds. A 20 ft protokinetics mat was used to provide spatio-temporal measures of walking and 3-D accelerometers were also placed on the legs, lower trunk, upper thoracic, and head segments to assess body motion. The root mean square (RMS) of acceleration amplitude was calculated in three directions to indicate segment control and gait variability (i.e., the SD of stride time and length) was calculated to provide an indicator of gait instability.

Results & Discussion Overall, the PD individuals showed increased walking instability during both he preferred and fast walking speed as indexed by increases in the SD of stride time and stride length. Further, the PD persons exhibited diminished control over the motion (i.e., acceleration) of the lower trunk, upper trunk and head segments in all three dimensions compared to the healthy elderly. Additionally, decreasing segment control was directly related to increasing walking instability for the PD persons. It is likely that the loss of control of the upper body and head for individuals with PD leads to interruption of sensory information processing, resulting in deteriorated walking stability.

Significance Besides our understanding that an increase in lower limb variability could affect walking performance, a loss of upper body and head control may be additional important factors contributing to increased walking instability in people with PD.

References

[1] Cole, M. H., Silburn, P. A., Wood, J. M., Worringham, C. J., & Kerr, G. K. (2010). Falls in Parkinson's disease: kinematic evidence for impaired head and trunk control. *Movement disorders: official journal of the Movement Disorder Society*, 25(14), 2369–2378.

[2] Morrison, S., Moxey, J., Reilly, N., Russell, D. M., Thomas, K. M., & Grunsfeld, A. A. (2021). The relation between falls risk and movement variability in Parkinson's disease. *Experimental brain research*, 239(7), 2077–2087.

[3] Latt, M. D., Menz, H. B., Fung, V. S., & Lord, S. R. (2009). Acceleration patterns of the head and pelvis during gait in older people with Parkinson's disease: a comparison of fallers and nonfallers. *The journals of gerontology. Series A, Biological sciences and medical sciences*, 64(6), 700–706.

VERTICAL GROUND REACTION FORCE SYMMETRY DURING A DROP VERTICAL JUMP TASK IS ASSOCIATED WITH PATIENT-REPORTED FUNCTION AFTER ANTERIOR CRUCIATE LIGAMENT RECONSTRUCTION

Michelle C. Walaszek[1*], Katherine Collins[2], Francesca Genoese[2], Elaine Reiche[3], Shelby Baez[3], Matthew Harkey[2], Christopher Kuenze[1]

[1]University of Virginia, Department of Kinesiology, Charlottesville, VA

[2]Michigan State University, Department of Kinesiology, East Lansing, MI

[3]University of North Carolina – Chapel Hill, Department of Exercise and Sport Science, Chapel Hill, NC

*Corresponding author's email: dpk9tk@virginia.edu

Introduction: Following anterior cruciate ligament reconstruction (ACLR), individuals undergo testing as early as 4-months post-ACLR to determine preparedness for successful return to sport (RTS). During RTS assessments, bilateral jump landing tasks are used to assess movement quality and symmetry during a sport-related task while patient-reported outcome measures (PROM) are used to assess knee-related symptoms, function, and psychological readiness [1]. However, the relationship between jump-landing vertical ground reaction force (vGRF) symmetry and PROM among individuals with ACLR is not well explored. Thus, the purpose of this study was to assess the relationship between vGRF LSI during a bilateral drop vertical jump (DVJ) task and PROM in individuals 4 to 12-months post-ACLR. Symmetrical quadriceps strength and single leg hop distance are associated with higher IKDC scores [2; 3] and as a result, we hypothesize higher vGRF LSI will be correlated with better PROM.

Methods: This was a sub-analysis of a large, longitudinal RTS study in individuals after ACLR. Individuals 12-30 years old with primary, unilateral ACLR 4-12 months prior to testing without prior medical history that prevented safe participation in testing were included in the current study. For the DVJ task, participants were asked to jump from a 30 cm box that was positioned at a distance ½ participant height (cm) away from the center of the force platform. Immediately upon landing, participants were asked to complete a vertical jump upward to attain maximal height. Participants completed 3 successful trials on each limb. vGRF data were collected using two embedded force platforms, sampled at 1200 Hz, and filtered with a 4th-order Butterworth filter with a cut-off of 12 Hz. Normalized vGRF data ($N*(BW)^{-1}$) were processed using the Motion Monitor software and a custom Matlab code. Normalized peak vGRF during the 1st landing were averaged for each limb and mean peak normalized vGRF symmetry was calculated: LSI (%) = (ACLR limb peak vGRF/uninvolved limb peak vGRF)*100% where LSI=100% indicates symmetrical vGRF. Participants completed the 1) Anterior Cruciate Ligament Return to Sport after Injury scale (ACL-RSI), 2) International Knee Documentation Committee (IKDC), and 3) Knee Osteoarthritis Outcome Score (KOOS) (Symptoms, Pain, Sport, Activities of Daily Living (ADL), and Quality of Life (QOL) subscales). Spearman's rho partial correlations were calculated for vGRF LSI and PROM controlling for time since surgery (months). Correlations were interpreted as: 0.0 to 0.19 = very weak, 0.20 to 0.39 = weak, 0.40 to 0.59 = moderate, 0.60 to 0.79 = strong, 0.80 to 1.0 = very strong. The patient acceptable symptom score (PASS) criteria were used to determine acceptable knee-related symptoms status (IKDC ≥ 75.9%; $KOOS_{symptoms} \geq 57.1\%$; $KOOS_{pain} \geq 88.9\%$; $KOOS_{ADL} \geq 100.0\%$; $KOOS_{Sport} \geq 75.0\%$; $KOOS_{QOL} \geq 62.5\%$) [4]. All statistical analyses were performed in an open-source statistical software (jamovi 2.3.19.0).

Results & Discussion: Forty-four participants were included in the current analysis (Females n=25; Age=18.6±3.4 years; Mass=77.7±19.9 kg; Height=172.6±9.0 cm; time since surgery=6.7±1.1 months). vGRF LSI was positively, weakly correlated to IKDC score (ρ=0.32, p=0.03) and KOOS Sport subscale (ρ=0.31, p=0.04). There were no other statistically significant correlations between vGRF LSI and the remaining PROM (Table 1). These findings indicate better patient-reported knee-function is correlated with more symmetrical vGRF during the 1st landing of the DVJ task 4-12 months after ACLR. Individuals report acceptable PASS on the IKDC and 4 of the 5 KOOS subscales (Table 1) but demonstrate 81.3±25.2% vGRF LSI during the DVJ task at a critical timepoint post-ACLR. Thus, a mismatch between patient-reported function and landing mechanics exists at a critical timepoint when individuals are progressed to sport-specific movements in preparation for RTS.

	Mean±SD	Spearman's Rho (ρ)	p-value
ACL-RSI	70.4±22.6	0.24	0.13
IKDC	87.6±9.0	0.32	0.03*
KOOS - Symptoms	67.5±13.1	0.08	0.60
KOOS - Pain	94.6±7.7	0.06	0.69
KOOS - ADL	96.8±13.7	0.47	0.11
KOOS - Sport	90.5±10.8	0.31	0.04*
KOOS - QOL	69.8±19.8	0.13	0.40

Table 1: Means and standard deviations (SD) of PROM and Spearman's Rho partial correlations between vGRF LSI during the DVJ task and PROM. *Indicates statistical significance p<0.05.

Significance: Better patient-reported knee function is weakly correlated with more symmetrical vGRF during a bilateral jump landing task 4 to 12-months post-ACLR. With the advancement in portable force sensing technology, vGRF LSI is an efficient and cost-effective clinical objective measurement to determine function following ACLR. As jump landing tasks are commonly used during RTS testing, integrating vGRF symmetry would provide the clinical team dynamic movement strategies employed by individuals recovering from ACLR. Addressing asymmetry in vGRF during a bilateral jumping task may improve patient-reported knee-function which may ultimately improve RTS success following ACLR. It is necessary to continue to investigate the relationships between PROM and high-level, dynamic tasks to improve success with post-ACLR rehabilitation and RTS following ACLR.

Acknowledgements: Thank you to the Michigan State University AIR Lab research, sports medicine staff, and participants.

References: [1] Greenberg EM et al. (2018), *J Ortho Sports Phys Ther* 48(10); [2] Zwolski C et al. (2015), *Am J Sports Med*, 43(9); [3] Logerstedt D et al. (2012), *Am J Sports Med*, 40(10); [4] Muller B et al. (2016), *Am J Sports Med*, 44(11)

ANTICIPATORY SYNERGY ADJUSTMENT DURING FINGER FORCE PRODUCTION SCALES IN GO-NO-GO TASKS

Anvesh S. Naik, Ruchika Iqbal, and Satyajit Ambike
Department of Health and Kinesiology, Purdue University, West Lafayette, Indiana
Email : naik20@purdue.edu

Introduction: In motor systems, synergies in redundant sets of biomechanical variables lead to the stability of salient performance variables. Furthermore, synergies weaken when the actor is informed that they need to perform an action by rapidly changing the performance variables [1]. This anticipatory synergy adjustment (ASA) reflects a reduction in the stability of the ongoing behavior that assists in producing the required change in that behavior [2]. So far, the magnitude of the ASA has been quantified in finger-force production tasks. However, it is not known whether the ASA scales with the likelihood of having to inhibit an expected change in the ongoing behavior.

We examined this issue in a force production task. Participants performed four-finger, isometric, force production tasks in a *go/no-go* paradigm. In the *go* (control) task, participants produced a constant force, and at a known time, produced a quick force pulse. In the *go/no-go* task, participants performed the control task in 80% of the trials (go trials). However, in the remaining 20% trials, they had to inhibit the pulse production (no-go trials). We hypothesized that the synergy stabilizing the total force will be stronger for the *go/no-go* task compared to the *go* task (H1). The higher stability will help inhibit the pulse production for the no-go trials. However, the higher stability for the *go/no-go* task will also make the pulse production for the go trials less efficient, resulting in slower changes in total force compared to the *go* task (H2).

Methods: Healthy young adults (N=30, 14 female, 24.4±2.5 years) participated in the study. Participants sat comfortably in a chair with their forearms resting on top of a table. They placed the distal phalanx of each finger of their dominant hand on a force transducer (Nano-17; ATI Automation). The transducers recorded each finger's downward vertical force at 1000 Hz. Visual feedback on the total force, F_T, computed as the sum of the downward forces of all fingers, was provided for all trials via a computer screen.

For the *go* task, participants produced a constant F_T value (10% of maximum voluntary contraction -MVC, measured earlier) for 5s (foreperiod). A target appeared at 25% MVC 1.5s before the end of the foreperiod. There were also three tones 0.75s apart during these 1.5s. At the 3rd tone, participants had to rapidly increase F_T to 25% MVC to hit the target and quickly return to 10% MVC and remain there till the end of the trial. There were 15 trials of the *go* task. In the *go/no-go* task, participants performed the go task for 80% of the trials. The remaining 20% no-go trials began like the go trials, however, at the 3rd tone, the target at 25% MVC vanished, and participants had to inhibit their pulse response and continue producing F_T equal to 10% MVC. There were 75 trials in the *go/no-go* task, out of which 60 (80%) were go and 15 (20%) were no-go trials (randomized). All trials in both task-types were 10s long.

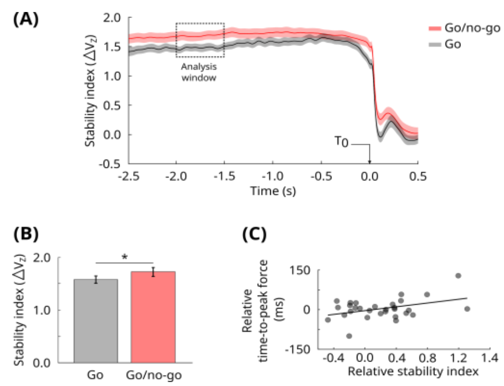

Figure 1: (A) Synergy index (ΔV_z) time series (T_0 is instant of change in force), (B) Average ΔV_z comparison, and (C) Relation between relative synergy index and relative time-to-peak force.

The individual finger forces (F_i) were filtered using a zero-lag, 4th-order, low-pass Butterworth filter (10-Hz cut-off). We chose only go trials for further analyses. The stability of F_T during the foreperiod, before the appearance of the target or the beeps, was quantified using the uncontrolled manifold (UCM) analysis [2]. This analysis provides a synergy index (ΔV_z), which quantifies the covariation in the digit forces that stabilize the value of the important performance variable F_T. A low value of ΔVz implies lower stability of F_T and vice-versa. To test H1, we averaged ΔVz within a 0.5s window before the first tone (box in Fig.1A) for the two tasks and analyzed this variable using a two-sample paired t-test. To quantify the force pulse performance, we computed time-to-peak force as the time between peak F_T and the first instance when F_T increased by more than 2% of peak F_T (T_0 in Fig. 1A) for the go trials in both tasks. To test H2, we performed linear regression between the across-task difference in ΔV_z and the across-task difference in time-to-peak force.

Results & Discussion: Compared to the go task, the average ΔVz was higher ($t(29)=2.3$, $p<.05$) for the go/no-go task (Fig.1B) indicating that participants stabilized F_T more when there was uncertainty regarding movement execution and inhibition could be required (consistent with H1). Moreover, the change in average ΔVz was positively correlated (R^2=0.3; slope=57 ms; $p<.05$,) with the change in time-to-peak force during the go/no-go task relative to the go task (Fig. 1C), indicating that individuals who were more stable during the go/no-go task were also slower in reaching the peak force (consistent with H2). This shows that a vigilant motor system accounts for the possibility of inhibiting a planned action by increasing the stability of the ongoing behavior; however, this likely leads to slower actions when they need to be executed.

Significance: These results indicate that the motor system may scale ASAs. Further work is required to quantify the sensitivity of ASA to the likelihood of inhibition, whether scalability of ASA is affected by aging or pathologies, and whether scalability appears in other motor behaviors. Furthermore, we aim to introduce motor coordinative processes and synergies in the description and understanding of inhibitory control, which is currently viewed as a cognitive process. Our work could inform the clinical assessment of inhibitory control in disorders like ADHD and schizophrenia and also inform interventions for arresting dexterity loss with aging.

References: [1] Tillman and Ambike (2018), J Neurophysiol, *119*(1); [2] Hasan (2005), J Mot Behav, 37.

IMU-BASED 3D SHOULDER AND ELBOW JOINT ANGLE ESTIMATION DURING BADMINTON, GOLF, DANCE, YOGA, AND SWIMMING

Kezhe Zhu[1*], Jinxuan Li[1], Peter B. Shull[1]
[1] Department of Mechanical Engineering, Shanghai Jiao Tong University, Shanghai, China
*Corresponding author's email: kezhe_zhu@sjtu.edu.cn

Introduction: Upper limb motion capture provides essential information for assessing human ability and intention, and serves as a foundation in rehabilitation, interactive games, and animation. While motion capture is traditionally performed with optical motion capture (OMC) system, inertial measurement units (IMUs) can potentially reduce the cost and enable portability. In this study, we developed and validated an IMU algorithm for 3D shoulder (thoracohumeral) and elbow angle estimation during badminton, golf, dance, yoga, and swimming.

Methods: Seven IMUs with magnetometers were used for 3D shoulder and elbow angle estimation. Six IMUs were placed on the sternum, upper arms, and forearms. An additional IMU was placed on the back of the pelvis to act as the static calibration reference. The IMU orientation q_{GS} was first estimated through a two-step complementary filter [1]. Then, the calibration offset q_{SB} was estimated from functional calibration data during the initial neutral pose. Finally, we calculated the relative orientation $q_{B_pB_d}$ between the proximal and distal segments. The 3D shoulder and elbow angles were derived from the ZXY Euler angle decomposition of $q_{B_pB_d}$.

Thirty health subjects (age: 22.83±0.90; height: 1.73±0.07 m; weight: 60.73±8.57 kg; gender: 20 males and 10 females) performed five 2-minute trials of sports activities, including badminton, golf, dance, yoga, and upper body swimming. Carbon fiber plates with three retro-reflective markers were manually aligned with IMUs mounted on the arms. These triple marker sets were used for segment tracking. Fourteen retro-reflective markers for segment definition and tracking were placed on each subject's thorax and upper arms (Fig. 1.). Once the markers and IMUs had been worn properly, subjects first performed elbow flexion/extension and pronation/supination, respectively, for functional calibration. Subjects were then instructed to perform the corresponding sports activities after a 5-sec static neutral pose at the beginning of each trial. We assumed the 3D joint angles were all zero in this initial state. A thirteen-camera stereophotogrammetric system (Vicon, Oxford, UK) and Visual3D (C Motion, MD, USA) were used for tracking segment movements and calculating reference shoulder and elbow angles. To achieve better repeatability in calibration, the upper arm medial-lateral axis and forearm longitudinal axis was defined by elbow flexion/extension axis and pronation/supination axis, respectively [2]. The IMUs and Vicon system were electronically synchronized, and both collected the data at 100Hz.

The RMSE of estimated elbow angles of all collected trials were calculated for analysis. However, due to the shoulder joint agility, the shoulder angle would frequently exceed the gimbal lock domain while the upper arms were horizontally elevated. Therefore, the estimated and reference shoulder angles were first transformed back into quaternions, $q^{est}_{B_pB_d}$ and $q^{ref}_{B_pB_d}$, respectively. Then their relative quaternion was decomposed into Euler angles as the error, as in Eq. (1).

$$q_{Est,Ref} = q^{est}_{B_pB_d} \otimes \left(q^{ref}_{B_pB_d}\right)^* \quad (1)$$

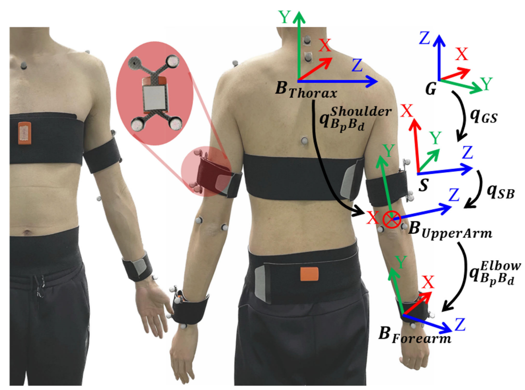

Figure 1: Experiment setup and the definitions of the segment body coordinate system.

Results & Discussion: Overall average and standard deviation shoulder and elbow angles estimation RMSE was 3.6 ± 1.8°, and 1.9 ± 1.7°, respectively, which is substantially more accurate than has been previously reported in sports activities [3]. The two main reasons for the accuracy improvement were likely the more consistent and repeatable functional calibration method and the quaternion-based error evaluation method. Due to the nonlinearity of the Euler angle decomposition, the shoulder joint Euler angle error could be nonlinearly amplified from the fixed calibration error and reached the maximum when the subjects horizontally elevated their upper arms. Quaternion-based error computation avoids this extreme nonlinear mapping.

Significance: The presented IMU-based 3D shoulder and elbow angle estimation algorithm is accurate and was validated for badminton, golf, dance, yoga, and swimming. The proposed algorithm may be useful for portable upper limb motion capture during dynamic sports-related activities.

Acknowledgments: This work is supported by the National Natural Science Foundation of China under grant 52250610217.

Table 1: RMSE of estimated shoulder and elbow joint angles during five sports activities. Left and right joints were both included. Values reported as group means± standard deviation.

	Activity	Badminton	Golf	Dance	Yoga	Swimming	Mean
Shoulder	Abduction/Adduction	2.5±1.0°	3.2±1.2°	3.7±2.0°	3.0±1.2°	3.9±2.4°	3.3±1.7°
	Internal/External	3.4±1.3°	2.8±0.9°	4.1±2.0°	4.0±1.8°	5.1±2.3°	3.9±1.9°
	Flexion/Extension	2.9±1.2°	3.3±1.1°	3.6±1.8°	3.3±1.8°	4.5±2.7°	3.5±1.9°
Elbow	Abduction/Adduction	1.7±1.0°	1.8±0.9°	1.7±0.9°	3.7±1.7°	1.5±0.9°	2.1±1.4°
	Internal/External	1.6±1.1°	1.7±1.0°	1.8±1.1°	4.0±2.4°	1.3±0.8°	2.1±1.7°
	Flexion/Extension	0.9±0.4°	0.9±0.3°	0.9±0.6°	3.6±3.3°	1.1±0.5°	1.5±1.9°

References:
[1] Fan et al. (2018). *Meas Sci Technol* 29(11);
[2] de Vries et al. (2010), *J Biomech* 43(10);
[3] Fantozzi et al. (2016). *J Sports Sci* 34(11).

ACTIVITY RECOGNITION IMPROVES LOWER-LIMB KINEMATICS PREDICTION USING A REDUCED IMU SENSOR CONFIGURATION

Jinxuan Li[1], Kezhe Zhu[1], Peiqi Kang[1], Peter B. Shull[1]
[1]School of Mechanical Engineering, Shanghai Jiao Tong University, Shanghai, China
Email: jinxli@sjtu.edu.cn

Introduction: Lower-limb kinematics prediction based on wearable sensors is essential for injury risk identification during sports and surgical outcome assessment by providing an objective analysis of kinematic parameters. In addition, a reduced-sensor-count configuration, where sensors are placed on a subset of the total number of lower-limb segments, will improve user comfort while reducing setup time and system cost [1]. However, traditional uniform deep-learning models fail to adapt to multiple human activities with reduced-sensor-count configurations, because different activity poses produce the same sensor orientations [2]. Thus, we aimed to utilize activity recognition to build new deep-learning models for bilateral hip and knee angle prediction under a reduced wearable inertial measurement unit (IMU) count.

Methods: Fifteen male subjects performed four physical activities (dance, golf, swimming, and yoga) while wearing three IMUs (MTw, Xsens, Netherlands) at the pelvis and both shanks. Subjects also wore 28 markers on their lower body. Four 4-marker clusters were used for motion tracking, placed on each thigh and shank, respectively. The other twelve markers were placed on both sides of the ankle, knee, and hip joints for segment definition. The reference hip and knee joint angles were computed by a camera motion capture system (Vicon, Oxford, UK) and Visual3D (C Motion, MD, USA). The IMU and optical motion capture system sampling rates were both 100 Hz. The length of each activity was two minutes.

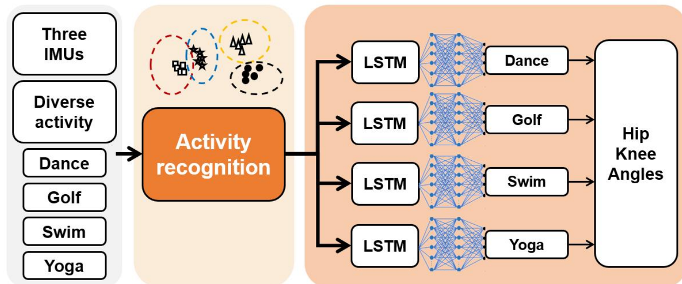

Figure 1: Architecture of the activity-aware-based hierarchical model. The first level was activity recognition based on feature extraction and Support Vector Machines, and the second level was four LSTM sub-models for joint angle prediction.

An activity-aware-based hierarchical model for accurate bilateral hip and knee angle prediction across all four activities was designed, which was only based on the inertial data of three IMUs (pelvis and both shanks). The first level of the proposed model is an activity-aware sub-model based on feature extraction and Support Vector Machines (Fig. 1). The second level is four long short-term memory (LSTM) sub-models inherited from the corresponding activity types for joint angle prediction [3] (Fig. 1). Additionally, a more complex uniform LSTM model trained on the same inertial data of IMUs was built for comparison. The prediction error of different models was represented by the normalized root mean square error (NRMSE), computed as RMSE (between predicted and true joint angles) divided by the range of true joint angles during different activities.

Results & Discussion: The activity-aware-based hierarchical model was 8% more accurate than the uniform model at most. For all twelve axes of bilateral hip and knee angles, the activity-aware-based hierarchical model was more accurate than the uniform model (Fig. 2).

One possible reason for the proposed model being more accurate is that the activity recognition decouples the motion pattern from the joint angle prediction process. The motion pattern information is provided as an additional constraint of human posture to the joint angle prediction sub-models.

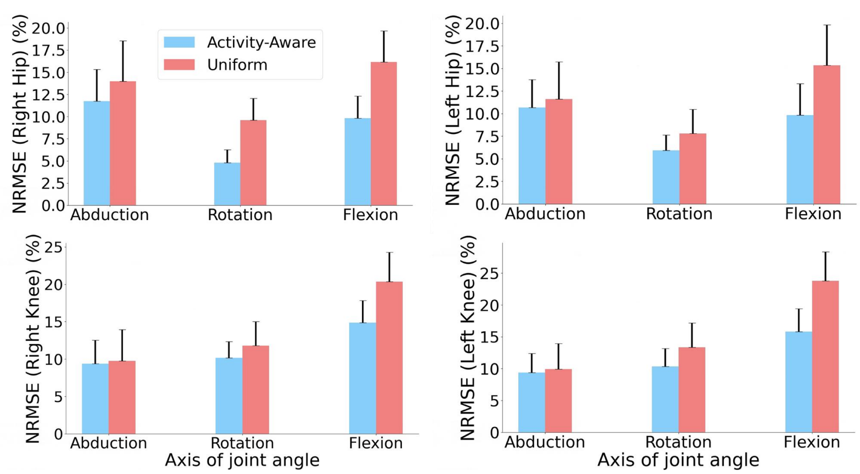

Figure 2: Joint angle prediction errors of the proposed model and traditional uniform model. NRMSE: Normalized Root Mean Square Error.

Significance: Activity recognition improves activity generalization of the lower-limb joint angle prediction model with a reduced sensor configuration. The proposed hierarchical model enables the lower-limb joint angle prediction for more diverse sports-related tasks in daily injury prevention and post-operative clinical rehabilitation.

References:

[1] Sy L et al. (2020). IEEE Transactions on Biomedical Engineering, 68(4): 1293-1304.
[2] Huang Y et al. (2018). ACM Transactions on Graphics (TOG), 37(6): 1-15.
[3] Mundt M et al. (2020). Sensors, 20(16): 4581.

WHAT YOU NEED TO KNOW ABOUT EXERCISE MONITORING WITH INERTIAL SENSING WEARABLES

Vu Phan[1*], Ke Song[2], Rodrigo Scattone Silva[3], Karin Silbernagel[3], Josh R. Baxter[2], and Eni Halilaj[1]
[1]Department of Mechanical Engineering, Carnegie Mellon University, Pittsburgh, PA, USA, [2]Department of Orthopaedic Surgery, University of Pennsylvania, Philadelphia, PA, USA, [3]Department of Physical Therapy, University of Delaware, Newark, DE, USA
*Author's email: vuphan@andrew.cmu.edu

Introduction: Monitoring rehabilitation exercises with low-cost wearables is a critical step in tracking remote physical-therapy compliance and delivering personalized treatment. While a multitude of commercial devices (e.g., Apple, Fitbit) can perform basic action recognition, few have been applied to improve healthcare delivery. Research in physical activity classification has been limited by small training data that include only a few exercises [1]. Practical factors like sensor number, modality, location, sampling frequency, data size, and feature engineering approaches could also impact classifier performance but have not been systematically studied. This study used wearable sensor data to (1) develop a deep learning model that generalizes to a broad array of exercises, (2) investigate the impact of sensor density and location for better product development, (3) research the influence of sensor type and sampling rate to optimize battery life, and (4) determine whether theoretical limits of performance would be met with more data and better feature engineering.

Methods: After obtaining IRB approval and informed consent, 19 healthy adults with no self-reported injuries were recruited to perform 37 lower-extremity exercises (Fig. 1b). Their motion was recorded with 10 inertial measurement units (IMUs; Fig. 1a) and a marker-based motion capture system. Motion data from both modalities were recorded at 100 Hz. IMU data were segmented, labelled, and then used to train a sequential convolutional neural network (CNN; Fig. 1c). A leave-one-subject-out scheme was used to evaluate model generalizability to test subjects. The training data were similarly split into train and validation sets to tune hyperparameters. We trained additional models to probe the impact of sensor density and location, modality and sampling rate, and state estimation. We also applied a curve fitting method to project the model's learning curve and determine the sample size required for optimal performance based on estimated theoretical limits.

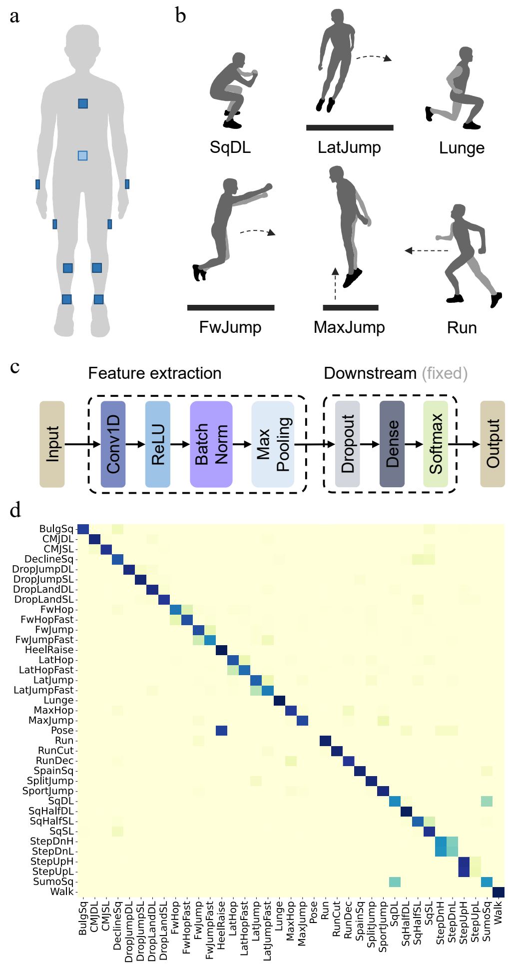

Figure 1: Study Overview. a. Sensor placement. **b.** Example exercises. **c.** Architecture of the classifier. **d.** Confusion matrix detailing classifier performance, with the predicted exercise in the x-axis and the true one in the y-axis (range: dark blue = 100%, yellow = 0%).

Results & Discussion: The classifier predicted exercise type with greater than 81% accuracy for new subjects. Misclassification was often due to exercise similarity (Fig. 1d). For example, "fast" and "normal" jump speeds (e.g., during forward jump vs. fast forward jump) vary among subjects, while the group means may not be substantially different for the two exercises. We additionally tested several important factors to gauge the trade-offs between usability and classifier performance. *Exercise Archetypes.* Grouping similar exercises using k-mean clustering improved the classifier by 14%, while still providing clinically relevant information on cumulative joint loading, which is similar across exercises grouped together. *Sensor Density and Location*. Removing upper-body sensors had minor effects on classifier performance. The model trained with five sensors on the pelvis, thighs, and shanks achieved comparable performance to that trained with the full sensor set. Reducing the number of sensors to one revealed that the pelvis provided the highest accuracy, at 61% compared to 59% for the thigh and 43% for the wrist. Single-sensor devices require subject-specific data to reach reasonable accuracies, if detecting specific exercises is desired, as implied in a past study [2]. *Battery and Memory Use.* Using accelerometery-only data (removing the battery-hungry gyroscope) or reducing the sampling rate to 20 Hz did not compromise performance. *Larger Data vs. Better Feature Engineering.* More data from the same population are not necessary since the fitted learning curve indicated that thousands of subjects would be needed to increase accuracy by less than 8%. Small data from more diverse populations, such as patients, however, could be beneficial. Instead, our analysis suggests that good feature engineering is a judicious and low-cost way to improve performance. When using joint angles, instead of linear accelerations and angular velocities, model performance improved by 7%.

Significance: As interest and need in remote therapy monitoring and coaching solutions (e.g., Hinge Health, Figure8) grows, the science that powers "patient coaching" remains opaque. In this study, we answered key questions that interested researchers, clinicians, and product developers should ask before engaging patients in remote exercise-monitoring programs. Our work increases transparency around the back-end models that will power remote monitoring solutions, now and in the not-too-distant future.

Acknowledgements: This study was funded by NIH/NIAMS R01AR078898 and NSF/CBET 2145473.
References: [1] O'Reilly et al. (2018), *Sports Med.* 48(5); [2] Um et al. (2017) *IEEE IROS*.

EXPLORING ASSOCIATIONS BETWEEN GAIT KINEMATICS-BASED CLASSIFICATION OF KNEE OSTEOARTHRITIS PATIENTS AND CLINICAL/RADIOGRAPHIC FEATURES: INSIGHTS FROM A BIOMECHANICAL STUDY

Felipe Gonzalez[1,2,3]*, Gustavo Leporace[1,2], Carlos Franciozi[2], Leonardo Metsavaht[1,2], Felipe P. Carpes [4], Jorge Chahla[5], Marcus Luzo[2]

1 Brazil Institute of Health Technologies (Instituto Brasil de Tecnologias da Saúde), Rio de Janeiro,RJ, Brazil.
2 Post Graduation Program of Clinical Radiology, Escola Paulista de Medicina, Federal University of São Paulo (Universidade Federal de São Paulo), São Paulo, SP, Brazil.
3 Department of Orthopedic Surgery, Galeão Air Force Hospital (Hospital de Força Aérea do Galeão), Rio de Janeiro, RJ, Brazil.
4 Laboratory of Neuromechanics, Federal University of Pampa (Universidade Federal de Pampa), Uruguaiana, RS, Brazil.
5 Division of Sports Medicine, Midwest Orthopaedics at Rush, Chicago, IL, USA.
*Corresponding author's email: felipegonzalez818@gmail.com

Introduction: Knee osteoarthritis (KOA) is a prevalent musculoskeletal condition that leads to a wide variability of gait characteristics among patients. To better understand the nature of this variability, previous authors [1] have utilized gait kinematics to categorize KOA patients into four distinct profiles: profile 1 (P1), flexed knee; profile 2 (P2), externally rotated knee; profile 3 (P3), stiff knee; and profile 4 (P4), knee varus thrust and rotational rigidity. Despite these efforts, the relationship between these kinematic gait profiles and their associated clinical and radiographic characteristics remains poorly understood. Thus, the aim of this study was to investigate whether differences in clinical and radiographic characteristics were associated with these four gait profiles. The identification of such associations has the potential to improve the clinical and surgical management of KOA patients by informing targeted interventions based on the unique characteristics of each profile.

Methods: This cross-sectional study used available data from a previous biomechanical study [1]. Data on the four gait profiles were collected from 42 KOA patients selected from a total knee arthroplasty waiting list. 3D kinematics of the knee was recorded during gait using an 8-camera optoelectronic system. Subjects were evaluated for knee strength, knee range of motion, tibial slope, femorotibial angle, radiographic severity, anthropometric measurements, and patient-reported outcomes: IKDC, LEFS, VAS-Pain. Multiple comparisons were made using Dunn's test with Sidák adjustment. The level of significance was set at 5%, and the effect size was calculated.

Results & Discussion: BMI was the only variable associated with a specific gait profile: profile 4 ($p = 0.01$; ES= P1xP4: -0.62; P2xP4: -0.41; P3xP4: -0.40). Our findings suggest that most clinical and radiographic characteristics commonly measured in clinical practice did not differ significantly among KOA patients with the four different gait profiles. The only exception was a higher BMI noted in those with gait profile 4; however, it remains unclear if this leads to varus thrust or rotation rigidity as reported by previous studies [2].

Significance: The significance of this article lies in its contribution to the understanding of KOA and the relationship between gait kinematics and clinical and radiographic characteristics of KOA patients. The article builds on previous research that has identified four distinct gait profiles among KOA patients and investigates whether these profiles are associated with differences in clinical and radiographic characteristics. This article may be particularly useful for clinicians and researchers working in the field of musculoskeletal conditions who are interested in understanding the relationship between KOA gait and clinical and radiographic characteristics.
Incorporating 3D gait analysis to identify different gait profiles provided additional insights beyond what conventional methods could offer. Moving forward, further research should validate these findings while examining if any modifiable characteristics are possibly associated with each identified gait pattern. In this way, better informed clinical and surgical decision can be done based in gait kinematics-based classifications.

Acknowledgements: We would like to acknowledge the support of Galeão Air Force Hospital (Hospital de Força Aérea do Galeão) staff in the development of this article.

References:
[1] Leporace G, Gonzalez F, Metsavaht L, Motta M, Carpes FP, Chahla J, et al. Are there different gait profiles in patients with advanced knee osteoarthritis? A machine learning approach. Clinical Biomechanics 2021;88. https://doi.org/10.1016/J.CLINBIOMECH.2021.105447
[2] Paterson KL, Sosdian L, Hinman RS, Wrigley T V., Kasza J, Dowsey M, et al. The influence of sex and obesity on gait biomechanics in people with severe knee osteoarthritis scheduled for arthroplasty. Clinical Biomechanics 2017;49:72–7. https://doi.org/10.1016/j.clinbiomech.2017.08.013.

GRASP TRAINING AFTER SPINAL CORD INJURY USING AUGMENTED FEEDBACK IN MIXED-MODE REALITY

Mingxiao Liu[1*], Samuel Wilder[1], Sean Sanford[1], Sophie Dewil[1], Noam Harel[2], Raviraj Nataraj[1]
[1]Department of Biomedical Engineering, Stevens Institute of Technology, Hoboken, NJ, USA
[2]Spinal Cord Damage Research Center, James J. Peters VA Medical Center, Bronx, NY, USA
*Corresponding author's email: mliu26@stevens.edu

Introduction: Neurotraumas can impair grasping capabilities used for activities of daily living, and physical therapy (PT) to rehabilitate hand function can be time- and effort-intensive [1]. Training processes to accelerate motor learning may be facilitated by employing technologies that naturally foster greater neural engagement. Virtual reality (VR) is increasingly prevalent in PT to engage users with customizable environments and enhanced feedback [2]. Our lab previously examined how performance positively correlates to engagement expressed as perceptions of control [3, 4]. In a subsequent study [5], we demonstrated how providing guidance cues during training to enhance such perceptions will improve post-training performance. In this same study, we established how training guidance with augmented feedback from our custom-built smart glove improved the performance of a grasp-and-place task. The glove provides sensory cues (visual, audio) to inform the user when a "secure" grasp was achieved. In the new study presented here, we added VR (mixed-mode reality) to enhance the augmented feedback, and we assessed the subsequent effects on performance and electroencephalography (EEG) with persons having a spinal cord injury (SCI).

Methods: Persons with incomplete cervical-level SCI (n=6) participated in this study after signing informed consent forms approved by the Bronx VA Medical Center IRB. Each participant wore a 64-channel scalp-surface cap for EEG recording (Brain Vision) and our smart glove with force and flex sensors. Participants performed a grasp-and-place task of a small cubic object onto a designated target (Figure 1). Participants executed three blocks of trials: 1) an initial block of 15 trials without feedback to establish baseline performance before training, 2) a block of 30 trials to train with augmented feedback (audio and visual), and 3) a block of 15 trials without feedback to determine effects *after* training. The three blocks of trials were repeated for three different feedback conditions. For "glove feedback," a beeper and LED onboard the glove were activated during secure grasp. For "VR feedback," participants experienced mixed-mode reality as they viewed a VR environment (Unity) through a headset (HTC Vive with LEAP) but continued to grasp the real object. Participants observed virtual representations of the object and the grasping hand in VR. The VR-enhanced audio and visual feedback cues were provided through earpiece sounds and changing the virtual object's color from red to green. Participants also completed a "no feedback" condition (control case) with no additional feedback about grasp during training.

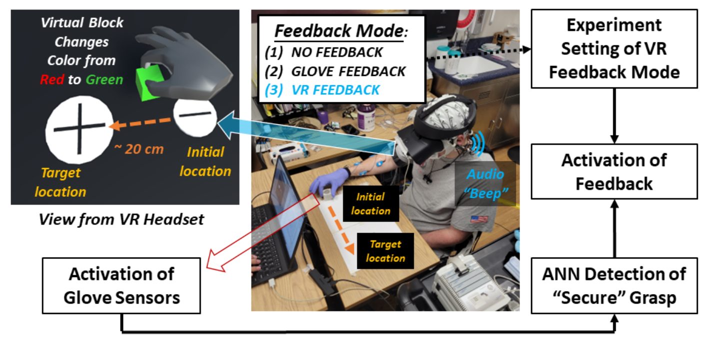

Figure 1: Experimental flow of training to perform a grasp-and-place task in mixed-mode reality.

Results & Discussion: Training feedback with VR produced a significant ($p<0.05$) improvement (reduction) in task completion time and the object's motion pathlength compared to no feedback. Glove feedback demonstrated intermediate results with inconclusive differences. Feedback with VR also significantly increased EEG power (overall and within alpha and beta bands) in the primary motor cortex (Figure 2) after training from baseline (pre-training) compared to other feedback conditions.

Significance: Our results suggest that enhancing augmented feedback with VR during training could facilitate better grasp function outcomes, especially for persons with SCI. In addition to immediately improved performance, increases in brain activity at regions associated with motor execution suggest the potential for desirable neuroplastic effects. In particular, the increases in alpha-band activity suggest early consolidation of motor learning features from a pre-learning state [6]. Our study's results should motivate future examination of computerized interfaces leveraging cognitively centered approaches (e.g., leveraging perceptions, learning with augmented feedback) for motor rehabilitation.

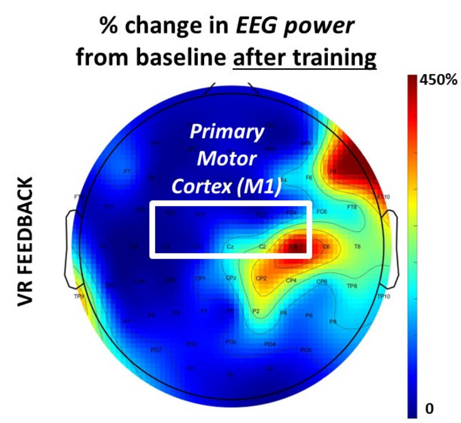

Figure 2: Brain activation (EEG power) map after training with VR feedback.

Acknowledgements: The authors acknowledge support from the Charles V. Schaefer School of Engineering and grant no. I21 RX003582-01 from the Department of Veterans Affairs.

References: [1] Woldag H. et al. J. Neurol. 2002; 249: 518-528. [2] Merians A.S. et al. Neurorehabil. Neural Repair. 2006; 20(2): 252-267. [3] Nataraj R. et al. Front. Hum. Neurosci. 2020; 14. [4] Nataraj R. et. al. PLOS ONE; 27. [5] Liu M. et al. Sensors. 2021; 21(4): 1173. [6] Henz D. et al. Front. Behav. Neurosci. 2016 10:199.

VALIDATING INERTIAL MEASUREMENT UNITS FOR MEASURING TRUNK KINEMATICS DURING OVER-GROUND TRIPS

Youngjae Lee[1], Neil B. Alexander[2], Christopher T. Franck[3], Michael L. Madigan[1*]
[1]Grado Department of Industrial and Systems Engineering, Virginia Tech, Blacksburg, VA, United States
[2]Department of Internal Medicine, University of Michigan, Ann Arbor, MI, United States
[3]Department of Statistics, Virginia Tech, Blacksburg, VA, United States
*Corresponding author's email: mlm@vt.edu

Introduction: Trip-induced falls are a major cause of non-fatal injuries in the United States. To investigate these events, researchers have traditionally used optical marker-based motion capture systems to measure trunk kinematics during over-ground trips in a laboratory setting. However, these systems are costly and typically require multiple fixed cameras. Small, wearable inertial measurement units (IMUs) may be an alternative given their lower cost and lack of need of fixed cameras. No studies to our knowledge have validated the use of an IMU to measure trunk kinematics during over-ground trips. Therefore, the goal of our study was to compare trunk flexion angle and angular velocity during over-ground trips measured by an IMU to those measured by an optical marker-based motion capture system. We hypothesized that the trunk flexion angle and angular velocity would be comparable between the two systems. These results are based upon a prior study that validated the use of an IMU to measure trunk kinematics during treadmill perturbations that simulated trips and slips [1].

Methods: A convenience sample of 10 healthy young adults (5 females; age 22.1 ± 2.4 years; height 1.7 ± 0.1 m; mass 71.8 ± 8.8 kg) was recruited for our study. Subjects completed a single experimental session during which they were exposed to two laboratory-induced trips while walking on a walkway. Trunk kinematics were recorded using an IMU on sternum and markers placed bilaterally at the acromion processes and greater trochanters. Failed recoveries (i.e., falls) occurred when the force applied to a safety harness exceeded 30% body weight. Trunk flexion angle and angular velocity at touchdown of the initial recovery step were calculated for the outcome measures. A Bland-Altman plot was created to show agreement of the two trunk kinematics estimates between the two systems.

Results & Discussion: A total of 19 trips resulted in 4 falls and 15 recoveries. One trip trial was excluded from the final analysis due to a missed trip. Bland-Altman plots show systematic differences between the two systems of 5.3 deg for trunk angle and 11.7 deg/s for trunk angular velocity (Figure 1). To evaluate the clinical relevance of these system differences, they were compared to mean differences between falls and recoveries after over-ground trips reported in other studies (Table 1). These results support our hypothesis that trunk kinematics were comparable between the two systems, and the differences between systems are small enough to still recognize clinically-relevant differences between falls and recoveries.

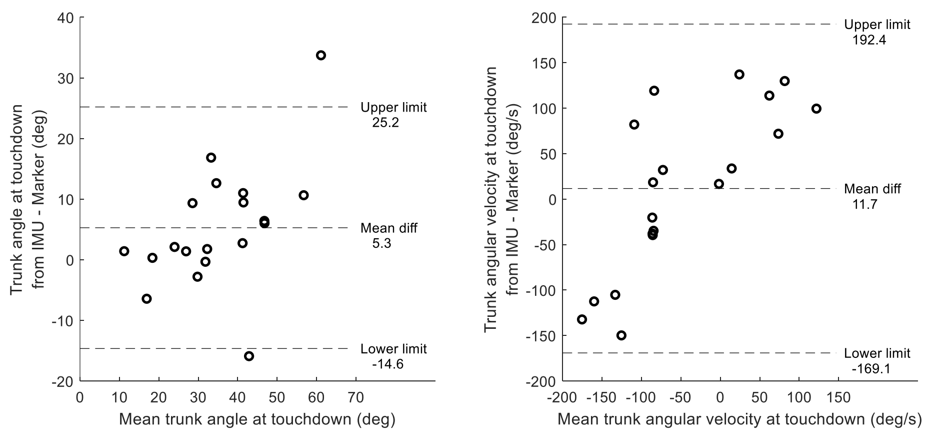

Figure 1. Bland-Altman plots with 95% limits of agreement. Each data point represents a single trip trial. Trunk angle and angular velocity are positive in flexion.

Table 1. Mean difference in trunk kinematics between falls and recoveries from prior and current studies.

Study	Trunk flexion angle (deg)	Trunk flexion angular velocity (deg/s)
Ref [2]	14	102
Ref [3]	15	53
Current markers	10	73
Current IMU	10	84

Significance: Although our sample size was limited, this study provides evidence that a single sternum-worn IMU is viable for capturing trunk kinematic responses to over-ground trips, and may enable trunk kinematics after real-world trips to be assessed outside the laboratory setting.

Acknowledgements: Research reported in this publication was supported by the National Institute On Aging of the National Institutes of Health under Award Number R21AG075430. The content is solely the responsibility of the authors and does not necessarily represent the official views of the National Institutes of Health. The authors also thank Michelle Morris for her contributions to data acquisition.

References: [1] Miller & Kaufman (2019), *Medical Engineering & Physics* 70; [2] Pavol et al. (2001), *The Journals of Gerontology Series A: Biological Sciences and Medical Sciences* 56(7); [3] Grabiner et al. (2012), University of Illinois at Chicago.

HUMAN ACTIVITY RECOGNITION BASED ON DEEP LEARNING MODEL

Bummo Koo, Seunghee Lee, Sumin Yang, Dongkwon Kim, Youngho Kim*
Department of Biomedical Engineering and Institute of Medical Engineering, Yonsei University, Wonju, Korea
*Corresponding author's email: younghokim@yonsei.ac.kr

Introduction: Human activity recognition (HAR) is an important research field with wide-ranging applications, including industrial automation, sports and entertainment assessments, and health care and rehabilitation tasks [1]. The highest proportion of one-person households in Asia is found in Japan, South Korea, and Taiwan, with rates of 32.4%, 23.9%, and 22%, respectively, representing a dramatic increase from their corresponding rates in 1980, which were 19.8%, 4.8%, and 11.8%, respectively [2]. In these societies with high rates of one-person households, HAR systems can help individuals maintain their health and prevent dangerous situations like fall. Falls are a common cause of injury and hospitalization, particularly among older adults. Accurate detection of falls can enable timely medical intervention and reduce the risk of serious complications [3]. In this study, HAR system based on deep learning was proposed and evaluated for its performance in recognizing 14 activities of daily living (ADLs) and 11 falls.

Methods: 20 healthy volunteers (10 males and 10 females 22.0±1.9 yrs, 164.9±5.9 cm, 61.4±17.1 kg) were recruited and performed 14 ADLs and 11 falls (Table1). An IMU sensor was positioned on the S2. All movements were labeled into 7 classes according to the movement characteristics and the direction of falls (Table 2). Data from the 16 subjects were used to train the deep learning model and those from the remaining 4 subjects were used to test the model. ResNet model [4] tuned for our dataset was applied for the activity recognition.

Table 1: Experimental movements

ADL	**D01**. Stand, **D02**. Sit and stand up from floor, **D03**. Squat, **D04**. Waist bending, **D05**. Walking, **D06**. Jogging, **D07**. Stumble while walking, **D08**. Jogging in place, **D09**. Jumping, **D10**. Walk upstairs and downstairs, **D11**.Sit and stand up from stool, **D12**. Collapse in a stool when trying to stand up, **D13**. Lying on the mattress, **D14**. Slowly sit and stand up from a low-height mattress
Fall	**F01**. Backward fall while walking caused by a slip, **F02**. Forward fall while walking caused by a trip, **F03**. Forward fall while jogging caused by a trip, **F04**. Backward fall when traying to sit down, **F05**. Forward fall while sitting, **F06**. Lateral fall while sitting, **F07**. Backward fall while sitting, **F08**. Forward fall when trying to get up, **F09**. Forward fall, **F10**. Lateral fall, **F11**. Backward fall

Table 2: Class of movements

Class	Movements
Class1	Stand (D01)
Class2	Sit and get up (D02,03,04,11,12,13,14)
Class3	Gait (D05,06,07,10)
Class4	Jump (D08,09)
Class5	Forward fall (F02,03,05,08,09)
Class6	Backward fall (F01,04,07,11)
Class7	Lateral fall (F06,10)

Results & Discussion: Figure 1 showed the results of the classification. Our proposed model represented an accuracy of 96.33% (289/300). However, the model showed a higher accuracy of 98.67% (296/300) for the binary classification (ADLs or Falls). Most movements except 4 movements were predicted well with ADLs and falls. These four movements were mistakenly recognized as partially similar movements. For example, F06(lateral fall while sitting) was mis-recognized as Class2(sit and get up).

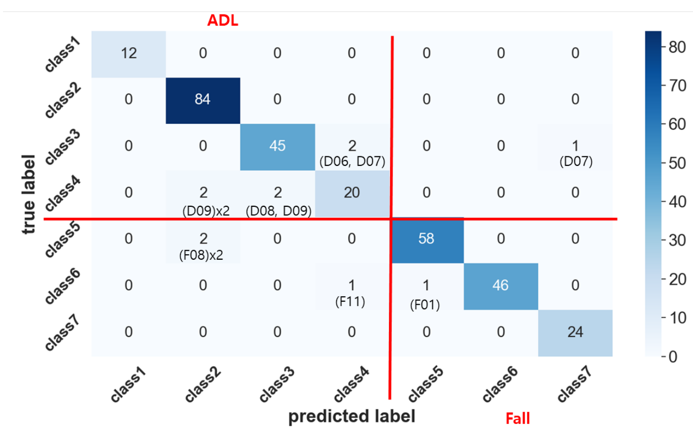

Figure 1: Confusion matrix

Significance: The proposed model showed good performances for HAR. Our system can be applied to wide fields such as health care and rehabilitation. In addition, it helps to maintain health and detects falls for people who are in one-person households. Overall, our study contributes to the growing body of research on HAR and underscores the importance of developing accurate and reliable systems for detecting human activities.

Acknowledgements: This research was partly supported by the Institute of Civil Military Technology Cooperation funded by the Defense Acquisition Program Administration and Ministry of Trade, Industry and Energy of Korean Government under grant No.21-SF-GU-07 and project for Cooperative R&D between Industry, Academy, and Research Institute (S3104657) funded by the Ministry of SMEs and Startups (MSS, Korea).

References:
[1] Bulling A et al. CSUR. 46.3, 2014.
[2] Yeung W et al. Demogr. Res. 32, 2015.
[3] Koo B et al. Sensors. 21.14, 2021.
[4] He, K et al. CVPR., 2016.

DEEP LEARNING BASED FALL RISK PREDICTION USING DATA AUGMENTATION

Seunghee Lee, Bummo Koo, Sumin Yang, Dongkwon Kim, Youngho Kim*
Department of Biomedical Engineering and Institute of Medical Engineering, Yonsei University, Wonju, Korea
*Corresponding author's email: younghokim@yonsei.ac.kr

Introduction: Falls are one of the fatal causes of death with the elderly [1]. Risk prediction in fall accidents is necessary for rescue and prevention after the accident. The peak acceleration value is one of the key measurement factors that can affect the severity of injury [2]. Kim et al. [3] proposed a study to predict the impact of falls of the elderly with the peak acceleration value. In this study, a deep learning regression model was used to predict the acceleration peak value that can represent the risk of activities of daily motions (ADLs) and falls.

Methods: 20 healthy adult subjects (24.8 ± 2.0 years old, 173.5 ± 6.1 cm, 76.6 ± 13.0 kg) were recruited from Yonsei University for the study and performed 14 ADLs and 11 falls (IRB No. 1041849-202204-BM-079-02) (Table1). An IMU sensor (Xsens Dot, Netherlands) was attached to the S2 position of the subject. The 6-axis IMU sensor data were measured at a sampling frequency of 60 Hz. Data from 0.2 s to 0.7 prior to the peak A_{SVM} value and eight features (Ax, Ay, Az, A_{SVM}, Gx, Gy, Gz, G_{SVM}) were extracted for the analysis. Data were split in a 4:1 ratio and used for the training and the testing of the model. The peak acceleration values were predicted by deep learning model consisted of 1D-CNN and LSTM layers. The model was trained by the mean squared error (MSE) and the mean absolute error (MAE). The data augmentation techniques such as noise injection, scaling, and window slicing were applied to solve data imbalance problem.

Table 1: Experimental movements

ADL	**D01**. Stand, **D02**. Sit and stand up from floor, **D03**. Squat, **D04**. Waist bending, **D05**. Walking, **D06**. Jogging, **D07**. Stumble while walking, **D08**. Jogging in place, **D09**. Jumping, **D10**. Walk upstairs and downstairs, **D11**.Sit and stand up from stool, **D12**. Collapse in a stool when trying to stand up, **D13**. Lying on the mattress, **D14**. Slowly sit and stand up from a low-height mattress
Fall	**F01**. Backward fall while walking caused by a slip, **F02**. Forward fall while walking caused by a trip, **F03**. Forward fall while jogging caused by a trip, **F04**. Backward fall when trying to sit down, **F05**. Forward fall while sitting, **F06**. Lateral fall while sitting, **F07**. Backward fall while sitting, **F08**. Forward fall when trying to get up, **F09**. Forward fall, **F10**. Lateral fall, **F11**. Backward fall

Results & Discussion: The non-augmentation model (MAE:1.25g, MSE: 3.00g^2) showed larger error in both cases than the augmentation model (MAE: 1.19g, MSE: 2.93g^2). Model performances were improved when data augmentation techniques were applied. In Figure 1, fall movements such as falls when trying to sit down on a chair and Lateral fall while sitting (F04, F06) showed lower peak acceleration value than other falls. Higher peak acceleration values were predicted in D02 and D09 among ADLs, representing relatively dangerous movements. Deep learning based data augmentation techniques such as GAN will be applied in the future study.

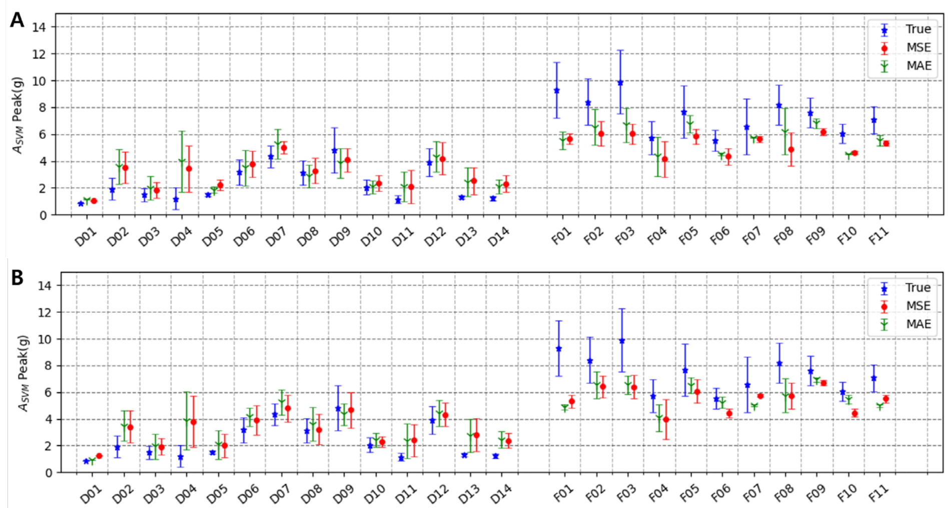

Figure 1: True and Predicted Values (MSE vs MAE): A is the augmentation model and B is not.

Significance: The risk prediction algorithm could be used as a device to warn risks and call for emergency support when applied to mobile application. Our algorithm would be applied to the real world in the future. The algorithm is expected to prevent fatal injuries in fall accidents by providing proper feedback.

Acknowledgements: This research was partly supported by the Institute of Civil Military Technology Cooperation funded by the Defense Acquisition Program Administration and Ministry of Trade, Industry and Energy of Korean Government under grant No.21-SF-GU-07 and project for Cooperative R&D between Industry, Academy, and Research Institute (S3104657) funded by the Ministry of SMEs and Startups (MSS, Korea).

References:

[1] Rubenstein, L. Z. Age and ageing 35.suppl_2, 2006
[2] Hajiaghamemar M et al. Annals of biomedical engineering 43, 2015
[3] Kim et al. Sensors 20.21, 2020

INFLUENCE OF GAIT RETRAINING ON RUNNING SPEED AND MECHANICS FOLLOWING MUSCULOSKELETAL INJURY IN MILITARY PERSONNEL

Nicholas Reilly[1,2], Amy Weart[1], Erin Miller[1,3], Paige McHenry[1,3], Maria Gonnella[1,2], Henry Haltiwanger[2], Kevin Ford[4], Michael Crowell[3], and Donald Goss[1,2,4]
[1] The Geneva Foundation, Tacoma, WA
[2] Womack Army Medical Center, Fort Bragg, NC
[3] Baylor University-Keller Army Community Hospital | Division I Sports Physical Therapy Fellowship, West Point, NY
[4] Department of Physical Therapy, High Point University, High Point, NC
Corresponding Author Email: nreilly@genevausa.org

Introduction: In accordance with training and fitness requirements, active-duty service members (ADSMs) regularly perform bouts of running and vigorous exercise. The frequency and cumulative strains of such activities are associated with higher risks of musculoskeletal injury when compared to the general population [1]. Numerous biomechanical parameters have been identified as precursors to running-related injury including greater average vertical loading rates (AVLR), excessive hip and knee frontal plane movement , and slower cadences [2,3]. As such, improving the understanding of the driving factors behind these biomechanical parameters can set the foundation for successful clinical management plans for rehabilitation and optimization of ADSM's physical readiness and ability to perform.

Structured gait retraining protocols have previously been utilized to modify kinematic and kinetic gait parameters to improve clinical outcomes for running-related injuries and reduce long-term re-injury risk [4,5]. In practice, strategic components for gait retraining include metrics such as corrections in postural alignment, utilizing a non-rearfoot strike pattern, and increasing cadence in efforts to mitigate mechanical strain and exerted forces on the joints and structures of the lower limbs. While the overall goal of gait retraining is to instil a self-selected gait pattern less conducive to injury risk, it remains uncertain what influence gait retraining has on preferred running speed, and what effects changes in preferred running speed may have on kinematic and kinetic parameters following completion of structured gait retraining. The purpose of the present study was to assess the influence of structured gait retraining on preferred running speed and corresponding kinematic and/or kinetic alterations indicative of musculoskeletal injury risk.

Methods: Following a referral to a physical therapist for a running-related injury, 24 ADSMs were recruited to participate in the study and were randomly allocated either to a return-to-run program consistent with Military Health System practices (n=13) or to receive supplemental gait retraining via telehealth consisting of corrective feedback on running form shared through a cloud-based coaching platform (n=11). Prior to and immediately following the completion of the eight-week intervention timeframe, participants ran at a self-selected pace on a force-plate instrumented treadmill to collect running kinetics data at 1200 Hz while having kinematic data tracked using a 16-camera three-dimensional motion capture system (Qualisys, Gothenburg, Sweden) at 120 Hz. Group and time differences for all variables were assessed using 2x2 ANCOVAs with running speed serving as a covariate. *a priori* levels of significance for all dependent variables were set at 0.05.

Results and Discussion: There were no significant differences between groups for peak sagittal and frontal hip and knee angles or preferred running speed between groups at baseline. Following the completion of the intervention period, the telehealth group demonstrated significantly reduced peak hip adduction angles compared to baseline ($p=0.044$). In addition, the telehealth group demonstrated significantly greater peak hip flexion angles compared to controls ($p=0.040$). The covariate, preferred running speed, was observed to be significantly related to peak hip abduction angle ($p=0.038$) and peak knee abduction angle ($p<0.001$). However, there were no significant changes in preferred running speed for both groups following the completion of the intervention period.

Telehealth gait retraining was shown to be an effective means to modify kinematic parameters following running-related injury. In addition, the results of the present study showed a significant association between preferred running speed and frontal plane kinematics at the hip and knee during gait. Given the association between frontal kinematics and injury risk, manipulating running speed should be considered if problematic frontal kinematics persist.

Significance: The ability to instil movement patterns associated with a reduced risk of injury without the need for laboratory-grade instrumentation presents a viable means to reach a larger cohort of patients spanning numerous running-related pathologies. Expediting recovery from and reducing incidence rates of running-related musculoskeletal injury would provide significant relief from the financial and temporal strains on individual patients and health care systems at large. Further research is required to assess the long-term adherence of the newly adopted kinematic patterns as well as long-term clinical outcomes and re-injury rates more comprehensively.

Acknowledgments: This work was funded in part by the Musculoskeletal Injury Rehabilitation Research for Operational Readiness (MIRROR), Department of Physical Medicine & Rehabilitation, Uniformed Services University, Bethesda, MD, (award HU00011920011).

References: [1] Grimm et al., 2019, *Sports Med and Arthroscopy*. 27: 84–91., [2] Futrell et al., 2018, *Med Sci Sports Exer.* 50: 1837–1841., [3] Kristianslund et al., 2014, *Br J Sports Med*. 48: 779–783., [4] Dunn et al., 2018, *Hum Mov Sci*. 58: 21–31., [5] Miller et al., 2020, *Mil Med*. 186: e1077-e1087.

DO INDIVIDUALS WITH LOWER LIMB OSTEOARTHRITIS REDSITRIBUTE PROPULSION PROXIMALLY?

Francesca E. Wade[1*], Chun-Hao Huang[1,2], Burcu Aydemir[1,3], Kharma C. Foucher[1]
[1]Biomechanics and Clinical Outcomes Laboratory, University of Illinois at Chicago
[2]Musculoskeletal Epidemiology and Biomechanics Laboratory, Northeastern University
[3]Division of Rheumatology, Northwestern University Feinberg School of Medicine
*Corresponding author's email: fwade21@uic.edu

Introduction: Typically, as individuals age, the musculature used to generate propulsive force leading to forward motion during walking is shifted proximally from the ankle to the hip [1]. However, lower limb osteoarthritis has associated impairments of the hip joints [2], which may alter individual joint contributions to forward propulsion. If people with osteoarthritis do generate forward propulsion differently to their age-matched peers, this could be a contributor to mobility disability in osteoarthritic populations whilst also providing evidence that redistribution of propulsion may be due to musculoskeletal impairment. Accordingly, in this study, we quantified the hip and ankle contributions to forward propulsion in individuals with hip or knee osteoarthritis and in healthy control participants, using the redistribution ratio [3]. We hypothesized that individuals with hip or knee osteoarthritis would have lower redistribution ratios than individuals without lower-limb pathologies during steady state walking.

Methods: Data were collected as part of a previous study. 19 individuals, who had 10 consecutive clean steps in the first 2.5 minutes of walking at a self-selected comfortable speed at the beginning of a 10-minute fatigability protocol, were selected for inclusion in this analysis. Passive markers were placed on the anterior and posterior superior iliac spine, greater trochanter, thigh, lateral femoral condyle, shank, lateral malleolus, calcaneus, 1st, 2nd, and 5th metatarsal heads. Additional medial markers were placed on the knee and ankle during static calibration. Marker position was captured by 8 cameras (120Hz, Eagle, Motion Analysis Corp.). Individuals walked on an instrumented split-belt treadmill (2040Hz, Treadmetrix). Ten consecutive steps for each individual were analysed. Marker trajectories and force data were filtered with a 4th order low-pass Butterworth filter at 6Hz and 25Hz cut-off frequencies respectively. Force data were used to identify gait events in Visual3D. A conventional gait model was applied to obtain ankle and hip power during the stance phase of each gait cycle. The individual joint contributions to forward propulsion were summarized with the redistribution ratio calculated as 1 – (positive ankle work – positive hip work)/(positive ankle work + positive hip work). A value of 0 indicates that all propulsion is generated about the ankle and a value of 2 indicates that all propulsion is generated about the hip [3]. The involved limb was that with osteoarthritis, or the worse side for bilateral diagnoses, and the non-dominant limb for control participants. A repeated measures ANOVA with a within-subject factor of limb (2 levels: 1) involved, 2) uninvolved) and a between-subject factor of group (3 levels: 1) control–CON, 2) knee osteoarthrosis–KOA, 3) hip osteoarthritis–HOA) was used to assess differences in redistribution ratio.

Results & Discussion: There were no differences in age, body mass, or self-selected walking speed across participant groups (CON: n=5, age=63±4y, BMI=27.42±2.79kg/m^2; KOA: n=7, age=55±4y, BMI=35.52±2.11kg/m^2; HOA: n=7, age=55±2y, BMI=32.00±1.91kg/m^2). Nor were there differences in redistribution ratio between the involved and uninvolved limbs ($p=0.301$, $\eta_p{}^2=0.067$) of the participants with osteoarthritis. We did, however, identify group differences ($p=0.010$, $\eta_p{}^2=0.438$). In contrast to our hypothesis, the involved limbs in KOA and HOA had significantly higher redistribution ratios compared to the control group (Figure 1). Notably, there were no differences between the affected limb redistribution ratios for the KOA and HOA group. While not significant, KOA participants had a greater redistribution ratio in their uninvolved limb compared with their involved limb (.17±.11), while there were minimal differences between limbs in the HOA participants (.04±.11). Our findings contrast with our initial hypothesis, instead indicating that lower limb osteoarthritis led to greater contributions of more proximal joint musculature to forward propulsion.

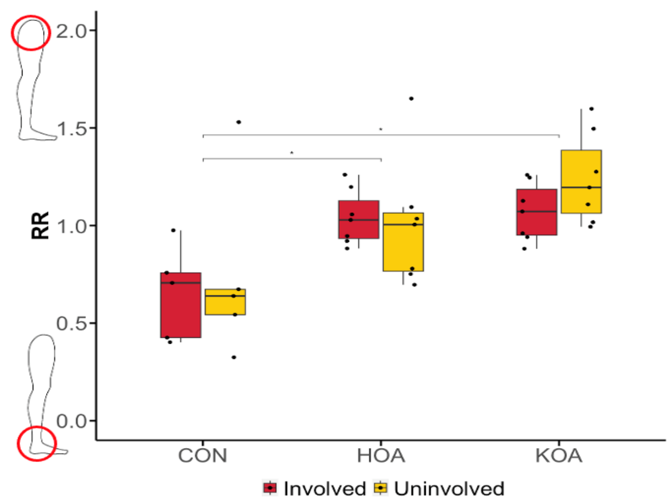

Figure 1: Boxplots with median, 1st and 3rd quartiles are provided for the redistribution ratio (RR). Data for involved (red) and uninvolved (yellow) limbs are provided in control participants (CON), people with hip osteoarthritis (HOA) and people with knee osteoarthritis (KOA).

Significance:
These findings suggest that osteoarthritis does not prevent the proximal redistribution of forward propulsion. Considering individuals may shift propulsion back to the ankle with biofeedback [3], it is still unclear whether the redistribution is maladaptive. Our findings in individuals with impairment in the proximal kinetic chain has given further evidence that this redistribution of propulsion is not mechanical in origin. Future work will investigate the impact of psychosocial factors and pain on the redistribution of propulsion.

Acknowledgements: This work was funded by R21AG052111-01 and UL1 TR002003.

References: [1] DeVita & Hortobagyi (2000), *J Appl Physiol* 88(5) 1904-11; [2] Alnahdi et al. (2012) *Sports Health* 4(4): 284-92; [3] Browne & Franz (2018), *PlOS One* 13(8): e0201407; [4] Bejek et al (2006), Knee Surg. Sports Traumatol. Arthrosc. 14:612-22

VALIDATING INERTIAL MEASUREMENT UNITS FOR MEASURING SLIPPING FOOT KINEMATICS DURING OVER-GROUND SLIPS

Michelle A. Morris[1], Youngjae Lee[1], Neil B. Alexander[2], Christopher T. Franck[3], Michael L. Madigan[1*]
[1]Grado Department of Industrial and Systems Engineering, Virginia Tech, Blacksburg, VA, United States
[2]Department of Internal Medicine, University of Michigan, Ann Arbor, MI, United States
[3]Department of Statistics, Virginia Tech, Blacksburg, VA, United States
*Corresponding author's email: mlm@vt.edu

Introduction: Slip-induced falls are a leading cause of injuries in the United States [1-2]. Slips have traditionally been studied in a laboratory-controlled environment with optoelectronic motion capture (MOCAP) systems. Inertial measurement units (IMUs) are less expensive wearable devices that can also capture body kinematics. The purpose of this study was to compare key slipping kinematic measures derived from IMUs with those derived from a gold standard MOCAP system. We hypothesized that these key slipping kinematic measures would be comparable between the two systems.

Methods: Ten young adults (5 female, age = 22.1 ± 2.4 years, BMI = 24.4 ± 2.5 kg/m^2) were slipped while walking at a self-selected purposeful speed along a 10-meter walkway. Slips were induced by spreading vegetable oil over a 0.9 x 0.9-m area on the walkway while participants were distracted. All participants had their dominant foot slipped at heel strike. Kinematic data were simultaneously collected from an IMU on the slipping foot and markers on the ankles, heels, and toes using MOCAP (Qualisys North America, Inc., Buffalo Grove, IL). IMU local frames were aligned with anatomical planes [3], and a zero-velocity correction was used to account for IMU drift [4]. Slip distance and peak slip speed in the anterior-posterior (AP) direction were calculated from both systems. A Bland-Altman analysis was used to determine the level of agreement of the two slipping measures between the two systems.

Results & Discussion: One subject was excluded from the analysis due to a missed slip. Bland-Altman plots show systematic differences between systems of 1.19 cm for AP slip distance and 9.43 cm/s for peak AP slip speed (Figure 1). To evaluate the clinical relevance of these system differences, they were compared to mean differences between falls and recoveries after over-ground slips reported in prior studies that used similar methods and MOCAP [5-6] (Table 1). These results support our hypothesis that slip kinematics were comparable between the two systems, and that the difference between the systems is likely small enough to still recognize clinically-relevant differences between falls and recoveries.

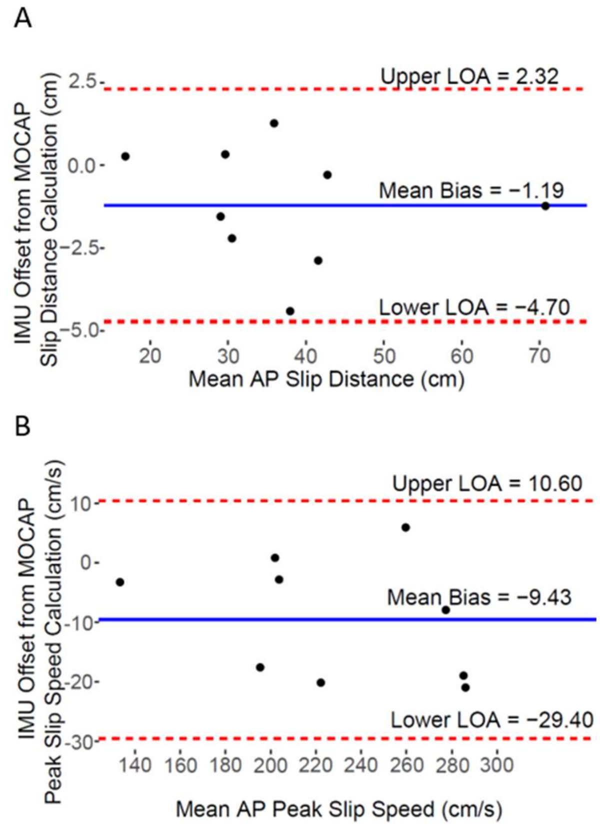

Fig. 1. Bland-Altman plot showing system differences and 95% limits of agreement (LOA) for A) AP slip distance and B) AP peak slip speed.

Table 1: Comparison of mean differences between slip-induced falls and recoveries.

	Brady 2000 [5]	Allin 2018 [6]	Current Study Results MOCAP	Current Study Results IMU
AP Slip Distance (cm)	25.29	15.21*	11.43	8.26
AP Peak Slip Speed (cm/s)	52.91	77.69*	109.13	94.86

* Mean value for falls was calculated as a weighted average of the three fall types reported in this study.

Significance: Although our sample size was limited, our results provided evidence that IMUs can be a viable form of portable motion-capture for slip kinematics. Moreover, IMUs have potential for accurate slip measurement outside of the laboratory environment, potentially leading to a better understanding of real-world slip events.

Acknowledgements: Research reported in this publication was supported by the National Institute On Aging of the National Institutes of Health under Award Number R21AG075430. The content is solely the responsibility of the authors and does not necessarily represent the official views of the National Institutes of Health.

References: 1. *WISQARS Leading Causes of Nonfatal Injury,* CDC (2020); 2. Courtney et al. *Ergonomics* (2001); 3. Cain et al. *Gait Posture* (2016); 4. Rebula et al. *Gait Posture* (2013); 5. Brady et al. *Journal of Biomechanics* (2000); 6. Allin et al. *Ergonomics* (2018).

DO BIOMECHANISTS REPRESENT THE GENERAL POPULATION? AN INVESTIGATION OF SELECTION BIAS AND HAND FUNCTION

Maximillian T. Diaz[1*], Joel B. Harley[2], Jennifer A. Nichols[1]
[1]J. Crayton Pruitt Family Department of Biomedical Engineering, University of Florida, Gainesville, FL, United States
[2]Department of Electrical & Computer Engineering, University of Florida, Gainesville, FL United States
*Corresponding author's email:mdiaz40@ufl.edu

Introduction: Biomechanical studies are highly susceptible to selection bias due to small study cohorts (n<30) [1]. In studies focusing on young adults, for example, it is common practice to include laboratory members and colleagues to ease subject recruitment burden. However, this recruiting practice can increase participant bias as a biomechanist's experience may influence their behavior due to *a priori* expectations [2]. An example of this would be a study focusing on running techniques that collected data primarily from biomechanists. In this case, biomechanists may subconsciously exaggerate their form in a manner that is not reflective of the population to favor a desired study outcome [3]. Unfortunately, data on recruitment methods and subject occupation are often not reported, so it is unknown how much of the literature has primarily been conducted on biomechanists and whether this practice leads to skewed results.

In this study, we evaluate if subject cohorts made primarily of biomechanists create skewed results by comparing the hand function of biomechanists to an age-matched population. Due to an understanding of common experimental techniques, we expect biomechanists will demonstrate increased hand function compared to naïve subjects. We specifically examined how the anthropometrics and hand strength of attendees at the 2022 North American Congress on Biomechanics (NACOB) compared to that collected from 15 different locations within our local community.

Table 1. Sample Size of Age Clusters from Mean Shift Clustering

Age Cluster	NACOB Population (Male/Female)	General Population (Male/Female)	Total (Male/Female)
18-39	167 (84/83)	262 (92/170)	429 (176/253)
40-62	3 (1/2)	35 (12/23)	38 (13/25)
63-73	0 (0/0)	48 (21/27)	48 (21/27)
74-95	22 (14/8)	31 (13/18)	53 (27/26)

Methods: To test for performance bias in the biomechanics community, we evaluated hand function from subjects (n=596) at 16 unique locations, including the 2022 North American Congress on Biomechanics (NACOB). Subjects participated in a 15-minute, IRB-approved survey, that consisted of demographics, the Michigan Hand Questionnaire [4], maximum grip and lateral pinch strength via dynamometry, and three five-second, maximum lateral pinch trials using a six-degree-of-freedom force sensor that records time-series data.

Given that hand strength is influenced by age, analyses were age stratified using mean shift clustering. The need for age stratification was confirmed with regression analysis (p<0.001). Importantly, use of the mean shift clustering algorithm reduced bias. As unlike k-means clustering, this algorithm does not require pre-defining the number of clusters to be identified [5]. As the majority (n=167) of NACOB participants fell within the 18- to 39-year-old cluster, initial analyses were limited to all subjects (n=429) within that age cluster (Table 1).

To determine if recruiting only biomechanists biases results, sex stratified comparisons were performed using a Mann-Whitney U comparison test. The need for sex stratification was confirmed with regression analysis (p<0.001). For each sex, we used a Mann-Whitney U comparison test to compare the distributions of nine metrics: height, weight, grip strength, lateral pinch strength, hand length, hand width, as well as the maximum, average, and standard deviation of the resultant 3D pinch force between NACOB attendees and the age-matched population.

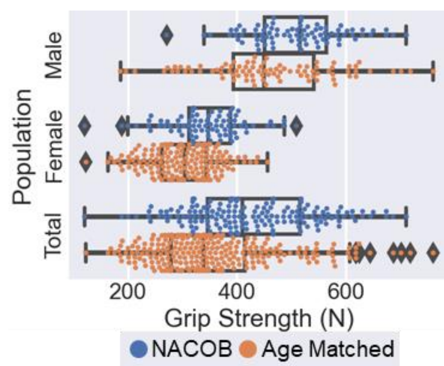

Figure 1: Comparison of grip strength when accounting for recruitment location and sex as biological variables. Male and female participant were found to significantly higher grip strength compared to age-matched non-biomechanists.

Results & Discussion: The NACOB cohort, which consisted of biomechanists, had skewed results for seven of the nine metrics. Specifically, population values for self-reported height, grip strength (Fig. 1), lateral pinch strength, hand length, and average resultant pinch force were significantly higher (p<0.05) for both male and female NACOB subjects as compared to age-matched individuals from our local community. Male participants at NACOB had grip and pinch strengths 11.1% and 5.9% above age-matched participants, respectively. Likewise, female NACOB participants had grip and pinch strengths that were 13.8 % and 8.0 % higher than the age-matched population. These findings agree with prior work that has shown subject's expertise can lead to altered performance [2], and that subjects who are biomechanists are often more athletic than the general population [3]. Thus, the increase in strength-based metrics may be a result of subject bias. However, whether this bias is due to biomechanists having more experience with directions, such as "squeeze as hard as you can", versus actual differences in physical strength is unknown.

Significance: These results indicate that findings from subject cohorts consisting primarily of biomechanists may represent skewed results compared to subject cohorts of naïve participants. This highlights the need to collect information on recruitment location and occupation as possible biological variables that should be controlled for in biomechanics research to increase generalizability.

Acknowledgements: Funding from NIH (R21 EB030068) and NSF GRFP. Thanks to NACOB 2022 for allowing us to collect data.

References: [1] Knudson (2011), *Percept. Mot. Skills* 112(3) [2] Stowell & Addison (2017), *APA* [3] Shorten et al. (2017) *ISBS Proceedings Archive*. 35(1) [4] Chung et al. (1998), *J Hand Surg Am.* 23(4) [5] Virupakshappa et al. (2019) *IEEE IUS*

NEURAL RESPONSES DURING A FORCE-CONTROL MOTOR TASK WITH ALTERED VISUAL FEEDBACK

Sophie Dewil[1*], Mingxiao Liu[1], Sean Sanford[1], Raviraj Nataraj[1]
[1] Department of Biomedical Engineering, Stevens Institute of Technology, Hoboken, NJ, USA
*Corresponding author's email: sdewil@stevens.edu

Introduction: After neurological trauma such as spinal cord injury, affected persons can undergo physical therapy (PT) to recover function. However, the slow progress and the monotony of PT [1] can dampen motivation and diminish performance [2]. Therefore, motor rehabilitation approaches with computerized interfaces, such as robotics and virtual reality (VR), have been increasingly adopted [3]. However, such interfaces may better support motor learning if designed to promote cognitive foundations of motor function, such as feelings of agency. Sense of agency is the perception of control [4], which is naturally aligned with motor actions. Our lab's prior works [5, 6] have shown that automating or adding noise to the visual feedback of motor performance will significantly and concurrently reduce agency and motor performance. Furthermore, there was a significant correlation between performance and agency across various modes with altered visual feedback. In the current study, we examined whether changes in neurological activity are discernible with these changes in visual feedback in a force-control task. In particular, we assessed alpha- and beta-band electroencephalography (EEG), given its association with changes in agency [7]. Understanding how changes in computerized interfaces dominated by visual feedback can affect neurological responses with motor training may be essential to optimizing functional outcomes.

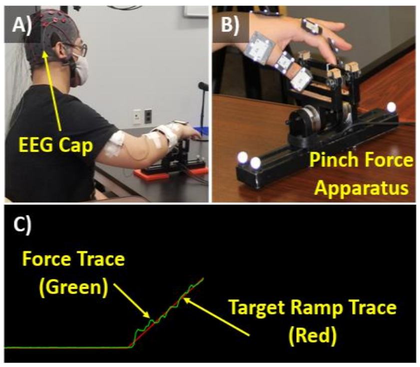

Figure 1: A) Experimental setup for the force-control task, B) device recording pinch forces, C) participant view of performance feedback.

Methods: Neurotypical participants (n=11) signed an informed consent form approved by the Stevens Institutional Review Board. Participants wore a 32-channel scalp-surface cap for EEG recording (USBamp g.tec). A custom pinch apparatus with two 6-DOF load cells (Mini40, ATI Industrial Automation) was used to record forces from precision pinch (thumb, index finger) (**Figure 1**). A total (magnitude) pinch force trace was displayed (SIMULINK, Mathworks) on a computer monitor against a target ramp trace (rises 1.25 N/sec) occurring over 4 sec. Participants repeated this force-tracking task in three 20-trial blocks. Performance was displayed within each block under a different mode of visual feedback, intended to represent perceived distortions in device control as previously done in [5]. The feedback modes were: *1) Default* = displayed force trace reflected true force applied; *2) Auto* = force trace automatically adhered to the target trace more so with ramp time; *3) Noise* = random low-level force (<0.5 N) was added to the displayed force trace.

Results: One-way ANOVA indicates significant ($p<.001$) differences in alpha- and beta-band power between feedback modes with post hoc differences, as observed in **Figure 2**. The Noise condition exhibited the greatest alpha and beta power across all three modes.

Discussion: This study demonstrated that altering visual feedback of performance during a force-control motor task can significantly affect neurological activity. Notably, EEG power was highest with the Noise mode, which imposes perceptional distortions from an accurate (i.e., Default) representation of performance. Such distortions can significantly impair agency and performance with motor tasks [5, 6]. An inverse relationship between agency and alpha activity has been observed in other work [7], which is consistent with our study's finding. Such results suggest that motor therapy with a computerized interface must carefully consider how feedback is presented in the complex interplay between cognitive, neurological, and motor responses.

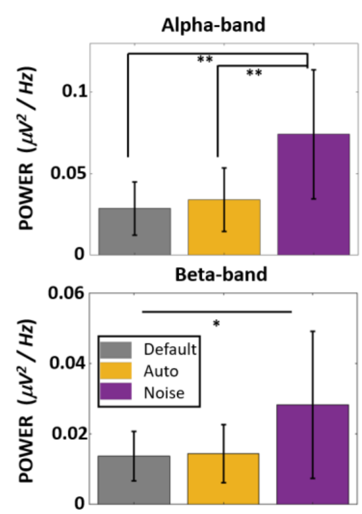

Figure 2: Neurological activity in the alpha (top) and beta (bottom) bands across visual feedback modes. * $p < 0.05$, ** $p < 0.001$.

Significance: This study observed significant changes in neural responses when only mildly manipulating the visual feedback of performance in a simple force-control task. This study's findings suggest the potency of computerized feedback to affect motor learning in indicators for performance *and* neuroplasticity. Ultimately, our study should inspire further investigation into how interfaces for motor rehabilitation, or similar computerized applications, can be more intelligently designed and deployed to optimize functional outcomes.

Acknowledgements: The authors acknowledge support from the Schaefer School of Engineering and Science at the Stevens Institute of Technology.

References: [1] Burke JW. Vis Comput. 2009;25(12):1085-1099; [2] Maclean N. Soc. Sci. Med. 1982;50: 495-506; [3] Howard MC. Comput. Hum. Behav. 2017;70:317-327; [4] Moore JW. Conscious Cogn. 2012;21(1):546-561; [5] Nataraj R. Front. Bioeng. Biotechnol. 2021;8:1544; [6] Nataraj R. Front. Hum. Neurosci. 2020;14:126; [7] Kang SY. PLoS One. 2015;10(8):e0135261

MUSCLE ACTIVATION DURING AQUATIC TREADMILL WALKING IN CHILDREN WITH CEREBRAL PALSY: PRELIMINARY EVIDENCE

Joseph W. Harrington[1*], Brian A. Knarr[1], Vivek Dutt[2], David C. Kingston[1]
[1]Department of Biomechanics, University of Nebraska at Omaha, Omaha, NE, USA
[2]Department of Orthopaedic Surgery, University of Nebraska Medical Center, Omaha, NE, USA
*Corresponding author's email: josephharrington@unomaha.edu

Introduction: Cerebral palsy (CP) is the most common cause of motor disability in juveniles occurring in 3.3/1000 live births [1]. Most children with CP have impaired gait due to muscle weakness and altered joint kinematics; key mechanisms that decreases walking efficiency [2]. Aquatic treadmill training is a promising rehabilitation method that promotes repetitive gait cycles in an environment that alters bodyweight support, passively increases resistance on the lower limbs, and assists postural stability. However, there is limited evidence investigating the effect of aquatic treadmill walking on muscle activation.

Therefore, the purpose of this study was to determine the effect of treadmill environment and walking speed on lower limb muscle activity in children with CP. We hypothesized that mean muscular activation, across all strides, would be the greatest during dry treadmill walking at a fast speed due to increased physical demand of fast walking and the increased body weight offloaded in water due to buoyancy.

Methods: To date, two children with CP have completed three 3-minute walking trials based on varying their self-selected walking speed determined using a previously described protocol [3]: Slow (75%), Normal (100%), and Fast (125%) walking speeds were used on a conventional (DRY) and aquatic (WET) treadmill. Children were instrumented with wireless waterproof surface electromyographic (EMG) sensors and inertial measurement units (Cometa srl., Milan, Italy) to detect initial contact events for data truncation. Specific muscle sites include the rectus femoris (RF), semitendinosus, tibialis anterior, and medial gastrocnemius (MG); muscles that contribute to the impaired gait of children with CP. Children completed block randomized DRY treadmill walking trials, followed by WET treadmill trials, and reported their rated perceived exertion (RPE), using a 0-10 scale, after each trial. During WET treadmill trials, the water level was set at the participant's xiphoid process. Raw EMG data were full wave rectified, filtered and normalized using the greatest magnitude found in the DRY Fast walking trial. The primary outcome variable was mean muscle activity across all strides. *C1:* A 14-year-old male with CP presenting with Gross Motor Function Classification System (GMFCS) I and a more affected right limb. *C2:* A 7-year-old male with CP presenting with GMFCS I and a more affected right limb.

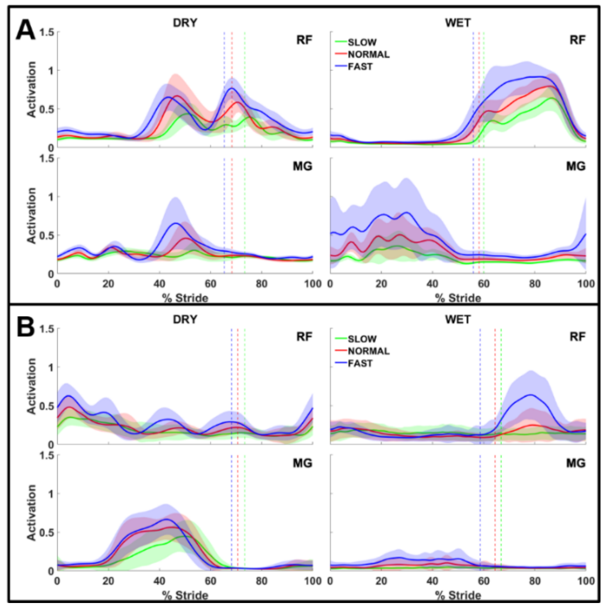

Figure 1: C1 (A) and C2 (B) mean muscle activation waveforms during DRY and WET treadmill walking trials. Speeds are defined in-text. Initial contact corresponds to 0% stride. Shaded areas represent one standard deviation and dotted vertical lines represent mean toe-off timing amongst speeds.

Results & Discussion: Mean RF muscle activation of C1 (DRY: 0.28, WET: 0.29) and C2 (DRY: 0.25, WET: 0.19) had minimal differences when comparing environments; however, elevated activation is observed in the swing phase in WET, opposed to stance in DRY (Fig 1). Interestingly, increased mean MG activation was observed during WET speed trials in C1, but a decrease in C2. However, C1 walked 0.09 m/s faster during WET trials. An increase in RF activation in swing phase and decreased MG activation during WET treadmill walking has been reported in typically developing children [3]. Furthermore, children with CP reported an 80.9% decreased RPE during WET treadmill trials (DRY: 3.5, WET: 0.67), while typically developing children reported 78.0% greater RPE [3], indicating children with CP found it easier than typically developing children to walk in water.

Significance: Aquatic treadmill walking reduced MG activation in one child while increasing swing phase RF activation in both children with CP. Preliminary data suggests muscle activation changes in children with CP trends towards typically developing controls [3] while also reducing perceived exertion in children with CP. However, to further investigate and provide additional evidence, we are actively recruiting children with CP for this study.

Acknowledgements: This work was supported by the University of Nebraska Collaboration Initiative Pilot Award (26246) and the National Institutes of Health (1R15HD109666).

References: [1] Kirby et al, *Res. Rev. Disabil.* 32, 462-469 (2011), [2] Dallmeijer et al, *Gait Posture* 31, 366-369 (2010), [3] Harrington et al, *J Electromyogr Kinesiol* 68, (2023)

PEAK MINUTE-LEVEL FREE-LIVING CADENCE IS ASSOCIATED WITH LABORATORY GAIT SPEED AND VERTICAL GROUND REACTION FORCES FOLLOWING ANTERIOR CRUCIATE LIGAMENT RECONSTRUCTION

Katherine Collins[1*], Caroline Lisee[2], Matthew Harkey[1], Dante D. Goss[3], Karin Pfeiffer[1], Jeemin Kim[1], Christopher Kuenze[3]
[1] Michigan State University, Department of Kinesiology, East Lansing, MI
[2]University of North Carolina at Chapel Hill, Motion Science Institute, Chapel Hill, NC
[3]University of Virginia, Department of Kinesiology, Charlottesville, VA
*Corresponding author's email: colli784@msu.edu

Introduction: Individuals with anterior cruciate ligament reconstruction (ACLR) exhibit asymmetrical vertical ground reaction forces (vGRFs) and slower walking speeds, which have been related to indicators of poor knee joint health and knee osteoarthritis (OA) development [1]. However, walking biomechanics and gait speed are often assessed in research laboratories that have limited ecological validity. Cadence (i.e., steps taken per minute) is a spatiotemporal component of gait speed that can be measured in free-living conditions using wearable devices (e.g., triaxial accelerometer). Monitoring free-living cadence may provide an ecologically valid avenue to assess and intervene on free-living ambulation. However, the relationship between accelerometer measured free-living cadence and laboratory-assessed gait speed and vGRFs has not been evaluated among individuals with ACLR. Therefore, the purpose of this study was to determine the association between mean and peak minute-level free-living cadences and laboratory-assessed gait speed and ACLR limb peak vGRF. We hypothesized that laboratory-assessed gait speed and peak vGRF would be related to free-living mean and peak minute-level cadences because previous studies have reported that individuals with ACLR who take fewer steps per day also exhibit lower vGRFs during overground walking.

Methods: Participants with history of primary, unilateral ACLR completed a single laboratory visit to assess walking speed and ACLR limb peak vGRF. Participants walked down a 6-meter walkway at a natural, comfortable pace 5 times. Gait speed was measured using a pair of timing gates (TracTronix, TF 100) and vGRFs were collected using 2 embedded force platforms (Advanced Medical Technology Inc., Watertown, MA) at 1000 Hz. ACLR limb peak vGRF was identified during the first 50% of stance and was normalized to participant body weight. Gait speed and ACLR limb peak vGRF are reported as the average across 5 trials. For the following 7 days, participants wore an Actigraph GT9X Link monitor (Actigraph, LLC, Pensacola, FL) on the right hip. Monitor data were collected at 30 Hz and wear-time was validated in accordance with Choi et al. [2]. Non-wear time was removed from analysis, and the remaining data were analyzed in 60-second epochs. Mean minute-level cadence is reported as the average number of steps taken each minute during wear periods of light-to-moderate cadence (60-130 steps per minute). Peak minute-level cadence is reported as the maximum number of steps taken during any 1-minute period of wear time. Four partial correlations evaluated the association between 1) laboratory gait speed and mean minute-level light-to-moderate cadence, 2) ACLR limb peak vGRF and mean minute-level light-to-moderate cadence, 3) laboratory gait speed and peak 1-minute cadence, and 4) ACLR limb peak vGRF and peak 1-minute cadence. Total monitor wear time and participant height were controlled for in analyses. Partial correlations were interpreted using Pearson's r as: < 0.39: weak, 0.40-0.69: moderate, and > 0.70 strong.

Results & Discussion: Forty-eight participants (age: 21.3 ± 6.0 years old, sex: 26 F/ 22 M, height: 174.0 ± 8.0 cm, mass: 77.5 ± 20.0 kg, time since ACLR: 13.9 ± 15.9 months, total monitor wear time: 5910 ± 2372 minutes) were included and their gait characteristics are outlined in Table 1. Mean minute-level light-to-moderate cadence was not significantly associated with laboratory-assessed gait speed (r_p=0.28, P=0.059) or ACLR limb peak vGRF (r_p=0.25, P=0.093). Laboratory-assessed average gait speed was moderately and positively associated with peak minute-level cadence (r_p=0.44, P=0.002) and ACLR limb peak vGRF was weakly and positively associated with peak minute-level cadence (r_p=0.33, P=0.025). These findings indicate a disconnect between average laboratory-assessed gait characteristics and average free-living cadence characteristics. However, the results of this study also indicate that participants who demonstrated greater walking speeds and vGRFs in the laboratory environment also exhibited greater peak minute-level cadences under free-living conditions.

Table 1. Laboratory and Free-living Gait Characteristics

Laboratory	
Gait Speed (m/s)	1.26 ± 0.24
ACLR Limb Peak vGRF (x BW)	1.10 ± 0.08
Free-living	
Peak 1-minute cadence (steps/min)	145 ± 25
Mean 1-minute light-to-moderate cadence (steps/ min.)	86.7 ± 6.8

Data are presented as mean ± standard deviation., ACLR=anterior cruciate ligament reconstruction, vGRF=vertical ground reaction force, BW=body weight

Significance: These findings highlight a disconnect between the average gait speeds and peak vGRFs of 5-10 steps in the laboratory environment with the average free-living cadences that participants spent > 90% of their time each day. However, wearable-device interventions delivered in free-living conditions that target peak 1-minute cadences may serve as an avenue to intervene on walking speeds and vGRFs that have been previously related to indicators of knee OA development and poor knee joint health following ACLR.

Acknowledgements: This work was partially supported by a grant from the Great Lakes Athletic Trainers' Association.

References: [1] Pietrosimone et al. Walking Speed As a Potential Indicator of Cartilage Breakdown Following Anterior Cruciate Ligament Reconstruction. Arthritis Care Res (Hoboken). 2016 Jun;68(6):793-800. PMID: 26502367. [2] Choi et al. Validation of accelerometer wear and nonwear time classification algorithm. Med Sci Sports Exerc. 2011 Feb;43(2):357-64. PMID: 20581716; PMCID: PMC3184184.

A KINEMATICS-BASED APPROACH TO FUTURE JOINT ANGLE PREDICTION

Ryan Pollard[1], David Hollinger[1], Michael Zabala[1]
[1]Auburn University, Auburn, AL, U.S.A
*Corresponding author's email: rzp0051@auburn.edu

Introduction: Machine learning models are powerful algorithms that can be used for predicting future joint angles in biomechanical applications [1]. However, their high computational demand makes near-future prediction difficult. Therefore, the use of more simplistic, kinematics-based models may be beneficial for predicting joint angles in a near-future application. Such kinematically-informed models would utilize trendline extrapolation techniques or physics-based kinematic equations in order to make predictions. Due to their simplicity, it is hypothesized that the kinematics-based prediction models would rival the machine learning prediction accuracy while having significantly lower computational demand for near-future applications (~100ms). Additionally, common performance metrics do not denote *agreement* with user intent, but rather merely indicate prediction error. It may be beneficial to denote whether a predicted angle precedes or lags behind the measured joint angle. Such a performance metric would seek to provide additional information about an algorithm's performance and prediction tendencies that cannot be captured though error metrics.

Methods: Lower-limb kinematics for nine healthy subjects were recorded using a ten camera Vicon motion capture system. Each subject performed three stair climb trails, consisting of the ascent of two seven-inch steps, and each participant provided informed consent approved by the Auburn University IRB. Musculoskeletal models for each trial were then developed within Visual3D to determine the joint angles of the left and right ankle. Seven prediction algorithms were developed from trendline extrapolations and kinematic forecasting techniques for future joint angle prediction. The models incorporated a sliding window of $t_{window} = 50ms$ of previous data to predict joint angles $t_{pred} = 100ms$ in the future. Each algorithm's offline performance was determined by comparing the predicted ankle angles to the measured ankle angles using a root-mean-square error (RMSE) and by recording the computational runtimes for each model. A Random Forest machine learning model was tested and trained on the same dataset to serve as a baseline for comparison.

Additionally, a novel performance metric – the *Agreement Factor* (AF) – was developed as a characterization of the fluency between the predicted angle and the observed motion of the joint. The AF metric indicates whether a predicted angle precedes (AF = 1.0) or lags (AF = 0.0) the measured angle temporally. This performance metric informs whether a model tends to predict joint angles that precede or lag behind the measure motion and serves as an additional measure, alongside RMSE, that seeks to compare the performance of varying prediction models. A repeated measures ANOVA followed by post-hoc paired t-tests were performed to compare the difference between each of the models' RMSEs, runtimes, and AFs.

Results & Discussion: The kinematics and extrapolation-based algorithms compute joint angle predictions ~50x faster than the Random Forest machine learning model (Fig.1C). The top performing kinematics-based models demonstrated comparable prediction errors to that of the Random Forest model (Modified Angular Acceleration = 7.6° RMSE; Linear Extrapolation = 8.1° RMSE; Random Forest ML model = 5.0° RMSE) (Fig.1A), confirming the hypothesis that kineamtically-informed prediction models could rival machine learning prediction errors with signifcantly lower computational demand. Additionally, the inclusion of the AF metric allows for the comparison of models with similar prediction errors. For example, although the Naïve extrapoaltion approach has a relatively low prediction error (RMSE = 8.7°, Fig. 1A), the model's predicted values tend to lag behind the measured angle (average AF = 0.0, Fig. 1B).

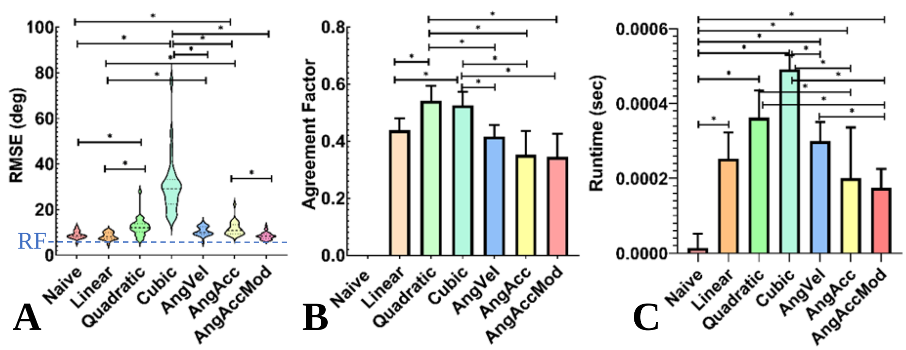

Figure 1: Prediction RMSE (A), agreement factor (B), and runtime (C) during stair ascent for kinematic-based modes. *denotes significant difference between groups ($p<0.05$)

Significance: Such results provide the basis for inclusion of kinematically-informed prediction models in real-time ankle exoskeleton applications. By using these kinematics-based algorithms, the computational demand of near-future joint angle prediction is significantly decreased when compared with common machine learning algorithms, allowing for additional time for exoskeleton actuation without comprising prediction accuracy. Additionally, because kinematically-informed models are not "trained" like machine learning models, they are task agnostic, and hence can be used for predicting future angles for several different actions without significant loss of accuracy, which may be beneficial for free-exploration exoskeleton applications that are not restricted to a single action in a laboratory setting.

References: [1] Tack (2019), *Musculoskelet Sci Pract* 39; [2] Andriacchi et al. (1998), *J Biomech* 120(6).

PR2023_19943

DOES ALTERING PD-AFO STIFFNESS AFFECT ANKLE MECHANICS IN INDIVIDUALS POST-STROKE: A PILOT STUDY

Shay R Pinhey[1*], Jacob Skigen[2], Zahra McKee[1], Elisa S Arch[1,3]
[1]Biomechanics and Movement Science Program, [2]Department of Biomedical Engineering, [3]Department of Kinesiology & Applied Physiology, University of Delaware, Newark, DE
*Corresponding author's email: spinhey@udel.edu

Introduction: It has previously been shown that use of passive-dynamic ankle-foot orthoses (PD-AFOs) as compared to other AFOs can improve walking biomechanics in individuals post-stroke, although there is variability across participants [1], [2]. PD-AFOs have a spring-like characteristic which allows them to help compensate for losses in muscle strength especially in the plantar flexors [1], [3]. In our previous studies, PD-AFO bending stiffness was customized for each participant based on his/her level of plantar flexor weakness. However, we do not know if that is the best prescription model, which may explain some of the variability in prior results. The purpose of this study was to gain an initial understanding as to whether or not changing the stiffness of a PD-AFO affects ankle biomechanics of individuals post-stroke during walking. Due to changes in the PD-AFO's spring-like characteristics with changing stiffnesses, we hypothesized that ankle biomechanics will differ among PD-AFO stiffnesses for individuals post-stroke.

		Self-Selected Walking Speed	Peak Dorsiflexion Angle	Peak Plantar Moment	Peak Positive Power
Percent Difference	Low:High	0.0%	7.6%	3.5%	32.9%
	Low:Medium	5.2%	10.4%	19.4%	50.7%
	Medium:High	5.2%	2.3%	16.0%	18.5%

Figure 1: One *example* participant is presented here. Percent difference comparisons between all stiffness levels are shown for each outcome variable. Boxes highlighted in orange indicate a percent difference greater than 10%. This subject exemplifies that, while which outcome variable is most affected and which stiffness level causes the biggest changes varies among subjects, ankle mechanics are changing across all subjects with stiffness.

Methods: In a single visit per participant, five participants (Age: 61.8 ± 6.8 yrs, Time since stroke: 5.6 ± 2.3 yrs, Height: 1.72 ± 0.13 m, Weight: 85.2 ± 17.0 kg) post-stoke walked on an instrumented split-belt treadmill (Bertec, USA) with three different PD-AFO stiffness conditions (low, medium, and high) while motion capture data (Qualisys, USA) were collected at 240 Hz and kinetic data were collected at 1200 Hz. PD-AFO stiffness conditions varied somewhat among participants in this study: one participant had PD-AFOs with low stiffness = clinically-prescribed stiffness, medium = half-way between low and high, and high = stiffness approximately customized to make up for the participant's level of plantar flexor weakness; one participant only had two PD-AFOs with low = 50% of the clinically-prescribed stiffness, medium = clinically prescribed stiffness; while three had PD-AFOs with low stiffness = 50% of the clinically-prescribed stiffness, medium = clinically prescribed stiffness, and high = stiffness approximately customized to make up for the participant's level of plantar flexor weakness. Each PD-AFO was worn for a one-minute trial at the participant's previously determined PD-AFO self-selected walking speed. Rest between trials was given as needed. Prior to each trial of treadmill walking, subjects performed a 10-meter walk test with each new PD-AFO to determine self-selected walking speed with that given PD-AFO stiffness. This walking speed was used only for analysis. Post-processing was performed in Visual 3D (C-Motion Inc., USA) to analyze four ankle biomechanical variables for each stiffness across stance phase: self-selected walking speed, peak ankle dorsiflexion angle, peak plantar moment, and peak positive power. For each variable, percent difference was calculated for each stiffness condition comparison within each participant.

Results & Discussion: Figure 1 shows the percent differences for one only one participant due to space constraints but results from all participants are summarized here. Percent differences above 10% were reached in many outcome variables across all stiffness comparisons for all participants. Percent changes reached as high as 50% for ankle angle and power comparisons in multiple participants. While there was variability across participants on which stiffness condition resulted in the greatest change in each outcome variable, these results show that an immediate change in ankle biomechanics occurs when PD-AFO stiffness is changed.

Significance: This study demonstrated that PD-AFO stiffness level can alter ankle joint mechanics and self-selected walking speed for individuals post-stroke. While the PD-AFO stiffness levels varied somewhat among participants in this study, this study still achieved its purpose in evaluating if stiffness level affects ankle joint mechanics for individuals post-stroke, which has never been shown before. It is clear from this study that PD-AFO stiffness level matters for individuals post-stroke. Future research should further evaluate changes in ankle biomechanics and other walking performance parameters elicited by a more regimented range of PD-AFO stiffness levels to provide insight into how stiffness can be optimized for each individual. If a prescription method for determining optimal PD-AFO stiffness can be determined, this could change the way clinicians prescribe AFOs for individuals post-stroke.

Acknowledgements: This work was supported in part by USAMRAA (Award No.W81XWH-18-1-0502).

References: [1] Arch and Reisman (2016), *J Prosthetics and Orthotics* 28(2); [2] Koller et al. (2021), *Prosthetics and Orthotics International* 45(4); [3] Davis and DeLuca (1996), *Gait and Posture* 4(3)

SMARTPHONE AND PAPER BASED DELIVERY OF BALANCE INTERVENTION FOR OLDER ADULTS IS EQUALLY EFFECTIVE, ENJOYABLE, AND OF HIGH FIDELTY

Vipul Lugade*, Molly Torbitt, Suzanne O'Brien, Patima Silsupadol
Division of Physical Therapy, Binghamton University
*Corresponding author's email: vlugade@binghamton.edu

Introduction: The older adult population is increasing dramatically across the globe, with the percentage of US adults over the age of 65 years estimated to rise to 21.6% by the year 2040 [1]. Concurrent with rapid population increases, falls among older adults are a significant health concern, with recent estimates indicating that 1 in 4 older adults experience a fall [2]. Interventions to improve balance and reduce fall risk are needed, and it is paramount that theses interventions be provided in an easy-to-follow and accessible manner. Home paper-based balance programs have, to date, been shown to be effective, feasible, and desirable [3]. However, it is unknown whether such interventions can be conducted effectively and remotely through a smartphone application. Therefore, the objective of this study was to investigate the utility and impact of a 4-week phone-based versus paper-based balance training among older adults. Due to the increased usage of smartphone technology, even in older adult populations, it was hypothesized that phone-based delivery of exercise would demonstrate similar fidelity, enjoyment, and effectiveness in improving walking and balance performance, when compared to paper-based intervention.

Methods: Adults over the age of 65 who were able to ambulate at least 10 meters without an assistive device, were cognitively intact based on scoring 18/22 or greater on the Montreal Cognitive Assessment-Blinded, and owned an Android or iOS smartphone were recruited into the study. Participants were asked to complete a sensory organization test, as well as three walking trials at a self-selected speed before and after the training sessions. All participants were randomly assigned to either a smartphone- or paper-based intervention program. A single trainer (SO) was blinded to participant performance, the testers (MT, PS) were blinded to the treatment condition, and participants were blinded to the presence of two treatment groups. The four-week intervention program prescribed twelve 30-minute sessions, including balance activities which followed Gentile's taxonomy of movement tasks (Figure 1). These tasks progressed from stance activities, stance activities with hand manipulation, gait activities, and finally gait activities with hand manipulation.

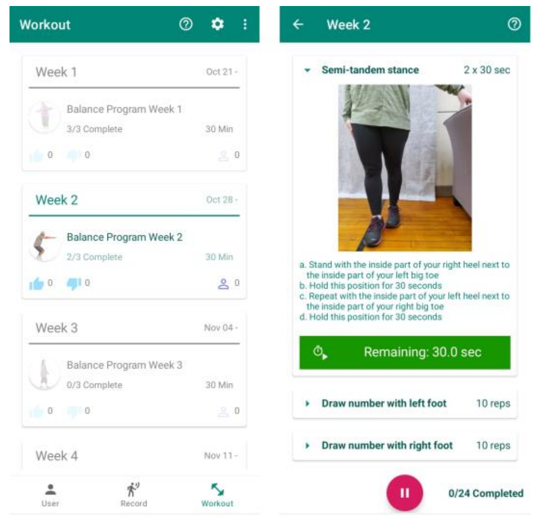

Figure 1: Smartphone-based delivery of the four-week exercise program. Detailed instruction, along with a visual representation of each exercise activity was provided in a similar format for participants receiving the paper-based version of the exercise program.

Fidelity was evaluated automatically through completion of exercise programs delivered on the phone and self-reported times among the paper group. Enjoyment of the intervention program was assessed through a 7-point Likert scale following completion of the study, with a 0 indicating "Did not enjoy at all" to 6 being "Enjoyed tremendously". Effectiveness was based on changes in gait velocity (GV) as well as standing strategy (SS) and equilibrium scores (ES) during the SOT between pre- and post-intervention for both groups. A two-way mixed effect ANOVA (group * visit) was performed for walking speed and SOT measures, while a Mann-Whitney U Test was utilized for assessing differences in self-reported enjoyment.

Results & Discussion: A total of 31 participants were recruited into the study, with 16 randomized into the smartphone (5 males; age: 75.2±8.6 years; BMI: 25.6±4.4 kg/m^2) and 15 into the paper (5 males; age: 78.2±8.4 years; BMI: 26.1±4.3 kg/m^2) intervention groups. Two participants from the smartphone group dropped out of the study, one immediately following the initial visit to the laboratory and another notifying the investigators two weeks into the intervention program due to feelings of dizziness and excessive fatigue. Among the remaining 29 participants, all completed the 4-week program, with an average of 44.6min spent on each session. Although no group*visit interaction or group main effect was found for GV, SS or ES, all participants demonstrated an approximately 0.03m/s increase in GV (p=0.041) and a 4.3% increase in SS (p=0.037) following the four-week balance intervention. No group differences were found for enjoyment in the program (p=0.403), with an average enjoyment of 3.96±1.66 reported. Furthermore, no safety concerns were raised during the home-based program. Increased gait velocity and standing strategy indicated effectiveness of the home-based program in improving both walking and standing performance. Improved SS is further indicative of greater use of an ankle strategy, in comparison to a hip strategy, in maintaining standing balance. Similar performance, adherence, and enjoyment across groups following intervention is indicative of the potential to deliver intervention to older adults using either smartphone or paper-based delivery methods.

Significance: Results from this study demonstrate the efficacy of delivering home-based intervention to older adults through either smartphone or paper-based delivery methods. Continued investigation and generalizability of these results can enhance telehealth services, promote healthy living through individualized intervention delivery, and allow clinicians to implement remote intervention in their usual care of older adults.

Acknowledgements: Funding provided by Transdisciplinary Area of Excellence-Data Science, Binghamton University.
References: [1] Administration for Community Living, 2021; [2] CDC, 2021; [3] Wongcharoen et al., 2017.

EXTERNAL FORCES DURING THE AMERICAN RUMBA BOX STEP ACROSS THREE DANCE LEVELS

Meredith D. Wells[1*], Feng Yang[2]
[1]Emory University School of Medicine, Department of Medicine, Division of Geriatrics and Gerontology, Atlanta, GA, USA
[2]Georgia State University, Department of Kinesiology and Health, Atlanta, GA, USA
*Corresponding author's email: mdwell2@emory.edu

Introduction: Ballroom dance is increasing in popularity [1] and has been reported to induce mental and physical benefits [2]. Possibly due to its multi-directional and complex movement patterns, ballroom dance has been used to improve balance in older adults and clinical groups [2-3]. However, limited biomechanical information about ballroom dance's many movement patterns is available. The purpose of this study was to determine if and to what extent the ballroom dance experience level affects the vertical ground reaction force (GRF) and loading rate (LR) during the rumba box step, a rhythm ballroom dance pattern (Figure 1). We hypothesized that the more experienced the dancers were, the lower the GRF and the LR would be, and the smaller the variance within the groups would be.

Methods: Fifty-six individuals participated – 20 inexperienced (NEW, age: 21.9 ± 4.6 years; ballroom dance experience: 0 years), 18 recreational (REC, age: 30.2 ± 5.1; experience: 2.3 ± 2.0) and 18 professionals (PRO, age: 30.8 ± 6.1; experience: 10.5 ± 8.6). After a 5-minute warm-up, participants performed the four movements that constitute a rumba box step: a back step with the right foot (BSR), a forward step with the left foot (FSL), and a sidestep to the right (SSR) and the left (SSL) in a random order. The closing of the feet was not collected due to the force plate set up. Three trials were collected for each. Participants performed the dance steps on a vinyl floor. GRFs were collected using two force plates (AMTI, MA). The outcome variables included peak vertical GRF and LR normalized to body weight (BW). Kruskal-Wallis (K-W) with post-hoc tests were conducted to compare measures among groups. Levene's test was used to assess the homogeneity within groups. SPSS v.27 (IBM, NY) with an alpha level of 0.05 was used.

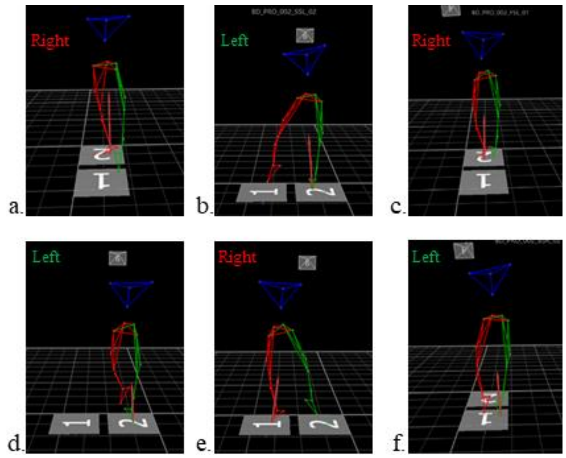

Figure 1: The rumba box step pattern from the follow's perspective where dancers step a) back on the R, b) to the side with the L, c) and together with the R, and then d) forward on the L, over on the R, and together with the L.

Results & Discussion: Results indicate that our hypothesese were partially correct (Table 1). Professional dancers demonstrated smaller LRs ($p < 0.001$) and GRFs ($p < 0.001$) during the BSR. The LR was also smaller in the more experienced levels during both the SSL ($p = 0.013$) and the SSR ($p = 0.260$), though it was not significant during the SSR. The GRF during the SSL, SSR, and FSL and the LR during the FSL were similar among groups ($p > 0.05$). The variance of the results tended to be greater in the less experienced levels in the GRF of the BSR ($p = 0.004$), the LR of SSL ($p < 0.001$), and both the GRF ($p = 0.001$) and the LR ($p = 0.015$) during the SSR. These results indicate that more experienced dancers may have greater control of their body and the rate of weight transfer, particularly when moving backward during this pattern. The GRF and the LR were more similar across the three levels when performing the FSL while the forces increased when performing the BSR, SSR and SSL in the less experienced levels. The variance within the levels was also significantly different. As dance experience and training increase, the consistency in the movement patterns appears to increase as indicated by the smaller standard deviations.

Significance: This study adds to the limited knowledge on the biomechanics of ballroom dance. Given ballroom dance's growing popularity, it is important to understand the mechanisms behind the movements so that correct information is communicated, dancers can train effectively while reducing the risk of injury, and rehabilitation protocols can be established. This study also indicates that professional dancers likely have the most accurate movement patterns, as indicated by the greatest consistency in the professional level.

Table 1. Comparisons of LR (BW/s) and the peak vertical GRF (BW) (in mean ± standard deviation) during the rumba box step components among experience levels using the Kruskal-Wallis test. Homogeneity of Variance was assessed using Levene's test.

Dance Element	Force	NEW	REC	PRO	*p*-value (K-W)	*p*-value (Levene's)
Backward Step R (BSR)	LR	5.51 ± 1.93	3.13 ± 1.73	1.95 ± 0.83	**< 0.001**	0.062
	GRF	1.23 ± 0.10	1.08 ± 0.09	1.04 ± 0.03	**< 0.001**	**0.004**
Forward Step L (FSL)	LR	1.81 ± 1.20	1.72 ± 0.90	1.51 ± 0.53	0.944	0.101
	GRF	1.02 ± 0.06	1.03 ± 0.03	1.03 ± 0.02	**0.009**	0.460
Sidestep to the L (SSL)	LR	3.44 ± 2.47	2.43 ± 1.47	1.56 ± 0.56	**0.013**	**< 0.001**
	GRF	1.09 ± 0.14	1.05 ± 0.04	1.01 ± 0.07	0.139	0.120
Sidestep to the R (SSR)	LR	2.62 ± 2.35	1.92 ± 0.87	1.49 ± 0.52	0.260	**0.001**
	GRF	1.06 ± 0.13	1.04 ± 0.04	1.03 ± 0.02	0.234	**0.015**

Acknowledgements: This research was supported by the Georgia State University Doctoral Dissertation Grant.

References: [1] "About DanceSport," (2010); [2] Sohn, Park & Kim, 2018, *Technology & Healthcare*; [3] Wells & Yang, 2021, *MDPI: Biomechanics*.

BALANCE CONTROL DURING BEAM WALKING IS NOT PREDICTIVE OF BACK HANDSPRING BALANCE CONTROL AND PERFORMANCE ON THE BALANCE BEAM

Gabriella H. Small* and Richard R. Neptune
Walker Department of Mechanical Engineering, The University of Texas at Austin, Austin, TX
*Corresponding author's email: gsmall@utexas.edu

Introduction: Despite the nearly 4.7 million gymnasts in the US [1], gymnastics remains an understudied sport [2]. The back handspring step out (BHS) in women's artistic gymnastics is a foundational skill that occurs in balance beam routines starting as young as 10 years old through the collegiate and Olympic levels [3]. Some studies investigating the BHS on the floor found unique biomechanical demands uncommon in daily activities, such as a higher wrist extension angle than the natural range of motion [4] and high valgus moments in the elbow [5]. However, fewer studies have investigated the specific balance control demands of a BHS when constrained to a balance beam [e.g., 6]. The small margin of stability (MoS) [7] available makes beam walking a challenging motor task that has previously been used as an indicator of balance control during walking [e.g., 10].

Balance control has been assessed using whole-body angular momentum (*H*) in a variety of different tasks [8], where higher ranges of *H* correlate with lower clinical balance scores and consequently poorer balance control [9]. While gymnasts are skilled at beam walking, it remains unclear if their balance control during beam walking is a predictor of their balance control during a BHS. Previous studies have found correlations between various measures of balance control and countermovement jump performance in other sports [11]. However, the specific demands of the countermovement in the take-off of the BHS require the gymnast to produce angular momentum as well as vertical and backwards momentum while tightly maintaining frontal plane balance [3]. Thus, the purpose of this study was to determine if beam walking balance control was predictive of BHS balance control and performance. We hypothesize that the more regulated a gymnast's frontal plane balance is during beam walking, the more regulated their balance control in a BHS will be and the better their scored performance.

Methods: A 12 camera system (Vicon, Oxford) recorded 3D full body kinematics for 20 gymnasts (age: 16.7 ± 4 years, skill level: 8.1 ± 1) during 3 beam walking trials and 3 BHS on a 9' long 4'' wide balance beam mounted on the floor. Motion data was then analysed in Visual3D (C-Motion, MD) and MATLAB (Mathworks Inc., MA). Dynamic balance was quantified using the range of *H*. To further understand the relationship with scored performance, performance deductions were calculated based off of the Code of Points [3]. Trials where the gymnast fell off the beam were not included in the analyses and the beam walking trials were cropped to only include steady-state walking. Linear regressions were performed between the range of *H* during beam walking and the BHS range of *H* and deductions to determine if correlations exist between balance control during beam walking and performance of the BHS.

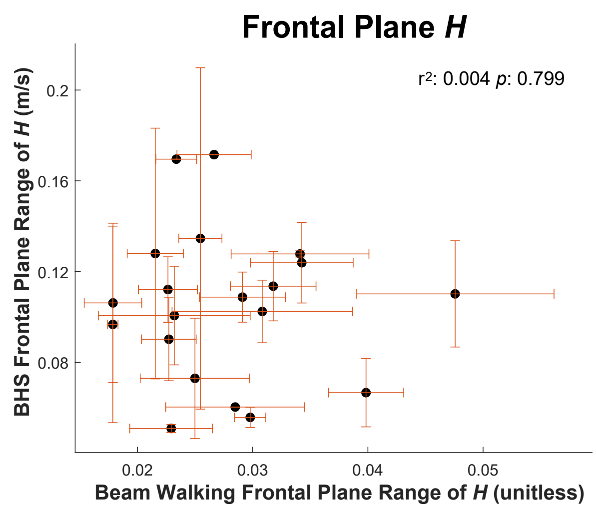

Figure 1: Normalized frontal plane range of whole-body angular momentum (*H*) for the back handspring step out (BHS) trials, which were normalized by height and mass. The beam walking trials were normalized by height, mass and walking speed.

Results & Discussion: Contrary to our hypothesis, frontal plane balance control during beam walking was not a predictor of balance control during the BHS (Fig. 1) or performance of the BHS, determined by deductions ($r^2 = 0.02$). While beam walking performance is a predictor of balance control in a number of populations [10], gymnasts are likely skilled enough at beam walking that differences between gymnasts cannot be used a metric of BHS skill. Interestingly, beam walking balance control was not affected by age ($r^2 = 0.20$) or years of participation in gymnastics ($r^2 = 0.06$). This lack of a difference is contrary to a previous study finding that differences in beam walking ability varies across skill levels in gymnastics [12], perhaps due to a wider age range of the gymnasts analysed in the present study.

Significance: Given the popularity and risks in gymnastics, more research is needed to understand the neuromuscular control and biomechanics of various skills. This work found that the simple motor task of beam walking was not sufficient at predicting balance control during the BHS and its subsequent scored performance. Furthermore, these results give more insight into dynamic balance and motor control in gymnasts that could give insights into other athletic populations.

Acknowledgements: This project was supported in part by the National Science Foundation Graduate Research Fellowship Program.

References: [1] SFIA (2019) Gymnastics Participation Report; [2] Farana et al., (2023), *Sports Biomech.* 22; [3] FIG Code of Points (2022); [4] Henrichs (2005), *WWU*; [5] Koh et al., (1992), *Am. J. Sports Med.* 20; [6] Ede et al., (2021), *Sports Biomech.*; [7] Hak et al., (2013), *Clin Biomech* 28; [8] Neptune & Vistamehr (2019), *J. Biomech. Eng.* 141; [9] Nott et al., (2014) *Gait Posture* 39; [10] Uematsu et al., (2018) *Exp. Gerontol.* 114; [11] Falces-Prieto et al., (2022) *Sci. Rep.* 12; [12] Peltenburg et al., (1982) *Int. J. Sports Med.* 3.

IMPROVING DATA EFFICIENCY AND ACCURACY OF IMU-DRIVEN BIOMECHANICAL ASSESSMENT VIA SELF-SUPERVISED LEARNING

Tian Tan[1*], Peter B. Shull[2], Akshay S. Chaudhari[1]
[1]Department of Radiology, Stanford University, Stanford, CA, USA
[2]School of Mechanical Engineering, Shanghai Jiao Tong University, Shanghai, Shanghai, China
*Corresponding author's email: alanttan@stanford.edu

Introduction: Biomechanical measurement traditionally relies on force plates and marker-based motion tracking, confining the measurement environment and limiting the scale of biomechanical studies. Wearable inertial measurement units (IMUs) could enable human movement monitoring in natural environments in larger cohorts. Recently proposed deep learning techniques hold promise to enable IMU-driven gait assessment, however these techniques typically require a large amount of IMU data as well as synchronized force plate and marker data that serve as labels for model training. Such datasets are rare because their collection requires trained personnel to operate in-lab devices, thus costly and time-consuming. Self-supervised learning may mitigate this challenge of data scarcity. It aims to pre-train deep learning models for representation extraction based on a vast amount of "unlabeled" data. Then, the pre-trained models can be fine-tuned to various downstream estimation tasks with "labeled" data. In this study, we evaluated the benefits of self-supervised learning based on an "unlabeled" IMU dataset with 6.6 hours of human movements, which reduced requirements on the size of downstream "labeled" datasets by 60% - 90% for loading rate, ground reaction force, and knee flexion moment estimation.

Methods: An "unlabeled" dataset [1] consisting of 90 subjects performing 21 movements while wearing 17 IMUs was segmented into windows for self-supervised model pre-training. The accelerometer and gyroscope data from the same window contain mutual underlying information, and pre-training aims to learn to extract this relationship using a convolutional neural network (ResNet-50 [2]). To accomplish this, the accelerometer and gyroscope data were first fed into the model to generate their respective representations. The model was then optimized to increase the similarity between the accelerometer and gyroscope representations of the same window while minimizing those from different windows using a contrastive loss [3].

To evaluate the performance of the self-supervised model, we used three downstream datasets that are substantially different from pre-training dataset in terms of subject numbers, IMU numbers, and gold-standard measurements, i.e., using 1 IMU for estimating loading rate among 15 subjects [3], using 2 IMUs for estimating peak ground reaction force among 21 subjects [4], and using 8 IMUs for estimating peak knee flexion moment among 17 subjects [5]. The self-supervised model was fine-tuned on each downstream dataset to estimate the corresponding biomechanical parameter. It was also compared against a randomly-initialized model that is used in conventional supervised learning. To ensure a fair comparison, both models were evaluated via five-fold cross validation, with subjects randomly assigned to folds. For each fold, models were trained with the same number of sufficiently large training steps.

Results & Discussion: The self-supervised model matched the performance of a conventional randomly initialized model while reducing training data requirements by 90% for loading rate estimation, by 60% for peak ground reaction force estimation, and by 75% for peak knee flexion moment estimation (Fig. 1). When using the entire datasets [4] – [6] for training, the self-supervised model significantly improved the mean correlation coefficients from 0.87 to 0.91 for loading rate estimation, 0.79 to 0.83 for peak ground reaction force estimation, and 0.87 to 0.90 for peak knee flexion moment estimation (Fig. 1).

Although the pre-training dataset we used was larger than downstream datasets, scaling the size of pre-training dataset may further improve the effectiveness of self-supervised learning. Future research may consider using synthetic IMU data or simulated human movement to generate large-scale data for self-supervised learning.

Significance: Self-supervised learning with a large "unlabeled" IMU dataset for model pretraining can substantially improve data efficiency or improve the accuracy of deep learning. This approach could unlock newer and broader use cases of IMU-driven assessment where only limited "labeled" data is available.

Acknowledgements: This work was supported by the Joe and Clara Tsai Foundation through the Wu Tsai Human Performance Alliance.

References: [1] Ghorbani et al. (2021), *Plos One* 16(6); [2] He et al. (2016) *IEEE CVPR*; [3] Alayrac et al. (2020) *NIPS*; [4] Tan et al. (2021), *IEEE JBHI* 25(4); [5] Camargo et al. (2021), *J Biomech* 119; [6] Tan et al. (2022), *IEEE TII* 19(2).

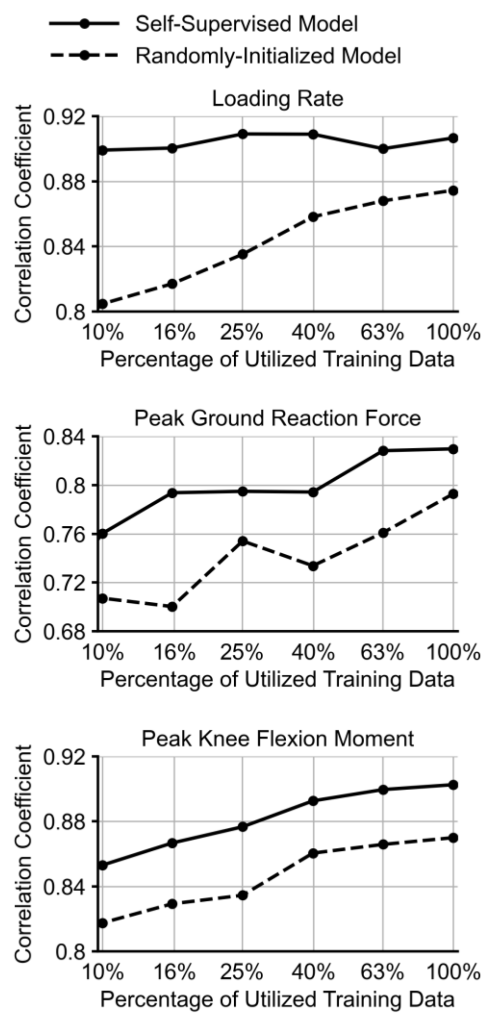

Figure 1: Correlation coefficients of biomechanical parameter estimation for a range of reduced training set sizes. Self-supervised models outperformed randomly-initialized models for all sizes.

THE ASSOCIATION BETWEEN GRIP STRENGTH AND UPPER BODY POWER IN U.S. MARINE INFANTRY

Luke Brown[1], Robert Murphy[1], Rebecca Zifchock[1], Douglas Jones[2], Pinata H. Sessoms[2], Amy Silder[2]*
[1]United States Military Academy, West Point, NY; [2]Naval Health Research Center, San Diego, CA
*Corresponding author's email: amy.b.silder.civ@health.mil

Introduction: U.S. Marines rely on upper body strength and power to accomplish tasks such as carrying heavy weapons and gear, rappelling, combat grappling, and marksmanship. Extended field training and operational missions in garrison often lead to inadequate nutrition and poor sleep, which ultimately lead to the warfighter's inability to optimally recover. Early identification of the factors that lead to reduced upper body strength and power would enable leadership to predict and mitigate factors that deter military operational readiness and increase injury risk.

Grip strength is cost effective and simple, making it valuable for use in the clinic or field. Numerous studies have associated grip strength with overall health and mortality in older adults [1], but little data exist on whether grip strength can be used to predict the health and performance of young, physically active adults. One study found that higher grip strength was predictive of better marksmanship in police academy recruits [2]. If similar associations exist between grip strength and muscular power, this will lend valuable insights into the performance of many physically demanding tasks required in military training and combat situations.

The purpose of this study was to investigate the relationship between grip strength and ballistic pushup performance in U.S. Marines. We hypothesized that higher grip strength would be strongly correlated with upper body peak power and ballistic pushup height.

Methods: A total of 71 male U.S. Marines [mean (standard deviation), age 22 (4) years; height 174 (6) cm; mass 80 (11) kg] provided informed consent to participate in this study. All participants did three ballistic pushups on a ForceDecks® dual force plate system (VALD Performance, Newstead, Australia). They were instructed to get their chest as high off the plate as possible. ForceDecks software was used to estimate peak power, peak power normalized to upper body mass, and pushup height. Participants also completed three maximum grip strength tests using a hand-held dynamometer with their dominant hand, defined as the hand they would use to shoot a weapon. Testing was conducted with their arm straight and slightly away from their body. Pearson's correlation was used to investigate the relationship between the maximum grip strength and ballistic pushup performance as represented by peak power, peak power normalized to upper body mass, and maximum ballistic pushup height.

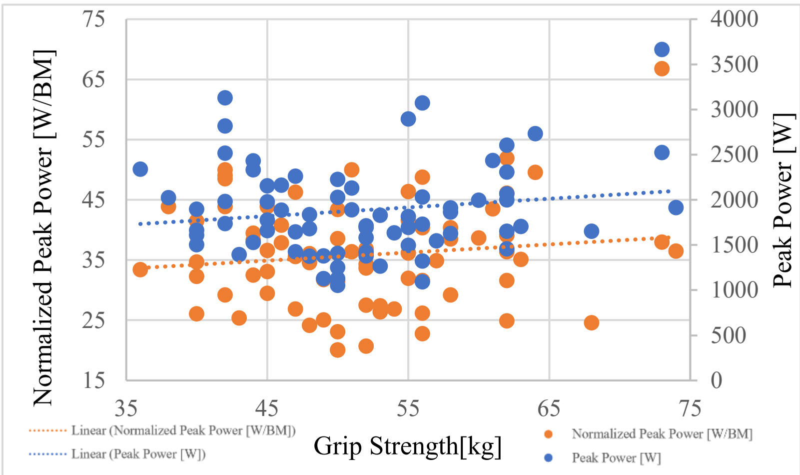

Figure 1: Association between grip strength, peak power normalized to upper body mass (BM), and peak power.

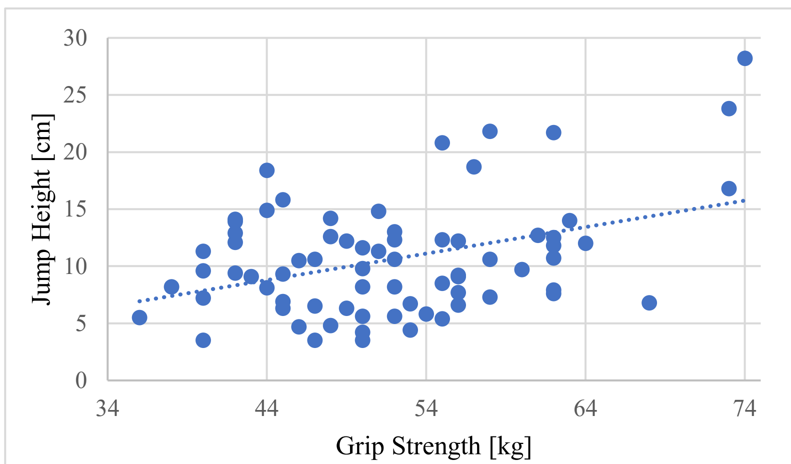

Figure 2: Association between ballistic pushup jump height and grip strength.

Results & Discussion: In contrast to our hypothesis, grip strength was weakly correlated with peak power (Figure 1, r=0.16, p<.001) and peak power normalized to body mass (Figure 1, r=0.13, p<.001). A moderate positive correlation was found between grip strength and pushup height (Figure 2, r=0.39, p<.001). The ballistic pushup has been shown to be a reliable assessment to predict upper body power [3], and grip strength has been shown to be a useful predictive assessment for overall health in older adults [1]. Despite the important predictive capabilities of each individual test in other populations, the results of our study indicate that grip strength may not be useful to assess dynamic upper body strength and power in warfighters.

Significance: Although grip strength is a simple, cost-effective test, it is likely not useful to assess upper body power in young, healthy adults. Given that grip strength has previously been correlated with better marksmanship [2], it is possible that correlations exist in military tasks that require motor skills such as throwing a grenade. Further analysis of asymmetry during the ballistic pushup and its relationship to arm dominance may lend insights into rappelling, physical fitness scores, and upper body injury risk.

References: [1] Bohannon (2019), *Clin Interv Aging* (14); [2] Orr et al. (2017), *Int. J. Environ. Res. Public Health* 14(8); [3] Wang et al. (2017), *J Strength Cond Res* 31(5).

Assessing Test-retest Reliability of Nonlinear Dynamic Outcomes from Functional Near-Infrared Spectroscopy Brain Measurement

Hector Flores[3]; Isabellah Mayoral Ortega[3]; Kelsi Petrillo, BS[3]; Bilaval Javed, MD[1,2,3]; Nima Toosizadeh, PhD[1,2,3]
[1]Arizona Center on Aging; [2]Division of Geriatrics, GIM and PM, Department of Medicine; [3]Department of Biomedical Engineering, College of Engineering; University of Arizona, Tucson
*Corresponding author's email: ntoosizadeh@arizona.edu

Introduction: Cognitive impairment, like Alzheimer's Disease (AD), is a prevalent issue in the United States that is expected to worsen in the coming years. Current screening methods for cognitive impairment rely on MRI which can be intimidating to patients, especially older adults. This creates the need for a simple, accurate, patient-friendly, and repeatable screening method to assess early onset symptoms of cognitive impairment. One way of assessing cognitive impairment is measuring nonlinear brain complexity using Sample Entropy and Multiscale Entropy (MSE) analysis. Studies show that AD is related to low levels of nonlinear complexity due to neural death and disconnections[1]. To measure complexity, functional Near-Infrared Spectroscopy (fNIRS) is used as a non-invasive tool for measuring blood oxygenation/deoxygenation levels in the brain in the form of a soft optode headcap (Figure 1). In our previous work, fNIRS was combined with a previously validated Upper Extremity Function (UEF) test to assess cognitive impairment[2,3]. The goal of the current study was to assess test-retest reliability of MSE outcomes from fNIRS with UEF dual-tasking.

Figure 1: Artinis Brite fNIRS optode headcap.

Methods: Ten healthy participants were recruited ranging from 19 to 28 years old. Participants completed the Montreal Cognitive Assessment (MoCA) to measure cognitive status. Then, they performed a variety of tasks which included resting, counting backwards from a number by intervals of 3, flexing and extending the elbow, and completing a dual task that combined both flexing and extending elbow and cognitive task of counting simultaneously. Participants completed each task once which was preceded and followed by a resting period while wearing the fNIRS headcap, which recorded data across 22 channels covering the temporal, parietal, and frontal regions of the brain for the entire duration of the test. The data across the channels was grouped by brain regions. One week later, the individuals were reevaluated using the exact same protocol. Sample entropy (Equation 1) was used to quantify complexity based on pattern reproducibility in a time series using logarithmic likelihood[1]. The MSE equation (Equation 2) was used to calculate sample entropy at 5 different time scales representing 5 different time windows for graining data. This includes Scales 1, 5, 10, 15, and 20 which represent dynamics across varying scale factors[3]. Statistical analysis was performed in JMP using Intraclass Correlation Coefficient (ICC), to assess test-retest reliability using two-way mixed effect models with an absolute agreement definition.

$$SampleEn\,(m, r, n) = -\ln \frac{P_{m+1}(r)}{P_m(r)}$$

Equation 1: Sample entropy formula, N is time series length, m is pattern length, r is tolerance radius, and P is probability of radius falling within tolerance.

$$y_j^l = \frac{1}{l} \sum_{i=(j-1)l+1}^{jl} x_i, 1 \leq j \leq \frac{N}{l}$$

Equation 2: MSE formula; N is time series length, l is time scale, and y is time

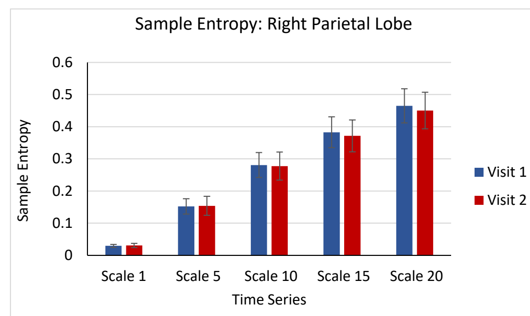

Figure 2: Average ICC with no bias across right parietal lobe between rest and dual task.

Results and Discussion: The maximum ICC values were achieved during Scale 5 which yielded an ICC value of 0.79 and scale 10 which yielded a value of 0.81 (Figure 2 and 3). According to the ICC thresholds, these values represent good reliability (above 0.75). The results from the statistical analysis showed that on average, ICC values increased from rest to dual task, with 8.8% difference for time scale 5 and 6.5% difference for time scale 10 (Figure 3).

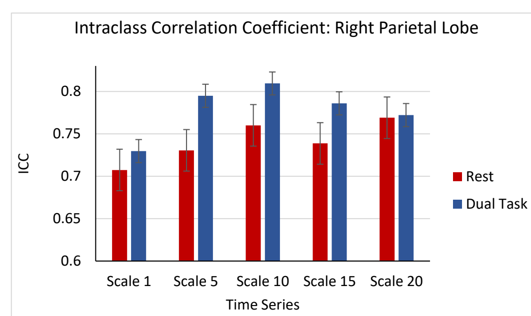

Figure 3: Average sample entropy values across right parietal lobe between rest and dual task.

Significance: ICC values indicate good test-retest reliability of fNIRS data. The increase in ICC values from rest to dual task suggests that the controlled stress on the brain increases the accuracy between fNIRS measure across two visits. It is important to assess the precision and accuracy of fNIRS as a screening tool to continue its use in clinical trials. This repeat study is part of a larger ongoing trial which compares readings from younger participants to older adults who vary in levels of cognitive impairment. ICC analysis will be revisited routinely as more subjects are recruited.

Acknowledgements: Funding from the Arizona Alzheimer's Consortium and The University of Arizona BIO5 Institute support this project. The findings of this manuscript are those of the authors and not of the sponsor.

References: [1] Pena et al. (2022) *J Neuroimaging* (1-13); [2] Ehsani et al. (2020), *Computers in Biology and Medicine* (103705); [3] Toosizadeh et al. (2019), *Scientific Reports* (10911)

APPLICATION OF MACHINE LEARNING ALGORITHMS TO PREDICT ELBOW BIOMECHANICAL EFFICIENCY

Richard J. Boergers*, Manfred Minimair, Michael Ciminiello, Emily Giannini, Natasha Rosa, Zachary Sylvester, Anthony Vischovich
Seton Hall University, South Orange, NJ
*Corresponding author's email: Richard.boergers@shu.edu

Introduction: Baseball pitching is a complex movement involving rotations of multiple body segments that are accelerated in sequential order through a kinetic chain. High pitch velocities are recognized as a metric to indicate performance, however it is known that there are concurrent high joint forces and torques to the elbow which have been linked to injury [1]. Motion analysis is useful for predicting what kinetic and kinematic factors are associated with large elbow torques and high pitch velocity. Recently, a research group applied a linear regression model to assess biomechanical efficiency which refers to fastball velocity per unit of normalized varus torque [2]. Another research group applied machine learning models to predict elbow varus torque [3]. The goal of this study was to utilize unique machine learning models to determine the importance of the features for approximating the biomechanical efficiency of pitching.

Methods: Nine collegiate pitchers (age = 20.4 ± 1.8 years, height = 1.85 ± 0.05 m, mass = 87.4 ± 7.6 kg) each threw a bullpen session of fastball pitches into a catch net at a regulation distance from the mound to home plate (18.4 m). Twenty-five fastballs (per pitcher) were extracted for this study in which 3D motion data was collected using a 47 reflective marker set and a 9-camera motion analysis system (Qualisys, Göteborg, Sweden) at a sampling rate of 240 Hz. Joint kinematic and kinetic data were calculated with a 14-segment, 6 degrees-of freedom (DOF) full-body model configured in Visual3D (C-Motion, Germantown, MD). The pitch cycle data began at lead leg foot contact (0%) and ended at ball release (100%). Data were divided into ten equal time intervals (0%-10%, 11%-20%…etc). For each feature (variable) in the data, each interval was assigned the average of the corresponding recorded values, resulting in a data set with 453 features and 220 rows, each representing the motion of a single pitch. Biomechanical efficiency was approximated by regression trees, providing scores for the feature importance [4], [5]. R^2 scores were used to measure the regression performance. For the current data set, the standard computational approach for regression trees led to R^2 ranging up to 0.79 with standard deviations (SD) of up to 0.28 of the R^2 scores computed for testing data obtained by cross-validation. Subsequently, the tree computation was enhanced with a search for relevant feature subsets by recursive feature elimination [4], resulting in trees with R^2 ranging from 0.84 to 0.85 with cross-validation standard deviations ranging from 0.17 to 0.19. Further reducing the SD, multiple trees were combined with bagging and with random forest procedures. Combining up to ten trees resulted in R^2 ranging from 0.77 to 0.85 and respectively from 0.83 to 0.90, both with SD ranging from 0.15 to less than 0.17, while larger tree ensembles did not exhibit any lower SD.

Results & Discussion: The computed regression trees approximate biomechanical efficiency with R^2 ranging from 0.77 to 0.90 and thus outperform reported linear methods having $R^2 = 0.27$ (explaining only 27% of the variance in biomechanical efficiency). The selections of features computed corresponds well to important aspects of the pitchers' motions. Maximal elbow torque is ranked as most important which is expected because biomechanical efficiency directly depends on maximal elbow torque, thus the ranking substantiates the interpretability of the trees. The models identified critical features often cited in the literature between 70%-80% of the pitch cycle which is known to be the time a pitcher transitions from the cocking phase to arm acceleration. By algorithmic design and due to the specific data available (220 pitches and 453 features), the different regression trees naturally emphasize different relationships among biomechanical efficiency and the features in the data. Table 1 illustrates importance of features from two of our best models.

Table 1. Features identified by best models from using regression trees with bagging and random forests

Model A	
Feature	**Relative Importance (range 0 to 1)**
Pitching shoulder abduction angle at 70-80% of pitch cycle	0.8681
Maximum elbow varus torque	0.0848
Elbow varus torque at 70-80% of pitch cycle	0.0453
Pitching elbow extension angular velocity at 70-80% of pitch cycle	0.0018

Model B	
Feature	**Relative Importance (range 0 to 1)**
Maximum elbow varus torque	0.9452
Lead hip angular flexion velocity at 70-80% of pitch cycle	0.0501
Pitching elbow extension angular velocity at 70-80% of pitch cycle	0.0018

Significance: This project applied a unique machine learning technique to analyze baseball pitching data for impactful factors related to elbow biomechanical efficiency. Previously, linear regression was typically applied to data at only 3 critical incidents (lead leg foot contact, shoulder maximal external rotation and ball release), however we used 10 equal time intervals between lead leg foot contact and ball release, which allows for inclusion of over 453 features. Our top models selected factors that have been found to be significant in previous studies that used more simplistic methods. This statistical approach may be advantageous in the future for evaluation of impactful factors.

Acknowledgements: This work was supported by the Opportunity Meets Innovation Challenge grant award made to Seton Hall University by the New Jersey State Office of the Secretary of Higher Education and the Academy for Applied Analytics and Technology at Seton Hall University.

References: [1] Chalmers et al. (2020), *Ortho J Sport Med* 8(3). [2] Crotin et al. (2022), *Am J Sport Med 50(12).* [3] Nicholson et al. (2022), *Am J Sport Med* 50(1). [4] James et al. (2021), *An Introduction to Statistical Learning: with Applications in R*. NY. Springer. [5] Pedregosa et al. (2011), *J Mach Learn Res* 12(85).

KNEE SYMPTOMS ARE NOT ASSOCIATED WITH FREE-LIVING CADENCE AMONG ADOLESCENTS WITH ANTERIOR CRUCIATE LIGAMENT RECONSTRUCTION

Christopher Kuenze[1*], Katherine Collins[2], Dante D. Goss[1], Karin A. Pfeiffer[2], Michelle C. Walaszek[1], Matthew Harkey[2]
[1]University of Virginia, Department of Kinesiology, Charlottesville, VA
[2]Michigan State University, Department of Kinesiology, East Lansing, MI
*Corresponding author's email: ckuenze@virginia.edu

Introduction: Anterior cruciate ligament reconstruction (ACLR), reduced gait speed, and persistent knee symptoms are risk factors for development of knee osteoarthritis (OA). ACL injury and ACLR most commonly occur in individuals who are less than 20 years of age. Young individuals who have undergone ACLR walk at slower average walking cadences during free-living when compared to heathy matched controls and slower gait speed is associated with biomarkers of cartilage degradation [1]. During the first year after ACLR, more than 40% of individuals report unacceptable knee symptoms [2]. However, it is unclear if walking cadence under free-living conditions is associated with knee-related symptoms among this population. Therefore, the purpose of this study was to compare accelerometer measured, free-living cadence between adolescents who report acceptable or unacceptable knee symptoms during the first year after ACLR. Due to the high prevalence of unacceptable symptoms and slow average free-living cadence among individuals with ACLR, we hypothesized that adolescents reporting unacceptable knee symptoms after ACLR would display slower free-living cadence.

Methods: Participants were recruited for this cross-sectional study from a single, university-affiliated orthopaedic sports medicine clinic. Participants were 13-18 years old and had undergone primary, unilateral ACLR 4-9 months prior to enrolment. Participants completed the Knee Injury and Osteoarthritis Outcome Score (KOOS) symptoms, pain, quality of life (QOL), and activities of daily living (ADL) subscales. Patient acceptable symptom state (PASS) for each KOOS subscale has been established as symptoms > 57.1%, pain > 88.9%, QOL > 62.5, and ADL= 100.0%. The Luyten PASS criteria operationally define unacceptable knee symptoms as scoring less than the PASS score on at least 2 of the subscales [2]. Participants were instructed to wear an Actigraph WGT3x or Link accelerometer (Actigraph, LLC., Pensacola, FL) for seven days during all waking hours. Data were collected at 30 Hz and processed in 60-second epochs [1]. Wear time was validated at 600 min/day for at least 4 days. Non-wear time was removed, and all remaining data were used to calculate the number of total minutes spent and the median cadences in light (60-100 steps per minute) and light to moderate (60-130 steps per minute) activity intensities. Independent samples t-tests or Fisher's exact tests compared demographics between individuals with and without unacceptable knee symptoms. One-way ANCOVAs and partial eta squared effect sizes compared time in light and light to moderate cadence as well as the median cadence observed within each cadence range between individuals with and without unacceptable knee symptoms while controlling for minutes accelerometer wear time.

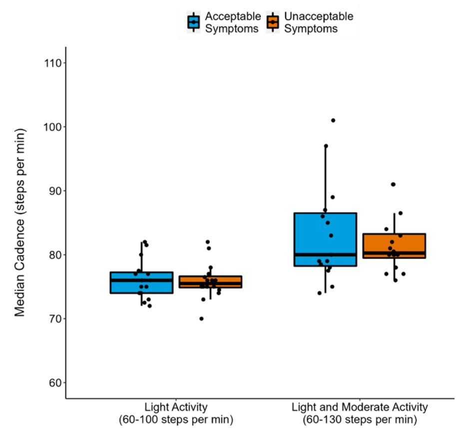

Figure 1: Comparisons of median cadence values between the acceptable and unacceptable symptoms groups when data are limited to light activities (i.e., slow walking) and light to moderate activities.

Results & Discussion: Thirty-one individuals were classified as having acceptable symptoms (N=15, sex=11 females, age=15.9±1.3 years, time since surgery=6.3±0.9 months) or unacceptable symptoms (N=16, biologic sex=9 females, age=16.0±1.1 years, time since surgery=5.9±2.2 months). Symptom groups did not differ based on age (p=0.880), sex (p=0.320), or time since surgery (p=0.454), but the unacceptable symptoms group wore their accelerometer 1,518 minutes more than the acceptable symptoms group (p=0.028). This finding justified including accelerometer wear time as a covariate because the number of minutes in a given activity intensity may be inflated if a participant had greater wear time. There were no between group significant differences in median cadence during light ($F_{1,28}$=0.003, p=0.954, η^2p=0.001) nor light to moderate intensity activities ($F_{1,28}$=0.148, p= 0.703, η^2p=0.005) (Fig 1.). Similarly, there were no significant between group differences in total minutes spent in light intensity activities ($F_{1,28}$=0.350, p=0.559, η^2p=0.012) nor light to moderate activities ($F_{1,28}$= 0.497, p= 0.487, η^2p= 0.017). These findings indicate that the presence of symptoms does not appear to influence walking cadence in this population.

Significance: The findings of this study indicate that while slower walking cadence and persistent knee symptoms are risk factors for OA development, the presence of unacceptable knee symptoms may not influence walking cadence among this adolescent patient population. Consequently, independent interventions (e.g., gait biofeedback, pain management) may be required to address persistent functional limitations and symptoms with the goal of enhancing quality of life and mitigating the long-term risk of OA development.

Acknowledgements: This work was partially supported by a grant from the Great Lakes Athletic Trainers' Association.

References: [1] Lisee CM, Montoye AHK, Lewallen NF, Hernandez M, Bell DR, Kuenze CM. Assessment of Free-Living Cadence Using ActiGraph Accelerometers Between Individuals With and Without Anterior Cruciate Ligament Reconstruction. J Athl Train. 2020 Sep 1;55(9):994-1000. [2] Harkey MS, Baez S, Lewis J, Grindstaff TL, Hart J, Driban JB, Schorfhaar A, Kuenze C. Prevalence of Early Knee Osteoarthritis Illness Among Various Patient-Reported Classification Criteria After Anterior Cruciate Ligament Reconstruction. Arthritis Care Res (Hoboken). 2022 Mar;74(3):377-385. Epub 2022 Feb 11.

PREDICTING WARFIGHTER PHYSICAL PERFORMANCE AND READINESS METRICS FROM SENSOR DATA COLLECTED DURING RUCK MARCH

Preetish Rath[1*], Seth Elkin-Frankston[2], Amy Silder[3], J. Josiah Steckenrider[4], Victoria G. Bode[2], Michael C. Hughes[1]
[1]Tufts University, Medford, MA; [2]Combat Capabilities Development Command (DEVCOM) Soldier Center, Natick, MA; [3]Naval Health Research Center, San Diego, CA; [4]United States Military Academy, West Point, NY
*Corresponding author's email: Preetish.rath@tufts.edu

Introduction: A ruck march is characterized by walking over rough terrain for a prolonged period, carrying military gear weighing approximately 50% of body weight. This activity is essential during military training and operations; however, there is limited research on the utility of time-series data collected from wearable sensors to assess warfighter mission performance and readiness. Our goal is to predict post-march warfighter physical performance and readiness metrics from inertial measurement unit (IMU) data collected during a loaded ruck march. A successful prediction model could enable commanders to monitor warfighters' data to identify individuals who are likely to exhibit decreased readiness (e.g., poor balance, torso strength) during operational missions.

Methods: Two cohorts of U.S. Army infantry warfighters (1st cohort: n=70; age: 22.9 ± 3.2 years; body mass index (BMI): 26.09 ± 3.5 kg/m^2, and 2nd cohort: n=71; age: 23.1 ± 3.1 years; BMI: 25.4 ± 3.9 kg/m^2) completed self-paced, 10.5–13.2 km (3.5–4.5 hour) ruck march on hard top. Physical performance and readiness metrics such as mid-thigh isometric pull and anterior-posterior balance (radius of the 95% center of pressure confidence ellipse with the warfighter's eyes closed) were collected after the ruck march. Warfighters achieved a mean mid-thigh isometric pull score of 115 N and a mean anterior-posterior balance score of 3.5 cm. Supervised regression was used to predict a warfighter's physical performance from a torso-mounted IMU (measuring torso lean in the medial-lateral and anterior-posterior directions over time) comparing two existing machine learning models (LASSO[1] and LightGBM[2]) and a novel probabilistic regression model called the prediction-constrained hidden Markov model (PC-HMM)[3,4]. All models were trained and evaluated separately on the 1st and 2nd cohorts to demonstrate model consistency on independent populations.

Results & Discussion: While predicting mid-thigh isometric pull and anterior posterior balance from IMU data, we found that our proposed PC-HMM performed better than other existing models. While predicting mid-thigh isometric pull on the 2021 cohort, our PC-HMM achieved a mean absolute error (MAE) of 20 N (with 95% bootstrap CI: 17–23) across squads (compared with a MAE of 25 N (95% bootstrap CI: 22–27) achieved by LASSO and MAE of 25 N (95% bootstrap CI: 22–28) achieved by LightGBM). Similarly, while predicting anterior-posterior balance on the 2021 cohort, our PC-HMM achieved a MAE of 1.1 cm (95% bootstrap CI: 1.0–1.3) across squads (compared with a MAE of 1.5 cm (95% bootstrap CI: 1.3–1.6) achieved by LASSO and MAE of 1.4 cm (95% bootstrap CI: 1.3–1.5) achieved by LightGBM). Similar performance was observed on the 2nd cohort of warfighters. Figures 1 and 2 illustrate the performance results on the 1st and 2nd cohorts, respectively.

Significance: Time-series data collected from wearable sensors during ruck march helps to predict warfighter balance and torso strength, which are critical factors in determining their readiness for operational missions. The capability to assess and predict warfighter readiness will have a profound impact on mission planning and operational performance. Decision leaders will have the ability to select the most capable warfighter for an objective based on individual current and future readiness levels, and mission demands.

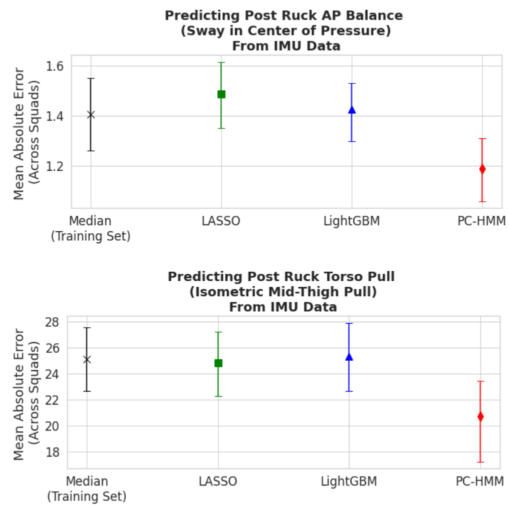

Figure 1: Performance of predicting A) anterior-posterior balance (AP balance; units: cm) and B) mid-thigh isometric pull (torso pull; units: N) (warfighter physical performance metrics) using different models on **1st cohort**. Our proposed PC-HMM achieves the least mean absolute error compared with other models.

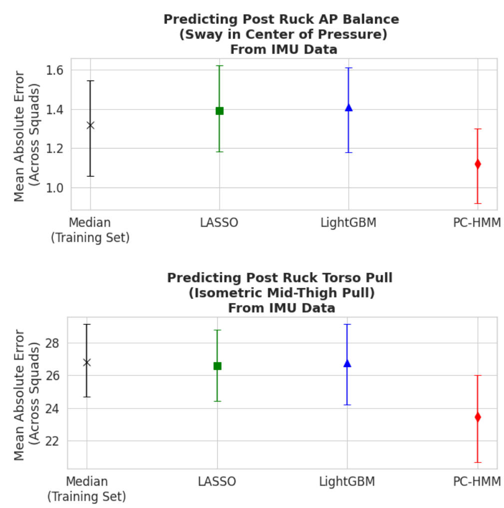

Figure 2: Performance of predicting A) anterior-posterior balance (AP balance; units: cm) and B) mid-thigh isometric pull (torso pull; units: N) (warfighter physical performance metrics) using different models on **2nd cohort**. Our proposed PC-HMM achieves the least mean absolute error compared with other models.

Acknowledgements: This work was supported by the U.S. Army Combat Capabilities Development Command Soldier Center (DEVCOM SC) as part of the Measuring and Advancing Soldier Tactical Readiness and Effectiveness (MASTR-E) program.

References: [1] Tibshirani, R. (1996) *J R Stat Soc Series B Stat Methodol* 58(1); [2] Ke et al. (2017) *Adv Neural Inf Process Syst* 30; [3] Rath et al. (2022) NeurIPS 2022 Workshop on Learning from Time Series for Health; [4] Hughes et al. (2018) AISTATS PMLR 84.

SLEEP QUALITY & ITS AFFECT ON DUAL TASK COST WHEN EXAMINING STEP LENGTH IN HEALTHY ADULTS

C. Mattie Higgins[1*], Hyeon Jung Heselton[2], Dawn Venema[3], Julie B. Boron[2], Jennifer M. Yentes[1]
[1]Department of Kinesiology & Sport Management, Texas A&M University
[2]Department of Gerontology, CAPACITY Lab, University of Nebraska at Omaha
[3]Physical Therapy Program, University of Nebraska Medical Center
*Corresponding author's email: mattiehiggins@tamu.edu

Introduction: Dual-task paradigms are defined as the ability to partake in two tasks concurrently, commonly a motor task paired with a cognitive task; it is vital to being able to perform daily tasks such as walking while talking on the phone. These paradigms are used to assess an individual's attentional resources[1]. Attentional capacity is commonly limited by the arousal of the individual, and persons with inadequate sleep will often observe attentional lapses[2]. The purpose of this study was to examine if sleep quality affects the ability to walk while carrying on phone conversations (common and uncommon topics such as favorite foods and qualities they most value in someone, respectively). It was hypothesized that sleep quality may predict the dual task cost of walking, especially when carrying on an uncommon conversation.

Methods: A total of 39 younger-, middle-, and older-adults (23.1±1.8; 45.1±7.2; 74.5±3.9 yrs) participated in two randomized visits: dual and single task. On the first visit, participants completed the Pittsburgh Sleep Quality Index (PSQI), consisting of 19 self-rated questions, where higher scores indicated worse sleep quality[3]. At the start of each visit, participants rated their interest, on a 5-point Likert scale, in different common and uncommon conversation topics.

During the dual task visit, participants walked around a 20 m loop in the laboratory where one of the straight sides of the loop was a 6 m gait mat (Zeno™Walkway, Protokinetics LLC, Havertown, PA). Participants completed two- randomized, 3-minute walking trials at their self-selected speed around the loop. Both trials consisted of walking and talking on the phone, one trial of each common and uncommon topic conversations. 5-minute rest was given between trials. Conversations were conducted over a cellular phone. Topics of the conversations were selected based upon the participants' ratings. During the single task visit, participants completed two 3-minute telephone conversations and then completed two 3-minute walking trials. Step length gait data were used to measure dual task cost (DTC) with the following equation: (conversation walking - no conversation walking) / no conversation walking)*100. ANCOVA analysis was run with DTC as the dependent variable, PSQI as the independent variable, and age as a covariate.

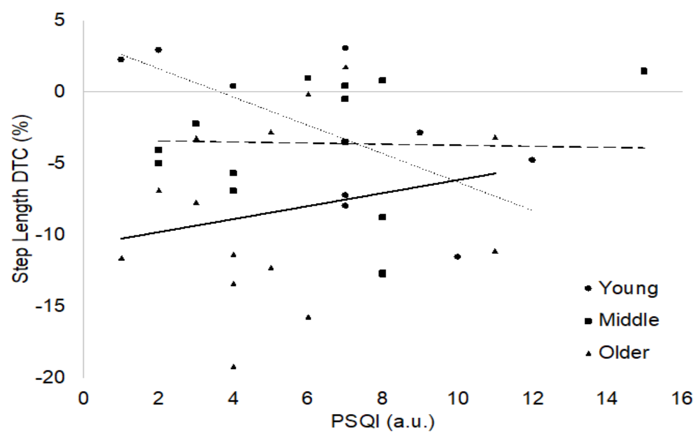

Figure 1: Scatter plot of PSQI and Step Length DTC for all age groups (circle=young; square=middle; triangle=older). Trendlines demonstrate best fit lines for common conversation topics

Results & Discussion: The current data did not provide significant evidence to accept our hypothesis. Before age was added to the model, there was indication that PSQI was predictive of DTC in the common conversation condition, especially in the older adults (Figure 1). However, after controlling age, PSQI did not indicate significant effect on DTC. During common conversations, the regression was significant ($p=0.037$); however, upon inspection of the coefficients, PSQI was not significant ($p=0.579$), while age was significant ($p=0.011$). Thus, age appeared to be the driving force for the association, not PSQI scores. During uncommon conversations, the overall regression was not significant ($p=0.067$).

In both cases, when the data were controlled for age, there was no significant relationship between PSQI and DTC. There are several potential reasons as to why PSQI was not a strong indicator of DTC. The gait measure of step length may not have been sensitive to attentional control. During walking, it has been found that more active control is needed for movement in the mediolateral plane, rather than the anteroposterior plane of movement[4]. Thus, step width might have been more sensitive to changes in attentional demands and should have been the gait measurement used to calculate DTC. Step length was used for this study; however, step width was one of many measurements collected by the gait mat and can be investigated in future studies. In this study, sleep quality was measured using a survey. Using an activity monitor, may provide more quantifiable sleep quality data rather than a subjective survey such as PSQI. Another limitation of this study was the small sample size which can explain the high variability seen within the participants. More participants would be needed for future studies to gain a clearer understanding of the association sleep quality has with dual task walking. In conclusion, this present study does not support that sleep quality has a negative effect on step length dual task cost. Future studies should consider examining step width, using an activity monitor to add an objective sleep quality indicator, as well as considering looking at the mental dual-task cost since this study only examined physical dual-task cost.

Significance: Performing multiple tasks concurrently is a common daily activity, and if poor sleep leads to decreased attentional capacity, adults with poor sleep habits may be at higher risk for falls and injury. This study highlights the needs to examine the association between DTC in more participants to better understand these risks.

Acknowledgements: Thank you to Judith Kim for collecting the data, the amazing team at the University of Nebraska Omaha for the data, and Dr. Jenna Yentes for the guidance and support.

References: [1] VanRullen, R., Reddy, L. & Koch, C. (2004), [2] Chua, E. C.-P., Fang, E. & Gooley, J. J. (2017), [3] Buysse, D. J., Reynolds, C. F., Monk, T. H., Berman, S. R. & Kupfer, D. J. (1989)., [4] Bauby, C. E. & Kuo, A. D. (2000).

REGULARITY OF CENTER OF PRESSURE REFLECTS TASK DIFFICULTY DURING STANDING DUAL-TASK

Jack Manning[1*], Emerson Sebastião[2], Jennifer M Yentes[1]
[1]Texas A&M University, Department of Kinesiology and Sport Management
[2]Northern Illinois University, Department of Kinesiology and Physical Education
[*]corresponding author's email: jackpmanning@tamu.edu

Introduction: Dual-tasking is a commonly used paradigm where a motor task (e.g. standing) is combined with a cognitive task (e.g. counting backwards), which tends to have negative effects on either the motor task, the cognitive task, or both.[1] Postural control is a cortically driven phenomena in which sensory information is integrated with estimates of body posture to coordinate upright stance.[2] The human body and it's subsystems (e.g. the postural control system) act in predominately nonlinear ways, presumably due to the enormous amount of components present in the body (e.g. amount of neurons and muscle cells).[3] Nonlinear mathematical algorithms have become popular in the analysis of postural control because they can provide important information about behavioral patterns.[4] Sample entropy (SEn) is one such nonlinear algorithm which has been used in postural control literature and has been shown to provide valuable information that is not available with traditional linear approaches. SEn provides a measurement of how regular a behavior is.[4] Many different types of cognitive tasks have been used in the literature, which use different cognitive resources.[5] This makes comparison between studies difficult or even dubious. Therefore, the purpose of this experiment was to test the differences that different commonly used cognitive tasks have on center of pressure dynamics. The primary hypothesis being that cognitive tasks which are more demanding will have more negative effects on center of pressure dynamics.

Methods: Twenty apparently healthy young adults (Mean age: 23.5±2.1 years) were recruited and enrolled in the study. During the balance assessment protocol participants were asked to stand barefoot on a force plate with feet shoulder width apart at a 15-degree angle from the midline. Participants were asked to stand on the force plate for 2 minutes during four trials under different conditions: 1) single task (ST), 2) linguistic DT (LDT), and 3) arithmetic DT counting backwards by one (DT1), and 4) counting backwards by seven (DT7). All trials were randomized prior to data collection. During DT1 and DT7 participants were asked to count down from 500 by either 1 or 7, respectively. During LDT participants were verbally presented 3- or 4-letter words and asked to spell those words backwards. Each word's frequency was checked using the Corpus of American English.

Center of pressure data were collected at 100 Hz and down sampled to 50 Hz for subsequent analysis in R software. Linear analyses were conducted to calculate root mean square, sway path, and range metrics. Sample entropy (SEn) values were then calculated in R using m=2 and r=0.2*standard deviation.[4] One-way ANOVAs were used in SPSS to evaluate the differences in linear metrics and SEn values in the anteroposterior direction between trials with significance set at $p<.05$.

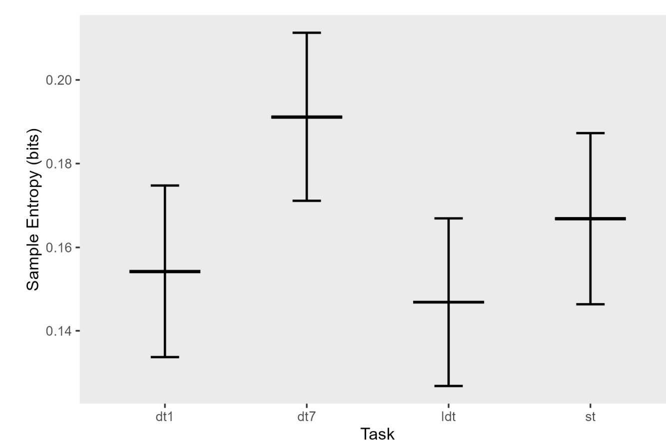

Figure 1: Comparison of mean sample entropy values ± standard error in the anteroposterior direction between different dual-task conditions. dt1: subtraction by 1; dt7: subtractions by 7; ldt: spelling words backwards; st: single task.

Results & Discussion: None of the ANOVAs using linear metrics reached significance (lowest p=.3). The one-way ANOVA with SEn also failed to reach significance (p=.383). Estimated marginal means indicated trends toward significance (**Figure 1.**). The mean values of DT1 (SEn=.154±.036) and LDT (SEn=.147±.035) were similar, and appear to be lower than DT7 (SEn=.191±.035), while ST (SEn=.16±.02) is in between those two ranges. Word count frequency was between 5,000 and 2 million.

There are many types of cognitive tasks currently used in the dual-task literature to probe different features of neural control.[5] Dual-tasking has been shown to affect center of pressure regularity under eyes closed condition, but not under eyes open condition in healthy young adults during a language-based dual-task.[6] Functional neuroimaging data has also shown that an auditory language comprehension dual-task shows different neural activation decrements than a visual detection task.[5] Type of task has received attention, while difficulty of task is not as heavily considered in design. The current results indicate that the cognitive task might affect the motor task differently depending on the difficulty of the task. SEn results indicate that DT1 and LDT are similar in difficulty, while DT7 may be more cognitively demanding, resulting in a slightly higher SEn value. Word difficulty has been shown to be tied directly to frequency of use in the Corpus of American English. The words used in the current study were relatively easy based on their frequency distribution.

Significance: It appears that counting backwards by one seems to have a similar cognitive load as spelling easy words backwards. This provides preliminary evidence that task difficulty is an important consideration in dual-task study design. Future work can use this information to better inform cognitive task selection for dual-task paradigms.

References: [1.] Woollacott, M. & Shumway-Cook. *Gait & Posture* **16**, 1–14 (2002). [2.] Rubega, M. *et al*. *Sci Rep* **11**, 14132 (2021). [3.] Kędziorek, J. & Błażkiewicz, M. *Entropy* **22**, 1357 (2020). [4.] Yentes, J. M. *et al*. *Ann Biomed Eng* **41**, 349–365 (2013). [5.] Leone, C. *et al. Neuroscience & Biobehavioral Reviews* **75**, 348–360 (2017). [6.] Donker, S. F., Roerdink, M., Greven, A. J. & Beek, P. J. *Exp Brain Res* **181**, 1–11 (2007).

PREDICTIVE KINEMATIC MODELING OF REACHING TASKS WITHIN A SPACESUIT

Kyra A. Lee[1*], Han Kim[2], Sudhakar Rajulu[3]
University of Puget Sound
National Aeronautics and Space Administration
kalee@pugetsound.edu

Introduction: During the Space Shuttle era (1981-2011), the National Aeronautics and Space Administration (NASA) astronaut selection requirements were relaxed to include females, and astronaut classes also began to represent a more diverse cross-section of the United States population. Compared to the Apollo era (1961-1972), which had 24 male crewmembers, the Space Shuttle era had 848 crewmembers, leading to NASA's current requirements to accommodate individuals who fall within a 1st to 99th percentile range on a variety of critical dimensions. Thus, since the 1960s, Extra-Vehicular Activity (EVA) spacesuits have progressed from soft fabric enclosures tailored to fit a small number of men to highly capable systems made from separable components that can be swapped out to allow re-sizing and customization, designed to fit a large portion of the population [1]. However, despite these needs of faster production rate and multiple spacesuit sizes, due to budget constraints, designers are usually limited to one size of a spacesuit prototype, which forces human performance issues, such as kinematic limitations, ergonomic concerns, and sizing problems, to be anticipated through other methods, such as kinematic models [2]. However, not only do we want to model existing movements, we seek to predict movements, as understanding the characteristic patterns is crucial for the design and operation of a spacesuit. Particularly, how does the hand within the spacesuit navigate? If the hand positions at the endpoints of a motion are already known, we believe it is possible to fill in the gaps and map an accurate trajectory. Thus, this project aims to build and test various mathematical functions to model tangential hand velocity, 3D orientation, and 3D location. With these techniques, it is thought that the Anthropometry and Biomechanics Facility's future spacesuit motion database will be able to not only categorize, search, and retrieve previously collected motion data efficiently, but also predictively generate new motions that do not exist in the collected data.

Methods: Using the existing Blender model of various right hand reaching motions within a spacesuit Hard-Upper Torso (HUT), x, y, and z coordinate locations of the right shoulder, elbow, and hand for all movements were first exported to a spreadsheet and individual motions were segmented. To model tangential hand velocity, 10 control points were used as input for a B-spline function. To predict a suited reaching motion, we first tested a spherical linear interpolation of quaternions, or *Slerp* for short. In this interpolation of a rotation, the shortest path between two unit quaternions is found and can be projected onto the unit sphere as the great arc visualizing rotation matrices. However, we observed large inaccuracies and decided to use a third, intermediate interpolation quaternion, which led to a spherical "quadrangular" interpolation algorithm, or *Squad* for short. This interpolation is similar to *Slerp*, except that we now produce a cubic spline interpolation due to the third, intermediate control point. After mathematically generating predicted reaching motions, tracking animations were built in Blender to display a visual representation of the comparison between reaching trajectories and bone segment paths.

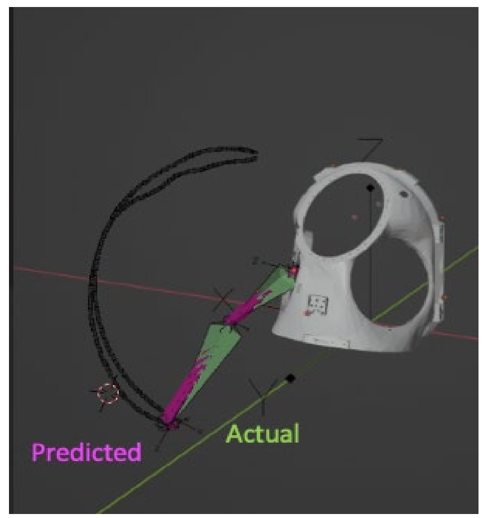

Figure 1: Actual vs. Predicted reaching motion trajectories for one specific motion path generated from tracking animations built in Blender that utilize the combined statistical models.

Results & Discussion: We successfully determined a way to statistically predict a variety of suited reaching motions using combined mathematical models of tangential hand velocity, elbow angle, 3D orientation, and 3D location. For all of the selected motion segments, the predicted movements were found to be roughly 7 or less inches away from the real movement. In terms of accuracy, it is believed that the wave-like patterns were primarily caused by time phase differences. During certain parts of a reaching motion, either the real or predicted arm segments would accelerate, but both did not experience this phenomenon at the same time. In addition, during the final stages of this work, we experienced the issue of quaternion sign flipping. Like with spherical coordinates, this issue can be resolved manually, and in the future, we hope to fix this problem. Overall, using this framework to build upon, our aim is to be able to predict even more complex motions, in order to work toward the ABF's goal of a generative spacesuit motion database.

Significance: Regarding functional task characterization and ergonomic risk factors, previous work has shown that virtual body modelling tools can be used to more accurately estimate various human body dimensions and human-spacesuit interactions that will be encountered in a population. By integrating biomechanical analyses with visualizations of likely postures, joint configurations, and movements, ergonomic concerns and design alternatives can be communicated early in the design and planning phases or during redesign for improvement.

References:

[1] Kim et al. (2019), Human modeling tools for spacesuit and hardware design and assessment *DHM and Posturography* 613-25;

[2] Vu et al. (2021), Assessment of biomechanical risk factors during lifting tasks in a spacesuit using singular value decomposition. *Proceedings of the 21st Congress of the International Ergonomics Association.*

EFFECTS OF HIGH-ALTITUDE TRAINING CONDITIONS ON LOWER BODY POWER

Robert Murphy[1], Luke Brown[1], Amy Silder[2]*, Pinata Sessoms[2], Douglas Jones[2], Tony Duong[2,3], Rebecca Zifchock[1]
[1]United States Military Academy, West Point, NY; [2]Naval Health Research Center, San Diego, CA; [3]Leidos Inc., San Diego, CA
*Corresponding author's email: amy.b.silder.civ@health.mil

Introduction: Marines and other armed service members are often exposed to cold weather and high-altitude conditions for long during training and dismounted movements. These conditions can induce significant physiological changes in the human body and can result in decremented physical and cognitive performance as well as injury [1]. This impacts military readiness, introduces significant financial cost, and affects the immediate and long-term health status of the individuals themselves. Previous work suggests that lower body performance metrics, such as running time trials as well as jump height, can *improve* in high-altitude, low-oxygen environments [2,3]. However, these studies were conducted in controlled environments and thus, have focused on individuals who have minimal changes to other factors such as sleep, nutrition, and stress. Marines often train for long durations with disrupted sleep, nutrition, and regimented daily schedules that can cause changes in body mass, specifically lean body mass (LBM).

The countermovement jump (CMJ) is a reliable tool to quantify lower body power [4]. However, it is unclear how muscle mass could influence an individual's capacity to maximize their lower-body power. In a study of elite swimmers, researchers found that CMJ force-time characteristics increased with increased lower body lean mass [5]. Similarly, Markovic et al. [6] proposed a body-size independent index of power by normalizing performance metrics to body mass, stature, and thigh-girth. While these studies normalized the performance metrics to multiple measures of body composition, they were also conducted in controlled environments where the participants were not exposed to environmental conditions that could result in changes in LBM. Therefore, the purpose of this study was to analyze the effects of a 28-day extended training at high-altitude conditions on the lower body power of U.S. Marines, normalized to their available LBM. Compared to before the start of the training exercise, it was expected that the participants would demonstrate a decrease in jump height and normalized peak power at the conclusion of their training, and that the decreases would be significantly correlated to their loss in LBM.

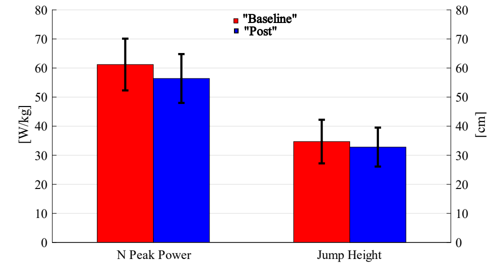

Figure 1: Mean (standard deviation) peak power normalized to lean body pass and jump height

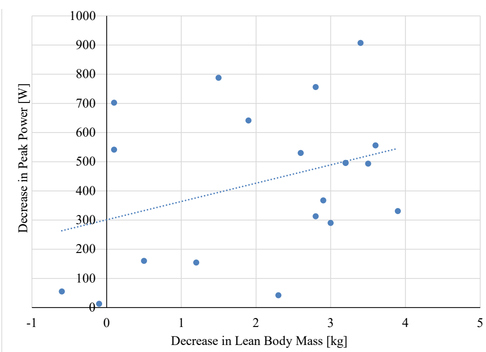

Figure 2: Decrease in peak power vs. decrease in lean body mass.

Methods: Twenty male U.S. Marine Infantrymen (19-25 years, 75.5 (7.1) kg provided informed consent to participate in this study. Participants reported to an indoor facility at their home training command, located at approximately sea level, where their total body mass (weight) and LBM were measured using a body composition analyzer (InBody, Cerritos, CA). LBM is defined as the sum of the total body water and dry lean mass. Participants were then asked to complete five CMJ's in standard issue boots on a dual force plate system (VALD Performance, Newstead, Australia), which was subsequently used to estimate subjects' peak power and jump height. Peak power was defined as the maximum power recorded out of five repetitions during the takeoff phase of the CMJ, and jump height was estimated from flight time. Lower-body power was normalized to LBM. Approximately 1-week after baseline testing, participants began a 28-day mountain training exercise at 2500-3000m elevation with day/night temperatures averaging 11/-9^{o} C. One day after completion of the training exercise, the testing protocol was repeated at a separate indoor facility, located at the mountain training command. Peak power normalized to LBM and jump height were compared between baseline (pre) and after completion of the high-altitude training exercise (post) using a paired, one-tailed t-test, and the relationship between the change in peak power and the change in LBM was assessed using Pearson correlation, $\alpha = 0.05$.

Results and Discussion: Throughout the 28 training days, participants lost an average of 4.0 (1.6) kg of total body mass ($p<.01$) and 2.1 (1.4) kg of LBM ($p<.01$). As hypothesized, both peak lower-body power normalized to LBM ($p<.01$) and jump height ($p=.02$) decreased from baseline to the completion of training (Figure 1). Contrary to our second hypothesis, the decrease in peak power over the course of the training was not correlated with the loss in LBM ($r=.34$, $p=.14$, Figure 2). The lack of strong correlation using the included sample size suggests that factors other than loss in LBM such as lack of sleep, inconsistent nutrition, and stress may have also influenced the decrease in lower-extremity dynamic performance in this physically intensive training environment at high-altitude.

Significance: The findings of this study present important considerations for tactical populations and defense organizations. The health, performance, and success of military members is imperative to maintain operational readiness. Improved methods of regulating injury and ensuring proper nutrition, hydration, and sleep are necessary to maintain the fitness and readiness of the force. Defense organizations, in conjunction with researchers in the field of biomechanics, must develop more significant and impactful methods to regulate the decrease in lower body performance of the military through training and field operations in hostile environments.

References: [1] Kramer, 1993, *Hum Factors;* [2] Rojas-Valverde, 2020, *MHSalud;* [3] Almeida, 2021, *Front Physiol;* [4] Markovik, 2004, *J Strength Cond Res;* [5] Thng, 2022, *Int J Sports Sci Coach;* [6] Markovic, 2007, *J Sports Sci.*

SAGITTAL PLANE COORDINATION STRATEGIES TO MITIGATE KNEE LOADING DURING LANDING BETWEEN MALES AND FEMALES

Justin D. Dennis[1*], Kevin H. Choe, Melissa M. Montgomery, Scott K. Lynn, Brock M. Crews, Derek N. Pamukoff
[1]Department of Exercise and Sports Science, University of North Carolina at Chapel Hill; Chapel Hill NC
*Corresponding author's email: jddennis@unc.edu

Introduction: Females rupture their anterior cruciate ligament (ACL) 2x more frequently than males,[1] which may be due to aberrant sagittal plane landing biomechanics.[2] Comparison of minimum or maximum kinematics or kinetics does not account for simultaneous joint motion or potential differences at various portions of landing. A modified vector coding technique can be used to determine if interjoint motion occurs in the same direction (in-phase), opposite direction (anti-phase), or independent of each other. Therefore, the purpose of this study was to compare lower extremity and trunk sagittal plane coordination patterns, kinematics, and kinetics between males and females during the landing phase of a drop vertical jump. Due to females displaying aberrant sagittal plane landing biomechanics, we hypothesized that females would land with less anti-phase motion between the ankle/knee coupling and knee/hip coupling, more in-phase motion between the knee/trunk coupling, and smaller sagittal plane angles and moments throughout the landing phase compared with males.

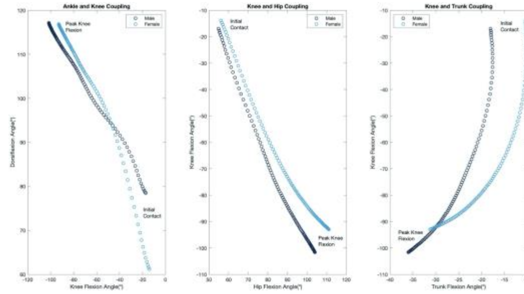

Figure 1: Angle-Angle plot of the sagittal plane ankle/knee, knee/hip, and knee/trunk couplings.

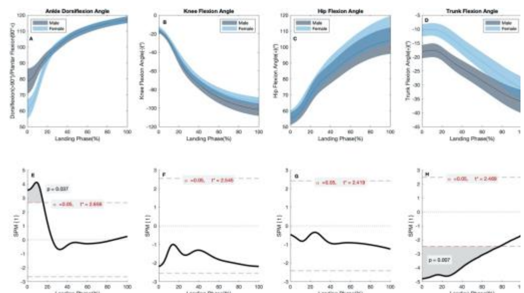

Figure 2: Dorsiflexion (A), Knee Flexion (B), Hip Flexion (C), and Trunk Flexion (D) comparisons via statistical parametric mapping.

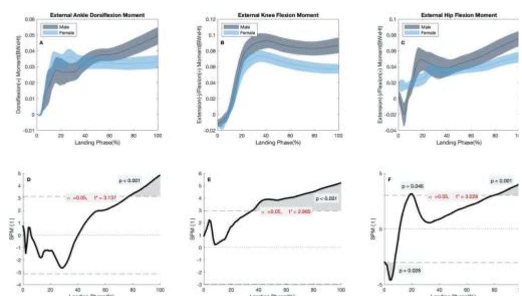

Figure 3: External Dorsiflexion (A), Knee Flexion (B), and Hip Flexion (C) moment comparisons across the landing phase via statistical parametric mapping.

Methods: 28 males (age:22.36±2.39, BMI:24.58±3.67) and 28 females (age:21.89±2.02, BMI:22.57±3.89) performed a drop vertical jump from a 30cm box placed half their height from force platforms. A modified vector coding technique (Fig.1) and binning analysis were used to compare coordination patterns between the sagittal plane ankle/knee, knee/hip, and knee/trunk couplings via Mann-Whitney U Tests. Joint angles and moments were compared throughout the landing phase via statistical parametric mapping.[3] All analyses were completed in MATLAB via custom scripts with an alpha of 0.05.

Results: The ankle/knee coupling revealed females landed with less isolated knee flexion (U=644.5, Z=-2.51, p=.012) and more simultaneous ankle dorsiflexion and knee flexion (i.e., anti-phase) (U=979.5, Z=2.97, p=.003) compared with males. The knee/hip coupling revealed females landed with less simultaneous knee flexion and hip extension (i.e., in-phase) (U=714, Z=-2.55, p=.011) and less isolated knee flexion (U=657, Z=-2.34, p=.019) compared with males. The trunk/knee flexion coupling revealed females landed with more simultaneous trunk and knee flexion (i.e., in-phase) (U=924, Z=2.06, p=.039) and less isolated knee flexion (U=654, Z=-2.36, p=.019) compared with males. Females landed with greater plantarflexion from 0-15% and smaller trunk flexion from 0-78% of landing (Fig. 2) compared with males. Females landed with smaller external ankle dorsiflexion moments from 78-100%, smaller external knee flexion moments from 35-100%, larger external hip flexion moments from 1-7%, and smaller external hip flexion moments from 19-20% and 80-100% of landing compared with males (Fig.3).

Discussion: Our primary findings partially supported our hypotheses and indicated that females landed with a strategy to limit isolated knee flexion motion and loading. This may be a compensatory strategy to limit the responsibility of the quadriceps to attenuate vertical and posterior ground reaction forces during the landing phase of a drop vertical jump. For example, eccentric quadriceps activity is required to attenuate landing forces, but females have previously demonstrated weaker relative quadriceps compared with males.[4] As such, females may land with greater ankle plantarflexion and smaller trunk flexion during the early portions of landing to allow for greater simultaneous ankle and knee flexion (i.e., anti-phase) and knee and trunk flexion (i.e., in-phase). Finally, females landed with smaller sagittal plane ankle, knee, and hip moments during the later portions of landing compared with males, which may indicate a reduction in relative force absorption from these joints.

Significance: Males and females utilize different sagittal plane interjoint coordination strategies and different biomechanics at various portions of the landing phase that may have implications for ACL injury discrepancies between sexes. Future studies should identify interjoint coordination risk factors for ACL rupture and landing interventions that increase isolated knee flexion motion in females such as landing with greater trunk flexion.

References: [1] Beynnon et al. (2014), *Am J Sports Med* 42 1806-1812; [2] Leppänen et al. (2017), *Am J Sports Med* 45 386-393. [3] Pataky et al. (2010), *J Biomech* 43 1976-1982. [4] Montgomery et al. (2012), *Med Sci Sports Exerc* 44 2376-2383.

FOOT PLACEMENT COVARIANCE IS UNAFFECTED BY AN EXPLICIT TARGET BEFORE OBSTACLE CROSSING

Ashwini Kulkarni[1], Chuyi Cui[1], Shirley Rietdyk[1], Satyajit Ambike[1]
[1]Department of Health and Kinesiology, Purdue University, West Lafayette, IN, USA
*Corresponding author's email: kulkar50@purdue.edu

Introduction: One way that humans maintain walking stability is by modulating their foot placement so that the relationship between the center of mass (CoM) state and the base of support (a body-centric constraint) is preserved [1]. However, when environmental features impose additional constraints, foot placements are altered so that both the body-centric and environmental constraints are simultaneously satisfied. For example, while approaching an obstacle, foot placement variance decreases monotonically up until the last foot placement before the obstacle. Foot placement before the obstacle is markedly consistent, as inappropriate foot placement increases the risk of tripping on the obstacle [2]. The last foot placement acts as an *implicit target for foot placement*. Additionally, we recently showed that, during the approach, the covariance in consecutive foot placements changes systematically over multiple steps. This reflects a shift towards prioritizing the environmental constraints imposed by the obstacle versus the body-centric constraint [3]. Here, we determine if this shift in the covariance is influenced when an explicit target is presented at the same location as the implicit target (green target in **Fig. 1A**). The explicit target is a new environmental constraint that is not different from the implicit target at the same location. We hypothesized that with an explicit target, the variance in the foot placement will be lower, and the covariance index will be lower (reflecting a shift to prioritizing the environment) for the steps that include this foot placement (Step$_{-1}$ and Step$_0$), but it will not be different at the other steps.

Methods: Fifteen young adults (22 $\pm$ 4 years) walked on an 8 m walkway and crossed the obstacle placed midway in the walkway. They performed two task: one without a target (implicit target) and one with an explicit target, where they stepped on a visual target on the ground (**Fig. 1A**). Each task was performed 20 times.
The across-trial variance structure in the distances of the trail and lead heel from the obstacle was quantified using the inter-step covariation (ISCz) index [3] for multiple steps. A higher ISCz index indicates a greater priority for foot placement relative to a body-centric constraint versus an environmental constraint, and vice versa. A task × step RM-ANOVA on the ISCz index was conducted.

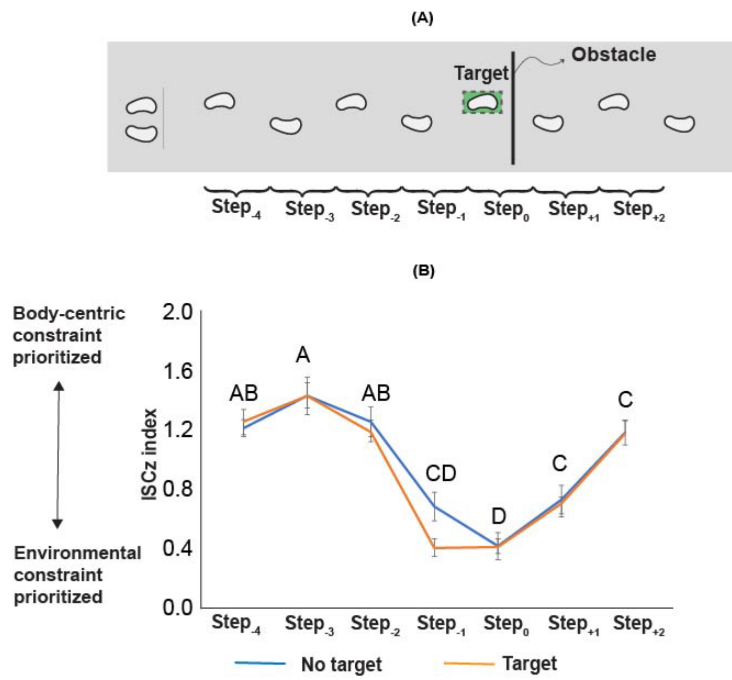

Figure 1: (A) Bird's eye view of the walkway along with the target and obstacle location**. (B)** Mean $\pm$ SE of the inter-step covariance (ISCz) index. Different alphabets indicate statistical significance ($p<0.05$).

Results & Discussion: The shift in the ISCz index observed in [3] was again observed here with an implicit and explicit target (significant effect of Step; $p<0.01$; **Fig. 1B**). However, counter to our hypothesis, presentation of an explicit target did not affect the ISCz index (no main or interaction effect of task; $p>0.4$), although there is a trend towards a significant difference for Step$_{-1}$. Furthermore, the foot placement variance tended to decline for the foot placement on the target ($p=0.06$). Overall, although we observe the hypothesized trends in the data, we did not observe the hypothesized effects of an explicit target, likely due to the size of our sample. It may also be that ISCz has reached a floor with Step$_0$; ISCz < 0 indicates that the step length is destabilized [3], and this may impact gait stability.

Significance: While foot placement modulation is a known strategy for maintaining gait stability, it is less clear how this strategy is altered while navigating environmental hazards. We recently identified an additional strategy of modulating inter-step covariance that humans employ to simultaneously manage body-centric and environmental constraints [3]. The ISCz index that we developed to identify this behavior also allows us to quantify changes in foot placement control in cluttered environments. Further work is warranted to identify the contribution of various sensory modalities (including vision, which is obviously essential for navigating cluttered environments) to this control strategy. Future work is also warranted to identify if the covariance signature can be utilized to identify fall risk or other motor deficits across age and in pathological populations. Our results here suggest that the covariance is not sensitive to the specific explicit target that we used, but more work is warranted to identify whether humans can be flexible with the covariance strategy in other situations and whether the strategy can be modified via interventions.

Acknowledgment: Bilsland Dissertation Fellowship

References: [1] Winter (1995). *Gait Posture,*3(4); [2] Muir et al (2015). *Gait Posture,* 41(1); [3] Kulkarni et al (2021). *Motor Control.* 27(1)

QUANTIFYING THE EFFECTS OF AMERICAN FOOTBALL SHOULDER PADS ON REACH DISTANCE AND PLAYER PERCEPTION OF COMFORT AND FIT

Claudia M. Town[1*], Ron Jadischke[2], David M. Andrews[1]
[1]University of Windsor, Department of Kinesiology, Windsor, Ontario, Canada
[2]Xenith, MI, USA
*Corresponding author's email: town1@uwindsor.ca

Introduction: The majority of sports equipment research to date has focused on their protective capabilities, and not on how they impact player performance and comfort while using them [1]. Evaluations of how sports protective equipment impacts player performance, as well as the comfort and fit of sport protective equipment, are relatively new and emerging concepts in the literature [2,3]. Frayne et al. [2] studied the effects that shoulder pads have on the reach envelopes of hockey goalie players. However, participants were sitting while they completed the reach envelope protocol, and their trunks were not secured. Consequently, it is not known what the contribution of the shoulder joints alone would have been to the reach envelopes while shoulder pads were worn. Evidence related to shoulder pad comfort and fit is also limited to date [3], but is important to understand since some players opt out of wearing recommended equipment if it is uncomfortable [4]. Therefore, the purpose of this study was to create a standardized methodology to quantify the effects of football shoulder pads on player reach distance and determine players' perceptions of comfort and fit for two models of shoulder pad (standard shoulder pad, prototype shoulder pad).

Methods: Ten current or former players (high school or university level) participated in this study. Five GoPro Hero 9 cameras recorded the movement sequences. LED lighting illuminated the retroreflective markers on the participants' middle fingers and helmets. A stabilizing apparatus was utilized to restrict trunk and head motion and to isolate the contribution of the shoulder joint during the reach distance protocol. Participants completed three trials of the movement sequence (flexion, extension, abduction, horizontal extension, horizontal flexion right arm, and horizontal flexion left arm), in each of three different pad conditions (no shoulder pad, standard shoulder pad, prototype shoulder pad). Part one of the questionnaire was completed (i.e., on breathability, weight, restriction, and discomfort) following each shoulder pad condition. Part two of the questionnaire was completed after the reach distance protocol and included open-ended questions regarding participants' likes and dislikes of the shoulder pads. Marker tracking was completed in ProAnalyst® and reach distance was measured for each of the conditions in every position. A Three-Way Repeated Measures Analyses of Variance was performed (dependent variable - maximum reach distance; independent variables - trial, condition, movement).

Results & Discussion: The prototype pad allowed for 23.1cm and 10.3cm more reach distance on average in abduction and flexion, respectively than the standard pads ($p<0.05$) (Fig. 1). These findings have meaningful practical implications given that the diameter of a standard size football is ~17cm, which is less than the mean difference in reach distance between the prototype and standard shoulder pads for abduction in the Z direction. This suggests that players may be able to make catches while wearing the new prototype shoulder pads that they would not have been able to make wearing the standard pads. There were no significant differences in reach distance in the no shoulder pad condition compared to the prototype shoulder pad condition for any movement in any direction. Some athletes will opt out of wearing important pieces of safety equipment because they feel that the equipment negatively impacts performance [4]. However, this study showed that the prototype pads enabled the participants to reach to a similar extent compared to when they were not wearing pads at all.

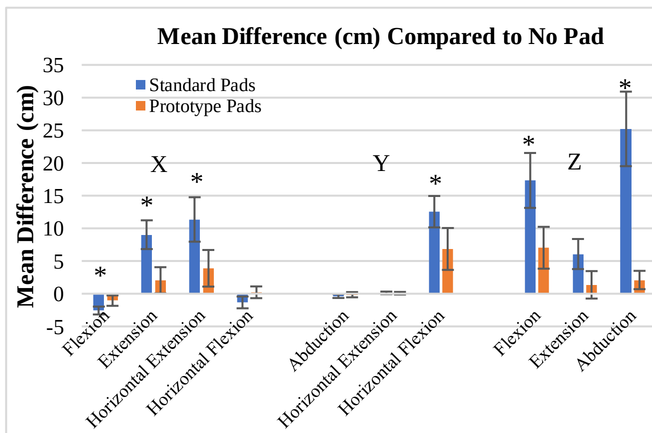

Figure 1: Mean (±SE) difference (cm) in reach distance between the no shoulder pad condition and the two pad conditions (standard, prototype) for each relevant movement in the X, Y, Z directions. *$p<0.05$ compared to no shoulder pad

Participants found the prototype shoulder pad to be significantly more breathable and comfortable than the standard shoulder pad ($p<0.05$). Better breathability may be attributed to the perforation in the material of the prototype shoulder pad. Participants also reported that the neck collar region was more comfortable in the prototype shoulder pad condition ($p<0.05$). The prototype shoulder pad was quite flexible, whereas the standard shoulder pad had a stiff shell that may cause the shoulder pad to shift upwards to the neck when participants reached above their heads.

Significance: Despite the fact that equipment can impact athletic performance and equipment comfort and fit can affect user compliance and safety, there is a lack of literature in these areas. This study began to address this gap as well as the limitations of what little work has been reported previously. In addition, the differences found in reach distances, comfort and fit between the two shoulder pads studied herein provide manufacturers with valuable insights from a redesign standpoint. They can also assist players and practitioners, such as equipment managers and coaches, when selecting equipment that may give players a performance advantage.

References: [1] Barstch et al. (2012), *J Neurosurg* 116; [2] Frayne et al. (2019), *ISB Conference Abstract*; [3] Virani et al. (2017), *Med Sci Sports Exer* 49; [4] Brisbine et al. (2020), *J Sci Med Sport* 23.

HUMAN GAIT ENTRAINMENT TO SOFT ROBOTIC HIP PERTURBATIONS ON A SELF-PACED TREADMILL : A PRELIMINARY STUDY

Omik Save[1], Sidhant Das[1], Evan Carlson[1], Hyunglae Lee[1*]
[1]School of Energy, Matter, and Transport Engineering, Arizona State University, Tempe, USA
*Corresponding author's email: hyunglae.lee@asu.edu

Introduction: Human walking can get synchronized to periodic pulses applied to the lower extremity joints at frequencies closer to their natural walking frequency, which is known as a gait entrainment phenomenon. Recent studies utilizing the entrainment paradigm in robot-assisted gait training have consistently demonstrated its potential to increase gait cadence and correct gait asymmetry[1,2]. Although promising, the previous studies on a fixed-speed treadmill showed that the success rate of entrainment decreases, and natural biomechanics are significantly altered with the increase in perturbation frequency. To address this issue, this study investigated whether self-paced walking on a variable-speed treadmill, which closely simulates overground walking, can improve the success rate of gait entrainment, and preserve the natural walking biomechanics under various perturbation conditions.

Methods: Seven healthy young adults (6 male, 1 female, mean age: 22 years, mean height: 1.83 m, mean weight: 86.9 kg) were recruited for this study which was approved by the Institutional Review Board of Arizona State University (STUDY00015183). The study utilized a lightweight, pneumatically actuated soft hip exosuit to provide periodic hip flexion perturbations, which has been verified to not interfere with the subject's natural biomechanics during walking[3].

A calibration experiment was first performed to determine the preferred walking speed of each subject and record the corresponding natural stride frequency (f_{gait}) and spatiotemporal walking parameters. The main study was composed of the two walking experiments that were evaluated on two separate days, at least five days apart. Four perturbations with different perturbation frequencies (specifically, $1.0 \cdot f_{gait}$, $1.08 \cdot f_{gait}$, $1.18 \cdot f_{gait}$, and $1.30 \cdot f_{gait}$) were tested on each subject in either i) a conventional Fixed-Speed Treadmill (FST) where the treadmill speed was set constant to the subject's preferred walking speed or ii) an active Variable-Speed Treadmill (VST) that simulated overground walking by matching the position and velocity of the subject's center-of-mass during self-paced walking.

Figure 1: A user wearing a soft robotic hip perturbation device while walking on the treadmill.

Each of the 4 perturbations was repeated 3 times in random order on both days of the experiments. Each walking trial was 180 seconds long and a mandatory rest period of at least 5 minutes was provided at every 4 trials. A trial was considered successfully entrained if the perturbation timing in at least the last 30 strides was confined within the ±10% gait phase of the averaged perturbation timing of this window.

The primary parameter investigated in this study was the success rate of entrainment at different perturbation conditions between the FST and VST experiments. Other parameters of interest were the percent change in mean treadmill speed during the VST experiment, percent change in mean stride length, and percent change in mean normalized propulsive impulse, which was calculated by integrating the shear force during propulsion and normalizing it by the weight of the subject.

FST [Mean (STD)]	**Perturbation Frequency**							
VST [Mean (STD)]	**0%**		**8%**		**18%**		**30%**	
Success of Entrainment (%)	100.0 (0.0)	100.0 (0.0)	93.3 (13.3)	93.3 (13.3)	80.0 (26.7)	93.3 (13.3)	33.3 (42.2)	73.3 (38.9)
Change in Mean Treadmill Speed (%)	0.0 (0.0)	6.8 (7.6)	0.0 (0.0)	16.1 (6.1)	0.0 (0.0)	27.4 (5.7)	0.0 (0.0)	39.4 (10.7)
Change in Mean Stride Length (%)	-1.1 (0.6)	5.2 (6.1)	-8.1 (3.6)	6.6 (4.4)	-15.5 (0.6)	7.6 (4.1)	-23.0 (0.2)	6.6 (8.2)
Change in Mean Normalized Propulsive Impulse (%)	3.9 (3.2)	12.4 (11.0)	-12.5 (4.5)	8.5 (7.5)	-26.2 (3.8)	3.4 (7.1)	-40.0 (4.1)	-2.5 (11.5)

Table I: Group average results (mean and standard deviation in parentheses) for each parameter investigated in both FST and VST experiments.

Results & Discussion: The group average results (Table I) showed a similar success rate of entrainment at perturbation frequencies closer to f_{gait} (i.e., $1.0 \cdot f_{gait}$ and $1.08 \cdot f_{gait}$) during both FST and VST experiments. However, the VST experiment showed a trend of the higher success rate than that of the FST experiment at higher perturbation frequencies (i.e., $1.18 \cdot f_{gait}$ and $1.30 \cdot f_{gait}$). There was a systematic increase in mean treadmill speed with the increase in perturbation frequency during the VST experiment. Furthermore, while the mean stride length and normalized propulsive impulse showed a consistent decrease with the increase in perturbation frequency during the FST experiment, they were relatively unchanged during the VST experiment. The results suggest that VST walking could preserves natural walking biomechanics better than FST walking during gait entrainment to perturbations with various frequencies.

Significance: The results of this preliminary study highlight the potential of using a self-paced variable speed treadmill and a soft robotic hip exosuit to extend the basin of entrainment while preserving the natural biomechanics of walking which could enhance the effectiveness of entrainment-based gait rehabilitation.

References: 1. J. Ahn et al. (2011), *IEEE Eng. in Medicine and Biology Society (EMBC).* 2. C. Thalman et al. (2021), *IEEE Robotics and Automation Letters (RA-L)*. 3. L. Baye-Wallace et al. (2022), *Robotics and Automation Letters (RA-L).*

The potential of the 180-degree cutting maneuver as an ACL injury assessment

Alejandro Ovispo-Martinez[1*], Henry Wang[2], Dorice Hankemeier[3], Clark Dickin[4].
Ball State University, Muncie, Indiana, USA[1-4]
*Corresponding author's email: alexovispo13@gmail.com

Introduction: An anterior cruciate ligament (ACL) injury is a serious injury an athletic team or athlete can experience as it brings many complications and barriers for both the athlete and the team. Studies have found that there is a high incidence of ACL injury among athletes and high injury rates observed in women's and male sports. (1) Studies have found that most ACL injuries have occurred during a non-contact rapid change of direction movements. (2,3) Rapid change of direction movements, including cutting maneuvers, jump landings, and their variations, have been investigated over the years to identify injury risk factors that may lead to this injury. Pivot-cutting maneuvers are common in sports such as soccer, football, and basketball. (4) The neuromuscular activation, kinetic, and kinematic factors have been studied in cutting maneuvers and jump landings, however, the pivot or 180-degree cutting maneuver has not been fully investigated. Therefore, the main purpose of this study is to compare the biomechanical ACL injury risk factors of a 180-degree cutting maneuver when compared to a sidestep cutting maneuver and a jump-landing task. A secondary purpose was to analyze the lower limb mechanics of the 180-degree cutting maneuver and its potential to be used as a screening tool for ACL injury. Due to the greater change of direction and multiplanar control required to perform the 180-degree cut, we expect that it will elicit similar or greater biomechanical risk factors compared to a 45-degree cut and a jump-landing task.

Table 1. Kinematic and Kinetic measurements are compared between all three tasks and during all three phases.

Initial Contact	**180-Cut**	**45-Cut**	**Jump-Landing**
Knee Flexion	20.5 ± 1.6	32.0 ± 2.1*	21.9 ± 2.1
Knee ABD Angle	-0.9 ± 1.8	-5.5 ± 2.4*	-8.5 ± 1.5
Hip Flexion	44.6 ± 4.1	60.4 ± 2.7*	44.6 ±5.6
Loading Phase	**180-Cut**	**45-Cut**	**Jump-Landing**
Peak Knee Flexion	63.4 ± 2.1	55.5 ± 2.6*	93.9 ± 2.7
Peak Knee Adduct M	1.5 ± .2	0.8 ± .1*	0.3 ± .1
Propulsive Phase	**180-Cut**	**45-Cut**	**Jump-Landing**
Peak Knee ABD Angle	2.9 ± 2.0	2.5 ± 2.2	3.2 ± 1.5
Peak GRF	1.6 ± .1	2.2 ± .1*	1.4 ± .1

*Asterisks indicate significant difference from the 180-degree cutting task

Methods: 12 healthy recreationally active participants (Age: 21.3 ± 1.2 yrs., height: 1.75 ± .10 m, weight: 72.4 ± 7.0 kg) performed 45-degree cuts and 180-degree cuts in a randomized order and under unanticipated conditions. Participants then performed vertical drop-jump landings on two AMTI ground-embedded force plates. Three successful attempts at each task were used for analysis and comparison. Biomechanical variables were collected during these tasks at the initial contact, loading, and propulsive phases of the dominant limb. Repeated measures of ANOVA were conducted for each variable and pairwise comparisons were compared between each task and a significance alpha level of .05 was used.

Results & Discussion: During the initial contact phase, there were decreased knee flexion angles ($p < .001$) and hip flexion angles ($p < .001$) during the 180-degree cut when compared to the 45-degree cut. This indicated that during the 180-degree cutting maneuver, the participants were in a more erect posture, placing the knee joint in a compromising position that could eventually lead to injury. During the loading phase, the 180-degree cut resulted in decreased peak knee flexion angles ($p < .001$) and increased knee adduction ($p < .001$) moments compared to the jump-landing task. During the loading or force absorption phase, the 180-degree cutting maneuver demanded more dynamic control and stabilization in both the frontal and sagittal planes when comparing it to a simple jump landing. The drop-jump landing has been used as an ACL pre-assessment and these results may indicate that a more dynamic movement such as the 180-degree cut could be included to uncover other risk factors in individuals that the jump-landing misses. During the propulsive phase, the 180-degree cut elicited greater knee adduction moments than the 45-degree cut ($p < .030$) and jump-landing ($p < .002$). Also, the 180-degree cut resulted in greater peak vertical GRFs when compared to the jump landing task ($p < .003$). The propulsive phase has not been previously analyzed during the 180-degree cutting maneuver, and these results suggest that during this phase it also demanded increased dynamic stabilization and control from the individual to reduce loading and prevent potential injury.

Significance: The 180-degree cutting maneuver displayed great loading and stress on the knee joint during all phases analyzed. Due to its distinctive mechanical characteristics and high demand for dynamic control required to perform this movement, it should be incorporated as a pre-screening assessment for ACL injury along with other common movements and tools used today.

Acknowledgments: N/A

References: [1] Gupta AS et al. Sex-Based Differences in Anterior Cruciate Ligament Injuries Among United States High School Soccer Players: An Epidemiological Study. Orthopaedic Journal of Sports Medicine. 2020 [2] Rothenberg P et al. Knee Injuries in American Football: An Epidemiological Review. 2016. [3] Alentorn-Geli E et al. Prevention of non-contact anterior cruciate ligament injuries in soccer players. Part 1: Mechanisms of injury and underlying risk factors. Knee Surg Sports Traumatol Arthrosc. 2009. Journal of sports medicine and physical fitness. 2019. [4] Robinson G et al. Path changes in the movement of English Premier League soccer players. Journal of Sports Medicine and Physical Fitness. 2011

THE ROLE OF KINEMATIC ESTIMATION ACCURACY IN LEARNING WITH WEARABLE HAPTICS

Nataliya Rokhmanova[1,2*], Owen Pearl[1], Katherine J. Kuchenbecker[2], Eni Halilaj[1]
[1]Carnegie Mellon University, Department of Mechanical Engineering, Pittsburgh, USA
[2]Max Planck Institute for Intelligent Systems, Haptic Intelligence Department, Stuttgart, Germany
*nrokhman@andrew.cmu.edu

Introduction: Gait retraining to modify the foot progression angle (FPA) with real-time feedback has been found to reduce the knee adduction moment and pain in people with medial knee osteoarthritis [1]. With the use of inertial measurement units (IMUs), this preventative approach could eventually be prescribed in the clinic and performed at home, instead of relying on frequent visits to the gait laboratory. However, kinematic estimation algorithms using IMUs are prone to subject-specific errors [2]; quantifying this error on a per-subject basis in the laboratory contradicts the notion that IMUs would facilitate clinical implementation. Here, we sought to understand how errors in IMU tracking impact a person's ability to learn a toe-in gait. We hypothesized that a higher error in tracking FPA would have a negative effect on retraining accuracy (H1) and a negative effect on learning rate (H2). Post-hoc, we hypothesized that foot size negatively correlates with tracking error.

Methods: Thirty adults (15F, 15M) were taught a toe-in gait (Fig. 1A). Two groups trained with vibration feedback for four 5-minute blocks, either on a laboratory treadmill or outdoors. The last group received no training but was verbally instructed to maintain a 5-degree toe-in gait. Subjects first performed 1-minute baseline and toe-in data collections in the laboratory. FPA was estimated from both a foot-worn IMU [3] and optical motion capture, which was used as ground truth for the root mean squared error (RMSE). Vibration feedback was provided to either the dorsal or medial shank if the FPA exceeded a ±2-degree deviation from the target toe-in angle (5 degrees medial of mean baseline FPA). Retraining accuracy was expressed as the percent of steps within the target toe-in range during the final 5-minute block. H1 was evaluated using the Spearman's rank correlation coefficient between RMSE and retraining accuracy. We grouped subjects by RMSE values using the silhouette criterion for *k*-means clustering. We evaluated H2 with a two-way repeated measures ANOVA, with RMSE group as the factor and accuracy at four retraining blocks as the repeated measure. Unpaired t-tests with a Bonferroni correction were used for paired comparisons. For post-hoc analysis of the relationship between foot size and RMSE, we used a Spearman's rank correlation coefficient.

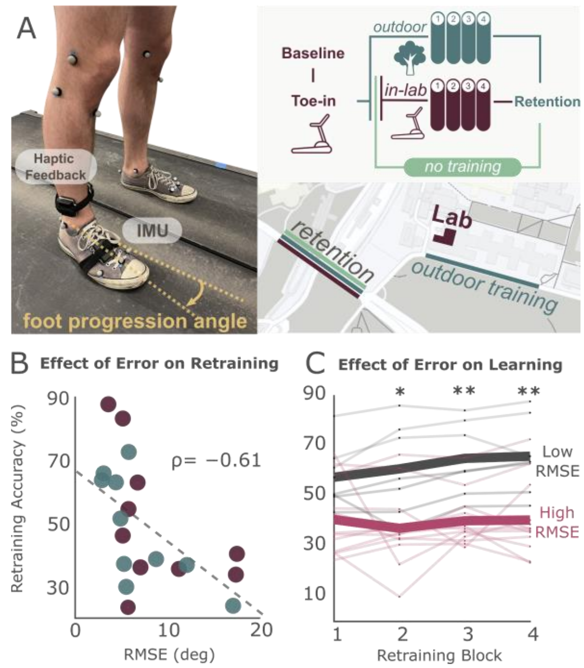

Figure 1: (A) The experiment took place indoors and outdoors. (B) Tracking error had a negative effect on retraining accuracy in the last block of retraining. (C) After grouping subjects based on their kinematic tracking accuracy, those with low error showed higher learning rates.

Results & Discussion: We found a negative correlation between tracking RMSE and average retraining accuracy ($\rho = -0.61$, $p = 0.0054$; Fig. 1B). This correlation was maintained after excluding five subjects outside of the interquartile range of RMSE values. The no-feedback group showed no correlation between retraining accuracy and device RMSE ($\rho = 0.061$, $p = 0.87$), suggesting that retraining accuracy is likely not corrupted by IMU error. These results indicate that inconsistent feedback, driven by kinematic tracking error, leads to low retraining accuracy—a trend that may be amplified in the patient population, whose proprioceptive and motor learning abilities tend to degrade with age [4]. After clustering subjects into two groups by RMSE, we found an effect of group on retraining accuracy ($p < 0.0001$) with significant differences in the last three retraining blocks ($p = 0.021$, 0.0012, 0.0069, Fig. 1C). The low-RMSE group had a final accuracy (M = 65.9%, SD = 15.2%) similar to successful gait-retraining studies using motion capture feedback [5]. In a post-hoc analysis, we found that foot size was negatively correlated with RMSE ($\rho = -0.48$, $p = 0.033$). Algorithms that use foot-mounted IMUs rely on gyroscope data for step segmentation; angular acceleration peaks are reduced with a smaller foot lever, resulting in missed steps. As knee osteoarthritis disproportionately affects females [6], who on average also have smaller feet than males, inconsistent FPA tracking may place this demographic group at a disadvantage for harnessing the benefits of wearable gait-retraining.

Significance: Errors in kinematic estimation have a cascading effect on feedback quality in gait retraining. Without knowledge of this feedback quality, clinicians could risk falsely classifying a patient as a non-responder if they failed to improve after a period of retraining. The effect of tracking error on learning may also extend to other forms of gait retraining that rely on IMUs for gait-event detection or kinematics estimation, such as reducing tibial shock in runners or improving gait symmetry in individuals with cerebral palsy or Parkinson's disease. In the future, algorithms that calibrate to the individual could enable reliable tracking for a diverse set of patients, ensuring efficient use of the time that patients and clinicians invest in retraining gait.

Acknowledgements: This work was supported in part by the NSF GRFP under grants DGE1745016 and DGE2140739.

References: [1] Wouda *JNER* 2021 [2] Richards *Arch Phys Med and Rehab* 2017 [3] Tan *IEEE EMBS* 2021 [4] Pai *Arth & Rheum* 2005 [5] Richards *Gait & Posture* 2018 [6] O'Connor *Clin. Orthop.* 2011

CONCURRENT VALIDITY OF FOUR MOTION CAPTURE SYSTEMS FOR MEASURING JOINT ANGLES AT DISCRETE TIMEPOINTS DURING DYNAMIC MOVEMENTS

Nathan A. Edwards[1,2*], Jaclyn B. Caccese[1,2], Ryan Tracy[1], Joshua A. Hagen[2], James A. Oñate[1,2]
[1]School of Health and Rehabilitation Sciences, The Ohio State University
[2] The Human Performance Collaborative, The Ohio State University
*Corresponding author's email: edwards.1614@osu.edu

Introduction: The gold standard for motion capture is systems utilizing infrared cameras and reflective markers. As motion capture technologies continue to develop, different clinical environments are utilizing these technologies for various tasks. Motion capture solutions with increased usability include markerless motion capture (MLMC), inertial measurement units (IMUs), and red-green-blue depth (RGBD) cameras. To measure movement kinematics, MLMC applies pose detection algorithms to synchronized video data. RGBD cameras similarly perform pose detection but applied on video data combined with infrared depth estimation. IMUs combine accelerometer, gyroscope, and magnetometer data to determine sensor orientation, and the orientation of multiple IMUs can be used to calculate segment or joint kinematics. The validity and reliability of MLMC has been established in gait,[1] but not for dynamic movements. IMUs and RGBD assessments have also been validated for spatiotemporal gait parameters[2] and shoulder range of motion[3,4] and for some dynamic movements,[2] but researchers recommend validating them for new data environments. Therefore, the purpose of this study was to compare the concurrent validity of MLMC, IMUs, and an RGBD camera to gold standard motion capture during 3 movements: lunges, overhead squats (OHS), and countermovement jumps (CMJ).

Methods: Thirteen healthy adults participated in this study. Participants completed nine lunges (on each leg), OHSs, and CMJs. Full-body kinematic data were collected concurrently by 10 Vicon MX-F40 cameras, 8 Optitrack Prime Color cameras, 15 Opal Gen 2 IMUs, and a HumanTrak RGBD camera system. Data were collected at 128Hz for Vicon, Optitrack, and the IMUs. Optitrack video data were analyzed in Theia Markerless software for pose estimation. Kinematic calculations were performed in Visual3D for Vicon and Theia data. Joint kinematics for IMU and RGBD data were analyzed using manufacturer algorithms. Critical events and kinematic comparisons were done in MATLAB with Vicon as the reference system. The outcomes for each movement task included peak measures of hip flexion, knee flexion, knee abduction/adduction, trunk flexion, and trunk lateral flexion. Coefficients of determination (R^2 agreement levels: good > 0.7, moderate 0.3-0.7, poor < 0.3) and mean absolute error values were calculated for each outcome.

Results & Discussion: The MLMC assessment had the highest agreement with the markered system, specifically for peak hip and knee flexion. The IMU measurements ranged from moderate to poor agreement, and the RGBD measurements were all poor (Table 1). To determine the effect of measurement errors within clinical environments, error values can be considered relative to the range of motion occurring for a joint during a movement. For example in the OHS, 6° of measurement error might constitute a 30% error for trunk flexion (20° of range of motion) while 6° of error is only a 6% error for knee flexion (100° of range of motion). These errors must also be considered relative to minimal clinically important differences for movements and joints of interest.

Table 1. Coefficients of determination and mean absolute error (MAE) values between each motion capture system and Vicon (right leg only).

	Lunge			Overhead Squat*			Countermovement Jump%		
	MLMC	IMUs	RGBD	MLMC	IMUs	RGBD	MLMC	IMUs	RGBD
Peak Hip Flexion	MAE = 6.1 R^2 = 0.70	MAE = 10.2 R^2 = 0.23	MAE = 18.5 R^2 = 0.007	MAE = 8.0 R^2 = 0.68	MAE = 18.9 R^2 = 0.21	MAE = 22.3 R^2 = 0.005	MAE = 8.4 R^2 = 0.88	MAE = 14.5 R^2 = 0.68	MAE = 27.3 R^2 = 0.07
Peak Knee Flexion	MAE = 5.6 R^2 = 0.34	MAE = 6.4 R^2 = 0.35	MAE = 13.7 R^2 = 0.23	MAE = 5.8 R^2 = 0.80	MAE = 10.2 R^2 = 0.36	MAE = 26.6 R^2 = 0.07	MAE = 5.3 R^2 = 0.90	MAE = 8.5 R^2 = 0.49	MAE = 21.3 R^2 = 0.01
Peak Knee Adduction/ Abduction	MAE = 2.6 R^2 = 0.39	MAE = 3.1 R^2 = 0.09	MAE = 3.2 R^2 = 0.03	MAE = 8.2 R^2 = 0.21	MAE = 16.8 R^2 = 0.19	MAE = 68.6 R^2 = 0.12	MAE = 5.1 R^2 = 0.21	MAE = 9.1 R^2 = 0.03	MAE = 32.5 R^2 = 0.005
Trunk Flexion	MAE = 5.2 R^2 = 0.35	MAE = 6.1 R^2 = 0.1	MAE = 7.2 R^2 = 0.002	MAE = 8.8 R^2 = 0.48	MAE = 11.8 R^2 = 0.67	MAE = 15.2 R^2 = 0.04	MAE = 7.5 R^2 = 0.26	MAE = 8.8 R^2 = 0.11	MAE = 7.5 R^2 = 0.04
Trunk Lateral Flexion	MAE = 2.3 R^2 = 0.47	MAE = 3.6 R^2 = 0.32	MAE = 5.8 R^2 = 0.07	MAE = 2.0 R^2 = 0.29	MAE = 6.0 R^2 = 0.17	MAE = 3.5 R^2 = 0.0002	MAE = 2.3 R^2 = 0.46	MAE = 3.6 R^2 = 0.11	MAE = 4.1 R^2 = 0.04

* Trunk measurements recorded at peak knee flexion **%** All reported values are after landing

Significance: Recent advances in motion capture give researchers and clinicians access to more information to support the health and performance of their respective populations. The accuracy of the MLMC system supports its use in applied settings. Future emphasis should be given to developing workflows that support high participant throughput, which will maximize utilization.

Acknowledgements: This work was supported by the U.S. Department of Defense/Office of Naval Research, Defense University Research Instrumentation Program, and Air Force Research Laboratory.

References: [1] Kanko et al. (2021), *J Biomech* 127; [2] Kobsar et al. (2020), *J Neuroeng Rehabil* 17(1); [3] Poitras et al. (2019), *Sensors* 19(7); [4] Huber et al. (2015), *Physiotherapy* 101(4).

POSTURAL CONTROL DEFICITS ON A CONTINUOUSLY MOVING PLATFORM IN PARTICIPANTS WITH CHRONIC ANKLE INSTABILITY

Xiaohan Xu[1*], Dr Genevieve K.R. Williams [1], Prof. Joanna Bowtell [1], Dr Will Young [1], Dr Daniel Fong [2]
[1]Public Health and Sport Sciences Department, Faculty of Health and Life Sciences, University of Exeter
[2] National Centre for Sport and Exercise Medicine, School of Sport Exercise and Health Sciences, Loughborough University
*Corresponding author's email: xx274@exeter.ac.uk

Introduction: Lateral ankle sprains, despite being extensively researched in terms of mechanisms and treatment, continue to be the most prevalent musculoskeletal injury in both athletics and general populations [1]. Postural control deficits are frequently reported following an acute lateral ankle sprain, and in individuals with chronic ankle instability (CAI) [2]. Studies that evaluate unilateral weight-bearing exercises in participants with CAI have identified significant alterations to lower extremity movement mechanics, during eyes-closed standing [3], drop landing [4] and lateral stepping down [5]. However, postural control in CAI on a continuous moving platform is unknown. By challenging balance through continuous perturbations, it is possible to provide information how these CAI individuals respond to external disturbances and adjust their posture to maintain stability accordingly. We hypothesized that individuals with CAI would demonstrate deficits in the Time-to-boundary (TTB) measure of postural control on a moving platform; CAI would exhibit greater changes in postural stability from static standing to a moving platform or when closing their eyes, compared to healthy controls.

Methods: Four physically active participants with CAI (age = 28.3±5.3years, height = 175.25±1.7cm, mass =83.1±12.0 kg) and five healthy controls (age=28.2±4.0 years, height =169.2±4.7 cm, mass =63.82±9.19kg) participated in this study. Each participant performed four conditions of 30-s single-leg standing, including standing with eyes open and closed on a stable surface, and with eyes open and closed on a moving platform on one leg (injured in CAI; side matched in control). The platform motion follows a mediolateral sinusoidal pattern with an acceleration at $1 m/s^2$, and the amplitude of its displacement at 5 mm (peak-to-peak displacement at 10 mm). The TTB measures were absolute minimum TTB, mean of the minimum TTB samples, and standard deviation of the minimum TTB samples. All measures were calculated in both the mediolateral (ML) and anteroposterior (AP) directions from the centre of pressure [6].

Results & Discussion:

To compare the effects of group, platform motion and eye condition on TTB measures, a series of 2 (group) $\times$ 2 (platform) $\times$ 2 (eyes) mixed analyses of variance (ANOVA) were computed (table 1). A significant interaction was observed for TTBML absolute minimum (p = 0.044 η_p^2 = 0.46). Significant group main effects were also observed and pairwise comparisons revealed that the CAI group on average demonstrated significantly less TTBML absolute minima (p=0.016; η_p^2 = 0.59; mean difference=-0.149; 95% CI=-0.26 to -0.038), TTBML mean of minima (p =0.011; η_p^2 = 0.62; mean difference=-1.33; 95% CI=-2.23 to -0.04) and TTBML SD of minima (p=0.030;η_p^2 =0.51; mean difference=-1.33; 95% CI=-2.23 to -0.04) compared to the control group regardless of vision or moving condition. There was no significant group main effect in TTB variables in AP direction. Moving platform decreased postural stability in both groups (figure 1). This is the first study to compare TTB on a moving platform between CAI and control. The main findings partially supported our hypothesis, that individuals with CAI have more unstable postural control than healthy control in overall conditions [6]. Moving platform decreased postural stability, especially in healthy control in TTBML absolute minima (p = 0.020; ES=0.17) and TTBML mean of minima (p=0.030; ES=2.07), which violated our hypothesis. This may reflect the possibility that people with CAI use a variety of compensatory mechanisms to maintain balance on a moving platform. For more difficult postural tasks, alternative biomechanical variables, such as time to stabilization, torque, and ankle stiffness could be computed to comprehensively measure the postural control in CAI. However, this abstracts reflects progress of PhD work, which renders the authors' findings tentative.

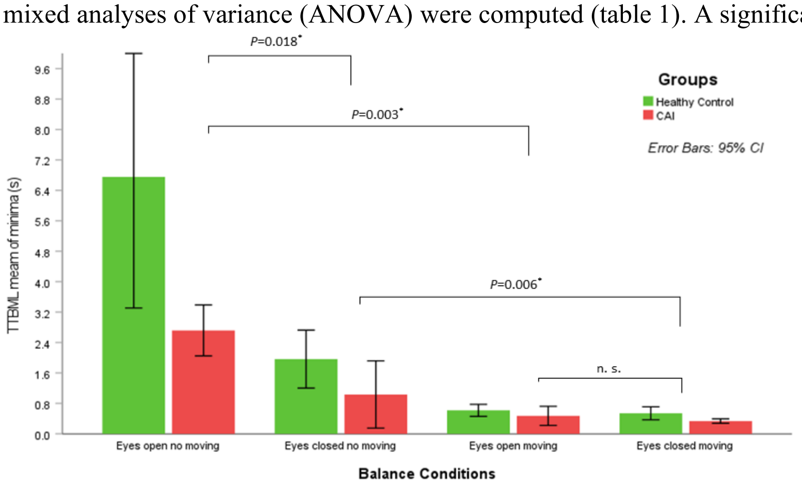

Figure 1. Comparison of Four Balance Conditions in CAI and Control Groups. The figure shows the mean and confidence interval of TTBML mean of minima (s) in four balance conditions. The p value reflects the main effect of balance conditions in both of group, with significance level adjusted using Bonferroni correction ($^* p < 0.05$). Overall, moving platform decreased postural stability in both groups, while the effect of visual disturbance on postural stability during continuous perturbation is not significant.

Table 1.
Time-to-boundary (TTB) measures (mean ± SD) for the unilateral stance in CAI and control groups on moving/non-moving platform with eyes open/closed

Measure		Non moving		Moving		Moving X group (p)	Eyes X group (p)	Group (p)
		Eyes open	Eyes closed	Eyes open	Eyes closed			
TTBML absolute minimum (s)	CAI	0.34 ± .12	0.24 ± .04	0.15 ± .06	0.11 ± .03	0.012*	0.036*	0.016*
	Control	0.78 ± .25 [a]	0.31 ± .09	0.22 ± .09	0.13 ± .05			
TTBML mean of minima (s)	CAI	2.72 ± .42	1.03 ± .56	0.47 ± .16	0.34 ± .04	0.015*	0.077	0.011*
	Control	6.76 ± 2.78 [a]	1.96 ± .61	0.62 ± .13	0.54 ± .14 [a]			
TTBML S.D. on minima (s)	CAI	3.26 ± .48	1.09 ± .82	0.32 ± .21	0.26 ± .18	0.033*	0.108	0.030*
	Control	12.07 ± 7.44	2.68 ± 1.24	0.42 ± .14	0.48 ± .20			

[a] Denotes significantly different than CAI group (p<0.05). ML: mediolateral, AP: anteroposterior, S.D.: standard deviation. * p <0.05. P value adjusted by Bonferroni correction

Significance: Participants with CAI demonstrated deficits in postural control compared to healthy control in overall balance conditions regardless of vision or moving effects. The moving platform decreased postural stability in both groups. The effect of visual disturbance on postural stability during continuous perturbation is not significant.

Acknowledgements: This work was funded by the China Scholarship Council (CSC).

References: [1] Doherty et al. (2014), *Sports Med* (44)1: 123-40; [2] Thompson et al. (2018), *Sports Medicine* 48(1); [3] Song et al.(2016), *Med Sci Sports Exerc* 48(10); [4] Simpson et al. (2019), *Phys Ther Sport* 37:210-219; [5] Simpson et al. (2019), Phys Ther Sport 39: 1-7; [6] Hertel et al. (2007), *Gait & Posture* 25: 33-39;

DETERMINING THE EFFECT OF ELBOW AND WRIST ANGLES ON MAXIMUM VOLUNTARY CONTRACTION SURFACE ELECTROMYOGRAPHY SIGNALS OF UPPER EXTREMITY MUSCLES

John P. Calisi[1], Anthony J. Zamarra[2], Benjamin B. Wheatley[3]*
Departments of [1]Psychology, [2]Biomedical Engineering, [3]Mechanical Engineering, Bucknell University
*Corresponding author's email: bbw008@bucknell.edu

Introduction: Surface electromyography (sEMG) is an effective, non-invasive technique for measuring muscle activity. sEMG can be implemented in many settings, such as in rehabilitation plans for stroke victims [1]. To effectively compare sEMG data taken from multiple sessions or individuals, the data must be normalized. One widely accepted technique of normalizing sEMG data involves referencing the maximum electrical voltage that is voluntarily produced by a contracting muscle, commonly referred to as the Maximum Voluntary Contraction (MVC) [2]. Although a significant amount of sEMG research is conducted on upper extremity muscles, it is not known the extent to which varying joint angles of the upper extremity contribute to differences in MVC results for such muscles. The present investigation aimed to determine how varying joint angles of the elbow and wrist during isometric contractions of the upper extremity contribute to differences in MVC of upper extremity muscles.

Methods: Ten healthy participants were included in this study (Mean age 22 ± 2.3 years). Upon arrival, participants were equipped with sEMG sensors and motion capture markers along the right upper extremity to record muscle activity and joint angles (Fig. 1A). Each participant completed a series of 18 isometric contractions, consisting of 9 flexion and 9 extension exercises at varying elbow and wrist angles. For each exercise, participants performed 3 trials at the start range of motion (~20° UE flexion), 3 trials in the middle range of motion (~90°), and 3 trials at the end range of motion (~130°) (Fig. 1B). For each of the 3 trials at a given elbow angle, wrist angle was manipulated such that one trial was conducted with a neutral grip, one with a supinated grip, and one with a pronated grip (Fig. 1C). To establish maximal isometric contraction, participants held an empty dumbbell handle while researchers provided manual resistance and sEMG data was acquired at a rate of 1,000 Hz. Following collection, raw sEMG data was processed by filtering, rectification, and conversion to a linear envelope with a time step of 0.2 seconds in MATLAB. Two-way ANOVAS on the maximum processed sEMG value from each trial were conducted for each muscle to examine the effects of elbow angle, wrist angle, and potential interactions on sEMG activity.

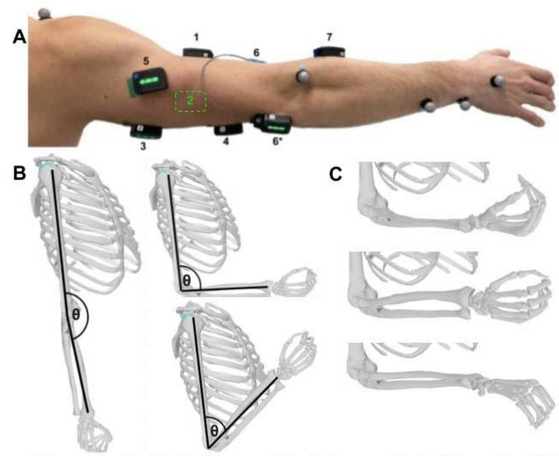

Figure 1: **A)** sEMG Sensors (black & green). 1. Biceps brachii long head (Bi L); 2. (Not pictured) Biceps brachii short head (Bi S); 3. Triceps brachii long head (Tri Lo); 4. Triceps brachii medial head (Tri M); 5. Triceps brachii lateral head (Tri La); 6. Brachialis (Bra); 6*. Anchoring sensor for specialized brachialis sensor, no sEMG data was collected from this; 7. Brachioradialis (BRad). **B)** Start (left), middle (top), and end (bottom) ranges for elbow flexion. **C)** Supinated (top), neutral (middle), and pronated (bottom) grip for wrist angle.

Results & Discussion: Greater MVC was observed at the start range of motion compared to the middle range of motion for the biceps brachii long head (0.64 at start versus 0.42 at middle, $p = 0.0032$), biceps brachii short head (0.67 at start versus 0.46 at middle, $p = 0.0043$), and brachialis (0.70 at start versus 0.50 at middle, $p = 0.030$). Greater MVC was observed at neutral wrist angles compared to both pronated and supinated for the biceps brachii short head (0.69 at neutral versus ~0.5 at others, $p = 0.015$ and 0.020), brachialis (0.74 versus ~0.6, $p = 0.022$ and 0.070), and at neutral versus pronated for the triceps brachii medial head (0.64 versus 0.47, $p = 0.020$). While other statistical comparisons were significant, these trends emerged as most consistent. For most upper extremity muscles involved in flexion, our results suggest that isometric contractions conducted at the start range of motion provide the highest MVCs compared to contractions at the middle and end ranges. A neutral grip also elicited higher average MVCs for select upper extremity muscles compared to trials conducted with pronated and supinated grips. Such findings can inform future methodologies that require the normalization of upper extremity sEMG data, as well as clinical applications seeking to target and elicit activity of such upper extremity muscles. While our sample size of $n = 10$ participants is small, the emergence of trends even among individual variability suggests meaningful conclusions can be made from this research. Further work to incorporate kinematic analysis, expand upon individual variability, and identify physiological mechanisms for these results is currently ongoing.

Significance: The findings of this research hold value in both research and clinical applications. Specific procedures proposed in this study (start range of motion during elbow flexion and a neutral grip) can help inform future sEMG research that requires the collection of MVC for upper extremity muscles, as well as providing a better understanding of how specific muscles and heads of the upper extremity can be targeted by manipulating joint angles. Our work also suggests that previously accepted procedures for eliciting MVC in other muscles might not be eliciting a true maximal contraction. Given the high incidence of upper extremity impairment following strokes, as well as the success of sEMG interventions in stroke rehabilitation [3], this work could be used by clinicians to better access patient upper extremity strength and neuromuscular coordination, thus improving rehabilitation plans and patient outcomes.

References: [1] Lawrence, E. S. et al. (2001). *Stroke*, *32*(6), 1279–1284. [2] Yang, J. F., & Winter, D. A. (1983). *Archives of Physical Medicine and Rehabilitation*, *64*(9), 417–420. [3] Munoz-Novoa, M. et al, (2022). *Frontiers in Human Neuroscience*, *16*, 897870.

CAN INSTRUMENTED INSOLES DETECT HIP AND KNEE MEDIAL COLLAPSE?

Aspen B. Chadderdon, Molly C. Shepherd, Marcie Harris-Hayes, Michael D. Harris*
[1]Washington University in St Louis
*Corresponding author's email: harrismi@wustl.edu

Introduction: Medial collapse is a movement pattern characterized by excessive thigh adduction and medial rotation combined with excessive knee valgus during weight-bearing.[1] Medial collapse is often observed during landing or squatting and has been associated with patellofemoral pain, chronic hip pain, and potentially with anterior cruciate ligament injuries.[1-3] Conversely, correcting medial collapse patterns has been associated with improved hip and knee-related patient reported outcomes.[4,5] A challenge when training patients to correct medial collapse is providing quantitative real-time feedback that is simple to understand, and can be captured in a variety of environments.[6] We hypothesize that the abnormal kinematics of medial collapse are accompanied by a shift of force distribution from the lateral to the medial side of the foot, and that shift can be detected in real-time with instrumented insoles. To test this hypothesis, the primary objective of this pilot study was to quantify the ratio of lateral-to-medial forces during medial collapse using instrumented insoles. The secondary objective was to determine if the amount of lateral-to-medial force shift can predict the amount of kinematic change at the knee during normal versus medial collapsing squats.

Methods: With consent, 11 subjects (7 female, 28 ± 7 y/o) completed normal and medial collapsing double and single-leg squats (Fig. 1). First, instrumented insoles with medial forefoot, lateral forefoot, and hindfoot force sensing areas ($f_{capture}$=100 Hz; loadsol, Novel Inc) were placed in subjects' shoes and calibrated to bodyweight. Reflective markers were placed on each subject's left and right anterior superior iliac spines and immediately superior to the patella (Fig. 1). Next, subjects completed three normal double-leg squats and three medial collapsing squats (Fig. 1), followed by three normal and three medial collapsing single-leg squats. Digital video ($f_{capture}$=25 fps; Vue, Vicon) was recorded from the frontal plane and the marker positions were used to measure knee valgus angles in Kinovea software (Fig. 1). For quality control, insole forces were compared to force plate signals to ensure errors ≤ 5% bodyweight; knee angle measurements were found to be highly repeatable between raters (ICC = 0.99).

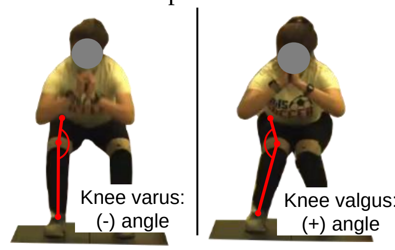

Figure 1: Double-leg normal (left) and medial collapsing (right) squats. During normal squatting, subjects controlled their motion to limit thigh adduction. During medial collapsing squats, subjects adducted the thigh during descent. Knee valgus angle was measured using reflective markers and the ankle center.

Our primary question was if the ratio of lateral-to-medial insole forces changed significantly when subjects switched from normal to medial collapsing squats. Analyses were performed at the point of deepest squat, identified using the digital video. Lateral-to-medial ratios were calculated as the lateral forefoot force divided by the medial forefoot force and tested using Welch's t-tests (α=0.05). Our secondary question was if force ratio changes were predictive of knee valgus angle changes when subjects switched from normal to medial collapsing squats. Lateral-to-medial ratios were averaged across the three squats for each subject and squat type. Linear regression was applied with lateral-to-medial force ratio as the independent variable and the change in knee valgus angle as the dependent variable.

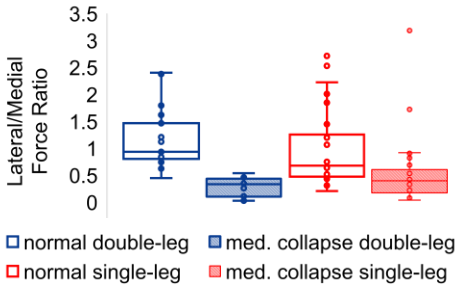

Figure 2: Force ratios during normal and medial collapsing squats.

Results & Discussion: Our hypothesis that lateral-to-medial force shifts occur during medial collapse was supported. During normal double- and single-leg squats, the average force ratios were 1.15 [95%CI: 0.96, 1.33] and 0.99 [0.73,1.24], respectively, which suggests nearly equal force distribution on the foot. During medial collapse, the force ratios were smaller for both double-leg ($p<0.001$) and single leg ($p=0.008$) squats, signifying a shift toward loading on the medial side of the foot (Fig. 2). These results are promising evidence that a simple to collect force measurement using instrumented insoles can detect a potentially harmful movement pattern. However, there was not a linear relationship between change in force ratio and change in knee valgus angle as subjects switched from normal to medial collapsing squats. The R^2 for regression during double-leg squats was <0.001 and was 0.04 for single leg squats, indicating that changes in force ratios poorly explained variation in changes to knee angle. A predictive relationship may exist between force and knee kinematics, but it is unlikely to be linear, and analysis was likely influenced by limitations inherent to 2D video analysis such as the inability to measure internal rotation of the thigh along with adduction. To further study these relationships, as well as other kinematic factors such as ankle stiffness, we plan to utilize 3D motion capture and more sophisticated analyses of predictive relationships.

Significance: Instrumented insoles can detect and measure medial collapse movement patterns during squatting. An advantage of instrumented insoles is that they provide real-time force data so patients can have a simple, quantitative, and interactive tool for correcting medial collapse either in the clinic or at home. While this is pilot data, it motivates more extensive study into the different activities and environments in which real-time, portable force measures can help detect and treat unhealthy movement patterns.

Acknowledgements: NIH R01AR081088.

References: [1] Hewett (2005), *J. Sports Med.* 33(4); [2] Schmidt (2019), *J Sport Health Sci*; 8(5) [3]Austin (2008), *J Orthop Sports Phys Ther*. 38(9); [4] Harris-Hayes (2018), *J Orthop Sports Phys Ther* 48(4); [5] Arhos (2021) *J ISAKOS* 6(5); [6] Hribernik (2022), *Sensors* 22(8).

Failure loads of suture anchors for Achilles tendon prosthesis in a rabbit model

Obinna P. Fidelis[1]*, Katrina L. Easton[1], David E. Anderson[2], Pierre-Yves Mulon[2], Dustin L. Crouch[1]
[1]College of Engineering and [2]College of Veterinary Medicine - University of Tennessee, Knoxville
*Corresponding author's email: ofidelis@vols.utk.edu

Introduction: Suture-anchor constructs, each consisting of a suture passed through an eyelet in a screw, are commonly used to reattach soft tissues, such as tendons and ligaments, to bones. The mechanical strength of suture-anchor constructs largely affects the overall integrity of the musculoskeletal reconstruction [1]. In a previous in vivo study, we surgically replaced the Achilles tendon in rabbits using a polyester silicone-coated artificial tendon. The artificial tendon was attached to the calcaneus bone using a suture-anchor construct. However, the suture-anchor constructs failed in several rabbits. The failure mode was suture breakage at the mid-substance (i.e., away from the knot). As part of a root cause analysis, we performed mechanical tensile testing of two types of suture-anchor constructs that we used in the surgeries and whose sizes were compatible with the rabbit model. The goal of the testing was to quantify the maximum tensile load to failure after cyclic tensile loading. The results of this study will inform future in vivo tests to reduce the risk of failure of suture-anchor constructs.

Methods: In this study, IMEX and Arthrex anchors (Figure 1A) used to attach artificial tendons in rabbits (Figure 1B) were tested. One anchor type (60-27-09, 2.7 mm x 11 mm, IMEX Inc., Longview, TX) has a raised eyelet and was accompanied by a USP size 5 Fiberwire suture (Arthrex Inc., Naples, FL), while the other (Mini Corkscrew AR-1319FT, 2.7 mm x 7 mm, Arthrex Inc., Naples, FL) has an eyelet that is embedded within the screw and was accompanied by a USP size 0 Fiberwire suture. The IMEX anchors were divided into two groups: modified (IM, n=5) and unmodified (IU, n=5). The IMEX anchor had sharp edges around the eyelet and head, which may have contributed to its failure. Therefore, in the IM group, we manually filed and smoothed sharp edges using a hand-held rotary grinder and file set. The Arthrex anchors (n=5) were tested in the third group (AT). The anchors were screwed into pre-drilled holes of 5/64 inches diameter on a simulated bone block (PCF 50 (0.8g/cc), Sawbones, Vashon, WA); this block density is commonly used for testing screw pullout, insertion, and stripping torques [2]. Using a universal material testing machine (Model 5965, Instron Inc., Norwood, MA), the samples were loaded from 0 N to 60 N uniaxially for 1000 cycles to mimic cyclic loading during hopping gait [3], then ramped to failure, all at a 4.5 mm/s extension rate. We hypothesized that (1) the IM group would have a higher average failure load than the IU group and (2) the AT group would have the lowest failure load among all groups due to its smaller suture size. An independent-sample, two-tailed Student's t-test was used to compare values between the groups, with $p<0.05$ considered significant.

Results and Discussion: All samples in each of the three groups completed 1000 cycles. The loads at failure of the IM, IU, and AT anchors were 400.54 ± 81.72 N, 473.24 ± 42.35 N, and 112.37 ± 4.99 N, respectively. Although it was hypothesized that the modified IMEX anchor (IM group) would have a higher average load at failure than the unmodified IMEX anchor (IU group), there was no statistically significant difference between these groups. The AT anchor group had a significantly lower load at failure ($p<0.05$) than both of the groups with IMEX anchors (Figure 1C), supporting our second hypothesis. In the IU group, two out of five samples failed at the knot, and the remaining three failed around the eyelet. All five samples in the IM group failed around the eyelets, whereas all five samples in the AT group failed at the knots, which may not have been unconnected with the size 0 suture used on the AT group.

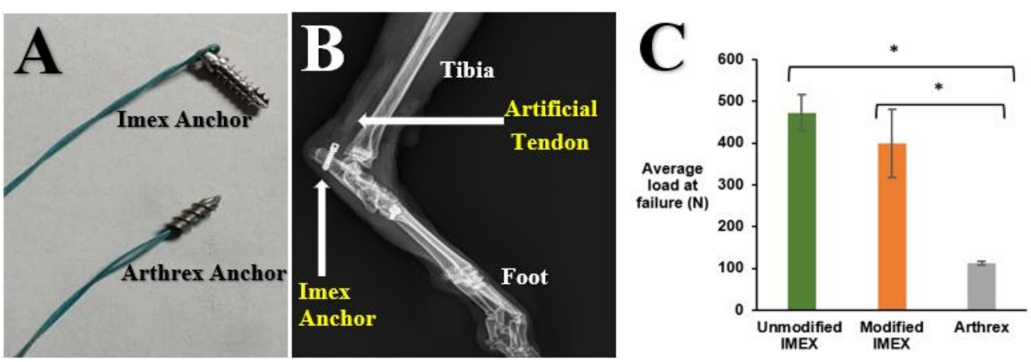

Figure 1 (A). Suture-anchor constructs that were tested in the study (B). Radiograph of the rabbit hindlimb (lateral view) showing attachment of artificial tendon using the IMEX-based suture-anchor construct (C). Bar plot showing the average failure loads of suture-anchor constructs across test groups; asterisks indicate a significant difference between groups ($p<0.05$).

Significance: Quantifying the mechanical strength of orthopedic implants improves our understanding of their in vivo performance and can inform device design and selection for specific clinical applications. Using an appropriate device is critical to avoid costly revision surgeries and patient hardship. We will also use these results to refine our animal model in future studies.

Acknowledgement: NSF CAREER 1944001.

References: [1] Barber FA *et al.* (1993) *Arthroscopy – The Journal of Arthroscopic and Related Surgery* 9(6): 647-654. [2] Sawbones (2023) Product information [3] West JR *et al.* (2004) *Journal of Biomechanics.* 37(11): 1647–1653.

DEEP LEARNING FOR AUTOMATIC SEGMENTATION OF QUADRICEPS CROSS-SECTIONAL AREA: VALIDATION IN PEOPLE WITH ANTERIOR CRUCIATE LIGAMENT INJURY

Beyza Tayfur[1*], Paul Ritsche[2], Jacob Leuteneker[1], Madison Wheeler[1], Olivia Sunderlik[1], Oliver Faude[2], Martino V Franchi[3], Alexa K Johnson[1], Riann Palmieri-Smith[1]
[1] University of Michigan, Ann Arbor, MI, USA
[2]University of Basel, Basel, Switzerland
[3] University of Padua, Padua, Italy
*Corresponding author's email: beyzat@umich.edu

Introduction: Quadriceps muscle cross-sectional area (CSA) is an important outcome measure to understand neuromuscular function in healthy and knee-injured populations. Panoramic ultrasound provides reliable and accessible measurements of muscle CSA. Obtained images are generally manually segmented, which is a time consuming process. Automation of image segmentation can enable large volumes of images to be analyzed in a reliable and efficient way. Previous research showed that deep learning approaches offer fast and objective segmentation of lower limb panoramic ultrasound images comparable with manual segmentation in healthy people.[1] However, muscle structure and quality may change in different knee conditions, such as following anterior cruciate ligament (ACL) injury [2], which may affect the validity of the automation procedures on muscle images of people with different knee conditions. Therefore, we aimed to train convolutional neural networks (CNN) with quadriceps images of people with an ACL injury and compare its validity to models using images from a combination of healthy and ACL-injured people. This will establish the validity of different models to automate muscle CSA segmentation in people with knee conditions.

Methods: We used an available convolutional neural networks (CNN) code, DeepACSA, which has been shown to be valid in healthy people to automate CSA measurement of the vastus lateralis.[1] DeepACSA is publicly available, including the healthy muscle images used to train their models.[1] We used vastus lateralis images of people with an ACL injury (n=116, age 23.25±8.22, 60 females), before (T01) and 2 months after their surgery (T02) since the muscle structure changes between these time points.[2] We trained 3 different models, using only ACL T01 muscle images (n=334, ACL1), using ACL T01 and T02 images (n=430, ACL2), and using the combination of healthy leg images of DeepACSA and ACL T01 and T02 images (n=974, Combined). The CNN used in DeepACSA uses a random 90/10% training/validation data split within the training data set during model trainings. CNN performance was evaluated using intersection-over-union (IoU) scores for the validation data set for all models. After model trainings, we also tested the three different models on all ACL T01 and T02 images for correct and erroneous prediction percentages, which included both seen and unseen images for the models. This was done by visual inspection of input image and model prediction CSA (Fig. 1). We also used the model from the original DeepACSA, which used only healthy leg muscles to train their models. Following visual inspections, best performing model (i.e. the model with the highest percentage of correct predictions) results were compared to manual segmentations results using intra-class correlation coefficients (ICC), 2-way mixed-effects model with absolute agreement and standard error of measurement (SEM). This was performed on 20 randomly selected ACL T01 and 20 T02 images, separately.

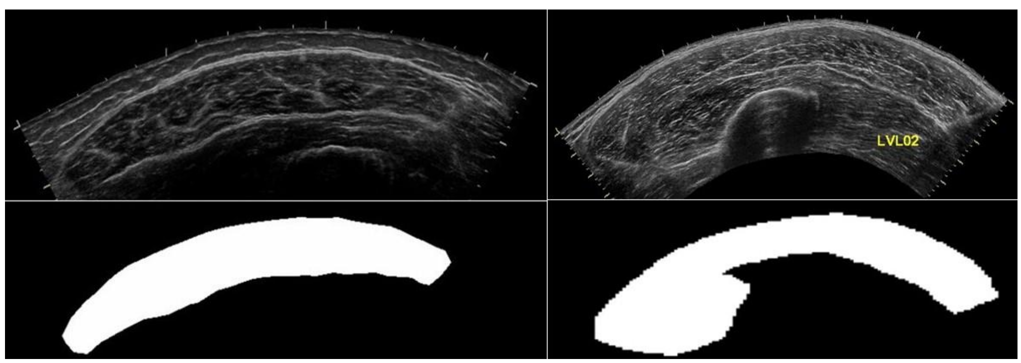

Figure 1. Input images and model predictions. Correct prediction (Left) and erroneous prediction (Right)

Results & Discussion: Overall, all models showed high validation IoU scores (>.995) and the best performing model was the Combined model for both ACL T01 and T02 images (83.24% and 71.87% accurate prediction, respectively). The ICC for T01 was 0.976 (95% confidence interval: 0.941 to 0.991) and for T02 0.953 (95% confidence interval: 0.872 to 0.982). The SEM was 1.05 and 1.17 cm^2 for T01 and T02, respectively. Overall, time to analyse each image was reduced to 5 seconds, with a high percentage of images being accurately analysed by the Combined model. Increased variability in images (Healthy and ACL muscles), and including the same data set for training resulted in high validity in our models for ACL muscles.

Significance: The Combined CNN model developed in this study enables the use of an automated approach in both healthy and ACL injured populations to measure quadriceps (vastus lateralis) muscle CSA in a valid and efficient way. Future studies are needed to validate these new models in other clinical datasets.

Acknowledgements: Research reported in this abstract was supported by the Eunice Kennedy Shriver National Institute of Child Health & Human Development of the National Institutes of Health under Award Number R01HD093626. The content is solely the responsibility of the authors and does not necessarily represent the official views of the National Institutes of Health.

References: [1] Ritsche et al. (2022), *Med Sci Sports Exerc* 54(12), [2] Garcia et al. (2020), *Sports Health* 12(3)

MEASURING VOLUME AND VOLUME CHANGE OF TRANSTIBIAL RESIDUAL LIMBS USING A HIGH-PRECISION LASER SCANNING SYSTEM

Mohammadreza Freidouny, Carson Squibb, Michael K. Philen, Michael L. Madigan*
Virginia Tech, Blacksburg, Virginia, USA
*mlm@vt.edu

Introduction: An estimated 1.6 million individuals in the U.S. have a lower limb amputation, and 185,000 amputations are performed every year [1]. Diurnal changes in residual limb volume can affect prosthetic socket fit, which in turn can cause discomfort, skin irritation, and restrict activities [2]. Accurately measuring these changes can facilitate improving socket fit [3]. Squibb et al. [4] reported the development of a novel high-precision laser scanning system (Figure 1) that measured the volume of a residual limb model with an absolute error less than 0.2%. This study demonstrated the use of this system to measure the volume and volume changes of transtibial residual limbs of human subjects.

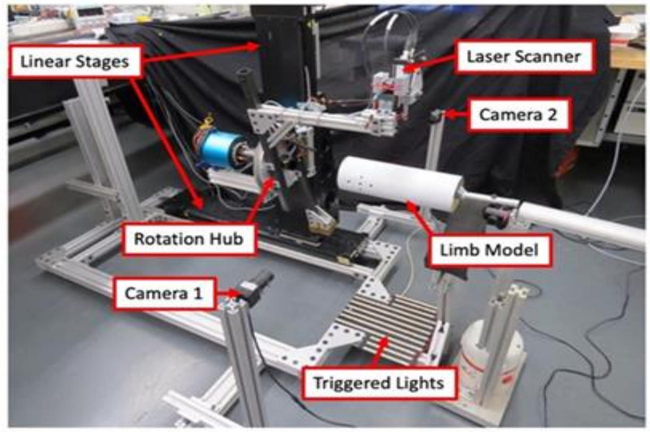

Figure 1: Laser scanner system with a 10 cm diameter model of a residual limb [4]. Each scan of residual limb required ~35 seconds to complete.

Methods: Three subjects (two males, age: 58-60) with unilateral transtibial amputations completed the study. Subjects initially doffed their socket for 20 minutes to allow limb volume to equilibrate. Three scanning phases were then completed using the laser scanning system. Phase 1 involved five consecutive scans between which the limb was held motionless, and enabled measures of scanner test-retest reliability and limb volume at baseline. Phase 2 involved three scans with the subject removing their limb from the scanning area and reinserting it prior to each scan. Phase 3 involved 10 consecutive scans at approximately one-minute intervals after standing for 15 minutes with their prosthesis and doffing the prosthesis. These scans provided a measure of both limb volume change resulting from the standing, and of limb volume recovery after doffing the prosthesis. Intraclass correlation coefficient (ICC) and Standard error measurement (SEM) were calculated from Phase 1 and 2 data to quantify scanner reliability.

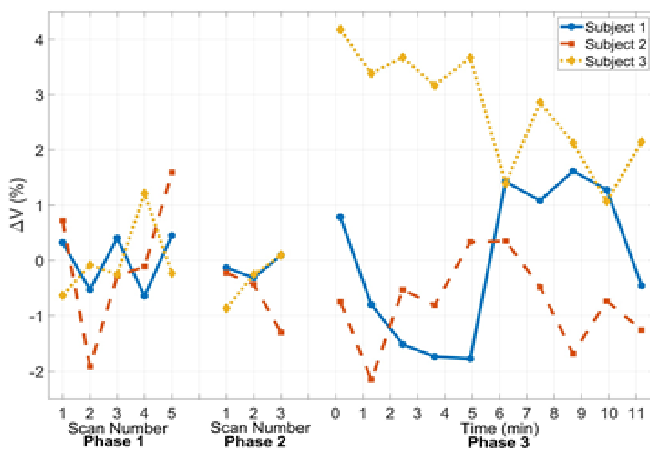

Figure 2: Volume change (ΔV) with respect to the average volume of the five scans in Phase 1.

Results & Discussion: In Phase 1, the maximum volume difference across all scans was less than 2% (Figure 2). In Phase 2, the volume difference was smaller (albeit over fewer scans), indicating the system can accommodate clinically-relevant variations in limb position and orientation. The ICC and SEM values [6] both showed excellent reliability of the laser scanner system for obtaining residual limb volume (Table 1). In Phase 3, the initial volume change from the mean of Phase 1 was less than 1% for subjects 1 and 2, and +4% for subject 3. For comparison, Zachariah et al. [5] reported volume changes of -1.1% to +12.6% after doffing the prosthesis immediately following 4-5 minutes of walking. Over 15 minutes of repeated scans during Phase 3, subjects 1 and 2 showed no consistent trend in volume change while subject 3 showed a decrease in volume. For comparison, Zachariah et al. [5] reported volume increases of 2.4 to 10.9 over 35 minutes after doffing the socket following 4-5 minutes of walking.

As mentioned by [4], movement of the limb toward and away from the cameras and difficulties associated with mesh alignment can be potential factors causing errors in the scans.

Table 1: ICC and SEM values of the volume measurements in phases 1 and 2.

Phase	ICC	SEM (cm^3)
1	0.99	7.13
2	0.99	3.95

Significance: This study demonstrated the use of a novel laser scanner to provide accurate measurements of residual limb volume. Such measurements can be used to better understand factors contributing to volume change, improve finite element analyses of residual limb stress and strain, and in the development of strategies to mitigate its effect on comfort, activities, and quality of life.

Acknowledgements: This work was supported by the National Science Foundation under Grant No. 1906132.

References: [1] Ziegler-Graham et al. (2008) *Arch Phys Med Rehabil 89*(3); [2] Sanders & Fatone (2011) *JRRD 48(8)*; [3] Tantua et al. (2014) *JRRD 51*(7); [4] Squibb et al. (2023) *Measurements: Sensors (In review)*; [5] Zachariah et al. (2004) *JRRD 41(5)*; [6] Portney & Watkins (2000) *Foundations of Clinical Research, Prentice Hall Health.*

MANUAL MUSCLE TESTING APPROACH FOR EMG NORMALIZATION IN YOUNG AND OLDER ADULTS

Skylar C. Holmes[1]*, Ericber Jimenez Francisco, Katherine A. Boyer[1]
[1]University of Massachusetts, Amherst
*Corresponding author's email: scholmes@umass.edu

Introduction: Natural variations in electromyography (EMG) signal intensity exist within and between individuals. To minimize this variation and allow for comparison between groups the EMG signal can be normalized to a reference signal [1]. Normalization to a maximal voluntary isometric contraction (MVIC) using a dynamometer is a common method but obtaining an accurate MVIC for EMG normalization can be time consuming and difficult in older adults. Walking is a submaximal activity and previous research has shown that during gait the peak EMG of the gluteus maximus, quadriceps, and hamstrings are between 5 and 15% of MVIC EMG while plantar flexors and dorsiflexors range from 27-43% of MVIC [2]. This indicates that even in healthy older adults the EMG during gait should not exceed 100% of MVIC. Manual muscle testing (MMT) is the current standard method for assessing strength in the clinical setting and previous research found MMT is comparable to the MVIC method in young adults, but it has not been assessed in older adults [3]. MMT may be a feasible alternative to the traditional MVIC approach to elicit a normalization criterion for gait EMG. Imperative to MMT is providing consistent resistance but whether manual resistance is sufficient to elicit a similar response as fixed resistance is unclear. Therefore, the purpose of this study was to 1) compare manual and fixed resistance MMT protocols and 2) assess an MMT protocol in older adults. We hypothesized that individuals would be able to produce a higher peak EMG with fixed resistance as compared to manual.

Methods: Eight healthy young adults (4 male, 4 female) and 7 healthy older adults (3 male, 4 female) without any musculoskeletal or neurological pathologies participated in the study. Surface EMG was recorded for ten lower limb muscles: Rectus Femoris (RF), Vastus Medialis (VM), Vastus Lateralis (VL), Biceps Femoris (BF), Semitendinosus (ST), Lateral Gastrocnemius (LG), Medial Gastrocnemius (MG), Soleus (SOL), Tibialis Anterior (TA), and Gluteus Maximus (GMA) (Trigno Wireless, Delsys Natick MA). The EMG electrodes were placed on the dominant limb, as indicated by the participant's preferred limb to "kick a ball". Each participant completed a maximal contraction protocol for each muscle and/or muscle group that relied on their ability to move against gravity during a static isometric contraction where resistance was applied. MMT1 relied on manual external resistance to elicit the maximal contraction while MMT2 relied on fixed resistance with the help of a belt (Figure 1). Young participants completed both MMT1 and MMT2 for the following muscle groups: quadriceps, hamstrings, and glutes. Older participants only completed MMT1. For all protocols participants completed two consecutive contractions with 60s of rest period between contractions. The MMT protocol was followed by five level walking trials at a preferred walking speed. EMG data were band-pass filtered at 20 – 500Hz, rectified, and linear envelopes were generated with a 10Hz low-pass filter (MATLAB, The MathWorks Inc, MA). The peak EMG magnitude for each muscle was the peak value of the linear envelope for each contraction. Maximum EMG amplitudes between MM1 and MMT2 were compared using paired samples t-test (α=.05). To assess the ability of the older adults to elicit peak EMG amplitude in MMT1 the peak EMG magnitude for each muscle was extracted and the maximum EMG from level walking trials was divided by the maximum EMG magnitude from MMT.

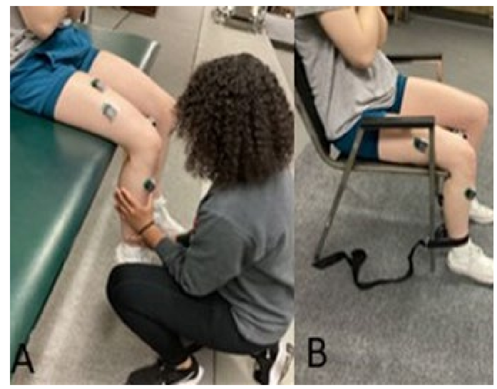

Figure 1: Participant positioning for knee extensor testing: A) using manual resistance B) using fixed resistance.

Results & Discussion: The RF, BF, and GMA did not show any significant difference in peak EMG envelope magnitude between MMT1 and MMT2 ($p>.05$). MMT1 (manual resistance) elicited a significantly higher EMG magnitude in the VM, VL, and ST ($p<.05$). EMG readings from 97.8% gait trials remained below 1.0. Values exceeded 1.0 in the SOL in 1 participant in the young group while values exceeded 1.0 in the MG, LG, and VM in the older group (all different participants), suggesting we didn't capture peak EMG during these contractions.

Muscle	Young	Older
Knee Extensors	0.23(0.2)	0.53(0.3)
Knee Flexors	0.40(0.4)	0.51(0.3)
Plantar Flexors	0.58(0.2)	0.59(0.3)
Dorsiflexors	0.50(0.1)	0.58(0.2)
Gluteus Maximus	0.19(0.1)	0.30(2)

Table 1. Ratio of Maximum EMG amplitude during gait to Maximum EMG amplitude during MMT, all values are Mean (SD)

Significance:

Manual resistance was not different and in some instances superior to belt fixation in eliciting a higher EMG amplitude. This indicates that belt fixation may not be needed to elicit a maximum EMG response when conducting MMT. The ratio of EMG from Gait/MMT was similar for young and older adults suggesting MMT may be a sufficient normalization criterion for gait EMG in older adults.

References: [1] Lehman et al. (1999), *J. Manip. Physiol. Ther.* 22; [2] Ericson et al. (1986), *Scand J Rehabil Med.* 18(4); [3] Tabard-Fougère et al. (2018), *Gait Posture* 60.

DEVELOPMENT AND ASSESSMENT OF A THREE-DIMENSIONAL COMPUTATIONAL MODEL OF THE NEONATAL BRACHIAL PLEXUS

Sarah J. Wright[1*], Michele J. Grimm[1,2]
[1]Departments of Biomedical Engineering and [2]Mechanical Engineering, Michigan State University, East Lansing, MI, USA
*trappsa1@msu.edu

Introduction: The brachial plexus is a complex set of nerves that begins from the cervical (C5-C8) and thoracic (T1) nerve roots. During the birthing process, vaginal or cesarean, these nerves are susceptible to an injury known as Neonatal Brachial Plexus Palsy (NBPP). It has been documented clinically and through research that, for cephalic presentations with the fetal arm adducted against or across the body, the injury initiates at C5 and progresses down to sequentially include the lower nerve roots. Conducting clinical or experimental injury analysis of NBPP is challenging due to the vulnerable population involved – infants. The use of computational modeling allows the exploration and analysis of this nerve complex to investigate the effect of maternal and neonatal parameters on brachial plexus stretch during the birth process. To date, there are no 3D neonatal brachial plexus models published. An anatomically accurate FEM model will allow in-depth analysis of NBPP injuries by providing a better understanding of stress distribution within the nerves. Furthermore, the model will provide knowledge of the progression of injury when force is applied. Our current analysis demonstrates (1) the injury progression along the plexus and (2) the location of stress values above the injury threshold limit (0.22 MPa) [1]. We anticipate our novel three-dimensional neonatal brachial plexus model can be used simulate and study specific brachial plexus injuries (Erb's Palsy, Klumpke's Palsy, etc.) to further investigate patterns of injury in NBPP.

Methods: The model was designed, meshed, and evaluated in Solidworks (Dassault Systemes). The dimensions of the brachial plexus's roots and trunks were collected during primary reconstructive surgery on infants. The diameter and length of the brachial plexus's cord's, divisions, and branches were determined based on the ratio of adult plexus's dimensions in relationship to the known neonatal dimensions. As there are no material properties published for human neonatal brachial plexus, the Young's modulus and Poisson's Ratio were taken from porcine samples [1,2].

Boundary conditions and loads were established within Solidworks static simulation. An encastré condition was applied to the midline of the spinal cord to constrain all active structural degrees of freedom. This condition was selected as the *in situ* spinal cord is encased within the foramen of the vertebrae.

As an initial determination of applied load for the ends of the distal nerve branches, the force needed to cause a maximum stress within a nerve root of 0.22 measured stress at failure (mean + 1 SD) for the nerve roots and trunks in an experimental study on piglets [1]. The necessary load was determined to be 0.2125 N – thus this value was applied perpendicular to the distal end of each terminal branch, equally distributed across the transverse cross-sectional area.

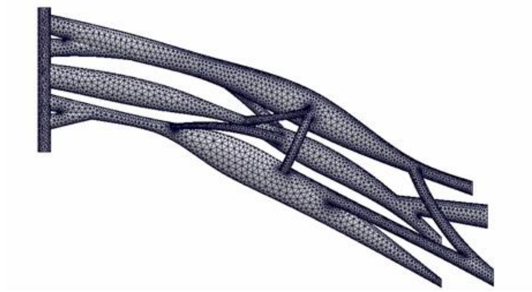

Figure 1: Mesh Quality Plot conducted within Solidworks of the anterior view of the left neonatal brachial plexus.

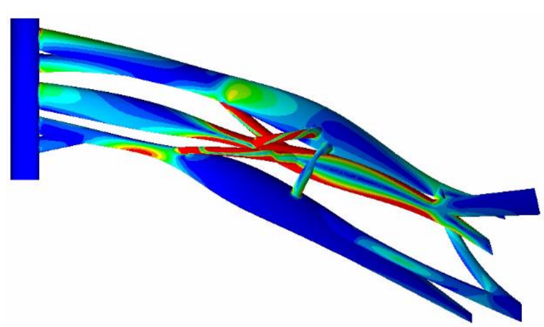

Figure 2: Von Mises Stress resulting from a perpendicular force applied to the nerve endings.

Results & Discussion: Clinical patterns of brachial plexus injury and some experimental work demonstrate that C5 and C6 experience higher stress under initial loading of the brachial plexus than do the lower roots, and that these levels of the complex are damaged first [3] [Fig 2]. Our model simulation confirms this outcome.

The stress at C5 within the initial (control) model was 0.2225 MPa – concluding that an injury has a reasonable likelihood of occurring as it is over the injury threshold of 0.22 MPa [1]. Within this control model, the C6 nerve root has a stress value of 0.113 MPa – below the threshold. When the C5 nerve is severed, the stress at C6 increases 7-fold. If the injury progresses to include C6, this pattern of injury is commonly known as Erb's Palsy. Further analysis indicates that as each successive nerve root fails (through rupture or avulsion), a constant applied force will cause the stress to increase in nerve roots that remain intact – increasing their risk of failure. If the injury progresses through all five nerve roots, this results in a total palsy.

An anatomically accurate FEM of a neonatal brachial plexus can be used to replicate and evaluate different NBPP injury patterns, as well as the progression of NBPP along the brachial plexus complex. Modeling these injuries can improve and advance the science of understanding the effect of key maternal and neonatal variables on injury risk during pregnancy and specifically the birthing process.

Significance: The stress patterns presented within these initial simulations may be an obvious result to biomechanical engineers, but they are not obvious to neurosurgeons or obstetricians. This model allows the progression of injury to be visually explained to medical professionals and will allow for the exploration of the effect of forces of labor and delivery on NBPP injuries.

Acknowledgements: We thank our colleagues from Lynda Yang's neurosurgery team at the University of Michigan for insight and expertise that assisted the research – including the infant nerve dimensions. Funding provided by NSF Award CBET 2028474.

References: [1] Singh et al. (2018), *J. Brachial Plex. Peripher. Nerve Inj*. 13, e8–e14; [2] Nishida et al. (2015), *Neural Regen Res*, 10(11), pp. 1869–1873; [3] Metaizeau et al. (1979), *Chir Pediatr*, 20(3), pp. 159–163.

DUAL TASK GAIT IS NOT ADVERSELY AFFECTED BY A CAREER OF COLLISION SPORTS

Thomas A. Buckley[1], Jessie R. Oldham[2], Barry A. Munkasy,[3] Kristen Williams,4
[1]University of Delaware, [3]Georgia Southern University, [2]Virginia Commonwealth University, [4]Vanderbilt University
Email: TBuckley@udel.edu

Introduction: Repetitive head impacts (RHI) are commonly described as head impacts which frequently and legally occur within contact sports, but do not elicit clinical signs or symptoms of concussion. These RHI may be associated with a variety of later life neuropathologies including elevated rates of dementia and associated neurodegenerative disorders which have been identified in RHI exposed athletes.[1] Gait is a highly stable motor task in generally healthy young adults and has been termed the "6th Vital Sign" based on strong associations between gait speed and numerous critical life outcomes. The use of gait overcomes limitations of prior studies which used either clinical tests with psychometric limitations and practice effects or neuroimaging outcomes which may lack clinical translation. Therefore, the purpose of this study was to assess dual task (DT) gait performance over the course of an intercollegiate athletic career. As exposure to high levels of RHI have been linked to neurological deficits, we hypothesized that RHI exposed athletes in collision/contact sports would show deficits in DT gait as compared to those in limited/non-contact sports.

Methods: We recruited 31 student-athletes who participated in either Collision/Contact (e.g., football, soccer; N=17, HT: 1.77 ± 0.11 m, WT: 77.7 ± 23.5 kg) or limited/non-contact (e.g., swimming, baseball, field hockey; N=15, HT: 1.72 ± 0.13 m, WT: 66.4 ± 8.0 kg) based on likely exposure to RHI from two institutions. Participants were assessed at PRE (i.e., prior to intercollegiate athletic participation) and POST (following a collegiate athletic career) and there was a mean of 1,324 days between assessments with no difference between groups (p=0.583). All participants completed five trials of dual task gait using working memory tasks (e.g., serial 7's, spelling a word backwards) which has previously been shown to be an effective cognitive challenge in a concussion populatuon.[2] The gait data was collected on two separate systems and there were no differences between sites at either time point. At one site, gait performance was assessed using a 4.9 m GAITRite instrumented walkways (CIR Systems, Sparta, NJ, USA). The second site used inertial measurement units (Opal Sensor, APDM, Inc, Portland, OR) with an accelerometer attached with elastic wraps on each foot and L5 and data was collected at 128 Hz.

To assess for changes over the course of a career, separate 2 (Group: RHI, Non-RHI) X 2 (Time: Pre, Post) mixed design ANOVA were performed for each dependent variable of interest and the model was adjusted for concussion history at the time of test and sex. Based on A-priori research questions, the mains effect for both group and time were also assessed and significant main effects were followed up with Cohen's d effect size calculations.

Results & Discussion: There were no significant group by time interaction for dual task gait velocity (Non-RHI: PRE: 1.15 ± 0.14 m/s and POST: 115 ± 0.16 m/s; RHI: PRE: 1.10 ± 0.17 m/s and POST: 1.12 ± 0.16 m/s; F=0.801, P=0.777). There were no DT Gait Velocity significant main effects for Time (F=0.238, P=0.631) or Group (F=2.33, P=0.133). (Figure) There were no significant group by time interaction for dual task stride length (Non-RHI: PRE: 64.8 ± 6.8 cm and POST: 64.3 ± 8.0 cm and RHI: PRE: 62.4 ± 9.2 and POST: 63.8 ± 9.5 cm; F=0.004, P=0.958). There were no DT Step Length significant main effects for Time (F=0.039, P=0.860) or Group (F=0.155, P=0.700). (Figure)

The long-term effects of RHI are a critical concern given the inherent nature of head impacts in contact sports along with the suspected associated later life neuropathology. College athletics is typically the highest level of participation for most athletes and the time they experience the largest number of RHI in their playing career. The primary finding of this study was no difference between RHI and non-RHI athletes dual task gait performance between the beginning and conclusion of their collegiate athletic careers. While the long-term effects of RHI remain to be elucidated, these results suggest that RHI do not adversely affect gait performance in the short-term when the individual is still young.

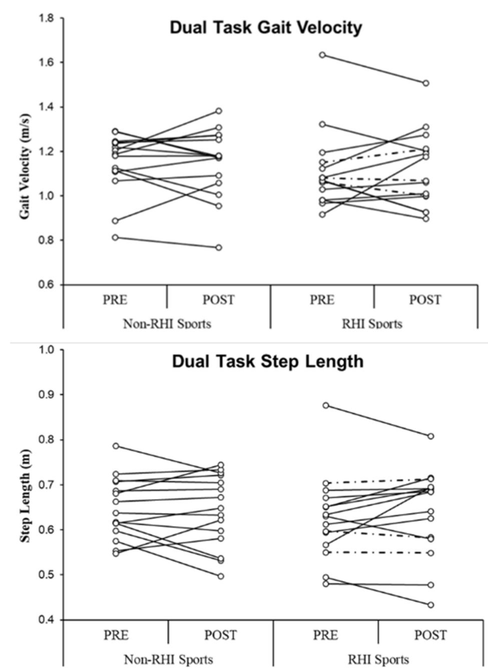

Figure. There were no significant group by time interactions for either Dual Task Gait Velocity or Step Length.

Significance: The long-term effects of RHI are a critical challenge to sports medicine providers and pose potential serious public health concerns. The results of this study suggest that participating in RHI exposure such as soccer and football as a collegiate student-athlete does not impair gait performance across their collegiate career or when compared to non-RHI exposed student-athletes. Subsequent studies should perform a more comprehensive assessment including cognition and mental health. Finally, prospective longitudinal studies are required to further elucidate the long-term effects of RHI on neurological health.

Acknowledgments: The project was funded, in part, by a grant from the NIH/NINDS (1R21NS122033).

References:

1. Russell et al, (2022) J Neurol Neurosurg Psychiatry 93(12)
2. Buttner et al, (2019) Br J Sports Med. 54(2)

LOST TO THE DECADES: A PROMISING VARIABLE FOR POSTURAL INTERVENTION

Katherine E. Feroben[1*], Nathan D. Schilaty[1], Nathaniel A. Bates[2], Takashi Nagai[3]
[1]University of South Florida, [2]Ohio State University, [3]USARIEM
*Corresponding author's email: fek@usf.edu

Introduction: For decades, 'frequency dispersion' has been labeled as insignificant for determining postural implications. Despite this variable being accurate when using inertial sensors, there is very little change between healthy, aged, and diseased individuals.[1] For many years, 'exercise capacity' has been used to determine health and aging risks. The chances of survival have been shown to increase with the capacity to have a more active lifestyle.[2] Even low intensity physical activity has been shown to improve symptoms associated with psychological disorders, thereby improving quality of life.[3] When measuring the effects of interventions in physical activity, inertial sensors are utilized to determine things such as movement angles, velocity, direction, and alignment while doing a standing balance task.[4] Frequency dispersion is a dimensionless measure of variability of the frequency content of the power spectral density.[5] Previous research has disregarded frequency dispersion due to the "unreliability" of its measures, noting that the subjects could have changed balance strategies between the two collections of data.[6] We speculate that this development of new or altered balance strategies could be the exact variable we should be looking at to determine reliability of intervention programs. Higher frequency dispersion after intervention could point to cognitive changes that help the body adapt to physical shifts more readily.

Methods: This study was approved by the Mayo Clinic Institutional Review Board (20-004586). Informed consent was obtained from each participant prior to data collection. Two cohorts were determined by the participant themselves into a control and an intervention group. Both groups participated in baseline data collection lasting approximately 30 minutes. The participants then returned after six weeks to have a post-intervention data collection. Data collection consisted of balance/gait assessments. Balance/gait assessment included three trials of balance repeated three times each and a 4-meter walk speed test, both using Opal IMUs (APDM Inc, Portland, OR, USA). Participants were asked to stand still with their arms by their side, and their feet were positioned by a standardized object. Two tasks were conducted with these specifications: Eyes Open (EO) for thirty seconds and Eyes Closed (EC) for thirty seconds. The third task completed for balance had the participants in a tandem position with one foot forward and the forward heel contacting the toes of the foot positioned behind. All trials of tandem were completed with eyes closed.

Results & Discussion: The intervention group of individuals had two sets of data collected: the first set was at the initial enrollment (Baseline) and the second set was after 6 weeks of participation in the intervention (Post) (see Methods). Compliance was based on at least 70% completion of the intervention exercises. Statistical analysis was run utilizing the program JMP 16 Pro. Upon statistical significance analysis, two tasks were determined to have a p-value < 0.01 for the same variable. Frequency dispersion was shown to be significantly greater in the post data collection for the individuals that complied with the 6-week intervention program consisting of low-intensity balance exercises. The two tasks showing this significant change were EO and EC. This significant increase in frequency dispersion suggests that the participants had adapted new or additional balance strategies to combat the physical task of balance. The significance noted in both EO and EC could suggest that the intervention program effects different aspects of balance. In the case of EO, we can speculate that the utilization of the intervention instructional videos was able to help the sensory inputs aside the visual sensory system. Shown in a previous study, the distraction of an external focus improved the balance of the individual. This visual sensory distraction seems to help the body adjust to the loss of visual attention, allowing the vestibular and somatosensory systems to make up the loss. [7] In the case of EC, this significant increase in frequency dispersion could validate that the EO increase relies on the vestibular and somatosensory systems when completing the task. This overall increase in frequency dispersion could indicate that the vestibular and somatosensory systems are adapting to the task in the event that visual input is lost. Thus, changing the prioritizing system in balance after the new adaptations had been subconsciously learned. Here, we suggest that the measure of frequency dispersion can be used when determining the positive effects associated with physical activity interventions. A significant change of frequency dispersion between the baseline data and the post intervention data in the cohort completing the intervention program was seen.

Significance: In the realm of biomechanics, prior research has shown that exercise or physical activity can reduce age-related pathologies after initial onset. The results of this study could point investigators to another variable that could lead to conclusions previously overlooked or conclusions that could be better validated with the additional parameter. For decades, frequency dispersion has been ignored for its inability to be re-testable, but the results of this study could implicate this variable in a new light moving toward a healthier future for both mind and body.

Acknowledgements: Funding for this study was provided by the NCMIC Foundation.

References: [1] Mancini et al. (2012), *J Neuroeng Rehabil* 9 (1); [2] Myers et al. (2002), *New England Journal of Medicine* 346 (11); [3] Izquierdo-Alventosa et al. (2020), *Int J Environ Res Public Health* 17 (10); [4] Rocchi et al. (2006), *Neurosci Lett* 394 (2); [5] Curtze et al. (2016), *Phys Ther* 96 (11); [6] Craig et al. (2017), *Neuroeng Rehabil* 14 (1); [7] Ma et al. (2022), *J Neuroeng Rehabil* 19 (1);

BIOMECHANICAL OUTCOMES ASSOCIATED WITH 3 COMMERCIALLY AVAILABLE MICROPROCESSOR KNEES DURING LEVEL GROUND AND STAIR ASCENT WALKING TASKS

Kinsey R. Herrin[1,2*], Sujay Kestur[1], Sixu Zhou[1,2], Aaron Young[1,2]
[1]George W. Woodruff School of Mechanical Engineering, Georgia Institute of Technology
[2]Institute of Robotics and Intelligent Machines, Georgia Institute of Technology
*Corresponding author's email: kinsey.herrin@gatech.edu

Introduction: The challenges which follow transfemoral amputation (TFA) significantly impact an individual's ability to function independently in the community and thus their overall quality of life. In addition to greater difficulties with community ambulation than those with below the knee amputation[1], these patients are also at greater risk for falls, have higher energy costs associated with walking, greater gait deficits and are less likely to be satisfied with their prosthesis. These challenges highlight a key difference between the above and below knee patient populations- loss of the anatomical knee, and the criticality of the prosthetic knee for effective rehabilitation following TFA. Microprocessor prosthetic knees (MPKs) are the gold standard for prosthetic intervention over non-MPK devices[2, 3] given their benefits in relation to improved gait, safety, comfort, confidence, reduced falls, balance, patient satisfaction and reduced energy expenditure, greater ease in negotiating varying terrains, and improvements in multi-tasking. However, despite this overwhelmingly long list of benefits, very little work has been done to understand specific benefits of individual MPKs. This approach limits evidence available to clinicians during the prescription process immediately following TFA, forcing clinicians to rely on experience, trial fittings or reimbursement factors when selecting a knee for a patient.
Therefore, in this study, we examine biomechanical outcomes associated with 3 commercially available knees- 2 passive knees and one powered knee during common community ambulatory tasks. We hypothesize that the lighter weight passive knees will show improved performance during level ground tasks which required little added power, while the powered knee will perform better in a stair ascent task which requires increased power injection to complete with normal biomechanics.

Methods: Eight participants with transfemoral amputation consented to an IRB approved protocol and then were fit and trained on either the Ossur Rheo, Ossur Power Knee or Ottobock C-leg 4 (in randomized order) by a certified prosthetist and wore each knee at home for a 1-week period. Following the acclimation period, participants completed a 10mwt (10-meter walk test) over level ground on an instrumented gait mat (PKMAS; ProtoKinetics LLC, Havertown, PA), and we collected full body biomechanics (Vicon; Denver, CO; Bertec; Columbus, OH) during a stair climbing task. Following completion of all performance tasks, participants were then fit and trained with the next MPK to wear at home for a week and returned to the lab for repeat testing until all three MPKs were completed.

Results & Discussion: As seen in *Figure 1*, during the level ground 10mwt, we observed that on average participants walked faster, had reduced asymmetry and reduced gait variability index (GVI, a correlate with fall risk) in the passive MPKs compared to the Power Knee. The C-leg showed significant improvements ($p<0.05$) in these outcomes compared to the Power Knee when looking at velocity and GVI, and both C-leg and Rheo had significantly improved stance time asymmetry compared to the Power Knee. In contrast, during the stair ascent task, we observed that the prosthetic side knee contributed significantly more positive energy in the Power Knee condition than either of the passive knees. Additionally, we observed more normal knee kinematics (improved knee flexion) in stair ascent in the Power Knee condition than either the C-leg or Rheo knees.All participants who enrolled in the study wore passive MPKs as their clinically prescribed prosthesis and 75% of the participants (n=6) wore C-legs. We accept our hypothesis as our data indicate that during level ground walking, the C-leg and Rheo both performed well for most users but as expected, do not provide any assistance for activities requiring active power such as stair climbing. For certain users, activities beyond level ground walking may represent an important aspect of complete rehabilitation and as such, clinical prescription should carefully weigh pros and cons associated with varying technologies to allow maximum benefit to the user.

Significance: Understanding outcomes associated with specific MPKs may allow clinicians to prescribe based on the anticipated activities and needs a patient will have following amputation. This data may also be useful in the development of future MPKs capable of passive mechanics during less demanding ambulatory tasks while allowing for the injection of power during more difficult tasks.

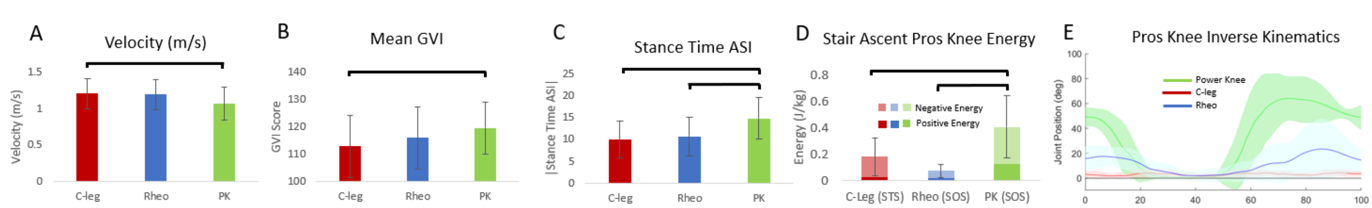

Figure 1. Horizontal black bars indicate significant differences at $p<0.05$. Participants A. walked significantly faster, and B. reduced Gait Variability Index in the C-leg compared to the Power Knee. C. Participants had reduced stance time asymmetry in the C-leg compared to the Power Knee and the Rheo compared to the Power Knee. D. The Power Knee prosthetic side knee joint contributed more positive joint energy during stair ascent, but no differences were seen in total energy between knees and E. had greater knee flexion than the C-leg or the Rheo.

Acknowledgements: This work is funded through a grant from the DoD CDMRP Award Number W81XWH-21-1-0686.

References: [1] Davies, et al. (2003) *POI* 27(3); [2] Kaufman, et al. (2006) *J Biomech* 39; [3] Kaufman et al. (2007) *Gait and Posture* 26(4)

OPTIMAL-PREP MOTOR LEARNING STRATEGIES IMPROVES QUADRICEPS PEAK TORQUE IN PATIENTS WITH ANTERIOR CRUCIATE LIGAMENT RECONSTRUCTION

Jennifer A. Hogg[1*], Ryan D. Mayfield[1], Evan T. Harper[1], Levi D. Grace[1], Jed A. Diekfuss[2,3,4]
[1]University of Tennessee at Chattanooga, Chattanooga, TN
[2]Emory Sports Performance And Research Center (SPARC), Flowery Branch, GA
[3]Emory Sports Medicine Center, Atlanta, GA
[4]Department of Orthopaedics, Emory University School of Medicine, Atlanta, GA
*Corresponding author's email: jennifer-hogg@utc.edu

Introduction: Following primary anterior cruciate ligament (ACL) injury, secondary injury rates to either the ipsilateral or contralateral ACL remain high despite concerted preventive and rehabilitative efforts [1]. Quadriceps muscle force output is a known shortcoming following ACL reconstructive surgery (ACLR). Approximately 1 in 3 ACLR patients attain symmetrical quadriceps muscle strength at 6 months post-ACLR [2], typically regaining full symmetry 4.5 years post-ACLR [3]. In addition to short-term effects of quadriceps dysfunction, lingering deficits increase risk of early osteoarthritis progression [4].

Historically, rehabilitation following ACLR has been limited to local joint function, focusing on range of motion and isolating the surrounding musculature [5]. Recent calls for more holistic treatment of knee injuries [6] advocate for the inclusion of centrally-driven processes to promote robust post-injury outcomes. Motor learning strategies may address this need. The OPTIMAL-PREP theory [6,7] includes 3 pillars, often employed simultaneously; enhanced expectancies and autonomy support to target motivation and external focus of attention to target automatic processes.

Due to the need to develop holistic rehabilitative strategies to address quadriceps deficits following ACLR, we hypothesized that compared to a control condition, an OPTIMAL-PREP condition would result in greater quadriceps and hamstring isokinetic peak torque and rate of force development and that these effects would be more pronounced in the surgical limb compared to the uninvolved limb.

Methods: We employed a two-treatment crossover design to test the acute effects of an OPTIMAL-PREP condition on isokinetic quadriceps and hamstrings torque output. Thirteen participants (10 females) 23 ± 19 months post-ACLR volunteered for this single session study (22.5 ± 3.0 yrs; 170.7 ± 8.3 cm; 71.5 ± 13.4 kg). All participants were cleared for full participation in activity. Patients with re-injuries or contralateral tears were excluded. Seven and six participants were allocated to the control and experimental conditions first, respectively, then switched and completed the remaining condition. Both conditions consisted of 5 repetitions at 60°/sec (concentric quadriceps + concentric hamstrings) on a Biodex isokinetic dynamometer outfitted with Humac NORM software. The uninvolved limb was tested first, followed by the involved. For the control condition, participants were instructed to perform the exercise "as hard and fast as possible." For the OPTIMAL-PREP condition, participants were additionally told that "Research shows that if you focus on moving the line on the screen (external focus pillar) you will exhibit greater quadriceps output (enhanced expectancies pillar)." Participants were also given a choice of which graph they wanted to view during the testing (autonomy support pillar). Peak torque (Nm) and rate of force development (RFD; Nm/s/kg) for the quadriceps and hamstrings were extracted from among the 5 repetitions. Four 2x2 (side by condition) RMANOVAs were conducted. *A priori* effect size of η_p^2 of 0.06 (moderate) was considered meaningful.

Results: Descriptive statistics for all dependent variables, stratified for side and condition, are presented in Table 1. For quadriceps peak torque, we observed moderate effects for the side by condition interaction (η_p^2 = 0.13, p = 0.21) and the main effect for side (η_p^2 = 0.06, p = 0.42) and a large effect for condition (η_p^2 = 0.23, p = 0.08). For hamstrings peak torque, we observed moderate effects for side (η_p^2 = 0.13, p = 0.22) and condition (η_p^2 = 0.10, p = 0.29). For quadriceps RFD, we observed no meaningful effects. For hamstrings RFD, we observed moderate effects for side (η_p^2 = 0.11, p = 0.25) and condition (η_p^2 = 0.11, p = 0.84).

Side	Condition	Quad Pk Torq (Nm)	Ham Pk Torq (Nm)	Quad RFD (Nm/s/kg)	Ham RFD (Nm/s/kg)
Involved	Control	154.0 ± 40.0	96.8 ± 20.0	3.4 ± 1.4	2.8 ± 0.8
	OPTIMAL-PREP	162.5 ± 43.4	99.5 ± 21.5	3.4 ± 1.4	2.8 ± 0.9
Uninvolved	Control	162.2 ± 27.9	99.6 ± 19.4	3.3 ± 1.0	3.0 ± 0.8
	OPTIMAL-PREP	162.9 ± 34.3	102.5 ± 16.8	3.3 ± 1.0	2.9 ± 0.8

Table 1: Descriptive statistics (mean ± SD) for all outcome variables for each limb and condition.

Discussion: Our hypothesis that the OPTIMAL-PREP condition would result in greater improvements on the involved surgical limb was partially supported. In particular, improvements in quadriceps peak torque were driven by the surgical limb. Quadriceps peak torque is a frequently used marker of quadriceps muscle function and we observed a mean improvement of 8 Nm for the involved limb between conditions. It is possible that the enhanced expectancies portion of our manipulation ("…you will exhibit greater quadriceps output") targeted the quadriceps more than the hamstrings, partially explaining our results.

Significance: Quadriceps strength deficit is a known shortcoming of current ACL rehabilitation. Motivational and attentional motor learning strategies may be beneficial for improving quadriceps muscle function in this population. We urge clinicians to consider implementing OPTIMAL PREP strategies when training and testing post-surgical leg muscle strength.

References: [1] Webster et al. (2021), *Orth J Sports Med* 9; [2] Cristiani et al. (2019), *KSSTA* 27; [3] Tsai et al. (2022), *KSSTA* 30(10); [4] Patterson et al. (2020), *Br J Sports Med;* [5] Sugimoto et al. (2012), *J Athl Train* 47(6); [6] Diekfuss et al. (2021), *J Sci Sport Exer* 3(1); [7] Wulf & Lewthwaite (2016), *Psych Bull Review* 23.

EFFECTIVENESS OF SOLID GEL AS AN ALTERNATIVE TO TRADITIONAL LIQUID ULTRASOUND GEL FOR MUSCULOSKELETAL ULTRASOUND IMAGING

Samuel T. Kwak[1*], Madison A. Gaines[1], W. Knox Pittman[2], Young-Hui Chang[1]
[1] School of Biological Sciences, Georgia Institute of Technology
[2] Wallace H. Coulter Department of Biomedical Engineering, Georgia Institute of Technology
*Corresponding author's email: samueltkwak@gmail.com

Introduction: Ultrasound imaging is a non-invasive way to measure muscle-tendon structures *in vivo*. Generating ultrasound images requires an intermediary medium, most commonly liquid ultrasound gel, to transmit sound waves from the ultrasound probe to the subcutaneous tissues. However, using liquid gel creates a low friction interface at the skin, which can lead to the probe moving relative to the muscle over time during movement. This requires readjusting the probe, which may alter its orientation relative to muscle fascicles and change their measurement in the scanned image. For example, imaging the muscle-tendon junction (MTJ) of the medial gastrocnemius (MG) muscle can be particularly troublesome as the 3D skin surface changes to become uneven with activation, causing the probe to lose contact with the skin.

Solid gel has similar acoustic properties to liquid ultrasound gel. In the context of ultrasound imaging, solid ballistics gel has been used as a phantom body part for medical training purposes [1]. Since it melts at temperatures greater than 150°F, solid gel is also moldable and reusable. Due to these properties, solid gel may be a promising alternative to liquid gel for ultrasound imaging of musculoskeletal structures. Some studies have compared the two types of gel in different contexts [2,3], but none have assessed its use during active movement. Here, we evaluated the effectiveness of a solid gel for musculoskeletal ultrasound imaging during a jumping task. We hypothesized that solid gel would reduce ultrasound probe movement while generating a comparable quality image of underlying musculoskeletal tissues. We also predicted that image quality would improve with a smaller solid gel thickness.

Methods: Preliminary data were collected on one subject that consented in accordance with a protocol approved by the Georgia Institute of Technology Institutional Review Board. We placed an ultrasound probe onto the MG MTJ and wrapped it with an elastic band. As an intermediary between the probe and the skin, we used either liquid ultrasound gel or a commercially available solid ballistics gel with a thickness of 2 mm or 20 mm. Markings were traced onto the skin so that the probe was placed on the same location between collections.

The subject performed 70 countermovement vertical jumps using each material. Ultrasound images were captured at 60 Hz on every 10th jump. We used the blind/referenceless image spatial quality evaluator (BRISQUE), which quantifies image distortion [4], to measure the image quality during quiet standing as well as at maximum shortening of the MG muscle, when the MTJ was most contracted during the jump. We measured probe movement relative to the skin by measuring the distance travelled by the MTJ relative to the first jump.

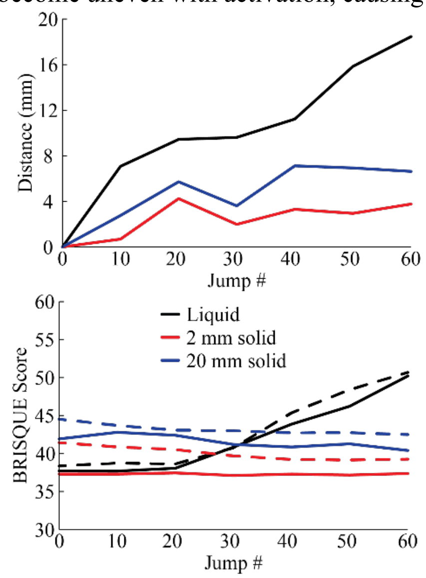

Figure 1: (a) Distance the probe moved relative to the leg; and (b) BRISQUE score before jumping when using liquid (black), 2 mm solid (red), and 20 mm solid (blue) gel. Dashed lines indicate BRISQUE score at maximum muscle shortening.

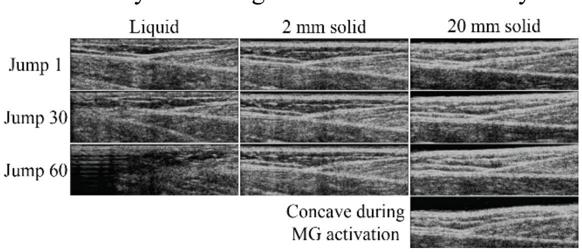

Figure 2: Ultrasound images of the MG MTJ during quiet stance before a jump using different gels.

Results & Discussion: Through 60 countermovement jumps using liquid ultrasound gel, the ultrasound probe moved 18.5 mm relative to the MTJ and no musculoskeletal structures were visible by the 70th jump (Fig. 1a). This movement was evident in the BRISQUE score which increased by 12.5 points during standing and 12.3 points during maximum shortening, indicating a decrease in image quality. The MTJ was no longer identifiable for scores above 48 (Fig. 1b, Fig. 2). When using the 2 mm and 20 mm solid gels, the probe moved 3.8 and 6.6 mm, respectively. Using solid gel either did not change or even increased the image quality by 1.5 to 2.2 points.

The natural uneven shape of the surface of the MG MTJ was apparent when using the 20 mm solid gel (Fig. 2, bottom right). In contrast, the skin is flattened when using either the liquid gel or a thin solid gel, most likely due to the flat ultrasound probe pressing against the leg. While more data are needed to confirm these preliminary results, all tested gels resulted in comparable results for a short-term activity. The thicker solid gel, however, may provide an advantage for producing clear repeatable images that more closely resemble natural muscle movements while also allowing for longer data collections without the need for probe readjustment.

Significance: Solid gel has the potential to improve current standards for ultrasound imaging due to its reusability, customizability, and greater friction against the skin without sacrificing image quality. This can help lower the barrier to expanded use cases of ultrasound imaging studies over a broad range of different activities.

Acknowledgements: This work was supported by the National Science Foundation though the NRI grant 1734416.

References: [1] Alves et al. (2020), *Ultrasound Med Biol* 46(8). [2] Klucinec. (1996), *J Athl Train* 31(4). [3] Tsui et al. (2012), *Can J Anaesth* 59(2). [4] Mittal et al. (2012), *IEEE Trans Image Process* 21(12).

A SINGLE SESSION VR BASED MIRROR THERAPY AFFECTS MOTOR CORTEX BUT NOT NEUROMUSCUALR ACTIVATIONS

Sheridan M Parker[1*], Brian Ricks[2], Nick Stergiou[1], Jorge Zuniga[1], Brian A Knarr[1]
[1]Department of Biomechanics, University of Nebraska at Omaha, Omaha Nebraska, USA
[2]Department of Computer Science, University of Nebraska at Omaha, Omaha Nebraska, USA
*Corresponding author's email: sheridanparker@unomaha.edu

Introduction: Previous research has shown that mirror therapy can promote neuroplasticity through visual feedback leading to decreased asymmetrical motor cortices activations and improved motor function [1-3]. However, there is a need for more accessible home-based rehabilitation programs, especially considering situations like the recent pandemic. Virtual Reality (VR) is a novel technology that allows for games to be performed remotely, for example in a home-based setting or remote from a rehabilitation clinic. We have developed a custom mirror-therapy based Balloon Simulation in VR where the game's purpose is to pop as many balloons as possible within a 1-minute time limit. We hypothesized that there would be an increase in peak whole motor cortex activation when performing the VR simulation with augmentation and post-augmentation for the affected hand (AFH) and bilateral hands (BLH) while there would be no difference between baseline, augmentation, and post-augmentation conditions for the less affected hand (LFH). We further hypothesized that there would be an increase in neuromuscular activation for the *wrist flexors, wrist extensors, biceps brachii, and lateral triceps* during the augmentation condition compared to baseline and post-augmentation conditions for the AFH, LFH, and BLH at 10%, 50% and 90% of amplitude probability distribution function (APDF).

Methods: Nine chronic post-stroke adults participated in the study. Participants were asked to complete the Balloon Simulation (Oculus Rift, Oculus) under observation with fNIRS (Nirsport2, Nirx). Participants completed the Balloon Simulation under 3 conditions, baseline, augmentation, and post-augmentation. The participants saw only the virtual hand avatars for the AFH, LFH and BLH that performed the task for baseline and post-augmentation conditions. For the augmentation condition, the participants saw both virtual hand avatars such that the contralateral hand avatar mirrored the tested hand for the AFH and LFH hand conditions. For the BLH augmentation condition, participants saw the virtual hand avatars mirror the LFH movements. BLH, AFH and LFH conditions were randomized within the baseline, augmentation, and post-augmentation conditions. Three trials were performed for each AFH, LFH and BLH during each condition for a total of 27 trials collected. A 3-minute rest period was provided between conditions, and a 1-minute rest period was provided between trials. To measure cortical motor cortex activations, fNIRS was used. The fNIRS cap was centered over the vertex (Cz) of the head with an 8x7 sensor-detector (S-D) montage and short-separation channels resulting in 20 measurement channels. The montage was placed over the motor cortices following the 10-20 international probe placement standard. The NIRS AnalyzIR toolbox was used to process fNIRS data [4]. The raw signals were resampled to 4Hz to account for high frequency data. The resampled signals were then converted to optical/ density with a partial path length factor of 1. The optical density signals were then converted to hemoglobin concentrations using the modified Beer-Lambert Law. A general linear model (GLM) analysis was applied to the hemoglobin concentration metric with an auto regressive-iterative least-squares function to obtain levels of activation, beta (β) values, for each measurement channel. A mixed effects model was performed comparing the baseline, augmentation, and post-augmentation conditions using beta values and fixing for participants. A Benjamini-Hochberg statistical significance correction was applied to account for multiple comparisons. Data and statistical analyses were performed in MATLAB R2018a with significance set at $q<0.05$. Neuromuscular activations were calculated using the APDF. A Friedman test with post-hoc Wilcoxon signed rank tests were performed for each condition-muscle at 10%, 50% and, 90% APDF. A Bonferroni statistical correction was applied with significance set to $p<0.003$. Data analyses were performed in MATLAB R2018a, and statistical analyses performed in SPSS.

Results & Discussion: No measurement channel was statistically significant for the LFH (figure 1A). There was 1 (D1-S1) measurement channel statistically significant for the left hemisphere for the AFH. This channel is associated with the trunk area of the motor cortex homunculus which indicated that participants could have been using different trunk strategies. There were 2 (D3-S1, D7-S7) measurement channels that were statistically significant for the BLH. These channels are associated with the trunk (D3-S1) and hand (D7-S7) areas. This could indicate that the brief augmentation condition could have affected the participants' trunk and hand strategies during the post-augmentation within a single session. There was no statistical difference between baseline, augmentation, post-augmentation for any AFH, LFH, or BLH wrist flexors, wrist extensors, biceps brachii, or lateral triceps on neuromuscular activations at 10% APDF (all: $p>0.003$, $\eta^2_p = 0.25$), 50% APDF (all: $p>0.003$, $\eta^2_p=0.09$) and 90% APDF (all: $p>0.003$, $\eta^2_p=0.076$). These results indicate that the Balloon Simulation does induce a change in neuromuscular activation.

Significance: The results of this study indicated that VR based mirror-therapy through the Balloon Simulation could affect participants' trunk and hand strategies within a single session while maintain the same neuromuscular activations. This Balloon Simulation may be beneficial for clinical populations of varying functional levels that could benefit from increased motor repetitions and home-based neurorehabilitation.

Acknowledgements: GRACA, NIHP20GM109090, R01NS114282, NASA EPSCOR, NSF2124918. Eduardo Montoya, Will Heller and, Lee Buhrmann for their work on the VR Balloon Simulation.

References: [1] Perez-Cruzado et al (2017), *Aust Occup Ther J* 64; [2] Gandhi et al (2020), *Ther Clin Risk Manag* 16; [3] Xiong et al (2022), *Aging Neuroscience* 14; [4] Santosa et al (2018), *Algorithms* 11.

ASSOCIATION BETWEEN HEART RATE RESTING STATE ENTROPY AND HEART RATE DYNAMICS IN PATIENTS WITH AORTIC STENOSIS.

Peggy Ackun[1], Patricio Arrue[1], Nima Toosizadeh[1*], PhD.
[1]Department of Biomedical Engineering, College of Engineering, University of Arizona
*Corresponding author's email: ntoosizadeh@arizona.edu

Introduction: Aortic Stenosis (AS) is a cardiovascular disease that restricts the blood flow from the left ventricle to the aorta and leads to a decline in physical activities in people with such conditions. Heart rate (HR) complexity has been implemented as a common method to assess cardiac autonomic dysfunction in cardiovascular diseases. The HR complexity is derived from the electrocardiogram (ECG) signals while the participant is resting for a minimum of five minutes. The focus of the current study was to compare the HR complexity during a 5-minute resting period and the HR dynamics, which is a novel approach to measure HR changes during a 20-second physical activity among healthy young adults and older adults with AS.

Methods: Healthy young adults (controls) aged 18-30 years and older adults (>64 years) with AS were recruited for this study. HR complexity was assessed by asking the participants to sit still with no interaction or movement, and HR was recorded for 5-minutes. HR dynamics were assessed when participants performed a physical task (20s baseline, 20s of rapid elbow flexion with the right arm, and 30s recovery). HR was recorded using an ECG sensor attached to the left side of the chest and upper rib. Multiscale entropy (MSE) method with a selected scale factor of 20 was used to measure complexity during the 5-minute resting trial using time series of intervals between the heartbeats. HR dynamics parameters included percent change in HR during the activity and the recovery period after the arm flexion task. ANOVA models were used with the groups, age, BMI, and sex as independent and HR dynamics and the MSE values as dependent variables. Pearson correlations between MSE and HR dynamics were calculated.

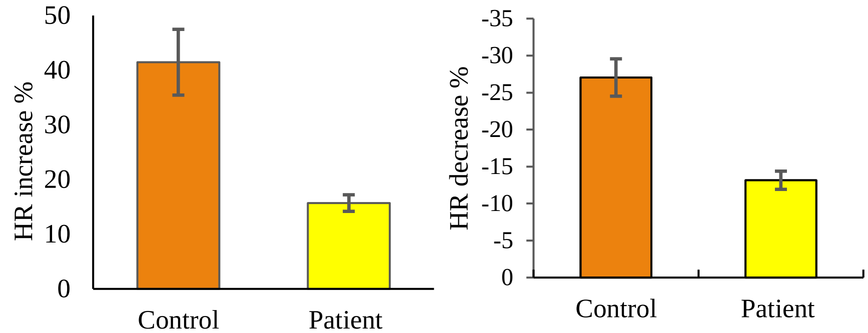

Figure 1: HR% increase and decrease among controls and AS Patients

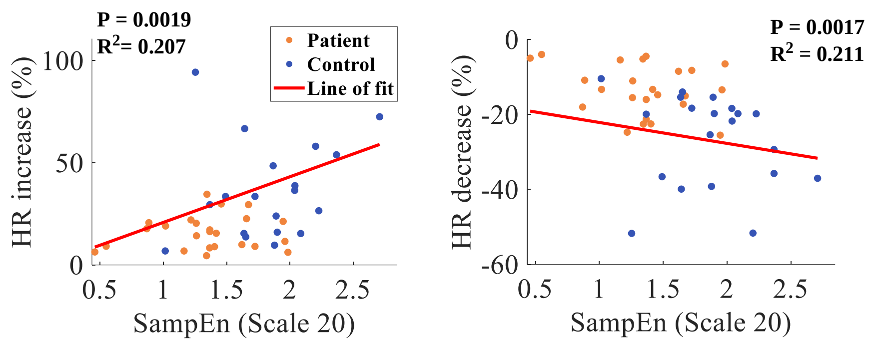

Figure 2: Correlation between the HR increase and decrease with MSE Scale 20 among controls and AS patients.

Results & Discussion: A total of 64 participants were recruited for this study, including 30 healthy controls (age=21±6 years) and 34 AS patients (age=71±11 years). There was a significant difference between HR dynamics (HR increase and decrease) between controls and AS patients (mean values of 41.46% and 15.70% for HR increase - p=0.0055 and mean values of -27.04% and -13.15% for HR decrease – p=0.0007, for controls and AS patients, respectively – Figure 1). The Pearson correlation between the HR dynamics and the MSE data among the two groups combined showed significant associations, "Figure 2" (p<0.0019, with r-values ranging between 0.2 to 0.37). Results suggest that the proposed HR dynamics can provide a quicker measure of autonomic control deficits in AS.

Significance: Current findings suggest that HR outcomes obtained from a quick 20s test during the physical activity can provide information on cardiac autonomic dysfunction in AS patient. AS is mostly associated with increased risk of frailty in older adults. Frailty is a syndrome associated with low physiological reserve, which leads to muscle loss and autonomic dysfunction. Currently there is no specific device or assessment tool available to detect frailty in AS patients, hence our current findings suggest that HR dynamics outcomes obtained could provide information in assessing frailty in AS. For future investigations, we will develop an easy-to-use app on a smart watch for identifying frailty with the use of simultaneous measures of HR dynamics and motor performance.

Acknowledgements: This project was supported by two awards from the National Institute of Aging (NIA/NIH 1R01AG076774-01A1 and 1R21AG059202-01A1).

References: [1] Costa M., Goldberger A.L., Peng C.-K. Multiscale entropy analysis of biological signals. Phys Rev E 2005; 71:021906 [2] Filter-based multiscale entropy analysis of complex physiological time series, Yuesheng Xu and Liang Zhao [3] Metelka, Rudolf. "Heart rate variability-current diagnosis of cardiac autonomic neuropathy. A review. "*Biomedical Papers of the Medical Faculty of Palacky University in Olomouc* 158.3 (2014). [4] Nima Toosizadeh, et al. 'Frailty assessment using a novel approach based on combined motor and cardiac functions: A pilot study'. BMC geriatrics, 22:199. 2022.

Can Physical Therapy Training Enhance Use of a Passive-Dynamic Ankle-Foot Orthosis for Individuals Post-Stroke?

Zahra McKee[1*], Jacob Skigen[2], Darcy Reisman[3,1], Elisa Arch[4,1]
[1]Biomechanics and Movement Science, [2]Biomedical Engineering, [3]Physical Therapy, [4]Kinesiology and Applied Physiology, University of Delaware
*Corresponding author's email: mckeezn@udel.edu

Introduction: Post-stroke muscle weakness limits motor performance with plantar flexor weakness being of particular concern [1,2]. Ankle-foot orthoses (AFOs) are commonly prescribed to assist with this muscle weakness and improve walking function. Passive dynamic ankle-foot orthoses (PD-AFOs) are designed to provide dynamic levels of assistance about the ankle joint by providing resistance to bending via rotational spring-like stiffness [3]. However, without proper loading of the PD-AFO by the user, the orthosis' spring-like assistance may not be activated, preventing the device's full benefits from being utilized. This pilot study aimed to investigate if physical therapy training could improve loading of the PD-AFO and if so, if the user's walking capabilities improved.

Methods: Two participants post-stroke with plantar flexor weakness who had previously participated in a one-month study where they were prescribed a customized PD-AFO participated in this case series. Participants each attended five training sessions conducted by a Research Physical Therapist. Since there are no established methods to train PD-AFO use, the tasks in these sessions were customized by the physical therapist based on their evaluation of what would work best for each participant, but overall training aimed to increase dorsiflexion during midstance on the PD-AFO side as to engage the PD-AFO's rotational spring. Some example tasks were prompting to take longer steps with their non-paretic leg, inclined treadmill walking, and walking with a weight on the non-paretic ankle. A full instrumented gait analysis was performed both before and after the training. Data were collected at the participant's fastest self-selected walking speed with the PD-AFO from the one-month study on a split-belt, force plate-instrumented treadmill where participants were outfitted with a six-degree-of-freedom pelvis and lower-extremity motion capture marker set. Data was processed through Qualysis Track Manager, followed by analysis in Visual 3D to calculate the inverse dynamics and energetics. After treadmill walking, participants performed a 10 Meter Walk Test to measure their self-selected walking speed.

Results & Discussion: The two participants had different gait patterns prior to training and responded differently to the training (Figure 1). Subject A experienced improved ankle biomechanics after training; paretic peak dorsiflexion angle increased 369.3%, paretic peak plantar flexion moment increased 58.5%, and paretic peak positive ankle power increased 90.3%. The ankle power also showed a marked storage-and-return of energy in late stance post-training, likely from improved loading of the PD-AFO. However, this did not translate to improved walking function, as self-selected walking speed was virtually unchanged (Pre: 0.32 m/s, Post: 0.35 m/s) and total mechanical cost of transport increased by 10% (Pre: 1.88 J/kg/m, Post: 2.07 J/kg/m). Additional research is needed to understand why ankle mechanics improved but more global walking function did not. Subject B had more mixed results; paretic peak dorsiflexion angle increased 5.19%, paretic peak plantar flexion moment decreased 3.84%, paretic peak positive ankle power decreased 14.0%, and total mechanical cost of transport increased by 13.0% (Pre: 2.24 J/kg/m, Post: 2.53 J/kg/m). Interestingly, however, self-selected walking speed doubled (Pre: 0.2 m/s, Post: 0.4 m/s) for Subject B. Notably, the gait analysis data were not collected at this faster walking speed - collecting data at this faster walking speed may have revealed post-training improvements in ankle biomechanics.

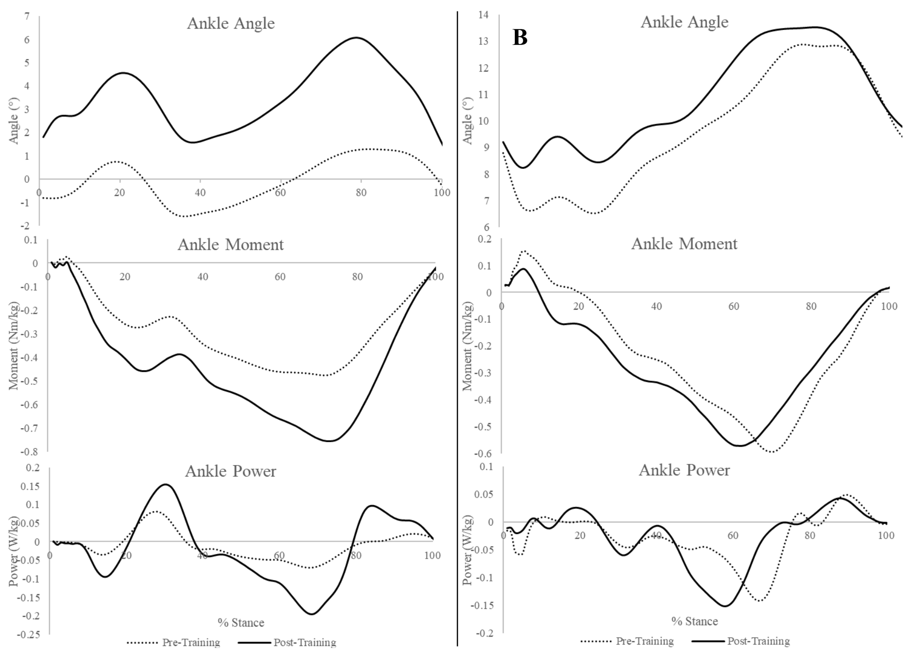

Figure 1: Graphs displaying paretic sagittal ankle angle, moment, and power for subjects A and B. All graphs are recorded with the x axis as percentage of stance with 0%=heel strike & 100%=toe off

Significance: Physical therapy training focusing on PD-AFO loading has the potential to improve ankle biomechanics and walking speed, although results varied across participants. With signals of improvement demonstrated, future research should address training paradigms to develop effective PD-AFO gait training methods to aim to optimize PD-AFO use for individuals post-stroke.

Acknowledgements: Thank you to Tamara Wright and Henry Wright for their physical therapy services. This work was supported in part by USAMRAA (Award No. W81XWH-18-1-0502).

References: [1] Nadeau et al. (1999), Clin Biomech 14(2). [2] Pak & Patten (2008), Top Stroke Rehabil 15(3). [3] Faustini et al. (2008), IEEE Biomed Eng 55(2).

THE EFFECTS OF CERVICAL SPINE IMMOBILIZATION AND DEFORMITIES ON WALKING BALANCE

Emily K. Eichenlaub[1], Aaron M. Gelinne[2], Deb Bhowmick[3], Jason R. Franz[1]
[1]Joint Department of Biomedical Engineering, University of North Carolina Chapel Hill and North Carolina State University
[2]Department of Neurosurgery, University of North Carolina Chapel Hill
[3]Department of Neurosurgery, Duke University
*Corresponding author's email: emeich@email.unc.edu

Introduction: Cervical spine injury is a common pathology encountered in the clinical setting [1]. Failure to properly identify and treat cervical injury can lead to severe neurologic deficits due to cervical instability and subsequent damage to the spinal cord. Cervical immobilization with an external orthosis, such as collars or halo vests, is a mainstay treatment for a large percentage of cervical spine injuries. Although the use of an external cervical orthosis is intended to restrict excessive joint rotation for the patient's safety, there is evidence that immobilization of the cervical spine is associated with numerous clinical co-morbidities and balance impairments [2-3]. These risks are generally considered acceptable due to the risk of neurologic damage in the setting of a non-stabilized cervical spine. However, we suspect that cervical immobilization and deformity changes a person's gait characteristics and predisposes them to higher prevalence of falls. To the best of our knowledge, no studies have characterized whether the acute effect of immobilization adversely changes gait mechanics relevant to future disability and falls. Walking balance perturbations are often used to emulate balance challenges faced in the real world and characterize the ability to accommodate instability relevant to risk of falls. This study aimed to identify characteristic changes in head-trunk kinematics and vulnerability to balance perturbations elicited by cervical immobilization and prescribed changes in posture to simulate cervical deformities. We first hypothesized that there will be characteristic changes in kinematics with cervical kyphosis and lordosis significantly altering head-trunk kinematics. We also hypothesized that, compared to walking with full cervical mobility, participants will exhibit greater vulnerability to balance perturbations when walking with cervical immobilization and artificially induced cervical impairments.

Methods: Fifteen young unimpaired adults participated in this study (5M, 10F; age: 24.3±4.4 yrs; preferred walking speed 1.31±0.13 m/s). Within each experimental block, we randomized four cervical conditions, including an unbraced condition and three braced conditions (kyphosis, neutral, and lordosis) using an adjustable universal cervical collar. Subjects first walked on the treadmill for two minutes at their preferred walking speed in each cervical condition. Subjects then completed a block randomized series of experimental walking perturbation trials, which included (1) 200 ms rapid treadmill belt decelerations of 6 m/s^2, (2) continuous mediolateral optical flow perturbations, and (3) reactive lateral stepping. Subjects wore 48 motion capture markers on their head, arms, trunk, pelvis, and legs, which provided whole-body 3D kinematics. The head angle was calculated relative to the vertical axis and the neck angle was calculated as the angle between the trunk and head in Visual3D. In this study, anterior-posterior margin of stability (MoS_{AP}) served as our measure of susceptibility to treadmill-induced perturbations. MoS_{AP} uses the position and velocity of the body's CoM as well as the anterior base of support (BoS). Using methods described by Young and Dingwell and adapted from Hof et al. [4-6], MoS_{AP} was calculated at the instant of the heel-strike following the perturbation as the distance between the extrapolated center of mass (xCOM) and the anterior BoS. Thus far, we have compared MoS_{AP} during unperturbed walking and in response to treadmill belt decelerations using a one-way repeated measures ANOVA for each spinal condition.

Results & Discussion: We successfully induced cervical kyphosis and lordosis, exemplified by anticipated changes in average head and neck angles during unperturbed walking (Fig. 1A). Specifically, the lordotic condition significantly increased neck extension compared to all other conditions (head angle p-values < 0.023, neck angle p-values <0.015) while the kyphotic condition significantly increased neck flexion compared to the other braced conditions (neck angle p-values <0.041). Thus, we confirmed kyphosis and lordosis can be artificially induced with the adjustable universal neck collar.

A smaller MoS_{AP} indicates that the extrapolated CoM, which incorporates CoM velocity, is closer to the boundary of the stepping foot base of support, thus decreasing stability. In agreement with our hypothesis, both kyphotic and lordotic cervical conditions increased vulnerability to treadmill belt decelerations, as evidenced by a significant decrease in MoS_{AP} (kyphosis $p = 0.028$; lordosis $p = 0.004$) (Fig. 1B).

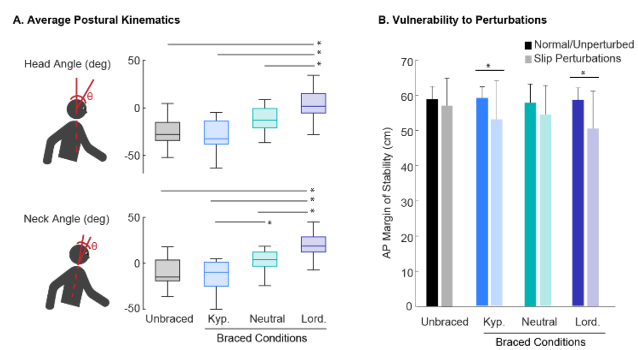

Figure 1. (A) Validation of our protocol to immobilize (neutral) and artificially induce kyphosis (Kyp.) and lordosis (Lord.). (B) MoS_{AP} as a measure of vulnerability to treadmill belt decelerations compared to normal, unperturbed walking. Asterisks (*) denote a significant difference with an alpha level of 0.05.

Significance: Our results suggest that cervical spine deformities increase vulnerability to walking balance challenges and may increase the risk of falling. Prescription of cervical immobilization should be used cautiously to help monitor balance and reduce falls risks.

References: [1] Lowery et al. (2001), *Annals of emergency medicine* 38(1); [2] Wewel et al. (2019), *J Neurosurg Spine*; [3] Richardson et al. (2000), *Archives of physical medicine and rehabilitation*, 81(3). [4] Hof et al. (2005), *J Biomech* 38(1); [5] McAndrew Young et al. (2012), *Gait & Posture* 36(2). [6] Hof et al. (2005), *J Biomech* 38(1).

EFFECT OF INVERSION AND EVERSION ANGLE ON ANKLE PLANTARFLEXION TORQUE

Zane A. Colvin[1*], Gabriela B Diaz[1*], & Alena M. Grabowski[1,2]
[1]University of Colorado Boulder, Boulder, CO
[2]VDepartment of Veterans Affairs Eastern Colorado Healthcare System, Denver, CO
*Authors both contributed equally to this work
Corresponding author's email: Zane.Colvin@colorado.edu

Introduction: A sprinter's maximum velocity (vmax) slows when running along a curve compared to a straightaway[1]. Curve-running vmax depends on the generation of vertical ground reaction force (vGRF) and centripetal GRF. During curve-sprinting, athletes lean their upper body inward towards the center of the curve to generate cGRF, placing the ankle joints of the inside and outside legs into eversion (up to 35°) and inversion (up to 15°), respectively[2,3]. Competitive sprint races are always run in the counterclockwise (CCW) direction, positioning the athletes left leg on the inside and right leg on the outside relative to the center of the curve. The inversion and eversion experienced by the right and left leg, respectively, when running CCW along a curve may result in differences in plantarflexion torque between legs.

A sprinter's vmax slows exponentially, while ankle inversion and eversion angles increase as the curve radius decreases[2,4]. Thus, ankle joint eversion and inversion angles of the inside and outside legs during curve sprinting likely contribute to the leg-specific differences in GRF production and plantarflexion torque. We hypothesized that compared to the contralateral limb, average peak ankle plantarflexion torque would be greater in the left leg (inside for CCW curves) for eversion, and greater in the right leg (outside for CCW curves) for inversion angles. We also hypothesized that peak ankle plantarflexion torque would be greatest for a neutral ankle angle (0°) and would decrease as ankle inversion or eversion angle increased.

Methods: Four subjects (1M, 3F) gave informed consent and completed 1 experimental session, which consisted of a series of maximum isometric plantarflexion contractions at 5 different ankle angles including: 0°, 10°, 20°, and 30° of ankle inversion and eversion per leg (Fig. 1). Subjects completed a 5 minute walking warm-up at 1.25 m/s on a level treadmill. After the warm-up, subjects were fit to an isokinetic dynamometer (Biodex System 3) in a seated, reclined position, where the plantarflexion axis of rotation of the ankle matched the dynamometer axis of rotation and included a custom part that allowed for set ankle inversion and eversion angles. Subjects performed 3 maximum isometric contractions at each ankle angle in a randomized order while we measured plantarflexion torque. We then used a custom Matlab script to calculate the 3-rep average peak torque at each angle and normalized it to bodyweight.

We constructed separate linear mixed effects models for peak plantarflexion torque for ankle inversion and eversion angles. Peak plantarflexion torque at a neutral ankle angle was included in both models. Ankle angle and leg were considered fixed effects, and subject was considered a random effect. Significance was determined with $\alpha = 0.05$

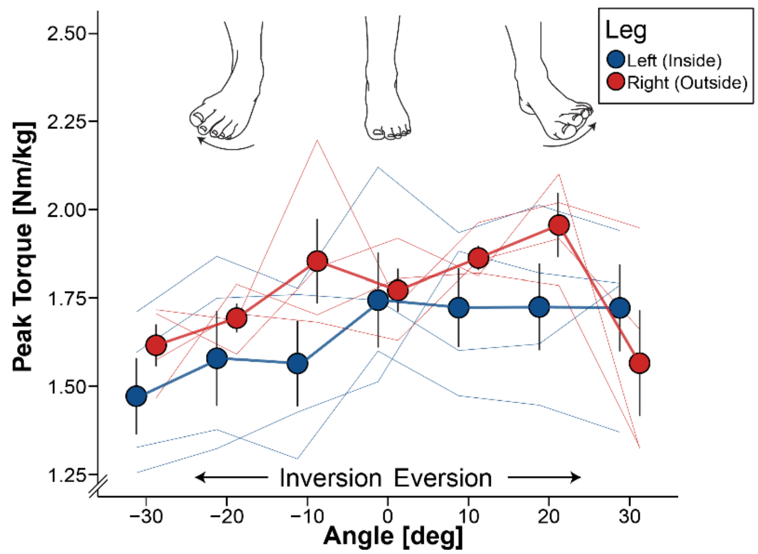

Figure 1: Figure 1. Average peak plantarflexion torque at different inversion and eversion angles. Small lines indicate individual subject data. Thick colored lines and circles indicate average peak plantarflexion torque for the left, or inside leg (blue), and right, or outside leg (red), relative to the center of the curve when running CCW. Error bars represent standard error.

Results & Discussion: For any given eversion angle, we found no significant difference in peak plantarflexion torque between the right and left leg ($p = 0.34$). For any given inversion angle, the right leg produced on average 10.7% (0.182 Nm/kg) greater peak plantarflexion torque compared to the left leg ($p < 0.05$). Our first hypothesis was partially supported, indicating that the right (outside) leg, which is inverted when running around a CCW curve, may influence plantarflexion strength compared to the left (inside) leg and thus performance.

As eversion angle increases, we found no significant difference in peak plantarflexion torque ($p = 0.11$). We found that for each 10° increase in inversion angle, peak plantarflexion torque in both legs decreased by 0.0825 Nm/kg ($p < 0.05$). Thus, our second hypothesis was partially supported, indicating that the slow in speed as curve radius decreases may be due to limitations in peak plantarflexion torque production of the outside leg as inversion angle increases.

Significance: These results can be used to inform training and performance for 200m and 400m track athletic competitions. Our results suggest that athletes should focus on training their outside leg plantarflexion torque to potentially mitigate the slowing of maximum velocity around a curve. Our data support a potential training effect, leading to an imbalance between legs and highlight potential limitations to curve sprinting performance such as a decrease in plantarflexion torque as ankle inversion increases.

References: [1] Y.-H. Chang and R. Kram, J. Exp. Biol., Mar. 2007; [2] T. Alt. et al, J. Sports Sci. Apr. 2015; [3] L. Judson et al, J. Sports Sci. Feb. 2020; [4] P.R. Greene, J. Biomech. Eng. May 1985

A sprinter's maximum velocity slows when running along a curve compared to a straightaway. Additionally, ankle inversion and eversion angles increase as the curve radius decreases, up to 35° eversion for the inside leg and 15° of inversion for the outside leg on a 400m track. Thus, ankle joint eversion and inversion angles of the inside and outside legs during curve sprinting likely contribute to the leg-specific differences in ground reaction force production and plantarflexion torque, likely contributing to a slow in sprinting velocity. With 4 subjects, we tested peak plantarflexion torque of both legs at a neutral ankle angle and 10°, 20°, and 30° inversion and eversion. For any given eversion angle, we found no significant difference in peak plantarflexion torque between the right and left leg. For any given inversion angle, the right leg produced on average 10.7% (0.182 Nm/kg) greater peak plantarflexion torque compared to the left leg. As eversion angle increases, we found no sig

HUMAN LOWER EXTREMITY MUSCLE FIBER LENGTHS DO NOT SCALE WITH BODY DIMENSIONS

Jongsang Son[1], Samuel R. Ward[2,3], Richard L. Lieber[4,5,6*]
[1]Department of Biomedical Engineering, New Jersey Institute of Technology, Newark, NJ; [2]Department of Orthopaedic Surgery, University of California San Diego, La Jolla, CA; [3]Department of Radiology, University of California San Diego, La Jolla, CA; [4]Shirley Ryan AbilityLab, Chicago, IL; [5]Departments of Physiology and Physical Medicine and Rehabilitation, Northwestern University, Chicago, IL; [6]Research Service, Hines V.A. Hospital, Maywood, IL
*Corresponding author's email: rlieber@sralab.org

Introduction: Muscle architectural design is the primary determinant of muscle function [1]. Many previous studies have clearly shown a scaling relationship between muscle mass and body mass across species with several orders of magnitude size difference [2]. However, it is not clear how much of the established scaling relationships are due to interspecies locomotion differences, muscle design differences, or a combination of the two. It is also not clear how muscle architecture should scale with size since muscle mass and muscle architecture are only loosely correlated [1]. For a few human muscles, scaling relationships were proposed [3] but, due to small sample sizes (n = ~10) and the relatively small amount of human size variation, it remains unknown as to whether the aforementioned scaling exists, and if so, whether such scaling patterns vary among functional groups. We collected a very large human dataset consisting of 952 individual human skeletal muscles from 34 cadaveric specimens with an age range of 36-103 years and a height range of 152-188 cm. Thus, the purpose of this study was to quantify the architectural properties of the largest human data set ever assembled to establish the scaling relationship(s), if any that exist across size.

Methods: The study protocol was approved by the Committee on the Use of Human Subjects at the University of California, San Diego and the Department of Veterans Affairs, San Diego. We removed 28 muscles from each of 34 formaldehyde-fixed human lower extremities (18F; 70.0 ± 18.1 years; 169.1 ± 10.0 cm; 78.5 ± 13.8 kg). Each muscle was removed from its most proximal origin to its most distal tendon attachment. After excision, anthropometric measurements (e.g., height and body mass) and representative skeletal measurements (e.g., femur length and tibial length) were made on each specimen. Muscle architecture was measured according to the methods developed by [4] as described by [5]. Of muscle architectural parameters, muscle mass (M^M), physiological cross-sectional area (PCSA), and fiber length (L^F) were used for further analysis. To explore scaling relationships, we computed correlation coefficients between muscle architectural parameters and anthropometric/skeletal measurements. Data are presented as mean ± standard deviation.

Results & Discussion: Among the tested 28 lower extremity muscles, the four muscles with the largest M^M were gluteus maximus (575.8 ± 194.2 g), vastus lateralis (385.7 ± 139.1 g), adductor magnus (341.9 ± 135.4 g), and soleus (283.0 ± 104.1 g). The muscles with the four longest L^F were sartorius (408.2 ± 40.2 mm), gracilis (232.6 ± 36.2 mm), semitendinosus (194.5 ± 29.6 mm), and gluteus maximus (162.8 ± 28.3 mm). As expected from previous studies, M^M and PCSA scaled well with body mass and height, whereas, surprisingly, there was no significant relationship between L^F and any of the bony dimensions measured nor height nor body mass for most muscles (Fig. 1). We confirmed that this lack of scaling relationships between L^F and body size was not due to the small amount of human size variation, by comparing the height distribution of the samples in this study with the distribution of the recent US population (> 90% overlapping area of the estimated normal distributions). These findings then suggest that human skeletal muscles have an intrinsic property that determines their muscle fiber length, and therefore, muscle design, that is independent of size. The data also clearly indicate that different sized individuals' muscles differ based on the number of muscle fibers contained in the muscle, increasing cross-sectional area and muscle mass as a result.

Significance: This study demonstrates that, while muscle mass and cross-sectional area scale with body size, muscle fiber length is independent of size, indicating that muscle function may differ based on the number of muscle fibers contained within the muscle.

Acknowledgements: This work was supported by NIH grants P30AR061303, R01HD048501 and Department of Veterans Affairs.

References: [1] Lieber and Ward (2011), *Philos. Trans. R. Soc. Lond. B. Biol. Sci.* 366(1570); [2] Alexander et al. (1981), *Journal of Zoology*. 194(4); [3] Charles et al. (2019), *PLOS ONE*. 14(10); [4] Sacks et al. (1982), *J. Morphol.* 173(2); [5] Lieber et al. (1990), *J. Hand Surg.* 15(2).

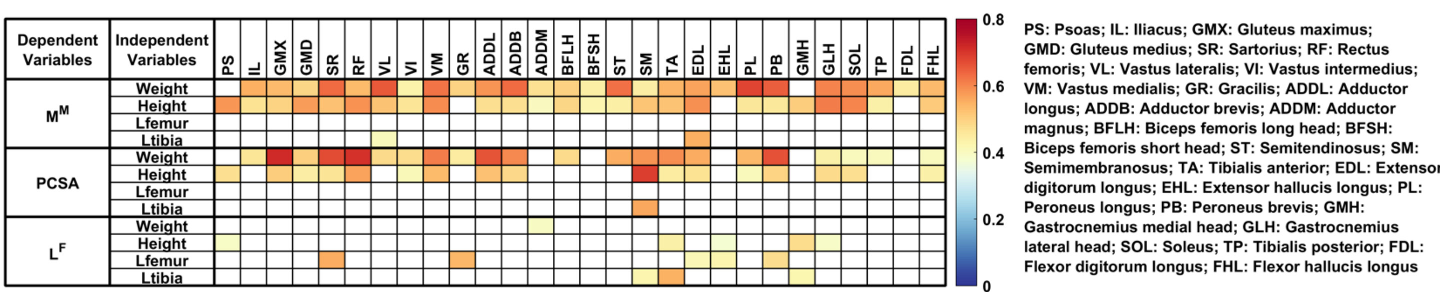

Figure 1: Color-coded correlation coefficients between independent variables (i.e., body mass, height, femur length, and tibia length) and dependent variables for each muscle. Note that empty cells indicate no significant correlation. Clearly, muscle mass scales best with body size while fiber length shows little or no correlation.

CYCLING CADENCE BUT NOT WORKRATE IMPROVES GAIT VELOCITY

Tanner A. Thorsen[1*], Christopher J. Keating[2], Rials J. Hester[1]
[1]The University of Southern Mississippi
[2]Univsersidad Católica De Murcia
*Corresponding author's email: tanner.thorsen@usm.edu

Introduction: Diminished walking ability linked to aging has been well documented [1]. Gait cadence and velocity are two key variables shown to decline with age. This decrease in walking ability leads to reduced physical independence, increased frailty, and greater risk of falling [2]. Stationary cycle ergometers offer a low-impact, affordable, and safe exercise modality which have been used to improve health parameters in older adults. During cycling, the work required of the rider is affected by both cycling cadence (speed) and cycling work rate (resistance). Recently, bouts of cycling exercise have been indirectly reported to increase gait cadence and improve gait velocity in different populations of older adults [3]. Cycling may deliver longer exposure to continual and relevant movement experiences, with a motor plan complementary to walking, manifesting in improved gait velocity after the exercise. Yet, the extent to which cycling cadence and cycling work rate, or their interaction, contributes to improved gait velocity remains unknown. Though it has not been explicitly tested, we suggest that a direct relationship exists between cycling cadence – measured in revolutions per minute and gait velocity – measured in meters per second, which may be responsible, in part, for improved gait velocity post-cycling exercise.

The primary objective of this research is to investigate the relationship between cycling cadence, work rate, and gait velocity. We posit that a cycling training program that increments cycling cadence above typical gait cadence (steps per minute), may be a safe, and effective mechanism to improve gait velocity, stride length, and double support time. In light of previously published gait velocity post cycling exercise, we hypothesized that cycling cadence training will improve post-exercise gait velocity greater than cycling work rate training.

Methods: Fifteen young healthy adults were randomly assigned to one of three cycling groups. All groups performed a single bout of cycling at prescribed settings. The control group (CONTROL) cycled at 55 RPM at a work rate of 1.0 W/kg. Those assigned to the cadence training group (CADENCE) cycled at 75 RPM at a work rate of 1.0 W/kg, while those assigned to the work rate training group (WORKRATE) cycled at 55 RPM at 1.5 W/kg. Both prior to (PRE) and immediately following (POST) each bout of cycling, gait velocity was recorded and spatiotemporal measures of gait (double support time, step width, step length, cadence) were calculated as participants completed a ten-meter walk test (10MWT).

Gait velocity was measured with a laser timing gate system set up to record the time participants took to complete the middle 6 meters of 10MWT (Dashr, Lincoln, NE, USA). Lower extremity kinematics were recorded with a 10-camera motion capture system (Qualisys, Gotenburg, Sweden). Spatiotemporal variables were computed as participants walked across consecutive in-ground force platforms in the motion capture volume. Pared samples t-test were performed between PRE and POST conditions for each group and effect size was calculated as Cohen's d (*d*).

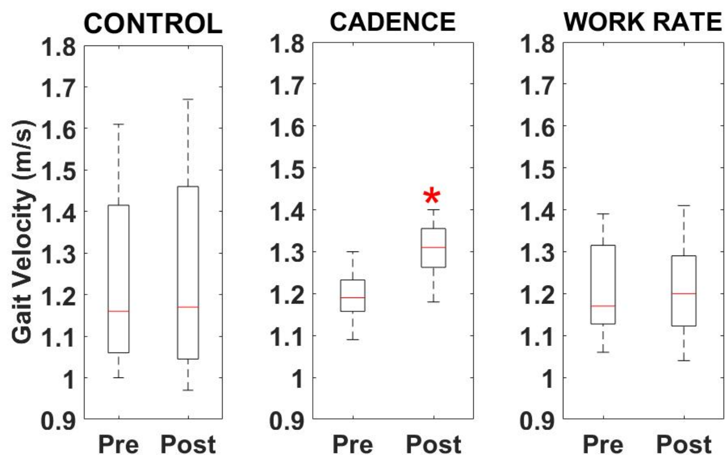

Figure 1: Gait velocity pre- and post- cycling exercise. CONTROL participants cycled at 1.0 W/kg and 55 RPM, CADENCE participants cycled at an increased cadence of 80 RPM at a work rate of 1.0 W/kg, and WORK RATE participants cycled at an increased work rate of 1.5 W/kg at 55 RPM. Red asterisk (*) denotes statistical significance.

Results & Discussion: Gait velocity was significantly increased from PRE (1.19 m/s) to POST (1.30 m/s, $p = 0.022$, $d = 0.17$) in the CADENCE group (Figure 1). Within the CADENCE group, only average step length changed significantly from PRE (0.64 m) to POST (0.68 m, $p = 0.020$, $d = 1.58$). Thus, our initial hypothesis, that performing bouts of cycling at RPM greater than self-selected gait SPM would improve over-ground gait velocity, was supported. Increased step length may be a contributing factor to increased gait velocity post-cycling. Our future analyses will examine changes in lower extremity joint kinematics, kinetics, and ground reaction forces to ascertain additional biomechanical factors that contribute to increased gait velocity.

Significance: These results carry implications for future rehabilitation and training protocols. When gait velocity falls below 1.0 m/s or 100 SPM, risk of falling and other secondary health complications increases. As such, cycling interventions that increment pedaling cadence above that of self-selected gait cadence may produce simple and regularly implementable exercise interventions for those who otherwise may feel unsafe performing gait training.

References: [1] Jerome et al. (2015), *Arch Gerontol Geriatr* 38(2); [2] Branch et al. (1985), *Amer Journal Public Health* 75(12). [3] Tsushima et al. (2015) Aging Clin Exp Res 27(1).

Development of an Automated Framework for a TinyML-Based Fall Detection System

Mojtaba Mohasel[1], Lindsey K. Molina[2], Shane R. Wurdeman[3], Richard R. Neptune[2], Corey A. Pew[1*]
[1]Department of Mechanical and Industrial Engineering, Montana State University, Bozeman, MT
[2]Walker Department of Mechanical Engineering, The University of Texas at Austin, Austin, TX
[3]Clinical and Scientific Affairs, Hanger Clinic, Austin, TX
Email:*Corey.Pew@montana.edu

Introduction: Falls pose a significant risk of injury and even mortality for individuals with lower limb amputations [1]. Although fall detection devices can objectively track fall incidence, they often have limited memory and low power. Therefore, many previous studies have relied on simple machine learning (ML) algorithms, which can suffer from high false alarms and low detection rates [2]. In contrast, deep learning (DL) models have the potential to reduce false alarms by automatically learning features from input data using neural networks. However, designing a TinyML [3] model architecture (i.e., to be run on low-power, small footprint devices) that achieves a high detection rate relies on multiple interdependent variables, making manual configuration challenging. This study aims to automate both ML and DL workflows and optimize their performance, thereby enabling the development of an efficient TinyML system.

Methods: Data was collected from 35 individuals, 30 intact controls (model training) and 5 lower limb amputees (model testing). Two inertial measurement unit sensors [4] placed on the anterior of each shank measured acceleration and angular velocity in the x, y, and z directions. Participants navigated a laboratory course that involved activities of daily living (ADL) and controlled falling movements.

Data were highly imbalanced, with 98.3% ADL versus 1.7% falls, requiring appropriate methods and metrics (F-score) for training and model comparison. RUSBoost [5] and Easy Ensemble [6] are designed for imbalanced data and represent ML models. For DL, a one-dimensional Convolutional Neural Network (CNN) has shown high accuracy on time series data [2]. CNNs extract features from input data with convolutional layers, allowing parallel processing and faster inference time compared to similar deep models. The final model was designed to be implemented on an ESP32 processor with onboard memory of 512 KB. Automation utilized a weighted sum approach [7] with F-beta score and the number of inference operations as objectives, and memory capacity as a constraint.

ML classifier data was segmented into windows of 15 consecutive samples based on hardware restrictions. Optimal performance of models considered several hyperparameters including the number of estimators, maximum depth of trees, minimum sample leaves, minimum number of samples required to split a node, the cost-complexity parameter (ccp_alpha), sampling strategy, and window size. A Bayesian optimization method [8] and 10-fold cross-validation techniques were employed to tune the hyperparameters and determine the optimal combination that yielded the highest F-beta score while minimizing the number of inference operations.

CNN data was segmented into fixed windows of 100 consecutive samples, representing the duration of a fall or ADL. A weighting method by percent of sample count was utilized to handle the class imbalance [9]. Hyperparameters including the number of convolutional, pooling, and dropout layers, as well as their order, filter size, number of fully connected layers, and number of neurons were fine-tuned using Bayesian optimization. The developed neural architecture search approach simultaneously scales all dimensions of the network (width, depth, and resolution) and constructs architectures that use memory below 512 KB.

Results and Discussion: The CNN model outperformed in all metrics except run time size (Table 1). The RUSboost model ranked second in fall detection with a 91% recall, but with a high false alarms rate (6% precision). The EasyEnsemble model lowered the false alarm rate but at the expense of misclassifying fall incidence (81% recall). The success of the CNN model can be attributed to three factors: 1) CNN employs time domain features to distinguish between falls and ADLs, whereas the raw data was directly used in the other models as generating features for traditional ML models was not feasible in real time due to the hardware constraint of our ESP32, 2) availability of 7 million samples for training favors deep models more, and 3) the weighting method utilized for CNN is effective for high imbalance ratios.

Table1: Comparison of developed models. Best performance bolded.

Model	RUSboost		EasyEnsemble		CNN	
Class	Fall	ADL	Fall	ADL	Fall	ADL
Recall	91%	79%	81%	93%	**97%**	**98%**
Precision	6%	100%	15%	100%	**43%**	**100%**
F-score	87%		95%		**98%**	
Run-time	**18 KB**		27KB		228 KB	

Significance: This study presents a novel automated framework that uses multi-objective optimization to train ML and DL models. It facilitates the deployment of these models on hardware with limited resources, which is ideal for settings where resources are constrained. The framework also addresses the persistent challenge of class imbalance in fall detection studies.

Prior research [2] developed a CNN architecture for TinyML, achieving a 96% recall rate without class imbalance, indicating our present work meets or exceeds previous methods. Building upon this work, the proposed automated framework can export TinyML with high detection rates without requiring tedious manual model tuning. Our CNN model can provide clinicians with accurate and objective information about patient falls, enabling them to develop appropriate interventions and prosthetic prescriptions to improve patient care and safety.

Acknowledgement: Funding provided by OPORP Grant W81XWH-20-1-0164. The authors thank Bryce Billings from Hanger Clinic for feedback on this work.

References: 1) Miller et al., Arch. Phys. Med. Rehab. 82(2001). 2) Salah et al, Int. J. Elect. Comp. Eng. 12, no. 4(2022). 3) Warden p et al, O'Reilly media 2016 4) Choi, A et al, IEEE TNSRE 30 (2022) 5) Seiffert et al, IEEE T-Systems, 1(2009) 6) Liu et al, IEEE IBSIC, (2009) 7) Kim et al, SMO, 29 (2005) 8) Wu et al, J. Electron. Sci. Technol.17 (1) 2019 9) King et al., Political Analysis 9 (2) 2001.

THE EFFECTS OF REAL TIME VISUAL FEEDBACK ON STEP-TO-STEP TRANSITION WORK DURING WALKING IN PEOPLE WITH TRANSTIBIAL AMPUTATION

Caelyn Hirschman[1], Janet Zhang[1,2] & Alena M. Grabowski[1,3]
[1]Applied Biomechanics Lab, University of Colorado Boulder, CO USA
[2]School of Nursing and Human Physiology, Gonzaga University, Spokane, WA USA
[3]Eastern Colorado Healthcare System, Department of Veterans Affairs, Denver, CO USA
email: Caelyn.Hirschman@colorado.edu

Introduction: During the step-to-step transition phase of walking, people with unilateral transtibial amputation (uTTA) using an elastic energy storage and return (ESAR) prosthesis have lower trailing affected leg (AL) push-off work and a greater magnitude of leading unaffected leg (UL) collision work than non-amputees walking at the same speed [1]. These differences may contribute to a greater risk of joint pain and osteoarthritis in the UL [2]. Use of a stance-phase powered ankle-foot prosthesis (BiOM) can increase trailing AL push-off work and reduce the magnitude of leading UL collision work to normative levels [3], but some studies found no change in leading UL collision work compared to use of an ESAR prosthesis [4]. Modifying step-to-step transition work by providing biomechanical feedback to people with uTTA could improve walking function and may reduce injury risk. For example, real-time visual feedback (VF) targets of AL peak propulsive horizontal ground reaction force ($hGRF_{peak}$) during walking could affect step-to-step transition work. We hypothesized that subjects with uTTA using their own ESAR prosthesis would: 1. increase trailing AL push-off work and decrease the magnitude of leading UL collision work when given VF targets of $hGRF_{peak}$ 20% and 40% above baseline (BL) levels and 2. not retain step-to-step transition work changes when VF was removed. We also hypothesized that subjects using the BiOM prosthesis would: 1. increase trailing AL push-off work and decrease the magnitude of leading UL collision work when given the same VF targets and 2. retain trailing AL push-off work and leading UL collision work when VF was removed.

Methods: Nine subjects (7M, 2F) with uTTA provided informed consent and walked on a dual-belt force treadmill (Bertec, Columbus. OH) at 1.25 m/s using their own ESAR prosthesis and the BiOM prosthesis while we measured vertical and horizontal GRFs (1000 Hz). We calculated trailing AL push-off work and leading UL collision work during the step-to-step transition using the individual limbs method [5]. We measured baseline (BL) AL $hGRF_{peak}$ during the first 5-min walking trial without VF. Then, during VF trials, we placed a monitor in front of each subject, plotted real time AL $hGRF_{peak}$, and asked subjects to match targets of 0%, +20% and +40% of their BL AL $hGRF_{peak}$. Each VF trial was 5 min, followed by a 5-min rest and a 5-min retention trial where VF was removed. We used two linear mixed effects models [6] with $p<0.05$ to determine whether prosthesis type, VF condition and retention condition had a main or interaction effect on trailing AL push-off work and leading UL collision work. In the models the fixed effects were VF condition (continuous), retention condition (categorical) and prosthesis type (categorical). Participant was a random effect. We report unstandardized model coefficients (B) (dependent variable = B*independent variable + intercept).

Results & Discussion: During VF trials (Fig 1a), we found a main effect of prosthesis type on trailing AL push-off work (B=5.41, $p<0.01$; Fig 1a). On average, when subjects used the BiOM during VF trials (Fig 1a), trailing AL push-off work was 5.41 J greater compared to using an ESAR prosthesis. During retention trials (Fig 1b), we found a main effect of prosthesis type on trailing AL push-off work (B=4.25, $p<0.01$; Fig 1b). On average, when participants used the BiOM during retention trials (Fig 1b), trailing AL push-off work was 4.25 J greater compared to using an ESAR prosthesis. We found no other significant main or interaction effects.

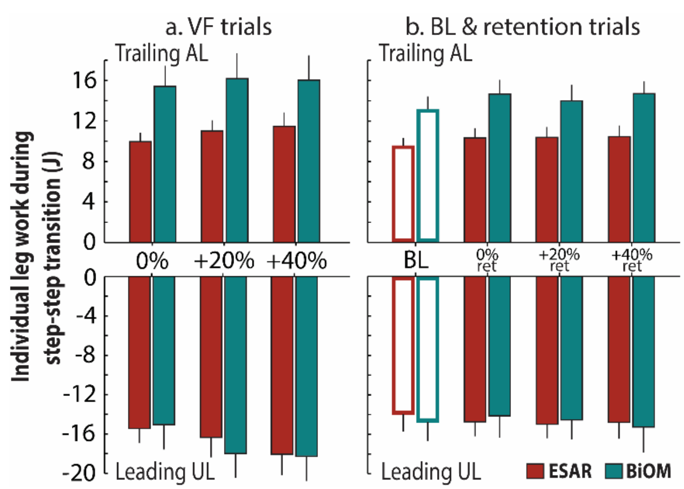

Figure 1. Average trailing affected leg (AL) push-off work and leading unaffected leg (UL) collision work (J) when subjects used elastic storage and return (ESAR; red) and stance-phase powered (BiOM; blue) prostheses during visual feedback (VF) (a) and retention (b) trials. Unfilled bars indicate baseline (BL) trials and filled bars indicate VF (a) and retention (b) trials. Error bars indicate standard error.

Significance: Our results suggest that use of the BiOM compared to an ESAR prosthesis increases trailing AL push-off work with or without VF. However, we found no significant changes in trailing AL push-off work or leading UL collision work when subjects received VF compared to BL. When using an ESAR prosthesis, on average subjects increased $hGRF_{peak}$ by 17.1% for the +20% VF target and 24.6% for the +40% VF target. When using the BiOM prosthesis, on average subjects increased $hGRF_{peak}$ by 18.2% for the +20% VF target and 25.5% for the +40% VF target. Use of VF of $hGRF_{peak}$ may not be effective in changing step-to-step transition work. A joint level analysis and/or greater sample size may provide further insight into the relationship between VF and step-to-step transition work.

Acknowledgements: Funding from the VA RR&D Service RX002943-01A2.

References: [1] Adamczyk et al., *Trans Neural Syst Rehabil Eng*, 2015; [2] Morgenroth et al., *Gait & Posture*, 2011; [3] Herr & Grabowski, *Royal Society B,* 2012; [4] Russell Esposito et al., *Prosthet Orthot Int*, 2016; [5] Donelan et al., *Journal of Biomechanics*, 2002; [6] Bates et al., *Journal of statistical software*, 2015.

WALKING SPEED AND FOOTWEAR ON GAIT KINEMATICS: A COMPARISON BETWEEN ELDERLIES AND ADOLESCENTS

Keven. Santamaría-Guzmán[1,2*], Tyrone. Loría-Calderón[2], Mynor. Rodriguez-Hernandez[2], Jaimie. Roper[1]
[1]School of Kinesiology, Auburn University, Auburn, Alabama.
[2]University of Costa Rica, Western Campus, San Ramón, Costa Rica
*Corresponding author's email: kevensant@gmail.com

Introduction: Aging is a natural process associated with changes such as loss of muscle strength, impaired balance, decreased joint mobility, and detriment of physical abilities[1-3]. These changes affect the functional independence of the individual due to reduced mobility, which in turn increases the risk of falls and limits the person to perform activities of daily living, such as walking or climbing stairs. In terms of mobility, the gait is the most susceptible to these changes in physical abilities, since aging has been related to changes in the kinematic patterns of gait, such as decreased range of motion in the ankle, knee, and hip[4], and lower gait length, cadence, and symmetry[5], compared to healthy and young individuals[6,7]. This causes older individuals to walk slower, decrease their stride length, or take longer in the double support period when walking. In this scenario, footwear plays a relevant role, since there is evidence that it improves stability during gait and reduces variability[8]. However, there is limited evidence on the effect that footwear has on gait kinematics in older adults and young people. Therefore, the purpose is to know if there is an effect of footwear and walking speed on gait kinematics in older adults and adolescents.

Methods: 13 older adults (7 females and 6 males) with mean age of 81 ± 4 yrs., mass 69.28 ± 7.95kgs., height 160.92 ± 7.33cm., and 12 adolescents (6 females and 6 males) with main age of 16 ± 1yrs., mass 62.88 ± 23.64kg, height 163.71 ± 10.59cm., were recruited from the Comprehensive Program for the Elderly and the Scientific High School in the University of Costa Rica. All participants provided a signed informed consent. Participants completed a 30-meter walk test four times at a preferred speed with self-owned sports shoes and barefoot and walking at maximum speed with and without sports shoes; these conditions were randomized. In each attempt the participant had two inertial measurement units (IMU) (WIMU PRO™, RealTrack Systems, Almería, Spain) with a sampling frequency of 100 Hz were used to calculate the stride length and time, cadence, and double limb support time. The IMU devices were attached over both ankles using a spandex belt. The 30-meter course was marked with lateral lines and a central line (Figure 1). Each participant started walking five meters behind the start line and finished their attempt five meters after the finish line (see figure 1). In both lines, there were timed photocells (WITTY, Microgate Chrono Systems, NY, USA) to measure the gait speed. Five three-way ANOVA was performed to identify the differences in the variables stride length and time, cadence, double limb support time, and gait speed, between elderlies and adolescents, wearing sports shoes or barefoot, in preferred walking speed or maximum walk speed.

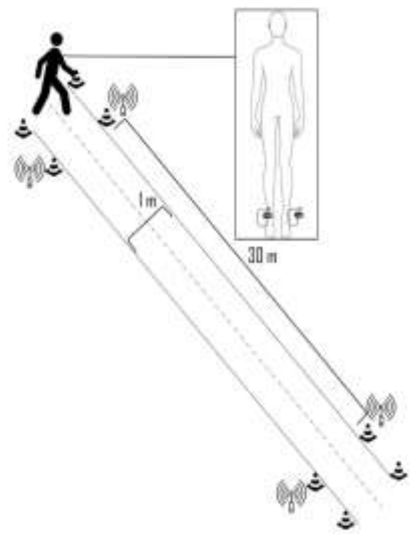

Figure 1: 30-meters walking test set up.

Results & Discussion: Regarding gait speed, older adults are capable to increase their walking speed using sports shoes (diff= 0.29m/s; F= 10.43; p= 0.002) and without shoes (diff= 0.29m/s; F= 10.48; p= 0.002), with respect to their preferred speed, which indicates the mechanical possibility of regulating kinematic changes to cover a segment with greater performance, without affecting their safety of movement. When adolescents were compared against older adults, in barefoot and at maximum speed, significant differences were found (diff= 0.25m/s; F= 7.35; p= 0.008), but in the same condition at normal speed, there were none. This indicates the advantage of young people to move more effectively without footwear. In stride length, adolescents showed more amplitude at normal speed with shoes (diff= 21.55cm; F= 18.45; p= 0.0001) and barefoot (diff= 23.25cm; F= 21.47; p= 0.0001), the same occurred at maximum speed with footwear (diff= 28.35cm; F= 31.93; p= 0.0001) and without (diff= 26.22cm; F= 27.30; p= 0.0001). This supports the notion that with increasing age the amplitude of the stride decreases. In addition, it was found that sports shoes allow a wider stride in adolescents (diff= 17.16cm; F= 11.25; p= 0.001) and older adults (diff= 15.03cm; F= 9.34; p= 0.003) at maximum speed compared to barefoot. At normal speed, there is no change in stride length. Double-limb support was higher in older adults at normal speed with footwear (diff= -32.96ms F= 17.95; p= 0.0001) and without (diff= -19.48ms F= 6.27; p= 0.014) and at maximum speed with footwear (diff= -55.45ms F= 50.82; p= 0.0001) and without (diff= -42.55ms F= 29.93; p= 0.0001), compared to adolescents. What added to the gait speed, reflects the requirements to regulate the balance with the age. Finally, the stride time and cadence did not show any change in the conditions.

Significance: The use of footwear allows the elderly to move with greater speed and amplitude without affecting their safety. More research is required on what footwear should have to enhance safety while walking and prevent events such as falls in older adults.

Acknowledgments: Thanks to the collaborators for their time devoted. This study was developed without external funding support.

References: [1] Zotz, T., et al. (2014). *Top Geriatr Rehabil*, *30*(4); [2] Papalia, G., et al. (2020). *J. Clin. Med.*, 9(8); [3] Gielen, E., et al. (2021). *Nutr. Rev.*, 79(2); [4] Boyer, K., et al. (2017). *Exp. Gerontol.*, 95; [5] Aboutorabi, A., et al. (2016). *Aging Clin Exp Res*, 28(3); [6] Osoba, M., et al. (2019). *Laryngoscope Investig. Otolaryngol.*, 4(1); [7] Madrid, J., et al. (2023). *Gait and Posture*, 99; [8] Petersen, E. (2020). *BMC Geriatr*, 20(1).

KNEE EXCURSION IS RELATED TO DYNAMIC POSTRUAL STABILITY AFTER ACL RECONSTRUCTION

Alexa K Johnson[1*], Riann M Palmieri-Smith[1,2]
[1]School of Kinesiology, University of Michigan, Ann Arbor, MI
[2] Department of Orthopedic Surgery, University of Michigan, Ann Arbor, MI
*Corresponding author's email: akjohns@umich.edu

Introduction: Anterior cruciate ligament (ACL) reconstruction regularly results in altered knee mechanics during landing, including reduced knee flexion angles and sagittal plane knee moments [1]. Landing, particularly on a single limb, requires more than just adequate mechanics to be successful (i.e., prevent injury and/or falling) [1]. Postural stability is another factor that contributes to a successful landing during athletic tasks and poor postural stability has been indicated as a contributing factor to reinjury risk following ACL reconstruction [2]. The dynamic postural stability index (DPSI) is a measure of an individual's ability to maintain balance while transitioning from a dynamic to static state via the dissipation of ground reaction forces [3]. Previous research has examined dynamic postural stability during landing from a single limb hop at the time individuals are cleared to return to sport after ACL reconstruction, but has presented conflicting results [4, 5]. Furthermore, previous research has also yet to examine how knee range of motion during landing is contributing to stability. Therefore, the primary purpose of this project was to assess if knee excursion during landing are related to dynamic postural stability in persons after ACL reconstruction. Secondarily, we examined whether between limb differences in dynamic postural stability and knee mechanics were present after ACL reconstruction.

Methods: Thirty-three individuals (14M,19F; Mass: 75.4± 18.8kgs; Height: 1.72±0.1m; Age:24.0±16.3yrs) with a unilateral ACL injury who had undergone surgical reconstruction and had recently been cleared to return to physical activity (9.5±1.7 months post-ACLR) completed one testing session conducting a biomechanical analysis of a single limb hop. For the single limb hop, individuals were instructed to hop as far as they could while still being able to stick the landing. Three-dimensional motion capture and in-ground force plates were used to assess bilateral kinematics and dynamic postural stability indices during the landing portion of the single limb hop. Dynamic postural stability, an index measuring mean square deviations assessing fluctuations around a 0 point, was quantified in three directions: medial lateral (MLSI), anterior posterior (APSI), vertical (VSI), and a combined total score. Pearson correlation coefficients were used to assess the relationship between patient function and knee excursion to DPSI scores. Paired t-tests were used to assess between limb differences (ACL limb vs Non-ACL limb) in DPSI scores and knee excursion. Significance was set a priori at $p < 0.05$ for correlations and at $p \leq 0.01$ for t-tests (corrected for multiplicity).

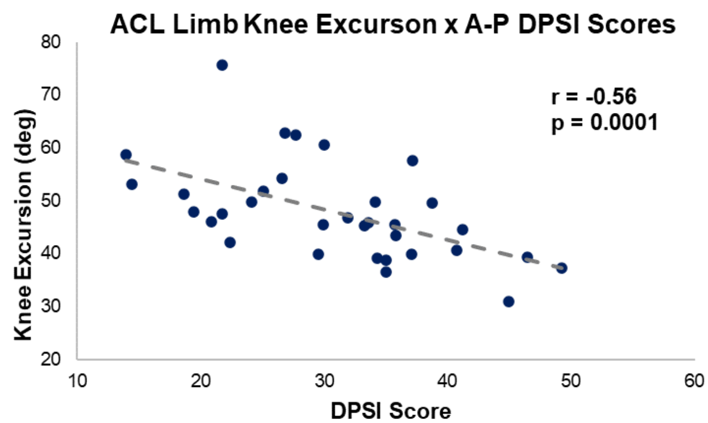

Figure 1: Scatterplot showing the relationship between knee excursion in the ACL limb and the anterior-posterior dynamic postural stability index during a single limb hop.

Results & Discussion: In the ACL limb, greater knee excursion was related to lower APSI scores (Figure 1; r = -0.56, p=0.0001). In the Non-ACL limb, greater knee excursion was related lower total DPSI (r = -0.44, p=0.010), MLSI (r = -0.38, p=0.03), APSI (r = -0.46, p=0.007), and VSI scores (r = -0.45, p=0.007). The ACL limb had significantly lower MLSI scores when compared to the Non-ACL limb (p=0.007). There were no between limb differences in knee excursion, DPSI, APSI, and VSI scores between limbs. Also, knee excursion was related to better stability scores, with greater excursion resulting in more stability. This was particularly true for the Non-ACL limb as it was related to all directions of stability, where in the ACL limb excursion was only related to anterior posterior stability. Landing on the ACL limb may require a greater number of strategies to stick a landing limiting the role of total knee excursion.

Significance: The strong relationship between Non-ACL limb stability and greater knee flexion during landing of a single limb hop indicates how important knee flexion excursion during landing is for stability and a reduction in injury risk. In the ACL limb we only found a relationship between knee excursion and anterior-posterior postural stability scores. Restoring knee flexion range of motion during landing activities should be a focus of late-stage ACL rehabilitation to improve this relationship with all directions of postural stability. This lack of knee flexion excursion during landing in the ACL limb is possibly putting individuals at a higher risk for additional for injury, especially when levels of higher performance are required for sport performance. As the stability during landing from jumping and hoping tasks are important for a successful and safe landing. Increased focus on knee excursion during landing is critical to safely return individuals with ACL reconstruction back to physical activity.

Acknowledgements: The authors would like to thank Mike Curran, MS, ATC for his assistance with data collection.

References: [1] Palmieri-Smith & Lepley (2015), *Am J Sport Med* 43(7); [2] Paterno et al (2010), *Am J Sports Med* 38(10). [3] Wikstrom et al., (2005) *J Athl Train,* 40(4). [4] Heinert et al., (2018) *IJSPT,* 13(3). [5] Head et al., (2019) *Phys Ther Sport,* 38.

DETECTING EVENTS TO DEFINE PHASES OF THE BASEBALL SWING

Sarah M. Hildreth[1], Christopher L. Camp[1], Kenton R. Kaufman[1*]
[1]Department of Orthopedic Surgery, Mayo Clinic, Rochester, MN, USA
*Corresponding author's email: kaufman.kenton@mayo.edu

Introduction: Baseball pitching has been studied extensively in a 3D motion capture setting. The baseball swing, while also having been studied with motion capture, has been analyzed using a more holistic approach. Just like pitching, batting data can be used to quantify the kinematics and kinetics of players' swings to improve performance and prevent injury. Previous studies have recognized events to define the loading phase and impact [1,2]. The phases following impact, however, are not as well defined. While previous studies have researched the kinematics of different follow through types [3], to our knowledge there is no explicit event which marks extension after impact or the end of follow through. To improve and focus analysis of the baseball swing, it needs to be further partitioned into phases of interest which include loading, approach, contact, extension, and follow through. Therefore, the purpose of this study was to identify objective kinetic and kinematic events that define these phases of interest and can be observed across multiple different hitting techniques.

Methods: 2 college baseball players participated in this study (2/2 Male, Age=18.5±0.5 years, Height=1.8±0.1 meters, Weight=81.3±3.1 kg, 1 right-handed hitter). Subjects performed batting swings at full effort during a free swing, off a tee, and during side toss. Fifty-eight reflective markers were placed on the subject, bat, and ball collectively and used to capture kinematic data at 400 Hz with a 14-camera motion capture system (Raptor 12HS, Motion Analysis, Rohnert Park, CA). Ground reaction forces (GRF's) for each foot were collected at 800Hz using embedded force plates (AMTI, Watertown, MA). Subject kinematics and event detection were analyzed in Visual3D (C-Motion, Inc., Germantown, MD), where marker data was filtered using GCVSPL and GRF data was filtered at 10 Hz using a low-pass filter.

Using previous literature and pilot data, the following events were created to define the phases of the swing: Foot off (*Foff*), foot on (*Fon*), impact, full extension (*Fext*), and end of follow through (*EOFT*). Keeping consistent with the literature, *Foff* and *Fon* were defined as the moment the vertical GRF signal of the front foot dropped to zero and increased above zero, respectively, and marked the beginning and end of the subject's loading phase. Impact was given two definitions, depending on whether a ball was included in the trial. When a ball was present, impact was defined as the peak acceleration of the ball in the forward direction. In the absence of a ball, such as during a free swing trial, impact was defined as the peak velocity of the distal end of the bat in the forward direction. The angle between the bat and the forearm of the subject's leading arm was used to define *Fext*, which occurred when this angle hit a minimum between impact and *EOFT.* The impact and *Fext* events mark the beginning and end of the extension phase. Lastly, the *EOFT* event was also given two definitions, depending on whether the subject used a one- or two-handed follow through. For one-handed follow throughs, *EOFT* was defined by an inflection point in the joint velocity of the front shoulder in the frontal plane of the batter's trunk, indicating that the batter is abducting their arm away from their body after the swing is done. For two-handed follow-throughs, the *EOFT* event was defined with an inflection point in the joint velocity of the rear shoulder in the frontal plane of the batter's trunk. Following a stretch when the back shoulder reaches its full range of motion, the batter begins to bring the arm back, indicating the end of the swing.

Results & Discussion: Using the definitions above, the events of *Foff, Fon*, impact, *Fext*, and *EOFT* events were successfully identified in both subjects across a variety of hitting techniques including free swings, tee swings, and side toss. Figure 1 shows an example of the consistency of these events during three tee swings, with a swing being defined as the time from *Foff* to *EOFT*. The consistent existence of these events across different hitting techniques provides the basis for objectively defining the different phases of the baseball swing that is quantitative and repeatable.

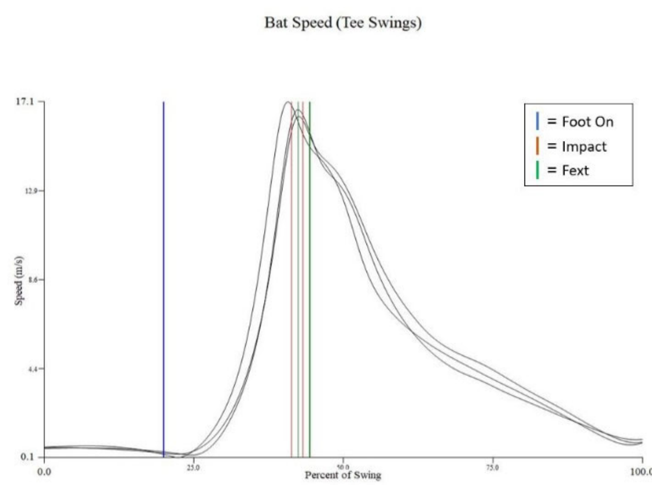

Figure 1. Bat Speed (m/s) of the distal end of the bat during three tee swings with observed events labeled.

Significance: Defining the phases of the baseball swing using objective timing events helps to improve the efficiency and repeatability of analysis. While certain events, like loading and impact are well established in the literature, other events such as extension and the end of follow through are less established. This work provides the definitions for objective, quantitative measures that can be used to define the different phases of the baseball swing. These events are repeatable across different hitting techniques. The implementation of these events can help to guide future studies of the baseball swing by creating universal timing measures.

Acknowledgements: This research was supported by an internal grant from Mayo Clinic.

References: [1] Punchihewa et al. (2019), *J Biomech* 87; [2] Welch et al. (1995), *J Ortho & Sports Phys Therapy* 22(5); Cross et al. (2019), ISBS 2019, Oxford, OH;

EFFECTS OF UNILATERAL ANKLE LOADING ON MUSCLE ACTIVITY DURING WALKING

Huaqing Liang[1]
[1]School of Physical Therapy, Marshall University, WV
*Corresponding author's email: liangh@marshall.edu

Introduction: Walking is a daily activity that requires constant adjustments to the changing environment. Humans can adapt their gait patterns when a new stimulus (such as a novel force applied on one leg) is added repeatedly or continuously. The removal of such a stimulus could result in aftereffects, where humans continue to walk as if the stimulus was still in place. Eventually, de-adaptation might occur after the stimulus is removed for several minutes and the original gait pattern would be adopted again.

When an asymmetrical perturbation is provided to people with an asymmetrical gait, it has the potential to augment the asymmetry, facilitate the recognition and the correction of this asymmetry. There were plenty of studies used a spit-belt treadmill to provide such an asymmetrical disturbance to walking [1]. These studies reported that split-belt treadmill walking could induce an asymmetrical gait pattern in young adults, and these young adults displayed a negative after-effect when returned to normal treadmill walking, indicating the learning of a new gait pattern [1]. Unilateral ankle load could be a more readily available tool in most clinical settings to provide asymmetrical disturbance to walking. However, only a few studies examined the effects of unilateral loading on gait pattern changes [2] and none of the studies explored the muscular activity changes when unilaterally loading or unloading the ankle during walking.

The purpose of this study was to investigate the immediate and late muscle activity adjustments when unilaterally loading and unloading the ankle during walking in young adults. We hypothesized that similarly to split-belt treadmill disturbance [3], muscle activities would increase immediately after unilaterally loading the ankle, and would return to baseline level during late adaptation.

Methods: Thirty young adults (15M/15F, 24.3±1.7 years of age) were recruited for this study. They were instructed to walk on a treadmill at their preferred walking speeds in 3 conditions: 1) a 2-minute trial with no load (Baseline); 2) 3 bouts of 5-minute trials with a load (3% of bodyweight, 2.3±0.3 kg) on the dominant ankle (Loading); and 3) a 5-minute trial with the load removed (Unloading). Eight EMG sensors were placed on bilateral vastus lateralis (VL), biceps femoris (BF), tibialis anterior (TA), and lateral gastrocnemius (LG). Data were extracted from 5 periods: the first 10 strides of the Loading and Unloading to assess early adaptation and early post-adaptation period; and the last 30 strides of the Baseline, Loading, and Unloading to assess the baseline, late adaptation, and late post-adaptation periods. EMG data were filtered and full-wave rectified. Then linear envelopes were created within each gait cycle.

Key durations within a gait cycle were selected for each muscle based on their functional phases during normal walking [4]. Specifically, these durations included loading response and the last 10% of the gait cycle for VL, loading response and the last 10% of the gait cycle for BF, loading response and the whole swing phase for TA, and the 20% of the gait cycle before toe-off to represent the push-off phase for LG. The integrated area of each duration was calculated, and was further normalized using the average value of the last 30 strides in the baseline condition for each muscle and each participant, respectively. Repeated measures ANOVA was conducted and post-hoc pairwise comparisons with Bonferroni adjustments were used when necessary. The statistical significance was set at $\alpha=0.05$, and eta-squared (η^2) was used to evaluate the effect size.

Results & Discussion: Our results supported our hypothesis and showed that young adults increased their muscle activities immediately after unilaterally loading the ankle: specifically in the loaded-side BF just before initial contact and both sides of TA right after initial contact to provide the braking force, and in the loaded-side LG to produce extra internal torque and achieve adequate push-off during walking. Our results also showed that the muscle activities during the examined durations all returned to or fell below baseline level during the late adaptation period. Additionally, several muscles displayed an after-effect and demonstrated a decrease of activities following removal of the unilateral load, such as both sides of BF around initial contact, and the loaded-side TA after initial contact.

Statistical analysis revealed that compared to baseline, there were increases in muscle activation integrals in early-adaptation period observed in loaded-side BF during the last 10% of the gait cycle, in both sides of TA during the loading response, and in loaded-side LG during the push-off phase (all $p<0.05$, η^2 ranges from 0.092 to 0.209). Moreover, compared to baseline, there were decreases in muscle activation integrals in early post-adaptation period observed in loaded-side BF during the last 10% of the gait cycle, in unloaded-side BF during loading response, and in loaded-side TA during loading response (all $p<0.05$, η^2 ranges from 0.061 to 0.209).

A previous study on gait spatiotemporal parameters showed that a unilateral ankle load could elicit the learning of a new gait pattern [2]. Additional, previous results on joint kinematics reported that when adding a unilateral load, young adults usually adjusted their ankle kinematics for immediate adaptation, and gradually made more proximal adjustments at the knee and hip joints during late adaptation period. In the current study, an early adaptation with increased muscle activities at the ankle joint was observed. However, not much late adaptation at the muscle activity level was required at the ankle or knee joints. This might indicate that young adults have the ability to fine tune their neuromuscular control and the new adapted gait pattern did not increase the demands on the muscle activity.

Significance: Unilateral loading could create unilateral perturbation to people with asymmetrical gait, thus has the potential to assist in error recognition and error correction, and stimulate the emergence of new gait patterns. Further studies are need to explore the muscle activity changes in clinical populations when adding or removing a unilateral load during walking, to explore the feasibility of using the unilateral load as an intervention tool in clinical populations without creating excessive demands to their muscles.

References: [1] Torres-Oviedo et al. (2011), *Prog Brain Res.* 191:65-74; [2] Nobe & Prentice (2006), *Exp Brain Res.* 169:482-495; [3] MacLellan et al. (2014) *J Neurophysiol.* 111:1541-1552; [4] Ounpuu & Winter (1988), *Electroencephalogr. clin. neurophysiol.* 72:429-438.

REGULARITY OF LOWER LIMB JOINT ANGLE MOTIONS DECREASED AFTER A SIX-MONTH SUPERVISED EXERCISE THERAPY.

Farahnaz Fallahtafti[1*], Zahra Salamifar[1], Iraklis Pipinos[2], Jason M. Johanning[2], Sara A. Myers[1,2]
[1] Department of Biomechanics, University of Nebraska at Omaha, Omaha, NE USA
[2] Department of Surgery and Research Service, Omaha Veterans' Affairs Medical Center, Omaha, NE USA
*Corresponding author's email: ffallahtafti@unomaha.edu

Introduction: Lower extremity peripheral artery disease (PAD) is a cardiovascular condition caused by narrowed or blocked arteries supplying the legs. Claudication is a cramping pain in the legs of patients with PAD, brought on by exertion and relieved with rest. Supervised exercise therapy (SET) is a conservative, non-operative treatment strategy for improving walking performance in patients with PAD. Gait variability is altered in patients with PAD [2], but whether SET restores gait variability is unknown. Gait variability is important because it can provide an overall metric for functional performance, and restored gait variability may indicate that SET improved overall gait as well as the distance patients can walk. This study investigated the effect of SET on gait variability in patients with PAD. We hypothesized that a six-month intervention with SET would improve gait variability in patients with PAD.

Figure 1: Supervised exercise therapy included five minutes warm-up, 50 minutes of intermittent exercise, and 5 minutes cool down. Treadmill walking exercise started at a low treadmill workload of 2 mph and 0% grade as soon as a patient was able to walk for 8 to 10 minutes at the initial load, the grade were increased by 2%, every two minutes. SET was done 3 times/week for 6 months.

Methods: Forty-three patients with PAD (Age: 63.79±6.21 years), height: 1.76±0.07 m, and body mass: 91.53±18.6 kg) were evaluated before and immediately after a six-month SET intervention (Figure 1). Participants walked on the treadmill at their preferred speed while kinematic data were recorded with motion analysis cameras (Motion Analysis Corporation, Rohnert Park, CA). Data were collected before the onset of claudication pain. Nonlinear measures of variability (i.e., sample entropy and Lyapunov exponent) were used to calculate the regularity and the ability to respond to movement perturbations from joint angle time series during walking. We used a fixed number (3500) of data points for analysis before claudication pain started for all participants. We used a two-way repeated measure ANOVA (intervention (pre/post) × joint (ankle/knee/hip).

Results & Discussion: Sample entropy differed significantly before and after the SET intervention (Figure 2). Sample entropy indicated a more regular pattern in the ankle, knee, and hip joint angle time series after SET. This change with SET means patients walked with gait patterns closer to those seen in older individuals without PAD. Ankle angles were still more irregular than the knee and hip joints, which could be related to the impaired calf muscles in patients with PAD [3]. The hip is a ball and socket as opposed to a hinge type of joint like a knee. There are different types of soft tissues around it, it is a deeper joint, and there are more muscles. The greater entropy in the hip could be the result of complex structure and muscle contributions.

According to the results of the current study, the largest Lyapunov exponent values were not significantly different before and after SET intervention (Figure 2). A potential explanation for the lack of significant changes could be the length of the dataset, which was 3500 data points.

Significance: Our results demonstrated that while SET improved walking distances and regularity of gait, all gait variability differences were not restored to values typical of older individuals without PAD. Patients may need additional rehabilitation to fully restore gait.

Acknowledgments: This research was funded by the National Institute of Health (R01AG034995, R01HD090333, R01AG049868), and the United States Department of Veterans Affairs (I01RX000604, I01RX003266)

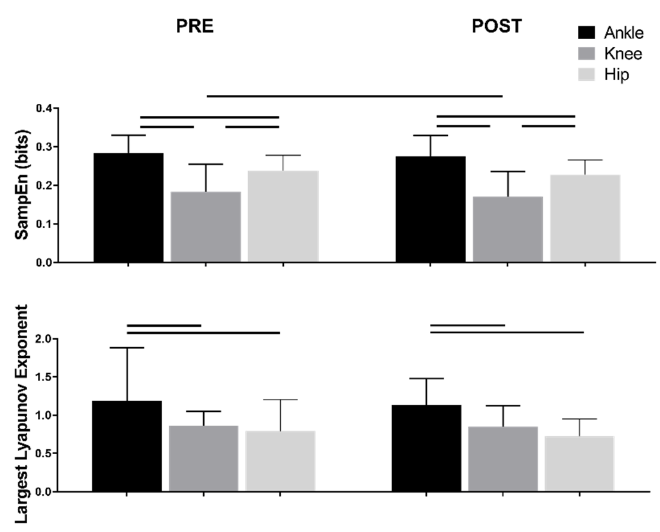

Figure 2: Nonlinear measures of sample entropy (top) and largest Lyapunov Exponent (bottom) of the sagittal angular motion for the ankle, knee, and hip before (Pre) and after (Post) SET. The horizontal bars represent the significant difference ($p < 0.05$).

References:

1. Aherne et al., 2015. Surg Res Pract, 960402.
2. Myers et al., 2009. J Vasc Surg. 49(4):924-931
3. McDermott, M.M., 2015. Circ. Res. 116, 1540–1550.

DIFFERENCES BETWEEN WINDUP AND STRETCH PITCHING BIOMECHANICS IN BASEBALL

Glenn S. Fleisig[1*], Rafael F. Escamilla[2], Jonathan S. Slowik[1]
[1]American Sports Medicine Institute
[2]California State University, Sacramento
*Corresponding author's email: glennf@asmi.org

Introduction: In baseball, a pitcher is allowed at any time to pitch from either the windup or set position (also known as pitching from the stretch). Some pitchers use the windup without runners on base and the stretch with runners on base, while other pitchers simply pitch from the stretch at all times. Some believe the windup is less stressful on the arm, while others believe it is easier to become consistent mastering just one technique. Remarkably, while pitching biomechanics have been reported in hundreds of publications, comparison of windup and stretch biomechanics has been limited to two small-sample studies few biomechanical variables [1,2]. The objective of this study was to a compare a large number of kinematics and kinetics between windup and stretch across a large sample of professional, collegiate, and high school baseball pitchers.

Methods: Biomechanical data were analyzed for 221 healthy baseball pitchers, including 105 professional, 52 collegiate, and 64 high school level athletes. A total of 39 reflective markers were placed on each subject before testing. After unrestricted warmup, the pitcher threw full-effort fastballs for data collection from a mound to a catcher or target strike zone above home plate at regulation distance from the pitching rubber (18.44 m). Fastball velocity was recorded with a radar gun (Stalker Sports Radar, Plano, TX, USA) while motion of the reflective markers was measured with a 12-camera, 240 Hz automated motion capture system (Motion Analysis Corporation, Santa Rosa, CA, USA). Each subject pitched 3 - 10 fastball trials from the windup and 3 - 10 from the stretch. For each pitch, 23 kinematic variables were calculated as previously described [1,3,4]. Elbow and shoulder kinetics were calculated using inverse dynamics [3]. Joint torques were divided by body-weight and by height to create normalized unitless variables [5]. Similarly, normalized forces were calculated by dividing joint force by body-weight. Data for the kinematic and normalized kinetic variables were compared across the two techniques (windup, stretch) and three competition levels (professional, collegiate, high school) using two-way repeated measures analyses of variance. All analyses were conducted in SigmaStat (Version 12.5, Systat Software, USA) with an *a priori* level of significance of $\alpha=0.01$.

Results & Discussion: There was a significant interaction between pitch technique and competition level for ball velocity. Velocity was significantly greater for windup than stretch at the collegiate and high school levels, but the difference of the means was relatively small (0.3 m/s for college; 0.2 m/s for high school). Scarborough et al. [2] found no differences between pitch techniques for college and high school pitchers. Dun et al. [1] previously reported a small, significant difference in fastball velocity between windup and stretch for professionals, but no such difference was found in the current study. Six angle parameters were statistically different between windup and stretch, however the magnitudes of these differences were clinically insignificant as each was less than 1 degree (Table 1). Although statistical differences were found for peak values of normalized shoulder anterior force, elbow flexion torque, and shoulder proximal force, the magnitude of the differences were negligible. Previous studies on smaller samples found no kinematic or kinetic differences between windup and stretch pitching [1,2].

Table 1. Kinematic differences ($p<0.01$) between pitching techniques

	Mean		Standard error of the mean
	Windup	Stretch	
Instant of Front Foot Contact			
Upper trunk tilt (º)	8.0	7.6	0.5
Knee flexion (º)	42.2	42.8	0.6
Foot angle closed (º)	8.6	9.3	0.8
Delivery			
Max. pelvis angular velocity (º/s)	569	561	5
Shoulder external rotation (º)	159.1	159.9	0.8
Max. upper trunk angular vel (º/s)	1107	1103	6
Max. shoulder IR vel (º/s)	6584	6653	69
Instant of Ball Release			
Elbow flexion (º)	24.5	24.2	0.4
Trunk forward tilt (º)	34.5	35.0	0.6

Significance: This study did not support the belief that pitching from the windup is less stressful (i.e., less force and torque at the elbow and shoulder). Furthermore, since kinematic differences were not found, it may not be more difficult to master both techniques instead of just one. Thus, this study indicates no benefits or disadvantages for using one or both techniques and pitchers should decide based upon their comfort and strategy considerations.

Table 2. Kinetic differences ($p<0.01$) between pitching techniques

	Mean		Standard error of the mean
	Windup	Stretch	
Max. shoulder anterior force	0.40	0.40	0.01
Max. elbow flexion torque	0.034	0.034	0.001
Max. shoulder proximal force	1.17	1.16	0.01

References:

[1] Dun et al. (2008), *AJSM* 36(1); [2] Scarborough et al. (2021), J Clin Sports Sci Med 20; [3] Escamilla et al. (2018), *J Appl Biomech* 34; [4] Fleisig et al. (1995), *AJSM* 23(2); [5] Crotin et al. (2022), *AJSM* online ahead of print

EXPLORING THE EFFECT OF PHYSICAL ACTIVITY LIFESTYLE ON *IN VIVO* PASSIVE STIFFNESS IN THE LUMBAR SPINE

Chelsea M. Dumasal[1*] & Kayla Fewster[1]
[1]School of Kinesiology, University of British Columbia, Vancouver, BC, Canada
*Corresponding author's email: cdumasal@student.ubc.ca

Introduction: Passive stiffness in the lumbar spine is a growing research area and an indicator of lumbar spine health, as passive stiffness properties contribute to spinal stability [1,2]. Deviations in baseline passive stiffness may provide insights into lumbar spine injury mechanisms or pain reporting, as changes in lumbar spine stiffness have been linked to factors such as age [3], chronic low back pain reporting [4], dynamic repetitive flexion [5], rear-end automobile collisions [6], prolonged sitting in office chairs [7], and prolonged driving [8]. A large number of studies have repeatedly shown that sustained static postures, including prolonged sitting and standing, can be detrimental to the lumbar spine [9,10]. As such, more recent findings have advocated for switching between postures for lumbar spine health, as opposed to simply replacing sitting with standing [11,12,13]. Despite this potential for movement to positively influence the lumbar spine, one limitation common to the aforementioned passive studies is that they do not control for physical activity or sedentary lifestyle behaviours across participants. To fill this gap in the literature, the purpose of the current investigation was to determine the effect of physical activity lifestyle on flexion passive stiffness in the lumbar spine. It was hypothesized that differences in passive stiffness would emerge across participants classified as having either an active (ACT) versus sedentary lifestyle (INACT).

Methods: 9 participants (5 ACT,4 INACT) were recruited. To measure physical activity lifestyle, participants completed the International Physical Activity Questionnaire - Short Form along with additional questions to quantify the duration and types of activity they engaged in [14]. Participants were classified as INACT if they routinely completed less than 150 minutes of moderate-to-vigorous aerobic activity and less than 2 sessions of total-body strengthening activities per week over the past year. Likewise, participants fell into the ACT group if they met or surpassed aerobic and strength activity thresholds. During passive stiffness testing, participants laid on their left side on a customized frictionless jig. The legs, pelvis and arms were secured in a fixed position while the torso was permitted to move through the full range of flexion motion. The experimenter then pulled the participant into maximum flexion. Throughout testing, motion capture was used to track motion of the trunk and pelvis (Optotrak Certus, NDI, Waterloo, Canada) at a rate of 20 Hz. A load cell (Model MLP-100, Transducer Techniques Inc., Temecula, CA) was attached in series to the top of the upper body cradle to measure the force applied by the experimenter. Surface EMG (2000 Hz, Noraxon, USA Inc., Scottsdale, Arizona, USA) monitored the lumbar erector spinae and rectus abdominus bilaterally to ensure muscle activation remained below 5% MVC. Applied moment was calculated by measuring the moment arm between the point of force application and the estimated location of the L4-L5 intervertebral disc. From passive trials, moment-angle curves were generated to quantify differences in passive stiffness. Moment-angle curves were partitioned into 3 linear regions (low, transition and high stiffness) for flexion [15]. Differences in the shapes of the passive moment-angle curves (slopes of the low, transition and high stiffness zones, moment-angle breakpoints) were quantified. A one-way ANOVA assessed the influence of Activity Level on Passive Stiffness parameters.

Results & Discussion:
A significant effect of Activity Level on Passive Stiffness in Lumbar Flexion was observed for the high stiffness slope (*p = 0.020*), indicating that active individuals have higher measures of passive stiffness in comparison to sedentary individuals. No other significant differences were seen across the low stiffness (*p = 0.286*) and transition zone slopes (*p = 0.596*) between groups. Although not significantly different, trends were observed in the low and high moment-angle breakpoints (% maximum flexion), such that the breakpoints of active individuals occurred at a greater percentage of their maximum range of lumbar flexion. In particular, mean low moment-angle breakpoints of active and sedentary individuals were 43 $\pm$ 6% and 34 $\pm$ 12% respectively. Mean high moment-angle breakpoints of active and sedentary individuals were 79 $\pm$ 7% and 74 $\pm$ 11% respectively.

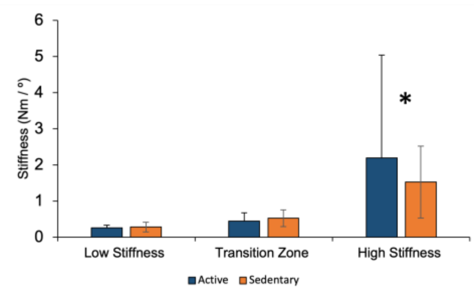

Figure 1: Mean stiffnesses of the active group from the low stiffness, transition, and high stiffness zones were 0.26$\pm$0.07, 0.45$\pm$0.23, and 2.20$\pm$2.85 Nm/º respectively. Mean stiffnesses of the sedentary group from the low stiffness, transition, and high stiffness zones were 0.28$\pm$0.13, 0.53$\pm$0.23, and 1.53$\pm$1.00 Nm/º respectively. Statistically significant differences are identified with an asterisk.

Significance: The current investigation demonstrated differences in *in vivo* passive stiffness in the lumbar spine between individuals with a physically active versus sedentary lifestyle. The findings of the study may have implications for injury risk to the lumbar spine. Further studies are warranted to investigate sex-based differences and different types of physical activities (e.g. acute versus long-term, aerobic versus resistance training).

References: [1] Panjabi et al. (1989), *Spine* 14(10); [2] Panjabi et al. (2005), *J Biomech* 38(8); [3] Gruevski & Callaghan (2019), *Ergo* 62(7); [4] Gombatto et al. (2008), *Clin Biomech*, 23(8); [5] Parkinson et al. (2004), *Clin Biomech*, 19(4); [6] Fewster et al. (2021), *Clin Biomech*, 90; [7] Beach et al. (2005), *TSJ*, 5(2); [8] DeCarvalho & Callaghan (2011), *IJIE*, 41(6); [9] Gallagher et al. (2014), *Ergo*, 57(4), [10] Sorensen et al. (2015), *Man Ther*, 20(4); [11] Fewster et al. (2019), *HMS*, 66; [12] Gallagher & Callaghan (2015), *HMS*, 44; [13] McKinnon et al. (2021), *Ergo*, 64(4); [14] Craig et al. (2003), *Med & Sci*, 35(8); [15] Barrett et al. (2021), *HMS*, 76

CHARACTERIZING MUSCLE FATIGUE IN SEMG DATA WITH TOPOLOGICAL DATA ANALYSIS

Allyson K. Clarke[1*], Benjamin B. Wheatley[2*], Chulhyun Ahn[3]
Departments of [1]Biomedical Engineering or [2]Mechanical Engineering, Bucknell University, Lewisburg, PA
[3] Department of Physical Medicine and Rehabilitation, Geisinger Health System, Danville, PA
*Corresponding author's email: bbw008@bucknell.edu

Introduction: Surface electromyography (sEMG) is a non-invasive method of recording the electrical signal of an individual muscle during activation. This signal can be interpreted as a combination of sine waves with varying frequencies and amplitudes. Muscle fatigue is defined as a decline in the maximum voluntary contraction (MVC), or a decrease in the maximal force-generating capacity of a muscle as it tires [1]. When a muscle contracts over an extended period, the median frequency (MDF) of the sEMG signal decreases, which is generally understood to indicate fatigue [2]. While MDF correlates to muscle fatigue, it cannot be used to reliably predict fatigue or muscle weakness, since an adequate representation of muscle activity includes both the frequency and amplitude of the electrical signal. Topological data analysis (TDA, a mathematical approach to studying the inherent characteristics of data) provides insights into time-series data that typical frequency-based processing methods cannot discern, such as the frequency and amplitude of a signal. We hypothesized that in sEMG data, TDA can provide a stronger correlation to fatigue than frequency-based analyses. TDA has proven useful in diverse applications, from monitoring gene expression to classification of neurological disorders in EEG signals [3, 4].

Methods: 31 subjects (ages 19-54, 15M, 16F) participated in the study. Each subject fatigued their first dorsal interossei (FDI) muscle by performing an isometric abduction at 50% of their MVC force for up to five minutes. Raw sEMG signal was divided into 15 second segments, and to discard initial transients the first segment was not included in analysis. For frequency analysis, the mean and median frequency were calculated for each segment by conversion to the frequency domain via a fast Fourier transform. For topological data analysis (TDA), a visibility graph was constructed from the raw data, which can then be used to determine the simplicial complex of each segment, which is a representation of the geometric shapes between points that are visible to each other (Figure 1). From each simplicial complex, single number characterizers of the data were extracted, as detailed in Chutani et al [5]. Linear regression was performed on all characterizers with respect to experiment time, which we interpret as fatigue.

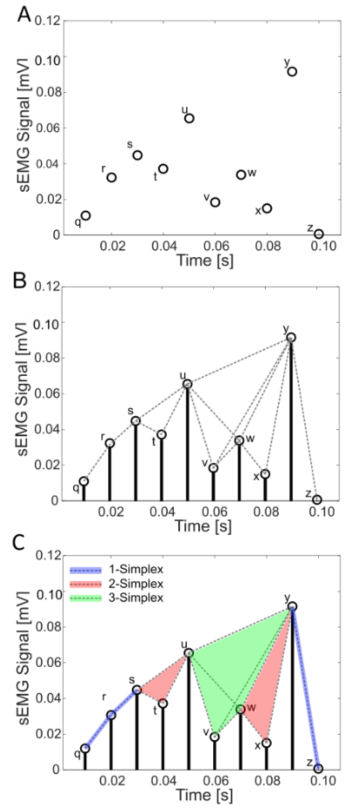

Figure 1. Representative TDA approach. A) Data from sEMG signal. B) Visibility graph constructed from sEMG signal. Nodes are connected if a straight line can be drawn between points without intersecting the intermediate height of another node. C) (Maximal) simplices resulting from visibility diagram.

Results & Discussion: Of 62 total trials, we selected 14 trials that met constant force screening criteria. For all data, the number of simplices showed a stronger correlation with time (R^2= 0.35) than the median frequency of the signal (R^2= 0.32). A multivariate on four frequency and topological characterizers provided an even stronger correlation with time (R^2= 0.47). The results followed a similar trend on an individual basis (Table 1). Our result that a regression performed on topological and frequency characterizers showed a stronger correlation to experiment time than MDF alone suggests that TDA could be a powerful tool in improving muscle fatigue measurement. However, more experimentation that directly measures muscle fatigue is needed to confirm this hypothesis.

Table 1. R^2 values for linear regressions on an individual trial basis. A multivariate regression showed the strongest fit for each individual.

	1	2	3	4	5	6	7	8	9	10	11	12	13	14	Mean
Number of Simplices	0.922	0.944	0.777	0.978	0.961	0.947	0.951	0.979	0.895	0.964	0.520	0.965	0.950	0.989	0.910
MDF	0.985	0.968	0.602	0.767	0.844	0.727	0.941	0.985	0.801	0.884	0.805	0.956	0.889	0.948	0.864
Multivariate	0.993	0.972	0.881	0.968	0.980	0.985	0.988	0.989	0.984	0.959	0.865	0.975	0.967	0.989	0.964

Significance: Half of stroke survivors require long-term rehabilitative care, which is complicated by the high degree of deficit variability. Quick and accurate fatigue characterization can allow for targeted treatment plans and improved rehabilitation for stroke survivors. This study provides evidence that the combination of topological data analysis and statistical methods can provide more accurate fatigue detection from surface electromyography data. Future work with machine learning algorithms is anticipated to provide even better fatigue characterization.

References: [1] Yousif, H. et al. IOP Conf. Ser.: Mater. Sci. Eng. 705, 012010 (2019); [2] Cifrek, M. et al. Clinical Biomechanics, 24, 327-340 (2009); [3] Dey, T. et al. BMC Bioinformatics, 22, 627 (2021); [4] Xu, X. et al. Frontiers in Neuroscience, 15, 761703 (2021); [5] Chutani, M. et al., Chaos, 30, 013109 (2020)

EFFECTS OF STATIC EXERCISES ON HIP MUSCLE FATIGUE ASSESSED BY SURFACE ELECTROMYOGRAPHY

Olivia L. Dyer[1], Benjamin B. Wheatley[2*], Mark A. Seeley[1]
[1]Geisinger Musculoskeletal Institute, Danville, PA.
[2]Bucknell University, Department of Mechanical Engineering, Lewisburg, PA.
*Corresponding author's email: b.wheatley@bucknell.edu

Introduction: To determine hip strength and fatigability, clinicians use a variety of tests including the HipSIT Test, which has patients perform a clam-shell exercise to measure hip abduction strength, and the Vail Sports Test, which has patients perform a single leg squat, lateral bounding, and jogging to assess hip and core strength [1,2]. However, these tests lack specific muscular measurements and require assessment from an individual. Surface electromyography (sEMG) has been used to characterize muscle fatigue by observing a decrease in mean (MNF) and median (MDF) frequency of the sEMG signal over time as a static exercise is performed [3]. Furthermore, while sEMG data has previously been used to characterize muscle fatigue, it remains unclear if accelerometer data from low-cost IMUs can be used as a quantitative substitute for sEMG to estimate muscle fatigue. This study aimed to determine the differences in hip muscle fatigue as measured by sEMG and knee accelerometer data across two commonly performed activities – a wall sit and a single leg squat. We hypothesized that there would be a decrease in the mean frequency and an increase in knee acceleration as the duration of the activity increased, and that there would be a correlation between mean frequency (muscle fatigue) and knee acceleration (wobble).

Methods: Twenty-four participants (14F, 10M) were recruited to participate in a fatigue analysis study. Three sEMG sensors were placed on each participant – one each on the gluteus medius, gluteus maximus, and the rectus femoris. A 6-axis accelerometer was placed on the lateral portion of the knee. Participants then performed five exercises for 90 seconds each, grouped into two sets, one including a wall sit and single leg squat (general activities) and the other set including a side leg raise, single leg superman, and knee raise (targeted muscle activities). The exercises within each set were randomized. Following data collection all data analysis was performed in MATLAB. All sEMG data was analysed using a fast Fourier transform (FFT) and the frequencies were averaged over 10 second intervals. The area under the resultant acceleration curves for each 10 second interval was also calculated. Linear regressions for each participant were performed on all the frequencies and acceleration data of the single leg squat and wall sit to determine the R^2, slope, and intercept for each exercise and muscle group. Only the results of single leg squat and wall sit are reported for simplicity.

Results & Discussion: There was a decrease in mean frequencies (MNF) across all muscle groups for the single leg squat and wall sit activities, although the coefficient of determination was generally low to moderate ($R^2 \approx 0.5$, Figure 1A). There was a slightly stronger correlation among MNF in the wall sit compared to the single leg squat activity suggesting that the wall sit exercise more reliably elicits fatigue of the gluteus medius, gluteus maximus and rectus femoris muscles (Figure 1A). In addition to an observed decrease in MNF, there was an increase in area under the acceleration curve for each 10 second interval in the wall sit and single leg squat activity, with a larger slope of 9.57 ± 0.70 observed in the wall sit. There was a very weak coefficient of determination between accelerometer area under the curve slope and muscle fatigue slope, with $R^2 = 0.20$ for gluteus medius (Figure 1B). Further analysis is needed to determine the extent to which individuals who exhibit greater muscle fatigue also exhibit greater knee accelerations (wobble).

A

Activity		Gluteus Medius	Gluteus Maximus	Rectus Femoris	Acceleration AUC
Squat	Slope	-0.17 ± 0.54*	-0.49 ± 0.73*	-0.21 ± 0.91*	1.26 ± 2.48*
	R^2	0.34 ± 0.29	0.52 ± 0.31	0.35 ± 0.24	0.39 ± 0.24
Wall Sit	Slope	-0.83 ± 1.09*	-1.36 ± 1.79*	-0.64 ± 0.59*	9.57 ± 0.70*
	R^2	0.44 ± 0.31	0.51 ± 0.32	0.43 ± 0.25	0.47 ± 0.31

B

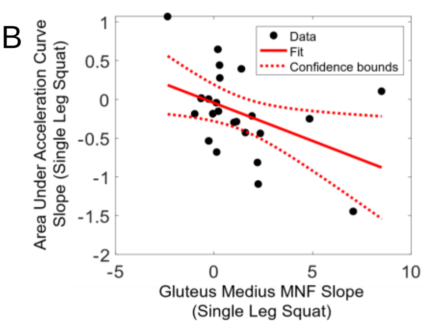

Figure 1: (A) Table of slopes and R^2 values (mean ± standard deviation) for muscle sEMG signal mean frequency versus time and accelerometer area under the curve versus time for both the single leg squat and wall sit activities. There was a more negative slope observed for all of the muscles and a more positive slope for the area under the acceleration curve for the wall sit activity compared to the sing leg squat (* denotes $p<0.05$ between activities). (B) Linear regression to observe the correlation between area under the acceleration curve slope compared to the gluteus medius MNF slope during the single leg squat activity ($R^2 = 0.20$).

Significance: Developing an accessible, low-cost, fast, and standardized method to measure the fatigability of hip muscles can allow for clinicians to successfully determine the strength of these muscles and determine if a person is able to return to normal activity levels following a lower limb injury. Our work suggests that the wall sit activity more reliably fatigues the gluteus medius, gluteus maximus, and rectus femoris muscles. While additonal data analysis is required, this work is a step towards implementing low-cost IMUs to estimate hip muscle fatigue by examining the relationship between aceeleration and sEMG fatigue data.

Acknowledgements: The authors would like to acknowledge the Bucknell-Geisinger Research Initiative for funding.

References: [1] Almeida GPL, et al. *J Orthop Sports Phys Ther*. 2017 [2] Garrison JC, et al. *Int J Sports Phys Ther*. 2012 [3] Cifrek M, et al. *Clinical Biomechanics*. 2009

ON DESIGNING AN IMPLANTABLE TRAPEZIUM REPLACEMENT BONE FOR MEASURING *IN VIVO* LOADS AT THE BASE OF THE THUMB

Joseph J. Crisco*, Julia A. Henke, Daniel McDermott, Rohit Badida, Amy M. Morton, Josephine M. Kalshoven, Douglas C. Moore
Department of Orthopaedics, Warren Alpert Medical School of Brown University and Rhode Island Hospital, Providence, RI
*Email: joseph_crisco@brown.edu

Introduction: A functional and pain-free thumb is critical to accomplishing many activities of daily living. The thumb is a common site for acute trauma, repetitive workplace injury, and the development of osteoarthritis (OA). Investigators have used musculoskeletal modeling to understand and mitigate workplace-associated injuries, while conservative therapy and arthroplasties are both treatments for thumb pathologies. For this project, it is notable that the standard of care for end-stage thumb base OA is surgical removal of the trapezium carpal bone (Fig. 1). Understanding the loads at the base of the thumb during activities of daily living would advance and validate musculoskeletal modelling and inform the approaches to clinical treatments, especially arthroplasty design and the scope of preclinical device testing for FDA clearance. The ultimate goal for this project is to develop an instrumented replacement trapezium capable of measuring the loads *in vivo*. In this abstract we present two strain gauge-based load sensor design options and report on the accuracy associated with two different approaches to calibration, with and without strain gauge drop out.

Methods: An initial ("Tube") design was based on previous successful designs in instrumented total knee arthroplasty developed to measure the loads across the knee joint during activities of daily living.[1] The Tube design incorporated a central sensing column with 3 circumferential rosette strain gauges (Fig. 2. 9 gauges, 120 Ω, VPG Sensors). Although well-established for larger joints, this approach affords limited space for internal electronics due to the small size of the trapezium (approx. 17x15x25mm^3). A subsequent design iteration incorporated a diaphragm as the sensing element. Five gauges (1000 Ω, VPG Sensors) were bonded to the underside of the Diaphragm (Fig. 3), designed to be welded to a container that houses the electronics (inductive power receiver, signal conditioner, amplifier and BLE). Calibration of the sensing elements was performed by securing both the Tube and Diaphragm designs to a 6 DOF load cell (Resolution: 0.25 N and 0.005 Nm. SI 580-20, ATI, Apex, NC), applying loads, and comparing the sensing element output to the 6 DOF load cell loads (the strain data was conditioned and amplified with a benchtop system). The maximum loads applied to the Tube and Diaphragm designs were, respectively, Fx: 48.8, 65.1, Fy: 125.4, 68.6, Fz: 15.8, 53.4, Mx: 0.97, 0.28, My: 0.42, 0.04, and Mz: 0.71, 0.26 (N and Nm). A supervised neural network with two cascade-forward nets (Levenberg-Marquardt and Bayesian Regularization training functions for the forces and moments, respectively) was employed for calibration using a 70/30 train/test and 10 k-fold validation on 68,228 and 444,335 data points, for the Tube and Diaphragm transducers, respectively. Loading along the longitudinal axis of the first metacarpal (Fy) was set as the most critical outcome measure (x: volar, z: radial). Accuracy was defined as the 95% CI of the limits of agreement (LOA) compared to the 6 DOF load cell using a Bland-Altman analysis.

Results & Discussion: The 95% CI LOA in Fy was significantly smaller in the Diaphragm design (1.9 N) than in the Tube design (19.7 N). Strain gauge removal had variable effects depending on sensor design and the number and locations of the gauges removed. For example: removing individual gauges in the Diaphragm design increased the 95% CI LOA for Fy by 3.0 N, 3.9 N, and 5.0 N, for three instances of individual gauge removal, respectively. On the other hand, removal of 2 of the 9 gauges in the Tube design (separately) increased the 95% CI LOA for Fy to 25.8 N and 28.1 N. We are moving ahead with the diaphragm design instrumented with 5 strain gauges with the goal of measuring loads across the thumb carpometacarpal joint *in vivo*, given its ability to measure axial loads with a 95% CI LOA of approximately 2 N. Many challenges remain before the device can be considered for FDA clearance and implantation in live humans. To minimize subject risk, the device will not be provided with a battery. The power and data systems are being developed and evaluated first in benchtop testing, followed by the miniaturization and installation of the components within the Diaphragm on a flexible circuit board. Mechanical components (fabricated from titanium (Ti6Al4V), Fig. 3) will be welded and hermetically sealed, followed by fatigue testing for structural and electrical integrity.

Significance: An instrumented trapezium capable of measuring loads at the base of the thumb will be immensely valuable to clinicians, researchers, and implant designers who need accurate load data to understand the role of joint loading in thumb pathophysiology, to refine musculoskeletal models, to standardize pre-clinical testing, and to develop more effective and cost-effective surgical treatments.

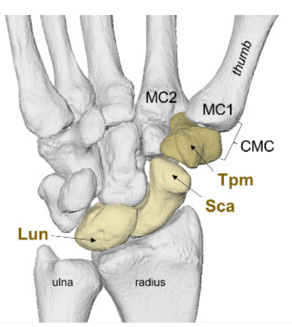

Fig. 1. Trapezium (Tpm) bone is replaced with the load sensing device in patients undergoing trapeziectomy for severe OA.

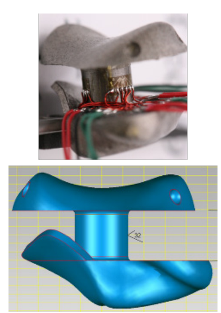

Fig. 2. Tube design showing strain gauges for benchtop calibration.

Fig 3. The underside of the distal component of the Diaphragm design instrumented with 5 strain gauges (L). A lateral view and cross-section of the Diaphragm design (R).

Acknowledgements: This research was funded in part by NIH/NIAMS R21AR077201. Portions of the data have been previously presented at the 2023 Annual Meeting of the Orthopaedic Research Society.

References: [1] D'Lima et al., 2013.

SHOULDER PAIN AND VARIABILITY OF WHEELCHAIR HANDRIM KINETICS IN SPINAL CORD INJURY

Caleb Cordes[1*], Josh Leonardis[2], Alyssa Schnorenberg[3], Shubhra Mukherjee[4], Karin Goodfriend[5], Amee Seitz[6], Lawrence Vogel[4], Brooke Slavens[1,3]
[1]University of Wisconsin-Milwaukee, Department of Rehabilitation Sciences & Technology
*Corresponding author's email: cmcordes@uwm.edu

Introduction: Manual wheelchair users with pediatric-onset spinal cord injury (SCI) are less likely to experience shoulder pain than their counterparts with adult-onset SCI [1]. Variability in manual wheelchair handrim kinetics may play an important role, as increasing variability is thought to limit shoulder pain by decreasing repetitive strain of the shoulder joint complex [2]. By establishing the relationship between variability of handrim kinetics and shoulder pain in wheelchair users across the lifespan, we hope to reveal mechanistic insights into shoulder pain to inform prevention and treatment strategies. The purpose of this study was to determine the relationships between variability in manual wheelchair handrim kinetics and intensity of shoulder pain in manual wheelchair users with pediatric- and adult-onset SCI. We hypothesized that increasing variability in peak resultant force and fraction of effective force (FEF) would be associated with decreasing pain intensity in those with pediatric-onset and adult-onset SCI.

Table 1: Participant demographics. Age, age at SCI, duration of wheelchair use, and pain scores given as mean± 1 standard deviation.

Group	Age (years)	Level of SCI	Age at SCI (years)	Duration of Wheelchair Use (years)	WUSPI Scores (0-150)	PROMIS T-Scores (Population mean 50±10)
Pediatric SCI (7, 4 females)	11±3.6	T3-L3	4±4	6.5±4.3	3±7	44±1
Adult-Ped Onset (6, 4 females)	21±0.9	C6-L3	12±6	9.1±6.9	11±15	50±8
Adult Onset (8, 1 females)	42±11.6	C6-L3	30±7	11.9±7.7	22±16	60±10

Methods: Twenty-one (21) manual wheelchair users with SCI (Table 1) participated in a single experimental session. Participants completed the Wheelchair Users Shoulder Pain Index (WUSPI, increasing score with increasing pain intensity) and the Patient-Reported Outcomes Measurement Information System Pain Interference (PROMIS-PI, increasing score with increasing pain interference) outcome questionnaires. Participants propelled their wheelchair at a self-selected speed while a SmartWheel instrumented handrim sampled 3-D dominant-side handrim kinetics during the contact phase of wheelchair propulsion. Handrim kinetics of interest were peak resultant handrim force (N) and fraction of effective force (FEF; ratio of peak tangential force to resultant handrim force, N:N), a measure that may indicate how effectively handrim forces are applied during propulsion [3,4]. The coefficient of variation (CV; standard deviation divided by the mean) was computed to quantify variability of handrim kinetics. Simple linear regression was used to assess relationships between handrim kinetics and WUSPI and PROMIS-PI scores.

Results & Discussion: Relationships between handrim kinetics variability and pain outcomes varied among groups. There was a trend of decreasing pain scores with increasing CV of peak resultant force while increasing CV of FEF was correlated with increasing pain scores across all groups (Fig. 1). Pediatric participants' PROMIS-PI scores increased with increasing CV of FEF, but pediatric scores otherwise had no relationship with variability of handrim kinetics (Fig. 1). Shoulder pain intensity in adults with pediatric onset increased with increasing CV of FEF (Fig. 1). While increasing variability in peak resultant force may result in reduced repetitive shoulder strain, increasing variability in FEF may indicate ineffective force application to the wheelchair handrim and greater demands on shoulder musculature [2,3]. Alternatively, individuals with shoulder pain may increase variability in FEF and other handrim kinetics such as peak resultant force to avoid exacerbations of discomfort. The role of FEF in wheelchair propulsion and shoulder pain warrants further investigation in a larger population.

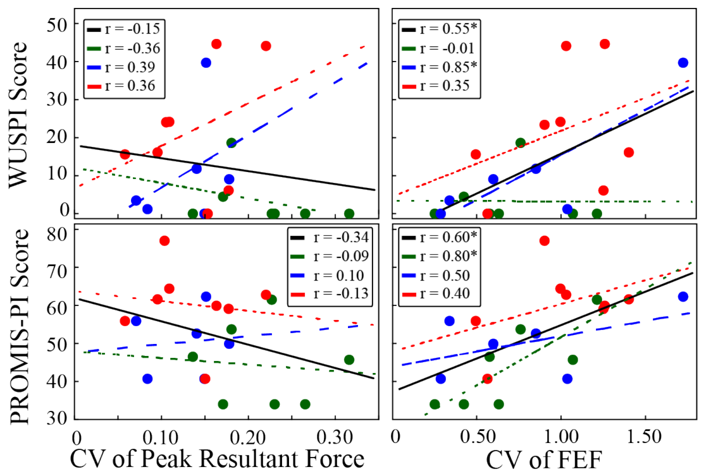

*Figure 1: Relationships between variability in handrim kinetics and pain. Pediatric participants are shown with green circles, adults with pediatric onset with blue circles, and adult onset with red circles. Regression lines are plotted for each group, with regression results for all participants shown in black. * denotes p<0.05.*

Significance: This novel study is an important step in our ongoing work exploring relationships between variability of handrim kinetics as an indicator of overuse and shoulder pain in persons with SCI across the lifespan [1,5]. Understanding why the prevalence of shoulder pain is lower among those with pediatric-onset SCI will provide insight into shoulder health and pain prevention for manual wheelchair users of all ages. Further investigation of potential biomechanical and shoulder architectural moderators of the relationship between handrim kinetics and shoulder pain is underway.

Acknowledgements: This research was supported by the Eunice Kennedy Shriver National Institute of Child Health and Human Development (NICHD) of the NIH (1R01HD098698). Thanks also to members of the UWM Mobility Lab and Shriners Children's Chicago research teams.

References: [1] Slavens et al. (2015), *Front Bioeng Biotechnol* 3:137; [2] Rice et al. (2014), *Arch Phys Med Rehabil* 95(4); [3] Bregman et al. (2009), *Clin Biomech* 24(1); [4] Rankin et al. (2010), *J Biomech* 43(14); [5] Cordes et al. (2022), *Proceedings of North American Congress on Biomechanics*

CHANGE IN PRE-SEASON TRAINING TIMING IMPACTS RUNNING METRICS IN DI FIELD HOCKEY

Kathleen A Bieryla[1*], Jared Miner[2], Ryan C. Snyder[2]
[1]Shiley School of Engineering, University of Portland, Portland, OR
[2]Department of Chemical Engineering, Bucknell University, Lewisburg, PA
*Corresponding author's email: bieryla@up.edu

Introduction: The COVID-19 pandemic presented an unprecedented challenge for collegiate sports. Due to the global pandemic the typical NCAA fall 2020 field hockey season for most teams was postponed until spring 2021 and played as a shortened season.[1] The pandemic restrictions, along with the change from fall to spring, produced a different pre-season for athletes compared to what they normally experience. Pre-season during a typical year consists of individual summer workouts with limited to no contact from coaches followed by an intensive approximately two-week practice and scrimmage schedule without a simultaneous class schedule before official games begin. For spring 2021, all athletes were on campus in weeks leading up to competitive games and partaking in general conditioning while also simultaneously in classes. The majority of athletes were also on campus in fall 2020. There was a notably less intense pre-season practice schedule before going into the shortened season. Previous research has examined GPS metrics in Division I (DI) field hockey players, but this was with a standard preseason, and prior to the game format changing from two halves to four quarters.[2] No study has examined the effect of changing the pre-season training timing on running metrics in DI field hockey players.

The purpose of the study was to examine how different pre-season regiments would affect GPS running metrics during the first six games of the season. It was hypothesized that a pre-season that was more consistent with ongoing training and stretched over a longer period of time would enable equal or higher running metrics during competitive matches in the 2020 season compared to the first six games of the 2019 season.

Methods: GPS data was recorded from a single DI women's field hockey team during the 2019 and 2020 (which occurred in spring 2021) season. Only the first six games of the 2019 season were analyzed to compare to the full season of 2020 which only consisted of six games. Data was collected from 20 players in 2019, over six weeks, and 22 players in 2020, over three weeks. The dependent measures included total time (TT, min), the amount of time the player spent in the game, total distance traveled by player (TD, m), low-speed running (LSR, m), distance traveled while the player's velocity < 10.99 km/h, and high-speed running (HSR, m), distance traveled while the player's velocity > 11.00 km/h. To allow for comparisons, measures were calculated relative to the TT for each player. A linear mixed model ANOVA was used to compare across seasons, with significance set at $p<0.05$. All statistical analyses were completed in JMP Pro 16.2 (Cary, NC).

Results & Discussion: There was no difference in TT between 2019 and 2020. Athletes played an average of 35.8 ± 12.7 min in 2019 and 35.8 ± 13.4 min in 2020 ($p=0.061$). The data supports the hypothesis of higher running metrics during 2020 compared to 2019. There was a significant increase in relative TD ($p<0.001$), LSR ($p<0.001$), and HSR ($p<0.001$) between the two seasons (Figure 1). Relative TD increased an average of 22.2 m/min, relative LSR increased an average of 10.8 m/min and relative HSR increased an average of 11.1 m/min. These increases suggest the difference in pre-season training did make a difference for the athlete's running metrics during competitive matches. Changing the training from two weeks of intense two-a-day workouts to longer, more sustained training improved the running metrics. In addition, the change in training may have made a major difference for the first-year athletes. During a normal season, first-year athletes only have the intense pre-season for training prior to starting the season. Furthermore, the first-year athletes are adjusting to college life which may affect their performance on the field and their overall conditioning[3]. In 2020, the first-year athletes were living on campus in the fall term so they may have adjusted better to college life and were able to train informally with team members throughout the semester. This combination may be the reason the first-year athletes increased relative TD by and average of 33 m/min from 2019 to 2020, while only increasing TT less than 1 min.

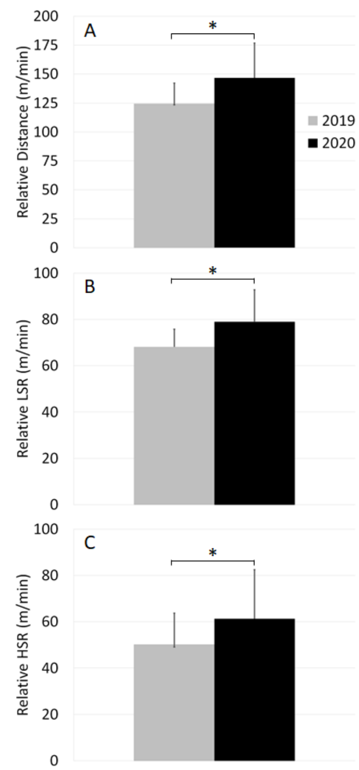

Figure 1: Mean values for relative distance (A), LSR (B), and HSR (C) for the first six games of the season with regular pre-season training (2019, gray) and less intense pre-season training (2020, black). Error bars represent standard deviation. * Indicates significant difference ($p<0.05$).

Significance: Coaches and trainers for fall sports may want to rethink how pre-season training occurs. The results of this study suggest the typical pre-season for fall sports may not be the best to increase the output of the athletes. Instead, having a less intensive pre-season with more touch points may increase the running metrics for athletes during a game. Major changes to pre-season timing would need to occur through a NCAA rule change.

Acknowledgements: The authors would like to thank the coaches of the women's field hockey team for help with the study.

References: [1] Johnson (2020), https://www.ncaa.org/news/2020/9/16/di-council-approves-moving-fall-championships-to-the-spring.aspx; [2] Vescovi & Frayne (2015), *Int J Sports Physiol Perform* 10(4). [3] Bieryla et al. (2021), *App Sci* 11(17).

STRATEGIES USED TO REDUCE KNEE LOADING IN SINGLE-LIMB SQUAT 3-4 MONTHS POST-ACLR

Jiaqi Wang[1*], Susan Sigward[1]
[1]Division of Biokinesiology and Physical Therapy, University of Southern California, Los Angeles, CA 90033
*Corresponding author's email: jwang388@usc.edu

Introduction: Literature supports the presence of reduced knee loading in the surgical limb following anterior cruciate ligament reconstruction (ACLr). Knee extensor moment (KEM) deficits have been found to persist [1] throughout recovery and [2-3] across a variety of tasks. The use of inter- and intra- limb compensations to reduce knee loading during double-limb tasks is well described in this population. [1] At 3 months post-ACLr, compensations that shift the demands to the non-surgical (NSx) limb (inter-limb) and to the hip in the surgical (Sx) limb (intra-limb) explain 85% of the variance in KEM during a double-limb squat. These compensations are observed in the absence of appreciable between-limb differences in knee flexion angle (KFA). Less is known regarding compensations to reduce knee loading during single-limb squats when a shift in demands to the NSx limb is not an option. Therefore, the aim of this study is to determine what strategies individuals 3-4 months post-ACLr use to reduce KEM during a single-limb squat. Given the inherent increase in demands during a single-limb squat, it is expected that individuals utilize intra-limb compensations along with reducing knee flexion to reduce knee extensor loading.

Methods: Seven individuals (sex, 4 female; age, 34.3±13.7 years; height, 1.75±0.08 m; mass, 73.3±14.0 kg; 111±23 days post-ACLr) performed non-paced single-limb squats to maximal depth with the contralateral limb extended out front. Kinematics (3D motion capture), ground reaction forces (force platforms) and anthropometrics were used in inverse dynamics equations to calculate sagittal plane moments at the hip, knee and ankle. KFA, ground reaction force (GRF) magnitude, knee, hip and ankle plantar flexor moments at the time of peak KEM were identified. Hip-to-knee (H:K) and ankle-to-knee (A:K) extensor moment ratios were calculated to represent the intra-limb distribution of moments. Between-limb ratios (Sx/NSx) were calculated for each variable to represent the difference between limbs. A ratio of 1 indicates no difference between limbs, and a ratio < 1 indicates that the Sx limb is smaller than the NSx limb. The average of three trials per limb was considered for analyses. Paired t-tests were used to examine between limb differences for all variables. Between-limb ratios were considered in a best subsets regression model to determine the best predictors of KEM ratio.

Results & Discussion: When compared to the Sx limb, KEM ($p < 0.05$), KFA ($p < 0.05$), and GRF ($p < 0.01$) were smaller; H:K ($p < 0.05$), and A:K ($p = 0.14$) were larger in the Sx limb (Table 1). Smaller H:K and A:K ratios indicate that the intra-limb distribution in the Sx limb was more hip and ankle dominant than in the NSx limb. The best predictor model for KEM ratio included three variables (H:K ratio, GRF ratio and A:K ratio), explaining 96% of the variance in KEM ratio. A larger between-limb H:K ratio (indicating a more hip dominant distribution in the Sx versus NSx limb) was related to a smaller KEM ratio (indicating a KEM deficit in the Sx limb). Similarly, a larger A:K ratio was related to a smaller KEM ratio. A smaller GRF ratio was related to a smaller KEM ratio. Between-limb ratio of KFA did not add to the prediction of the KEM ratio.

Significance: In this small sample, individuals adopted intra-limb compensations by shifting the demands to the hip and ankle, and modulating the GRF magnitude to reduce KEM in the Sx limb. Despite the fact that shifting the force to the other limb was not an option, individuals appeared to manipulate the same variables to compensate during double- and single-limb squats. Manipulation of the GRF magnitude was accomplished by lowering squat velocity. Compensations may differ when squat speed is controlled for.

References: [1] Sigward et al. (2018), *J Orthop Sports Phys Ther* 48(9); [2] Hughes et al. (2020), *J Athl Train* 55(8); [3] Lepley & Kuenze (2018), *J Athl Train* 53(2).

Table 1. Descriptive statistics and between-limb comparisons. *Significant main effect of limb.

	Limb	Mean (SD)	Significance	Mean Difference	95% CI
pKEM (Nm/Kg)	Sx	1.19 (0.46)	<0.05*	-0.39	(-0.70, -0.07)
	NSx	1.58 (0.57)			
KFA (Degrees)	Sx	75.84 (14.29)	<0.05*	-10.25	(-18.43, -2.08)
	NSx	86.10 (7.72)			
GRF (N)	Sx	751.38 (136.27)	<0.01*	-32.46	(-53.84, -11.08)
	NSx	783.84 (134.09)			
H:K Ratio	Sx	1.15 (0.26)	<0.05*	0.27	(0.00, 0.55)
	NSx	0.87 (0.26)			
A:K Ratio	Sx	0.64 (0.31)	0.14	0.15	(-0.07, 0.38)
	NSx	0.48 (0.22)			

THE EFFICACY AND FEASIBILITY OF BIOFEEDBACK IN ERGONOMICS

Demir J. Tuken[1*], Ian Silva[2], Rachel V. Vitali[3]
[1]Univeristy of Iowa Department of Biomedical Engineering, Heartland Center for Occupational Health and Safety
[2,3]University of Iowa Department of Mechanical Engineering
*Corresponding author's email: demir-tuken@uiowa.edu

Introduction: Healthcare workers, primarily those in the surgical field and dentistry, have a high risk of developing musculoskeletal disorders (MSD) due to maintaining prolonged awkward or unsafe postures induced by environmental working conditions that have generated few new worker safety regulations throughout the decades [1-3]. The associated chronic, debilitating pain significantly impacts their careers and lives, and it frequently leads to early retirement and, ergo, a critical loss of talent and productivity that required years of expensive training to obtain [4]. Previous work has provided a wealth of subjective data (e.g., [1]), which indicates a certain level of negation of the prevalence and impact of these medical conditions. Although a problem has been identified, an objective, quantifiable method of determining the key factors contributing toward injury or tracking improvements resulting from interventions is missing [5]. The purpose of this study is to provide pilot data supporting the feasibility and efficacy of a wearable sensor-based monitoring and biofeedback system for training the user to adopt specific postures or switch postures after extended periods of time. Participants are asked to engage in a simple typing task while maintaining different postures. Two approaches are utilized to ensure that participants maintain the desired posture: 1) a physical guide that will be removed prior to testing, and 2) a biofeedback system that provides haptic feedback. The purpose is to evaluate if the wearable sensors, inertial measurement units (IMUs) and surface electromyography (EMG) sensors, can quantify differences in spine orientations and muscle activity, respectively, for different postures and/or throughout the duration of a trial. The specific hypotheses for this study include the following: 1) Trials with an engaged posture have increased muscle activation than trials in a neutral posture, 2) Deviations from a neutral sitting posture will cause increased rates of muscle activation and fatigue, and 3) Trials using biofeedback will conform more to experimental testing configurations (i.e., postures) than trials without biofeedback.

Methods: On 11 March 2023, IRB permission was granted to study 35 healthy adults with no history of MSD, vestibular disorders, and heart conditions recruited via email. For each participant, five postural test conditions [1. neutral posture, 2. engaged posture, 3. neck at 30^{o} relative to back, 4. head at 30^{o} relative to back, and 5. neck plus head at 30^{o} relative to back] distributed in a randomized order were conducted. Each condition had 6 trials, 3 with haptic biofeedback and 3 without biofeedback. During each trial, participants will complete a generic one-minute typing test to capture cognitive ability. Muscle activation from shoulder muscles [left descending trapezius (LT), right descending trapezius (RT), left infraspinatus (LI), and right infraspinatus (RI)] were collected using surface EMGs (Cometa). Isometric maximum voluntary contractions (MVCs) were measured for each muscle via the SENIAM protocol. Post processing of EMG data included low pass filtering, 4^{th} order Butterworth bandpass filtering, and rectification as well as a fast Fourier transform (FFT) to inspect frequency content. The RMS for each trial was taken in 50 millisecond intervals. The EMG data was then normalized to the highest post processed reading in the MVC test. Posture analysis for the back and neck was conducted using lightweight, wireless IMUs (SageMotion) that were taped to participants' L5, C7, and skull. Each IMU includes a tri-axial accelerometer, gyroscope, and magnetometer that a proprietary Kalman filter fused together to provide orientation estimates in quaternion form. The roll Euler angle was calculated according to θ = (arctan(t_0, t_1)*180/pi -90°) where t_0 and t_1 are elements of the quaternion and -90° accounts for relating the sensor's orientation to vertical. The IMUs also include vibrotactile motors capable of providing haptic biofeedback (e.g., when the participant's neck angle exceeds some threshold angular deviation). The posture analysis was conducted in real time using Python whereas the muscle activation analysis and all post processing was conducted using MATLAB. The average normalized moving RMS for each muscle was evaluated for each condition and compared to the neutral average normalised moving RMS. Orientation differences between trials with and without feedback were compared for the average angle deviation from desired test condition.

Results & Discussion: Preliminary data for one participant has been collected and analyzed. These early results indicate an increase in muscle activation when compared to neutral posture. On average across all muscles with feedback, engagement increased by 32.89%, back at 30° increased by 39.77%, neck at 30° increased by 19.25%, and back plus neck at 30° increased by 19.66%. For the participant, angle deviation for trials without haptic biofeedback did not increase compared to trials with biofeedback. Following the collection of all 35 participants, t-tests will be conducted for the following three cases: 1) comparing the difference in muscle activation between engaged posture trials versus neutral posture trials, 2) comparing the difference in muscle activation between neutral posture trials and the three postures with 30^{o} deviations, and 3) comparing the difference in angle deviations between trials with and without haptic biofeedback. The increase in muscle activation across all trials compared to neutral postures indicate that unsafe postures may be correlated to muscle activation [6]. The increase in magnitude of activation during trials when compared to normal indicates greater muscle fatigue in awkward or unsafe postures. Future data collection will be completed to support or refute theses hypotheses.

Significance: Developing an objective measure for studying the relationship between posture and muscle activation is crucial toward determining root causes for MSD in medical professionals. Preliminary results suggest that the methods proposed in this study are a feasible way to collect and determine the relationship between muscle activation and posture orientation. The efficacy of the study will allow for procedural implementation in a healthcare setting as a means toward determining the key factors of chronic pain in medical professionals through quantifiable, objective data.

References: [1] Kitzman et al. (2012), *J Ophthalmology* 119(2). [2] Epstein et al. (2018), *J JAMA* 153(2). [3] Hayes et al. (2009), *J IJDT* 7.3. [4] Yamalik (2007), *J IDJT* 57. [5] Lietz et al. (2018), *J PLoS ONE* 13(12). [6] Sterling et al. (2001), *J Pain* 2.3

RELATIONSHIP OF HIP MUSCLE STRENGTH TO WALKING AND BALANCE PERFORMANCE IN UNILATERAL TRANSTIBIAL PROSTHESIS USERS

Andrew Sawers[1*], Stefania Fatone[2]
[1]University of Illinois Chicago, Department of Kinesiology and Nutrition
[2]University of Washington, Department of Rehabilitation Medicine
*Corresponding author's email: asawers@uic.edu

Introduction: Improved walking and balance is a commonly stated goal of lower limb prosthesis (LLP) users [1]. Restoring or improving locomotor skills is therefore a priority of prosthetic rehabilitation [2]. Although 26-62% of LLP users regain the ability to walk outdoors [3], gait impairments, particularly reduced speed, endurance, and balance [3] diminish LLP users' safety and mobility.

There is growing evidence that muscle weakness is a major factor limiting safe and efficient locomotion in LLP users [4]. Hip muscles play a particularly prominent role, compensating for lost ankle propulsion, stabilization, and body weight support [5]. There is however no consensus regarding the causal relationship between hip muscle strength and LLP users' walking and balance performance [4]. Identifying the contribution of hip strength to LLP users' walking and balance performance would provide a focus to the assessment and treatment of gait impairments that is currently lacking. The objective of this study was therefore to determine how much variance in walking and balance performance could be explained by hip strength in unilateral transtibial (TT) prosthesis users. We hypothesized that due to the loss of ankle propulsion and medial-lateral stabilization, greater residual limb hip extension and abduction strength would be associated with greater walking speed, endurance, and balance in unilateral TT prosthesis users.

Methods: Unilateral TT prosthesis users were recruited from local prosthetic clinics. A motor-driven dynamometer was used to measure maximum voluntary isometric hip extension and flexion torque in a supine position with the hip flexed 20°, as well as abd- and adduction torque in a side lying position with the hip abducted 10° [6]. Testing order (i.e., leg and muscle group) was randomized. Participants completed 15 five-second trials with 10s rest between trials. Measures of hip muscle strength, including peak torque, average torque, torque impulse, and torque steadiness were calculated from the processed torque signal, and scaled to body mass x thigh length [7]. Walking speed, endurance, and balance were assessed by administering the 10-meter walk test (10mWT), 2-minute walk test (2MWT), and Narrowing Beam Walking Test (NBWT), respectively. Forward stepwise multiple linear regression was used to evaluate the relationship between isometric measures of residual and intact limb hip strength and walking and balance performance.

Results & Discussion: 13 TT prosthesis users were recruited, provided informed consent, and enrolled in the study (mean age: 53 yrs, mean time since amputation: 20 yrs, 8 males, 10 traumatic amputations). In support of our hypothesis, modeling of causal relationships between hip strength and walking and balance performance revealed that two measures, residual limb (RL) peak hip extension torque and RL hip abduction torque steadiness, were consistently and significantly associated with better walking and balance. Together, RL peak hip extension torque and hip abduction steadiness explained 69%, 60%, and 68% of the variance in TT prosthesis users' walking speed, endurance, and balance, respectively (Fig. 1). Individually, RL peak hip extension torque and hip abduction steadiness explained 51% and 18% of the variation in speed, 36% and 24% of the differences in endurance, and 17% and 51% of the variance in balance, respectively. Deficits in RL hip extensor torque generating capacity primarily impaired walking speed and endurance [8], while a decrease in the RL hip abductors' ability to maintain a consistent torque mainly reduce walking balance.

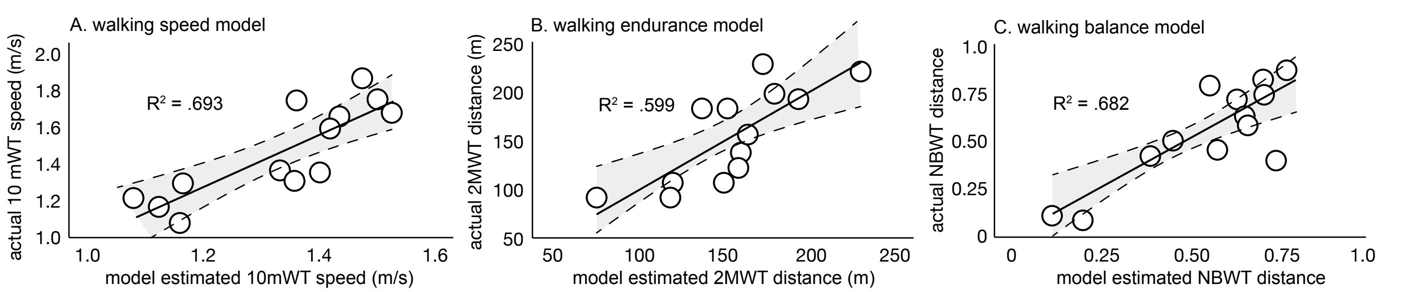

Figure 1: Multivariate models based on residual limb peak hip extension torque and residual limb hip abduction torque steadiness reconstructed TT prosthesis users' walking speed (A), endurance (B), and balance (C), explaining 69%, 60%, and 68% of the variance, respectively.

Significance: Deficits in RL peak hip extension torque and RL hip abduction torque steadiness may serve as modifiable factors that clinicians can assess and treat to improve unilateral TT prosthesis users' walking and balance performance. 30-40% of the variance in walking and balance performance was not explained by isometric hip muscle function. Further research that considers other muscles, their functions (i.e., rate of torque development), actions (i.e., isokinetic), and coordination is needed to advance rehabilitation.

Acknowledgements: This work was supported by the Department of Defense under award number W81XWH-19-1-0547.

References: [1] Manz et al. (2022), *JNER* 19(119); [2] Meier (2014), *Phys Med Rehab Clin N Am* 25(1); [3] van Velzen et al. (2006), *Clin Rehabil* 20(11); [4] Hewson et al. (2020), *POI* 44(5); [5] Seroussi et al. (1996), *Arch Phys Med Rehab* (77); [6] Powers et al. (1996), *Phys Ther* 76(4); [7] Sawers & Fatone (2022), *Clin Biomech* (97); [8] Raya et al. (2010), *POI* 34(1).

IS IT THE VIRTUAL ENVIRONMENT OR JUST THE HEAD-MOUNTED VIRTUAL REALITY DEVICE THAT INDUCES POSTURAL INSTABILITY?

Harish Chander[1*], Hannah Freeman[2] & Adam Knight[1]
[1]Neuromechanics Laboratory, Department of Kinesiology, Mississippi State University
[2]Department of Occupational Therapy, The University of Alabama at Birmingham
*Corresponding author's email: hchander@colled.msstate.edu

Introduction: Virtual reality (VR) has been proven to be very effective and is commonly used in various health-related interventions and rehabilitation, specifically in balance and fall prevention training. The use of a head mounted display device (HMD) for VR exposure has been reported to cause postural instability, similar to standing with eyes closed with lack of visual feedback [1]. More recently, in assessing postural stability with exposure to different altitudes in VR, greater postural instability was reported in VR conditions, regardless of the altitude and even at ground level, compared to a real environment not wearing HMD [2]. The detrimental effects of immersive VR on postural stability have been attributed to distorted visual feedback, reduced visual field and sensory conflict during postural control. Due to constant evolution of VR technology, the HMD's mass has been consistently lowered, yet the addition of an extra mass to the head, essentially to the distal end of the inverted pendulum model during quiet standing, can impose postural instability, merely from the mass added by the HMD. Therefore, the purpose of this study was to assess postural stability, both with and without visual feedback in a real environment and in a virtual environment. With immersive VR capable of causing visual field limitation, distortion, and sensory conflict, as well the HMD capable of causing instability to the inverted pendulum model, it was hypothesized that exposure to the virtual environment and wearing the VR HMD will increase postural instability.

Methods: A total of 30 apparently healthy male and female participants (age: 21 ± 1 years; height: 166.5 ± 7.3 cm; mass: 71.7 ± 16.2 kg) after clearing physical activity readiness and simulator sickness questionnaires (SSQ), completed the study. Immediately following familiarization with postural stability and VR HMD exposure, participants completed another SSQ, and if the SSQ score was > 5, the participant was excluded. After a 10-minute break, three trials of bilateral static postural stability were recorded using the BTrackS™ balance platform, in four postural stability conditions; in real non-virtual environment with no HMD with eyes open (EO_NoVR) and eyes closed (EC_NoVR) and in a virtual room VE with an HMD with eyes closed (EC_VR) and eyes open (EO_VR). Participants were advised to stand as erect as possible without moving and to look straight at the front wall of the room and completed SSQ. Center of Pressure (COP) postural sway velocity (SV) (cm/s) was used as the outcome variable and comparison of SV during all four postural stability conditions were analyzed using a one-way repeated-measures analysis of variance (RM ANOVA) at an alpha level of 0.05.

Results & Discussion: Results revealed a significant main effect between four postural stability conditions for SV, (F (3,87) = 64.465, $p < 0.001$, $\eta p^2 = 0.690$). Pairwise comparisons revealed that EO_NoVR demonstrated significantly lower SV compared to both EC_NoVR and EC_VR, but not EO_VR, while EC_NoVR demonstrated significantly greater SV compared to EC_VR and EO_VR, along with EC_VR demonstrating significantly greater SV than EO_VR (Fig. 1). Findings revealed that eyes open condition in the real environment without HMD promoted greater postural stability compared to both eyes closed conditions, without and with HMD, which could be explained by the lack of visual feedback; but also demonstrated similar postural stability compared to eyes open with VR HMD, suggesting that the virtual environment did not negatively affect postural stability as originally hypothesized. This can be attributed to the more realistic virtual scene/room used in the current study compared to our previous, which may have resulted in a less distorted visual feedback and lower sensory conflict. Additionally, the effects of VR induced postural instability could be minimized when the virtual environment is created as much as a duplicate of the real environment [3]. While the virtual and real environment were not an exact replica, they were similar with same dimensions. When both eyes closed conditions were compared, wearing the HMD resulted in a better postural stability than not wearing one, which was also contrary to the original hypothesis. Proprioception plays a vital role in postural control especially when visual feedback is absent, and increased proprioception when something is wrapped around a body part, has been reported to improve postural stability by increasing one's awareness to their body position in space [4]. Wearing the HMD might have provided more proprioceptive feedback to the postural control system and resulting in better postural stability. Finally, wearing the HMD with eyes open compared to closed, still demonstrated better postural stability suggesting that the availability of visual feedback, even from a virtual environment was beneficial to the postural control system.

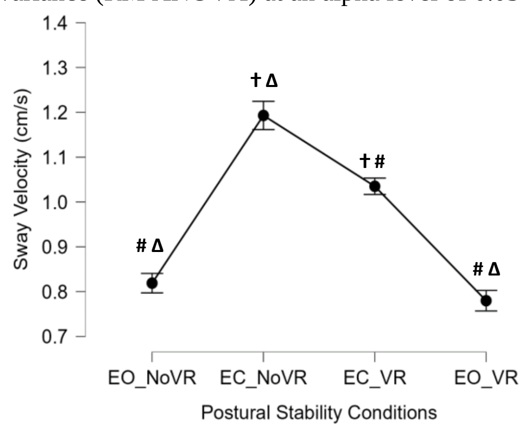

Figure 1: COP sway velocity (cm/s) during four postural stability conditions. †: significant difference from EO_NoVR; #: significant difference from EC_NoVR; Δ: significant difference from EC_VR and bars represent standard error.

Significance: Findings offer insights into the positive impact of VR and the use of an HMD on postural stability, which can be applied not to just health-related applications, but also on broader use of VR for teaching, learning, and interaction without any negative consequences of postural instability and simulator sickness, at least on healthy younger population.

References: [1] Horlings et al. (2009), *Neuroscience Letters*, 451(3), 227-231; [2] Chander et al. (2021), *Workplace Health & Safety*, 69(1), 32-40; [3] Cleworth et al. (2012), *Gait & Posture*, *36*(2), 172-176; [4] Gur et al. (2015), *Gait & Posture*, *41*(1), 93-99.

COMPARISON OF JOINT ANGLES BETWEEN HEALTHY AND OSTEOARTHRITIC TRAPEZIOMETACARPAL JOINTS USING DYNAMIC COMPUTED TOMOGRAPHY

Michael T. Kuczynski[1,2*], Charley Hasselaar[2], Gurpreet Dhaliwal[3,4], Neil J. White[2,3,4], Sarah L. Manske[1,5]
[1]Biomedical Engineering Graduate Program, Schulich School of Engineering, University of Calgary, Canada
[2]McCaig Institute for Bone and Joint Health, Cumming School of Medicine, University of Calgary, Canada
[3]Depatment of Surgery, Cumming School of Medicine, University of Calgary, Canada
[4]South Campus Research Unit for Bone and Soft Tissue, Calgary, Canada
[5]Department of Radiology, Cumming School of Medicine, University of Calgary, Canada
*Corresponding author's email: mkuczyns@ucalgary.ca

Introduction: Osteoarthritis (OA) commonly affects the trapeziometacarpal (TMC) joint at the base of the thumb, which can cause pain and functional impairments. While the etiology of OA is not fully understood, joint biomechanics are known to play a role in the development and progression of OA. Further, biological factors, such as female sex, may increase one's risk for the development of hand OA. While the TMC joint is challenging to study with traditional kinematic methods, new advancements in computed tomography (CT) imaging, known as dynamic CT, allow for the quantification of joint motion *in vivo*. The purpose of this study is to compare TMC joint biomechanics in women with OA to a sample of young, healthy controls using dynamic CT.

Methods: All methods were performed in accordance with guidelines set by the Conjoint Health Research Ethics Board at the University of Calgary (REB21-0508). Seven women with no signs of TMC OA (age 20 – 40), and five women with clinically diagnosed TMC OA (age > 50) were scanned. Only TMC joints with Eaton-Littler stages 1-3 (mild to moderate OA) were included in the OA group. Dynamic CT (Revolution HD GSI, GE) scanning consisted of a radial abduction-adduction movement (functional flexion-extension) with the following scanning protocol: 120 kVp, 100 mA, 0.293x0.293x2.5 mm voxels, 15 s scan time, 40 mm longitudinal coverage, 4 vol/s gantry rotation, and 3 movement cycles per participant. Due to limitations in the dynamic CT scan coverage area, CT scans of the full hand were obtained using a cone-beam CT (CBCT) scanner to assist in image processing and landmark selection for segment coordinate system (SCS) definition. CBCT scanning protocol was as follows: 120 kVp, 5 mA, and 0.25 mm^3 voxels (HiRise, Curvebeam). Image processing was performed using a previously described Python workflow [1]. Abduction-adduction, flexion-extension, and axial rotation joint angles were then computed. Statistical analysis was performed using Statistical Parametric Mapping (SPM) in MATLAB [2]. For each participant, a single movement cycle was manually extracted for analysis. Angle curves were first filtered using a fourth order Butterworth filter and then resampled to ensure the number of data points between participant movement cycles is equal. Finally, angle curves were matched by peak angle before applying SPM to compare between groups (Mann-Whitney U test, $\alpha = 0.05$).

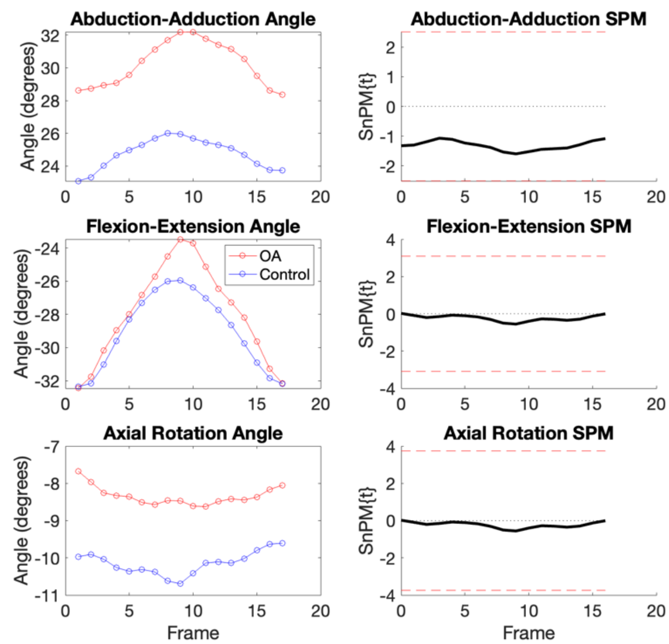

Figure 1: Mean joint angle (left) and SPM t-statistic (right) plots as a function of dynamic CT frame for the radial abduction-adduction movement. No statistical significance is seen between OA and control groups for each joint angle measured ($P > 0.05$). Red dashed lines in the SPM plots indicate the critical threshold values for statistical significance.

Results & Discussion: SPM results of TMC joint angles between the OA and control groups showed no statistically significant difference between groups, at any stage of the radial abduction-adduction cycle ($P > 0.05$) (Fig. 1). These results suggest that there may be no significant difference between radial abduction-adduction movements of healthy and OA TMC joints, however, a small sample size likely affects these results. While statistical significance was not observed in this preliminary work, additional analysis is currently being performed on more clinically relevant thumb movements (thumb opposition and key pinch). Previously, clinically measured lateral key pinch strength has been shown to be associated with early TMC OA [3], even before the development of radiographic findings. An automated SCS definition approach that has been previously defined for the TMC joint [4] is also being explored to investigate if manual SCS definition has a large effect on joint angle results. Future work will incorporate bone proximity mapping to investigate TMC joint stress distribution between groups. Moreover, using high-resolution CT imaging (61µm isotropic voxels), bone microarchitecture analysis will be performed to explore microstructural bone changes in TMC OA and their effects on joint function.

Significance: As TMC OA is often asymptomatic in early disease states, investigating *in vivo* TMC joint biomechanics using dynamic CT has potential to quantify differences in TMC joint biomechanics that may otherwise go undetected until clinical symptoms present.

References: [1] Kuczynski *et al*. (2022), *BMC Med Imaging* 22(1); [2] Pataky. (2010), *J. Biomech* 43(10); [3] McQuillan, *et al*. (2015), Clin. Orthop. Relat. Res. 474; [4] Halilaj *et al*. (2013), *J Biomech* 46(5).

IMPACT FORCE ON FIVE COMMON RUNNING SURFACES

Thomas Urrunaga[1], Kurt M DeGoede[1*], and Brian Falk[2]
[1]School of Engineering, Mathematics and Computer Science, Elizabethtown College
[2]Athletics Department, Elizabethtown College
*Corresponding author's email: degoedek@etown.edu

Introduction: Casual runners and semi-pro athletes alike fall victim to misconceptions that are handed down across generations. One of the misconceptions runners of all calibers tend to cling to, is the idea that the surface they run on will affect the peak force of impact [1 2]. However, a spring in series model indicates that this persistent guiding principle may be misguided. As in a foot, shoe, and ground interaction, the 'softest' spring in a series of springs, in our case the shoe, dominates the interaction. The stiffness of the shoe predicts the impact dynamics, rather than the stiffness of the less-compliant ground surface. In-shoe measurements on several common running surfaces have confirmed this analysis [3, 4]. However, some of this work was conducted at slower non-competitive paces (and thereby lower impact forces) and stride-to-stride variation in impact force introduced uncertainty in the measurements. Therefore, this study was introduced to mechanically simulate heel strike in running in controlled impacts across several common running surfaces.

Methods: This study was completed with the use of a strain gauge load cell and a cue ball to represent the spherical shape of a human heel at the end of a falling arm. A shoe was then constrained to the cue ball and a 2kg mass was attached above the load cell. The release angle and height of the impactor allowed for the arm of the impactor to strike the ground at 2 meters per second. The load cell output was set to a range voltage between -5 and +5 volts into a strain gauge amplifier transducer. This information was then received into a NI-USB6211 which translated the output to NI-express. The data was processed in Octave, where average peak force was determined for 15 trials between 5 common synthetic running surfaces (concrete, asphalt, indoor Mondo, outdoor Mondo, and crushed gravel) for 3 different shoes (225 total trials). On each surface, a different location was used within the boundaries of the same surface decrease systematic error.

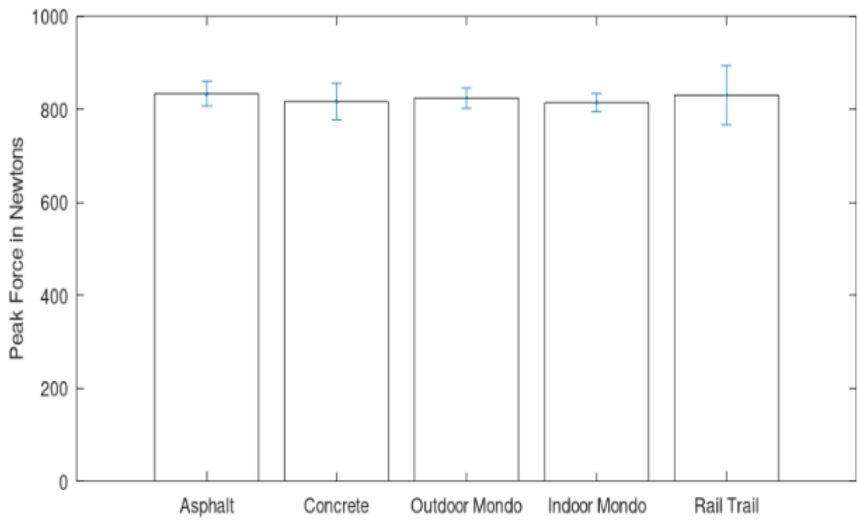

Figure 1: Average peak force on shoe 1 across the five surfaces.

Results & Discussion: These results validate the trials completed with human subjects with higher precision than our human subject trials [4]. We measured no significant differences between the surfaces on the same shoe ($p > 0.05$, Figure 1), suggesting that impact force while running in cushioned training shoes does not depend on the ground surface. However, it is important to note that there were larger variations in the concrete and rail trail data due to difficulty in sighting these two surfaces – it was more difficult to locate level uniform testing sites. There was a significant difference in the impact force of each shoe measured on all surfaces ($p < 0.05$, Figure 2).

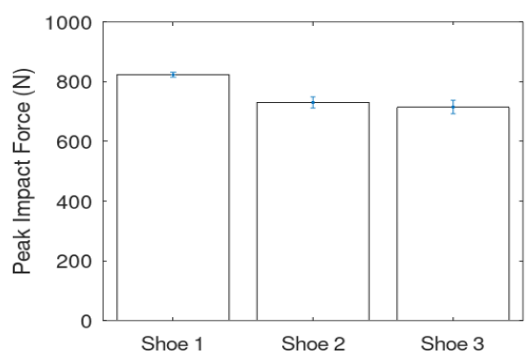

Figure 2: Average peak force across each shoe.

Significance: When running in well cushioned training shoes, ground surface play's little role in determining impact forces. The location for training runs among running groups and individuals should be decided on factors other than running surface for surfaces ranging from Mondo to Concrete.

Acknowledgements: Thank you to Mark Gatti for assistance with designing and fabricating the testing device. This project was funded through the Bollman Fund for Engineering Research and the SCARP program at Elizabethtown College.

References:

[1] Bloom, Marc https://www.runnersworld.com/uk/health/ injury/a760152/top-10-running-surfaces/ [Accessed 8 11 2022].
[2] Wingenfeld, Sascha https://www.runtastic.com/blog/en/best-surface-running-training/ [Accessed 8 11 2022].
[3] H Boey, et al, Sports Biomechanics, 16:2, pp. 166-176, 201.
[4] K DeGoede, et al, ASB 2021

MEASURES OF LIMB CLEARANCE SUGGEST ALL OBSTACLES ARE NOT CREATED EQUAL

Ashlyn M. Jendro[1*], MaryAnn Gundlach[1], Hope M. Hanson[1], Tiphanie Raffegeau[2], and Abigail C. Schmitt[1]
[1]University of Arkansas, [2]George Mason University
Email: amjendro@uark.edu

Introduction: Unintentional falls are the leading cause of non-fatal injury and emergency department visits among all ages in the United States (52.8%).[1] Most falls in young adults occur when walking, and approximately 25% of falls were a result of a trip.[2] Current literature agrees that when young adults are unsuccessful at crossing obstacles, there is typically insufficient toe elevation over the obstacle, usually with the trailing foot.[3] However, there seems to be no significant difference in clearance measures or approach/landing distances among young adults when crossing obstacles of differing heights up to 30% of limb length.[4]

Obstacle crossing is extensively studied in the laboratory,[4] however many studies are limited by using obstacles that may not be found in real-world situations. A better understanding of how individuals cross obstacles with differing appearances and dimensions is needed to better understand potential strategies to prevent injuries and inform future fall prevention strategies. The purpose of this study is to compare measures of obstacle crossing behaviour across four obstacles; one commonly used in laboratory-based obstacle crossing studies (a dowel) and three obstacles that can be found in real-world scenarios (a branch, a parking curb, and a rope).

Methods: Twenty-three (5 men, 18 women) healthy, young adults (23±4 yrs, 1.65±0.10 m, 68.9±16.9 kg, 20 right leg dominant), completed a series of obstructed walking tasks while barefoot and wearing the Plug-in Gait marker set (Vicon Motion Systems). 3D motion capture recorded trajectories while participants completed 10 obstacle crossing trials walking along an 8-meter walkway and crossing with their self-selected lead limb. The obstacles presented were a dowel (crossing height: 150mm), a branch (crossing height: 165mm), a parking curb (crossing height: 120mm), and a caution rope (crossing height: 300mm) (Fig. 1). Participants were asked to *"walk across the walkway at a comfortable pace and step over the obstacle along the way."*

Measures of foot clearance and approach/landing distances were used to assess obstacle crossing strategy. Toe clearance, for both the leading and trailing limbs, was defined as the minimum vertical distance between the toe marker and the obstacle when the toe marker was directly above the obstacle. Approach and landing distances were defined as the horizontal difference between the obstacle and the toe marker of the trail limb when the lead limb was crossing over the obstacle and the heel marker of the lead limb when the trail limb was crossing over the obstacle, respectively. Obstacles were identified by markers placed on the obstacles (Fig. 1). Repeated-measures ANOVAs were used to compare means between obstacles, alpha set to .05.

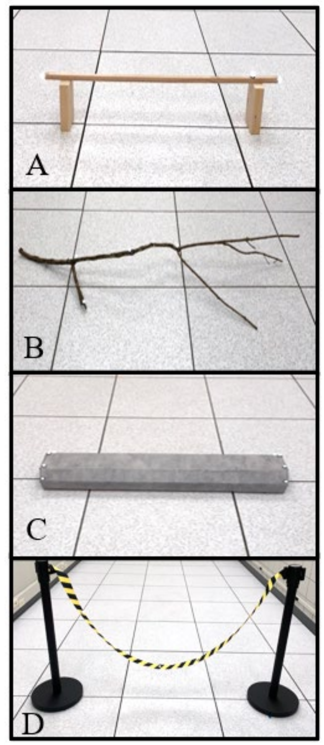

Figure 1: Obstacles used: (A) dowel, (B) branch, (C) parking curb, and (D) rope.

Results & Discussion: Trials in which the participant contacted the obstacle and the subsequent trial were removed from the final analysis. Approach distance ($F(2.01)= 32.01$, $p< .001$), landing distance ($F(2.77)= 49.19$, $p< .001$), lead toe clearance ($F(2.35)= 22.15$, $p< .001$), and trailing toe clearance ($F(2.47)= 54.84$, $p< .001$) all showed significant differences based on Greenhouse-Geisser adjustment for the repeated measures ANOVA between obstacles (Table 1). Major findings indicate that approach and landing distances were smaller in the curb compared to the other obstacles ($p< .001$). Additionally, landing distance was also smaller for the rope compared to the dowel and branch ($p< .001$). Lead toe clearance was smaller for the branch and curb compared to the dowel ($p= .001$; $p< .001$ respectively) and the rope ($p= .040$; $p< .001$, respectively). Trailing toe clearance was different across all obstacle combinations ($p< .010$). These results suggest that young adults use different crossing strategies to successfully clear obstacles with different appearances/dimensions. These differences in obstacle crossing strategy may be a result of some obstacles being more familiar and other obstacles being perceived as intimidating.

Significance: These data reinforce the need for a more robust variety of obstacles in future obstacle crossing studies. Considering significant differences were seen in the trailing toe clearance measures across all obstacles, which is where young adults typically have unsuccessful crossings, it appears there is more to learn about how young adults cross obstacles in real world settings.

Acknowledgements: Funding for this project was provided by a University of Arkansas Honors College Research Grant.

References: [1] WISQARS (2020), CDC; [2] Heijnen & Rietdyk (2016), *Hum Mov Sci*. 46:86-95. [3] LoJacono et al. (2018), *J Mot Learn Dev.* 6(2):234-249. [4] Lu et al. (2006), *Gait Posture.* 23(4):471-479.

Table 1: Mean ± SD of measures of obstacle crossing in mm.

	Approach Distance (TL)	Landing Distance (LL)	Lead Toe Clearance	Trail Toe Clearance
Dowel	258 ± 48	238 ± 45	153 ± 34	180 ± 40
Branch	247 ± 46	240 ± 54	127 ± 30	146 ± 40
Curb	180 ± 51	157 ± 45	117 ± 27	104 ± 20
Rope	261 ± 42	197 ± 49	145 ± 34	208 ± 42

DESIGN AND USE OF A NOVEL DEVICE FOR PERTURBING FOOT PLACEMENT DURING OVERGROUND WALKING

Richard W. Smith[1*], Michelle J. Karabin[1], Mark R. Redfern[1]
[1]University of Pittsburgh Corresponding Author: *ris55@pitt.edu

Introduction: Many studies utilize perturbations to explore the strategies people use to maintain balance during walking [1]. Foot placement has been shown to be the primary strategy used for walking balance, particularly in the mediolateral direction where walking is unstable [2,3]. By perturbing foot placement, the dynamic relationship between the center of mass (COM) and base of support (BOS) is disturbed, requiring an active recovery response. These types of perturbations generally require ground shifting, which is most easily accomplished with treadmills because they are already motorized and can be instrumented to provide kinetic data. However, treadmill walking has been shown to be biomechanically different than overground walking [4,5]. The objective of this study was to develop a simple and inexpensive device capable of delivering consistent mediolateral foot placement perturbations of varying magnitudes during overground walking. This work describes the design and development of this device and demonstrates its ability to evoke stepping responses for balance recovery.

Methods: The device consists of a 44.5” x 25.5” x 7” box containing a plate (1) on a bed of rollers (2) (Fig. 1). The box is set in a recessed floor so that the plate is flush with the walking surface. Springs (3) and electromagnets (4) are set inside the box on either side of the plate. The plate can be pulled against the springs until it contacts the electromagnets, which hold the plate in place when powered. When power to the magnets is removed, the plate is released and slides to the center, creating the foot placement perturbation. The perturbation distance is varied by inserting crossbeams (5) of different thicknesses into the stopper slots (6), stopping the plate at different points. The device is triggered at heel contact using a capacitive touch system consisting of wires adhered to the top of the plate (7) that are connected to a capacitive touch sensor. When a participant’s shoe contacts the plate, the sensor triggers a switching circuit to remove power to the magnets, initiating the perturbation.

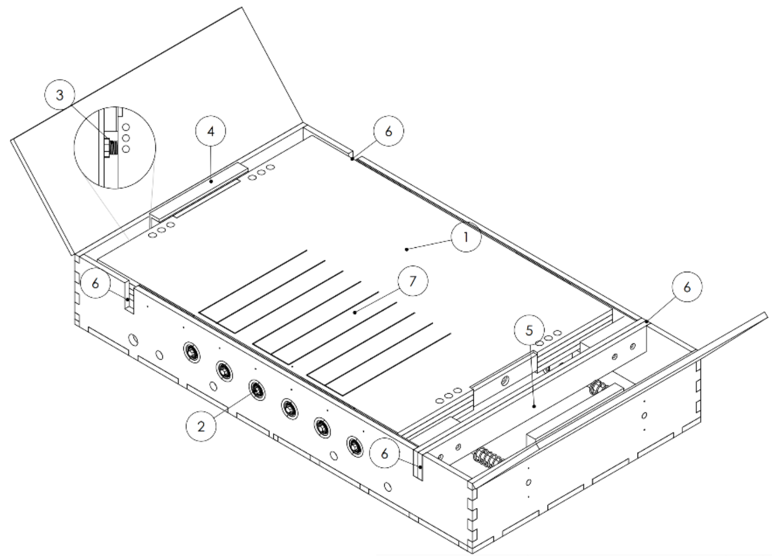

Figure 1: Schematic of the foot placement perturbation device.

The device is being used as part of a larger study to assess balance recovery in response to foot placement perturbations. Participants walk along a 5-meter walkway capture volume with and without perturbations. Specifically, participants complete three baseline trials of normal walking, followed by three trials of each perturbation type (small/large medial; small/large lateral). The perturbations consist of 3.5 cm and 6.5 cm displacements with peak velocities of 4.5 cm/s and 5.5 cm/s, respectively. All perturbations occur at right heel strike. A 14-camera Vicon motion capture system is used to collect kinematic data. Data from 4 subjects are reported here. Step width on the first recovery step following the perturbation was analyzed to evaluate the balance response to the perturbations.

Results & Discussion: Table 1 shows the step width on the first recovery step following the perturbation. Responses that were significantly different from baseline are marked with an asterisk. Medial perturbations elicited narrower steps than normal walking. In fact, small and large medial perturbations led to crossover steps, as indicated by the negative step widths. Lateral perturbations led to wider steps compared to normal walking. For both perturbation directions, the large perturbations evoked larger responses than the small perturbations. These responses are consistent with existing literature demonstrating that foot placements are adjusted based on whole body COM accelerations [6]. Medial BOS shifts lead to increased lateral COM acceleration, necessitating a narrower (or crossover) recovery step. Conversely, lateral BOS shifts lead to increased medial COM acceleration, requiring a wider recovery step.

Table 1: Step width on first recovery reported as mean ± SD

	Step Width (cm)
Baseline	9.0 ± 3.1
Small Medial	-0.3 ± 2.8*
Large Medial	-8.8 ± 2.7*
Small Lateral	15.6 ± 3.0*
Large Lateral	22.8 ± 1.2*

Significance: This work documents the design of an overground foot placement perturbation device that is simple and inexpensive to manufacture and operate. This increases the feasibility of overground walking studies, which are more biomechanically similar to real-world walking than treadmill studies. Future work can use this device to investigate other outcome measures, such as kinematics, muscle activity, or accelerometry, which are likely to show greater differences between treadmill and overground walking [7].

Acknowledgements: Funding: NIDCD/NIH: F311DC020110.

References: [1] Brough et. al, 2021, *J Biomech* 116; [2] Bauby & Kuo, 2000, *J Biomech*, **33**(11); [3] Bruin et. al., 2018, *J. R. Soc. Interface. 15: 20170816;* [4] Hollman et. al., 2016, *J Biomech* 43; [5] Parvataneni et. al., 2009, *J Biomech* 24(1); [6] Reimann et. al., 2018, *Kinesiology Review* 7(1); [7] Semaan et. al., 2022, *J Biomech,* 92.

GENERALIZED JOINT HYPERMOBILITY AND NECK PAIN: EFFECTS ON RANGE OF MOTION AND STRENGTH

Rebecca Abbott[1], Kyle Dalske[2], Carly Molenaar[2], David Oriala[2], Brett Volin[2], Arin Ellingson[1,2]
[1]University of Minnesota Department of Rehabilitation Medicine, [2]Division of Physical Therapy. * ellin224@umn.edu

Introduction: Generalized joint hypermobility (GJH), excessive range of motion (ROM) of joints throughout the body, affects approximately 20% of the U.S. population and is associated with an increased risk for injury and chronic joint pain [1-2]. Neck pain is the 3rd most common chronic pain condition in the U.S. and is associated with poor health outcomes [3]. Partially due to the heterogeneity of chronic neck pain (cNP), treatment is difficult and often ineffective. Elucidation of the role of GJH and neck pain/disability on clinical measures of neck function are needed to develop improved diagnosis and targeted treatments. The purpose of this study is to 1) define the prevalence of cNP in those with GJH, and 2) determine the relationships of GJH and cNP on neck ROM and strength. We hypothesize that GJH is associated with a higher prevalence of cNP, increased neck ROM, and decreased neck and grip strength.

Methods: Data collection took place at the University of Minnesota Research Facility at the 2022 Minnesota State Fair (eligibility = 18+). GJH was assessed by a physical therapist using the Beighton Score (BS), a 0-9 scale with a point added for each hypermobile body area. Survey data included demographics, musculoskeletal pain (body area, pain intensity, chronicity), and Neck Disability Index (NDI). Clinical measures for neck function were collected on a subset of participants, including neck active ROM with an inclinometer, and neck and grip strength with handheld dynamometers.

Multiple linear regression analyses were performed to determine the relationship between physical measures of neck function and GJH. To enable exploration of multiple factors, we were liberal in our consideration of predictors and interactions. A forward stepwise regression approach was used to select predictor variables for each model. Potential predictor variables included age, sex, body mass index (BMI), Neck Disability Index (NDI), number of painful areas, and cNP. Interaction effects were also explored. Necessary assumptions for each model were verified and met.

***Table 1**: Multiple Linear Regression model for each ROM and strength outcome (n=266). Significant predictors (p<0.05) are indicated by arrows (up/green: positive effect, down/red: negative effect). R^2, F-ratio, and p-values are reported in reference to model fit and variance. ROM for lateral bending (Lat Bend) and axial rotation (Axial Rot) are summed across left and right directions, while strength is averaged.*

		Age	Sex (Male)	BS	BMI	NDI	BS*NDI	Sex*BMI	Sex*BS	Age*BMI	Age*BS	R^2	F-ratio	p-value
ROM	Flexion			▲								0.032	9.2	0.0026
	Extension	▼		▲	▼	▼	▲					0.284	21.5	<.0001
	Lat Bend	▼		▲		▼						0.408	62.8	<.0001
	Axial Rot	▼		▲		▼	▲					0.260	24.0	<.0001
Strength	Flexion	▼	▲	▲	▲	▼		▲			▼	0.591	46.0	<.0001
	Extension	▼	▲	▲	▲	▼		▲	▲	▼		0.524	35.1	<.0001
	Lat Bend	▼	▲	▲	▲	▼		▲	▲	▼		0.501	32.0	<.0001
	Grip Left	▼	▲	▲	▲							0.534	78.2	<.0001
	Grip Right	▼	▲	▲	▲	▼			▲			0.553	55.9	<.0001

Results & Discussion: 555 participants (219/336 male/female, age: 18-86 years) were enrolled. The overall prevalence of cNP was 10.4% (6.4% for males, 13.1% for females). Prevalence of cNP increased with each BS cut-off. The commonly used BS≥5 cut-off resulted in a cNP prevalence of 20.7% vs. 9.3% for those with vs. without GJH - supporting CNP is more prevalent in those with GJH.

A subset of participants (n=266) had additional measures collected including neck ROM and neck and grip strength. The multivariate linear regression models are summarized in **Table 1**. The forward stepwise regression approach resulted in inclusion of different predictor variables and interaction effects for each model. In general, these variables better accounted for variance in neck strength (all R^2>0.5) than neck ROM measures. Preliminary analyses revealed that BS was a significant, but weak, independent predictor of each neck ROM measure, but did not significantly independently predict strength measures.

When considering the full models, BS continued to be a significant positive predictor of neck ROM, with additional negative influence of age, BMI, and NDI. These results support the hypothesis that GJH is associated with increased neck ROM. Of note, little of the flexion ROM variance was attributed to the predictor variables, which hints that other factors or interactions may be missing from the analysis. The interaction of BS x NDI was found to be significant for extension and axial rotation ROM, accounting for the interesting result that as BS increases, neck disability has less of a negative effect on neck ROM.

BS becomes a significant predictor of neck and grip strength when age, sex, BMI, and NDI are accounted for. However, BS was found to have a positive association with strength, which is contrary to our original hypothesis that GJH is associated with decreased neck and grip strength. Definitive conclusions from these models should be made with caution, as up to 8 predictors and interactions were included in this exploratory analysis, increasing the difficulty of interpretation and risk of overfitting.

Significance: This study is the first to define the relationship between GJH and chronic neck pain prevalence and to assess their roles in clinical measures of neck function. The finding of a two-fold increase in the prevalence of chronic neck pain in those with a BS≥5 highlights the need for targeted treatments for those with GJH. The significant associations and interactions of GJH, age, sex, BMI, and NDI on neck ROM and strength will guide further investigations to improve diagnosis and targeted treatments in GJH and cNP.

Acknowledgements: RA is supported by NIH NCATS TL1R002493 and UL1TR002494
References: [1] Juul-Kristensen et al. (2017), *BMC Msk Disord* 18(1); [2] Mulvey et al. (2013) *Arthritis Care Res* 65(8); [3] Nahin et al. (2015) *J Pain* 16(8)

Load Variability during a Stop Jump is Higher in Female Patients with an ACLR

Jenna K. Mesisca[1*], Sara L. Arena[1], and Robin M. Queen[1]
[1]Virginia Tech, Department of Biomedical Engineering and Mechanics
*Corresponding author's email: jkmesisca@vt.edu

Introduction: Anterior Cruciate Ligament (ACL) injuries continue to rise with over 200,000 occurrences each year, with approximately 90% of patients electing to undergo ACL reconstruction (ACLR) [1-3]. Females are approximately four times more likely to suffer an ACL injury and twice as likely to sustain a reinjury following ACLR compared to males [4,5]. Movement variability can be crucial when athletes need to adapt to changing conditions during sports, specifically when cutting or pivoting [6,7]. Previously, variability was seen as noise or random error [8]. Recently, movement variability has been reported to be essential for an athlete to be able to react to changing conditions appropriately during sports practices and competition [9]. The optimal level of variability is still unclear; when variability is too high the movement is seen as unstable and when it is too low the movement is seen as stiff and unforgiving [10]. Specifically, understanding movement and limb symmetry variability during a bilateral landing task may provide insight into potential injury risk factors. Therefore, the goal of this study was to examine posterior and vertical ground reaction force (GRF) and loading rate intra-subject variability between patients with an ACLR and healthy controls (HC) during a stop jump. Due to the previous sex-disparities in ACL injury rates, it is hypothesized that female patients with an ACLR will have greater variability when compared to male patients with an ACLR and HC females.

Methods: Forty patients with an ACLR and 67 HC completed seven trials of a stop jump task that required the participants to land on embedded force places (AMTI, Watertown, MA, USA) sampling at 1920 Hz. An intra-subject coefficient of variation (CV) was calculated for each participant for posterior GRF, vertical GRF, and loading rate. The limb symmetry index (LSI) CV was calculated for each of the previously stated measures [11]. A linear mixed effects model was used to examine the effects of the CV between group (HC, ACLR), sex (male, female), and limb (surgical, nonsurgical). Due to non-normal distributions of residuals, the analysis was performed on the ranks. Significant interactions or main effects were explored with Tukey's Honestly Significant Difference (HSD). All analyses were conducted in JMP (SAS Institute Inc., Cary, NC) with $p<0.05$.

Results & Discussion: There was a group by sex interaction for the vertical GRF CV ($p<0.001$) and loading rate CV ($p=0.018$). Vertical GRF CV was higher in female patients with an ACLR compared to female HC ($p<0.001$) and male patients with an ACLR ($p=0.032$). Loading rate CV was higher in female patients with an ACLR compared to female HC ($p=0.005$) and male HC ($p=0.032$). A limb by sex interaction was found for posterior GRF CV ($p=0.049$), with the surgical/nondominant limb being greater than the nonsurgical/dominant limb in males only ($p=0.047$). There was also a limb by sex interaction for vertical GRF CV ($p=0.012$), but all pairwise comparisons were nonsignificant. A group by sex interaction was found for vertical GRF LSI CV ($p=0.001$), with female patients with an ACLR having greater asymmetry than female HC ($p=0.024$). Posterior GRF LSI CV ($p=0.002$) was higher in patients with an ACLR compared to HC. The higher mean CV values in patients following ACLR is likely the result of increased variability on the surgical limb and greater between-trial variability. The difference between female HC and female patients with an ACLR in vertical GRF LSI is a direct result of asymmetric bilateral landings.

Table 1: Measures (mean ± standard deviation) with a significant group by sex interaction.

	HC		**ACLR**	
	Male	**Female**	**Male**	**Female**
Vertical GRF CV	18.01 ± 0.87	**15.32 ± 0.91***	**17.12 ± 1.05***	21.67 ± 1.28
Loading Rate CV	**30.74 ± 2.04***	**27.45 ± 2.13***	29.06 ± 2.44	37.28 ± 2.98
Vertical GRF LSI CV	24.20 ± 4.33	**19.58 ± 4.53***	21.43 ± 5.25	42.43 ± 6.44

* Indicates significantly different from female ACLR ($p<0.05$).

Significance: The results support the sex disparity in the incidence of ACL injuries. The higher variability in patients following ACLR demonstrates the need to assess variability when determining an athlete's readiness to return to sport following surgery and rehabilitation. These results indicate the importance of combining bilateral landing tasks with a limb symmetry measurement to understand the variation in movement. Future work should also examine kinematic variability to more deeply understand group and sex differences to help minimize ACL injury and reinjury rates in female athletes.

Acknowledgements: The author would like to acknowledge Alexander Peebles for his contributions to data collection. Support for this study was provided by grants from the National Institutes of Health: R21AR069865-01A1.

References: [1] Rockwood et al. (2016) *Clinical Journal of Sports Medicine*, [2] Beaumont Health Org, [3] Harilainen et al. (2015) *Cochrane Database of Systematic Review*, [4] Paterno (2015) *Journal of Athletic Training*, [5] Schilaty et al. (2017) *Orthopedic Journal of Sports Medicine*, [6] Hamill et al. (1999) *Human Movement Science*, [7] Heiderscheit et al. (2011) *Med Sci Sports Exerc.,* [8] Schmidt (1984) *Research Quart for Exerc. & Sport*, [9] Ryssegam (2014) *Inst. of Phys. Ed. International Conf.*, [10] Pease (2006) *Academia,* [11] Rohman et al. (2015) *The American Journal of Sports Med.*

Does the distal-to-proximal redistribution of joint mechanics affect walking economy?

Negin Fallah* & Owen N. Beck
Dept. of Kinesiology and Health Education, University of Texas at Austin, Austin, Texas, USA
*Corresponding author's email: nfallah@utexas.edu

Introduction: Older adults (≥65 years) exhibit a "distal-to-proximal shift" in joint mechanics [1, 2]. During walking, older adults produce relatively greater hip extension moments and relatively lower ankle extension moments than young adults [1, 2]. This distal-to-proximal shift in older adult joint moments correlates with their greater metabolic cost of walking versus young adults [2]; we wonder whether these correlations are spurious. After all, other aspects of aging physiology may explain the metabolic increase in older versus young adults. And biomechanically, hip extensor muscles have longer muscle-to-joint center moment arms than ankle extensors, enabling hip muscles to produce less force per unit joint moment (F=M/r). Hip extensors also have stiffer tendons than ankle extensors, which reduces the in-series muscle shortening per unit tensile force (x=F/k). Both reduced muscle force production and less muscle fiber shortening typically need yield less metabolic energy per contraction. While there are other differences between the ankle and hip extensors, based on moment arm and tendon stiffness data, we hypothesized that producing hip extensor moments requires less metabolic energy than producing ankle extensor moments.

Methods: To test our hypothesis, after we obtained informed written consent, we quantified the metabolic energy expended from a 28-year-old male while they produced hip- and ankle- extension moments on a dynamometer. The participant arrived to the lab ≥3 hours postprandial. The participant sat on a chair with their right leg secured in a fixed position: ankle at 85°, ankle joint aligned with the dynamometer's axis of rotation, and knee at 165° (90° = perpendicular segments). In this position, the participant performed a 5-min trial where they cyclically produced ankle extension moments following visual and audio feedback (0.75 Hz, 0.5 duty, 28 Nm peak moment). Next, the participant performed the same 5-min trial using their hip extensors while laying with their hip joint at 160° and aligned with the dynamometer's axis of rotation. We measured net rates of oxygen uptake and carbon dioxide production via open circuit spirometry. We averaged the rates of oxygen uptake and carbon dioxide production over the last minute to calculate net metabolic power [3].

Results: The participant produced similar extension moments at the hip and ankle while consuming dissimilar rates of metabolic energy. The participant produced an average net hip extension moment of 16.8 Nm over 1.3 seconds per cycle and an average net ankle extension moment of 18.6 Nm over 1.2 seconds per cycle (Fig. 1). The participant's cycle average peak joint extension moment for the hip and ankle were 36.6 Nm and 35.3 Nm, respectively. Despite producing similar moment profiles, the participant expended more than twice as much net metabolic power to produce hip moments (62.9 W) than ankle moments (16.7 W) (Fig. 2).

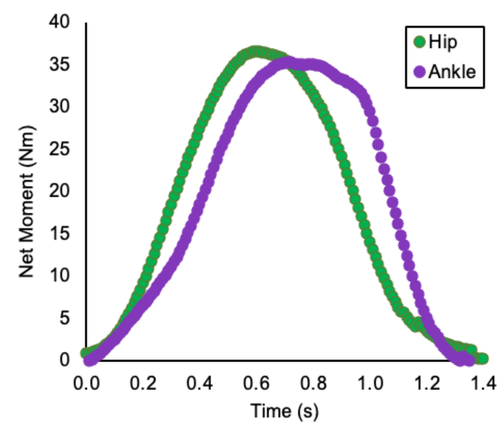

Figure 1. Average ankle (purple) and hip (green) extension moment cycle while producing a peak moment of 35.3 and 36.6 Nm, respectively.

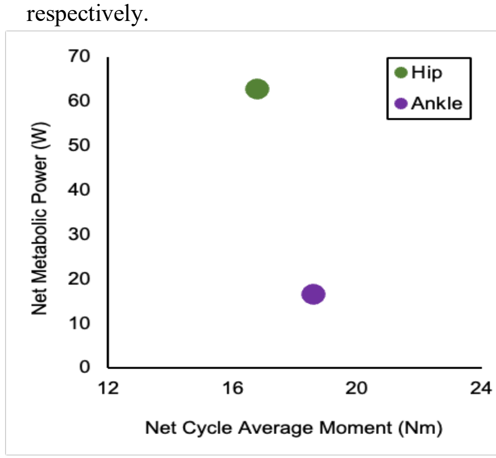

Figure 2. Net metabolic power while repeatedly producing the ankle (purple) and hip (green) extension moments seen in Figure 1.

Discussion & Significance: Even though hip extensors have longer moment arms and stiffer tendons than ankle extensors, we found that the metabolic cost of producing extension moments is greater at the hip than ankle; rejecting our hypothesis. Accordingly, other muscle-tendon characteristics must underpin our metabolic findings. Perhaps hip extensor muscle contractile properties (e.g., fiber type) and longer muscle fibers contribute to their increased metabolic cost of producing moments compared to ankle extensors. Regardless of the mechanism(s), our finding supports the notion that the distal-to-proximal redistribution of joint mechanics increases the metabolic cost of walking [2]. Based on our data, interventions that reduce biological hip extension moments, such as exoskeletons, will enable more economical walking than reducing biological ankle extension moments. Therefore, to mitigate the age-related increase in walking metabolism, biomechanical interventions should prioritize reducing older adult hip extension moments before reducing ankle extension moments.

References: [1] Boyer et al. (2017) *Exp Gerontol*; [2] Delabastita et al. (2021) *Scand J Med Sci Sports*; [3] Peronnet and Massicotte (1991) *Can J Sport Sci*.

Kinetic Variability Differences During a Single Hop between ACLR and Healthy Control Cohorts

Jenna K. Mesisca[1*], Sara L. Arena[1], and Robin M. Queen[1]
[1]Virginia Tech, Department of Biomedical Engineering and Mechanics
*Corresponding author's email: jkmesisca@vt.edu

Introduction: Female athletes are more likely to sustain a primary and a second ACL injury when compared to men, with approximately 60% of all female ACL injuries resulting from a non-contact mechanism [1,2]. Athletes need a level of variability in their movement to effectively react to changing situations in their sport, and this variability may play a role in injury risk. Cutting or landing tasks are commonly used in ACL injury analysis as the quick changes in the movement require shifts in the athlete's load [3,4]. Specifically, the single hop is a common unilateral loading task used in return to sport assessments [5]. Understanding load variability and between limb asymmetries during this task will help to better understand ranges of variability within ACLR patients and inform interventions that seek to reduce reinjury rates. Therefore, the goal of this study was to examine peak force, loading rate, and impulse variability during the single hop test between patients following an ACLR and healthy controls. Due to the previous sex-disparities in ACL injury rates, it is hypothesized that ACLR females will have greater variability when compared to ACLR males and control females.

Methods: Twenty-five patients with an anterior cruciate ligament reconstruction (ACLR) and 30 healthy controls (HC) completed seven trials of the single hop task on each limb while wearing in-shoe loadsol® sensors (Novel Electronics, St. Paul. Minnesota, USA) sampling at 100 Hz. An intra-subject coefficient of variation (CV) in peak impact force, loading rate, and impulse was calculated for each participant. The limb symmetry index (LSI) CV was calculated for each of the previously stated measures [6]. The CV values were compared between groups (HC, ACLR), sex (male, female), and limb (dominant/non-surgical, non-dominant/surgical) using a linear mixed effects model with hop distance included as a covariate. The residuals that showed non-normal distributions had the analysis performed on the ranks. Significant interactions or main effects were explored with Tukey's Honestly Significant Difference (HSD). All analyses were conducted in JMP (SAS Institute Inc., Cary, NC) with $p<0.05$.

Results & Discussion: Loading rate CV was higher in HC compared to patients with an ACLR ($p=0.006$), in males compared to females ($p<0.001$), and in the dominant(D)/non-surgical (NSG) compared to the non-dominant (ND)/surgical (SG) limb ($p=0.046$) (Figure 1). Loading rate LSI and impulse LSI were higher in males compared to females ($p=0.004$ and $p=0.009$, respectively). The ACLR group showed lower variability, regardless of limb or sex, compared to controls, indicating a stiffer unilateral landing. The lower variability could result in increased reinjury rates following return to sport as the knee is unforgiving and has less ability to react in changing environments. Future work should explore the role of movement variability on second ACL injury risk when returning to sport.

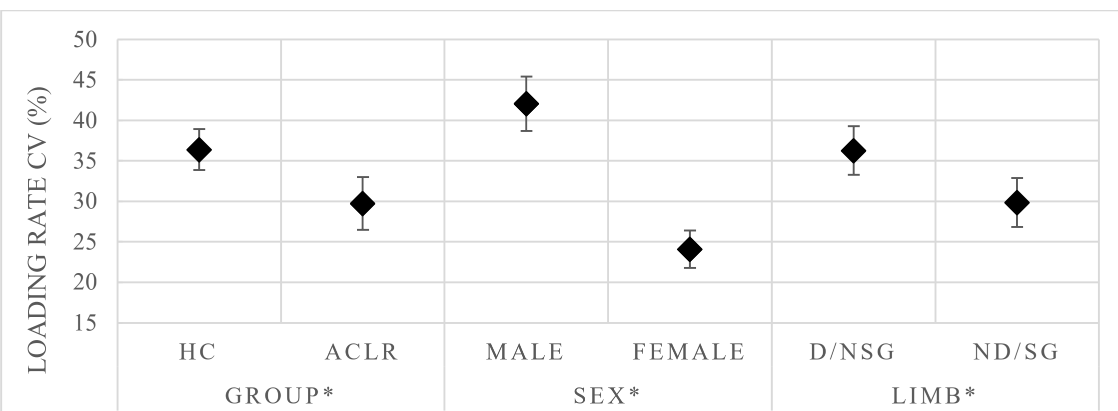

Figure 1: Loading rate (mean ± SD) CV outcomes (*indicates significantly different $p<0.05$)

Significance: The results support the idea that individuals are going to land with greater force on their preferred (dominant/nonsurgical) limb during a unilateral landing, since unilateral landings do not allow for compensation with the contralateral limb as is possible during bilateral landings. These results indicate that unilateral hop testing, in this case the single hop task, should continue to be implemented in return to sport criteria to better understand between limb symmetry and movement variability and their association with ACL injury risk.

Acknowledgements: The author would like to acknowledge Lindsey Maguire, Adam Heilmann, Evan McConnell, and Laura Dickerson for their contributions to data collection.

References: [1] Luque-Seron et al. (2016) *Sports Health*, [2] Giugliano et al. (2007) *Physical Medicine and Rehabilitation Clinics of North America,* [3] Hamill et al. (1999) *Human Movement Science*, [4] Heiderscheit et al. (2011) *Med Sci Sports Exerc*, [5] *Massachusetts General Brigham Sports Medicine*, [6] Rohman et al. (2015) *The American Journal of Sports Med.*

INDIVIDUALS EARLY AFTER ACLR SHOW MOTOR LEARNING OF KNEE MECHANICS DURING GAIT

Elanna Arhos[1,2*], Jonathan M. Wood[2], Lynn Snyder-Mackler[2], Karin Grävare Silbernagel[2], Susanne M. Morton[2]
[1]Ohio State University, Columbus, OH
[2]University of Delaware, Newark, DE
*Corresponding author's email: elanna.arhos@osumc.edu

Introduction: After ACL reconstruction (ACLR), reduced peak knee flexion (PKFA) and peak knee extension (PKEA) joint angles are common and persists for years [1]. Clinical interventions are not successful in restoring gait symmetry post-operatively, suggesting there may be an underlying neural mechanism. These gait asymmetries are of particular importance as they may be associated with the consequent development of post-traumatic knee joint osteoarthritis after ACLR. [2] Reduced afferent feedback following ligamentous injury and ACLR may be implicated in limiting the capacity for motor learning of a symmetric gait pattern, given motor learning requires appropriate sensorimotor feedback. [3] It is unknown whether this type of sensory impairment affects learning. Therefore, the purpose of this study was to determine the motor learning capacity of individuals after ACLR. We assessed one common form of motor learning, sensorimotor adaptation, of both step length and knee joint kinematics (PKFA and PKEA) during gait using the split-belt treadmill adaptation paradigm.[4] While spatiotemporal variables are not directly implicated in the development of post-traumatic knee joint osteoarthritis in individuals after ACLR, step length symmetry is considered the gold standard gait parameter to quantify sensorimotor adaptation capacity and magnitude on the split-belt treadmill. [4] Due to previous literature supporting the adaptation of spatiotemporal variables in this population [5], we hypothesized individuals after ACLR would be able to adapt and retain a novel step length symmetry pattern, but not to the same extent as controls. Secondly, due to the described sensory impairments after ligament injury, we expected that individuals after ACLR would be able to adapt knee joint kinematics, but to a lesser extent than uninjured controls.

Methods: 15 individuals 6.2 ± 1.8 months after ACLR (9 females, 20.8 ± 3.5 years) and 15 age, sex, and activity level matched controls were included in the study. Participants were significantly different in PKFA during baseline gait (Table 1). Participants underwent a split-belt treadmill adaptation paradigm consisting of treadmill walking during baseline, learning, and washout periods. During baseline and washout, the belts were moving the same sped (tied). During learning, the belts moved and two different speeds, in a 2:1 ratio, to induce adaptation. The fast belt remained at the self-selected walking speed for the uninvolved limb (dominant limb for controls), and the slow belt was set at half that speed. Kinematic data were collected using an 8-camera motion analysis system (Vicon MX) and a sampling rate of 100 Hz and calculated using commercial software (Visual 3D, C-Motion, and MATLAB, TheMathWorks). Step lengths were calculated as the distance between the leading and trailing calcaneus markers at the time of heel strike.

We characterized learning as the magnitude of asymmetry remaining at the end of the learning period. We characterized storage of the newly learned pattern as the magnitude of the aftereffects in asymmetry at the beginning of the washout period. Primary variables of interest were step length asymmetry index ((involved limb step length-uninvolved limb step length/involved limb step length + uninvolved limb step length) x100), and PKFA and PKEA interlimb differences (involved minus uninvolved limb) during the stance phase of gait. We used a 2x5 ANOVA with repeated measures on the factor time period to compare differences between groups across time periods.

	ACLR (n=15)	**Control (n=15)**	**P-value**
Tied Treadmill Gait Speed (m/s)	1.05 ± 0.17	1.06 ± 0.082	0.78
Peak Knee Flexion Angle ILD (degrees)	-4.33 ± 3.41	-0.92 ± 4.16	0.010
Peak Knee Extension Angle ILD (degrees)	-0.59 ± 2.97	0.39 ± 5.19	0.27

Table 1: Baseline gait speed and interlimb differences in individuals after ACLR and controls for kinematics. Values are mean ± SD. ILD, interlimb difference.

Results & Discussion: Both groups demonstrated learning of step length ($p<0.001$) with no interaction or main effect of group ($p\geq0.56$). Both groups demonstrated learning of PKFA and PKEA (main effect of time: $p<0.001$). Individuals after ACLR demonstrated similar PKFA and PKEA during the learning and washout phases compared with the group of control individuals (main effect of group: $p>0.67$; interaction effect: $p>0.091$). For both PKFA and PKEA there was a significant aftereffect ($p<0.001$), which suggests the central nervous system learned and stored a new gait symmetry pattern. We found individuals after ACLR can adapt step length in response to the split-belt perturbation, however the amount of adaptation and retention did not differ between groups as we expected. We also found individuals after ACLR were able to adapt their PKFA and PKEA interlimb symmetry in response to the split-belt perturbation to a similar magnitude as controls, indicating an ability to learn new gait patterns through sensorimotor adaptation of knee kinematics.

Significance: These results suggest that PKFA and PKEA are malleable and that gait-specific, motor learning-based interventions to restore interlimb gait symmetry may be feasible following ACLR. There is a need to develop gait-specific interventions, applied early on in rehabilitation, that appropriately target these gait mechanics.

Acknowledgements: This study is supported by the National Institutes of Health (F31-AR078580, S10-RR028114) and the Foundation for Physical Therapy Research (PODS Level II Scholarship).

References: [1] Hart et al. (2016) *Br J Sports Med* 50(10); [2] Wellsandt et al., (2016), *Am J Sports Med* 44(1); [3] Needle et al. (2017), *Sports Med* 47(7); [4] Helm et al. (2015), *Phys Med Rehabil* 26(4); [5] Roper et al. (2016) *Orthop J Sport Med* 4(2).

INDIVIDUALS WITH A VENTRAL HERNIA WHO REPORT MODERATE TO HIGH FEAR HAVE WORSE PRE-OPERATIVE CLINICAL OUTCOMES THAN THOSE WITH LOW FEAR

Elanna K. Arhos[1*], Kiana Shannon,[1] Savannah Renshaw,[1] Benjamin Poulose[1], Stephanie Di Stasi[1], Ajit Chaudhari[1]
[1]Ohio State University, Wexner Medical Center, Columbus, OH
*Corresponding author's email: elanna.arhos@osumc.edu

Introduction: Ventral hernia repairs (VHR) are one of the most common surgeries performed in the United States.[1] Even once surgery has restored the abdominal wall, patients demonstrate major impairments of the musculoskeletal system including poor strength and abdominal core function, and ultimately a lower self-reported quality of life.[2] Fear of movement, or kinesiophobia, may develop in patients with ventral hernia due to pain and functional impairments. Higher levels of kinesiophobia have been shown to impact function and self-reported outcomes in a variety of patient populations.[3,4] Kinesiophobia has also been linked to changes in movement strategies, primarily manifesting as restricted movement and muscle activation patterns.[5] Understanding the relationship between kinesiophobia and clinical outcomes in individuals with ventral hernia may assist clinicians in assessing compensatory movement during functional tasks. The purpose of this study was to assess clinical outcomes in patients with ventral hernia between different categories of kinesiophobia. Due to the established relationship between kinesiophobia and functional outcomes in other patient populations, we hypothesized that clinical outcomes would be worse in patients who report higher levels of kinesiophobia.

Methods: Participants were involved as part of an ongoing randomized controlled trial designed to test the efficacy of post-operative physical therapy (PT). Participants must be between 18-70, diagnosed with a ventral hernia, and scheduled for elective VHR. Participants were excluded if they had a transverse hernia width <2cm, have a movement disorder, use assistive devices, or had current PT. Participants included in this analysis were at the pre-operative timepoint and had not yet received surgery or randomization to PT. Primary outcomes included the Five Time Sit to Stand (5xSTS), Quiet Unstable Sitting Test (QUeST) and the Hernia-Related Quality-of-Life (HerQLes). The 5xSTS was assessed as the time taken to stand up and sit down from a standard height chair five times. The QUeST is an assessment of abdominal core function using postural sway while seated on an unstable surface, eyes closed, with a cognitive dual task. The QUeST assesses mean center of pressure path length during sitting balance using a force plate under a BOSU® over 3 averaged trials. The QUeST core stability score reported is the absolute difference from the normative population mean in multiples of the 95% confidence interval of the standard error of measurement, where 0 represents normal and <0 represents lower core stability [6]. The HerQLes is a 12-item survey of quality of life for patients with hernia disease scored from 0-100, where higher scores indicate higher quality of life.[7] Participants were split into 3 groups based on their Tampa Scale of Kinesiophobia (TSK-11) score, an 11-item self-reported questionnaire score out of 44 possible points asking about fear of movement and physical activity participation restrictions due to pain. Groups were minimal (TSK ≤ 22), low (TSK 23-28), or moderate to high kinesiophobia (TSK ≥ 29) [8]. A one-way ANOVA with a Bonferroni correction was run to compare QUeST, 5xSTS, and HerQLes results between groups.

Results & Discussion: There was a statistically significant difference between groups with QUeST (p=0.016, Table 1) and 5xSTS (p=0.002) but not HerQLes (p=0.45). Post-hoc comparisons revealed that the moderate to high fear group performed significantly worse than the low fear group (p=0.014) on the QUeST and significantly worse than both the minimal (p=0.003) and low fear (p=0.013) groups on the 5xSTS. We found individuals with moderate to high kinesiophobia have significantly worse pre-operative core stability and function than those in the minimal and low kinesiophobia groups. Minimal clinically important differences (MCIDs) have not been established for QUeST, but in 5xSTS the difference far exceeds the MCID of 2.3s. While group differences in the HerQLes were not statistically significant, the difference between the minimal and moderate to high kinesiophobia groups exceeded the MCID of 15.6 and may be clinically meaningful. Assessing kinesiophobia is of relevance as patients may develop fear-avoidant behavior, which ultimately can lead to reduced physical activity and changes in movement [5,8]. Future work will assess if PT is effective in reducing kinesiophobia and increasing physical function in those in the moderate to high group.

	Minimal (n=10)	Low (n=17)	Moderate to High (n=10)	p-value
Age	46.4 ± 12.6	51.2 ± 8.8	51.7 ± 10.0	0.4
Sex (F)	2	7	4	0.5
BMI	34.9 ± 4.4	33.7 ± 6.0	33.6 ± 6.5	0.8
QUeST	-3.7 ± 2.8	-2.6 ± 3.2	-7.30 ± 5.7	0.02
5xSTS (s)	11.2 ± 2.1	13.9 ± 3.3	21.7 ± 11.7	0.002
HerQLes	56.3 ± 28.4	47.5 ± 29.4	39.8 ± 28.2	0.5

Table 1: Mean ± standard deviation of demographic and clinical outcomes across minimal, low, and moderate to high kinesiophobia groups. F, female; QUeST, Quietly Unstable Sitting Test; HerQLes, Hernia-Related Quality-of-Life; 5xSTS, Five Times Sit to Stand.

Significance: These results suggest that kinesiophobia may be an important patient-related factor in individuals with ventral hernia that may help to distinguish those with poor physical function and core stability. While TSK-11 has not previously been measured in this patient population, clinicians treating individuals with ventral hernia may consider assessing for kinesiophobia and its consequent relationship to physical function and compensatory movement strategies to direct effective rehabilitation.

Acknowledgements: This study is supported by the National Institute of Diabetes, Digestive and Kidney Diseases (R01-DK131207).

References: [1] Poulose et al. (2012) *Hernia* 16(2); [2] Cherla et al. (2018) *World J Surg* 42(10; [3] Lentz et al. (2009) *J Orthop Sports Phys Ther.* 39:270-7; [4] Vlaeuyen et al. (1995) *Pain* 62:363-72; [5] Trigsted et al. (2018) *Knee Surg Sports Traumatol Arthrosc.* 26(12). [6] Chaudhari et. al (2022), *Clin Biomech* 93; [7] Krpata et al. (2012) *J Am Coll Surg* 215(5); [8] Chimenti et al. (2021), *Front. Pain Res.* [9] Baez, Hoch & Hoch. (2020) *Knee Surg Sports Traumatol Arthrosc* 28(6);

HOW HEALTHY OLDER ADULTS ADAPT STEPPING TO ENACT LATERAL MANEUVERS

David M. Desmet[1*], Meghan E. Kazanski[1,2], Joseph P. Cusumano[3], Jonathan B. Dingwell[1]
[1]Department of Kinesiology, Pennsylvania State University, University Park, PA, USA
[2]Department of Medicine, Division of Geriatrics and Gerontology, Emory University School of Medicine, Atlanta, GA, USA
[3]Department of Engineering Science & Mechanics, Pennsylvania State University, University Park, PA, USA
*Email: dmd78@psu.edu

Introduction: Walking requires frequent maneuvers to navigate changing environments and shifting goals. Humans accomplish maneuvers and maintain balance primarily by modulating their foot placement [1]. For lateral maneuvers, however, a direct trade-off between stability and maneuverability has been proposed [2]. Therefore, it is important to better understand how humans adapt stepping to simultaneously maintain balance and perform lateral maneuvers.

We previously developed a theoretical framework to describe how humans regulate stepping from each step to the next while walking [3]. This framework proposes goal functions to define the walking task and identify solutions as Goal Equivalent Manifolds (GEMs). During straight-ahead walking, humans multi-objectively regulate primarily step width (w) and secondarily lateral body position (z_B) [4]. During lateral maneuvers, young healthy adults adapt stepping regulation at each step to directly trade off w-regulation for z_B-regulation [5]. Thus, our lateral stepping regulation framework quantifies the proposed stability / maneuverability trade-off [2].

As older adults rely more on foot placement to maintain lateral balance [6], we hypothesized that they would be less able to adequately adapt stepping to perform lateral maneuvers. As such, we expected older adults to exhibit a lesser w- for z_B-regulation trade-off.

Methods: Twenty young (YH; 21.7 ± 2.6 yrs) and 18 older (OH; 71.6 ± 6.0 yrs) healthy adults walked on a motorized treadmill in a virtual environment. Following an audible and visual cue, participants switched between two parallel paths centered 0.6m apart.

We computed stepping variability ellipses at each maneuver step for each group as 95% prediction ellipses from all left (z_L) and right (z_R) lateral foot placements plotted in the [z_L, z_R] plane [7]. We characterized each ellipse by its aspect ratio, area, and orientation: aspect ratio reflects the relative weighting of w and z_B regulation, area characterizes overall [z_L, z_R] stepping variability, and orientation reflects the degree of alignment to the constant-w GEM [5]. As all stepping data from each group at a given step were used to construct a single prediction ellipse, we compared ellipse characteristics between groups using a previously established two-sample statistical procedure for bootstrapped data (α=0.05) [7].

Results & Discussion: OH participants typically used the same four-step strategy as YH to perform the lateral maneuver [5]. OH participants exhibited less stepping variability than YH at the transition step, but remained more variable for longer after the maneuver. Ellipse orientations did not differ between Groups (Fig. 1).

The aspect ratios of the OH and YH ellipses did not significantly differ at the transition step, and both ellipses were more isotropic than during straight-ahead walking (Fig. 1). This result indicates that OH and YH participants similarly traded off w-regulation for z_B-regulation to enact the transition.

However, the OH stepping ellipse became significantly more isotropic at the preparatory step prior to the maneuver, while YH participants did not substantially deviate from their continuous stepping regulation strategy until the transition step. In addition, the OH ellipses were slightly but significantly more isotropic than the YH ellipses during continuous walking both before and after the maneuver (Fig. 1).

In summary, while the maximum w- for z_B-regulation trade-off was similar among OH and YH participants, OH participants enacted this trade-off over a greater number of steps. Furthermore, OH participants maintained a slightly altered stepping regulation strategy throughout the trial in anticipation of the frequent maneuvers. Thus, OH participants adapted their stepping *less quickly* during this lateral maneuver task.

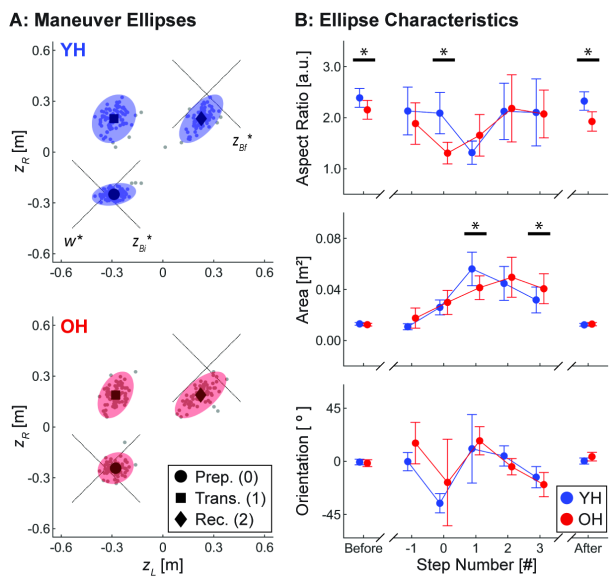

Figure 1: (A) Stepping data and 95% prediction ellipses for YH and OH participants at the preparatory, transition, and recovery steps of the lateral maneuver. (B) Ellipse aspect ratio (top), area (center), and orientation (bottom) during straight-ahead walking and at each step of the maneuver for YH and OH participants.

Significance: Goal-directed walking, including the lateral maneuver assessed here, requires humans to make decisions related to the task of walking itself. During lateral maneuvers, these decisions include how and when to adapt lateral stepping to enact a stability / maneuverability trade-off [2]. Here, our results demonstrate that older adults chose to distribute this trade-off over a greater number of steps. In this sense, older adults appeared less able to adapt their stepping as quickly as young adults during lateral maneuvers.

Acknowledgements: NIH / NIA Grant # R01-AG049735 & R21-AG053470

References: [1] Bruijn & van Dieën (2018), *J R Soc Interface* 15(143); [2] Acasio et al. (2017), *Gait Posture* 52; [3] Cusumano & Dingwell (2013), *Hum Mov Sci* 32(5); [4] Dingwell & Cusumano (2019), *PLoS Comp Bio* 15(3); [5] Desmet et al. (2022) *PLoS Comp Bio* 18(11); [6] Vistamehr & Neptune (2021), *J Biomech* 128; [7] Desmet et al. (2023), *bioRxiv* 2023.02.24.529927

HOW HEALTHY OLDER ADULTS DECIDE BETWEEN COMPETING WALKING MANEUVERS

David M. Desmet[1*] and Jonathan B. Dingwell[1]
[1]Department of Kinesiology, Pennsylvania State University, University Park, PA, USA
*Email: dmd78@psu.edu

Introduction: Falls among older adults most often occur while walking, and many occur during non-steady-state actions like incorrect weight-shifting during maneuvers [1]. Given the frequency of such maneuvers [2], it is important to assess the nature of age-related declines in walking maneuver performance.

Humans enact maneuvers and simultaneously maintain balance primarily by modulating their foot placement [3]. However, it has been proposed that lateral maneuvers require humans to trade-off stability for maneuverability [4]. We have since determined that humans adapt lateral stepping during maneuvers in a manner consistent with this trade-off [5].

Here, we aimed to determine how older and young adults prioritize these competing stability and maneuverability objectives. Participants were asked to decide between two presented paths: a narrow path designed to challenge stability, and a lateral path designed to challenge maneuverability. We hypothesized that, relative to their ability, older adults would select more conservative stepping strategies that prioritize stability [6]. Thus, we predicted that older adults would more often choose to traverse the lateral path.

Methods: Twenty young (YH; 24.7 ± 3.9 yrs) and 18 older (OH; 71.2 ± 6.3 yrs) healthy adults walked on a 1.2m wide motorized treadmill in a virtual environment. Participants first completed single path trials, during which they traversed narrow (NARR) and lateral (LAT) paths individually. Five difficulties (01-05; 01 = easiest) were assessed by varying NARR path widths and LAT path lateral displacments from the initial path (Fig. 1A). To quantify ability, we calculated errors for each path and difficulty as the percentage of steps outside of the path boundaries.

Participants then completed decision trials (DECN), during which they chose between simultaneously presented narrow and laterally displaced paths (Fig. 1A). Five difficulties were assessed, consisting of narrow and lateral paths of the same relative difficulty (01-05). To quantify decisions, we calculated the percentage of narrow paths chosen for each difficulty.

Group differences in single-path errors and the percentage of narrow decisions were assessed using two-factor (Group x Difficulty) mixed-effects ANOVA (α=0.05). Individual Group and Difficulty differences were determined using Tukey's pairwise comparisons.

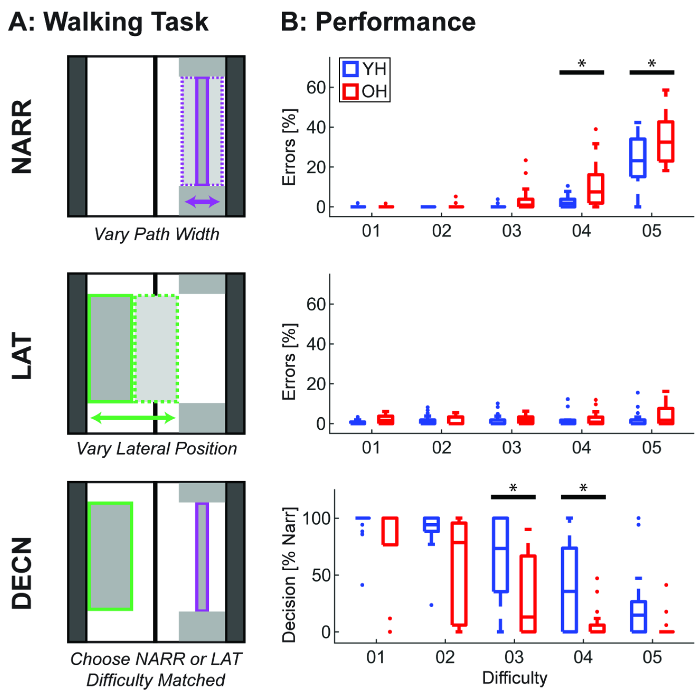

Figure 1: (A) Depictions of experimental conditions. (B) Errors while traversing NARR (top) and LAT (center) paths, and the percentage of narrow paths chosen during DECN trials (bottom), for each group and difficulty. Asterisks (*) denote significant Group differences.

Results & Discussion: Group differences in single-path errors (i.e., ability) were observed only at the most difficult NARR paths; OH participants made significantly more errors at NARR paths 04 & 05 (both $p < 0.004$; Fig. 1B [top]). No significant Group differences in errors were observed for NARR paths 01-03 (all $p > 0.834$) or any LAT paths ($p = 0.293$; Fig. 1B [center]).

Across DECN difficulties, OH participants chose to traverse the lateral path more often than YH ($p = 0.001$; Fig. 1B [bottom]). Individual Group x Difficulty comparisons were significant at DECN 03 & 04 (both $p < 0.026$). More OH than YH participants selected the lateral path at DECN 02 as well, but this difference did not reach statistical significance ($p = 0.106$).

Furthermore, at DECN 03, OH participants made significantly fewer narrow path decisions despite no significant group differences in ability to traverse the respective NARR and LAT paths. These results support our hypothesis that older adults select more conservative stepping strategies when deciding between competing walking maneuvers. Additional analyses are being conducted to quantify these stepping strategies and determine age-related differences in the prioritization of stability vs maneuverability.

Significance: A stability-maneuverability trade-off has been proposed to explain how humans adapt stepping to enact lateral maneuvers [4,5]. However, while older and young adults *can* similarly adapt stepping to enact maneuvers [7], they may *choose* to do so in different ways. Here, we begin to identify how older and younger adults weigh competing stepping objectives when making walking-related decisions.

Acknowledgements: NIH / NIA Grant # R01-AG049735 & R21-AG053470

References: [1] Robinovitch et al. (2013), *Lancet* 381(9860); [2] Glaister et al. (2007), *Gait Posture* 25(2); [3] Bruijn & van Dieën (2018), *J R Soc Interface* 15(143); [4] Acasio et al. (2017), *Gait Posture* 52; [5] Desmet et al. (2022) *PLoS Comp Bio* 18(11); [6] Arvin et al. (2016), *J Biomech* 49(7); [7] Desmet et al. (2023), *bioRxiv* 2023.02.24.529927

COMPARISONS BETWEEN IN-LAB AND OUT-OF-LAB FREE-LIVING DERIVED GAIT PARAMETERS

Matthew C. Ruder[1*], Monica Malek[2], Kim Madden[3], Anthony Adili[3], Dylan Kobsar[1]
[1]Department of Kinesiology, McMaster, University, Hamilton, ON
[2]Department of Biomedical Engineering, McMaster, University, Hamilton, ON
[3]Department of Surgery, McMaster, University, Hamilton, ON
*Corresponding author's email: ruderm@mcmaster.ca

Introduction: Knee osteoarthritis (OA) is a debilitating degenerative disease that results in decreased quality of live. Over time, the changes in bone and surrounding tissues in the knee can require a total knee arthroplasty (TKA) as an end-stage treatment. Gait analysis can inform clinicians with important information as to the progression of knee OA, but these lab-based assessments may not fully reflect how the patient moves in the real world. In recent years, wearable inertial measurement units have provided an opportunity to researchers to collect more ecologically valid data outside of lab settings, in patients' real life. However, very few studies have directly assessed the relationship between in-lab gait measures, such as stride time, against longer-term free-living gait assessments using wearable sensors. Therefore, the purpose of this study was to compare in-lab derived gait parameters to out-of-lab free-living derived gait parameters. It was hypothesized that out-of-lab free-living stride time would be longer than in-lab gait, and that there would be differences in gait asymmetry between in-lab and out-of-lab free-living assessments.

Methods: As part of a larger study related to the effects of the timing of total knee arthroplasty surgery, 10 older adults (Range: 50-71 years old) with moderate-to-severe knee OA were recruited from an orthopedic clinic at the time of their surgical decision. Following consent, patients had one wearable inertial sensor (AX6, 100 Hz, Axivity Ltd, Newcastle, UK) on placed on each leg at the anterior-medial aspect of the proximal tibia using medical grade adhesive tape. Following sensor placement, 52 retroreflective markers were placed on lower body anatomical landmarks and then patients were instructed to walk up and down a hallway 4-5 times while being captured by optoelectronic motion capture system (14 camera Optitrack system, 120 Hz, NaturalPoint, Corvallis, OR, USA). Following motion capture collection, the retroreflective markers were removed but the patient continued to wear the sensors for one week of free-living collection. At the end of the sensor collection period, patients removed the sensors and mailed them back in a pre-addressed envelope. Upon receipt of the sensors, data were downloaded and processed using a custom Python script. Briefly, walking segments were identified through harmonic frequency analysis for each side before individual strides were identified through gyroscope and accelerometer events [1][2]. Outliers and non-strides were identified through use of calculating the correlation of multiple correlation of the average of the first 100 strides against each individual strides waveform followed by a principal competent analysis [3]. Mean stride time was then calculated on the remaining strides. For the in-lab data, data were processed using custom Visual3D pipelines to segment walking trials. Gait parameters, including stride time, were calculated for each side. For both in-lab and free-living data, asymmetry index (ASI) was calculated between mean stride times.

Results & Discussion: Several notable differences between in-lab and free-living data were observed (Table 1). An average of 14.0 strides per patient were analysed from the in-lab gait analysis compared to 6187.2 strides per patient from out-of-lab gait. Mean in-lab stride times were not significantly less than mean free-living stride times (in-lab=1.18 s, free-living=1.22 s; p = 0.17), but mean standard deviation of stride times were significantly greater in free-living stride times than in-lab (in-lab=0.07, free-living=0.44; p=0.0056). ASI was also seen to be significantly greater in free-living data compared to in-lab (in-lab=2.21, free-living=10.7; p=0.04). This suggests that while a limited number of strides collected in-lab are generally consistent, free-living assessment has a much greater number of strides with a greater range of strides collected. The lack of agreement between the in-lab and free-living data could also be due to the OA patient population known to have a high degree of variability due to fluctuation in daily pain that cannot be captured with in-lab systems. Further refinement of free-living collections with wearable sensors could lead to more representative patient data to be used in treatment decisions in clinical populations.

Significance: While in-lab systems are highly accurate systems, their cost and time commitment often limit their utility in clinical settings. Further development and refinement of wearable systems such as outlined in this preliminary study will facilitate more accessible data collections in clinical settings more representative data.

Acknowledgements: Arthritis Society of Canada provided salary support for MR through Training Graduate PhD Salary Award.

References: [1] Ullrich, et al. (2020). *IEEE J Biomed*. 23(7), 1869-78. [2] Mariani, et al. (2013). *Gait &Posture*. 37, 229-34. [3] Ferrari, et al. *Gait & Posture*. 31, 540-2.

Table 1: In-lab vs free-living stride time comparisons

	Mean Patient Strides	Mean Stride Time (s)	Mean St. Dev. of Stride Time (s)	Mean ASI
In-Lab	14.0	1.18 (0.10)	0.07 (0.03)	2.21 (1.3)
Free-Living	6187.2	1.22 (0.17)	0.44 (0.59)	10.7 (13.5)
T-Test		0.17	0.0056	0.04

TIME EVOLUTION IS A SOURCE OF BIAS FOR THE CALCULATION OF LARGEST LYAPUNOV EXPONENTS DURING GAIT

Kolby J Brink, Tyler Wiles, Nick Stergiou, and Aaron D. Likens
Department of Biomechanics, University of Nebraska at Omaha, Omaha, NE USA
Corresponding author's email: kolbybrink@unomaha.edu

Introduction: Human movement is inherently variable by nature. However, the term *variability* is often interpreted in various ways in movement science. Here, we recognize variability as the fluctuations in repeated processes (e.g., steps). Observing variability through this lens reveals that natural processes and human movement alike share a rich complexity. One of the most common analytical tools for assessing movement complexity is the largest Lyapunov exponent (LyE) which quantifies the rate of trajectory divergence or convergence in an *n*-dimensional state space. Previous studies have demonstrated differences in LyE in kinematic signals during walking between healthy controls and ACL-deficient patients, peripheral artery disease patients, unilateral transtibial amputees and more[1].

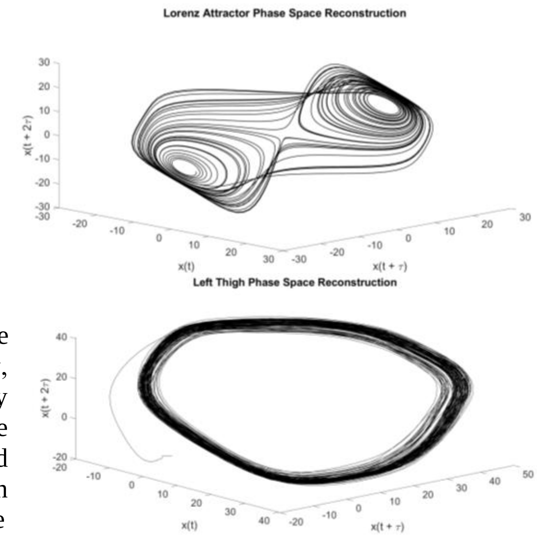

Figure 1. Phase space reconstruction of (top) simulated data (i.e., Lorenz attractor) and (bottom) experimental data (i.e., left thigh pitch).

One popular method for assessing LyE is the Wolf et al algorithm[2]. Many studies have investigated how Wolf's calculation of the LyE changes due to sampling frequency, filtering, data normalization, and stride normalization. However, a surprisingly understudied parameter needed for LyE computation is evolution time. Evolution time is the number of sample intervals by which each pair of neighboring points is followed before a new neighboring pair is chosen. For instance, chaotic systems require an evolution time that is not too large for convergence to theoretical values. The purpose of this study is to investigate how the LyE changes as a function of evolution time in simulated and experimental data (Fig. 1).

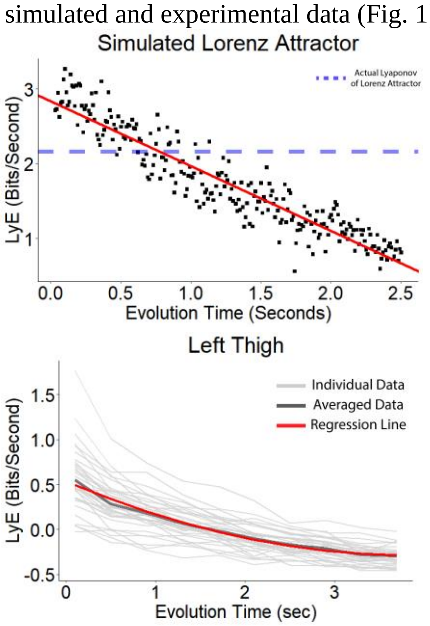

Figure 2. LyE values as a function of evolution time during (top) simulated data and (bottom) experimental data.

Methods: *Subjects.* The data from 36 healthy subjects (M/F = 18/18, age = 24.6 ± 2.66 yrs, BW = 71.9 ± 7.99 kg, HT = 1.73 ± 0.08 m) were utilized.
Experimental Procedure. Kinematic data during self-paced overground walking was collected on a ~200m indoor track. The data was captured at 200 Hz using Noraxon Ultium Motion™ inertial measurement unit (IMU) sensors (Noraxon, Inc., Scottsdale, AZ). Sensors were placed on the head, upper thoracic, lower thoracic, pelvis, upper arm, forearm, hand, thigh, shank, and foot. The subjects performed nine four-minute overground walking trials at their self-selected walking speed. The trials were spread over three blocks of three trials each. The subjects then completed the same experimental procedure one week later, totaling two sessions overall.
Data Analysis. Segment pitch angles from the left and right thigh, shank, and foot were extracted from the first 2-minutes of each trial to calculate LyEs. Simulated data consisted of values from a reconstructed Lorenz attractor sampled at 50 Hz. All experimental data was also downsampled to 50 Hz due to computational requirements. The time delay, τ, and embedding dimension, *m*, needed to reconstruct the state space were found using Average Mutual Information and False Nearest Neighbor functions, respectively[3,4]. Evolution time was calculated by multiplying a fixed constant by the sampling rate and applying the ceiling function (ceil()) in MATLAB to round up to the nearest whole integer. For simulated data, evolution time was systematically increased by increasing the fixed constant from 0.05 to 5 by 0.01, totaling 496 evolution time values. For experimental data, the same procedure occurred but the fixed constant increased from 0.05 to 1.85 by 0.2 due to computational constraints. The Wolf et al[2] algorithm was then run with each evolution time (Fig. 2).

Results & Discussion: Multi-level models were used to assess whether linear and quadratic evolution time improved prediction of LyE over and above an intercept only model for experimental and simulated data, respectively. *Exp. Data:* A fixed effect of evolution time and fixed effect of a quadratic time improved the model fit when predicting LyE ($p= <0.0001$), with LyE values decreasing 0.43 SDs for every 1 second increase in evolution time, $t = -14.7$, $p = <.0001$. *Sim. Data:* LyE values decreased 2.0 SDs for every 1 second increase in evolution time, $t=-24.6$, $p=<.0001$. Large evolution times negatively biased LyE values for both simulated and experimental data, although there is some indication of a plateau with higher values. An evolution time of 0.8 seconds produced estimates closest to theoretical values for the Lorenz system.

Significance: The findings from this study ought to be considered for future research using the Largest Lyapunov exponent obtained by the Wolf et al. algorithm. The present results provide a reference point for choosing evolution time values based on simulated and experimental results rather than potentially arbitrary rules of thumb.

Acknowledgements: This work was supported by NIH P20GM10909, NSF-2124918, & UN Collaborative Initiative.

References: [1] Raffalt et al. (2018); [2] Wolf et al. (1985); [3] Kennel et al. (1992); [4] Abarbanel et al. (1993)

EFFECTS OF MOVEMENT-BASED INTERVENTIONS ON SPINAL MUSCLE FATIGUE AND SPINE ORIENTATION DURING SITTING OFFICE TASKS: A COMPARATIVE STUDY

Zeinab Kazemi[1]*, Maryam Mohammadalizade[2], Mohammad Sadegh Ghasemi[2], Alireza Shaghaghi[2], Divya Srinivasan[1]
[1] Department of Industrial Engineering, Clemson University, Clemson, SC 29634, USA
[2] Department of Ergonomics, Iran University of Medical Sciences, Tehran, Iran
*Corresponding author's email: zkazemi@clemson.edu

Introduction: Millions of individuals worldwide spend a significant portion of their time sitting in front of visual display terminals, which has further increased for various activities since the COVID-19 pandemic. Prolonged sitting can lead to trunk muscle fatigue due to continuous deep muscle contractions which may subsequently reduce spinal stability and increase stress on the spine [1].
Interventions to alleviate musculoskeletal symptoms due to prolonged sitting can be divided into two main categories: work-rest programs and interventions that target the mechanisms responsible for such symptoms. The latter is usually preferred [2] since the work-rest programs are often impractical in many work environments. Postural changes which aim to increase postural variability and muscle fatigue while reducing the spinal load [3] have been suggested. Dynamic sitting postures have been shown to be beneficial by intermittently activating motor units, increasing nutrient and fluid flow to muscles, and facilitating spinal movements [4]. In this sense, feedback sensors and stretching exercises are suggested interventions, but their effectiveness varies in the literature [5]. Although previous research has investigated sitting tasks and potential interventions, none have compared alterations in the spine biomechanical behavior during computer-based tasks under movement-based interventions. Hence, this study aims to fill this gap by comparing neck and trunk muscle fatigue and trunk global orientation during computer tasks under three conditions: i) control, ii) performing a set of stretching exercises, and iii) wearing a sensor to provide feedback. Our hypothesis is that specific intervention- and task-related responses to muscle fatigue and spine orientation will exist.

Methods: A total of 20 healthy subjects were asked to perform four 10-min tasks (editing, n-back memory test, typing, and video watching) under three test conditions: control, performing a set of stretching exercises before each task, and wearing a low-cost sensor on C7 vertebrae to provide feedback and improve posture and trunk mobility. The sensor provided an audible alarm when the neck angle was between -10 and +20 degrees for more than 91 seconds or when the neck was bent forward more than 20 degrees and remained in that position for more than 30 seconds. Electromyographic activities of right and left upper trapezius (UTR, UTL), cervical erector spinae (ESCR, ESCL), thoracic erector spinae (ESTR, ESTL), and lumbar erector spinae (ESLR, ESLL) were continuously recorded over the tasks. Reflective markers were adhered to the T1 and S2 vertebrates to measure the global orientation of the spine [6]. The effects of *intervention* and *task* were analyzed using two-way repeated measure analysis of variance (ANOVA), followed by post hoc multiple comparison test.

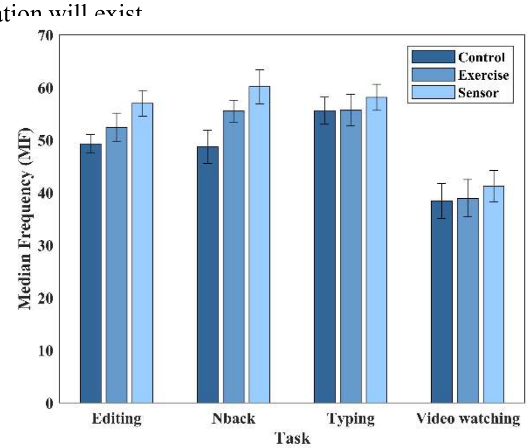

Figure 1: Median frequency of right upper trapezius while doing four computer-based tasks under three conditions: control, performing a set of stretching exercises before each task, and wearing a low-cost sensor on C7 vertebrae to provide feedback

Results & Discussion: The study found significant main effects of *intervention* ($p=0.017$) and *task* ($p=0.001$) on the median frequency of UTR muscle. The sensor condition showed %13.5 higher median frequency than the control ($p=0.045$), while watching showed a lower median frequency than editing (%30.12, $p=0.037$), nback (34.33%, $p=0.004$), and typing (36.8%, $p=0.010$) tasks. No significant effect of *intervention* and interaction of *intervention*×*task* was found for UTR. A significant main effect of *task* was observed for UTL. Specifically, as compared with watching, higher median frequency was obtained for editing ($p=0.000$), nback ($p=0.000$), and typing ($p=0.003$). ESCR did not show significant main effects for *task*, *intervention*, or their interaction. However, the ESCL muscle had a higher median frequency with sensor than with the control condition ($p=0.027$). As compared with typing, editing significantly reduced median frequency for ESLR (%13.61). Also, watching showed a lower median frequency than nback ($p=0.043$) and typing (0.014). Finally, ESLL showed a main effect of *task* ($p<0.001$), with a lower median frequency during watching than nback ($p=0.015$) and typing ($p=0.026$). The greatest forward lean was in the 10-min computer task, less lean occurred in 'correct' sitting, and the least in standing. The greatest forward lean was in the exercise condition and for the editing task, while the least in the sensor condition and video-watching task. Overall, the median frequency was increased using the sensor, suggesting the promising effect of postural variability on muscle fatigue reduction. This observation is consistent with a decreased trunk lean forward angle to sustain the same sitting posture over the computer-based tasks. Moreover, watching and editing were associated with higher median frequency, likely due to their higher visual and motor coordination requirements.

Significance: The effects of movement-based interventions (stretching exercises and feedback sensor) and task type on postural behaviour were examined over seated computer work. The results suggest that both interventions can positively impact postural behaviour, but the mobility-based intervention may be more effective in improving overall posture. Additionally, the type of task can have a significant impact on muscle fatigue, with certain tasks, such as editing and video-watching leading to higher levels of muscle fatigue compared to more dynamic task like typing. The results may provide practical insights for practitioners to promote healthy postural behaviour among individuals engaged in prolonged computer work.

References: [1] Ng, D., et al., Applied ergonomics, 2014. 45(3); [2] Waters, T.R. and R.B. Dick, Rehabilitation Nursing, 2015. 40(3); [3] Falla, D., et al., Physical therapy, 2007. 87(4); [4] Bontrup, C., et al., Applied ergonomics, 2019. 81; [5] Johnston, V., et al., Applied Ergonomics, 2019. 76; [6] Claus, A.P., et al., Applied ergonomics, 2016. 53.

SHOULDER MUSCLE ACTIVATION TIMING IN INDIVIDUALS WITH REDUCED SCAPULAR UPWARD ROTATION

Gaura Saini[1*], Jarred Frisk[2], Madeline Goodson[2], Matthew Heiling[2], Lauren Reimers[2], Paula Ludewig[1,2]
[1]Division of Rehabilitation Science, University of Minnesota
[2]Division of Physical Therapy, University of Minnesota
*Corresponding author's email: saini041@umn.edu

Introduction: The prevalence of shoulder pain is high in the adult population, and these individuals may demonstrate altered motion and muscle activity patterns.[1,2] Reduced scapular upward rotation is of particular concern as it may contribute to compression of the rotator cuff tendons.[3] Upward rotation is driven by the serratus anterior (SA) and lower trapezius (LT) muscles, and altered activation of either muscle may correspond to specific movement patterns. Biomechanically, individuals with insufficient (i.e., reduced magnitude or delayed) SA activity are expected to have reduced upward rotation and excessive scapular anterior tilt whereas those with insufficient LT activity are expected to have reduced upward rotation and lateral translation of the scapula.[4,5,6] The purpose of this study was to determine if differences in timing of muscle activation exist between the SA, LT, and the primary muscle driving humeral motion - anterior deltoid (AD) - during overhead reaching in two groups of adults with shoulder pain: 1) those displaying reduced scapular upward rotation and excessive scapular anterior tilt (anterior tilt group) and 2) those with reduced upward rotation and lateral translation of the scapula (lateralization group). Due to the biomechanical role of each muscle, we hypothesized that the SA would activate significantly later in the ROM compared to AD in the anterior tilt group and the LT would activate significantly later in the ROM compared to AD in the lateralization group.

Methods: 42 participants aged 18-60 with non-traumatic shoulder pain who demonstrated reduced scapular upward rotation (defined as ≤35° by inclinometer at 120° humerothoracic (HT) elevation) were enrolled in this study. 20 were classified into the anterior tilt group (≥10° by inclinometer at 90° HT elevation), and 22 were classified into the lateralization group (≥1 cm lateral translation of the root of the spine of the scapula from rest to 90° HT elevation). Participants were instructed to simulate reaching for an item on a high shelf while HT elevation kinematics were assessed with optical motion capture and muscle activity was captured with surface electromyography (EMG) of SA, LT, and AD. EMG data were normalized to maximum voluntary contractions. The initiation of muscle activation was operationally defined as 5% of maximum contraction[7] and was scaled from 0 to 100% of the range of motion. EMG data were normally distributed, and a two-way ANOVA with factors of group and muscle was performed (a = 0.05).

Results & Discussion: No interaction of group and muscle was found, and the main effect of group was not significant ($p = 0.159$). There was a significant main effect of muscle ($p < 0.001$) indicating that across all participants, the SA activated significantly later than the AD. Although the main effect of group was not significant, group data are provided descriptively in Fig. 1. The SA activates later in the ROM compared AD in both groups (anterior tilt: 17% vs. 8%, lateralization: 24% vs. 9%), and the LT activates later than AD in the lateralization group (17% vs. 9%). These data suggest that SA may be delayed in participants with reduced scapular upward rotation regardless of concomitant scapular movement patterns, emphasizing the SA's role in producing upward rotation. Participants with the lateralization pattern also appear to have delayed LT activation. Participant data were compared to a small cohort of asymptomatic controls with sufficient upward rotation. Descriptively, the SA activates earlier in the control group than both symptomatic groups (10% ROM). The LT activates earlier in the control group (14%) than the symptomatic lateralization group.

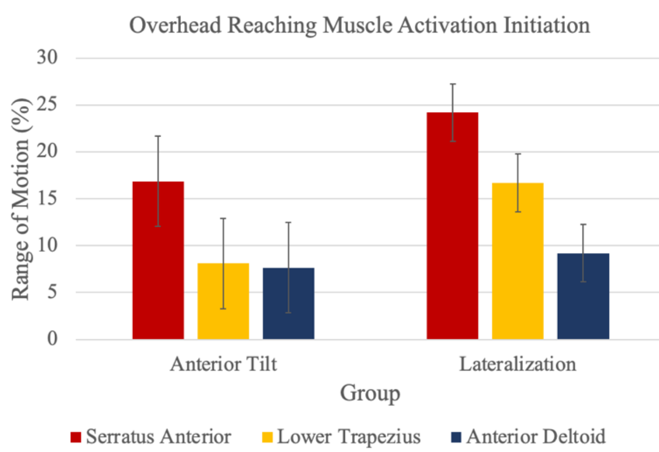

Figure 1: Muscle activation initiation as a percent of range of motion presented by group (anterior tilt, lateralization). Data are presented as mean with standard error.

Significance: Similar timing of the scapular muscles (SA and LT) and the deltoid are necessary to prevent reverse action of the deltoid and achieve sufficient scapular upward rotation to maintain optimal muscle lengths and conserve the glenohumeral joint space. These findings identify delays in key scapular muscle activation in individuals with shoulder pain and reduced scapular upward rotation. Neuromuscular training of SA and LT may be helpful in improving scapular biomechanics in these individuals.

Acknowledgements: Funding provided by NIH/NIAMS F31 F31AR079259, Promotion of Doctoral Studies II Scholarship from the Foundation for Physical Therapy Research, and Midwest Center for Occupational Health and Safety Pilot Projects Research Training Program.

References: [1] Lefèvre-Colau (2018), *Ann Phys Rehabil Med*; [2] Michener (2016), *J Shoulder Elbow Surg*; [3] Lawrence (2019), *J Orthop Sports Phys Ther*; [4] Didesch and Tang (2019), *J Hand Surg Am*; [5] Roren (2013), *Clin Biomech*; [6] Seror (2018), *Muscle Nerve*; [7] Wadsworth (1997), *Int J Sports Med*

A Battle of Balance: Differences in postural stability among cross-country runners, trail runners, and healthy non-runners

Cabel J. McCandless[1*], Christopher A. Aiken[1], and Kevin D. Dames[2]
[1]Kinesiology Department, New Mexico State University, Las Cruces, NM, USA
[2]Kinesiology Department, SUNY Cortland, Cortland, NY, USA
[*]Email: ccmand1@nmsu.edu

Introduction: Current research on balance with runners focuses on track and field athletes or road runners [1,2]. However, the cross-country and trail running population have seldom been examined in the literature. It is particularly impactful to examine these athletes as they run on a variety of surfaces (trails, dirt, uphill, downhill, etc.). Running on these uneven surfaces can put the runners at a higher risk of ankle sprains [3], so it is important to study these populations to reduce such injury. Poor static balance is associated with increased lower limb injury, specifically at the ankle [4]. Therefore, the purpose of this study is to assess differences in postural stability among cross-country and trail runners, and healthy non-runners. We hypothesized that consistent training on uneven, unpredictable terrain would promote better balance in the trail runners.

Methods: Healthy college students (Control), NCAA DI collegiate cross-country runners (XC), and age-matched trail runners (Trail) participated for this study (Table 1). Trail runners were those who had competed in a trail race within the last year. All participants had to be between the ages of 18-35, and free of any diagnosed neurological conditions. Participants also had to be free of any lower extremity injuries from the past 6-months, which would impact balance. Participation included a single testing session including three 15-second single leg stance trials on a force plate, for both their dominant and non-dominant limb, under two conditions: eyes-open and eyes-closed. The minimum Time to Boundary (TTB) were calculated among the three trials and averaged within each leg and condition. TTB is the amount of time the individual has to make postural corrections to maintain balance [5]. Participants also completed the International Physical Activity Questionnaire (IPAQ) and had active ankle range of motion assessed via goniometry. These were both collected to contextualize any observed differences in TTB across the groups.

Results & Discussion: Through a MANOVA, significant differences were found between condition, group and condition * group for the TTB variables. Subsequent One-way ANOVAs were run to follow up these findings. Significant differences in TTB minima were observed within groups (Table 2). This indicates that all participants, regardless of running background, had worse stability when their eyes were closed. A significant difference was observed among the groups for the TTB AP minimum, with the trail runners having the greater stability during the EO-DL condition. This aligns with previous research seen in novel runners [2]. No significant differences were observed between groups in ankle range of motion to help better understand this TTB difference, but significant differences from the IPAQ did show that the XC group was participating in vigorous physical activity more frequently and for longer durations than the other two groups.

Table 1. Participant Demographics. Mean (SD)

Parameter	Control, N= 11	Trail, N=12	XC, N=10
Age (years)	21.1 (.6)	23.5 (2.1)	20.1 (1.9)
Mass (kg)	73.2 (15.8)	68.3 (6.9)	58.9 (7.6)
Height (cm)	169.7 (9.5)	174.5 (6.4)	171.7 (12.2)
Vigorous Days	2.8 (1.7)	4.3 (1.7)	5.8* (1.4)
Vigorous Time (min)	50.5 (24.4)	47.5 (15.0)	90** (20.0)
AROM-DL-S (deg)	83.3 (12.2)	91.3 (4.8)	78.0 (12.9)
AROM-DL-F (deg)	35.2 (14.4)	38.8 (12.5)	30.6 (7.2)
AROM-NDL-S (deg)	75.0 (15.6)	87.5 (16.6)	70.2 (7.9)
AROM-NDL-F (deg)	34.4 (11.8)	41.75 (19.8)	32.0 (11.8)

Note: AROM: Ankle Range of Motion, DL: Dominant Leg, NDL: Non-dominant Leg S- Sagittal, F- Frontal. * Indicates a significant difference from Control group and ** indicates a significant difference from Control and Trail group.

Significance: Trail runners exhibited better static stability than the other two groups. Trail running may promote proprioceptive ability or engage non-sagittal plane muscle groups for stabilization to a greater extent than level, unobstructed running. Further research into training and ankle strength should be conducted to determine what causes this difference amongst similar runners (XC group).

Table 2. Minimum Time to Boundary (TTB) variables. Mean (SD)

Parameter	Control, N=11	Trail, N=12	XC, N=10
Mediolateral TTB (s)			
EO-DL	0.47* (0.14)	0.54* (0.18)	0.43* (0.19)
EC-DL	0.16 (0.07)	0.24 (0.10)	0.20 (0.14)
EO-NDL	0.44* (0.14)	0.55* (0.10)	0.59* (0.24)
EC-NDL	0.22 (0.08)	0.22 (0.08)	0.34 (0.14)
Anteroposterior TTB (s)			
EO-DL	1.14* (0.36)	1.69*ᵀ (0.25)	1.16* (0.6)
EC-DL	0.35 (0.17)	0.66 (0.29)	0.57 (0.47)
EO-NDL	1.14* (0.29)	1.47* (0.33)	1.49* (0.54)
EC-NDL	0.48 (0.16)	0.58 (0.30)	0.56 (0.47)

Note: EO: Eyes-Open, EC: Eyes-Closed, DL: Dominant Leg, NDL: Non-dominant Leg. * Indicates a significant difference within the group from the EC condition on the same leg and ᵀ indicates a significant difference from Control and XC group.

References: [1] Knight et al. (2016), *Sports Biomech* 15(2); [2] Drum et al. (2023), *IJOERPH* 20; [3] Bressel et al. (2007), *J of AT* 42(1); [4] Plisky et al. (2006), *JOSPT* 36(12); [5] Hertel & Kramer (2005), *Gait & Posture* 25(1).

SURVEYS OF SELF-PERCEIVED BALANCE INTEGRITY ARE POOR PREDICTORS OF VULNERABILITY TO BALANCE PERTURBATIONS

Andrew D. Shelton[1*], Jessica L. Allen[2], Vicki S. Mercer[3], Jeremy R. Crenshaw[4] and Jason R. Franz[1]
[1] Joint Department of Biomedical Engineering, UNC Chapel Hill & NC State University, Chapel Hill, NC, USA [2]Department of Mechanical and Aerospace Engineering, University of Florida, Gainesville, FL, USA [3]Division of Physical Therapy, UNC Chapel Hill, Chapel Hill, NC, USA [4]Department of Kinesiology and Applied Physiology, University of Delaware, Newark, DE, USA
E-mail: adshelt@email.unc.edu

Introduction: Falls in our rapidly aging population are a significant public health challenge. An understanding of an individual's risk for falls is necessary for the prescription of preventative measures to combat this challenge. Self-reported questionnaires of fear, self-efficacy, and confidence are commonly used as a proxy measure to gauge an individual's risk for falls. It is an important goal of rehabilitation to not only prevent falls, but to also promote mobility and independence [1]. To effectively accomplish both sides of this goal, we must understand the relationship between self-reported or perceived balance integrity and objective vulnerability to walking balance perturbations. However, there is a disconnect between walking instability (a significant correlator of falls) and self-reported neuropsychological measures [2]. Any disconnect between perceived balance integrity and objective vulnerability may predispose older adults to disadvantages for their safety or for their independent mobility. For example, individuals reporting low perceived integrity but who present with a low vulnerability to perturbations may unnecessarily limit their mobility or participation in daily activities. Conversely, individuals reporting high perceived integrity but who present with a high vulnerability to perturbations may participate in higher risk situations. However, this disconnect has yet to be explored using walking balance perturbations to elicit objective vulnerability associated with falls. Therefore, the purpose of this study was to determine the relationship between self-reported balance integrity (i.e., fear, self-efficacy, confidence) and objective measures of vulnerability to a series of walking balance perturbations. First, we hypothesized that older adults would be more vulnerable than younger adults to walking balance perturbations. Second, we hypothesized that older adults would have a lower perceived balance integrity than younger adults. Finally, we hypothesized that surveys of self-perceived balance integrity would be poor predictors of vulnerability to balance perturbations.

Methods: 29 younger adults (22.4±2.0 yrs, 14 F) and 28 older adults (73.0±5.9 yrs, 15 F) completed three common self-reported surveys: Activity-specific Balance Confidence (ABC), Falls Efficacy (FE), and the Fear of Falling Questionnaire-Revised (FFQ-R). They also completed four treadmill walking trials at their preferred overground walking speed in randomized order, including unperturbed walking, and: (i) treadmill-induced slip perturbations applied at heel strike [2], (ii) lateral waist-pull perturbations applied toward the swing leg at toe off, and (iii) continuous mediolateral optical flow perturbations. Using measured motion data, we calculated margins of stability in the anteroposterior (MoS_{AP}) and mediolateral (MoS_{ML}) directions at the instant of heel strike (that directly following perturbation onset for slip and waist-pull perturbations). Vulnerability to balance perturbations was calculated as percent change in MoS from the participants unperturbed walking trial to the perturbation trial.

Results & Discussion: As hypothesized, AP vulnerability to perturbations was significantly higher for treadmill-induced slips and lateral waist pulls in OA versus YA ($p \leq 0.018$). The same was true in ML vulnerability for optical flow perturbations and lateral waist pulls ($p \leq 0.039$)(Fig. 1A&B). Regarding surveys of self-perceived integrity, only the FFQ-R scores were worse in OA than in YA ($p = 0.007$)(Fig. 1C). Also, as hypothesized, we found no correlation between surveys of self-perceived balance integrity and vulnerability to balance perturbations ($r \leq 0.309$, $p \geq 0.109$). Our four-quadrant analysis added that roughly half of our participants (54% of OA and 42% of YA) reported levels of self-perceived integrity that were disassociated from their vulnerability to perturbations (Fig. 1D&E).

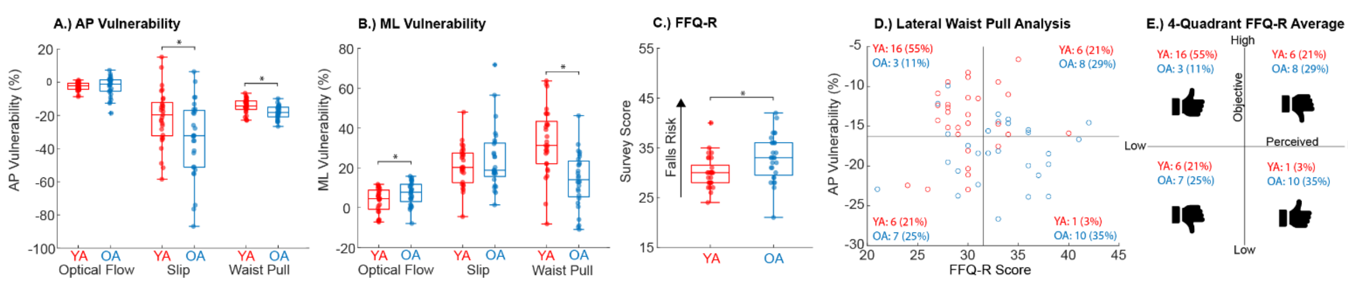

Figure 1: (A) AP vulnerability, ΔMoS, and (B) ML vulnerability across the three walking balance perturbation trials. Self-reported survey scores for the (C) FFQ-R scores (D) Representative four quadrant analysis of AP vulnerability to lateral waist pulls. (E) Averages of four quadrant analysis for FFQ-R survey responses. Asterisks (*) indicate significant differences ($p<0.05$).

Significance: OA are objectively more vulnerable than YA to various perturbation paradigms. However, this vulnerability may be missed using self-reported questionnaires. To best inform personalized rehabilitative training, we must understand this fundamental disconnect, not only to prevent falls, but also to promote as independent of a lifestyle as possible for those in our aging population.

Acknowledgements: Supported by a grant from NIH (R21AG067388).

References: [1] Gallagher, E.M. (1994) *The Center on Aging, U of Victoria, British Columbia* [2] Whipple M. O., et al. (2018) *Geriatr Nurs,* **39** p.170-7 [3] Crenshaw J, et al. (2014) *Gait & Posture*, **40** p. 363-8

LOWER EXTREMITY MUSCLE CONTRIBUTIONS TO 3-DIMENSIONAL GROUND REACTION FORCES DURING UNANTICIPATED CUTTING

Shelby A. Peel[1*], Jake A. Melaro[2], Joshua T. Weinhandl[2]
[1]School of Kinesiology and Nutrition, The University of Southern Mississippi, Hattiesburg, MS, USA
[2]Department of Kinesiology, Recreation, and Sport Studies, The University of Tennessee, Knoxville, TN, USA
*Corresponding author's email: shelby.peel@usm.edu

Introduction: Anticipatory effects on cutting mechanics have been reported and suggest that unanticipated cutting could lead to a higher risk of injury compared to anticipated cutting [1]. Previous work has quantified how muscle contributions to 3-dimensional (3D) GRFs have been used to understand specific lower extremity muscles role in bodyweight support, braking, and propulsion during cutting in healthy males [2]. However, it is unknown how lower extremity muscles contribute to 3D GRFs in females. Examining muscle contributions may offer insight in understanding task demands and improve technique in females that often perform unanticipated cutting in their respective sport. Therefore, the purpose of this study was to examine lower extremity muscle contributions to 3D GRFs during unanticipated cutting in healthy females.

Methods: Ten healthy, recreationally active female participants (24.3 ± 2.8 yrs, 65.1 ± 7.5 kg; 1.68 ± 0.05 m) complete five 45° unanticipated cuts that were randomly selected via a computer stimulus using a custom LabVIEW program (v17.0, National Instruments Corporation). During the cutting task, participants were asked to plant on their right foot and cut 45° to the left. A 12-camera motion capture system (200Hz, Vicon) and a force platform (2000Hz, AMTI, Inc) were used to collect marker coordinate and GRF data, respectively. Two timing gates (Lafayette Instrument) were placed before the force plate to trigger the visual stimulus and to monitor participant entrance velocity. Modified gait2392 musculoskeletal models [3] were scaled to the specific participants, and static optimization was used to obtain estimated net muscle forces. An induced acceleration analysis [4] was used to decompose the 3D GRFs into individual lower extremity muscle contributions. Individual muscles of the vasti, gluteus maximus, gluteus medius, and gastrocnemius were then summed together for each respective muscle group. Means and standard deviations were calculated for peak muscle group GRFs that made meaningful contributions to the overall 3D GRFs.

Results & Discussion: The soleus (247.2 ± 51.4 N) and gastrocnemius (401.1 ± 42.4 N) were primary contributors to propulsion with the soleus peaking during the first ~50% of stance, while the gastrocnemius peaked during the last ~40% of stance (Fig 1). The vasti group (-365.5 ± 63.9 N) was the primary contributor to braking during the majority of stance in the anteroposterior direction. The soleus (653.6 ± 132.8 N), gastrocnemius (482.6 ± 65.6 N), vasti group (379.6 ± 89.8 N), and gluteus maximus (137.2 ± 74.7 N) were all primary contributors to bodyweight support during cutting. The gluteus maximus peaked in its contribution within the first ~20% of stance, while the soleus and vasti group contributed the most during the first ~60% of stance. As the soleus and gastrocnemius declined in their contributions, the gastrocnemius became the dominant contributor during the last ~40% of stance. Finally, the soleus, gastrocnemius, vasti group, and gluteus medius were the primary contributors to the medially directed GRF. The soleus (-216.9 ± 72.7 N) acted as the primary contributor to the medially directed GRF during the first ~50% of stance. Once the participants started the push off portion of stance, the soleus contribution declined as the gastrocnemius (-279.5 ± 67.2 N) took over as the primary contributor during the last ~40% of stance. The vasti group (-94.5 ± 92.7 N) and the gluteus medius (-43.2 ± 18.5 N) contributed to medial GRF during the entirety of stance, while the gluteus maximus (30.1 ± 16.9 N) and tibialis posterior (72.7 ± 27.5 N) acted as antagonists in the mediolateral direction.

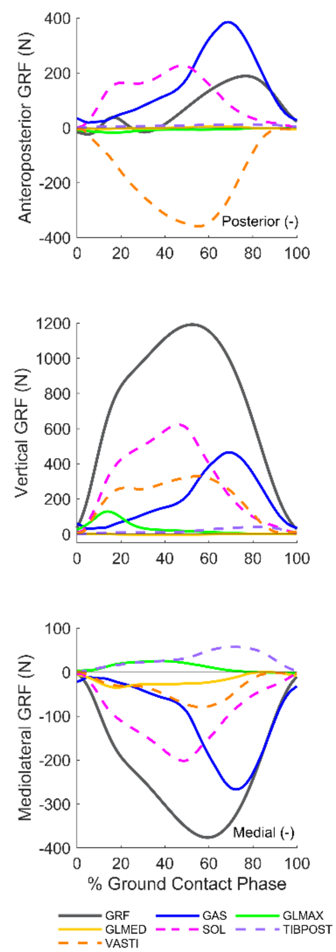

Figure 1: Ensemble averages of muscular contributions to 3D GRFs. GRF: ground reaction force; GAS: gastrocnemius; GLMAX: gluteus maximus; GLMED: gluteus medius; SOL: soleus; TIBPOST: tibialis posterior; VASTI: vasti group

In previous work, the soleus worked with the vasti group as a primary contributor to braking GRF, while the vasti group, gluteus maximus and gluteus medius contributed to medial GRF [2]. This conflicts with our findings as the soleus was a major contributor to propulsion, as well as both the soleus and gastrocnemius acting as primary contributors to medially directed GRF. This might indicate a sex difference exists in muscle contribution during unanticipated cutting. However, it is also possible that a difference in methodology, specifically in the cutting task used between the two studies, might have led to these discrepancies.

Significance: The results of the current study may help inform neuromuscular training interventions specifically targeted to females in an effort to ultimately minimize injury risk and increase performance during unanticipated cutting. These findings also suggest that muscle contributions between males and females are currently unclear, and future research is warranted.

References: [1] Griffin LY, et al. (2006) *Am J Sports Med.* 34:1512-1532; [2] Maniar N, et al. (2019) *J Biomech* 82:186-192; [3] Lai AM, et al. (2017) *Ann Biomed Eng.* 45:2762-2774; [4] Hamner SR, et al. (2010) *J Biomech.* 43:2709-2716.

A MATHEMATICAL MODELLING APPROACH TO THE MECHANICS OF MULTIARTICULAR MUSCLES

Jessica L. Tingle[1*], Derek J. Jurestovsky[2], Henry C. Astley[1]
[1]The University of Akron,
[2]Pennsylvania State University
*Corresponding author's email: jtingle@uakron.edu

Introduction: Muscles spanning multiple joints play important functional roles in a huge diversity of systems across tetrapods. Numerous structures owe their dexterity to multiarticular muscles, including hands, feet, and prehensile tails [1-2]. Beyond prehension, some multiarticular muscles function in force production and/or postural control during locomotion [3-4]. These include trunk muscles that contribute both to bending and to stabilization in diverse body plans. Despite the ubiquity and importance of multiarticular muscle systems, we still lack a thorough understanding of fundamental mechanics. Snakes can serve as excellent study organisms for advancing this topic for two major reasons: 1) they rely on their axial musculoskeletal system for a huge range of activities, and 2) their muscles span from one or a few vertebrae to >30, with other details of muscle architecture varying among muscles and among species [5] (Fig. 1A). The main goal of this study was to derive a general equation relating muscle force production and shortening to torque generation and postural change, which can clarify the mechanical consequences of different anatomical arrangements of multiarticular muscles.

Methods: We examined the relationship between anatomical arrangement and mechanical function in several major epaxial muscles, using the corn snake (*Pantherophis guttatus*) as a study species. We first characterized the anatomy of four major epaxial muscles (Fig. 1A and 1B). We then used cross products to determine relative contributions of each muscle to torque and its components based on their lever arms (Fig. 1C). This approach has commonly been used to deepen scientific understanding of monoarticular systems [6]; however, it assumes that only one joint is moving, which is clearly inaccurate for multiarticular systems. Therefore, we next derived an explicitly multiarticular equation that relates muscle length changes to postural changes. To do so, we modelled the vertebral column and the hypothetical muscle as the arcs of a circle and an Archimedean spiral, respectively, with identical origins (Fig. 1D). The arc length equations provided a starting point for our derivation. Our final equation uses anatomical traits to relate muscle length to curvature. We used this new equation to compare the function of the four epaxial muscles.

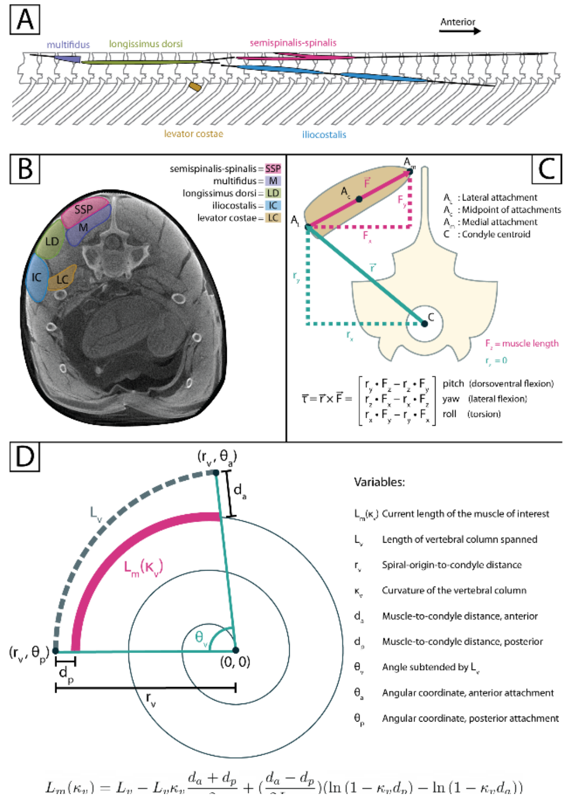

Figure 1: Corn snake muscle anatomy and calculations, generalizable to other multiarticular systems. A) Schematic showing a lateral view of the axial muscles of interest. B) Transverse section of a contrast-enhanced μCT scan showing the same muscles. C) Diagram showing the lever approach for calculating the potential relative contributions of each muscle to torque and its components (pitch, yaw, and roll). D) Diagram of our model accounting for changing curvature in a multiarticular system, which relates epaxial muscle length $L_m(\kappa_v)$ to the curvature of the vertebral column (κ_v) in a way that can be generalized to other multiarticular systems.

Results & Discussion: The equation we derived has an interesting property: its first half represents an "arc approximation" for determining muscle length in the case where the muscle runs parallel to the vertebral column (its anterior and posterior attachments are at the same distance from the vertebral column), and its second half of the equation represents a "spirality adjustment" accounting for the fact that the anterior and posterior muscle attachments are often different distances from the vertebral column. We found that the spirality adjustment term made a negligible contribution for all of the epaxial muscles under consideration: the calculated muscle lengths with and without the spirality adjustment were always within 0.5% of each other. This result would hold for any system in which the offset of muscle attachment points from the joints is small relative to the resting length of the muscle. Ignoring the spirality adjustment makes possible the derivation of additional equations putting muscle shortening (relative or absolute) in terms of either body curvature or intervertebral joint angles. We then went on to determine the relative contributions of each muscle to forceful vs. fast movements in various planes of motion, which can help us understand the role of different muscles in various behaviors, that have different force vs. speed requirements in different planes.

Significance: This study compares the potential contributions of different epaxial muscles to torque in different planes of motion (pitch, yaw, and roll), which provides a baseline for hypotheses regarding the expected evolution of different muscles with respect to behavior. In so doing, we created a new analytical tool that can be applied to other multiarticular muscle systems. Our results contribute to knowledge of snake muscles specifically and multiarticular muscle systems generally, providing a foundation for future investigation of potential trade-offs between mechanical output and locomotor control.

Acknowledgements: This work was funded by NSF Award #2045581 to HCA.

References: [1] Sustaita et al. 2013, *Biol Rev* 88(2); [2] Luger et al. 2021, *ICB* 61(2); [3] Gramsbergen et al. 1999, *Dev Brain Res* 112(2); [4] Schilling & Carrier 2010, *J Exp Biol* 213(9); [5] Greene 1997, U. of California Press; [6] Vogel 2003 Princeton U. Press.

DYNAMICALLY MEASURING PLANTAR TISSUE STIFFNESS WITH THE ULTRASHOE (AN ULTRASOUND EMBEDDED SANDAL)

Ellen Y. Li[1*], Scott Telfer[1,2,3], Brittney Muir[1,3], William R. Ledoux[1,2,3]
[1]RR&D Center for Limb Loss and MoBility (CLiMB), VA Puget Sound, Seattle, WA
Departments of [2]Orthopaedics & Sports Medicine, [3]Mechanical Engineering, University of Washington, Seattle, WA
*Corresponding author's email: eli17@uw.edu

Introduction: Individuals with diabetes mellitus are often at a higher risk for plantar tissue ulceration and subsequently lower limb amputation. Some researchers hypothesize that this increased risk is related to changes in plantar tissue properties, which lead to increases in plantar tissue stiffness and pressure. Measuring plantar tissue stiffness requires identifying the amount of load applied to a region and subsequent tissue compression. Previous studies that simultaneously measured plantar pressure and compression used either fluoroscopy during gait trials [1], exposing subjects ionizing radiation, or ultrasound but in static conditions by applying a known load to the foot through indentation tests [2]. One study embedded an ultrasound probe into a set of shoes and captured both plantar pressure and tissue compression dynamically [3], but the pressure sensels covered a larger surface area, minimizing the accuracy of the load measurements. The goal of this study was to develop a novel sandal (Ultrashoe) that embeds an ultrasound probe with load cells directly below it to safely and accurately measure plantar tissue stiffness during gait.

Methods: A sandal sole was casted with liquid polyurethane plastic (Smooth-On Simpact 60A) in a 3D printed mold. It was designed to contain a forefoot and heel cut-out to hold load cells and an ultrasound probe below the second or third metatarsal head and the calcaneus, respectively (Fig 1A). Adjustable Velcro straps and Dacron padding were incorporated to maximize adherence between the foot and the sandal surface, and to reduce skin irritation (Fig 1B). Four load cells (Model 13, Honeywell) were placed in the forefoot cut-out under an uncased ultrasound probe (SLH20-6, Aixplorer), secured with custom 3D printed parts. A layer of Dacron was used as a thin insole padding and a 0.5mm thick ultrasound gel pad was placed on top of the ultrasound probe and case cover to allow for a consistent imaging interface with the plantar surface (Fig 1C). The ultrasound (SuperSonic Imagine's Aixplorer) was set to its maximum frame rate, 45 Hz, and load cell data was collected through LabVIEW software (National Instruments) at 100 Hz.

Figure 1: **Ultrashoe design.** (A) Polyurethane molded shoe and straps. (B) Prosthetic foot secured for visual. (C) Ultrashoe with load cells, ultrasound probe, insole liner, and gel pad.

Preliminary data were collected from a male subject with diabetes mellitus. The subject was fitted with a size 11 men's Ultrashoe with an ultrasound probe centered on the second metatarsal head. An AMTI split-belt treadmill was used for data collection and the speed was set to 0.4 m/s, comparable to his measured unassisted overground walking speed. Once the treadmill reached its target speed, Ultrashoe data were collected for 30 seconds, which included a deceleration phase during the last 5 seconds. Data were synchronized during post-processing and plantar thickness was semi-automatically tracked using a custom script in MATLAB (MathWorks). Plantar tissue force-deformation data were calculated by averaging the loading curves, with the first and last two steps removed. Subsequently, plantar tissue stiffness was determined with a linear regression in the last 30% of the loading curve.

Results & Discussion: One 30 second walking trial was analysed, and 11 of the 13 steps were used to estimate plantar stiffness (Fig 2). Without filtering, the raw data estimates a plantar stiffness of 114.5 N/mm and elastic modulus of 2.9 MPa. The forefoot stiffness and elastic modulus measured are higher than those reported in other studies [2,4]. Other studies often used low applied forces (<10N) during indentation tests [2], which would lead to the analysis of only the toe region of loading curve and lower predicted moduli. Additionally, our study may include an initial compression due to shoe strapping, lowering the maximum compressive strain recorded.

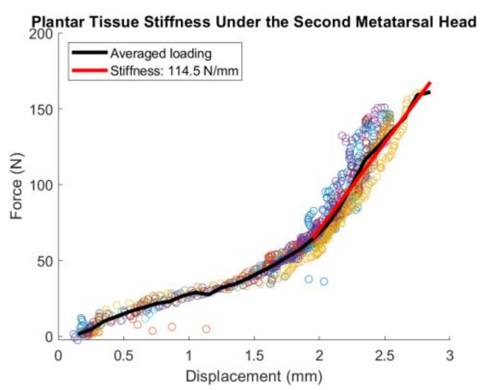

Figure 2: **Plantar tissue stiffness under the second metatarsal head.** Loading curves from 11 steps are plotted as unfilled, colored circles with displacement (mm) and force (N) along the x- and y-axis, respectively. Solid lines are used to represent the average loading curve (black) and plantar tissue stiffness within the final 30% of strain (red).

Significance: The Ultrashoe allows researchers to measure plantar tissue properties across dynamic gait trials, providing insight on variations in plantar tissue stiffness, strain rate, and energy loss across individuals with and without pathologies that may affect the plantar tissues. Such data can inform subject-specific finite element modelling of the feet, be incorporated into designing custom orthotic devices, and advise early diagnostic and treatment techniques.

Acknowledgements: Funding for this study was provided by NIH grant AR072216-01 and VA award A3539R. Preliminary research was conducted by Tony Huynh.

References: [1] Wearing, CS, et al., Clin Biomech, 24:397-402, 2009. [2] Klaesner, JW, et al., Arch. Phys. M. 83(12):1796-1801, 2002. [3] Telfer, S, et al., Gait & posture 39(1)1: 328-332, 2014. [4] Chao, CY, et al. (2011) Ultrasound Med Biol. *37*(7): 1029-1038, 2011.

Changes in ankle power during walking at different speeds with powered ankle exoskeleton

Meredith K. Owen[1*], Tereza Janatova[1], Kelsey Reeves[1], Benjamin Brightwell[1], Justin Pol[2], Junfei Tong[3,4], Anup Pant[3,4], Jacques Reifman[3], Michael A. Samaan[5], Brian Noehren[1]
[1]Department of Physical Therapy, University of Kentucky, Lexington, KY, [3]Department of Defense Biotechnology High Performance Computing Software Applications Institute, Telemedicine and Advanced Technology Research Center, United States Army Medical Research and Development Command, Fort Detrick, MD, USA, [4]The Henry M. Jackson Foundation for the Advancement of Military Medicine, Inc., Bethesda, MD, USA
*Corresponding author's email: mow229@uky.edu

Introduction: Military rucking is a strenuous task requiring long-distance marching while carrying heavy loads of combat equipment, often in complex terrains where mechanical transportation would not be feasible. The additional weight and difficult topography can lead to a rise in energy expenditure and changes in gait mechanics leading to an increased risk for both acute and chronic injuries. Powered exoskeletons, which produce an external torque to provide a mechanical advantage at the targeted joint, have been shown to reduce energy expenditure during walking by increasing power output at the ankle joint [1,2]. The autonomous exoskeleton selected for this study required controller training at a speed of 3.0 mph; however, maintaining a set speed during overground walking can be challenging, especially for longer durations. The purpose of this study was to evaluate changes in ankle power while walking at varying speeds with a powered autonomous ankle exoskeleton.

Methods: 5 healthy active individuals (5 male, age = 22.2 ± 3.5, height = 1.77 ± 0.04 m, weight = 85.2 ± 8.5 kg) completed two study visits. Walking gait biomechanics were determined for baseline (no exoskeleton) and while wearing a powered ankle exoskeleton (EB60, Dephy, Inc., Maynard, MA). Participants completed a training session with the ankle exoskeleton prior to the data collection visit. Prior to each use, the exoskeleton was calibrated at a set walking speed of 3 mph (1.34 m/s), per manufacturer recommendation.

Ankle joint kinetics and vertical ground reaction forces were measured using an instrumented 13-camera motion capture system. Fifty-two reflective markers were placed at specific anatomical and tracking locations on the trunk, and lower extremities. A static standing calibration was recorded first, followed by walking trials at five set speeds (2.0, 2.5, 3.0, 3.5, and 4.0 mph). Kinematic and kinetic data were collected at 200 and 2000 Hz, respectively, and filtered with a 4th order Butterworth filter with a cutoff frequency of 8 Hz for kinematic data and 35 Hz for kinetic data. Peak ankle plantar flexor moment and peak ankle power were calculated in Visual3D and compared across all speeds between the two walking conditions with two-way repeated measures ANOVAs. Significance was set at 0.05. For trials with the powered exoskeleton, ankle power is considered to be representative of the biological contribution and exoskeleton contribution.

Results & Discussion: Average values are reported in Table 1. Peak ankle power was significantly higher with the powered ankle exoskeleton for walking speeds of 3.0 mph ($p = 0.0003$), 3.5 mph ($p = 0.0017$), and 4.0 mph ($p < 0.0001$). Ankle power increased by 0.13 W/kg (15%) at 2.0 mph, 0.18 W/kg (17%) at 2.4 mph, 0.42 W/kg (31%) at 3.0 mph, 0.36 W/kg (21%) at 3.5 mph and 0.55 W/k (28%) at 4.0 mph. There were no significant differences in peak plantar flexor moment between walking with and without the exoskeleton at any speed. Largest percent increase in ankle power occurred at the calibration speed of 3.0 mph, potentially indicating that the exoskeleton is most effective at the trained speed.

Table 1. Peak Ankle Power and Peak Ankle Plantar Flexor Moment (Mean ± SD)

	Ankle Power (W/kg)		Ankle Moment (Nm/kg)	
Speed	No Exoskeleton	Powered Exoskeleton	No Exoskeleton	Powered Exoskeleton
2.0 mph	0.82 ± 0.17	0.94 ± 0.22	0.85 ± 0.09	0.82 ± 0.07
2.5 mph	1.08 ± 0.40	1.26 ± 0.26	0.92 ± 0.09	0.88 ± 0.04
3.0 mph	1.34 ± 0.33	1.75 ± 0.34*	0.97 ± 0.10	0.97 ± 0.08
3.5 mph	1.68 ± 0.59	2.04 ± 0.48*	1.06 ± 0.09	1.01 ± 0.10
4.0 mph	1.95 ± 0.54	2.50 ± 0.69*	1.11 ± 0.10	1.09 ± 0.12

Significance: Powered ankle exoskeletons are designed to give the wearer a mechanical advantage during a designated task (i.e. walking) and can reduce overall energy expenditure. Power generation by the ankle during push-off is a significant contributor to overall power output during walking [3] and so, supplementing the energy production at the ankle joint via powered exoskeleton could help decrease the overall load on the ankle joint and plantar flexor muscles. For this study, the ankle exoskeleton required training at a consistent specific gait speed on a treadmill (3.0 mph); however, overground walking over long-distances inevitably causes variability in speed. Characterizing the changes in ankle power while wearing an autonomous exoskeleton over various speeds provides useful information about the functionality of the exoskeleton. Future work should seek to expand upon these findings by investigating longer walking durations.

Acknowledgements: The project described was supported by the U.S. Army Medical Research and Development Command under contract No. W81XWH-20-C-0031. The opinions and assertions herein are the private views of the authors and are not to be construed as official or as reflecting the views of the U.S. Army, the U.S. Department of Defense, or the Henry M. Jackson Foundation for the Advancement of Military Medicine, Inc. This abstract has been approved for public release with unlimited distribution. The authors would also like to thank Grace Brooks and Delaney McNeese for their assistance with data processing.

References: [1] Mooney, Rouse, & Herr (2014) *J Neruoeng Rehabil*,3(11); [2] Mooney & Herr (2016), *J Neruoeng Rehabil* 13(1); [3] Farris & Sawicki (2012), *J. R. Soc. Interface* 9(66)

ASSESSMENT OF TWO NOVEL FORCE CONTROL VARIABILITY TASKS

Madison Mingo[1*], Lindsey Remski[1], Amelia S. Lanier[1], Brian A. Knarr[1]
[1]Department of Biomechanics, University of Nebraska at Omaha, Omaha, NE USA
*Corresponding author's email: mmingo@unomaha.edu

Introduction: In the United States, more than 200,000 anterior cruciate ligament (ACL) injuries occur each year [1]. Greater than 70% of ACL injuries occur through noncontact maneuvers [2]. This includes cutting or pivoting movements. The prominence of these noncontact maneuvers among ACL injury incidences suggests the presence of motor control deficits. There exists a methodology to detect these deficits that utilizes shear force control and nonlinear analysis, specifically the largest Lyapunov exponent (LyE) [3]. Previously, this force control task has been used to compare the control strategies among uninjured recreational athletes, uninjured high-performance athletes, those with ACL injury who had not undergone reconstruction (ACLD), and those with ACL injury who had undergone reconstruction (ACLR) [4]. A baseline measure with a healthy population would show the effectiveness of the LyE and demonstrate test-retest reliability with this method. Furthermore, in a clinical setting, isokinetic dynamometry is often used to monitor a patient's progress during rehabilitation [5]. The clinical translation of the force control task to isokinetic dynamometry requires further evaluation.

The purpose of this study was to determine the test-retest reliability of the novel force control task and to determine the correlation between the force plate task and an isokinetic dynamometer task. In accordance with the results of previous studies [3-4], we first hypothesized that the shear force control variability would demonstrate high retest reliability in healthy individuals. Secondly, as both tasks were developed to measure force control variability in populations with knee injury risk, we hypothesized that a strong correlation would exist between the LyE values for the two tasks.

Methods: A total of 12 healthy participants completed both the force plate task and the isokinetic dynamometer task at two sessions, which occurred one week apart (Figure 1). For the force plate task, participants stood on force plates and watched the visual feedback screen. Participants generated shear forces bi-directionally to the beat of a metronome set at 60 bpm and tried to align the slider on screen with stationary indicators set at 50% of the participant's maximal force in that direction. For the isokinetic dynamometer task, participants laid on one side and watched the visual feedback screen. With the top leg resisted, participants raised and lowered the top leg to the beat of a metronome set at 60 bpm and tried to align the slider on screen with a stationary indicator set at 50% of the participant's maximal force in that direction.

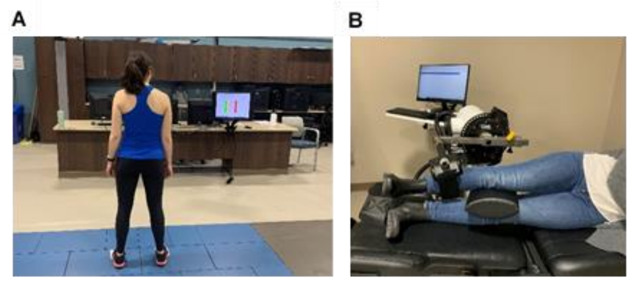

Figure 1: Experimental setup of the force control variability tasks. **(A)** Force plate task; **(B)** Isokinetic dynamometer task.

Force data was kept unfiltered to maintain subtle changes in the force signals. Force control variability was measured using LyE, which was calculated using the algorithm from Wolf and colleagues [6]. The reliability of the LyE from the average of the trials at each session was evaluated using interclass correlation coefficients (ICC) for a two-way random effects model for consistency of a single rating. Pearson's correlation coefficient was used to evaluate the correlation between the force plate task and the isokinetic dynamometer task.

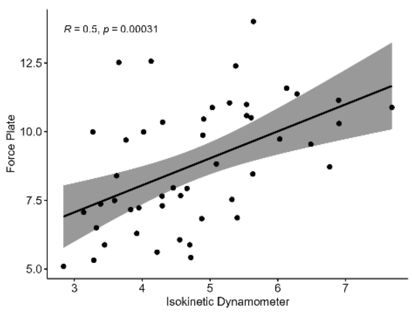

Figure 2: Correlation between the LyE scores for each task.

Results & Discussion: The first hypothesis that the shear force control variability would demonstrate high retest reliability in healthy individuals was not supported. The ICC value for each condition fell within 0.60 to 0.80, indicating that the force plate task has moderate reliability. These results suggest that some error may exist within day-to-day measurements. The second hypothesis that a strong correlation would exist between the LyE values for the two tasks was not supported. While the correlation between the two tasks was significant (Figure 2), the magnitude of the variance indicates that these two tasks are not heavily related. This result suggests that each task may present different information regarding force control variability with knee function.

Significance: This study demonstrated the ability of two novel tasks to evaluate an aspect of knee function through force control variability. Additionally, this is the first study to show the feasibility of utilizing an isokinetic dynamometer to assess force control variability. The results of this study may provide clinicians with a more accessible way to obtain force control variability. Future work should aim to develop minimum detectable changes (MDC) and minimal clinically important differences (MCID) for each of these tasks.

Acknowledgements: This project was funded through the University of Nebraska Omaha's Office of Creative Activity and Research.

References: [1] Benjaminse A et al. (2006), *JOSPT* 36(5); [2] Boden BP et al. (2000), *Phys Sportsmed* 28(4); [3] Lanier A et al. (2018), *Sensors* 18 (8); [4] Lanier A et al. (2020), *J Orthop Res* 38(8); [5] Habets B et al. (2018), *BMC Res Notes* 11(1); [6] Wolf A et al. (1985), *Physica D: Nonlinear Phenomena* 16(3).

VALIDATING A RESISTIVE ANKLE POWERED EXOSKELETON FOR AT HOME REHABILITATION AMONG INDIVIDUALS WITH CEREBRAL PALSY

Collin D. Bowersock[1*], Jenna R. Moeckly[1], Shanpu Fang[1], Zachary F. Lerner[1]
[1]Northern Arizona University | Mechanical Engineering
*Corresponding author's email: collin.bowersock@nau.edu

Introduction: An estimated 50% of children living with cerebral palsy (CP) utilize an ankle-foot orthosis [1]. These devices are implemented to improve function and postural control during gait. However, there is limited evidence on the effectiveness of these devices to improve gait function over an individual's life. There is a great need for a biomedical device that can be used by individuals with CP as a long-term functional gait training tool. Our previous treadmill-based work has shown the utility of a wearable ankle-powered exoskeleton as a functional gait training tool by resisting ankle plantar flexion during the stance phase of gait [2]. However, little to no evidence is available from a free-living setting. The purpose of this study was to validate an ankle-powered exoskeleton for at-home functional gait training. An overground walking environment was used as a simulated free-living setting as many individuals do not have access to a treadmill to conduct gait training at home. We hypothesize that individuals with CP will have similar plantar flexor muscle engagement when walking with the device during a simulated free-living setting when compared to treadmill walking.

Methods: To validate the device for at-home functional gait training, seven participants with CP used the resistive ankle-powered exoskeleton in two walking environments, overground and treadmill. In each environment, participants walked in four different conditions, shod (no exoskeleton), exoskeleton (exo), exoskeleton and biofeedback (exo + bio), and biofeedback (bio). The purpose of the multiple conditions was to compare the devices' ability to recruit the ankle musculature with another common gait rehabilitation technique, biofeedback. During the exoskeleton conditions, the device applied an ankle dorsiflexor torque during the stance phase of walking at 12% of the participant's peak baseline value. During the biofeedback conditions, a chime from a speaker was delivered when the participant reached a peak ankle plantar flexor torque that was 8% greater than their baseline. Unilateral tibias anterior (TA), medial gastrocnemius (MG), vastus lateralis (VL), and biceps femoris (BF) EMG was collected to quantify the device's effect on lower limb musculature recruitment. The peak EMG magnitude of each muscle was taken during six stance phases of gait for each participant after applying a 4th-order low pass filter. A 2-way repeated measures ANOVA was used to test for significance between walking environments and conditions as well as any interaction effects.

Results & Discussion: Average peak muscle activations across participants during each condition are shown in Figure 1. Results of the statistical analysis showed TA peak to be dependent on the walking environment and condition. Post hoc analysis revealed overground walking to result in increased TA peak activity and TA peak activity was significantly greater during shod than exo + bio and bio conditions. BF peak EMG was dependent on the walking condition with post hoc testing revealing increased BF peak EMG during exo + bio when compared to exo and bio independently. The changes in TA muscle activity between conditions could be due to the inherent properties of the device, helping to lower the foot to the ground and reducing TA activation. Changes in BF activity could be a result of an altered gait caused by the device and the biofeedback. The lack of significant MG peak differences between the two walking environments supports our hypothesis. Surprisingly, no walking condition was found to increase peak MG activation which is the muscle that is being targeted by the exoskeleton and biofeedback. The previous work using the device on a treadmill found plantar flexor improvements when paired with biofeedback however this was after 15 minutes of device acclimation [2]. As mentioned, the exoskeleton may have altered the participants' gait, acutely reducing the ankle range of motion and thus the amount of plantar flexion activity. Continued analysis will investigate these possible alterations in gait kinematics. Longer acclimation and more instructive biofeedback may be necessary to yield participants' habitual gait kinematics and to increase the recruitment of the plantar flexor muscles.

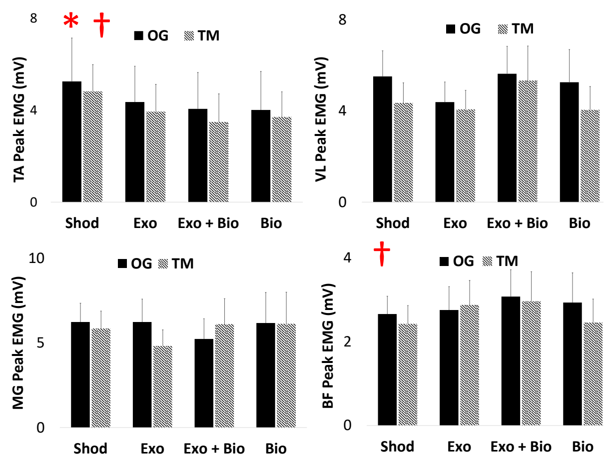

Figure 1: Average peak EMG for medial gastrocnemius (MG), tibias anterior (TA), biceps femoris (BF) and vastus lateralis (VL) for the 7 participants during overground (OG) and treadmill (TM) walking in each of the conditions; Shod, exoskeleton (Exo), exoskeleton and biofeedback (Exo + Bio), Biofeedback (Bio). Error bars represent the average SD.
* denotes a significant difference between walking environments across conditions. † Denotes a significant difference between condition across environments.

Significance: Our overarching goal is to provide a device that can be easily used in a real-world setting and to provide functional gait training environments that result in long-term improvements in the walking ability of individuals with gait deficits. This work helps to validate our device for community use while also revealing areas that can be improved before deployment. This work demonstrates that while walking aids and biofeedback may be developed to target certain muscles they may result in a large effect on other muscles without appropriate instruction, practice, and feedback.

References: [1] Wingstrand, Hägglund & Rodby-Bousquet. (2014), *BMC Musculoskeletal Disorders 15, 327.* [2] Conner & Lerner (2022), *IEEE Int Conf Rehabil Robot. 1-6*

JOINT KINEMATICS IN INFANTS WITH DOWN SYNDROME DURING EARLY TREADMILL INTERVENTION: PRELIMINARY RESULTS

Robert Zeid II[1*], Patrick Underwood[1], Jackelyne Perez[1], Jianhua Wu[1]
[1]Georgia State University, Department of Kinesiology and Health
*Corresponding author's email: rzeid1@gsu.edu

Introduction: Down syndrome (DS) is a genetic disorder that causes significant motor, cognitive, and language delays. While typically developing (TD) infants begin to walk around 12 months of age, infants with DS begin to walk approximately around 24 months. Walking is a fundamental skill that provides infants with access to interact with their environment, and facilitates their motor, social, and cognitive development [1]. Early treadmill intervention allows infants to practice bodyweight-supported stepping on a treadmill and has been shown to attain an early onset of walking. Joint kinematics is typically used to measure joint biomechanics when studying stepping pattern during the intervention and gait development after the intervention. Our previous study demonstrated that infants with DS who received either a high-intensity and a low-intensity treadmill intervention increased peak knee flexion, hip flexion, and hip extension within one year after the onset of independent walking [2].

The preliminary results reported here are part of a comprehensive, longitudinal study which assesses motor, cognitive, and language development in infants with DS who all receive an early treadmill intervention and one half for the "sticky mittens" training. For the treadmill stepping intervention, we expect that the infants will increase peak knee flexion, hip flexion, hip extension, knee angular velocity, and hip angular velocity over time. Additionally, we expect that the infants will increase step length and step frequency.

Methods: Three infant subjects (3 males), aged about 10 months, were recruited in this study when they were able to sit independently for 30 seconds. Parents were provided a mini treadmill at home and instructed to practice treadmill training for 8 minutes/day, 5 days /week, with a belt speed of 0.1 m/s. As step frequency increases to 10 steps/min, the parents increased the belt speed. Additional external ankle load will be added bilaterally above the ankles when the infant is able to produce consistent stepping at the belt speed of 0.2 m/s. The treadmill intervention will be terminated when the infant is able to walk three steps independently.

We visited the infant's home once a month to record their bodyweight-supported stepping on the treadmill. We recorded two 3-minute treadmill stepping bouts, one with four reflective markers and one markerless. The four reflective markers were placed on the infant's right hip, knee, ankle, and foot. One Noraxon ® Ninox-125 camera and an iPad were used to record treadmill stepping from the sagittal view of the infant's right side. Here we focused on the marker-based trials from the preliminary data collected at our second and four monthly visits. Noraxon ® MyoResearch 3 software was used to process the marker-based trials. A custom MATLAB ® program was used to calculate joint kinematics and step length and frequency. Hip joint angle was defined with respect to a vertical line. Knee joint angle was defined with full knee extension as 180 degrees. Mean and standard deviation of the variables was used to quantify the changes between visit 2 and visit 4 of each subject.

Results: Preliminary results revealed that all 3 subjects increased their step frequency between visit 2 and 4 (subject 1: 4.67 to 8 steps/min, subject 2: 1.33 to 3.33 steps/min, and subject 3: 5.67 to 20.33 steps/min). Subject 3, who presented with a larger increase in step frequency between visits, also increased peak knee flexion (mean±SD: 64.9±18.86 to 72.75±20.04 degrees), peak knee velocity (142.97±71.3 to 276.87±126.38 deg/s), peak hip velocity (155.01±58.41 to 162.12±53.89 deg/s), and step length (125.79±38.82 to 179.36±51.71 mm) from visit 2 to visit 4. In contrast, subjects 1 and 2 presented with reduction in these variables from visit 2 to visit 4 although they increased step frequency.

Discussion: The preliminary results showed the high variability of joint kinematics and spatiotemporal variables during the early phase of the treadmill training, as the infants began to learn the new stepping skills on a moveable belt. Previous studies have shown that infants with DS produce fewer steps and of multiple types early in the treadmill training, compared to typically developing infants [3]. The production of consistent alternating steps takes several months of practice and may be associated with other motor milestones such as pull to stand. Although subjects 1 and 2 had an increased step frequency at visit 4, they presented with reductions in kinematic and spatiotemporal variables. This suggests that infants with DS display different developmental trajectories even though the ultimate goal is to achieve alternating stepping and eventually walking independently. These preliminary results coincide with the developmental cascade framework. One limitation to this study is the use of 2D motion analysis to capture spatiotemporal and kinematic variables. Another limitation is a small sample size given the ongoing data collection. We are hopeful that our continued subject recruitment will help verify our preliminary findings.

Significance: The trajectory of joint kinematics during the treadmill training provides important information to enhance our understanding on the development of joint motion and coordination in infants with DS. This information is vital to help revise and adjust the intervention protocol to achieve the best training outcomes. This knowledge will provide further evidence that the home-based, body weight-supported treadmill intervention is essential for infants with DS to enhance their interaction with the environment and improve motor, social, and cognitive development.

Acknowledgements: We thank NIH (R21HD105879) for funding and all the participants and their parents for their participation.

References: [1] Angulo-Barroso et al. (2007), *Gait & Posture* 27; [2] Wu, et al. (2010), *Physical Therapy* 90(9); [3] Ulrich, et al. (2001) *Pediatrics* 108(5).

FROM SUBTLE TO SEVERE: MAPPING THE CONTINUUM OF SYMPTOM EXPRESSION IN ROTATOR CUFF TEARS WITH BIOMECHANICS

Sarah M. Barron[1*], Joseph J. King[2], Federico Pozzi[2,3], Jennifer A. Nichols[1,2]
[1]J. Crayton Pruitt Family Department of Biomedical Engineering, [2]Department of Orthopaedic Surgery & Sports Medicine, [3]Department of Physical Therapy, University of Florida
*Corresponding author's email: sgormley@ufl.edu

Introduction: Some individuals with rotator cuff tears (RCT) experience poor clinical outcomes, with symptoms persisting after conservative treatments and high failure rates for surgical repairs. Yet, other individuals with RCT do not experience any significant symptoms [1]. This suggests that compensatory mechanisms, such as muscle activation patterns and joint kinematics, play an important role in symptom expression. However, despite various research efforts [e.g., 1-3], to what extent biomechanical compensations influence symptom expression in RCT is not fully understood. For this study, we employed a variety of biomechanical methods, including electromyography (EMG) and motion capture, to comprehensively investigate the relationship between RCT symptom expression and temporal biomechanical data during a diverse range of tasks. We hypothesized that the data from individuals with RCT would show considerable heterogeneity, but also elucidate differences in symptom expression.

Methods: To date, this IRB-approved study includes 4 participants (3 male, 66.8 ± 7.1 years old) with RCT (full-thickness supraspinatus) and 13 controls (6 male, 67.4 ± 6.4 years old). Each participant completed the Shoulder Pain and Disability Index (SPADI) questionnaire to measure symptom expression. Participants then completed 4 range of motion (ROM) (flexion, abduction, scaption, 5-lb weighted scaption) and 5 functional (drink, axilla wash, hair comb, back pocket reach, seatbelt reach) tasks following a 0.75 Hz metronome, with five repetitions per trial and two trials per task. Motion-capture data were collected at 120 Hz using a marker-set with 31 markers on the trunk and arm, including a 3-marker cluster on the acromion for scapular tracking [4]. Muscle activations were collected at 3000 Hz from 12 locations [Surface EMG: anterior/middle/posterior deltoid (A./M./P. Del), upper/lower trapezius (UT/LT), serratus anterior (SA), pectoralis major (Pec), latissimus dorsi (Lat). Intramuscular EMG: supraspinatus (Sup), infraspinatus (Inf), teres minor (TM), subscapularis (Sub)]. Maximum voluntary contraction (MVC) tasks [5] were collected for signal normalization.

Joint angles were calculated in OpenSim (v4.4) using inverse kinematics and scaled versions of the thoracoscapular shoulder model, which can describe pathological scapular motion [6]. Shoulder joint angles were transformed to reflect net scapular and humeral rotations relative to the trunk. EMG data were filtered and EMG envelopes from each trial were normalized to peak activations from MVC tasks. Statistical parametric mapping ($\alpha = 0.05$) was performed in Python (spm1d package [7]) to compare humeral and scapular kinematics and muscle activations over time between the RCT and control groups. Mean normalized muscle activation for each participant near end ROM (25-50% task completion), where the largest activations tended to occur, was also calculated for each muscle and task.

Results & Discussion: Glenohumeral kinematics and muscle activations differed significantly between RCT and control participants in all tasks. Scapular differences were the most prominent, with considerable heterogeneity present across RCT participants (Fig. 1). To fully understand the heterogeneity observed and identify commonalities between participants with similar symptoms, more data are needed. However, examination of the individual RCT participants collected to date is illuminating. Notably, the participants with the lowest (21) and highest (47) SPADI scores (0 is no pain/disability) demonstrated contrasting compensations. During abduction, the higher-SPADI participant (Fig. 1, dashed orange) had decreased lateral winging near end ROM compared to controls (Fig. 1, blue), while the lower-SPADI participant (Fig. 1, dotted orange) had increased winging. Similarly, near end ROM of seatbelt reach, the higher-SPADI participant was within 1 standard deviation of controls, while the lower-SPADI was again higher. Activations of the scapular rotators during end range abduction (Fig. 2, rectangles) of each RCT participant were also unbalanced in ways that mapped onto the kinematics. For example, the lower-SPADI participant (Fig 2., dotted) had decreased LT activation compared to controls, while the higher-SPADI participant (Fig. 2, dashed) had increased LT and UT activation. Past studies have shown increases in Sup activation for RCT patients compared to controls [1], but this was only seen in the lower-SPADI participant and was coupled with large increases in Pec activation (Fig. 2, dotted). These results, in combination with the fact that the difference in SPADI score between the two highlighted participants represents a clinically important difference [8], suggest muscle activations and scapular kinematics align with RCT symptom expression.

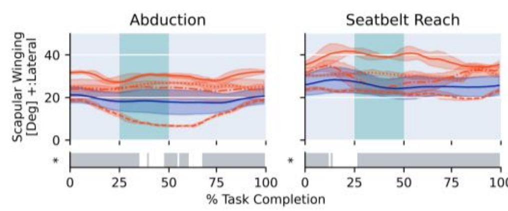

Figure 1: Scapular rotations for individual tear participants (orange) and control group (blue) during a selected ROM (left) and functional (right) task. Teal region represents where EMG averaging occurred.

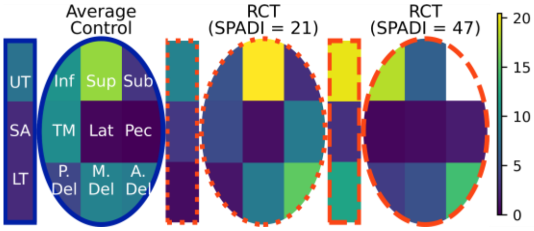

Figure 2: Muscle activations (scapular insertion: rectangle, humeral insertion: ellipse) near end abduction ROM for two tear (orange border) and all control (blue border) participants.

Significance: Viewing symptom expression as a dichotomous variable oversimplifies the complexity of RCT and the nuances of time-series biomechanical data can be lost in the process of averaging. Thus, this study highlights a need for personalized evaluation of individuals with RCT.

References: [1] Kelly et al. (2005) *J Shoulder Elbow Surg* 14(2); [2] Duc et al. (2014) *Physiol Meas* 35(12); [3] Alenabi et al. (2016) *Clin Biomech* 32; [4] Karduna et al. (2001) *J Biomech Eng* 123(2); [5] Boettcher et al. (2008) *J Orthop Res* 26(12); [6] Seth et al. (2016) *PloS One* 11(1); [7] Pataky (2010) *Comp Meth Biomech Biomed Eng* 15(3); [8] Roy et al. (2009) *AC&R* 61(5).

ACCURACY OF SKILL ACQUISITION DURING AN 8-WEEK GAIT INTERVENTION STUDY TO REDUCE KNEE JOINT LOAD IN PATIENTS WITH KNEE OSTEOARTHRITIS

Kelly Poretti*[1], Oladipo Eddo[1], Bryndan Lindsey[1] Nelson Cortes[2,3]
[1]Sports Medicine Assessment, Research & Testing Laboratory, George Mason University, Manassas VA
*Corresponding author's email: kporetti@gmu.edu

Introduction:
Knee osteoarthritis (KOA) is one of the most common causes of chronic disability [1]. Gait modifications have been used as a treatment intervention due to their ability to reduce knee load as well as pain and progression of KOA [2]. Although modifications have been proven to be effective in reducing knee loads, successful intervention requires both skill acquisition and retention [3]. Gait modifications are often learned through a 6–12-week training program offering real-time visual feedback to the patient [4,5,6], but recent literature has explored the use of real-time haptic feedback for training [5,6]. There is a lack of research on motor learning outcomes, such as accuracy and retention, of these delivery methods. Therefore, the purpose of this study was to explore the accuracy of trunk lean and foot progression gait modifications after an 8-week haptic feedback training period.

Table 1: Accuracy, residual angles, and time of pattern change over the 8-week training period. Accuracy is calculated as the percentage of steps within the prescribed range. The residual angle is calculated as the difference between the participant's executed angle and the prescribed angle. Time is defined as the time at which the accuracy during the 20-minute session becomes variable.

Session Number	Subject 1 – Trunk Lean			Subject 3 – Trunk Lean			Subject 2 – Foot Progression			Subject 4 – Foot Progression		
	Accuracy	Residual Angle	Time	Accuracy	Residual Angle	Time	Accuracy	Residual Angle	Time	Accuracy	Residual Angle	Time
2	89%	-3.311	5min	99%	-2.73	7min	80%	2.74	10min	79%	2.81	10min
3	95%	-4.43	7min	57%	-3.98	7min	77%	3.43	10min	89%	2.82	10min
4	100%	-3.15	8min	75%	-4.46	8min	98%	0.31	10min	87%	3.23	10min
5	85%	-3.91	10min	98%	-3.64	10min	86%	3.69	10min	93%	1.92	10min
6	73%	-3.77	10min	96%	-3.41	13min	74%	3.63	10min	94%	1.94	10min
7	82%	-4.22	10min	78%	-4.22	13min	54%	2.47	10min	97%	1.00	10min
8	97%	-2.85	7min	93%	-4.61	13min	42%	3.70	12min	97%	0.66	12min
9	91%	-3.81	7min	98%	-2.93	13min	65%	3.89	11min	96%	1.02	11min

Methods: Four participants with medial KOA volunteered for this study. Two participants completed a trunk lean gait modification (TLM), while the other two participants completed a foot progression gait modification (FPM). SageMotion inertial measurement units were used to provide haptic feedback as well as measure kinematic variables during each session (SageMotion MT USA). Participants completed 20 minutes of treadmill training once a week for a total of 8 weeks. Feedback was provided following a faded feedback design. A custom MATLAB code was used to calculate the accuracy for each step, which was defined as the difference between the participant's trunk lean angle or foot progression angle and the boundaries of the prescribed modification (TLM: +8° to +23°, FPM: -5° to -20°). A descriptive analysis was conducted to assess the accuracy of the prescribed modification over the course of the training period as well as between FPM and TLM.

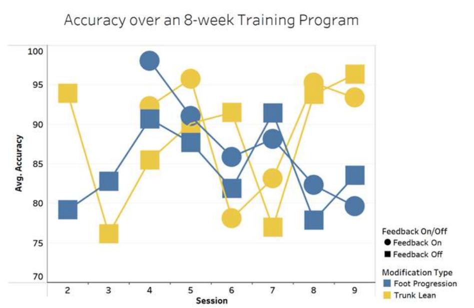

Figure 1: Average accuracy of modification execution over the course of the 8-week training period. Accuracy is calculated as the percentage of steps within the prescribed range.

Results & Discussion: In general, the accuracy of executing the prescribed modification showed no distinct patterns of change (Figure 1). Changes in accuracy showed patterns of improvement for one FPM participant but showed no change for the other FPM participant and were inconsistent for TLM participants (Table 1). Therefore, it is hypothesized that the acquisition of these motor skills is participant- and modification-dependent. Further investigation into the patterns of accuracy during each 20-minute training session revealed a general pattern of improvement during the first 10 minutes of the training session for FPM participants followed by an increased variability in accuracy for the remaining 10 minutes. For TLM participants, during each 20-minute training session, a pattern of decreased accuracy during the first 10 minutes of the training session was followed by an increase in randomness for the remaining 10 minutes of the training session. It is hypothesized that the length of the training period may result in fatigue that causes an increased variation in the participants' gait.

Significance: This study provides a preliminary analysis of the ability for KOA patients to acquire the necessary motor skills to implement this treatment outside of a laboratory setting. Based on this preliminary analysis, training programs for gait modification should be individualized to each participant and modified based on the gait modification used. Participants may need to modify training to their motor learning preferences such as the length of the training period, the delivery mode of the feedback they are receiving, and the type of feedback they are receiving so that they can obtain the best outcomes from this treatment method.

Acknowledgements: This work was supported in part by the NSF grant DGE: 1922598.

References: [1] Richards et al. (2017), *Arch of Phys Med and Rehab* 98(1); [2] Hunt et al. (2011), *J Biomech* 44(5); [3] Charlton et al. (2020), *Phys Ther* 101(2); [4] Eddo et al. (2017), *Int J of Kines and Sports Science* 5(3); [5] Shull et al. (2011), *J Biomech* 44(8); [6] Lindsey (2021), *J Biomech Eng* 143(4)

OBSTACLE CROSSING IN HEALTHY YOUNG AND OLDER INDIVIDUALS

Hope M. Hanson[1], Ashlyn M. Jendro[1], Tiphanie E. Raffegeau[2], Abigail C. Schmitt[1]
[1]University of Arkansas, [2]George Mason University
email: acs063@uark.edu

Introduction: In the United States, the average population age is rising and will continue to increase in the coming years.[1] With an increasing population of older individuals comes greater risk of fall-related injuries associated with activities of daily living. Falls are considered a leading cause of injury and death in older individuals, and the majority of falls are caused by body imbalance or obstacle collision due to a clearly visible stationary object (e.g., rug, chair, branch).[3,4,5] The aging process leads to worse balance and coordination and decreased stumble recovery ability.[2] Older adults tend to cross obstacles with increased toe clearance in order to prevent tripping and remain safe during obstacle crossing, suggesting they may see the obstacle as a greater challenge compared to healthy young individuals.[2]

Much of what is known about obstacle crossing in older adults is limited to artificial obstacles that are unique to the laboratory. Currently, there is little data available about how older adults cross the varied types of obstacles that are likely encountered in the real world. Thus, the purpose of this study was to compare measures of obstacle clearance between young and older adults for two different obstacles: a dowel and a branch.

Methods: Nine (4 men, 5 women) healthy, older adults (69±4 yrs, 1.68±1.04 m, 77.1±22.0 kg) and nine gender-matched healthy, young adults (23±3 yrs, 1.68±0.11 m, 72.9±17.7 kg) completed a series of obstructed walking trials in the laboratory while barefoot. 3D motion capture was used to track participants wearing the Plug-in-Gait Full-body marker set (Vicon Motion Systems, bottom panels, Fig.1).

Each participant completed ten trials of walking for each obstacle along an 8-meter walkway. Obstacle order was randomized. Participants were instructed to "*walk at a comfortable pace, stepping over the obstacle along the way*". The obstacles included a branch (max crossing height: 160 mm), and a dowel rod, the traditional obstacle in laboratory studies (crossing height: 150 mm) (Fig. 1).

Toe clearance was measured to assess crossing strategies. Vertical toe clearance of the leading and trailing limbs was measured directly above each obstacle, from the toe marker to the marker placed on each obstacle. Approach distance was measured as the horizontal distance between the toe marker of the trailing limb and the obstacle when the leading limb was crossing over the obstacle. Landing distance was measured as the horizontal distance between the heel of the leading foot and the obstacle when the trailing limb was crossing over the obstacle.

Results & Discussion: Older individuals crossed both the branch and the dowel with increased margins of safety when compared to younger adults, evidenced by higher toe clearances for both the lead ($p= .008$) and trail ($p= .001$) limbs. The older adults also exhibited smaller leading limb landing distances than the younger adults ($p= .040$).

Regardless of age, participants crossed the dowel with more toe clearance than the branch, on both the lead and trail limbs ($p= .003$, $p= .047$, respectively). Suggesting that, based on the toe clearances, the branch appears to be a less threatening obstacle to avoid than the dowel.

These results are consistent with previous literature showing that older individuals increase foot clearance in both the leading and trailing limbs to prevent tripping, supporting the idea that the obstacle is perceived as a greater risk by older individuals. The smaller landing distance indicates a shorter step which suggests a strategy to increase stability during obstacle crossing.

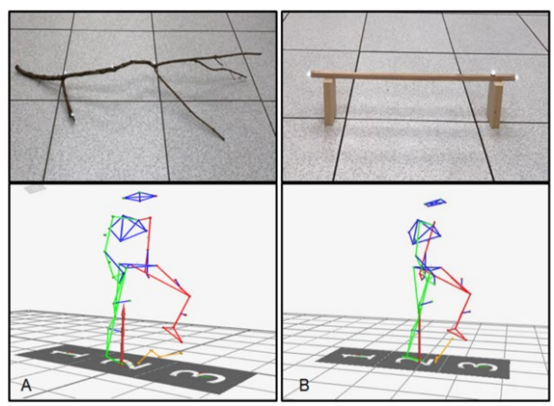

Figure 1: Branch (A) and dowel (B) obstacles. Bottom panels show the participant and obstacle marker sets.

Significance: These results better our understanding of how obstacle crossing changes with age and support the notion that balance is a priority during safe obstacle crossings. Further, this information could help inform fall prevention strategies during obstacle crossing in real-world situations.

Acknowledgments: Funding provided by a University of Arkansas Honors College Research Grant.

References: [1] Medina et al., 2020. *US Census.* 25-1145. [2] Lu et al., 2006. *Gait Posture.* 23(4):471-479. [3] Hahn & Chou, 2004. *J Biomech*. 37(6):837-844. [4] Overstall et al., 1977. *Br Med J.* 1(6056):261-264. [5] Tismina et al., 2017. *PLOS ONE*. 12(5).

Table 1: Mean ± SD of measures of obstacle crossing in mm.

		Approach Distance (TL)	Landing Distance (LL)	Lead Toe Clearance	Trail Toe Clearance
Older Adults	Branch	270 ± 58	232 ± 60	156 ± 29 +	200 ± 53 +
	Dowel	270 ± 58	210 ± 58	193 ± 41 +	242 ± 53 +
	Combined	270 ± 56	221 ± 59 *	175 ± 39 *	221 ± 56 *
Younger Adults	Branch	268 ± 52	264 ± 57	129 ± 18 +	151 ± 46 +
	Dowel	281 ± 49	258 ± 49	160 ± 36 +	175 ± 36 +
	Combined	274 ± 49	261 ± 52 *	144 ± 32 *	163 ± 42 *

* Indicates a significant main effect of group, + Indicates a significant main effect of obstacle

What can jumping tasks teach about long-term compensations in joint power after an ACL reconstruction?

Tereza Janatova[1]*, Kelsey Reeves[1], and Brian Noehren[1]
[1]Department of Physical Therapy, University of Kentucky, Lexington, KY
*Corresponding author's email: t.janatova@uky.edu

Introduction: Significant effort has focused on restoring functional abilities during recovery following an anterior cruciate ligament (ACL) reconstruction. However, it is unclear whether deficits remain long-term for more strenuous activities such as jumping. Deficits could be either due to a lack of ability to generate sufficient power or other psychological factors, such as a learned behavior or a fear-avoidance pattern. One way to test this is to evaluate the ability to generate knee joint power in both the injured and non-injured limbs during a single-leg jumping task in comparison to a double-leg task. Comparing symmetry between tasks would provide insight into the contribution of the ability to generate power (unilateral limb symmetry comparison) to a learned or fear-avoidant trait response (bilateral limb symmetry comparison). Thus, the purpose of this study was to evaluate the limb symmetry differences for power generation between bilateral and unilateral jumping long-term post-ACL reconstruction. We hypothesized that there would be significant differences in knee joint power in the bilateral but not the unilateral task. As a secondary analysis to better understand the factors directly affecting power generation during jumping tasks, we examined whether knee extension moment and knee flexion excursion angle were significantly different in each task.

Methods: Nineteen individuals (13 females, age 25.1 ± 7.3, height 1.71 ± 0.09 m, weight 76.4 ± 14.0 kg, BMI 26.1 ± 3.8 kg/m^2) 6.5 ± 3.6 years after ACL reconstruction completed a one-time visit to assess jumping biomechanics.

Sagittal plane knee joint kinematics, kinetics, and vertical ground reaction force (vGRF) were collected using a 13-camera motion capture system (Motion Analysis Corp, CA) and 2 force plates (Bertec Corp., OH). Following standard laboratory setup, fifty-two reflective markers were placed on the trunk and lower extremities (27 on anatomical landmarks and 25 tracking markers). All participants performed a static standing calibration and a dynamic hip trial to determine the hip joint center, followed by two jumping tasks. Each participant completed four double-leg countermovement jump (DL CMJ) trials with one foot on each force plate, and four trials of single-leg countermovement jump (SL CMJ) trials on each limb, starting with the uninvolved limb. Participants were instructed to jump as high as possible while still maintaining a stable landing.

Kinematic and kinetic data were collected at 200 Hz and 2000 Hz, respectively. All data were filtered using a 4th order Butterworth low-pass filter with a cutoff frequency of 8 Hz for kinematic data, and 35 Hz for kinetic data. Knee extension moment, knee flexion excursion angle, and knee joint power during the concentric phase of each jump were computed in Visual 3D, averaged across all four trials for each task, and extracted using a custom MATLAB code for each participant (MATLAB R2022a, MathWorks, Inc., MA). Knee joint excursion angle was calculated as peak knee flexion angle minus knee flexion angle at take-off. Knee extension moment and knee joint power were normalized to participants' body weight. The limb symmetry index (LSI) was determined by dividing the value for the involved limb by the uninvolved limb for each of the listed variables, and reported as a percent value. All variables for the involved vs. uninvolved limb were compared using a paired t-test, with the significance set at 0.05.

Results & Discussion: Average values for knee joint power, knee extension moment, and knee flexion excursion angle during the concentric phase for both SL CMJ and DL CMJ are reported in Table 1. We found a significant difference in knee joint power ($p<0.001$) during DL CMJ but not during SL CMJ ($p=0.200$). When evaluating the component parts of knee joint power during DL CMJ, significant differences between limbs were noted for knee extension moment ($p=0.012$) but not for knee flexion excursion ($p=0.190$). There were no significant differences for any variable between limbs during SL CMJ.

The results show that individuals post-ACL reconstruction are capable of equal knee joint power production at long-term follow-up visits. However, the significant reduction in knee joint power in the involved limb during bilateral jumping suggests that they prefer to underutilize their injured limb when the task allows. These findings indicate that the deficits in bilateral jumping are likely not due to a lack of ability but rather a learned behavior or a fear-avoidant compensation. When we further evaluated the factors that affect knee joint power generation, we discovered that knee flexion excursion angles are nearly identical. However, knee extension moment during the bilateral jump showed significantly lower values in the involved joint, indicating that they did not change the movement pattern but rather utilized the quadriceps less. Potentially, neuromuscular reeducation interventions to better maximize the capabilities of the involved limb during bilateral tasks could be developed to help maximize long-term outcomes.

Table 1. Jumping mechanics during the concentric phase (Mean ± SD)

Variable	Single-Leg Counter Movement Jump				Double-Leg Counter Movement Jump			
	INV	**NON**	**LSI %**	***p* value**	**INV**	**NON**	**LSI %**	***p* value**
Knee Joint Power (W/kg)	4.1 ± 1.3	4.3 ± 1.3	96.6	0.200	4.0 ± 1.2	4.7 ± 1.3	86.8	**<0.001***
Knee Extension Moment (Nm/kg)	0. 92 ± 0.23	0.92 ± 0.22	100.3	0.835	0.66 ± 0.17	0.74 ± 0.15	90.8	**0.012***
Knee Flexion Excursion (Deg)	69 ± 8	71 ± 9	98.4	0.219	86 ± 11	87 ± 11	98.4	0.190

Note: * indicates significance at $p < 0.05$

Significance: Findings from the unilateral task show that the capacity to generate concentric power at the knee joint is restored long-term. However, individuals choose to favor the non-injured limb during bilateral tasks. These results suggest that targeted neuromuscular movement strategies may be needed more than improving muscle power to fully restore jumping mechanics long-term.

References: [1] Gardinier et al. (2012), *J Orthopaedic Research* 31(3); [2] Slater et al. (2017), *J Athl Training* 52(9).

Load Symmetry During Gait following Total Knee Arthroplasty Compared to Controls

Jorjie Wilson[1*], Kelli Allen[2], Sara Arena[1], Robin Queen[1]
[1]Department of Biomedical Engineering and Mechanics Virginia Tech, Blacksburg, VA, USA
[2]Department of Medicine, University of North Carolina, Chapel Hill, NC, USA
Email: jorjiemw@vt.edu

Introduction: Total knee arthroplasty (TKA) is one of the most common surgical procedures performed in the U.S. with rates rising rapidly. The demand for this surgery is expected to rise to 3.48 million by 2030 [1]. TKA surgery results in decreased pain, increased range of motion, and improvements in physical function for many patients. However, it has been reported that some patients suffer from persistent functional deficits and gait asymmetry following TKA surgery. Patients continue to load their non-surgical leg more heavily during walking, even when the post-surgical leg is pain free [2]. This places the contralateral limb at risk for developing osteoarthritis, with approximately 40% of patients with unilateral TKA needing TKA on the contralateral side within 10 years [3,4]. Assessing asymmetries is beneficial when assessing lower limb injury risk and functional deficits following surgery. However, there is a gap in knowledge regarding how gait asymmetry post-TKA compares to healthy older adults. Therefore, the objective of this study was to examine load symmetry during self-selected speed walking captured in a clinic-like setting in healthy older adults (HC) and patients post-TKA. Identifying lingering deficits can improve post-TKA outcomes through better rehabilitation processes that directly address these underlying asymmetries. It is hypothesized that patients post-TKA will exhibit greater asymmetry during gait when compared to HC participants.

Methods: A sample of 98 participants were used for this study (49 TKA, 49 healthy controls). TKA patients who were 12 weeks post-surgery and approaching the end of their physical therapy visits were recruited and tested at UNC-Chapel Hill, while control participants were recruited and tested at Virginia Tech. All data was collected under an approved Institutional Review Board protocol and all participants signed informed consent. All participants were instructed to complete three 10-meter walking trials at a self-selected speed. Participants had loadsol® sensors (novel® USA, St. Paul, MN) placed bilaterally to collect plantar loads at 200 Hz. Data were analyzed using the Load Analysis Program (LAP), a custom-built MATLAB user interface that identifies individual steps [5]. Ten consecutive steps from each trial were used to calculate the outcome measures of interest. The Normalized Symmetry Index (NSI) was calculated for peak weight acceptance force, peak propulsive force, stance time, and impulse. The NSI is a bounded index where a NSI value of ±100% expresses the maximum level of asymmetry, with a positive value indicating the non-surgical limb metric was larger, and a NSI value of 0 indicates perfect symmetry [6]. The NSI was calculated for each trial and averaged across trials for each participant. An independent t-test was used to compare participant demographics between TKA and HC groups. A mixed effects model including average walking speed as a factor was used to compare NSI values between the two groups. All statistical analyses were conducted in JMP (SAS Institute Inc., Cary, NC) with $p<0.05$.

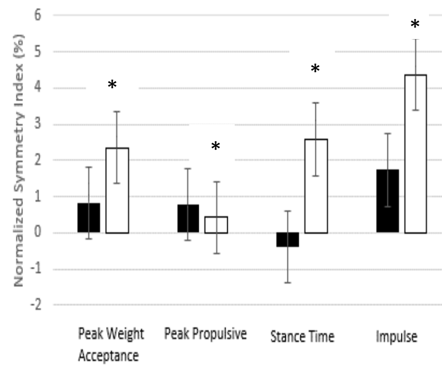

Figure 1: NSI values for HC (black) and TKA (white) for the following measures: Peak Weight Acceptance Force, Peak Propulsive Force, Stance Time, Impulse. (*indicates significantly different)

Results & Discussion: The age (HC: 63.3±8.4yrs, TKA: 66.2±6.9yrs; $p>0.05$) and height (HC: 1.7±0.1m, TKA: 1.7±0.1m; $p>0.05$) were similar between groups. However, weight was greater (HC: 75.7±20.1kg, TKA: 86.4±17.6kg; $p=0.006$) and average walking speed was lower (HC: 1.4±0.2m/s, TKA: 0.8±0.2m/s; $p<0.001$) in the TKA group. The NSI for peak weight acceptance force ($p = 0.005$), peak propulsive force ($p=0.025$), stance time ($p=0.004$), and impulse ($p<0.001$) were higher in TKA patients (Figure 1). These results show that load asymmetry during gait persists in TKA patients 12 weeks post-surgery in data that were collected in a clinic-like setting. These results support the hypothesis demonstrating persistent gait asymmetries in TKA patients. Overall, these results agree with literature that suggests that asymmetrical gait patterns in this population may be due to compensatory patterns that are implemented to reduce heavily loading the surgical limb.

Significance: Due to the gait deficits following TKA surgery, it is essential for clinicians and researchers to develop a novel approach to improve post-surgical outcomes. This study has implications for post-surgical physical therapy evaluation and treatment to help patients begin to develop more symmetrical loading as they increase their physical activity. One possible intervention could include the use of the loadsol® to retrain load symmetry during gait in patients following TKA. This research also creates a baseline comparison for future work to further investigate asymmetry measures between these two groups during walking and other tasks.

Acknowledgements: Support for this study was provided by grants from the National Institutes of Health: **1R21AR074149.** The data collection was completed with the help of Theresa Libera, Kimberlea Grimm and Katie Huffman

References: [1] Feng et al. (2018), *J Multidiscip Healthc.* 11; [2] Milner (2008), *Gait & Posture* 28(1); [3] McMahon (2003), *J Rheumatol.*30(8);[4] Ritter(1997),*J Arthroplasty*12(3);[5] Luftglass et al(2021), *Clin Biomech* 88;[6] Queen et al.(2020), *J Biomech 99*

SELF-SELECTED HANDRAIL USE REDUCES COMPLEXITY OF LOWER LIMB JOINT MOVEMENTS DURING TREADMILL GAIT IN CHRONIC STROKE SURVIVORS

Emily A. Steffensen,[1] Joel H. Sommerfeld,[1,2] Aaron D. Likens,[1,2] & Brian A. Knarr[1]
[1]Department of Biomechanics, University of Nebraska at Omaha, Omaha, NE;
[2]Nonlinear Analysis Core, Center for Human Movement Variability, Omaha, NE
email: easteffensen@unomaha.edu

Introduction: Stroke is a leading cause of adult long-term disability and survivors often have significant gait impairments[1]. Stroke survivors also often present with altered weight distributions and greater postural sway[2]. These presentations result in gait asymmetries that affect balance, and physical therapists often implement handrail use when conducting treadmill training paradigms[3]. Some evidence has demonstrated that stroke survivors have more normalized step parameters and reduced energy cost of walking on the treadmill while using the handrail with self-selected support rather than light-touch support [3,4]. Despite this, in terms of variability, the paretic side limb has been shown to have greater divergence at the joint-level than the non-paretic side during post-stroke treadmill walking, which is associated with reduced mechanical stability [5]. However, the effects of handrail support on lower limb joint movement variability during post-stroke treadmill walking have not been investigated. Therefore, the purpose of the study was to investigate the effects of handrail use during treadmill walking in individuals post-stroke on lower limb joint dynamics using recurrent quantification analysis (RQA). We hypothesized that complexity in the lower limb joint movements would decrease with increased handrail use during ambulation on a treadmill due to increased constraints imparted on the system.

Methods: 26 adults with chronic stroke walked at their self-selected walking speed on a steady state, instrumented treadmill for three minutes for each of the three conditions: walking without handrails (NoHR), walking with handrails at less than 5% body weight support (5%HR), and walking with handrails with self-selected support (SSHR). Handrails were used with the participants' less affected arm. During the 5%HR condition, visual biofeedback of force application on the handrail was utilized. If participants were unable to walk on the treadmill without handrails, the no-handrail condition was excluded. Full kinematic data were collected. Specifically, bilateral hip flexion and extension, hip adduction and abduction, knee flexion and extension, and ankle dorsiflexion and plantarflexion were extracted. RQA was conducted on the lower limb joint angles to determine the recurrence to regions in state space reconstructed from joint range of motion over time. Mean line length (MeanL), which represents the average bout of recurrent trajectories, was the primary outcome variable. Effect sizes are described by conventional standards.

Results & Discussion: In each of the joints and planes examined, handrail use significantly affected the MeanL of the ranges of motion (Table 1, Fig. 1). In flexion and extension of the hip, SSHR produced higher MeanL than did NoHR and 5%HR, with a moderate to large effect and moderate effect, respectively. The difference between NoHR and 5%HR, however, was not significantly different. Similarly, in hip adduction and abduction, SSHR produced higher MeanL than did NoHR and 5%HR, with a moderate to large effect and moderate effects, respectively. However, the difference between NoHR and 5%HR was not significantly different and had only a small to moderate effect. In knee flexion and extension, SSHR produced higher MeanL than did NoHR with a moderate effect. However, the differences between SSHR and 5%HR and NoHR and 5%HR were both non-significant and had small effects. In ankle plantarflexion and dorsiflexion, the difference between SSHR and 5%HR was non-significant with a small effect. However, SSHR and 5%HR both produced significantly higher MeanLs than NoHR, with moderate to large and small to moderate effects, respectively. Overall, SSHR use significantly reduces the complexity of motion in lower limb joints, especially compared to NoHR use, supporting our hypothesis. It is possible that greater reliance on the handrail during SSHR, compared to 5%HR or NoHR, could be inducing greater constraints on the system, resulting in reduced complexity of the lower limb joint angles.

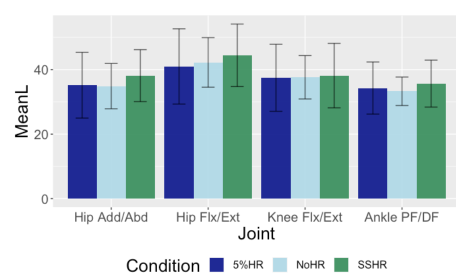

Figure 1: MeanL of each joint and plane of interest, by condition.

	Hip Flexion/Extension		Hip Adduction/Abduction		Knee Flexion/Extension		Ankle Plantarflexion/Dorsiflexion	
SSHR	44.7 ± 1.89		38.3 ± 1.54		38.8 ± 1.72		35.9 ± 1.24	
5%HR	41.0 ± 1.88		35.2 ± 1.53		37.5 ± 1.71		34.3 ± 1.23	
NoHR	38.5 ± 2		32.5 ± 1.67		34.9 ± 1.82		31.6 ± 1.34	
	P-value	Effect Size	P-value	Effect Size	P-value	Effect Size	P-value	Effect Size
SSHR-5%HR	**0.0110**	0.36	**0.0275**	0.36	0.6286	0.11	0.2029	0.23
SSHR-NoHR	**0.0010**	0.61	**0.0001**	0.67	**0.0170**	0.39	**0.0003**	0.61
5%HR-NoHR	0.1943	0.24	0.1205	0.31	0.1115	0.28	**0.0295**	0.39

Table 1: Summarized results of MeanL at each joint and plane of interest per handrail condition, and differences between handrail conditions. $P < 0.05$ was considered significant. Values that exceeded significance are indicated in bold.

Significance: Self-selected handrail use generally reduces complexity of motion in the lower limb joints compared to light touch or no handrail use, which may have implications for the transferability of treadmill training paradigms to overground gait stability in stroke survivors. These results may suggest that handrail use during treadmill training in post-stroke populations should be prescribed strategically according to rehabilitation goals.

References: [1] C.M. Cirstea, *Stroke*. (2020) 2892–2894. [2] S.F. Tyson, et. al, *Phys Ther.* **86** (2006) 30–38. [3] T. Ijmker, et. al, *J Neuroeng Rehabil*. **12** (2015). [4] T. Ijmker, et al., *Arch Phys Med Rehabil*. **94** (2013) 2255–2261. [5] K. Kempski, et. al, *J Biomech*. **68** (2018) 1–5.

The reliability of an IMU-based motion capture system for dynamic margins of stability and ranges of total body angular momentum: effects of walkway length and number of strides

Jackson Lordall[1*], Atabak Mehrabani[2], Sunny Bui[1], Alison R. Oates[1], Joel L. Lanovaz[1,2]
[1]College of Kinesiology, [2]Division of Biomedical Engineering, University of Saskatchewan, SK, CA
*Corresponding author email: Jackson.Lordall@usask.ca

Introduction: Multi-sensor inertial measurement unit- (IMU) based motion capture systems enable recording of 3D whole body kinematics outside of lab environments. Ranges of total body angular momentum (H) reflect control over angular motion about the center of mass (COM) [1]. Margins of stability (MOS) describe the motion state of the COM relative to the base of support edges [2]. The reliability of IMU-based motion capture systems for ranges of H and average MOS during walking have not been established. A recent systematic review and meta-analysis [3] suggested that including more steady state strides in an analysis may improve reliability outcomes. Since the number of steady-state strides captured per trial may differ between experimental set-ups due to different walkway lengths, this study investigated the influence of walkway length and number of steady state strides captured on the test-retest reliability of an IMU-based motion capture system for estimating ranges of H and average MOS during overground walking.

Methods: Young adults completed two study visits (>48 hours apart) consisting of 10 walking trials in a lab (walkway length: 8m) and a hallway (walkway length: 20m) (40 trials total over both visits). Participants wore a full-body 17 sensor IMU-based kinematic data collection system (Xsens Awinda, Enschede, NL, fs=60Hz). The ranges of anterior-posterior (AP) and medial-lateral (ML) H over a stride were computed with a 16-segment model [4] and normalized to height, walking speed, and mass [5,6]**.** Average ML MOS over a stride was computed based on Hof et al. [2]. Relative reliability was assessed using intraclass correlations (ICC) (3, k) [7]. ICC values were interpreted as poor (<0.5), moderate (0.5-0.75), good (0.75-0.9), and excellent (>0.9) [8]. Absolute reliability was assessed using minimal detectable change at a 95% confidence level (MDC95) expressed as a percentage of the mean [9]. Mean H and MOS were calculated using consecutive strides at incremental increases in the number of strides (maximum strides: lab 20; hall 50). ICC and MDC95 values were calculated at each stride count.

Results & Discussion: 28 young adults (12 male, 16 female, age=24±4yrs, height=171±9.5cm, mass=76±21kg) participated with an average of 4±2 days between data collections. For most participants, two to three and five to eight steady state strides per trial were captured in the lab and hallway respectively.

The ICCs indicated good to excellent reliability for normalized H ML ranges and moderate to excellent reliability for normalized H AP ranges in the lab and hallway and moderate to excellent reliability for average ML MOS in the hallway (Fig. 1). The hallway and lab had similar ICCs for normalized H ranges after 10 strides were completed (4-5 trials in the lab, 2 trials in the hallway) (Fig. 1). The ICCs indicated better reliability for average ML MOS in the lab compared to the hallway which may be related to the number of strides captured per trial and, potentially, variability in walking over longer distances. The ICC for average ML MOS in the hallway reduced as more strides were added to the analysis. ICCs may be reduced due to low between-subject variability [9] caused by normalizing the ranges of H AP and the chosen study population for average MOS ML. Low between-subject variability may also explain the reduction in ICCs for average MOS ML in the hallway compared to the lab. Future work could look at the ICCs for these variables in populations with more between-subject variability and with non-normalized data.

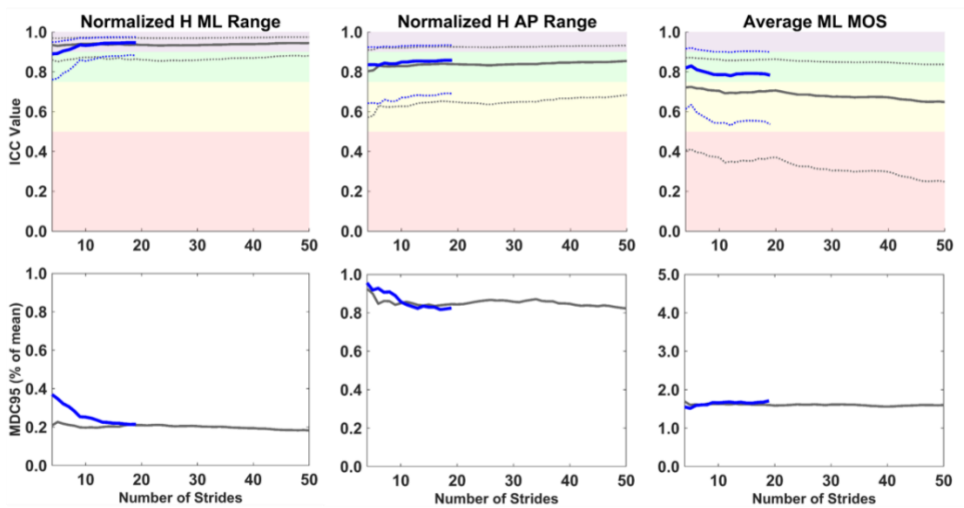

Figure 1: ICC (± 95%CI) (upper) and MDC95% (lower) for outcomes at each stride captured in the lab (blue) and the hallway (grey). ICC shading: >0.9 (purple), 0.75-0.9 (green), 0.5-0.75 (yellow), <0.5 (red).

The MDC95 values were less than 2% of the mean values for normalized ranges of H and average MOS ML and were not largely affected by the number of strides included in the analysis or walkway length (Fig. 1). These results suggest that an IMU-based motion capture is a reliable instrument for walking balance research. The concurrent validity of an IMU-based motion capture system for measures of COM control during walking needs to be established and is the subject of further work in our lab.

Significance: These results are encouraging for walking balance research involving repeated measurements and different walkway lengths outside of lab environments.

References: [1] Begue et al. (2019), *Exp Gerontol* 127; [2] Hof et al. (2005), *J Biomech* 38(1); [3] Kobsar et al. (2020), *JNER* 17; [4] De Leva (1996), *J Biomech* 29; [5] Herr et al. (2008), *J Exp Biol* 211; [6] Bennet et al. (2020), *Hum Mov Sci* 29; [7] McGraw & Wong (1996), *Psycholog Methods* 1(1); [8] Shrout & Fleiss (1979), *Psychol Bull* 86(2); [9] Weir (2005), *J Strength Cond Res* 19(1).

Neck muscle fatigue from experienced soldiers wearing head-borne systems

Theresa D. Hardin[1], Marina G. Carboni[1], John W. Ramsay[1], and Clifford L. Hancock[1]
[1]U.S. Army DEVCOM Soldier Center, Natick, MA, USA
Email: theresa.d.hardin.civ@army.mil

Introduction: Soldiers wear heavy head-borne systems for extended periods of time to support mission requirements. The effects of neck and shoulder muscle fatigue have been studied primarily in aviation pilots [1,2] who experience greater accelerations than a dismounted soldier. However, little research has been performed to understand the impact of head-borne systems on dismounted soldiers where weight often exceed the 2.5kg recommended limit for aviation pilots. In this study, the effects of head-borne load configurations on neck and shoulder muscle activation while performing a prone static marksmanship task were investigated using surface electromyography (sEMG). Head-borne load configurations varied in total mass and mass distribution (forward or rear offset from the midline). We hypothesized that neck muscle fatigue would increase, as demonstrated by a decreased median sEMG frequency, over the 3-hour data collection. Furthermore, it was expected that the subjects would become more fatigued from heavier helmets and helmets with a center of mass further from the midline resulting in greater sEMG power spectrum shifts compared to the lighter head-borne systems and midline-aligned systems. The data reported are preliminary results from an ongoing study.

Methods: Eleven experienced soldiers, defined as those who have been deployed at least once, performed dismounted soldiering tasks while wearing five different weighted head-borne load configurations. The soldiering tasks consisted of static and dynamic marksmanship and a portion of the sprint-drag-carry (SDC) from the Army Combat Fitness Test (ACFT), performed before and after a 1-hour walk on a treadmill at 60% of their Froude velocity [3]. The static marksmanship task was selected because it is an isometric activity that soldiers perform frequently and isolates the neck muscles due to the soldier's prone position. The task required the soldier to take 5 shots at their own pace while focusing on maximizing shooting accuracy. The 5 shots were repeated in succession for 5 trials totaling 25 shots. The participant repeated the entire soldiering task 5 times over the course of 5 days, wearing a different head-borne configuration each session and having at least one day of rest between each session. The 5 different load configurations were: 1) LMRO, low-mass (1.5kg) rear-offset (-2cm), 2) MMFO, mid-mass (2.5kg) forward-offset (3.5cm), 3) MMM, mid-mass (2.5kg) midline (0cm), 4) HMM, high-mass (3kg) midline (0cm), and 5) HMFO, high-mass (3kg) forward-offset (3cm). Offsets were relative to the subject's tragion notch. During each session, sEMG was collected at 2000 Hz (Trigno Quattro Sensor, Delsys, Natick MA) on the sternocleidomastoid (sterno), splenius capitis (scap), semispinalis (semi), and upper trapezius (trap). sEMG signals from the static marksmanship task were post-processed with custom MATLAB scripts (MathWorks, Natick MA) using the following method: 1) discard data where EMG signal had frequent clipping, 2) detrend by removing the DC offset, 3) bandpass between 6 and 500 Hz using a 2nd-order Butterworth filter, 4) use the acceleration measurement from the sEMG to identify when shots were being taken and remove data where the subject was firing the weapon, 6) average the median frequencies across pre- and post-walk trials for a given session, 7) execute a 2-factor repeated-measures ANOVA ($p<0.05$) to test the main effects of time (pre-walk vs post-walk) and load condition (LMRO, MMFO, MMM, HMM, and HMFO).

Results & Discussion*:* Decrease in median frequency of the power spectrum of sEMG signals is associated with increased muscle fatigue during isometric contractions. Median frequency was used as opposed to mean frequency because it is less influenced by random noise and more sensitive to fatigue [4]. The median frequency from the static marksmanship task post-walk was significantly lower than pre-walk for both the sterno ($p=0.049$) and the scap ($p<0.001$), as shown in Table 1. The shift to lower frequencies within the power spectrum indicate that the muscles fatigued as a result of the soldiering tasks while wearing the head-borne loads. No significant differences were found in median frequency in the trap and data was discarded for the semi due to sensor error. To acquire the target and take shots during the prone static marksmanship task, the soldiers laterally flexed and extended their neck and braced the weapon against their shoulder while aiming down the sights. The sterno contributes to neck flexion and helps obliquely rotate the head, and the scap laterally flexes and rotates the neck. Although the trap does contribute to neck extension, the data suggested that it did not fatigue as much as the sterno and the scap. The trap is a larger muscle whereas the sterno and scap are smaller muscles and are therefore likely more subject to fatigue. It is expected that the semi will have a lower median frequency post-walk, but additional data will need to be collected to increase our sample size. Furthermore, there were no significant differences in median frequency between head-borne configurations. Test subjects were soldiers experienced in wearing heavy load conditions which could be a significant factor in why no differences were found between configurations.

Table 1: Median Frequency Descriptive Statistics Pre- and Post-Walk*

Muscle	Time	Mean	Std. Dev
Sternocleidomastoid	Pre	87.8	1.3
	Post	74.0	6.5
Splenius Capitis	Pre	88.8	1.6
	Post	68.6	3.1

*Only statistically sig. differences are shown

Significance: Regardless of helmet load configuration, participant neck muscles fatigued between pre- and post-walk marksmanship tasks as evidenced by the shifts in the power spectrum of the sEMG signals. However, no differences in muscle fatigue between helmet load configurations were found. Ultimately, with a greater sample size to improve statistical power, this data will help inform our knowledge of neck muscle fatigue for dismounted soldiers wearing head-borne systems so that standards for sustainable loads can be established. Future areas of research include whether various head-borne loads and distributions affect marksmanship scores and whether level of experience wearing load and/or neck strength correlates with median frequency outcomes and marksmanship performance.

References: [1] Albery, C.B. et al. (2008), Tech. Rep. AFRL-RH-WP-TR-2008-0096; [2] Thuresson, M. et al. (2003). Aviation, Space, and Envr. Med., 74(5), 527-532; [3] England, SA. Et al. 2007 February; 25(2): 172–178 [4] Stulen, FB et al. (1981) IEEE Trans Biomed Eng. 28(7):515-23.

A FORCE-PLATE INSTRUMENTED PUSH-AND-RELEASE TEST CAN ESTIMATE KEY KINEMATIC OUTCOMES

Michael Christensen[1], James Tracy[2], and Jeremy Crenshaw[1*]
[1]University of Delaware; [2]University of Colorado Anschutz Medical Campus
email: [*]crenshaw@udel.edu

Introduction: Reactive balance, or the body's rapid reaction to maintain stability after a perturbation, is a specific domain of postural control that is related to the risk of falling [1]. Currently, there exists a dichotomy in tests of reactive balance: research versus clinical settings. Tests conducted in research settings, such as Stepping Thresholds [2], are precise, repeatable, and allow for analyses of the underlying mechanisms of impaired reactions. These tests, however, have limited feasibility outside of well-equipped laboratories. Clinical tests of reactive balance are low-cost and efficient, but do so with less precision, repeatability, and mechanistic insight [3]. One such test is the Push-and-Release Test (PRT) which broadly categorizes performance based on the number of steps need to recover [4].

We propose adding basic force-plate instrumentation to the PRT. Force-plates are commonly found in laboratories and potentially feasible for clinical spaces, as they require minimal space and set-up. We aim to validate a force-plate-instrumented PRT as a means to precisely assess reactive balance, quantifying the relationship between key kinematic outcomes and force-plate-derived variables.

Methods: Ten unimpaired participants (4M/6F, mean (SD) Age: 25.4 (3.6) years; BMI: 21.9 (2.1) kg/m^2) were administered six to eight trials of the instrumented PRT in the anterior, left, right, and posterior directions on two force plates (1200 Hz; Figure 1). Three-dimensional motion capture data (120 Hz) was also recorded to estimate ankle-joint center (AJC) and whole-body center of mass (COM). Lateral trials where a crossover stepping strategy was used were excluded from our analysis. The following were determined from kinetic data:

- Anterior ground reaction force at release (GRF_{AP}; %Body Weight) as an indicator of initial lean conditions, or perturbation difficulty.
- Peak vertical GRF of the initial force plate ($GRF_{V\text{–}Stance}$; %Body Weight) as an indicator of the stance-limb or pre-stepping response.
- Peak step-limb GRF ($GRF_{V\text{–}Step}$; %Body Weight) as an indicator of support from the stepping limb after taking a step.
- Step length (SL; %Height) as estimated from the COP locations of the two forces plates.
- Step time (ST; Seconds) as estimated by force-plate determined perturbation onset time and step contact time.

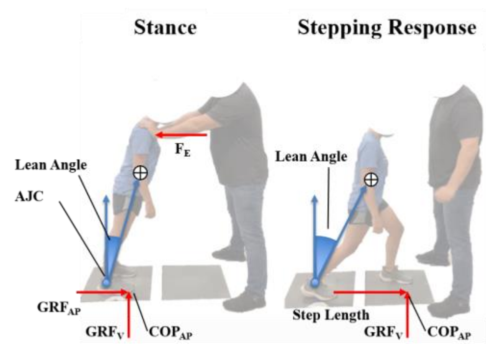

Figure 1: An example of the force-plate-instrumented Push-and-Release test administered in the anterior direction. Kinetic and force-plate derived variables collected are also noted here. Force provided by the examiner (F_E) is also noted, but is not included in our analysis.

Using motion-capture data, peak lean angular velocity (ω; deg/second) after release was defined by the rotation of the vector from the trail-limb ankle-joint center to the whole-body COM in the sagittal or frontal plane [5,6]. Backwards elimination multiple regressions were used to determine the relationships between peak lean angular velocity and force-plate derived variables.

Results & Discussion: Force-plate derived measures during the Push-and-Release Test held significant relationships with the angular velocity of the balance reaction (Equations 1-3). These results are evidence that we can reasonably estimate key kinematic features of the balance-reaction solely from kinetic measures. Thus, we can provide more precise outcomes than those of the Push-and-Release Test while still maintaining feasibility for clinical settings. Our equations, however, do not readily inform how to improve the balance reaction. For example, reducing the perturbation difficulty (GRF_{AP}) or shortening ST should reduce the angular velocity of the response if all other variables are held constant (EQ3). On the other hand, we do not recommend a reduction in SL or vertical GRF of the stepping limb, as short steps and insufficient lower-extremity support have been associated with failed responses [7]. However, we can recommend rehabilitation targeting the ankle plantar flexors, as increasing vertical force under the trailing stance limb reduced angular velocity during the recovery step (EQ1). We will further develop these equations by cross-validating them with additional data including a greater variety of stepping responses and participants.

$$Anterior\ (r^2 = 0.51):\quad \boldsymbol{\omega} = 15.8 + 61.3\,(\boldsymbol{SL}) + 8.1\,(\boldsymbol{GRF_{V-Step}}) - 19.7(\boldsymbol{GRF_{V-Trail}}) \qquad \textbf{EQ1}$$

$$Lateral\ (r^2 = 0.72):\quad \boldsymbol{\omega} = -11.5 + 88.4\,(\boldsymbol{SL}) + 6.1\,(\boldsymbol{GRF_{V-Step}}) \qquad \textbf{EQ2}$$

$$Posterior\ (r^2 = 0.83):\quad \boldsymbol{\omega} = -31.0 + 66.1\,(\boldsymbol{ST}) + 42.3\,(\boldsymbol{SL}) + 19.2\,(\boldsymbol{GRF_{V-Step}}) + 67.2(\boldsymbol{GRF_{AP}}) \qquad \textbf{EQ3}$$

Significance: Our results suggest that we can estimate key kinematic aspects of a balance reaction from force plate data. In doing so, we have insight on the specific aspects of the stepping response that can be modified to improve performance. This analysis is feasible in many settings, and it allows us to assess balance reaction beyond the outcome of one or more steps.

Acknowledgements: Funding from the UD KAAP Department and a contribution from Magnitude Express supported this work.

References: [1] Mansfield et al., 2015. *Phys Ther.* 101; [2] Crenshaw & Kaufman, 2014, *Gait Posture*. 39(2); [3] Smith BA, et al., 2016, *Physiother Res Int.* 21; [4] Jacobs et al., 2006. *J neurol.* 253; [5] Allum and Carpenter, 2005. *Curr Opini Neurol.* 18(1); [6] Grabiner et al., 2008. *J Electromyogr Kinesiol*. 18(2); [7] Patel and Bhatt, 2015. *Psychol Repo.* 3(2).

COMPARISON OF THREE PORTABLE IMUS' ORIENTATION ACCURACY DURING DYNAMIC SHOOTING

Martin Fultot[1*], Aidan Gross[1], Brian Higginson[1]
[1]Galvion Ballistics
*Corresponding author's email: martin.fultot@galvion-usa.com

Introduction: Estimating 3 DoF orientation without motion capture systems represents a crucial capability in many research applications. Attitude and Heading Reference Systems (aka IMUs) combined with sensor fusion constitute the preferred approach in most cases. However, the accuracy of results depend on three factors: hardware quality, filter algorithm and motion profile. Most human behavior research applications use commercial "plug and play" IMU solutions with important technical specifications hidden within proprietary black boxes. For this reason it is important to carry out empirical studies that assess the accuracy of particular models within the context of the motion profile type the system will be applied to. Highly accurate positional tracking systems like Vicon's infrared provide a valid orientation estimate ("Ground Truth", or GT) which is then compared with the IMU *cum* Sensor Fusion estimate. The quaternion distance between both orientations represent the overal angular error, which can be used to compare benchmarks [1].

In the field of dynamic shooting, when the goal is to track the orientation of a pistol or rifle, the particular challenge is to handle a) the high angular velocities, b) the jerky accelerations due to recoil, and c) the variable magnetic disturbances due to ferrous influence from the gun and armor. In this study we tested the accuracy of three different models from three different brands: Shimmer's Shimmer3, APDM's Opal and Vicon's BlueTrident. To control for the sensor fusion aspect, we used the same open source Madgwick algorithm [2] on all of their raw data rather than their proprietary sensor fusion outputs. Given the lack of rich details about their hardware and software specifications, it was difficult to come up with strong a priori hypotheses about their accuracy. However three factors drove the following expectations: 1) Blue Trident's integration with Vicon's mocap through Nexus should ensure high accuracy; 2) Opal's low output sample rate (128 Hz) could incur a cost in accuracy; 3) 6 DoF Sensor fusion without magnetic reference should have *better* results than 9 DoF alternative given the sheer amount of magnetic variability associated with the motion profile in question.

Methods: The three IMU units were mounted on top of the Picatinny rail of an M4 airsoft rifle. The centre and axis of each sensor was aligned to the barrel's longitudinal axis and rifle's "up" vector. Vicon retroreflective markers where placed around each sensor to obtain the rigid body orientation of the rifle. A 32 second trial was then recorded which included high-paced dynamic linear and angular motions in all directions but mostly on the horizontal plane and 22 shots fired. Timestamps were aligned using sharp accelerometer recoil peaks. All raw data was collected as 9 DoF magnetometer, accelerometer and gyroscope time series. Shimmer was resampled from 512 Hz to GT's 120Hz using linear interpolation. Opal was equally resampled from 128 Hz to 120 Hz. Gyro and accelerometer data was low-passed with a Butterworth filter at 0.05 Nyquist ratio to dampen the recoil peaks on the signal. Magnetometer data were de-biased and all axes realigned to match the initial GT orientation. The resulting signals were fed to a Madgwick filter adjusting for the best gain per sensor (0.005 for Shimmer3 and Opal and default 0.14 for BlueTrident), with (9DoF) and without (6 DoF) the magnetometer signal. The resulting quaternions were matched against GT orientation and the time-dependent angular quaternion distance was computed for each in degrees. Finally the mean angular distance or Mean Absolute Error (MAE) [1] was computed for each.

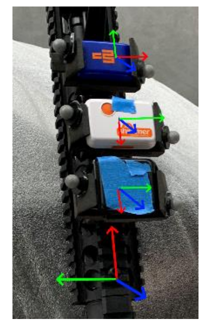

Figure 1: IMUs and mocap markers aligned on rifle.

Results & Discussion: The MAEs were: Opal (6 DoF): 2.89˚, Shimmer3 (6 DoF): 7.68˚, BlueTrident (6 DoF): 13.36˚; Opal (9 DoF): 4.01˚, Shimmer3 (9 DoF): 8.96˚, BlueTrident (9 DoF): 7.73˚. The best performer was Opal on 6 DoF and the worst was BlueTrident on 6 DoF. All estimates were better without magnetometer except BlueTrident which improved more than 5 degrees with it. Shimmer and Opal were slightly better without the magnetometer with barely more than one degree improvement. Hypothesis 1) was invalidated as, despite its integration with the same system used for mocap, Blue Trident was the worst performer. Hypothesis 2) was invalidated as Opal was by far the best performer despite the low sample rate. Hypothesis 3) was validated as the inclusion of the magnetometer did not improve estimation, especially for Opal which was the best performer. These results suggest that Opal's under-the-hood smoothing and resampling down to 128 Hz is extremely efficient in that the "raw" data coupled with a fine-tuned Madgwick filter can produce a virtually drift-less estimate, at least for 30ish second motion trials. On the other hand, given the small improvement over 9 DoF, it would still be worth leaving magnetometer data in the sensor fusion estimate to prevent drift accumulation over longer trials.

Significance: The present study shows very promising results regarding the reliability of AHRS use for orientation estimation in highly dynamic research including high impact events such as recoil. A small, light, wireless unit combined with even a "vanilla" sensor fusion algorithm in relatively short trials can provide accurate data for many applications even when discarding magnetometer's heading anchor. The next step should consist in testing longer trials to allow for drift accumulation and assessing Visual Inertial alternatives that replace magnetometer reference with visual information for world reference.

References:

[1] Justa, J., Šmídl, V., & Hamáček, A. (2020). Fast AHRS filter for accelerometer, magnetometer, and gyroscope combination with separated sensor corrections. *Sensors*, 20(14), 3824; [2] Madgwick, S. (2010). An efficient orientation filter for inertial and inertial/magnetic sensor arrays. *Report x-io and University of Bristol (UK)*, 25, 113-118.

ADULTS WITH AND WITHOUT KNEE OSTEOARTHRITIS DIFFER MORE ON STAIRS THAN LEVEL WALKING

Julien A. Mihy[1*], Mayumi Wagatsuma[1], Jenna A. Mlecko[1], Stephen M. Cain[2], Jocelyn F. Hafer[1]
University of Delaware[1], West Virginia University [2]
Corresponding author's email: mihyj@udel.edu

Introduction: Knee osteoarthritis (OA) is an irreversible degenerative joint disease that affects more than 19% of Americans over the age of 45 and is one of the leading causes of musculoskeletal pain in older adults [1]. The effects of knee OA on gait mechanics are typically evaluated using level overground walking measured with optical motion capture, which is regarded as the gold-standard and is limited to controlled laboratory settings. Inertial measurement units (IMUs) also provide measurements that can reliably quantify movement during level overground walking. However, existing IMU-derived metrics may not be sensitive enough to reveal differences between those with mild knee OA and healthy adults [2]. Stair walking is a particularly challenging daily task for those with knee OA, and may be useful for eliciting larger group differences in gait mechanics [3]. However, knowledge of gait mechanics during stair walking outside of laboratory settings is limited. Therefore, the purpose of this study is to determine whether there is a greater difference between adults with and without knee OA during stair ascent, descent, or overground walking using IMUs.

Methods: Ten older adults (5 with symptomatic knee OA: 60.2±2.2 years; 5 healthy: 65.2±3.6 years) were recruited. Four inertial measurement units (IMUs) were placed on the sacrum and right (healthy) or symptomatic (knee OA) thigh, shank, and foot. The medial-lateral axes (functional axes) of body segments relative to IMU sense axes were determined using data from a functional calibration [4]. Pelvis, thigh, shank, and foot motion were collected as individuals performed roughly 20 walking trials across an overground runway and then completed two flights of stairs (ascending and descending) all at their preferred pace.

Gait events were identified using continuous wavelet transform to enable calculations of joint ranges of motion and a zero-velocity update algorithm was employed to calculate stride length and speed [2]. Stair stance was manually identified using subject specific linear acceleration and angular velocity magnitude thresholds [2].

Walking variables of interest were stride speed, stride length, and joint ranges of motion (ROM) about the functional axis during steady state strides. Stride length during walking was calculated as the net horizontal displacement between consecutive stance onsets. Stride speed was calculated as the stride length divided by the time between consecutive stance onsets.

Stair variables during ascent and descent were time to completion, percent stance on stair, and joint ROMs during stance. For stairs, we extracted all strides excluding the first and last step for each flight. Time to completion was calculated as the first onset of stance to the last end of swing for the entirety of stair walking. Joint ROM for walking and stairs were calculated as the maximum minus minimum joint excursion across stance.

Stride length, stride speed, and joint excursion ranges of motion were averaged across all strides for each condition. Variables of interest were compared between groups (healthy and knee OA) using independent t-tests ($\alpha=0.05$) for each condition (overground walking and ascending and descending stairs).

Results and Discussion: This study evaluated different methods to assess joint health in older adults that could feasibly be used outside of the lab. Hip ($p=0.01$), knee ($p<0.001$), and ankle ($p<0.001$) ROM differed between groups for stair descent (fig 1.). Time to completion and percent stance did not differ between groups during stair descent ($p>0.05$). No significant differences between groups were found for any variable during overground walking and stair ascent ($p>0.05$). These results demonstrate that simple IMU-derived metrics during stair descent were able to detect differences between groups unlike the same variables measured during level overground walking. Increasing task difficulty may be required for distinguishing joint health status in those with mild knee OA outside of the lab using IMUs. Time to completion may not be sufficient for evaluating stair mechanics to detect mild differences in function in adults with knee OA. Stance phase joint ROM during stair descent may be a better tool for assessing function in those with knee OA.

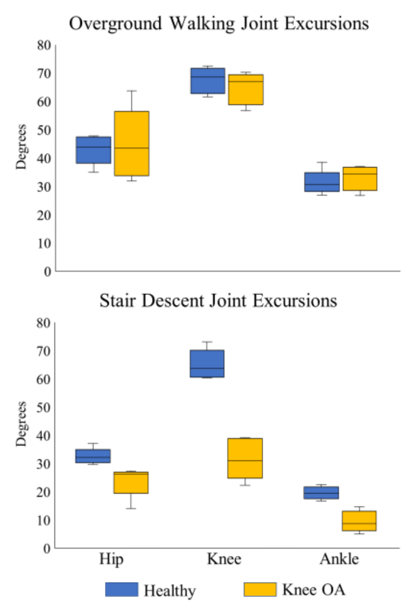

Figure 1. Sagittal joint excursions during stance for overground walking and stair descent. All joints were significantly different ($p<0.05$) between groups during descent. No differences during overground walking.

Significance: Our results demonstrate that IMU-derived metrics can reveal differences in gait mechanics due to knee OA. The IMU-derived metrics in this study are analogous to marker and force plate based stair mechanics and were sensitive enough to detect differences between groups. Increased knowledge about how stair walking mechanics differ in those with varying degrees of knee OA may inform interventions that aim to increase performance and decrease pain during stair walking, which is a common difficult activity of daily living.

References: [1] Kaufman et al., J Biomech, 2001; 34 907-915; [2] Hafer et al, Journal of Biomechanics, 2020; 99 109567; [3] Whitchelo et al., Disabil Rehabil, 2014; 36(13) 1051-1060; [4] Mihy et al., medRxiv 2022.11.29.222828

ACHILLES TENDON PATHOLOGY AND FUNCTIONAL IMPAIRMENTS IN ADOLESCENTS WITH HEEL PAIN

Kayla D. Seymore[1,2*], Shawn Hanlon[3], Bradley Bley[4], Karin Grävare Silbernagel[1,2]
[1]Biomechanics and Movement Science Program, University of Delaware, Newark, DE, USA
[2]Department of Physical Therapy, University of Delaware, Newark, DE, USA
[3]Department of Physical Medicine and Rehabilitation, University of Colorado, Aurora, CO, USA
[4]Delaware Sports Medicine, Wilmington, DE, USA
*Corresponding author's email: seymorek@udel.edu

Introduction: The incidence of Achilles tendon injuries in youth sports has increased [1], yet Achilles tendon pathology in adolescents has been poorly studied, potentially leaving the youth population at risk of long-term health issues. In adults, the overuse injury of Achilles tendinopathy is clinically diagnosed by tendon/heel pain with loading and loss of function [2], while the same symptoms in adolescents are instead considered a growth plate disorder called calcaneal apophysitis. With no clear difference in the clinical diagnosis of apophysitis and tendinopathy for patients under 18 years old with heel pain, Achilles tendon injury may be overlooked in adolescents. Inappropriate diagnosis and treatment of Achilles tendon injury in adolescents can reduce quality of life and impede the development of a physically active lifestyle into adulthood [3]. Before new approaches to treatment can be developed for adolescents with heel pain, research is needed to determine the presence of Achilles tendon pain and/or altered tendon structure that may contribute to functional deficits. The purpose of this study was to evaluate Achilles tendon symptoms, structure, and function in adolescents with heel pain.

Methods: Thirteen adolescents (6 F, 11.5 ± 2.5 yrs) with clinically confirmed heel pain were included in the study. Symptom severity was measured via Achilles tendon pain on palpation (scale of 0-10) and the Victorian Institute of Sport Assessment-Achilles (VISA-A) questionnaire. Achilles tendon length (calcaneus to soleus myotendinous junction), cross-sectional area (CSA), and thickness were measured using B-mode ultrasound, according to previously published protocol [4]. Mechanical properties of shear modulus and viscosity were measured using continuous shear wave elastography (cSWE) [5]. A test battery was used to assess lower limb functional performance [6]. Total repetitions and work for a maximum endurance single-leg heel-rise test were measured using a linear encoder affixed to the heel. Average plyometric quotient (PQ = flight time/contact time) was calculated for the middle 20 hops (out of 25) during a single-leg hopping test using a light-mat. The maximum counter-movement jump (CMJ) and drop CMJ height from 3 single-leg jumps were also measured with the light-mat. Participants were divided into three groups based on pain location: calcaneus (CAL), Achilles tendon (ACH), and both (DUAL). Absolute values for the most symptomatic limb (determined by VISA-A) and limb symmetry index (LSI = most symptomatic/least symptomatic limb*100) values were reported for each group. LSI calculations allowed for a comparison of degree of difference between limbs amongst groups. All results were reported descriptively.

Results & Discussion: Eleven out of thirteen adolescents with heel pain presented with Achilles tendon pain, altered tendon structure, and functional deficits. The CAL group (n=2) had the most insertional (4±4) and least midportion (0±0) pain on palpation, highest VISA-A scores (68±28 pt), longest tendon length, smallest tendon CSA and thickness, highest shear modulus, lowest viscosity, and worst function in the most symptomatic limb (**Fig. 1**). The ACH group (n=3) had the least insertional (1±1) pain on palpation, shortest tendon length, largest tendon CSA and thickness, and lowest shear modulus in the most symptomatic limb (**Fig. 1**). The DUAL group (n=8) had the most midportion (6±2) pain on palpation, lowest VISA-A scores (58±17 pt), highest viscosity, and similar or better function in the most compared to least symptomatic limb (**Fig. 1**). Achilles tendon structural impairments were most frequently observed in adolescents with midportion tendon pain, while functional impairments were most frequently observed in adolescents with calcaneus pain. In early years of adolescence, it may be important to assess Achilles tendon structure and lower limb function in relation to heel pain symptoms.

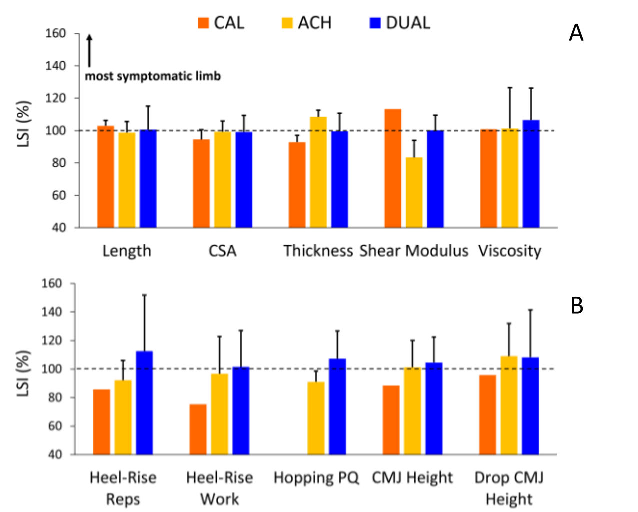

Figure 1: Mean (SD) structural (A) and functional (B) outcomes for each group. Note: 1 CAL participant did not complete full evaluation.

Significance: Identifying Achilles tendon structure and function in adolescents will help improve understanding of Achilles tendinopathy development in the youth population. With proper injury diagnosis, adolescents with heel pain may receive better and more appropriate clinical care to maintain physically active lifestyles into adulthood.

Acknowledgements: Research reported in this abstract was supported by the National Institute of Arthritis and Musculoskeletal and Skin Diseases of the National Institutes of Health under award number R01AR072034, the National Athletic Trainers' Association Research Foundation Doctoral Grant number 1920DGP08, and the Eastern Athletic Trainer's Association Grant number 001_2021.

References: [1] Simpson et al. (2016), *Sports Medicine* 46:545-57; [2] Scott et al. (2020), *Br J Sports Med* 54:260-2; [3] James et al. (2016), *Health Qual Life Outcomes* 14:95; [4] Zellers et al. (2019), *J Orthop Res* 37:933-41; [5] Cortes et al. (2015), *Ultrasound Med Biol* 41:1518-29; [6] Silbernagel et al. (2006), *Knee Surg Sports Traumatol Arthrosc*, 14:1207-17.

ADDITION OF INDEPENDENT SCAPULAR MOTION TO ENHANCE THE BIOFIDELITY OF A MUSCULOSKELETAL MODEL

Joshua Pataky[1*], Meghan E. Vidt[1,2]
[1]Biomedical Engineering, Pennsylvania State University, University Park, PA, USA
[2]Physical Medicine and Rehabilitation, Penn State College of Medicine, Hershey, PA, USA
*Corresponding author's email: jjp6192@psu.edu

Introduction: Computational models are powerful tools that can be used to investigate the biomechanical underpinnings in different clinical populations that are not feasible to study experimentally [1]. As computational model use increases in shoulder mechanics research, it is necessary to include features that make these models more biofidelic [2], including representation of degrees of freedom and arthrokinematics that can vary across the population and be impacted by injury. Current models, such as the upper limb model in OpenSim [3] (MoBL-ARMS [4]) represent the glenohumeral joint as a ball-and-socket joint with 3 rotational degrees of freedom and scapular motion is defined by regression equations. However, scapular kinematics are known to change after injury and influence upper extremity function [5]. Recently, researchers have developed an upper extremity model (Scapulothoracic Joint model) that includes independent scapular motion [6]. Our objective was to enhance the biofidelity of the MoBL-ARMS model by incorporating independent scapular degrees of freedom.

Methods: The MoBL-ARMS upper extremity model in OpenSim (v3.3) was used as a baseline. The Scapulothoracic Joint model, which includes a custom plug-in describing the scapulothoracic joint and independent scapular motion, was used as a foundation for incorporating scapulo-thoracic articulations into the MoBL-ARMS model. Scapular motion is defined by 4 degrees of freedom, including: abduction, elevation, upward rotation, and winging (Fig. 1A). The plug-in describing these degrees of freedom and the axes about which scapular rotations occur, and the constraints defining the scapulothoracic joint were identified, extracted, and implemented into the MoBL-ARMS model to replace the regression equations previously defining scapular kinematics as a function of thoracohumeral elevation. To validate the addition of independent scapular degrees of freedom, bone pin marker data of humeral abduction derived from human subjects performing humeral elevation tasks in the frontal plane were evaluated [7]. Notably, this data set was the same that was used by researchers to validate the Scapulothoracic Joint model [6]. The bone pin data were used as inputs to the scale tool, followed by the inverse kinematics tool in OpenSim. The same procedures were performed with both the Scapulothoracic Joint model and the model (New Model) developed here. Results from inverse kinematics were smoothed with a zero-phase 4th order Butterworth filter with a 6Hz cutoff. The maximum difference and RMSE of the 4 scapular degrees of freedom were separately computed and compared between the New Model and the Scapulothoracic Joint model.

Results & Discussion: Simulations were successfully run with each of the models. Maximum differences were computed (Fig. 1B), with positive values indicating that the New Model had a greater joint angle than the Scapulothoracic Joint model. Scapular degrees of freedom of the New Model compared to the Scapulothoracic Joint model were: 4.33° in scapular abduction, -0.33° in scapular elevation, -2.51° in scapular upward rotation, and 1.21° in scapular winging. RMSEs were: 2.42° in scapular abduction, 0.17° in scapular elevation, 1.38° in scapular upward rotation, and 0.73° in scapular winging. The New Model matches the kinematics calculated with the Scapulothoracic Joint model with a maximum angle difference of 4.33° or less for each degree of freedom and RMSE values of 2.42° or less for each scapular degree of freedom, providing initial model validation.

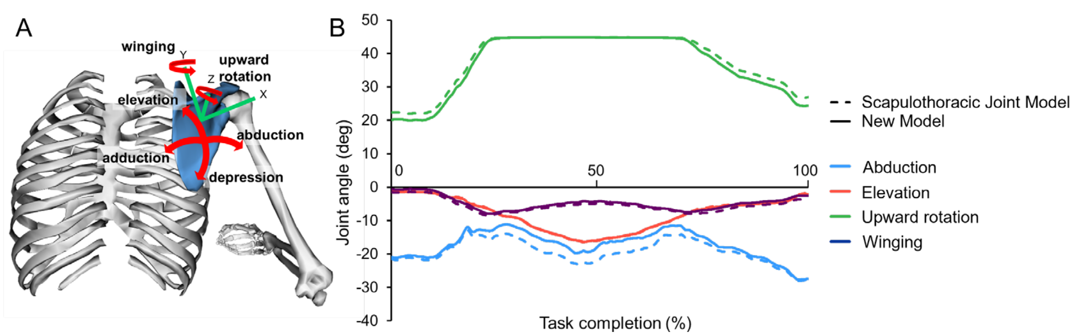

Figure 1: (A) Four degrees of freedom defining independent scapular motion, including: abduction, elevation, upward rotation, and winging. (B) Inverse kinematics predicted joint angles of humeral abduction for the existing Scapulothoracic Joint model (dashed) and the New Model (solid).

Significance: The development of more biofidelic computational models is necessary for detailed study of functional implications across populations and in the context of injury. The enhanced robustness of the model will also facilitate future clinical translation of modelling tools. Ongoing work seeks to further improve model tracking and validate against other recorded data [8, 9]. We will also combine these advancements with our other prior work which has added humeral head translation and glenohumeral ligaments into the model [10].

Acknowledgements: NSF-CBET #2103440

References: [1] Magermans et al. (2004), *Clin Biomech* 19(4):350-357; [2] Morrow et al. (2022), *J Electromyogr Kinesiol* 62:102409; [3] Delp et al. (2007), *IEEE* 54(11):1940-1950; [4] Saul et al. (2015), *Comput Methods Biomech Biomed Eng* 18(13):1445-1458; [5] Huang et al. (2015), *J Shoulder Elb Surg* 24(8):1227-1234; [6] Seth et al. 2016, *PLoS ONE* 11(1):e0141028; [7] Ludewig et al. (2009), *J Bone Joint Surg AM* 91:378-389; [8] Borstad & Ludewig (2002), *Clin Biomech* 17(9-10):650-659; [9] Karduna et al. (2001), *J Biomech Eng* 123(2):184-190; [10] Khandare & Vidt (2022), *Comput Methods Biomech Biomed Eng* 27:1-8.

MINIMIZING THE EFFECT OF CAMERA BUMP ON 3D DLT MOTION CAPTURE

William P. Moynihan[1*], Suzanne M. Konz[1], Brian M. Morgan[2], and Steven Leigh[1]
[1]Biomechanics and [2]Computer and Information Technology Departments, Marshall University, Huntington, WV, USA
*Corresponding author's email: moynihan@marshall.edu

Introduction: When modeling movement using the direct linear transformation (DLT) procedure, physical handling of the camera and environmental conditions such as wind and vibrations can cause slight unintended camera movement, which is enough to invalidate any measurements. The relationship between image and physical coordinates is only maintained when the cameras' viewing angles do not change between recordings of the calibration and trials. Applying 2D affine transformations to misaligned image coordinates could restore the consistency between calibration and trial data. The purpose of this study was to test a method to correct image coordinates from cameras bumped during recording using rotation, scale, and translation transformations. Error magnitudes and patterns were compared among measured and reconstructed lengths of both a rigid object and survey poles defining a 3D object space.

Methods: Two video cameras placed at roughly perpendicular angles recorded a rigid object consisting of three orthogonal pipes and survey poles defining a cuboid object space onto their image planes. A calibration and 129 trials were recorded, with each trial using a different combination of camera translation (±2.5 cm, 5 cm, 10 cm in eight radially symmetric directions (Fig. 1)), yaw (±2.5°, 5°, 10° left and right), and magnification (±150% zoom in to 40 mm and out to 90 mm focal length). Landmarks at the intersection and ends of the rigid object's pipes and along the survey poles were digitized using Motus (Vicon, Oxford, UK). The physical coordinates of the rigid object and survey poles were reconstructed from the image coordinates using the DLT procedure [1] in MS2016 (Motionsoft, Durham, NC) into an X (forward), Y (left), and Z (up) coordinate system. Twenty-four trials were reprocessed to assess inter- and intra-rater reliability.

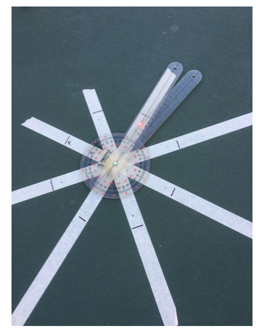

Figure 1: Radially symmetrical tape strips with marks used to measure camera translation.

Two static landmarks that were always present within the object space formed a reference line in the calibration and each trial. Custom-written code was used to rotate, then scale, and then translate the trial coordinates in so that the reference line coordinates in each trial matched that of the calibration. Rotation was calculated as $u = u_0\cos(\theta) - v_0\sin(\theta)$ and $v = u_0\sin(\theta) + v_0\cos(\theta)$, scale was calculated as $(u, v) = k(u_0, v_0)$, and translation was calculated as $u = u_0 + u_t$ and $v = v_0 + v_t$, where u was the horizontal image coordinate in pixels, v was the vertical image coordinate in pixels, and k was the ratio between reference line lengths.

The minimum detectable change (MDC) was estimated using inter- and intra-rater comparisons as described by Stratford [2]. The correlation and agreement of the errors in the rigid object's and survey poles' reconstructed lengths were tested with Bland-Altman and regression plots and a 3-way ANOVA. The MDC was used as a threshold for clinical significance of distance errors.

Results & Discussion: Among all trials, the transformations consistently reduced distance errors of the rigid object and distance and location errors of the survey poles to below the MDC of 36 mm. Average relative distance errors were 0.04% in X, 0.53% in Y, and 0.29% in Z for the survey poles and 2.78% in x, 0.18% in y, and 0.26% in z for the rigid object. We identified no correlations in error patterns among the corrected trials ($F = 0.0$, n.s.). There were some notable trends when evaluating error magnitude along different dimensions.

Greater perturbations resulted in greater errors. Object errors in dimensions that were close to parallel to the bumped camera's optical axis were greater than object errors in dimensions perpendicular to the optical axis (y error = 0.18% vs. x error = 2.78%). The landmarks defining the 3D coordinates of the object were projected onto specific pixels of the cameras' image planes. Similar line projections perpendicular to the optical axis have more pixels than those parallel to it. This results in larger relative changes in parallel projections when a camera is bumped. The quantization of projection distances also explains why zooming out introduced greater reconstruction error than zooming in (40 mm = 0.66% vs. 90 mm = 0.45%).

Survey pole errors were greater in dimensions perpendicular to the bumped camera's optical axis (Y error = 0.53% vs. X error = 0.04%). The vertical axis of the camera was not aligned with the vertical axis of the object space or tripod. Rotational perturbations of the camera were made about the tripod's vertical axis. The camera perturbations were therefore a combination of yaw and pitch. These combined rotations caused greater relative errors in distances measured in Y and Z, the axes about which pitch and yaw occur. This axis misalignment can result in disproportionate errors across dimensions.

Significance: Motion capture with 3D DLT can be error-prone because of multiple environmental factors that may bump the camera and invalidate the calibration. Since DLT is mostly used in outdoor environments where real-time motion capture systems are impractical, these environmental factors cannot be eliminated completely, and a slight change in viewing angle or zoom can render the results unusable. Correcting the marker image coordinates with simple 2D transformation equations may reduce reconstruction error due to bumped cameras enough to produce reasonably valid results. The only change required for the motion capture process is to find two static markers that form a reference line in both the calibration and trial videos, which can be used to align the trial even if the camera is bumped. Researchers will thus have fewer discarded trials and more reliable results from data collected with DLT.

References:
[1] Abdel-Aziz, Karara, & Hauck (2015), *Photogrammetric Engineering & Remote Sensing* 81(2).
[2] Stratford (2004), *Physiotherapy Canada* 56(1).

The reliability of an IMU-based motion capture system for spatiotemporal walking parameters: effects of walkway length and number of strides

Atabak Mehrabani[1], Jackson Lordall[2*], Sunny Bui[2], Alison R. Oates[2], Joel L. Lanovaz[1,2]
[1]Division of Biomedical Engineering, [2]College of Kinesiology, University of Saskatchewan, SK, CA
*Corresponding author email: Jackson.Lordall@usask.ca

Introduction: Inertial measurement units (IMUs) allow for the assessment of spatiotemporal walking parameters during different biomechanical tasks and settings and the use of IMUs for gait assessment has increased in recent years [1,2]. The common practice in gait analysis; however, is having participants walk in lab environments with limited walkway lengths. Despite all the research conducted with IMU-based motion capture systems, the test-retest reliability of such systems has been a matter of debate specifically in terms of ideal walkway length and the number of strides required, with some studies suggesting an increased number of steady state strides could improve reliability outcomes [3]. The main purpose of this study was to investigate whether walkway length and number of steady state strides impact the reliability of spatiotemporal parameters when using an IMU-based system for overground walking.

Methods: 28 young healthy adults (12 males, 16 females, age =24 ± 4 years, height = 171 ± 9.5 cm, mass = 76 ± 21kg) completed two study visits (>48 hours apart) consisting of 10 walking trials in a lab (walkway length: 8m) and a hallway (walkway length: 20m) (40 trials over both visits). Participants wore an IMU-based full body kinematic data collection system with 17 sensors (Xsens Awinda, Enschede, NL, fs = 60Hz). The following spatiotemporal walking parameters were computed from steady state gait in each trial: stride velocity, stride length, stride cadence, and step width. Test-retest reliability was assessed using intraclass correlations (ICC) (3, k) [4]. ICC values were interpreted as poor (<0.5), moderate (0.5-0.75), good (0.75-0.9), and excellent (>0.9) [5]. Absolute reliability was assessed using minimal detectable change at a 95% confidence level (MDC95) and expressed as a percentage of the mean [6]. Mean spatiotemporal parameters were calculated using consecutive strides at incremental increases in the numbers of strides (maximum strides: lab 20; hall 50) and ICC and MDC95 values were calculated at each stride count.

Results & Discussion: For most participants, two to three steady state strides per trial were captured in the lab while five to eight strides per trial were recorded in the hallway.

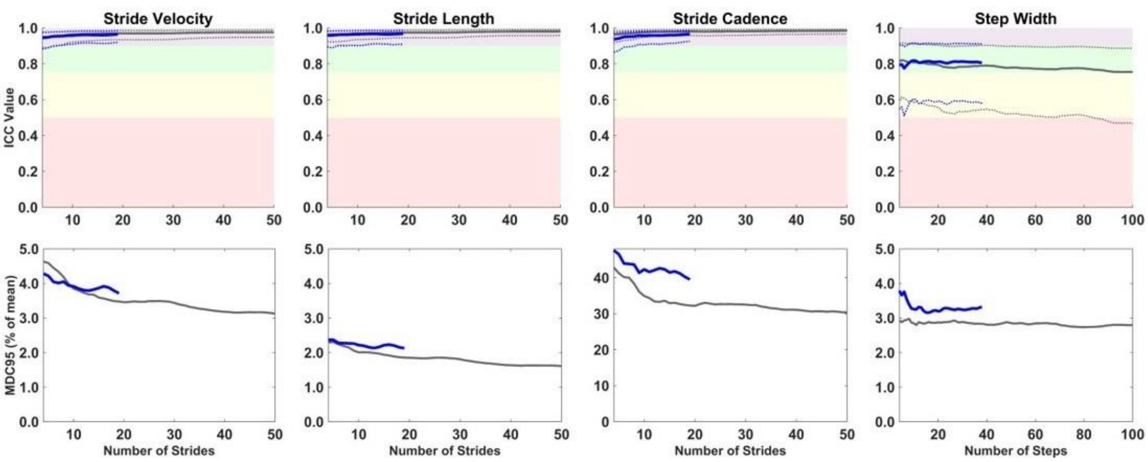

Figure 1: ICC (± 95%CI, top row) and MDC95 (bottom row) for spatiotemporal parameters at each stride/step count in the lab (blue line) and the hallway (grey line). ICC shading: >0.9 (purple), 0.75-0.9 (green), 0.5-0.75 (yellow), <0.5 (red).

ICCs indicated excellent test-retest reliabilities for all spatiotemporal parameters except step width which was moderate to good (Fig. 1). ICC values were similar to Teufl et al [7] for stride length, slightly better for cadence, but significantly greater in our study for step width (ICC = ~0.80 vs. ICC = 0.25). MDC95 values were <5% of the mean for all parameters except stride cadence (Fig. 1). Larger MDC95 for stride cadence may be related to the sampling frequency of the system (fs = 60 Hz). Differences in reliability between the lab and hallway converged at around 10 strides for stride velocity and stride length (4-5 trials in lab, 2 trials in hallway), while differences between walkway lengths were small but still evident after 20 strides for step width and stride cadence (8-10 trials in lab, 4 trials in hallway). Considering acceptable MDC95 values for step width, ICC outcomes and wider confidence interval bands in step width might be attributed to lower between-subject variability in our study. Reliability outcomes were consistent and acceptable after 10 strides regardless of the walkway length and number of strides per trial.

Significance: Portable IMU kinematic systems can be very reliable for spatiotemporal parameters with a relatively small number of strides. This is encouraging for those who wish to assess walking performance in non-laboratory environments.

References: [1] Hamacher et al. (2014), *Gait Posture* 39(4); [2] Donath et al. (2016), *Gait Posture* 49; [3] Kobsar et al. (2020), *JNER* 17; [4] McGraw & Wong (1996), *Psycholog Methods* 1(1); [5] Shrout & Fleiss (1979), *Psychol Bull* 86(2); [6] Weir (2005), *J. Strength Cond. Res.* 19(1); [7] Teufl et al. (2019), *J. Sens* 19(1).

THE EFFECTS OF COMBINING SELF-CONTROLLED PRACTICE AND FOCUS OF ATTENTION ON JUMP PERFORMANCE

Joei R. Velten[1*], Logan T. Markwell[1,2], Jared M. Porter[1]
[1]University of Tennessee, Knoxville
[2]Jósef Piłsudski University of Physical Education in Warsaw, Biała Podlaska, Poland
*jvelten@vols.utk.edu

Introduction: When performing a task, individuals can direct their attention internally, toward characteristics of their body mechanics, or externally, toward their desired movement outcomes. Numerous studies have demonstrated positive performance effects associated with adopting an external focus of attention across a variety of skills. In a recent systematic review and meta-analysis focused specifically on jumping, adopting an external focus of attention resulted in superior jumping performance when compared to both an internal focus of attention and control conditions[1].

Learner autonomy is also an important aspect of the practice context. Previous studies have found when learners are given the choice of when they want to receive feedback, they perform better on retention and transfer tests than their non-choice counterparts[2].

Recent studies suggest that providing instructions that direct attention externally or allowing participants to choose where they direct their attention results in similar performance[3]. Additionally, pilot data suggests when self-controlled practice is combined with internal focus of attention, performance differences may be marginal compared to self-controlled practice combined with external focus of attention. However, further research is needed to gain a better understanding of how these two constraints interact with one another. Therefore, the purpose of this study was to expand on previous research and compare motor performance between self-controlled, yoked, and control practice groups practicing the same skill. It was hypothesized that the self-controlled practice group with an external focus of attention would jump the furthest distance and the yoked condition instructed to focus their attention internally would jump the shortest distance.

Methods: Participants (n = 61) were randomly assigned to a self-control group (n = 21), yoked group (n = 20), or control group (n = 20) in which they performed a standing long jump task. All participants completed a total of 10 jumps. The self-control group was given the choice of which attentional cue (i.e., internal or external) they wanted to focus on prior to each jump. Participants in the yoked group were instructed how to focus their attention (i.e., internally or externally) prior to each jump. Participants in the control group were instructed to jump to the best of their ability without any explicit instructions directing their attention.

Results & Discussion: A 2 (focus of attention condition) x 2 (gender) x 3 (group) mixed repeated measures ANOVA was conducted to evaluate potential performance differences. Statistical analysis revealed a significant main effect for the attentional focus condition and gender (fig. 1), but no group or interaction effects were observed. These results align with the attentional focus literature and show that an external focus resulted in a further jump distance compared to an internal focus. Additionally, these results did not show a motor performance improvement during the self-controlled group. Such findings are congruent with recent meta-analyses questioning the effectiveness of self-controlled practice[4]. Future studies should continue to investigate this phenomenon to further develop effective practice strategies and improve our understanding of the skill acquisition process. Additionally, future research should include additional measures of kinematics, kinetics, and muscle activation to better understand how altering focus of attention results in changes in movement mechanics.

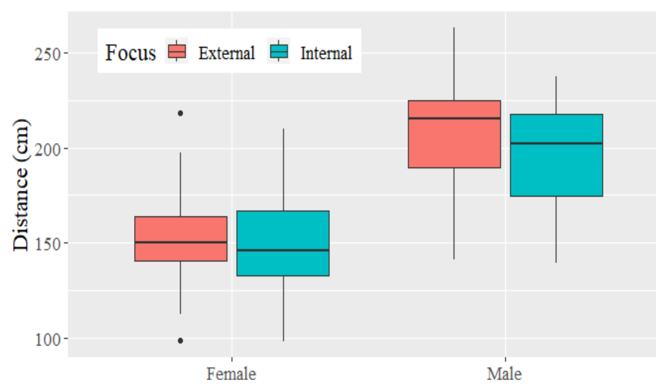

Figure 1. The boxplot displays standing long jump distance (cm) separated by gender and attentional focus condition. The bold lines represent the median, the boxes show the 25th and 75th percentile (upper and lower quartile), the whiskers show the minimum and maximums, and the dots represent outliers.

Significance: Research shows that most of the information provided in sport and rehabilitation contexts promotes an internal attentional focus[5,6]. However, the empirical evidence is quite clear that an internal attentional focus hinders performance and learning, whereas at external focus enhances motor performance and learning[1]. The findings of this study demonstrate the robustness of the focus of attention effect while also highlighting the limited effects of self-controlled practice. From a practical perspective, coaches, clinicians, and instructors should explicitly instruct movers to direct their attention externally when executing a gross motor skill such as the standing long jump. Also, the results of our experiment add to a growing body of work which has consistently reported that instructing a person to think about their mechanics has null, and potentially depressing effects on movement outcomes such as jump distance.

References: [1] Makaruk, et al. (2021), *J Hum Kin, 75(1)*; [2] Chiviacowsky, S., & Lessa, H. T. (2019), *JMLD, 7(2)*; . [3] Asadi et al. (2019), *JMLD, 7(2)*; [4] McKay et al. (2022), *Meta Psyc, 6;* [5] Hussein & Ste-Marie (2023*), JMLD*; [6] Porter et al. (2010), *Sport Sci Rev*

ERROR-STATE KALMAN FILTER FOR LOWER-LIMB KINEMATIC ESTIMATION: AN EVALUATION FOR RUNNING

Jamie Ferris[1*], Noel C. Perkins[1], Michael V. Potter[2]
[1]University of Michigan, Ann Arbor, MI, USA
[2]Francis Marion University, Florence, SC, USA
*Corresponding author's email: jcferris@umich.edu

Introduction: Inertial measurement units (IMUs) are relatively accessible, easy to wear on a day-to-day basis, and can be used 'in the field' to unobtrusively capture over ground running mechanics in a variety of training and racing environments. However, the estimation of traditional position-domain measures such as foot inclination angle or stride length from IMU measurands (linear acceleration and angular velocity) requires robust sensor fusion algorithms which reduce the accumulation of drift and other error during integration.

Sensor fusion methods such as extended Kalman filters or complementary filters often leverage task-specific information (e.g., zero-velocity updates) to better correct for drift. While many algorithms have been developed or are accurate for only lower body sagittal plane kinematics, few have accurately estimated 3-dimensional lower body kinematics [1, 2], and those have typically made assumptions that limit their application to 'in the field' running (e.g., the assumption of level ground).

Potter et al. recently developed an error-state Kalman filter (ErKF) method for a 7-body representation of the lower limbs to estimate 3-dimensional lower body kinematics using data from seven wearable IMUs. The algorithm leveraged numerous correction methods including zero-velocity, gravitational, joint center, and joint axis based corrections [2, 3]. Potter et al. validated the model on fast and slow walking data, reporting root mean square error (RMSE) of the flexion/extension and abduction/adduction joint angle estimates of generally $\leq 5°$ compared to motion capture estimates. The RMSE of stride length and step width estimates were generally ≤ 0.13 m and ≤ 0.07 m, respectively, for the fastest walking gaits [3].

However, the model has not yet been evaluated during running gait. In this study, we aimed to evaluate the accuracy of this ErKF for lower-limb kinematic estimation during treadmill running.

Methods: Six male recreational runners (36.8 ± 10.6 years) completed 6 min of treadmill running at 14 km/hr. Kinematic data were collected at 200 Hz via the current standard (i.e., marker-based motion capture with the Plug-In-Gait marker set) and seven inertial measurement units placed on the feet, shanks, thighs, and pelvis (IMUs; Opal, APDM).

The IMU-based estimates were calculated for approximately 3.5 min of steady-state running via the ErKF algorithm. The initial state (positions, orientations) and joint centers and axes were first calculated from the marker data [3]. Note that in order for this algorithm to be used exclusively 'in the field', joint centers and axes would need to be estimated without relying on marker data. After adapting the algorithm to running data (e.g., midstance detection [4]), we tuned the ErKF parameters (e.g., initial state uncertainty, accelerometer noise [2]) to minimize the RMSE of the joint angle, step width, and step length estimates during running.

The marker-based joint angle estimates were computed using methods which decreased the impact of marker collinearity on internal/external rotation estimates. In addition, the stability of these estimates to small perturbations was evaluated in order to aid in the comparison of marker and IMU-based estimates.

Results & Discussion: The ErKF algorithm successfully arrested drift in the joint angle estimates. As reported by prior studies, the resulting IMU-based angle estimates were most accurate in the sagittal plane. Stride length estimates were at times offset from marker-based estimates, suggesting that the incorporation of GPS data may improve estimates. Improved sensor-to-segment calibration may also improve both joint angle and stride metric estimates. This study also demonstrated a limitation of a common method for lower body joint angle estimation (the Plug-In-Gait marker set), suggesting that moderate errors in IMU-based internal/external rotation estimates may still be comparable to current methods.

Significance: The ErKF algorithm developed by Potter et al. may yield useful estimates of some of the lower-limb kinematics during running. Future work may develop methods for estimating joint centers and axes from inertial data and evaluate the algorithm in additional running conditions.

Acknowledgements: This project was supported by Dr. Christine Agresta and the University of Michigan Rackham Graduate Student Research Grant.

References: [1] Moore et al. (2019). *Curr Sports Med Rep* 18(12); [2] Potter et al. (2021). *PLoS One* 16(4). [3] Potter et al. (2022). *Sensors* 22. [4] Skog et al.(2010). *IEEE Trans Biomed Eng* 57(11).

WEARABLE SENSOR DETECTION OF TREADMILL-INDUCED SLIP PERTURBATIONS

Jordan N. Feldman[1], Constantin W. Beyer[2], Jessica L. Allen[3], Jason R. Franz[1*]
[1] UNC Chapel Hill and NC State University, Chapel Hill, NC, USA [2]Technische Universität Ilmenau, Ilmenau, Germany
[3] University of Florida, Gainesville, FL, USA
*Corresponding author's email: jrfranz@email.unc.edu

Introduction: Monitoring instability is critical for the prevention of dangerous falls. Recent developments in the use of wearable sensors (i.e., inertial measurement units – IMUs) have shown promise in their application to monitor physical activity [1]. Currently, there is less research in their application to monitor locomotor instability. Those studies that are available use a wearable sensor to detect fall events [2]. However, the biological signals associated with preclinical instability that could precipitate a first fall are much more subtle. It is unclear whether and the extent to which wearable sensor thresholds for detecting locomotor instability resemble the biological threshold for perceiving that instability, even in otherwise healthy younger adults. This study in young adults aimed to build on previous studies using small-amplitude treadmill-induced slip perturbations [3] to establish and objectively compare a conscious threshold for perceiving instability and wearable-sensor based thresholds for detecting that instability. We hypothesized that: (1) wearable sensors have the capacity to detect the instability elicited by treadmill-induced slip perturbations, with (2) thresholds for conscious perception that will be indistinguishable from thresholds for wearable sensor detection. Ultimately, our anticipated outcomes can be used as a basis for developing and deploying wearable sensor technology to detect instability and prevent falls.

Methods: 15 young adults (8F, 23.4 ± 3.7 years) participated and completed treadmill walking at their preferred overground walking speed (1.37 ± 0.11 m/s). Subjects were fit with seven wearable IMU sensors (APDM Opal) placed on their sacrum and left and right wrists, shanks, and feet. While walking, a custom Matlab treadmill controller rapidly decelerated (6 m/s^2) one foot at initial contact during the stance phase every 12-15 strides at random. Eight perturbation magnitudes delivered in randomized order five times each ranged from 0.02 m/s to 0.3 m/s, after which the belt immediately returning to the subject's preferred speed. After each perturbation, subjects were asked to respond "Yes" or "No" if they felt a balance disturbance. Subjects wore wear noise-cancelling headphones to prevent them hearing the treadmill velocity changes. We used pairwise statistical parametric mapping (SPM) to analyze perturbation-induced differences between IMU-derived outcomes (accelerations, orientations, and ankle joint angles) versus unperturbed walking.

Results & Discussion: The threshold perturbation amplitude for perceived instability averaged 0.061 m/s, which is highly consistent with previous work (Fig. 1A) [3]. We found statistically significant differences in most acceleration signals in response to treadmill-induced slips (Fig. 1B). These effects increased in amplitude and duration with perturbation magnitude and were most pronounced for a wrist-worn accelerometer on the side of the slip. However, acceleration signals had a higher threshold for instability detection compared to the biological perception threshold, reaching significance for magnitudes ≥ 0.100 m/s. Analysis of the goniometer signals is ongoing, and will be evaluated in a similar manner to determine the veracity of those signals to detect perturbation-induced instability. Conversely, IMU-derived ankle joint kinematics were highly sensitive to all perturbation magnitudes, evidenced by a significant increase in dorsiflexion near midstance compared to unperturbed walking. These effects increased in amplitude and duration with perturbation magnitude, with a threshold for detecting treadmill-induced instability as low as 0.02 m/s.

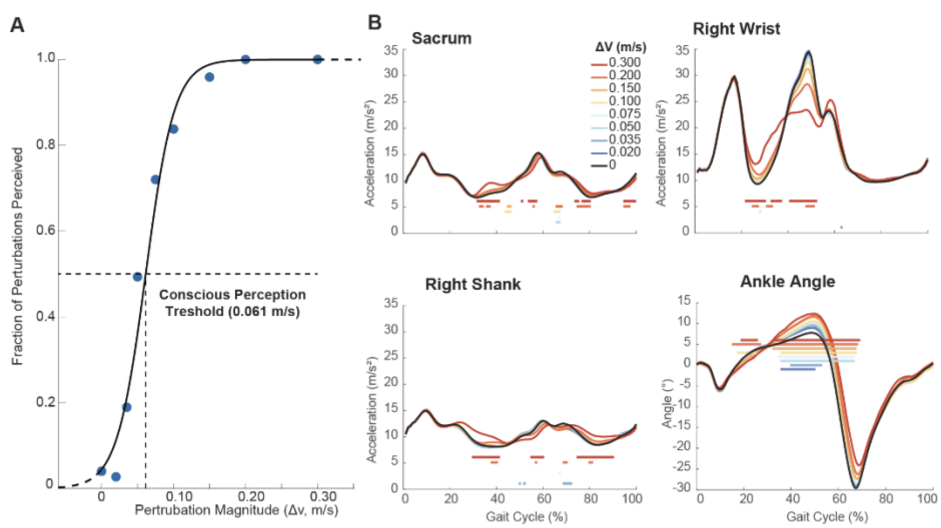

Figure 1. (A) Conscious perception thresholds using a psychometric curve fit and (B) acceleration signals and IMU-derived ankle joint angle across all perturbation magnitudes. Horizontal bars represent regions of significant SPM results versus unperturbed walking.

Significance. Acceleration signals alone perform worse than conscious perception in detecting the instability elicited by treadmill-induced slip perturbations, at least in a group of otherwise healthy younger adults. However, IMU-derived ankle joint kinematics are highly sensitive to even the smallest amplitude perturbation, with thresholds ~3x smaller than conscious perception. Continued work in this area seeks to investigate the generalization of these conclusions to individuals more representative of those at risk of falls.

Acknowledgments. Supported by a grant from the NIH (R21AG067388).

References: [1] Kristoffersson & Lindén (2022), *Sensors* 22(2); [2] Khojasteh et al. (2018), *Sensors* 18(5). [3] Liss et al. (2022) *Gait& Posture* 91.

THE IMPACT OF REGULATING THE RESISTANCES OF AN ARTICULATED ANKLE FOOT ORTHOSIS ON THE PARETIC LEG MUSCLES OF STROKE SURVIVORS.

Oluwaseye Odanye[1*], Emily Steffensen[1], Lindsey Remski[1], Elisa Arch[2], Brian Knarr[1]
[1]Department of Biomechanics, University of Nebraska at Omaha, Omaha, NE USA
[2]Department of Kinesiology and Applied Physiology, University of Delaware, Newark, DE USA
*Corresponding author's email: oodanye@unomaha.edu

Introduction: Ankle foot orthoses (AFOs) are devices prescribed for assistive or rehabilitative purposes to augment the function of weak plantarflexor and/or dorsiflexor muscles in stroke survivors. These devices function through a characteristic bending stiffness graded as the AFO's resistance to plantarflexion (PF) and/or dorsiflexion (DF) in different AFO types [1]. AFOs with PF resistance aid dorsiflexor function through the loading response and prevent dragging of the toe at the swing phase of gait [2]. Also, the weak plantarflexor muscle function is augmented at the mid – to – late stance phase of the gait cycle through the AFO DF resistance [1]. Evidence exists on how different AFOs impact the gait cycle and walking ability of stroke survivors [1], [3], although, there are reservations on the use and clinical prescription of the device due to a purported loss in muscle mass with long-term use [4]. Our study looked to investigate this using an individual-specific articulated ankle foot orthosis (A-AFO) assembled with a triple action joint. The goal of this study was to see how regulating the PF and DF resistances of the A-AFO will impact the activity of the lower leg muscles of the participants, and we hypothesized that increasing the DF resistance would decrease the tibialis anterior (TA) muscle activity in swing and the soleus muscle activity at the terminal stance while increasing the PF resistance will increase the tibialis anterior (TA) activity and rectus femoris (RF) activity both at the swing phase of the gait cycle. These hypotheses were based on existent evidence in studies like that of Lairamore et al. 2011[5] where they found decreased TA activity at the swing phase of gait with a dynamic AFO.

Methods: The study was done in two sessions with a minimum of 1-week interval. We recruited four subjects (S01 – S04; 3M and 1F) between the ages of 19 – 80 (63.5 ± 5.9 years) who had a stroke more than 6 months prior and could walk independently with or without a walking aid. We customized the A-AFO's footplate and calf section for each subject using a 3D scanner to scan the shank-to-foot of the participants with the EMG sensors placed on the paretic leg muscles to create sensor orifices. The scanned image was fitted in a predetermined design which we 3D printed using polylactic acid printing material, before assembling the prints with a commercially available triple-action joint used in a Kobayashi et al study [1]. These fabrication processes were completed between the first and second visits. Participants were fitted with the AFO at the 2nd visit and a 2-minute walking trial was done before we randomly tested three PF (PF1-low; PF2-medium; PF3-High) and three DF (DF1-low; DF2-medium; DF3-High) resistance settings as the participants walked in a straight line at their comfortable speed in the lab while recording the muscle activity for the TA, RF, and soleus muscles through the gait phases. EMG data were collected with the sensors synchronized with a 20-camera motion capture system. Analog data were processed in Visual 3D, before comparing the magnitudes of the peaks between resistance settings with Friedman's non-parametric test in SPSS *version 26* (IBM SPSS Statistics, Chicago, IL, USA).

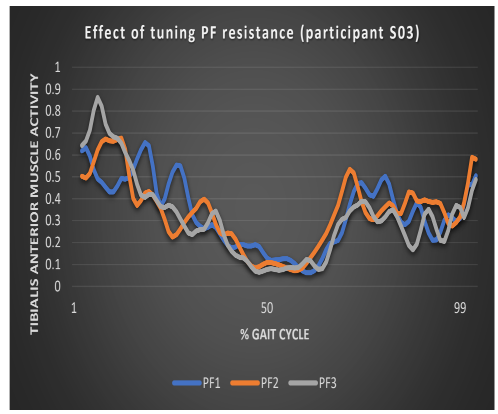

Figure 1: The effect of tuning the plantarflexion resistance settings of the A-AFO on the TA muscle activity of participant 2's paretic leg.

Results & Discussion: Our preliminary results showed mean differences in the mean rank of muscle activity level when we tuned the PF and DF resistances, but none were statistically significant. The TA muscle activity in swing at PF3 was lower compared to PF1 and PF2 (figure 1 shows sample TA activity for S03), although not statistically significant [(χ^2 = 1.5, p = 0.472); *small effect size* (Kendall W = 0.188)], and the RF mean rank muscle activity differences at the swing phase were also not statistically significant [(χ^2 = 0.5, p = 0.779); *small effect size* (Kendall W = 0.0625)]. There was no statistically significant difference in the means of the TA muscle activity [(χ^2 = 1.5, p = 0.472); *small effect size* (Kendall W = 0.188)] at the swing phase and the soleus muscle activity [(χ^2 = 3.5, p = 0.174); *moderate effect size* (Kendall W = 0.438] at the stance phase when the DF resistance of the AFO was tuned. Despite the non-significance in the data, we noted trends indicating an increased or decreased muscle activity with resistance variation. These trends showed the AFO's tendency to impact the activity level of the lower leg muscles of stroke survivors, albeit in a distinct manner. The heterogeneous clinical presentation and the different characteristics of the stroke population was our inferred reason for the different activation patterns observed. Though, we believe an improved sample size may give a clearer picture of the A-AFOs impact enabling further insight into the research question.

Significance: This study showed the tendency of the articulated AFO to impact the activity of the lower leg muscles of stroke survivors during assistive function; although, further research is necessary with a larger sample size to give a more clearcut picture.

Acknowledgments: Funded by University of Nebraska Omaha Graduate Research and Creative Activity grant - 31254.

References: [1] Kobayashi et al. (2017), Med Eng Phys, Vol. 44, pp. 94-101; [2] Yamamoto et al. (2020), IEEE TNS and Rehab Eng, vol. 28, pp. 21904-2202; [3] Arch and Reisman (2016), Journal of P and O, vol. 28, pp. 60-67; [4] Hesse et al. (1999), Stroke, vol. 30, pp. 1855-1861; [5] Lairamore et al. (2011), P and O International, Vol. 35, pp. 402-410.

HIP, KNEE, AND ANKLE JOINT FORCES DURING EXOSKELETAL-ASSISTED WALKING USING A SUBJECT-SPECIFIC VIRTUAL SIMULATOR

Vishnu D. Chandran[1], Gabriela B. de Carvalho[2], Ann M. Spungen[3,4], Noam Y. Harel[3,4], William A. Bauman[4], and Saikat Pal[2,3*]
[1]Hospital for Special Surgery, New York, NY; [2]New Jersey Institute of Technology, Newark, NJ;
[3]James J. Peters Veterans Affairs Medical Center, Bronx, NY; [4]Icahn School of Medicine at Mount Sinai, New York, NY
*Corresponding author's email: pal@njit.edu

Introduction: Robotic exoskeletons have vast potential to restore upright mobility in individuals who have diverse neurological, rheumatological, or age-related impairments. The growing demand for these devices necessitates the development of technology to characterize human-robot interaction during exoskeletal-assisted walking (EAW). Parametric studies to characterize human-robot interaction during EAW using experimental methods are cost-prohibitive and often not feasible. For instance, joint contact forces provide a surrogate measure of bone loading, but experimental methods to quantify joint forces during EAW are invasive. *In vivo* data on joint forces during EAW do not exist. Computational simulation is the only viable alternative. Accordingly, the **goal** of this study was to develop a computational framework to quantify the hip, knee, and ankle joint forces using a subject-specific virtual simulator that reproduced EAW.

Methods: An able-bodied man (41 years, 178 cm, 86.2 kg) was recruited for study participation. The participant was trained in a ReWalk™ P6.0, and his 3-D motion was analyzed during unassisted walking (without the exoskeleton) and EAW maneuvers (Fig 1A). 3-D motion data included simultaneous measurements of marker trajectories, ground reaction forces, electromyography (EMG), and exoskeleton motor angle and torque data.

We adapted a full-body OpenSim model [1] to simulate unassisted and EAW maneuvers. A full-scale geometry of the ReWalk was integrated with the musculoskeletal model (Fig 1B). The human-robot model had 10 DoF to represent the exoskeleton and 37 DoF to represent the human. The human-robot model represented interaction using OpenSim's bushing forces (three linear spring-damper systems, two for lower legs, two for upper legs, and one at the torso) [2]. The bushing element's stiffness parameters were calibrated based on forces from instrumented knee brackets. The generic musculoskeletal model was scaled to match the anthropometry of the subject. Inverse kinematics was performed to obtain joint angles, and inverse dynamics to obtain joint moments. Exoskeleton interaction forces were quantified using OpenSim's force reporter [2].

EMG-tracked muscle-driven simulations were performed using OpenSim Moco [3] to compute the hip, knee, and ankle joint forces. Lower extremity motion was reproduced using the DeGrooteFregly2016 muscle model [4]. Ideal torque actuators were used to displace the torso and the upper body. In our simulations of EAW, the exoskeleton interaction forces (Bushing Forces) were included and applied to a model without the exoskeleton geometry. In addition to this approach, EAW was simulated using two other approaches: 1) exoskeleton motor torques prescribed directly at each joint (Prescribed Torque), and 2) excluding exoskeleton interaction forces or motor torques (w/o Interaction).

Results & Discussion: The virtual simulator reproduced unassisted and EAW within acceptable tolerances (average RMSE 1.2 cm for unassisted and 1.3 cm for EAW). Our joint force results from unassisted walking compared well with prior *in vivo* studies (Figs 1C-F), especially at the knee joint (Figs 1E-F) [5, 6]. Peak compressive hip forces ranged from 3.2-3.8 body weights (BW) for unassisted walking, and 3.5-4.9 BW during EAW. Peak compressive knee forces ranged from 3.1-3.4 BW for unassisted walking, and 2.5-5.4 BW during EAW. Peak compressive ankle forces ranged from 4.5-5.0 BW for unassisted walking, and 4.0-4.2 BW during EAW.

In vivo data on joint forces during EAW do not exist. As part of model validation, we compared computed joint forces from unassisted walking with available *in vivo* data. We used all model parameters from the unassisted trials as input to our EAW trials. Furthermore, we quantified joint forces using three different approaches to maximize confidence in our computational framework. All three approaches produced similar trends in joint forces; the increased peaks observed in the Prescribed Torque approach (green lines in Figs 1C-H) were due to additional torques applied by the exoskeleton's motors at the hips and knees to overcome directional changes.

Significance: This is the first study to quantify hip, knee, and ankle joint forces during EAW in an FDA-approved exoskeleton. These joint forces during EAW may serve as input to computational models to quantify the mechanical competence of bone, which may serve as a surrogate measure to determine fracture risk in individuals with severe osteoporosis, such as in those with chronic spinal cord injury.

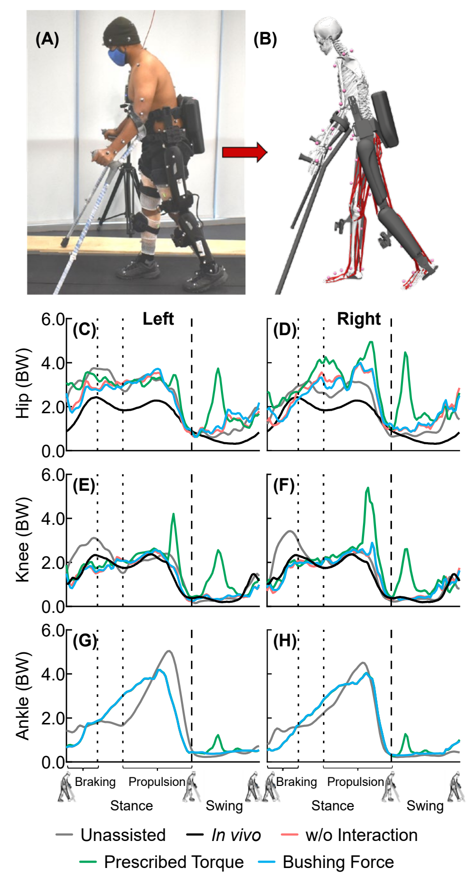

Figure 1: Motion capture experiment (A) and corresponding virtual simulator of EAW (B). Resultant compressive hip (C, D), knee (E, F), and ankle (G, H) forces from unassisted and EAW. *In vivo* joint forces during unassisted walking from prior studies [5, 6] are shown for comparison. BW = body weight.

Acknowledgements: The Department of Veterans Affairs RR&D #1 I01 RX003561.

References: [1] Rajagopal et al. 2016, *IEEE Trans Biomed Eng* 63; [2] Seth et al. 2018, *PLoS Comput Biol* 14; [3] Dembia et al. 2020, *PLoS Comput Biol* 16; [4] De Groote et al. 2016, *Ann Biomed Eng* 44; [5] Bergmann et al. 2001, *J Biomech* 34; [6] Fregly et al. 2012, *J Orthop Res* 30.

COMPARISON OF ACCELERATION IN PRE- AND POST-SEASON YOUTH MALE SOCCER PLAYERS

Taliah J. Carlson[1*], Jake A. Melaro[1], Joshua T. Weinhandl[1]
[1]University of Tennessee Knoxville, TN, U.S.A
*Corresponding author's email: tcarlso3@vols.utk.edu

Introduction: Soccer players experience high rates of rapid acceleration and deceleration as they change directions during matches and training [6]. Optimal training load will maximize performance and decrease the risk of injury. Undertraining may not adequately prepare the individual for matches while overtraining can have unnecessary loads, and both may increase the risk of injury [1]. Investigation of acceleration performance at pre- and post-season provides insight into managing the player's training load to reduce the risk of injury and develop training interventions [2]. The purpose of this pilot program research was to investigate the difference in the pre-season and post-season peak accelerations and acceleration integrals of youth male soccer players.

Methods: Fifteen male soccer players (age: 14.94 ± 0.56 years) voluntarily engaged in the following agility and jumping drills: a 36.6-meter jog, 5-10-5-meter lateral shuffle, the M-cone drill in both directions for emphasis on each leg, and a bilaterally performed single leg triple jump. In the-10-5-meter lateral shuffle drill participants shuffled 5 meters, changed directions, and shuffled 10 meters, and then shuffled 5 meters back. In the M-cone drill the participants sprinted around the cones changing direction rapidly and this was completed in both directions to primarily place the load on the right and then left leg. In the single leg triple hop participants were told the goal was maximum horizontal displacement. Data was collected through inertial measurement units (IMUs) rigidly attached to participants distal tibias (1600 Hz; Vicon Blue Trident, Vicon Motion Systems Ltd, Oxford, UK). Data was processed utilizing Python. Examined variables were peak accelerations and acceleration integrals, which represent maximum tibial loading and the lower extremity cumulative loading. Utilizing R, an independent t-test with a 0.05 alpha level was completed.

Results & Discussion: None of the drills had statistical significance for either peak accelerations or acceleration integrals in the comparison between pre- and post-season (Fig. 1).

The implementation of a high-intensity speed-based training program, that had appropriate loads and duration, has shown improvements in the acceleration phase and agility in females aged 13 and males aged 11 to 12 [3, 4]. A systematic review found that 79% of the studies examined found that in youth soccer there was a positive relationship between cumulative load (measured by GPS) and injuries and there was support for supplementary training interventions that utilize load management strategies [5]. The current data shows that the cumulative loading of the lower extremity (measured by IMUs) is noticeably smaller in the single leg triple hop task compared to the other tasks. This shows that drill selection may be another factor to consider when developing training interventions. Therefore, future research should examine sex comparisons, other age groups, potential pubertal effects, and task selection, to determine if statistically significant differences suggest training programs that are more individualized with appropriate trainings load to reduce the risk of injury and maximize performance.

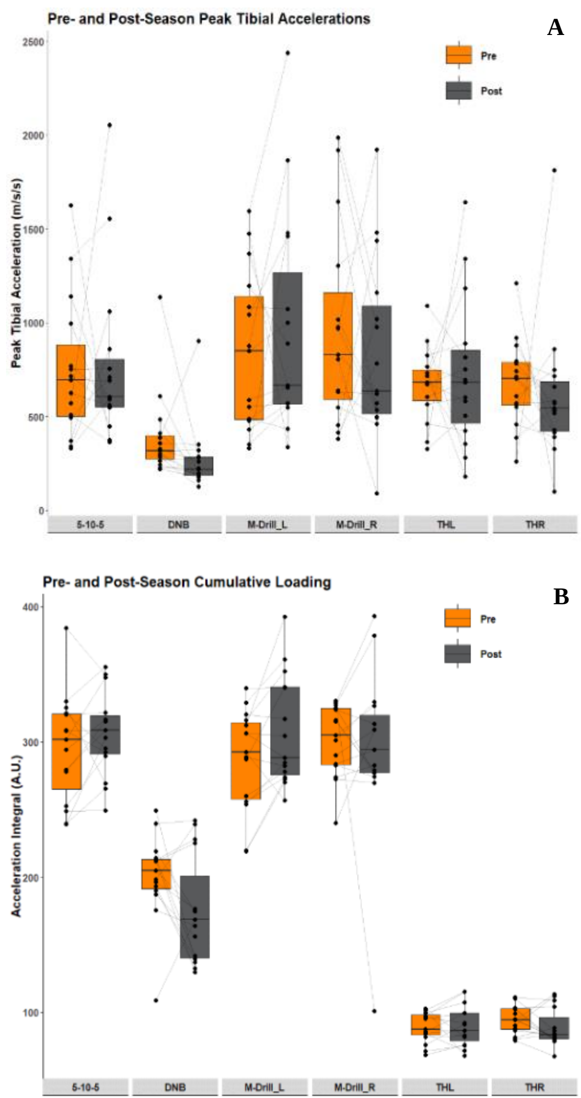

Figure 1: Peak tibial accelerations (A) and acceleration integrals (cumulative loading) (B) for pre- and post-season high school-aged males.

Significance: Although there was no statistical significance, the results of this pilot program prove the feasibility of collecting lower extremity acceleration data during a youth soccer practice. Future research aims to gain insight into managing training load, so it is important to examine other factors, such as sex and age, to find the training load sweet spot that maximizes performance and has limited injury risk.

Acknowledgements: We would like to thank the Knoxville Crush Football Club for allowing us to use their indoor facility and the opportunity to work with their teams.

References: [1] Gabbett, T. J. (2016), *British J of Sports Medicine*, 50(5); [2] López-Sagarra, A., et al. (2022), *Applied Sciences*, 12(24); [3] Mathisen, G.E., & Danielsen, K.H. (2014), *J of Physical Education and Sport*, 14, 471; [4] Pettersen, S. A., & Mathisen, G. E. (2012), *J of Strength and Conditioning Research*, 26(4); [5] Sniffen, K., et al. (2022), *Sports Med* 8, 117; [6] Zhang, Q., et al. (2022), *Frontiers in Physiology*, 13.

DIFFERENCES IN LOAD SYMMETRY BETWEEN HEALTHY OLDER ADULTS AND TOTAL KNEE ARTHROPLASTY PATIENTS

Tyana Scott[1*], Kelli Allen[2], Sara Arena[1], Robin Queen[1]
[1]Department of Biomedical Engineering and Mechanics, Kevin Granata Biomechanics Lab, Virginia Tech, Blacksburg, VA, USA
[2] Department of Medicine, University of North Carolina, Chapel Hill, NC, USA
*Corresponding author's email: tyscott1@vt.edu

Introduction: Total Knee Arthroplasty (TKA) is intended to restore knee joint function and relieve pain. More than 750,000 TKA operations are performed in the United States annually[1]. In the next seven years, the number of TKA procedures are projected to increase by 673%, reaching 3.48 million operations[2]. Bourne et al.[3] reported overall high satisfaction with the procedure, however, up to 18% of patients were dissatisfied with the outcome of their TKA operation. Gait mechanics can be used to assess surgical outcomes, and more specifically a limb symmetry index can be used to check for between limb discrepancies in limb loading. Clinicians use side-to-side limb symmetry during activities of daily living to measure intervention success, recovery during rehabilitation, and potential injury risk[4]. The purpose of this study was to compare load symmetry during activities of daily living between healthy older adults and patients following TKA. Based on previous literature it was hypothesized that the patients with a TKA would have greater asymmetry.

Methods: Forty-seven healthy adults (C) and 47 patients with a TKA, 50 years or older, were recruited, signed IRB approved informed consent and completed testing. Participants were asked to wear their own footwear that they typically used for walking[5]. Each participant completed one 30 second sit-to-stand[6] (STS) trial and one timed-up-and-go[7] (TUG) trial. Load data was processed using the Load Analysis Program[5] (LAP), to determine peak force (PkF) and impulse (Imp) for each limb. The Normalized Symmetry Index[8] (NSI) was used to quantify symmetry, where values range from -100 to 100, with values closer to 0 representing perfect symmetry. An independent t-test was used to compare STS PkF NSI and Imp NSI between C and TKA groups. Due to non-normal distributions, a Wilcoxon Rank-Sum test was used to compare TUG PkF NSI and Imp NSI between C and TKA groups. All analyses were conducted in JMP (SAS Institute Inc., Cary, NC) with $p<0.05$.

Results & Discussion: No significant difference existed in load symmetry for the TUG between the two groups for the PkF NSI ($p=0.806$) nor the Imp NSI ($p=0.450$) (Table 1). However, there was a significant difference in PkF NSI ($p<0.001$) and Imp NSI ($p<0.001$) for STS. The purpose of this study was to compare load symmetry during daily functional tasks between patients with a TKA in comparison to a healthy older adult population. As expected, during the STS task, the healthy, control population had greater symmetry (values closer to 0) when compared to patients with a TKA. The patients with a TKA had higher loads on non-surgical limb. The lack of differences between groups during the TUG could be the result of gait changes that occur with aging and increased variability in movement patterns, however, additional research would need to be completed to assess variability and age-related changes in gait mechanics when completing the TUG. This study demonstrates the feasibility of using the loadsol to capture symmetry metrics and track recovery during the rehabilitation process following TKA in a clinical setting. By monitoring changes in load and loading symmetry across time, clinicians will be able to assess rehabilitation progression and potentially alter treatment plans to potentially improve patient outcomes.

Table 1. NSI during STS and TUG (Mean ± SD)

		STS	TUG
PkF NSI	Control	-0.32±12.55*	6.12±15.83
	TKA	23.37 ± 16.05*	9.16±10.54
Imp NSI	Control	2.31±13.59*	6.88±19.97
	TKA	28.79±19.26*	12.80±12.80

* p<0.001 between groups

Significance: This study developed the first side-to-side load symmetry database in healthy older adults during activities of daily living. This information could be invaluable as a comparison to patient populations when trying to determine therapeutic targets. The results from the patients with a TKA demonstrate a need to continue to assess side-to-side symmetry following surgery and to develop interventions that seek to restore symmetry during the recovery process. In addition, future work could explore the ability to utilize symmetry to assess rehabilitation progression and surgical recovery to develop individualized treatment plans. This research lays the groundwork for understanding how clinically assessed loading metrics can be captured and integrated into clinical practice. In future work, loading symmetry and other measures could be analysed to determine their association with patient reported outcomes.

Acknowledgements: The authors would like to thank Theresa Libera for her contribution to healthy control data collection and the study team at the UNC Chapel Hill, particularly Kimberlea Grimm and Katie Huffman for completing data collection for the patients with a TKA. Support for this study was provided by a grant from the National Institutes of Health: 1R21AR074149.

References: [1] *American Academy of Orthopaedic Surgeons. (2020, June). Total knee replacement – orthoinfo – aaos.* [2] *Kurtz S et al., J. Bone and Joint Surgery, 2007. 89(4), p.780–785.* [3] *Bourne R. B. et al., Clin. Ortho and Rel Res., 2010. 468(1), p.57–63.* [4] *Alrawashdeh W. et al., J. Musculo & Neuro Inter., 2022. 22(1), p.102-112.* [5] *Luftglass A. et al., Clin Biomech., 2021. 88, p105421.* [6] *Alnahdi A.H. et al., Knee Surg Sports Trauma Arthrosc., 2016. 24, p.2587-2594* [7] *Yoshida Y. et al., Clin Biomech., 2008. 23(3), p.320-328* [8] *Queen R. et al., J. Biomech., 2020. 99, p. 109531.*

Effect of unanticipated constraint on lower extremity energy absorption during jump landings following ACL reconstruction

Brendan P. Silvia[1], Fatemeh Aflatounian[1], James N. Becker[1], Keith A. Hutchinson[1], Janet E. Simon[2], Dustin R. Grooms[2], and Scott M. Monfort[1]
[1]Montana State University, Bozeman, MT, USA, [2]Ohio University, Athens, Ohio, USA
Email: scott.monfort@montana.edu

Introduction: Nearly a quarter of athletes younger than 25 years old who have undergone anterior cruciate ligament reconstruction (ACLR) suffer a second ACL injury [1]. Athletes who have undergone ACLR demonstrate altered patterns of bilateral energy absorption in the joints of the lower limbs through greater hip extension and ankle plantar flexion [2]. Return to sport (RTS) tests have found that although limb symmetry in single leg hop distance may be >90%, it is achieved through compensation from the hip and ankle of the injured limb [3]. Additionally, it is unknown how these compensations might change when individuals are subjected to sport-like constraints, such as rapid decision making [4]. The purpose of this study was to examine the differences in energy absorption across each of the joints of the lower body during unanticipated jump landings. Specifically, this study investigated how an unanticipated directional cue influenced the relative proportion of negative work performed at the ankle, knee, and hip joints during a jump landing. We hypothesized that, due to previously reported compensatory mechanisms following ACLR, added cognitive challenge during a jump landing task would cause a decrease in the negative work done at the injured knee during landing.

Methods: 36 participants (10M/26F; 19.8 ± 1.76yr; 69.57 ± 12.81kg; 1.71 ± 0.10m; 1.46 ± 0.62 years since surgery, Tegner: 6.8±1.8) with prior ACLR and having been cleared for RTS performed a series of jump-land-jump trials from a 30 cm box set at half the participants' height from the force plates. Participants were instructed to jump as high as they could upon landing from the initial jump. This abstract focuses on a subset of data from a larger study. Specifically, we focused this analysis on baseline (BL) and unanticipated conditions (UA – a visual cue given ~250 msec prior to the initial landing of which a secondary direction to jump was given: up, 45° left, 45° right). The average of 5 successful conditions for the secondary jump direction of straight up for both the BL and UA were used for the analysis. Lower extremity kinematics and kinetics were estimated, and then negative work for each lower extremity joint for both limbs were calculated for the initial landing by integrating the sagittal plane joint power curves. Percent of negative work at each joint was used as the dependent variable, with the primary analysis focusing on the percent of negative work at the involved knee. Mixed effects models were used to test for differences between conditions (BL vs. UA), with participants as random factors and covariates of age, gender, mass, and time since surgery also included in the statistical models.

Results & Discussion: Consistent with prior studies, the uninvolved knee and limb absorbed more energy compared to the involved knee and limb (both p<0.001) [3]. The tendency to use the uninvolved limb more to absorb energy during jump landings may highlight maladaptive landing techniques following ACLR considering the increased risk of a second ACL injury on the uninvolved limb after passing RTS criteria [2, 5]. However, our hypothesis was not supported as there was not a significant change in energy absorption at the involved or uninvolved knee due to changing conditions (p=0.908 and p=0.392, respectively). When expanding analysis to include other joints, the hip (involved: p=0.001; uninvolved: p=0.024) and ankles (involved: p=0.007; uninvolved: p<0.001) experienced significant differences between conditions, **Figure 1**. For the UA trials, ankles demonstrated an increase in relative energy absorption, while the involved hip demonstrated a decrease in relative energy absorption. The increase in relative energy absorption at the ankle requires greater involvement from the ankle plantar flexors, which has previously been correlated to reduced hip strength and an increased loading of the ACL through the action of the gastrocnemius [6].

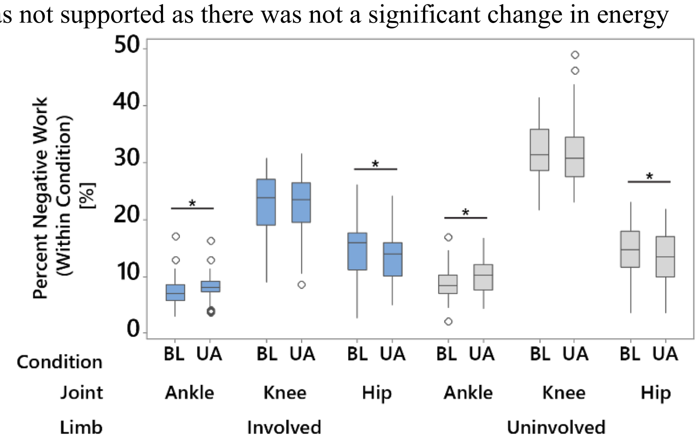

Figure 1. Distribution of negative joint work at each joint (bilaterally) for anticipated (BL) and unanticipated (UA) conditions. Significant differences between conditions are indicated with an *.

Longer time since surgery was associated with greater energy absorption by the involved knee (p=0.015) and involved ankle (p=0.015), while a decrease in energy absorption was exhibited at the uninvolved hip (p=0.048). The increase of energy absorption in the involved knee with increased time since surgery suggests that as this time increases, so does the tendency for patients to involve the surgical knee during jump landings.

Significance: Participants shifted the relative energy absorption from the hip to the ankles when faced with an unanticipated jump landing constraint. As increased gastrocnemius contraction has been shown to cause greater peak anterior shear force on the ACL [7], these findings highlight how sport-relevant scenarios can elicit ACL-injury relevant shifts in energy absorption during a jump landing.

Acknowledgements: This research was supported by the NIH award R03HD101093. We would also like to thank Ezekiel Barden and Patrick Fischer for their help with the study and physical therapy and orthopedic clinics in Bozeman for recruitment support.

References: [1] Wiggins et al. (2016) AJSM 44(7). [2] Decker et al.(2002) MSSE 34(9). [3] Kotsifaki et al. (2022) BJSM 56(5). [4]. Mohammad et al. (2021) IJATT 26(3). [5] Webster et al. (2019) SM (49)6. [6] Romanchuk et al. (2020) JB 113. [7] Navacchia et al. (2019) ABE 47(12).

COMPARISON OF ACCELERATION FREQUENCY BINS BETWEEN PRE- AND POST-SEASON YOUTH MALE SOCCER PLAYERS

Taliah J. Carlson[1*], Jake A. Melaro[1], Joshua T. Weinhandl[1]
[1]University of Tennessee, Knoxville, TN, U.S.A
*Corresponding author's email: tcarlso3@vols.utk.edu

Introduction: In soccer, players experience high rates of quick accelerations and decelerations as they change directions in games and training [5]. Through investigating acceleration performance at pre- and post-season testing insight can be providing to work towards managing the athlete's training load to reduce the injury risk and develop training interventions to maximize performance [3]. Therefore, it is important to examine the effects of acceleration, an external load, on performance (fitness) and negative consequences, such as injury rates and fatigue. Number of impacts that result in higher accelerations during speed and agility drills might provide insight to help prevent overuse injuries over the course of a season.

One study on elite team rugby players utilized GPS systems to measure acceleration, which was organized into discrete acceleration bands of mild (0.55-1.11 m/s^2), moderate (1.12-2.78 m/s^2), and maximal ($\geq$ 2.79 m/s^2) [2]. This study found there was an association between the mild, moderate, and maximum accelerations occurring over greater distances and a reduction in risk of injury, with lower accelerations being associated with lower risk of soft-tissue injury [2]. The current research aimed to analyze tibial impact accelerations and categorize them into smaller 1g bins so future research can examine how those tibial loads are related to injury risk. The purpose of this pilot program research was to investigate the qualitative differences in acceleration frequency bins between pre-season and post-season youth male soccer players during an agility drill.

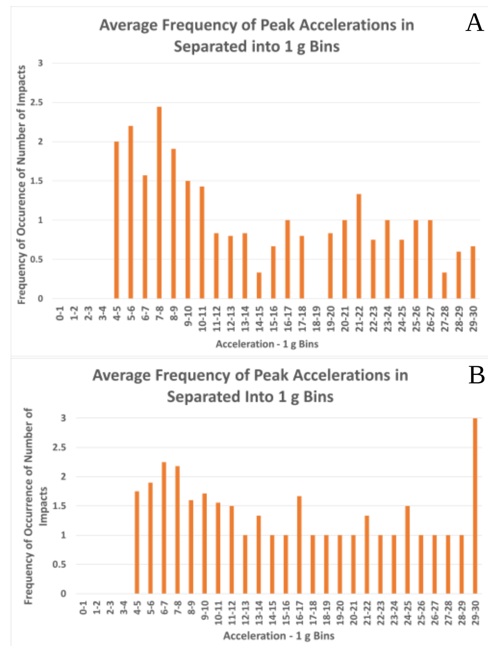

Figure 1: Peak tibial accelerations per step (ground contact) across the trial organized into frequency bins to compare the differences between pre-season (A) and post-season (B). The frequency bins are set to 1 g bins.

Methods: Twelve male soccer players (age: 15.07 ± 0.49 years old) voluntarily engaged in a M cone drill. In the M-cone drill the participants sprinted around the cones changing direction rapidly. The data was collected through inertial measurement units (IMUs) (1600 Hz; Vicon Blue Trident, Vicon Motion Systems Ltd, Oxford, UK) rigidly attached to the participants distal tibia and slightly superior to the medial malleolus of both legs. The data was processed utilizing Matlab (R2022b, MathWorks Inc., USA). Resultant acceleration was calculated and filtered with a 4^{th} order low pass Butterworth filter with a cut-off frequency of 60 Hz [4]. The peak accelerations during ground contact and locations of those peaks were then found to bin the acceleration into 1 g bins. The bins were averaged across the participants to compare differences between pre- and post-season.

Results & Discussion: Qualitatively, there appears to be a slight shift from pre- to post-season in the acceleration frequency bins. In the pre-season there is a higher frequency of peaks occurring in the lower acceleration bins compared to the post-season. From pre- to post-season, there is a shift where the frequency bins mostly level out across the middle acceleration bins. In the post-season there is an increase in the frequency of peak tibial accelerations in the 30 g bin, the highest peak acceleration across the participants trial, compared to the pre-season.

The current research shows shifts from pre-season to post-season in how often different levels of peak tibial accelerations during ground contact are occurring throughout a singular sport-specific task. Investigating peak tibial accelerations helps to provide insight into the effects of training load on the athlete from pre-season to post-season and therefore provides insight into how to manage training loads and develop training interventions that work towards balancing maximizing performance (fitness), while reducing fatigue and the risk of injury [1]. Previous research has shown that reducing the amount sprinting, meaning high accelerations, when preparing for competition, may reduce the athlete's risk of soft-tissue injuries [2]. This shows the importance of examining how often different levels of accelerations are occurring throughout tasks to gain a better understanding of the athlete's risk of injury during training.

Significance: This research was part of an exploratory pilot program to investigate the categorization of acceleration into frequency bins and to prove the feasibility of collecting lower extremity acceleration data during a youth soccer practice. Future research aims to gain insight into managing training load, so it is important to refine the process for coding and categorizing frequency bins.

Acknowledgements: We would like to thank the Knoxville Crush Football Club for allowing us to use their indoor facility and the opportunity to work with their teams.

References: [1] Gabbett T.J. (2016), *British Journal of Sports Medicine* 50, 273-280; [2] Gabbett & Shahid (2012), *Journal of Strength and Conditioning Research*, 26(4), 953-960; [3] López-Sagarra, A., et al. (2022), *Applied Sciences*, 12(24); [4] Sheerin, K. R., et al. (2019), *Gait & Posture*, 67, 12–24; [5] Zhang, Q., et al. (2022), Frontiers in Physiology, 13.

ASSESSMENT OF VARUS THRUST USING INERTIAL MEASUREMENT UNITS

Millissia A. Murro*, Julien A. Mihy, Mayumi Wagatsuma, Jocelyn F. Hafer
Department of Kinesiology & Applied Physiology, University of Delaware, Newark, DE
*Corresponding author's email: murrom@udel.edu

Introduction: Knee osteoarthritis (KOA) is a degenerative joint disease that affects approximately 23% of individuals 60 years or older, causing pain with movement, stiffness, and a lower quality of life [1]. Individuals with KOA tend to have specific movement traits associated with the disease such as varus thrust, or a bowing-out of the knee during walking. Clinicians can quantify the presence of varus thrust during walking through a subjective, visual analysis. Visually-identified varus thrust determined by well-trained clinicians has been correlated to high peak external knee adduction moment and knee adduction angular velocity during the first half of stance as assessed using optical motion capture (MoCap) [2]. Thus, these laboratory measurements provide an objective assessment of varus thrust and therefore assist in identifying those who either have KOA or are at risk for KOA.

MoCap assessments of varus thrust are helpful, but not ideal for a setting other than a lab. Inertial measurement units (IMUs) can measure angular velocity and linear acceleration and are more affordable with less required time for assessment than MoCap. In a clinical setting, IMUs could provide a way for clinicians to objectively measure varus thrust and KOA in a more efficient manner. Recently, researchers showed that optical motion capture measures of varus thrust correlated with peak thigh and shank angular velocities measured using IMUs in individuals with KOA [3]. However, IMUs have not been used to examine the difference in varus thrust between those with KOA and healthy older adults or the relationship between IMU derived knee velocity and varus thrust. The primary goal of this study was to compare estimates of varus thrust between MoCap and IMU data. We hypothesized that IMU measures of varus thrust would correlate with those estimated with MoCap. The secondary goal of this study was to compare measures of varus thrust between those with KOA and healthy older adults. We hypothesized that varus thrust measures would be significantly different between those with KOA and healthy older adults.

Methods: Sixteen subjects (10 Healthy:61.8±2.7 years, BMI:25.7±3.8; 6 KOA:65±2.8 years, BMI:27.5±3.4) walked at a self-selected speed in our over-ground laboratory. Each subject walked until we achieved 10 successful force plate strikes (left limb for Healthy, symptomatic limb for KOA). Standard MoCap methods were followed to assess lower extremity kinetics and kinematics. MoCap data were collected simultaneously with two IMUs that were placed on the shank and the thigh. IMU data were functionally oriented using walking and upright standing data [4].

All variables were assessed in the frontal plane. The MoCap variables examined were peak external knee adduction moment and knee angular velocity during the first half of stance and the IMU variables examined were peak shank, thigh, and knee angular velocity during the first half of stance. All data visualization and processing were done using Visual3D (Boyds, MD) and custom Matlab scripts (Natick, MA). A one-tailed independent t-test was used to examine the MoCap variables between groups (KOA and healthy older adult). Linear correlations were then used to examine the relationship between each MoCap variable and each of the IMU variables.

Results & Discussion: Between groups there was no significant difference in either external knee adduction moment (Healthy:2.8±.007%BW*height, KOA:2.5±.01%BW*height) or knee velocity (Healthy:40.4±16.2deg/s, KOA:36.7±19.2deg/s). This indicates that neither group showed differences in varus thrust. No significant relationships were found between any of the IMU variables and the MoCap variables (Table 1, all p>0.05). Since our MoCap results suggested our subjects did not have a large range of varus thrust magnitude, it is reasonable that we were unable to find an IMU correlate of varus thrust in this dataset. These findings may be due to the fact that our subjects with KOA were relatively high-functioning. In a previous study done by Costello et al. [3] where they were able to detect varus thrust via IMU measurements, they had subjects with severe KOA with low functioning knees (KOOS: 59.2±11.1) whereas our subjects had higher functioning knees (KOOS: 76.0±15.8) and potentially less severe KOA. Costello et al. [3] also screened those with KOA with radiographs, whereas we did not. Varus thrust may be more related to structural than functional KOA.

Correlations Between MoCap and IMU Variables

		MoCap Variables	
		Knee Adduction Moment	**Knee Angular Velocity**
IMU Variables	**Shank Angular Velocity**	-0.02	0.23
	Thigh Angular Velocity	0.56	-0.004
	Knee Angular Velocity	0.25	0.10

Table 1: Pearson's correlation coefficients (r) between the MoCap variables and each of the IMU variables. No significant relationships were found for any variables.

Significance: Assessing mild KOA or early onset of KOA may not be feasible using these IMU measures. These findings indicate that varus thrust may not be the best measure to assess KOA in such cohorts. Alternative strategies should be examined to allow for accurate detection of individuals at-risk for KOA or those with early onset KOA. A limitation to our data was that we had a small KOA sample. Increasing the variety of KOA subjects may provide more variance in the outcome variables, allowing for differences to be seen.

References:

[1] Zhang Y et al., *Clin Geriatr Med* 2010, 26(3):355-369 [2] Chang AH et al., *Osteoarthritis Cartilage* 2013, 21(11):1668-1673 [3] Costello KE et al., *J Clinical Biomech* 2020, 80, 105232 [4] Mihy JA et al., *medRxiv* 2022, 11.29.22282894 (preprint)

BOTULINUM NEUROTOXIN INJECTIONS IMPROVE HIP ROTATION IN CHILDREN WITH CEREBRAL PALSY

Archisha Kanchan[1], Gabriela B. De Carvalho[1], Vishnu D. Chandran[2], Catherine A. Mazzola[3], JenFu Cheng[4,5], O. Folorunsho Edobor-Osula[5], Hannah A. Shoval[6], and Saikat Pal[1*]

[1]New Jersey Institute of Technology, Newark, NJ; [2]Hospital for Special Surgery, New York, NY; [3]NJ Pediatric Neuroscience Institute, Morristown, NJ; [4]Pediatric Rehabilitation Specialists, Watchung, NJ; [5]Rutgers-New Jersey Medical School, Newark, NJ; [6]Atlantic Health System, Summit, NJ

*Corresponding author's email: pal@njit.edu

Introduction: Cerebral Palsy (CP) is the most common childhood onset disability often characterized by different forms of gait abnormalities. Botulinum neurotoxin type A (BoNT-A) is a common intervention to improve gait in children with CP. BoNT-A blocks the release of acetylcholine neurotransmitters, which inhibits a muscle's ability to contract. CP is typically characterized by high tone and spasticity; targeted delivery of BoNT-A to the affected muscles is theorized to reduce tone and spasticity, thus improving gait [1, 2]. However, the effects of BoNT-A in improving joint kinematics and achieving gait more representative of typically developing (TD) children is not well-understood. Accordingly, the **goal** of this study was to evaluate the effects of BoNT-A on joint kinematics and gait deviation (compared to TD) in children with CP.

Methods: We recruited six children with CP for this study (Fig 1). Participants provided written informed consent prior to participation. Participants' gait was evaluated pre and post a single session of BoNT-A injections performed by their clinicians. 3-D motion of participants was collected during over ground walking at self-selected speeds, including simultaneous measurements of marker trajectories, ground reaction forces, and electromyography (EMG) data (Fig 1A-B). A 17-camera motion capture system (Vicon V8, Vicon Motion Systems, Oxford, UK) was used to track the retro-reflective markers. 3-D motion was tracked using 61 retroreflective markers following the Conventional Gait Model (CGM) 2.5 [3]. Joint kinematics during gait were extracted from Vicon's inverse kinematics framework. Next, we quantified gait deviation from TD children using the Movement Analysis Profile (MAP), which provides a single score of deviation at each joint [4]. A custom MATLAB script was used to calculate the MAP scores. Improvements in joint kinematics during the stance and swing phases were quantified using root mean square error (RMSE) calculated with respect to average results from TD children [4]. Improvements in mean MAP scores were tested using a one-sided Wilcoxon signed-rank test (alpha = 0.05).

Results & Discussion: The BoNT-A intervention improved left hip rotation in children with CP (Fig 1). The mean MAP score for left hip rotation decreased by 40.4% (pre 15.6°, post 9.3°, $p = 0.019$, Fig 1C). We observed a decrease in MAP scores in 5 out of 6 children with CP (Fig 1C). Next, we evaluated improvements in left hip rotation angles independently during the stance and swing phases (Fig 1D-I). We observed near equal improvements in both the stance and swing phases, with average decrease in RMSE values being 38.4% (pre 15.6°, post 9.2°) and 41.9% (pre 15.1°, post 9.0°) for the stance and swing phases, respectively (Fig 1D-I). These improvements were limited to the left hip rotation angle. Although we observed subject-specific improvements in joint kinematics and MAP scores in the other degrees of freedom at the hip, and at the pelvis, knee, ankle, and foot joints, these improvements were not statistically significant.

Significance: Increased hip internal rotation decreases movement efficiency because it affects foot alignment distally. Our results provide evidence in support of BoNT-A to improve hip rotation in children with CP. Such quantitative data enables clinicians to provide evidence-based treatment and long-term care for children with CP.

Acknowledgements: New Jersey Health Foundation (PC 23-21).

References: [1] Kerr et al. 2003, *J Bone Joint Surg Br* 85; [2] Multani et al. 2019, *Paediatr Drugs* 21; [3] Leboeuf et al. 2019, *Gait and Posture* 69; [4] Baker et al. 2009, *Gait and Posture* 30.

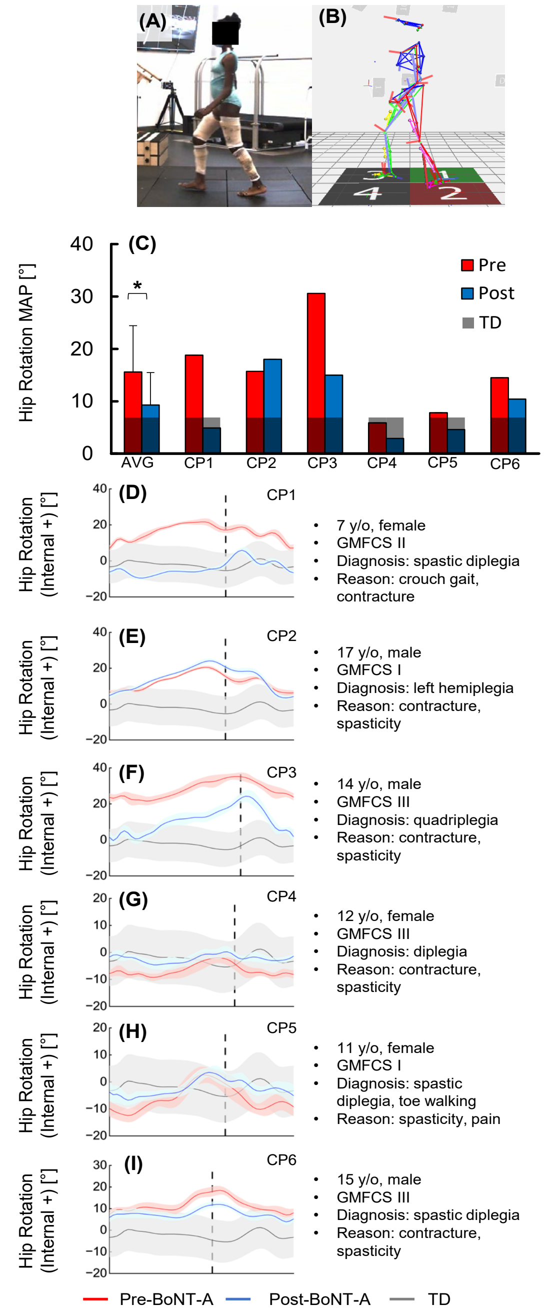

Figure 1: Gait analysis of a representative child with CP (A) and their gait model (B). The average and subject-specific MAP scores for left hip rotation pre and post BoNT-A injections. The black bars represent average MAP score from TD children. The error bars represent one standard deviation (C). (D-I) Average±1SD left hip rotation angles as a function of gait cycle pre and post BoNT-A injections are compared to mean angles from TD children. The vertical lines represent toe-off. Participant demographics, clinical diagnosis, and clinical reason for BoNT-A intervention are included.

BOTULINUM TOXIN TYPE A INJECTIONS MAY IMPROVE GAIT KINEMATICS TOWARDS TYPICALLY DEVELOPING VALUES IN CHILDREN WITH CEREBRAL PALSY: A PRELIMINARY REPORT

Stephanie N. Mace[1*], Hope Voto[2], Brian Knarr[1], David C. Kingston[1]
[1]Department of Biomechanics, University of Nebraska at Omaha, Omaha, NE USA
[2]Univeristy of Nebraska Medical Center, Omaha, NE, USA
*Corresponding author's email: smace@unomaha.edu

Introduction: Cerebral palsy (CP) is the most common cause of motor disability in childhood [1], with many cases presenting with spastic musculature that impairs walking. Botulinum toxin type A (BoNT-A) injections can mitigate muscle spasticity with maximal effects occurring 6-8 weeks post-injection [2,3]. Additional treatments can be administered 3-6 months following the initial injection [3] due to spasticity returning. Current assessments of BoNT-A's efficacy in the lower limb primarily rely on clinical and physical examinations, like the Modified Ashworth and Tardieu Scales which specifically measure spasticity in the involved musculature [4]. Though helpful, these clinical assessments cannot quantify the effectiveness of BoNT-A on gait kinematics. Therefore, the purpose of this study is to quantify changes in gait kinematics, specifically in the ankle, knee, and hip joints at three-time points of BoNT-A treatment: before injection (baseline), 6 weeks, and 3 months post-injection. We hypothesized that improvements would occur in gait kinematics for specific joints depending on the muscle that was injected (monoarticular versus biarticular), with most improvements presenting at 6 weeks and a decrease in improvements from 6 weeks to 3 months due to the injection's diminishing effects over time.

Methods: Thus far, three children with spastic CP (age: 11.33 ± 7.02 years, height: 140.55 ± 27.16 cm, weight: 55.12 ± 26.92 kg) have completed gait analyses at baseline and 6-week follow-up. Trials consisted of barefoot overground walking on a 10 m path with eight embedded force plates (AMTI, Watertown, MA) measuring kinetics at 1000 Hz. Kinematics were recorded via 20 motion capture cameras (Raptor/Kestrel 4200, MAC, Rohnert Park, CA) at 100 Hz. Each child was instrumented with 54 reflective markers to capture lower extremity and trunk kinematics. At least five independent force plate contacts for each leg were required for each visit. The more and less affected sides were separately averaged to calculate the root mean square (RMS) difference via custom MATLAB code (The Mathworks, Natick, MA) for each anatomical plane of lower limb joints during stance. The RMS differences with a positive value indicate an increase in range of motion and a negative value indicates a decrease in range of motion during stance.

Results & Discussion: Preliminary results are reported using a ΔRMS above 5° and below -5° threshold criterion. Differences observed for T02 revealed a reduction in less affected frontal ankle (ΔRMS = -5.15°), an increase in less affected sagittal hip (ΔRMS = 5.64°), more affected sagittal ankle (ΔRMS = 10.02°), more affected frontal ankle (ΔRMS = 5.24°), more affected sagittal hip (ΔRMS = 15.14°; Fig 1A), and more affected transverse hip (ΔRMS = 8.37°). The differences observed for T03 revealed a reduction in more affected sagittal ankle (ΔRMS = -7.05°), more affected transverse ankle (ΔRMS = -28.11°), more affected sagittal knee (ΔRMS = -16.34°), more affected sagittal hip (ΔRMS = -19.29°; Fig 1B), and an increase in less affected frontal knee (ΔRMS = 6.13°). The differences observed for T07 revealed a reduction in more affected frontal knee (ΔRMS = -5.37°), more affected transverse knee (ΔRMS = -8.58°), less affected sagittal hip (ΔRMS = -7.87°; Fig 1C), and an increase in less affected transverse ankle (ΔRMS = 9.36°), left transverse knee (ΔRMS = 5.67°), and less affected transverse hip (ΔRMS = 6.49°). Though specific joints showed differences in magnitude and direction of change, it is valuable to observe the changes that are occurring to all joints that impacts overall walking ability since BoNT-A can impact joints and planes differently depending on targeted musculature and pre-treatment mobility of the child.

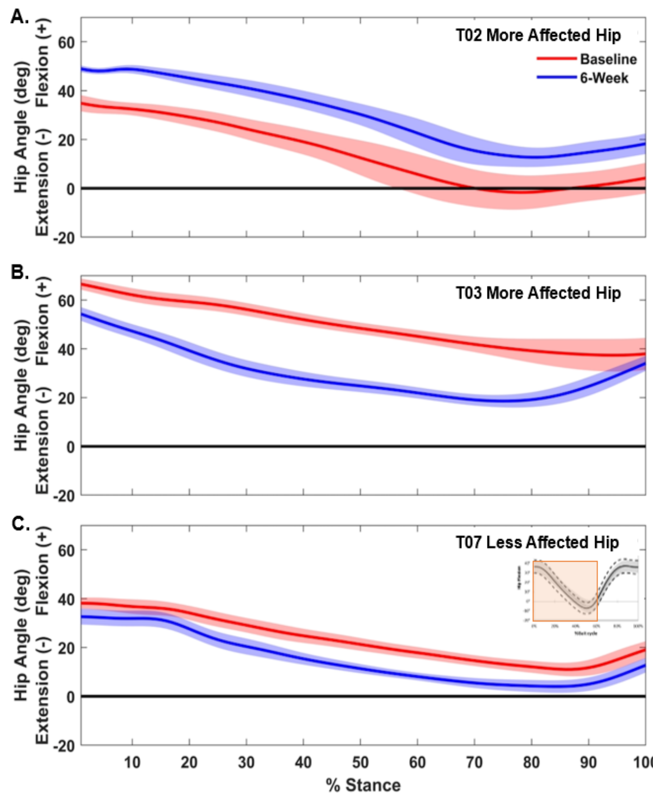

Figure 1. Panels represent the sagittal hip joint angle for each child. C) The upper left figure is typically developing values for sagittal hip kinematics [5]. The orange region represents the stance phase that is the region of interest and depicted in each panel. Solid lines represent the average across all strides with shaded regions being 1 standard deviation. Red indicates baseline kinematics prior to BoNT-A injection. Blue indicates kinematics from a 6-week follow up.

Significance: Preliminary results suggest BoNT-A affects several planes of lower limb joint kinematics 6 weeks post BoNT-A injection and improved overall gait kinematics towards typically developing values. To gain insight into the effects of the BoNT-A over typical clinical interventions, additional 3-month follow-up data will provide inferences of the drug's short-term efficacy.

References: [1] Kirby et al, (2011), *Res. Rev. Disabil.* 32; [2] Hastings-Ison et al, (2018), *J. Child. Orthop.* 12; [3] Multani et al, (2019), *Pediatr. Drugs* 21; [4] Sarathy et al, (2019), *Ind. J. Orthop.* 53; [5] Pixone et al, (2014), *Gait&Posture* 39.

ABILITY OF A COMERCIAL INERTIAL MEASUREMENT UNIT SYSTEM TO QUANTIFY TEMPORAL DISTANCE MEASURES: A PILOT STUDY

Farwa Ali M.B.B.S.[1*], Cecilia A. Hogen M.S.[2], Keith A. Josephs M.D.[1], Jennifer Whitwell Ph. D.[3], Kenton R. Kaufman Ph.D.[2]
[1] Department of Neurology, Mayo Clinic, Rochester, MN
[2] Department of Orthopedic Surgery, Mayo Clinic, Rochester, MN
[3]Department of Radiology, Mayo Clinic, Rochester, MN
*Corresponding author's email: ali.farwa@mayo.edu

Introduction: Inertial measurement units (IMUs) are increasingly being used for measuring temporal-distance gait features. The ease of use and low cost are attractive. However, it is important to consider the measurement validity when making any decisions based on the data. Due to the readily available nature of processed data, clinical investigators are highly likely to rely on proprietary software solutions accompanying the device. Data on external validity of the commercially available software accompanying IMU systems is limited. In this pilot study, we explored the differences between temporal distance features in young normal individuals measured with an IMU compared to gold standard video motion capture (MoCap).

Methods: Reflective markers were placed on each subject using a modified Helen-Hayes marker system. [1] Three-dimensional marker trajectories were captured at 120Hz with a 14-camera motion capture system (Raptor 12HS, Motion Analysis Corporation, Rohnert Park, CA) while subjects walked barefoot on level ground (10m in length) for 5 trials. Motion capture data was analysed using Visual 3D (C-Motion Inc Germantown MD). The APDM Opal IMU system and their custom software Mobility Lab (Version 4, APDM Wearable Technologies, Inc, Portland, OR) was simultaneously used for acquiring temporal distance measures. The steady walk paradigm in the software was tested for each of the 5 trials. The IMUs were affixed to the sternum, lumbar, bilateral wrist and bilateral dorsal foot using double sided tape. Spatial features of velocity (cm/s), cadence (steps/m), stride length (cm), stability using gait stability ratio (GSR) (steps/m) and temporal features of step time (sec), limb support time (% of gait cycle) and limb swing time (% of gait cycle) were assessed for each system. Measures of variability for stride length, step time, velocity, cadence, and GSR were also evaluated. Differences between the two systems were assessed with Bland-Altman plots. All statistical analysis was performed using Blue Sky.

Results & Discussion: 7 healthy controls gave written consent for the study. Median age: 36 (IQR = 27-44) years, median height: 171.6 (IQR = 164.3-177.1) cm, median weight: 70.4 (IQR = 67.85-81.90) kg). There was a high degree of agreement between MoCap and IMU acquired time measurements such as support and swing time durations. Variability as measured by standard deviations was comparable. Significant differences were seen in velocity which was on average 10.8 cm/s slower for IMU compared to MoCap (95%CI 8.8-12.7), stride length was on average 12.4 cm shorter (95%CI 8.5-16.4), (Figure 1) and GSR was slightly higher as measured by the IMU by on average 0.135 steps/m (95%CI 0.04 – 0.233). Cadence was comparable with the IMU producing slightly higher values with a mean difference of 0.126 steps/min (not statistically significant). While the IMU software closely approximates MoCap for time-based variables, it is not highly accurate for distance. Significant errors were noted in the
IMU measurement of velocity, stride length and GSR compared to MoCap in normal healthy volunteers. A previous assessment of Mobility Lab software, using three sensors (lumbar, bilateral foot) and a pressure sensor walkway as gold standard, found high degree of agreement on velocity, stride length and cadence but poor agreement on support and swing times in normal subjects.[2] The APDM Opal system has been evaluated in Parkinson's disease [3], cerebellar ataxia [4] and multiple sclerosis [5], with variable degrees of agreement on different variables. A systematic review concluded that step and stride time had excellent reliability, while other measures had lower reliability [6]. Magnitude of error is rarely reported. Our goal was to evaluate the accuracy of APDM Mobility Lab software compared to MoCap and report the error in the readings to be considered when applying IMUs to different disease states.

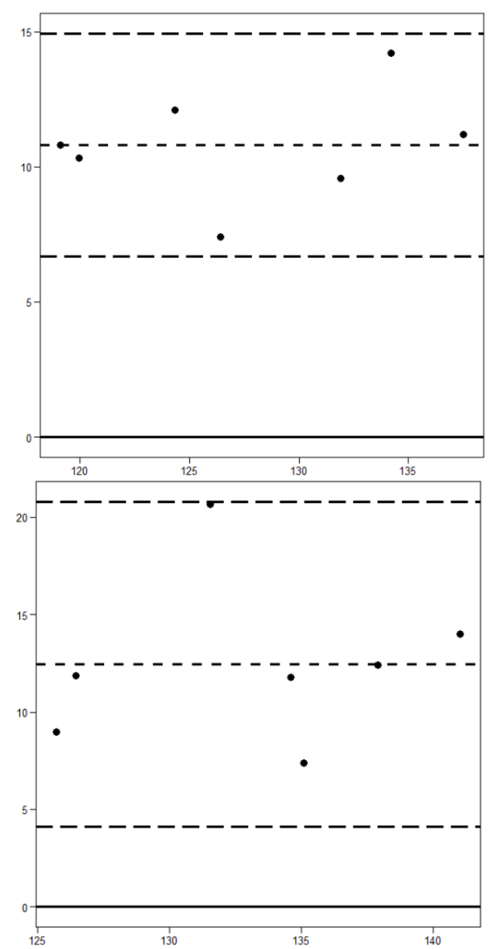

Figure 1: Bland-Altman plots for velocity cm/s (upper) and stride length cm (lower). 95% CI range is shown, x-axis=mean, y-axis=difference between

Significance: This pilot study demonstrates that IMU measurements may have an error compared to gold standard motion capture. With a rapid increase in the use of digital mobility outcomes, it is essential to assess validity of devices, and commercially available software used for acquiring and processing data. This will enable readers to assess validity of measurements, compare results across studies and evaluate scientific conclusions drawn from the data.

Acknowledgements: NIH NINDS R01 NS089757 and NIH NINDS K23 NS124688.

References: [1] Wooten 1990 J Orthop Res 8(3), [2] Morris 2021Physiol Meas 40(9) [3] Mancini 2016 Exp Rev Med Devices 13(5) [4] Brandt 2016 Gait and Posture [5] Storm 2018 PLOS One 13(5) [6] Kobsar 2020 J of Neuroeng Neurorehab 17(62)

MULTI-SEGMENT KINETIC FOOT MODEL SHOWS CORRECTION OF HINDFOOT ABDUCTION MOMENT IN FRONTAL PLANE AFTER HIGH TIBIAL OSTEOTOMY (HTO) SURGERY FOR KNEE VARUS

Songlin Zhu[1], Thomas Jenkyn[1,2*]
[1]School of Kinesiology, Faculty of Health Sciences, University of Western Ontario
[2]Department of Mechanical and Materials Engineering, Faculty of Engineering, University of Western Ontario
*Corresponding author's email: tjenkyn@uwo.ca

Introduction: A high tibial osteotomy (HTO) is a surgery that corrects the alignment of a varus knee. A varus knee tends to have increased adduction moment during walking which increases the incidence of osteoarthritis in the medial compartment [1]. What is unclear is the effect of a varus knee alignment on loading of the foot and ankle. It is hypothesized that increased knee adduction moment is accompanied by an increased abduction moment at the hindfoot (calcaneus). HTO corrects a varus knee alignment and reduces medial compartment compression. So, it is also hypothesized that HTO partially corrects hindfoot abduction moment. To measure hindfoot abduction moment, a multi-segment kinetic foot model (MSKFM) is used with optical motion capture and floor-mounted force plates. The MSKFM used is a novel modification of the Dupont foot model [2], which subdivides the foot into independently tracked hindfoot, midfoot, forefoot and hallux segments (Figure 1). Incorporating the force plate kinetic and motion capture kinematic data enables the moments and powers between foot segments to be calculated.

Methods: Testing occurred in a 12-camera motion capture laboratory (Motion Analysis Corp.) equipped with two floor-mounted force plates (AMTI). A total of 15 auto-reflective markers were placed in a modified Helen Hayes configuration except for the right foot, which had 10 auto-reflective markers for the MSKFM. Each test subject walked at preferred pace over the two force plates, striking them with the right foot. Kinematic data was collected at 50 Hz and kinetic data at 1500 Hz. These were combined to calculate moments and powers between each foot segment in the sagittal, frontal and transverse planes. Moments and powers were external and reported as distal segment relative to proximal. Only frontal plane moment at the hindfoot (with respect to the lower leg) is reported here.

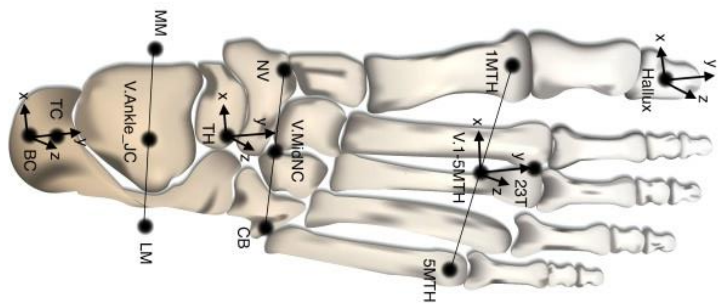

Figure 1: Bones and axes of the hindfoot, midfoot, forefoot and hallux segments of the MSKFM.

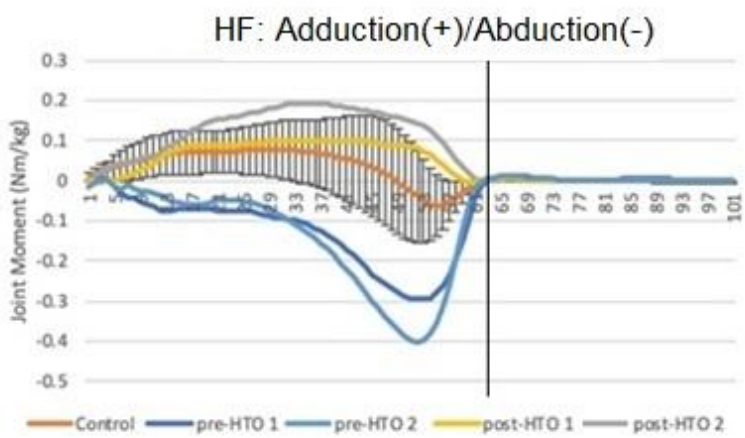

Figure 2: Frontal plane moment of the hindfoot with respect to the lower leg during one gait cycle (1 to 101% of gait). Stance phase occurs first, followed by swing phase. Toe-off is indicated with a vertical black line.

Results & Discussion: A total of 20 test subjects comprised the normal cohort. Figure 2 shows the frontal plane moment acting on the hindfoot (calcaneus) relative to the lower leg. The normal abduction-adduction moment is shown in orange with error bars of plus/minus one standard deviation. Two HTO candidates with knee varus prior to surgery are the light and dark blue lines. The same two candidates post-HTO are the yellow and grey lines. Normal hindfoot moment tends to be inverting until just before toe-off in stance phase. Prior to HTO surgery, the moment on the hindfoot of HTO candidates significantly differed from normal and was abducting throughout stance phase, with peak abduction moments just before toe-off. After HTO surgery, the hindfoot moment was restored to adduction throughout stance phase. However, the two candidates did not show the same trend toward an abduction moment just before toe-off as did the normal population. The HTO surgery has previously been shown to correct knee adduction moment [3], but this study shows that the more distal hindfoot abduction moment is also partially corrected by the surgery.

Significance: Increased abduction moment at the hindfoot is a compensation for the increased adduction moment of the varus knee. Left uncorrected and this hindfoot moment likely leads to foot pathology and difficulty in locomotion. This pilot study has demonstrated that correction of the knee varus also partially corrects the large hindfoot abduction moment, suggesting that pedorthic care can be avoided post-HTO surgery.

Acknowledgements: This research is supported by the Natural Science and Engineering Research Council of Canada (NSERC)

References: [1] Cho Y, Ko Y, Lee W. (2015), *J Physical Therapy 27*(1); [2] Lee DY, et al (2017), *J Foot and Ankle Res* 10(29); [3] Choi GW et al (2015), *Knee Surg, Sport Traumatology, Arthroscopy* 25.

THE USE OF SMARTPHONES IN MEASURING STATIC POSTURAL STABILITY

Jun G. San Juan,[1] Emily Lovekin[1], April Davis[1], and Vipul Lugade[2]
[1]Department of Health and Human Development, Western Washington University
[2]Division of Physical Therapy, Binghamton University, Binghamton, NY
*Corresponding author's email: jun.sanjuan@wwu.edu

Introduction: Having proper balance is essential for maintaining the overall quality of life as it is necessary for independent living and the performance of daily activities. Postural sway is often observed in clinical settings, as it can provide important context in determining mortality, injury and re-injury risk of the lower extremity, and cognitive status. While the usage of force platforms to assess postural sway has proven to be a highly reliable[1,2] and valid [3] method, they yield several practical disadvantages. In addition to being highly expensive pieces of equipment, force platforms also require testing in a laboratory or clinic, which limits the ability for testing outside of a controlled environment. To date, very few studies have suggested strong and feasible methods of balance assessment that could be utilized in the patient's living environment. Current guidelines to assess balance require the skill and expertise of healthcare professionals, resulting in variable practice patterns that often rely on measurements under ideal clinical conditions. The purpose of the study was to test the feasibility of using a smartphone with a custom app to measure human balance during quiet standing in the lab and home environment. We hypothesized that a smartphone with a custom app would exhibit concurrent validity when compared to the force plate data and would also show high repeatability in measuring static postural stability.

Methods: A total of 16 healthy participants, 9 Females, (age = 28.1 ± 10.3 years; height = 1.68 ± 5.5 m; mass = 77.0 ± 22.1 kg) were included in this study. All participants possessed an Apple iPhone 6S (SP) or newer that had an operating system of iOS13 or newer. Participants were given a code to download the IMPROVE custom app for free in the Apple App store. A force plate (FP) (AMTI Inc., Watertown, MA) captured ground reaction forces and center of pressure (COP) data at 1000 Hz. During each trial, two iPhones using the IMPROVE app collected tri-axial acceleration (100 Hz). One was placed in a smartphone belt on the lower back around the waist, at the level of the L3 lumbar spine. The other iPhone was placed in the participant's right front pocket facing forward. During the quiet standing balance trial, participants were asked to stand barefoot with their self-selected feet position on a foam pad (Yes4ALL) placed on top of the force plate for a total of 45 seconds. A squat movement was utilized to synchronize the FP and the SP data. The foot placement was marked and measured to ensure that the same position was achieved for each data collection session. Three sessions were held within 7 days. Sessions 1 and 3 were held in the lab using both iPhones. Session 2 was completed at the participant's home using just the iPhone placed in their front pocket. To assess the concurrent validity of the smartphone with the force plate, a Pearson Product moment correlation was utilized. The Intra-class Correlation (ICC = 2,1) was used to evaluate inter-day reliability between sessions 1 and 3. Also, a paired t-test was used to examine the difference between smartphones on the waist and in the pocket. The alpha level was set to 0.05 and SPSS v28 was used for all statistical analysis. ICC values below 0.5 indicate poor reliability, 0.5 – 0.75 moderate reliability, 0.75 – 0.9 good reliability, and above 0.9 exceptional reliability [4].

Results & Discussion: Most of the smartphone acceleration sway measurements were significantly correlated to the COP measures of sway using the force plate. Only the RMS and Range A-P showed no significant correlation (Table 1). Overall, the smartphone in the pocket and force plate showed moderate to good test-retest repeatability (r = 0.63 to 0.81). Only Range A-P showed poor repeatability (r = 0.39 and 0.46). Other than sway area (p = 0.04), no significant differences were found between the smartphone on the waist and in the pocket in measuring the trajectory measures (p > 0.05). The result of the current study showed that smartphones with a custom app are a repeatable and valid measurement for assessing static postural stability. Also, smartphones used to measure postural stability can be placed in the front pocket instead of using a smartphone belt placed around the waist.

Table 1. Concurrent validity of the Smartphone in measuring static postural stability.

Trajectory Measures	Force Plate (m)		Smartphone in Pocket (m/s^2)		Correlation	
	Mean	SD	Mean	SD	r	p
Distance	**0.010**	**0.002**	**0.011**	**0.003**	**0.53**	**0.04**
RMS	0.011	0.002	0.013	0.004	0.49	0.06
Path	**0.792**	**0.202**	**1.495**	**0.474**	**0.69**	**0.003**
Range A-P	0.030	0.010	0.054	0.021	0.40	0.13
Range M-L	**0.051**	**0.013**	**0.050**	**0.013**	**0.82**	**< 0.001**
Range	**0.052**	**0.012**	**0.070**	**0.019**	**0.51**	**0.04**
Sway Area (m^2/s; m^2/s^2)	**9.1×10^{-5}**	**4.0×10^{-5}**	**2.1×10^{-4}**	**1.1×10^{-4}**	**0.75**	**< 0.001**

Significance: The current study can provide clinicians and patients with the ability to improve intervention and assessment of static postural stability. The smartphone with the custom app can be deployed in a safe, and easy-to-use manner. Clinicians and patients will have the ability to track the results of their intervention progress in the comfort of their living environment.

Acknowledgments: We would like to thank Dr. Barbara Lehman for her assistance with the statistical analysis.

References: [1] Quatman-Yates et al. (2013), *Int J Sports Phys Ther* 8(6); [2] Harro & Garascia (2019), *J Geriatr Phys Ther* 42(3); [3] Harro et al. (2016), *Phys Ther* 96(12); and [4] Koo & Li My (2016), *J Chiropr Med* 15(2).

Stroboscopic Visual Disruption Alters the Neuromotor Control and Biomechanics of Depth Jumping

Kenny D Harrison[1], Jaimie A Roper[1], Christopher J Dakin[2], Anne Z Beethe[2], Talin J Louder[2]

[1]Auburn University, Auburn, AL, U.S.A, [2]Utah State University, Logan, UT, U.S.A

Kdh0077@auburn.edu

Introduction: During a landing impact, ground reaction forces (GRF) are applied from the ground to the feet, resulting in a distribution of internal stress through musculoskeletal kinetic chains. The magnitude of stress applied to the various structures of the body upon landing may depend on the pattern and magnitude of activation of agonist and antagonist skeletal muscle occurring during the fall but prior to impact[1,2]. Vision, as well as other sensory systems, modulate this muscle activity, which plays an important role in controlling overall landing mechanics. The aim of this study was to investigate vision's impact on depth jump landings by disrupting vision via stroboscopic goggles.

Methods: 20 participants (11 male, 9 female) completed 6 trials of depth jumping (0.51 m) in each of two visual conditions (full vision vs stroboscopic vision). Ground reaction force, rate of force development (RFD), and unilateral surface electromyography (EMG) measurements were collected from Tibialis Anterior (TA), Vastus Medialis, Vastus Lateralis, Biceps Femoris, and Gastrocnemius Medialis (GM). Root-mean-square EMG for these muscles was calculated over specific time-bins (150ms pre touchdown, 30-60 ms, 60-85 ms, and 85-120 ms post touchdown). Main effects of condition, and interactions between visual condition and trial number were assessed using repeated measures analysis of variance (α=0.05).

Results and Discussion: Participants peak GRF, normalized to body weight, was 6.4% greater when jumping with stroboscopic goggles compared to the jumping condition with full vision (Table 1 below). During the stroboscopic condition, Tibialis Anterior activation during the 60-85ms post-touchdown period was reduced compared to the full vision condition. VL activation during the 85-120ms post-touchdown period was reduced compared to the full vision condition (Figure A).

Significance: Visual disruption decreased TA and VL muscle activity during the touchdown phase of a depth jump. This presented as altered landing mechanics and lower limb muscle activation patterns. During visual disturbance, healthy young adults may alter their TA and VL activity to land successfully. Future work should examine full body kinematics and center of mass control in this movement as it will lead to better understanding of how vision contributes to depth jumps and potentially provides insight into using visual training mechanisms to reduce the risk of lower extremity injury such as Anterior Cruciate Ligament tears.

Measure	Full Vision	Stroboscopic Vision
Peak GRF (BW)	4.66 (1.26)	4.96 (1.64) *
RFD (BW*s^{-1})	94.27 (49.74)	97.34 (43.72)

Table 1. Central Tendency and dispersion for GRF measures.

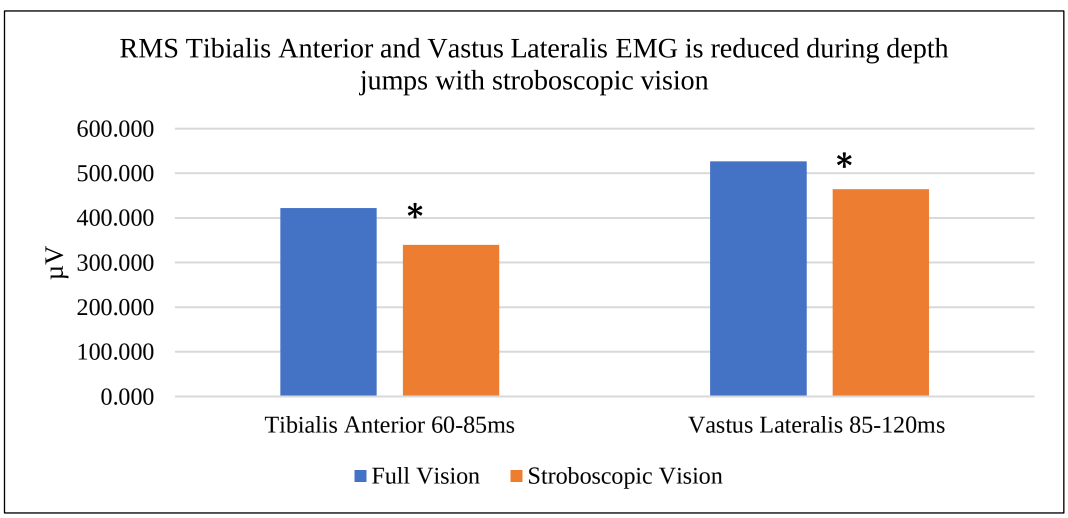

Figure A. Surface EMG changes according to visual condition

*Significantly different from full vision ($p < 0.05$).

References: [1] Baudry & Duchateau (2012), J Physiology 590(21) ; [2] Santello et al. (2001), J Physiology 537(1)

THE EFFECTS OF UNILATERAL ANKLE LOADING ON SPATIOTEMPORAL GAIT PARAMETERS DURING TREADMILL WALKING IN CHILDREN AND ADULTS

Yeon-Joo Kang[1*], Haneol Kim[1], Matthew Beerse[2], Robert Zeid[1], Patrick Underwood[1], Jianhua Wu[1]
[1]Georgia State University, [2]University of Dayton
*Corresponding author's email: ykang9@student.gsu.edu

Introduction

Walking is an essential physical activity for daily life and is a complex activity that requires coordinated motions at the lower limbs to move the body forward while maintaining balance in an upright position. While a healthy population often displays a relatively symmetrical pattern between the left and right sides, this gait symmetry can be compromised due to pathology or injury. One method of augmenting gait asymmetry is to introduce loading on one leg but keeping the other leg intact [1].

Children's gait pattern is different from that of adults due to differences in body proportion and neuromuscular control. Children showed significantly shorter step time and higher step frequency compared to adults [2].Our previous study on unilateral ankle loading has shown that young adults increase step length on both sides and increase step time on the loaded side but decrease it on the unloaded side [3]. We hypothesize that with unilateral loading, children will show similar patterns as adults in step length and time.

Methods

Twenty healthy young adults (aged 18 to 35 years, ten males and ten females) and eleven children (aged 6 to 12 years, five males and six females) participated in this study. The subjects walked straight along a 10-meter walkway three times at their comfortable speed and the average speed was used for treadmill walking. The subjects completed 5-minute treadmill walking under each load condition in a random order: A0, A25, A50, and A75 representing the increase of moment of inertia of the leg about the knee joint by 0%, 25%, 50% and 75%, respectively. The Vicon lower-body model with 16 markers was used to collect data. The marker data were processed using the Vicon Nexus software. Step length was normalized by leg length and step time was normalized by leg length and gravitational acceleration. Three-way (2 group x 2 side x 4 load) mixed ANOVA was conducted on step length and step time. Pairwise comparisons with Bonferroni adjustments were conducted if necessary. For all statistical processes, R package 'afex' and 'emmeans' were used, and the significance level was set as alpha = 0.05.

Results and Discussion

Children showed a longer step length and step time than the adult group from both sides across all loading conditions. The average treadmill speed was 1.26 m/s in adults and 0.98 m/s in children. However, normalized step speed was not different between the two groups. While step length did not show a significant difference or interaction between the two groups (Fig. 1), step time (Fig.2) showed a group by condition interaction (p <0.05), a group by side interaction (p <0.01), and a side by condition interaction (p <0.001). Post-hoc analysis indicated that (1) children display a longer step time than adults across all loading conditions, (2) only adults showed asymmetry in step time between the loaded and unloaded sides, and (3) asymmetry in step time was significant at A50 and A75 conditions in adults.

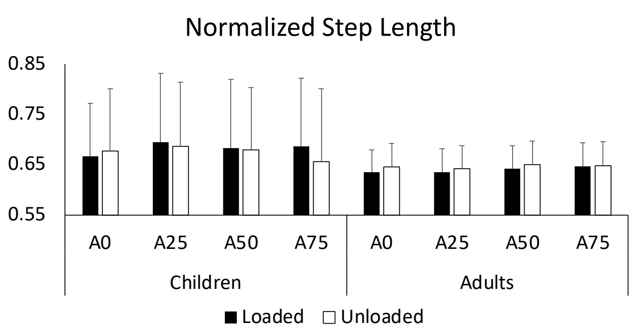

Fig 1: Mean and standard deviation of normalized step length

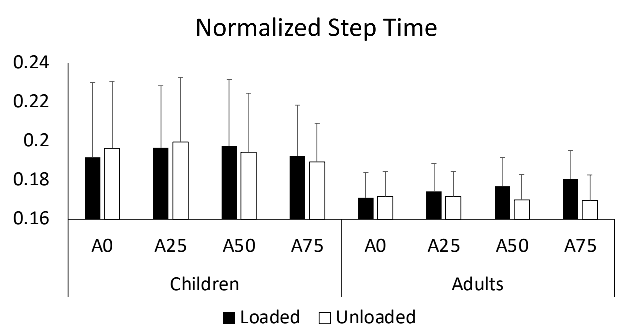

Fig2: Mean and standard deviation of normalized step time

Significance

This study demonstrated the effect of unilateral load on step length and step time is different in children and adults. Children showed longer step length and step time than adults and did not show asymmetry between loaded and unloaded sides which was displayed in the adult group. It suggests that children and adults may use different motor strategies while adapting to a weight perturbation on one leg. Our results present important knowledge on motor adaptation to weight perturbation and can serve as a reference to the design and implementation of future motor rehabilitation in children with disabilities.

Acknowledgments

We are grateful to all the participants for their participation. There is no funding support and no conflict of interest in this study.

Reference

[1] Smith and Martin (2007). *Hum Mov Sci*, 26(3); [2] Aloba et al. (2019). UAHCI 2019; [3] Kim et al. (2021). ASB 2021.

A PRELIMINARY ANALYSIS OF TIMED UP AND GO PERFORMANCE IN PEOPLE WITH ESSENTIAL TREMOR

Patrick G. Monaghan[1,] Kenneth Harrison[1], Julia A. Christl[1], Jaimie A. Roper[1]
[1]Auburn University School of Kinesiology
*Corresponding author's email: pgm0011@auburn.edu

Introduction: Our daily environments are dynamic and require flexibility in performing different postural transitional movements. This may be even more pertinent for people with Essential Tremor (ET), who exhibit walking and balance impairments [1-3]. Failure to adequately perform such vital strategies may severely impede mobility, hinder independence, and increase fall risk [4]. The Timed Up and Go (TUG) test is a well-established clinical assessment of dynamic gait and balance and reflects critical postural transitional movements [5]. Examining specific phases of the TUG (rather than the total TUG time) may be more sensitive [6]; however, few studies have examined and compared performance on each phase of the TUG in people with ET. Therefore, this study sought to compare phases of a standard and complex TUG between people with and without ET.

Methods: 14 people with ET (7 females, 7 males, 65 ± 16 years) and 9 people without ET (6 females, 3 males, 65 ± 18 years) completed a standard and complex TUG. Participants were equipped with six wireless inertial measurement units (Opal, Generation 2, APDM, Inc, Portland, OR.), with three-dimensional sensors placed at the sternum and lumbar spine and one at each foot and each wrist. For the complex TUG tasks, participants completed the typical TUG task; however, they also carried a tray containing a cup filled with 325ml of water. The total TUG time, duration of each phase (sit-to-stand, turning, and stand-to-sit), and turning velocity were derived and used in the analysis. A repeated measures ANOVA with mixed effects were then conducted to compare the effect of condition (standard TUG and complex TUG) and group (ET and Non-ET) for derived outcomes.

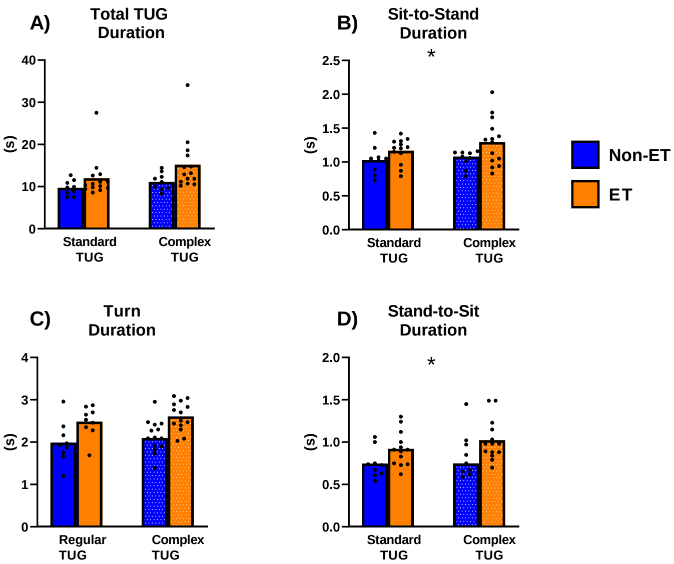

Figure 1. Duration of total and phases of the standard and complex TUGs. Shaded circles reflect individual data points. A) total TUG duration (s), B) sit-to-stand duration (s), C) turn duration (s), D) stand-to-sit duration (s) * indicates main effect of group.

Results & Discussion: A significant main effect of group was found for the duration of the sit-to-stand ($F(1,20) = 6.046$, $p = .02$) and stand-to-sit phase ($F(1,20) = 8.057$, $p = .01$) of the TUG. In contrast, no group differences were observed for total TUG duration ($F(1,20) = 3.027$, $p = .09$), turn duration ($F(1,20) = 1.726$, $p = .20$), or turn velocity ($F(1,20) = 3.826$, $p = .07$). People with ET took on average 0.194s longer to complete the sit-to-stand phase and 0.179s longer to complete stand-to-sit phase of the TUG compared to those without ET. The total TUG duration, a commonly used clinical screening metric [7], was not different between people with and without ET. At the same time, specific phases (sit-to-stand and stand-to-sit) of the TUG provided such distinction. These outcomes support previous literature highlighting the increased sensitivity of assessing particular phases of the TUG rather than simply the overall duration [6]. We also observed a main effect of condition for the total TUG duration ($F(1,20) = 19.566$, $p < .001$), turn duration ($F(1,20) = 37.675$, $p < .001$), and turn velocity ($F(1,20) = 52.749$, $p <.001$). Both groups took 2.37s longer to complete the total TUG during the complex task compared to the standard task. No significant group and condition interaction was observed ($F(5,16) = .914$, $p = .497$).

Significance: While the overall TUG duration may be a beneficial clinical outcome, it is plausible that analysis of specific components of the TUG assessment may exhibit increased sensitivity to detect those most at risk for mobility disability. Outcomes may provide more patient-specific targeted therapeutic approaches, focusing on the elements of the TUG where performance was most impacted. In addition, a hallmark of ET is the distinct heterogeneity of clinical characteristics. Therefore, future work should examine the relationship between clinical characteristics of ET and performance of components of the TUG. Such work will be critical in permitting the earlier identification of those most at risk for mobility impairment, thus helping to reduce potential fall risk.

Acknowledgments: Participants with Essential Tremor were paid from a pilot grant program awarded from the Center for Clinical and Translational Science (CCTS).

References: [1] Arkadir, et. al. (2013), *Therapuetic adv in neuro disorders,9*(4). [2] Louis et. al. (2010), *Movement Disorders, 25*(11). [3] Rao et. al. (2011), Gait&Posture, *34*(8). [4] Shumway-Cook et. al. (2000), *Physical Therapy, 80*(9). [5] Podsiadlo et. al. (1991), *J American Geriatics Society, 125*(2). [6] Mirelman et. al. (2014), *J American Geriatics Society*, 62(4), [7] Herman et. al. (2011), *J Gerontology*, 57(3)

BOUT DURATION DURING OUT-OF-LAB WALKING AFFECTS GAIT VARIABILITY

Mayumi Wagatsuma[1], Julien A. Mihy[1], Stephen M. Cain[2] and Jocelyn F. Hafer[1]
[1]Kinesiology & Applied Physiology, University of Delaware, [2] Chemical and Biomedical Engineering, West Virginia University
Email: mayumiw@udel.edu

Introduction: Gait variability is the stride-to-stride variance during walking. Stride-to-stride variability increases with age and is associated with gait and stability impairments, potentially leading to an increased risk of falls [1,2]. Previous studies have examined gait variability during either out-of-lab walking or a 6-min walk using inertial measurement units (IMUs) [3,4] or force-sensitive insoles [2]. However, the selection of bout duration was varied (e.g., selected only bouts from a 5-10m walking distance or all bouts). In the lab, gait variability is usually estimated on a treadmill or during short overground bouts. In daily life (Out-of-lab), walking bout duration is highly variable [5]. There is no standardized method for grouping or selecting walking bouts (e.g., by time, speed, or step count) and therefore the impact of bout characteristics on gait variability is not well understood. Therefore, the purpose of this study was to compare the effects of walking bout duration on gait variability among healthy young adults and older adults with and without knee osteoarthritis (OA).

Methods: Ten healthy younger (28.1±3.5yrs) and older (60.8±3.3yrs) adults and seven older adults with knee OA (64.1±3.6yrs) participated in this study. Four IMUs [Opal v2, APDM] were placed on the pelvis, and right or more affected limb's thigh, shank, and foot. Participants walked a prescribed ~10 min route in a campus building. A zero-velocity update algorithm was used to calculate spatiotemporal variables from foot-mounted IMU data [6]. Medial-lateral axes for the pelvis, thigh, shank, and foot were defined using a functional sensor-to-segment orientation method [7]. Level strides without turns were selected and standard deviations of walking velocity, stride length, and knee, hip, and ankle angular excursion (ROM) were calculated per bout and averaged for each subject. Variables were compared between short bouts (S) (≤60 secs), long bouts (L) (>60 secs), and all bouts (S+L) for young and older with and without knee OA using a 3 (Group) x 3 (Bout duration) repeated measures ANOVA (α=0.05).

Results & Discussion: Short bouts were 32.1±19.1 sec and long bouts were 188.8±137.6 sec, on average. An effect of bout duration was found for walking speed, stride length, and hip, knee, and ankle ROMs variability. Post-hoc analyses showed short bouts had greater walking speed, stride length, hip, knee, and ankle ROM variability compared to long and all bouts respectively, and all bouts had greater variability than long bouts (p<0.05: L< S+L <S) (Figure 1). Group main effects showed that only knee ROM variability had a significant difference among groups. Young adults had smaller knee ROM variability compared to older adults with and without knee OA (p=0.015, p=0.025, respectively). Although increased variability with shorter bouts agrees with a previous study that compared in and out-of-lab gait, short bouts in our study were not short enough to represent in-lab walking.

Significance: We found that measures of gait variability were significantly different depending on the length of the walking bout (≤60 s, >60 s, or all bouts). Therefore, consideration of bout characteristics is critical for responsibly interpreting measures of gait variability. Without understanding how the selection of walking bout duration changes gait variability, one could misinterpret gait variability in real-world walking. The out-of-lab setting in this study may not characterize real-world bout duration effectively. It might be more meaningful to observe a variety of walking durations from free-living and non-prescribed walking routes to explain gait variability. Out-of-lab gait duration selection criterion is important and should be carefully considered depending on the research question.

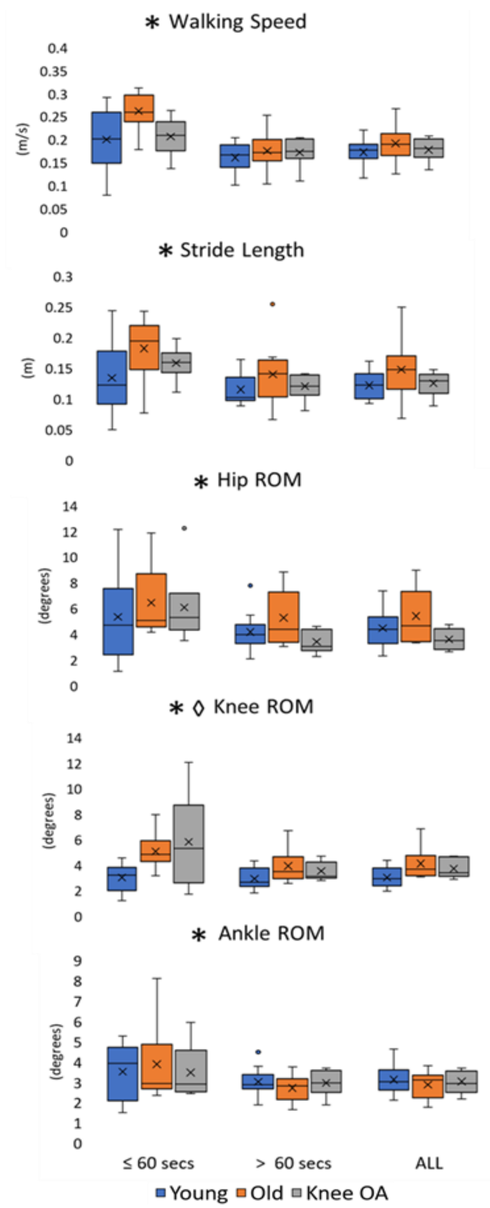

Figure 1: Comparison of gait variability among short (≤60 secs), long (>60 secs), and all (ALL) bouts among healthy young and older adults and older adults with knee OA. *Significant differences among short, long, and all bout durations ◊Significant differences among young adults, and older adults with and without knee OA.

References: [1] Kang, Gait & Posture 2008, 27.4, 5720577; [2] Hausdorff et al., Arch Phys Med Rehabil 2001, 82(8), 1050-1056; [3] Carcreff et al., Sci Rep 2020, 10(1), 2091; [4] Del Din et al., J Neuroeng Rehabil 2016, 13(1):46; [5] Baroudi, Gait & Posture 2022,98, 69-77; [6] Rebula et al., Gait Posture 2013, 38, 974-980; [7] Mihy et al., medRxiv 2022.11.29.22282894

THE INFLUENCE OF STEP WIDTH ON BALANCE RESPONSE STRATEGIES DURING PERTURBED WALKING

Lindsey K. Molina[1,2]*, Gabriella H. Small[1], Richard R. Neptune[1]
[1]Walker Department of Mechanical Engineering, The University of Texas at Austin, Austin, TX, USA
[2]Exponent, Inc., Phoenix, AZ, USA
*Corresponding author's email: lmolina@exponent.com

Introduction: Compared to healthy young adults, individuals with neuromuscular deficits are at an increased risk of falling [e.g., 1] and walk with wider step widths [e.g., 2]. Understanding how step width affects the mechanisms used to restore balance following balance perturbations could guide rehabilitation aimed at reducing fall rates.

The purpose of this study was to determine if altered step widths change the balance response strategies following mediolateral surface perturbations in healthy young adults. Following a perturbation, we hypothesized that walking with increasingly wider steps will require the recruitment of additional strategies to restore balance. Specifically, we expected that following medial/lateral surface translation perturbations, walking with a wider step width will require greater joint moment deviations (i.e., difference in joint moment between the perturbed and unperturbed steps across the gait cycle), with the magnitude of the deviations increasing at the wider steps.

Methods: Kinematic and kinetic data were collected from 15 healthy young adults (7 male, age: 25 ± 4 years). Each subject performed eight 30-second walking trials on an instrumented treadmill, consisting of steady-state walking at narrow (25% narrower), self-selected (SS), wide (50% wider) and extra-wide (100% wider) step widths. A custom script (D-flow, Motek, Amsterdam, NL) determined heel strike timing [3] and projected foot placement targets on the treadmill at the desired step width. During four of the eight trials, the treadmill provided a medial and lateral 2.5cm surface translation lasting 0.25s to each stance foot midway through single-leg-stance when the rate of change of frontal-plane whole-body angular momentum was at a maximum.

A 13-segment inverse dynamics model was created for each subject (Visual3D, C-Motion, Germantown, USA) to calculate joint moments on the recovery step, normalized by subject mass. Balance response strategies [4] were quantified using deviations of ankle inversion moment (lateral ankle strategy), ankle plantarflexion moment (ankle push-off strategy), and hip abduction moment (lateral hip strategy). A one-way repeated-measures Statistical Parametric Mapping (SPM) ANOVA and follow-up SPM paired t-tests with a Bonferroni correction [5] evaluated differences in deviation measures between SS and all other step widths.

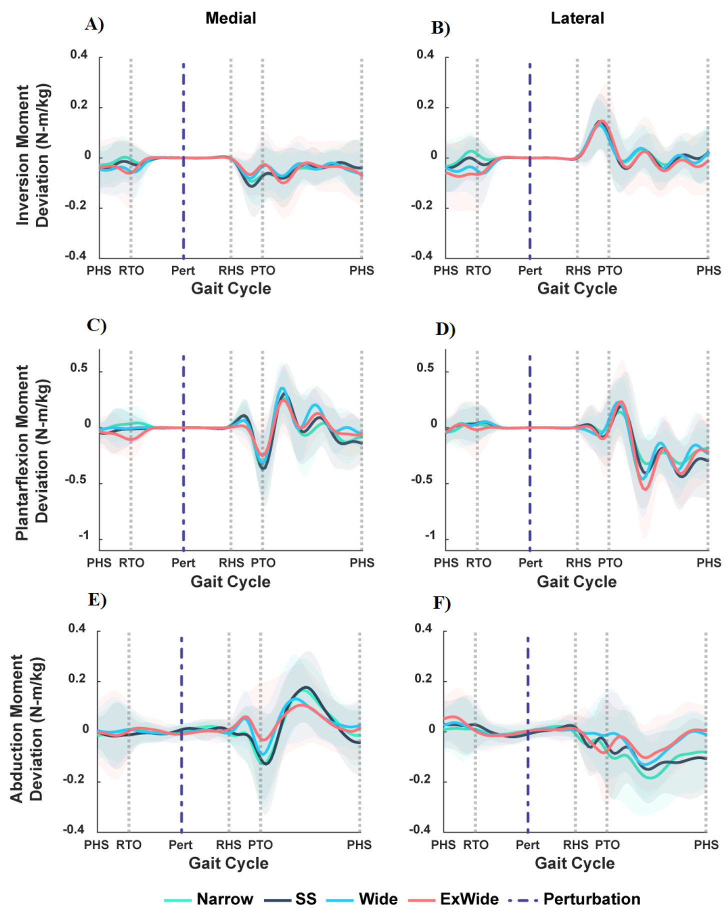

Figure 1: Ankle inversion (A, B), ankle plantarflexion (C, D) and hip abduction (E, F) moment deviation (± standard deviation) after medial (A, C, E) and lateral (B, D, F) perturbations walking at narrow, self-selected (SS), wide and extra-wide (ExWide) step widths. Vertical grey dashed lines indicate perturbed side heel strike (PHS) and toe off (PTO) and recovery side heel strike (RHS) and toe off (RTO). No significant differences were found between SS and all other step widths.

Results & Discussion: There were no differences between the SS and other step widths for ankle inversion, ankle plantarflexion, or hip abduction moment deviation (Fig. 1). Therefore, step width did not affect the response strategies used, which suggests that healthy young adults have the capacity to respond similarly to surface translation perturbations at a wide range of step widths.

Significance: Individuals with neuromuscular deficits may respond differently to these surface translation perturbations. Muscle structure and functional changes in these individuals can lead to reduced muscle strength (e.g., hip abductors [6]). Thus, at wider steps, these individuals may not be able to produce the required joint moments, which may help explain their increased fall risk. Investigating differences in balance response strategies at different step widths in clinical populations remains an area of future work.

A better understanding of balance control can help improve rehabilitation outcomes for those susceptible to falling. These results highlight the relationship between step width and balance response strategies following mediolateral perturbations in healthy young adults and provide a baseline for comparing balance response strategies to those with neuromuscular deficits.

Acknowledgements: This work was supported in part by the National Science Foundation Graduate Research Fellowship Program.

References: **[1]** Forster and Young, 1981. *BMJ* 311(6997):83–86. **[2]** Roerdink et al., 2007. *Phys. Ther.* 87:1009-1022. **[3]** Zeni Jr. et al., 2008 *Gait Posture* 27:710-714. **[4]** Reimann, et al., 2018. *Kinesiol Rev* 7:18-25. **[5]** Pataky, 2012. *Comp Meth Biomech Biomed Engr* 15:295-301 **[6]** Neckel et al., 2006. *J NeuroEngr Rehab*. 3:17.

THE CHRONIC EFFECTS OF A STRETCHING PROGRAM ON RANGE OF MOTION AND VELOCITY OUTPUT OF AN OVERHAND THROW IN COLLEGIATE BASEBALL PLAYERS

Keaton R. Hamilton[1*], Brooke M. Odle[1], Maureen Dunn[1]
Hope College, Holland, MI, USA
Corresponding author's email address: *keaton.hamilton@hope.edu

Introduction: Acute and chronic stretching programs have been reported to increase shoulder range of motion (ROM) utilizing the cross-body stretch and the sleeper stretch [1] but no prior study has examined how this increase may affect throwing velocity in overhead athletes. Few methods have been shown to consistently increase throwing velocity with the exception of various weighted ball and strength training programs [2], often associated with high rates of injury [3]. This study aimed to determine if a nine-week stretching protocol completed during season in collegiate baseball players would result in improvements in shoulder ROM and/or increases in overhand throwing velocity. Since methods to increase throwing velocity are often associated with increased shoulder ROM, it was hypothesized that a 9-week stretching program would increase the ROM of the glenohumeral joint and subsequently increase the throwing velocity in collegiate baseball players.

Methods: Participants' baseline shoulder ROM (goniometer) and overhand throwing velocity (radar gun) were assessed manually and using wearable motion capture sensors. Participants were then matched into either a control group (n=8) or an experimental group (n=8) based on pretest manual velocity measures. The experimental group then performed four sets of sleeper and cross-body stretches, 30 seconds each, five times per week for a duration of nine weeks prior to post testing.

Results & Discussion: A significant interaction was observed in the manually recorded velocity data (p=0.017) as seen in Fig. 1. The control group's velocity decreased over the testing period and the stretching group's velocity slightly increased. There were main effects over time for both active and passive internal rotation and horizontal abduction. Analysis of the sensor data indicated an interaction in extension (p=0.04) and a trend towards interaction in flexion (p=0.054). No significant interactions were found between groups from pre to post test with respect to manually measured ROM in both active and passive flexion, extension, internal rotation, external rotation, or horizontal abduction (p>0.05). Further analysis suggests differences in throwing techniques, which may have impacted the results. Future work should focus on throwing technique.

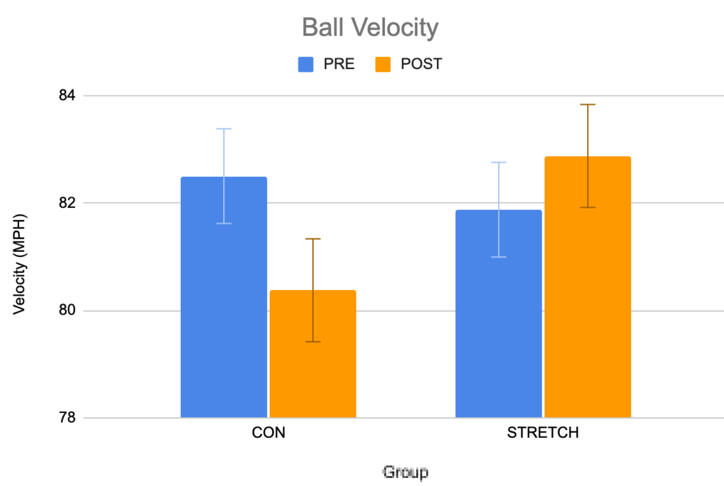

Figure 1. Ball velocity before and after a nine-week shoulder stretching program. A significant interaction occurred between groups over time (p=0.017).

Significance: Although the stated hypothesis was not supported, this study paves the way for future research regarding both ROM and velocity measures of overhead throwing athletes. It furthers the use of wearable data capture systems in the relevant field and when studying motions involving the overhead throwing motion. It was also seen that these wearable motion capture systems may allow for data collection outside of a laboratory setting as seen in the present study. The current study also implies the need to consider small variations in throwing mechanics when collecting and analyzing data associated with the overhead throwing motion.

References: [1] Yavanika et al. (2020). *Int Physiother.* 7(2). [2] Escamilla et al. (2012). *J Strength Cond Res.* 26(7). [3] Bullock et al. (2018). *J Athl Train.* 53(12).

HAMSTRINGS WORK DEMANDS DEPEND ON WALKING SLOPE AND HEAVY LOAD CARRIAGE

Jordan T. Sturdy[1*], Hedaya N. Rizeq[2,3], Amy Silder[2], Pinata H. Sessoms[2], Anne K. Silverman[1]
[1]Colorado School of Mines, Department of Mechanical Engineering, USA
[2]Naval Health Research Center, San Diego, CA, USA; [3]Leidos, Inc., San Diego, CA, USA
*Corresponding author's email: sturdy@mines.edu

Introduction: Hip muscle weakness contributes to risk of distal lower limb and lumbar spine injury [1], which comprise 60–80% of all musculoskeletal overuse injuries among military service members [2]. Carrying heavy backpacks and walking on sloped surfaces require modified hip joint power generation and absorption relative to level, unloaded walking [e.g., 3,4]. Muscle activity achieves these net joint powers; however, the mechanical work performed by individual muscles cannot be directly measured. In addition, while concentric (shortening) and eccentric (lengthening) muscle work both result in acute reduction in force-producing capability, repetitive eccentric work causes greater and longer lasting strength deficits [5]. Thus, the purpose of this study was to quantify hamstring muscle work during sloped and loaded walking while using different backpack implementations.

Methods: Six (5M, 1F) participants (height: 1.74±0.08 m, mass: 78.5±9.5 kg, age: 29±7 y) volunteered for this study. Optical motion capture (120 Hz), ground reaction forces (1200 Hz), and electromyography (EMG, min 1200 Hz) were collected while participants walked on −10° (Down), 0° (Level), and +10° (Up) slopes at 1.15 m/s. Three load conditions on each slope included participants wearing only body armor and a helmet (~6.5 kg, No Pack) and two 40% body weight conditions where the remaining backpack mass was supported by shoulder straps only (Shoulder) or shoulder straps and a hip belt (Hip Belt).

A model containing the lower limbs [6] and a detailed torso with lumbar rhythm [7] and torque-driven arms [6] was developed in OpenSim 4.3 [8] (simtk.org) for the No Pack condition. A backpack attachment model [9] represented the Shoulder and Hip Belt conditions. Inverse kinematics and ground reaction forces from Visual3D were used to drive sloped walking simulations using calibrated models of each participant and backpack condition. Residual errors were reduced and muscle states were solved with computed muscle control. Positive and negative musculotendon power from biceps femoris long head (BFLH) and semimembranosus (SEM) were integrated over right strides to obtain concentric and eccentric work, respectively. We compared muscle work using ANOVA ($\alpha = 0.05$) with main effects of backpack, slope, and the Backpack × Slope interaction. Pairwise comparisons using Tukey's HSD were performed as indicated by main effects.

Results and Discussion: Simulations were verified for low residuals and kinematic tracking errors, and agreement between model muscle activations and EMG of 11 muscles was validated. Concentric work (Fig. 1) by BFLH and SEM increased with walking slope ($p < .005$ for all pairwise comparisons). BFLH concentric work was ~45% greater in both Hip Belt and Shoulder compared with No Pack ($p < .001$ for both pairwise). The Backpack × Slope interaction was significant for BFLH eccentric work ($p = .031$). In all three backpack conditions, BFLH eccentric work during Up was greater than during both Down and Level ($p < .030$ for all comparisons). In addition, BFLH eccentric work was greater during Hip Belt ($p = .001$) and Shoulder ($p < .001$) compared with No Pack while walking Up. In contrast, SEM eccentric work decreased with increasing walking slope ($p < .005$ for all comparisons) and was not affected by backpack condition.

These results illustrate the large hamstring demand during uphill walking. However, other than the slope effect on concentric work, the walking conditions produced different responses between BFLH and SEM. While SEM work progressively shifted from eccentric to concentric with walking slope, BFLH work, both eccentric and concentric, increased with walking slope and added backpack weight. These different responses may be due to differences in muscle architecture and geometry for these biarticular muscles.

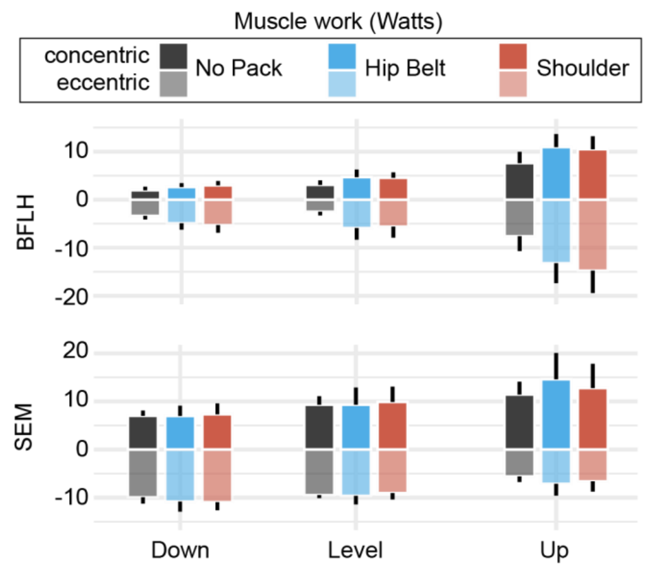

Figure 1. Averaged concentric (+) and eccentric (-) muscle work performed in each slope and backpack condition. Error bars represent 1 standard deviation.

Significance: BFLH is more frequently injured than the other hamstring muscles [10], and injuries are attributed to eccentric strain and greater eccentric work relative to medial hamstrings [11]. These preliminary findings can improve training recommendations for occupations requiring load carriage on varied terrains.

References: [1] Niemuth, (2007) *Int Sport J*, 8(4), 179-192; [2] U.S. Army Public Health Center, 2018;
[3] Huang & Kuo, (2014) *J Exp Biol*, 217(4), 605-613; [4] McIntosh et al., (2006) *J Biomech*, 39(13), 2491-2502
[5] Newham et al., (1983) Clin Sci, 64(1), 55-62; [6] Lai et al., (2017) *Ann Biomed Eng*, 45(12), 2762-2774
[7] Christophy et al., (2012) *Biomech Model Mechanobiol*, 11(1-2), 19-34; [8] Seth et al., (2018) *PLoS Comput Biol*, 14(7)
[9] Sturdy et al., (2021) *Appl Ergon*, 90, 103277; [10] Ekstrand et al., (2012) *Br J Sports Med*, 46(2), 112-117
[11] Schuermans et al., (2016) *Am J Sports Med*, 44(5), 1276-1285

EFFECTS OF CONSTANT LOAD EXERCISE ON KNEE MECHANICS IN AT-RISK WEIGHT INDIVIDUALS

Mariana V. Jacobs*, Kylie Cochran, Justin Pol, Trey Naylor, Jody L. Clasey, Michael A. Samaan
[1]University of Kentucky, Lexington, KY
*Corresponding author's email: mariana.jacobs@uky.edu

Introduction: The recent increased prevalence of obesity has led to an increase in obesity related adverse health effects including osteoarthritis (OA) [1]. Normative weight measures can be defined using several different strategies including body mass index (BMI; $kg \cdot m^{-2}$) [2], total body fat percentage (%Fat) [3], and fat free mass index (FFMI; $kg \cdot m^{-2}$) [4]. Individuals that exhibit body composition measures higher than normative ranges, regardless of the method used to classify weight, are at a higher risk of becoming obese and/or developing OA. Obese individuals exhibit higher incidence of knee OA due to altered gait patterns including higher peak knee adduction angles [5] and lower knee abduction moments [6]. The American College of Sports Medicine (ACSM) recommends aerobic exercise in at-risk (overweight and obese) populations to reduce excess total body and regional fat mass and correspondingly, reduce the risk of obesity related comorbidities yet it is unclear how obesity impacts knee mechanics during prolonged walking (aerobic exercise). Prior work has shown that utilizing BMI to classify obesity results in inconsistent assessment of knee mechanics in obese individuals [7]. It is also unclear whether differing weight-based classifications result in similar group changes in knee mechanics during aerobic exercise. The purpose of this study was to assess if at-risk weight individuals exhibit alterations in knee mechanics during constant load exercise across varying weight classification strategies. We hypothesized that changes in knee mechanics would be inconsistent between varying weight classification strategies.

Methods: Thirty-eight participants (18F; 23.6 ± 3.4 yrs; BMI 27.1 ± 6.7 $kg \cdot m^{-2}$) underwent a total body DXA scan and a 3D gait analysis during a 30-minute walking task (self-selected speed) on an instrumented treadmill. DXA was used to measure total fat mass, % body fat (%Fat) and FFMI and subsequently used to divide participants into healthy and at-risk weight using a BMI $> 25 < 30$ $kg \cdot m^{-2}$[2] (commonly classified as overweight), BMI ≥ 30 $kg \cdot m^{-2}$[2] (commonly classified as obese), sex and age specific %Fat groupings of healthy and at-risk [3], and FFMI [4]. Between group differences in the changes in peak knee joint angles and internal joint moments over a 30-minute walking task were assessed for each of the 4 weight classifications using unpaired t-tests or Mann-Whitney U-tests as needed ($p \leq 0.05$). Knee flexion, abduction and external rotation angles and moments were considered negative.

Results & Discussion: Knee mechanics were similar between healthy and at-risk groups when a BMI > 25 $kg \cdot m^{-2}$ (combining overweight and obese BMI) was used to group subjects. However, when the groups were categorized by combining healthy + overweight BMI (BMI ≤ 25 $kg \cdot m^{-2}$) versus the obese BMI (BMI ≥ 30 $kg \cdot m^{-2}$), the obese group exhibited significantly greater increases in knee adduction angle (p=0.05), greater decreases in knee adduction moment (p<0.001) and a larger increase in knee abduction moment (p=0.03). The at-risk %Fat group had significantly larger decreases in knee adduction (p=0.04) and larger increases in abduction moments (p=0.02) than the healthy %Fat group. When categorized based on the FFMI, the above the 50th percentile group had significantly lower increases in adduction (p=0.02), lower decreases in flexion (2nd half stance; p<0.01), and larger decreases in internal rotation (p=0.005) moments compared to the below the 50th percentile FFMI group (Table 1). Our results support our hypothesis that changes in knee mechanics would differ when different weight classification strategies are employed.

Significance: Although excess body mass is associated with increased knee joint loading and may lead to onset of knee OA in obese individuals [8], the changes in knee joint mechanics that occur during prolonged walking in at-risk and/or obese populations have not been fully elucidated. Our study results indicate that identifying significant alterations in knee joint mechanics during prolonged walking are dependent on the strategies for healthy versus at-risk or obese weight classifications, and thus varying results were obtained when participants are classified using BMI, %Fat or FFMI criteria. Determination of an optimal strategy to classify healthy and at-risk weight individuals will allow exercise specialists and biomechanists to better understand the impact of constant load exercise on knee joint mechanics and to develop effective aerobic exercise and gait-related interventions to reduce body mass and preserve knee joint health in at-risk weight individuals.

Acknowledgements: UK Pediatric Exercise Physiology Lab Endowment and NIH (UL1TR001998 & K01AG073698).

References: [1] Pi-Sunyer F. X. (1999). *Med Sci Sp Exc*, *31*(11 Suppl); [2] Donnelly et al., (2009). *Med Sci Sp Exc*, *41*(2). [3] Gallagher et al., (2000). *The Am J Clinic Nutrition*, *72*(3); [4] Schutz et al., (2002). *Int J Ob & Rel Met Dis*, *26*(7). [5] Lai et al., (2008). *Clin Biomech*, *23 Suppl 1*; [6] McMillan et al., (2010) *Gait Posture*, *32*(2); [7] Capodaglio et al., (2021) *Sensors*, 21,7114 [8] Messier et al., (2014). *OAC*, *22*(7)

	BMI ($kg \cdot m^{-2}$)		%Fat		FFMI ($kg \cdot m^{-2}$)	
Change in peak knee angles (°) and moments ($Nm \cdot kg^{-1}$)	Healthy + OW (N=29)	Obese (N=9)	Healthy (N=19)	At-Risk (N=19)	< 50th % (N=8)	> 50th % (N=30)
Adduction Angle	-0.16±0.71^a	0.55±1.34	-0.11±0.83	0.13±1.02	-0.30±0.40	0.08±1.03
Adduction Moment	0.05±0.07^a	-0.06±0.09	0.06±0.07^b	-0.01±0.01	0.09±0.09^c	0.01±0.09
Abduction Moment	0.02±0.07^a	-0.04±0.05	0.03±0.08^b	-0.02±0.06	0.04±0.09	-0.01±0.07
Flexion Moment (2nd Half Stance)	0.06±0.06	0.04±0.05	0.05±0.07	0.06±0.06	0.10±0.07^c	0.04±0.03
Internal Rotation Moment	-0.03±0.07	-0.05±0.05	-0.03±0.08	-0.04±0.05	0.02±0.06^c	-0.05±0.06

Table 1: Group means ± SD and statistical differences ($p \leq 0.05$) for: ^{a} Obese BMI; ^{b} At-risk %Fat; ^{c} FFMI > 50th percentile. OW: overweight

FALL CIRCUMSTANCES AMONG WALKER USERS IN LONG-TERM CARE INDICATE DEFICIENCIES IN WALKER DESIGN

Kimberly A. Nickerson[1,2*], Kailey Diaz[1,2], Brittney C. Muir[1,2]
[1]RR&D Center for Limb Loss and MoBility (CLiMB), Department of Veterans Affairs, Seattle, WA
[2]Department of Mechanical Engineering, University of Washington, Seattle, WA
*Corresponding author's email: kanick@uw.edu

Introduction: In individuals over the age of 65, falls are the leading cause of fatal and nonfatal injuries with 30% of this population falling each year [1][2]. Walkers are common mobility aids prescribed to reduce fall risk, however, the role of walkers in risk reduction is limited as walker users and non-users alike experience similar fall incidence rates [3]. Improvement to clinical user device training is often suggested as a method to reduce falls with walkers. However, modified training regimens may not be applicable to many walker users who self-obtain the devices commercially or receive them from family, friends, or long-term care facility staff rather than from medical professionals who provide user training [4]. The limited access to device training suggests that fall mitigation efforts should address device deficiencies in addition to training deficiencies. Walker deficits remain largely unknown, therefore the purpose of this study was to identify the common circumstances of falls in older adult walker users and the associated deficits in walker designs.

Methods: 41 videos from a public data set capturing real-life falls of walker users in two retirement facilities were reviewed independently by two researchers [5]. For each video, the circumstances leading up to the fall were evaluated. Qualitative codes were established to describe three fall mechanism categories: walker type (two-wheeled walker or rollator), fall direction (forward, backward, or sideways), and activity at the time of the fall (forward walking, turning, standing, transferring from standing to sitting on the walker's seat or stationary chair, transferring from sitting on the walker's seat to standing, transferring to an upright position after bending over, collapsing the walker's seat, misuse of walker or walker not used). The researchers coded each video separately, compared codes, and then came to a consensus through discussion and video review following any discrepancies. Falls with the activity at the time of fall coded as "misuse of walker" (n=5) or "walker not used" (n=2) were excluded from further analysis. For the remaining 34 falls, a frequency analysis was performed to assess the frequency of falls associated with each combination of walker type, fall direction, and activity at the time of fall. Combinations with high-frequency rates were identified as common fall scenarios.

Results & Discussion: Of falls that occurred during two-wheeled walker use (n=7), users mostly fell sideways while turning (Table 1). Turning with a two-wheeled walker is often reported as a difficult maneuver [6]. Due to the fixed nature of the front wheels, users frequently pick up the walker to complete a turn, reducing their base of support and lateral stability. Since turning may be necessary for the safe navigation of many environments, improvement to the turning functionality of two-wheeled walkers is needed to mitigate sideways falls.

Of falls that occurred during rollator use (n=27), users primarily fell backwards during transfer activities (Table 2). The percentage of backward falls was 16 % higher in rollator users than in two-wheeled walker users, while the percentage of sideways falls was 17% lower for rollator users. Compared to two-wheeled walkers, the implementation of two fixed back wheels and rotatable front wheels in rollators may improve mediolateral maneuverability but at a cost to anteroposterior stability. Backward falls with rollators were often a result of individuals neglecting to lock the wheels while transferring. These findings emphasize the need for a more accessible, easily controlled braking mechanism. The challenges users may face in engaging rollator brakes should be further investigated.

Table 1: Percentages of falls involving two-wheeled walkers by activity and fall direction

	Fall Direction			
Activity	Forwards	Backwards	Sideways	**Total**
Turning	0	0	43	**43**
Walking	14	0	0	**14**
Standing	0	14	0	**14**
Transferring	0	29	0	**29**
Collapsing seat	0	0	0	**0**
Total	**14**	**43**	**43**	**100**

Table 2: Percentages of falls involving rollators by activity and fall direction

	Fall Direction			
Activity	Forwards	Backwards	Sideways	**Total**
Turning	0	11	15	**26**
Walking	7	0	7	**15**
Standing	7	0	4	**11**
Transferring	0	44	0	**44**
Collapsing seat	0	4	0	**4**
Total	**15**	**59**	**26**	**100**

Significance: The use of two-wheeled walkers and rollators do not completely mitigate fall risk in older adults. The poor maneuverability, lateral stability, and braking mechanisms of these devices contributed to falls in our study. These results may be used to inform the design of an improved walker that specifically addresses current walker deficiencies, ultimately reducing the number of falls that occur while using wheeled walkers.

References: [1] Bergen et al. (2016), *MMWR Morb Mortal Wkly Rep* 63(37); [2] Hartholt et al. (2011), *J Trauma – Inj, Inf, Crit Care* 71(3); [3] Gell et al. (2015), *J Am Ger Soc* 63(5); [4] Sloot and Komisar (2022), *Gait & Posture* 97; [5] Robinovitch et al. Databrary (2018); [6] Lindemann et al. (2016), *Aging Clin & Exp Res* 28(2).

RELIABILITY OF ISOKINETIC TRANSVERSE PLANE HIP STRENGTH TESTING IN SUPINE

Vered Arbel[1*], Maeve Gobeyn[2], Kharma C. Foucher[3]
[1]Department of Kinesiology and Nutrition, University of Illinois at Chicago
*Corresponding author's email: varbel2@uic.edu

Introduction: Transverse plane movements of the hip are used during activities of daily living (ADL), such as getting into and out of a car, turning, and even advancing the contralateral limb during walking. Hip internal rotation (IR) and external rotation (ER) are also important in performance testing such as the timed-up-and-go or the figure of eight test. These activities are mostly performed with the hip in a neutral or near-neutral position in the sagittal plane, however transverse plane strength testing is often performed with the hip and knee at 90 degrees and/or in a seated position. [1,2,3,5] This is a potential problem because the moment generating capacity is different at different degrees of hip flexion. [4] Thus, hip strength measured with the hip at 90 degrees likely will not accurately reflect functional strength. Arguably, strength should be tested in a position where it simulates how it is functionally used. Accordingly, the purpose of this study was to develop and assess the reliability of an isokinetic strength testing protocol during which the hip is tested in a supine position with the hip and knee in a neutral anatomical position.

Methods: Twelve adults without acute or chronic lower extremities injuries, participated in the study (8 men and 4 women, 22.8±2.4 years; 65.1±17.5 kg, 164.9±9.5 cm). First, participants completed a 10- minutes warm up on the treadmill at a self-selected speed. Next, to prepare for testing, a restrictive brace was placed on the knee and the ankle to minimize any contribution of the knee and the ankle joint. Participants were then positioned in a supine position on an isokinetic dynamometer [Biodex System 4 Pro, Medical Systems, Inc., Shirley, NY], with hip and knee in extension and feet against the footplate. (Figure 1). Participants were given one practice trial to familiarize themselves with the testing procedures and equipment. Finally, three measurements of ER and IR torque were measured at 60º/s with a one-minute rest interval between each set. The highest peak isokinetic torque score (Nm) of the three attempts was used. Participants returned seven days later for a second testing session, which was identical to the first session. Statistical analysis was conducted using SPSS statistical package version 28 (SPSS Inc, Chicago, IL). Test-Retest reliability was determined by using intraclass correlation coefficients (ICC), based on single-rating, absolute agreement, and two-way mixed effects model. By convention, values between 0.75-0.9 indicated good reliability, >0.9 indicated excellent reliability.


Figure 1 Isokinetic Transverse Testing in Supine with Restrictive Knee and Ankle Braces

Results and Discussion: The ICC was good for right hip internal rotation torque and excellent for all other measures. (Table 1). Peak torque ranged from 2.4-30.6 Nm in internal rotation and 3.3-37.7 Nm in external rotation. One previous report evaluated similar participants in a similar position and found mean values of 36.5 Nm in internal rotation and 33.5 Nm in external rotation in men and 25.4 Nm in internal rotation and 21.1 Nm in external rotation for women [5]. While these values are within the range of those from the present study, the mean values are higher. This could be due to differences in testing such as the use of braces and the lack of use of hand grips in this study, which limited assistive contribution from other muscle groups. These rigorous testing conditions are a key strength and contribution of this study. Limitations of the study included that the majority of participants were men and the total sample size precluded sex comparisons. This matters because transverse peak torque may differ between women and men [4]. Future research will include larger groups balanced between men and women. Nevertheless, this study presents a novel testing protocol designed to mimic the position of the hip and knee joint during upright activities that shows good to excellent reliability and preliminarily good validity with the limited comparisons possible. Future work should also assess reliability for any special populations of interest.

Table 1: Isokinetic Hip Transverse Peak Torque and Interclass correlation Coefficient.

Variables	Peak Torque Nm Session 1	Peak Torque Nm Session 2	Intraclass Correlation	95 % Confidence Interval		Sig
				Lower Bound	Upper Bound	
R hip internal rotation	15.8 ±9	15.6 ±8	.875	.621	.962	< .001
R hip external rotation	18 ±12	18 ±10	.924	.756	.977	< .001
L hip internal rotation	13.5 ±13	14.3 ±14	.953	.850	.986	< .001
L hip external rotation	15.3 ±15	16.7 ±16	.929	.777	.979	< .001

Significance: Transverse strength testing in a supine position may provide relevant norms to employ when assessing function. Because the moment arms, and thus moment generating capacity, for hip rotators change with sagittal plane hip angle, it is essential to consider their torque production in the ranges of flexion seen during common movements. This protocol can further be used to inform effective interventions and individualized programming. Examples of populations in which this is important include people with hip osteoarthritis and other hip pathologies, as well as athletes and dancers who utilize transverse plane motions.

References: [1] Baldon et al. (2013), *J Appl Biomech 29(5), 593-599;* [2] Claiborne et al. (2009), *J Electromyogr Kinesiol* 19(5), e345-e352; [3] Dugailly et al. (2005), *Isokinet Exerc Sci* 13(2), 129-137; [4] Delp et al. (1999) *J Biomech* 32, 493—501; [5] Lindsay et al.(1992) *J Orthop Sports Phys Ther* 16(1), 00043-00050

BIOMECHANICAL BASIS OF INTERVAL THROWING PROGRAMS IN BASEBALL: A SYSTEMATIC REVIEW

Travis Dias[1*], Benjamin G. Lerch[2], Jonathan S. Slowik[3], Kevin E. Wilk[4], James R. Andrews[3], E. Lyle Cain, Jr[3], Glenn S. Fleisig[3]

[1]University of South Carolina School of Medicine Greenville, Greenville, SC, USA, [2]Pennsylvania State University Harrisburg, Middletown, PA, USA , [3]American Sports Medicine Institute, Birmingham, AL, USA, [4]Champion Sports Medicine, Birmingham, AL, USA

* Corresponding author's email: tdias@email.sc.edu

Introduction: Baseball continues to grow in popularity throughout the United States and worldwide. Accordingly, elbow surgeries, such as ulnar collateral ligament surgery ("Tommy John Surgery"), have seen a disproportionate rise with studies reporting two to sixfold increases in performed procedure [1]. An interval throwing program is commonly used in the rehabilitation process following throwing-related injuries. This program, designed to build strength, flexibility, and endurance to facilitate a safe return to play, consists of two phases: throwing on flat ground at increasing distance ("long-toss") and pitching at partial effort from the mound. The purpose of an interval throwing program is to progressively build up joint kinetics, specifically elbow varus torque, and maintain kinematics similar to the kinematics of full-effort baseball pitching [1-4]. To date, there have been no systematic reviews looking at the biomechanics of interval throwing programs. The purpose of this review was to summarize literature that analyzed the kinematics and kinetics of interval throwing programs for baseball players. Specifically: (1) Does an interval throwing program progressively build joint kinetics (specifically, elbow varus torque) up to the level produced in full-effort baseball pitching? and (2) Are the kinematics produced during interval throwing similar to baseball pitching kinematics?

Methods: A systematic review was conducted following PRISMA guidelines. Electronic databases (PubMed and Google Scholar) were systematically searched from 1987 to 2022. Two reviewers independently screened articles according to inclusion criteria. Eligible articles were included if they were peer-reviewed and included biomechanical data of baseball throws used in interval throwing programs, specifically flat-ground throwing and/or partial-effort pitching from the mound.

Results & Discussion From the 750 articles, 83 were selected for full text review, and 12 met the inclusion criteria. Five studies used optical motion capture data [2, 4-6,11], and seven reported data from inertial measurement unit (IMU) sensors [1-3, 7-10, 12]. Most studies showed increased elbow varus torque with increased flat-ground throwing distance. Elbow varus torque for most flat-ground throws did not exceed full-effort pitching torque, and elbow varus torque during partial-effort pitching was less than during full-effort pitching [1, 2, 4-8, 11, 12]. As shown in Figure 1, this indicates that an interval throwing program progressively builds joint kinetics as the elbow varus torque increases throughout this program. In general, flat-ground throwing produced similar kinematics to full-effort pitching. As flat-ground throwing distance increased, shoulder external rotation angle and shoulder internal rotation velocity increased while arm slot above horizontal decreased [3, 5]. Partial-effort pitching significantly reduces joint torques and rotational velocities but produces kinematic differences from full-effort pitching; shoulder external rotation angle, shoulder internal rotation velocity, elbow extension velocity, and ball velocity increased as effort increased [4].

Figure 1: Elbow varus torque versus (A) flat-ground throwing distance (m) and (B) pitching effort (percent of full effort).

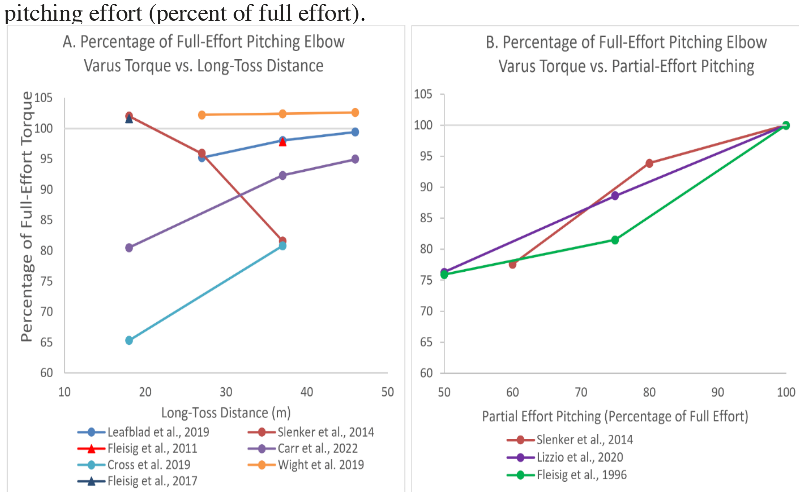

Significance: Interval throwing programs systematically build up joint torques and velocities while maintaining generally similar kinematics to full-effort pitching. This systematic review contributes to the necessary biomechanics literature supporting the use of an interval throwing program for the safe rehabilitation of injured baseball players, especially following ulnar collateral ligament surgery.

References:

[1] Carr et al. (2022), *Arthroscopy*; [2] Cross et al. (2019), *37th Int. Soc. of Bioimech. in Sport Conf*; [3] Dowling et al. (2018) *AJSM*; [4] Fleisig et al. (1996), *ASB*: Proc. of the 20th Annual Meeting; [5] Fleisig et al. (2011), *JOSPT*; [6] Fleisig et al. (2017), *Sports Health*; [7] Leafblad et al. (2019), *Sports Health*; [8] Lizzio et al. (2020), *JSES*; [9] Lizzio et al. (2021), *AJSM*; [10] Melugin et al. (2019), *AJSM*; [11] Slenker et al. (2014), *AJSM*; [12] Wight et al. (2019), *Int. J. Phys. Educ. Fit. Sports*.

BIOMETRICS USING FULL BODY HUMAN MOVEMENT VARIABILITY GAIT DATA

Tyler M. Wiles[1*], Seung Kyeom Kim[1], Nick Stergiou[1], Aaron D. Likens[1]
[1]Department of Biomechanics, University of Nebraska at Omaha
*Corresponding author's email: tylerwiles@unomaha.edu

Introduction: At a visual perceptual level, humans readily distinguish between familiar and unfamiliar people at far distances based on their gait or with minimal information cues [1]. Based on these observations, numerous techniques and datatypes have been used to identify individuals based on their physical characteristics [2,3]. While many approaches generate good performance in terms of identification, very few have considered the problem from a fundamental biomechanics perspective [4]. We hypothesized that there are gait characteristics intrinsic and unique to everyone, so that everyone has a unique "gaitprint", similar to humans possessing unique fingerprints. We further hypothesized that principled gait features that measure human movement variability should provide keys to uncovering this gaitprint [5]. Here, we investigate those hypotheses by pairing simple biometric techniques with detailed, multi-day measurements of gait features for the purpose of identifying each person's gaitprint.

Methods: Thirty healthy young adults between the ages 19-35 were sampled from the NONAN GaitPrint dataset [6]. Between 2 days, participants completed 18, 4-minute, self-paced overground walking trials (n = 540 total trials) on a 200-meter indoor track while wearing 16 Noraxon Ultium Motion inertial measurement units (200Hz). Participants were also given a short, optional break after every 3 trials. A total of 74 variables were calculated including bilateral spatiotemporal variables consisting of distance traveled, average speed, cadence, stride and step lengths, widths, and times, supplemented by percentage of stance, swing, and support phases. Bilateral lower body joint angles (hip, knee, ankle) were also calculated as mean and standard deviations of peak flexion, extension, range of motion, and velocity. We used three methods to split our data into training and test sets. Split 1 (70/30) included a random 70%/30% split of all trials to be placed in the training and test set, respectively. Split 2 (Day 1) used all trials from Day 1 as the training set, and the remaining trials were used as the test set. Split 3 (Trial 1) used the very first trial from Day 1 as the training set, and the remaining 17 trials per participant were used as the test set. Identification was performed using 4 methods: Euclidean distance (ED), cosine similarity (CS), random forest (RF), and support vector machine (SVM) classifiers. Accuracies for various methods are given in Table 1. CS and ED methods allow for determination of Rank 1, Rank 5, and Rank 10 accuracies and are also given in Table 1.

Results & Discussion: Identification performance was best in the 70/30 split with the SVM approach generating the best Rank 1 Accuracy, followed by RF, CS, and ED, in that order. Our results also demonstrate that the simple approach of comparing gait feature vectors (ED and CS) resulted in relatively good identification, with the CS method outperforming the ED method. Unsurprisingly, accuracy deteriorates when less training data is used, especially in the Trial 1 condition. For example, ED performance dropped precipitously when training data contained only a single trial of data, as did CS, albeit to a lesser extent. Machine learning approaches (RF & SVM) fared better, although performance still dropped. Considering our results, a general implication is that a person's identity is indeed related to patterns of gait variability produced when walking overground. One potential limitation of the current work is that metrics included were limited to linear measures of angular and spatiotemporal features of gait. Currently, we are exploring the value of including nonlinear measures as additional gait features, as human movement variability seems to contain both linear and nonlinear characteristics [7]. In addition, we are investigating a larger array of machine learning classifiers and study variable importance in machine learning outcomes.

Table 1: Correct identification results as percentage accuracy for all data splits and methods of analysis

Distribution	ED Rank 1	ED Rank 5	ED Rank 10	CS Rank 1	CS Rank 5	CS Rank 10	RF	SVM
70/30	93.21%	98.15%	98.15%	93.83%	99.38%	99.38%	96.91%	99.38%
Day 1	68.89%	88.52%	92.59%	80.37%	91.48%	95.93%	95.93%	94.74%
Trial 1	46.27%	65.29%	77.84%	60.78%	84.11%	88.43%	75.88%	82.55%

Significance: We provide preliminary evidence that gait variability could be a distinguishing feature in humans. We were able to correctly identify individuals with near perfect accuracy (99.38%) using Rank 5 and 10 cosine similarity and support vector machine learning. Expectedly, using a single trial per participant resulted in the least accurate identification but still reached respectable accuracy from CS Rank 10. The advancement of identification using gait is important considering varied clothing, changing facial features, or distorted images create challenges for biometrics based on those features. Furthermore, gait-based identification is especially useful for use with markerless motion capture systems that extract gait features, regardless of apparel, without direct measurement using sensors.

Acknowledgements: NSF 212491, NIH P20GM109090, R01NS114282, University of Nebraska Collaboration Initiative, the Center for Research in Human Movement Variability at the University of Nebraska at Omaha, NASA EPSCoR, IARPA.

References: [1] Cutting & Kozlowski (1977), *Bull. Psychon. Soc.* 9(5); [2] Wang et al. (2010), *DICTA*. 320-327; [3] Cao et al. (2018), *IET Radar Sonar Navig.* 12(7); [4] Nixon (2005), *Human Identification Based on Gait*. [5] Stergiou & Decker (2011), *Hum. Mov. Sci.* 30(5); [6] Wiles et al. (2023), *Sci. Data*. Preprint Under Review; [7] Gibbons et al. (2020) *Motor Control*. 24(1).

EFFECT OF PROSTHETIC FOOT SELECTION ON METABOLIC COST AND KNEE JOINT LOADING IN TRANSTIBIAL AMPUTEE GAIT DURING DIFFERENT LOAD CARRIAGE CONDITIONS

Aude S. Lefranc [1*], Glenn K. Klute [2], and Richard R. Neptune [1]
[1] Walker Department of Mechanical Engineering, The University of Texas at Austin, Austin, TX
[2] VA Center for Limb Loss and MoBility and Department of Mechanical Engineering, University of Washington, Seattle, WA
*Corresponding author's email: lefranc@utexas.udu

Introduction: Individuals with unilateral transtibial amputations (TTA) are likely to develop secondary disorders such as osteoarthritis (OA) in their intact limb[1] and experience significantly greater metabolic costs and fatigue than non-amputees[2]. Studies have shown that the ankle plantarflexors play a critical role when individuals carry a load[3]. Thus, load carriage presents a significant challenge to individuals with TTA since they lack plantarflexor functionality in their residual leg and prosthetic foot stiffness cannot be modulated to accommodate the load changes. Those using a clinically prescribed passive prosthetic foot during altered load conditions experience greater metabolic cost, increased intact limb power generation and absorption, and increased prosthetic foot dorsiflexion during late stance[4-6]. The purpose of this study was to use a modelling and simulation framework to investigate the effects of various prosthetic feet and load conditions on metabolic energy expenditure and joint loading. We hypothesized there would be an optimal prosthetic foot and load carriage position that minimized energy expenditure and joint loading.

Methods: Kinematic and kinetic data were collected from five individuals with TTA at their self-selected walking speed. 20 trials were collected for each individual, consisting of five loading conditions (no load; 13.6 kg carried as a front load, back load, intact-side load and residual-side load) while wearing four prosthetic feet (a passive clinically prescribed foot, a passive foot one category stiffer than prescribed, their prescribed foot with a heel stiffening wedge and a dual-keel foot). Two participants also wore a powered-ankle foot prosthesis (Empower, Ottobock, Austin, TX) for all loading conditions, thus completing an additional five trials each. A generic musculoskeletal model (OpenSim gait2392) was modified to create a three-dimensional TTA model by removing the segments distal to the residual knee and replacing them with a transected tibia, pylon-socket and ankle-foot prosthesis. In the loaded simulations, the interface between the mass and the torso was modelled using a linear spring and damper along the vertical translational degree of freedom. Total average metabolic power was determined by calculating metabolic power for each muscle based on the metabolic model by Umberger et al.[7] and summing the contributions from individual muscles. Intact knee axial contact loads were determined using computed muscle controls followed by OpenSim's joint reaction analysis algorithm, and then computing the impulse over the gait cycle.

Results & Discussion: The front load condition generally resulted in the greatest total metabolic cost across a gait cycle while the no load condition resulted in the least (Fig. 1A). The optimal prosthesis for minimizing metabolic cost was the dual-keel foot for the no load condition, the one category stiffer foot for the front load, the prescribed foot with a heel-stiffening wedge for the intact-side load, and the prescribed foot for the back and residual-side loads. The intact-side load resulted in the greatest intact knee loads across all prostheses; conversely, the no load condition resulted in the least (Fig. 1B). The optimal foot for minimizing intact knee loads was the powered foot for the no load and intact-side load conditions, the prescribed foot for the residual-side load, the one category stiffer foot for the front load, and the prescribed foot with a heel-stiffening wedge for the back load. It should be noted that large variability was observed across all conditions. This suggests that individuals with TTA may rely on a variety of compensatory strategies to overcome plantarflexor loss under the various load conditions. Further, these results suggest the need for patient-specific prescription as there seems to be a large range of responses to each prosthetic foot. Increases in knee joint loads resulting from a prosthetic foot or loading condition did not always correspond to increased metabolic cost and vice-versa. This suggests that a prosthetic foot that is optimal for one metric may not be optimal for the other, and foot prescription should be modified in order to target specific objectives. These results also suggest that TTAs who present with fatigue should avoid carrying front loads, while those at risk of OA should avoid intact-side loads.

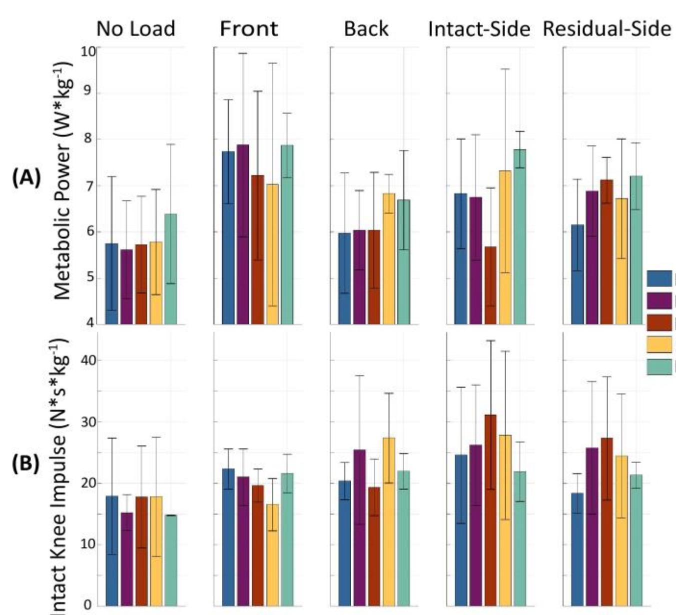

Figure 1 – Average metabolic power (A) and average intact axial knee impulse (B) across a gait cycle for no load, front, back, intact-side and residual-side loads. Prostheses evaluated include prescribed (PR), dual-keel (DK), prescribed with heel-wedge (HW), one category stiffer (SF) and Empower (Ottobock, Austin, TX) powered foot (PW).

Significance: This study provides insight into the effects of load carriage and prosthetic foot selection on metabolic cost and average axial intact knee impulse. Further studies with more participants are needed to generalize these findings.

Acknowledgements: Supported in part by VA awards RX003138 and RX002974.

References: [1] Struyf et al. (2009), *Arch Phys Med Rehabil* 90(3); [2] Gailey et al. (1994), *Prosthet Orthot Int* 18(2); [3] McGowan et al. (2008), *J Appl Physiol* 105(2); [4] Doyle et al. (2014), *Clin Biomech* 29(2); [5] Schnall et al. (2012), *J Rehabil Res Dev* 49(4); [6] Schnall et al. (2014), *J Rehabil Res Dev* 51(10); [7] Umberger et al. (2003), *Comput Methods Biomech Biomed Engin* 6(2).

The Effect of Light Touch Induced Sensory Feedback on Postural Stability in Unilateral Lower Limb Prosthesis Users

Moaz Tobaigy[1,2], Julie Ferrell-Olson[1], Andrew Sawers[1]
[1] Department of Kinesiology, University of Illinois at Chicago, Chicago, IL 60612
[2]Faculty of Medical Rehabilitation Science, King Abdulaziz University, Jeddah, KSA 21589
*Corresponding author's email: mtobai2@uic.edu

Introduction: Balance control relies on proprioceptive and cutaneous sensory feedback [1]. Such inputs are lost or impaired after lower limb amputation [2,3], reducing postural stability and increasing fall risk. To enhance stability while standing or walking, lower limb prosthesis (LLP) users describe seeking out intermittent contact with nearby objects and surfaces [4,5]. It is unclear if this intermittent contact is consistent with the light touch paradigm (i.e., contact force <1N) and the need for additional sensory feedback [6], or a desire for additional mechanical support, and a motor deficit. Previous studies have demonstrated that sensory feedback regarding the motion state of the body derived from light touch significantly enhances postural and dynamic stability in other clinical populations [7,8]. The efficacy with which light touch feedback can similarly improve LLP users' stability is uncertain due to the considerable loss of peripheral sensorimotor function [2,3] and reorganization of the somatosensory cortex after amputation [9]. Therefore, the objective of this pilot study was to determine if light touch sensory feedback is sufficient to improve unilateral LLP users' postural stability. We hypothesized that due to its efficacy in other clinical populations, light touch-induced sensory feedback would improve postural stability in unilateral transtibial (TT) prosthesis users.

Methods: A cross-sectional pilot study was conducted with 3 unilateral TT prosthesis users. Each participant performed two quiet stance tasks: no touch (NT) with crossed arms, and light touch (LT) with the index finger of their dominant arm contacting a stationary surface with a force not to exceed 4 N. Postural stability was assessed by calculating the mean distance (MDIST), velocity (MVELO), and 95% confidence ellipse area (AREA) of the center-of-pressure trajectory derived from limb-specific ground reaction forces [10]. To identify within-subject differences in postural stability, 95% confidence intervals (CI) were computed for each COP metric and compared between NT and LT tasks. Non-overlapping CI were taken as a conservative estimate of a significant difference between NT and LT.

Results & Discussion: Light touch did not reduce participants' vertical ground reaction force (mean vertical GRF no touch = 793 ± 151N, light touch = 792 ± 151N), indicating that light touch did not provide mechanical support, but rather sensory feedback. In general, 95% CIs for the resultant COP mean distance, mean velocity, and area did not overlap between NT and LT tasks (Table 1). Light touch was also more effective at improving AP rather than ML postural stability (Table 1). Despite the loss and impairment of sensory feedback in their residual and intact limbs, our results suggest that light touch sensory feedback is sufficient to improve TT prosthesis users' postural stability. These preliminary findings suggest that postural instability in TT prosthesis users may be attributable to sensory rather than motor deficits.

Table 1. Effect of light touch on postural stability in 3 unilateral transtibial prosthesis users.

	Subject 1: traumatic amputation		Subject 2: traumatic amputation		Subject 3: dysvascular amputation	
COP metrics	no touch	light touch	no touch	light touch	no touch	light touch
Resultant MDIST (mm)	4.1 (3.7, 4.5)	2.5 (2.2, 2.9)*	3.5 (3.2, 3.9)	1.5 (1.4, 1.6)*	8.6 (6.2, 11)	4.3 (4.1, 4.4)*
AP MDIST (mm)	3.9 (3.6, 4.2)	2.4 (2.0, 2.8)*	3.4 (3.2, 3.7)	1.5 (1.4, 1.6)*	8.1 (6.1, 10)	4.1 (4.0, 4.2)*
ML MDIST (mm)	1.0 (.65, 1.4)	.67 (.61, .72)	.31 (.28, .34)	.30 (.26, .33)	1.9 (.56, 3.2)	.77 (.66, .88)
Resultant MVELO (m/s)	9.6 (9.2, 10.0)	8.5 (7.7, 9.2)	10 (10, 10)	9.2 (8.9, 9.5)*	19 (15, 22)	13.6 (13.5, 13.8)*
AP MVELO (m/s)	8.3 (8.2, 8.4)	7.2 (6.6, 7.9)*	8.9 (8.8, 8.9)	7.7 (7.2, 8.1)*	17 (14, 21)	13 (12, 13)*
ML MVELO (m/s)	3.3 (3.2, 3.4)	3.2 (2.9, 3.5)	3.7 (3.7, 3.8)	3.7 (3.6, 3.8)	4.9 (4.3, 5.5)	3.72 (3.5, 4.0)*
AREA (mm^2)	38 (23.8, 52.5)	15 (12, 19)*	26 (24, 29)	11 (9.7, 12)*	414 (311, 518)	72 (68, 77)*

*Non-overlapping 95% confidence intervals

Significance: The results of this pilot study provide preliminary insight into whether postural instability in LLP users can be attributed to sensory or motor deficits. Ongoing data collection will increase sample size and test the effect of light touch versus heavy touch (i.e., unconstrained force contact) on LLP users' postural stability, further probing the need for and role of sensory feedback versus mechanical support. Determining the contribution of sensory versus motor deficits to postural stability could have important implications for rehabilitation strategies and technologies that seek to improve the safety of LLP users. Such interventions could include modifications to amputation procedures, prosthetic componentry, and balance-related sensory re-training.

References: [1] Kavounoudias et al., (2001), *J Physiol* 532(3; [2] Kavounoudias et al., (2005), *Arch Phys Med* 86(4); [3] Kosasih et al., (1998), *JRRD* 35(1) [4] Murray et al., (1969), *Am J Phys Med* 48(1); [5] Kim et al., (2022), *Disabil Rehabil* 44(15); [6] Jeka et al., (1994), *Exp Brain Res* 100(3); [7] Dickstein et al., (2001*), Gait & Posture* 14(3); [8] Oates et al., (2021), *Spinal Cord* 59(2); [9] Schwenkries et al., (2003), *Neuroscience Letter* 349(3); [10] Prieto et al., (1996), *IEEE Trans Biomed Eng*. 43(9).

WEARABLE ROBOTIC EXO-THERAPY CAN IMPROVE GERIATRIC MOBILITY: A CASE STUDY

Jack R. Williams[1*], Jenna C. Hylin[1], Ying Fang[2], Julie L. Stone[1], Zachary F. Lerner[1]
[1]Northern Arizona University, [2]Rosalind Franklin University
*jack.williams@nau.edu

Introduction: Mobility deficits are prevalent among older adult populations. It is thought that these deficits stem from reduced ankle plantar flexor strength during the push-off portion of walking gait, resulting in less ankle power generation, slower walking speeds, and an increased metabolic cost of walking. Together these outcomes can lead to a reduced quality of life and additional health complications. Thus, there is a critical need to explore therapies aimed at promoting mobility among this population. Wearable robotic exoskeletons offer a unique opportunity to explore novel rehabilitation strategies. Our lab has developed an untethered ankle exoskeleton and demonstrated its utility as a resistive gait training tool to promote increased strength and mobility among those with cerebral palsy[1]. This device was conceived with the core-concepts of motor learning in mind, specifically aiming to allow participants to train within the functional context of walking and to be able to do so beyond a clinical setting. While we have recently demonstrated the efficacy of the device to promote plantar flexor muscle usage among an older adult population[2], it is unknown if a multi-week exo-therapy training protocol using this device can promote increased strength and mobility among this population and if there are biomechanical alterations post-training. Thus, the purpose of this preliminary study was to explore the viability of this device as a resistive exo-therapy tool to promote improved mobility among a geriatric population. We hypothesized that 4 weeks of exo-therapy would lead to increased plantar flexor strength, faster walking speeds, a lower metabolic cost of walking, and increased ankle plantar flexor moments and powers.

Methods: One individual (Male, Age: 82) completed four weeks of resistance exo-therapy. This included 14 overall visits consisting of a pre-training session, 12 training visits, and a post-training session. The following measures were assessed pre- and post-training: plantar flexor strength (using a handheld dynamometer), self-selected and fastest walking speeds (during a 30-meter overground walk test), and the metabolic cost of walking (during the last two minutes of a six-minute treadmill walk)[1]. Additionally, for the treadmill session, the participant was outfitted with retroreflective markers and both kinematic and kinetic data were recorded during the final minute of walking. Both pre- and post-training biomechanical variables of interest were determined after scaling a generic musculoskeletal model in OpenSim (v3.3) and performing inverse kinematics and dynamics analyses[3]. The twelve training sessions consisted of 20 total minutes of treadmill walking while receiving resistance from the exoskeleton device. During this the participant also received audio-visual biofeedback in the form of peak plantar-pressure which aimed to encourage increased plantar flexor usage during the push-off phase of gait[2]. Changes in the variables of interest were quantified as percent change relative to the pre-training values. Biomechanical symmetry was quantified pre- and post-training using an interlimb ratio (ILR = right/left, 1.00 = symmetry).

Results & Discussion: Our hypotheses were partially supported. All functional measures of interest displayed beneficial changes post-training (**Table 1**). This included increases in plantar flexor strength, increases in walking speeds, and decreases in the metabolic power associated with walking. Together, these results indicate that this exo-therapy device and paradigm has the potential to promote increased and more efficient mobility. Interestingly, despite bilateral increases in plantar flexor strength, bilateral increases in ankle biomechanical features were not observed. Ankle moment and power increased in the left leg, but the right leg had a consistent plantar flexor moment and demonstrated a considerable decrease in power post-training. This was contrary to our hypothesis, but it is not necessarily a negative outcome. In fact, it appears as if these changes post-training actual resulted in a more symmetric biomechanical movement pattern, as the participant initially presented with an asymmetric gait (Moment: $ILR_{Pre} = 1.37 \pm 0.40$; $ILR_{Post} = 1.03 \pm 0.18$; Power: $ILR_{Pre} = 2.32 \pm 1.45$; $ILR_{Post} = 0.98 \pm 0.62$). This aligns with participant feedback, as they initially reported high fatigue within the left but not the right leg. It may be that the participant overly relied on the right leg during gait pre-training and that, by performing this functional gait exo-therapy, they may have increased functional usage of the left leg leading to a reduced reliance on the right. This could suggest that this device and the exo-therapy paradigm may promote beneficial changes in functional neuromuscular control, however future work is needed to explore this idea. The results of this study should be interpreted with extreme caution as this was performed in a single individual. Future work will examine the efficacy of this exo-therapy strategy among a much larger older adult population.

Significance: Resistive exo-therapy has the potential to promote strength, mobility, and biomechanical symmetry among older adults.

References: [1] Conner et al. (2020), *IEEE J Eng Med Biol.* (1); [2] Fang et al. (2022), *Wearable Technol.* (3); [3] Delp et al. (2007), *IEEE Trans Biomed Eng.* 54(11).

Table 1: Pre-Training and Post-Training Measures of Interest.

Variable		Pre	Post	Percent Change (Pre vs. Post)
Plantar Flexor Strength (N)	**Left**	127.1 ± 10.9	176.6 ± 5.1	+39%
	Right	128.4 ± 6.2	171.6 ± 13.9	+34%
Walking Speed (m/s)	**Self-Selected**	1.22 ± 0.05	1.38 ± 0.01	+13%
	Fastest	1.56 ± 0.05	1.81 ± 0.06	+16%
Metabolic Power (W/kg)		3.49	3.19	-9%
Ankle Plantar Flexion Moment (Nm/kg)	**Left**	1.20 ± 0.17	1.55 ± 0.13	+30%
	Right	1.59 ± 0.37	1.59 ± 0.25	0%
Ankle Power (W/kg)	**Left**	2.33 ± 0.43	3.38 ± 0.50	+45%
	Right	5.10 ± 3.02	3.28 ± 2.29	-36%

3D-PRINTED DUAL-DENSITY METAMATERIALS FOR USE IN ACCOMMODATIVE INSOLES

Kimberly A. Nickerson[1,2*], Ellen Y. Li[1,2], Scott Telfer[1,3], William R. Ledoux, [1,2,3], and Brittney C. Muir[1,2]
[1]RR&D Center for Limb Loss and MoBility (CliMB), Department of Veterans Affairs, Seattle, WA
Departments of [2]Mechanical Engineering, and [3]Orthopaedics and Sports Medicine, University of Washington, Seattle, WA
*Corresponding author's email: kanick@uw.edu

Introduction: Individuals with diabetic neuropathy are at high risk for lower limb amputation due to plantar ulcers caused by loss of protective sensation and high plantar pressures [1]. Custom insoles are often prescribed to redistribute plantar loads and offload regions of high pressure. Considered the standard of care (SoC), these insoles are typically made from multi-layer foams consisting of an accommodative top layer for pressure reduction and a rigid bottom layer for support and pressure redistribution [2]. However, with recent developments in additive manufacturing, 3D-printed elastomer metamaterials may be a more durable and customizable choice for insole fabrication. Previous work by our group has advanced the development of subject-specific 3D-printed insoles with the goal of matching the full-contact and multilayer design of SoC insoles [3]. One challenge of a full contact design is that the insole may vary in thickness, for example, to conform to the shape of a high arch. Little is known about the relationship between thickness of 3D-printed dual-density lattices and their mechanical properties. The purpose of this study was to investigate how thickness influences the behavior of dual-density lattices for use in 3D-printed accommodative insoles.

Methods: Two lattices of differing strut diameters (0.6 mm, 1.03 mm) were designed by Carbon (Carbon Inc., Redwood City, CA) to match the stiffness profiles of bilaminate (accommodative) and EVA (rigid) foams, both are components of a tri-layer foam (Amfit Inc., Vancouver, WA) commonly used for SoC insole fabrication. A third lattice with a uniform strut diameter (0.85 mm) designed to have mechanical properties equal to the average of the accommodative and rigid lattice struts was also generated. Dual-density lattices comprised of a rigid bottom layer and an accommodative top layer were designed to model the multilayer configuration of the SoC insole. Pucks of three different compositions were printed with Carbon® Elastomeric Polyurethane (EPU) 41 at thicknesses of 7, 10, and 13 mm, each 30 mm in diameter, to represent insole regions of varying thicknesses [4]. Across puck heights, two types of dual-density lattices and a single-density lattice were printed. The average single-density (ASD) pucks had the average strut diameter lattice across their full thickness. Equal dual-density (EDD) pucks had equal ratios of rigid and accommodative regions across puck thicknesses. Lastly, the consistent dual-density (CDD) puck had an accommodative region kept at 4 mm thick across all puck thicknesses, matching the bilaminate layer (nominally 4 mm) in SoC insoles. Each puck underwent 1000 cycles of compression testing in an E3000 materials testing machine (Instron, Norwood, MA) following the procedures detailed by Hudak et al. [3]. Local linear stiffnesses for each puck were calculated at three instances during the final loading cycle, equal to plantar pressures of 50, 150, and 250 kPa. The range in local stiffnesses and loading curves for each puck configuration (ASD, EDD, CDD) were compared across puck thickness.

Results & Discussion: For ASD pucks, as thickness increased, local stiffness decreased (Table 1), exhibiting behaviors consistent with single-density foam insoles [4]. The stiffness of EDD pucks also decreased as puck thickness increased, suggesting that overall puck thickness and stiffness are inversely related for single and dual-density pucks. In addition to puck thickness, layer thickness impacted the stiffness of dual-density pucks as CDD pucks of all thicknesses had similar stiffness curves for applied pressures less than 250 kPa (Figure 1). The small range of stiffness values across CDD pucks shows that accommodative region thickness may have a more pronounced effect on stiffness for pressures under 250 kPa than total puck thickness. To produce an insole of variable thickness with consistent properties under equal loading, a CDD lattice should be utilized. Although the range in local stiffness values for CDD pucks starts to increase at 250 kPa, a CDD lattice may be sufficient for use in an insole as plantar pressures greater than 200 kPa are considered high-risk for developing ulcers and may require additional offloading [5].

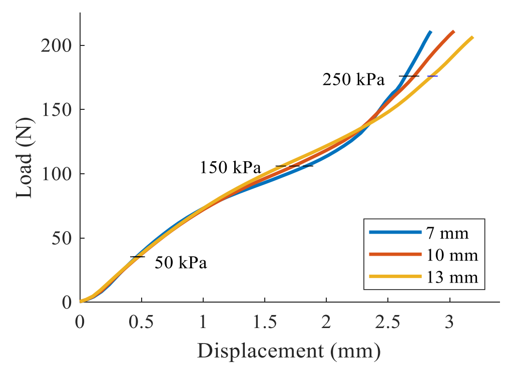

Figure 1: CDD pucks' load-displacement curves for the final cycle of pressure application to 300 kPa

Table 1: Local stiffness values (N/mm) and stiffness range for ASD, EDD, and CDD pucks of multiple thicknesses

		ASD				EDD				CDD			
		7 mm	10 mm	13 mm	Range	7 mm	10 mm	13 mm	Range	7 mm	10 mm	13 mm	Range
Applied Pressure	50 (kPa)	133.80	91.38	69.75	64.05	261.44	129.77	81.69	179.76	87.29	80.40	79.73	7.55
	150 (kPa)	76.16	56.43	46.02	30.14	242.24	91.35	44.77	197.47	42.63	43.92	45.02	2.39
	250 (kPa)	75.54	61.19	44.05	31.49	212.49	86.23	78.02	134.48	151.54	105.74	87.15	64.39

Significance: 3D-printed dual-density lattices with a constant accommodative and variable rigid region thickness may be sufficient for use in accommodative insoles. Continuing to investigate 3D-printed metamaterials in future work may inform the design of 3D-printed accommodative insoles and ultimately improve patient outcomes.

Acknowledgments: Funding for this study was provided by VA Award A3539R.

References: [1] Stress R, et al. Diabetes Care 20(5), 1997; [2] Janisse D and Janisse E, Pro Orth Int 39(1), 40-47, 2015; [3] Hudak Y, et al. Med Eng & Phys 104, 2022; [4] Lemmon D, et al. J Biomech 30(6), 1997; [5] Owings TM, et al. Diabetes Care 33(5), 2008.

MUSCLE ADAPTATION TO SPEED CHANGES DURING WALKING IN YOUNG AND OLDER ADULTS

J.T. Lin[1*], T. Shields[1], H. Dennerlein[1], A. Patel[2], L. Coar[1], J. Betancourt[2], A. Greenberg[2]
[1]Seton Hall University Doctoral of Physical Therapy Department; [2] Seton Hall University College of Nursing
*Corresponding author's email: juite.lin@shu.edu

Introduction: Functions of sensorimotor systems are critical to control movements and maintain balance, but these functions could be compromised by age [1]. Generally, falls happen when the motor system fails to adjust body posture and maintain balance in changing standing and walking conditions. As two-legged species, we evolve motor strategies in order (i.e., ankle then hip strategies) to maintain standing balance. However, a limited number of studies have addressed what motor strategies people, especially older adults would involve when changing walking conditions, such as changing walking speeds. Muscle co-contraction is necessary to provide stability to prevent falls while experiencing perturbation [2], but it is contradicted by dynamic movements and flexibility. With the normal aging process, sarcopenia is characterized by a decline in muscle strength and power because of losing Type II muscle fibers. Neurodegeneration is also part of normal aging that affects motor coordination through a reduction in brain activity and function. Therefore, there is a need to investigate how motor strategies (e.g., muscle coordination mechanism) would change in the face of speed perturbation and whether these changes are different with an aging population.

Methods: This study was an observational study design. We recruited 3 young adults (22 y/o) and 3 older adults (71±7 y/o) in the study. Walking speeds, including self-selected comfortable and fast walking speeds, and step lengths were measured by the GaitRite system. Participants then walked on the split-belt treadmill, which was utilized to provide speed perturbations. Specifically, participants walked at comfortable and fast speeds for 1 minute, then one side of the belt (i.e., the side where subjects have a shorter step length) increased the speed for 5 minutes, then both belts were returned to the comfortable speed for another 2 minutes. Real-time kinematic and surface electromyography (EMG) data were collected during the entire walking section. A VICON Plug-in-Gait Lower-limb 16 marker set was used to obtain lower extremity kinematics data in 3D. Muscle activities, including tibialis anterior, gastrocnemius medialis, rectus femoris, and hamstrings were monitored using wireless EMG. All EMG signals were normalized by the peak EMG value of each muscle, which is collected at individual maximum walking speeds. The co-contraction index (CCI) was used to quantify the level of selective leg movements (i.e., muscle coordination). Specifically, CCI is the ratio of EMGs to EMGl*(EMGs+EMGl), where EMGs is the level of muscle activities for the less active muscle and EMGl is the level of muscle activities for the more active muscle during the stance phase of the gait cycle. A higher value of CCI represents a higher level of simultaneous activation of the counter-acting muscles.

Results & Discussion: When participants walked at self-selected maximum walking speeds, we found that young adults had a higher muscle co-contraction on leg muscle than on hip muscles (*p*=.05) (Fig. 1). However, older adults had a comparable muscle co-contraction between leg and hip muscles. When participants walked on the split-belt treadmill, all participants had a longer step length on the slower belt sides during the perturbation period, then the step length pattern was reversed after removing the perturbation (Fig. 2). As expected, compared to CCI during comfortable walking, both age groups showed an increased CCI on both leg and hip muscles on the slower belt side at the beginning of perturbation (i.e., early adaptation period) and smoothly decreased till the end of perturbation (Fig. 3). Interestingly, compared to older adults, young participants had a higher muscle co-contraction at the hip muscles, especially during the early post-adaptation period (*p*<.01), where the leg muscle coordination pattern was not different between age groups (Fig. 3). It is possible that young adults primarily involve leg but not hip muscles to provide walking stability when they anticipated speeds changes. Under unanticipated speed changes (i.e., speed perturbation), young adults could effectively involve and adjust both hip and leg strategies to maintain walking stability, whereas older adults solely rely on leg strategy that limits their ability to maintain balance and the older adults take a longer time to adapt to a new walking condition.

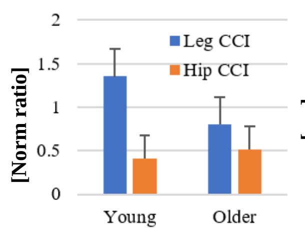

Figure 1. Max walking speeds

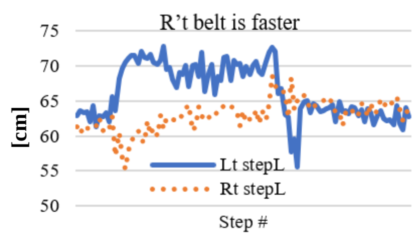

Figure 2. Illustration of gait adapt.

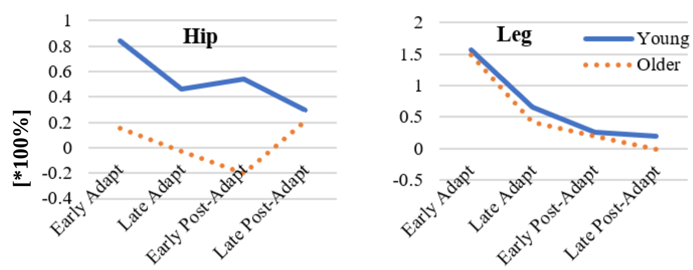

Figure 3. The change of hip and leg CCI on the slower belt side

Significance: Neuromuscular coordination is one of the most common intrinsic factors contributing to fall risks in older adults. By identifying the neuromuscular changes with aging during walking and changing speeds, we can further develop a rehabilitation program that specifically targets these muscles and movements that need to be improved.

Acknowledgments: The study was supported by Seton Hall University Opportunity Meets Innovation Challenge Grant program

References:

[1] Fasano A, Plotnik M, Bove F, Berardelli A. The Neurobiology of Falls. Neurological Sciences. 2012;33(6):1215-1223.
[2] Falk, J., Strandkvist, V., Pauelsen, M. et al. Increased co-contraction reaction during a surface perturbation is associated with unsuccessful postural control among older adults. BMC Geriatr 22, 438 (2022).

Sit-to-Stand Balance Control in Diabetic Peripheral Neuropathy

Mohsen Alighanbari[1*], Hao-Yuan Hsiao[1], Lisa Griffin[1]
[1] Department of kinesiology and health education, The University of Texas at Austin
*Corresponding author's email: m.alighanbari@utexas.edu

Introduction: Diabetic peripheral neuropathy (DPN) is a neuronal disease that affects the distal extremities and progresses proximally [1]. DPN complications increase the risk of falling up to 64%, with the highest incidence of falling during transitional tasks like sit-to-stand (STS) [2]. Although balance control was found to be compromised during walking and quiet standing [3,4], previous literature found no significant difference between healthy and DPN groups during STS while assessing the whole-body center of mass movement [5]. The STS is a bilateral task in which both the left and right limbs contribute to its successful execution. Recent studies have shown a significant difference in nerve conduction velocity of the right and left limb in older adults with DPN [6] and lower perturbation detection capability in only the left leg in older adults with DPN [7], therefore it is possible that peripheral neuropathy may affect each limb differently. The variation in how neuropathy affects each limb may compromise balance control of one leg and not the other, resulting in impaired balance in frontal plane rather than sagittal plane of motion. However, this is yet to be tested. Therefore, the present study aims to test our hypothesis that older adults with DPN have an abnormality in their balance control on the left leg compared to healthy older adults.

Methods: A total of 8 older adults (2 DPN age: 72.0 ± 9. 9 years and 6 control age: 70.3 ± 9.6 years) were recruited. For the DPN group, older adults with mild peripheral neuropathy were selected. The presence of neuropathy was assessed by Michigan Neuropathy screening questionnaire and Biothesiometer. Participants performed STS tasks with 90° hip flexion and 105° knee flexion. Participants placed each foot on one force plate symmetrically and shoulder-width apart. Participants kept their hands on their waists during all the experimental procedures and performed the task with self-selected speed. Kinematic and kinetic data were collected using 12 Vicon cameras (100Hz) and 3 Bertec force plates (2,000Hz). The third force plate was used under the adjustable chair to identify the seat-off instant. The motion of the sternum marker identified STS initiation. The maximum hip extension was marked as STS termination. Center of pressure (CoP) data was filtered using zero lag 5th order Butterworth filter with the cut-off frequency of 25Hz. The resultant CoP distance was calculated using the Parito et al. equation $[Resultant\ distance[n] = (AP[n]^2 + ML[n]^2)^{1/2}]$. The 95% confidence ellipse area was enclosed to the CoP path for each limb and normalized with the duration of the STS tasks. Finally, the maximum and average of the CoP resultant distance for each limb were calculated. All the procedures were performed in MATLAB using custom code. A one-way MANOVA was used with a group as a factor (DPN and Healthy) and CoP area, CoP maximum distance, and CoP average distance as dependent variables. The statistical test was performed in SPSS (version 27) with the level of significance set to 0.05.

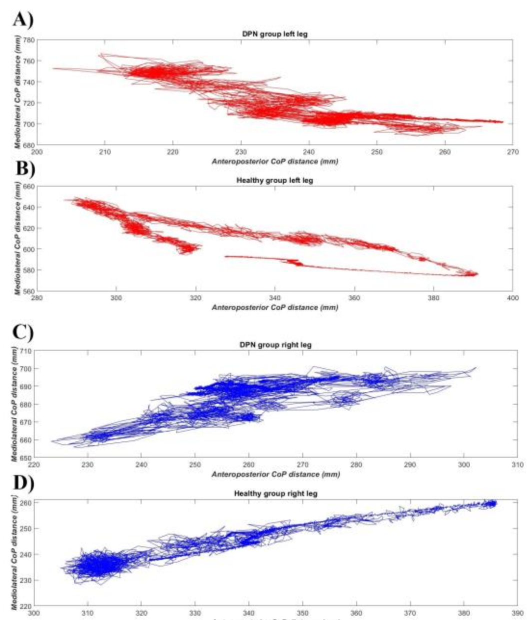

Figure 1: A) CoP sway area for left leg in DPN population in mm. **B)** CoP sway area for left leg in healthy population color for left leg is set to red **C)** CoP sway area for the right leg for DPN in blue color **D)** Healthy adults CoP sway area for the right side.

Results & Discussion: Assessment of CoP enclosed elapsed area for the left limb showed a significantly higher sway in old adults with DPN than healthy old adults (P = 0.001). However, no statistical difference was found for the right leg CoP area between DPN and healthy adults (P = 0.309). Also, the maximum of the resultant CoP distance (P = 0.036) and the mean of the resultant CoP distance (P = 0.027) are statistically different for the left leg between DPN and healthy adults. In contrast, no statistical significance was found in the maximum and average resultant CoP for the right leg between DPN and healthy control. Our results demonstrate that older adults with DPN have abnormalities in their balance control in the left leg compared to healthy old adults during STS task. Combining our results with previous findings on motor nerve conduction velocity showed that peripheral neuropathy affects the left leg more than the right leg, which may reduce the overall balance control and increases the risk of falling. Further investigation is required to identify other mechanical alterations due to variation in peripheral neuropathy's effect on the left and right limbs.

Significance: We observed balance control abnormalities in the left leg of the DPN population compared to healthy controls. This result may offer potential explanations to the higher incidence of falling in the DPN population during transitional tasks. Thus, future rehabilitation protocols should address interlimb differences in this population.

Acknowledgements: This study is supported by College of Education small grant at the University of Texas at Austin.

References: [1] Greene et al. (2021), *Annual review of medicine* 41(1) 303-320; [2] Yang et al. (2016), *Age Aging* 45(6) 761-767; [3] Sawacha et al. (2009), *Clinical biomech.* 24(9) 722-728; [4] Lafond et al. (2004), *Diabetes care* 27(1) 173-178; [5] Lim et al. (2014), *Pm&r* 6(3) 209-214; [6] Younesian et al. (2020), *J. Applied biomech.* 36(3) 171-177; [7] Kim & Robinson (2006), *International J. Occupational safety and ergonomics* 12(3) 1065-1085.

SAGITTAL PLANE TESTING FOR INFANT PRODUCT SAFETY: PROOF OF CONCEPT STUDY

Sarah M. Goldrod[1*], Erin M. Mannen PhD[1]
[1]Department of Mechanical and Biomedical Engineering, Boise State, Boise, ID, USA
*Email: sarahgoldrod@u.boisestate.edu

Introduction: Approximately 3,400 infants die of sudden unexpected infant death (SUID) each year, and some of these deaths occur in commercial infant products like bouncers or swings when infants are asleep or unattended [1]. To promote safe sleep, the American Academy of Pediatrics (AAP) recommends that caregivers place infants on their backs on a firm sleep surface without soft bedding, and that infants sleep on a non-inclined surface. While a crib is the undisputed safest place for an infant to sleep, commercial infant products like bouncers or swings can provide a contained space for parents to place a baby for attended play. However, many infants are left unattended or fall sleep in commercial products that are not designed for nor adhere to the AAP's safe sleep guidelines. Thus, ensuring that infants are as safe as possible in every infant product is critical.

Previous research has established that head/neck and trunk posture are important for normal breathing. Reiterer et al. found that at 45° of head/neck flexion, the mean lung resistance of the preterm infants increased by 34% compared to a neutral position [3], and extreme head/neck flexion can cause complete airway occlusion in infants lacking head control. Lin et al. found that slumped sitting significantly decreased lung capacity and expiratory flow compared to a normal sitting position [4]. Another study found that a slumped posture affected ribcage and chest wall motions during breathing compared to a normal sitting position [5]. Clearly, head/neck flexion and trunk flexion are postural characteristics which can negatively influence breathing, yet current regulatory standards governing commercial infant products like a bouncer or swing do little to evaluate infant body posture within products. Two devices currently exist to measure body position – the hinged weight gage (~$500) and the CAMI dummy (~$12,000). The purpose of this proof-of-concept study is to evaluate current test devices and a 4-segment anthropometric device (~1,000) [6], all compared to an actual infant's body position.

Methods: Testing was divided into two experiments: mechanical testing of with the sagittal plane devices (hinged weight gauge, CAMI dummy, and 4-segment device) and motion capture human subject testing. The Fisher-Price Rock N' Play (Fig. 1) was used for both experiments. This product was chosen because it features a design similar to some bouncers and swings, and our previous research has shown that inclined sleep products result in ~16° of trunk flexion during normal supine lying [7]. Each sagittal plane device was placed in the Rock N' Play in the intended position for a total of three times. We used a Wixey Digital Angle Gauge to measure the segment angles and then computed the difference between segment angles to determine the flexion/extension angles of each hinge/joint. Human testing was conducted on one participant in our IRB approved study (126-MED20-005). We used an eight-camera motion capture system, (Qualisys, Gothenburg, Sweden), to collect data. A marker set of nine retroreflective markers was placed on the participants to track motion. Each participant was placed supine on a flat surface and in a Rock N' Play product for 2 to 3 minutes. The flat surface was used to normalize subject data and each trial was trimmed to a single frame for this proof-of-concept study. A custom MATLAB 2022a code was created to process the data and calculate the head/neck and trunk flexion of the infants.

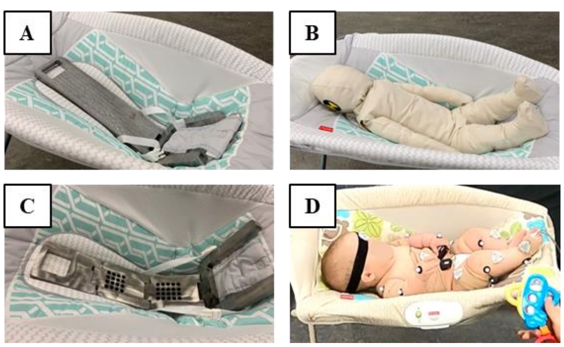

Figure 1: Testing in the Fisher-Price Rock N' Play, (A) hinged weight gauge, (B) CAMI dummy, (C) 4-segment, and (D) participant.

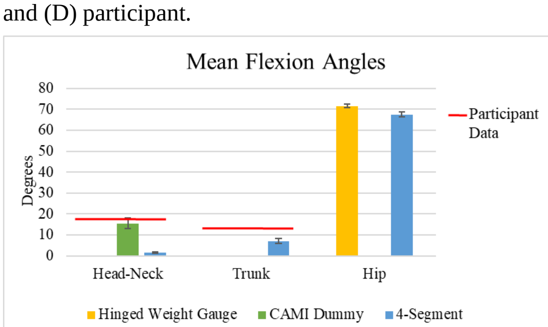

Figure 2: Mean flexion angles of 2-segment infant hinged weight gauge, CAMI dummy, and 4-segment device.

Results & Discussion: The infant exhibited head/neck flexion of 17° and trunk flexion of 14°. The results revealed several limitations with current testing devices (Fig. 2). The hinged weight gauge cannot model head/neck or trunk flexion angles. The CAMI dummy is ideal for modelling head/neck geometry and flexion but cannot model trunk or hip angles. The 4-segment device was able to measure head-neck, trunk, and hip angles though the head/neck results did not compare well with the infant data. The addition of a pelvis segment to the 4-segment device may facilitate consistent positioning between devices and between tests, and addition of three-dimensional head geometry may improve accuracy of results. A larger data set with more participants and time, with many categories of infant products will provide a more robust comparison on the accuracy of sagittal plane devices. This proof-of-concept study shows that sagittal plane devices are able to replicate infant body position measurements consistent with *in vivo* data, but that improvements are required to obtain both head/neck flexion and trunk flexion in a single device.

Significance: Safe body positioning is critical for healthy breathing, and manufacturers would benefit from a simple mechanical device to enable them to measure these parameters in infant products. This study compared three mechanical devices to *in vivo* data from an infant to evaluate accuracy and inform development of improved sagittal plane testing devices.

References: [1] CPSC (2022); [2] Moon et al. (2022), *Pediatrics*, *150*(1); [3] Reiterer (1994), *Pediatric Pulmonology*, *17*; [4] Lin et al. (2006), *Phys. Med. and Rehab*, *87(4)*; [5] Lee et al. (2010), *Resp. Phys. and Neuro.*, *170(3)*; [6] Mannen et al. (2022) *CPSC*; [7] Wang et al. (2018), *J Biomech. 128*.

COMPARISON OF DIFFERENT HIP JOINT CENTER PREDICTION METHODS

Natesan K, Lu H-C, Likness A, Atkins LT, Yang HS, James CR
Center for Rehabilitation Research, Texas Tech University Health Sciences Center, Lubbock, TX, USA
Email: knatesan@ttuhsc.edu

Introduction: The hip joint center (HJC) is a critical coordinate that must be accurately estimated when quantifying lower extremity biomechanics. HJC accuracy influences downstream calculations of the hip, thigh, and knee angles. Numerous HJC estimation methods exist, such as the greater trochanter (GT) method [1] or regression equations from Bell [2], Davis [3], Vaughan [4], Hara [5], and Harrington [6]. The regression methods use whole-body or pelvis measurements as regression inputs. Most HJC prediction methods use medical imaging or cadaveric studies for validation. In a systematic review, Kainz [7] recommended Harrington's method. In this study, we aimed to compare selected HJC prediction methods to Harrington's method and determine their relative similarity for estimating the HJC coordinate and hip, thigh, and knee angles. We sought to provide insight into how the chosen prediction method influences the HJC coordinate and its dependent angles.

Methods: Ten subjects (five women; age: 23.6 ± 1.9 yrs.; BMI: 21.6 ± 2.97 kg/m^2) were drawn from a prior study [8]. Three-dimensional marker trajectories were acquired from the pelvis, thigh, and leg using an eight-camera Vicon system (Nexus 2.6.1, Centennial, CO; 200 Hz). Anthropometric data were also measured. Marker positions were recorded while subjects assumed a static standing position. Raw trajectories were low pass filtered (6 Hz; Butterworth, fourth order) and processed using a custom MATLAB (The MathWorks, Inc., Natick, MA, USA) program that calculated HJC coordinates using the six [1-6] prediction methods, and their corresponding hip, thigh, and knee angles in the standing pose. Pearson correlation (*r*) was used to quantify covariation across subjects between Harrington's and the other five methods. Root mean square error (RMSE) in each dimension and spatial distance (NormD) were calculated to examine agreement with Harrington's method. Results were reported visually and descriptively.

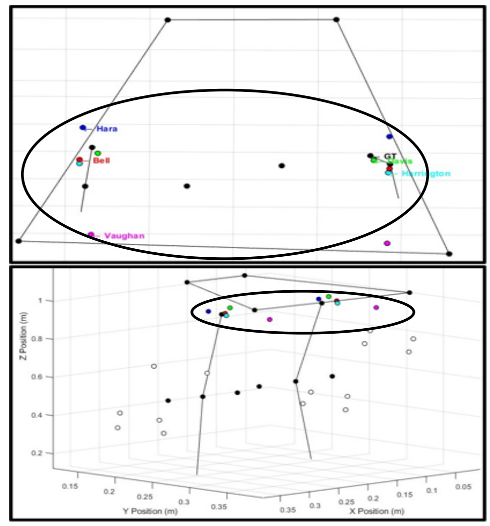

Figure : Predicted HJC locations (inside the black ovals) from the six methods. Color legend: GT=black, Bell=red, Davis=green, Vaughan=magenta, Hara=blue, Harrington=cyan.

Results & Discussion: Bell's method produced HJC coordinates most like Harrington's method (RMSE: 0.001-0.010 m; NormD: 0.012 m; *r*: 1.00-1.00), while Vaughan's method was least similar (RMSE: 0.004-0.037 m; NormD: 0.039 m; *r*: 0.89-1.00; **Figure** and **Table**). Additionally, Bell's method produced the most similar hip, thigh, and knee angles (RMSE: <0.01-0.5 deg; *r*: 0.97-1.00), whereas Vaughan's method produced the least similar angles (RMSE: 0.3-5.0 deg; *r*: 0.84-1.00). The other methods' similarity to Harrington varied based on the comparison metric. After Bell's method, Hara's method predicted the most similar HJC coordinates (**Table**), but Davis's method produced the lowest average hip (RMSE: 0.628 deg; *r*: 0.99-1.00), thigh (RMSE: 0.627 deg; *r*: 0.94-1.00), and knee (RMSE: 0.637 deg; *r*: 0.99-1.00) angle errors. By coordinate dimension (X, Y, Z), the anteroposterior (Y) direction had the greatest error, explained by the 0.037 m error in Vaughan's HJC coordinate prediction, which propagated to the downstream angles. Without Vaughan's data, the average error was similar for Y (RMSE: 0.013 m) and Z (vertical; RMSE: 0.014 m). The average X error (mediolateral; RMSE: 0.005 m) was the least overall.

Significance: The results suggest that Harrington's and Bell's methods result in similar hip, thigh, and knee angles with a maximum difference of 0.5 degrees. However, Vaughan's method should be used cautiously because of the 5-degree sagittal plane hip, thigh, and knee angle differences from Harrington's method. Vaughan's large anteroposterior (Y) coordinate error appears to result from using pelvis width instead of pelvis depth to predict the HJC's Y-coordinate. Alternate calculations that replaced pelvis width with depth improved the estimation substantially, making Vaughan's method more similar to the other methods. In conclusion, the HJC prediction method affects the HJC coordinate and its dependent hip, thigh, and knee angles. Following Kainz [7], we recommend Harrington's method, but Bell's method produces similar results.

Table: HJC coordinate error (RMSE), absolute spatial distance (NormD), and relationship (Pearson *r*) to Harrington's method.

	RMSE (m)			NormD (m)	Pearson *r*		
Method	**X**	**Y**	**Z**		**X**	**Y**	**Z**
GT	0.006	0.022	0.008	0.027	0.86	0.99	0.98
Hara	0.003	0.019	0.008	0.021	0.92	1.00	1.00
Vaughan	0.004	0.037	0.006	0.039	0.89	0.98	1.00
Bell	0.001	0.004	0.010	0.012	1.00	1.00	1.00
Davis	0.009	0.007	0.031	0.034	0.98	1.00	1.00

Note: X is the mediolateral axis; Y is the anteroposterior axis; Z is the vertical axis.

References: [1] Graci V et al., 2016. *J Sports and Health Sci.* 5:95-100. ; [2]. Bell AL et al., 1990. *J Biomechanics.* 23:617-621. ; [3]. Davis RB et al.,1991. *Human Movement Sci.* 10:575-587. ; [4]. Vaughan CL et al., 1999. *Dynamics of Human Gait*. ; [5]. Hara R et al., 2016. *Scientific Reports.* 6:37707. ; [6]. Harrington ME et al., 2007. *J Biomechanics.* 40:595-602. ; [7]. Kainz H et al., 2007. *Clinical Biomechanics.* 30:319-329. ; [8]. Atkins LT et al., 2019. *Gait & Posture.* 74:121-127.

COMPREHENSIVE GAIT ASYMMETRY METRICS RELATE TO GAIT SPEED AND NOT MOTOR IMPAIRMENT

Aria Haver-Hill[1], Sarah A. Kettlety, Natalia Sanchez, Kristan A. Leech
[1]Viterbi School of Engineering, University of Southern California
email: haverhil@usc.edu

Introduction: Numerous biomechanical impairments are common post-stroke [1]. Given this, recent work has developed measures of overall gait asymmetry to provide a comprehensive assessment of biomechanical impairment [2,3]. Two such metrics are interlimb asymmetry (ILA) [2] and the Combined Gait Asymmetry Metric (CGAM) [3]. ILA measures asymmetries in the contribution of individual segments to the step length in the sagittal plane. Whereas, CGAM is based on a modified Mahalanobis distance and can include any number or type of gait metric. It is unclear whether these overall gait asymmetry metrics are capturing a similar measure of gait asymmetry, or if the addition of frontal plane, spatiotemporal, and kinetic measures in the CGAM allows us to capture gait asymmetry more comprehensively. Additionally, it is unclear whether these overall gait asymmetry metrics relate to motor impairment and walking function. Therefore, we have two research questions: 1) what is the relationship between ILA and CGAM in people post-stroke, and 2) how do these metrics relate to motor impairment and walking function? Because both metrics capture gait asymmetry and because the CGAM captures asymmetry indices not represented in ILA, we hypothesized that ILA and CGAM would be moderately and positively associated. In addition, based on data that suggests motor impairment is related to individual metrics of kinematic asymmetry [4,5], we hypothesize that ILA and CGAM as measures of gait quality will be negatively associated with motor impairment and gait speed.

Methods: Twenty-six participants post-stroke walked on a treadmill for two minutes at their self-selected gait speed. Kinematic and kinetic data were recorded bilaterally using a motion capture system. We calculated ILA and the CGAM and averaged each variable across the trial. In the CGAM calculation, we included asymmetry indices for circumduction, hip hiking, double limb support time, single limb support time, step length, peak swing knee angle, trailing limb angle, peak hip extension, peak hip flexion, and propulsion. To explore the relationship between the different metrics of gait asymmetry, we correlated average CGAM with average ILA. To understand the relationship between these gait asymmetry values and measures of motor impairment and walking function, we also correlated CGAM and ILA against Lower-Extremity Fugl-Meyer (LE-FM) scores and self-selected treadmill speed.

Results & Discussion: We found a positive correlation between CGAM and ILA ($r = 0.52$, $p = 0.007$; Figure 1A). We found negative correlations between CGAM and gait speed ($r = -0.44$, $p = 0.02$; Figure 1C) and ILA and gait speed ($r = -0.78$, $p < 0.0001$; Figure 1E). This suggests that participants who walk at faster speeds also have more symmetric gait than those walking at slower speeds. In addition to this, we found no relationship between CGAM and LE-FM scores ($r = -0.28$, $p = 0.16$; Figure 1B) and ILA and LE-FM scores ($r = -0.15$, $p = 0.46$; Figure 1D). Consistent with our hypothesis, these results demonstrate a positive relationship between two metrics that capture overall gait asymmetry post-stroke and that people with lower asymmetry scores exhibit faster walking speeds. In contrast to our hypothesis, gait asymmetry was not related to motor impairment.

Significance: Here we found that comprehensive measures of gait asymmetry post-stroke are more related to gait speed than motor impairment measured via the LE-FM score. In addition, the relationship between ILA and gait speed was stronger than CGAM and gait speed, suggesting that measures of sagittal plane asymmetries are more related to gait speed than frontal plane metrics. Future work is necessary to understand the relationship between gait function and frontal plane asymmetries.

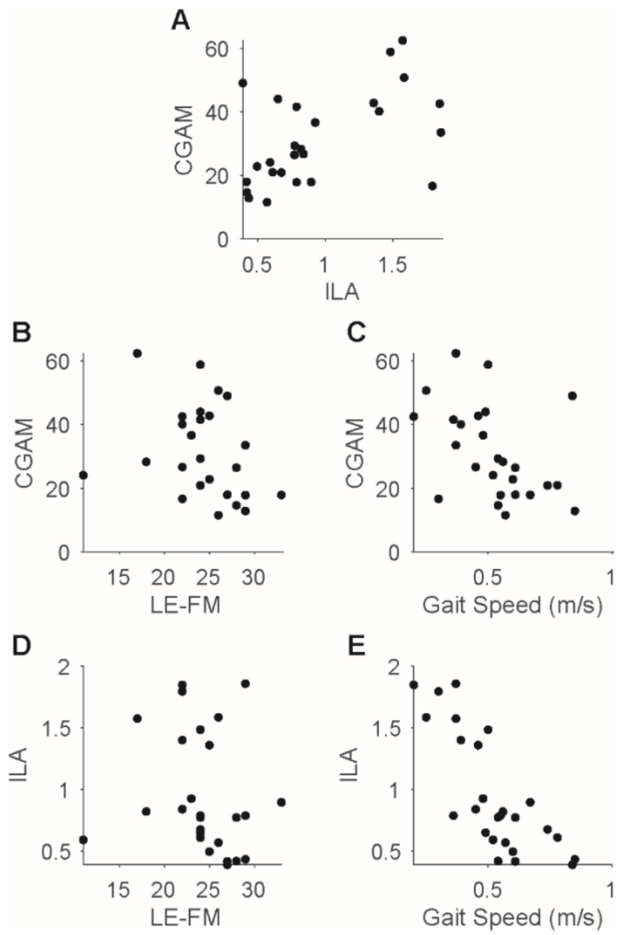

Figure 1. Correlations between gait asymmetry metrics, motor impairment, and gait speed. Abbreviations: ILA, interlimb asymmetry; CGAM, combined gait asymmetry metric; LE-FM, Lower-Extremity Fugl-Meyer.

Acknowledgments: This research was supported by NIH grant R03 HD104217-01 and the Magistro Family Foundation Research Grant from the Foundation for Physical Therapy Research.

References: [1] Chen et al. *Gait & Posture 22(1)* ; [2] Padmanabhan et al. (2020) *J Neuroeng Rehabil.* 17(1); [3] Ramakrishnan et al. (2018) *Frontiers in Neurorobotics* 12(1), [4] Shin et al. (2021) *J Neuroeng Rehabil.* [5] Patterson et al. (2010) *Neurorehabil Neural Repair*. 24(9).

EFFECTS OF GROWTH MINDSETS ON ACADEMIC PERFORMANCE IN KINESIOLOGY

Stephanie Scoville[1], Brian P. Selgrade[1*]
Dept. of Sports Medicine and Human Performance, Westfield State University
*Corresponding author's email: bselgrade@westfield.ma.edu

Introduction: There is limited research surrounding the impacts of growth mindset in kinesiology students. In kinesiology, students have one semester to learn how the muscles move in the body. Students must to learn and apply physics to help explain how the muscles in the body work, and the course has a focus in math and physics that students generally find challenging. A growth mindset is a belief that your intelligence can be shaped by training and practice [1]. People with growth mindsets see challenges as something that they can grow and learn from. In contrast, someone who believes their intelligence is innate and permanent would be considered to have a fixed mindset [1]. Someone with a fixed mindset would see challenges as something that might hurt their confidence or make them feel inferior to their peers. The purpose of this study was to give insight on the correlations between growth mindset and students success in undergraduate kinesiology. We hypothesized that students would not alter their mindsets over the course of the semester. We also hypothesized that mindsets towards math would be more fixed than student's general mindset. A growth mindset may be the difference between a student dropping a class and giving up and the student persevering through their challenging courses [2]. In doing this study we wanted to fill in some of the gaps that the limited research had provided for us about the effects of growth mindset on students.

Methods: During the fall 2022 semester, the students took 3 surveys. Each survey was the same but at different points in the semester, first day of class, mid semester, and before their final exam. We used a modified Implicit Theories of Intelligence Self Scale (ITI-SS) with additional questions to understand specific mindsets towards math, writing and computer skills [3]. There were 4 additional questions for each specific category. These additional questions were written similarly to the general questions but specified growth in certain fields (e.g. "I believe I can always substantially improve on my abilities *to solve math problems"*). Question responses were on a 5-point Likert scale ranging from strongly disagree to strongly agree, and average mindset was coded such that lower numbers indicated a more fixed mindset. We used Wilcoxon signed-ranks tests to compare initial and final survey results for each category and to compare initial results in each category to initial general scores.

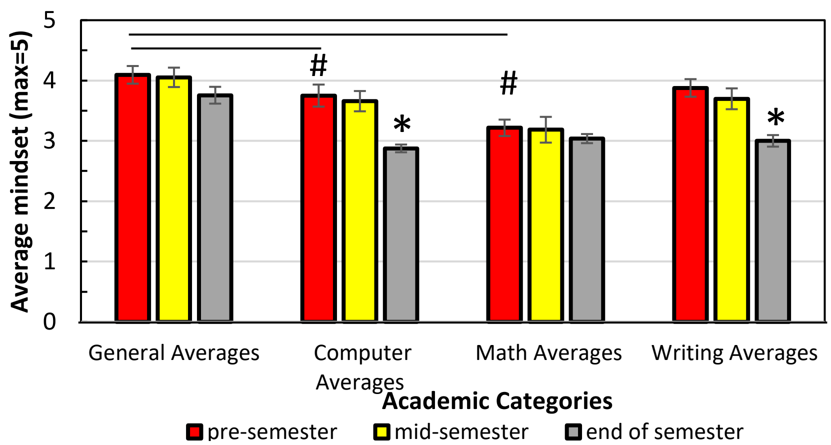

Figure 1: Averaged mindset survey answers for each academic category at three different times in the semester. * Signifies significant differences from the pre-semester survey for the same category. # signifies significant difference from the initial general average for the same survey time. Error bars signify standard error.

Results & Discussion: Twenty students completed each survey. Students' general mindset decreased from 4.05 in the initial survey to 3.76 in the final survey, although this difference was not significant (fig. 1, p=0.093). Contrary to our hypothesis, mindsets towards computer skills and writing significantly decreased by 0.89 and 0.78, respectively, from the beginning to the end of the semester (p=0.001 for both), indicating that students drifted toward a fixed mindset. However, even at the end of the semester, all mindset scores except for computer skills were above 3, indicating that students still had more of a growth mindset for each category. Prior research has shown that, in challenging science courses, students' mindsets become more fixed, especially if they struggle in the course [4]. Mindsets may have become more fixed for computer skills and writing specifically because students found the class's spreadsheet assignments and lab reports to be difficult. Math mindset was significantly lower than general mindset pre-semester, supporting our second hypothesis (p=0.001). Pre-semester mindset towards computer skills was also significantly lower than general mindset (p=0.010), but pre-semester writing mindset was not (p=0.11). These data indicate students' mindsets were more fixed towards math and computer skills than in general.

Significance: These findings suggest that, without interventions, kinesiology students' mindsets will not improve and could become more fixed, particularly in regard to computing skills and writing. Kinesiology at Westfield State University is a challenging class that Movement Science majors typically take as sophomores. Shifting students towards a fixed mindset could affect their motivation and potentially, academic performance in kinesiology and future courses. Similarly, more fixed initial mindsets towards math and computer skills could explain why students tend to be less motivated towards portions of kinesiology class that require these skills. Future work should teach kinesiology students to adopt a growth mindset to determine if this can improve academic performance.

Acknowledgements: This research was funded by a Scholarship of Teaching and Learning Grant from Westfield State University.

References: [1] Zappe, S. et al. *(2017), Frontiers in Ed Conf*. 10.1109/FIE.2017.8190685. [2] Frary, M. (2018), *Proc 125th ASEE Annual Conf.* [3] De Castella, K., Byrne, D. (2015), *Eur J Psychol Ed*. 30 (245); [4] Limeri et al. (2020), *Int J STEM Ed*. 7 (35).

THE TRAMPOLINE AFTEREFFECT IN YOUNG ADULTS AND TYPICALLY DEVELOPING CHILDREN

Matthew Beerse[1*], Jianhua Wu[2]
[1]University of Dayton
[2]Georgia State University
*Corresponding author's email: mbeerse1@udayton.edu

Introduction: Motor adaptation is an important function enabling the production of consistent movement patterns under varying environmental constraints [1]. The presence of an adapted movement pattern after removal of the external stimuli has been termed an aftereffect and has been employed to study motor adaptation [2]. The trampoline aftereffect paradigm has been demonstrated in young adults [3] and has the potential to provide insight to the control of stiffness parameters of the neuromuscular system. Following sixty seconds of hopping on a trampoline, young adults demonstrated increased whole-body vertical stiffness and reduced jump height during the performance of the first countermovement jump (CMJ) [3]. These variables returned to baseline magnitudes during the performance of the second CMJ, after thirty seconds of rest. Perceptual sensitivity changes of the muscle spindles and/or vestibular system have been postulated to contribute to the trampoline aftereffect. While typically developing children have the capacity to adapt and re-adapt in the presence of an aftereffect, it is not always to the same extent as young adults [4], and their capacity to navigate the trampoline aftereffect is unknown. Therefore, the purpose of this study was to compare the trampoline aftereffect between children and young adults. We hypothesized that following trampoline hopping exposure, both groups will increase whole-body vertical stiffness and decrease jump height while performing the first CMJ and this effect might persist in the next CMJs in children but not young adults.

Methods: Fifteen young adults (7F/8M, 23.39±1.42 years old) and fifteen children (9F/6M, 9.62±1.59 years old) participated in this study. Kinetic data were collected using two floor-embedded force plates (AMTI, MA, USA), sampled at 1000 Hz. Subjects performed two sets of five CMJs, separated by 30 seconds of rest each, as their baseline task. Following the baseline sets, subjects hopped on a minitrampoline (JumpSport, Model 550F 44"), with an estimated stiffness of 7.85 kNm^{-1}, at a frequency of 1.5 Hz, cued by a metronome. Subjects hopped for three durations: 30, 60, and 120 seconds in a random order. Immediately after the completion of each bout of trampoline hopping, subjects performed a set of five CMJs, as described in the baseline task. Subjects rested for at least five minutes before their next trampoline hopping exposure.

Vertical ground reaction force (GRF) was used to calculate vertical acceleration of the center-of-mass (COM), which we double integrated to vertical displacement. Whole-body vertical stiffness was calculated as the quotient of peak vertical GRF and peak vertical COM displacement. Vertical COM velocity at take-off was used to estimate vertical jump height. Dependent variables were vertical COM displacement normalized by leg length, vertical GRF normalized by bodyweight, and jump height normalized by subject height. We conducted three-way (2 group x 3 duration x 6 CMJ) mixed ANOVAs on the dependent variables.

Results & Discussion: Our hypothesis was partially supported in that both the adult and children groups demonstrated increased whole-body vertical stiffness following trampoline hopping exposure in all five CMJs, and the trampoline aftereffect was not different between groups nor across exposure durations and jump height was unaffected. In addition, both the adult and children groups demonstrated a trampoline aftereffect during the performance of CMJs that manifested with reduced vertical COM displacement and increased peak vertical GRF. The effects on stiffness and displacement persisted through all five CMJs in both groups, while peak vertical GRF disappeared after the first CMJ.

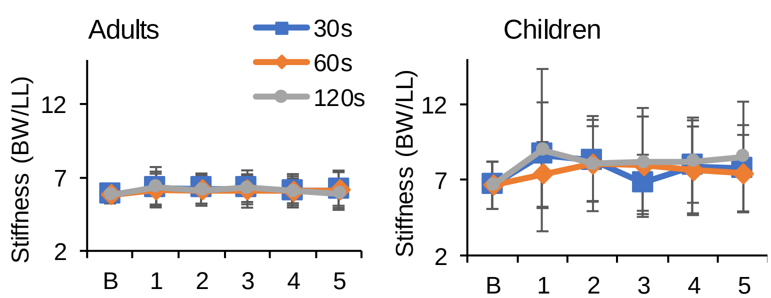

Figure 1: Mean (SD) of whole-body vertical stiffness normalized by bodyweight (BW) and leg length (LL) for adults and children with baseline (B) and five CMJs post trampoline exposure (1-5).

Significance: Our findings suggested that typically developing children aged 5-11 years old might have an adult-like perceptual system for the maintenance of whole-body vertical stiffness. Not only was the trampoline aftereffect found in this population, but the persistence of the aftereffect was not different between groups following different durations of trampoline exposure. Interestingly, our results were dissimilar from previous evaluations of the trampoline aftereffect in young adults [3], where adaptation and re-adaptation occurred following the first CMJ only. In our study, average whole-body vertical stiffness increased by 6% and 11% in adults and children, respectively, compared to 18% in the prior study, suggesting a tolerable range of stiffness control. We propose that appropriate application of trampoline exposure might facilitate the performance of movements requiring adequate whole-body vertical stiffness, which might be particularly beneficial for populations with atypical stiffness control.

Acknowledgements: This study was supported by a Georgia State University Dissertation Grant and CEHD Doctoral Dissertation Support Grant. We would like to thank all the participants for their volunteering participation.

References: [1] Damiano et al. (2017), *Front Hum Neurosci* 11; [2] Michel et al. (2007), *Cog Neuro Sci* 19; [3] Marquez et al. (2010), *Exp Brain Res* 204; [4] Musselman et al. (2011), *J of Neurophys*, 105.

AUTOMATED MOVEMENT SCREEN: DEVELOPING A DATA-DRIVEN SCORING TOOL TO ASSESS SPINE MOTOR DYSFUNCTION

Carl Alano, Shawn Beaudette
Kinesiology, Brock University, St. Catharines, ON

Introduction: Low back pain (LBP) is the leading cause of disability worldwide, affecting over 500 million people annually across the globe [1]. Many of these cases (up to 90%) are classified as 'non-specific' [2], meaning that the pain cannot be attributed to any specific injury or pathology. It is understood that those affected by LBP present with heterogeneous motor control phenotypes that are indicative of dysfunction and pain development [3]. Through assessment of motor behaviours, it is believed that specific subgroups of dysfunction may be distinguished, which can help clinicians objectively administer a more personalized and effective standard of care [4]. As such, although objective assessments of movement may help to streamline the management of LBP, current methods of quantification, such as using a 3D motion-capture studio, can be costly and limit the practical use of the technology. As a result, the scalability and accessibility of these technologies in real-world settings is restricted. Recent advancements in computer vision and smartphone availability have made human motion capture more accessible. The purpose of this study is to leverage open-source human pose estimation software (MediaPipe™, Google) to understand the relationship between motor patterns derived from cell-phone inputs, and participant reported outcomes related to low back dysfunction. Although any previous research studies have distinguished motor features between those with/without LBP. It is hypothesized that principal components derived from the pose data will be capable to objectively discriminate levels of motor dysfunction (movement patterns or characteristics) that are more common in one group compared to the other.

Methods: To the study purpose, we have a proposed sampling 1000 participants into an online study (185 currently sampled to date). Participants enrolled in the online study will complete validated questionnaires related to disability (Oswestry Disability Scale, Quebec Disability Scale), fear of movement (Tampa Scale for Kinesiophobia), and physical activity (International Physical Activity Questionnaire), while also uploading videos where they complete standardized movement tasks (i.e., object pick-up, squatting, spine flexion). Pose data from the spine movement trials will be processed (i.e., aligned, scaled, and time-normalized) and reduced using principal components analysis (PCA) to facilitate further analyses. Specifically, spine movement features (principal components) will be used as inputs to predict functional outcomes related to disability, fear of movement and physical activity history.

Results and Discussion: Preliminary data representing the difference in body-weight squat motor phenotype are being reported. Of the 185 sampled participants 81 completed video-based movement assessments. Principal components (PC) scores of self-declared LBP (n = 13) and healthy (n = 68) participants were compared using t-tests, assuming two samples with unequal variances. Of the 10 PCs tested, PC5 and PC6 were significantly different between the groups ($p<0.05$), with PC4 and PC9 nearing significance ($p<0.1$). It is possible that the variation captured by these PCs are related to clinically meaningful information related to movement range-of-motion, or spatiotemporal coordination.

Table 1. t-test results comparing PC scores of LBP and Healthy participants.

	LBP		Healthy				
	Mean	**SD**	**Mean**	**SD**	**df**	**t**	**p**
PC1	-0.46	21.65	0.09	27.77	18	-0.38	0.35
PC2	-0.51	20.88	0.10	19.27	17	-0.44	0.33
PC3	0.11	8.24	-0.02	13.39	20	0.15	0.44
PC4	-1.20	10.13	0.23	8.29	16	-1.50	0.08
PC5	-0.91	3.59	0.17	7.02	22	-1.75	0.05
PC6	-1.37	3.43	0.26	3.91	18	-2.87	0.01
PC7	0.47	3.33	-0.09	3.52	17	1.01	0.16
PC8	0.27	3.45	-0.05	3.20	17	0.56	0.29
PC9	0.89	4.95	-0.17	2.43	14	1.64	0.06
PC10	0.03	1.29	-0.01	2.34	21	0.10	0.46

Significance: The results of this preliminary analysis suggest modes of variation present in video-derived pose data are capable of distinguishing those with self-reported LBP. Future work will quantify the relationship between video-based pose data and self-reported measures of disability, kinesiophobia, and physical activity.

Acknowledgements: This research was funded, in part by the Natural Sciences and Engineering Research Council (NSERC) of Canada (RGPIN-2020-05195). The authors wish to thank the Ontario Kinesiologists Association (OKA) and the Ontario Chiropractic Association (OCA) for their assistance with recruitment.

References:
[1] Vos, T., et al. 2016.. Lancet 388, 1545–1602; [2] Maher, C et al. 2017. Lancet 389, 736–747; [3] Hemming, R et al. 2018. Eur. Spine J. 27(1): 163–170; [4] Fritz, J.M. et al. 2007. J. Orthop. Sports Phys. Ther. 37(6): 290– 302.

PLANTAR KINETICS DURING WALKING AID USE IN PERSONS WITH TYPE 2 DIABETES MELLITUS

Holton Gwaltney[1*], Joseph Harrington[1], Jose Anguiano-Hernandez[1] & David Kingston[1]
[1]Department of Biomechanics, University of Nebraska at Omaha, Omaha, NE USA
*Corresponding author's email: hgwaltney@unomaha.edu

Introduction: Type 2 Diabetes Mellitus (DM) is an endocrine system disorder that can cause changes in the central nervous system, neuropathy, and loss of sensation in the foot leading to foot ulceration, with the forefoot being the most commonly affected area [1,2]. Treatment of plantar ulcers involves casting, removable walking boots, half-shoes, and non-weight-bearing prescriptions that rely on walking aids such as crutches, walkers, and Wheeled Knee Walkers (WKW) [3]. Previous studies have investigated alterations to compressive forces on the foot when using walking aids, but shear forces require additional analyses [4]. Therefore, this study aimed to compare the effect of walking aid use on shod propulsive foot shear forces in patients with Type 2 DM. We hypothesized that propulsive foot shear forces would differ between walking aids and unassisted walking, with unassisted being the lowest, followed by WKW, standard walker, and crutches, respectively. Our second hypothesis was there would be a moderate positive correlation (0.3-0.5) between bodyweight unloaded (BWU) onto assistive devices and shear forces.

Methods: Twenty participants (12:8 F:M, 59.63±10.57 years, 91.75±13.8 kg) with Type 2 DM performed four walking conditions with different walking aids in randomized order. Walking conditions were axillary crutches, a standard walker, WKW, and unassisted walking. Participants walked back and forth on a 10 m track for 200 m at a self-selected pace or until electing to stop. Eight embedded force plates measured shod foot kinetics (AMTI Inc., Watertown, MA). Trunk and lower limb kinematics were recorded by a 20-camera motion capture system (Motion Analysis Corp, Rohnert Park, CA). Walking data were split into stance periods in Visual3D (Version 2022, C-Motion, Germantown, MD) using a 50 N threshold for consistency with prior insole studies [5]. Kinetic data at the outsole were filtered with a zero-lag 4th-order low-pass Butterworth filter using a cutoff frequency of 6 Hz. Custom MATLAB (R2022b, Mathworks, Natick, MA) software was used to average mediolateral (M/L), anteroposterior (A/P), and vertical forces per condition (Figure 1). Three separate one-way repeated measures ANOVAs with Bonferroni post-hoc comparisons were used to assess hypotheses. Three Pearson correlations were conducted to assess the relationship of BWU onto assistive devices and shear forces.

Results & Discussion: Significant main effects ($p<0.001$) were observed in M/L forces with post-hoc analyses revealing a significant difference between the WKW and all other modalities ($p<0.001$) for peak lateral shear with the WKW mean peak of –66.2 N compared to approximately -15 N in all other conditions. Mean peak medial shear was also different ($p<0.001$) between the WKW (12.4 N) and unassisted (65.8 N). Trends were similar in braking shear ($p<0.001$) with mean WKW values of 14.6 N compared to 158.4 N, 137.8 N, and 99.3 N from crutches, unassisted, and standard walker, respectively. Peak propulsive shear differed ($p<0.001$) between WKW (-76.0 N), crutches (-113.6 N), and unassisted (-142.3 N) as well as between WKW and standard walker (-96.5 N) ($p=0.033$). The WKW also had significantly less ($p<0.001$) mean peak vertical force (501.483 N) compared to crutches, unassisted, and standard walker (911.7 N, 942 N, and 967.7 N, respectively) at the outsole, which is similar to prior results from insole data [5].

BWU onto the WKW had a moderate negative correlation ($r = -0.318$) with peak braking shear and a weak positive correlation ($r = 0.121$) with peak propulsive shear. Also, BWU onto the WKW had a weak negative correlation ($r = -0.235$) with peak medial shear and a weak positive correlation ($r = 0.149$) with peak lateral shear. BWU onto the crutches had negligible correlations with peak medial, propulsive, and braking shear, but a weak positive correlation ($r = 0.228$) with peak lateral shear. BWU onto the standard walker had weak positive correlations ($r = 0.290$ and $r = 0.166$) with peak lateral and braking shear, respectively. A moderate positive correlation ($r = 0.357$) was found with peak medial shear, and a weak negative correlation ($r = -0.173$) was found with peak propulsive shear.

Participants unload an average of 57-63% body weight onto walking aids, but this does not correlate well with changes to A/P or M/L shear forces at the outsole. The significantly lower A/P peaks for the WKW indicate less braking force is needed compared to other walking aids with a consistent load throughout the stance period (Figure 1). Although walking aid use resulted in less stress overall, the outsole experiences substantial lateral forces, which may still result in ulceration issues for this population.

Significance: The M/L and A/P shear significantly differed between walking aids and the unassisted condition, but values were not substantially lower. Only the standard walker had a moderate positive correlation with peak medial shear. This implies that BWU magnitude is poorly related to changes in outsole kinetics.

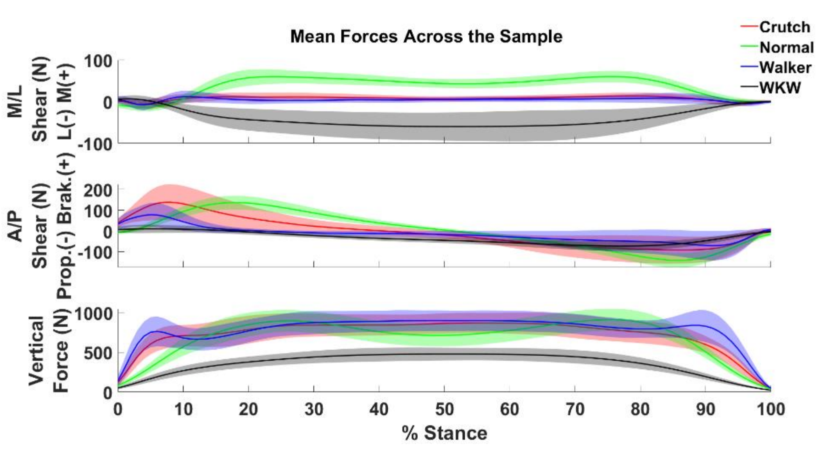

Figure 1: Sample means for mediolateral (top), anteroposterior (middle), and vertical (bottom) forces. Shaded regions are one standard deviation from the mean. Stance is defined from initial contact to final contact on an ipsilateral limb.

References: [1] Ko et al. *Gait & Posture*, *34*(4), 548–552, 2011. [2] Bus et al. *Dia./Met. and. Res. Rev.*, *36*, 2020. [3] Bus et al. *D/M and Res. Rev.*, *32*, 99–118, 2016. [4] Giacomozzi et al. *J. of Foot and Ankle. Res.*, *1*(S1), O3, 2008. [5] Anguiano-Hernandez et al. *Gait & Posture*, 98, 5-61, 2022.

EFFECTS OF ADDED-MASS ON THE GAIT OF MIDDLE-AGED ADULTS: ASSESSED USING STATISTICAL PARAMETRIC MAPPING

Vinayak Vijayan[1], Shanpu Fang[1], Timothy Reissman[1], Megan E. Reissman[1], Allison L. Kinney[1*]
[1]EMPOWER Lab, Department of Mechanical and Aerospace Engineering, University of Dayton, Dayton, OH, USA
*Corresponding author's email: akinney2@udayton.edu

Introduction: To accurately quantify and improve the performance of an exoskeleton, we must first be able to quantify human performance. This is especially true in the case of "assist as needed" control algorithms. In the case of exoskeletons that employ "assist as needed" control strategies, it is expected that the user can walk unhindered when the assistance is not active [1]. However, the added mass of the exoskeleton device itself will affect the user's gait. To improve the performance of such exoskeletons, it is important to quantify the effects of added mass across the whole gait cycle with a method such as statistical parametric mapping (SPM) [2].

Prior studies have focused mainly on a cohort of healthy younger adults to characterize the effects of added mass on gait [3][4]. To our knowledge, there is no study that quantifies the effects of added mass on middle-aged adults. Nevertheless, aging is related to changes in the musculoskeletal system as well as changes in the central and peripheral nervous systems [5]. These changes in musculoskeletal capabilities and proprioceptive feedback could affect an older individual's ability to tolerate and adapt to the added mass indicative of an exoskeleton. This study will focus on the gait-related adaptive behaviors of middle-aged adults when mass is added around the waist and the thigh. As such, this study's design will help bolster the basic science behind the design of hip exoskeletons and provide insight into how middle-aged adults respond to walking with added mass. Based on the modeling simplification that gait can be modeled as a coupled pendulum, we hypothesize that loading at the pelvis and thigh will have different characteristic impacts on gait parameters, with pelvis loading having a greater impact on stance and thigh loading having a greater impact on swing. Based on prior literature [4], we also expected the young and middle-aged adults to have different responses to the added mass during walking.

Methods: Fourteen middle-aged and fourteen younger adults participated in this study [6]. The participants walked at their selected speed on an instrumented treadmill for 1 minute under 9 different loaded conditions. The conditions represented a full-factorial combination of low (+3.6 lb), medium (+7.2 lb), and high (+10.8 lb) mass amounts at the thighs and pelvis. Muscle activity was recorded for medial gastrocnemius, soleus, tibialis anterior, vastus lateralis, vastus medialis, biceps femoris and semitendinosus muscles. Hip, knee, and ankle joint kinematics and kinetics were analyzed for the sagittal plane. Joint angles, moment, and reaction forces and muscle activations were evaluated using SPM [2]. Two 2-way repeated measures ANOVAs were used to evaluate the effects of pelvis load (low, medium, or high) and thigh load (low, medium, or high) on the gait parameters separately for the younger and the middle-aged adults. Post hoc paired t-tests were used to compare pairs of conditions.

Results & Discussion: Increased ankle moments were observed as a general response to added mass (Fig. 1). Hip exoskeleton designers should consider modifying the control approaches at the hip and knee joints to reduce the effects on ankle moments. Our hypotheses that loading at the pelvis and thigh will have characteristically different impacts on gait parameters and that young and middle-aged adults will have different responses to added mass were supported. We observed that, under pelvis loading, middle-aged adults had a preferred adaptive strategy to avoid increased hip flexion at heel strike and increased knee flexion during weight acceptance.

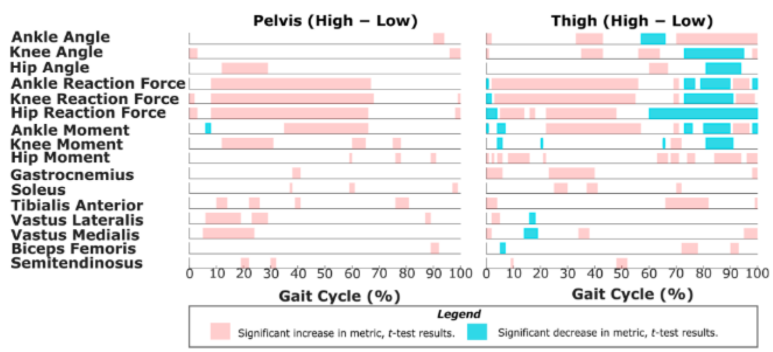

Figure 1: Map of SPM results for middle-aged adults, showing comparisons between low and high added mass levels at the pelvis and thigh.

Under thigh loading, a general strategy of limb stiffening was observed in the case of middle-aged adults. Without exoskeleton modification, these responses could cause increased joint reaction forces and loading rates for middle-aged adults. A low magnitude of mass on the thigh seems to be well tolerated by all healthy adults. However, we observed that thigh loading created steeper loading rates and had caused higher activation of tibialis anterior. Therefore, it is important to consider the toe-clearance requirements, and the steeper loading rates that have been shown to be associated with thigh loading. In the case of thigh loading, ideally the hip exoskeleton should be capable of providing an additional external hip extension moment during contralateral toe-off, to meet the demands of propelling the added mass forward.

Significance: This study comprehensively characterizes the effects of added mass across the whole gait cycle, in both young and middle-aged adults. This can help improve exoskeleton design by accounting for the important element of human performance under added mass representative of a hip exoskeleton. The SPM analysis approach may inform control strategies for exoskeletons with "assist-as-needed" by highlighting the regions of the gait cycle over which particular joint assistance is likely to be required and even the regions where active control is not required. Overall, as the user's age may impact their response to an exoskeleton, designers should aim to include sensors to directly monitor user response and adaptive control approaches that account for these differences.

References: 1] Naghavi et al. (2020), *Robot Auton Syst* 134; [2] Pataky et al. (2012), *Comp Meth Biomech Biomed* 15; [3] Dames et al. (2016), *Gait & Posture* 50; [4] Vijayan et al. (2022), *Gait & Posture* 92; [5] Herssens et al. (2018), *Gait & Posture* 54; [5] Vijayan et al. (2022), *Sensors* 22.

CHANGES IN STIMULATION AMPLITUDE ARE CORRELATED TO CHANGES IN GAIT MECHANICS

Margo C. Donlin[1*], Jill S. Higginson[1,2]
[1]University of Delaware Departments of [1]Biomedical and [2]Mechanical Engineering
*Corresponding author's email: donlinm@udel.edu

Introduction: After stroke, impaired motor control often causes increased foot drop [1] and decreased forward propulsion [2]. Functional electrical stimulation (FES) is a common rehabilitation technique that can improve foot drop and forward propulsion when applied to the dorsiflexor and plantarflexor muscles [3, 4]. However, FES is not effective for all individuals post-stroke, with some seeing clinically meaningful improvements and others not responding to the stimulation [3, 5]. To address the limitations of current FES protocols, we developed a novel adaptive FES (AFES) system that iteratively updates the stimulation amplitude to the dorsiflexor and plantarflexor muscles in response to measured real-time gait variables to target individual-specific impairments at every stride.

The purpose of this work is to characterize the relationship between varying stimulation amplitudes and ankle dorsiflexion angle error and peak propulsive force asymmetry. Because stimulation increases dorsiflexion angle and propulsive force, we hypothesize that dynamic increases in stimulation amplitude will result in decreased ankle dorsiflexion angle error and peak propulsive force asymmetry.

Methods: At every stride, the AFES system measures real-time dorsiflexion angle and propulsive force and calculates an error value relative to a healthy reference value, which is used to update the stimulation amplitudes. Dorsiflexion angle error (DF_{Error}) is the percent difference between the real-time dorsiflexion angle and a neutral dorsiflexion angle. Peak propulsive force asymmetry ($AGRF_{Asym}$) is the difference between the nonparetic and paretic peak propulsive forces divided by the sum of the nonparetic and paretic peak propulsive forces. Then, the next (k+1) values of dorsiflexor (DF $Stim_{k+1}$, Eq. 1) and plantarflexor (PF $Stim_{k+1}$, Eq. 2) stimulation are calculated based on the current (k) values (DF $Stim_k$, PF $Stim_k$) and the maximum stimulation limits (DF_{Max}, PF_{Max}). Within a threshold defined by healthy gait variability, the stimulation amplitude does not change, and the magnitude of the calculated stimulation is decreased to remove the discontinuity around these thresholds. Increased angle error and asymmetry result in increased stimulation, which directly counteracts the increased angle and asymmetry to promote healthier gait.

$$DF\ Stim_{k+1} = DF\ Stim_k + (DF_{Error} \times DF_{max}) - (sign(DF_{Error}) * 0.02 * DF_{Max}) \quad (1)$$

$$PF\ Stim_{k+1} = PF\ Stim_k + \left(AGRF_{Asym} \times PF_{max}\right) - (sign(AGRF_{Asym}) * 0.05 * PF_{Max}) \quad (2)$$

One young healthy individual (M, 26 years, 1.72 m, 70.23 kg) walked for two minutes on an instrumented treadmill (Bertec Corp., Columbus, OH, USA; 2000 Hz.) with motion capture (Qualisys AB, Göteborg, Sweden; 100 Hz.) markers bilaterally on the lower body [5]. Stimulation (Digitimer Ltd., Welwyn Garden City, England) was delivered to a randomly selected leg acting as the paretic limb using bilateral footswitches [4] with updated stimulation amplitudes at each stride. Stimulation amplitudes, dorsiflexion angle error, and peak propulsive force asymmetry were recorded at each stride. A linear regression was performed on the change in stimulation amplitude from one stride to the next and the angle error or asymmetry between the same two strides.

Results & Discussion: The purpose of this study was to characterize the relationship between changing stimulation amplitudes and real-time gait variables. When the stimulation amplitude did not change, there was some variation in dorsiflexion angle error (Fig. 1A) and peak propulsive force asymmetry (Fig. 1B), likely due to normal gait variability. When the stimulation amplitude increased from one stride to the next, dorsiflexion angle error and peak propulsive force asymmetry decreased, as hypothesized. Decreases in angle error and asymmetry with increased stimulation indicate trends toward healthy gait patterns and suggest that the AFES system may be a useful rehabilitation tool capable of adjusting to real-time gait variations and promoting healthy gait.

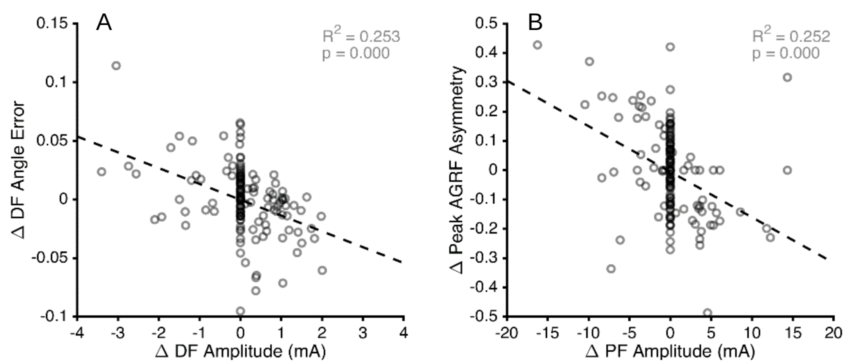

Figure 1: (A) Change in DF angle error versus change in DF stimulation amplitude. (B) Change in peak propulsive force asymmetry versus change in PF stimulation amplitude.

One limitation of this study is the use of a single young healthy subject rather than individuals post-stroke. Future work will expand on this pilot study to characterize the relationship between changes in stimulation amplitude and real-time gait variables in individuals post-stroke to determine if this trend holds true with the increased variability and decreased motor control associated with chronic stroke.

Significance: Characterizing the relationship between stimulation amplitude and biomechanical response is important for post-stroke gait rehabilitation to verify that the stimulation is having the desired effect. Additionally, a known relationship between changes in stimulation amplitude and changes in functional gait measures may help clinicians translate desired biomechanical outcomes into prescribed stimulation patterns for more efficient and effective treatment selection.

Acknowledgements: NIH-NIGMS (P20 GM103446) and the State of Delaware; NIH GM 103333; University of Delaware Doctoral Fellowship. This content is solely the responsibility of the authors and does not necessarily represent the official views of NIH.

References: [1] Li et al. (2018) *Front Physiol* 9(Aug); [2] Roelker et al. (2018) *Gait Posture* 68; [3] Dickstein (2008) *Neurorehabil Neural Repair* 22(6); [4] Kesar et al. (2009) *Stroke* 40(12); [5] Ray, N. et al. (2021) *J Biomech* 124(April)

IMPULSE GENERATION OF EACH LEG IN HIGH SCHOOL BASEBALL PITCHERS

Samantha Gajda[1], Jun Liu[1], Christopher Knowlton[2], Roy Iverson[1], Alex Smith[1], Zach Tropp[3], Matthew Gauthier[4], Nikhil Verma[2], Gregory Nicholson[2], Anthony Romeo[5], Antonia Zaferiou[1*]
[1]Department of Biomedical Engineering, Stevens Institute of Technology, New Jersey, USA
*Corresponding author's email Antonia.Zaferiou@stevens.edu

Introduction: In baseball pitching, ground reaction forces (GRFs) are controlled by the pitcher to generate the whole-body momenta required to throw a baseball. This study investigated the roles of the lead (front) and lag (back) legs in generating linear and angular impulse before ball release during fastballs. It was suggested that the role of the lag leg was to drive the body forward and the lead leg to act as a stable base for the rotation of the hips and pelvis [1]. Our recent study found that the lag leg generates positive linear impulse, the lead leg generates negative linear impulse, and the lag leg generates a significantly greater angular impulse than the lead leg in four professional pitchers [2]. In this study of high school pitchers, we expected similar trends such that the lag leg will generate greater forward linear impulse and greater angular impulse about each leftward and vertical axes vs. the lead leg.

Methods: Male high school pitchers (n = 19) volunteered (self-reported >75 mph pitch speed) for this study in accordance with the IRB. Each pitcher performed warmups and reflective markers were affixed to calculate the total body center of mass (CoM) position [3]. Force plates (1000 Hz, Bertec, OH, USA) were built into a practice mound and adjusted according to individual stride lengths. The mound replicated dimensions used in a Major League Baseball mound. 3D kinematics were captured (250 fps, Optitrack, OR, USA). Participants pitched fastballs 18.44 m from a strike zone target and trials rated "poor" by the pitcher were excluded. Additionally, some trials had poor marker tracking, resulting in 4-9 trials per pitcher. The orthogonal global axes were defined by forward axis from the mound to home plate, an upward vertical axis, and a leftward axis from the rubber to first base. Left-handed pitchers' angular impulse about vertical was transformed to be consistent with right-handed pitchers. Linear impulse was the time integral of GRFs. Angular impulse was the time-integral of the moment about the CoM. The sign test was used to compare impulses between legs for each subject.

Results & Discussion: For all pitchers, the lag leg generated forward linear impulse and the lead leg generated backward linear impulse (for 15 pitchers, statistically greater; **Fig. 1A).** Additionally, for all pitchers, the lag leg generated greater angular impulses about vertical vs. the lead leg (for 15 pitchers, statistically greater; **Fig. 1B**). These results for forward linear impulse and angular impulse about vertical were consistent with our previous study of professional pitchers [2]. In our prior study of professional pitchers all four pitchers generated greater angular impulse about leftward with the lag leg [2]. However, in this study 13 out of 19 pitchers generated greater angular impulse about leftward with the lag leg (for nine pitchers, statistically greater) and some pitchers did not generate greater angular impulse with their lag leg (gray boxes; **Fig. 1C**). For example, **Fig. 1D** shows the body positions of two pitchers at peak moment with similar net angular impulse about leftward, but opposite leg-dominance with respect to angular impulse generated about leftward. Subject 5 releases the ball with the lag leg remaining on the force plate while subject 6 releases the ball after the lag leg departed the force plate. Pitchers using either strategy achieved ball speeds ranked in the bottom, middle, or top third of ball speeds in this study (ranged from 63-82 mph). Thus, this study initially shows that different strategies can achieve similar outcomes. While it is beneficial to investigate within-subject patterns when more than one pattern is used across participants (e.g., **Fig. 1C**), the use of the sign test when there were fewer than six trials is a current limitation. Only participants with greater than five trials had statistically significant differences detected, despite apparent differences in impulse generation between legs (e.g., **Fig. 1A**). Therefore, our next step is to use more advanced statistical approaches that enable investigating how impulse patterns relate to ball-speed and accuracy outcomes.

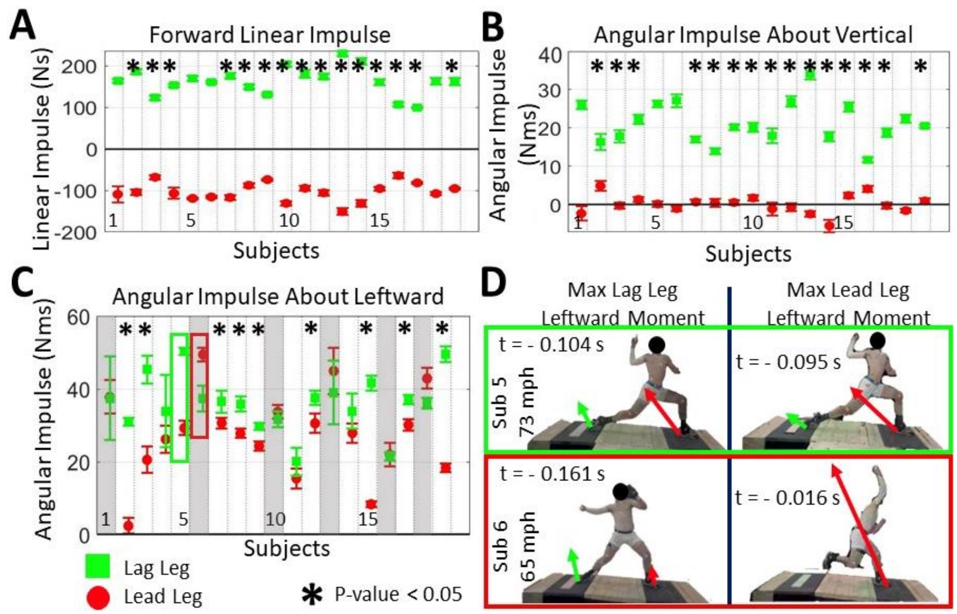

Figure 1: Mean (SD) **(A)** forward linear impulse, **(B)** angular impulse about vertical, and **(C)** angular impulse about leftward for each leg and each subject. Gray boxes indicate when the mean angular impulse about leftward generated by the lead leg > lag leg. **(D)** Example GRFs during each leg's application of peak moment about a leftward axis through the CoM (t = 0 s is ball release).

Significance: This study reveals strategies used by high school pitchers to generate linear and angular momenta during fastballs.

Acknowledgements: We thank the participants of the study and financial support from a Major League Baseball research grant.

References: [1] Elliott et al. (1988), *Int J Spo Biomech* [2] Liu et al. (2022), *Sports Biomech*. [3] De Leva (1996), *J Biomech*

TEMPORAL ALIGNMENT OF GAIT PHASES IS NECESSARY BEFORE COMPUTING COORDINATION MEASURES

Elham Alijanpour[1], Abed Khosrojerdi[2], Daniel M. Russell[1*]
[1]School of Rehabilitation Sciences, Old Dominion University, Norfolk, VA, USA.
[2]Department of Mechanical and Aerospace Engineering, Old Dominion University, Norfolk, VA, USA.
*Corresponding author's email: dmrussel@odu.edu

Introduction: Interest in the coordination of joint or segment kinematics and its variability has grown in recent decades [1]. However, there are inconsistent results for coordination and its variability (CaV) in the literature for the same joint couples (e.g., hip/knee) during the same task (e.g., walking) [2-4]. Differences between studies may arise from limitations and problems in the calculation methods. Two common methods to quantify CaV are continuous relative phase (CRP) and vector coding (VC) [5]. Both methods begin with curve registration [6], where typically curve registration involves normalizing each gait cycle (GC) to one hundred percent [7]. However, variation in the proportional duration of gait phases could lead to a quasi-periodicity problem where different phases of the cycle are averaged together and then compared between conditions or groups [8]. Recently, temporal alignment (TA) of gait phases has been proposed to solve this problem [9]. In the current study, we used two different methods to quantify CaV (CRP and VC) on both temporally aligned by phase and unaligned data. We hypothesized that whether the GCs were temporally aligned or not would influence the CaV data.

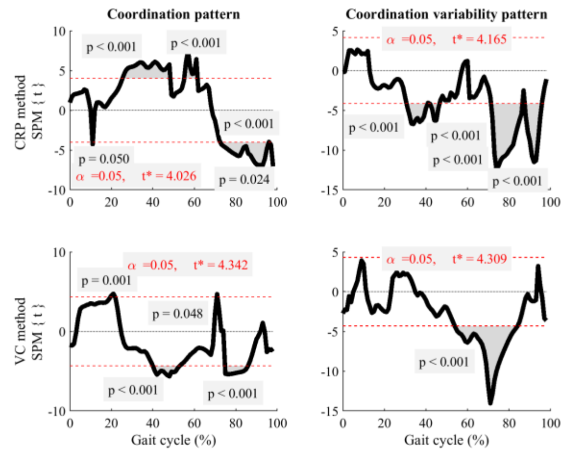

Figure 1: T-statistic results of SPM t-test for sagittal hip-knee coordination and its variability between aligned and unaligned data of walking at preferred speed.

Methods: Seventeen healthy adults (ten young adults, age: 25.2 ± 3.25 years, weight: 74.08 ± 12.27 kg, height: 1.72 ± 0.83 m, gait speed: 1.32 ± 0.10 m/s, seven older adults, age: 70.57 ± 3.50 years, weight: 71.03 ± 13.42 kg, height: 1.71 ± 0.14 m, gait speed: 1.33 ± 0.18 m/s) walked on an instrumented treadmill based on their preferred overground speed measured on an instrumented mat. Ten VICON motion capture cameras and conventional lower extremity gait model 2.4 were used to record the gait data. CaV for one hundred GCs (both temporally aligned and unaligned) for the sagittal plane lower extremity joints of each participant were calculated using both CRP and VC methods. Statistical parametric mapping (SPM) analysis, using paired t-tests, was employed to determine significant differences in CaV between aligned and unaligned data at each percentage of the gait cycle.

Results & Discussion: SPM analysis revealed significant differences in CaV between the temporally aligned and unaligned GCs (See Figure 1). TA changes CaV values for both CRP and VC calculations. Figure 2 reveals that mean coordination values are similar for temporally aligned and unaligned data, but there is a temporal shift, particularly evident in the swing phases for both CRP and VC measures. Coordination variability reveals an approximately similar pattern for temporally aligned and unaligned data, but variability was significantly higher in unaligned data, especially during the swing phase. This effect is particularly large for CRP variability. These findings are likely due to a quasi-periodicity problem in unaligned data, where kinematics from different phases is averaged together (e.g., pre- and initial swing phases). The greater differences later in the GC (swing phase) could arise from an accumulation of changes in proportions of the gait phases unaccounted for when only the whole GC is aligned. Similar results were found for the knee-ankle, and hip-ankle couples but the figures for only the hip-knee couple are provided for illustration.

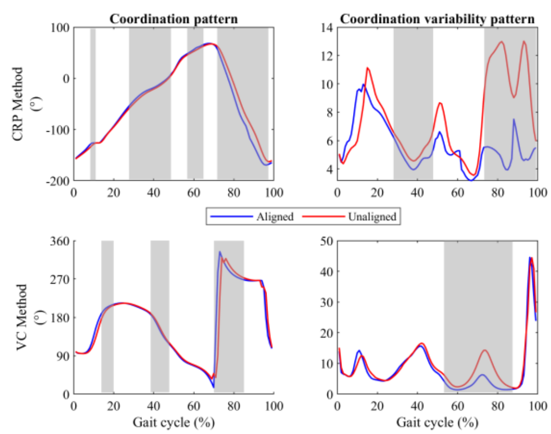

Figure 2: The mean curves of coordination and its variability for sagittal hip-knee coordination and its variability between aligned and unaligned data of walking at preferred speed. Gray rectangles show the significant points in the gait cycle.

Significance: Time normalization over the GC can lead to averaging data together from different phases, which alters CaV measures, potentially resulting in misleading findings. Temporal alignment of phases before computation of CaV can help to mitigate this concern for gait analysis and possibly other motor skills.

References: [1] Alijanpour et al. (2021), *Journal of Biomechanics* 120; [2] Hafer et al. (2018), *Gait & Posture* 62; [3] Ippersiel et al. (2021), *Gait & Posture* 85; [4] Byrne et al. (2002), *Perceptual and Motor Skills* 94(1); [5] Robertson et al. (2013), *Human Kinetics*; [6] Honert et al. (2021), *Journal of Biomechanics* 119; [7] Pecoraro et al. (2006), *Journal of NeuroEngineering and Rehabilitation* 3; [8] Forner-Cordero et al. (2006), *Journal of Biomechanics* 39(5); [9] Helwig et al. (2011), *Journal of Biomechanics* 44(3).

STATISTICAL PARAMETRIC MAPPING AND DYNAMIC TIME WARPING ANALYSIS OF AGE AND GAIT SPEED

Vinayak Vijayan[1], Shanpu Fang[1], Timothy Reissman[1], Allison L. Kinney[1], Megan E. Reissman[1*]
[1]EMPOWER Lab, Department of Mechanical and Aerospace Engineering, University of Dayton, Dayton, OH, USA
*Corresponding author's email: mreissman1@udayton.edu

Introduction: Gait speed is a sensitive indicator of overall health. Interventions which improve gait speed by even 0.1 m/s are considered clinically relevant [1]. To properly evaluate gait alterations, and develop successful rehabilitative interventions, it is important to characterize the relationships between speed and gait parameters. Discrete metrics have been used primarily to describe gait changes with speed [2]. However, there is limited data on the effects of gait speed across the entire gait cycle. Discrete point analysis can highlight certain changes but may not represent the scale of the effect across the gait cycle [3] or temporal shifts in the profile.

Statistical parametric mapping (SPM) can be used to examine the effects of speed changes across the whole gait cycle [4]. However, SPM could be affected by differences in timing of gait events [5]. A curve registration algorithm, like dynamic time warping (DTW), could be used to reduce the effects of timing differences and isolate magnitude differences [5]. Additionally, age could be a confounding factor that could affect responses to changes in speed. The purpose of this study is to characterize the effects of speed changes and age on gait across the whole gait cycle. We utilized classical peak analysis, SPM, and DTW SPM techniques to quantify both the magnitude changes and the timing differences that occur as a result of changing gait speed or age. Based on previous literature [5], we hypothesize that an increase in speed will cause timing shifts and magnitude changes in both groups. However, we expect the main differences between the groups to arise as magnitude changes, being a consequence of the deterioration of physical capabilities with age.

Methods: Twelve middle-aged and twelve younger adults participated in this study. A 2-minute overground walking test was used to determine the baseline walking speed. The medium speed and fast speed were fixed as 115% and 130% of the baseline walking speed. The participants walked on a split-belt instrumented treadmill for 1 minute per trial. Sagittal plane joint angles, moment, and muscle activations were evaluated using SPM, as described by Pataky [4]. DTW was implemented to isolate the changes in magnitude caused by variations in speed. DTW algorithm reduces the total cumulative Euclidean distance between two signals.

Results & Discussion: SPM and DTW SPM generally agreed suggesting that changes due to gait speed have both magnitude and temporal impacts, supporting our hypothesis for both age groups. Using SPM and DTW SPM in tandem helps isolate and analyze the characteristic temporal and magnitude changes caused by a change in gait speed.

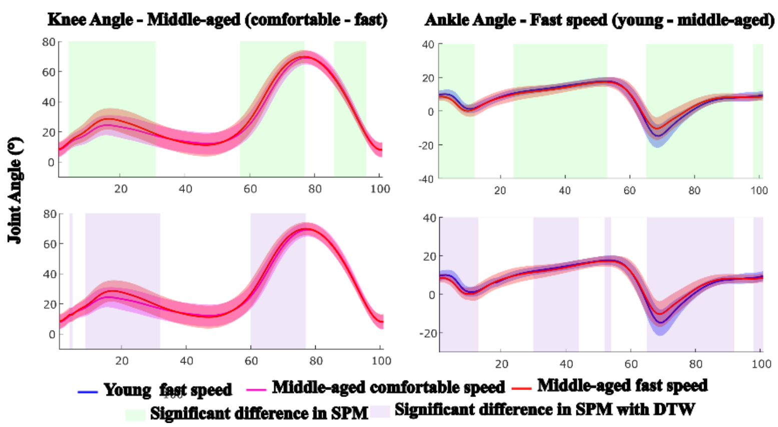

Figure 1: Representative results from SPM and SPM DTW

Younger adults' stride lengths were higher than the middle-aged adults for all speeds. This was associated with a significant increase in stance, but not swing, time. Increased stance time is related to better stability and could indicate changes in gait quality happening in middle-aged adults [6].

The hypothesis that the main differences between the two groups will arise as magnitude changes is more complicated. Ankle range of motion and peak ankle plantarflexion are significantly lower for middle-aged adults at the fast speed (Fig 1). This is consistent with previous findings that range of motion decreases with age [7]. Increasing ankle mobility should be explored as a possible intervention to help middle-aged adults safely increase gait speed. SPM and DTW SPM revealed that both groups increase ankle plantarflexion moment with speed. However, middle-aged adults demonstrated greater ankle moment magnitude in mid-stance and preferentially activated Gastrocnemius whereas younger adults activated Soleus. The largest knee flexion magnitude changes due to speed were in mid-stance, where both groups responded similarly to speed increases and had similar magnitudes (Fig 1). Knee moments also increased for both groups with speed but younger adults produced greater mid-stance knee moments despite having similar knee angles. In mid-stance, middle-aged adults had a stronger recruitment of the Vasti and then Gastrocnemius which likely stiffens the knee but reduces overall knee moment. Knee range of motion was significantly different between the two groups at the low and medium speed, but not at the fast speed. Increasing gait speed helps middle-aged adults adopt a knee range of motion comparable to younger adults. The hip remains generally more flexed throughout the gait cycle for the middle-aged adults. This change in positioning may underlie the observation that middle-aged adults had greater early stance extension moment and decreased late stance flexion moment.

Significance: Interventions that help improve gait speed are considered clinically relevant. Ideally, the rehabilitation should focus on safely improving gait speed. Our results show improving joint mobility could help middle-aged adults adapt a strategy of increasing speed that is closely matched with younger adults. Some of the characteristic differences, like the difference in strategic activation of plantar flexors or the characteristic increase in knee flexion in the stance phase in both groups, observed by SPM would have been overlooked by discrete peak analysis.

References: [1] Lusardi et al. (2003), *J Geri Phy Ther*; [2] Fukuchi et al. (2019), *Syst Rev* 8; [3] Fang et al. (2022), *Sensors* 22; [4] Pataky et al. (2012), *Comp Meth Biomech Biomed* 15; [5] Hornet et al. (2021), *J Biomech* 119; [6] Blaszczyk et al. (2011), *Acta Neurobio Exp* 71; [7] Bell et al. (1981), *J Appl Sport Sci* 6;

Knee Effusion and Pain are Not Related to Quadriceps Avoidance Gait in Individuals with ACL Injury

Reagan R. Recchia[1], Taylor McCollin[1], Michael J. Angelini[1], Alexa K. Johnson[1*], Riann M. Palmieri-Smith[1]
[1]University of Michigan, Ann Arbor, Michigan
* Corresponding author's email: akjohns@umich.edu

Introduction: Knee joint effusion and pain are common clinical sequalae accompanying an acute anterior cruciate ligament (ACL) injury and may contribute to the altered biomechanical function present in this population. Prior research utilizing a joint effusion model (i.e., where sterile saline is injected into the knee joint capsule to produce artificial joint swelling) has shown that knee effusion results in a quadriceps avoidance gait pattern, characterized by decreased knee excursions, knee extension moments, and ground reaction forces (vGRF)[1]. Additionally, increased pain has been associated with decreased vGRF and peak knee moments following ACL reconstruction [2], though this has not been characterized after ACL injury. The relationship between knee effusion, pain, and biomechanical adaptations that are typical of quadriceps avoidance gait, in individuals with ACL injury has not previously been characterized and warrants consideration. Therefore, the purpose of this study was to investigate the relationship between knee effusion, pain, and knee mechanics during gait in individuals with an ACL injury. We hypothesized that individuals with greater magnitudes of effusion and pain in their ACL-injured limb would display mechanics characteristic of a quadriceps avoidance gait pattern.

Methods: Forty-four participants (20 males and 24 females; Age: 23.3 ± 9.0yrs; Height: 1.7±0.1m; Mass: 73.4 ±16.4kgs) with a primary ACL injury were included in this study. We quantified subjective pain using the pain scale subsection of the Knee Injury and Osteoarthritis Outcome Score (KOOS). Suprapatellar knee joint effusions were quantified using ultrasound (GE LogiqE, GE Healthcare, Chicago, IL). Patients were in the supine position, with the knee rested at 30 degrees of knee flexion. The ultrasound probe was placed longitudinally approximately 2cm proximal to the superior border of the patella, along the quadriceps tendon. The probe was carefully placed on the skin to not place pressure on the suprapatellar pouch compressing the effusion. The cross-sectional area of the effusion in the suprapatellar pouch was measured using ImageJ (Figure 1) and the average of three images computed. A three-dimensional motion capture system (Oqus Cameras, Qualisys AB, Sweden) and two in-ground force plates (AMTI OR6-7, AMTI, Watertown, MA) were used to ascertain knee kinematics and kinetics. Kinetics were calculated utilizing inverse dynamics. Participants walked at their self-selected speed over the force plates and knee excursion, peak internal knee extension moment, and peak vGRF were determined within the first 50% of stance for both the ACL-deficient and the contralateral limb. Paired t-tests were used to assess differences between limbs (ACL and Non-ACL) for knee excursion, peak knee extension moment, and vGRF. Significance for t-tests were set at $p \leq 0.016$ (corrected for multiplicity). Multiple linear regressions were run to determine how pain and effusion contributed to gait mechanics. Analyses were considered significant at $p \leq 0.05$.

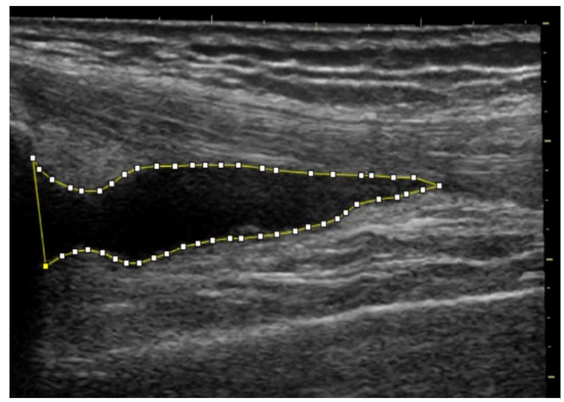

Figure 1: Representative image of a suprapatellar knee joint effusion. Effusion was traced in ImageJ software to calculate the cross-sectional area.

Results & Discussion: The ACL-injured knee had an average effusion size that was 129.5±85.4mm^2 and average KOOS pain score of 77.5±10.4. The ACL-injured limb presented with significantly lower knee excursion (ACL: 16.0±4.0°, Non-ACL: 19.1±3.7°; p=0.0001), peak knee extension moments (ACL: 0.4±0.1 Nm/kg*m, Non-ACL: 0.5±0.2 Nm/kg*m; p=0.012), and peak vGRFs (ACL: 1.11±0.08xBW, Non-ACL: 1.15±0.11 xBW; p=0.0001) when compared to the Non-ACL limb. Effusion size and pain did not influence ACL limb peak vGRF (R^2=0.002; p = 0.366), knee excursion (R^2 = -0.027; p = 0.638), or peak knee extension moment (R^2 = -0.049; p = 0.951). Previous research with simulated knee joint effusions have shown that knee effusion can result in knee mechanics reflective of a quadriceps avoidance gait pattern. This data has contributed to the idea that effusion was at least partially responsible for these same gait adaptations in individuals with ACL rupture. While the ACL-injured limb in our subjects did present with characteristics of a quadriceps avoidance gait, our data indicate that knee effusion and pain are not contributing to the reduced knee excursions and knee and limb loading during walking in individuals after ACL injury.

Significance: Current treatment following ACL injuries emphasizes reducing effusion and pain quickly after the initial injury to improve movement. However, our findings suggest that the effusion and pain in the ACL-deficient leg, while they may occur in tandem with changes in knee mechanics, are not the factors causing gait modifications. Quadriceps neuromuscular dysfunction (i.e., deficits in strength, activation, and rate of torque development) may explain the altered gait patterns after ACL injury [6], however more research is necessary to confirm the association.

Acknowledgements: Research reported in this abstract was supported by the Eunice Kennedy Shriver National Institute of Child Health & Human Development of the National Institutes of Health under Award Number R01HD093626. The content is solely the responsibility of the authors and does not necessarily represent the official views of the National Institutes of Health.

References: [1] Torrey et al., 2000, *Clin Biomech* 15, [2] Azus et al., 2018, *PM&R* , 20, [3] Gardinier et al., 2013, *J Orthop Res,* 31;[4] Thomson et al. 2018, *J Sci Med Sport,* 20; [5] Capin et al., 2017, *Clin Orthop Relat Res*, 475; [6] Lewek et al., 2002, *Clin Biomech*, 17.

INTEGRATED WHOLE-BODY ANGULAR MOMENTUM DURING NARROWING BEAM WALKING TEST USING PASSIVE AND POWERED KNEE PROSTHESES

Sixu Zhou[1,2*], Sujay Kestur[2], Aaron Young[1,2], Kinsey Herrin[1,2]
[1]Institute of Robotics and Intelligent Machines, Georgia Institute of Technology
[2]George W. Woodruff School of Mechanical Engineering, Georgia Institute of Technology
*Corresponding author's email: szhou357@gatech.edu

Introduction: Falls are one of the most frequent and common risks that prosthesis users experience in daily life [1]. The consequences can result in both physical and psychological harm to the user, including severe injuries and fear of falling. Commercially available microprocessor prosthetic knees (MPKs) restore the ability to walk on varying community terrains (level ground, stairs, and ramps). Passive prostheses provide users with limb support and damping control in walking. Powered prostheses provide users with active joint extension power to reduce residual limb biological joint load. Providing balance stability for individuals with transfemoral amputation (TFA) wearing either passive or powered lower limb prosthesis is a goal in the field. Whole-body angular momentum (WBAM) is a common measure to evaluate human balance, where previous studies suggest that WBAM is highly regulated during locomotion while maintaining dynamic stability [2]. The integration of WBAM (iWBAM) is a physical quantity that indicates the net body rotation or flexion from the starting pose. The narrowing beam walking test (NBWT) is designed to evaluate the balance ability for individuals with TFA where the goal of the test is walk as far down the beam as possible [1]. The NBWT is composed of four six-yard-long beams with sequentially decreasing widths starting from 18.6cm, 8.6cm, 4.0cm to a final 2.0cm. From previous studies, the NBWT provides sufficient test difficulties without ceiling or floor effects. However, there are few studies that have evaluated the stability of individuals with TFA, especially in beam walking. Due to the step width restriction on the beam in the frontal plane, we hypothesized that 1) iWBAM would be highly regulated in the frontal plane instead of the sagittal or transverse planes. We hypothesized that 2) distance traveled would affect iWBAM in the frontal, sagittal and transverse planes. Since powered knee prostheses can generate active power assistance, we hypothesize that 3) powered knee prostheses would perform better at regulation of iWBAM than passive knee prostheses.

Methods: Eight subjects with TFA consented to an IRB approved protocol and were fit and trained on three different commercially available knees. Each participant wore the Ottobock C-Leg 4, Ossur Rheo Knee or Ossur Power Knee at home for a one-week acclimation period in a randomized order. Following acclimation, motion capture data (Vicon; Denver, CO) was collected as the participants completed the NBWT for five trials with arms crossed at the waist to limit contribution of arms to balance. The first three trials were used as practice trials and only the last two trials were included in the data analysis. Following completion of data collection, participants were then fit and trained on a different knee and repeated the protocol until all three knees were completed.

Results & Discussion: As shown in Fig 1A, frontal plane iWBAM showed significant differences ($p<0.05$) and was more regulated compared to the sagittal and transverse plane (Fig 1B and 1C) as participants walked further on the beam, therefore allowing us to accept Hypothesis 1. The distance travelled in the frontal plane did not affect iWBAM ($p=1.0$). However, there are significant differences ($p<0.05$) between the iWBAM of the first half and iWBAM of the second half of the beam in both sagittal and transverse planes allowing us to partially accept Hypothesis 2. In addition, the powered prosthesis, the Power Knee, did not show significant differences ($p>0.05$) compared to the passive prostheses, the C-leg and Rheo, in regulation of iWBAM, therefore forcing us to reject Hypothesis 3. However, the Rheo showed significant differences ($p<0.05$) compared to the C-leg in regulation of iWBAM in all planes. Higher regulation in the frontal plane indicated that participants used strategies during NBWT such as hip rotation to adjust the center of mass (COM) back to the neutral position. Lower regulation in the sagittal and transverse planes indicated that participants had difficulty controlling forward speed and body rotations in the transverse plane. The loss of the anatomical knee and ankle make the body rotation in the transverse plane at each heel contact more challenging for participants without direct control of the prosthetic knee/ankle and proprioceptive feedback. We believe the powered prosthesis did not perform better than passive prostheses as a result of a common feature across the devices which allows the user to lock the knee in a flexed position when staying in the same pose for over two seconds to provide single stance support.

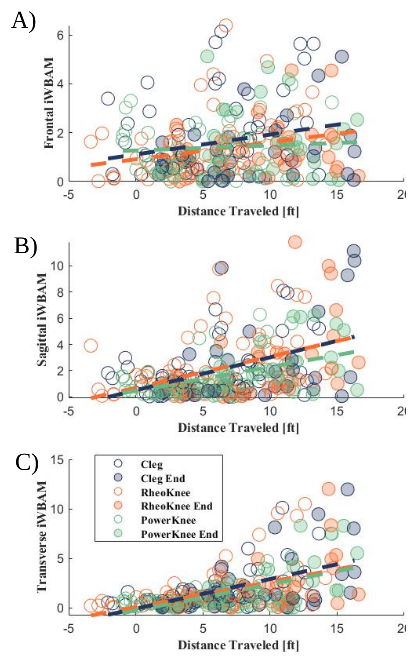

Figure 1: A) Frontal, B) sagittal and C) transverse plane integrated whole-body angular momentum changes across C-leg, Rheo and Power Knee in narrowing beam walking test.

Significance: A better understanding of how individuals with TFA control balance and the relationship between stability and different types of knees may allow engineers to design more robust controllers for stability.

Acknowledgements: This work is funded through a grant from the DoD CDMRP Award Number W81XWH-21-1-0686.

References: [1] Sawers et al. *J Rehabil Med* 50(5): 457-464; [2] Herr et al. (2008) *J Experimental Biology* 211, 467-481

MEDIOLATERAL GAIT VARIABILITY IN RESPONSE TO SENSORY PERTURBATIONS

Skyler Miller[1], Vinayak Vijayan[1], Sydney Lundell[1], Timothy Reissman[1], Megan E. Reissman[1*]
[1]EMPOWER Lab, Department of Mechanical and Aerospace Engineering, University of Dayton, Dayton, OH, USA
*Corresponding author's email: mreissman1@udayton.edu

Introduction: It has previously been proposed that the variations in lateral foot placement to stabilize movement is actively controlled by the CNS in response to the visual, vestibular, and proprioceptive sensory feedback [1]. Whereas the fore-aft foot placement is more dependent on the pendulum like dynamics of the leg [2]. Thus, changing the sensory weighting may in effect act like a perturbation which could impact the stability, or foot placement, of the person. Examining the literature, it has been previously found that sensory perturbations could affect balance during gait [3]. However, variations in foot placement could be due to changes in speed, or it could be due to changes in sensory input. A prior study has also tested detrending variations in foot placement into speed-related trend and variations due to changes in sensory perturbation, under eyes-open and eyes-closed conditions [4]. However, to our knowledge there are no previous studies that comprehensively reports the effects of sensory perturbation on foot placement, decoupled from the variations due to speed changes. Therefore, the purpose of this study is to quantify the effects of sensory perturbation on variability of foot placement, or step-to-step balance, using a multitude of conditions.

Methods: 23 healthy participants without any gait abnormalities participated in this study. Participants walked on an instrumented split belt treadmill during a variety of conditions. The conditions included a Baseline (no sensory perturbation), Blurry (blurred safety glasses), Brown (brown noise from headphones), Dark (all lights turned off), Dark-Brown (combination of Dark and Brown conditions), and Head-Turn (~135° left to right head motion set to a metronome with 50 bpm). Each condition was 150 seconds long followed by 150 seconds of washout, denoted by a prefix Wash for each of the conditions. To quantify variations in foot placement due to sensory perturbations, step length and step width were decomposed into speed-related variations [step length speed (SLS), step width speed (SWS)] and variations due to changes in conditions [step length condition (SLC), step width condition (SWC)].

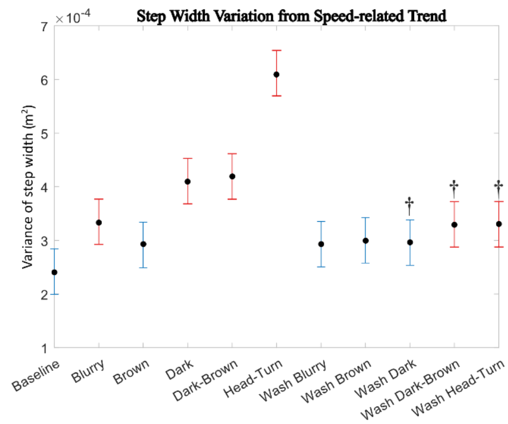

Figure 1: Mean and error bar showing variation due to changes in conditions (SWC). Red color represents significant difference from baseline and † represents significant difference of wash trial from the corresponding trial.

Results & Discussion: SLS and SWS showed no significant results in the pairwise comparisons, showing that the detrending was effective. As such all results discussed here are variations due to changes in conditions and are with respect to the Baseline condition. The Head-Turn condition caused the largest significant change in both SLC and SWC. Further, SWC during the wash trials was reduced but still maintained a significantly higher variation. This indicates that some of the lasting effects of vestibular perturbation were not washed out after 150 seconds of treadmill walking. Disorientation caused by vestibular perturbation has been previously established in the literature [5]. Vestibular cues have been identified as being particularly important in maintaining balance at high velocities of movement [6]. Our results show that vestibular cues are important to step-to-step balance, independent of gait speed. Both the Blurry condition and Dark condition caused a significant increase in SWC. As expected, the Dark condition caused a greater increase in SWC. The Dark condition is likely a stronger effect on the visual spatial orientation than the Blurry condition. The wash trials for both Blurry and Dark conditions were not significantly different. Such findings indicate that the subjects were able to resume their normal gait pattern when the visual perturbations were removed. Similar to the Dark condition, the Dark-Brown condition also showed an increase in SWC. However, the addition of auditory perturbation resulted in a longer effect, wherein the wash trial for the Dark-Brown condition was reduced but remained significantly different. Interactions between visual and auditory cues have previously been reported; postural sway was observed to be significantly improved with an addition of auditory stimulus to visual cues [7]. The addition of Brown noise to the dark condition in this study, takes away the existing environmental spatial orientation auditory cues, like the sound of the treadmill. Brown condition on its own did not cause any significant difference in step width.

Significance: This study successfully demonstrates the effects of sensory perturbations on healthy adults, decoupled from speed-related changes. We identified that a majority of changes in foot placement occurred in the mediolateral direction. The Head-Turn condition, or vestibular perturbation, resulted in the most variation in foot placement. A major goal of vestibular rehabilitation is returning to normal function of the vestibular sensory system. Our results could help define the normal range of variations in response to vestibular perturbations, detrended from speed-related changes. We also identified that brown noise had no impact on foot placement but integrating brown noise with visual perturbations caused lasting effects, which were not observed under each of the conditions alone. These insights about step-to-step balance could help in further understanding human motor control of balance during gait.

Acknowledgements: This work was funded by the Multiloop Cybernetic System Multidisciplinary University Research Initiative (MURI, N000142012163).

References: [1] Peterka RJ et al. (2002) *J Neurophysiol* 88; [2] O'Connor et al. (2009) *J Neurophysiol* 102; [3] Chien et al. (2014) *Ann Biomed Eng* 42; [4] Collins et al. (2013) *PLoS ONE* 8; [5] Black et al. (2003) *Curr op otolar head neck surgery* 11; [6] Horak (2010) *Restor Neurol Neuros* 28; [7] Madelyn et al1. (2016) *J Vesti Res* 26.

Comparative Analysis of Novel Wearable Ultrasound Sensors and Kinetic Assessments to Monitor Muscle Function

Erica L. King [1,2*] Ahmed Bashatah[1], Brian M. Guthrie [3,4], Margaret T. Jones [3,4,5], Qi Wei [1], Siddhartha Sikdar [1,2], Parag V. Chitnis [1,2]

[1] Department of Bioengineering, George Mason University, Fairfax, VA, USA

[2] Center for Adaptive Systems of Brain-Body Interactions, George Mason University, Fairfax, VA, USA

[3] Frank Pettrone Center for Sports Performance, George Mason University, Fairfax, VA, USA

[4] Kinesiology, George Mason University, Fairfax, VA, USA

[5] School of Sports, Recreation, and Tourism Management, George Mason University, Fairfax, VA, USA

*Corresponding author's email: eking20@gmu.edu

Introduction: Understanding musculoskeletal injuries (MSKIs) effects on synergistic muscle recruitment has the potential to improve rehabilitation techniques and provide personalized treatment [1]. Current laboratory techniques, like surface electromyography (sEMG), lack the ability to differentiate between activation of deeper muscles, providing limited knowledge on muscle recruitment and synergy during natural dynamic movements [2]. MSK ultrasound (MSK-US) imaging is emerging as an effective assessment technique for rehabilitation and biomechanics by providing an in-depth assessment of muscle structure, composition, movement, and overall function through imaging muscle groups at varying depths in real time. Muscle-level outcome measures such as fascia pennation angle, contraction velocities, and muscle activation can be utilized in ultrasound-base assessment of MSKIs.

Despite certain advantages, current clinical MSK-US devices are inadequate due to probes being bulky, hand-held, tethered, and needing custom holders to maintain skin contact making them unamenable to imaging muscle tissues during dynamic tasks. Our lab has developed a specific Motion-mode (M-mode) MSK-US paradigm that employs wearable sensors strategically placed over muscles of interest to sense movement of MSK tissue in real time. Each wearable MSK-US sensor provides a single scan line placed directly over the muscle to capture changes over time [3]. ~~We have developed a specific Motion-mode (M-mode) MSK-US paradigm that employs wearable sensors strategically placed over muscles of interest to sense movement of MSK tissue in real time, and proved single scan lines placed directly over muscles of interests to capture changes in muscle status over time [3].~~ This miniaturized, wearable MSK-US enables rapid imaging during rehabilitation exercises via hands-free operation and is un-inhibiting to patient movement.

Commented [QW1]: It was an incomplete sentence. Does this edit make sense?

Commented [ELK2R1]: Yes it does

Methods: A single MSK-US sensor was attached on the right vastus lateralis (VL) of four participants (23-28 years of age). Participants were asked to perform three countermovement jump (CMJ) trials on a force plate (AccuPower; AMTI, Watertown, MA, USA) with a data acquisition system utilizing custom LabVIEW (National Instruments, Austin, TX, USA). All data were collected synchronously, and image analysis was performed using a custom MATLAB (MathWorks, Natick, MA, USA) program to estimate MSK-US mean pixel value (MPV) and normalized pixel difference (NPD) of the VL during CMJ. MPV was found by taking the average mean pixel intensity along the columns of the region of interest (ROI), which was selected manually, excluding fascia interference. NPD was determined by averaging the pixel intensities across the same ROI to measure a relative change of muscle state between scan lines. The signals were filtered using the Teager-Kaiser Energy Operator (TKEO) and then normalized to their root-mean square baseline. The percent change was calculated by dividing the peak values for jump take-off and landing by baseline. The correlation coefficient was calculated to determine if there was a relationship between the metrics.

Results & Discussion: Force data showed that the mean $\pm$ SD of percent change during take-off and landing was 0.28%$\pm$0.09 and 0.66%$\pm$0.17 relative to baseline for each peak, respectively. MPV values changed 0.42%$\pm$0.29 and 0.81%$\pm$0.17, and NPD changed 0.41%$\pm$0.32 and 0.84%$\pm$0.12 for the corresponding peaks. Overall results indicate there was significant correlation between the CMJ force data and MSK-US metrics ($p < 0.05$).

The wearable MSK-US system has shown the ability maintain skin contact and acoustic coupling during complex movements while collecting quantitative MSK-US data. Data from our sensors can provide semi-real-time quantitative feedback that is comparable to results from traditional kinetic measurements (Fig 1).

Commented [MTJ3]: complex what?

Significance: Wearable MSK-US offers potential for assessing muscle injury and facilitating assessment during treatment and rehabilitation periods, thereby yielding new quantitative information on healing progression. The wearable MSK-US system will enable the monitoring muscle performance during functional activity and exercises informing return to play decisions in new ways previously unobservable.

Acknowledgements: These efforts were sponsored by the Government under Other Transactions Number MTEC-MPAI W81XWH-15-9-0001 and MOMRP RESTORE W81XWH-21-1-0190.

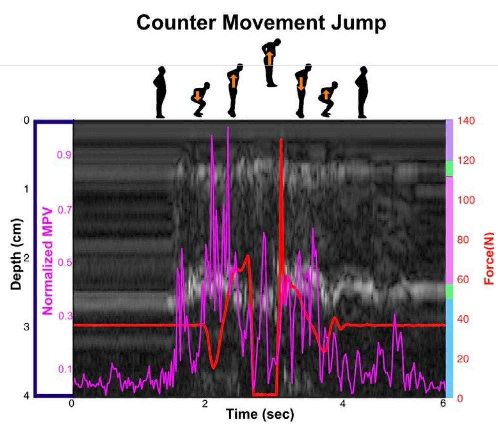

Figure 1: MPV can be used in comparative analysis to force plate measures to depict muscle activation patterns in the VL during CMJ.

References: [1] S. Safavynia, *et al.,* (2011). *TSPIR*; [2] S. Delaney, *et al.,* (2010). *M& N*; [3] P. Chitnis, *et al*., (2021). US Patent 10,935,645 B2

MUSCLE OXYGENATION PATTERNS DURING AT-HOME AND LABORATORY LIGHT INTENSITY WALKING

Zachary J. Wilson[1*], Noah S. Rick[2], Daniel J. Methven[1], April J. Chambers[1,2]
[1]Health and Human Development, School of Education, University of Pittsburgh, Pittsburgh, PA, USA
[2] Department of Bioengineering, Swanson School of Engineering, University of Pittsburgh, Pittsburgh, PA, USA
*Corresponding author's email: zjw17@pitt.edu

Introduction: Current wearable fitness monitors are limited to global estimates of activity. These devices do not directly measure muscles' physiological responses to activity, which is influenced by intensity and duration. [1] Near-infrared spectroscopy (NIRS) is a non-invasive technology that emits light into underlying tissue to measure muscle oxygenation (SmO_2). [2] The use of NIRS in a free-living environment has yet to be explored. Muscle oxygenation dynamics measured at-home will provide information on the usefulness of the NIRS tool to be used outside of controlled, laboratory settings. The purpose of this study was to describe muscle oxygenation dynamics during light intensity walking in a controlled and uncontrolled environment.

Methods: Seven healthy subjects (22.71 ± 2.43 years; 26.68 ± 1.81 kg/m^2) completed a 1-hour laboratory light intensity walk (RPE 1-3) and 1-hour at-home light intensity walk (RPE 1-3) on non-repeating days. Intensity was subjectively monitored by the OMNI-RPE scale. [3] SmO_2 was recorded by a MOXY NIRS device placed on the subject's dominant medial gastrocnemius muscle. Muscle oxygenation variables of interest were adopted from previous literature. [4]

Results & Discussion: Medial gastrocnemius muscle oxygenation during light intensity at-home and laboratory walking had visually similar patterns shown in Figure 1. Baseline muscle oxygenation, SmO_{2B}, started around 52% and gradually rose to a higher plateau, identified as steady state, SmO_{2SS}, around 78% and remained elevated for the duration of the walking session. The change in muscle oxygenation from baseline to steady state, ΔSmO_2, was around 26% for both walking settings. The time to reach steady state, SmO_{2SS}Time, appeared to be quicker during the at-home walking session. Paired t-tests were conducted to evaluate the differences between the SmO_2 variables of interest between walking settings. There were no statistically significant differences between SmO_{2B} (p=0.938), SmO_{2SS}, (p=0.954), ΔSmO_2 (p=0.927), or SmO_{2SS}Time (p=0.079). In general, the influx of SmO_2 seen during the onset of light intensity walking suggests there is an abundance of oxygen within the tissue, compared to the usage of oxygen to fuel muscle metabolism. [5] Eventually, when the SmO_2 curve reaches steady state, this is interpreted as the dynamic equilibrium of the oxygen supply meeting the oxygen demand/usage of the muscle tissue to perform the walking activity. The similar visual patterns and lack of statistical differences seen between the walking settings can imply the practical use of NIRS technology to be effective in measuring muscle oxygenation patterns outside of controlled environments.

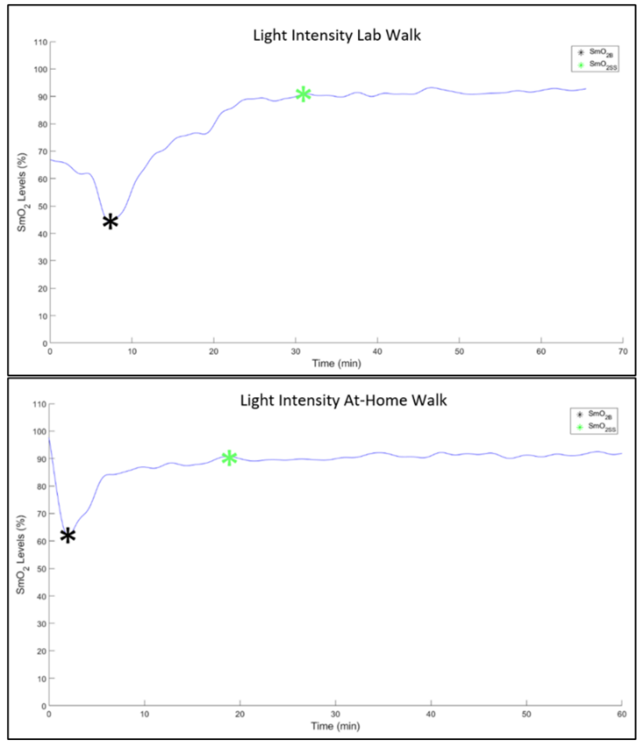

Figure 1: Muscle oxygenation patterns during light intensity walking in the laboratory (Top) and at-home (Bottom) setting. Black asterisk denotes SmO_{2B}. Green asterisk denotes SmO_{2SS}.

Significance: Walking activity is the most often prescribed form of exercise from clinical settings. [6] However, there have been no studies that evaluated local physiological parameters, i.e., muscle oxygenation, between controlled and uncontrolled walking environments. Additionally, the use of wearable NIRS technology has been limited to laboratory trials, sports settings, and activities of higher intensities. Therefore, the current study not only describes in detail the muscle oxygenation patterns during light intensity walking, but also shows that wearable NIRS can be used in uncontrolled environments to measure muscle oxygenation. The addition of NIRS in the at-home setting can lead to better exercise prescription and health monitoring.

Acknowledgements: Research supported by the University of Pittsburgh School of Education Research Fund

References: [1] Belardinelli et al. (1995), *Eur J Appl Physiol Scand* 70(6); [2] Barstow (2019), *J Appl Physiol* 126(5); [3] Robertson (2004), Human Kinetics. [4] Ferrari et al. (2011), *Philos Trans A Math Phys Eng Sci* 369(1955); [5] Hargreaves & Spriet (2020), *Nat Metab* 2(9); [6] Franklin (2006), *Prev Cardiol* 9(1)

THE DESIGN, FABRICATION, AND TESTING OF A JOINTED FOOT-ANKLE, MUSCLE-DRIVEN ENDOPROSTHESIS: WHITE RABBIT AMPUTATION MODELS

Heidi E. Seuss[*,1], Morteza Asgari[1], Katrina L. Easton[1], David E. Anderson[2], Dustin L. Crouch[1]
College of Engineering and College of Veterinary Medicine, University of Tennessee-Knoxville
*Corresponding author's email: hseuss@vols.utk.edu

Introduction: Limb amputation affects over 2 million people in the US and causes devastating sensorimotor impairment [1]. Patients are often prescribed an external prosthesis to partly replace the form and function of the missing limb. However, as many as 45% of patients reject external prostheses, in part, because they fail to restore natural sensorimotor function [2]. To address this problem, we propose to develop jointed endoprostheses that can be completely implanted within living skin and physically attached to muscles to leverage the innate sensorimotor capabilities of these tissues. To test the feasibility and potential effectiveness of this concept, we have designed, fabricated, and implanted endoprosthesis prototypes to replace the hindlimb ankle and foot in a rabbit model of amputation. We have previously reported study outcomes related to wound healing and tissue interface [3, 4]; ongoing studies are investigating biomechanical function. This abstract describes the design and fabrication of a jointed foot-ankle endoprosthesis prototype.

Methods: The endoprosthesis prototype was designed to replace the skeletal structure of the distal end of the tibia and foot. The tibial segment of the prototype included a 316L stainless steel stem (feature 3, Figure 1) that was inserted into the distal end of the tibia and secured with PMMA bone cement. An ultra-high molecular weight polyethylene hinge pin was used to join the shank and foot segments to form a one-degree-of-freedom hinged ankle joint. The foot segment had two loops (features 1 and 2, Figure 1) that served as attachment points for tendons. The assembled segments, excluding the stem portion, were first cast with a base layer of a stiff two-part silicone (hardness = 40 Shore A LSR BIO M340, Elkem Silicones), which also made up the "toe" portion of the foot so that it was flexible. The base layer was then dip coated with a softer two-part silicone (hardness = 1 Shore A, LSR 4301, Elkem Silicones) to reduce the severity of fibrous capsulation due to the foreign body response [5].

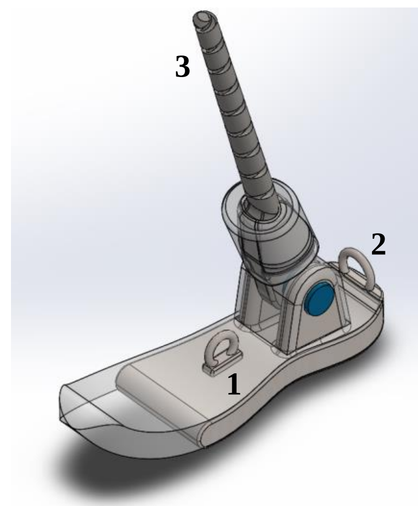

Figure 1: CAD model of the endoprosthesis assembly. Features 1 and 2 are the tendon attachment loops and feature 3 is the stem that interfaces with the tibia.

The component computer-aided design (CAD) models of the endoprosthesis were created using commercial software (Solidworks, Dassault Systems). Test pieces of prototypes were iteratively printed using an Anycubic Photon X stereolithography printer, which permitted rapid design changes. The test pieces enabled us to better visualize design features to ensure they were appropriate for the *in vivo* study. Once the prototype designs were finalized, the CAD models were used to print the segments via selective laser melting (SLM) from powder stock stainless steel. Since the prosthesis was small and intricate, SLM proved to be the most reliable option for detailed prints. Once the printed parts were received, any rough surfaces were sanded down; particular attention was paid to the tendon attachment loops to prevent wear. Both silicones used were quite viscous, so the mixing process of the two parts introduced a lot of bubbles into the material. To combat this, the silicone was subjected to a vacuum (VEVOR 8 CFM vacuum pump) in a 2-gallon sealed chamber until all of the bubbles were released. The higher shore rated silicone was applied to the endoprosthesis via a custom resin mold printed with the Photon X. After pouring the silicone into the mold around the endoprosthesis, the filled mold was introduced to the vacuum one more time to remove bubbles before being cured in a high-temperature oven. The softer silicone was applied immediately afterwards by dipping the entire assembly into the material and curing it in the oven.

Results & Discussion: The fabrication of the endoprosthesis was challenging but successful. Silicone can be difficult to work with but is effective in emulating the texture of skin. Our fabrication technique improved with each iteration, but there are still a few areas that could be improved for the next fabrication attempts. For example, the method for coating the endoprosthesis with silicone should be streamlined. While the stiff silicone toe does allow for more flexibility of the endoprosthesis, casting silicone in a mold is more challenging and time consuming than dip coating. Further research into alternate silicone casting methods, especially ones suitable for prototyping, would be helpful to assess the feasibility of simplifying this process. Additionally, it will be helpful to add extra stock material to certain features, such as tendon attachment loops, so that they can be sanded without compromising their mechanical strength.

Significance: This study will enable successful *in vivo* testing of the muscle-driven endoprosthesis concept. This is necessary to develop the technology as well as assess the safety and efficacy of the concept on its path to commercialization and clinical use.

Acknowledgements: Tickle College of Engineering, University of Tennessee, Knoxville. NSF Award #1944001.

References: [1] Ziegler-Graham K, et al. (2008) *Arch Phys Med Rehabil*, 89(3). [2] Salminger S, et al. (2022) *Disabil Rehabil*, 44(14). [3] Hall PT, et al. (2021) *Ann Biomed Eng*, 49(3). [4] Crouch DL, et al. (2022) *Bioeng*, 9(8). [5] Noskovicova N, et al. (2021) *Nat Biomed Eng*, 5.

VOCABULARY SLIP-UPS IN REPORTING SURROGATE SLIPS

Gaspard Diotalevi, Cécile Smeesters*
Research Centre on Aging, Sherbrooke, QC, Canada
Department of Mechanical Engineering, Université de Sherbrooke, Sherbrooke, QC, Canada
*Corresponding author's email: Cecile.Smeesters@USherbrooke.ca

Introduction: Among postural perturbations, slips have been extensively investigated for their prevalence as well as for the human and financial cost of injury [1]. To that end, several different experimental setups have been used in laboratories around the world to induce slips to participants with varying rates of ecological validity. This leads to recurrent ambiguity in reporting results, as wording is often misleading and methods used hinder the generalization of results. Based on a recent literature review of 47 papers on "slips" published between 2015 and fall 2022 [2], we assessed the magnitude of these issues in current research, highlighted a worthy example of clear and faithful writing [3] and proposed a way to avoid the slippery slope of surrogate slip vocabulary slip-ups.

Methods: 47 papers published between 2015 and fall 2022 were extracted from a recent literature review on "slips" [2] and scrutinized. Four main experimental designs were identified: two surrogate slips and two true slips (Table 1). We then noted in which part of the paper authors first acknowledged experimenting on surrogate slips instead of true slips. Every instance of the word "slip" was searched for and pondered considering its context in the title, the abstract and the bulk of the text. Clear enough wording found in those papers were "simulated slip", "surrogate slip", "slip-like", "emulated slips" and ""slip" (in quotes)". Finding at least one of these wordings in the title or the abstract deemed them clear enough, while three or more were required for the bulk of the text. Finally, we also checked whether limits to the generalization of results were explicitly stated regarding the fact that the postural perturbation was not a true slip.

Table 1: Fundamental differences between surrogate slips and true slips for experimental setups published between 2015 and fall 2022.

	− Ecological validity +			
	Surrogate slip (Surface translation)		**True slip**	
Characteristics	Treadmill acceleration (18 papers)	Uniaxial platform (19 papers)	Lubricated sheets† (1 paper)	Lubricated/ icy surface (9 papers)
Allows for medio-lateral displacement and planar rotation of the foot	No	No	Yes	Yes
Free foot dynamics along unconstrained degrees of freedom	No	Yes	Yes	Yes
Ecological friction at the sole-lubricant-floor interface	No	No	No	Yes

† Two layers of overlain lubricated sheets, one static with regard to the floor and the other static with regard to the shoe. Due to the negligible inertia of the sheet directly under the shoe, this experimental design is independent of footwear effects.

Results & Discussion: Only 10 of 47 reviewed papers (21.3%) dealt with true slips, while 37 (78.7%) used surrogate slips. Among the latter, only 5 (13.5%) immediately acknowledged experimenting with surrogate slips in their title, 7 others (18.9% of surrogate slips) became explicit while reading their abstract and 2 more (5.4%) only admitted to experimenting with surrogate slips in the bulk of the text. 23 papers (62.2% of surrogate slips) never explicitly mentioned it, leaving it to the reader to exert some critical thinking when reading the Methods of the paper. Finally, some of those studies mostly used clear enough wording in sections or figure captions obviously heavily inspired from other work.

More importantly, only 9 (24.3% of surrogate slips) tried to explain how those postural perturbations differ from a true slip. Surprisingly, most studies about training programs using treadmill accelerations implicitly consider passive uniaxial movable platforms as the gold standard for overground slips, to the point that one gets the impression that a true overground slip is induced in real life by such a device instead of a more ecologically valid method such as a lubricated or icy surface. Yet treadmill accelerations and movable platforms constrain by design two of the three degrees of freedom of a slipping foot, i.e., the medio-lateral displacement and planar rotation of the foot. Very rarely is any mention of the issue this poses for the generalization of results found [4].

One worthy paper [3] aptly used "support-surface perturbation" to qualify their postural perturbations induced on passive uniaxial movable platforms, correctly classifying them as surface translations rather than true slips. Papers using the acceleration of the belt of a treadmill could also be classified as surface translations.

Significance: This abstract empathises the need for precise and unequivocal wording when reporting findings on true human slips. Not only can incorrectly worded titles and abstracts set up wrong expectations for the reader, but routinely calling surrogate slips "slips" (not in quotes) in papers makes us blind to the inherent limitations that some experimental setups possess. Treadmill accelerations and passive uniaxial moving platforms hold very interesting advantages, notably in terms of control and repeatability of trials. Moreover, they definitely compliment the set of tools both researchers and clinicians can use to understand and prevent falls. However, we advise using "surrogate slip" or "surface translation" instead of "slip" to describe the postural perturbation they induce.

Acknowledgements: The Fonds de recherche du Québec – Nature et Technologies (FRQNT) and the Natural Sciences and Engineering Research Council of Canada (NSERC) for their financial support.

References: [1] Parachute (2021), *The Cost of Injury in Canada*. [2] Ferreira et al (2022), *Sensors* 22(23), 9254; [3] Inkol et al (2019), *J Mot Behav* 51(3), 318-330; [4] Troy and Grabiner (2006), *Gait & Posture* 24(4), 441-447.

ENHANCING MODEL GENERALIZABILITY VIA TRANSFER LEARNING FOR MULTI-ACTION INTENT RECOGNITION

David S. Hollinger[1*] & Michael E. Zabala[1]
[1]Department of Mechanical Engineering, Auburn University, Auburn, AL
*Corresponding author's email: dzh0063@auburn.edu

Introduction: Human movement encompasses a variety of dynamic actions. Human intent recognition is often used to sense the user's desired movement and is beneficial because it can monitor and analyze human behavior, detect abnormalities, and offer feedback to enhance exercise routines. Despite physical activity guidelines recommending adults to participate in at least 150 minutes of moderate to strenuous activity per week, approximately 46.9% of U.S. adults were sufficiently active to experience meaningful health benefits [1]. Personalizing a wearable device to a user's gait can increase user engagement and encourage habits of daily movement. Smartphones and smart watches are often used to track physical activity. One way to encourage physical activity among the general population is through wearable robotic assistance [2]. Additionally, it is difficult to predict movement intent using a single model. However, a model based on machine learning may be more suitable to achieve this objective [3]. Here, we propose a multi-action intent recognition machine learning model to predict joint angles across a variety of movements. We hypothesized that the prediction accuracy for a specific model would have a lower prediction error compared to a general model. Despite a smaller training dataset, we speculated that the specific model provides more relevant training data compared to the general model and, therefore, provide better more accurate predictions on the test set.

Methods: Twenty-five subjects performed three repetitions of 13 actions while wearing 16 EMG and IMU sensors (Trigno by Delsys Inc.). The protocol was approved by the Auburn University IRB (protocol no. 17-279-MR 1707), and all study participants provided written informed consent. A random forest model was used to predict ankle angles 100 ms into the future. Thirteen models were trained and tested for the same action (action-specific) while one model was trained on all 13 actions (action-generic). RMSE was used to evaluate model performance. An ANOVA was performed, and a significant result prompted post-hoc paired t-tests ($p<0.05$). We also performed a secondary analysis by training action-specific and action-generic models on five high-level actions (e.g. backward walk, kneel down, kneel up, running, and walking).

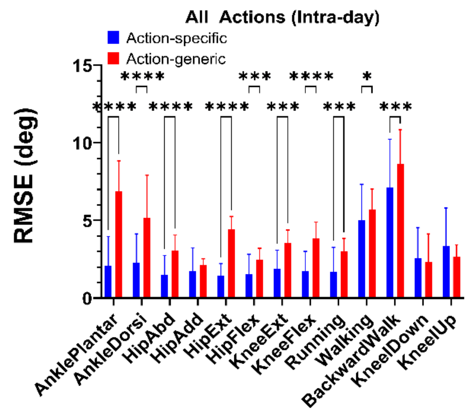

Figure 1: Action-specific vs. action-generic models tested on 13 different activities. ***: denotes a significant difference between activities ($p<0.001$)

Results & Discussion: The significant ($p<0.05$) ANOVA test prompted post-hoc paired t-tests with nine action-specific models significantly outperforming the action-generic model (Fig 1). Since prediction RMSE for high-level activities, such as kneel down and kneel up, were not statistically different, we performed a secondary analysis by training action-specific and action-generic models on five high-level actions (Fig 2). The results for the secondary analysis showed that action-specific models were not significantly different than the action-generic model for this particular dataset (Fig 2). Therefore, training a model on high-level actions is suggested because of the benefits of reducing model complexity and runtime during online testing. Additionally, training on similar high-level activities may provide greater model generalizability compared to training on as many activities as possible.

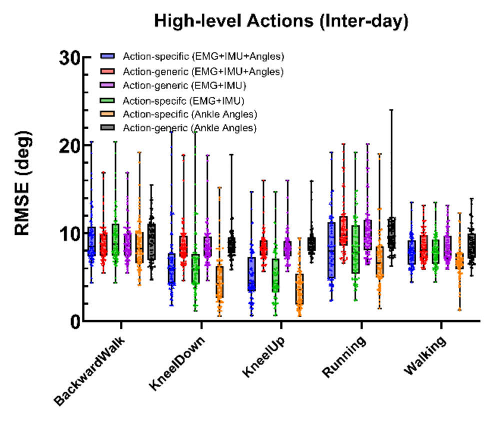

Figure 2: inter-day testing during five high-level activities.

Significance: Models trained on task-specific data including joint angles can effectively predict future joint angles for the same task. Therefore, the type of data included during training can influence the model to generalize to unseen activities. Therefore, an action-specific random forest model may be preferred for controlling a robotic exoskeleton when the user is expected to encounter various activities. Future work will leverage deep learning models trained on large and diverse datasets which can generalize for multi-action intent recognition.

Acknowledgements: We would like to thank the Combat Capabilities and Development Command (CCDC) for funding this study (Project: W15QKN-17-9-1025, PAO Number: PR2023_24581).

References:
[1] Boudali et al (2017), *39th Annual Int. Conference of IEEE EMBC* pp. 1889-1892.
[2] J. D. Omura, et al. (2019), *Prev. Chronic. Dis.*, vol. 16, p. E66, doi: 10.5888/pcd16.180690.
[3] Hollinger et al., 2023. The Influence of Gait Phase on Predicting Lower-limb Joint Angles. IEEE Transactions on Medical Robotics and Bionics – In Press

A LIGHTWEIGHT AND COMPLIANT EXOSKELETON FOR HUMAN AUGMENTATION IN REAL WORLD

Israel Dominguez[1*], Shuangyue Yu[1], Antonio Di Lallo[1], Hao Su[1*]

[1]Israel Dominguez, Shuangyue Yu, Antonio Di Lallo, and Hao Su are with the Lab of Biomechatronics and Intelligent Robotics, Department of Mechanical and Aerospace Engineering, North Carolina State University and Joint NCSU/UNC Department of Biomedical Engineering, North Carolina State University, Raleigh, NC, 27695; University of North Carolina at Chapel Hill, Chapel Hill, NC 27599, USA.

*Corresponding author's email: hao.su796@ncsu.edu

Introduction: The field of powered exoskeleton technology has seen considerable development in recent years, with the potential to greatly enhance human mobility. Numerous studies have focused on developing optimized control profiles to reduce energy expenditure [1], utilizing a variety of methods such as human-in-the-loop strategies, and data-driven approaches. However, few studies successfully achieved the design and development of an untethered and versatile device that satisfies the requirements for real-world applications [2], [3]. In addition to mechanical design, the electronics architecture employed in exoskeletons plays a crucial role in their performance. State-of-the-art electronics solutions provide limited reliability, compromised processing power, or slow communication with sensors and actuators outside the lab environment. Designing an effective exoskeleton requires balancing multiple attributes of the mechatronic system, including weight, power, torque capability, and compliance, while also being able to compute the implemented algorithm and provide energy to the knee joint at the right time. These challenges emphasize the importance of a comprehensive and holistic approach to the design and development of powered knee exoskeletons for outdoor scenarios.

Methods: In this study, we present a design for a lightweight (unilateral: 1.4 kg, total: 3.6 kg) and compliant robot knee exoskeleton that aims to enhance human capabilities in real-world applications. Figure 1 shows our lightweight and compliant knee exoskeleton system for outdoor applications. Our design achieves high torque density (10 Nm/kg) while maintaining a lightweight and compliant system and the battery lasts more than 1.5 hours, which makes it suitable for outdoor exoskeleton applications. Additionally, we developed a reliable portable electronics architecture that enables users to run complex control strategies in outdoor settings. We used a versatile control that read kinematics data (IMU sensors) and classify activities among squatting, stair-climbing, and incline walking, and then generate an assistive torque profile through a quasi-static model (squatting) or gait-cycle-based assistance (walking and stair-climbing). To verify the effectiveness of the exoskeleton to augment mobility in a real-world setting, we evaluated the metabolic cost and heart rate required to traverse a 1 km hiking route, with a 60 m increase in elevation in the no-exo, assist-on, and assist-off conditions. Furthermore, we carried out laboratory experiments with 9 able-bodied participants to perform squatting, stair-climbing, and loaded incline walking tasks.

Unilateral weight (kg)	1.4
Actuation torque (Nm)	14
Torque density (Nm/kg)	10
Backdrive torque (Nm)	0.22 (low)
Battery life	>1.5 hrs

Figure 1: Our lightweight and complaint knee exoskeleton design during loaded incline walking on the treadmill and real-world overground.

Results & Discussion: Our findings revealed that the average metabolic cost of the user was reduced by 9.8% when using the assist-on exoskeleton compared to the no-exo condition. Additionally, the average normalized heart rate was reduced by 13.8% when using the assist-on exoskeleton. The results of our performance testing demonstrate the effectiveness of the exoskeleton in augmenting human movement and highlight its potential to benefit individuals in outdoor activities such as hiking. The laboratory experiments showed that the assist-on condition resulted in an average metabolic reduction of 22.2% for squatting, 12.8% for stair-climbing, and 5.5% for loaded incline walking when compared to the no-exo condition. These results highlight the crucial role of exoskeleton design in maximizing user benefit by reducing mass penalties and optimizing actuator compliance on user performance.

Significance: The proposed lightweight and compact exoskeleton can reduce energy expenditure during outdoor activities such as hiking, and its effectiveness was evaluated through performance testing. Our conclusions demonstrate that the knee exoskeleton can significantly increase performance while reducing human energy consumption, representing a breakthrough in the field of human-robot interaction. This work highlights the potential of knee exoskeleton technology to augment human movement and expand our horizons, benefiting individuals with gait impairments and those undertaking physically demanding activities such as warehouse workers, firefighters, and hikers.

Acknowledgments: This work is in part supported by National Science Foundation CAREER award CMMI 1944655.

References: [1] T. Huang, S. Zhang, S. Yu, M. MacLean, J. Zhu, A. Lallo, C. Jia, T. Bulea, M. Zheng and H. Su, "Modelling and Stiffness-Based Continuous Torque Control of Lightweight Quasi-Direct-Drive Knee Exoskeletons for Versatile Walking Assistance," in IEEE Transactions on Robotics, vol. 38, no. 3, pp. 1442-1459, Jun. 2022; [2] S. Yu, T.H. Huang, D. Wang, B. Lynn, D. Sayd, V. Silivanov, Y.S. Park, Y. Tian, H. Su. "Design and Control of a High-Torque and Highly-Backdrivable Hybrid Soft Exoskeleton for Knee Injury Prevention during Squatting". IEEE Robotics and Automation Letters, 2019. [3] S. Yu, T.H Huang, X. Yang, C. Jiao, J. Yang, Y. Chen, J. Yi, H. Su. "Quasi-Direct Drive Actuation for a Lightweight Hip Exoskeleton with High Backdrivability and High Bandwidth", IEEE/ASME Transactions on Mechatronics. vol. 25, no. 4, pp. 1794-1802, Aug. 2020. (ASME Mechatronics TC 2020 Best Student Paper)

SURVEY OF REQUIREMENTS FOR EXOSUITS AND EXOSKELETONS FOR AT-HOME STROKE REHABILITATION

Philippe Malcolm[1*], Siena Senatore[1], Marco Gonzalez-Castellon[2], Mukul Mukherjee[1]
[1]Department of Biomechanics, University of Nebraska at Omaha, Omaha, NE, USA
[2]Department of Neurology Sciences, University of Nebraska Medical Center, Omaha, NE, USA
email:*pmalcolm@unomaha.edu

Introduction: Stroke affects approximately 800,000 Americans annually[1]. This disease results from a cerebrovascular event that causes brain cell death, paralysis, speech problems, and numbness. In addition, more than half of the patients experience motor impairment[2]. Regaining walking mobility requires regular physical therapy[3]; however, lack of access to rehabilitation facilities is an important cause of disparity in treatment outcomes for various diseases. This is particularly concerning in states such as Nebraska, where patients often live more than 15 minutes from the nearest clinic[4].

Different groups are developing wearable devices to help with rehabilitation exercises in the clinic and at home. Over the years, we have seen different new types being developed (passive, active, rigid, soft)[5]. Regardless of the material used, these devices can be used to either resist or assist specific joints during locomotion. While these devices are being implemented as a rehabilitative measure, it is unclear what patients would be most willing to use[6]. In this abstract, we describe preliminary results from a survey to get stakeholder input regarding therapeutic needs and preferred types of wearable devices.

Methods: We conducted an anonymous online stakeholder survey to quantify preferences while using assistive devices. We contacted patients using two registries. While this is an ongoing study, current results are based on preliminary data from 5 female and 3 male stroke patients ranging between 30 and 79 years of age.

Results & Discussion: The preliminary results show that patients are highly interested in solutions for additional exercise therapy at home (Table 1). Preferences from patients support the recent direction of wearable robotics toward soft exosuits since 75% of the participants prefer soft exosuits over rigid exoskeletons (Table 2). Furthermore, the majority prefers elastic devices over powered devices and devices that strike a balance between adjustability and ease of use over those that prioritize adjustability or ease of use. Finally, while previous literature suggests that the ability to wear exoskeletons and exosuits below clothing could be essential to remove societal barriers[7], our survey did not support this hypothesis since most prefer wearing devices as an overgarment. These preferences are largely confirmed by another part of the survey, where we ask patients to rank several existing wearable devices.

Although alignment with patient preference is essential to ensure that a device will be used, the fact that specific devices are preferred does not imply that they are effective. Furthermore, the present results are based on relatively limited data. We are now taking surveys from other stakeholders (caregivers, clinicians, researchers, etc.) to gain additional perspectives.

Significance: An online survey of stroke patients shows strong interest in new solutions for additional at-home therapy. Stroke patients prefer elastic soft exosuits that are adjustable, easy to use, and worn as overgarments compared to other wearable devices. Gathering this information could provide insight into how to positively integrate these at-home therapy devices.

Acknowledgments: We would like to thank NIH COBRE, P20GM109090, and The University of Nebraska Collaboration Initiative for funding this research.

References: [1] Tsao CW et al., 2022. *Circulation*. **145**: 153-639; [2] Schaechter. 2004. *Progress in Neurobiology*. **73**: 61–72; [3] Klassen et al., 2020. *Stroke.* **26**: 39-48; [4] Parker et al., 2018; [5] Siviy C et al., 2022. *Nature Biomedical Engineering.* 1-17; [6] Wolff J et al., 2014. *Journal of NeuroEngineering and Rehabilitation.* 11: 169; [7] Yandell et al., 2019. *IEEE Transactions on Neural Systems and Rehabilitation Engineering.* **27**: 712-23.

Question	Most common answer	%
Preferred therapy location	Home	86%
Need for extra home therapy	Strongly agree	63%

Table 1: Data on needs for stroke patients

Feature	Most common answer	%
Device type	Soft	75%
Actuation type	Elastic	75%
Adjustability	Adjustable + quick to don	50%
Wearability	Overgarment	63%

Table 2: Data on preferences for wearable devices for at-home therapy

FRONTAL PLANE BALANCE PATTERNS OF OLDER ADULTS DURING PRE-PLANNED AND LATE-CUED TURNS

Zahava Hirsch[1*], Mitchell Tillman[1], Jun Liu[1], Allison Clark[1], Antonia Zaferiou[1]
[1]Stevens Institute of Technology, Biomedical Engineering Dept., Hoboken, NJ USA
* email: ZHirsch@stevens.edu

Introduction: Up to half of walking steps are turns [1] and for older adults, a fall during a turn is eight times more likely to result in a hip fracture [2]. The purpose of this ongoing study is to understand how older adults maintain balance while walking and turning. We looked at two measures of balance: whole-body frontal plane angular momentum (Hf), which can convey mediolateral balance regulation information [3]; and lateral distance (LD), which describes if the center of mass (COM) remains within the base of support [4]. Based on findings from young adults [5], we hypothesized that during pre-planned and late-cued turns vs. straight line gait, older adults will: 1) use a larger Hf range, and 2) use a larger LD range.

Methods: This study included four healthy older adults (3 female; age 74 ± 8 years; mass: 74 ± 7 kg; height 1.70 ± .05 m) who provided informed consent in accordance with the IRB. Participants passed cognitive and dynamic balance assessment tests and did not fall within 6 months preceding their participation. A 13-segment whole-body kinematic model [6] was built using optical motion capture data (250 fps; OptiTrack, USA). A grocery store aisle intersection was simulated with a taped T-shaped walkway that was 0.915 m wide, including a 10 m straight-way with a 90° turn in the center. Three tasks were performed 12-14 times in an order of increased challenge as a safety precaution. First, participants walked straight for 10 m. Next, they performed 90° pre-planned left turns. Finally, they performed 90° late-cued left turns visually cued by a display at the end of the 5 m aisle (mixed with 50% catch trials; one participant did not have time to complete the late-cued turns). A Physical Therapist followed closely behind the participants for "standby assistance". Hf about the COM was normalized to a dimensionless form [3]. LD was calculated as the distance from the COM to the closest lateral edge of the base of support (mediolateral was defined by the frontal plane of the pelvis). LD is positive when the COM is medial to the lateral edges of the feet (as in straight-line gait) and negative if the COM is lateral of the lateral edge of the foot. Hf and LD ranges were found during the turn phase (defined by a pelvis rotation threshold) or steady-state straight-line gait. A percentile bootstrap statistical test was used to compare the ranges within-participant across the three tasks performed (conditions were dependent with non-normal distributions).

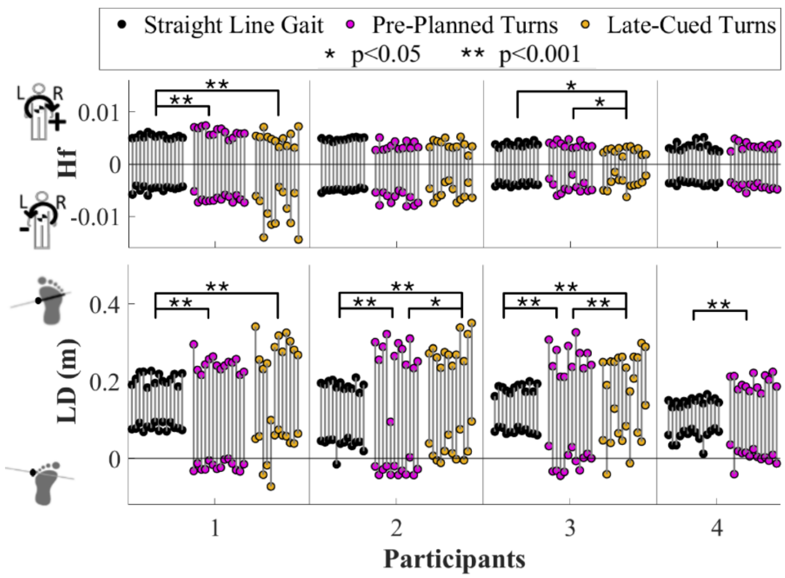

Figure 1: Min, max, and range **(A)** Hf and **(B)** LD for all trials and participants during straight-line gait, pre-planned, and late-cued turns. Asterisks indicate significant differences within-participant in the ranges across tasks.

Results & Discussion: Only Participant 1 had significantly larger Hf ranges during turns vs. straight-line gait (**Fig. 1A**). While more participants are needed to understand group trends, none in this study demonstrated the group trends we previously found in young adults, who progressively significantly increased their Hf ranges from straight-line gait to pre-planned to late-cued turns [5]. In fact, it is notable that the Hf range of Participant 3 was significantly *smaller* during late-cued vs. pre-planned turns, which could be a protective strategy. All participants showed a significant increase in LD range between straight-line gait and pre-planned turns (**Fig. 1B**). All three participants who performed late-cued turns used a significantly larger LD range than in straight-line gait. Participants 2 and 3 used a significantly smaller LD range during late-cued vs. pre-planned turns. Of note, Participant 1 had the most negative LD minima for a few trials and generally the most negative Hf minima during late-cued turns, which may indicate a specific late-cued turn strategy. Though there was no hypothesis related to gait speed, the average gait speed was progressively slower from straight-line to pre-planned to late-cued turns, which may provide context for these initial frontal-plane balance findings. This is an ongoing study that we will expand to include more participants, including fall-prone older adults. We plan to explore both within and across-participant trends, including gait speed and turn strategies as covariates or moderators. Further, we will investigate if the baseline factors we measure, such as physical activity levels, fall history, fear of falling, clinical balance scores, or sensorimotor abilities affect balance patterns during turns.

Significance: These findings suggest that healthy older adults may regulate their frontal plane balance during turning using strategies that are person-specific and may differ from healthy young adults [5]. Using these initial findings, we expect that as the study expands, we may find divergent strategies in the extent to which older adult participants control their angular momentum and COM positioning during turns. Overall, this research advances our understanding of how balance strategies during turns may change with age.

Acknowledgements: We thank the participants and acknowledge the financial support from NSF Award #1944207.

References:[1] Glaister (2007), *Gait & Posture.* 25; [2] Nevitt & Cummings (1994), *Osteoporosis Int.* 4; [3] Vistamehr et al. (2021). *J Biomech*. 128; [4] Dixon et al (2016). *Clin. Biomech*. 32; [5] Tillman et al. (2021). *J Biomech*. 141; [6] de Leva (1996). *J Biomech*. 29

COMBINED EFFECTS OF TAI-CHI GAIT WITH LATERAL GROUND SUPPORT PERTURBATIONS ON DYNAMIC BALANCE CONTROL: A PIOLET STUDY IN YOUNGER AND OLDER ADULTS

Jacob Smith[1*], Hao-Yuan Hsiao[1], Troilyn Jackson[1], Donald Prible[1], Wei Liu[2]
[1]The University of Texas at Austin, Department of Kinesiology and Health Education, TX, USA
[2]The University of Texas Science Center at San Antonio, Department of Physical Therapy, TX, USA
*jacobmsmith@utexas.edu

Introduction: Approximately one third of older adults fall every year and those who are hospitalized or live in a nursing home fall more often [1]. Deficits in dynamic stability and limb support are key risk factors for falls [2,3]. Developing exercise and intervention approaches that improves dynamic stability control and limb support force production may reduce the risk of falls among older adults. Although Tai-Chi (TC) has been broadly used for fall prevention, the findings from previous Tai-Chi studies are inconclusive [4] with limited long-term success. This is partly because the direct balance control mechanisms that were involved during TC practice are unknown and therefore the ability to apply certain TC forms to target specific balance deficits is limited. In addition, although many falls occur due to external balance perturbations, TC movements typically do not emphasize rapid reactions that are needed for balance recovery following perturbation. Combining TC gait with external perturbation may develop a new approach that engages both voluntary and reactive mechanisms of balance control. Accordingly, this study aimed to compare the dynamic stability and limb support force impulse during normal walking, TC gait, and TC with medial (MED) and lateral (LAT) ground support perturbations in younger and older adults. It was hypothesized that compared to regular walking, conditions involving TC will show decreased dynamic stability with increased limb support force impulse in both younger and older adults. In addition, we hypothesized that MED will induce least MOS amongst all conditions tested, indicating that MED further challenges dynamic stability.

Methods: Methods: Ten (n=10) healthy younger (age 27.8 ±5.05 year; 4 female; height 1.73±0.11 m; weight 70.08±14.57 kg) and ten (n=10) healthy older adults (age 69.7±5.35; 5 female; height 1.67±0.06 m; weight 69.46±10.5 kg) performed three tasks on a split-belt treadmill: comfortable speed walking, TC gait, and TC gait with treadmill medial-lateral perturbation. Body segment position data were recorded by using a 10-camera motion capture system (Vicon-USA, Denver, CO) sampled at 120 Hz. *Ground* reaction forces were measured by an instrumented treadmill (M-gait, Motek, Netherland) sampled at 1000 Hz. Three 30-second trials for the comfortable walking speed (CWS) and the TC gait conditions were recorded. During the TC gait with perturbation, the treadmill translated medially (MED) or laterally (LAT) (3 cm within 370 ms) during single leg stance phase. The direction of the perturbation is pseudo-randomized to minimize anticipation. A customized program was used to ensure that 2 medial and 2 lateral perturbations were induced to each leg during each trial. The time interval between each perturbation was at least 3 seconds to allow recovery to regular TC gait. Three 2-minute TC gait with perturbation trials were recorded. Minimum lateral margin of stability [5] was calculated to characterize dynamic stability. Vertical ground reaction force-time intergral during single stance phase was used to charaterize limb support. Two-way (condition X age group) mixed model analysis of variance was performed to analyze MOS and vertical force impulse.

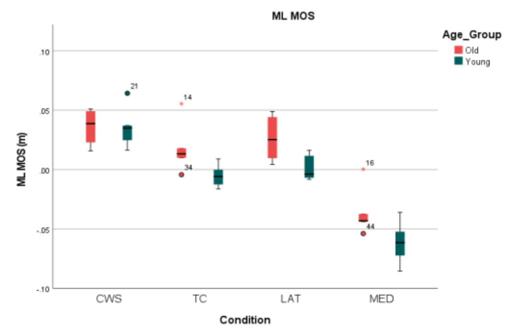

Figure 1: For ML MOS, Post Hoc analysis revealed that CWS had greater MOS compared to all other conditions ($p < 0.01$) and MED has reduced MOS compared to all other conditions ($p < 0.01$).

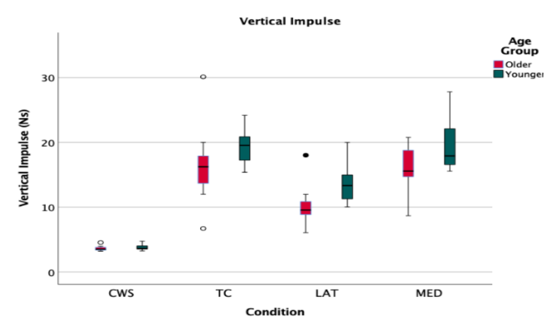

Figure 2: For vertical force impulse, a main effect of condition was detected ($F = 146.548$, $p < 0.01$).

Results & Discussion: A main effect of condition was detected for both MOS and vertical impulse. Compared to regular walking, all other conditions that involved TC gait showed decreased MOS (Fig. 1) and increased vertical force impulse (Fig. 2). In addition, the MED condition induced the smallest MOS (Fig. 1). These findings indicate that combining treadmill surface perturbation with TC gait may be an effective and feasible approach to challenge lateral dynamic stability and limb support force production. Furthermore, a main effect of age was detected for MOS. Older adults exhibited a larger MOS compared to young. This may reflect a conservative strategy adopted by the older adults when learning TC.

Significance: These findings provided insight into how balance control mechanisms are modulated during TC exercise and indicated that combining ground support perturbation with TC may further challenge dynamic stability. Future research will investigate the effects of various perturbation intensities on postural reactions during TC gait.

References: [1] Stevens et al. (2008), *J Safety Res.* 39(3); [2] Tajali et al. (2018), *International J MS Care* 20(4); [3] Pavol & Pai (2007), *J Biomech* 40(6); [4] Huang et al. (2017), BMJ Open 7(2); [5] Hof et al. (2005), *J Biomech* 38(1)

THE IMPACT OF PARTICIPANT MASS AND HEIGHT ON REGRESSION-BASED HIP JOINT CENTER CALCULATIONS ASSESSED WITH MRI-BASED MODELS

Emily M. McCain[1*], Mario E. Garcia[1], Evan A. Dooley[1], W. Brody Hicks[1], Xiao Hu[1], Shawn D. Russell[1], Silvia S. Blemker[1]
[1]University of Virginia, Charlottesville, VA, USA
*Corresponding author's email: emily.mccain@virginia.edu

Introduction: Scaling musculoskeletal models to individual subjects often requires determination of the hip joint center (HJC) which is typically located at the center of the femoral head. HJC locations are determined either with predictive, regression-based relationships contingent on 3D locations of surface markers or with functional methods that consider relative motion of the pelvis and femur. While functional methods are more accurate [1], they require participants to complete movements that are difficult for clinical populations. However, regression-based equations often do not account for sex differences in bone size or the impact of increased mass [2-4], and therefore may not accurately predict HJC across the general population. In persons with higher masses, marker placement can be more difficult as increased adipose tissue makes accurate palpation challenging and because after palpation, placed markers may shift when tissue is no longer compressed. In addition, changes in bone shape, which may be independent of size could also lead to errors in HJC placement. Inaccurate HJC locations affect simulated joint angles, moments, muscle activity, and joint reaction forces. Improved understanding of how body size (mass and height) affects joint centers and therefore model scaling would improve the usability of musculoskeletal models. This research will characterize the impact of participant mass and height on HJC accuracy by comparing three common regression-based HJC calculations (Harrington[2], Davis[3], Bell[4]) to MRI-determined HJC.

Methods: Twelve bony landmarks at the pelvis (left/right posterior superior iliac spine (PSIS), anterior superior iliac spine (ASIS)), knee joint (lateral and medial tibial plateau (LKNE & MKNE)), and ankle joint (lateral (LMAL) and medial malleoli (MMAL)) were located using palpation, and the skin superficial to each landmark was physically marked using a surgical marker for four subjects (4F, mass: 66.43±14.87 kg, height 1.65±0.07 m, BMI: 24.21±4.51 kg/m^2). Vitamin E tablets were placed with the major ellipsoid radii in the superior/inferior direction for all 12 markers. Subjects were scanned on a 3T Siemens (Munich, Germany) Trio MRI Scanner in a three-point Dixon Sequence with a field of view: 280 mm × 450 mm (which may be adjusted for larger subjects), slice thickness: 5 mm, and in-plane spatial resolution: 1.1 mm × 1.1 mm. T1-weighted DIXON scans were processed using a combination of an artificially intelligent (AI)-based algorithm and manual vetting by a team of segmentation engineers (Springbok Analytics, Charlottesville, VA).The AI algorithm segmented all lower extremity bones from MRI axial slices [5, 6]. Vitamin E tablets were manually segmented in Slicer 3D, and the center of segmented tablets were determined in MATLAB by fitting an ellipsoid to the segmented shape. HJC was calculated using three common methods [2-4] and then measured as the center of a sphere fit to the MRI-determined femoral head in MATLAB. The magnitude of the error between calculated and measured HJC was determined and averaged across left and right HJCs for each subject and method. The relationship between error magnitude and participant mass*height was defined for each HJC calculation using a linear regression model in MATLAB.

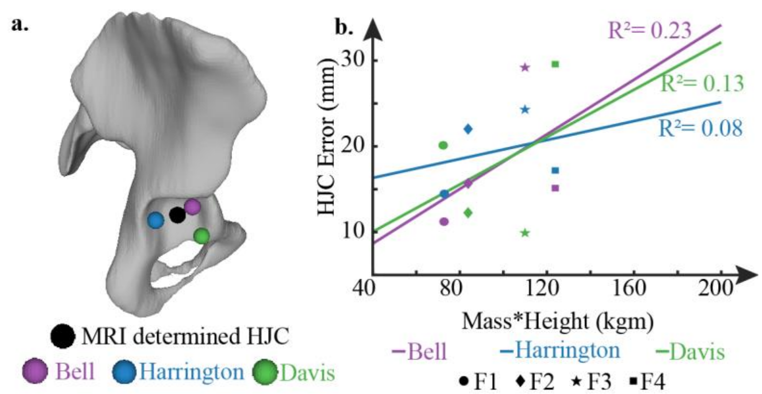

Figure 1: a. MRI- segmented pelvis and calculated and measured HJC locations for F1 and **b** HJC error plotted with mass*height for all three regression-based

Results & Discussion: Visual inspection of marker placement relative to bony landmarks in MRI scans demonstrated good agreement (Fig.1a). We did not find a relationship between the participant mass*height and HJC error for any of the three regression-based models tested (Fig 1b; $p>0.05$ for Bell, Harrington, and Davis). The errors in HJC were within the range reported previously [1]. Interestingly, none of the methods take a measure of the pelvis in the superior/inferior direction; instead the superior/inferior location of HJC is defined with respect to pelvic width+ limb length [2, 3] or pelvic width alone [4]. Therefore, it is possible that rather than height and mass, HJC error scales with the aspect ratio between pelvic width and pelvic height, with higher errors accrued as ratios deviate from ratios implicit in regression-based calculations. Future work will investigate the influence of pelvis aspect ratios and an increased sample size more representative of the general population and including both male and female subjects to allow us to investigate potential sex differences in HJC calculations.

Significance: Identifying the etiology of HJC error can improve accuracy of musculoskeletal models and broaden their applicability to people of all body sizes.

Acknowledgements: NIH Grant #R01AR078396a

References: [1] Fiorentino et al. (2016), *Gait Posture* 50. [2] Harrington et al. (2007), *J Biomech* 40(3); [3] Davis III, et al. (1990), *Hum. Mov. Sci.* 10(5). [4] Bell et al. (1990), *J Biomech* 23(6); [5] Ni et al. (2019), *J Med Imaging* 6(4); [6] Handsfield et al. (2014), *J Biomech* 47(3).

IMPACT OF OSTEOARTHRITIS AND SURGERY ON THE FEMALE CARPOMETACARPAL JOINT OF THE THUMB

Adam J. Chrzan[1], Nicole D. Arnold[1], Kevin Chan[2], Tamara Reid Bush[1*]
[1]Mechanical Engineering, Michigan State University, East Lansing, MI, USA
[2]Orthopedic Hand and Upper Extremity Surgery, Spectrum Health, Grand Rapids, MI, USA
Email: *reidtama@egr.msu.edu

Introduction: Osteoarthritis (OA) in the hand affects 27% of Americans ages 50-54, and prevalence steadily increases to 84% when 70-74 years of age [1]. The thumb carpometacarpal (CMC) joint is one of the most likely hand joints to develop OA, and to cause symptoms like reduced motion, pain, and weakness, which make daily tasks challenging to perform [1,2]. This is particularly true for females, who are up to 1.8x more likely than males to develop CMC OA, and 3.8x more likely to undergo surgical intervention [3,4]. The ligament reconstruction with tendon interposition (LRTI) surgery is the most common, but the primary indicator of a successful surgery is a reduction in pain, and limited motion and strength data are investigated. It is unknown whether the motion and strength are restored to the level of healthy adults. Research is not available to determine if differences occur across the several other available surgical procedures. Thus, the goals of this work were to 1) identify the thumb CMC motion capabilities of older healthy females, 2) investigate kinematic differences in a population with severe CMC OA, and 3) determine the kinematic effects of LRTI surgery on CMC kinematics at 3- and 6-months post-surgery.

Methods: Older healthy (OH) (40+ years) female participants had no prior surgery or injury to the thumb, did not have thumb CMC OA, were not pregnant, and were tested once. Female participants that had a diagnosis of CMC OA and consented to LRTI surgery were the second population, and all OA participants were tested pre-surgery, 3-, and 6-months post-surgery. Healthy and OA participants reported their visual analog scale (VAS) pain score for the tested thumb. A higher score denoted more pain (0-100).

A six-camera motion capture system (Qualysis, Gothenburg, Sweden) gathered motion data at 100 Hz. A rigid marker pod containing four markers was placed on the thumb metacarpal, and individual markers were placed on the ulnar styloid, distal radial tubercle, and the distal end of the 2nd metacarpal. Participants performed a maximum circumduction motion to explore their thumb movement boundaries. Flexion and abduction angles at the CMC joint were calculated using the Grood and Suntay method with local coordinate systems constructed on the thumb metacarpal as well as the dorsum of the hand from their respective markers [5]. By plotting the CMC abduction (x-coordinate) and flexion (y-coordinate) angles across the entire circumduction motion, CMC motion boundaries were determined and later averaged across each population. CMC motion boundaries represented the limits of joint motion, and were used to determine the 1) area, 2) centroid, and 3) shape of participant's motion using MATLAB (MathWorks, Natick, MA). A mixed-effects model tested for the effects of study group (OH, Pre-surgery, 3-, and 6-months post-surgery) on kinematics using a Tukey adjustment.

Results & Discussion: 13 OH females (average age 58.0 ± 9.3 years), and 10 CMC OA females (average age 62.1 ± 8.9 years) participated. All CMC OA participants were tested before surgery (20.4 ± 30.4 days before surgery), 3-months (92.2 ± 6.0 days post-surgery) and 6-months post-surgery (183.0 ± 9.1 days post-surgery). All CMC motion area pairwise comparisons were statistically significant ($p<0.045$), except the OH/pre-surgery ($p=0.957$) and 3-months/6-months ($p=0.999$) comparisons (Fig. 1). While OH and pre-surgery areas were similar, the CMC motion shapes showed a redistribution of motion, likely due to compensatory biomechanics and anatomical changes in the joint as a result of OA [6]. Pre-surgery participants had larger VAS pain scores than OH ($p<0.001$), but both 3- and 6-months post-surgery pain was lower than pre-surgery ($p<0.001$), and comparable to OH pain ($p>0.124$). While LRTI surgery reduced CMC joint motion and yielded altered motion patterns, pain was also significantly reduced, however motion abilities were not restored to that of the healthy females. All study groups had similar centroid abduction coordinates ($p>0.416$), but OH participants had a greater flexion coordinate than all OA timepoints ($p<0.030$). This migration of motion towards negative flexion among all OA timepoints may indicate reduced joint stability and increased ligament laxity [7].

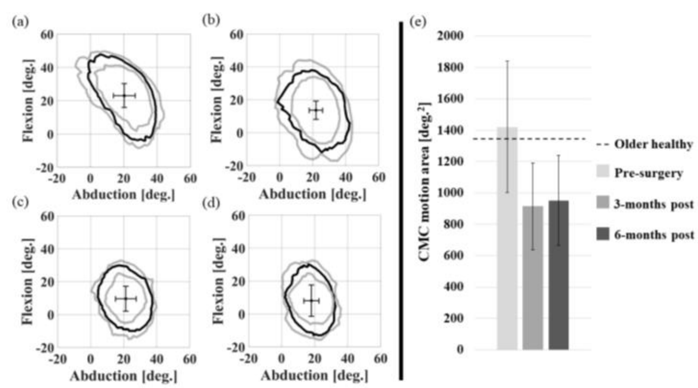

Figure 1: Average (solid black line) and ±1 standard deviation (light gray lines) CMC motion boundaries for (a) OH, (b) pre-surgery, (c) 3-month post-surgery, and (d) 6-months post-surgery, with average centroid locations and standard deviations. (e) CMC motion boundary areas.

Significance: This study is novel because averaged female motion boundaries are presented for multiple populations and timepoints, which enables comparison of motion shapes between groups. This is particularly relevant when used to compare the outcomes of thumb CMC surgeries. These data provide insight into the kinematic changes of the female thumb CMC joint due to arthritis and LRTI surgery and can be used by both patients and surgeons to select the most optimal, and improve, thumb CMC OA surgeries.

Acknowledgements: Funding was received from the Spectrum health – Michigan State University Alliance Grant.

References: [1] Haugen et al. (2011), *Ann Rheum Dis* 70; [2] Matullo et al. (2007), *Hand* 2; [3] Dahaghin et al. (2005), *Ann Rheum* Dis 64(5); [4] Lane et al. (2021), *BMJ Open* 11(7); [5] Grood & Suntay (1983), *J Biomech Eng* 105; [6] Halilaj et al. (2014), *J Biomech* 47(11); [7] Li & Tang (2007), *J Biomech* 40(3)

Musculoskeletal Injury Risk Stratification Using Wearable Lower-Limb Sensors in Active-Duty Military Populations

Don Goss[1,2,3], Ignacio Gaunaurd[4], Matthew Helton[5], Maria Gonnella[1,3], Nicholas Reilly[1,3], Henry Haltiwanger[1], Robert Gailey[4]

1. Womack Army Medical Center, Fort Bragg, NC
2. Department of Physical Therapy, High Point University, High Point, NC
3. The Geneva Foundation, Tacoma, WA
4. Miller School of Medicine, University of Miami, Miami, FL
5. United States Army 82nd Airborne Division, Fort Bragg, NC

Corresponding Author's Email: dgoss@highpoint.edu

Introduction: By the nature of their work, active-duty Soldiers are at an inherently higher risk of sustaining a musculoskeletal injury compared to the general population. Musculoskeletal injuries (MSI) affect approximately 800,000 service members annually and contribute to approximately 25 million days of limited duty [1]. While numerous biomechanical and performative parameters have been identified as precursors to increased musculoskeletal injury risk [2,3], assessments to identify these factors require laboratory-grade instrumentation and analytical techniques that are often not available to military populations. As a result, Soldiers at a higher risk of injury are often not recognized until an injury occurs, leaving the window to identify predictive metrics for injury risk and opportunities for proactive approaches to mitigate such risk unexplored.

There is an emphatic need for the development and implementation of quick screening assessments that can classify and predict the risk of lower extremity (LE) MSI prior to activity. Prior research has utilized specialized instrumentation to identify and stratify injury risk via a composite score (i.e., Injury Risk Index (IRI)) in collegiate athletes based on a fifteen-minute testing battery assessing static and dynamic stability [4,5]. As such, implementation of IRI could facilitate improved decision-making and reduce the negative impact associated with selected MSI in highly active populations. However, these approaches have yet to be thoroughly explored within military or tactical athlete populations. The purpose of this study is to determine the frequency and distribution of Soldiers' risk of MSI after performing sensors-based objective LE tests for static and dynamic stability.

Methods: As of December 2022, 263 (92% male, 8% female) United States Army Soldiers were recruited, and completed demographic and previous joint-specific injury history intake. Soldiers donned a sleeve with two inertial measurement unit sensors over each knee. They performed single limb stance (SLS) to obtain Region of Limb Stability (ROLS) values, which measures static LE stability. Subsequently, the four-meter sidestep test (FmSST) was obtained measuring the Transitional Angular Displacement of Segments (TADS) values. TADS is a measure of dynamic joint stability. The ROLS and TADS symmetry values between LEs is calculated for both tests and the values are used to determine IRI category as low, moderate or high risk for injury. Total assessment time was ≤ 15 minutes per Soldier. Descriptive statistics and frequency distributions were used to characterize the study population.

Results & Discussion: Of the 263 participants, 113 (43%) reported previous injuries, distributed as, 11% hip, 26% knee, 35% ankle, and 28% injuries to multiple joints. The ROLS IRI classified Soldiers with either high or moderate risk as follows: prior hip injuries 58%, prior knee injuries 62%, prior ankle injuries 66%, and multiple joints 66%. For TADS IRI classified Soldiers with high and moderate risk as follows: prior hip injuries 25%, prior knee injuries 20.5%, prior ankle injuries 37.5%, and multiple joints 50%.

Significance: The number of Soldiers with prior lower limb MSI had lower static and dynamic stability symmetry could be a concern for reinjury and/or less than ideal physical performance while on duty. The ability to identify the risk of injury in Soldiers, athletes or people with previous injuries may promote preventative interventions or pre-habilitation to reduce re-injury.

Acknowledgements: This work was funded in part by the Musculoskeletal Injury Rehabilitation Research for Operational Readiness (MIRROR), Department of Physical Medicine & Rehabilitation, Uniformed Services University, Bethesda, MD, (award HU00011920011).

Disclaimer: The opinions and assertions expressed herein are those of the author(s) and do not necessarily reflect the official policy or position of the Uniformed Services University or the Department of Defense.

References:

[1] K.G. Hauret et al. (2015), The American Journal of Sports Medicine. [43] 2645-2653.
[2] S.A. Kliethermes et al, (2021), Br J Sports Med. [55] 851–856.
[3] E. Kristianslund et al, (2014), Br J Sports Med. [48] 779–783.
[4] L.A. Feigenbaum et al, (2020), Med Sci Sports Exerc. [52] 2483–2488.
[5] I. Gaunaurd et al, (2018), J Biomech. [84] 252–256.

QUASI-STIFFNESS AS A MEASURE FOR EVALUATING BIOMECHANICAL CHANGES ACROSS STEP WIDTHS

Stephanie L. Molitor* and Richard R. Neptune
Walker Department of Mechanical Engineering, The University of Texas at Austin, Austin, TX, USA
*Corresponding author's email: stephanie.molitor@utexas.edu

Introduction: Previous studies investigating biomechanical responses to altered step width conditions have largely focused on changes in joint moments [1]. However, joint angles, namely frontal-plane hip angle, are also subject to change across step widths. Dynamic quasi-stiffness quantifies the simultaneous changes in joint angle and moment throughout the progression of a task and is used to define controllers for assistive devices (e.g., prostheses, exoskeletons) [2]. Although current devices primarily focus on emulating sagittal-plane ankle dynamics, frontal-plane hip quasi-stiffness remains largely unexplored but has important implications for the development of exoskeletons since clinical populations often walk with wider steps [3]. Therefore, the objective of this study was to investigate how frontal-plane hip quasi-stiffness in healthy individuals changes when walking at different step widths. Given that frontal-plane hip moment changes with altered step widths [1], we hypothesized that hip quasi-stiffness would also change across step widths.

Methods: Kinematic and kinetic data were collected from 15 healthy young adults (7 male; age: 25 ± 4 years; height: 169 ± 13 cm; mass: 69 ± 12 kg) walking at four step width conditions: narrow (25% narrower), self-selected (SS), wide (50% wider) and extra-wide (100% wider). Frontal-plane hip joint angles and moments were computed for each leg in Visual3D (C-Motion, Germantown, USA) and then used to determine quasi-stiffness using a custom-built MATLAB (MathWorks, Natick, USA) script. Quasi-stiffness during the late-stance phase [4-5] was calculated as the linear slope between angle and moment [5]. A linear mixed-effects model was used to evaluate the relationship between step width and quasi-stiffness, where quasi-stiffness was the dependent variable, fixed effects included the step width condition and leg (left or right), and subject was the random effect. In the case of a significant main effect ($\alpha = 0.05$), Bonferroni-adjusted pairwise t-tests were performed to compare quasi-stiffness of each step width condition to the SS width.

Results & Discussion: Compared to walking at SS step width, walking at wider step widths was associated with decreased frontal-plane hip quasi-stiffness during late-stance (Fig. 1). Walking at narrower step widths did not result in a significant change in quasi-stiffness. These results are consistent with previous work showing the frontal-plane hip moment decreases at increased step widths [1]. The agreement between quasi-stiffness and joint moment, which is a standard measure used to evaluate joint mechanics, supports the use of quasi-stiffness to describe the hip response across step widths. Although frontal-plane hip quasi-stiffness agrees with joint moment in the case of altered step widths, it may be beneficial to verify this agreement in other locomotor tasks where simultaneous changes in joint angle and moment may be less clear. Future work will expand this investigation by characterizing quasi-stiffness of the other lower-limb joints (knee and ankle) throughout the gait cycle in both frontal and sagittal planes.

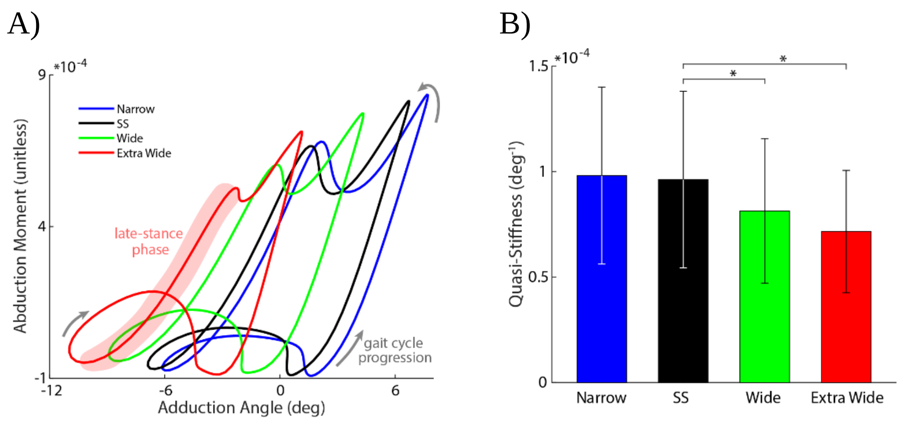

Figure 1: Frontal-plane hip quasi-stiffness was derived from the angle-moment curve during late-stance (**A**). Compared to self-selected (SS) step widths, quasi-stiffness decreased with increased step width (**B**).

Significance: Results from this study provide insight into the frontal-plane hip quasi-stiffness response to step width, which is directly applicable to the development of biomimetic controllers for assistive devices. Furthermore, our finding that frontal-plane hip quasi-stiffness changes across step widths provides a foundation for comparisons in different clinical populations and other locomotor tasks.

Acknowledgements: This work was supported in part by the National Science Foundation Graduate Research Fellowship Program. The authors thank Gabriella H. Small and Lindsey K. Molina for collecting the data used in this study.

References: **[1]** Molina et al. *in review*; **[2]** Caputo & Collins, (2014). *J. Biomech.*, *136*(3).; **[3]** Hof et al., (2007). *Gait & Posture, 25*(2); **[4]** Crenna & Frigo, (2011). *Hum. Mov. Sci.*, 30(6); **[5]** Shamaei et al., (2013). *PLOS ONE, 8*(3).

DETECTING CHANGES IN VARUS THRUST GAIT USING AN IMU – A PILOT STUDY

Halime E. Gulle[1*], Torstein E. Dæhlin[1], Irene Davis[1]
[1]School of Physical Therapy and Rehabilitation Science, University of South Florida, FL, USA
*Corresponding author's email: halimegulle@usf.edu

Introduction: Knee osteoarthritis (KOA) affects over 19% of Americans aged 45 years or older [1]. The etiology of KOA is multifactorial. However, lower extremity mechanics are known to play a significant role. Specifically, the knee adduction moment (KAM), and associated varus (outward) thrust of the knee, has been related to the development and progression of KOA. Thus, reducing the KAM may improve the overall health of the knee. An effective way to reduce KAM is through altering the gait pattern [2]. For example, studies have demonstrated an indirect reduction in the KAM by increasing foot toe-out and by increasing lateral trunk lean [3]. However, these changes result in an abnormal gait pattern that may adversely load other musculoskeletal tissues. In another study, Barrios et al. [4] put participants though an 8-session, faded feedback, retraining that focused directly on reducing the varus malalignment of the knee. The authors provided real-time feedback on the frontal plane knee angle using a motion analysis system. They reported a significant reduction in both the knee varus angle and KAM without causing an abnormal gait pattern [4].

Previous interventions to alter the gait of those with KOA have primarily been conducted in laboratory environments, limiting their ecological validity. Wearable sensors, such as inertial measurement units (IMUs), allow us to take our interventions outside of the laboratory environment and provide feedback and monitor gait in the natural environment. For example, IMUs can be used to measure the abduction velocity of the thigh, which may serve as a surrogate measure of lateral thrust of the knee. However, it is currently unknown whether these measures correspond to frontal plane angles and moments.

Methods: This is an on-going pilot study to investigate if changes in knee biomechanics caused by using a medial thrust gait have corresponding signatures in thigh and shank angular velocities. Participants were screened for having a varus thrust gait. One male (age:32 yrs., mass:80.5 kg., ht:1.70 m) was deemed eligible for this study. The participant with a varus thrust gait completed 7 habitual and 7 medial thrust walking trials while instrumented with an IMU affixed to their lateral thigh. The participant walked along a 30-meter walkway traversing two embedded force plates (AMTI Optima, Watertown, MA, USA) at its center, while being recorded by a 10-camera motion analysis system (Vicon Vantage V5, Oxford, UK). After data collection, kinematic and kinetic data were processed using Visual 3D (Version 6, Germantown MD) to compute knee angles as well as KAM. Time series data from the thigh adduction velocity, along with the knee adduction angle and moment were extracted. Ensemble averages were generated for the stance phase of the 7 trials in each condition. Peak knee adduction angle and peak KAM during the first 50% of stance (loading phase) were determined for comparison between conditions. Mean ± standard deviations were calculated across the 7 trials in each condition. The remaining number of participants (10) will be completed prior to ASB 2023.

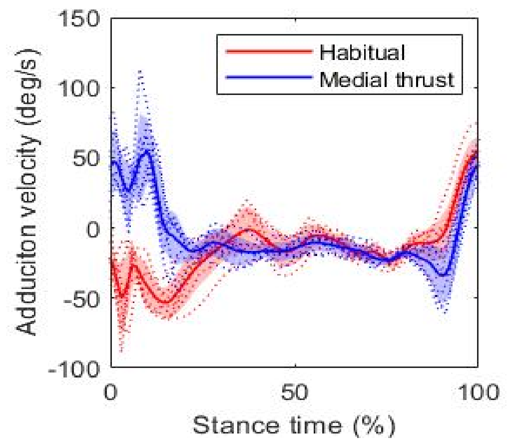

Figure 1: Thigh velocity measured from the IMU between habitual and medial thrust gaits.

Results & Discussion: The participant walked at a similar speed in both his habitual gait (1.16 ± 0.02 m/s) and the medial thrust gait (1.14 ± 0.03 m/s). His medial thrust gait resulted in a change from a thigh abduction velocity to a thigh adduction velocity during the first 20-30% of stance (Figure 1). This led to a change in the knee angle from an adduction (varus) angle to a more neutral angle (Figure 2a). As a result of these changes, the peak knee adduction moment was reduced during medial thrust gait (Figure 2b). Collectively, these data suggest that an IMU can be used to detect changes in thigh adduction with a medial thrust gait. This change may be used to provide visual feedback for retraining purposes. Additionally, the reduced external knee adduction moments during medial thrust gait suggests that the changes induced can lead to a decrease in medial joint loading. This is significant as reducing medial knee joint loading may improve the prognosis of individuals with medial knee OA.

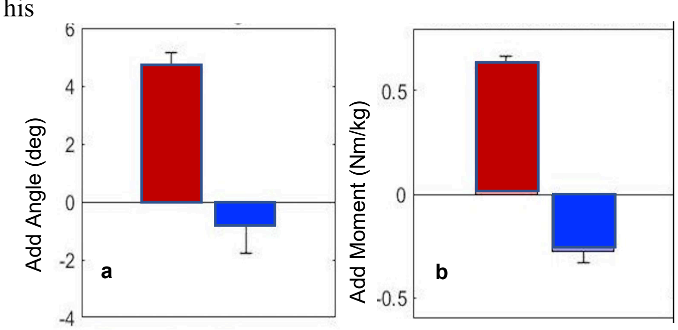

Figure 2: Comparison of **a**. peak knee adduction angle and **b**. adduction moment between habitual and medial thrust gaits.

Significance: The current results suggests that an IMU can be used to move the gait retraining for knee OA patients from specialized laboratories to clinics and more natural environments. The potential to conduct some of the retraining out of the clinic will result in greater efficiency in terms of time as well as costs.

References:

[1] Wallace et al. (2017), PNAS, 114(35); [2] Chang et al. (2004) Arthritis & Rheumatism, 50(12); [3] Mündermann et al.(2004) Arthritis & Rheumatism, 50(4); [4] Barrios et al (2010), Journal of biomechanics, 43(11).

Analysis of subjective and objective measures in assessing fall risk status in adults with Essential Tremor and adults without Essential Tremor

Julia A. Christl[1*], Patrick G. Monaghan[1], Kenneth D. Harrison[1], Sarah A. Brinkerhoff[1], Harrison C. Walker[2], Jaimie A. Roper[1]
[1]Auburn University School of Kinesiology, Auburn AL
[2]University of Alabama in Birmingham Heersink School of Medicine, Birmingham AL
*Corresponding author's email: jac0151@auburn.edu

Introduction: People with Essential Tremor (ET) are at an increased risk of falls or near falls when engaged in complex tasks due to tremors and impaired gait and balance performance [1]. There are many ways to categorize a fall risk including ways used commonly in research and in clinical practice (e.g. self-reported falls, balance confidence, balance and walking assessments in specialized biomechanics laboratory settings) but there is no standardized categorization for those in people with ET. Therefore, purpose of this study was to examine self-reported measures and objective measures in people with ET to better assess their fall categorization. We used the Falls Efficacy Scale (FES), a questionnaire designed to assess the participant's fear of falling while doing certain tasks [2]. We also measured the overall Timed Up and Go (TUG) duration, as it has previously been incorporated as a clinical screening tool for fall risk [3].

Methods: Thirteen participants diagnosed with ET (Males=6 Females=7 avg. age=63) and 8 participants without a diagnosis with ET (CTRL) (Males=2 Females=6 avg. age=64) participated in this study. Movement sensors (Opal, Generation 2, APDM, Inc, Portland, OR.), were placed on participant's ankles, wrists, sternum and lumbar to measure TUG duration in seconds. The FES was administered to assess fear of falling and then participants completed the TUG assessment. Lastly, the participants were asked about their fall history in the previous 3 months (retrospective) in addition to a weekly check in for prospective falls or near falls via text for 4 weeks. Participants were classified as a faller (F) if they had experienced a fall within the last 3 months during intake or 1 month after the study, or a non-faller (NF) if they did not fall during the prospective or retrospective period. Pearson correlation analyses were conducted to examine the relationship between FES scores and TUG duration in the following groups: ET, ET-F, ET-NF, CTRL, CTRL-F and CTRL-NF.

Results & Discussion: Eight participants with ET reported at least 1 retrospective or prospective fall. Three participants without ET reported at least 1 retrospective or prospective fall. Average FES score for participants with ET was 15. Average FES score for participants without ET was 11. Average TUG duration for participants with ET was 11.78 seconds. Average TUG duration for participants without ET was 9.33 seconds. We observed a positive correlation between FES and TUG duration in ET-F ($r(6) = .85$, $p = .01$), ET-NF ($r(3) = .76$, $p = .08$) and all ET participants ($r(11) = .86$, $p < .001$). (Figures 1a-1c). There was no significant correlation between FES and TUG duration in CTRL-F ($r(1) = .22$, $p = .86$) or in all non-ET (CTRL) participants regardless of fall ($r(6) = .53$, $p = .18$). (Figures 1a and 1c). The correlation was influenced by 1 participant in the ET faller population and 2 participants in the ET non-faller population. These participants had increased FES scores as well as increased TUG durations putting them at an increased risk of falling.

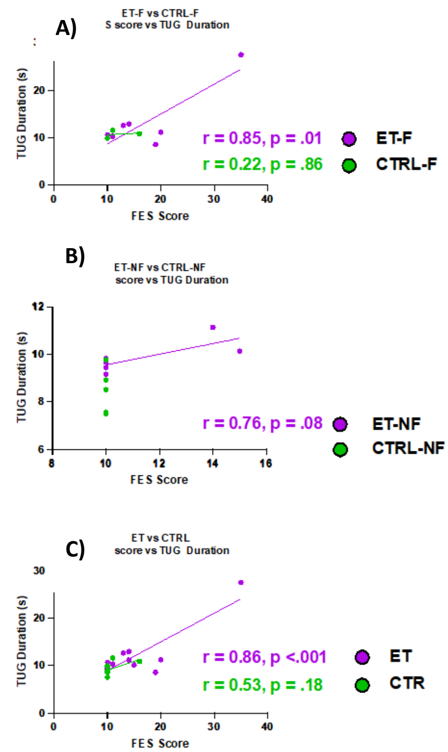

Figures A-C. FES score TUG duration in ET and CTRL groups.

Significance: Based upon our results, people with ET are considered to be at a higher fall risk than those without ET. Categorization of whether adults are at an increased fall risk is important in clinical settings as well as in research laboratories to better design an intervention for the participant. The use of both self-reported (FES) and objective (TUG duration) measures was demonstrated to be important in analyzing fall risk status in adults with ET in this study. An increased FES score in addition to an increased TUG duration demonstrated a strong correlation in fallers and non-fallers in the ET population.

References: [1] Ashwini K. Rao, et. al., (2011), *Gait & Posture* 38(3), [2] Lucy Yardley, et. al., (2005) *Age and Ageing*, 34(6), [3] Shumway-Cook et. al. (2000*), Physical Therapy, 80*(9).

EXAMINING IMU-DERIVED CHANGES IN ARM MOBILITY DURING DAILY LIVING FOLLOWING MASTECTOMY AND IMMEDIATE BREAST RECONSTRUCTION

Barrett Bongiorno[1*], Stephen M. Cain[2], David B. Lipps[1]
[1]School of Kinesiology, University of Michigan; [2]Department of Chemical and Biomedical Engineering, West Virginia University
*Corresponding author's email: bongiobp@umich.edu

Introduction: Mastectomy rates in the U.S. are increasing, driven by more breast cancer patients opting for a mastectomy with breast reconstruction to manage future cancer recurrence and restore the natural breast mound [1]. While breast reconstruction patients commonly report shoulder pain and restricted mobility in the months and years following surgery [2], new surgical approaches to breast reconstruction may lessen the shoulder morbidity associated with mastectomy and breast reconstruction. For example, prepectoral placement of the implant provides comparable psychosocial and aesthetic outcomes for patients as subpectoral implant placement without the need to disinsert the pectoralis major. Prepectoral placement of an implant can also significantly lower patient-reported pain scores compared to subpectoral implant placement [3]. However, the effect of immediate breast reconstruction on shoulder mobility during daily life has yet to be quantified. Therefore, we examined how breast cancer patients use their arms during everyday life using multiple body-worn inertial measurement units (IMUs) following surgery. We hypothesize that women undergoing mastectomy and immediate breast reconstruction with a prepectoral implant will display no change in arm mobility after surgery, indicating this growing surgical approach has an added functional benefit to patients.

Methods: Seven women undergoing mastectomy (six bilateral and one left unilateral) and immediate breast reconstruction with prepectoral implants (mean age 48.1 years, mean height 1.65 m, mean weight 74.4 kg) were enrolled in this study and provided informed written consent to the study procedures. Participants completed two home monitoring sessions both prior to their initial reconstruction surgery and prior to implant exchange (3-months post-op). For each session, participants were mailed a package of five Opal IMUs (APDM Inc.) to wear for two consecutive days. Each morning, participants secured these IMUs bilaterally on the forearms and upper arms, along with the thorax. Participants were instructed to wear the sensors for a minimum of 10 hours during the day. At the end of the day, participants placed the sensors in a charging station overnight and repeated the research activities for a 2nd day before mailing back the sensors. Measures of upper arm angle and forearm angle (with respect to the vertical) and wrist height (with respect to shoulder height) were calculated for the first day of observation of each home session. We excluded data from non-wear times and analyzed only data from when participants were upright (torso angle < 30°) and when an arm was moving (vertical speed of wrist > 0.01 arm lengths per second). The median upper arm angle, forearm angle, and wrist height across each full day was calculated. Paired t-tests evaluated time and arm differences for each outcome measure, with $p < 0.05$ considered significant.

Results & Discussion: Analysis of the data from seven participants reveals several trends. In comparing the difference in arm angle from the first to second visits, women did exhibit a trend towards a reduction in their median wrist height over the entire day for both their left ($p = 0.064$, Cohen's $d = -0.86$) and right arms ($p = 0.072$, Cohen's $d = -0.83$) approximately three months after the prepectoral breast reconstruction was performed when compared to pre-surgery. This trend indicates that women could adopt less elevated arm postures after mastectomy and breast reconstruction. However, no significant difference in forearm angle or upper arm angle were observed for the left or right arm between pre-surgery and three-months post-surgery (all $p > 0.18$, Cohen's $d < 0.57$). We did observe a potential trend where upper arm angle differed between the left and right arms before surgery ($p = 0.08$, Cohen's d=-0.79) but was similar after surgery ($p = 0.84$).

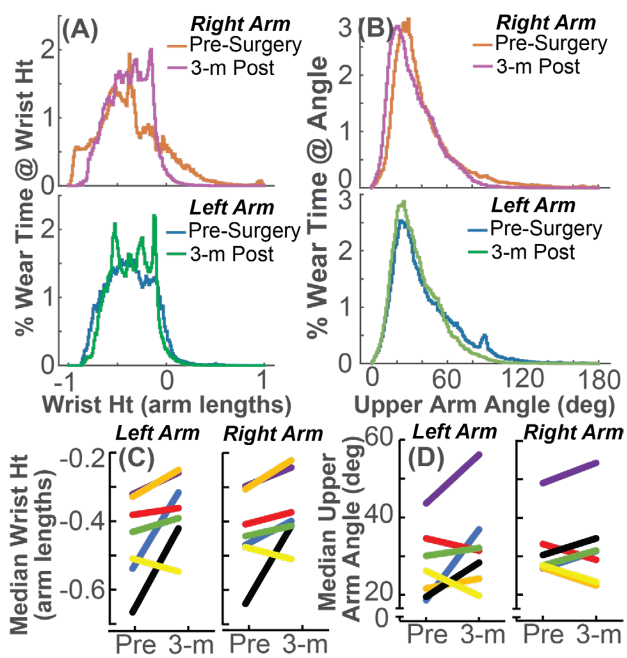

Figure 1: Representative histograms display the range of (a) wrist heights with respect to shoulder (height = 0; height < 0 is wrist below shoulder) and (b) upper arm angles with respect to the vertical for each arm of one patient across an entire day before breast reconstruction and after 3 months. The change in median (c) wrist height and (d) upper arm angle across the entire day are shown for each patient (N=7, differing colors).

Overall, these findings could indicate adaptions in arm use during everyday life following breast reconstruction. In terms of limitations, the data are highly dependent on the lifestyle of the participant and their daily tasks and obligations, which could drastically affect the time spent in different upper limb positions from day to day. Future research may consider including patient-reported measures of daily activity level and pain to contextualize the data relative to a typical day for the patient.

Significance: To our knowledge, this is the first study of its kind to utilize wearable IMU sensors to analyze upper limb position in mastectomy patients in an at-home setting throughout a typical day.

Acknowledgements: American Cancer Society RSG-20-016-01-CCE.

References: [1] Kummerow et al. (2015) *JAMA Surg* 150(1). [2] Tarantino et al. (2006) *Plast Reconstr Surg* 117(5). [3] Walia et al. (2018) *Plast Reconstr Surg Glob Open* 6(4).

CHANGES IN LOWER EXTREMITY WORK DURING PROLONGED WALKING IN INDIVIDUALS WITH KNEE OSTEOARTHRITIS

Samantha Price,[1] Joshua J. Stefanik,[2] Cara L. Lewis,[3] Irene S. Davis,[4] David T. Felson,[3] Patrick Corrigan[1]
1 – Saint Louis University; 2 – Northeastern University; 3 – Boston University; 4 – University of South Florida
*Corresponding author's email: Patrick.corrigan@health.slu.edu

Introduction: Individuals with single-joint osteoarthritis (OA) commonly develop OA in neighboring joints [1]. Aberrant walking patterns are known to increase the likelihood of OA development. Yet, it remains unclear if biomechanical compensations occur during prolonged walking that hasten the development of OA [2]. This is important because walking programs are recommended for managing pain in individuals with OA. Thus, the purpose of this study was to describe the biomechanical changes that occur at the hips, knees, ankles, and feet during prolonged walking in individuals with knee OA.

Methods: Twelve participants (5 female) with clinically defined knee OA in at least one knee based on the National Institute for Health and Care Excellence (NICE) criteria were included. Mean (SD) age, height, body mass, and BMI were 61 (8) years, 170.0 (10.8) cm, 88.5 (24.1) kg, and 30.2 (6.3) kg/m^2, respectively. Participants walked at a consistent self-selected speed (1.21 (0.13) m/s) on a treadmill for a 3 minute warm up, 30 minute walking period, and 3 minute cool down. During the last minute of the warm up (pre) and first minute of the cool down (post), lower extremity marker data were sampled (300 Hz) with an 12-camera motion capture system and force data were sampled (1200 Hz) with force-instrumented split-belt treadmill. After reducing each condition to 10 gait cycles, the Constituent Lower Extremity Work (CLEW) approach was applied [3]. In short, the CLEW approach includes determining positive and negative work during stance and swing phases for the hips, knees, ankles, and feet through integration of 6 degree-of-freedom power waveforms, which account for rotational and translational segment power [3-6]. To visualize the distribution of work within a limb, pie charts are developed by calculating the work performed by each constituent relative to the total absolute work of the limb. Finally, the charts are scaled to the mechanical cost of transport (CoT), which is the absolute limb work per stride length. This process was completed on both the most and least symptomatic limbs, which was determined using scores (VAS; 0-100) from the question "How bad has the pain been in your knee, on average, in the past week?"

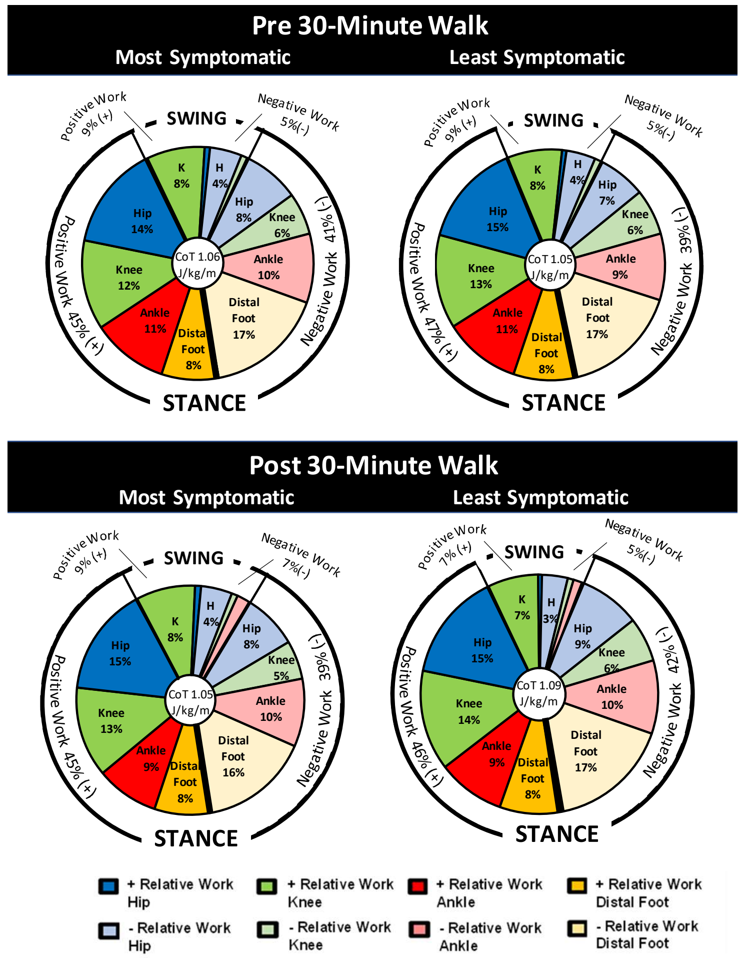

Figure 1: CLEW Approach – Relative constituent work scaled to the mechanical cost of transport (CoT) per limb pre and post a 30 minute walk.

Results and Discussion: Mean (SD) VAS pain scores for the most and least symptomatic limbs were 56 (14) and 32 (26), respectively. The mean (SD) absolute limb work (J/kg) for the most symptomatic and least symptomatic limbs were 1.44 (0.46) and 1.37 (0.35) in the pre condition and 1.39 (0.57) and 1.47 (0.51) in the post condition. CoT was similar between limbs and conditions (Figure 1). Mean (SD) absolute knee work (J/kg) for the most and least symptomatic limbs were 0.18 (0.06) and 0.19 (0.06) in the pre condition and 0.26 (0.18) and 0.21 (0.09) in the post condition. Distribution of work appeared to be relatively similar between limbs and conditions (Figure 1), but it is unclear what constitutes a meaningful difference in work. When looking at only those with unilateral knee OA (n=5), results did not change, with relative work being within 2% for each constituent. In summary, prolonged walking did not appear to induce biomechanical compensations in individuals with knee OA. This may be important to consider when prescribing walking programs for those with OA.

Significance: Distribution of work remained relatively symmetrical at the hip, knee, ankle, and foot before and after a 30 minute walk in individuals with knee OA. To identify mechanisms that explain single to multi-joint OA progression further research is needed.

References: [1] Metcalf et al. (2013) *J Bone Jt Surgery* 95 B(3); [2] Corrigan et al. (2020) *Osteoarthritis and Cartilage Open* 2(4); [3] Ebrahimi et al. (2017), *Gait and Posture* 56; [4] Ebrahimi et al. (2017), *J Biomech* 58; [5] Zellers et al. (2019) *J of Orthopaedic Research* 37; [6] Zelik et al. (2015) *J of Experimental Biology* 218(6).

COMPUTATIONAL EVALUATION OF NON-CONTACT ACL INJURY MECHANISMS

Trent M. Guess[1*], Jacob Thomas[1], Rob Wissman[1]
[1]University of Missouri, Columbia, MO
*Corresponding author's email: guesstr@health.missouri.edu

Introduction: Injury to the anterior cruciate ligament (ACL) of the knee is a major life event, often requiring surgical reconstruction and subsequent long-term rehabilitation. Videos of athletes sustaining injury and the location of bone bruising can elucidate body and tibiofemoral position near the time of injury. However, the specific mechanisms that result in failure level stress in ACL fibers is not precisely known. Greater knowledge of ACL injury biomechanics would enhance prevention, reconstruction, and rehabilitation efforts. Computational models of the knee can predict ACL loading in response to muscle and external knee forces and may provide important insight into ACL injury mechanisms that enhance evidence provided by injury videos and bone contusion patterns. This project used a computational knee model and design of experiments (DOE) methods to systematically explore the relationship between knee loading and ACL strain for the purpose of connecting the known and unknown biomechanical factors of ACL injury.

Methods: A multibody computational model was created from medical imaging and experimental biomechanical testing of a left cadaver knee (male, 49 yrs, 72 in, 133 lbs) (Fig. 1). Acquired MRIs were segmented to produce geometries of the tibia, fibula, femur, and patella including bone and articular cartilage. MRI was also used to determine insertion and origin footprints for the cruciate ligaments. Multi-axis tibiofemoral force/displacement relationships were measured with a 6-axis robotic tester with SimVITRO orthopaedic biomechanical testing software. The experimental data was used to determine zero-load lengths and modify ligament stiffness in the computational model. The ACL was represented by 3 bundles [1] and the posterior cruciate, lateral collateral, medial collateral, anterolateral, and patellofemoral ligaments were included. The menisci were not represented. Deformable contacts were defined between tibiofemoral and patellofemoral articular cartilage [2]. The linear and toe regions of ligament bundles were modelled with a piecewise function. During simulations, the femur was constrained while the tibia was free to move with six degrees of freedom. Quadriceps muscle forces were used to maintain desired flexion angle through a feedback controller. Hamstring and gastroc forces were included along with vertical, anterior/posterior, and medial/lateral forces applied at the ankle. DOE methods were used to determine the effects of flexion angle and muscle and ground reaction force inputs on ACL strain. Vertical compression force was held constant (500 N) and the DOE included 5 factors and 2 levels (Table 1) resulting in 32 simulations for a full factorial design. A multi-factorial ANOVA was used to examine the contribution of each factor on ACL strain and orthogonal contrasts were used to determine the directionality of each factor's effect on strain.

Table 1: DOE inputs

Factor	Upper	Lower
Flexion (deg)	20	5
Ant/Post (N)	100	-100
Med/Lat (N)	70	-70
Gastroc (N)	400	5
Hamstring (N)	400	5

Results & Discussion: 12 simulations resulted in knee hyperextension and were not included in this analysis. For the remaining 20 simulations, medial/lateral force ($F = 10.8$, $p = 0.005$), anterior/posterior force ($F = 6.5$, $p = 0.02$), and gastrocnemius force ($F = 4.1$, $p = 0.06$) had the largest influence on ACL strain level. The lateral and posterior directions for the ground reaction force produced the highest ACL strain. The combination of 20 deg knee flexion, posterior and lateral ground reaction force, 400 N gastrocnemius force, and 5 N hamstring force produced the highest ACL strain. This combination of inputs resulted in the lateral femur sliding past the lateral posterior tibia plateau creating a mechanical wedge that results in high strain on the ACL and a compressive force sufficient to crush bone at the contact location. This location matches the most commonly seen bone bruise site [3]. For simulation with the lateral force switched to medial and otherwise identical inputs, the femur stays on the tibial plateau and ACL strain is low.

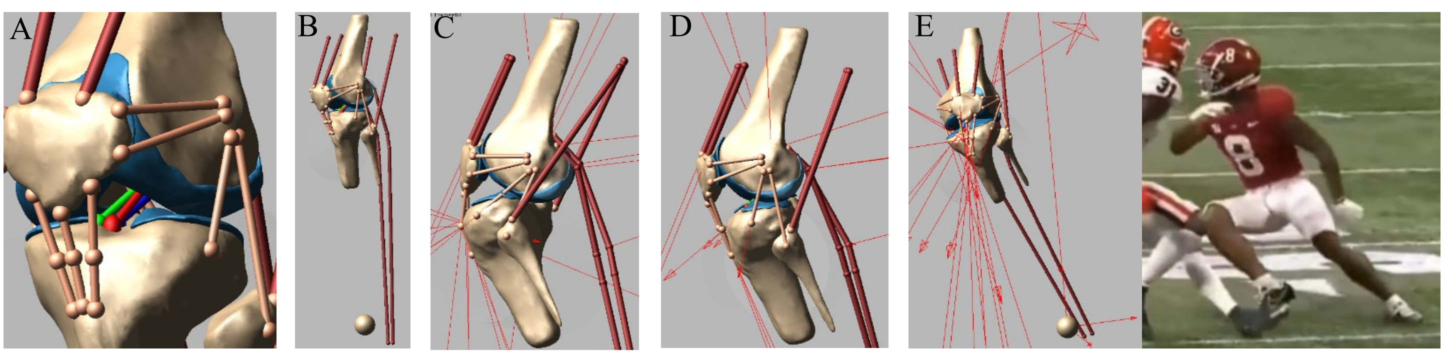

Figure 1: Knee model with 3 ACL bundles (A), muscle forces, and ankle forces (B). Simulation with highest ACL strain (C) and simulation with identical inputs except a medial ground reaction force (D). Inputs to the high ACL strain simulation are consistent with the "dynamic valgus" injury mechanism (E) seen in ACL injury videos. It also generates high contact forces localized at lateral ACL injury bone bruise locations.

Significance: The worst-case ACL loading simulation is consistent with body and tibiofemoral position commonly observed with non-contact ACL injury. This injury mechanism is also consistent with concomitant tissue injury and known anatomical risk factors. Our simulations indicate bone bruising that occurs at the time of ACL injury and a wedging mechanism that generates high ACL loading through mechanical advantage. The lateral force creates a valgus moment, however in our simulation the lateral force enables high strain through the observed wedging effect, not through direct application of valgus moment force on the ACL.

Acknowledgements: This research was funded by the Kansas City Consortium for Musculoskeletal Diseases.

References: [1] Butler, et al. (1992) *J Biomech*, [2] Guess et al. (2017) *Med Eng Phys,* [3] Shi et al. (2021) *Ann Biomed Eng*

KINEMATIC COMPARISON OF THE LOWER EXTREMITES IN SPORT-SPECIFIC AND LABORATORY ENVIRONMENTS FROM LACROSSE ATHLETES

Pratham Singh[1*] and Timothy Burkhart[1]
[1] Faculty of Kinesiology, University of Toronto, Toronto, ON
*Corresponding author's email: Pratham.singh@mail.utoronto.ca

Introduction: An athlete's goal is optimize performance while minimizing the risk of injury. However, the neuromuscular coordination of the bi-articular lower extremity muscles is complex [1] and the synchronous motion of the joints requires a functional-mechanical propagation through the kinetic chain. While lower extremity kinematics data has been accurately collected using equipment in a laboratory setting, the ecological validity of the data may be reduced as it does not reflect an environment that is experienced during sport. Therefore, the purpose of this study is to compare lower extremity kinematics in lacrosse athletes between their field environment and within the lab. We hypothesized that lacrosse athletes will have a greater range of motion (ROM) when completing similar multiplanar tasks in the sport specific environment compared to the laboratory environment for comparable tasks.

Methods: Five varsity level lacrosse athletes were recruited (M: 2, F: 3; Age: 21.6 [4.27]). On the field, the lacrosse athletes performed a three-cone drill. In the laboratory, they performed a sidestep cut (run for 5 meters, decelerate, and perform a 90˚ cutting manoeuvre with the contralateral limb). Motion capture data was collected for each kinematic evaluation using a markerless motion capture system (Theia Markerless, Kingston, ON). Motion data was recorded using eight motion capture cameras sampling at 120 Hz (Sony, Tokyo, Japan). Kinematic data was processed using Visual 3D (C-Motion Inc., Boyds, MD). The range of motion (RoM) was calculated as the difference between the minimum and maximum angles for the cutting phase of each task. A one-way repeated measures ANOVA was used (IBM SPSS, V28; Armonk, NY, USA) to quantify differences between tasks ($\alpha=0.05$).

Table 1: Right and left knee ROM for knee flexion/extension, abduction/adduction and internal/external rotation were all greater in the sport specific environment than in the laboratory

Right Knee	**Flexion/ Extension (˚)**	**Abduction/ Adduction (˚)**	**Internal/ External Rotation (˚)**
Cut Left	83.98 [7.46]	27.96 [4.20]	38.32 [8.90]
Cut Right	96.59 [8.10]	36.40 [5.02]	40.49 [5.47]
Three Cone Drill	109.81 [9.38]	57.01 [2.69]	59.83 [0.96]

Left Knee	**Flexion/ Extension (˚)**	**Abduction/ Adduction (˚)**	**Internal/ External Rotation (˚)**
Cut Left	93.29 [6.87]	34.24 [5.52]	39.13 [10.73]
Cut Right	83.72 [7.21]	30.78 [5.96]	36.01 [3.77]
Three Cone Drill	116.24 [10.00]	58.28 [1.10]	60.58 [0.27]

Results: The right and left knee RoMs for knee flexion/extension, abduction/adduction and internal/external rotation were all significantly greater during the cutting phase of the three-cone drill on the field in comparison to performing a sidestep cut to the right or left in a laboratory environment (Right: $F(2,4) = 53.23$, $p < 0.05$; Left: $F(2,4) = 129.70$, $p < 0.05$) (Table 1). The RoMs for the contralateral limb during a cut in the laboratory environment were not significantly different for either the right or left side (Right: $F(1,2) = 6.50$, $p > 0.05$; Left: $F(1,2) = 6.60$, $p > 0.05$).

Discussion: The increased knee RoM in the lacrosse athletes on the field suggests that they may be at an increased level of performance when compared to the laboratory environment. They are expanding the use of the lower extremity kinetic chain that involves the knee to achieve task completion in an environment they are familiar with. Having the athletes on the field rather than in a laboratory environment to perform similar tasks may help sustain improved knee joint performance. This further suggests that researchers and clinicians should consider the environment and the type of task used for assessment when quantifying an athlete's risk of injury or readiness to return-to-sport.

Significance: Given that lacrosse athletes are at an increased risk of ACL injuries [2], performing injury risk, or return to sport assessments on the field, with sport relevant tasks may provide a more accurate kinematic assessment. This could result in better identification of those athletes that are at a higher risk for injury and could better identify when an individual is truly ready to return to sport.

Acknowledgements: The research is funded by an NSERC Discovery Grant.

References:

[1] Webster K et al. (2019), *Sports Med* 49(6)
[2] Braun H et al. (2015), *Knee Surg. Sports Traumatol. Arthrosc.* 23(4)

CAMERA-BASED VS. CAMERA-LESS (IMU-BASED) KINEMATICS FOR ESTIMATES OF LUMBAR SPINE LOADS USING A FULL BODY MUSCULOSKELETAL MODEL

Maria Prado[1], Sakiko Oyama[2], Hugo Giambini[1]*

[1]Department of Biomedical Engineering and Chemical Engineering, University of Texas at San Antonio, San Antonio, TX, USA

[2]Department of Kinesiology, University of Texas at San Antonio, San Antonio, TX, USA.

*Corresponding author's email: hugo.giambini@utsa.edu

Introduction: Wertebral loads acting on the human spine can be estimated using computer-based musculoskeletal (MSK) models. This is a common method for non-invasive analyses of human motion and loads estimations using an inverse dynamic approach [1]. The gold standard for human kinematic analysis is based on optical motion capture that is limited to laboratory environments. Inertial measurement unit (IMU)-based motion capture systems are an alternative to obtaining body kinematic in real-life environments without the need for cameras; however, they have not been extensively validated [2 – 4]. MSK-based estimates of spine loads based on camera-less (IMU-based) systems have not been compared to the gold standard camera-based system. The aims of this study were: (1) to compare the kinematics obtained using camera-based and camera-less systems; (2) to compare the estimated spine loads obtained using a MSK model based on the camera-based and camera-less kinematic inputs. Successful outcomes using the camera-less system could facilitate the estimation of spine loads in natural environments and for diverse populations allowing for its implementation in the clinical setting to evaluate pathologies and conditions, and their association with spine curvature and balance disorders without the need for complicated experimental set-ups.

Methods: Eleven healthy volunteers were instructed to perform static postures (standing, standing with arms at chest holding weights, and standing with arms extended holding weights) and dynamics tasks (flexion-extension [F-E], lateral bending [LB], axial rotation [AR], walking, and walking with weights; **Fig. 1**) using the two motion capture systems, camera-based and camera-less, simultaneously. A full-body MSK model was implemented using the AnyBody modelling software to estimate loads acting in the L4-L5 spine segment. For each task, the compressive reaction force was obtained. The data from one of the male participants (Age: 24 yrs., Height: 1.7 m, Body mass: 72 kg) whose height and body mass closely matched the participant in a previous study (Wilke et al. [5]) that reported *in-vivo* measurements of pressures of the L4-L5 spine was used to compare and validate the model. To minimize the effect of abnormal posture on outcomes, normal ranges of thoracic kyphosis, lumbar lordosis, and sacral inclination angles were confirmed by evaluating all subjects in an upright standing position using the Spinal Mouse (SM), that allow for surface curvature measurements of the spine to be obtained non-invasively.

Results & Discussion: Pressures matched those previously obtained *in-vivo* (F-E: 0.70, 0.95, and 0.91 MPa; AR: 0.60, 0.60 and, 0.40 MPa; LB: 0.60, 0.73, and 0.69 MPa; standing: 0.50, 0.50, and 0.48 MPa; walking: 0.60, 0.6., and 0.64 MPa; for in vivo, camera-based, and camera-less, respectively. Bland-Altman and statistical analyses on kinematics showed LB to exhibit the highest agreement between the two systems (p = 0.74), while F-E and AR showed weak agreements with significant differences (p<0.0001). While the trend in the kinematics was the same for both motion capture systems, statistical differences were found between them when estimating spine loads during F-E (p=0.005), LB (p=0.01), AR (p=0.04), walking (p=0.02), and walking with weights (p=0.0005). Seven of the eight tasks showed excellent correlations (R^2 = 0.74 to 0.99) in estimates of L4-L5 compressive loads between systems. Spine curvature assessment showed no significant differences between female (45.3 ± 3.6) and male (42.7 ± 2.9) thoracic kyphosis angles (p=0.49), and between female (35.2 ± 4.4) and male (27.4 ± 8.2) lordotic angles (p=0.23).

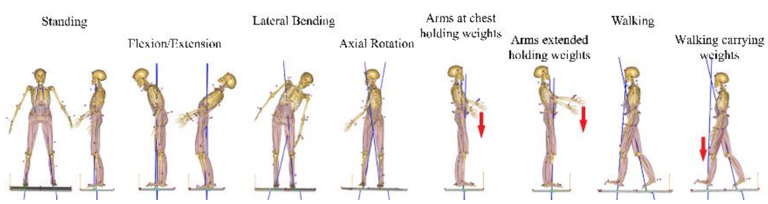

Figure 1: Static postures and dynamics tasks.

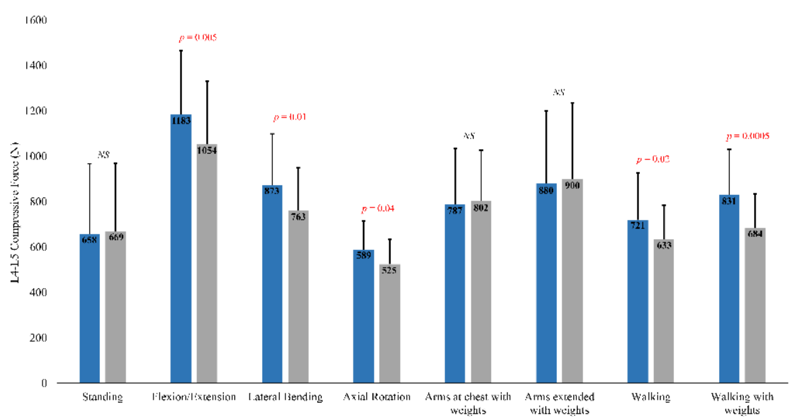

Figure 2: Summary of L4-L5 predicted loads.

Significance: Our study proved that we could successfully implement a camera-less system to accurately obtain forces acting in the spine. While statistically different, differences in predicted loads might not be clinically different, and the camera-less system can be a robust tool to obtain loads from activities of daily living, allowing for fast and convenient evaluation, which is conducive to longitudinal assessment of subjects inside and outside the laboratory setting. Future studies should evaluate the clinical significance of the systems.

Acknowledgements: This study was supported in part by The University of Texas at San Antonio, and the Office of the Vice President for Research, Economic Development, and Knowledge Enterprise.

References: [1] Fluit et al. (2014); [2] Pedro et al. (2021); [3] Zhang et al. (2013); [4] Cloete and Scheffer, (2008); [5] Wilke et al. (2001).

Learning to Balance on the Stability Platform: Individual Differences in Motor Learning

Simon M. Cone[1*], Dr. Rajiv Ranganathan[1,2]
[1]Department of Kinesiology, Michigan State University, East Lansing, MI, USA
*Corresponding author's email: conesimo@msu.edu

Introduction: Given the exact same amount of practice, some individuals can improve quickly at new motor skills while other individuals improve much more slowly. Prior research has explored reasons for these individual differences in motor learning but has focused mainly on simple motor tasks offering limited solutions, such as sequence learning or adaptation tasks [1]. Complex motor tasks offer greater task-space redundancy, which means that the performer must choose from many possible movement solutions in order to perform the motor task.

Learning a complex new balance task can be difficult because many different joint movements can produce an equivalent change in the performance variables of interest [2]. In order to learn a new dynamic balance skill, a performer must first discover, and then refine, a coordination pattern that allows them to stabilize a task-specific relationship between their center of mass and base of support. While we know that individuals can improve their balance across weeks of practice, it is poorly understood why some individuals are able to quickly improve their performance while other individuals improve much slower. The purpose of this study is to investigate how frontal plane balance control is improved across weeks of practice and to analyze individual differences in the learning processes.

Methods: Participants were asked to practice balancing on the stability platform during 10 practice sessions across 10 weeks of practice (Fig. 1). During each stability platform trial, participants were instructed to keep the platform balanced in the horizontal position for as long as possible [3]. Performance changes were measured using a multivariate set of dependent variables. Whole body kinematics, muscular activation patterns from 8 muscles in each leg, and video recording data was collected to analyze changes in coordination on multiple levels to investigate how balance was improved [4]. Non-negative matrix factorization was used to analyze how lower body "muscle synergies" developed across practice [5].

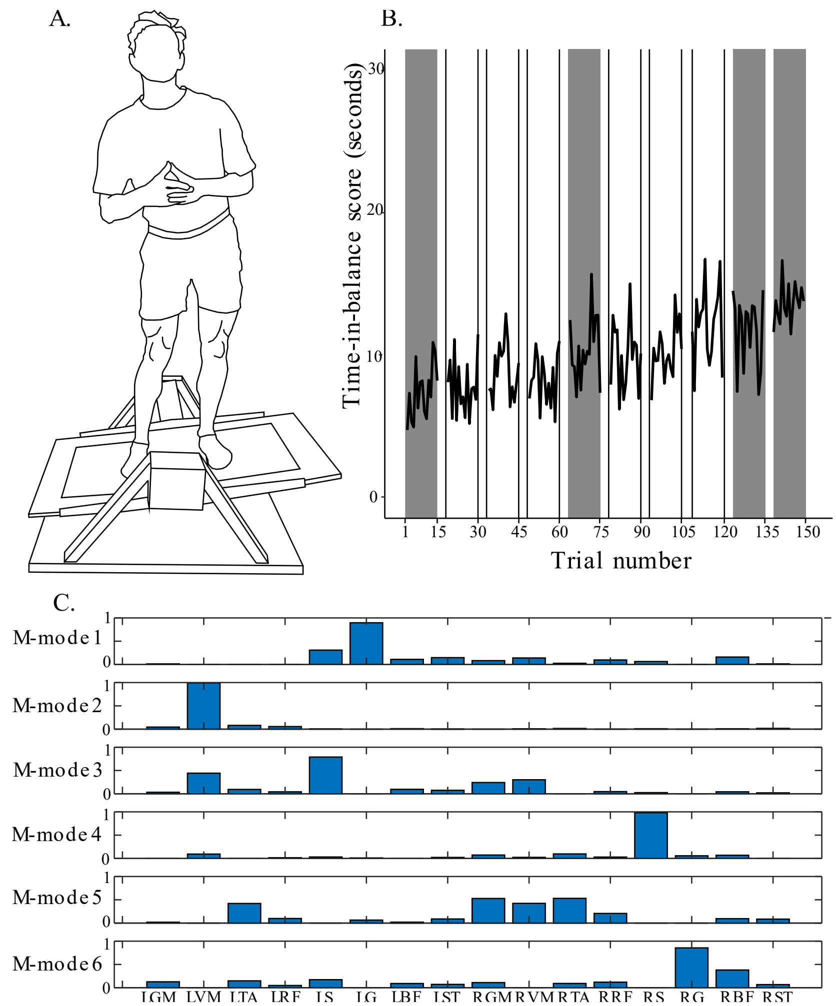

Figure 1 A. Participants are asked to stand on the stability platform and attempt to keep the platform balanced in the frontal plane for as long as possible during each trial; **B)** The performance curve for participant 4 **C)** During session 10, there were 6 "muscle synergies" that accounted for 90%of the variance in 16 lower body muscles.

Results & Discussion: Balance performance improved significantly for all participants. Preliminary behavioral data demonstrated that most participants used a similar motor strategy during the first trial, but quickly developed their own unique coordination patterns. Generally, participants either constrained their arm movements while balancing, displaying a "lower-body strategy" (Fig. 1) or they freed their arm movements to help them balance displaying a "upper-body strategy". Preliminary data suggested that developing an upper-body strategy early in practice benefit final performance.

Significance: Understanding how individual differences influence motor learning is important for understanding how redundancy is utilized by the human motor control system. Additionally, how balance control is improved, and why some individuals improve balance faster are critical questions that must be answered in order to design effective balance training interventions.

References: [1] Ranganathan et al. (2022) *Neurosci Biobehav Rev*; [2] Ko et al., (2003) *Hum Mov Sci*; [3] Taubert et al., (2010) *J Neurosci*; [4] Wade et al., (1972) *J Mot Behav*; [5] Ting (2007) *Prog Brain Resl*; [6] King et al., (2012) *Neurosci Lett*

DEVIATIONS IN JOINT LOADING WHEN ENCOUNTERING UNEXPECTED UNEVEN TERRAIN FOR HEALTHY INDIVIDUALS AND INDIVIDUALS WITH A TRANSTIBIAL AMPUTATION

Kristen M. Stewart[1*], Glenn K. Klute[2], Richard R. Neptune[1]
[1] Walker Department of Mechanical Engineering, The University of Texas at Austin, Austin, TX
[2] VA Center for Limb Loss and MoBility and Department of Mechanical Engineering, University of Washington, Seattle, WA
*Corresponding author's email: kristen.stewart@utexas.edu

Introduction: Walking over an unexpected uneven surface is often encountered during daily activities and requires recovery strategies to maintain balance. Healthy individuals often use a hip or lateral ankle strategy when recovering from balance perturbations [e.g., 1], and they also conform their foot to the surface and alter their ankle inversion/eversion moments when encountering uneven surfaces [2]. However, individuals with a unilateral transtibial amputation (TTA) have fewer residual limb muscles and relatively stiff ankle-foot prostheses, which require different balance recovery responses [e.g., 3].

While joint loading is a potential indicator of joint pain and injury [e.g., 4], it is difficult to measure experimentally. Joint loading is affected by muscle activity [5], and therefore different recovery responses would likely affect joint loading. In contrast, musculoskeletal modeling and simulation, which can be used to estimate joint contact forces, is a promising approach to assess the influence of stepping on an uneven surface on joint loading.

The purpose of this study was to identify differences in joint loading between healthy individuals and individuals with TTA when stepping on an uneven surface and the subsequent recovery step using musculoskeletal modeling and simulation. We expect deviations in joint loading between the uneven surface and flush conditions will be larger for individuals with TTA compared to healthy individuals.

Methods: Five healthy individuals and five individuals with TTA walked over-ground while kinematic and kinetic data were collected. The middle step of the walkway was either flush or rotated $\pm 15°$ in the frontal plane for an inverted or everted condition. The orientation of the plate was blinded to the subjects.

Models for each subject were scaled in OpenSim 4.2 [6] from the "gait2392" model, and the inertial properties of the residual limb for those with TTA were modified and muscles spanning the ankle joint were removed [7]. The simulations included the uneven step (with the dominant or residual limb for healthy individuals and individuals with TTA, respectively) and the subsequent recovery step. A computed muscle control algorithm [8] was used to solve for the muscle activations and a joint reaction analysis was performed to determine the axial loading at the hip, knee and ankle joint of each limb during the respective stance phase. Deviations in joint loading were computed as the difference between the joint contact forces during each uneven surface condition and flush condition.

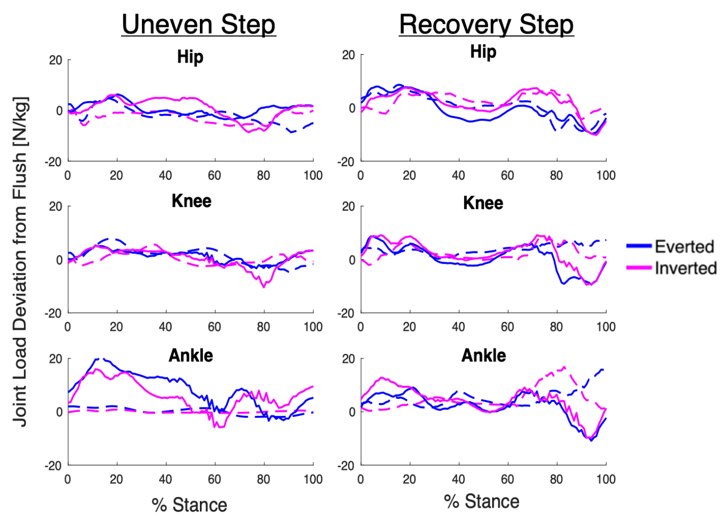

Figure 1: Joint loading deviations from the flush condition during stance of each uneven and recovery steps. Solid lines represent healthy individuals and dashed lines represent individuals with TTA. Joint contact forces were normalized by body mass and averaged across subjects for each group.

Results & Discussion: The largest joint loading deviations between the uneven surface and flush conditions for healthy individuals were present at the ankle (Fig. 1), consistent with a lateral ankle strategy, where ankle muscles activate to make small adjustments to the center of pressure [1]. Conversely, there were no deviations for individuals with TTA at the prosthetic ankle (Fig. 1). This difference at the ankle led to higher joint loading at the knee, where there is already a high risk for osteoarthritis in individuals with TTA [e.g., 9], but lower joint loading deviations at the hip. In either uneven surface condition, healthy individuals experienced increases in joint loading at all joints in early stance of both steps, but often decreases in late stance of the recovery step relative to flush (Fig. 1). In contrast, the recovery step had larger deviations from mid-stance on for individuals with TTA compared to healthy individuals (Fig. 1), suggesting individuals with TTA had a greater reliance on their intact limb after initial contact.

Significance: These results highlight joint loading differences between individuals with TTA and healthy individuals, suggesting there is a need to integrate more compliance in the ankle-foot prostheses to provide more natural adaptations on uneven terrains.

Acknowledgements: Funded in part by US Dept. of Veterans Affairs (I50 RX002357, IK6 RX002974, I01 RX001840).

References: [1] Reimann et al. (2018), *K.R.* 7(1); [2] Segal et al. (2018), *J. Biomech. Eng.* 76; [3] Miller et al., (2018), 76; [4] Maly (2009), *Exerc Sport Sci. Rev.* 37(1); [5] Shelburne et al. (2006), *J. Orthop. Res.* 28(10); [6] Delp et al. (2007), *IEEE Trans. Biomed. Eng.* 54; [7] LaPrè et al. (2018), *Int. J. Num. Method. Biomed. Eng.* 34; [8] Thelen & Anderson (2006), *J. Biomech.* 39(6); [9] Burke et al. (1978) *A.R.D.* 37(3).

TRANSFER OF GRAVITY ADAPTATION BETWEEN END-EFFECTORS: JUMPING IN SIMULATED REDUCED GRAVITY INDUCES ALTERED REACHING BEHAVIOR

Chase G. Rock*, Angela Luo, Xiao Yang, Young-Hui Chang
School of Biological Sciences, Georgia Institute of Technology, Atlanta, GA, USA
*Corresponding author's email: crock@gatech.edu

Introduction: Humans possess incredible motor adaptability, allowing for successful movement under various physical contexts. New physical contexts can range from simple (wearing a backpack) to complex (driving in a race car), with adaptation to each context being facilitated by integration of sensory, motor, and cognitive systems. With such multi-level adaptation, transfer of learning can occur between different end-effectors (right-handers can write with their left hand, and vice versa [1]) or between different tasks (prism goggle adaptation of reaching can affect locomotion [2]). The goal of the current work was to test transfer of motor learning from one motor system to another, specifically by using a gravity manipulation.

In previous work, we have characterized the adaptation of lower limb muscle activity to reduced gravity exposure (ASB 2020) across different reduced gravity levels (NACOB 2022). We found that following targeted jumps in reduced gravity, there is a change in leg muscle activity prior to landing that reflects an expectation of lower gravity. In other words, adaptation to simulated reduced gravity in a single context (i.e., jumping) will lead to adaptive after-effects in that same context. What is currently unknown is if a gravity exposure in one motor context (jumping with legs) will transfer to another distinct motor context (reaching with arms). The motor control and adaptability of arm reaching movements has been well-characterized in previous research [3]–[5]. Lateral reaches typically show symmetrical velocity profiles, but upwardly directed reaches show a slight asymmetry, with peak velocity occurring earlier in the movement [4]. With increases in gravity, peak velocity occurs even earlier [5].

Hypothesis: Following a lower-limb adaptation protocol in simulated reduced gravity, the neuromechanical system will adopt an expectation of lower gravity, causing upper-limb reaches to resemble movement in hypogravity. We tested the prediction that the time to peak arm angular velocity would occur later after exposure to jumping in reduced gravity.

Methods: Ten participants (5M/5F) gave informed consent prior to participating in a protocol approved by the Georgia Tech IRB.

Targeted Jumping: Participants performed two-legged countermovement jumps to a target set at 75% of their personal maximum jump height. This target was used for all 70 jumps, in this order: 10 at 1g, 50 in simulated reduced gravity, and 10 at 1g. Reduced gravity was simulated using a selection of constant force springs mounted above the participant and attached via a harness (ASB2020). For all jumps, arm involvement was minimized by crossing them or holding on to the straps of the reduced gravity simulator.

Targeted Reaching: A physical target was placed at arm's length in front of the participant, at shoulder height. Starting from a resting position with their dominant arm pointing down at their side, we instructed participants to point to the target, rotating only about the shoulder (i.e., keeping the elbow and wrist straightened) and to move at a comfortable speed. Sets of twenty reaches were performed prior to (PRE) and immediately following (POST) jumping in simulated reduced gravity. Retroreflective markers on the hand, forearm, and upper arm provided 3D position of the limb, which was collected and tracked using Vicon Nexus. Angular limb velocity and peak velocity timing were calculated in Visual3D. MATLAB was used to statistically compare PRE vs POST conditions.

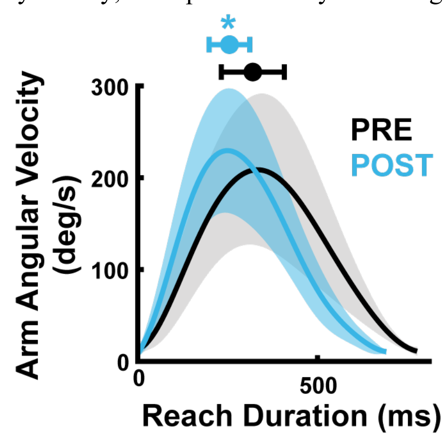

Figure 1: Participants achieved peak velocity earlier following exposure to simulated reduced gravity. Group mean velocity profiles (shading: ± SD) for the final reach performed prior to (PRE; black) and the first reach immediately after (POST; blue) jumping in simulated reduced gravity. Circles show mean peak velocity timing (error bars: ± SD); * denotes sig. difference from PRE

Results & Discussion: We observed a significant shift in the time to peak arm angular velocity. Contrary to our prediction, however, the time to peak velocity occurred significantly earlier in POST trials compared to PRE trials (Fig. 1). In this study, participants only made reaches in normal gravity, but we aimed to affect their expectation of gravity through jumping in simulated reduced gravity. This appears to have been successful, but the shift in reach velocity moved in the opposite direction than expected. In fact, the POST reaches resemble movements that occur during exposure to hypergravity [5], rather than hypogravity. To interpret this finding, we speculate the following chain of events: 1) reduced gravity jumping leads to task-specific adaptation of central and peripheral systems, resulting in reduced force production and higher sensitivity to proprioceptive information in the legs; 2) following jumping adaptation, initiating an arm reach in 1g results in 'normal' gravity sensory feedback from the arms; 3) a heightened sensory weighting may lead the central nervous system to misinterpret the transition from reduced gravity to normal gravity sensory information as an exposure to hypergravity, resulting in movement dynamics that resembles a reach in hypergravity.

Significance: Gravity represents a universal force that affects the control of most movements of the human body. This study supports the hypothesis that gravity is represented by the neuromechanical system centrally, making it accessible by multiple end-effectors for different behaviors. It appears that the central nervous system incorporates both recent sensorimotor experience and live feedback from multiple behaviors to build a prediction of the effects of gravity. When these are in conflict, erroneous behavior can be induced.

References: [1] N. Bernstein, Pergamon P., 1967. [2] A. Bakkum *et al.*, *Journal of Neurophysiology*, 2020 [3] R. Shadmehr *et al.*, *J. Neurosci.*, 1993 [4] R. Gentili *et al.*, *Neuroscience*, 2007 [5] F. Crevecoeur *et al.*, *Journal of Neurophysiology*, 2009

CO-CONTRACTION ABOUT THE ANKLE INCREASES WITH THE THREAT OF A WALKING PERTURBATION

Nancy T. Nguyen[1*], James B. Tracy[2], Jeremy R. Crenshaw[1]
[1]University of Delaware, Newark, DE; [2]University of Colorado Anschutz Medical Campus, Aurora, CO
*Corresponding author's email: nanguy@udel.edu

Introduction: The ability to prevent a fall after a walking perturbation is not only dependent upon reactive balance, but also the initial, potentially modifiable conditions related to stability. We previously investigated how unimpaired young adults proactively modify their gait kinematics when anticipating large anterior or posterior perturbations [1]. When anticipating a perturbation, participants took shorter, more frequent steps in a manner that benefitted stability margins at foot strike, but not midswing. Another manner in which an individual may protect against a perturbation is by increasing co-contraction about the ankle, in effect increasing the resistance at the base of the inverted pendulum. The purpose of this study was to investigate if such pro-active ankle co-contraction occurs when walking under the threat of large anterior and posterior perturbations.

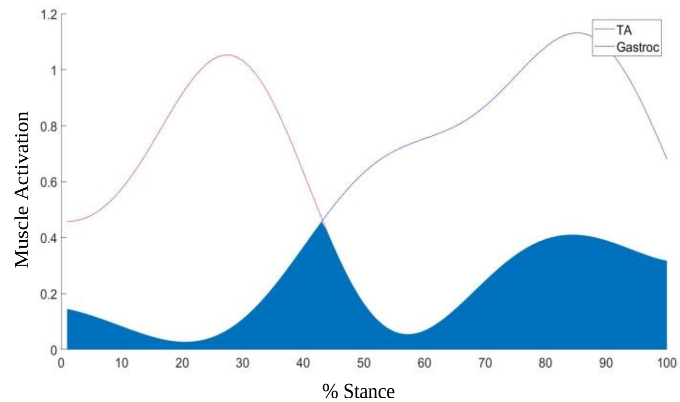

Figure 1. Example area under the curve graph for the fast condition with an anticipated anterior "trip" perturbation. The shaded region indicates the common area of the TA and Gastroc muscles. The x axis represents % stance from heel-strike to toe-off. The y axis represents muscle activation relative to unperturbed walking at 0.8 statures/s.

Methods: This is a secondary analysis of data from our previous study [1]. Equipped with a safety harness, eight participants (5 Female/3 Male; Age 26.8(5.26) years; BMI 21.3(2.39) kg/m^2) walked on a computer-controlled treadmill (ActiveStep®, Simbex). Participants walked under nine randomly-ordered task conditions with combinations of three walking speeds (0.6, 0.8, and 1.0 statures/s) and three perturbation conditions (anterior simulated trips, posterior simulated slips, and none). A perturbation occurred occasionally (12±2 steps) through rapid treadmill-belt accelerations. The participant was informed of the speed and perturbation type at the beginning of the trial, but not the timing of each perturbation. The perturbation magnitudes were intended to create credible threats to stability but not induce falls into the safety harness. Full-body motion capture (Qualisys, 120 Hz) and EMG of the bilateral tibialis anterior (TA) and medial gastrocnemius (Gastroc; Delsys, 1200 Hz) were recorded. We analysed co-contraction indices (CCI) [2] of these muscles separately for right and left stances prior to a perturbation, as follows (Figure 1):

$$\%\ CoCon = 2\ x\ \frac{common\ area\ TA\ \&\ Gastroc}{area\ TA + area\ Gastroc}\ x\ 100\%$$

The effects of walking speed, perturbation condition, and limb on CCI were assessed using a 3x3x2 repeated measures ANOVA.

Results & Discussion: There was a significant interaction of perturbation condition and limb ($p=0.036$, $\eta^2= 0.38$) on CCI. Regardless of the limb, and relative to unperturbed walking, co-contraction was elevated when anticipating anterior ($p<0.03$) and posterior ($p<0.01$) perturbations (Figure 2). A large, non-significant effect size ($p = 0.26$, $\eta^2 = 0.167$) was observed for the interaction of speed x perturbation x limb which suggests speed may influence these results.

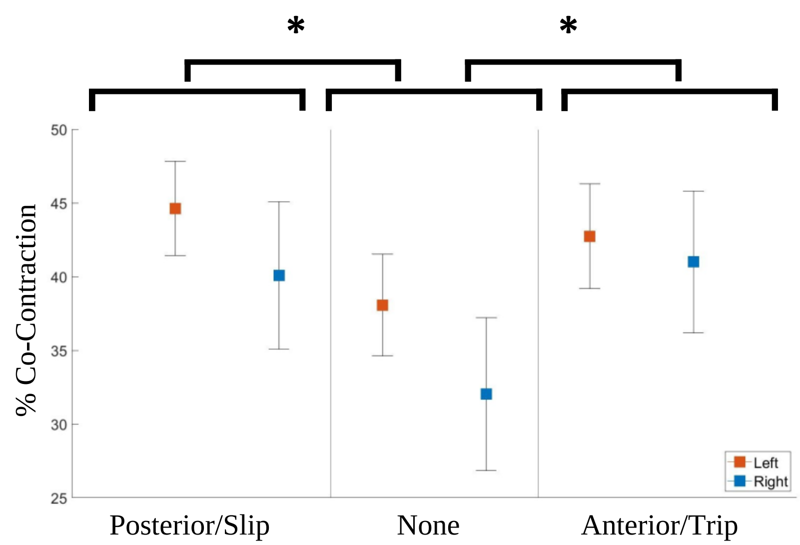

Figure 2. Average estimated mean co-contraction indices and standard errors before anticipated posterior "slip", no perturbation, and anticipated anterior "trip". Left limb is represented by red squares and right limb is represented by blue squares. * indicates p≤0.05.

Significance: Unimpaired individuals may be limited in how they can modify gait kinematics to improve stability when anticipating large perturbations [1]. These results suggest that co-contraction occurs in a manner that may increase resistance to perturbations. Future studies will determine the extent to which populations with a high risk of falling and/or neuromuscular impairment are able to proactively modify their gait kinematics and muscle activity in anticipation of a perturbation. That information may provide insight on underlying mechanisms of fall risk in these groups.

References: [1] Tracy (2022), University of Delaware Dissertation; [2] Winter (2009), *J Wiley & Son, Inc (4).*

THE EFFECTS OF TRAMPOLINE HOPPING ON SOLEUS H-REFLEX AND TENDON TAP REFLEX

Zac Wicks*[1], Robert Zeid[1], Briana Finch[1], Jianhua Wu[1]
[1]Department of Kinesiology and Health, Georgia State University
*Corresponding author's email: zwicks2@gsu.edu

Introduction

The Hoffman's Reflex (H-reflex) is a low threshold reflex that is alike to the typical stretch reflex, except that it bypasses the muscle spindles by being activated by a percutaneous electric stimulus. Eliciting the H-reflex in the soleus muscle allows to determine the spinal cord's reflexive capabilities and the ability of the α-motorneuron to excite a specific motor pool. It has been found that the H-reflex can be either suppressed or enhanced via different acute bouts of exercise [1]. Tendon tap reflex is another form of stretch reflex and has been used to assess neuromuscular response with a light mechanical touch on a tendon. Hopping is a common format of continuous movement and has been shown to modify joint kinematics and kinetics on different surfaces and conditions. The purpose of this study was to assess whether the H-reflex and tendon tap reflex are affected by hopping on two different surfaces: on the hard floor vs. on a trampoline. We hypothesized that hopping on a trampoline might recalibrate the neuromuscular response of the soleus, to a greater extent, to the H-reflex and tendon tap reflex than hopping on the floor.

Methods

Nine subjects were recruited (age: 21-32 years, M = 2, F = 7). Mean and SD of the subject characteristics were: height (155.7 ± 31.9 cm), weight (77.8 ± 37.3 kg), and leg length (89.9 ± 6.0 cm). Subjects lay prone on a massage table. Electrodes were attached to the skin on the top of the foot, and on the lateral aspect of the soleus muscle. The EMG data were recorded with iWorx LabScribe v3.63 (iWorx, Dover, NH).

Two stimulating electrodes were attached to the subject: one was placed superior to the patella, and the other was placed on the posterior aspect of the knee to stimulate the posterior tibial nerve. This posterior electrode was repositioned until a clear H-reflex EMG signal was obtained from the soleus. Electrical current was increased until M_{max} was achieved, and then reduced until the M-wave reached roughly 20% of M_{max} (133.1 ± 30.7 mA) to normalize the H-reflex response [1]. Once this electrical current intensity was determined, 10 baseline stimulations of the H-reflex were elicited and recorded from the soleus as a baseline. Subjects then performed the following series of hopping tasks: hopping on the floor at 2.2Hz for 41s for two bouts and on a trampoline at 1.5Hz for 60s for two bouts. After each bout, 10 H-reflex stimulations were elicited and recorded from the soleus at random intervals of 5-10s. The subjects were then given a 5-minute rest period before the next bout of hopping. Next, an Achilles tendon tap was utilized to repeat the same order and collect neuromuscular responses at baseline and after two bouts of hopping on the ground and on a trampoline. A reflex hammer with an attached plethysmograph was used to striking the Achilles tendon and elicit the stretch reflex. EMG amplitude was normalized by the corresponding baseline data. Two-way (2 surface x 2 bout) repeated measures ANOVAs were performed on the normalized EMG data for the H-reflex and tendon tap reflex separately.

Results and Discussion

For the H-reflex, EMG amplitude reduced from bout 1 to bout 2 for both floor and trampoline conditions (Fig. 1). Also, EMG amplitude had lower values for hopping on a trampoline than for hopping on the floor. For the Achilles tendon tap reflex, EMG amplitude decreased from bout 1 to bout 2 after hopping on the floor while it increased after hopping on a trampoline.

Based on these results, it appears that the H-reflex decreases significantly after trampoline hopping, and the stretch reflex increases significantly after trampoline hopping. Our hypothesis was partially supported such that the tendon tap reflex is recalibrated after a bout of hopping on a trampoline, but not on the hard floor.

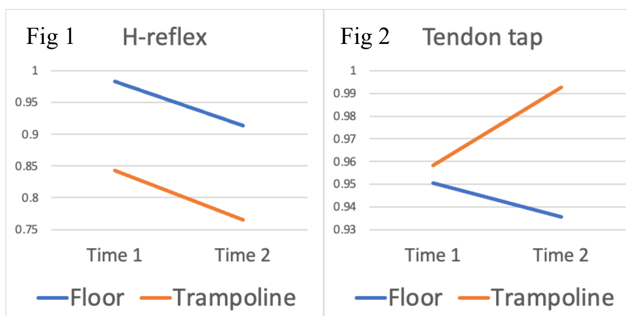

Significance

A diminished H-reflex is indicative of an improvement in postural control [2]. Our data demonstrate that hopping on a trampoline appears to modulate this spinal reflex and might be able to enhance postural control. By modulating the stretch reflex with an exercise modality that many people can perform, we can create simple, new interventions to help improve postural control in individuals with neurological movement disorders. This may eventually enhance their mobility and quality of life.

Acknowledgements

We would like to thank all the participants for volunteering their participation.

References

[1] Armstrong, et. al. (2008). *J. Strength Cond. Res.*, *22*(2); [2] Keller, et. al. (2012). *Scand J Med Sci Sports*, *22*(4).

EVALUATING NOVEL PLANTAR PRESSURE-BASED 3D PRINTED ACCOMMODATIVE INSOLES -A PILOT STUDY

Brittney C. Muir[1,2], Jing-Sheng Li[1,2], Yuri F. Hudak[1,2], G. Eli Kaufman[2], Scott Cullum[1,2], Patrick M. Aubin[1,2]
[1] Department of Mechanical Engineering, University of Washington, Seattle WA, USA
[2]VA RR&D Center for Limb Loss and MoBility (CLiMB), Seattle WA, USA
*Corresponding author's email: bcmuir@uw.edu

Introduction: Custom accommodative insoles are commonly prescribed to people with diabetes to redistribute plantar pressure and decrease the risk of ulceration [1]. Advances in 3D printing, materials science, and software have enabled our group to create new latticed 3D printed metamaterials whose properties are derived not only from the base material but also from the lattice microstructures within the metamaterial. Insoles manufactured using personalized metamaterials (PMM) have both patient-specific geometry, stiffnesses and structural behavior. However, the biomechanical effect of our PPM novel accommodative insoles have not yet been tested clinically. The purpose of this study is to investigate the effect of the SoC diabetic insoles, two types of 3D printed diabetic insoles with PMM, and no custom insole (research shoe; RS) on walking plantar pressure in adults without existing ulcer(s). A description of the insole design workflow and mechanical testing of the 3D printed material can be found here [2].

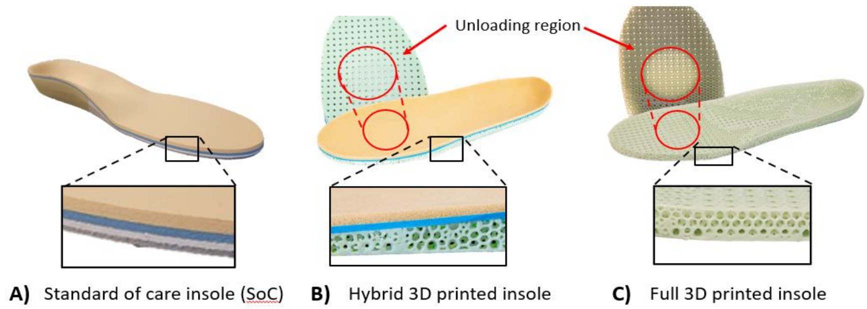

Figure 1: The three types of insoles that were fabricated. A) standard of care insole (SoC). B) Hybrid 3D printed insole with bilaminate foam top (Hybrid). C) full 3D printed insole (Full).

Methods: Twelve individuals (3 with diabetes) were recruited for this study. In-shoe walking plantar pressure (pedar-X, novel GmbH, Munich, Germany) in the research shoe (RS, Dr. Comfort® Men's Stallion or Women's Refresh, DJO LLC, Lewisville, TX) at the baseline visit was taken and sensels with pressure over 200 kPa were used to define an offloading region. Three pairs of custom insoles (two 3D printed insoles with personalized metamaterials (Hybrid and Full) designed based on foot shape and plantar pressure mapping and one standard-of-care (SoC) insole as a comparator). The Full insole was printed on a Carbon® L1 3D printer using the EPU41 material using a custom lattice structure that mimics the compressive properties of the SoC. The Hybrid insole was similarly designed but with the top 4 mm consisting of a Poron-Plastazote bilaminate sheet glued to the surface to attain the same overall geometry of the fully-3D printed version, but with a surface feel of the SoC (Figure 1). At a second visit, in-shoe plantar pressure measurements during walking were recorded and compared across the RS and the three insoles (SoC, Hybrid, Full).

Results & Discussion:
No adverse events occurred during testing. Maximum peak plantar pressure and the pressure time integral were reduced in the offloading regions in the Hybrid and Full but not in the SoC compared to the research shoe (Figure 2). This is not surprising as the 3D printed insoles had regions of sparse lattice in the RoI. However, this is encouraging as even participants without elevated plantar pressure can show a reduction in plantar pressure with the sparse lattice. Since the insole must support body weight when walking, a reduction in pressure in one region (e.g., the RoI) must be balanced by an increase in pressure in other regions. A concern of ours was that we would reduce pressure in the RoI only to have greatly increased pressure in the ADJ region. Prior studies have shown that the custom insoles reduce peak plantar pressure [e.g., 3] or PTI in the diabetic foot with neuropathy or ulceration, however this is inconsistent with our findings.

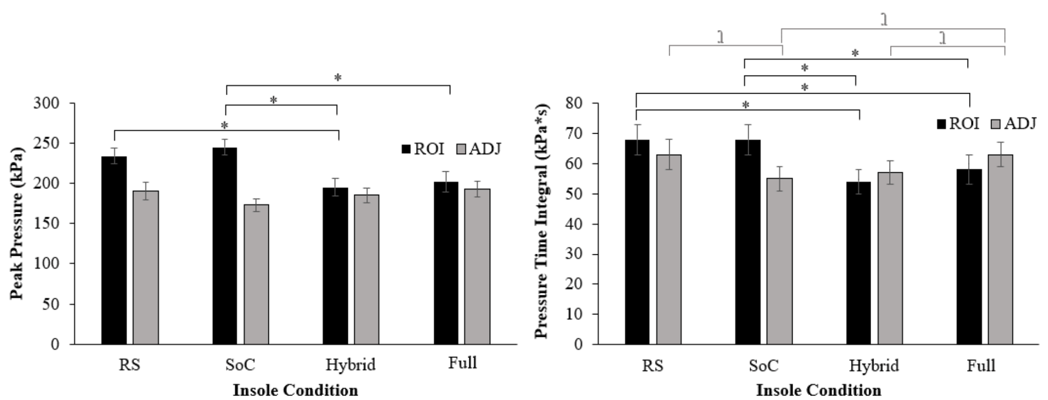

Figure 2: Peak plantar pressure during walking across the four insole conditions (left). Pressure-time integral during walking across insole conditions (right). Region of interest (RoI; black), adjacent region (ADJ; grey). * indicates p-value < 0.05 for RoI, ℩ indicates p-value < 0.05 for ADJ. Error bars represent standard error.

Significance: This pilot study confirms our ability to manufacture the 3D printed personalized metamaterials insoles, demonstrates their ability to reduce plantar pressure, and identifies our ability to modify the 3D printed design to offload certain parts of the foot using plantar pressure. The advance in 3D printed technology has shown its potential to improve current care.

Acknowledgments: Funding for this study was provided by VA award A3539R.

References:[1] Bus et al., 2016, *Diabetes Metab J 32*; [2] Hudak et al., 2022, *Med Eng Phys 104*; [3] Arts et al., 2015, *Diabet. Med. 32*

Effects of a step-rate based gait training on running gait mechanics: A systematic review and meta-analysis

Dante D. Goss[1*], Jennifer Xu[1], Jay Hertel[1]
[1]University of Virginia, Department of Kinesiology, Charlottesville, VA
*Corresponding author's email: nxq9uz@virginia.edu

Introduction: Running is a common activity that also carries a risk of injury, with an injury incidence of 7.7 per 1000 hours in recreational runners [1]. Braking ground reaction force impulse (BGRFI) and knee flexion angle at initial contact are key variables found to be risk factors for some of the most common running-related injuries (RRIs) [2]. Gait training has been used as a method of mitigating and treating these injuries [3]. Increasing step rate is a common method of gait training, though it is unclear how these interventions specifically affect biomechanical risk factors of RRIs. The primary aim of this study was to perform a systematic review with meta-analysis to investigate the effects of step-rate based gait training interventions on biomechanical risk factors for RRIs, namely BGRFI, knee flexion angle at initial contact, peak knee flexion angle, and ankle sagittal plane angle at initial contact. Increasing step rate has been previously purported to modify these risk factors of RRI, thus we hypothesized that step-rate based gait training would have a potentially protective effect on these risk factors.

Methods: A systematic literature search was performed on PubMed and Web of Science to identify studies meeting inclusion criteria and published before October 2022. Included studies sought to increase step rate during running in adult runners and measured associated changes in gait biomechanical measures. Methodological quality was assessed using the Physiotherapy Evidence Database (PEDro) scale. Pre-post comparisons of reported kinetic and kinematic variables were made for each intervention condition and meta-analyses with random effects model were performed to calculate pooled mean differences when possible, otherwise standard mean differences were calculated.

Results & Discussion: Nineteen original studies were included with a total of 422 individuals enrolled and a mean PEDro score of 4.95 (SD: 1.39) on a 10-point scale. Two studies measured changes in BGRFI in acute interventions, with a moderate standard mean difference decrease of 0.64 (95% CI: 0.29 to 1.00, I^2=0%, p=0.0004). This is a positive result and points to the effectiveness of the step rate intervention at decreasing this risk factor. Four studies measured the effect of a multisession intervention on knee flexion angle at initial contact, with a pooled increase of 4.32° greater knee flexion (95% CI: 0.92° to 7.73°, I^2=69%, p=0.01). Four studies measured the effect of a multisession gait training intervention on peak knee flexion angle with a pooled decrease of 3.31° less knee flexion (95% CI: 1.51° to 5.10°, I^2=0%, p=0.0003). Taken together, these changes point to a running pattern change with the knee being less flexed at peak and more flexed during touchdown. Considering decreased knee flexion angle at initial contact is a risk factor for RRI, this is a positive result. Five studies measured the effect of a multisession intervention on sagittal plane ankle angle at initial contact, with a pooled decrease of 2.29° less ankle dorsiflexion (95% CI: 0.80° to 3.78°, I^2=11%, p=0.003). This points to the adaptation of a footstrike pattern closer to the midfoot than the rearfoot.

Significance: Step-rate based gait training was effective at decreasing loading, as measured by BGRFI, and caused potentially beneficial changes in measures of peak knee flexion angle, knee flexion angle and sagittal plane ankle angle at initial contact. These results support the use of gait training aimed at increasing step rate to modify biomechanical measures associated with increased risk of RRIs, however prospective studies monitoring injury occurrence in runners before and after gait training are needed to determine if step-rated based gait training actually reduces the incidence of RRIs.

References: [1] Videbæk et al. (2015). *Sports Medicine*, 45(7), 1017–1026. [2] Willwacher et al. (2022). *Sports Medicine*, 52(8), 1863–1877. [3] Davis et al. (2020). *Current Reviews in Musculoskeletal Medicine*, 13(1), 103–114.

A SIMPLIFIED POINT-MASS FOOT PLACEMENT ESTIMATOR: EVALUATION AND POTENTIAL APPLICATIONS

Corbin M. Rasmussen[1*], Nathaniel H. Hunt[1]
[1]Department of Biomechanics, University of Nebraska at Omaha, Omaha, NE USA
*Corresponding author's email: cmrasmussen@unomaha.edu

Introduction: Compensatory stepping to stabilize the center of mass (CoM) is a crucial recovery strategy following balance perturbations [1]. As such, quantifying the compensatory stepping demands given destabilized CoM dynamics may be a useful proxy for perturbation severity and fall risk. One approach to identifying an "ideal" step location is the Foot Placement Estimator (FPE_D), which presumes physical pendulum dynamics and returns the step location that balances post-step total energy with peak potential energy at the unstable equilibrium point (i.e. vertical), resulting in a one-step recovery [2]. However, this method is labor- and computationally-intensive due to its basis in a distributed mass inverted pendulum model, which requires full-body kinematics. Therefore, as a first step, our aim was to derive a simplified point-mass FPE (FPE_P) attainable with simple marker sets [3,4] and compare it to the original FPE_D via simulation and in unperturbed walking to assess its relative potential for calculating ideal step locations.

Methods: FPE_P is grounded in the same assumptions as FPE_D (no double-limb support, sufficient friction at step contact, plastic step collisions, conservation of angular momentum) to calculate the step location that balances post-step total energy with peak potential energy [2]. However, only pre-step CoM vertical position z_1, vertical velocity $\dot{z}_1$, horizontal velocity $\dot{y}_1$, mass m, and gravity g are required to calculate FPE_P. Ideal step locations for a one-step recovery (y*) were compared across ranges of simulated z_1, $\dot{z}_1$, $\dot{y}_1$, and m values while other variables were held constant at 1.0 m for z_1, -0.2 m/s for $\dot{z}_1$, 1.2 m/s for $\dot{y}_1$, and 80 kg for m (Fig. 1). CoM motion state ranges spanned beyond those expected during walking to examine if model divergence occurred at the extremes. Maximum, mean, and minimum moments of inertia about the CoM (I_{CoM} =19.30, 13.37, and 5.15 kgm^2) and mean angular velocities (ω =3.17, 0.03, and -2.15 rad/s) from walking and slipping data were used to assess their influence on FPE_D-derived ideal step placements. Anteroposterior (AP) and mediolateral (ML) FPE_P and FPE_D time series were also calculated during unperturbed walking trials and normalized to the gait cycle. To assess the utility of a simplified marker set, two FPE_P models were built: one utilizing a full body marker set (FPE_P-full) and one using only anterior and posterior superior iliac spine markers (FPE_P-pel) [3] to estimate CoM kinematics. Model behaviors and predictions during walking were compared using Pearson correlation coefficients (R) and mean absolute errors (MAE) between each pair of FPE models within each trial, summarized here by means and standard deviations of each across all trials.

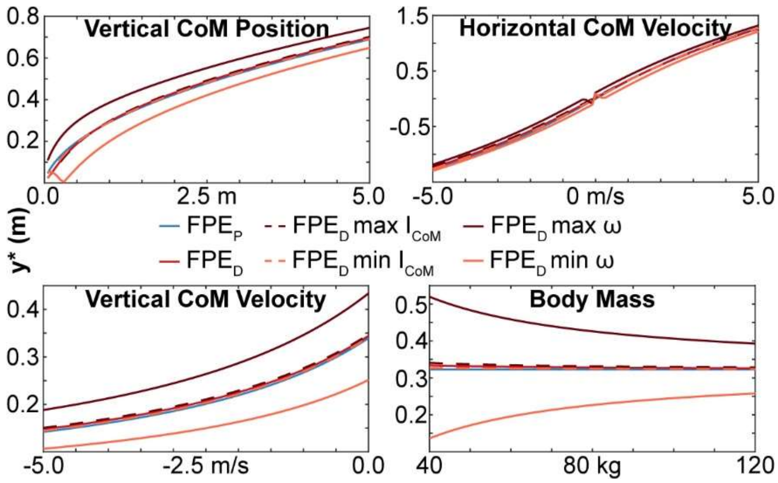

Figure 1: Ideal step positions calculated from the point mass model FPE_P and distributed mass model FPE_D across ranges of CoM motion state variables. Mean I_{CoM} and ω were used for FPE_D unless otherwise specified.

Results & Discussion: FPE_P and FPE_D models showed similar behaviors and close alignment across the simulated CoM motion state variable ranges at all levels of I_{CoM} and typical levels of ω, although extreme values of ω drove large deviations between models (Fig. 1). Body mass imparted a growing influence on FPE_D as it decreased, but had no effect on FPE_P predictions. During unperturbed walking, all models were in close agreement in the ML direction (Table 1). Correlations were generally weaker in the AP direction, but all mean MAEs were less than three centimeters (Table 1). These results suggest that simplified FPE_P models may provide sufficiently similar ideal step locations to the more comprehensive FPE_D, though caution may be needed during recovery from severe perturbations (i.e. when ω may be large).

Significance: We believe FPE_P could have utility for providing stepping targets, monitoring perturbation balance training progress, and quantifying perturbation severity all in a more accessible, user-friendly manner than provided by FPE_D. Planned next steps include evaluating models on compensatory stepping data and implementing FPE_P in a perturbation severity metric that provides a more complete picture of destabilization.

Acknowledgements: Research funded by NIH grants R15AG063106 and P20GM109090.

References: [1] Te et al. (2023), *Gait Posture* 100; [2] Wight et al. (2008), *J Comput Nonlinear Dyn* 3; [3] Whittle (1997), *Hum Mov Sci* 16; [4] Havens et al. (2018), *Gait Posture* 59.

Table 1: Summary statistics for FPE model comparisons during unperturbed walking.

Model Comparison	ML R (mean ± SD)	ML MAE	AP R	AP MAE
FPE_D to FPE_P-full	0.945 ± 0.111	0.007 ± 0.002 m	0.955 ± 0.036	0.027 ± 0.007 m
FPE_D to FPE_P-pel	0.915 ± 0.129	0.010 ± 0.004 m	0.656 ± 0.191	0.029 ± 0.006 m
FPE_P-full to FPE_P-pel	0.975 ± 0.017	0.006 ± 0.002 m	0.772 ± 0.145	0.015 ± 0.004 m

Portable instrumented assessment of dual task gait in mild cognitive impairment

Jamie B. Hall[1*], Jacob Thomas[1], Rylea Ranum[2], Andrew M. Kiselica[2], Rebecca Bliss[1], Trent M. Guess[1]
[1]Department of Physical Therapy, University of Missouri
[2]Department of Health Psychology, University of Missouri
[*]Corresponding author's email: halljami@health.missouri.edu

Introduction: 6.5 million Americans over 65 years of age have Alzheimer's disease (AD). Direct costs of care are estimated at $321 billion annually. [1] Developing detection methods for early disease stages, including mild cognitive impairment (MCI) are vital to addressing this public health crisis. Recent studies have demonstrated the ability of dual task gait assessment to discriminate between healthy older adults, older adults with mild cognitive impairment (MCI), and those with dementia. [2] Dual task assessment pairs a motor task with a cognitive task, often resulting in degradation of performance in 1 or both tasks. [3] A recent meta-analysis reported significant differences in velocity, stride length, and stride time between healthy older adults and those with MCI in a single task condition but reported even greater differences in a dual task condition (DT). [4] Authors reported counting tasks (e.g. serial subtraction by sevens) were more sensitive than verbal fluency tasks (e.g. listing months of the year) in the dual task paradigm. [4] Many studies using instrumented gait analysis during dual tasking in this population rely on expensive measurement systems such as marker-based capture systems or inertial motion unit systems which are not feasibly implemented in the general population. The inexpensive, portable Kinect Azure spatial sensor has been shown to accurately measure spatiotemporal gait parameters when compared with the gold standard Vicon marker-based motion capture system. [5] The purpose of this study was to assess the ability of a portable measurement platform using the Azure Kinect to detect differences in dual task gait between healthy older adults and older adults with a diagnosis of MCI.

Methods: Adults over 60 years old with and without a diagnosis of MCI were recruited for this study. Exclusion criteria included neuromuscular disease, recent injury or surgery which interferes with functional mobility, and use of assistive devices or above ankle orthoses. Participants were placed in the experimental group if they had a previous diagnosis of MCI or their Montreal Cognitive Assessment (MOCA) score was less than 24. [6] 20 healthy older adult controls (70.5 ± 5.4 years old, 13 females, 168.9 ± 9.5 cm, 81.35 ± 24.07 kg, MOCA score 27.8 ± 1.3) and 12 older adults with MCI (75.3 ± 6.4 years old, 8 females, 167.44 ± 13.14 cm, 76.85 ± 23.0 kg, MOCA score 24.6±2.7) participated. Data were collected using the Azure Kinect spatial sensor with body tracking SDK and custom algorithm to identify walking spatiotemporal parameters including bilateral stride length, step length, and stride time. Participants were instructed to walk 7.6 meters while performing serial subtraction by 7 from a random number. All participants completed 2 dual task walking trials. Data analysis was performed using IBM SPSS 28 software. Data from trials for each participant were averaged. Because data were not normally distributed, Mann Whitney U tests were used to compare groups. Post hoc testing included the Benjamini-Hochberg test to control for the false discovery rate. [7]

Results & Discussion: There was a significant difference between groups for left stride and step length (p=0.04, 0.04) during dual task gait; those with MCI having a significantly shorter left stride and step length than controls (p=0.04). Right stride and step length were also shorter but after post hoc adjustment were no longer statistically significant (p=0.06). [Table 1] Preliminary data suggest even with a small sample size, dual task gait differences are detectable between individuals with MCI and healthy older adult controls using the portable, inexpensive Azure Kinect spatial sensor. This study was likely underpowered and future work will include increasing sample sizes for both groups and using machine learning to better understand the relationship between dual task walking performance and other variables including age, MOCA score, health history, as well as measures of other motor/balance constructs.

Table 1: Dual Task Gait Spatiotemporal Parameters

Variable	**Median_Controls**	**Median_MCI**	**Unadjusted p-value**	**p-value**
Left Stride Length (mm)	1169.74	945.64	0.01*	0.04*
Right Stride Length (mm)	1168.70	1070.45	0.04*	0.06
Left Stride Time (sec)	1.20	1.22	0.82	0.82
Right Stride Time (sec)	1.16	1.25	0.21	0.28
Left Step Length (mm)	573.97	503.10	0.01*	0.04*
Right Step Length (mm)	594.00	522.25	0.03*	0.06

*****Statistically significant with $\alpha<0.05$

Significance: An inexpensive, portable measurement platform using the Azure Kinect spatial sensor was able to detect dual task differences between older adults with MCI and healthy controls. The ability to detect cognitive impairment associated with risk for AD with an inexpensive, portable measurement device may improve access to assessment, detection, and diagnosis of AD in the future. Ultimately, our goal is to use motor/balance function measures to increase early intervention, improving overall disease management, decreasing costs, and improving quality of life.

References: [1] 2022 Alzheimer's disease facts and figures [2022] *Alzheimers Dement* 18(4); [2] Åhman et al. (2020) *BMC Geriatrics* 20:258*;* [3] Bayot et al. (2018) *Clin Physiol* 48; [4] Bahureksa et al. (2017) *Gerontology* 63(1); [5] Guess et al. (2022) *Gait Posture* 96; [6] MOCA website at https://www.mocatest.org/faq/ ; [7] Benjamini (1995) *J R Stat Soc* 57(1)

DYNAMIC POSTURAL CONTROL WITH COGNITIVE TASK TEST IN FEMALE ATHLETES AND NON-ATHLETES

Alyssa Klump[1], Anisha Moorthy[1], Rianna Pfau[1], Yunju Lee[1,2*]
[1]Department of Physical Therapy and Athletic Training, Grand Valley State University, Grand Rapids, MI, USA
[2]School of Engineering, Grand Valley State University, Grand Rapids, MI, USA
*Corresponding author's email:leeyun@gvsu.edu

Introduction: Balance and postural control are key skills in athletic performance. Many intrinsic and extrinsic factors influence balance at various levels of sports as well as in different sports. Some of these extrinsic factors include the processing of cognitive information while the body's postural control measures are challenged. These can be referred to as cognitive perturbations, or external distractors. Successfully maintaining balance involves interactions between the visual, vestibular, and somatosensory systems. Equally important is the proprioceptive information from the joint which can be affected by factors such as injury. Competing in sports requires varied levels of dynamic balance depending on sport type, level, and playing conditions and involves input from these different systems constantly. The American College of Sports Medicine recently added balance performance as a part of its guideline for physical fitness and balance training has recently become a regular part of many sports training programs [1]. Howell et al. studied tandem gait speed with dual cognitive tasks between collegiate male and female athletes [2]; however, there was a lack of studies for balance control among female athletes. Hof et al. [3] suggested that an extrapolated center of mass (XCoM), which accounts for the velocity of the COM, could be a better parametric measure in dynamic measures of balance. So, the purpose of this study was to quantify dynamic postural control in female collegiate athletes and compare these findings to postural control in healthy non-athlete counterparts. We hypothesized that female athletes would demonstrate greater dynamic postural control as evidenced by quicker task completion times and better accuracy with added cognitive distractors compared to non-athlete peers.

Methods: Female athletes and non-athlete controls aged 18-30 were recruited from GVSU and the Grand Rapids area. Thirty-two female subjects were recruited; 16 athletes (20.3±1.13 yrs; 70.2±10.70 kg; 168.4±7.03 cm), 16 non-athletes, (22.1±2.25 yrs; 62.6±8.61 kg; 165.7±6.12 cm) and participated in data collection. To increase external validity, athletes from different sports and experience levels were recruited. In order to qualify as an athlete, participants had to be actively involved in a club or varsity sporting team on campus. Each participant completed dynamic balance tasks with single and dual task conditions while wearing seventeen Xsens sensors on major anatomical landmarks. Dynamic balance tasks included overground gait at a self-selected pace over force plates as well as tandem gait along a 3-meter-long piece of tape. Cognitive tasks for both tandem and normal gait included spelling 5-letter words backwards, subtracting by 7's, or reciting months of the year in reverse order. A combination of single and dual trials was completed for each task ensuring proper contact with force plate and piece of tape. Data was collected using force plates for center of pressure (COP), Xsens sensors for center of mass (COM) and a combination for calculation of margin of stability (MOS) in the anterior-posterior (AP) direction and the medial-lateral (ML) direction. Two-way repeated measures ANOVA was performed with alpha level set at 0.05.

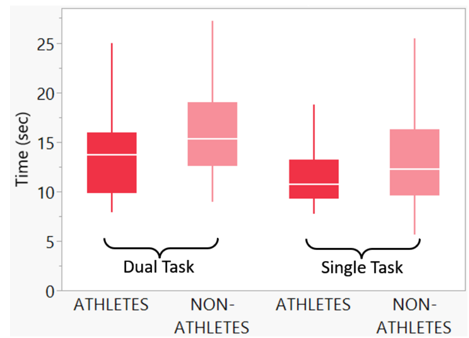

Figure 1: Box and whisker plot of time to complete tandem walking by athletes and non-athletes performing single and dual tasks.

Results & Discussion: The time to complete tandem walking between athletes and non-athletes was statistically significant (12.5±0.46 vs. 15.55±0.46 sec, $p<0.01$) as well as between all subjects performing a dual vs. single task (15.52±0.46 vs.12.54±0.46 sec, $p<0.01$). The result showed that the athletes had quicker completion times compared to non-athletes and all subjects took longer to complete tandem walking while performing a cognitive task. There is no interaction effect between group and task although the trend appears to be towards athletes having quicker completion times for both single and dual tasks compared to non-athletes (Fig. 1). These findings supported our hypothesis that female athletes demonstrated greater dynamic postural control during tandem walking. During gait, the excursion and range of COP-AP were significantly larger among female athletes than non-athletes, while the same outcomes of COP-ML were reduced in female athletes. The MOS-AP and MOS-ML showed reverse results comparing to the COP data. The finding in gait with dual-task tests supported that the female athletes walked faster and towards AP direction therefore they performed greater margin of stability and better dynamic control in the walking direction comparing to the female non-athletes.

Significance: Our goal with this research was to establish a baseline data set of postural control measures in female athletes at the collegiate level to understand how dynamic postural control ability differs among athletes and non-athletes. The results of this study could be used to guide future research looking at various types of balance and postural control in female athletes as well as between different sports. Ultimately, we will have an increased understanding of if and how postural control is different in female athletes in various contexts. This information can be used for clinical practice as well as for training and coaching of athletes on the field.

Acknowledgements: This study was supported by a research grant program of the American Physical Therapy Association (APTA) Michigan Institute for Education and Research, Inc.

References: [1] Chander et al. (2015), *J Sports Sci 2;* pp.13-20. [2] Howell et al. (2017), *Clin J Sport Med 27(5)*; pp. 444-449. [3] Hof, et al. (2005), *J Biomech* 38; pp. 1-8.

THE EFFECT OF ACUTE CERVICAL TRACTION EXERCISES ON THE STIFFNESS OF THE UPPER TRAPEZIUS AND MIDDLE SCALENE MUSCLES

Elise Walker[1*], Constantin Heinemann[2], Whitney L. Wolff[3], David B. Lipps[1]
[1]School of Kinesiology, University of Michigan; [2]Department of Kinesiology, East Carolina University; [3]Department of Kinesiology and Community Health, University of Illinois Urbana-Champaign;
*Corresponding author's email: welise@umich.edu

Introduction: Idiopathic chronic neck pain is one of the most common musculoskeletal disorders, with an annual prevalence rate exceeding 30 percent of adults worldwide [1]. Increased stiffness of neck musculature is a common symptom of idiopathic chronic neck pain [2]. Cervical traction is a common intervention used in physical therapy to manage idiopathic chronic neck pain. Cervical traction decreases muscular and radicular pain in the neck by increasing the intervertebral space between the cervical vertebrae [3]. However, the effect of cervical traction on muscle stiffness remains unclear. The stiffness of individual neck muscles can be estimated by recording shear wave velocity over the muscle belly with ultrasound shear wave elastography [4]. The purpose of this study was to determine the effect of supine cervical traction on shear wave velocity of the upper trapezius (UT) and middle scalene (MS) in participants with idiopathic chronic neck pain and to quantify the load relaxation relationship response of the UT and MS within a single set of five-minute traction applications. We hypothesized that the shear wave velocity of the UT and MS would decrease in response to cervical traction in participants with idiopathic chronic neck pain and healthy controls. Additionally, we hypothesized that muscle stiffness of the UT and MS would be higher in the idiopathic chronic neck pain participants before and after cervical traction.

Methods: This study enrolled 18 participants with self-reported chronic neck pain (4 M, 14 F; age: 55.2(20.4) yrs; height: 170.2(11.6) cm; weight: 66.9(11.6) kg; Neck Disability Index (NDI) score 11.6(.1)) and 17 healthy matched controls (5 M, 12 F; age: 60.7(17.1) yrs; height 169.1(8.9) cm; weight: 65.5(11.6) kg; NDI score .71(1.1)). The study was approved by our local IRB, and all participants provided written informed consent. Shear wave velocity data were collected with an ultrasound shear wave elastography machine (Supersonic Mach 30, Hologic) in the UT and MS muscles in all participants. Two locations from the UT were examined: UTN was measured slightly lateral and inferior to the spinous process of the C4 vertebrae, and UTS was found at the midpoint between the C7 spinous process and the acromion process. Before beginning cervical traction, passive unloaded shear wave elastography images were collected. Participants then laid supine within a cervical traction device (Evertrac CT800). Six sets of cervical neck traction were applied in 5-minute increments at 9 kg. During each set of traction, images were acquired from one unilateral muscle location after 2.5 and 5 minutes of traction. The order of the six muscle locations was randomized, with five minutes of rest between each bout. Following the traction sets, another unloaded set of images was collected. Linear mixed effects models for each muscle (MS, UTN, UTS) assessed the influence of time (pre-traction, 2.5 minutes, 5 minutes, and post-traction), sex (male, female), side (left and right), and group (chronic neck pain, healthy controls) on the magnitude of shear wave velocity. Bonferroni adjustments were made for any multiple comparisons.

Results & Discussion: Mean shear wave velocity of both portions of the UT were significantly affected by time during neck traction (both $F_{3,55}>12.8$, $p<0.001$) **(Figure 1A)**. Compared to before traction, the shear wave velocity of UTN and UTS were significantly reduced after 2.5 minutes and 5 minutes of traction (all $p<0.001$). The shear wave velocity of UTN and UTS then increased from the 5-minute mark to the post-test measurement (both $p<0.001$), returning to values that were not significantly different from the pre-traction collection (both $p>0.339$). There was also a significant interaction between sex and time for the shear wave velocity of UTS ($F_{3,55}=2.8$, $p=0.043$). This interaction revealed that women had lower UTS stiffness when compared to men both before traction and after traction **(Figure 1B)**. There were no significant effects of time, sex, or group on the shear elastic modulus of the MS in response to neck traction.

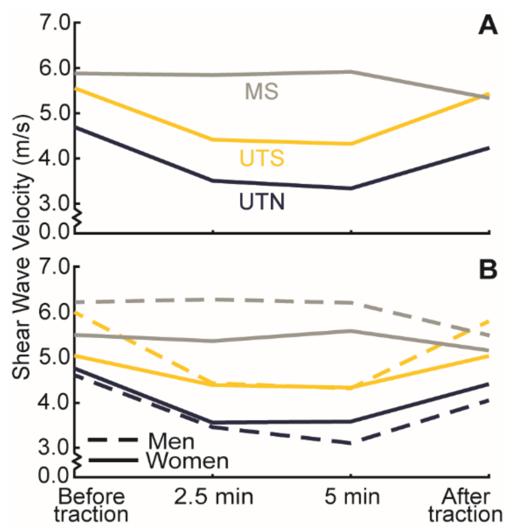

Figure 1: Mean shear wave velocity before, during, and after cervical traction for (A) all participants and (B) separated by sex.

Our findings agreed in part with our hypotheses. Cervical traction exercises decreased muscle stiffness in UTN and UTS in individuals with chronic neck pain and matched healthy controls. However, no significant differences were found within the MS muscle. Interestingly, men were seen to have a greater change in muscle stiffness due to an acute bout of traction when compared to women. However, women had an overall lower UTS muscle stiffness. A limitation of this study is that shear wave velocity was only recorded from one traction session. Future research could expand upon the long-term results of the change in muscle stiffness across multiple recurring traction sessions.

Significance: This study supports cervical neck traction as an intervention to reduce stiffness of the upper trapezius muscles during physical rehabilitation. The significant decrease in muscle stiffness found here provides new mechanistic insights into how cervical traction can benefit clinical care and pain management.

Acknowledgements: University of Michigan Rackham Graduate Student Research Grant

References: [1] Cohen (2015), *Mayo Clin Proc.* 90(2); [2] Tas et al. (2018), *J Manipulative Physiol Ther.* 41(7); [3] Jellad et al. (2009), *Ann Phys Rehabil Med.* 52(9); [4] Wolff et al. (2016), *J Biomech*, 141.

BIOMECHANICAL DIFFERENCES BETWEEN RECREATIONAL AND COLLEGIATE RUNNERS

Ryan J. Evans[1*], Tyler J. Moffit[2], Peter K. Mitchel[3], Derek N. Pamukoff[1]
[1]Western University, London ON
[2]California State University, Bakersfield; Bakersfield CA
[3]California State University, Fullerton CA
*Ryan Evans email: revans44@uwo.ca

Introduction: Running is a popular form of physical activity due to its high level of accessibility [1,2,3], and serves as a recreational and competitive activity. The summed action of the ankle, knee, and hip extensors (i.e. total support moment, TSM) contribute to propulsion during running [3,4]. Moreover, the ankle plantar flexors contribute the largest component of extensor work compared with the knee and hip extensors in distance running [3]. As such, lower ankle plantar flexor moments during propulsion and increased reliance on the knee and hip extensors in recreational runners may contribute to performance deficits, varying injury risk, and slower speed when participating in distance running [3]. Identifying joint distribution proportions of the TSM could provide insight into locomotive strategies of different populations. The purpose of this study was to compare the total support moment and extensor moment distributions during running between recreational and collegiate distance runners. We expected that all moments would be higher in the collegiate group with the proportion of ankle moment as a percent of the total support moment would also be higher in the collegiate group.

Methods: A sample of 35 collegiate (male=26, female=9) and 28 recreational (male=23, female=5) runners between the ages of 18 and 35 from the university cross country team, student population, and local running groups that were free from lower body injuries were recruited for the study. Collegiate runners were on an intercollegiate team or had been in the preceding year while recreational runners were those running up to 3 times a week for a minimum of 16 km. Participants underwent a single visit including a 5-minute treadmill running warmup, familiarization trails, and 5 overground running trials at a self-selected speed. Participants wore standardized footwear and were outfitted with reflective markers on their dominant limb. Running trials took place on a 20-meter runway using a 9-camera motion capture system (240Hz) and force pate (2400Hz) that recorded running biomechanics of the dominant limb at a self-selected pace (±5%). Visual 3D was used for model construction. Marker trajectories and ground reaction forces were low pass filtered at 20Hz. Inverse dynamics procedures were used to derive internal hip, knee, and ankle joint moments. One-way multivariate analyses of variance were used to compare extensor moments (BWxHt and %TSM) between groups that were and were not adjusted for running speed.

Results & Discussion: Normalized extensor moments differed between groups (Pillai's trace = 0.342, $F(58,4)=7.5421$, $p<0.001$). Post hoc comparisons indicated that the TSM ($p<0.001$), plantarflexor moment ($p=0.004$), knee extensor moment ($p=0.033$), and hip extensor moments ($p=0.040$) were greater in the collegiate group compared with the recreational group (Table 1). When adjusted for speed, the normalized knee extensor moments differed between groups (Pillai's trace = 0.204, $F(57,4)= 3.648$, $p=0.01$). Post hoc comparisons indicated that the TSM ($p=0.002$) and plantarflexor moment ($p=0.029$) were greater in the collegiate group. However, the knee extensor moment ($p=0.984$) and hip extensor moment ($p=0.064$) did not (Table 1). Individual joint contributions to TSM did not differ when unadjusted for speed (Pillais's trace = 0.073, $F(60,2)=2.349$, $p=0.104$) for the plantarflexor moment ($p=0.033$), knee extensor moment ($p=0.235$), and hip extensor moment ($p=0.468$). When adjusted for speed, the extensor contributions to TSM differed between groups (Pillai's trace = 0.106, $F(59,2)=3.503$, $p=0.037$). The plantarflexor moment was greater ($p=0.037$) but the knee extensor moment was lower ($p=0.018$) in the collegiate compared with recreational runner group (Table 1). This difference in joint contributions between recreational and collegiate level runners may contribute to differences in running ability. Greater proportional use of the ankle joint in collegiate runners rather than the knee seen in recreational runners during propulsion may be a more efficient propulsive strategy.

Significance: A larger contribution from the ankle joint during propulsion may allow for a larger capacity to increase running speed. In faster running and sprinting, the use of larger muscles groups such as the hip extensors are more prevalent [5]. Therefore, at slower running speeds, the use of the ankle joint may be a more efficient propulsion strategy by allowing for larger muscle groups to contribute less. Recreational runners may be able to increase their running speed through greater plantarflexion during propulsion.

References: [1] Ceyssens et al. (2019), *Sports Medicine 49*(7); [2] Derrick TR. (2004), *Med Sci Sports Exerc* (36); [3] Novacheck TF. (1998) *Gait & Posture*; [4] Winter DA. (1980), *J Biomechanics* (13); [5] Schache et al. (2015), *J Experimental Biology* (218)

Table 1: Mean (95% confidence interval) of TSM, Plantar Flexor Moment, Knee Extensor Moment, and Hip Extensor Moment controlled for body weight and height and the Plantar Flexor Moment, Knee Extensor Moment, and Hip Extensor Moment as a percentage of TSM for collegiate and recreational groups adjusted and unadjusted for speed.

	Not Adjusted for Speed		**Adjusted for Speed**	
	Rec (n=28)	Collegiate (n=35)	Rec (n=28)	Collegiate (n=35)
Total Support Moment (BWxHt)	0.319 (0.299, 0.339)	0.393 (0.375, 0.411)	0.329 (0.305, 0.352)	0.385 (0.365, 0.406)
Plantar Flexor Moment (BWxHt)	0.125 (0.109, 0.141)	0.156 (0.142, 0.170)	0.125 (0.107, 0.144)	0.156 (0.140, 0.172)
Knee Extensor Moment (BWxHt)	0.176 (0.162, 0.189)	0.196 (0.183, 0.208)	0.187 (0.172, 0.202)	0.187 (0.173, 0.200)
Hip Extensor Moment (BWxHt)	0.019 (0.002, 0.035)	0.041 (0.027, 0.056)	0.016 (-0.003, 0.036)	0.043 (0.026, 0.060)
Plantar Flexor Moment (%TSM)	0.354 (0.325, 0.382)	0.395 (0.370, 0.421)	0.347 (0.314, 0.381)	0.4 (0.371, 0.429)
Knee Extensor Moment (%TSM)	0.519 (0.486, 0.552)	0.493 (0.464, 0.522)	0.541 (0.504, 0.578)	0.475 (0.443, 0.507)
Hip Extensor Moment (%TSM)	0.127 (0.096, 0.159)	0.112 (0.084, 0.140)	0.111 (0.075, 0.147)	0.125 (0.093, 0.156)

EFFECT OF WALKING SPEED AND RHYTHMIC AUDITORY STIMULATION ON SPATIOTEMPORAL PARAMETERS DURING TREADMILL WALKING IN CHILDREN AND ADULTS

Haneol Kim[1*], Zac Wicks[1], Robert Zeid[1], Jianhua Wu[1]
[1]Georgia State University
*Corresponding author's email: hkim162@student.gsu.edu

Introduction: One adapts to the environment and task constraints during walking with complex neuromuscular coordination (muscle activation and joint coordination) [1]. Since walking is a rhythmic/cyclic movement, rhythmic auditory stimulation (RAS) has been shown to affect gait patterns, to a greater extent, compared to other sensory stimulation. Despite the complexity of gait, healthy individuals can synchronize rhythmic movement to auditory cueing or external rhythm [2] and produce consistent movement patterns under different environmental conditions [3]. Previous RAS studies reported beneficial effects on spatial and temporal gait parameters in clinical populations. However, few studies have been conducted to compare spatiotemporal variables between children and adults while walking on the treadmill at different speeds and/or under various RAS frequencies.

The purpose of this study was to compare the effect of treadmill walking speed (TWS) and RAS frequencies on spatiotemporal gait parameters between healthy children and young adults. We hypothesized that stride length will increase but will decrease with increasing walking speed. Also, we hypothesized that stride time will decrease with increasing TWS and RAS frequency.

Methods: Twenty healthy young adults aged 18 to 35 years (YA: 10M/10F) and ten typically developing children aged 7 to 11 (TD: 6M/4F) participated in this study. Participants walked at their preferred speed on a 10-meter walkway three times. The average walking speed across three trials was used to set treadmill speeds. A 9-camera Vicon motion capture system and a lower-body model of marker placement were used to collect the kinematic data. A Zebris FDMT-S instrumented treadmill was used to collect the kinetic data.

A baseline trial with 100% TWS and 100% RAS was collected first. In study 1, only walking speed was manipulated: 75% TWS and 125% TWS at the same 100% RAS. In study 2, only the RAS frequency was manipulated: 75% RAS and 125% RAS at the same 100% TWS. Adequate rest was provided between trials to minimize fatigue.

Spatiotemporal gait parameters included normalized stride length, stride time, stance time, and swing time. Two-way (2 Group × 3 Condition) mixed ANOVAs were conducted for each study at a significance level of α = 0.05. Post-hoc pair-wise comparisons were completed if necessary.

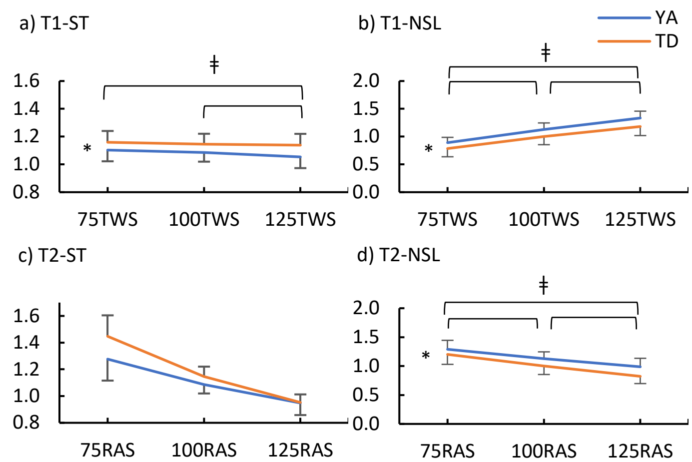

Figure 1: Mean and SD of stride time (ST) and normalized stride length (NSL) with various treadmill walking speeds at preferred metronome cueing conditions in study 1 (T1: a and b) and with various rhythmic auditory stimulation frequencies at a preferred walking speed in study 2 (T2: c and d). The symbol * indicates a group difference and ǂ indicates a condition difference at $p < 0.05$. YA: young adults; TD: typically developing children.

Results & Discussion: In study 1, stride time decreased across the three TWS conditions for healthy young adults and typically developing children (Fig. 1a). There was a group effect (p=0.028) and a condition effect (p=0.003). Children showed a longer stride time than adults across the TWS conditions. Normalized stride length increased across the TWS conditions for both groups (Fig. 1b). Healthy young adults showed a greater normalized stride length than children (p=0.011) across TWS conditions. There was a condition effect in normalized stride length with increased TWS (p<0.001).

In study 2, stride time decreased across the three RAS conditions for both groups (Fig. 1c). There was an interaction effect (p=0.004). Children showed a longer stride time than adults in the lower RAS conditions. Normalized stride length decreased across the RAS conditions for both groups (Fig. 1d). Young adults had a greater normalized stride length than children (p=0.016) across RAS conditions and there was a condition effect in normalized step length with increased RAS (p<0.001). Overall, both healthy young adults and typically developing children demonstrated similar patterns with various TWS and RAS.

Significance: Spatiotemporal variables such as stride time and normalized stride length were affected by various TWS and RAS frequencies in young adults and children. Increasing TWS induced increased stride length and decreased stride time. However, increasing RAS induced opposite trends such that both children and adults decreased stride time. Further, a significant difference between children and adults indicates that age is an important factor in gait development and adaptation. These preliminary results provided important baseline data on how children and adults adjust their gait patterns to adapt to various TWS and RAS conditions. This can be helpful when analyzing auditory-motor synchronization in people with disabilities.

Acknowledgements: We are grateful to all the participants for volunteering their participation. This study was partially supported by the Georgia State University Provost's Dissertation Fellowship program.

References: [1] Desrochers & Gill (2021). *Hum Mov Sci*. 77: 102798; [2] Hunt et al. (2014). *Sci Rep*. 4: 1-6; [3] Musselman et al. (2011). *J Neurophysiology*. 105: 2195-2203.

WHAT IS THE INTERACTION AMONG MEASURED MUSCLE VOLUME, JOINT TORQUE, AND JOINT POSITION AT THE ANKLE, KNEE, AND HIP?

Mario E. Garcia[1*], Emily M. McCain[1], Xiao Hu[1], Shawn D. Russell[1], Silvia S. Blemker[1]
[1]University of Virginia, Charlottesville, VA, USA
*Corresponding author's email: nfq3bd@virginia.edu

Introduction: Computational modeling has become a ubiquitous tool for examining musculoskeletal injury and disease, and according to lumped parameter models [1], muscle volume is a major determinant of force. Empirical studies have shown that, across individuals, maximum voluntary joint torques correlate with the summation of corresponding muscle volumes [2]. Height and mass have also shown a correlation with muscle volumes [3], however these relationships are influenced by sample populations (predominantly males/athletes/disease states). The relationship between muscle volume and joint torque varies across joints, and advancements in *in vivo* magnetic resonance imaging (MRI) allow for improved accuracy in individual and grouped muscle volumes. Reduced scanning time allows for lower limb assessment in a single MRI session; permitting large-scale studies of musculoskeletal structure. The musculoskeletal modeling community can now move to large scale questions such as: do correlations between muscle volume and torque differ across joints and joint angles? **This study probes the interaction among muscle volume, joint torque, and joint position by measuring lower extremity muscle volumes as well as ankle, knee, and hip joint torque at varied angles.**

Methods: Five female subjects were recruited between the ages of 20-39 (26.2±2.28 years) within five height (1.63±0.07 m) and BMI (70.44±26.95 kg) categories [4]. <u>Dynamometry</u>: Following a five-minute self-selected walking speed trial, subjects completed 2 repetitions of a three-second maximal isometric voluntary contraction (MVIC) for ankle plantar/dorsiflexion ($\theta_{Ankle,PF}$), knee extension/flexion ($\theta_{Knee,E}$), standing hip extension/flexion ($\theta_{Hip,F}$), and standing hip ab/adduction ($\theta_{Hip,AB}$) of the right leg (**Fig 1B**) using Biodex System 4 dynamometer (Biodex Medical Systems Inc.). Each trial and joint angle was randomized and followed with a one-minute recovery. During each standing hip trial, a Donjoy T-ROM knee brace locked the knee at 0°. <u>Muscle volumes:</u> Subjects laid supine during a two-point Dixon sequence with a field of view: 280 mm x 450 mm, slice thickness: 5 mm, and in plane spatial resolution: 1.1 mm x 1.1 mm, 3T MRI scanner (Trio, Siemens, Munich Germany) to identify bone and muscle boundaries. This scan allowed for volume calculations of muscle and non-contractile tissue through a deep convolution neural network-based segmentation method, previously developed by the PI and collaborators [5], and manual vetting (Springbok Analytics, Charlottesville, VA). Individual muscle volumes were determined from the segmentations, and then summed across functional groups. <u>Analysis:</u> Peak torques were extracted from raw dynamometry data using MATLAB (MathWorks), where average peak torque was calculated for each angle and joint direction (n=5). Muscle group volume as a predictor of peak torque was analyzed using linear regression (MATLAB). Corrected muscle volumes were calculated by removing fat infiltration mass from muscle group volumes.

A) Averaged Joint Torque (Nm)

PF Angle	ANKLE PF	ANKLE DF	EX Angle	KNEE EX	KNEE FX	FX Angle	HIP FX	HIP EX	AB Angle	HIP AB	HIP AD
0°	78.22	10.08	15°	30.88	82.80	0°	89.76	69.18	0°	76.94	34.40
15°	51.16	19.14	40°	74.52	73.30	15°	88.38	79.62	10°	60.66	69.26
30°	38.70	25.84	65°	123.82	64.68	30°	79.20	112.96	20°	42.78	95.38
45°	25.86	22.22	90°	153.06	50.18						

Torque to Volume (Nm/mL) Regression R^2 Values

PF Angle	ANKLE PF	ANKLE DF	EX Angle	KNEE EX	KNEE FX	FX Angle	HIP FX	HIP EX	AB Angle	HIP AB	HIP AD
0°	0.430	0.409	15°	0.936	0.938	0°	0.359	0.664	0°	0.321	0.623
15°	0.682	0.820	40°	0.881	0.899	15°	0.489	0.433	10°	0.233	0.360
30°	0.822	0.858	65°	0.286	0.743	30°	0.741	0.700	20°	0.083	0.517
45°	0.451	0.765	90°	0.130	0.003						

Max Torque Min / Min R^2 Max

B)

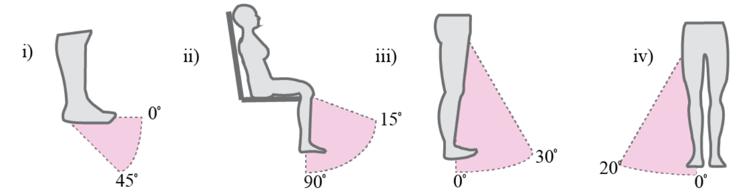

Figure 1: A) Visual representation of the average torque (n=5) and linear regression values for all joint directions at measured angles (R^2 p-values < 0.05 shown in white). **B)** Complete range of motion and torque direction for the ankle plantar flexion (i), knee extension (ii), hip flexion (iii), and hip abduction (iv).

Results & Discussion: Correlations between peak torques did not always align with increased R^2 (**Fig 1A**). For θ_{Knee}, peak torque occurs at 90° in extension and at 15° for flexion, while the highest R^2 occurs at 15° for each joint direction. Corrected muscle volumes were also considered; however, these volumes led to lower R^2 values for $\theta_{Ankle,PF}$, $\theta_{Knee,E}$, and $\theta_{Hip,AB/AD}$. These results suggest scaling relationships between muscle size and strength are complicated by each muscles force-length properties at a given joint angle. Decreased correlation between volume and torque in a female population may be due to sex differences in storage of adipose, where females traditionally store adipose in peripheral regions such as the lower limb [6].

Significance: A substantial repository of sex specific muscle volumes and MVICs for a healthy normal distribution of the US population has not been collected. This study is the beginning of a larger project aiming to generate a sex-specific repository of muscle volumes and MVICs across N=50 males and N=50 females and through collection and analysis, we plan to address the importance of sex as a biological variable.

Acknowledgments: Research funded by NIH Award T32GM145443 and NIH Grant #R01AR078396.

References: [1] Zajac et al. (1990), *Mult. Musc. Sys. Biomech.* [2] Holzbaur et al. (2007), *J Biomech* [3] Handsfield et al. (2014), *J Biomech* [4] Fryar et al. (2016), *Vital Health Stat* [5] Ni et al. (2019), *J Med Imaging* [6] Karastergiou et al. (2012), *Biol Sex Differ*

DIFFERENT CONTEXTS CONSTRAIN COORDINATION DYNAMICS BETWEEN WINNING AND LOSING TEAMS

Seung Kyeom Kim[1*], Nicholas Stergiou[1], Aaron D. Likens[1]
[1]Department of Biomechanics, University of Nebraska at Omaha, Omaha, NE USA
*Corresponding author's email: seungkyeomkim@unomaha.edu

Introduction: Inter-team team coordination dynamics (TCD) that emerge within the context of invasion team sports (e.g., basketball, soccer) provide rich information about landmark game events [1]. Previous research has studied inter-team TCD by applying analyses that quantify team dynamics as having unvarying, periodic behavior [2]. However, the interactions that occur in the constantly changing context of invasion team sports are nested within multiple scales (inter-individual, intra-team, inter-team). Hence, understanding inter-team TCD requires investigations that account for those multi-scale relationships. Following previous work [3], we hypothesized that inter-team TCD vary as a function of temporal scale. To investigate that hypothesis, we studied scale-wise relative phase dynamics between winning and losing basketball teams prior to scored baskets.

Methods: The time series of players' coordinates and critical game events of each game were analyzed from the 2015-2016 NBA season [3]. On both long and short axes, the arithmetic means of each team's player coordinates were utilized as a collective measurement to capture each team's dynamics. To investigate the inter-team TCD, continuous relative phase (ϕ) between the two centroids of both teams was computed. ϕ was then averaged ($\bar{\phi}$) for scales from 1 second up to 23 seconds, depending on the length of each scoring sequence. Scoring sequences shorter than 3 seconds (e.g., fast break after steals) were excluded to focus the analysis on gameplays driven by team coordination. Finally, the joint effects of time scales, point values (2-point shots and 3-point shots), scoring teams (winning teams and losing teams) on $\bar{\phi}$ were examined via linear mixed effect models on both axes. Our baseline model contained linear, quadratic, cubic trend of time scales. The fixed effects of point values and scoring teams and all possible interactions among the predictor variables were sequentially added. Model improvement was evaluated with likelihood ratio tests.

Results: Our models seem to fit observed data well, except for at large time scales (> 20 seconds; Fig. 1). Due to limited space, we only summarize the highest order interaction that was observed in the best fitting model for each axis. As follow-up analyses, we performed simple slope analyses and simple slope comparisons. On the long axis, the acceleration of $\bar{\phi}$ across time scales was greater when scoring 3-points compared to when scoring 2-points ($p < .001$). In addition, the acceleration of $\bar{\phi}$ across time scales was larger when losing teams scored relative to when winning teams scored ($p = 0.034$). The rate at which $\bar{\phi}$ changed across time scales when winning teams scored 3-points was greater when they scored 2-points ($p < .001$). Lastly when scoring 3-points, $\bar{\phi}$ increased faster when winning teams scored compared to when losing teams scored ($p < .001$). On the short axis, $\bar{\phi}$ of the winning teams was closer to 0 when they scored 2-points relative to when they scored 3-points ($p < .001$).

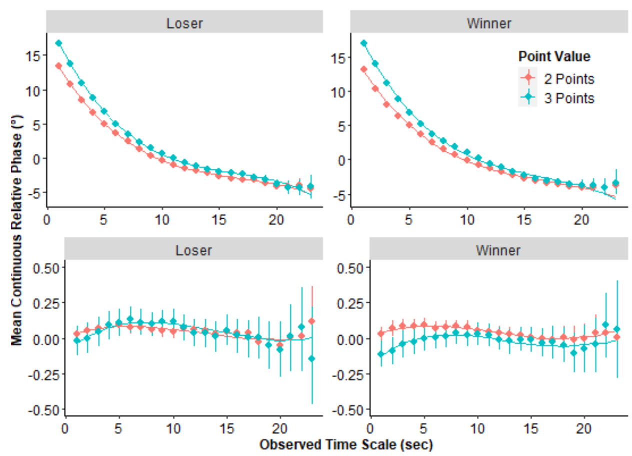

Figure 1: Mean continuous relative phase ($\bar{\phi}$) at each time scale and the best fitting models. Top panels: mean $\bar{\phi}$ on the long axis. Bottom panels: mean $\bar{\phi}$ on the short axis.

Discussion: Consistent with our hypothesis, $\bar{\phi}$ seems to rely on the time scale at which it is observed, along with point values and scoring teams. The dissimilar effect of scoring teams on the inter-team TCD infers that winning teams and losing teams use different game tactics. The difference in the acceleration of $\bar{\phi}$ may hint to distinct temporal features of strategies that break the balance between the two teams. Specifically, losing teams may be typically using strategies that aim to shake off their opponent's defence in a shorter time scale compared to the strategies of winning teams. Gameplay differences also seems to be determined by point values. Compared to scoring two points, the goal of scoring three points as a constraint may have led the scoring team to adopt strategies that increases the rate of change in phase leading on the long axis. Our results suggest that there may be specific TCD that enhance efficacy of scoring and determine the game outcome.

Significance: The current results reveal fundamental information about inter-team coordination TCD in invasion team sports. By analyzing the behaviors across multiple scales, we will be able to answer questions on how certain behaviors of teams lead to superior outcomes in different contexts of invasion team sports while others fail. Ultimately, the answers to those questions will help sports teams design tactics that are optimal to their team and let them win their games. Implications of our results are not limited to invasion team sports but may generalize to environments where a number of teams have to achieve a common goal, such as medical and military teams.

Acknowledgements: NSF 212491, NIH P20GM109090, R01NS114282, University of Nebraska Collaboration Initiative, the Center for Research in Human Movement Variability at the University of Nebraska at Omaha, NASA EPSCoR, IARPA.

References: [1] Duarte, R., et al (2012), *Human Movement Science* 31(6); [2] Gorman, J. C., et al (2022), *Human Factors*; [3] Likens, A. D., et al (2014); [4] https://github.com/sealneaward/nba-movement-dat

ASSOCIATION BETWEEN LOWER EXTREMITY MUSCULAR RECOVERY AND PHYSCOLOGICAL IMPROVEMENT IN PATIENTS WITH POST-ACUTE SEQUELAE OF SARS-COV-2 UNDERGOING NEUROMODULATION: A DOUBLE-BLIND RANDOMIZED CONTROLLED TRIAL

Myeounggon Lee[1,†], Alejandro Zulbaran-Rojas[1,†], Rasha Bara[1], Areli Flores-Camargo[1], Ram kinker Mishra[1], Gil Spitz[2], Dipaben Modi[3], Fidaa Shaib[3], Bijan Najafi[1,*]

1 Interdisciplinary Consortium on Advanced Motion Performance (iCAMP), Division of Vascular Surgery and Endovascular Therapy, Michael E. DeBakey Department of Surgery, Baylor College of Medicine, Houston, Texas, USA
2 Baylor St Luke's Medical Center, Exercise Physiology, Liver Transplant Program, Houston, Texas, USA
3 Pulmonary Care Medicine, BCM, Houston, TX
† Both authors shared first-authorship
*Corresponding author's email: bijan.najafi@bcm.edu

Introduction: Post-Acute sequelae of SARS-CoV-2 (PASC) can lead to persistent symptoms of muscle deconditioning in the lower extremities (LE) among COVID-19 patients who have a history of severe illness and currently have no evidence-based treatment options [1]. As a result, affected individuals may experience reduced physical activity and psychological distress [2]. Studies have shown that lower extremity (LE) electrical stimulation (E-Stim) can effectively activate muscles and enhance endurance and strength [3,4]. In this 4-week double-blinded, randomized controlled trial, we investigated if the potential efficacy of daily home LE E-Stim in addressing muscle deconditioning can lead to an improvement of psychological distress in COVID-19 patients with a history of severe illness.

Methods: Eligible participants who had a history of severe COVID illness and persistent lower extremity (LE) PASC were randomly assigned to either an intervention group (IG) or a control group (CG). The IG self-administered daily one-hour E-Stim to the gastrocnemius muscle (GAS) using a wearable functional E-Stim device (Tennant Biomodulator®, Avazzia Inc., Dallas, TX, USA) with four-electrode adhesive pads, placed on each leg's proximal and distal regions, for a 4-week period. The CG used an identical but non-functional device (placebo) during the same period. Primary outcomes were assessed using surface electromyography sensors (sEMG, Delsys Trino Wireless EMG System, MA, USA) placed on both lateral GAS, measuring GAS strength (GASs) during a maximum voluntary contraction (MVC) test [3,5], and GAS endurance (GASe) during 5-min of E-Stim [4]. Secondary outcomes included psychological characteristics such as anxiety and cognitive function, evaluated using the Beck Anxiety Inventory (BAI) and Montreal Cognitive Assessment (MoCA) questionnaires, respectively. Data were collected at baseline and four weeks, and delta (Δ) change was obtained. Pearson's correlation was used to explore the association between Δprimary and Δsecondary outcomes through time.

Results & Discussion: A total of 18 participants completed all assessments and interventions, with 10 participants in the IG and 8 participants in the CG. The mean age and body mass index (BMI) in the IG were 51.1 ± 9.9 years and 30.3 ± 5.2 kg/m^2, respectively, with seven females (70%). In the CG, the mean age and BMI were 52.4 ± 7.4 years and 37.0 ± 5.4 kg/m^2, respectively, with six females (75%). A total of 36 independent samples were analyzed for both left and right lower limbs, with 20 in the IG and 16 in the CG. The IG demonstrated a significant correlation between greater ΔGASs and less ΔBAI score (r=-0.495, p=0.027, Figure 1 a), as well as a correlation between greater ΔGASe and higher ΔMOCA score (r=0.601, p=0.023, Figure 1 b). However, no such associations were observed in the CG between lower extremity and patient-reported outcomes (p>0.05).

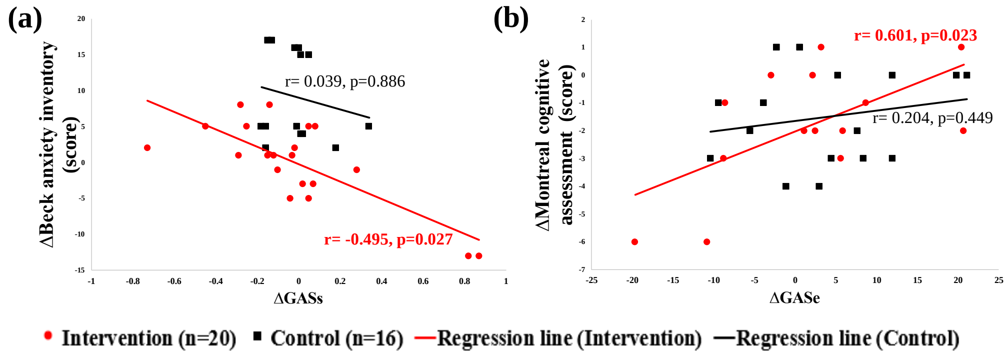

Figure 1. Results of the correlation analysis between Δprimary and Δsecondary outcomes: (a) negative association between ΔGASs and Δanxiety; and (b) positive association between ΔGASe and Δcognitive function.

Significance: This study's findings suggest that self-administered E-Stim may be a promising treatment option for PASC-related muscle deconditioning, leading to improvements in anxiety and cognitive function among individuals with a history of severe COVID illness. The results highlight the feasibility and potential of E-Stim as a valuable addition to the current treatment options for PASC. Further studies evaluating the effectiveness of E-Stim in restoring physical features such as gait and balance in PASC patients are necessary to validate these findings.

References: [1] McClafferty et al. (2020), *Journal of Clinical Neuroscience*, 79; [2] Aiyegbusi et al., (2021). *Journal of the Royal Society of Medicine*, 114(9); [3] Zulbaran-Rojas et al., (2022), *Frontiers in Medicine, 9;* [4] Zulbaran-Rojas et al., (2023). *Physiological reports*, 11(5); [5] Konrad, P. (2005).

EARLY MACROSTRUCTURAL CHANGES TO THE GLENOHUMERAL JOINT FOLLOWING BRACHIAL PLEXUS BIRTH INJURY

Vivian Mota[1], Kyla B Bosh[1,2], Jacqueline H. Cole[1,2], and Katherine R. Saul[1]
[1]North Carolina State University, [2]University of North Carolina at Chapel Hill
Email: vmmota@ncsu.edu

Introduction: Brachial plexus birth injury (BPBI) is a nerve injury with a prevalence of 1-3 in 1000 live births[1]. Effects of BPBI may include impairment of arm function such as muscle paralysis, shoulder contracture, joint dislocation, and deformed scapular and humeral growth[2-4]. Preliminary studies of BPBI in rodent models have shown that altered limb loading may directly affect glenoid formation and growth[5-7]. Our goal is to better understand the development of glenohumeral deformities and how they impact the early stages of the bone growth process following nerve injury and disarticulation. Because there is no clinical consensus as to the proper timing of intervention for BPBI, this ongoing study to elucidate the timecourse of bone deformity post-nerve injury is crucial to developing effective therapeutic interventions. We hypothesize that postganglionic injury will have a larger impact on the joint-level macrostructure and will be detectable as early as 4 weeks post-injury.

Methods: Seventy-four Sprague Dawley rats received one of four surgeries 3-6 days post-birth. Two surgical neurectomy procedures were applied to the C5-C6 nerve roots to capture different injury locations relative to the dorsal root ganglion: postganglionic (distal, n=20) and preganglionic (proximal, n=20) neurectomy. The disarticulation group (n=20) underwent amputation of one forelimb at the elbow to induce altered and reduced limb usage consistent with the neurectomy groups but without nerve injury[6]. Sham control group (n=14) underwent similar incisions as for neurectomy, but the plexus was kept intact[6]. The unaffected contralateral limbs were used as an additional control. Animals were euthanized 4 weeks post-surgery, and the upper torso and forelimbs were fixed and immersed in 70% ethanol. Macrostructural scans of the intact shoulder were obtained with micro-CT (SCANCO Medical μCT 80, 0.5-mm Al filter, 70 kVp, 114 μA, 800 ms integration time, voxel size = 36 μm x 36 μm x 36 μm).

Bone scans of the glenohumeral joint were reconstructed, and measures of bone deformity 4 weeks post-injury of the postganglionic surgeries were quantified using Mimics (Materialise), a 3-D medical imaging software. Specific clinical measures of glenoid and humeral morphology included glenoid version angle, glenoid inclination angle, glenoid radius of curvature, humeral head thickness and width, and humeral head curvature (**Figure 1**). Image analysis is ongoing; when complete, statistical analysis will assess the effects of nerve injury group (preganglionic, postganglionic, disarticulation, and sham), limb comparisons (injured and uninjured), and within-group factors (4 and 8 weeks) using mixed linear models (SAS).

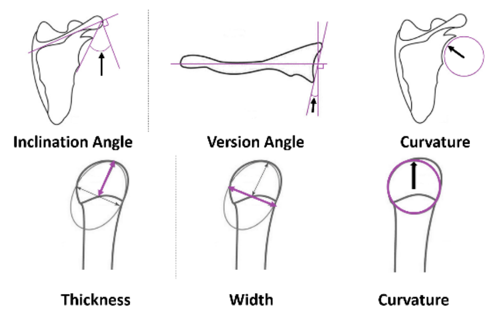

Figure 1: Morphologic measurements on the scapula and humerus[6]

Results & Discussion: Initial analyses have been made for the postganglionic group between the injured and uninjured limb and compared to prior measurements made for animals undergoing the same procedures and analyzed 8 weeks post-surgery[6]. At both weeks 4 and 8, the injured-side glenoid was more declined than in the uninjured limb (n=2) (**Figure 2**). Specifically, at 4 weeks, compared to the uninjured side, the injured side showed a smaller glenoid curvature (-26%), the glenoid inclination angle was more declined (-27%, **Figure 2**), the glenoid version angle was more retroverted (-144%), and the humeral head thickness was smaller (-18%), whereas the humeral head curvature and humeral head width had little difference. These glenoid changes are initially consistent with prior measurements made at 8 weeks for postganglionic neurectomy, in which glenoid inclination was more declined and glenoid curvature was increased[6]. At 8 weeks, no significant alterations in humeral head thickness and width or glenoid version angle were observed. Image analysis, when completed for all animals at 4 weeks, will allow for direct comparison with the statistical analyses.

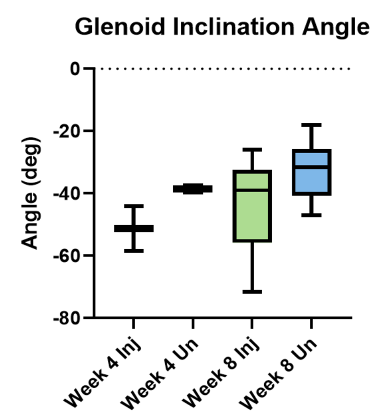

Figure 2: Glenoid inclination angle of injured (Inj) and uninjured (Un) limbs at 4 and 8 weeks.

Significance: This ongoing study sheds light on how nerve injury directly influences macro-structural changes of the scapula and humerus at 4 weeks post-injury and the timecourse of changes. Our initial evidence shows that glenohumeral deformity is detectable at 4 weeks after postganglionic injury. Identifying the timeline of the bone deformity gives us insight into when clinical intervention may be most effective for the different types of nerve injury and disarticulation. Ongoing analyses examine 2-, 3-, and 16-weeks post-injury time points following preganglionic, postganglionic, disarticulation, and sham surgeries.

Acknowledgments: NIH R01HD101406. We thank Dr. Kerry Danelson and Dr. Roger Cornwall for their surgical support.

References: [1] Foad et al. (2008), *J Bone Joint Surg* Am 90(6):1258-64; [2] Pearl et al. (1998), *J Bone Joint Surg Am* 80(5):659-67; [3] Poyhia et al. (2005), *Pediatr Radiol* 35(4):402-9; [4] Cheng et al. (2015), *J Hand Surg Am* 40(6):1170-6; [5] Dixit (2021), *J Hand Surg Am* 46:146; [6] Fawcett (2021), Doctoral Dissertation https://www.lib.ncsu.edu/resolver/1840.20/39052; [7] Crouch et al. (2014), *J Hand Surg Am* 39(2):303-11

Segmental power analysis of a round off in a pediatric gymnast: A case study

Avery Takata, John Collins, Emma Caringella, Henry G Chambers, Patrick Curran
Rady Children's Hospital, San Diego, CA, USA
Motion Analysis Laboratory, Southern Family Center for Cerebral Palsy, Rady Children's Hospital, San Diego, CA, USA

Introduction: In gymnastics, the upper extremities withstand high impact loads during weight-bearing exercises where female athletes most frequently injure their wrists [1]. Floor exercises cause the most frequent incidence of wrist injury during more basic skills (e.g. round off, back handspring) [2]. The distal radial physis is a common injury site where stress injury can have damaging affects to the growth plate in youth gymnasts [1]. Because the distal radius bears 80% of the load placed on the extended wrist, researchers have evaluated high axial compressive forces and loading rates and found that when applied to an extended wrist, these variables are associated with wrist injury risk [1-3]. Previous studies have identified compression joint reaction forces and moments occurring at the wrist and elbow joints also related to injury risk [1-4]. However, radiographs of youth radial stress injuries display a volar widening of the distal radial epiphysis suggesting a distraction force causing injury to the growth plate [3]. Therefore, a gap remains in understanding the kinetic contribution to this etiology. This study sought to explain rates of energy generation, absorption, and transfer through the upper extremity segments by their respective joints during roundoff to explore their role during a basic gymnastic floor skill.

Methods: One 12-year-old female gymnast was recruited and enrolled prospectively to participate in the study (Height=1.48, mass=44.6 kg). 51 reflective markers were placed on standard upper and lower extremity bony landmarks. Data was collected on a 10-camera Qualisys Arqus system (Qualisys, Inc, Gothenburg, Sweden) at 120 Hz. The participant performed two roundoffs with hands placed in the T-position over two in-ground force plates (AMTI, Watertown, MA) collecting at 1200 Hz and were included if the athlete landed with one hand on each force plate. Visual 3D (C-Motion, Inc, Boyds, MD) was used to create a model and calculate upper extremity forces, moments, joint torques, and angular velocities during each hands' contact phase. The rates of energy generation, absorption, and transfer through the hand, forearm, upper arm, and trunk segments and their respective joints using a method to calculate segmental power analysis previously described [4].

Results & Discussion: The closed chain kinetic movement pattern of the roundoff requires a balance of energy flow through the first and second contact limbs to propel the athlete into and out of an inverted position in preparation for more advanced skills. The joint moments at the elbow calculated in this study are comparable to those in previous youth female analyses, but have yet to report wrist joint moments (elbow internal flexor moment = 0.57±0.03 N/kg, 0.61±0.11 N/kg, respectively, elbow internal adduction moment = 0.34±0.03m N/kg, 0.40±0.29 N/kg, respectively, wrist internal flexor moment = 0.29±0.07 N/kg, wrist internal adduction moment = 0.05±0.03 N/kg) [4]. The rates of energy transfer by segment torque powers (STP), and generation and absorption by joint torque powers (JTP) are displayed in Figure 1. The first and second contact wrist both absorb energy to eccentrically control the initial weight acceptance at the forearm. However, the first contact limb transfers energy proximally to the forearm while the second contact limb transfers distally from the forearm. This is due to the differing hand positions where parallel position requires the hand to rotate faster than the forearm into the dorsiflexed position, whereas the forearm rotates out of dorsiflexion in the T-position faster than the fixed hand segment. At the elbow, the first contact limb alternates between generating and absorbing energy and delivers energy from the upper arm distally to create a stable base at the forearm for the rest of the body to rotate and propel the athlete into double-limb support then into an upright position. The second contact elbow transfers energy proximally to the upper arm and absorbs energy to eccentrically control the fall of the center of mass and push the body into an upright position. Previous studies have found the second contact limb experiences higher moments, net loads and loading rates compared to the first contact limb in the T hand positions [2]. The current finding suggests increased eccentric contractions in the forearm of the second limb compared to the first which are known to increase stresses of these structures.

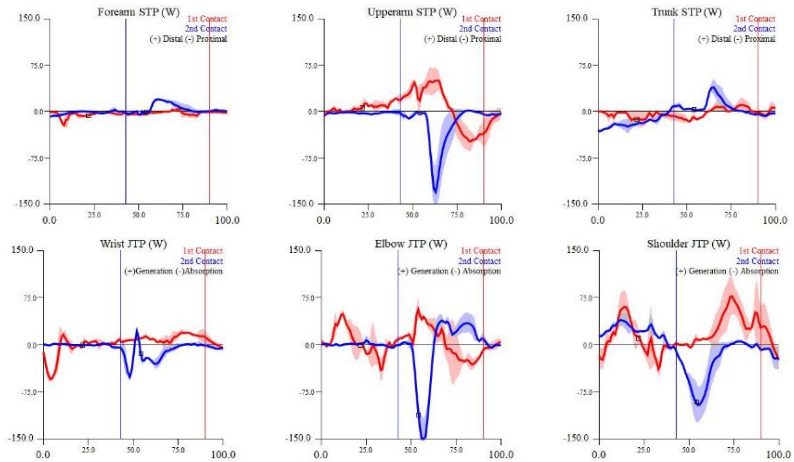

Figure 1:Mean ±SD bands of STP and JTP from 1st contact to 2nd contact (vertical blue) to 1st off (vertical red) to 2nd off.

Significance: These initial findings may describe the flow of energy through a roundoff and give a more complete picture of what is occurring at each joint and segment in this closed kinetic chain movement pattern. Although these data cannot answer clinical questions surrounding specific structures of the wrist and elbow joint without making large assumptions, they add insight into the repetitive, high stress movement pattern of a round off. With more subjects, the rates of energy generation, absorption, and transfer can be confirmed through the different phases of the round off in order to better understand their relationship to joint moments and reaction forces.

References: [1] Webb, B.G., et al. (2008). *Current Sports Med. Reports*. 7(5), 289-295.
[2] Farana, R., et al. (2017). Journal of Sports Sciences. 35(2), 124-129.
[3] DiFiori, J. P., et al. (2006). *The American Journal of Sports Medicine*. 34(5), 840–849.
[4] Farana, R., et al. (2014). Sports Biomechanics. 13(2), 123-134.
[5] Aguinaldo, A.L, et al. (2021). *ISBS Proceedings Archive*, 39(1) Article 36.

The effect of midsole stiffness and measurement method on ground reaction forces during running

Eleanor E. Scripps[1*], Brian Noehren[2], Meredith K. Owen[2]
[1]Department of Mechanical Engineering, University of Kentucky, Lexington, KY,
[2]Department of Physical Therapy, University of Kentucky, Lexington, KY,
*Corresponding author's email: eesc232@uky.edu

Introduction: Changing a shoe's construction (i.e. compressive stiffness of the midsole) can alter loading during running [1], which has important implications for performance and injury risk. Typically, loading as measured by vertical ground reaction force is determined using standard laboratory-based force platforms. These methods are considered to be the gold standard, but limit testing to activities that can be performed within a laboratory setting. For in-field monitoring, instrumented insoles placed within the shoe allow for feasible measurement of ground reaction forces. Previous work has indicated shoe type affects ground reaction forces during running when measured with lab-based force platforms [1] and during jumping when measured with instrumented insoles [2]. However, the effects of shoe construction on ground reaction forces measured with instrumented insoles during running is unknown. The purposes of this study were to first, evaluate the effect of shoe stiffness on peak ground reaction force (PGRF), impulse, and loading rate as measured by instrumented insoles secondarily, to compare the measurements methods across the different shoe types.

Methods: Three shoe types with varying midsole stiffness combinations were assessed: A/B has low stiffness in the forefoot and medium stiffness in the rearfoot, B/B has medium stiffness throughout, and C/B has high stiffness in the forefoot and medium stiffness in the rearfoot. 12 active individuals (weight: 61.52±3.86 kg) with no current lower-limb injuries completed one study visit. Ground reaction forces were measured with both a force plate embedded treadmill (Bertec, Columbus, OH) and the instrumented insoles (loadsol®, Novel Electronics, St. Paul, MN). The loadsols were calibrated after a brief accommodation period following manufacturer guidelines. Calibration was repeated until bodyweight determined by the loadsols was within ±5% of the participant's measured body weight [3]. Participants ran on the force embedded treadmill at 3 m/s, and three trials of 10 seconds were recorded simultaneously for both the force plate and the insoles. This process was repeated for each shoe type. The order of the shoe was randomized using a random number generator. Data were filtered and processed using custom MATLAB code (v2020b, MATLAB, Natick, MA). Individual steps were isolated and PGRF, impulse, and loading rate were calculated for each step. The middle eight steps were averaged for each metric. PGRF was defined as the overall maximum vertical ground reaction force during stance phase. Impulse was calculated as the area under the force-time curve. Loading rate was defined as the rate of increase in force during the early phase of stance. When an impact peak was present, loading rate was calculated from 20% to 80% of the time to impact peak. If there was no clear impact peak, loading rate was calculated using one of two methods (1) from 20% to 80% of the time to the point the instantaneous slope change is less than -15 N/s and the vGRF is greater than participant body weight [4] or (2) from 10% to 15% of the time to PGRF. Method two was implemented if both of the qualifiers from method one were not met. Differences between shoe types and between measurement methods were assessed with two-way repeated measures ANOVAs. Significance was set at 0.05.

Results & Discussion: Table 1 lists the average values for all variables of interest. No between shoe differences were noted for any metric when measured by the loadsols. When measured by the force plates, PGRF was significantly higher in shoe C/B than shoe A/B ($p=0.017$). Between measurement methods, impulse was significantly higher for loadsol measurements than force plate measurements for each shoe type ($p<0.001$ for every shoe type). Loading rate was significantly lower when measured with the loadsols than with the force plate for each shoe type ($p<0.001$ for every shoe type). These findings potentially suggest that altering the stiffness of running shoes does not have a substantial effect on ground reaction force as measured with insoles, but large changes in midsole compressive stiffness do affect ground reaction force as measured with the force plates. Also, they may suggest that impulse and loading rate are more affected by measurement technique.

Table 1: PGRF, Impulse, and Loading Rate (Mean ± SD) *Denotes significance between shoe type A/B and C/B
^Denotes significance between measurement devices

	PGRF (BW)		Impulse (BW*s)		Loading Rate (BW/s)	
Shoe Type	Force plate	Loadsol	Force plate	Loadsol	Force plate	Loadsol
A/B	2.43±0.04*	2.40±0.05	0.35±0.004	0.37±0.01^	68.21±5.47	57.68±6.94^
B/B	2.45±0.06	2.47±0.05	0.36±0.004	0.38±0.01^	66.20±6.10	54.91±5.89^
C/B	2.48±0.04	2.46±0.05	0.36±0.004	0.37±0.01^	67.07±5.42	56.71±6.20^

Significance: Loadsols and other instrumented insoles provide clinical utility in their ability to be used outside of standardized environments. Our results may support the use of loadsols for studies that are unable to standardize footwear or do not want to standardize footwear to increase translatability. Differences noted between measurement methods may be a result of the location of measurement and/or the sampling frequency [5]. Loadsols measure ground reaction forces above the midsole and at a lower sampling frequency than the instrumented treadmill, which could have a greater impact on time-based measurements such as impulse and loading rate. Future studies should investigate the effects of altering other shoe properties on ground reaction forces measured with instrumented insoles, as well as include other kinematic and kinetic outcomes to assess overall biomechanical effects of shoe type.

References: [1] Sun et al. (2020) J Sports Sci Med 19. [2] Luftglass et al. (2021) *Clin Biomech* 105421. [3] Peebles et al. (2018) Sensors 18. [4] Futrell et al. (2020) J Sport Health Sci 9. [5] Renner et al. (2019) *Sensors* 19.

EARLY STANCE NEGATIVE KNEE POWER CAN BE TRACKED USING IMUS

Fany Alvarado*, Julien A. Mihy, Mayumi Wagatsuma, Jocelyn F. Hafer
Graduate Program in Biomechanics and Movement Science; Kinesiology & Applied Physiology University of Delaware
*Corresponding author's email: fany@udel.edu

Introduction: Early stance knee kinetics may provide insight into knee joint health. Knee joints affected by weak quadriceps, such as those post-anterior cruciate ligament reconstruction (ACLR) or with knee osteoarthritis (OA), have altered knee kinetics [1,2]. Peak negative knee power may indicate deficits in quadriceps strength and gait alterations in early stance [1,3]. The current standard to assess knee kinetics is optical motion capture (MoCap) and force plates. Estimating knee joint powers outside the lab, without MoCap, might allow us to track changes in joint function in individuals post ACLR or with knee OA [4]. Inertial measurement units (IMUs) can be used outside the lab but cannot directly quantify kinetics, including joint power. However, IMUs can measure angular velocity, a component of joint power. We have previously shown that IMU-derived angular velocity can track peak propulsive powers [5]. If IMUs can be used similarly to track negative knee joint power, this may be useful for assessing changes in knee joint function due to injury, pathology, or rehabilitation [1,3]. The purpose of the study was to determine if we can use IMU-measured joint and segment angular velocity to evaluate negative knee joint power.

Methods: Ten healthy young (27.9±4.7 years), 10 healthy older adults (72.3±3.3 years), and 9 older adults with knee OA (69.2±4.5) performed ten walking trials at preferred and fast speeds. Motion capture (Vicon) and force plate (AMTI) data were collected using standard methods. MoCap data were used to calculate early stance peak negative knee power. Two IMUs (APDM) were placed on the lateral thigh and shank. IMU data were functionally oriented to a segment reference frame where one axis was approximately sagittal [6]. All IMU outcome variables were calculated about this axis. IMU outcome variables included early stance peaks in negative and positive knee angular velocity, positive thigh angular velocity, and negative shank angular velocity, as well as the times of these peaks. Data were averaged for each subject and walking speed. Pearson correlations were calculated between peak negative knee power and each IMU outcome variable across all speeds for the combined young, older healthy, and OA groups.

Results & Discussion: There were significant correlations between peak negative knee power and both negative ($p=0.001$, $r=0.416$) and positive ($p<0.001$, $r=-0.616$) knee angular velocity. Negative knee angular velocity (39.2±5.8% stance) corresponds to the direction of rotation that contributes to negative knee joint power, however, this peak velocity did not occur at a similar time compared to negative knee joint power (15.0±2.6% stance). Positive knee angular velocity does not correspond to the direction of rotation that contributes to negative knee joint power, but this peak velocity did occur at a similar time compared to negative knee joint power (10.2±2.4% stance). Negative knee power also correlated with negative shank angular velocity ($p<0.001$, $r=0.687$). Here, peak negative shank angular velocity had similar timing to negative knee joint power (9.2±2.6% stance) and segment movement that would contribute to negative knee joint power (Fig 1). This finding agrees with a previous study that found a relationship between shank angular velocity and knee loading [4]. No significant correlation was found between negative knee power and positive thigh angular velocity ($p=0.516$, $r=-0.087$).

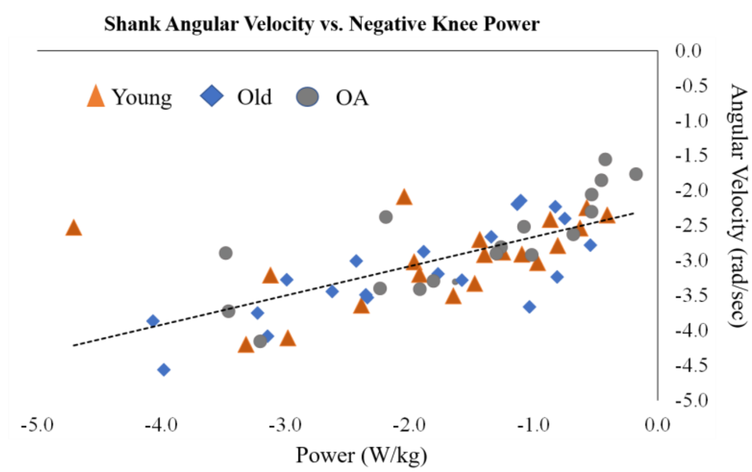

Figure 1: Correlation between negative shank angular velocity and knee power across all groups ($p<0.001$).

Significance: This study aimed to test whether IMU-measured joint or segment angular velocities were associated with negative knee joint power. Our findings suggest that IMU-measured angular velocity could track negative power. This finding supports testing whether free-living angular velocities captured with IMUs correspond to longitudinal changes in knee joint power observed in the lab.

Acknowledgements: These data were collected at the University of Michigan.

References: [1] Sigward et al. (2016). *Clin Biomech*. 32,249-254; [2] Mills et al. (2013) *Arthritis Care Res* 65(10); [3] Winter. (1983) *Clin Orthop Relat Res* 175; [4] Sigward et al. (2016), *Gait Posture* 49; [5] Hafer (2020), *J Biomech* 106; [6] Mihy et al., medRxiv 2022.11.29.22282894

VALIDATION OF A REMOTE UPPER EXTREMITY FRAILTY ASSESSMENT: UTILIZING GOOGLE'S MEDIAPIPE ALGORITHM FOR TELEHEALTH APPLICATIONS

Mohammad Dehghan Rouzi[1,†], Myeounggon Lee[1,†], Nesreen El-Refaei[1], Anmol Momin[1], Bijan Najafi[1,*]

1 Interdisciplinary Consortium on Advanced Motion Performance (iCAMP), Division of Vascular Surgery and Endovascular Therapy, Michael E. DeBakey Department of Surgery, Baylor College of Medicine, Houston, Texas, USA
† Both authors shared first-authorship
*Corresponding author's email: bijan.najafi@bcm.edu

Introduction: Remote frailty assessment holds great potential in healthcare by increasing accessibility, enabling early detection and intervention, reducing costs, empowering patients, and improving care coordination and research. We previously validated a 20-second repetitive elbow flexion-extension test, the Frailty Meter (FM), which measures frailty index (FI), frailty phenotypes (slowness, weakness, exhaustion, rigidity) [1,2], and dual-task performance, an indicator of cognitive performance [3], using a wrist-worn sensor. However, the wrist-worn sensor limits FM's applicability in telemedicine. Google's machine-learning model "Mediapipe"[4] has been widely used to identify human body movements from video recordings [5, 6]. In this study, we aim to employ Mediapipe to measure elbow velocity from standard video recordings (video-based FM, **Figure 1**) and validate its accuracy compared to the sensor-based FM.

Methods: A total of 65 adults, aged 20 to 85, were enrolled in the study (IRB #: H-43917, Clinical Trial#: NCT05754021). Following our previously validated procedures, participants completed the upper extremity test using sensor-based FM while being video-recorded from a sagittal view with a standard webcam. They were instructed to flex and extend their dominant arm for 20 seconds during single-task (ST) and dual-task (DT) assessments, counting backwards from 50 during DT. A pairwise t-test was employed to compare the 20-second angular velocity and frailty phenotypes (weakness, slowness, rigidity, exhaustion) [7] between sensor-derived and video-derived data. To determine the absolute agreement between the two outcomes, an intra-class coefficient (ICC(2,1)) analysis was performed. ICC values are classified as follows: 1) below 0.50, poor; 2) 0.5 – 0.75, moderate; 3) 0.75 – 0.90, good; and 4) above 0.90, excellent.

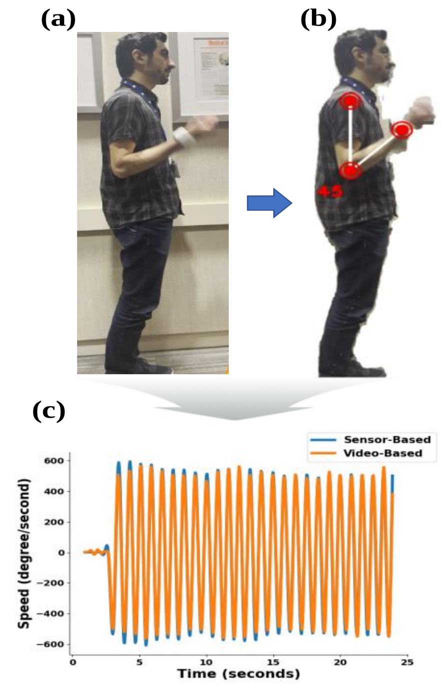

Figure 1. 20-second FM test: (a) is describing the upper extremity test wearing wrist-sensor in the sagittal view; (b) is estimated the body position based on the landmark; and (c) is a calculated angular velocity by the video and sensor-based recording.

Results & Discussion: All participants (Age: 56.0 ± 18.7 years; Body mass index: 28.6 ± 6.1; Female: 49 (75.4%)) successfully completed both tests, demonstrating the high feasibility of the proposed method. A good to excellent agreement was observed between video-based and sensor-based FM in measuring elbow angular velocity during both testing conditions (ST: ICC(2,1) range: 0.887 – 0.999; average: 0.983; DT: ICC(2,1) range: 0.914 – 0.998; average: 0.980). Moreover, excellent agreement was achieved between video-based and sensor-based approaches for measuring frailty index and phenotypes, with no significant differences between outcomes during both ST and DT conditions (ST: ICC(2,1) range: 0.990 – 0.999; DT: ICC(2,1) range: 0.976 – 0.999). These findings support the validity of the video-based FM for measuring frailty and its phenotypes.

Significance: Our study introduces a tele-medicine solution that monitors frailty remotely with high feasibility and accuracy. This solution utilizes videoconferencing between patients and physicians, which is increasingly accepted by healthcare payers and convenient for older adults who may have difficulty traveling to clinics. Our proposed software can be integrated into any telehealth platform, making it accessible for clinicians to use during telehealth visits. Furthermore, our video-based frailty monitoring technology has potential applications in clinical trials, particularly for remote capture of biomarkers to minimize risk to vulnerable populations during the COVID-19 pandemic. By reducing the need for in-clinic visits, this technology could facilitate remote tracking of frailty over time during clinical trials.

Acknowledgements: We thank the iCAMP staff for their assistance with data collection.

References: [1] Toosizadeh et al., (2015). Journal of the American Geriatrics Society, 63(6); [2] Toosizadeh et al., (2017). PloS one, 12(2); [3] Najafi et al., (2020). JAMA Network Open, 3(11); [4] Bazarevsky et al., (2020). arXiv preprint arXiv; [5] Halder, A., & Tayade, A. (2021). Journal homepage: www. ijrpr. Com; [6] Subramanian et al., (2022), Scientific Reports, 12(1), 1-16;
[7] Lee, H., Joseph, B., Enriquez, A., & Najafi, B. (2018). Gerontology, 64(4).

Anticipatory postural adjustment size is not related to first step length and speed during gait initiation for people with Parkinson disease

Chelsea "CJ" Duppen, [1] Nina Browner [2], Michael D. Lewek [1,3]
(1) Human Movement Science Curriculum, University of North Carolina at Chapel Hill
* Corresponding author's email: chelsea_parker@med.unc.edu

Introduction: Small amplitude movements are a hallmark of advanced Parkinson disease (PD), and present across a variety of motor tasks including reaching, hand use, speech, and gait. Impaired ability to initiate and maintain gait in people with PD is especially pertinent, as these activities are associated with increased risk for falls [1], decreased functional independence [2], and decreased health-related quality of life [3]. As a necessary precursor to walking, the process of initiating gait is critical to support safe, independent ambulation. While initiating gait, people with PD demonstrate a decrease in anticipatory postural adjustment (APA) amplitude [4], and a decrease in first step length and speed [5]. APAs consist of a center of pressure (COP) shift posterior and towards the initial swing limb, which allows for a shift of center of mass forward and towards the initial stance limb [6], such that the first step forward can occur. As the initial feature of gait initiation, it seems likely that the decreased APA amplitude is responsible for the diminished first step length and speed in people with PD. However, despite copious research on impairments in gait initiation for people with PD, the relationship between APA size and first step length and speed has not been reported. The purpose of this study was to examine these relationships to inform potential treatment targets. We hypothesized that there would be a positive relationship between APA size and first step length and speed in people with PD.

Methods: Ten adults with idiopathic PD (4, 1, and 5 in Hoehn & Yahr stages I-III, respectively) (67 $\pm$ 11 y/o) were asked to initiate gait, of their own volition, while standing on two adjacent force plates. To best mimic movements outside the laboratory, participants self-selected their starting position, so long as one foot was on each force plate and weight distribution was approximately equal. Participants completed a total of six trials. COP time series were determined from ground reaction forces, while first step length and speed were calculated using heel marker position data from a motion capture system. APAs were calculated as peak lateral COP excursion towards the initial swing limb prior to toe off. Trials without an APA, or with multiple APAs, were removed from analysis. We then completed two-tailed bivariate correlation analyses for 1) APA size and first step length, and 2) APA size and first step speed.

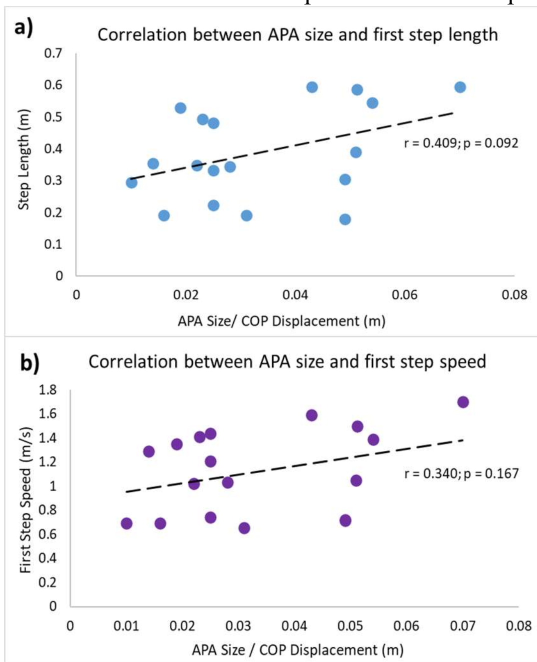

Figure 1:Correlation between APA size and **a)** first step length and **b)** first step speed. Each data point represents a trial, with a dashed regression line.

Results and Discussion: The average APA size across all participants was 0.034 $\pm$ 0.016 m, which is consistent with previous literature on gait initiation for people with PD [1]. Average first step length and speed were 0.388 $\pm$ 0.142 m and 1.123 $\pm$ 0.34 m/s, respectively. Correlation analyses revealed no significant relationship between APA size and first step length ($p = 0.092$; $r = 0.409$) or first step speed ($p = 0.167$; $r = 0.340$) (Figure 1). Despite a general consensus in the literature that APAs are responsible for the transition from steady stance to dynamic movement (such as walking), our results suggest that in our group of people with PD, they are not as closely related to first step length and speed as originally hypothesized. Importantly, of the 60 total trials, 4 trials were removed for failure to achieve steady stance prior to gait initiation, 11 were removed for absence of APA, and 22 were removed for having 2+ APAs. While it is customary to remove trials with either absent or multiple APAs, this highlights the importance of finding a way to retain these data in analyses, as they may be crucial for determining factors influencing impaired gait initiation for people with PD.

Significance: Difficulty initiating and maintaining gait are grouped under the umbrella term "freezing of gait", which is associated with worse outcomes and high risk for falls for people with PD [1]. Therefore, it is essential to know how best to treat this phenomenon. Our study found that while APAs precede gait initiation, it appears they may not be a contributing factor for gait initiation deficits for people with PD. Future research should focus on other potential biomechanical factors contributing to the reduced first step length and speed to inform treatments aimed at improving freezing of gait for this population.

Acknowledgements: This work was supported in part by the National Center for Advancing Translational Sciences, National Institutes of Health TL1 Postdoctoral Training Program [5TL1TR002491-05] and the Foundation for Physical Therapy Research Promotion of Doctoral Studies I Award.

References: [1] Okuma (2014), *J Parkinsons Dis.*4(2); [2] Santos-Garcia et al. (2020) *Neurol Sci;* [3] Moore, Peretz, Giladi (2007) *Mov Disord* 22(15); [4] Halliday et al (1998) *Gait Posture* 8(1); [5] Roemmich et al (2012) *Gait Posture* 36(3); [6] Martin et al. (2002), *Physical Therapy* 82(6)

A ROBOTIC LOWER LIMB SURROGATE FOR MEASURING THE EFFECT OF IDEO STRUT STIFFNESS ON TIBIAL STRAIN

Robert McGrath PhD[1,2*], Michael Poppo MS[1,2], Brett Johnson PhD [2,3], Lee Childers PhD CP[2,3]
1. The Henry M. Jackson Foundation for the Advancement of Military Medicine, Bethesda, MD.
2. Center for the Intrepid, Brooke Army Medical Center, JBSA Ft. Sam Houston, TX.
3. DoD/VA Extremity Trauma and Amputation Center of Excellence, USA.
*Corresponding author's email: robert.l.mcgrath30.ctr@health.mil

Introduction: Stress fractures account for up to 20% of injuries observed in sports medicine clinics and 49% of stress fractures occur in the tibia [1]. To expedite return to activity following tibial stress fracture, we are investigating orthoses to reduce stresses experienced by the tibia. A popular existing ankle foot orthosis is the Intrepid Dynamic Exoskeletal Orthosis (IDEO); an energy storing and returning device which unloads the lower leg. Muscle activity is a significant contributor to tibial stress [2], however the relationship between strut stiffness and tibial stress is unclear. Standard medical device testing, prior to human participant testing, would typically involve a cadaveric model. However, a cadaver cannot capture the significant contribution of muscle activity on tibial stress. Therefore, the objective is to develop a robotic lower extremity surrogate to mimic plantarflexor muscle force and load bearing while quantifying the effect of IDEO strut stiffness on tibial strain as measured by the robotic surrogate. We hypothesize that under consistent cyclical tendon force and body weight application, tibial strain will decrease as the strut stiffness category is increased.

Methods: The robotic surrogate (Fig. 1A) is composed of a 3D printed tibia and fused foot bone from Rigid 10K resin (Formlabs Inc., Somerville, MA), which has a Young's modulus comparable to that of bone [3]. The tibia and foot bone are joined by a custom aluminum rotary joint. To replicate Achilles tendon force, a Caplex System driven Bowden cable (Humotech, Pittsburgh, PA) and in-line load cell (FuTek, Irvine, CA) were installed with the inner cable terminating at the posterior side of the calcaneus. Strain gauge rosettes (VPG, Inc., Raleigh, NC) were bonded to five locations on the tibial shaft: at mid-length lateral, medial, and posterior locations and medial side distal and proximal locations. This entire apparatus was set in Dragon Skin silicone rubber (Smooth-On Inc., Macungie, PA) casted in the shape of a male leg sized within the 50th percentile of male US Army Service members [4]. To model external loads due to walking, the surrogate was placed in a material testing system (MTS) (Instron Corp., Norwood, MA). A digital trigger coordinated the cyclical application of loads from the MTS and Caplex System driven Bowden cable, both of which were controlled using force feedback.

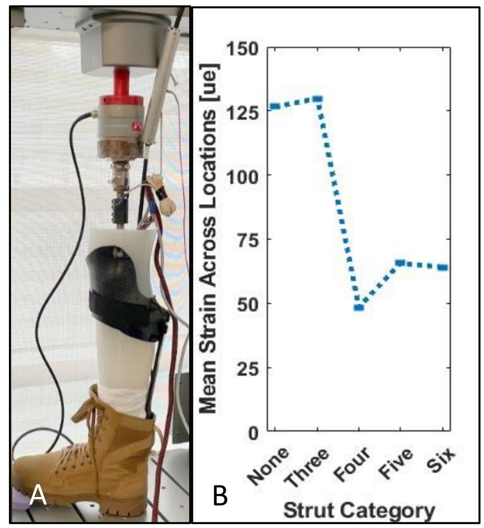

Figure 1:(A) the robotic surrogate mounted in the material testing machine and (B) the mean strain across the five sensor locations for each IDEO strut condition.

The robotic surrogate was fitted with an IDEO and standard issue army boot. Five commercially available 300mm carbon fibre struts from different clinical stiffness categories (3, 4, 5, 6, whereas 3 is the least stiff) were fitted to the IDEO separately for testing and a no strut condition served as a control. For each trial, the Bowden cable load was applied sinusoidally from 0 to 375 N at 1 Hz, and the MTS loaded the surrogate sinusoidally from 0 to 225 N at 1 Hz to replicate 25% of anatomical loads. Each trial was 20 cycles and the peak maximum principal strain values at each strain gauge location were assessed using a custom MATLAB script for the last 10 cycles (MathWorks, Inc., Natick, MA). A two-way ANOVA was performed on the data with post-hoc Tukey-HSD pairwise comparisons between conditions and gauge location in JMO Pro (SAS Institute Inc., Cary, NC).

Results & Discussion: The main effects and two-way interaction of strut category and strain gauge location were significant ($p < 0.001$). These results indicate that measured strain changes according to strut stiffness and sensor location and there is an interaction of these effects. All post-hoc pairwise comparisons of least squared mean strain of gauge locations across strut category conditions (Fig. 1B) were significant ($p < 0.001$). In these comparisons, the category three strut yielded the highest mean strain, and the category four strut yielded the lowest mean strain. These findings are contrary to our hypothesis, indicating that there may be an optimal strut stiffness for reducing tibial strain that is of an intermediate category and therefore stiffness. Further experimentation can be performed at higher percentages of anatomical loads to further elucidate the relationships between AFO properties and tibial strain.

Significance: This experiment shows the feasibility of using a robotic surrogate to evaluate the effects of AFO attributes, such as strut stiffness, on tibial strain. The results of this experiment suggest that the category of AFO stiffness may not have a simple inverse relationship with tibial strain and that higher stiffnesses may result in lower tibial strains.

Acknowledgements: Funded by Department of Defense Grant No. W81XWH2120013. The views expressed herein are those of the author(s) and do not reflect the official policy or position of Henry M. Jackson Foundation for the Advancement of Military Medicine, Inc., Brooke Army Medical Center, the Department of Defense, or any agencies under the U.S. Government.

References: [1] Abbott, A, 48(1), 2020, [2] Matijevich, ES, PLoS ONE, 14(1), 2019, [3] Wu, D, Acta Biomaterialia 78, 2018, [4] Gordon, CC, Natick/TR 15/007, 2012, [5] Ishikawa, M, J Appl Physiol 99, 2005.

EFFECT OF WALKING SPEED AND RHYTHMIC AUDITORY STIMULATION ON KINETIC GAIT PARAMETERS DURING TREADMILL WALKING IN CHILDREN AND ADULTS: A PILOT STUDY

Haneol Kim[1*], Jianhua Wu[1]
[1]Georgia State University
*Corresponding author's email: hkim162@student.gsu.edu

Introduction: Human gait is affected by various external constraints such as visual, tactile, auditory, task, and environmental constraints but healthy individuals can adapt to these constraints [1]. For instance, healthy young adults can respond to external auditory constraints immediately and effectively [2]. Based on the ability to synchronize gait with auditory cueing, rhythmic auditory stimulation (RAS) has been applied to clinical populations with Down syndrome, cerebral palsy, stroke, or Parkinson's disease and showed improvements in step length, walking velocity, and gait symmetry [3, 4]. However, it is not fully understood to what degree RAS as an external constraint affects human gait in children and adults, particularly during treadmill walking in terms of kinetic variables [5]. There were no studies investigating the effect of treadmill walking speed (TWS) with various RAS or the effect of RAS with various TWS. Additionally, it is meaningful to investigate the differences in kinetic gait variables between children and adults. Children may use different strategies because the locomotor system for children has not matured yet.

The purpose of this study is to compare the kinetic gait characteristics between children and adults while walking on the treadmill with various treadmill walking speeds and rhythmic auditory stimulation frequencies. We hypothesized that children would show a similar trend but lower amplitude in response to different treadmill walking speeds at the same RAS frequency and in response to different RAS frequencies at the preferred treadmill walking speed compared to adults. We hypothesized that kinetic variables such as vertical ground reaction forces (vGRF) and impulses would decrease with decreasing TWS and with increasing RAS frequency.

Methods: Five healthy young adults (2M/3F) aged between 18 and 35 years and five children (3M/2F) aged between 7 and 11 years participated in this study. Participants walked on a 10-meter walkway at their self-selected speed three times, and the average speed was used for treadmill walking. A Zebris FDMT-S instrumented treadmill was used to collect the vGRF data and calculate braking and propulsive impulses.

First, participants completed a 5-minute baseline trial with 100% TWS and 100% RAS. In study 1, walking speed was manipulated but not the RAS frequency: 75% TWS and 125% TWS at the same 100% RAS. In study 2, the RAS frequency was manipulated but not walking speed: 75% RAS and 125% RAS at the same 100% TWS. At least five minutes of rest was provided between trials to minimize fatigue. Vertical GRF data were processed and exported in the Zebris software and then analyzed using a customized MATLAB program. Dependent variables included normalized first and second peak forces and normalized braking and propulsive impulses. Two-way (2 Group x 3 Condition) mixed ANOVAs were conducted for each study at a significance level of $\alpha = 0.05$. Post-hoc pair-wise comparisons were completed if necessary.

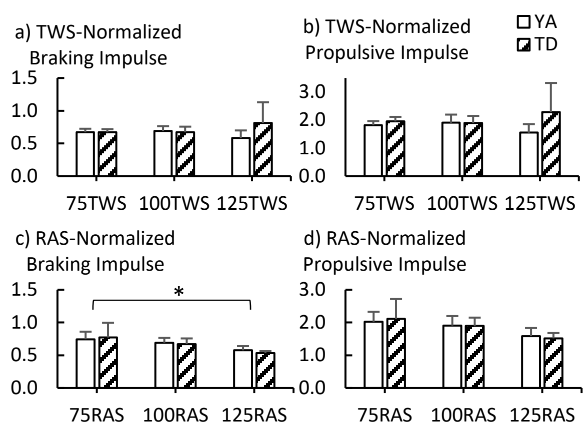

Figure 1: Mean and SD of braking and propulsive impulse for study 1 (T1: a and b) and for study 2 (T2: c and d). Symbol * indicates a condition difference at $p < 0.05$. YA: young adults; TD: typically developing children.

Results & Discussion: In study 1, no significant difference was found in normalized first and second peak vGRF between children and adults. Further, no significant difference was found in normalized braking (Fig. 1a) and propulsive (Fig. 1b) impulse. Both groups showed similar values in 75TWS and 100TWS; however, children increased normalized braking impulse while adults decreased it at 125TWS (Fig 1a). Similarly, children increased normalized propulsive impulse while adults decreased it at 125TWS (Fig 1b).

In study 2, there were no significant differences in normalized first and second peak vGRF. There was a condition effect in normalized braking impulse ($p = 0.025$, Fig 1c). Post-hoc pairwise comparisons revealed there was a significant difference between 75RAS and 125RAS ($p = 0.008$). There was no significant difference in normalized propulsive impulse (Fig. 1d). Both groups decreased braking impulse with increasing RAS frequencies while walking at a preferred walking speed.

Significance: Kinetic variables such as normalized first peak vGRF, second peak vGRF, braking impulse, and propulsive impulse were not affected by various TWS with the same RAS frequency in young adults and children. Increasing TWS while maintaining RAS increased braking and propulsive impulses for children but decreased these variables for adults. However, increasing RAS while maintaining TWS decreased braking and propulsive impulses in both children and adults. These preliminary results provided important baseline data on gait adaptation to various TWS and RAS conditions. This knowledge can be helpful when studying auditory-motor synchronization in people with disabilities.

Acknowledgements: This study was partially supported by the Georgia State University Provost's Dissertation Fellowship program.

References: [1] Desrochers & Gill (2021). *Hum Mov Sci*. 77: 102798; [2] McKay et al. (2017), *Gait & Posture.* 58: 78-87; [3] Bastian et al. (2008). *Curr Opin Neurol*. 6: 628-633; [4] Leow et al. (2014). *Front Hum Neurosci.* 8: 811; [5] Wu & Ajisafe (2014). *Gait & Posture*. 39: 241-246.

Multi-dimensional assessment of age-related changes in gait and balance

Jamie B. Hall[1*], Jacob Thomas, Sam Weiss, Trent M. Guess
[1]Department of Physical Therapy, University of Missouri
[*]Corresponding author's email: halljami@health.missouri.edu

Introduction: Age-related changes in gait and balance are well documented. [1,2] Adding a cognitive task to a motor task in a dual task (DT) paradigm may magnify these changes. [3] Gait and balance studies across the life span use expensive technologies which are often unidimensional and not easily implemented. We have developed a portable, inexpensive, multi-dimensional measurement platform, Mizzou Point-of-care Assessment System (MPASS) which integrates a custom forceplate, Kinect Azure spatial sensor, and interface board. The purpose of this study was to assess MPASS' ability to detect age-related changes in gait and balance.

Methods: The healthy older adult (HOA) group consisted of 19 community-dwelling adults (70.45±5.93 years old, 168.91±9.5cm, 7 males). The healthy young adult (HYA) group consisted of 15 NAIA athletes (19.8±1.66 years old, 180.5±6.03cm, 15 males). For gait assessment, participants walked at self-selected speeds while recorded by the Kinect Azure spatial sensor with body tracking SDK. For balance assessment, participants stood on our custom forceplate with eyes closed, arms crossed, and feet shoulder width apart. DT condition included serial subtraction by 7. [3] 2-3 trials of tasks were completed and averaged for analysis. Custom code calculated gait spatiotemporal parameters and center of pressure (CoP) balance measures. Gait measures were normalized to height. Data were not normally distributed, therefore, we used Mann Whitney U tests with Benjamini Hochberg correction for data analysis.[4]

Results & Discussion: There were significant differences for CoP balance measures in both single and DT conditions with HOA having greater total, mediolateral (ML), and anteroposterior (AP) 95% sway area and mean total velocities.[Table 1] In addition, there were significant differences for dual task gait stride and step lengths.[Table 2] Interestingly, HOA's median step/stride length was greater than that of HYA. Upon further analysis, HOA's minimum step/stride lengths were less than that of HYA but maximum values were greater for HOA. Overall range of values and variance were greater in HOA. Anecdotally, we noted levels of physical activity and fitness varied for HOA participants during data collection; some individuals reporting being largely sedentary and others teaching senior exercise classes 3 times per week. HYA were a more homogenous group. Despite this surprising finding between groups in gait, CoP measures of eyes closed standing on a firm surface discriminated between groups. By employing multiple postural control systems during gait, HOA may have compensated for physiological age-related changes that was not possible during eyes closed balance assessment. Future work will include larger sample sizes and more robust demographic, health history, and physical activity questionnaires to allow for stratification of subsets within groups to help control for heterogeneity.

Table 1: Eyes Closed on Firm Surface				
Single Task Condition	**Median HYA**	**Median HOA**	**Unadjusted p-value**	**p-value**
95% Area CoP (mm^2)	183.71	280.67	0.017	0.041*
Mean Total velocity CoP (mm/s)	12.06	29.99	<0.001	<0.001*
Mean Total velocity CoP-ML (mm/s)	5.35	8.69	<0.001	<0.001*
Mean Total velocity CoP-AP (mm/s)	9.48	27.07	<0.001	<0.001*
Dual Task Condition	**Median HYA**	**Median HOA**	**Unadjusted p-value**	**p-value**
95% Area CoP (mm^2)	204.81	281.10	0.190	0.323
Mean Total velocity CoP (mm/s)	13.03	31.56	<0.001	<0.001*
Mean Total velocity CoP-ML (mm/s)	5.87	9.11	0.002	0.006*
Mean Total velocity CoP-AP (mm/s)	11.83	27.11	<0.001	<0.001*

Table 2: Dual Task Gait Spatiotemporal Parameters											
	Healthy Older Adults					**Healthy Young Adults**					**Group Comparison**	
Variable	**Median**	**Max**	**Min**	**Range**	**Variance**	**Median**	**Max**	**Min**	**Range**	**Variance**	**Unadjusted p-value**	**p-value**
Left Stride Length (mm)	6.76	8.12	4.2	3.92	1.234	5.78	7.4	5.11	2.29	0.579	0.012	0.032*
Right Stride Length (mm)	6.97	8.2	4.34	3.86	1.173	5.73	7.09	5.27	1.83	0.436	0.003	0.024*
Left Step Length (mm)	3.38	4.27	2.02	2.25	0.338	2.94	3.7	2.61	1.09	0.123	0.006	0.024*
Right Step Length (mm)	3.48	4.63	2.16	2.47	0.462	2.87	3.7	2.6	1.1	0.147	0.02	0.04*

Significance: In our small sample, MPASS eyes closed balance assessment on a firm surface detected age-related changes in motor control despite the heterogeneity of our older adult sample. In contrast, DT gait assessment detected differences but not those typically associated with advancing age. Based on the results of this study, measurement systems which assess multiple constructs related to motor control such as MPASS may be best practice when the goal is to discriminate between populations with heterogeneity.

References: [1]Herssens et al. (2018) *Gait Posture* 64; [2] van Humbeeck et al. (2023) *Sci Rep* 13; [3] Bahureksa et al. (2017) *Gerontology* 63(1); [4] Benjamini (1995) *J R Stat Soc* 57(1)

THE EFFECT OF DUAL TASK ON DYNAMIC POSTURAL CONTROL DURING GAIT INITIATION

Angeloh Stout[1*],Ke'Vaughn Waldon[1] Kaye Mabbun[1], Miguel Barcellano[1], Sandra Cuenca[1], Gu Eon Kang[1,2**]
[1]The University of Texas at Dallas, Department of Bioengineering, Richardson, TX
[2]The University of Texas Southwestern Medical Center, Department of Plastic Surgery, Dallas, TX
Email: *Angeloh.Stout@utdallas.edu, **GuEon.Kang2@utdallas.edu

Introduction

The effect of cognitive dual task on gait is crucial in understanding the connection between the motor and cognitive functions [1]. Although previous studies reported an interaction between cognitive dual task and steady state gait, gait initiation, which requires relatively dramatic postural transition (i.e., from standing to walking) compared to steady state gait, has not yet been investigated [2]. We aim to investigate the effects of cognitive dual task on gait initiation by examining the anticipatory postural adjustment (APA) onsets of the force onset and onset times for the stance and stepping limb during gait initiation in healthy young adults. We hypothesize that dual tasking will cause an increase in the vertical force response, and longer onset times.

Methods

The study included 23 healthy young adults (age=22.56±3.89 years, 16 male, body-mass index= 24.49 ± 2.39 kg/m2; no history of neurological and orthopaedic condition) recruited from the University of Texas at Dallas community. Participants performed gait on a 10-meter walkway, located in the Neuromuscular and Musculoskeletal Biomechanics Laboratory on the University of Texas at Dallas campus. We used a 3D optoelectronic motion capture technology (sampling rate = 100 Hz; VICON, Oxford, UK) synchronized with two force plates (sampling rate = 1000 Hz, Kistler, Winterthur, Switzerland) to collect kinematic and ground reaction force (GRF) data. Prior to data collection, we attached reflective markers (n = 74) on each participant's anatomical landmark.

Participants were asked to stand still on each force plate with one foot, then start to walk along the walkway at their comfortable pace (single task; ST), and while subtracting backwards by a random number (dual task; DT). Visual3D was used to analyse marker and GRF data. We investigated APA onsets of GRF and onset times for the stance and stepping limb. The APA force outcomes investigated were Onset stepping max, Onset stance min, Onset stance max, while APA onset times were Onset stepping max, Onset stance min, and Onset stance max. Magnitude of force was calculated by the difference between the variable and the initial APA onset and normalized to their body weight (BW), similarly the onset times were calculated from the APA onset time as the origin of difference. Figure 1 shows the landmarks of the APA response. The two conditions (ST vs. DT) were compared using a paired t-test (1 tailed) where significant difference was identified via p value ($p < 0.05$).

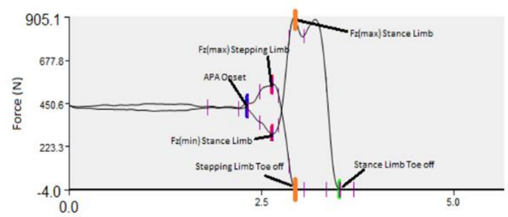

Figure 1: Vertical GRF versus time graph of gait initiation. Blue = APA Onset, Pink = Onset stepping max/Onset stance min, Orange = Onset stance Max, Green = Stance limb toe off (TO).

Results and Discussion

We found no significant differences for APA force Onset Stance Max, and the APA onset Stepping Max and Stance Max times (Table 1). Significant differences were found for APA force Onset Stepping Max and Stance min, and APA onset Stance toe off.

Table 1. Gait initiation outcomes of ST versus DT. * *p <0.05; DTE (%): dual task effect = |single-dual| / single *100*

APA Force (% BW)	ST	DT	p value	DTE	APA Time (seconds)	ST	DT	P value	DTE
Onset Stepping Max	13.00±8.06	17.41±9.02	0.003*	33.9	Onset Stepping Max	0.30±0.12	0.31±0.14	0.34	3.1
Onset Stance Min	-14.00±8.41	-18.36±9.21	0.004*	-31.1	Onset Stance Max	0.71±0.21	0.76±0.27	0.14	6.9
Onset Stance Max	48.70±7.13	48.32±5.80	0.38	0.8	Onset Stance TO	1.37±0.26	1.52±0.34	0.01*	10.8

Significance

Our study revealed the postural adjustment exchange from the initial transition phase of Onset to Stepping Max. These indicators of delayed step times and postural adjustment could assist in developing intervention methods to improve gait initiation strategy and prevent fall risks.

References

[1] Goh et al., 2021. *BMC Geriatrics* 510: s12877-021-02464-8, [2] Bayot et al., 2020. *Neurophysiol Clin* 51(6):554-568

COMPARISON OF JOINT ANGLE PREDICTION ALGORITHMS TO CONTROL A LOWER-LIMB EXOSKELETON EMULATOR

Sarah M. Bass[1*], David S. Hollinger[1], Ryan S. Pollard[1], Michael E. Zabala[1]
[1]Department of Mechanical Engineering, Auburn University, Auburn, AL, USA
smb0186@auburn.edu

Introduction: Exoskeletons are at the forefront of assistive technology research for their rehabilitation and performance enhancement potential. In rehabilitation, exoskeletons allow users to regain mobility and more easily perform everyday tasks in an effort to improve the user's health and independence.[1] Performance enhancing exoskeletons allow users to complete tasks at an elevated level. This can be accomplished by reducing the metabolic cost of an activity or by enhancing the activity while maintaining the same metabolic cost.[2] For example, an exoskeleton can reduce the user's muscle and respiratory efforts while walking or enable the user to carry a heavier load while maintaining the same muscle and respiratory efforts as carrying a lighter load. A primary challenge for performance enhancing exoskeletons is predicting the operator's intent to actuate the exoskeleton accordingly. This research effort involves integrating sensor feedback and motor control to actuate an ankle exoskeleton emulator with the objective of evaluating two ankle angle predictive algorithms: a random forest machine learning algorithm and a kinematic extrapolation algorithm. It is hypothesized that the random forest model will have greater angle accuracy but a longer actuation delay between the determination of the desired angle and it being realized in the emulator.

Methods: An exoskeleton emulator was designed and built to test the software. Bowden cables attached to a servo motor actuate the emulator about the ankle joint. A potentiometer attached to the ankle joint tracks current joint angle. The ankle angle predictive algorithms and motor control were implemented to actuate the emulator to evaluate the RMSE and delay associated with each algorithm. The current emulator joint angle was compared to the predicted joint angle to calculate the motor control logic to actuate the emulator. A baseline mechanical accuracy and delay were collected by streaming the operator angle directly to the emulator. The random forest algorithm uses a machine learning model trained on ankle angles from 30 walking trials and the kinematic extrapolation algorithm uses basic kinematic equations to predict ankle angle based on the three previous angle data points. These algorithms use ankle angle as their sole input. The algorithms' input data, referred to as the operator angle, was obtained using inverse kinematic software (Visual 3D) from treadmill walking trials and fed to the algorithm. The walking data from three subjects (obtained IRB approved consent) were tested three times on each method for a total of nine trials per method. An ANOVA and paired t-tests were used to determine significance.

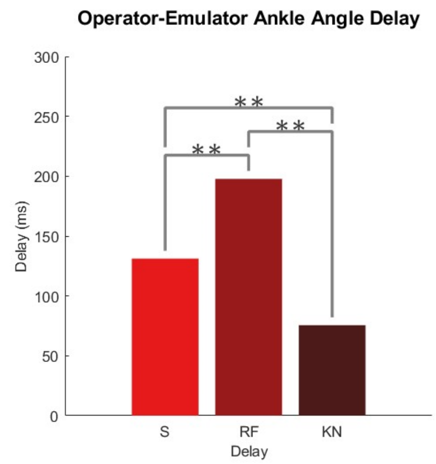

Figure 1: Statistical analysis results of paired t-tests of the delay between streaming (S), random forest (RF), and kinematic extrapolations (KN). NS – no significance, * (p<0.05), ** (p<0.01)

Results & Discussion: To determine the mechanical delay between the operator angle and the emulator angle, the signals were shifted in time according to maximal reduction of RMSE. The average delay for streaming, random forest, and kinematic extrapolation were 131 ms, 198 ms, and 76 ms, respectively. High significance ($p<0.01$) was determined between each method (Fig. 1). The RMSE was calculated on unshifted data and the shifted RMSE was calculated after the signals were shifted using the previously established delay. The average RMSE and average shifted RMSE values for streaming, random forest, and kinematic extrapolation were 8.5°, 13.0°, 8.8° and 4.9°, 9.3°, 7.5°, respectively. The corresponding levels of significance are shown in Fig. 2. These results partially support the hypothesis. Between the random forest and kinematic extrapolation algorithms, the random forest algorithm had a longer delay, but also had a higher unshifted and shifted RMSE. The kinematic extrapolation algorithm had a shorter delay compared to both the baseline and random forest algorithm, and lower unshifted and shifted RMSE compared to the random forest algorithm.

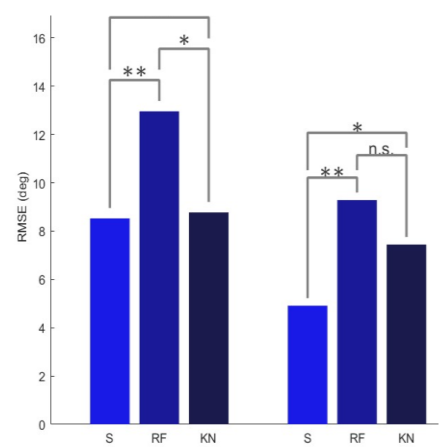

Figure 2: Statistical analysis results of paired t-tests of the RMSE and shifted RMSE between streaming (S), random forest (RF), and kinematic extrapolations (KN).
NS – no significance, * (p<0.05), ** (p<0.01)

Significance: The results suggest that a machine learning model that requires training is not necessary for ankle exoskeleton emulator control because the shifted RMSE between the random forest algorithm and kinematic extrapolation model is not significant, but the kinematic model has a significantly lower delay. This would reduce the time required to create algorithms for ankle angle predictions. With additional refinement, the kinematic extrapolation model may eventually outperform the accuracy of the baseline streaming method and further reduce the operator-emulator delay.

References: [1] Tsukahara et al. (2010), *Advanced Robotics* 24(11);
[2] Zoss et al. (2006), *IEEE/ASME Transactions on Mechatronics* 11(2).

A NOVEL APPROACH TO QUANTIFY MANUAL WHEELCHAIR PROPULSION PATTERNS

Kathylee Pinnock Branford[1*], Meegan G. Van Straaten[2], Omid Jahanian[2], Melissa M. B. Morrow[3], and Stephen M. Cain[1†]
[1]West Virginia University, Morgantown, WV, [2]Mayo Clinic, Rochester, MN and [3] Univ. of Texas Medical Branch, Galveston, TX
[*]kp0107@mix.wvu.edu and [†]stephen.cain@mail.wvu.edu

Introduction: Wheelchair propulsion is the primary mode of mobility for manual wheelchair (MWC) users, who wheel approximately 10% of the time they are seated in their wheelchairs during a typical day [1]. The MWC propulsion stroke cycle is comprised of a propulsive push phase and recovery phase. During the push phase, the hand is in contact with the rim and exerts force to increase or maintain wheelchair velocity. The arms are brought back in preparation for the next push during the recovery phase, which follows the push phase. Previous studies have identified four patterns for the hand trajectory during the recovery phase: semicircular (SC), single looping over (SLOP), double looping over (DLOP), and arcing (ARC) [2,3]. A SC pattern is recommended to prevent upper limb injuries [4]. The equipment used to quantify wheelchair propulsion in lab-based approaches (instrumented push rims, optical motion capture, and dynamometers) can alter MWC propulsion kinematics and is not adaptable to study propulsion during daily life. In contrast, inertial measurement units (IMUs) enable continuous measurements of linear acceleration and angular rate in free-living environments and can be easily attached to the user and MWC with minimal impact on propulsion dynamics. Therefore, we aim to develop an IMU-based approach to 1) calculate wrist trajectories during different wheelchair propulsion and 2) identify push and recovery phases.

Methods: We utilized a total of three IMUs (APDM Opal; linear acceleration range ±160m/s^2, angular velocity range ±2000deg/s, sampling frequency 240Hz): one on the right wrist, one above the right elbow, and one on the hub of the right rear wheel. This pilot study collected data from one able-bodied individual propelling a MWC (TiLite ZR) on an instrumented treadmill (Bertec Corporation; Columbus, Ohio) at 1.2m/s using three different propulsion patterns (SC, SLOP and ARC) for approximately 30 pushes. Instantaneous wheelchair speed was calculated using the known radius of the rear wheel and the measured angular velocity. Orientations of the upper arm and forearm were calculated from measured linear accelerations and angular velocities. We defined position vectors from the shoulder to the elbow and the elbow to the wrist using calculated orientations and the measured limb lengths of the upper arm and forearm. Principal components analyses of the two position vectors ensured that the vectors were resolved in the same inertial reference frame; orientation drift was corrected by applying rotations about the vertical axis. Summing the two position vectors yielded estimates of the wrist position relative to the shoulder; velocity of the wrist relative to the shoulder was obtained by differentiating position. We automated the identification of push phases by using the calculated wrist kinematics and wheelchair speed; a push phase begins when the wrist has a forward velocity and ends when the wrist has a backward velocity or an upward velocity.

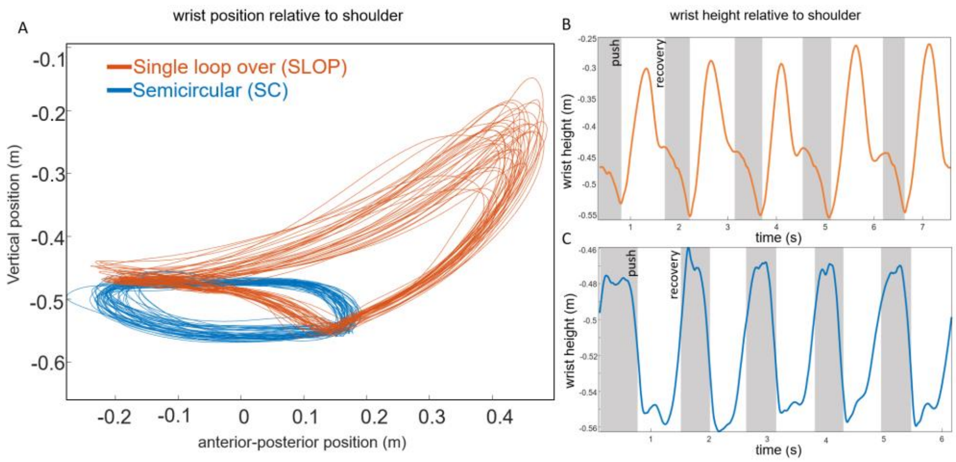

Figure 1. A) Wrist trajectories relative to the shoulder from single loop over (SLOP) and semicircular (SC) propulsion **B)** SLOP and **C)** SC wrist height relative to the shoulder versus time; shaded region is the push phase, and the white region is the recovery phase.

Results & Discussion: Figure 1A illustrates the wrist trajectory relative to the shoulder for the SC and SLOP propulsion patterns. Different propulsion patterns have different changes in wrist height relative to the shoulder during the recovery phase (Figs. 1B and 1C) and can be used to automate the identification of propulsion patterns: SC (mean height -0.49m, max. height -0.47m, min. height -0.57m), SLOP (mean height -0.24m, max. height -0.15m, min. height -0.53m), and ARC (mean height -0.47m, max. height -0.46m, min. height -0.54m). Future work will evaluate the accuracy of our approach across a range of MWC users and implement our approach to identify propulsion patterns during daily life.

Significance: We calculate the position of the wrist relative to the shoulder during MWC propulsion using measured data from IMUs secured to a rear wheel of a MWC and an MWC user's upper arm and forearm. These kinematic data can be used to robustly identify propulsion patterns and push and recovery phases of each propulsion cycle, which is important for quantifying upper extremity loading during the daily life of MWC users.

Acknowledgments: NIH Eunice Kennedy Shriver National Institute of Child Health and Human Development (R01HD084423)

References: [1] Sonenblum et al. (2012) *Rehabilitation research and practice*, 753165; [2] Boninger et al. (2002) *Physical Medicine and Rehabilitation*, 83(5); [3] Boninger et al. (2005) *Journal of rehabilitation research and development*, *42*(3). [4] Boninger et al. (2005) *The journal of spinal cord medicine*, *28*(5), 434–470

PREDICTING PERFORMANCE EFFECTS OF APPLIED PROPULSIVE FORCE IN OVER-GROUND WALKING

Evan A. Dooley[1, 2*] and Shawn D. Russell[1, 2, 3]
[1]University of Virginia, Motion Analysis and Motor Performance Laboratory, Charlottesville, Virginia, USA
*Corresponding author's email: dooley@virginia.edu

Introduction: Over 6 million people in the US use assistive devices to improve their walking performance (US Dept. of Ed.). Typically, these devices are prescribed to improve the user's stability, but use of assistive devices also affects the users' energetic cost of walking [1]. We are investigating how forces that could be applied to a person via a powered posterior walker (i.e. horizontal propulsion and breaking forces applied to the pelvis) change the energetic cost of walking. Experimentally measuring the energetic effects of assistance is challenging given the need for devices to be instrumented to capture all forces acting on the human, as well as the ability of participants to be able to walk continuously for at least five minutes. To address these challenges, we developed a simulation framework that predicts lower-body joint work required as assistive forces are applied to a human model walking. Joint work is used as the key performance metric in this study as it has been shown to relate to the energetic cost of human movement [2].

Methods: Using the OpenSim Moco environment [3], we defined an optimization scheme that enables a torque-driven human body model to interact with the ground while following the motion of over-ground walking. This optimization scheme has no a priori knowledge of ground reaction forces that match the walking motion. A foot-floor contact model [4] has been implemented to enable the prediction of ground reaction forces as external loading on the human model changes. Subject-specific models were made of 4 participants (14±7.0 y.o.; 57±33.7 kg; 1.6±0.27m; 2F, 2M). The motion to be tracked in the predictive simulations came from 3D motion capture (Vicon) of each participant walking continuously over level-ground at their self-selected walking speed. Multiple walking trials were simulated for each subject. To predict the effect of applied propulsive forces, constant point-to-point forces were created in each model between the human body model's pelvis and a point at the average pelvis height at least five meters beyond the end of the simulated walkway. Forces of -4, 0, 4, 8, 12, and 16% bodyweight (BW) were applied to each walking simulation. The predicted joint moments were then used to calculate lower-body joint work done under each of the applied force conditions. Utilizing the tracking task of the optimization implemented in these simulations, we held the motion of each trial constant while the external forces were varied. Consequently, any change seen in joint work is a result of only change in the applied force and not due to changes in walking motion.

Results & Discussion: On average, the predicted cost of walking can be minimized with the addition of 8% constant propulsive force (*Fig. 1*). While this trend agrees with values from literature, the predicted reduction is only 7% the cost of walking with no applied force, as opposed to 36% found experimentally [5]. When a -4% force is applied, this method predicts an increase of 5% in the cost of walking, agreeing with literature in both trend and value [6].

When considering each person individually, we find two groups: (1) where the unassisted condition requires the least work and (2) another where work without assist force is greater than all forward assists applied (*Fig. 1*). For the two participants where forward assist did predict a decrease in work, the minimum work needed was found with 8% BW forward assist and the reduction in that work was 25%, matching much more closely with literature experiments [5].

Initial results of this method are very promising as the group trend matches trends reported in the literature. More work is needed to fully explain differences between participants and determine whether they capture existing variance within the population, or if there is a systemic reason for why these predictions differ from the literature experiments. Even with these current limitations due to small sample size, this work still details a significant step forward in using simulations to predict walking performance of activities that could not be collected in a laboratory setting. Both simulation and experimental work is needed to validate whether this holds when considering pathologic populations.

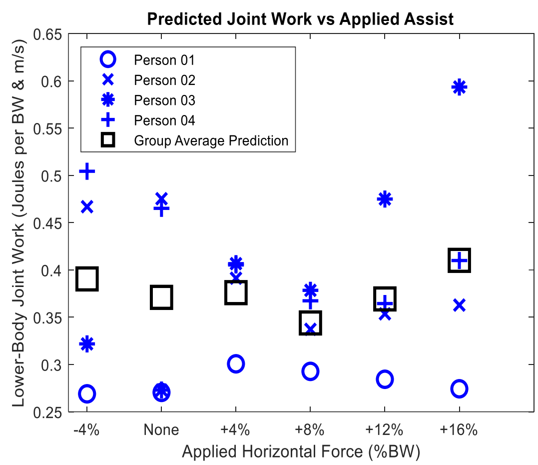

Figure 1. Average predicted lower- body joint work at each level of applied force. Each person shown as a unique blue mark, with the group as black squares.

Significance: In order to develop assistive devices that apply optimal assistance forces to their users, we must be able to predict how applying assistance forces change the users' walking performance. Ultimately, this work results in a predictive simulation framework to assess how assistive forces may alter walking performance. This will dramatically increase the assistance methods that can be investigated to improve the aid provided to users by their devices. This framework will be used to develop a posterior walker with motorized rear wheels to reduce the effort required for walking without losing the device's stability benefits; keeping this population walking longer, providing critical exercise and continued muscle development. Developing a way to better improve assistive devices will help users stay active longer, improving their quality of life and providing key physiological, mental, and social benefits.

Acknowledgements: The authors would like to thank Nick Bianca as well as the rest of the Moco forum contributors for their help and support throughout this project. This work was funded in part by NIH-SBIR 5R44HD082863-03.

References: [1] Park, *Yonsei Med. J.*, 2001, 42:180-4. [2] Russell, *Sports Tech.*, 2012, 5: 120-31. [3] Dembia, *PLoS Comput. Biol.*, 2020, 16(12). [4] Miller, *PeerJ*, 2021, 9:e11960. [5] Antonellis, *Sci. Robot.*, 2022, 7(64). [6] da Silva, *J. App. Phys.*, 2022, 133(3).

POWERED KNEE EXOSKELETON IMPROVES SYMMETRY AND REDUCES MUSCLE EFFORT DURING SIT-TO-STAND TRANSITIONS IN INDIVIDUALS POST-STROKE: A CASE SERIES

Andrew J. Gunnell[1,3,4*], Sergei V. Sarkisian[1,3,4], and Tommaso Lenzi[1,2,3,4]
[1] Department of Mechanical Engineering at the University of Utah, [2] Department of Biomedical Engineering at the University of Utah, [3] Robotics Center at the University of Utah, [4] Rocky Mountain Center for Occupational and Environmental Health
*Corresponding author's email: andy.gunnell@utah.edu

Introduction: An estimated 7 million Americans reported having a stroke making it one of the leading causes of long-term disability in the US [1]. About 80% of stroke survivors experience hemiparesis, resulting in difficulty or inability to move one side of the body [2]. Even with the best rehabilitation, most stroke survivors have permanent mobility impairments, impacting their ability to live independently [3]. Sit-to-stand is an essential daily activity that challenges stroke survivors with hemiparesis. Often, this population uses compensatory movements during sit-to-stand, resulting in asymmetric weight-bearing and knee extension torque, leading to falls and muscle fatigue [4]. Powered knee exoskeletons aim to address this problem by actively generating torque as needed to supplement the residual strength of the affected user's knee [5][6]. Despite more than two decades of research in powered exoskeletons, no study has so far investigated whether a knee exoskeleton can effectively assist stroke survivors during sit-to-stand transitions. We hypothesize that a powered knee exoskeleton can supplement the torque generated by the affected leg of hemiparetic stroke survivors, improving knee torque symmetry while reducing muscle effort and improving weight-bearing symmetry.

Methods: We recruited three stroke survivors with hemiparesis to perform sit-to-stand transitions from an armless bench in a motion capture lab without (*No Exo* condition) and with an assistive knee exoskeleton worn on the affected lower limb (*Exo* condition). During the *Exo* condition, the exoskeleton provided proportional EMG control assistance to extend the knee. Our main variables of interest were knee extension torque, knee extensor (vastus medialis, vastus lateralis, and rectus femoris) EMG, and weight-bearing symmetry. Weight-bearing symmetry was determined using the degree of asymmetry (DOA) [7]. Paired t-tests compared *No Exo* and *Exo* conditions for each outcome measure, and all results are reported as across-subject (mean ± standard error).

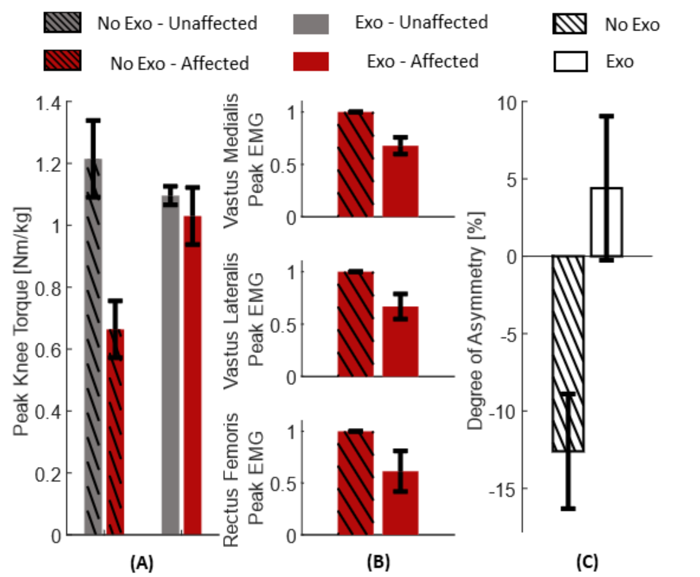

Figure 1: (A) Peak knee torque during sit-to-stand for both legs and conditions. **(B)** Affected side normalized peak EMG for three quadricep muscles. **(C)** Degree of asymmetry at point of maximum vertical GRF during sit-to-stand transition.

Results & Discussion: During the *Exo* condition, the affected-side peak knee torque was 1.03 ± 0.092 Nm/kg, compared to 0.66 ± 0.091 Nm/kg during *No Exo*, resulting in a 56% increase between (Fig. 1(A)). The affected-side peak EMG values during the *Exo* condition were all lower than the *No Exo* condition for all three knee extensors. The percentage change between *Exo* and *No Exo* affected-side peak EMGs from the vastus medialis, vastus lateralis and rectus femoris was -32.2 ± 7.98%, -33.2 ± 11.9%, and -38.6 ± 19.6%, respectively (Fig. 1(B)). The DOA during the *Exo* condition was 4.40 ± 4.65%, indicating more weight on the affected side, whereas the DOA during the *No Exo* condition was -12.6 ± 3.71%, indicating more weight on the unaffected side (17.0% change) (Fig. 1(C)). These results support our hypothesis. The powered knee exoskeleton increased the knee torque produced at the affected-side knee, while reducing knee extensor EMG on the affected-side, indicating reduced muscle effort and fatigue with the device. The weight-bearing symmetry also improved with the exoskeleton, indicating that the users put more weight on their affected-side and allowed the device to support and lift them.

Significance: Our powered knee exoskeleton increased affected-side knee torque, improved knee-torque symmetry, reduced muscle effort on the affected side, and improved weight-bearing symmetry in three stroke survivors with hemiparesis during sit-to-stand transitions. Powered exoskeletons have the potential to assist millions of stroke survivors, improving their quality of life and independent mobility.

Acknowledgements: Funded by NIOSH under grant # T42/CCT810426, and the NSF under grant # FRR-2046287.

References

[1] Benjamin, E. J. *et al.* (2019) *Circulation* 139(10); [2] Hoffman, H. (2022); [3] Mozaffarian, D. *et al.* (2016) *Circulation* 133(4); [4] Cheng, P. T. *et al.* (2001) *Arch Phys Med Rehabil* 82(12); [5] Shepherd, M. K. *et al.* (2017) *IEEE/ASME Trans on Mech* 22(4); [6] Sarkisian, S. v. *et al.* (2021) *IEEE Trans on Neur Sys and Rehab Eng* 29; [7] Highsmith, M. J. *et al.* (2011) *Gait Pos* 34(1)

SCALING MUSCULOSKELETAL MODELS USING DNYAMOMETRY

Varun Joshi[1*], Katherine A. Boyer[2], Brian R. Umberger[1]
[1]School of Kinesiology, University of Michigan, Ann Arbor, MI
[2]Department of Kinesiology, University of Massachusetts, Amherst, MA
*Corresponding author's email: varunjos@umich.edu

Introduction: Generalized musculoskeletal models are often used to represent a broad range of humans with differing levels of muscle strengths and sizes. To do this, a base set of model parameters are determined, typically from cadaveric or imaging data, and then scaled to an individual based on their height and body mass. However, such scaling methods do not guarantee that the resulting musculoskeletal models will have the dynamic motion and force production capabilities of the individuals they are meant to represent. Often, these musculoskeletal models are far stronger than the people they are based on.

In dynamometric experiments, participants are instructed to produce their maximum joint moments or velocities under controlled movement conditions, thus providing an upper limit of their movement capabilities. Previous work has tried to match the maximum moment generated in such tests to those produced by models [1]. Here, we propose using the entire task to estimate muscle parameters that allow a model to track not just the maximum joint moment but also the rate at which these moments are developed.

Methods: We used a MATLAB-based bilevel optimization method [2] with OpenSim Moco [3] to solve for the lowest ankle strength, i.e., the weakest muscles that would allow a musculoskeletal model to accurately track the results of an isometric plantarflexion strength test and a maximum ankle joint velocity test.

The following steps were performed:

1. The segment lengths and masses of the model were scaled to the dimensions of a participant.
2. The model pose was set to match that of the dynamometric task being performed.
3. All joints other than the one being tested were locked at their target pose.
4. The outer optimization loop used a genetic algorithm to select a scaling factor for the muscles.
5. The inner optimization used the scaling factor to weaken or strengthen the model and solved for the muscle excitations that most accurately tracked the measured joint angle and joint moment.
6. The results of the inner optimization were used to adjust the scaling factor in the outer loop.

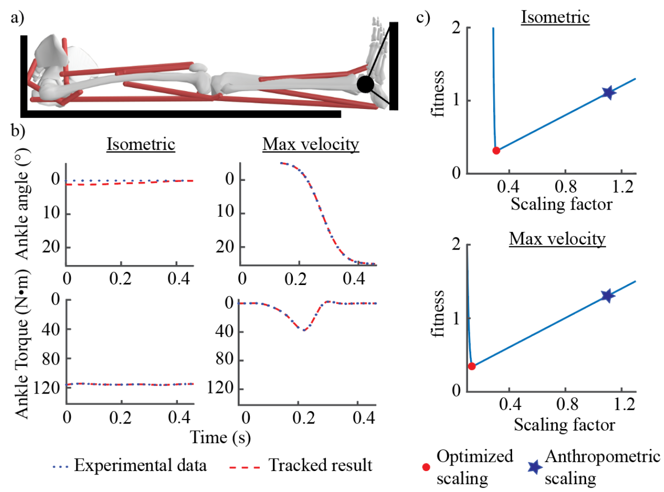

Figure 1: Tracking simulation results for maximum isometric strength and maximum joint velocity dynamometric tests for the ankle. The panels show a) the pose of the musculoskeletal model (matching experimental conditions), b) torque and angle data from the tests, and c) the inner loop cost as a function of the plantar flexor muscle scaling factor. Red circle: optimized scaling factor for the model, and blue star: anthropometric scaling factor.

Steps 4-6 were repeated until the outer loop converged to the lowest possible scaling factor (as stronger muscles can match or exceed the performance of weaker muscles) that tracked the data accurately. The cost function for the inner loop was:

$$J_{\text{inner}} = \int_o^T \left(w_{\text{ang}}\, r_{\text{ang}}(t) + w_{\text{mom}} r_{\text{mom}}(t) + w_{\text{exc}} \sum_{i=1}^{n_{\text{mus}}} e_i^2(t)\right) dt$$

where, $r_{\text{ang}}(t)$ and $r_{\text{mom}}(t)$ are the absolute tracking errors for the joint angle and joint moment respectively, and $e_i(t)$ is the excitation of the i$^{\text{th}}$ muscle at time t. The weights w_{ang} , w_{mom} , and w_{exc} were set heuristically to 100, 100 and 1 respectively. The cost function for the outer loop was:

$$J_{\text{outer}} = w_{\text{scale}} s + w_{\text{track}} J_{\text{inner}}$$

Where, s is the scale factor and the weights w_{scale} and w_{track} were set to 1 and 0.1, respectively.

Results & Discussion: Figure 1 shows the results from tracking an example data set for ankle plantarflexion. The optimization selects an ankle strength scaling factor of 0.3 for an isometric strength test, and 0.14 for a maximum velocity test. A more conventional anthropometric scaling approach [4] yielded a scaling factor of 1.1, over 3 times stronger than needed to match the isometric strength test. Given these two scaling factors (0.3 and 0.14), the higher of the two should be selected to allow the model to match the capabilities of the subject in all tests. Natural extensions to this work include adding data from isokinetic or isotonic tests, and optimizing other muscle model parameters, such as maximum contraction velocity or muscle fiber length.

Significance: Individualized muscle scaling methods allow musculoskeletal simulations to, more accurately, represent the capabilities of the individual being modelled.

Acknowledgements: This work was funded by NIH grant 5R01AG068102-02.

References: [1] Bobbert and van Ingen Schenau, (1990), *J. Biomec* 23(2), [2] Nguyen et al. (2019) *IEEE TNSRE* 27(7); [3] Dembia et al. (2020) *PLOS Comput. Biol.* 16(12); [4] Luis et al. (2022) *Front. Bioeng. Biotechnol.* 10.

Adaptation of anterior cingulate theta-band synchronization parallels adaptation to small discrete treadmill perturbations

Jinfeng Li[1*] and Helen J. Huang[1]
[1]Department of Mechanical and Aerospace Engineering, University of Central Florida, Orlando, FL 32816, USA;
*email: jinfeng@knights.ucf.edu

Introduction: Mobile electroencephalography (EEG) studies have revealed an active involvement of the anterior cingulate cortex during perturbed walking. When individuals experienced external perturbations during walking, theta (3-8 Hz) power increased within the anterior cingulate cortex, suggesting its role in error detection or monitoring [1]. However, most perturbed walking studies used large and infrequent perturbations. We recently found that small perturbations applied on a stride-by-stride basis could still disrupt gait balance and that young adults differentially adapted foot placement and center of mass control as they experienced more perturbations [2]. The purpose of this study was to investigate the adaptation of electrocortical responses to stride-by-stride small treadmill belt perturbations (acceleration and deceleration) to explore to what extent the anterior cingulate is involved in locomotor adaptation. We hypothesized that the anterior cingulate cortex would be involved in error detection to small stride-by-stride gait perturbations. We expected that anterior cingulate theta power would increase when subjects first experienced the perturbations due to perturbation induced balance disruption, and the anterior cingulate spectral fluctuations would decrease as subjects gained more experience with perturbations. We also expected distinct electrocortical responses to belt acceleration and deceleration perturbations, due to the different balance strategies subjects employed during small directional treadmill perturbations.

Methods: Fourteen young, healthy subjects (8 males, 6 females) walked on a split-belt treadmill (M-Gait) at a speed of 1.0 m/s, while we briefly accelerated (Slip) or decelerated (Stick) the left belt speed either immediately after left heel strike or at left mid-stance to create four types of perturbations. Each trial began with a 2-minute unperturbed walking (pre), followed by 8-minute perturbed walking (perturbation), and finished with another 2-minute unperturbed walking (post). Each trial included one type of perturbation, and a no-perturbation catch stride occurred randomly 1 out of every 5 strides during perturbed walking. We recorded body kinematics using a motion capture system (OptiTrack) and brain dynamics using a custom-built dual-layer EEG system (BioSemi ActiveTwo). We performed dipole source localization, time-frequency analyses, and compared electrocortical responses between early (first 33% of the strides) and late (last 33% of the strides) during the 8-minute perturbed walking.

Results & Discussion: We identified an anterior cingulate cluster with a dipole from 8 out of 14 subjects. Increased anterior cingulate theta power (synchronization) occurred after all types of perturbations (Fig. 1A), which aligns with previous studies that have reported increased anterior cingulate theta power following external perturbations [1,3]. This adds evidence that the anterior cingulate cortex is involved in error detection during locomotor adaptation. As subjects gained more experience with perturbations, theta spectral power decreased from early to late perturbed for all conditions (Fig. 1A). The theta-band average event-related spectral perturbation (ERSP) waveforms also showed significant decrease of spectral power from early to late perturbed in all conditions except for the left heel strike slip perturbation (Fig. 1B). These results suggest anterior cingulate adaptation occurred, supporting our hypothesis and first expectation.

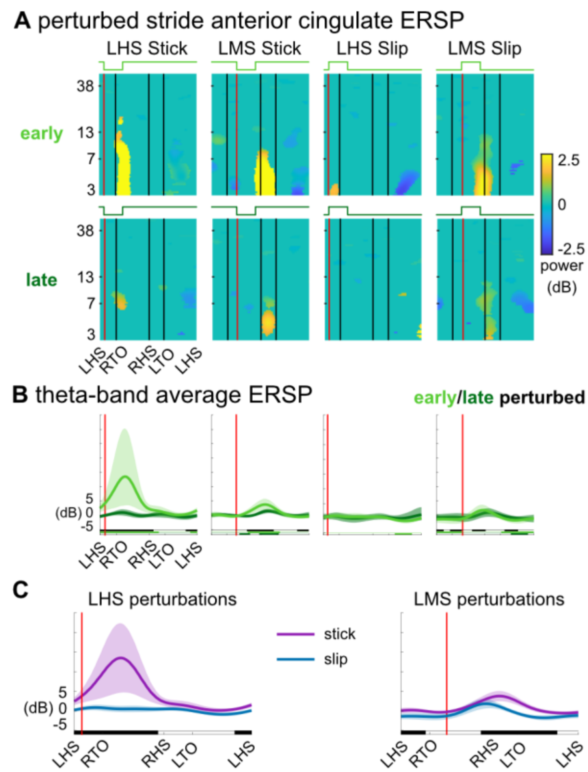

Figure 1: A, anterior cingulate event-related spectral perturbation (ERSP). B and C, theta-band average ERSP. Black bars indicate significant difference between early and late perturbed in B, while significant difference between stick and slip perturbations in C. Gait events: left heel strike (LHS), left mid-stance (LMS), right toe off (RTO), right heel strike (RHS), left toe off (LTO).

Stick perturbations elicited greater anterior cingulate theta-band average ERSP than slip perturbations, regardless of perturbation timing (Fig. 1C). This finding also supports our hypothesis and second expectation. The electrocortical responses parallel our previous study that showed that stick perturbations induced greater changes in gait stability than slip perturbations [2]. The increased anterior cingulate response for stick perturbations may reflect that falling backwards, which tends to occur with belt decelerations, is more difficult to counteract than falling forwards, which tends to occur with belt accelerations [4].

Significance: Our findings expand the understanding of the electrocortical processes involved in locomotor adaptation, highlighting the ability of the anterior cingulate to monitor errors related to small treadmill belt perturbations during walking. These findings also suggest the possibility of using perturbation direction as a means of modulating these dynamics.

Acknowledgements: This work was supported by NIH R01AG054621 (to H.J.H.).

References: [1] Peterson & Ferris (2018), *eNeuro.* 2018(5); [2] Li & Huang (2022), *J Neurophysiol.* 127: 38–55; [3] Shirazi & Huang (2021), *IEEE Trans Neural Syst Rehabil Eng.* 29: 468–477; [4] Patel & Bhatt (2018), *Exp Brain Res.* 236: 619–628.

AGE GROUP CLASSIFICATION WITH TIME-SERIES GAIT DATA

Shanpu Fang[1], Vinayak Vijayan[1], Megan E. Reissman[1], Timothy Reissman[1], Allison L. Kinney[1]*
[1]EMPOWER LAB, Department of Mechanical and Aerospace Engineering, University of Dayton, Dayton, OH, USA
*Corresponding author's email: akinney2@udayton.edu

Introduction: With increasing age populations come an expected rise in aging related injuries, with some believing that accelerated aging is closely connected to age related diseases [1]. To help mitigate this rise, research has been done to quantify the degradation of gait. These studies have shown that the degradation of gait in an elderly population, compared to that of a young population, can be recognized by purely data-driven techniques such as machine learning [2,3]. Aging is a continuous process, and the continuum from aging to its related diseases means there does not exist a clear boundary between the two [1]. Thus, it is critical to reveal this degradation during the aging process. This study focuses on not only recognizing continuous gait degradation with aging but also in an environment close to the real-world environment: at different walking speeds and with various body loads. Using the temporal, or time-series, data directly, machine learning techniques are used to classify the ages of healthy participants based on their lower limb joint kinematics and kinetics during short walking trials. Success of such an approach can help our understanding of body function degradation.

Methods: Joint kinematics and kinetics were collected and analyzed during treadmill walking of 29 healthy participants (age 34.7 ± 13.2 years, body mass 73.7 ± 12.0 kg, BMI 25.0 ± 3.6 kg/m^2, comfortable walking speed 1.06 ± 0.13 m/s, all mean ± SD; 15 were female). The study was IRB approved. Participants each walked on a treadmill at 100%, 115%, and 130% of their participant-specific, comfortable walking speed, with 10 different loads distributed at their pelvis and thighs (0 – 9.8 kg). A 60-second trial was collected for each walking speed level and load distribution, during which data were collected using motion capture (150 Hz) and force plates (1500 Hz). Time-series 3D hip, knee, and ankle angles and moments were calculated using Visual3D (C-motion Inc., Germantown, MD USA), after which a machine learning pipeline, "timesias" [4,5], based on LightGBM, was used to train machine learning models (5-fold cross validation). Each participant was placed in one of the six age groups, with 10-year increments. Models had no knowledge of walking speed and body load. A model made its classification decision for a specific 60-second trial based only on the time-series joint angles and moments. Model accuracies of age group classification were compared between "3D angles + 3D moments", "3D angles only", and with reduced dimensions (for example, sagittal plane only). SHAP analysis was conducted to highlight feature contributions.

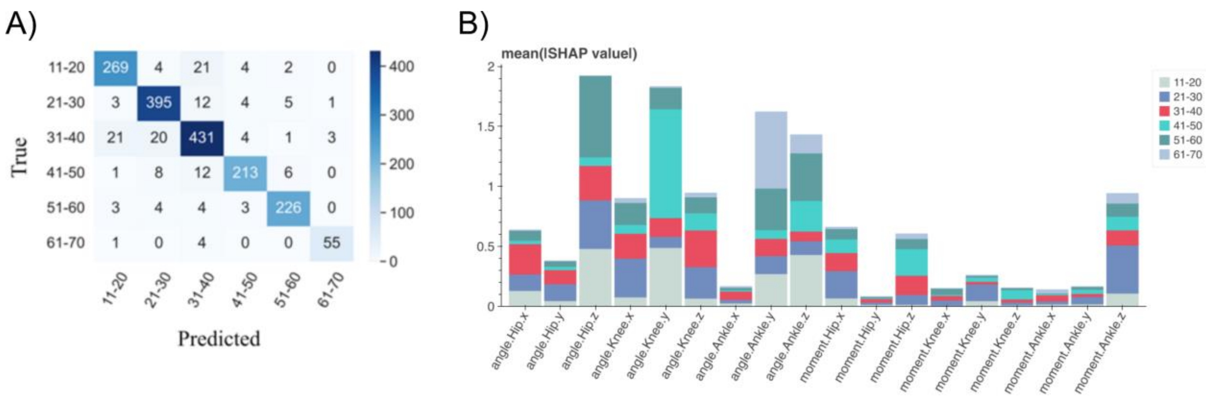

Figure 1: A): Numbers of model predicted classification versus true classification for 10-year age groupings. Sagittal, frontal, and transverse plane angles and moments were included. B): Mean absolute SHAP values for each age group and angle or moment feature. x: Sagittal, y: Frontal, and z: Transverse.

Results & Discussion: High classification accuracies were achieved by the time-series machine learning models. With both joint angles and moments in all 3 planes, the classification accuracy was 91.3%. This accuracy was achieved over 1740 trials. The confusion matrix (Fig. 1A) shows that most incorrectly classified trials were placed in age groups close to their true values. This supports the argument that aging is a continuous processing, which can be demonstrated via this machine learning approach. The high accuracy also demonstrates that even with different gait speeds or different body loadings, the age group gait discrepancies are maintained. The SHAP values (Fig. 1B) show that for most age groups, the contributions were distributed across multiple features. This explains why the accuracy drops dramatically to 66.3% with only sagittal plane joint angles included. Joint moments overall make less contributions, and even when excluded, a high accuracy of 88.8% was still achieved. This shows that lower limb joint angles alone are sufficient for obtaining a relatively high classification accuracy. This is encouraging since the estimation of joint moments requires expensive equipment including force plates, as opposed to less expensive IMUs for joint angles.

Significance: The machine learning approach taken here has demonstrated that aging as a continuous process can be classified by time-series gait data. Since joint angle data are sufficient for performing accurate classification, a remote health monitoring system could utilize devices such as IMUs to monitor a patient's gait and provide clinical references to mitigate aging related injuries/diseases [6].

References: [1] Franceschi et al. (2018). *Front Med* 5(61); [2] Zhou et al. (2020). *Sci Rep* 10(1); [3] Rehman et al. (2019). *Sci Rep* 9 (1); [4] Guan et al. (2021). *iScience* 24(2); [5] Zhang et al. (2021), *STAR Protocols* 2(3); [6] Vegesna et al. (2017). *Telemed e-Health* 23(1).

A COMPARISON OF NERVE AND NERVE ROOT NONLINEAR ELASTIC MECHANICAL BEHAVIOR IN HUMAN, PORCINE, RABBIT, AND MURINE SPECIMENS

Rachel E. Bruns[1*], Mackenzie A. Hoey[2*], Zac Domire, PhD[2], Alex Vadati, PhD[1]

[*] These authors contributed equally to this work.

[1]Department of Engineering, East Carolina University, Greenville, NC

[2]Department of Kinesiology, East Carolina University, Greenville, NC

Introduction: Radiculopathy of the spine is a prevalent chronic disorder, affecting up to 10% of individuals over the age of 50[1]. It is caused by a wide number of pathologies, such as disc herniation, sciatica, degenerative lumbar scoliosis, ligament ossification, spinal stenosis, and other acute injuries. Nerve roots, which are vulnerable to damage within the spinal column, often are a direct source of pain in these various conditions. To find better treatments, the mechanisms of nerve root pain within the spine must be more fully understood. These mechanisms can be investigated using mathematical methods to create realistic models of the spine and simulate both static and dynamic loading through finite element (FE) modeling. One of the main components of any FE model is realistic mechanical properties and behavior of the tissue. While the mechanical properties of nerves and nerve roots have been investigated for decades, there are few examples of studies that report their stress-strain relationship prior to failure, and even fewer studies fit this experimentally-derived load response to the corresponding constitutive material models. Moreover, the species, age, health, size, and type of nerve highly influences their mechanical properties[2]. The purpose of this research is to compare uniaxial tension test data from several different species and types of nerves by calibrating hyperelastic material models for the purpose of credible FE model development. As the application of bio-fidelic finite element models in biomechanics is growing exponentially, this information is necessary to develop more accurate models that investigate nerve root biomechanical interactions in a wide variety of chronic spine disorders.

Materials and Methods: Following a literature search for uniaxial tensile test studies of human and animal nerves, constitutive hyperelastic material models were calibrated for each dataset found. Uniaxial tension stress-strain relationship datasets were extracted using PlotDigitizer for nerve roots from rats[3], rabbit tibial perineurium[4], porcine nerve roots[5], and human tibial and peroneal nerves[6]. The rabbit tibial perineurium dataset was obtained at a faster strain rate 10 orders of magnitude greater than the other datasets. MCalibration version 7.1.1 (Veryst Engineering Needham, MA, USA) was used to run optimization of coefficients for a hyperelastic Ogden material model with stress-strain relationship for uniaxial tension shown below.

$$\sigma_u = \sum_{k=1}^{N} \frac{2\mu k}{a_k}\left[\lambda^{a_k} - \left(\frac{1}{\sqrt{\lambda}}\right)^{a_k}\right],$$

where σ_u represents uniaxial principal stress, N is the order of the model (set to 3), μ and a_k are material constants, and λ is the first principal stretch. Optimization was based on maximizing the R^2 value between the model and stress-strain experimental data. To ensure model stability in a wide range of strains, Drucker stability tests were run for all cases. The calibrated Ogden hyperelastic models were also compared to previously reported Ogden models for human ulnar and median nerves[7].

Results and Discussion: The stress-strain curves and R^2 values of each dataset is shown in Figure 1. R^2 values for all the datasets were greater than 0.96, with the highest being the human peroneal model at 0.995. One of the main take aways from Figure 1 is the wide range of reported stiffness of nervous tissue between species and type of nerve. Tissues closer to the spinal cord, like nerve roots, were reported to be less stiff than peripheral nerves, potentially resulting in higher deformability of nerve roots and increased vulnerability to developing radiculopathies. Additionally, the shape of the stress-strain curve varies among different specimens as stiffness increases. Less stiff nerves demonstrated a strain-stiffening behavior while the stiffer nerves show a strain-softening behavior. This could be due to the differences in the size of the nerves, histological composition, or variations in testing techniques. In general, datasets including rate dependent behavior in the literature are limited and need to be investigated in order to account for viscoelastic properties of nerve tissue. In conclusion, our results demonstrate that biomechanical modeling of nervous tissue is highly nuanced, and it is critical to understand the variety of experimental conditions that contribute to differences in mechanical behavior before creating credible FE models for a specific application.

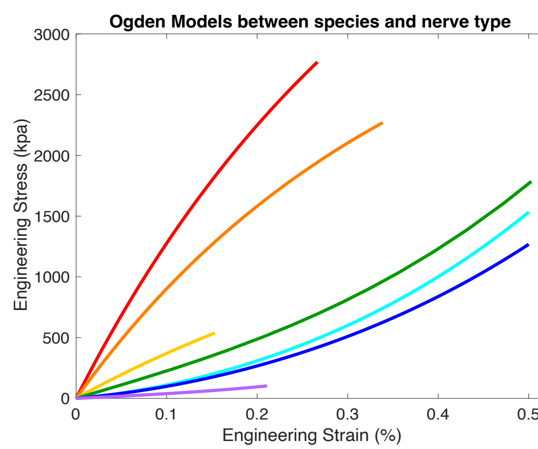

Color	Nerve	R^2
	Human Tibial	0.980
	Human Peroneal	0.995
	Pig Nerve Fibers	0.962
	Rabbit Tibial-Perineurium	0.975
	Human Ulnar	~
	Human Median	~
	Rat L4 Nerve Root	0.978

Figure 1-*Ogden stress-strain hyperelastic relationship of different nerve tissues and R^2 values*

Significance: As FE modeling of biological tissues grows in popularity, it is important to have a robust and accurate understanding of the mechanical properties of the modeled tissues. This study has provided hyperelastic constitutive models for a variety of different nerves and species. The results from this study allow us to implement more accurate material models into human and animal FE models. With more accurate models, we can further explore and understand the mechanisms for chronic radiculopathic conditions.

Acknowledgements: This work was supported by the Office of Naval Research [N000142112649].

References: [1] Mansfield et al. (2020). *Musculoskeletal Care*. [2] Paggi et al. (2021). *J of neural engineering* [3] Singh et al. (2006). *J of biomechanics*. [4] Koppaka et al. (2022). *J of Biomechanics.* [5] Tamura et al. (2015). *J of Sustainable Research in Engineering.* [6] Kerns et al. (2019). *Anatomical record*. [7] Ma et al. (2013). *J of Biomedical Material Research*.

MOTOR CONTROL ASSESSMENT USING WEARABLES DURING POST-STROKE GAIT

Azarang Asadi[1*], Jill S. Higginson[2], Jeffrey A. Reinbolt[1]
[1]Department of Mechanical, Aerospace, and Biomedical Engineering, University of Tennessee-Knoxville
[2]Department of Mechanical Engineering, University of Delaware
*Corresponding author's email: aasadi1@vols.utk.edu

Introduction: Stroke is a leading cause of disability worldwide and nearly 795,000 people annually suffer strokes in the U.S [1]. Stroke-related motor control impairments, such as post-stroke gait, severely limit daily life activities. Improving motor control of gait is one of the main goals of post-stroke rehabilitation; however, residual impairments remain for some despite treatment efforts. Gait performance is assessed by functional biomechanical measures, which are *effects* of motor control. Muscle synergies are weighted groups of muscles coactivated to *cause* a movement and have been associated with functional walking ability [2], which may provide a better measure for treatment outcomes. To monitor outcomes during and after treatments, Inertial Measurement Units (IMUs) have successfully assessed the functional performance of individuals with gait disabilities. In this simulation study, we aim to investigate post-stroke gait motor control assessment using virtual IMUs placed bilaterally on lower limbs. Our objective is to identify the relevant measures from IMUs that best explain the variance in motor control to develop a predictive model for motor control assessment.

Methods: Subject-specific musculoskeletal models and dynamic gait simulations were created using OpenSim [3] for 8 individuals post-stroke before and after 12-weeks of FastFES retraining. Virtual IMUs (6 units with 3 axes each) were placed bilaterally on the thighs, shanks, and feet segments. IMU signals (linear acceleration, a, and angular velocity, ω) were generated using the Body Kinematics and Point Kinematics tools and defined relative to the anterior-posterior (AP), superior-inferior (SI), and medial-lateral (ML) axes in a global reference frame. Computed Muscle Control determined muscle activations and, to compare with EMG studies, 5 muscles (rectus femoris, semimembranosus, biceps femoris long head, medial gastrocnemius, anterior tibialis) were used to calculate one muscle synergy related to motor control ability [2]. The Variance Not Accounted For ($VNAF_1$) by this one synergy was used as the motor control index, and the entire cohort's $VNAF_1$ median categorized 182 gait cycles into 2 groups with either low or high motor control. Distinguishing regions between the groups were identified with Statistical Parameter Mapping (SPM), addressing shortcomings of 0D methods by analyzing the entire signal trajectory, and the peak values of each region were extracted [4]. Stepwise multiple linear regression with 10-fold cross validation was carried out to identify the best performing measures and develop the predictive model.

Results & Discussion: The cross-validated, stepwise regression model identified 10 IMU measures for motor control assessment (Table 1). The predictive model indicated that IMUs may be utilized to assess post-stroke gait motor control (Figure 1, $R^2 = 0.77$, adj. $R^2 = 0.75$, $p < 0.001$). Two IMU measures of angular velocity (ω) for the paretic thigh about the ML axis show consistency with previous studies indicating lower peak hip flexion rates are observed in post-stroke gait [5]. This observation may be associated with limited hip flexion/extension following stroke, which contributes to the appearance of circumduction. Future studies may use clustering analysis to better categorize different gait cycles according to their extent of motor control impairment, such that similar gait patterns are grouped together, resulting in a better identification of distinguishing regions.

Significance: These results demonstrate the utility of IMUs for motor control assessment of individuals with post-stroke gait, which may translate to assessments outside of the gait treatment laboratory. Our findings will facilitate and benefit healthcare to advance individualized rehabilitation by allowing providers to monitor treatments and maximize outcomes. To our knowledge, this work is the first to combine biomechanical simulations, muscle synergy analysis, and IMUs to develop a predictive model for motor control assessment. Our approach for post-stroke gait may extend to other populations with motor control impairments.

References: [1] Centers for Disease Control and Prevention; [2] Steele et al. (2015), *Dev Med Child Neurol*, 57(12); [3] Delp et al. (2007), *Biom. Eng. IEEE*, 54(11); [4] Patakay et al. (2015), *J Biomech.*, 48(7); [5] Rybar et al. (2014), *Gait & Posture*, 39(4)

Table 1. Identified IMU measures for motor control assessment.

Limb	Measure	Gait Region	Estimate	Std. Err.	*P*
Non-paretic	ML ω foot	Mid-stance	0.00065	0.00021	0.00256
	SI ω foot	Mid-swing	0.00009	0.00003	0.00711
Paretic	ML ω foot	Terminal stance	-0.00036	0.00010	0.00072
	ML a shank	Mid-stance	0.01028	0.00305	0.00092
	SI a shank	Initial swing	-0.00368	0.00076	<0.00001
	AP a shank	Terminal swing	-0.00616	0.00106	<0.00001
	AP a thigh	Initial contact	-0.01052	0.00509	0.04021
	ML ω thigh	Mid-swing	0.00054	0.00011	<0.00001
	ML ω thigh	Terminal swing	-0.00024	0.00007	0.00048
	SI a thigh	Pre-swing	0.00625	0.00205	0.00265

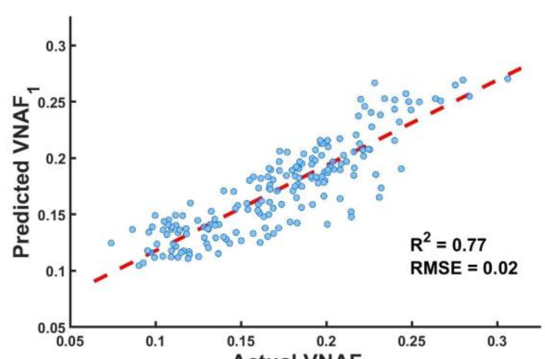

Figure 1. Regression results of motor control predicted by IMUs.

THE INFLUENCE OF SEX AND BODY SIZE ON HIP JOINT CENTRE ESTIMATION METHODS ON KNEE KINEMATICS

Harry S. Battersby[1*], Skylar C. Holmes, Steven A. Garcia, and Derek N. Pamukoff[1]
[1]Western University, London ON, Canada
email: hbatters@uwo.ca

Introduction: Joint center location is essential when using motion capture to measure accurate kinematic and kinetic data during gait. Due to subcutaneous tissue joint geometry, the hip joint center (HJC) must be estimated using estimation methods based on externally placed anatomical landmarks. Common methods use a regression model with pelvic landmarks such as the ASIS, PSIS, and Sacrum as inputs [1] (e.g., Coda) or a system using 25% the intertrochanteric distance (GT). However, different methods result in different HJC estimations [2]. A difference in HJC location influences kinematics knee kinetic and kinematic [3]. The influence of the HJC method on hip kinematics during gait has been assessed [4], but little is known about the effects of HJC estimation methods on knee biomechanics. The knee adduction angle (KAA) and knee flexion angle (KFA) are widely reported in the literature because they influence knee osteoarthritis progression [5]. Moreover, anatomical differences that further remove marker placement from accurate anatomical landmark positions, such as high BMI individuals [6], or differences between sexes, such as pelvis shape [7], have not been examined when looking at the effects of different HJC estimation models. The purpose of this study was to compare knee kinematics during gait in individuals with and without obesity and between males and females using two different HJC estimation methods. We hypothesized a KFA using the GT method compared with the Coda HJC method. We also hypothesized a lower level of agreement in sagittal and frontal plane knee kinematics between the HJC methods in individuals with obesity compared to individuals without obesity and in females compared to males.

Methods: Twenty-four males and 24 females with obesity (BMI>30) (Age=22.8±3.5 years, BMI=33.1±4.1 kg*m^2, body fat %=37.91±7.15) and 24 males and 24 females without obesity (BMI: 18.5-30) (Age=22.0±2.6 years, BMI=21.6±1.7 kg*m^2, body fat %=19.88±6.57) participated. Gait biomechanics were assessed over 5 trials along a 10m walkway. Calibration markers from the ASIS and PSIS were used to derive the HJC using the Coda method, and from the GTs to derive the HJC using the GT method. Marker trajectories were sampled at 240 Hz and force plate measurements were sampled at 2400hz. Visual 3D was used to create 2 right HJCs could be obtained. Gait outcomes included the peak KAA and KFA. Gait outcomes were compared between HJC methods using a 2(Method) by 2(Sex) by 2(BMI group) repeated measures ANOVA. Intraclass correlation coefficients (ICC: two-way mixed, absolute agreement, average measures) were used to quantify the agreement between HJC estimation models.

Results and Discussion: Peak values for KFA and KAA for groups can be found in Table 1. There were no significant interaction effects between BMI, sex, and method. A main effect of method was found for the KAA ($p<0.01$). Peak KAA was greater (2.28°) in the Coda method than in the GT method across all groups. ICCs indicated excellent agreement for both HJC models in the KAA for Males without obesity (ICC: 0.92, 95%CI: 0.06-0.98), Females without obesity (0.88, 95%CI: 0.05-0.97), Males with obesity (0.86, 95%CI: 0.04-0.96), and Females with obesity (0.89, 95%CI: 0.16-0.97). ICCs also indicated excellent agreement for both HJC models in the KFA for Males without obesity (0.95, 95%CI: 0.89-0.98), Females without obesity (0.92, 95%CI: 0.70-0.97), Males with obesity (0.90, 95%CI: 0.78-0.96), and had good agreement for Females with obesity (0.72, 95%CI: 0.37-0.88).

Significance: The Coda and GT HJC estimation methods showed excellent agreement for peak KAA in all groups. Despite excellent agreement, the confidence intervals for each group were large and caution should be taken when assessing the reliability of these results. Further, the Coda method produced a significantly greater KAA than the GT method suggesting a more medial HJC estimation when using Coda. This systemic difference in methods however was only 2.28° and should be interpreted with caution due to the small magnitudes of difference when examining frontal plane kinematics that could be attributed to measurement error. Excellent agreement was found between methods for peak KFA in all groups other than females with obesity. This increases confidence when comparing sagittal plane knee kinematics between HJC methods in males with and without obesity. However, females have more adipose tissue distributed throughout the pelvis segment than males [8]. Researchers should be cautious when comparing knee kinematics between studies that used different HJC estimation techniques, particularly in females with obesity.

References

1. Davis, (1991). *Human Movement Science*, *10*(5), 575–587. **2**. Bennett, (2016). *Journal of Biomechanics*, *49*(13), 3047–3051. **3**. Stagni, (2000). *Journal of Biomechanics*, *33*(11), 1479–1487. **4**. Sangeux, (2014). *Gait & Posture*, *40*(1), 20–25. **5**. Pamukoff, *Gait and Posture*, 65, 221–227. **6**. Browning (2007). *Medicine & Science in Sports & Exercise*, *39*(9), 1632–1641. **7**. Tague, (1989). *American Journal of Physical Anthropology*, *80*(1), 59–71. **8**. Simpson, (2010). *Sleep*, *33*(4), 467–474.

	Males without obesity	Females without obesity	Males with obesity	Females with obesity
KFA Coda (degrees)	26.58°± 5.98	24.01° ± 5.83	24.52° ± 5.96	25.22° ± 4.25
KFA GT (degrees)	26.64° ± 6.76	22.92° ± 8.38	26.84° ± 7.84	26.81° ± 5.29
KAA Coda (degrees)	1.45° ± 3.96	3.04° ± 4.96	0.36° ± 3.96	3.07° ± 4.05
KAA GT (degrees)	-0.47° ± 3.93	0.01° ± 5.28	-1.80° ± 3.80	1.06° ± 3.91

Table 1: Peak KFA and KAA (Mean ± SD) from stance phase within all groups.

ACCURACY AND PRECISION OF A PRESSURE SENSITIVE WALKWAY MEASURING SPATIOTEMPORAL GAIT PARAMETERS ACROSS DIFFERENT FOOT STRIKE PATTERNS

Samuel Hockett[1], Spencer Stinson[1], Caleb Williams[1], Brian Garner[1], Jonathan Rylander[1]
[1]Department of Mechanical Engineering, Baylor University, Waco, TX
samuel_hockett1@baylor.edu

Introduction: Spatiotemporal gait parameters are commonly used to quantify physical functioning in health care, athletics, engineering, and more. Notably, these parameters are used to track patient progress in populations with atypical gait patterns such as cerebral palsy [1], amputation [2], and joint replacement [3]. For gait analysis, the gold standard is marker-based motion capture and floor mounted force plates [4]. While this equipment is reputable, it can be quite expensive and time-consuming. Alternatively, pressure-sensitive walkways (PSW) are typically more affordable, simpler, and more portable. However, for a PSW to be useful for application, the accuracy and precision of these devices must be evaluated for various foot strike patterns. Therefore, the purpose of this study was to evaluate the error of a recently developed PSW with different foot strike patterns to emulate atypical gaits by comparing its measures of step width, step length, and step time with those measured using a gold standard system.

Methods: The study was deemed exempt by the Baylor University IRB. Data from adults (N=10, Mean Age: 23.5) with no lower-limb impairments was collected. The gold standard (GS) was a twelve camera Vicon™ Vantage™ motion capture system (250Hz) synced with three floor-mounted AMTI force plates (500Hz). Reflective markers were placed according to the Vicon Lower-Body Plug-in-Gait model. A high resolution, four-tile Tekscan® Strideway™ (TS) system (250Hz) was placed over the force plates to create three consecutive foot strike locations over a distance of 260cm. Force plate locations were outlined with tape on the TS to indicate where subjects' feet must strike to ensure direct comparison of gait events. Each subject recorded 10 left and 10 right steps for each of five foot strike patterns: 1) self-selected normal walking speed with normal (heel-to-toe) foot strike (N); 2) same as normal strike pattern but at a self-selected faster speed (F); 3) normal speed and strike but the foot at a toe-out angle (prompted at 45deg) (TO); 4) toe-walking (forefoot strike only) at a normal speed with no toe-out foot angle (TW); 5) toe-walking at a normal speed with a toe-out foot angle (TO+TW). For the TS system, the standard software automatically detected and boxed foot strikes. For both TS and GS, stepping parameters were calculated according to heel-based line of progression methods used by the standard TS software [5]. Within each strike pattern group, accuracy error was defined as the mean difference between TS and GS values from the 10 left or 10 right steps of a single subject. Precision error was defined as the difference between the calculated standard deviation by the TS and GS from the same right and left step groups. This led to 20 samples for each strike pattern group. A one-way ANOVA on strike pattern was performed to elucidate the effect it has on the performance of the TS.

Results & Discussion: Accuracy and precision errors are shown in Table 1 and Table 2. Within the normal (N) strike pattern, the TS had good accuracy and precision. However, step width accuracy was strongly dependent on heel contact as the toe-walking strike patterns performed worse (Fig. 1). Without heel contact, the TS is only estimating heel position while the GS can track true heel position. This discrepancy is most evident in the TO+TW strike pattern since the heel is not contacting and is displaced mediolaterally compared to the forefoot due to the toe-out angle. Opposite to step width, step time error is increased for strike patterns with heel contact (N, F, TO). This is due to boxing errors in which the TS software does not box the foot properly and the most common error is when only the forefoot is boxed while excluding the heel. For step length, data shows excellent accuracy and precision across strike patterns.

	N	F	TO	TW	TO+TW	p-value
SW	-2.6%	1.4%	42%	39%	177%	<0.0001
SL	3.5%	2.3%	2.0%	3.5%	2.5%	0.787
ST	-1.0%	-7.8%	-4.0%	-1.4%	-0.7%	0.009

Table 1: Accuracy errors across the five foot strike patterns listed as percent of gold standard mean values for step width (SW), step length (SL), and step time (ST). The p-values listed are for the one-way ANOVA on foot strike pattern effect.

	N	F	TO	TW	TO+TW	p-value
SW	2.8%	6.4%	21%	5.0%	7.9%	0.224
SL	1.1%	1.6%	0.3%	0.7%	1.0%	0.501
ST	4.6%	11.4%	6.3%	-0.5%	-0.1%	0.0003

Table 2: Precision errors across the five foot strike patterns listed as percent of gold standard mean values for step width (SW), step length (SL), and step time (ST). The p-values listed are for the one-way ANOVA on foot strike pattern effect.

Significance: The results presented in this abstract indicate that a pressure-sensitive walkway can be used to accurately and precisely measure step width, step length, and step time under normal strike patterns, but the user needs to be aware that errors can substantially increase with certain foot strike patterns. The results of this study will help inform users about potential issues when using a PSW for testing populations with atypical gait patterns.

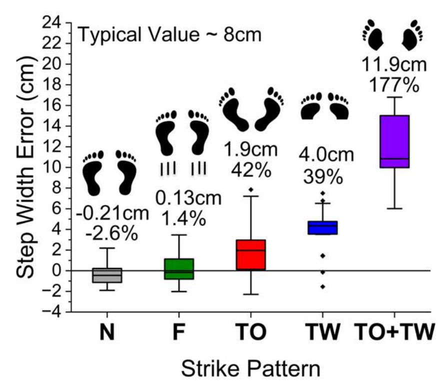

Figure 1: Step width accuracy error of the Tekscan Strideway across the five foot strike patterns.

Acknowledgements: This work was supported by a grant from the Texas Higher Education Coordinating Board (THECB). The opinions and conclusions expressed in this document are those of the authors and do not necessarily represent the opinions of the THECB.

References: [1] Corsi et al. (2019), *Dis & Rehab* 43(11); [2] Wong et al. (2016), *Pros & Orth Intl* 40(1); [3] Kolk et al. (2014), *Clin Biomech* 29(6); [4] Goldfarb et al. (2021), *Comp Meth & Prog in Biomed* 212; [5] Tekscan® Strideway™ Help File Sys. Ver. 7.7x

Development of a low-cost biocompatible EMG electrode: sensitivity, validity, and instructions for fabrication

Stoneback L[1*] and Fullano GD[2], White MS[1], Naaz S[1], Lepley LK[1]
[1]School of Kinesiology, University of Michigan, Ann Arbor, MI.
[2]Department of Molecular and Integrative Physiology, University of Michigan, Ann Arbor, MI
*Corresponding author's email: lukeston@umich.edu

Introduction: Electromyography (EMG) is a valuable diagnostic tool for detecting neuromuscular abnormalities that can be especially useful in preclinical models during the development and testing of interventions. In these models, implantable biocompatible electrodes are commonly used, however their use can be cost-prohibitive. To remedy this issue, we sought to fabricate a low-cost biocompatible electrode that matches the rigor of the current industry standard.

Methods: The main objective of this investigation was to produce a low-cost EMG electrode that matches the sensitivity and validity of the current industry standard (EP105, Chronic EMG Patch, MicroProbe). Detailed instructions regarding low-cost biocompatible electrode construction are provided in Figure 1. The rigor of these electrodes was tested using a series of *ex vivo* and *in vivo* procedures. The *ex-vivo* procedure used a saline bath to mimic physiological conditions to compare our custom-fabricated electrode to that of the industry standard on measures of sensitivity (i.e., signal agreement). The *in-vivo* procedure consisted of the surgical implantation of the electrode into the vastus lateralis (VL) muscle of 16-week-old age female Long Evans rat (Envigo) to test signal validity during uphill and downhill gait. The *in-vivo* procedure was conducted with approval (IACUC #PRO00009166) and in accordance with the NIH animal care guidelines.

All data were analysed using Prism ($P<0.05$). For *ex-vivo* testing the level of sensitivity between electrodes was assessed using a series of Pearson correlation coefficients and Bland-Altman plots. These statistical tests were applied to 8000 samples from sine, triangle and square waveforms that were produced by a signal generator (4005DDS 5MHz Function Generator, B&K Precision) in the saline bath. The validity of the custom electrode was assessed via *in-vivo* testing, where the rat's gait was perturbed and a reduction or increase in VL EMG would be expected. These data were rectified and smoothed using a RMS algorithm in MATLAB. Mean EMG values during stance (i.e., paw-on to paw-off) during 25 seconds of free walking (at 16m/min) were compared using welch two-sample t-test between incline and decline walking conditions.

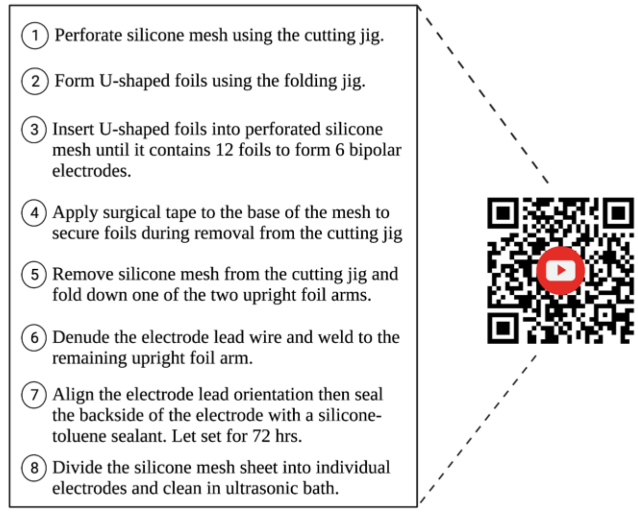

Figure 1. Instructions for the fabrication of biocompatible EMG electrodes with video demonstration.

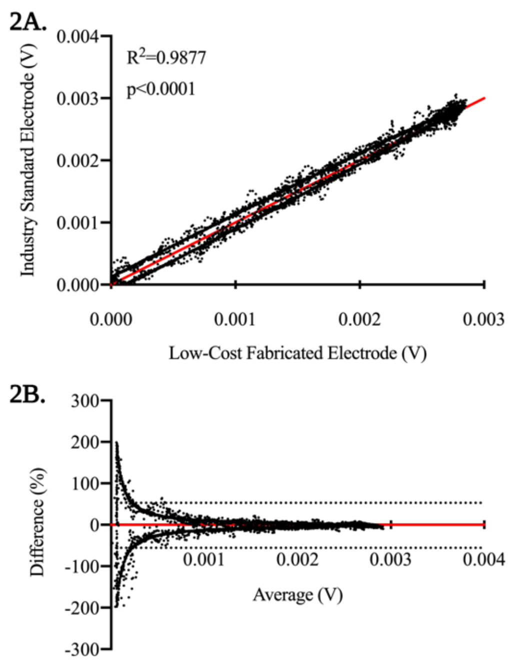

Figure 2. Representative waveform analysis. A. Pearson correlation between the low-cost fabricated and industry standard electrode for a 5 Hz sine wave. B. Bland-Altman plot of the percent difference between the custom and industry standard electrodes across average voltages.

Results & Discussion: *Ex-vivo* testing revealed high levels of signal agreement between the custom and industry standard electrode across all tested waveforms (sine [$R^2 = 0.987$], square [$R^2 = 0.990$], triangle [$R^2 = 0.931$] representative plots, Figure 2). Mean EMG activity during stance was found to be significantly lower during downhill walking (0.113 ± 0.035, $p = 0.011$) than uphill (0.176 ± 0.066). This *in-vivo* observation is consistent with previous studies [1], that report concentric contractions (i.e., uphill walking) to be characterized by higher levels of EMG signaling than eccentric contractions (i.e., downhill walking). Collectively, these findings support the sensitivity and validity of our low-cost biocompatible electrode with detailed instructions for assembly.

Significance: Quantification of electrical activity of muscle is fundamental to understanding the underlying mechanisms of disorder and the effectiveness of potential treatments. Our custom fabricated electrode represents a cost-effective alternative (approx. $32/unit) to the industry standard (approx. $300/unit) that can be used by others in the field to quantify this important metric of musculoskeletal health.

Acknowledgements: This work was supported NIH/NIAMS K01AR071503 to Lepley LK.

References: [1] Butterfield TA, Leonard TR, Herzog W. J Appl Physiol (1985). 2005.

SEX DIFFERENCES IN INDIVIDUAL MUSCLE ASYMMETRY LEVELS OF THE LOWER EXTREMITY IN HEALTHY ADULTS

Olivia DuCharme, ME[1*], Matthew Cousins, BS[1], Silvia S. Blemker, PhD[1,2], Lara Riem, PhD[1]
[1]Springbok Analytics, Charlottesville, VA
[2]University of Virginia, Charlottesville VA
*Corresponding author's email: olivia.ducharme@springbokanalytics.com

Introduction: The purpose of this study was twofold: (1) establish normative asymmetry ranges for individual muscles of the lower extremity in healthy adults and (2) examine if sex differences in asymmetry exist in healthy adults. Understanding muscle asymmetry is crucial for contextualizing performance adaptations, understanding compensation during recovery, and developing predictive indices for injury. Muscle asymmetry can indicate compensation following injury recovery [3], exhibiting heterogenous patterns across patients as observed following ACL surgery [4]. Therefore, restoration of muscle symmetry after injury is of great interest [7,8]. However, understanding normative ranges of asymmetry is important for interpreting asymmetry levels in injured individuals. Asymmetry prevalence can be performance dependent. Previous research has demonstrated interlimb asymmetries are common in soccer players (asymmetrically demanding sport) [5,2], while low interlimb asymmetries are found in symmetrically demanding sports, such as track athletes [6]. Lastly, asymmetry is a predicator for incidence of injury. Previous work has found a muscle asymmetry threshold of 15% or higher to be linked with increased injury [1,2]. While these thresholds help create basic guidelines to help predict injury and understand possible performance adaptations, it fails to individualize expected asymmetry by muscle function, performance, and related to sex. Current work has begun to investigate and define individual muscle asymmetry characteristics in the quadriceps and hamstring muscles [10], however, to our knowledge, this has not yet been established for muscles throughout the lower extremities, while examining sex differences. To measure asymmetry in the currently proposed study, volumes were measured in 54 lower extremity muscles obtained from MRI scans. We hypothesize that muscle-level asymmetry will vary between muscles and between sexes.

Methods: A total of 96 healthy adults participated in this study: 46 females (25.7 ± 8.8 years) and 50 males (24.0 ± 8.7 years). Lower body axial T1 weighted sequence magnetic resonance imaging (MRI) scans were collected for all participants to acquire images of the entire lower limbs from T12 to the fibular malleoli with a minimum resolution of 1.9 x 1.9 x 5 mm. Automated segmentation [11] was performed to quantify 27 muscle volumes bilaterally, and final segmentations were vetted by a team of trained segmentation engineers to ensure consistency and accuracy across patients. Muscle volumes were calculated by summing voxel volumes from segmented images. To assess asymmetry of limb muscles, the absolute percent difference in muscle volume between muscles sides was found. To compare differences in asymmetry between sexes and individual muscles, a two-way mixed repeated ANOVA was used with sex being the between-subject effect and muscle being the within-subject effect. The data was skewed to the right (as asymmetry value was an absolute value) and therefore a log10 transformation was used before analysis. A statistical significance level of $\alpha = 0.05$ was used.

Results & Discussion: There was no statistically significant interaction between muscle and sex. The main effect of muscle demonstrated a significant difference in asymmetry between muscles ($F(24, 2444) = 5.96$, $p < .001$, $\eta 2 = 1.00$). The main effect of sex showed that there were significantly larger asymmetries in females than males ($F(1, 94) = 9.74$, $p = .002$, $\eta 2 = .87$). Post-hoc comparisons revealed asymmetry was significantly greater in females than males for the gluteus minimus ($p = .034$), sartorius ($p = .048$), and fibulari ($p = .026$). The results illustrate normative ranges of muscle asymmetry are muscle dependent, and differences due to sex occur. The dataset presented in this study can be used as a preliminary reference for expected asymmetry levels for use in rehabilitation, injury prediction, and observation of performance adaptations.

Significance: Upon examining muscle volume asymmetries in 27 lower extremity muscles in healthy adults, normative asymmetry bounds significantly vary depending on muscle and sex. The results presented in this study further support patient-specific healthcare and can be used to help establish muscle and sex-specific approaches to rehabilitation, injury predication, and training.

Acknowledgements: We wish to acknowledge Bryan Heiderscheit and Wim Derave for contributing data to this normative database.

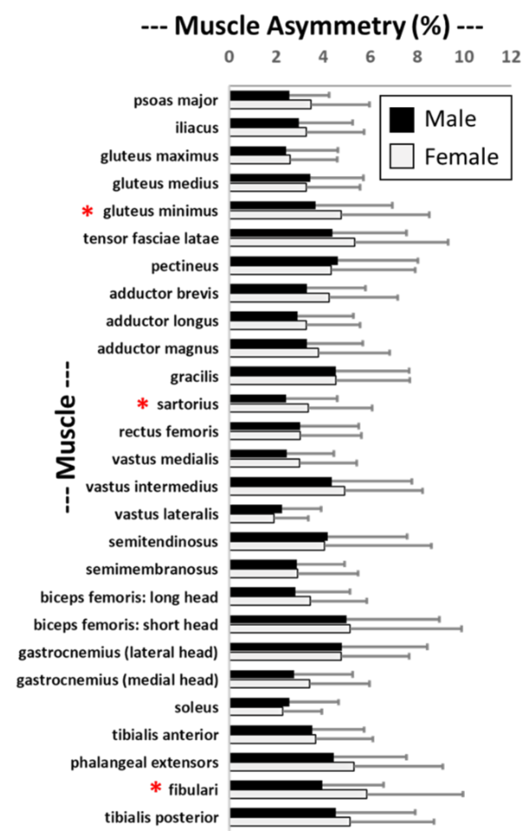

Figure 1: Asymmetry of muscles (mean and standard deviation) for males (black) and females (white).

References: [1] Knapik et al. (1991), *AM J Sports Med* 19; [2] Croisier et al. (2008), *AM J Sports Med* 36; [3] Silder et al. (2008), *Skeletal Radiol* 37;[4] Hart; [5] Rahnama et al. (2005), *Ergonomics* 48; [6] Handsfield et al. (2017), *Scand J Med Sci Sports* 27; [7] Zwolski et al. (2015), Am J Sports Med 43; [8] Lepley et al.(2015), Sports Health 7; [9] Fukunaga et al. (2001), *Acta Physiol Scand* 172; [10] Kulas e al. (2018), *J Ortho. Research* 36(3); [11] Ni et al. (2019), *J Med. Img*. 6(4);

PATIENT REPORTED AND BIOMECHANICAL OUTCOMES FOR SERVICEMEMBERS WITH ANTERIOR CRUCIATE LIGAMENT RECONSTRUCTION UNDERGOING REHABILITATION AT A MILITARY TREATMENT FACILITY

Julia A. Lytle[1*], Tyler Cardinale[1], Andrew Plows[1], Tatiana Djafar[2], Joshua Winters[2], Trevor Kingsbury[1]
[1]Naval Medical Center San Diego, San Diego, CA, USA
*Corresponding author's email: julia.a.lytle2.ctr@health.mil

Introduction: Return to duty following anterior cruciate ligament reconstruction (ACLr) can be challenging and many Servicemembers (SMs) may experience long term dysfunction that may lead to permanent restriction from some military duties [1]. Within a Military Treatment Facility (MTF), the ACLr treatment protocol has a focus on early weightbearing and range of motion to facilitate speed of recovery, based on current literature [2]. This includes progressive goals of jogging within 3-6 months, ~90% strength for quadriceps, and hop test and Y-Balance Test (YBT) limb symmetry >90%. At generally 9-month post op, patients are looking to enter the return to sport phase. Patient reported outcomes (PRO) such as the Tampa Scale of Kinesiophobia (TSK-11) and Knee Injury and Osteoarthritis Outcome Score (KOOS) are commonly utilized tools in ACLr that were used to evaluate a SMs perception of their injury. Patients following ACL injuries often demonstrate lower-limb asymmetries in vertical ground reaction force (VGRF) with compensatory increased loading of the uninjured leg during double-leg squats and other functional tasks [3]. There is a paucity of studies evaluating biomechanical and PRO data in a military population during rehabilitation as part of a clinical program. Therefore, the purpose of this study was to assess PRO and biomechanical data in SMs in rehabilitation at an MTF after ACL reconstruction over the first 12 months of clinical care.

Methods: This study is an IRB approved, retrospective review of a feedback-based rehabilitation program in place at the MTF over the last 12 months. 33 SMs after ACLr underwent PRO and biomechanical assessment at standard timepoints throughout their clinical care. SMs are clinically evaluated every 3 months (3, 6, 9, and 12 months) after reconstruction and feedback is provided to the SMs and their providers. SMs were given the TSK-11, KOOS, and the Y-balance test (YBT). The biomechanical assessment consisted of subjects performing five cued body weight squats on two force plates (Kistler Instrument Corp, Novi, MI, USA). Data was collected and processed using ForceDecks software (VALD, Newstead, AU). Scores were recorded, and leg length was used to normalize scores. Variables of interest for the PRO included overall TSK-11 score and KOOS overall score and sub scores. YBT was used to assess percent limb differences. For the squat protocol, concentric and eccentric mean and peak forces and bilateral mean and peak force asymmetry were assessed. A one-way ANOVA was performed to examine the effect of time on the outcome variables of interest (PRO and biomechanics) with an alpha set to .05.

Results & Discussion: There was no significant difference between TSK-11 scores at any time point. In this population there was a low overall prominence of kinesiophobia. The mean score across all timepoints were 34, with a score of 37 or higher is what is clinically considered to have kinesiophobia. There were significant improvements in KOOS sport and rec scores between 3 months (43.8±26.1, $p=0.004$) and 9 months post op (71.8±14.9, $p=0.004$). Y-balance limb difference was significantly improved between 3 months (11.9±7.6, $p=.031$) and 6 months (7.3±4.0, $p=.031$) post op as well as between 3 (11.9±7.6, $p=.002$) and 9 months (4.3±3.2 $p=.002$) post op. Significant biomechanical improvements in concentric and eccentric force asymmetry were observed during squatting. Concentric mean force asymmetry significantly improved between 3 months (24.9±9.9, $p=0.005$) and 9 months post op (13.2±9.7, $p=0.005$) as well as 3 months (24.9±9.9, $p=.002$) and 12 months post op (9.4±8.3, $p=.002$) and 6 months (19.3±11.9, $p=.041$) and 12 months (9.4±8.3, $p=.002$) post op. Similarly, eccentric mean force significantly improved between 3 months (19.3±10.1, $p= 0.03$) and 6 months (12.45±9.765 $p=.033$) as well as 3 months and 9 months (11.6±7.1, $p=0.03$) and lastly at 3 months post op (19.3±10.1, $p=.01$) and 12 months post op (7.7±5.5, $p=.01$) during the squat task. However, there were no significant improvements in mean concentric ($p=.45$) or eccentric force ($p=.38$) asymmetry between 9 months post op and 12 months post op suggesting a possible barrier for SM's later in rehabilitation.

Significance: This retrospective review evaluated the implementation of an ACLr rehabilitation program with PRO and biomechanical assessments to inform on rehabilitation progress at an MTF over the last 12 months. KOOS improvements indicate that across time there is a significant trend in the ability to perform higher level activities due to progress in recovery. These PRO differences are important because the scores reflect a significant change in function with higher level activities such as squatting, running, jumping, twisting and kneeling. Biomechanically, early asymmetries are to be expected and with feedback and a focus on early weight bearing, ideally the goal of <10% limb asymmetry is achieved at the 9-month mark. It is interesting to note that improvements drop off after the 9-month mark and there are still some PRO and biomechanical differences present. Given that there is focus on both readiness to return from limited duty and a SMs job duties, focused rehabilitation at the MTF commonly drops off after the 6-9-month mark. Due to no (statistically) significant improvement between 6- and 9-months post op could suggest that the biggest improvements happen earlier in rehab, emphasizing the importance of early engagement. If SMs were allowed increased access to rehabilitation even after coming off limited duty, continued improvements may be seen and is a focus of future research.

Acknowledgements: Thank you to General Dynamics Information Technology for support.

References: [1] Antosh (2018). *Military medicine*, *183*(1-2), e83-e89. [2] Peebles, Liam (2019). Sports Medicine and Arthroscopy Review. 27. 10.1097/JSA. [3] Sanford BA (2016). *The Knee*, 23(5), 820–825.

UNDERSTANDING MOTOR ADAPTATION IN DOMIANT VS NON-DOMINANT LOWER LIMB

Stephanie B. Hernández Hernández[1*], Peter G. Adamczyk[1]
[1]Department of Mechanical Engineering, University of Wisconsin - Madison
*email: hernandezher@wisc.edu

Introduction: Most interventions for the lower limbs follow the traditional model of simple experimentally controlled tasks that provide high repetition on movements directly related to functional goals, like body weight supported walking. In contrast, some modern approaches aim to improve rehabilitation through interventions informed by more nuanced principles of motor control and motor learning. Such principles are mainly studied in the upper limb. Therefore, we aim to better understand lower limb motor control and motor learning with the goal of narrowing the gap between current poststroke rehabilitation techniques and principles of motor control.

NOTTABIKE, a one degree of freedom custom haptic leg robot, was built to train and test novel motor tasks [1]. The system has a motor to drive the crank and sensors that measure crank angle, pedal angle, and foot forces. Haptic environments – computer programs connecting pedal force and motion – are programmed to simulate different physical systems the user can interact with. Preliminary work in our lab consisted of having a young cohort perform a reaching task with the right leg against a virtual spring with varying stiffnesses [1]. Blocks of reaching trials with different sequences of stiffness settings were designed to test aspects like the effect of the training environment's stiffness on reaction time, rise time (time to reach from 5 deg to 30 deg), settling time (time to stabilize at 45 deg) and overshoot or undershoot angles. We learned that the human motor system plans each movement expecting a stiffness matched to the trial immediately prior; that unanticipated stiffness changes lead to over- or under-shoot with characteristic errors and correction patterns; and that individuals exhibit personal preferences in strategy reflecting a speed vs. accuracy trade-off. For this study we want to explore difference in motor adaptation between dominant (DL) and non-dominant (NDL) leg on a young cohort. We hypothesize that the DL will have better motor performance (lesser reaction and rise times, lesser over and undershoot in catch trials) when compared to the NDL. This study is the first of three where we will be performing similar tests on chronic stroke and age-matched cohorts.

Methods: Three healthy right-dominant subjects between the ages of 22 and 28 were recruited (1 female, 2 male). They were instructed to use NOTTABIKE to reach from 0 to 45 degrees (Fig. 1A) as quickly as possible. The study took two days to complete, with subjects using their DL (right) on the first day and their NDL (left) on the second day. *Reaching Experiment*: NOTTABIKE rendered one of three virtual spring stiffnesses (10, 20 or 30 Nm/rad). The experiment consisted of blocks with 80 reach trials each. The first block trained the subject to reach against a low stiffness spring but presented randomly-spaced catch trials with medium stiffness.The second block trained high stiffness reaches with medium stiffness catch trials. An auditory motivational system was used throughout all blocks based on the time taken to settle at the target (excellent, good, poor = coin clink, beep, buzz sound) to keep the subjects engaged and prevent slacking.

Results & Discussion: Averages for the three subjects tested are presented in **Figure 1**. When subjects trained in a low stiffness environment and encountered high stiffness catch trials, they tended to undershoot their target position. A bigger undershoot was seen in the DL (8.3°±2.4°) when compared to the NDL (7.2°±2.0°). When subjects trained in a high stiffness environment and encountered medium stiffness catch trials, they tended to overshoot their target position. The NDL (8.7°±1.8°) had higher overshoot when compared to the DL (6.9°±1.8°). When comparing reaction times, we saw that for all blocks subjects had slower reaction times with their NDL (Block1: 0.41±0.02 s (DL) vs. 0.43±0.02 s (NDL); Block2: 0.4±0.02 s (DL) vs. 0.43±0.03 s (NDL)). Lastly, rise time did not exhibit differences between DL and NDL. A potential reason why we didn't see difference in rise times could be due to subject preference between accuracy and speed trade-off. Even though they were instructed to reach the target position as fast as they could, they had individual preferences. The results from this study demonstrate that subjects coordinate their movement based on their prior trained stiffness and that this has an effect on overshoot and undershoot. When completing the full study we hope to find if dominance has an effect on motor performance. Similar tests in stroke and age-matched cohorts will explore how aging affects control and how neural injury interacts with limb dominance to affect performance and adaptation.

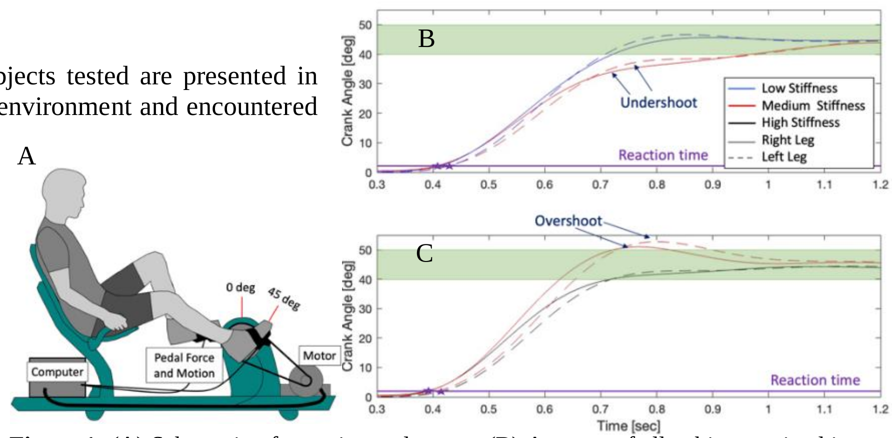

Figure 1: (A) Schematic of experimental set up. (B) Average of all subjects trained in a low stiffness environment, encountering high stiffness catch trials and (C) trained in high stiffness environment, encountering medium stiffness catch trials.

Significance: The objective of this research project is to explore and characterize lower limb motor control to inform future development of stroke rehabilitation protocols. Studying motor control and learning can help us understand the mechanisms and processes behind movement coordination, skill acquisition and motor task complexity. Studying these concepts in chronic stroke cohorts vs. age matched and young adults will help us identify key differences that can guide the development of rehabilitation tasks that exploit these concepts.

Acknowledgements: NSF grants (CMMI-1830516, HRD-1612530), and UW-Madison OVCRGE with funding from WARF.

References: [1] Dawson-Elli, A. R. (2022). (Doctoral dissertation, The University of Wisconsin-Madison).

MOTOR SEGMENTATION PREDICTS MOTOR SYMPTOMS IN PEOPLE WITH PARKINSON'S DISEASE

Rebecca J. Daniels[1*], Christopher A. Knight[1]
[1]Department of Kinesiology and Applied Physiology, University of Delaware, Newark, DE
*Corresponding author's email: rdaniels@udel.edu

Introduction: Clinical research in Parkinson's disease (PD) needs objective, easy-to-implement measures to quantify the underlying pathophysiology and progression of motor symptoms. Rapid isometric and dynamic single-joint contractions have often been used to study disease-related slowing in people with PD (PwPD). Force and surface electromyograms in these tasks indicate that disruptions in neuromuscular excitation in some PwPD cause abnormal, segmented, force-time curves and exaggerated slowing [1,2]. We call these irregularities motor *segmentation* which can be measured from a time-efficient and highly-reliable protocol [3]. However, it is unknown whether segmentation relates to measures of disease severity and function in PwPD. Aim 1 was to determine whether segmentation can predict motor symptom severity comparably to other measures of disease severity. We hypothesized that segmentation would significantly predict motor symptom severity similarly to disease duration and levodopa medication intake (LED). Aim 2 was to determine whether PwPD with segmentation (Seg) differ from people without segmentation (No Seg) in disease duration, motor symptom severity, function and rapid force performance. We hypothesized that Seg would have greater disease duration and motor symptoms as well as poorer timed measures of function and force performance.

Methods: This study included 23 PwPD (aged 69.6 ± 7.1 years, 25.5 ± 4.0 kg●m^{-2}, 5.7 ± 5.3 years since diagnosis, 503.8 ± 361.1 mg LED). All subjects were assessed using the motor subsection (part III) of the Movement Disorder Society-Unified Parkinson's Disease Rating Scale (UPDRS) [4] while on their usual medications. They also performed the 3 m timed up and go (TUG).

The subjects performed approximately 50 rapid isometric finger abduction force pulses to 30-50% of their maximal voluntary contraction force (MVC) against a force transducer while they viewed their force feedback on a computer monitor. The first (RFD) and second-time derivatives of force (F"(t)) were calculated. An RFD threshold of 20% MVC/s determined the start and end of each force pulse. The number of segments was calculated from the number of zero crossings in F"(t) [3]. Segmentation quantified from force onset to 90% of the peak force (F90) was used for analysis, and subjects with segmentation≥2 were classified as Seg. The median time from force onset to F90 was also measured (ttF90).

Multiple linear regression was used to test whether segmentation, time since diagnosis, and LED significantly predicted UPDRS score. Mann-Whitney U was used to test for group differences in force measures, measures of disease severity, and function.

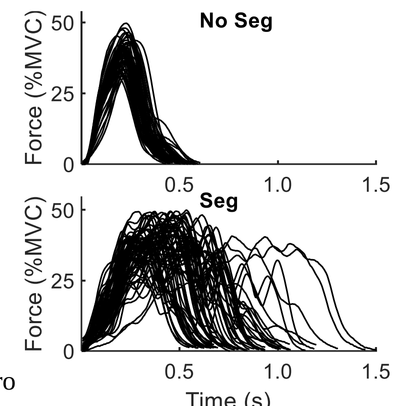

Fig. 1: Force pulse overlay for a subject without segmentation (No Seg) and a subject with segmentation (Seg).

Results & Discussion: The overall regression was statistically significant (R^2=0.40, F=4.3, p=0.018). Segmentation significantly predicted UPDRS score (β=7.4, p=0.004), while time since diagnosis, and LED did not (β≤0.2, p≥0.685). Nine PwPD were classified as No Seg and 14 were classified as Seg. Seg had greater ttF90 (U=123.0, p<0.001), greater TUG (U=98.5, p=0.023), greater UPDRS scores (U=104.5, p=0.007) and a longer time since diagnosis (U=101.5, p=0.013) compared to No Seg. Though preliminary, these results suggest that segmentation may be a useful measure to assess disease severity and slowing in PwPD.

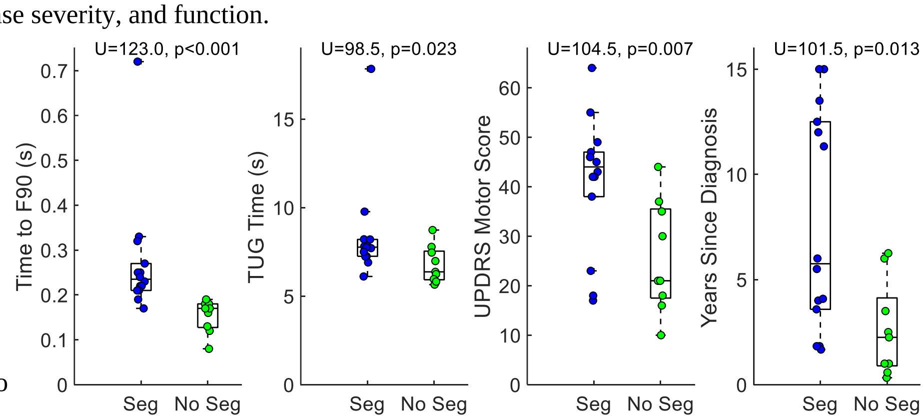

Fig. 2: Box plots show different distributions of dependent variables in groups with seg (Seg) and without seg (No Seg).

Significance: Segmentation provides a precise measure of neuromuscular control impairment during rapid movement that may contribute to motor symptoms in PwPD. Considering this, and the ease and reliability of the protocol, segmentation may be a potential disease marker or outcome measure during intervention studies.

Acknowledgements: This research was funded by Shake It Off Inc., West Chester, PA.

References:
[1] Wierzbicka, Wiegner, Logigian et al (1991), *J Neurol Neurosurg Psychiatry* 54(3); [2] Pfann, Buchman, Comella et al (2001), *Mov Disord* 16(6); [3] Howard, Grenet, Bellumori et al (2022), *Exp Brain Res* 240(7-8); [4] Goetz, Tilley, Shaftman et al (2008), *Mov Disord* 23(15).

OPENSIM MODEL FOR BIOMECHANICAL ANALYSIS WITH OPEN-SOURCE LEG

Sixu Zhou[1,2*], Sujay Kestur[2], Kinsey Herrin[1,2], Aaron Young[1,2]
[1]Institute of Robotics and Intelligent Machines, Georgia Institute of Technology
[2]George W. Woodruff School of Mechanical Engineering, Georgia Institute of Technology
*Corresponding author's email: szhou357@gatech.edu

Introduction: Musculoskeletal modeling is a common practice that allows analysis of human joint kinematics and kinetics using motion capture systems and force plates. OpenSim is an open-source software that allows users to run scaling, inverse kinematics and inverse dynamics pipelines using markers and ground reaction force data. The scaling process uses 3-dimensional marker coordinates and scales the baseline model to match the actual participant's body size with distributed mass and inertia. The inverse kinematics process further uses the 3-dimensional marker coordinates in locomotion to compute the joint angles. After exporting ground reaction forces and centers of pressure from force plates, the inverse dynamics are calculated to compute the joint load during ambulation. Furthermore, joint powers can be calculated using joint velocity from the inverse kinematics results and joint load from the inverse dynamics results. The open-source leg (OSL) is a robotic prosthesis with two actuators located at the knee and ankle joints designed by the University of Michigan allowing researchers to study various controllers on the same prosthetic device hardware [1]. The simplest solution to generate biomechanical outcomes of individuals with lower limb amputation is to use models of able-body individuals. However, modeling prosthetic devices after an able-body individual's morphology may not provide an accurate representation of the human and device interaction. Therefore, we hypothesize that the biomechanical model using a lower limb prosthesis will perform better than the biomechanical model using able-body morphology in both the 1) inverse kinematics and 2) inverse dynamics calculations.

Methods: The biomechanical model was modified from a baseline model designed by Rajagopal, et al [2] using the CAD model of the OSL. The knee and ankle assembly replaced the anatomical shank and foot segments and constrained the joint contact locations. The prosthetic knee center was aligned to match with the sound side knee center, and the ankle was aligned in the same method before the scaling process. Both devices were connected using a prosthetic pylon to replace the shank, which can be lengthened or shortened based on the user's residual limb length and sound side knee center. In addition, the mass, moments of inertia and center of mass of the model were modified from the readings in the Solidworks.
Eight subjects with transfemoral amputation (TFA) consented to an IRB approved protocol and were fit and trained on the OSL. Each participant was asked to walk on a slope with an incline angle at 5.8° for ten trials while full body biomechanics were recorded (Vicon, Denver, CO; Bertec, Columbus, OH). The inverse kinematics and inverse dynamics results are computed using OpenSim.

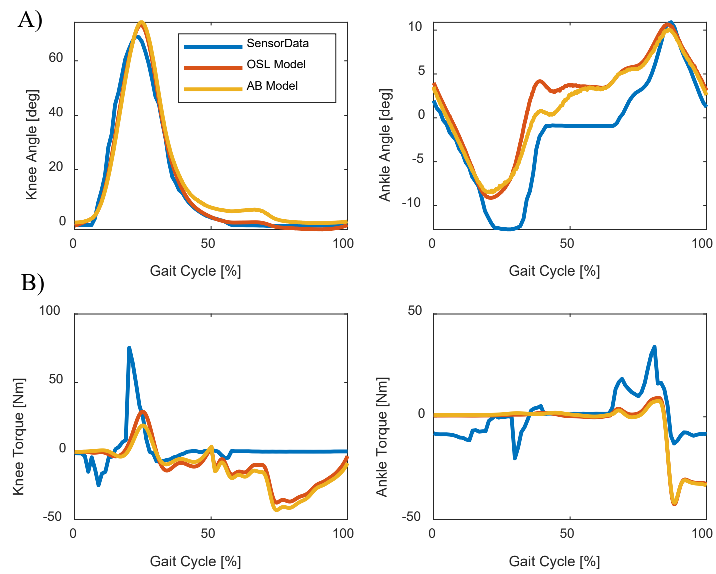

Figure 1: A) Inverse kinematics and B) inverse dynamics results using various biomechanical models on a staircase in timeseries.

Results & Discussion: As shown in Fig 1A, the inverse kinematics of the knee shows similar results between the sensor data and able-bodied model or the OSL model. The able-bodied model shows an RMSE value of 4.866° and an R-squared value of 0.952, while the OSL model shows an RMSE value of 3.297° and an R-squared value of 0.978. However, the inverse kinematics of the ankle did not show similar results. The abled-bodied model shows an RMSE value of 3.484° and an R-squared value of 0.693, while the OSL model shows an RMSE value of 4.241° and an R-squared value of 0.545 allowing us to partially accept Hypothesis 1. The inverse dynamics of both the knee and ankle, as shown in Fig 1B, show small R-squared values, but the OSL model shows slightly better results than the able-bodied model in the knee with RMSE values of 19.67 Nm and 22.11 Nm, respectively. Our biomechanical model with the OSL generates more accurate results in the inverse kinematics and inverse dynamics than the able-bodied model in the knee but does not perform equally well in the ankle. The large errors in the inverse dynamics may be the result of the missing interactions from human joints and devices (the dynamic effects between the residual limb and socket interface). In addition, the motor power transmission loss, such as friction effects and losses in transmission efficiency, is not included in the model with lower limb prostheses.

Significance: Research collaborations studying the OSL can use the model to generate biomechanical outcomes of individuals with TFA in any ambulatory task.

Acknowledgements: This work is funded through a grant from the DoD CDMRP Award Number W81XWH-21-1-0686

References: [1] Azocar et al., *Nature Biomedical Engineering* 4.10; [2] Rajagopal et al., *IEEE Transactions on Biomedical Engineering* 63. 10

BILATERAL ASSESSMENT OF SHOULDER OVERUSE IN MANUAL WHEELCHAIR USERS WITH SPINAL CORD INJURY USING IMU DATA DURING DAILY LIFE

Omid Jahanian [1], Meegan G. Van Straaten [1], Kathylee Pinnock Branford[2], Emma Fortune Ngufor[1], Stephen M. Cain[2], and Melissa M. B. Morrow[3*]
[1]Mayo Clinic, Rochester, MN, USA; [2]West Virginia University, Morgantown, WV, USA;
[3]University of Texas Medical Branch, Galveston, TX, USA
email: jahanian.omid@mayo.edu memorrow@utmb.edu

Introduction: Manual wheelchair (MWC) users with spinal cord injury (SCI) rely heavily on their upper limbs for both mobility and activities of daily living, thereby exposing themselves to a significant risk of shoulder overuse and accelerated rate of shoulder pathology progression beyond what occurs naturally with aging [1]. To address this issue, our study introduces a novel approach, a combined risk score, that utilizes inertial measurement unit (IMU) data to quantitatively assess the extrinsic factors contributing to shoulder overuse, such as upper-arm posture, arm overuse, and rest time in the dominant and non-dominant arms.

Methods: Under Mayo Clinic IRB approval, 16 MWC users (14 males, age (SD): 41(12) years, injury level: C6–L1, median years of MWC use (IQR): 6(4, 12) years) were recruited. IMUs (Opal, APDM Inc., USA) were worn on the upper arms and chest for one or two days in the free-living environment, and our established method was used to calculate the humeral elevation angle [2]. We used our previously developed algorithm to detect active and resting bouts of repetitive arm motion throughout the day [3]. In summary, one movement cycle was defined as an arm elevation greater than 10° followed by arm lowering of greater than 10°. The movements with smaller ranges of motion that occurred between successive elevation and lowering events were treated as a part of the movement cycle. The intervals between the consecutive cycles were calculated, and a bout of activity was defined as the consecutive movement cycles with intervals of less than 7 seconds [4]. The intervals greater than 7 seconds were considered resting bouts. Finally, the combined shoulder risk score, defined based on the ergonomic literature and observations in our previous studies [2, 5], was calculated for each active bout (Table 1). Parameters of interest, including number and total time of active bouts, total resting time, median combined shoulder risk score, and cumulative combined shoulder risk score were calculated and compared between dominant and non-dominant arms using Wilcoxon Signed-Rank tests ($\alpha = 0.05$).

Table 1. Definition of combined shoulder risk score.

Parameter	Definition
Duration Score (DS) T_{AB}: Duration of active bout (sec)	$T_{AB} \leq 10$ Sec → DS = 0 Else → DS = $\lceil T_{AB} / 30 \rceil$
Repetition Score (RS) $Freq_{AB}$: frequency of movement cycles per an active bout (1/min)	RS = $\lfloor Freq_{AB}/4 \rfloor$
Posture Score (PS) HEA: median humeral elevation angle per an active bout	HEA ≥ 90° → PS = 3 60° ≤ HEA ≤ 90° → PS = 2 30° ≤ HEA ≤ 60° → PS = 1 HEA ≤ 30° → PS = 0
Combined Shoulder Risk Score (CSRS)	CSRS = (1 + DS * (RS+PS))

Results & Discussion: The average (SD) total active time for the dominant arm was 8065 (4754) seconds, including 340 (184) active bouts, and the average (SD) total resting time was 30594 (9169) seconds. The average (SD) total active time for the non-dominant arm was 7215 (4114) seconds, including 330 (167) active bouts, and the average (SD) total resting time was 31349 (9462) seconds. The total active time was significantly longer ($p = 0.011$), and the total resting time was significantly shorter ($p = 0.049$) for the dominant arm than the non-dominant arm. The median combined shoulder risk score was not significantly different between the dominant and non-dominant arm; however, the cumulative combined shoulder risk score throughout the day was significantly ($p = 0.03$) higher for the dominant arm (Table 2). These results indicate that this approach was sensitive enough to detect the asymmetries in arm use between dominant and non-dominant arms in MWC users. The larger cumulative shoulder risk score and shorter total resting time for the dominant arm demonstrate the more extensive exposure of the dominant side to potential shoulder overuse in comparison to the non-dominant side.

Table 2. Group mean (SD) and median (Q1, Q2) for dominant and non-dominant arm median combined shoulder risk score and cumulative combined shoulder risk score throughout the day, and statistical results for the comparison between dominant and non-dominant arms.

	Median Combined Shoulder Risk Score			**Cumulative Combined Shoulder Risk Score**		
	Dominant Arm	Non-Dominant Arm	p	Dominant Arm	Non-Dominant Arm	p
Average (SD)	4.6 (0.8)	4.4 (1.2)	0.852	3697 (2693)	3302 (2288)	0.030*
Median (Q1, Q2)	4.5 (4, 5)	5 (4, 5)		3210 (2192, 4656)	3019 (1963, 4026)	

Significance: The results from this study indicate the feasibility and potential of the proposed approach to capture the repetitive movements and resting periods to understand the risk to the shoulder that can be linked with shoulder pathology development in MWC users with SCI. These preliminary results suggest that MWC users may be at greater risk for shoulder pathology on their dominant side due to the repetitive and prolonged use of their arm during daily life. Data collections and analyses with larger sample sizes of MWC users and age- and sex-matched able-bodied individuals, and more days of IMU data collection are warranted to improve the definition of the combined shoulder risk score and confirm the findings of this study.

Acknowledgements: This research was supported by the NIH (R01 HD84423).

References: [1] Jahanian et al. (2022), *J Spinal Cord Med* 45(4); [2] Goodwin et al. (2021), *PLoS One* 16(4); [3] Jahanian et al. (2022), *NACOB2022*; [4] Tolerico et al. (2007), *JRRD* 44(4); [5] Lind et al. (2020), *Ergonomics* 63(4).

THE EFFECTS OFWEAKNESS, CONTRACTURE, AND ALTERED CONTROL ON WALKING ENERGETICS DURING CROUCH GAIT

Elijah C. Kuska[1*], Michael H. Schwartz[2], Katherine M. Steele[1]
[1]Department of Mechanical Engineering, University of Washington, Seattle, WA
[2]Center for Gait & Motion Analysis, Gillette Children's Specialty Healthcare, St. Paul, MN
kuskae1uw.edu

Introduction: Cerebral palsy is the result of a neurologic injury at or near the time of birth that results in altered motor control. Individuals with CP often develop secondary, progressive musculoskeletal impairments like weakness and contracture. Interactions between neuromuscular impairments impart complex restrictions on gait which are difficult to understand experimentally, limiting treatment efficacy. For example, individuals with CP consume on average 2x the energy of their non-disabled peers when walking; however, we remain unable to improve energy consumption [1]. Furthermore, CP is a heterogenous populations which further limits our understanding of factors that impact energy and treatment efficacy.

Machine learning (ML) enables parsing of complex interactions within heterogenous populations but requires a significant amount of data [2]. Musculoskeletal modelling and simulation offer a non-resource intensive way to rapidly evaluate hypothetical relationships and generate synthetic data which can be used to inform ML algorithms [3]. However, these methods have rarely been combined to examine energetics during gait, let alone in individuals with CP.

The purpose of this study was to investigate the effects of neuromuscular impairments on walking energetics in CP.

Methods: We utilized a previously developed 2D sagittal-plane musculoskeletal model and direct collocation framework [4] to generate tracking simulations of common gait patterns in CP—moderate and severe crouch—and nondisabled (ND) gait [5]. Simulations of each gait pattern were perturbed by altering control, weakness, and contracture. Altered control was simulated by reducing the number of muscle synergies controlling each leg from 8 (individual muscle control or IMC) to 5 and 3, where fewer synergies reflect reduced control complexity which is associated with worse function and treatment outcomes in CP [6]. Weakness was simulated by reducing a muscle's maximum isometric force and contracture was simulated by reducing a muscle's tendon slack length; both were imposed in muscles commonly affected in CP [7]. Altered control and weakness or contracture were simulated combinatorial and the severity of each was increased while the simulation minimized deviations from the desired gait pattern and cost of transport (CoT).

A Bayesian Additive Regression Trees (BART) model predicted resultant CoT values from simulated neuromuscular impairments and enabled us to parse the simulated impairments accumulated local effects (ALEs) on CoT [8]. Greater effects indicate impairments that were major drivers of CoT. Then, by comparing crouch to ND gait, we elicit advantages and disadvantages of walking in crouch.

Results & Discussion: Simulations closely tracked crouch and ND kinematics (RMSE < 2.5°) and BART accurately predicted CoT for all gait patterns ($R^2 > 0.97$). Almost all simulated neuromuscular impairments had a larger impact on CoT during ND gait than crouch gait (Figure 1), highlighting possible advantages of walking in crouch. Vasti weakness had a larger effect on CoT as crouch severity increased; stemming from increased demand placed on, and reduced capacity of, the knee extensors when walking in crouch [9]. Thus, addressing vasti weakness in crouch may effectively reduce CoT.

Control complexity had a smaller effect as crouch severity increased highlighting possible advantages of walking in crouch with altered control. Surprisingly, control complexity had a smaller effect on CoT relative to the other simulated neuromuscular impairments which contrasts common clinical assumptions [10].

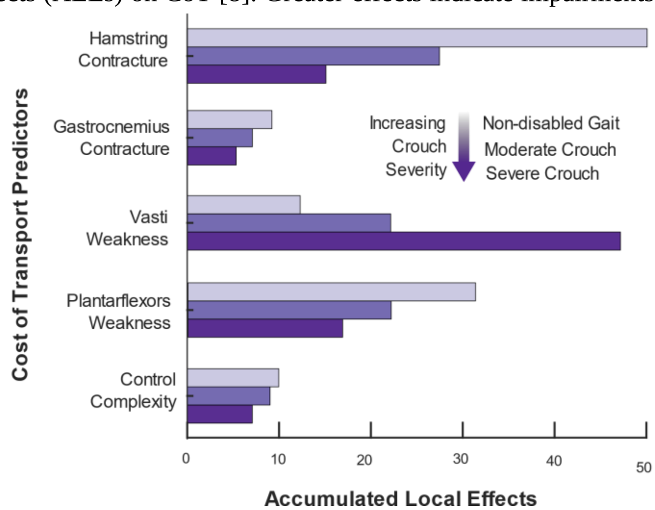

Figure 1: Accumulated local effects of neuromuscular impairments on cost of transport (CoT) during non-disabled and crouch gait.

Significance: This study demonstrated that altered gait patterns like crouch—considered inefficient and disadvantageous—may reduce the effect of common neuromuscular impairments highlighting potential advantages of gait patterns in CP. Furthermore, the effects of neuromuscular impairments were gait-pattern specific and understanding such can provide insight into how and why individuals with neurologic injuries select their gait pattern. Additionally, by informing machine learning with synthetic data generated from modelling and simulation we can probe and identify mechanisms contributing to elevated energetics during gait, highlighting advantages of ML, modelling and simulation, and both in combination. Similar work extended to patient-specific data could improve the efficacy of neurorehabilitation by identifying neuromuscular impairments that have large effects on CoT, which could then be targeted by interventions to more effectively improve energetics.

Acknowledgements: This work was supported by NIH Award R01NS091056 and R21HD104112.

References: [1] Ries et al. (2018), *Hum. Mov. Sci.* 57; [2] Halilaj et al. (2018), *J. Biomech* 81; [3] Renani et al. (2021), *Sensors* 21; [4] Mehrabi et al. (2019), *J. Biomech* 90; [5] Rozumalski et al. (2009), *Gait Posture* 30; [6] Schwartz et al. (2016), *Dev Med Child Neurol* 58; [7] Kuska et al. (2022), *J. Biomech* 134; [8] Chipman et al. (2010) *Ann App Stat* 4; [9] Steele et al. (2012) *J. Biomech* 42; [10] Gill et al. (2023), *medRxiv*

DOES A RUNNING STROLLER AFFECT 3D JOINT KINEMATICS?

Amy Lista[1], Diego Carbajal[1], Lauryn Morgan[1], Benjamin W. Infantolino[1], Allison R. Altman-Singles[1,2,*], Joseph M. Mahoney[1,2,3]
[1]Kinesiology, Penn State Berks, Reading PA 19610
[2]Mechanical Engineering, Penn State Berks, Reading PA 19610
[3]Mechanical Engineering, Alvernia University, Reading PA 19601
*Corresponding author's email: ara5093@psu.edu

Introduction: Running is an effective method to maintain health, but half of regular runners are injured each year [1]. 80% of running-injuries are related to loading and form [2]. During early parenthood, it is critical to maintain physical activity, but this can be challenging. A running stroller can be used while running outdoors, but it is important to understand its effects on running mechanics.

Significant changes in lower limb kinematics while running with a stroller have been reported [3,4], but these findings are inconsistent and incomplete. Full 3D kinematics at the knee and ankle have not been determined for stroller running and may be meaningful indicators of running injury risk [5]. The purpose of this study is to examine the 3D kinematics of the hip, knee, and ankle when running with and without a stroller. It is expected that motion analysis will reveal a more flexed posture upon landing while pushing a stroller, due to limited space and forward lean into the handlebars.

Methods: Healthy local runners (aged 18-45, running > 8 km/week) were recruited. Runners ran across an 18 m runway with embedded force plates (Bertec, Columbus, OH). Lower extremity reflective marker motion was tracked using 12 Vicon cameras (Vicon, Centennial, CO). A self-selected speed was determined after a warmup, then maintained within 10% for 5-10 satisfactory trials with and without the stroller. Force (2000 Hz) and marker position (200 Hz) were recorded using Nexus (Vicon, Centennial, CO).

Marker trajectories were lowpass filtered at 6 Hz and 3D joint kinematics of the hip, knee, and ankle were calculated using Visual 3D (C-Motion, Germantown, MD). Custom MATLAB (Mathworks, Natick, MA) code was developed to determine stance phase. The mean value of each kinematic curve at initial contact, max, and min were extracted to perform a two-tailed paired bootstrapped t-test with 10^6 resamples to determine the difference between conditions. A Bonferroni correction was performed, resulting in an $\alpha = 0.0042$.

Results & Discussion: 23 healthy runners age 26.4±7.9 yrs, 167.6±9.4 cm, 65.84±11.94 kg participated in this study (6 male, 17 female). Participants ran 20.7±19.5 km on average each week. The ankle, knee, and hip were all more flexed at initial contact and at the peak during stroller running (Table 1). This indicates a flexed posture due to increased pelvic tilt, and likely trunk tilt while grasping the stroller. The hip and knee also had less peak extension, indicating a shift in overall joint excursion.

Increased ankle eversion at initial contact and peak indicates a more pronated foot when running with a stroller. This may increase the risk of overuse injuries [6]. It is possible this is due to the increased attention given to foot placement when pushing a stroller. Increased hip abduction and external rotation can cause a slight increase in varus posture of the lower extremity. While this effect was not visible at the knee, altered secondary plane motion at the hip can be associated with increased joint injury risk [5]. The changes in hip motion were observed previously [4], but this work may not have been powered to detect changes at the ankle and knee.

Table 1. Mean value for each kinematic variable. A % difference in **bold*** indicates a significant difference between stroller and control ($p<0.0042$).

	@ Initial Contact			@ Max			@ Min		
Joint	**Control**	**Stroller**	**% Diff**	**Control**	**Stroller**	**% Diff**	**Control**	**Stroller**	**% Diff**
Ankle DF	71.25°	73.47°	**3%***	86.48°	89.33°	**3%***	40.58°	40.66°	0.2%
Ankle ADD	-2.91°	-2.80°	4%	1.94°	1.28°	-41%	-13.29°	-13.18°	1%
Ankle EV	-8.43°	-6.97°	**19%***	0.55°	3.53°	**146%***	-9.83°	-8.77°	11%
Knee EXT	-11.74°	-18.22°	**-43%***	-9.58°	-11.96°	**-22%***	-44.22°	-47.83°	**-8%***
Knee ADD	4.47°	5.07°	13%	7.78°	7.90°	2%	2.24°	1.85°	-19%
Knee IR	-11.11°	-9.79°	13%	1.21°	1.88°	44%	-12.44°	-11.64°	7%
Hip FLX	32.51°	43.09°	**28%***	34.17°	43.46°	**24%***	-15.53°	-11.00°	**34%***
Hip ADD	4.73°	5.19°	9%	9.29°	9.62°	4%	-4.33°	-3.14°	**32%***
Hip IR	8.30°	8.97°	8%	9.77°	10.46°	7%	-1.90°	0.24°	**256%***

Significance: A more flexed posture was observed during stroller running along with changes in the secondary plane of the ankle and hip. Previous work indicated that GRF was decreased when pushing a stroller due to load sharing with the stroller [7]. Taken together, it is unlikely that altered joint motion with decreased loading would substantially increase injury risk, but it is important to continue to characterize these mechanics to determine a full picture of injury risk. This work may inform future stroller design.

Acknowledgements: This work received funding from the Franco, Cohen-Hammel, MC REU, and RDG Awards from PSU.

References: [1] Tschopp & Brunner (2017) *Z Rheumatol* 76(5); [2] van Poppel et al. (2021) *J Sport Health Sci* 10(1); [3] Alcantara et al. (2017) *PLOS ONE*, 12(7); [4] O'Sullivan et al. (2016) *Gait Posture,* 43; [5] Heinert et al. (2008) *J Sport Rehab* 17(3); [6] Nigg et al. (2019) *Footwear Sci*, 11(3); [7] Mahoney et al. (2022) *NACOB*, Ottawa, ON

MUSCLE PROPERTIES IN RABBITS WITH AN END-LIMB, MUSCLE-ATTACHED ENDOPROSTHESIS

Fisher S. Adkisson[1*], Dustin L. Crouch[1], Katrina L. Easton[1], Caleb Stubbs[1], Obinna P. Fidelis[1], Kristin Bowers[2], Cheryl B. Greenacre[2], Stacy M. Stephenson[3], David E. Anderson[2]
[1]College of Engineering, [2]College of Veterinary Medicine, [3]Graduate School of Medicine, University of Tennessee, Knoxville (UTK)
*Corresponding author's email: fadkisso@vols.utk.edu

Introduction: Endoprosthetic limbs that physically attach to muscles may restore more natural sensorimotor function to people with amputation than current prostheses that are worn externally on the body. The function enabled by such a prosthesis is expected to depend partly on the force-generating behavior of the attached muscles. Muscle force-generating behavior is strongly related to muscle properties, such as mass and length, according to well-characterized (e.g., force-length-velocity) relationships [1]. Amputation, muscle-endoprosthesis geometry (e.g., moment arms), endoprosthesis material properties, endoprosthetic limb use, and other factors may affect muscle properties and, thus, muscle force-generating behavior. The objective of this study was to quantify two muscle properties, mass, and length, of muscles in the hindlimb of rabbits with a foot-ankle muscle-attached endoprosthesis prototype. The leading hypothesis for this study was that muscles on the operated side with the endoprosthesis would have lesser mass and length than muscles on the contralateral intact side.

Methods: In four 16-week-old New Zealand white rabbits, we surgically replaced the left hindlimb with a jointed foot-ankle endoprosthesis prototype. The rabbits were part of an iterative, developmental, proof-of-concept study and, therefore, interventions were not the same across all rabbits. For example, the tibialis cranialis and triceps surae muscles were sutured to the endoprosthetic foot across the ankle joint with either the biological tendons (n=2) or polyester, silicone-coated artificial tendons (n=2) [2]. Also, the rabbits were euthanized at either 8 (n=1), 16 (n=2), or 24 weeks (n=1) post-surgery. For all rabbits, both hindlimbs were removed at the hip, skinned, then fixed in 10% neutral buffered formalin for at least 5 days with the knee at 90° flexion and the ankle in neutral dorsi/plantar flexion. The fixed limbs were transferred to 70% ethanol for at least 2 days. From six muscles on each side (Figure 1), we measured muscle mass and length using a digital scale and caliper, respectively. For each rabbit, muscle, and variable, we computed the percent difference between sides. We then computed the mean and standard deviation of percent differences across rabbits. We performed one-tailed, one-sample Student's t-tests to identify percent differences that were significantly different from zero ($p \leq 0.05$).

Results & Discussion: On average, muscle mass was less on the operated side than on the intact side for all muscles; however, the percent difference in muscle mass between sides was statistically significant only for LG = 36% (p=0.001), MG = 32% (p<0.001), and Sol = 77% (p<0.001) (Figure 1). That muscle mass being lower on the operated side was likely due to disuse atrophy; though muscles were attached across the endoprosthetic ankle, the ankle range of motion was substantially lower than that of an intact ankle due to fibrotic encapsulation of the endoprosthesis. We are currently testing strategies to reduce fibrotic encapsulation to increase endoprosthetic ankle range of motion and, subsequently, muscle use to prevent atrophy. Muscle length for all the muscles was significantly less on the operated side compared to the intact side, even for muscles that were attached to the endoprosthesis (Figure 1). The percent differences in muscle length between sides were LG = 18% (p=0.004), MG = 19% (p=0.004), Sol = 30% (p<0.001), TA = 18% (p=0.001), ED = 21% (p=0.004), FD = 26% (p=0.002). The muscles may have retracted during the surgical amputation and, in the case of attached muscles, not stretched back to their pre-amputation lengths when attached to the endoprosthesis. Muscles in a chronically shortened position may become functionally shorter by losing sarcomeres in series [3], limiting the muscle's excursion capacity. In future surgeries, we will monitor muscle lengths intraoperatively to see if restoring muscle length during surgery can preserve muscle length post-surgery.

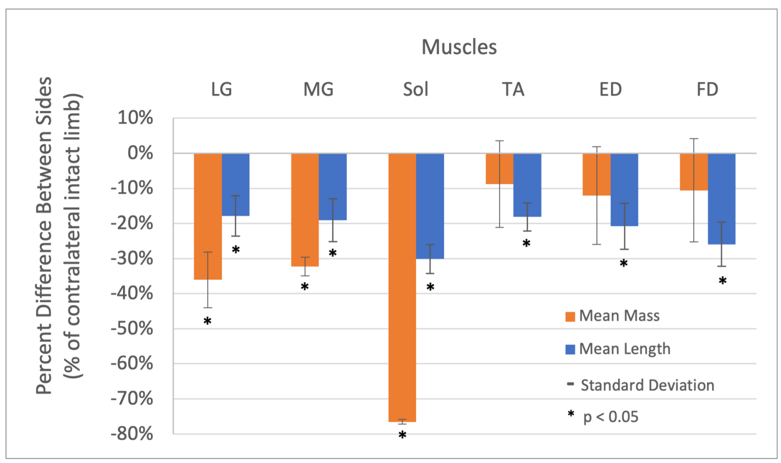

Figure 1: Percent differences in muscle mass and length between operated (endoprosthetic) and contralateral intact sides, relative to the intact side. LG = Lateral gastrocnemius; MG = Medial gastrocnemius; Sol = Soleus; FD = Flexor digitorum; TC = Tibialis cranialis; ED = Extensor digitorum.

Significance: A loss of muscle mass and length will likely reduce the ability of muscles attached to an endoprosthesis to generate force and change length during muscle contraction, limiting the force and movement output of an endoprosthetic limb. Future work will investigate factors that contribute to loss of muscle mass and length and potential strategies to avoid such loss.

Acknowledgements: UTK Office of Laboratory Animal Care. NIH R61AR078096.

References: [1] Zajac FE, 1989. *Crit Rev Biomed Eng*, 17(4):359-411. [2] Hall PT, et al., 2023. *J Biomech* (Accepted). [3] Abrams RA, et al., 2000. *Musc Nerve*, 23:707-714.

EVALUATING POSTURAL CONTROL OF PATIENTS WITH DIABETES USING A VIRTUAL REALITY-BASED SENSORY ORGANIZATION TEST

Zachary Van Dorn[1,2], Kai Cheng[1,2], Sodiq Fakorede[1,2], John Miles[3], Chun-Kai Huang[1,2*]
[1]Department of Physical Therapy, Rehabilitation Science, and Athletic Training; [2]KU Mobility Consortium;
[3]Department of Endocrinology, Diabetes and Clinical Pharmacology; University of Kansas Medical Center, Kansas City, KS, USA
*Corresponding author's email: chuang7@kumc.edu

Introduction: Impaired balance or postural control is one of the most complications in patients with diabetes mellitus (DM) that leads to the increased risk of falls. The balance impairment in DM may stem from deficits in the sensory system such as visual, somatosensory, or vestibular sensations. To evaluate sensory organization, virtual reality (VR) technology has been broadly applied to recent rehabilitation research with its immersive, feasible and applicable features. Our previous work using the Virtual Reality Comprehensive Balance and Training (VR-ComBAT) tool presented the feasibility and safety of the VR-ComBAT in healthy individuals. Moving forward, the objective of this study is to compare balance and postural control in patients with DM and their age-matched controls.

Methods: Two patients with Type 2 DM and two age-matched healthy adults participated in this study. Participant's balance and postural control was recorded through (1) clinical assessment tools such as the Berg Balance Scale and Mini-BESTest; (2) center-of-pressure (COP) measures using VR-ComBAT. The VR-ComBAT consists of a VR headset and a force plate (Figure 1) can emulate the equivalent testing conditions of a formal SOT: (1) eyes open on a firm surface; (2) eyes closed on a firm surface; (3) eyes open together with sway referenced visual surround; (4) eyes open on a soft surface; (5) eyes closed on a soft surface; and (6) eyes open on a soft surface with sway visual surround. Participants were instructed to maintain their balance for 60 seconds in each condition while standing using VR-ComBAT. The COP displacement and velocity in anteroposterior and mediolateral directions were calculated on each condition utilizing the NetForce Ver. 3.5.3 and MATLAB software.

Figure 1:VR- ComBAT.

Results and Discussion: Compared to healthy adults, patients with DM showed lowered functional balance scores, higher movement frequency (1.08 ± 0.3 Hz vs. 0.68 ± 0.13 Hz), and greater center-of-pressure displacements in both anteroposterior and mediolateral directions. Adopting VR-based SOT is promising by showing possible DM-induced sensory deficits that leads to imbalance. The preliminary outcomes also indicate altered postural control during quiet standing in patients with DM compared with age-matched healthy adults. Continued data collection from DM patients would better interpret the way of how DM patients compensate differently than healthy age-matched controls.

Significance: Our study prompts the VR application in the balance assessment. As a relatively low-expense method to perform the SOT, the popularity of VR-ComBAT in both the research and clinical settings are warranted. Also, our findings can help researchers and clinical practitioners to better understand the postural control of DM patients, which also guide them about the future study and tailor-made interventions.

Acknowledgements: Research reported in this publication was supported by the Kansas University Training Program in Neurological and Rehabilitation Sciences (NIH T32HD057850).

References:

[1] Moon S, Huang CK, Sadeghi M, Akinwuntan AE, Devos H (2021), *Front Bioeng Biotechnol* 9:678006.
[2] Kim, Y.-G. and S.-H. Kang, *The Effect of Virtual Reality-Based Exercise Program on Balance, Gait, and Falls Efficacy in Patients with Parkinson’s Disease.* Journal of The Korean Society of Physical Medicine, 2019. **14**(4): p. 103-113.
[3] Parry, J., *The use of virtual reality environments for medical training.* Digital Medicine, 2019. **5**(3): p. 100-101.
Niki, K., et al., *A Novel Palliative Care Approach Using Virtual Reality for Improving Various Symptoms of Terminal Cancer Patients: A Preliminary Prospective, Multicenter Study.* J Palliat Med, 2019. **22**(6): p. 702-707.
[4] Schultheis, M.T. and A.A. Rizzo, *The application of virtual reality technology in rehabilitation.* Rehabilitation Psychology, 2001. **46**(3): p. 296-311.

USER-CENTRIC ITERATIVE DESIGN OF AN ANKLE EXOSUIT TO REDUCE ACHILLES TENDON LOAD DURING RUNNING

Cameron A. Nurse*, Derek N. Wolf, Katherine M. Rodzak, Rachel H. Teater, Shimra J. Fine, Chad C. Ice, Karl E. Zelik
Department of Mechanical Engineering, Vanderbilt University, Nashville, Tennessee, United States
*Corresponding author's email: Cameron.a.nurse@vanderbilt.edu

Introduction: Ankle exoskeletons and exosuits (exos) are an emerging technology with the potential to improve locomotor performance and health; however, these benefits will only be realized if exos are designed to be practical and acceptable for specific users and use cases. Ankle exos can provide an assistive plantarflexion torque during walking and running. Prototypes have been shown in laboratory experiments to reduce calf muscle activity and Achilles tendon load [1,2]. However, a major challenge for the exo field has been moving from lab-based feasibility to real-world empirical evidence of efficacy. Real-world testing requires the development of exos that are well-suited (e.g., practical, comfortable, acceptable) for specific users. To date, no such ankle exo has been developed for runners. The overarching goal of our work is to develop an ankle exo for runners, which could be used in real-world testing to explore the effects of reduced Achilles tendon loading on reducing injury risk, accelerating recovery post-injury, or enhancing performance. The specific purpose of this abstract (and conference presentation) is to summarize the user-centric, iterative design process that we are using to try to develop a usable, practical, and biomechanically effective solution. Dissemination of this design process may be beneficial for other researchers and engineers developing wearable assistive devices.

Methods: We identified long-distance runners as a key group of users who might benefit from biomechanical assistance, for instance, to help mitigate risk of overuse injury resulting from the cumulative strain on their Achilles tendon during running [3]. We are using a variation of the Modified Agile for Hardware Development framework, which starts with cross-disciplinary collaborative activities to define user needs, technical requirements, project objectives, and risks. For us, this work began with a scientific literature search and interviewing 24 stakeholders: 12 runners (competitive and recreational), 6 collegiate track coaches, 4 physical therapists, and 2 physicians. We used the interviews to define user stories (i.e., what users say they want or need). We then compiled technical requirements based on interviews and biomechanics literature. Next, we used a focus matrix to better understand the intersection of user needs and technical requirements. Finally, we performed a series of design iterations; design cycles comprised of smaller design sprints with highly focused objectives and success metrics.

Results and Discussion:
To date, we have completed 6 design iterations, each of which culminates in one or more testable prototypes that are tested with users. Learnings from each iteration are used to identify the design objectives and sprints within the next iteration. To achieve a lightweight but assistive design, we adapted a quasi-passive ankle exosuit that was previously shown to be feasible to assist walking in the lab [1]. This design uses an under-the-foot clutch and a soft, sleeve-like shank interface. An elastic member (assistive spring) then operates in parallel to the user's calf muscles to offload the Achilles tendon (Fig 1). Our current prototype weighs less than 500 g while providing over 20 Nm of ankle plantarflexion torque assistance during stance phase and less than 1 Nm during the swing phase of running (Fig 1B). Improvements concerning thermal and physical comfort, and footwear integration, are the focuses of upcoming/ongoing design iterations. Details about the iterative design process and the ankle exo design will be shared at the conference.

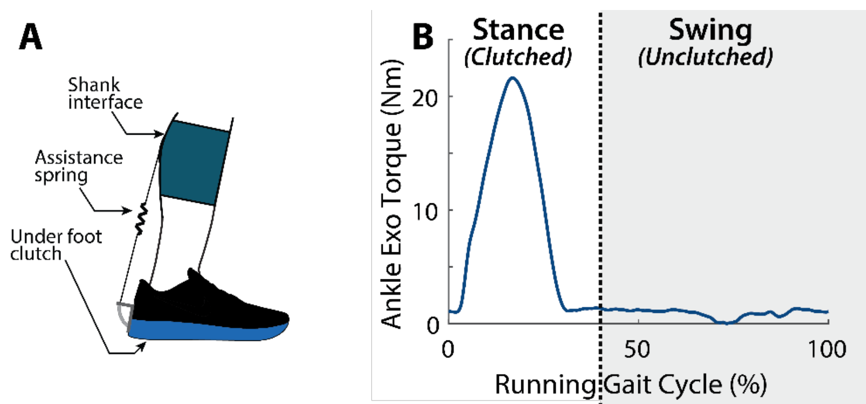

Fig 1: Exo architecture (A) and ankle assistance provided during running (B)

Significance: This user-centric design approach may be useful for others seeking to develop practical, effective wearable assistive devices that can be tested and translated outside the lab. Successful development of this ankle exosuit would establish a new, lightweight, practical tool for offloading the Achilles while running, which would enable novel real-world and longitudinal studies, and may help reduce injury risks, accelerate recovery, or enhance performance.

Acknowledgements: This research is funded by the Wu Tsai Human Performance Alliance.

References: [1] Yandell et al (2019), *IEEE Trans Neural Syst Rehab* 24(4); [2] Witte et al (2020), *Sci Robot* 5(40); [3] Van der Vlist et al (2019), British Journal Sport Med 53

A NEGATIVE RELATIONSHIP BETWEEN HUMAN MOVEMENT VARIABILITY AND MIND WANDERING

Anaelle E. Charles[1*], Aaron Y. Wong[2], Caitlin Mills[2], Nick Stergiou[1,3] and Aaron D. Likens[1]

[1]Department of Biomechanics, University of Nebraska at Omaha, Omaha, NE USA

[2]Department of Educational Psychology, University of Minnesota, Minneapolis, MN USA

[3]AUTH Biomechanics, Department of Physical Education and Sport Science, Aristotle University of Thessaloniki, Greece

*Corresponding author's email: anaellecharles@unomaha.edu

Introduction: Mind-wandering (MW) is a cognitive phenomenon occurring when the mind drifts off task and occupies up to 30-50% of our daily thoughts[1]. MW has been associated with a decrease in cognitive performance in various tasks such as reading, driving, and memory retention. The intermittent nature of MW, fluctuating from an attentive state to an inattentive state, raises fundamental questions about its effect on movement variability. Previous work associated higher MW responses with an increase in the amount of variability during a finger tapping task when taps were paced by a periodic metronome[2]. However, evidence also suggests that periodic metronomes tend to decrease the natural variation of healthy movements, effectively mimicking movement patterns associated with movement pathologies[3]. The relationship between MW and time varying movement patterns, however, remains unclear. Therefore, in this study we investigated the extent to which MW is related to the changes in movement patterns over time.

Methods: One hundred and twenty undergraduates from the University of New Hampshire completed an online finger tapping experiment. Participants performed a self-selected paced finger tap condition to determine their preferred tapping speed (mean inter-tap interval; ITI) and tapping variability (standard deviation; SD). Then, participants performed a metronome response task under four randomized conditions using a variable (*Persistent*), a traditional (*Periodic*), an unstructured (*Random)*, and no (*Free)* metronome. Mean and SD ITI were used to scale metronomes to each participant's preferred pace. **Figure 1** depicts the experimental protocol. ITI time series was divided into 7 periods in which the *Hurst exponent* (H) was computed to capture the temporal structure of the tapping behavior. A series of logistic linear mixed effect (LMEs) models were used to determine if changes in H predicted the likelihood of MW. The dependent variable, MW, was a binary variable (no MW = 0; MW = 1). Model improvement was assessed by the likelihood ratio test and revealed that the best-fitting model contained linear and quadratic effects of time, condition, H, and their interactions.

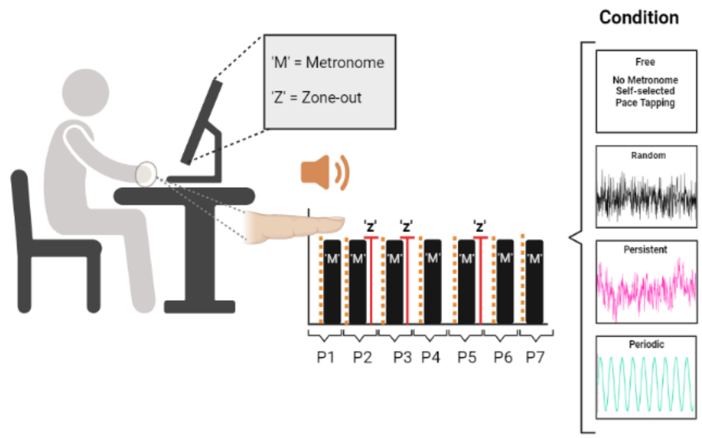

Figure 1: Experimental set up. Participants pressed the 'M' key when hearing the metronome tone and pressed the 'Z' key every time they caught themselves zoning out ('Z').

Results & Discussion: As a manipulation check, we computed a linear mixed model to verify that the metronome manipulation did alter the natural temporal structure. The results showed that relative trends of H aligned with the literature (Free: H = 0.58; SD = 0.14, Persistent: H = 0.61; SD = 0.15; Periodic: H = 0.37; SD = 0.19; Random: H = 0.48; SD = 0.14). A surprising result showed that H was on average lower than typically observed. In terms of MW, our results implied a negative relationship between MW and H, such that, for a one SD increase in the H, the log likelihood of MW decreased by 0.37 (β = -0.37, SE = 0.17, p = .025). The results also suggest that, on average, the Persistent condition led to the largest increase of MW (β = 0.79, SE = 0.28, p = .004). The other conditions showed no significant differences between Free and Random (β = 0.01, SE = 0.24, p = .956) nor between Free and the Periodic condition (β = 0.18, SE = 0.26, p = .493). Overall, our findings suggest a negative relationship between MW and H, such that an increase in MW results in a decrease in movement patterns H, becoming less persistent over time. In addition, this relationship is moderated by the type of metronome, which indicates that changes in MW rate is task dependent.

Significance: Due to the prevalence of MW and its negative consequences on human movement variability (low values of H), we hypothesize that MW could also negatively impact gait. In term, MW could reduce a walker's ability to process essential information, leading to fatal injuries, especially in older adults and individuals with neurodegenerative diseases.

Acknowledgements: Funded by the NIH awards P20GM109090 and R01NS114282, NSF 212491, Nebraska Collaboration Initiative, NASA EPSCoR, GRACA 3063

References:

[1] G. K. Smith, C. Mills, A. Paxton, and K. Christoff, "Mind-wandering rates fluctuate across the day: evidence from an experience-sampling study," *Cogn. Research*, vol. 3, no. 1, p. 54, Dec. 2018, doi: 10.1186/s41235-018-0141-4.; [2] P. Seli, J. A. Cheyne, and D. Smilek, "Wandering minds and wavering rhythms: linking mind wandering and behavioral variability.," *Journal of experimental psychology: human perception and performance*, vol. 39, no. 1, p. 1, 2013.; [3] N. Stergiou and L. M. Decker, "Human movement variability, nonlinear dynamics, and pathology: is there a connection?" *Human movement science*, vol. 30, no. 5, pp. 869–888, 2011.

HOW DOES A RUNNING STROLLER AFFECT TIBIAL ACCELERATION DURING A RUN?

Diego Carbajal[1], Amy Lista[1], Joseph M. Mahoney[1,2,3], Allison R. Altman-Singles[1,2,*]
[1]Kinesiology, Penn State Berks, Reading PA 19610
[2]Mechanical Engineering, Penn State Berks, Reading PA 19610
[3]Mechanical Engineering, Alvernia University, Reading PA 19601
*Corresponding author's email: ara5093@psu.edu

Introduction: Running with a stroller has health and wellness benefits for caregivers of young children. However, little is known about how running with a stroller changes the risk of running-related injuries. Previous laboratory work indicated that the ground reaction force and impact loading, known contributors to running injury risk [1,2], were reduced when running with a stroller, potentially due to load sharing between the runner and stroller [3]. However, running in the lab with only a short runway revealed that it was difficult to achieve a constant running speed while pushing a stroller.

Tibial acceleration has often been used as a surrogate measure of impact loading [4], which is then used to assess impact-related injury risk [1,2]. This measure could be used during outdoor stroller running to determine if the reduction in loading is maintained. Running outdoors on more variable terrain more accurately captures what is done in practice and should be used as such to determine injury risk while running with a stroller. Therefore, the purpose of this study was to determine tibial acceleration during outdoor stroller running compared to running without a stroller. It was expected that stroller running would result in a lower peak magnitude of tibial acceleration, in part due to load sharing between the stroller and runner.

Methods: Healthy runners between 18-45, running at least 8 km per week were recruited from the local community; experience with a stroller was not a requirement to participate. Blue Trident Inertial Measurement Units (IMUs) (Vicon, Centennial, CO) were fixed to the anteromedial aspect of the distal tibia with tape and wrapped tightly to the leg. The IMU was aligned with the long axis of the tibia. Participants ran a set, asphalt, 1 km course three times. The first was considered a warm-up and accommodation to stroller running, and the second and third were randomized to running with or without the stroller (*i.e.*, stroller vs. control). Participants were asked to run at a comfortable "talking" speed and to run both stroller and control trials at the same speed.

High-g linear acceleration data were collected at 1600 Hz and extracted from the IMUs using CaptureU (Vicon, Centennial, CO). Custom MATLAB (Mathworks, Natick, MA) code was developed to filter the accelerations using a 4^{th}-order low-pass Butterworth filter at 60 Hz and calculate the resultant acceleration using the x, y, and z components. The resultant peak tibial acceleration (R-PTA) was extracted for each footstrike and the median for each person and condition was determined. This median was used to perform a paired bootstrapped t-test ($\alpha = 0.05$) with 10^6 resamples to determine the difference between conditions.

Results & Discussion: 13 healthy runners age 28.4±9.1 yrs, 169.1±8.0 cm, 66.56±13.53 kg participated in this study (5 male, 8 female). Participants ran 13.5±12.0 km on average each week. The median R-PTA decreased 9% when running with a stroller ($p = 0.006$, Fig. 1A).

The speed for the control condition was 3.4±0.7 m/s and stroller 3.3±0.6 m/s. However, the speeds for each person *between* conditions fluctuated between 0.3% and 13.7%. Based on previous studies investigating the relationship between speed and R-PTA [5], speed was used as a correction factor (Fig. 1B). Once corrected, stroller R-PTA remained reduced compared to the control by 5% ($p = 0.028$).

While speed *did* play a role in the reduction in R-PTA, there was still a consistent reduction when speed was accounted for. These results suggest that the stroller did indeed reduce R-PTA. R-PTA is associated with reduced impact loading, which confirms what was measured in the laboratory [1].

Reduced tibial acceleration could be caused by a reduction in the joint forces and a change in movement pattern. Concurrent work in this lab has confirmed that there is a more flexed lower extremity strategy at the hip, ankle, and knee when running with a stroller [6]. In addition, when the runner holds onto the stroller's handlebars, they transmit load from their body into the stroller, slightly unweighting their lower extremities, thus reducing the force on the tibia, and therefore the acceleration.

This combination of kinematic and kinetic mechanisms may explain the reduction in R-PTA that could be protective against impact-related overuse injuries.

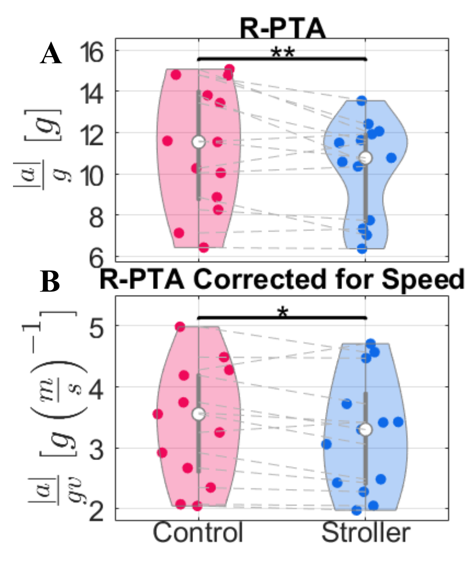

Figure 1. Resultant peak acceleration (R-PTA) for control (red) and stroller (blue) conditions. Median R-PTA for each person and condition are represented as a dot within each violin plot. Paired control and stroller dots for each participant are connected by a dashed gray line. * indicates $p<0.05$, and ** $p<0.01$.

Significance: Reduced R-PTA may indicate a reduction in risk of overuse injuries in runners while pushing a stroller. This may be beneficial for this caregiving population, especially due to changes in physiological- and lifestyle-related risk factors.

Acknowledgements: This work received funding from the Franco, Cohen-Hammel, MC REU, and RDG Awards from PSU.

References: [1] Milner et al., (2006) *MSSE*, 38; [2] Pohl et al., (2008) *J Biomech* 41; [3] Mahoney et al. (2022) *NACOB*, Ottawa, ON; [4] Sheerin et al., (2019) *Gait Posture*, 67; [5] Sheerin et al. (2020) *Sport Biomech*, 19(6); [6] Lista et al. (2023) *ASB*, Knoxville, TN

EVALUATION OF INNER, CLOSE-TO-BODY UPPER EXTREMITY FUNCTION USING A REAL-TIME FEEDBACK REACHABLE WORKSPACE APPROACH IN CHILDREN WITH BRACHIAL PLEXUS BIRTH INJURY

R. Tyler Richardson[1*], Stephanie A. Russo[2], Ross S. Chafetz[3], Spencer Warshauer[3], Emily Nice[3], James G. Richards[4], Dan A. Zlotolow[3], Scott H. Kozin[3]
[1]Pennsylvania State University Harrisburg, Middletown, PA, USA
* email: rtr12@psu.edu

Introduction: Brachial plexus birth injury (BPBI) frequently results in lifelong impairments in upper extremity (UE) function [1]. Evaluation of the entirety of an individual's UE function is critical for informing patient-specific decision making. Reachable workspace quantifies global UE function by measuring regions in space that patients can reach with their hands [2] and may offer a more complete understanding of function than traditional clinical assessments. Existing workspace approaches only report outer, far-from-body function [3] or are limited in characterizing the inner, close-to-body function needed for essential activities of daily living [4]. The purpose of this study was to evaluate the ability of a real-time feedback reachable workspace tool to assess inner, close-to-body function in children with BPBI. Due to the presence of the unilateral injury, we expected that the affected limb would have less workspace than the unaffected limb in regions corresponding to common functional impairments in BPBI – shoulder elevation, external rotation, and extension.

Methods: Trunk and UE segment orientations of 8 children with unilateral BPBI (ages 3-10 years; various injury levels and surgical histories) were measured with motion capture. An array of virtual targets surrounding the participant was created using cylindrical coordinates with radii scaled to be close-to-body. Custom software displayed targets and real-time visual feedback from motion capture with movements of a red cursor sphere controlled in real-time based on the position of the hand relative to the trunk (**Fig. 1A**). Targets were displayed sequentially by primary region (head, thorax, abdomen) (**Fig. 1 A/B**) until all targets were reached or until the participant was unable to reach any more. Participants completed trials on their affected and unaffected limbs. Percent workspace reached was calculated for three sub-regions (anterior/ipsilateral, anterior/contralateral, posterior/ipsilateral) within each primary region (**Fig. 1B**). A two-way repeated measures ANOVA with post hoc analyses was used to assess interlimb differences in percent workspace reached for each sub-region.

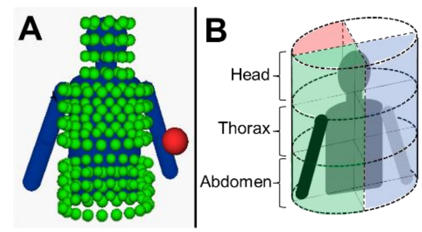

Figure 1: A) real-time feedback displayed. B) 3 regions (head, thorax, abdomen) each with 3 sub-regions - anterior/ipsilateral (green), anterior/contralateral (blue), posterior/ipsilateral (red).

Results & Discussion: The affected limb had less workspace for all regions surrounding the head (**Fig. 2**). This result supports the hypothesis as the head regions require sufficient shoulder elevation or elevation and external rotation both of which are common movement deficits in BPBI. The affected limb had less workspace for two abdominal regions (**Fig. 2**); the anterior/ipsilateral region necessitates shoulder abduction or extension to reach the most lateral portions of this region while the posterior/ipsilateral region requires shoulder extension, both of which are frequently limited in BPBI. The regions with no significant differences either did not require any of the common movement deficits in BPBI (abdominal anterior/contralateral, thoracic anterior/ipsilateral, thoracic anterior/contralateral) or only had little available workspace (thoracic posterior/ipsilateral) (**Fig. 2**). Together these results support the hypothesis that reachable workspace can detect deficits in close-to-body UE function that are consistent with movement limitations in BPBI.

Significance: These findings show that reachable workspace is capable of assessing inner, close-to-body UE function in BPBI and will supplement existing outer, far-from-body workspace evaluations [5] to help guide clinical decision making and outcomes assessment.

Acknowledgements: 2022 Shriners Hospitals for Children Clinical Research Grant (71005-PHI-22).

References: [1] Russo et al. (2014), *J Shoulder Elbow Surg* 23(3); [2] Abdel-Malek et al. (2004), *Ergonomics* 47(13); [3] Han et al. (2013), *PLoS Currents*; [4] Matthew et al. (2020), *IEE J Biomed Health Inform* 24(11). [5] Richardson et al. (2022), *J Biomech* 132.

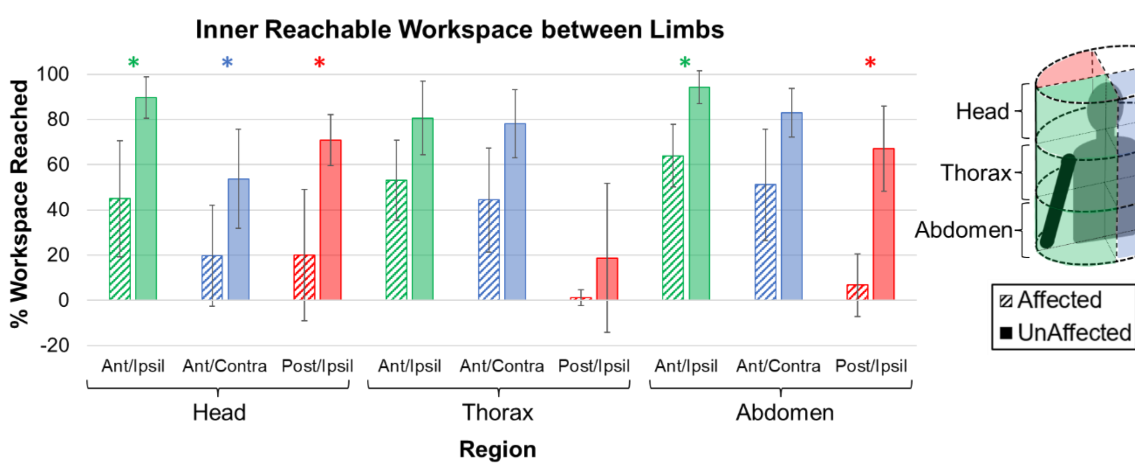

Figure 2: Interlimb differences (mean±1SD) in percent workspace reached by region. * indicates significant difference.

FOCUSED ULTRASOUND STIMULATON OF SCIATIC NERVE INDUCES PERIPHERAL MUSCLE CONTRACTION IN A MURINE MODEL

Zoe M. Moore[1*], Jake Elliott[2], Julianna C. Simon[1,2], Meghan E. Vidt[1,3]
[1]Biomedical Engineering, Pennsylvania State University, University Park, PA, USA
[2]Graduate Program in Acoustics, The Pennsylvania State University
[3]Physcial Medicine and Rehabilitation, Penn State College of Medicine, Hershey, PA, USA
*Corresponding author's email: zmm5238@psu.edu

Introduction: Low back pain (LBP) is common, affecting up to 30% of adults in the United States [1]. Increased sitting and poor posture are primary contributors to the development of LBP, which is characterized by pain in the lumbar and sacral spine. Muscle disuse, or lack of activity to avoid pain, is one of the main side effects of LBP. Current treatments for LBP include medication and physical therapy, but these have shown mixed success [2], with low patient compliance [2] and no specific treatment showing superiority [2]. There is a need to develop an alternative treatment that can strengthen deep spinal muscles and alleviate pain. Previous work has shown that focused ultrasound (fUS) has an excitatory or inhibitory effect on neurons, depending on the fUS parameters [3], suggesting that fUS can be used to activate muscle. The aim of this study is to evaluate whether fUS can activate muscle via peripheral nerve stimulation in an *in vivo* murine model and examine how successful fUS stimulation affects muscle mechanical properties.

Methods: The sciatic nerve of 19 Sprague-Dawley rats (IACUC #202101801) was treated with fUS on a randomly selected side. Indwelling electromyography (EMG) electrodes were inserted into the gastrocnemius muscle belly prior to being submerged in a water bath at body temperature (~37°C). The rats were randomly split into 3 treatment duration groups (30 s, 90 s, 180 s), and all rats were treated every other day for 2 weeks. After the final treatment, animals were euthanized, and bilateral gastrocnemius muscles (treated side, contralateral control) were harvested for mechanical testing and histology. Thirty gastrocnemius muscles (15 treated; 15 control) were potted and underwent mechanical testing using a previously reported protocol [4, 5, 6]. Briefly, the muscle was tested with a 585 MiniBionix (MTS Systems, Eden Prairie, MN) preloaded at 0.08 N, followed by 10 cycles of preconditioning, then rested for 300 s. Next, a stress-relaxation test was performed for 600 s, followed by a load-to-failure test with a load application rate of 0.0015 mm/s. An automated algorithm developed by our group [7] was used to calculate strain of the tissue and determine the Young's modulus for each group. The Shapiro-Wilk test was used to test for data normality. Then, separate paired t-tests were used to evaluate Young's modulus between treatment groups and across treatment durations; Young's modulus between treated and control groups; and Young's modulus between successful and unsuccessful stimulations. All analyses were performed with MATLAB with significance set at $p<0.05$. The other four rats were randomly selected for histological analysis (4 treated; 4 control) to determine whether tissue damage occurred due to fUS application. Skin and soft tissue from the treatment site were dissected, fixed in formalin for 7 days, then processed using standard paraffin wax techniques. All samples were sectioned and stained using Hematoxylin and Eosin (H&E) and qualitatively analyzed.

Results & Discussion: Muscle activation, defined as measurable signal above baseline EMG measures, was observed in 15 of 19 rats with fUS application, which is consistent with previous work[3]. There was no difference in Young's modulus when comparing between treatment duration for either the treated ($p=0.6305$) or control ($p=0.3998$) groups, so groups were combined into a single group for remaining analyses. No difference was seen in Young's modulus between treated (119.9 ± 43.1 kPa) and control (101.3 ± 37.8 kPa) groups ($p=0.2442$) (Figure 1A). There was no difference in Young's modulus between successful and unsuccessful stimulations ($p=0.4487$) (Fig. 1A). No histological evidence of morphological changes near the fUS target area or surrounding muscle was observed (Figure 1B). In summary, these results show no change in Young's modulus for the gastrocnemius muscle following 2 weeks of muscle activation via targeted fUS stimulation. It is possible that a 2-week time frame is insufficient for muscle remodeling and resultant changes to mechanical properties to occur. Ongoing work continues to examine how fUS can be used to stimulate muscle, including targeting more peripheral locations in the muscle bulk and evaluating whether fUS can control the level of muscle activation.

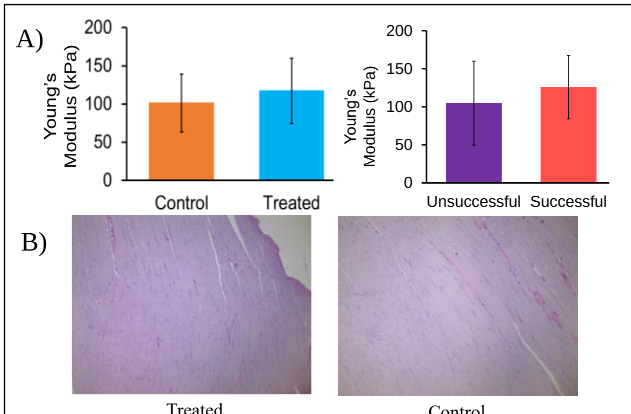

Figure 1: A) Young's modulus for treated (119.9 ± 43.1 kPa and control (101.3 ± 37.8 kPa) ($p=0.2442$) groups (left) and Young's modulus for unsuccessful and successful stimulation ($p=0.4487$) groups (right). B) Histology of the treated and control groups at the fUS target location of the sciatic nerve, showing no evidence of thermal or focal damage.

Significance: This study demonstrated that fUS can be used to stimulate muscle activation. fUS has potential for application in rehabilitation for LBP and other diseases that cause muscle disuse. Successful muscle stimulation with fUS motivates ongoing studies to determine dosing of fUS intervention for treatment of LBP and muscle disuse.

Acknowledgements: Penn State College of Engineering Multidisciplinary Seed Grant (PIs: Vidt, Simon).

References: [1] Shmagel et al. (2016), Arthritis Care Res. [2] Uritis et al. (2019), Current Pain and Headache Reports. [3] Downs et al. (2018), Phys Med Viol. 63(3). [4] Huang et al. (2004) Ann Biomed Eng. [5] Toscano et al. (2010), Clin (Sao Paulo). [6] Khandare et al. (2020) J Biomech.. [7] Elliott et al. (2022), Ann Biomed Eng. 50(5).

EXAMINATION OF AGE- AND SEX-BASED DIFFERENCES ON MUSCLE COMPENSATION FOLLOWING A ROTATOR CUFF TEAR DURING A LOADED DYNAMIC TASK

Zoe M. Moore[1*], Lilla Caton[1], Mitchell Vanden Heuvel[1], Joshua Pataky[1], Meghan E. Vidt[1,2]
[1]Biomedical Engineering, Pennsylvania State University, University Park, PA, USA
[2]Physcial Medicine and Rehabilitation, Penn State College of Medicine, Hershey, PA, USA
*Corresponding author's email: zmm5238@psu.edu

Introduction: Rotator cuff tears (RT) are common in adults, with increasing prevalence with more advanced age [1]. RT can influence an individual's ability to complete functional tasks, such as reaching and lifting a weighted object [2]. These tears are characterized by partial- or full-thickness tearing of the supraspinatus tendon, which is often accompanied by infraspinatus and subscapularis tendon tears in more severe injury presentations. Previous work by our group showed that the middle and posterior deltoid and teres minor increase muscle force with increased RT severity in a cohort of older males and females [3]. Other work showed that performing a functional task with increased load influences joint kinematics [4]. However, no work has examined the separate effects of age, sex, and load on muscle compensation strategies in the context of RT severity. Thus, the goal of this study was to determine the effect of age, sex, load, and RT severity for a forward reach task using a computational model.

Methods: Four models were developed in OpenSim software (v.3.3) [5] representing young (30.5±6.5 years) and older (74.5±3.5 years) adult males and females, using muscle force-generating properties defined in literature [6, 7]. Peak isometric force of muscle actuators in the model were reduced to represent 3 RT severities, consistent with our previous work [3]. Forward reach kinematics from a prior study [2] were used as inputs to a Computed Muscle Control [8] simulation, followed by a point kinematics analysis to determine hand deviation. For all simulations, external loads (0N; 4.5N; 13.3N; 22.2N; 44.5N; 53.4N; 66.7N) were separately applied to the hand in the global negative vertical direction. Outcomes included: root mean squared error (RMSE) for hand kinematic deviation and average normalized muscle force relative to the peak isometric force definition of each muscle path. After determining that the data was non-parametric using a Kolmogorov-Smirnov test, model-predicted outcomes were separately compared across age, sex, load, and RT severity using a Kruskal-Wallis test, with significance set at $p \leq 0.05$.

Results & Discussion: Results revealed that in general, predicted hand deviation compared to the input kinematics was preserved for all models with increasing load and RT severity, with an average RMSE=0.015 for the no tear, 0N load model, and RMSE=0.023 for the massive tear, 66.7N load model. All external loads were combined to look at the effect of RT severity. Normalized muscle force in the middle deltoid, posterior deltoid, infraspinatus, and teres minor muscles increased with increasing RT severity for all groups (young adult males/females, older adult males/females) (all $p<0.001$) (Fig. 1). Other trends observed included an increase in normalized force for the ribs compartment of pectoralis major muscle path for young adult females ($p=0.0155$) and older adult females ($p<0.001$), an increase in normalized anterior deltoid muscle force for the young adult males ($p=0.0438$), and an increase in normalized subscapularis muscle force for older adult males ($p<0.001$). All RT severities were combined to look at the effect of load. Muscle force contributions were similar across all groups (young adult males/females, older adult males/females) with increasing load. A significant increase was seen in normalized muscle force for anterior deltoid, middle deltoid, and infraspinatus (all $p<0.001$). An increase in normalized teres minor muscle force with increasing load was also seen for young adult females ($p<0.001$) and older adult females ($p<0.001$). These findings indicate that females are using a larger proportion of their muscle activation capacity than males to perform a loaded forward reach. It also suggests that older adult males recruit different muscles than young adult males to complete the task, which may indicate that older adults have a different muscle force-generating profile than young adults.

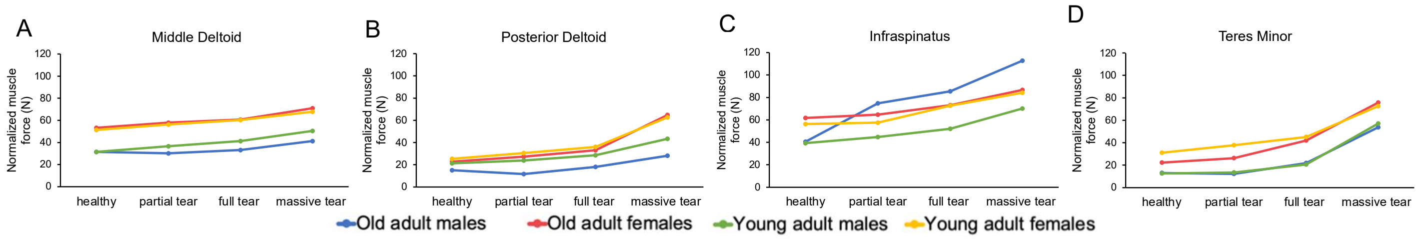

Figure 1: Normalized muscle force for A) middle deltoid, B) posterior deltoid, C) infraspinatus, and D) teres minor muscles for young adult males/females and older adult males/females with increasing RT tear severity (all $p<0.001$).

Significance: Regardless of age, females recruit muscles similarly to complete a forward reach with increased load and RT severity. Males recruit different muscles than females with increased RT severity, which could be due to sex-based differences in muscle force-generating profiles. This work found that the deltoid muscle compensates in all model groups evaluated, making it a potential target for RT rehabilitation. The sex- and age-based differences identified here also suggest that there may be additional opportunities to customize rehabilitation. Ongoing work is examining the relationships identified here in other functional tasks.

References: [1] Yamamoto et al. J Shoulder Elbow Surg. 2010;19(1). [2] Vidt et al. J Biomech. 2016;49(4). [3] Pataky et al. Clin Biomech. 2022. [4] Li et al. J Biomech. 2016;6;49(13). [5] Delp et al. IEEE Trans Biomed. Eng. 2007;54(11). [6] Holzbaur et al. J Biomech. 2006; 40(2007). [7] Vidt et al. J Biomech. 2012; 45(2). [8] Thelen et al. J Biomech. 2003;36(3).

AGE RELATED DIFFERENCE IN HEAD CONTROL DURING FALLING

James R Fang[1], Lingjun Chen[1], Emilia Potts[1], Nathanael Garcia[2], Andrew Luzania[2], Danya Pradeep Kumar[1], Neil B Alexander[3], Jacob J Sosnoff[1*,]
[1] Department of Physical Therapy, Rehabilitation Sciences and Athletic Training, University of Kansas Medical Center
[2] School of Medicine, University of Kansas Medical Center
[3] Department of Internal Medicine, Division of Geriatric and Palliative Medicine, University of Michigan
*Corresponding author's email: jsosnoff@kumc.edu

Introduction: Falls are the leading causes of accidental injury and injury-related death among the elderly[1]. Fall-related head injury is common and associated with morbidity and mortality. Fall-related head injury occurs when the head strikes the ground or other surface. Older adults have elevated risk for head impact during a fall[2]. It is postulated that this elevated risk stems in part from declines in neck muscle activation compare to young counterparts [3]. However, there is a lack of direct evidence linking age-related difference in neck muscle activation latency to the risk of fall-related head impact. The current study aims to fill this knowledge gap by investigating age-related differences in neck muscle activation during falls. We hypothesize that older adults will have H1) higher occurrence of head impact during fall, and H2) longer neck muscle activation latency in response to fall.

Methods: Three older adults at risk for fall related injury(age 77±7 yr; 1/3 female) and three healthy young adults (age: 29±4 yr; 1/3 female) participated in the study. All participants underwent experimentally induced falls in multiple directions (backwards, left, and right falls). Participant underwent two falls in each direction for a total of six falls. Figure 1 visualizes the experimental set-up and data streams. The falling movement was quantified using 8 camera optical marker base motion capture system sample at 100Hz (MotionAnalysis, Inc). Electrical activity of the head stabilizers musculature, specifically bilateral sternocleidomastoid and upper trapezius [3] were collected using surface electromyograms (EMG; Delsys, Inc) sample at 2148Hz. The primary outcomes were occurrence of head impact and the muscle activation latency during fall. The occurrence of the head impact were identified using standardized visual inspection of fall videos [2]. The muscle activation latency was determined as the difference between the fall initiation and the onset time of the muscle, where the onset of the EMG was determined using method of [3]. Chi-square test was used to assess the effect of age on occurrence of head impact, and independent t-test was used to test the difference of muscle activation latency between older and young adults.

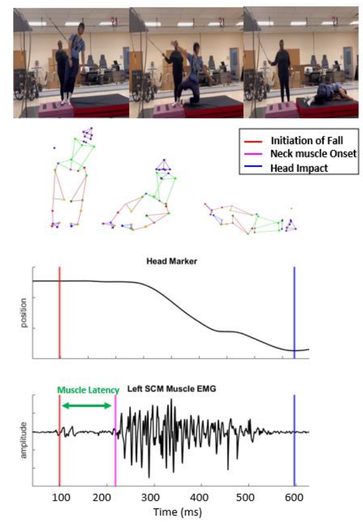

Figure 1: Experimental Fall Paradigm: Participants were supported by a harness. Falls were initiated via a pseudorandom release of the support. The motion of the body was captured by the motion capture system and the time of the fall initiation, and the head impact were determined by the corresponding marker position. Then the onset time of the synchronized EMG signal was calculated in this time range and used to determine the muscle activation latency.

Results & Discussion: Older adults had higher occurrence of head impact compared to young adults (11/18 falls = 61% vs. 3/18 falls = 17%, $p = .006$, Cohen's $w = 0.91$). There was no difference on muscle latency between old and young adults (see Table 1). These results are in contrast to Choi et al.[4] who reported that muscle latency was related to head impact in self-initiated falls in young adults. The discrepancy could result from differences in self-initiated falls vs. experimentally induced falls. The discrepancy highlights the need to further investigate induced falls and caution should be used when generalizing from self-initiated falls. It is also possibility that the current preliminary sample is under-powered. The null result also raises the possibility that other factors such as muscle strength or stiffness are contributing to age-related differences in head impact during falls. Further investigation on factors that may elevate the risk of head impact during fall is needed.

Table 1. Muscle activation Latency of old and young adults (mean±SD)

	LSCM (ms)	RSCM (ms)	LUT (ms)	RUT (ms)
Old Adults	89.47±219.90	52.69±158.81	22.57±174.95	52.45±215.00
Young Adults	3.93±9.59	55.68±163.94	76.56±150.95	42.44±79.54
p-value	0.55	0.71	0.55	0.49
Cohen's d	0.49	-0.02	-0.32	0.23

Significance: The current study collected preliminary data to investigate the relation between head impact and neck muscle control. Overall, the results are distinct from previously reported head control during self-initiated falls. The null result raises the possibility that other factors besides muscle activation relate to age-related differences in head control.

Acknowledgements: This project is supported by Grant T32HD057850-13 and R21AG073892.

References: [1].Prevention CfDCa. Important facts about falls. 2017 [Available from: https: // www.cdc. gov / homeandrecreationalsafety / falls / adultfalls.html.; [2].Wood TA, Moon Y, Sun R, Bishnoi A, Sosnoff JJ. BioMed research international. 2019. [3].Wood TA, Hernandez ME, Sosnoff JJ. Journal of electromyography and kinesiology. 2020;51:102405. [4].Choi W, Robinovitch S, Ross S, Phan J, Cipriani D. Clinical biomechanics. 2017;49:28-33.

CLOSED-LOOP CONTROL FOR HUMAN LAND AND STOP TASKS

Rodolfo Amezcua-Cerda[1*], Henryk Flashner[1], Jill L. McNitt-Gray [2,3]
[1]Departments of Aerospace and Mechanical Engineering, [2]Biological Sciences, [3]Biomedical Engineering
University of Southern California, Los Angeles, CA. *Corresponding author's email: amez875@usc.edu

Introduction: Human land-stop tasks are fundamental in various biomechanical contexts, such as gymnastics. During a landing, gymnasts execute a multi-joint control strategy to regulate ground reaction forces (GRFs) and achieve balance. Previous modeling efforts have suggested that land-stop tasks are intrinsically open-loop [1]. This work, in contrast, proposes that the body employs a closed-loop feedback control configuration during land-stop tasks. A closed-loop controller is designed for a planar four-link model along with a rigid impact ground model. The novelty of this modeling effort is including the foot, ankle torque, and the transition from underactuation to full actuation in the model, Figure 1. The controller and model are validated with experimental data during a series of landings where the participant intentionally regulated the magnitude of the GRFs upon contact.

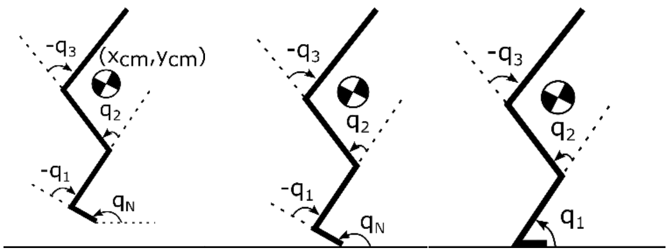

Figure 1: Planar four-link model used to study a land-stop task. Generalized coordinates q_i denote absolute and relative angles of the body segments. (Left) Flight phase model in free fall. (Middle) Underactuated model used upon toe contact. (Right) Fully actuated model upon heel contact. Transitions between phases of the model are achieved with instantaneous rigid impact ground events.

Methods: A female participant with a background in gymnastics provided informed consent and performed a series of self-regulated landings from a 0.445 meter platform. The three types of landings were characterized as normal, soft, and hard according to the magnitude of the GRF. Kinematic data in the sagittal plane was captured at 11000 frames per second with a 1.5mm/pixel resolution. Ankle, knee, hip, and shoulder points were tracked. A cubic smoothing spline was applied to the data to attenuate high frequency noise.

The dynamics of the human body are derived under rigid body assumptions using coordinates described in Figure 1. The land-stop task is partitioned into flight, impact (defined as twice the time to peak vertical GRF observed in data), and post-impact. The impact phase begins when the toes contact the ground. At this point a rigid impact ground model [2], that assumes an instantaneous change of angular velocities but no change in angular positions, is used. When the heel contacts the ground, the rigid impact ground model is applied once more. The model is underactuated until the heel impact event because there is no actuation about the toe.

A closed-loop controller is designed for this model by tracking the experimental joint angles during flight and post-impact phases, and tracking the experimental GRFs during the impact phase. To do so, a nominal state and control trajectory is obtained using tools from trajectory optimization. Then the model is locally stabilized about this nominal trajectory using the state feedback solution to the time-varying linear quadratic regulator.

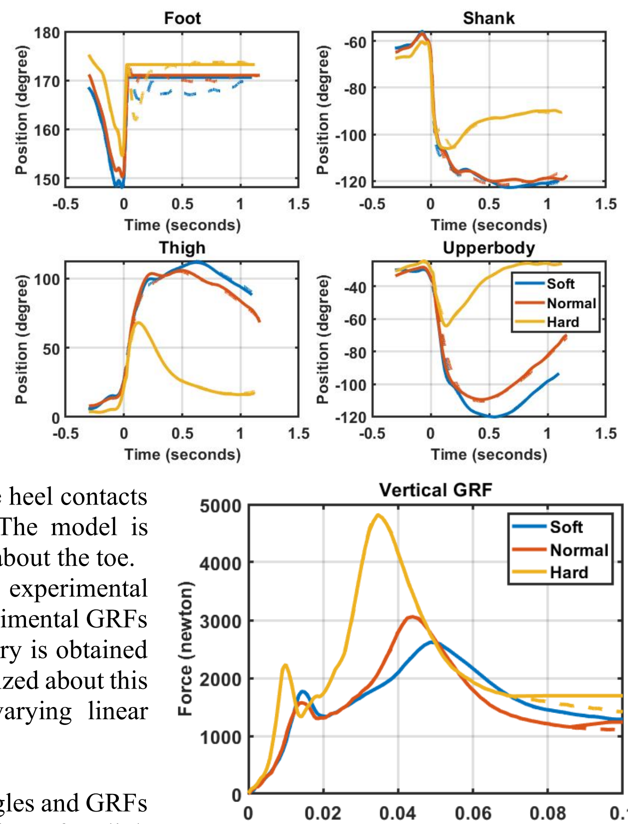

Figure 2: In all plots dashed is data, solid is simulation. (Top) Joint angles. (Bottom) GRF.

Results & Discussion: The model reproduces the experimental joint angles and GRFs well across the three landing conditions, Figure 2. This suggests that a planar four link model and rigid impacts is a sufficient model to capture land-stop task dynamics. Furthermore, as in experiments, the model can regulate GRFs using feedback control; this suggests that humans use a closed-loop control configuration during land-stop tasks.

Significance: This modeling effort captures key principles during a land-stop task. During the flight phase, the body must configure itself to prepare for landing. It must then appropriately regulate the GRFs and reduce momentum during impact, while achieving balance during post-impact. Furthermore, the optimization used to find the nominal state trajectory could be interpreted as a learning process humans undergo. Moreover, dealing with underactuation is feature that is often not addressed. Future questions to be posed with this type of model could be how would the joint angles and GRFs change if the task objective were a land-and-go situation?

References: [1] Gruber. Wobbling mass model v. rigid body models. (1998). [2] Westervelt, E.R. (2018). *Feedback Control*, CRC.

ARTICULAR SURFACE MORPHOLOGY AND THE RELATIONSHIP TO FRONTAL-PLANE ANKLE STIFFNESS UNDER LOADING IN INDIVIDUALS WITH AND WITHOUT CHRONIC ANKLE INSTABILITY

Zoe Villamar[1,2*], Ali Serhal[3], Eric J. Perreault[1,2,4], Daniel Ludvig[1,2]
[1]Department of Biomedical Engineering, Northwestern University, Evanston, IL
[2]Shirley Ryan AbilityLab, Chicago, IL, [3]Department of Radiology [4]Department of Physical Medicine and Rehabilitation, Northwestern University, Chicago, IL
*Corresponding author's email: zoevillamar2018@u.northwestern.edu

Introduction: Ankle sprains are the most common musculoskeletal injury. Up to 40% of individuals go on to develop chronic ankle instability (CAI) after a first-time sprain, resulting in recurring sprains, the ankle giving way, and feelings of instability. CAI is associated with articular surface abnormalities, particularly in the talus [1]. The talus is an articulating bone of the subtalar and the tibiotalar joints, both of which allow for frontal plane motion. Cadaver studies demonstrate that the articular surfaces are an important component within the ankle that provide stability in the frontal plane. Under high axial loads, they provide greater resistance to frontal plane motion. In fact, at full body weight, the articular surfaces may provide up to 100% of the resistance to motion [2]. Consistent with cadaver studies, axial loading has been shown to be a significant modulator of frontal-plane ankle stiffness *in vivo* [3]. As axial loading increases, frontal-plane ankle stiffness increases, thereby reducing the probability of a sprain. However, the effect of abnormalities in talar morphology to frontal-plane ankle stiffness under loading *in vivo* remain unknown. We hypothesize that individuals with CAI will have a reduced effect of load on ankle stiffness compared to individuals without ankle impairments, and this will be correlated to measurements quantifying abnormalities of talus morphology. If this correlation exists, it could mean that talar morphologies predispose individuals to developing CAI after a first-time sprain, which could be taken into account for more conservative rehabilitation.

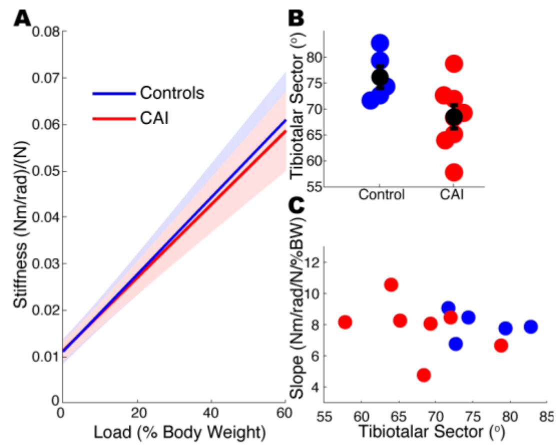

Figure 1: (A) Group average of frontal-plane stiffness under passive load. Shaded areas are 95% confidence intervals. (N = 9 controls, 8 CAI). (**B**) Tibiotalar sector values for controls (N = 5) and CAI (N = 8). Error bars are SEM. (**C**) Stiffness-load slope values against tibiotalar sector values (N = 5 controls, 7 CAI).

Methods: To date, we have collected data from eight females with chronic ankle instability, selected using guidelines based on subject history established by the 2014 International Ankle Consortium, and 9 females without ankle impairments. We estimated ankle stiffness under passive loading using our established protocol [1]. Briefly, subjects were seated with their ankle fixed to a rotary motor via a fiberglass cast. The knee and ankle angle were at 90 degrees of flexion. The desired load was set by applying pressure to the knee. Electromyographic (EMG) data were collected from the tibialis anterior (TA), lateral gastrocnemius (LG), medial gastrocnemius (MG), soleus (SOL), peroneus longus (PL), and peroneus brevis (PB) to assess any load-dependent changes in muscle activity. Small rotational perturbations were applied to the ankle in the frontal plane to estimate stiffness. To characterize the talus morphology, a subset of participants (8 CAI, 5 controls) had standard anterior-posterior and lateral weight-bearing x-ray images. A radiologist blinded to subject group (Control vs. CAI) made measurements according to those previously established to be different in CAI [3]. These include the frontal curvature of the talus, the talar radius, and the tibiotalar sector. We used linear mixed-effects models to test the hypothesis that individuals with CAI have a reduced effect of load on frontal-plane ankle stiffness. Ankle stiffness was the dependent variable, load as a percent of body weight was a continuous factor, subject was a random factor, and subject group was a fixed factor. We also used linear mixed-effects models to (1) test if there are differences in the talus morphology metrics between groups, and (2) test the hypothesis that the stiffness-load slope is correlated to the talus morphology.

Results & Discussion: Individuals with chronic ankle instability had a load-stiffness slope that was only 5% less than that in individuals without ankle impairments, demonstrating that the effect of load did not differ greatly between the two groups (Fig. 1A). The frontal curvature of the radius was 22% smaller, the talar radius was 8% smaller which was opposite trends in a previous report [1]. The tibiotalar sector was 10% smaller in CAI (Fig. 1B), which was consistent with previous findings [1]. These differences in articular surface morphology showed moderate to weak correlation with the load-stiffness slope (frontal curvature: r = 0.26; talar radius: r = 0.03; tibiotalar sector: r = -0.24, Fig 1C). Our ongoing data collection will provide the statistical power to determine which of these trends are statistically significant, and if there are differences based on sex.

Significance: This is the first study to quantify the effects of load and articular surface geometry on frontal-plane ankle stiffness in individuals with CAI. Upon completion of data collection, we will be able to determine if altered talus morphology is associated with a reduced ability to resist a sprain, thereby clarifying the significance of previous results demonstrating that individuals with CAI also have altered talar morphology.

Acknowledgements: NIH T32 HD07418. American Society for Biomechanics Grant-In-Aid.

References: [1] Frigg et al., 2007. *Br J Sports Med* 41:420–424 [2] Stormont et al., 1985. *Am J Sports Med*, 13(5): p. 295-300. [3] Villamar et al., (2022) *J Biomech* 143: 111282.

INTEGRATING WEARABLE IMU SENSORS TO COLLECT AND ANALYZE HUMAN MOVEMENT OUTSIDE THE LAB

Anthony Wash [1,2], Eric G. Meyer*[1]
[1]Biomedical Engineering, Lawrence Technological University, Southfield, MI, USA
[2]Functional Athletic Sequence Training LLC, Troy, MI, USA
*Corresponding author's email: emeyer@ltu.edu

Introduction: There are a variety of tests and movement screens used to identify human biomechanical movement patterns. For example, the overhead deep squat screen or drop jump landing can assess lower extremity movement and may identify biomechanical patterns that may contribute to injury risk [1]. The Function Movement Screen (FMS) is one of the common movement screens used to assess human movement and potential injury risk [2]. They were developed to observe movement asymmetry and dysfunctional movement patterns of the upper and lower extremity and trunk. However, the qualitative FMS score (on a scale of 0-3 points) may be limited in its ability to predict injury incidence, due to inaccuracies or reliability issues with the scoring criteria. Quantitative analysis of human movement and joint reaction forces has typically been performed in a motion capture biomechanics laboratory which produce more reliable and accurate kinematic results [3]. However, kinesiology professionals and coaches do not have the access, time or expertise to use this equipment to track athletes, physical therapy patients or other clients. Another approach to quantifying human movement is with inertial measurement unit (IMU) sensors, which are relatively cheap, more accessible, can be set up easily and work outside of the motion capture laboratory, in real-world environments [4]. This project compares the lower extremity kinematic data from five mBient wireless IMU sensors (model MMRL, https://mbientlab.com/) with FMS scores while participants perform three movements; Overhead Deep Squat, Hurdle Step (right and left sides) and In-Line Lunge (right and left sides). The hypothesis was that quantitative kinematic measurements from wearable sensors would correlate with specific qualitative lower extremity FMS scores.

Methods: Eight participants (13-42 years old) with no lower extremity injury and a range of movement backgrounds were included in the study according to the University IRB approved procedure and with signed informed consent. IMU sensors were attached to the torso, thighs, and distal tibias using Velcro straps. Data collection was controlled from a smartphone app with quaternion orientations and Euler angle data recorded at 100 Hz for the entire session of approximately 10 minutes. The IMU data was then post-processed to quantify the lower extremity kinematics during each FMS movement. A Certified Athletic Trainer (AW) scored each participant using the standard qualitative method. Kinematic variables of interest included hip (HF) and knee flexion (KF) as well as hip ab/adduction (HA), knee valgus/varus (KV) and torso angle (TA) relative to ground. Qualitative and quantitative scores were compared using linear regression statistics.

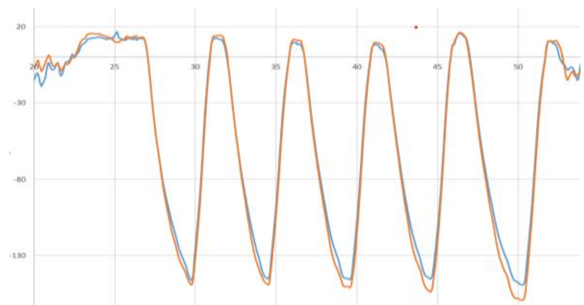

Figure 1: Representative deep squat FMS trial showing right (blue) and left (orange) hip flexion angles from IMU sensor data.

Participant	1	2	3	4	5	6	7	8
HF_R	151	138	162	164	151	69	91	116
HF_L	141	130	167	158	141	113	75	116
FMS	3	3	3	3	3	1	1	1
KF_R	150	120	153	145	150	114	105	98
KF_L	137	128	154	131	137	104	81	89
FMS	3	2	3	3	3	1	1	1
HA_R	41	25	37	20	20	15	29	10
HA_L	22	22	14	17	18	17	47	18
FMS	1	1	1	2	2	2	1	2
KV_R	24	9	23	9	10	10	21	31
KV_L	8	30	14	11	8	18	15	18
FMS	1	1	1	3	3	2	1	1

Table 1: Deep squat kinematic angles (right and left) from IMU sensor data and FMS scores.

Results & Discussion: A representative time series graph of the kinematic data computed from IMU sensors is shown (Fig. 1). Kinematic results had moderate predictive value after regression analysis depending on the FMS activity (Table 1). In Deep Squat, participants who scored a 3 had greater HF and KF values for all movements compared to those who scored a 2 or 1. Kinematic values varied slightly between left and right sides, so the minimum ranges of motion were used. These parameters were chosen because during qualitative scoring of FMS, comparing left and right sides, the minimum score is the final score. However, the maximum values of HA and KV were used to compare those FMS scores because in order to score a 3, participant has to have less than 15° of HA and KV [2]. Kinematic angles for Hurdle Step and Lunge were also compared with FMS scores.

Significance: The qualitative and quantitative results in this study show some consistent trends. However, more data and analysis methods would be required to fully establish the biomechanical parameters for the optimal angles during the FMS or other types of performance assessment [5]. Wearable sensors with automated data analysis could allow for accurate diagnosis and/or exercise prescription [6]. This technology would give movement professionals a more consistent and detailed analysis of how an individual is moving and may help them determine or confirm asymmetries that may be hidden to the qualitative eye. The study's correlations between wearable sensors and FMS scores are relevant to kinesiology professionals, coaches and individual athletes because these methods would allow real world analysis of human movement and performance tracking outside of traditional motion capture laboratories.

References: [1] Heredia et al. (2021), *J Sports Sci Med* 20; [2] Cook et al. (2014), *Int J Sports Phys Ther* 9(3). [3] O'Reilly et al. (2018), *Sports Med* 48. [4] Shull et al. (2014), Gait Posture 40. [5] Whiteside et al. (2016), *J Strength Cond Res* 30(4). [6] Wu et al. (2021), *Applied Sci* 11(96).

DO PHYSICAL OUTCOME MEASURES OF FORCE AND VELOCITY CORRELATE WELL WITH RATING OF TENNIS PERFORMANCE IN COLLEGIATE MALE ATHLETES? A PILOT STUDY

Gouresh M. Powar*, Michael W. Olson
Biomechanics Lab; Department of Athletic Training and Exercise Physiology; Midwestern State University, Wichita Falls, TX
*Corresponding author's email: gouresh.powar@gmail.com

Introduction: Tennis is one of the most watched sports across the globe. Tennis involves high speed serves, reactive ground strokes, and extremely agile movement which needs extraordinary levels of fitness [1]. Studies have been conducted on junior athletes assessing on-court performance variables, med-ball throws, and counter-movement jump, strength parameters, and serve velocity [2, 3, and 4] but research on collegiate athletes is minimal. Collegiate coaches have been using 'Universal Tennis Rating' (UTR) and 'World Tennis Number' (WTN) for several years to recruit athletes. The UTR is calculated based on competition, score, opponents, and win/lose history [5]. Many countries have different ratings of tennis performance and recruiting the athletes from these counties becomes subjective without a quantitative data. Previous studies have reported correlation results between isometric strength and stroke velocity, but very few have looked at relationships between isokinetic strength, stroke velocity, and rating of tennis performance [6]. Coaches need quantifiable variables that are easy to measure, such as ball velocity, and tie it to important performance variables that can only be measured with a research lab or if a rating system is absent for certain athletes. Our aim was to establish relationships between isokinetic strength, med-ball throws, UTR, WTN, and stroke velocity (StV) for ground strokes (backhand and forehand) and serve in collegiate tennis players. Due to isokinetic movements, med-ball throws mimicking the serve and ground strokes, we hypothesized a strong correlation between them. As skill and physical outcome measures of force and velocity were not found correlated in the previous studies, we hypothesized no correlation between the physical outcome measures, UTR and WTN.

Methods: Six male (n = 6) participants volunteered for the study (age: 20.3 ± 1.6 year, training age: 14 ± 1.3 years, height: 177.8 ± 4.6 cm, body mass: 75.7 ± 5.8 kg, dominant limb length: 76.5 ± 1.72 cm). Participants were athletes from a collegiate men's tennis team which participates in division 2 of National Collegiate Athletic Association (NCAA). The study conducted was a cross-sectional study. The data collection was done during off-season and within 2 weeks' time period over two separate sessions. The two sessions: 1) laboratory and 2) on-court were separated by 24-hour period and done on a day with minimal to no training load. During the laboratory session: anthropometric data (height, mass, chronological age, training age, dominant limb length) were collected along with 1) two trials and 4 total measurements of Isokinetic strength (60 deg/s) in 8 different movements [1) Shoulder internal (IsokIR), external rotation (IsokER), 2) shoulder horizontal adduction (IsokAdd), abduction (IsokAbd), 3) wrist flexion (IsokFx), extension (IsokEx), 4) wrist pronation (IsokPro), supination (IsokSup)] on Biodex System 3 dynamometer (Biodex, Corp., Shirley, NY). The participants were asked to do 5 min of warm-up on treadmill at self-selected speeds and upper-extremity mobility exercises. Only the dominant arm was tested. During the on-court session: 1) Velocity for six serves (S. StV), six forehand (F. StV), and six double backhand (B.StV) and 2) distance for two trials of three medicine ball throw (MBT) types: overhead (O.MBT), forehand (F.MBT), and backhand (B.MBT) were collected . The participants were asked to perform upper-extremity mobility exercises and at least 6 serves, forehands, and backhands as a warm-up. The peak ball velocity was measured by a hand-held radar gun [Pocket radar ball coach, US]. The radar was positioned 2m behind the player and an approximate height of 1.5m. The UTR and WTN data was acquired from the coaching staff. Pearson correlations (2-tailed) were used to assess the relationships between variables, primarily the isokinetic, StV, medicine ball throw, and UTR/WTR. The alpha was set at $p < 0.05$.

Results: A significant positive correlation was found between IsokER peak torque (24.24 ± 4.48 Nm), F.StV (79.72 ± 5.05 m/s) ($r = 0.894$, $p < 0.05$) and B.StV (83.98 ± 5.52 m/s) ($r = 0.846$, $p < 0.05$). Similarly, a significant positive correlation was found between IsokER average torque (24.24 ± 4.48 Nm), F.StV (79.72 ± 5.05 m/s) ($r = 0.927$, $p < 0.01$) and B.StV (83.98 ± 5.52 m/s) ($r = 0.919$, $p < 0.01$). A significant negative correlation was found between IsokER peak torque (24.24 ± 4.48 Nm) and UTR (11.14 ± 0.08) ($r = - 0.826$, $p < 0.05$). A significant negative correlation was found between IsokEx average torque (7.06 ± 2.27 Nm) and UTR (11.14 ± 0.08) ($r = - 0.820$, $p < 0.05$). Lastly, A significant positive correlation was seen between F.StV (79.72 ± 5.05 m/s) and B.StV (83.98 ± 5.52 m/s) ($r = - 0.937$, $p < 0.01$). No significant correlation was found between any of the isokinetic movements, all MBT types and WTN. No significant correlation was found between any of the MBT types, S.StV, F.StV, B.StV and UTR.

Discussion: The isokinetic movements such as shoulder external rotation that mimic on-court movement was highly correlated to both forehand and backhand strokes, which shows support to the first hypothesis. It can be seen that no other isokinetic movement nor med-ball throw had a significant correlation due to the restrictive nature of movements compared to the serve and ground strokes, which shows lack of support to our first hypothesis The isokinetic external rotation and wrist extension was negatively correlated with UTR, which shows lack of support to our second hypothesis. Further data are needed to corroborate these finding.

Significance: The results of the study highlight the importance and quantification of movement-specific strength training, general strength training and skill training. The data can be used to analyse performance, targeted diagnostics, and for rehabilitation programs.

Acknowledgements: Midwestern State University Men's Tennis Team

References: [1] Fernández-Fernández et al. (2014). Br. J. Sports Med. 48(Suppl. 1); [2] Colomar et al. (2020). Front Physiol. 11:196; [3] Baiget et al. (2016). J Hum Kinet. 53:63-71; [4] Fett et al. (2020) J Strength Cond Res. 34 (1):192-202. [5] Howell et al. (2013). US 8,548,610 B1. [6] Signorile et al. (2005) J Strength Cond Res. 19(3):519-26

COMPARING SPATIAL-TEMPORAL STRATEGY IN OLDER ADULTS CLASSIFIED AS FALL RISK UNDER DUAL-TASK GAIT CONDITIONS

Peoples, Brandon M.[1], Kenneth Harrison[1], and Jaimie Roper[1]
School of Kinesiology, Auburn University[1]
bmp0049@auburn.edu

Introduction: Walking speed is known as "the 6th vital sign" due to its ability to predict future health status, functional ability, balance confidence, and fall risk[1]. Furthermore, walking requires precise muscle activation across multiple joints and sensory integration to ambulate through ever-changing environments[2]. Although walking speed decreases as we age, older adults have the capability to adjust parameters of gait to meet the demands of an environment (i.e., hurrying across a crosswalk prior to the walking indicator change). Length-Time difference (LTD) evaluates the spatial-temporal strategy during varying walking conditions (i.e., fast walking vs. comfortable walking)[3]. Older adults who employ a temporal strategy (quicker steps) have greater propulsion and braking; however, they are more likely to have lower functional ability, and are at tripping risk which in turn increases fall risk. Conversely, older adults who employ a spatial strategy (longer steps) to modulate speed may have an increased propulsive reserve which allows them to adapt their gait to meet the needs of their environment[3]. Understanding the spatial-temporal strategy utilized by community-dwelling adults classified as a fall risk while performing dual-task walking in a non-laboratory setting is unknown. Since the temporal strategy is associated with lower functional ability, we hypothesize there will be a difference in the spatial-temporal strategy amongst older adults classified as fall-risk during different walking speeds and dual task conditions.

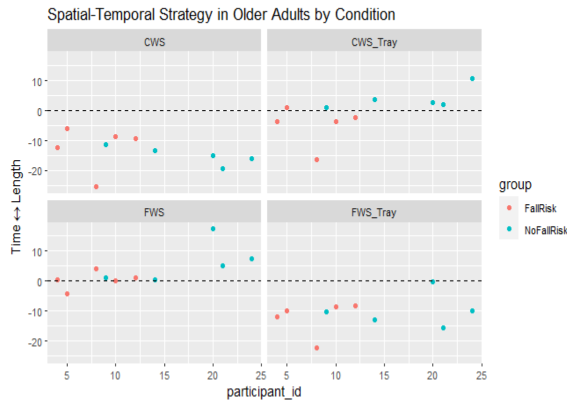

Figure 1: Spatial-Temporal Strategy by fall risk group and Length-Time Difference (LTD). 1) CWS (Fast Walk vs. Comfortable Walk 2) CWS_Tray (Comfortable Tray vs. Comfortable Walk) 3) FWS (Fast Tray vs Fast Walk) 4) FWS_Tray (Fast Tray vs Comfortable Tray. A negative value for LTD indicates a temporal strategy, while a positive value indicates a spatial strategy.

Methods: Ten older adults (3 M, 7 F, 70±8yrs.) performed the 5R-STS test while wearing 6 IMU sensors located on the sternum, lumbar (L5), wrists, and feet prior to walking across an 8-meter instrumented walkway during a community health fair. The 5-rep sit to stand (5R-STS) test is a simple clinical assessment of functional ability, lower body strength, and fall risk[4,5]. Fall risk was classified as a duration greater than 15 seconds during the 5R-STS using the IMU sensors[4,5]. Testing was performed in a designated area and controlled for interference. All participants were exposed to the non-laboratory environment and given the same instructions prior to each assessment. Participants completed four walking trials under the following conditions: 1) Comfortable Walking 2) Comfortable Walking while holding a tray with a glass of water (Comfortable Tray) 3) Fast Walking 4) Fast walking while holding a tray with a glass of water (Fast Tray). Walking speed variables (e.g., step length and time) were calculated from the instrumented walkway. Spatial-temporal strategy was calculated using Length-Time Difference. The formula for Length-Time difference is: $LTD = \frac{(Step\ Length_{Condition} - Step\ Length_{Walking\ Speed})}{Step\ Length_{\ Walking\ Speed}} + \frac{(Step\ Time_{Condition} - Step\ Time_{Walking\ Speed})}{Step\ Time_{Walk\ Speed}}$.

Results & Discussion: We conducted a 2 (groups) X 4 (tasks) Repeated Measures ANOVA to compare the effect of LTD on fall risk group. We observed a significant main effect between LTD and fall risk group (F (3, 6) = 7.60, p = 0.02). Additionally, we observed a significant within-subject effect for LTD (F (3,24) = 4.55, p = 0.04). A pairwise comparison using Bonferroni correction showed there was a significant difference between groups when walking with a tray at a comfortable speed (F (1,8) =6.872, p = 0.03), the fall-risk group utilized a temporal strategy (M = -4.99, ± 6.69) while the non-fall risk group utilized a spatial strategy (M = 4.07, ± 3.86). Regardless of fall risk, all older adults utilized a temporal strategy in the fast-walking condition compared to the comfortable walk condition (fall risk: M = -12.35, ± 7.65) (non fall-risk: M = -14.97, ± 3.03) there was not a significant difference between groups F (1,8) =.505, p = .50). When walking fast with a tray there was not a significant difference between groups F (1,8) =3.09, p = .12), both utilized a spatial strategy, (fall-risk group: M = 0.38, ± 3.01; non fall-risk group: M = 6.29, ± 6.90), compared to walking fast without a tray. When walking fast with a tray, both groups utilized a temporal strategy but there was not a significant difference between groups F (1,8) = 3.40, p = .10), (fall-risk group: M = -7.5, ± 2.25; non fall-risk group: M = 13.13, ± 6.44), compared to walking at a comfortable speed with a tray. Generally, our study demonstrates that LTD is a simple way to calculate changes in spatial-temporal strategy amongst older adults regardless of fall risk status when coupled with a dual task (**Fig. 1)**.

Significance: The ability to adapt walking speed under various conditions and in different environments is important for community dwelling older adults. Length-Time Difference is a quick simple way to assess maladaptive gait strategies in older adults and can be easily calculated by clinicians to address underlying issues in gait patterns such as a decline in lower body strength or functional ability.

References: [1] Fritz, Stacy PT, PhD1; Lusardi, Michelle PT, PhD2. White Paper: "Walking Speed: the Sixth Vital Sign". Journal of Geriatric Physical Therapy 32(2):p 2-5, **[2]** Sato, Sumire, and Julia T. Choi. "Neural control of human locomotor adaptation: lessons about changes with aging." The Neuroscientist 28.5 (2022): 469-484. **[3]** Baudendistel, Sidney T et al. "Faster or longer steps: Maintaining fast walking in older adults at risk for mobility disability." Gait & posture vol. 89 (2021): 86-91. doi:10.1016/j.gaitpost.2021.07.002 **[4]** Buatois, Severine et al. "A simple clinical scale to stratify risk of recurrent falls in community-dwelling adults aged 65 years and older." Physical therapy vol. 90,4 (2010): 550-60. doi:10.2522/ptj.20090158 **[5]** Buatois, Severine, et al. "Five times sit to stand test is a predictor of recurrent falls in healthy community-living subjects aged 65 and older." Journal of the American Geriatrics Society 56.8 (2008): 1575-1577.

PRELIMINARY STUDY OF STEP WIDTH PREDICTABILITY IN OLDER ADULT WALKING ACROSS SPEEDS

Aaron Fleming[1*], Abbas Alili[2], Varun Nalam[1], He (Helen) Huang[1*]
[1] Joint Department of Biomedical Engineering, NC State University, Raleigh, NC 27695-7115; University of North Carolina at Chapel Hill, Chapel Hill, NC 27599 USA
[2]Department of Electrical and Computer Engineering, NC State University, Raleigh, NC 27606, USA
*Corresponding author's email: hhuang11@ncsu.edu

Introduction: Changes in walking stability in older adult populations are often accompanied by increases in gait variability (e.g., step width). Abnormal gait variability is thought to be a result of deteriorating sensorimotor integration [1]. Recent work investigating step width behavior in young, able-bodied adults has demonstrated the existence of a relationship between pelvis dynamics and step width behavior, where pelvis position and velocity during walking can significantly predict variation in step-width [2]. For neurological populations with deficits in walking stability (i.e., stroke) this pelvis state to step width relationship is altered compared with able-bodied adults [3]. Additionally, stroke survivors with altered step-width predictability have poorer functional and self-reported balance scores [4]. Thus, the application of this particular step width analysis may hold potential to uncover step width strategies in other populations, that is older adults, compared with younger able-bodied adults and predict changes in function. As a preliminary study we investigated differences in step-width predictability between older (>65 years old) and younger adults. This preliminary study will lay the groundwork for future inclusion of older adults with fall-risk.

Methods: We recruited 5 Older adults (OA) (3 males, age: 70±3.32, height: 1.68±0.11m) and 5 younger adults (YA) (5 males, age: 30.4±3.36, height: 1.76±0.07m) to participate in this study. This experimental protocol was approved by the University of North Carolina at Chapel Hill Institutional Review Board, and all participants provided written informed consent before participating in the study. We asked participants to walk on a split-belt treadmill (Bertec, 1000Hz) at multiple speeds (0.2m/s, 0.4m/s, 0.6m/s, 0.8m/s and 1.0ms) in a randomized order for two minutes per speed. We allowed participants to walk on the treadmill with all speeds to provide initial acclimation before testing. During testing we collected whole-body motion capture (Vicon, 100Hz, 30 markers). To investigate the relationship between step width and pelvis dynamics we performed multiple linear regressions [2]:

$$SW = A\, x_{sacrum} + B\, v_{sacrum} + C\, SW_{mean} \tag{1}$$

where SW is step width at each heel-strike, x_{sacrum} is the difference between the average mediolateral position between PSIS markers and stance heel marker position, v_{sacrum} is the mediolateral velocity of the sacrum, and SW_{mean} is used as the intercept term and is the average SW for the given trial [2]. We quantified the strength of this pelvis to step width relationship using R^2 from the regression. We performed MLR separately for each subject and walking speed. We compared differences in R^2 at step start and step end time points using a one-way ANOVA for each population with walking speed as the main effect. We conducted pair-wise comparisons using Tukey HSD, with $p<0.05$ as significance threshold.

Results & Discussion: We observed a consistent step width strategy across walking speeds for OA participants (i.e., no significant differences in R^2 value between walking speeds at step start ($p=0.29$) or step end ($p=0.28$), Fig. 1). This contrasts with YA participants, who modified their step width strategy for slower walking speeds, which aligns with previous study of YA walking. Walking speed was a significant effect for YA participant R^2 at step start ($p=0.008$) and step end ($p=0.001$), and significant pair-wise comparisons are shown in Fig. 1.

These observations point to potential changes in walking behaviour in older adults, specifically in the step-by-step control of step width. Previous study in YA population argues that higher R^2 during faster walking speed may be a result of faster mediolateral center-of-mass (CoM) acceleration [2], requiring quicker steps, which may force individuals to pre-plan step width behaviour at toe-off. Hence, pelvis-foot dynamics at step start provide better prediction of step width at faster speeds. OA participants applied the same step width strategy across all speeds, which may suggest an increase reliance on pre-planning step width for slower speeds. This pre-planning may be a result of increased CoM acceleration at slower speeds for OA, which we will investigate in future study.

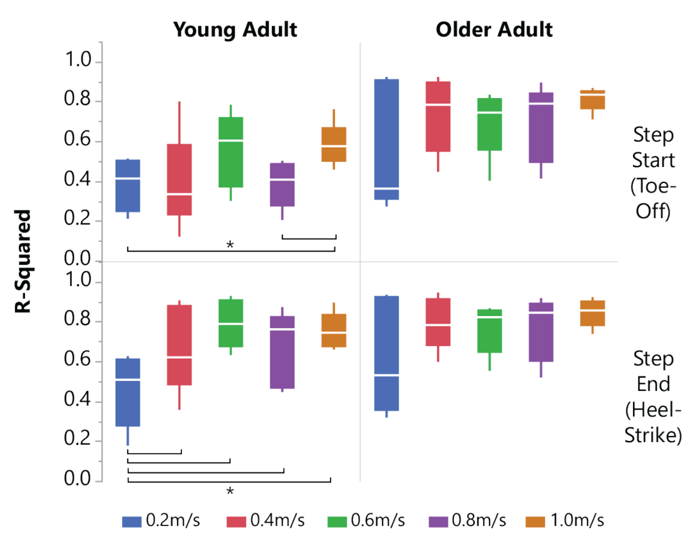

Figure 1: R-squared value of step width prediction for older and younger adults at step start and end. Significant pair-wise differences are shown with *.

Significance: This is the first study to investigate step-width predictability in healthy OA and provides the groundwork to investigate step-width predictability in OA with a history of falls. This work could lead to a better understanding of the mechanisms behind older adult falls and provide the opportunity for interventions for targeted rehabilitation of walking behaviour with systems like an abduction/adduction, powered hip exoskeleton [5].

Acknowledgements: Funding for this research project was provided by NSF1954587.

References: [1] Dean & Kuo (2007) *IEEE TBME* 54.11; [2] Stimpson & Dean (2018) *J Biomech 68*; [3] Stimpson & Dean (2019), *Gait & Posture 70*; [4] Howard & Dean (2022) *BioRxiv 2.489530* [5] Ting & Huang (2018) *IEE Trans. Mech. 23.1*

COMPLETERS OF TANDEM TASK AND DOPAMINE MEDICATION HAVE BETTER POSTURAL STABILITY IN PARKINSON'S DISEASE

Moll AN, Kuhman DJ, Walker HC, Lima C, Gonzalez C, and Hurt CP[1]
[1]University of Alabama at Birmingham, 1705 S. University Blvd, Birmingham, AL 35205
email: *amoll@uab.edu

Introduction: As Parkinson's Disease (PD) progresses individuals are at a greater risk for developing postural instability and falls. In fact, for individuals with PD, falls are the leading cause of injuries, hospitalization and even death [1,2]. Addressing functional balance declines with disease progression are major unmet needs in PD therapeutics. Maintenance of balance requires that the nervous system is able to effectively respond to external postural disturbances that are encountered in everyday life. Responding to postural disturbances is a multifactorial problem the nervous system must solve to maintain stability. Additionally, individuals with PD have difficulties in scaling their postural responses due to abnormal sensorimotor integration. We collected both static balance data as well as dynamic balance on a group of individuals who were part of a larger study. We performed a study to test the effect of medication on the capacity of individuals with PD to reduce the amount of sway performed during increasingly more challenging balance tests for static balance control and to avoid taking a step in response to scaled external postural disturbances to measure dynamic balance control [3]. We hypothesize that individuals on dopaminergic medications would be more stable to complete the hardest balance "tandem" test reflecting in an increase in dynamic balance response.

Methods: Forty individuals with PD (mean age: 61 years, UPDRS off medication: 49) participated in this study. Participants stood quietly on a force platform for 60 seconds with feet shoulder width apart, feet together, semi-tandem, and tandem postures while we quantified their sway area as the task of balance became more challenging. Additionally, participants experienced progressively increasing balance disturbances while standing on a treadmill with a range of small belt displacements. We instructed participants to avoid taking a step to these increasing postural disturbances. Treadmill belt acceleration was incrementally increased 0.5 m/s^2 at per trial and increased until individuals were unable to avoid stepping 4 times in a row at a given magnitude resulting in their step threshold [3]. A two-way ANOVA repeated measures was performed to determine if medication state (OFF vs. ON) and task (quiet standing, feet together, semi-tandem) had a significant effect on sway (mm). Paired samples t-tests were used to compare step threshold magnitude and balance capability between all static posturography positions. Paired samples t-tests were used to compare step threshold magnitude and balance capability between "off" and "on" medication states. Based on previous work in our lab, we were also interested in assessing the extent that being able to complete a tandem stance task would differentiate our participants into distinct groups for the step threshold tasks [4].

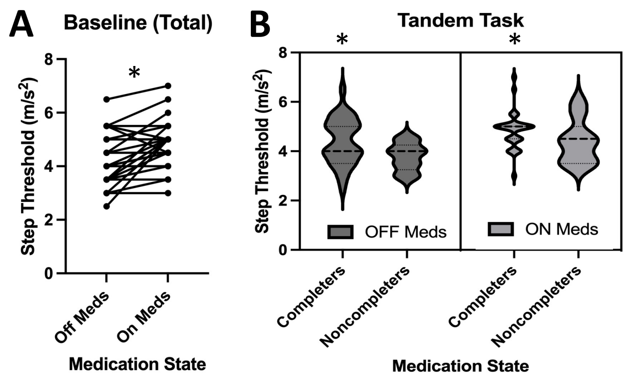

Figure 1: Step threshold magnitude results comparing "off" and "on" medication states (A) and comparing "off" and "on" medication states for completers and noncompleters of tandem static posturography (B). Results show a significant difference between the "off" and "on" medication state for step threshold in total (A) as well as completers of the tandem task (B). * $p < 0.001$

Results & Discussion: A two-way ANOVA revealed that tasks ($p < 0.001$) and not medication state ($p = 0.694$) had a statistically significant effect on the sway balance test. The participants have a medium effect size from tasks ($\eta^2 = 0.509$). The participant performing the more challenging balance test experienced significantly higher sway than participants performing the less demanding task. Further, a Bonferoni post hoc analysis's test for multiple comparisons found that participants that performed the semi-tandem balance test had significantly higher sway than participants that performed the quiet stance task ($p < 0.001$). Also, a Bonferoni post hoc analysis's test for multiple comparisons found that participants that performed the feet together balance test had significantly higher sway than participants that performed the quiet stance task ($p < 0.001$). However, there was no significant difference between participants that performed the feet together and semi-tandem tasks. There was also no statistically significant interaction effect between medication state and tasks ($p=0.79$).

For participants "off" and "on" medication states, step threshold magnitude was significantly higher "on" medication. ($p < 0.001$; Figure 1A). The effect size for the "on" medication state in comparison to the "off" medication state was medium to large ($\eta^2 = 0.72$). Based on previous findings from our lab, we wanted to assess whether the ability to complete a tandem stance balance task affected the results of the step threshold task (Figure 1B). Participants that completed the tandem balance test had larger step thresholds ($p < 0.001$; Figure 1B), which resulted in a medium to large effect size between the "on" and "off" medication state ($\eta^2 = 0.73$).

Significance: Although our preliminary data and prior research studies show dopaminergic medications allow individuals to withstand greater amounts of instability during dynamic balance testing, these results also support our hypothesis that individuals on dopaminergic medications experience a greater dynamic balance response if they can complete the most challenging balance "sway" tandem test. This is important for clinical purposes, especially to inform evidence-based perturbation-based training intervention programs for individuals with Parkinson's Disease.

References: [1]Horak FB, et al. Physical Therapy. 1997; 517-33.; [2]Allen NE, et al. Parkinsons Dis. 2013; doi.org/10.1155/2013/906274; [3]Kuhman D, et al. Gait & Posture. 2020; 68-74.; [4] Hurt Cet al., *International Society of Biomechanics*. 2019: Calgary CA.

HOW DO CHANGES IN MUSCLE STRUCTURE AND TISSUE QUALITY RELATE TO STRENGTH CHANGES OVER TIME IN DUCHENNE MUSCULAR DYSTROPHY?

Allison N. McCrady[1*], Chelsea D. Masterson[2], Robert J. Gutierrez, PhD[3], Sarah A. Tolman[3], Laura E. Barnes[3], PhD, Rebecca J. Scharf, MD, MPH[2], and Silvia S. Blemker, PhD[1]
[1] Department of Biomedical Engineering, University of Virginia, Charlottesville, VA, USA
*Corresponding author's email: anm9xd@virginia.edu

Introduction: Duchenne muscular dystrophy (DMD) is a progressive neuromuscular disorder where fatty infiltration and fibrosis contribute to severe muscle weakness and functional decline[1]. Clinical assessments measure disease progression using subjective ratings of participatory functional tasks, infeasible for 45% of DMD patients diagnosed with a cognitive disorder, do not directly quantify muscle structure and tissue quality[2], [3]. Previous studies have demonstrated the use of ultrasound, a clinically accessible imaging modality, to measure muscle size in healthy persons and tissue quality (echogenicity) in DMD to estimate disease progression[4], [5]. The biceps brachii is easily accessible for *in vivo* measurements and heavily impacts the upper limb function essential to patient independence. Establishing a relationship between muscle and functional measurements, we can objectively track disease progression in clinic. **The goal of this study is to 1) examine the changes to muscle structure and tissue quality over time in patients with DMD and typically developing (TD) controls, and 2) relate changes in muscle size, shape, and tissue quality to muscle function.**

Methods: The dominant arm biceps brachii muscle of 12 participants (DMD: n = 7 – treatments: 2 Exon skipping, 5 steroid, TD: n = 5) was imaged with a linear array transducer (H9.0/40, Telemed LS 128 CEXT) at multiple time points (two or three visits between 6, 12, or 18 months after the first visit) at the midsection of the muscle in the longitudinal and transverse planes (**Fig. 1A**). An image processing algorithm was developed to measure the cross-sectional area (CSA), average echogenicity (pixel gray scale value intensity), maximum feret diameter (largest distance between two parallel tangential lines), thickness (largest distance perpendicular to maximum feret diameter), and diameter ratio (muscle thickness/maximum feret diameter) of the muscle on five images (**Fig. 1A**). Maximum voluntary elbow flexor torque was measured using a handheld dynamometer (Chatillon DFS II) placed on the forearm with the elbow positioned at 90 degrees (n=5). Ultrasound measurements were analyzed and compared to maximum voluntary elbow torque.

Results & Discussion: The majority of participants have a positive relationship between CSA and maximum voluntary elbow torque as expected (**Fig. 1B**). Three participants (2 DMD, 1 TD) demonstrate a negative relationship, which may suggest submaximal effort or additional measurements beyond CSA, such as echogenicity, influence torque generation and must be considered. TD participants and younger patients with DMD fall within a normal range of muscle echogenicity, whereas older patients with DMD show increased echogenicity and decreased torque (**Fig. 1C**). TD participants generally had a positive relationship between increasing diameter ratio (more circular) and elbow torque, whereas the patients with DMD had a larger range of diameter ratios with varying relationships to torque (**Fig. 1D**). This may suggest an ideal range of diameter ratio exists for peak functional capacity. Further integration of the shape and size of the muscle may further elucidate insights to the functional capacity of muscles. Muscle measurements are affected by patient treatment type and disease progression. For example, *DMD3*, 5-year-old with exon skipping therapeutic, follows TD trends, but the *DMD7,* a more progressed patient with the same treatment, does not. In summary, we have found that, as expected, healthy and dystrophic muscle change differently over time during periods of growth and there is not a singular variable that best relates to functional changes for all participants. Future analyses will examine the relationship between muscle 3D morphological and functional changes.

Significance: Relating ultrasound measurements to function, we can observe and track functional changes objectively and easily in the clinic, overcoming the limitations of current assessments. Our future work will continue to track subject measurements over time to develop a novel imaging based functional assessment to improve the clinical care of patients with DMD and neuromuscular disease.

Acknowledgements: Funded by NIH Award T32GM136615, Coulter Foundation, and UVA Center for Engineering in Medicine.

References: [1] Yiu, et al. (2015), *J Paediatr Child Health* 51(8), [2] Mazzone, et al. (2009), *Neuromuscul Dis* 19(7), [3] Mirski, et al. *J Pediatr* 165(5), [4] Jansen, et al. (2012), *Neuromuscul Dis* 22(4), [5] Ikai, et al. (1968), *Eur J Appl Physiol* 26(1)

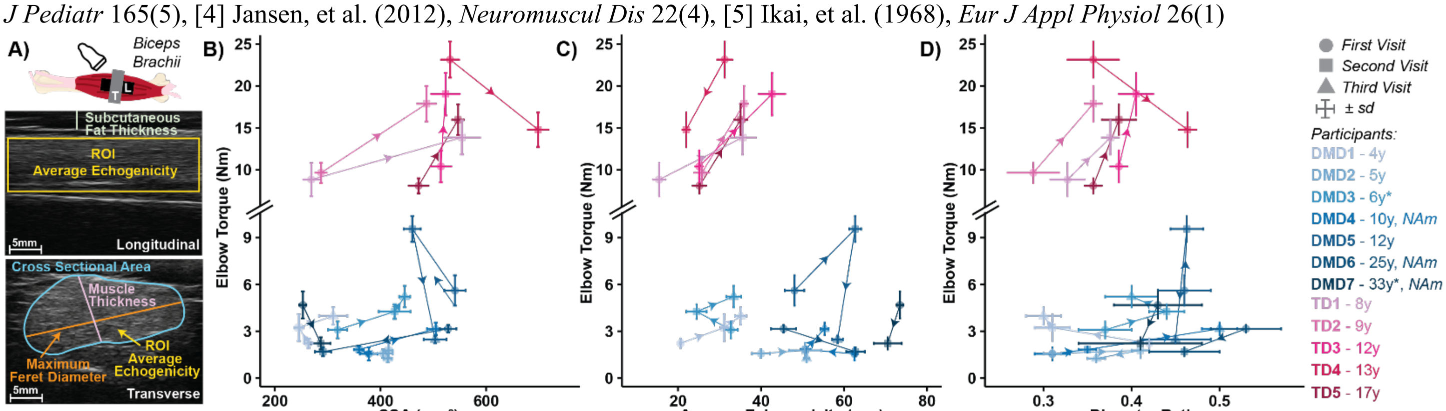

Figure 1: A) Overview of ultrasound measurements of biceps brachii, B) Cross-sectional area (CSA), C) diameter ratio, and D) average echogenicity for each subject versus torque. Points are mean with error bars as the standard deviation. *NAm* = Non-Ambulatory, *Exon Skipping treatment

INCREASED POSTURAL THREAT ALTERS CONTROL OF DYNAMIC STABILITY FOLLOWING EXTERNAL PERTURBATIONS THAT INDUCE A STEP

Marco A Avalos*, Shirali Shah, Noah J Rosenblatt
Center for Lower Extremity Ambulatory Research (CLEAR), Dr. William M. Scholl College of Podiatric Medicine at Rosalind Franklin University of Medicine and Science, North Chicago, IL
*Corresponding author's email: marco.avalos@rosalindfranklin.edu

Introduction: Fear of falling (FoF) affects almost 35% of older adults and can lead to self-imposed activity restrictions that negatively impact their quality of life [1]. Older adults with FoF may perceive everyday environment challenges (e.g., uneven surfaces, curbs) as threatening to posture, which may negatively impact postural control during daily activities and contribute to the increased fall risk. For example, a study found that inducing postural threat in young adults by having them stand at height provokes a stiffening strategy to maintain tighter control over posture [3] and more conscious control while standing [4]. What needs to be clarified is whether postural threat elicits inappropriate reactive balance responses following a perturbation. Therefore, this study aimed to evaluate the effects of postural threat on the compensatory stepping response in healthy young adults as a model for older adults with FoF. It was hypothesized that under increased postural threat, younger adults would demonstrate a change in the control of reactive balance responses requiring a step, as demonstrated by altered kinematics of the recovery stepping responses.

Methods: We recruited ten healthy young adults. Participants donned a waist-mounted spring scale that was pulled while they resisted. Upon release of the load, participants were instructed to try to recover balance without taking a step. Loads were applied in one-pound increments in the posterior (provoking a forward step) and anterior (provoking a backward stepping) directions until steps were required to restore balance upon load release (stepping thresholds). Reflective passive markers placed on the participant according to the Plug-in Gait model were tracked using an 8-camera motion capture system. The loading protocol was performed overground (OG) and over a 1 m elevated platform (PF). After each condition, a Spielberg State-Anxiety Scale (STAI) was filled out. The stepping threshold (ST) was recorded for each height and direction of the pull, and only the stepping threshold trials were analyzed.

For the stepping trial only, we extracted the time for foot-off (tFO) relative to release of the load, recovery step length (SL), time for step recovery (tSR) relative to foot-off, margin of stability (MOS) at recovery foot-off (MOS_{FO}) relative to the MOS at release (MOS_{rel}), both taken relative to the non-stepping foot, and MOS at recovery foot contact (MOS_{FC}) taken relative to the stepping foot. We first performed a two-way repeated ANOVA on the ST. In the event of a significant difference between conditions, then, for each condition, we planned to correlate changes in ST with changes in kinematics; in the event of significant associations, we would covary for ST in the subsequent step. We planned to compare the set of kinematic measures using a two-way repeated measures MANOVA with kinematics as the dependent variables to establish condition differences. Spearman correlations were run to assess relationships among MOS variables and all other spatiotemporal stepping parameters.

Results & Discussion: A significant direction by height interaction on ST that was of medium-sized effect [F (1, 9) = 5.375, p = 0.046; partial η2 = 0.37]. Post hoc comparisons indicated an effect of condition on ST for only the posterior ST, which may reflect the fact that visual information is more heavily weighed under threatening conditions. Since vision can not be relied upon to direct backward steps, people are more cautious (step sooner). Differences in ST were unrelated to between-condition kinematic changes during backward stepping, such that ST was not included as a covariate for kinematic comparisons.

Regardless of the stepping direction, MOS tended to be more negative during OG compared to the PF condition (Fig. 1). There was less change of MOS from release to FO ($MOS_{FO\text{-}rel}$ [F (1, 9) = 20.59, p = 0.001]), and during the step itself (from FO to before FC) in the PF condition. While the recovery step was initiated sooner during the PF condition, i.e., smaller tFO [F (1, 9) = 8.16, p = 0.019; partial η2 = 0.48] and SL was significantly shorter [F (1, 9) = 13.63, p = 0.005; partial η2 = 0.60] compared to OG condition. The diminished need for a longer recovery step in the PF condition may be due to a less destabilized system at foot-off during the PF condition. Similarly, MOS_{FC} was significantly higher [F (1, 9) = 7.14, p = 0.026] in the PF condition compared to the OG condition, despite a shorter SL due again to a lower degree of instability during the step. Overall, an increase in threat appears to induce a more conservative behavior (i.e., less time in single support) with less willingness to experience instability.

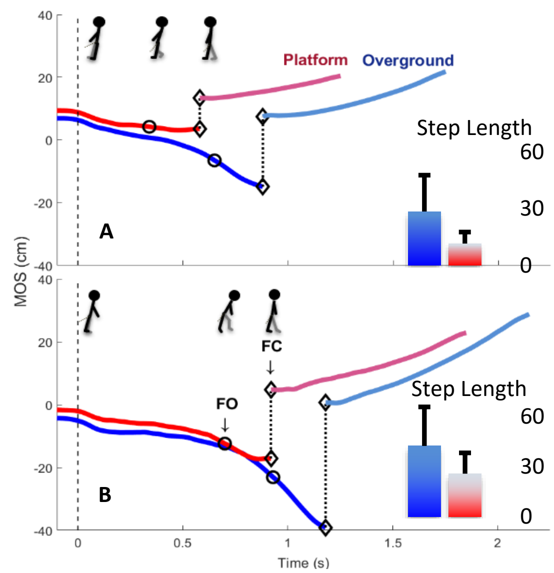

Figure 1. Comparisson of margin of stability between surfaces during A) posterior and B) anterior stepping. Time 0 is the moment of load release. FO = Time of Foot-Off; FC = Time to Foot-Contact; ○ FO event; ◊ FC event; ◊···◊ transition from monopedal to bipedal support.

Significance: If postural threat negatively impacts the effectiveness of recovery response when steps are elicited, then it may be necessary to address the underlying cognitions that lead to perceived threats before addressing physical limitations to improve stepping response in older adults with FoF.

References: [1] Young et al. (2015), *Gait Posture* 41(1); [2] Carpenter et al. (2001), *Exp Brain Res* 138(2); [3] Carpenter et al. (2004), *J Neurophysiology* 92(6); [4] Huffman et al. (2009), *Gait Posture* 30(4).

ALTERED MANUAL WHEELCHAIR PUSH RIM POSITIONING: THE EFFECT ON SUBACROMIAL DISTANCE DURING PROPULSION

Gaura Saini[1*], Aaron Hellem[1], Cyrus Rezvanifar[1], Amanuel Nigatu[1], Denzel Godwin[1], Teresa Bisson[1], Arin Ellingson[1], John Looft[2], Andrew Hansen[2], Paula Ludewig[1]
[1]Department of Rehabilitation Medicine, University of Minnesota
[2]Minneapolis Adaptive Design & Engineering (MADE) Program, Minneapolis VA
*Corresponding author's email: saini041@umn.edu

Introduction: Individuals using manual wheelchairs (MWCs) as their primary form of mobility have a high prevalence of shoulder pain.[1,2] Propulsion requires repetitive shoulder motion within the range of motion thought to pose the greatest risk of rotator cuff subacromial compression.[3-5] A modeling study determined that the theoretical biomechanically optimal position for MWC push rims is with the center of the push rims anterior to the shoulder to minimize muscle stress, co-contraction, and metabolic cost.[6] A novel MWC was designed separating the push rims from the drive wheels. The design allows the rims to be anteriorly positioned without affecting chair stability. This pilot study assessed the distances between the coracoacromial (CA) arch and the supraspinatus insertion (SSI) during MWC propulsion in order to test the *in vivo* biomechanics of an anterior push rim position as compared to the standard position (push rim axis below the shoulder joint). We hypothesized that the theoretical position would result in increased SSI to CA arch distances compared to the standard position during the push phase of MWC propulsion.

Methods: Six full-time manual wheelchair users with spinal cord injuries of thoracic level 1 (T1) and lower (ensuring full upper extremity function) were tested. Humeral and scapular motion was assessed using biplane video radiography and thoracic motion was captured using an 8-camera Vicon optical motion capture system. A custom MWC simulator allowed independent push rim positioning and simultaneous capture of propulsion kinematics within the x-ray field of view. Data were collected while participants propelled the simulator in: 1) standard position, with the center of the push rim aligned with the shoulder joint and 2) anterior position, with the center of the push rim 10° anterior to the shoulder joint using a goniometer. MRIs or CT scans were obtained to create participant-specific 3D models of the humerus and scapula. The bone models were projected onto the video x-rays to obtain 3D kinematics (2D/3D shape-matching), and humeral kinematics were described with respect to the thorax (humerothoracic (HT) kinematics). Kinematic data and SSI-to-CA arch minimum distance were extracted using a custom algorithm developed in MATLAB.

Results & Discussion: The minimum distance was located between the SSI and the anterolateral acromion for all participants. Regardless of push rim position, minimum distances occurred near the end of the push phase coinciding with maximum HT flexion. Minimum distances ranged from 2.8-9.4mm (mean = 6.7 ± 2.5mm) in the standard position and from 1.1-8.9mm (mean = 5.8 ± 3.0mm) in the anterior position. Descriptively, smaller minimal distances were found in the anterior position compared to the standard position, though the change was <2 mm in all participants.

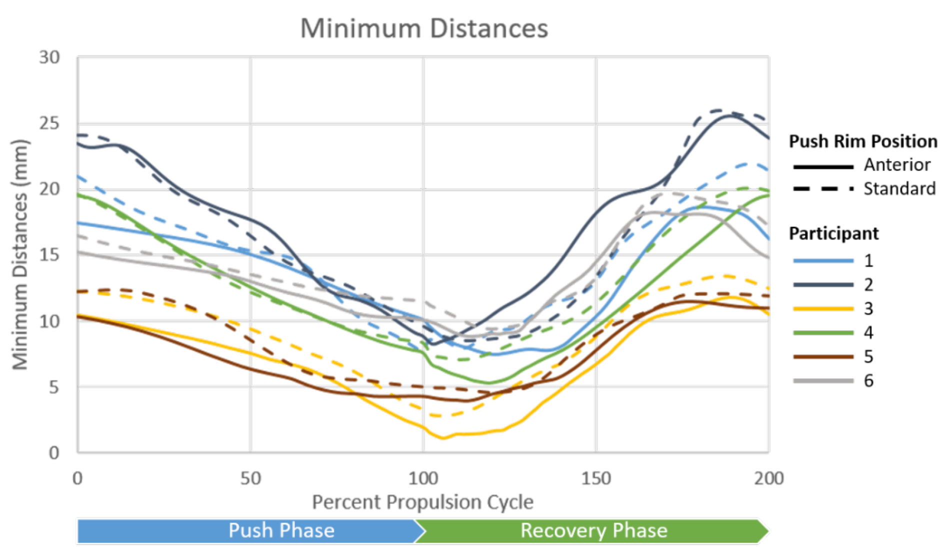

The theoretical optimal anterior push rim position appears to decrease rather than increase the subacromial space during wheelchair propulsion. It is not yet known if this results in increased supraspinatus compression which could contribute to shoulder pain or repetitive cuff microtrauma. However, these preliminary results suggest that, although a theoretically optimal anterior push rim position may decrease muscle stress, co-contraction, and metabolic cost, it may not be biomechanically advantageous with regard to kinematics. Considering actual soft tissue structures rather than only bone-to-bone distances as well as considering alternate wheelchair designs are important future areas of investigation.

Significance: Individuals who use MWCs rely on repetitive motion at their shoulders for mobility. It is critical to understand shoulder biomechanics during MWC propulsion given the high prevalence of shoulder pain in this population. Adjusting the push rims to minimize muscle stress may also reduce the subacromial space, although the implication on rotator cuff subacromial compression is not yet known. Additional *in vivo* testing will determine if benefits of an anterior push rim position exist.

Acknowledgements: Funding provided by the Maslowski Charitable Trust; wheelchair simulator provided by the MADE Program

References: [1] Soo Hoo (2022), *PM R*; [2] Kentar (2018), *Spinal Cord*; [3] Mozingo (2020), *Clin Biomech*; [4] Mozingo (2022), *J Electromyogr Kinesiol*; [5] Lawrence (2017), *J Orthop Res*; [6] Slowik (2013), *Clin Biomech*

A BOTTOM-UP MODELLING APPROACH FOR AN OPENSIM THORACOLUMBAR SPINE MODEL

Jacob J. Banks[1,2*], Neal E. Wiggermann[1], Dennis E. Anderson[2]
[1] Baxter Int., Deerfield, IL, USA; [2] Beth Israel Deaconess Medical Center / Harvard Medical School, Boston, MA, USA
*Corresponding author's email: jacob_banks@baxter.com

Introduction: Quantifying the kinetic demands of the spine is important for clinical and occupational injury risk assessments [1]. Mathematical musculoskeletal models are used to estimate spine loads because direct *in vivo* measurement is infeasible [1]. Spine models vary but are generally based on principles of linked segment dynamics, Newton-Euler equations, and anatomical properties. The central location of the spine within the body allows for the kinetic demands to be modeled by either a top-down (TD) or bottom-up (BU) segmental analysis approach. A TD approach solves reactionary forces and moments starting at the hands/head segments and progresses down through the spine. Conversely, a BU approach solves forces and moments from the feet and up to the spine.

In the popular biomechanics modeling software OpenSim [2] the kinetics are solved by beginning distally and progressing in the direction of the base segment, typically the pelvis in full body models. Therefore, spine kinetics are solved with a TD approach in existing OpenSim models. To our knowledge there is not an OpenSim model that solves the kinetics of the spine in a BU approach. Comparing results from both approaches serves as a form of validation [3], as theoretically kinetic results from either approach should be the same given accurate external forces (e.g., ground reaction forces; GRFs) and body segment properties. Further, while early models have been validated by comparing both approaches at the lower lumbar level [3], the overall trade-offs between TD and BU approaches have not previously been examined at more superior levels of the thoracolumbar spine.

Therefore, the aim of this study was to construct and then validate an OpenSim thoracolumbar model that solves the kinetic demands from the BU. We hypothesize that the intervertebral joint (IVJ) moments from the BU model will reflect those from the traditional TD model [4] it was based on. The new BU model will be useful when external hand forces are not well defined or upper limb kinematics data are missing, further validate the existing TD model, and provide confidence in the assigned rigid-segment properties of both models.

Methods: To date, three participants (2 males and 1 female, 22 ± 2 years of age, 172.8 ± 4.9 cm in stature, and 70.0 ± 7.9 kg in mass) have consented and participated in this Institutional Review Board (Advarra, USA) approved laboratory study protocol.

In brief, 53 markers were placed over participant's skin and clothing in accordance to palpated bony landmarks and reference points. An initial standing static calibration pose and four lift-lower trials were recorded (50 Hz; Motion Analysis Corp., USA) while the participant's feet were positioned on individual force plates (AMTI Inc., USA). Trials composed of two-hand sagittal and one-hand lateral lift types from the floor-to-waist height of an instrumented milk crate across lift weights of 0% and 15% of body weight. The 48 × 33 × 28 cm milk crate was instrumented with load cells (Omega Eng. Inc., USA) in line with handles. During the 0% bodyweight condition, participants did not lift the crate but moved their hands to the handles of the crate. Three repetitions of each of the four randomly presented lift scenarios were performed.

Net joint moments were calculated from the measured kinematics and external forces using standard OpenSim procedures[2] with two distinct models: 1) an existing and validated full-body thoracolumbar model which solves the kinetics in the spine using a TD approach[4], and 2) an alteration of the first model that solved in a BU direction by moving the base segment from the pelvis to the T1 vertebrae.

Three-dimensional orthogonal T5/T6 and L5/S1 IVJ moments from each lifting trial and modelling approach were compared in magnitude and temporally using root mean square (RMS) and cross-correlation (R^2) analyses, respectively.

Results & Discussion: The IVJ moments from the newly presented OpenSim thoracolumbar BU approach model agreed well with those from the previously validated TD model (Table 1). The agreement at the thoracic level was relatively similar as that between the lumbar moments, which supports the use of either approach to estimate thoracic loading. Poor temporal correlations for axial and lateral moments during sagittal lifts reflect their relatively low magnitude and linearity. With no direct measurement of *in vivo* loading to compare to, it is unknown which approach provides the most accurate results, which emphasizes the importance of being able to demonstrate a satisfactory degree of agreement between them.

Table 1: Average (±SD) RMS (in N×m) and R^2 of BU vs. TD IVJ orthogonal moments (rows) for sagittal and lateral lifts of 0 and 15% bodyweight.

		Sagittal 0%		Sagittal 15%		Lateral 0%		Lateral 15%	
		RMS	R^2	RMS	R^2	RMS	R^2	RMS	R^2
T5/T6	F/E	10.2 ± 2.8	.90 ± .11	11.2 ± 3.4	.97 ± .03	7.4 ± 2.7	.91 ± .13	8.3 ± 1.4	.92 ± .08
	Lat.	2.4 ± 0.5	.17 ± .13	2.4 ± 0.5	.31 ± .21	3.4 ± 1.3	.50 ± .28	4.0 ± 1.0	.97 ± .01
	Axl.	3.1 ± 0.7	.05 ± .06	3.3 ± 0.6	.06 ± .05	3.6 ± 0.8	.51 ± .19	4.9 ± 0.8	.92 ± .03
L5/S1	F/E	10.2 ± 2.8	.99 ± .01	10.5 ± 2.2	.99 ± 0	8.6 ± 3.9	.99 ± 0	10.2 ± 3.7	.99 ± 0
	Lat.	2.7 ± 0.6	.38 ± .23	3.1 ± 0.4	.44 ± .19	3.8 ± 1.7	.98 ± .03	4.5 ± 1.0	.99 ± .01
	Axl.	3.0 ± 0.8	.47 ± .30	3.2 ± 0.5	.58 ± .33	3.5 ± 0.7	.84 ± .04	5.9 ± 1.4	.96 ± .01

Future work will build on this work and include additional participants and crate masses, different lifting speeds, the analysis of all IVJ levels, and the impact of the BU approach on IVJ joint reactions.

Significance: The newly presented BU model of the thoracolumbar spine complements the existing TD model and provides an alternative approach when upper extremity kinematics or external forces are inaccurate or absent. The relatively strong agreement between the two modelling approaches further validates the rigid-body properties assigned to the model(s). Additionally, for the first time, TD and BU modelling approaches of the spine have been compared at the thoracic level. The BU model presented here will be made available on the open-source SimTK website [2].

Acknowledgements: This work was in part funded by a DoD CDMRP: W81XWH-20-1-0608 (awarded to DEA & BIDMC)

References: [1] Dreischarf et al. (2016) *J. Biomech.* 49(6); [2] Delp et al. (2007) *IEEE Trans.* 54(11); [3] Kingma et al. (1996) *HMS* 15(6); [4] Bruno et al. (2015) *J. Biomech. Eng.* 137(8)

THE EFFECT OF AGE ON LOWER LIMB MUSCLE ACTIVITY DURING SINGLE TRANSITION STEP DESCENT

Zahra Mollaei[1*], Emily E. Gerstle[2], Hanieh Pazhooman[1], Mohammed S. Alamri[1], Stephen C. Cobb[1]
[1]Gait & Biodynamics Laboratory, Department of Kinesiology, University of Wisconsin-Milwaukee, Milwaukee, WI, USA
[2]Human Motion Laboratory, Department of Health and Human Performance, University of Scranton, Scranton, PA, USA
*Corresponding author's email: zmollaei@uwm.edu

Introduction: Falls among older adults are a significant public health problem due to their high prevalence and associated costs. This may be especially true for older women, who experience approximately 63% of older adult falls [1] and three times the medical costs [2]. Falling in older adults occurs most commonly during ground level activities and step negotiation [3]. Although falls occur more frequently during level ground activities, the incidence of fall-related injury is higher during step negotiation [4]. Most previous transition step descent studies have reported increased lead limb agonist/antagonist muscle co-activation and/or individual muscular activity in healthy active older adults compared with young adults [5–8]. Only one study has investigated lead and trail limb muscle co-activation between young adults and old adults with a fall history [9].Therefore, the purpose of this study was to investigate the influence of age and fall history on trail and lead limb lower extremity muscle activation during single transition step negotiation. Due to age-related decreases in strength, we hypothesized that older adults lead and trail limb would have greater muscle activity (an indicator of greater muscular effort) compared with young adults. In addition, due to older adults with a fall history having decreased strength compared to older adult non-fallers, we postulated older adults with a fall history would demonstrate the greatest muscle activity.

Methods: 15 young adults aged 18-40 years (YA), 15 older adults ≥ 65 years with a fall history (OF), and 15 older adults ≥ 65 years without a fall history (ONF) provided informed consent and participated in the study. Muscle activity was assessed using bipolar surface electrodes placed bilaterally on the tibialis anterior, medial gastrocnemius, rectus femoris, and lateral hamstrings. Participants completed five self-selected speed barefoot trials along a 5.5-m long raised walkway, descended a 17-cm step (right foot lead), and continued to walk 3 m. A force plate embedded at the base of the step recorded lead limb initial contact and GRF during lead limb weight acceptance. After the stepping trials, EMG activity during maximum voluntary contractions (MVC) were assessed. Each muscle's activity during the step trials was normalized to the peak MVC EMG activity and multiplied by 100. Trail limb man muscle activity was calculated from lead toe-off before the step until lead limb initial contact after the step. Lead limb mean muscle activity was calculated from lead limb initial contact after the step through lead limb weight acceptance.

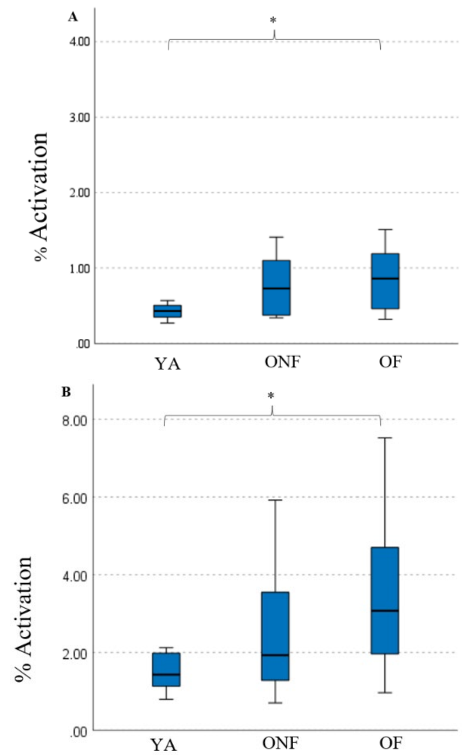

tibialis anterior (B) muscle activity (% MVC) in young (YA), older without history of fall (ONF), and older with history of fall (OF). The median value was utilized to indicate the central tendency of each group.

Results & Discussion: Follow-up group pairwise comparisons performed following significant Kruskal-Wallis tests showed significantly increased activity in the trail limb biceps femoris in OF vs YA (adj. p-value = 0.016), and the trail limb tibialis anterior in OF vs YA (adj. p-value = 0.029) (Fig 1). As hypothesized, there were significant increases in muscle activity between the YA and the OF group. Trail limb differences were both associated with muscles likely acting as antagonists at the knee and ankle. This may be consistent with the increased duration of ankle and knee musculature co-activation in older adults reported by Chandran et al. [8]. Interestingly, Gerstle et al. [9] using the same data set as this study did not report significant knee or ankle coactivation differences between the groups. The difference may be due to Gerstle et al. [9] calculating co-activation using the integrated EMG during the lowering period versus this study that quantified the individual muscle activity as the mean activity. The lack of significant lead limb knee and ankle muscle activation between the groups is inconsistent with previous studies [6,7]. The differences may be due to the differing group inclusion criteria, stepping tasks, and/or variable of interest calculations.

Significance: Although increased trail limb biceps femoris and tibialis anterior activity may function to increase joint stiffness to compensate for decreased muscle strength during step negotiation, it may also result in less efficient movement. This may lead to earlier muscle fatigue and increased risk of falling. Changes in the activity of these trail limb muscles could be used as additional outcome variables to assess the effectiveness of fall intervention programs that aim to improve function during step negotiation.

Acknowledgements: UW-Milwaukee, CHS, Student Research Grant Award; ASB Graduate Student Grant-in-Aid.

References: [1] Florence et al. (2018), *J Am Geriatr Soc* 66(4);[2] Burns et al. (2016), *J Safety Res* 58;[3] Choi et al (2019), B*MC Geriatrics* 19(1);[4] Duckham et al. (2013), *BMC Geriatrics* 13(1);[5] Hortobagyi et al (2000), *J Electromyogr Kinesiol* 10(2); [6] Larsen et al. (2008), *J Electromyogr Kinesiol* 18(4);[7] Buckley et al. (2013), *Exp Gerontol* 48(2);[8] Chandran et al. (2019), *Gait Posture* 73;[9] Gerstle et al. (2022), *J Aging Phys Act.* DOI 10.1123/japa.2021-0521.

SENSOR AND CROSS-MODAL KNOWLEDGE DISTILLATION FOR KINETICS ESTIMATION

Md Sanzid Bin Hossain[1], Zhishan Guo[2], Hwan Choi[3*]
[1]Electrical and Computer Engineering Department, University of Central Florida, Orlando, Florida, 32816, USA
[2]Computer Science Department, North Carolina State University, Raleigh, North Carolina, 27695, USA
[3]Mechanical and Aerospace Engineering Department, University of Central Florida, Orlando, FL 32816, USA
*Corresponding author's email: hwan.choi@ucf.edu

Introduction: Joint kinetics, such as ground reaction forces and joint moments, provide crucial information for clinical treatments and assistive devices. Currently, force plates and motion capture systems are the only tools used to process such data, and mostly in a lab setting. This method's drawbacks include high expense and extensive space requirements. Computational models with wearable sensors have been attempted but require many sensors and subject-specific data. Data-driven kinetic estimation using deep learning algorithms is suggested to solve these issues to estimate kinetics with fewer sensors. However, reducing the number of sensors drops prediction accuracy, making it difficult to ensure accurate kinetic estimation with limited information.

Knowledge distillation (KD) is a deep learning technique for compressing models by transferring knowledge from a large teacher network to a smaller student network. Additionally, this method can be extended to share knowledge between various input data modalities. Inspired from this, we are proposing a method of distilling knowledge from eight inertial measurement unit (IMU) sensors on the body and two 3rd person's view video cameras to three IMU sensors on the thigh, shank, and feet to estimate knee flexion moment (KFM), knee abduction moment (KAM), mediolateral, vertical, anterior-posterior (A-P) ground reaction forces (GRFs). Thus, the two techniques in our suggested method (Figure 1) include "Sensor Distillation (SD)," which transfers knowledge from eight IMU sensors to three IMU sensors, and "Cross-Modal Knowledge Distillation," which transfers knowledge from trajectories of joint center to three IMU sensors. The experiments in Table 1 demonstrates that our proposed method of sensor and cross-modal knowledge distillation significantly improves the kinetics estimation performance while using three IMU sensors in test condition.

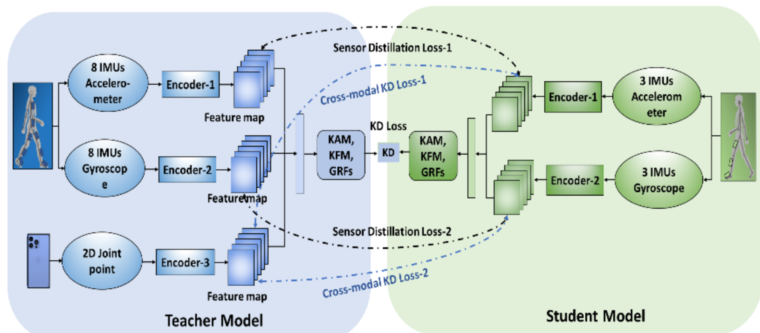

***Figure 1:** Overall process of sensor and cross-modal knowledge distillation from teacher to student model*

Methods: We used a publicly available dataset [1] to train the kinetics estimation model. In this dataset, 17 male subjects' (age: 23.2 ± 1.1 years; height: 1.76 ± 0.06 m; mass: 67.3 ± 8.3 Kg) data were collected with different walking speeds, foot progression angles, step widths, and trunk sway angles in the treadmill condition. Two cell-phone camera videos were used to get the 2D joint point of the human body using OpenPose library [2]. Our student model is trained with three IMUs, while the teacher model is trained with 8 IMUs and 2D joint point. For the encoder, we utilized two stacked bi-directional long short-term memory networks (LSTM). We utilized the following total loss to train the student model. We conducted Repeated Measures Analysis of Variance (ANOVA) with a least significant difference correction post hoc test for normalized root mean square error (NRMSE) and Pearson correlation coefficient (PCC) separately with a p-value less than 0.05 to determine if our proposed distillation technique significantly improves the performance compared to the model with three IMUs.

$$Total\ loss = Student\ loss + \alpha \times KD\ loss + \beta \times (Sensor\ Distillation\ loss - 1 + Sensor\ Distillation\ loss - 2) + \Upsilon \times (Cross - modal\ KD - 1 + Cross - modal\ KD - 2)$$

***Table 1:** Mean NRMSE and PCC of different kinetics components when using different approaches. * shows statistically significant differences. Bold represents the best result between model with 3 IMUs and 3 IMUs + KD + SD*

Metric	Model	KFM	KAM	Mediolateral	Vertical	A-P	Mean
NRMSE	**8 IMUs + 2D Point**	4.26 ± 1.70	5.66 ± 1.59	5.65 ± 0.68	3.65 ± 0.45	3.76 ± 0.46	4.60 ± 0.49
	3 IMUs	4.47 ± 1.47	**5.98 ± 1.79**	6.66 ± 1.40 *	**4.19 ± 0.45**	4.11 ± 0.49	5.08 ± 0.57 *
	3 IMUs + KD + SD	**4.36 ± 1.42**	6.06 ± 1.71	**6.09 ± 1.21**	4.22 ± 0.59	**4.02 ± 0.50**	**4.95 ± 0.54**
PCC	**8 IMUs + 2D Point**	0.952 ± 0.041	0.939 ± 0.025	0.938 ± 0.010	0.992 ± 0.002	0.967 ± 0.007	0.958 ± 0.011
	3 IMUs	0.946 ± 0.042	0.922 ± 0.026	0.922 ± 0.011 *	**0.990 ± 0.002**	0.961 ± 0.009	0.948 ± 0.011 *
	3 IMUs + KD + SD	**0.949 ± 0.038**	**0.922 ± 0.026**	**0.929 ± 0.011**	0.989 ± 0.003	**0.963 ± 0.011**	**0.951 ± 0.010**

Results & Discussion: There are significant improvements in overall mean NRMSE and PCC of all the components when KD and SD are used in the model. This strategy helps to gain information from a large number of IMUs and other modalities while using a smaller number of wearable sensors

Significance: This study introduces a novel strategy to infuse different modalities' information to reduce the number of IMU sensor to guarantee better kinetics estimation performance. It opens future research for narrowing the performance gap between the teacher and student model using an advanced method and algorithm.

References: [1] Tan, Tian et al. (2022), IEEE Trans. Industr. Inform, 19(2); [2] Z Cao et al. (2019). IEEE PAMI, 43(1): 172-186

SHAPE VARIATION OF THE FIRST METATARSAL AND IMPLICATIONS FOR BONE COORDINATE SYSTEMS

Eric D. Thorhauer[1,2*], William R. Ledoux[1,2,3]

[1]Center for Limb Loss and Mobility (CLiMB), Department of Veterans Affairs, VA Puget Sound Health Care System, Seattle, WA

Departments of [2]Mechanical Engineering and [3]Orthopaedics & Sports Medicine, University of Washington, Seattle, WA

*Corresponding author's email: ericthor@uw.edu

Introduction: Natural variation in the shape of the metatarsals has been observed across primates [1]. In humans, distal metatarsal heads that guide first metatarsal phalangeal joint (MTPJ1) motion may be everted in 11-13 degrees (range: -2 to 25) of torsion relative to the shaft [2]. As maturing technology like biplane fluoroscopy facilitates precise quantification of in vivo MTPJ1 motion, there is growing need for metatarsal joint coordinate systems that are sensitive to these natural variations. The goals of this study were to identify anatomical regions of shape variation in the first metatarsal that may affect the fitting of bone coordinate systems, and to compare two candidate methods for fitting metatarsal coordinate systems in a larger, more diverse cohort [3].

Methods: Subjects (N = 73, 33 females, 40 males, age: 49.6 ± 9.6 years) with neutrally aligned (21), planus (38), and cavus (14) feet underwent computed tomography (CT) scans of the foot and ankle (voxel size 0.9 x 0.9 x 0.5 mm). Scans were segmented to produce subject-specific first metatarsal models using custom software (MultiRigid) [4]. Segmented bone volumes were imported into ShapeWorks Studio to generate a statistical model of metatarsal shape variance (1500 particle samples, Procrustes alignment) [5]. The mean metatarsal was reconstructed along with the shapes representing ± 2 standard deviations along the primary modes of variation. These models were inspected to identify anatomical regions and variations associated with each mode. A bone model was generated representing each mode/standard deviation level, and coordinate systems were embedded using two methods: 1) principal component analysis of the bone surface (PCA) and 2) fitting cylinders to the bone shaft and distal articular surface to define the bone axes [3]. The angular deviations between these resultant coordinate systems across the mode/variance levels were compared in the three anatomical planes.

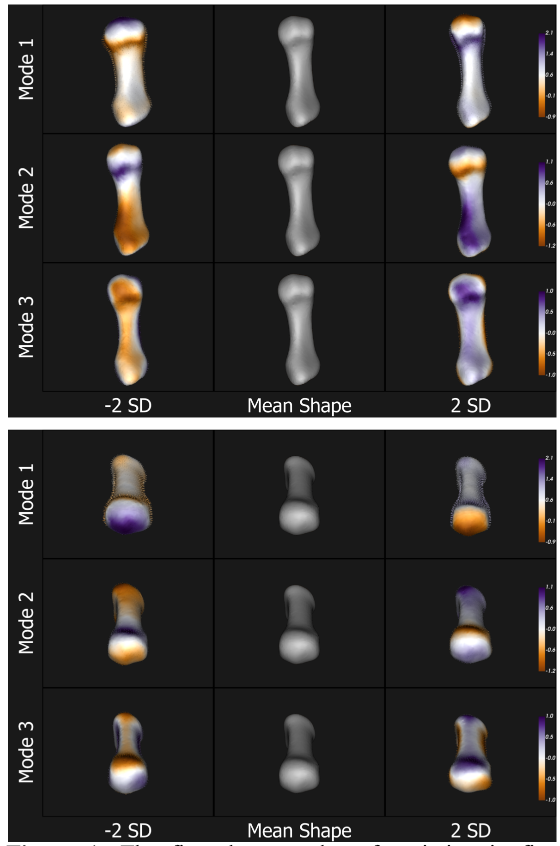

Figure 1: The first three modes of variation in first metatarsal bone shape. Two standard deviations from the mean shape are depicted for each mode, viewed from the plantar aspect (top) and from the anterior aspect (bottom).

Results & Discussion: The resulting model described 56.2% of the total shape variance in the first three modes. The first three modes revealed variation in both the gross metatarsal shape and the extent of the distal head's cam shape (Figure 1). Mode 2 variations were associated with changes in the metatarsal aspect ratio (long and thin vs short and broader). Mode 3 exhibited varying degrees of prominence in the region of the distal head crista. The standard deviations of the inclination angles in the frontal, sagittal, and transverse planes were smaller for PCA (0.5°, 0.1°, 0.2°, respectively) than CYL (2.7°, 2.6°, 1.2°, respectively). This suggests that the PCA coordinate systems were less sensitive to the observed variations in metatarsal head shape.

Significance: This study demonstrated natural variations in first metatarsal shape and highlighted the anatomical regions of greatest variance. These regions include the articular surfaces of the distal head directly responsible for guiding and determining the MTPJ1 kinematics. Algorithms for automated coordinate system embedding must be sensitive to these metatarsal variations. These data may also aid in the cam design of MTPJ1 joint replacement hardware or in planning osteotomies.

Acknowledgements: Supported in part by VA Rehabilitation Research and Development Grants A2180R, A3030R, and RX002970.

References:

[1] Drapeau, M. S., et al., "Metatarsal Torsion in Monkeys, Apes, Humans and Australopiths," J. Hum. Evol., 2013.
[2] Kitashiro, M., et al., "Age- and Sex-Associated Morphological Variations of Metatarsal Torsional Patterns in Humans," Clin. Anat., 2017.
[3] Thorhauer E, et al., "A Cadaveric Comparison of the Kinematic and Anatomical Axes and Arthrokinematics of the Metatarsosesamoidal and First Metatarsophalangeal Joints". J. Biomech. Eng., 2023.
[4] Hu Y, et al. "Multi-rigid image segmentation and registration for the analysis of joint motion from three-dimensional magnetic resonance imaging". J. Biomech. Eng. 2011.
[5] Cates, J., et al., Statistical Shape and Deformation Analysis, Elsevier Academic Press, Cambridge, MA, pp. 257–298.

HIP AND KNEE KINEMATICS AT PEAK ANTERIOR FOOT POSITION INFLUENCES ADAPTATIONS AT INITIAL CONTACT DURING GAIT WITH VISUAL FEEDBACK

Erik T. Hummer[1*], Melvin Mejia[2], Xuan Liu[2], Peter Barrance[2]
[1]Department of Kinesiology and Health, Rutgers University, New Brunswick, NJ, USA
[2]Center for Mobility and Rehabilitation Engineering Research, Kessler Foundation, West Orange, NJ, USA
*Corresponding author's email: Erik.Hummer@Rutgers.edu

Introduction: Augmented visual feedback provided during treadmill gait training promises to increase its clinical benefits [1]. Understanding gait adaptations adopted in response to feedback stimuli is critical to refine and improve feedback formulation and technology. We have previously reported [2] on gait adaptations in paediatric cerebral palsy (CP) while providing visual feedback on relative foot position [3], with a scoring mechanism based on peak anterior foot position (AFP_{Peak}). The intent of this feedback is to increase AFP_{Peak}, which in habitual gait coincides with initial contact, by adopting greater knee extension and/or hip flexion kinematics. Preliminary findings have shown that while most subjects increased AFP_{Peak}, some displayed unintended adaptations that did not promote a greater anterior foot position at initial contact (AFP_{IC}), due to decoupling of the timing between AFP_{Peak} and initial contact. Understanding the kinematic strategies used to increase AFP_{Peak} may inform how to further improve such a feedback system and guide its implementation. The purpose of this study was to characterize the adaptations in knee flexion angle (θ_{Knee}) and hip flexion angle (θ_{Hip}) at AFP_{Peak} in order to shed light on how potential strategies may influence changes in outcomes at initial contact.

Methods: Four participants (13.8 ± 5.1 yrs) diagnosed with CP displaying increased knee flexion angle at initial contact walked at a self-selected speed on a treadmill with synchronized collection of lower extremity kinematics from four IMUs (60 Hz) and 3-dimensional motion capture (120 Hz). Baseline kinematics were collected for 1 minute followed by four 6-minute bouts of walking with visual feedback. IMU data from the more involved limb were used in a kinematic model to determine relative AP foot position displayed as a red dot moving vertically [2]. The display incorporated scoring zones and awarded points in ascending order based on AFP_{Peak} for each step. Data were collected for each step at initial contact and at AFP_{Peak} for all trials. Average values for the primary outcomes (AFP_{IC}, θ_{Knee} and θ_{Hip} at AFP_{Peak}) were determined for baseline. Two hundred feedback steps were randomly selected for each participant and aggregated to create an 800-step dataset. Primary outcomes were processed as percent change from baseline average (%). 3D k-means clustering was used to select each step into one of two unique clusters.

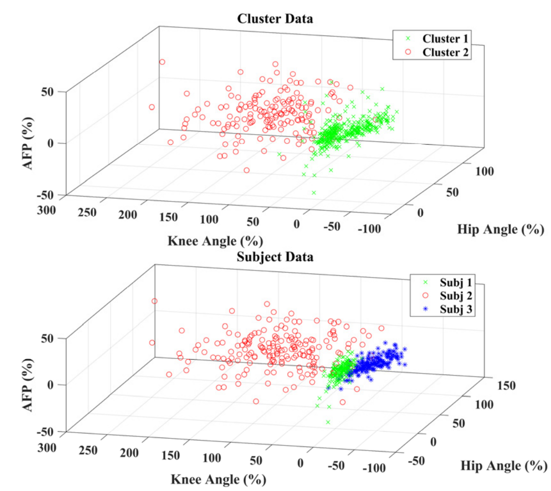

Figure 1: (Top) Results from k-means cluster analysis across subjects S1-3 based on adaptations to AFP_{IC}, and θ_{knee} and θ_{hip} at AFP_{Peak}. (Bottom) Subject specific data utilized for k-means cluster analysis.

Results & Discussion: The initial analysis selected clusters that almost exclusively selected subject 4 (S4) into a cluster separated from S1-3. This was primarily due to a much greater increase in AFP_{IC} for S4 (mean 850%) than S1-3 resulting from a greater change from baseline to feedback pattern as well as a lower baseline AFP_{IC}. We conducted a second cluster analysis on S1-3 who demonstrated more similar adaptations in AFP_{IC} (-1.4% - 15.4%). Two clusters (I and II) were formed from the 600 steps from S1-3. Cluster I included all steps from S1 and S3 and 25 steps from subject 2. Therefore, cluster II consisted of 175 steps from subject 2. Cluster I displayed increases in AFP_{IC} (14.1%), contrary to a decreased AFP_{IC} in cluster II (-3.4%, Fig 1). θ_{Knee} at AFP_{Peak} was in a more extended position than baseline for cluster I (-20.6%) in contrast to a more flexed position in cluster II (120.8%). Finally, θ_{Hip} at AFP_{Peak} saw a moderate increase in flexion for cluster I (6.9%) and a large increase for cluster II (78.5%). S4's strategy to achieve large AFP_{IC} increases was qualitatively overall similar to cluster I.

Our results suggest that steps classified within cluster II, which predominantly derived from a single subject, had exaggerated increases in both hip and knee flexion angles at AFP_{Peak}, resulting in no positive adaptation at initial contact. Most likely, this excessive hip flexion allowed the participant to prolong the terminal swing phase and to reach their foot further anteriorly, allowing for an increased score. This unintended adaptation appears to deviate from a natural gait pattern and may not be a desired result. Refining the visual feedback interface to emphasize or "weight" the scoring mechanism to favour increasing knee extension adaptations may be beneficial in deterring patients from unintended gait adaptations including excessive increases in θ_{Hip} at AFP_{Peak}. Conversely, additional cues by trained clinical staff may also be appropriate in improving the implementation of the current visual feedback system while maintaining the easy-to-use real-time stimulus as currently designed.

Significance: We identified specific kinematic adaptations prompted by a wearable sensor based visual feedback system that may mitigate potential benefits for individuals with CP. With this knowledge, refinements can be made to bolster the clinical effectiveness of this system for gait training that does not require extensive research equipment and that is designed for direct use in clinical settings.

Acknowledgements: Funding for this study was provided by Kessler Foundation and Children's Specialized Hospital.

References: [1] Booth et al. (2018), *Dev Med Child Neurol* 60(9); [2] Hummer et al. (2022), *NACOB*: Ottawa, CA 2022. [3] Balasubramanian et al. (2010), *Clin Biomech* 25(5).

THE EFFECTS OF DAMPING COMPONENTRY ON STANCE PHASE PROSTHETIC WORK

Seth R. Donahue[1*], Trevor Kingsbury, Kota Z. Takahashi, Matthew J. Major[1]
[1] Department of Physical Medicine & Rehabilitation, Northwestern University, and Jesse Brown VA, Chicago IL, USA
*Corresponding author's email: seth.donahue@northwestern.edu

Introduction: Mechanical work and power are crucial measures for the characterization of prosthetic foot function during locomotion of persons with transtibial amputation as they affect mobility outcomes. The systematic evaluation of commercial componentry with damping properties are essential to help inform prosthetic prescription. Componentry with damping properties include but are not limited to hydraulic ankle units and shock absorbing pylons (SAPs). Hydraulic ankles are a passive damped articulation between the prosthetic foot and pylon, and they have been linked to an increase in walking speed and reduced compensatory intact ankle-foot kinetics [1]. SAPs comprise of a shank with viscoelastic properties that can compress and/or twist about the longitudinal axis and have been shown to increase the magnitude of negative work during load acceptance in early stance [2]. The purpose of this project was to evaluate the effects of systematically including damping components on stance-phase mechanical work during transtibial prosthetic gait. Given their design intention, we expect that damping components will increase energy dissipation during prosthetic gait.

Methods: Two participants (1f/1m, 47/72 yrs, 1.70/1.70 m, 84.7/55.4 kg) with unilateral transtibial amputation participated. Both participants experienced traumatic amputation over 20 years prior. Both were able to walk independently without assistance. Participants walked over ground along a 10 m level walkway at their self-selected speed under four different prosthesis conditions: 1) dynamic response carbon-fiber prosthetic foot (Horizon, College Park, USA), 2) dynamic response prosthetic foot with SAP (Fillauer, USA), 3) dynamic response foot with a hydraulic ankle (Odyssey K3, College Park), 4) dynamic response foot with the hydraulic ankle and SAP. Participants walked using their customary socket and suspension system and all distal components were selected according to manufacturer guidelines. Low profile standardized laboratory shoes were used to account for possible shoe effects. A custom 6-degree of freedom marker set was utilized with 37 markers. Kinematic and Kinetic data were collected using a 12-camera motion capture system (Motion Analysis Corporation, USA) at 120 Hz, and 6 floor embedded force plates at 1200 Hz (AMTI, USA). Kinematic and kinetic data were processed using Visual3D (C-motion, USA) and were filtered with a frequency cutoff of 6 Hz and 25 Hz, respectively. Mechanical power (Wkg^{-1}) of the prosthesis (i.e. components distal to the socket) and the anatomical foot-ankle complex were calculated using the unified deformable power analysis [3]. Positive, negative, and net mechanical work (Jkg^{-1}) were calculated by integrating power with respect to time using custom MATLAB code (Mathworks, USA). As only a case series, the mean and 95% Confidence Intervals (CIs) were calculated across five steps for each prosthetic condition of both participants for statistical comparison.

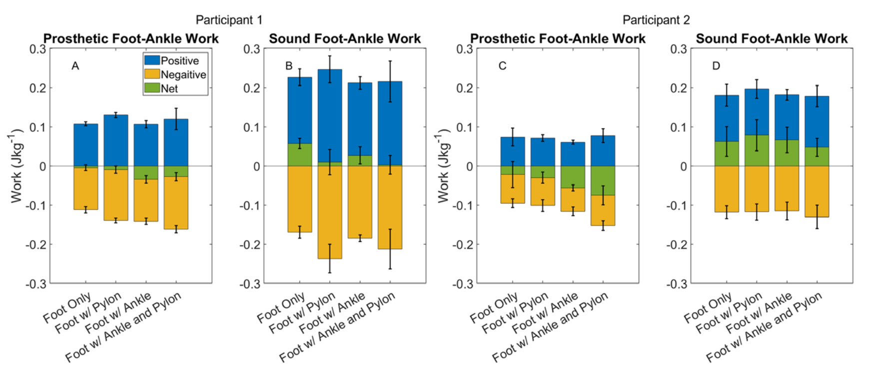

Figure 1: Stance-phase work (mean and 95%CI) for the prosthesis (A, C) and sound ankle-foot complex (B, D).

Results & Discussion: Mechanical work for each participant is shown in Figure 1. As expected, these results suggest that addition of damping components increased prosthesis energy dissipation as reflected by decreased net mechanical work for both participants. This increased dissipation was primarily due to the increased magnitude of energy absorbed (negative work), as adding damping components had no measurable effect on energy generated/returned (positive work). Participants demonstrated unique responses on the sound ankle-foot to each prosthetic condition that emphasizes need to consider subject-specific effects. Participant 1 expressed symmetric increases in positive and negative work with the use of the SAP, while Participant 2 effectively demonstrated no change between conditions. This study was limited by the small sample size, although data collection is ongoing. Additionally, while these results support the use of damping components to increase prosthesis energy dissipation, these results are currently limited to ankle-foot structures and do not reflect how the energy is transmitted to the residual limb.

Significance: Here we report novel data from a systematic analysis of the effects of prosthetic damping components on prosthesis and sound ankle-foot complex work. Our preliminary results suggest that adding a hydraulic ankle and SAP to a dynamic response foot can increase the absorbed and dissipated energy of a prosthesis throughout the stance phase of walking while having little influence on prosthesis energy return. Results may help inform prosthetic prescription when the clinical goal is to enhance prosthetic damping.

Acknowledgements: This work was supported by funding from the DOD Orthotics and Prosthetics Outcomes Research Program (award# W81XWH2120007). Content does not reflect views of the US Dept. of VA, US Dept of Defense, or US Government. We would also like to thank Rebecca Stine, M.S. and Wendy Beattie, CPO, for their assistance with data collections.

References: [1] De Asha et al. (2013), *J Neuroeng. Rehabilitation* 10(3);
[2] Maun et al. (2021), *J Neuroeng. Rehabilitation* 18(1);
[3] Takahashi et al. (2012), *J Biomech,* 45(15);

ASSESSING THE ACUTE EFFECTS OF WEARABLE SENSOR DERIVED AUDITORY BIOFEEDBACK ON GROSS LUMBAR PROPRIOCEPTION

Aurora Battis, Shawn M. Beaudette
Department of Kinesiology, Brock University, St. Catharines ON
*Corresponding author's email: ab15rd@brocku.ca

Introduction: Patients experiencing low back pain (LBP) exhibit impaired motor control patterns and proprioceptive deficits and may benefit from proprioceptive retraining [1]. Proprioception is typically quantified by assessing conscious control (e.g., active or passive re-matching tasks) or subconscious control (e.g., vibration evoked reflexes) [2]. The neuromuscular control of the spine operates in a feedback loop by incorporating afferent feedback to inform on a motor response [3]. The use of supplemental sensory inputs has become an area of importance for sensorimotor (re)training, with potential utility to optimize movement patterns, reverse central maladaptation(s), and aid with rehabilitation for those affected with chronic LBP. Augmented biofeedback can be used as a training method that provides additional information to enhance performance through changed behaviors [4]. The **purpose** of this study is to explore the potential utility of wearable sensor derived auditory biofeedback to enhance conscious proprioception of the lumbar spine in a sample of young, healthy participants. Due to the success of augmented biofeedback as a training method for other sensorimotor impairments (e.g., visual feedback in balance training) [4], it is **hypothesized** that auditory biofeedback training will be effective at acutely improving accuracy (Constant Error [CE], Absolute Error [AE]) and precision (Variable Error [VE]) of the gross lumbar spine during sagittal plane repositioning.

Methods: 28 healthy young adults (14 females) participated (mean age = 22.9 ± 3.4 yrs; height = 172.8 ± 9.5 cm; mass = 73.4 ± 13.9 kg). Participants were instrumented with a wireless electrogoniometer spanning T12-S1 and remained in an ergonomic kneeling chair for all interventions and assessments (Figure 1). Three maximum flexion ROM trials were completed to derive four targets: 20%, 40%, 60%, and 80% of their peak flexion ROM. Participants were familiarized with each target prior to the pre-training test. The pre-training test consisted of an active flexion repositioning task five times/target, with all repetitions and targets assessed in a random order. Two of the four targets were then randomly selected (one each ± 50% ROM) and trained for five minutes each with supplementary auditory feedback, derived from the wireless electrogoniometer. Following training, participants completed a post-training test which mirrored the pre-training test to evaluate acute effects of the supplementary auditory training.

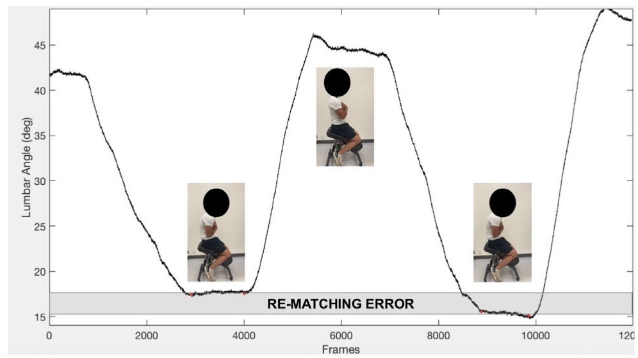

Figure 1: Representative data depicting the repositioning task and error for a single participant.

Results & Discussion: Although the majority of CE, AE and VE PRE/POST group comparisons were insignificant ($p > 0.05$), positive group effects were observed across all targets. The targets with the strongest effects were the mid-range targets (i.e., 40% and 60% max ROM). To assess the relationship of any acute benefits of the training session with baseline proprioceptive abilities, bivariate linear regressions were conducted comparing any apparent changes in proprioceptive abilities with baseline performance. Moderate-to-strong negative linear regressions indicate that those with the poorest re-matching abilities at baseline demonstrated the strongest benefits (i.e., reductions in CE, AE, and VE) of the acute auditory biofeedback. The findings reported here represent a proof of principle that acute auditory biofeedback training has the capacity to improve lumbar proprioception in a population of healthy young participants. Although baseline proprioception varied, significant effects may be masked by the elevated abilities in this sample of young, healthy participants. These findings suggest that this type of proprioceptive re-training technique may be of use in a clinical population where proprioceptive deficits are present.

Significance: Collectively, the findings of this research lay the groundwork for further research into sensory biofeedback as a training tool to enhance conscious proprioception of the lumbar spine. Acute auditory biofeedback training appears to have merit as a means to improve proprioceptive abilities in those with apparent proprioceptive deficits. Given this, further assessment of auditory biofeedback training is warranted by potentially evaluating a clinical population, and the retention of training benefits. Further, additional work is warranted to assess the utility of this paradigm on complimentary, subconscious aspects of proprioception, across a wide range of potential sensory feedback modalities (i.e., haptic, visual, etc.).

Acknowledgements: This research was funded, in part by the Natural Sciences and Engineering Research Council (NSERC) of Canada (RGPIN-2020-05195). The authors wish to thank Hannah McMaster for her contributions to the research project.

References: [1] van Dieën et al., 2019. J Orthop Sports Phys Ther. 49(6): 380–88; [2] Brumagne et al., 2000. Spine. 25(8): 989-94; [3] Reeves et al., 2007. Clin Biomech. 22(3): 266-274; [4] Alhasan et al., 2017. Clin Interv Aging. 12: 487-497.

LOCOMOTOR ADAPTION TO A MOVEMENT AMPLIFICATION ENVIRONMENT IN PEOPLE WITH CHRONIC STROKE

Shamali Dusane[1], Anna Shafer[2], Keith E. Gordon[1, 2]
[1]Department of Physical Therapy and Human Movement Sciences, Northwestern University, Feinberg School of Medicine, Chicago, IL 60611, [2]Research Services, Edward Hines Jr. VA Hospital, Hines, IL 60141
keith-gordon@northwestern.edu

Introduction: Balance is a strong predictor of the number of steps people with chronic stroke (PwCS) take each day [1]. Most PwCS have significant balance impairments that contribute to gait deficits [2] and alarmingly low levels of physical activity [3]. Thus, there is a compelling need to develop effective interventions to enhance walking balance in ambulatory PwCS. We have developed an innovative approach to train walking balance that is similar in principle to error augmentation, a motor learning framework known to accelerate skill acquisition of reaching movements in PwCS [4, 5]. Specifically, we used a cable-driven robot to apply smooth and continuous lateral forces to the pelvis during treadmill walking. The applied forces were proportional in magnitude and in the same direction as a participant's real-time lateral whole-body center-of-mass (COM) velocity [6]. The effect is that when a participant moved to the right, the robot pulled them to the right. The resulting *Movement Amplification Environment* (*MAE*) challenged walking balance by increasing the difficulty to maintain straight walking. Exaggerating a participant's own movements may aid in re-learning balance by enhancing sensory feedback that makes it easier to perceive small movements. The control of lateral walking balance is particularly challenging for PwCS and believed to require considerable contributions from the nervous system. Therefore, we 1) directly challenged lateral balance to maximize nervous system engagement and to provide task specific training and 2) focused our evaluation of gait adaptations on changes in lateral motion. This preliminary study aimed to evaluate how PwCS control their lateral COM excursion while walking in a *MAE* (adaptation) and immediately after this practice (after-effects). We hypothesized that PwCS would adopt control strategies that result in a reduced lateral COM excursion after the *MAE* is removed.

Methods: Three ambulatory individuals with chronic, hemiparetic stroke were included in the study (60.7 ± 11.3 years). Participants performed 2-min of walking on an oversized treadmill (Tuff Tread, Willis, TX) at their preferred walking speed to familiarize themselves with the treadmill (*Baseline*). Next, participants performed five 2-min bouts of walking in the *MAE* separated by short rest breaks. At the completion of the fifth bout of walking in the *MAE*, the applied forces were removed on-the-fly without stopping the treadmill and participants walked for another 2-min to evaluate *After-Effects*. (*Post*) The Movement Amplification gain (strength of the lateral force) was adjusted during the first 2 minutes of the Amplification Field to be challenging while still allowing successful forward progression (*MAE* gain ranging from 25 to 45). Participants' 3D kinematic data was collected using 19 reflective markers placed on the pelvis and lower limbs and a 12-camera motion capture system (Qualisys, Gothenburg Sweden). To quantify control of lateral COM motion, we used motion capture data to calculate lateral COM excursion each step and then identified the minimum average lateral COM excursion occurring during five consecutive gait cycles.

Results & Discussion: We found that all PwCS were able to successfully walk in the *MAE*. During the first 2 minutes of walking in the *MAE* (Early Field) participants' lateral COM excursion was 9% greater than baseline and participants were observably challenged to control their walking direction. During the last 2 minutes of walking in the *MAE* (Late Field), participants' lateral COM excursion was 9% smaller than Baseline and participants demonstrated improved ability to control their lateral motion in the *MAE*. When the *MAE* was removed, there was a significant 28% decrease in lateral COM excursion compared to baseline ($p<0.05$) (Figure 1). This rapid adaptation indicates that PwCS changed their walking pattern in response to the *MAE* in a manner that improved control of lateral motion. We postulate that the enhanced sensorimotor feedback created by walking in the balance-challenging *MAE* may help PwCS to identify small movement errors and adapt anticipatory balance control strategies that improve walking balance.

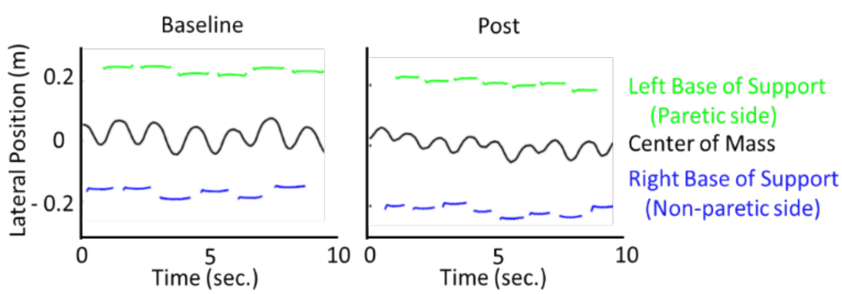

Figure 1: After-Effect of Walking in a Movement Amplification Environment. Lateral COM and base of support (5th metatarsal) position during walking for a representative participant. Data show walking immediately before (Baseline) and after 10-min of walking in the *MAE* (Post). Note, no external forces were applied during the Baseline and Post periods. Lateral COM excursion decreased after walking in the *MAE*.

Significance: Our preliminary data finds that in response to walking in a *MAE* PwCS adapt their gait in a manner that improved control of their lateral COM motion. Training walking balance of PwCS by amplifying a person's self-generated movements is a radical departure from current practice and could create effective new clinical interventions. These findings motivate further research to better understand the mechanisms of balance control PwCS adapt in response to walking in a *MAE*.

Acknowledgements: This study was funded by the United States Department of Veteran Affairs, Rehabilitation Research and Development, #1 I01 RX003371 and the Northwestern University Department of Physical Therapy and Human Movement Sciences.

References: [1] Handlery et al. (2021), *Stroke*, 52 (5); [2] Tyson (2006), *Physical Therapy*, 86(1); [4] Fini et al. (2017), *Physical Therapy,* 20(1); [4] Patton et al. (2006), *Exp Brain Res*, 168(3); [5] Huang et al. (2013), *IEEE Trans Biomed Eng*, 60(3); [6] Brown et al. (2017), *39th Annual International Conference of the IEEE EMBC*.

PRELIMINARY RESULTS FROM MEASURING THE DYNAMICS OF MILITARY TASKS

W. Brett Johnson[1, 2*], Jaqueline Villanueva[3], Joshua Childress[4], W. Lee Childers[1, 2]
[1]DoD/VA Extremity Trauma and Amputation Center of Excellence, USA, [2]Center for the Intrepid, Brooke Army Medical Center, JBSA Ft. Sam Houston, TX, [3]The Henry M. Jackson Foundation for the Advancement of Military Medicine Inc., Bethesda, MD, [4]Glacier Support Services, San Antonio, TX
*Corresponding author's email: william.b.johnson462.civ@health.mil

Introduction: Understanding the loads military Service members experience is essential for designing safe and effective exoskeletons for them. One current design effort is to create an assistive exoskeleton for casualties with lower leg injuries to enable mobility until they can be evacuated to higher levels of medical care. While a casualty with a lower leg injury using an exoskeleton will likely have a diminished capacity to perform normal military tasks, understanding the dynamics of those tasks can establish threshold criterion to ensure the designs are robust enough to withstand loads the Service members may encounter. Therefore, the purpose of this pilot study is to quantify the dynamics of common military tasks that may have unique combinations of lower limb forces and moments. This information will inform the design requirements of future devices, including assistive exoskeletons for austere environments.

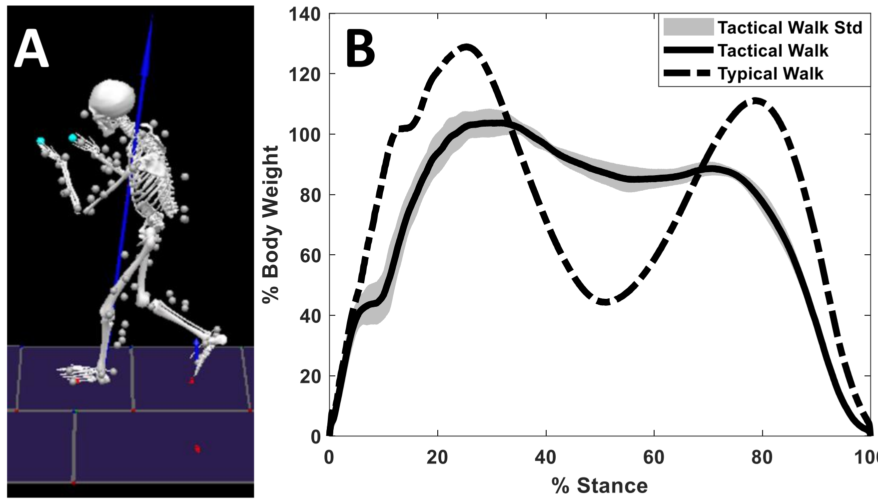

Figure 1: A) Visual 3D model of a participant performing a tactical walk. **B)** Average ground reaction force for tactical walking during the stance phase (black line, gray shading represents ± 1 std). The peaks of the force profile appear to be smaller than those of typical able-bodied gait (dashed line).

Methods: One able-bodied subject gave their informed consent (Female, Height: 1.4 m, Weight: 52 kg). They were fitted with standard issue US Army body armor including a helmet and plate carrier. Subjects were given a mock M4 rifle and asked to perform the following common military tasks: entering a kneeling firing position and return to standing, entering a prone firing position and return to standing, ammo can carry, and tactical walking at a self-selected speed (a gait pattern adopted to prevent tripping on uncertain terrain during dismounted patrols). Additionally, participants performed other regular tasks such as running, walking at a self-selected speed, and a Timed Up and Go test. Embedded force plates measured the ground reaction forces during these tasks while a motion capture system tracked the position of reflective markers placed on the participant. A set of five plate strikes where collected for each task, and ground reaction forces were ensemble averaged together and normalized to the participant's weight.

Results & Discussion: While analysis is ongoing, a notable preliminary finding are the distinct features of the ground reaction force profile for the tactical walk compared to that of typical gait. The peaks and heel strike transient were smaller than typical gait. While some of these differences may be attributable to changes in walking speed, (the participant walked at 1.6 m/s for the typical walk and 1.1 m/s for the tactical walk), the second peak of the ground reaction force for the tactical walk is almost non-existent. The tactical walk is a crouched gait pattern that minimizes vertical motion of the upper body to facilitate targeting with a rifle. The smaller second peak may be a means to reduce the vertical excursion of the body center of mass.

Results are currently limited to one participant, and these findings may not extrapolate to the broader population of Service members. However, the target enrollment for this ongoing study is twenty-three subjects and will be able to provide a more generalizable data set.

Significance: Quantifying the loads acting on Service members as they perform common tasks will guide specifications for wearable equipment. These specifications will ensure that devices are able to endure the vigorous activities of service members.

Acknowledgements and Disclaimer: Funded by the Dept. of Defense Combat Casualty Care Research Program, Project ID: CO210052. The views expressed herein are those of the author(s) and do not reflect the official policy or position of the Brooke Army Medical Center, the Department of Defense, or any agencies under the U.S. Government.

References: [1] US Army Training and Doctrine Command, TRADOC Pamphlet 525-3-1

THE EFFECT OF THREE-MONTH ANKLE FOOT ORTHOSIS (AFO) ON SPATIOTEMPORAL GAIT CHARACTERISITCS OF PATIENTS WITH PERIPHERAL ARTERY DISEASE

Salamifar Z[1*], Fallahtafti F[1], Kaeli S[2], Johanning J[3,4], Pipinos I[3,4], Myers SA[1,3]
[1] Department of Biomechanics, University of Nebraska at Omaha, Omaha, NE USA
[2] Department of Biostatistics, University of Nebraska Medical Center at Omaha, Omaha, NE USA
[3] Department of Surgery and Research Service, Omaha Veterans' Affairs Medical Center, Omaha, NE USA
[4] Department of Surgery, University of Nebraska Medical Center, Omaha, NE USA
*Corresponding author's email: ssalamifar@unomaha.edu

Introduction: Peripheral artery disease (PAD) is a manifestation of the blood vessels supplying the legs becoming narrowed or blocked. Insufficient blood flow causes claudication (pain) during walking and chronic PAD leads to myopathy which impairs gait prior to the onset of claudication pain. Gait impairments includes reduced velocity, torques, and power generation, particularly at push-off [1,2,3,4]. Ankle foot orthoses (AFO) have previously been showed to enhance gait in patients with neurological disease and to increase walking distances in patients with PAD[5]. The spatiotemporal parameters of gait are often used to identify pronounced and consistent gait differences in clinical populations. Linear variability, such as standard deviation, can provide additional insight by quantifying the amount of variation in the temporal and spatial characteristics. Increased variability has been found in patients with PAD[6]. This study evaluated the effect of initial AFO use and a three-month AFO intervention on spatiotemporal gait parameters of patients with PAD. We expected that spatiotemporal gait characteristics may improve in patients with PAD after a three-month AFO intervention.

Methods: This study used a control-crossover design to assess the impact of AFOs at first use and after a three-month AFO intervention (Figure 1). Subjects were randomized into control and AFO groups. Patients in the AFO group wore an AFO each day for three-months (immediate intervention group) while the control group followed the standard of care for the first three months (delayed intervention group) (Figure 2,3). Both groups returned for a second evaluation, "crossed over" to the other group for three months, then returned for a final assessment. Patients were instructed to wear the AFOs at all the times except in bed and showering during AFO intervention. During the assessment, patients walked with (AFO)/without AFO(NAF) while kinematic data were recorded. Mean and standard deviation (variability) of spatiotemporal gait data (step velocity, step length, step time, and step width) were calculated.

Figure 1: Study Protocol – Subject walked over the defined path overground on force platforms with and without the carbon-composite AFO, for at least five trials. The spring-like properties of carbon composite allows energy to be stored during heel strike and returned at the point of toe-off.

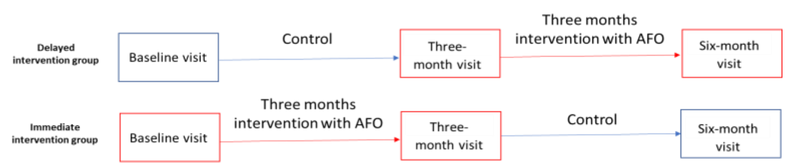

Figure 2: Red outlines define the visits from delayed and immediate intervention groups which were included in the comparison analysis between the dependent variables for before and after-intervention.

Figure 3: Red outlines define the visits from control (no intervention) and intervention groups which were included in the comparison between the dependent variables at baseline

Results & Discussion: While wearing AFOs, patients with PAD had increased step time compared to the NAF condition in a single session. However, after a three-month AFO intervention, patients' step time decreased, indicating the AFO had a beneficial effect on gait adaptation after intervention. The immediate intervention group preserved the amount of step width variability following three months of intervention, however, the delayed intervention group experienced significantly reduced amount of step width variability when walking without the AFO. Reduced step width variability is associated with increased sensory impairment and marked as a deviation from healthy walking pattern [5]. Amount of variability of step length and step velocity were reduced at three months' visit compared to baseline. These changes indicate gait patterns moved closer to healthy controls, which can be related to AFO adaptation after three months.

Significance: The mean and variability of spatiotemporal gait characteristics were significantly improved after a three-month AFO intervention. AFOs may allow patients with PAD to walk with patterns more like older controls without PAD.

Acknowledgements: This study was supported by NIH grants (R01AG034995, R01HD090333, RO1AG049868) and VA grants (I01RX000604, I01RX003266).

References: [1] J. D. Hooi et al. (2001), Am J Epidemiol, vol. 153, no. 7, pp. 666–672; [2] M. N. Schieber et al. (2017) J Vasc Surg, vol. 66, no. 1, pp. 178-186.e12; [3] M. N. Schieber et al. (2017) J Vasc Surg, vol. 71, no. 2, pp. 575–583. [4] A. Gouelle et al. (2017) Handbook of Human Motion (pp.1-20); [5] Brach, J. S et al. (2007) Gait Posture 27, 431-439; [6] S. A. Myers, et al. (2009). J Vasc Surg, vol. 49, no. 4.

THE EFFECTS OF AN INCLUSIVE BADMINTON PROGRAM ON UNILATERAL STATIC BALANCE FOR YOUNG ADULTS WITH INTELLECTUAL AND DEVELOPMENTAL DISABILITIES

Alana J. Turner[1*], Isabelle Farm[1], Sachini N K Kodithuwakku Arachchige[2], Aaron Griffith[3], Po-Lin Chen[3], Chih-Chia Chen[3], Adam C. Knight[3], Chad Smith[1], & Harish Chander[3] [1]Coastal Carolina University, Conway, SC [2]Weber State University, Ogden, UT, [3]Mississippi State University, Mississippi State, MS*Corresponding author's email: aturner4@coastal.edu

Introduction: For the general population, 1-3% of individuals have an Intellectual and Developmental Disability (IDD) [1]. Individuals with IDD present an array of postural control and locomotor deficits which results in a higher prevalence of falls when compared to peers [2]. Previous literature has reported the fall prevalence for adults with IDD is over 40% [2]. Thirty-two percent of these falls result in injury or death [2]. Efforts to create or find interactive balance interventions to delay or limit these deficits are essential for people with disabilities to improve their quality of life and overall movement. Badminton is a popular sport worldwide that requires fast and powerful shots and agile footwork [3]. Agility, which is defined as a rapid whole-body movement with a change of velocity or direction in response to a stimulus, is a crucial variable for outstanding performance in badminton competitions [3]. Agility-type training during badminton could not only improve balance for young adults with disabilities but could improve postural control mechanisms for this population. The purpose of this research was to examine static postural control/balance in young adults with IDD and typical developing (TD) young adults before, during, and after an inclusive badminton intervention. Due to the type of agility training incorporated into a badminton program which is similar to therapeutic balance training (i.e., anterior-posterior weight shifts and unilateral stances), the researchers expected to see improvements for both groups in the badminton intervention.

Methods: Eight participants (four IDD-BADM and four TD-BADM) participated in a 12-week inclusive badminton intervention, with the other eight participants as matched controls (four IDD-CONTR and four TD-CONTR) (74.19kg ± 9.8kg, 171.96cm ± 5.4cm; 21.7 ± 1.8 years of age; 9 females and 7 males; 8 with IDD and 8 TD). The study followed a repeated measures design (pre, mid, post) before the intervention, at 6 weeks, and after 12 weeks. Static balance measurements included dominant leg unilateral stance- eyes open (1LEO) (10s) balance tests on an AMTI® (Waterford, MA) force plate. Sway measurements included: average anterior/posterior (A/P) displacement (in), average medial/lateral (M/L) displacement (in), average 95% ellipsoid area (EA) (in^2), and average velocity (AV) (ft/s). Post-hoc comparisons were performed using a Greenhouse-Geisser correction if significant main effects were identified. The badminton group followed the Special Olympics Individual Badminton Skills Assessment and the Badminton World Federation (BWF) guidelines and was designed as a bi-weekly 50-minute, inclusive badminton adapted physical education class, including 24 sessions.

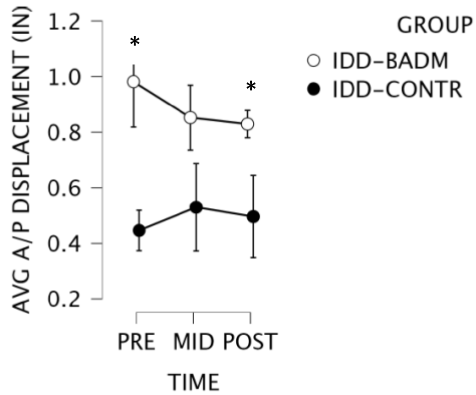

Figure 1: 1LEO Average A/P Displacement (in.) Group x Time Interaction for IDD-BADM from Pre-Test to Post-Test. "*" indicates group x time interaction for IDD-BADM showing greater descreases in displacement compared to IDD-CONTR,; standard deviation bars displayed.

Results & Discussion: A significant group x time interaction was reported for IDD-BADM for average COP displacement in the A/P direction during 1LEO, post-hoc simple effects comparisons revealed greater decreases in COP displacement, improvements in balance performance, from pre-test to post-test for the badminton intervention group ($p = 0.036$) while the control group increased COP displacement, defecits in balance performance, from pre-test to post-test (Fig 1). These results align with the type of movements and skills that are acquired from playing badminton. For instance, badminton players react to the moving shuttlecock and adjust their body position rapidly and accordingly throughout the game [3]. Badminton players are constantly shifting their center of gravity (COG) outside and within their base of support (BOS) while performing very quick, unilateral upper limb movements [4]. This constant movement of the COG with asymmetrical upper body movements while playing badminton over the course of 12-week biweekly classes is challenging and trains the postural control system by integrating and organizing changing sensory information while utilizing a feedforward process for quick response times, especially for those with postural control deficits. This type of intervention is also training anticipatory postural adjustments, which assists in the A/P displacement of the individual's COP while moving forwards and backwards throughout the court while the individual is contacting the shuttlecock with rapid change of the six degrees of freedom of the dominant arm's glenohumeral joint. Even though these are training dynamic balance movements, static balance, like during the 1LEO condition, is also being challenged during training and improving. However, no significant main effects for time, group, nor significant group x time interactions were found for average displacement in the M/L direction, 95% ellipsoid area, average velocity, or average length for the other test groups (Fig 1).

Significance: These results align with the need to create fall prevention programs to reduce the prevelance of falls for this population [1]. By creating inclusive exercise programs, this could motivate those with IDD to not only improve balance but to become physically active with TD peers which could improve other areas of wellness like psychylogical aspects of diability. Moving froward, it could be possible to promote social inclusivity through exercise while lowering an individal's biomechanical constraints. **References:**

[1] Maulik et al. (2011), *Res Dev Disabil* 32(2); [2] Willgoss et al. (2010), *J. Clin. Nurs.* 19(15-16); [3] Faude et al. (2007), *Eur J Appl Phys* 100(479-86); [4] Teu et al. (2005), *Sports Eng* 8(171-8).

USING LOADSOL DATA TO ESTIMATE KNEE JOINT MOMENTS IN STATIONARY CYCLING

Walter G. Menke*, Songning Zhang
University of Tennessee, Knoxville, TN
*Corresponding author's email: wmenke@vols.utk.edu

Introduction: Kinetic calculations for important clinical classifications of joint moments, such as knee moments, has historically been limited to laboratory settings that require high-value equipment such as force plates to appropriately measure kinetics. With less expensive and more portable solutions, such as the loadsol (novel), the ability to measure kinetics has become more feasible for clinicians. Stationary cycling is an activity recommended by clinicians for management and rehabilitation of knee pathologies such as knee osteoarthritis [1]. While previous studies have validated the loadsol for measuring vertical ground reaction forces, there has been no literature that implements the vertical loadsol data to estimate joint moments [2]. The purpose of this research was to investigate if measured vertical pedal reaction force (PRFz) and knee joint moments calculated from the loadsol can be used to estimate joint moments when compared to a gold standard set of force-sensing instrumented pedals. It was hypothesized that the knee joint moments estimated from loadsol PRF and the maximum PRFz would not be significantly different from those computed from the instrumented pedals.

Methods: Nine subjects participated in stationary cycling that was conducted at workloads of 1kg, 2kg, and 3kg and at 80 RPM for 2-minute bouts on a Monark cycle ergometer with each participant in standardized shoes. Data were recorded for the final 10 seconds of the 2-minute period and divided into five trials of one full cycle trial. Kinematic data using a 12-camera system (240Hz, Vicon) and kinetic data from the customized instrumented pedals (1200Hz, Kistler) were recorded using Vicon Nexus. The loadsol data (100Hz, novel) collection were synchronized with the Vicon Nexus using the *loadsync* device. The knee joint moments were computed using the only PRFz for the loadsol conditions and assuming the center of pressure (COP) is fixed at the center of pedals while these values for the instrumented pedal conditions were computed using all three PRF components and computed COPs in Visual 3D. Minimum sagittal knee moment (Min KMx), minimum frontal knee moment (Min KMy), maximum internal rotation moment (Max KMz), and maximum PRFz (Max PRFz) were determined for each trial and averaged for each condition per subject. A 2 x 3 (method x workload) repeated measures ANOVA was performed for the variables (SPSS v29). Only data from the participant's right side were assessed. Normality was assessed using Shapiro Wilkes tests. The significance level was set at 0.05 a priori.

Results & Discussion: The majority of conditions were significantly different from each other for all variables presented except for KMz 1kg and 2kg workloads (Table 1). Knee extension moments, classified as positive, are usually seen in the power phase of cycling. The mean differences show that Min KMx was overestimated with the loadsol compared to the instrumented pedals to the point that no extension moment was present. The loadsol underestimated the Min KMy compared to the instrumented pedals. In addition, the loadsol overestimated the peak internal rotation moment in the 3kg condition. Peak PRFz recorded by the loadsol were consistently 45-60N lower than the instrumented pedals, which may be a result of the sampling rate being insufficient to truly capture reaction forces during this activity. The data for the loadsol peaks were calculated using only the vertical vector that is always oriented perpendicular to the pedal interface and its COP does not move mediolaterally. As a result, during the power phase, the pedal tilts to face anteriorly and so does the vector from the loadsol. The lack of anteroposterior PRF component in the loadsol method, which keeps the PRF vector anterior to the knee, resulted in a lack of extension moment that is typically seen the power phase with the instrumented pedal method. These present data do not support the hypothesis that the knee moments and PRFz peaks would be similar between the two calculation methods.

Table 1: Two-way ANOVA results comparing both methods of knee moment calculations. MD: mean difference, SE: standard error, p: significance and CI: confidence interval (Lower, Upper).

	MD	*SE*	*p*	*95% CI*
Min KMx 1kg	15.3	3.7	0.003	6.9, 23.8
Min KMx 2kg	20.0	5.0	0.004	8.6, 31.4
Min KMx 3kg	27.9	6.3	0.002	13.5, 42.3
Min KMy 1kg	-7.4	1.67	0.002	-11.3, -3.5
Min KMy 2kg	-10.2	2.4	0.003	-15.8, -4.7
Min KMy 3kg	-14.4	2.2	0.000	-19.4, -9.4
Max KMz 1kg	-0.4	2.4	0.890	-5.9, 5.2
Max KMz 2kg	3.1	2.2	0.199	-2.0, 8.3
Max KMz 3kg	10.0	2.5	0.004	4.3, 15.7
Max PRFz 1kg	60.1	13.27	0.002	29.5, 90.7
Max PRFz 2kg	45.8	13.72	0.010	14.2, 77.5
Max PRFz 3kg	50.4	12.20	0.003	22.2, 78.5

Significance: The current research covers the inception of implementing more cost effective and feasible solutions for clinicians wanting to assess patient kinetics without the use of an instrumented pedal in a laboratory setting. Our findings do not currently support the usage of the loadsol in estimating joint moments at the knee during stationary cycling, especially for sagittal-plane moments. Future research should involve finding a way to adjust the missing planes of PRFs; perhaps utilizing a machine learning algorithm that can relate anteroposterior force directions from instrumented pedals to pedal angle to better estimate knee joint moments with loadsol data. Utilizing more user friendly equipment to estimate clinically relevant data for practitioners may be a future path to acquiring this data easily for the development of rehabilitation strategies and interventions.

Acknowledgements: Kaileigh E. Estler (data collection) and Austin P. Abbott (data collection and processing).

References: [1] Kutzner, I et al. *Journal of Orthopedic and Sports Physical Therapy 42:1032-1038, 2012*
[2] Renner KE et al, *Sensors* 19: 265, 2019

INDUCED TRANSIENT MOOD TASK TO INVESTIGATE THE RELATIONSHIP BETWEEN EMOTION AND POSTURAL CONTROL IN ADULTS WITH GLAUCOMA

Natalie Bick[1*], Helmet T. Karim, Howard Aizenstein, Mark Redfern[1], and Rakié Cham[1]
[1]Department of Bioengineering, University of Pittsburgh, Pittsburgh, PA
*Corresponding author's email: nab173@pitt.edu

Introduction: Glaucoma is a leading cause of blindness, and adults with glaucoma fall at a greater rate than similarly aged adults without glaucoma [1, 2]. While glaucoma-related changes in vision certainly contribute to falls, other risk factors may be at play. Depression occurs at a higher rate in people with glaucoma and is an important fall risk factor in older adults [3]. *The impact of depression on balance in this population has not been studied.* As depression is a mood disorder, the mechanisms of mood states are important to understand how sensory information is processed. Thus, the overarching goal of this study is to understand how mood induction contributes to balance deficits and fall risk in glaucoma. We expect individuals with glaucoma to display a different relationship between emotions and postural control than those without.

Methods: Four adults with glaucoma (2F) and four similarly aged adult without (2F) were enrolled after screenings to exclude any vestibular, somatosensory, or neurological condition that impacts balance. Participants underwent questionnaires to characterize mental and physical health. Based on previous work in mood-focused gait studies [4] and a worry-rumination task [5], participants were asked to "Think of a time in your life when you felt extremely [happy or sad]." Participants were asked to rate how strongly they felt emotion during each memory on a scale of 1-5, where 1=no emotion and 5=extreme emotion. Each personalized memory was shortened to a cue phrase and converted to an audio file (<10 s) using text-to-speech software. These cues were repeated back to the participants during balance testing, creating induced transient mood (ITM) states. ITM cues (4 happy, 4 sad) were created for each participant, each with a rating of ≥3. Balance testing was performed using the Bertec® CDP/IVR™ platform with a full factorial design consisting of 4 balance conditions, each comprised of a *floor* and *vision* condition: floor conditions were fixed platform and sway-referenced (SR) platform with a gain of 1; vision conditions were eyes open and closed. During each balance condition, participants were asked to focus on their feelings about a happy ITM and a sad ITM (order randomized), separated by a neutral fact (evoked emotions rated ≤2). Each balance condition lasted about 6 minutes, with the participant focusing on each ITM cue (happy, neutral, sad) for 2 minutes.

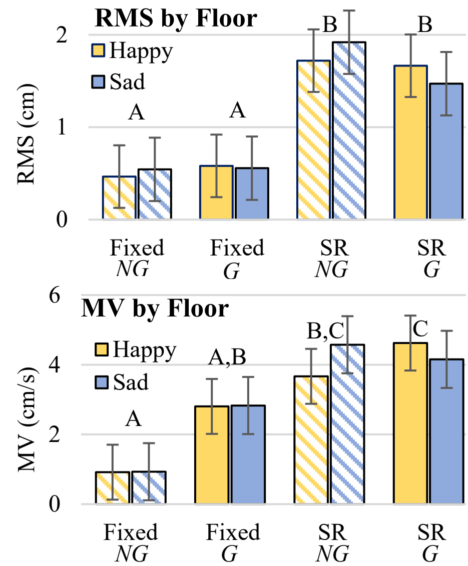

Fig 1: Averaged results separated by participant type, floor, and ITM. Significance marked by letters. Error bars are standard error.

Center-of-pressure (COP) data were collected at a sampling frequency of 1000 Hz and filtered using a 4th order Butterworth filter with a cut-off frequency of 2.5 Hz. Root-mean-square (RMS) and mean velocity (MV) of the anterior-posterior COP data were calculated and transformed using a Box-Cox transformation to ensure normality assumptions were met. Mixed linear regression models were constructed, with fixed effects of *floor, vision, ITM, patient* group, and the first order interactions, with *subject* as a random effect; dependent variables were transformed RMS and MV, fit separately. Statistical significance was set at α=0.01 to reduce chances of type I errors. Post-hoc student's t-tests were conducted with α=0.05.

Results & Discussion: The MV model revealed *floor* (*p<0.0001*) and *floor x patient* (*p=0.01*) were significant. Post-hoc analyses revealed that fixed floor resulted in significantly smaller MV values than SR floor, within each patient group and across groups (Fixed-NG vs SR-NG *p<0.0001*, Fixed-G vs SR-G *p<0.0001*, Fixed-NG vs SR-G *p=0.04*). This also occurred in the RMS model (*floor p<0.0001* and *floor x patient p=0.01).* RMS was significantly smaller during fixed floor than SR floor across and within groups (Fixed-NG vs SR-NG *p<0.0001*, Fixed-G vs SR-G *p<0.0001*, Fixed-NG vs SR-G *p=0.006*, Fixed-G vs SR-G *p=0.002*). In both models, *vision, ITM,* and the other interactions did not reach significance. It is worth noting a trend in *ITM, patient,* and *floor* is emerging (***Fig 1***). During the SR floor condition, the control participants had larger RMS and MV values during sad ITM than during happy ITM, but the glaucoma group had the opposite trend, where happy ITM resulted in larger values than sad ITM. This may indicate a previously unobserved relationship between mood and balance in people with glaucoma that impacts balance performance during sensory challenging conditions. There was also a *patient* trend in MV during the fixed floor condition: the glaucoma group had larger MV than the control group. Together, these results indicate that somatosensory input is an important factor in postural control in glaucoma.

Significance: As this study continues, the contribution of emotions to balance performance in those with glaucoma, and how that differs from those without glaucoma, will continue to emerge. This knowledge may be useful in reducing fall risk in adults with glaucoma.

Acknowledgements: Bioengineering in Psychiatry T32 Fellowship & Lendvay-Newton Balance Disorder Research Philanthropic Gift

References: [1]Lamoureux et al., 2008. *Invest Ophthalmol Vis Sci*. 49(2). [2]Ramulu, 2009. *Curr Opin Ophthalmol*. 20(2). [3] Biderman et al., 2002. *Journal of Epidemiology and Community Health*. 56(8). [4] Kang and Gross, 2016. *J Biomech*.. 49(16). [5] Andreescu et al., 2011. *Depress Anxiety*. 28(3).

ENHANCING COMFORT AND FUNCTIONALITY: A CROSS-OVER RANDOMIZED CONTROLLED TRIAL INVESTIGATING THE EFFECTS OF AN INNOVATIVE FOOTWEAR INTERVENTION ON PAIN REDUCTION AND FUNCTIONAL PERFORMANCE

MG Finco, Myeounggon Lee, Nesreen El-Refaei, Anmol Momin, Bijan Najafi
Department of Surgery, Baylor College of Medicine, Houston, TX, USA
*Corresponding author's email: Graci.Finco@bcm.edu

Introduction: As we age, our feet tend to flatten and the fat padding on the soles of our feet becomes stiffer, leading to excessive foot pronation and resulting foot pain [1]. It is estimated that this affects approximately 24% of older adults [2]. In this study, we evaluated the effectiveness of an innovative footwear intervention (Orthofeet, NY, USA) [3] designed to address these issues and improve foot function. Specifically, Orthofeet is designed to enhance arch support, align the body, and prevent excessive pronation, potentially reducing foot pain. We hypothesized older adults wearing innovative shoes designed to reduce foot pain, compared to those who wore their own shoes, would show improvements in self-reported foot function, faster walking speeds, and longer stride lengths.

Methods: People over the age of 50 years with self-reported moderate to severe foot pain were included (IRB #:H-51229, Clinical Trial#: NCT05434078). Participants were randomized into control and intervention groups, and were assessed at baseline and 6-week visits. Participants in the control group wore their own shoes at both baseline and 6 week visits. Participants in the intervention group wore their own shoes at the baseline visit, were given the intervention shoes and asked to wear them for the subsequent 6 weeks, and returned wearing the intervention shoes for their 6-week visit. Demographics were collected at baseline. At both visits, self-reported foot function according to the Foot Functional Index (FFI) and gait characteristics according to wearable sensor-derived data, were collected. Gait characteristics included stride velocity and stride length at the participant's habitual walking speed over a 10-meter level-ground walkway. This was completed for single-task (ST) walking and dual-task (DT) walking (participant also counted backwards aloud). General linear modelling was used to compare within (repeated measures) and between (generalized estimating equations) groups. Significance of $p<0.05$ was considered statistically significant. Partial eta squared (η_p^2) determined effect sizes.

Results & Discussion: Data from 38 participants (19 in each group; 5 males; 63.5 ± 6.8 years of age) were included in the analyses.

Table 1. Within and Between-Group Comparisons

	Control Group (n=19)				Intervention Group (n=19)				Group effects
	Baseline	6-week	*p*-value	η_p^2	Baseline	6-week	*p*-value	η_p^2	*p*-value
FFI Pain Score	49.3±15.9	41.2±20.9	0.078	0.107	34.0±12.6	21.6±14.7	**<0.001***	0.238	**<0.001***
FFI Disability Score	49.1±26.3	38.2±20.7	**0.002***	0.384	33.5±23.1	21.9±20.9	**<0.001***	0.471	**0.037***
FFI Limits in Activity Score	15.1±12.7	14.3±8.0	0.116	0.081	12.4±10.6	10.3±9.2	0.085	0.360	0.483
FFI Total Score	113.5±50.6	86.5±36.8	**0.005***	0.381	87.0±53.8	53.8±41.3	**<0.001***	0.378	**0.004***
ST Stride Velocity (m/s)	0.99±0.2	1.13±0.2	**0.021***	0.263	1.03±0.2	1.13±0.2	**<0.001***	0.544	0.723
ST Stride Length (m)	1.12±0.2	1.24±0.2	**0.002***	0.412	1.12±0.1	1.21±0.2	**0.039***	0.253	0.962
DT Stride Velocity (m/s)	0.84±0.3	1.04±0.2	**0.028***	0.240	0.90±0.2	1.04±0.2	**0.004***	0.437	0.585
DT Stride Length (m)	1.09±0.2	1.19±0.2	0.050	0.197	1.12±53.8	1.16±0.2	0.262	0.083	0.981

Table 1: Mean ± standard deviations. Significance (bold, *)= $p<0.05$. FFI=Foot Functional Index, ST=single-task, DT=dual-task, Int.=Intervention, m=meters, s=seconds. Partial eta squared (η_p^2) determined effect sizes.

Table 1 presents significant improvements in foot function, faster stride velocity, and longer stride lengths at 6-week compared to baseline in both control and intervention groups. The intervention group showed significant reductions in FFI Pain Score, while the control group did not. While both control and intervention groups exhibited a significant time effect, the intervention group showed larger effect sizes indicative of greater improvement. Between-group differences showed that the intervention group had significantly more foot function than the control group, with the exception of FFI Limits in Activity Score. Supportive of our hypothesis, the intervention group showed more pronounced improvements in foot function, walking speed, and stride lengths with the innovative shoes compared to controls who wore their own shoes.

Significance: While both groups showed significant improvements, the intervention group showed more pronounced improvements in foot function, stride velocity, and stride length than the control group. Ultimately, these innovative shoes could be recommended to older adults to help improve foot function and gait characteristics. This clinical trial is still recruiting participants. Future work will determine if these results are generalizable to a larger sample size, and examine the crossover effect.

Acknowledgements: Thanks to Josh White and Ron Bar from Orthofeet for providing the shoes used in this study.

References: [1] Neville et al. (2020), *J Am Podiatr Med Assoc* 110(5); [2] Muchna et al. (2018), *J Am Podiatr Med* 108(2); [3] Innovative shoes provided by the company Orthofeet.

TIBIAL ACCELERATION COMPLEXITY VIA IMUS ON VARIOUS TURF SURFACES

Joshua M. Lardie[1*], Jake A. Melaro[1], Kyley H. Dickson[2], John C. Sorochan[2], Joshua T. Weinhandl[1]
[1]Kinesiology, Recreation, and Sport Studies, University of Tennessee, Knoxville, TN
[2]Department of Plant Sciences, University of Tennessee, Knoxville, TN

*Corresponding author's email: jlardie@vols.utk.edu

Introduction: The use of synthetic turf fields has increased over recent years due to increased durability, decreased maintenance, and reduced environmental effects compared to natural turfgrasses [1]. A consensus has not been reached, however, on the impact of synthetic turf on musculoskeletal injury rates [2]. Lower-extremity injuries have been assessed and correlated via tibial shock measured accelerometry [3, 4]. The ability to quantify the complexity in a movement of a biological system using entropy analysis may highlight the differences between greater injury risk factors, disease states, or levels of experience in training [5, 6]. Therefore, the purpose of this study is to determine if the tibial acceleration complexity changes on various turf surfaces. We hypothesize that there will be no significant differences in tibial acceleration complexity between surfaces.

Methods: 24 healthy participants (13 males, mass: 71.15kg ± 12.98, height: 1.73m ± 0.11) performed a variety of drills to show dynamic sprinting, change of direction, lateral agility, and single leg bounding. This included a self-selected jog, the M-drill, the 5-10-5 drill, and triple hop. The M drill navigated 5 cones, 5 meters from one another, in the shape of an uppercase M with focus on change of direction at each vertex, completed in both directions. The 5-10-5 consisted of a lateral shuffle 5 meters to the right, then 10 meters to the left, followed by 5 meters back to the original starting position. Triple hop began on a single leg and 3 bounds were taken, with the final landing position maintained, completed on both legs as well. Each set of drills were completed on 3 different surfaces: synthetic turf, warm season turfgrass, and cool season turfgrass. The synthetic turf (SYN) was a 3rd generation synthetic turf with a crumb rubber infill and a foam-based shock pad underneath. The warm season turfgrass was Bermuda (BER) and the cool season turfgrass was Kentucky Blue Grass (KBG). IMUs (IMeasureU, Auckland, New Zealand) were used with a rubber strap secured to the medial & distal tibia, superior to the medial malleolus. Participants were shown a demonstration of the drill and provided with verbal instructions. All drills were performed in participants non-provided athletic shoes. Data processing and statistical analysis took place in Python (3.10.7). Acceleration due to gravity was removed and oversaturation of the low G sensors was replaced with the output of the high G sensors [7]. Data was down sampled from 1000Hz to 100Hz [5]. The complexity index (CI), or area under the curve of multiscale entropy, was calculated using sample entropy of the resultant tibial accelerations. Multiple one-way repeated measures ANOVA ($\alpha = 0.05$) were conducted to compare the effect of SYN, KBG, and BER on tibial acceleration CI by turf of each leg. If significance was discovered, a Tukey's HSD post-hoc analysis was performed to determine the significant group differences.

Results & Discussion: There were no significant differences between tibial resultant acceleration CI for surfaces for all tasks for both legs. Right leg triple hop showed significance between the SYN and KBG surfaces but failed to pass the assumption of sphericity. This was adjusted using a Greenhouse-Geiser correction, resulting in no significant difference [$F(2,46) = 3.05$, $p = 0.07$]. Table 1 refers to the CI average and standard deviations.

Table 1: Complexity average and standard deviation for left and right tibial resultant accelerations for each task on each surface.

	Task	Left	Right
SYN	**5-10-5**	6.86 ± 6.92	9.50 ± 7.99
	DNB	19.95 ± 11.97	25.63 ± 9.35
	M-Drill	7.65 ± 6.40	12.91 ± 10.98
	TH	4.57 ± 2.64	3.13 ± 2.02
KBG	**5-10-5**	7.11 ± 6.43	5.87 ± 5.89
	DNB	24.31 ± 10.39	27.20 ± 6.35
	M-Drill	6.52 ± 5.46	7.68 ± 6.59
	TH	6.01 ± 3.69	4.75 ± 2.65
BER	**5-10-5**	6.62 ± 5.82	7.84 ± 6.58
	DNB	25.46 ± 9.74	26.42 ± 7.76
	M-Drill	8.51 ± 8.07	9.32 ± 8.95
	TH	6.16 ± 2.95	4.19 ± 2.05

Significance: A change in CI has been associated with fatigue (decreased CI) and can be used to identify trained versus untrained runners [8]. Those with movement disorders can be identified based on CI compared to healthy controls. A sudden change or decrease may serve as a warning of a detrimental change in the athlete's biological system [5]. The greater CI is typically a characteristic of a healthy system and higher adaptive capacity [9]. Our findings help support that synthetic turf does not significantly alter the tibial accelerations during change of direction movements, lateral shuffling, or single leg support during dynamic athletic movement. Future research is needed on more heavily trafficked surfaces, more athletically trained populations, as well as additional drills and surface types.

References: [1] Elvidge et al. (2022), *Footwear Science* 14(3). [2] Gould et al. (2022), *Foot & Ankle Ortho* 7(1). [3] Milner et al. (2006), *MSSE* 38(2). [4] Shelburne et al. (2004), *J Biomech* 37(3). [5] Gruber et al. (2021), *F Sprt Act Living* 3. [6] Schutte et al. (2018), *Gait Posture* 59. [7] van Hees et al. (2013), *PLOS* 8(4). [8] Parshad et al. (2012), *Math Biosci Eng* 9(1). [9] Costa et al. (2002), *Phys Rev Lett* 89(6).

STRIDE TO STRIDE VARIABILITY THROUGHOUT A PROLONGED TREADMILL WALK

Athulya A. Simon*, Kiichi Ash, Katherine A. Boyer
Department of Kinesiology, University of Massachusetts Amherst, USA
*Corresponding author's email: athulyasimon@umass.edu

Introduction: An increase in variability of gait characteristics such as stride length and width have been associated with increased fall risks in older adults [1]. Gait alterations in older adults due to muscle weakness and neural changes with age may be further compounded by muscle fatigue [2]. Muscle fatigue associated with activities of daily living may also exacerbate mobility deficits in older adults. Prior work has found that a 30-min treadmill walk (30MTW) can induce knee extensor muscle fatigue that results in greater changes in gait mechanics for older as compared to younger adults [3]. Muscle fatigue induced by a repeated sit-to-stand task is shown to alter gait stability by increasing step width and step length variability [4]. With respect to age, stride to stride variability in response to the fatiguing walk is not known. The aim of this study was to quantify age-related differences in both mean values and stride to stride variability of spatiotemporal gait parameters (stride time, step length, and step width) and center of mass (COM) motion throughout a 30MTW. We hypothesized that older adults, as compared to younger adults, would experience greater increases in mean values and greater increases in stride to stride variability in response to the 30MTW.

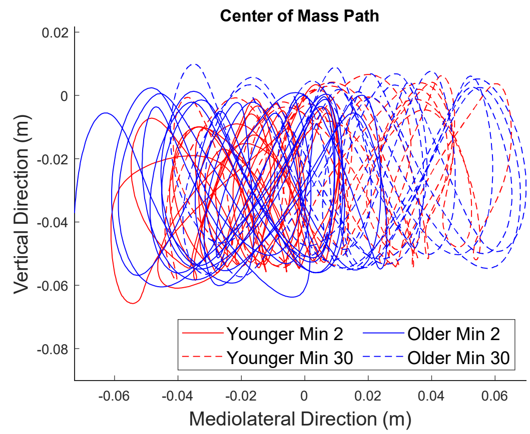

Figure 1: Sample participants' COM path projected into the frontal plane.

Methods: Motion capture data were collected on 7 younger (Y; 36.7 ± 3.4 years, 2 female) and 8 older (O; 71.5 ± 1.2 years, 4 female) healthy adults during a 30MTW at a preferred speed. Data were collected at 200 Hz in 10 second increments at minutes 2, 10, 18, and 30. At minutes 7, 14, and 20 the treadmill was raised to a 3% incline for a 1-minute challenge period to mimic environmental challenges. Motion capture markers were placed on the pelvis (left and right PSIS and sacrum) and feet to estimate center of mass (COM) motion and calculate spatiotemporal gait parameters. The university IRB approved all procedures.

Heelstrike timepoints, calculated from the velocity of the foot markers, were used to segment out individual strides. COM position was calculated as the average position of the pelvis markers. COM path length is the total 3D distance travelled by the COM in a complete stride. ROM corresponds to the anteroposterior (AP), mediolateral (ML), and vertical ROM of the COM. Mean and max acceleration of COM are calculated from the 2nd derivatives of the COM position data. Step length and width were normalized to leg length. The coefficient of variation (COV), the measure of stride to stride variability, was calculated for all variables using the mean and standard deviation of the respective measures. The mean and COV were compared between age groups and across time using repeated measures ANOVAs with $\alpha \leq 0.05$. Post-hoc analyses were run where significant interaction effects were found.

Results & Discussion: The impact of the 30MTW was similar for younger and older adults with only time effects seen for vertical ROM ($F(3,39)=24.95$, $p<.0001$), COM path length ($F(3,39)=22.83$, $p<0.0001$), step width ($F(3,39)=3.43$, $p=0.03$), and mean COM acceleration ($F(3,39)=9.86$, $p<0.0001$). For the vertical ROM (Fig. 1) and COM path length there was a slight increase over time, while the step width decreased over time. Of note, the mean COM acceleration only increased from minutes 2 to 10 ($F(1,13)=9.24$, $p=0.0095$) and then had no significant changes ($F(2,26)=0.27$, $p=0.7667$) at the remaining timepoints. This may be due to participants adapting to walking on a treadmill. Age effects were seen for the AP ROM ($F(1,13)=5.43$, $p=0.0365$), where younger adults had a greater ROM compared to older adults suggesting greater movement about the treadmill belt. Age x time interaction effects were seen for stride time ($F(3,39)=7.33$, $p=0.0005$). The older adults increased their stride time ($F(3,21)=8.89$, $p=0.0005$) over the course of the 30MTW while younger adults did not significantly change ($F(3,18)=2.31$, $p=0.1109$). The treadmill speed remains fixed, therefore an increase in stride time suggests the older adults are shifting to a slightly slower stride frequency, possibly due to fatigue. No significant differences were found for the COVs suggesting that there is minimal change in stride to stride variability over the course of the 30MTW.

Few differences were found in the mean values of the spatiotemporal parameters or COM motion between the younger and older groups. On average the physical activity of the older group was much higher than the younger group and neither group exhibited any mobility deficits on a standardized physical performance battery. Together with the lack of differences in any of the gait variability measures perhaps it is not surprising that there was not a difference in the response to the 30MTW. In the future, as our sample size increases, we plan to separate our older population into subsets based on activity and mobility levels as our active older adults may be too similar to our younger adults.

Significance: Maintaining mobility is fundamental to extending our healthspan. Walking is a possible exercise to maintain mobility and the lack of significant change in variability over time suggests that for healthy active adults prolonged treadmill walking does not elevate falls risks as a function of walk duration.

Acknowledgements: This work was supported by NIH R01 AG068102

References: [1] Maki (1997), *J Am Geriatr Soc* 45(3) [2] Kent-Braun et al. (2014), *Muscle Nerve* 49(2); [3] Hafer J and Boyer K. (2020), *J App Biomech* 36(3); [4] Helbostad et. Al (2007) *J Gerontol A* 62(9)

ANALYZING INTRALIMB GAIT COORDINATION IN STROKE SURVIVORS: A MODIFIED VECTOR CODING TECHNIQUE TO COMPARE PARETIC AND NON-PARETIC SIDES

Nikolaos Aggelousis[1*], Christos Kokkotis[1], Evangeli Karampina[1], Evangelos Karakasis[1], Maria Protopapa[1], Suzana Kordosi[1], Giorgos Giarmatzis[1], Konstantinos Vadikolias[2]
[1]Department of Physical Education and Sport Science, Democritus University of Thrace, Greece
[2]Department of Medicine, Democritus University of Thrace, Greece
*Corresponding author's email: nagelous@phyed.duth.gr

Introduction: Stroke survivors' paretic limb is frequently marked by diminished strength, restricted range of motion, and spasticity, which may contribute to differences in intralimb gait coordination between their paretic and non-paretic sides. These differences can result in an uneven and inefficient gait pattern, leading to further mobility impairments and an increased risk of falls. Understanding the underlying mechanisms and addressing these differences through targeted rehabilitation interventions is essential for improving outcomes for individuals with stroke.

Previous research on intralimb gait coordination of stroke survivors revealed spatiotemporal asymmetries and reduced bilateral coordination between the paretic and non-paretic limb. A recent study utilized the vector coding method to investigate coordination in the sagittal plane during gait in stroke survivors. This study demonstrated a shift towards proximal control during the stance phase of both legs, and an inability to separate segment coordination during the swing phase of the affected limb [1]. The current study aims to expand on the previous research by utilizing a modified vector coding technique to analyze intralimb gait coordination across all planes of motion in chronic stroke survivors. Our hypothesis was that there would be similarity in intralimb coordination between the paretic and non-paretic limbs, as human gait is bipedal in nature. However, we expected to observe greater coordination variability in the paretic limb because of its motor control deficits.

Methods: Eight chronic stroke patients having mild right paresis voluntarily participated in the study. Position-time data and ground reaction forces were recorded using a 3D-motion capture system consisting of 10 infrared cameras (Vicon) and an instrumented treadmill (Bertex) with a sampling rate of 100 and 1000 Hz, respectively. Retro-reflective markers were also attached to specific body landmarks according to the Conventional Gait Model 2.4 full body marker protocol. Each participant was requested to walk on the treadmill at their preferred walking speed, and data were collected for 10 successive gait cycles for each limb. After filtering, the kinematic data was normalized to represent 100% of the gait cycle, which was defined as the period between foot strikes of the same limb. A modified vector coding (VC) technique [2] was used to quantify thigh-shank and shank-foot intralimb coordination in both limbs during gait.

Results & Discussion: Mean (± SD) values of frequency of the four coordination patterns for thigh-shank and shank-foot couplings throughout the gait cycle are presented in Fig 1. During the gait cycle, there were no significant differences found in the frequency of coordination patterns between the thigh-shank and shank-foot coupling angles of the paretic and non-paretic limbs, as indicated by the ANOVA results. This could be attributed to the improvement of intralimb coordination in the paretic limb that could have resulted from the repetitive practice of gait-specific movements and/or the use of auditory cues as part of their rehabilitation interventions.

Furthermore, no significant differences in coordination variability were observed between the paretic and non-paretic limbs for any segment-segment coupling as revealed by the statistical parametric mapping analysis. Our hypothesis was contradicted by this finding, which could be attributed to the significant inter-individual variability observed in both limbs.

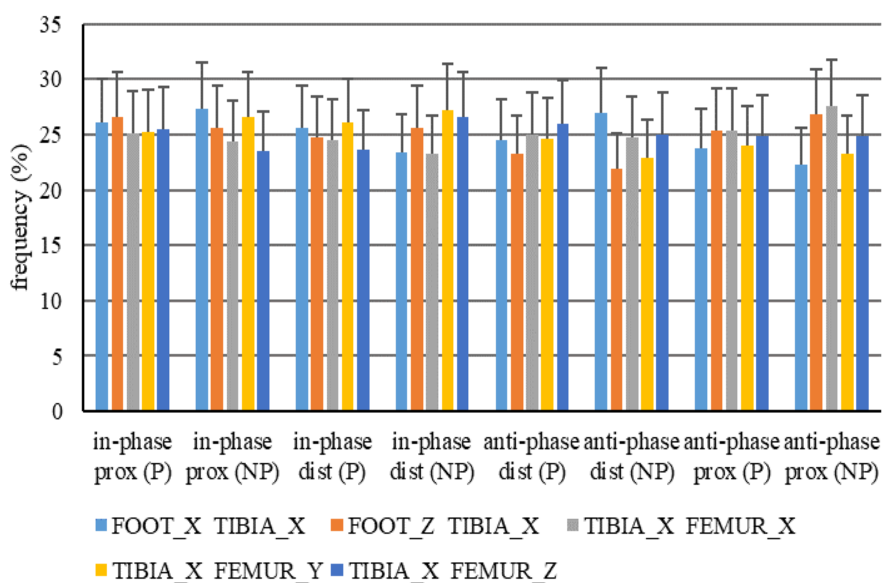

Figure 1. Mean (±SD) values of frequency of coordination patterns for the thigh-shank and shank-foot coupling angles during the gait cycle.

Significance: Using the VC technique to measure the variations in intralimb coordination between the paretic and non-paretic sides can provide valuable insights for designing efficient rehabilitation programs for stroke survivors.

Acknowledgements: This work was supported by grant MIS 5047286 from Greek and European funds (EYD-EPANEK).

References: [1] Celestino et al. (2019), *Hum Mov Sci* 68; [2] Needham et al. (2015), *J Biomech* 48(12)

VALIDATION OF BPNET FOR HUMAN MOTION DATASET PREPARATION FOR GAIT FEATURE EXTRACTION

Bibash Lama[1], Jaerock Kwon[2], Yunju Lee[1,3*]

[1]School of Engineering, Grand Valley State University, Grand Rapids, MI, USA

[2]Department of Electrical and Computer Engineering, University of Michigan, Dearborn, MI, USA

[3]Department of Physical Therapy and Athletic Training, Grand Valley State University, Grand Rapids, MI, USA

*Corresponding author's email:leeyun@gvsu.edu

Introduction: Detection of accurate key joint positions during normal human motion is critical for the development of intelligent systems that can recognize individuals based on their unique gait pattern, with applications in fields such as sports science, medical diagnosis, security, and surveillance. Deep learning excels in detecting key joint positions and has a significantly greater potential for extracting human gait features, making it a promising tool for integrating gait analysis into real-world applications [1]. Deep learning frameworks such as NVIDIA TAO offer the opportunity to develop customized models based on our own dataset and adapt them to our purpose, including human key point detection. The objective of this study was to develop and validate the platform using the NVIDIA TAO for accurately inferring human body joint positions from 2D images without using markers and the high-tech motion capture system. To achieve the goal, we collected a high-resolution dataset using a 3D motion capture system. The dataset consisted of 2D images from three different view angles: 0, 45, and 90 degrees with 3D ground truth positions of human body joints. Also, the study aimed to improve the accuracy of the machine learning model using high-resolution human motion datasets synchronized in 2D and 3D, and to complete the pilot study to investigate the feasibility of the prediction models of the inference engine using newly created datasets.

Methods: The 3D ground truth data were obtained for 25 human subjects using VICON system (5 trials of 2~3 seconds walking per each subject at 120 Hz) and three RGB cameras (30 Hz) positioned at three different angles (0, 45, and 90-degree angles) relative to the subjects to simultaneously capture 2D images. Total images of 21,500 were collected and annotated for key points. Calibration matrixes estimated using Zhang's Method [2] were used to compute the 2D projected points for all captured images. The annotated key point positions extracted from those images were used to prepare the dataset for 2D feature detection. The NVIDIA TAO's Body Pose Net (bpnet) was used to train two neural network models using two sets of data: one with publicly available COCO-2017 dataset [3], and our purposed dataset (3D joint positions using VICON and images from RGB cameras in three different angles). To validate that our dataset improved a neural network model, we evaluated the estimation accuracies of the two trained models by comparing predictions with the projected points obtained from the VICON system as ground truth values.

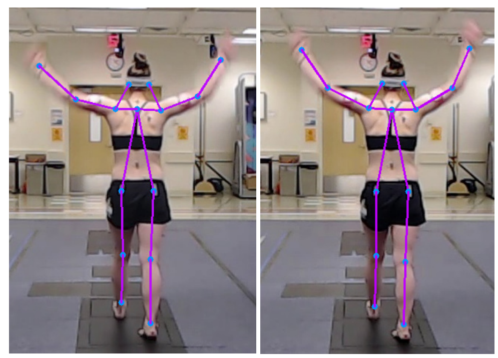

Figure 1: Human motion detection results of two trained models are shown in each joint position during gait. (Left: with the proposed dataset vs. Right: COCO-2017 dataset.)

Results & Discussion: Two bpnet models were successfully trained with one model trained using the COCO-2017 dataset and the other using the proposed dataset. The performance metric used was Mean Per Joint Position Error (MPJPE). The results of the study show that the MPJPE (mean ± SD) for the COCO-2017 trained model was 12.27 ± 11.27 mm, while the model trained with the proposed dataset yielded 18.24 ± 14.38mm. The average MPJPE values for each joint were further categorized into upper body and lower body joints. Specifically, the MPJPE value recorded for the COCO-2017 trained model was 15.08 ± 17.39 mm for the upper body and 9.47 ± 5.16 mm for the lower body. On the other hand, the MPJPE value recorded for models trained with the proposed dataset was 26.19 ± 20.62 mm for the upper body and 10.29 ± 8.15 mm for the lower body. Overall, the results suggested that the proposed dataset was able to achieve comparable results with the COCO-2017 dataset. Importantly, the proposed dataset was able to achieve the similar results as the COCO dataset using only one-fourth the number of images, thereby saving a significant amount of computational time and resources. It is anticipated that with the inclusion of more data, the proposed dataset would achieve greater accuracy.

Significance: The human motion dataset we collected and the proposed integrated framework for estimating key joint positions are unique because the dataset is (1) higher resolution than other datasets such as Human3.6M [4], Microsoft COCO [5], and MARS [6], (2) a specific motion focused on gait, so that the integrated framework would have a higher accuracy in predicting key joint positions for gait motions in 3D from the 2D video images, thus (3) the integrated prediction system can be used to re-identify people by their gait pattern in view-invariant and markerless settings, which are common in practical cases. The applied cases can be (1) identification of a person from CCTV video footage without worrying about privacy issues since no facial identity is required and (2) detection of concussion of players by temporal analysis of their gait pattern during a game in a non-invasive way since the proposed system does not require markers or any sensors on the players.

References: [1] Sepas-Moghaddam et al. (2023), *IEEE Trans. Pattern Anal. Mach. Intell.* 45(01); pp.264-284

[2] Zhang (2000), *IEEE Trans. Pattern Anal. Mach. Intell.* 22(11); pp. 1330-1334.

[3] https://cocodataset.org/#download

[4] Ionescu et al. (2013), *IEEE Trans. Pattern Anal. Mach. Intell.* 36(7); pp. 1325-1339.

[5] Lin et al. (2014), *European Conference on Computer Vision*, pp 740–755.

[6] Zheng et al. (2016), *European Conference on Computer Vision*. (http://zheng-lab.cecs.anu.edu.au/Project/project_mars.html)

THE IMPACT OF BIOFEEDBACK ON LIMB STIFFNESS AND KNEE JOINT POWER IN ACLR PATIENTS

Bryana N. Vasquez[1*], Michael A. Teater[1], Sara L. Arena[1], and Robin M. Queen[1]
[1]Department of Biomedical Engineering and Mechanics, Virginia Tech, Blacksburg, VA
*Corresponding Author's Email: bvasquez@vt.edu

Introduction: In the first year following anterior cruciate ligament reconstruction (ACLR), athletes are 15 times more likely to sustain a second ACL injury when compared to a non-injured athlete [1]. Many of the athletes who are cleared to return to sport (RTS) display muscle weakness in the surgical limb and asymmetrical loading patterns during dynamic movements, which increases their risk of re-injury [2, 3]. Following ACLR, patients will commonly experience decreased voluntary muscle activation, resulting in increased muscle stiffness and limited eccentric activation of the quadricep muscles, both of which play an important role in knee joint stability during landing [4, 5]. A biofeedback intervention focused on neuromuscular control has the potential to improve these biomechanical measures during the rehabilitation process. Therefore, the purpose of this study was to determine the impact of a biofeedback intervention on surgical limb stiffness and eccentric knee joint power among patients following ACLR during the landing phase of a stop-jump task. It was hypothesized that following the completion of a biofeedback intervention, the biofeedback group would have decreased surgical limb stiffness and increased surgical limb eccentric knee power compared to controls.

Methods: The ACL-Biofeedback Trial was an assessor-blinded, single-center, parallel design randomized controlled trial (ClinicalTrials.gov: AR069865), with participants following an ACLR and intending to RTS randomized into a biofeedback (BF) or attention control (C) group (n=40; 18 BF, 22 C) [2]. The BF group underwent a 6-week training program that involved visual and tactile feedback during a series of controlled squats while the C group completed several online and in-person educational sessions. Each participant completed 10 stop-jump landing trials prior to (pre), immediately after (post), and 6 weeks after (ret) both interventions concluded. The 3D marker data from a modified Helen-Hayes marker set [6] was collected at 240 Hz using a 10-camera motion capture system (Qualisys, Gothenburg, Sweden) and the ground reaction forces (GRF) were collected at 1920 Hz from embedded force plates (AMTI, Watertown, MA, USA). The data was processed in Visual 3D (C-Motion, Bethesda, MD, USA) and imported into a custom MATLAB (MathWorks, Natick, MA, USA) script for analysis. Peak resultant GRF (peak rGRF) was normalized by the resultant kinetic energy at initial contact [7]. Limb stiffness was then defined for the surgical limb as the ratio of normalized peak rGRF to change in limb length from initial contact to peak rGRF. Additionally, peak eccentric knee joint power (EccKP) was quantified during landing and normalized by body weight. A linear mixed effects model (p<0.05) was used to examine the effect of an intervention (BF, C) and time (pre, post, ret) on normalized peak rGRF, change in limb length, limb stiffness, and EccKP. Due to the non-normal distribution of residuals for surgical limb stiffness and normalized peak rGRF, the analysis was performed on the ranks. The Cohen's d effect size was calculated by BF compared to the C group and considered small, medium, or large if the value exceeded 0.2, 0.5, or 0.8, respectively [8]. All analyses were completed in JMP Pro 16 (SAS Institute Inc., Cary, NC, USA).

Results & Discussion: All 40 participants were present for the pre-intervention assessment. Four BF participants and two C participants did not complete post and ret assessments, and one C participant was removed from ret testing due to data collection errors. Normalized peak rGRF, change in limb length, and limb stiffness (Table 1) were not significantly different between groups (p>0.090), nor did they significantly change with time (p>0.270). There was no increase in EccKP for the BF group compared to the C group (p=0.529, d=-0.203), however, there was a main effect of time on EccKP (p=0.002). A Tukey's HSD analysis indicated a difference in EccKP between pre and ret (p=0.001), with the knee power increasing by 18.5%. Contrary to our hypotheses, our results suggest that biofeedback training with squats did not result in changes to limb stiffness during landing, but that over time, the eccentric action of the quadriceps improved independent of the intervention. Participants were given real-time biofeedback on squats during the intervention, and while this type of eccentric motion is similar to the stop-jump tasks assessed at each time point, differences in speed and power between landing and squatting may make it difficult to transfer biomechanical improvements between these tasks to alter landing mechanics.

Table 1: Summary of Intervention Results

Variable	Biofeedback	Control	Cohen's d
Normalized Peak rGRF (N/J)	0.508 ± 0.15	0.471 ± 0.1	0.296 (small)
Change in Limb Length	0.052 ± 0.02	0.058 ± 0.02	-0.367 (small)
Limb Stiffness (N/J)	11.7 ± 4.9	9.39 ± 3.7	0.522 (medium)
Peak Knee Power (W/kg)	14.8 ± 5.3	16.0 ± 6.8	-0.203 (small)

Significance: Efforts to restore surgical limb stiffness and knee power during landing are important for athletes following ACLR to return to sport successfully by reducing their risk of re-injury, which in turn will reduce the healthcare costs associated with ACLR. Biofeedback interventions aimed at improving surgical limb neuromuscular control can still be a beneficial contribution to an athlete's rehabilitation program following ACLR, but ultimately may be task-specific and require a larger enrollment as we did not find any improvements in limb stiffness or eccentric knee power in the biofeedback group when compared with the attention control program.

Acknowledgments: The author would like to acknowledge Alexander Peebles for his contributions to data collection. Support for this study was provided by grants from the National Institutes of Health: R21AR069865-01A1.

References: [1] Paterno (2015), *J Athl Train.* 50(10); [2] Queen et al. (2021), *CCTC* 100769; [3] Paterno et al. (2014), *Clin J. Sport Med.* 22(2); [4] Granata (2002), *J Electromyogr Kinesiol.* 12(2); [5] Ward et al. (2018), *J Athl Train.* 52(2); [6] Renstrom et al. (2008), *Br J Sports Med.* 42(6); [7] Mesisca et al. (2021), *Clin Biomech*. 105443; [8] Lakens (2013), *Front Psychol.* 863.

EFFECTS OF CUSTOM DYNAMIC ORTHOSIS PROXIMAL CUFF DESIGN ON FOOT LOADING

Jason M. Wilken[1*], Sara Magdziarz[1], Kirsten M. Anderson[1], Molly S. Pacha[1], Donald D. Anderson[2]
[1]Department of Physical Therapy and Rehabilitation Science, The University of Iowa, Iowa City, IA
*Corresponding author's email: jason-wilken@uiowa.edu

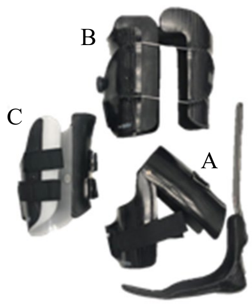

Figure 1: Participants walked with no CDO and 3 CDOs with different proximal cuff designs.

Introduction: Carbon fiber custom dynamic orthoses (CDOs) consist of a proximal cuff that wraps around the lower leg below the knee, a posterior carbon fiber strut, and a semi-rigid footplate. CDOs have been shown to reduce forces acting on the foot, improve function, and reduce pain for individuals with lower extremity impairments.[1,2] During gait, forces are transferred away from the foot to the tibia through the proximal cuff, which may explain observed improvements in pain and function.[1] Up to 60% offloading has been reported with robust CDOs using a proximal cuff specifically designed to offload the limb.[1] However, it is unknown if or how proximal cuff design influences offloading. The effects of proximal cuff design on peak and cumulative foot loading during gait were investigated in this study.

Methods: Activities were approved by the local Institutional Review Board and all participants provided written informed consent. 5 individuals with no history of function limiting lower extremity injuries (3Male/2Female, 45.6(16.5)yrs, 1.78(0.08)m, 73.1(3.1)kg) and 1 individual who had experienced an intra-articular ankle fracture in the last five years and had elevated articular contact stress (1Female, 59yrs, 1.74m, 80.8kg) participated.[3] *CDO conditions*: Participants completed testing without a CDO (NoCDO) and with CDOs that had the same footplate and posterior strut but different proximal cuff designs in a randomized order (Figure 1): clamshell cuff connected by a Chicago screw and secured with Velcro (CDOA), clamshell cuff secured with a BOA dial (CDOB), clamshell cuff secured with Velcro (CDOC). *Procedures*: Loadsol insoles (Novel Electronics) were used to measure forces between the foot and the shoe (NoCDO) or the foot and the footplate (CDOA/B/C) as participants walked at a controlled speed.[4] *Data Analysis*: Data were processed in Visual 3D (C-motion Inc.) and Matlab R2020 (The MathWorks Inc.). Average peak and cumulative loading from a minimum of five walking trials were calculated for the hindfoot, forefoot, and midfoot (proximal 30%, middle 30% and distal 40% of insole, respectively), and all regions (total foot). Cumulative loading was calculated as the indefinite integral over the stance phase of gait.

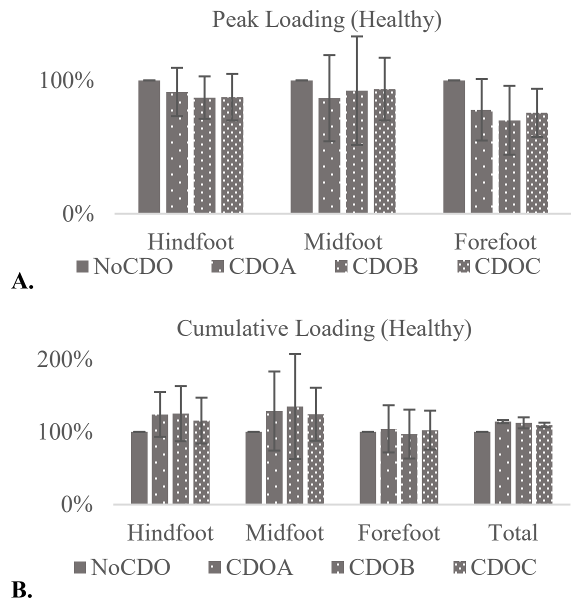

Figure 2: Peak (A) and cumulative (B) hindfoot, midfoot, forefoot, and total foot loading for healthy participants.

Results & Discussion: For healthy individuals, peak forefoot and hindfoot forces with the CDO decreased by more than 22% and 8%, respectively, compared to walking without a CDO (Figure 2A). Cumulative loading increased for multiple cuff conditions and regions compared to walking without a CDO (Figure 2B). Similar peak offloading was seen for the participant who had experienced an intra-articular ankle fracture (Figure 3). The study CDOs reduced forces under the foot to a lesser extent than those previously investigated.[1] Previous work has shown that the center of pressure travels a shorter distance when walking with a CDO than without, which may explain the increased cumulative loading observed in the hindfoot and midfoot in some conditions.[1]

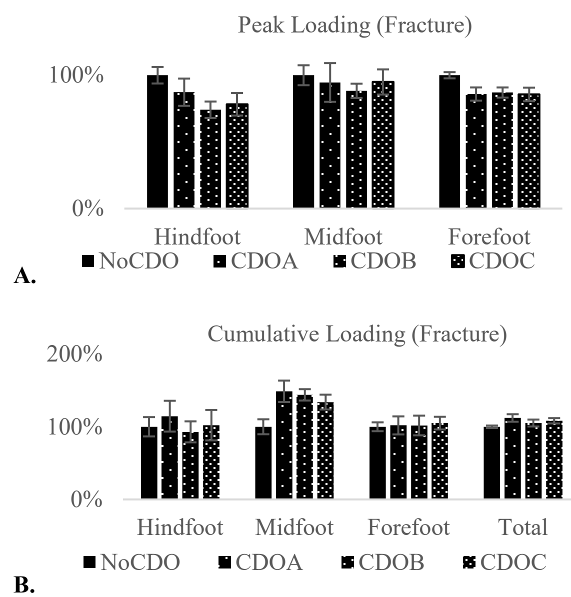

Figure 3: Peak (A) and cumulative (B) hindfoot, midfoot, forefoot, and total foot loading for the study participant with an intraarticular fracture.

Significance: All proximal cuff designs included in this study reduced peak forefoot forces, supporting their use for individuals experiencing pain with limb loading. However, the increases in cumulative loading should be taken into account when considering CDOs as an intervention for individuals with altered sensation or poor skin or tissue health.

Acknowledgements: This work was supported by a Department of Defense grant (W81XWH-18-1-0658).

References: [1] Stewart, et al. (2020), *JPO* 32(1). [2] Bedigrew, et al. (2014), *CORR* 472. [3] Anderson, et al. (2011), J Orthop Res 29(1). [4] Renner, et al. (2019), *Sensors* 19(2).

EXTERNAL ATTENTIONAL FOCUS CUES ON TIBIAL ACCELERATION COMPLEXITY VIA IMUS

Joshua M. Lardie[1*], Jake A. Melaro[1], Kevin A. Valenzuala[2], Joshua T. Weinhandl[1]
[1]Kinesiology, Recreation, and Sport Studies, University of Tennessee, Knoxville, TN
[2]Department of Kinesiology, California State University, Long Beach, CA

*Corresponding author's email: jlardie@vols.utk.edu

Introduction: External attentional focus cues (EAFC) center on the result of the movement or the interaction with the environment or implements with notably higher learning benefits [1]. Iliotibial band syndrome (ITBS) is a repetitive motion injury characterized by altered hip and knee kinematics in runners [2]. Little to no consensus has been reached on rehabilitation plans for ITBS, although gait retraining has shown promise in other knee injuries [3]. The ability to quantify the complexity in a movement of a biological system using entropy complexity analysis may highlight the differences between healthy and afflicted populations [4,5]. Therefore, the purpose of this study is to determine if the tibial acceleration complexity changes between conditions with EAFCs. We hypothesize that there will be a significant decrease in tibial acceleration complexity in experimental conditions compared to control.

Methods: Seven healthy participants (4 males, age: 24.86yo ± 3.34, height: 1.73m ± 0.07, mass: 68.20kg ± 8.68) ran on an instrumented split belt treadmill for a duration of 5 minutes per condition, following a warmup of 5 minutes at a self-selected pace on the same treadmill. Each participant wore an IMU (IMeasureU, Auckland, New Zealand) on each leg, secured to the medial distal tibia. A differing-colored piece of tape was placed on each participants lateral malleolus and base of the 5th metatarsal of their right foot. During the control condition (CON), no EAFCs were given. During the metatarsal condition (MET), participants were instructed to "push the [colored] piece of tape to the right", matching the color of tape on the base of the 5th metatarsal. During the malleolus condition (MAL), participants were instructed to "push the [colored] piece of tape to the right", matching the color of the tape on the lateral malleolus. Verbal cues were repeated twice before beginning and thrice during the 5-minute trial for the MET and MAL condition. Colors of tape were chosen by researchers to contrast participants running shoes and participants were verbally asked what colors the tape were on application, prior to using the term during testing to ensure clarity. Running velocity was self-selected during the warmup by gradually increasing belt velocity until it was at a "long run" pace, then starting at a faster belt velocity and gradually reducing until a similarly comfortable pace was selected. If the two paces were within a 5% difference, this would be the trial running velocity (3.17m/s ± 0.45). Data processing and statistical analysis took place in Python (3.10.7). Acceleration due to gravity was removed and oversaturation of the low G sensor (±16g) was replaced with the output of the high G sensor (±200g) [6]. Data was down sampled from 1000Hz to 100Hz [4]. The complexity index (CI), or area under the curve of multiscale entropy, was calculated using sample entropy of the resultant tibial accelerations. A two-way repeated measures ANOVA ($\alpha = 0.05$) was conducted to compare the effect of EAFC on tibial acceleration complexity for leg and condition. If significance was discovered, a Tukey's HSD post-hoc analysis was performed to determine the significant group differences.

Results & Discussion: No leg difference was observed right versus left for condition as the independent variable. The MAL group had a mean difference of +3.62 units of complexity ($p = 0.04$) compared to the CON group for combined legs. There were no significant differences observed for condition [$F(2,12) = 2.07$, $p = 0.17$] or leg and condition [$F(2,12) = 2.05$, $p = 0.17$]. We expected to see a decrease in complexity in EAFC conditions compared to control due to the altered gait kinematics associated with the EAFC as it was designed to reduce ITBS symptoms.

Significance: A change in complexity has been associated with fatigue (decrease CI) or those with disease states compared to healthy controls. The greater complexity is typically a characteristic of a healthy system and higher adaptive capacity [4,7]. Since these were experienced runners (30.3 mi/wk ± 14.5), it is likely they were highly adaptive to the change in gait. 85% of the participants complexity increased during EAFCs compared to control (Figure 1). Further research is needed to explore the type of entropy performed, length of experiment, length of entropy sample, and an increase in sample size.

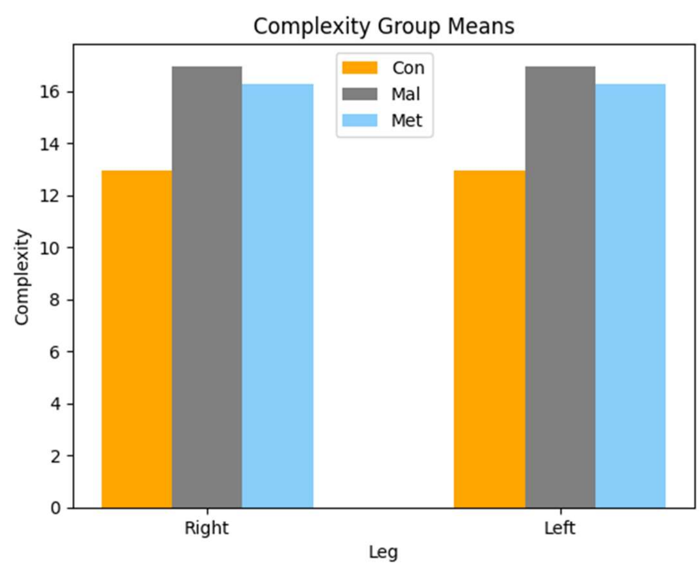

Figure 1: Group means of complexity of tibial acceleration resultant for each leg and condition.

References: [1] Marchant et al. (2009), *J of Stren Con* 23(8). [2] Baker et al. (2018), *PM&R* 10(10). [3] Shull et al. (2013), *J of Ortho Re* 31(7). [4] Gruber et al. (2021), *F Sprt Act Living* 3. [5] Schutte et al. (2018), *Gait Posture* 59. [6] van Hees et al. (2013), *PLOS* 8(4). [7] Costa et al. (2002), *Phys Rev Lett* 89(6).

CURVE ANALYSIS OF LOWER LIMB TRANSITION STEP NEGOTIATION KINEMATICS IN OLDER ADULTS

Mohammed S. Alamri[1*], Emily E. Gerstle[2], Hanieh Pazhooman[1], Zahra Mollaei[1], Stephen C. Cobb[1]
[1]Gait & Biodynamics Laboratory, Department of Kinesiology, University of Wisconsin-Milwaukee, Milwaukee, WI, USA
[2]Human Motion Laboratory, Department of Health and Human Performance, University of Scranton, Scranton, PA, USA
*Corresponding author's email: msalamri@uwm.edu

Introduction: Step negotiation is a leading contributor to falls, especially as individuals age. Approximately one-third of step-related falls occur on the first step, or the last step during the switch to level walking [1]. However, few studies have investigated single transition step negotiation [2-3]. The studies conducted have shown closer lead limb foot placement [2-3], greater ankle plantar flexion [2], and greater knee flexion [3] at initial contact of the transition step in older compared to younger individuals. While discrete analyses such as these can be used to investigate kinematics at important predetermined instances during the step negotiation, they are not able to assess potentially important joint position differences over the entire time series. Statistical parametric mapping (SPM) enables assessment of an entire time series [4]. Therefore, the purpose of this study was to use SPM to investigate ankle, knee, and hip joint angle differences between older and young female adults during step negotiation. Due to the decreased strength and balance associated with aging, we hypothesized that older females would demonstrate increased positions of hip flexion and adduction, knee flexion, and ankle dorsiflexion of the trail limb as the lead limb is lowered to initial contact of the transition step. We postulated the same changes in the lead limb during lead limb weight acceptance of the transition step. Finally, to successfully navigate the transition step without falling, we hypothesized there would be compensatory lead and trail limb changes during the lowering and landing periods, respectively.

Methods: 15 older female adults (71.5 ± 5.0 y) with a fall history (OF) and 15 young female adults (22.6 ± 3.2 y) (YA) participated in the study. Following written informed consent, each participant performed 5 self-selected speed barefoot walking trials along a 5.5 m raised walkway, descended a 17 cm step (right foot lead), and continued walking 3 m. Marker position data were collected using a 14-camera motion analysis system and a force plate located at the base of the step recorded. Kinematic and GRF data were processed from lead limb toe-off prior to the step, through lead limb weight acceptance of the transition step. The spm1d package for one-dimensional SPM was then used to assess the normality of the data and perform independent t-test or non-parametric analysis of the 3D ankle and hip time-series, and the sagittal plane knee time-series [4].

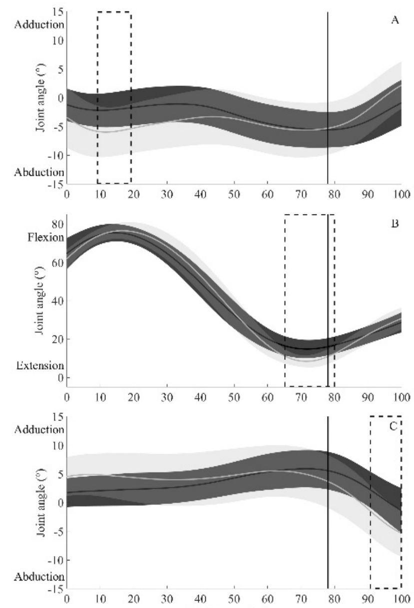

Fig 1. Lead limb hip frontal plane (a), lead limb knee sagittal plane (b), and trail limb hip frontal plane (c) transition step kinematics. Black line is OF group mean; grey line is YA group mean. Shaded areas are ± 1 SD. Vertical bar at 78% is lead limb initial contact. Dashed boxes indicate areas of significant group differences.

Results & Discussion: Lead limb independent t-test results revealed significantly decreased lead hip abduction position from 9-19% (mean difference: 3.74°; $p = 0.045$) and increased knee flexion position from 65-80% (mean difference 5.8°; $p = 0.012$) of the step negotiation in the OF group (Fig 1). Trail limb independent t-test results revealed significant between group hip frontal plane differences from 91-100% of the step negotiation (mean difference: 3.92°; $p = 0.046$). Both groups abducted during the period, however, the OF group transitioned from an adducted position to a slightly abducted position, while the YA group was in an abducted position the entire period (Fig 1).

The decreased OF group lead limb hip abduction occurred during lead limb swing phase. Without other trail or lead limb compensatory movements, the position may result in lower foot clearance during lead limb swing. The increased OF group lead limb knee flexion at initial contact is consistent with discrete analysis of this same data [3]. The SPM analysis, however, revealed the increased knee flexion began during the late swing phase of the step negotiation. This may have been a compensatory movement to ensure adequate lead limb step clearance. Finally, the increased trail limb hip adduction position at the end of the lead limb weight acceptance period may have been related to the increased lead limb knee flexion during late swing and early weight acceptance. Lead limb knee flexion would effectively shorten the lead limb. Thus, increased trail limb hip adduction may function with the increased lead limb knee flexion to enable lead limb foot placement closer to the step [3]. Although the OF group trail limb hip adduction position difference was not significant until late weight acceptance, it was more adducted at the beginning of weight acceptance.

Significance: If decreased lead limb hip abduction in older adults with a fall history does result in decreased clearance during lead limb swing, it could be utilized as an outcome variable in training programs aimed at decreasing step-related falls. Similarly, if the increased lead limb knee flexion in late swing and early weight acceptance, and the increased trail limb hip adduction during lead limb weight acceptance in the OF group are compensatory changes to minimize time in single limb stance due decreased strength/balance [3]; they too could be utilized as outcome variables to assess fall prevention program effectiveness.

Acknowledgements: UW-Milwaukee, CHS, Student Research Grant Award & ASB Graduate Student Grant-in-Aid.

References: [1] Templer (1992), *MIT Press*, Cambridge, MA; [2] Lythgo et al. (2007), *Gait Posture* 26 (1); [3] Gerstle et al. (2021), *Clin Biomech* 89; [4] Pataky (2012), *Computer Comput Methods Biomech Biomed Engin*, 15(3).

QUANTIFYING THE EFFECTS OF VICTIMIZATION ON GAIT: AN EXPLORATORY STUDY

Marco A. Avalos*, Andrew Costa, Saaniya Farhan, David S Kosson, Noah J. Rosenblatt,
Center for Lower Extremity Ambulatory Research (CLEAR), Dr. W. M. Scholl College of Podiatric Medicine at Rosalind Franklin University of Medicine and Science, North Chicago, IL
*Corresponding author's email: marco.avalos@rosalindfranklin.edu

Introduction: In 2019 it was reported that 22% of students ages 12-18 were bullied [1]. How offenders like bullies select victims has been widely researched [2]. Surprisingly, offenders may use nonverbal cues in walking style to identify victims [3]. Previous studies have shown a correlation between how easily a person would be subject to attack and movements during gait using qualitative parameters [4]. This study aimed to explore quantitative differences in three-dimensional aspects of gait between adults with and without a history of victimization. In light of prior work in which qualitative parameters focused on weight shifting and smoothness of movement [4,5], we also concentrate our analysis on smoothness since it is considered a measure of coordinated movement [6].

Methods: We recruited 31 young females (age: 26.2 ± 5.0 years; height: 160 ± 5.2 cm; mass: 64.1 ± 11.7 kg). Reflective markers were placed following the plug-in gait model and tracked by an 8-camera motion capture system. We recorded participants' gait as they walked between tasks that served as deceiving study objectives. Gait was unknowingly recorded as participants walked across a 10m walkway to move from task to task. At the end of data collection, participants filled out a survey asking if they had been victimized, the frequency, and if this was in-person or online. Victimization was not explicitly defined unless asked by the participant, in which case researchers indicated that victimization should be considered "as being equal to or greater than bullying," as per prior work [2].

We calculated the smoothness of the pelvis, torso, head, and whole body center of mass from the motion capture data and the smoothness of upper and lower body joint angles. We calculated smoothness using the normalized jerk scores (NJS, Eq. 1) [6], where lower NJS indicates greater smoothness. T-tests were used to compare variables between those who identified as victims and those who did not. Effect sizes (Cohen's d) are provided for comparison with d-values of at least 0.50 (moderate strength).

$$\boldsymbol{NJS} = \sqrt{\frac{\mathbf{1}}{\mathbf{2}}\frac{\boldsymbol{T}^{\mathbf{6}}}{\boldsymbol{D}^{\mathbf{2}}}\int \boldsymbol{J}^{\mathbf{2}}\,\mathbf{dt}}$$

Equation 1 Smoothness formula. NJS = Normalized Jerk Score; T = stride time; D = movement distance; J = Jerk.

Results & Discussion: Unexpectedly, 55% of females (17 participants) identified as victims, which is considerably higher than prior reports with victimization rates of 25% in school-aged students [1]. Of all of the smoothness measures considered, only NJS for the whole body COM in the frontal plane showed a significant effect of the group with higher values (more jerky motion) in the victimized group (Fig. 1). There were moderate, non-significant effects for some other smoothness measures. In a previous study, emotion affected smoothness in the sagittal and transverse planes [7]. The effects of victimization appear to differ from emotion, which may reflect a less transient impact of the former vs. latter.

Previous work has shown that persons with psychopathic traits can better identify gait cues in persons with a history of victimization [8]. As the whole body COM is not something that is apparently visible, either: i) this is something that those individuals can visualize more easily; and/or ii) other objective measures may differentiate the two groups; or iii) measures need nod show significant individual differences to fall within the "unspoken language" that the perpetrators read and that the victimized person communicates. As with any other language, body language may reflect the complexity of many small coordinated cues that may collectively tell a story to the trained listener. Our next step to better decode this language is to follow prior work and have persons with psychopathic traits view motion capture videos of our targets to see if they can distinguish those with and without a history of victimization. If so, future research can focus on developing interventions to improve variables that distinguish victims from non-victims.

SMOOTHNESS DOMAIN	VARIABLE	*p* VALUE	EFFECT SIZE
Sagittal Plane	Pelvis COM	0.947	
	Head COM	0.477	
	Whole COM	0.297	
	Torso COM	0.27	
Frontal Plane	Head COM	0.305	
	Torso COM	0.213	
	Pelvis COM	0.188	
	Whole COM	**0.019**	**0.893**
Transverse Plane	Pelvis COM	0.745	
	Torso COM	0.337	
	Whole COM	0.319	
	Head COM	0.145	0.541
Flexion/Extension Angle	Elbow	0.949	
	Wrist	0.417	
	Ankle	0.405	
	Hip	0.243	
	Knee	0.113	0.591
	Shoulder	0.085	0.644

1 0.9 0.8 0.7 0.6 0.5 0.4 0.3 0.2 0.1 0.075 0.05 0.025 0.01

Figure 1. Above shows the variables tested and the P values with effect size that were significant or within marginal significance. Heat map indicate the movement jerkiness.

Significance: Identifying and quantifying variables that differentiate the gait of persons with and without victimization may serve as cues to point offenders and may provide a tool to help those victimized feel more empowered and less likely to experience future assault.

Acknowledgments: This project was supported by Grant number 2T35DK074390 from the National Institute of Diabetes and Digestive and Kidney Diseases of the National Institute of Health.

References: [1] Irwin et al. (2021), *NCES*; [2] Book et al. (2013), *J Interpers Violence* 28(11); [3] Grayson & Stein (1981), *J Commun* 31(1); [4] Gunns et al. (2002), *J Nonverbal Behav* 26(3). [5] Ford et al. (2007), *Gait Posture* 26(1); [6] Hogan & Sternad (2009), *J Mot Behav* 41(6); [7] Montepare et al. (1988), *J Pers Soc Psychol* 55(4); [8] Ritchie et al. (2018), *J Crim Psychol* 8(2).

REAL-TIME FEEDBACK RESULTS IN GREATER OUTER, FAR-FROM-BODY AND INNER, CLOSE-TO-BODY UPPER EXTREMITY REACHABLE WORKSPACE IN HEALTHY ADULTS

Benjamin G. Lerch, Kristen Guarneschelli, Grigorios Papachristos, R. Tyler Richardson
Pennsylvania State University Harrisburg, Middletown, PA, USA
Email: rtr12@psu.edu

Introduction: Adequate upper extremity (UE) function is essential for activities of daily living. Assessment of the entirety of an individual's UE function is needed to guide clinical decision making in pediatric and adult populations. Reachable workspace quantifies global UE function by measuring regions in space that can be reached with the hand [1] and may offer a more complete understanding of function than traditional clinical assessments. Existing reachable workspace approaches evaluate a limited set of motions with visual guidance and feedback from a researcher or camera system [2]. A recent workspace approach incorporated more engaging and interactive real-time (RT) visual feedback with motion capture into data collection which elicited a "best effort" acquisition of function compared to traditional instructions from a researcher [3]. The benefit of RT feedback, however, has only been measured for outer, far-from-body workspace in young children [3], thus it is unclear if this benefit extends to adults or to inner, close-to-body UE function. The purpose of this study was to determine the effect of RT visual feedback on outer, far-from-body and inner, close-to-body UE reachable workspace in healthy adults. Due RT feedback resulting in more workspace reported in children, we expect that both outer and inner workspace collected with RT feedback will be greater than traditional verbal and basic visual feedback in healthy adults.

Methods: Trunk and UE segment orientations of 19 healthy adults (ages 19-25 years) were measured with motion capture for workspace trials under two conditions: with and without RT feedback. For RT feedback trials, arrays of virtual targets surrounding the subject were created for the outer and inner workspace regions. Custom software displayed targets and RT visual feedback from motion capture with movements of a red cursor sphere controlled in RT based on the position of the hand relative to the trunk (**Fig. 1A/B**). Targets were displayed sequentially by outer (**Fig. 1C)** or inner region (**Fig. 1D**) until all targets were reached or could not be completed. For no RT feedback trials, subjects received verbal and basic visual instructions like those of clinical assessments. Subjects were asked to trace out large circles with their hand that encompassed their furthest and closest reach within a plane of arm elevation. They traced circles in all planes of elevation before reaching around their head/neck and all around their thorax and abdomen. Percent workspace reached was calculated for each outer and inner workspace region (**Fig. 1C/D**). A two-way repeated measures ANOVA with post hoc analyses was used to assess differences in percent workspace reached between conditions for each sub-region.

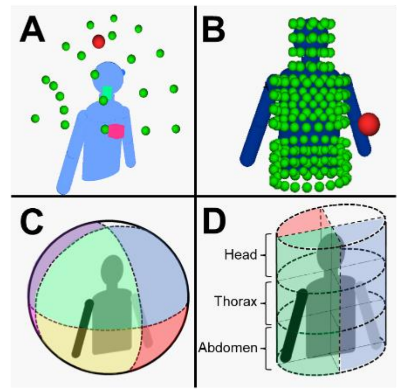

Figure 1: Real-time feedback for outer (A) and inner (B) workspace and regions within outer (C) and inner (D) workspace.

Results & Discussion: RT feedback elicited significantly greater workspace for all outer regions with the mean differences ranging from 15.8% to 37.8% (**Fig. 2**). Increases in outer workspace from RT feedback were similar to those previously found in children [3]. All inner regions reported more workspace with RT feedback (mean differences from 6.6% to 50.2%), however, some of these differences did not reach significance (**Fig. 3**). The lack of significant differences in the anterior/ipsilateral regions of the head and thorax likely are due to the large amount of workspace in these regions, while the lack of a significant difference in the posterior/ipsilateral thoracic region is likely due to the minimal workspace in this region (**Fig. 3**). Together these findings support the hypothesis that RT feedback elicits greater workspace for both the outer and inner regions compared to traditional instructions.

Significance: Reachable workspace collected with RT feedback offers a more complete measure of both outer and inner UE function in healthy adults. Normative workspace values for adults will aid with interpretation of workspace values for clinical populations.

Acknowledgements: 2022 Penn State Harrisburg Smart Home Research Initiative Research Development Grant**.**

References: [1] Abdel-Malek et al. (2004), *Ergonomics* 47(13); [2] Han et al. (2013), *PLoS Currents*; [3] Richardson et al. (2022) *J Biomech* 132.

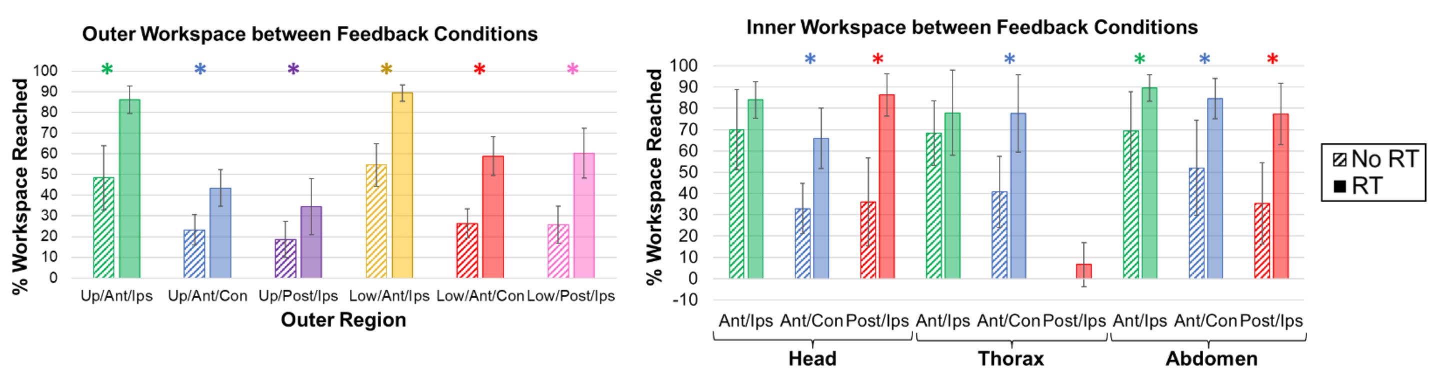

Figure 2: Differences in workspace between conditions (mean±1SD) for outer and inner regions. * indicates significant difference.

EXTERNAL ATTENTIONAL FOCUS CUES ON TIBIAL ACCELERATIONS AND SYMMETRY VIA INERTIAL MEASUREMENT UNITS DURING TREADMILL RUNNING

Joshua M. Lardie[1*], Kevin A. Valenzuela[2], Joshua T. Weinhandl[1]
[1]Kinesiology, Recreation, and Sport Studies, University of Tennessee, Knoxville, TN
[2]Department of Kinesiology, California State University, Long Beach, CA
*Corresponding author's email: jlardie@vols.utk.edu

Introduction: An external attentional focus cue (EAFC) centers on the result of the movement, or the interaction with the environment or implements. This has been shown to increase muscle force production and decrease overall electromyography activity compared to internal attentional focus cues or cues that center on the movement itself [1]. Learning benefits as measured by performance in retention testing are notably higher while using EAFC as well [2]. Iliotibial band syndrome (ITBS) is a repetitive motion injury and the leading cause of lateral knee pain amongst runners with an incident rate reported from 12-16% [3,4]. Little consensus has been reached on identification tests or rehabilitation plans for ITBS, especially with gait retraining. Vertical and resultant accelerations have been associated with running injuries across all foot strike patterns using inertial measurement units (IMU) [5]. However, little research investigating ITBS with IMUs has been conducted. Therefore, the purpose of this study was to examine the effects of multiple EAFCs designed to reduce ITBS symptoms on acceleration during running. We hypothesize there will a significant difference in acceleration metrics between conditions.

Methods: Seven healthy participants (4 males, age: 24.86yo ± 3.34, height: 1.73m ± 0.07, mass: 68.20kg ± 8.68) ran on an instrumented split belt treadmill for a duration of 5 minutes per condition, following a warmup of 5 minutes at a self-selected pace on the same treadmill. Each participant wore an IMU (IMeasureU, Auckland, New Zealand) on each leg, secured to the medial distal tibia. A differing-colored piece of tape was placed on each participants lateral malleolus and base of the 5th metatarsal of their right foot. During the control condition (CON), no EAFCs were given. During the metatarsal condition (MET), participants were instructed to "push the [colored] piece of tape to the right", matching the color of tape on the base of the 5th metatarsal. During the malleolus condition (MAL), participants were instructed to "push the [colored] piece of tape to the right", matching the color of the tape on the lateral malleolus. Verbal cues were repeated twice before beginning and thrice during the 5-minute trial for the MET and MAL condition. Colors of tape were chosen by researchers to contrast participants running shoes and participants were verbally asked what colors the tape were on application, prior to using the term during testing to ensure clarity. Running velocity was self-selected during the warmup by gradually increasing belt velocity until it was at a "long run" pace, then starting at a faster belt velocity and gradually reducing until a similarly comfortable pace was selected. If the two paces were within a 5% difference, this would be the trial running velocity. Data processing and statistical analysis took place in Python (3.10.7). Acceleration due to gravity was removed and oversaturation of the low G sensor (±16g) was replaced with the output of the high G sensor (±200g) [6]. All three axes were filtered using a 4th order, zero-lag, recursive Butterworth lowpass filter with a cut-off frequency of 50Hz. The resultant acceleration was calculated and used for analysis. The peak acceleration (AccP) per trial was an average of all peaks following manual visual assessment of trial. Acceleration integrals (AccI) were taken using these peaks. Symmetry was defined as the difference of the right and left leg divided by the average of the right and left leg. A two-way repeated measures analysis of variance (ANOVA) ($\alpha = 0.05$) was conducted by condition and leg for AccP and AccI. A one-way repeated measures ANOVA ($\alpha = 0.05$) was conducted for symmetry analysis. If significance was discovered, a Tukey's HSD post-hoc analysis was performed to determine the significant differences.

Condition	AccP (g)	AccI (g*s)	Sym AccP	Sym AccI
Control	11.26	641.19	0.08	0.01
Mal	11.50	653.16	0.05	0.02
Met	12.36	668.52	0.09	0.02

Table 1: AccP, AccI, Sym AccP, and Sym AccI of the resultant tibial acceleration of the right leg for each condition.

Results & Discussion: No significant differences were observed for right tibial AccP [$F(2,12) = 0.87$, $p = 0.44$], AccI [$F(2,12) = 3.13$, $p = 0.081$], symmetry of AccP [$F(2,12) = 0.29$, p = 0.0.75], or symmetry of AccI [$F(2,12) = 0.24$, $p = 0.79$]. See Table 1. This may demonstrate a relatively unchanged loading profile even though kinematic alterations were made via EAFCs for the MET and MAL conditions. Resultant and vertical accelerations have been associated with vertical loading in running injuries; however, it is unclear whether the runners were diagnosed with ITBS [5]. Loading rates may not be associated with ITBS, or an emphasis in a different axis may be necessary [7].

Significance: Repetitive motion injuries such as ITBS have a lack of consensus for identification or rehabilitation practices. Instrumented force treadmills and motion capture analysis are often used in biomechanical research, however field-based approaches are advancing rapidly. IMUs allow the subjects to be in a natural environment, on their usual running routes and surfaces where the injuries are occurring. Since tibial acceleration may differ between field and laboratory conditions [8], more research is needed on associating IMU data to ITBS. This study has shown that a healthy populations acceleration profile does not differ significantly when an EAFC designed to alter the kinematics to reduce pain associated with ITBS is introduced. Future research should include more IMU measured variables as well as an afflicted population. Additionally, classification techniques may be constructed from field-based IMU measurements once the relationship is further established or they may be used to measure the efficacy of a rehabilitation plan to retrain subjects with EAFCs.

References: [1] Marchant et al. (2009), *J of Stren Con* 23(8). [2] Wulf et al. (2001), *Exp Psych Soc* 54A(4). [3] Baker & Fredericson (2016), *Phys Med Rehab Clin N Am* 27. [4] Benca et al. (2020), *J Clin Med* 9(2). [5] Tenforde et al. (2020), *PM&R* 12(7). [6] van Hees et al. (2013), *PLOS* 8(4). [7] de Souza Junior et al. (2023), *Appl Sci* 13(6). [8] Milner et al. (2020), *Med Sci Sports Ex* 52(6).

TEMPORARY LOSS OF VASTI LATERALIS FUNCTION NORMALIZES IN VIVO KNEE JOINT KINEMATICS AND REDUCES PAIN IN PATIENTS WITH PATELLOFEMORAL PAIN

Frances T. Sheehan* and Katharine E. Alter
*Rehabilitation Medicine, Clinical Center, National Institutes of Health
*Corresponding author's email: gavellif@cc.nih.gov

Introduction: Chronic idiopathic patellofemoral (PF) pain, a potential precursor to osteoarthritis, is one of the most common knee problems. The widely accepted theory regarding the etiology of PF pain is that a force imbalance around the knee leads to static PF malalignment and dynamic PF maltracking. In turn, this malalignment/maltracking leads to elevated joint contact stresses, which ultimately leads to PF pain (Fig 1). The source of this imbalance and the validity of this model is still open to debate. Two of the largest issues hindering our understanding of PF pain etiology are our inability to directly, non-invasively measure muscle force and the lack of studies evaluating the connectivity between the elements that are hypothesized to lead to pain (Fig 1). It remains unknown if medializing the force balance around the knee can normalize PF kinematics and/or reduce PF pain. Thus, the purpose of this study is to test the hypothesis that a temporary iatrogenic loss of vastus lateralis (VL) muscle force normalizes (medializes) aberrant patellar kinematics and reduces pain in patients with PF pain.

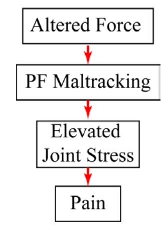

Fig 1: PF pain Diagram

Methods: To date, 23 patients diagnosed with idiopathic PF pain (duration > 6 months) have been enrolled, with 9 being disqualified after visit 1. During visit 1 all required paperwork and clinical evaluations were completed. Patients rated their current pain (100-pt visual analog scale - VAS). We then acquired a dynamic cine-phase contrast (CPC) MR image set (x,y,z velocity & anatomic images) during cyclical extension-flexion [1]. Patients rated their pain during the dynamic MRI (VAS). High-resolution static MR images were also acquired. The scanning protocol was saved to allow identical scanning parameters and locations for visit 2 [2].

For visit 2 (within 4 weeks), patients again rated their current pain (VAS) and completed a pain/strength assessment (rating their pain after ascending/descending 3 flights of stairs, performing 3 squats to their maximal depth, and an isometric knee extension task with maximum isometric strength being measured). Using ultrasound guidance and electrical stimulation, the peripheral femoral nerve motor branch to the distal third of the VL was localized and temporarily blocked using 1-5 cc of 0.5% solution of bupivacaine. A post-injection pain/strength assessment was completed once the block was confirmed effective. The patient was then transported to the MR scanner. Using reference marks on both the coil holder and the skin over the subject's knee, the subject was placed in as similar a position as possible to the visit 1. The dynamic scanning was repeated. The patient rated their pain (VAS) during the dynamic MRI and then completed a post-MRI pain/strength assessment.

We quantified PF and TF kinematics, pre- and post-injection (pre-I and post-I) by integrating the CPC data and interpolated to single knee angle (KA) increments. Changes in kinematics were evaluated using a repeated ANOVA followed by Wilcoxon signed rank test (if the null hypothesis was rejected), as was done previously [2]. Pain and strength changes were evaluated using a paired Student's t-test. To date, 11 datasets have been fully analysed (the remaining 3 are awaiting kinematic analysis).

Results & Discussion: The study hypotheses were supported. The temporary block of the distal VL normalized PF kinematics and reduced pain in our patient cohort (Fig 2). Post-I, the patella consistently (across subjects and KAs) shifted medially 2.1 to 2.3 mm (KA=10-35º, p=0.003-0.021). Tilt medialized less consistently 3.2 to 3.8º (KA=20-35º, p=0.016 to 0.041). Post-I, patients reported lower pain during exercise (37-50%, p<0.05). There was no difference in pain at the start of visits 1&2 (Fig 2). Maximum extensor isometric force capacity reduced post-I (14%, p<0.01, Fig 2). These reductions in pain and max isometric torque were maintained after the MR exam in visit 2.

This *in vivo* data collection with patients in active pain, allowed us to demonstrate causal links crucial for understanding the etiology of PF pain (Fig 1) and for designing interventions. The medial kinematic changes post-I were larger than those seen in a previous control study, where the VMO was temporarily blocked [2]. The next step in the study is to combine the dynamic and static images [3], to evaluate if medializing the patella, which reduced pain, alters PF joint contact.

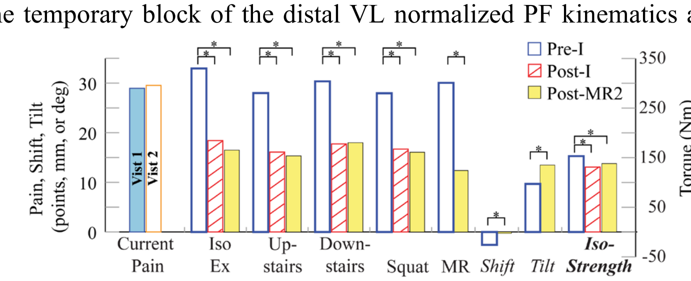

Fig 2: **Pain, Kinematic, and Strength Changes pre- and post-Injection**. Pain was rated using a 100-pt VAS. Significant differences are denoted with a *. Current pain was recorded at the start of visits 1&2. During isometric exercise (Iso Ex), while going up/down 3 flights of stairs, and during 3 deep squats pain was assessed at 3-time points (pre- and post-injection and post-MRI). Pain was assessed after dynamic MR during both visits. Patellar shift(mm) and tilt(deg) values are from KA with maximum change pre-to-post-I (35º and 30º) provided for a knee angle of 15 degrees. Maximum isometric torque was assessed at the same 3 time points as above.

Significance: This study advances our clinical understanding of PF pain etiology by providing the first *in vivo* data pertaining the effects of reducing the lateral quadriceps force producing capacity on PF kinematics, isometric extensor torque production, and pain. Unlike past studies that have demonstrates associations between individual measurements (e.g., alignment, EMG, etc) and PF pain, this study provides direct *in vivo* evidence in support of the causal link between extensor force balance, altered kinematics, and PF pain (Fig 1). This reinforces the current interventional focus on vasti medialis strengthening and the use of a longer acting muscle block (e.g, botulinum toxin) combined with quadriceps strengthening to medialize PF kinematics and reduce pain.

References: [1] Behnam et al (2010) *JOB* 44(1), [2] Sheehan et al (2012) *Clin Biomech* 27(6), [3] Borotikar et al *JOB* (2012) 45(6).

SIAMESE CONVOLUTIONAL NEURAL NETWORKS FOR STROKE DIAGNOSIS AND EXPLAINABILITY BASED ON GAIT ANALYSIS

Christos Kokkotis[1*], Kyriakos Apostolidis[1], Evangelos Karakasis[1], Evangeli Karampina[1], Serafeim Moustakidis[1], Evangelia Makri[1], Giorgos Giarmatzis[1], Konstantinos Vadikolias[2], Nikolaos Aggelousis[1]
[1]Department of Physical Education and Sport Science, Democritus University of Thrace, Greece
[2]Department of Medicine, Democritus University of Thrace, Greece
*Corresponding author's email: ckokkoti@affil.duth.gr

Introduction: Stroke is one of the leading causes of death and disability worldwide. In fact, it is estimated that every year, more than 15 million people worldwide suffer a stroke. One of the most devastating consequences of stroke is the loss of motor function, which can significantly impact a person's quality of life. Depending on the location and severity of the stroke, individuals may experience weakness, paralysis, or difficulty with coordination and balance. Rehabilitation and physical therapy are often necessary to help stroke survivors regain motor function and improve their overall well-being. In order to achieve this aim, personalized treatments which are based on quantitative measurements are necessary. Thus, gait analysis is used to evaluate the way a person walks, including the movement and coordination of different body parts. Hence, personalized treatments based on gait analysis can be particularly beneficial for stroke survivors, as the extent and location of the brain damage can vary widely from person to person, leading to different types of motor impairments. By analyzing a patient's gait, healthcare professionals can identify specific areas of weakness or asymmetry in their movement patterns and develop targeted interventions to address those issues.

However, the relatively small number of stroke survivors in each area presents a challenge for healthcare professionals in terms of accurately diagnosing and treating this population. This challenge has led to a need for new approaches that can improve the accuracy of stroke diagnosis and enable earlier intervention and treatment. One such approach is the use of Siamese convolutional neural networks (CNNs). Siamese CNNs are a type of neural network architecture that has shown great potential in the field of biomechanics for clinical use. Biomechanics is the study of the mechanics of living organisms, including humans, and is critical in assessing and treating musculoskeletal injuries and diseases. Hence, the aim of the study is the development of Siamese CNNs based on biomechanical time series in order to i) investigate the diagnostic accuracy of the proposed approach for stroke versus non-stroke and ii) identify specific areas of weakness or asymmetry in the movement patterns of stroke survivors.

Methods: Eleven chronic stroke survivors and eleven healthy subjects were included in this study. Motion capture data were recorded at the Biomechanics Lab – DUTH, Greece. All participants walked on a split-belt, instrumented treadmill. All the employed subjects walked at their preferred walking speed (10 gait cycles/each). Kinematic data were calculated throughout according to the Conventional Gait Model 2 (CGM2) (Nexus 2.14, Vicon Metrics Group Ltd, Oxford, UK). Image representation is based on the kinematic data (ankle plantarflexion/dorsiflexion, knee flexion/extension, hip flexion/extension, hip abduction/adduction and hip internal and external rotation for paretic and non-paretic leg respectively and center of mass in three dimensions) for 10 gait cycles per subject. A Siamese CNN with contrastive loss function, which is a distance-based loss function, was trained on treadmill images in order to classify the images into stroke survivors and healthy. As a similarity index, the Euclidean distance was used. For the evaluation of the model, we used the accuracy metric. We also studied the explainability of our method by applying GradCAM in test images. GradCAM is a visualization technique that shows where a CNN is looking to make its decision.

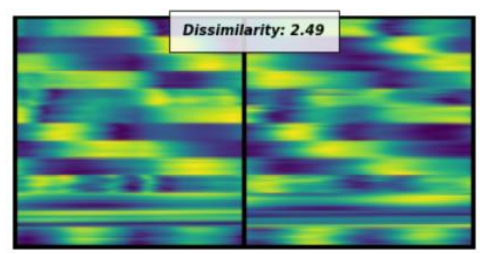

Figure 1: Figure 1 consists of a stroke survivor (right) and a non-stroke image (left).

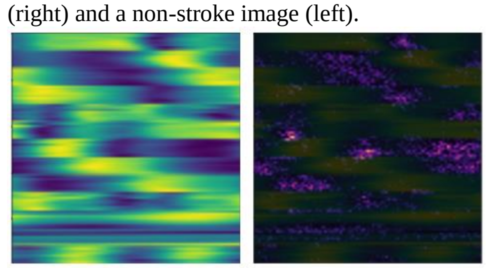

(a) (b)

Figure 2: (a) Treadmill image of stroke survivor and (b) GradCAM on this image.

Results & Discussion: In our approach, we used a small model with three convolutional blocks where each block consists of a convolutional layer, a dropout, and a batch normalization layer. The model finally results in a feature vector with 5 values. Our model was trained for 20 epochs presenting 100% testing accuracy and loss 0.211. Figure 1 is shown that images from different classes have a big `dissimilarity value (2.49). Figure 2 presents the application of GradCAM in test images. Specifically, the bright regions show where the model looks to classify an image. Overall, personalized treatments based on gait analysis and AI tools can help stroke survivors to regain their mobility and improve their quality of life,

Significance: By using Siamese CNNs, clinicians and researchers can more accurately track changes in patients' conditions over time, allowing for earlier personalized intervention and better treatment outcomes. Specifically, Siamese CNNs can be used to identify abnormal movement patterns in gait analysis, which can be used to diagnose and treat a variety of conditions in stroke. Thus, using Siamese CNNs in clinical biomechanics can greatly improve the accuracy and efficiency of clinical diagnosis and treatment even with little data, leading to better patient outcomes and improved quality of life.

Acknowledgements: This work was supported by grant MIS 5047286 from Greek and European funds (EYD-EPANEK).

References: [1] Li et al. (2020), npj Digit. Med. 48(3).

IMUS REQUIRED FOR VARYING LEVELS OF DETAIL FOR HUMAN ACTIVITY CLASSIFICATION

Samuel J. Murphy[1*], Rachel V. Vitali[1]
[1]University of Iowa, Iowa City, IA, USA
*email: samuel-murphy@uiowa.edu

Introduction: The ability to monitor and understand human activity in the real world has important implications for health, behaviour, and performance. While optical motion capture may have the advantage of accurate position data and controlling for confounding variables, it can also affect a person's natural motions and types of movements that can be captured [1]. On the other hand, inertial motion capture, which utilizes inertial measurement units (IMUs), allows for more natural movement and activities outside of a laboratory setting. While IMUs are naturally unobtrusive and portable, processing IMU data can require advanced signal processing techniques and are often task- or activity-specific to acquire meaningful metrics [1]. As a result, the first step in that post processing pipeline is activity classification. An interesting open research area concerns the number and placement of IMUs needed to achieve appropriate levels of accuracy as well as sufficient detail in what types of activities are being conducted. Studying scientists conducting scientific fieldwork will lead to a better understanding of work cadence, metabolic costs, and navigation of rough terrain. This study considers IMUs attached to body segments as well as tools, which is a departure from previous research that largely considers one or the other [2]. The purpose of this study is to investigate the first step of the activity classification framework, which is to establish when different IMUs are moving and when pairs of IMUs are exhibiting similar movement patterns.

Methods: A convenience sample of 15 participants (9 female, 6 male; 25.9 ± 6.1 years old) were recruited for this study. All study activities were approved by the University of Iowa Institutional Review Board, and participants gave written informed consent prior to participation. Three representative tools were chosen as typical for a scientist conducting scientific fieldwork: 1) backpack, 2) tablet, and 3) rock hammer [3]. A total of eight IMUs were placed on feet (2), hands (2), and sternum (1) in addition to the backpack, tablet, and hammer. Ground truth data was labelled manually from collected data. After a static standing calibration, participants performed trials around a predesignated course.

Table 1: Sensor Placement for each Group

Group #	# of Sensors	Sensors Added to Group
1	1	Right Foot
2	2	Backpack
3	4	Hammer, Tablet
4	6	Right Hand, Left Hand
5	8	Left Foot, Sternum

The IMUs were distributed into five increasingly more inclusive groups (Table 1). For Groups 1 and 2, only motion was considered since their signals should realistically only match during static periods. Motion classification was performed using a Support Vector Machine (SVM) with a linear kernel. The features were extracted from 0.25 second time windows with 50% overlap. The features included the maximum, minimum, mean, and standard deviation of the acceleration and angular velocity magnitude data [2]. Prior to training the motion classifier, the features were standardized. An 80-20 training-test split was used for a 5-fold cross validation.

For signal matching between pairs of IMUs, dynamic time warping (DTW) was used to extract features for an SVM with a linear kernel. DTW is a time series analysis that can quantify how similar two signals that may be shifted in time are. One signal is a reference signal while the other is manipulated in time and magnitude to match said reference signal. These DTW features were extracted from 1-second time windows with 50% overlap. In total, the features include the DTW outputs (i.e., distances) between each IMUs acceleration magnitude, angular velocity magnitude, product of the acceleration and angular velocity magnitudes, and the sensor labels. Note that the reference signals for each are extracted from the static standing calibration data. The sensor labels were added to capture pair-specific patterns. The features were similarly standardized and split as for the motion classifier features and used for a 5-fold cross validation.

Results & Discussion: The preliminary results reported here consider the activities performed by a single participant and are shown in Table 2, which includes Groups 1-3 (Table 1). These results show promise with all motion classifiers having a test accuracy greater than 90% and the signal matching classifier achieving close to 90% accuracy. Next steps include feature selection (e.g., minimum redundancy maximum relevance algorithms) and reduction (e.g., principal component analysis). Future work will extend this work to include Groups 4 and 5 (Table 1). Other classifier models will also be considered (e.g., k-nearest neighbour and logistic regression).

Table 2: Classification Accuracy of IMU Groups

Classifier - Group	Training Accuracy	Test Accuracy
Motion - 1	94.7%	94.0%
Motion - 2	92.6%	92.2%
Motion - 3	91.5%	91.0%
Signal Matching - 3	89.9%	89.7%

Significance: This work supports longitudinal, unstructured, and unconstrained human activity classification in the real world. Current studies focus on sensors placed on subjects with limited (often no) use of sensors placed on tools. This proposed work investigates the number and placement of IMUs for appropriate accuracy and details to distinguish between activities with finer detail. This work supports efforts to conduct activity classification on NASA scientists executing fieldwork to glean information about metabolic cost, work cadence, and navigation of rough terrain to support decision-making protocols related to future missions [3].

Acknowledgments: This material is based upon work supported by a Rajyalakshmi & Shankar N Planjery Scholarship.

References: [1] Kitagawa et al., 2016, Gait and Posture, 110-114, 45, [2] Demrozi et al., 2020. IEEE Acess, 210816-210836, 8, [3] Vitali et al., 2020. ICES-2020-163

THE INFLUENCE OF SIMULATED LABRAL QUALITY CONDITION ON SHOULDER MUSCLE ACTIVATION PATTERNS DURING ISOMETRIC AND FUNCTIONAL TASKS

Fergus TH. Lam[1]*, Clark R. Dickerson[1]
[1]Department of Kinesiology of Health Sciences, University of Waterloo, ON, Canada
*Corresponding author's email: fthlam@uwaterloo.ca

Introduction: Glenohumeral joint stability depends on a combination of shoulder muscular action and the glenoid labrum labral injuries and degenerations can affect glenohumeral joint reaction forces and potentially increase shoulder muscle efforts [1]. However, the relationship between shoulder labral condition and muscle demands was unclear as compensatory muscle strategies accompanying labral compromise lacked identification. Targeted analysis was required to determine the activation pattern of each muscle which traditional non-invasive biomechanical physical measurements cannot easily achieve. The purpose of this study was to determine how simulated labral statuses influence shoulder muscle activation patterns using a mathematical biomechanical shoulder model. Secondarily, we investigated potential links between observed variations in muscle recruitment patterns and potential muscle overuse. We expected the within-task differences in muscle activation patterns would depend on the locations and severity of the simulated labrum deficits, due to the directional changes in joint reaction forces while performing both functional and physical tasks [1]. Also, we expected degenerative conditions and torn labrum conditions would cause increased activation levels in defined muscle groups. Lastly, the magnitude of muscle activation levels would increase with the severity of the labral condition [2].

Methods: Isometric and functional movement tasks kinematic data were collected using a VICON MX20 passive motion capture system (VICON, Oxford, UK) to provide geometric inputs to the shoulder model using a single male participant. Muscle forces (%MVC) and glenohumeral joint contact forces were predicted by the Shoulder Loading Analysis Modulus (SLAM) model [3]. A total of 12 compromised labral conditions, including no labrum, age-related labral degeneration, athletic labral damage, and various types of labral reconstructions, were simulated for every task by altering the glenoid stability constraints of the SLAM model. The glenohumeral joint stability ratio was decreased by an average of 6%, 12% and 20% in eight equally spaced compass directions of the glenoid to simulate ages 61 to 80 [4], ages over 80 [4] and the condition with no labrum [1], respectively. An average of 16% decrease was applied to the stability constraints at 0°, 45° and 315° to simulate Type II Superior Labrum Anterior and Posterior (SLAP) lesions [5-7].

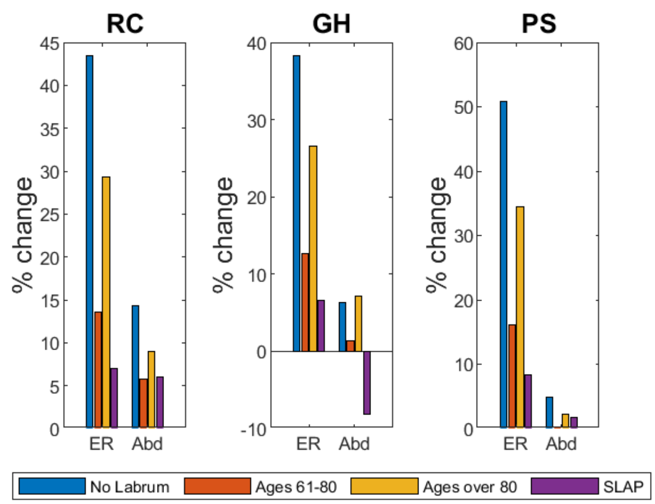

Figure 1: Means of percentage changes of rotator cuff (RC), glenohumeral (GH) and periscapular (PS) muscles %MVC in isometric tasks.

Results & Discussion: For brevity, this abstract highlights outcomes from the external rotation and abduction isometric tasks. Rotator cuff muscles (RC), glenohumeral muscles (GH), and periscapular muscles showed more than a 10% increase in %MVC levels in conditions with no labrum, ages between 61 to 80, ages over 80, and SLAP lesions for the external rotation when compared to intact labrum condition (Figure 1). In abduction, rotator cuff muscles also showed an increase in %MVC levels for the same labral conditions and a slight increase in the other two muscle groups (Figure 1). Similar muscle recruitment patterns existed in both degenerative and torn labrum conditions during external rotation, but only rotator cuff muscles experienced similar muscle recruitment patterns in both conditions in abduction. Further, muscle activation levels increased with the severity of the compromised labral conditions in external rotation for all muscle groups. However, the increasing behaviour in glenohumeral and periscapular muscle levels in abduction misaligned with our hypothesis but revealed some of the complexity of the interconnected activation of the complex shoulder musculature. This glenohumeral stabilization behaviour of the rotator cuff coincided with previous work [8]. In summary, simulated joint stability ratios reflective of labral damage increased muscle demands, suggesting more likely fatigue in their performance.

Significance: This study provides insight into the muscle strategies that patients may use to compensate for directional shoulder instabilities. Previously, relationships between muscle recruitment patterns and the quality of the labrum were unidentified. The current study can help to inform and advise clinicians about the challenges that patients with defective labrum may face when performing specific activities in certain postures. This information can be used as a guideline for secondary injury prevention by identifying connections between tissue overload, such as muscle fatigue, and previously reported potential shoulder injuries. Finally, the results could provide suggestions to improve postoperative strengthening and flexibility training. In conclusion, this study can help raise awareness and inform considerations relative to compromised labral management and mechanistic bases for functional capacity.

References: [1] Lippitt & Matsen (1993), *Clin Orthop Relat Res*. (291); [2] Pfahler et al. (2003), *J Shoulder Elbow Surg.* 12(1); [3] Dickerson et al. (2007), *Comput Methods Biomech Biomed Engin.* 10(6); [4] Alashkham et al. (2020), *Anatomy* 14(3); [5] Clavert (2015), *Orthop Traumatol Surg Res.* 101(1); [6] Panossian et al. (2005), *J Shoulder Elbow Surg.* 14(5); [7] Patzer et al. (2012), *J Shoulder Elbow Surg.* 21(11); [8] Mulla et al. (2020), *J Biomech.* 100.

STAND-UP AND SIT-DOWN WITH POWERED KNEE-ANKLE PROSTHESES: BETTER, BUT NOT PERFECT – WHY?

Grace R. Hunt[1,4*], K. Bo Foreman[3], Tommaso Lenzi[1,2,4,5]
[1] Department of Mechanical Engineering, [2] Department of Biomedical Engineering, [3] Department of Physical Therapy & Athletic Training, and [4] Robotics Center at the University of Utah; [5] Rocky Mountain Center for Occupational and Environmental Health
*Corresponding author's email: grace.hunt@hsc.utah.edu

Introduction: Most lower-limb prostheses can provide some support during tasks like sit-down but cannot assist during activities like stand-up. As a consequence, above-knee amputees must rely on their intact leg and upper body to compensate for the lack of assistance from their prostheses. These compensatory movements result in weight-bearing asymmetry, which negatively affects balance, increases fall risk, and exacerbates secondary conditions such as osteoarthritis and back pain [1]. Powered prostheses can actively assist users during both stand up and sit down. However, we do not know the "optimal" level of powered assistance, so we cannot maximize the benefits of powered prostheses. Our previous study found that weight-bearing symmetry improves with increasing assistance from a powered knee prosthesis when standing up [2]. A second previous study found that subjects improved weight-bearing symmetry while standing up with direct neural EMG control of the powered prosthesis torque [3]. In a third study under review, we find that a powered prosthesis improves weight bearing symmetry during sit-down [4]. Here we compare data from our previous studies, aiming to understand the relative improvements due to different controllers and activities, and to identify essential questions to guide the research and development of powered prosthesis technologies.

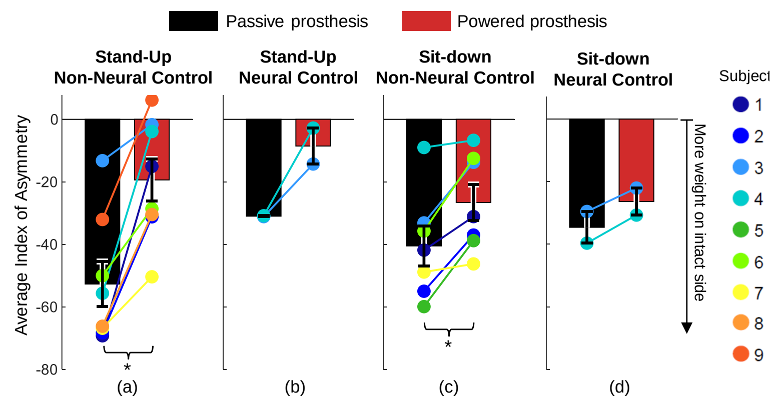

Figure 1: Index of asymmetry (IOA). Bars show across-subject means and standard errors. Dots show single-subject means. Asterisks indicate significant differences ($p < 0.05$). **(a)** *Stand-up, non-neural* (N = 8). **(b)** *Stand-up, neural* (N = 2). **(c)** *Sit-down, non-neural* (N = 7). **(d)** *Sit-down, neural* (N = 2).

Methods: Nine above-knee amputees provided informed consent. During every activity, we recorded a passive trial with the subject's prescribed prosthesis. During *Stand-up, neural* and *Sit-down, neural*, subjects controlled the powered prosthesis torque directly using EMG [2]. During *Stand-up, non-neural*, the powered prosthesis provided 1.6 Nm/kg, twice the non-amputee stand-up knee torque [3]. During *Sit-down, non-neural*, each subject preferred different levels of assistance [4]. Our outcome measure is the average index of asymmetry (IOA), a measure of weight-bearing symmetry. $IOA = (GRF_{prosthesis} - GRF_{intact})/(GRF_{prosthesis} + GRF_{intact}) * 100$. An IOA of 0 is "perfect". Negative IOA indicates more weight on the intact side. Results are reported as across-subject mean ± standard error. Paired t-tests compare passive and powered IOA during the four activities.

Results : During *Stand-up, non-neural* (N = 8), the powered prosthesis significantly improved IOA by 63%, from -52.71 ± 14.39 with passive to -19.40 ± 13.45 ($p = 0.00107$) (Figure 1(a)). During *Stand-up, neural* (N = 2), the powered prosthesis improved IOA by 72% ($p = 0.31$), from -31.00 ± 0.15 with passive to -8.56 ± 5.76 (Figure 1(b)). During *Sit-down, non-neural* (N = 7), the powered prosthesis significantly improved IOA by 34% ($p = 0.0112$), from -40.52 ± 12.00 with passive to -26.61 ± 10.90 (Figure 1(c)). During *Sit-down, neural control* (N = 2), the powered prosthesis improved IOA by 24% ($p = 0.11$), from -34.60 ± 5.06 with passive to -26.36 ± 4.32 (Figure 1(d)). Notably, subject 9 achieved positive IOA (more weight on the prosthesis) during stand-up (Figure 1(a)), and every subject's symmetry improved with the powered prosthesis (Figure 1).

Discussion: The powered prosthesis improved IOA more during stand-up (63% non-neural, 72% neural) than during sit-down (34% non-neural, 24% neural). We believe this is because passive prostheses provide some assistance during sit-down, but no assistance during stand-up, so there is more opportunity for improvement during stand-up. The powered prosthesis improved symmetry during all four activities, but never achieved "perfect" symmetry – even when we provided 2 times the knee torque produced by healthy knees, and even when subjects directly controlled the torque using their own muscles, subjects still put more weight on their intact leg on average. These results raise several important questions for future research: *Can* IOA be zero? What will it take to get IOA to zero? Is it an issue of control? Is it the prosthetic socket? Is it the lack of sensory feedback from the prosthetic foot? What is the role of subject training? What is the role of the powered ankle? We need to address these multi-faceted questions before powered prosthetics can leave the laboratory and begin improving real-life mobility for above-knee amputees.

Significance: Powered prosthetics have the potential to improve mobility, independence, and quality of life for millions of above-knee amputees – but first, we must understand the limitations of current technologies. We show that even with advanced prosthetics, powerful torque assistance, and volitional neural control, above-knee amputee's symmetry is improved, but not "perfectly" symmetric.

Acknowledgements: We thank Suzi Creveling, Sarah Hood, Selena Cho, Lukas Gabert, and Minh Tran. Funded by NIH grant R01 HD098154/HD/NICHD, NIOSH grant T42/CCT810426, the US DOD grant W81XWH2110037 and NSF grant 1925371.

References: [1] Gailey, R. *et al.* (2008) *J Rehabil Res Dev* 45(1); [2] Hunt, G. R. *et al.* (2022) *IEEE Trans Neural Syst Rehabil Eng;* [3] Hunt, G. *et al.* (2021) *IEEE Open J Eng Med Biol* 2(May); [4] Hunt, G. R. *et al.* (2023) *J Neuroeng Rehabil*

CHANGES IN OLDER ADULT OBSTACLE CROSSING KINEMATICS AFTER LOWERING OBSTACLE HEIGHT

Gabrielle Torrijos*, Patrick Fleming[1], Rahul Bashyal[1], Abigail Schmitt[2], & Tiphanie Raffegeau[1,3]
[1]George Mason University, Manassas, Virginia, USA
[2]University of Arkansas, Fayetteville, Arkansas, USA,[3]Ohio University, Athens, Ohio, USA
[1*]Corresponding author's email: Gtorrijo@gmu.edu

Introduction: Psychomotor impairments are prevalent in adults with depression and are associated with poor treatment outcomes [1]. Compared to healthy older adults, those with depression are at a higher risk of falling, developing a fear of falling and avoiding physical activity, which can lead to a decline in mobility and increase the risk of early mortality. Depression is considered a clinical risk factor for falls [2], yet it remains unclear how psychomotor impairments such as diminished obstacle avoidance during everyday walking may contribute to fall risk in older adults with depression. Avoiding obstacles is crucial in daily walking as movement in everyday life requires walking on uneven terrain and crossing obstacles, making it imperative to examine obstacle avoidance so that we can better target and reduce fall risk in older adults with depression [3]. The purpose of this study was to investigate the role of locomotor adaptation of the lower extremities during obstacle crossing tasks to better understand mobility deficits that resemble everyday walking challenges in older adults with depression. We started by assessing how healthy older adults would adjust steps to cross a shorter obstacle in an effort to develop more targeted gait interventions that improve daily mobility. We hypothesized that older adults would not change crossing kinematics when crossing a large versus small obstacle due to diminished capacity to adapt.

Methods: Nine adults (three men and six women, mean age = 71 ± 4 yrs, mean height = 1.67 ± 0.10 m, mean mass = 69.1 ± 8.2 kg) performed a series of obstructed walking tasks. Participants were fitted with 39 lightweight reflective markers in accordance with the Plug in-Gait model (Vicon Motion Systems). 3D motion capture recorded trajectories while the participants crossed a dowel set at 17.9 cm in the center of a 10-meter path, participants approached the dowel from both sides for a total of ten laps. Participants then completed a dual task obstacle crossing to serve as a distraction (results not included). In full view of the participant, the obstacle height was dropped to 13.9 cm and the participant similarly crossed the shorter dowel ten times. Foot trajectories and obstacle coordinates were used to calculate the horizontal distance between the toe marker and the obstacle (obstacle approach), the vertical distance between the toe and heel marker and the obstacle (toe/heel clearance) and the horizontal distance between the heel marker and the obstacle (obstacle landing) for the lead (first limb to cross the obstacle) and the trail (second limb to cross the obstacle) crossing foot. To assess our hypothesis, we calculated effect sizes for small samples with Hedge's *G* and examined the effects of obstacle height (small vs large) and crossing foot (lead vs trail) on approach, clearance, and landing distances.

Results & Discussion: The data showed small to medium effects of lowering the obstacle on crossing kinematics, primarily for the trail limb crossing outcomes. For obstacle approach, the lead foot approach was shorter for the small than large obstacle (Mean difference = 8.60 mm, Hedge's *G* = -0.126) whereas the trail limb exhibited a larger trail limb approach distance despite a lower obstacle height (Mean difference = -20.65 mm, Hedge's *G* = -0.220). Toe clearance was similarly higher for the lead foot after lowering the obstacle height (Mean difference = 6.01 mm, Hedge's *G* = 0.142) but the trail limb slightly decreased toe clearance after lowering the obstacle (Mean difference = -9.14 mm, Hedge's *G* = -0.222). While changes to heel clearance was similar for both limbs across both obstacles (Lead heel clearance: Mean difference = 9.94 mm, Hedge's *G* = 0.232, Trail heel clearance: Mean difference = -9.81 mm, Hedge's *G* = -0.262), changes to obstacle landing difference were relatively limited to the trail limb, where lead landing difference was farther for the smaller obstacle (Mean difference = 16.18 mm, Hedge's *G* = 0.189) but the trail limb landed closer to the smaller obstacle (Mean difference = -15.67 mm, Hedge's *G* = -0.350). The results suggest older adults approached the smaller obstacle with larger steps across and lower toe clearances, supporting this sample effectively adopted a different strategy to cross the smaller obstacle.

Table 1. Obstacle Crossing Kinematics (Mean and Standard Deviations) for Older Adults at Obstacles of Different Heights

		Approach Distance	Toe Clearance	Heel Clearance	Landing Distance
Large Obstacle (179 mm)	Lead foot	580 ± 36	209 ± 37	133 ± 33	219 ± 71
	Trail foot	317 ± 79	219 ± 36	421 ± 34	578 ± 37
Small Obstacle (139 mm)	Lead foot	571 ± 63	216 ± 40	143 ± 45	236 ± 84
	Trail foot	297 ± 57	209 ± 38	411 ± 33	562 ± 45

Significance: When the obstacle height dropped, older people took longer steps with lower clearances, effectively adapting their strategy to the lower obstacle. Our findings contribute to the understanding of how older adults adapt their gait patterns when navigating obstacles of varying sizes and exploring the impact of different types of obstacles (e.g., height, width) on gait adaptations may identify potential challenging environments and aid in the ability to navigate through environments for older adults. Future samples will include more older adults with depression for a more comprehensive understanding of the complex interplay between cognitive processes for everyday locomotor adaptations. Quantifying lower limb adaptation can contribute to the development of effective fall prevention programs tailored to the unique needs of older individuals with depression.

References: [1] Damme KSF. *Eur Arch Psychiatry Clin Neurosci*. 2020. doi:10.1007/s00406-019-01059-0, [2] Sobin C. *Am J Psychiatry*. 1997. doi:10.1176/ajp.154.1.4, [3] Anstey KJ *Journals Gerontol - Ser B Psychol Sci Soc Sci*. 2008. doi:10.1093/geronb/63.4.P249

Dynamic visual acuity during asymmetric walking

C. Dane Napoli[1*], Joseph Hamill[1], Wouter Hoogkamer[1], Richard E.A. van Emmerik[1]
[1]University of Massachusetts Amherst
*Corresponding author's email: dnapoli@umass.edu

Introduction: Research on shock attenuation has pointed to both active (e.g., kinematic alterations) and passive (e.g., tissue deformation) mechanisms as ways in which the head is stabilized during gait [1,2]. Importantly, these mechanisms appear to respond adaptively to varying degrees of impact shock, such that greater amplitudes are attenuated to a greater extent [3]. As a result, the head remains relatively stable across many locomotor conditions, thereby facilitating visual field stability [3,4,5].

Much of the research on shock attenuation and head stability, however, has not directly measured visual perception and has instead inferred how it might be affected by head movement during locomotion. Moreover, little research has considered how such adaptations might manifest when individuals locomote under perturbing conditions.

Accordingly, we investigated the effects of imposed locomotor asymmetry on dynamic visual acuity, head stability, and shock attenuation [6]. We expected that when locomotor asymmetry was imposed, individuals would exhibit decrements in shock attenuation, head stability, and dynamic visual acuity. Further, we expected that individuals would adapt to this asymmetry over time, and that this adaptation would be reflected by a partial return in the dependent variables described above during the adaptation period [7].

Methods: Fifteen young, healthy adults were recruited for this study. Participants were instrumented with retroreflective markers and had accelerometers secured to the tibiae and frontal bone. Participants walked on an instrumented split-belt treadmill while reporting the orientations of Landolt-C optotypes that were projected at heel strike.

Participants first walked on the treadmill with both belts set to 1.2 $m \cdot s^{-1}$ for the baseline condition. The left and right belts were then set to 0.6 $m \cdot s^{-1}$ and 1.8 $m \cdot s^{-1}$, respectively, for the adaptation condition. Finally, both belts were again set to 1.2 $m \cdot s^{-1}$ for the washout condition. The following results and discussion will be limited to the baseline and adaptation conditions.

Step length asymmetry, shock attenuation, head stability (i.e., high- and low-frequency head acceleration power), and dynamic visual acuity (i.e., visual task performance) were measured throughout each condition. All dependent measures were averaged across the first and last fifty strides and were assessed using repeated measures analyses of variance [6].

Results: Consistent with prior literature, step length asymmetry was greater in the adaptation condition than in the baseline condition across both the first and last fifty strides (Figure 1). Shock attenuation was greater in the baseline condition than in the adaptation condition across the first fifty strides, but not across the last fifty strides. Both high- and low-frequency head acceleration power were greater in the adaptation condition than in the baseline condition across both the first and last fifty strides. Dynamic visual acuity was greater in the baseline condition than in the adaptation condition across the first fifty strides, as indicated by a moderate effect size. Dynamic visual acuity was also found to increase from the first to the last fifty strides of the adaptation condition ($p=0.030$; $d=-0.530$) [6].

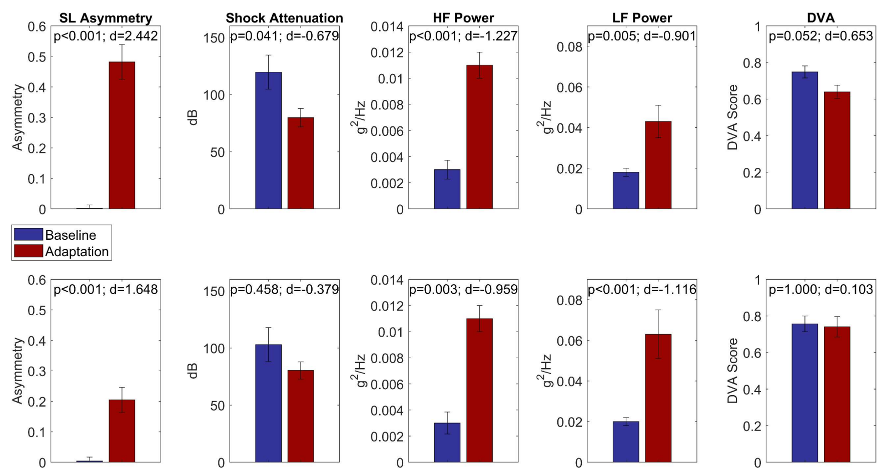

Figure 1: Step length (SL) asymmetry, shock attenuation, high- and low-frequency (HF; LF) head acceleration power, and dynamic visual acuity (DVA) across the first (top panel) and last (bottom panel) fifty strides.

Discussion: These results confirmed our expectation that locomotor asymmetry would lead to decrements in shock attenuation, head stability, and dynamic visual acuity. Of particular importance is the tendency of these variables to partially return to baseline values after a period of adaptation, even when an external perturbation persists. Many of the differences observed between the baseline and adaptation conditions across the first fifty strides were either smaller in magnitude or no longer present when measured across the last fifty strides. It is worth noting that the increased low-frequency head acceleration power in the adaptation condition may reflect an increase in compensatory head movement that aids in visual perception, as dynamic visual acuity increased across the adaptation condition (Figure 1) [6,8].

Significance: Our results illustrate the adaptive nature of the locomotor system by examining the maintenance of dynamic visual acuity when the body is constrained to asymmetry. Further, we caution against the conflation of low-frequency head acceleration power with a lack of head stability, as the former may reflect compensatory movement that aids in visual perception.

References: *[1] Boyer & Nigg (2004), J Biomech 37(10); [2] Paul et al. (1978), J Biomech 11(5); [3] Hamill et al. (1995), Hum Mov Sci 14(1); [4] Derrick et al. (1998), Med Sci Sport Exerc 30(1); [5] Mercer et al. (1995), J Athl Train 45(3); [6] Napoli et al. (2022), Hum Mov Sci 85(11); [7] Roemmich & Bastian (2018), Annu Rev Neurosci 41(1); [8] Pozzo et al. (1990) Exp Brain Res 82(1).*

ELEPHANT TRUNK BIOMECHANICS AND MUSCLE MECHANICS USING HUMAN-BASED TECHNIQUES

Andrew Schulz[1,2,*], Margaret Zhang[2], Cassandra Shriver[3], Krishma Singal[4]
School of Biological Sciences[3], Mechanical Engineering[2], and Physical Sciences[4], Georgia Tech, Atlanta, GA
Max Planck Institute for Intelligent Systems[1], Stuttgart, Germany
*Email: aschulz@is.mpg.de

Introduction: The elephant trunk is an immensely complex appendage with deeply folded skin on the dorsal portion for protection and intermediate wrinkles for gripping slippery objects with asymmetric trunk elongation between these sections [1]. The skin covers the inner portion of the trunk, comprised of several thousand muscle fibers that, through actuation, can erect vibrissae or whiskers for added sensing [2]. With no bones or joints, this hydrostat is an infinite degree of freedom system, as any two constraints will have a third in between them [3]. In this abstract, we discuss a preliminary experiment to determine the amount of muscular work capable in a living elephant trunk utilizing an actuated peg board and collaborating with Zoo Atlanta.

Methods: The methods described will be that of two different sets of experiments, including both with living African elephants (L*oxodonta africana*) at Zoo Atlanta, as well as diseased African and Asian elephant trunk specimens taken at Humboldt University in Berlin, Imperial College London, and Icahn School of Medicine at Mount Sinai. The living elephants were both 38-year-old elephants, and the deceased elephant specimens ranged from 2 years old to 45 years old. We utilized uniaxial strain testing of elephant trunk skin to determine the mechanical properties of the different load-bearing layers of the skin as they develop with age as well as to understand the specific muscle output of the elephant trunk muscle. All experiments and dissections were under approved research by Georgia Tech's IACUC and Zoo Atlanta's ethics team.

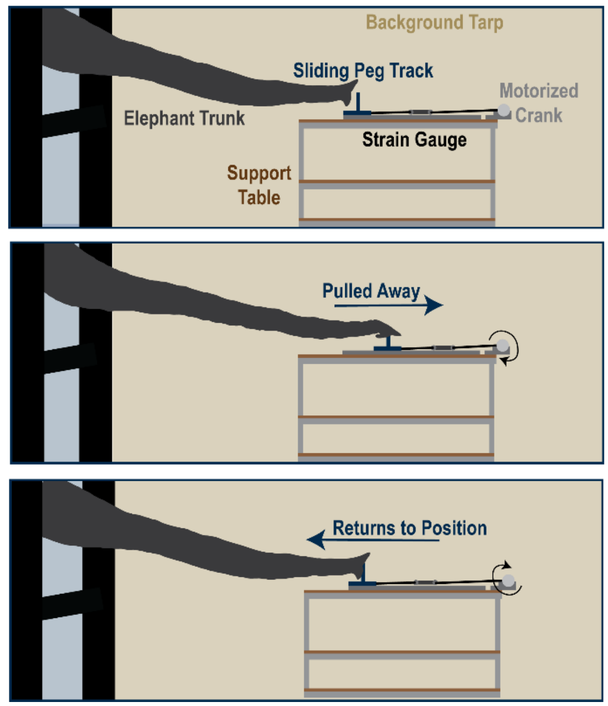

Figure 1. Schematic of an elephant experiment showing an in-vivo work loop technique of hydrostats.

Results & Discussion: The elephant trunk has asymmetries in function from the micro to the macro levels. Preliminary elongation trials with the elephant displayed that the elongation capabilities of the trunk are upwards of 20% with asymmetries of dorsal and ventral stretching. When performing uni-axial tests of the elephant skin, we see a divergence of strain stiffening versus strain softening behaviour, with the dorsal skin exhibiting strain softening due to the wrinkled geometry. In contrast, the ventral skin is strain stiffening with shifting moduli of elasticity throughout different trunk sections due to asymmetric wrinkles and folds. Additionally, in working with Zoo Atlanta, we have worked to understand the elephant trunk using an in-vivo work loop technique **Figure 1.** This in vivo- work loop setup uses an actuated peg board with an elephant to determine the amount of network of an elephant during elongation cycles. Current results are preliminary in showing that an elephant can output upwards of 30N of force to the peg gripping and exhibit 40 N mm of work during a pulling cycle. Additional experiments will be performed with varying distances between the elephant trunk, and we believe that the utilization of this in-vivo work loop technique could help advance the comparative biomechanics field utilizing human-based techniques. As the elephant trunk is pure muscle with no bones, joints, or additional assistive mechanics, the work loop technique creates a uniquely applicable technique for a comparative understanding of purely muscular appendages like hydrostats and skeletons.

Significance: Overall, the ability of engineers and biologists to share knowledge and techniques allows more scientifically encompassing comparative biomechanics studies to occur. Using uni-axial strain tests, complex materials mimic, advanced microscopy, and work-loop techniques can all be applied to various biological organisms to help advance biomechanics, bio-inspired robotics, and even wildlife conservation. By utilizing these engineering-based techniques and collaborating with biologists, we can discover connections between a macro function and micron-sized discovery, such as the non-homogeneity of elephant skin explained by collagen entanglement in the skin.

Acknowledgments: Thank you to those who assisted in making this work possible, including early influencers of G. Sawicki, C. Higgins, J. Reidenberg, and Y. Chang. Thank you to the Haptic Intelligence Department and Max Planck Institute for Intelligent Systems for travel support.

References: [1] Schulz AK et al. PNAS 119: 31, 2022. [2] Schulz AK et al. Bioinsp. & Biom. 113: 110845, 2023. [3] Kier B. et al. Zoo. Jour. of Lin. 130: 1985

DYNAMIC TRACKING OF KNEE KINEMATICS USING ULTRASOUND: A CADAVERIC VALIDATION

Matthew B. Blomquist[1*], Everett Cartier[1], Joshua D. Roth[2]
Departments of [1]Biomedical Engineering and [2]Orthopedics and Rehabilitation, University of Wisconsin-Madison, Madison, WI
*mbblomquist@wisc.edu

Introduction: There are key limitations of current methods for assessing knee kinematics in the clinic despite their universal importance for diagnosing injuries, tracking healing, and guiding treatments. For example, to check for a torn ligament, clinicians manually apply loads to the knee and qualitatively assess whether the relative motion between the femur and tibia is abnormal [1]. This subjective assessment works for severe injuries, but not for more subtle changes due to progressive disease or healing. In a research setting, optical motion capture and fluoroscopy are commonly used to measure joint kinematics. However, several limitations, such as skin-motion artifacts (motion capture), ionizing radiation and costly infrastructure (fluoroscopy), and burdensome set-up (both), limit their use in the clinic. Thus, there is a critical need for a novel method to quantify knee kinematics in the clinic that is accurate, precise, safe, accessible, and broadly familiar to both clinicians and researchers. Accordingly, *our objective for this study* was to develop and validate an ultrasound (US)-based bone-tracking algorithm to assess knee kinematics during standard clinical assessments.

Methods: *Robotic Testing:* In five fresh-frozen human cadaveric knees (1F/4M, 66.2 ± 3.4 years), we simulated varus, valgus, anterior, and posterior laxity assessments at 0°, 20°, and 45° of knee flexion using a six degree-of-freedom (DOF) robotic simulator (KR300 2700-2, KUKA; ***Figure 1a***). During each assessment, we placed an US transducer (LF11-5H60-A3, ArtUS, TELEMED) over the lateral (during varus loading), medial (during valgus loading), or anterolateral (during anterior-posterior (A-P) loading) aspects of the knee. We performed all laxity assessments using two different loading trajectories: (1) uni-directional loading to simulate an ideal laxity exam with no off-axis loads, and (2) multi-directional loading to simulate a realistic laxity exam with off-axis loads [2]. Max forces/torques for both trajectories were ±89 N (rate of 4.5 N/s) for A-P and ±15 Nm (rate of 0.75 Nm/s) for varus-valgus (V-V).

US-based bone-tracking algorithm: We used B-mode cine loops and a custom, normalized cross-correlation method to track bone motion. After defining the region of interest (ROI) around both the femur and the tibia (***Figure 1b***), we found the peak correlation between each ROI in successive frames to track distance changes. To determine the V-V angle changes, we converted the distances to rotations by measuring the medial-lateral width of the tibial plateau and assuming the varus or valgus rotation occurred about an axis through the middle of the plateau [3]. To determine the A-P translation changes, we divided the distance changes by the cosine of the angle between the transducer plane and the A-P axis.

Analysis: For each laxity assessment, we computed the errors between the US-measured kinematics and the time-synched robot-measured kinematics at each US frame (***Figure 1c***). We pooled errors across specimens and flexion angles and computed the root-mean-square errors for each clinical assessment.

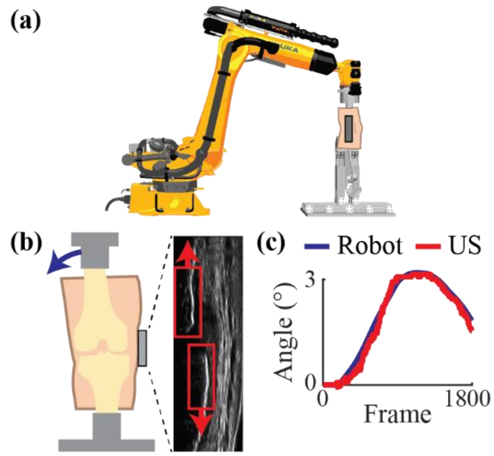

Figure 1: ***(a)*** We used a Kuka robot to simulate clinical laxity exams and measure resulting robot kinematics. ***(b)*** We estimated bone kinematics using our ultrasound-based bone-tracking algorithm. ***(c)*** Representative plot of ultrasound (US) vs robot kinematics.

Table 1: Root-mean-square errors (RMSE) and maximum translation/rotation measured by the robot (mean ± std) for each loading trajectory.

		RMSE	Max motion
Anterior (mm)	Uni	0.92	5.9 ± 2.2
	Multi	1.44	7.1 ± 1.8
Posterior (mm)	Uni	1.47	5.1 ± 1.7
	Multi	0.84	4.5 ± 1.5
Varus (°)	Uni	0.77	3.7 ± 1.3
	Multi	0.47	2.3 ± 0.5
Valgus (°)	Uni	0.51	3.3 ± 0.8
	Multi	0.78	2.6 ± 1.2

Results & Discussion: The largest RMSEs for rotations and translations were 0.77° and 1.47 mm, respectively, for uni-directional loading and 0.78° and 1.44 mm, respectively, for multi-directional loading (***Table 1***). Even though errors in multi-directional loading increased in some of the DOFs, the measurement errors were still lower than differences in laxity between intact and ligament injured knees by three to four fold [4, 5].

Additionally, the errors in V-V are on par with previous errors determined for biplane fluoroscopy during simulated walking in one human cadaver, with RMSEs reaching 0.77° for V-V rotations [6]. However, A-P translation errors are greater in our study compared to the 0.35 mm for A-P translations in the prior study [6]. Our ongoing work is expanding this evaluation to include a variety of functional daily activities (e.g., walking, stair climbing, and stair descent). Additionally, we are currently evaluating the sensitivity of these US-measured kinematics to transducer placement, definition of bone ROIs, and loading rates.

Significance: Measuring kinematics using ultrasound will enable widespread assessments of knee kinematics because ultrasound is a safe, non-radiating method that is already familiar to clinicians. This study showed that our ultrasound-based bone-tracking algorithm is a promising approach to assess joint kinematics for a range of applications including diagnosing disorders, monitoring healing, and informing rehabilitation.

References: [1] Torg et al. (1976), *Am J Sports Med* 4(2); [2] Arant et al. (2023), *ORS Conference*, Paper #1982; [3] Dhaher et al. (2003), *J Biomech* 36(2); [4] Robinson et al. (2006), *Am J Sports Med* 34(11); [5] Stephen et al. (2016), *Am J Sports Med* 44(2); [6] Guan et al. (2016), *IEEE Trans Med Imaging* 35(1).

SHOOTING DYNAMICS IN A QUASI FITTS TASK UNDER MECHANICAL AND PERCEPTUAL LOADS

Martin Flament Fultot PhD[1*], Aidan Gross B.S.[1], Brian Higginson PhD[1]
Galvion Ballistics Ltd., Warfigther Systems Integration Laboratory
*Email: martin.fultot@galvion-usa.com

Introduction: Marksmanship is a dynamic aiming task in which a target needs to be acquired and then the gun needs to be moved and aligned so as to place a round accurately. Several extrinsic and intrinsic factors can affect the performance of the aiming task, which is usually measured by accuracy and time. However, the underlying biomechanical dynamics can reveal adaptive patterns that stabilize performance. For instance, in canonical Fitts' tasks the velocity profile of the aiming effector shows changes as a function of difficulty. Such changes are supposed to reflect a strategy shift in how the target is honed in. In order to better predict aiming behavior under such circumstances, dynamical model of underlying biomechanics have been proposed. In particular [1] have attempted to model the aiming system in a Fitts' task as a complex Hookean spring or oscillator, where the neuromuscular system modulates parameters such as stiffness as well as Duffing and Rayleigh terms as a function of factors affecting difficulty. The model transforms the data into Hooke's portrait where acceleration is a function of position and velocity. The model successfully predicts the traditional Fitts' law and velocity profiles. In non-oscillatory tasks such as aiming towards a target with a rifle and engaging it, though, the same model can still predict the observed dynamics, assuming a sufficiently overdamped oscillation will fail to show the repetitive feature of Fitts'-like aiming.

Moreover, the concept of "difficulty" in traditional Fitts' task can be extended to include factors beyond target distance and size. In the case of military applications, an important source of task difficulty comes from mechanical and perceptual load. More specifically, in this study we assess the effects of Night Vision Goggles (NVGs) both as an inertial alteration to head rotation and as form of perceptual encapsulation that reduces the participants Field of View (FOV) and thus access to peripheral information about the shootability of targets. In a "shoot, no shoot" task, participants need to choose between two equidistant targets before they have visual information about its "shoot" or "no shoot" state and at the same time rotate their rifle towards it to aim. To separate the mechanical from the perceptual effect on aiming, the task was performed wearing either a helmet only (HEL), a helmet with NVGs deployed (NVG-NOCW), or a helmet with NVGs deployed and a counterweight on the back (NVG-CW). We hypothesized that, akin to a Fitts' task, the different conditions would influence the coefficients of a Hookean model that reproduces the angular dynamics of the rifle with NVG-NOCW constituting the most difficult condition and HEL the least once.

Methods: Seven participants with shooting experience were recruited. They stood about 15 feet away from two equidistant targets situated at nearly 45 degrees left and right from a third centre target in the forward direction. Participants were instructed to aim and shoot at the centre target then pivot as quickly as possible to one of the two other targets and shoot at it if it was tagged "shoot" or aim at the other and shoot it. The two peripheral targets would not pivot and show their tag until the first centre target was shot. They were randomized so that the participant could not predict which of the two was the "shoot" target. All participants repeated the task four times per condition (HEL, NVG-NOCW, NVGCW). Angular data was collected using an IMU aligned with the rifle's barrel and "up" vector to extract angular velocity from the gyroscope. The gyroscope data was filtered using first order Savitzky-Golay filter, resampled, and trimmed so all trials begun with the first shot and ended with the last shot. Hooke's portraits were then generated by integrating the angular velocity to obtain angular position and differentiating angular velocity to obtain angular acceleration. The three variables were then used to create incrementally more complex dynamical models by regressing position, velocity (damping), cubic position (Duffing) and cubic velocity (Rayleigh) on acceleration with R's lme4 mixed effects modelling until further terms didn't significantly improve the fitness of the model. Lastly the effect of the three different conditions was added to the model incrementally to assess their modulatory effect on the different parameters.

Results & Discussion: The final unconditional model contained the following coefficients (intercept = 0.352, position = -4.777, Duffing = 3.622, and velocity = -0.003) with p-value < 2.2e-16 and Chi-square = 1060.3. From this unconditional basis we next looked to test whether controlling for condition in our model improved the fitness. We found that adding condition as a fixed term and interaction term continued to improve the model fitness. The final conditional model contained the following coefficients (intercept = 0.228, position = -4.509, Duffing = 3.343, velocity = -0.002, condition = 0.107, position:condition = -0.232, Duffing:condition = 0.238, velocity:condition = -0.0007) with p-value < 1.623e-15 and Chi-square = 63.47. These results show that the different mechanical and perceptual conditions affected the dynamics in a similar way to difficulty parameters in traditional Fitts. However, the similarity is not straightforward as the departure from linearity affected mostly the acceleration phase and not so much the deceleration phase. HEL showed a higher stiffness profile. This could be due to higher "confidence" both in the status of the target (thanks to more peripheral information) and in the controllability of the head towards the honing in phase, as opposed to the NVG-NOCW condition, in which information was not available and inertial conditions would make the honing more unstable.

Significance: The present study shows the value of dynamical modelling applied to aiming tasks. In particular the traditional divide between aiming with and without repetition can be dissolved by a model that encompasses both. Similarly, the concept of difficulty can be extended from the traditional Fitts' distance and size parameters to a variety of factors that don't always result in the same Hookean profiles. It is possible that an even more encompassing model predicts Hooke's profiles and performance metrics directly as a function mechanical and cognitive load, as well as extrinsic parameters such as target distance and size.

References:

[1] Mottet, D., & Bootsma, R. J. (1999). The dynamics of goal-directed rhythmical aiming. *Biological cybernetics*, 80(4), 235-245.

RELATIONSHIP BETWEEN MEAN VELOCITY IN BIPEDAL, TANDEM AND UNIPEDAL STANCES

Ruth Ann Miller[1]*, Jett Mattison[1], Ken Pitetti[2], Nils Hakansson[1]
[1]Department of Biomedical Engineering, Wichita State University, Wichita, KS
[2]Department of Physical Therapy, Wichita State University, Wichita, KS
*Corresponding author's email: ramiller@shockers.wichita.edu

Introduction: Stable balance is a prerequisite for basic mobility and impaired balance is a known factor in unintended falls. A common field test used to assess balance is the unipedal stance in the BESS[1] and BOT-2[2] tests. However, the unipedal stance, especially for the elderly population, is an unstable stance liable to adverse events during testing. Populations susceptible to falling would benefit from a clinical test that provides the similar information as the unipedal test but using a more stable stance such as a bipedal stance. Therefore, the objective of this study was to determine whether a correlation exists between the center of pressure (COP) mean velocity of the unipedal, tandem, and bipedal stance postures. The existence of such a correlation would afford the benefits of unipedal stance information acquired through the more stable bipedal posture.

Methods: To fulfill the aforementioned objective, the mean velocity of the COP was measured from thirty-five (19 females, 16 males; age = 23.7 ± 2.8 years) neurotypical young adults as they stood as still as possible on an ATMI force plate in each of six stances comprised of three postures (i.e. bipedal, tandem, and unipedal) under two conditions (i.e. with eyes open and eyes closed) for 30 seconds. The data collection order was randomized by the six stances and repeated in four blocks of testing (A, B, C, and D). Loss of stance start and stop times were identified and not used in the calculations. Mean velocity of the COP (MVelocity, mm/sec) was calculated using the equations provided by Prieto[3]. An Anderson-Darling test for normality was performed on the mean velocity data in for all stances *a priori*. Correlation was assessed using Kendall's Tau. Kendall's Tau is a non-parametric statistic that is it more efficient with non-normal data.[4] Statistical significance was set at $p<-0.05$.

Table 1 Kendall's τ Mean Velocity

Stance	2FEO		2FEC		TDEO		TDEC		1FEO	
2F EC	**0.5242**	*								
TD EO	*0.2692*	*	**0.4028**	*						
TD EC	*0.2294*	*	*0.3914*	*	**0.4845**	*				
1F EO	*0.3169*	*	**0.4344**	*	**0.5178**	*	**0.4292**	*		
1F EC	*0.2536*	*	*0.3720*	*	**0.4616**	*	**0.4377**	*	**0.5373**	*

* P<0.000; 2F indicates bipedal, TD indicated tandem, 1F indicates unipedal, EO indicates eyes open, EC indicates eyes closed.

Results & Discussion: The Anderson-Darling test rejected normality for the mean velocity data in all stances. A positive correlation was shown between the mean velocity in bipedal and unipedal stances. Moderate correlation ($0.4<\tau<0.69$)[5] between stance is indicated by bold type in Table 1, and was found between (a) unipedal eyes closed (1FEC) and unipedal eyes open (1FEO) stance, (b) 1FEC and both tandem stances, (c) 1FEO and both tandem stances, (d) 1FEO stance and the bipedal stance with eyes closed (2FEC), (e) tandem stances with eyes open and eyes closed, (e) 2FEC and tandem eyes open, and (f) between the bipedal stances with eyes open (2FEO) and eyes closed. A weak correlation ($0.1<\tau<0.39$)[5] is indicated by italicized type and is found between (a) 2FEO stance and both tandem stances and the (b) 2FEO stance and both unipedal stances. All stance pairs showed either weak or moderate correlation. In all cases, the p-value was statistically significant. The safest and most commonly used stance when measuring balance, 2FEO, had its highest tau correlation with 2FEC and showed low tau correlations to 1FEO and 1FEC.

Significance: The unipedal stance, while being an effective tool for assessing balance in healthy populations, is an unstable stance. If it can be shown that the mean velocity correlations sufficiently well between unipedal and other more stable stances, perhaps clinical criteria can be developed to effectively assess balance using only the bipedal stance. A limitation of this study concerned age of participants. Future research needs to determine correlations between stances in the 4th to 9th decades of life.

References:

[1] Balance Error Scoring System (BESS), University of North Carolina, Sports Medicine Research Laboratory; [2] Bruininks-Oseretsky test of motor proficiency (2nd ed.). NCS Pearson, Minneapolis, MN 2005; [3] Prieto et al. (1996), *IEEE Trans Biomed Engr* 43(9); [4] Fielden et al., Nonparametric measures of association. No. 91. Sage, 1993; [5] Schober et al. (2018), *Anesthesia & Analgesia* 126(3).

KNEE ANGLE AND ANGULAR VELOCITY DURING A PROGESSIVE LATERAL STEP-UP TEST IN CHILDREN WITH CEREBRAL PALSY

Sydni V.W. Whitten[1], Shelley Jakiel[1], Trevor Batson[1], Gavin Colquitt[2], Li Li[2], Joshua Vova[3], Ye Shen[1], Christopher M. Modlesky[1*]
[1]Department of Kinesiology, University of Georgia, Athens, GA
*Corresponding author's email: christopher.modlesky@uga.edu

Introduction: Cerebral palsy (CP) is a neurological disorder associated with muscle weakness, increased muscle stiffness, poor muscle quality, and spasticity [1,2] which impair lower extremity movement and execution of physical activities. The lateral step-up test (LSUT) has been used to assess gross motor function, mobility, and functional strength in individuals with CP [3]. However, no studies have assessed the joint kinematics that may affect LSUT performance in children with CP. One purpose of the study was to explore the differences in knee joint kinematics (angle and angular velocity) during a LSUT between children with CP and typically developing control children. It was hypothesized that at the point of push-off, children with CP exhibit less extension, more adduction, less extension velocity, and less abduction velocity of the stationary knee than controls. A second purpose of the study was to determine if the expected differences in knee joint kinematics are related to LSUT performance. It was hypothesized that greater knee extension and knee extension velocity are related to better LSUT performance.

Methods: Twenty-three children with mild spastic CP (5-11 y; I-II on the Gross Motor Function Classification Scale) and 23 age-, sex-, and race-matched typically developing controls participated in the study. Anthropometrics were collected, and 53 retroreflective markers were placed on the bony landmarks following a standard Qualisys AIM model (Qualisys, v 2022.1, Lincolnshire, IL) for the LSUT. The LSUT consisted of 4 trials, progressed in step height (0, 10, 15, and 20 cm), and lasted 20 s/trial. Participants stood with feet shoulder-width apart with the more affected limb as the stationary limb and were instructed to complete as many steps as possible within a trial. Motion capture (100 Hz; Qualisys) was used to capture kinematic data. Using Visual 3D (C-motion, Germantown, MD), a 14 Hz low-pass Butterworth filter was applied and the knee joint angle and angular velocity of the stationary limb were assessed at the point of push-off from the ground of the moving (less-affected) limb. Data were analyzed using IBM SPSS Statistics (v 24, Armonk, NY). Differences in group characteristics were determined using independent t-tests if data were normally distributed and Mann-Whitney U tests if data were non-normally distributed. A linear mixed effect model, with participant height as a covariate, was used to assess group differences in angle and angular velocity and differences between step heights. Analysis of covariance were used for the post-hoc analyses. Spearman rho correlations (r_s) were used to assess the relationship between knee joint kinematics and LSUT performance.

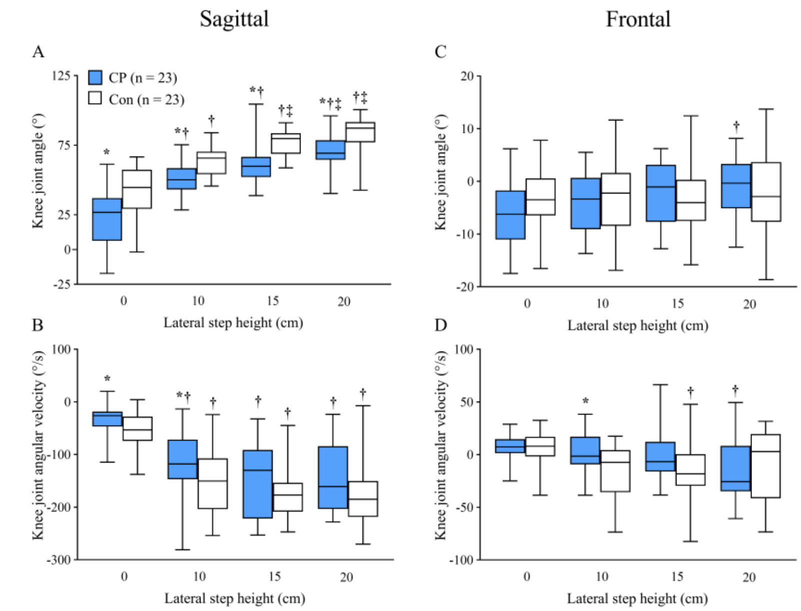

Figure 1: Knee joint kinematics at push-off during a progressive LSUT. *Group differences, †Different form 0 cm, ‡Different from 10 cm.

Results & Discussion: There were no group differences in age, height, body mass, or body mass index. Knee joint kinematic results are presented in Fig 1. At the point of push-off, children with CP exhibited greater knee extension of the stationary limb at all step heights compared to controls. For both groups, there was less extension at 10, 15, and 20 cm compared to 0 cm and also at 20 cm compared to 10 cm. Children with CP exhibited less extension velocity compared to controls at 0 and 10 cm. Both groups had greater extension velocity at 10, 15, and 20 cm compared to 0 cm. Children with CP exhibited less abduction velocity at 10 cm compared to controls and exhibited greater abduction velocity at 20 cm compared to 0 cm. Greater knee extension velocity was related to greater LSUT performance at 10 cm (r_s = -0.555, p = 0.006) and 15 cm (r_s = -0.480, p = 0.020). Both groups exhibited less extension and greater extension velocity at the higher step heights compared to the lowest step height. Although both groups exhibited greater extension velocity at the higher step heights, greater extension velocity was related to greater LSUT performance only in children with CP.

Significance: This is the first study to assess the relationship between knee joint kinematics and LSUT performance in children with CP. The relationship between knee extension velocity and LSUT performance suggests that increases in knee extension velocity may improve the ability to step laterally in children with CP. Studies are needed to identify rehabilitation techniques that increase the velocity at which a child with CP can move through the full knee range of motion.

Acknowledgements: This research study was funded by the National Institutes of Health (HD090126).

References: [1] Elder et al. (2003), Dev Med Child Neurol 45(8); [2] Johnson et al., (2009), J Pediatr 154(5); [3] Chrysagis et al. (2013), *Disabil Rehabil* 35(11).

CURVE ANALYSIS OF FOOT KINEMATICS IN RUNNERS WITH PLANTAR HEEL PAIN

Hanieh Pazhooman[1*], Mohammed S. Alamri[1], Zahra Mollaei[1], Stephen C. Cobb[1]
[1]Gait & Biodynamics Laboratory, Department of Kinesiology, University of Wisconsin-Milwaukee, Milwaukee, WI, USA
*Corresponding author's email: pazhoom2@uwm.edu

Introduction: Plantar heel pain (PHP) is one of the most common overuse injuries in runners, and is associated with diminished general health-related quality of life [1,2]. PHP is generally believed to be caused by mechanical overload of the plantar fascia during gait that leads to microtrauma and subsequent degeneration [3]. Although foot kinematics in patients with PHP during walking has been investigated [4], the kinematics during running has not. Moreover, all the studies conducted have investigated differences in predetermined discrete variables during gait. Statistical parametric mapping (SPM) on-the-other hand allows investigation of joint angle differences over an entire time series [5]. Therefore, the purpose of the current study was to use SPM to investigate foot joint angle differences between runners with and without PHP during running. Due to the degeneration of the plantar fascia associated with PHP, we hypothesized that runners with PHP would exhibit increased joint angles in the foot consistent with inadequate tension in the plantar fascia. Specifically, we postulated that runners with PHP would demonstrate increased dorsiflexion, abduction, and eversion (angles associated with pronation) in the rearfoot (RC) and the medial and lateral midfoot (MMF, LMF). Based on the pronation twist concept of the forefoot [6] and the relative independence of the medial and lateral forefoot (MFF, LFF), we hypothesized the MFF would exhibit increased dorsiflexion and inversion positions and the LFF would demonstrate increased plantar flexion and inversion positions.

Methods: 14 females and 16 males (age: 18-45 y) provided written consent and participated in the study. A seven-segment foot model that defines six functional articulations (RC, MMF, LMF, MFF, LFF, 1MTP) was used to quantify foot motion [7]. 15 runners with common clinical symptoms of PHP, and 15 uninjured runners completed 5 running trials. A 10-camera system captured marker positions, and a force plate identified initial contact and toe-off events. A MATLAB program was used to filter the data, perform rigid body transformation procedures, and calculate angular positions of the articulations during the stance phase. Next, the spm1d package for one-dimensional SPM was used to assess the normality of the data and then perform independent t-test, or non-parametric, analysis of the three-dimensional RC, LMF, MMF, LFF, MFF functional articulation time series and the 1MTP functional articulation sagittal plane time series.

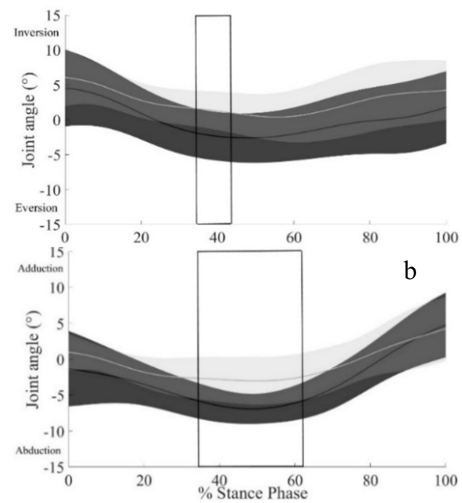

Fig 1: LFF frontal (a) and transverse (b) plane stance phase joint angles. Black line: Uninjured runners (mean ± 1SD); Grey line: PHP runners (mean ± 1SD). Boxes indicate areas of significant group differences.

Results & Discussion: Independent t-test results showed significantly greater LFF inversion angle in the PHP group from 34% - 43% of stance phase (mean difference: 3.57°; $p = 0.043$) and significantly greater LFF adduction angle in the PHP group from 34% - 62% of stance (mean difference: 3.64°; $p = 0.008$) (Fig 1).

The LFF of the PHP runners was in a position of greater inversion for the entire stance phase, but the significant increase occurred during midstance as the rearfoot was transitioning from pronation to supination. The increased position of LFF inversion as the foot transitions from pronation to supination could be due to insufficient tension in the plantar fascia. Interestingly, although the period during which the significant difference in the time series occurred differed, Takabayashi et al. [8] reported an increased forefoot inversion position in runners with flatfoot (excessive pronation) compared to those with normal foot structure. The increased LFF adduction position in PHP runners during mid-late midstance and early propulsion was not anticipated. The transverse plane motion of the forefoot during running gait has not been well defined, however, although the difference was not significant, runners with flatfoot in the Takabayashi et al. [8] also demonstrated an increased position of forefoot adduction compared to runners with normal foot structure. So, the increased LFF adduction position in PHP runners may also be consistent with increased position of forefoot pronation.

Significance: Many common PHP interventions, such as functional foot orthoses, focus on rearfoot function. The increased LFF inversion and adduction positions in runners with PHP identified in the current study suggest that it may be may also be important to assess and address function of the joints distal to the calcaneus.

Acknowledgements: UW-Milwaukee, CHS, Student Research Grant Award; ASB Graduate Student Grant-in-Aid.

References: [1] Di Caprio et al. (2010), J Sport Sci Med 9(4); [2] Irving et al. (2008), J Am Podiatr Med Assoc 98(4); [3] Tountas et al. (1996), Clin Orthop Relat Res; [4] Harutaichun et al. (2021), J. Assoc.Chart.Physiother.Sports Med 50; [5] Pataky et al. (2012), Comput Methods Biomech Biomed Engin 15(3); [6] Hicks et al. (1953), Journal of anatomy 87(4); [7] Cobb et al. (2016), J Appl Biomech 32(6); [8] Takabayashi et al. (2021), J Orthop Res 39(3).

ANKLE AND REARFOOT ANGLE AND ANGULAR VELOCITY IMPACT ON PERFORMANCE IN A PROGRESSIVE LATERAL STEP-UP TEST IN CHILDREN WITH CEREBRAL PALSY

Shelley Jakiel[1], Sydni V.W. Whitten[1], Trevor Batson[1], Gavin Colquitt[2], Li Li[2], Joshua Vova[3], Ye Shen[1], Christopher M. Modlesky[1*]
[1]Department of Kinesiology, University of Georgia, Athens, GA
*Corresponding author's email: christopher.modlesky@uga.edu

Introduction: Cerebral palsy (CP) is characterized by motor disability, muscular spasticity, contractures, and altered mechanical loading [1-3]. The lateral step-up test (LSUT) has been used to assess gross motor function, mobility, and functional strength, which are necessary for activities of daily living in individuals with CP [4]. The aims of this study were to determine if ankle joint kinematics of the more affected limb (MAL; stationary limb) during a progressive LSUT are different in children with CP compared to typically developing control children and if the expected differences are related to LSUT performance. It was hypothesized that during the concentric push-off phase of the LSUT, children with CP will have more plantarflexion, more rearfoot eversion, and less plantarflexion velocity in the MAL. In addition, greater plantarflexion angle and velocity will be related to better LSUT performance.

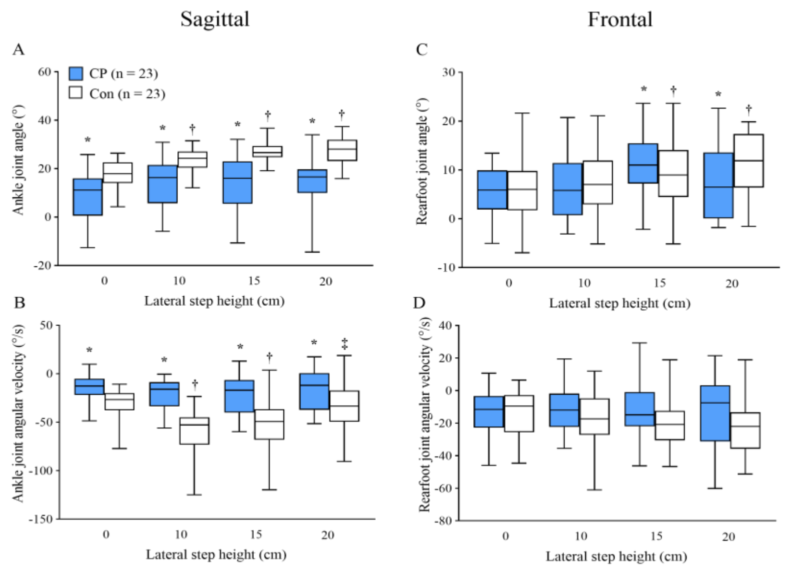

Figure 1: Ankle and rearfoot joint kinematics at push-off during the progressive LSUT. *Group differences. †Different form 0 cm. ‡Different from 10 cm.

Methods: Twenty-three children with mild spastic CP (5-11 y; I-II on the Gross Motor Function Classification Scale) were matched by age, sex, and race with 23 typically developing controls. Participants were outfitted with 53 passive reflective markers placed on bony prominences based on a Qualisys AIM model (Qualysis, v 2022, Lincolnshire, IL). The LSUT consisted of four 20 s trials, each corresponding to an increase in step height (0, 10, 15, and 20 cm). Participants were instructed to stand with feet shoulder-width apart with the MAL stationary on the elevated surface and the LAL resting on ground level. Participants were to complete as many repetitions as possible during each trial. Kinematic data were collected through motion capture (100 Hz, Qualisys) and processed through Visual 3D (C-motion, Ontario, Canada). A 14 Hz low-pass Butterworth filter was applied, and joint angles and angular velocities of the ankle and rearfoot were calculated at each push-off from the ground by the LAL. Data were analyzed via IBM SPSS Statistics (v24, Armonk, NY). Differences between groups were assessed using independent t-tests for normally distributed variables and Mann-Whitney U tests for nonnormally distributed variables. A linear mixed effect model with subject height as a covariate was used to assess group differences in angle, angular velocity, and differences between step heights. Analysis of covariance was used for post hoc analyses. Spearman rho correlations (r_s) were utilized to assess the relationship between joint kinematics and LSUT performance.

Results & Discussion: Groups were not significantly different in age, height, body mass, or body mass index. Ankle and rearfoot joint kinematics are presented in Figure 1. During concentric push-off, children with CP had less dorsiflexion at all step heights (all $p \leq 0.001$). Rearfoot eversion in children with CP was less than controls at 15 and 20 cm ($p = 0.021$ and 0.048, respectively). Children with CP demonstrated less plantarflexion velocity at all step heights (all $p < 0.005$). There were no significant correlations between ankle and rearfoot angles and LSUT performance during concentric push-off at any step height for either group (rs range =-0.169 to 0.358, all $p > 0.05$). As step height increased, plantar flexion velocities in children with CP were correlated with LSUT performance (rs range = -0.456 to -0.611; all $p < 0.05$). Consistent with the hypothesis, children with CP displayed more plantarflexion and less plantarflexion velocity compared to controls. However, higher plantarflexion velocity was associated with better LSUT performance in children with CP.

Significance: This study assessed ankle and rearfoot specific angles, angular velocities, and their relationships with LSUT performance in children with CP. The relationship between plantarflexion velocity and LSUT performance suggests that increases in plantarflexion velocity may improve LSUT performance. Further research is warranted to determine potential treatment strategies that increase plantarflexion velocity to lead to greater performance on the LSUT and physical function in children with CP.

Acknowledgments: This research study was funded by the National Institutes of Health (HD090126).

References:[1] Arneson et al. (2009), *Disabil Health J* 2(1); [2] Bax et al. (2005), *Dev Med Child Neurol*, 47(8); [3] Mohagheghi et al. (2007), *Clin Biomech*, 22(6); [4] Chrysagis et al. (2013), *Disabil Rehab*, 31(11);

QUADRICEPS STEADINESS AND JERKY KNEE MOTION FOR INDIVIDUALS WITH KNEE MUSCULOSKELETAL INJURY AND DISEASE

Nicholas L. Hunt[1*], Matthew V. Robinett, Tyler N. Brown
[1]Boise State University, Boise, ID, USA
*Corresponding author's email: nichunt@u.boisestate.edu

Introduction: Knee instability, characterized as joint buckling, shifting, or giving way during weight-bearing activity, is reportedly a pathogenic factor for joint musculoskeletal injury and disease [1]. Adequate quadriceps strength and contraction steadiness may prevent knee instability to mitigate injury and disease development. Although quadriceps steadiness is related to poor physical function, it is unknown if it decreases with knee musculoskeletal injury and disease, or whether it is related to "jerky" knee motion that may characterize joint instability [2]. We hypothesize that individuals with knee injury and disease will exhibit less quadriceps steadiness and jerkier sagittal and frontal plane knee motions, and quadriceps steadiness would exhibit linear relation to jerkiness of knee motion.

Methods: Four groups (1: adults with confirmed knee musculoskeletal injury (ACL-R), 2: disease (OA), and sex- and age-matched controls (3: to ACLR and 4: to OA)) were recruited. Each participant performed three knee extensor maximal voluntary isometric contractions (MVIC) on an isokinetic dynamometer (HUMAC NORM, CSMI, Stoughton, MA, USA) and three walk trials at a self-selected speed through the motion capture volume.

The MVIC trial with highest maximal voluntary torque was bandpass filtered (3.9 to 31.2 Hz), linearly detrended, and submitted to a Fast Fourier Transform. Then, quadriceps steadiness measures, including peak power frequency (PPF), defined as frequency with the highest power, and coefficient of variance (CV), defined as the ratio of filtered torque standard deviation by mean of raw torque, were calculated according to [3].

For the walk task, 3D marker trajectories were collected using ten high-speed optical cameras (240 Hz, Vantage, Vicon Motion Systems LTD, Oxford, UK). For each trial, the marker data was lowpass filtered (12 Hz, 4th order Butterworth) and processed in Visual 3D (C-Motion, Rockville, MD) to obtain frontal and sagittal plane jerk cost, according [2].

For statistical analysis, quadriceps steadiness (CV and PPF), and sagittal and frontal plane knee jerk cost during early (0-17%), mid (17-34%), and full stance (0-100%) measures were submitted to a one-way ANOVA. Correlation analysis determined relation between quadriceps steadiness and knee jerk cost for all participants and each cohort. Alpha level was $p<0.05$.

Results & Discussion: Knee injury and disease impacted every quadriceps steadiness and knee jerk measure except CV (all: $p<0.005$). In partial agreement with our hypothesis, the ACLR cohort exhibited 66% greater PPF ($p=0.047$), and a 33-42% reduction in sagittal and frontal plane knee jerk cost than matched controls (all: $p<0.001$); whereas, the OA cohort exhibited no difference in quadriceps steadiness, yet a 34-45% reduction in sagittal and frontal plane jerk cost compared to matched controls (all: $p<0.001$). Individuals with knee injury and disease may adopt gait biomechanics to increase joint stability and protect from further soft-tissue degradation, however, it is unclear whether these knee mechanics are adopted to overcome neuromuscular deficits.

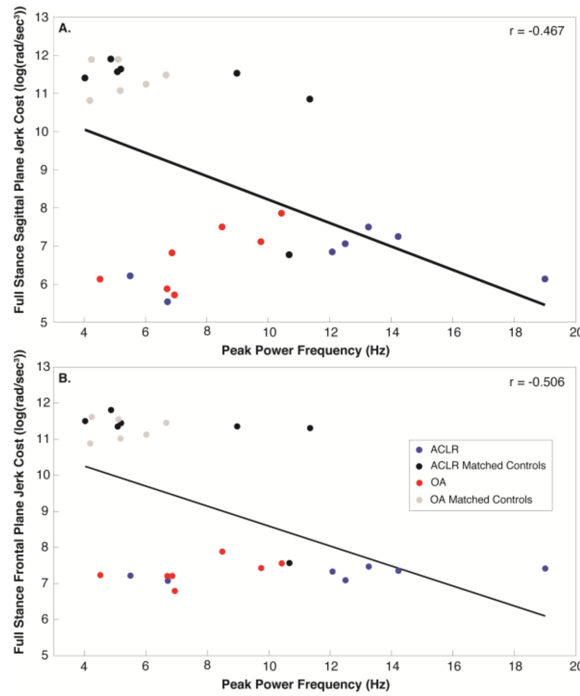

Figure 1: Depicts relation between PPF and full stance sagittal (A) and frontal plane (B) jerk cost.

Individuals with less steady quadriceps contraction may minimize knee joint motion to provide stability and protect from hazardous soft-tissue loading. Participants exhibited a significant positive relation for CV with midstance sagittal plane jerk cost ($r=0.482$, $p=0.011$), and contrary to our hypothesis, a significant moderate, negative relation between PPF to sagittal and frontal plane knee jerk cost during each stance phase (**Fig. 1**) (all: $r=-0.440$ to -0.539, $p<0.022$). Yet, following knee injury, individuals with less steady quadriceps contraction may exhibit jerkier knee motion when loading the limb in early stance. The ACLR cohort exhibited strong, negative correlations between CV and early stance frontal plane jerk cost ($r=-0.774$, $p=0.041$), but strong, positive correlation between PPF and early stance frontal plane jerk cost ($r=0.835$, $p=0.020$). The OA cohort exhibited strong, positive correlations between PPF and sagittal plane jerk cost during each stance phase ($r=0.784$ to 0.830, $p<0.037$), but further work is needed to determine whether this is a consequence of joint disease or age-related changes to muscle, as OA participants were significantly older than the ACLR cohorts.

Significance: These results provide valuable insight on quadriceps function, and their relatedness to gait, in individuals with musculoskeletal injury and disease. These insights may be employed to develop targeted interventions to mitigate acceleration of knee musculoskeletal disease. Yet, future work is needed to determine the specific neuromuscular deficits to reduce hazardous joint motions that may contribute to the development and progression of degenerative joint disease.

Acknowledgements: NIH NIA (R15AG059655) and NIGMS (2U54GM104944) supported this work.

References: [1] Blalock, *C Med Ins Arth Musc Disord*, 2015; [2] Krammer, *Gait Posture* 2021. [3] Satam, *Clin Biomech* 2022

PERSONALIZED CONTROL IN POWERED KNEE PROSTHESIS: A NOVEL FRAMEWORK EMPLOYING CONTINUOUS IMPEDANCE FUNCTIONS AND PCA-BASED TUNING

Woolim Hong[1], He (Helen) Huang[1*]
[1]Joint Department of Biomedical Engineering, NC State University, Raleigh, NC & University of North Carolina, Chapel Hill, NC
*Corresponding author's email: hhuang11@ncsu.edu

Introduction: Lower-limb amputation significantly impacts an individual's mobility and agility, leaving them vulnerable to falls and injury [1]. This is particularly true for transfemoral amputees, who face greater mobility challenges and a higher risk of falling due to their more significant portion of limb loss compared to transtibial amputees. Powered prostheses have been developed and studied over the years as a treatment to restore the amputees' gaits as closely as possible to those of healthy people. However, most of these studies still lack personalized control for amputees [2] or require a demanding tuning process for each individual and walking scenario to achieve an appropriate walking performance [3]. In this study, we propose a novel framework for powered knee prostheses that can deliver personalized control to amputees, potentially enhancing user-prosthesis coordination and the functionality of the prosthesis. The main objective of this study is to facilitate personalized knee prosthesis control while reducing the effort of tuning parameters.

Methods: We propose a continuous impedance control framework for knee prostheses, which requires continuously varying stiffness, damping, and equilibrium angle throughout the gait cycle [2, 4]. This is referred to as 'continuous impedance functions (CIFs)' in this study. To obtain the CIF set for each individual, we utilized a convex optimization problem that fits the estimated knee joint torque to a given able-bodied human dataset [5]. For personalization purposes, the CIFs need to be fine-tuned for each user, so we developed a new tuning space using Principal Component Analysis (PCA). This helps us to identify common features (i.e., principal components (PCs)) while reducing the dimensionality of the original data. By adjusting the weights of the PCs, we can reconstruct the CIFs, which we use as tuning parameters to refine the initial CIFs for each individual.

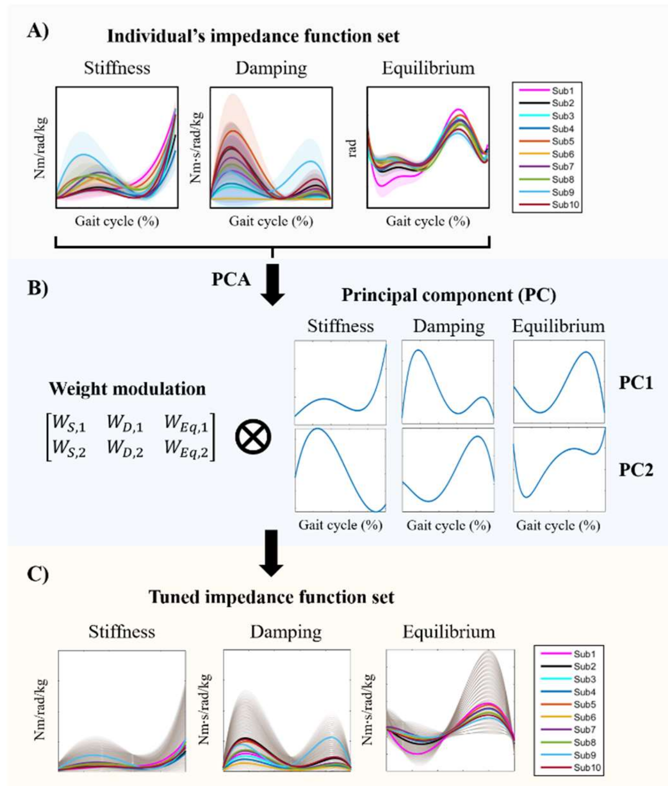

Figure 1. Study overview: The colors represent each subject's result. (A) Individual knee impedance function set by fitting them to human data. (B) PCs are extracted using PCA. (C) Personalized impedance function sets are obtained by adjusting the weights of the PCs; transparent lines indicate the newly generated impedance functions resulting from the modulation of the PCs' weights.

Results & Discussion: Figure 1(A) illustrates the continuous knee joint impedance functions (i.e., CIFs) for ten able-bodied subjects obtained through convex optimization. As shown in Figure 1(B), PCA is used to extract the 1st and 2nd PCs, reducing the dimensionality of the original CIF dataset. PC1 accounts for 95.91%, 93.67%, and 96.06% of the total variance in stiffness, damping, and equilibrium angle, respectively, while PC2 accounts for 3.09% (stiffness), 6.09% (damping), and 3.04% (equilibrium angle). This indicates that PC1 captures the majority of the information in the original impedance functions, while PC2 provides additional variation for impedance function modulation. To assess the feasibility of using PC weight modulation to fine-tune the impedance functions, we adjusted the weights of PC1 and PC2 and observed the resulting variations in impedance functions. Figure 1(C) presents the reconstructed impedance functions based on varying weights of the PCs. The weights of PC1 (i.e., $W_{S,1}$, $W_{D,1}$, $W_{Eq,1}$) were modulated from 0 to 1 in increments of 0.1, while the weights of PC2 (i.e., $W_{S,2}$, $W_{D,2}$, $W_{Eq,2}$) were modulated between -1 and 1 in increments of 0.1. The newly generated impedance functions cover the actual impedance functions, demonstrating their potential for fine-tuning by adjusting the corresponding weights of the PCs. Consequently, our framework requires only six tuning parameters for each joint (based on two PCs), in contrast to the current finite state machine-based impedance control framework, which necessitates 12 parameters for each joint [3].

Significance: The significance of this study lies in reducing the effort for the personalization of knee prostheses by 1) presenting continuous functions for stiffness, damping, and equilibrium angle, and 2) incorporating a novel, smaller-dimensional tuning space through the application of PCA, which facilitates the personalization of the specified continuous impedance functions.

Acknowledgements: This work was supported in part by the National Institute on Disability, Independent Living, and Rehabilitation Research (NIDILRR; #90ARHF0004), and in part by National Science Foundation (NSF; #2211739).

References: [1] Miller et al. (2001), Arch Phys Med Rehab 82(9); [2] Best et al. (2023), IEEE Trans Robotics; [3] Li et al. (2021), IEEE Trans Robotics 38(1); [4] Anil Kumar et al. (2021), ICRA, pp. 3219–3225; [5] Embry et al. (2018), IEEE Trans Neural Sys Rehab Eng 26(12).

THE ANTICIPATION AND DIRECTION OF TREADMILL-INDUCED SLIP PERTURBATIONS AFFECTS THE NEUROMECHANICAL BEHAVIOR OF DISTAL LEG MUSCLES

Emily Eichenlaub[1*], Jessica Allen[2], Vicki Mercer[3], Jeremy Crenshaw[4] and Jason R. Franz[1]
[1]Joint Dept. of Biomedical Engineering, UNC Chapel Hill and NCSU, USA, [2]Dept. of Mechanical and Aerospace Engineering, UF, USA, [3]Division of PT, UNC Chapel Hill, USA, [4]Dept. of Kinesiology and Applied Physiology, University of Delaware, USA
*Corresponding author's email: emeich@email.unc.edu

Introduction: The timing and magnitude of local muscle neuromechanics can yield insight into proactive and reactive balance control during walking and changes thereof due to aging or disease. Moreover, when combined with walking balance perturbations, we can establish cause-effect relations between the presence of instability and specific changes in local neuromechanics. Intuitively, anticipation of a balance perturbation should provide a means to disproportionately probe proactive vs. reactive changes in muscle activations, lengths, and velocities. This notion is supported by some studies reporting evidence of proactive adjustments for an anticipated walking balance perturbation [1]. However, studies have either investigated a single perturbation direction [1-2], analyzed only reactive responses [3], or omitted ultrasound data critical to understand the origins of sensory signals and the vigor of motor responses. Our purpose was to determine how muscle neuromechanics influence susceptibility to anticipated and unanticipated walking balance perturbations. We hypothesized that, compare to unperturbed walking, both anticipated and unanticipated balance perturbations would elicit greater local muscle adjustments, evidenced by greater activations. We also hypothesized that (i) unanticipated balance perturbations would elicit greater reactive local muscle responses evidenced by greater requisite activation, while (ii) anticipated balance perturbations would elicit greater proactive local muscle responses via greater preactivation.

Methods: Twenty young adults participated in this single-visit study (8 M/12 F; mean ± standard deviation; age: 22.8±3.3 years; preferred walking speed: 1.39±0.14 m/s). Participants responded to treadmill belt perturbations delivered at the instant of heel-strike in which the belt accelerated or decelerated over 200 ms at 6 m/s^2 controlled using a custom Matlab script. We delivered perturbations either unexpectedly (i.e., unanticipated) or at the end of a three second verbal countdown (i.e., anticipated). We collected electromyographic (EMG) activities from the left medial gastrocnemius (MG) and tibialis anterior (TA) using wireless electrodes at 1000 Hz (Delsys). We calculated integrated EMG (iEMG, V*s) for: early stance (0-50%, ESt), late stance (50-100%, LSt), early swing (0-50%, ESw), and late swing (50-100%, LSw) for each stride.

Results & Discussion: Participants showed increased MG activity during LSt, ESw, and LSw in preparation for anticipated accelerations and during ESt in preparation for decelerations compared to unperturbed walking and unanticipated perturbations ($p<0.01$) (Fig. 1). Conversely, we found no anticipatory changes for TA activation in the preceding stride for either perturbation direction. Independent of anticipation for decelerations, participants showed higher TA activity during Est and LSt of the perturbed stride compared to unperturbed walking, to resist the rapid plantarflexion ($p<0.01$). During the perturbed stride, anticipated decelerations resulted in increased MG activity during LSw, while unanticipated decelerations resulted in decreased MG activity during Est and ESw compared to unperturbed walking. During the perturbed stride following anticipated accelerations, we found higher MG activity compared to unperturbed and unanticipated accelerations in ESt, LSt, and ESw ($p<0.01$) to resist the rapid dorsiflexion. Unanticipated accelerations only resulted in higher MG activity than unperturbed walking during ESw ($p<0.01$). Regardless of direction/anticipation, we found delayed MG activity in the perturbed stride. During the recovery stride, anticipated decelerations yielded higher Est, LSt, and ESw TA activity while anticipated treadmill accelerations resulted in significantly higher LSt and ESw MG activity compared to unperturbed walking and unanticipated perturbations (TA, $p<0.01$; MG, $p<0.01$). We are now quantifying MG and TA muscle lengthening from cine ultrasound images to understand the origins of sensory signals and the vigor of the EMG responses.

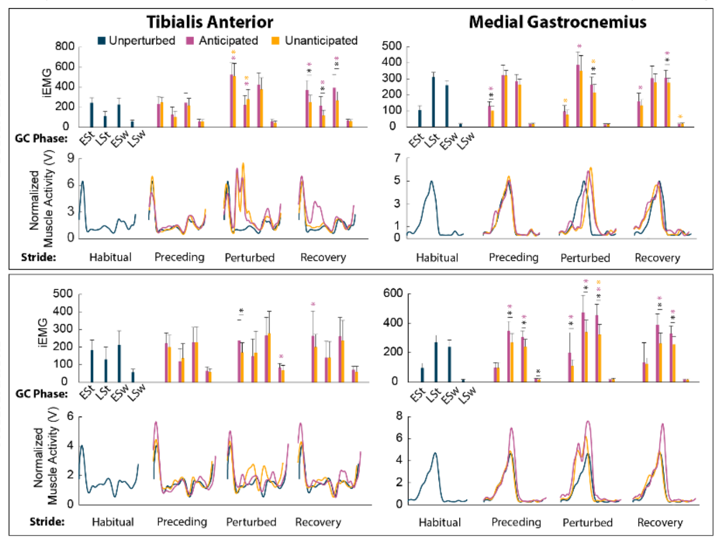

Figure 1. iEMG and normalized activities prior to and following a walking balance perturbation. Black asterisks (*) denote significant effects of anticipation. Pink and yellow asterisks denote differences from unperturbed.

Significance: We reveal effects of anticipation on perturbation-induced balance responses at the local muscle level that were not evident in our previous work using measures of whole-body instability in the same subjects [4]. Although speculative, this suggests that more subtle effects of age, cognitive decline, or neurodegenerative disease on motor planning (i.e., anticipation) or execution to mitigate the instability elicited by perturbations may manifest in local muscle neuromechanics prior to being detected by whole-body vulnerability.

Acknowledgements: Supported by NIH (R21AG067388). We thank Daniel Duque Urrego/Sahaj Sapovadia for their contributions.

References: [1] Chambers et al. (2007), *Gait & Posture*; [2] Marigold et al. (2002), *American Physiological Society*; [3] Brodie et al. (2018), *Journal of Biomechanical Science and Engineering;* [4] Eichenlaub et al. (2023), *Human Movement Science.*

CAREER PROGRESSION IN TACTICAL ATHLETES: EFFECT ON BIOMECHANICAL AND PERFORMANCE OUTCOMES

Tyler C. Cardinale[1], Andrew Plows[1], Julia A. Lytle[1], Tatiana E. Djafar[2], Joshua D. Winters[2], Trevor D. Kingsbury[1]
[1]Clinical Biomechanics Laboratory, Naval Medical Center San Diego, San Diego CA, USA
[2]University of Kentucky, Sports Medicine Research Institute, Lexington KY, USA
Email: tyler.c.cardinale.ctr@health.mil

Introduction: Navy Explosive Ordnance Disposal (EOD) technicians are tactical athletes with demanding performance requirements. These demands require higher levels of athletic ability, and these technicians can be more severely impacted by injury than other military roles. Due to the specialized nature of their occupation, this population was identified to need embedded providers and strength coaches within their training environment, but these additional resources have only been available for the last 3-5 years [1]. As a result, there is continued considerable interest in understanding the current function and career progression of these technicians. Previous work has highlighted the potential for loss of readiness in the later stages of a warfighter's career [2]. To monitor the function of EOD technicians and provide real-time feedback and data to coaches and providers, the use of portable force plates has emerged as a valuable tool. This technology allows for comprehensive, rapid assessments of technicians. When combined with previous injury history and years of service, it allows for a retrospective analysis of EOD technicians. The purpose of this study was to evaluate the effect of career progression defined by years of service on biomechanical and performance outcomes in EOD technicians.

Methods: 168 EOD technicians were assessed using a full battery of biomechanical tests on portable force plates (Kistler Instrument Corp, Novi, MI, USA), and data were collected and processed using ForceDecks software (VALD, Newstead, AU) during their deployment training cycle. All technicians~~s~~ were fit for full duty at the time of assessment. This assessment included a countermovement jump (CMJ), repetitive hopping test (HT), and isometric mid-thigh pull (IMTP). Variables of interest included CMJ take-off and landing forces, concentric peak power, jump height, and take-off force asymmetry; IMTP peak vertical force and peak vertical force asymmetry; and HT reactive strength index (RSI). General demographic information was also recorded for these technicians including years of service (yr). They were categorized into groups based on phase of career (early 0-6 yr, N=84, mean age 25.6 yrs; mid 7-14 yr, N=58, mean age 32.3 yrs; and late 15+ yr, N=26, mean age 39.6 yrs). A one-way ANOVA was used to determine if there were differences in the biomechanical variables between career phases with alpha = 0.05.

Measure	Group	Mean	StD	F	Sig.
CMJ Takeoff Peak Force (N)	Early Career (0-6 yr)	2205.96	422.10	0.01	0.99
	Mid Career (7-14 yr)	2193.84	412.79		
	Late Career (15+ yr)	2200.35	485.95		
CMJ Peak Landing Force (N)	Early Career (0-6 yr)	5480.40	1497.56	0.32	0.73
	Mid Career (7-14 yr)	5305.98	1406.27		
	Late Career (15+ yr)	5249.35	2157.73		
CMJ Peak Power (W)	**Early Career (0-6 yr)**	**4478.67**	**771.91**	**4.00**	**0.02**
	Mid Career (7-14 yr)	**4412.17**	**1095.81**		
	Late Career (15+ yr)	**3896.46**	**998.20**		
CMJ Jump Height (Flight Time) (In)	**Early Career (0-6 yr)**	**13.15**	**2.36**	**14.77**	**0.00**
	Mid Career (7-14 yr)	**11.65**	**2.48**		
	Late Career (15+ yr)	**10.33**	**2.93**		
CMJ Peak Takeoff Force Asymmetry (%)	Early Career (0-6 yr)				
	Mid Career (7-14 yr)				
	Late Career (15+ yr)				
IMTP Peak Vertical Force (N)	Early Career (0-6 yr)	3043.27	452.53	1.04	0.35
	Mid Career (7-14 yr)	3142.53	495.13		
	Late Career (15+ yr)	2999.42	569.01		
IMTP Peak Vertical Force Asymmetry (%)	Early Career (0-6 yr)				
	Mid Career (7-14 yr)				
	Late Career (15+ yr)				
HT RSI (Flight/Contact Time)	**Early Career (0-6 yr)**	**1.75**	**0.42**	**4.91**	**0.01**
	Mid Career (7-14 yr)	**1.65**	**0.39**		
	Late Career (15+ yr)	**1.48**	**0.33**		

Figure 1: Descriptive statistics and ANOVA results for career phase data. Significant differences in bold.

Results & Discussion: There were no significant performance differences in technicians when performing strength tasks. There were significant differences in both ballistic tasks. Later career technicians had significant biomechanical and performance decreases compared to younger technicians [Figure 1]. Decreases in jump height were detected at the mid and late career point compared to early, while CMJ power and HT RSI were significantly decreased at the late career point.

Significance: The population's overall performance was excellent, as anticipated. However, there was a significant decline in ballistic performance and lower body power among technicians in the later stages of their careers, despite maintaining their performance in strength-based tasks. These findings may highlight the importance for technicians to engage in diverse strength and conditioning programs that prioritize maintaining plyometric capacity and ballistic performance, particularly as they advance to later stages of their careers. Specifically, the late career RSI of <1.50 would indicate the need for corrective plyometric work. Additionally, across all measures, asymmetry was present at all timepoints (>10%). As a result, continued engagement throughout the technician's career with strength and conditioning coaches and providers may be beneficial to deter career phase performance drop-offs seen in this large cohort and maintain or improve symmetry and other musculoskeletal health metrics.

Acknowledgements: Thank you to General Dynamics Information Technology for support. The views expressed herein do not necessarily reflect those of the Department of the Navy, Department of Defense, DHA or the U.S. Government.

References: [1] Stump, Jeremiah et al. "EOD Warrior Athlete Working Group: Recommendations for an Evidence-Based, Forcewide, EOD Warrior Athlete Program." (2014). [2] Apt, John et al. (2016) Mil Med, 181, 2:173.

UNDERSTANDING DYNAMIC POSTURAL REACTIONS IN BLIND PEOPLE USING AN AUDITORY STIMULUS

Lauren A. Luginsland, Kiara Barrett, Justin A. Haegele, Hunter J. Bennett
Department of Human Movement Sciences, Old Dominion University, VA USA
*Corresponding author's email: llugi001@odu.edu

Introduction: Visual cues have been shown to play a key role in human balance [1]. During a quiet-standing task, sighted individuals rely on proprioception ~70%, vestibular system ~20%, and visual feedback ~10% to maintain their overall balance [2]. Alterations to the environment may alter the recruitment of sensory information in sighted individuals; this has been referred to as the 'reweighting' of sensory information [2, 3]. However, research investigating the influence of 'reweighing' in populations lacking one of these sensory feedback mechanisms is necessary. Blindness, a visual acuity <3/60, has been estimated to affect 0.48% of people in the world [4]. Blind individuals must rely on their senses quite differently than sighted peers due to their lack of visual information. As humans living in a dynamic environment, it is crucial to be able to adapt to environmental changes quickly and efficiently, whereby postural reaction time can be paramount to overall safety. Dynamic postural reaction time tasks provide important information about underlying cognitive and sensory processing [5] as well as provide an assessment of overall motor program function used to initiate and complete tasks [6]. The timing of sensory processes are crucial evaluation factors when investigating reaction time (initiation of stimulus to start of physical movement), movement time (initiation of physical movement to completion of task) and overall response time (initiation of stimulus to completion of task) [7]. Despite typically being referred to as "deficient" in some capacity, 'reweighting' of sensory processes in blind people could become streamlined over the lifespan by experiences to accommodate for environmental changes [8]. The purpose of the study was to investigate postural reaction time tasks in blind and sighted persons using an auditory stimulus. We hypothesized there would be no significant differences in any temporal component (reaction, movement, response) of the postural reaction tasks.

Methods: Five blind people (i.e., no light perception in either eye or some light perception with the inability to recognize the shape of a hand at any distance or in any direction) and five age, sex, and body mass index (BMI) matched sighted controls (AGE: 29.00±11.53yrs. vs. 30.20±12.28yrs., BMI: 30.93±6.16 vs. 29.06±7.54) participated in the study. All participants were right leg dominant. Kinematic and kinetic data was collected using a 10 camera VICON motion capture system with two Bertec force plates. Simple auditory (stimulus presented as "left" or "right" -> tap stated foot) and complex auditory (same stimulus presented -> tap opposite foot) postural reaction time tasks were performed. Data was analyzed in Visual 3D (Version 6, C-Motion, Inc.). Reaction, response, and movement times were calculated using the anterior-posterior center of pressure (COP) data for each task. The start of the response was determined at the instance the COP exceeded (3*Standard Deviation) + Mean of the baseline at the fore period. The response end was determined based on a 10-N cut-off applied to the vertical ground reaction force used to detect the foot tap; the immediate value greater than 10-N was used to determine the event. A 2 x 2 (Group x Task) mixed model ANOVA was utilized to determine reaction, movement, and response time differences (SPSS Version 27, IBM Corp; alpha level 0.05).

Results & Discussion: There were no significant interactions for reaction, movement, or response time (F: 0.38, p=.58; F=0.08, p=0.79; F=0.27, p=.62, respectively). The simple task had shorter reaction time (F=7.04, p=.03; η_p^2 = 0.47) but no difference in movement (F=0.13, p=.73) or response (F=2.73, p=.14) times compared to the complex task. The blind group had increased response (F=5.45, p=.048, η_p^2 = 0.41) but not reaction (F=3.32, p=.11) or movement (F=1.70, p=.23) times compared to sighted controls (Fig.1). The lack of group differences in reaction and movement times partially supports our hypothesis. Differences in the summation of those times (i.e., response time) may be due to the visual advantage of the CON group to see the overall location of the force plate in the lab. Therefore, they were able to tap the force plate in front of them without extending their limb as deliberately compared to the blind group. These findings may be indicative that 1) vision is not as important in dynamic postural reaction tasks as 'reweighting' of the senses can overcome the lack of feedback and 2) blind people should not be viewed as 'deficient' in these tasks. These findings are supported by the tendency of our anatomical structure of our brain pathways whereby visual stimuli is processed slower compared to auditory [9].

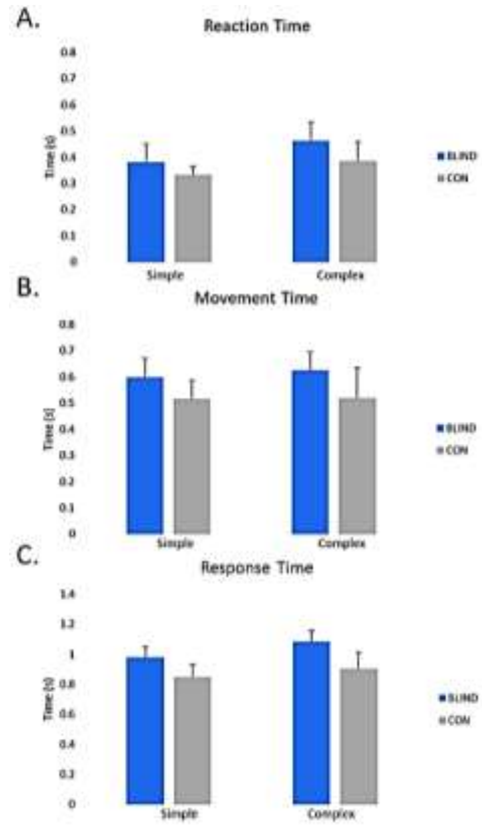

Figure 1. Depicts mean and standard deviation of (A) Reaction Time, (B) Movement Time, and (C) Response Time across groups: BLIND (Blue), CON (Gray)

Significance: The vision status of healthy individuals does not appear to influence dynamic postural reaction time. Blind people achieved similar times compared to their sighted peers which should be a consideration used in therapeutic and rehabilitation settings.

References: [1] Lee & Lishman (1975), *J Hum Mov Stud* 1(2); [2] Peterka (2002), *J Neurophysio* 88(23); [3] Braddick & Atkinson (2020), *Perception* 49(8); [4] Bourne et al. (2017), *Lan Glob Hlth* 5; [5] Molholm et al. (2002), *Cogn Brain Res* 14; [6] Keele (1968), *Psych Bul* 70(6); [7] Armitano-Lago et al. (2020), *Scan J Med & Sci* 30(8); [8] Huxham et al. (2001), *Aus J Physio* 47(2); [9] Brebner (1980), *Reaction Times.*

LOW-PROFILE WEARABLE SUIT FOR SENSING HUMAN DYNAMICS

Ryan T.F. Casey[1*], Christoph P.O. Nuesslein[1], Anirban Mazumdar[1], Gregory S. Sawicki[1], Aaron J. Young[1]
[1]Georgia Institute of Technology
*Corresponding author's email: rcasey9@gatech.edu

Introduction: The current state of the art for collecting biomechanical data of humans is to use high precision motion capture systems and force plates. While these systems are very accurate, their drawbacks include inaccessibility, inability to study certain movements in their correct contexts, and significant data processing to achieve results. The field has developed alternatives that utilize wearable technology and developed approaches including the XSens IMU based motion capture system and Harvard's strain sensor-based suit, which can characterize the kinematics of human motion [1][2]. However, no wearable system to date is capable of characterizing dynamics of human motions.

The ability to accurately quantify ground reaction forces as well as kinematics with low-profile wearable technology would enable dynamics data to be collected in many new contexts outside of lab environments. The development of such a sensing suit would be an enabling technology for exoskeleton controllers which are often in a torque control paradigm. Furthermore, real-time feedback could be employed to help users minimize potentially dangerous joint loading consequences of their motions, whether via active exoskeleton assistance, or through sensory feedback to the user, to make them cognizant of dangerous postures. We present and characterize a wearable biomechanics sensing suit that incorporates pressure sensing insoles as a means of characterizing ground reaction forces.

Methods: The Second-Skin is a wearable sensing suit consisting of compression pants and a modified running backpack. Onboard are eight total sensors, six inertial measurement units (IMUs), and two pressure sensing insoles. The IMUs are 3DM®GX5-AHRS series IMUs from Parker Hannifin Corporation©, which are industrial grade precision IMUs that are small and lightweight, and the pressure sensing insoles are OpenGo™ insoles from zFlo. Each IMU is placed on a different segment of the body (Figure 1A), which allows for each segment of the body to be measured independently. Onboard the backpack a NVIDIA® Jetson Nano handles communication and syncing between all the sensors via ROS. Each IMU connects to the Jetson Nano via serial USB and can send its linear accelerations, angular velocities, and Euler angles. Additionally, each Insole connects to the Jetson via Bluetooth, and can send its vertical ground reaction force, center of pressure, linear accelerations, and Euler angles. Lastly, the compression pants and insoles can be easily swapped out for different sizes, and the running backpack can be easily adjusted, allowing the Second-Skin to be correctly fitted to most people.

A simple experiment was performed using the Second-Skin to validate its ability to measure segment angles (sagittal thigh and shank) and vertical ground reaction forces compared to conventional motion capture. One subject performed level ground walking for 45 seconds on a Bertec® instrumented treadmill while being recorded by both the Second-Skin and a Vicon® motion capture system (ground truth). RMSE of kinematic angles were calculated between these systems for the entire duration of the trial. Likewise, the vertical ground reaction forces on the left foot and right foot were measured by the instrumented treadmill and the insoles, and RMSE was calculated between these values for the entire 45 second trial.

Results & Discussion: RMSE of the sagittal plane segment angles of the left shank, right shank, left thigh, and right thigh were .095, .109, .173, and .178 (rad), respectively (Figure 1C). It is possible that the higher error of thigh segment angles relative to shank segment angles is due to the placement of the IMU being further from bone, and thus more affected by changes in soft tissue. RMSE of the vertical ground reaction forces of the left insole and right insole were 31.38 and 36.56 (N), respectively (Figure 1C). IMU measurements were able to be recorded at a rate of 200hz, and insole data was able to be recorded at a rate of 50hz, which is sufficiently fast enough to do sensing for wearables [3].

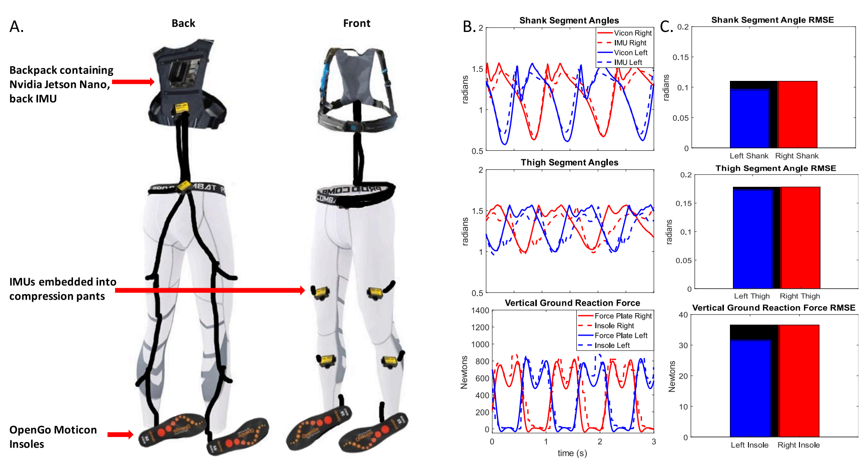

Figure 1. A: Conceptual diagram of the Second Skin. **B:** Timeseries data of recorded shank segment angles, thigh segment angles, and vertical ground reaction forces for three seconds of walking trial. **C:** RMSE between measurements from the Second Skin and measurements from Vicon motion capture system of entire walking trial.

Significance: The results indicate it may be possible to characterize dynamics of human motion with wearable technology. Doing so would potentially extend the practice of biomechanics research to new environments, and facilitate improvements in the effectiveness of wearable robots.

Acknowledgements: Supported by US Department of Energy (DOE), Sandia National Labs, DE-NA0003525.

References: [1] Mavor et al. (2020). *Sensors*, *20*(15); [2] Menguc et al. *2013 IEEE International Conference on Robotics and Automation*; [3] Santoyo-Ramón et al. (2022). *Measurement*, *19.*

RELIABILITY AND VALIDITY OF THE 3-SENSOR LOADSOL® INSOLE IN POST-STROKE PARTICIPANTS: A CURVE AND TIME-SERIES ANALYSIS

Nicole K. Rendos[1], Michael C. Rosenberg[1], Trisha M. Kesar[1]
[1]Emory University, Atlanta, GA
*Corresponding author's email: nrendos@emory.edu

Introduction: In-shoe sensors support data-driven clinical gait analysis where force platforms are unavailable. The loadsol® (novel electronics inc. St. Paul, MN) is a wireless in-shoe device with three capacitive sensors (forefoot, midfoot, hindfoot) used to measure the plantar force between the foot and the shoe. Burns et al. [1] demonstrated a single-sensor loadsol® had good-to-excellent test-retest reliability and agreement with a force plate during walking for peak ground reaction force (GRF), contact time, and impulse in able-bodied individuals. Though Burns et al. [1] utilized a step-by-step analysis of peak data during gait, a time-series and curve analysis would address remaining questions regarding both test-retest reliability and validity of the loadsol® with three sensors, rather than a single capacitive sensor. Additionally, participants with chronic post-stroke hemiparesis display aberrant gait patterns which adversely impact propulsion, gait speed, gait symmetry, and walking function [2]. Thus, the purpose of this study was to evaluate point estimate and time-series reliability and validity of the 3-sensor loadsol® in the paretic and non-paretic limbs of individuals post-stroke.

Methods: Eleven individuals with chronic post-stroke hemiparesis (5 males, 6 females, age = 57.0 ± 12.0 years, 70.0 ± 57.2 months post-stroke) walked on a split-belt instrumented treadmill with loadsols® in both shoes. Participants completed two 60-second walking trials (T1, T2) each at their self-selected (SS), medium (MS), and fast (FS) walking speeds. Loadsol® data were normalized to 100% of the gait cycle and averaged. Peak plantar force (PPF, N) and integral (INT) were calculated from the full foot sensor for each trial. Test-retest reliability was determined by intra-class correlation coefficients (ICC) for PPF and INT, and statistical parametric mapping (SPM) over the average normalized loadsol® curves for trials at the same speed. Validity was established by identifying within-trials similarity of the continuous time-series plantar force data measured by the loadsol® versus the vertical ground reaction force measured by the forceplates. The accuracy and similarity of shape of the force plate and loadsol® time-series were quantified using variance accounted for (VAF) and linear regression coefficient of determination (r^2), respectively.

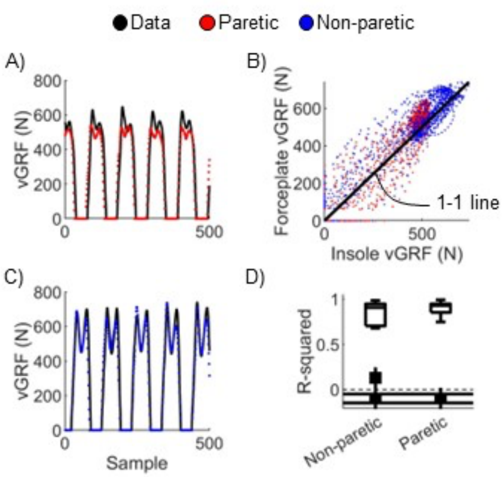

Figure 1. Example of agreement between the force plate and loadsol® time-series. A) Paretic leg force plate (black) and loadsol® (red) data for an example trial with strong correlation. B) Alignment of estimated forces in the force plate and insoles for the paretic (red) and non-paretic (blue) legs for the same trial as in (A). Perfect alignment would correspond to all data falling on the 1-1 line. vGRF = vertical ground reaction force. C) Non-paretic leg force plate (black) and loadsol® (blue) data for the same trial as in (A). D) R^2 values in the paretic and non-paretic legs across all trials. Low R^2 values were due to variable sampling rates in the loadsols® preventing alignment of the time-series.

Results & Discussion: The loadsol® demonstrated excellent test-retest reliability when examining PPF in the paretic (SS ICC = .999; MS ICC = 1.0; FS ICC = .999) and non-paretic (SS ICC = .996; MS ICC = .999; FS ICC = .999) legs. Similarly, the loadsol® also demonstrated excellent test-retest reliability for INT in the paretic (SS ICC = .995; MS ICC = .999; FS ICC = .997) and non-paretic (SS ICC = .996; MS ICC = 1.0; FS ICC = .999) legs. SPM indicated no time-series differences in average loadsol® curves between T1 and T2 at any speed for the paretic or non-paretic leg (p = 1). Additionally, forceplate and loadsol® time-series trajectories (Fig. 1 A & C) were highly similar in shape for the paretic (slope = 1.02 ± 0.25; r^2 = 0.94 ± 0.12), and non-paretic (slope = 0.96 ± 0.34; r^2 = 0.87 ± 0.26) legs (Fig. 1 B & D) legs. Differences in overall similarity between legs was lower in both the paretic (VAF = 0.80 ± 0.34) and non-paretic (VAF = 0.70 ± 0.47) legs. Differences between forceplate and loadsol® time-series were not significant for either leg ($p > 0.08$).

Overall, the loadsol® displayed near perfect test-retest reliability when examining PPF and INT point estimates at various speeds in a population with impaired gait mechanics. SPM analysis of average loadsol® curves further demonstrated no differences among normalized gait curves between trials of the same speed. The time-series similarity of forceplate and loadsol® data suggest that loadsol® inaccuracies are primarily due to differences in the scale, but not shape, of the time-series, which may stem from loadsol® calibration. The similarity of loadsol® validity between legs supports the insoles' utility in post-stroke gait analysis.

Significance: The excellent test-retest reliability of the loadsol® and similarity of the shape of the loadsol® sensors and forceplate time-series force estimates support the insoles' validity as a measurement tool for clinical gait analysis in gait impaired populations. However, differences in scale between loadsol® and forceplate time-series data may prevent direct comparison of the measures.

Acknowledgements: The authors would like to thank Emory DPT III students Badel N, Bufkin K, Chan B, Christianson H, Lionberger G, Mould O, Ogbonna N, Proppe B, Spraker J, and Tarnacki E for their assistance with data collection.

References: [1] Burns GT et al. *J Sport Sci*. 2019; 37(10). [2] Awad LN et al. *Neurorehabil Neural Repair*.2015; 29(6).

HOW DOES USE OF AN ADJUSTABLE PROSTHETIC SOCKET AFFECT PEAK VERTICAL GROUND REACTION FORCE ASYMMETRY DURING WALKING IN PEOPLE WITH TRANSFEMORAL AMPUTATION?

Gabriela B. Diaz[1], & Alena M. Grabowski[1,2]
[1]University of Colorado Boulder, Boulder, CO
[2]Department of Veterans Affairs Eastern Colorado Healthcare System, Denver, CO
Corresponding author email: Gabriela.Diaz@colorado.edu

Introduction:
To enable walking, people with a transfemoral amputation (TFA) are typically fit with a rigid prosthetic socket attached to prosthetic components such as articulating knees and passive-elastic prosthetic feet. However, use of such prostheses can result in functional impairment and secondary injury such as osteoarthritis, osteoporosis, and chronic leg and back pain [1]. These secondary conditions likely result from peak vertical ground reaction force (vGRF) asymmetry between the affected leg (AL) and unaffected leg (UL). Also, walking at faster speeds requires greater vGRF production, which may contribute to greater asymmetry between the AL and UL [2].

A prosthetic socket is perhaps the most important part of a prosthesis [3] because it allows force and energy transfer between the residual limb and prosthesis, and its fit and function influence successful rehabilitation following TFA [4]. People with TFA are typically fit with a rigid socket but commonly experience residual limb volume fluctuations of up to 18% throughout a day [5]. A prosthetic socket that adjusts to residual limb volume changes may provide a more secure attachment to the residual limb, improve force and energy transfer, and reduce socket pistoning compared with a rigid socket.

A new modular adjustable socket (Quatro, Quorum Prosthetics, Windsor, CO) has been developed to accommodate residual limb volume changes of up to 12%. The Quatro socket has adjustable panels that could decrease movement of the residual limb within the socket and improve comfort, which could allow users to walk with more symmetric peak vGRFs. Use of an adjustable socket could therefore enhance rehabilitation and improve function [2], which in turn could reduce comorbidities such as osteoarthritis and leg and back pain [1] in people with TFA. We hypothesized that due to a better fit, 1: the first and second peak vGRFs would be less asymmetric between the AL and UL when subjects with a TFA use the Quatro socket compared to a rigid socket during walking, 2: At faster walking speeds, asymmetry between the AL and UL will increase more when using the rigid socket versus the Quatro socket.

Methods: Two male subjects with TFA provided informed consent and completed three fitting sessions and one experimental session. During the fitting sessions, each subject was fit with an adjustable socket using Quatro technology that mimics their existing prosthetic socket suspension system. During the experimental session subjects walked on a dual belt force-measuring treadmill (1000 Hz; Bertec, Columbus, OH) on level ground at 0.75, 1.0, 1.25, and 1.5 m/s using a rigid socket and Quatro socket (4 trials per socket) with the same prosthetic components for each socket.

We determined peak vGRFs from ten steps for the AL and UL. Then, we calculated the 1st and 2nd peak vGRF symmetry index (SI), which is expressed as a percentage, to establish the magnitude of asymmetry between the AL and UL, where 0% is perfect symmetry [6]. SI was calculated using the following equation. SI (%) = $|(vGRF_{UL} - vGRF_{AL})/(0.5*(vGRF_{UL} + vGRF_{AL}))| * 100\%$ (Fig. 1). Due to the current small sample size, we used inferential statistics to compare peak vGRF SI between sockets.

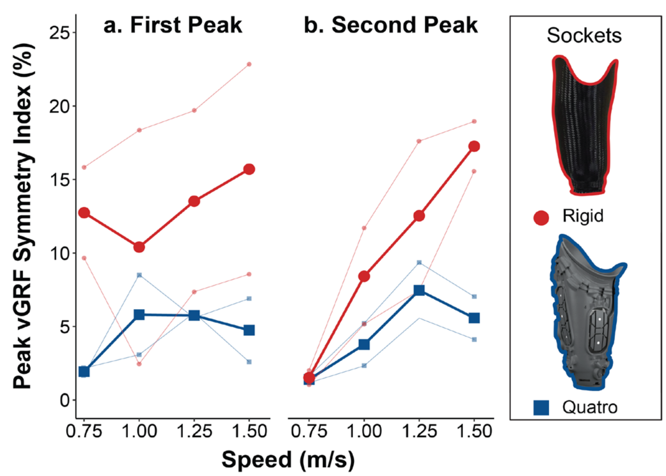

Figure 1: Average 1st (a) and 2nd (b) peak vertical ground reaction force (vGRF) symmetry index while subjects used a conventional rigid socket (Red) and adjustable Quatro socket (Blue). Bold lines represent the mean, and faded lines show each subjects data.

Results & Discussion:
Compared to using the rigid socket, use of the Quatro socket reduced 1st peak vGRF asymmetry from 13% to 5% and reduced the 2nd peak vGRF asymmetry from 10% to 5% across all walking speeds (Fig. 1). At faster speeds, the 1st peak vGRF SI increased from 2% to 6% when subjects used the Quatro socket, however SI increased from 13% to 16% when subjects used the rigid socket (Fig. 1). At faster speeds, the 2nd peak vGRF SI increased from 1% to 7% when subjects used the Quatro socket and from 1% to 17% when subjects used the rigid socket (Fig 1).

Significance:
Our results suggest that use of an adjustable prosthetic socket may decrease peak vGRF asymmetry, which could improve function and reduce secondary injury for people with TFA.

Acknowledgements:
Funding from the VA RR&D Service RX003643

References:
[1] Gailey, R., et al., *JRRD*, 2008, [2] Sanderson, D.J. and P.E. Martin, *Gait Posture*, 1997, [3] Aydin, A. and S.C. Okur, *Med. Sci. Mont.*, 2018, [4] Pirouzi, G., et al., *Sci. World J.*, 2014, [5] Sanders, J.E. and S. Fatone, *JRRD,* 2011, [6] Robinson, R.O., et al., *J. Manip. Physiol. Ther.*, 1987.

HIP MOMENT RESPONSE TO MEDIOLATERAL ASSISTANCE PROVIDED BY POWERED HIP EXOSKELETON DURING WALKING

Zhenyuan Yu[1*], Abbas Alili[2], Varun Nalam[1], Aaron Fleming[1], Helen Huang[1]
[1]Department of Biomedical Engineering, NC State University, Raleigh, NC,27695-7115; University of North Carolina at Chapel Hill, Chapel Hill, NC 27599 USA.
[2]Department of Electrical and Computer Engineering, NC State University, Raleigh, NC, 27606 USA.
*Corresponding author's email: zyu27@ncsu.edu

Introduction: Wearable robotic hip exoskeletons carry huge potential in aiding balance and locomotion for people with deficits in sensorimotor integration or with weakened muscle strength. Although a large number of hip exoskeletons are developed to provide assistance in the sagittal plane, very few have been reported for assistance in the frontal plane. Thus, we have developed a robotic hip exoskeleton that can provide assistance torque in the frontal plane and showed how it can be used to modulate the step width during walking [1]. An important aspect of this development is to analyze how human-robot interactions affect the mechanics of the hip joint and how this response differs from volitional step width increases during walking. These observations would provide insights into the underlying neuromuscular responses that the robot generates and would guide the development of the assistance and rehabilitation protocols aimed at providing personalized intervention to each user's needs.

Methods: We developed a fully powered and compliant robotic hip exoskeleton, which provided assistance in the mediolateral (ML) direction. The stiffness parameter of the admittance controller implemented on the hip exoskeleton was increased to apply the abduction torque. The direction of the applied torque was determined by changing the equilibrium angle parameter. During the study, the participant (weight: 55 kg, height:1.70 m; age: 33) was asked to walk for two minutes while wearing the exoskeleton. The participant experienced two levels of stiffness (K): 0 and 80 N·m/rad during these walking trials. It should be noted that the exoskeleton applies no torque during K=0 trial, with hip mechanics being contributed only by the user. Each stiffness level was applied for one minute of the walking trial at both joints. Visual markers were attached to the lower limb, pelvis, and torso to estimate lower-limb mechanics while wearing the exoskeleton using Vicon Nexus and Visual 3D software. Lower limb kinematic and kinetic data were then compared using statistical parametric mapping (SPM) [2] for continuous signal. The right hip joint abduction/adduction angle and moment (human and hip exoskeleton combined) averaged over the gait cycle for both trials and reported here.

Results & Discussion: Fig. 1a, b. shows the results of the right hip abduction/adduction angle and moment for two conditions namely, without (K=0) and with (K=80) abduction assistance. Fig. 1c, d shows the corresponding SPM results demonstrating the range of the gait cycles where aforementioned metrics were significantly different. From Fig 1a. it is observed that the hip abduction/adduction angle increased after applying assistance torque, which is also observed as step width increase. For abduction/adduction moment, the abduction assistance profile was similar for most stages of the gait cycle or larger (i.e., 25%-45%, 75%-90% of the gait cycle) than the no assistance case.

More importantly, we observed a different hip joint moment behavior of the user walking with wider step width due to exoskeleton assistance when compared to previous studies where users volitionally increased step width with those studies reporting a significant decrease in human hip moment [3]. Our interpretation of this finding is that the mediolaterally acting hip exoskeleton provided extra torque assistance which is added to the human generated moment. While this is an interesting result with implications for both assistance and rehabilitation, further subjects have to be analyzed to confirm consistent trends. Further, the observed joint torque is combined torque of user and exoskeleton and individual user behavior could provide further insights into how the interaction affects human joint responses, which could be used in training for rehabilitation.

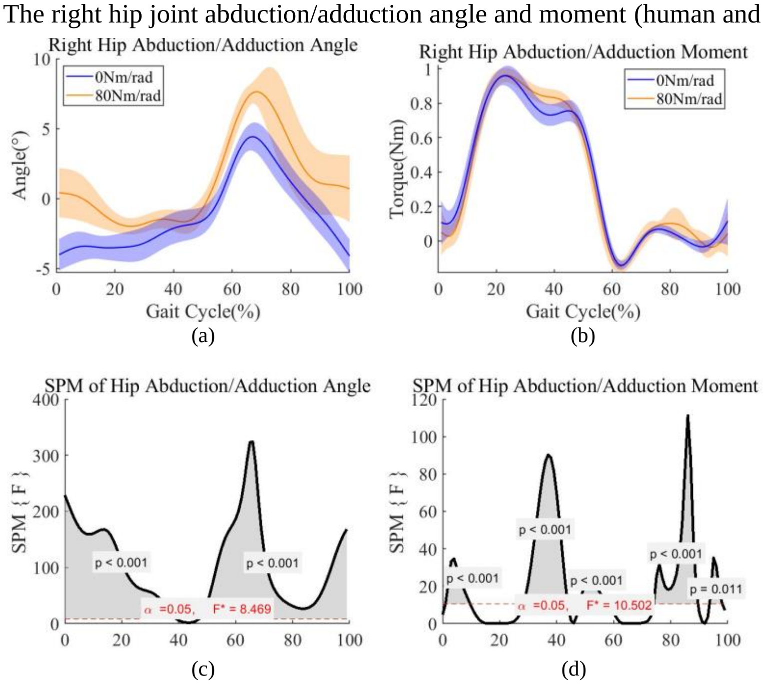

Figure 1: (a), (b) Hip joint angle and moment response to no assistance (K=0) and assistance (K=80) from the hip exoskeleton. (c), (d) SPM analysis results for hip abduction/adduction angle and moment for both cases.

Significance: The results show that the mediolaterally active hip exoskeleton used in this study can provide hip abduction torque assistance, which carries a great potential for patients with weakened hip joint (e.g., lower-limb amputees and elder people). Further, the exoskeleton can preserve torque behavior observed during normal walking while volitionally increasing step width reduces hip torque moment.

Acknowledgements: Research supported by NIDILRR 90REGE0017 and IBM.

References: [1] Alili et al. (2023), TechRxiv 3, (7); [2] Pataky et al. (2017), Proceedings of the International Society of Biomechanics 7 (23-27); [3] Stief et al. (2021), Gait & Posture, Elsevier. 89 (161-168).

REAL-TIME 3D BIOFEEDBACK CAN IMPROVE DYNAMIC BALANCE CONTROL ON THE Y BALANCE TEST

Martin P. Kilbane*, Melina R. Canter, Kaitlyn J. Bresingham, Edgar A. Bolívar-Nieto, and James P. Schmiedeler
University of Notre Dame
*Corresponding author's email: mkilban4@nd.edu

Introduction: The Y Balance Test (YBT) is a common clinical dynamic balance assessment that exhibits favorable validity and reliability [1]. The YBT has subjects stand on one leg while reaching out with the other in three directions – anterior (ANT), posteromedial (PM), and posterolateral (PL) (Fig. 1a). The reach distances are one way to quantify subject flexibility. While the task is appropriately challenging, measurement of only maximal reach distance in three directions lacks the resolution to identify the degree of control exerted over the subject's center of mass (COM), so it reveals nothing about the smoothness of movement or quality of postural control. Instrumenting subjects with an inertial measurement unit (IMU) can fill this void. The authors are aware of no work examining the effects on YBT performance of real-time biofeedback using IMU data. The 95% ellipsoid volume of sway (95EV) is a comprehensive 3D measure of balance formed from linear acceleration in the medio-lateral and anterior-posterior directions and the transverse plane rotational acceleration (Fig 1b) [2]. Real-time accelerometer and gyroscope data for a point near the COM can be used to calculate the subject's current COM point of sway in 3D (95EV point). Sensitive, intuitive, and easy-to-visualize metrics, such as the 95EV, have the potential to provide useful information that can be easily interpreted and thus, leveraged in clinical practice [3]. The aim of this study is to explore, for a single pilot subject, whether real-time 3D biofeedback based on the 95EV can help improve YBT performance as measured by both the maximal reach distances and the 95EV. The hypothesis tested is that real-time 3D biofeedback based on the 95EV will lead to improved YBT performance according to both metrics.

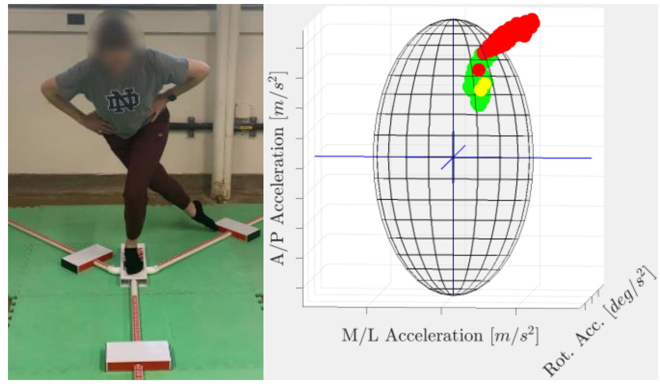

(a) **(b)**

Figure 1: a) Subject performing posterolateral (PL) reach during Y Balance Test. **b)** Baseline 95EV (wireframe) for PL reach with current 95EV point (colored dots) plotted atop it in 3D. 95EV is formed from linear acceleration in medio-lateral (M/L) & anterior-posterior (A/P) directions & transverse plane rotational acceleration.

Methods: One pilot subject (1 female; age 21, height 173 cm; weight 67 kg) completed 4 practice YBT reach excursions to eliminate the test's training effect [4]. As an intervention, the researcher showed the subject a video of these trials and explained the relationship of the movements to the simultaneous plotting of the 95EV. A 5° offset of the linear acceleration in the medio-lateral and anterior-posterior directions was implemented to realize the 3rd dimension of the 95EV. The subject then completed 3 trials in each of 3 directions (order randomized) standing on each foot while receiving real-time 3D biofeedback of the 95EV, as generated from data collected with an inertial sensor (Shimmer3) placed on the subject's lumbar region. This sensor was calibrated and configured to stream tri-axial accelerometery ($\pm 2\ g$), gyroscope ($\pm 500\ deg/s$), and magnetometer ($1.9\ gauss$) data to a computer running a custom MATLAB (R2022b) script at a frequency of 51.2 Hz. The baseline 95EV was calculated from the average of the initial 4 trials, and the current 95EV point was traced atop it on a 46" screen in front of the subject (Fig. 1b). The traced point was displayed as green when within 75% of the 95EV, yellow when between 75 and 95%, and red when outside the 95EV. Dynamic balance was assessed using both the standard reach distance normalized by leg length and the 95EV. The average of the three biofeedback trials was compared to the pre-biofeedback performance in terms of both normalized reach distance (%) and 95EV ($deg \times m^2 s^{-6}$).

Results & Discussion: The subject performed repeated YBTs without fail, and results were similar for both legs. For the right leg, the average normalized reach distances with biofeedback were 54.8% (ANT), 88.2% (PM), and 89.6% (PL) compared to 52.7% (ANT), 81.7% (PM), and 83.9% (PL) pre-biofeedback. The subject achieved farther reach distances in all trials with the biofeedback. The average 95EVs with biofeedback were 15.5 $deg \times m^2 s^{-6}$ (ANT), 11.5 $deg \times m^2 s^{-6}$ (PM), and 34.4 $deg \times m^2 s^{-6}$ (PL) compared to 22.7 $deg \times m^2 s^{-6}$ (ANT), 24.6 $deg \times m^2 s^{-6}$ (PM), and 55.2 $deg \times m^2 s^{-6}$ (PL) pre-biofeedback, so the subject also demonstrated a greater degree of control of COM accelerations with the biofeedback. The subject may have prioritized improvement in 95EV more so than in normalized reach distance because the biofeedback was explicitly in terms of 95EV.

Significance: This study demonstrates that real-time 3D biofeedback using an inertial sensor has the potential to improve dynamic balance control and reach distances on the YBT. The results suggest the need for a full study with a control group to determine if the pre- to post-biofeedback YBT performance gains observed herein were due primarily to just repetition of the task or can be linked specifically to the biofeedback. Such a full study could also examine the training effects to validate if performance enhancements are retained once biofeedback is removed. Positive results from this broader study would inform how clinicians could implement real-time 3D biofeedback using the 95EV to both promote controlled movements and improve flexibility for subjects with balance deficits.

Acknowledgements: This study was funded by a Naughton Faculty Research Accelerator Grant from the University of Notre Dame.

References: [1] Plisky et al. (2009), *N Am J Sports Phys Ther* 4(2); [2] Alberts et al. (2015), *Med Sci Sports Exerc* 47(10). [3] Johnston et al. (2018), *Digit Biomark* 1(2); [4] Gribble et al. (2012), *J Athl Train* 47(3).

IMPACTS OF FATIGUE ON NEUROMECHANICAL STRATEGIES IN SINGLE-LEG JUMPING

Melody S. Modarressi[1*], Chase G. Rock[1], Gregory S. Sawicki[1,2], Young-Hui Chang[1]
[1]School of Biological Sciences, [2]School of Mechanical Engineering, Georgia Institute of Technology, Atlanta, GA, USA
*Corresponding author's email: mmodarressi3@gatech.edu

Introduction: Fatigue has a profound influence on neuromuscular and biomechanical properties in humans, particularly regarding the risk of injury around joints [1]. The behavior of joints and their corresponding muscles can be altered following physical exertion, via factors such as muscle activation and coactivation, force production capacity, motor control and movement patterns, and kinetics and kinematics, among many other properties [1]. Although fatigue is known to ultimately reduce force production capacity of the affected muscles, humans can maintain their performance level over long periods through compensatory strategies; multi-joint motor tasks use a range of neuromechanical strategies to prolong an activity at a given performance output [2]. This study aims to characterize changes in these strategies within the context of single-legged jumps (SLJs) following fatigue; this task is common across many sports and is often associated with injuries at the knee joint [3]. By investigating the subtle changes of measurable biomarkers before and after fatiguing the lower limbs, we hypothesized that humans rely less on joints and muscles that have been fatigued when performing explosive tasks involving power production and absorption, such as jumping. Therefore, we predict that the joints associated with muscles that experience a greater degree of fatigue contribute less to the net mechanical work of the task, and that less fatigued neuromuscular components act synergistically to compensate via a redistribution of energy within and between joints in an attempt to preserve net mechanical work done on the center of mass.

Methods: We collected preliminary data from one participant (30-year-old male, height =185.9cm, mass =111.1kg), with the goal of fatiguing to a point just before task failure, which may provide more ecologically relevant results. The participant performed three maximal SLJs using his dominant leg on a force platform. The maximum vertical displacement of these three jumps was recorded and used to calculate the target height for subsequent SLJs (75% of maximum height). After sufficient rest, the participant was tasked with a fatigue protocol in which he squatted repeatedly to a knee flexion angle of 90 degrees, with the goal of inducing targeted fatigue of the major muscle groups in the leg. Squatting occurred at a pace of 50 bpm until one of two possible criteria was met: the participant squatted for three consecutive minutes or failed to complete two successive squat cycles to the target flexion angle on beat. At this point, he attempted three maximal SLJs to the target height. If the target was reached in any of these jumps, the fatigue protocol was repeated until all three SLJs failed to reach the target height. Joint kinetics and kinematics were compared between the pre-fatigue and the penultimate cycle of the post-fatigue conditions.

Results & Discussion: We observed reduced net power production and absorption, and a redistribution of joint contributions to total mechanical work following fatigue (Fig. 1). The ankle was the principal power producer in the lift-off stage of the jump in both conditions. However, positive contributions of the knee were reduced by 15% post-fatigue. The positive power contributions of the ankle and hip increased by 13% and 2%, respectively, to counterbalance changes at the knee. In the landing stage, power absorption at the knee was reduced post-fatigue and the negative work contribution by the knee decreased by 14%. This reduction was offset by an increase in negative work performed at the hip and ankle by 4% and 10%, respectively. We speculate from these results that the knee experienced greater fatigue than the ankle or hip, resulting in the ankle's increased contribution to propulsion after neuromuscular fatigue. Similarly, the reduced contribution of the knee to the total negative work during landing points to greater fatiguability of knee extensor muscles. Moreover, the subject adopted a jumping control strategy that spared the knee through greater power absorption at the hip and ankle. The joint-level compensatory trends observed prior to SLJ performance decline were also observed after fatigue to task failure was established, highlighting the benefits of a progression-to-fatigue protocol. Previous research has found that humans exploit kinetic redundancies to maintain functional motor outputs, so the variance in joint work contributions seen in our findings provide motivation to further investigate the underlying mechanisms of motor abundance in SLJs and similar explosive tasks [4].

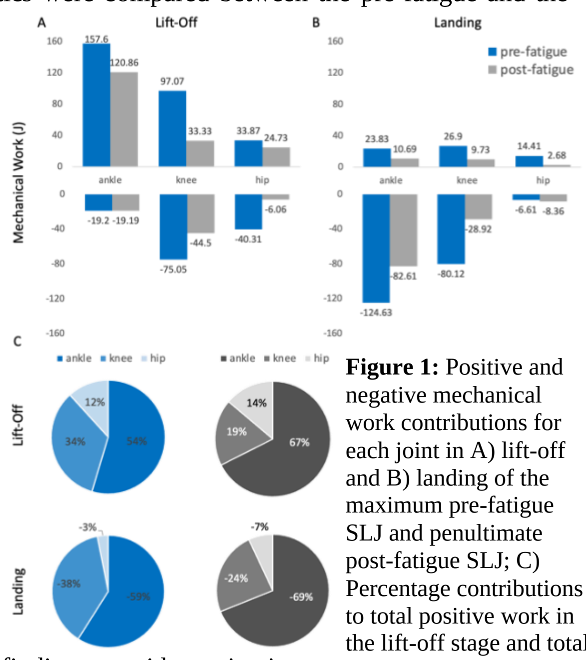

Figure 1: Positive and negative mechanical work contributions for each joint in A) lift-off and B) landing of the maximum pre-fatigue SLJ and penultimate post-fatigue SLJ; C) Percentage contributions to total positive work in the lift-off stage and total negative work in the landing stage.

Significance: These preliminary results highlight the presence of built-in dynamic control strategies to maintain performance outputs following neuromuscular fatigue. The involuntary modifications to joint coordination we observed allow performance to be maintained despite fatiguing conditions. The broader application of these results suggests the utility of identifying early biomarkers of fatigue to better understand the state of lower limb components during continuous, strenuous activities well before the point of injury. The characterization of such biomarkers in tasks such as single leg jumps will provide a framework for improved prediction and mitigation of fatigue-related injuries.

References: [1] Padua et al. (2006), *J Athl Train* 41(3); [2] Bonnard et al. (1994), *Neurosci Lett* 166; [3] Laughlin et al. (2011), *J Biomech* 44(10); [4] Yen et al. (2009), *Exp Brain Res* 196(3).

JOINT WORK COMPENSATIONS IN UNILETRAL TRANSTIBIAL PROSTHESIS USERS DURING GAIT ACCELERATION AND DECELERATION

Shay R. Pinhey[1*], Ethan Chen[2], Anna Shafer[4], Amanda L. Shorter[2], and Keith E. Gordon[3, 4]
[1]Biomechanics and Movement Science Program, University of Delaware, Newark, DE
[2]Department of Biomedical Engineering, Northwestern University, Chicago, IL
[3]Physical Therapy and Human Movement Sciences, Northwestern University, Chicago, IL
[4]Research Service, Edward Hines Jr. VA Hospital, Hines, Illinois
*Corresponding author's email: spinhey@udel.edu

Introduction: Unilateral transtibial prosthesis users (UTPUs) often exhibit gait asymmetries that may result from the prostheses' inability to match intact ankle joint power. Prosthesis users compensate for reduced prosthetic ankle power with increased work on the sound limb during the step-to-step transition from prosthetic limb stance to sound limb stance and increased positive power at the hip on the prosthetic side [1], [2]. Many studies have focused on steady-state walking, but little is known about compensation strategies during non-steady-state activities (starting, stopping, etc). Our purpose was to better understand the compensatory strategies UTPUs employ during two non-steady state walking tasks: acceleration and deceleration. Similar to the compensations seen during steady-state walking, we hypothesize that 1) work on the prosthetic limb will be driven by the hip joint and 2) work on the sound limb will be driven by the ankle joint.

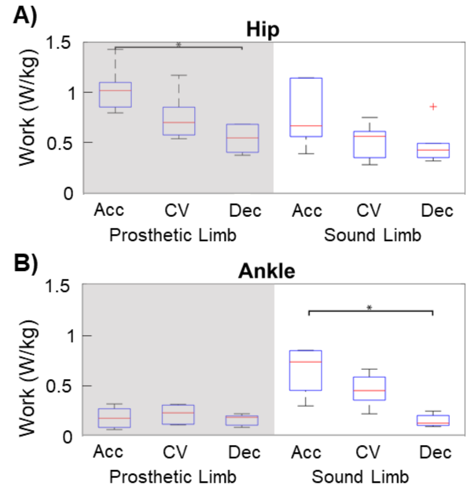

Figure 1: Positive work is shown for each condition for the hip (A) and ankle (B) joints. Significant differences between conditions are denoted with a *.

Methods: Six K3 level UTPUs (4 Male, Age: 55.2±17.3 years, Height: 1.74±0.11 m, Mass: 84.4±18.2 kg, Time since amputation: 13.5±11.4 years) walked on their own non-articulated dynamic prosthetic foot wearing their own socket. Participants walked over ground across six force plates which collected ground reaction forces at 1000 Hz while motion capture data was collected at 100 Hz. Participants were instructed to walk straight ahead across force plates which cued one of the following tasks via audio and visual prompts on contact: rapidly decelerate (DEC), remain at constant velocity (CV), or rapidly accelerate (ACC). Participants walked for four alternating blocks of 10 trials with two conditions per block (ACC and CV or DEC and CV) in randomized order. To reduce cognitive load, participants were informed at the beginning of each block which pair of conditions they might be instructed to perform. Analysis was performed using Visual 3D (C-Motion, MD) and MATLAB (Mathworks, MA) to calculate joint work (positive and negative) at the ankle, knee, and hip during stance phase. Separate one-way repeated measures ANOVAs were used to identify significant differences in joint work ($p<0.05$) between conditions (DEC, CV, ACC). If significance was found, post-hoc t-tests were used to assess differences ($p<0.0167$, Bonferroni-correction) between conditions.

Results & Discussion: Joint work comparisons for the hip and ankle across all conditions are displayed in Figure 1. Participants exhibited greater positive hip work in ACC than DEC on the prosthetic limb ($p=0.003$). No significant differences were found in negative work for the prosthetic hip or in the sound limb hip for positive or negative work across all three conditions. The change in hip work from ACC to DEC only on the prosthetic side supports our hypothesis that joint work compensations are being modulated by the hip on the prosthetic limb side. For the sound limb, positive ankle work was greater during ACC than DEC ($p<0.001$). Post-hoc comparisons showed no significant difference in the negative work performed by the sound limb ankle or in positive or negative work at prosthetic ankle across all three conditions. Changes in the sound limb ankle work from ACC to DEC conditions support our hypothesis that joint work compensations on the sound limb are occurring at the ankle. We found no significant differences in knee work between conditions.

Significance: Asymmetries in joint work are important because they can be indicative of increased demand on a joint which can increase risk of injury and can lead to overuse effects. Is has been found that increased load on the hip joint in UTPUs contributes to lower back pain [3] and that similar risks can be indicated at the ankle joint of the sound limb. These findings have important implications in prosthetic design and clinical training. It may be beneficial to use a powered ankle-foot prosthesis to help compensate for the lost ankle power and help reduce burden on the prosthetic limb hip and sound limb ankle. Additionally, physical therapy to strengthen the prosthetic side hip may be beneficial. Future work should continue to assess compensatory strategies during non-steady-state walking with consideration of using uniform prosthetic components in all subjects to reduce potential confounding factors and additional variability.

Acknowledgements: Support by The Orthotic and Prosthetic Foundation for Education and Research.

References: [1] Houdijk et al. (2009), *Gait and Posture* 30(1); [2] Silverman et al. (2008), *Gait and Posture* 28(4); [3] Kusljugic et al. *Bosn J Med Sci* 6(2).

TIBIAL SHOCK COMPLEXITY DIFFERENCES BETWEEN SOCCER ATHLETES AT DIFFERENT PEAK HEIGHT VELOCITIES AND ACROSS A SEASON

Jake A. Melaro[1], Joshua M. Lardie[1], Joshua T. Weinhandl[1*]
[1]1University of Tennessee, Knoxville, TN, U.S.A
*Corresponding author's email: jweinhan@utk.edu

Introduction: Sport-related lower-extremity injuries increase steadily from age 6-12 for boys and girls, particularly apophysitis overuse injuries [1,2]. though these and other injury rates increase substantially at and immediately following peak height velocity (PHV) during puberty [3,4]. Tibial shock measured via accelerometer has been used for load monitoring during training and linked with both stress fractures and tibiofemoral shear forces [4,5]. Physiological changes and fatigue effects from a competitive season may induce changes in lower-extremity loading during training that could potentially lead to injury. Differences and changes in movement complexity computed via entropy analysis may potentially be used to identify athletes at risk of injury [6,7]. Considering the rapid yet differential timings of puberty-related changes to body segment inertial properties, coordination, and strength, we suspect differences in tibial shock complexity between athletes relative to PHV and pre- to post-season will be present. Observable differences in lower-extremity loading complexity may provide insight into thresholds at which these non-contact and overuse injuries occur.

Methods: Tibial accelerations were measured for A) 15 male soccer athletes (1.17±0.64 years post-PHV) before and after a competitive season and B) 10 pre-, circa-, and post-PHV (30 total) male athletes during preseason training. Multiscale entropy curves and complexity index (CI – area under entropy curves) were computed for an easy jog (DNB), M-drill in both directions (M-Drill-L and M-Drill-R), 5-10-5, and triple hop drills for both legs (THL and THR). Mean CI differences were compared for each drill via paired t-tests for pre-post comparisons and ANOVAs for PHV group comparisons.

Results & Discussion: Pre-post season differences revealed CI was lower at post-season testing for all drills except 5-10-5 and THL (Fig A and B). Differences between PHV group were only found in the DNB whereby CI was greater in pre-PHV compared to PHV and post-PHV athletes (Fig C and D).

Pre-post and PHV group statistical comparisons suffered from low sample size and power. Further work is needed to understand the influence of other factors (i.e., sex, parameter selection, sensor location, etc.) on complexity results, though these data show time-series entropy analysis may be an appropriate discriminatory tool for loading complexity differences during these field drills.

Significance: Complexity differences between athletes across a season or stemming from PHV status may not be apparent at conventional time scales. Multiscale entropy may potentially be a useful tool used to monitor athlete movement quality and complexity near PHV to reduce injury associated with puberty.

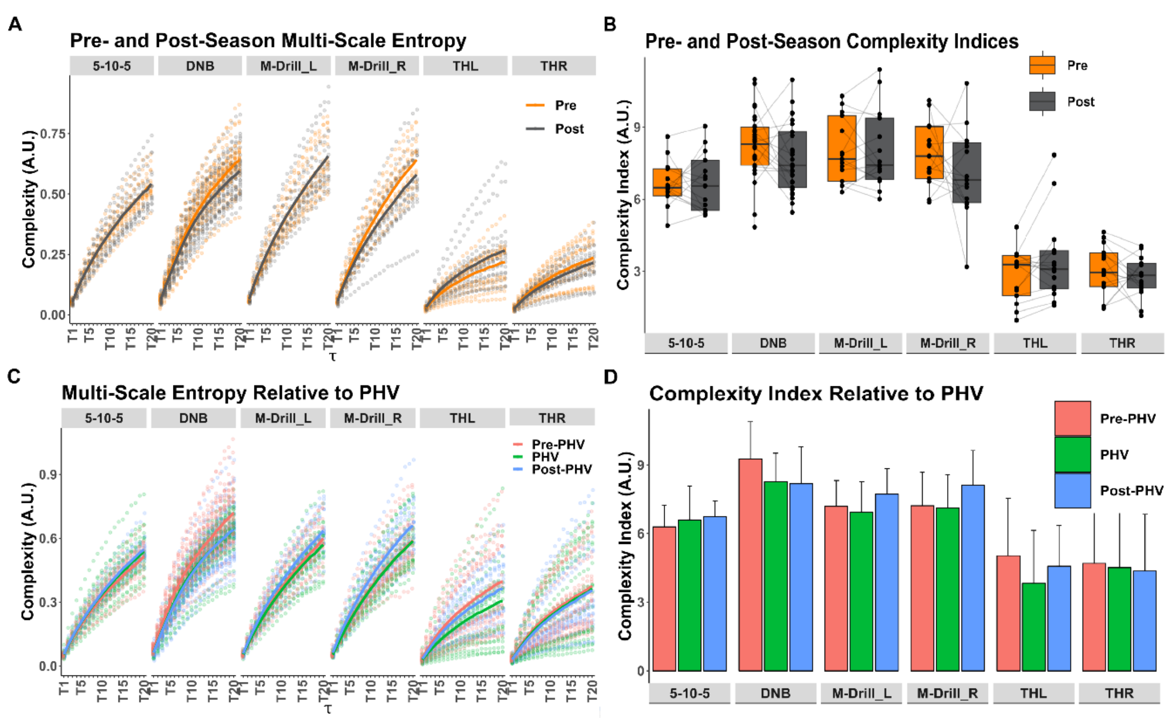

A) Multiscale entropy across 20 timescales by drill between testing sessions **B)** CI by drill between testing sessions
C) Multiscale Entropy results across 20 timescales by drill and PHV status **D)** CI by drill and PHV status

References: [1] Sørensen & Röck (1996), *Scand J Med Sci Sports, 6*(5). [2] Tursz & Crost (1986), *Am J Sports Med, 14*(4). [3] Gupta et al. (2020). *Ortho J Sports Med, 8*(5). [4] Van Der Sluis et al. (2014), *Int. J. Sports Med., 35*(4). [5] Milner et al., (2006), *MSSE, 38*(2). [6] Shelburne et al. (2004), *J Biomech, 37*(3). [6] Gruber et al. (2021). *Front. sports act. living, 3*. [2] Schütte et al. (2018). *Gait Posture, 59*. [2] Tursz & Crost (1986), *Am J Sports Med, 14*(4).

THE IMPORTANCE OF JOINT CENTER LOCATION IN SCALING SEXUALLY DIMORPHIC MUSCULOSKELETAL MODELS

Joseph Dranetz[1], Shuo Chen[1], Hwan Choi[1*]
[1]University of Central Florida Department of Mechanical and Aerospace Engineering
*Corresponding author's email: hwan.choi@ucf.edu

Introduction: The accurate use of generic musculoskeletal models to represent the dynamics of individual subjects relies on quality model scaling. The scaling process serves as a link between the generic model, developed with extensive imaging and cadaveric study of the general population, and the movement and reaction force data, collected from individual subjects experimentally. However, the linear scaling of generic models introduces error into representations of subject specific biomechanics. The mass distribution, bone morphology, and joint center locations of individual subjects may differ from those of the generic model. For example, as popular generic models are based exclusively on male data, sexual dimorphic structural differences found in female subjects may not be represented. The purpose of this work was, therefore, (1) to generate gendered generic musculoskeletal models and compare the differences in model geometry between male, female, and previous generic models and (2) to illustrate the sensitivity of the body segment parameters and joint center locations on the performance of each of the models in inverse kinematic/dynamics analysis.

Methods: Segment mass/inertial and anatomical landmark/joint center location data from Dumas et al. [1] were combined to generate sexually dimorphic generic musculoskeletal models. The models were adapted from a generic Rajagopal model [2], altering the segment mass and inertial properties to match the Dumas data. Joint definitions were moved to match Dumas joint center locations, and the Dumas anatomical landmarks were used to define new marker positions. To further improve upon the musculoskeletal modeling, the locations of the hip, knee, and ankle joint centers were adjusted to match locations found with Symmetrical Center of Rotation Estimation or Symmetrical Axis of Rotation Analysis operations within Vicon. Each subject is represented with four models: two scaled Rajagopal models (with and without joint center adjustment) and two scaled gendered Dumas models (with and without joint center adjustment).

Walking data from 4 subjects (2M and 2F) were collected to compare the 4 models. For motion data collection, subjects wore 46 reflective markers following a modified Helen-Hayes set and were tracked by a 12-infrared camera motion capture system (Vicon). Force plates (AMTI) were used to measure ground reaction forces. The root mean square (RMS) marker errors associated with each model scaling were compared to assess model accuracy. The results of inverse kinematics and inverse dynamics from each model were compared to demonstrate the effect of model formulation on model outputs.

Results & Discussion: The RMS marker error for scaling all the models varied between 2.09 cm and 3.63 cm. Most of this variance occurred between participants as the variance between which model was used was less than 0.25 cm and the variance between whether the joint centers were adjusted was less than 0.1 cm. For all models, the marker with the highest error was either an acromial marker or a greater trochanter marker. As neither of these markers were used in determining scale factors, the error is likely due to subject specific differences in bone morphology and does not indicate poor model scaling.

Figure 1 shows sagittal joint kinematics were similar when using the different female models. Differences in Rajagopal and Dumas model hip kinematics were due to differences in coordinate definitions for the pelvis and not necessarily differences in kinematic predictions. Differences in kinematics were only found in late swing in both ankle flexion and hip adduction. These differences may have been due to differences in model marker definitions for the foot and pelvis.

Differences were also found in sagittal plane dynamics between the two models during swing only. This was likely due to differences in the models' mass/inertial segment properties. The most pronounced impact that joint center adjustment had on dynamics was found in hip adduction during stance. This is consistent with the hip joint center adjustments which placed the hip joint centers more laterally. While the gendered Dumas models' hip joint centers were located more laterally than the Rajagopal models', they still moved laterally during the hip joint center adjustment. Consequently, greater hip abductive moments were observed in models with more laterally placed hip joint centers.

Significance: The results of this study identify potential sources of error in subject specific musculoskeletal model kinematics and dynamics. Discrepancies in hip joint center location led to error in estimations of hip abductive moment, and differences in mass/inertial properties led to error in estimations of dynamics during swing. These errors would likely be more pronounced when modeling subjects with movement disabilities where changes in bone and muscle morphology have occurred.

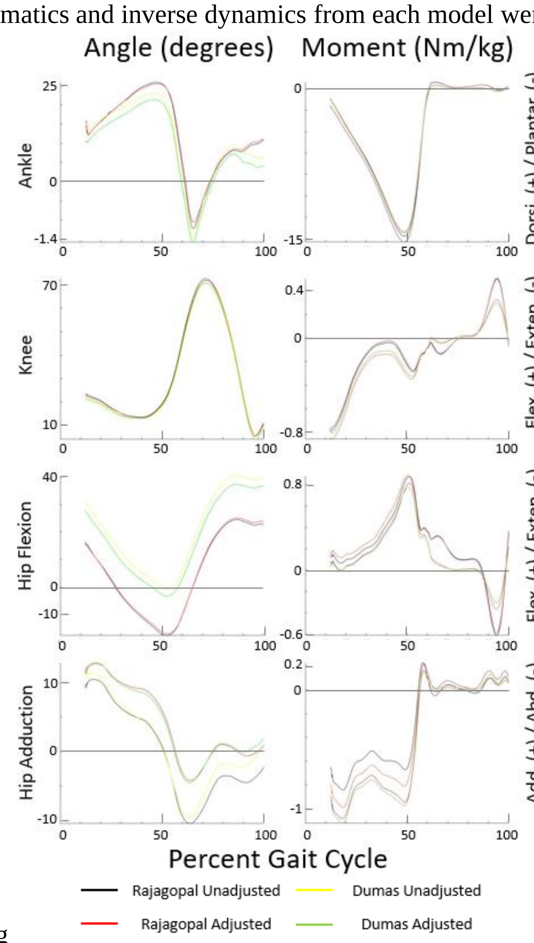

Figure 1: Kinematics (Left) and Dynamics (Right) estimated from each of the 4 different musculoskeletal models of a female subject.

References: [1] Dumas et al. (2007), *J Biomech* 40(3); [2] Rajagopal et al. (2016), *IEEE Trans. on Biomed. Eng.* 63(10)

REAL WORLD GAIT TRAINING WITH A HYBRID ANKLE EXOSUIT IN INDIVIDUALS WITH CEREBRAL PALSY

Emmanuella A. Tagoe[1*], Ying Fang[2], Jack R. Williams[1], Zachary F. Lerner[1,3]
[1]Northern Arizona University, [2]Rosalind Franklin University, [3]University of Arizona
*eat277@nau.edu

Introduction: Individuals with neurological conditions, such as cerebral palsy (the most prevalent childhood motor disorder), suffer strength and motor control impairments that negatively affect their walking ability [1]. Individuals with CP walk at a much slower rate with reduced stride length and stride-to-stride muscle repeatability across all walking terrains compared to healthy individuals [2]-[4]. Thus, increasing walking speed, stride length and muscle repeatability are crucial clinical goals for treating gait abnormalities [4],[5]. Over the years, exosuits and exoskeletons have proven to be beneficial for individuals with neurological impairments during treadmill walking or in highly controlled overground environments [6],[7]. Treadmills, however, do not accurately represent real-world terrains encountered in daily life. Moreso, practical application of these devices will occur on real-world terrains rather than on treadmills or in other laboratory settings. To date, only one study has demonstrated benefits using exoskeleton assistance during walking on level real-world terrain in healthy young adults. It is unknown if exosuit assistance translates to real-world settings for individuals with neurological disorders. Thus, the purpose of this study was to investigate the benefits of real-world gait training with hybrid ankle exosuit assistance in individuals with CP. We hypothesized that, following training, ankle exosuit assistance will increase walking speed, stride length and muscle repeatability without increasing muscle work compared to unassisted walking. We also hypothesized that, there will be some improvements in unassisted walking after training.

Methods: Six individuals with CP completed two training sessions of 20- minute exosuit-assisted walking on a 409 m outdoor route consisting of level surfaces, stairs, inclines, and declines. They also completed pre- and post-training assessments of assisted (Exo) and unassisted walking (Shod) on the same route while recording spatiotemporal outcomes and muscle activity to assess any benefits of training sessions *(Figure 1a)*. Data was only processed and analysed for the level portion of walking; however, future work will explore the other terrains. We used two-tailed paired t-tests to compare normally distributed parameters and Wilcoxon signed-rank test to compare non-parametric data for the pre- and post-training visits for both assisted and unassisted walking.

Results & Discussion: There was no significant difference in all measurable outcomes between conditions on the pre-training visit. Following training, however, walking with assistance significantly increased walking speed by 8% ($p = 0.028$) and stride length by 7% ($p = 0.028$) compared to unassisted post-training walking *(Figure 1b and c)*. Additionally, exosuit assistance resulted in improvements in stride-to-stride repeatability of the soleus (decreased variability of 29%; $p=0.152$) muscle that carried over to unassisted walking (decreased variability of 29%; $p=0.046$) *(Figure 1d)*. This suggests that benefits of walking with exosuit assistance can be achieved after acclimation to the device. Stance phase integrated muscle activity was similar across all conditions and visits *(Figure 1e)*. There was no significant increase in walking speed nor stride length within condition across pre- and post- trainings. This may be due to an inadequate amount of training sessions for the highly variable number of terrains used in study. Future studies will investigate outcomes using more repeated training sessions.

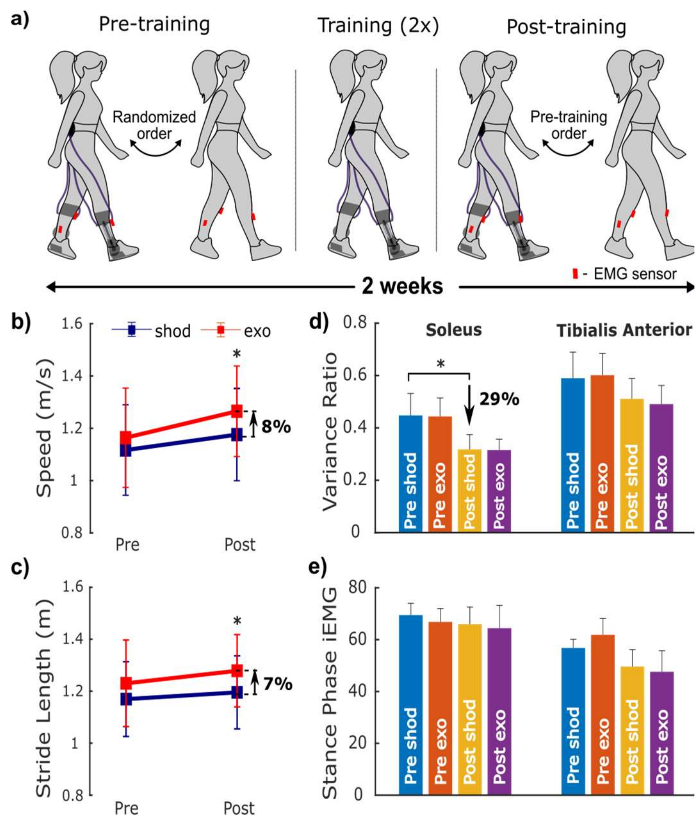

Figure 1: a) Overview of experimental protocol used in this study. b) Walking speed c) Stride length d) Variance ratio (VR) of Soleus and Tibialis Anterior muscles and e) Stance phase integrated EMG (iEMG) of Soleus and Tibialis Anterior muscles for pre-and post-training Shod and Exo conditions across visits. * indicates a significant difference between conditions and/or visits.

Significance: Individuals with CP can safely and effectively navigate real-world terrains using an ankle exosuit. Ankle exosuit assistance can lead to improvements in walking speed, stride length and stride-to-stride muscle repeatability following training, setting the stage for home, school, and community-based testing.

Acknowledgements: The authors would like to thank the members of the Biomechatronics laboratory at Northern Arizona University for their assistance during data collection for this study.

References: [1] A. Michael-Asalu (2019), *Adv. Pediatr.*(66); [2] C. Kim and S. Son (2014), *J Phys Ther Sci 26(9)*; [3] Y. Ma (2019), *Appl. Bionics Biomech*; [4] Y. Kim et al (2020), *Neurorehabil Neural Repair;* [5] F. N. Todd *et al.(1989)*, *JBJS* (71); [5] Y. Fang et al.(2020), *Gait Posture* (95); [6] L. N. Awad *et al.(2017)*, *Sci. Transl. Med.(9)*

EMG ACTIVITY OF KNEE MUSLCES DURING INCLINED WALKING ON DIFFERENT SLOPES FOR PATIENTS WITH TOTAL KNEE AHROPLASTY

Songning Zhang*, Chen Wen
Biomechanics/Sports Medicine Lab, The University of Tennessee, Knoxville, TN
*Songning Zhang: szhang@utk.edu

Introduction: Patients with unilateral total knee arthroplasty (TKA) has been shown to have reduced peak knee extension moment (KEM) [1] and total knee compressive force (TCF) [2] of their replaced limb compared to healthy participants during incline ramp walking. However, knee joint related muscle activity level has not been examined in ramp walking for this patient population, and it is unknown if electromyographic (EMG) activation of knee joint muscles support the findings of KEM and TCF. Therefore, the purpose of this study was to examine electromyographic (EMG) activities of knee joint related muscles in the replaced and the non-replaced limbs of TKA patients during walking on level (0°) and inclined surfaces of 5°, 10° and 15°. The hypothesis was that the EMG activation levels would be lower in the replaced limbs compared to the non-replaced limb based on the previous results of KEM and TCF.

Methods: Twenty-five TKA patients participated in this study from a local orthopedic clinic (68.8 ± 4.9 years, 1.70 ± 0.11m, 83.2 ±15.6 kg, 22.1 ± 11.72 months from surgery). Ten healthy participants served as healthy controls (69.1 ± 4.5 years, 1.74 ± 0.12 m, 75.0 ± 23 kg). 3D kinematic data were collected using a 12-camera system (240 Hz, Vicon) and EMG activity of vasus medialis (VM), vastus lateralis (VL), semitendinosus (ST), biceps femoris long head (BF), and medial gastrocnemius (MG) were collected using a wireless EMG system (1200 Hz, Delsys). An adjustable and instrumented ramp system with two separate walking surfaces bolted onto two force platforms (1200 Hz, AMTI) was used to collect ground reaction force. Participants performed five trials each in level (0°) and uphill walking on 5°, 10° and 15° inclined surfaces. The EMG signals were bandpass filtered at 10 Hz and 450 Hz, full-wave rectified and filtered with a moving root-mean-squared filter (RMS). The EMG values were normalized to the maximal value of the respective functional movement tests. The RMS values were computed during the stance phase. A 2 x 4 (limb x slope) repeated measures ANOVA was used to examine the interactions and main effects of the RMS EMG variables. Post-hoc comparisons with Bonferroni adjustments were used to detect limb and slope differences.

Results & Discussion: No significant limb effects were found but significant slope effects were found for all muscles. Two knee extensors muscles, VM and VL, increased their RMS values with each increase of incline from 0° (level walking) to 15° (Table 1). These increases of VM and VL, compared to 0°, are similar at 5°, but greater for the non-replaced limbs at 15° (110% and 119%) and 10° (56% and 56%) compared to the replaced limbs at 15° (86% and 68%) and 10° (47% and 38%), respectively. The RMS EMG values of three knee extensor muscles, ST, BF and MG, were also increased with increased incline slopes from 0° to 15° (Table 1). The RMS EMG increases of two hamstring knee flexors were similar at 5°,10° and 15°. However, the increases of MG RMS value were greater for the non-replaced limbs than the replaced limbs at 5° (39% vs 29%), 10° (81% vs 49%) and 15° (108% vs 67%).

Table 1. RMS EMG values (% activation) of replaced and non-replaced limbs across different incline slopes: mean±std.

	Replaced				Non-replaced			
	0°	5°	10°	15°	0°	5°	10°	15°
VM [a-f]	21.3±10.3	25.6±12.4	31.3±14.1	39.5±17	18±11.4	21.4±12.4	28.1±13.4	37.9±19.8
VL [a-f]	21.1±12.3	24±13.2	29.1±14	35.5±15.8	17.2±8.9	21.2±9.6	26.8±12.7	37.7±18.3
ST [a-f]	23±12.9	30.1±15.5	33±16.2	33.5±15.2	24.1±14.5	31.9±17.5	36.3±18.8	40±22
BF [a-f]	22.6±13.6	28.2±15.7	35±18.7	38.6±19.7	21.1±15.9	29.1±20.3	31.8±19.9	34±22.6
MG [a-f]	19.5±9.1	25.3±10.4	29±10	32.6±10.8	16.5±8.8	22.9±9.4	29.9±11.6	34.3±11.8

[a]: different between 0° and 5°; [b]: different between 0° and 10°; [c]: different between 0° and 15°; [d]: different between 5° and 10°; [e]: different between 5° and 15°; [f]: different between 10° and 15°, std: standard deviation.

The EMG activation results provide support for the knee joint kinetic results. Wen at al. [1] found that the peak KEM was greater in the replaced limbs at 10° and 15° of ramp walking. Tanner et al. [2] found the TCF in the not-replaced limb was greater compared to the replaced limbs at 10°. Although our EMG results did not show limb effect, greater percentage increases were observed for the knee extensors (VM and VL) in the non-replaced limbs, lending partial support of the knee joint moment results. These results also support the notion that the replaced limbs of TKA patients are still not fully recovered during daily gait ambulation tasks with greater mechanical demand, even after 22 months after their knee surgery.

Significance: The ramp walking is commonly employed in the post-surgery rehabilitation of TKA patients. The ramp incline of 5° offers moderately increased mechanical demands on knee extensors and flexors for these patients during their rehabilitation which seems to be reasonable to progress TKA patients to greater intensity from level to ramp walking during their earlier rehabilitation. The usage of an incline greater than 5°, e.g. 10° or higher, places much greater mechanical demands to the knee joint and its musculature and may only be suitable during the later stage of the rehabilitation process.

Acknowledgements: Patients with TKA in the study and graduate students assisting the equipment setup during data collection.

References: [1] Wen, C. Cates, H.E., and Zhang, S. (2019) *J Biomech* 89: 40-47. [2] Thorsen, T., Wen, C., Zhang, S. (2021) *J Biomech Eng* 143: 101005-2.

VALIDITY OF A POLHEMUS PORTABLE MOTION TRACKING SYSTEM FOR KINEMATICS OF REACHING

Jennifer Gerst, B.S.[1*], John Fox, Ph.D. [2], Amanda Ransom, Ph.D.[3], and Matthew Foreman, Ph.D.[4]
[1,4]Methodist University Doctor of Occupational Therapy Program
[2]Methodist University Doctor of Physical Therapy Program
[3]Methodist University Department of Kinesiology
*Corresponding author's email: jgerst20@student.methodist.edu

Introduction: The use of optoelectronic motion capture cameras is typically considered a gold standard in objective, lab-based reaching assessment for neurological conditions such as stroke. Such assessments utilize motion capture cameras and retroreflective marker arrangements to examine kinematic parameters including reach distances, joint angles, reach path ratios, and smoothness during reach-to-target tasks [1]. Movements can be performed in various directions to targets at different distances to comprehensively measure motor impairment related to limited range of motion (ROM), impaired interjoint coordination, slower speed of movement, and excessive use of compensatory movements [1] [2]. However, such methods often lack context for activity-based reaching performed during daily life, and thus it may be important to consider more portable motion capture systems that could be used outside of a laboratory in more ecologically valid settings. Reaching to a single marker on a tripod does not have the same meaning and salience as reaching, for example, to a cabinet to retrieve a coffee mug when thirsty.

The purpose of this study is to investigate the validity of a portable, electromagnetic motion capture system (Polhemus G4) compared to an optoelectronic system (Vicon Bonita) for measuring the kinematics of a reach-to-target task within a laboratory setting. The long-term goal of this research is to use evidence from this investigation to justify the use of the portable motion capture system for a novel, ecologically valid reaching assessment performed within a simulated activities of daily living laboratory.

Methods: A convenience sample of healthy participants (n=7) were recruited to participate in a seated reaching assessment in a lab-based setting at the Methodist University Motion Analysis Laboratory. Participants completed reach-to-target movements while simultaneously being measured by a 14-camera Vicon Bonita camera system and a Polhemus G4 EMT motion tracking system. Participants completed two sets of five reaches to a shoulder height target marker in three directions: the sagittal, scaption, and frontal planes. Two sets of reaching movements were performed: one set at arm's length (non-extended) and one set at 20cm beyond arm's length (extended). Extended reaches were utilized to elicit maximal range of motion (ROM) and compensatory movement at the trunk [2]. Twenty-one retroreflective markers were placed on C7, sternal notch, xyphoid process, and bilateral iliac crests, shoulders, medial/lateral epicondyles, ulnar/radial styloids, and dorsal hands. An arrangement of three markers were placed at the shoulder anteriorly, laterally, and posteriorly to estimate glenohumeral joint center. Twelve Polhemus G4 sensors were placed at C7, L5, and bilateral shoulders, mid-humeri, elbows, mid-forearms, and wrists. Data were cleaned, reduced, and exported from Vicon Nexus (2.6.1) and the The Motion Monitor xGen softwares for analysis in Matlab (r2021b). Clinically relevant variables including reach distance, shoulder flexion and abduction, and trunk flexion and abduction were analyzed relative to reach direction. Mean differences and standard deviations were calculated across all repetitions. Pearson's correlations were used to establish relationships between measurement characteristics. Correlations were not performed on trunk variables during non-extended reaches due to lack of variance. Correlation coefficients were considered strong (r>0.75), moderate (r=0.5-0.75), weak (r=0.25-0.5), and no relationship (r<0.25).

Table 1. Mean differences (MD), standard deviations of mean differences (SD), and Pearson's correlation coefficients (r) between Vicon and Polhemus data for all reaching repetitions across participants.

		Non-Extended		Extended	
		MD (SD)	r	MD (SD)	r
SAGITTAL	Reach Distance (cm)	2.23 (1.49)	0.88	1.30 (1.78)	0.90
	Shoulder Flexion°	-14.30 (4.32)	0.94	-5.03 (7.74)	0.75
	Trunk Flexion°	1.09 (0.74)	-	4.84 (2.62)	0.88
FRONTAL	Reach Distance (cm)	-3.17 (1.83)	0.94	-4.44 (3.14)	0.77
	Shoulder Abduction°	-9.21 (4.44)	0.95	0.95 (6.07)	0.93
	Trunk Lateral Flexion°	-0.98 (1.99)	-	5.95 (2.87)	0.82
SCAPTION	Reach Distance (cm)	-0.93 (2.00)	0.97	-2.89 (3.58)	0.75
	Shoulder Flexion°	-16.33 (8.34)	0.64	-11.03 (9.34)	0.69
	Shoulder Abduction°	-18.02 (5.94)	0.85	-9.26 (5.24)	0.92
	Trunk Flexion°	0.40 (0.61)	-	3.32 (1.76)	0.89
	Trunk Lateral Flexion°	-0.91 (1.37)	-	4.07 (3.47)	0.53

Results & Discussion: When comparing reach distances, mean differences between Vicon and Polhemus ranged from 0.93-4.44cm (Table 1). For shoulder angles, mean differences ranged from 0.95-18.02°. For trunk angles, differences ranged from 0.40-5.95°. Correlations showed moderate-strong relationships between systems for all variables (r=0.53-0.97).

Significance: In summary, the Polhemus G4 system was moderately-strongly correlated with the Vicon system and measured relative wrist displacement within 5cm, trunk angles within 6°, and shoulder angles within 18° for simple reach-to-target tasks. While correlations signify some validity, it is significant to note that the mean differences ranged widely and beyond what might be considered clinically acceptable, particularly for shoulder flexion and abduction. These findings are supported by similar investigations in the sport biomechanics literature, where the Polhemus G4 system has been shown to be, at worst, poorly correlated with optical motion capture for kinematics of the pelvis and trunk [3]. Limitations to this study include interference from metal structures during electromagnetic tracking and differences in sensor and marker placement between systems. Future work will incorporate a portable motion tracking system for development of a novel, contextual based, ecologically valid reaching assessment.

References: [1] Wagner et al. (2008), *Physical Therapy, 88*(5), 652-663; [2] Foreman & Engsberg (2020), *Sensors, 20*(24); [3] Wheare et al. (2021), *Sensors, 21*(13)

OLDER ADULTS BENEFIT MORE THAN YOUNGER FROM ACTIVE, BUT NOT PASSIVE, ANKLE EXOSKELETONS

Lindsey H. Trejo[1*], Jason R. Franz[2], Greg S Sawicki[1]
[1]School of Mechanical Engineering and Bio Sciences, Georgia Institute of Technology, Atlanta, GA, USA
[2]Department of Biomedical Engineering, University of North Carolina – Chapel Hill and North Carolina State, Raleigh, NC USA
*Corresponding author's email: ltrejo@gatech.edu

Introduction: Older adults consume metabolic energy faster during walking than young adults. Age-related changes in muscle-tendon units (MT) spanning the ankle are thought to cause reduced muscle power and force economy [1]. For example, due to reduced Achilles tendon stiffness (k_t), older adults walk using shorter, less economical muscle operating lengths and higher muscle activations than younger adults [2]. Previous literature in younger adults has shown passive ankle exoskeletons can reduce metabolic cost by altering the ankle muscle-tendon dynamics [3]. Additionally, active exoskeletons have shown even larger reductions in metabolic cost in real-world settings [4]. The purpose of this study was to compare passive and active ankle exoskeleton assistance strategies across age. Since older adults exhibit lower baseline economy, we predicted ankle exoskeleton assistance would result in larger metabolic benefits for older versus younger adults regardless of assistance strategy (i.e., passive vs active).

Methods: Seven young (5 M, 2F, 21 ± 2.2 yrs) and three older adults (3F, 73 ± 7 yrs) have thus far walked on a treadmill at 1.25 m/s. We programmed commercially-available portable ankle exoskeletons (Dephy Inc, Maynard, MA) to deliver spring [3] or motor-like assistance [5]. For each participant, we compared 6 exoskeleton assistance conditions: no exoskeleton, exoskeleton with zero torque (i.e., added mass), spring-like assistance (k_{exo} = 70 Nm/rad), and motor-like assistance at low, medium, and high magnitudes (T_{peak} = 10, 20, 30 Nm) (Fig. 1 inset). We measured $\dot{V}O_2$ and $\dot{V}CO_2$ using a portable indirect calorimetry system (COSMED, Italy) and converted to metabolic power using Brockway's equation.

Results & Discussion: Consistent with previous literature, we found ankle exoskeletons that applied both spring-like (~5% reduction) and motor-like (~7-18% reduction) assistance reduced metabolic cost for younger adults when compared to zero torque (Fig. 1a). In partial support of our hypothesis, older adults *only* benefited from motor-like assistance (~12-24% reduction) (Fig. 1b, blue). Surprisingly, metabolic cost increased (~5%) with spring-like assistance for older adults (Fig. 1b, pink). For motor-like assistance, older adults exhibited, on average, 5% larger metabolic benefit than young adults.

A potential mechanism driving larger improvements from motor-like assistance could reside at the muscle level [7], by shifting muscle dynamics to more economical operating points (i.e., longer lengths, slower velocities). Additionally, these results are from 41 (spring-like) – 57 (motor-like, 19 min at low, medium and high) min of exoskeleton assistance, and literature suggests full benefits take up to 218 min [8]. We believe the spring-like assistance was unable to provide a metabolic benefit for older adults because the k_{exo} needs to be optimized to their physiology. We would predict that a stiffer spring would be needed to offset known reductions in biological k_t in older adults.

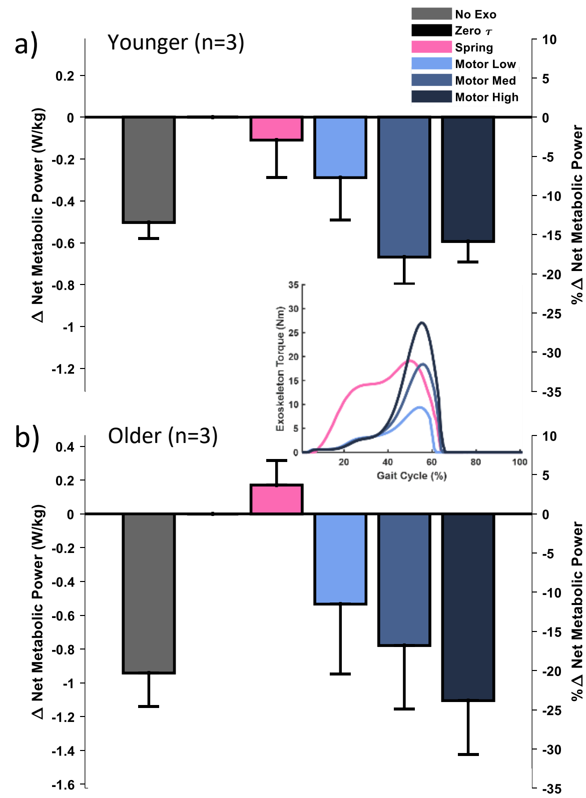

Figure 1: The absolute change (left axis) and percent change (right axis) in net metabolic power (mean ± SE) from the exoskeleton zero torque condition for young (a) and older (b) adults. The inset plot is average exoskeleton torque patterns from one participant. Change in net metabolic power young: -0.503, 0, -0.110, -0.289, -0.668, -0.594 W/kg; older: -0.942, 0, 0.170, -0.534, -0.779, -1.105 W/kg respectively. Percent change in net metabolic power young: -13.437, 0, -2.925, -7.719, -17.856, -15.860 %; older: -20.305, 0, 3.669, -11.516, -16.794, -23.832 % respectively. This means motor-like but not spring-like ankle exoskeleton assistance was more metabolically beneficial for older adults.

Significance: Given the clear performance gap between motor-like over spring-like assistance, our results should motivate engineering developers to focus on creating powered solutions in leaner form factors at more equitable price points. This is particularly important when considering adoption of exoskeletons as assistive technology for people with mobility challenges. Age-related differences in performance suggest a person's physiological properties may need to be considered when prescribing exoskeleton assistance. Future work will explore which physiological properties (e.g., k_t, soleus force-length-velocity properties) are most closely related to our observed age-related differences in metabolic benefit due to ankle exoskeleton assistance.

Acknowledgements: National Institute On Aging of the National Institutes of Health (R01AG058615), Alfred P. Sloan Foundation Graduate Scholarship, and Goizueta Foundation Fellowship

References: [1] B. Krupenevich et al. (2021), *Gerontology;* [2] F. Panizzolo et al. (2013) *Gait & Posture;* [3] R. Nuckols et al. (2020), *Sci Rep;* [4] Slade et al. (2022), *Nature;* [5] Shepard et al. (2022) *IEEE RA-L* [6] Zhang et al. (2017) *Robotics.* [7] Jackson [8] K. Poggensee & S. Collins (2021), *Sci Rob.*

Strategies utilized by nulliparous women while negotiating stairs during four modes of infant carriage

Holly Olvera[1*], Abigail R. Brittain[1], Erin M. Mannen[1], Safeer F. Siddicky[1,2]
[1]Mechanical and Biomedical Engineering, Boise State University, Boise, ID
[2]Kinesiology and Health Education, The University of Texas at Austin, Austin, TX
*Corresponding author's email: hollyolvera@u.boisestate.edu

Introduction: For the first year of life, infants rely heavily on their caregivers to transport them. While some infant carriage strategies such as carrying infants in arms, in wraps, and in baby carriers on a parent's body have been prevalent through history, modern infant product design has introduced alternative methods to carry infants including car seats and strollers. However, it is unclear how these different carrying methods may impact caregivers' biomechanics or injury risk. The objective of this pilot study is to identify the strategies utilized by nulliparous women when negotiating stairs while carrying an infant manikin.

Methods: An outdoor obstacle course was designed, representing typical activities required to navigate urban architecture: ascending and descending stairs and ramps, entering and exiting buildings, and crossing curbs. The course was completed by ten healthy female participants (age: 22.3±1.4 years; height: 65.2±2.5 inches; weight: 142.7±17 lbs.). All participants were injury and pain free. No participant was a mother or had been previously pregnant. Participants carried an infant manikin in a body-worn baby carrier, car seat, stroller, and in arms through the outdoor obstacle course. Each carrying method was completed six times, three times forward and three times backwards through the course. High-speed video cameras filmed each obstacle along the course. Three investigators analyzed 50 randomly selected trials to identify movement strategies for each carrying condition based on defining characteristics. A total of 480 trials were collected. Twenty-two trials were excluded due to equipment malfunction. This abstract focuses on data from the stairs in the obstacle course.

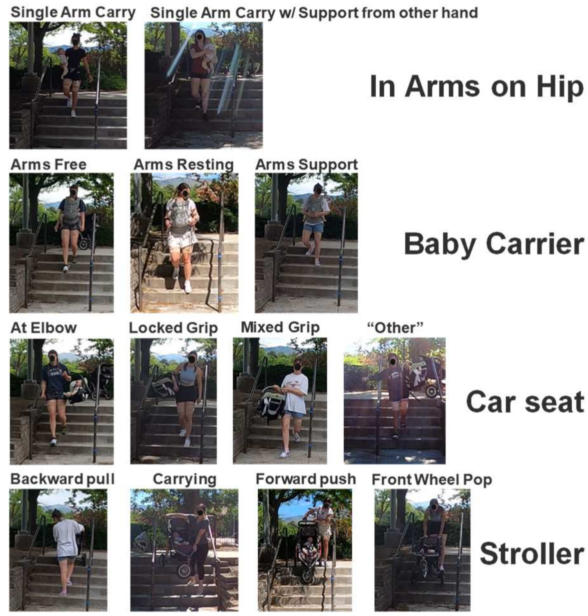

Figure 1: Photos of some distinct carrying strategies.

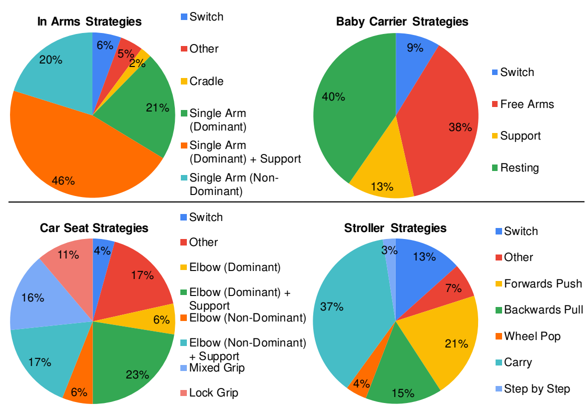

Figure 2: Frequency of all carrying strategies.

Results & Discussion: Of the 458 trials completed by participants, 112 were in arms, 114 in a baby carrier, 115 in a car seat, and 117 in a stroller. The following results are from stair negotiation, with some common strategies demonstrated in Fig. 1, and all observed strategies and their frequencies of utilization presented in Fig. 2. When carrying the infant manikin in arms, five main strategies were identified: cradling and carrying on the hip with a single arm (dominant or non-dominant) with and without support from the second arm. When carrying the manikin in a baby carrier, three main strategies were observed: arms hanging freely, arms wrapped around the baby carrier providing additional support, and arms resting on the baby carrier providing little to no support. Six strategies were identified in the car seat condition: carrying the car seat at the elbow (dominant and nondominant) with and without support from the second arm (support), a mixed grip, and a single arm "lock" grip. Five strategies were identified in the stroller condition: a forward push, a backwards pull, a front wheel pop, carrying, and a step-by-step carry. A "switch" and an "other" category was added to each condition for cases when a participant transferred between strategies or used a strategy not defined above (but not observed commonly). For the in arms condition, participants preferred to carry the manikin on the dominant hip and with the dominant arm while the non-dominant arm provided support (41/112 trials). This was an unexpected observation since a left sided bias exists when carrying infants and inanimate objects alike [1], and 9/10 of our participants were right-dominant. The most employed strategy when carrying the manikin in baby carriers was resting the hands on the carrier (46/114 trials), followed closely by free hanging arms (43/114 trials). This observation is well aligned with recent findings [2] that indicate that caregivers primarily utilize babywearing for the ability to multitask and be "hands free". The most common strategy for carrying the car seat was carrying at the elbow (dominant) with support from the non-dominant arm (26/116 trials). Carrying the stroller was the most common strategy used in the stroller condition (45/117 trials). Carrying the manikin in car seats and strollers showed more variability in carrying strategies chosen, compared to the in arms or carrier conditions. This may be attributed to a relative lack of infant care experience in the participants. Car seats and strollers are also fairly heavy, which may have contributed to participants altering their carrying strategies. Our future work involves exploring spatiotemporal and EMG data of all infant carriage modes and strategies.

Significance: Research involving mother-infant dyads have often focused on the infants, regarding how best to provide care for that vulnerable population. The needs of the perinatal population are vastly understudied. This feasibility study provides the basis for a full experimental exploration of the impact of various common infant transport methods on caregivers' biomechanics in real-world scenarios.

References: [1] Ellis et al. (2013), 37:231-44, *J Nonverbal Behav*. [2] Havens et al. (2022), 46:25-34, *J Womens Health Phys Therap*.

A novel controller for belt accelerations during late stance to modulate propulsion mechanics at multiple speeds

Hannah N. Cohen[1*], Fabrizio Sergi[1*]
[1]Department of Biomedical Engineering, University of Delaware
* Corresponding author: fabs@udel.edu

Introduction: Propulsion is a major subtask of walking, which is critical for completing activities of daily living. Our lab has previously developed AccelBelt, a novel protocol that aims to modulate propulsion mechanics by accelerating the treadmill belt supporting the trailing limb as the subject is pushing off. The acceleration creates a fictitious inertial force that subjects must work against by increasing their propulsive force. This protocol was previously tested on healthy participants, demonstrating an increase in propulsive force during and after exposure to AccelBelt [1]. The perturbation controller for this experiment was tuned for baseline walking speeds that are typical for healthy adults (1 – 1.6 m/s), but the previous controller was not consistent nor safe across a wide range of speeds. Future work with AccelBelt aims to use the paradigm to modulate propulsion mechanics in post-stroke individuals, where walking speeds can be as slow as 0.4 m/s. This presents a need to update the AccelBelt controller to provide consistent and safe exposure to belt accelerations at slower speed.

In general, AccelBelt controllers aim to accelerate the belt supporting the trailing limb during late stance (to specifically modulate propulsive force), and preferably during double support (for safety). Due to inherent delays in treadmill acceleration (~75 ms), and due to the short duration of double support at normal walking speeds (~125 ms), the previous AccelBelt controller sent an acceleration signal in anticipation of the occurrence of contralateral heel strike, predicted using information from the previous gait cycle. At slow speeds, because double support duration increases at lower walking speeds, this predictive algorithm would accelerate the belt for a longer time compared to faster speeds, making it difficult to control the "dose" of exposure to belt accelerations. Also, high variability in the timing of gait events, likely in a neuromotor impaired population [2], may make prediction of gait events less reliable and compromise the safety of the protocol. In this study, we present and validate AccelBelt 2.0, a new logic for applying belt accelerations during late stance that makes it possible to control the duration of exposure to accelerations across multiple speeds, while allowing these accelerations to primarily occur during double support.

Methods: The AccelBelt 2.0 controller, designed to operate as desired at low speeds ($v < 0.5$ m/s), is primarily based on predicting toe-off (TO) events, and on accelerating the belt for a certain amount of time (T_{TOT}) prior to the predicted TO event if heel strike (HS) of the contralateral leg has been detected. T_{TOT} will depend on the desired acceleration duration (T_{des}) and on intrinsic actuation delays of the treadmill (T_{del}). For our system, T_{rt} is 40 ms. Targeting T_{des} of 180 ms, T_{TOT} was set to 220 ms (Fig. 1). At speeds where the duration of double support is comparable with T_{des}, it would be important to send the acceleration command based on predicted HS, and not after detection to minimize the effect of actuation delays. As such, the AccelBelt 2.0 controller implements additional logic for the protocol at higher velocities (between 0.5 m/s and 1 m/s). Rather than waiting to detect HS, the controller sends the acceleration signal if the current time is within T_{ant} seconds of predicted HS. Due to the negative association between the duration of double support and gait speed, we scaled parameter T_{ant} with velocity to achieve consistent timing across speeds ($T_{ant} = 2T_{ant,1} * v - T_{ant,1}$), with $T_{ant,1}$=0.175 s.

To validate the developed controller, three participants participated in a walking experiment. Subjects performed 5 separate walking trials where they walked at a baseline of 0.4, 0.5, 0.6, 0.8, and 1 m/s and experienced 20 consecutive perturbations (magnitude: 5 m/s^2). To measure real-time velocity, three groups of five circular pieces of reflective tape were placed on each treadmill belt. Movements of the belts were detected via a ten-camera Vicon T40-S passive motion capture system (Oxford Metrics, Oxford, UK). Real-time HS and TO events were identified as the vertical force crossing a 125 N threshold. Change in belt velocities $v_{L/R}$ relative to baseline v_{BL} were estimated from motion-capture data. To quantify the "dose" of exposure, parameter $d_R = \int_{t_{HS,L}}^{t_{TO,R}} (v_R - v_{BL})dt$ was calculated. A mixed-model ANOVA was fit to the data with velocity as a fixed effect and participant as a random effect to test the hypothesis that d_R would not be significantly different across velocity conditions. Pairwise comparisons were performed between parameters d_R at all velocities.

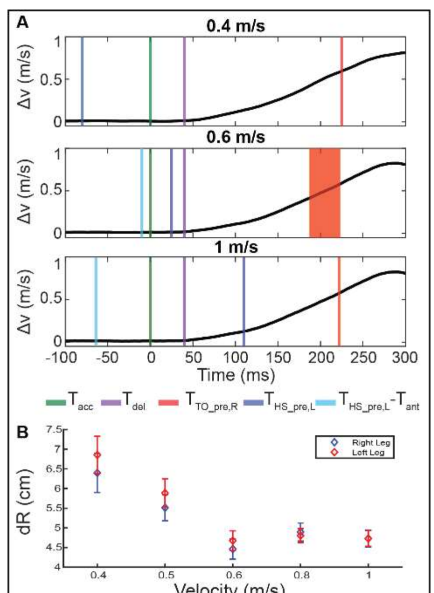

Figure 1: (A) Timing diagram describing the operation of the developed controller at multiple speeds. (B) Incremental displacement d_R measured for each speed condition.

Results & Discussion: There was a significant effect of speed (p = 0.0425; p = 0.0068) on d_R and d_L. The most significant difference was between 0.4 and 0.6 m/s (mean$_R$ = 0.0193, p = 0.0388; mean$_L$ = 0.0216, p = 0.0116). A second mixed-model ANOVA was run without the 0.4 m/s data. In the second model, speed was not a significant effect (p = 0.0956; p = 0.112).

Significance: The main objective of this work was to develop a new controller that provided consistent exposure to belt accelerations across multiple speeds. The developed controller provided consistent accelerations for speeds between 0.5 and 1 m/s, but not for 0.4 m/s. The reason for such a mismatch is likely due to biases in predicting toe-off events at low speeds. Future work will include testing the paradigm with post-stroke individuals and studying modulation of propulsive force using the AcceltBelt 2.0 controller.

References: [1] Farrens et al. (2020), *IEEE T Neur Sys Reh* 28(2). [2] Wang et al. (2020) *Int J Rehabil Res* 43(1).

INVARIANCE OF FORCE PLATE INDEPENDENT A2 PROXIES ACROSS GAIT SPEED AND PATHOLOGY

Theresa E. McGuirk[1,2*], Carolynn Patten[1,2]
[1]Biomechanics, Rehabilitation, and Integrative Neuroscience Lab, Dept PM&R, University of California Davis, Sacramento, CA
[2]Veterans Affairs Northern California Health Care System, Martinez, CA
*Corresponding author's email: temcguirk@ucdavis.edu

Introduction: Features of internal joint power data convey how kinetics are used across lower limb joints while walking. The timing and magnitude of these features (maxima and minima) at key points in the gait cycle inform energy transfer during normal and pathological gait [1]. However, joint power derivation requires a motion capture system and 6-degree-of-freedom (DOF) force plates, tools not typically accessible in clinical or daily living environments where these metrics could inform regarding disease progression and rehabilitation. Here, as a first step, we focus on peak ankle plantarflexion power (A_2) which quantifies a significant proportion of kinetic energy during gait [2]. We decompose the Newton-Euler equations of motion derivation for ankle moment into 6 subcomponents (eq.1) and investigate features which parallel A_2 across a range of gait speeds yet are calculated without force plate data.

Methods: Kinematic and kinetic data acquired through 3D motion capture were extracted from 126 cases (76 post-stroke, 63.5±10.1 years, 50 age-matched controls, 61.2±9.1 years) during walking on a split-belt treadmill instrumented with two 6-DOF force plates. Participants walked at a range of speeds (control: 0.2-2.0m/s, post-stroke: 0.1-1.35m/s). Data were modelled as linked rigid-body segments, scaled to subject-specific parameters (height and mass) with assigned segment geometry and inertial properties [3,4]. Ankle joint power ($P_{ANK,X}$) was defined as the product of joint angular velocity and ankle moment ($M_{ANK,X}$, eq.1) derived using Newton-Euler equations of motion and the free body diagram [5]. We have rearranged these terms to form 6 moment components; MC_1 – MC_3 require force plate data while MC_4 – MC_6 utilize foot segment position, acceleration and inertial properties, thus can be derived without force plate data. Features of MC_4 – MC_6, including maxima and minima, were identified in terminal stance through mid-swing for each individual gait cycle. Results were averaged per subject by leg for analysis and compared to maximum $P_{ANK,X}$ (A_2).

[eq.1]
$$M_{ANK,X} = \overbrace{M_{FP,X}}^{MC_1} + \overbrace{F_{FP,Y} \times (CP_{FT,Z} - JC_{ANK,Z})}^{MC_2} - \overbrace{F_{FP,Z} \times (CP_{FT,Y} - JC_{ANK,Y})}^{MC_3} - \underbrace{IXX_{FT} \times \alpha_{FT,X}}_{MC_4} - \underbrace{(m_{FT} \times a_{FT,Y}) \times (CM_{FT,Z} - JC_{ANK,Z})}_{MC_5} + \underbrace{[m_{FT} \times (a_{FT,Z} - g_Z)] \times (CM_{FT,Y} - JC_{ANK,Y})}_{MC_6}$$

Results & Discussion: When examining features of the control data, the maximum of MC_5 revealed a strong correlation with corresponding A_2 values (R^2 = 0.801). Peak MC_5 also maintained a consistent time lag relative to A_2 (9.16±2.01 %GC) over a range of walking speeds. This time lag is maintained for MC_5 in data acquired from the less affected leg post-stroke (9.54±2.09 %GC) and increases slightly, but consistently, in the more-affected leg (12.84±4.21 %GC). This strong association between A_2 and peak MC_5 in both timing and magnitude suggest peak MC_5, derived without force plate data, is an excellent candidate for an A_2 proxy.

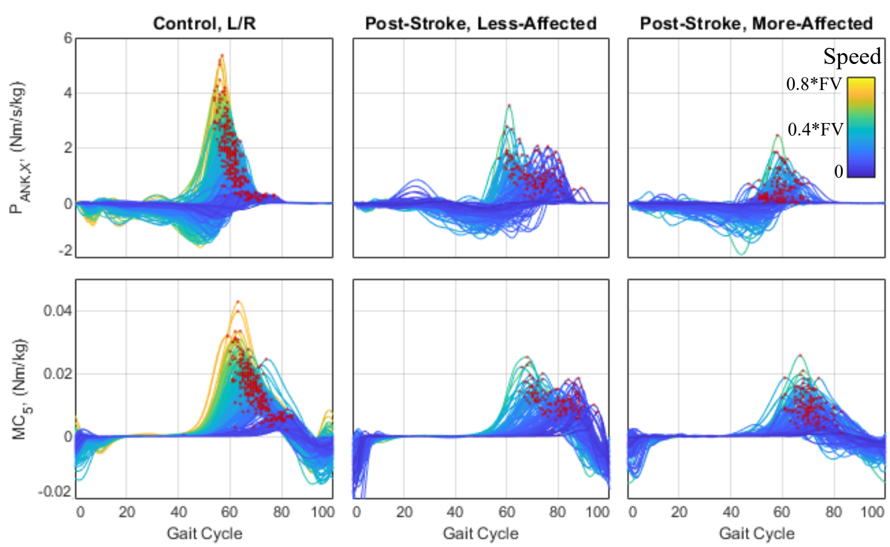

Figure 1: Row 1: Ankle plantarflexion power ($P_{ANK,X}$) across the gait cycle; A_2 is marked with red dot. Row 2: Moment component driven by linear acceleration (MC_5), peak value marked with red dot. Column 1: Control data from both legs. Column 2: Post-stroke data from less-affected leg. Column 3: Post-stroke data from more-affected leg. Data vectors are color coded to walking speed relative to Froude velocity (FV). FV = $\sqrt{g*LL}$, where g = gravity, LL = leg length. The walk-to-run transition for bipeds occurs at Speed ≈ 0.707*FV [6].

Significance: The ability to estimate joint power without force plates has myriad applications for clinical settings or daily activity monitoring [7]. Our method leveraged the physics on which internal joint moment is derived and examined the contributing signals measured without force plates (i.e. segment position, acceleration, inertial properties). This approach maintains the contextual link of the source to the original power calculation, providing relevant insight into the behaviour of candidate A_2 proxies. These findings expand the utility of tools accessible outside motion capture labs (i.e. markerless motion capture, inertial measurement sensors), and may accelerate their translation for use in clinical and free-living settings.

References: [1] Sutherland DH. *Gait Posture*. 2005 Jun; 21(4):447-461. doi:10.1016/j.gaitpost.2004.07.008; [2] Winter DA. *Crit Rev Biomed Eng*. 1984;9(4):287-314. [3] Chen G, Patten C. *J Biomech*. 2008;41(4):877-883. doi:10.1016/j.jbiomech.2007.10.017; [4] Hanavan EP. *AMRL TR*. 1964 Oct;1-149. [5] Winter DA. *Biomechanics and Motor Control of Human Movement. 4th Ed*. Sep 2009. doi:10.1002/9780470549148; [6] Usherwood JR. *Biol Lett*. 2005 Sep 22; 1(3): 338-341. doi:10.1098/rsbl.2005.0312; [7] McGuirk TE, et al. *Front Hum Neurosci*. 2022;16. doi:10.3389/fnhum.2022.867485.

AN ANALYSIS OF SPATIOTEMPORAL PARAMETERS UNDER VARIOUS NON-SLIP SOCK IN WALKING GAIT

Christopher M. Wilburn[1], John L. Grace[1], Jordan E. Tompkins[1], Brandi E. Decoux[2], John W. Fox[3], Jerad J. Kosek[1] Hannah Houde[1], Bahman Adlou[1], Meghan Hancock[1], Kennedy Drake[1], Evelyn Iturradle[1] & Wendi H. Weimar[1]

[1]Auburn University, Auburn, AL

[2]Southeastern Louisiana University, Hammond, LA

[3]Methodist University, Fayetteville, NC

email: czw0043@auburn.edu

Introduction: Approximately 700,000 to 1,000,000 falls occur within hospital settings each year [1]. Injuries associated with at-risk falls populations can induce fractures soft tissue damage, ultimately producing pathological gait patterns and increasing morality rates. Thus, non-slips socks have recently become an effective and affordable methods for fall prevention [2]. However, the composition properties associated with these socks often result in an unfitted location of the embedded slip-resistant material on the sock on other areas of the foot [3]. Thus, the functionality of the non-slip sock is altered and the occurrence of falls still occur. While there are socks that are manufactured with various non-slip compositional properties, research investigating its influence on gait mechanics has not been thoroughly investigated. Therefore, this project investigated how various non-slip socks impact the spatiotemporal parameters of walking gait.

Methods: Twenty-five participants (height: 1.84 ± 0. 06 m; mass: 88.4 ± 12.1 kg) consented, indicated good self-reported health, and absence of a lower extremity injury within the last six months participated in the IRB approved study. Participants completed three successful gait trials under three randomized footwear conditions, barefoot (BF), traditional non-slip socks (HNS; Medline Industries LP, Northfiel, IL), and compressed non-slip socks (ANS; Pembrook Appareal, Vancouver, WA) across an instrumented walkway (ProtoKinetics LLC, Havertown, PA). The ANS condition consisted of a non-slip socks composed of elastic materials and a reinforced arch band that promoted a more secure fit. Spatiotemporal variables, such as normalized stride length, double and single stance time, single and double stance center of pressure distance, cadence, and velocity, were exported and analyzed in SPSS (IBM, NY). A series of repeated measures ANOVAs were employed to determine the effect the sock conditions.

Results & Discussion: Main effects were observed amongst double support center of pressure and single support time (*Table 1)*. Specifically, the ANS yielded a shorter center of pressure trajectory when compared to HNS. Additionally, the ANS condition resulted shorter single support time when compared the BF and HNS while, the BF obtained shorter single support time compared to HNS. These findings suggest that non-slip socks of various compositional properties improve some gait parameters without inducing mechanics that increase falls.

Significance: The combination of shorter single support time and double support center of pressure in the ANS condition reduces the likelihood of compromised balance and promotes gait efficiency. While this project investigated healthy individuals, these findings have imperative implications for fall prevention strategies. Future research should be conducted to examine the benefits of various non-slips socks have on clinical populations and additional biomechanics.

References: [1] Gu et al. (2016), Chin. Nurs. Res. 3 (1) 7-10; [2] Jazayeri et al (2021), IJQHC. 33(2); [3] Richie (2017), Athletic footwear and orthoses in sports medicine, 91-105.

	Barefoot		Hospital Non-Slip		Compressive Non-Slip				
	M	*(SD)*	*M*	*(SD)*	*M*	*(SD)*	*F*	*p*	η^2
Cadence (step/sec)	105.01	(7.06)	106.38	(10.48)	106.28	(8.65)	.614	.545	.026
Double Support (s)	.28	(.04)	.28	(.06)	.28	(.07)	.229	.796	.010
Double Support COP (cm)	52.94	(5.38)	53.66	(4.70)*	52.34	(4.42)*	3.741	(.044)*	.140
Normalized Stride Length (% body height)	76.63	(4.27)	89.644	(3.546)	95.654	(5.381)	1.298	.279	.053
Single Support (s)	.42	(.03)$^{+}$	.43	(.03)*	.414	(.03)$^{*,+}$	10.805	<.001	.320
Single Support COP (cm)	12.27	(1.46)	12.29	(1.40)	12.22	(1.40)	.232	.794	.10
Velocity (cm/s)	118.16	(14.05)	119.76	(14.24)	120.65	(15.26)	1.861	.167	.075

Table 1. Comparisons in spatiotemporal parameters of walking gait under the barefoot, traditional hospital non-slip sock and compressive non-slip sock conditions.

THE INCREASE IN FRONTAL-PLANE ANKLE STIFFNESS WITH WEIGHT-BEARING IS SENSITIVE TO ANKLE POSTURE

Zoe Villamar[1,2*], Prakash Jayabalan[2,3], Eric J. Perreault[1,2,3], Daniel Ludvig[1,2]
[1]Department of Biomedical Engineering, Northwestern University, Evanston, IL
[2]Shirley Ryan AbilityLab, Chicago, IL, [3]Department of Physical Medicine and Rehabilitation, Northwestern University, Chicago, IL
*Corresponding author's email: zoevillamar2018@u.northwestern.edu

Introduction: Ankle sprains are the most common musculoskeletal injury, typically resulting from excess inversion. A decreased level of frontal-plane ankle stiffness could increase the possibility of a sprain. Stiffness increases greatly with axial loading of the ankle [1] providing a mechanism to help stabilize the ankle during weight-bearing conditions. However, this effect of load has only been studied in neutral postures in which sprains are less common. Cadaveric studies have shown that there is less resistance to motion, and hence lower stiffness, when the ankle is loaded in plantarflexion [2], a posture in which sprains are common, though it is unclear how these cadaveric results relate to *in vivo* properties of the ankle. Our objective was to determine how sagittal plane postures alter the relationship between axial loading and frontal-plane ankle stiffness. We hypothesized that the plantarflexed posture would have less of an effect of load on ankle stiffness.

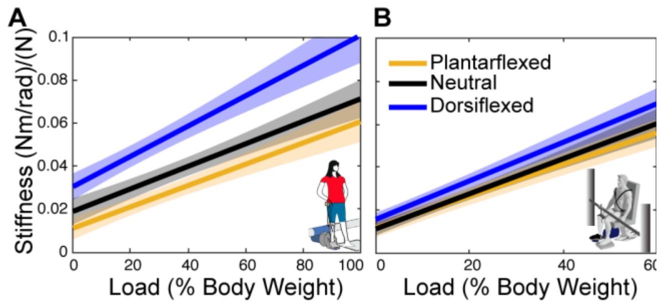

Figure 1: (A) Effect of sagittal plane posture during weight-bearing. (B) Effect of sagittal plane posture during passive loading. All figures are group averages of stiffness from linear mixed-effects models. Shaded areas are 95% confidence intervals.

Methods: Our goal was to investigate the effect of sagittal plane posture on loaded frontal-plane ankle stiffness. We performed 2 experiments to accomplish this. In the first experiment, 18 participants (10 females) completed a functional weight-bearing task. While standing, they voluntarily shifted their body weight onto their tested ankle while the sagittal plane angle of their ankle was altered systematically. As muscle activity can confound estimates of frontal-plane ankle stiffness, we designed a 2nd experiment to isolate the effect of load. A different set of participants (4 males, 10 females) were seated as the ankle was axially loaded externally while subjects relaxed their muscles. For both experiments, postures of neutral, 15 degrees plantarflexion, and 15 degrees dorsiflexion were tested. Small rotational perturbations were applied to the ankle in the frontal plane to estimate stiffness. To determine whether posture or load related to changes in muscle activity could contribute to any differences in stiffness, electromyographic (EMG) data were collected from the tibialis anterior (TA), lateral gastrocnemius (LG), medial gastrocnemius (MG), soleus (SOL), peroneus longus (PL), and peroneus brevis (PB). We used linear mixed effects models to test our hypotheses that plantarflexed postures would result in reduced frontal-plane ankle stiffness. Stiffness was the dependent variable, load was a continuous factor, subject was a random factor, and sagittal plane posture was a categorical factor that interacted with load. Since muscle activity is known to affect ankle stiffness, we wanted to determine if muscle activity increased with loading to see if it could be a confounding factor. To do this, we computed separate models for each muscle with EMG as the dependent variable.

Results & Discussion: During standing, across all subjects, sagittal plane posture had a significant effect on non-weight-bearing frontal-plane ankle stiffness ($F_{2,25} = 20.5$, $p < 0.0001$) and on how stiffness changes with weight-bearing load ($F_{2,19} = 5.6$, $p = 0.01$). Stiffness was less sensitive to load when the ankle was in a plantarflexed posture ($4.9 \pm 0.6\text{x}10^{-4}$ Nm/rad/N/%BW) compared to when it was in a dorsiflexed posture ($7.2 \pm 0.7\text{x}10^{-4}$ Nm/rad/N/%BW; $t_{18} = 3.1$, $p = 0.006$), though not when compared to neutral posture ($5.2 \pm 0.6\text{x}10^{-4}$ Nm/rad/N/%BW; $t_{20} = 0.46$, $p = 0.65$) (Fig 1A). As a result, we found that the frontal-plane ankle stiffness was greatest in dorsiflexion and least in plantarflexion throughout the entire range of weight-bearing. Muscle activity during standing may have contributed to the differences, as the MG, SOL, PL and PB significantly increased in activity with weight-bearing by 0.04–0.39 %MVC/%BW (all $p < 0.05$). This increase in muscle activity with weight-bearing may contribute to the increased stiffness with weight-bearing, and differences in muscle length between the three postures might be the reason for the differences in the load-stiffness slopes between postures.

During the seated task, in which there were no changes in muscle activation, there was a significant effect of sagittal plane posture on unloaded frontal plane ankle stiffness ($F_{2,20} = 5.4$, $p = 0.01$) but there was no significant effect of sagittal plane posture on how stiffness changes with load ($F_{2,16} = 2.8$, $p = 0.09$). Stiffness in the dorsiflexed posture was greatest, while there was no significant difference between neutral and plantarflexed posture over the range of loads tested (Fig 1B). There were no effects of posture or passive load in activity for any muscle (all $p>0.05$). These results demonstrate that a dorsiflexed posture increases frontal plane stiffness independent of joint loading, and joint loading could not be the reason for the increased sensitivity of stiffness to weight-bearing when the ankle is dorsiflexed.

Significance: The ankle is less stiff in plantarflexed postures compared to dorsiflexed postures at all levels of load, making it more susceptible to injury. The altered sensitivity to weight-bearing load but not with passive load with posture suggests that muscle activation plays a role in modulating the effect of the axial loading with sagittal plane posture.

Acknowledgements: NIH T32 HD07418

References: [1] Villamar et al., (2022) *J Biomech* 143: 111282 [2] Stiehl et al., 1993. *J Orthop Trauma.* 7(1): p. 72-7.

INTEGRAL RECONSTRUCTION AND STAIRS&RAMPS DETECTION USING ONE FOOT-MOUNTED IMU

Yisen Wang[1*], Katherine H. Fehr[1], Peter G. Adamczyk[1]
[1]University of Wisconsin-Madison
*email: ywang2557@wisc.edu

Introduction: Foot trajectory reconstruction using an Inertial Measurement Unit (IMU) enables biomechanics studies on human locomotion in both in-lab and out-of-lab settings. Kalman Filter based reconstruction, including Extended Kalman Filter (EKF) or Error State Kalman Filter (ESKF) are powerful methods. However, they suffer from the drift in height [1] without the correction of other sensors. One reason is due to the limited bandwidth and/or range on the IMU: heel strike impact can't be captured perfectly [2], thus causing error, especially in the vertical direction, which is not well-modeled as Gaussian noise. The inaccurate height information makes it difficult to detect ramps and stairs from only a foot-mounted IMU. In this abstract, we propose an enhancement to integral-based reconstruction that has more accurate height information and can detect ramps and stairs using only one foot-mounted IMU. Although we produce a 3D trajectory reconstruction in post-processing, here we only focus on the height information, therefore ignore the common heading drift issue. We also assume that the orientation of the IMU sensor at each moment can be obtained by any orientation filter.

Methods: We take the same sensor error model as in ESKF [3], but only keep the accelerometer bias term $b = [b_x, b_y, b_z]^T$. We introduce the heel strike velocity error Δv_{hs} to describe the discontinuity in the world z-axis velocity at the heel strike instant, k_{hs}. The velocity update from time k to time $k+1$ is computed as the following:

$$\begin{bmatrix} v'_x(k+1) \\ v'_y(k+1) \\ v'_z(k+1) \end{bmatrix} = \begin{bmatrix} v_x(k) \\ v_y(k) \\ v_z(k) \end{bmatrix} + \left(\begin{bmatrix} R_{11}(k) & R_{12}(k) & R_{13}(k) \\ R_{21}(k) & R_{22}(k) & R_{23}(k) \\ R_{31}(k) & R_{32}(k) & R_{33}(k) \end{bmatrix} \begin{bmatrix} a_{m,x} - b_x \\ a_{m,y} - b_y \\ a_{m,z} - b_z \end{bmatrix} + g \right) \Delta t \qquad (1)$$

Where $R(k)$ is the rotation matrix representing the sensor orientation at time k, a_m is the measured accelerometer signal in sensor body frame, and g is the gravity vector.
We define $\Delta v(n)$ as the accumulated velocity difference due to acceleration bias up to time n. For a single stride, we can represent the accumulated velocity difference as:

$$\Delta v(n) = \sum_{k=0}^{n} (R(k)) b \Delta t = R_v(n) b \Delta t \qquad (2)$$

Where $R_v(n) = \sum_{k=1}^{n} R(k)$ is the sum of rotation matrix from $R(1)$ to $R(n)$. We can follow the same idea to compute for position difference due to acceleration bias, because of the second order term in integrating position, we define $R_p(n) = \sum_{k=1}^{n} (R_v(k) + \frac{1}{2} R(k))$.
The heel strike velocity error Δv_{hs} will contribute to the z-axis velocity at heel strike moment as $v_z(k_{hs}) = v_z(k_{hs}) + \Delta v_{hs}$, and to z-axis position as $\Delta p_z = \Delta v_{hs}(N - k_{hs})\Delta t$, where N is the length of samples for that stride and Δt is sample period.
In the case of walking on level ground, double integrating the raw data yields residual velocity and residual height at the end of the stride. Combining the equations for velocity difference, position difference and heel strike velocity error, we obtain the system of equations (3), which can be solved to find $[b_x, b_y, b_z, \Delta v_{hs}]$, corrections that yield zero residual velocity and height.

$$\begin{bmatrix} -V_{residual,x}(N) \\ -V_{residual,y}(N) \\ -V_{residual,z}(N) \\ -H_{residual,z}(N) \end{bmatrix} = \begin{bmatrix} R_{v,11}(N) & R_{v,12}(N) & R_{v,13}(N) & 0 \\ R_{v,21}(N) & R_{v,22}(N) & R_{v,23}(N) & 0 \\ R_{v,31}(N) & R_{v,32}(N) & R_{v,33}(N) & 1 \\ R_{p,31}(N)\Delta t & R_{p,32}(N)\Delta t & R_{p,33}(N)\Delta t & (N - k_{hs}) \end{bmatrix} \begin{bmatrix} b_x \\ b_y \\ b_z \\ \Delta v_{hs} \end{bmatrix} \Delta t \qquad (3)$$

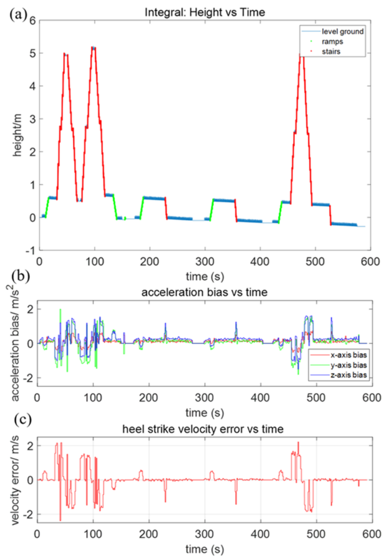

Figure 1: (a) height change on 10-minute walk, including stairs with 4.5m height; (b) acceleration bias on each step; (c) velocity error on each step.

In the case of non-level ground, there will be large deviation in the acceleration bias and heel strike velocity error from equations (3), as shown in Fig 1 (b)(c). We can apply a simple criterion to separate the ramp and stairs from level ground. For non-level ground steps, we only solve for the zero residual velocity conditions to get acceleration bias and use average heel strike velocity error from previous steps. Finally, we can use the trajectory results to separate any mix between ramp and stairs.

Results & Discussion: We tested the new method on 3 unimpaired subjects and one with unilateral amputation, using an APDM Opal sensor on top of the shoe. Subjects walked a random route, including level ground, up and down ramps, and three times up and down stairs to the upper floor, plus short stairs, then returned to the same spot. One testing result is shown in Fig 1. The stable distribution of acceleration bias demonstrates that some pattern of imperfect measurement exists in that condition. Because we do not model the sensor noise explicitly, the acceleration bias here contains effects due to both imperfect measurement of the movement and sensor noise. Table 1 summarizes the reduction in height error due to the proposed method. In general, the new method works very well on natural legs, and less well on prosthetic foot, partly because much bigger heel strike impact occurred on prosthetic leg. The main remaining height error happens on ramps and stairs.

Table 1: testing results on four subjects

Subject	Distance	Integral: Residual Height	ESKF: Residual Height
1-left	695 m	1.49 m (0.21%)	5.79 m (0.83%)
1-right	705 m	1.07 m (0.15%)	11.32 m (1.61%)
2-left	313 m	2.74 m (0.88%)	8.77 m (2.80%)
2-right	309 m	0.25 m (0.08%)	5.85 m (1.89%)
3-right	602 m	-0.27 m (0.05%)	10.64 m (1.77%)
4-prosthetic	518 m	1.54 m (0.29%)	7.79 m (1.50%)
4-unimpaired	527 m	0.38 m (0.07%)	18.85 m (3.58%)

Significance: The novel integral reconstruction provides more accurate height information, it can also detect level ground vs. ramps and stairs reliably using only one foot-mounted IMU, which is not easy only using Kalman Filter based reconstruction.

Acknowledgements: This project is funded by DOD W81XWH-19-2-0024.

References: [1] Hsu, et al. 2017 *IEEE Sensors* [2] Ju, et al. 2015 *Measurement Sci & Tech* [3] Solà 2017 *arXiv.*

CONTROLLING ANKLE MOTION USING TAYCO BRACE AND AN ORTHOPEDIC WALKING BOOT DURING WALKING

Amber Aultman[1], Meghan Haser[1], Ben VonGunten[1], Henry Wang[1], D. Clark Dickin[1*]
[1] Ball State University, Muncie, IN, USA
*email: dcdickin@bsu.edu

Introduction: Ankle fractures are relatively common and take weeks to months before full recovery is achieved. To assist in the recovery process, orthopedic walking boots (OWB) have widely been used as an alternative to casting the injured limb to immobilize the joint and provide overall stability to the limb. Using OWBs has been shown to significantly decrease the recovery time in individuals suffering from ankle fracture [1]. While the OWB has become standard practice of care for those suffering from ankle and foot injuries, the design of the boot can cause alterations in gait mechanics [2]. The OWB creates a leg length discrepancy resulting in pelvic tilt away from the affected limb and can lead to low back pain and contribute to the development of osteoarthritis at the hip and knee [3]. To offset the resulting limb length discrepancies, a heel lift on the unaffected limb has been used to correct pelvic tilt and improve overall gait, but the lift introduced frontal plane hip asymmetry compared to the OWB [4]. As an alternative to the OWB, the TayCo ankle brace (TAB) was designed to achieve joint immobilization analogous to the OWB while eliminating the discrepancy in leg length. Previous research demonstrated minor changes and asymmetries on temporal-spatial measures of gait when using the OWB, [5] but the efficacy of the TAB in controlling ankle motion has not been compared to the OWB during locomotion. The purpose of this study was to 1) assess the effectiveness of the TAB in stabilizing the ankle and subtalar joint, in the sagittal and frontal planes during gait in healthy adults; and 2) determine the overall impact of the TAB on the mechanics of walking relative to both the OWB and to a control shod condition.

Methods: Twenty-one younger adults (21 ± 2.62 years) performed a series of level walking trials under three different ankle support conditions (Figure 1); TayCo Brace (TAB), orthopaedic walking boot (OWB) and cross training running shoes (Shod). Participants attended a one-day session that involved 3-4 walking trials across a 10m walking for each condition while walking at a self-selected pace. A 15-camera Vicon motion capture system (VICON Inc., Denver, CO, USA) using and a modified Plug-In Gait marker set was used to quantify gait speed and kinematic data.

Figure 1: Picture of the Shod, TayCo brace, and walking boot including marker placement.

Results & Discussion: Significant differences ($p \leq .03$) were revealed between OWB (1.33m/s) and both Shod (1.46m/s) and TAB (1.44m/s) conditions. Summary kinematic data are illustrated in Table 1 for all testing conditions. In contrast to the Shod condition, both the OWB and the TAB significantly reduced ankle motion in all three planes ($p \leq 0.001$). No differences were revealed for ankle motion between the OWB and the TAB in the frontal or transverse planes of motion, however significant differences between TAB and OWB occurred in the sagittal plane ($p = 0.01$). Across all subjects, 2.85° more dorsi/plantarflexion occurred in the TAB than the OWB. While the OWB was shown to limit sagittal plane motion slightly more than TAB, the difference was relatively small. These findings indicate that practitioners can prescribe the TAB for their patients requiring ankle immobilization. The TAB provided comparable control in two out of three planes of motion with relatively minor differences in ankle dorsi/plantarflexion when compared to OWB. Since the TAB allows the patient to wear their own footwear, there is no change in their limb length.

		Shod	TAB	OWB
Sagittal	YA	30.17 *	16.13 †	12.11
Frontal	YA	20.34 *	8.39	8.15
Transverse	YA	13.43 *	7.32	7.98

Table 1: Overall range of motion at the ankle during stance while walking at a self-selected pace. ROM in all three planes show total motion (degrees) occurring at the ankle. (indicates a significant difference between Shod and both TayCo and the Walking boot) († indicates a significant difference between TayCo and the Walking boot).*

Significance: As expected, during level ground walking, the ankle joint experienced reductions in ROM for all three planes of motion during the bracing conditions (TAB or OWB) which are designed to limit ankle mobility. When comparing TAB and OWB, significant differences were observed in the sagittal plane with TAB permitting 2.85 degrees more range of motion than OWB. While statistically significant, these results reveal that the TAB and OWB perform similarly and accomplish the same basic goal of ankle immobilization with only a slight difference in plantarflexion and dorsiflexion movement.

Acknowledgements: Partial funding to support participant compensation was received from TayCo Brace, Inc.

References: [1] Amaha et al. (2017), *AP-SMART* [2] Gulgin et al. (2018), *Gait and Posture* 59 [3] Murray et al. (2017) *JMPT* 40 [4] Severin et al. (2019) *Gait and Posture* 73. [5] Gordon & Smith (2018) *Whitepaper*

CHANGE OF DIRECTION TASK PARAMETERS ACROSS DIFFERENT TURF SURFACES

Wendi H. Weimar[1*], John Fox[3], Christopher Wilburn[1], Brandi Decoux[2]
[1]School of Kinesiology, Auburn University
*Corresponding author's email: weimawh@auburn.edu

Introduction: The prevalence of artificial turf surfaces has increased in recent years, with some estimates putting the number of artificial fields installed to be as high as 6000 [1]. Most of the research has focused on performance and injuries on different surfaces, but relatively little research has investigated the influence of the surface on the consistency of the performer on that surface. It was hypothesized that performers would be more variable on the artificial surfaces and less variable on the natural surface because the performers are more familiar with natural surfaces and will have a preferred method for changing direction.

Methods:
Thirteen college aged participant were recruited and provided voluntary consent. Each participant performed three trials of a 5-10-5 drill on four surfaces, as quickly as possible. The four turfs included three artificial sport surfaces (with different shock-pad and infill conditions) and one natural sport surface. There were four variables of interest: time to complete the 5-10-5 drill (COD Time), plant leg angle with the ground (Approach Angle), time foot was in contact with the ground (Contact time) and distance between foot and target to turn about (Distance to Fitlight). Kinematic data was collected with an Xsens MVN Awinda inertial motion capture system, timing data was collected with a Fitlight timing system and video analysis was used to determine foot contact time. ICC calculations were performed to estimate consistency of performance on each surface.

Results & Discussion: The ICC of the participants' COD Time is good to excellent [2] with the exception of performance on the natural surface (Table 1). The ICC on the artificial surfaces is in line with previous work [3], however the previous project did not consider a natural surface. The hypotheses were that the participants would perform with more consistency on the natural surfaces and not as consistent on the artificial surfaces. The opposite was the case, it would seem that the participants adopted a less consistent performance/pattern on the natural surface perhaps because the artificial surface is more predictable and they did not need to deviate as much to adjust to natural fluctuations. The finding between the artificial and natural surfaces is what prompted us to consider the other variables present project. ICC of the participants performance for foot contact time and distance to Fitlight® were moderate to excellent [2] for the Art1 & Art3, and Nat, but not Art2. It was anticipated that at least one of the follow up variables would display concomitant consistencies as the COD time. However, that was not the case, indicating that the follow up variables were not the reason for the inconsistency between the natural and artificial surfaces COD time. However, the large inconsistencies noted on Art2 do require further consideration. Furthermore, the consistency of the approach angle may imply that this a stable variable and is not adjusted based on the frictional constraints of the surface. Further research is needed to identify how the body does adjust to manage the frictional characteristics between the shoe and surface.

COD Time			
	ICC	LB	UB
Art1	0.943	0.806	0.987
Art2	0.873	0.527	0.976
Art3	0.928	0.755	0.984
Nat	0.492	-0.586	0.875
Contact time			
	ICC	LB	UB
Art1	0.553	-0.308	0.879
Art2	-0.155	-2.382	0.688
Art3	0.89	0.678	0.97
Nat	0.568	-0.264	0.883
Approach Angle			
	ICC	LB	UB
Art1	.929	0.793	0.981
Art2	.933	0.79	0.984
Art3	.928	0.79	0.981
Nat	.887	0.669	0.969
Distance to Fitlight®			
	ICC	LB	UB
Art1	0.89	0.677	0.97
Art2	0.552	0.959	6.543
Art3	0.88	0.648	0.967
Nat	0.899	0.704	0.973

Table 1: Data for each variable of interest. Art1, Art2, Art3 are the artificial surfaces and Nat refers to the natural surface.

Significance:
The alignment of the ICC's for COD time between the present and previous project is interesting, for several reasons. While the ICCs are the very similar, the confidence intervals are much larger for the present project, suggesting that the participants were consistent within themselves, but not within the group. This finding is enhanced by the distribution of best performances. For example, 46% of the participants posted their fastest time on Art1, 38% on Art2, 8% on Art3 and 8% on Nat. This may be explained by the difference in the turf installation procedures between the two projects which may alter the timing of the ground reaction force being applied to the person. Last, research should consider why participants performed with less consistency on a natural surface vs artificial surfaces, when natural surfaces are often considered the preferred surface.

Acknowledgements: Funding provided by Shaw Industries Group, Inc and by the Auburn University Sport Biomechanics Laboratory

References:
1. Synthetic Turf Council Synthetic Turf 360: A guide for today's synthetic turf (2016). https://www.actglobal.com/research/STC-SyntheticTurf360.pdf
2. Koo & Li (2016). *J of Chiro Med* 15(2).
3. Wannop et al. (2020), *Life* 10(12).

LINKING THE TERRADYNAMICS, MECHANICS AND ENERGETICS OF DISSIPATIVE TERRAIN LOCOMOTION

Jonathan R. Gosyne[1, 3*], Qingyi Lou[1], Claudia Vitale[1], Gregory S. Sawicki[1, 2],
[1]The George W. Woodruff School of Mechanical Engineering, [2]The School of Biological Sciences, Georgia Institute of Technology, Atlanta, GA, USA, [3]Exponent Inc.
*Corresponding author's email: jonathan.gosyne@gatech.edu

Introduction: The mechanics and energetics of human locomotion on deformable media have been studied for decades, with works examining the metabolic expenditure and joint level effects across various forms of locomotion. While these works have linked whole body mechanics to energetics, little has been done to understand the underlying causes associated with the increased cost of transport in humans at the joint, muscle and ground surface level [1,2]. Much of this has been attributed to the limitations of instrumentation and sensing. Even so, it has been shown [1-3] that energy expenditure is not linearly scalable to actual mechanical work, with potential causation at the muscle level, however, there have been no human studies that allows for direct inverse dynamics from human locomotion over these substrates that directly link these mechanics to muscular function.

Our study presents a first step toward linking energetics to joint level mechanics, using a customized in-lab apparatus to perform the first comprehensive analysis of the joint-level inverse dynamic relationships for human locomotion on sand. The goal of this study was to understand why, at the joint level, it is more metabolically costly to locomote on sand, when compared to a similar task on hard ground. To this end, we hypothesized that participants would (1) show an increase in metabolic cost when performing a mechanically comparable task on sand versus hard ground, (2) Show increasing powers at across the joints of the leg, and (3) show that the increase in mechanical changes are not sufficient to account for metabolic rate differences.

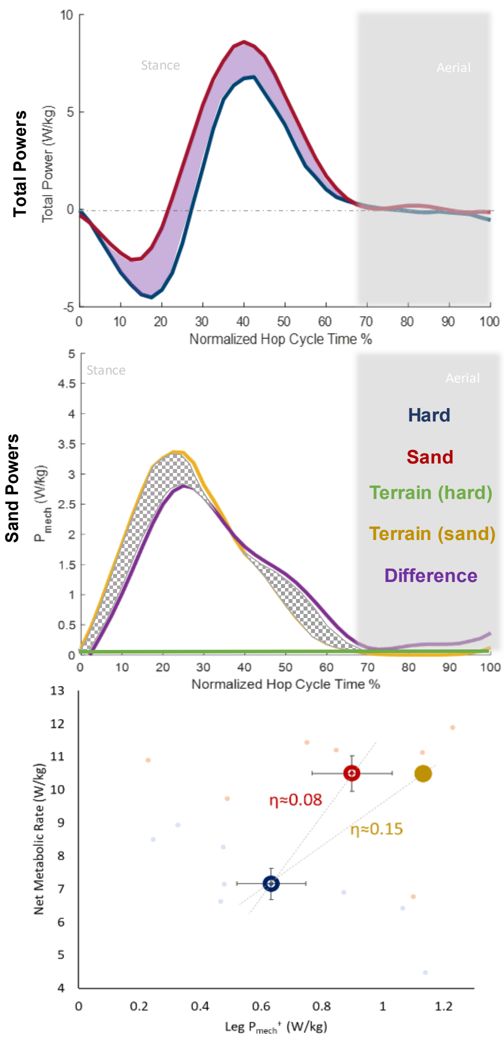

Figure 1: (Top) Power over the cycle for the leg on hard ground and sand, (middle) difference in powers over the cycle between the leg on hard ground as well as the actual terrains, (bottom) efficiency of P^{+}_{mech} of the leg from hard ground to sand.

Methods:

After obtaining informed consent, eight volunteers (average ± standard deviation; age: 23.63 ± 2.67 years; height: 1.78 ± 0.05 m; mass: 81.5 ± 10.1 kg; resting metabolic rate 1.48 ± 0.14 W/kg) were asked to fast overnight, and a 10-minute standing metabolic baseline was taken using an indirect calorimetry system. Participants were asked to don a pair of force sensing insoles and were prepared by administering a full lower body marker set. Participants were then asked to perform 2 x 5-minute hopping trials at 2.5Hz to matched height using biofeedback from the insoles and reflective markers on hard ground and on sand. Terrain conditions were randomized, and metabolic expenditure was measured through the same means as the resting trial.

Results & Discussion:

We found an increase in $\bar{P}_{met}$ of approximately 22% when comparing the mechanically matched hard ground and sand conditions. When the $\bar{P}_{mech}$ of the entire leg is considered, some interesting trends emerge. We found the total leg power developed over hard ground to be $\bar{P}_{mech\ hard}{}^{+}$ = 0.6399 W/kg increasing on sand to $\bar{P}_{mech\ sand}{}^{+}$ = 0.89 W/kg, leading to an increased mechanical work input of $\Delta\bar{P}_{mech\ leg}{}^{+}$ = 0.253 W/kg. Comparatively, the power lost to the sandy terrain was given as $\bar{P}_{mech\ sand}{}^{+}$ = 0.302 W/kg over the cycle. This leaves a discrepancy of $\bar{P}_{mech\ sand}{}^{+} - \Delta\bar{P}_{mech\ leg}$ = 0.05. We hypothesize that these discrepancies were due to work done at joints not covered by our marker set, the midfoot. As such, investigation at the full body level set is needed to further determine the magnitude contribution of the additional joints. Finally, we found that the efficiency η≈ 0.08, lower than the expected efficiency of positive work, 0.25. When accounting for positive work contributed by other systems, η increases to only 0.15, assuming $\bar{P}_{mech\ total}{}^{+}$ to be equivalent to the total mechanical power performed on the sand over a cycle. This highlights inefficiencies in the lower limb muscles, and prompts deeper investigation into the muscle level effects of dissipative terrain locomotion.

Significance: We have presented a novel joint level energetic analysis that links the whole-body metabolic energy cost of hopping in sand, to the work done by the primary movers of the leg, and the work done on the surface itself. These results serve to further the scope of knowledge of bipedal locomotion in dissipate substrates and can further inform future studies at the muscle level, as well as the design of wearable devices that allows users to go further and farther than ever before.

References: [1] Lejeune et al, (1998) *JEB*, [2] Gosyne and Sawicki, (2021), *APS*; [3] Gosyne and Sawicki, (2022); *ASB*.

DEVELOPMENT OF A FOOT-ANKLE EXOSKELETON TO REDUCE THE METABOLIC COST OF DISSIPATIVE TERRAIN LOCOMOTION

Jonathan R. Gosyne[1, 3*], Claudia Vitale[1], Qingyi Lou[1], Gregory S. Sawicki[1, 2],
[1]The George W. Woodruff School of Mechanical Engineering, [2]The School of Biological Sciences, Georgia Institute of Technology, Atlanta, GA, USA, [3]Exponent Inc.
*Corresponding author's email: jonathan.gosyne@gatech.edu

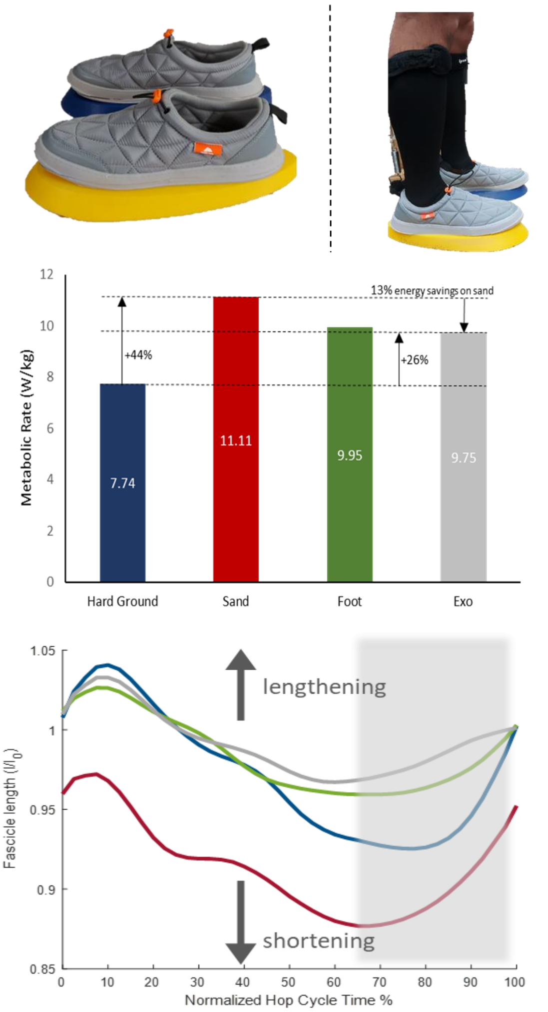

Figure 1: A picture of the foot-ankle exoskeleton (top), **n**ormalized metabolic rate for hard ground, sand, and augmented hopping (middle) and fascicle length relationship (l/l_0) (bottom) for the tested participant.

Introduction: Sand, gravel, and other surfaces consisting of granular media have more complex interactions with a human's walking gait than static surfaces (like a paved road). These surfaces often show non-linear and dissipative behavior, resulting in them being sensitive to applied forces, dynamically changing over time, and energy intensive to traverse. Currently, lower-limb exoskeletons are not designed or optimized for these surfaces. This gap in functionality was the focus of this study; the goal being to design an exoskeleton meant specifically to handle the challenges posed by sandy terrain, while reducing the energetic cost of movement.

Our previous work [1] has shown that much of the increase in metabolic cost of dissipative terrain locomotion is due to unfavorable muscle length operating points and higher muscle velocities. Additionally, *in-silico*, we have shown that a foot-ankle exoskeleton with optimized geometry and stiffness can eliminate the metabolic penalty associated with energy dissipation during locomotion on dissipative substrates. Now, we seek to translate these ideas into a bioinspired physical prototype that combines added area and added stiffness around the ankle joint, that we will used to comparatively investigate assisted and unassisted human hopping in sand. To this end, based on previous findings from modelling and human walking studies, we hypothesized that participants would (1) show a decrease in metabolic cost when performing a mechanically matched task with our exoskeleton on sand versus without and (2) operate at more favorable (longer) muscle lengths and lower fascicle velocities.

Methods: After obtaining informed consent, one participant (age: 22 years; height: 1.784m; mass: 88.8kg; resting metabolic rate 1.53 W/kg) was asked to fast overnight, and upon arriving in the morning, a 10-minute standing metabolic baseline was taken using an indirect calorimetry system. The participant was asked to don a pair of force sensing insoles and reflective makers were placed at the left and right posterior superior iliac spine to provide height biofeedback and validation through motion capture. A B-mode ultrasound probe was then placed on the skin superficial to each participant's right soleus, and the subject was then asked to perform 4 x 5-minute hopping trials. Trials were performed at 2.5Hz to matched height on hard ground, on sand, with only the exoskeleton foot on sand, and with the entire exoskeleton on sand. Terrain conditions were randomized, and metabolic expenditure was measured through the same means as the resting trial.

Results & Discussion: In agreement with our previous modelling and pilot results, we found a decrease in metabolic cost when performing a mechanically matched task with the exoskeleton on sand versus without. We found decreases in fascicle operating lengths on sand of when compared to mechanically comparable hopping on hard ground, with the fascicle lengths shown as a function of l_{CE}/l_0. Additionally, we found that the addition of the foot and the exoskeleton returned the operating length of the muscle to a similar region as that of hard ground. Unlike the terrain-length relationship, we found no appreciable changes in the fascicle shortening velocities. We expected to see a reduced shortening velocity due to the reduction in metabolic cost, and thus will continue to investigate this as the number of enrolled subjects increase. We found little difference between the hard ground and assisted conditions, prompting the investigation of additional MTU systems around the knee and hip.

Significance: This study presents the first metabolic-cost-reducing device designed for use over dissipative terrain. These results serve to further the scope of knowledge of bipedal locomotion and are a first step in the design of wearable devices that can mitigate energetic penalties associated with 'real-world' locomotion over dissipative terrain for applications in healthcare, agriculture, and beyond.

Acknowledgements: I would like to thank each and every member of the GT PoWeR lab for their support during this study series.

References: [1] Gosyne and Sawicki, APS 2021, [2] Gosyne and Sawicki, ASB 2022

Assessing methods to immobilize the ankle and its influence on joint motion during stair descent

Caroline Ashton[1], John Ethan Andamasaris[1], Emma Burns[1], , Henry Wang[1], D. Clark Dickin[1]

[1]**Biomechanics Laboratory, Ball State University, Muncie, IN, USA**

Introduction: The orthopedic walking boot (OWB) has been widely used as an alternative to casting an injured limb to immobilize and stabilize the joint. OWB has been shown to reduce recovery time in individuals with an ankle fracture or injury [1]. While the OWB is frequently used when treating individuals with ankle and foot injuries, the design of the boot has been shown to alter gait and postural stability [2]. The design of the OWB effectively creates a leg length discrepancy and causes the pelvis to be offset away from the affected limb, leading to low back pain and osteoarthritis at the hip and knee [3]. Despite these risks, the OWB continues to be prescribed for the treatment of ankle and foot injuries. As an alternative to the OWB, the TayCo Brace (TAB) is designed to immobilize the ankle joint to reduce recovery time without creating a leg length discrepancy. Preliminary studies have determined that the TAB provided more stability to both ankle eversion and inversion [4] while showing marginal alterations to gait compared to the OWB [5]. Stair negotiation is an essential task required for daily living that places high demand on the lower extremity musculature and is often associated with high fall risk [6]. Few research studies have investigated the use of joint immobilization devices during stair negotiation. Thus, the purpose of this study was to assess the effectiveness of the TAB in stabilizing the ankle and subtalar joint, in the sagittal and frontal planes during stair descent in healthy adults.

Figure 1: Shown from left to right: shod, TAB, and OWB. Each condition presented includes the designated retro-reflective marker configuration for both the shank and foot

Methods: 21 young adults (21±2.62 years) were assessed during stair descent trials across three lower extremity conditions (Shod, OWB, and TAB – Figure 1) performed in a randomized order. Descent trials were collected on a 3-step staircase (17cm step height) and participants were instructed to step down without using the handrail for assistance. Each footwear condition was assessed 3-5 times, and kinematic data were collected using a 3D motion analysis system to assess ankle, knee, and hip joint motion.

Results and Discussion: Figure 2 illustrates the differences in ankle motion occurring when using the TAB or the OWB in comparison to the Shod condition. As expected, both the TAB and OWB were able to control all three planes of ankle motion significantly compared to Shod ($p<0.001$). There were no significant differences between TAB and OWB in the sagittal or transverse plane in the ankle during stair descent. However, the OWB did permit a greater amount of ankle ab/adduction during stair descent than the TAB ($p=0.048$). Additionally, differences in joint motion were observed at the knee and hip when using the OWB. At the hip, the OWB resulted in greater amounts of flexion/extension than both the TAB ($p = 0.031$) and the Shod ($p=0.003$) condition, and greater amounts of hip ab/adduction than the TAB ($p = 0.013$) and Shod ($p = 0.006$) conditions. In contrast, the knee joint went through less flex/ext in the OWB than either the Shod ($p=0.001$) or TAB ($p=0.007$) conditions. While both the TAB and OWB controlled the ankle similarly, the OWB resulted in altered joint motion at the knee and hip. These modifications to stair descent mechanics when using a OWB should be considered when prescribing them as a therapy tool for ankle recovery. The TAB allowed participants to have similar ankle immobilization compared to the OWB, while not altering hip and knee mechanics of stair descent.

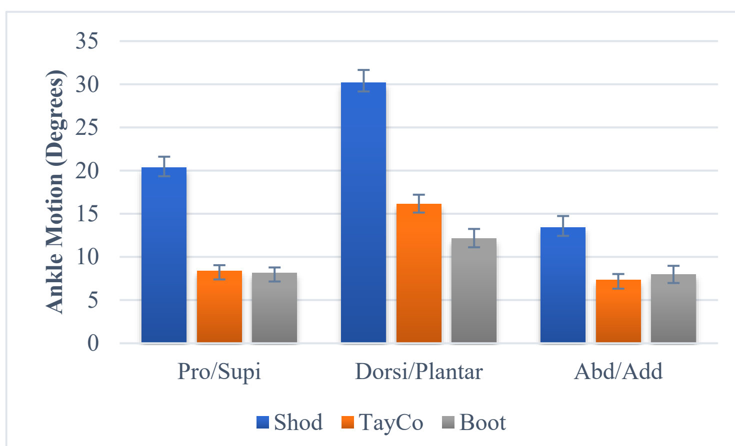

Figure 2: Ankle motion during stair descent. Significant differences were revealed between Shod and both TAB and OWB ($p<0.001$). Significant difference also occurred between OWB and TAB in the frontal plane (ab/adduction)(† $p=0.048$).*

Significance: The TAB offers health care professional an alternative to the OWB when prescribing ankle immobilization devices. Additionally, the TAB does not alter leg length since the patient is able to wear the same shoe on both feet without the need for a lift for the non-braced ankle. The results provided from this study revealed that TAB is as effective as the OWB in controlling ankle motion in both the sagittal and transverse planes, while simultaneously reducing the concomitant gait alterations caused through using an OWB.

Acknowledgements: Partial funding to support participant compensation was received from TayCo Brace, Inc.

References: [1] Amaha et al. (2017), *Asia-Pac J Sports Med Arthrosc Rehabil Technol* 7(10–14); [2] Gulgin et al. (2018), *Gait Posture* 59(76–82); [3] Murray et al. (2017), *J Manipulative Physiol Ther* 40(5):320–9; [4] Niebur & Requet. (2022), *TayCo Brace Report 042;* [5] Gordon & Smith. (2022), *TayCo Brace Report 041;* [6] Samuel et al. (2011), *Gait Posture* 34(2):239-44

QUADRICEPS STRENGTH SYMMETRY IS NOT A PREREQUISITE TO AUGMENTING PEAK KNEE EXTENSOR MOMENT IN INDIVIDUALS WITH ANTERIOR CRUCIATE LIGAMENT RECONSTRUCTION

Amanda E. Munsch[1*], Carly M. Rauch[1], Brian Pietrosimone[2], Jason R. Franz[1]
[1]Joint Department of Biomedical Engineering, UNC Chapel Hill and North Carolina State University, Chapel Hill, NC, USA
[2]MOTION Science Institute, Department of Exercise and Sport Science, UNC Chapel Hill, Chapel Hill, NC, USA
*Corresponding author's email: aemunsch@live.unc.edu

Introduction: Altered gait biomechanics that persist after anterior cruciate ligament reconstruction (ACLR) are thought to precipitate osteoarthritis (OA) development through a change in tibiofemoral joint loading [1]. Specifically, individuals with ACLR often exhibit reduced peak knee extensor moment (pKEM), a surrogate for quadriceps mechanical output, that likely emerges from quadriceps dysfunction [2]. Quadriceps muscles contribute more force than any other muscle group to tibiofemoral joint loading [3]. Thus, restoring quadriceps function is likely an important step in reestablishing homeostatic joint loading. It remains unclear if quadriceps strength deficits must be overcome first before implementing interventions that augment the mechanical output of the quadriceps during walking. Biofeedback is a method used to cue specific, real-time gait changes and could be used for precision rehabilitation. However, there is a critical gap in our understanding of how quadriceps strength deficits affect individual limb strategies used to augment lower extremity loading during gait. Elucidating the neuromuscular strategies instinctively used by individual after ACLR to modulate quadriceps output has important translational implications for the development of interventions to mitigate OA. Our purpose was to evaluate the bilateral capacity of individuals after ACLR to modify pKEM in the context strength asymmetries. We hypothesized that pKEM biofeedback would elicit increases and decreases in pKEM with systematic accompanying changes in vertical ground reaction force (vGRF), knee flexion angle (KFA), and quadriceps muscle activation with lesser changes in the ACLR limb compared to the contralateral limb.

Methods: We recruited 15 individuals with unilateral ACLR to participate in the study (9 females; 11 bone-patellar tendon-bone grafts, 4 quadriceps tendon grafts; mean±s.d.; age: 22.7±5.9 years, BMI: 25.3±4.5, post-ACLR: 2.3±1.4 years). We measured bilateral knee extensor strength via a Biodex dynamometer while participants performed maximum voluntary isometric contractions (MVICs) with their knee positioned at 90° flexion. We then fitted participants with electromyography (EMG) sensors bilaterally on the vastus medialis and lateralis and retroreflective markers on the lower limbs, pelvis, and torso. Participants completed five two-minute walking trials on the treadmill, beginning with a habitual walking trial. We immediately analyzed this trial to estimate baseline bilateral average pKEM values using a real-time inverse dynamics model of the lower limb described previously [4]. We found the bilateral average pKEM during the first half of stance during the two-minute trial and established target values at ±40% and ±20% for use in biofeedback trials. During biofeedback trials, we encouraged participants to modify their gait to match the height of a ball representing their real-time pKEM projected on a screen in front of the treadmill to the height of a horizontal line representing the target value. We evaluated main effects of limb, condition, and limb × condition interaction on pKEM. vGRF, KFA, and integrated EMG for each muscle using two-way statistical parametric mapping (SPM, α=0.05) and performed paired t-tests on bilateral torque measurements from MVICs.

Results & Discussion: During habitual walking, ACLR limb pKEM was 0.39±0.31 Nm/kg and contralateral limb pKEM was 0.50±0.44 Nm/kg, a between-limb difference that was not significant (p=0.430). We found no main effect of limb on pKEM (p=0.457, Fig 1A), but we found a main effect of biofeedback condition on pKEM ($p<0.001$) and pairwise differences between all four biofeedback conditions and habitual walking (all $p<0.001$). Specifically, pKEM increased 56% (ACLR) and 47% (contralateral) during the +40% conditions. Between-limb differences in pKEM percent change during the +40% condition were not significant (p=0.116). We found smaller KFAs in the ACLR limb during early stance (p=0.016, Fig 1B) and a limb × condition interaction around the region of first peak vGRF where the ACLR limb exhibited a floor effect with no decrease in vGRF during the -20% and -40% conditions ($p>0.05$, Fig 1C). We found ACLR limb quadriceps weakness evidenced by smaller peak torque (p=0.017) but no between limb-differences in percent change in quadriceps muscle activation during the +40% condition (p=0.524).

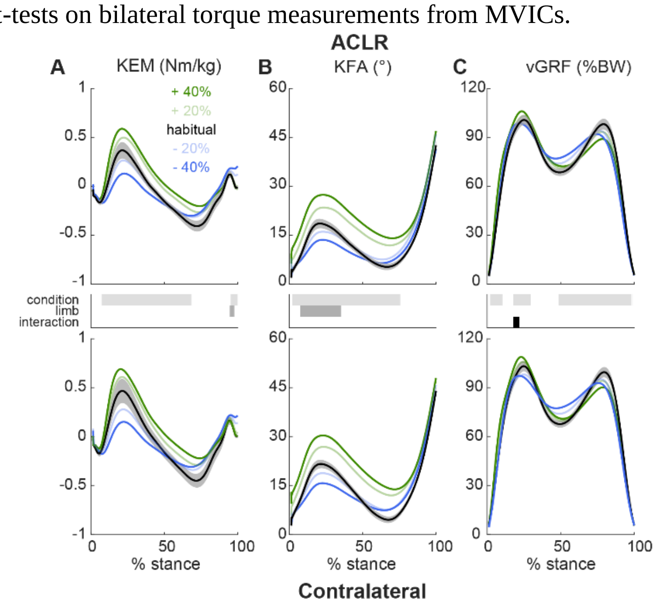

Fig 1. (A) knee extension moment, (B) knee flexion angle, (C) vertical ground reaction force. Row 1: ACLR limb outcomes; Row 2: regions of stance with a significant main effect; Row 3: contralateral limb outcomes

Significance: Despite quadriceps weakness in the ACLR limb, both limbs demonstrated a capacity to increase and decrease pKEM with no between-group differences in quadriceps muscle activation or percent change in pKEM. We conclude that quadriceps weakness need not be overcome before more functional interventions target quadriceps mechanical output.

Acknowledgements: Supported by two grants from NIH (R21AR074094 and F31AR078013).

References: [1] Andriacchi et al. (2009), *J Bone Jt Surg* 91(1); [2] Roewer et al. (2011), *JBiomech* 44(10); [3] Sasaki et al (2010), *JBiomech* 43(14); [4] Munsch et al (2020), *PeerJ* 8:e9505.

CAN STATIONARY CYCLING AT INCLINED SLOPES MITIGATE KNEE JOINT MOMENT?

Kaileigh E. Estler*, Sean A. Brown, Walter G. Menke, and Songning Zhang
Kinesiology, Recreation, and Sport Studies, University of Tennessee, Knoxville, TN, USA
*Corresponding author's email: kestler1@vols.utk.edu

Introduction: During daily activities (e.g. walking and knee bending.), the knee joint is subjected to large magnitudes of repetitive loading; therefore, consequent degradation of knee cartilage may lead to knee osteoarthritis (KOA). Gait modifications have been of interest for mitigating/altering the magnitude of KJ loading [1]. To reduce knee joint loading with respect to walking, stationary cycling is a common exercise prescription for patients with KOA and total knee replacement, post-surgery. However, there has been limited research with the intention for clinical applications of inclined stationary cycling both as a preventative exercise modality and rehabilitative prescription for KOA patients. Previous work observed an increased mean peak knee extension moment when cycling uphill, similar to the trends reported during incline walking [2,3]. However, no studies have investigated the effect of incline cycling on internal abductor moment as it is related to medial knee loading. Therefore, the purpose of this study was to explore the effect of four different incline settings of stationary cycling on peak frontal and sagittal knee moments. It was hypothesized that peak knee extension moment would increase with a change in inclines. Given this is the first study to examine the frontal knee joint moments, the effect of inclined cycling on the knee abduction moment was hypothesized to be unchanged.

Methods: Eleven healthy and recreationally active participants (Age: 22.7±3.2 years, BMI: 26.5±2.6, 5 females) completed a total of eight 2-minute bouts of stationary cycling using a smart bike (Kickr, Wahoo) at four incline conditions (0%, 5%, 10%, 15%), each at two workrates (60W and 90W) in a randomized order. During last 10 seconds of the 2-minute bout, 3-dimensional kinematic and pedal reaction force (PRF) data were recorded using a 13-camera motion capture system (240 Hz, Vicon Motion Analysis Inc., Oxford, UK) and a pair of customized instrumented pedals (1200 Hz, Kistler). Three-dimensional kinematic and kinetic variables were computed using Visual3D (6.0, C-motion Inc.). A 2 (Workrate) x 4 (Incline) repeated measures analysis of variance was conducted to examine the variables of interest: peak vertical PRF, and the internal peak knee extensor (KEM) and abductor (KAM) moments. A Greenhouse-Geisser correction was performed if the assumption of sphericity was violated. Only the variables from the right side (dominant side) were included in the analyses.

Results & Discussion: The ANOVA results indicated no significant incline effect for vertical PRF (p=0.636), knee abduction moment (p=0.235), and KEM (p=0.736). These results are congruent with the unchanged peak vertical ground reaction , but against the observed increases in peak KEM found in the previous uphill cycling study [2]. Significantly higher peak PRF and KEM were found at the 90 W compared to 60 W (p=0.05). However, no significant interactions of workrate and slope were observed on any of the observed variables. It is worth noting the decreasing trend of peak knee abduction moment from 0% to 15% incline (Table 1). The high variability in the 0% and 5% conditions and small sample size may have prevented the results from being statistically significant.

Table 1: Mean peak vertical PRF, knee extensor and abductor moment across conditions: Mean ± STD.

	Workrate (W)	0%	5%	10%	15%
Vertical PRF (N)	60	202.5±42.2	198.3±38.9	202.6±27.1	203.9±31.9
	90	222.5±26.7	222.7±26.7	224.6±27.8	206.4±39.7
Knee Extensor Moment (Nm)	60	19.5±8.1	18.6±7.7	20.3±6.7	17.4±6.2
	90	25.6±8.9	26.0±7.9	27.9±5.6	23.5±7.4
Knee Abductor Moment (Nm)	60	-14.3±26.1	-10.6±13.7	-6.9±5.3	-7.1±5.4
	90	-13.6±19.1	-10.0±10.0	-8.5±6.1	-10.1±6.1

Note: vertical PRF (Newtons), knee moment (Newton*meters). All data are for the subjects' right limb.

Significance: These results are not statistically encouraging to present the argument that inclined stationary cycling should be implemented as a rehabilitative exercise for KOA patients. Rather, this could be an alternative form of exercise for those that seek a preventative KOA activity (i.e. lower knee joint loading compared to walking or running). Furthermore, clinicians may be able to prescribe inclined cycling to increase exercise intensity without overloading the knee joint. These data are of the first to provide evidence for possible application Examination of knee joint electromyography may provide greater insight for future work relevant to this study.

Acknowledgments: Thank you to Austin Abbott and Shawn Wheeler for their assistance in data collection.

References: [1] Bennett et al. (2017), *Med Sci Sports Exerc* 49(3); [2] Caldwell et al. (1999), *J Biomech* 15, [3] Wen et al. (2019), *J Biomech* 39

AGING-RELATED DECLINES IN STRENGTH AFFECT THE CAPACITY TO RECOVER FROM A FORWARD BALANCE LOSS

Gabriel J. Haberly[1*], Michael J. Pavol[2]
[1]College of Allied Health, George Fox University, Newberg, OR
[2]College of Public Health and Human Sciences, Oregon State University, Corvallis, OR
*Corresponding author's email: ghaberly@georgefox.edu

Introduction: Forward falls, such as from tripping, are common among older adults and can lead to serious injury [1]. A modifiable factor that may contribute to these falls is aging-related declines in muscle strength. Sarcopenia is associated with an elevated risk of falls [2], and correlations have been found in older adults between weaker muscles and lesser ability to recover from a forward balance loss [3]. However, associations do not prove causation. This study therefore used a mathematical modeling approach to examine the extent to which aging-related declines in muscle strength affect the capacity to restore static balance after a recovery step from a forward balance loss. We hypothesized that aging-related declines in strength would result in a lesser capacity to restore static balance relative to young adults, as the declines in strength would adversely affect the ability to arrest the body's forward and downward motion.

Methods: Restoration of static balance after touchdown of a forward recovery step was simulated in the sagittal plane using a six-link musculoskeletal model, adapted from Kadono and Pavol [4]. The front foot of the model was fixed to the ground. Motions of the leg and thigh of the front limb and of the head-arms-torso were controlled by 10 Hill-type musculotendon actuators. The rear foot and rear lower limb moved passively, with the metatarsal heads of the rear foot pinned to the ground at a fixed pivot point. Actuator force was controlled by a set of six parameterized neural excitation signals. Angle-dependent passive moments constrained joint ranges of motion.

An integrated optimization and forward-dynamics simulation procedure was used to map the feasible region for balance recovery for an initial forward and downward velocity of 20% body height/s of the body center of mass (COM) and hips, respectively. Mapping was performed for selected initial hip heights (Z_{HIP}) and COM horizontal positions (X_{COM}) by using simulated annealing to search for the initial state and pattern of neural excitation corresponding to the most anterior X_{COM} or the lowest or highest Z_{HIP} from which the model could achieve a quasi-static, stable state within 1 s, without violating the anatomical and mechanical constraints.

The anterior boundary of the feasible region for balance recovery was mapped for typical strength values of young and older adults. Aging-related declines in strength were simulated by adjusting parameters of the model's musculotendon actuators. Maximum isometric force was decreased by 32.5% from that of young adults to represent older adults in their 70's. In addition, the deactivation time constant was increased by 26%, the maximum muscle strain rate was decreased by an average of 11%, passive muscle stiffness was increased by 10%, and normalized tendon stiffness was decreased by 42%.

Results & Discussion: Aging-related declines in strength were found to impair the capacity to restore static balance after a recovery step from a forward balance loss (Fig. 1). The model-determined anterior boundary of the feasible region for balance recovery was similar in shape for young and older adults; however, the boundary for older adults was shifted posteriorly by 11.2% of foot length, on average, for Z_{HIP} of 44-52% of body height. A posterior shift indicates that the COM cannot be as far anterior to the heel of the front foot at step touchdown if the step is to be effective in restoring COM stability and static balance. Essentially, for a forward balance loss of the same extent, the minimum required step length for a single-step recovery was about 3 cm larger for older adults in their 70's than for young adults.

Surprisingly, there were minimal age-differences in the anterior boundary of the feasible region for balance recovery for Z_{HIP} of 39-42% of body height (Fig. 1). The boundaries for both young and older adults reached the anatomical limits on Z_{HIP}. This would suggest that despite aging-related declines in strength, older adults in their 70's are not impaired in their ability to arrest their downward motion and support their weight after a recovery step from a forward balance loss.

Consistent with previous epidemiological [2] and experimental [3] studies, the present results indicate that aging-related declines in strength do result in a lesser capacity to recover from a forward balance loss. The present results confirm this is a causal relationship. Furthermore, they indicate that one cause of this lesser capacity to recover is an impaired ability to arrest the body's forward motion after step touchdown by generating a backward-directed braking force from the ground.

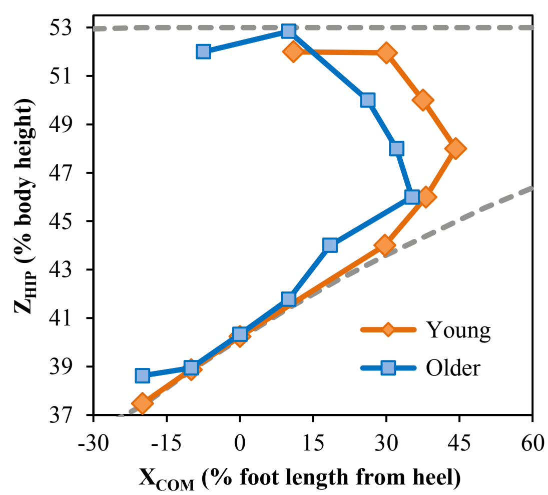

Figure 1: Model-derived anterior boundary of the feasible region for balance recovery for muscle strengths representative of young adults and older adults in their 70's. Static balance should be able to be restored if, at touchdown of a recovery step, X_{COM} relative to the heel of the front foot and Z_{HIP} are within the enclosed area to the left of the displayed boundary. Dashed lines are the anatomical limits on Z_{HIP}.

Significance: Aging-related declines in muscle strength negatively impact the capacity to recover from forward balance losses at older ages by impairing the ability to re-establish anteroposterior stability of the COM. As such, interventions to prevent forward falls by older adults should include strength training aimed at preventing or reversing aging-related declines in strength. Furthermore, this strength training should include exercises that target muscle groups involved with arresting the forward motion of the COM.

References: [1] Berg et al. (1997), *Age Ageing* 26(4); [2] Gadelha et al. (2018), *Arch Gerontol Geriatr* 79; [3] Graham et al. (2015), *Exp Gerontol* 66; [4] Kadono & Pavol (2013), *J Biomech* 46(1).

AGING AND SPEED ADAPTATIONS IN FUNCTIONAL DEMAND OF THE KNEE EXTENSORS DURING WALKING

Ross J. Brancati[1*], Jane A. Kent[1], Kate L. Hayes[1], Fany Alvarado[1], Katherine A. Boyer[1]
[1]Department of Kinesiology, University of Massachusetts, Amherst, MA
*Corresponding author's email: rbrancati@umass.edu

Introduction: The knee extensor (KE) muscle group is critical for gait and mobility as these muscles support the center of mass, provide joint stability, and assist with push-off during ambulation. [1], [2] Aging-related structural changes to the knee extensors can include smaller muscle volume and greater fat fraction. [3] Changes in size and composition of the KEs lead to reductions in maximal torque and specific torque (strength/muscle size) during dynamic contractions in older adults. [4], [5], [6] In turn, smaller KE muscle size and strength can result in a greater functional demand (FD), which is measured as the percentage of maximal strength used during a task, [7] or a modification in gait mechanics to mitigate increases in FD due to reduced muscle strength.

Hafer et a. (2020) investigated the impact of age, habitual physical activity, and walking speed on FD in midlife (aged 55-70 yr) and younger adults. They found greater FD at peak knee flexion moment (KFM) in inactive older adults compared with younger adults, and a main effect of walking speed for the FD at peak KFM. [8] Age-related declines in mobility, muscle structure, and strength are accelerated beyond 70 years [9], so the goal of this study was to compare FD in younger (30-40 yr) and older (70-80 yr) adults during overground walking and quantify potential structural or functional factors in the KEs that may impact FD.

Methods: Nine younger (Y, 36±3 yr, 24.0±3.4 kg·m^{-2}, 6 female) and five older (O, 74±2 yr, 26±4.0 kg·m^{-2}, 3 female) healthy adults underwent traditional gait analysis at self-selected (SS) and SS+30% (Fast) walking speeds using the point cluster technique [10], motion capture (Qualysis, Sweden), and force plates (AMTI, MA, USA). External knee joint moments were calculated using an inverse dynamics approach with Visual 3D (C-Motion, MD, USA). Strength was determined as peak torque from KE maximum voluntary isometric contractions (MVIC, Nm) using dynamometry (Biodex, NY, USA). Fat-water magnetic resonance images obtained in a 3-tesla scanner (Siemens, Germany) were used to quantify quadriceps muscle maximal fat-free contractile cross-sectional area (CSA, cm^2) and fat fraction (%) using a custom-written MATLAB script. Specific torque (ST, Nm·cm^{-1}) was calculated by dividing MVIC by CSA. FD (%) was calculated for peak knee flexion and second peak knee extension moments by dividing moments by MVIC. [8] Habitual physical activity was quantified as the 7-day average for uniaxial counts (arb. units) from a waist-worn accelerometer (ActiGraph, FL, USA). A 2x2 ANOVA was used to test for effects of age and walking speed on FD. Statistical differences in fat fraction, MVIC, specific torque, and physical activity were quantified with independent t-tests.

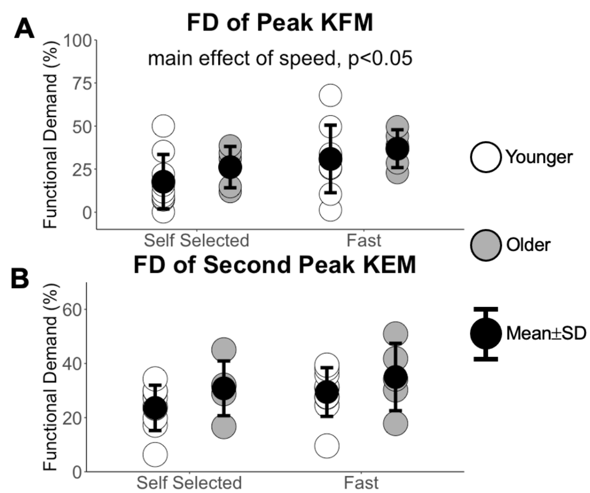

C

Descriptive Data

Variable	Younger Adults	Older Adults	p-value
Walking Speed (m/s)	1.01 (0.15)	1.09 (0.08)	0.23
Fat Fraction (%)	8.83 (1.76)	8.48 (1.81)	0.73
MVIC (Nm)	169.34 (47.91)	134.40 (50.03)	0.22
Specific Torque (N/cm)	297.21 (66.10)	269.71 (66.70)	0.47
Physical Activity (ct/day)	158.44 (52.25)	213.40 (58.32)	0.09

Figure 1: FD for the peak KFM (A) and second peak KEM (B). A significant effect of speed was found for the FD at the peak KFM. SS walking speed, fat fraction, MVIC, specific torque, and physical activity levels are shown in Figure 1C, presented as mean (standard deviation)

Results & Discussion: An effect of speed (SS: 20.7±14.7%, Fast: 33.0±16.8%, p=0.04), but not age (Y: 24.3±18.6%, O: 31.5±12.2%, p=0.25), was found for the FD of the peak KFM (Fig. 1A). No effect of age (Y: 26.5±9.0%, O: 32.9±10.9%, p=0.09) or speed (SS: 26.2±9.4%, Fast: 31.4±10.2%, p=0.15) was found for the FD of the second peak KEM (Fig. 1B). No effects of speed or age were found for peak knee joint moments; and neither MVIC nor specific torque differed by age (p=0.22; p=0.47, Fig. 1C).

In agreement with previous findings in mid-life adults [8] our results show that faster walking speeds require greater relative demands of the KEs during overground walking. FD at the peak KFM was comparable to the cohort investigated by Hafer et al. (2020), but FD at peak KEM in our study was on average 10% greater for both age groups. Notably, SS walking speed was 30% lower in our cohort. The effect of speed on FD at the KFM suggests that adopting a slower walking may be one mechanism to reduce FD during weight acceptance. FD may be an important measurement to consider when probing mechanisms for altered gait in older adults with weaker KEs, impairment, or who are less physically active.

Significance: FD is important for understanding how much of an individual's capacity is used during an activity. Older adults may modify gait or walking speed to reduce demands on the KEs during walking. This is especially important to consider as older adults experience aging related changes to KE size and composition, along with fatigue during activities of daily living.

Acknowledgements: Funding: NIH AG058607. Aidan Gross, Omar Abdelaal, and Amir Shah for data processing.

References: [1] Pandy et al. (2010), *J Biomech* 43(11); [2] Whittington et al. (2008), *Gait & Posture* 27(4); [3] Farrow et al. (2011), *Aging Clin Exp Res* 33(2); [4] Lanza et al. (2003), *J Appl Physiol* 95(6); [5] Callahan & Kent-Braun (2011), *J Appl Physiol* 111(5); [6] Fitzgerald et al. (2021), *J Physiol* 599(12); [7] Macdonald et al. (2007), *Univers Access Inf Soc* 6(2); [8] Hafer & Boyer (2020), *J Appl Biomech* 36(3); [9] Cameron et al. (2023), *Eur J Appl Phsyiol*; [10] Andriacchi et al. (1998), *J Biomech Eng* 120(6)

OBSTACLE CLEARANCE STRATEGIES OF OLDER ADULTS IN MIXED REALITY ENVIRONMENT

Srikant Vallabhajosula[1]*, Pratheep Paranthaman[2], Alys Giordano[1], Alexander Japit[1], Christopher Go[1], Alicia Wilson[1], Matthew Lawler[1], Stacey Walton[1], Oliver Tuisa[1]
[1] Department of Physical Therapy Education, Elon University, Elon, NC
[2] Department of Computer Science, Elon University, Elon, NC
*Corresponding author's email: svallabhajosula@elon.edu

Introduction: Falls due to tripping is a serious concern among older adults.[1] Biomechanics of obstacle clearance is a well-studied topic as it gives insight into factors associated with tripping. Previously, obstacle clearance was studied by using obstacles of different heights and surfaces relative to physical reality (PR).[2] A relatively novel method of studying obstacle clearance is to use immersive technologies like Virtual Reality (VR) and Mixed Reality (MR) in which users wear a head mounted display unit to visualize and interact with computer-generated content. While VR offers a totally immersive environment, MR offers a hybrid environment where participants can visualize both PR and virtual objects. The purpose of our study was to compare obstacle clearance strategies used by healthy young adults and older adults with low fall risk in these three environments (PR/VR/MR). We hypothesized that the obstacle clearance strategies of older adults would be different compared to younger adults and would depend on the environment of obstacle clearance.

Methods: Eleven older adults (7 males, 4 females; Age, 75.2+/-7.6 years; low fall risk screened using STEADI) and 12 healthy, younger adults (3 males, 9 females; Age, 23+/-3 years) participated. Participants walked in PR, MR and VR environments while crossing a 15in. (38.1cm) obstacle. The order of environments was randomized between the participants. Reflective markers were placed bilaterally on the 2nd metatarsal head and posterior calcaneus. Toe and heel clearance from obstacle, and distance of toe and heel from the obstacle before and after clearing the obstacle were used as dependent variables. This was done for both leading and trailing legs. An average of the three trials was used for statistical analyses. A two-way mixed ANOVA with environment (PR vs. MR vs. VR) and group (younger adults vs. older adults) as factors was performed.

Results & Discussion: For leading leg, significant interaction was observed for toe and heel clearance, distance of toe, and heel before crossing the obstacle (all $p<=0.021$; Table 1). Older adults displayed greater toe and heel clearance while crossing the obstacle in PR, yet less clearance in MR environment. Both groups displayed similar behaviour in VR environment. Furthermore, both groups placed their foot at similar distances from the obstacle in PR and VR environments but in MR environment, older adults placed their foot further from the obstacle. Significant group main effect showed that older adults placed their foot closer to the obstacle after clearance (both $p<=0.026$). For trailing leg, significant interaction was observed for toe and heel clearance, distance of toe and heel before crossing the obstacle (all $p<=0.017$; Table 1). Specifically, older adults showed similar toe and heel clearance while crossing the obstacle in PR and VR but showed lesser values in MR environment. Further, older adults placed their trailing foot further from the obstacle in MR environment. Significant group main effects showed that older adults placed their foot further from the obstacle before clearing it and closer to the obstacle after clearing it (all $p<=0.012$). Significant main effects for environment were observed for all variables (all $p<=0.031$). Together these results suggest that older adults used different strategies while clearing the obstacle in MR environment. For instance, older adults placed their feet farther from the obstacle before stepping over yet did not raise their trailing leg toe to sufficient height and barely cleared the obstacle with their trailing leg heel in MR environment. This could be due to differences in perception of the risk associated with not clearing the obstacle in MR environment or the focus on clearing with leading leg and not with trailing leg.

Table 1. Mean (SD) foot clearance and distance values from obstacle

	Physical Reality		Mixed Reality		Virtual Reality	
Dependent Variables	**Younger adults**	**Older adults**	**Younger adults**	**Older adults**	**Younger adults**	**Older adults**
LL Toe Clearance	17.9 (4.3)	25.8 (6.4)	28.6 (8.1)	22.4 (17.1)	28.8 (11.2)	29.6 (8.0)
LL Heel Clearance	20.7 (3.6)	22.4 (4.5)	26.8 (4.7)	20.5 (9.9)	26.3 (7.1)	24.3 (6.7)
LL TDBCO	89.1 (12.9)	91.5 (12.4)	86.9 (16.3)	108.9 (19.6)	80.7 (19.2)	81.1 (18.1)
LL HDBFO	112.7 (13.2)	116.0 (13.6)	110.7 (16.2)	131.3 (19.3)	104.3 (19.6)	102.8 (17.0)
LL TDACO	46.1 (6.5)	41.6 (5.3)	43.3 (13.4)	34.2 (14.4)	58.4 (13.5)	47.2 (11.6)
LL HDACO	22.3 (6.4)	17.1 (5.0)	19.4 (13.4)	11.1 (13.6)	34.9 (13.8)	25.3 (7.5)
TL Toe Clearance	22.3 (4.4)	22.0 (5.7)	12.7 (15.6)	-3.6 (18.5)	20.8 (15.9)	22.3 (9.8)
TL Heel Clearance	43.5 (3.2)	41.4 (4.5)	30.6 (12.1)	13.4 (16.3)	38.8 (15.8)	39.4 (7.8)
TL TDBCO	23.5 (4.7)	30.0 (6.0)	29.2 (7.9)	49.3 (14.6)	17.3 (10.3)	24.7 (9.2)
TL HDBFO	47.2 (4.5)	54.2 (7.6)	52.8 (7.4)	72.9 (13.9)	41.1 (10.8)	47.5 (9.2)
TL TDACO	120.5 (9.4)	106.3 (13.7)	105.0 (26.2)	91.7 (18.5)	122.6 (17.3)	100.8 (17.2)
TL HDACO	96.7 (9.6)	81.2 (13.2)	81.4 (25.7)	68.3 (16.8)	99.3 (16.8)	77.2 (16.5)

LL – Leading Leg; TL – Trailing Leg; TDBCO – Toe Distance Before Clearing the Obstacle; HDBFO - Heel Distance Before Clearing the Obstacle; TDACO – Toe Distance After Clearing the Obstacle; HDAFO - Heel Distance After Clearing the Obstacle

Significance: Studies have shown beneficial applications of these virtual environments as effective interventions when working with older adults.[3] While VR has been used more for training purposes and studies using MR are scarce, there has been limited use of both VR and MR as tools for physical therapy assessment.[3] VR/MR apparatus could potentially be a cost-efficient tool that is easy to store and can be customized to fit different physical therapy assessment needs. Virtual obstacles in a real environment can be space efficient and minimize fall-risk during patient-therapist interactions Results of the current study could help in creating and using such VR and MR environments. Results from the current study suggest that while training older adults in MR could have practical relevance to reducing fall-risk, special attention needs to be given to clearance strategies they can use to successfully negotiate obstacles.

Acknowledgements: Elon Faculty Research and Development Funds

References: [1] Hausdorff et al., *APMR*. 2001;82(8):1050–6. [2] McFadyen et al. *J Gerontol A Biol Sci Med Sci*. 2002; 57(4):B166-74. [3] Phu et al., *Clin Interv Aging*. 2019; 28(14):1567-1577)

AGING AND COGNITIVE DEFICITS DIFFERENTIALLY IMPACT THE ABILITY TO MODULATE SPATIAL AND TEMPORAL FEATURES OF WALKING IN ADULTS WITH MILD COGNITIVE IMPAIRMENT

Michael C. Rosenberg[1*], Alexandra Slusarenko, Ke Cao, J. Lucas McKay, Laura Emmery, Trisha M. Kesar, Madeleine E. Hackney
[1]W.H. Coulter Dept. Biomedical Engineering, Emory University and Georgia Institute of Technology, Atlanta, GA, USA
*Corresponding author's email: mcrose3@emory.edu

Introduction: Dance-based movement therapies aim to restore or mitigate age-related declines in balance, mobility, and cognitive function in adults with neurodegenerative diseases, such as in those with mild cognitive impairment (MCI) [1]. During therapy, participants modulate spatial (*i.e.*, joint kinematics) and temporal (*i.e.*, step timing) features of movement to match prescribed target movements. Current design of spatial and temporal targets is subjective; personalizing these targets based on participants' motor and cognitive function may enhance therapy efficacy [1, 2]. However, it is unclear how age-related motor [3] and cognitive deficits [4] in adults with MCI impact their abilities to modulate spatial and temporal features of movement.

Here, we investigated the relationship between age-related motor and cognitive deficits and the ability to accurately modulate spatial and temporal features of walking. We hypothesized that motor and cognitive deficits would differentially impact the ability to modulate spatial and temporal features of walking [5, 6]. We predicted that (1) healthy older adults (HOA) would perform spatial modifications less accurately than healthy young adults (HYA), reflecting differences associated with age-related motor deficits, and (2) HOA would perform temporal modifications more accurately than adults with MCI, reflecting differences associated with cognitive deficits.

Methods: We estimated hip, knee, and ankle kinematics using inertial sensors (APDM, Inc., Portland, USA) in 12 HYA, 12 HOA, and 12 adults with MCI while performing diverse modifications to the spatial and/or temporal features of their gait. In ballet-based spatial modifications (N=9), participants altered typical hip-knee-ankle kinematic patterns (e.g., 90° hip extension with maximal ankle plantarflexion during swing; Fig 1A) asymmetrically in stance or swing, or unilaterally in stance and swing. In temporal modifications (N=9), participants walked in 2- to 6-step sequences of quick and slow steps, synchronized to either Tango (2-count) or Waltz (3-count) music. In spatiotemporal modifications (N=4), participants performed spatial and temporal modifications simultaneously.

For each trial, we quantified movement performance as the percent error relative to spatial (peak joint angles) or temporal (step timing) targets, averaged across all targets from the movement. We compared movement performance between HYA and HOA (reflecting aging-related motor differences), and HOA and MCI (reflecting cognitive function differences) using linear regression with the HYA and MCI groups as indicator variables and the HOA group as the reference variable. We also report effect sizes (Cohen's *d*) and percent differences in performance between groups (Δ).

Results & Discussion: As predicted, HOA performed spatial modifications significantly less accurately than HYA ($p=0.010$; $d=1.1$, Δ=4.0%; Fig 1B & C). Differences between HOA and HYA were largest during swing-phase gait modifications ($p=0.006$, $d=1.3$, Δ=5.8%), suggesting that age-related balance deficits may limit gait modulation capacity [6]. Across all temporal modifications, HOA and MCI performance was not statistically different ($p=0.160$; Fig 1B). However, HOA performed long step sequences (6 steps) more accurately than adults with MCI ($p=0.030$, $d=0.9$, Δ=6.5%). Deficits in working memory in MCI may, therefore, limit individuals' abilities to accurately modulate temporal features of walking during training [7]. Spatiotemporal modifications elicited larger differences between HOA and MCI ($p=0.017$; $d=1.3$, Δ=2.6%), suggesting additional demand on cognitive resources or an interaction between motor and cognitive function [7].

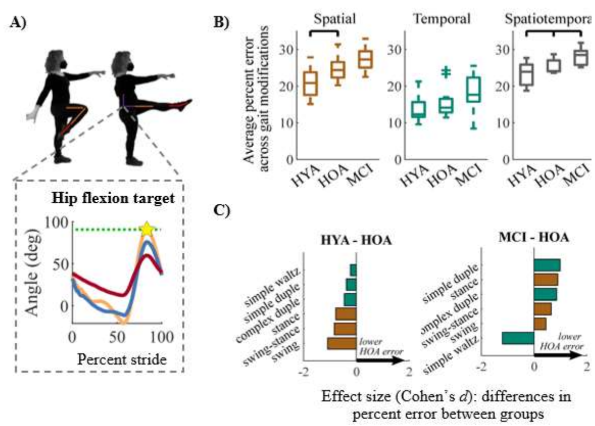

Figure 1: Gait modification example and results. A) Spatial gait modification example (top) and one corresponding biomechanical target (bottom; star). Waveforms represent one participant from each of the HYA (orange), HOA (blue) and MCI (red) groups. B) Group differences in spatial, temporal, and spatiotemporal modification performance, C) Effect sizes of group differences in performance.

Significance: Our findings represent a step toward objectively personalizing movement therapies to improve mobility and cognitive function in adults with MCI. Group differences in gait modification performance highlight how cognitive, not just motor, deficits can impact movement performance in adults with MCI and may impact therapy efficacy in other populations with cognitive impairment (e.g., Parkinson's). Further, our dance-based experimental paradigm's ability to reveal relationships between movement performance and motor or cognitive deficits supports its potential as a tool to track therapy efficacy.

Acknowledgements: Supported by the National Institute for Child Health and Human Development of the National Institutes of Health under award numbers F32HD108927 and R01AG062691, and a Goizueta Alzheimer's Disease Research Center Innovation Seed Grant.

References: [1] Hackney, et al. (2007) *Am J Dance Ther* 29(2); 74; [2] Guadagnoli & Lee, T.D. (2004) *J Motor Behav* 36(2); [3] Booth, et al., (1994) *Med Sci Sport Exerc* 26(5); [4] Gauthier, et al. (2006) *Lancet* 367(9518). [5] Rosenberg, et al., (2023) *Front Hum Neurosci* 17; [6] Bahureksa, et al., (2017) *Gerontology* 63(1); [7] Montero-Odasso, et al., (2011) *Arch Phys Med Rehabil* 93(2).

GAIT EXPLORATION WITH HAPTIC FEEDBACK ASSISTANCE

Paula Simo Higueras[1*], Alexandra S. Voloshina[1]
[1]Department of Mechanical and Aerospace Engineering, University of California –Irvine, CA USA
*psimohig@uci.edu

Introduction: Current rehabilitation approaches primarily rely on performing simple, repetitive movements. However, increasing movement variability during rehabilitation training has been linked to improved balance and stability in everyday gait [1]. This is possibly a result of variability training positively affecting the development of new motor commands, similar to how toddlers learn to walk by engaging in gait exploration [2]. Introducing variability into gait training for adults after motor impairment would likely also benefit the development of new motor control pathways [3, 4, 5]. To this end, we propose a wearable system that relies on user tracking and haptic feedback to direct participants to explore a variety of gait movements. The device relies on a foot-mounted Inertial Measurement Unit (IMU) to track user location and a belt with vibrotactile motors which provides feedback and instructions to the wearer. We use data from the IMU to evaluate participant direction of movement on a stride-by-stride basis. Depending on user performance of the previous steps, vibrotactile cues guide the user to perform additional, diverse movements. This device can effectively track and analyze the most common gait movements of a person and encourage the user to perform movements outside of their typical range. In this work, we present the preliminary designs for the wearable device. We have tested device tracking abilities while performing a range of walking tasks and have effectively dictated movements to one neurologically healthy participant. Future work will focus on implementing real-time tracking and analysis, individualized vibrotactile feedback, and testing with participants after stroke.

Methods: The IMU on the device tracks user location while the motors provide instructions to perform specific movements. In preliminary experiments, the IMU was placed on only one foot of the user. We integrated acceleration data from the IMU, and calculated user trajectories and movement patterns on a stride-by-stride basis. Specifically, we evaluated the angle between all consecutive strides, as well as the stride length and width. Plotting all stride vectors together provides a summary of the variability of movement.

The vibrotactile motors were placed on the left and right sides of the waist and dictated vibrational cues at 121 Hz and a duration of 1.5 sec. Motor vibration indicated to the participant to turn in the direction of vibration as long as the vibration continued. Verbal feedback was provided to the user to make ‘sharp’ or ‘smooth’ turns, although only ‘sharp’ turns are presented here.

Data collection was conducted with one participant who walked at three pre-determined trajectories (rectangular trajectory, front and backwards walking, and zig-zag walking) and was then asked to follow vibrational cues sent every 3 or 5 seconds.

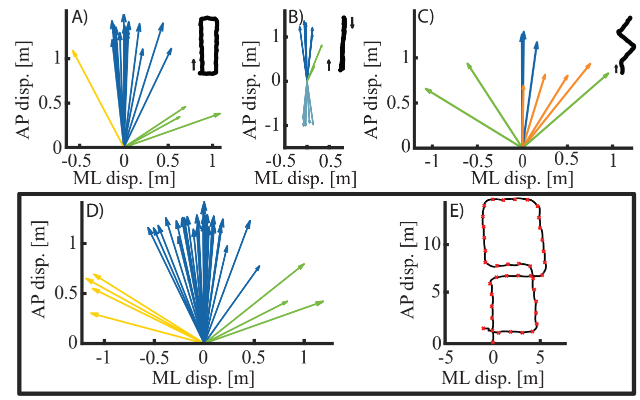

Figure 1: Movement vectors relative to the anteroposterior (AP) and mediolateral (ML) displacement for three walking trajectories: (A) rectangular walking trajectory, (B) forward and backward walking, and (C) zigzag walking. The overall walking trajectory for each experiment is shown in black. Movement vectors (D) and gait trajectory (E) during walking with vibrotactile feedback. Vector colors indicate preliminary clustering of similar movements.

Results & Discussion: IMU tracking successfully identified the pre-defined walking trajectories and indicated the direction of each stride for both parts of the data collection (Fig. 1). Stride trajectories for the pre-defined movement patterns had an average stride angle of 10.57±24.88 deg, 3.66±10.14 deg, 5.15±37.31 deg (mean±std) with respect the vertical displacement, for the rectangular, back and forth, and zigzag movements, respectively. The walking trajectory defined by vibrational cues had an average stride angle of -4.38±29.28 deg (mean±std). These results are consistent with the expected results, where we see greater movement variability in trajectories requiring more diverse movements. Preliminary k-means clustering analyses have successfully identified several groups of movements in different types of activities. Future work will include developing more robust clustering techniques in order to more effectively quantify movement variability. Future work will also focus on developing individualized vibrational cues based on user performance and average trajectories, in order to encourage movement variability.

Significance: We have presented the preliminary designs of a wearable device that can track and quantify user gait and guide them to perform more variable movements. Gait exploration can potentially accelerate and amplify the effects of rehabilitation by informing patients about the movements they should perform, as well as allow them to train at home. In addition, further development of the device could lead to more effective training with assistive devices and during sport activities, as well as improvements in quantifying and categorizing movement. Finally, further experiments focusing on the benefits of gait exploration during rehabilitation will advance understanding of motor learning and task adaptation.

Acknowledgments: The authors thank Chi-Shih Jao and Dr. Andrei M. Shkel for their assistance in implementing the inertial navigation algorithm. This research was supported in part by the Balsells Fellowship.

References: [1] Beauchet et al. (2009), *Gerontology*, 55(6); [2] Adolph et al. (2012), *Psychological science* 23 (11); [3] Shea et al. (1990), *Research quarterly for exercise and sport* 61(2); [4] Wulf et al. (1997), *Journal of Experimental Psychology: Learning, Memory, and Cognition* 23(4); [5] Krakauer et al. (2021), *Neurorehabilitation & Neural Repair* 35 (5).

INFLUENCE OF SURFACE TYPES ON LOWER EXTREMITY ACCELERATION PROFILES DURING ATHLETIC MANEUVERS

Rebecca C. Waite[1*], Joshua M. Lardie[1], John C. Sorochan[1], Kyley H. Dickson[1], Joshua T. Weinhandl[1]
[1]University of Tennessee Knoxville, TN, U.S.A
Corresponding author's email: rwaite2@vols.utk.edu

Introduction: With the use of both natural and artificial turf becoming common in sports, many athletes believe artificial turf could increase injury risk, and they have reported a higher level of muscle soreness after playing on artificial surfaces when compared to playing on natural grass [1,2]. Overuse injuries are often considered to be created by excessive, repetitive loads [3]. Therefore, it is important to determine how differing surface types will impact lower extremity loading characteristics and injury risk. The purpose of this study was to determine the differences in peak acceleration and acceleration integrals in both natural and artificial turf. As artificial turf has been designed to emulate the properties of natural grasses, we hypothesized that there would be no significant differences in peak acceleration or acceleration integrals across varying surfaces.

Methods: Twenty-five recreationally active individuals (age: 18-35 years) voluntarily engaged in agility and jumping drills, including a 36.6-meter jog and a single leg triple hop on the right leg, across three surfaces. In the 36.6-meter jog, participants were instructed to jog at a comfortable pace. In the single-leg triple hop, participants were instructed to maximize their horizontal displacement through three consecutive hops on the right leg, starting the first hop while balancing on the right leg at standstill and halting after the final hop while maintaining balance on the ipsilateral leg. Each test was conducted on Bermuda Turfgrass (BER), Kentucky Bluegrass (KBG), and artificial turf (SYN) with the order of completion counterbalanced across participant groups. Accelerometer and gyroscopic data was collected using inertial measurement units (IMUs, IMeasureU, Auckland, New Zealand) securely attached to the distal tibias of each participant. Maximal tibial load was measured through peak acceleration, and cumulative load of the lower extremities was determined through acceleration integrals. Python (3.10.7) was used to process data. Acceleration due to gravity was removed; manual visual assessment of each trial was completed before averaging all peaks to find the peak acceleration value of each trial. To determine statistical significance, repeated measures ANOVA (RMANOVA, $\alpha = 0.05$) and Tukey's HSD tests were applied.

Results & Discussion: There were no significant differences in peak tibial acceleration or acceleration integrals between the three different surfaces during jogging and a single-leg triple hop. While the RMANOVA analysis of peak acceleration in the jogging condition (Table 1) initially showed a significant difference across the varying surfaces, a subsequent Tukey's HSD analysis did not show significance in peak acceleration between the surfaces.

Table 1: Differences in Peak Tibial Acceleration (m/s/s) and Tibial Acceleration Integrals in Self Selected Jogging (DNB) and Triple-Hop (TH) Trials

Task	Turf Type	Peak Acceleration (g)	Acceleration Integrals (g*s)
DNB	SYN	8.99±2.33	32.89±3.14
DNB	KBG	10.29±3.35	32.63±5.53
DNB	BER	8.58±2.51	32.87±3.98
TH	SYN	19.54±5.23	-
TH	KBG	18.65±5.66	-
TH	BER	20.76±6.30	-

Our hypothesis of no significant differences in peak acceleration and acceleration integrals between SYN, KBG, and BER was supported. A limitation of this study is that, during the time of the study, the Bermuda grass was not in its active growing season. Additionally, participants gathered were not trained athletes, but healthy, recreationally active individuals. Future research should investigate the differences in performance of artificial turf and natural grass in both its growing and dormant seasons while using trained athletes.

Significance: Our results support that there is no significant difference between artificial and natural turf in tibial acceleration and may not pose an increased risk of lower extremity injuries due to impact load. Therefore, artificial turf appears to be a reasonable alternative to natural grass for sporting facilities.

Acknowledgements: We would like to thank the UTK Plant Sciences Department for allowing us to use the UT Farms facility to conduct this research.

References: [1] Poulos et al. (2014) *BMC Sports Science, Medicine & Rehabilitation*, 6(1); [2] Williams, S. et al. (2016) *Scandinavian Journal of Medicine & Science in Sports*, 26(1); [3] McGhie & Ettema (2013) *The American Journal of Sports Medicine* 41(1)

SUBCUTANEOUS FAT CONTRIBUTION TO ECHO INTENSITY VERSUS PEAK TORQUE IN YOUNG ADULTS

Nathan Q. Holland[1], Hunter J. Bennett[1], Stacie I. Ringleb[1*]
[1]Old Dominion University, Norfolk, VA, USA
*Corresponding author's email: sringleb@odu.edu

Introduction: B-mode ultrasonography (US) is a non-invasive and cost-effective way to assess muscle quality. Echo intensity (EI) is a gray-scale analysis of US images which allows for muscle quality to be expressed numerically. A study investigating male firefighters found that a higher corrected EI value correlated to an increase in percent decrease in peak torque (PT) from slow to fast velocities [1]. Percent decrease in PT is thought to demonstrate crucial information on fast-twitch muscle fiber function [2, 3]. A relationship between EI and percent decrease in PT was also observed in research concerning aging populations; strength reductions were attributed to a decrease in fast-twitch fibers, increase in intramuscular fat, and muscle belly stiffness from fat infiltration [2]. To the authors' knowledge, literature has not confirmed this relationship in young adults or determined if the relationship varies with biological sex. Additionally, there is uncertainty if correcting for subcutaneous fat in muscle quality analysis is needed; using Pearson's product moment correlation coefficient may help decide its necessity. This research attempts to address such limitations by comparing young adult female and male subcutaneous fat contribution to EI values and determining its relation to percent decrease in PT measures.

Methods: *Participants*. Ten females (23.70 ± 3.34 y/o, 25.07 ± 5.49 kg/m^2 BMI) and eleven males (22.27 ± 3.04 y/o, 25.70 ± 3.93 kg/m^2 BMI) participated in this study. *Muscle Quality*. US images were obtained on the ipsilateral limb corresponding to the dominant hand of the subject using a GE Logiq e BT12 (GE Healthcare, Milwaukee, WI) in panoramic mode. Device settings were 68 dB gain, 6.0 cm depth, 10 MHz frequency, and 72 dynamic ratio. EI was determined using Fiji is Just ImageJ (Fiji 2.3.0/1.53q version, National Institutes of Health, Bethesda, MD). The polygon function was used to select the rectus femoris (RF) while minimizing the inclusion of the surrounding fascia. A mean value between 0 (black) and 255 (white) arbitrary units was found. The uncorrected EI value was adjusted for subcutaneous fat thickness (SCF) influence using the equation: corrected EI = uncorrected EI + (SCF x 40.5278). *Strength Assessment*. A calibrated HUMAC Norm dynamometer (Computer Sports Medicine, Inc., Stoughton, MA) was used for strength assessment. Participants were seated with their dominant leg secured to the dynamometer lever arm using a padded strap. The dynamometer axis of rotation was aligned with the dominant leg's lateral femoral epicondyle. Restraining straps were placed over the chest, pelvis, and thigh and participants utilized the left and right handlebars of the chair during testing. Strength was tested during range of motion. Each participant completed two trials of five maximal voluntary isokinetic muscle actions of the leg extensors at 60 and at 120 deg/s with 1-minute rest between reps for each testing velocity. Over the duration of each muscle action, participants received verbal encouragement. Isokinetic peak torque (PT) percent decrease was calculated using the average of peak torque across trials. *Statistical Analysis*. Pearson product-moment correlations (r) of EI and % decrease in PT (IBM SPSS Statistics Version 28, Armonk, NY) was performed. Statistical significance was determined using an alpha of $p \leq 0.05$.

Results & Discussion: Statistical analysis demonstrated minimal correlation and no statistical significance ($p>0.05$) when examining the relationship of uncorrected EI and % decrease in PT for females and corrected EI and % decrease in PT for males. A strong linear relationship was found for females between corrected EI and % decrease in PT ($r = 0.761$ and $p = 0.011$) (Fig. 1a). For males, a relationship was found for uncorrected EI instead. Notably this relationship yielded a strong negative linear correlation ($r = -0.624$ and $p = 0.040$) (Fig. 1b).

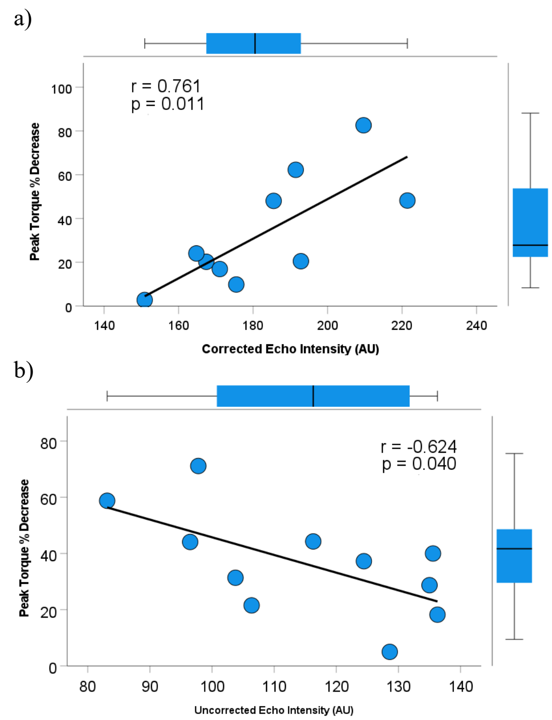

Figure 1: a) Relationship between corrected echo intensity (AU) and the % decrease in PT for young adult females. b) Relationship between uncorrected echo intensity (AU) and the % decrease in PT for young adult males.

Significance: Results showed that correcting for subcutaneous fat for EI measures may be needed for young women as uncorrected yielded no relationship of EI to PT. For young men, the EI correction may be unneeded as corrected EI showed no relationship of EI to PT. Sample size may have biased the results and as a result a larger sample population of females and males may be required to investigate these findings further.

Acknowledgements: Student support is provided by the G-RISE Program (NIH grant number: 1T32GM140911-01 and matching funds by ODU) and the Koerner Family Foundation. Special thanks to G.R. Gerstner, PhD for insight and to I. Kumi and K. Parrish for data collection assistance.

References: [1] Gerstner et al. (2018), *J Strength & Cond Rsrch* 32(10); [2] Gerstner et al. (2017), *Exp Gerontol* 99; [3] Jenkins et al. (2015), *Muscle Nerve* 52; [4] Ryan et al (2016), *Appl Physiol Nutr Metab* (2016) 41(10)

3-D HUMAN MOTION TRACKING WITH A SINGLE CAMERA

Soyong Shin[1*], Zhixiong Li[1], Eni Halilaj[1]
[1]Department of Mechanical Engineering, Carnegie Mellon University, Pittsburgh, PA USA
*Corresponding author's email: soyongs@andrew.cmu.edu

Introduction: Vision-based motion tracking is gaining traction in biomechanics, but interest can be dichotomized into either high-accuracy multi-camera applications that require calibration (e.g., Theia3D [1], OpenCap [2]) or planar single-camera ones that do not capture three-dimensional (3-D) kinematics (e.g., DeepLabCut [3], OpenPose [4]). In addition, current computer vision models have limited ability to capture human motion with temporal consistency, and often suffer from high jittering and unrealistic kinematics. To improve motion tracking with a single video, in this study we built a deep learning model that leverages a large motion capture dataset to accurately reconstruct 3-D kinematics from a single red-green-blue (RGB) video. We hypothesized that this model's accuracy would surpass the performance of prior single-video models and match that of OpenCap, which uses two videos and a biomechanical model.

Methods: The proposed deep learning model is trained to predict 3-D kinematics from two-dimensional (2-D) joint centres retrieved with off-the-shelf neural networks such as OpenPose (Fig. 1). To train this model, we generated synthetic pairs of 2-D joint centers and 3-D kinematics using a large marker-based motion dataset that includes 500 subjects performing a wide range of activities [5]. To generate 2-D joint centers, we created virtual cameras with random positions and projected 3-D joint centers obtained from the marker data into 2-D space, followed by the addition of noise that encompassed jittering, occlusion, and bias. We used Recurrent Neural Networks (RNNs) to predict 3-D motion from 2-D joint centers and evaluated the model's accuracy using real data from 5 subjects performing overground walking and squatting. Marker-based motion capture was used as ground truth, VIBE [6] and PARE [7] as the state of the art in single-video approaches, and OpenCap [2] with two calibrated cameras as the state of the art for biomechanical modelling with video data. We tested our leading hypothesis with a repeated measures ANOVA, using the mean root-mean-squared errors (RMSEs) for both kinematics and angular accelerations as performance metrics, since the later captures the dynamical consistency of the solutions. Here we focused on the lower extremity.

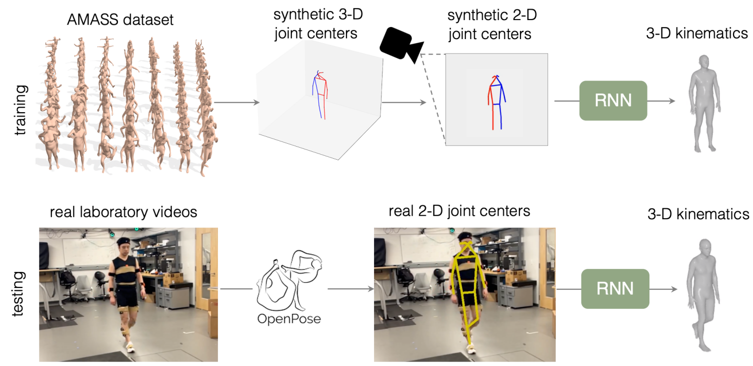

Figure 1: Overview. The RNN is trained on synthetic 2-D joint center data (input) generated from the AMASS dataset, which also contains 3-D kinematics (output). On videos from new subjects, OpenPose (an off-the-shelf model) predicts 2-D joint centers and the RNN trained here predicts the 3-D kinematics.

Results & Discussion: In estimating 3-D kinematics, the proposed model outperformed single-camera approaches and matched OpenCap, which currently uses two calibrated cameras and a biomechanical model (Table 1). During walking, our model outperformed VIBE, PARE, and OpenCap across joints and degrees of freedom ($p < 0.0001$). During squatting, our model outperformed VIBE by 2.8 ± 2.4° ($p < 0.0001$) and PARE by 0.9 ± 2.3° ($p = 0.0021$) but underperformed compared to OpenCap by 2.1 ± 3.6° ($p < 0.0001$). This is likely due to the limited activities in the training dataset, which did not include squatting. Across activities and joints, our model provided better temporal consistency than VIBE, PARE, and OpenCap ($p < 0.0001$). Although mean joint angle curves were generally smooth (Fig. 1A), single gait cycles from the three state-of-the-art methods often exhibited noise, which lead to higher angular acceleration errors than our approach (Fig. 2B). Our model, on the other hand, learned the distribution of human motion robustly, showing promise for future dynamics analyses.

Table 1: The proposed model performed better than the single-view and matched multi-view approaches that use biomechanical models.

Activity	Metric	OpenCap	VIBE	PARE	Ours
Walking	Angle (°)	7.8 ± 3.0	9.8 ± 3.7	7.2 ± 2.3	**4.9 ± 1.6**
	Accel (rad/s^2)	56.0 ± 20.5	91.8 ± 41.1	150.8 ± 65.1	**28.9 ± 9.1**
Squatting	Angle (°)	**4.8 ± 2.4**	9.6 ± 2.4	7.7 ± 2.2	6.9 ± 2.4
	Accel (rad/s^2)	24.1 ± 9.0	79.3 ± 40.3	101.1 ± 41.0	**12.4 ± 5.4**
All	Angle (°)	6.2 ± 3.1	9.7 ± 3.0	7.4 ± 2.8	**6.0 ± 2.3**
	Accel (rad/s^2)	35.7 ± 13.4	86.0 ± 50.0	121.1 ± 54.2	**18.4 ± 6.9**

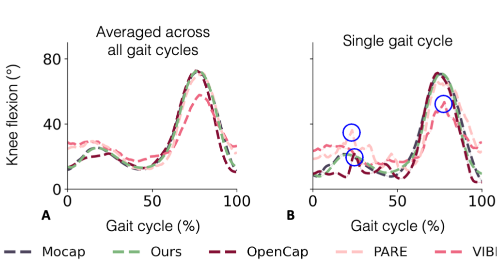

Figure 2: Temporal Consistency. (A) The proposed model showed the best match to the mocap data across entire gait cycles. (B) Our model maintained superior temporal consistency.

Significance: While existing multi-video algorithms suffer from time-consuming calibration steps, single-video algorithms suffer from low accuracy. The proposed model overcomes these challenges by enabling 3D gait analysis from a single RGB video with comparable accuracy to multi-camera approaches, improving feasibility for clinical settings, where time is of essence.

Acknowledgements: This study was funded by a Korean Government Fellowship, CMU Center for Machine Learning and Health Fellowship and NSF/CBET 2145473.

References: [1] Kanko *et al.*, 2020, *J. Biomech.;* [2] Uhlrich *et al.*, 2022, *BioRxiv;* [3] Mathis *et al.*, 2018, *Nature Neuroscience;* [4] Cao *et al.*, 2019, *IEEE PAMI;* [5] Mahmood *et al.*, 2019, *ICCV*; [6] Kocabas *et al.*, 2020, *CVPR*; [7] Kocabas *et al.*, 2021, *ICCV*.

PYLON MOMENT OF CIRCLE WALKING WITH INVERSION AND EVERSION OF A PROSTHETIC ANKLE

Rebecca A. Roembke, Kieran Nichols, Sophya Akhetova, Peter G. Adamczyk
University of Wisconsin – Madison Mechanical Engineering Dept
email: rroembke@wisc.edu

Introduction: Existing adaptable prostheses can change their sagittal plane mechanics to accommodate different behaviors and terrains. But much of the stability challenge to locomotion is in the frontal plane. The natural ankle can both conform to unlevel terrain and provide active torque to help control lateral balance. The two-axis adaptable ankle (TADA) is a semi-active prosthesis that aims to restore some ankle adaptability and control in the frontal plane. It provides the ability to change ankle angle during swing phase. One use of this functionality is to augment turning, in which the ankle inverts or everts to modulate the frontal ankle torque and accommodate the lean of the trunk and legs. Circle walking has been studied with amputees and fixed ankle angles in the transverse plane [1], but we are looking to explore circle walking in a prosthesis with the ability to change inversion and eversion angle. We hypothesize that pylon moment will be minimized when the ankle is in the configuration that conforms to level ground when the body leans towards the inside of the circle: inversion when the prosthesis is the outside leg as shown in Fig 1, eversion when the prosthesis is the inside leg.

Figure 1: Example of ankle conforming to level ground

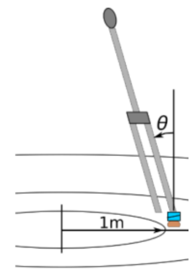

Methods: The data reported are from two participants (n=2) wearing the TADA with a right-side ankle bypass orthosis [2]; additional data will be collected on ten participants in the next few months. The participants walked in three Clockwise (CW) and Counter clockwise (CCW) circles with radius of 1 m and configurations of -10˚ (Inversion, IV), 0˚ (Neutral, N), and +10˚ (Eversion, EV). A metronome was played at 75 beats per minute to regulate speed and timing of steps. A lower body set of inertial motion capture sensors (XSENS MVN) was worn to record approximate walking speed and a pylon load cell (Europa+, Orthocare Innovations) was used to collect pylon moment data. We quantified the mean of the frontal plane pylon moment during each stance phase, for each angle condition (IV, N, EV) and each direction of walking (CW, CCW).

Figure 2: TADA ankle

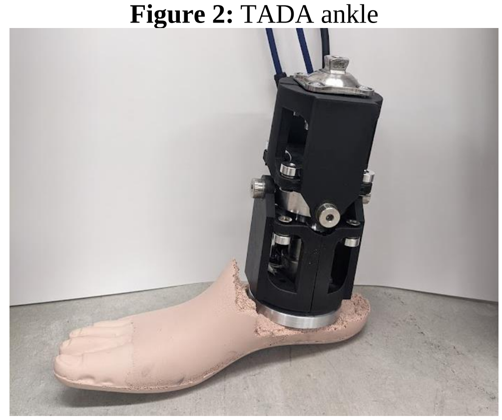

Results & Discussion: Five of the six cases had higher frontal ankle moment magnitude when the prosthesis was the outside foot (CCW) compared to when it was in the same angle configuration as the inside foot (CW) (Fig 3). However, contrary to the hypothesis, frontal moment was smallest in the eversion condition and not when the prosthesis conformed to level ground.

It is thought that frontal plane instability might appear in other ways such as speed changes, step length [1], or step width. Subjects noted it was more difficult to keep moving in the desired direction when using the eversion condition in CCW circles, meaning it may not be the ideal configuration even though the frontal moment is smaller than both the neutral and inversion conditions. Future directions for this study are to find the optimal ankle angle while walking around corners and finding other methods in addition to pylon moment to measure success for finding optimum ankle angle.

Figure 3: Mean Ankle Moment during stance phase

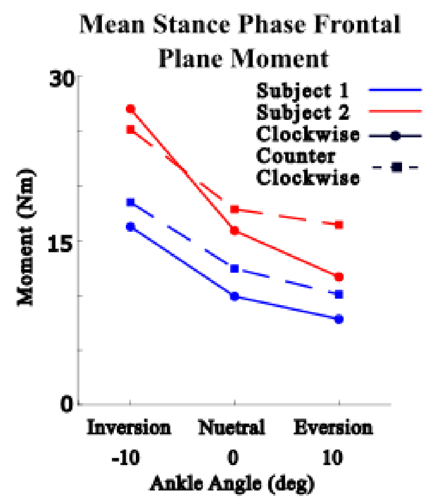

Significance: These results will help to better understand how ankle angle affects prosthetic ankle moment while turning corners of different radii. The hope is that an ankle with the ability to change frontal plane angle can augment turning, to improve balance and stability for users of future prosthetics.

Acknowledgements: This material is based upon work supported by the National Science Foundation Graduate Research Fellowship Program under Grant No. DGE-1747503. Any opinions, findings, and conclusions or recommendations expressed in this material are those of the author(s) and do not necessarily reflect the views of the National Science Foundation. DOD grant W81XWH2010884

References: [1] Ava D. Segal et al. (2011) *Gait & Posture*, Volume 33, Issue 1, 2011, Pages 41-47, [2] Grimmer, M., Holgate, M., Holgate, R. *et al.* (2016) *BioMed Eng OnLine* 15 (Suppl 3), 141

PHYSICAL THERAPY ASSESSMENT WITH UNCALIBRATED CAMERAS AND INERTIAL SENSORS

Soyong Shin[1*], Jessica Hodgins[2], Adam Popchak[3], Keelan Enseki[3], Eni Halilaj[1,2]
[1]Department of Mechanical Engineering, Carnegie Mellon University, Pittsburgh, PA USA, [2]The Robotics Institute, Carnegie Mellon University, Pittsburgh, PA USA, [3]Department of Physical Therapy, Pittsburgh, PA USA
*Corresponding author's email: soyongs@andrew.cmu.edu

Introduction: Automated assessment of physical therapy exercises could help support more personalized care by enabling clinicians to track patient performance and tailor care accordingly. Current single-camera solutions primarily focus on detecting repetitions of an exercise and not correctness in execution. While multi-modal algorithms that combine multiple videos and inertial sensors could resolve these shortcomings, the calibration steps required for both data sources limit clinical translation. To inspire clinical translation, we need to be able to work with uncalibrated data that can be easily collected by busy clinicians. Here we describe an end-to-end approach for estimating exercise correctness using uncalibrated video and inertial measurement unit (IMU) data and test this approach on 25 patients performing a step-up exercise. Our hypothesis was that the proposed approach would be more accurate than single-camera or IMU-only models at detecting whether a subject performed the exercise correctly.

Methods: Vision-based motion tracking in three dimensions (3-D) typically involves fitting a statistical meshed model of the human body to video data using two steps: (1) a neural network that extracts joint centers from the video and (2) an optimization step that deforms the mesh to best match the joint centers extracted in (1). Multi-view approaches optimize mesh fitting across different videos simultaneously and require calibration parameters, which increases data collection time. Here we extract calibration parameters automatically during the optimization approach, in a process we call auto-calibration (Fig. 1). Additionally, we refine the proposed solutions by adding a reprojection term to the cost function that minimizes the difference between signals from virtual IMUs attached to the meshed model and real IMU data collected in the experiments.

To test this proposed approach, we used data from 25 subjects performing a step-up exercise (340 correct and 195 incorrect repetitions). Two physical therapists labeled each repetition as correct or incorrect, and an adjudicated score was used as the ground truth label. We then trained Random Forest classifiers to predict error. The baseline classifiers used two-dimensional (2-D) joint centers from the front camera (single-view), front and side cameras (multi-view), IMU acceleration and orientation (IMU-alone), and both multi-view video and IMU signals (fusion). Our classifiers used joint angles from the mesh fitting from each modality. We used a leave-5-subjects-out cross-validation (L5SO-CV) scheme to evaluate the models.

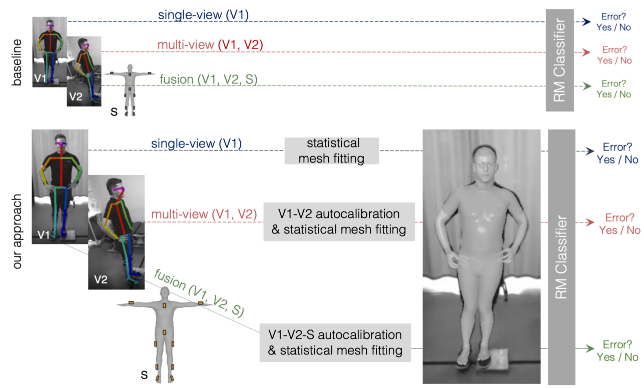

Fig 1: Overview. The baseline models use video joint centers and IMU orientations from Xsens to predict exercise error with a Random Forests (RM) classifier. Our approach is to first fit a 3-D statistical mesh of the human body to derive 3-D kinematics, which are then used as features in the classifier. Data from multiple videos (V1, V2) and IMU sensors (S) are calibrated automatically.

Results & Discussion: Our classifiers, which used auto-calibration, were more accurate than the baseline classifiers (Table 1) and favorable compared to clinician agreement reported in prior work [1]. Our algorithms improved classification performance (F1 score) by approximately 50% for all input modalities compared to the baseline classifiers. This improvement is likely due to our approach of extracting kinematics, rather than using joint centers. While our single-view model suffered from ambiguity, models leveraging data from two videos and IMUs led to the best performance (Fig. 2). Given that clinician agreement has a mean kappa score of 0.18, and that uncalibrated data were used, we believe that these classifiers showed reasonable accuracy. Typically, performance evaluation is subjective to what a clinician sees rather than measures. Because our proposed models enable quantitative assessments of 3-D kinematics, they provide the opportunity for even more objective assessment if combined with heuristics, instead of machine learning models trained on clinician assessment as the ground truth.

Table 1: Our classifiers outperform all the baseline models.

Metric	Models	Input modality: single-view	multi-view	IMU-alone	fusion
Precision	baseline	0.23	0.36	0.54	0.46
	our	0.45	0.61	–	**0.66**
Recall	baseline	0.18	0.30	0.42	0.33
	ours	0.36	0.48	–	**0.56**
F1 score	baseline	0.20	0.33	0.47	0.38
	ours	0.40	0.54	–	**0.60**

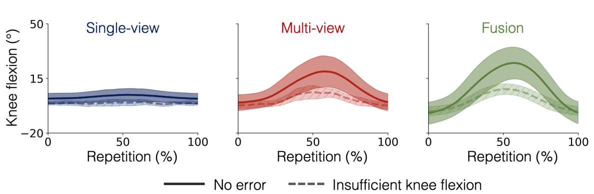

Fig 2: Qualitative Comparison. Our fusion model was better able to distinguish exercise repetitions with insufficient knee flexion from normal repetitions than vision-only approaches.

Significance: The proposed approach for assessing physical therapy performance with uncalibrated cameras and IMUs can encourage adoption because of its ability to outperform single-camera methods, such as those embedded in commercially available solutions (e.g., Kaia Health), while still maintaining data collection time within similar limits.

Acknowledgements: This study was funded by a Korean Government Fellowship and a pilot project from the Restore Center at Stanford University (funded via NIH P2CHD101913). We would like to thank A.S. Whitford and E. Kim for their contributions.

References: [1] Whelan *et al.*, 2019, *PTRJ*; [2] Loper *et al.*, 2015, *SIGGRAPH Asia*; [3] Cao et al., 2018, *IEEE PAMI.*

Prolonged Load Carriage During Walking Induces Fatigue and Redistributes Lower Limb Muscle Effort

Qingyi Lou[1*], Amro Alshareef[1, 2] & Gregory S. Sawicki[1,2,3]
[1]The George W. Woodruff School of Mechanical Engineering, [2]Institute for Robotics and Intelligent Machines,
3The School of Biological Sciences, Georgia Institute of Technology, Atlanta, GA, USA
*Corresponding author's email : qlou8@gatech.edu

Introduction

Load carriage, muscle fatigue or a combination of both could increase falls risk because of changes in gait parameters that lead to balance challenges. For example, populations that engage in activity involving navigation through unstructured terrain while carrying body-borne load, such as soldiers, EMTs, and hikers, may be especially susceptible to falls because added mechanical demand could induce and neurological fatigue over time [1]. A previous study of muscle-level fatigue compared the max effort force and muscle activation magnitude before and after an acute bout of walking with 40% body weight and failed to establish significant changes in biomarkers of fatigue for muscles around the knee joint [1]. However, that study did not examine muscles around the ankle, knee and hip together during a prolonged walking trial, in conditions with vs. without load carriage. Here we begin to address this gap, setting up an experiment with the goal to characterize the *(re)distribution* of muscle fatigue across the lower-limb during load carriage over an ecologically-relevant timescale. We hypothesized that due to a higher relative demand for force and work to propel the body with added load, the distal muscles (e.g., ankle plantarflexors) would fatigue at a faster rate than proximal muscles (e.g., hip extensors) over a 30 min walking bout.

Methods

One healthy participant walked at 1.2 m/s on a split-belt treadmill mounted on a fixed-platform (CAREN, Motek Inc., Netherlands) for 31 minutes with (Session 1) and without (Session 2) a body-borne load. For the load carriage session, the participant donned a weighted vest with added mass equivalent to 20% of body weight. In the no-load session, the participant donned the weighted vest with no added mass. Lower-limb muscle electromyography (surface EMG), joint kinematics (motion capture), and ground reaction forces (force platforms) were collected every 5-minutes during each session. Gait cycles from each 1-minute recording were identified using the on/offset of the ground reaction force of a single leg. EMG data were bandpass filtered, offset by mean value, rectified, and smoothed prior to analysis. We calculated the mean power frequency and mean amplitude across the last 8 gait cycles of each minute long trial from EMG records taken from key muscles of the ankle (TA, Sol, MG) and hip (BF, Gmax).

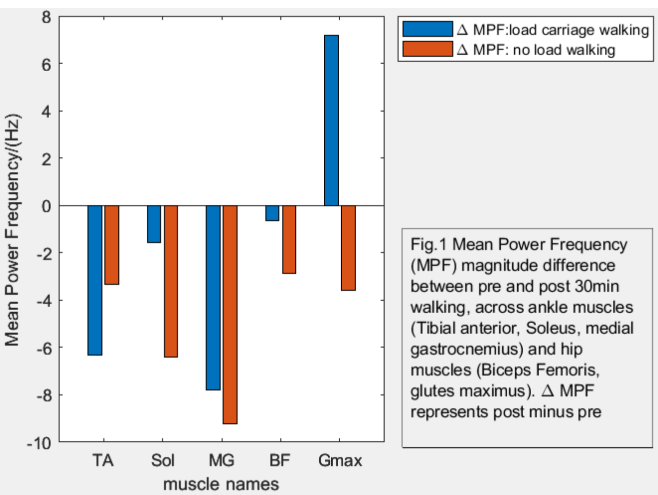

Fig.1 Mean Power Frequency (MPF) magnitude difference between pre and post 30min walking, across ankle muscles (Tibial anterior, Soleus, medial gastrocnemius) and hip muscles (Biceps Femoris, glutes maximus). Δ MPF represents post minus pre

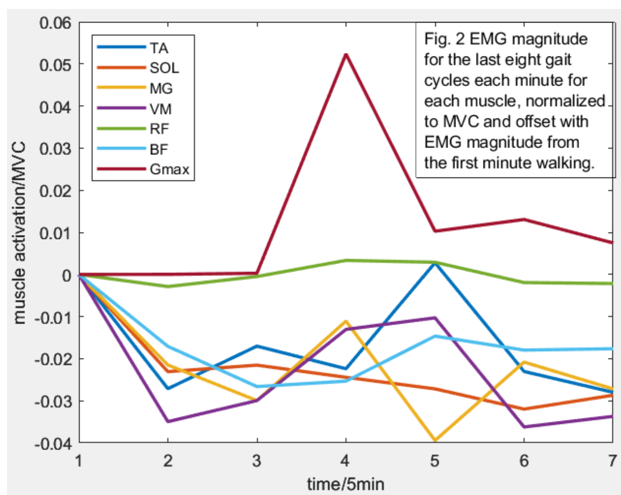

Fig. 2 EMG magnitude for the last eight gait cycles each minute for each muscle, normalized to MVC and offset with EMG magnitude from the first minute walking.

Results and Discussion

We observed a decrease in mean power frequency over the 30-minute walking bouts with (Session 1 – blue) and without body-borne load (Session 2 – orange) for *all* the muscles of interest except for gluteus maximus (Gmax) during the load carriage session (Fig. 1). This trend in our initial pilot data indicates that 30 minutes walking can induce muscle fatigue, even without added load [2]. In addition, during Session 1 with body-borne load, we found decreases in EMG magnitude for the ankle muscles (TA, Sol, MG) that was accompanied by increases in EMG magnitude for hip muscles (Gmax) (Fig. 2). This trend indicates a distal to proximal shift from using ankle muscles to using hip muscles that builds and persists as fatigue accumulates while walking with a body-borne load.

Significance

Characterizing the progression of fatigue over time during walking is a crucial first step that will help engineers develop assistive devices and develop training protocols that specifically target muscles that tire quickly. Our preliminary data suggests targeting the ankle muscles may be an effective means to mitigate local and global effects of muscle fatigue during load carriage. Future work will aim to extend these data and more comprehensively explore how joint-level neuromechanical effects of muscle fatigue impact dynamic balance.

References

[1] Simpson et al. (2011) *J Electromyogr Kinesiol* [2] Zhang et al. (2022) J Eng Med

A MACHINE LEARNING APPROACH TO EXAMINE THE ROLE OF GAIT AND PHYSICAL ACTIVITY PARAMETERS ON RISK OF KNEE REPLACEMENT: THE MULTICENTER OSTEOARTHRITIS STUDY

Kerry E. Costello[1,2,3*], David T. Felson[3], S. Reza Jafarzadeh[3], Neil A. Segal[4], Cora E. Lewis[5], Michael C. Nevitt[6], Vijaya B. Kolachalama[2,3], Deepak Kumar[2,3]
[1]University of Florida
*Corresponding author's email: k.costello@ufl.edu

Introduction: Rates of knee replacement (KR) due to knee osteoarthritis (OA) are rising exponentially and projected to reach as many as 3.5 million/year in the U.S. by 2040 [1]. Thus, there is an urgent need to identify risk factors for KR that can be easily assessed in large samples and addressed with scalable interventions. Abnormal joint biomechanics are a risk factor for knee OA and can be modified by changing gait and/or physical activity [2]. Spatiotemporal gait metrics and daily physical activity metrics can be captured quickly and easily with pressure sensing mats and wearable sensors. However, these measures are not independent, and demographic and clinical factors such as age and limb alignment can affect biomechanics and are also independent risk factors for knee OA (i.e., confounders), making traditional analysis approaches challenging. Applying machine learning approaches to large datasets can help with understanding the effect of this complex set of inter-related predictors on risk of KR. The objectives of this study were to 1) build and evaluate a machine learning model to predict KR at 8-year follow-up from gait, physical activity, demographic, and clinical inputs, 2) identify influential predictors of KR from the model, and 3) quantify the effect of these predictors on KR.

Methods: The Multicenter Osteoarthritis Study is a large, observational cohort of individuals with and at risk for knee OA that includes spatiotemporal gait data, activity monitor data, KR outcome data, demographic, and clinical data for n=1683 knees [3]. Gait data were collected during 4 trails of 'usual' speed walking using a GaitRite walkway, with metrics averaged across all strides. Daily average activity parameters (step count, minutes in low intensity, and minutes in high intensity) were extracted from 7 days of ankle worn StepWatch Activity Monitor data. An ensemble machine learning model (Fig. 1) was trained to predict the binary KR outcome from 16 gait, 3 physical activity, and 16 demographic/clinical parameters and evaluated on a held-out test set. A variable importance measure statistic was used to identify parameters that most frequently appeared as top contributors to prediction. Parametric g-computation was then used to calculate the marginal cause risk differences across quantiles or categories of each top contributing predictor [4,5].

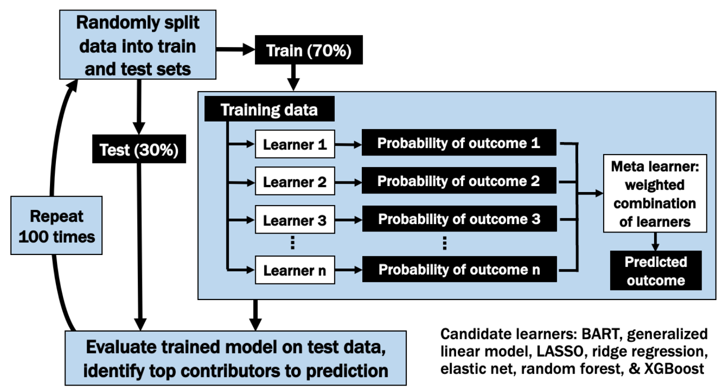

Figure 1: Super learning [9], an ensemble machine learning approach, was used to predict the binary KR outcome from gait, physical activity, clinical, and demographic features.

Results & Discussion: The median (2.5th-97.5th percentile) AUC was 0.84 (0.79-0.88), comparable to a deep learning model predicting KR at 9 years from knee radiographs [6]. Spatiotemporal gait parameters were not top contributors to prediction of KR; structural signs of knee OA (Kellgren-Lawrence grade [KLG]), limb alignment, age, knee pain, willingness for surgery, depressive symptoms, body mass index, education, step count, contralateral KLG, and contralateral knee pain were top contributors to prediction. However, of these, our g-computation analysis only identified higher structural severity, varus knee alignment, greater knee pain, and greater contralateral KLG as associated with higher risk of KR, and lower willingness to undergo surgery and presence of depressive symptoms with lower risk of KR. Thus, the relationship between step count and risk of KR was inconclusive. Spatiotemporal parameters may be less relevant to KR than knee-specific biomechanics (i.e., knee joint moments, muscle activation), which have previously been associated with KR at a similar follow-up length [7,8]. Additionally, only 3 summary measures were used to characterize physical activity, potentially losing relevant information about cumulative exposure to knee joint loads. These results may also indicate that common demographic and clinical risk factors for OA are more important to risk of KR than gait and physical activity.

Significance: This novel study was the largest to look at gait and physical activity predictors of KR, assessed multiple inter-related predictors by using a machine learning approach, utilized an independent test set for model evaluation, and used g-computation to explore causal relationships. While the model performed well, we did not find conclusive evidence for the association of spatiotemporal gait and daily average physical activity features with risk of KR at 8-year follow-up. These results could indicate that clinical and demographic measures are more important in determining risk of KR but could also suggest that these gait and physical activity measures are too simplistic to describe knee biomechanics in the context of future KR risk and potential intervention targets.

Acknowledgements: MOST participants and clinic staff, NIH NIA (AG18820, AG18832, AG18947, AG19069), NIH NIAMS (P30AR072571), Rheumatology Research Foundation (Investigator Award).

References: [1] Singh (2019), *J Rheumatol* 46(9); [2] Hinman et al. (2013) [3] Segal et al. (2013), *PMR* 5(8); [4] Snowden et al. (2011) *Am J Epidemiol* 173(7); [5] Grembi et al. (2022) *PLoS One* 17(7); [6] Leung et al. (2020) *Radiology* 296(3); [7] Hatfield et al. (2015) *Arthritis Care Res* 67(7); [8] Hatfield et al. (2021) *Arthritis Care Res* 73(4); [9] https://github.com/tlverse/sl3.

EFFECTS OF MATURATION ON TIBIAL ACCELERATION PROFILES DURING SPEED-&-AGILITY DRILLS IN MALE YOUTH SOCCER PLAYERS

Kavon Bonakdar[1], Jake A. Melaro[1], Joshua T. Weinhandl[1]
[1]University of Tennessee, Knoxville
Kbonakda@vols.utk.edu

Introduction: Sport-related injuries increase in males throughout high school, with ~68% of adolescent injuries occurring in the lower extremity [1, 2]. This is likely due to rapid, physiological changes during puberty such as bone growth and increased muscle mass, which can increase the forces experienced by the body and be a factor for higher prevalence of lower extremity injuries [3]. According to a recent study, growth-related injuries account for 30% of all severe injuries that require at least 40 days of participation time lost in soccer academies. Thus, the reduction of growth-related injuries can be important in the prevention of long-term repercussions and maximize players' potential development [4]. Investigating acceleration performance throughout puberty can provide insight into managing training load to reduce injury while also optimizing performance [5]. Therefore, the purpose of this study was to investigate the peak acceleration and acceleration integral in youth soccer players when performing agility drills between maturation groups. It was hypothesized that peak acceleration and cumulative loading would increase as males experience puberty.

Methods: Thirty male youth soccer players were recruited from a local soccer club to voluntarily participate in this study. The Mirwald equation was used to determine how close the players were to their peak height velocity (PHV) and then stratify them into groups of pre-PHV, PHV, and post-PHV based on their relative proximity to PHV [6]. Inertial measurement units were placed on the participants bilaterally on the distal-medial tibia (1600 Hz; Vicon Blue Trident, Vicon Motion Systems Ltd, Oxford, UK). The first drill was a 36.6-meter jog followed by an M-cone drill in which the participants ran in an M shape and made sharp cuts at each cone (completed in both directions). Next was a 5-10-5-meter lateral shuffle drill where participants shuffled 5 meters, changed directions to shuffle 10 meters in the other direction, and then back 5 meters towards the middle. The final drill was a single leg triple jump in which the participants goal was maximum horizontal displacement. Data was analyzed using Python v3.10.4 (Python Software Foundation, Beaverton, OR, USA). An independent t-test (α=0.05) was used to determine the statistical significance with R 4.2.1 (R Foundation for Statistical Computing, Vienna, AUST).

Results and Discussion: For average peak acceleration, the post-PHV group had significantly higher values in the 5-10-5 drill when compared to the PHV and pre-PHV groups. The post-PHV group had significantly higher cumulative loading rates in the 5-10-5, M-drill left, and triple hop right when compared to the pre-PHV group. The PHV group also had higher cumulative loading when compared to the pre-PHV group in the 5-10-5, M-drill left, and triple hop right. The post-PHV boys experienced higher cumulative loading in some drills but higher peak acceleration in only one drill. Thus, the hypothesis that peak acceleration and cumulative loading during agility drills was not supported. Even though the differences between the groups were not significant in the cumulative loading, there is a trend of gradual increase in load as throughout maturation in all drills except for down and back. This suggests that males approaching their peak velocity are gradually increasing their peak tibial acceleration, but this slight increase leads to a significantly larger cumulative load throughout the span of a training session.

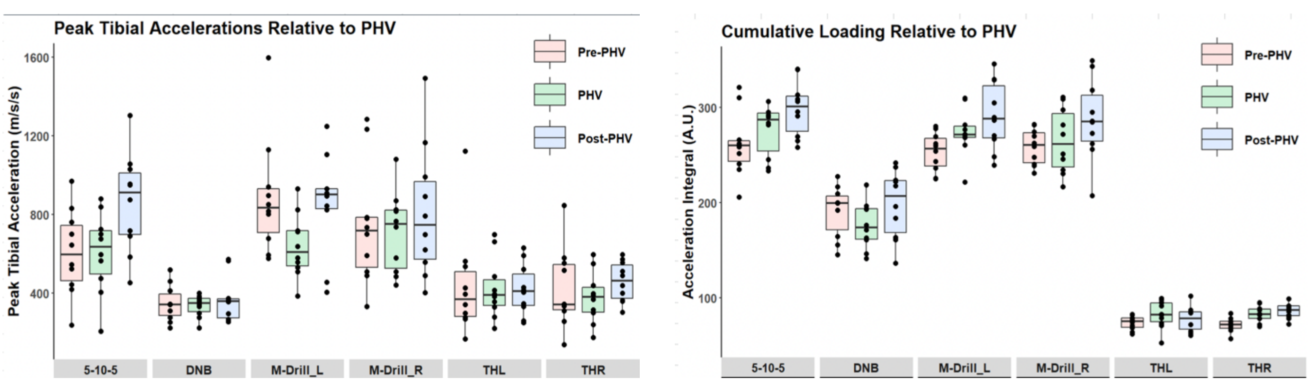

Figure 1. Box plot of the average peak tibial accelerations (A) and cumulative loading rate (B) relative to the maturation group in each agility drill.

Significance: There were observed changes in cumulative load throughout maturation in this study, which previous literature has identified as an increased risk factor for youth sport injuries. Therefore, monitoring this metric as male soccer athletes mature could help prevent injuries [7]. One such way would be by controlling week-to-week changes in load to detect early growth-related conditions so that practitioners can training modify content for high-risk players and detect growth-related conditions before an injury occurs [4].

References

[1] Comstock, R.D., Pierpoint, L.A. National high school sports-related injury surveillance study 2018-2019. 2020; [2] Verhagen, E. A. L. M., et al. BJSM, 43(13),1031-1035. 2009; [3] Dupré, T., & Potthast, W. Sports Biomechanics, 1-13. 2022; [4] Monasterio, X., et al. IJSM, 44. 2023; [5] Gabbett, T. J. BJSM 50(5), 273-280. 2016; [6] Mirwald, R. L. et al. MSSE, 34(4), 689-694. 2002; [7] Sniffen, K. et al. Sports Med – Open, 8, 117. 2022

OCCUPANT CHARACTERISTIC RISK FACTORS FOR WHIPLASH COMPLAINTS IN MOTOR VEHICLE COLLISIONS

Kjeryn A. Soetaert[1*], Julia E. de Lange[2], Chad E. Gooyers[2], Kayla M. Fewster[1]
[1]School of Kinesiology, University of British Columbia, Vancouver, BC, Canada
[2]Forensic Engineering, Toronto, ON and Vancouver, BC
*Corresponding author's email: k.soetaert@alumni.ubc.ca

Introduction: Whiplash associated disorders (WAD) are frequent complaints following low velocity rear-end motor vehicle collisions (MVC) and are considered one of the highest financially burdening musculoskeletal injuries due to the wide range of symptoms and variable recovery rates [1]. With up to 50% of individuals with WAD experiencing chronic symptom reporting, current research has focused on prognostic risk factors [2]. Despite substantial research on WAD injury mechanisms, definitive factors of elevated injury risk and likelihood of chronicity of symptoms remain inconclusive. Characteristics such as pre-existing cervical intervertebral disc (IVD) degeneration, cervical facet joint degeneration or generalized neck pain have been suggested to influence WAD symptom reporting, duration, and overall prognosis [3,4]. Additionally, prior neck pain or injury, increased age and female biological sex have been reported to significantly increase risk of poor WAD prognosis via increased severity of present symptoms and prolonged recovery times [2,4]. To further elucidate prognostic risk factors for WAD following MVCs, we utilized redacted and deidentified medical records from individuals involved in low to moderate severity MVCs to shift reliance from self-reported symptoms and subjective collision recall to medical documentation and collision severity. It was hypothesized that a greater proportion of occupants with evidence of cervical degeneration (e.g., facet joint osteoarthritis and/or IVD degeneration) would experience WAD symptoms following a low to moderate severity MVC.

Methods: This study incorporated a secondary analysis of data provided by a Canadian forensic engineering firm (30 Forensic Engineering). Files were indexed in a searchable (internal) electronic database, which contained 23 years of cases (2000-2022), with only cases with a collision severity below 20km/hr being further evaluated. A summary of useable case data was reviewed, de-identified and summarized to ensure anonymity by the partner organization. Cases were cataloged by specific collision and occupant characteristics including age, sex, collision severity and type, direction of collision forces, restraint use, vehicle make and model, seating position in the vehicle, prior collisions, injuries claimed, and pre-existing medical documentation. Across all cases, percentages of total cases or descriptive statistics (means and standard deviation) were calculated for seating position, collision severity, collision configuration, biological sex, presence of pre-existing cervical degeneration (degeneration grade and location) and whiplash or WAD injury claims. Paired t-tests were completed on all mean outcome measures.

Results & Discussion: In total, 166 cases met the inclusion criteria, with 83.1% involving a claim of whiplash. Across all 166 cases there were more female than male claimants; 59.6% of all claimants were female and 40.4% were male. The mean collision severity (SD), defined as the change in velocity or 'delta-v', was 11.92 (5.26) km/hr across all collision types. The most common pre-existing medical condition was cervical degeneration; 40.6% of claimants had medical evidence of cervical spine degeneration (Figure 1). Incidence of WAD was equally distributed between biological males and females with 83.8% of female claimants and 82.1% of males claiming a WAD. A rear-end impact was found to be the most common collision configuration, accounting for 74% of all claims, with 84% of those cases having associated whiplash claims. The mean collision severity across all WAD claims was 11.34 (5.57) km/hr. There was no significant difference in rear-end mean collision severity between whiplash claimants and those without. When controlling for medical evidence of cervical spine degeneration, the average collision severity associated with subjective WAD complaints was observed to decrease from 12.7 km/h (without degeneration) to 10.7 km/h with evidence of cervical spine IVD degeneration, and further to 7.7 km/h when the combination of both facet and IVD degeneration was present.

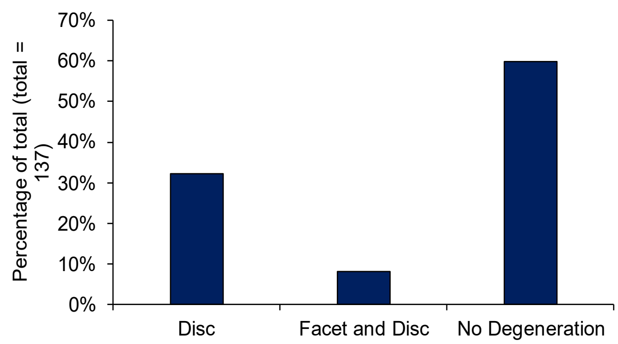

Figure 1. Percentage of WAD claims as a function of cervical spine degeneration.

Significance: Results indicate that claimants with medical evidence of cervical spine degeneration may report subjective WAD complaints at lower collision severities. This finding was evident for claimants with medical evidence of both IVD and facet degeneration. This preliminary research can be used to direct additional further investigations on prognostic risk factors for WAD following a low to moderate speed MVC. Last, it is important to note that the complaints included in this investigation are on the basis of symptom reporting in the context of litigation. It also does not include individuals who may or may not have been exposed to a MVC but did not make an injury claim.

References: [1] Stemper & Corner (2016), *J Biomech* 36(9); [2] Walton et al. (2013), *J Orthop Sports Phys Ther* 43(2); [3] Malik et al. (2021), *Int J Spine Surg* 15(4); [4] Yoganandan et al. (2013), *Semin Spine Surg* 25(1)

THE EFFECTS OF TIBIALIS ANTERIOR FATIGUE ON BALANCE

Hailey Musgrove[1], Joseph Mallillin[1], Noelle Tuttle[1], Marco A. Avalos[2], Young-Hoo Kwon[1]
[1]Texas Woman's University
[2]Rosalind Franklin University of Medicine and Science
email: Hmusgrove@twu.edu

Introduction: The tibialis anterior (TA) is a muscle in the anterior portion of the lower leg. It is responsible for dorsiflexion at the talocrural joint and inversion at the subtalar joint. The TA assists gait through force absorption during heel strike and eccentrically decelerates the foot during loading response [1]. The TA is also the main muscle involved in dorsiflexion (DF) for toe clearance during the swing phase and is an important contributor to balance during stance. To safely and efficiently complete activities of daily living, proper balance during ambulation must be maintained [2]. Daily activities include safely changing directions, standing up from sitting, and single-leg balance (e.g., normal gait, walking upstairs).

Muscle fatigue can affect the ability to properly perform activities of daily living. There is little research on the effect fatigue has on the TA alone with regard to gait and balance. The limited research involving fatigue in gait and balance is in conjunction with the TA and plantar flexors or the latter alone [3,4]. Therefore, this study aims to investigate TA fatigue's effects on balance. It is hypothesized that balance ability will decrease after TA fatigue.

Methods: This preliminary analysis includes 17 participants (10 females, 16 right-leg dominant, 24.6 ± 5.9 yrs, 165.6 ± 8.6 cm, 73.6 ± 15.0 kg). After a warm-up, Pre-fatigue (PRF) kinematic data were collected on the NeuroCom Balance Master. PRF measures included a Unilateral Stance (US) on the dominant leg, Step Quick Turn (SQT) turning on the dominant leg over the non-dominant shoulder, and Sit-To-Stand (STS) with a ten-second hold. PRF measures for range of motion (ROM), proprioception (PRO), and force outputs were measured on the Biodex, followed by a fatigue protocol. The fatigue protocol consisted of a maximum of 10 sets of five repetitions of eccentric and concentric contraction of the TA against 10 Nm. There was a ten-second break between each set. Participants followed this protocol until failure before completing the post-fatigue (POF) measurements. A repeated measures MANOVA was used to compare condition mean differences and Cohens-d test for effect size was also performed.

Results & Discussion: Though changes in sway velocity were seen, only the STS sway had a significant change with a medium effect size (Table 1). A possible reason for this increase may be due to a decreased ability to maintain the body from a back sway (TA eccentric contraction) balance because of muscle fatigue. An effect of familiarization may have reduced the significance on SQT, but from observation, there was a large amount of individual variability in turn technique. Also, because the SQT is a more complex task, increased concentration was required, leading to increased control of movement during the turn. On the other hand, STS is a task that we consider autonomic in our daily activities, and therefore, is easily affected by the TA fatigue.

	PRF	**POF**	***p***	***d***
US sway (deg/sec)	0.83±0.18	0.92±0.16	.152	-.365
SQT sway (deg/sec)	19.34±8.4	16.54±7.0	.085	.446
STS sway (deg/sec)	4.29±1.1	4.92±1.0	**.025**	-.598
STS weight trans (sec)	0.37±0.2	0.30±0.2	.179	.341
STS Sym (%BW)	2.55±7.3	2.56±7.9	.996	-.001
Torque (Nm)	21.71±8.9	15.29±8.5	**.014**	.667
DF ROM (deg)	17.12±7.1	11.82±9.3	**.001**	.947
Proprioception (deg)	2.27±5.5	3.60±6.2	**.026**	.261

Table 1. PRF and POF averages. **Bold** represents statistically significant changes.

The other two STS parameters did not show significant differences; nevertheless, there was a reduction in the weight transfer time during POF (Table 1), We assume that due to TA fatigue, the participant will avoid holding postures that demand high TA activity, and therefore, will rise faster to achieve a more comfortable position. The lack of changes in the symmetry load was unexpected, but it was noticed that following fatigue, some participants loaded more on their dominant leg and others on their non-dominant leg to achieve balance, thus not showing significant changes. It should be noted, however, that during STS, the TA functions mainly in the sagittal plane, and the symmetry load is a frontal load function.

As expected, significant changes were seen in torque and DF ROM (Table 1), as fatigue can reduce the ability to produce force and therefore can affect active ROM. Together, these will affect the ability to raise the toes during ambulation, leading to foot drop, and evoke a compensatory body sway to avoid dragging the foot, as seen in the SQT sway. During POF measurements, seven participants tripped once and six had multiple trips while walking between machines, and all participants demonstrated gait changes. Multiple trips have been shown to lead to greater fall risk in healthy older adults [5]. This further proves that the POF movements were cautious and changes may not be only due to learning effects. These findings imply that fatigue of the TA could influence fall risk, balance, and other activities.

Significance: Results in this study had a significant impact with medium to high effect size in a healthy population, which could become more pronounced in populations with high fall risk (i.e., older adults). The results from this study could indicate the necessity to include ankle DF strengthening in therapy and regular strengthening routines, especially in clinical populations. Future research could benefit from understanding the extent TA fatigue has on balance in clinical populations.

References: [1] Brockett & Chapman (2016), *Orthop Trauma*, 30(3); [2] Mancini & Horak (2010), *Eur J Phys Rehabil Med*, 46(2); [3] Salavati et al. (2007), *Gait Posture*, 26(2); [4] Rojhani-Shirazi et al. (2019), *J Biomed Phys Eng*, 9(2). [5] Srygley et al. (2009), *Arch Phys Med Rehabil*, 90(5)

STRATEGIES FOR INCREASING GAIT SPEED IN FEMALES WITH HIP PAIN

Fang-Yu Syu[1*], Zoe Perkins,[1] Cara Lewis[1]
[1]Human Adaptation Lab, Boston University, Boston, MA, USA
*Corresponding Author Email: fangyu@bu.edu

Introduction: Changes in gait speed are beneficial in daily life. In healthy individuals, modifications in cadence, stride length or a combination of both are used to regulate the change in walking speed [1]. The cadence-stride length relationship can represent central gait control and gait abnormalities [2]. Individuals with hip pain have been found to walk differently than controls with less hip extension angle and total hip range of motion (RoM) at the same walking speeds [3]. Moreover, at faster walking speeds, individuals with hip osteoarthritis who increased their cadence have a smaller increase in hip joint moment than individuals who increase their stride length. This highlights the importance of selecting an appropriate strategy when regulating gait speed in individuals with hip joint diseases [4]. Therefore, the aim of this study was to investigate the characteristics of individuals with hip pain who mainly increase their cadence compared to those who increase stride length during walking at a faster speed.

Methods: This study was a secondary analysis of 90 female participants from previously collected data. Each participant walked at a preferred (i.e., self-selected) and a fast (25% faster than preferred) speed. Kinematic data were collected using a motion capture system, while kinetic data were collected using an instrumented treadmill to determine heel strike and toe-off. Participants rated their pain in real-time on an 11-unit numerical rating scale (NRS) and completed the WOMAC pain scale. Visual3D was used to calculate gait parameters, including cadence and stride length during preferred and fast speeds, which were then used to calculate the gait index:

$$\Delta\text{Cadence} = \frac{Cad^{fast} - Cad^{prefer}}{Cad^{prefer}} \text{x}100\% \qquad \Delta\text{Stride} = \frac{Stride^{fast} - Stride^{prefer}}{Stride^{prefer}} \text{x}100\% \qquad \text{Gait index} = \frac{\Delta\text{Cadence} - \Delta\text{Stride}}{(\Delta\text{Cadence} + \Delta\text{Stride})/2}$$

Tertiles were used to divide participants into three groups based on their gait index: the cadence group, combination group, and stride length group. The two divergent groups (cadence and stride length) were compared using independent t-tests, with an alpha level of 0.05 to determine differences in demographic, kinematic, and pain data.

Results & Discussion: The cadence group gait index ranged from -0.25 to 0.69, while the stride length group index ranged from -1.02 to -0.49. There were no significant differences in age, height, or weight between groups (Table 1). The cadence group had a higher score on the WOMAC pain subscale (p=0.02); there was no difference in real-time pain during tasks (p=0.077). The cadence group walked with a higher preferred speed (p<.001) with a greater peak hip extension angle and greater total hip RoM during both preferred (p≤0.004) and fast walking speeds (p≤0.007) compared to the stride length group (Fig 1). The cadence group demonstrated a smaller increase in total hip RoM (p=0.019) during fast walking speeds, but there was no difference in the speed-related increase in peak hip extension angle (p=0.735) compared to the stride length group (Fig 1). The results suggest that individuals who mainly increase their cadence when walking faster, experience greater pain during daily activities and may already be at the end of their available hip extension.

Table 1. Demographics data

Group	N	Age (years)	Height (cm)	Weight (kg)	Preferred gait speed (m/s)*	Index*	NRS	WOMAC pain scale*
Cadence	30	28.77±8.24	167.72±7.38	63.96±10.15	1.36±0.18	0.01±0.21	1.80±1.91	5.80±3.75
Stride length	30	26.60±9.01	166.29±6.25	64.74±10.21	1.22±0.13	-0.72±0.16	1.03±1.31	3.87±2.30

*: p<0.05

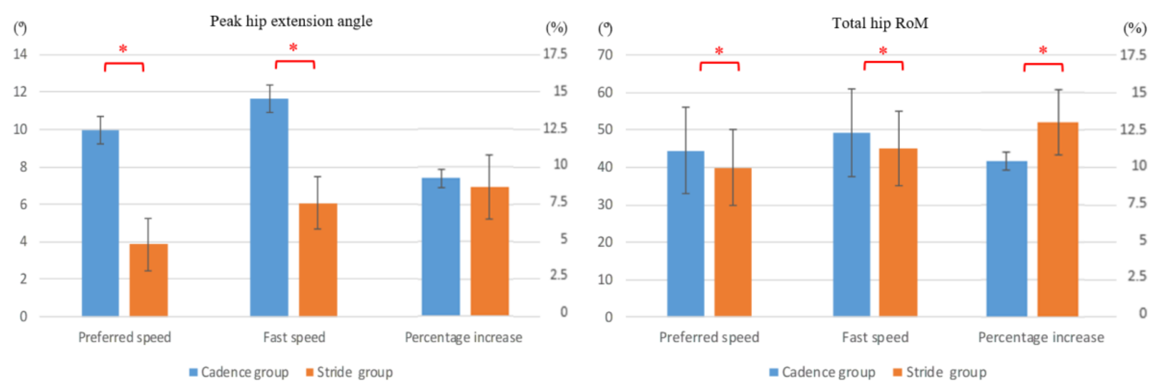

Figure 1. Peak hip extension angle and total hip RoM in cadence and stride length group during preferred and fast walking speed. *: p<0.05

Significance: This study may provide the insight into strategies individuals with hip pain use to increase walking speed. Clinicians may consider these different strategies when developing treatment plans for patients with hip pain.

Acknowledgments: This work was supported by NIH R21 AR061690 and K23 AR063235.

References: [1] Charla et al., (2013), *Gait Posture*; [2] Thorlene et al., (2011), *Gait Posture*; [3] Lewis et al., (2021), *Front Sports Act Living*; [4] Tateuchi et al., (2021), *Arthritis Res Ther*.

EFFECTS OF MATURATION ON LOWER LIMB LOADING SYMMETRY DURING SPEED-&-AGILITY DRILLS IN MALE YOUTH SOCCER PLAYERS

Kavon Bonakdar[1], Jake A. Melaro[1], Joshua T. Weinhandl[1]
[1]University of Tennessee, Knoxville
Kbonakda@vols.utk.edu

Introduction: Sport-related injuries increase in males throughout high school, with ~68% of adolescent injuries occurring in the lower extremity [1, 2]. According to a recent study, growth-related injuries account for 30% of all severe injuries that require at least 40 days of participation time lost in soccer academies. Thus, the reduction of growth-related injuries can be important in the prevention of long-term repercussions and maximization of players' potential development [3]. Asymmetries can represent a potential constraint that limits an athlete’s movement strategies which can in turn lead to motor behaviors adaptations that increase injury risk [4]. It has been shown that youth athletes tend to be more asymmetrical relative to experienced players [5]. Investigating loading asymmetries throughout puberty is especially important since children can experience delays or even regressions in some sensorimotor mechanisms [6]. Therefore, the purpose of this study was to evaluate symmetry in tibial accelerations in youth soccer players performing agility drills between maturation groups. It was hypothesized that peak acceleration and cumulative loading asymmetries would decrease as males experience puberty.

Methods: Thirty male youth soccer players were recruited from a local soccer club to voluntarily participate in this study. The Mirwald equation was used to determine how close the players were to their peak height velocity (PHV) and then stratify them into groups of pre-PHV, PHV, and post-PHV based on their relative proximity to PHV [7]. Inertial measurement units were placed on the participants bilaterally on the distal-medial tibia (1600 Hz; Vicon Blue Trident, Vicon Motion Systems Ltd, Oxford, UK). Participants completed a M-cone drill in which the participants ran in an M shape and made sharp cuts at each cone, before completing the drill again starting with a cut on the opposite leg. Peak accelerations and cumulative loading (acceleration integrals) were identified. Limb symmetry index was then calculated [8]. Data was analyzed using Python v3.10.4 (Python Software Foundation, Beaverton, OR, USA). A 2-way ANOVA (between=PHV group, within=drill direction) with a Holm correction was used to determine the statistical significance with R 4.2.1 (R Foundation for Statistical Computing, Vienna, AUST).

Results and Discussion: ANOVA results showed no interaction effect between drills and PHV groups for acceleration integral or peak accelerations, while only revealing a significant main effect between PHV groups for the acceleration integral ($F=6.380$, $p=0.005$). Post hoc t-tests showed that the PHV ($p=0.014$) and post-PHV ($p=0.014$) group asymmetries were statistically different from the pre-PHV group. No statistical trend regarding acceleration asymmetry was present.

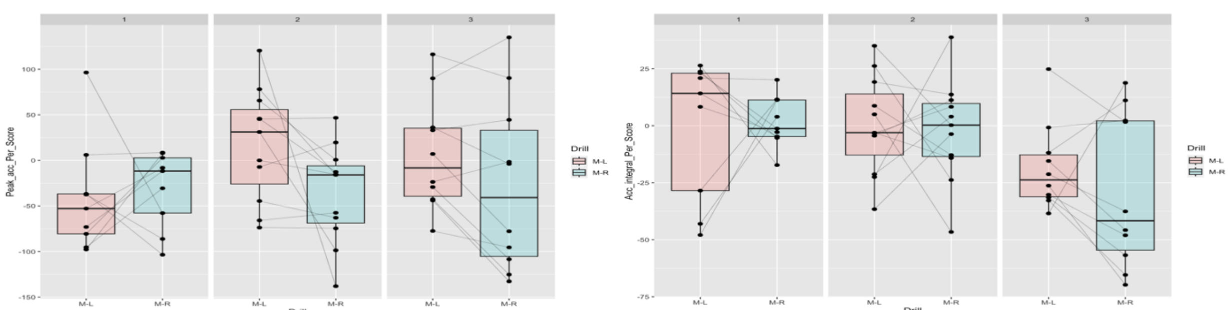

Figure 1. Box plot of the individual peak acceleration asymmetry (A) and cumulative loading asymmetry (B) between the lower limbs in each different of M-drills (M-drill left=pink and M-drill right=blue) relative to the maturation groups.

Significance: The large individual differences suggest that the players have inconsistent movement patterns. This could be a result of a lack of neuromuscular control that is prevalent during puberty. Therefore, specialized training in motor control strategy could be an effective measure for preventing injuries during puberty [5].

References [1] Comstock, R.D., Pierpoint, L.A. National high school sports-related injury surveillance study 2018-2019. 2020; [2] Verhagen, E. A. L. M., et al. BJSM, 43(13),1031-1035. 2009; [3] Monasterio, X., et al. IJSM, 44. 2023; [4] Newell, K. M., et al. Human Movement Science, 8(4), 403-409.1989; [5] Fousekis, K., et al. JSSM, 9(3), 364. 2010; [6] Quatman-Yates, C. C., et al., BJSM; 46(9), 649–655. 2012; [7] Mirwald, R. L. et al. MSSE, 34(4), 689-694. 2002; [8] Cuk, T., Variability and Evolution, 9(1), 19-32. 2001

DOES A FATIGUING OVERHEAD TASK ALTER TRUNK MUSCLE RESPONSES TO DYNAMIC MOVEMENTS?

Sam S. Vasilounis[1], Matthew S. Russell[1], Jaclyn N. Chopp-Hurley[1], and Janessa D.M. Drake[1]
[1]Kinesiology and Health Science, York University, Toronto, ON

Introduction: Overhead work poses substantial musculoskeletal stress in the upper extremities and trunk due to detrimental postures and sustained loading, which are risk factors associated with work-related musculoskeletal disorders (MSDs) [1]. The region of the pelvis and trunk that joins the lower and upper extremities in the kinetic chain is known as the lumbopelvic-hip complex (LPHC) [2]. Reduced physical demands on the upper extremity's distal segments depend on adequate energy transfer from the lower extremity through the trunk. The trunk musculature may have an impactful role on maintaining energy output during the overhead drilling task to fatigue. Dynamic control of the LPHC in this research refers to a level of stiffness that allows for the optimal production, transmission, and control of forces and motion to the distal limbs of the kinetic chain [2]. This may influence the dynamic control of the LPHC during dynamic tasks since one's capacity to stabilize the trunk heavily influences their capacity to control the lower extremity [2]. The purpose of this research was to examine the effect of an overhead drilling task to fatigue on trunk and lower limb kinematic and kinetic responses to dynamic tasks post overhead fatigue.

Methods: 12 healthy, right-handed adults (19-35yr; BMI 22.4 ± 1.7 kg/m^2) were instrumented with Xsens Awinda wireless motion tracker system (Xsens TM Technologies B.V. CA, USA) on the lower limb. Using a Delsys Trigno System (Delsys Inc., Natick, MA), a total of eight surface and two fine-wire intramuscular electrodes were used in quantify trunk and lumbopelvic electromyography (EMG). Specifically, surface EMG was collect from the left and right thoracic erector spinae at T4 and T9, lumbar erector spinae at L3 and gluteus medius. Moreover, indwelling EMG of the right thoracic erector spinae at T4 and T9. Further, trunk and right upper limb kinematics using a Vicon® MX system (Vicon Motion Systems Limited, Hauppauge, NY).

Participants executed a fatiguing overhead drilling (FOD) task while standing until volitional fatigue [3]. A single round of the FOD task consisted of a 50% duty cycle of 32 seconds of drilling and 32 seconds of rest. Prior to the FOD protocol, participants completed three sets of one maximum vertical drilling force (MVDF) measured with an ErgoFET push-pull force gauge (Hoggan Scientific, Salt Lake City, Utah, USA) affixed to the drill, where the maximum value between the three trials was used to determine the target force (50% of MVDF). During a FOD round, participants completed two sets of four postures, each consisting of four seconds of drilling while maintaining a the target force. Participants completed as many rounds as able until volitional failure confirmed via verbal communication or the inability to maintain target force during a FOD round.

Prior to and following the FOD, participants a series of dynamic tasks. These tasks included: single leg balance task (eyes open and eyes closed), single-leg squat (SLS), and single-leg drop landing (SLDL) task [2, 4]. For the single leg balance task, participants completed a fifteen-second unilateral quiet stand for the right and left leg. Individuals completed the SLS were instructed to place their hands on their hip and the floating limb was required to move posteriorly. Participants completed the SLDL by jumping from a 31cm box onto the force plate. Three successful trials of each task per leg were performed. A trial was considered successful for each dynamic task when participants regained or maintained balance and were able to return to their starting postures. Foot position was marked on the force plate for all dynamic tasks to ensure repeatability.

Results and Discussion: Results indicate that individuals displayed decreased peak left hip flexion during right SLS task POST-FOD (63.7º ± 4.5) compared to PRE-FOD (100.7º ± 5.8, p = 0.03). Furthermore, after the FOD task participants displayed increased peak centre of pressure displacement in the anterior-posterior axis (Figure 1, 34.1mm ± 5.4 and 55.9mm ± 3.7, p = 0.006) and increased knee varus during right SLDL task compared to prior the FOD task (-11.11º ± 2.2 and 8.3º ± 2.5, p = 0.01). In Figure 1 details the PRE and POST FOD task of the left foot SLDL and right foot SLDL for the left leg (left bars) and right leg (right foot), respectively.

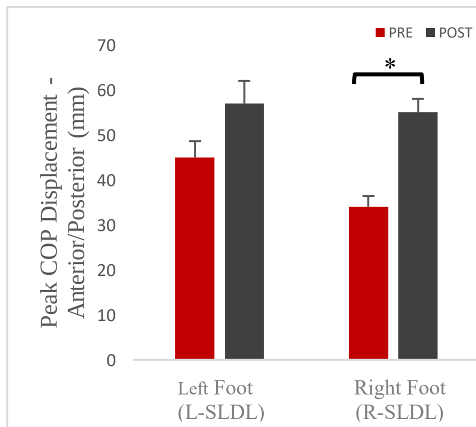

Figure 1: A comparison of peak COP-AP displacement in the left and right foot during the SLDL task pre and post FOD, respectively (*p = 0.006).

These initial results suggest there may be a decrease in LPHC dynamic control as displayed through the SLS and SLDL tasks as a result of overhead drilling task to volitional fatigue. Moreover, the difference between limbs in these dynamic tasks could be due to a deficit in unilateral LPHC control. Further examination between these changes in trunk and lower limb kinematics and kinetics, and trunk and hip electromyography are to be determined.

Significance: If preliminary findings are confirmed, it may provide insight into the role of the trunk on sustained overhead work to fatigue and the impact this fatigue plays on the dynamic control of the LPHC. This research may uncover data that individuals working in fields that maintain overhead drilling work may be at risk population for unknown deficits in LPHC dynamic control. Overall, these results should allow researchers could inform the use of rest and job rotation in relevant industries so as to not repeat exposures.

Acknowledgments: The authors wish to acknowledge the Centre of Research Expertise for the Prevention of Musculoskeletal Disorders (CRE-MSD) for financial support.

References: [1] Grive, J. et al. (2008). *Occupational Ergonomics* (8) 53-66.; [2] Kibbler, W. et al. (2006). *Sports medicine* (36); 189-98.; [3] Sood, D. et al. (2017) *Ergonomics* (10), 1405-1414.; [4] Cannon, J. et al. (2021). *Journal of Biomechanics* (116) 11024.

SEX DIFFERENCE IN LOWER EXTREMITY JOINTS' KINEMATICS COORDINATION DURING THE GAIT CYCLE PHASES

Abed Khosrojerdi[1], Nathan Q. Holland[1], Elham Alijanpour[2], Hunter J. Bennett[3], Stacie I. Ringleb[1*]
[1]Department of Mechanical & Aerospace Engineering, Old Dominion University, Norfolk, VA, USA
[2]School of Rehabilitation, Old Dominion University, Norfolk, VA, USA
[3]Department of Human Movement Science, Old Dominion University, Norfolk, VA, USA
*Corresponding author's email: sringleb@odu.edu

Introduction: In recent decades, kinematics coordination research has moved gait analysis literature from examining gait as a dynamic system to focalized analysis of joint coordination [1]. Researchers and clinicians can examine coordination patterns (CP) to better understand neuromuscular changes following various gait interventions or in comparing populations with neuromuscular disorders [2]. On the other hand, sex differences are also one of the important characteristics that should be considered in gait interventions [3-4]. Literature suggests sex differences in gait parameters [5-6]. For instance, Ko et al found that females have a greater ankle range of motion (ROM) while males have a greater hip ROM [7]. Although sex differences in CP have been reported during cutting maneuvers [8] and running [9-10] to our knowledge, there is no study to investigate sex differences in kinematics CP at each phase of the gait cycle. Hence, in this abstract, we aimed to investigate sex differences in lower extremity joints' kinematics coordination during the gait cycle phases. We hypothesize that coordination patterns might be different between males and females due to physiological and anatomical differences.

Methods: Five females (age: 23.6±3.64 years, mass: 73.99±21.61 kg, height: 167±4.5 cm) and five males (age: 20.2±2.16 years, mass: 87.74±24.5 kg, height: 184±1.2 cm) were asked to walk on a walkway five times. A nine-camera VICON motion capture system and plug-in gait model were used to record lower extremity kinematics. Three gait cycles were manually separated by loading response (LR), mid-stance (MSt), terminal stance (TSt), pre-swing (PS), initial swing (ISw), mid-swing (MSw), and terminal swing (TSw) for each participant. After pre-processing kinematics data in Nexus software, ankle/knee, knee/hip, and ankle/hip kinematics CP in the sagittal plane were computed using a modified vector coding method [11] by a custom MATLAB code (The Mathworks, Natick, MA). Then the average of CP in each gait phase was extracted for statistical analysis. The independent t-test was employed using SPSS software to investigate differences between sexes.

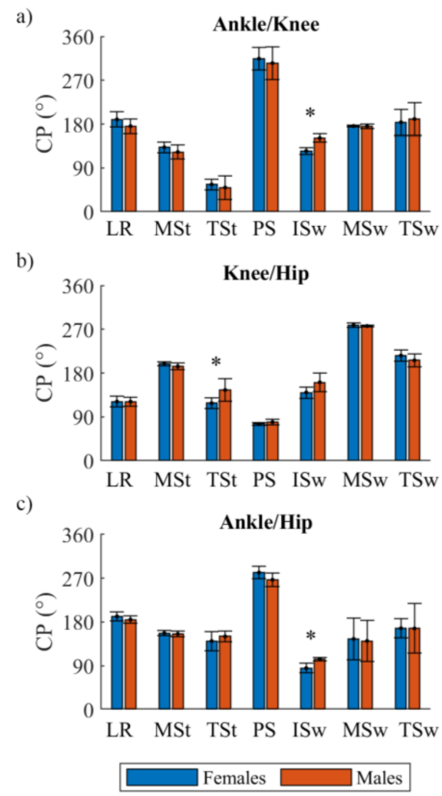

Figure 1: The average CPs of ankle/knee (a), knee/hip (b), and ankle/hip (c) during each phase of the gait cycle.
* Shows the significant difference between males and females.

Results & Discussion: The results showed that the ankle/knee CP is anti-phase (ankle dorsi flexion and knee extension) during the ISw in both groups; however, females use the ankle more than the knee for foot clearance, but males use the knee more than the ankle for this purpose, $p=0.001$, (Fig 1.a). In addition, the knee/hip CP is anti-phase (knee flexion, hip extension) during the TSt in both groups; however, females use the knee more than the hip for heel rise, but males use the hip more than the knee, $p=0.046$, (Fig 1.b). These results revealed that females use the distal joint for foot rise, while males use the proximal joint, which is similar to findings that females had greater ankle ROM while males had more hip ROM in males. Lastly, in ankle/hip, females have an in-phase CP (ankle dorsi flexion and hip flexion) while males have an anti-phase CP (ankle dorsi flexion and hip extension) during the ISw phase, however, both groups use the ankle more than hip, $p=0.004$, (Fig 1.c). The difference in hip motion during the ISw phase may be due to pelvic anatomical differences between males and females. For example, because the position of the hip joint center is different in males [12], they may reach extension sooner than females during ISw.

Significance: The results indicated males and females employ different CPs during TSt and ISw phases. Females' gait kinematics CP is characterized by distal joint dominancy while males use to have proximal joint dominancy. These differences should be considered in the clinical setting and gait interventions.

References: [1] Krasovsky et al. (2010), *Neurorehabilitation and neural repair* 24(3); [2] Needham et al. (2015), *J Biomechanics* 48(12); [3] Kerrigan et al. (1998), *American Journal of Physical Medicine & Rehabilitation* 77(1); [4] McKean et al. (2007), *Clinical Biomechanics* 22(4); [5] Cronstrom et al. (2016), *Gait & posture* 49; [6] Frimenko et al. (2015), *Physiotherapy* 101.3; [7] Ko eat al. (2011), *J Biomechanics* 44(10); [8] Pollard et al. (2005), *J applied biomechanics* 21(2); [9] Takabayashi et al. (2018), *J Foot and Ankle Research* 11(1); [10] Boyer et al. (2017), *J Sports Sciences* 35(22); [11] Needham et al. (2014), *J Biomechanics* 47(5); [12] Lewis et al. (2017), *The Anatomical Record* 300(4).

THE EFFECT OF DUAL TASK ON MUSCLE ACTIVITY DURING GAIT INITIATION

Ke'Vaughn Waldon[1*], Angeloh Stout[1], Kaitlin Manning[1], Brandon Nunley[2], Aakriti Jaiswal[1], Gu Eon Kang[1,3**]
[1]The University of Texas at Dallas, Department of Bioengineering, Richardson, TX
[2]The University of Texas at Austin, Department of Biomedical Engineering, Austin, TX
[3]The University of Texas Southwestern Medical Center, Department of Plastic Surgery, Dallas, TX

Email: *Ke'vaughn.Waldon@utdallas.edu, **GuEon.Kang2@utdallas.edu

Introduction

Cognitive dual task is known to lead to disrupted balance control of gait (i.e., dual task gait) across people of all ages [1,2]. Several studies examined potential causal factors of the disrupted balance control during dual task gait such as activation of lower extremity muscles. For example, it has been reported that older adults increase muscle coactivation as a response to cognitive dual task while in steady state gait [3]. Although such studies provided valuable insights of possible roles of lower extremity muscles during dual task gait, studies that have examined probably more important phase of gait in terms of balance control, such as gait initiation, is sparse. Here, we studied the effects of dual task on muscle coactivation in healthy young adults during the gait initiation phase.

Methods

Eleven healthy young adults (age=20±2 years; 7 male; body mass index=23.58 ±2.90 kg/m^2; no history of neurological or orthopedic condition that might affect gait) were recruited from the university community. Eight Delsys Trigno Wireless Electromyography sensors sampling at 2000Hz were placed bilaterally on the Vastus Lateralis (VL), Biceps Femoris (BF), Tibialis Anterior (TA), and Gastrocnemius Lateralis (GL). A maximum voluntary contraction (MVC) was collected for each muscle. Muscle activity was calculated based on normalizing MVC data to dynamic trial data.

Each participant was asked to stand with one foot on each Kistler force platform (n=2, sampling = 1000Hz). Then, participants were instructed to walk over a 10-meter walkway at a self-selected speed without an additional task (single task; ST) and repeat that walk while being provided a starting number to count downward (dual task; DT). We used Visual3D to identify the phases of gait initiation using ground reaction forces (GRF). Gait initiation was identified through the onset (step max) of the GRF and offset (toe off, step min). The calculation of muscle co-contraction activation comparison was defined as, Co-contraction = ((Low EMG/ High EMG) x (Low EMG + High EMG) x100) [2]. The two task conditions were compared (ST vs DT) using a paired two tailed t-test ($p<0.05$).

Results and Discussion

Results are summarized in Table 1. Overall, muscle activity decreased during dual task compared to single task. Muscle co-contraction increase during dual task. However, significant differences were found only in GL/TA muscles.

Table 1. Comparisons of muscle activity (%) and co-contraction (%) between ST and DT conditions. *Swing = Stepping Limb**

		ST	DT	P-value			ST	DT	P-value
Activity	Swing BF	7.02±4.46	6.30±3.26	0.43	Activity	Swing VL	4.29±1.31	6.04±3.05	0.06
	Stance BF	7.61±5.12	6.40±3.94	0.12		Stance VL	5.87±3.92	5.45±3.28	0.51
Activity	Swing GL	10.83±10.35	6.47±4.27	0.18	Co-contraction	Swing BF/VL	0.40±0.11	0.404±0.115	0.985
	Stance GL	28.31±20.85	29.98±28.35	0.74		Stance BF/VL	0.44±0.16	0.424±0.137	0.752
Activity	Swing TA	9.19±4.05	9.32±4.17	0.93	Co-contraction	Swing GL/TA	0.48±0.12	0.478±0.152	0.919
	Stance TA	15.12±11.51	11.29±8.02	0.06		Stance GL/TA	1.18±0.25	0.915±0.288	0.004

Significance

The study had one significant difference ($p<0.05$) for Stance GL/TA in the muscle co-contraction during dual task, which provides some perspective on the effects of the dual task condition. Though, the participants were young and healthy, the knowledge gained can be used as a benchmark for guiding discernment quantification for lack of balance under cognitive load in aging adults.

References

[1] Uemura, K et al., (2012). Gait & Posture, 35(2), 282–286.;[2] Khanmohammadi, R et al., (2016). Gait & Posture, 43, 148–153.;[3] Hortobágyi, T et al., (2009). Gait & Posture, 29(4), 558–564.

BIOMECHANICS DISTINGUISH PEOPLE WITH VS WITHOUT MILD COGNITIVE IMPAIRMENT DURING MOTOR-COGNITION TESTS.

Madeleine E. Hackney[1*], Meredith D. Wells, Clara Beth La Follette, Meghan Kazanski, Michael Rosenberg
[1]Department of Medicine, Division of Geriatrics and Gerontology, Emory University, Atlanta, GA
*Corresponding author's email: mehackn@emory.edu

Introduction: Mild cognitive impairment (MCI) results in motor and cognitive impairments that interact to affect function. The four-square step test (FSST) is a validated assessment of motor-cognition and mobility for older adults and clinical populations such as Parkinson's, involving multidirectional stepping over obstacles. Participants are asked to step around a grid made of 1" canes, placing both feet in each square. Participants step in a clockwise direction immediately followed by the counterclockwise direction. Typically, faster FSST times indicate better balance and mobility. The FSST has high utility because time to complete is easily measured. [1] Yet, little is known about the biomechanics of performing the FSST. This study's goal was to determine the effect of age and cognition on lower limb joint angles during the FSST.

Methods: Eight healthy young adults (HYA: 22.7±3.4 years), 7 healthy older adults (HOA: 66.3±11.3 years), and 8 adults with MCI (MCI: 69.3±7.3 years) completed three FSSTs while wearing inertial sensors. Outcome variables included peak hip flexion, hip abduction, knee flexion, and ankle dorsiflexion angles of leading and trailing limbs during lateral stepping, and time to complete. Lateral steps were selected as the steps of interest due to the inherent instability during side stepping. Independent *t*-tests were used to compare variables between HYA and HOA, and between HOA and MCI.

Results & Discussion: Completion time was significantly different between HYA and HOA (p=0.002), but not between HOA and MCI. Peak hip flexion was not different in the leading or trailing limbs between HYA and HOA, but MCI showed less peak hip flexion in both the leading (p=0.038) and trailing (p=0.032) limbs than HOA. MCI also showed a trend toward less peak knee flexion in the leading and trailing limbs than HOA. Differences in time to complete between HYA and HOA may indicate an effect of age, while differences in joint angles between HOA and MCI may illustrate an effect of cognition.

Significance: These results suggest that cognitive status may impact the kinematic strategies used to perform multidirectional tests of motor-cognition. Biomechanical analyses are critical because they are more sensitive and can detect differences in balance and mobility as well as completion strategy that time to complete cannot. Future investigations should examine additional biomechanical variables that may have led to the differences in joint flexion and completion time including step width and time spent in stance vs. swing.

Acknowledgements: This project was supported by Emory Office of the Senior Vice President for Research and by the NIH/NIA R01 AG062691-01 and NIH/NIA 3R01AG062691-02S2 (PI: Hackney).

References:

[1] Dite W & Temple VA. *Arch Phys Med Rehabil.* 2022;83(11): 1566-1571.

HOW DOES MUSCLE SYNERGY RECRUITMENT CHANGE AFTER KNEE EXOSKELETON GAIT TRAINING

Siddharth R. Nathella[1*], Dawit Lee[1], Aaron J. Young[1], Lena H. Ting[1,2]
[1]George W. Woodruff School of Mechanical Engineering, [2]Wallace H. Coulter Department of Biomedical Engineering, Georgia Institute of Technology
*Corresponding author's email: snathella@gatech.edu

Introduction: Genu recurvatum is a condition characterized by hyperextension of the knee joint during walking, which can impede mobility. Here, we investigate how gait training using a knee exoskeleton and visual biofeedback affects muscle coordination in children with genu recurvatum. Previous studies have shown that children with cerebral palsy undergoing exoskeleton rehabilitation exhibit an increase in the number of muscle synergies used and a decrease in the variability accounted for by a single muscle synergy (VAF_1) after training [1] and have indicated that VAF_1 can be a valuable metric in gait rehabilitation as it provides insight into the complexity of motor control [2]. However, it remains unclear whether similar outcomes in VAF_1 are observed in other populations undergoing exoskeleton biofeedback training, and if the changes observed in VAF_1 indicate an individual relying less on a specific muscle synergy. We hypothesize that as the subjects complete the training targeting a specific knee-kinematic profile, VAF_1 will decrease over the course of the training and as VAF_1 decreases, the contributions each required synergy will become more similar.

Methods: Two subjects participated in a training protocol involving knee exoskeleton assistance and a visual biofeedback game based on real-time knee flexion. Each subject completed 4-6 visits, which included a 30-minute training session with 90 seconds of non-intervention baseline and post-training walking. During the training sessions, the subject walked on a treadmill at their own pace while the knee exoskeleton would assist the subject as needed. The visual biofeedback game rewarded the subject for achieving the target knee flexion profile and provided feedback for hyperextension or premature flexion. Electromyography (EMG) data was analysed from 5 muscles on each subject during three visits. Non-negative matrix factorization (NMF) was used to extract a single muscle synergy, and the VAF1 was computed comparing single synergy reconstruction to the original EMG data. Additionally, three synergies were extracted to reach 90% VAF and the VAF for each synergy was computed in order to evaluate changes to the muscle synergy recruitment. A bootstrapping approach was used to evaluate the robustness of the synergy analysis, where a significant change was considered for non-overlapping 90% confidence intervals.

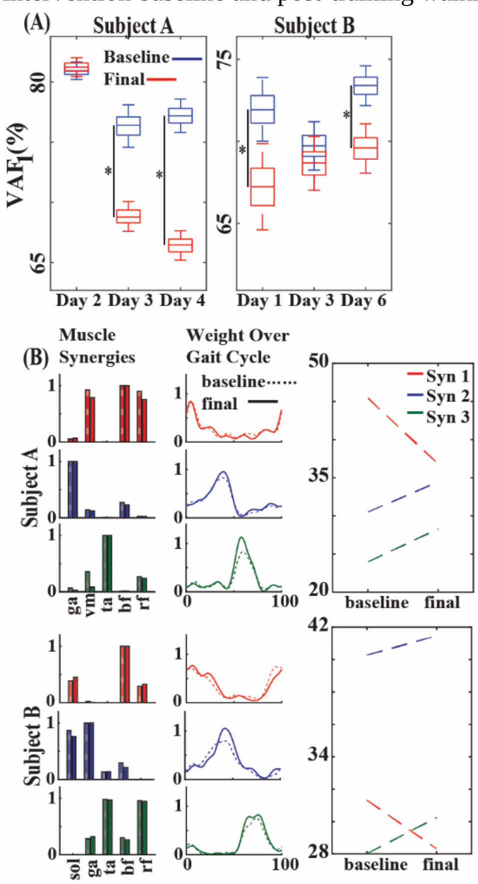

Figure 1: A) VAF1 on each collected day for Subjects A & B. significant reductions are noted by a *. B) Representative muscle synergies with the change in VAF for each synergy, from the days with the largest VAF1 change.

Results & Discussion: A significant decrease in VAF_1 was observed on two visits for both subjects (Fig.1A), suggesting increased motor control complexity after training. Both subjects needed three muscle synergies to achieve a 90% VAF (Fig.1B), which along with the structure of the muscle synergies, remained constant over the training for each subject. The constant synergies suggest that during the training, changes to the VAF_1 are due to changes in the recruitment of the existing synergies during the gait cycle. Looking at how the total VAF was spread out over the three synergies, we see differing results between Subject A and Subject B. On days with a decrease in VAF_1, we see Subject A has a significant decrease in the VAF of the most contributing synergy with increased recruitment of the plantar flexor synergy, and a more even contribution of the three synergies (Fig.1B). With Subject B, there was a slight but ultimately insignificant increase in the plantar flexor synergy VAF, and no trend towards more even VAFs between the three synergies. This suggests that despite the VAF_1 changes observed, this does not necessarily translate to less reliance on a particular synergy overall. This difference between the subjects could be explained by different levels of effectiveness of the training, as Subject A saw larger VAF_1 changes.

Significance: Understanding changes in motor control during exoskeleton/robot-assisted rehabilitation is crucial for evaluating the effectiveness of these therapies for motor learning. Overall, this work shows that training with the knee exoskeleton and visual biofeedback can result in reduction in VAF_1 for children with genu recurvatum. However, the reduction in VAF_1 in does not guarantee a tendency for an individual to rely less on one specific synergy, and that a further analysis of the synergy recruitment can give some insight into the particular strategy encouraged by the training.

Acknowledgements: *The authors would like to acknowledge Shriner's International Hospital for Children and the Imlay Foundation for their contributions to funding this work.*

References: [1] B. C. Conner et al. (2021), Journal of Biomechanics. [2] M. H. Schwartz et al. (2016) Developmental Medicine & Child Neurology

APPROPRIATENESS OF LIMB SYMMETERY CALCULATIONS AND CUTOFFS IN FUNCTIONAL TESTING

Kristen Renner[1*], Alexis Henderson
[1]University of Arizona College of Medicine Department of Orthopaedic Surgery
*Corresponding author's email: kristenrenner@arizona.edu

Introduction: Limb symmetry index (LSI) for functional tasks such as hopping, jumping, walking and running has been used to assess a patient's injury risk and/or readiness to return to sport. The majority of clinic-based return to sport testing calculates LSI as the operative side divided by the non-operative side times 100%, in a healthy population this translates to non-dominant (ND) divided by dominant (D) times 100% [1]. An LSI outside of the 90-110% range has been used in many clinics and research laboratories as the cutoff value used to determine readiness to return-to-sport (RTS) and/or indicates an increased injury risk [2-4]. However, some groups use 5% or other unspecified cutoff values. Additionally, many different approaches are taken to calculate the same LSI including the best attempt, the average of multiple trials prior to calculating LSI, the average of trial-by-trial LSI and many articles do not specify which approach was used. Therefore, the purpose of this study is to investigate the impact of various approaches to calculating LSI and the potential impact on RTS criteria and injury risk assessment in functional testing. We anticipate categorizations of individuals who are "at risk" will vary depending on the approach of LSI calculation.

Methods: 20 healthy recreationally active young adults (10M/10F) completed 5 trials of a triple hop (TH) and single hop (SH) and 3 trials of the 6m hop (6m), peak knee flexion during single limb squat (SLS), and the Y-balance anterior (YAnt), posteromedial (YPM), posterolateral (YPL) and composite (YComp) scores. TH, SH, YAnt, YPM and YPL were normalized to height. LSI was then calculated with the best trial (Best), worst trial (Worst), the average of trials and the median of trials. Participants were then categorized as "low risk" with an LSI 95% and 105%, "moderate risk" with an LSI between 90-95% or 105-110%, or "high risk" with an LSI less than 90% or greater than 110%.

Results & Discussion: The mean and standard deviation for each task is reported in Table 1. There is large variability in how an individual is categorized depending on how the LSI is calculated. In the SH categorization only 5 of the 20 participants had consistent categorization across all four methods. When looking at just the "best" and "average" methods of calculating 15/20 participants had agreement. Similarly, in TH 7 participants had different categorization between "best" and "average" methods of calculating LSI (SLS=7, 6m=6, YAnt=3, YPM=11, YPL=6, YComp=5). This study should be repeated with patient populations undergoing RTS testing to better understand how LSI calculation method may impact clearing patients to RTS.

Significance: While it may seem fair or kind to the patient undergoing RTS testing to take their best score, we question if that is the method of calculating LSI that is most indicative of readiness to RTS, or in the case of a healthy individual if it is predictive of injury risk. An argument could be made for using the median or even the worst trial of the testing series as the median of 7 attempts would remove outliers and would have the benefit keep the calculation of LSI in the clinic simple. Future investigations into task specific and injury specific cutoff values for LSI would be beneficial.

Table 1: Mean and standard deviation for the nondominant (ND) and dominant (D) limbs for each task

	6m	TH	SH	SLS	YAnt	YPM	YPL	YComp
ND	2.38±0.75	0.34±0.05	0.14±0.03	87.1±13.0	0.69±0.08	1.04±0.14	0.7±0.08	1.08±0.16
D	2.27±0.66	0.35±0.04	0.15±0.03	89.4±12.9	1.06±0.13	93.13±9.73	1.08±0.13	95.65±10.03

Table 2: Limb symmetry index for each participant calculated with the Best trial (B), Worst trial (W), median (M) and average of trials (A) for each task. Red indicates "high risk" categorization, yellow is "moderate risk" and green is "low risk". White cells indicate that the participant did not complete the task according to instructions.

SH				TH				SLS				6m				YAnt				YPM				YPL				YComp			
B	A	M	W	B	A	M	W	B	A	M	W	B	A	M	W	B	A	M	W	B	A	M	W	B	A	M	W	B	A	M	W

Acknowledgements: This research was supported in part by the University of Arizona's Undergraduate Research Program.

References: [1] Reid et al. (2007), *Phys Ther* 37(3). [2] Toole et al. (2017), *JOSPT* 47(11). [3] Gokeler et al (2016), *KSSTA* 25. [4] Adams et al. (2012), *JOSPT* 42(7). [5] Queen et al. (2020), *J Biomech* 99:109531.

DEEP LEARNING-BASED CONTROL OF A POWERED KNEE-ANKLE PROSTHESIS

Christoph P. O. Nuesslein[1*], Aaron J. Young[1]
[1]Exoskeleton and Prosthetic Intelligent Controls Lab, Woodruff School of Mechanical Engineering, Georgia Institute of Technology
*Corresponding author's email: cnuesslein3@gatech.edu

Introduction: Semi- and fully-active lower-limb prosthetic controllers attempt to span the gap between robust operation and ease of scalability to new wearers or environmental contexts. Unfortunately, designing controllers that can be finely adjusted to a specific user or locomotion mode typically makes them more robust to that context, but less generalizable overall. Existing devices will often employ finite state machines (FSMs) that split up the gait phase into stance and swing impedance controllers, like that developed by Bhakta et al. [2]. However, these controllers typically require much hand-tuning of each of their component variables, an issue that is only compounded when using a separate controller for different locomotion modes (e.g. level-ground walking, movement on stairs, inclines, and so on). In particular, the stance phase often requires particular care in its controller adjustment to achieve operation robust enough for the user to move comfortably. There is thus a clear necessity for controllers that can provide assistance that is both robust and generalizable.

Deep learning techniques could provide a solution to this control issue because of their ability to synthesize outputs by finding underlying patterns in time-series sensor data. They have already been shown to accurately estimate joint torques based on reduced sensor information [3]. Here, we present a similar approach by replacing the stance phase controller(s) of the FSM on an active knee-ankle prosthesis with a deep learning model that takes the device's sensors as input and outputs direct torque control to the motors. We expect that a deep learning model trained on this sensor data will be able to closely match the performance of an FSM-based set of discrete impedance controllers (FSM-IC).

Methods: Prosthesis sensor data collected on the Open-Source Leg (OSL) (Fig. 1B) [1] from level-ground walking trials at varying speeds with four male transfemoral amputees were analyzed. These sensors included inertial measurement units (IMUs) on the foot, ankle, knee, and thigh of the prosthesis, as well as an in-series 6-axis load cell and motor encoder angles at the knee and ankle joints (Fig. 1A). The ground truth labels were the torque commands for the knee and ankle joints generated by a hand-tuned FSM-IC [2].

The models used here were temporal convolutional networks (TCNs) adapted from Molinaro et al. [3]. One model was trained per joint, so the ankle model used commanded ankle joint torque as its ground truth while the other model used commanded knee torque as its target data (Fig. 1A). Each model comprised five residual blocks with a channel size of 50 and a kernel size of four. Performance of the models was determined using leave-one-subject-out validation.

Results & Discussion: Leave-one-subject-out validation resulted in torque estimates with R^2 values of 0.68 ± 0.06 at the knee and 0.55 ± 0.12 at the ankle, as well as subject weight-normalized RMSE of 0.26 ± 0.04 Nm/kg and 0.11 ± 0.03 Nm/kg at the knee and ankle respectively (Fig. 1C). Representative averages of these stance-phase estimates compared to the FSM-IC torques are shown in Fig. 1D. This level of performance error between the FSM-IC controller output and the TCN-generated commanded torque estimates is in line with our expected result, implying that properly tuned TCNs can provide suitable commanded torque to a knee-ankle prosthesis during level-ground walking. Since this estimation encompasses only walking data, it would be intriguing to explore TCN performance across a range of locomotion modes. Expanding the dataset explored might allow the TCN to leverage its nature as a continuous estimator to provide more seamless transitions between locomotion modes compared to the ones employed by FSM-ICs.

Significance: TCN-based control shows promise as an alternative to typical impedance-controlled prosthesis operation. Here, we showed that TCNs can not only capture the complexity of commanded torque at all actuated joints, but that they can also generalize well to new subjects. With these capabilities, deep learning-based torque control could help to make prostheses more robust, easier for new users to adapt to, and more readily scalable to new environmental contexts.

Acknowledgements: Funding supplied by NDSEG fellowship and NIH Director's New Innovator Award DP2-HD111709.

References: [1] Azocar et al. (2020), *Nature Biomed. Eng.* 4, 941-953, [2] Bhakta et al. (2020), *Military Medicine*, Vol. 185, Issue Supp. 1, pp. 490-499, [3] Molinaro et al. (2022), *IEEE TMRB*, Vol. 4, No. 1, pp. 219-229.

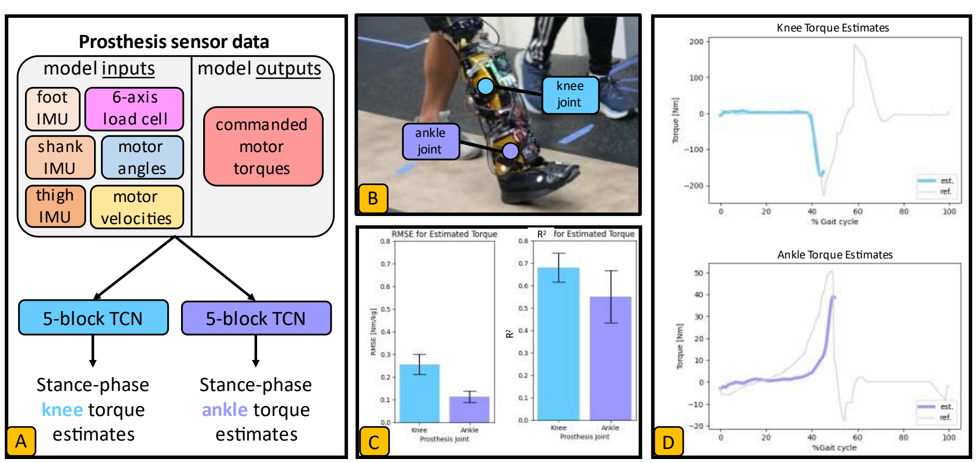

Figure 1: (**A**) The training pipeline of the Temporal Convolutional Networks (TCNs) used here take sensor data from the Open-Source Leg (OSL) [1] and use the joint torques from an impedance controller [2] as the training labels. (**B**) The OSL is an active knee-ankle prosthesis, shown here during level-ground walking. (**C**) RMSE and R^2 values are shown for each joint's torque predictions. (**D**) Preliminary results of stance phase torque estimates are mapped over representative assistance profiles.

EFFECTS OF GENDER ON RUNNING ECONOMY AND PLANTARFLEXOR FUNCTION IN MIDDLE-AGED RUNNERS

Zoey C. Kearns[1*], Eduardo Martinez III[2], Max R. Paquette[2]
[1]University of Maryland, College Park
[2]University of Memphis
*Corresponding author's email: zckearns@umd.edu

Introduction: Comparisons of running biomechanics between men and women of different ages have been scarce and inconsistent as some studies find that women run with equal or lower magnitude of plantarflexor kinetics[1,2] or the opposite.[3] In older runners, changes in biomechanical function (e.g., muscle and tendon characteristics, joint kinetics) may contribute to declines in performance,[4–6] but previous investigations have not measured Achilles Tendon (AT) stiffness. Lower AT stiffness may require more plantarflexor force and higher rate of muscle force production to sufficiently power the muscle-tendon unit during propulsion. These age-related factors may contribute to higher relative metabolic costs and as a result, higher perceived running effort and less enjoyment in aging runners that could differ between the genders. The **purpose** of this study was to assess the influence of gender on running economy (RE), plantarflexor function, and AT stiffness in middle-aged runners and identify associations between AT stiffness and RE and measures of ankle plantarflexor function. We hypothesized that women would run with a lower magnitude of ankle plantarflexor torque, positive ankle power and work, and AT stiffness. Additionally, we expected that a stiffer AT would be associated with more efficient running economy and improved plantarflexor function.

Methods: 20 middle-aged runners (10 women, 51±5 yrs) underwent laboratory testing for RE, spatiotemporal, ankle joint kinetic and kinematic variables, isometric plantarflexor torque, and AT stiffness during isometric contractions. Running variables were collected at preferred speed and 5% faster than preferred speed. Independent t-tests were used to compare dependent variables between genders. Pearson correlation coefficients were calculated to assess the associations between AT stiffness and $\dot{V}O_2$max, RE, and measures of plantarflexor function.

Results & Discussion: There were no significant differences in preferred speed, running economy, isometric plantarflexor torque, peak ankle positive power, hip to ankle positive work ratio, and AT stiffness between genders. Women had a lower $\dot{V}O_2$max ($p=0.03$) and ran with lower peak ankle PF torque, peak ankle negative power, ankle positive work, ankle negative work, and total negative and positive work ($p<0.05$; **Figure 1**). There was no correlation between AT stiffness and $\dot{V}O_2$max, running economy, and measures of plantarflexor function ($p>0.05$). Both genders ran at similar effort (RE) and preferred speed (2.7±0.4 m/s), making their ankle plantarflexor characteristics and biomechanics easily comparable. Additionally, there was no difference in strike pattern between the genders, so the different plantarflexor demands of varying strike patterns should not be considered a confounding variable. Previously, 50-70 year old women runners (2.7 m/s) ran with higher peak positive ankle power and ankle positive work than men of the same age.[3] This speed corresponded to 103% and 94% of preferred for women and men, respectively. Thus, the conflicting findings may suggest that gender differences could be speed dependent.

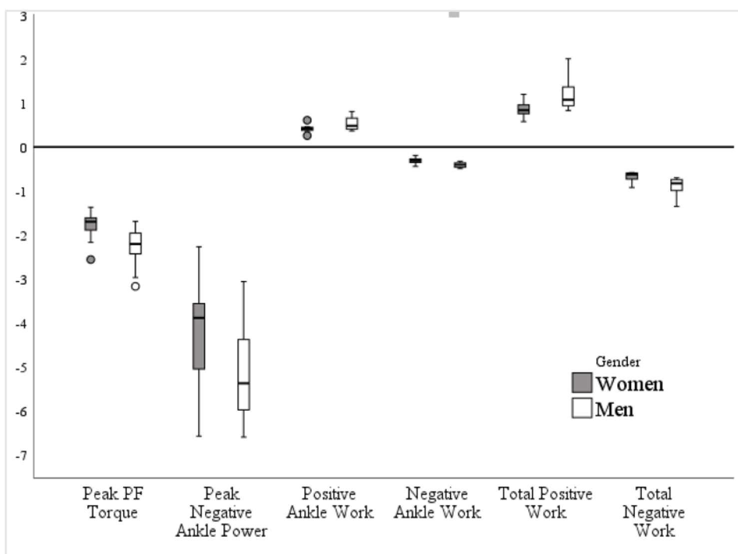

Figure 1. Peak ankle plantarflexor (PF) torque ($Nm \cdot kg^{-1}$), peak negative ankle joint angular powers ($W \cdot kg^{-1}$), positive and negative ankle joint angular work ($J \cdot kg^{-1}$), and total positive and negative work ($J \cdot kg^{-1}$) at the runner's preferred speed.

Significance: Our findings, compared to previous literature, suggest that gender differences in ankle biomechanics of middle-aged runners may be speed dependent. This informs future investigations, with the testing demands being a factor in predicting gender differences in running biomechanics, as well as recommendations for footwear and training.

References: [1] Boyer at al. (2017) *J Sports Sci* 35(22); [2] Willson et al. (2015) *J Biomech* 48(15); [3] Paquette (2017) *World Congress of Biomechanics* [4] Paquette et al. (2018) *Med Sci Sports Exerc* 98(3); [5] Paquette et al. (2021) *Scand J Med Sci Sports* 31(2); [6] Willy & Paquette (2019) *Sports Med Arthrosc Rev* 27(1).

TRUNK POSTURE VARIATIONS DURING WALKING WITH ROLLING PERTURBATIONS

Kierstin L. Niemeyer[1*] & Nathaniel H. Hunt[1]
[1]Department of Biomechanics, University of Nebraska at Omaha, Omaha, NE USA
*Email: kierstinniemeyer@unomaha.edu

Introduction: Auditory feedback may augment spatial perception of dynamic posture and inform improved feedback control and stability of walking. Human walking is inherently unstable and requires active feedback control to maintain upright posture in the frontal plane, especially when subjected to reduced sensory information such as restricted vision [1]. The trunk accounts for almost half of an individual's body mass and thus is one of the largest contributors to the CoM control [2]. To design an effective mapping from dynamic posture to auditory feedback requires better understanding of the ranges of posture during normal and perturbed walking. Therefore, the purpose of this was to measure the effect of continuously rolling walking surface perturbations (range = ± 10 deg) on the range of trunk angles exhibited. This is the first of a series of studies towards our long-term goal of designing an auditory sensory augmentation device to improve frontal plane stability during destabilized walking conditions.

Methods: One healthy female, age 23, participated in this pilot study. The participant walked on the Computer Assisted Rehabilitation Environment (CAREN) (Motek Medical BV, Amsterdam, The Netherlands) treadmill at a speed on 1.0 m/s in two different conditions—(1) normal, unperturbed and (2) platform perturbed. Perturbations were randomly generated along a standard normal distribution, spanning $\pm 10^{\circ}$ of platform roll and delivered continuously during the perturbed trial to create a destabilizing walking environment. Trunk and lower body kinematics were measured using ten motion capture cameras (Vicon, Oxford Metrics Inc., Oxford, UK) and reflective markers. Trunk angle was defined as the angle of the thorax relative to the pelvis in the frontal plane, with positive values indicating rightward lean and negative values indicating leftward lean [3]. Step width was calculated as the mediolateral distance between heel markers at instances successive heel strikes [2] while standard deviation of these values during each condition defined step width variability [4].

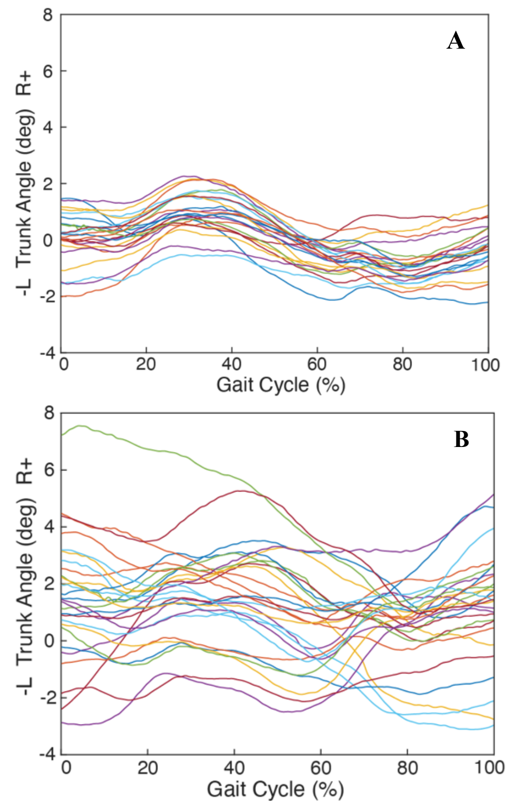

Figure 1: Gait cycle is defined as right heel strike to right heel strike. **(A)** Trunk angle in frontal plane during 30 seconds of normal treadmill walking normalized gait cycle; **(B)** Trunk angle in frontal plane during 30 seconds of platform perturbed treadmill walking normalized gait cycle.

Results & Discussion: Frontal plane trunk angle increased during walking with continuous rolling perturbations compared to normal walking. Absolute mean peak trunk angle during normal walking was found to be $1.44^{\circ} \pm 0.96^{\circ}$ (Fig. 1A), while absolute mean peak trunk angle during perturbed walking conditions was $3.64^{\circ} \pm 1.08^{\circ}$ (Fig. 1B). During normal walking frontal plane trunk angle spanned a range of -2.71° to 2.76° compared to a range of -6.20° to 7.55° during perturbed walking. Mean step width and step width variance increased during perturbed walking compared to normal walking. Normal walking resulted in an average step width and step width standard deviation of 130.00 ± 19.98 mm (mean $\pm$ std, Fig. 2). Perturbed walking conditions resulted in an average step width and step width variability of 141.63 ± 98.59 mm (Fig. 2). Absolute mean peak platform slope during the perturbed condition was found to be $4.46^{\circ} \pm 2.95^{\circ}$.

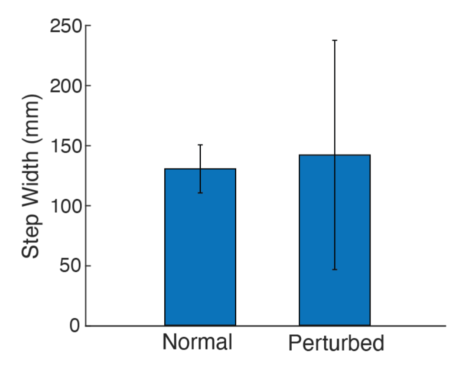

Figure 2: Rolling perturbations increase the range of step widths. Step width and step width variability during normal walking compared to conditions of platform perturbed walking.

Significance: Results from this study demonstrate that frontal plane trunk lean and step width are increased by continuous rolling perturbations to the walking surface. More so, the results suggest that the trunk lean is correlated with the severity of perturbations delivered. The results from this study will be used for determining design parameters for a future study. For this study we are developing a real-time biofeedback system that delivers auditory cues with information representing trunk motion in the frontal plane during walking. Thus, the aim of the future study is to investigate the efficacy of using real-time auditory feedback that system during destabilizing walking conditions to minimize side-to-side trunk lean and improve dynamic balance.

Acknowledgments: We would like to acknowledge the University of Nebraska Omaha COBRE grant for funding this research.

References: [1] Bauby & Kuo (2000), *J Biomech* 33; [2] Arvin et al (2016), *J Biomech* 49; [3] Shih et al. (2021), *J Biomech* 114; [4] Rosenblatt & Grabiner (2010), *Gait & Posture* 31.

QUADRICEPS STRENGTH BUT NOT MUSCLE SIZE IS RELATED TO UNDERLOADING DURING WALKING IN ACL-INJURED INDIVIDUALS

Zoe Barnett[1], Beyza Tayfur[1], Reagan Recchia[1], Alexa K. Johnson[1*], Riann M. Palmieri-Smith[1,2,]
[1]School of Kinesiology, University of Michigan, Ann Arbor, MI
*Corresponding author's email: akjohns@umich.edu

Introduction: Following a tear of the anterior cruciate ligament (ACL), it is commonplace for individuals to shift mechanical demands away from their injured knee and limb. This manifests as diminished knee moments and vertical ground reaction forces in the ACL limb during walking and can be characterized as limb underloading [1, 2]. It is also well established that following ACL injuries, individuals have decreased quadriceps strength and muscle size that is contributing to their reports of instability and weakness [4]. While previous research has identified that quadriceps strength is associated with underloading after ACL reconstruction [1], there is little information regarding how quadriceps strength and muscle size may contribute to underloading after an ACL injury. The purpose of this study was to investigate how quadriceps strength and muscle size contributed to underloading during walking. We hypothesized that those with decreased strength and smaller muscle size would be more likely to underload after ACL injury.

Methods: Thirty individuals (15 females and 15 males; Age: 22.9 ± 9.2; Height: 173.6 ± 9.3; Mass: 71.2 ± 16.0;) who had sustained a primary ACL tear were included in this study. Individuals completed a single testing session following their ACL injury that included quadriceps strength and muscle size assessments, as well as over ground gait biomechanics. Quadriceps maximal isometric strength was recorded using an isokinetic dynamometer (Humac, CSMI, Inc.) with the knee positioned at 60 degrees. The average peak of three maximal effort trials was recorded and normalized to body mass. Images of the vastus lateralis muscle were gathered using panoramic ultrasound (GE LogiqE, GE Healthcare, Chicago, IL) in which patients were in the supine position, with the knee rested at 30 degrees of flexion. Cross sectional area (CSA) was measured using Image J (NIH, Bethesda, MD). Three dimensional motion capture (Qualisys AB, Sweden) and two in-ground force plates (AMTI OR6-7, AMTI, Watertown,MA) were used to assess gait biomechanics. The impulse of the sagittal plane knee moment (from initial contact to peak knee flexion), and VGRF impulse during stance phase were recorded bilaterally. Paired t-tests were used to evaluate differences in muscle size, quadriceps strength, sagittal knee moment impulse and the VGRF impulse between ACL and non-ACL limbs, significance for t-tests were set at $p \leq 0.0125$ (corrected for multiplicity). While controlling for gender, multiple linear regressions were run to determine how quadriceps size and strength contribute to knee and limb loading during walking. Regression analyses were considered significant at $p \leq 0.05$.

Results & Discussion: The ACL limb had significantly smaller vastus lateralis CSA (Table 1; p=0.004) and lower peak torque (Table 1; p=0.0001) in comparison to the non-ACL leg. The ACL limb also exhibited a smaller VGRF impulse (Table 1; p=0.0001) compared with the Non-ACL limb. There were no between limb differences in sagittal plane knee moment impulse (p>0.01). When assessing the relationship between quadriceps strength, muscle size, and limb loading (while controlling for gender) on the ACL limb, it was found that gender and muscle strength were significant predictors of VGRF impulse during the stance phase of gait (R^2=.704, p=0.001). Gender was a significant contributor itself (R^2=0.340, p=0.0001) to VGRF impulse, and ACL limb quadriceps strength contributed a significant R^2 change of 0.362 (p=0.0001). Further, there was no significant model for gender, quadriceps strength and muscle size contributing to knee moment impulse during walking. These results partially support our hypothesis in that decreased muscle strength, but not muscle size, is associated with ACL limb underloading. Additionally, males were more likely to walk with increased VGRF impulse. Our data also reveal asymmetries in quadriceps size and strength between limbs, similar to previous research, [4] and also identifies ACL limb underloading after ACL injury.

Variable	**ACL** (Mean ± SD)	**Non-ACL** (Mean ± SD)
Strength (Nm/kg)*	2.35 ± 0.6	2.88 ± 0.6
Vastus Lateralis CSA (cm^2/kg)*	3.14 ± 0.5	3.75 ± 1.1
Sagittal Knee Moment Impulse (Nm/kg*m/s)	0.02 ± 0.01	0.03 ± 0.02
VGRF Impulse (xBW/s)*	5.39 ± 0.4	5.57 ± 0.4

Table 1: ACL limb and Non-ACL limb quadriceps muscle strength, muscle morphology, knee moment impulse and VGRF impulse. * indicates signficant between limb difference at p <0.0125

Significance: The relationship between muscle strength and VGRF impulse during walking suggests that declines in quadriceps strength following injury may contribute to increased underloading in the ACL limb. Simultaneously, the stronger individuals are after ACL injury the less likely they are to underload, highlighting the importance of rehabilitation following ACL injury in preparation for surgery. Our data may also suggest that females who present with lower quadriceps strength may be more susceptible to limb loading deficits after ACL injury. Given that limb and knee underloading are known to be associated with post-traumatic knee osteoarthritis [3], it appears warranted to implement therapies aimed at enhancing quadriceps strength prior to ACL reconstruction in order to potentially improve underloading thereby improving long-term knee joint health.

Acknowledgements: Research reported in this abstract was supported by the Eunice Kennedy Shriver National Institute of Child Health & Human Development of the National Institutes of Health under Award Number R01HD093626. The content is solely the responsibility of the authors and does not necessarily represent the official views of the National Institutes of Health.

References: [1] Pietrosimone B, et al., (2018), *J Orthop Res*. 36(11); , [2] Gardinier et al., 2013, *J Orthop Res,* 31; [3] Pfeiffer SJ, et al., (2019), *Med Sci Sports Exerc.* 51(4); [4] Williams G, et al., (2005), *J Biomech* 38(4);

PENNATION ANGLE CHANGES DURING SUCCESSIVE LOADING CYCLES

Joshua Swift[1] and Benjamin W. Infantolino[1*]
[1]Kinesiology, The Pennsylvania State University - Berks
*Corresponding author's email: bwi100@psu.edu

Introduction: Traditionally, models of muscles assume that the pennation angle change experienced by a muscle is linked to the joint angle change. Azizi et al. [1] demonstrated a variable gearing can be seen in muscle which is dependent on the loading condition. In these situations, pennation angle can differ between different load conditions even if the muscle moves through the same range of motion. Eng et al. [2] described possible mechanisms for this and some in vivo experiments which have demonstrated variable gearing in human muscle. Mercer and Infantolino [3] demonstrated a change in the anterior tibialis pennation angle during successive submaximal contractions though a fixed ankle range of motion. However, not all subjects demonstrated a change in pennation angle through successive contractions. Additionally, for subjects who did demonstrate a change in pennation angle, it was not clear how many cycles was required for the pennation angle to stop changing since it clearly cannot change with each cycle over tens or hundreds of cycles.

The purpose of this research was to use a more familiar muscle activity (squatting) under two loading conditions which allowed subjects to complete enough cycles to determine when pennation angle stopped changing over successive cycles.

Methods: Five subjects (4 male, 1 female, 1.79 ± 0.1m, 82 ± 23kg, 21 ± 1 year) who regularly performed squats during their workout routines participated in the study. Knee range of motion was controlled for each subject by moving the safety bars in a squat rack so that the bar touched the safety bars when the knee reached 90º of flexion. Subjects were instructed to just touch the safety bars for each of their 8 repetitions. A linear flat ultrasound probe (LV8, Telemed) was attached to the lateral thigh using medical tape and elastic wraps in order to visualize the vastus lateralis. Subjects were asked to perform 8 repetitions for a back squat under two loads: body weight plus an empty bar and with the bar weighted to 50% of the subject's self reported 1RM.

Ultrasound videos were analysed using custom written Matlab code which measured the pennation angle of all detectable fascicles in each frame of the ultrasound video. Pennation angle vs. time graphs were used to initially determine if pennation angle changes took place during successive cycles and when pennation angle stopped changing.

Results & Discussion: In three of the ten total videos (two body weight and one 50% 1RM), the image quality was poor so that pennation angle could not be reliably measured using Matlab. For the remaining 7 videos, three had no trend (figure 1) but 4 did have a change in pennation angle during successive cycles (figure 2). For those that showed changes, all changes stopped by the 5th cycle.

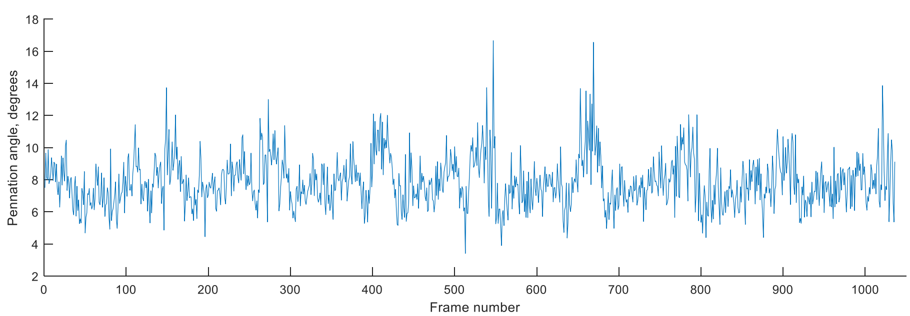

Figure 1

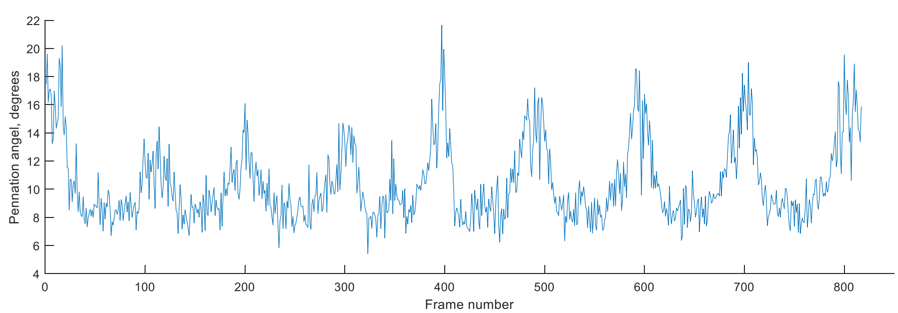

Figure 2

The inconsistency in pennation angle changes across subjects is consistent with the results of Mercer and Infantolino [3]. The fact that some subjects showed changes in both the body weight and 50% of 1RM conditions indicate that this pennation angle shift occurs at various loads. Why some subjects exhibit this shift and others do not is still not clear as no differences in subjects seemed to explain the inconsistency in pennation angle shift.

Significance: The finding that some subjects exhibited a shift in pennation angle without a shift their knee joint range of motion indicate that something is changing in their vastus lateralis force output capability. This is worth investigating both in terms of how and what mechanical advantage or disadvantage it may provide to those individuals. Future studies will look to determine if the shift occurs in the same muscle under different conditions and if shifts occur in different muscles of individuals exhibiting pennation angle shifts.

References: [1] Azizi, Brainerd, and Roberts (2008) *PNAS* 105(5); Eng, Azizi, and Roberts (2018) *Int Comp Bio* 58(2); [3] Mercer and Infantolino (2020) 44th ASB conference

DYNAMIC STABILITY DURING FIXED SPEED TREADMILL, SELF-PACED TREADMILL, AND OVERGROUND WALKING

Shawanee' Patrick, Daniel Richie, Ajit Chaudhari
Ohio State University
*Corresponding author's email: patrick.436@osu.edu

Introduction: Utilizing treadmills for walking studies is beneficial in that it can create a controlled, safe environment for repeatable gait studies and gait training. Treadmill walking can also allow you to collect data over a large number of steps. Fixed-speed treadmills (FST) are commonly used, but they are not well suited to creating walking conditions that are similar to overground walking (OGW). Overground walking has variations in gait parameters that fixed-speed treadmills are not capable of capturing [1]. Previous research has shown that there are significant differences in gait parameters and stability measures for overground walking and fixed-speed treadmills. Self-paced treadmills (SPT) have been looked to as a way to allow for variances in walking speed more similar to overground walking[1]. Self-paced treadmills vary walking speed based on the natural speed of the user, theoretically making walking more like natural overground walking.

Local dynamic stability is a measure that refers to sensitivity to small perturbations during gait [2]. Natural fluctuations as we walk reflect these perturbations. Therefore, utilizing a self-paced treadmill or overground walking may be beneficial in getting the most accurate measure of local stability. In studies comparing the variance of gait parameters, dynamic stability measures are commonly measured using data collected on fixed-speed treadmills at a self-selected speed or overground walking [3]. However, fixed-speed treadmills have been shown to result in less variance of gait parameters and more stability during walking compared to overground walking [3]. Self-paced treadmills have not been compared to overground walking and fixed-speed treadmills when observing local dynamic stability measures. This study aims to compare local dynamic stability (short-term Lyapunov exponents) for overground walking, self-paced treadmill walking, and fixed-paced treadmill walking.

Methods: 15 healthy participants (age: 32 ± 10y; 2 females; BMI 26 ± 3) gave informed consent in accordance with procedures of the Institutional Review Board of The Ohio State University. Participants walked for 5 minutes (~300 gait cycles) under three different conditions: outdoor OGW on a straight and level path and indoor walking on a FST and SPT; the treadmill being a Bertec split-belt treadmill (Bertec, Columbus, OH). Treadmill trials began at a subject-specific overground self-selected speed (1.32 ± 0.11 m/s). Gait cycle data was collected on 9-axis accelerometers (3 sensors) at 500Hz located at the pelvis and both ankles for all three test conditions. For each test condition, participants were instructed to walk at a comfortable pace (without regard for maintaining any specific pace) over the 5-minute trial. For the SPT condition, participants were first given a 5-minute acclimation trial.

Local dynamic stability was quantified by the short-term Lyapunov exponent (λ_s). A 12-dimensional state space was defined using linear accelerations and angular velocities of the pelvis and their time-delayed copies using standard methods [4]. The λ_s represents the average divergence of nearby trajectories in the state space [5]. This value tells us about the sensitivity to perturbations. The maximum λ_s was calculated for FST, SPT, and OGW for each participant. ANOVA was used to test for significant differences between the different conditions for the short-term Lyapunov exponent λ_s for each walking trial.

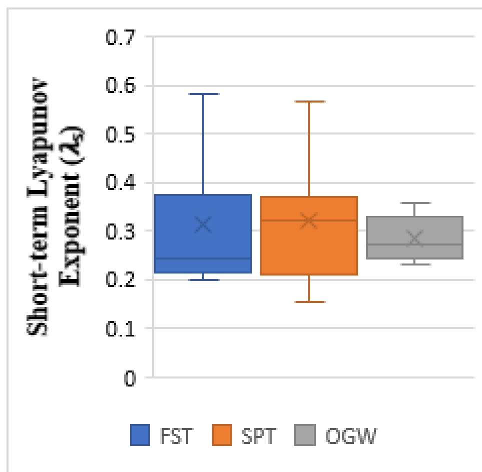

Figure 1: Maximum Short-term Lyapunov exponent for 5-min walking trial for FST, SPT, and OGW.

Results & Discussion: The results for the average max short-term Lyapunov exponent (λ_s) can be seen in Figure 1. There was no significant difference in the short-term Lyapunov exponent between the three walking trials. This was unexpected due to previous studies that observed lower short-term Lyapunov exponent values for FST than SPT [3]. It is possible that participants modulate their gait parameters to maintain the same dynamic stability. This warrants a further investigation of corelations of various gait parameters and their variances with dynamic stability measures for FST, SPT and OGW. This result also may not be the same for those who have conditions that impact balance and gait. It is possible that for those with gait deficits there is an inability to maintain local stability across FST, SPT and OGW. Further exploration of dynamic stability measures and gait parameters during FST, SPT and OGW for those with gait deficits may be beneficial in understanding changes in gait that result in maintained or changes dynamic stability.

Significance: Local dynamic stability measures hold promise for assessing sensitivity to perturbation, but it is critical to understand how and whether the collection method impacts the measured local dynamic stability. Identifying best-practices for gait conditions to measure local dynamic stability will enable future studies of fall risk and gait interventions to reduce that risk.

References: [1]J. Kim et. al (2013)*35th Annual International Conference of the IEEE (EMBC)*. [2] J. B. Dingwell, et. al.(2000) *Journal of Biomechanical Engineering* [3] Y. Qian et. al.(2020), *Journal of Biomechanical Engineering*[4] H. Kantz et. al (2003) Cambridge University Press. [5] J. B. Dingwell and H. G. Kang, (2006) *Journal of Biomechanical Engineering*.

Shape Analysis of Glenohumeral Bone Surfaces by Gender and OA Severity

Reilly Stafford[1*], Morgan Dalman, M.S.[2], Katherine R. Saul, Ph.D.[3]
[1]Department of Mechanical and Aerospace Engineering, North Carolina State University, Raleigh, NC, USA
*Email: rlstaff2@ncsu.edu

Introduction: Osteoarthritis (OA) is a common disease of the joints that has an influence on bone shape over time. This occurs through a loss of cartilage at the inflicted joint leading to remodeling of the adjacent bone. As OA progresses with severity, analyzing the differences in humerus and glenoid geometry is important when determining treatment options for OA of the glenohumeral joint [1]. Better understanding of bone degradation would allow for more robust detection of OA and informed treatment options. Currently, there is not a universal method for predicting both OA progression and injury risk/impact for patient specific cases [2]. This research leverages mathematical analysis and computational modeling with musculoskeletal models and FE modeling, two of the most popular computational methods [3] to understand the differences in OA progression architecture and loading patterns. Using a Generalized Procrustes Analysis (GPA), this research implements a shape analysis to construct a musculoskeletal model of the glenohumeral joint to analyze changes to bone geometry over time after injury for OA patients. This will allow severity of OA to be distinguished by determining specific markers for severity level in bone geometry changes. Doing so will enable more informed treatment plans in patient specific cases to be formulated for better recovery after injury.

Methods: A GPA with a sliding landmark method [4] was constructed in MATLAB to perform a shape analysis on segmented humerus bone files from magnetic resonance (MR) images of both male and female patients (Fig. 1). MATLAB has a built-in function for a GPA, however due to the complex shape of bone, a sliding landmark method is needed to be able to evaluate the same location on each bone. The GPA involves calculations to perform scaling, rotation, and translation operations while returning a Procrsutes distance (PD) value. Scaling is performed by taking the root mean square distance (RMSD) between points and their centroid, rotation by using a rotation matrix on the shape, and translation by adding/subtracting centroid differences to the shape being translated. A PD value is then obtained by taking the sum of squared differences (SSD) of all landmark data points between the two shapes and standardizing that value by the reference scale. PD minimization was performed to superimpose landmarks between subjects and compute the deviations [5].

Results & Discussion: To validate the custom 3D GPA implementation, a PD was performed for an analytic shape and compared to the PD output and scaling factors of the MATLAB's Procrustes function; accuracy was confirmed between the constructed GPA and MATLAB's GPA (Fig. 2). A PD of 0.0364 and scaling factor of 1.2861 was obtained for both the constructed GPA and MATLAB's GPA. Ongoing work with development of GPA will serve to further verify significance in application of bone shape analysis. This will allow nuanced differences in bone shape geometry to be determined across different levels of OA. In addition, bending energy (BE) will be implemented to make landmark data homologous from subject to subject by sliding landmarks across tangential planes until BE is minimized [5].

Significance: The constructed GPA will be used to determine scaling rules that consider sex as a factor, and identify morphological features on the humerus and glenoid associated with OA severity. This work provides an initial foundation for constructing a bone growth model for OA of the glenohumeral joint. Continued work will focus on characterizing OA development to help identify risk of injury and improve treatment for patients with OA after rotator cuff injury.

References:
[1] NICE (2020), *Clinic. Guid.* [2] Rasanen et al. (2012), *J Orthop Res.* **31**(1): 10-22. [3] Mukherjee et al. (2020), *Front Bioeng Biotechnol.* **8**: 93. [4] Danelson et al. (2008), *Stapp Car Crash J.* [5] Perez et al. (2006), *Div Antro.*

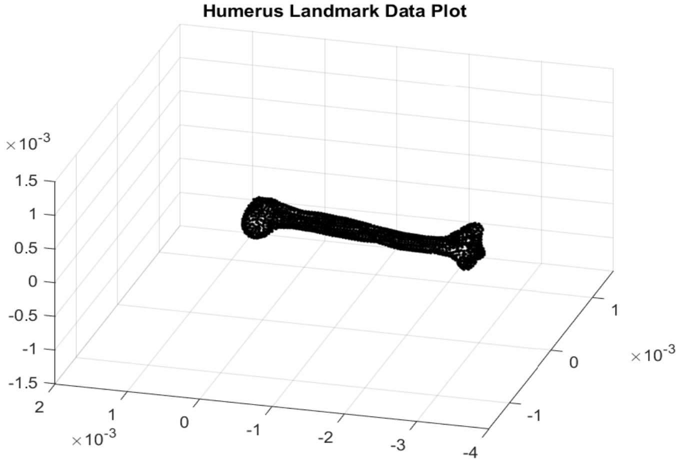

Figure 1: Healthy humerus segmented landmark data points

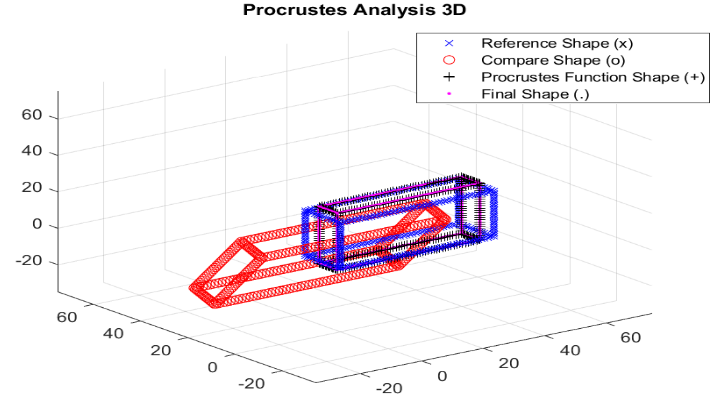

Figure 2: Analysis performed on simple 3D shape to minimize deviations between landmark data points on compare and reference shapes. Results compared with MATLAB's analysis on the same shape, with both matching

A KINEMATIC AND KINETIC COMPARISON TO IDENTIFY A BEST PRACTICE FOR MULTISEGMENTED FOOT MODELS

Julia Nicolescu[1*], Andrew Wilzman[1], Karen L. Troy[1]
[1]Department of Biomedical Engineering, Worcester Polytechnic Institute, Worcester, MA
*Corresponding author's email: jnicolescu@wpi.edu

Introduction: The human foot is complex, yet it is often represented as a single segment in biomechanical modeling. Such models are unable to capture the kinematic and kinetic data of specific regions of the foot. To understand injuries in the feet, such as bone stress injuries, plantar fasciitis, Achilles tendonitis, and arthritis, a multisegmented foot model is necessary. Multisegmented foot models (MSFMs) have become a core part of extracting biomechanical information in research and in the clinic.[1] However, across all the models that have been developed, each differs by the number of segments included and how they are defined, so there is no consensus for best practice. It is unknown whether the various MSFMs available yield the same kinematic and kinetic data and what level of detail is necessary to accurately measure such values. Here, we compared three MSFMs using the same input data set to understand how the assumptions and boundaries of each one may influence the results. We measured tibiotalar and metatarsophalangeal joint angle, moment, and force in each model. We expected that increasing the number of model segments would decrease the force and moment at individual joints because it will be spread across the various segments.

Methods: We selected two MSFMs for inclusion based upon the number of segments included, how the segments were defined, whether they included a medial/lateral split, and if they contained a segment that started/ended at the distal or proximal ends of the metatarsals. We also designed a three-segment foot model according to these criteria. All models were then constructed in Visual 3D (V3D). Table 1 shows the models used in this project, how they differentiate from each other, and how they were constructed.

Table 1. The MSFMs included in the study, the segment number and segment definition, and how they were designed in V3D.

Model Name	**Number of Segments and Segment Definition**	**Construction in Visual 3D**
Oxford Foot Model [2]	4: Shank, rearfoot, forefoot (excluding distal tarsals), hallux	C-Motion tutorial [4]
Milwaukee Foot Model [3]	4: Shank, rearfoot, forefoot (including distal tarsals, hallux	Adapted from Oxford
Three-Segment Model	3: Shank, rearfoot, forefoot	Original construction

Twenty young adults (age: 20.55 years ± 1.5 years; 10/10 male/female) who ran an average at least 24 km/week provided written informed consent to participate in this institutionally approved study. Participants performed a fast jog along a 10-meter runway. Force and motion data were collected using two AMTI force platforms (AMTI, USA; 1000 Hz) and 10 Vicon Vantage cameras (Vicon, UK; 100 Hz). The cameras tracked the movement of 16 reflective markers on each foot and 6 reflective markers on each lower leg. For this abstract, a subset of 9 participants (5 male, 4 female) were analysed. The angle, moment, and force of the tibiotalar and metatarsophalangeal joints were calculated for each MSFM based on the same input data set.

Results & Discussion: Figure 1 shows the force at the tibiotalar joint as determined by each of the three models. The joint force in the left and right foot of each participant is shown and the average for each model is graphed in bold. We first observed that there is a minimal difference between the results of the Oxford and the Milwaukee models. This indicates the midfoot region containing the distal tarsals did not have a significant impact on the results. We also observed that the three-segment model yielded similar results to the other two models, but overall appeared to show higher forces. This supports the idea that having fewer segments leads to greater joint force calculations. Overall, the observed relationships between the three models cause us to wonder how many segments are necessary for MSFMs. We plan to continue this work to include more MSFMs with varying segment numbers and definitions to determine the necessary level of detail.

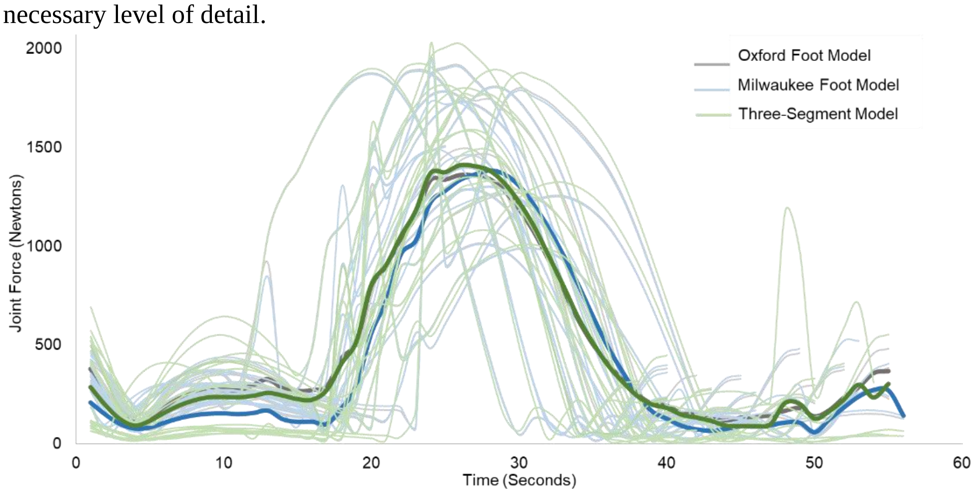

Significance: Multisegmented Foot Models are a necessary biomechanical model for understanding the complexities of the foot and its associated injuries. Determining the best practice for MSFMs will allow for greater validation and widespread use instead of continued publications of novel models. We hope to use the results of this work to predict metatarsophalangeal joint kinematics and kinetics to aid in our research of metatarsal bone stress injuries.

References: [1] Leardini et al. (2019) *Gait & Posture, 69* [2] Carson et al. (2001) *Journal of Biomechanics, 34* [3] Myers et al. (2001) *23rd Annual International Conference of the IEEE* [4] C-Motion Inc. Tutorial: Oxford Foot Model

EXPLORING THE LIMITS OF MECHANICAL BUFFERING IN A PENNATE MUSCLE

Daisey Vega[1*], Christopher J. Arellano[1]
[1]Department of Health and Human Performance, University of Houston, Houston, TX, USA
*Corresponding author's email: dvega2@cougarnet.uh.edu

Introduction: The ability of a muscle-tendon unit (MTU) to absorb energy without damage to muscle fascicles relies on two basic mechanisms: mechanical buffering via tendon stretch [1] and architectural gearing via muscle shape change [2]. While these energy absorbing mechanisms can be thought of as independent, the question remains as to how these two mechanisms might interact or be limited when rapid rates of MTU lengthening occur at varying levels of contractile force conditions.

We suspect that when MTU lengthening occurs at higher contractile force levels, there may be a biological limit to a muscle's ability to architecturally gear and/or tendon's ability to stretch and absorb energy. This limit would be reflected by muscle fascicle lengthening and thus, an increase in muscle fascicle power input. Therefore, we hypothesized that when lengthening occurs at a greater level of contractile force, the MTU will rely more heavily on muscle fascicles to absorb power input.

Methods: We used previously established *in situ* protocols [3] on the lateral gastrocnemius (LG) muscle-tendon unit of wild strain turkeys (n = 2). To change the initial force level conditions, we varied the timing of MTU lengthening relative to the start of maximal muscle force activation. A total of 10 time delays were determined starting from 0 ms to the time of peak tetanus force. For all trials, we measured dynamic shape changes (fascicle length and thickness via sonomicrometry), muscle force (load cell), and MTU lengthening (potentiometer) integrated with a linear actuator (Kollmorgen) that stretched the MTU at a fixed rapid rate (50 mm/s) and magnitude (10 mm).

Peak MTU and muscle fascicle power input were calculated by taking the product of the MTU force by the velocity of the linear actuator and the velocity of the muscle fascicle length change, respectively. Power was then normalized by LG muscle mass. Figure 1 shows power inputs (W/kg) of two out of the ten experimental conditions: 0 ms delay (lengthening of the MTU occurs at the onset of muscle activation) and 360 ms delay (lengthening of the MTU occurs at the time corresponding to peak tetanus force). To account for differences in initial MTU power input due to the increase in force level conditions, peak power inputs of muscle fascicles were expressed as a percentage of total MTU power input.

Results & Discussion: Across a range of time delays, the percentage of total power input into the MTU that was absorbed by the muscle fascicles ranged between ~6-20% (n = 2). This leaves approximately 84-90% of the total power input into the MTU unaccounted for, which must be owed to elastic elements and muscle shape changes. These observations indicate that the MTU did not rely more heavily on muscle fascicles to absorb power input and thus, our preliminary findings do not support our hypothesis. Instead, it seems that the MTU was robust in dealing with rapid power inputs across a range of contractile force level conditions.

We aim to collect a full data set for this study (n=4) and our future analysis will focus on uncovering the contribution of muscle shape change (e.g., architectural gearing) and tendon stretch as mechanisms to deal with rapid rates of energy inputs. Such analysis will give us insight into <u>*how*</u> the MTU can deal with absorbing energy across a range of contractile force conditions.

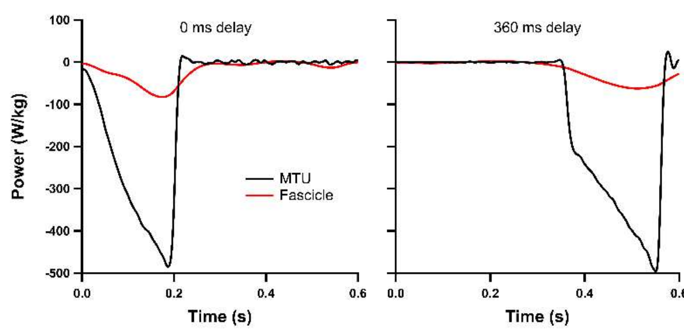

Figure 1. Total power input at the whole MTU level and fascicles of the lateral gastrocnemius muscle of a turkey during *in situ* lengthening experiments (n=1). During the 0 ms delay condition, total power into the MTU was 485 W/kg and 83 W/kg was absorbed by the fascicles (~17% total power input). During the 360 ms delay condition, total power into the MTU was 495 W/kg and 62 W/kg was absorbed by the fascicles (~13% total power input).

Significance: During locomotion, the level of muscular contractile force and the rate of energy that must be absorbed can profoundly change between agile maneuvers such as deceleration, landing, fast speed running, and instantaneous redirection of the body. Understanding how the tendon's buffering mechanism and muscle's architectural gearing interact could reveal a feature of muscle-tendon mechanical behavior that is intrinsically robust to dealing with energy inputs that can vary unpredictably with respect to its contractile state. These insights will broaden our basic understanding of the mechanisms that facilitate energy absorption in the lengthening domain, an area that remains to be fully explored.

Acknowledgments: This work is supported by the National Science Foundation CAREER grant awarded to Dr. Christopher J. Arellano.

References: [1] Roberts and Azizi (2010), *J Appl Physiol* 109(2); [2] Azizi and Roberts (2014), *J Exp Biol* 217(3); [3] Arellano et al. (2016), *J Biomech* 49(9)

RUN MECHANICS IN INDIVIDUALS WITH RESOLVED VERSUS NO HISTORY OF PLANTAR FASCIITIS

Lukas Krumpl[1*], Nickolai J. P. Martonick[1], Joshua P. Bailey[1]
[1]Department of Movement Sciences, University of Idaho, Moscow, ID, USA
*Corresponding author's email: lkrumpl@uidaho.edu

Introduction: The plantar fascia (PF) plays an integral part in maintaining foot and arch control during the stance phase of the gait cycle [1]. The dynamic role of the PF allows it to react to ground contact by coiling around the toes and providing tension within the foot to prevent increased midfoot extension and eversion, and decreased forefoot dorsiflexion under weightbearing conditions [1,2]. This function is impaired in people with plantar fasciitis [3].

Despite plantar fasciitis being a frequently diagnosed overuse running injury, only one study has evaluated foot mechanics in people with resolved plantar fasciitis [5]. There were no differences in multi-segment foot kinematics between individuals with resolved plantar fasciitis and individuals with no injury history [5]. Information on foot and run mechanics during prolonged running is missing in a population recovered from plantar fasciitis. The overall interaction between the foot and ground during stance phase would benefit from more than discrete events through the phase. Waveform analyses of the stance phase have shown the capability to indicate differences between forefoot and midfoot kinematics [5]. Thus, the purpose was to evaluate how multi-segmental foot mechanics and lower extremity stiffness in runners with resolved plantar fasciitis respond to a prolonged submaximal treadmill run.

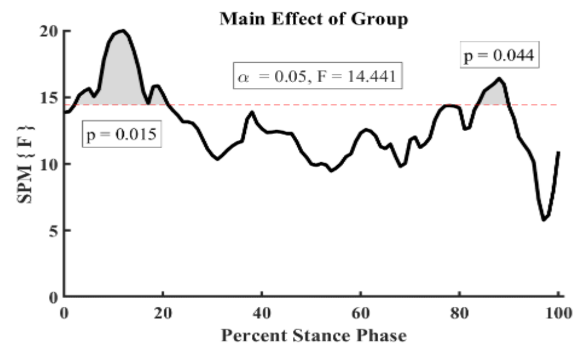

Figure 1: SPM repeated measures ANOVA for midfoot angle in the sagittal plane. The dashed red lines indicate the threshold for significant differences.

Methods: Sixteen participants completed the study. Eight participants had resolved plantar fasciitis (RPF) (3 females; age: 25.5yrs [±9.3]; mass: 69.1kg [±11.2], height 180.1cm [±11.1]). Resolved plantar fasciitis was defined as having had no symptoms for at least one month [4]. Eight participants had no plantar fasciitis (NPF) history (2 females; age: 22.9yrs [±5.1]; mass: 70.1kg [±8.1], height 177.9cm [±6.3]). Participants performed a maximal effort GXT to determine ventilatory threshold 2 (VT2). 80% of the speed at VT2 was used as relative velocity for the 30-minute run. Participants were equipped with a multi-segment foot [4,5] and full body model. Three-dimensional marker trajectories were collected with an eight-camera motion capture system (250 Hz; VICON, Oxford Metric Ltd., Oxford, UK). Motion capture data were collected at minutes 1:30, 15, and 29:30 of the run. Vertical & leg stiffness, and foot mechanics were analyzed by multiple mixed model (2 group x 3 time) repeated measures ANOVAs, followed by *post-hoc* two-sample t-tests. Midfoot and forefoot sagittal and frontal angles were analyzed as waveforms via statistical parametric mapping (SPM) at each percentage of the stance phase. Alpha level was set at .05. Stiffness statistical analyses were completed via SPSS (v. 29.0) & SPM analyses were completed in MATLAB.

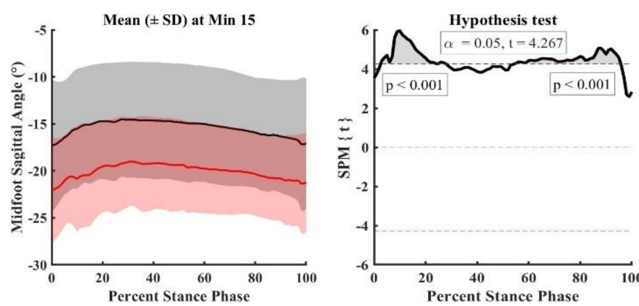

Figure 2: SPM post-hoc pairwise comparisons for midfoot angle in the sagittal plane. A more positive value suggests greater midfoot sagittal angle. RPF (red) and NPF (black) group showed significant differences twice ($p<0.001$) during the stance phase at the 15-minute measurement.

Results & Discussion: SPM analyses showed no significant differences for group or time for forefoot, and midfoot frontal angles. SPM analysis revealed a significant main effect of group for midfoot sagittal angles (Fig 1). *Post-hoc* pairwise comparisons revealed that the RPF and NPF group had different midfoot sagittal angles at 15-minutes (Fig 2). There were no group differences in leg ($p=0.072$) and vertical ($p=0.297$) stiffness, and no time differences ($p=0.30$ & $p=0.22$, respectively) during the run.

These findings suggest that the NPF group displayed greater midfoot plantarflexion angles during the stance phase. Increased midfoot plantarflexion coincides with a more pronounced lowering of the medial longitudinal arch (MLA). This was specifically visible at min 15, where the NPF group showed more midfoot plantarflexion after initial contact and prior to toe off. A potential explanation for the sole difference halfway through the run may be gait adaptations associated with an understanding that the end of the run is approaching; a 'finish strong' mindset. Diminished MLA lowering is present in plantar fasciitis and decreases the foot's capacity to return stored potential kinetic energy [6]. Thus, the present results indicate that, similarly to symptomatic people, resolved plantar fasciitis may alter midfoot sagittal angles throughout the stance phase, as presented by a decreased ability of MLA lowering.

Significance: This outcome provides information for understanding how foot mechanics of resolved plantar fasciitis individuals reacts to mechanical loading. RPF may have long-term effects on midfoot plantar- and dorsiflexion. The reduced lowering of the MLA did not appear to affect leg and vertical stiffness during the run. However, the run conducted on a treadmill at submaximal effort may explain unchanged run and foot mechanics and warrant further investigations at greater intensities to increase structural demands.

References: [1] Gefen (2003), *Foot & Ank Int 24*; [2] Stecco et al. (2013), *J Anat 223*; [3] Crary et al. (2003), *Foot & Ank Int 24*; [4] Wiegand et al. (2022), *Clin Biomech* 97; [5] Leardini et al. (2007), *Gait & Post 25*; [6] Wearing et al. (2004), M Sc Sports

TRICEPS SURAE ACTIVATION DOES NOT AFFECT ANKLE MECHANICAL ENERGY EXPENDITURE DURING THE PROPULSION PHASE OF UNIPEDAL HOPPING IN PERSONS WITH ACHILLES TENDINOSIS

David Ortiz-Weissberg, MSc*; Kornelia Kulig, PhD, PT, FAPTA
Jacquelin Perry Musculoskeletal Biomechanics Research Laboratory
Division of Biokinesiology and Physical Therapy, University of Southern California, Los Angeles, CA, USA
*Corresponding author's email: ortizdav@pt.usc.edu

Introduction: Achilles tendinosis (ATx), a stage of tendinopathy characterized by advanced degeneration in the tendon core[1], presents an exemplary model for studying how the human body adapts to tissue pathology. Notably, persons with Achilles tendinosis demonstrate a reduction in the contribution of the triceps surae to plantar flexor activation during unipedal hopping[2]. Considering that the triceps surae comprise approximately 66% of the plantar flexor force production capacity[3], reduced dependence on these muscles may impair ankle joint kinetics. Given that the ankle is the predominant source of energy generation during hopping[4], relating the altered activation magnitudes to ankle mechanical energetics will provide further insight into function and adaptations in persons with Achilles tendinosis.

The purpose of this research is to investigate the relation between triceps surae activation magnitudes and ankle mechanical energetics during the propulsion phase of unipedal vertical hopping in persons with Achilles tendinosis. Due to the triceps surae accounting for the majority of plantar flexor force production capacity, we hypothesize that reduced activation of the triceps surae in persons with tendinosis will reduce ankle mechanical energy expenditure (MEE) relative to healthy controls.

Methods: Thirteen persons (6 with Achilles tendinosis) were tasked with unipedal hopping on an AMTI force plate at 2.33 Hz, prescribed via metronome. 2.33 Hz is near the maximum self-selected unipedal hopping frequency and is thus likely to uncover deficits in ankle function. Participants were instrumented with a full lower extremity retroreflective marker set and surface EMG (sEMG) of the gastrocnemii and the soleus. Seven to ten hops were analysed for the involved limb of the tendinosis group and the matched limb of the controls.

The propulsion phase was segmented from the ground contact phase based on the minimum vertical position of the L5-S1 marker. Ankle MEE was calculated via rectification and integration of the mechanical power time series. MEE was chosen to account for all ankle work, regardless of sign. The sEMG was band-pass filtered, rectified, smoothed via a low-pass Butterworth filter with a 3.5 Hz cut-off, and normalized to the EMG from a maximum height single leg vertical jump. The total triceps surae activation was quantified as the sum of the integrated EMG.

A robust linear mixed effects models was used to assess the effect of total triceps surae activation on ankle MEE, permitting usage of all hops while down-weighting influential points. The composite regression equation was Ankle MEE ~ $\beta_0 + \beta_1$TS Activation + β_2Group + β_3(TS Activation*Group), where the tendinosis group was coded as 0 and the control group as 1.

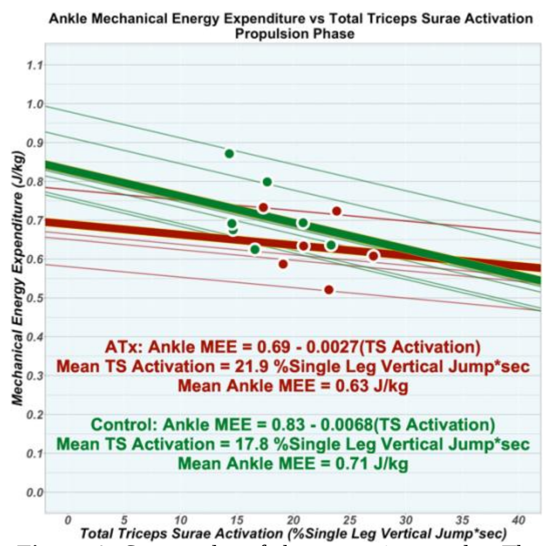

Figure 1: Scatter plot of the regression results. The thick lines represent the group regression lines while the thinner lines are participant specific. Each data point represents the average for one participant.

Results & Discussion: The mean triceps surae (TS) activation, mean ankle MEE, and regression coefficients for each group are displayed in Figure 1. The intercepts indicate that, in the absence of triceps surae activation, the average ankle MEE was 0.69 J/kg ($p < 0.001$) for Achilles tendinosis participants and 0.83 J/kg for the control group. The group difference was not statistically significant ($p = 0.78$). There was no significant influence of triceps surae activation on ankle MEE for either group ($p = 0.33$, 0.36). The data do not support our hypothesis: persons with Achilles tendinosis are able to maintain ankle MEE and this maintenance does not depend on the degree of triceps surae activation. The absence of a relation between triceps surae activation and ankle MEE indicates that the propulsion phase MEE stems from sources other than triceps surae active force. We recommend that future work investigate the possible sources.

Our findings differ from previous research[5] in that our participants did not display a reduction in triceps surae activation. These discrepancies may be due to our inclusion of the soleus and lateral gastrocnemius. This then suggests that adaptations may occur even within the triceps surae, such that the soleus and/or lateral gastrocnemius compensates for reduced medial gastrocnemius activation.

Significance: Our research indicates that persons with Achilles tendinosis can produce similar levels of ankle MEE as persons without a history of Achilles pain/injury. Synthesizing our results with previous reports of reduced ankle joint work during single-leg heel raises[6] presents an exciting implication for our understanding of Achilles tendinopathy: ankle joint kinetics are not necessarily impaired in persons with tendinosis, but rather the body balances task performance and protection of the tendon from further damage.

Acknowledgements: This research is supported by the American Society of Biomechanics Graduate Student Grant-In Aid and the International Society of Biomechanics Matching Dissertation Grant.

References: [1] Kulig et al. (2020), *Front. Physiol.* 11(651); [2] Chang & Kulig (2015), *J. Physiol.*, 593(15); [3] Ward et al. (2009), *Clin. Orthop. Relat. Res.*, 467(4); [4] Dick et al. (2019), *J. R. Soc. Interface*, 16(159); [5] Baur et al (2011), *J Electromyogr Kinesiol* 21(3); [6] Silbernagel et al (2006), *Knee Surgery, Sport Traumatol Arthrosc* 14(11).

AUTOMATED GENERATION OF BILATERAL PERSONALIZED FOOT-GROUND CONTACT MODELS

Spencer T. Williams*, Claire V. Hammond, Marleny Vega, Geng Li, and Benjamin J. Fregly
Department of Mechanical Engineering, Rice University, Houston, TX, United States
*Email: stwilliams@rice.edu

Introduction: One of the driving goals of musculoskeletal modeling is the optimization of treatments for individual patients with movement impairments [1-3]. For this to be possible, it must be feasible to create personalized musculoskeletal models. When predicting the effect of a treatment on walking, these models require an accurate representation of a patient's foot-ground contact mechanics to predict the ground reaction forces (GRFs) and moments produced by the new gait pattern [1,2]. Unfortunately, creating subject-specific foot-ground contact models is difficult and time-consuming, and most models do not account for ground reaction moments [1,2]. This study presents a new Matlab-based software tool for automatically generating bilateral and unilateral subject-specific foot-ground contact models calibrated to experimental ground reaction force and moment data.

Methods: The software isolates two-segment foot models from a full-body OpenSim [3] model and places linear viscoelastic elements in a grid on the bottom of the shoe. It uses MATLAB's nonlinear least squares optimization algorithm to optimize stiffness coefficients, a damping coefficient, a dynamic friction coefficient, a viscous friction coefficient, a spring resting length, and deviations from spline-fitted experimental kinematics. The cost function penalizes kinematic changes, ground reaction errors, and each stiffness coefficient's deviation from a Gaussian weighted average of its neighbors to reduce discontinuities in stiffness profile. Users provide input data files and model settings through an XML file, which enables modification of included design variables, cost function terms, and allowable errors. The software may calibrate one or multiple foot-ground contact models at one time. If models are optimized simultaneously, they will share a damping coefficient, coefficients of friction, a spring resting length, and stiffness coefficients; the models will each be calibrated using their own respective kinematics and ground reactions, and the stiffness profile of a left foot will be mirrored about the sagittal plane relative to a right foot to ensure bilateral symmetry of physical properties. To validate the method, we generated right-side, left-side, and bilateral personalized foot-ground contact models for one subject.

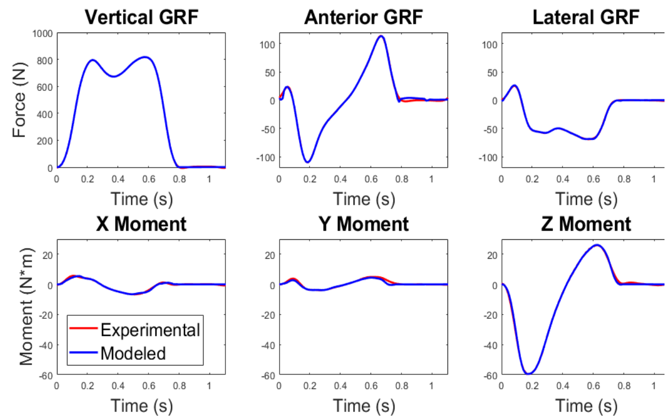

Figure 1: Modeled and experimental ground reactions for a right-side model.

Results & Discussion: All models accurately reproduced experimental kinematics and ground reactions (Table 1). An example of the match between modeled and experimental ground reactions is shown in Figure 1. Ground reaction and kinematics tracking were both slightly less accurate for the bilateral model, though not to a significant degree. As expected, the stiffness properties of the bilateral model were between those of the two unilateral models. Generating each of the unilateral models in Table 1 required 4 to 4.5 hours of CPU time, while the bilateral model needed 16 hours due to approximately doubling both the number of design variables and tracking quantities to model for the cost function.

Table 1: RMS errors for ground reactions and kinematics with viscoelastic element stiffness distributions (mean ± standard deviation).

Side modeled	GRF RMSE (N)	Moment RMSE (N*m)	Rotation RMSE (°)	Translation RMSE (mm)	Stiffness (N/m)
Right	1.838	0.736	2.087	6.072	3601.7 ± 1796.2
Right (bilateral)	2.383	0.753	2.128	6.381	3156.3 ± 1359.7
Left	2.006	0.497	1.935	7.525	2501.5 ± 1199.0
Left (bilateral)	2.062	0.524	2.166	7.269	3156.3 ± 1359.7

Significance: This new tool automates the complex process of modeling foot-ground contact with a two-segment foot model on one or multiple feet, a critical step toward practical personalized musculoskeletal modeling. As the process to create these models becomes more accurate and accessible, musculoskeletal modeling will enable more researchers to study the effects of potential treatments for movement impairments and empower clinicians and patients to make more informed decisions about those therapies. These results indicate that optimizing models for the right and left feet simultaneously can generate models with similar physical properties without significantly impacting tracking of ground reactions and kinematics. Source code and tutorials for this tool will be available on SimTK.org as part of a model personalization pipeline plugin for OpenSim.

Acknowledgements: This research was funded by the U.S. National Institutes of Health (grant R01 EB030520 to B. J. Fregly).

References: [1] Jackson J et al. J Biomech Eng 138,9, 2016; [2] Meyer A et al. Front Bioeng Biotech 4, 2016; [3] Seth A et al. PLoS Comput Biol 14(7), 2018

THE EFFECT OF INCREASED SENSORY FEEDBACK FROM NEUROMODULATION AND EXOSKELETON USE ON ANKLE CO-CONTRACTION IN CHILDREN WITH CEREBRAL PALSY

Charlotte D. Caskey[1]*, Siddhi Shrivastav, Heather Feldner, Kristie Bjornson, Chet T. Moritz, Katherine M. Steele[1]
[1]Department of Mechanical Engineering, University of Washington, Seattle, WA
*Corresponding author's email: cdcaskey@uw.edu

Introduction: Children with cerebral palsy (CP) have a brain injury around the time of birth that impairs motor control. As a result, children with CP often have increased co-contraction of antagonistic muscles during activities such as walking, altering movement and increasing energy costs [1]. Increased sensory feedback, via methods like repetitive, task-specific gait training and neuromodulation, prompts greater supraspinal input during tasks and improves control of muscle activity [2-3]. New methods to support and provide sensory feedback may help reduce co-contraction and improve walking in CP.

Transcutaneous spinal cord stimulation (tSCS) is a novel, non-invasive neuromodulation technique that activates sensory pathways to amplify communication in the nervous system. Prior studies in animals and humans showed tSCS targets sensory feedback largely via 1a afferent pathways [4]. In addition, ankle exoskeletons that can apply resistance or assistance to the ankle during walking have shown to alter motor control in CP and may support sensorimotor integration by amplify the sensory feedback to spinal and cortical networks during walking [5]. This study sought to evaluate the effect of increased sensory feedback from tSCS and a resistive ankle exoskeleton (Exo) on ankle co-contraction during walking. Due to increased supraspinal input from greater sensory feedback during the walking task, we hypothesized ankle co-contraction would decrease when walking with tSCS and the ankle exoskeleton.

Methods: We quantified co-contraction during walking with (1) no devices, (2) tSCS, (3) Exo, and (4) tSCS and Exo together for five children with CP (10.4±4.5 yrs, GMFCS I-II; 4 male). All walking was performed on a treadmill (Bertec) and totalled 20 minutes at a self-selected speed (.91±.22 m/s), kept consistent for each child across sessions. Walking tasks were performed on separate days a minimum of five days apart in a convenience randomized order. Electromyography (EMG) data were recorded bilaterally (2000 Hz; Delsys, Inc.) on the soleus and tibialis anterior muscles. EMG data were high-pass filtered (20 Hz), rectified, low-pass filtered (10 Hz), normalized to the 95th percentile, and segmented by gait cycle. Results report co-contraction of these muscles during stance, defined as the first 60% of the gait cycle, during the final one minute of each session. Co-contraction index (CCI) was calculated as:

$$CCI\ (\%) = \frac{2I_{ant}}{I_{tot}} \times 100$$

Where I_{ant} is the is antagonistic muscle activity and I_{tot} is the sum of both the agonist and antagonist EMG activity [6].

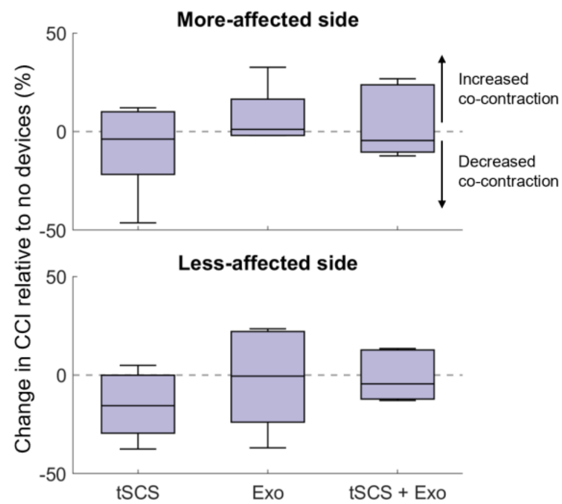

Figure 1: Change in co-contraction index (CCI) of the soleus and tibialis anterior muscles for walking with spinal stimulation (tSCS), the resistive ankle exoskeleton (Exo), both the tSCS and Exo together (tSCS + Exo), relative to walking with no devices.

Results & Discussion: Children with CP displayed higher levels of co-contraction, 40-80%, during walking with no devices compared to prior reports of nondisabled children [1]. Compared to walking with no devices, tSCS and tSCS + Exo reduced ankle co-contraction, with the greatest reduction on the less-affected side when walking with tSCS (Figure 1). Ankle co-contraction remained about the same during the Exo only conditions. These results suggest tSCS may lead to reduced ankle co-contraction in just one walking session, but the less-affected side of the body may be responding faster than the more affected limb. Gad et al. (2021) also reported a 20% reduction in ankle co-contraction with tSCS applied in a single 30-min session for 9 children with CP [4]. Repeated visits may be needed to reach a response on the more-affected side. The Exo did not have the same effect as tSCS, which may be because the Exo makes the walking task more challenging while also increasing sensory feedback. As a results, participants may fatigue faster or maintain high co-contraction to provide extra stability at the ankle. These results also suggest there may be an interaction between the Exo and tSCS. Thus, how the user responds to each device individually may not accurately predict how they respond when devices are used together. Overall, participants had highly variable responses to each walking task, especially on the more-affected side. This suggests there may be other factors affecting responses, such as age, GMFCS level, or mental focus during training.

Significance: This study demonstrates the potential of combining the Exo and tSCS for treadmill gait training and the effect on coordination of ankle muscle activity for children with CP. We highlight the importance of considering device interactions in rehabilitation and how changes in neuromuscular activity in a single visit may inform long-term, rehabilitative impacts of multimodal device use.

Acknowledgements: This work is supported by NSF GRFP Award DGE-1762114 and SCH CP Research Pilot Study Fund 2022 Award.

References: [1] Unnithan et al. (1996), *Med Sci Sports Exerc* 28(12); [2] Côté et al. (2004), *J Neurosci Res* 24(50); [3] Samejima et al. (2022), PTJ 103; [4] Gad et al. (2021), *Neurotherapeutics* 18(3); [5] Conner et al. (2020), *Ann Biomed Eng* 48(4); [6] Falconer and Winter (1985), *Electromyogr Clin Neurophysiol* 25(2-3).

THE IMPACT OF DESIGN FACTORS ON USER BEHAVIOR IN A VIRTUAL REALITY HOSPITAL ROOM FOR ENHANCED FALL PREVENTION STRATEGIES

Nooshin Seddighi[1*], Ying-Ching Chen[1], Andrew S. Merryweather[1,2], K. Bo Foreman[1], Alan Kuntz[1], Edoardo Battaglia[1], Haohan Zhang[1], Ellen Taylor[3], Bob Wong[1], Peter C. Fino[1]
[1]The University of Utah, Salt Lake City, UT, USA
[2]Amazon, LLC, Seattle, WA, USA (contribution made prior to employment)
[3]The Center of Health Design, Concord, USA
*Corresponding author's email: Nooshin.Seddighi@utah.edu

Introduction: Falls and resulting injuries in the hospital setting are considered a challenge and profound concern for patients, families, and hospital staff. Hospitalized patients are particularly vulnerable to falls, with nearly one-third experiencing minor injuries, and a smaller proportion experiencing severe soft tissue wounds, fractures, or head trauma [1]. These injuries can lead to longer and costlier hospital stays, long-term disability, or death. One strategy to mitigate risk of falling is to consider hospital room design. However, it is often not feasible to construct physical iterations of various designs. Virtual reality (VR) technology is increasingly being used for healthcare interventions including simulations of medical procedures and therapy sessions [2], and VR may have particular benefits in the design of healthcare facilities, such as hospitals and clinics to test the factors that may influence user behaviour in these spaces. In this study, we aimed to investigate the impact of various design factors on user behaviour in a VR hospital room.

Methods: Ten participants (5M / 5F) with a mean (SD) age, weight, and height of 26.2 (3.5) years, 72.6 (10.2) kg, and 169 (10.5) cm, respectively, were recruited and provided informed written consent for this IRB-approved study. Our VR environment consisted of four hospital room layouts each with a distinct layout determined by the positioning of various objects, including a bed, chair, sofa, toilet with grab bars, sink, and IV pole. To enhance the realism of the virtual reality experience, the room in which the study was conducted contained physical versions of the bed, toilet, sink, and IV pole, enabling participants to fully immerse themselves in the environment. The VR environment was developed using Unity 3D software and was experienced through an HTC Valve Index headset, which allowed participants to move around and interact with objects in the virtual space. Positional data was captured at 2 Hz during the study from the headset, hand controllers, and trackers located on the lumbar spine and both feet of the participants. Participants began each trial seated on the bed, and were instructed to stand up and walk toward the bathroom, sit on the toilet, wash their hands, and walk back to the bed. A total of 64 trials were completed to test varying room configurations (8 configurations), door type (swing or sliding), starting side of the bed (left or right) and presence of an IV pole (IV or no IV). The 64 trials were divided into two sets and randomized in order. To quantify the influence of these parameters on behavior that are likely associated with falls, we assessed the total trial time, time spent in the bathroom, and the percentage of each trial traveled in backwards and sideways directions, defined using the angle θ between the instantaneous orientation and velocity of the lumbar tracker (forward: $-\frac{\pi}{4} < \theta < \frac{\pi}{4}$; sideways: $\frac{\pi}{4} < |\theta| < 3\frac{\pi}{4}$; backwards: $3\frac{\pi}{4} < |\theta| < \pi$). Linear mixed effect regression models assessed each outcome with fixed effects of room configuration, door type, presence of an IV pole, set number, and two- and three-way interactions using a 0.05 significance level.

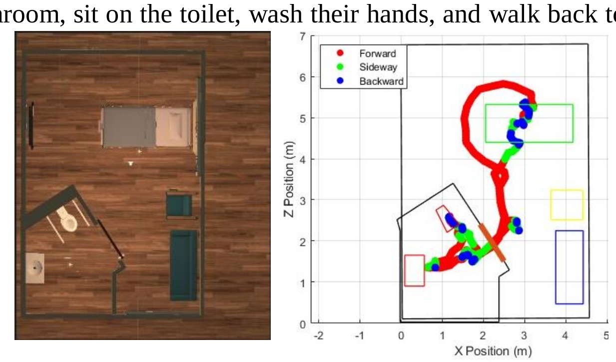

Figure 1: (Left) Top-down view of one of the hospital rooms designed in virtual reality, and (Right) sample participant trajectory colored by the three types of participant motion (forward, sideways, backwards).

Results & Discussion: The room configuration had a significant effect on the amount of backward ($p < 0.001$) and sideways ($p < 0.001$) motion. The type of door had a significant effect on several variables; sliding doors were associated with faster trials ($p = 0.019$), less time in the bathroom ($p = 0.005$) and a smaller percentage of backwards ($p < 0.001$) and sideways ($p < 0.001$) motion compared to swing doors. The presence of an IV was associated with slower trials ($p < 0.001$), longer time spent in bathroom ($p < 0.001$), and a greater percentage of the trial spent traveling sideways ($p < 0.001$). There were also several significant interaction effects, including between door type and the presence of an IV on distance motion ($p < 0.001$) and between room configuration and IV on the sideways motion ($p < 0.001$). These results suggest that the room configuration, type of door, and presence of medical equipment such as IV poles can significantly impact user performance and experience. These findings provide valuable insights for healthcare professionals and designers to optimize the design of spaces to enhance user experience and performance. Further research will build physical environments based on these results for more comprehensive biomechanical assessments of fall-risk.

Significance: The results of this study provide valuable insights into the effect of environmental factors on movement patterns in a simulated hospital room. These results highlight the importance of considering environmental factors when designing healthcare facilities, particularly with regards to fall risk. Using virtual reality can present an efficient and cost-efficient method to vary room configuration across a wide variety of designs before proceeding to testing physical iterations of spaces.

Acknowledgments: Funding from AHRQ R18HS025606.

References: [1] Spoelstra SL, et al. Clinical nursing research. 2012 [2] Burdea GC, Coiffet P. Virtual reality technology. 2003

INFLUENCE OF OPTIMIZATION INFORMED MUSCLE PARAMETERS ON FINGER KINETICS

Christopher T. Jadelis[1*], Carter K. Wang[1], Katherine R. Saul[1]
[1]Department of Mechanical and Aerospace Engineering, North Carolina State University, Raleigh, NC, USA
*Corresponding author's email: ctjadeli@ncsu.edu

Introduction: Musculoskeletal (MSK) models of the hand and fingers [1], [2] have been effective tools studying hand function and elucidating underlying biomechanics of clinical finger deformities [3]. This is of specific interest in stroke rehabilitation, since accurate prediction of hand kinetics is essential for control of wearable devices such as soft exoskeletons used in robotic rehabilitation [4], [5]. However, the use of MSK models in wearable devices has been limited because conventional MSK models are typically informed by cadaver or sparse in-vivo measurements and may be limited in patient specific applicability due to kinetic predictions that are not personalized. Subject-specific musculoskeletal parameters are essential to address this, but can be challenging to obtain, requiring extensive and invasive examinations. Indirect prediction of musculoskeletal parameters using electromyography (EMG)-informed optimization, and non-invasive measurements have been successfully applied in the lower limb [6], [7]; however, limited work has applied or validated this technique in the hand. To address this, we explored EMG-informed optimization techniques to predict subject-specific parameters in muscles governing index finger motion to assess the applicability of this method to the hand. We expect an MSK model informed by EMG optimization to predict muscle forces that differ from those predicted using from generic MSK models for the same kinematics due to altered muscle parameters.

Methods: An open-source dataset of finger kinematics and matched EMG were used in this study [8]. This dataset includes individual and concurrent flexion of the fingers for ten subjects, with five repetitions. These kinematics and EMG data were pre-processed for use with an existing MSK model of the hand and fingers implemented in OpenSim (v3.3) [2], [9]. We considered 7 muscles crossing the index finger: the extensor digitorum communis (EDC), extensor indices (EI), flexor digitorum superficialis (FDS), flexor digitorum profundus (FDP), first palmar interosseous (FPI), first dorsal interosseous (FDI), and the lumbrical of the index finger (LUM). The joints of the index finger in the model included the metacarpal phalangeal joint (MCP), proximal interphalangeal (PIP) and distal interphalangeal joint (DIP). To assess the conventional MSK model, the existing model was linearly scaled based on marker data indicating segment lengths, and computed muscle control (CMC) was applied to predict muscle forces for 5 trials of index finger flexion for a single subject. A subject-specific MSK model was created using the EMG-informed optimization toolbox titled "Calibrated EMG-Informed Neuromusculoskeletal Modelling Toolbox" (CEINMS) [6]. CEINMS was used to generate optimized muscle parameters for a single subject using the same 5 trials to calibrate the model. Maximum isometric force, tendon slack length, and optimal fiber length parameters were chosen for optimization, based on prior sensitivity analyses [10]. To evaluate the effect of the optimized parameters, CMC was applied to the optimized model, and predicted muscle forces were compared to that of the linearly scaled model without optimized parameters.

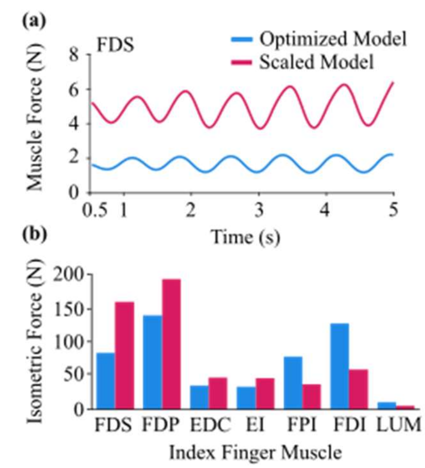

Figure 1. Predicted muscle forces of the FDS during the second trial (a) and changes in maximum isometric force (b) between the optimized and scaled models.

Results & Discussion: The optimized model was successfully calibrated using the five index finger flexion trials. Resulting parameters differed from the scaled model. The extrinsic muscles (EDC, EI, FDP, and FDS) were reduced in force-generating capacity, with the FDS maximum isometric force reduced by 48%. Conversely, the intrinsic muscles (FPI, FDI, and LUM) increased in maximum isometric force, with a 114% increase for the FDI, suggesting that intrinsic muscle strength required for stabilization is greater in the calibrated subject (**Fig. 1b**). Tendon slack length changes were less substantial; the FDI tendon slack length which was reduced by 14.8%. Optimal fiber lengths were unchanged from the scaled model. This variation in parameters resulted in a reduction in muscle forces during finger flexion in comparison to the scaled model. The largest effect was observed for the FDS muscle for trial 2 (**Fig. 1a**) with an average reduction of 3.23 N, representing a 65.8% change, suggesting that calibration of muscle parameters may enable more accurate subject-specific muscle force predictions in comparison to the scaled model alone. These analyses will be expanded to multiple subjects to assess generalizability of this method, and muscle parameters will need to be evaluated to assess physiologic validity.

Significance: This work demonstrates the novel application of EMG informed model optimization to a musculoskeletal model of the hand to predict subject-specific parameters that influence finger kinetics. The techniques demonstrated in this work can be expanded to calibrate a full MSK model of the hand as a study tool for subject specific hand biomechanics, and control of wearable devices.

Acknowledgements: NSF IIS- 2106747

References:
[1] A. J. Barry., *J. Biomech*, **77**, Aug. 2018 **[2]** D. C. McFarland., *IEEE Trans Biomed Eng*, Oct. 2022 **[3]** B. I. Binder-Markey., *J. Hand Surg*, **44**, Sep. 2019 **[4]** D. L. Crouch., *J. Neural Eng.*, **14**, Mar. 2017 **[5]** D. L. Crouch., *J Biomech*, **49**, Dec. 2016 **[6]** C. Pizzolato et al., *J Biomech*, **48**, Nov. 2015 **[7]** H. Kainz., *Clin Biomech*, **87** Jul. 2021 **[8]** S. K. Dwivedi., *IEEE Trans Biomed Eng*, **67** Sep. 2020 **[9]** S. L. Delp., *IEEE Trans Biomed Eng*, **54**, Nov. 2007 **[10]** R. Hinson., J Biomech, **141** Aug. 2022

DOES DIRECTION MATTER? AN ANALYSIS OF THE VOLLEYBALL ATTACK

Kiara Barrett[1*], Kyle Parrish[1], Lauren Luginsland[1], Hunter J. Bennett[1]
[1]Old Dominion University, Norfolk, Virginia
*Corresponding author's email: kbarr011@odu.edu

Introduction: Volleyball is a popular sport played around the globe. The main offensive movement in volleyball is the attack, in which players attempt to contact the ball in such a way that it cannot be returned resulting in a point scored. Typically, a ball that is hit with a greater velocity is more difficult to return. Many aspects of the attack can influence ball velocity and injury risk, as increases in shoulder flexion and abduction at ball contact are hypothesized to heighten injury risk [1]. For example, players can alter approaches, follow-throughs, and attack direction to elicit better performance. Research has shown no difference in ball speed when comparing attack direction [1], but a significant influence of technique on shoulder angles [2]. It is unknown how follow-through, or a combination of direction and follow-through, can influence ball velocity and shoulder kinematics. From a motor learning perspective, research shows motions we plan to do in the immediate future have an impact on the motor memory in the present [4]. In support of motor learning perspectives, previous research has shown that modifications to the follow-through can affect kinematic properties of an overhead movement prior to the beginning of follow-through, including ball velocity [3]. The purpose of this study is to compare kinematic parameters of the volleyball attack across direction and follow-through. We hypothesize that there will be no differences in kinematics across direction [1], however hitting the ball straight ahead with the same-side follow-through will result in greater degrees of shoulder abduction and internal rotation at ball contact.

Methods: 13 experienced volleyball players participated in this study. Participants performed a self-selected warmup and familiarization trials. Next, participants performed 5 successful trials of a volleyball attack off a stationary ball under four commonly performed conditions in a randomized order: a combination of attacking the ball in two directions (angle vs line) and following-through to different sides of the body (same-side vs cross-body). When hitting angle, the participants were instructed to hit towards the dominant arm side. Hitting line consisted of hitting straight ahead. The same-side follow-through consisted of the participant completing the attack with their dominant hand finishing on the ipsilateral side. When performing the cross-body follow-through, participants finished their swing with the dominant hand on the contralateral side. A 12-camera Vicon system (Vicon Vantage, 400Hz) was used to record 3D motion capture data of the upper trunk (thoracic & scapula), upper arm, forearm, and hand of the attack limb. Data was filtered with a low-pass Butterworth filter at 30Hz. Elbow (flexion and abduction) and shoulder angles (flexion, abduction, internal rotation), and hand velocity (resultant and multi-axial) at the point of ball contact were determined via Visual 3D (C-Motion, Inc.), using an XYZ rotation sequence. A 2x2 (direction by follow-through) Repeated Measures ANOVA was used to evaluate the effect of direction and follow-through on elbow and shoulder angles; dependent t-tests were used to compare multi-axial hand velocity (SPSS, IBM, Inc.; alpha $< .05$).

Results & Discussion: No significant interactions or main effects were found in hand velocity, elbow angle, shoulder flexion or shoulder abduction ($p>.05$). A significant effect of direction was found for shoulder rotation ($p=.04$) but not follow-through ($p>.05$). Averages and standard deviations of each variable are reported in Table 1. Our findings agree with previous research [1], suggesting no differences between shoulder abduction and elbow flexion at ball contact between ball trajectory directions. This is unsurprising, as players strive to attack in a similar manner each time to mask their intention from the defender. It has been hypothesized that smaller angles of shoulder flexion and abduction at ball contact decreases risk of injury [1,2]. Based on our results, no major differences in these angles exist between ball trajectory direction or follow-through. However, we did find a significant difference in rotation angle at ball contact. Participants presented with lower shoulder rotation angles when hitting "line", however the effect of internal rotation on injury risk has yet to be examined. Future research should investigate kinetics at the shoulder and its relationship with shoulder loading and injury.

Significance: This information has implications for injury risk and prevention as well as sport performance. Volleyball players can choose to hit in either direction, with any follow-through without fear of decreases in velocity. In addition, no differences exist between hypothesized indicators of injury risk, promoting the selection of any direction or follow-through deemed ideal for task success.

References: [1] Reeser et al. (2010), *Sports Health* 2(5). [2] Seminati et al. (2015), *Sports Biomech* 14(2). [3] Beseler et al. *J. Mot Learn and Dev* 10(2). [4] Howard et al. (2015) *Current Biology* 25(3).

		Cross		Line	
		CB	SS	CB	SS
Hand Velocity (m/s)	Resultant	12.57(2.61)	11.44(3.12)	12.86(2.95)	12.67(3.03)
	Mediolateral	0.15(3.25)	0.49(3.03)	-0.90(2.32)	-0.78(1.86)
	Ant/Posterior	11.06(2.38)	10.46(2.28)	11.81(2.40)	11.71(2.52)
	Vertical	-4.97(1.89)	-4.80(2.15)	-4.67(2.31)	-4.60(2.09)
Elbow Angle (deg)	Flexion	18.35(8.28)	19.20(9.85)	18.04(9.82)	17.77(9.94)
	Abduction	-7.59(7.34)	-6.66(6.75)	-7.44(8.54)	-6.16(7.22)
Shoulder Angle (deg)	Flexion	138.52(16.90)	139.23(13.37)	139.86(12.86)	141.36(12.88)
	Abduction	-41.04(12.56)	-39.09(10.23)	-38.38(8.00)	-37.57(8.65)
	In Rotation	**66.36(23.62)**	**70.10(20.65)**	60.44(21.65)	66.41(19.77)

Notes: Mean(SD). CB: Cross-Body, SS: Same-side. Bolded values are statistically different across direction

A COMPARISON OF MEDIOLATERAL SURFACE TRANSLATION AND FOOT PLACEMENT PERTURBATIONS ON BALANCE CONTROL AND RESPONSE STRATEGIES

Lydia G. Brough[1]* and Richard R. Neptune[2]
[1]New York Yankees Performance Science, Tampa, FL, USA
[2]Walker Department of Mechanical Engineering, University of Texas at Austin, Austin, TX, USA
*Corresponding author's email: lydia.brough@utexas.edu

Introduction: Balance perturbations can be used to gain insight into the underlying mechanisms of balance control in both healthy and pathological populations. Mediolateral surface perturbations [1] and foot placement perturbations [2] may produce similar balance responses since both apply a force at the foot to produce a mediolateral balance disturbance. However, the effects of these perturbations have not been directly compared. Lateral hip and ankle strategies have been observed following medial foot placement perturbations [2] while bilateral hip reactions have been observed after mediolateral surface perturbations [1]. Others have shown that trunk muscles are active in response to mediolateral slips [3]. During mediolateral surface perturbations, some individuals allow their whole body to translate with the perturbation rather than attempting to keep their center of mass stationary [4], which is a strategy that is not possible with foot placement perturbations.

The purpose of this study was to compare the influence of two similar mediolateral perturbations (foot placement versus surface translation) on balance control and responses strategies at the hip, ankle and trunk. Because surface perturbations allow whole body translation over the foot while foot placement perturbations do not, we hypothesized that foot placement and surface translation perturbations of similar magnitude and timing would produce different balance response strategies.

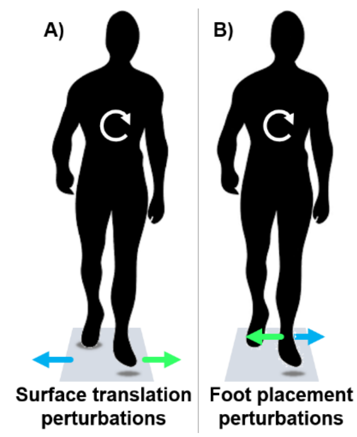

Figure 1: Medial (green) and lateral (blue) balance perturbations were produced by treadmill surface translations and by a force applied to the ankle. The white arrows indicate the direction of positive rotation in the lab reference frame.

Methods: Kinetic and motion capture data were collected during two separate studies, each with 15 young, healthy participants walking on an instrumented treadmill. In both studies, medial and lateral balance perturbations were applied at 80% of the gait cycle (~200 ms before heel strike). For the surface translations, a custom D-flow (Motek, Amsterdam, NL) script was developed to produce 3.0 cm medial and lateral surface translations applied to the stance leg (Fig. 1A). For the foot placement perturbations, a pneumatic device released compressed air medially or laterally at the swing ankle to perturb their foot placement by approximately 3.5 cm from the unperturbed trajectory (Fig. 1B). Joint muscle moments and frontal plane whole-body angular momentum (*H*) were calculated in Visual 3D (C-Motion, Germantown, MD). Differences between perturbed and unperturbed gait cycles were assessed using one-dimensional statistical parametric mapping two-tailed paired t-tests [5].

Results & Discussion: Both medial surface perturbations and foot placement perturbations produced an increase in *H*, indicating a disruption to balance control [6]. However, the increases in *H* were more dramatic and were sustained longer into the gait cycle after the foot placement perturbations compared to surface perturbations (Fig. 2). Changes in joint moments were much lower for the foot placement perturbations compared to the surface translation perturbations.

Thus, as hypothesized, the perturbations produced different balance response strategies. Moreover, the effects of the surface translation perturbation were less disruptive to balance control than the foot placement perturbation. Although both types of perturbations had similar magnitude and timing, during the treadmill surface perturbations, participants could translate their body center of mass with the treadmill, which limited the body rotational effects and changes to frontal plane angular momentum. In contrast, the foot placement perturbations were applied to the swing foot, which limited the body's translation due to the constraint of the stance foot on the ground and instead produced a whole-body rotational effect.

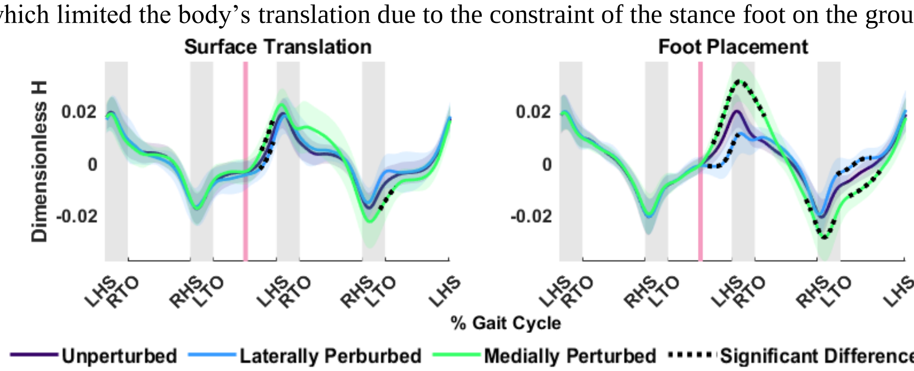

Figure 2. Frontal plane whole-body angular momentum during unperturbed steps and after medial and lateral surface and foot placement perturbations. The vertical solid line indicates the timing of the perturbation. Dotted lines indicate a significant difference between the perturbed and unperturbed trials.

Significance: These results have implications for developing perturbation-based balance training, as mediolateral surface translation perturbations may not produce the desired response strategies to help reduce fall risk in clinical populations.

Acknowledgements: This research was supported in part by the NSF Graduate Research Fellowship Program.

References: [1] Afschrift et al., 2018, *Sci. Rep. 8.* [2] Brough et al., 2021, *J Biomech* 116, 110213 [3] Oliveira et al., 2012, *J. Neurophysiol*. 108, 1895–1906 [4] Brady et al., 2009, *Gait Posture* 29, 645–649 [5] Pataky, 2012, *Comp Methods Biomech Biomed Eng*, 15(3):295-301 [6] Neptune and Vistamehr, 2019, *J Biomech Eng* 141, 070801.

DO HUMANS USE MUSCLE ACTIVATION OR ENERGY COST TO SELECT WALKING SPEED? WHAT WE CAN LEARN FROM ANKLE EXOSKELETON INTERVENTIONS

Benjamin A. Shafer[1*], Kiandra Peart, Richard So, Aaron J. Young, Gregory S. Sawicki
[1]George W. Woodruff School of Mechanical Engineering, Georgia Institute of Technology, Atlanta, GA
*Corresponding author's email: Ben.Shafer@gatech.edu

Introduction: Although the cause of slower walking with age is still unknown, exoskeletons may provide a viable solution for rapid increases in mobility for older adults. Walking speed declines as we age and has been correlated to reductions in quality of life and independence. Humans typically walk at speeds that minimize energy consumed per unit distance (cost of transport; COT) but this may not hold in older adults [1]. Changes in metabolic cost per unit muscle activation accompanying the distal-to-proximal shift in lower-limb joint power output with age [2] may dissociate the relationship between COT and lower-limb cumulative muscle activity per distance (CMAPD) in older adults. The resulting divergence in CMAPD vs. COT cost landscapes could help identify the underlying mechanism driving self-selected walking speed (SSWS) in humans. Exoskeletons provide a tool to modulate the COT [3] and muscle activity needed to walk at a given speed. Together, measuring changes in COT and CMAPD with exoskeleton assistance applied to younger and older adults could determine whether COT or CMAPD better correlates with changes in SSWS. We hypothesize that changes in the CMAPD rather than COT optimal speed will better correlate with changes in SSWS due to exoskeleton assistance.

Methods: We used Dephy ExoBoots to apply assistive ankle torque to 3 younger adults (YA) and measured their overground SSWS without the exoskeletons (NoExo) and with optimized assistance (Exo). To compare optimal COT and CMAPD speeds, we measured whole-body metabolic cost and muscle activity in 8 lower limb muscles (tibialis anterior, soleus, medial gastrocnemius, vastus medialis, rectus femoris, biceps femoris, gluteus maximus, gluteus medius) across 5 different speeds ($SSWS_{NoExo}$, $SSWS_{NoExo}$ +/- 33% & 67%, and $SSWS_{Exo}$). We fit a quadratic curve to the COT & CMAPD data across speeds for each Exo condition per each participant. Using the optimal speed (i.e., speed at minimum COT or CMAPD) for each curve, we plotted the percentage difference (Exo from NoExo) in COT and CMAPD vs. percentage difference in SSWS and fit a linear regression to the across participant data.

Results & Discussion: Despite tuning to optimize exoskeleton (Exo) assistance for increased SSWS, upon validation we found that Exos did not change SSWS (Fig. 1 A&C). Nevertheless, Exo assistance did lead to measurable changes in the speed for min COT and min CMAPD (Fig. 1, A-D). Optimal speeds for min COT and min CMAPD were slower than the associated SSWS, likely due to measurement location (treadmill for COT and CMAPD, overground for SSWS). Overall, Exo use decreased COT at optimal speeds, increased COT at the slowest and fastest speeds (Fig. 1A) and did not have a large effect on CMAPD across speeds (Fig. 1C). Changes in optimal COT speed were negatively correlated with changes in SSWS (Fig. 1B), while changes in CMAPD were positively correlated (Fig. 1D). Overall, CMAPD more strongly correlated with changes in SSWS than COT.

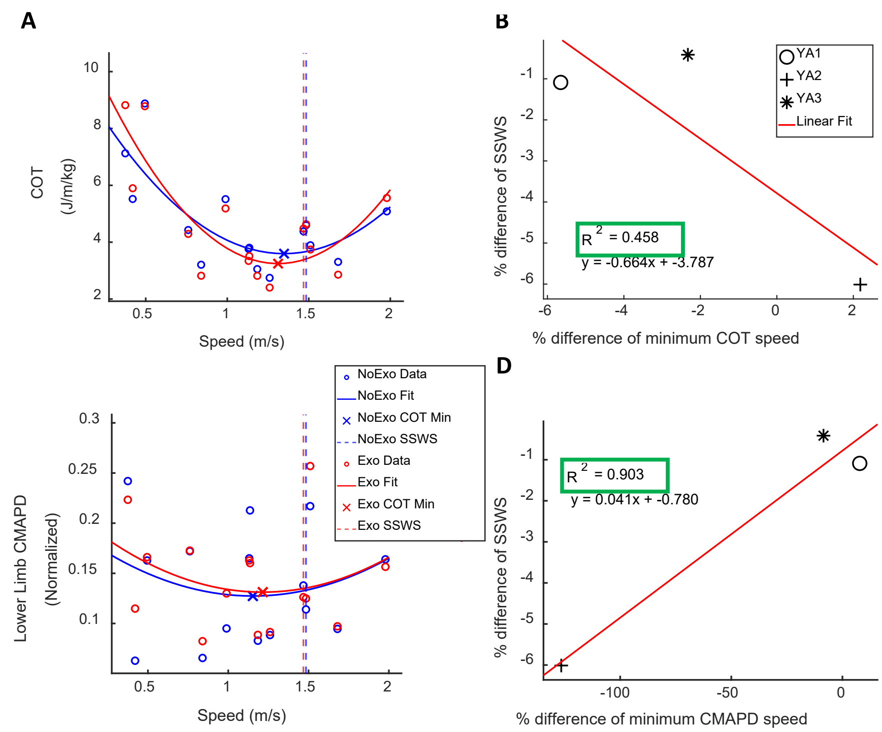

Figure 1: (A) COT vs Speed for all subjects (N = 3) for Exo (red) and NoExo (blue), each fit with a quadratic curve and its minimum marked. (B) Linear regression between percentage change between Exo and NoExo in optimal COT speed and SSWS per subject. (C) Lower Limb CMAPD vs Speed for all subjects (N = 3) for Exo (red) and NoExo (blue), each fit with a quadratic curve and its minimum marked. (D) Linear regression between percentage change between Exo and NoExo in optimal Lower Limb CMAPD speed and SSWS per subject.

Significance: Exoskeletons can be used to understand more about human behaviour by driving changes in users' physiological response. Here we have shown that COT may not be the best predictor for SSWS compared to CMAPD. This may be intuitive, as the body has no way of directly measuring energy consumption, but does have sensory organs that correlate with muscle loading (e.g., spindles, Golgi tendons). Interventions that reduce relative muscle activation (i.e., making muscles 'stronger') could more directly affect walking speed selection. A follow-up study with older adults that includes hip Exo assistance will compare changes in SSWS across target joints.

Acknowledgements: This work was supported in part by the NSF NRI (1830215) to A.J.Y. and the NIH NIA (R01AG058615) to G.S.S.

References: [1] Martin et al. (1992), *J App Phys* 71(1); [2] Delabastita (2021) *Scand J Med Sci Sports.* [3] Slade et al. (2022) *Sci Rob* 610

EMG Based Optimization for Squat Assistance with Ankle-Foot Exoskeleton

Hyeongkeun Jeong[1], Ashutosh Tiwari[1], Myunghee Kim[1*]
[1]University of Illinois at Chicago, Chicago, Illinois, U.S.
*Corresponding author's email: myheekim@uic.edu

Introduction: Personalized assistance by ankle-foot exoskeleton could help users squat by enhancing user's work profitability and by relieving fatigue compared to non-assistance. A Conventional method for assistance personalization has adopted the human-in-the-loop (HIL) optimization [1], which usually uses a respiratory sensor to estimate metabolic cost. However, its optimization term was too long, resulting in fewer parameter explorations. Previous research [2, 3] revealed rectus femoris activation and quadriceps dominant synergy activation reduced in squatting compared to non-assisted conditions and showed a meaningful correlation. We aimed to evaluate a cost estimation method by muscle activity when squatting in the HIL optimization. In this study, we conducted the HIL optimization process (N = 1) while using Rectus femoris (RF) activation as a cost function and found optimal parameters for the ankle-foot exoskeleton. During validation, quadriceps muscle activations in the optimal condition were compared to unpowered and no-device conditions.

Methods:
The experimental study protocol includes a single male subject (Weight: 69.5 Kg, Age: 35, Height: 175 cm) equipped with the modular ankle-foot exoskeleton (AFE). The AFE was developed in-house using additive manufacturing which incorporates the active plantarflexion and passive dorsiflexion range of motion. The plantarflexion power was provided using the dual cable-transmission portable setup, whereas the elastic band was used to provide passive dorsiflexion assistance. The motor actuation was controlled using the PC-based real-time control TwinCAT software (Beckhoff Automation, Germany). The TwinCAT integrates with the custom-designed Simulink controller model in MATLAB to decide the logic for the motor operation. In addition to the exoskeleton, the subject was equipped with three electromyography sensors (TrignoEMG, AD Instruments, USA) to record the muscle activity of the rectus femoris (RF), vastus lateralis (VL), and vastus medialis (VM). The ankle torque, ankle angle, and EMG data were time-synchronized and collected in real-time using the MATLAB code.

The experimental study was conducted during two different sessions, namely, Day1 and Day2. Day1 was acclimation day and on Day2, the human-in-the-loop optimization of the AFE parameter was executed. On Day1, the baseline data were collected while the subject was asked to squat without wearing the AFE for 3 min. Subsequently, the subject was asked to squat while wearing the AFE for three different assistive conditions, i.e., unpowered, low plantarflexion (26 Nm), and high plantarflexion (40 Nm) assistance in a random manner. The subject was instructed to squat for a total of 8s per squat cycle, which includes 1 s descent, 1 s ascent, and 6 s rest standing between each squat. A total of 12min rest time was provided between the conditions.[2] On Day2, we conducted the EMG-based human-in-loop (HIL) optimization, which was largely composed of two sessions. ***Session 1 (HIL optimization):*** In this session, we determine the personalized stiffness parameters of the AFE for the ascent and descent stages of squatting using real-time EMG cost measurements. This involved employing the HIL Bayesian optimization technique [1] with EMG as a cost. The selected stiffness parameters for both ascending and descending phases were subsequently used to validate the optimization-based assistance. After completing the HIL optimization for 15min, the subjects were allowed to rest for 45 minutes. ***Session 2 (Personalized assistance):*** In the validation study, the stiffness condition identified as optimal (personalized) through the HIL optimization procedure was compared to both the unpowered and no-device conditions. The detailed validation study protocol has been outlined in Kantharaju et al. [2]. For analysis, only the last three minutes of the data collected were considered.

Results & Discussion: In our preliminary study, on the assisted leg, the personalized condition affected quadriceps muscles, including the RF, VL, and VM activities. The personalized assistance reduced rectus femoris activity by 41% and 40% compared to the unpowered and no-device conditions, respectively (Fig. 1.A). The VL decreased by 8.8% and 11.7% compared to the unpowered and no-device conditions, respectively (Fig. 1.B). The VM decreased by 20% and 12.3% compared to the unpowered and no-device conditions (Fig. 1.C).

This reduced activity on quadriceps muscles by the ankle-foot exoskeleton supports the results [2, 3]. The squat activity is a closed chain exercise, so ankle-foot assistance decreases quadriceps muscle activity [3]. The future work includes full data collection to evaluate the effect of the EMG-based optimization on the physical effort during the squat exercise. If successful, this method could potentially help reduce muscle activity and increase overall squat efficiency and performance.

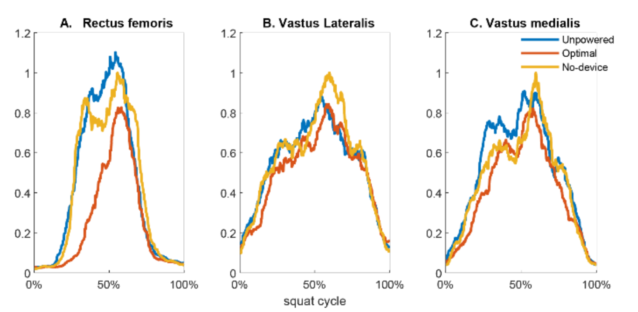

Figure 1. The mean trajectory of each muscle activity during unpowered, optimal and no-device conditions during squat cycle. The last 7 squat was selected for the mean trajectory of each muscle. 0% is the stand phase, 50% is the squat bottom phase, and 100% is the stand-back phase. Each data was normalized by the peak value of the mean trajectory of muscle activities in the no-device condition.

Significance: In the future, we can integrate EMG and exoskeleton within a wearable device to personalize the assistance in real-time. This could be potential because the conventional method using a respiratory sensor is not feasible and uncomfortable to use daily.

References:: [1] Ding et al. (2018), *Science Robotics* 3(15); [2] Kantharaju et al. (2022), *IEEE TNSRE* 30; [3] Hyeongkeun Jeong (2023), *Scientific reports* 13(1).

EFFECT OF MOTION AND OXYGENATION LEVEL ON HUMAN-IN-VEHICLE ROLL TILT TASKS

Lanna Klausing[1], Molly Fenik[1], Paige Kompa[2], Timothy Reissman[1], Anne Crecelius[2], Megan Reissman[1*]
[1]EMPOWER Lab, Department of Mechanical and Aerospace Engineering, University of Dayton, Dayton, OH, USA
[2]HP Lab, Department of Health and Sports Science, University of Dayton, Dayton, OH, USA
*Corresponding author's email: mreissman1@udayton.edu

Introduction: Upper extremity human motor control has largely focused on tasks presented under stationary conditions [1]. However, many related real-world tasks involve controlling a vehicle, such as a car or aircraft. In such cases the visual and vestibular influence of vehicle movement on the operator must also be considered [2]. Of particular interest is aircraft pilot disorientation, in which the human has reduced or incorrect perception of their orientation in space [3-4]. The use of Virtual Reality (VR) headsets and motion platforms allows for simulation of both the visual and vestibular sensory information during a vehicle orientation task. In this work our focus was on human performance of vehicle roll tilt angle, as this is a critical task for aircraft pilots when executing coordinated heading changes. The purpose was to determine the role of vestibular sensory information on human motor control by testing with the motion active (Motion) and stationary (No Motion). Our first hypothesis was that task performance would be improved when matched vestibular sensory input was provided, as multiple sensory inputs have been shown to strengthen spatial orientation estimates [5]. Additionally, as reduced brain oxygenation (hypoxia) is thought to be a possible contributor to pilot disorientation, we aimed to study the impact of oxygenation level (Oxygen Level) for the same roll tilt task. Our second hypothesis was that hypoxia would increase roll tilt error due to prior work showing that hypoxia significantly lowers alertness levels in pilots over time [6].

Figure 1: Experimental setup showing motion simulator, VR headset, joystick, and neck brace arrangement. Note gas mask is not shown.

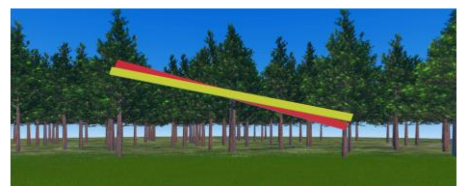

Figure 2: Custom VR environment showing roll tilt target bar (red) and the final vehicle angle orientation feedback (yellow).

Methods: Healthy participants (n=12) sat in a motion platform (YawVR) while wearing a VR headset (Vive Pro) [Figure 1]. A custom VR simulation (Unity) presented roll tilt angle targets which appeared as a visual bar tilted to either 10° or 20° [Figure 2]. Participants controlled a joystick (Thrustmaster Airbus), where leftward stick displacements caused left roll tilt in the virtual vehicle and vice versa. Participants were instructed to adjust their vehicle roll angle to align with the visual target within 10 seconds per trial and click a trigger on the joystick to indicate their finalized vehicle orientation selection. Visual orientation, in VR headset, was shown for all trials. For Motion trials, the visual roll tilt angle was also commanded to the motion simulator. For No Motion trials the motion simulator was on but held in a fixed, level position. Participants wore an oro-nasal breathing mask which provided 21% oxygen during normoxic trials and 10% oxygen (equivalent to 14,000 ft altitude) during hypoxic trials. Inspired O_2 and expired CO_2 were monitored on a gas analyzer (ADInstruments). All participants completed the full set of trials under normoxic conditions to train (data not included here). After training, a hypoxic set and a normoxic set were completed, with presentation order randomized, and a 20 minute break between. All Unity based data was exported (90 Hz) and analyzed (Visual3D) to determine metrics of final roll tilt error and task completion times.

Results & Discussion: The magnitude of the tilt task resulted in different characteristics. For low roll (10°) tasks, factors of Motion or Oxygen Level were not significant for roll tilt error ($p>0.05$). However, Motion trials were significantly longer for task completion time ($p=0.031$, $P=0.58$), while the factor Oxygen Level had no significance for this metric. This suggests that for small vehicle corrections, the impact of the vestibular sensory information and brain oxygenation on human motor control performance is likely low.

For high roll (20°) tasks, Motion and Oxygen Level were significant factors for roll tilt error ($p<0.001$, $P>0.99$ and $p=0.021$, $P=0.64$ respectively). For Motion trials, participants undershot their roll tilt target by -2.6° on average versus -0.1° for No Motion trials. While hypoxic, participants undershot their roll tilt target by -1.6° on average versus -1.1° under normoxic conditions. With respect to roll tilt variability, Motion was significantly greater ($p<0.001$, $P=0.93$), while Oxygen Level was not significant for this metric. Additionally, Motion trials were significantly shorter for task completion time ($p=0.014$, $P=0.69$), while the factor Oxygen Level had no significance. This suggests that with a larger roll tilt, the vestibular input may have a greater negative impact on human motor control performance, which refutes our first hypothesis. Further, our second hypothesis is accepted but only when also exposed to larger body tilt.

Significance: While Motion did not improve the roll tilt task performance, it did highlight that the presence or absence of motion is a significant factor when larger changes in body orientation are performed. Oxygen Level also was shown to be an important but seemingly smaller factor than that of Motion, and only relevant at a higher roll tilt magnitude. Thus, studies of human-in-vehicle performance should prioritize including vehicle motion to better characterize human motor control of tasks such as aircraft piloting maneuvers.

Acknowledgements: This work was funded by the Multiloop Cybernetic System MURI (MURI, N000142012163).

References: [1] Rosenbaum (2009), *Human motor control*; [2] Gillingham & Previc (1993), Spatial orientation in flight; [3] Ledegang & Groen (2018), *Aero Med & Human Performance*, *89*(10); [4] Boril et al. (2020), *Aero Med & Human Performance*, *91*(10); [5] Zupan et al. (2002), *Bio Cybernetics* 86(3); [6] Steinman et al. (2017), *Aero Med & Human Performance* 88(8)

IMPACT OF CLASSIFICATION ON TRUNK KINEMATICS IN JUNIOR WHEELCHAIR BASKETBALL ATHLETES

Hannah Houde, Jerad Kosek, Jordan Tompkins, John Grace, Meghan Hancock, Christopher Wilburn and, Wendi Weimar

Auburn University, School of Kinesiology, Auburn, AL, U.S.A

Introduction:
Participation in sports activities for people with a disability has increased over the past years, yet literature is limited regarding wheelchair propulsion in sports. Most studies on wheelchair propulsion have investigated able-bodied participants or individuals using wheelchairs for daily use instead of a sport specific wheelchair. Additionally, research inclusive of specific populations, such as junior wheelchair athletes, also remains limited. Therefore, the purpose of this study was to assess how wheelchair basketball classification (based on function) affects sport specific reaction time and sprinting performance in junior wheelchair athletes while in sport-specific wheelchairs.

Methods: 15 athletes volunteered to participate in this project and performed two sprinting conditions; a linear 15-meter sprints (three trials) and a "Go-Stop-Go" 15-meter sprints (three trials). During the "Go-Stop-Go" task, participants were told to stop at a random point during the 15-meter sprint. After coming to a full stop, the participants were told to complete the sprint trial. Athletes were given a proposed classification score (PCS) by a certified classifier. The lower the number the less function and the greater the impact individual's disability has on their propulsion and play. Due to the relatively small sample size per classification level, the participants were grouped into high classification (2.5-4.5) and low classification (1-2.0) groups. Each participant used their own sports wheelchair that they used for competition and practice. Reaction and sprint times were collected utilizing a timing watch (Jawku®, Pheonix, AZ).

Results A series of repeated measures ANOVA'swere performed using SPSS (Version 27, IBM. Armonk, NY) to determine if proposed classification score influences trunk kinematics, overall time and reaction time during various sprinting tasks. The results demonstrated significance for time during the linear sprinting (LS) condition $F (7,12) =5.6363$, $p =.005$; $\eta^2=767.$). There was also significance between classification and reaction time $F (3,12) =9.954$; $p =.001$; $\eta^2=341$). There was no statistical significance found between the LS task, trunk maximum ($p=0.60$) or trunk minimum angle ($p=.037$). For the go-stop-go condition, there was no statistical significance for trunk maximum angle, ($p=.056$). No statistical significance was found for trunk velocity when compared to classification ($p=.021$), however, trunk maximum velocity during the go-stop-go condition when compared to classification $F (3,12) = 7.108$, $p=.005$, $\eta^2=.753$. but no statistical significance found in trunk minimum velocity ($p=.030$, $\eta^2=.493$).

Discussion: This sample of data demonstrated significance of time, classification group and velocity. These variables are impactful when determining training techniques for junior wheelchair basketball athletes and developing proper pushing mechanics. Although other results were not statistically significant these results can be interpreted as athletically significant because the magnitude of the difference between classification groups would inform and influence training protocol differences between these two groups. Further research is needed to identify if the classification process is sensitive enough to stratify junior athletes by function and not by talent.

References:[1] Bergamini, et al., 2015. BioMed Research International. 2015: 275965. [2] Mukherjee, et al., 2005. Indian Journal of Medical Research.121, 747:758. [3] Zhao, et al., 2003. Journal of Engineering in Medicine 217:405

MUSCULAR AND KINEMATIC ADAPTATIONS TO A SHOULDER EXOSUIT

Kaleb Burch[1], Jill Higginson[1,2]
[1]Mechanical Engineering, University of Delaware, Newark, DE, USA
[1]Biomedical Engineering, University of Delaware, Newark, DE, USA
email: kburch@udel.edu

Introduction: Activities of daily living (ADLs) such as reaching for a high shelf are vital for independent living [1-2]. Unfortunately, many individuals struggle to perform these tasks independently due to conditions such as stroke [2-3]. Technologies such as exosuits have the potential to empower these individuals to perform ADLs independently by assisting limb motion: for example, post-stroke walking speed has been improved with a lower extremity exosuit [4]. However, exosuits that assist shoulder motion are less common and little has been done to assess the effect of these exosuits on muscle activity and kinematics during functional tasks such as a high reach.

Figure 1: Shoulder exosuit pictured from behind with major components labelled.

Methods: The exosuit in this study (Fig. 1) consists of an upper arm wrap and torso harness composed of a backplate, shoulder pad, and adjustable straps around the shoulders and waist. The exosuit assists shoulder motion using a cable driven by a motor-pulley actuation system (motor: Maxon EC flat 45, 70W) which winds the cable around a spool to produce tension. A load cell (ATO) sits at the junction between the cable and arm wrap to measure forces applied to the arm.

A single subject performed a series of self-paced reaches to a tripod positioned according to the subject's hand position at 90˚ shoulder flexion and 30˚ elbow flexion. First, the subject performed 20 reaches without wearing the exosuit (NO_EXO). Then, the subject put on the exosuit and performed a 120-reach assisted phase (EXO_ON) in twelve 10-reach increments with rest periods of 1-3 minutes, followed by a 20-reach unassisted phase while still wearing the exosuit (EXO_OFF). During the EXO_ON trials, the subject used a switch with their left hand which triggered a pre-set assistive force pattern up to 40N.

Kinematics of the shoulder, elbow, and wrist were recorded via motion capture with retroreflective markers placed on the torso, upper arm, and forearm, and hand. Muscle activity of the deltoid heads (anterior, middle, and posterior) was recorded using surface EMG (Delsys Trigno Avanti). This data was filtered with a 20-450Hz 4th order bandpass Butterworth filter, rectified, and filtered again with a 6th order 5 Hz lowpass Butterworth filter.

Mean muscle activity and movement duration was compared across NO_EXO, EXO_ON, and EXO_OFF. We hypothesized that muscle activity during the EXO_ON phase would be lower than the other phases for all muscles.

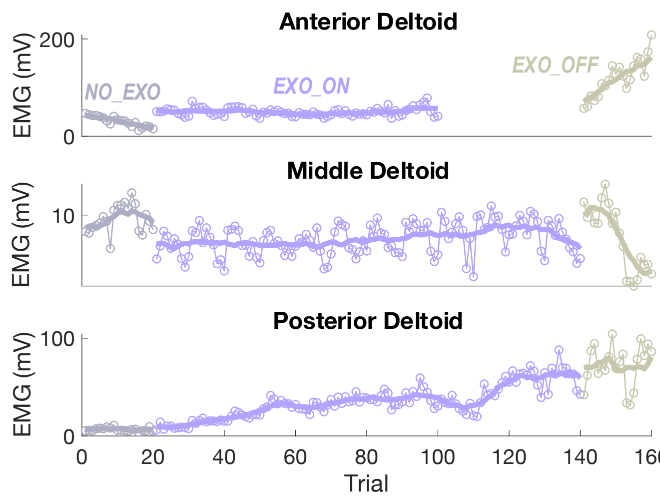

Figure 2: Mean muscle activity of each reach for the anterior, middle, and posterior deltoid heads. Each reach is represented by an open dot. The NO_EXO condition is indicated with grey dots, EXO_ON with purple dots, and EXO_OFF with gold dots. The thick lines represent 10-reach moving averages for the corresponding condition. For the anterior deltoid, trials 91-120 were excluded since the EMG electrode had poor skin contact which altered the signal.

Results & Discussion: Mean anterior deltoid muscle activity during EXO_ON was greater than NO_EXO (64.7% increase) but less than EXO_OFF (58.4% decrease) (Fig. 2). Mean middle deltoid muscle activity during EXO_ON was less than NO_EXO (21.1% decrease) and than EXO_OFF (4.7% decrease). Mean posterior deltoid muscle activity during EXO_ON was greater than NO_EXO (320% increase) but less than EXO_OFF (61.6% decrease). The contrast between the mixed effects of assistance on the anterior deltoid and the decrease in middle deltoid activity is counterintuitive since the cable is more closely aligned to the line of action of the anterior deltoid than the middle deltoid. Furthermore, the increases in posterior deltoid activity were not anticipated. These patterns were further evaluated by considering movement duration. Movement duration was faster in EXO_ON trials compared to NO_EXO by 74ms (5.9% decrease) and compared to EXO_OFF by 163ms (12.2% decrease). These results indicate that the subject did not necessarily reduce effort expended when assisted by the exosuit, but instead moved at a faster pace. Posterior deltoid activity increased, which might indicate that this muscle was controlling the acceleration of the upper arm. This effect could be a response to the stiff force transmission of this exosuit which resisted movement against the cable.

Significance: These initial results demonstrate that a shoulder-assistive exosuit can reduce muscle activity in some muscles and accelerate movement duration during a functional reaching task.

Acknowledgements: UNIDEL Foundation, Inc.

References: [1] Oosterwijk et al., (2018), *Physioth Theory & Pract.* 34(7); [2] Lai et al., (2002), *Stroke* 33(7); [3] Kwakkel et al., (2003), *Stroke* 34(9); [4] Awad et al. (2020), *J NeuroEng & Rehab* 17(1).

TRANSTIBAL PROSTHESIS USERS LUNGING AND REACHING: EVALUATING FUNCTIONAL ABILITY AND LOWER LIMB LOADING

Rachel H. Teater*, Derek N. Wolf, Karl E. Zelik
Department of Mechanical Engineering, Vanderbilt University, Nashville, TN
*Corresponding author's email: rachel.h.teater@vanderbilt.edu

Introduction: Many lower limb prosthesis users (LLPUs) have mobility challenges that make it difficult to independently perform activities of daily living [1]. Surveys of transtibial LLPUs have found that 25% cannot pick up an item off the floor, 41% cannot get up from the floor, and 40% do not have independent household mobility [1,2]. Even users with a high level of functional ability struggle with daily tasks such as bending down or shifting weight from one limb to the other without losing their balance [3]. Performing a lunge or reaching forward to pick up an item are movements that require a significant amount of lower limb strength and coordination. These movements are common in daily life and are also the foundation of more complex movements required for independent living, recreational activities, and some occupations. Characterizing the performance and movement patterns of LLPUs during these movements could inform interventions to increase the safety and ability of users to complete daily tasks. Therefore, the objective of this study was to characterize the functional ability and lower limb force distribution of transtibial prosthesis users during reaching and lunging.

Methods: Eight unilateral transtibial LLPUs (7M/1F, 39 ± 14yrs, 1.78 ± 0.13m, 85.8 ± 14.1kg, all K4) participated in this study wearing their prescribed prosthesis. Participants performed three repetitions of lunging and reaching with each limb leading. An example image for each task is pictured in Figure 1. For lunging, participants were instructed to lunge to a comfortable depth. For reaching, participants were instructed to reach for a light object (approximately 1.5m in front of them and 0.25m off the ground) by stepping forward with one foot while leaving the other foot in place. If a participant could not complete a task, this was documented before proceeding to the next task. Ground reaction force (GRF) data were recorded under each foot using in-ground force plates (AMTI) during all tasks. Participant feedback on perceived effort, stability, and comfort for each task was collected using a scale of 0 to 10. We computed the percentage of force in the front limb by dividing the vertical GRF under the front limb by the total vertical GRF under both limbs. We computed this percentage for each task iteration either at the bottom of the lunge or at the moment the object was picked up. The percent force in the front limb was compared between the two versions of each task, the intact limb leading and the prosthetic limb leading, using a paired t-test or Wilcoxan sign-rank test ($\alpha=0.05$). Eight able-bodied controls (5M/3F, 35.9 ± 9.7yrs, 1.77 ± 0.09m, 78.4 ± 14.6kg) were also recruited and tested with the same protocol to provide a reference for interpretation of LLPU results.

Results & Discussion: All eight LLPUs were able to complete a lunging motion with both limbs leading. However, two participants were unable to complete the reaching task. The oldest participant (66 years) required a handrail for support. Another participant needed the object moved closer for him to complete the reach with his prosthetic limb in front. Overall, participants reported that they felt unstable and that the tasks required a high amount of effort (most users rated effort a 7 out of 10 or greater). Six of eight participants reported they preferred to lunge and reach with their intact limb leading. On average, LLPUs put 85% of their force through their intact limb during lunging when it is in front. This is significantly more than when they lunge with their prosthetic limb in front where they put 63% of their total GRF in their front limb ($p<0.001$, Fig. 1). Similarly, during reaching, LLPUs put more force through their front limb when their intact limb is leading (91%) compared to when their prosthetic limb is in front (78%, $p<0.02$). During lunging and reaching, able-bodied controls put the majority of force through their front limb (Fig. 1). LLPUs also put more force in their front limb, but the proportion of force between limbs is different depending on which limb is in front. LLPUs put a greater percentage of force in their front limb when it is their intact limb. During unstable movements, LLPUs may prefer to rely on their intact limb more and adopt movement patterns that place greater demand on their intact limb, which may increase risk for degenerative joint disorders, which occur frequently in LLPUs. This is also likely why most participants preferred to perform these tasks with their intact limb leading.

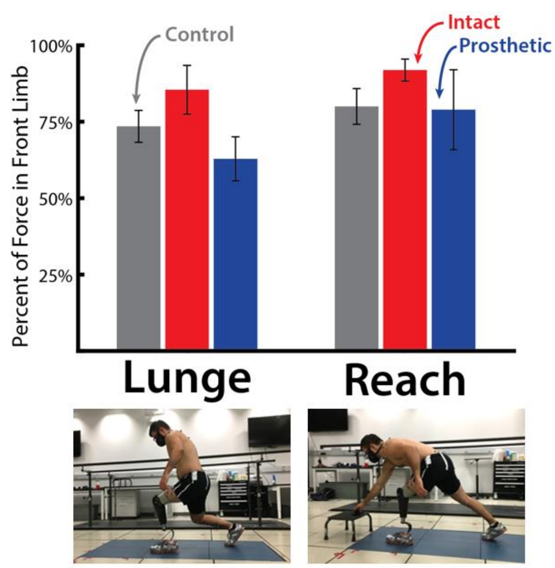

Figure 1: Percent of vertical ground reaction force in the front limb during lunging and reaching. LLPU data are in red for intact limb leading and blue for prosthetic limb leading. Control participant data are in grey.

Significance: This is one of the first investigations into the performance of LLPUs performing lunging and reaching movements which are essential for daily life. We found that LLPUs prefer to load their intact limb more than their prosthetic limb during these tasks that they found both challenging and unstable. Understanding how LLPUs currently do these movements is an important step towards developing prosthetic device or rehabilitation interventions. Interventions that enable LLPUs to feel more stable when loading their prosthetic limb could increase their ability to complete lunging and reaching movements in addition to other activities of daily living.

Acknowledgements: This research was supported by NIDILRR (90IFRE0001), NIH (T32EB021937), and NSF GRFP (1937963).

References: [1] Gauthier-Gagnon et al. (1999). *Arch Phys Med Rehabil* 80. [2] Davies and Datta (2003). *Prosthet Orthot Int* 27(3). [3] Morgan et al. (2022). *Disabil Rehabil* 44.

A NEURAL NETWORK'S JOURNEY IN UNDERSTANDING BONE STRENGTH

Andrew R. Wilzman[1*], Karen L. Troy[1]
[1] Worcester Polytechnic Institute, Worcester, Massachusetts 01609
*Corresponding author's email: arwilzman@wpi.edu

Introduction: Finite Element Analysis (FEA) was heavily developed in the 20th century for structural analysis of everything from buildings and dams to airplanes and spacecraft. Today, biomedical engineers rely on the accurate estimations of FEA in areas such as providing patient-specific medical devices. In our work, we use FEA as a tool to assess and understand bone mechanical behavior both as a research method and to inform clinical practice. The FEA process is not accessible to many researchers and most clinicians because it requires specialized knowledge, equipment, and sometimes days to compute a result whose accuracy depends on the diligence of the user. Deep Learning (DL) offers a unique approach to this challenge by allowing us to train a 'black box' algorithm to compute a single or multi-dimensional result from a large dataset of predictors. In this exploratory study, we examined the potential of DL techniques to establish direct relationships between 3D computed tomography images and FEA-estimated axial stiffness of bone. We hypothesized that all neural network approaches would outperform linear regression in predicting axial stiffness of human tibias. We further hypothesized that the performance of the neural networks would increase with the quality of the information given.
Methods: To train our DL model, we used a previously collected density-calibrated CT dataset comprised of 119 individuals with spinal cord injury. This included images of the proximal tibia up to three times during an intervention aimed to increase lower extremity bone mass. Another de-identified dataset supplied ten quantitative micro-CT images of knees from able-bodied participants. Our lab previously processed these images using Mimics (Materialise, Belgium) software to create density-weighted point clouds of the tibias. From these, we calculated 65 strength and mineralization variables such as bone mineral density, cross sectional area, and buckling ratio at various regions within each bone. We then employed FEA techniques to estimate each bone's compressive stiffness[1].

Using unsupervised learning, we developed one neural network to represent the 65-variable dataset with ten or less variables, and another network to represent the large point cloud dataset using 100 variables. We then compared linear regressions of the calculated strength and mineralization variables to three DL networks. The first network's (NN-A) only predictors are from the previously learned representation of the density-weighted point clouds. The second network (NN-B) adds the ability to learn how the point clouds are related to the strength and mineralization parameters. The final network (NN-C) is awarded information on the learned representation of each bone's strength and mineralization parameters.

We analysed the predictive power of each approach by calculating the coefficient of determination (R^2) and Mean Absolute Error (MAE) of the predictions with respect to the FEA outcome. We used LASSO (Least Absolute Shrinkage and Selection Operator), which is a supervised dimension-reduction technique, to optimize the bias and variance of the linear regression model. To reduce our chances of overfitting, we decided to use a k-fold cross validation scheme with five split datasets repeated ten times.

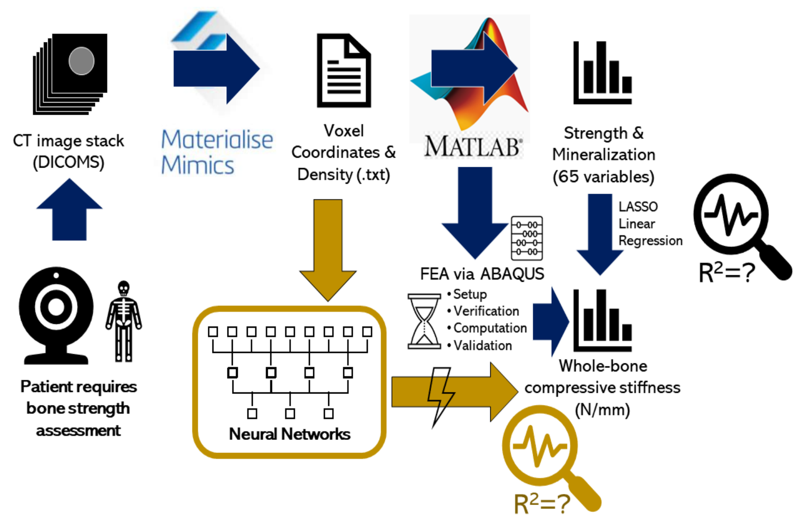

Figure 1. The current procedure to calculate whole-bone compressive stiffness requires FEA. In this study, we explored the accuracy of neural networks to explain bone stiffness to LASSO regression of strength & mineral variables.

Results & Discussion: The results of fitting each model are outlined in Table 1. The stiffnesses estimated by FEA ranged from 954 to 8002 N/mm. The LASSO regression model performed reasonably with almost three-quarters of the variance explained, and a MAE spanning roughly ten percent of the dataset. The first neural network, NN-A, regularly overfit the training data and was unable to provide reliable testing accuracy. The informed networks, NN-B and -C, performed better on the testing sets but was unable to reach the same amount of explained variance as the LASSO model. Lower errors indicate promise in developing informed neural networks to produce reliable FEA outcome estimates. We partially accepted both hypotheses with NN-B and -C outperforming LASSO regression in testing error, and with latter neural networks outperforming the first, but without a clear difference between B and C.

Table 1. Testing accuracy of each model

Model	R^2	MAE (N/mm)
LASSO Regression	0.747	646.6
NN-A	0.084	949.9
NN-B	0.647	224.3
NN-C	0.557	261.3

Significance: In this study we examined the efficacy of neural networks in predicting FEA outcomes of human bone with and without the knowledge of its physical attributes measured by CT. We were able to create two neural networks that outperformed an optimized LASSO linear regression model by reducing MAE by 60-65%. We hope that these models can provide steps towards developing networks that accept raw CT images as an input and output accurate FEA outcome predictions in seconds.

References: [1] Edwards WB, Schnitzer TJ, Troy KL. J Biomech. 2013 doi: 10.1016/j.jbiomech.2013.04.016.

INVESTIGATING THE ALIGNMENT OF BALANCE METRICS TO USER PERCEPTION USING ROBOTIC KNEE PROSTHESIS

Amirreza Naseri[1], Ming Liu[1*], I-Chieh Lee[1], Helen (He) Huang[1]
[1] UNC/NCSU Joint Department of Biomedical Engineering, NC State University, Raleigh, NC, USA
*Corresponding author's email: mliu10@ncsu.edu

Introduction: Balance is an important aspect of physical and mental well-being, and its monitoring during walking can provide valuable information on walking behavior. Several balance metrics including subjective and objective measurements have been introduced [1]. These metrics have been utilized to evaluate the performance of assistive devices used by individuals with walking-related physical impairments [2]. Integration of balance information into the controller of assistive devices carries the potential to improve their functionality in terms of walking balance. However, there is no clear guidance on which balance metrics would be most beneficial in improving these types of human-robot systems. Metrics aligned with users' own perception of balance have the potential to be a promising option due to the fact that 1) Users' perception of balance is subjective and varies significantly between individuals, making it crucial to understand how they perceive their own balance and how it relates to objective measures. 2) Aligning balance metrics to user perception ensures meaningful and relevant balance assessments. 3) Previous research has shown a disconnect between objective measures and user perception, highlighting the need to identify quantitative balance measurements that align with users' perception for a comprehensive understanding of users' subjective experience of assistive devices [3].
In this study, we aim to systematically evaluate the alignment of balance metrics with the users' own perception of balance.

Methods: Data was collected based on the previous experiment in which the subjects walked with robotic knee prosthesis [4]. We manually triggered the control disturbance torques for 200 ms applied at different timing (different states of stance phase), type (flexion or extension), and intensity levels. The perception of the users regarding their balance disruption was recorded via their verbal feedback ("perceivable", "non-perceivable"). We considered common balance metrics: 1) spatial parameters (i.e., step length and step width); 2) stability parameters including the margin of stability, the inclination angle, and whole-body angular momentum, and 3) postural control parameters (i.e., vertical displacement of the center of mass and anterior-posterior progression of the center of pressure). We also analyzed 4) the angular momentum of the adjacent segments at the prosthetic knee joint (residual thigh and prosthetic shank).
To perform the comparison, we categorized disturbed walking conditions (collected from five subjects with unilateral transfemoral foot amputation) based on the timing, type, and intensity levels. For each balance metric, we determined the difference between normal and disturbed profiles using the root mean squared error (RSME). We then conducted a non-parametric Friedman test to determine the viability of each balance metric for representing the difference in intensity level perceived by the user. After identifying the potential candidates among the balance metrics, we developed a multinomial exponential regression model to determine which metrics are better correlated and aligned with the users' perception of balance disruption. To compare the fitting model of different balance metrics, we used AIC (Akaike Information Criterion) which measures the trade-off between goodness of fit and model complexity. The model with the lower AIC value shows a better fit.

Results & Discussion: The results of the Friedman test indicated that postural control parameters, knee momentum, and inclination angle are viable parameters that can differentiate different walking conditions, including normal/non-perceivable and perceivable disturbances. The other metrics did not indicate a clear separation between different disturbed walking conditions. In general, the knee momentum and A-P CoP were most closely aligned with users' perception of balance when experiencing internal disturbances (Fig.1).

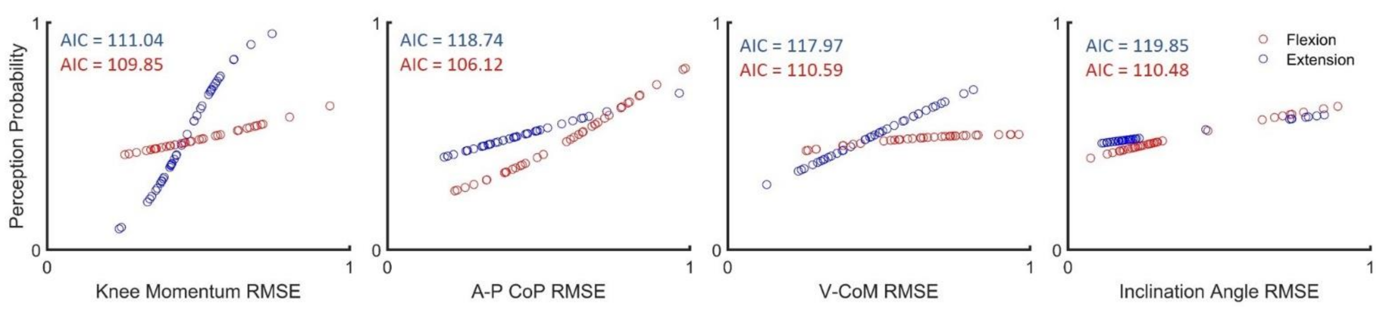

Figure 1: Multinomial logistic regression model to predict the probability of the perceivable flexion and extension disturbances when the probability exponentially fits the normalized RMSE of different balance metrics.

Significance: The findings show that 1) a higher correlation observed between user perception and balance metrics measured closed to the disturbed joint. 2) Some of the full body balance metrics may not be sensitive enough to reflect short time disturbance at a distal joint. 3) Identified balance metrics have implications to be used to monitor disturbances while using robotic prosthesis.

Acknowledgements: The authors would like to thank NIH (Grant R01EB024570) for the support of this work.

References: [1] Siragy and Nantel (2018), Front. Aging Neurosci. 10:387.; [2] Chiu, Raitor, and Collins (2021), IEEE Trans. Med. Robot. Bionics 3(3).; [3] Zhang, Liu & Huang (2014), IEEE Trans. Neural Syst. Rehab. Eng. 23(1): 64-72.; [4] Lee et al. (2022), IEEE Trans. on Neural Systems and Rehab. Eng. 30:2773–2782.

Age related lower extremity strength and power changes in preschool children during their preschool program

Bahman Adlou*, Christopher Wilburn[1], Brandi Decoux[2], Danielle Wadsworth[1], Wendi Weimar[1]
[1]Auburn University
[2]Southeastern Louisiana University
*Corresponding author's email: bza0058@auburn.edu

Introduction: Physical development in preschool children is an important topic of interest for many researchers. Preschool years are crucial for the development of gross motor skills and lower extremity strength and power. Thus, understanding the changes in lower extremity development during preschool years is important for developing effective interventions that promote healthy growth in young children, and in establishing the groundwork for fitness throughout their future lives. In this study, we aimed to measure the changes in lower extremity power in preschool children years before and after their 9-month preschool program. This research is important in providing insights into the growth and development of preschool children and informing the development of interventions that promote healthy physical development in this population.

Methods: Twenty-eight 3- to 5-year-old preschool children (mean±SD: 4.14±0.65) were recruited to partake in the study. Informed consent and assent were obtained for and by each participant. Participants were asked to sprint up a ramp at an incline of 27 degrees for 3 trials initially, and repeated the same protocol after 9 months in their preschool program. Step length and time parameters were obtained to calculate lower extremity (LE) strength and power for age group comparisons across their 9 months program. Age was used as a predictor to explain the potential changes in LE peak and average work and power using one-way Analysis of Variance (ANOVA) tests. Analysis was done using SPSS (version 25, IBM).

Results and Discussion: Average power (4%) and work (<1%) minimally changed (4 and <1%, respectively) across the program, with 3-year-olds changing the most for both power (4.7%) and work (1%) compared to 4- and 5-year-old children (power and work percent differences: 3.9, 0.4% and 2.6, 0.6%, respectively). Age group explained less than 10% of the variance in all four variable comparisons between the initial and follow up tests and did not reach a statistical significance. Results showed no evidence for age-related changes in LE power in preschool children. Children's bodies at this age grow rapidly, and such structural changes and their associated neuromechanical adaptations could explain the observed variance in this study. Furthermore, this project may point to the need for the development of a directed fitness protocol to improve the strength and power of our young children. Encouragement of physical activity may provide a foundation for a more healthy lifestyle and life.

Significance: This study's findings are interesting since average lower extremity strength and power of the preschool children did not change significantly with their overall increase in size and mass. Therefore, the consistent average work and power could be indicative of the children's proper growth through their program while they grow rapidly and their coordination adapts.

EFFECTS OF A 6-WEEK TRAINING PROTOCOL ON LOWER LIMB KINETICS DURING CUTTING MANEUVERS

Paige M. Agnew, Hunter J. Bennett, Zachary A. Sievert
[1]Old Dominion University, Norfolk, Virginia
*Corresponding author's email: pagne002@odu.edu

Introduction: ACL injury risk and occurrence of injury is highly present in non-contact sport related injuries with nearly one out of four youth athletes having not one but two ACL injuries [1]. The risk associated with these movement patterns is highly correlated to an increase in knee valgus and a decrease in hip muscle strength [2]. ACL reconstruction surgery is prevalent and imperative for athletes to return to play however the risk of reinjury or injury to the unaffected ACL is increased post-surgery [3]. Previously, researchers have focused on sex-based differences in ACL loading during cutting movements and found that females had greater ACL loading during a 45-degree cutting movement [4]. Although anticipated cuts put athletes at a greater risk for ACL overloading leading to injury, unanticipated cuts also present similar risk to ACL injury. The purpose of this study was to determine if a 6-week plyometric and strength training program emphasizing hip and ankle strength, could reduce knee loading and subsequently ACL load during both unanticipated and anticipated cuts. With the implementation of a lower limb strengthening program, we expect to see an increase in hip and ankle moments, to redistribute the load from knees to hips and ankles, after the 6-week intervention in both anticipated and unanticipated cuts.

Methods: 8 (4 male, 4 female) participants volunteered for this study (Age 23yr±2, Height 1.75m±0.08, Mass 78.36kg±7.3). A three day per week periodized training protocol was implemented for 6-weeks consisting of two strength focused days and one dynamic plyometric day between the two strength days. Strength days included back and front squats followed by a plyometric movement and accessory work for the hamstring and quadriceps muscle groups. The plyometric day included bipedal and unipedal broad jumping and central nervous system activation. There was a 4-week preparatory phase followed by a hypertrophy phase for the next two weeks. Participant's performed unanticipated and anticipated cuts, pre and post training, at a 45° angle to a force plate. 3-D lower extremity kinematic data were collected using a Vicon Nexus system and data were low-pass filtered at 12Hz cut. Joint moments were normalized to each participant's mass * height. 2 x 2 within-subjects ANOVAs were used to analyze peak ankle plantarflexion, ankle inversion, knee flexion, knee abduction, hip flexion, and hip adduction angles during stance across cutting tasks and pre/post training. In addition, the knee extensor and abduction knee load relative to the full lower extremity (sum of hip, knee, and ankle) were examined.

Results & Discussion: Mean and standard deviations for each variable are reported in the table. A significant task main effect was found for knee flexion (F=14.46, p<0.01, η_p^2=0.71) and abduction (F=11.95, p=0.01, η_p^2=0.67) angles. Knee flexion and abduction were larger by 6.7 and 1.4 degrees, respectively. This increase in knee flexion could be a result of decreased hip muscle activation, of the hip flexors, during the active flexion period in cutting. A significant interaction was found for hip flexion angles (F=7.29, p=0.03, η_p^2=0.55). An increase in hip flexion between pre- and post-training indicates there is a shift is muscle activation of the lower limb during this movement pattern. Pre-training, hip flexion angles were significantly greater during unanticipated cuts (T=3.81, p<0.01); however, differences in hip flexion angles were not different post-training (p>0.05). The disappearance of a difference between cutting conditions indicates that there was an effect of the training intervention that allowed participants to flex the hip more similarly across both cutting conditions versus having a greater increase in hip flexion as seen pre-training. This indicates a positive adaptation to training as the decrease in variations between the two cutting maneuvres allows for more similar repeated movement patterns and consistency of athlete movement. These results indicate that a 6-week strength training intervention does improve kinematic differences in hip flexion angles; however, knee sagittal and frontal plane loading remained unaffected, limiting the likely effects on reducing ACL loading.

VARIABLE	AXIS	PRE		POST	
		AC	UAC	AC	UAC
ANKLE	PLTFLX	-25.3 (7.7)	-27.0 (7.8)	-29.5 (8.0)	-32.0 (10.2)
	INV	25.8 (8.6)	30.3 (8.8)	26.9 (8.1)	27.0 (7.7)
KNEE	FLX	-50.2 (7.4)	-58.4 (8.4)	-54.5 (8.7)	-59.6 (10.0)
	ABD	-8.3 (5.7)	-9.6 (6.1)	-6.3 (3.2)	-7.9 (3.4)
HIP	FLX	45.7 (8.4)	52.4 (9.6)	45.9 (10.1)	48.8 (7.9)
	ADD	-4.0 (7.0)	-4.7 (7.0)	-4.8 (4.2)	-6.4 (4.5)
KNEE	EXT	39.4 (8.9)	40.7 (8.9)	44.1 (4.3)	44.0 (3.7)
LOAD	ABD	34.0 (9.6)	32.3 (10.0)	37.0 (8.8)	37.1 (8.5)

Table. Mean (SD) for each variable across tasks and training.

Significance: The results of this study aim to improve the strength training protocols used by coaches and rehabilitation specialists to prevent the instance of ACL loading resulting in injury. Further investigation into muscle electromyography will aid in understanding the changes in muscle contraction during anticipated and unanticipated cutting maneuvres. Additionally, clinicians and sports professionals should consider strength training interventions to decrease the variability of hip flexion across both conditions to reduce the risk of injury due to ACL overloading in multi-directional sport.

References: [1] Nessler, T., Denney, L. & Sampley, J. ACL Injury Prevention: What Does Research Tell Us?. *Current Reviews in Musculoskeletal Medicine* Med 10, 281–288 (2017)
[2] Khayambashi, K., Ghoddosi, N., Straub, R., Powers, C. (2016) Hip muscle strength predicts noncontact anterior cruciate ligament injury in male and female athletes, *American Journal of Sports Medicine,* 44(2) 355 – 361
[3] White, K., Di Stasi, S., Smith, A., & Snyder-Mackler, L. (2013) Anterior cruciate ligament-specialized post-operative return-to-sports (ACL-SPORTS) training: a randomized control trial, BMC Musculoskeletal Disorders, 14(108)
[4] Sinclair, J., Brooks, D., Stainton, P. (2019) Sex differences in ACL loading and strain during typical athletic movements: a musculoskeletal stimulation analysis, European Journal of Applied Physiology, 19, 713 – 721

TAKING OPENSIM INTO THE WILD WITH WEARABLE SENSORS

Jonathan D. Mortensen*, Scott G. McLean
Exponent
*Corresponding author's email: jmortensen@exponent.com

Introduction: Both OpenSim, an open source musculoskeletal modeling software, and wearable sensor technologies continue to improve and expand capabilities. OpenSim has introduced a workflow for processing Inertial Measurement Unit [IMU] sensor data referred to as OpenSense [1]. The goal of this new workflow is providing high-quality biomechanics analysis in settings that traditional optical motion capture would be limited, but looks to the users to collect high quality IMU data. Vicon Blue Trident IMUs now include automated sensor fusion, providing global orientation in the form of time synchronized quaternions across multiple sensors. This data provides the input required to drive OpenSim through OpenSense. We have developed methods to effectively and efficiently collect and process the IMU data required to drive full-body kinematics in OpenSim. We have demonstrated these methods in challenging environments associated with such activities as fly fishing, mountain biking, skiing, and swimming. The purpose of our submission is to share these general methods and to demonstrate how OpenSim can now be taken into the wild to study biomechanics in novel ways.

Methods: Kinematic data were collected for fly fishing, mountain biking, skiing, and swimming. For each of these activities, up to 16 Blue Trident IMUs were used. Data collection was carried out through use of the Capture U iPhone application, which provides a simple interface to the IMUs. After data collection began, the IMUs were calibrated to the local magnetic fields. The IMUs were then secured to the participant with athletic tape. A static posture in a known pose was performed, following which the activity of interest was performed. Data collection was then stopped, and the data were downloaded. Custom MATLAB scripts assisted in segmenting the data into specific regions of interest, filtering the data, formatting the data as required by OpenSense, and running inverse kinematics within OpenSense.

Results & Discussion: Synchronized video confirmed that realistic kinematic data was obtained within OpenSim for each of the activities. Fly fishing data can clearly indicate casting technique, total arm movement, and even the kinematics of catching a fish miles away from any motion capture lab. The mountain biking data displays cycling speed and how the rider adapted his body posture as he progressed through various terrain over a large area. The skiing data captured number of turns made down the run, as well as knee and torso angle. The swimming data provided the ability to analyse stroke technique, count number of kicks, and display the body angle as the swimmer completed laps (**Figure 1)**.

This type of data collection and processing is challenging, but the tools in OpenSim and provided by the Vicon Blue Trident IMUs is making it more reliable and accessible. The OpenSim MATLAB API makes it possible to streamline much of the required processing. Several lessons were learned during data collection and processing. These included calibration techniques, best practices for collecting data, and methods for more efficiently processing the data. We are encouraged by our success of full-body kinematics data collection in settings that traditional optical motion capture is not yet possible.

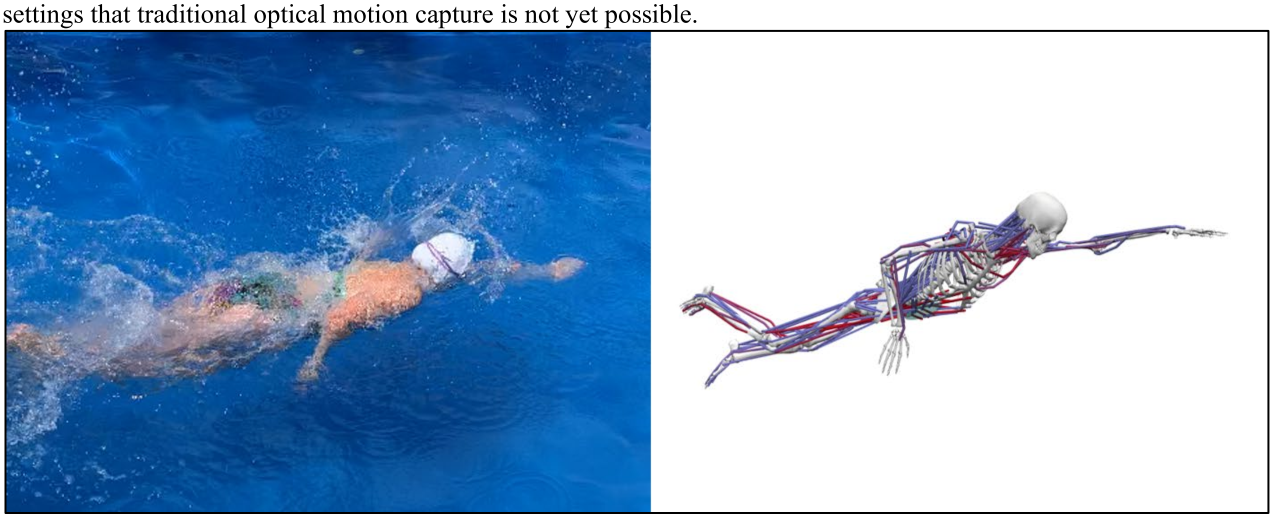

Figure 1: Demonstration of swimming IMU data driving an OpenSim model

Significance: To our knowledge, this is the first time IMU data has been used to drive OpenSim models in any of the four activities discussed. These techniques open the door for exciting new analyses. We believe sharing our techniques and progress will save other researchers significant time and effort in attempts to study human biomechanics away from the lab an in the wild.

Acknowledgements: We'd like to thank all of our data collection participants including Spencer Mortensen, Carter Hesterman, Anna Quist, and Bryan Marshall

References: [1] Borno, et al., Journal of NeuroEngineering and Rehabilitation 19.1 (2022): 1-11.

Tibiofemoral joint contact forces with slip perturbations during symmetric and asymmetric walking

Alexander S. Clark[1], Madison Deanes[1], John D. Willson[1], Ryan D. Wedge[1*]
[1]Department of Physical Therapy, East Carolina University
*Corresponding author's email: wedger19@ecu.edu

Introduction: Gait asymmetry is common in people following musculoskeletal injuries such as lower limb amputation [1,2]. There is some evidence that this gait asymmetry contributes to altered knee joint contact forces [3] and more detrimental long term consequences such as increased incidence of knee joint OA [4] and increased risk of falls [5]. Perturbations during gait elicit gross motor responses to avoid falls that may affect knee joint contact forces and also be affected by the presence of gait asymmetry. The purpose of this study was to examine differences in tibiofemoral joint contact forces before, during, and after slip perturbations when walking with symmetric and asymmetric belts. We hypothesized that contact forces would be greater with asymmetric walking and post-perturbation steps would be greater than baseline steps for both conditions.

Methods: Five able-bodied participants (2 females, 72.1 ± 9.1 kg, 1.78 ± 0.1 m) between 18-30 years old walked on an instrumented split-belt treadmill with symmetric (1.3 $m \cdot s^{-1}$ each belt) and asymmetric (1.3 $m \cdot s^{-1}$ right belt and 0.8 $m \cdot s^{-1}$ left belt) belt speeds. The conditions were separated by a five-minute rest. After two minutes of walking without perturbations the participants experienced a 50% decrease in belt speed at a rate of 4.0 $m \cdot s^{-2}$ at heel strike ten times on each limb for each condition, given at randomized intervals over the next 25 minutes. 3D segmental motion (200 Hz) and ground reaction force data (2000 Hz) for 20-25 individual stance phases pre-perturbation (baseline), during perturbation, for the non-perturbed limb immediately after perturbation (contralateral), and the first and second steps for the perturbed limb after perturbation (post-pert 1 and 2) were recorded. Those data were filtered using a 15 Hz cutoff, 4th order, zero-lag, low pass Butterworth and used for inverse dynamics calculations (c-motion Inc, Boyds, MD). Peak tibiofemoral joint contact force was calculated using a previously validated model [6] informed by inverse dynamics solutions. The limbs were lumped together for baseline stance phases, and the leg being analyzed depended on the condition (e.g., right belt perturbation meant right limb for perturbation, post-pert 1 and 2, and the left limb for contralateral). A two-way 2 (condition) X 5 (step) ANOVA was performed with Tukey HSD post-hoc tests in the case of significant main effects ($\alpha = 0.05$).

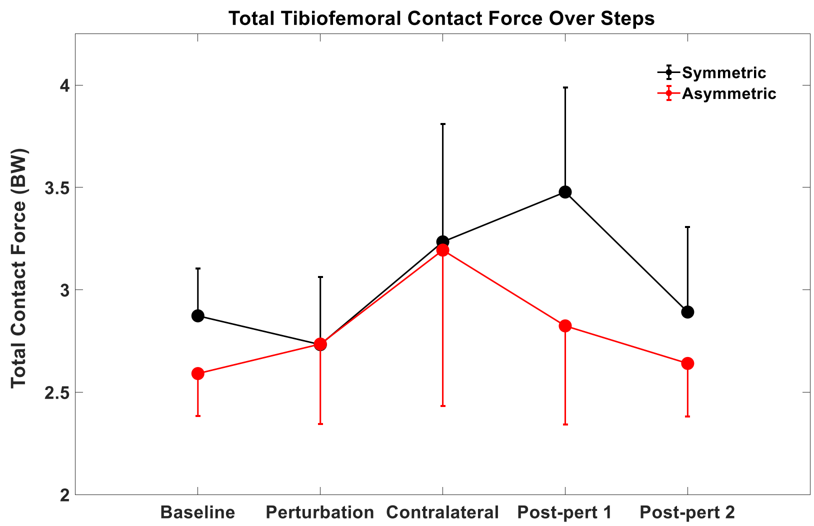

Figure 1: Tibiofemoral contact force (means + 1 SD) for symmetric (black) and asymmetric (red) walking for 5 different steps pre-perturbations (baseline), the perturbation step, the non-perturbation side step after perturbation (contralateral), and the two steps of the perturbation side following perturbation (post-pert 1 and 2).

Results & Discussion: The tibiofemoral joint contact forces were greater for symmetric walking compared with asymmetric walking ($p < 0.001$) which was contrary to our hypothesis (Figure 1). The contralateral and post-pert 1 steps were greater than baseline contact forces ($p < 0.001$), and the second step post-pert was not greater than baseline for symmetric walking ($p = 0.135$) but was greater for asymmetric walking ($p = 0.003$) (Figure 1). The greater contact forces for symmetric walking may be explained by both belts moving at 1.3 $m \cdot s^{-1}$ and the slower left belt with the asymmetric condition led to lower contact forces even though it was a non-preferred pattern [7]. The contact forces for the first step by the contralateral (non-perturbed) side and perturbed side (post-pert 1) were both greater than baseline contact forces which indicates it takes multiple steps to recover from a perturbation and return to near baseline mechanics even in an able-bodied population.

Significance: Able-bodied individuals have greater loads with symmetric walking than asymmetric walking even when exposed to perturbations during gait. This appears to contrast with the finding that people with unilateral lower limb amputation prefer to walk with asymmetric characteristics and have greater joint contact force on the intact limb. How symmetric walking would affect joint contact force in people with lower limb amputation needs to be investigated to understand if their preferred, asymmetric, pattern leads to the lowest joint contact forces.

Acknowledgements: Part of this work was supported by NSF REU (#1950507).

References: [1] Wedge et al. (2022), *Clin Biomech* 94(April); [2] Sanderson & Martin (1997), *Gait & Post* 6(2); [3] Ding et al. (2020), *J Ortho Res* 39(4); [4] Norvell et al. (2005), *Arch Phys Med Rehabil* 86(3) ;[5] Kulkarni et al. (1996), *Physiotherapy* 82(2); [6] Barrios & Willson (2017), *J Appl Biomech* 33(2); [7] Lenton et al. (2018), *PLoS One* 13(11).

Implementing a Muscle Model Driven Robotic Arm

Rauf A. Iftikhar[1*], Surabhi N. Simha[2], Lena H. Ting [2]
[1]Emory College of Arts and Sciences
[2] Department of Biomedical Engineering, Emory University and Georgia Institute of Technology, Atlanta, USA
*Corresponding author's email: riftikh@emory.edu

Introduction: A robotic emulator of spasticity based on physiological mechanisms may improve clinical assessments and our understanding of spasticity. Spasticity is a motor disorder characterized by increased muscle tone and exaggerated muscle activation in response to passive stretching, affecting patients with conditions such as cerebral palsy and stroke. Clinicians manually move a patient's limb at different speeds to differentiate degrees of muscle resistance to assess spasticity. Although the mechanisms of resistance are not well understood, recent computational models show that increased muscle short-range stiffness coupled with a short-latency reflex based on force feedback can mechanistically reproduce quantitative measurements of spasticity. However, it is not clear whether these mechanisms reproduce that resistance felt by the clinician. Implementing computational models on a physical robot could help bridge that gap. Towards this, we emulated a Hill-type muscle model on a robot platform. Here we aim to design a robotic emulator of an arm driven by a Hill-type muscle model. We aim to add to this model by introducing short range stiffness and both a velocity-based and force-based activation reflex to simulate spasticity.

Methods: We used four models to validate the implementation of muscle forces by the KinArm End-Point Lab robot [1]. The robot has a graspable handle that can apply forces to the user and measures the applied force well as the position of the handle in 2D space (Fig. 1). Above the plane of the handle, a virtual reality screen displays the position of the hand and the simulated limb. We validated the accuracy of the forces at the handle when programmed based on the motion of the handle. Using feedback of the hand position and the musculoskeletal geometry, the controller estimates the instantaneous length of the muscle. For a spring model, the force output is the product of the muscle length and a spring stiffness. For a spring-damper model, the force is also dependent on the velocity of the muscle (Fig. 1). We also implemented a Hill-type muscle model, where force is non-linearly related to muscle length, velocity, and activation to evaluate implementation of muscle mechanics; the muscle endpoint was located at the handle. Finally, we added limb mechanics such that the handle was at the end of a virtual limb where the force was based on a Hill-type muscle model generated a torque at a simulated joint (Fig. 1).

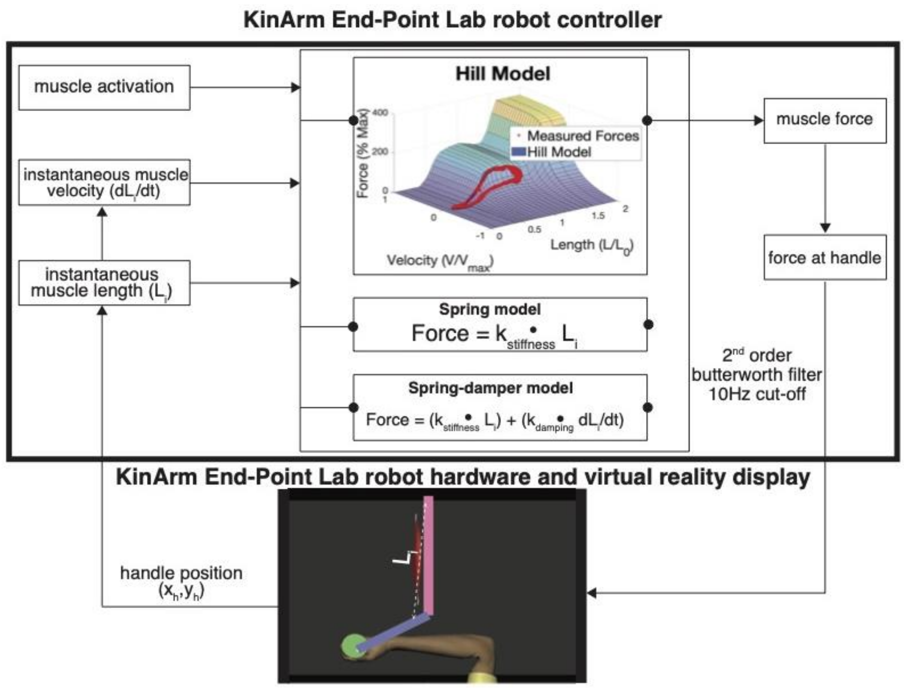

Figure 1: Muscle model implementation on KinArm End-Point Lab

Results & Discussion: The Mean Squared Error (MSE) was 0.03N, 0.3 N, 0.3 N, and 0.16 N for the spring, spring-damper, Hill model, and Hill-model with limb mechanics respectively. The center block of the controller in Fig. 1 illustrates that the forces applied on the user when the limb model was implemented (red lines) matches the predicted forces from the Hill-type muscle model (blue-yellow surface). Next, to emulate muscular reflex characteristic of spasticity, we will next add and compare models with activation as a function of force and velocity feedback from muscle spindles.

Significance: The KinArm robotic platform can emulate muscle forces when it is manipulated by a human user. The controller can be augmented to evaluate proposed mechanisms of spasticity by implementing force, length, and velocity-based feedback reflexes and comparing the force profiles of these models to results from instrumented biomechanical measures [2]. Further, the spasticity emulator can be used to allow clinicians to assess the feel of the robot and could ultimately assist in the training and standardization of spasticity assessment.

Acknowledgements: This work was supported by NIH grant R01HD046922 and the Emory SURE Program.

References: [1] KinArm End-Point Robot, BKIN Technologies Ltd, Kingston, Canada; [2] L. Bar-On et al., "A Clinical Measurement to Quantify Spasticity in Children with Cerebral Palsy by Integration of Multidimensional Signals," Gait & Posture 38, no. 1 (May 2013)

EFFECT OF SELF-PACING TREADMILL BELT MOTOR SOUNDS ON GAIT SPEED

Trevor Evans[1], Ajit M.W. Chaudhari[1]
[1]Health and Rehabilitation Sciences, The Ohio State University
Corresponding author's email: evans.2374@osu.edu

Introduction: Motorized treadmills are commonly used in research to analyze gait. Assessing treadmill walking offers the main advantage of a decreased space required for walking, which allows for longer and more reliable periods of data collection. It also allows researchers to better control environments which could otherwise alter movement patterns. Traditional fixed-speed treadmills eliminate the speed fluctuations observed in overground walking, and self-pacing treadmills were developed to address this shortcoming by continually adjusting belt speed based on user position while walking. While the self-pacing design is an improvement, there are still mixed findings regarding the similarity of self-pacing and overground walking paradigms, suggesting a need to further examine reasons for potential differences in spatiotemporal gait parameters [1,2]. One explanation that hasn't been pursued is the incorporation of the treadmill belt motor sounds as auditory feedback while walking. The belt motors make noises with sound characteristics such as pitch and amplitude that vary based on the user's front-back position on the treadmill. Past research has demonstrated that auditory feedback can influence balance and gait behavior [3]**,** therefore we want to explore the possibility that self-pacing treadmill walkers utilize the information from the belt motor sound characteristics in their movement patterns, which will be reflected in altered gait parameters. We hypothesize that the gait speed and gait speed variability of the walkers on a self-pacing treadmill will be significantly different when the sounds from the treadmill belt motors are heard versus when they are not.

Methods: Healthy adult participants (N=11) were first given a brief introduction of how a self-pacing treadmill functions and a guideline to walk at a comfortable speed for the duration of the study. Participants underwent an acclimation period of at least five minutes of walking on the self-pacing treadmill, and then data collection began. Participants walked for five minutes while being able to hear the sounds from the belt motors, and directly after were given noise-cancelling headphones to wear while they walked for another five minutes. To ensure that the motor sounds were not heard during the noise-cancelling condition, brown noise was played through the headphones for the duration of the trial, and volume was adjusted until participants confirmed that they could not hear external sounds.

Gait speed and gait speed variability were the parameters of interest for this study. We used paired t-tests to compare the gait speed averages and coefficients of variation observed between the inclusion and exclusion of belt motor sounds during self-paced treadmill walking. α =0.05 was assigned as the level of statistical significance.

Results & Discussion: The results for gait speed and variability can be seen in Table 1. The paired t-tests showed a significant difference in average walking speed between the two conditions, but the coefficients of variation did not show significant differences.

Table 1: Outcome Parameters Summary

Variable		Sound Condition	No Sound Condition	P-value
Gait Speed (m/s)	Average	1.187 (0.091)	1.258 (0.106)	.027*
	CV	0.079 (.033)	0.086 (0.043)	0.451

This study aimed to determine the effect that auditory feedback from the belt motors on a self-pacing treadmill has on gait speed and variability. It was observed that average gait speed significantly increased when the belt motor sounds were no longer heard by the participant. Previous literature regarding auditory stimulus effects on walking has supported the findings from this study in that gait parameters changed while walkers were listening to an external sound [4]. We believe that this study furthers previous work by suggesting that walkers on a self-pacing treadmill are incorporating sounds from belt motors that affects their gait speed. One potential explanation for this is that the sound constantly presents spatial information about relative position on the treadmill, leading to the walker having to adapt their walking in a manner that results in decreased gait speed. Qualitatively, participants noted that they preferred the headphone condition, which could relate to 1) the lack of any external auditory feedback experienced during overground walking or 2) the decreased speed seen in the sound condition, indicative of a more cautious walk from an increased awareness of changing belt speeds. A limitation of this study is the sample size of the data. This is a preliminary study, and more participants will be recruited to ensure the validity of the results shared here.

Significance: This study shows that motor sounds are a factor that should at least be considered for future studies when doing gait analysis on a self-pacing treadmill, particularly if the researchers are interested in gait speed. Gait speed is shown to be a significant clinical indicator for falls and other pathologies, therefore we should be ensuring that the movements we observe in labs translate to real-world settings [5]. Future work will be to analyze other gait parameters, as well as compare both of these conditions to overground walking.

Acknowledgements: This study was funded through MURI #12731926.

References: [1] Van der Krogt, 2018 – Gait &Posture [2] Plotnik, 2015 – JNER [3] Sejdic, 2012 – PLOS [4] Tajadura, 2015 – CHI [5] Kyradalen, 2018 – Physio Research

FRONTAL AND SAGITTAL ANKLE KINEMATICS DURING HOPPING AND RUNNING DIFFER BETWEEN NATURAL AND ARTIFICIAL TURF SURFACES

Brandi E. Decoux[1*], Christopher M. Wilburn[2], Megan A. Gordon[1], Wendi H. Weimar[2]
[1]Southeastern Louisiana University, Hammond, LA
[2]Auburn University, Auburn, AL
*Corresponding author's email: brandi.decoux@southeastern.edu

Introduction: Many sports traditionally played on natural grass are now taking place more frequently on artificial turf. Thus, a thorough understanding of the human-surface interaction on artificial turf versus natural grass has become increasingly important. While much of the previous research in this area has focused on maximal effort athletic tasks (e.g., sprinting and agility drills), the extent to which key biomechanical parameters of fundamental movements like hopping and running differ between surfaces remains unknown. Of the lower extremity joints, the ankle is considered to be one of the most important during fundamental and athletic movements due to the crucial role it plays in maintaining balance and absorbing and generating force. Therefore, the purpose of this study was to compare frontal and sagittal plane ankle kinematics during hopping and running across different artificial turf surfaces and natural grass. Due to the varying stiffness characteristics of the artificial turf and natural grass surfaces, we hypothesized that ankle range of motion and angular velocities in the frontal and sagittal planes would be greater on the less stiff surfaces compared to the stiffer surfaces. These differences are expected due to the nature of stiff surfaces returning more energy than pliant surfaces.

Methods: Seventeen healthy male recreational athletes (age: 23.1 ± 2.9 years; height: 1.81 ± 0. 06 m; mass: 77.8 ± 9.9 kg) were recruited from the surrounding community to participate in this study. All participants indicated their voluntary involvement by signing an informed consent document approved by the Institutional Review Board prior to participation. Using an inertial motion capture system (MTw, Xsens Technologies B.V., Enschede, the Netherlands), kinematic data were obtained at 100 Hz during three single-leg hopping trials and three 35m submaximal running trials on each of the four surfaces Data was exported from Xsens MVN Analyze (Version 2019.0, Enschede, the Netherlands) and imported into Visual3D (C-Motion, Germantown, Maryland, USA) for reduction. Frontal and sagittal plane ankle angular velocities and range of motion during the middle four stance phases of the dominant foot for each hopping and running trial were extracted for analysis. For each variable of interest, the mean of all trials in each condition were statistically analysed in SPSS (Version 29.0, SPSS Inc, Chicago, IL, USA) with the significance level set a priori at $\alpha = .05$. Due to data failing to meet the assumption of normality, repeated measures Friedman ANOVA by Ranks tests were conducted to assess for differences across the four surfaces, and Dunn's pairwise analyses were carried out post hoc with a Bonferroni correction for multiple comparisons when necessary.

Table 1. Stance phase frontal and sagittal plane ankle kinematic variables (mean ± SD) during hopping and running on each artificial turf (AT) surface and natural grass (NG) for the statistically significant variables.

		AT 1	AT 2	AT3	NG
Hopping	Sagittal Plane ROM (°)	40.9 ± 5.7	42.6 ± 5.8	42.4 ± 4.9	39.4 ± 4.0
Running	Peak Eversion AV (°/s)	372.4 ± 167.2	361.7 ± 177.5	461.2 ± 200.7	379.2 ± 157.4
	Sagittal Plane ROM (°)	37.7 ± 4.9	37.8 ± 4.6	38.3 ± 4.2	35.2 ± 4.4
	Peak Plantarflexion AV (°/s)	384.7 ± 335.5	493.5 ± 318.5	519.9 ± 341.0	305.7 ± 330.7

Notes: ROM = range of motion; AV = angular velocity.

Results & Discussion: Descriptive statistics for all variables of interest are summarized in Table 1. A significant effect of surface on sagittal plane ROM was observed during hopping (χ^2 (3) = 10.341, p = .016, W = .203) and running (χ^2 (3) = 17.541, p = <.001, W = .344). Natural grass demonstrated smaller sagittal plane ROM values than AT 3 during hopping (Z = 1.353, p = .013) and running (Z = 1.824, p = <.001) in addition to smaller sagittal plane ROM values than AT 2 during running (Z = 1.176, p = .047). Greater sagittal plane ROM has been suggested to be indicative of an impact attenuation strategy [1]. During running, significant effects of surface on peak eversion AV (χ^2 (3) = 11.471, p = .009 , W = .225) and peak plantarflexion AV (χ^2 (3) = 14.294, p = .003, W = .280) were observed. Peak eversion AV was found to be greater on AT 3 than AT 1 (Z = 1.294, p = .021) and AT 2 (Z = 1.235, p = .032), while peak plantarflexion AV was less on NG than AT 2 (Z = 1.235, p = 0.32) and AT 3 (Z = 1.294, p = .021). These differences in angular velocity may suggest that compensation in ankle joint motion are necessary a response to maintain balance and generating propulsion for in response to varying levels of surface stiffness and material deformation during stance. In addition, previous research has suggested that eversion angular velocity may be related to the development lower extremity injury [2,3], but consensus has not been reached on whether greater or smaller values are of more concern.

Significance: Differences in ankle frontal and sagittal plane kinematics observed between artificial turf and natural grass surfaces during hopping and running are important to consider since the ankle joint serves as a key shock absorber, transmitting forces from the ground up through the leg and into the rest of the body.

References: [1] Kuhman et al. (2016), *Hum Mov Sci* 47; [2] Willems et al. (2006), *Gait Posture* 23; [3] Chambon et al. (2014), *Gait Posture* 40(1);

WALKING STABILITY AND KINEMATIC VARIABILITY FOLLOWING PHYSICAL FATIGUE INDUCED BY INCLINE TREADMILL WALKING

Pei-Chun Kao[1, 2*], Colin Lomasney[1, 2]
[1]Department of Physical Therapy and Kinesiology, [2]New England Robotics Validation and Experimentation (NERVE) Center
University of Massachusetts Lowell, Lowell, Massachusetts
*Email: PeiChun_Kao@uml.edu

Introduction: Physical fatigue has been shown to affect neuromuscular performance such as reduced ability of generating a desired force level, decreased joint position sense, and deteriorated movement coordination. However, the methods to induce physical fatigue, using a general exercise involving the whole body (i.e., whole-body fatigue) (e.g., running, walking, ironman triathlon) versus using a local muscular exercise involving particular muscular groups (i.e., localized fatigue), may cause various extent of changes in performance. For the effects of physical fatigue on walking performance, previous studies showed that healthy individuals walked with a more cautious gait pattern by reducing walking speed or increasing step width. In terms of the changes in gait variability and stability following motor fatigue, there is more consensus on the increased variability in step spatiotemporal parameters but less consensus on the changes in walking stability [1-4]. In a prior study from our laboratory [1], we used leg presses and isolated ankle movements to induce "localized" fatigue and we found that healthy young subjects increased kinematic variability but adjusted their steps to maintain similar level of walking stability. The objectives of this study are to (1) examine the effects of whole-body physical fatigue induced by the incline treadmill walking on gait stability and variability, and (2) compare the results with our previous findings on the effects of localized physical fatigue. We hypothesize that whole-body fatigue would affect gait variability and stability to a greater extent than the localized fatigue because whole-body activities could disturb more sensory systems (e.g., visual, vestibular, the plantar cutaneous mechano-receptors) than the localized muscular exercises [5].

Methods: Twenty healthy young participants (9F and 11M) walked on an instrumented treadmill at 1.25 m/s and 0° of incline for 5 minutes before (PRE) and after (POST) physical fatigue. Treadmill walking with progressively increased incline gradient (2.5° every five minutes) was used to induce physical fatigue. The criteria of reaching physical fatigue include a Borg rating of perceived exertion (RPE) > 17/20, reaching ~85% of their maximum age-predicted heart rate, and a 20% reduction in the vertical jump height. We computed dynamic margins of stability (MOS), step and joint kinematic variability, and short-term local divergence exponent (LDE) of the trunk motion for each trial. To compare with our previous results on the effects of localized fatigue [1], we computed the percentage of change between POST and PRE for all parameters.

Results & Discussion: Compared to PRE, participants had significantly smaller values of short-term LDE for the trunk motion in all directions during POST (A-P: $p<0.01$, M-L: $p=0.04$, VT: $p=0.01$), indicating that participants became more locally stable after being fatigued. Participants walked with significantly greater mean MOS_{AP} ($p<0.001$) but had similar mean MOS_{ML} during POST. The variability in MOS_{AP} and MOS_{ML} was also significantly greater during POST than during PRE ($p<0.01$ and $p=0.02$, respectively). Participants had significantly smaller mean step width ($p=0.05$) but greater step width variability ($p<0.01$) during POST. There was no difference between PRE and POST in the mean and variability of step length and stride time, or the variability of ankle, knee, and hip joint angle. For the center of mass (COM) velocity, participants walked with significantly greater mean peak COM velocity in the A-P direction ($p<0.01$) but had similar A-P COM velocity variability during POST. On the contrary, participants walked with similar mean peak COM velocity in the M-L direction but had significantly greater M-L COM velocity variability ($p<0.01$) during POST. These results indicate that participants walked with greater amplitude of A-P trunk movement but had greater stride-to-stride variability of M-L trunk movement after being fatigued.

When comparing the effects of localized fatigue versus whole-body fatigue, there were similar changes in majority of the gait parameters except for the mean step width, mean MOS_{ML}, knee joint angle variability, mean peak M-L COM velocity, and short-term LDE for the A-P trunk motion. We found that mean step width ($p<0.01$), mean MOS_{ML}($p=0.01$), knee joint angle variability ($p<0.01$), and mean peak M-L COM velocity ($p<0.01$) were significantly increased to a greater extent after localized fatigue than after whole-body fatigue. However, short-term LDE value for the A-P trunk motion was significantly reduced to a greater extent after whole-body fatigue ($p=0.02$) than after localized fatigue, indicating that local stability of the A-P trunk motion was improved following whole-body fatigue. Our findings do not support our hypothesis. Instead, these results indicate that localized fatigue affects gait variability and stability to a greater extent than the whole-body fatigue.

Significance: Having the capability to detect and monitor physical fatigue of an individual from performing rigorous physical activities (e.g., prolonged walking, running, or activities requiring repetitive lifting or squatting) can help reduce the risk of musculoskeletal injuries or falls. Researchers have been put in substantial effort into developing a physical fatigue index or model by incorporating the movement information collected from wearable sensors. The findings of this study provide important insights on how physical fatigue is being induced, whole-body fatigue versus localized fatigue, could cause various extent of changes in gait performance.

Acknowledgements: Supported by NSF IIS-1955979

References: [1] Kao et al. (2018), *PLoS One* 13(7):e0201433; [2] Arvin et al. (2015), Gait Posture 42:545-9; [3] Yoshino et al. (2004) J Biomech 37:1271-80; [4] Suzuki et al. (2014), J Phy Ther Sci 26:1637-40; [5] Paillard (2012), Neurosci Biobehav Rev 36(1):162-76.

EVALUATING THE EFFICACY OF STROBE GOGGLES FOR CHALLANGING STANDING BALANCE

Madeleine E McCreary, Ryland D Swearinger, Sarah E Stenberg, Daniel P Ferris, Erika M Pliner*
Department of Biomedical Engineering, University of Florida
*Corresponding author's email: erikapliner@ufl.edu

Introduction: Falls account for most of injury related hospitalizations in older adults, and roughly 40% of all injury deaths [1]. As the global population ages, the number of injuries due to falls is expected to double by 2030 [1]. Yet, falls are preventable incidents [2,3]. Diet, exercise, and home modifications reduce fall risk [2], but additional falls prevention interventions are needed to combat this major public health problem [1]. Balance training paradigms are a promising intervention to decrease fall incidents. Physical perturbations during balance training (e.g. moving platform, waist pulls) reduce fall risk, but the implementation of these paradigms require costly, custom equipment and fall-arrest systems [4]. There is a need for accessible balance training paradigms. Balance control requires integration of the visual, vestibular, and sensorimotor systems. The visual system can easily be perturbed through affordable eyewear. Thus, this study investigates the effectiveness of visual perturbations via strobe goggles in challenging standing balance. We hypothesized that visual perturbations via strobe goggles would reduce standing balance stability compared to standing balance with no visual perturbations. This work is a necessary step towards the design of a balance training paradigm that is both globally accessible and beneficial towards reducing fall incidents.

Methods: 50 healthy younger adults have completed a balance training paradigm with strobe goggles. This study analyses a subset of the balance training paradigm, comprising of two standing balance tasks. Specifically, participants stood for two six-minute trials, one in a bilateral stance and one in a tandem stance. The order of the stance was randomly assigned to each participant. The participants wore strobe goggles. The strobe goggles were programmed for no strobe (goggle lens remained transparent) and strobe (goggle lens flipped between 0.067 s opaque and 0.1 s transparent) periods. Each trial consisted of an initial one-minute no strobe period, a four-minute strobe period, and a final one-minute no strobe period. Participants were instructed to look at a fixation target, set 10 feet away and at eye level. Participants stood on one (bilateral stance) or two (tandem stance) force places (AMTI, collected at 1000 Hz). The participant's center of pressure (COP) was calculated from the force plate data [5]. The COP 95% confidence ellipse was quantified for each trial-minute [6]. A greater elliptical area is likely to indicate reduced stability, suggesting challenged balance. This abstract presents data of the participants processed to date (n=5). When data processing is completed for all participants, an ANOVA will be performed on the COP 95% confidence ellipse area with stance (bilateral, tandem), trial-minute and visual perturbation (no strobe, strobe) as independent variables.

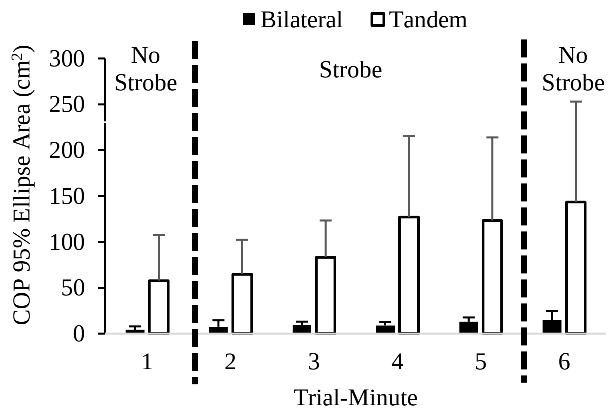

Figure 1: Average COP 95% confidence ellipse area by trial-minute for bilateral (black) and tandem (white) stances, n = 5. Error bars denote standard deviation.

Results & Discussion: Preliminary results show greater elliptical area during tandem stance than bilateral stance (Fig. 1). Greater elliptical area for the tandem stance compared to the bilateral stance suggests tandem stance to be more challenging and agrees with pervious literature [7]. Elliptical area is potentially increased due to visual perturbations and time into trial (based off graphical trends, n=5). For both bilateral and tandem stance, there was an increase in the elliptical area (cm^2) from the no strobe (trial-minute 1 – bilateral mean: 4.20; std=3.65 and tandem mean: 57.81; std=49.86) to the strobe (trial-minute 2 – bilateral mean: 7.97; std=6.92 and tandem mean: 64.69; std=37.67) periods. However, more participants are needed to determine whether this increase, suggesting reduced standing balance stability, is statistically significant. This would confirm our hypothesis and indicate that visual perturbations via strobe goggles challenge balance. Surprisingly, elliptical area may not decrease in the last minute with no visual perturbations. We expected the elliptical area to decrease to a level similar to the first minute of no visual perturbations. The observed effect may be due to disorienting effects due to the visual perturbations and/or participant fatigue. Additional data is needed to confirm these trends. To date, this study is limited by sample size (the number of participants processed) and standing stability metrics. Only the COP 95% confidence ellipse area is presented in this abstract. Presenting a more comprehensive set of standing balance metrics (e.g. sway range, frequency, velocity) can aid in improving this study's definition of stability and challenged balance.

Significance: In order to make balance training paradigms more accessible, it's crucial to develop cost-effective methods that can be easily distributed. The strobe goggles are relatively inexpensive and simple to use; if they are found to effectively challenge balance, they can be used to develop more accessible balance training paradigms.

Acknowledgements: This study is funded by the NIH – National Institute on Aging (Grant #: 1F32AG072808-01).

References: [1] WHO 2007 Global report on Fall Prevention in Older Populations; [2] NIH Falls and Fractures in Older Adults: Causes and Prevention; [3] CDC Older Adult Fall Prevention; [4] Mansfield et al. (2015). *Physical Therapy & Rehabilitation Journal*; [5] Borrelli et al. (2020). *Journal of Biomechanics*; [6] Prieto et al. (1996) *IEEE Transactions of Biomedical Engineering*; [7] Jonsson et al. (2005). *Clinical Biomechanics*.

QUANTIFYING DAILY HEAD TURNS AND HEAD-TRUNK COUPLING IN HEALTHY ADULTS

Selena Cho[1*], Peter C. Fino[1]
[1]University of Utah, Salt Lake City, Utah
*Email: selena.cho@utah.edu

Introduction: Continuous activity monitoring has been popular in quantifying how many steps people have to take, hours of sleep, and even the number of full-body turns a person needs to do in a day.[1] In recent years, the focus has shifted from not only quantity, but the quality (i.e., kinematics) of movement. For example, on top of the number of full-body turns, we can now characterize kinematics like peak angular velocity or turning amplitude.[1] These qualitative measures for daily living have only recently become possible due to the development of small, minimally obtrusive inertial measurement units (IMUs). Many continuous monitoring studies place an IMU at the waist for full body turn metrics, but quantifying head movements is also important; the head houses our visual and vestibular system responsible for vision, postural control, and gaze stability, and head motion can be an important marker of rehabilitation for people with impaired vestibular function.[4,5] Yet, there are few, if any, studies quantifying rotations of the head, during daily life.[1,2,3] The purpose of this study was to determine the feasibility of capturing kinematics of the head during daily life, with an end goal of providing normative data on head-trunk coupling and distributions of the number, speed, and amplitude of head turns.

Methods: Four healthy (3F, mean (SD) age = 28 (3.2) yrs) participants signed an informed written consent approved by the University of Utah IRB. Three IMUs (Axivity, Newcastle, UK) were placed behind the right ear just superior to the mastoid process, neck (T2), and lumbar area (L3) and collected tri-axial linear acceleration and angular velocity data at 100 Hz. Participants were asked to wear the sensors for seven days. Participants were asked removed the head sensors before showering and sleeping, and upon replacing the head sensor, calibrate it by shaking, nodding, and jumping three times for synchronization with anatomical axes. All data were processed through a custom MATLAB script (Mathworks, Natick, MA).

Data were segmented into the separate days from 8AM to 9PM. Raw angular velocity from the head sensor was filtered with a 4th order recursive low-pass Butterworth filter with a cutoff frequency of 3 Hz. Head turns were defined when peak yaw angular rate was greater than 15 °/s.[1] Turns occurring within 1/3s in the same direction were combined, but those less than 1/6s were excluded.[5] Head-on-body turns refers body turns when the head is rotating with respect to the body reference frame, which can be identify if the head rotation with respect to trunk ($\dot{H}_t$), defined as the magnitude in the difference of head rotation ($\dot{H}_s$) and trunk rotation ($\dot{T}_s$), is greater than 10 °/s.[6] Full-body turns refer to turns in which both head and trunk are rotating together or equivalently, defined anytime $|H_t| < 10$ °/s.[6] Outcomes were the number of head turns, the peak angular rate, angular displacement, and the percentage of head-on-body and full-body turns.

Table 1: Head turning characteristics

	S01	S02	S03	S04
Head Turns Mean (SD)	2076 (1070)	4535 (2092)	9831 (3492)	7958 (2937)
Peak Angular Rate (°/s)	47.9 (44.2)	43.8 (43.2)	56.2 (51.4)	64.9 (59.1)
Angular Displacement (°)	27.4 (40.8)	20.4 (36.4)	22.1 (31.9)	26.6 (36.4)
Full-Body (%) Mean (SD)	10 (4)	4 (2)	7 (2)	7 (4)
Head-on-trunk (%) Mean (SD)	90 (4)	96 (2)	93 (2)	93 (4)

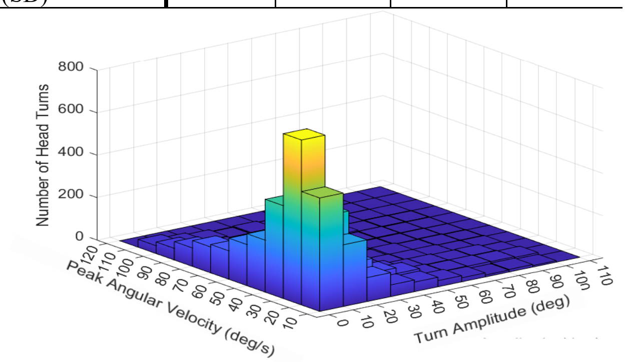

Figure 1: Distribution of head turn amplitude and peak angular velocity during a day.

Results and Discussion: Three participants wore the sensors for seven days. One participant ended data collection early after five days because they did not want to continue. Participants completed an average (SD) of 5976 (3930) head turns per day (Table 1). Of these head turns, most were performed with an angular displacement of <10° and peak angular rate of <40°/s (Figure 1). The average percentage (SD) of full-body turns across all participants were 7% (4) while the average percentage of head-on-body turns were 93% (4) (Table 1). The number of head turns is almost 10 times greater than the number of full-body turns.[1] Daily head turn counts also varied for each participant due to different activities. For example, Subject S01 was sick for a couple of days which may have contributed to a lower head turn count. The 8AM-9PM window may have missed some head turns due to early risers or late sleepers, but these results suggest there is substantial head motion that is not being captured through standard methods and may be important for monitoring daily activity.

Significance: To our knowledge, this is the first study to measure head kinematics for a week in healthy individuals. Our findings find that head turns occur nearly ten times more frequently than full-body turns, with the majority of daily turns being head-on-body turns. Head movements during daily life may provide important information that could guide clinical decisions related to diagnosis and rehabilitation.

Acknowledgements: This research was supported by the National Science Foundation Graduate Research Fellowship Program.

References: [1] Stuart, S. et al., 2020. *J Neurotrauma*. 37(139-145). [2] El-Gohary, M. et al., 2013. *Sensors.* 14(356–369). [3] Paraschiv-Ionescua, A. et al., 2018. *Gerontology.* 64(601-611). [4] Minor, L. B., 1998. *Otolaryngol Head Neck Surg* 188(s5-s15). [5] Paul, A. et al, 2017. *IEEE Trans Neural Syst Rehabil Eng*. 25(2347-2354). [6] Solomon, D. et al., 2006. *Exp Brain Res.* 173(475–486).

WHICH HIP MODEL BEST PREDICTS BIOLOGICAL TORQUES ACROSS LOCOMOTION MODES? A SIMULATION STUDY

Po Chuan Chen, Benjamin A. Shafer[1*], Wei-Lin Du, Aaron J. Young, Gregory S. Sawicki
[1]George W. Woodruff School of Mechanical Engineering, Georgia Institute of Technology, Atlanta GA, USA
*Corresponding author's email: ben.shafer@gatech.edu

Introduction: Wearable assistive devices can augment people's mobility but lack a robust control strategy that can adapt to the various locomotion modes (speeds, slopes, and gaits) of everyday life. Human-in-the-loop optimization methods can find effective assistance at each mode, but these methods are time-consuming and exhausting for both the user and experimenter. Knowing that biological torque changes for each mode, we believe an analytical controller that could predict biological torque (BioTorque) across modes without user adjustment would address this issue. We simulated how well three optimized hip exoskeleton control models (impedance control (IMP), proportional myoelectric control (PMC), and muscle activity driven neuromuscular model-based control (NMM)) could mimic BioTorque across 26 different locomotion modes using only joint kinematics (angle and its derivative) and/or muscle activity (gluteus maximus and rectus femoris) as inputs (Fig. 1A). We hypothesized that the NMM would better predict BioTorque than IMP or PMC, as it leverages both kinematics and muscle activity.

Methods: We drove each model and comparison using previously recorded locomotion data from 5 participants including 4 speeds (1.25 m/s, 2 m/s walking, 2 m/s running, and 3.25 m/s running) across 7 slopes (±15° (except at 3.25 m/s running), ±10°, ±5°, and 0°). Each model was driven by the appropriate signals for that mode and the model torque output was compared against the measured, ground-truth BioTorque (Fig. 1C) using mean absolute error (MAE). The model parameters were tuned to minimize the MAE. To ensure we found the best tuning for each model, we compared three optimization algorithms (Surrogate, Bayesian, and CMAES) with enough iterations for each to converge within 5% MAE. We chose Surrogate, as it yielded the lowest error and the fastest convergence rate. IMP model took joint angle as input and then implemented a virtual spring and damper to generate an output torque (Fig. 1B). On the other hand, PMC model took measures EMG as input, amplified it (G_{EMG}) and concatenated it with a delay unit (Fig. 1B). Lastly, EMG-driven NMM-based controller [1] took in both joint angle and EMG as inputs, and implemented a Hill-type muscle-tendon model for each muscle, including a linear tendon spring in series with a contractile element representing muscle force and a non-linear spring in parallel (Fig. 1B). To calculate how well each model could mimic BioTorque at each trained mode, we split the data by gait cycles in a 3:1 training-to-validation ratio and measured the MAE only on the validation data. These results were averaged across participants and then the 26 modes for each model (Fig. 1D left). To determine how each model could predict BioTorque without retraining, we trained the model on one mode, measured MAE on the other 25 modes, and calculated the average per mode. We repeated this for all 26 modes and then averaged MAE across modes for each model (Fig. 1D right).

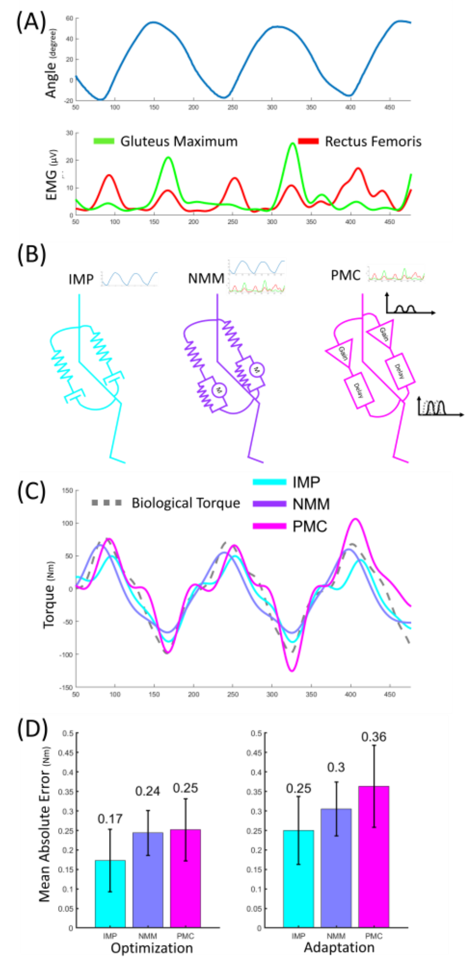

Figure 1: (A) Experimental angle and EMG data for model inputs. (B) Diagram of each model. The number of model parameters are 6 for IMP, 32 for NMM, and 4 for PMC. (C) Comparison between BioTorque and output torques of models. (D) MAE of optimization and adaptation.

Results & Discussion: The IMP model best mimicked measured BioTorque, showing the lowest optimization (training) MAE at 0.17 Nm (Fig. 1D left) on average across participants and modes. PMC showed worst performance, with the highest MAE. Furthermore, IMP model, with only 6 tunable parameters, also outperformed the more complex NMM and PMC models in terms of adaptability, with an MAE of 0.25 Nm (Fig. 1D right). It seems incorporating measured gluteus maximus and rectus femoris muscle activity actually hinders BioTorque estimates, possibly due to their high variability and differences in peak timing compared to BioTorque. On the contrary, joint kinematics provide a less variable and more effective signal to drive analytical models.

Significance: IMP model, a simpler architecture with fewer parameters, can better predict BioTorque than more physiologically complex models. Leveraging this understanding will help design exoskeletons controllers focused on motion sensors, with controller based on joint kinematics to provide continuous assistance across modes.

Acknowledgements: This research was supported by grants to A.J.Y. from the NSF National Robotics Initiative (Award#1830215).

References: [1] Markowitz et al. (2011) Philosophical Transactions

DYNAMIC SPORTS VISION AND BASEBALL SWING PERFORMANCE METRICS

Kaitlyn Armstrong[1], Kasey Murphy[1], Ann Claire Blalock[1] , Thomas Andre[1], Corbit Franks[1], Chip Wade[1*]
[1]University of Mississippi, University, MS, Human Movement and High Performance Laboratory
*Corresponding author's email: cwade@olemiss.edu

Introduction: Sports are dynamic activities that requires significant visual abilities for high performance on a consistent basis. The implications of vision on sports performance have gained significant interest over the last decade (Laby. 2021). Understanding how visual abilities influence on-field performance, on a daily basis and throughout the day, is an area that requires further clarification. Liu et al. (2020) highlighted the predictability of batting performance from visual and oculomotor abilities. Their results suggested faster processing speeds, oculomotor speeds and smooth pursuit accuracy translated to improved batting performance specifically when considering the decision-making at the plate of professional baseball players. Although certain aspects of visual and oculomotor skills have been assessed, parafoveal visual skills require further assessments. Shekar et al. (2020) assessed the use of digital sports vision training programs for improving certain aspects of vision among baseball players and softball players. Their results suggested no significant differences between experimental and placebo groups, however, each variable achieved minimal clinical relevance. Furthermore, the use of vision data for player selection in the professional baseball settings has previously been investigated (Kirschen et al. 2021). The authors highlighted the relevance of the vision score as a tool for player selection. The aim of the proposed study is to assess the association between oculomotor variables and baseball related metrics on quantitative swing performance metrics.

Methods: 9 male baseball position players between the ages of 15-18 participated in this study on a single testing day consisting of vision and swing testing in a single session. Participants will be recruited from a high school baseball program. Individuals with a current upper extremity injury, head injury, or visual/ocular impairment will be excluded from the study. The assessments consisted of the RightEye visual assessments and the Trackman assessment for hitting performance. The RightEye visual metrics consisted of a quantitative eye tracking assessment for: Brain Overall Score, Fixation Score, Pursuit Score, Saccade Score, Sports Score, Onfield Score, Mindeye Score, Functional Score, Mechanics Score. The Trackman metrics consist of quantitative swing (Exit Speed, Spin Rate, Launch Angle, Distance) and plate discipline (O-Swing , Z-Swing % and Z-Miss %) variables. A preliminary analysis was first performed to check for violations of statistical assumptions. First, we compared oculomotor variables by Trackman measures with separate univariate ANOVAs. Next, we conducted a series of multiple regression analyses to evaluate how well the visual variables predict swing and plat discipline variables. The data was analyzed using STATA 17(STATA, College Station USA). A value of $p < 0.05$ was considered statistically significant, and when appropriate we used Bonferroni adjustments for p-value.

Results & Discussion: Using separate univariate ANOVAs, we compared vision variables by Trackman metrics. There were significant correlations between Trackman metrics for all Righteye assessment variables (Table 1.). A stepwise multiple regression of Brain Overall Score, Fixation Score, Pursuit Score, Saccade Score, Sports Score, Onfield Score, Mindeye Score, Functional Score, Mechanics Score was performed to predict quantitative swing and plate discipline measures. The findings revealed a significant predictive relationship between Righteye vision metrics and Trackman swing and plate discipline metrics.

Significance: The results demonstrated that several dynamic vison measures were good predictors of swing and plate discipline metrics in high schools' players. Additional research is needed to provide a more thorough understanding of the relationship between oculomotor function and performance and develop effective player develop methods that improve these swing qualities player performance outcomes.

Acknowledgements: No outside support was provided for the completion of this study
References: Liu, S., Edmunds, F. R., Burris, K., and Appelbaum, L. G. (2020a). Visual and oculomotor abilities predict professional baseball batting performance. Int. J. Perform. Anal. Sport 20, 683–700. doi: 10.1080/24748668.2020.177 7819
Laby, D. M., Kirschen, D. G., Govindarajulu, U., and DeLand, P. (2019). The effect of visual function on the batting performance of professional baseball players. Sci. Rep. 9:16847. doi: 10.1038/s41598-019-52546-2

	Exit Speed	Spin Rate	Launch Angle	Distance	O-Swing %,	Z-Swing %	Z-Miss %	p-value
Brain Overall Score	97(13)	84(11)	84(17)	99(18)	86(21)	83(12)	88(17)	0.001
Fixation Score	96(21)	84(11)	87(11)	84(15)	91(12)	87(21)	87(17)	0.003
Pursuit Score	98(11)	94(12)	91(15)	81(23)	94(17)	87(17)	84(13)	0.001
Saccade Score	97(12)	92(17)	87(19)	91(11)	93(21)	83(16)	88(12)	0.05
Sports Score	88(17)	84(22)	97(19)	95(17)	85(17)	88(12)	94(11)	0.002
On field Score	87(19)	97(11)	82(76)	96(16)	81(21)	98(17)	91(18)	0.05
Mindeye Score	92(23)	88(17)	84(21)	94(21)	90(22)	91(19)	99(8)	0.05
Functional Score	98(13)	91(13)	94(11)	87(13)	91(13)	85(26)	96(13)	0.001
Mechanics Score	96(7)	96(24)	97(17)	95(12)	92(16)	92(14)	95(17)	0.001

Table 1: Mean (sd) comparison of RightEye vision metrics by Trackman swing and plate discipline metrics.

A CENTER OF PRESSURE TRANSFORM FOR COMMERCIAL SMART INSOLES

Jeromy D. Miramontes[1*], Catherine W. Bowyer[2], Suzanne M. Konz[1], and Steven Leigh[1]
[1]Biomechanics and [2]Physical Therapy Departments, Marshall University, Huntington, WV, USA
*Corresponding author's email: miramontes1@marshall.edu

Introduction: Many different types of wearable technology are commercially available and only about five percent of wearable technology in the current market has been validated formally [1]. Wrist-worn fitness trackers have poor to moderate validity when measuring simple factors such as step count but exhibit greater validity at jogging and running speeds [2]. Force sensitive insoles allow more complex variables to be measured in-the-field and have previously been calibrated to the gold standard of force platforms [3]. A commercially available and relatively affordable force sensitive insole system may be applicable for in-the-field kinetic data collection. There is uncertainty if there is biomechanical similarity among level, uphill, and downhill running performed in a lab setting versus overground. To gather the most ecologically valid data regarding running technique, researchers may conduct analyses of the activity in the same setting as the typical performance. The purpose of this study was to compare the normal force and center of pressure as measured by a commercially available and relatively affordable force sensitive insole system with a force platform and 3-D infrared camera motion analysis system during running in a lab setting, and then to compare running in a lab setting to running on a trail outside. We hypothesized that the force sensitive insoles would provide similar kinetic data to a force platform, and that kinetic data would be different in a lab setting compared with an outdoor trail.

Methods: Fifteen people who ran at least five miles regularly were recruited from a collegiate running club and running groups from the surrounding community. All participants had established running patterns and no current injuries or other injuries to the lower extremities in the six months prior to the study. Participants wore their own running shoes and were given ARION (ato-gear, Eindhoven, NL) insoles to wear underneath their own insoles. After completing the informed consent process, participants familiarized themselves with running in a lab, including establishing step patterns to be able to land completely on a force platform with one foot without changing stride length. Participants then ran across the lab five times, and then immediately went outside to complete a one mile loop of a campus running trail.

While they were in the lab, kinematic data of the participants running were collected using ten Vantage cameras (Vicon, Oxford, UK), kinetic data were collected with a force platform embedded in the floor (AMTI, Watertown, MA), and all data were recorded into a Vicon Nexus system. Marker clusters were placed on the participants toe and heel, and markers were placed on their medial and lateral ankles, mid-calf, and knees such that the markers could be used to define the outline of the foot and anatomically relevant planes for the forefoot, rearfoot, and shank, and joint axes could be defined for the toe, ankle, and knee. Insole data were collected during the lab and the outdoor trials, and time-synchronized to the motion analysis system data recorded by Vicon using the unix time stamp.

The Center of Pressure location as measured by the force platforms was transformed from the force platform coordinate system to a foot coordinate system defined by the toe and heel marker clusters using custom written code in MatLab (MathWorks, Natick, MA). The center of pressure location and vertical ground reaction force was compared between the motion analysis system and insoles and between in-lab and outdoor running with cross-correlation analyses.

Results & Discussion: Center of pressure location was similar between that calculated by the insoles and that calculated by the motion analysis system ($R = 0.845$, lag = 19). Normal force time history was similar between the insoles and the motion analysis system ($R = 0.916$, lag = 14). The normal force time history was different between running in a lab versus running outside ($R = 0.659$, lag = 44). These data suggest that the normal force measured by the insoles had a pattern consistent with the ground reaction force measured with the motion analysis system. The timing of the change of location of the center of pressure and timing of the rise and fall of the normal force was similar between both systems, however, the data from the insoles lagged the data from the motion analysis system, which might indicate a delayed response from the insole, or a cushioning effect due to the insole being worn within a shoe. The shoe also appeared to attenuate the maximum force measured by the insole. These results indicate that a force sensitive insole may be useful to conduct within-subject analyses in-the-field.

Significance: Ground reaction forces cannot be observed visually, provide critical information for movement assessments, and are inputs to inverse dynamic calculations of joint loads. The use of force plates to measure ground reaction forces is limited by their cost and specific location requirements. Alternative devices, such as force sensitive insoles, are generally cheaper and allow for measurements to be made in the environment in which typical performances occur. This study presents a method to estimate vertical ground reaction force and center of pressure for a commercially available force sensitive insole. This may be an affordable option to collect kinetic data in-the-field.

References:
[1] Peake, J.M., Kerr, G., & Sullivan, J.P. (2018), *Front. Physiol.,* 9.
[2] Ming-De, C., et al. (2016), *Med Sci Sports Exerc,* 48(10).
[3] Chumanov, E.S., Remy, C.D., & Thelen, D.G. (2010), *Comput Methods Biomech Biomed Engin,* 13(5).

STATIC POSTURAL CONTROL IN PEOPLE WITH DIABETES: AN COMPARISON BETWEEN CENTER OF MASS AND CENTER OF PRESSURE

Kai Cheng[1,2], Zachary Van Dorn[1,2], Sodiq Fakorede[1,2], John Miles[3], Chun-Kai Huang[1,2*]
[1]Department of Physical Therapy, Rehabilitation Science, and Athletic Training; [2]KU Mobility Consortium; [3]Department of Endocrinology, Diabetes and Clinical Pharmacology; University of Kansas Medical Center, Kansas City, KS, USA
*Corresponding author's email: chuang7@kumc.edu

Introduction: The numerous incidents of fall and its pertaining cost give rise to the need for a comprehensive sensory organization test (SOT) for postural control, especially in fall-prone populations [1,2]. The impaired postural control and increased fall incidents have been noted in the population with diabetes mellitus (DM) [3]. For example, the increase in center-of-pressure (COP) displacement and velocity using a force plate during quiet standing has been interpreted as varied postural sway and impaired balance in DM patients. The inertial measurement unit (IMU) that captures target objects' position and orientation data in space has been adopted for clinical balance assessment with the advantages of portability and cost-effectiveness [4]. With the question and interest of whether the IMU data can somehow equivalently represent the COP data during quiet standing, the objective of this study is to compare the COM data obtained from an IMU system to the concurrent data recorded by a force place during quiet standing from patients with DM.

Methods: Eight recruited participants with type 2 DM were instructed to stand on the AMTI force plate (Watertown, MA) with the Solo Step harness system (Sioux city, SD). The force plate was used to measure the COP data while one APDM sensor (Portland, OR) was used to measure the COM data. A virtual reality-based SOT (i.e., VR-ComBAT) paradigm that emulated the SOT conditions (e.g., normal, occluded, and conflicted visions) was adopted [5]. The COM and COP data were processed in terms of the displacement, velocity, frequency, and sway area in anteroposterior and mediolateral directions. The Wilcoxon's signed-rank test was used to compare differences between COM vs. COP and Spearman's rank correlation was used for the correlation.

Table 1. The comparison between COP and COM displacement in quiet standing

	COP		COM		p-value
	Mean	SD	Mean	SD	
Average velocity (mm/s)	55.85	32.89	35.84	18.01	0.09
Velocity AP (mm/s)	47.89	30.32	30.88	14.97	0.16
Velocity ML (mm/s)	20.6	9.6	11.7	7.48	0.01*
Average frequency (mm)	1.2	0.4	1.26	0.93	0.01*
Frequency AP (Hz)	1.4	0.5	0.78	0.13	0.02*
Frequency ML (Hz)	1.31	0.34	1.13	0.2	0.05*
RMS distance (mm)	8.23	2.59	11.53	5.18	0.02*
RMS distance AP (mm)	7.36	2.49	10.49	4.75	0.02*
RMS distance ML (mm)	4.32	1.55	4.43	2.13	0.78

*There has the statistically significant difference (p-value = 0.05).

Table 2. The correlation between COP and COM in quiet standing

	COP		COM		p-value
	Mean	SD	Mean	SD	
Average velocity (mm/s)	55.85	32.89	35.84	18.01	0.29
Average frequency (mm)	1.2	0.4	1.26	0.93	<0.01*
Frequency AP (Hz)	1.4	0.5	0.78	0.13	<0.01*
RMS sway area (mm/s^2)	176.46	164.46	142.36	178.28	0.03*
RMS distance (mm)	8.23	2.59	11.53	5.18	0.03*
RMS distance AP (mm)	7.36	2.49	10.49	4.75	<0.01*

*There has the statistically significant difference (p-value = 0.05).

Results & Discussion: Our results show that there shows some similarity and correlation between COP and COM displacement measurement in the balance assessment in population with DM. The similar average velocity especially in the anteroposterior direction of both COP and COM displacement can be observed (Table.1). As for the average frequency, sway area and root mean square (RMS) of distance, significant correlations can be found between two measurements (Table.2).

In our study, both the COP measurement and COM measurement show some similarity and correlation during the static balance assessment. Considering the correlation between COP and COM, the change of frequency, distance and area of postural sway may be able to be investigated through COM instead of COP. Specifically, the variables in the AP direction with lower variation may have the higher validity to measure postural sway using COM.

Significance: The COM measurement via IMU might be similar and equivalent to COP measures using a force plate. Future clinical balance assessment might adopt COM measures to quantify postural control in patient population with the advantages of feasibility, portability and cost-effectiveness. More sample sizes and in-depth analysis are warranted to consolidate this statement.

Acknowledgements: Research reported in this publication was supported by the Kansas University Training Program in Neurological and Rehabilitation Sciences (NIH T32HD057850).

References:
[1] Bergen, G., Steven, M.R., Burns, E.R. (2016), *Morbidity and Mortality Weekly Report* 65 (37).
[2] Hart LA et al., (2020), *J Am Geriatr Soc* 68(6).
[3] Hewston P, Deshpande N (2016), *Can J Diabetes* 40(1).
[4] Moon S, Huang CK, Sadeghi M, Akinwuntan AE, Devos H (2021), *Front Bioeng Biotechnol* 9:678006.
[5] Zilliox LA, Chadrasekaran K, Kwan JY, Russell JW (2016), *Current Diabetes Reports*. 16(9).

ANKLE EXOSKELETONS MITIGATE CALF MUSCLE FATIGUE OVER 30 MINUTE WALKING BOUTS

Amro A. Alshareef[1,3*], Olivia Moore[2], Jason Franz[4], Gregory S. Sawicki[1,2,3]
[1] Woodruff School of Mechanical Engineering [2] Wallace H. Coulter Dept. of Biomedical Engineering
[3] Institute for Robotics and Intelligent Machines, Georgia Institute of Technology, Atlanta GA, USA
[4] Joint Department of Biomedical Engineering, UNC at Chapel Hill and NC State University, Chapel Hill, NC, USA
*Corresponding author's email: aalshareef6@gatech.edu

Introduction

Balance assistance for clinical populations or for older adults is becoming increasingly necessary to support rehabilitation and prevent injury. To this end, walking balance control, fatigue analysis on a metabolic and muscular level, and exoskeletal device assistance have all garnered individual attention. Muscle fatigue correlates with reduced balance integrity – likely due to reduced force responsiveness on the muscular level [1]. Fortunately, exoskeletal assistance has been shown to decrease walking metabolic cost [3] and, at least with passive assistance under stationary loading tasks, mitigate fatigue [2]. Furthermore, it has been shown that proper ankle exoskeletal control can improve balance during walking [4]. Yet, the mechanisms by which exoskeletal assistance influences fatigue, and thereby fatigue-induced imbalance, remains unclear. We hypothesize that ankle exoskeletons assistance will offload force required for locomotion from the calf muscles to the exoskeleton motors, attenuate the onset of muscle fatigue, and result in reduced measures for biomarkers of fatigue in ankle plantar flexors.

Methods

Two participants (18-20 years) walked for a 30-minute period on a dual-belt instrumented treadmill platform (CAREN, Motek) on two days. A full body reflective marker set was applied to participants for motion capture, allowing for calculation of joint kinematics and kinetics. We applied surface electrodes to capture electromyographic (EMG) signals from the muscles depicted in Figure 1A. In session one the participant wore Dephy EB60 ankle exoskeletons, utilizing the optimized torque assistance profile controller developed Zhang et al. [3] with a 20 Nm peak torque. In session two the participant completed the same 30-minute walking bout without an exoskeleton. The order of the sessions was randomized between participants. We used two metrics to catalog evidence for muscle fatigue – namely, (i) mean power frequency (MPF) from each EMG signal and (ii) the ratio of integrated joint moment per integrated unit muscle activation for the muscles acting on that joint.

Results and Discussion

We have thus far found that ankle moment per unit soleus (SOL) activation and per unit medial gastrocnemius (MG) activation is greater with exoskeleton assistance than without, indicating reduced calf muscle fatigue with assistance (Fig. 1B). This result is consistent with the difference in MPF of the SOL and MG from minute 1 to minute 30, where exoskeleton assistance results in a higher MPF at the end of the walking bout compared to without assistance (Fig. 1A). Interestingly, we are finding that hip moment per unit gluteus maximus (GMAX) activation and per unit rectus femoris (RF) activation is less with than without exoskeleton assistance (Fig. 1B), indicating greater fatigue in the hip flexors and extensors with exoskeleton assistance. This result is consistent with the GMAX and RF shift toward a lower MPF from minute 1 to minute 30 of the walking bout with exoskeleton assistance compared to without (Fig. 1A). This seems to indicate an offloading of demand from the ankle to the hip with exoskeleton assistance.

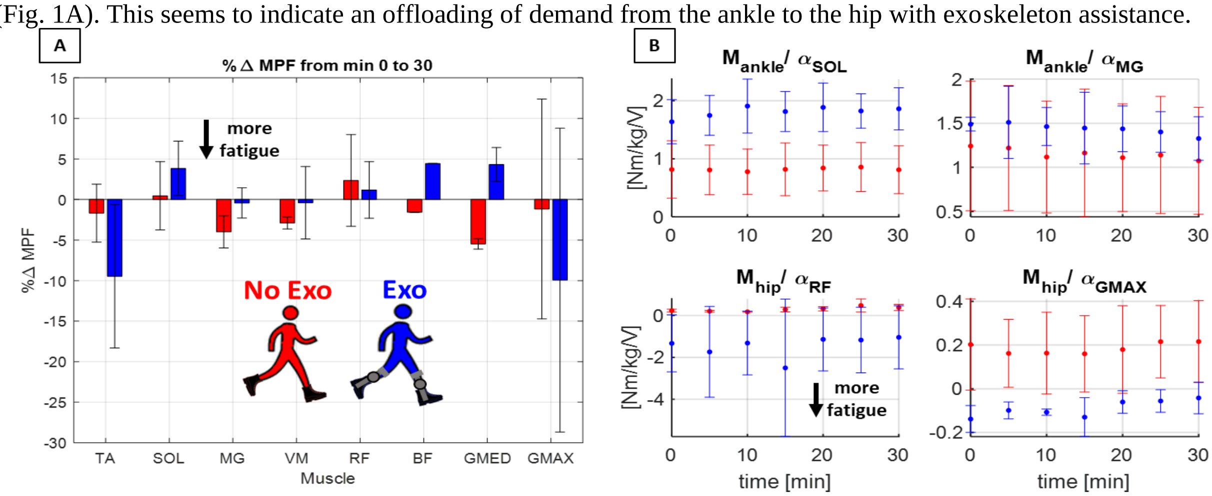

Figure 1: A) Mean Power Frequency (MPF) for 8 proximal and distal leg muscles. B) Joint moment per unit muscle activation at the ankle and hip.

Significance

Using the data set from this study, we will be able to better map the influence of exoskeletal assistance on muscle fatigue, providing a roadmap for the use of exoskeletons to mitigate fatigue not only to prolong walking capacity, but also to improve resilience to balance challenges and mitigate falls. We will also continue to investigate the effects of muscle level fatigue on locomotor stability during functionally relevant walking tasks, which is currently a gap in our exploration of fatigue and assistance in both younger and older adults, by incorporating various destabilizing perturbations during the 30-minute walking trial.

Acknowledgments

We would like to thank Qingyi Lou, Lauren Harris, and Jenny Leestma, for their feedback and support during this experiment. Support from the National Institute on Aging of the National Institutes of Health, R01AG058615.

References

[1] Lacey et al. (2019) IJES [2] Lamers et al. (2020) Sci Rep. [3] Zhang et al. (2017) Science. [4] Bayon et al. (2022) JNR

EFFECTS OF STROBOSCOPIC PERTURBATIONS ON GAIT PARAMETERS

Elizabeth S Ray, Chloe M Lapish, Nora M Lewis, Kathryn S Kalouf, Daniel P Ferris, Erika M Pliner*
Department of Biomedical Engineering, University of Florida
*Corresponding author's email: erikapliner@ufl.edu

Introduction: Approximately 36 million falls occur every year among older adults [1]. These falls lead to 3 million hospitalizations and 32,000 deaths in the U.S [1]. Falls pose a threat to physical health and have psychological consequences such as developing a fear of falling [2]. A common reason for falling in older adults is due to gait disturbances [3]. Thus, various training paradigms that aim to challenge gait have been developed. Perturbation-based gait training is known to reduce fall risk [4]. Unfortunately, most perturbation-based gait training systems (e.g. CAREN) require costly equipment. There is a need for affordable perturbation-based gait training paradigms that maintain high efficacy in falls prevention. Visual feedback is a critical component to balance control that is easily perturbed. Therefore, using visual perturbations during gait training is a promising paradigm for an affordable intervention that reduces fall risk. Goggles that strobe from transparent to opaque (stroboscopic perturbations) reduce visual feedback [5] and are likely to challenge balance. The goal of this study is to determine if visual perturbations from strobe goggles challenge balance during gait training. We hypothesized that stroboscopic perturbations during gait training would challenge balance. Knowledge from this work will aid in guiding more affordable perturbation-based gait training interventions for falls prevention.

Methods: 50 healthy younger adult participants completed a balance training paradigm for this study**.** The balance training paradigm comprised of walking on a beam (1-inch in height) that was connected to a treadmill moving at 0.3 m/s. Participants wore strobe goggles during balance training and the width of the beam was adjusted to each participant's baseline balance ability. This abstract assesses a subset of data after a 30-minute balance training period. Specifically, one 7-minute balance training trial is assessed. This 7-minute trial comprises of a two-minute no strobe (goggles remained transparent), four-minute strobe (goggles flipped between 0.067 s opaque and 0.1 s transparent), and one-minute no strobe period. Kinematic data was captured from 14 reflective markers that were placed on the participant's feet and recorded with a 20-camera motion capture system (OptiTrack, collected at 100 Hz). Custom Matlab and Python code was written to determine heel contact, toe-off, foot location, and temporal gait parameters from the kinematic data. This abstract presents a subset of analyzed gait parameters: the percent of beam strikes (i.e. number of foot strikes on the beam over the total number of foot strikes) and the percent of double support time (i.e. percent of time both feet are in contact with the beam over the total time of consecutive foot strikes on the beam). This data was quantified for each trial-minute. A lower percentage of beam strikes and double support time would suggest challenged balance during gait. A portion of the participants' motion data has been processed for analysis (n=5). When data processing is completed for all participants, ANOVA tests will be performed on the gait parameters (dependent variables) with visual perturbation (no strobe, strobe) and trial-minute as independent variables.

Results & Discussion: Percent of beam strikes was highest during the first no strobe period (x=0.69, std=0.21) and lowest during the strobe period (x=0.62, std=0.16). There was a small increase in the percent of beam strikes from strobe to the final no strobe period (x=0.64, std=0.17). Similarly, the percent of double support time was highest during the first no strobe period and lower during the strobe period (Fig. 1). The percent double support time was lowest during the final no strobe period, corresponding to the last minute of the trial. These data trends suggest the stroboscopic perturbations to challenge balance during gait, but additional data is required to confirm these results and support our hypothesis. Interestingly, gait parameters vary between the initial no strobe and final no strobe periods (mean differences of 0.05 and 0.06 for the percent of beam strikes and double support time, respectively). These results may be due to disorientating effects from the stroboscopic perturbations or participant fatigue, but additional data is required to better assess this trend. The current results are limited by the number of processed participants. Future analyses will comprise a greater number of participants, temporal gait parameters and spatial gait parameters to better assess the effects of stroboscopic perturbations on challenging balance during gait.

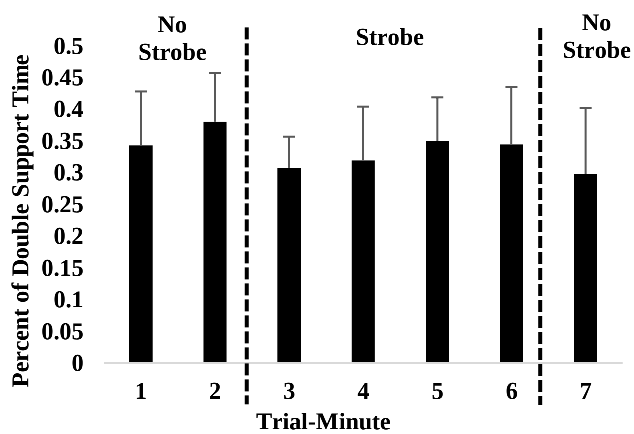

Fig 1: Average percent of double support time by trial-minute, n = 5. Error bars denote standard deviation.

Significance: There is a need to make perturbation-based gait training more affordable while maintaining efficacy in reducing fall risk. Thus, assessing the challenged balance effects of a perturbation that can be made more affordable (i.e. stroboscopic perturbations) during gait training is a necessary step towards this goal.

Acknowledgements: This study is funded by the NIH – National Institute on Aging (Grant #: 1F32AG072808-01).

References: [1] CDC. Keep in Your Feet–Preventing Older Adult Falls; [2] Schoene et al. (2019), *Clinical interventions in aging* vol. 14 701-719; [3] Jahn, Klaus et al (2010), *Deutsches Arzteblatt international* vol. 107,17 306-15; [4] Rieger, Markus M et al. (2020) *BMC geriatrics* vol. 20,1 167; [5] Bennett et al. (2018), *Frontiers in Psychology* vol. 9.

Muscle Contribution and Torque Generation During Dart Throwing Motion

Tyler Mason[1*], Morgan Dalman, M.S.[1], Katherine R. Saul, Ph.D.[1]
[1]Department of Mechanical and Aerospace Engineering, North Carolina State University, Raleigh, NC, USA
*Email: trmason2@ncsu.edu

Introduction: The Dart Throwing Motion (DTM) [1] is a key motion to everyday life. Everytime a drinking glass is picked up, a hammer is swung, or a dart is thrown, the wrist articulates in an oblique plane requiring both flexion and deviation. Prior research has been performed studying the planes through which the DTM acts, and on the skeletal components of the motion. Specifically, prior work has described the motion of the scaphoid and lunate during DTM [2], as well as importance of the midcarpal joint in through the DTM [3]. Muscle contributions to wrist function have largely been characterised with respect to the anatomical flexion and deviation planes rather than the functional DTM orientation. The goal of this research was to evaluate muscle demands needed to generate the DTM motion and assess the moment generated about the wrist during the motion.

Methods: A motion capture system (Motion Analysis Corporation, Santa Rosa, CA) was used to collect the kinematics for a single subject performing a DTM. Data was post-processed and smoothed with a 6 Hz Butterworth filter (Cortex, Motion Analysis Corporation, Santa Rosa, CA). Retroreflective markers (1 cm) were placed on anatomical locations of the upper limb and hand. Markers include the 7th cervical vertebra (C7), the most ventral aspect of the sternoclavicular joint (SC), xiphoid process (XP), the most lateral aspect of the acromial angle (AA), the bicep belly (BC), the lateral epicondyle of the humerus (LE), the medial epicondyle of the humerus (ME), the middle of the forearm (FC), the styloid process of the radius (RS), the styloid process of the ulna (US), the 2nd metacarpophalangeal joint (2MP), and the 5th metacarpophalangeal joint (5MP). Because prior work has established that the skeletal positioning of the hand bones are mostly unchanged throughout the DTM [4], the participant was instructed to hold their finger tips together. The kinematic data was used to scale and perform inverse kinematics and computed muscle control analyses with an upper limb musculoskeletal model [5] in OpenSim (v3.3)[6]. Simulations were used to calculate muscle forces and lengths produced throughout the DTM. The wrist postures and corresponding force and length data were used in a custom Matlab program (r2021b) (The Mathworks, Natick, MA) to compute the torque about the DTM wrist rotational axis throughout the motion. The method is shown in Figure 1.

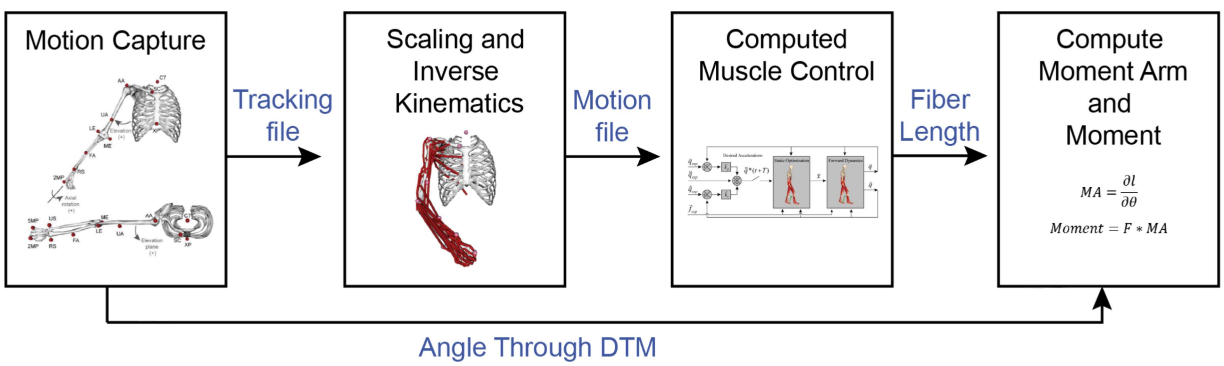

Figure 1: The methods diagram for computing the moment about the wrist during the dart throwing motion.

Results & Discussion: The moment about the wrist along the DTM plane was nearly constant throughout most of the motion, with a the largest deviation occurring during the throw. The minimum moment during the task was 4.29 Nm. Limitations of this study include the small sample size as this is currently based on a single subject. Future work will include additional data collection on subjects with varying anthropometrics and strength, along with additional motion (drinking from a glass, and hammer swing), to reveal further information about the applied moments throughout the oblique plane. As the oblique plane varies in orientation as a function of flexion and deviation of the wrist, further data collection may reveal coordinated muscle activity during a DTM and other coordinated wrist motions.

Significance: This work provides greater understanding of the Dart Throwing Motion, and evaluates the torque about the wrist during the DTM. Further research is needed to explore all forms of oblique wrist plane movement (DTM, hammer swing, drinking, etc.). This work is ongoing, with collection from additional participants planned.

Acknowledgements: Special thanks to Morgan Dalman, Ph.D Candidate and MoBL Research Assistant, NC State University. This research is funded by the Office of Undergraduate Research at NC State University.

References: [1] Palmer et al. (1985), *J Hand Surgery* 39(10); [2] Werner et al. (2004), *J Hand Surg* 29A(418-422); [3] Mitsukane et al. (2018), *J Phys Ther Sci.* 3(355-360); [4] Li et al. (2005), *Clinical Biomechanics* 20(177-183); [5] Holzbaur et al. (2005). *Ann Biomed Eng. 33*:829-840. [6] Delp, S.L. et al. (2007). *IEEE Trans Biomed Eng*. 55(1940-1950)

KINEMATICS OF THE FIRST METATARSOPHALANGEAL JOINT: BAREFOOT VS SHOD

Eric D. Thorhauer[1,2*], William R. Ledoux[1,2,3]
[1]Center for Limb Loss and Mobility (CLiMB), Department of Veterans Affairs, VA Puget Sound Health Care System, Seattle, WA
Departments of [2]Mechanical Engineering and [3]Orthopaedics & Sports Medicine, University of Washington, Seattle, WA
*Corresponding author's email: ericthor@uw.edu

Introduction: More precise quantification of first metatarsal phalangeal joint (MTPJ1) kinematics is permitted with the development of biplanar fluoroscopy systems dedicated to foot and angle imaging. Among the strengths of biplane systems over conventional motion capture systems are their ability to track bone motion in shoes.

Methods: Following IRB approval, subjects underwent bilateral computed tomography scans which were segmented to produce subject-specific first metatarsal and proximal phalanx models (Mimics v20, Materialise, Leuven, Belgium). Bone embedded coordinate systems were defined using the inertial axes of the bone surfaces. Subjects performed both barefoot and shod gait trials at self-selected speeds through the capture volume of a biplane imaging system (ISSI, Painesville, OH, USA) while pulsed X-ray video fluoroscopy sequences (120Hz) were collected. A strain gauge embedded in the X-ray transparent walkway was used to detect the gait cycle events. MTPJ1 bone motion was reconstructed using the model-based method of optimally aligning digitally reconstructed radiographs to the stereo fluoroscopy images in custom software (Figure 1) [1,2]. Kinematic results were smoothed with a second-order Butterworth filter with a cut-off frequency of 20Hz.

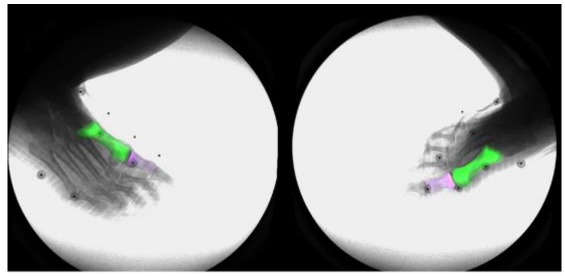

Figure 1: MTPJ1 model-based tracking on biplane fluoroscopy sequences.

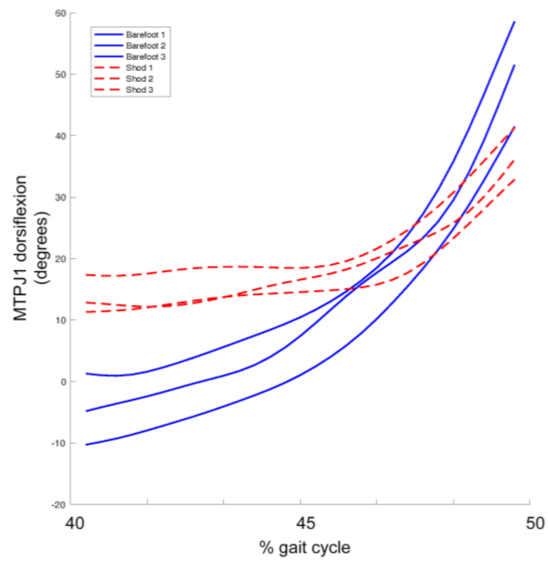

Figure 2: MTPJ1 dorsiflexion angle (degrees) during terminal stance phase for both shod (red dashed lines) and barefoot (solid blue lines) trials.

Results & Discussion: Currently the MTPJ1 motion for one subject has been tracked in both conditions. The resultant MTPJ1 dorsiflexion kinematics from late midstance to terminal stance phase were calculated (Figure 2). In the shod condition, the MTPJ1 started 15 degrees more dorsiflexed than during barefoot. On average, range of motion was 23.0 degrees for shod and 55.1 degrees for barefoot. Peak dorsiflexion angles were 13.8 degrees higher in barefoot trials on average. This study demonstrated that unlike traditional motion capture systems, biplane fluoroscopy can track foot bone kinematics while shod.

Significance: This study demonstrated the ability to track foot bone motion during shod trials and began quantifying within-subject differences in MTPJ1 kinematics between shod and barefoot gait. Previous studies have found extensive differences between barefoot and shod gait in healthy populations [3,4]. Given that most people spend most of their time in shoes, further research into the kinematics of the foot in these conditions is warranted.

Acknowledgements: Supported by VA Rehabilitation Research and Development Grants RX002008 and RX002970.

References:
[1] Iaquinto JM, Tsai R, Vu QB, Haynor DR, Sangeorzan BJ, Ledoux WR. Preliminary model-based validation of a biplane fluoroscopy system. J Foot Ankle Res. 2014.
[2] Thorhauer, E., & Ledoux, W. R. (advisor). MS Thesis, Calibration and optimization of a biplane fluoroscopy system for quantifying foot and ankle biomechanics. University of Washington Libraries, 2020.
[3] Stone AE, Shofer JB, Stender CJ, Whittaker EC, Hahn ME, Sangeorzan BJ, Ledoux WR. Ankle Fusion and Replacement Gait Similar Post-surgery, But Still Exhibit Differences Versus Controls Regardless of Footwear, JOrthop Res. 2021 Jan 17. doi: 10.1002/jor.24988. Online ahead of print. PMID: 33458862
[4] Keenan GS, Franz JR, Dicharry J, Croce UD, Kerrigan DC. Lower limb joint kinetics in walking: the role of industry recommended footwear. Gait Posture. 2011;33(3):350-355.

PREDICTION OF UPPER LIMB INCAPACITATION AS A RESULT OF CROSS-SECTIONAL MUSCLE TISSUE LOSS

Morgan J. Dalman, M.S.[1*], Haley Geithner.[1], Katherine R. Saul, Ph.D.[1]
[1]Department of Mechanical and Aerospace Engineering, North Carolina State University, Raleigh, NC, USA
*Corresponding author's email: mdalman2@ncsu.edu

Introduction: Injuries to the extremities are common among military combat casualties and can limit mobility. From 2005-2009, 82% of musculoskeletal wounds from combat casualties were explosion related [1]. From 2000-2009, 4,693 service members had sustained a gunshot wound related to combat [2], and 73% of gunshot wounds affected the extremities, potentially limiting mobility [3]. Despite the frequency of these injuries, the level of resulting incapacitation that can be expected is not yet clear. Blast and penetrating wound injuries cause volumetric loss of muscle tissue, which inherently reduces the mechanical capacity of muscle due to loss of contractile material. While other factors - such as blood loss, neurological injury, bone fracture and pain - can additionally impact function, the mechanical deficits can provide an estimate of functional deficits expected from wounds of a particular size. Using computational musculoskeletal modeling, this study evaluates potential incapacitation experienced by an individual as a result of cross-sectional muscle tissue loss in the upper extremity.

Methods: Two typical functional movements were chosen for evaluating upper limb incapacitation (lift weight to head height and hair comb). The range of required joint moments for performance of each upper extremity functional task was obtained from prior literature [4]. An existing upper limb computational musculoskeletal model representing a 50th percentile male [5] was used to simulate effects of muscle loss using OpenSim (v3.3) [6] and MATLAB (r2022b) (The Mathworks, Natick, MA). We systematically decreased muscle cross-sectional area from 0-100% (10% increments) for functional muscle groups and the individual muscles comprising them (e.g. **Fig 1**). Simulated joint moments were calculated for the shoulder and elbow.

Results & Discussion: The simulations suggest that isolated injury to single muscles at the shoulder and elbow (**Fig. 1 a-d**) is unlikely to directly limit functional performance, but significant injury to a functional group, as is common in penetrating/blast injuries, may limit ability to perform important mobility tasks when >90% of cross-sectional area is disrupted. However, injury to deltoid in isolation results in a more marked deficit than that associated with other muscles. Limitations of the current work include that we have initially considered effects of cross-sectional muscle loss in isolation and injury to single muscles and functional groups rather than more complex patterns of injury or concomitant factors such as nerve or bone injury; these will be addressed in future work. In addition, an individual's nominal anthropometry, age, and strength will also affect outcomes. Future work will consider these limitations and extend analysis to the upper limb.

Significance: These simulations provide insight into whether functional deficits for upper limb functional movement are likely to occur following injury causing volumetric muscle loss, based on the mechanical consequences of lost contractile material.

Acknowledgement: Research funded by NIH-1F31AR081691-01.

References: [1] Belmont, et al. (2013). *J Orthop Trauma*. 27: 107-113. [2] Walker, et al. (2012). *Int J Surgery* 10: 140-143. [3] Laughlin, et al. (2017). *Int J Surgery 48*: 286-290. [4] Murray et al. (2004), Clinical Biomechanics 19(6):586-594. [5] Holzbaur et al. (2005). *Ann Biomed Eng. 33*:829-840. [6] Delp, S.L. et al. (2007). *IEEE Trans Biomed Eng*. 55(1940-1950)

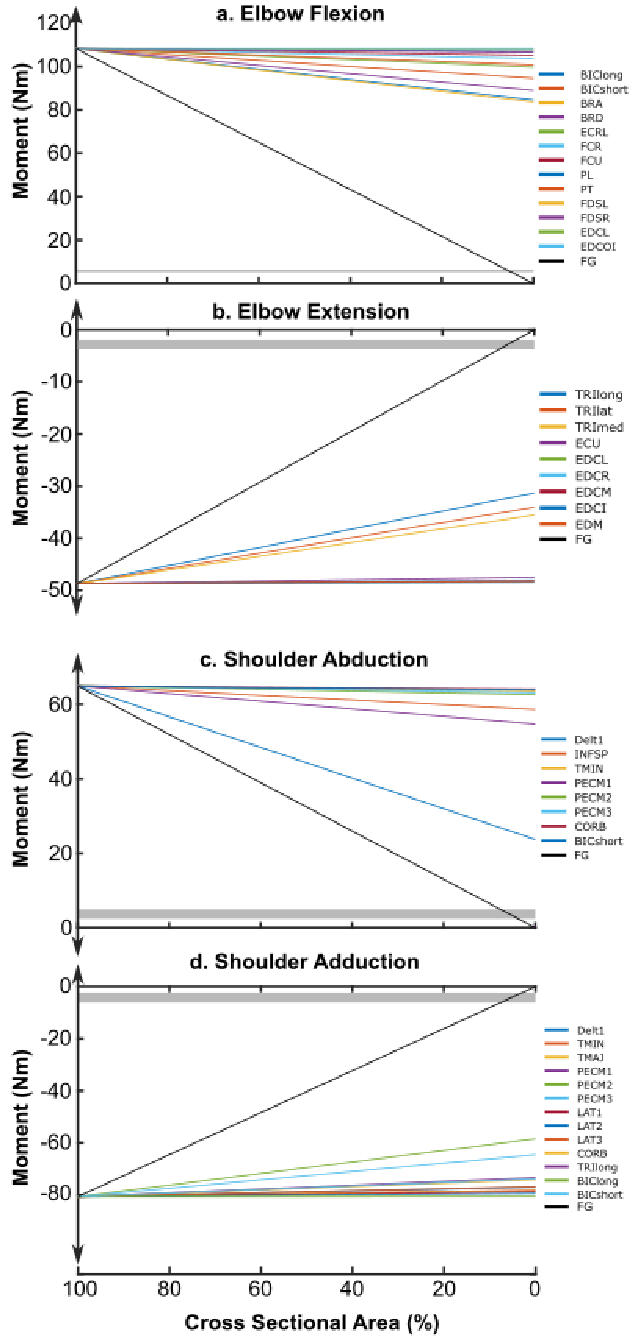

Figure 1: Joint moment across decreasing physiological cross-sectional area for individual muscles and function group as a whole.

ACCURACY OF A 2D CAMERA FOR RUNNING DUAL SIDED KINEMATIC DATA

Luke VanKeersbilck[1*], Jared Steele[1], Iain Hunter[1]
[1]Brigham Young University, Provo Utah
email: *lvank@byu.edu

Introduction: Previously three-dimensional motion capture data required multiple cameras and an expensive motion capture system. With the rise in machine learning pose estimation algorithms, it is becoming possible to obtain three-dimensional data of human movement with a single smart phone camera. One issue with this method is often one side of the body is partially occluded from view by the rest of the body. Previous studies have gotten around this by using a camera on the right and the left sides of the body (1). The purpose of this study was to compare the accuracy of a pose estimation algorithm at estimating joint angles on both the side that is full yin view and the one that is partially occluded as compared to the gold standard motion capture system.

Methods: Ten subjects (6 men, 4 women) ran on a treadmill while being filmed by a traditional 12 camera motion capture system (Qualysis and Visual 3D) and a single cell phone camera (iPhone SE 2020, Apple Corp) at 240 Hz. The cell phone was placed 30° forward from completely sagittal. MediaPipe Pose and Visual 3D were used to produce 3D positions of anatomical landmarks for the cell phone video and motion capture system respectively. MediaPipe unlike other pose estimation algorithms can calculate 3D angles for 33 anatomical points (1,2). This data was used to calculate sagittal plane angles for the hip, knee, and ankle. The MediaPipe angles were compared to the motion capture system using a Pearson-r correlation for both the fully visible side and the partially occluded side. Differences between the sides were evaluated using a one-sided dependent t test, $\alpha=0.05$.

Results & Discussion: Overall, the correlations between MediaPipe and motion capture were very good with the hip and knee being better than the ankle. There were some notable differences between the two when looking at the angles overlayed. The angles from Mediapipe were often slightly less extreme at the ends of the range of motion. The ankle overall was not predicted well by MediaPipe. This may be because of the motion of the foot and the range of motion it goes through. It may also be related to the colour of the subject's shoes being like the colour of the treadmill making it more difficult to differentiate between their shoes and the treadmill. Looking at the differences in the two legs the data demonstrates that they are not significantly different despite the partially occluded side having slightly lower correlation values. This illustrates that MediaPipe can accurately estimate angles from a single camera view even when the leg is not fully in view.

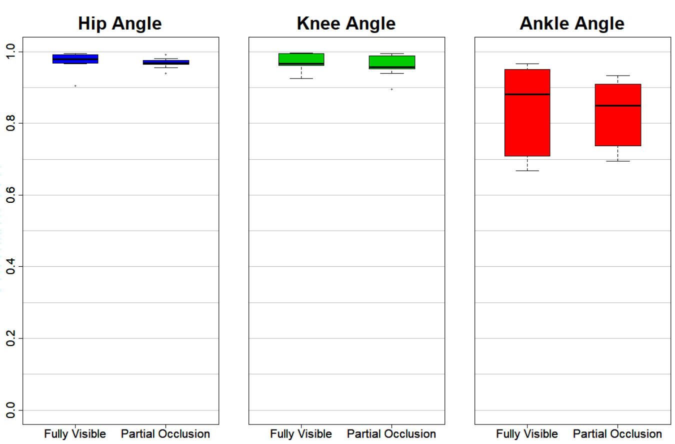

Figure 1: Graph of the correlation coefficients for the Hip, knee, and Ankle for the two sides

		Correlation	p values
Hip	Fully visible	0.974± 0.026	0.865
	Partial Occlusion	0.968±0.014	
Knee	Fully visible	0.971±0.237	0.988
	Partial Occlusion	0.962±0.031	
Ankle	Fully visible	0.841± 0.118	0.695
	Partial Occlusion	0.825± 0.085	

Table 1: Mean correlation coefficients between the single camera view and motion capture system as well as p values for the comparison between the two sides

Significance: These results indicate that MediaPipe can provide accurate sagittal plane angles from a single camera view; however, some caution should be taken when interpreting data at the ends of the range of motion. This technology may allow researchers to collect large data sets from subjects that have not been possible in biomechanics research, allowing us to answer questions we have not been able to in the past.

References:[1] Stenum et al., 2022. PLoS Comput Biol , PMC8099131
[2] Garg S et al. J Ambient Intell Human Comput 13: 2022.
[3] Singh AK. Advances in Intelligent Systems and Computing 1413: 2021.

IMPLEMENTATION OF A STEPPING INHIBITION TASK DURING TURNING GAIT

Nicholas Kreter[1*] and Peter C. Fino[1]
[1]University of Utah Department of Health and Kinesiology
*Corresponding author's email: nick.kreter@utah.edu

Introduction: Humans regularly walk in complex environments that require precise foot placement to maintain stability and forward progress. Typically, foot placement is planned 2-3 steps in advance to identify upcoming obstacles and plan trajectory [1]. However, directing vision 2-3 steps ahead leaves time for new obstacles to appear in planned foot placement locations. To maintain stability and forward progress when obstacles suddenly appear in planned stepping locations, humans must rapidly inhibit their initial stepping plan and rapidly select a new one.

During straight-line gait, humans demonstrate a systematic process for selecting alternate foot placement locations that prioritizes forward progress over stability [2]. However, it remains unclear whether this systematic process is consistent for turning gait where stability is at greater threat. Turning gait complicates the design and analysis of locomotion studies because forward progress and stability are no longer aligned with the global reference frame. The purpose of this project is to explore the feasibility of investigating stepping inhibition and alternate foot placement strategies during turning gait with a virtually projected walkway synced with a motion capture system.

Methods: Five young adults (3F, mean age 24.4 years) completed 10 blocks consisting of 22 randomly ordered walking trials along a virtually projected walkway displaying a series of stepping stones oriented in a straight line (0°), or with a single 60°, 90°, or 120° turn. Stepping stone distribution was adjusted based on participant leg length. Participants were asked to walk briskly and accurately so that a motion capture marker on their second metatarsophalangeal joint was placed in the center of each virtual stepping stone. Twelve trials in each block featured normal black stepping stones. For eight trials, the stepping stone in the middle of the turn changed color during foot placement one-step before the apex of the turn, signaling that the stepping position was not safe and that participants should select a different foot placement location. Two trials in each block were catch trials where a non-turn stepping stone changed color and had to be avoided. Trials were split evenly between step turns and spin turns.

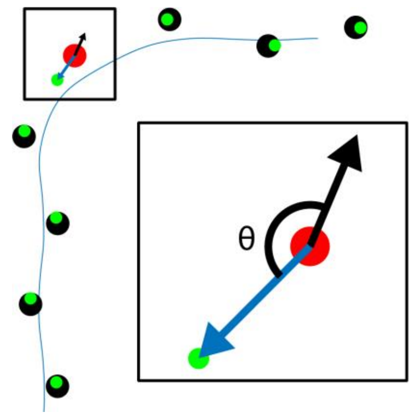

Figure 1: Trial layout and calculation of stepping strategy. Participants were shown a walkway with black stepping stones. On some trials when entering within one step of the turn, the central stepping stone of the turn changed color to red. Participants had to adjust foot placement location (green dots) to avoid the suddenly unsafe stepping stone. The angle (θ) between the alternate step vector and the vector of AP CoM trajectory at the step determined our outcome of stepping strategy.

Motion capture data were collected with a 13-segment model. The position of the stepping stones in the walkway were recorded before testing and between each block. All data were rotated to align with the instantaneous center of mass (CoM) trajectory, which defined the anteroposterior direction. The vector normal to the CoM trajectory and a vertical vector defined the ML axis. Positional marker data from each foot was used to determine stepping position relative to the stepping stones for all steps. For inhibited steps, the vector connecting the original planned stepping location (the center of the projected stepping stone) and the executed foot placement position was calculated. The angle between the alternate foot placement vector, and a vector centered on the projected step and aligned with CoM trajectory was then used to define alternate stepping strategy. Means and standard deviations of foot placement angle were calculated for step turns and spin turns of each angle.

Results & Discussion: For inhibited steps during straight gait (0°) participants demonstrated a varied strategy that trended towards a medial alternate foot placement [θ = 115.8° (50.8)]. During 60° [step turn θ = 140.2° (49.4°); spin turn θ = 135.2° (43.8°)] and 90° turns [step turn θ = 132.9° (49.5°); spin turn θ = 142.1° (53.2°)] participants adjusted alternate foot placement closer towards a short and medial stepping strategy. For the sharpest turns (120°) participants shifted strategy even closer to a short stepping strategy and also exhibited the least variance [step turn θ = 147.6° (30.4°); spin turn θ = 162.1° (27.6°)].

This study aimed to show that investigating foot placement during a stepping inhibition task with turns is feasible. Alternate foot placement strategies for stepping inhibition tasks have previously only been investigated during straight line gait [2] and on treadmills [3]. Here, we show that 1) implementing a stepping inhibition task during is feasible, and 2) that alternate foot placement strategies may be scaled by instantaneous stability, which changes for different types of turns.

Significance: This new experimental method demonstrates the ability to investigate stepping inhibition, or other complex gait tasks, with turns. Moving forward, our system for projecting non-linear walkways will allow for investigations of real-world gait and perturbations in a controlled lab setting for both healthy and pathologic groups, leading to insights about the organization of foot placement decisions in human locomotion.

Acknowledgements: This project was supported by the University of Utah Graduate Research Fellowship.

References: For example: [1] Matthis et al. (2015), *J Vision 15*(3); [2] Patla et al. (1999), *Exp Brain Res* 128; [3] Potocanac et al. (2014), *G&P* 39 (1).

AUTOREGRESSIVE MODELING REVEALS DISRUPTION IN MOTOR COORDINATION DURING DUAL TASK WALKING PROTOCOL

Yannis K. Halkiadakis[1], Joseph DePalma[1], Jasmine Johnson[1], Carmen Lo[1], Alyssa Pearce[1], Emily Schillinger[1], Ainsley Svetek[1], Noah Davidson[1], and Kristin D. Morgan[1*]

[1]Department of Biomedical Engineering, University of Connecticut, Storrs, CT 06269, USA
*Corresponding author's email: kristin.2.morgan@uconn.edu

Introduction: Individuals operating in demanding environments are often challenged to make critical decisions while receiving and processing high volumes of information. Over time, the repeated exposure to these challenging situations can be cognitively taxing and as a result could impact individuals motor function. Dual task walking experiments, where individuals simultaneously perform a cognitive and walking task, serves as a way to evaluate the influence cognitive load has on motor coordination. The psychomotor vigilance task (PVT) is an established task used to evaluate individuals' reaction time and attention switching capabilities in response to visual stimuli [1]. Here, visual stimuli were used to cognitively engage the individuals while they walked on a treadmill. We coupled the cognitive task with a walking task as gait is good measure of motor coordination and is sensitive to changes in cognitive impairment [2]. Autoregressive (AR) modeling, a time series analysis technique, was used to detect changes in gait dynamics as it has been shown to be effective in identifying changes in gait variability in response to altered cognitive function [3]. Therefore, this study evaluated how increasing cognitive load altered motor coordination in healthy controls. We hypothesized that individuals would exhibit more variable gait dynamics as measured via stance time based on their AR model coefficients.

Methods: Ten healthy controls (mean ± standard: age: 21.5±3.0yrs; height 1.7±0.1m; mass 73.3±10.5kg) performed a dual task walking protocol on an instrumented split-belt Bertec treadmill (Bertec Corporation, Columbus, Ohio). First, participants performed a practice PVT task and a 5-minute warm-up on the treadmill prior to get acclimated to the tasks and equipment. For the ***single task trial,*** participants walked on the treadmill at a self-selected speed for 3-minutes. For the ***dual task trial,*** participants walked on the treadmill while performing the PVT task for 3-minutes. To complete the PVT task, the participants wore a headset device that was affixed push buttons and blue and yellow LED lights that sat approximately 8 inches in front of their face. The participants were instructed to push the right button when the blue light lit up and the left button yellow light lit up.

To evaluate changes in gait dynamics, the stance time data was collected for each stride for each participant. The mean stance time was calculated for each participant. To conduct the AR model analysis a second order AR model was fit to the stance time waveforms [4-5]. The two AR model coefficients, AR1 and AR2, were extracted from each stance time waveform and plotted in the AR triangle to evaluate stance time variability. A t-test was performed to determine if there were significant differences in the variables of interest between the single and dual task trials ($\alpha = 0.05$).

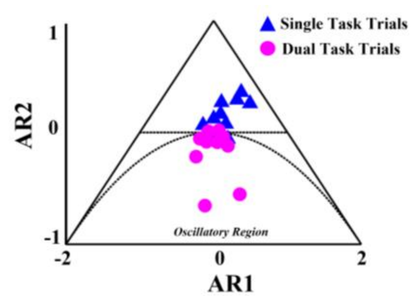

Figure 1. An illustration of how the individual's stance time dynamics during the single and dual task trials separated them on the AR triangle. The cognitive demand of the PVT increased their stance time variability and shifted them into the oscillatory region.

Results & Discussion: The results of study indicated that the participants exhibited increased stance time variability as measured by the AR model coefficients. The participants produced significantly lower AR2 values during the dual task trial (p=0.001) which placed the participants in the oscillatory region of the AR triangle (Fig. 1). The placement in the oscillatory region indicates that the individual's stance time dynamics were highly variable. Prior studies have shown individuals with significant cognitive impairment often reside in this region of the AR triangle [3]. There were no differences in mean stance time. The participants completed the PVT with an accuracy of 98.7% and with a reaction time of 4.5 ± 0.04 seconds.

Significance: This work is significant as it demonstrates how gait can be used to identify changes in cognitive function in individuals. This can be extremely beneficial to organizations whose members spend significant time monitoring screens as these findings suggest that we could use changes in gait patterns to detect when an individual is cognitively fatigue and identify a different member to perform the monitoring duties. The success of the AR modelling analysis to identify these changes in gait dynamics, when the mean stance time did not, suggests that more non-traditional analyses should be implemented to evaluate changes in motor control.

Acknowledgements: This work was supported by the Department of Defense/Office of Naval Research N00014-20-1-2708.

References: [1] Matsangas et al. (2020) *Sleep*, *43*(12), zsaa118; [2] Ko et al. (2018) *Gait & posture*, *63*, 63-67; [3] Alzakerin et al. (2019) *BMC neurology*, *19*, 1-6; Box & Jenkins (1976) Time series analysis; Montgomery et al.(2008) Intro to Time Series.

Table 1. Comparison of Stance Time and Performance Measures during Single and Dual Task Trials

	Single Task	Dual Task	P-value
Mean Stance Time (sec)	1.1 ± 0.4	1.1 ± 0.3	0.88
AR 1 Coefficient	0.16 ± 0.19	0.0 ± 0.18	0.08
AR 2 Coefficient	0.15 ± 0.14	-0.18 ± 0.24	0.001*
Reaction Time (sec)	–	4.5 ± 0.04	–
Percent Correct (%)	–	98.7 ± 1.6	–

ADAPTATING LATERAL STEPPING REGULATION ON CURVILINEAR PATHS

Anna C. Render[1*], Joseph P. Cusumano[2], Jonathan B. Dingwell[1]
[1] Department of Kinesiology, Pennsylvania State University, University Park, PA, USA
[2] Department of Engineering Science & Mechanics, Pennsylvania State University, University Park, PA, USA
*Corresponding author's email: acr313@psu.edu

Introduction: A person's ability to adapt their gait to meet specific environmental demands, is essential for safe locomotion. On straight paths, people prioritize maintaining their step width ($\boldsymbol{w}$) over lateral body position ($\boldsymbol{z_B}$) [1] but can make $\boldsymbol{w}$ and $\boldsymbol{z_B}$ regulation trade-offs to adapt to a given task [2,3]. However, curvilinear paths could require greater $\boldsymbol{z_B}$ control that introduces competition between $\boldsymbol{w}$- and $\boldsymbol{z_B}$-regulation. To navigate curvilinear paths, we hypothesize that people increase $\boldsymbol{z_B}$-regulation at the cost of decreased $\boldsymbol{w}$-regulation.

Methods: Twenty-four people (aged 18-35) walked on different paths projected onto the surface of a treadmill [4] (Fig. 1A). Paths were straight (NIL_; top), slowly winding/low oscillation frequency (LOF_; middle), and quickly winding/high oscillation frequency (HIF_; bottom). Each path was presented both wide (_W=0.6 m) and narrow (_N=0.3 m). Stepping parameters $\boldsymbol{w}$ and $\boldsymbol{z_B}$ were calculated in a path-defined local coordinate system [5].

For each trial, we plotted left ($\boldsymbol{z_L}$) and right ($\boldsymbol{z_R}$) lateral foot placements in the [z_L, z_R] plane and constructed 95% prediction ellipses (Fig. 1B) [3] and computed the aspect ratio (λ_1/λ_2) and area of each ellipse.

Then, we mapped how errors in $\boldsymbol{w}$ & $\boldsymbol{z_B}$ (i.e., $\boldsymbol{w'}$ & $\boldsymbol{z_B'}$) were corrected on the next step (i.e., $\Delta\boldsymbol{w}$ & $\Delta\boldsymbol{z_B}$) ([1]; Fig. 1C). We quantified the degree of step-to-step error correction by the slopes ($\boldsymbol{M_w}$ and $\boldsymbol{M_{zB}}$) of the least-squares fits [1].

We conducted 2-factor (Frequency x Width) ANOVAs on each of the above dependent measures (Fig. 1B-C).

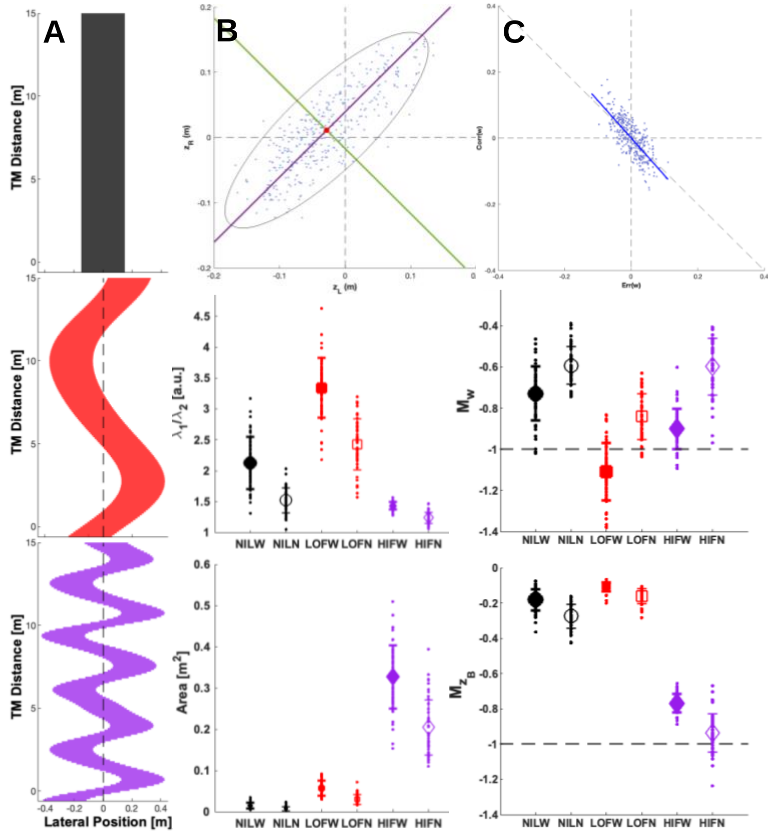

Figure 1. A: *Curvilinear walking paths*. **NIL** (top), **LOF** (middle), **HIF** (bottom). **B:** *Ellipse Characteristics*. Example stepping data with 95% prediction ellipse (top); mean ± SD of ellipse aspect ratio (middle), and area (bottom) for each path. **C:** *Step-to-step error correction*. Example error correction plot with least-squares fit (top); mean ± SD of the error correction slopes for $\boldsymbol{\Delta w}$ **vs.** $\boldsymbol{w'}$ (middle) **and** $\boldsymbol{\Delta z_B}$ **vs.** $\boldsymbol{z'_B}$ (bottom) for each path. The black dashed lines indicate a slope of −1: i.e., "perfect" error correction.

Results & Discussion: On the narrower paths (_N vs. _W), λ_1/λ_2 decreased (more isotropic), ellipse area decreased, and $\boldsymbol{M_w}$ increased away from -1.0 while $\boldsymbol{M_{zB}}$ decreased toward -1.0 (all p<0.001). Thus, when paths narrowed, people's steps were less variable, and they corrected their $\boldsymbol{z_B}$ more and their $\boldsymbol{w}$ less, thereby trading off some $\boldsymbol{w}$-regulation for increased $\boldsymbol{z_B}$-regulation to remain within the path bounds.

There is a significant main effect of path Frequency for all dependent measures (all p<0.001). On the slowly winding paths (LOF_ vs. NIL_), λ_1/λ_2 increased (more elongated in the direction of the $\boldsymbol{w^*}$ manifold), ellipse area increased, and $\boldsymbol{M_w}$ decreased toward -1.0 while $\boldsymbol{M_{zB}}$ increased away from -1.0. Thus, when paths oscillated slowly, people's steps were more variable, and they corrected their $\boldsymbol{w}$ more and their $\boldsymbol{z_B}$ less, thereby further reducing $\boldsymbol{z_B}$-regulation for increased $\boldsymbol{w}$-regulation.On the quickly winding paths (HIF_ vs. LOF_), λ_1/λ_2 decreased (more isotropic), ellipse area increased, and $\boldsymbol{M_w}$ increased away from -1.0 while $\boldsymbol{M_{zB}}$ decreased toward -1.0. Thus, when paths oscillated quickly, people's steps were even more variable, and they corrected their $\boldsymbol{z_B}$ more and their $\boldsymbol{w}$ less, thereby trading off $\boldsymbol{w}$-regulation for increased $\boldsymbol{z_B}$-regulation that enabled greater maneuverability on the path.

Significance: Here, we investigated how people adapt their foot placements to negotiate a real-world context that challenges their $\boldsymbol{w}$ and $\boldsymbol{z_B}$. The important finding here is that on both narrow and quickly winding paths, people traded off control of their $\boldsymbol{w}$ for increased control of their $\boldsymbol{z_B}$. This complementary inverse coupling between $\boldsymbol{w}$ and $\boldsymbol{z_B}$ agrees with our previously developed lateral stepping regulation framework [1,2,3]. If people are sacrificing lateral stability for increased maneuverability to navigate these more complex paths, it is also important to investigate how balance is affected in these contexts to better understand if/when our stability is compromised.

Acknowledgements: NIH / NIA Grants # R01-AG049735 & R21-AG053470, and Sloan Foundation Grant # G-2020-14067.

References: [1] Dingwell et al. (2019), *PloS Comp. Bio.* 15(3); [2] Render et al., 2020. *J Biomech.* 119: 110314; [3] Desmet et al. (2022) *PLoS Comp Bio* 18(11); [4] Render et al. (2022), *N. Am. Congr. Biom.*; [5] Dingwell et al. (2023), *Am. Soc. Biom.*

Muscle Parameter Perturbation Simulations of Rotator Cuff Repair

Morgan Dalman, M.S.[1], Katherine R. Saul, Ph.D.[1]
[1]Department of Mechanical and Aerospace Engineering, North Carolina State University, Raleigh, NC, USA
*Corresponding author's email: mdalman2@ncsu.edu

Introduction: Rotator cuff tears can occur due to acute injury, age-related wear, and/or degeneration of the tendon; resulting in increased shoulder weakness and pain, reduced range of motion, and difficulty independently completing activities of daily living [1]. The common treatment for rotator cuff tears is surgical reattachment of the tendon; however, surgery is not always advisable. To select patients for surgical repair, approximations of the parameters affecting retear likelihood and future functional capacity - including muscle atrophy, intramuscular fat, and tendon retraction distance - are derived from 2D medical imaging; however, recent research has demonstrated that 2D approximations do not correlate with quantitative muscle measured from 3D muscle volumes [2,3]. When estimated measurements of repair tension, defined as the passive force transferred through the muscle-tendon unit after surgical repair, are exceedingly high, there is a high probability (20-70%) of post-surgical retear, limited functional capacity, and/or shoulder instability due to altered joint contact forces that can happen at larger values of repair tension [4-6]. Thus the goal of this work was to evaluate the sensitivity of muscle parameters affected by rotator cuff tears and repairs using computational musculoskeletal modelling.

Methods: Kinematic data for abduction, scapular abduction, forward flexion, internal/external rotation, and axilla wash movements via optical motion capture [2]. Data were post-processed and smoothed with a 6 Hz Butterworth filter (Cortex, Motion Analysis Corporation, Santa Rose, CA). An existing upper limb computational musculoskeletal model representing an adult male [7] was used to run perturbation simulations to vary muscle parameters most commonly altered with rotator cuff tears and repairs.The model shoulder degrees of freedom are defined according to the ISB standards [8]. Muscle changes including tendon slack length and tendon stiffness were represented by altering the corresponding force-generating parameters of the Hill muscle model. Peak muscle force is proportional to muscle volume. Retraction was represented by shortening the tendon slack length [9], and stiffness of the muscle tendon unit can be computationally represented by altering the spline governing the passive force-length curve in the muscle model [10]. For each simulation, the parameter values were decreased by 5%. Glenohumeral joint reaction force was evaluated using a Computed Muscle Control (CMC) simulation based on previously collected kinematic data. Glenohumeral joint reactions were compared across simulations to identify which parameters were most sensitive.

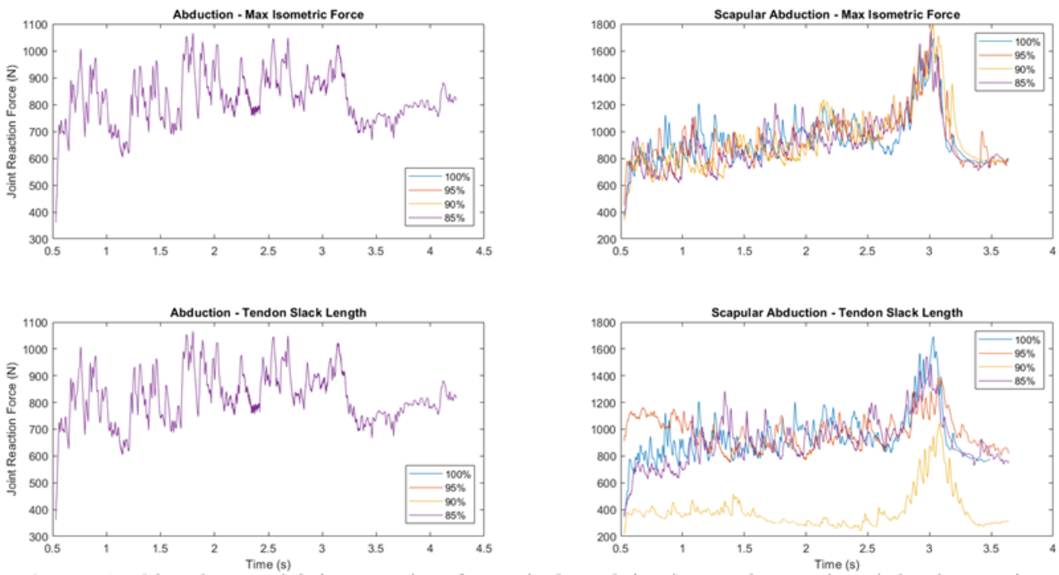

Figure 1: Glenohumeral joint reaction force during abduction and scapular abduction under decreasing max isometric force and tendon slack length conditions.

Results & Discussion: Abduction tasks were insensitive to both max isometric force and tendon slack length. Scapular abduction was most sensitive to tendon slack length with max joint reaction force decreasing by 8.8% for a 15% reduction in tendon slack length of the supraspinatus muscle. This suggests supraspinatus tensioning during repair is more critical than possible atrophy in determining post operative loads on the glenohumeral joint. Future work will expand this simulation framework to include MonteCarlo simulations to examine physiologic distribution of parameters and examine possible interactions between parameters and the effects on both joint reaction force and contact location.

Significance: This work provides a framework for understanding the sensitivity of muscle parameters affected by rotator cuff injury and the reference for future change to operative technique and selection process changes for rotator cuff repairs.

Acknowledgements: Research funded by NIH-1F31AR081691-01

References: [1] Dang et al. (2018). *Sports Med Arthrosc Rev.* **26**(3). [2] Vidt et al. (2016). *Arthroscopy.* **32**(1). [3] Goutallier et al. (1994). *Clin Orthop Relat Res.* (304). [4] Bigliani et al. (1992). *J Bone Joint Surg Am*. **74**(10). [5] Murray et al. (2002). *J Shoulder Elbow Surg*. **11**(1). [6] Galatz et al.(2001). *J Bone Joint Surg Am.* **83**(7): 1052-6. [7] Holzbaur et al. (2005). *Ann Biomed Eng. 33*. [8] Wu et al. (2005). *J Biomech*. **38**(5) [9] Saul et al. (2011). *Clin Biomech (Bristol, Avon)*. **26**(8) [10] Millard et al. (2013). *J Biomech Eng*. **135**(2).

RELATIVELY SMALL CHANGES IN FOOT-ANKLE MECHANICS OVER MONTHS ALTER MUSCULOSKELETAL STRUCTURE

Jordyn N. Schroeder[1*], Owen N. Beck, Gregory S. Sawicki[1]
[1]Georgia Institute of Technology, George W. Woodruff School of Mechanical Engineering
*Corresponding author's email: jschroeder9@gatech.edu

Introduction: Form follows function. Under lengthening conditions, skeletal muscle fascicles lengths increase by adding sarcomeres in series [1]. Following concentric or eccentric exercise, skeletal muscles hypertrophy[2]. On the other hand, muscle atrophy has been observed in chronic unloading and disuse studies. Tendons also adapt to their mechanical environments and are sensitive to several factors; strain magnitude, cycle duration, cycle frequency and intervention duration. Increases in tendon stiffness and cross-sectional area have been observed in exercise studies and tendon atrophy has been observed in chronic unloading and disuse studies. Most muscle and tendon adaptation knowledge comes from exercise intervention studies that include low cycle numbers and large strains. Literature suggests tendon is not likely to remodel unless interventions are above ~4.5-6.5% strain[3]. However, cross sectional studies of habitual high wearers report sizable increases in kt decreases in muscle length. This indicates that even with small changes in loading (i.e. low strain), muscle-tendon remodeling may occur if the number of cycles is plentiful.

The purpose of this study was to determine how relatively small changes in foot ankle mechanics remodels the underlying MT structure following relatively large number locomotion cycles. We altered foot ankle mechanics in daily activities over a 14-week intervention via modified footwear and measured leg MT structural properties pre and post intervention. We hypothesized that footwear that increased/decreased muscle operating lengths during daily use would lead to muscles that were relatively longer/shorter after intervention. We also hypothesized that devices that decreased/increased force on the calf MT over a large number of cycles would lead to tendons that were less/more stiff after intervention.

Methods: We recruited n=6 in the high toed footwear group and n=8 in the high heeled footwear group. Participants wore their experimental shoes during their daily activities for 12-16 weeks. We measured cross sectional area of the distal Achilles tendon (AT) using ultrasound. We used a dynomometer, ultrasound, and EMG to collect tendon and soleus muscle force-length relationships. AT stiffness is taken from the slope of the AT FL curve from 50-100% of MVC.

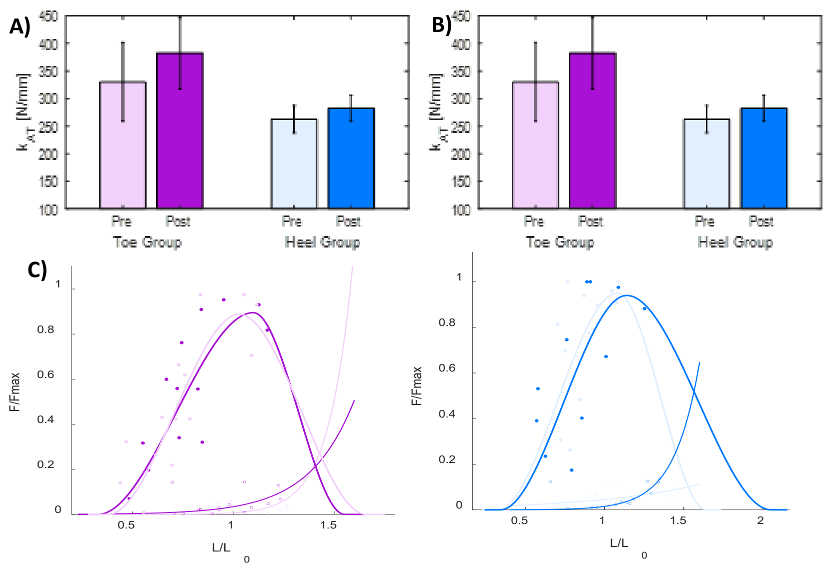

Figure 1: A) Achilles tendon stiffness (k_{AT}) pre and post intervention, n=4 toe group, n=8 heel group. **B)** Achilles tendon cross-sectional area (CSA) pre and post intervention, n=6 toe group, n= 8 heel group. **C)** Normalized soleus force-length relationships pre (light) and post (dark) intervention, n=3 toe group, n=2 heel group

Results: During walking in daily life, our intervention increased fascicle operating length in the high toes and decreased fascicle operating length in the high heels [Abstract 146952]. Peak muscle tendon (MT) force increased in high toes by 21% and decreased in high heels by 8% [Abstract 146952]. Overall, tendon stiffness did not change in either the high toes (p=0.456) or the high heels (p=0.449) groups (Fig. 1A). AT CSA did not change in the high toes group (p=0.133), while high heels decreased AT CSA by 10% pre vs. post intervention ($p<0.001$) (Fig. 1B). Preliminary analyses suggest that shifts in soleus l_0 of the muscle for both high toes and high heels (Fig. 1C). Participants varied in the number of daily steps they look in their experiment shoes. In high heels, participants took avg ± sd: 1442 ± 1257 steps/day; range: 0 to 3704 steps/day. In high toes participants took avg ± sd: 3768± 1626 steps/day; range: 1179 to 5998 steps/day. For every 1000 steps/day participants took in high heels their k_{AT} increased 7-8% (β= 19 kN/m; p=0.008) and their CSA increased 5% (β= 3 mm^2 ; $p<0.001$). For every 1000 steps/day participants took in high toes their k_{AT} increased 7% (β= 22 kN/m; p=0.019) and their CSA did not significantly change (p=0.535).

Discussion: Although the high heel and high toe interventions changed triceps-surae MT force in opposite directions, AT stiffness increased in both groups when accounting for avg. steps/day in the intervention shoes. Further investigation of muscle-tendon dynamics and joint mechanics may reveal how tendon loading in the high heels led to increased k_{AT} and CSA despite reducing MT force.

Significance: Results from this study indicate that small changes in foot-ankle mechanics can result in changes in musculoskeletal structure with a high number of loading cycles. This study can increase our knowledge on musculoskeletal adaptation outside of exercise training and disuse protocols. It can also inform the wearable device field on how using devices that change foot-ankle mechanics over long-time scales can impact users.

References: [1] Hinks et al (2022) *Jappl* [2] M. V. Franchi et al (2014) *Acta Physiol* [3] Mcmahon (2022) *J Strength Cond Res*

COMPARING DOMINANT AND NONDOMINANT SHOULDER GRIDLE JOINT RANGES OF MOTION

Ola Alsaadi[1], Moira Pryhoda[1], Michelle B. Sabick[1]
Department of Mechanical and Materials Engineering[1], University of Denver, Denver, CO
Email: ola.alsaadi@du.edu

Introduction: Subtle differences in anatomy and patterns of usage between the dominant and nondominant upper extremities may result in musculoskeletal dysfunction [1]. This work focuses on the kinematics of the upper extremity joints, given their essential role in performing activities of daily living. The shoulder girdle has six degrees of freedom, which describe the range of movements possible at its various joints[2]. The purpose of this study was to measure glenohumeral (GH) scapulothoracic (ST) and humerothoracic (HT) motion during different activities of daily living in the sagittal, coronal, and transverse planes, comparing the minimum and maximum joint angles, and the range of motion between their dominant and nondominant arm joints.

Methods: Five right-arm dominant subjects without shoulder pathology (3M, 2F, 30.8 ± 5.36 yrs.) participated in the study. Upper extremity motion was captured using a marker-based motion capture system (Vicon Hauppauge, NY, USA) at 100 Hz. Markers were placed on bony landmarks for both left and right upper extremities and trunk following ISB recommendations [3] Each subject performed four controlled movements with each arm: (1) shoulder abduction to maximum elevation, (2) shoulder flexion to maximum elevation, (3) internal/external (IE) shoulder rotation with the shoulder in neutral elevation and the elbow flexed to 90°, (4) IE with the shoulder abducted to 90°, and the elbow flexed to 90° (Figure 1). Kinematic analysis was performed in Visual 3D (C-motion, Germantown, MD). Anatomical coordinate systems were assigned following the ISB standard convention [3] GH joint kinematics were calculated as a Y-X-Z Cardan sequence of the humerus orientation relative to the scapula [4] ST joint kinematics were calculated as a Z-Y-X Cardan sequence of scapula orientation relative to a neutral scapular position with the shoulder at rest against the body. HT joint kinematics were calculated as follows: Z-Y-Z Cardan sequence of the humerus orientation relative to the trunk. The joint range of motion (ROM) was quantified as the magnitude of the difference between the maximum and minimum joint angle in each plane during each trial. Range of motion of the GH, ST, and HT joint elevation angles for the arm flexion and abduction motions and rotation angles for both IE rotations were compared using a paired t-test.

Figure 1: Starting (left) and ending (right) positions of dominant arm during the maximum abduction movement.

Results & Discussion: Total ROM was not significantly different between the dominant and nondominant arms (p>0.05). However, the dominant arm tended to exhibit smaller ROM for GH, HT, and ST elevation during the abduction and flexion movements, and also in both IE rotation positions (Figure 2). The subtle differences in ROM could be due to adaptations of the musculoskeletal system to differences in usage or strength between the dominant and nondominant upper extremities. A larger subject population will be needed to determine whether the trends represent significant or functional differences. Changes in ROM could also be due to undetected osteoarthritis [5] in the dominant arm because it’s utilized more than the left arm, which will reduce flexibility and ROM, although that seems unlikely given the age of the subject population.

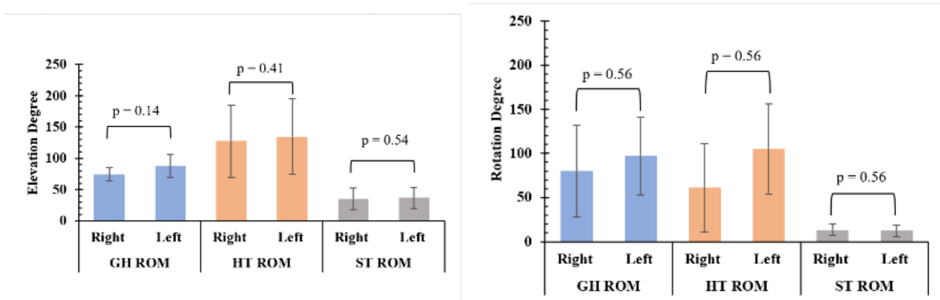

Figure 2: Comparison of range of Motion (Left figure) arm during abduction, (Right) arm during internal and external rotation, p < 0.05 signify statistical significance. GH signifies Glenohumeral. HT signifies humerothoracic. ST signifies scapulothoracic.

Significance: This study quantified the ROM of the GH, HT, and ST joints of the dominant and nondominant arms during four isolated movements. The next step of this study will be comparing the joint kinematics collected with motion capture to joint kinematics obtained through bi-planar fluoroscopy to quantify the accuracy of skin-mounted markers. To provide a mechanistic understanding of shoulder function under normal and pathologic settings and to evaluate the outcomes of non-surgical and surgical clinical interventions, it is crucial to measure in-vivo joint mobility. This research will provide more understanding of how the shoulder girdle of the upper limbs and the trunk interact and the patterns needed for various combinations of trunk and arm movements.

Acknowledgements: This work was made possible by the collaboration of Thor E. Andreassen and Kevin Shelburne, PhD.

References: [1] H. Jee & J. Park (2019), Iranian J of Public Health 48(10); [2] T. K. Gill et al. (2020), BMC Musculoskelet Discord 21(1); [3] G. Wu et al. (2020), J Biomech 28(5); [4] V. Phadke et al. (2011), J Biomech 44(4); [5] D. M. Spranz et al. (2019), Orthopaedics & Traumatology: Surgery & Research 105(8).

USE OF INERTIAL MEASUREMENT UNITS FOR LOWER LIMB PROSTHESIS ALIGHNMENT DURING WALKING

Luke Nigro, PhD[1*], Janet Zhang-Lea, PhD[2], Alena M. Grabowksi, PhD[1,3]
[1]University of Colorado Boulder, Department of Integrative Physiology, Boulder, CO, USA
[2]Gonzaga University, Department of Human Physiology, Spokane, WA, USA
[3]Department of Veterans Affairs, Eastern Colorado Healthcare System
*Corresponding author's email: luke.nigro@colorado.edu

Introduction
To walk, people with a transtibial amputation (TTA) are fit and aligned to a prosthesis by a prosthetist to subjectively maximize function and comfort. Lower limb prostheses typically consist of a rigid socket that surrounds the residual limb and connects to a prosthetic foot via a pylon. Alignment of these prosthetic components refers to the relative orientation of the pylon and prosthetic foot with respect to the socket. Prosthesis alignment affects socket reaction moment impulse [1], which might affect knee joint loading patterns. Improper prosthesis alignment may worsen knee joint loading and could therefore be a contributing factor to the prevalence of osteoarthritis (OA) in people with lower limb amputations, which could be mitigated by improving alignment. Individuals with TTA experience a greater prevalence of OA compared to non-amputees [2], which is likely due to an altered distribution of knee joint loading, evidenced by higher knee abduction moments in intact limbs compared to residual limbs [3]. Currently, prosthesis alignment relies on a prosthetist's visual inspection of walking, which can be prone to error. This study aims to employ a novel method that uses wireless inertial measurement unit (IMU) sensors to assess lower limb prosthetic alignment accuracy in a cost-effective way (<$200). We hypothesized that the root mean squared error (RMSE) between IMU-calculated angles and marker-based motion capture segment angles for each prosthesis alignment would be less than 6° in the sagittal plane, which is within two standard deviations of previously reported similar data [4], for different prosthetic alignment conditions.

Methods
Two subjects with a TTA provided written informed consent to participate in this study. Subjects walked on a dual-belt force-measuring treadmill (Bertec Corporation, Columbus, OH, USA, 1000Hz) while using a prosthesis with five different sagittal plane alignments. Prior to walking, we secured three IMUs (Blue Trident, Vicon, Oxford, UK; 1000Hz) to the subjects' legs in such a way as the axes of the IMUs coincided with the anatomical functional axes of the lower limbs. We placed tracking clusters of ≥3 markers on the prosthetic foot, pylon, and socket, and used a 10-camera motion capture system (Vicon, Oxford, UK; 100Hz) to measure 3D marker positions. Prior to each trial, a certified prosthetist aligned the subjects' prostheses at the pylon/socket interface using standard practices ("neutral" alignment, 0°). The subjects stood in place on the treadmill for calibration. Then, the subjects walked for three minutes with each of five different sagittal plane prosthetic alignments: neutral, ±3° and ±6° (within ±10% of target angle) compared to the subjects' neutral alignment. We verified each alignment using a custom MATLAB (Mathworks, Natick, MA, USA) program. IMU, motion, and force data were captured simultaneously. We processed motion capture data in Visual 3D (C-Motion, Germantown, MD, USA) to obtain angular orientations of the socket, pylon, and prosthetic foot. We integrated IMU gyroscopic data with respect to time (MATLAB 'cumtrapz') to obtain IMU angles. All reported angles are in reference to the static calibration (0°).

Results & Discussion
The IMU data consistently over-estimated peak positive and negative sagittal angle values for each segment by an average ±SD of 7.65±5.41° across all conditions (Fig. 1). RMSE of the angles obtained from the IMUs compared to the marker-based motion capture system throughout the entire trial was 20.98±11.11° in the sagittal plane, which greatly exceeded our target threshold of 6°. However, the timing and overall shape of the segment angle profiles generated from the IMUs vs. marker-based motion capture were similar between the peak values for each stride.

Significance: While IMUs may exhibit substantial RMSE compared to marker-based motion capture computing body segment angles, the errors were consistent per stride. Thus, IMUs could be used to detect changes in timing, or changes in segment angle profiles over time for an individual. Moreover, functional alignment tasks during calibration could decrease overall RMSE by allowing more accurate alignment of the IMUs' coordinate systems with the anatomical axes [5], and thus providing prosthetists with an inexpensive tool for objective prosthesis alignment.

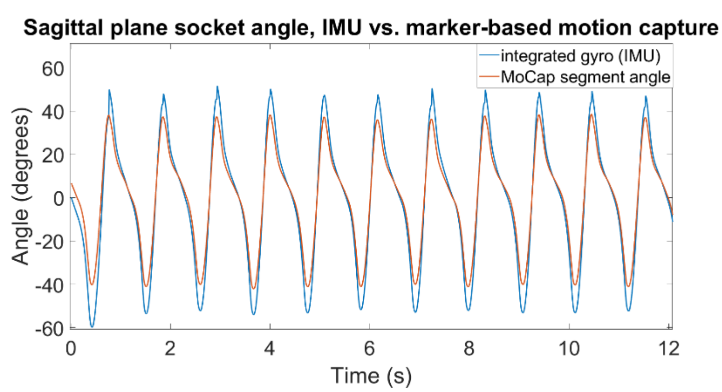

Figure 1: Portion of data comparing sagittal plane prosthetic socket angles calculated from IMU gyroscopic data (blue) and marker-based motion-capture methods (orange).

Acknowledgments: Funding from the VA RR&D Service RX003861.

References: [1] Kobayashi et al. J. Biomech. 47 (2014), [2] Struyf et al. Arch. Phys. Med Rehabil. 90 (2009), [3] Royer & Wasilewski, Gait Posture 23 (2006), [4] de Jong et al., J. Biomech. 108 (2020), [5] Vitali & Perkins, J. Biomech. 106 (2020).

TRADING OFF STABILITY, AGILITY AND EFFICIENCY OF MOVEMENT ACROSS A BROAD RANGE OF MUSCLE-TENDON MORPHOLOGIES

Laksh Kumar Punith[1*], Gregory S Sawicki[1]
[1]Georgia W Woodruff School of Mechanical Engineering, Georgia Institute of Technology
*Corresponding author's email: lpunith@gatech.edu

Introduction: Animals care about multiple locomotion objectives, and yet are stuck with one version of their bodies at any given time. This produces a conundrum, which physiological properties should animals pick? While answering this question is subjective, as it depends on the animal's specific needs and its ecological context, we can however start to discover what tradeoffs the animal does face in making this decision. Previous studies have compared different breeds of dogs [1] or different types of athletes [2] performing the same task to make conclusions about the relative pros and cons of one musculo-tendon parameter set over another. However, since this is correlational and not causal, and since it's difficult to experimentally change one parameter of an animal's morphology while keeping others constant, it makes it difficult for us to generate maps of physiological parameters to functional performance across multiple objectives/tasks. Therefore, in this study, we used a mathematical modeling approach. In particular, we asked – given a simple one-dimensional cyclic task such as hopping with your ankles – how does tendon stiffness affect the stability, agility and economy of the task independently and what are the tradeoffs animals face when picking one value of tendon stiffness over another over the objective space? Since previous work has shown that hopping energetics is optimal when the system is in resonance, we hypothesized that there exists a tendon stiffness that generates resonant hopping which is metabolically efficient – but difficult to deviate from and therefore less stable and agile. And that, as you move to higher or lower tendon stiffness from that optimal region, we would observe lower metabolic efficiency but higher stability and agility – an unavoidable fundamental trade-off.

Methods: We modified a previously published model of human hopping to include an aerial phase [3]. The model consisted of a mass in gravity that is cyclically actuated by a compliant muscle-tendon unit that is stimulated by a square wave of 2.5Hz and 10% duty factor. Once the model achieved stable hopping, we either (a) did nothing or (b) perturbed the height of the ground or (c) perturbed the timing of stimulation for a large range of tendon stiffnesses. We measured the metabolic efficiency of hopping without a perturbation (measured by mechanical work/metabolic work), the stability of the system over various changes to ground height (measured by average cumulative mechanical work 5 hops after the perturbation/work injected by the change in ground height) and agility of the system (measured by maximum positive and negative work done by changing stimulation pattern/mechanical work without a perturbation).

Results & Discussion: We found that biological tendon stiffness values (represented by the black vertical line in the figure) coincided with maximum metabolic efficiency, intermediate stability, lowest agility (in terms of generating positive work) and close to highest agility (in terms of generating negative work). Reducing tendon stiffness from that point, reduced metabolic efficiency, increased stability, increased positive agility and first increased and then decreased negative agility. Subsequently, increasing tendon stiffness from the biological value, drastically reduced efficiency, drastically reduced stability, increased positive agility, and drastically reduced negative agility. Thus, there lies a pareto optimal front going from low tendon stiffness values up to biological values, where humans may trade efficiency for higher positive agility and stability.

Significance: Our finding of pareto optimality is particularly interesting because previously most studies focused on evaluating populations and interventions based on a single metric. For example, it was believed that older adults having lower tendon stiffnesses than young adults is a maladaptive trait as it may reduce efficiency [4] and thus needs to be corrected by exercise or exoskeletons. However, if our results could extend to other tasks like running and walking, then we may find that older adults are simply trading metabolic efficiency to gain higher agility and stability – which is a reasonable assumption as falls are highly risky in terms of health outcomes for older adults. Thus, an intervention to alter their tendon stiffness or account for it may in fact hamper their objectives. Thus, future research needs to contend with the multitudes of animal objectives and how it relates to their underlying morphology.

References: [1] Pasi et al (2003) *J Evolutionary Biology* [2] Cooper et al (2021) *J Biomechanics* [3] Robertson et al (2014) *Bioinspiration & Biomimetics* [4] Lichtwark et al (2007) *J Biomechanics*

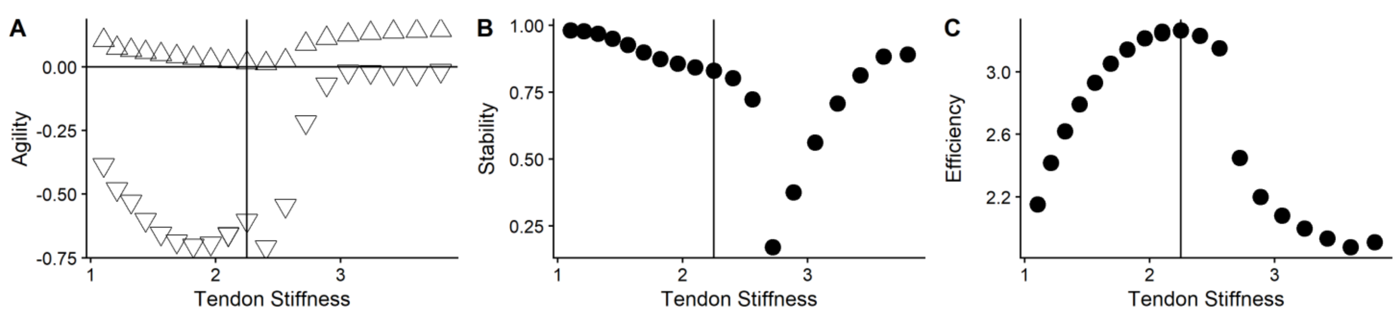

Figure 1: (A) Positive (triangle) and negative (downward facing triangle) agility, (B) Stability and (C) Efficiency of hopping across a broad range of tendon stiffness values. Note : Tendon stiffness on the X axis is normalized such that 2.25 relates to 180000N/m.

BIOMECHANICAL COMPARISON BETWEEN SUMO AND CONVENTIONAL STYLE DEADLIFTS

Madelyn Henning[1], Arnel Aguinaldo[1*], Jacob Goodin[1], Rafael Escamilla[2]
[1]Department of Kinesiology, Point Loma Nazarene University, San Diego, CA
[2]Department of Physical Therapy, California State University, Sacramento, CA
*Corresponding author's email: arnelaguinaldo@pointloma.edu

Introduction: Strength athletes, such as American football players and powerlifters, often employ the barbell deadlift to enhance hip, thigh, and back strength and is considered one of the most common resistance exercises for strengthening the thigh and posterior chain muscles [1]. The starting position for the deadlift is with the lifter in a squat position and is then lifted upwards in a continuous motion by extending the knees and hips until the lifter is standing erect with knees locked and the shoulders thrust back [2-3]. From this position, the barbell is slowly lowered back to the ground by flexing the knees and hips. This deadlift motion can be performed using either a conventional or sumo style, the difference between which stems primarily due to a greater stance width and narrower grip width in the sumo deadlift. Biomechanical evidence in the current literature indicate that sumo lifters maintain a more upright position and therefore can deadlift with reduced lumbosacral (L5S1) joint forces and moments compared to conventional lifters [2-3]. Previous research also suggests that differences in the angles, mechanical work, and moments at the lower body joints exist between the two deadlift styles [2-3]. However, previous biomechanical comparisons of the two deadlift styles were limited to 2D or manually digitized 3D kinematic analysis and kinetic estimations without incorporating ground reaction force (GRF) data. Therefore, we aimed to compare sagittal plane trunk and lower body kinematic and kinetic metrics between sumo and conventional deadlifts in competitive powerlifters.

Methods: Eleven male and one female experienced powerlifters without a history of lower extremity or trunk pathology participated in this study with a mean (±SD) age, mass, and height of 25.8 ± 7.2 y, 86.9 ± 11.6 kg, and 179.2 ± 6.3 cm, respectively. Inclusion criteria included all participants being able to perform both sumo and conventional deadlifts pain-free with proper technique using their 6-repetition maximum (6-RM) intensity and have at least five years' experience in performing both sumo and conventional deadlifts in their resistance training regimens. All participants provided written informed consent in accordance with the Institutional Review Board affiliated with the research lab in which the data for this study was collected. Each subject's 6-RM was determined for both the sumo and conventional deadlifts. A standard 20.5 kg Olympic barbell and Olympic discs (Standard Barbell) were used while performing the deadlift during data collection, which was facilitated using 3D marker-based motion capture and force platform systems at sampling rates of 120 Hz and 1200 Hz, respectively. Sagittal kinematics and kinetics of the L5S1, hip, knee, and ankle joints were calculated using Visual3D (C-Motion, Boyds, MD). Discrete metrics at the lift-off (LO), knee passing (KP), and lift completion (LC) events were extracted from each lift and statistically compared using paired t-tests at a significance level of 0.05 using R and RStudio (2022.12).

Results & Discussion: No differences in mean bar velocity between the conventional (0.4 ± 0.1 m/s) and sumo (0.4 ± 0.1 m/s, $p = 0.57$) deadlifts were found. Stance width was larger in the sumo deadlift (0.9 ± 0.1 m) as compared to that of the conventional deadlift (0.4 ± 0.1 m, $p < .001$). There were also differences in several kinematic and kinetic variables (Table 1). Notably, knee flexion at LO was lower in the sumo deadlift (63.1 ± 14.4°) than it was in the conventional deadlift (72.7 ± 12.9°, $p = .02$) while ankle plantar-flexion at LC was greater in the sumo deadlift (15.3 ± 7.6°) than it was in the conventional deadlift (5.0 ± 3.9°, $p < .001$). The L5S1 joint moment at KP was higher in the conventional deadlift as compared to that of the sumo deadlift (41.9 ± 49.7 Nm vs. 35.6 ± 46.0 Nm, $p = .009$) as well as in the hip joint moment at KP (267.2 ± 64.7 Nm vs. 213.5 ± 88.4 Nm, $p = .003$).

Table 1: Select discrete kinematic and kinetic metrics between conventional and sumo deadlift (N=12)

Variable	**Conventional**	**Sumo**	**Difference (95% CI)**	***p***
Mean Bar Velocity (m/s), Mean (SD)	0.4 (0.1)	0.4 (0.1)	0.01 (-0.03 to 0.06)	0.57
Max Bar Velocity (m/s), Mean (SD)	0.7 (0.1)	0.7 (0.1)	0.04 (-0.03 to 0.10)	0.22
Trunk Flexion (°) @ LO, Mean (SD)	77.2 (10.9)	69.7 (14.0)	7.5 (3.4 to 12)	0.002
Trunk Flexion (°) @ KP, Mean (SD)	67.9 (5.3)	54.4 (7.3)	14 (9.2 to 18)	<0.001
Hip Moment (N) @ LO, Mean (SD)	-301.6 (75.7)	-258.8 (114.9)	-43 (-94 to 8.1)	0.091
Hip Moment (N) @ KP, Mean (SD)	-267.2 (64.7)	-213.5 (88.4)	-54 (-85 to -23)	0.003

Significance: These findings provide further insights as to the specific mechanisms by which the lumbar and hip extensor muscles produce the torques required to properly perform conventional and sumo deadlifts. Furthermore, they reinforce the notion that sumo deadlifts may be more effective in strengthening lower body muscles while minimizing the risk of lower back and joint injuries.

References:

[1] Martin-Fuentes et al. (2020), *PLoS ONE,* 15(2).
[2] Escamilla et al. (2000), *Med Sci Sports Exec,* 32(7).
[3] McGuigan and Wilson (1996), *J Strength and Cond Research,* 10(4).

THE EFFECTS OF A CONVERSATIONAL SPEECH ON DUAL-TASK OBSTACLE CROSSING IN OLDER ADULTS

Rahul Bashyal[1], Patrick Fleming[1], Gabrielle Torrijos[1], Abigail Schmitt[2], Tiphanie Raffegeau[1,3]
[1]George Mason University, Manassas, Virginia, USA
[2]University of Arkansas, Fayetteville, Arkansas, USA,[3]Ohio University, Athens, Ohio, USA
[1*]Corresponding Author's Email: rbashya2@gmu.edu

Introduction: Falls pose a significant risk of fatal and non-fatal injuries among individuals aged 65 and older [1] and many falls occur when people trip while walking [2]. Difficulties in avoiding obstacles and preventing tripping while performing a concurrent cognitive task such as walking while talking have been described in older adults at risk of falling [3-4]. Despite this, current evidence on the combination of dual-task walking (e.g., walking while talking) and obstacle crossing kinematics is limited [5], with existing studies primarily focusing on laboratory-based gait tasks rather than activities resembling realistic scenarios [6]. Therefore, the purpose of this study was to quantify changes in obstacle crossing during an activity designed to mirror a real-world conversational speech task (walking while talking) in adults aged 65 and older. We hypothesized that older adults would maintain larger crossing distances relative to the obstacle during a concurrent conversational speech task compared to obstacle crossing alone.

Methods: Nine adults (three men and six women, mean age = 71 ± 4 yrs, mean height = 1.67 ± 0.10 m, mean mass = 69.1 ± 8.2 kg) participated in a series of walking tasks on an obstructed pathway. Motion capture technology (Vicon, Nexus) recorded locomotor walking tasks using 39 reflective markers placed on the participants body, adhering to the Plug-in-Gait model. Trials were recorded at 120 Hz, with participants walking at self-selected speeds along a 10-meter walkway, crossing a dowel (18 cm) in the center of their path from both directions with their preferred limb (Fig 1). While performing the dual-task, participants discussed randomly assigned topics from six selected options (e.g., places traveled, first job, favorite sport) 'as if talking with a friend' for one minute, continuously traversing the walkway and avoiding the obstacle while speaking. Foot trajectories and obstacle coordinates were analyzed in MATLAB to calculate horizontal and vertical distances between toe markers and the obstacle during the crossing step, as well as the horizontal distance between the heel marker and the obstacle for both the lead (the first foot to cross the obstacle) and trail (the second foot to cross the obstacle) crossing foot. Effect sizes corrected for small samples (Hedge's *G*) were calculated to compare differences between lead and trail foot crossing kinematics and obstacle crossing with and without a dual-task.

Figure 1: Image of 18cm tippable dowel obstacle with reflective markers positioned in the center of the walkway.

Results & Discussion: Participants demonstrated few changes in their obstacle crossing parameters during conversational speech as compared to obstacle crossing without speech. The largest changes were detected during dual-task obstacle approach, where the lead foot approached the obstacle at a farther distance than obstacle crossing (Mean difference = 28.6 mm, Hedge's G = 0.570). Small changes in toe clearance were detected during the dual-task, where participants raised their toe clearance higher during a dual-task (Mean difference = 8.3 mm, Hedge's G = 0.184) with slightly greater effects on trail limb clearance (Mean difference = 7.7 mm, Hedge's G = 0.182) than the lead limb (Mean difference = 8.9 mm, Hedge's G = 0.147). Lead foot landing was decreased moderately with a dual-task (Mean difference =-18.7mm, Hedge's G = -0.225) supporting a shorter crossing step while speaking. However, the remaining crossing kinematics showed little change from single to dual-task or between the lead and trail foot (all G's < 0.170).

Table 1. Obstacle Crossing Kinematics (Mean and Standard Deviation) for Older Adults During Single and Dual-task Obstacle Crossing

		Approach (mm)	Toe Clearance (mm)	Heel Clearance (mm)	Landing (mm)
Single task	Lead foot	571 (64)	216 (40)	143 (45)	236 (84)
	Trail foot	297 (57)	209 (38)	411 (33)	562 (180)
Dual task	Lead foot	600 (27)	224 (69)	143 (49)	217 (69)
	Trail foot	285 (58)	217 (39)	412 (32)	560 (20)

Significance: Despite being a well-practiced cognitive task, conversational speech led to gait adaptations in older adults during obstacle crossing that may be attributed to the increased cognitive demand. A further approach distance, increased toe clearance, and closer landing suggests that the conversational speech task influenced older adults to take a more cautious approach when navigating obstacles, perhaps allowing for more time to gather visual and sensory feedback about the obstacle shape and position. These findings highlight the importance of considering everyday cognitive tasks on mobility in older adults, particularly in complex real-life environments that require simultaneous step adjustments to avoid obstacles. Future dual-task research should consider aspects of cognitive demands when examining cognitive and motor demands in older adult mobility.

References: **[1]** Burns et al. (2018), *Morb Mortal Wkly Rep* 67(18); doi:10.15585/mmwr.mm6718a1 **[2]** Robinovitch et al. (2013), *The Lancet* 381(9860); doi:10.1016/S0140-6736(12)61263-X **[3]** Becker et al. (2022) *Braz J Mot Behav* 16(5); doi:10.20338/bjmb.v16i4.317 **[4]** Ayers et al. (2014), *Gerontology* 60(2); doi:10.1159/000355119 **[5]** Raffegeau et al. (2022), *Exp Gerontol* 161. doi:10.1016/j.exger.2022.111710 **[6]** Beauchet et al. (2005), *J Mot Behav*. 37(4).

APPLYING BIOMECHANICAL APPROACHES AND TECHNOLOGY TO ACCIDENT INVESTIGATIONS AND 3D VISUALIZATIONS

Rosemarie Figueroa Jacinto, PhD, CHFP[1], Jessica Marie Zendler, PhD[1,2*], VJ Tanwar,CFVT[1], Richard V. Baratta, PE, PhD, ACTAR[1]
[1]Rimkus, Houston, TX; [2] University of Michigan, Ann Arbor, MI
*Corresponding author's email: jzendler@rimkus.com

Introduction: Biomechanical professionals are not only equipped to evaluate human body dynamics and mechanics as they relate to a specific incident, but they also are in a unique position to contribute their knowledge and experience with tools and technology often used in academia/research, to enhance accident investigation as a whole. Stakeholders, such as attorneys, jurors, mediators, and judges, benefit vastly from scientific-based visuals to understand certain aspects of the case. With that said, some of these tools can be leveraged not only to explain the biomechanical areas of a case but also to assist other experts in multidisciplinary teams and to create powerful animations that visualize the sequence of events leading up to the subject incident. The goal of this paper is to outline how various biomechanical approaches, tools, and equipment can be applied in forensic investigations and multidisciplinary approaches. To this aim, this paper discusses a case involving biomechanics in the operating room and outlines how some of these tools were deployed.

Methods: A thorough review of the information available was performed to understand all the case-specific factors, including:

- After 90 minutes into laparoscopic surgery, a 30-year-old nurse claimed that his hand extensor tendon ruptured while he was holding an endoscopic camera during the surgery.
- Injury was allegedly caused by a forceful grasp from a surgeon.
- Surgeon was over 60 years old, suffered from carpal tunnel syndrome, and was standing on a step stool throughout surgery.
- Manual examination of the subject endoscopic tool indicated that if the tip touches skin it can burn.
- There was no evidence of claims from the patient related to subsequent issues or burns after the surgery.
- Nurse was involved in a vehicle collision one week prior to the subject incident, in which all airbags were deployed.
- Nurse's mechanical engineering expert involved in the case opined that the injury occurred from a localized force through a soft fiber optic cable passing over the dorsal side of the nurse's hand. Nurse's medical expert (hand surgeon) opined that the fiber optic cable had nothing to do with how the extensor tendon ruptured but that the injury mechanism was possible. They compared it to a rugger jersey finger injury during flag football and to a bicep rupture during flexion.

A detailed analysis and experimentation with the subject tool and fiber optic cable was conducted to determine the plausibility of the injury through the claimed mechanism. To assess the motions and forces based on the incident description provided by the Nurse, several tools were used during the inspection and analysis, including motion capture (MoCap), photo matching techniques, video-based photogrammetry, force gauges, and tactile pressure sensors. Additionally, an extensive literature review was performed to understand the mechanism of injury for an extensor tendon and to identify all factors affecting hand force exertions.

Results & Discussion: Analysis revealed that the claimed biomechanical mechanism of injury for an extensor tendon rupture – which involves an acute traumatic event or chronic injuries – was not present at the time of the subject incident. Results from the inspection and analysis demonstrated that many factors affect grip strength and pulling/pushing forces, that grasping forces are not localized in only one zone, and that hand movement in this specific scenario can be achieved only if the reaction forces in extension exceed the external forces forcing flexion. This case study presents a subset of tools that can be used to evaluate kinematics and other factors involved in biomechanical assessments. These and other biomechanical and visualization tools can be used in a host of capacities to enhance forensic investigations beyond the biomechanical analysis scope.

For example, MoCap can be used to demonstrate certain interactions of a person and specific environment/tool/product, such as in the dynamics of a fall or manual lifting task, or the relative position of a person's center of mass with respect to a handrail or the edge of a seat at an amusement ride. MoCap data also can provide kinematic inputs to estimate kinetics via simulation techniques (e.g., MADYMO) or to create realistic 3D animations with the sole purpose of serving as visual aids to explain technically complex interactions in a simple and compelling manner. Surveillance video, photo matching, and photogrammetry techniques (e.g., PF Track) can be used to compute individuals' speed, position, and movements. These can also be deployed to determine the speeds, movements, and relative positions of vehicles, bicycles, pedestrians, and other objects and products and to assist in conducting gait analysis of the events leading up to a slip, trip, misstep, and fall. Customizable, interactive, and realistic applications can be developed by leveraging the use of and knowledge in 3D scanning (e.g., FARO), gaming animation tools (i.e., Unreal and Unity), and human modeling techniques. Realistic 3D surrogates (characters) can be created based on the anthropometrics of the involved individuals, placed in the actual environment, and produced as interactive animations, simulations, and physical models to answer critical questions and help a layperson visualize key findings. These tools can also be used to develop 3D Environments that can then be depicted in Virtual, Augmented, and Mixed Reality (VR/AR/XR) environments and head-mounted displays (HMDs) to be used for forensic evaluations and as compelling scientific-based demonstrative aids [1,2].

Significance: This study aims to close the gap between academia and industry by showcasing how biomechanical tools and knowledge, typically confined to research settings, can be leveraged in a forensic setting. We present a method and discussion whereby biomechanical and physics-based visual tools can turn complex science into efficient, digestible knowledge for lay stakeholders.

References: [1] Figueroa-Jacinto et al., (2020), *HFES Proceedings*; [2] Figueroa-Jacinto et al., (2019), *HFES Proceedings*.

BIOMECHANICAL RESPONSES OF OLDER BALLET DANCERS FOLLOWING STANDING SLIPS

Caroline Simpkins[1*], Jiyun Ahn[1], Sangwon Shin[1], Sara Mahmoudzadeh Khalili[1], Feng Yang[1]

[1]Georgia State University

*Corresponding author's email: claubacher1@gsu.edu

Introduction: Falls are common in older adults [1]. Dance interventions have low attrition and high satisfaction rates [2]. Ballet training emphasizes whole-body coordination, movement fluidity, and postural control while also challenging flexibility and strength [3]. Ballet could be an attractive option to reduce older adult fall risk [4]. Dynamic gait stability is a novel method to measure a person's fall resistance [5]. Based on a conceptual framework (the Feasible Stability Region theory, or FSR), dynamic gait stability is quantified by the kinematic relationship between the body's center of mass (COM) and base of support (BOS) [6]. No study has examined how older ballet dancers maintain stability after an external perturbation, particularly a standing slip. The purposes of this study were to 1) examine how older ballet dancers respond to the first unexpected standing slip perturbation compared to non-dancers and 2) determine if older dancers adapt to repeated standing slips more quickly than non-dancers. We hypothesized that dancers would be more stable at recovery step liftoff (LO) and adapt quicker to repeated standing slips compared to non-dancers.

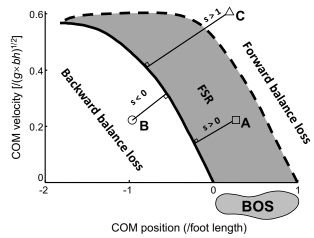

Fig. 1: Stability (s) defined by the FSR theory is calculated as the shortest distance from the COM motion state to FSR's lower limit. A larger stability indicates a more stable state resisting backward falling.

Methods: Seventeen older adult females were recruited: 7 ballet dancers (age: 63.00 ± 5.86 years, body height: 1.62 ± 0.07 m, mass: 58.01 ± 3.63 kg) and 10 non-dancers (63.30 ± 5.85 years, 1.60 ± 0.07 m, 69.49 ± 15.35 kg). Participants with 26 reflective markers attached to the bony landmarks wore a safety harness on the ActiveStep treadmill (Simbex, NH). One marker was placed on the treadmill to record the belt movement. After 3 standing trials (told no belt movement would occur), participants were told a slip may or may not occur on any of the following trials. Following 3 more standing trials where participants anticipated a slip, but no slip occurred, the first unexpected slip occurred ensued by 9 more slips. The standardized slips were created by suddenly accelerating the belt forward to 1.2 m/s over 300 ms, and then diminishing to zero over another 300 ms. The total belt slip distance was 36 cm. The first (S1) and last (S10) slip trials were analyzed. Full-body kinematics were collected from reflective markers through a motion capture system (Vicon, UK). The primary outcome was dynamic gait stability. Secondary variables were the slip outcome (fall vs recovery), and trunk angle and rotation velocity in the sagittal plane. LO was identified using the foot kinematics. The body's COM kinematics were computed using sex-dependent segmental inertial parameters based on filtered marker paths. The two components of the COM motion state (position and velocity) were calculated relative to the BOS and normalized by foot length (l_{BOS}) and $\sqrt{g \times bh}$, respectively, where g is the acceleration due to gravity and bh the body height. Stability (a unitless variable) at LO was calculated using the COM motion state according to the FSR. When the COM motion state is within the FSR limits (**A**, Fig. 1), balance can be maintained without changing the BOS. A COM motion state below/above the lower/upper FSR limit indicates an unstable state against backward/forward falling (**B/C**, Fig. 1). Slip outcome was a fall if the hip height decreased by 4.5% *bh* or more. Trunk angle (deg) at LO was formed by the trunk segment and the vertical reference line (negative angle = backward lean). Trunk velocity (deg/s) at LO was the first derivative of the trunk angle with respect to time. Independent t-tests compared stability and trunk kinematics between groups. Fisher's exact test compared slip outcome. All analyses were conducted using SPSS 28.0 (IBM, NY) with an α of 0.05.

Results & Discussion: The results partially support our hypothesis. At LO, both groups had similar stability for S1 ($p = 0.49$), but dancers were more stable than non-dancers for S10 ($p = 0.04$, Fig. 2a). Dancers had a lower fall rate than non-dancers for S1 (29% vs 90%, $p = 0.04$) and S10 (14% vs 50%, $p = 0.30$, Fig. 2b). Dancers exhibited a more upright trunk than non-dancers at LO for S1 ($p = 0.02$) but not S10 ($p = 0.37$, Fig. 2c). Both groups had comparable trunk velocity at S1 ($p = 0.63$), but dancers had higher forward velocity at S10 than non-dancers ($p = 0.05$, Fig. 2d). The findings indicate that older dancers react more favorably than non-dancers to the first unexpected standing slip as evidenced by their lower fall rate. After repeated standing slip exposure, ballet dancers displayed a lower fall rate and better stability at LO than their non-dancer peers. Group differences could be attributed to dancers having better trunk movement control.

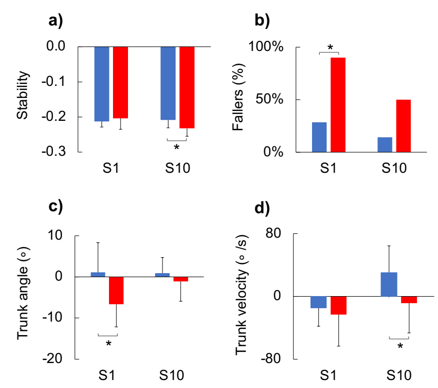

Fig. 2: Comparisons between **ballet dancers** ($n = 7$) and **non-dancers** ($n = 10$) for **a)** stability at liftoff (LO), **b)** slip-faller rate, **c)** trunk angle at LO, and **d)** trunk velocity at LO on the first (S1) and last (S10) slips. * indicates $p \leq 0.05$.

Significance: Our study suggests that older ballet dancers have a significantly lower fall rate than non-dancers when exposed to an unexpected standing-slip. Dancers also could adapt more quickly to repeated standing slips than non-dancers. The findings could provide insight into the underlying mechanisms of ballet practice reducing falls in persons at a high fall risk.

Acknowledgements: This project was supported by the American Society of Biomechanics Grant-in-Aid and the Scott Lilienfeld Injury Prevention Scholarship from Emory University.

References: [1] Bergen et al. (2016), *MMWR* 65. [2] Sharp & Hewitt (2014), *Neurosci Biobehav Rev*. 47. [3] Houston & McGill (2013), *Arts Health*. 5. [4] Simpkins et al. (2022), *J Biomech*. 145. [5] Yang et al. (2009), *J Biomech*. 42. [6] Yang et al. (2007), *J Biomech*. 40.

EFFECTS OF VISION AND KNOWLEDGE OF LANDING CONDITIONS ON PRE-LANDING AND EARLY LANDING MECHANICS ASSOCIATED WITH ACL LOADING

Ling Li[1], Yu Song [1], Peyton Hatcher [1], Raychl Fairbanks[1], Boyi Dai[1]*
[1] Division of Kinesiology and Health, University of Wyoming, Laramie, WY, USA
*Corresponding author's email: bdai@uwyo.edu

Introduction: Knee flexion angles typically start to increase shortly prior to initial ground contact, and peak anterior cruciate ligament (ACL) strain could occur during pre-landing in non-injury landings [1]. Disruption to sensory input and motor planning during pre-landing might result in limited knee flexion along with increased impact forces to cause ACL injuries during early-landing [2]. Single-leg landings demonstrated decreased pre-landing knee flexion angles and flexion velocities compared with double-leg landings [3]. Interestingly, the removal of vision did not appear to affect pre-landing muscle activities and impact landing forces as long as individuals had knowledge of the drop height before the landing task. However, how a lack of vision and knowledge of landing conditions might affect pre-landing knee kinematics and landing forces was unknown [4]. Thus, the aim of the study was to assess the effects of continuous vision and knowledge of drop heights on knee kinematics and peak vertical landing forces when participants landed from three drop heights.

Methods: Nine male and nine female recreational athletes (age: 22.4±2.4years; height: 1.7±0.1m; weight: 70.5±12.6kg) participated. Participants performed single-leg drop landings from three different landing heights controlled by a lifting table (11cm, 22cm, and 33cm) under three experimental conditions: having continuous vision and knowledge of the drop height (VK), having no continuous vision but having knowledge of the drop height (NK), and having no continuous vision or knowledge of the drop height (NN) (Figure 1). In the NN condition, the drop heights were adjusted after participants were blindfolded. The pre-landing and early-landing phases were defined as 100ms before and after initial contact. Dependent variables included the minimal knee flexion angles (MKFA) during pre-landing, knee flexion angles (KFA) and knee flexion angular velocities (KFV) at initial contact and peak vertical ground reaction force (PVF) during early-landing.

Figure 1. NN condition.

Results & Discussion: There were generally no significant differences between the VK and NK conditions (Figure 2). Compared to VN and NK conditions, the NN condition resulted in the greatest MKFA during pre-landing and KFA at initial, the smallest KFV at initial contact, and the greatest PVF at heights of 22cm and 33cm (Table 1). In the VN and NK conditions, participants had a more active knee extension-flexion movement pattern during pre-landing, resulting in greater knee flexion velocities at initial contact. The active knee flexion and accurate anticipation of initial contact prepared the body to decelerate more gradually to decrease impact forces during early-landing. On the other hand, the removal of vision and knowledge of drop heights changed pre-landing motor programming, shown by increased knee flexion angles but decreased knee flexion velocities near initial ground contact. As participants could not predict initial ground contact, they kept their knees at a greater flexion position but decreased flexion velocities during pre-landing, which may serve as a protective mechanism to passively prepare for initial ground contact. However, the less active knee flexion resulted in greater vertical forces.

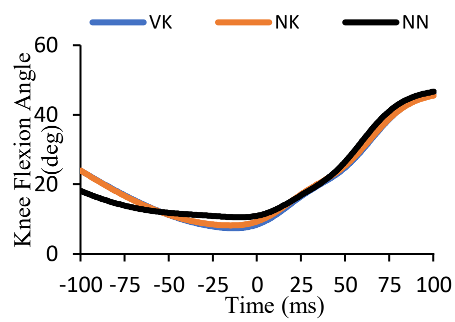

Figure2. knee angles at 33 cm.

Significance: These findings highlighted a lack of knowledge of landing heights could cause disruption to the preparation of pre-landing and result in less knee flexion velocities and increased impact forces. In sports situations, limited knowledge about the relative position between the body and ground could be caused by multiple tasking, action-reaction, and mid-flight perturbation. Therefore, it would be important to train athletes in such situations to prepare for safe landings.

Acknowledgements: Ling Li's graduate assistantship was provided by the Wyoming INBRE, supported by the NIH (P20GM103432).

References: [1] Englander et al., 2019. Am. *J. Sports Med*, 47(13), 3166-72; [2] Hughes & Dai. 2023. *Sports Biomech.* 22(1), 30-45; [3] Li et al., 2022. *J.Appl. Biomech*. 1(39), 34-41;[4] Liebermann & Goodman. 2007. *J. Electromyogr Kinesiol*.17(2), 212-22

Table 1. Means and standard deviations of dependent variables for different landing conditions.

	11 cm			22 cm			33 cm		
	VK	NK	NN	VK	NK	NN	VK	NK	NN
MKFA (deg)	14.7±6.7B	14.4±6.1B	19.9±6.9A	11.5±4.9	11.2±4.9	13±5.2	7.7±4.4B	8.3±4.5B	10.6±3.8A
KFA (deg)	14.9±6.6B	14.7±5.7B	20.1±6.6A	12±4.7B	12.1±4.3B	13.9±4.8A	9.4±3.7C	10.4±3.8B	12.2±3.2A
KFV (deg/s)	6.0±84.7A	27.8±74.5A	-81.6±123.2B	82.9±79	108±74.7	92.1±51.4	197.9±63.6A	195.8±61.3A	113.7±58.3B
PVF (BW)	2.8±0.4B	3.0±0.4A	2.4±0.4C	3.4±0.4B	3.7±0.4A	3.7±0.6A	4.5±0.5B	4.6±0.7B	5.2±0.6A

Note: The effect of drop conditions for three landing heights is grouped, where A > B > C.

MARKERLESS MOTION CAPTURE AND BIOMECHANICAL ANALYSIS PIPELINE FOR REHABILITATION

R. James Cotton[1,2,*]
[1]Shirley Ryan AbilityLab [2]Department of Physical Medicine and Rehabilitation, Northwestern University
*Corresponding author's email: rcotton@sralab.org

Introduction: There is a substantial need for novel tools to enable routine, precise, movement analysis of rehabilitation patients, both for research and for clinical practice. Advances in computer vision show much promise and have enabled commercially available markerless motion capture systems, but there is limited work optimizing pipelines from multi camera views to fitted biomechanical models with kinematics. This process can be roughly divided into two stages. The first stage uses human pose estimation (HPE) algorithms to detect a set of keypoints for each camera and time point and then reconstructs the temporal trajectories of virtual markers, similarly to marker-based motion capture. Like marker-based methods, these trajectories must be sufficiently cleaned up prior to fitting biomechanical models, including ensuring reasonable constraints on smoothness and anatomical plausibility. Additionally, there are many HPE algorithms available, but the majority are not designed to locate a viewpoint invariant virtual marker. The second stage includes skeleton scaling, marker positioning, and inverse kinematics, which must be adapted to work with the HPE keypoint set and be robust to noise in the trajectories. Finally, any such system must be validated on clinical populations to ensure the human pose estimation algorithms generalize to these populations. In this work, we describe optimization of the first two stages and validation of the final system on videos of walking collected from both inpatient and outpatient participants seen in a rehabilitation hospital. The optimized system showed good performance for a range of clinical conditions and was able to detect clinically meaningful changes in walking.

Methods: This study was approved by the Northwestern IRB. Thirty-two participants were recruited from both inpatient and outpatient clinics with a range of diagnoses including stroke, spinal cord injury, amputation, and neuropathy. Video was acquired from our multicamera acquisition system while they walked on an instrumented gaitway. We used 10 Blackfly GigE cameras that with calibrated intrinsic and extrinsic parameters that were network synchronized to submillisecond accuracy.

We varied two aspects of the pipeline. 1) The HPE algorithm used to detect the keypoints. We compared OpenPose, MMPose, and a recent version MeTRAbs trained on multiple different 3D datasets [1]. The second aspect we varied was how the virtual marker trajectories were reconstructed from the keypoints from different cameras [2]. We compared a robust triangulation algorithm to an optimization approach to find trajectories that were consistent with the detected keypoints while also being smooth and anatomically consistent. We also performed this optimization using an implicit representation of the trajectory, where a neural network was optimized to learn a mapping from time to the virtual marker locations in 3D. We measured the performance by the geometric consistency of the reconstructed virtual markers and the detected keypoints. We also measured the trajectory noise and bone length variations.

Biomechanical fitting used the nimblephysics library with a bilevel optimization approach [3] that optimizes over multiple dynamic trials. We used a modification of the Rajapogal skeleton [4] that included a neck joint and markers that matched the virtual keypoints. The marker locations were refined with multiple rounds of adjusting the unscaled model by the average marker offsets from all the trial fits. We modified the nimblephysics python interface to enable soft joint limits with regularization and explored a range of hyperparameters for the inverse kinematics. Performance was also measured by the geometric consistency with the model markers and the image keypoints, by the noise in the pose trajectories, and the different between the calcaneus location and the GaitRite heel locations.

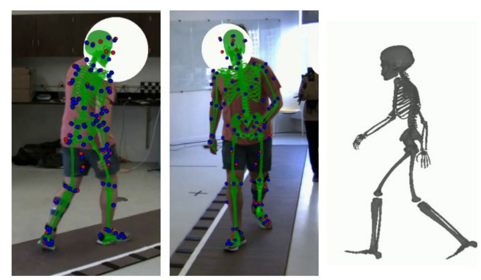

Figure 1: Example model fit.

Results & Discussion: *Trajectory reconstruction:* We found that the keypoint algorithm and the representation used for reconstructing the trajectories were both important factors. MeTRAbs showed the greatest geometric consistency, followed by MMPose with OpenPose performing the worst. Both optimization approaches resulted in substantial improvements in both trajectory smoothness and anatomic consistency, with the implicit representation providing the best fits. *Biomechanical fits:* Fig 1 shows a representative example overlay of the skeleton reconstruction on the image view, showing the good alignment to the image, and between the model-based markers and detected keypoints. The iterative optimization of the biomechanical model improved the resulting fits. We found a number of hyperparameters were important for obtaining a good fit, including adding soft-joint regularization to allow occasional violations of the model joint limits and increasing the weight on the anthropomorphic prior. Using the dense keypoint matching the MOVI dataset using [1] was also critical for constraining the torso and hip. The geometric consistency of the fitted model markers with the detected keypoints remained high (more than half the markers reprojected within 5 pixels and more than 90% within 20 pixels). The calcaneus position aligned within a centimeter of GaitRite heel events. Importantly, the system was sensitive to clinically meaningful interventions like changes in ankle and knee kinematics when walking with the use of an AFO or FES.

Significance: Markerless motion capture greatly reduces the barrier to kinematic analysis and can extend this practice into more realms of rehabilitation. We tested and optimized several algorithmic components for obtaining accurate fits and validated this pipeline on rehabilitation patients. It builds on open and accessible tools, making it very affordable to replicate through a hospital.

Acknowledgements: Thanks to Allison DeLillo, Anthony Cimorelli, Kunal Shah, Shawana Anarwala for help with participant recruitment and data collection. Thanks to Tasos Karakostas for the use of the GaitRite. Thanks to the developers of nimblephysics, EasyMocap, aniposelib, and Jax for developing Open-Source tools that enabled this work.

References: [1] Sárándi, Hermans, Leibe. WACV 2023. [2] Cotton et al., Improved Trajectory Reconstruction for Markerless Pose Estimation. arXiv 2023. [3] Werling, Raitor, et al., bioRxiv 2022. [4] Rajagopal, et al., TBME 2016.

DOES PROSTHETIC FOOT TYPE INFLUENCE CONTRALATERAL KNEE LOADS DURING WALKING AMONG INDIVIDUALS WITH UNILATERAL TRANSTIBIAL AMPUTATION?

Pawel R. Golyski[1,2*], Jonathan R. Gladish[1,2], Jason T. Maikos[3], Brad D. Hendershot[1,2,4]
[1]Extremity Trauma and Amputation Center of Excellence, Falls Church, VA, [2]Walter Reed National Military Medical Center, Bethesda, MD
[3]Veterans Affairs New York Harbor Healthcare System, New York, NY, [4]Uniformed Services University of Health Sciences, Bethesda, MD
*Corresponding author's email: pawel.golyski.civ@health.mil

Introduction: Individuals with vs. without unilateral transtibial amputation (UTTA) are 17 times more likely to develop osteoarthritis (OA) in the contralateral knee, potentially due to repetitive exposures to abnormal forces during ambulation [1]. Advanced prosthetic foot designs that aim to mimic the biological ankle-foot, such as powered ankle-foot prostheses (POW), may mitigate OA risk by reducing reliance on the contralateral limb. However, results can vary with the methodology for estimating knee loads; at the overall limb level, vertical ground reaction force (vGRF) peak and loading rate are common measures, while at the joint level, knee adduction moment (KAM) peak and loading rate are thought to relate more closely with forces on the medial condyle [2]. A major limitation of these measures is that external forces alone (i.e., neglecting muscle forces) comprise only ~50% of the total load borne by the knee [3]. In this analysis, we overcame this limitation by using participant-specific neuromusculoskeletal models to estimate medial condylar force (MCF) in the contralateral knee of individuals with UTTA during walking with energy storing and returning (ESR), ESR with articulation (ART), and POW devices. We hypothesized that the early stance peak MCF and loading rate would be smallest with the POW vs. ESR and ART device types. Secondarily, we analyzed early stance vGRF and KAM peaks and loading rates to investigate whether results would be different based on the level of analysis (i.e., relative to overall limb or joint).

Methods: Nine individuals with UTTA (7 males/2 females, mean±SD age: 40±8yr, stature: 179±5cm, body mass: 89.7±14.1kg, time since UTTA: 63±96mo, etiology: 1 cancer, 8 trauma) wore three different prosthetic feet (ESR, ART, POW), in a randomized sequence for ~1 week each. At the end of each acclimation period, full-body motions (120Hz) and bilateral GRFs (1200Hz) were collected as participants walked overground at three targeted speeds (1.0, 1.3, 1.5 m/s). A full-body model with UTTA was scaled to each participant [4], and muscle forces were estimated using static optimization, in OpenSim 4.4 [5]. These muscle forces, together with GRFs, were used to estimate MCF peaks and loading rates during early stance, while GRFs alone were used to calculate early stance vGRF and KAM peaks and loading rates. A linear mixed model with a fixed effect of prosthetic foot type and a covariate of walking speed (measured during each individual walking trial, as opposed to using explicit bins) assessed the main and interactive effects of prosthetic foot type and walking speed ($p<0.05$). All activities were approved by the local IRB, and participants provided informed consent.

Results & Discussion: Across all loading measures (vGRF, KAM, MCF), there were no effects of prosthetic foot type ($p>0.07$), or interactions between foot type and walking speed ($p>0.09$; Fig 1). Thus, our hypothesis was not supported, suggesting that more advanced prosthetic feet (i.e., POW vs. ESR with or without ART) may not reduce contralateral knee loads during walking. Our findings contrast with those of previous studies comparing POW and ESR feet [6-7], which may be attributable to differences in prosthesis acclimation, alignment, and/or fit. Additionally, since our conclusions did not vary by the level of analysis (leg and joint vs. condyle), this tentatively suggests that external loads are sufficient for understanding the relative effects of different prosthetic feet during walking, noting the important caveat that we did not measure muscle activations, and thus estimated activations could not be directly validated.

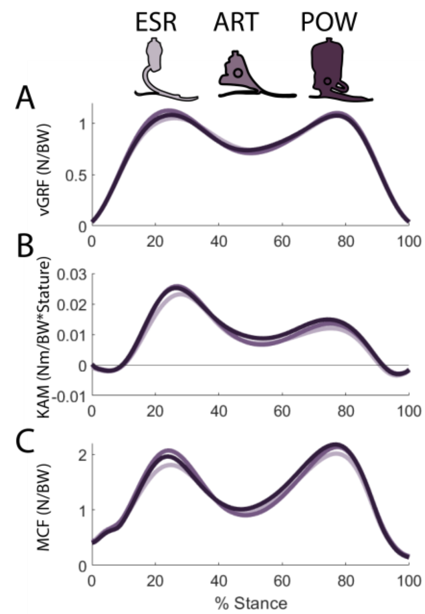

Figure 1: Time-series plots of contralateral limb: A) vGRF, B) knee adduction moment (KAM), and C) medial condylar force (MCF). Each curve represents the ensemble average across all speeds and all participants for each prosthetic foot type. BW = body-weight including prosthesis mass.

Significance: This work represents a systematic and multi-scale effort to combine experimental and computational approaches to understand the influence of different prosthetic foot types on contralateral limb loads associated with knee OA risk. To enable a more complete understanding of how device type may influence knee OA risk, future studies should 1) investigate whether proximal (e.g., trunk) compensations may explain the lack of load differences across devices [8], and 2) expand to activities associated with larger limb loads (e.g., non-steady state walking), in conjunction with wearable sensing/activity monitoring outside the laboratory.

Acknowledgements: Support was provided by the Congressionally Directed Medical Research Programs, Orthotics and Prosthetics Outcomes Research Program (Award #W81XWH-17-2-0014). The views expressed in this abstract are those of the authors, and do not reflect the official policies of the Uniformed Services University of the Health Sciences, U.S. Departments of the Army, Navy, Defense, nor the U.S. Government.

References: [1] P.A. Struyf et al. *Arch Phys Med Rehabil* 2009. [2] I. Kutzner et al. *PLoS One* 2013. [3] B.J. Fregly et al. *J Orthop* 2012. [4] A.M. Willson et al. *Comput Methods Biomech Biomed Engin* 2022. [5] S.D. Uhlrich et al. *Sci Rep* 2022. [6] A.M. Grabowski & S. D'Andrea *JNER* 2013. [7] E. Russell Esposito & J.M. Wilken *Clin Biomech* 2014. [8] A. Mündermann et al. *J Biomech* 2008.

Markerless motion capture estimates of lower extremity biomechanics are comparable to marker-based across 8 movements

Ke Song[1*], Todd J. Hullfish[1], Rodrigo Scattone Silva[2], Karin Grävare Silbernagel[2], Josh R. Baxter[1]
[1]University of Pennsylvania, Philadelphia, PA; [2]University of Delaware, Newark, DE
*Corresponding author's email: ke.song@pennmedicine.upenn.edu

Introduction: Accurate motion capture and analysis are essential for assessing human biomechanics [1-3]. Marker-based motion capture is the standard, but marker misplacement [2], skin artifact [3], cost, experimental setup, and processing time all limit its utility in large-scale and real-world applications. Markerless motion capture potentially overcomes these barriers, but its fidelity in quantifying human biomechanics has not been verified across common human movements. The few validation studies to date have focused on walking [4], running [5], or kinematic-only measures [4, 6]. In this study, we directly compared lower extremity kinematics and kinetics estimated from marker-based and markerless motion capture across 8 movements. We hypothesized that markerless estimates would match marker-based at the ankle and knee during most movements, while differences would be larger at the hip and during faster movements.

Methods: We quantified lower extremity kinematic and kinetics in 10 healthy subjects (5M/5F, 22 ± 2 y/o, BMI = 23.8 ± 2.4 kg/m^2) in this IRB-approved study. We concurrently recorded data using 12 marker-based cameras, 8 markerless video cameras (both 100Hz), and 3 force platforms (1000Hz) while subjects performed 8 movements: heel raises, walking, step-down, running, double-leg squat, sumo squat, countermovement jump, and run-and-cut. We used a marker-based link-segment model [7] and a markerless deep learning algorithm (*Theia3D*) [4] to simultaneously estimate 5 pairs of right leg kinematic (angle) and kinetic (moment) measures: ankle dorsi-plantarflexion, knee flexion, hip flexion-extension, ad-abduction, and internal-external rotation. We calculated Pearson correlation (R_{xy}) and root-mean-square difference (RMSD) between markerless and marker-based estimates of each angle and moment in each movement. We averaged each R_{xy} and RMSD across 10 subjects to determine an overall between-system agreement (R_{xy}) and magnitude difference (RMSD). We defined $R_{xy} \geq 0.7$ strong and ≥ 0.9 very strong [8], RMSD $\leq 5°$ small for joint angles, $\leq 2.5\%$ Height × Weight for moments.

Results: Markerless kinematic and kinetic estimates both matched marker-based for most movements (**Figure** shows running). We found strong correlations in ankle, knee, and hip sagittal angles ($R_{xy} \geq 0.877$) and moments ($R_{xy} \geq 0.785$). Hip ad-abduction angle ($R_{xy} \geq 0.739$) and moment ($R_{xy} \geq 0.819$) also strongly correlated, while transverse rotation angle had weaker correlation ($R_{xy} \leq 0.601$). RMSD was small for most angles ($\leq 5.9°$) except hip sagittal or transverse angles (6.7° – 15.9°), and moments ($\leq$ 2.66% H×W) except running / run and cut (up to 7.15%).

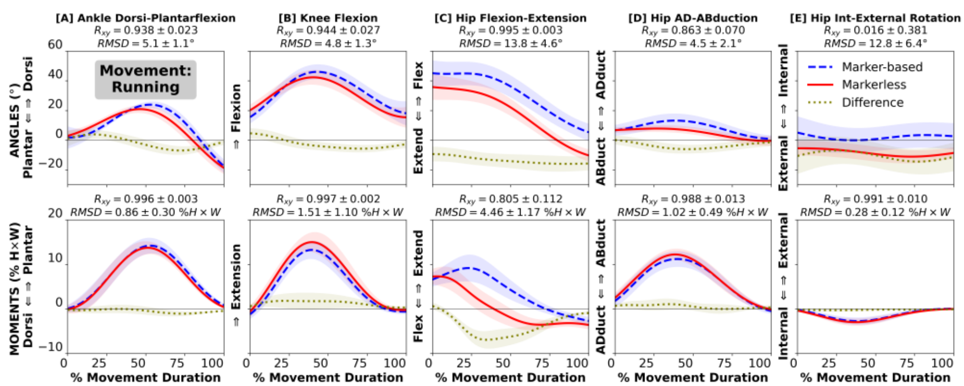

Figure: Joint angles (top) and moments (bottom) during *running*: [A] ankle dorsi-plantarflexion, [B] knee flexion, [C] hip flexion-extension, [D] ad-abduction, and [E] internal-external rotation. Waveforms = group mean (line) ± 1SD (shade) for marker-based (dash), markerless (solid), and their difference (dot). *Full results of all 8 movements can be found in our preprint article (link in **Acknowledgements**).*

Discussion: The results confirmed our hypothesis that markerless estimates of lower extremity kinematic and kinetics match marker-based during most movements, with strongest agreements in sagittal joint angles. Our finding supports prior evidence on the kinematic fidelity of markerless motion capture [4] and is the first to show that joint moments from markerless also match marker-based during most movements. Thus, we conclude that marker-based and markerless motion capture are comparable when estimating lower extremity biomechanics. Larger between-system disagreements during faster movements can be explained by marker-based skin artifacts. Such errors are expected at the hip given the known artifacts and difficulties to identify bony landmarks [2, 3]. We speculate that the markerless system better characterized hip kinetics such as late-stance flexion (**Figure**, bottom C), but verifying its accuracy requires comparison to gold-standard fluoroscopy. Our results are limited by model differences between systems, which may have caused hip angle offsets (**Figure**, top C/E). Future studies should match model definitions to confirm whether markerless systems reliably estimate hip measures.

Significance: Markerless motion capture can facilitate large-scale and real-world analyses not previously feasible with marker-based techniques. The biomechanics community should continue to verify, validate, and establish best practices for markerless motion capture, thereby advancing collaborative research and expanding real-world assessments needed for clinical translation.

Acknowledgements: NIH R01AR078898, R01AR072034, R37HD037985. We thank Madison Woods, Audrey Lehneis, and Liliann Zou for data processing. A preprint associated with this study is on *bioRxiv* at biorxiv.org/content/10.1101/2023.02.21.526496v1.

References: [1] Camomilla 2017 *Biomed Eng Online*; [2] Della Croce 2005 *Gait Post*; [3] Leardini 2005 *Gait Post*; [4] Kanko 2021 *J Biomech*; [5] Tang 2022 *Bioengineering*; [6] Ito 2022 *JSAMS+*; [7] Slater 2018 *BMC Musculoskelet*; [8] Schober 2018 *Anesth Analg*.

PERSONS WITH UNILATERAL TRANSTIBIAL AMPUTATION EXPERIENCING INTACT LIMB JOINT PAIN EXHIBIT ASYMMETRIC PEAK TIBIAL ACCELERATION DURING WALKING

Therese E. Parr[1a,3], Shawn Farrokhi[1a,2], Brad D. Hendershot[1b,2], Courtney M. Butowicz[1b,2*]
[1]Extremity Trauma and Amputation Center of Excellence [1a]Naval Medical Center, San Diego, CA, USA; [1b]Walter Reed National Military Medical Center, Bethesda, MD, USA; [2]Uniformed Services University of the Health Sciences, Bethesda, MD, USA; [3]Oak Ridge Institute for Science and Education, Oak Ridge, TN, USA
*Corresponding author's email: courtney.m.butowicz.civ@health.mil

Introduction: Persons with lower limb loss are at an increased risk of secondary musculoskeletal joint pain and degeneration [1], which can be debilitating and limit everyday function [2]. Among persons with unilateral transtibial amputation (TTA), greater incidences of intact side knee and hip pain have been previously associated with greater loading magnitude and rates in the intact limb during walking (vs. persons without TTA) [1], especially during foot strike/initial loading response [3]. Peak tibial axial acceleration (PTA) has been strongly correlated with vertical loading rates during walking and running, and knee joint pain during walking [5]. Recent evidence suggests that wearable sensors, such as inertial measurement units (IMUs), may be a feasible option to accurately quantify PTA without the need for force platforms [4, 5] in many populations. However, PTA and its relationship to lower limb joint pain has yet to be examined in persons with TTA. Therefore, the aim of this study was to assess the differences in PTA between persons with TTA with vs. without self-reported intact (contralateral) lower limb joint pain. We hypothesized that persons with intact side limb pain (ILP) experience greater PTA on their intact side, and lesser PTA on their prosthetic side, resulting in a more bilaterally asymmetric PTA.

Methods: Fifty-one persons with unilateral TTA were divided into two groups based on self-reported daily presence of intact-side limb pain (ILP): (1) 26m/9f with no ILP (age = 37.8 ± 10.8 yr, height = 175.7 ± 7.33 cm, mass = 87.8 ± 20.5 kg) and (2) 9m/7f with ILP (age = 42.1 ± 14.8 yr, height = 174.9 ± 10.1 cm, mass = 86.0 ± 16.9 kg). Each participant performed three repetitions of the 10-meter walk test at a self-selected speed while wearing triaxial IMUs (Opal, Generation 2, APDM, Inc, Portland, OR) placed bilaterally on the feet and shanks (Fig 1). Tibial accelerations were filtered through a fourth-order Butterworth filter with a 20 Hz cut-off frequency and then time-normalized using the foot strikes identified from the foot angular velocities [6,7]. PTA for both intact and prosthetic sides were extracted for each step and a symmetry index was established between limbs. Symmetry index defined a ratio of 1.0 as perfect symmetry, while a ratio greater than 1.0 indicated PTA was larger on the prosthetic side, and a ratio less than 1.0 indicated PTA was larger on the intact side. Statistical analysis was performed using an ANCOVA with the covariate of gait speed ($p < 0.05$). All values are reported as means ± standard deviations.

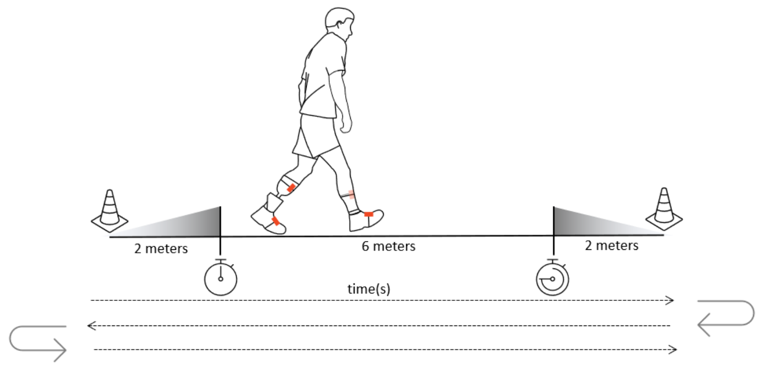

Figure 1: Participants wore IMUs on their feet and shanks while performing three repetitions of the 10-meter walk test

Results & Discussion: Gait speed was similar between ILP and no ILP groups (1.34 ± 0.2 vs. 1.35 ± 0.2 m/s, p = 0.853, F = 0.03). Persons with vs. without ILP had lesser prosthetic side PTA (0.64 ± 0.2 vs. 0.81 ± 0.3 g, p = 0.042, F = 4.37), and similar intact side PTA (0.82 ± 0.2 vs. 0.78 ± 0.2 g, p = 0.533, F = 0.40), resulting in a more asymmetrical PTA (0.81 ± 0.2 vs. 1.0 ± 0.3, p = 0.015, F = 6.43). Lesser prosthetic-side PTA among those with vs. without ILP suggest those with pain asymmetrically and preferentially loaded the intact side. These findings were also supported by persons with TTA, with vs. without ILP, having a symmetry index less than 1.0, indicating greater PTA asymmetry in favor of the intact limb. The results support previous work that suggests persons with TTA often have higher incidences of intact limb joint pain and preferential loading of the intact side [1,5,7].

Significance: This study identified asymmetries in PTA between persons with TTA with vs. without ILP, with the ILP group tending to preferentially load their intact side (despite reporting ILP). Future research should work towards further establishing whether PTA is a reliable metric for prediction and classification of ILP among persons with TTA, as well as persons with transfemoral amputation. Given the feasibility of PTA measurement using commercially available wearable sensors, this measure could provide clinicians with a useful guidance for implementation of unloading strategies to improve symmetry and help mitigate secondary musculoskeletal pain in persons with TTA.

Acknowledgements: This work was supported, in part, by an appointment to the DoD Research Participation Program administered by ORISE (contract number DE-SC0014664). The views expressed herein do not reflect the official policy of USUHS, U.S. Departments of the Army/Navy/Air Force, DoD, nor the U.S. Government.

References: [1]Gailey R, *J Rehabil Res Dev* 2008; 45: 15–30. [2]Sions JM, *Scand J Pain* 2022; 22: 578–586. [3]Norvell DC, *Arch Phys Med Rehabil* 2005; 86: 487–493. [4]Pohl MB, *J Biomech* 2008; 41: 1160–1165. [5]James K, *Arthritis Rheumatol.* p. 74 (suppl 9). [6]Grimmer M, *Front Neurorobot* 2019; 13: 1–15. [7]Tirosh O, *J Sci Med Sport* 2019; 22: 91–95.

EFFECTS OF FATIGUE ON LOWER-LIMB COORDINATION AND COORDINATION VARIABILITY DURING RUNNING IN HIGHLY TRAINED ENDURANCE RUNNERS

Yiyang Chen[1,2*], Gleydciane Alexandre Fernandes[1,2], Henri Lajeunesse[1,2], Isabella Sierra[1,2], Caroline Paquette[1,2], and Julie N Côté[1,2]
[1]Department of Kinesiology and Physical Education, McGill University, Montreal, Canada
[2]Centre for Interdisciplinary Research in Rehabilitation, Jewish Rehabilitation Hospital, Laval, Canada
*Corresponding author's email: yiyang.chen3@mail.mcgill.ca

Introduction: Sustained repetitive strides in long distance running induce fatigue, which is one of the risk factors of lower limb running injuries[1]. Abnormalities in coordination and its variability have been proposed to be associated with running injuries[2], as they reflect the flexibility of the locomotor system to develop adaptive or maladaptive patterns in response to external and internal factors, such as skill level and fatigue[3]. Continuous relative phase (CRP) is one of the tools developed to assess movement coordination and has the advantage of incorporating both the displacement and velocity of the joint. Therefore, it has been suggested to reflect higher-order coordination information compared to other techniques[4]. Using CRP analysis, research has shown that fatigue induced an increased coordination amplitude and variability during toe-off and initial swing phases in recreational runners[3]. It is still unclear if running-induced fatigue could influence lower-limb coordination patterns in highly trained endurance runners. Hence, the aim of this study was to investigate the effects of running-induced fatigue on lower-limb coordination and coordination variability among highly trained endurance runners using CRP analysis. Similar to recreational runners, we hypothesized that the endurance runners would increase their lower-limb coordination amplitude after fatigue. Since coordination variability is influenced by levels of skill, we expected that highly trained endurance runners may display different variability strategies to adapt to fatigue.

Methods: Twelve highly trained male endurance runners who had a minimum weekly running volume of 40 km and had been competing for at least three consecutive years participated in this study (age: 29 ± 7 years, weight: 69.1 ± 5.7 kg, height: 177.6 ± 7.0 cm). A VO2max treadmill test was conducted to induce fatigue. The participant ran at 10 km/h for 30 seconds before and after the test, defined as non-fatigue and fatigue-terminal conditions, respectively. They were instructed to rate their perceived exertion on a Borg CR20 scale at the beginning of each condition. Lower-limb kinematic data were acquired at 128 Hz using inertial measurement units (IMUs; APDM, Inc., Portland). The IMUs were placed on the main landmarks of the lumbar, bilateral thighs and shanks, and feet. Joint angles of the right leg in the sagittal plane were calculated using OpenSim software (4.4, Sim TK). CRP analysis based on the Hilbert transform approach was used to quantify coordination for the Hip-Knee and Knee-Ankle joint pairs. The resulting CRP values are between 0 and 180, where 0 represents full in-phase coupling, while 180 represents full out-of-phase coupling. Mean absolute relative phase (MARP) and deviation phase (DP) were further calculated to quantify coordination amplitude and variability in stance, swing, and four subphases of stance. Generalized estimating equations were used to compare MARP and DP before and after fatigue.

Results & Discussion: No significant difference was found in MARP of Knee-Hip and Knee-Ankle couplings before and after fatigue. As for DP, fatigue led to a significant increase in DP of the Knee-Hip joint pair after fatigue during pre-swing (Wald Chi-Square = 4.11, df = 1, p = 0.04; Fig.1), suggesting more interactions between knee and hip joints during the transition phase after fatigue. These results of the current study strengthened the notion that highly trained endurance runners may use consistent but more flexible coordination strategies to maintain performance in response to fatigue.

To date, the current study is the first to investigate the changes of CRP variability with fatigue in highly trained endurance runners. A previous study observed that both recreational and experienced runners increased their Knee-Hip coordination variabilities and displayed more out-of-phase Pelvis-Thigh coordination patterns after fatigue during stance[5]. However, the coordination in that study was quantified using vector coding technique, which only included the information of angular displacement and entailed loss of higher-order information compared to CRP analysis[4].

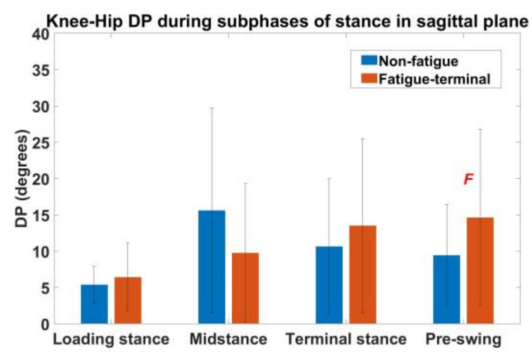

Figure 1. Knee-Hip deviation phase (DP) in subphases of stance in sagittal plane. *F* represents significant effects of fatigue.

Significance: The information on lower-limb coordination and coordination variability extracted by CRP technique has the ability to reveal higher-order dynamics for detecting performance changes with fatigue during running. These findings could help further explain the mechanisms of fatigue and injury development in running for high-level endurance runners. The potential long-term application of this study is to advance software design using wearable sensor technology. Especially, incorporating population-specific analyses will improve the personalization of these technological applications and contribute to personalized science.

Acknowledgements: We would like to thank the participants for their contributions and the Sylvan-Adams Sports Science Institute at McGill University for providing partial funds to support this study.

References: [1] Kluitenberg et al. (2015), *Sport. Med*, 45; [2] Palmer & van Emmerik (2012), *Sports Med Arthrosc Rehabil Ther Technol*, 4(1); [3] Bailey et al. (2020), *Sports Biomech*, 19(5); [4] van Emmerik et al. (2012), *Research Methods in Biomech*, second ed; [5] Mo & Chow (2019), *J Sports Sci*, 37(9).

LONGITUDINAL CHANGES IN COLLEGIATE RUNNER BIOMECHANICS

Elizabeth A. Schmida[1,2*], Mikel R. Stiffler-Joachim[2], Bryan C. Heiderscheit[2,3]
[1]Department of Mechanical Engineering, University of Wisconsin-Madison
[2]Department of Orthopedics and Rehabilitation, Badger Athletic Performance, University of Wisconsin-Madison
[3]Department of Biomedical Engineering, University of Wisconsin-Madison

*schmida@ortho.wisc.edu

Introduction: Experienced runners are often thought to demonstrate more efficient running mechanics. However, cross-sectional studies have shown no association between running experience level and differences in lower extremity running biomechanics [1]. Longitudinal changes in running biomechanics have not yet been studied and may be more likely to occur among runners involved in consistent training programs, such as collegiate cross country. Understanding the typical differences in running biomechanics from year-to-year may help monitor athlete-specific gait changes throughout a runner's collegiate career. Therefore, the purpose of this study was to determine if commonly assessed running biomechanics in collegiate cross country runners change as year of eligibility increases.

Methods: Preseason running gait analyses were collected on Division 1 cross country runners, while running at their preferred training pace, over six seasons (2015-2021; 2020 season excluded). For a gait collection to be included in the analysis, the runner must have had no prior lower extremity surgeries, be healthy at time of collection, and be rostered for the given cross country season. Whole body kinematics and ground reaction forces (GRFs) were collected and processed using a standard procedure [2]. Year of athletic eligibility was used to describe the number of years a runner was exposed to a collegiate running program. Running variables commonly related to performance and injury risk were included in the analysis (Table 1). Separate linear mixed effects models assessed the influence of year of eligibility on each running variable while controlling for sex and running speed. Runner and limb were included as random effects to account for within-subject correlation due to repeated measures across years. Model estimates and 95% confidence intervals (CIs) were calculated. P-values ≤ 0.05 were considered significant.

Results: One-hundred and ninety-nine gait collections, with 103 unique runners (62 females) met the inclusion criteria. As collegiate running experience increased, a statistically significant decrease was observed in duty factor, heel-to-center of mass (COM) distance, and peak hip adduction while a statistically significant increase in peak vertical GRF was also observed (Table 1). Foot inclination angle at initial contact also decreased marginally with increased runner experience (p = 0.07, Table 1).

Table 1: Linear mixed effects model results as estimates and 95% confidence intervals (CIs) for each running variable of interest.

Running Variable	Estimate (95% CI)	p-value
Step Rate [steps/min]	0.29 (-0.22, 0.79)	0.27
Duty Factor [%]	-0.11 (-0.21,-0.01)	**0.03**
Anterior-Posterior Heel-to-COM Distance (initial contact) [cm]	-0.27 (-0.42,-0.12)	**<0.01**
Vertical COM Excursion [cm]	0.01 (-0.05, 0.07)	0.65
Foot Inclination Angle (initial contact) [°]	-0.36 (-0.74, 0.02)	0.07
Peak Hip Adduction (stance phase) [°]	-0.27 (-0.49, -0.04)	**0.02**
Peak Knee Flexion (stance phase) [°]	-0.15 (-0.36, 0.06)	0.17
Peak Vertical GRF [N/kg]	0.12 (0.03, 0.21)	**0.01**
Braking Impulse [Ns/kg]	0.000 (-0.002, 0.001)	0.52
Vertical Impulse [Ns/kg]	-0.005 (-0.014, 0.004)	0.26

Discussion: As collegiate running experience increased, foot strike occurred closer to the body's COM with a smaller proportion of the stride cycle spent in contact with the ground. To maintain the same vertical impulse while ground contact time decreased, peak vertical GRF also increased. Despite statistical significance, the meaningfulness of these changes is questionable. For example, heel-to-COM distance decreased by 0.27 cm per year of eligibility, indicating approximately a 1 cm decrease over a typical collegiate runner's career compared to their first year of eligibility. Similar magnitudes of change for each additional year of eligibility were observed for duty factor (0.11% decrease/year), peak hip adduction (0.27 degree decrease/year), and peak vertical GRF (0.12 N/kg increase/year).

Significance: This study provides initial evidence that running biomechanics are unlikely to substantially change throughout a collegiate runner's career. Further research is required to determine the relationship between these factors and running efficiency. Performance and injury risk implications for runners who exhibit greater-than-typical changes in running biomechanics from one year to the next should also be investigated.

Acknowledgements: The authors would like to acknowledge the Sports Medicine staff in the University of Wisconsin-Madison Division of Athletics for their commitment to the welfare of the student-athletes and contributions to the Badger Athletic Performance program.

References: [1] Agresta et al. (2018), *Gait Posture*, vol. 61; [2] Stiffler-Joachim et al. (2019), *Med Sci Sports Exerc*, vol. 51.

ANTICIPATORY SYNERGY ADJUSTMENT DURING CURB DESCENT IN HEALTHY OLDER ADULTS

Chuyi Cui[1], Ashwini Kulkarni[1], Shirley Rietdyk[1], Satyajit Ambike[1]
[1] Department of Health and Kinesiology, Purdue University, West Lafayette, IN, USA
Email : cui111@purdue.edu

Introduction: Community ambulation often requires quick adaptations in gait in response to changes in the environment. It has been argued that although stability is essential for safe locomotion, high stability may hurt maneuverability, and animals may frequently have to trade stability for maneuverability [1]. We previously quantified this potential tradeoff between stability and maneuverability in young adults during curb descent [2]. We observed robust synergies in the ground reaction forces and moments that stabilized whole body motion during the double support phase of curb descent. Furthermore, the synergies were minimally affected when they expected to adjust the subsequent foot placement. Thus, young adults either prioritized stability during curb descent over future stepping adjustment, or they have the capacity to simultaneously manage stability and maneuverability demands. Here, we quantify the ability of older adults to manage the stability-maneuverability tradeoff in the curb descent task. There is evidence that older adults prioritize the planning of future steps over execution of the ongoing movements when the upcoming steps are challenging [3]. Therefore, we hypothesized that in older adults, the stability while descending a curb will reduce to facilitate a quick change in the subsequent foot placement.

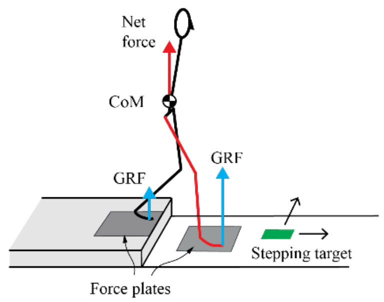

Fig 1. In target-shift tasks, the green target shifts forward or laterally in 50% of the trials when the leading foot contacts the ground. Blue arrows represent GRFs under the feet, and the red arrow at the CoM represents the net effect of the GRFs.

Methods: 24 healthy older adults (68.5±5.4 years, 9 males) walked on an 8 m walkway and stepped down a 15 cm curb at 4 m. For some tasks, a visual target was projected on the ground at the preferred foot location for the step immediately after stepping down. Participants first performed baseline trials without a target. Participants then performed three tasks in block-randomized order: Fixed target, Anterior-shift target, and Lateral-shift target (Fig. 1). In the latter two conditions, the probability of target shift was 50%. Kinematics and ground reaction forces (GRFs) were recorded. We used 15 trials when the target did *not* shift to examine the effect of an anticipated maneuver while holding other factors relatively invariant.

We quantified gait stability during double support using a synergy analysis we recently developed [2,4]. We computed six synergy indices, one for net force in each coordinate direction, and one for net moment about each coordinate direction. A synergy index is the normalized covariance in the bilateral GRFs and moments that contribute to and stabilize the corresponding net force or moment. Stabilization of the net force and moment implies stabilization of the whole-body linear and angular accelerations, respectively, and thereby quantifies gait stability. Separate one-way ANOVAs were conducted to examine the effect of task on each synergy index.

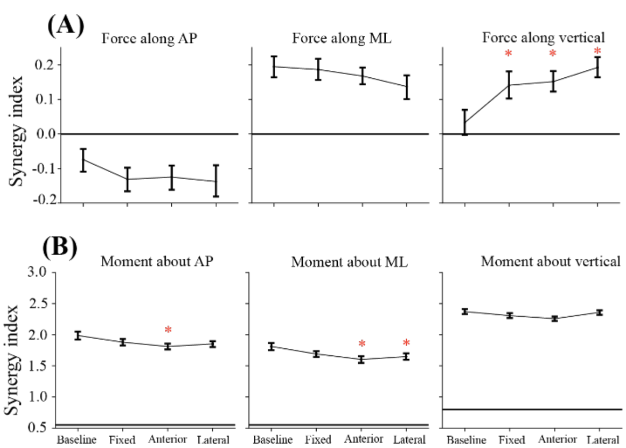

Fig 2. Synergy index for stabilizing resultant forces (A) and resultant moments about CoM (B). Horizontal lines in each plot show discriminating threshold indicating presence/absence of synergy. Asterisks indicate significant difference compared to baseline according to post-hoc comparisons with Tukey corrections.

Results & Discussion: The double support duration was longer for both target shift tasks ($p<0.01$). Gait speed was lower for the three target conditions compared with baseline ($p<0.01$).

A significant effect of task was observed for the synergy index for synergy stabilizing net force along vertical direction ($p<0.01$), and net moments about the AP and ML axes ($p<0.02$). The synergy index for net vertical force was higher for the three target conditions compared with baseline (Fig. 2A). The synergy index for the net moment about the AP axis was lower for the anterior target shift condition compared to baseline. The synergy index for the net moment about the ML axis was lower for both target shift conditions (Fig. 2B), thus partially supporting our hypothesis.

Significance: The higher synergy index for the net vertical force assists in lowering the synergy index for the net moments about the AP and ML axes [2,4]. Our key finding is the weakening of the AP and ML moment synergies, and hence the stability of angular motions in those directions, for the target shift tasks. While these synergy declines might assist the performance of the subsequent stepping task, the declines might also increase the risk of losing balance during curb descent, as it is crucial to regulate body angular motion during descent [5]. These adjustments by older adults were not observed in young adults [2], reflecting an age-related increase in anticipatory locomotor control involving bilateral kinetic synergies. Kinetic synergies allow the investigation of the stability-maneuverability trade off in gait and can quantify gait adaptability in older and pathological populations.

References: [1] Hasan (2005), *J. Mot Behav* 37(6); [2] Cui et al (2022), *PLoS ONE* 17(10); [3] Chapman & Hollands (2007) *Gait & Posture* 26(1); [4] Cui et al (2020), *J Biomech* 106; [5] Silverman et al (2014), *Gait & Posture* 39(4).

STEP WIDTH AND STEP LENGTH RESPONSE TO ACTIVE ABDUCTION/ADDUCTION ASSISTANCE PROVIDED BY POWERED HIP EXOSKELETON

Abbas Alili[1*], Aaron Fleming[2], Varun Nalam[2], Helen Huang[2]
[1]Department of Electrical and Computer Engineering, NC State University, Raleigh, NC, 27606 USA.
[2]Department of Biomedical Engineering, NC State University, Raleigh, NC,27695-7115; University of North Carolina at Chapel Hill, Chapel Hill, NC 27599 USA.
*Corresponding author's email: aalili@ncsu.edu

Introduction: Falls are a major concern for older people and individuals affected by stroke, and is generally caused by compromised balance due to poorer sensorimotor integration [1]. The compromised balance is critical in mediolateral direction (ML) which requires active control of step width to achieve balance [2]. Older adults, lower limb amputees and individuals after stroke fail to accurately integrate the position of their stance limb and pelvis to place their swing foot appropriately, due to poor abduction-adduction hip movement control [3]. Several systems have been developed to regulate step width for clinical populations to address these limitations. However, these systems are fixed immobile systems which cannot be utilized during functional tasks. Thus, in this study we investigate the validity of a wearable robotic approach to modulate the human step width and length response through abduction/adduction assistance provided by ML acting robotic hip exoskeleton, which could then be implemented during functional tasks.

Methods: This study involved ten non-disabled adults (six males, four females) with an average age of 25.2 ± 4.6 years, mass of 70.8 ± 11.6 kg, and height of 1.72 ± 0.06 m. We developed fully powered and compliant robotic hip exoskeleton acting in ML direction and utilized it in the study. To apply adequate ML torque, we adjusted the stiffness parameter of the admittance controller governing the hip exoskeleton, with the direction of the applied torque determined by changing the equilibrium angle parameter. The participants were instructed to walk for three trials while wearing the exoskeleton, under both abduction and adduction assistance conditions. Each walking trial lasted 5.5 minutes, with the first thirty seconds no torque applied. During each trial, the participants experienced five levels of stiffness (K): 0, 20, 40, 60, and 80 N·m/rad. We applied each stiffness level for one minute of the walking trial for both the left and right joints, and the order of K levels was randomized for each individual trial. Ultimately, each participant experienced the same level of K thrice for each of the abduction or adduction assistance sessions.

Results & Discussion: Fig. 1. shows the influence of stiffness K of active hip exoskeleton abduction or adduction assistance on step width and step length. In average participants walked with wider steps (Fig. 1a.) during the abduction assistance session due to the applied abduction torque and narrower steps (Fig. 1b.) due to the adduction torque applied to both limbs over the whole gait cycle. One-way ANOVA showed that change of K value in hip abduction and adduction significantly ($p < 0.001$) influences step width across participants, compared to no torque applied (K=0) mode. In contrast, calculated step length results did not show any statistical significance for various values of K for both sessions, as shown in Fig. 1c. (blue and red error bars). Participants responded almost linearly to applied abduction/adduction torque until the saturation reached. This can shed light on developing ML hip models that can be used to understand the step width behaviour in ML balance context. The study found that the step length of hip exoskeleton users did not change with either abduction or adduction assistance at various stiffness levels. This supports previous research indicating no relationship between anterior-posterior and mediolateral foot placements during walking [2].

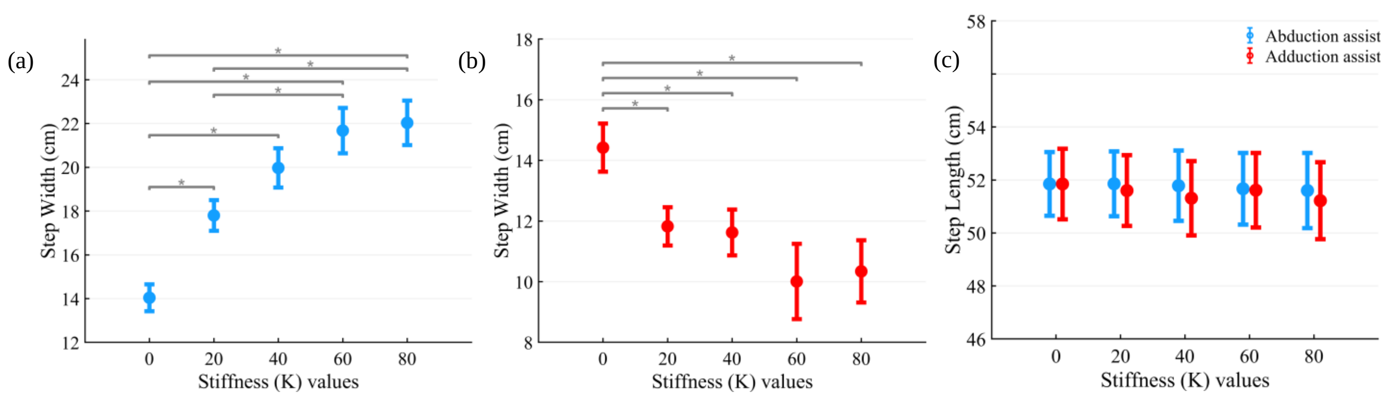

Figure 1: Influence of stiffness K of hip exoskeleton abduction (blue) and adduction (red) assistance on step width and step length. (a) Step width increased across K levels for abduction assistance mode. (b) Step width decreased across K levels for adduction assistance mode. (c) Step length did not change for the hip exoskeleton assistance regardless the assistance direction and applied stiffness. The data points represent the mean and error bars show the standard error mean, and asterisks (*) indicate significant ($p<0.05$) results of post-hoc tests.

Significance: The hip exoskeleton and control presented in this study have exciting potential applications. They could enhance ML balance control in populations with sensorimotor dysfunction and serve as a research platform to study ML balance control mechanisms and step width modulation. This would improve our understanding of the neuromechanical aspects of motion control during walking both inside and outside of the lab.

Acknowledgements: Research supported by NIDILRR 90REGE0017 and IBM.

References: [1] Morrison et al. (2016) Gait & posture, Elsevier 49, pp.148-154; [2] C. E. Bauby et al. (2000), J. Biomech. 33 (11).; [3] N. K. Reimold et al. (2021), IEEE Trans. Neural Syst. Rehabil. Eng., vol. 29, pp. 134–143.

CHANGES IN MULTI-MUSCLE COORDINATION DURING A 30-MINUTE WALK DIFFER BY FATIGABILITY

Jocelyn F. Hafer[1*], Sarah A. Roelker[2], Katherine A. Boyer[2]
[1]Kinesiology and Applied Physiology, University of Delaware, [2]Kinesiology, University of Massachusetts Amherst
*Corresponding author's email: jfhafer@udel.edu

Introduction: Muscle fatigue can affect gait mechanics [1-2]. Muscle activity (i.e., EMG) may change in response to fatigue, and such changes could be associated with altered joint loads or metabolic cost. To date, most studies of fatigue and EMG have fatigued all participants equally, often using non-ecological tasks such as repeated contractions on a dynamometer [e.g., 3]. While such protocols show that fatigue can influence EMG during gait, they do not reveal the extent to which fatigue-induced changes in EMG may occur during daily life. This question is particularly relevant for older adults, who experience greater magnitudes of dynamic muscle fatigue compared to their peers when exposed to the same exercise stimulus (i.e., they are more fatigable) [4]. During an extended bout of walking, individual muscles may fatigue to different extents, and there may be a redistribution of EMG to account for fatigued muscles. This change in multi-muscle coordination may vary depending on an individual's fatigability. The purpose of this study was to determine whether multi-muscle coordination (i.e., muscle modules) during gait changed differently between older adults who did or did not fatigue in response to a 30-min walking bout. We hypothesized that multi-muscle coordination at the end of the walk would be more similar to that at the beginning of the walk for adults who did not fatigue compared to those who did fatigue. We also aimed to explore whether changes in individual muscle coordination explained multi-muscle coordination differences pre- to post-walk.

Methods: Forty adults aged 55-70 years completed a study that included knee extensor power testing on an isokinetic dynamometer before and after a 30-min treadmill walk [5]. We collected EMG data for 8 muscles during the walk: vastus lateralis and medialis, rectus femoris, lateral and medial hamstrings, lateral and medial gastrocnemii, and tibialis anterior. We bandpass filtered, rectified, and lowpass filtered all data, and then extracted 10 strides from the 2nd and 30th minutes of the walk. We normalized EMG amplitude to each muscle's average stance-phase activation during the 2nd minute of walking. For both the 2nd and 30th minutes of the walk, we used non-negative matrix factorization to create muscle weightings and activation profiles (modules) that explained ≥90% of the variance of each subject's original EMG signal [6]. We explored whether these modules changed from the beginning to the end of the treadmill walk by computing the total variance in the 30th minute's EMG signal accounted for by the 2nd minute's muscle modules (30by2VAFt). We computed 30by2VAFt for each subject and compared it between individuals who did or did not fatigue in response to the walking protocol (fatigue = drop in knee extensor power ≥20%) using a one-tailed t-test (α=0.05). For each group, we also explored the contribution of changes in individual muscles to 30by2VAFt using linear regressions between each muscle's variance accounted for in the 30th minute by the 2nd minute's muscle modules (30by2VAFm) and 30by2VAFt.

Results & Discussion: Of the 40 participants, we excluded 9 due to incomplete muscle power data (n=1) or EMG signal quality issues (n=8). Final participants included 16 who did fatigue (63±3 yrs, 4F/12M, walking speed 1.3±0.1 m/s) and 15 who did not (62±4 yrs, 8F/7M, walking speed 1.3±0.1 m/s). Muscle modules constructed from minute 2 EMG data accounted for significantly more variance in minute 30 EMG for the group that did not fatigue compared to the group that did (Fig 1; mean 30by2VAF 53.8±14.1% and 44.0±15.6% for non-fatigue and fatigue groups, respectively; p=0.04). This result suggests that the coordination of lower extremity muscle activation changes more during a walking bout in individuals for whom the walking bout induces fatigue. For the group that did not fatigue, there were significant associations between 30by2VAFm and 30by2VAFt for all muscles except the gastrocnemii (r 0.54-0.78, p<0.05). For the group that did fatigue, significant associations between 30by2VAFm and 30by2VAFt existed only for the vastus lateralis, rectus femoris, and lateral hamstrings (r 0.50-0.59, p<0.05). These results may indicate that a small group of proximal muscles drove changes in multi-muscle coordination for the group that fatigued, while changes in muscle activity were more evenly distributed for the group that did not fatigue.

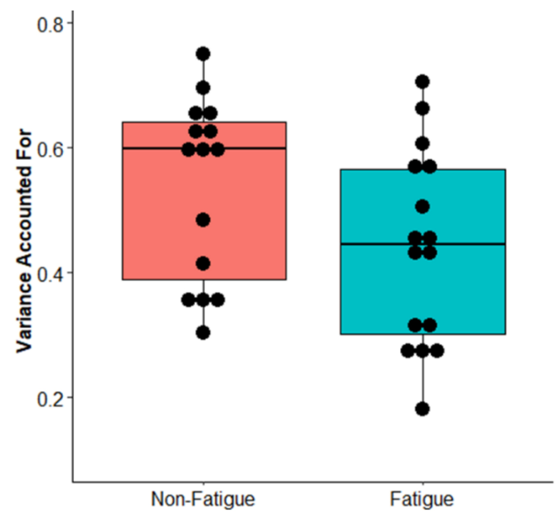

Figure 1. Distribution of total variance in min. 30 EMG accounted for by min. 2 muscle modules (30by2VAFt) for adults who did (blue) or did not (red) fatigue after a 30 minute walk. Dots represent individual participants.

Significance: Increased fatigability (susceptibility to fatigue in response to activity) could affect gait and mobility during daily life for older adults. Our results suggest that individuals who are more fatigable have larger changes in lower extremity muscle activity in response to a walking bout compared to their less-fatigable peers. The distribution of changes in individual muscle activity appeared to be different between groups, potentially indicating that changes in multi-muscle coordination are driven by a smaller set of muscles in fatigable individuals. In the current study, changes in gait mechanics were minimal, regardless of fatigability or changes in muscle coordination [5,7]. Future work should determine whether the observed changes in muscle activity relate to the fatigue of specific muscles (rather than just the knee extensors) or translate to changes in joint loading or metabolic efficiency.

References: [1] Murdock & Hubley-Kozey, 2012, *Eur J Appl Physiol*; [2] Dos Santos et al., 2019, *PLoS ONE* 14(12); [3] Longpre et al., 2013, *Clin Biomech*; [4] Paris et al., 2022, *J Appl Physiol*; [5] Hafer et al., 2019, *Gait Posture*; [6] Roelker et al., 2021, *PLoS ONE*; [7] Hafer & Boyer, 2018, *Gait Posture*

JOINT KINEMATICS AND GROUND REACTION FORCES FROM SPINAL CORD INJURED AND ABLE-BODIED PARTICIPANTS WALKING IN A SELF-BALANCING EXOSKELETON

Gabriela B. De Carvalho[1*], Vishnu D. Chandran[2], Ann M. Spungen[3,4], and Saikat Pal[1,3]
[1]New Jersey Institute of Technology, Newark, NJ, USA; [2]Hospital for Special Surgery, New York, NY, USA;
[3]James J. Peters Veterans Affairs Medical Center, Bronx, NY, USA; [4]Icahn School of Medicine at Mount Sinai, New York, NY, USA
*Corresponding author's email: gbd5@njit.edu

Introduction: Robotic exoskeletons have vast potential to restore upright ambulation in persons with spinal cord injury (SCI). However, widespread use of such devices has been limited due to several reasons, with one important reason being the need for hand-held crutches or a walker. Recently, a new self-balancing exoskeleton (Atalante, Wandercraft, Paris, France) received Food and Drug Administration approval for rehabilitation. The **goal** of this study was to quantify human-robot kinematics and ground reaction forces (GRF) during exoskeletal-assisted walking (EAW) in the self-balancing exoskeleton from controlled experiments with SCI and able-bodied (AB) participants.

Methods: We recruited three (two SCI, one AB) participants for this study. Participants performed unassisted walking (only AB) and four modes of EAW (Fig 1A): Early Gait (EG: 0.18±0.01 m/s) and Real Gait (RG1: 0.33±0.02 m/s; RG3: 0.39±0.02 m/s; RG5: 0.43±0.02 m/s). 3-D motion of the human-robot system was analyzed during EAW and unassisted walking, including simultaneous measurements of marker trajectories, GRF, and exoskeleton encoder data. 3-D motion was tracked using 61 markers on the human following the Conventional Gait Model (CGM) 2.5 template [1], 54 markers on the exoskeleton following a custom template, and an additional 6 offset markers on the human to reconstruct occluded anatomical markers during EAW.

We developed a custom pipeline in Vicon Nexus (Vicon Motion Systems, Oxford, UK) to determine human-robot kinematics during EAW and unassisted walking. To calculate joint angles of the human, we modified the CGM 2.5 template to include the offset markers. A static trial with the human outside the exoskeleton provided the pose of the CGM 2.5 and offset markers. This information was input to Vicon's *replaceMissingMarker* MATLAB script [2], which estimated the instantaneous position of the occluded markers during dynamic trials based on the offset and other CGM 2.5 markers of the same segment. This modified CGM 2.5 marker set was input to Vicon's inverse kinematics framework to determine the joint angles of the human. Next, joint angles of the exoskeleton were calculated using a custom marker set. A custom script was developed to define the exoskeleton pose and segments that utilized Vicon modules *NexusTrajectory* and *NexusSegment*, respectively. We used data from a static trial with the human in the exoskeleton to add the exoskeleton joint centers and segments to create a combined human-robot model. This combined human-robot model was input to a custom script that utilized the *NexusAngle* module to calculate exoskeleton joint angles during dynamic trials.

Results & Discussion: Participants with SCI experienced greater thorax and pelvic tilt during EAW compared to the AB participant (Figs 1B-E). Mean thorax flexion angles ranged from 11.9° to 19.3° in the SCI participants, compared to -2.0° to 1.0° in the AB participant (Figs 1B-C). Mean pelvic flexion angles ranged from 13.5° to 16.5° in the SCI participants, compared to 8.9° to 10.0° in the AB participant (Figs 1D-E). Next, participants with SCI experienced greater hip flexion during EAW compared to the AB participant (Figs 1F-G). Mean peak hip extension angles ranged from -9.7° to -19.0° in the SCI participants, compared to -1.6° to -6.0° for the AB participant (Figs 1F-G). In addition, SCI participants experienced greater knee flexion during the stance phase (Figs 1H-I). In general, RG modes were more representative of normal walking compared to the EG mode (Figs 1B-K). The GRF results demonstrate that all participants were completely weight-bearing during EAW (Fig 1L).

Significance: This is the first study in the United States to train people with SCI in EAW in a self-balancing robotic exoskeleton. This study provides new insight into human-robot kinematics and GRF during EAW. The ability for individuals with SCI to perform weight-bearing walking has important implications for the preservation of bone health in this chronic osteoporotic population.

Acknowledgements: National Institutes of Health grant 1S10OD032226-01.

References: [1] Leboeuf et al. 2019, *Gait and Posture* 69; [2] Pires 2020, *Vicon Manual*.

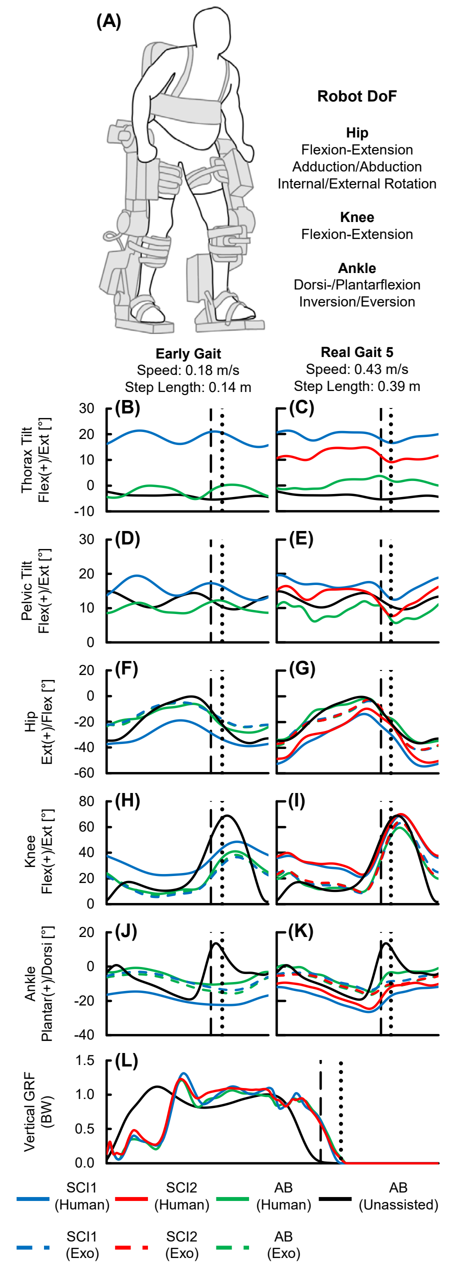

Figure 1: (A) A representative participant with SCI during EAW in the self-balancing exoskeleton (Exo). Average human thorax (B-C), pelvic (D-E), hip (F-G), knee (H-I), and ankle (J-K) angles from EAW and unassisted walking. Average Exo hip (F-G), knee (H-I), and ankle (J-K) angles from EAW. Joint angles from only EG and RG5 are shown. (L) Average left leg vertical GRF during EAW and unassisted walking for RG5 trials. The GRFs from EAW were normalized to the combined weight of the user and the exoskeleton; GRFs from unassisted walking were normalized to the user's body weight (BW). Vertical lines (dotted: EAW; dashed: unassisted) represent toe-off.

Cognitive-motor function during jump landings following anterior cruciate ligament reconstruction

Fatemeh Aflatounian[1], Ezekiel Barden[1], James N. Becker[1], Keith A. Hutchison[1], Janet E. Simon[2], Dustin R. Grooms[2], and Scott M. Monfort[1]
[1]Montana State University, Bozeman, Montana, USA, [2]Ohio University, Athens, Ohio, USA
Email : fatemehaflatounian@montana.edu

Introduction: Second ACL injury risk remains high following ACL reconstruction (ACLR), indicating a need to improve rehabilitation and return-to-sport assessment [1]. Common assessments often do not probe for deficits in cognitive-motor function that can lead to higher-risk biomechanics during sports [2]. The clinical relevance of cognitive-motor function is further emphasized by ACL injuries commonly occurring in sports where athletes need to devote attention externally [3]. Dual-task screening provides a unique chance to detect movement impairments by testing cognitive and motor skills simultaneously [4]. Therefore, to improve ACLR outcomes, it is crucial to investigate the role of cognitive-motor function in secondary ACL injury risk and assess its impairments. This study aimed to evaluate the spectrum of dual-task impairments that persist following ACLR. We hypothesized that adding cognitive tasks would elicit the riskier biomechanical predictors of second ACL injuries for ACLR patients compared to matched healthy controls.

Methods: 20 individuals who had undergone primary ACL reconstruction surgery and cleared to return to sports (**AR,** 16F/4M, 19.8±1.4 yrs; 1.69±0.10 m; 68.0±14.9 kg, 1.6±0.6 yrs post ACLR; Tegner: 6.9±1.9; Marx: 11.3±4.8) and 20 healthy controls (**HC,** 16F/4M, 20.0±1.8 yrs; 1.70±0.08 m; 66.0±7.4 kg; Tegner: 6.2±1.6; Marx: 11.2±4.4) who were matched at an individual level on gender, age, dominant limb, BMI, sports activities, Tegner score and Marx activity score participated in this study. Kinematics and ground reaction force data were collected as participants performed a jump landing from a 30 cm box followed instantly by a secondary jump (straight up, 45° right, 45° left). We used an inverse kinematics model in Visual 3D to calculate kinematic and kinetic outcomes [5]. Conditions included: Baseline (**NAD,** anticipated direction, no cognitive task, no visual gaze constraint), Baseline with Visual Constraint (**NAF,** same as NAD but with constraining visual gaze forward), Visual Unanticipated (**VUF,** secondary jump direction cue (arrow) was presented ~250 msec prior to initial contact with looking at the fixation), Auditory Unanticipated (**AUD,** secondary jump direction verbal cue was completely played ~250 msec to initial contact), Auditory Unanticipated with Visual Constraint (**AUF,** same as AUD but with constraining visual gaze forward), and Visual Memory (**VAM,** anticipated secondary direction with visual working memory task). Dependent variables were second ACL injury predictors [6], including uninvolved hip rotation net moment impulse (**HM-Impulse [Nm-s/kg]**), limb asymmetry in knee flexor moment at initial contact normalized to the body weight and height (**KFM-IC [%BW-HT]**) and range of knee abduction angle for the involved limb (**KAbA-range [°]**) [6]. We considered age, height, time since surgery, Tegner scale, Marx activity scale, and maximum jump height as potential covariates for each dependent variable, with those reaching bivariate correlations of r≥0.2 included in the statistical models. Mixed effect statistical models tested for Group*Condition interactions as well as Group differences between ARs and HCs, with age and time since surgery for **KAbA-range**, and height and maximum jump height for **HM-Impulse** as covariates.

Results & Discussion: No significant Group*Condition interaction was detected for any of the second ACL injury biomechanical predictors. Significant Group differences were observed for **KAbA-range** (p = 0.04) and **KFM-IC** (**Figure 1,** p = 0.002), but not for **HM-Impulse** (p = 0.069). Post-hoc analysis showed that the AR had riskier knee mechanics compared to HC, as evidenced by increased frontal plane knee motion (**KAbA-range**: 16.4±4.8° for AR and 15.71±4.6° for HC), and more knee extensor moment of uninvolved relative to involved limb (i.e., decreased **KFM-IC:** $-3.1*10^{-3}\pm11.0*10^{-3}$% for AR and $0.6*10^{-3}\pm8.4*10^{-3}$% for HC), aggregated across conditions. Although the Group*Condition interaction did not reach significance, our preliminary data appear to show clustering of group differences for conditions with anticipated versus unanticipated directional constraints for KFM-IC (**Figure 1**), where AR individuals demonstrated the largest deleterious differences compared to HC during unanticipated conditions (Cohen's d: from -0.64 to -0.70) relative to anticipated conditions (Cohen's d: from -0.06 to -0.04). It is noteworthy that data collection is ongoing for this study, highlighting the preliminary nature of the findings reported here.

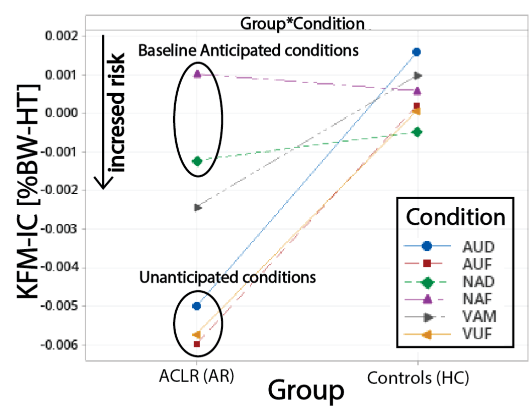

Figure 1: Interaction plot of KFM-IC, Group and Condition

Significance: The study results suggest that individuals with ACL reconstruction exhibit riskier knee mechanics than healthy controls during jump landing movements that included various additional constraints. This finding is consistent with previous research, highlighting the need for effective rehabilitation to improve knee mechanics and reduce the risk of further ACL injuries. However, further research is needed to confirm these preliminary findings, as data collection is ongoing.

Acknowledgements: This research was supported by the NIH award R03HD101093. We would also like to thank Patrick Fischer, Kaylan Wait, and Brendan Silvia for their help and physical therapy and orthopaedic clinics in Bozeman for their recruitment support.

References: [1] Wiggins et al. (2016) *Am J Sports Med* 44(7): 1861–1876, [2] Bertozzi et. al. (2023) *Sports Health*, [3] Vargas et al. (2023) *IJSPT* 18(1): 122-131, [4] Monfort et. al. (2019) *Am J Sports Med* 47(6):1488–1495, [5] Fischer et al. (2021) *J Applied Biomech* 37(4), [6] Paterno et al. (2010) *AJSM* 38(10)

RELATIONSHIPS BETWEEN PATIENT-REPORTED OUTCOMES AND BIOMECHANICAL PREDICTORS OF SECOND ACL INJURIES DURING UNANTICIPATED JUMP LANDINGS

Scott M. Monfort[1*], Fatemeh Aflatounian[1], Ezekiel Barden[1], Patrick D. Fischer[1,2], James N. Becker[1], Keith A. Hutchison[1], Janet E. Simon[3], Dustin R. Grooms[3]

[1]Montana State University; Bozeman, MT; [2]Shriners Children's Northern California; Sacramento, CA; [3]Ohio University; Athens, OH

*Corresponding author's email: scott.monfort@montana.edu

Introduction: Lack of psychological readiness following anterior cruciate ligament reconstruction (ACLR) is associated with increased risk of a second ACL injury [1-2]. However, relationships between patient-reported outcome measures (PROMs) and ACL loading mechanics have been mixed [3-5]. The inability to robustly link PROMs to injury-relevant biomechanics could be due in part to the biomechanical assessments not incorporating reactive and external visual demands that are prevalent in sport and ACL injury scenarios [6]. The additional cognitive demands of these scenarios may exacerbate neuromuscular impairments and generate a robust and reliable movement biomarker of fear following ACLR. Therefore, the purpose of this study was to characterize relationships between PROMs and dual-task interference for biomechanical predictors of second ACL injuries during jump landings that involved rapid decision making (i.e., unanticipated). We hypothesized that worse scores on PROMs would be associated with greater cognitive-motor interference for biomechanical predictors of second ACL injury.

Methods: Thirty-six persons (26F/10M, 19.8±1.8 years; 1.71±0.1 m; 69.6±12.8 kg, 1.5±0.6 years post ACLR; Tegner: 6.8±1.8) who completed rehabilitation from a primary ACLR participated. PROMs of ACL-Return to Sport after Injury (ACL-RSI), Knee injury and Osteoarthritis Outcome Score (KOOS) Pain, and the Forgotten Joint Score-12 Knee (FJS-12) were selected to assay psychological readiness, pain, and joint awareness related to knee (dys)function, respectively. Lower scores on the PROMs indicate worse outcomes. 3D kinematics and ground reaction forces were collected as participants performed jump landing tasks [7] under conditions with anticipated and unanticipated secondary jump directions. Unanticipated conditions were introduced through three approaches: visual (arrow) and auditory (verbal audio clip; with and without constraining visual gaze away from the landing area). Biomechanics of the initial landing from the box for trials with a straight up secondary jump direction were selected for analysis. Biomechanical predictors of second ACL injury were selected as dependent variables of interest [8]. These variables were: 1) uninvolved hip internal/external rotator impulse within the first 10% of stance (**Uni-HRot_Imp**), 2) asymmetry of knee flexor/extensor moment at initial contact (**KFM_Asym**), and 3) range of knee abduction angle for the involved limb (**Inv-KAbA_range**) [8]. Larger **Uni-HRot_Imp** (less external rotator moment) and **Inv-KAbA_range** (more frontal plane motion) values and smaller **KFM_Asym** values (relatively more uninvolved knee extensor moment) were interpreted as 'riskier' [8]. The dual-task change for each of the three unanticipated conditions (DTC: unanticipated – anticipated) for these variables were used to characterize the relationships of PROMs to cognitive-motor function. Regression models tested for relationships between DTC in second ACL injury predictors and PROMs, with predictors of 'Condition' and relevant covariates also included in the models. Significance was set at α=0.016 to control for the three dependent variables (0.05/3).

Results & Discussion: After controlling for age, gender, mass, and time since surgery, several significant relationships were identified (**Table 1**). ACL-RSI, KOOS-Pain, and FJS-12 each associated with DTC in the biomechanical variables; however, the direction of the relationships varied. ACL-RSI and KOOS-Pain scores had expected relationships (worse PROM → riskier DTC) with **Inv-KAbA_range** and **KFM_Asym,** respectively. However, ACL-RSI (**Uni-HRot_Imp, KFM_Asym**) and FJS-12 (**KFM_Asym**) also had significant relationships with DTC in the opposite direction (worse PROM → less DTC). Interestingly, a follow-up analysis indicated that DTC were generally inversely correlated with the baseline biomechanical variable estimates (riskier single-task biomechanics → less DTC) for **Uni-HRot_Imp** and **KFM_Asym**. The collective results are consistent with higher functioning participants (better PROMs) displaying desirable biomechanics during single-task conditions, but then also demonstrating the greatest risk-associated DTC in unanticipated scenarios. In contrast, lower functioning participants struggled to mitigate risky biomechanics during single-task conditions and maintained similar biomechanics (less DTC) with additional challenge. 'Condition' did not reach significance.

Table 1. Outcomes of regression analyses. Standardized coefficients with p-values are presented for each PROM.

Dual-Task Change	β_{std} ACL-RSI	β_{std} KOOS-Pain	β_{std} FJS-12	Model Summary
Uni-HRot_Imp [Nm-s/kg]	**$1.4*10^{-3}$ (p<0.001)**	$0.7*10^{-3}$ (p=0.043)	$0.5*10^{-3}$ (p=0.16)	R^2_{adj} = 31% (p < 0.001)
KFM_Asym [%BW-HT]	**$-3.9*10^{-1}$ (p=0.001)**	**$3.1*10^{-1}$ (p=0.010)**	**$-3.7*10^{-1}$ (p=0.002)**	R^2_{adj} = 21% (p < 0.001)
Inv-KAbA_range [°]	**-0.94 (p<0.001)**	0.25 (p=0.291)	-0.48 (p=0.041)	R^2_{adj} = 12% (p = 0.01)

Significance: ACLR patients with apparent high functional ability and normalized PROMs demonstrated higher injury risk mechanics with the additional of an unanticipated cognitive challenge. These findings may indicate value to include cognitive-motor challenges in ACLR RTS assessments, which are currently absent in common RTS criteria.

Acknowledgements: This research was supported by NIH award R03HD101093. We would also like to thank Kaylan Wait and Brendan Silvia for their help and physical therapy and orthopedic clinics in Bozeman for their recruitment support.

References: [1] Paterno et al. (2018) *Sport Health* 10(3), [2] McPherson et al. (2019) *AJSM* 47(5), [3] Baez et al. (2023) *MSSE* 55(3), [4] Dudley et al. (2022) *Phys Ther Sport* 56, [5] Trigsted et al. (2018) *Knee Surg, Sports Traum, Arthro* 26, [6] Vargas et al. (2023) *IJSPT* 18(1), [7] Fischer et al. (2021) *J Applied Biomech* 37(4), [8] Paterno et al. (2010) *AJSM* 38(10).

OLDER ADULTS USE A MORE CAUTIOUS STRATEGY TO NAVIGATE TURNS WHILE WALKING

Kevin Lima[1], Andrew D. Shelton[1], Jessica L. Allen[2], Vicki S. Mercer[3], and Jason R. Franz[1]*
[1]Biomedical Engineering, UNC Chapel Hill & NC State University, Chapel Hill, NC, USA [2]Mechanical and Aerospace Engineering, University of Florida, Gainesville, FL, USA [3]Physical Therapy, UNC Chapel Hill, Chapel Hill, NC, USA
E-mail: jrfranz@email.unc.edu

Introduction: Falls among older adults are a highly prevalent health risk with potential for severe consequences. Falls occur most frequently during locomotor activities such as walking. However, there are many locomotor activities performed each day with a higher risk for falls than walking along a straight path – a task that dominates our studies of age-related instability. As a pivotal example, the quality of turning mobility can distinguish recurrent older adult fallers from non-fallers [1]. The figure-8 walk test (F8W) is a clinically-feasible activity that focuses exclusively on turning mobility [3] and involves different cognitive processes compared to straight-path walking [4]. Previous work has shown that the time taken to complete the F8W correlates with outcomes such walking speed, physical function, and walking confidence among older adults. Despite the clinical relevance of these discoveries, aging-effects on turning mobility remain understudied and thus poorly understood. The goal of this project was to investigate the effects of age (older versus younger adults) on key metrics of performance during the F8W. As a particularly novel contribution, we specifically aimed to quantify age-related differences in the "smoothness" of turning mobility, quantified herein using jerk – the first time derivative of acceleration. We hypothesized that older adults would complete the F8W with longer path lengths and slower speeds but with increased jerk and thus lesser smoothness than younger adults.

Methods: 33 younger adults (22.6 ± 3.5 yrs, 18F) and 34 older adults (72.6 ± 6.1 yrs, 18F) completed 5 repetitions of the F8W. The F8W involves completing a figure 8 pattern defined by two cones set 5 feet apart. For each repetition, participants started and ended from a standing position at the center of the figure 8 (Fig. 1A). Subjects wore 36 motion capture markers on their trunk, pelvis, legs, and feet. For our analyses, we used only the sacrum marker. Specifically, we used the sacrum marker trajectory to calculate: (*i*) total path length, (*ii*) the length along the major, longitudinal axis, (*iii*) the width along the minor, transverse axis, and (*iv*) jerk, calculated as the time derivative of sacrum acceleration and reported as a vector magnitude using the non-vertical components [2]. For jerk, we analyzed the absolute maximum and minimum values and the trial average. We compared outcomes between younger and older adults using independent samples t-tests and an alpha of 0.05.

Results and discussion: As hypothesized, older adults walked further, on average, by 8.3% than younger adults when completing the F8W ($p<0.038$) (Fig. 1). We found that this longer total path length in older adults was the result of their taking a ~14% wider path ($p=0.01$) rather than any difference along the major, longitudinal axis ($p=0.06$) compared to younger adults. However, contrary to our hypothesis, we found that older adults walked with 13.4% less average and 14.6% less peak jerk than younger adults ($p < 0.05$) (Fig. 1B). Jerk is a hallmark biomechanical outcome used to describe the smoothness of gait. We originally anticipated that older adults would complete the F8W with higher average and peak jerk than younger adults, which we would have interpreted in the context of more erratic kinematics indicative of instability during turning. This unanticipated result is equally informative. The F8W test requires complex coordination and at least some additional cognitive processing, and observed behavior is determined not only by sensorimotor integrity and the automatic neural signals central to locomotion, but also by neuropsychological aspects of cognition, perception, and self-efficacy. In other words, participants have a capacity for choice that may be less obvious or relevant during straight-line walking.

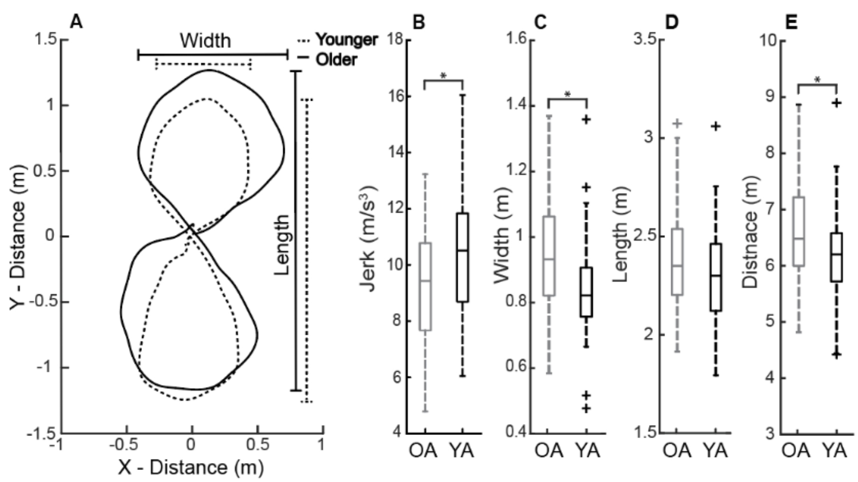

Figure 1: (A) Representative subject completing the F8W. (B-E) Differences in performance metrics between older and younger adults. Asterisks (*) indicate significant difference ($p<0.05$)

Significance: Older adults use a more cautious strategy than younger adults when completing a figure-8 walking task. The consistency with which older adults take this smoother and wider approach is evidence for neuropsychological differences in turning mobility that warrants further investigation.

Acknowledgements: Supported by NIH 1R21AG067388.

References: [1] Mancini M., et al. (2016) *J of Gerontology*, **71** p. 1102-8 [2] Balasubramanian S., et al. (2015) *J of NeuroEngineering and Rehabilitation*, **12** [3] Rebecca J. Hess, et al. (2010) *Physical Therapy*, **90** p. 89-99 [4] Kristin A. Lowry, et al. (2012) *Archives of Physical Medicine and Rehabilitation*, **93** p. 802-807

THE EFFECT OF DIFFERENT COMBINATIONS OF PASSIVE-MECHANICAL PROSTHETIC KNEE AND ANKLE-FOOT COMPONENTS ON GAIT SAFETY IN TRANSFEMORAL PROSTHESIS USERS

Miguel Vaca[1,2*], Rebecca Stine[2], Matthew J. Major[1,2], Steven A. Gard[1,2]
[1]Northwestern University, Chicago, IL; [2]Jesse Brown VA Medical Center, Chicago IL
*Corresponding author's email: miguelvm@u.northwestern.edu

Introduction: There is strong evidence to suggest that persons with lower limb loss experience a high prevalence of falls and fall-related injuries [1]. Furthermore, previous studies have identified that the majority of falls in transfemoral prosthesis users (TFPUs) occur while walking [2]. To facilitate gait safety during walking, motor control of the legs must achieve certain objectives during the two phases of gait: 1) prevent buckling while weight-bearing during stance [3] and 2) avoid limb collision with the ground during swing [4]. TFPUs must rely on their intact hip and leg prosthesis comprised of a prosthetic knee and ankle-foot mechanism. Several studies have examined the individual effect of prosthetic knees and feet on gait safety, however there is a gap in knowledge about the interaction and combined effects of this componentry. The current study examined the effects of commonly prescribed prosthetic knee and ankle-foot components on factors of gait safety in TFPUs to help inform prescription guidelines and hence contribute to evidence-based practice.

Methods: This study was approved by the Jesse Brown VA Medical Center Institutional Review Board. Three TFPUs (1 female, 29-36 years old, 68.28±39.24 kg; 1.69±.15 m) completed four testing sessions. During each session, the participants were randomly fitted with one of the four different combinations of prosthetic knee and ankle foot components (Fig. 1). Following accommodation, participants performed three tasks: 1) walking at level ground along 10-meter walkway; 2) walking on an incline surface; 3) walking on a decline surface. The tasks were repeated until five clean foot strikes on a force plate (or isolated pedestal mounted to a force plate in the case of ramp walking) were recorded for both limbs. Reflective markers were positioned on anatomical landmarks of the arms, legs, and pelvis according to a modified Helen Hayes set to define a 12-segment body model. Kinematic data were collected using a 12-camera motion capture system (Motion Analysis Corp., Santa Rosa, CA) and kinetic data were acquired using six floor-embedded force plates (AMTI, Watertown, MA). Gait data were processed using CORTEX and analyzed using Visual 3D (C-Motion, Germantown, MD) and custom software in MATLAB (Mathworks, Natick, MA).

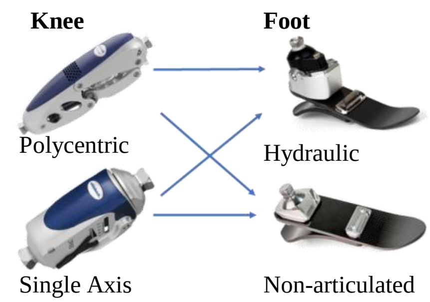

Figure 1: Knee-foot combinations tested:
1) Polycentric Knee - Hydraulic Foot;
2) Polycentric Knee - Non-articulated Foot;
3) Single-axis Knee - Hydraulic Foot;
4) Single-axis Knee - Non-articulated Foot.

Results & Discussion: The results for level walking are displayed in Figure 2, along with outcome definitions. KMAI and PSKM are related to gait safety during stance phase, while TKSE, TC, and HC are related to gait safety during swing phase. These results suggest that gait safety is improved (i.e., more negative KMAI, smaller PSKM, later TKSE and increased TC) for the two prosthetic setups including the polycentric knee. However, the results are more nuanced when considering the knee-foot combination. Contrary to our expectations, the characteristics of the polycentric knee and hydraulic foot were not necessarily additive for improving gait safety across all the variables. For PSKM, TKSI and TC, the second combination appeared to offer the most advantages. Additionally, the results suggest a similar effect of combination 1 and 4 on PSKM. These preliminary results might also suggest the possibility of functionally equivalent combinations of prosthetic knees and feet, which may be related to user compensatory mechanisms and requires further investigation. Data collection on additional participants is ongoing.

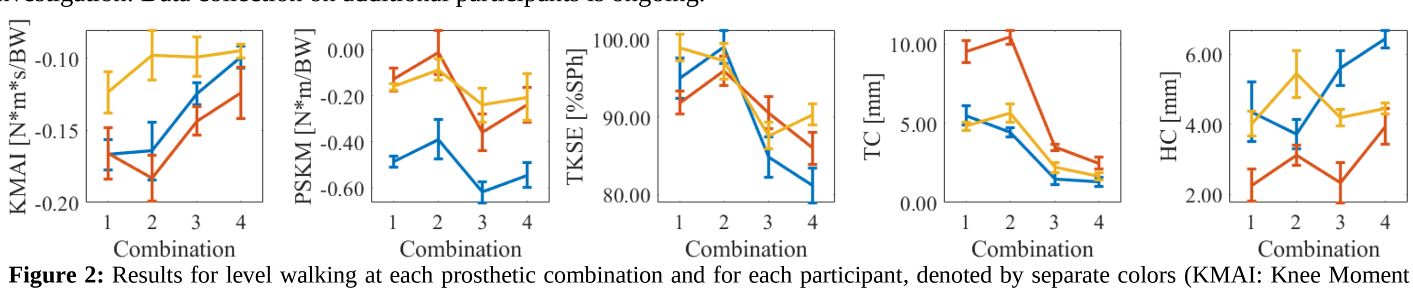

Figure 2: Results for level walking at each prosthetic combination and for each participant, denoted by separate colors (KMAI: Knee Moment Angular Impulse, PSKM: Pre-swing Knee Moment, TKSE: Timing of Terminal Knee Swing Extension, TC: Toe clearance, HC: Heel Clearance).

Significance: This study examined the effects of different combinations of two primary, commonly prescribed designs of prosthetic knees and feet on TFPU gait safety. These results contribute to the body of knowledge on prosthetic design effects to inform evidence-based practice and improve our understanding of the motor response of persons with transfemoral limb loss to changes in prosthetic design, which has important implications for design and control of transfemoral prostheses to facilitate gait safety and minimize falls.

Acknowledgements: This study was supported by the Department of Defense (grant no. W81XWH1910447).

References: [1] Wong et al. (2016), *J Rehabil Med* 48(1); [2] Kim et al. (2001), *PM&R* 11(4); [3] Hisano et al. (2020), *Gait & Posture* 77; [4] Rosenblatt et al. (2017), *Prosthet Orthot Int* 41(4).

INCREASED HAMSTRING STRETCH AND STRETCH RATE IN ACCELERATIVE VS CONSTANT SPEED RUNNING

Reed D. Gurchiek[1*], Zachary Teplin[1], Jennifer Hicks[1], Scott Delp[1]
[1]Department of Bioengineering, Stanford University
*Corresponding author's email: gurchiek@stanford.edu

Introduction: Hamstring strain injuries are a major time-loss injury for many athletes [1, 2] with high re-injury rates [3] and increasing incidence [4]. Understanding injury mechanisms will help identify athletes at risk and design interventions. It was recently shown that hamstring injuries often occur when athletes are accelerating and not necessarily at high speeds [5]. However, investigations of hamstring mechanics during running have been mostly limited to constant speeds on a treadmill. We aimed to compare hamstring kinematics during accelerative running to running at a constant speed.

Methods: Three iPhones were used to record videos of eight participants (4 women, 4 men) running overground on an outdoor running surface. They performed six constant speed running trials, each at a different speed. They also performed six accelerative running trials, called flying sprints, wherein the participant begins running at a constant speed and, when given a verbal cue, accelerates forward as fast as possible. The constant speeds that preceded the six accelerations were the same as those in the six constant speed running trials. Video recording, synchronization, and processing as well as the scaling and kinematic analysis of a three-dimensional musculoskeletal model was performed in OpenCap [6]. We isolated individual steps from each trial and characterized the peak length and average lengthening velocity in late swing of the biceps femoris (long head) muscle-tendon unit (MTU). To compare between the two conditions, we used a linear regression with step-average running speed (normalized by the subject-specific maximum observed running speed across all trials) as the independent variable.

Results & Discussion: We observed peak MTU lengths (normalized by the length in neutral pose) during constant speed running at 80-100% of top speed (mean ± s.d. = 1.089 ± 0.026) that were comparable with observations from treadmill running [7] (1.098 ± 0.026 and 1.098 ± 0.028 at 80% and 100% of top speed, respectively). Data for speeds less than 80% of top speed were not reported in [7]. While biceps femoris peak MTU lengths were not significantly different at top speeds ($p=0.23$ for the linear model intercept), the accelerative condition resulted in greater peak lengths at lower running speeds ($p<0.01$ for the linear model slope). We found similar results for the lengthening velocities ($p=0.51$ for the intercept; $p<0.01$ for the slope). For example, the lengthening velocities in the accelerative condition at 50% top speed were the same as the constant speed condition at 75%.

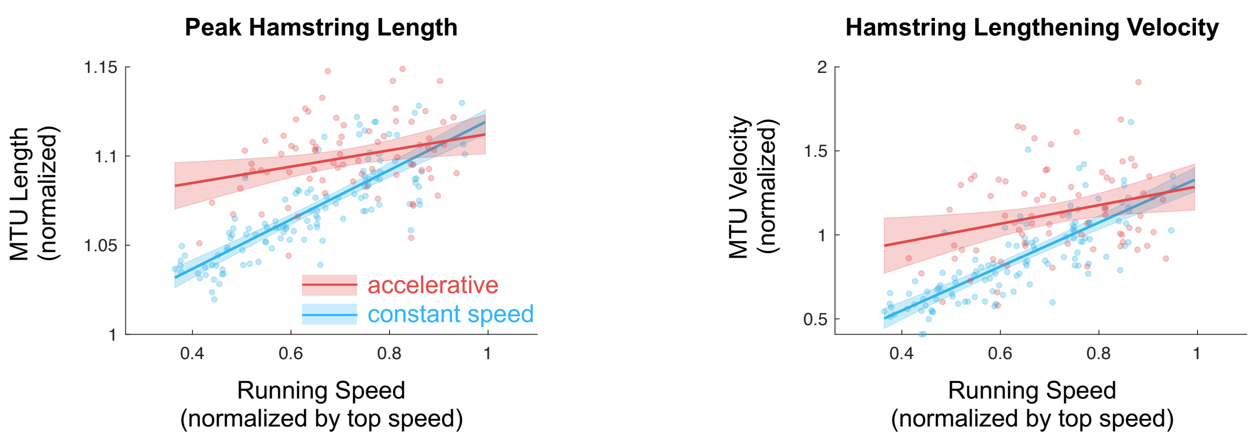

Figure 1: Peak biceps femoris MTU length (left) and lengthening velocity (right) vs. normalized running speed during both accelerative (red dots) and constant speed (blue dots) running. MTU lengths and velocities were normalized by the length in neutral pose (thus MTU length data are unitless and MTU velocity data are in units s^{-1}: normalized lengths per second). Each data point represents a single step. Solid lines depict linear regression lines, and the shaded area illustrates the 95% confidence intervals.

Significance: Our results provide a biomechanical explanation for the recent observation that hamstring strain injuries often occur during accelerative running [5]. They also suggest that metrics used to monitor athletes and their exposure to high-risk circumstance (long lengths, fast lengthening velocities) in practices and games (e.g., using GPS) should incorporate both running speed and acceleration.

Acknowledgements: This work was supported by the Wu Tsai Human Performance Alliance at Stanford University and the Joe and Clara Tsai Foundation.

References: [1] Ekstrand et al. (2011), *Br J Sports Med* 45:553-8; [2] Edouard et al. (2016), *Br J Sports Med* 50:619-30; [3] de Visser et al. (2012), *Br J Sports Med* 46:124-30; [4] Ekstrand et al. (2022), *Br J Sports Med* doi:10.1136/bjsports-2021-105407; [5] Kerin et al. (2021), *Br J Sports Med* 56:608-15; [6] Uhlrich et al. (2022), *bioRxiv* doi:10.1101/2022.07.07.499061; [7] Thelen et al. (2005), *Med Sci Sports Exerc* 37(1):108-14

KINEMATIC ANALYSIS OF LIVE OCTOPUS: APPLICATION TO SOFT ROBOTICS AND HUMAN BIOMECHANICS

Garrett S. Weidig[1], Brittany Bush[1], Fermin Jimenez[1], Galit Pelled, PhD[1], Tamara Reid Bush, PhD[1],
[1]Department of Mechanical Engineering, Michigan State University, East Lansing, MI, USA
*Corresponding author's email: reidtama@msu.edu

Introduction: Octopus arms and their unique flexibility have inspired the design of certain soft robots [1]. These soft robots were often flexible grippers capable of manipulating objects, whether that be in a surgical suite or on an assembly line [2]. Many soft robotic devices modeled after the octopus could only bend in one direction, even though the animal they emulated was capable of much more complex movements. Previous work quantified octopus arm movements, particularly bending and twisting, because those movements had the greatest effect on the overall posture [3]. However, researchers focused on movements that were kinematically simpler, and thus, so were their definitions. Curvature calculations were used to measure the magnitude of the bend that was occurring in the direction of the suckers [3]. Twist was used to quantify the amount of torsion in the arm, responsible for changing the plane on which curvature was occurring [3]. However, these definitions were not sufficient for quantifying the arm in more complex postures, such as bending in multiple directions (not just toward the suckers). There is a need for movement calculations that capture the full kinematic abilities of octopus arms and the devices they inspire in order to influence more complex soft robot movements. Thus, the goals of this work were to 1) create and 2) test new movement definitions using data from a live, swimming octopus to fully quantify the arm posture in three dimensions. Additionally, a previous method for reporting twist was used as a comparison.

Methods: A four-camera underwater motion capture system was used to collect 3D movement data on five markers attached to the arm of a live octopus, species *Octopus bimaculoides*. Data were collected at a sampling rate of 150 Hz and for as long as all five markers remained on the octopus' arm. For analysis, the arm was segmented into proximal and distal parts. Each segment consisted of three markers and the two segments shared the middle marker. The overall posture was characterized by the magnitude of bending (defined as an angle of curvature) and the direction of bending (defined either by twist or planar orientation). Twist (Fig 1b.), which was reported in the literature, was calculated as the angle between the two normal vectors associated with the proximal and distal segments and reported as θ. Planar orientation (Fig 1a.) was calculated by creating two, independent local coordinate systems on the proximal and distal segments and measuring the three kinematic angle differences that separated them (α, β, and γ, also known as flexion/extension, abduction/adduction, and internal/external rotation). Thus, perfectly planar movements (e.g., only bending toward the suckers) would result in non-zero values for α, but exactly zero for θ, β, and γ. Whereas more complex movements like bending in multiple directions or twisting would result in non-zero values for all outcome measures.

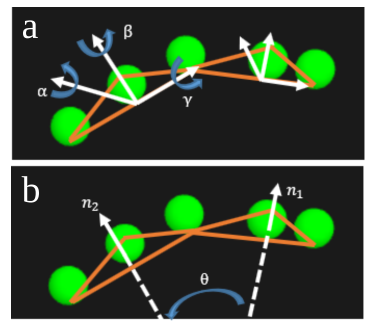

Figure 1: Markers on swimming octopus arm. (a) Planar orientation (α, β, and γ) determined by local coordinate systems created on the proximal and distal segments. (b) Twist (θ) determined by the angle between normal vectors on the proximal and distal segments.

Results & Discussion: During swimming, sections of arm movement were analysed, one where the arm appeared to exist on one plane (simple bend) and one where the arm demonstrated a complex set of motions (complex bend). The direction of the curvature for the distal segment relative to the proximal were represented by the novel method (α, β, and γ) and the twist method from the literature (θ). Relative to the simple bending posture, values for β, γ, and θ were larger in the complex bending posture (Table 1). This meant the movement was not planar and that twisting or bending in multiple directions occurred. This data point emphasized that it is not possible to quantify the overall posture of the octopus arm using only the magnitude of the curvature and angle of twist. Instead, it is necessary to describe the magnitude of the bending on each segment and exactly how the planes are oriented in 3D space, especially in instances of complex postures. It is important to note that even when the arm seemed to be all on one plane (as it was in the simple bending posture), there were still non-zero values for β, γ, and θ meaning that the full planar orientation analysis was required, instead of just curvature and twist. Additionally, the methods used for α, β, and γ are directly relatable to 3D human biomechanics, whose definitions will be necessary for soft robots in human settings.

Table 1: Analysis for complex and simple bending postures that occurred during swimming. Shaded columns provide data for new approach, which provides details on α, β, and γ, while the standard single angle approach of θ provides much less information. The new planar orientation method is necessary to fully define the complex nature of these arm movements.

Posture	Prox. Curve	Dist. Curve	α (°)	β (°)	γ (°)	θ (°)
Simple Bend	19.4	2.1	32.4	-9.9	-8.8	18.2
Complex Bend	8.3	35.0	20.9	17.6	-74.9	72.3

Significance: Because soft robots have taken inspiration from octopus arm movements, it was crucial that complex postures be measured and communicated in 3D space. Whether it be a live octopus, an octopus inspired upper extremity prosthesis, or a human performing a common task, perfectly planar movements are rarely seen. As the soft robotic field grows and the use of complex postures becomes more practical, previous methods are less applicable. Now, there is an effective way of understanding the overall posture in 3D space.

Acknowledgements: This work was supported by NIH grant UF1NS115817 and is under IACUC# PROTO201800092.

References: [1] She et al. (2016), *Soft Robotics* 3(2); [2] Rateni et al. (2015), *Meccania* 50; [3] Zelman et al. (2013), *Front. Comput. Neurosci.* 7(60)

OPTIMIZING EXOSKELETON ASSISTANCE TO IMPROVE WALKING SPEED AND ENERGY ECONOMY FOR OLDER ADULTS

Ava Lakmazaheri[1,*,†], Seungmoon Song[1,2,*], Brian B. Vuong[1], Blake Biskner[1], Deborah M. Kado[3,4], and Steven H. Collins[1]

[1] Department of Mechanical Engineering, Stanford University, Stanford, CA, USA. [2] Department of Mechanical and Industrial Engineering, Northeastern University, Boston, MA, USA. [3] Geriatrics Research Education and Clinical Center, Veterans Affairs, Palo Alto, CA, USA. [4] Department of Medicine, Stanford University, Stanford, CA, USA.

[*] These authors contributed equally to this work.

[†] Corresponding author's email: avalak@stanford.edu

Introduction: Forty percent of Americans aged 65 and older report mobility challenges [1], marked by declines in gait speed and energy economy. Lower-limb exoskeletons have demonstrated potential to improve either measure, but primarily in studies with healthy younger adults [2-4]. Promising techniques like optimization of exoskeleton assistance may provide the greatest benefits in walking performance but have yet to be tested with older populations. Multi-objective exoskeleton optimization is another critical step: speed and energy consumption have yet to be simultaneously targeted for any population. The primary objectives of our study were to: (1) assess the extent to which trained older adults can garner speed and energy benefits from ankle exoskeleton assistance and (2) extend human-in-the-loop optimization [4] to target both self-selected walking speed and metabolic energy consumption in a multi-objective paradigm. We also aimed to characterize older adults' adaptation to exoskeleton use and gain initial insights into the effects of aging on response to exoskeleton assistance.

Methods: We investigated the effectiveness of human-in-the-loop optimization [4] of ankle exoskeletons in ten older adults, aged 65 and older (5 females; mean age: 72 ± 3 years). Participants walked on a self-paced treadmill [5] wearing an indirect calorimetry device and ankle exoskeleton emulators [6] that provided an assistive plantarflexion torque once per step. Participants were instructed to walk at a comfortable speed during testing. A human-in-the-loop optimizer varied torque profiles every two minutes in search of parameters that maximized the user's self-selected walking speed and minimized the user's metabolic rate according to a multi-objective cost function. After four hours of training and optimization, a validation session was conducted to compare self-selected speed, metabolic rate, metabolic cost of transport, optimized exoskeleton mechanics, and spatiotemporal gait parameters between unassisted and assisted walking conditions.

Results & Discussion: Optimized exoskeleton assistance improved walking performance for older adults. On average, participants experienced an 8% (0.10 m/s, p = 0.001) increase in self-selected walking speed, a 19% (0.68 W/kg, p = 0.007) decrease in metabolic rate, and a 25% (0.71 J/kg/m, $p = 7.5e{-4}$) decrease in metabolic cost of transport due to optimized ankle plantarflexion assistance (Fig. 1). These speed and energy benefits are clinically meaningful [7,8] and show that human-in-the-loop optimization can effectively target multiple aspects of walking performance.

Optimized exoskeleton parameters varied between participants (peak of 0.54 ± 0.10 Nm/kg at $52.3 \pm 1.1\%$ stride, rise time of $27.3 \pm 7.0\%$, and fall time of $10.4 \pm 2.6\%$), indicating the importance of personalizing assistance. Step frequency and peak plantarflexion angle increased with assistance, while other gait features were unchanged, suggesting that benefiting from exoskeleton assistance did not require many changes that could compromise older adults' comfort and stability. Older adults' optimal exoskeleton parameters and biomechanical responses to assistance appeared distinct from those previously established for younger adults [2,3]; smaller and lighter-weight exoskeletons may be more appropriate for older adults.

Participants adopted an improved motor control strategy with training but did not fully adapt to walking with exoskeletons within the study duration. Both age and self-paced treadmill use appeared to slow motor adaptation, motivating targeted familiarization and training protocols for older exoskeleton users.

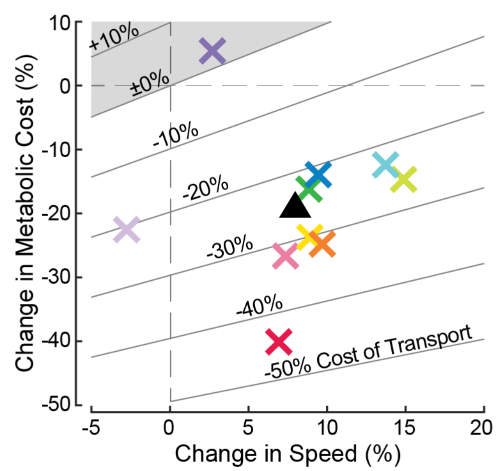

Figure 1. Changes in self-selected walking speed, metabolic cost, and metabolic cost of transport with exoskeleton assistance. Participants plotted in unique colors and mean plotted in black.

Significance: Our results demonstrate that (1) exoskeletons can provide clinically meaningful improvements in walking performance for older adults and (2) multiple objectives can be simultaneously addressed through human-in-the-loop optimization. Our findings point to the potential of portable, commercial exoskeletons that enable older adults to walk comfortably at faster speeds with reduced energy consumption, helping them navigate everyday environments with increased ease, independence, and satisfaction.

Acknowledgements: This work was supported by the National Science Foundation (1828993 and DGE-1656518), the National Institutes of Health (R00AG065524), and the Stanford Institute for Human-Centered Artificial Intelligence (203112).

References: [1] HHS (2022), "2021 Profile of Older Americans"; [2] Poggensee & Collins (2021), *Sci Robot* 6(58); [3] Song & Collins (2021), *IEEE TNSRE* 29; [4] Zhang et al. (2017), *Science* 356(6344); [5] Song et al. (2020), *JNER* 17(68); [6] Witte & Collins (2020), *Wearable Robotics*; [7] Perera et al. (2006), *J Am Geriatr Soc* 54(5); [8] Darter et al. (2013), *Res Q Exerc Sport* 84(2).

SURFACE, BUT NOT AGE IMPACT LOWER LIMB JOINT WORK DURING WALK AND STAIR ASCENT

Wenzel, TA[1], Hunt, NL[1], Holcomb, AE[2], Fitzpatrick, CK[2], Brown, TN[1]
[1]Department of Kinesiology, Boise State University, Boise, ID, USA
[2]Department of Mechanical and Biomedical Engineering, Boise State University, Boise, ID, USA
email: thomaswenzel@u.boisestate.edu

Introduction: Older adults (> 65 years) often fall when navigating a slick or uneven challenging surface [1]. During common locomotor activates, such as walk or stair negotiation, older adults exhibit unfavorable lower limb biomechanical changes, including diminished joint torque and power, and proximal mechanical work redistribution that may increase their fall risk [2,3]. Yet, it is currently unknown whether traversing a challenging slick or uneven surface exacerbates older adults' unfavorable lower limb work and power changes. We hypothesize that older adults will produce less limb and joint work, but greater work contribution from proximal joints than younger adults to walk and ascend stairs, while all participants (young and older) will increase proximal joint work contribution when navigating a challenging surface during the walk and stair ascent.

Methods: Twelve young (18 to 25 years) and 12 older (> 65 years) adults performed a walk and stair ascent task on a normal, slick, and uneven surface. The slick surface consisted of a wood panel covered by a smooth, plastic material fixed atop of the force platform or stairs, while the uneven surface consisted of a wood panel composed of nine painted wooden blocks of differing heights fixed atop the force platform or stairs.

For each walk and stair ascent trial, synchronous 3D marker trajectories and GRF data were collected using ten high-speed optical cameras (240 Hz, Vantage, Vicon Motion Systems LTD, Oxford, UK) and a single force platform (2400 Hz, OR6, AMTI, Watertown, MA). For each trial, the marker and GRF data were lowpass filtered (12 Hz, 4th order Butterworth), and processed in Visual 3D (C-Motion, Rockville, MD) to obtain lower limb sagittal plane joint power. Then, limb, and hip, knee and ankle positive mechanical work and each joint's percent of contribution to total limb work (joint work divided by limb work and multiplied by 100) were determined.

Stance phase positive limb and joint work, and relative joint work were submitted to statistical analysis. Two-way mixed model ANOVAs tested main effects and interaction between age (young and older adults) and task (walk and stair ascent), age and surface (normal, slick, and uneven) for each task. Alpha level was < 0.05.

Results & Discussion: Ascending the stairs required greater positive limb, and hip, knee, and ankle work than walking (all: $p < 0.001$; Fig. 1). Participants increased hip contribution 37% to total positive work at the hip during the walk ($p < 0.001$), which shows that in a basic movement like walking, individuals rely on the hip to be the primary mover and stabilizer. Knee contribution increased 48% during the stair ascent ($p < 0.001$). This increased work contribution by the knee musculature to lift the center of mass up during the ascent task may accelerate muscular fatigue and increase likelihood of a fall, particularly for the older adults.

In partial agreement with our hypotheses, surface, but surprisingly not age, impacted positive limb work. When walking over a challenging surface, limb ($p < 0.001$), hip ($p = 0.010$), and knee ($p < 0.001$) positive work increased. Specifically, limb and knee work increased on the uneven, and hip work increased on the uneven and slick surfaces. Hip ($p = 0.015$), knee ($p < 0.001$), and ankle ($p = 0.010$) work increased when navigating the challenging surfaces during the stair ascent. Hip and ankle work were greater on the slick surface, while knee work increased when ascending stairs with an uneven surface. The instability of the challenging surfaces may require greater contribution from large hip and knee musculature to maintain stability, and forward or vertical propulsion (Fig. 1.). In fact, navigating the challenging surfaces lead to approximate 9% and 4% decrease in percent ankle contribution to total work during the walk and stair ascent; but an approximate 4% increase in hip during walk and a 6% increase in knee contribution during the stair ascent and both tasks.

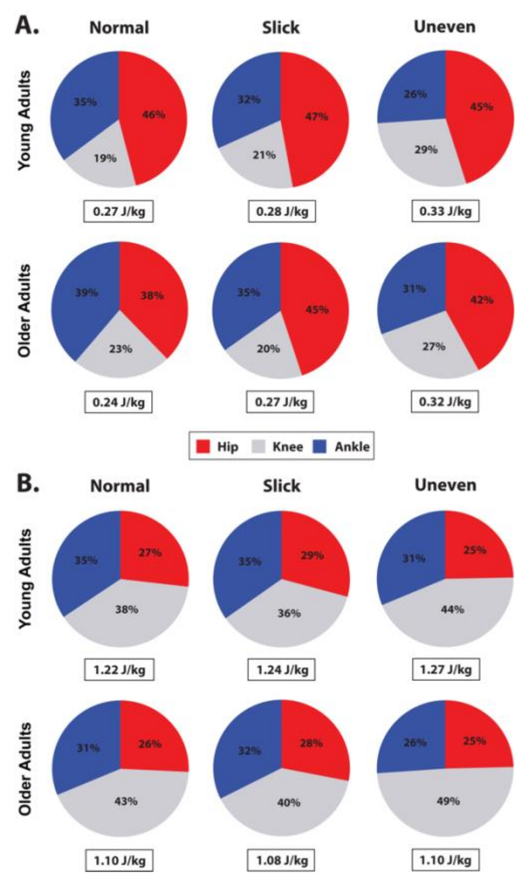

Figure. 1. Limb positive work (J/kg), and hip (red), knee (gray), and ankle (blue) contribution to total limb work for young and older adults during the walk (A) and stair ascent (B) task on each surface.

Significance: With falls being a prominent issue, experimental evidence showing that both young and older adults walk and/or ascend stairs with a challenging surface by redistributing work proximally to the large hip and knee musculature may be a critical step towards development of effective fall prevention programs. The sole difference in power generation between age groups was deficit in the older adult's ankle. Identifying whether an impairment is due to age related differences or stems from functional limitations could be critical for effective treatment in older adults.

Acknowledgements: NIH Institute on Aging (R15AG059655) supported this work.

References: [1] Li. *Am J Public Health* **96**, 2006. [2] DeVita. *J Appl Physiol* **88**, 2000. [3] Franz. *Gait Posture* **39**, 2014.

Young adults accelerate their arms significantly faster than older adults in response to a slip perturbation

Jonathan S. Lee-Confer[1*], Matthew K. Lo[1,2] & Karen L. Troy[3]
[1]Verum Biomechanics, Tucson, Arizona 85716
[2]University of California Irvine, Irvine, California 92697
[3]Worcester Polytechnic Institute, Worcester, Massachusetts 01609
*Corresponding author's email: jonathan@verumbiomech.com

Introduction: Slips and falls are a serious health concern for older adults. Prior work has shown that arm movements reduce falls by 70% in young adults during a slip incident [1]. Furthermore, arm movements are reported to reduce trunk extension velocity during a slip [2]. However, sideways falls can also occur and are linked to severe injuries such as hip fractures [3]. Older adults are reported to delay their reactive arm responses by 60 ms compared to young adults during a slip [4]. Fortunately, reactive-based exercises are shown to improve the response times of older adults [5]. Currently, it is not known whether older adults move their arms as fast as young adults in response to a slip incident. It is possible that they move their arms slower compared to young adults, which would diminish the positive effect of arm movement on balance. Due to older adults experiencing strength deficits over time, we expected that older adults would exhibit significantly slower arm movement responses compared to younger adults when experiencing a slip incident.
t

Methods: We reanalyzed data from a subset of 11 healthy older adults (72.0 ± 5.0 years old) and 11 healthy young adults (25.2 ± 5.9 years old) who participated in previously reported study [2]. Briefly, participants were fitted into a full-body harness attached to a low-friction trolley to prevent falling and injuries during the perturbation. Twenty-three reflective markers placed on anatomical locations were tracked using 8 motion capture cameras. Participants traversed a 12.8 m walkway with a Plexiglas sheet embedded mid-way. Young adults slipped on oil and older adults slipped on a water-soluble lubricant. In this data subset, all younger adults recovered, and all older adults fell after the slip, as determined in previous work [6]. Here, we analyzed the arm contralateral to the slipping foot [7] for both groups. Arm abduction angles were obtained and acceleration was calculated in Matlab. Independent t-tests were conducted between the peak arm acceleration of the older and younger adults with an alpha level set to 0.05.

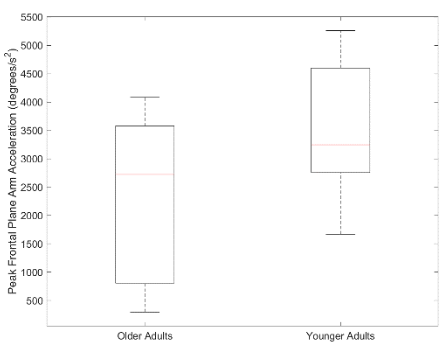

Figure 1. Box plot showing the peak frontal plane arm acceleration between the older adults (n = 11) and younger adults (n = 11)

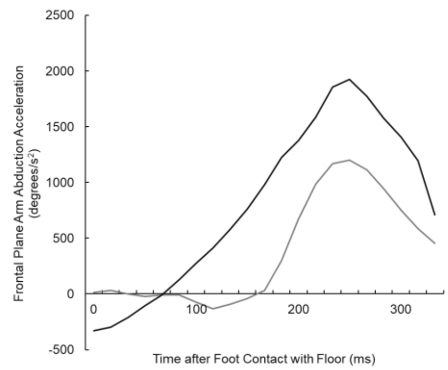

Figure 2. Average arm angular acceleration in the frontal plane between the older adults (gray line, n = 11) and younger adults (black line, n = 11)

Results: 3 of the 11 older adults (27%) and 1 of 11 younger adults (9%) experienced a fall. Young adults' peak arm abduction acceleration was significantly greater than older adults' peak arm abduction acceleration (3593.2 ± 1144.8 vs. 2309.8 ± 1428.5 degrees/s^2, $p = 0.02$). We observed a non-significant delayed response in arm abduction in older adults (197.0 ± 109.0 vs. 131.8 ± 65.6 ms, $p = 0.07$).

Discussion: The results of this study support the hypothesis as older adults' peak arm acceleration was significantly less when compared to younger adults. The results of this study were expected as older adults tend to lose muscle mass as they age, and this would translate to decreases in their ability to produce ballistic movements. Current ACSM guidelines suggest 150 minutes of moderate-intensity aerobic exercise and 2x/week of strength training of major muscle groups for older adults [8]. However, it is unknown whether exercise protocols that target ballistic movements using the deltoids to produce abduction may be beneficial for regaining balance from a slip. While previous studies [5] have shown that neuromuscular responses may be improved in older adults, future studies could investigate whether strengthening exercises targeting the deltoids can improve muscular performance of responses to a slip perturbation.

Significance: This study opens up the possibility to exploring targeted exercises that may directly improve slip responses. There is no question that whole-body exercises are beneficial, however this study and previous work show that arm abduction may be important for balance during a slip. This work has the potential to influence physical therapy fall prevention protocols to include simple exercises that can provide older adults with more tools to regain balance when necessary during a slip incident.

References: [1] Lee-Confer et al. (2022), *Hum Mov Sci* 86; [2] Troy et al. (2009), *J Biomech* 42(9); [3] Nankaku et al. (2005), *Osteo Int.* 16; [4] Merrill et al. (2017), *J Biomech* 58; [5] Arnold et al. (2022) *Clin Rehab* 36(7); [6] Beschorner et al. (2009) *Ergonomics* 51; [7] Lee-Confer et al. (2022), *J Biomech* 133; [8] ACSM Guidelines for Exercise Testing and Prescription, 11th edition

THE INFLUENCE OF STEP WIDTH ON INDIVIDUAL MUSCLE CONTRIBUTIONS TO FRONTAL-PLANE BALANCE CONTROL

Lindsey K. Molina[1,2]* and Richard R. Neptune[1]
[1]Walker Department of Mechanical Engineering, The University of Texas at Austin, Austin, TX, USA
[2]Exponent, Inc., Phoenix, AZ, USA
*Corresponding author's email: lmolina@exponent.com

Introduction: Clinical populations walk with wider step widths compared to healthy young adults [e.g., 1]. Walking with wider steps has been linked to a higher destabilizing frontal-plane external moment ($\dot{H}$) and greater range of frontal-plane whole-body angular momentum (H) [2], which are indicators of poor balance control [3,4]. Therefore, understanding the effect of walking with wider steps on individual muscle contributions to balance response strategies could provide clinicians with muscular targets for rehabilitation.

The purpose of this study was to investigate the influence of step width on muscle contributions to frontal-plane balance control following lateral surface translation perturbations using musculoskeletal modelling and simulation. We hypothesized that following perturbations at wider steps, there will be increased contributions from the gluteus medius and plantarflexors, which are primary contributors to frontal-plane balance control [5].

Methods: Kinematic and kinetic data collected from 15 healthy young adults (7 male, age: 25 ± 4 years) were used to create the musculoskeletal models and simulations of the walking tasks. Each subject performed two 30-second walking trials on an instrumented treadmill, consisting of steady-state walking at self-selected (SS) and wide (100% wider) step widths. A custom D-flow (Motek, Amsterdam, NL) script determined heel strike timing [6] and projected foot placement targets on the treadmill at the desired step width. During the trials, the treadmill provided lateral 2.5cm surface translations lasting 0.25s to the stance foot midway through stance. A representative gait cycle for each subject and condition was chosen for the simulation analysis using a functional depth method [7].

A total of 30 simulations (15 subjects, 2 conditions: SS and wide steps) were performed in OpenSim 4.4 [8] using a 12-segment musculoskeletal model with 23 degrees-of-freedom and 92 Hill-type musculotendon actuators [9]. A residual reduction algorithm minimized dynamic inconsistencies [8], and computed muscle control estimated muscle excitations required to track the joint kinematics [10]. Individual muscle contributions to $\dot{H}$ were calculated to determine their overall contribution to frontal-plane balance control [5]. Contributions were combined into functional muscle groups and averaged over single-leg-stance on the first recovery step following the perturbation. Paired t-tests found differences in muscle contributions between step widths.

Results & Discussion: Contrary to our hypothesis, the stance plantarflexors (soleus and gastrocnemius) decreased their contributions to average positive $\dot{H}$ at wider steps ($p = 0.013, 0.036$) (Fig. 1). To gain further insight into this finding, we separated the contributions to $\dot{H}$ into vertical and mediolateral (ML) ground reaction force (GRF) components (muscle contributions to vertical GRF*ML moment arm and ML GRF*vertical moment arm). As expected, the plantarflexors increased the magnitude of their contribution to the vertical GRF component of $\dot{H}$ at wider steps. However, the plantarflexors switched their contributions from the lateral to the medial GRF at wider steps, which led to an overall decrease in plantarflexor contribution to average positive $\dot{H}$. This change also corresponded with a decrease in average negative contribution to $\dot{H}$ from the foot extensors and tibialis anterior, which could be beneficial for individuals with distal muscle weaknesses and may explain their preference for walking with wider steps.

Also contrary to our hypothesis, the stance gluteus medius ($p = 0.242$) did not change its average contribution to $\dot{H}$. With the increased hip abduction angle at the wider steps, the gluteus medius muscle fibers were shorter and shifted further from their optimal length, which adversely affected its ability to meet external moment demands following the perturbations.

Significance: Plantarflexor and gluteus medius contributions to frontal-plane balance control did not increase which corresponded with a reduction in $\dot{H}$ demands from some distal muscles. Simulations were essential to explain these results and understand why those with distal muscle weakness may prefer walking with wider steps.

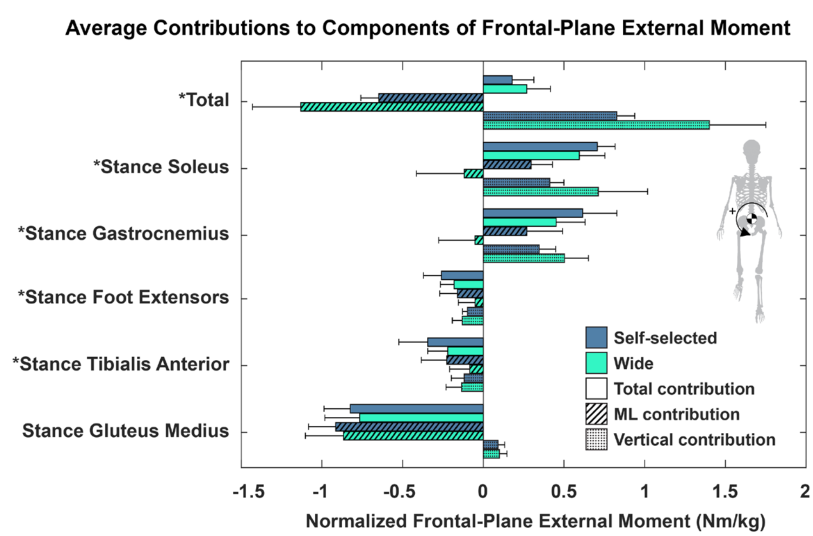

Figure 1: Primary contributors to frontal-plane external moment ($\dot{H}$) during single-leg-stance on the recovery step following a lateral perturbation while walking at self-selected and wide step widths, separated into vertical and mediolateral (ML) ground reaction force components. Error bars represent one standard deviation. "*" denotes a significant difference in average contributions to $\dot{H}$ at different step widths.

References:

[1] Forster and Young, 1981 *BMJ.* 311:83–6. **[2]** Vistamehr et al., 2016 *J Biomech.* 49:396-400. **[3]** Neptune and Vistamehr, 2019 *J Biomech.* 141:1-10. **[4]** Nott et al, 2014 *Gait Posture.* 39:129-34. **[5]** Neptune and McGowan, 2016 *J Biomech.* 49:2975-81. **[6]** Zeni Jr. et al., 2008 *Gait Posture.* 27:710-4. **[7]** Sangeaux and Polak, 2015 *Gait Posture.* 41:726-30. **[8]** Delp, et al., 2007 *IEEE Trans Biomed Eng.* 54:1940-50. **[9]** Delp, et al., 1990 *IEEE Trans Biomed Eng.* 37:757-67. **[10]** Thelen, et al, 2003 *J Biomech*. 36:321-8.

AN IMPLANTABLE ACTUATOR FOR MUSCLE FORCE ASSISTANCE IN A BIPEDAL ANIMAL MODEL

Sean Thomas[1*], Ravin Joshi[1], Bo Cheng[2], Huanyu Cheng[3], Michael C. Aynardi[4], Gregory S. Sawicki[5], Jonas Rubenson[1]

Department of [1]Kinesiology, [2]M. Eng., [3]Eng. Mech and Sci., [4]Orthopedics, The Pennsylvania State University, PA 16802, USA, [5]School of Mech. Eng., Georgia Tech, GA 30332, USA *email: sean.thomas@psu.edu

Introduction: Mobility, a key metric for quality of life, is often rehabilitated using basic aids (e.g. walkers). Wearable robotics, such as exoskeletons, offer a sophisticated solution, but often results in non-adherence [1] due to their impracticality, limiting their efficacy. Furthermore, externally-worn devices make precision and control challenging. Here, using a bipedal animal model (*Numida meleagris*), we present a concept for a fully implantable assistive limb actuator that can provide assistive torque at the ankle and reduce muscular demand at no additional energy cost. Rather than adopting an actuator that inputs mechanical power, we emulate the *in vivo* mechanics of leg muscles functioning isometrically that use tendons to store and release mechanical power [2]. This approach is similar to the externally-worn synthetic Achilles tendon used to reduce metabolic costs in humans [3]. Specifically, our aims are to develop a surgically-implanted actuator capable of: a) tight integration with biological tissues to replace one of the calf muscles and assist the remaining native calf muscles during gait; b) emulating native *in vivo* isometric loads and tendon energy storage/release; c) precise and rapid length and load adjustment (i.e. adaptable to shifting mechanical requirements) and clutching (force engagement/disengagement).

Methods: The basic control principle applied here consists of engaging an assistive actuator strut that replaces part of the native calf musculature during the stance phase, and subsequently disengaging the strut during the swing phase. Actuator design: a micro-DC motor paired with an encapsulating lead screw was used to change the length of the actuator body, while keeping the actuator volume low. The lead screw is designed to hold the actuator length static whilst under axial force applied by the biological tendon, without the need for actuator activation and energetic cost, while also providing rapid length changes during unloading (limb swing). The lead screw design was chosen with a nominal diameter of 8 mm and a thread pitch of 1.25 mm (Fig. 1). Implantation: implantation was developed on cadaver specimens (n = 3) and in survival surgery (n = 3). Animals were obtained as day-old animals from a commercial hatchery and cage reared to skeletal maturity. All experiments were approved by the PSU Institutional Animal Care and Use Committee. Surgeries were performed under standard aseptic and general anesthesia techniques (isoflurane inhalation and epinephrine/lidocaine injection for bleeding control). A blunt dissection was used to access the lateral aspect of the proximal tibia for the proximal actuator-to-bone attachment using a 2.2 mm micro corkscrew bone anchor with an integrated 2.0 FiberWire (Arthrex Inc.). The lateral gastrocnemius (LG) muscle was resected, creating functional deficit and freeing space for the actuator implant and room on the LG tendon for the distal attachment of the actuator. A Kessler suture technique was used to secure the distal actuator to the native LG tendon. *In situ* testing: A setup using cadaveric specimens was used to validate the mechanical feasibility of the micro-actuator. A stereotactic rig was designed to record forces and displacement prescribed to the biological tendon with and without the implantable actuator. The test bench consisted of a dual-mode force-length transducer (Aurora Scientific 310CLR lever, Aurora, ON, Canada; Fig. 1) mounted on linear rails and motion systems that allow the lever arm multiple degrees of freedom and adjustability. Lowman bone clamps were used to attach the femur to the rigid structure (Fig. 1). With the actuator inserted, the common Achilles tendon was severed distal of the ankle joint. The free tendon was attached to the Aurora lever arm using inextensible suture. The actuator was tested under ramp loading and tendon loading profiles simulating gait mechanics (OpenSim; [4]).

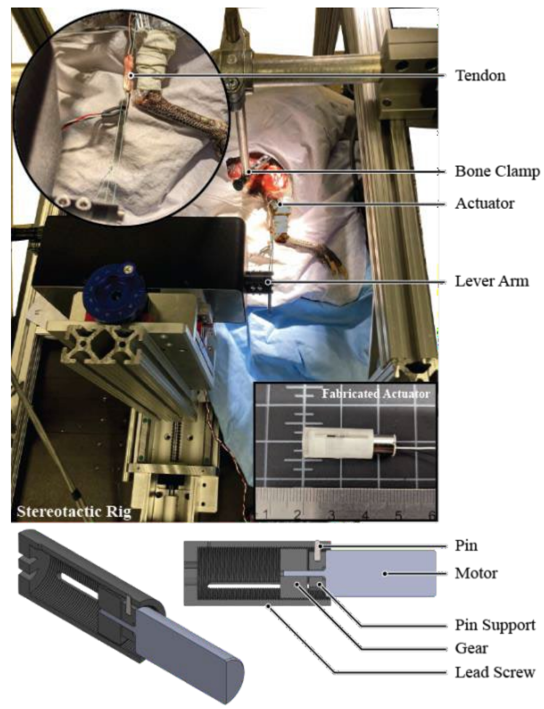

Figure 1: Characterization of micro-actuator within a cadaveric setup using a custom stereotactic rig.

Results & Discussion: We have developed a variable length actuator based on the concept of 'strutlike' biological muscle function (measuring ⌀9 x 30 mm) that can be fully implanted within the leg via a bone anchor and tendon fixation, replacing the lateral gastrocnemius muscle. The actuator is able to generate isometric force similar to the *in vivo* force of the native muscle during gait (~40N). The device has a stroke of 10 mm that operates up to 770 mm/s (77 stroke lengths/s; on an order of magnitude faster than biological muscle), capable of rapid contraction and elongation under low load. The stroke characteristics permits rapid clutching (disengaging when needed) and a tunable slack length to modulate the timing and level of assistive force during gait. Surgical viability has been established using survival surgeries, showing no signs of device rejection.

Significance: This work establishes the feasibility of an implantable assistive limb actuator using an animal model. Ongoing development aims at actuator miniaturization, sensor integration, and dynamic real-time actuator control in gait trials.

Acknowledgements: This work was supported by a seed grant from The Huck Institutes of the Life Sciences, The College of Health and Human Development, The College of Engineering, and The College of Medicine, at The Pennsylvania State University.

References: [1] N. Gutierrez et al., (2023) doi: 10.2139/ssrn.4361395. [2] T. J. Roberts (2016), *Journal of Experimental Biology* 219(2) [3] S. H. Collins et al., (2015), *Nature* 522(7555) [4] S. M. Cox et al., (2019) *Integr Org Biol*, 1(1).

GAIT SMOOTHNESS AS A MEASURE OF MOVEMENT QUALITY AFTER LOWER LIMB LOSS

Courtney M. Butowicz[1-3*], Julian C. Acasio[1,2], Brad D. Hendershot[1-3]
[1]Defense Health Agency: Extremity Trauma and Amputation Center of Excellence, Bethesda, MD, USA
[2]Walter Reed National Military Medical Center, Bethesda, MD, USA
[3]Uniformed Services University of Health Sciences, Bethesda, MD, USA
*Corresponding author's email: courtney.m.butowicz.civ@health.mil

Introduction: For persons with lower limb amputation (LLA), altered or missing muscles and joints reduce sensory feedback (i.e., proprioception) used to assist with motor planning. As a result, persons with LLA demonstrate altered coordination strategies that tend to manifest as abnormal gait mechanics. These altered motor strategies and gait mechanics are associated with highly prevalent secondary pain conditions (e.g., at the low back or intact knee) [1]. While there are kinematic differences observed during walking between persons with transfemoral (TF) vs. transtibial (TT) amputation [2], exploring different features of gait kinematics may further elucidate underlying coordination or motor strategies adopted by persons with LLA; for example, recent evidence suggests the smoothness of ankle, knee, and hip joint rotations can detect differences in the organization of movement control in relation to an external load in children with autism [3]. Thus, the purpose of this study was to explore the application of gait smoothness to persons with LLA and determine differences in joint rotation smoothness between persons with unilateral TF vs. TT limb loss, and non-limb loss controls. We hypothesized that persons with more proximal limb loss would demonstrate the least smoothness (i.e., greater normalized jerk cost) than those with TT or no limb loss, as more smoothness would be associated with a higher degree of proprioceptive input [4].

Methods: Twelve individuals with TT limb loss (mean [standard deviation] age: 31.8 [6.6] yr, stature: 179.5 [4.3] cm, body mass: 92.3 [14.6] kg, time since injury 86.7 [54.9] months), five with TF limb loss (age: 41.0 [5.1] yr, stature: 175.3 [4.3] cm, body mass: 78.5 [3.0] kg, time since injury 160.0 [148.2] months), and fifteen without limb loss (CT; age: 29.2 [8.9] yr, stature: 175.2 [7.0] cm, body mass: 72.8 [12.6] kg) completed biomechanical gait evaluations at 1.3 m/s across an overground walkway. Bilateral hip and knee kinematics were tracked (120Hz) via optical motion capture (Qualisys, Göteborg, SE) and angular jerk was determined as the 3rd derivative of sagittal-plane joint angles. Normalized jerk cost (JC) for each joint were calculated according to previous reports [5]; briefly, JC was normalized to both stride time and angular range of motion. One-way ANOVAs ($p<0.05$) assessed the effect of limb loss (i.e, CT, TT, TF) on hip and knee JC of both the intact and prosthetic limb (right limb of CT). Post-hoc bonferroni-corrected t-tests assessed pairwise differences ($p<0.0167$) and Cohen's d assessed effect sizes.

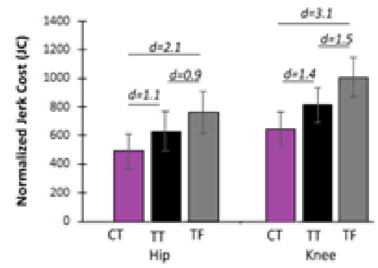

Figure 1: Normalized jerk cost (JC) of intact-side hip and knee identify gait smoothness differences between controls (CT) and persons with transtibial (TT) and transfemoral (TF) amputation. Effect sizes (Cohen's d) are indicated for each pairwise comparison.

Results & Discussion: There was a significant main effect of limb loss level on intact hip ($p=0.001$) and knee ($p<0.001$) JC. Supporting our hypothesis, post-hoc comparisons (Figure 1) revealed differences between hip JC of CT vs. TT ($p=0.03$), CT vs. TF ($p=0.001$), and knee JC of CT vs. TT ($p=0.01$), CT vs. TF ($p<0.001$), and TT vs. TF ($p=0.01$). Large effect sizes ($d>0.8$) were observed for each post-hoc comparison, indicating a practical significance of between-group differences, regardless of sample size. There were no differences by level of limb loss for prosthetic-side hip ($p=0.8$) and knee ($p=0.12$). These findings suggest that normalized JC is capable of distinguishing quality of movement between individuals with varying levels of proprioceptive feedback (largest JC with most proximal limb loss). Together, JC of the intact hip and knee joints establish differences in gait smoothness by level of limb loss and support previous work that suggests persons with vs. without TF amputation walk with altered and perhaps less efficient coordination strategies [6]. It is also likely that greater JC of the intact-side hip and knee (i.e., less smooth motion) are associated with both rigid and larger trunk-pelvic kinematics often observed in perons with TF limb loss.

Significance: Quantifying the smoothness of gait kinematics may help explain motor strategies adopted after LLA. While our findings preliminarily support JC for differentiating movement quality after LLA, future work should connect these JC measures to activity in proprioceptive regions of the brain to fully understand this relationship. Future work may also explore how surgical amputation techniques designed to increase proprioceptive feedback influence gait smoothness.

Acknowledgements: This work was supported, in part, by National Center for Medical Rehabilitation Research (NIH-NICHD; Award #5R03HD086512-02) and the Peer Reviewed Orthopaedic Research Program (PRORP; Award #W81XWH-14-2-0144). The views expressed are those of the authors, and do not necessarily reflect the official policy or position of the USUHS, U.S. Departments of the Army, Navy, Defense, nor the U.S. government.

References: [1] Butowicz (2017) *Adv Wound Care* 6(8); [2] Sagawa (2011) *Gait & Posture* 33(4); [3] Harry (2019) *Human Mvmt Science* 63; [4] Blanche (2012) *Am J Occup Ther* 66(5); [5] Romero (2003) *Exp Brain Res* 151; [6] Chang (2022) *Intern J of Prec Eng and Man* 23(3).

VALIDITY OF SPINE LOADING ASSESSED USING MARKERLESS VIDEO-BASED 3D MOTION ANALYSIS

Andrew C. Lynch[1], Jacob J. Banks[1,2*], Joanna N. James[1], Andrew P. White[1,2], Dennis E. Anderson[1,2*]
[1]Center for Advanced Orthopaedic Studies, Beth Israel Deaconess Medical Center, Boston, MA, United States
[2]Department of Orthopaedic Surgery, Harvard Medical School, Boston, MA, United States
*Corresponding author's email: danders7@bidmc.harvard.edu

Introduction: Understanding spinal loads is of interest for research, clinical, and ergonomic purposes. Advanced musculoskeletal modeling allows computational estimates of spinal loads based on measured motions, but obtaining motion data remains a barrier for applications outside of motion labs [1]. Some recent studies [e.g., 2, 3] have shown the use of single-video (2D) motion analysis to evaluate gait metrics and kinematics in clinical populations. To enable 3D reconstruction of motion and kinetic analyses, approaches using multi-view video as inputs to musculoskeletal models are of increasing interest [4], but their validity for evaluating spinal loads has not been examined. Here we evaluate the validity of multi-view video analyses to quantify spine loading compared to "gold standard" marker-based analyses [4], and whether it depends on the activity performed or vertebral level examined. We hypothesized that video-based loads would be larger than marker-based loads due to lower precision inducing more spurious movement.

Methods: Seven participants (4 men, 3 women, mean±SD age 29±7 years, height 173±8 cm, weight 69±10 kg) provided written informed consent. A full-body set of 97 motion capture markers (Vicon Motion Systems, UK), and two video cameras capturing frontal and left lateral images were recorded simultaneously. Participants performed: 1) a 2-handed sagittal plane lift (floor to waist height and return to floor) of a crate with 10% body weight, 2) self-paced walking, and 3) sit-to-stand. Videos were analysed with OpenPose software [5] to identify 25 anatomical landmarks in each view, and combined via direct linear transformations with custom MATLAB (The Mathworks, USA) scripts to estimate 3D positions. Inverse kinematics analyses were performed with both measurement approaches using scaled full-body thoracolumbar spine musculoskeletal OpenSim models [1, 6] followed by static optimization with low-pass filtering of the input kinematics at 6 Hz. Compressive loads at vertebral levels T8, T12, and L3 were extracted for evaluation and video-based loads were further filtered at 3 Hz. These results were time-normalized (0 – 100% of activity) and magnitude normalized to percent body weight (%BW). Peak and average loads for each level and task were calculated for each participant, as were root mean square errors (RMSE) and zero-lag cross correlation coefficients (*r*-values) were made between video and marker-based approaches. Mixed-model regressions were constructed to examine whether average loads and peak loads differed between the motion approaches. Two-way repeated measures ANOVAs examined whether RMSEs and cross-correlations varied with activity or vertebral level.

Results & Discussion: Peak vertebral loads during each activity (Fig. 1) as evaluated by video-based analyses were higher than marker-based analyses by an average of 107 %BW ($p < 0.001$), and similarly average loads during activities were higher by an average of 43 %BW ($p < 0.001$). Temporal correlations (Table 1) were affected by activity ($p < 0.001$), but not vertebral level ($p = 0.145$), and were higher for lifting ($p < 0.001$) and sit to stand ($p < 0.001$) than for walking. Mean RMSEs (Table 1) ranged from 30 to 92%BW and varied with activity ($p < 0.001$) and level ($p<0.001$), but without a significant interaction ($p = 0.070$). RMSEs for sit-to-stand were greater than for lifting ($p = 0.025$) and walking ($p < 0.001$), and RMSEs for lifting were greater than for walking ($p < 0.001$). RMSEs at L5 were greater than at T12 and T8 (both p-values < 0.001). Overall, we found video-based analyses over-estimate loading magnitudes, supporting our hypothesis, and accounting for a large proportion of the overall error. Temporal patterns were good for lifting and sit-to-stand, with significant spine motion, but were low to moderate for walking, when spine motion is more subtle. The OpenPose output currently lacks distinct trunk or spine points, which might limit its accuracy for spine motion, while additional cameras or processing of video-based kinematics might also improve performance.

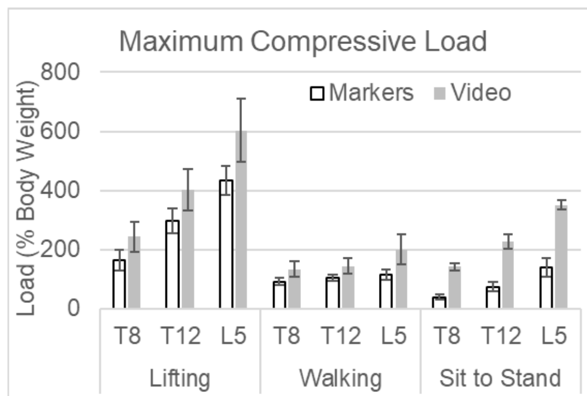

Figure 1: Maximum vertebral compressive loads (Mean ±SD) for three activities at three vertebral levels, as evaluated using marker-based motion data and video-based motion data.

Table 1: Mean (standard deviation) of correlation coefficients and RMSEs between video-based and marker-based spinal compressive loads for three activities at three vertebral levels.

	Correlation			RMSE (%BW)		
Activity	**T8**	**T12**	**L5**	**T8**	**T12**	**L5**
Lifting	0.72 (0.12)	0.79 (0.26)	0.80 (0.31)	37.7 (4.9)	50.6 (14.9)	89.6 (33.1)
Walking	0.39 (0.29)	0.50 (0.26)	0.36 (0.31)	33.4 (11.1)	30.8 (10.3)	52.5 (22.5)
Sit-to-Stand	0.59 (0.20)	0.82 (0.10)	0.83 (0.11)	57.9 (6.3)	75.3 (4.5)	91.8 (17.7)

Significance: This analysis demonstrates video-based motions have potential for estimating of spine loading in functional activities. However, additional development is needed to improve accuracy and validity, particularly for spine loading during walking, which is of interest for clinical conditions such as spinal stenosis [7].

Acknowledgements: Funded by a Faculty Grant from the BIDMC Department of Orthopaedic Surgery.

References: [1] Banks et al. (2023), *Appl Ergo*, 106:103869; [2] Lonini et al. (2022) *Digit Biomark* 6(1); [3] Rupprechter et al., (2021) *Sensors (Basel)*, 21(16). [4] Uhlrich et al. (2022) *bioRxiv*, 2022.07.07.499061; [5] Cao et al. (2021) *IEEE Trans Pattern Anal Mach Intell*, 43(1); [6] Alemi et al. (2021) *Front Bioeng Biotech* 9:688041; [7] Mousavi et al. (2021) *Front Bioeng Biotech* 9:751155

VALIDATION OF A MARKERLESS MOTION CAPTURE SYSTEM IN THE PRESENCE OF AN ORTHOPAEDIC KNEE BRACE

Joshua Taylor[1], Ikeade Adeyinka[1], Timothy Burkhart[1]
[1]Faculty of Kinesiology, University of Toronto, Toronto, ON
*Corresponding author's email: timothy.burkhart@utoronto.ca

Introduction: Marker-based (MB) motion capture systems are the current gold-standard of motion capture technology. The primary limitations associated with MB motion capture include errors in marker and/or rigid body placement and soft-tissue motion artifact [1, 2]. MB motion capture also requires participants to wear minimal or tight-fitting clothing for accurate marker placement, which can make participants feel uncomfortable or lead to unnatural movement [3]. Accurate marker placement is further challenged when the research requires participants to wear a device that obstructs anatomical landmarks required for marker placement. For example, knee braces restrict access to the femoral condyles. An alternative to MB motion capture is markerless (ML) motion capture technology that estimates 3-dimensional human joint kinematics based on a deep-learning algorithms [4]. While, this technology has been validated against MB systems, no research has quantified the effect of on-body devices on the accuracy of ML motion capture. Therefore, the purpose of this study was to validate ML motion capture against a MB system for measuring hip and knee kinematics when in the presence of a knee brace.

Methods: 14 healthy participants were fitted with an ÖSSUR Rebound Knee Brace (ÖSSUR Canada, British Columbia, Canada) and equipped with a unilateral reflective marker set up (bilateral on the anterior superior iliac spines, lateral iliac crests, and posterior superior iliac spines; unilateral on the femoral condyles, tibial plateau, malleoli, calcaneus, first metatarsal head, fifth metatarsal head, and between the second and third metatarsal heads). The femoral condyle markers were placed on the bony landmarks requiring them to be placed between the bony anatomy and the hinges of the knee brace. Three trials each of gait, walking lunges, and squat jumps were performed. An 18-camera Qualisys MB motion capture system (Qualisys AB, Gothenburg, Sweden) was used as the gold-standard and eight synchronized Sony RX0 II cameras (Sony Group corporation, Tokyo, Japan) were used for the ML system. Data was exported to Visual3D (C-Motion, Maryland, USA) and frame shifted using cross-correlation of knee flexion/extension angles to synchronize the two data sets. 3D kinematics were extracted at task-relevant times from the braced side: i) the gait analysis examined knee and hip angles at the end of the swing phase and during mid-stance phase; ii) the lunge analysis examined knee and hip angles at peak lunge depth when the braced limb was the front foot and the back foot; and iii) the jump analysis examined knee angles during the takeoff and landing phases at peak depth and the hip angles prior to ground contact. Bland-Altman plots (BA) were created, root mean squared error (RMSE) values were calculated, and cross correlation values were quantified.

Results & Discussion: Mean (SD) cross-correlation values for gait, squat jumps, and lunges were 0.98 (0.01), 0.99 (0.01), and 0.98 (0.02), respectively. RMSE values ranged from 4.14º (gait mid stance knee flexion/extension) to 20.46º (jump landing hip flexion/extension). Overall, RMSE values reported here are comparable to those from previous Theia3D validation research on gait where they found a maximum RMSE of 13.2º (knee internal/external rotation) and a minimum RMSE of 2.6º (hip abduction/adduction) [4]. BA plots demonstrated good agreement between Theia3D and Qualisys, with ~95% of differences in measurements falling within 1.96 standard deviations of the mean bias. The larger errors in this study compared to previous literature are likely attributable to the MB system's difficulty tracking semi-occluded markers from the knee brace.

Significance: The results presented here suggest that the Theia3D ML motion capture system generates valid representations of 3D knee and hip kinematics compared to a traditional MB system. In research or clinical settings where participants/patients are required to wear a knee brace, the use of ML motion capture is justified as it addresses some of the common limitations associated with traditional MB motion capture.

Acknowledgements: This research was funded by ÖSSUR Canada through a MITACS Accelerate Grant.

References:

[1] Della Croce D et al. (2005). Gait & Posture 21(2); p. 226–237.
[2] Dumas R et al. (2013). Journal of Biomechanics 47 (2); p. 476–481.
[3] Kanko RM et al. (2021). Journal of Biomechanics 121; p. 110422
[4] Kanko RM et al. (2021). Journal of Biomechanics 127; p. 110665

COMPARISON OF GAIT DEVIATION INDEX MEASURED BY MARKER-BASED AND MARKERLESS MOTION CAPTURE SYSTEMS IN CHILDREN WITH CEREBRAL PALSY(CP)

Jutharat Poomulna[1*], Brian Knarr[1], Vivek Dutt[2], David C. Kingston[1]
[1]Department of Biomechanics, University of Nebraska at Omaha, Omaha, NE, USA
[2]University of Nebraska Medical Center, Omaha, NE, USA
email: jpoomulna@unomaha.edu

Introduction: The gait deviation index (GDI) is a dimensionless measure of overall gait pathology used to compare kinematic data to a normative sample that is a key metric in the assessment of children with cerebral palsy (CP) [1,2]. The GDI score indicates overall gait pathology, with a score of 100 or higher representing typically developing gait and every 10-point difference indicating one standard deviation (SD) from the mean [2]. Clinical gait analysis (CGA) has been used for assessing gait disorders and evaluating treatments in ambulatory children with CP as a standard of care [3]. Marker-based motion capture is the gold standard for 3D gait analyses, but it has limitations in clinical use. Video-based markerless motion capture software is now commercially available that is easy to use, less expensive to operate, and reduces data collection time. Previous work [4] highlights Theia3D's accuracy and reliability compared to marker-based systems in healthy adult subjects, but it has not been verified for children with CP. This study aimed to quantify the effect of different motion capture systems and the severity of impairment on GDI outputs. Our primary hypothesis was that GDI measured using markerless will not differ from marker-based motion capture system due to its reliability in measuring kinematic data compared to the marker-based system. Our secondary hypothesis was that markerless GDI calculations will be different based on the limb assessed using the markerless approach.

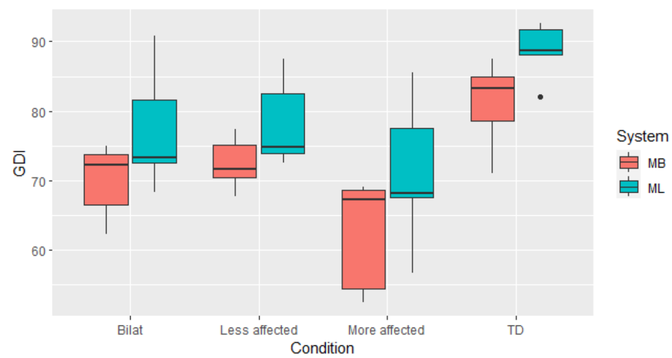

Figure 1: Box plots (minimum, first quartile, median, third quartile, and maximum) of GDI values amongst typically developing (TD) and children with CP, separating by more-affected leg, less-affected leg,

Methods: Five children with CP (GMFCS I: II (3:2), M:F (3:2), age 13.5±4.6 yrs., height 1.4±0.2 m, weight 36.7±10.0 kg), and five typically developing (TD) children (M:F (3:2), age 7.6±1.1 yrs., height 1.3±0.1 m, weight 34.0±11.5 kg) took part in this study. A marker-based camera system (Oqus, Qualisys AB, Gothenburg, Sweden) and a markerless camera system (Miqus Hybrid) were used to synchronously record video and motion data from 48 markers on the pelvis and lower limbs at 100 Hz. Video and marker trajectory data were processed using Theia3D (Theia Markerless Inc., Kingston, ON) and Visual3D (C-Motion, USA), to compute 3D lower limb joint angles. The GDI was calculated from one barefoot stride in the following conditions; more/less affected, and both legs for CP, and left/right, and both leg for TD (Figure 1). Baseline data from 166 controls (collected in a different laboratory [2]) were used to compare GDI scores of TD and CP children using: pelvic and hip angles (all three planes), knee flexion-extension, ankle dorsiflexion-plantarflexion, and foot progression angles following established methods [2]. Paired *t*-test and one-way repeated ANOVA were used to examine GDI scores between two systems in TD and CP, respectively. A separate one-way repeated ANOVA with Bonferroni corrections was used to investigate the differences in GDI score between limb assessed.

Results & Discussion: The markerless system generated higher GDI values than the marker-based system with the more-affected limbs having lower GDI values (Figure 1). Statistical tests indicated significant different in GDI scores between two systems in TD (t = -3.467, p < 0.05, r = 0.649) and significant difference in GDI score between systems in CP (F (1,4) = 9.968, p < 0.5, η^2 = 0.71). Pairwise comparisons among limb assessed measured using markerless system indicated no difference GDI score between more and less affected leg of CP (p = 0.182), while there was significant difference in GDI score (p < 0.05) when assessed using marker-based system. Therefore, the results refuted our first hypothesis that would be no differences in GDI scores between the two system. Similarly, our second hypothesis was rejected as there was no difference in GDI amongst limb assessed in markerless data. Both of systems had lower GDI values when the severity of impairment increased showing general agreement. However, the GDI score less than 100 in TD in this study may be attributed to differences of TD sample and reference database.

Significance: Differences in GDI values exists for both TD and CP children between markerless and marker-based system. This suggests a need to further investigate the reliability in measuring kinematic between motion capture systems. However, practical benefits of markerless motion capture this technology could overcome measurement differences as a viable alternative to marker-based system for acquiring the kinematic data in children with CP.

Acknowledgements: The University of Nebraska Omaha supported this work under the Graduate Research and Creative Activity (GRACA) program [grant number:31240]. Equipment for this study was supported by the Center of Research in Human Movement Variability of University of Nebraska Omaha and the National Institute of Health [grant number PGM109090]

References: [1] Massaad et al., 2014, *Gait & Posture* 39(1); [2] Schwartz & Rozumalski, 2008, *Gait & Posture* 28(3); [3] Wren et al., 2020, *Gait & Posture* 80(3)3; [4] Kanko et al., 2021, *J. Biomechanics* (3).

CLINICAL USE OF MARKERLESS MOTION CAPTURE IN PATIENTS RECOVERING FROM ACLR

Devin K. Kelly[1*], Adam W. Kiefer[1], Robin M. Queen[2], Gabrielle M. DelBiondo[1], Joe M. Hart[1]
[1]University of North Carolina at Chapel Hill, Chapel Hill, NC, USA
[2]Virginia Tech, Blacksburg, VA, USA
*Corresponding author's email: devin_kelly@med.unc.edu

Introduction: Athletes who rupture their anterior cruciate ligament (ACL) commonly elect reconstruction surgery (ACLR) to reestablish joint stability and return to unrestricted activity (RTA). Physical testing protocols, including single leg hop tasks, are often used to determine patient progress through post operative rehabilitation and readiness to RTA [1]. Despite the growing use of objective testing, patients are at a 6 times greater risk for subsequent knee injury post-ACLR [2]. Thus, there remains a critical need for improved RTA criteria. Kinematic evaluation has been proposed as a more precise method to determine recovery post-ACLR [3] however, this method requires expensive motion capture systems, expert operators, and lengthy processing times. Recently, an open source markerless motion capture system, OpenCap (https://www.opencap.ai/), requiring the use of only two iPads has become publicly available. OpenCap provides an easy and clinically accessible method of kinematic assessment [4] that is necessary to establish better processes for monitoring progress post-ACLR and RTA criteria. Therefore, the purpose of this study is to determine the feasibility of using an open source markerless motion capture system in a real clinical setting by comparing lower extremity sagittal plane kinematics between limbs during single leg hop tasks in patients recovering from ACLR.

Methods: Data were collected on five patients (Sex:2F,3M;Age:21±3years;Height:177±10cm;Mass:76.1±11.3kg) during point-of-care functional assessments post-ACLR (10±2months post-op). Patients completed 3 single leg hops for distance bilaterally in an Orthopaedic clinic setting. Kinematic data were collected using OpenCap and two iPads oriented at 45-degree angles to the hop direction. Peak sagittal plane kinematics and excursions of the hip, knee, and ankle, averaged over 3 trials for 4 patients and 1 trial for 1 patient, were determined for the propulsion and landing phases for the involved (ACLR) and uninvolved (healthy contralateral) limbs. The propulsion phase was defined as initial knee flexion to the first frame of flight. The landing phase was defined from the first frame of foot contact to the end of the trial. Cohen's d effect sizes (and associated 90% confidence intervals) were used to determine clinically meaningful differences between limbs (small (d=0.2), medium (d=0.5), large (d=0.8) (Table 1) [5].

Results & Discussion: OpenCap successfully measured kinematics during the single leg hop for distance in patients post-ACLR. Further, it was able to distinguish between involved and uninvolved limbs similarly to differences reported from controlled laboratory settings [3][6]. There were large effect size differences between limbs for peak knee flexion during propulsion, hip excursion, peak knee flexion, and knee excursion during landing with the involved limb smaller than the uninvolved limb. There were medium effect size differences between limbs for knee excursion and peak dorsiflexion during propulsion with the involved limb smaller than the uninvolved limb (Table 1). These results indicate potentially altered motion of the involved limb in the propulsion and landing phases including a reduced knee flexion stiff landing which may put the knee at greater risk for subsequent injury [3][6].

Table 1: Peak and excursion sagittal plane lower extremity kinematics. Cohen's d differences: small (d=0.2), medium (d=0.5), large difference (d=0.8). CV: coefficient of variation. CI: confidence interval.

Propulsion (degrees)	**Involved (Mean±SD)**	**CV**	**90% CI**	**Uninvolved (Mean±SD)**	**CV**	**90% CI**	**d**
Hip flexion	57.35±8.96	0.16	48.80-65.90	58.70±4.76	0.08	54.16-63.25	0.19
Hip excursion	57.89±14.86	0.26	43.73-72.06	58.38±4.16	0.07	54.41-62.35	0.04
Knee flexion	58.94±10.61	0.18	48.82-69.09	68.76±6.99	0.10	62.10-75.43	1.09
Knee excursion	50.53±16.37	0.32	34.92-66.14	60.10±12.05	0.20	48.61-71.58	0.67
Ankle plantarflexion	18.54±11.84	0.64	7.25-29.83	19.22±13.55	0.71	6.29-32.14	0.05
Ankle dorsiflexion	32.00±7.80	0.24	24.57-39.44	36.19±3.25	0.09	33.09-39.29	0.70
Ankle excursion	50.54±17.60	0.35	33.76-67.32	55.41±15.90	0.29	40.25-70.57	0.29
Landing (degrees)							
Hip flexion	60.69±22.40	0.37	39.34-82.05	63.49±14.61	0.23	49.61-77.36	0.15
Hip excursion	42.45±14.58	0.34	28.55-56.36	54.53±11.17	0.20	43.87-65.18	0.93
Knee flexion	50.08±20.04	0.40	30.98-69.18	65.52±13.05	0.20	53.08-77.96	0.91
Knee excursion	44.29±19.71	0.45	25.49-63.08	60.38±11.82	0.20	49.12-71.65	0.99
Ankle plantarflexion	21.13±8.55	0.40	12.97-29.28	17.82±9.14	0.51	9.10-26.53	0.37
Ankle dorsiflexion	16.15±4.23	0.26	12.12-20.19	18.03±6.38	0.35	11.94-24.11	0.35
Ankle excursion	37.32±7.31	0.20	30.35-44.29	35.84±11.49	0.32	24.89-46.80	0.15

Significance: The results of this study demonstrate the feasibility of kinematic data acquisition using OpenCap in a real clinical setting to successfully differentiate involved and uninvolved limbs. This presents the opportunity to integrate quantitative measures previously relegated to a laboratory setting into clinical practice such that improvements in monitoring progression through post operative rehabilitation and RTA testing can be made.

References: [1] Abrams et al. (2014), *Orthop J Sports Med* (2)1; [2] Paterno et al. (2014), *Am J Sports Med* 42(7); [3] Johnston et al. (2018), *Sports Med* 48; [4] Uhlrich et al. (2022), *bioRxiv*; [5] Cohen (1988), Statistical Power Analysis for the Behavioral Sciences; [6] Xergia et al. (2013), *J Orthop Sports Phys Ther* 43(3)

DEFINING MAMMALIAN CLIMBING GAITS AND THEIR INFLUENTIAL CRITERIA

Cassie Shriver[1*], Andrew Schulz[2], Dylan Scott[3], Jennifer Elgart[4], Joseph Mendelson III[1,4], David Hu[1,3], Young-Hui Chang[1*]
Georgia Tech School of Biological Sciences[1], Atlanta, GA; Max Planck Institute[2] for Intelligent Systems, Stuttgart, Germany; Georgia Tech School of Mechanical Engineering[3], Atlanta, GA; Zoo Atlanta[4], Atlanta, GA
*Email: cshriver7@gatech.edu

Introduction: In comparison to terrestrial locomotion, climbing presents a couple unique challenges. First, organisms must move upwards, meaning they lack a "restoring force" to bring them back into contact with the climbing surface as they continuously overcome gravitational forces. Second, organisms must possess morphology capable of gripping the climbing surface and perform appropriate contact patterns to prevent falling. While recent studies have examined climbing via van der Waals forces [1] and capillary adhesion [2], these are often limited to non-mammalian species less than 500 grams. Even amongst the studies for mammals, many are focused on primates, which take advantage of highly specialized opposable thumbs, elongated digits, and/or prehensile tails [3]. Despite the phylogenetic diversity of mammalian climbers, basic concepts like climbing gaits are still limited to insects, primates, and robots [4]. In this work, we attempt to translate the foundational descriptions of terrestrial gaits by Hildebrand [5] to mammalian climbing gaits. We performed kinematics analyses to identify common mammalian climbing gaits and discerned some underlying criteria influencing these gaits. Due to the aforementioned biomechanical constraints specific to climbing, we predict non-primate, mammalian climbing gaits will all fall within and occupy a smaller subspace of the known terrestrial gaits described by Hildebrand [5].

Methods: Preliminary kinematics analyses were conducted via video tracking. Videos were either acquired from online media sources (YouTube, documentaries, existing camera trap footage) or collected at Zoo Atlanta. For video data from Zoo Atlanta, climbing behaviour was encouraged by placing food atop structures within habitats or passively observed during hours of high activity. Once collected, videos were digitized using the DLTdv8 software [6] in MATLAB to track points of interest including all four limbs and the center of mass. By producing 2D coordinates for singular videos and 3D coordinates for paired (sagittal and frontal) videos, we determined limb contact patterns, duty factor, stride time, stride frequency, and identified gaits according to terrestrial standards [5].

Results & Discussion: We identified two fundamental gait patterns for mammalian climbing: 1) a climbing trot with alternating diagonal limb contacts and, 2) a climbing bound where both forelimbs or both hindlimbs exhibited alternating synchronous contact (Fig 1). While most observed mammals displayed the bounding gate more often, they would occasionally adopt the trotting gait during periods of deceleration or when navigating obstacles. However, the trotting gait did appear more frequently than the bounding gait amongst younger animals, with few seemingly capable of performing the bounding inchworm gait. Both gaits, as observed in an *Ursus arctos* cub and an *Ursus americanus* adult, fell within Hildebrand's phase plot describing terrestrial gaits (Fig 2).

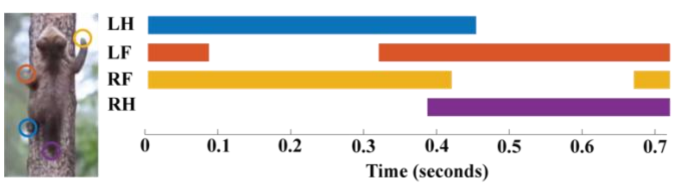

Figure 1: Representative gait cycles for an *Ursus arctos* cub (left side) and an *Ursus americanus* adult (right side). For the brown bear cub, diagonal limbs made synchronous contact with the climbing surface. The adult black bear exhibited a bounding gait with both forelimbs and both hindlimbs making alternating synchronous contact with the tree.

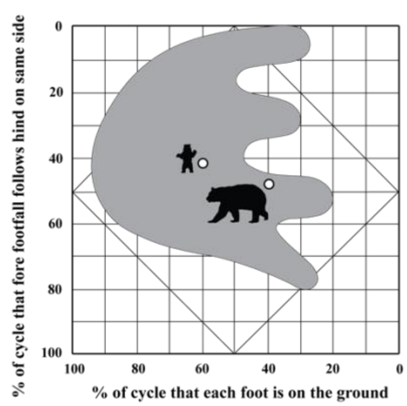

Figure 2: Preliminary analyses revealed that an *Ursus arctos* cub climbed with a duty factor and a same-side limb phase of 60% and 42%, respectively. An *Ursus americanus* adult climbed with a mean duty factor of 39% (forelimbs = 57%, hindlimbs = 22%) and a same-side limb phase of 47%. Both climbing gait patterns fell within those of terrestrial gaits (grey region) [5].

Significance: Larger mammals present intriguing scaling challenges that have yet to be understood in the context of how biomechanics scale with size or may be constrained by terrestrial locomotor control strategies. Here, we identified two fundamental gaits: a climbing trot and a climbing bound. Understanding mammalian climbing gaits and the principles dictating them is critical to behavioral insights and can inform habitat protection in the wild and design in zoological settings. This work also has great potential to aid in the development of bio-inspired climbing robotics capable of carrying larger loads.

Acknowledgements: We thank the Zoo Atlanta keepers, curators, and research team for their assistance in collecting data on their animals. We acknowledge the Wildlife Conservation Society and members who provided camera trap videos from Tikal National Park in Guatemala, and those who made climbing videos available online. C. Shriver was supported in part by the ARCS foundation.

References: [1] Autumn, K. et al. (2002), *PNAS* 99(19). [2] Dirks, J.H. and Federle, W. (2011), *Soft Matter* 7. [3] Hanna, J.B. et al. (2011), *Int. J. Primatol.* 145. [4] Brown, J.M. et al. (2019), *Bioinspir. Biomim.* 14. [5] Hildebrand, M. (1989), *Bioscience* 39(11). [6] Hedrick, T.L. (2008) *Bioinspir. Biomim.* 3.

A ROBOTIC EMULATOR FOR EXPLORING TRANSTIBIAL BIARTICULAR PROSTHESIS DESIGNS

Anthony Anderson[1,2*], Kira Gauthier, Mathew Sunil Varre, Kimberly Nickerson, Brittney Muir, Patrick Aubin
[1]Department of Mechanical Engineering, University of Washington, Seattle, WA
[2]Center for Limb Loss and Mobility (CliMB), VA Puget Sound Health Care System, Seattle, WA
*Corresponding author's email: ajanders@uw.edu

Introduction: People with transtibial limb loss face challenges related to the loss of ankle and foot musculature. Transtibial amputees (TTAs) have reduced mobility in terms of slower walking speeds, lower daily step counts, and higher rates of falling compared to the general population. Further, they experience a high prevalence of secondary musculoskeletal disease (e.g., knee osteoarthritis) due to cumulative loading from altered gait patterns. Improvements to ankle-foot prosthesis technology may improve walking patterns for TTAs, but functional outcomes are limited even when state-of-the-art powered prosthetic ankles are prescribed [1].

One potential factor that may explain the limitations of powered ankle-foot prostheses is that modern designs do not reflect the anatomical layout of the human plantarflexor muscles. Modern ankle-foot prostheses do not replicate the biarticular nature of the gastrocnemius muscle at the ankle and knee. It has been well-established through simulation and experimental studies that the soleus and gastrocnemius play synergistic but distinct functional roles during locomotion [2]. It is possible that ankle-foot prostheses that include knee flexion assistance through an exoskeleton or exosuit could provide the functional role of the gastrocnemius muscle and improve walking outcomes for people with transtibial limb loss.

Researchers are starting to explore the potential benefits of biarticular prostheses in improving walking outcomes for people with limb loss [3]. However, the design space for these prostheses is vast and requires careful consideration of optimal design and control strategies. The purpose of this study was to develop a robotic biarticular prosthesis emulator (i.e., a tethered research prosthesis) that can facilitate future studies in this area, allowing for the exploration and testing of different device embodiments and control strategies.

Methods: We designed and built a robotic biarticular prosthesis emulator by combining two custom wearable robotic devices - a knee flexion assistance exoskeleton and a previously developed powered ankle prosthesis (Fig 1). Each device is actuated with an independent off-board motor, Bowden cable transmission, and a high-performance control system. The exoskeleton was made using fiberglass struts, heat-formed plastic body interfaces, and custom-machined aluminum components. Both devices were equipped with wearable sensors that measure joint torque and angle and operate under joint torque control mode. The exoskeleton was designed with a dual frontal-plane hinge to improve comfort and alignment between the exoskeleton, the prosthetic socket, and the user's thigh.

The robotic performance of the knee exoskeleton was evaluated with benchtop tests. These tests were conducted with the exoskeleton rigidly mounted in a test stand. The biarticular prosthesis's torque production capabilities and tracking bandwidth were measured during these tests. We also conducted a preliminary walking experiment with one participant with transtibial amputation to test the biarticular prosthesis emulator. The participant walked in two conditions: a uniarticular condition and a biarticular condition. In the uniarticular condition, the ankle prosthesis emulated a linear torsion spring, and the knee exoskeleton behaved transparently (i.e., tracked zero torque). In the biarticular condition, the exoskeleton tracked a pre-defined torque trajectory over every stride, where the peak torque and peak torque timing were iteratively tuned through conversation with the participant.

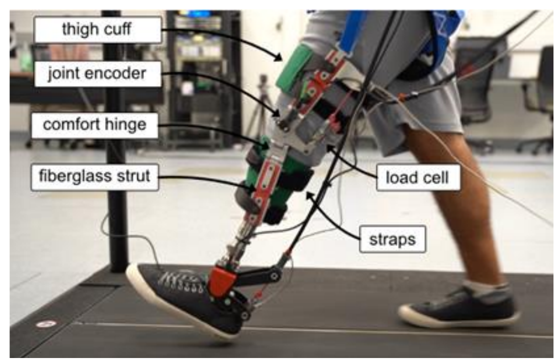

Figure 1: A participant with transtibial limb loss walking with the biarticular prosthesis emulator. Key components of the robotic knee exoskeleton are labeled.

Results & Discussion: The benchtop experiments showed that the peak knee flexion assistance torque for the exoskeleton is greater than 30 Nm and the torque tracking bandwidth is 5 Hz. The peak plantarflexion torque for the ankle prosthesis was greater than 150 Nm and the torque tracking bandwidth was previously found to be greater than 6 Hz. These benchtop tests indicate that the biarticular prosthesis emulator has sufficiently high joint torques and controller responsiveness to provide biomechanically-relevant levels of assistance.

During the preliminary walking experiment, the participant walked comfortably in the biarticular prosthesis emulator. The peak torque provided by the exoskeleton was 3 Nm in the uniarticular condition and 7 Nm in the biarticular condition. The walking experiment demonstrated that the hardware and software of the biarticular prosthesis emulator function as intended and that the device is capable of synchronizing its torque profiles with the user's gait.

Significance: This work is significant because it presents the design and evaluation of a novel research tool for designing biarticular prostheses that can potentially improve the walking patterns and quality of life of people with transtibial limb loss. By combining a powered ankle prosthesis with a knee flexion exoskeleton, the design can mimic the gastrocnemius muscle's functional role during locomotion. The robotic emulator developed in this study can facilitate future research to optimize the design and control of biarticular prostheses before devoting the significant resources required to develop untethered prototypes.

Acknowledgements: This work was funded in part by VA RR&D grants A9243C, RX002357, and RX002130.

References: [1] Kim et al. (2021), *J NeuroEng Rehabil* 18(1); [2] Lenhart et al. (2014), *J Biomech* 47(12). [3] Eilenberg et al. (2018), *J Robotics*.

DIRECTIONAL ASYMMETRIES IN STABILITY-MANEUVERABILITY TRADE-OFFS DURING WALKING

Rucha Kulkarni[1*], Francis Grover[2], Anna Shafer[3], Xenia Schmitz[1], Keith E. Gordon[2,3]

[1]Department of Biomedical Engineering, Northwestern University, [2]Physical Therapy and Human Movement Sciences, Northwestern University, [3]Research Service, Edward Hines Jr. VA Hospital

*Corresponding author's email: ruchakulkarni2023@u.northwestern.edu

Introduction: Walking in complex environments often requires gait patterns that are stable (resistant to unpredictable perturbations) and also allow for rapid change of direction (maneuver reaction time). However, how people accomplish both these goals is unclear. For example, increasing resistance to perturbations by increasing lateral margins of stability (i.e., taking wide steps or reducing whole-body center of mass lateral excursion or velocity) may increase maneuver reaction time by increasing the volitional impulse a person must generate to initiate a lateral maneuver (stability-maneuverability trade-off) [1,2]. Conversely, other research suggests that wider steps could also improve a medial maneuver reaction time by placing the body in desirable state to generate lateral ground reaction forces [3]. Our objective was to quantify the impact of complex environments on lateral and medial maneuver reaction times and its interactions with mechanisms to create lateral stability. We hypothesized maneuver reaction time would increase in complex environments.

Methods: Twenty-four healthy adults (25.6 ± 2.9 years, 14 males) performed 240 discrete stepping trials, moving quickly from a standing position to a projected end target 1.5 leg lengths ahead. During half of the trials, the end target location shifted 8° to the right (N=12) or left (N=12) once forward walking began (Fig. 1A). We used a cable-driven robot to apply lateral forces to the pelvis on select trials. Participants performed 60 baseline trials (null field, no force applied) followed by 180 trials in a complex environment (120 trials with random mediolateral forces applied interspersed with 60 null trials) (Fig. 1B). Participants always stepped first with their right leg and were not informed if any forces would be applied or whether the target would shift location during the trial. We calculated the minimum lateral margin of stability (MOS) for the first right step on trials when the target did not shift location and no forces were applied (60 trials during both baseline and complex fields). The minimum MOS is a function of the extrapolated COM and the base of support, and a higher value corresponds to greater lateral stability.[4] We calculated maneuver reaction time (Fig. 1C) only for trials when the target shifted location and no forces were applied (60 trials during both baseline and complex fields).

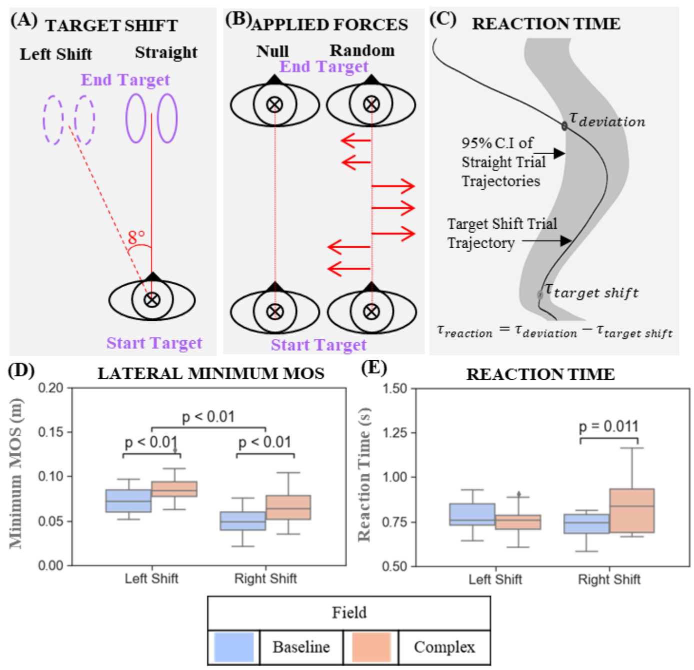

Figure. 1 (A) Representation of a left target shift trial. On select trials the target was instantaneously moved after the participant began forward walking. A right target shift trial not shown here. (B) Types of forces applied by the cable robot during select trials. (C) Calculation of reaction time for a representative participant for a single left target shift trial (D) Box plots and statistical results for lateral minimum MOS. These were calculated from all participants. (E) Box plots and statistical results for maneuver reaction time. The data represent average values for all participants.

Results & Discussion: The minimum MOS was significantly affected by both field (greater in complex than baseline) and target shift direction (greater for left than right) (Fig. 1D). This suggests people adopt strategies to increase stability in complex environments that are affected by potential requirements to change direction. We found a significantly longer maneuver reaction time in the complex environment than baseline when moving to the right and no change when moving to the left (Fig. 1E). This implies that positioning the body in a way that increases the lateral MOS on the right step hinders maneuvers to the right but places the body in an advantageous position to generate lateral forces to move to the left. Thus, the results find an interaction between environment, lateral margin of stability, and maneuver reaction time. Our findings partially support our hypothesis - increasing lateral margin of stability delayed lateral maneuvers but did not affect medial directed maneuvers. This suggests a more novel interpretation - the stability-maneuverability trade-off during human walking may be directional.

Significance: Our results provide insight into how the external environment influences a person's maneuverability and body positioning for lateral stability. The asymmetric effect of lateral margin of stability on maneuver direction may have important implications for gait training following neurologic injury. Often, impaired populations experience challenges in creating stable walking patterns and adapting quickly to the demands of their environment. Future research exploring how these populations respond to complex walking environments would benefit the design of interventions to enhance stability and maneuverability.

References: [1] Acasio et al. (2017), *Gait & Posture* 52; [2] Dickinson et al (2000), *Science* 288(5463); [3] Wu et al. (2015), *PloS One* 10(7); [4] Hof et al. (2005), *Journal of Biomechanics* 38(1)

BIOMECHANIAL DISADVANTAGE OF AMPUTATED LIMB GLUTEUS MEDIUS IN PATIENTS WITH UNILATERAL TRANSFEMORAL AMPUTATION

Galen F. Roda[1], Mohamed E. Awad[2], Danielle H. Melton[2], Cory L. Christiansen[2,3], Jason W. Stoneback[2], Brecca M. M. Gaffney[1,2]
[1]University of Colorado Denver, Denver, CO; [2]University of Colorado Anschutz Medical Campus, Aurora, CO; [3]VA Eastern Colorado Health Care System, Aurora, CO
email: brecca.gaffney@ucdenver.edu

Introduction: Patients with transfemoral amputation (TFA) are predisposed to develop hip osteoarthritis (OA) in either or both hips [1, 2]. Hip abductor weakness is a known primary mechanical factor in hip OA, as it influences muscles' ability to properly load and control the joint [3]. Patients with TFA demonstrate amputated limb hip abductor weakness due to limb disuse within the socket, which is commonly quantified using muscle volume [4, 5]. However, a muscle's ability to produce stabilizing forces and torques about a joint is affected by several additional factors, including muscle composition (fatty infiltration) and moment arm [6, 7]. We have recently demonstrated differences in proximal femur morphology in patients with TFA compared to controls, most evident in the torsional rotation of the greater trochanter [8]. While this likely affects the abductor muscle paths, quantification of all parameters that influence a muscle's ability to load a joint have not been quantified in patients with TFA. Thus, our objective was to compare bilateral muscle quality (volume and fatty infiltration) and moment arm of the gluteus medius (GMED) in patients with TFA.

Methods: With IRB approval, quantitative magnetic resonance (MR) images were collected in two sequences from the iliac crest to distal lesser trochanter from seven patients with unilateral TFA (2M/5F; age: 45.7±15.2 y/o; BMI : 24.7±5.3 kg/m^2; time since amputation: 23.7±14.5 years) on a 3T GE Signa PET/MR Scanner (GE Healthcare). T1-weighted LAVA fast-spin echo images with fat suppression followed by 3D IDEAL IQ images with a 6-point Dixon sequence were collected [9]. From the MR images, the GMED was bilaterally segmented via semi-automatic thresholding (Amira) and used to calculate muscle volumes (normalized by body mass (kg) and height (mm)) [10]. Muscle composition was quantified by separating water and fat signals based on the IDEAL algorithm [11]. Percent fat content was calculated as the fat signal divided by the sum of the fat and water signal multiplied by 100. Six of the seven patients (one patient was non-ambulatory) then participated in an instrumented gait analysis session that collected whole-body kinematics during overground walking at self-selected speeds (F_s=120 Hz, Vicon). Subject-specific musculoskeletal models were created by modifying a pre-existing model with 23 degrees of freedom and 92 muscles, while subject specificity was achieved using patient-specific MR images and motion capture data, with methods previously described [12]. GMED reconstructions were used to guide the attachment sites within the model. Bilateral abduction moment arms of the GMED were calculated across three gait cycles [13]. Bilateral differences in volume, fatty infiltration, and peak abduction moment arms were compared between limbs using paired Cohen's *d* effect sizes (medium effect: 0.5≤*d*<0.8; large effect: *d*≥0.8).

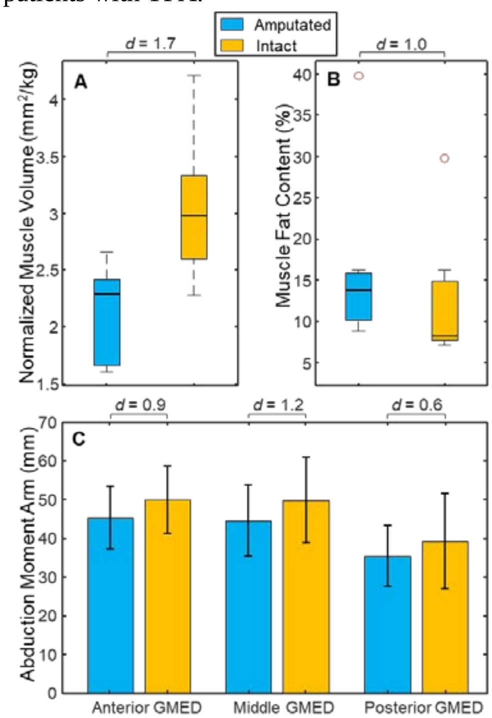

Figure 1. Boxplots of bilateral GMED **A)** volume, **B)** muscle fat content, and **C)** Mean ± 1 S.D peak GMED abduction moment arm.

Results & Discussion: Muscle volume was smaller and fatty infiltration was larger in the amputated limb GMED compared to the intact limb, indicating atrophy of the amputated limb [14] (Fig. 1). However, differences in muscle volume (*d*=1.7) were more pronounced than differences in fatty infiltration (*d*=1.0) which may be explained by prior evidence showing increased duration of activation of amputated limb GMED in patients with TFA compared to controls [15]. Additionally, we found the amputated limb GMED abduction moment arm was smaller compared to the intact limb (Fig. 1), which represents a biomechanical disadvantage of the amputated limb GMED. With this disadvantage, the amputated limb GMED would need to generate a larger amount of force to produce the same stabilizing torque about the joint for the amputated limb compared to the intact limb [16]. This indicates that GMED strengthening alone may not be sufficient to restore hip abductor function and normalize the force and torques that load the hip joint.

Significance: To our knowledge, these are the first results to comprehensively quantify bilateral GMED volume, composition, and abduction moment arm. Understanding all components that influence muscle force production may advance future interventions aimed at improving function and normalizing joint loading through targeted strengthening and movement retraining in patients with TFA.

Acknowledgements: This project was supported by the Colorado Clinical and Translational Sciences Institute (NIH/NCATS UL1 TR002535-04) and the University of Colorado Osseointegration Research Consortium.

References: [1] Ziegler-Graham et al. (2008) *Arch PMR.* [2] Kulkarni et al. (1998) *Clin Rehab*. [3] Amaro et al. (2007) *IJSM.* [4] Heitzmann et al. (2020) *PLoS One*. [5] Ryser et al. (1988) *Arch PMR.* [6] Gerber et al. (2007) *JSES.* [7] Ackland et al. (2012) *JOB.* [8] Roda et al. (2022) *ORS.* [9] Gaffney et al. (2023) *ORS.* [10] Handsfield et al. (2014). *JOB.* [11] Reeder et al. (2005) *MRM.* [12] Gaffney et al. (2020). *Clin Biomech.* [13] Sherman et al. (2013) *ASME Des. Eng. Tech. Conf.* [14] Goutallier et al. (2003) *JSES.* [15] Wentink et al. (2013) *JNER.* [16] Song et al. (2020) *JOB.*

HIGH FUNCTIONING OLDER ADULTS CAN IMPROVE BALANCE REGULATION DURING FAST WALKING

Sarah A. Roelker*, Athulya A. Simon, Katherine A. Boyer
Department of Kinesiology, University of Massachusetts Amherst
*Corresponding author's email: sroelker@umass.edu

Introduction: During locomotion, the whole-body angular momentum (H) about the center of mass must be regulated to maintain balance [1], such that a smaller peak-to peak range of H (H_R) is associated with better balance regulation [2]. Previous research suggests young adults decrease H_R with increasing walking speed [3]. However, compared to young adults, older adults have greater frontal plane H_R at preferred and fast walking speeds [4], suggesting greater fall risk [2]. Thus, older adults are thought to reduce walking speed to maintain balance [5]. The regulation of H is thought to be achieved by a small set of neural "primitives" (i.e., motor modules or muscle synergies) that simplify neural control [6]. The loss of an independent plantarflexor module due to reduced complexity (fewer modules) has been associated with increased frontal H_R in individuals post-stroke [7]. However, the relationship between modular control and balance regulation, and how walking speed or exercise influence this relationship, remains unclear for typically aging adults. The purpose of this study was to determine the effect of walking speed before and after a 30-minute bout of walking on balance regulation and modular control in young and older adults.

Methods: Five young (1 female, 38.6 ± 1.1 y, 1.8 ± 0.1 m, 85.4 ± 12.9 kg) and 9 older (4 female, 73.3 ± 3.2 y, 1.7 ± 0.1 m, 67.9 ± 12.6 kg) adults walked overground at a preferred (PWS) and fast (FAST) walking speed before (PRE) and after (POST) a 30-minute treadmill walking exercise. Three-dimensional marker data were collected at 200 Hz for each walking condition (PRE-PWS, PRE-FAST, POST-PWS, POST-FAST). Electromyography (EMG) data were simultaneously collected at 2000 Hz from 10 lower extremity muscles on the dominant leg. In Visual3D, marker data were lowpass filtered at 8 Hz and H was calculated about the center of mass. Peak-to-peak H_R was computed in the frontal, sagittal, and transverse planes and normalized to height, mass, and walking speed. In MATLAB, EMG from 3-5 gait cycles were bandpass filtered, rectified, and lowpass filtered. The EMG was normalized to the peak value from a maximum voluntary contraction and concatenated across gait cycles into a matrix (EMG_o) for input into a non-negative matrix factorization algorithm [8]. A bootstrapping approach with 500 samples with replacement [9] was used to determine the number of modules required to reconstruct EMG_o such that the lower bound of the confidence interval for the variability accounted for was greater than 80% for each muscle and 90% for all muscles combined. Walking speed, H_R in each plane, and number of modules were compared between age-groups and across conditions using two-factor ANOVAs. Post-hoc tests assessed for pairwise differences with Bonferroni corrections for multiple comparisons. For all tests $\alpha = 0.05$.

Results & Discussion: There were no differences in walking speed ($p \geq 0.19$) between age-groups (Table 1). In contrast to previous work, older adults walked with smaller frontal H_R than young adults in the PRE-PWS (p=0.04) and POST-FAST (p=0.02) conditions (Fig. 1). Older adults also walked with a smaller transverse H_R than young adults during the PRE-FAST (p=0.04). Sagittal H_R did not differ between age groups ($p \geq 0.27$). From the PWS to FAST speed, older adults reduced sagittal H_R PRE (p=0.02) and POST (p<0.01) exercise. The older adults' reduced frontal H_R at the FAST vs PWS speed POST exercise (p=0.03) only, which may have been due to reduced muscle capacity after exercise, as previous work suggests H_R minimization as a strategy to reduce muscle work [1]. The young adults' H_R did not differ between conditions in any plane ($p \geq 0.05$). There was no change in H_R from PRE to POST exercise at either speed, suggesting our high functioning participants' balance regulation was robust to the exercise. Number of modules did not differ by age or condition ($p \geq 0.19$). Interestingly, a secondary analysis revealed an independent plantarflexor module in all participants and conditions, further supporting the importance of an independent plantarflexor module for balance control [7].

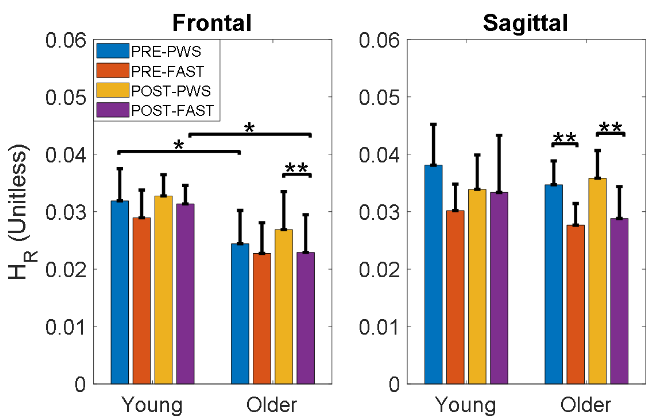

Figure 1. Frontal and sagittal planes H_R for young and older adults. Symbols indicate difference between: * age groups; ** conditions.

Table 1: Walking speed and module number by age and condition

Condition	Walking Speed (m/s) *		# of Modules	
	Young	Older	Young	Older
PRE-PWS	1.57 ± 0.18	1.48 ± 0.10	2.6 ± 0.5	3.0 ± 0.5
PRE-FAST	1.98 ± 0.21	1.89 ± 0.16	2.8 ± 0.4	3.0 ± 0.7
POST-PWS	1.56 ± 0.21	1.48 ± 0.12	2.8 ± 0.4	3.0 ± 0.5
POST-FAST	1.94 ± 0.20	1.82 ± 0.15	3.0 ± 0.7	2.7 ± 0.9

*POST-PWS and -FAST speeds were matched to PRE conditions.

Significance: Maintaining a small H_R is necessary to regulate balance [2] and older adults are thought to reduce walking speed to maintain balance [5]. However, our older adults reduced sagittal and frontal H_R at the FAST speed and walked with smaller frontal H_R than young adults at similar speeds, suggesting high-functioning older adults can improve balance regulation in response to walking demands. Future work will identify mechanisms (e.g., reduced step width [4]) older adults used to reduce H_R with increased walking speed.

Acknowledgements: The authors thank Kiichi Ash for assisting with data collection and funding from NIH 5R01AG068102.

References: [1] Herr & Popovic (2008), *J Exp Biol*; [2] Neptune & Vistamehr (2019), *J Biomech Eng*; [3] Bennett et al (2010), *Hum Mov Sci*; [4] Vistamehr & Neptune (2021), *J Biomech;* [5] Menz et al (2003), *Age Ageing*; [6] Popovic et al (2004), *IEEE/RSJ Int Conf on IROS*; [7] Brough et al (2019), *J Biomech*; [8] Lee & Seung (1999), *Nature*; [9] Roelker et al (2021) *PLOS One*.

BODYWEIGHT SUPPORT DECOUPLES THE BIOMECHANICAL AND PHYSIOLOGICAL DETERMINANTS OF EXERCISE TOLERANCE DURING HUMAN RUNNING

Shernice A. Thomas[1*], Francisco Espinoza[1], Christopher J. Arellano[1]
[1]Department of Health and Human Performance, University of Houston, Houston, TX, USA
*Corresponding author email: sathomas5@uh.edu

Introduction: Body weight-supported (BWS) running elicits changes in the biomechanics and physiology of running that make it possible for individuals to experience the benefits of running in a safer environment. At a given speed, running at a reduced body weight (BW) decreases the metabolic cost of running as well as the peak forces generated by the lower limbs [1]. This 'decoupling' benefit of BWS running has led to its increased use as a training tool to maintain cardiorespiratory fitness (CRF) levels among various populations. However, to maintain or improve CRF, exercise has to occur at the same metabolic rates achieved at 100% BW. To achieve this at a lower BW, one must run at much faster speeds by generating ground forces at higher rates, placing a higher mechanical burden on the lower limbs. It is possible that the need to generate ground forces at higher rates may limit one's ability to tolerate high-intensity exercise during BWS running, which has implications for exercise prescription under such conditions. To define exercise tolerance during running, we use the critical velocity (CV) framework which is based on a simple model of the human bioenergetic system [2]. According to this model, CV represents the maximum work rate one can sustain for a very long time primarily through aerobic metabolism. CV also represents the *critical metabolic rate* that demarcates the heavy and severe exercise intensity domains [2]. Given that the physiology and biomechanics of running are inherently linked, we sought to understand how altering the mechanical demands on the lower limbs (via BW support) influences one's ability to tolerate high-intensity exercise during running. We hypothesized that running with BW support will cause one's critical metabolic rate (i.e. CV) to occur at a lower relative intensity (expressed as %VO_2 max). The rationale underlying this hypothesis was based on our presumption that running at CV under 50% BW would necessitate faster running, resulting in greater reliance on less oxidative, more fatigable muscle fibers to sustain faster contraction rates [3]. We also hypothesized that the mechanical means to achieve one's CV at a lower BW will be accompanied by faster rates of force generation (i.e. shorter ground contact times) and lower magnitudes of force.

Methods: Twelve young, healthy runners participated in this study (3 W, 9M; age = 28.00 ± 5.29 years; mass = 69.68 ± 11.39 kg; height = 1.77 ± 0.08 m; mean ± SD). All subjects completed VO_2 max and CV trials (on separate days) at 100% BW and 50% BW. BWS running was achieved via a custom-built device that applied a lifting force on subjects as they ran on a force-measuring treadmill [4]. To determine CV, subjects ran at three fixed velocities equivalent to 90%, 100% and 105% of their velocity at VO_2 max (randomized) while we recorded their time to exhaustion (TTE) at each speed. We then fit subjects' resulting velocity and time data into the CV model: $V = CV + (D'/t)$, where V = velocity; CV = critical velocity, D' = the total distance one can run above CV, and t = TTE. Independent variables included treadmill velocity and BW level, and primary dependent variables included VO_2, CV, peak vertical GRF (vGRF), and ground contact time.

Results & Discussion: As hypothesized, CV occurred at a lower %VO_2 max at 50% BW (83.3%) compared to 100% BW (87.8%) ($p < 0.05$). On average, individuals also achieved lower VO_2 max values at 50% BW (44.9 ml/kg/min) compared to 100% BW (49.5 ml/kg/min, $p < 0.01$). These findings are functionally significant because they suggest that BWS alters exercise tolerance during running by prompting individuals to cross into their severe exercise intensity domain at a lower %VO_2 max, and altering one's CRF capacity. Therefore, it will be necessary to adjust exercise prescriptions under BWS running conditions, as an individual's critical fatigue threshold is not conserved. If we assume that an individual's relative critical fatigue threshold does not change under lower BW, then pushing an individual to exercise at fast speeds could lead to them prematurely reaching their fatigue limit. Additionally, our preliminary results (n=7) for our second hypothesis indicate that running at CV at 50% BW decreased peak vGRFs by ~22% and ground contact time by ~21%, on average, compared to 100% BW (Fig. 1). Our future research will explore the potential of high-intensity BWS running as an alternative training tool to maintain or improve running performance.

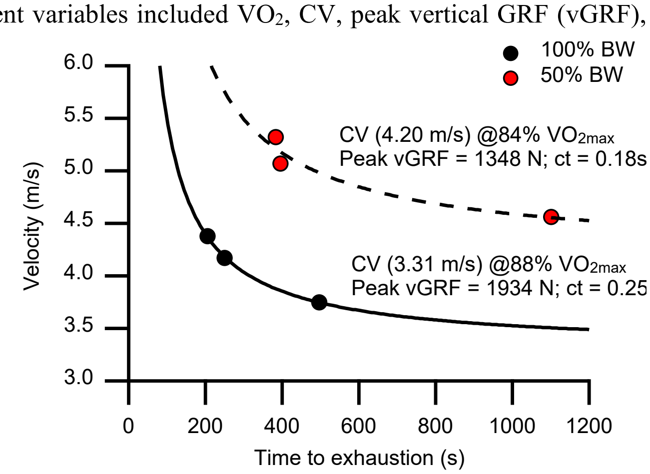

Figure 1. Data for a representative subject. Although CV occurs at a higher absolute velocity at 50% BW, it occurs at lower relative intensity (%VO_2 max) compared to 100% BW, indicating that individuals enter their severe intensity domain at an earlier point. Furthermore, running at 50% BW reduces peak vGRFs and ground contact time (ct), highlighting the need to generate ground forces more rapidly.

Significance: The insights gained from this study have both fundamental and applied implications for exercise interventions using BWS running. On a fundamental level, this study provides insights into the magnitudes to which BWS alters VO_2 max levels and exercise tolerance during running. On an applied level, this study shows that BWS may be used as a tool to train muscle fibers that generate forces more rapidly, in a safe environment with lower peak vertical ground reaction forces, potentially decreasing the risk of lower limb injury.

References: [1] Grabowski & Kram (2008), *J. Appl. Biomech* 24(3):288-97; [2] Monod & Scherrer (1965), *Ergonomics* 8(3):329-38; [3] Copp et al. (2010), *J Physiol* 588(24): 5077-87; [4] Teunissen et al. (2007) *J Exp Biol* 210(24):4418-27.

CAN MINIMUM TOE CLEARANCE PREDICT COMMUNITY-BASED, TRIP-RELATED STUMBLES BY OLDER ADULTS?

Marco A Avalos*, Noah J Rosenblatt
Center for Lower Extremity Ambulatory Research (CLEAR), Dr. W. M. Scholl College of Podiatric Medicine at Rosalind Franklin University of Medicine and Science, North Chicago, IL
*Corresponding author's email: marco.avalos@rosalindfranklin.edu

Introduction: Falls represent the leading cause of unintentional injuries in older adults [1], costing approximately $39,000 per fall [2]. Most falls occur after a trip event, which theoretically occurs when foot clearance, quantified as minimum toe clearance (MTC), is insufficient to avoid an obstacle [3]. Indeed, research has identified that a low MTC and a highly variable MTC theoretically increase the risk of tripping events [4]. Those who self-report multiple stumbles, including tripping events, are more likely to fall [5]. To our knowledge, no evidence relates to MTC and trip-related stumbles (tripping events) in older adults. This study aimed to quantify the extent to which MTC and its variability differed among older adults who did and did not prospectively report trip-related stumbles. Participants who prospectively reported multiple trip-related stumbles were expected to have lower and more variable MTC.

Methods: We analyzed data from 50 older adults with a BMI of 18.5-24.9 kg/m2 or BMI $\geq$ 30 kg/m2 recruited as part of a larger study on obesity and falls. Participants self-reported the number of falls in the prior year. They then walked across an 8 m walkway at a comfortable pace while the motion of a marker on the second metatarsal head ("toe marker") was tracked using motion capture. We normalized the vertical trajectory of the toe marker during the swing phase to its value at the prior midstance, and MTC was identified in each swing phase as a local minimum in the trajectory. For each participant, we calculated the mean MTC, median MTC, interquartile range (IQR), and standard deviation (SD) of MTC. Based on the participant's distribution of MTC across all steps, we also calculated skewness and kurtosis from each participant. We chose to describe MTC and its variability with both normal and non-normal descriptors in accordance with the literature, which has suggested that MTC distribution, at least within subjects, may be non-normal [6] and that measures of the non-normal distribution (i.e., skewness and kurtosis) may be essential in describing tripping probability [4].

Every other week for one year following data collection, participants completed a survey [7] that asked about their stumbles and the cause of stumbles. We categorized participants as "stumblers" if they reported two or more trip-related stumbles; otherwise, we defined them as "non-stumblers." A multivariate analysis of covariance was used to quantify group differences in the set of six MTC variables, covarying for demographics found to differ between groups.

Results & Discussion: 14 participants were categorized as stumblers, in which the proportion with a history of falls was more than twice that of the non-stumblers ($p=0.034$). A total of 107 trip-related stumbles were reported by stumblers (8.2 $\pm$ 9.4 trip-related stumbles per stumbler; maximum of 29). None of the six MTC-related variables significantly differed between stumblers and non-stumblers (Wilks' $\lambda = 0.916$, $F(6, 42) = 0.638$, $p = 0.699$).

Although no significant differences were found between groups, trip-related stumblers showed a tendency of diminished skewness and a negative kurtosis (Table 1). Collectively, these suggest that stumblers may less often reach MTC values on the high end of their utilized range. The absence of group differences may reflect the fact that assessing MTC during level ground walking within a sterile (without hazards) lab environment lacks ecological validity to assess the risk of community-based trip-related stumbles. The ability to adapt MTC in response to environmental challenges may be more relevant to dictating the risk of stumbling. Future work to identify older adults at greatest risk of experiencing a community-based trip-related fall should consider assessing MTC under various conditions (e.g., with and without obstacles and/or indoors and outdoors) combined with assessments of fall-recovery abilities. These studies may also consider including measures to account for individual levels of exposure to tripping hazards.

	Non-Stumblers (n=36)	***Stumblers (n=14)***	***Effect Size***
Median MTC (cm)	1.58 ± 0.62	1.44 ± 0.46	-0.028
Mean MTC (cm)	1.65 ± 0.64	1.47 ± 0.44	0.293
MTC-IQR (cm)	0.79 ± 0.27	0.77 ± 0.23	0.242
MTC-SD (cm)	0.60 ± 0.24	0.54 ± 0.13	0.279
Skewness	0.53 ± 0.44	0.32 ± 0.32	0.499
Kurtosis	0.29 ± 0.93	-0.20 ± 0.70	0.553

Table 1 Summary of average outcomes of the stumble groups. *Data is presented as M ± SD.*

Significance: Laboratory assessments may not capture the ability of a person's adaptability towards the challenges presented in the real world and may lack the ability to assess the risk of community-based trip-related stumbles. Also, the assessments of MTC distribution may provide a better picture of the person's risk of trip-related events than measures of central tendency MTC.

Acknowledgments: This study was supported by the National Institute of Arthritis and Musculoskeletal and Skin Diseases.

References: [1] Moreland et al. (2020), *MMWR* 69(27); [2] Blackwell et al. (2018), *http://www.cdc.gov/nchs/nhis/SHS/tables.htm*; [3] Barret et al. *Gait Posture* 32(4); [4] Begg et al. (2007), *Gait Posture* 25(2); [5] Srygley et al. (2009), *Arch Phys Med Rehabil* 90(5); [6] Best & Begg (2008), *J Biomech* 41(5); [7] Rosenblatt et al. (2017), *Prosteth Orthot Int* 41(4).

How Healthy Older Adults Maintain Lateral Balance On Narrowing Walking Paths

Meghan E. Kazanski[1,2*], Joseph P. Cusumano[3], Jonathan B. Dingwell[1]
[1]Department of Kinesiology, The Pennsylvania State University, University Park, PA, USA
[2]Department of Medicine, Division of Geriatrics and Gerontology, Emory University School of Medicine, Atlanta, GA, USA
[3]Department of Engineering Science & Mechanics, The Pennsylvania State University, University Park, PA, USA
[*]email: mek79@psu.edu

Introduction: Navigating non-straight walking paths (e.g., cluttered living spaces, crowded sidewalks) requires humans to maintain balance while adjusting stepping to accommodate their changing path (e.g., varying path width, location). Older adults' abilities to execute appropriate balance adjustments on continuously varying paths may be limited. These limitations may cause older adults to exhibit elevated instability risk, and possibly to avoid some walking paths entirely [1].

It is unclear *how* older adults perform ongoing side-to-side balance adjustments on continuously varying paths, and how these adjustments impact their lateral instability risk and ability to stay on their path.

Here, healthy young and older adults traversed a continuously-narrowing path, before voluntarily switching to a wider path [2]. We characterized participants' lateral stability margins [3] and instability risk [4] as paths narrowed. We hypothesized that all participants would exhibit gradually smaller stability margins that would be coincident with increased instability risk. We further hypothesized that older adults, *despite* larger stability margins, would exhibit elevated instability risk. We expected that older adults would transition off the narrowing path sooner than young adults [2], but with comparable instability risks at this earlier transition.

Methods: 20 young (YH; 21.7 ± 2.6 yrs) and 18 older (OH: 71.6 ± 6.0 yrs) healthy adults performed treadmill walking along a gradually narrowing virtual path. Participants chose when to switch to an adjacent, wider path [2]. We extracted step-to-step time series of participants' frontal-plane CoM states and path widths.

We compiled CoM states for each YH and OH groups, then separated states into a series of overlapping bins based on corresponding path widths (W_P).

For all steps in each bin, we computed participants' minimum lateral Margin of Stability (*MoS*) [3]. Each bin's *MoS* data were sub-sampled 50 times using a random 95% of bin data. We computed the lateral Probability of Instability (*PoI*) for each sub-sample by integrating the probability density function of the group-wise *MoS* over the lateral instability range (*MoS* < 0) [4]. *PoI* thereby directly measured each group's instability risk on any step enacted at a given W_P.

We characterized YH and OH *MoS* and *PoI* by plotting these changes across W_P. We then mapped the average path width at instants when participant switched paths onto these group-wise curves to define each participant's $(MoS)_{switch}$ and $(PoI)_{switch}$ thresholds. We evaluated age effects on these thresholds.

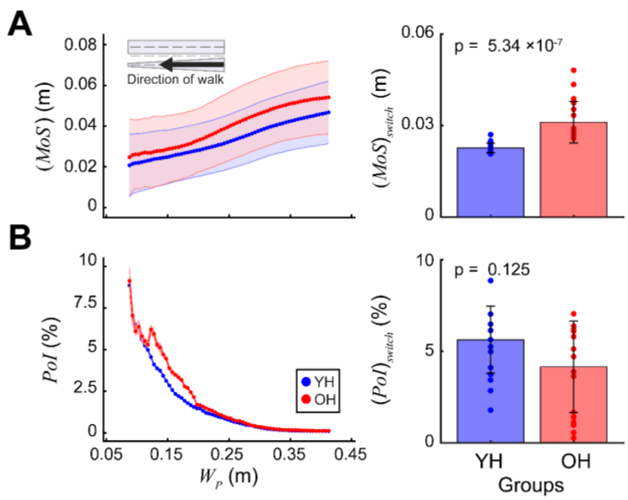

Figure 1: Across path widths (W_P), OH exhibited consistently larger lateral Margins of Stability (*MoS*) (**A**, left), and larger Probability of Instability (*PoI*) at narrower W_P (**B**, left) compared to YH. OH transitioned from the narrowing path sooner than YH [2], at wider stability margins, $(MoS)_{switch}$ (**A**, right; p<0.001) while retaining similar lateral instability likelihoods, $(PoI)_{switch}$ (**B**, right; p = 0.125).

Results & Discussion: All participants exhibited gradually smaller *MoS* as paths narrowed (Fig. 1A, left), indicating that CoM motion became progressively *closer* to a laterally unstable position. However, *MoS* cannot independently quantify *likelihood* of lateral instability at any given step [4]. These insights required the complementary *PoI* analysis [4], which revealed that both groups exhibited increased *PoI*, indicating elevated instability risk as paths narrowed (Fig. 1B, left).

As, expected, OH tended to exhibit higher *PoI* on narrower W_P compared to YH, which indicated their elevated instability risk *despite* consistently larger *MoS* (Fig. 1A-B). Thus, older adults' compensatory *MoS* did not fortify them against elevated lateral instability risk.

OH opted off of the narrowing paths sooner than YH (p = 0.022) [2]. OH left narrowing-paths while exhibiting *PoI* comparable to YH (Fig. 1B, right; p = 0.125), despite exhibiting larger *MoS* (Fig. 1A, right; $p = 5.34{\times}10^{-7}$). Thus, OH and YH opted off the narrowing-path walking at different levels of difficulty (i.e., path widths) *per se*, but did so while retaining similar lateral instability risk.

Significance: This work directly connects age-impaired *continuous* balance adjustments to elevated instability risk on narrowing walking paths. We characterized how humans adjust ongoing balance to manage changing path demands. We demonstrated that the nature of the narrowing path required participants to accept progressively greater lateral instability risk. Older adults' larger *MoS* compensations did not offset their elevated instability risk compared to young adults. Older adults left the narrowing path sooner, at low and similar *PoI*, suggesting that sensitivity to instability risk may be preserved with healthy aging.

Acknowledgements: NIH / NIA Grant #: R01-AG049735.

References: [1] Butler et al. (2015). *J. Gerontology*, 70.; [2] Kazanski at al. (2021). *Gait and Posture*, (88).; [3] Hof et al. (2005). *J. Biomech.* 38(1).; [4] Kazanski et al. (2022). *J. Biomech.* (144).

HOP DISTANCE LIMB SYMMETRY REFLECTS LANDING KNEE KINEMATIC SYMMETRY

Stefano Di Paolo[3], Naoaki Ito[1,2], Kayla D. Seymore[1,2*], Laura Bragonzoni[3], Stefano Zaffagnini[4], Lynn Snyder-Mackler[1,2], Karin Grävare Silbernagel[1,2]
[1]Biomechanics and Movement Science Program, University of Delaware, Newark, DE, USA
[2]Department of Physical Therapy, University of Delaware, Newark, DE, USA
[3]Department for Life Quality Studies, University of Bologna, Bologna, Italy
[4]2nd Orthopaedic and Traumatologic Clinic, IRCCS Rizzoli Orthopaedic Institute, Bologna, Italy
*Corresponding author's email: seymorek@udel.edu

Introduction: Limb symmetry index (LSI) from the commonly administered single-leg hop test battery [1] is widely used by clinicians to identify readiness to return to sport (RTS) after injuries like anterior cruciate ligament injury and subsequent reconstruction (ACLR) [2,3]. Landing with poor knee biomechanics (e.g., shallow knee flexion angle) may be a risk factor for ACL injury [4]. Whether LSI measured in a clinical setting accurately reflects lower limb biomechanical asymmetry after injury is unclear [5]. Advancements in markerless motion capture (mocap) technology may allow clinicians to readily obtain relevant biomechanics during hop testing, such as knee kinematics [6]. While clinically it makes sense that LSI scores from the hop test battery capture patients' ability to land safely, no work has quantitatively compared LSI scores obtained during the hop test battery to natural landing kinematic symmetry (i.e., without the potential movement constraints from clothing adjustments and/or marker fixation during traditional mocap). The purpose of this study was to investigate the correlation between hop test battery LSI and sagittal plane knee kinematic symmetry during landing using markerless mocap technology.

Methods: Forty-four participants with and without a history of knee surgery (23 female, 21 male, 32 healthy, 12 knee surgery, 28±8 years, 1.7±1.0 cm, 72.2±11.9 kg, 7±4 years since surgery) performed single hop (SLH), crossover hop (COH), and triple hop (TRH) tests as part of the hop test battery [1]. Eight high speed cameras (Sony RX0-II, Sony Corp., Minato, Japan, 120Hz) were used to collect motion data. Participants were asked to hop as far as possible, starting with their toes behind a marked point, and "stick the landing". Landing position of the heel was used to measure distance hopped. Each hop was performed first on the uninvolved (UN) then involved (IN) limb. The IN limb was defined as the injured or non-dominant limb. Two practice trials preceded two successful hop trials.

Theia 3D (Theia Markerless Inc., Kingston, Canada) was used to generate 3D model files for each trial. The model files were processed in Visual 3D (v6, C-Motion Inc., Germantown, USA). Take-off and landing events were defined from the velocity of foot segment heel and toe positions. The end of movement was identified as the furthest horizontal center of mass position within 0.5 sec of the last landing. Peak knee flexion angle was extracted from each landing phase (i.e., landing to take-off/end of movement), then averaged across landings (for COH and TRH) using two successful trials for each participant. Hop distance (clinical) and peak knee flexion angle (kinematic) LSI was calculated (LSI = [IN limb / UN limb] * 100) and averaged across two successful trials for each participant.

Spearman's rank correlation coefficient ρ was used to determine the relationship between clinical and kinematic LSI. Correlations were considered weak, moderate, and strong for $\rho < 0.40$, 0.40-0.70, and >0.70, respectively [7]. All statistical analyses were performed in Matlab (v9.13, The MathWorks Inc., Natick, USA). Alpha was set at 0.05.

Results & Discussion: Clinical LSI showed a moderate positive correlation with kinematic LSI at peak landing for the SLH and TRH (**Table 1**). The COH had a weak non-significant correlation with kinematic LSI during landing (**Table 1**), which was unsurprising due to the stronger knee frontal/transverse plane control required to perform this hop compared to the primarily sagittal plane movement for the SLH and TRH. Asymmetrical hop distance reflected asymmetrical knee sagittal plane kinematics during landing. Further research should assess if markerless mocap could be used to detect knee kinematic asymmetries in the ACLR population after RTS.

Table 1: Hop test battery metrics and limb symmetry index (LSI) correlations.

	Hop distance (m)		Peak knee flexion (°)		Clinical LSI (%)	Kinematic LSI (%)	Correlation	
	IN Limb	UN Limb	IN Limb	UN Limb			ρ [95% CI]	p-value
SLH	1.1 ± 0.3	1.2 ± 0.3	51.8 ± 11.3	53.6 ± 9.7	98.6 ± 15.9	97.3 ± 15.5	0.40 [0.11, 0.63]	0.008
COH	3.2 ± 1.1	3.3 ± 1.1	50.8 ± 6.6	52.9 ± 6.1	98.0 ± 12.6	96.3 ± 9.4	0.16 [-0.17, 0.46]	0.326
TRH	4.0 ± 1.0	4.0 ± 1.0	53.4 ± 6.4	53.3 ± 5.4	99.2 ± 9.9	100.9 ± 10.6	0.60 [0.34, 0.78]	<0.001

Significance: Symmetry scores on the hop test battery reflect knee landing biomechanics symmetry, emphasizing the importance of continuing to use the hop test battery as part of clinical RTS decision making. Markerless mocap is an exciting new technology that may provide useful information beyond current clinical symmetry metrics, allowing for better precision rehabilitation after knee injury.

Acknowledgements: Theia Markerless Inc. provided the cameras and software used in this research study.

References: [1] Noyes et al. (1991), *Am J Sports Med* 19:513-18; [2] Adams et al. (2012), *J Orthop Sport Phys Ther* 42:601-14; [3] Grindem et al. (2016), *Br J Sports Med* 50:804-8; [4] Della Villa et al. (2020), *Br J Sports Med* 54:1423-32; [5] Wellsandt et al. (2017), *J Orthop Sports Phys Ther* 47:334-8; [6] Ito et al. (2022), *JSAMS Plus* 1:100001; [7] Akoglu (2018), *Turk J Emerg Med* 18:91-3.

ALLIGATORS USE ELASTIC ENERGY STORAGE IN ANKLE EXTENSORS DURING STEADY STATE WALKING

Adrien A. Arias*, Elizabeth Mendoza, Emanuel Azizi
[1]Dept. of Ecology & Evolutionary Biology, University of California, Irvine
*Corresponding author's email: adriena@uci.edu

Introduction: Most legged animals have evolved a suite of musculoskeletal adaptations to reduce the energetic cost of terrestrial locomotion. Specifically, cursorial animals (i.e. adapted for running) have large proximal limb muscles that shorten to produce mechanical work (= force × muscle strain) while smaller distal muscles contract isometrically to generate force economically (but perform zero work) [1]. This mechanism is possible through the use of elastic elements in-series with distal limb muscles that stretch and recoil during locomotion, allowing muscle to contract isometrically. Most legged animals studied so far (e.g. humans, turkeys, goats) have distal free tendons that are well-suited for storing elastic strain energy, but it remains unclear whether alligators and other sprawling animals are capable of using elastic energy storage during locomotion or whether the lack of long, compliant tendons imposes additional work requirements on muscle fibers *in vivo*. Through a combination of *in situ* muscle preparations, joint-level analyses, and *in vivo* muscle function measurements during walking, we show 1) the gastrocnemius externus (GE) of alligators is capable of storing significant elastic energy in its tendon during supramaximal contractions, 2) surprisingly, GE develops force mostly isometrically while the ankle joint performs negative and positive work during ground contact, and 3) *in vivo* operating lengths of GE fall on the ascending limb of its force-length curve. Together these results show the GE's external free tendon stores and releases elastic energy at the ankle while GE muscle fibers contract isometrically— even at the low locomotor speeds used during alligator walking. This work expands the range of animals known to use elastic energy storage to reduce the metabolic cost of locomotion and suggests energy saving mechanisms during locomotion are more widely spread than previously assumed.

Methods: A total of 16 juvenile alligators (*A. mississippiensis*, Daudin 1801) were used for this study (range of body mass = 0.5-2.5 kg). For joint-level analyses (n=5), alligators were trained to walk across a trackway instrumented with a force plate and high-speed video cameras. An open-source MATLAB script [2] was modified to calculate instantaneous ankle joint forces and torques from 3D force and kinematic data using quaternion algebra and inverse dynamics. For *in situ* muscle preparations (n=8), the gastrocnemius externus (GE) muscle-tendon unit was isolated from adjacent muscles and securely attached to a dual-mode servomotor with Kevlar thread. Isolated GEs were then supramaximally stimulated across a range of lengths via silver electrode nerve cuff (on the tibial branch of the sciatic nerve) to quantify elastic energy stored during peak contraction. For *in vivo* muscle measurements (n=3), we implanted a leaf spring force transducer on GE's free tendon (to measure muscle force), sonomicrometry crystals (fascicle length), and electromyography (activation timing) to measure dynamic muscle function during steady state walking on a motorized treadmill.

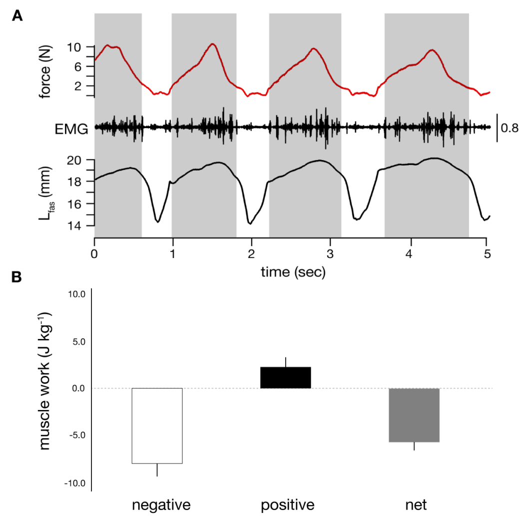

Figure 1: (A) Representative force, electromyography, and fascicle length (L_{fas}) data from an alligator walking steady state. Stance phases are denoted by grey shaded regions. (B) Pooled averages (n=32) of normalized muscle work during an entire stride. The gastrocnemius externus of alligators performs some negative work early in stance, followed by essentially isometric force development. Bars represent mean $\pm$ sem.

Results & Discussion: Isolated gastrocnemius externus (GE) muscles of alligators were found to shorten 19.0 $\pm$ 2.8 % of optimal fiber length (Lo) during maximum "isometric" contractions (muscle-tendon unit length was held constant). This significant shortening allowed 6.3 $\pm$ 1.8 J kg^{-1} of energy (normalized to muscle mass) to be stored in elastic elements, representing GE tendon's capability to store elastic energy during supramaximal contractions. Results of inverse dynamics analysis showed negative and positive power generation by the ankle joint during stance phase of walking, whereas *in vivo* fascicle strain data revealed that GE undergoes a period of eccentric contraction followed by isometric force development (Fig. 1A). Mechanical work performed by GE ranged between -2.0 and -7.2 J kg^{-1} during an entire stride across all animals used in this study (Fig. 1B), falling within the range of normalized work values performed by gastrocnemii in cursorial animals during terrestrial locomotion. Together these data suggest that GE's external free tendon stores and releases elastic energy at the ankle while GE muscle fibers contract isometrically to develop force economically. Additionally, we found that GE muscle fibers begin stance phase at 0.83 $\pm$ 0.19 Lo and reach maximal fascicle length (0.95 $\pm$0.10 Lo) near midstance, indicating operating ranges exclusively on the ascending limb of its force-length curve.

Significance: This work shows that alligators are not only capable of storing elastic energy in their distal tendons during supramaximal muscle contractions, but use this energy saving mechanism during steady state walking. Elastic energy storage is typically associated with highly derived morphological features, impulsive movements, and bouncy gaits, but our findings show that energy saving mechanisms are more widespread than previously assumed and likely apply to other sprawling species. It is surprising that alligators perform similar levels of mechanical work as more derived taxa [3,4,5,6], suggesting patterns of work generation (i.e. proximal limb muscles perform work and distal muscles transmit force) hold true across most legged animals studied to-date. This work will be of broad interest to those studying the evolution of complex integrated movements like walking and establishes an important baseline locomotor condition for alligators to test future muscle-level hypotheses based on variable terrain in sprawl-postured animals.

Acknowledgements: The authors thank MA Daley for use of their servomotor and treadmill. We also thank undergrad researchers ME Pena, A Arrita, and M Arreguin for help with data collection and digitizing.

References: [1] Dickinson et al. 2000, *Science* 288(5463); [2] Dumas et al. 2004, *Comput Methods Biomech Biomed Engin* 7(3); [3] Eng et al. 2019, *J of Exp Bio* 222(24); [4] Daley and Biewener 2003, *J of Exp Bio*, 206(17); [5] McGuigan et al. 2009 *J of Exp Bio*, 212(13); [6] Roberts et al. 1997, *Science* 275(5303)

MUSCULOSKELETAL SPECIALIZATION FOR SPRINTING AND MARATHON RUNNING

Tom Van Wouwe1, Jennifer Hicks1, Scott Delp1 and Karen Liu 2
1 Department of Bioengineering, Stanford University, Stanford, USA.
2 Department of Computer Science, Stanford University, Stanford, USA.
*email: tvwouwe@stanford.edu

Introduction: Sprinting and endurance running are fundamental to many forms of sport. Athletes excelling in either of these typically exhibit a specialized skeletal geometry and muscular morphology. For example, elite sprinters differentiate themselves from sub-elite level sprinters mainly by an increased volume of the hip muscles [1] and a high leg length-to-height ratio has been associated with better distance running performance [2]. We used musculoskeletal simulation to analyze the effects of musculoskeletal geometry, muscle volume, and muscle volume distribution on sprinting and marathon running performance. We enabled these simulations with 3D muscle-driven models by extending an existing simulator such that the musculoskeletal dynamics were differentiable with respect to the skeletal geometry. With this new simulator we first performed predictive simulations of sprinting and marathon running where we optimized musculoskeletal geometry (i.e., the 3D dimensions of each segment). While scaling segment dimensions and their mass, we increase total muscle for all muscles proportionally to the overall increase in mass. Next, we mimicked a selective strength training intervention in simulation (i.e., optimal distribution when 5% of the total muscle volume is added).

Methods: We performed predictive simulations of a running gait using a muscle-driven (92 muscles) three-dimensional musculoskeletal model with 31 degrees-of-freedom. To simulate marathon running, we imposed a running speed of 3.33m/s and minimized energy expenditure. To simulate sprinting, running speed was maximized. We optimized muscle coordination and musculoskeletal geometry or optimal distribution of added muscle volume (5% of total muscle volume at baseline), for both sprinting and marathon running.
To enable efficient simulation, we developed the first musculoskeletal simulator that is differentiable with respect to both muscle properties and musculoskeletal geometrical properties. Two adaptations were important. First, we formulated muscle wrapping (insertion points, muscle lengths and moment arms) as a differentiable function of the musculoskeletal geometry. This was achieved by a neural network that outputs muscle wrapping variables as a function of the 3D dimensions of the body segments and the joint kinematics. Ground truth for training the neural net was sampled from OpenSim. Second, we formulated the skeletal dynamics to be differentiable with respect to the segment dimensions and densities. By having a fully differentiable simulator we can exploit automatic differentiation during optimization which has been shown to speed up gradient computation by up to x20 for simpler problems [3]. Avoiding finite differencing for the expensive computation of muscle wrapping is the key to enabling these simulations in a reasonable time (optimizations took between 30 minutes and 4 hours).

Results & Discussion: Overall, our findings regarding skeletal geometry and optimal strength training align well with experimental observations. From a skeletal geometrical perspective, taller and heavier (i.e. more muscle volume) individuals with a deep pelvis increasing the capacity of the hip muscles are likely to be better sprinters. From a muscular perspective, training focused on improving the hip musculature helping to increase step frequency at similar step lengths and improving ankle extensor strength which was required to meet the demands of sustaining impact at higher speed. Strength training was not beneficial for marathon performance. Our workflow would extend to informing strength training interventions for other athletic tasks including jumping tasks, cutting movements and accelerative locomotion
Optimizing skeletal geometry improved marathon performance and was characterized by lower height and mass, a high leg length-to-height ratio, and a deep pelvis, maintaining the capacity of the hip muscles.

Significance: Our new musculoskeletal simulator enables the use of simulation to answer new research questions regarding effects of anthropometry, muscles strength and muscles wrapping and insertion on human motion. While the present study focused on athletic performance, with the possibility to optimize for the skeleton geometry and muscle wrapping we open a new avenue to predict optimal surgery in silico.

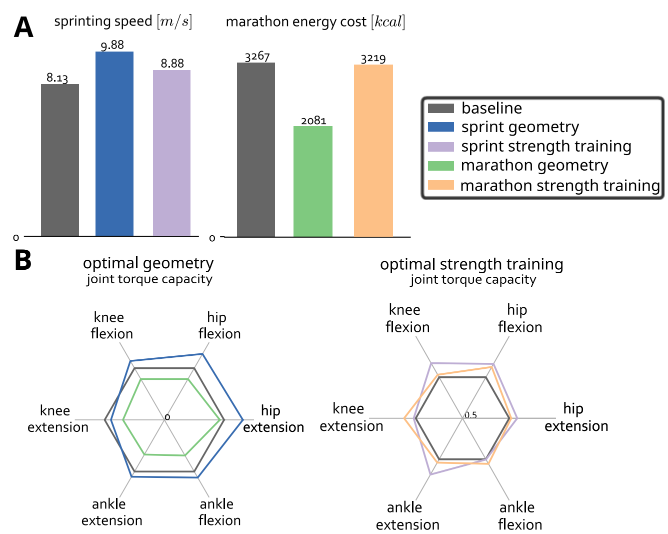

Figure 1 (A) Optimizing musculoskeletal geometry improves sprinting (22%) and marathon performance (36%). Specialized strength training, increasing total muscle volume by 5%, increases sprinting performance by 9% but does not affect marathon performance. (B) joint torque capacity adaptations for optimal skeletal geometries and optimal strength training

Acknowledgements: Supported by the Joe and Clara Wu Tsai Foundation through the Wu Tsai Human Performance Alliance.

References: [1] Miller R et al. (2019) *MSSE* **53**: 804-815; [2]Ueno H et al. (2019) *J Hum Kin* **70**: 165-172; Falisse A et al. (2019) PLoS One **14**(10), 2019

ENERGY REGULATION IN RESPONSE TO SUBSTRATE ENERGY LOSS

Brooke A. Christensen[1*], Monica A. Daley[1]
[1]Department of Ecology and Evolutionary, University of California, Irvine, Irvine CA, USA
*Corresponding author's email: brookec1@uci.edu

Introduction: Deformable substrates, such as sand, mud, and leaf litter, are common throughout nature and present a general challenge for terrestrial organisms. When an animal steps on a yielding surface, mechanical energy can be absorbed and dissipated by the substrate. Substrate energy dissipation creates an energetic imbalance. To maintain desired speed and direction of movement, deformable substrates demand rapid, situationally accurate management of limb and body mechanical energy.

Guinea fowl (*Numida meleagris*), a common bipedal model, employ a combination of 'passive' intrinsic mechanical and reflex mediated responses to maintain stability in response to unexpected terrain variation [1-3]. When perturbed during running, guinea fowl exhibit a posture-dependent stabilizing mechanism in which limb contact angle shifts to facilitate recovery though negative limb work [1]. If the rate of leg retraction is too slow, limb forces can quickly surpass musculoskeletal safety factors and result in injury [4-6]. Therefore, coordination of swing and stance dynamics is essential for maintaining stability, efficiency, and injury avoidance in complex terrain. Here, we develop a simple, physical model to mimic linear energy loss, enabling us to perturb mechanical energy in stance, without altering the preceding flight phase and initial contact dynamics. Through this approach, we aim to gain insight into the principles underlying stance phase mechanisms of force and energy regulation. We hypothesized guinea fowl would prioritize load regulation over gait steadiness when subject to within-stance energy loss perturbations.

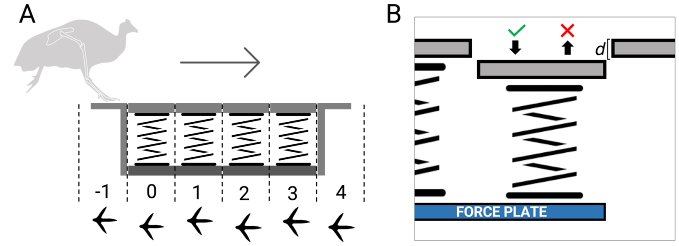

Figure 1: Schematic illustration of (A) trackway setup and (B) linear energy loss mechanism.

Methods: High-speed video and force plate data were collected as guinea fowl (n = 8) ran across a custom trackway (Fig. 1A) under three perturbation conditions: 1) late energy loss, 2) early energy loss, and 3) control. Conditions allow measurement of steps both preceding and following the perturbation. The middle section of the trackway consists of four custom built horizontal platforms, each capable of unidirectional motion in the vertical plane. Attached to each platform is a precision compression spring of known stiffness (k = 0.74 N/mm) which rests directly on a force plate (Kistler 926900AA6). At a predetermined limb penetration depth (d), the platforms lock into a compressed state to approximate linear energy loss (Fig. 1B), allowing the controlled removal of energy of a consistent magnitude. Video data were digitized using DeepLabCut [7]. All data were analyzed with a custom MATLAB script (2019b, MathWorks, Natick, MA, USA).

Results & Discussion: Our data support the hypothesis that guinea fowl prioritize load regulation over gait steadiness when navigating energy loss perturbations at a high speed. Peak vertical force and vertical loading rate remained consistent across pre-perturbed and perturbed strides (Fig. 2A), but decreased an average of 18% and 36%, respectively, during post-perturbed steps (Fig. 2B). Simultaneously, perturbed steps elicited a lower center of mass with deceleration in early stance. In the initial recovery step, center of mass was immediately raised despite continuing deceleration. However, the second recovery step reflected a shift toward acceleration with increased propulsive forces in late stance.

By preserving collisional dynamics at the instant of perturbation contact, results indicate force and energy regulation during stance are governed by a dynamic interplay of both passive and active mechanisms. In ongoing work, we are investigating how specific musculoskeletal mechanisms contribute to energy management and perturbation recovery, such as the intrinsic mechanics of viscoelastic tissues in the distal hindlimb.

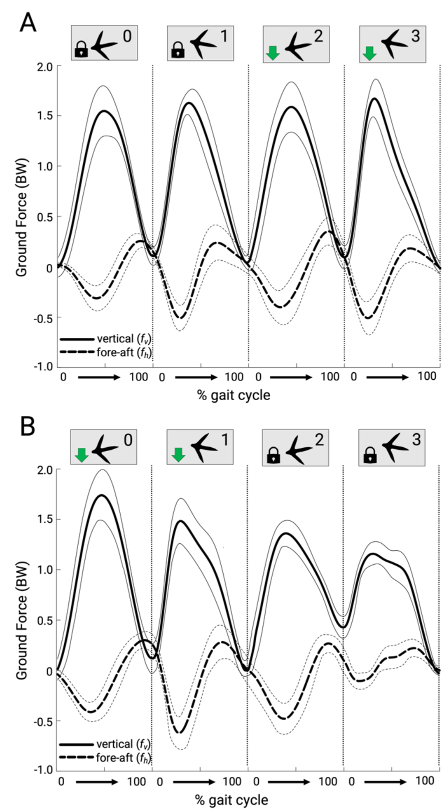

Figure 2: Mean ground reaction forces (± s.e.m.) for guinea fowl running across (A) late and (B) early energy loss perturbation conditions (n = 8).

Significance: Through integrating across energetics, body dynamics, and limb-ground interaction forces, we aim to promote technological innovation in the development of enhanced navigation capabilities for lower limb prostheses and legged robotic models.

Acknowledgements: This research was funded by NSF grant 2016049 (MAD). All experimental protocols were approved by the University of California, Irvine IACUC.

References: [1] Daley et al. (2006), *J Exp Biol*; [2] Daley et al. (2009), *J Physiol*; [3] Daley & Biewener (2011), *Philos Trans R Soc*; [4] Daley & Usherwood (2010), *Biol Letters*; [5] Blum et al. (2014), *PLoS One*; [6] Daley & Birn-Jeffery (2018), *J Exp Biol;* [7] Mathis et al. (2018), *Nat Neurosci*

THE IMPACT OF SEX AND VARYING HORIZONTAL APPROACH ON LIMB STIFFNESS AND LIMB STIFFNESS ASYMMETRY DURING LANDING

Michael A. Teater[1*], Daniel Schmitt[2], and Robin M. Queen[1]
[1]Department of Biomedical Engineering and Mechanics, Virginia Tech, Blacksburg, VA, USA
[2]Department of Anthropology, Duke University, Durham, NC, USA
*Corresponding author's email: michaelt20@vt.edu

Introduction: Female athletes are at increased risk for lower extremity injuries, especially ACL injuries [1]. Previous research has shown that female athletes use stiffer [2], more asymmetric [3] landing strategies. Experimental tasks used to assess landing mechanics are not uniform across the literature, and tasks that vary specifically based on horizontal approach prior to initial ground contact elicit differing posterior ground reaction force (GRF), knee flexion [4] and vertical GRF asymmetry [5]. It is possible that limb stiffness and between-limb stiffness asymmetry will differ based on sex and landing task during early impact when ACL injuries are believed to occur [6]. The purpose of this study was to compare leading limb stiffness, limb stiffness asymmetry, and related landing mechanics measures of male and female athletes across three tasks that varied by the horizontal approach prior to ground contact. Based on previous studies that determined sex- and task-specific differences during landing, it was hypothesized that there would be sex-by-task interactions for all outcome measures, with female athletes experiencing 1) greater leading limb stiffness and leading limb impact peak resultant GRF (rGRF) and lesser change in leading limb length as the tasks became more upright and less horizontally demanding, and 2) greater asymmetry in limb stiffness, peak impact rGRF, and change in limb length as the tasks incorporated a greater horizontal demand.

Methods: Twenty-eight healthy recreational athletes (14 male and 14 female) (Table 1) were recruited and signed IRB-approved informed consent prior to testing. Each participant completed seven trials of each bilateral landing including the drop vertical jump (DVJ), forward-drop vertical jump (F-DVJ), and stop-jump (SJ) in a randomized order. Three-dimensional motion capture (240Hz) (Qualisys, Goteborg, Sweden) and force plate data (1200Hz) (AMTI, Watertown, MA, USA) were collected for each participant during each trial. A modified Helen-Hayes marker set was used for data collection. Participants were provided form fitting athletic clothing and neutral shoes (Air Pegasus; Nike Inc., Beaverton, Oregon) to use during testing. Kinematic and kinetic energy-normalized kinetic measures were analyzed between initial ground contact and the peak impact resultant GRF (rGRF) during the first landing for each task. Asymmetry values indicating magnitude and direction of asymmetry were calculated as normalized symmetry index (NSI) values using previously reported methods [7], with the leg that initiated the tasks (leading limb) as the dominant limb in the formula and the leg used to push off the surface (trailing limb) as the non-dominant. A linear mixed effects model ($p<0.05$) was run in JMP Pro 16 (SAS Institute, Inc., Cary, NC, USA).

Demographic	Male	Female
Age (years)	20.8±2.29	22.1±2.14
Height (m)	1.77±0.070	1.68±0.070
Weight (kg)	72.8±5.50	68.4±11.1
BMI (kg/m²)	23.2±1.92	24.3±3.26

Table 1: Participant demographics (mean ± SD).

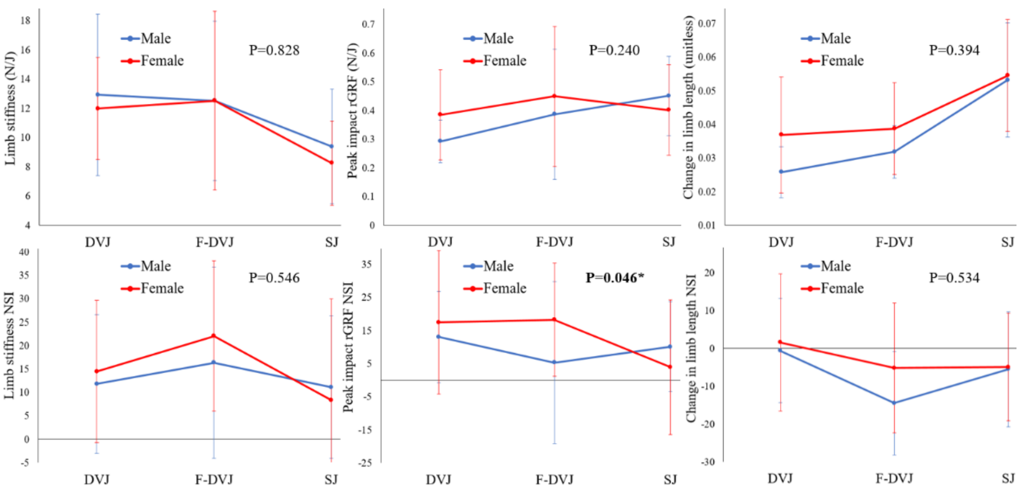

Figure 1: Interaction plots for each outcome measure. **Bold*** indicates a significant interaction ($p<0.05$).

Results & Discussion: A sex-by-task interaction existed for peak impact rGRF asymmetry; however, the largest sex-specific difference occurred during the F-DVJ, which did not support our reasoning for this hypothesized interaction. No other interactions existed between sex and task (Figure 1). While there appeared to be task-specific variation overall for each measure, sex-specific differences seemed to be consistent.

Significance: Limb stiffness and limb stiffness asymmetry have not been used to determine if sex differences in landing mechanics are exacerbated when experimental tasks better mimic the horizontally dynamic landings seen in sports. The only measure that produced a sex-by-task interaction was peak impact rGRF asymmetry. It appears that sex-specific landing mechanics differences reported in previous research may develop later in the landing phase of these tasks, as this study specifically examined the immediate landing phase that coincides with the proposed timing of ACL injuries [6], while previous work has examined the entire landing phase. Future sex-specific landing studies should explore tasks that vary by other sport-specific components, such as the inclusion of an overhead target mimicking a ball in mid-air or a fatigue protocol that includes game-like movements, to determine if sex-by-task interactions exist during early impact that can improve our understanding of the mechanism associated with sex-specific ACL injury risk.

References: [1] Powell & Barber-Foss (2000) *Am J Sports Med* 28(3); [2] Schmitz et al. (2007) *Clin Biomech* 22(6); [3] Gu et al. (2021) *Int J Environ Res Public Health* 18(11); [4] Peebles et al. (2020) *J Biomech* 105; [5] Britto et al. (2015) *Braz J Kinathrop Hum Perform* 17; [6] Koga et al. (2010) *Am J Sports Med* 38(11); [7] Queen et al. (2020) *J Biomech* 99

ENHANCING HUMAN NAVIGATION ABILITY USING AN ACTIVE WEARABLE EXOSKELETON

Carlos Carrasquillo[1*], Aakash Bajpai[1], Divya Iyengar, Killian Collins, Aaron Young[1], Anirban Mazumdar[1]
[1]Institute for Robotics and Intelligent Machines, Georgia Institute of Technology
*Corresponding author's email: ccarrasquillo3@gatech.edu

Introduction: The U.S. Department of Labor's 2020 data indicates that ~15% of reported deaths and ~17% of nonfatal occupational injuries occur due to "contact with objects and equipment" [1]. Worker situational awareness can be improved by providing intuitive and timely information about the environment via wearable devices. Previous studies utilize combinations of visual, auditory, and tactile stimuli to communicate threat information to wearers, but most require specialized hardware and have varying levels of effectiveness [2]. As active exoskeletons become increasingly viable for use in construction and warehouse settings, we propose a novel approach that leverages existing exoskeleton platforms to help individuals navigate around workplace hazards. Specifically, we developed an exoskeleton controller influenced by local fractional potential field information to generate a continuous torque profile intended to redirect a user to a safer path. To select the optimal field parameters, we tested several repulsive fractional orders for three different obstacle radius of influences. Due to the more immediate torque increase generated by higher fractional order fields, we hypothesized that larger fractional orders would cause larger path deviations than lower fractional orders given the same exoskeleton controller.

Methods: A master computer hosted a virtual reality scene and computed the repulsive field for a set fractional order, n, and radius of influence, r_{inf}. The artificial potential field (APF) magnitude and direction of the negative gradient at the subject's position were computed and relayed to the exoskeleton. Three independent mid-level hip exoskeleton controllers are summed to obtain an aggregate reference torque. The torques are scaled by the APFs to encourage movement away from high potentials and towards low potentials.

- Resist: A damping controller, intended to slow the wearer as they approach an obstacle.
- Assist: A simple impedance-based walking controller, intended to assist the user in moving away from the obstacle.
- Rotate: A differential controller, intended to rotate the user toward the direction of the negative gradient of the potential field. The magnitude of the rotate torque command depends on the normalized error between the user's heading and the safe heading.

Five able-bodied subjects were placed in an 8.5 m x 8.5 m level ground area and fitted with the exoskeleton. Subjects were tasked with walking from a start position to a goal position while navigating around a static obstacle. 9 combinations of potential field shape (n = 1,3,5) and radius of influence (r_{inf} = 1.5, 2.85, 4.2 m) were tested (6 trials per condition) (Fig. 1). To prevent oscillations about the ±180° heading error non-linearity, the rotate controller was biased left for half of the trials and right for the remaining half. A health metric [0, 100] was used as a measure of path safety, where the damage taken at each time step was proportional to the inverse of the squared distance from the subject to the obstacle. Trajectories were averaged by condition and across all participants.

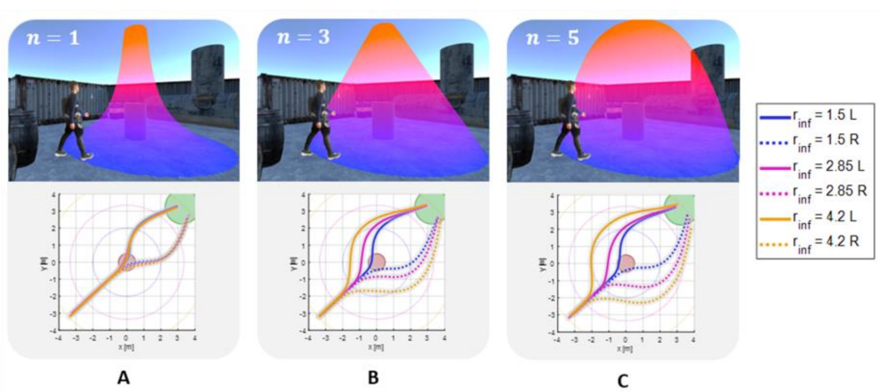

Figure 1: Potential field visualization and resulting averaged trajectories for repulsive field order (A) n = 1, (B) 3, (C) 5. Solid and dashed lines indicate left and right-biased trials, respectively.

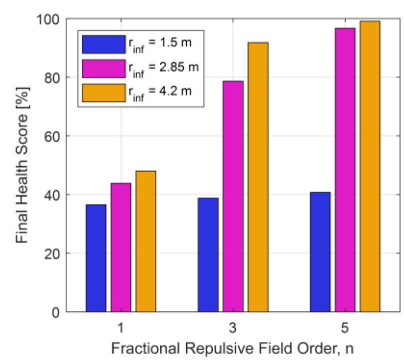

Figure 2: Average final health scores for repulsive field shape parameters n = 1, 3, 5.

Results & Discussion: Conditions with larger fractional orders resulted in consistently higher final health scores for the same r_{inf} (Fig. 2), with the biggest increase in performance occurring between n = 1 and n = 3. This likely occurs because larger potentials near the obstacle's effective radius generate perceptible torque magnitudes faster. Large sudden increases in torque magnitude also convey a heightened sense of urgency and allow the wearer more time to respond. Larger r_{inf} values also correlate with better trial performance but are overall less influential than varying fractional orders. However, large values of n and r_{inf} are not always beneficial; a value of n that is too large effectively acts more like a step response, which is (perhaps) unnecessarily abrupt and can cause instability to the wearer. Large values of r_{inf} can also cause the user to deviate unnecessarily from their path, resulting in excessively long path durations.

Significance: As exoskeletons become more prevalent in industrial settings, this work has the potential to decrease overall workplace injuries that result from collisions with objects and equipment. This technology may also help those with impaired visual and auditory senses by enhancing their ability to detect and evade incoming objects with more success than native human perceptual ability alone.

Acknowledgements: This research is supported by the NSF (NRI) 1830498 and an ARO-awarded NDSEG fellowship.

References: [1] Bureau of Labor Statistics, USDL-22-2139 (2022); [2] Bajpai et al., IEEE Trans. on Haptics (2020)

PARALLEL LEARNING AND RETENTION OF BALANCE CONTROL STRATEGIES WHILE WALKING THROUGH A NOVEL VISCOUS FORCE FIELD

Francis M. Grover[1*], Anna Shafer[2], Keith E. Gordon[1,2]

[1] Physical Therapy and Human Movement Sciences, Northwestern University Feinberg School of Medicine, Chicago, IL

[2] Edward Hines Jr. VA Hospital, Hines, IL

*Corresponding author's email: francis.grover@northwestern.edu

Introduction: Daily walking in complex environments involves anticipating and countering varying obstacles that threaten balance. Specific obstacles require specific strategies to counter them and often must be practiced while also encountering other obstacles that require different strategies. Learning and retention of multiple motor skills has been studied for a large variety of motor behaviors [1] under conditions of *massed practice* (repetitive practice under consistent conditions) versus *distributed practice* (intermittent practice involving frequent breaks or switches in practice conditions). Massed practice has typically been associated with faster learning rates but worse retention, while distributed practice has been associated with slower learning rates but better retention. We sought to test this hypothesis for balance control during walking as outcomes would have immediate and important implications for the design of physical therapy interventions to retain balance after injury. In the current study, healthy participants repetitively performed a discrete stepping task during which they experienced a novel balance-disrupting force field that could be delivered in two different directions. As each force field direction required a different control strategy to resist it, participants were implicitly tasked with learning two balance control strategies in the same experiment. We investigated parallel learning rates as participants practiced each force field direction according to a massed or distributed practice schedule.

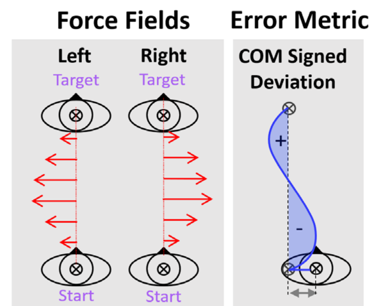

Figure 1: (Left) Depiction of the viscous force field delivered by the cable robot. Arrow lengths indicate forces scaled according to forward velocity. (Right) depiction of the COM error metric used to assess balance performance.

Methods: Eight healthy adults performed a series of discrete goal-directed stepping trials where they stepped quickly from a start location to an end location (located roughly three steps ahead) while experiencing balance-disrupting forces created by a cable-driven robot. The forces were delivered towards the participant's right or left side as a viscous force field that was proportional in magnitude to the participant's forward walking velocity (Figure 1). As the participant was required to step with the right foot for every trial, the force field disrupted balance asymmetrically depending on the direction, and therefore required qualitatively different movement strategies to resist. Participants were informed of the force field direction before every trial.

Participants performed 185 trials with different force field direction scheduling protocols. One group (n=4) received distributed practice of each direction where direction switched on every trial. A second group (n=4) received a more massed practice schedule, where force field direction switched every five trials. To assess adaptation to the force fields, we quantified error in balance performance as deviations in the participant's center-of-mass (COM) trajectory from COM trajectories during baseline walking (COM signed deviation) (Figure 1).

Results & Discussion: COM signed deviation indicated equivalent initial errors across learning conditions, for both force field directions. Participants in the massed practice condition exhibited steeper learning within clusters of trials with the same force field direction, reaching a performance ceiling quickly (performance tapering out after 2-3 trials within a cluster), but showed poor retention of that direction as indicated by high errors when switching directions. Participants in the distributed practice condition showed consistently higher errors and slower overall learning rates but exhibited more positive retention of each side as indicated by smaller increases in error after switching.

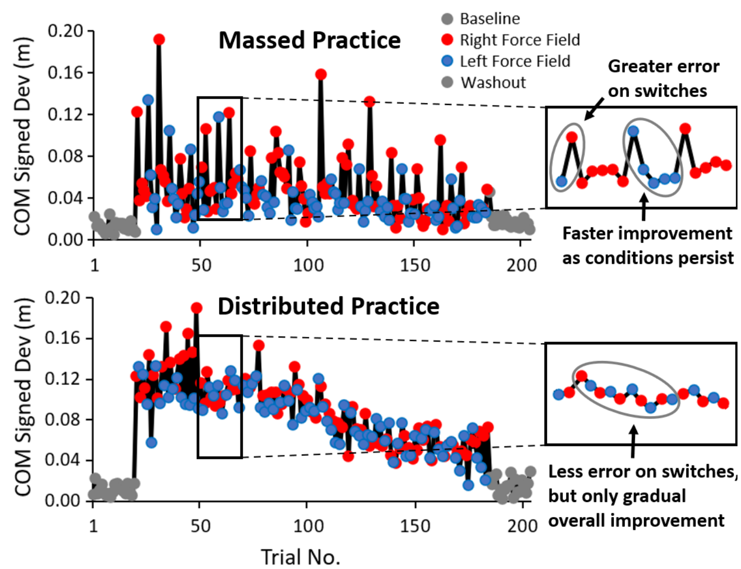

Figure 2: COM signed deviation (i.e., error) results. Participants in the massed practice condition showed steeper learning rates but worse retention during direction switches, while participants in the distributed practice condition showed more gradual learning but better retention of each direction. Each data point indicates the mean across participants (n=4).

Significance: These preliminary results suggest that the massed practice vs. distributed practice model of motor learning holds for control of walking balance in novel movement environments and indicates that this paradigm can be used to study aspects of motor learning that follow from that model. Moreover, it presents a paradigm to study other aspects of trial scheduling that could affect balance learning. For example, the influence of uncertain trial schedules (i.e., trial schedules where the participant does not know what condition they will receive each trial) has not been studied and warrants investigation to examine how balance learning unfolds in uncertain walking environments.

References: [1] Schmidt & Lee (2011), *Motor control and learning—A behavioral emphasis (2nd ed)*. 38(3)

Influence of knee morphology on the unipedal stance of flamingos

Charles Hammer, Skylar Taylor, Young-Hui Chang*
Comparative Neuromechanics Laboratory, Georgia Tech School of Biological Sciences, Atlanta, GA USA
*Email: yh.chang@ap.gatech.edu

Introduction: While many of the nearly 10,000 species of birds are known to exhibit a one-legged standing posture, flamingos and other long-legged birds are among the most well-known examples [1,2]. One peculiar aspect of unipedal stance is the potential for high energetic cost and fatigue. Flamingos have a crouched posture and the horizontally oriented femur means knee extensor muscles should be at a poor effective mechanical advantage for generating the knee torque required for body weight support [3]. The ability of flamingos to sleep on one leg is suggested to involve a passive mechanism to stabilize the joints for weight support [4]. Yet, the biomechanical mechanism within the knee joint to passively support flamingo unipedal stance is unknown. We hypothesized the flamingo knee to have distinct morphology that supports passive stabilization. Here, we aimed to characterize and demonstrate how the flamingo knee joint acts as a passive stay during unipedal stance.

Methods: We obtained five carcasses from two species: three were Chilean flamingos (*Phoenicopterus chilensis*) and two were Caribbean flamingos (*Phoenicopterus ruber*). All birds had previously died or been euthanized for reasons unrelated to this study and were received fresh frozen. All specimens were completely thawed prior to data collection. Preliminary data from three specimens are presented here. We used a custom high-speed biplanar x-ray radiography system to image and analyze the passive stay mechanism of the flamingo knee joint *in-situ*. Using x-ray motion analysis, we recorded flamingo knee joint kinematics as a function of frontal plane tibiotarsus angle as the specimen transitioned from a stable unipedal state (30° from vertical) to an unstable disengaged state (vertical tibiotarsus). We dissected the flamingo legs to characterize the morphology of the proximal (femur) and distal (tibiotarsus) bones that make up the knee joint.

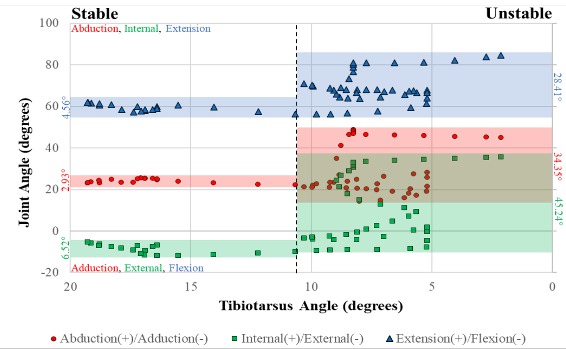

Figure 1: Knee joint angles (markers) and ROM (shading) as a function of tibiotarsus angle. The vertical dashed line indicates the transition between stable and unstable states.

Results & Discussion: Knee joint angles during *in-situ* destabilization revealed a period of rapid abduction and internal rotation along with a large knee extension (**Fig 1**). As tibiotarsus became more vertical, a large increase in knee range of motion occurred at 11°. The femur exhibited a notable mediolateral asymmetry. The lateral condyle had a greater mean anteroposterior depth (21.7±0.8mm) versus the medial condyle (14.5±0.8mm, 2-tailed t-test, N=6, p<<0.001). A corresponding asymmetric invagination existed on the proximal tibiotarsus. Manual manipulation revealed the lateral femoral condyle easily fit into the space formed by the fusion of tibia and fibula allowing free flexion-extension, but providing resistance when out of plane motion was introduced (i.e., knee adduction and external rotation).

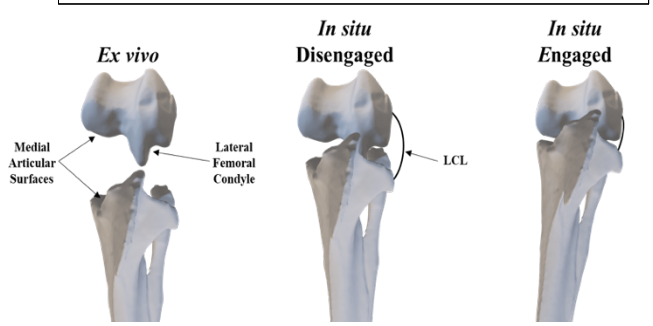

Figure 2: Frontal view of femur (upper) and tibiotarsus (lower) 3D models reveals asymmetric femoral condyles. Knee adduction and external rotation create impingement to resist knee motion.

As Chang & Ting [4] showed, manipulation of tibiotarsus toward a vertical orientation emulating bipedal stance leads to rapid disengagement of the knee mechanism and destabilization of the joint. When the tibiotarsus is adducted in the frontal plane to emulate a unipedal stance, however, the knee joint remains stable. We hypothesize the highly asymmetric morphology and coupling of the femur with the tibiotarsus provides a bony stay mechanism that binds and prevents further movement in the knee when an off-axis motion is introduced, as with adduction during unipedal stance. It is likely some connective tissues, such as the lateral collateral ligament, may also play an assistive role in this passive stay, but more study is needed to confirm this.

Significance: The asymmetry and size of the flamingo lateral femoral condyle suggests morphological adaptation for passive unipedal stance on a species scale. The presence of this same biomechanical mechanism on a class-wide scale would have important evolutionary implications as unipedal stance during sleep appears to be a ubiquitous behavior that is unique to birds.

Acknowledgements: We thank Zoo Atlanta and the Birmingham Zoo for providing cadaveric materials; Georgia Tech Invention Studio for use of 3D scanners, Nathan Kirkpatrick for XMA assistance and GT CNL colleagues for their support.

References:
[1] Clark, G. A. (1973), *Bird Banding*, *44*(1), 22–26; [2] Necker, R. (2010); [3] Biewener A. A. (1989), *Science* 245(4913), 45–48; [4] Chang, Y-H, Ting, L.H. (2017), *Biol. Lett.* 13: 20160948

ELASTIC EXOSKELETON INFLUENCE ON MUSCLE SPINDLE FIRING IN-VIVO

Amro A. Alshareef[1,4*], Paul Nardelli[2], Timothy Cope[2,3], Lena Ting[3,5], Gregory S. Sawicki[1,2,4]
[1] Woodruff School of Mechanical Engineering [2] School of Biological Sciences [3] Wallace H. Coulter Dept. of Biomedical Engineering
[4] Institute for Robotics and Intelligent Machines, Georgia Institute of Technology, Atlanta GA, USA
[5] Department of Rehabilitation Medicine, Emory University, Atlanta GA, USA
*Corresponding author's email: aalshareef6@gatech.edu

Introduction

With significant advancement in wearable technologies for assisting locomotion and augmenting balance, there is a growing need to understand how such devices affect sensorimotor control of movement. Exoskeletons act mechanically in parallel to a joint (e.g., elastic exoboots) and may alter sensory feedback during in gait. Most models for the firing of muscle spindles, the sensory organs in muscles that signal joint motion, rely on joint kinematics, with the sensory firing rates driven by Muscle Tendon Unit (MTU) length and velocity. Due to the connective tissues in parallel and series to the intra/extrafusal muscle fibers, however, whole MTU kinematics likely do not well represent the force or length changes experienced by spindles. Recent work suggests that the contractile force and yank acting on the intrafusal fibers may more accurately predict spindle instantaneous firing rate (IFR) during passive MTU stretches [1]. Whether a muscle spindle responds to kinematic versus kinetic signals is critical to predicting how exoskeletons in parallel with the MTU would alter sensory signals. Based on a simple modeling framework we developed [2], if spindle firing depends on fascicle kinematics, we should expect firing to increase because of added spring stiffness in parallel during eccentric contractions. If it is based on fascicle kinetics, however, then firing should decrease. As we cannot measure spindle firing in humans, we translated our model to an acute rat preparation, where we are able to directly measure spindle firing and fascicle kinematics and dynamics in-vivo.

Methods

We directly measured how muscle spindle IFR is influenced by added exoskeletal assistance during an eccentric contraction in an acute rat preparation. We measured IFR through the dorsal root while imparting a predetermined sinusoidal length change ($f = 2$ Hz, amp = 1.5 mm) using a motor attached to the gastrocnemius MTU. We attached 4 springs (0.066 – 0.33 N/mm) in parallel to the medial gastrocnemius MTU and vary activation through the ventral root during stretch. Starting with a high parallel stiffness, passive stretch condition, we gradually decreased the parallel stiffness while increasing muscle activation so that the peak MTU+spring system force is matched across spring stiffnesses ($\pm$ 2.5%). The result was a length clamped, force-matched eccentric contraction across various exoskeleton stiffness conditions, akin to a locomotion cycle.

Results and Discussion

Figure 1A shows a select two stiffnesses and their effects on the contractile muscle force and fascicle length change, with the yellow bars indicating location of muscle stimulation. The IFR more closely aligns the muscle force over the stretch period than fascicle length. Figure 1B shows that the fascicle length (measured with sonos imbedded in muscle tissue) decreases with reduced parallel stiffness while the muscle force (measured by subtracting the spring force from the total MTU+spring force) increases. Figure 1C overlays the in-vivo measured IFR over the kinematic-based and kinetic-based model predictions, indicating a clearer correlation of the measured with the kinetic-based, rather than kinematic, IFR prediction.

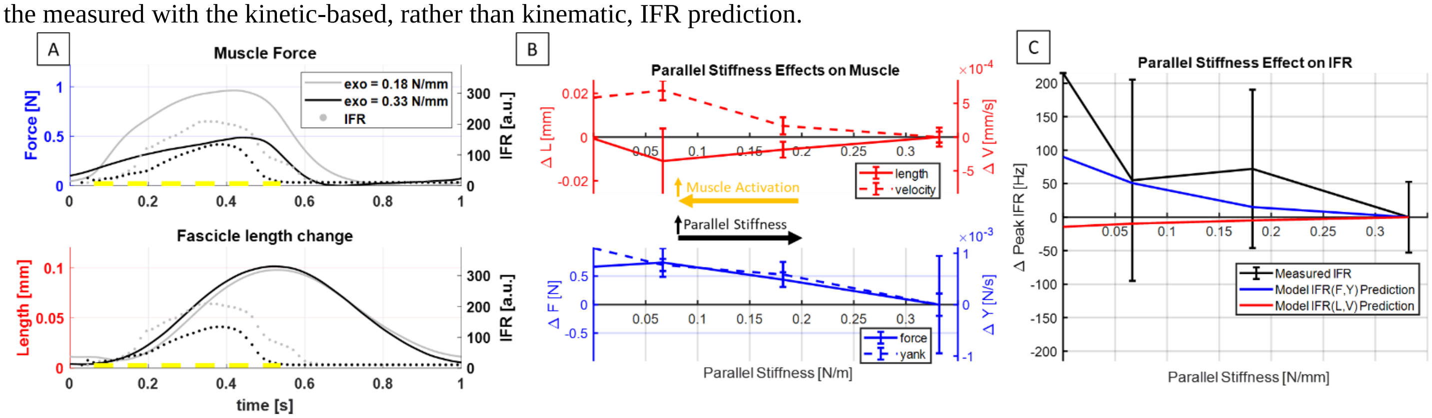

Figure 1: A) Muscle dynamics and IFR over 1 sinusoidal stretch across two exoskeleton conditions, B) Effects of varying exoskeleton stiffness across 4 conditions on kinematic (length and velocity change) and kinetic (force and yank change) factors experienced by the muscle fascicles, and C) Change in IFR measured versus model predictions. Results illustrated are from n=1 rat models.

Significance

As assistive devices become increasingly complex, an understanding of how they affect sensory feedback is critical if we are to develop exoskeletons more adept at addressing clinical challenges in motor learning and rehabilitation. Our approach allows for direct measurements of spindle response to known external loading, which can help reveal which muscle states contribute to spindle firing. Further collection in animal models, and eventually in humans, augmented with exoskeletal assistance, will help further illuminate the relationship between exoskeleton assistance, muscle mechanics, and resulting neural feedback [3].

Acknowledgments

This research was supported by funding from National Institutes of Health (NIH), Eunice Kennedy Shriver National Institute of Child health and Human Development (NICHD), R01HD090642.

References

[1] Blum et al. (2017) PloS Comput. Biol. [2] Alshareef et al. (2022) NACOB [3] Vincent et al. (2017) J Neurophysiol.

Thank you to our Sponsors

AMTI
FORCE AND MOTION

BERTEC

BETA
SIMULATION SOLUTIONS

KINATRAX

Motek
a DIH brand

novel

OptiTrack®

utmb Health

Center for Health Promotion,
Performance and
Rehabilitation Research

XSENSOR